

Yinping Zhang
Philip K. Hopke
Corinne Mandin
Editors

Handbook of Indoor Air Quality

Handbook of Indoor Air Quality

Yinping Zhang • Philip K. Hopke •
Corinne Mandin
Editors

Handbook of Indoor Air Quality

With 420 Figures and 219 Tables



Springer

Editors

Yiping Zhang
Department of Building Science
Tsinghua University
Beijing, China

Philip K. Hopke
Institute for a Sustainable Environment
Clarkson University
Potsdam, NY, USA

Corinne Mandin
Scientific and Technical Center for
Building (CSTB)
Marne-La-Vallée, France

ISBN 978-981-16-7679-6

ISBN 978-981-16-7680-2 (eBook)

<https://doi.org/10.1007/978-981-16-7680-2>

© Springer Nature Singapore Pte Ltd. 2022, corrected publication 2022

This work is subject to copyright. All rights are reserved by the Publisher, whether the whole or part of the material is concerned, specifically the rights of translation, reprinting, reuse of illustrations, recitation, broadcasting, reproduction on microfilms or in any other physical way, and transmission or information storage and retrieval, electronic adaptation, computer software, or by similar or dissimilar methodology now known or hereafter developed.

The use of general descriptive names, registered names, trademarks, service marks, etc. in this publication does not imply, even in the absence of a specific statement, that such names are exempt from the relevant protective laws and regulations and therefore free for general use.

The publisher, the authors, and the editors are safe to assume that the advice and information in this book are believed to be true and accurate at the date of publication. Neither the publisher nor the authors or the editors give a warranty, expressed or implied, with respect to the material contained herein or for any errors or omissions that may have been made. The publisher remains neutral with regard to jurisdictional claims in published maps and institutional affiliations.

This Springer imprint is published by the registered company Springer Nature Singapore Pte Ltd.
The registered company address is: 152 Beach Road, #21-01/04 Gateway East, Singapore 189721,
Singapore

Foreword

This book opens with editors Yiping Zhang, Philip Hopke, and Corinne Mandin explaining not only the purpose of this Handbook but also why it is so timely. In fact, indoor air quality (IAQ) has never been more important in terms of sustaining human health, well-being, and productivity. As we have seen so vividly with the COVID-19 outbreak, having buildings thoughtfully designed to appropriately protect their occupants and increase resilience is an essential public health requirement.

As the science of detection, simulation, analysis, and prediction has advanced, so has our understanding of the complex interactions among physical systems, human behavior, and the consequences of exposures. This Handbook will serve a new generation of investigators, designers, and practitioners as well as update those in the field since the first handbook was published in 2001.

So, how did the modern era of indoor air science begin? As the period of cheap energy ended, largely triggered by the oil embargo of 12 OPEC nations in October 1973, there were concerted efforts to conserve energy. Many decisions were made by individuals, professional organizations, and governments that compromised ventilation and degraded indoor air quality. To start to address these emerging issues, the US Department of Energy began to sponsor research on energy and IAQ at Lawrence Berkeley National Laboratory (LBNL). At LBNL, Greg Hollowell, David Grimsrud, John Girman, Tony Nero, and others were the first scientists and engineers in the USA to focus their efforts on indoor environments. Further afield, researchers in the UK, Europe, and the Nordic countries were engaged in research on radon, molds, thermal comfort, NO₂, odors, and optimizing ventilation.

At that time, I was on the faculty at Harvard working with Ben Ferris on the Six Cities Study. We were researching the long-term effects of ambient air pollution in adults and children across six US cities. We were characterizing ambient pollutants and tracking respiratory health. In our study, we saw a high prevalence of smoking among participants, many of whom lived in damp homes where gas-fired appliances were used. In industrialized Steubenville, Ohio (the city with the dirtiest outdoor air in our study), some 75% of the children lived in homes where one or more of their parents/caregivers smoked cigarettes. In the much cleaner city of Topeka, Kansas, over half the homes cooked with natural gas. These simple observations stimulated our curiosity to expand our research on the health effects of residential indoor pollution.

A seminal moment early in my academic career was co-chairing the National Research Council Committee on Indoor Pollutants with Michael Lebowitz. Our committee drew together what was known about the emerging field of indoor environments (National Research Council 1981). Collaborating with two committee members, Greg Hollowell and Demetrious Moschandreas, led to an *International Symposium on Indoor Air Pollution, Health and Energy Conservation* held on the campus of the University of Massachusetts Amherst (1981). Attracting over 500 participants from Europe, Asia, and North America, the Amherst symposium helped to establish indoor air science at the nexus of health, engineering, and design. What began as curiosity-driven research was now a research community open to ideas and to making a difference. Organizations led by Ole Fanger, Thomas Lindvall, Ib Andersen, Brigitte Berglund, and Tony Pickering encouraged many disciplines to convene around critical questions of IAQ. The interdisciplinary nature of IAQ science and practice persists and continues to draw in new disciplines, as reflected in the contributions to this new *Handbook of Indoor Air Quality*.

Twenty years on from these foundational gatherings, I collaborated with colleagues Jon Samet and John McCarthy to edit the first *IAQ Handbook*, published in 2001 by McGraw Hill (Spengler et al. 2001). By that time, many studies had been published on indoor contaminants in office buildings, homes, schools, and vehicles. The connection between the indoor environment and health was established with authoritative reports on passive exposures to tobacco smoke, radon, formaldehyde, asbestos, and molds (see the first chapter: History and Perspective on Indoor Air Quality Research). Universities and governmental agencies established research centers focused on ventilation, filtration, source mitigation, measurement and modeling, health, comfort, and productivity. Over time, indoor air science became more sophisticated as it incorporated the complex interactions among building systems and occupants. With the shift from a focus on air quality to total indoor environmental quality, the demand for professional consulting services grew as building managers, companies, and homeowners realized the potential impact of non-optimal indoor environmental quality.

In 2000, the US Green Building Council began what became an influential rating system for new buildings—the Leadership in Energy and Environmental Design, commonly known as LEED. This system has developed and now includes evidence-based credits on indoor environmental quality (IEQ) for occupants. Ventilation credits reference ASHRAE Standard 62.1 for non-residential buildings as a minimum prerequisite. Additional IEQ credits address contaminants emanating from cleaning practices, pest control, materials, and smoking, while others seek to improve the thermal, acoustic, and visual conditions. The World Green Building Council is now promoting more efficient and healthier buildings through 73 national green building organizations.

To scientists and engineers entering the field of IEQ today, I applaud your foresight in joining such a dynamic community. Indoor environments will continue to be important to the health, comfort, and productivity of people. There is much more to know and to do. Our COVID-19 pandemic experience may be the most widely publicized and broad-based event on our mind right now.

The pandemic has certainly advanced the importance of ventilation and filtration for keeping people well. Technologies such as *computational fluid dynamics*, advanced chemical analytical capability, human biomarkers, and genetic sequencing all have a part to play in unravelling IEQ and health. Devices built into our cell phones that track locations while measuring aspects of our physiological and cognitive performance, and emotional tone, or the use of virtual and augmented reality to indoor research is just beginning. Creating immersive experiences (visual, olfactory, auditory, and tactile) of indoor environments opens imaginative research avenues and new design opportunities.

Before the end of this century, the built environment is forecasted to double. Better buildings for our communities, both from an energy and materials standpoint can serve to sustain and improve the human condition and our natural world. To meet the challenges of rapid urbanization, depletion of natural resources, climate change, and the wide-scale threats posed by disparities, the United Nations Sustainable Development Goals (SDGs) present a path to a world that leaves no one behind. These goals call upon governments, the public and private sectors, and non-governmental organizations to work in partnership. To advance sustainable equitable with environmentally conscious development, our IEQ community needs to be included in these partnerships since many of the SDGs relate to the built environment (U.N. Sustainable Development Goals). The 2022 *Handbook of Indoor Air Quality* is a critical contribution to the journey ahead for humanity.

Akira Yamaguchi Professor of Environmental Health
and Human Habitation, Harvard T.H.
Chan School of Public Health
Boston, MA, USA

John (Jack) D. Spengler

References

- National Research Council (1981) Indoor pollutants. The National Academies Press, Washington, DC. <https://doi.org/10.17226/1711>
- Spengler JD, Samet JM, McCarthy JF (2001) Indoor air quality handbook. McGraw-Hill
- The Nexus of Green Buildings, Public Health, and the U.N. Sustainable Development Goals, Health Buildings for Health Program, Harvard T.H. Chan School of Public Health. <https://sdgs.forhealth.org/>

Preface

In 2001, McGraw-Hill published the *Indoor Air Quality Handbook* whose editors-in-chief were J.D. Spengler, J.M. Samet, and J.F. McCarthy. The handbook has contributed greatly to the development of indoor air quality research and has been a major contribution to providing the available knowledge regarding indoor air quality. Since then, new indoor air quality issues have been identified, and many achievements in the science and technologies of indoor air quality investigation and control have been accomplished, accompanied by the maturing of a new young generation of researchers. At the same time, the world has changed deeply: Internet, Wi-Fi, social media, Internet of Things, etc. are part of our lives and greatly influence research in every field. Climate change, increasing urbanization, energy-efficient buildings, low-carbon technologies, and social inequities also characterize what defines our world today. A handbook introducing the research advances in indoor air quality since 2001 was strongly needed as a new stepping stone to improved indoor environmental quality. Springer Nature invited us in 2016 to prepare such a handbook. We were very glad to accept this invitation, and we contacted three young researchers in the field of indoor air science to join the project as associate editors. A total of 136 authors from 19 countries have contributed to the handbook that you are now reading.

People live in indoor environments over 85% of their lifetime, and an adult inhales about 15 m^3 (17.5 kg) of air each day, which represents over 70% of the daily mass intake of the human body. Therefore, indoor air quality is very important to human health. The handbook presents our basic understanding of indoor air quality and the research achievements since 2001. It is divided into 12 sections: introduction to indoor air quality, indoor air chemicals, indoor air particles, measurement and evaluation, source/sink characteristics, indoor chemistry, human exposure to indoor pollutants, health effects and health risk assessment, indoor air quality and cognitive performance, standards and guidelines, indoor air quality control, and air quality in various indoor environments. It involves the fields of built environment, building energy, atmospheric environment, exposure science, public health, chemistry, fluid dynamics, etc., and highlights the diversity of disciplines engaged in indoor air science. Note that thermal comfort and biological contamination are not included because they represent fields of research too large to also be effectively addressed here. To have a handy reference on the current state of knowledge is

essential for researchers and practitioners working in indoor air and the related fields. It is also useful for the experts in other domains, policymakers, and general public to obtain basic knowledge on indoor air and be aware of recent advances, particularly in the context of the massive amount of information available online including unreliable reports.

This handbook was designed to be a dynamic resource. That is, in addition to the print version, the book is also published online and will be updated by the authors as needed to keep it aligned with updated knowledge. This salient feature can make the handbook current with research developments and various responses from the readers.

Last but not least, now that the handbook is ready for publication, we want to express our many thanks to all the contributors. To avoid duplication, those thanks are expressed in the “Acknowledgments” section.

Beijing, China
Potsdam, USA
Marne-La-Vallée, France
November 2022

Yinping Zhang
Philip K. Hopke
Corinne Mandin

Acknowledgments

The *Handbook of Indoor Air Quality* has been published with the assistance of many people. We would like to express our deep gratitude to those contributors who have provided their assistance over the past few years to make this Handbook possible. First, we are grateful to Dr. Yeung Siu (Stephen) Wai, editor of Major Reference Works, Springer Nature, who provided us the opportunity to launch the handbook. In making the production process effective, Haiqin Dong and Salmanul Faris Nedum Palli of Springer Nature have spent much time on monthly meetings and supporting services. Second, we are grateful to all the authors (over 130 from 19 countries) and all the reviewers (their names are in List of Reviewers on a separate page). Their knowledge, research experience, and achievement together with their great efforts guarantee the quality of the book. Third, we are grateful to Prof. C. Weschler, Rutgers University, USA, for the very helpful suggestions on the book framework, providing considerable detailed information and advice. We are also grateful to the following experts (arranged according to alphabet order of family names) for their helpful suggestions and information on Chap. 1.1, History and Perspective on Indoor Air Quality Research: W.P. Bahnfleth (USA), C. Chao (Hong Kong, China), Q.Y. Chen (USA), L. Fang (Denmark), X.B. Guo (China), F. Haghhighat (Canada), O. Hänninen (Finland), Y.G. Li (Hong Kong, China), J. Little (USA), L. Liu (China), L. Morawska (Australia), G. Morrison (USA), W.W. Nazaroff (USA), J.L. Niu (Hong Kong, China), A. Persily (USA), T. Salthammer (Germany), B. Singer (USA), S. Tanabe (Japan), K.W. Tham (Singapore), L. Wallace (USA), P. Wargocki (Denmark), P. Wolkoff (Denmark), X. Yang (China), J(ensen) Zhang (USA), and J(im) Zhang (USA). Last but not the least, we would like to express our heartfelt thanks to Prof. J. Spengler, Harvard University, USA, for writing the foreword of the current *Handbook of Indoor Air Quality*, both as a pioneer and leading scientist who has contributed greatly to indoor air science and as a Co-Editor-in-Chief of the *Handbook of Indoor Air Quality* 2001, 1st ed. New York: McGraw-Hill. Without their contributions, this handbook would not have attained its present status.

Editors-in-chief of Handbook of Indoor Air Quality

June 24, 2022

Contents

Volume 1

Part I Introduction to Indoor Air Quality	1
1 History and Perspective on Indoor Air Quality Research	3
Yinping Zhang, Philip K. Hopke, and Corinne Mandin	
Part II Indoor Air Chemicals	35
2 Very Volatile Organic Compounds (VVOCs)	37
Haimei Wang and Jianyin Xiong	
3 Volatile Organic Compounds (VOCs)	71
Xiong Jianyin and Shaodan Huang	
4 Semi-volatile Organic Compounds (SVOCs)	99
Jianping Cao	
5 Fragranced Consumer Products as Sources	129
Nigel Goodman and Neda Nematollahi	
6 Appliances for Cooking, Heating, and Other Energy Services	163
Tami C. Bond and Zachary Merrin	
7 Vaping and Secondhand Exposure	199
Liqiao Li and Yifang Zhu	
Part III Indoor Air Particles	231
8 Introduction to Particles in Indoor Air	233
Philip K. Hopke and Cong Liu	

9	Introduction to Aerosol Dynamics	247
	Andrew Maynard and Philip K. Hopke	
10	Impact of Outdoor Particles on Indoor Air	275
	Chen Chen and Bin Zhao	
11	Deposition	299
	Robert F. Holub and Michal Beneš	
12	Resuspension	331
	Andrea R. Ferro	
13	Interaction Between Gas-Phase Pollutants and Particles	349
	Jianping Cao	
14	Cooking Aerosol	387
	Mehdi Amouei Torkmahalleh	
Part IV Measurement and Evaluation		427
15	Sampling and Analysis of VVOCs and VOCs in Indoor Air	429
	Jinhan Mo and Yingjun Liu	
16	Sampling and Analysis of Semi-volatile Organic Compounds (SVOCs) in Indoor Environments	441
	Zidong Song, Jianping Cao, and Ying Xu	
17	Passive Samplers for Indoor Gaseous Pollutants	467
	Jianping Cao	
18	Real-Time Monitoring of Indoor Organic Compounds	493
	Yingjun Liu and Jinhan Mo	
19	Measuring Particle Concentrations and Composition in Indoor Air	517
	Lance Wallace and Philip K. Hopke	
20	Visualization and Measurement of Indoor Airflow by Color Sequence Enhanced Particle Streak Velocimetry	569
	Huan Wang and Xianting Li	
21	Measurements of Perceived Indoor Air Quality	609
	Pawel Wargocki and Krystyna Kostyrko	
Part V Source/Sink Characteristics		645
22	Source/Sink Characteristics of VVOCs and VOCs	647
	Tao Yang, Ningrui Liu, Xiaojun Zhou, John C. Little, and Yinping Zhang	

23	Source/Sink Characteristics of SVOCs	695
	Yili Wu, Jianping Cao, John C. Little, and Ying Xu	
24	Reference Materials for Building Product Emission Characterization	741
	Dustin Poppendieck, Wenjuan Wei, and Mengyan Gong	
25	Predicting VOC and SVOC Concentrations in Complex Indoor Environments	771
	Jianyin Xiong, Xinke Wang, and Yinping Zhang	

Volume 2

Part VI	Indoor Chemistry	809
26	Framing Indoor Chemistry Topics	811
	Michael S. Waring and Glenn C. Morrison	
27	Indoor Air Quality Through the Lens of Outdoor Atmospheric Chemistry	819
	Jonathan P. D. Abbatt and Douglas B. Collins	
28	Indoor Gas-Phase Chemistry	837
	Nicola Carslaw	
29	Indoor Photochemistry	855
	Tara F. Kahan, Cora J. Young, and Shan Zhou	
30	Indoor Surface Chemistry	885
	Glenn C. Morrison	
31	Occupant Emissions and Chemistry	903
	Gabriel Bekö, Paweł Wargocki, and Emer Duffy	
32	Analytical Tools in Indoor Chemistry	931
	Delphine K. Farmer, Matson Pothier, and James M. Mattila	
33	Indoor Chemistry Modeling of Gas-, Particle-, and Surface-Phase Processes	955
	Michael S. Waring and Manabu Shiraiwa	
Part VII	Human Exposure to Indoor Pollutants	983
34	Fundamentals of Exposure Science	985
	Andrea R. Ferro and Philip K. Hopke	
35	Exposure Routes and Types of Exposure	1003
	Elisabeth Feld-Cook and Clifford P. Weisel	
36	Role of Clothing in Exposure to Indoor Pollutants	1027
	Dusan Licina, Gabriel Bekö, and Jianping Cao	

37	Time-Activity Patterns	1057
	Xiaoli Duan, Beibei Wang, and Suzhen Cao	
38	A Modular Mechanistic Framework for Assessing Human Exposure to Indoor Chemicals	1113
	Clara M. A. Eichler and John C. Little	
	Part VIII Health Effects and Health Risk Assessment	1139
39	The Health Effects of Indoor Air Pollution	1141
	Jonathan Samet, Fernando Holguin, and Meghan Buran	
40	Epidemiology for Indoor Air Quality Problems	1189
	Shaodan Huang, Wenlou Zhang, Wanzhou Wang, and Furong Deng	
41	Animal Tests to Determine the Health Risks of Indoor Air Pollutants	1219
	Junfeng Zhang, Xu Yang, Xinyue Zheng, and Rui Li	
42	Application of Biomarkers in Assessing Health Risk of Indoor Air Pollutants	1251
	Jing Huang, Jiawei Wang, Teng Yang, and Junfeng Zhang	
43	The Full Chain Model: Linking Chemical Exposure from Indoor Sources to Human Health Effects	1301
	Anna-Sofia Preece, Huan Shu, and Carl-Gustaf Bornehag	
44	Disease Burden of Indoor Air Pollution	1325
	Otto Hänninen, Corinne Mandin, Wei Liu, Ningrui Liu, Zuoohui Zhao, and Yiping Zhang	
	Part IX Indoor Air Quality and Cognitive Performance	1369
45	Metrics and Methods (Performance Indicators, Methods, and Measurement)	1371
	David P. Wyon	
46	Postulated Pathways Between Environmental Exposures and Cognitive Performance	1397
	Kwok Wai Tham, Pawel Wargocki, and Shin-ichi Tanabe	
47	Effects from Exposures to Human Bioeffluents and Carbon Dioxide	1407
	Xiaojing Zhang, Asit Mishra, and Pawel Wargocki	
48	Effects of IAQ on Office Work Performance	1419
	Jose Ali Porras-Salazar, Stefano Schiavon, and Kwok Wai Tham	
49	Effects of Classroom Air Quality on Learning in Schools	1447
	Pawel Wargocki	

50 Sleep and Indoor Air Quality	1461
Li Lan and Zhiwei Lian	

51 Economic Consequences	1477
Jerzy Sowa, Shin-Ichi Tanabe, and Paweł Wargocki	

Volume 3

Part X Standards and Guidelines	1489
--	-------------

52 WHO Health Guidelines for Indoor Air Quality and National Recommendations/Standards	1491
Lidia Morawska and Wei Huang	

53 ASTM and ASHRAE Standards for the Assessment of Indoor Air Quality	1511
Xiaoyu Liu	

54 IEC/ISO Standards of Air Cleaners	1547
Dejun Ma and Shanshan Li	

55 IAQ Requirements in Green Building Labeling Systems and Healthy Building Labeling Systems	1565
Li Jingguang, Wei Jingya, and Ji Siyu	

Part XI Indoor Air Quality Control	1589
---	-------------

56 Testing and Reducing VOC Emissions from Building Materials and Furniture	1591
Jianshun Jensen Zhang, Wenhao Chen, Ningrui Liu, Bing Beverly Guo, and Yiping Zhang	

57 Influence of Ventilation on Indoor Air Quality	1637
Mengqiang Lv, Sumei Liu, Qing Cao, Tengfei Zhang, and Junjie Liu	

58 Evaluating Ventilation Performance	1675
Andrew Persily	

59 Control of Airborne Particles: Filtration	1715
Brent Stephens, Andrew Maynard, and Philip K. Hopke	

60 PCO and TCO in Air Cleaning	1737
Jinhan Mo and Enze Tian	

61 Managing IAQ at Multiple Scales: From Urban to Personal Microenvironments	1773
Jianshun Jensen Zhang, Jialei Shen, and Zhi Gao	

62 Simulations for Indoor Air Quality Control	
Planning	1815
Mengqiang Lv, Weihui Liang, Xudong Yang, and Jianshun Jensen Zhang	
Part XII Air Quality in Various Indoor Environments	1855
63 Indoor Air Quality in Day-Care Centers	1857
Shuo Zhang, Elizabeth Cooper, Samuel Stamp, Katherine Curran, and Dejan Mumovic	
64 Indoor Air Quality in Schools	1891
Chryssa Thoua, Elizabeth Cooper, Samuel Stamp, Anna Mavrogianni, and Dejan Mumovic	
65 Indoor Air Quality in Offices	1935
Andrea Cattaneo, Andrea Spinazzè, and Domenico M. Cavallo	
66 Indoor Air Quality in Elderly Care Centers	1961
Joana Madureira and João Paulo Teixeira	
67 Inhalation and Skin Exposure to Chemicals in Hospital Settings	1987
M. Abbas Virji, Lauren N. Bowers, and Ryan F. LeBouf	
68 Exposure to Air Pollutants in Ground Transport Microenvironments	2023
S. M. Almeida and V. Martins	
69 Indoor Air Quality in Commercial Air Transportation	2057
Florian Mayer, Richard Fox, David Space, Andreas Bezold, and Pawel Wargocki	
70 Indoor Air Quality in Industrial Buildings	2095
Yi Wang, Tengfei Zhang, Zhixiang Cao, and Zhichao Wang	
71 Household Air Pollution in Rural Area	2125
Zhihan Luo and Guofeng Shen	
72 Indoor Air Quality in the Context of Climate Change	2145
Patrick L. Kinney	
Correction to: Disease Burden of Indoor Air Pollution	C1
Otto Hänninen, Corinne Mandin, Wei Liu, Ningrui Liu, Zhuohui Zhao, and Yiping Zhang	
Index	2163

About the Editors



Yinping Zhang
Tsinghua University
Beijing, China

Yinping Zhang, Ph.D., is a professor in the Institute of Built Environment, Tsinghua University, Beijing, China. He is chairman of the Association of Indoor Environment and Health of China, director of the Beijing Key Laboratory of Indoor Air Quality (IAQ), head of the Building Environment Test Center, Tsinghua University, and president of the Academy of Fellows of the International Society of Indoor Air Quality and Climate (ISIAQ).

Zhang received his Bachelor (1985), Master (1988), and Ph.D. degrees (1991) from the University of Science and Technology of China (USTC). He has been a visiting scholar or professor in Stuttgart University, Germany (1994.5–95.5); Tokyo University, Japan (1996.10–12); and the Technical University of Denmark (DTU) (2004.10–12) and the Otto Mønsted visiting professor at DTU, Denmark (2007/2008, 3 months).

His principal research interests are indoor air quality and building energy efficiency. He has been the PI for over 40 research projects whose budgets were over 10 million \$US. He has published more than 10 books or book chapters, and more than 280 papers in international journals. His H index is 66 (Web of Science Core Collection). He is editor-in-chief or a key member of the editorial boards for over 20 Chinese IAQ-related standards. He has given over 20 plenary and keynote speeches in International Conferences including four International Conferences of Indoor Air (Copenhagen,

Denmark, 2008; Hong Kong, China, 2014; Ghent, Belgium, 2016; Seoul, Korea, 2020).

He serves as an associate editor of *Energy and Buildings* and *Carbon Neutrality* and is a member on the editorial boards of *Indoor Air*, *Environmental International*, *Sustainable Cities and Society*. He received the 1st Prize from the Natural Science Ministry of Education of China (2010), the 1st Prize from the Science and Technology Development Ministry of Beijing (2020), and the Inoue Uichi award (Japan, 2022).



Philip K. Hopke
Clarkson University
Potsdam, NY, USA

Dr. Philip K. Hopke is the Bayard D. Clarkson Distinguished Professor Emeritus at Clarkson University, former Director of the Center for Air Resources Engineering and Science (CARES), and former Director of the Institute for a Sustainable Environment (ISE). He is the head of the Aerosol Technologies Lab at Novosibirsk State Technical University and also holds an adjunct professorship in the Department of Public Health Sciences at the University of Rochester School of Medicine and Dentistry. Dr. Hopke is a past Chair of EPA's Clean Air Scientific Advisory Committee (CASAC) and has served on the EPA Science Advisory Board (SAB). Professor Hopke is a Past President of the American Association for Aerosol Research (AAAR) and was a member of more than a dozen National Research Council committees. He is a member of the NRC's Board of Environmental Studies and Toxicology. He is a fellow of the International Aerosol Research Assembly, the American Association for the Advancement of Science, and the American Association for Aerosol Research. He is an elected member of the International Statistics Institute and was the recipient of the Eastern Analytical Symposium Award in Chemometrics and the Chemometrics in Analytical Chemistry Conference Lifetime Achievement Award. He is also a recipient of the David Sinclair Award of the AAAR. He served as a Jefferson Science Fellow at the U.S. Department of State during the 2008–09 academic year.

Professor Hopke has extensive experience in indoor air quality issues including radon and radon decay product behavior, indoor atmospheric chemistry and secondary particle formation, in-room aerosol dynamics, and cooking and other sources of primary indoor particulate matter. He has been editor-in-chief of *Aerosol Science and Technology*, an editor of *Health Physics*, an editor of *Atmosphere, Air Quality, and Health*, and is currently an editor of *Aerosol and Air Quality Research* and *Chemometrics and Intelligent Systems*. He has written 1 book, edited 5, and published over 640 peer-reviewed journal papers.

Professor Hopke received his B.S. in Chemistry from Trinity College (Hartford) and his M.A. and Ph.D. degrees in Chemistry from Princeton University. After a postdoctoral appointment at M.I.T. and 4 years as an assistant professor at the State University College at Fredonia, NY, Dr. Hopke joined the University of Illinois at Urbana-Champaign, rising to the rank of professor of environmental chemistry, and he subsequently came to Clarkson in 1989 as the first Robert A. Plane Professor with a principal appointment in the Department of Chemistry. He moved his principal appointment to the Department of Chemical and Biomolecular Engineering in 2000. In 2002, he became the Clarkson Professor and Director of CARES. On July 1, 2010, he became Director of ISE that houses Clarkson's undergraduate and graduate environmental science degree programs as well as managing its sustainability initiatives. In May 2016, he moved to emeritus status.

**Corinne Mandin**

Scientific and Technical Center for Building (CSTB),
Marne-La-Vallée, France

Dr. Corinne Mandin earned her PhD in environmental chemistry from the University of Rennes, France. Previously she received an MSc in organic chemistry from the National School of Chemistry at the University of Montpellier and an MSc from Mines ParisTech in environmental engineering. She has been working on human exposure to chemicals in indoor environments, first at INERIS (French national institute for industrial environment and risks) for 8 years, and now at CSTB (French

scientific and technical center for building) that she joined in 2009.

She leads the French Indoor Air Quality Observatory, a research program created by the French government in 2001 to carry out nationwide surveys on indoor air quality in buildings. Her research interests include human exposure to volatile and semi-volatile organic compounds, particles, and fibers, especially in dwellings, schools, and office buildings.

She is a member of the “expert committee related to air” at the French Agency for Environmental Health and she previously chaired the “IAQ Guidelines Expert Committee” from 2009 to 2013. She collaborates with the World Health Organization and the European Joint Research Center. She was involved in several EU research projects (SINPHONIE, OFFICAIR, ALDREN). After having served as the Vice-President for Research (2016–2018), she currently serves as the President of the International Society for Indoor Air Quality and Climate (ISIAQ) (2020–2022).

Section Editors



Bin Zhao
Department of Building Science
School of Architecture
Tsinghua University
Beijing, China



Clara M. A. Eichler
Virginia Tech
Department of Civil and Environmental Engineering
Blacksburg, VA, USA

**Corinne Mandin**

Scientific and Technical Center for Building (CSTB)
Marne-La-Vallée, France

**Glenn Morrison**

Environmental Sciences and Engineering
Gillings School of Global Public Health
University of North Carolina
Chapel Hill, NC, USA

**Jianshun “Jensen” Zhang**

Building Energy and Environmental
Systems Laboratory, Department of Mechanical
and Aerospace Engineering
Syracuse University
Syracuse, NY, USA



Jianyin Xiong
Beijing Institute of Technology
School of Mechanical Engineering
Beijing, China



Jinhan Mo
Department of Building Science
Tsinghua University
Beijing, China



John C. Little
Department of Civil and Environmental Engineering
Virginia Tech
Blacksburg, VA, USA

**Kwok Wai Tham**

Department of the Built Environment
College of Design and Engineering
National University of Singapore
Singapore, Singapore

**Lidia Morawska**

International Laboratory for Air Quality and Health
Queensland University of Technology
Brisbane, Australia

**Michael S. Waring**

Department of Civil
Architectural and Environmental Engineering
Drexel University
Philadelphia, PA, USA

**Otto Hänninen**

Unit of Environmental Health
Department of Health Security
Finnish Institute for Health and Welfare
Kuopio, Finland

**Paweł Wargocki**

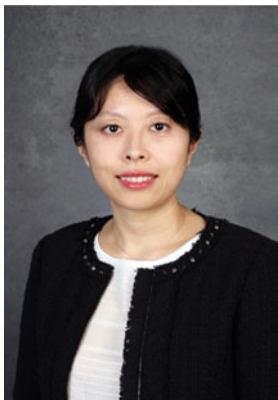
International Centre for Indoor
Environment and Energy
Department of Environmental and Resource
Engineering, DTU SUSTAIN
Technical University of Denmark
Kongens Lyngby, Denmark

**Philip K. Hopke**

Institute for a Sustainable Environment
Clarkson University
Potsdam, NY, USA



Wei Huang
School of Public Health
Department of Occupational and Environmental Health
Peking University
Beijing, China



Ying Xu
Department of Building Science
Tsinghua University
Beijing, China



Yiping Zhang
Department of Building Science
Tsinghua University
Beijing, China

About the Associate Editors



Cong Liu
School of Energy Engineering
Southeast University
Dhaka, Bangladesh

Dr. Cong Liu earned his Ph.D. in civil engineering from Tsinghua University, China. Before that, he received a Bachelor degree in thermal engineering from Southeast University, China. He was a visiting scholar in Missouri University of Science and Technology (2011–2012) and a postdoc in Georgia Institute of Technology (2014–2016). He is now an associate professor and vice dean in the Department of Refrigeration and Building Environment. His research covers transport and measurement of air pollutants, interaction of energy with environment and health, and heat and mass transfer. He is a member of the International Society of Indoor Air Quality and Climate.



Wenjuan Wei
Scientific and Technical Center for Building
Marne-la-Vallée, France

Dr. Wenjuan Wei is a research scientist in the Scientific and Technical Centre for Building (CSTB) since 2018. She received her B.S. in Energy and Power Engineering from Huazhong University of Science and Technology (HUST, 2005–2009) and her Ph.D. in Civil Engineering from Tsinghua University (2009–2014). She was a guest researcher at the National Institute of Science and Technology (NIST, 2011–2012) and a postdoctoral researcher at CSTB (2016–2018). During her

postdoctoral appointment, she was a Marie Skłodowska-Curie Fellow of the European Commission's Marie Skłodowska-Curie Actions and a PRESTIGE Fellow of Campus France. Dr. Wei is a specialist in indoor environmental quality (IEQ). Her research interests include emission and transport of (semi) volatile organic compounds (S)VOCs, indoor heat and pollutant exposures, and IEQ index. She has participated in several European and French research projects, such as ALDREN and PARC. She has published 37 peer-reviewed journal articles, and her h-index is 19. She got the Yaglou Award in 2022.

**Jianping Cao**

School of Environmental Science and Engineering
Sun Yat-sen University
Guangzhou, China

Dr. Jianping Cao got his Bachelor degree (2012) from the University of Science and Technology of China and his Ph.D. degree (2017) from Tsinghua University. After a 1-year postdoctoral experience at Virginia Tech., he jointed Sun Yat-sen University (Guangzhou, China) as an associate professor in 2018. He is now an associate professor in the School of Environmental Science and Engineering and the deputy director of the Department of Environmental Science in Sun Yat-sen University. His researches focus on the quantitative analysis, transport characteristics, exposure assessment, and mitigation of indoor air pollutants, especially focusing on semi-volatile organic compounds (SVOCs), one of the ubiquitous pollutants in indoor environments. He has published 32 research papers in international peer-reviewed journals since 2016. He currently serves as a Secretary in Youth Committee of Indoor Environment and Health Branch of the Chinese Society for Environmental Science, a Youth Editor of *Building Simulation: An International Journal*, and a Guest Editor of *Atmosphere* (Special Issue: Characterization and Mitigation of Indoor Air Pollution). For detailed information, please visit: <https://scholar.google.com.hk/citations?user=O-aUVmAAAAAJ&hl=en>, <https://www.researchgate.net/profile/Jianping-Cao>

List of Reviewers

Jianping Cao
Chun Chen
Hugo Destaillats
Clara M. A. Eichler
Lei Fang
Otto Hänninen
Philip K. Hopke
Wei Huang
Olivier Le Bihan
John C. Little
Corinne Mandin
Jinhan Mo
Lidia Morawska
Glenn C. Morrison
Kwok Wai Tham
Pawel Wargocki
Michael S. Waring
Charles Weschler
Jianyin Xiong
Ying Xu
Yiping Zhang
Jianshun “Jensen” Zhang
Bin Zhao

Contributors

Jonathan P. D. Abbatt Department of Chemistry, University of Toronto, Toronto, ON, Canada

S. M. Almeida Centro de Ciências e Tecnologias Nucleares, Instituto Superior Técnico, Bobadela, Portugal

Mehdi Amouei Torkmahalleh Division of Environmental and Occupational Health Sciences, School of Public Health, University of Illinois Chicago, Chicago, IL, USA

Gabriel Bekö International Centre for Indoor Environment and Energy, Department of Civil Engineering, Technical University of Denmark, Kongens Lyngby, Denmark

Michal Beneš Department of Mathematics, Faculty of Nuclear Sciences and Physical Engineering, Czech Technical University in Prague, Prague, Czechia

Andreas Bezold Environmental Control Systems, Airbus Operations GmbH, Hamburg, Germany

Tami C. Bond Department of Mechanical Engineering, Colorado State University, Fort Collins, CO, USA

Carl-Gustaf Bornehag Division of Public Health Sciences, Institution of Health Sciences, Karlstad University, Karlstad, Sweden

Icahn School of Medicine at Mount Sinai, New York, NY, USA

Lauren N. Bowers Respiratory Health Division, National Institute for Occupational Safety and Health, Morgantown, WV, USA

Meghan Buran Colorado School of Public Health, Aurora, CO, USA

Jianping Cao School of Environmental Science and Engineering, Sun Yat-sen University, Guangzhou, China

Qing Cao School of Civil Engineering, Dalian University of Technology, Dalian, China

Suzhen Cao University of Science and Technology, Beijing, China

Zhixiang Cao School of Building Services Science and Engineering, Xi'an University of Architecture and Technology, Xi'an City, China

State Key Laboratory of Green Building in Western China, Xi'an University of Architecture and Technology, Xi'an City, China

Nicola Carslaw Department of Environment and Geography, University of York, York, UK

Andrea Cattaneo Department of Science and High Technology, Università degli Studi dell'Insubria, Como, Italy

Domenico M. Cavallo Department of Science and High Technology, Università degli Studi dell'Insubria, Como, Italy

Chen Chen Department of Building Science, School of Architecture, Tsinghua University, Beijing, China

Wenhao Chen Environmental Health Laboratory Branch, California Department of Public Health, Richmond, CA, USA

Douglas B. Collins Department of Chemistry, Bucknell University, Lewisburg, PA, USA

Elizabeth Cooper Institute for Environmental Design and Engineering, University College London, London, UK

Katherine Curran Institute for Sustainable Heritage, University College London, London, UK

Furong Deng Department of Occupational & Environmental Health Sciences, Peking University School of Public Health, Beijing, China

Xiaoli Duan School of Energy and Environmental Engineering, University of Science and Technology Beijing, Beijing, China

Emer Duffy Insight SFI Research Centre for Data Analytics, School of Chemical Sciences, Dublin City University, Dublin, Ireland

Clara M. A. Eichler Department of Civil and Environmental Engineering, Virginia Tech, Blacksburg, VA, USA

Department of Environmental Sciences and Engineering, University of North Carolina at Chapel Hill, Chapel Hill, NC, USA

Delphine K. Farmer Department of Chemistry, Colorado State University, Fort Collins, CO, USA

Elisabeth Feld-Cook Chemical Terrorism, Biomonitoring Laboratory, Environmental and Chemical Laboratory Services, Public Health and Environmental Laboratories, New Jersey Department of Health, Trenton, NJ, USA

Andrea R. Ferro Department of Civil and Environmental Engineering, Clarkson University, Potsdam, NY, USA

Institute for a Sustainable Environment, Clarkson University, Potsdam, NY, USA

Richard Fox Aircraft Environment Solutions Inc., San Tan Valley, AZ, USA

Zhi Gao School of Architecture and Urban Planning, Nanjing University, Nanjing, China

Mengyan Gong National Institute of Standards and Technology (NIST), Engineering Lab, Gaithersburg, MD, USA

Nigel Goodman School of Property, Construction and Project Management, RMIT University, Melbourne, VIC, Australia

Bing Beverly Guo Building Energy and Environmental Systems Laboratory, Department of Mechanical and Aerospace Engineering, Syracuse University, Syracuse, NY, USA

Otto Hänninen Finnish Institute for Health and Welfare, Environmental Epidemiology, Environmental Health, Health Security, Kuopio, Finland

Fernando Holguin University of Colorado School of Medicine, Aurora, CO, USA

Robert F. Holub Center for Air and Aquatic Resources Engineering and Sciences, Clarkson University, Potsdam, NY, USA

Philip K. Hopke Institute for a Sustainable Environment, Clarkson University, Potsdam, NY, USA

Department of Public Health Sciences, University of Rochester School of Medicine and Dentistry, Rochester, NY, USA

Jing Huang Department of Occupational and Environmental Health Sciences, Peking University School of Public Health, Beijing, China

Shaodan Huang Department of Occupational & Environmental Health Sciences, Peking University School of Public Health, Beijing, China

Wei Huang Department of Occupational and Environmental Health, School of Public Health, and Institute of Environmental Medicine, Peking University, Beijing, China

Xiong Jianyin School of Mechanical Engineering, Beijing Institute of Technology, Beijing, China

Li Jingguang Shanghai Research Institute of Building Sciences (Group) Co. Ltd, Shanghai, China

Wei Jingya Tsinghua University, Beijing, China

Tara F. Kahan Department of Chemistry, University of Saskatchewan, Saskatoon, SK, Canada

Patrick L. Kinney Department of Environmental Health, Boston University School of Public Health, Boston, MA, USA

Krystyna Kostyrko Building Research Institute, Department of Thermal Physics, Acoustics and Environment, Warsaw, Poland

Li Lan Department of Architecture, School of Design, Shanghai Jiao Tong University, Shanghai, China

Ryan F. LeBouf Respiratory Health Division, National Institute for Occupational Safety and Health, Morgantown, WV, USA

Liqiao Li Department of Environmental Health Sciences, Jonathan and Karin Fielding School of Public Health, University of California, Los Angeles, CA, USA

Rui Li School of Life Sciences, Central China Normal University, Wuhan, China

Shanshan Li China Household Electric Appliance Research Institute (CHEARI), Beijing, China

Xianting Li Department of Building Science, Beijing Key Laboratory of Indoor Air Quality Evaluation and Control, Tsinghua University, Beijing, China

Zhiwei Lian Department of Architecture, School of Design, Shanghai Jiao Tong University, Shanghai, China

Weihui Liang School of Architecture and Urban Planning, Nanjing University, Nanjing, China

Dusan Licina Human-Oriented Built Environment Lab, School of Architecture, Civil and Environmental Engineering, École polytechnique fédérale de Lausanne, Fribourg, Switzerland

John C. Little Department of Civil and Environmental Engineering, Virginia Tech, Blacksburg, VA, USA

Cong Liu School of Energy and Environment, Southeast University, Nanjing, China

Junjie Liu Tianjin Key Laboratory of Indoor Air Environmental Quality Control, School of Environmental Science and Engineering, Tianjin University, Tianjin, China

Ningrui Liu Department of Building Science, School of Architecture, Tsinghua University, Beijing, China

Beijing Key Laboratory of Indoor Air Quality Evaluation and Control, Beijing, China

Sumei Liu Tianjin Key Laboratory of Indoor Air Environmental Quality Control, School of Environmental Science and Engineering, Tianjin University, Tianjin, China

Wei Liu Institute for Health and Environment, Chongqing University of Science and Technology, Chongqing, China

Xiaoyu Liu Office of Research and Development, Center for Environmental Measurement & Modeling, U.S. Environmental Protection Agency, Research Triangle Park, NC, USA

Yingjun Liu Department of Environmental Health, College of Environmental Sciences and Engineering, Peking University, Beijing, China

Zhihan Luo Laboratory of Earth Surface Processes, College of Urban and Environmental Sciences, Peking University, Beijing, China

Mengqiang Lv Tianjin Key Laboratory of Indoor Air Environmental Quality Control, School of Environmental Science and Engineering, Tianjin University, Tianjin, China

Dejun Ma China Household Electric Appliance Research Institute (CHEARI), Beijing, China

Joana Madureira Environmental Health Department, National Institute of Health, Porto, Portugal

EPIUnit, Institute of Public Health, University of Porto, Porto, Portugal

Laboratory for Integrative and Translational Research in Population Health (ITR), Porto, Portugal

Corinne Mandin Scientific and Technical Center for Building (CSTB), Marne-La-Vallée, France

V. Martins Centro de Ciências e Tecnologias Nucleares, Instituto Superior Técnico, Bobadela, Portugal

James M. Mattila Department of Chemistry, Colorado State University, Fort Collins, CO, USA

Anna Mavrogianni Institute for Environmental Design and Engineering, University College London, London, UK

Florian Mayer Department Environment, Hygiene, Sensor Technology, Fraunhofer Institute for Building Physics IBP, Valley, Germany

Andrew Maynard Arizona State University College of Global Futures, Arizona State University, Tempe, AZ, USA

Zachary Merrin Indoor Climate Research and Training, University of Illinois at Urbana-Champaign, Urbana, IL, USA

Asit Mishra SinBerBEST, Berkeley Education Alliance for Research in Singapore, Singapore, Singapore

Jinhan Mo Department of Building Science, School of Architecture, Tsinghua University, Beijing, China

Lidia Morawska International Laboratory for Air Quality and Health, Queensland University Technology, Brisbane, QLD, Australia

Global Centre for Clean Air Research, Department of Civil and Environmental Engineering, Faculty of Engineering and Physical Sciences, University of Surrey, Guildford, UK

Glenn C. Morrison Environmental Sciences and Engineering, University of North Carolina, Chapel Hill, NC, USA

Dejan Mumovic Institute for Environmental Design and Engineering, University College London, London, UK

Neda Nematollahi Department of Infrastructure Engineering, Melbourne School of Engineering, The University of Melbourne, Parkville, VIC, Australia

Andrew Persily National Institute of Standards and Technology, Gaithersburg, MD, USA

Dustin Poppendieck National Institute of Standards and Technology (NIST), Engineering Lab, Gaithersburg, MD, USA

Jose Ali Porras-Salazar Berkeley Education Alliance for Research in Singapore, Singapore, Singapore

Matson Pothier Department of Chemistry, Colorado State University, Fort Collins, CO, USA

Anna-Sofia Preece Division of Public Health Sciences, Institution of Health Sciences, Karlstad University, Karlstad, Sweden

Jonathan Samet Colorado School of Public Health, Aurora, CO, USA

Stefano Schiavon Center for the Built Environment, University of California, Berkeley, CA, USA

Guofeng Shen Laboratory of Earth Surface Processes, College of Urban and Environmental Sciences, Peking University, Beijing, China

Jialei Shen Building Energy and Environmental Systems Laboratory, Department of Mechanical and Aerospace Engineering, Syracuse University, Syracuse, NY, USA

Manabu Shiraiwa University of California—Irvine, Irvine, CA, USA

Huan Shu Division of Public Health Sciences, Institution of Health Sciences, Karlstad University, Karlstad, Sweden

Ji Siyu Shanghai Research Institute of Building Sciences (Group) Co. Ltd, Shanghai, China

Zidong Song Department of Building Science, Tsinghua University, Beijing, China

Jerzy Sowa Faculty of Building Services, Hydro, and Environmental Engineering, Warsaw University of Technology, Warsaw, Poland

David Space Environmental Control Systems, Retired, Boeing, Everett, WA, USA

Andrea Spinazzè Department of Science and High Technology, Università degli Studi dell'Insubria, Como, Italy

Samuel Stamp Institute for Environmental Design and Engineering, University College London, London, UK

Brent Stephens Department of Civil, Architectural, and Environmental Engineering, Illinois Institute of Technology, Chicago, IL, USA

Shin-ichi Tanabe Department of Architecture, Waseda University, Tokyo, Japan

João Paulo Teixeira Environmental Health Department, National Institute of Health, Porto, Portugal

EPIUnit, Institute of Public Health, University of Porto, Porto, Portugal

Laboratory for Integrative and Translational Research in Population Health (ITR), Porto, Portugal

Kwok Wai Tham Department of the Built Environment, College of Design and Engineering, National University of Singapore, Singapore, Singapore

Chryssa Thoua Institute for Environmental Design and Engineering, University College London, London, UK

Enze Tian Department of Building Science, School of Architecture, Tsinghua University, Beijing, China

M. Abbas Virji Respiratory Health Division, National Institute for Occupational Safety and Health, Morgantown, WV, USA

Lance Wallace United States Environmental Protection Agency (Retired), Santa Rosa, CA, USA

Beibei Wang University of Science and Technology, Beijing, China

Haimei Wang School of Mechanical Engineering, Beijing Institute of Technology, Beijing, China

Huan Wang Department of Building Science, Beijing Key Laboratory of Indoor Air Quality Evaluation and Control, Tsinghua University, Beijing, China

Jiawei Wang Department of Occupational and Environmental Health Sciences, Peking University School of Public Health, Beijing, China

Wanzhou Wang Department of Occupational & Environmental Health Sciences, Peking University School of Public Health, Beijing, China

Xinke Wang School of Human Settlements and Civil Engineering, Xi'an Jiaotong University, Xi'an, China

Yi Wang School of Building Services Science and Engineering, Xi'an University of Architecture and Technology, Xi'an City, China

State Key Laboratory of Green Building in Western China, Xi'an University of Architecture and Technology, Xi'an City, China

Zhichao Wang China Academy of Building Research, Beijing, China

Pawel Wargocki International Centre for Indoor Environment and Energy, Department of Civil Engineering, Technical University of Denmark, Kongens Lyngby, Denmark

Michael S. Waring Drexel University, Philadelphia, PA, USA

Wenjuan Wei Scientific and Technical Centre for Building (CSTB), Health and Comfort Department, French Indoor Air Quality Observatory (OQAI), University of Paris-Est, Champs-sur-Marne, France

Clifford P. Weisel Environmental and Occupational Health Sciences Institute, Rutgers, The State University of New Jersey, Piscataway, NJ, USA

Yili Wu Department of Building Science, Tsinghua University, Beijing, China

David P. Wyon International Centre for Indoor Environment & Energy (ICIEE), Department of Civil Engineering, Technical University of Denmark (DTU), Kongens Lyngby, Denmark

Jianyin Xiong School of Mechanical Engineering, Beijing Institute of Technology, Beijing, China

Ying Xu Department of Building Science, Tsinghua University, Beijing, China
Department of Civil, Architectural and Environmental Engineering, The University of Texas at Austin, Austin, TX, USA

Tao Yang Department of Building Science, Tsinghua University, Beijing, China
Beijing Key Laboratory of Indoor Air Quality Evaluation and Control, Beijing, China

Teng Yang Department of Occupational and Environmental Health Sciences, Peking University School of Public Health, Beijing, China

Xu Yang School of Life Sciences, Central China Normal University, Wuhan, China

Xudong Yang Department of Building Science, School of Architecture, Tsinghua University, Beijing, China

Cora J. Young Department of Chemistry, York University, Toronto, ON, Canada

Jianshun Jensen Zhang Building Energy and Environmental Systems Laboratory, Department of Mechanical and Aerospace Engineering, Syracuse University, Syracuse, NY, USA

School of Architecture and Urban Planning, Nanjing University, Nanjing, China

Junfeng Zhang Nicholas School of the Environment, Duke University, Durham, NC, USA

Global Health Research Center, Duke Kunshan University, Kunshan, Jiangsu Province, China

Duke Global Health Institute, Durham, NC, USA

Shuo Zhang Institute for Environmental Design and Engineering, University College London, London, UK

Tengfei Zhang Tianjin Key Laboratory of Indoor Air Environmental Quality Control, School of Environmental Science and Engineering, Tianjin University, Tianjin, China

School of Civil Engineering, Dalian University of Technology, Dalian, China

Wenlou Zhang Department of Occupational & Environmental Health Sciences, Peking University School of Public Health, Beijing, China

Xiaojing Zhang Beijing Key Laboratory of Green Built Environment and Energy Efficient Technology, College of Architecture and Civil Engineering, Beijing University of Technology, Beijing, China

Yinping Zhang Department of Building Science, School of Architecture, Tsinghua University, Beijing, China

Beijing Key Laboratory of Indoor Air Quality Evaluation and Control, Beijing, China

Bin Zhao Department of Building Science, School of Architecture, Tsinghua University, Beijing, China

Beijing Key Laboratory of Indoor Air Quality Evaluation and Control, Tsinghua University, Beijing, China

Zhuohui Zhao Department of Environmental Health, School of Public Health, Fudan University, Shanghai, China

Xinyue Zheng School of Life Sciences, Central China Normal University, Wuhan, China

Shan Zhou Department of Civil and Environmental Engineering, Rice University, Houston, TX, USA

Xiaojun Zhou School of Human Settlements and Civil Engineering, Xi'an Jiaotong University, Xi'an, China

Yifang Zhu Department of Environmental Health Sciences, Jonathan and Karin Fielding School of Public Health, University of California, Los Angeles, CA, USA

Part I

Introduction to Indoor Air Quality



History and Perspective on Indoor Air Quality Research

1

Yinping Zhang, Philip K. Hopke, and Corinne Mandin

Contents

Introduction	4
Early Stage Development Before 1970s	5
Modern Developments Since the 1970s	6
Indoor Air Conferences	7
The Academy of ISIAQ Fellows	8
International Society of Indoor Air Quality and Climate (ISIAQ)	9
Indoor Air journal, the Official Journal of ISIAQ	9
Representative Events or Works on Indoor Air Quality Field in the Modern Stage Since the 1970s	10
Quantitative Analysis of the General Information in Web of Science	10
The Number of Indoor Air Quality–Related Papers has Increased Rapidly Since 1990	10
Number of Papers Related to Specific Indoor Air Pollutants Since 1990	10
International Journals That Have Published the Most Indoor Air–Related Papers	19
Institutions That Published the Most Indoor Air–Related Papers	19
Averaged Citations Per Paper of the Ten Institutions Publishing the Most Indoor Air Quality Papers	19
On the Research Advances Since 2001	22
Perspectives on Indoor Air Quality Research Related to Chemicals	23

Y. Zhang (✉)

Department of Building Science, School of Architecture, Tsinghua University, Beijing, China

Beijing Key Laboratory of Indoor Air Quality Evaluation and Control, Beijing, China

e-mail: zhangyp@mail.tsinghua.edu.cn

P. K. Hopke

Institute for a Sustainable Environment, Clarkson University, Potsdam, NY, USA

Department of Public Health Sciences, University of Rochester School of Medicine and Dentistry, Rochester, NY, USA

e-mail: phopke@clarkson.edu

C. Mandin

Scientific and Technical Center for Building (CSTB), Marne-La-Vallée, France

e-mail: corinne.mandin@gmail.com

Conclusions	26
Appendix	27
References	28

Abstract

Modern indoor air science started in the 1970s. The reasons for separating the modern and old eras are: (1) building energy conservation became important due to the oil embargo in the Middle East in 1973 that had a great impact on building design and operation and in turn indoor air quality; (2) ambient air pollution became a topic of concern in many developed countries; (3) “modern diseases” were found to be associated with “modern exposure” during this period; (4) many new computational and measurement technologies such as computational fluid dynamics (CFD) and gas chromatography-mass spectrometry (GC-MS), respectively, occurred with the development of computer and the related technologies; and (5) a series of international societies and conferences related to indoor air science with worldwide impact were launched and recognized beginning in the 1970s. Modern indoor air science has been driven by two forces. One driver is the demands to fix important indoor air problems arising from a broad variety of pollutants: radon, asbestos, environmental tobacco smoke, particles (PM_{10} , $PM_{2.5}$, ultrafine particles), formaldehyde, volatile organic compounds, semi-volatile organic compounds, house dust mites, mold, bacteria, and associated health effects, e.g., sick building syndrome symptoms, asthma and allergies, Legionnaires’ disease, lung cancer, and airborne infections such as SARS and nowadays COVID-2019. The second driver is the new technologies such as CFD, big data analysis, advanced chemical analytical capability, sensing, control, and human biomarker analysis, which have contributed greatly to modern indoor air science. By understanding the influences of these two drivers on the development of indoor air science over the past decades, we can also perceive its future. In this first chapter, we summarize the history of indoor air science and outline some major challenges for the coming years.

Keywords

Indoor air quality · Health · VOCs · SVOCs · Particulate matter · History

Introduction

Although indoor air pollution has been a problem since people moved into caves and started fires for heat and cooking, it is only relatively recently that there has been extensive scientific study of indoor air quality (IAQ), its origins and potential mediation methods. The purpose of this chapter is to describe the development of the field of IAQ research and summarize our current state of efforts to address IAQ issues and improve human health.

Early Stage Development Before 1970s

Air, water, and food are necessary bodily intakes for human life. Their average intake (mass) for an adult per day for air, water and food are about 15 kg (ca. 13 kg inhaled indoors), 2 kg, and 2.3 kg for an 80 kg person, respectively (USEPA 2011). According to time-activity pattern investigations in 12 European countries, the USA, and China, people spend about 90% of their time indoors, including the enclosed environment of transportation, during their whole life (Szalai 1972; Klepeis et al. 2001; Duan et al. 2013). Therefore, indoor air quality (IAQ) can greatly influence human comfort, health, productivity, creativity, and well-being.

The history of our understanding on breathing is relatively short with respect to human history (Fitting 2015). Priestley (1733–1804), von Scheele (1742–1786), and Lavoisier (1743–1794) revealed the mystery of breathing. Priestley and van Scheele independently discovered oxygen (https://en.wikipedia.org/wiki/Carl_Wilhelm_Scheele). von Scheele and Lavoisier found air to be a mixture of gases. Lavoisier pointed out the role of oxygen in breathing, including the quantitative association between oxygen consumption and carbon dioxide (CO₂) release. As a result, the concentration of CO₂ was regarded as a measure of the freshness of air. Pettenkofer (1818–1901) noted that the unpleasant sensations of stale air were not due merely to warmth or humidity or to CO₂ or oxygen deficiency, but to the organic species emitted from the skin and exhaled from the lungs. He viewed CO₂ as not important itself, but an indicator of the concentration of other noxious or unpleasant substances emitted from people. In 1858, he published a book on ventilation in dwellings and stated that in order to keep people comfortable, the concentration of CO₂ should not be higher than 1000 ppm (the limit value was later referred to as the Pettenkofer number) (Sundell 1994, 2017). Billings (1889) published a book on the principles of ventilation and heating comfort. At that time, the study of ventilation mainly addressed comfort and not health. Odors, mainly body odors, and thermal comfort were regarded as the factors in setting guidelines for ventilation. A milestone study from this time was from Yaglou et al. (1936) about the perception of odor by building occupants, and the ventilation rate needed to make the air acceptable. Their research results have been used in numerous standards for ventilation (Sundell 1994; Janssen 1999; Persily 2015).

In Sweden in the 1950s and 1960s, “Light concrete” using alum shale with high radium content was a very common building material. Rolf Sievert investigated the risks of radium radiation exposure in the homes in Sweden from 1950. It was found that the ventilation rate influences indoor concentration of radon (Sundell 1994, 2017).

In 1952, the severe ambient air pollution in London, called the Great London Smog later, killed thousands of people in a few weeks (Bell et al. 2004). In 1962, the book “Silent Spring” about synthetic pesticides like DDT (dichlorodiphenyltrichloroethane) brought further attention to outdoor environments (Carson 1962). In addition,

pollutants emitted by many industries to ambient environments and pollutants in workplaces were also becoming of increasing interest. Therefore, in the 1960s and 1970s in many developed countries like the USA, organizations such as the US Environmental Protection Agency (EPA) and US Occupational Safety and Health Administration (OSHA) were established. Indoor environments were starting to be regarded as potentially protective against bad ambient air.

Subsequent attention turned to pollutants of indoor origin, including formaldehyde, radon, asbestos, tobacco smoke, and many volatile organic compounds. Wittmann (1962) published the first paper on the release of formaldehyde from particleboard. An early box model on passive (nonreactive) pollutants was developed (Turk 1963). Biersteker et al. (1965) simultaneously collected 800 paired indoor and outdoor air samples from 60 homes. They found that the I/O ratios of “smoke” and SO₂ were about 80% and 20%, respectively. Newer homes had lower SO₂ concentrations due to lower outdoor air change rates. The early focus on indoor particulate matter (PM) was generally on environmental tobacco smoke (ETS) and its related pollutants (Repace and Lowry 1980). Repace and Lowry defined a range of exposures to ETS and suggested that ventilation would not be the best solution given diminishing returns and the associated energy costs. Instead, they suggested smoking was incompatible with indoor spaces. The issues related to particulate matter in indoor air expanded with the increased interest in ETS (Repace and Lowry 1980), the role of particles in exposure and dose to radon decay products (Hopke et al. 1995), and the identification of indoor cooking (especially using solid fuel) as a major source of particles (Smith 1987).

Researchers from the Netherlands (Voorhorst et al. 1963, 1967; Pepys et al. 1968) found that house dust-mites were a major cause of allergies, which changed the research interest from “dust” to allergens in dust, and to pollen, pets, and most importantly house dust-mites.

In 1970, the Swedish Building Research Institute and the Swedish Radiation Protection Institute carried out a study of hundreds of homes in Gavle. They found that concentrations of radon were inversely correlated with the ventilation rate and possibly with the incidence of lung cancer. A key finding was that the lower the rate of ventilation, the higher risk of lung cancer (Sundell 2017).

With the development of additional analytical instruments and techniques, the number and types of compounds measured indoors increased. This provided the basis for indoor air quality research for “modern stage development.”

Modern Developments Since the 1970s

It can be considered that the modern indoor air science started in the 1970s, as suggested by Sundell (2017). According to our understanding, the main reasons for his statement are as follows: (1) building energy conservation became important due to the oil embargo in the Middle East in 1973, which had a great impact on building design and operation in turn indoor air quality; (2) ambient air pollution

became a topic of concern in many developed countries; (3) some diseases, later called “modern diseases,” were found to be associated with the exposure to newly man-made chemicals (Sundell 2017), later called “modern exposure”; (4) many new computational and measurement technologies such as computational fluid dynamics (CFD), gas chromatography-flame ionization detection (GC-FID), and gas chromatography-mass spectrometry (GC-MS), respectively, occurred with the development of desktop computers and the related technologies; and (5) a series of international societies and conferences related to indoor air science with worldwide impact were launched and recognized beginning in the 1970s (Appendix, Table A1).

Indoor Air Conferences

The first International Conference on Indoor Air was held at Copenhagen in 1978. About two hundred people took part in it. Quoting from the proceedings, “The purpose was to study the effect of the indoor air climate on man’s comfort, performance and health.” This conference was the inaugural event in what was to become the Indoor Air conference series (Nazaroff 2012). The first paper presented at this conference was by the Harvard group (Ferris, Speizer, Spengler, et al.) on the “six cities study.” As Sundell (2017) stated, “We recognized from the start that data from central station monitoring might not provide adequate detail of exposure, how is the exposure modified by indoor levels and what are the implications on health.” The “six cities study” had a great impact on subsequent indoor air quality studies. Starting in 1978 in Copenhagen, the Indoor Air conference series were held triennially through 2014, and biannually since then (Appendix, Table A1). A Healthy Buildings conference series was launched by the International Society of Indoor Air Quality and Climate (ISIAQ, see below) in 1988 to focus on the application of indoor air science in practice.

Sundell (2017) introduced the major research topics and the number of presentations for each of these major topics of every Indoor Air conference through 1978–2014. It’s interesting to follow the changes in research interests. It should be noted that much information cannot be found by searching the Web of Science because the conference proceedings for this early period are not readily available.

The Indoor Air conferences impacted IAQ studies and control strategies greatly. The second Indoor Air conference in Amherst, Massachusetts (USA) in 1981 was the first large indoor air conference open to all and had over 500 attendees. The third Indoor Air conference in Stockholm, Sweden, in 1984 had over 700 attendees from more than 40 nations and five volumes of conference proceedings.

Japan launched a sanitation law for buildings over 3,000 m² in the 1970s. Mandatory measurements of CO₂, carbon monoxide (CO), temperature, humidity, etc., every 2 months were required. However, for those new houses that had been insulated and air tightened to improve energy efficiency without mechanical ventilation systems, indoor concentrations of formaldehyde and some typical VOCs were very high and caused “Sick House Syndrome.” Indoor Air 1996 in Nagoya had

impact on changing the situation: the building code was changed in 2002. The tenth international conference was held in Beijing, China, in 2005. With over 1000 participants, Indoor Air 2005 was the first conference series held in a developing country, which greatly stimulated the development of indoor air-related research in China as can be seen in Fig. 3. A highlight of Indoor Air 2014 was the publication of a special topic issue of Indoor Air journal (2016, issue one) consisting of ten review papers written by the keynote speakers. Some of them have been highly cited. Due to COVID-2019, the Indoor Air 2020 (Seoul, Korea) conference was held online for the first time in the history of the Indoor Air Conference Series. The informal feedback has been very positive as the presentations remained available online for 6 months, which might be more impactful than usual conferences.

During this period, there were also many important conferences on indoor air quality, which were quite impactful: International Conference on Indoor Air Quality, Ventilation and Energy Conservation (IAQVEC) series (launched in 1992 in Montreal, Canada, initiated and organized by Profs. Francis Allard and Fariborz Haghishat), ROOMVENT series (launched in 1987 in Stockholm), International Symposium of Heating, Ventilating and Air-Conditioning (ISHVAC) series (launched in 1991 in Beijing by Tsinghua University), International Workshop on Energy and Environment of Residential Buildings (EERB) series, International Conference of Built Environment and Public Health (BEPH) series, American Society of Heating, Refrigerating and Air-Conditioning Engineers (ASHRAE) IAQ conference series, symposia/workshops of American Society for Testing and Materials (ASTM) as well as the US EPA. In addition, joint conferences with other scientific societies were organized such as the ISSEE-ISES-ISIAQ joint conference held in Basel, Switzerland, 2013 and the ISES-ISIAQ joint conference held in Kaunas, Lithuania, 2019. The multidisciplinary academic exchange at these two joint conferences was very impressive.

The Academy of ISIAQ Fellows

The experience of the 1980s encouraged community leaders to create formal structures to replace informal processes. In 1991, leaders of the first five Indoor Air conferences (Appendix, Tables A1 and A2) founded the International Academy of Indoor Air Sciences (IAIAS). Its purpose was to “promote international scientific cooperation in the field of indoor air science.” IAIAS invited new members who by invention, research, or other activities had contributed significantly to indoor air science. In the late 1990s, the IAIAS established two major awards to recognize outstanding achievements in indoor air science: the Yaglou award honors Professor C.P. Yaglou’s pioneering work on thermal comfort, indoor air quality, and requirements for acceptable ventilation; the Pettenkofer award honors Professor M. Pettenkofer who is regarded as the founder of modern hygiene science and whose accomplishments included pioneering work on carbon dioxide and indoor air quality (Nazaroff 2012). In 2005, the IAIAS merged with ISIAQ (see below) and became the Academy of Fellows of ISIAQ (the Academy). Table A2 lists the

executive committee of the Academy of Fellows of ISIAQ (1991–2022). Currently, the Academy retains primary responsibilities to nominate and elect new Fellows and to promote and select awardees. Becoming a member of the Academy is a recognition of research, practice, and/or outstanding service in the field of indoor air science.

The academic awards were extended later and now include: Lifetime Achievement Award – bestowed as appropriate on occasion to scholars who have made seminal contributions to indoor air science through their career's work; Pettenkofer Gold Medal – awarded to an individual in recognition of outstanding work in advancing the indoor air science; Yaglou Award – acknowledge outstanding work of young promising researchers within the indoor air science and to encourage them to continue their career in this field; Best Paper Awards – granted to the top papers published in Indoor Air journal during the previous 3 years, as judged by the editors and editorial board; and Student Awards – established in 2008 and granted in two categories: Student Achievement Awards are given to students based on their commitment and dedication to the field for any combination of academic, professional, and research achievements; Student Paper Awards are given to students who have published an outstanding paper in the field of indoor air quality during the past year.

International Society of Indoor Air Quality and Climate (ISIAQ)

ISIAQ was founded in 1992 by 109 international scientists and practitioners following the 5th International Conference on Indoor Air Quality and Climate (Toronto, 1990). It is an international, independent, multidisciplinary, scientific, nonprofit organization whose purpose is to support the creation of healthy, comfortable, and productivity-encouraging indoor environments. As a Society, its major role is to facilitate international and interdisciplinary communication and information exchange by publishing and fostering publication on indoor air quality and climate. It organizes, sponsors, and supports initiatives such as meetings, conferences, and seminars on indoor air quality and climate. It also co-operates with government and other agencies and societies with interests in the indoor environment and climate (Nazaroff 2012). The presidents of ISIAQ since 1992 are listed in Appendix, Table A3.

Indoor Air journal, the Official Journal of ISIAQ

In the late 1980s, professors Fanger from Denmark and Thomas Lindvall from Sweden, leaders in the indoor environment field, proposed to publish a new journal titled Indoor Air. Professor David Grimsrud served as the first editor-in-chief (EIC). The inaugural issue of the journal was published in March, 1991 (Grimsrud 2011). With the great contributions of the EICs, David Grimsrud (1991–2000), Jan Sundell (2001–2010), William W Nazaroff (2010–2018), and Yuguo Li (2019–present) and with many members in the editorial board, the journal becomes more and more

impactful, which can be seen from its increasing published paper number and impact factor. The journal has enjoyed high visibility both within and beyond the indoor air science community.

Representative Events or Works on Indoor Air Quality Field in the Modern Stage Since the 1970s

Many research topics have been explored starting in the 1970s and many studies have advanced our understanding of indoor air science. Table 1 lists selected representative examples. The selection is based on: original works having impacted later studies as a paradigm or later important applications and standards; review papers with novel insights having driven later studies; important events having significant impact on later studies or practice. Some important events and excellent studies may have been omitted due to our limited historical memory and knowledge. We wish that the readers could suggest other seminal studies in the future. Considering this chapter is being published online, we have chances to periodically revise it.

Quantitative Analysis of the General Information in Web of Science

In Web of Science Core Collection (WoS-CC), we searched the indoor air quality paper information on August 23, 2021. Some major conclusions are presented here.

The Number of Indoor Air Quality–Related Papers has Increased Rapidly Since 1990

We searched the number of papers by using the topic keyword “indoor air quality” by publication year. Figure 1 shows that the number of papers has increased rapidly since 1990. Many indoor air quality–related papers can only be identified by searching the keywords such as “formaldehyde”, “benzene”, “ventilation”, etc., instead of by “indoor air quality” on WoS-CC. Thus, Fig. 1 may underestimate the number of published papers.

Number of Papers Related to Specific Indoor Air Pollutants Since 1990

From a search similar to the one mentioned above, the numbers of papers covering indoor air pollutants since 1990 are shown in Fig. 2. Although many indoor air quality–related papers may not be fully identified by searching on these topic words in WoS-CC, the trend shown in Fig. 2 should still be illustrative.

Table 1 Selected representative events or works on indoor air quality (1971–2021)

Year	Events or works	References
1971	Measurements showing the impact of indoor chemistry, driven by nitrate containing particles from outdoors, on indoor telephone switching equipment	Hermance et al. (1971)
1972	Earliest strong work on time-activity pattern investigations in 12 European countries	Szalai (1972)
1973	First rate constants for ozone removal by surfaces reported	Mueller et al. (1973) Sabersky et al. (1973) Thompson et al. (1973)
1973	First box model of indoor chemistry published	Sabersky et al. (1973)
1973	First version of ASHRAE Standard 62, Standards for Natural and Mechanical Ventilation, published	Persily (2015)
1974	First Computational Fluid Dynamics (CFD) book report and paper in indoor air field	Nielsen (1974a, b)
1974	It was observed that ozone reactions indoors occurred largely on surfaces, presented model for indoor-outdoor pollutant relationship, and called out the potential to remove ozone from indoor air	Shair and Heitner (1974)
1975	Article showing formaldehyde pollution due to chipboard used as building material in Danish homes	Andersen et al. (1975)
1978	First international indoor climate symposium launched, which led to the series of Indoor Air conferences	Fanger and Valbjørn (1978)
1978	First labeling system for indoor material and furniture, German “Blue Angel,” in the world. A series of labeling systems for indoor material and furniture occurred later, such as M1 and AgBB in Europe (Committee for Health-related Evaluation of Building Products 2018; The Building Information Foundation RTS 1996); BIFMA in the USA (BIFMA International 2011), and more recently in Asian countries, including Japan, Korea, and Singapore	Blue Angel (2002), Zhang et al. (2022)
1979	Early major work on indoor-outdoor relationships for airborne particulate matter of outdoor origin	Alzona et al. (1979)
1979–1985	US EPA TEAM Study measured personal exposures (800 people in 8 cities) to numerous toxic/carcinogenic chemicals and found that organic pollutants were much higher indoors than outdoors and that exposures occurred mostly indoors	Wallace et al. (1987)
1979	First WHO report on indoor air quality	WHO (1979)
1980	SVOCs (phthalates, organophosphates and adipates) reported in indoor airborne particles; their relative abundance in indoor PM larger than that typically reported for outdoor PM	Weschler (1980)

(continued)

Table 1 (continued)

Year	Events or works	References
1981	The US National Academy of Sciences produced a landmark report: “Indoor Pollutants.” The committee was chaired by Spengler JD and co-chaired by Lebowitz MD	NRC (1981)
1981	ASHRAE ventilation standard distinguishing between smoking and nonsmoking spaces published	Weschler (2009)
1981	A concept for evaluating the effect of fresh air distribution indoors on indoor air quality, air age, was put forward	Sandberg (1981) Sandberg and Sjöberg (1983)
1982	Consumer Product Safety Commission banned urea-formaldehyde foam insulation in homes/schools	Weschler (2009)
1982	First paper on health effects related to buildings	Kröling et al. (1982)
1984	WHO defined the term “Sick Building Syndrome”	Sick building syndrome-Wikipedia; Finnegan et al. (1984)
1984	US EPA restricted indoor use of pentachlorophenol (PCP) in paints and wood	Weschler (2009)
1984	Recognition that soil gas could penetrate into buildings carrying with high levels of radon generated naturally by radioactive decay of radium	Nero and Nazaroff (1984)
1985	US EPA established Office of Indoor Air Quality	Weschler (2009)
1986	Asbestos Hazard Emergency Response Act signed into law	Weschler (2009)
1986	US National Academy of Sciences published “The airliner cabin environment: air quality and safety”, which called for a ban on tobacco smoking in passenger cabins of commercial aircraft. This changed indoor smoking habits and likely contributed to the later series of indoor smoking bans	Weschler (2009)
1986	First comprehensive indoor chemistry model developed. Results from the model agreed with measurements of pollutants in a museum gallery	Nazaroff and Cass (1986)
1986	Early study of sensory reactions of 62 human subjects exposed to a low concentration mixture of 22 VOCs emitted by building materials and furnishings	Mølhave et al. (1986)
1987	First Air Quality Guidelines published	WHO (1987)
1987	Publication of seminal book “ <i>Biofuels, Air Pollution, and Health: A Global Review</i> ” establishing that household pollution from biofuels had a worldwide health impact comparable or larger than outdoor pollution	Smith (1987)
1987	Researchers from US EPA and China CDC showed that the coal combustion indoors was a major cause of lung cancer especially for women in Xuanwei county of Yunnan province in China	Mumford et al. (1987); He et al. (1991)

(continued)

Table 1 (continued)

Year	Events or works	References
1987	A large study published on SBS symptoms among office employees, called the Danish Town Hall Study	Skov and Valbjørn (1987)
1988	Indoor Radon Abatement Act directed US EPA to identify areas with potential for high indoor radon	Weschler (2009)
1988	First conference in the Healthy Buildings series held in Sweden	Berglund et al. (1988)
1988	Fanger proposed “Olf and decipol” units for perceived air quality	Fanger (1988a, b)
1989	WHO recommends “source control” as best means of reducing indoor air pollution due to VOCs	WHO (1989)
1989	ASHRAE standard eliminated distinction between smoking and nonsmoking spaces	Persily (2015)
1989	Publications of the European Directive for construction products, the so-called “Construction Product Directive”. This was later amended by a Council Directive in 1993, again in 2011 through Regulation (EU) No 305/ 2011	European Commission (EC) (1989, 1993, 2011)
1989	First published analysis indicating that indoor ozone exposure (concentration × time) is often comparable to or larger than outdoor exposure	Weschler et al. (1989)
1989	The International Society of Exposure Analysis (ISEA) (subsequently renamed the International Society of Exposure Science (ISES)) created in 1989	https://www.ises.org
1989	First report (No 1) from the “European Concerted Action on Indoor Air Quality and Its Impact on Man” program about Radon. There followed another 29 reports about various aspects of VOCs and emission testing, and labeling. Important reports for European research	1989–2013 European Commission, Luxembourg https://op.europa.eu/en/publication-detail/-/publication/34beabd5-f38b-4336-ac69-3eec614bbad4
1989	First international course on indoor air quality and health held in Copenhagen and organized by Nordic Advanced Training in Occupational Health	Later held in 1992, 1996, 1999, 2003, 2006, and 2018 (endorsed by ISIAQ and Int Comm on Occup Health (ICOH))
1990	US EPA bans mercury in interior latex paint	Weschler (2009)
1990	Sources of indoor air pollution begin to be evaluated	Tichenor et al. (1990)
1991	Indoor Air, official journal of ISIAQ, was launched	Grimsrud (2011)
1991	Exposure science occurs as an independent science branch	Lioy and Weisel (2014)
1991	Introduction of the Field and Laboratory Emission Cell (FLEC), to be used both on-site and in the laboratory for controlled emission testing. Later achieved international standardization, ISO, ASTM, NORDTEST, China, etc.	Wolkoff et al. (1991a)

(continued)

Table 1 (continued)

Year	Events or works	References
1991	The first human provocation studies in climate chambers with typical building materials	Johnsen et al. (1991) Wolkoff et al. (1991b)
1992	International Society of Indoor Air Quality and Climate (ISIAQ) was founded in 1992 by 109 international scientists and practitioners following the 5th International Conference on Indoor Air Quality and Climate, Indoor Air '90 (Toronto, 1990)	https://www.isiaq.org/about_us.php
1992	The reaction products of ozone reacting with an indoor surface (new carpets) were observed for the first time, which stimulated studies on indoor chemistry and building products. It's the first paper on indoor chemistry and building products	Weschler et al. (1992)
1992	First international workshop bringing together experts from different disciplines to address indoor air as a multidisciplinary field of applied science. A monograph based on the event: Morawska L, Bofinger ND and Maroni M (Editors). Indoor Air – An Integrated Approach, Elsevier Science Limited, 1995, was published	Morawska et al. (1995)
1993	“Six cities study” starting in 1974 was published in the top journal, New England J Med, which investigated in six communities the health effects of air pollutants. Although the study was not focused on indoor air per se, it had a great impact on later indoor air quality studies	Dockery et al. (1993)
1993	Recognition that indoor combustion of solid fuels for heating and cooking in developing countries produced PM concentrations that can be an order of magnitude or higher than observed in Europe and North America. Thus, two areas of research on indoor particles have evolved with one focused on built environments in higher income countries (WHO 2010) and the other on the use of solid fuel combustion for indoor heating and cooking (WHO 2014)	Smith (1993)
1993	NIOSH and BASE study, the first major studies of office buildings (>100) in the USA, started in 1993	Brightman et al. (2008)
1994	A mechanistic model for emissions of VOCs from indoor materials was presented and formed the basis of later developments in VOC emission mechanistic modeling studies	Little et al. (1994)
1994	The Danish Indoor Climate Labeling system was launched, which is the first system to introduce odor and health based on VOC emissions	Wolkoff and Nielsen (1996)
1994	First meeting of ISO/TC146/SC6 (Indoor Air) held in Berlin, Germany by Prof. Bernd Seifert. Since then, 44 standards including ISO-16000 Part.1-40 (indoor) and 122919 Part 1-10 (interior air of road vehicles) have been published and updated	Tanabe (2017) https://www.iso.org/committee/52822.html

(continued)

Table 1 (continued)

Year	Events or works	References
1995	Residential air exchange rates in the USA: Empirical and estimated parametric distributions by season and climatic region was published	Murray and Burmaster (1995)
1996	The German Committee on Indoor Air Guide Values publishes its first Indoor Air Guide Value for toluene. Since then, values for about 53 VOCs/SVOCs have been derived	https://www.umweltbundesamt.de/en/topics/health/commissions-working-groups/german-committee-on-indoor-air-guide-values#german-committee-on-indoor-air-guide-values-air Fromme et al. (2019)
1996	Finland launched labeling system on formaldehyde and TVOC for building materials, which was called “M1”	The Building Information Foundation RTS (1996)
1996	Prediction of elevated indoor hydroxyl radical concentrations ($\sim 2 \times 10^5$ molecules/cm ³ at 20 ppb O ₃) because of indoor ozone/terpene reactions. Confirmed with experiments a year later	Weschler and Shields (1996, 1997a)
1996	Publication of the results of the “European AUDIT project” of 56 offices	Bluyssen et al. (1996)
1996	Early comprehensive review on indoor particles, which has strongly impacted later studies	Wallace (1996)
1996	PTEAM Study of 189 Los Angeles residents’ personal and indoor exposures to PM _{2.5} and PM ₁₀ published	Özkaynak et al. (1996)
1997	Detailed examination of potential chemical reactions among indoor pollutants (indoor chemistry)	Weschler and Shields (1997b)
1997	First Japanese guideline value for formaldehyde. Since then, guidelines for 13 chemicals and TVOC (tentative) were published	Azuma et al. (2020)
1998	Publication of the LEED (Leadership in Energy and Environmental Design) Green Building Rating System for New Construction (LEED v1.0). The VOC emissions for paints and coatings, adhesives and sealants, flooring, wall panels, ceilings, insulation, composite wood, and furniture are evaluated. Besides VOC emissions, the VOC content for paints, coatings, adhesives, and sealants are also evaluated	USGBC (2021) Zhang et al. (2022)
1998	European EXPOLIS study: first (and still remaining the only one) random working age population sample-based study on personal exposures including indoor measurements at homes and workplaces in Europe (seven cities in total)	Jantunen et al. (1998), Hänninen et al. (2004)
1998	Impact of temperature and humidity on the perception of indoor air quality was published. Lower temperature and dryer air make air quality perceived better under test conditions. The finding has influenced some ventilation standards for the limiting criteria of low humidity exposure	Fang et al. (1998)

(continued)

Table 1 (continued)

Year	Events or works	References
1999	Indoor air quality shown to have an impact office work	Wargocki et al. (1999)
1999	Ozone/terpene reactions recognized as source of secondary organic aerosols (SOA)	Weschler and Shields (1999)
2000	WHO published the report on the right to healthy indoor air	WHO (2000), Mølhave and Krzyzanowski (2000)
2001	First Indoor Air Quality Handbook published by McGraw-Hill	Spengler et al. (2001)
2001	The first study on the US time-activity patterns named as The National Human Activity Pattern Survey (NHAPS) was published, which have subsequently been applied worldwide to exposure assessment	Klepeis et al. (2001)
2001	China launched a mandatory standard on indoor air pollution control of civil building engineering, GB 50325-2001	https://www.chinesestandard.net/ PDF/English.aspx/ GB50325-2001
2001	Dampness in building and health (DBH) study reported the association between the dampness and mite exposure in buildings and health effects, which led to studies in Bulgaria, Singapore, USA (Texas), South Korea, Denmark, and mainland of China	Bornehag et al. (2001)
2001	A long-term research program dedicated to indoor air is funded by the French Government with the objective to perform regular nationwide measurement surveys in buildings: the French IAQ Observatory	Kirchner et al. (2011)
2002	China launched Indoor Air Quality Standards (GB/T18883-2002), which is for indoor air quality of nonindustry buildings	China CDC (2002)
2003	Biomonitoring of phthalate esters as a routine method. An estimation of the daily intake of di (2-ethylhexyl)phthalate (DEHP) and other phthalates in the general population was reported	Koch et al. (2003)
2003	The first approach using dimensionless analysis to obtain the generalized VOC emission correlations for building materials	Xu and Zhang (2003)
2004	First thorough study to show DEHP emission from PVC flooring and uptake of DEHP in floor dust	Clausen et al. (2004)
2005-2007	Reports on Relationships of Indoor, Outdoor, and Personal Air (RIOPA) were published. 48-h integrated indoor, outdoor, and personal air samples were collected between summer 1999 and spring 2001 at three different locations in the USA. Samples were analyzed for VOCs and particles	Weisel et al. (2005), Turpin et al. (2007)
2006	The first field study of indoor surface chemistry was published	Wang and Morrison (2006)

(continued)

Table 1 (continued)

Year	Events or works	References
2006	The first mechanistic model for emissions of SVOCs from indoor material was presented, which formed the basis of later developments in SVOC emission modeling studies	Xu and Little (2006)
2006	EU adopted Registration, Evaluation, Authorization, and Restriction of Chemicals (REACH)	Weschler (2009)
2007	Textbook on Exposure Analysis published	Ott et al. (2007)
2008	The first assessment of acid/base chemistry on indoor surfaces was published	Ongwandee and Morrison (2008)
2009	WHO Guidelines for Indoor Air Quality: Dampness and Mould	WHO (2009)
2009	Publication of a review paper on the changes in indoor pollutants since the 1950s, which attracted interest from many related disciplines	Weschler (2009)
2009	Ultrafine particle emissions from printers were found, which was considered as a turning point for printer design worldwide	Morawska et al. (2009)
2010	Studies with human subjects identified the major gas-phase products resulting from reactions of ozone with human skin lipids	Wisthaler and Weschler (2010)
2010	WHO Guidelines for Indoor Air Quality: Selected Pollutants	WHO (2010)
2010	Publication of a review paper on formaldehyde in the indoor environment, which attracted much interest of many related disciplines on the topic	Salthammer et al. (2010)
2011	Burden of disease of indoor air pollutants reported with DALY (disability-adjusted life years put forward by Murray and Lopez (1996)), which can be compared with other damage or loss for the first time. Researchers in Lawrence Berkeley National Lab (LBNL), USA estimated the health risks of typical indoor air pollutants, which got close to the idea as a pioneer work	Hänninen and Knol (2011), Hänninen et al. (2013) Logue et al. (2011, 2012)
2011	First major report on “Climate Change, The Indoor Environment, and Health”. It shows that climate change will affect indoor air pollutant concentrations, which shifts human exposure and influences public health	The committee was chaired by Spengler JD. The Institute of Medicine of the US National Academies (2011), Nazaroff (2013)
2013	ECA Report No 29: Harmonization framework for health-based evaluation of indoor emissions from construction products in the European Union using the EU-LCI concept	Kephalopoulos et al. (2013)
2013	First study showing that e-cigarettes release nicotine, aromatic compounds and nanoparticles. The publication triggered many other scientific studies and serves as a basis for discussions on legal measures	Schripp et al. (2013)

(continued)

Table 1 (continued)

Year	Events or works	References
2013	Human reference limits for key terpene ozone-initiated reaction products are derived for the first time	Wolkoff (2013)
2014	WHO Guidelines for Indoor Air Quality: Household Fuel Combustion	WHO (2014)
2014	Formaldehyde was confirmed to be a human carcinogen by the National Research Council of the United States because there is sufficient evidence of carcinogenicity from studies in humans that indicates a causal relationship between exposure to formaldehyde and at least one type of human cancer	US-NRC (2014)
2014	The WELL Building Standard® Version 1.0 (WELL v1.0) was launched for the Commercial and Institutional Office building sector. It applies to office spaces, where well-being is related to worker health, performance, and motivation. Indoor air quality is an important part in it. Later, a series of addendum on residential buildings was published	International WELL Building institute (2014)
2015	The ratios of inhalation and dermal exposure to phthalates (and later other SVOCs) were experimentally determined via an intervention study in a room for the first time, which provided a starting point for combined indoor/biomonitoring studies of SVOCs	Weschler et al. (2015)
2015	First publications of research funded by Sloan Foundation's <i>Chemistry of Indoor Environments (CIE)</i> program occurred	https://sloan.org/programs/research/chemistry-of-indoor-environments
2016	Assessment standard for healthy building (T/ASC 02-2016) was launched in China. Indoor air quality score contributed to roughly 25% of the total score. Since 2017, buildings with 30 million square meters have been certificated	ASC (2016)
2017	First assessment of the socioeconomic costs of indoor air pollution at the national scale, i.e., in France. The six target pollutants were benzene, radon, particles ($PM_{2.5}$), trichloroethylene, CO, and environmental tobacco smoke (ETS). It was found that the annual cost due to indoor air pollution was €20 billion (particles accounted for 70%), which was about 1% French GDP	Boulanger et al. (2017)
2017	First results of the European OFFICAIR study: seasonal and spatial variability of indoor air quality in 37 newly built or recently retrofitted office buildings across Europe	Mandin et al. (2017)
2017	First book on the inverse design approach in indoor air field	Chen et al. (2017)

(continued)

Table 1 (continued)

Year	Events or works	References
2018	On the development of health-based ventilation guidelines: principles and framework	Carrer et al. (2018)
2020	Use of a negative ion device can effectively reduce PM _{2.5} concentrations indoors. However, exposure to negative ions and/or ion-induced reaction products was significantly associated with increases in some biomarker levels indicative of increased cardiovascular health risks. Referring to this finding, Indoor Air Quality Standards of School Classrooms in China suggests to take caution in using negative ionization device to mitigate indoor PM _{2.5} exposure	Liu et al. (2020)
2021	WHO global air quality guidelines update: Particulate matter (PM _{2.5} and PM ₁₀), ozone, nitrogen dioxide, sulfur dioxide, and carbon monoxide. The WHO states that the same standard guidelines apply to both indoor and ambient air quality	WHO (2021)

International Journals That Have Published the Most Indoor Air-Related Papers

Indoor air quality-related papers are published in many international journals. Table 2 shows the number of papers of the top ten journals publishing the most papers since 1991. We searched on 15 August 2021 in WoS-CC by using the keyword “indoor air quality.”

Many excellent international journals such as Environmental Health Perspectives, The Lancet Public Health, Journal of Hazardous Materials, Environmental Science and Technology Letters also published indoor air quality-related research articles and review papers. Some indoor air quality-related papers are also published in top journals such as The New England Journal of Medicine, The Lancet, Science, Nature, Chemical Review, and Journal of American Medicine Association (JAMA).

Institutions That Published the Most Indoor Air-Related Papers

The top ten institutions in producing the most indoor air quality papers are shown in Fig. 3. Papers produced in all these institutions have increased rapidly since 2000 especially for Tsinghua U, U London, and Tianjin U.

Averaged Citations Per Paper of the Ten Institutions Publishing the Most Indoor Air Quality Papers

The average citations per paper of the top ten institutions in publishing the most indoor air quality papers are shown in Fig. 4. The ranks of the average

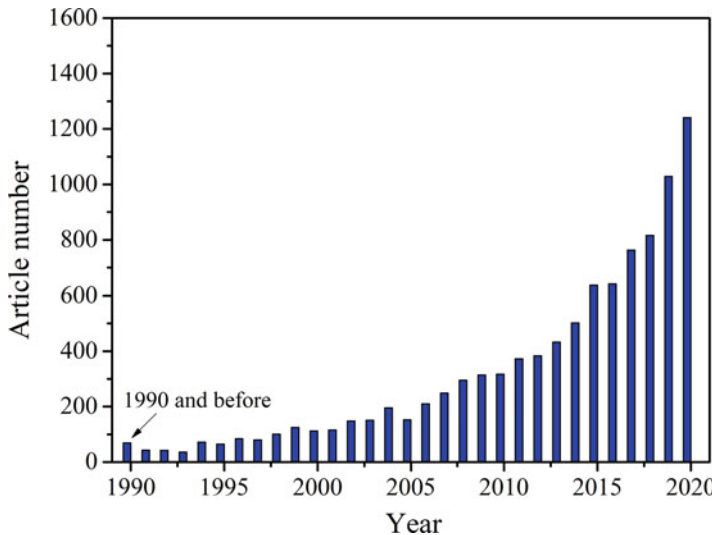


Fig. 1 Evolution of the annual number of peer-reviewed papers on indoor air quality since 1990. (Website: WoS-CC; Keyword: indoor air quality; Document type: articles; Date of analysis: Aug.23, 2021)

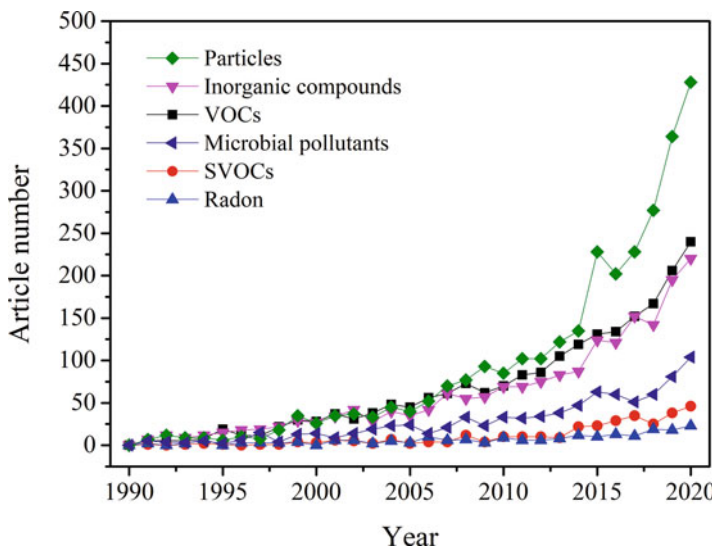
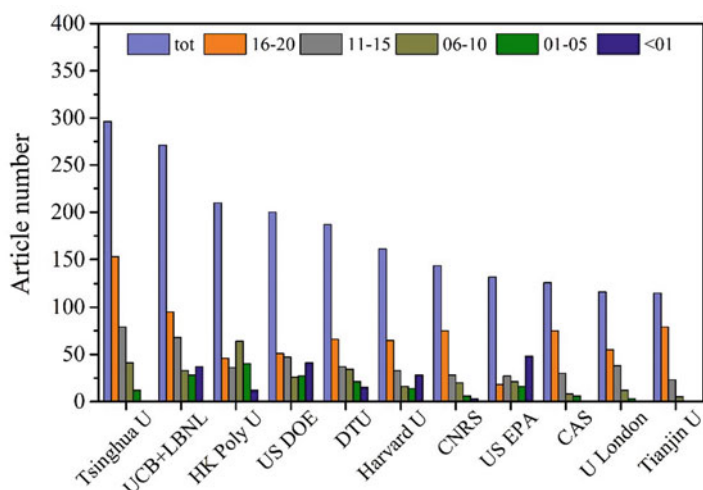


Fig. 2 Evolution of the annual number of peer-reviewed papers related to specific indoor air pollutants since 1990 (Website: WoS-CC; Keyword: “indoor air quality” AND pollutant name; Document type: articles; Date of analysis: Aug.23, 2021)

citations per paper for the total periods of these ten institutions are: DTU, USEPA, US DOE, UCB+LNBL, HK Poly U, Harvard U, U London, Tsinghua U, Tianjin U, CNRS. The average citation per paper of DTU before

Table 2 List of journals and their respective number of IAQ papers published during the period in WoS-CC (Totally 33120 papers were found in the searching)

Journals	Number of papers	Percentage (%)
Building and Environment	1103	3.33
Indoor Air	678	2.05
Atmospheric Environment	537	1.62
Energy and Buildings	512	1.55
Indoor and Built Environment	480	1.45
The Science of the Total Environment	375	1.13
International Journal of Environment Research and Public Health	288	0.870
Environment International	197	0.595
Environmental Science & Technology	191	0.577
Environmental Science and Pollution Research International	188	0.568

**Fig. 3** Number of indoor air science articles published by authors from different institutions. Ranked by total number of articles published. **Tsinghua** University, **UCB** (University of California, Berkeley)+**LBNL** (Lawrence Berkeley National Laboratory), **HK Poly U** (Hong Kong Polytechnic University), **US DOE** (United State Department of Energy DOE), **DTU** (Technical University of Denmark), **Harvard** University, **CNRS** (Centre National de la Recherche Scientifique, France), **US EPA** (United States Environmental Protection Agency), **University of London**, **Tianjin** University. Bars represent different publication year intervals: before 2001, during 2001–2005, during 2006–2010, during 2011–2015, during 2016–2020, and for all articles (tot, highest bar)

2001 is substantially higher than that of the other nine institutions. During 2011–2020, the difference of the average citations per paper of the ten institutions is not so large.

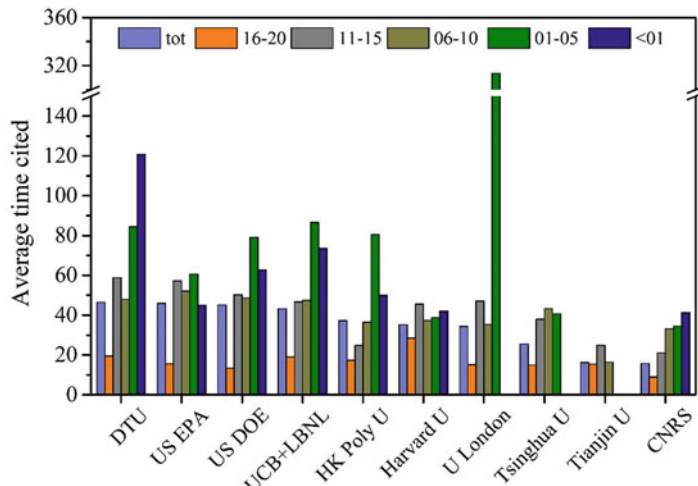


Fig. 4 Number of average citations per paper of the ten institutions in Fig. 3. Ranked by citations per paper for all articles (tot). Bars represent different publication year intervals: before 2001, during 2001–2005, during 2006–2010, during 2011–2015, during 2016–2020, and for all articles (tot)

On the Research Advances Since 2001

Spengler, Samet, and McCarthy as editors-in-chief published the *Indoor Air Quality Handbook* in 2001 (Spengler et al. 2001). To avoid overlaps, the present handbook focuses on those research advances that have occurred since 2001. Moreover, thermal comfort and indoor air quality studies related to biological aerosols are not included in the present handbook although they were included in the previous one.

In addition, by referring to the contents of the previous handbook and by considering the research advances in the past two decades, the contents of the present handbook are arranged by sections and chapters. The research advances are classified into the following sections: indoor air chemicals, indoor air particles, measurement and evaluation, source/sink characteristics, indoor chemistry, human exposure to indoor pollutants, health effects and health risk assessment, indoor air quality and cognitive performance, standards and guidelines, indoor air quality control, and air quality in various indoor environments.

By design, each handbook chapter is a review paper on the chapter's topic. The authors are experts on the chapter's topic. Therefore, we avoid repeating their reviews in this chapter. Our intent has been to provide a very brief introduction to the “broad view”, as well as isolated “snapshots” for selected representative work by using Figs. 1, 2, 3, and 4 and Tables 1 and 2. Although some important “milestones” in the history of indoor air research may have been omitted, we hope that the historical track can be clearly discerned from this chapter.

Multidisciplinary Co-operation. Compared with previous periods, more studies in this period are multidisciplinary. As Rawlings et al. (2005) stated, such multidisciplinary collaborations were often led by some “star” researchers. Additionally, there are many social networks of scholars that researchers can join to disseminate and find new studies, which are very helpful for such multidisciplinary studies (Li 2019).

Targeting Health Effects. For human-centered space, the purpose of indoor air quality study is to improve human health. Those research studies on indoor air quality without an association to health can be quite important. However, the whole “chain” is complete only if the health risk is included. To some extent, the risk can be regarded as the metrics of the problem importance. Certainly, it is not necessary for every researcher to do health risk analysis. Instead, the purpose should be accomplished with the co-operation of multiple disciplines. Therefore, more multidisciplinary co-operation studies should address IAQ and health issues.

Focus on Exposure. Both the concentrations of pollutants and people’s time-activity patterns govern exposure to pollutants (Morawska et al. 2013; Salthammer et al. 2018). Some major elements regarding human exposure and indoor air in the research studies carried out since 2001 are: (1) the development of human biomonitoring and the understanding of the contribution of indoor air compared to other sources such as diet; (2) the consideration of ingestion and dermal exposure in addition to inhalation only; all the exposure pathways are now addressed; (3) the development of the exposome concept (Wild 2012) in which indoor exposure throughout life is a major piece.

Financial Support. Compared to ambient air quality research studies, financial support of indoor air quality studies has been very limited. The reasons for these limitations include: (1) ambient air quality is regulated in many countries such as USA, EU, and China, while indoor air quality is not; (2) various indoor environments, especially homes are regarded as private spaces in which governments should not interfere; (3) ambient air pollution data measured in a few central locations can represent the likely exposures across a large area that can then be associated with public health within that area. In indoor research, it is necessary to measure air quality in a large number of indoor spaces with limited health data available for the specific people occupying those spaces; (4) controlling ambient air quality could be done on a large scale by governing bodies, while controlling indoor air quality involves the “entire” building environment, e.g., building materials, furniture, furnishings, consumer products, air cleaners and outdoor air, as well as the occupants themselves (Sundell 2017).

Perspectives on Indoor Air Quality Research Related to Chemicals

Find important problems to tackle in indoor air fields. Kirk Smith (1947–2020) made seminal contributions by studying the impact of indoor air pollution from household combustion on human health in developing countries such as India, China, Mongolia, Mexico, and Guatemala. He found that in India and China

alone, over one million premature deaths can be attributed to using biofuels indoors (Smith 2000). One reason for his substantial research success is that he always aimed at important problems to study. As he used to say, researchers should “follow the risk”. His career provides an excellent example of that way of choosing important problems.

Use burden of disease as a measure of the “importance” and “risk”. How to find those important or high-risk problems in indoor air fields to tackle? How to prioritize research, remediation initiatives, and public policies? In 1996, Murray and Lopez (1996) put forward the concept of the “burden of disease” to express diverging health loss, whose unit was the “disability-adjusted life year” (DALY). DALYs provide an estimation of the equivalent number of healthy life-years lost in a population due to premature mortality and morbidity (DALY). It can also be converted into economic loss by estimating the cost of a DALY to the society in which the analysis is being made. Smith and Mehta (2003) reported the seminal work on the burden of disease from indoor air pollution in developing countries. We suggest to use the burden of disease approach in the indoor air field to assess the “importance” or the “risk” for those pollutants for which the toxicity is known as illustrated by Hänninen et al. (2014, 2022). By using DALYs, indoor air pollutants can be targeted and suitable thresholds can be clearly defined as relevant standards for different countries, regions, and buildings. In addition, we define here a new concept, coefficient of investment (COI) (that is the ratio of reduction of the cost of the DALYs to the invested cost needed to mitigate the risk) to be a core parameter in evaluating the effectiveness of indoor air quality control system or approach. By using COI, suitable engineering control approaches can be assessed. Under this framework, many studies should be performed in the near future.

Apply machine learning system and big data analysis technology. Past studies used questionnaires and sampling methods that are difficult to implement on a large scale and obtain accurate information. Therefore, it is difficult to identify the associations between indoor environmental characteristics and human responses. In recent years, sensor systems and corollary machine learning approaches and big data analysis technology have rapidly developed. A revolutionary event is that “Alpha Go” developed by Google defeated the top human Go player (Fig. 5). With various online sensors that are also quickly improving, big data of extensive indoor environment information can be obtained conveniently. Temporal and spatial variabilities of indoor air pollution can be better characterized. Moreover, many techniques to obtain human biomarkers of exposure are also developing very rapidly. Big data on human responses in the indoor environment can also be obtained. With the help of powerful machine learning tools applied with big data analysis skill, associations between indoor environment information, and human responses can be isolated that would be impossible to obtain using the traditional approaches. However, data quality is always very important to get reliable results. Standardized measuring protocols with documented and validated methods will still be important problems to tackle in the future.

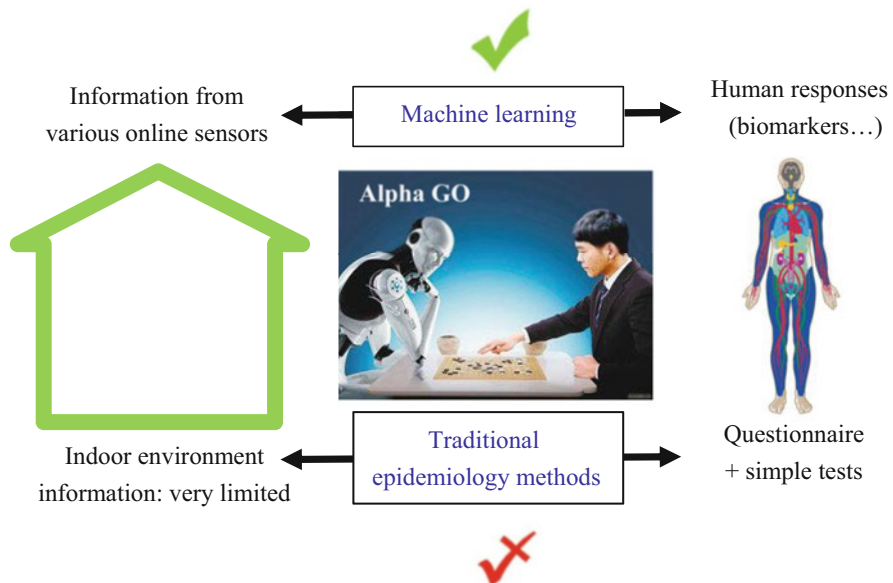


Fig. 5 Machine Learning System with Knowledge and Skill will be powerful in finding associations between indoor environment information and human responses

Understand and fix problems from the whole system (or integrated) view. A holistic view can reveal more links and associations than a partial view. For intercontinental travel, “flying” is much more efficient than surface transportation although it does not allow seeing the details of the surface. In the future, instead of detailed study of part of a well-defined problem, large questions related to the whole indoor environmental system can be solved using systematic approach. For example, the interplay between chemical exposure and both indoor and outdoor climatic conditions coupled with occupational exposures and personal risk factors such as host vulnerability that may enhance the impact of the chemicals needs to be integrated into the study design (Wolkoff 2020). Wild (2012) introduced the concept of exposome: the human exposome encompasses exposures to environmental factors throughout life, starting from conception and pregnancy. Indoor air science must be an integral part of exposome research to provide a comprehensive evaluation of human exposure to chemicals. Moreover, indoor air quality control should also receive attention as soon as energy efficiency or energy retrofits are addressed. Building or renovating buildings with a tighter envelope to remove air leakages and improve energy efficiency must absolutely involve considering the ventilation in the building.

Understand how to improve health via improved indoor air quality. Today, healthy buildings are not really “healthy” buildings but rather “not-sick” buildings. We know much about the effects of many targeted indoor air pollutants on human health. However, we know little about the effects related to improve indoor air

quality on improving health. For many developed countries, indoor air pollution problems can be neglected because they are not deemed important relative to development priorities. However, development should also include improved public health that comes from better indoor air quality. Study of this problem needs to be done in the near future given the size of the affected population. It would be the basis for developing truly “healthy” buildings. Moreover, vulnerable populations, i.e., pregnant women, unborn children, children, elderly, sick persons (in particular immune deficient individuals), are the ones for which healthy buildings are even more crucial.

Understand the serious indoor air problems in the rural or poor areas of developing countries and fix them. Identification and understanding the indoor air quality problems in rural or poor areas of developing countries such as in India, China, Mongolia, sub-Saharan Africa, and Central America remains very important. Research achievements can save millions of premature deaths in those countries. The problem of severe indoor pollution from solid fuel combustion in cooking/heating stoves has been known since the 1980s (Bonjour et al. 2013), but remains a significant issue for a large fraction of the world’s population. It produces more DALYs than any single biological agent (microbe or parasite). Both China and India have recently instituted programs to change to cleaner fuels, but much of the developing world still require cleaner cooking methods as discussed in ► Chap. 6, “[Appliances for Cooking, Heating, and Other Energy Services](#).“ It will take a concerted global effort to provide culturally appropriate solutions to the problem of clean cooking/heating appliances and the resulting improvement of indoor air quality.

Anticipate what will be the indoor environment in the context of global warming. There is now clear evidence that projected climate change will have major impacts on our lives, and particularly on our indoor environment (Vardoulakis et al. 2015). The risks are not yet fully described, but we can expect various outcomes, e.g., that higher temperatures will lead to higher building materials emissions and consequently higher indoor concentrations. Higher outdoor ozone concentrations may lead to more indoor chemistry and formation of secondary products. Mitigation and adaptation policies are needed, and, before that, a better understanding on how buildings will be impacted and used is needed. The indoor climate researchers have a key role to play.

Conclusions

Indoor air studies have become a well-defined component of scientific research. However, many challenges are yet to be met by the indoor air quality research community. Over the past decades, an innovative and dynamic research community has grown and proved its ability to develop understanding of indoor air quality

issues and provide solutions. In the future, using a multidisciplinary, holistic, and creative approach, multiple challenges related to indoor air quality will be addressed.

Appendix

Table A1 1st -16th Indoor Air International Conferences from 1978 to 2020

Year	Host city/country	Chairs
1978	Copenhagen/Denmark	PO Fanger, O Valbjørn, I Andersen
1981	Amherst/USA	JD Spengler, CD Hollowell, D Moschandreas
1984	Stockholm/Sweden	T Lindvall, B Berglund, J Sundell
1987	Berlin/Germany	B Seifert, H Esdorn, M Fischer, H Ruden, J Wegner
1990	Toronto/Canada	D Walkinshaw
1993	Helsinki/Finland	O Seppänen
1996	Nagoya /Japan	S Yoshizawa, K-I Kimura, K Ikeda, S-I Tanabe, T Iwata
1999	Edinburgh/UK	G Raw, C Aizlewood, P Warren
2002	Monterey/USA	H Levin, WJ Fisk, WW Nazaroff
2005	Beijing/China	L Wu, Y Jiang, R Zhao, Q Chen
2008	Copenhagen/Denmark	BW Olesen
2011	Austin/USA	RL Corsi, GC Morrison, D Weekes
2014	Hong Kong/China	Y Li, C Chao, J Niu, ACK Lai
2016	Ghent/Belgium	J Laverge, T Salthammer, M Stranger
2018	Philadelphia/USA	M Waring, B Stephens, WW Nazaroff
2020	Seoul/Korea	H Han, YG Lee
2022	Kuopio/Finland	P Pasanen

Table A2 Executive committee of the Academy of Fellows of ISIAQ (1991–2022)

Years	President	Vice president	Secretary
1991–1993	Demetrios Moschandreas	Bernd Seifert	Birgitta Berglund
1993–1996	Bernd Seifert	Birgitta Berglund	Kevin Teichman
1996–1999	P Ole Fanger	Anthony Pickering	Shin-ichi Tanabe
1999–2002	P Ole Fanger	Anthony Pickering	Shin-ichi Tanabe
2002–2005	John D. Spengler	Jan Sundell	Shin-ichi Tanabe
2005–2008	Jan Sundell	Shin-ichi Tanabe	William Nazaroff
2008–2011	Shin-ichi Tanabe	William Nazaroff	Tunga Salthammer
2011–2014	William Nazaroff	Tunga Salthammer	Yuguo Li
2014–2016	Tunga Salthammer	Yuguo Li	Richard Corsi
2016–2018	Yuguo Li	Richard Corsi	Pawel Wargocki
2018–2020	Richard Corsi	Pawel Wargocki	Yinping Zhang
2020–2022	Pawel Wargocki	Yinping Zhang	Shelly Miller
2022–2024	Yinping Zhang	Shelly Miller	Corinne Mandin

Table A3 Presidents of ISIAQ (1992–2022)

Years	President	Years	President
1992–1994	Douglas Walkinshaw	2009–2012	Richard Shaughnessy
1994–1997	Olli Seppanen	2012–2014	Pawel Wargocki
1997–2000	Marco Maroni	2014–2016	Glenn Morrison
2000–2003	Lidia Morawska	2016–2018	Marcel Loomans
2003–2006	Nadia Boschi	2018–2020	Marzenna Dudzinska
2006–2009	Kwok-Wai Tham	2020–2022	Corinne Mandin
		2022–2024	Ying Xu

References

- Alzona J, Cohen BL, Rudolph H et al (1979) Indoor-outdoor relationships for airborne particulate matter of outdoor origin. *Atmos Environ* 13:55–60
- Andersen I, Lundqvist GR, Mølhave L (1975) Indoor air pollution due to chipboard used as construction material. *Atmos Environ* 9:1121–1127
- ASC (2016) Assessment standard for healthy building (ASC/T 02-2016). Architecture Society of China
- Azuma K, Jinno H, Tanaka-Kagawa T, Sakai S (2020) Risk assessment concepts and approaches for indoor air chemicals in Japan. *Int J Hyg Environ Health* 225:113470
- Bell ML, Davis DL, Fletcher T (2004) A retrospective assessment of mortality from the London smog episode of 1952: the role of influenza and pollution. *Environ Health Perspect* 112:6–8
- Berglund B, Lindvall T, Måansson LG (1988) Healthy Buildings' 88 (No. BFR-D-14-1988). Swedish Council for Building Research
- Biersteker K, de Graaf H, Nass CAG (1965) Indoor air pollution in Rotterdam homes. *Air Water Pollut* 9:343–350
- BIFMA International (2011) ANSI/BIFMA M7.1, Standard Test Method for Determining VOC Emissions from Office Furniture Systems, Components and Seating
- Billings JS (1889) The principles of ventilation and heating and their practical application, 2nd edn. Engineering and Building Record, New York
- Blue Angel (2002) RAL-UZ 38. Low-emission wood products and wood-based products. German Institute for Quality Assurance and Certification
- Bluyssen PM, De Oliveira FE, Groes L et al (1996) European indoor air quality audit project in 56 office buildings. *Indoor Air* 6:221–238
- Bonjour S, Adair-Rohani H, Wolf J et al (2013) Solid fuel use for household cooking: Country and regional estimates for 1980–2010. *Environ Health Perspect* 121:784–790
- Bornehag CG, Blomquist G, Gyntelberg F et al (2001) Dampness in buildings and health. *Indoor Air* 11:72–86
- Boulanger G, Bayeux T, Mandin C, Kirchner S et al (2017) Socio-economic costs of indoor air pollution: a tentative estimation for some pollutants of health interest in France. *Environ Int* 104: 14–24
- Brightman HS, Milton DK, Wypij D, Burge HA, Spengler JD (2008) Evaluating building-related symptoms using the US EPA BASE study results. *Indoor Air* 18:335–345
- Carrer P, De Oliveira FE, Santos H et al (2018) On the development of health-based ventilation guidelines: principles and framework. *Int J Environ Res Public Health* 15:1360
- Carson R (1962) Silent Spring. Houghton Mifflin, Boston
- Chen QY, Zhai ZQ, You XY, Zhang TF (2017) Inverse design methods for the built environment. Swales & Willis Ltd, Exeter, Devon

- China CDC, Indoor Air Quality Standards (GB/T18883-2002)
- Clausen P, Hansen V, Gunnarsen L, Afshari A, Wolkoff P (2004) Emission of di-2-ethylhexyl phthalate from PVC flooring into air and uptake in dust: emission and sorption experiments in FLEC and CLIMPAQ. *Environ Sci Technol* 38(9):2531–2537
- Committee for Health-related Evaluation of Building Products (2018) AgBB, Evaluation procedure for VOC emissions from building products. <https://www.umweltbundesamt.de/en/document/agbb-evaluation-scheme-2018-1>. Accessed 20 Apr 2021
- Dockery DW, Pope CA, Xu X et al (1993) An association between air pollution and mortality in six U.S. cities. *N Engl J Med* 329(24):1753–1759
- Duan X, Zhao X, Wang B, Chen Y, Cao S (2013) Exposure factors handbook of Chinese population (adults). China Environmental Science Press, Beijing, China.
- European Commission (EC) (1989) Directive 89/106/EEC. OJ L40/12. EC Commission, Brussels. <https://eur-lex.europa.eu/legal-content/EN/TXT/?uri=CELEX:31989L0106>
- European Commission (EC) (1993) Council Directive 93/68/EEC of 22 July 1993. <https://eur-lex.europa.eu/legal-content/en/ALL/?uri=CELEX%3A31993L0068>
- European Commission (EC) (2011) Regulation (EU) No 305/2011 of the European Parliament and of the Council of 9 March 2011 laying down harmonised conditions for the marketing of construction products and repealing Council Directive 89/106/EEC Text with EEA relevance. <https://eur-lex.europa.eu/eli/reg/2011/305/oj>
- Fang L, Clausen G, Fanger PO (1998) Impact of temperature and humidity on the perception of indoor air quality. *Indoor Air* 8(2):80–90
- Fanger PO (1988a) Introduction of the OLF and the DECIPOL units to quantify air-pollution perceived by humans indoors and outdoors. *Energy Build* 12(1):1–6
- Fanger PO (1988b) Olf and decipol, new units for perceived quality. *Build Serv Eng Res Technol* 9(4):155–157
- Fanger PO, Valbjørn O (1978) Indoor climate: effects on human comfort, performance and health in residential, commercial and light-industry buildings. In: Proceedings of the first international indoor climate symposium. Danish Building Research Institute, Copenhagen
- Finnegan MJ, Pickering CA, Burge PS (1984) The sick building syndrome: prevalence studies. *Br Med J (Clinical Research Edition)* 289:1573–1575
- Fitting JW (2015) From breathing to respiration. *Respiration* 89(1):82–87
- Fromme H, Debiak M, Sagunski H et al (2019) The German approach to regulate indoor air contaminants. *Int J Hyg Environ Health* 222:347–354
- Grimsrud DT (2011) Indoor Air: the first 10 years. *Indoor Air* 21:179–181
- Hänninen O, Knol A (2011) European perspectives on environmental burden of disease: estimates for nine stressors in xix Countries. Available: <http://www.thl.fi/thl-client/pdfs/b75f6999-e7c4-4550-a939-3bccb19e41c1>. Accessed 7 Mar 2013
- Hänninen O, Alm S, Katsouyanni K et al (2004) The EXPOLIS study: implications for exposure research and environmental policy in Europe. *J Expo Anal Environ Epidemiol* 14:440–456
- Hänninen O, Sorjamaa R, Lippinen P et al (2013) Aerosol-based modelling of infiltration of ambient PM_{2.5} and evaluation against population-based measurements in homes in Helsinki, Finland. *J Aerosol Sci* 66:111–122
- Hänninen O, Knol A, Jantunen M et al (2014) Environmental burden of disease in Europe: assessing nine risk factors in six countries. *Environ Health Perspect* 122(5):439–446
- Hänninen O, Mandin C, Liu W, Liu N, Zhao Z, Zhang Y (2022) Disease burden of indoor air pollution, Handbook of Indoor Air Quality, SpringerNature. https://doi.org/10.1007/978-981-10-5155-5_48-1.
- He XZ, Chen W, Liu ZY, Chapman RS (1991) An epidemiological study of lung cancer in Xuan Wei county, China: current progress. Case-control study on lung cancer and cooking fuel. *Environ Health Perspect* 94:9–13
- Hermance HW, Russell CA, Bauer EJ, Egan TF, Wadlow HV (1971) Relation of airborne nitrate to telephone equipment damage. *Environ Sci Technol* 5(9):781–785

- Hopke PK, Jensen B, Li CS, Montassier N, Wasiolek P, Cavallo AJ, Gatsby K, Socolow RH, James AC (1995) Assessment of the exposure to and dose from radon decay products in normally occupied homes. *Environ Sci Technol* 29:1359–1364
- International WELL Building Institute (2014) The WELL Building Standard® Version 1.0 (WELL v1.0). The WELL Building Standard® is a registered trademark of Delos Living LLC. Delos Living LLC 22 Little West 12th Street, 4th Floor New York, NY 10014
- Janssen JE (1999) The history of ventilation and temperature control. *ASHRAE J* 41:47–52
- Jantunen M, Hänninen O, Katsouyanni K, Knöppel H, Künzli N, Lebret E, Maroni M, Saarela K, Srám R, Zmirou D (1998) Air pollution exposure in European cities: the EXPOLIS-study. *J Expo Anal Environ Epidemiol* 8(4):495–518
- Johnsen CR, Heinig JH, Schmidt K et al (1991) A study of human reactions to emissions from building materials in climate chambers. Part I: clinical data, performance and comfort. *Indoor Air* 1:377–388
- Kephalaopoulos et al (2013) European Commission, Joint Research Centre Institute for Health and Consumer Protection. Publications Office of the European Union, Luxembourg
- Kirchner S, Mandin C, Derbez M, Ramalho O (2011) Quality of indoor air, quality of life, a decade of research to breathe better, breathe easier. CSTB Press, Paris. 208p
- Kleppeis NE, Nelson WC, Ott WR, Robinson JP, Tsang AM, Switzer P, Behar JV, Hern SC, Engelmann WH (2001) The national human activity pattern survey (NHAPS): a resource for assessing exposure to environmental pollutants. *J Expo Anal Environ Epidemiol* 11:231–252
- Koch HM, Drexler H, Angerer J (2003) An estimation of the daily intake of di(2-ethylhexyl) phthalate (DEHP) and other phthalates in the general population. *Int J Hyg Environ Health* 206: 77–83
- Kröling P, Dirnagl K, Drexel H (1982) Gesundheits und befindlichkeitsstörungen in vollklimatisierten räumen. *Z Phys Med* 11:241–244
- Li YG (2019) Finding the most valuable references for interdisciplinary research. *Indoor Air* 29: 3–4. <https://doi.org/10.1111/ina.12519>
- Lioy P, Weisel C (2014) Exposure science. Elsevier, Amsterdam
- Little JC, Hodgson AT, Gadgil AJ (1994) Modeling emissions of volatile organic compounds from new carpets. *Atmos Environ* 28(2):227–234
- Liu W, Huang J, Lin Y et al (2020) Negative ions offset cardiorespiratory benefits of PM_{2.5} reduction from residential use of negative ion air purifiers. *Indoor Air* 30:31–39. <https://doi.org/10.1111/ina.12728>
- Logue JM, McKone TE, Sherman MH, Singer BC (2011) Hazard assessment of chemical air contaminants measured I residences. *Indoor Air* 21:92–109
- Logue JM, Price PN, Sherman MH, Brett C, Singer BC (2012) A method to estimate the chronic health impact of air pollutants in U.S. residences. *Environ Health Perspect* 120:216–222
- Mandin C, Trantallidi M, Cattaneo A et al (2017) Assessment of indoor air quality in office buildings across Europe – the OFFICAIR study. *Sci Total Environ* 579:169–178
- Mølhave L, Bach B, Pedersen OF (1986) Human reactions to low concentrations of volatile organic compounds. *Environ Int* 12(1–4):167–175
- Mølhave L, Krzyzanowski M (2000) The right to healthy indoor air. *Indoor Air*, 10(4): p 211
- Morawska L, Bofinger ND, Maroni M (1995) Indoor air – an integrated approach. Elsevier Science Limited
- Morawska L et al (2009) Characteristics and formation mechanisms of particles originating from the operation of laser printers. *Environ Sci Technol* 43(4):1015–1022
- Morawska L, Afshari A, Bae GN, Buonanno G et al (2013) Indoor aerosols: from personal exposure to risk assessment. *Indoor Air* 23:462–487
- Mueller F, Loeb L, Mapes W (1973) Decomposition rates of ozone in living areas. *Environ Sci Technol* 7:342–353
- Mumford JL, He XZ, Chapman RS et al (1987) Lung cancer and indoor air pollution in Xuan Wei, China. *Science* 35:217–220

- Murray DM, Burmaster DE (1995) Residential air exchange rates in the United States: empirical and estimated parametric distributions by season and climatic region. *Risk Anal* 15:459–465
- Murray CJ, Lopez AD (1996) The global burden of disease. Harvard University Press, Cambridge, MA
- National Research Council (NRC) (1981) Indoor pollutants. National Academy Press, Washington, DC
- Nazaroff WW (2012) ISIAQ and the academy of fellows. *Indoor Air* 22:353–355
- Nazaroff WW (2013) Exploring the consequences of climate change for indoor air quality. *Environ Res Lett* 8:015022
- Nazaroff WW, Cass GR (1986) Mathematical modeling of chemically reactive pollutants in indoor air. *Environ Sci Technol* 20:924–934
- Nero AV, Nazaroff WW (1984) Characterizing the source of radon indoors. *Radiat Prot Dosim* 7:23
- Nielsen PV (1974a) Flow in air conditional rooms: model experiment and numerical solution of the flow equations, book report. <https://vbn.aau.dk/en/persons/109176/publications/?ordering=publicationYearThenTitle&descending=false>
- Nielsen PV (1974b) Prediction of air distribution in a ventilated room. *Build Serv Eng* 41:219–222
- Ongwandee M, Morrison GC (2008) Influence of ammonia and carbon dioxide on the sorption of a basic organic pollutant to carpet and latex-painted gypsum board. *Environ Sci Technol* 42:5415–5420
- Ott WR, Steinemann AC, Wallace LA (2007) Exposure analysis. CRC Press, Taylor and Francis Group, Boca Raton
- Özkaynak H, Xue J, Spengler JD, Wallace LA, Pellizzari ED, Jenkins P (1996) Personal exposure to airborne particles and metals: results from the particle TEAM study in Riverside, CA. *J Expo Anal Environ Epidemiol* 6:57–78
- Pepys J, Chan M, Hargreaves FE (1968) Mites and house-dust allergy. *Lancet* 291:1270–1272
- Persily A (2015) Challenges in developing ventilation and indoor air quality standards: the story of ASHRAE Standard 62. *Build Environ* 91:61–69
- Rawlings CM, McFarland DA, Dahlander L, Wang D (2005) Streams of thought: knowledge flows and intellectual cohesion in a multidisciplinary era. *Soc Forces* 93:1687–1722
- Repace JL, Lowry AH (1980) Indoor air pollution, tobacco smoke, and public health. *Science* 208: 464–472
- Sabersky RH, Sinema DA, Shair FA (1973) Concentrations, decay rates and removal of ozone and their relation to establishing clean indoor air. *Environ Sci Technol* 7:347–353
- Salthammer T, Mentese S, Marutzky R (2010) Formaldehyde in the indoor environment. *Chem Rev* 110:2536–2572
- Salthammer T, Zhang YP, Mo JH, Koch HM, Weschler CJ (2018) Assessing human exposure to organic pollutants in the indoor environment. *Angew Chem Int Ed* 57:12228–12263
- Sandberg M (1981) What is ventilation efficiency? *Build Environ* 16(2):123–135
- Sandberg M, Sjöberg M (1983) The use of moments for assessing air quality in ventilated rooms. *Build Environ* 18(4):181–197
- Schröpp T, Markewitz D, Uhde E, Salthammer T (2013) Does e-cigarette consumption cause passive vaping? *Indoor Air* 23:25–31
- Shair FH, Heitner KL (1974) Theoretical model for relating indoor pollutant concentrations to those outside. *Environ Sci Technol* 8(5):444–451
- Skov P, Valbjørn O (1987) The “sick” building syndrome in the office environment: the Danish Town Hall Study. *Environment International*, 13(4-5):339–349
- Smith KR (1987) Biofuels, air pollution, and health: a global review. Springer, Boston
- Smith KR (1993) Fuel combustion, air pollution exposure, and health: the situation in developing countries. *Annu Rev Energy Environ* 18:529–566
- Smith KR (2000) National burden of disease in India from indoor air pollution. *Proc Natl Acad Sci* 97(24):13286–13293
- Smith KR, Mehta S (2003) The burden of disease from indoor air pollution in developing countries: comparison of estimates. *Int J Hyg Environ Health* 206(4–5):279–89. <https://doi.org/10.1078/1438-4639-00224>

- Spengler JD, Samet JM, McCarthy JF (2001) Indoor air quality handbook. 1st ed. New York: McGraw-Hill
- Sundell J (1994) On the association between building ventilation characteristics, some indoor environmental exposures, some allergic manifestations, and subjective symptom reports. *Indoor Air* S2:7–49
- Sundell J (2017) Reflections on the history of indoor air science, focusing on the last 50 years. *Indoor Air* 27:1–17
- Szalai A (1972) The use of time: daily activities of urban and suburban populations in twelve countries. Mouton, The Hague
- The Building Information Foundation RTS (1996) M1-Emission Classification of Building Materials. <https://www.greenbuildingsupply.com/core/media/media.n1?id=411494&c=772072&h=d447753ebd140a0896b3&xt=.pdf>. Accessed 20 Apr 2021
- The Institute of Medicine of the US National Academies (2011) Climate change, the indoor environment, and health. The National Academies Press, Washington, DC (pdf file available: http://www.nap.edu/catalog.php?record_id=13115).
- Thompson CR, Hensel EG, Kats G (1973) Outdoor indoor levels of six air pollutants. *J Air Pollut Control Assoc* 23:881–886
- Tichenor BA, Sparks LA, White JB, Jackson MD (1990) Evaluating sources of indoor air pollution. *J Air Waste Manage Assoc* 49:487–492
- Turk A (1963) Measurements of odorous vapors in test chambers: theoretical. *ASHRAE J* 5:55–58
- Turpin BJ, Weisel CP, Morandi M et al (2007) Relationships of indoor, outdoor, and personal air (RIOPA): part II. Analyses of concentrations of particulate matter species. Research Report (Health Effects Institute). 2007(#130 Pt 2):1–77
- US Environmental Protection Agency (USEPA) (2011) Exposure factors handbook: 2011 Edition, Chapter 14, Report No. EPA/600/R-09/052F, National Center for Environmental Assessment, Office of Research and Development, Washington, DC 20460, pp 43
- US Green Building Council (USGBC) (2021) Where LEED began. <https://www.usgbc.org/about/brand>. Accessed 17 Aug 2021
- US National Research Council (NRC) of the National Academies (NS) (2014) Review of the formaldehyde assessment in the national toxicology program 12th report on carcinogens ISBN 978-0-309-31127-1. This PDF is available from The National Academies Press at http://www.nap.edu/catalog.php?record_id=18948
- Vardoulakis S, Dimitroulopoulou C, Thornes J, Lai KM, Taylor J, Myers I et al (2015) Impact of climate change on the domestic indoor environment and associated health risks in the UK. *Environ Int* 85:299–313
- Voorhorst R, Spieksma-Boezeman MI, Spieksma FT (1963) Is a mite (*Dermatophagoides* sp.) the producer of the house-dust allergen. *Allergy Asthma* 10:329–334
- Voorhorst R, Spieksma FTM, Varekamp H et al (1967) The house-dust mite (*Dermatophagoides pteronyssinus*) and the allergens it produces. Identity with house-dust allergen. *J Allergy* 39:325–339
- Wallace LA (1996) Indoor particles: a review. *J Air Waste Manag Assoc* 46:98–126
- Wallace LA, Pellizzari ED, Hartwell TD et al (1987) The TEAM study: personal exposures to toxic substances in air, drinking water, and breath of 400 residents of New Jersey, North Carolina, and North Dakota. *Environ Res* 43(2):290–307
- Wang H, Morrison GC (2006) Ozone initiated secondary emission rates of aldehydes from indoor surfaces in four homes. *Environ Sci Technol*:5263–5268
- Wargocki P, Wyon DP, Baik YK, Clausen G, Fanger PO (1999) Perceived air quality, sick building syndrome (SBS) symptoms and productivity in an office with two different pollution loads. *Indoor air*, 9(3): 165–179
- Weisel CP, Zhang J, Turpin BJ, et al (2005) Relationships of indoor, outdoor, and personal air (RIOPA). Part I. Collection methods and descriptive analyses. Research Report (Health Effects Institute). 2005(#130 Pt 1):1–107
- Weschler CJ (1980) Characterization of selected organics in size-fractionated indoor aerosols. *Environ Sci Technol* 14:428–431
- Weschler CJ (2009) Changes in indoor pollutants since the 1950s. *Atmos Environ* 43:153–169
- Weschler CJ, Shields HC (1996) Production of the hydroxyl radical in indoor air. *Environ Sci Technol* 30(11):3250–3258

- Weschler CJ, Shields HC (1997a) Measurements of the hydroxyl radical in a manipulated but realistic indoor environment. *Environ Sci Technol* 31(12):3719–3722
- Weschler CJ, Shields HC (1997b) Potential reactions among indoor pollutants. *Atmos Environ* 31(21):3487–3495
- Weschler CJ, Shields HC (1999) Indoor ozone/terpene reactions as a source of indoor particles. *Atmos Environ* 33(15):2301–2312
- Weschler CJ, Shields HC, Naik DV (1989) Indoor ozone exposures. *J Air Pollut Control Assoc* 39(12):1562–1568
- Weschler CJ, Hodgson AT, Wooley JD (1992) Indoor chemistry: ozone, volatile organic compounds, and carpets. *Environ Sci Technol* 26:2371–2377
- Weschler CJ, Beko G, Koch HM et al (2015) Transdermal uptake of diethyl phthalate and di(n-butyl) phthalate directly from air: experimental verification. *Environ Health Perspect* 123:928–934
- WHO (1987) Air quality guidelines for Europe. Copenhagen: WHO Regional Office for Europe
- WHO (1989) Indoor air quality: organic pollutants. EURO reports and studies no. 111. World Health Organization, Copenhagen
- WHO (2000) The right to healthy indoor air: report on a WHO meeting, Bilthoven, The Netherlands 15–17 May 2000 (No. EUR/00/5020494). Copenhagen: WHO Regional Office for Europe
- WHO (2009) Development of WHO guidelines for indoor air quality: Dampness and mould, Bonn. <https://www.who.int/publications/i/item/9789289041683>
- WHO (2010) WHO guidelines for indoor air quality: Selected pollutants, Bonn. http://www.euro.who.int/_data/assets/pdf_file/0009/128169/e94535.pdf
- WHO (2014) WHO indoor air quality guidelines: household fuel combustion. Geneva. <https://www.who.int/publications/i/item/9789241548885>
- WHO (2021) Global air quality guidelines. particulate matter (PM_{2.5} and PM₁₀), ozone, nitrogen dioxide, sulfur dioxide and carbon monoxide. World Health Organization, Geneva. <https://apps.who.int/iris/handle/10665/345329>
- Wild CP (2012) The exposome: from concept to utility. *Int J Epidemiol* 41:24–32
- Wisthaler A, Weschler CJ (2010) Reactions of ozone with human skin lipids: sources of carbonyls, dicarbonyls, and hydroxycarbonyls in indoor air. *Proc Natl Acad Sci (PNAS)* 107(15):6568–6575
- Wittmann O (1962) Die nachträgliche Formaldehydabspaltung bei Spanplatten. *Holz Roh Werkst* 20:221–224
- Wolkoff P (2013) Indoor air pollutants in office environments: assessment of comfort, health, and performance. *Int J Hyg Environ Health* 216:371–394
- Wolkoff P (2020) Dry eye symptoms in offices and deteriorated work performance – a perspective. *Build Environ* 172:106704
- Wolkoff P, Nielsen PA (1996) A new approach for indoor climate labeling of building materials – emission testing, modeling, and comfort evaluation. *Atmos Environ* 30:2679–2689
- Wolkoff P, Clausen PA, Nielsen PA, Gustaffson H, Jonsson B, Rasmussen E (1991a) Field and laboratory emission cell: FLEC. In: Healthy buildings, IAQ-91. American Society of Heating, Refrigerating and Air Conditioning Engineers Inc (ASHRAE), Washington, DC, pp 160–165
- Wolkoff P, Nielsen GD, Hansen LF et al (1991b) A study of human reactions to building materials in climatic chambers. Part II: VOC measurements, mouse bioassay, and decipol evaluation in the 1–2 mg/M³ TVOC range. *Indoor Air* 1:389–403
- World Health Organization (WHO) (1979) Health aspects related to indoor air quality, EURO Reports and Studies 21, Copenhagen
- Xu Y, Little JC (2006) Predicting emissions of SVOCs from polymeric materials and their interaction with airborne particles. *Environ Sci Technol* 40:456–461
- Xu Y, Zhang YP (2003) An improved mass transfer based model for analyzing VOC emissions from building materials. *Atmos Environ* 37(18):2497–2505
- Yaglou CP, Riley EC, Coggins DI (1936) Ventilation requirements. *ASHVE Trans* 42:133–162
- Zhang JS, Chen WH, Liu NR, Guo BB, Zhang YP (2022) Testing and reducing VOC emissions from building materials and furniture to improve indoor air quality. *Handbook of Indoor Air Quality*, SpringerNature, https://doi.org/10.1007/978-981-10-5155-5_53-2

Part II

Indoor Air Chemicals



Very Volatile Organic Compounds (VVOCs)

2

Haimei Wang and Jianyin Xiong

Contents

Introduction	38
Properties and Hazards of Formaldehyde	38
Properties	38
Hazards	41
Usages and Pollution Levels of Formaldehyde	43
Methods for the Determination of Formaldehyde	46
Standard Test Methods	46
Analysis of Formaldehyde	47
Emission Models of Formaldehyde	49
Short-Term Emission Models	49
Long-Term Emission Model	53
Measurement of Key Emission Parameters of Formaldehyde	57
Introduction of Measurement Methods for the Key Emission Parameters	57
Introduction of the C-History Method	58
Impact of Environmental Factors on Formaldehyde Emissions	60
Impact of Temperature on C_0	62
Impact of Temperature on D_m	62
Impact of Temperature on K	63
Impact of Relative Humidity	64
Combined Effect of Temperature and Humidity on the Emission Rate	64
Conclusions	66
Cross-References	66
References	66

Abstract

High volatility organic compounds (or very volatile organic compounds, VVOCs) are an important category of indoor air pollutants, and the most-known VVOC is formaldehyde. Formaldehyde is ubiquitous in indoor

H. Wang · J. Xiong (✉)

School of Mechanical Engineering, Beijing Institute of Technology, Beijing, China
e-mail: xiongyj@bit.edu.cn

environment and mainly originates from the emissions of indoor materials and furniture. The existence of formaldehyde poses severe adverse health effect on people. This chapter introduces the formaldehyde properties and hazards, usages and pollution levels, determination methods, as well as the short-term and long-term emission models, the measurement of key emission parameters in the models, and the impact of environment factors on the key emission parameters and emission rate. This chapter attempts to provide a screen-level impression for the readers, to understand the formaldehyde, which should be helpful for the source characterization and control of formaldehyde in the indoor environment.

Keywords

VVOCs · Formaldehyde · Emission model · Key parameters · Impact factors

Introduction

High volatility organic compounds, or the so-called very volatile organic compounds (VVOCs), are an important subgroup of indoor pollutants and cover a wide spectrum of chemical substances (Salthammer 2016). Table 1 summarizes some typical VVOCs in the indoor environment. Among them, formaldehyde is by far the well-known VVOCs, which is also recognized as the most important compound in indoor environment. Therefore, this chapter just introduces formaldehyde as a typical representative of VVOCs. Formaldehyde is an important chemical for the global economy, widely used in construction, wood pressing, furniture, etc. Formaldehyde has been classified as a human carcinogen that causes nasopharyngeal cancer and probably leukemia, contributing significantly to global burden of disease.

This chapter will introduce the formaldehyde properties and hazards, usages and pollution levels, determination methods, emission models, key parameters measurement methods, and impact factors.

Properties and Hazards of Formaldehyde

Properties

Formaldehyde (CH_2O) is also known as methanal, methyl aldehyde, oxymethylene, oxomethane, methylene oxide, and formic aldehyde. The three-dimensional structure of formaldehyde is shown in Fig. 1. The molecular structure of formaldehyde (shown in Fig. 2) includes two carbon-hydrogen single bonds (C-H) and a carbon-oxygen double bond (C=O), where the angle between the C-H bond is 116.5° , and the angle between the C=O bond and the C-H bond is 121.8° . At normal temperature and pressure, formaldehyde is a colorless and highly toxic gas with a pungent, irritating odor. It is readily reactive, readily polymerizable, and highly flammable and can decompose into methanol and carbon monoxide at temperatures above

Table 1 List of very volatile organic compounds (Salthammer 2016)

Group	Compound	Formula	Group	Compound	Formula
C1	Methanol	CH ₃ OH	C4	n-Butane	C ₄ H ₁₀
	Formaldehyde	HCHO		2-Methylpropane	CH ₃ CH(CH ₃)CH ₃
	Formic acid	HCOOH		1,3-Butadiene	CH ₂ CHCHCH ₂
	Chloromethane	ClCH ₃		Butanal	C ₄ H ₈ O
	Dichloromethane	CH ₂ Cl ₂		2-Methylpropanal	CH ₃ CH(CH ₃)CHO
	Trichloromethane	CHCl ₃		2-Methyl-2-propanol	CH ₃ C(CH ₃)OHCH ₃
	Trichlorofluoromethane	CCl ₃ F		Methacrolein	CH ₂ C(CH ₃)CHO
	Dichlorodifluoromethane	CCl ₂ F ₂		2-Butanone	CH ₃ COCH ₂ CH ₃
	Dichlorofluoromethane	CHCl ₂ F		Methyl vinyl ketone	CH ₃ C(O)CHCH ₂
	Chlorodifluoromethane	CHClF ₂		2,3-Butanedione	CH ₃ C(O)C(O)CH ₃
	Methyl bromide	CH ₃ Br		Vinyl acetate	CH ₃ C(O)OCHCH ₂
	Phosgene	COCl ₂		Furan	C ₄ H ₆ O
C2	Ethane	C ₂ H ₆	C5	2-Chloro-1,3-butadiene	CH ₂ CHCClCH ₂
	Ethanol	C ₂ H ₅ OH		n-Pentane	C ₅ H ₁₂
	Acetadehyde	CH ₃ CHO		Cyclopentane	C ₅ H ₁₀
	Chloroethane	C ₂ H ₅ Cl		2-Methylbutane	CH ₃ CH(CH ₃)C ₂ H ₅
	1,1-Dichloroethene	Cl ₂ CCH ₂		Isoprene	CH ₂ C(CH ₃)CHCH ₂
	Vinyl chloride	C ₂ H ₃ Cl		2-Methylfuran	(C ₄ H ₃ O)CH ₃
	Glyoxal	CHOCHO	C6	2-Methylpentane	CH ₃ CH(CH ₃)C ₃ H ₇
	Ethylene oxide	C ₂ H ₄ O		3-Methylpentane	C ₂ H ₅ CH(CH ₃)C ₂ H ₅
C3	Propane	C ₃ H ₈	Other	Carbon disulfide	CS ₂
	1-Propanol	CH ₃ (CH ₂) ₂ OH		Methylsulfide	HSCH ₃

(continued)

Table 1 (continued)

Group	Compound	Formula	Group	Compound	Formula
	2-Propanol	CH ₃ CH(OH)CH ₃		Dimethylsulfide	S(CH ₃) ₂
	Propanal	C ₃ H ₆ O		Trimethylsilanol	Si(CH ₃) ₃ OH
	2-Propenal (Acrolein)	CH ₂ CHCHO		Acrylonitrile	CH ₂ CHCN
		CO(CH ₃) ₂		Acetonitrile	CH ₃ CN
	2-Propanone (Acetone)	CH ₂ (OCH ₃) ₂		Dimethylamine	HN(CH ₃) ₂
	Dimethoxymethane	CH ₃ COOCH ₃		Trimethylamine	N(CH ₃) ₃
	Methylacetate	CHOCOCH ₃		Diethylamine	HN(C ₂ H ₅) ₂
	Methylglyoxal				
	2-Chloropropane	CH ₃ CHClCH ₃			

Fig. 1 The three-dimensional structure of formaldehyde

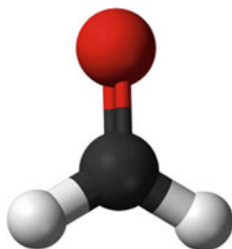


Fig. 2 The structure of formaldehyde



150 °C, but the uncatalyzed decomposition rate is very slow below 300 °C. The high chemical reactivity of formaldehyde makes it possible to carry out a variety of self-association reactions and forms a variety of chemical substances with water association (WHO 2002). Formaldehyde is highly soluble in polar solvents such as water and ethanol. In an aqueous solution, formaldehyde usually combines with water to form methylene glycol or self-polymerizes to form paraformaldehyde. Therefore, formaldehyde aqueous solution (commonly known as formalin) with a concentration of 37% is usually prepared and used for anticorrosion and sterilization. At room temperature, when the formaldehyde content is above 30%, the polymer will precipitate and make the solution turbid. Formaldehyde gas can form explosive mixtures with air under atmospheric pressure. The reported flammability is between 12.5% and 80% by volume, a 65–70% formaldehyde-air mixture being the most readily flammable (WHO 2002). The reported values for the physical and chemical properties of formaldehyde are shown in Table 2.

Hazards

Acute lethality. No reports of humans die from high levels of formaldehyde in the short term. Experiments using rats and mice with formaldehyde exposure have shown that the lowest dose usually produces a 0% mortality rate, and the highest dose usually produces a 100% mortality rate, but no clear limits have been reported (CAS 2008).

Nonlethal toxicity. Low-concentration formaldehyde exposure experiments on humans (≤ 20 ppm) and animals (≤ 31.7 ppm, nonhuman primates, rats, mice, and guinea pigs) showed nose/throat and eye irritation (CAS 2008). There were skin hypersensitivities in human experiments, and in animal experiments at 20 ppm and 30 ppm; it was observed that the hair around rats' genital area turned yellow

Table 2 Physical and chemical properties of formaldehyde (CAS 2008; Salthammer et al. 2010; WHO 2002)

Property	Range of reported values
Relating molecular mass	30.03
Melting point (°C)	-118 to -92
Boiling point (°C, at 101.3 kPa)	-21 to -19
Vapor pressure (calculated) (mm Hg, at 25 °C)	3883
Vapor density (air = 1)	1.067
Liquid density (g/mL, water = 1)	0.815
Water solubility (mg/L, at 25 °C)	Very soluble, up to 55% 980 L/L water
Henry's law constant (atm·m ³ /mol, at 20 °C)	3.27×10^{-7}
Autoignition temperature (°C)	300
Log octanol/water partition coefficient ($\log K_{ow}$)	0.35
Log organic carbon/water partition coefficient ($\log K_{oc}$)	0.70 to 1.57
Conversion factor	1 ppm = 1.23 mg/m ³ 1 mg/m ³ = 0.813 ppm

(Tobe et al. 1985). It should be noted that experiments on humans are short term, while experiments on animals are long term.

Neurotoxicity. Studies have tested the relationship between formaldehyde exposure and short-term memory, ability to concentrate, and changes in psychomotor functions, but no concentration-response relationship was found. However, the researchers did attribute the poor performance at 0.33 ppm exposure to irritation or central nervous system effects caused by the exposure. No report on neurotoxicity in animals (CAS 2008).

Developmental/reproductive toxicity. There is no evidence that formaldehyde exposure affects human development or reproduction. Inhalation, oral gavage, dietary, and drinking water studies have been used to investigate the effects of formaldehyde on animal reproduction and development, and it has been found that formaldehyde concentrations of 40 ppm are maternal toxicity, reflected in significant maternal weight loss; while concentrations of 20 ppm and 40 ppm are fetal toxicity, reflected in fetal weight loss (CAS 2008).

Genotoxicity. According to International Agency for Research on Cancer (IARC 2006), formaldehyde demonstrates positive effects in a large number of in vitro tests for genotoxicity, including bacterial mutation, DNA strand breaks, chromosomal aberrations, and sister chromatid exchange. Studies in humans showed inconsistent results with regard to cytogenetic changes (micronuclei, chromosomal aberrations, and sister chromatid exchange). The IARC reviewed some studies that showed increased DNA-protein cross-links in workers exposed to formaldehyde, which is consistent with the results of inhalation studies in mice and monkeys (IARC 2006; CAS 2008).

Carcinogenicity. According to the pollutant hazard list of IARC and WHO, formaldehyde is classified as a category A carcinogen. A study by the U. S. Environmental Protection Agency (U.S. EPA 2003) shows that there is a

significant statistical association between respiratory tumors in specific parts of the human body and formaldehyde exposure; formaldehyde exposure can induce cancer in rats and mice (nasal squamous cell carcinomas). The IARC (2006) stated that “sufficient epidemiological evidence that formaldehyde causes nasopharyngeal cancer in humans. There is strong but not sufficient evidence for a causal association between leukemia and occupational exposure to formaldehyde.”

Usages and Pollution Levels of Formaldehyde

Formaldehyde is an important economical chemical. The use of formaldehyde covers a wide range in people's lives. Urea formaldehyde resins, melamine formaldehyde resins, and phenol formaldehyde resins (UF, PF and MF resins) accounted for nearly 70% of global formaldehyde demand in 2017 (HIS Markit 2019). Particleboard, hardwood plywood, and medium-density fiberboard are the mostly manufactured wood-based boards with the use of urea formaldehyde resins; melamine formaldehyde resins, and phenol formaldehyde resins are largely used in composite wood products industry as glues. These resins are also molded to create different products, such as insulating layers, facial wipes, paper napkins, and paper product coatings.

Formaldehyde can completely negate or kill the activities of bacteria, fungi, yeast molds, viruses, and parasites, so that it is widely used in preservative and disinfectant. In the agricultural industry, formaldehyde is used as a fumigant to prevent mildew and rot in plants and vegetables. Formaldehyde has been also used in the medical fields. Some of the early medicinal applications of formaldehyde included its use in vasectomy, and as a disinfectant before hydatid cyst removal surgery. In the textile industry, in order to achieve anti-wrinkle, anti-shrink, and flame retardant effects, or to maintain the durability of printing and dyeing, it is necessary to add formaldehyde to the auxiliary agent in the production of clothing fabrics. Polyacetal made from formaldehyde can be used in thermoplastics in electrical and electronic applications, or in parts of motor vehicles and machines that are subjected to mechanical or thermal stress, and in household articles, such as light switches, sockets, lamps, plumbing parts, and motors.

According to report, worldwide annual production of formaldehyde is approximately 52 million tons in 2017 (Iabal et al. 2018). Products containing formaldehyde will gradually emit free formaldehyde in the process of use, and formaldehyde in the ambient air will damage human health through respiratory tract and skin contact. Formaldehyde levels between 0.1 and 0.5 ppm (about 0.12–0.6 mg/m³) can be detected by the human senses, 0.5–1.0 ppm (about 0.6–1.2 mg/m³) can cause eye irritation, and more than 1.0 ppm (about 1.23 mg/m³) can irritate the nose and throat (NICNAS 2006). A number of investigators have shown that formaldehyde exposure levels are generally higher indoors than outdoors. In the indoor environment, general sources of formaldehyde include: formaldehyde-containing resin products, cooking, various consumer products, such as furniture, carpets, glass fibers, permanent press cloth, paper products, cosmetic, perfumes, and some household cleaners.

Smoking is also an important source of indoor formaldehyde. Poor ventilation, high temperature, and residential renovation will increase the indoor formaldehyde concentration. In the outdoor environment, formaldehyde mainly comes from the exhaust gas produced by the combustion of diesel vehicle engines, the smoke produced by cigarettes and burning forests and wood products, as well as the formaldehyde emitted by indoor ventilation (Goldstein et al. 2021).

The indoor guideline values of formaldehyde regulated by different countries or organizations are summarized in Table 3, which can be categorized into two groups: short-term exposure (about 0.5–1 h) and long-term exposure (mostly 8 h). The short-term exposure limits are used to prevent acute health effects, such as sensory stimulation in a short period of time, while the long-term exposure limits are used to prevent chronic health effects. The short-term exposure limit recommended by the WHO (1987) is 0.08 ppm ($100 \mu\text{g m}^{-3}$).

Worldwide indoor and outdoor formaldehyde concentrations in air in several countries are summarized in Table 4. Indoor formaldehyde concentration levels in most countries are below or close to the limit ($100 \mu\text{g m}^{-3}$) recommended by the WHO (1987), but the levels reported in Cairo and Beijing are higher than this threshold, and the level reported in Beijing is more than two to three times the value. There is a uniform finding in different seasons and different cities: the concentration of formaldehyde in the indoor environment is higher than that in the outdoor environment. Previous studies have shown that the emission rate of formaldehyde increases with increasing temperature, so seasonal changes will lead to an increase in formaldehyde concentration in summer (Kinney et al. 2002; Ohura et al. 2006).

Table 3 International guideline values for formaldehyde in indoor air (Salthammer et al. 2010)

Country	Value		Comments
Australia	0.1 ppm	$120 \mu\text{g m}^{-3}$	Short duration
	0.08 ppm	$100 \mu\text{g m}^{-3}$	
Canada	0.1 ppm	$123 \mu\text{g m}^{-3}$	1 h
	0.04 ppm	$50 \mu\text{g m}^{-3}$	8 h
China	0.08 ppm	$100 \mu\text{g m}^{-3}$	1 h average
France		$50 \mu\text{g m}^{-3}$	2 h (proposed)
		$10 \mu\text{g m}^{-3}$	Long-term exposure (proposed)
Singapore	0.1 ppm	$120 \mu\text{g m}^{-3}$	8 h
Japan	0.08 ppm	$100 \mu\text{g m}^{-3}$	0.5 h
Korea	0.1 ppm	$120 \mu\text{g m}^{-3}$	8 h
Norway	0.05 ppm	$60 \mu\text{g m}^{-3}$	24 h average
	0.05 ppm	$100 \mu\text{g m}^{-3}$	30 min average
Poland	0.04 ppm	$50 \mu\text{g m}^{-3}$	24 h
	0.08 ppm	$100 \mu\text{g m}^{-3}$	8–10 h
UK		$100 \mu\text{g m}^{-3}$	0.5 h
USA (California)	0.027 ppm	$33 \mu\text{g m}^{-3}$	8 h
WHO	0.08 ppm	$100 \mu\text{g m}^{-3}$	0.5 h average

Table 4 Indoor and outdoor formaldehyde concentrations in various countries

Country	Concentration ($\mu\text{g}/\text{m}^3$)		References
	Indoor air	Outdoor air	
Uppsala	8.3 \pm 1.5 ^a	1.3 \pm 1.8	Sakai et al. 2004
Nagoya	17.6 \pm 1.8	5.8 \pm 1.5	Sakai et al. 2004
Shimizu (winter)	12.4 \pm 1.8	1.4 \pm 1.6	Ohura et al. 2006
Shimizu (summer)	18.7 \pm 2.6	2.5 \pm 1.4	Ohura et al. 2006
New York (winter)	11.5 \pm 4.9	2.1 \pm 0.9	Kinney et al. 2002
New York (summer)	28.5 \pm 13.8	5.3 \pm 2.3	Kinney et al. 2002
Los Angeles (winter)	21.0 \pm 11.0	3.9 \pm 1.3	Sax et al. 2004
Los Angeles (fall)	16.0 \pm 6.2	4.4 \pm 1.6	Sax et al. 2004
Mexico City	15.7 \pm 15.7	5.1 \pm 1.5	Serrano-Trespalacios et al. 2004
Paris	34.4 \pm 1.9		Clarissee et al. 2003
Quebec	29.5 \pm 1.6		Gilbert et al. 2006
Prince Edward	33.2 \pm 22.4		Gilbert et al. 2005
Cairo (spring)	117.5 \pm 49.6	38.9 \pm 9.5	Khoder et al. 2000
Cairo (summer)	141.6 \pm 63.0	49.6 \pm 12.7	Khoder et al. 2000
Beijing (winter)	228.0 \pm 160.9		Yao et al. 2005
Beijing (summer)	308.4 \pm 228.0		Yao et al. 2005

^ageometric mean \pm geometric standard deviation

The indoor and outdoor formaldehyde concentration levels in Shimizu, New York, Cairo, and Beijing in the summer season are higher than those in the winter season, which is consistent with the above pattern. Formaldehyde had a slightly higher concentration in the winter compared to that in the fall in Los Angeles, which could be interpreted as a lower exchange rate since people close windows in winter and less so during much of the rest of the year in Los Angeles.

As mentioned above, formaldehyde is widely used in a variety of industries in people's lives, including paint industry, the glue, dyes, rubber, metal, wood, leather, petroleum, pesticides, fertilizer, agricultural industries, medical, cleaning agents, preservatives, cosmetic, perfumes, vitamins, food, etc., which also leads to many people being exposed to formaldehyde in occupations. According to the pathological analysis data of humans and animals after exposure to formaldehyde for a certain period of time and some health hazard assessments, some safety and occupational health authorities have stipulated the formaldehyde occupational exposure limits (OELs, shown in Table 5): threshold value (TLV), time-weighted average (TWA), and short-term exposure limit (STEL). The indoor guideline value is lower than the occupational limit because people stay in the nonoccupational space for longer, and there are more vulnerable groups in the nonoccupational space, such as babies, the elderly, pregnant women, and children. The formaldehyde occupational exposure limit has had a downward trend over time as more information on its health risks has become available.

Table 5 Formaldehyde occupational exposure limits (OEL) of several countries (Zhang et al. 2009; Salthammer et al. 2010)

Country	OEL (ppm)		
	TWA ^a	STEL ^a	TLV ^a
Australia	1	2	
Canada			0.3
China			0.4
Germany	0.3		
Japan	0.1		
Sweden	0.5		1
South Africa	1	2	
UK	2	2	
USA			
The federal standard	0.75	2	
Recommended exposure limits ^b	0.016	0.1	0.3

^aTWA uses 8 h; STEL uses 30 min by most countries, except for the USA (15 min)

^bRecommended exposure limits (RELS as TWA and STEL) were recommended by NIOSH, and TLV by ACGIH

Methods for the Determination of Formaldehyde

Standard Test Methods

Perforator Method

The perforator method developed by the former European Particleboard Federation in the late 1960s has become the European standard EN 120 since 1984. EN 120 (1993) is used to determine the formaldehyde content of unlaminated and uncoated wood-based panels. Its extraction process is as follows: the formaldehyde is extracted from the test piece by boiling toluene, and then transferred to distilled water or desalinated water; and then the formaldehyde content in the aqueous solution is determined by the acetylacetone photometric method. EN 120 states that the correlation between the perforator value and the amount of formaldehyde emission depends on the density, porosity, and humidity of the test sample. The total running time of the perforator method is relatively short, so it is widely used in production quantification, classification, and control.

Flask Method

The flask method was standardized as EN 717-3 (1996). The main principle of the flask method is to hang a known amount of test panels above the water in a closed container kept at a constant temperature. The formaldehyde emitted from the test panels within a certain period time is absorbed by the water, and the formaldehyde content in the water is determined photometrically by the acetylacetone method.

Desiccator Method

The desiccator method is used to determine the amount of formaldehyde emitted by particleboard, fiberboard, plywood, oriented strand board (OSB), and wood laminate flooring. The main principle of the desiccator method is to put a certain exposed area of wood-based panels on the support of a clean dryer, and the bottom of the dryer contains a certain amount of distilled water. The wood-based panels are placed in a prescribed environment for a certain period time (about 24 h) and then analyzed by spectrophotometry to get the formaldehyde content.

Gas Analysis Method

The gas analysis method (EN 717-2 1994) can be used to determine the formaldehyde emitted from uncoated or coated wood-based panels, sidebands, floor coverings, foams, foils, laminated wood products, veneer wood products, and coated wood products. Formaldehyde emitted from test pieces of wood-based panels placed in the airtight chamber where the environmental conditions (temperature, humidity, airflow, pressure) are controlled, mixing with the air. This air is continually drawn off and passes through gas wash bottles containing water, which absorbs formaldehyde. The concentration of formaldehyde was determined by spectrophotometry or fluorescence method. The amount of formaldehyde released is calculated by the formaldehyde test concentration, sampling time, and sample exposure area of the test pieces. The procedure has been standardized in accordance with the EN ISO 12460-3:2015 standard.

Analysis of Formaldehyde

Spectrophotometric Method

Spectrophotometry is the most commonly used method in the determination of formaldehyde, and it has simple operation, low cost, strong selectivity, and high sensitivity (Hladova et al. 2019). According to different absorbers, the method can be divided into: acetylacetone method, MBTH method, AHMT method, chromotropic acid method, pararosaniline method, etc., and each spectrophotometric method has its advantages and disadvantages.

The acetylacetone (acac) method is a formaldehyde determination method based on Hantzsch reaction. The Hantzsch reaction refers to the cyclization of one kind of β -diketones with formaldehyde and ammonia in a slightly acidic solution to form dihydropyridine derivatives, which are generally colored and often fluorescent. Nash (1953) used 2,4-pentanedione (PD, acetylacetone) for the first time for formaldehyde determination based on Hantzsch reaction. Since then, this chemical reaction using PD has been used by many others and has been recommended in Europe and Japan for the determination of formaldehyde emissions from wood materials (Salthammer et al. 2010). The principle of acetylacetone method is that formaldehyde reacts with acetylacetone to form a yellow compound (dihydropyridine 3,5-diacetyl-1,4-dihydrolutidine (DDL)) under the action of ammonium salt and can be quantified

by ultraviolet/visible spectrophotometry under the wavelength of 412 nm. This method is simple in principle, easy to operate, stable in color, and not interfered by acetaldehyde, but its analysis process is relatively slow.

Since 1961, 3-methyl-2-benzothiazolone hydrazone hydrochloride (MBTH) has been introduced into the quantitative measurement of aldehyde compounds. Adding excessive amounts of MBTH to samples containing formaldehyde can trigger a variety of reactions. MBTH firstly reacts with formaldehyde to form an azine. Excess MBTH is oxidized with the addition of developer (Fe (III)). The oxidized MBTH reacts with the azine to form a strong blue color, and the resulting blue complex has the maximum characteristic absorption at 628 nm. The intensity of the blue color is proportional to the initial concentration of formaldehyde. The method is simple and easy to implement, with high sensitivity and low detection limit. However, MBTH is rarely used because of its high cost, interference with other lower aliphatic aldehydes, and instability of MBTH-formaldehyde intermediates.

The principle of AHMT method (Hladova et al. 2019) is that formaldehyde and 4-amino-3-hydrazino-5-mercaptop-4H-1,2,4-triazole (AHMT) are condensed under alkaline conditions, and then oxidized by potassium iodate to a purple red 6-mercaptop-5- triazolo [4,3-b]-s-tetrazine (MTT) compound. The depth of its color is proportional to the formaldehyde content. The concentration of formaldehyde is calculated by measuring the absorbance at 550 nm with a spectrophotometer. The AHMT method is more affected by aldehydes than the acetylacetone method.

The chromotropic acid method is that formaldehyde reacts with chromotropic acid in a concentrated sulfuric acid solution to form a red-violet hydroxydiphenylmethane derivative. The absorption maximum at 580 nm is used for UV/visible detection. This method has been standardized by the National Institute of Occupational Safety and Health (NIOSH) and is used to determine formaldehyde in large-scale chambers, in small-scale chambers, and in the desiccator method (Salthammer et al. 2010). Chromotropic acid method has the advantages of simple operation, rapid and sensitive, but it also has some shortcomings. It is not easy to handle in concentrated sulfuric acid, and the coexistence of phenols, aldehydes, alkenes, and NO₂ compounds has positive or negative interferences to the determination of formaldehyde (Hladova et al. 2019).

The pararosaniline method (Mikscha et al. 1981) is that formaldehyde and para-rosaniline form a magenta dye in the presence of sulfite ions, which is a unique reaction of formaldehyde. Its strong absorbance at 570 nm is used for UV/visible detection. In a strong acid medium, the pararosaniline method is a unique reaction of formaldehyde, and it is not interfered by other aldehydes and phenols during the measurement. However, this method also has some shortcomings: fast fading, susceptible to temperature, and the use of toxic mercury reagents.

Chromatographic Method

The chromatographic method (Li et al. 2007) for the determination of formaldehyde has a powerful separation function, simple operation, and good selectivity. It can be directly used for the determination of formaldehyde in indoors, textiles, and food. 2,4-Dinitrophenylhydrazine (DNPH) has been identified as a standard reagent for the determination of formaldehyde by many national and international standards bodies. DNPH reacts with formaldehyde in the presence of an acidic catalyst to form stable

and colored hydrazone derivatives. The hydrazone derivatives are separated by high-performance liquid chromatography (HPLC), and then the HCHO-DNPH derivative is detected by ultraviolet spectrum (UV) at 360 nm. The DNPH method has been used for different environmental samples, including automobile exhaust, waste and drinking water, and air pollution. In order to monitor air quality, a sampling tube based on DNPH coated solid adsorbent was developed. The DNPH method is described in EPA Method TO-11A, ASTM D 5197150 and has been accepted as an international standard by ISO (Salthammer et al. 2010).

Some interference should also be considered when using the DNPH method to monitor formaldehyde: ozone interference (Schulte-Ladbeck et al. 2001). Ozone easily reacts with DNPH and derived hydrazone compounds to interfere with the determination of formaldehyde. Therefore, an appropriate scrubber/descaler should be used to remove ozone. There are commercially available products, for example, ozone removal columns, which are used to remove ozone before DNPH sampling. The ozone removal column is filled with granular potassium iodide. When the ozone-containing air passes through the device, the iodine ions are oxidized to iodine, and the ozone in the air is consumed at the same time.

The analysis of aldehyde samples using HPLC follows these procedures (Wang et al. 2020a): (1) Extraction of aldehyde-DNPH derivatives: a quantitative acetonitrile solvent was accurately added to the DNPH sampling tube, which was then collected in a colorimetric tube, filtered with a membrane, and treated with an ultrasonic cleaner; subsequently, it was placed in a brown volumetric bottle and divided into a sample vial for use; (2) test and analysis: the prepared standard fluids and extractions of aldehyde-DNPH derivatives were analyzed by HPLC. The quantification is based on the retention time and peak area.

Sensors

Traditional formaldehyde measurement methods require well-trained operators to provide services and are expensive, and the system is large and difficult to carry, which promotes the application of sensor technology to formaldehyde measurement research (Chung et al. 2013). Descamps et al. (2012) proposed a colorimetric device based on the acetylacetone (acac) method to measure the concentration of gaseous formaldehyde in a nanoporous film doped with fluorine-P. Based on an ammonium sulfate derivatization reagent and a capillary electrophoresis-electrochemical detection (CEED) system, Deng et al. (2012) proposed a formaldehyde gas sensor with the minimum detection limit of 0.12 ppb and found that the detection signal strength was linearly correlated with the formaldehyde concentration in the concentration range of 0.4–770 ppb.

Emission Models of Formaldehyde

Short-Term Emission Models

Prediction of formaldehyde emissions in different indoor settings under various environmental conditions promote the development of modeling approach, which could be divided into short-term emission models and long-term emission models.

The short-term emission models mainly refer to the physical process of formaldehyde from indoor building materials and furniture, which include empirical models and physics-based models. The long-term emission models consider both the physical and chemical processes that occur inside the materials.

The empirical models are generally obtained through experimental observation and summarization of the test data and mainly include the power-law model, single-exponential (first-order) model, and double-exponential (second-order) model. Liu et al. (2015) applied the power-law model and single-exponential model to investigate formaldehyde emissions from composite wood and solid wood furniture and found that the power-law model worked better than the single-exponential model. The empirical models are simple and easy to use and are therefore frequently used in engineering applications, for example, in the BIFMA standard. However, these empirical models include empirical parameters, which do not have physical meanings and can just be obtained through nonlinear curve fitting of the model with test data. These empirical parameters are only applicable to the specific test conditions and cannot be extended to predict emissions in other scenarios. This limitation hinders wider use of empirical models, especially in real indoor environments where the environmental conditions change frequently. Therefore, Little et al. (1994) proposed the classic physics-based mass transfer model to characterize VOC emissions from single-layer building materials. This model considers two physical mass transfer processes for the VOC emissions: the internal diffusion process (characterized by D_m), and the interface partition process (characterized by K); while the external convective process is ignored. The key parameters (C_0 , D_m , K) in this model are the characteristic parameters, which reflect the essence of the emission process, and can be used in other emission scenarios (e.g., different ventilation rates or loading ratios). Some follow-up studies improved the application range of the Little's model and proposed various mass transfer models, for example, by considering the external convective process, by extending the model to multilayer materials, or by incorporating more general conditions. Here we will introduce some typical physics-based models.

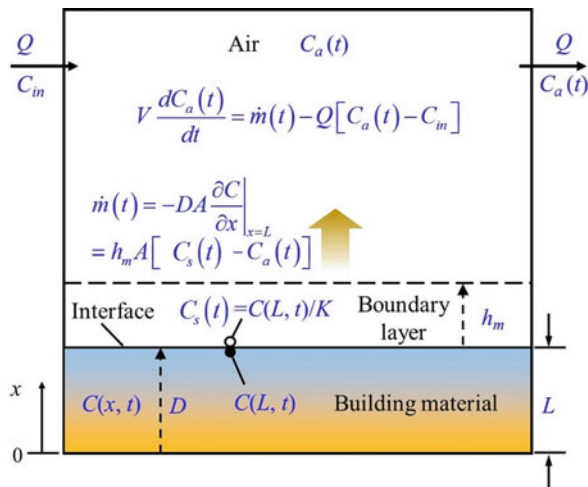
Formaldehyde emission from building material in a chamber or indoor environment is schematically shown in Fig. 3. The following assumptions are made: (1) the initial concentration of formaldehyde in the building material, C_0 , is uniformly distributed; (2) the inlet and initial formaldehyde concentrations of the chamber are zero; (3) mass transfer is one dimensional, vertical to the material surface; (4) the diffusion coefficient D_m and the partition coefficient K are constant; (5) the chamber air is well mixed; and (6) equilibrium always exists at the material/air interface.

Based on the above assumptions, the emission process of formaldehyde inside the material can be described by the one-dimensional diffusion equation:

$$\frac{\partial C_m}{\partial t} = D_m \frac{\partial^2 C_m}{\partial x^2} \quad (1)$$

where C_m is the VOC concentration inside the material, $\mu\text{g}/\text{m}^3$; t is the emission time, s ; D_m is the diffusion coefficient, m^2/s ; y is the coordinate, m .

Fig. 3 Schematic of formaldehyde emission from building material in a chamber



Since the material is placed on a stainless-steel chamber, no mass flux exists at the bottom of the material, or:

$$\frac{\partial C_m}{\partial x} = 0, \quad x = 0 \quad (2)$$

At the material/air interface, a third type of boundary condition can be used to describe the convective mass transfer process:

$$-D_m \frac{\partial C_m}{\partial x} = h_m (C_{as} - C_a), \quad x = L \quad (3)$$

where h_m is the convective mass transfer coefficient, m/s, which can be calculated using the empirical correlation; C_a is the formaldehyde concentration in the chamber and C_{as} is the formaldehyde concentration in the air at the interface, $\mu\text{g}/\text{m}^3$; L is the thickness of the material, m. Assume that an equilibrium exists at the material/air interface, that is:

$$C_m = K C_{as}, \quad x = L \quad (4)$$

where K is the material/air partition coefficient.

The initial condition for Eq. (1) is given as:

$$C_m(x, t) = C_0, \quad t = 0, \quad 0 \leq x \leq L \quad (5)$$

where C_0 is the initial VOC concentration inside the material, $\mu\text{g}/\text{m}^3$.

The above Eqs. (1)–(5) describe the emission process inside the material, together with the boundary conditions and the initial condition. These equations are not

closed because of the existence of C_a . An equation containing C_a is given as follows based on mass conservation of formaldehyde in the chamber:

$$V \frac{dC_a}{dt} = -AD_m \frac{\partial C_m}{\partial x} - QC_a, \quad x = L \quad (6)$$

where V is the volume of the chamber, m^3 ; A is the emission area of the material, m^2 ; Q is the ventilation rate, m^3/s .

Now the system of Eqs. (1)–(6) is closed. The formaldehyde concentrations in the material and the air phases can be solved simultaneously. In Little's model (Little et al. 1994), the external convection mass transfer resistance is neglected; that is, h_m is Eq. (3) is assumed to be infinity. Huang and Haghigat (2002) later developed an analytical model by neglecting the formaldehyde concentration in the air because of its low value relative to the concentration in the material by neglecting C_a in Eq. (3). After that, Xu and Zhang (2003) presented an improved mass transfer model by considering the full version of Eq. (3) and derived a semi-analytical model. The obtained solution is as follows:

$$C_m(x, t) = KC_a(t) + \sum_{m=1}^{\infty} \frac{\sin(\beta_m L)}{\beta_m} \cdot \frac{2(\beta_m^2 + H^2)}{L(\beta_m^2 + H^2) + H} \cdot \cos(\beta_m x) \cdot \left[(C_0 - KC_a(0))e^{-D\beta_m^2 t} + \int_0^t e^{-D_m \beta_m^2 (t-\tau)} \cdot K dC_a(\tau) \right] \quad (7)$$

where $H = h_m/D_m K$, β_m ($m = 1, 2, \dots$) are the positive roots of the following equation:

$$\beta_m \tan(\beta_m L) = H \quad (8)$$

Xu and Zhang's (2003) model is not a full analytical model since the solution of C_m in Eq. (7) is coupled with the air concentration C_a . By applying the Laplace transformation, Deng and Kim (2004) later derived a full analytical solution for the chamber formaldehyde concentration:

$$C_a(t) = 2C_0\beta \sum_{n=1}^{\infty} \frac{q_n \sin q_n}{G_n} e^{-D_m L^{-2} q_n^2 t} \quad (9)$$

with $G_n = [K\beta + (\alpha - q_n^2)KBi_m^{-1} + 2]q_n^2 \cos q_n + [K\beta + (\alpha - 3q_n^2)KBi_m^{-1} + \alpha - q_n^2]q_n \sin q_n$; $Bi_m = h_m L / D_m$; $\alpha = QL^2 / VD_m$; $\beta = AL / V$.

where Bi_m is the Biot number for mass transfer representing the ratio of the diffusion mass transfer resistance inside the material to the convective mass transfer resistance outside the material; α is the dimensionless air exchange rate; β is the ratio of the material volume to the chamber volume; q_n are the positive roots of the following equation:

$$q_n \tan q_n = \frac{\alpha - q_n^2}{K\beta + (\alpha - q_n^2)KBt_m^{-1}}, \quad n = 1, 2, \dots \quad (10)$$

In Deng and Kim's model, the initial VOC concentration in the chamber ($C_{a,0}$) and the inlet VOC concentration by ventilation (C_{in}) are zero. Later, Hu et al. (2007) developed a general analytical model for predicting emissions from arbitrary-layer building materials. It can estimate the formaldehyde emissions from arbitrary layered building materials whose mass transfer resistance through the gas-phase boundary layer on each side of it is not neglected and the initial distribution of material-phase formaldehyde concentration in each layer of building material is not necessarily uniform.

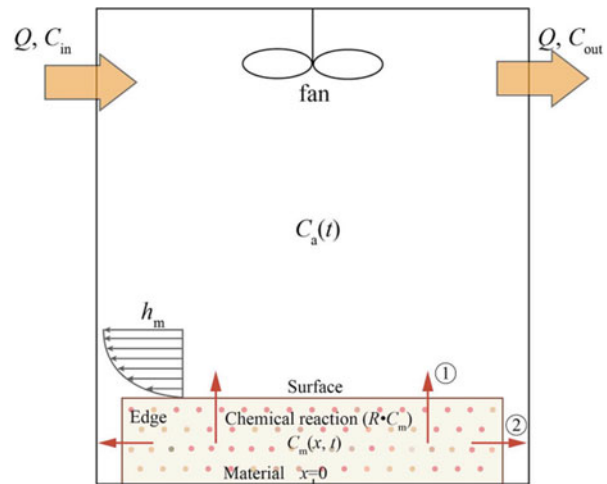
Long-Term Emission Model

The above physics-based models used short-term emission data to validate the effectiveness; whether these models can be extended to predict long-term emissions needs further investigation. In addition, these models generally consider the physical emission process only but neglect the chemical reaction process that is likely to occur in the long-term emissions especially for formaldehyde from composite wood panels (e.g., hydrolysis). Given this background, He et al. (2019) recently developed an improved mechanism-based model (long-term emission model) to predict the long-term behaviors of formaldehyde from composite wood materials with exposed edges and seams. One merit of the model lies in that it has a full analytical solution. Here we will briefly introduce this model.

A schematic of formaldehyde emissions from building material in a ventilated chamber or indoor environment is shown in Fig. 4. The formaldehyde emissions can originate from the top surface or the exposed edges. In most chamber tests, the edges are sealed. In these regions, emission occurs only from the top surface and can be treated as one-dimensional emission (the diffusion path perpendicular to the flat surface). By defining the diffusion path perpendicular to the edge surface, such one-dimensional emission can also describe the emission from the exposed edges and seams when they account for most of the emission quantity of the finished product. He et al.'s study mainly focuses on the latter emission scenario. Similar to other existing physical-based models, it is assumed that the formaldehyde distribution inside the material is uniform before testing, and the partition process at the material/air interface is governed by Henry's law. Further, it is assumed that the hydrolysis of UF resin inside the composite wood panel will continuously occur and produce new formaldehyde.

The chamber formaldehyde concentration for long-term emission can derive from both free formaldehyde initially in the material and hydrolysis of the UF resin. For the former, the emission rate of formaldehyde is described by physical mass transfer

Fig. 4 Schematic of formaldehyde emissions from building material in a ventilated chamber. (Scenario ① represents emission from top surface; scenario ② represents emission from exposed edges and seams)



process, and for the hydrolysis process, the reaction between UF resin and water vapor can be described by the following chemical reaction:



where P stands for the products except for formaldehyde. The formation rate of formaldehyde can then be written as

$$\frac{\partial C_m^F}{\partial t} = k \cdot C_{\text{UF}} \cdot C_{\text{water}} \quad (12)$$

where C_m^F is the concentration of formaldehyde in the building material originated from hydrolysis; k is the second-order rate constant; C_{UF} is the concentration of the UF resin in the building material; and C_{water} is the concentration of water vapor in the gas phase. Under the controllable chamber conditions (constant T and RH), the concentration of water vapor in the gas phase can be treated as a constant so that Eq. (12) is simplified to pseudo-first-order with regard to the concentration of UF resin:

$$\frac{\partial C_m^F}{\partial t} = k' \cdot C_{\text{UF}} \quad (13)$$

where k' is the pseudo-first-order rate constant.

As applied in previous studies based on experimental observation and theoretical analysis, the concentration of UF resin (C_{UF}) is assumed to be linearly correlated with the formaldehyde concentration in the material (C_m), that is:

$$C_{\text{UF}} = m \cdot C_m \quad (14)$$

where m is a constant and C_m is the concentration of formaldehyde in the building material including both physically free formaldehyde and chemically produced formaldehyde, $\mu\text{g}/\text{m}^3$.

By substituting Eq. (14) into Eq. (13):

$$\frac{\partial C_m^F}{\partial t} = R \cdot C_m \quad (15)$$

where $R = k' \cdot m$.

Based on the above analysis, the governing equation representing the physical diffusion and chemical reaction processes inside the material can be described by Eq. (16):

$$\frac{\partial C_m}{\partial t} = D_m \frac{\partial^2 C_m}{\partial x^2} + R \cdot C_m \quad (16)$$

The boundary conditions and initial condition, as well as the mass balance equation in the chamber, are the same to the above Eqs. (2)–(6). By virtue of the Laplace transform, an analytical solution is derived:

$$C_a(t) = 2C_0 \beta \sum_{n=1}^{\infty} \frac{q_n \sin q_n}{A_n} e^{(R - D_m \delta^{-2} q_n^2)t} \quad (17)$$

where

$A_n = [K\beta + (\alpha + G - q_n^2)KBi_m^{-1} + 2]q_n^2 \cos q_n + [K\beta + (\alpha + G - 3q_n^2)KBi_m^{-1} + \alpha + G - q_n^2]q_n \sin q_n$; $G = RL^2/D_m$; q_n are the positive roots of

$$q_n \tan q_n = \frac{\alpha + G - q_n^2}{K\beta + (\alpha + G - q_n^2)KBi_m^{-1}} \quad (n = 1, 2, \dots) \quad (18)$$

Equation (18) establishes the explicit relationship between the gas-phase formaldehyde concentration and four parameters, that is, C_0 , D_m , K , and R , which comprehensively considers the effect of physical and chemical processes.

In He et al. (2019)'s study, they compared empirical models and the long-term emission model. Two empirical models, a power-law model and a double-exponential model, are used. Both models have been widely used in previous studies. In addition, a pure physical model without chemical reactions is also included in the comparison. The values of coefficients in the empirical models are derived from least square regression by fitting the experimental data (gas-phase formaldehyde concentrations) for 3 months. For the physical model, the 3-month data are used to get the key parameters (C_0 , D_m , K). Figure 5 shows the comparisons of predicted gas-phase formaldehyde concentrations among the different models with experimental data. This figure indicates that the prediction from the

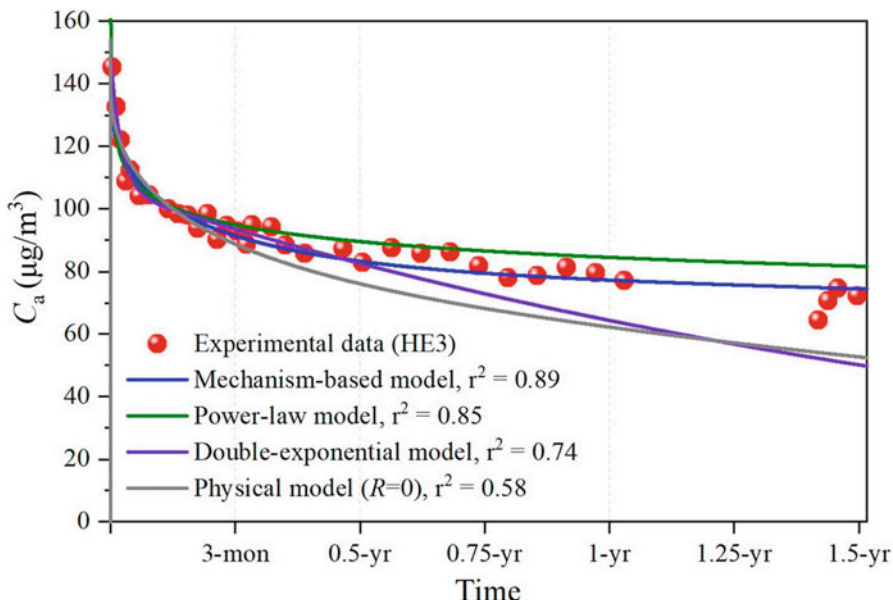


Fig. 5 Comparison of predicted gas-phase formaldehyde concentrations among different models with experimental data (He et al. 2019)

mechanism-based model or long-term emission model agrees well with the measured data over the whole period (1.5 year), while the prediction from the power-law model agrees well over about 1 year. The predictions of the double-exponential model and the physical model are a little lower than the measured data, especially for the long-term period (after 0.5 year). The square of the correlation coefficients (r^2) for the mechanism-based model, power-law model, double-exponential model, and physical model with experimental data are 0.89, 0.85, 0.74, and 0.58, respectively. These values are consistent with the above analysis. From this figure, we can further observe that the prediction of the mechanism-based model is between those of the double-exponential model and the power-law model. The power-law model agrees well with the data in the short- and mid-term emission periods, but for the relatively long-term emission period (i.e., after 1 year), the prediction of this model becomes close to equilibrium (decrease fairly slowly), which is not consistent with the pollutant emission behaviors. The double-exponential model represents exponential decay, and the trend of model is below the data observed in the long-term emission period. This trend is similar to that of the physical model. Therefore, for the long-term emissions from building materials and products, the existing empirical models and physical model are not able to accurately capture the formaldehyde emission characteristics. The good agreement for the short-, mid-, and long-term emissions between the model and experimental data demonstrates the effectiveness of the long-term emission model.

Measurement of Key Emission Parameters of Formaldehyde

Introduction of Measurement Methods for the Key Emission Parameters

The initial emittable concentration (C_0), the diffusion coefficient (D_m), and the material/air partition coefficient (K) are the three key emission parameters controlling the emission behaviors of formaldehyde from building materials or furniture. It is necessary to measure these parameters to understand the emission behaviors and how to control them. These key emission parameters are also the input of the above-mentioned short-term and long-term emission models. Many methods have been proposed to measure these three key emission parameters.

To measure the diffusion coefficients of VOCs in building materials, Kirchner et al. (1999) developed diffusion metric method, Bodalal et al. (2000) developed cup method, Meininghaus et al. (2000) proposed twin-compartment methods, Haghigat et al. (2002) proposed a dual-chamber method, and Blondeau et al. (2003) developed porosity methods. Generally speaking; all these methods produced large errors due to experimental disadvantages or took a long time. Cox et al. (2001b) measured K and D_m separately using a microbalance. However, the tests for K and D_m were based on a small sample of the material, which may not be different from the bulk material. Li and Niu (2005) used the inverse method to determine K and D_m for VOCs in building materials, but C_0 must first be known to use this method.

To measure C_0 of formaldehyde from dry building materials, traditional methods generally use solvent extraction or heat desorption methods (EN 120 1993). However, the methods only measured the total concentration instead of the emittable concentration of formaldehyde in the materials. Cox et al. (2001a) used free volume theory and a dual-mobility model to show that the total VOC concentration can be apportioned to mobile and partially immobilized fractions (C_0 in the aforementioned mass transfer models should be the concentration of the emittable compound or mobile fraction). They developed a fluidized-bed desorption (FBD) method to measure the C_0 of VOCs in vinyl flooring. The main merit of this method lies in that the application of cryogenic milling (CM) and FBD technique could accelerate the VOC emission greatly thus decreasing the experimental time. However, the apparatus of this method was relatively complicated, and the grinding process might change the physical or chemical properties of the material-VOC pairs, which might cause unpredictable measurement error of C_0 . The material was milled to powder at -140°C and the VOCs were then extracted from the powder at room temperature using FBD. The VOCs in the gas extracted from the fluidized-bed desorption and analyzed using GC/MS were assumed to be the mobile VOCs in the materials. Smith et al. (2009) applied the CM technique and developed an extraction method to determine C_0 . This method involved multiple equilibrium cycles and entailed flushing the chamber formaldehyde/VOCs multiple times once each emission process had reached equilibrium in a closed chamber. The tests often took a long experimental time (about 4 weeks). Furthermore, during the last few cycles of the extraction method, the uncertainty of measurement might increase due

to the very low formaldehyde/VOC concentrations in the chamber. The aforementioned methods target at extracting most of the formaldehyde/VOCs from the materials and then obtain the C_0 . In fact, it is not always necessary to extract most of the formaldehyde/VOCs. If it is enough to get the emission characteristic parameters just by extracting some of the formaldehyde/VOCs, it will undoubtedly reduce the test time. Later, Xiong et al. (2011a) developed a C-history method to rapidly, accurately, and simultaneously measure the three key emission parameters, which will be briefly introduced here. The summarization on some typical measurement methods is given in Table 6.

Introduction of the C-History Method

C-history method focuses on the emission process of formaldehyde from building material in a closed chamber (Xiong et al. 2011a), which can be used to

Table 6 Some measurement methods of the key emission parameters

Reference	Measurement method
Kirchner et al. (1999)	Cup method with measured parameter D_m Just one VOC can be tested at a time due to the use of purified VOC liquid Extraordinarily higher concentration inside the cup may overestimate D_m
Meininghaus et al. (2000)	Twin chamber method with measured parameters D_m and K Concentration level can be controlled at a required level Several VOCs can be tested in one experiment External convection is ignored, which will underestimate D_m when the airflow is slow
Yang et al. (2001)	Nonlinear regression method with measured parameters C_0 , D_m , and K K is predetermined by empirical correlations Maximum concentration in the chamber is difficult to detect, which may result in uncertainties for the measured C_0 and D_m
Cox et al. (2001a)	FBD method with measured parameters C_0 Short experimental time (within 7 h) Complicated experimental system Grinding process changes the physical properties of the material-VOC combination, which may cause unpredictable measurement errors
Cox et al. (2001b)	Microbalance method with measured parameters D_m and K Independent approach to measure the two parameters External convection is ignored
Li and Niu (2005)	Nonlinear regression method (inverse method) with measured parameters D_m and K There is a risk of multiple solutions due to the inter-dependence of the two parameters when they are estimated/fitted at the same time
Xu et al. (2009)	Twin chamber method with measured parameters D_m and K A similarity relationship between VOC and water vapor transport is established
Smith et al. (2009)	Extraction method with measured parameter C_0 Simple experimental system

(continued)

Table 6 (continued)

Reference	Measurement method
	Long experimental time (about 4 weeks) Grinding process changes the physical properties of the material-VOC combination, which may cause unpredictable measurement error
Wang and Zhang (2009)	A method measuring the parameters C_0 , D , and K Experiments take about 7 days Peak concentration after injection is hard to detect, which will affect the measurement accuracy
Xiong et al. (2011a)	C-history method for a closed chamber with measured parameters C_0 , D_m , and K Short experimental time (1 ~ 3 days) High measurement accuracy (RSD < 10%) Multiple samplings in airtight conditions may result in VOC mass loss if the chamber volume is small, which may result in uncertainty (this is not the case for large chambers)
Xiong et al. (2011b)	VVL method with measured parameters C_0 and K Performing tests in parallel can decrease the experimental time (within 24 h) With some improvements this method can be used to measure D_m and h_m
Xu et al. (2012)	Determination of D and K of formaldehyde in selected building materials and the impact of relative humidity
Huang et al. (2013)	C-history method for a ventilated chamber with measured parameters C_0 , D_m , and K Experimental time is less than 12 h and R^2 ranges from 0.96 to 0.99 One test is performed in airtight conditions, while other tests are performed in ventilated conditions, thus some commonly measurement instruments (e.g., GC/MS, HPLC) can be used
Ye et al. (2014)	Simple method for estimating the ranges of D_m and C_0 using gas-phase VOC concentration data obtained from ventilated chamber tests Validated using the Monte Carlo method and the National Research Council of Canada's emissions database This simple method has more benefits when only a few data points are available K is not determined
Wang et al. (2020b)	A general regression method for measuring the C_0 , D_m , and K of VOCs from building materials/furniture

simultaneously determine the three key emission parameters, C_0 , D_m , and K . This method needs to measure the change tendency of formaldehyde concentration in the chamber ($C_a(t)$) and the equilibrium concentration (C_{equ}). When the emission process reaches equilibrium, by assuming the material/air partition process conforming Henry's law, C_{equ} can be derived as follows based on VOC mass conservation between the material phase and air phase:

$$C_{equ} = \frac{C_0}{K\beta + 1} \quad (19)$$

By virtue of mass transfer analysis for the emissions in closed chamber, the following equation yields:

$$\ln \left(\frac{C_{\text{equ}} - C_a(t)}{C_{\text{equ}}} \right) = \text{SL} \cdot t + \text{INT} \quad (20)$$

where SL and INT are the functions of D_m and K , described by the following two equations:

$$\text{SL} = -D_m L^{-2} q_1^2 \quad (21)$$

$$\text{INT} = \ln \left(-\frac{2(K\beta + 1) \sin q_1}{q_1 A_1} \right) \quad (22)$$

Therefore, if the chamber formaldehyde concentration is treated as the form of the logarithm of dimensionless excess concentration in Eq. (20), the SL and INT can be obtained by doing linear curve fitting. The two parameters D_m and K can be obtained directly because they are functions of SL and INT, and we have two equations with two unknown parameters. Combining Eq. (19) and the known value of K , C_0 can be calculated. Since the main characteristic of this method is to apply the concentration history of formaldehyde in a closed chamber, this method is called as the C-history method for a closed chamber.

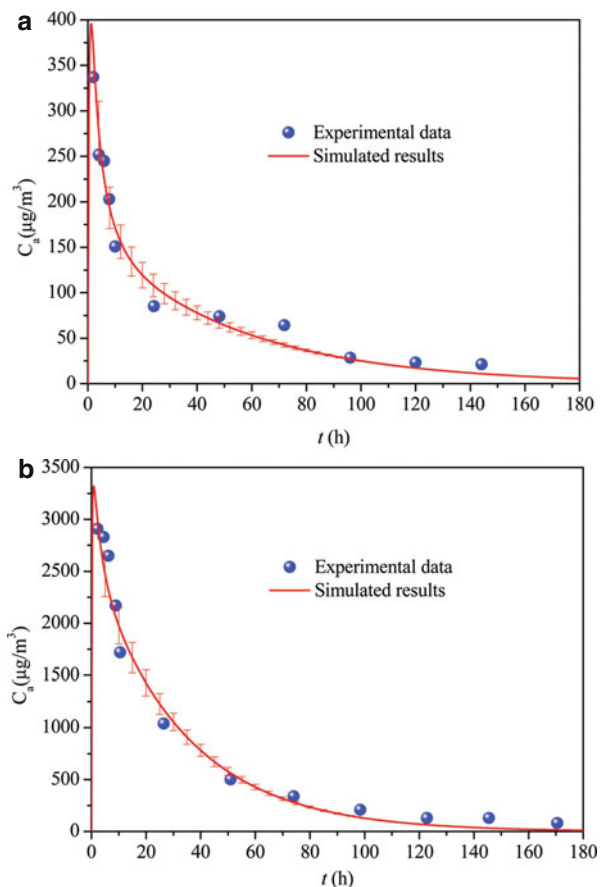
Independent experiments are performed to validate the measured key emission parameters. Based on the determined key emission parameters from the closed chamber and the analytical results for a ventilated chamber, the formaldehyde concentrations in the ventilated chamber were calculated and compared to the experimental data (Fig. 6). For the tested experimental time (within 180 h), the simulated results are in very good agreement with the observed data, suggesting that the measured parameters in the closed chamber are reliable and can be used to estimate formaldehyde emission in real ventilated conditions.

The C-history method just performs one emission process in closed chamber, making it very time-saving, with the experimental time generally less than 3 days, while the traditional methods tend to require 7 ~ 30 days. This is the main advantage of the C-history method. It is therefore a very convenient and effective method for rapid measurement of VOC emissions from building materials and for furniture labeling. In this method, the formaldehyde concentration in a closed chamber is sampled several times to determine the parameters. If the chamber volume is small, the multiple sampling may result in a change in the target formaldehyde concentration in the closed chamber, which may increase the measurement error. This drawback has been overcome by the C-history method for a ventilated chamber (Huang et al. 2013).

Impact of Environmental Factors on Formaldehyde Emissions

The three key emission parameters not only depend on the physical properties of the material-VOC combinations but also rely heavily on the experimental conditions especially the temperature and relative humidity. This combination is one of the most important features of these parameters. In general, indoor temperature varies within a

Fig. 6 Comparison of simulated results with the ventilated chamber experimental data for formaldehyde concentration of (a) medium-density fiberboard and (b) particle board (Xiong et al. 2011a)



temperature range, which is related to outdoor temperature, solar radiation, etc. Hunt and Gidman (1982) measured the temperature in 1000 buildings in the UK and observed an average temperature of 16 °C and a maximum temperature of 29 °C. McLaren et al. (2005) investigated the temperature in cars, and a maximum temperature of 67 °C was found in hot days. These temperature variances will cause a corresponding change to the three key emission parameters, which is one of the main reasons why formaldehyde and VOCs emit more rapidly in summer. The impact of temperature on the emission rate is a comprehensive effect of temperature impact on the key parameters since the emission rate is a function of the three parameters. The increase of emission rate with increasing temperature has been observed by many researchers. Myers (1985) reported that the emission rate of formaldehyde from particleboard increased by a factor of 5.2 between 23 °C and 40 °C. Lin et al. (2009) showed the emission rate and concentration increased 1.5–12.9 times when the temperature increased from 15 °C to 30 °C. Similar phenomena were also investigated by other researchers (Parthasarathy et al. 2011).

Impact of Temperature on C_0

It is found that the initial emittable concentration of formaldehyde (C_0) in a building material is much less than the concentration measured by the perforator method (C_{total}) under room temperature condition (Wang and Zhang 2009) and C_0 changes with the environmental conditions especially temperature. This phenomenon can be explained using statistical physics (Huang et al. 2015). From a microcosmic aspect, the formaldehyde molecules are bonded in the material surface by adsorption, and a molecule is emittable only when the kinetic energy of this molecule is high enough to overcome the bonding forces, that, to overcome an energy barrier. The sum of these molecules constitutes C_0 , which is obviously less than C_{total} . Considering that the average kinetic energy of the molecules increases with increasing temperature, it undisputedly leads to higher C_0 at higher temperatures. By using statistical physics theory, the correlations between the emittable ratio ($P = C_0/C_{\text{total}}$) and temperature, and between C_0 and temperature, are derived as follows:

$$\ln \left(P \sqrt{T} \right) = -\frac{A}{T} + B \quad (23)$$

$$C_0 = \frac{C}{\sqrt{T}} \exp \left(-\frac{A}{T} \right) \quad (24)$$

where A , B , and C are constants, which are not dependent on temperature but are only related with the physical properties of the material-formaldehyde combinations.

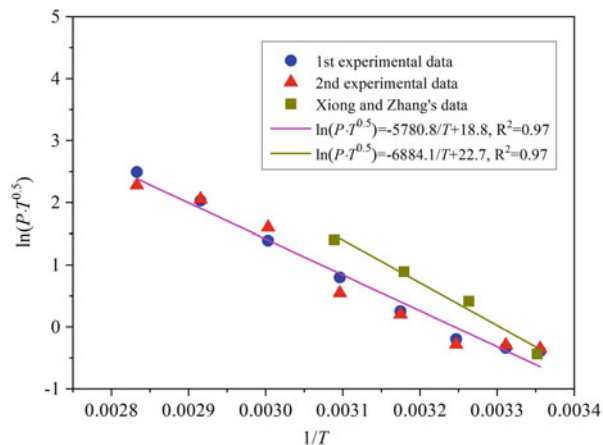
The two assumptions deriving these two equations are: (1) the energy barrier (ϵ_0) is a constant for a given material-formaldehyde combination; (2) chemical reactions are ignored and only physical interactions between formaldehyde and material molecules are considered. The derived correlations are thus applicable for emission scenarios meeting these conditions. When the parameters A , B , C in Eqs. (23) and (24) are obtained based on available results, the correlations can then be used to predict P and C_0 at other temperatures, which are very helpful and convenient for engineering applications.

Figure 7 shows the good agreement between the theoretical correlations and the experimental data (Huang et al. 2015), which demonstrates the effectiveness of the theoretical correlations. It should be noted that, up to now, the phenomenon of increased C_0 with increasing temperature is recently found in the formaldehyde emissions. Whether it is applicable for other VOCs is still not known or reported, and more experimental study is required.

Impact of Temperature on D_m

Diffusion of formaldehyde in building material is related with the heat motion of molecules, so the diffusion coefficient is significantly dependent on temperature. This effect is commonly assumed to follow with an Arrhenius-like behavior.

Fig. 7 Linear regression results by treating the experimental data with theoretical Eq. (23) and its comparison with the full relationship (Xiong and Zhang 2010; Huang et al. 2015)



However, the correlation lacks strong theoretical foundations. For VOC diffusion in porous materials, if the molecular diffusion is dominant, Deng et al. (2009) derived a theoretical correlation to characterize the influence of temperature on D_m :

$$D_m = B_1 T^{1.25} \exp\left(-\frac{B_2}{T}\right) \quad (25)$$

where B_1 and B_2 are positive constants for a given material-VOC combination.

This correlation indicates that D_m increases with increasing temperature. The calculations based on Eq. (25) agree well with the experimental data for four kinds of building materials (Deng et al. 2009). Once the parameters B_1 and B_2 are determined, the correlation can then be used to predict D_m at other conditions.

Impact of Temperature on K

Formaldehyde emission or adsorption in building materials is found to obey the Langmuir kinetic equation in many cases. By applying this equation, a theoretical correlation between the partition coefficient and temperature is deduced as (Zhang et al. 2007)

$$K = A_1 T^{1/2} \exp\left(\frac{A_2}{T}\right) \quad (26)$$

where A_1 and A_2 are positive constants for a given material-VOC combination.

Equation (26) indicates that K decreases with increasing temperature. Experimental tests of formaldehyde emissions from four kinds of building materials at temperatures 18–50 °C validates the reliability of the temperature correlation (Zhang et al. 2007).

Impact of Relative Humidity

Besides temperature, relative humidity (RH) also plays an important role in the emission behaviors. It should be noted that the influence of RH on the emissions of formaldehyde from composite wood products can be quite different from VOCs due to the hydrolysis of urea-formaldehyde adhesives. The impact of RH on the key emission parameters is a little more complicated. The increase of C_0 and K with increasing RH for formaldehyde from some building materials was reported (Xu and Zhang 2011). However, the impact of RH on K for VOCs indicates inconsistent outcomes, which is significantly related with the material-VOC combinations. Xu and Zhang (2011) investigated the sorption of toluene into calcium silicate and found that K decreased with the increase of RH . Deng (2010) examined the sorption of five VOCs into carpet and observed that K of ethylbenzene, undecane, and dodecane decreased with the increase of RH , while K of benzaldehyde and 1,2-dichlorobenzene firstly increased (in the RH range of 25–50%) and then decreased (in the RH range of 50–80%). In addition, the effect of RH on D_m for formaldehyde and VOCs is generally regarded as ignored (Farajollahi et al. 2009; Deng 2010; Xu and Zhang 2011).

The positive effect between the emission rate and RH for formaldehyde emissions has been observed in many experimental studies. Andersen et al. (1975) reported that the emission rate of formaldehyde from particleboard increased one fold in the RH range of 30–70%. For some VOCs, Lin et al. (2009) observed the similar phenomenon in the experiment that the emission rates of toluene, n-butyl acetate, ethylbenzene, and m,p-xylene increased 1.1–5.4 folds when RH increased from 50% to 80%.

Combined Effect of Temperature and Humidity on the Emission Rate

As mentioned above, the emission rate of formaldehyde from building materials are significantly influenced by the temperature and relative humidity. These two factors not singly but comprehensively affect the emission characteristics. The combined effect of temperature and relative humidity on the three key emission parameters C_0 , D_m , and K is the basis for obtaining the combined effect on the emission rate. According to the idea of variable separation method or the Berge equation, the combined effect of temperature and relative humidity can be regarded as the multiplication of effect of single variable. Based on this, the following correlation can be derived (Xiong et al. 2016):

$$E = E_1 T^{0.75} \exp \left(E_2 \cdot RH - \frac{E_3}{T} \right) \quad (27)$$

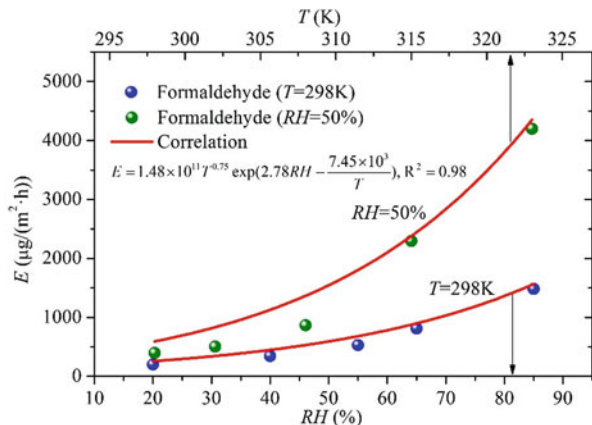
This equation explicitly characterizes the relationship between the steady-state emission rate and T , RH . Further analysis indicates that, with the increase of T or RH , the emission rate increases accordingly. Once the emission rate for a given material-pollutant combination is measured at three or more sets of environmental conditions, the three parameters E_1 , E_2 , and E_3 can be determined from nonlinear curve fitting

and the derived correlation (Eq. (27)) can then be applied to predict the emission rate at other T and RH different from the test conditions, which will be very helpful for engineering applications as well as for scientific researches. By combining ten sets of data for emission rates under varied temperature (25°C , 29°C , 35°C , 42°C , 50°C at $50\% RH$) and relative humidity (20% , 40% , 55% , 60% , 85% at 25°C) in prior studies, correlation (27) is applied to perform nonlinear regression. Fitting results between the emission rate and T , RH for formaldehyde from medium density fiberboard are shown in Fig. 8 (Xiong et al. 2016). The bottom x axis + y axis and the top x axis + y axis in Fig. 8 represent the results at a certain temperature ($T = 298 \text{ K}$) and a certain relative humidity ($RH = 50\%$), respectively. The time point for the emission rate at steady state in this figure is 40 h. Good regression accuracy is also obtained ($R^2 = 0.98$). The correlation between E and T , RH for formaldehyde from medium density fiberboard is represented as

$$E = 1.48 \times 10^{11} T^{0.75} \exp \left(2.78RH - \frac{7.45 \times 10^3}{T} \right) \quad (28)$$

With this quantitative correlation, the E of formaldehyde emissions from medium density fiberboard at different T and RH can be predicted. Take Beijing in China as an example. The indoor temperature and relative humidity of Beijing in summer and winter (with HVAC system) can be approximately taken as 24°C , 50% , and 20°C , 45% , respectively. Based on these data, the ratio of E in summer to that in winter is about 1.63, and this ratio can be regarded as the ratio of formaldehyde concentration in indoor environment in the two seasons. Yao et al. (2005) surveyed the indoor formaldehyde concentration levels in Beijing in 2003 and found that the formaldehyde concentration in summer is about 1.32 times to that in winter. This value is approximately consistent with the results based on prediction with Eq. (28), thus demonstrating the effectiveness of the correlation.

Fig. 8 The correlation between emission rate and T , RH for formaldehyde from medium density fiberboard (Xiong et al. 2016)



Conclusions

This chapter briefly introduces the formaldehyde properties and hazards, usages and pollution levels, determination methods, emission models, key parameter measurement methods, and impact factors. On the whole, the behavior of formaldehyde is now well understood. Nevertheless, so far, other very volatile organic compounds are seldom considered, and there are two main reasons for this: (1) the lack of a clear and internationally recognized definition of VVOCs; (2) the lack of a unified analysis method to identify and quantify VVOCs. In the past few years, VVOCs have increasingly become the focus of regulatory and health-related construction product emission assessments, which shows the importance of these substances. It is likely that the other VVOCs can be treated in a similar way to formaldehyde both experimentally and theoretically. However, work is still needed to obtain the necessary information on their presence in indoor air and their emission characteristics so that they are no longer “understudied.”

Cross-References

- ▶ [Source/Sink Characteristics of VVOCs and VOCs](#)
 - ▶ [Volatile Organic Compounds \(VOCs\)](#)
-

References

- Andersen I, Lundquist R, Molhave L (1975) Indoor air pollution due to chipboard used as a construction material. *Atmos Environ* 9:1121–1127
- Blondeau P, Tiffonnet AL, Damian A, Amiri O, Molina JL (2003) Assessment of contaminant diffusivities in building materials from porosimetry tests. *Indoor Air* 13:302–310
- Bodalal A, Zhang JS, Plett EG (2000) A method for measuring internal diffusion and equilibrium partition coefficients of volatile organic compounds for building materials. *Build Environ* 35: 101–110
- CAS Reg. No. 50-00-0. Interim acute exposure guideline levels (AEGLs) for formaldehyde. 2008
- Chung PR, Tzeng CT, Ke MT, Lee CY (2013) Formaldehyde gas sensors: a review. *Sensors* 13: 4468–4484
- Clarisse B, Laurent AM, Seta N, Le Moullec Y, El Hasnaoui A, Momas I (2003) Indoor aldehydes: measurement of contamination levels and identification of their determinants in Paris dwellings. *Environ Res* 92:245–253
- Cox SS, Little JC, Hodgson AT (2001a) Measuring concentrations of volatile organic compounds in vinyl flooring. *J Air Waste Manag Assoc* 51:1195–1201
- Cox SS, Zhao D, Little JC (2001b) Measuring partition and diffusion coefficients for volatile organic compounds in vinyl flooring. *Atmos Environ* 35:3823–3830
- Deng QQ (2010) Modeling VOC sorption of building materials and its impact on indoor air quality. Ph.D. Thesis, Tsinghua University, Beijing, China
- Deng BQ, Kim NC (2004) An analytical model for VOCs emission from dry building materials. *Atmos Environ* 38:1173–1180
- Deng QQ, Yang XD, Zhang JS (2009) Study on a new correlation between diffusion coefficient and temperature in porous building materials. *Atmos Environ* 43:2080–2083

- Deng B, Liu Y, Yin H, Ning X, Lu H, Ye L, Xu Q (2012) Determination of ultra-trace formaldehyde in air using ammonium sulfate as derivatization reagent and capillary electrophoresis coupled with on-line electrochemiluminescence detection. *Talanta* 91:128–133
- Descamps MN, Bordy T, Hue J, Mariano S, Nonglaton G, Schultz E, Tan-Thi TH, Vignoud-Despond S (2012) Real-time detection of formaldehyde by a sensor. *Sensors Actuat B Chem* 170:104–108
- EN 120 (1993) Wood-based panels –determination of formaldehyde content-extraction method called perforator method. European Standard
- EN 717-2 (1994) Wood-based panels – determination of formaldehyde release – part 2: formaldehyde release by the gas analysis method. European Standard
- EN 717-3 (1996). Wood-based panels – determination of formaldehyde release – part 3: formaldehyde release by the flask method. European Standard
- Farajollahi Y, Chen Z, Haghishat F (2009) An experimental study foreexamining the effects of environmental conditions on diffusion coefficient of VOC in building materials. *Clean-Soil Air Water* 37:436–443
- Gilbert NL, Guay M, David Miller J, Judek S, Chan CC, Dales RE (2005) Levels and determinants of formaldehyde, acetaldehyde, and acrolein in residential indoor air in Prince Edward Island, Canada. *Environ Res* 99:11–17
- Gilbert NL, Gauvin D, Guay M, Heroux ME, Dupuis G, Legris M, Chan CC, Dietz RN, Levesque B (2006) Housing characteristics and indoor concentrations of nitrogen dioxide and formaldehyde in Quebec City, Canada. *Environ Res* 102:1–8
- Goldstein AH, Nazaroff WW, Weschler CJ, Williams J (2021) How do indoor environments affect air pollution exposure? *Environ Sci Technol* 55:100–108
- Haghishat F, Lee CS, Ghaly WS (2002) Measurement of diffusion coefficients of VOCs for building materials: review and development of a calculation procedure. *Indoor Air* 12:81–91
- He ZC, Xiong JY, Kumagaib K, Chen WH (2019) An improved mechanism-based model for predicting the long-term formaldehyde emissions from composite wood products with exposed edges and seams. *Environ Int* 132:105086
- HIS Markit (2019) Formaldehyde. *Chemical Economics Handbook*
- Hladova M, Martinka J, Rantuch P, Necas A (2019) Review of spectrophotometric methods for determination of formaldehyde. *Res Papers Faculty Mater Sci Technol Slovak Univ Technol* 27: 105–120
- Hu HP, Zhang YP, Wang XK, Little JC (2007) An analytical mass transfer model for predicting VOC emissions from multi-layered building materials with convective surfaces on both sides. *Int J Heat Mass Transf* 50:2069–2077
- Huang HY, Haghishat F (2002) Modelling of volatile organic compounds emission from dry building materials. *Build Environ* 37:1127–1138
- Huang SD, Xiong JY, Zhang YP (2013) A rapid and accurate method, ventilated chamber C-history method, of measuring the emission characteristic parameters of formaldehyde/VOCs in building materials. *J Hazard Mater* 261:542–549
- Huang SD, Xiong JY, Zhang YP (2015) Impact of temperature on the ratio of initial emittable concentration to total concentration for formaldehyde in building materials: theoretical correlation and validation. *Environ Sci Technol* 49:1537–1544
- Hunt DRG, Gidman MI (1982) A national field survey of house temperatures. *Build Environ* 17: 107–124
- Iabal K, Mehmood N, Baber AA, Ali Z, Zeeshan M, Anjum W (2018) Production of 6600 TPY of formaldehyde from methanol using silver catalyst. Department of Chemical Engineering, Wah Engineering College, University of Wah, Islamabad
- IARC (International Agency for Research on Cancer) (2006) IARC monographs on the evaluation of carcinogenic risks to humans. Formaldehyde, 2-Butoxyethanol and 1-tert-Butoxypropane-2-ol. World Health Organization, Lyon, vol 88, pp 39–325
- Khoder MI, Shakour AA, Farag SA, AbdelHameed AA (2000) Indoor and outdoor formaldehyde concentrations in homes in residential areas in Greater Cairo. *J Environ Monit* 2:123–126
- Kinney PL, Chillrud SN, Ramstrom S, Ross J, Spengler JD (2002) Exposures to multiple air toxics in New York City. *Environ Health Perspect* 110:539–546

- Kirchner S, Badey JR, Knudsen HN, Meininghaus R, Quenard D, Sallee H, Saarinen A (1999) Sorption capacities and diffusion coefficients of indoor surface materials exposed to VOCs: Proposal of new test procedures. In: Proceedings of the 8th Inter. Conf. of Indoor Air 1999, Edinburg, pp 430–435
- Li F, Niu J (2005) Simultaneous estimation of VOCs diffusion and partition coefficients in building materials via inverse analysis. *Build Environ* 40:1366–1374
- Li Q, Sritharathikhun P, Motomizu S (2007) Development of novel reagent for Hantzsch reaction for the determination of formaldehyde by spectrophotometry and fluorometry. *Anal Sci* 23:413–417
- Lin CC, Yu KP, Zhao P, Lee GWM (2009) Evaluation of impact factors on VOC emissions and concentrations from wooden flooring based on chamber tests. *Build Environ* 44:525–533
- Little JC, Hodgson AT, Gadgil AJ (1994) Modeling emissions of volatile organic compounds from new carpets. *Atmos Environ* 28:227–234
- Liu XY, Mason MA, Guo ZS, Krebs KA, Roache NF (2015) Source emission and model evaluation of formaldehyde from composite and solid wood furniture in a full-scale chamber. *Atmos Environ* 122:561–568
- McLaren C, Null J, Quinn J (2005) Heat stress from enclosed vehicles: moderate ambient temperatures cause significant temperature rise in enclosed vehicles. *Pediatrics* 116:109–112
- Meininghaus R, Gunnarsen L, Knudsen HN (2000) Diffusion and sorption of volatile organic compounds in building materials-impact on indoor air quality. *Environ Sci Technol* 34:3101–3108
- Miksich RR, Anthon DW, Fanning LZ, Hollowell CD, Revzan K, Glanville J (1981) Modified pararosaniline method for the determination of formaldehyde in air. *Anal Chem* 53:2118–2123
- Myers GE (1985) The effects of temperature and humidity on formaldehyde emission from UF-bonded boards: a literature critique. *For Prod J* 35:20–31
- Nash T (1953) The colorimetric estimation of formaldehyde by means of the Hantzsch reaction. *Biochem J* 55:1470–8728
- NICNAS (2006) National Industrial Chemicals Notification and Assessment Scheme: formaldehyde, priority existing chemical assessment report no 28. Department of Health and Ageing, Australian Government
- Ohura T, Amagai T, Senga Y, Fusaya M (2006) Organic air pollutants inside and outside residences in Shimizu, Japan: levels, sources and risks. *Sci Total Environ* 366:485–499
- Parthasarathy S, Maddalena RL, Russell ML, Apté MG (2011) Effect of temperature and humidity on formaldehyde emissions in temporary housing units. *J Air Waste Manag Assoc* 61:689–695
- Sakai K, Norback D, Mi Y, Shibata E, Kamijima M, Yamada T, Takeuchi Y (2004) A comparison of indoor air pollutants in Japan and Sweden: formaldehyde, nitrogen dioxide, and chlorinated volatile organic compounds. *Environ Res* 94:75–85
- Salthammer T (2016) Very volatile organic compounds: an understudied class of indoor air pollutants. *Indoor Air* 26:25–38
- Salthammer T, Mentese S, Marutzky R (2010) Formaldehyde in the indoor environment. *Chem Rev* 110:2536–2572
- Sax SN, Bennett DH, Chillrud SN, Kinney PL, Spengler JD (2004) Differences in source emission rates of volatile organic compounds in inner-city residences of New York City and Los Angeles. *J Expo Anal Environ Epidemiol* 14:S95–S109
- Schulte-Ladbeck R, Lindahl R, Levin JO, Karst U (2001) Characterization of chemical interferences in the determination of unsaturated aldehydes using aromatic hydrazine reagents and liquid chromatography. *J Environ Monit* 3:306–310
- Serrano-Trespalacios PI, Ryan L, Spengler JD (2004) Ambient, indoor and personal exposure relationships of volatile organic compounds in Mexico City Metropolitan Area. *J Expo Anal Environ Epidemiol* 14:S118–S132
- Smith JF, Gao Z, Zhang JS, Guo B (2009) A new experimental method for the determination of emittable initial VOC concentrations in building materials and sorption isotherms for IVOCS. *Clean-Soil Air Water* 37:454–458

- Tobe M, Kaneko KT, Uchida Y (1985) Studies of the inhalation toxicity of formaldehyde, U.S. Environmental Protection Agency translation, TR-85-0236. U.S. EPA, Washington, DC
- U.S. EPA (U.S. Environmental Protection Agency) (2003) Integrated risk information system
- Wang X, Zhang Y (2009) A new method for determining the initial mobile formaldehyde concentrations, partition coefficients, and diffusion coefficients of dry building materials. *J Air Waste Manage Assoc* 59:819–825
- Wang HM, Zheng JH, Yang T, He ZC, Zhang P, Liu XF, Zhang MX, Sun LH, Yu XF, Zhao J, Liu XY, Xu BP, Tong LP, Xiong JY (2020a) Predicting the Emission Characteristics of VOCs in A Simulated Vehicle Cabin Environment based on Small-scale Chamber Tests: Parameter Determination and Validation. *Environ Int* 142: 105817
- Wang YZ, Yang T, He ZC, Sun LH, Yu XF, Zhao J, Hu YJ, Zhang SH, Xiong JY (2020b) A general regression method for accurately determining the key parameters of VOC emissions from building materials/furniture in a ventilated chamber. *Atmos Environ* 231:117527
- WHO (1987) Air quality guidelines for Europe. WHO Regional Office for Europe, Copenhagen
- WHO (2002) Formaldehyde: concise international chemical assessment document (40). World Health Organization
- Xiong JY, Zhang YP (2010) Impact of temperature on the initial emittable concentration of formaldehyde inbuilding materials: experimental observation. *Indoor Air* 20:523–529
- Xiong JY, Yao Y, Zhang YP (2011a) C-history method: rapid measurement of the initial emittable concentration, diffusion and partition coefficients for formaldehyde and VOCs in building materials. *Environ Sci Technol* 45:3584–3590
- Xiong J, Yan W, Zhang Y (2011b) Variable volume loading method: a convenient and rapid method for measuring the initial emittable concentration and partition coefficient of formaldehyde and other aldehydes in building materials. *Environ Sci Technol* 45:10111–10116
- Xiong JY, Zhang PP, Huang SD, Zhang YP (2016) Comprehensive influence of environmental factors on the emission rate of formaldehyde and VOCs in building materials: correlation development and exposure assessment. *Environ Res* 151:734–741
- Xu Y, Zhang Y (2003) An improved mass transfer based model for analyzing VOC emissions from building materials. *Atmos Environ* 37:2497–2505
- Xu J, Zhang JS (2011) An experimental study of relative humidity effect on VOCs' effective diffusion coefficient and partition coefficient in a porous medium. *Build Environ* 46:1785–1796
- Xu J, Zhang J, Grunewald J, Zhao J, Plagge R, Ouali A, Allard F (2009) A study on the similarities between water vapor and VOC diffusion in porous media by a dual chamber method. *CLEAN–Soil Air Water* 37:444–453
- Xu J, Zhang JS, Liu X, Gao Z (2012) Determination of partition and diffusion coefficients of formaldehyde in selected building materials and impact of relative humidity. *J Air Waste Manag Assoc* 62(6):671–679
- Yang X, Chen Q, Zhang J, Magee R, Zeng J, Shaw C (2001) Numerical simulation of VOC emissions from dry materials. *Build Environ* 36:1099–1107
- Yao XY, Wang W, Chen YL, Zhang WL, Song Y, Liu SL (2005) Seasonal change of formaldehyde concentration in the air of newly decorated houses in some cities of China. *J Environ Health* 22: 353–355
- Ye W, Little JC, Won D, Zhang X (2014) Screening-level estimates of indoor exposure to volatile organic compounds emitted from building materials. *Build Environ* 75:58–66
- Zhang YP, Luo XX, Wang XK, Qian K, Zhao RY (2007) Influence of temperature on formaldehyde emission parameters of dry building materials. *Atmos Environ* 41:3203–3216
- Zhang L, Steinmaus C, Eastmond DA, Xin XK, Smith MT (2009) Formaldehyde exposure and leukemia: a new meta-analysis andpotential mechanisms. *Mutat Res* 681:150–68.



Volatile Organic Compounds (VOCs)

3

Xiong Jianyin and Shaodan Huang

Contents

Introduction	72
Properties and Hazards of VOCs	72
Classes of VOCs	72
Properties of VOCs	73
Hazards	74
Typical Indoor VOCs	75
Benzene	75
Toluene	77
Xylene	79
Measurement Methods	80
Gas Chromatography	81
High-Performance Liquid Chromatography	81
Emission Models for VOCs	81
Characteristic Emission Parameters	81
Model for Prediction of Indoor VOC Concentration	84
Influential Factors of VOCs Emission	92
Conclusions	94
Cross-References	94
References	94

Abstract

Volatile organic compounds (e.g., benzene, toluene, xylene) are important indoor pollutants. Indoor VOCs mainly originate from furniture and building materials. VOCs can produce adverse health effects and therefore have drawn the attention of researchers of indoor environments and public health. This chapter introduces

X. Jianyin

School of Mechanical Engineering, Beijing Institute of Technology, Beijing, China

S. Huang (✉)

Department of Occupational & Environmental Health Sciences, Peking University School of Public Health, Beijing, China

e-mail: shhuang@bjmu.edu.cn

properties, hazards, guidelines, measurement methods, emission characteristic parameters, emission models, and influencing factors of VOCs, and is helpful for understanding the VOCs emission characteristics, concentrations, and their adverse effects on human health.

Keywords

VOCs · Emission character · Characteristic parameters · Emission models · Influencing factors

Introduction

Volatile organic compounds (VOCs) are organic chemical compounds whose composition makes it possible for them to evaporate under normal indoor atmospheric conditions of temperature and pressure. Different organizations have different definitions of VOCs. According to a World Health Organization (WHO) classification system, VOCs are defined by a boiling point range with a lower limit between 50 and 100 °C and an upper limit between 240 and 260 °C (WHO 1989). According to the ASTM International standard D3960-05, VOCs refer to any organic compound that can participate in atmospheric photochemical reactions (ASTM D3960-05 2018). The US Environmental Protection Agency (U.S. EPA) defines it as: volatile organic compounds are any carbon compound that participates in atmospheric photochemical reactions except for CO, CO₂, H₂CO₃, metal carbides, metal carbonates, and ammonium carbonate (U.S. EPA 1992). In China, VOCs refer to organic compounds with saturated vapor pressure greater than 70.91 Pa at room temperature, boiling point below 50–260 °C at standard atmospheric pressure of 101.3 kPa, and initial boiling point equal to 250 °C, or any organic solid or liquid that can volatilize at room temperature (GB 18582-2008 2008).

In the indoor environment, VOCs are introduced into the air mostly through the emissions from building materials, including flooring, paints, adhesives, wood protection agents, wall and roof coverings, sealants, wall plasters, bricks and concrete, etc. In addition, the use of detergents, deodorants, pesticides, cosmetics, the burning of household fuels in the kitchen (such as natural gas stoves), cooking fume, smoking, the use of printers, photocopiers, human breathing, and metabolism will also produce VOCs. VOCs not only pollute the environment but also affect human health (Soni et al. 2018).

The chapter will introduce properties and hazards of VOCs, measurement methods, emission characteristic parameters, emission models, and influencing factors.

Properties and Hazards of VOCs

Classes of VOCs

VOCs can be classified according to molecular structure or functional groups. These include aliphatic hydrocarbons (including those which are chlorinated–halocarbons), aromatic hydrocarbons, alcohols, ethers, esters, aldehydes, etc. (Anand et al. 2014).

At present, more than 300 types have been identified, and many of them are primarily found in indoor air. Table 1 presents the types and compositions of common VOCs. Common indoor VOCs include benzene, toluene, xylene, styrene, trichloroethylene, chloroform, trichloroethane, diisocyanate (TDI), diisocyanotoluene, etc. Table 2 lists typical indoor VOCs and their boiling points and vapor pressures.

Properties of VOCs

VOCs are a group of compounds that have some common physical-chemical properties (Cicolella 2008): (1) VOCs contain carbon, and most VOCs also contain nonmetallic elements such as H, O, N, P, S, and halogens; (2) their relative vapor density is heavier than air; (3) there are millions of species, most of which are

Table 1 Types and compositions of common VOCs

Type	Compositions
Aliphatic hydrocarbon	Methane, ethane, propane, cyclohexane, methylcyclopentane, hexane, 2-methylpentane, 2-methylhexane
Aromatic hydrocarbons	Benzene, toluene, ethylbenzene, xylene, n-propylbenzene, styrene, 1,2,4-trimethylbenzene
Halogenated compounds	Trichlorofluoromethane, dichloromethane, chloroform, carbon tetrachloride, 1,1,1-trichloroethane, trichloroethylene, tetrachloroethane, chlorobenzene, 1,4-dichlorobenzene
Phenol, ether, epoxy compounds	Cresol, phenol, ether, ethylene oxide, propylene oxide
Ketones, aldehydes, alcohols, polyols	Acetone, butanone, cyclohexanone, formaldehyde, acetaldehyde, methanol, isobutanol
Nitrile, amine compounds	Acrylonitrile, dimethylformamide
Acid, ester compounds	Acetic acid, ethyl acetate, butyl acetate
Polycyclic aromatic hydrocarbons	Naphthalene, phenanthrene, benzopyrene
Others	Methyl bromide, chlorofluorocarbons

Table 2 Typical indoor VOCs and their boiling point and vapor pressure

Name	Boiling point (°C)	Vapor pressure (below 20 °C, Pa)
1,1,1-trichloroethane	74.0	1.31×10^4
1,1,2-trichloroethane	114	2.35×10^3
Benzene	80.1	9.95×10^3
Chloroform	61.1	1.94×10^4
o-xylene	144	6.47×10^2
p-xylenes	138	8.75×10^2
Styrene	145	5.92×10^2
Toluene	111	2.89×10^2
Trichloroethylene	87.2	7.69×10^3
Toluene-2,4-diisocyanate	115–120	1.08

flammable and explosive, and some are toxic or even highly toxic; (4) most of them are insoluble or sparingly soluble in water, but easily soluble in organic solvents; (5) most of them are colorless with many having pungent or special odors; (6) low melting point, easy to decompose, and volatile, can participate in atmospheric photochemical reaction and thereby produce photochemical smog under irradiation with sunlight.

Hazards

The harm to human health and living environment is mainly reflected in the following aspects:

1. Most VOCs are malodorous gases, with pungent odors or odors, which can cause people's sensory discomfort and seriously reduce people's quality of life. Malodorous gas refers to all gas substances that stimulate the olfactory organs and cause people's dissatisfaction.
2. The special smell and the characteristics of penetration, volatilization, and fat solubility can cause many uncomfortable symptoms in the human body. It also has toxic, irritating, teratogenic, and carcinogenic effects, especially benzene, toluene, xylene, and formaldehyde are the most harmful to human health. Long-term exposure to VOCs can cause people to suffer from anemia and leukemia. In addition, VOCs can also cause diseases of the respiratory tract, kidneys, lungs, liver, nervous system, digestive system, and hematopoietic system. As the concentration of VOCs increases, the human body will experience symptoms such as nausea, headache, convulsions, and coma. Existing guidance for Environment Agency Inspectors is given in a series of Process Guidance Notes which divide VOCs into three categories (Marlowe et al. 1995): extremely hazardous to health, such as benzene, vinyl chloride, and 1,2-dichloroethane; class A compounds: those organic compounds that may cause significant harm to the environment including acetaldehyde, aniline, benzyl chloride, carbon tetrachloride, CFCs, ethyl acrylate, halons, maleic anhydride, 1,1,1-trichloroethane, trichloroethylene, trichlorotoluene; and class B compounds: organic compounds of lower environmental impact than class A compounds.
3. Most VOCs are flammable at fairly low concentrations, such as benzene, toluene, acetone, dimethylamine, and thiohydrocarbons. When the emission concentration of these substances is high and they encounter static sparks or other sources of ignition, they may easily cause fires. In recent years, fires and explosions caused by VOCs have occurred from time to time, especially in petrochemical companies.
4. Some VOCs can destroy the ozone layer, such as hydrochlorofluorocarbons (HCFC) (Solomon et al. 1992). When it is exposed to ultraviolet radiation from the sun, it can undergo a photochemical reaction to produce chlorine atoms that catalytically destroy ozone in the ozone layer. The decrease in the amount of

ozone and the destruction of the ozone layer increase the amount of ultraviolet radiation reaching the ground. Ultraviolet rays are harmful to human skin, eyes, and immune system.

5. Most VOCs are photochemically reactive (Yuan et al. 2012). Under sunlight, VOCs will chemically react with NO_x in the atmosphere to form secondary pollutants (such as ozone, etc.) or strong chemically active intermediate products (such as free radicals, etc.). Increasing the surface concentration of smog and ozone will endanger people's lives. It will also endanger the growth of crops and even cause the plant death. The haze caused by photochemical reaction (Song et al. 2019), in addition to reducing visibility, the generated ozone, peroxyacetyl nitrate (PAN), peroxybenzoyl nitrate (PBN), aldehydes, and other substances can irritate people's eyes and respiratory system, endangering people's health. The first photochemical smog episode was recorded in Los Angeles in 1943. Tokyo from 1970 to 1974 (Fukuoka 1975) and other cities have seen major photochemical smog pollution incidents.

Typical Indoor VOCs

Benzene

General Description

Benzene (CAS Registry Number 71-43-2; C₆H₆; molecular weight 78.1 g/mol) is an aromatic compound with a single six-member unsaturated carbon ring. It is a clear, colorless, volatile, highly flammable liquid with a characteristic odor and a density of 874 kg/m³ at 25 °C (HEI 2007).

At 1 atmosphere of pressure, benzene has a melting point of 5.5 °C, a relatively low boiling point of 80.1 °C and a high vapor pressure (12.7 kPa at 25 °C), causing it to evaporate rapidly at room temperature. It is slightly soluble in water (1.78 g/l at 25 °C) and is miscible with most organic solvents (WHO 2000). Benzene is soluble in lipids, has a log K octanol-water partition coefficient of 2.14 (HEI 2007) and a log K soil organic carbon-water partition coefficient of 1.85 at 25 °C. Its Henry's Law constant is 550 Pa.m³/mol at 25 °C, implying that it will have a tendency to volatilize into the atmosphere from surface water (IEH 1999).

Benzene in air exists predominantly in the vapor phase, with residence times varying between 1 day and 2 weeks, depending on the environment, the climate, and the concentration of other pollutants. Reaction with hydroxyl radicals is the most important means of degradation, with a rate constant of 1.2×10^{-12} cm³ molecule⁻¹ s⁻¹ at 298 K (IUPAC 2008a).

Other oxidants such as ozone and nitrate radicals can also contribute to a lesser extent to the degradation of benzene indoors, with rate constants of 2.7×10^{-17} cm³ molecule⁻¹ s⁻¹ at 298 K for nitrate radicals (IUPAC 2008b) and 1.7×10^{-22} cm³ molecule⁻¹ s⁻¹ at 298 K for ozone (WHO 2000, 2010; HEI 1999, 2007; IUPAC 2008c; NIST 2005).

Indoor Sources

Benzene in the family home mainly comes from the large amount of chemical raw materials used in building decoration, such as coatings, fillers, and various organic solvents. It can also infiltrate from attached garages where it has evaporated from stored vehicles such as cars or power lawn equipment. They all contain a large amount of organic compounds, which volatilize indoors after decoration. It is mainly contained in the following decorative materials: (1) Paint. Benzene which is an indispensable solvent in paint can volatilize from paint. Some low-grade and counterfeit paints are an important cause of excessive benzene content in indoor air; (2) Additives in various paints and coatings. The main components of additives are benzene, toluene, and xylene; (3) Various adhesives. In particular, solvent-based adhesives still have a certain market in the decoration industry, and most of the solvents used are toluene, which contains more than 30% benzene, but because of price, solubility, adhesiveness, and other reasons, it is still used by some companies. The sofas purchased by some households releases a large amount of benzene, mainly due to the use of adhesives with high benzene content in the production; (4) Waterproof materials. Waterproof materials contain a large amount of adhesives, and formaldehyde, benzene, etc. are the major components of adhesives (WHO 2010). Another major source of benzene is attached garages and vaporization from cars and household equipment like lawn mowers.

Hazards

It is generally believed that the origin of benzene's toxicity is caused by its metabolites, which means that benzene must be metabolized before it can cause harm to life (McHale et al. 2012). Benzene can be metabolized in the liver and bone marrow. The bone marrow is the formation site of red blood cells, white blood cells, and platelets. Therefore, benzene entering the body can form blood-toxic metabolites in the hematopoietic tissue itself. Long-term exposure to benzene can cause bone marrow and genetic damage. The blood test can find leukopenia, thrombocytopenia, pancytopenia, and aplastic anemia, and even leukemia. Someone investigated the health status of workers exposed to low-concentration benzene. The results showed that although the number of white blood cells in peripheral blood was within the normal range, it was significantly lower than that of the control group. In the benzene exposure group, the lymphocyte micronucleus rate of the observation population in the benzene production workshop was significantly different from that of the control group; with the increase of the benzene concentration in the work environment, the number of white blood cells decreased, and the lymphocyte micronucleus rate increased (EPA 2002). All these indicate that low concentrations of benzene are harmful to the health of the working population, and special attention should be paid to the damage to human genetic material. Inhalation of more than 4000 ppm of benzene for a short period of time not only has mucosal and lung irritation but also has inhibitory effects on the central nervous system. At the same time, it will be accompanied by headache, vomiting, gait instability, coma, cramps, and arrhythmia. Inhalation of more than 14,000 ppm of benzene will cause immediate death (WHO 2010; IARC 2012).

Guidelines

Guidelines on exposure levels are needed for indoor air, because indoor air is a significant source of benzene exposure and inhalation is the main pathway of human exposure to benzene. Benzene is present in both outdoor and indoor air. However, indoor concentrations are generally higher than concentrations in outdoor air owing to the infiltration of benzene present in outdoor air and to the existence of many other indoor sources. Typically, indoor concentrations are below the lowest levels showing evidence of adverse health effects. Considering benzene is present indoors and taking into account personal exposure patterns, which are predominantly indoors, indoor guidelines for exposure are needed.

Benzene is a genotoxic carcinogen in humans and no safe level of exposure can be recommended. The risk of toxicity from inhaled benzene would be the same whether the exposure was indoors or outdoors. Thus, there is no reason that the guidelines for indoor air should differ from ambient air guidelines (WHO 2010).

Previous WHO benzene guidelines for ambient air were calculated using the Plioform cohort studies (Crump 1994). Since these studies, new data have become available, such as those on the large Chinese workers cohort (Hayes et al. 1997). However, the unit risks and risk assessment analysis based on these data are still not available. Hence, we recommend continuing to use the same unit risk factors calculated from the Plioform cohort studies. The geometric mean of the range of the estimates of the excess lifetime risk of leukemia at an air concentration of 1 µg/m³ is 6×10^{-6} . The concentrations of airborne benzene associated with an excess lifetime risk of 1/10,000, 1/100,000, and 1/1000,000 are 17, 1.7, and 0.17 µg/m³, respectively.

As noted above, there is no known exposure threshold for the risks of benzene exposure. Therefore, from a practical standpoint, it is expedient to reduce indoor exposure levels to as low as possible. This approach will require reducing or eliminating human activities that release benzene, such as smoking tobacco, using solvents for hobbies or cleaning, or using building materials that off-gas benzene. Adequate ventilation methods will depend on the building location. In modern buildings located near heavy traffic or other major outdoor sources of benzene, inlets for fresh air should be located at the least polluted side of the building (WHO 2010).

Toluene

General Description

Toluene (CAS Registry Number 108–88–3; C₇H₈; molecular weight 92.1 g/mol) is a substituted aromatic hydrocarbon. It is a colorless, water-insoluble liquid with the smell associated with paint thinners. It is a monosubstituted benzene derivative, consisting of a methyl group (CH₃) attached to the phenyl group. As such, its systematic IUPAC name is methylbenzene. Toluene is predominantly used as an industrial feedstock and a solvent. It is also a common component of gasoline.

As the solvent in some types of paint thinner, permanent markers, contact cement, and certain types of glue, toluene is sometimes used as a recreational inhalant and has the potential of causing severe neurological harm (Streicher et al. 1981).

Indoor Sources

Exposure to toluene is generally via indoor air (Héroux et al. 2008). Indoor sources of toluene include building materials (e.g., solvent- and water-based adhesives, floor coverings, paint, chipboard), consumer and automotive products (e.g., cleaners, polishes, adhesive products, oils, greases, lubricants). The amount of toluene produced by smoking in the indoor environment is also considerable. According to statistics from the US EPA, the toluene content in mainstream cigarettes of unfiltered cigarettes is about ~100–200 µg, and the ratio of toluene concentration inside/mainstream cigarettes is 1.3 (EPA 1992). In attached garages, toluene generated by running engines or by product storage may also infiltrate into the indoor environment.

Hazards

Exposure to toluene has been shown to cause eye, nose, and throat irritation as well as headaches, dizziness, and feelings of intoxication. It has also been linked to neurological effects including poorer performances in tests of short-term memory, attention and concentration, visual scanning, perceptual motor speeds, and finger dexterity in the completion of physical tasks as well as negative effects on color vision and auditory capacity (Health Canada 2011).

In controlled exposure studies, healthy adults exposed to toluene for 4.5–7 h reported increased eye, nose, and throat irritation as well as headaches, dizziness, or feelings of intoxication at concentrations ranging from 189 to 566 mg/m³ (Andersen et al. 1983; Baelum et al. 1990), but not at 38 or 151 mg/m³ (Andersen et al. 1983).

Several occupational studies have reported effects of toluene on neurobehavioral endpoints (tests of manual dexterity, visual competency, and attention span) at concentrations ranging from 264 to 441 mg/m³ (Foo et al. 1988, 1990; Boey et al. 1997; Eller et al. 1999; Kang et al. 2005). No effects were seen at concentrations ranging from 75 to 113 mg/m³ (Kang et al. 2005), nor was any difference seen between exposed workers (98 mg/m³) and a reference group (11 mg/m³) (Seeber et al. 2004, 2005).

After toluene enters the body, about 48% is metabolized in the body and finally excreted from the body through the liver, brain, lungs, and kidneys. In this process, it will harm the nervous system. Volunteer experiments have shown that when the concentration of toluene in the blood reaches 1250 mg/m³, the short-term memory ability, attention span, and sensorimotor speed of the contacts are significantly reduced.

Guidelines

The lowest-observed-adverse-effect level for effects on the central nervous system from occupational studies is approximately 332 mg/m³ (88 ppm). A guideline value of 0.26 mg/m³ is established from these data adjusting for continuous exposure

(dividing by a factor of 4.2) and dividing by an uncertainty factor of 300 (10 for interindividual variation, 10 for use of a lowest-observed-adverse-effect level rather than a no-observed-adverse-effect level, and an additional factor of 3, given the potential effects on the developing CNS). This guideline value should be applied as a weekly average. This guideline value should also be protective for reproductive effects (spontaneous abortions). The air quality guideline could also be based on the odor threshold. In this case, the peak concentrations of toluene in air should be kept below the odor detection threshold level of 1 mg/m³ as a 30 min average (WHO 2000).

Xylene

General Description

Xylene (CAS Registry Number: 1330-20-7; C₈H₁₀; molecular weight: 106.16 g/mol) is any one of three isomers of dimethylbenzene, or a combination thereof. They are all colorless, flammable, slightly greasy liquids. They are of great industrial value (Fabri et al. 2000). The mixture is referred to as both xylene and, more precisely, xylenes. Mixed xylenes refers to a mixture of the xylenes plus ethylbenzene. Mixed xylenes are used widely as gasoline additives; as solvents in manufacturing and laboratory processes; in glues, adhesives, printing inks, paint thinners, and sealants; and as carrier solvents for delivery of some pesticides. The four compounds have identical empirical formulas C₈H₁₀. Typically, the four compounds are produced together by various catalytic reforming and pyrolysis methods (Cannella 2000).

The physical properties of the isomers of xylene differ slightly. The melting point ranges from –47.87 °C (m-xylene) to 13.26 °C (p-xylene). The para isomer's melting point is much higher because it packs more readily in its crystal structure. The boiling point for each isomer is around 140 °C. The density of each isomer is around 0.87 g/mL and thus is less dense than water. The odor of xylene is detectable at concentrations as low as 0.08–3.7 ppm and can be tasted in water at 0.53–1.8 ppm (Kandyala et al. 2010).

Indoor Sources

Indoor air sources of xylene include building and consumer products, such as adhesives and paints, and also tobacco smoke (ATSDR 2007). It can also infiltrate from attached garages.

Hazards

Xylene can be absorbed through the respiratory tract, skin, and digestive tract. Its vapor enters the human body through the respiratory tract, and part of it is discharged through the respiratory tract. The absorbed xylene is distributed in the body mostly in adipose tissue and adrenal glands, followed by bone marrow, brain, blood, kidneys, and liver. The toxicity of the three isomers of industrial xylene is slightly different, and all of them belong in the low-toxicity category. According to reports, three workers inhaled xylene with a concentration of 1000 ppm. One died 18.5 h

later. Autopsy showed pulmonary congestion and cerebral hemorrhage. The other two workers lost consciousness for 19–24 h, accompanied by memory loss and kidney functional changes (NIOSH 1978). In addition, inhalation of high concentrations of xylene can cause loss of appetite, nausea, vomiting, and abdominal pain, and sometimes can cause reversible liver and kidney damage. At the same time, xylene is also an anesthetic, and long-term exposure can cause nervous system dysfunction (CDC 2017).

Guidelines

According to OSHA, the permissible airborne exposure limit (PEL) is 100 ppm averaged over an 8-hour work shift. According to NIOSH, the recommended airborne exposure limit (REL) is 100 ppm averaged over a 10-hour work shift and 150 ppm, not to be exceeded during any 15-minute work period (EPA 2012).

Measurement Methods

VOCs measurement methods mainly include real-time monitoring and integrated sampling/analysis. These methods usually include sampling, pre-concentration, separation, and detection of several processes. The sampling methods of VOCs in the air can be divided into direct sampling, powered sampling, and passive sampling. Sample pretreatment methods include solvent analysis method, solid phase micro-extraction method, low temperature pre-concentration-thermal analysis method, etc.

Several real-time monitors for VOCs have been developed, and these utilize continuous detectors such as a photo-ionization detector (PID) or semiconductor sensor. These monitors can determine the total VOC (TVOC) concentration within approximately several seconds. However, their response depends on the nature of the organic constituents. Furthermore, proton transfer reaction-mass spectrometry (PTR/MS) has drawn great deal of attention for near real-time monitoring. These techniques allow immediate and continuous monitoring of the variation in TVOC concentration with time. PTR/MS can determine individual compound if the compounds have different masses and can produce ions via proton transfer reactions.

In integrated analysis, VOCs are collected into a sorbent tube with an air pump and analyzed using methods such as gas chromatography/mass spectrometry (GC/MS), gas chromatography/flame ionization detection (GC/FID), or high-performance liquid chromatography (HPLC). This method provides qualitative and quantitative information for each VOC in the collected air sample. Integrated analysis is recommended by some organizations for official VOC measurements. However, air samples have to be taken over at least half an hour and up to a few hours. Therefore, only time-averaged information can be obtained. Although integrated analysis is more accurate in qualitative and quantitative, and has high sensitivity in analysis and testing, the monitoring frequency and timeliness of monitoring results are obviously insufficient, and they cannot reflect the changes in gas concentration in time. The transport of the sample to the analytical lab may

result in sample loss and cross-contamination. The test process is tedious and time-consuming, the number of test samples is limited, and the test cost is high. Common methods for integrated analysis include gas chromatography and high-performance liquid chromatography.

Gas Chromatography

The most common technique used to detect, identify, and quantitate VOC is gas chromatography with flame ionization (FID), electron capture (ECD), or mass spectrometry (GC-MS) detection. Selection of a detection method requires consideration of various analytical parameters and regulatory requirements. Common stand-alone GC detectors used in VOC analysis include flame ionization detectors (FIDs), thermal conductivity detectors (TCDs), thermionic detectors (TIDs), electron capture detectors (ECDs), and atomic emission detectors (AEDs). The details of the detector including detectable compound and detection limit are listed in Table 3 (Dewulf et al. 2002).

High-Performance Liquid Chromatography

High-performance liquid chromatography (HPLC) is also widely used for separation, identification, and quantification of each component in a mixture. This technique is based on the logic of advancing a pressurized liquid solvent as well as a solid adsorbent at stationary phase at high pressure. Off-line VOCs are sampled using active air sampling through a 2,4-dinitrophenylhydrazine (DNPH)-coated solid sorbent cartridge for carbonyls, and XAD-2 (naphthyl isocyanate) sorbent tube, Tenax, or activated charcoal for a broader suite of polar VOCs. After that, the VOCs are analyzed by high-performance liquid chromatography (HPLC) (Salameh et al. 2018).

Emission Models for VOCs

Characteristic Emission Parameters

Three characteristic emission parameters are used to predict material emissions by virtue of physical models (Little et al. 1994). They are: the initial emittable concentration (C_0), the diffusion coefficient of the target VOC in material (D_m), and the material/air partition coefficient (K). These three key parameters are the physical property parameters, which are dependent on the species of pollutants and the test materials, as well as external environmental factors, such as temperature and relative humidity (Xiong et al. 2016).

Table 3 The details of detectors

Detector	Detectable compound	Detection limit
General-purpose detectors		
Flame ionization detector (FID)	Organic compounds (other than formaldehyde and formic acid)	0.1 ppm (0.1 ng)
Thermal conductivity detector (TCD)	All compounds other than the carrier gas	10 ppm (10 ng)
Barrier discharge ionization detector (BID)	All compounds other than He and Ne	0.05 ppm (0.05 ng)
Selective, high-sensitivity detectors		
Electron capture detector (ECD)	Organic halogen compounds Organic metal compounds	0.1 ppb (0.1 pg)
Flame thermionic detector (FTD)	Organic nitrogen compounds Inorganic and organic phosphorus compounds	1 ppb (1 pg) 0.1 ppb (0.1 pg)
Flame photometric detector (FPD)	Inorganic and organic sulfur compounds Inorganic and organic phosphorus compounds Organic tin compounds	10 ppb (10 pg)
Sulfur chemiluminescence detector (SCD)	Inorganic and organic sulfur compounds	1 ppb(0.1 pg)

The detection limits are approximations. Actual values will vary depending on the compound structure and analytical conditions

To illustrate the influence of these parameters, Guo et al. (2020) performed three sets of simulations to determine the influence of these parameters on the VOCs concentrations from multiple dry building materials. In each experiment, both size and emission surface area were kept constant for the two types of building materials under investigation, but with varying key parameters. Figure 1 shows the results from the simulations for single and multiple building materials. According to Fig. 1, higher C_0 and D_m lead to increased VOCs concentrations in the air, and higher K gives lowered VOCs concentrations. When there were more than one type of dry building materials existing, the change of VOCs concentrations in the air would be closer to that of the dry building material with higher C_0 , higher D_m , and lower K , especially at later stages.

In addition, convective mass-transfer coefficient (h) and air exchange rate (N) also affect the VOCs emissions. It was found that h only had significant influences at the start of the VOCs emission process, but at later stages, the influence of this parameter can be neglected. Lower h is associated with shorter time to reach steady state. When the magnitude of h was less than 10^{-4} , the VOCs emission would reach steady state quickly as shown in Fig. 2. Different values of N affect the whole VOCs emission from building materials (Fig. 3). At the later stages of VOCs emission process, it was observed that the VOCs concentration in the air was linearly correlated with N .

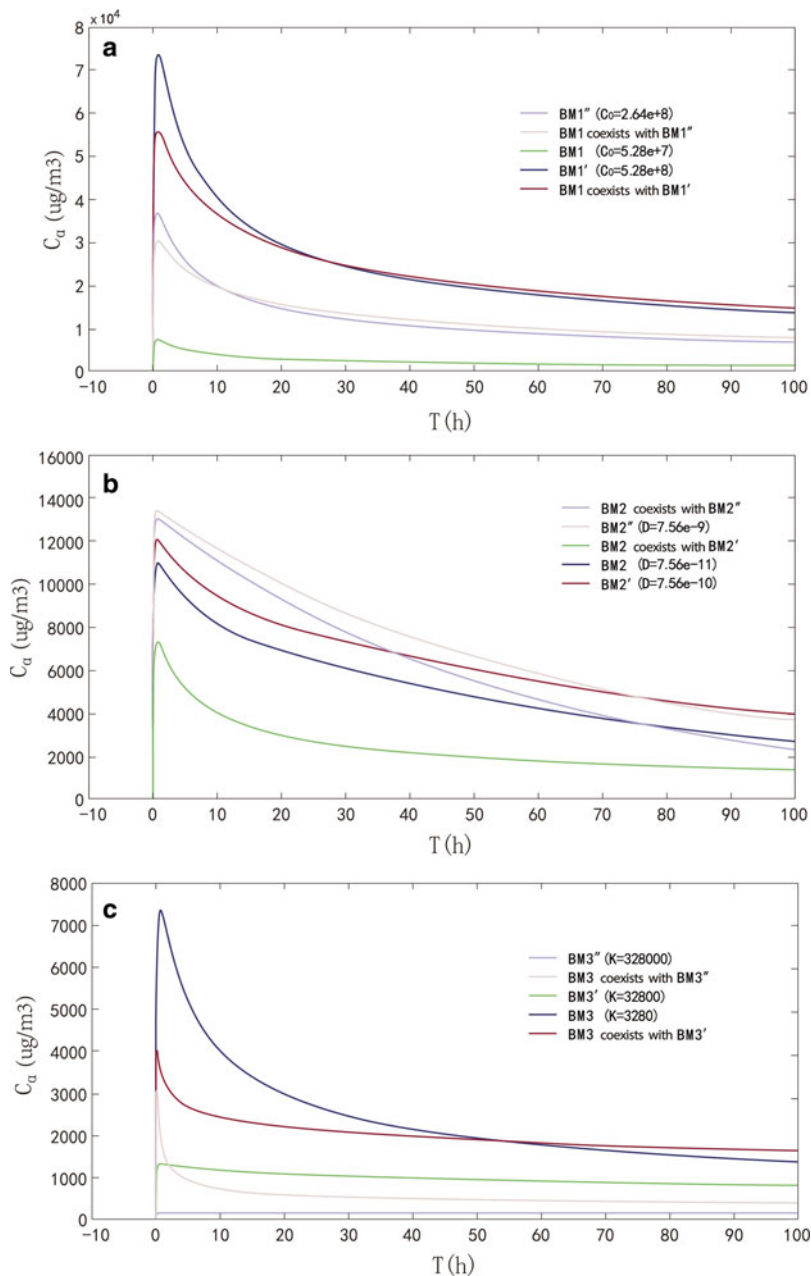


Fig. 1 Comparison of VOC concentrations over time for different values of (a) C_0 , (b) D_m , and (c) K . (Figure taken from Guo et al. (2020))

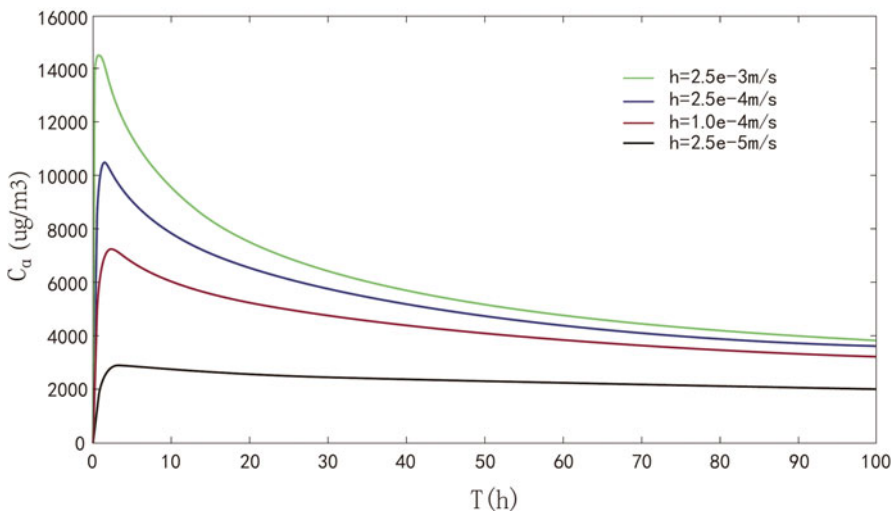


Fig. 2 Comparison of VOC concentrations with varying convective mass-transfer coefficient (h). (Figure taken from Guo et al. (2020))

Model for Prediction of Indoor VOC Concentration

Emission source models conventionally express the emission rate or emission factor as a function of time. The emission rate of the entire source, $R(t)$ (mg/h), is defined as the total amount of VOC or TVOC emitted per unit of time from the entire source. The emission factor (emission rate per unit), $E(t)$, is defined as follows (Zhang et al. 1997):

1. For a surface source with a defined area, $E(t)$, is the amount of VOC or TVOC emitted per unit time and per unit surface area of the source. Therefore,

$$R(t) = A \times E(t) \quad (1)$$

where A is area of the emitting surfaces, m^2 .

2. For a non-surface source or a source whose surface area cannot be easily measured or calculated (e.g., when an office workstation module is tested in a full-scale chamber), $E(t)$ is the amount of emissions per unit time and per unit source. In this case,

$$R(t) = n \times E(t) \quad (2)$$

where n is number of units of the source.

Emission source models for building materials may be divided into two categories: statistical models and mass transfer models. The following subsections will

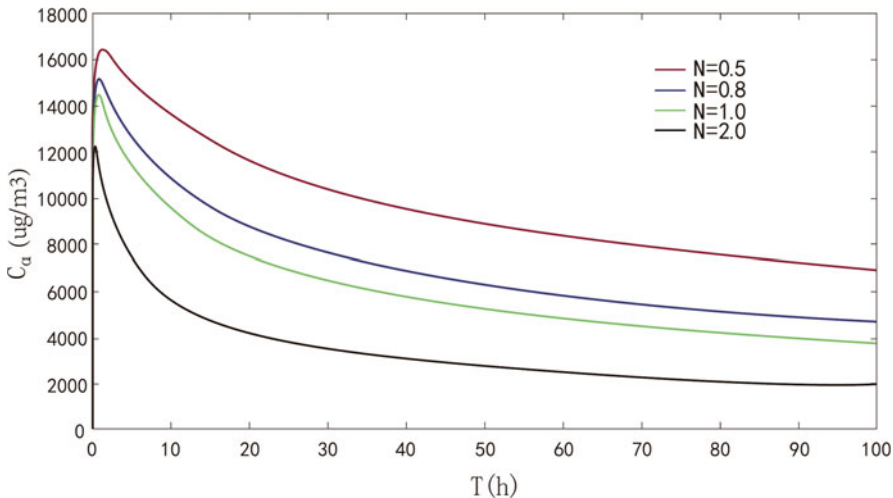


Fig. 3 Comparison of VOC concentrations with varying air exchange rate (N). (Figure taken from Guo et al. (2020))

introduce some common statistical and mass transfer models. In the following part, what we call emission rate is the emission factor (emission rate per unit), $E(t)$ ($\text{mg}/(\text{m}^2 \text{ h})$).

Statistical Models

These models are proposed/derived based on the observation and statistical analysis of emission data obtained from environmental chamber testing. The coefficients (or parameters) of these models are determined entirely by regression analysis of emission data obtained from chamber tests.

Constant Emission Factor Model

$$E(t) = \text{constant} \quad (3)$$

Chang and Krebs (1992) showed that this model described the emission of *p*-dichlorobenzene from moth cakes. In practice, it may also be used to approximate the emission rates from building materials that have nearly constant emission rates for a given period of time. For example, emission tests are often conducted by taking a single air sample after the test specimen is placed in a dynamic (i.e., ventilated) chamber for a fixed period of time (e.g., 24 h or a week) for the purpose of comparing emission strength of different products (Levin and Hodgson 1996). These test data may be used for evaluating the exposure of occupants to VOCs in a worst case scenario, assuming that the emission rates of these products are approximately constant.

First-Order Decay Model

$$E(t) = E(0) \exp(-k t) \quad (4)$$

where $E(0)$ is the initial emission rate, $\text{mg}/(\text{m}^2 \text{ h})$; k is first-order decay constant (or exponential decay constant), l/h ; and t is the emission time, h .

It is called a first-order decay model, because it can be derived from $d[E(t)]/dt = -k E(t)$ with the initial conditions: $E(t) = E(0)$, at $t = 0$. Both $E(0)$ and k are determined from the concentration data, $C(t)$, obtained in a dynamic chamber test. Several different calculation procedures are available for determining the model coefficients (ASTM 1990; Zhang et al. 1997).

A single first-order decay model is generally adequate for analyzing (representing) the VOC emission data from chamber test for a given time period. This time period is longer for a dry material or a “wet” material that is sufficiently dried than a “wet” material (e.g., from a week to 1 month for dry materials vs. 12 h for the initial emission period of “wet” materials). The validity of the model to predict the emission rate beyond the testing period has to be justified by some longer-term emission testing data for the same type of materials considered.

Double Exponential Model

$$E(t) = E_{01} \exp(-k_1 t) + E_{02} \exp(-k_2 t) \quad (5)$$

where E_{01} is the initial emission factor for the first (fast) decaying period, $\text{mg}/(\text{m}^2 \text{ h})$; and E_{02} is the initial emission factor for the second (slow) decaying period, $\text{mg}/(\text{m}^2 \text{ h})$.

With this model, the total initial emission factor is $E_{01} + E_{02}$, and the total emittable mass can be calculated by $E_{01}/k_1 + E_{02}/k_2$.

This model is adequate for representing chamber test data for both “wet” and dry individual materials. The coefficients of the model are determined by nonlinear regression analysis, but several procedures have been used by different researchers (Colombo et al. 1991; Chang and Guo 1992).

Second-Order Decay Model

$$E(t) = E(0)/[1 + k_2 E(0)t] \quad (6)$$

where k_2 is second-order decay constant, m^2/mg .

It is called a second-order decay model, because it is derived from $d[E(t)]/dt = k_2 E^2$ with the initial condition: $E(t) = E(0)$ at $t = 0$. It gives a very high initial emission rate followed by low and long-lasting emissions. Tichenor and Guo (1991) showed that this model well described the emissions from wood finishing materials. Clausen et al. (1993) represented k_2 as k_{21}/L to account for the effect of the thickness of a vinyl flooring (k_{21} is the second-order decay constant for unit thickness, L is the thickness of the source) and showed a good fit between the model and the test data. However, the model coefficients were not reproducible based on the results of three replicate

tests for the same material. The authors suggested that further validation of the model with better characterized data was necessary.

The *n*th-Order Decay Model

$$E(t) = E(0) / \left[1 + (n - 1) k_n E(0)^{(n-1)} t \right]^{1/(n-1)}, n > 1 \quad (7)$$

where k_n is the *n*th-order decay constant.

The *n*th-order decay model is a generalization of the second-order decay model. The additional parameter, *n*, provides a slight improvement in fitting the emission data (Tichenor et al. 1991).

Mass Transfer Models

These models are derived partially or entirely by applying the mass transfer theory to the emission processes. The coefficients (or parameters) in these models have more distinct physical meanings than those of statistical models. The model coefficients may be determined by regression analysis of data from the dynamic emission testing and/or experiments that are independent of the environmental chamber tests.

Interfacial Mass Transfer Models

The interfacial mass transfer across the boundary layer was described by Kays and Crawford (1981):

$$r(t) = K[C_s(t) - C(t)] \quad (8)$$

where r is rate of interfacial mass transfer, mg/(m²h); C_s air-phase concentrations at the interface of the surface, mg/m³; C is air-phase concentrations in the “free stream” over the surface, mg/m³; K is mass transfer coefficient, m/h; and t is the emission time, h.

Equation (8) states that the interfacial mass transfer rate (i.e., the emission factor in this case) is proportional to the concentration differential between the emitting surface and the ambient air. This principle has been applied successfully to model the initial period of the VOC emissions from “wet” materials, which are mainly controlled by the evaporative process.

Different assumptions about $C_s(t)$ have led to different interfacial mass transfer models as described below.

1. Constant Vapor Pressure Model:

$$E(t) = K[C_v - C(t)] \quad (9)$$

where C_v is VOC concentration in air corresponding to the saturated vapor pressure at the temperature of testing, mg/m³.

In this model, the concentration on the material surface is assumed to be constant and equal to the saturated vapor concentration in air. Chang and Krebs (1992) used this model to describe the emission of para-dichlorobenzene from a solid moth

repellent. They assumed that C_v was equal to the measured headspace concentration, while K was determined by regression analysis on the VOC concentration data from dynamic chamber testing. The model is only applicable to evaporative sources with a constant vapor pressure.

2. VB (Vapor Pressure and Boundary Layer) Model:

$$E(t) = K[C_v M(t)/Mo - C(t)] \quad (10)$$

where $M(t)$ is amount of VOC mass in the source, mg/m²; and total emittable VOC mass in the source, mg/m².

This model assumes that $C(t)$ is proportional to the VOC amount remained in the source (Guo and Tichenor 1992). When the VB model is applied to a well-mixed chamber space that has a constant air change rate and zero concentration at time zero, this model results in the following equation for the concentrations in the chamber:

$$C(t) = [L C_v K/(r_1 - r_2)][\exp(r_1 t) - \exp(r_2 t)] \quad (11)$$

where L is the loading ratio, m²/m³; N is air exchange rate, h⁻¹; and $r_{1,2} = \{[-(N + L K + C_v K/Mo) + [(N + L K + C_v K/Mo)^2 - 4 N C_v K/Mo]^{1/2}\}/2$.

The concentration of the most abundant VOC measured in the headspace analysis was used as C_v . Mo was the total amount of VOC emitted during the dynamic chamber testing. K was determined by fitting the model to the concentration data from the dynamic chamber testing (K was expressed as D_f/δ , where D_f is average diffusivity based on the most abundant compound, and δ is apparent laminar boundary layer thickness). The model was found to predict well the initial period (up to first 20 hours) of TVOC emissions from wood stains, polyurethane varnish, and wax.

3. VBX Model: VB Model for the Emissions of Individual VOCs

To quantify emission rate of individual VOCs from paints, Guo et al. (1998) developed the VB model to predict the emission rates of each individual compound:

$$E_i(t) = K_i(Cp_i - C_i) \quad (12)$$

where $E_i(t)$ is the emission factor of VOC_i, mg/m²; K_i is the mass transfer coefficient for VOC_i, m/h; Cp_i is the partial pressure for VOC_i expressed in mass concentration unit, mg/m³, $Cp_i = Cv_i x_i$, x_i is the molar fraction of VOC_i remaining in the solvent, dimensionless; $x_i = \Pi_i/\Pi$, and $\Pi = \sum \Pi_i$; Cv_i is the vapor pressure for pure VOC_i expressed in mass concentration unit, mg/m³; C_i is the vapor pressure for VOC_i expressed in concentration in the air, mg/m³; Π_i is the molar amount for VOC_i remaining in the source, moles/m²; and Π is the molar amount for TVOC remaining in the source, moles/m².

To simplify the implementation of the model, Guo et al. (1996) also proposed to use the original VB model instead of the summation for calculating the molar amount for TVOC and that the average molecular weight of TVOC was approximated by that of the compound with the highest vapor pressure in the mixture. The method was evaluated by experimental data from a small chamber and test houses

for “wet” materials including wood stain, polyurethane wood finish, and floor wax, and was found to be suitable for predicting the emissions from these materials during the initial period (up to first 20 h of testing).

4. A Semiempirical Model for Evaporative Sources

$$E(t) = K[C_s(0) \exp(-k_s t) - C(t)] \quad (13)$$

where $C_s(0)$ is the initial VOC concentration on the emitting surface, mg/m²; and k_s is the first-order constant for the VOC concentration on the surface, l/h.

This model assumes that $C_s(t)$ decreases exponentially with time. When applied to a well-mixed chamber space that has a constant air change rate, this model results in the following equation for the concentrations in the chamber:

$$C(t) = a[\exp(-b t) - \exp(-c t)] \quad (14)$$

where $a = L K C_s(0)/(L K + N - k_s)$; $b = k_s$; and $c = L K + N$.

Zhang et al. (1996) used this model to describe the initial period (first 12 h) of VOC emissions from wood stains applied on oak wood substrates. Nonlinear regression analysis was used to determine a , b , and c , and then solve the algebraic equations for K , $C_s(0)$, and k_s . The value of $C_s(0)$ was found to be significantly less than the saturation (equilibrium) concentration measured in the headspace analysis. This difference was attributed to the time delay (about 10–15 min) between applying the material onto the substrate and placing the specimen in the dynamic testing chamber.

The above interfacial mass transfer models are only applicable to evaporative sources such as during the initial period of emissions from “wet” building materials. In practice, the initial emission period is always followed by a second period during which the internal diffusion becomes the controlling process. A transition period is also expected between the two periods. Therefore, the surface concentration $C_s(t)$, in general, needs to be solved in conjunction with equation for the internal diffusion process within materials. This area needs further studies.

Internal Diffusion Mass Transfer Models

Considering that most interior building materials have a much larger surface area than their thickness, we limited our discussion to 1-D models:

For nonporous solid materials, Fick’s law may be used:

$$\rho_s A_s \frac{\partial C}{\partial t} = \rho_s A_s D_m \frac{\partial^2 C}{\partial x^2} + \rho_s A_s r_s \quad (15)$$

where A_s is the area of the surface, m²; C is the concentration in the solid, mg-species/mg-solid; D_m is the diffusion coefficient in the solid, m²/h; r_s is the local generation rate, mg-species/mg-solid; and ρ_s density of the bulk solid, mg/m³.

Assuming a zero local generation rate and a uniform initial VOC concentration within the material, Little et al. (1994) used the above model to describe the VOC emissions from carpets. The diffusion coefficients were estimated to be of the order

of 10^{-14} to $10^{-11} \text{ m}^2/\text{s}$, and the model was found to reasonably well fit the emission data over a period of about 150 h.

Christiansson et al. (1993) derived the following simplified model based on the above Fick's law:

$$E(t) = C_0(D_m/\pi t)^{0.5}, \text{ when } M(t)/M_0 \geq 50\% \quad (16)$$

$$E(t) = 2 C_0 D_m/z \exp(D_m \pi t/4z^2), \text{ when } M(t)/M_0 < 50\% \quad (17)$$

where C_0 is the initial pollutant concentration in the source, mg/m^3 ; D_m is the diffusivity of the pollutant in the source, m^2/h ; $\pi = 3.14159$; $M(t)$ is the amount of pollutant remaining in the source, mg/m^2 ; M_0 is the initial amount of pollutant remaining in the source, mg/m^2 ; and z is the thickness of the source.

Their results show that the above model described successfully the VOC emissions from PVC flooring materials tested.

For porous solid materials, diffusion within the solid can be attributed to three types: (1) diffusion in the air-phase, which can be characterized by an effective diffusion coefficient, D_e , in analogous to the Fick's law; (2) diffusion along the surfaces of the solid phase (surface diffusion), in which the diffusion coefficient is usually dependent on the concentration of the sorbed phase on the surfaces; and (3) diffusion through the solid. The partial differential equation for describing the diffusion within porous materials is much more complicated. For example, for sheet-like porous solids, assuming (a) the sorbed-phase concentration remains in equilibrium with the porous air-phase concentration, and (b) the surface and solid-phase diffusions are negligible, we have (Axley 1995):

$$\rho A_s e \frac{\partial C}{\partial t} + \rho_s A_s \frac{\partial C}{\partial t} = \rho_s A_s D_e \frac{\partial^2 C}{\partial x^2} + \rho_s A_s r_s \quad (18)$$

where D_e is the effective diffusion coefficient in the porous gas-phase, m^2/s ; ρ is the gas-phase density, $\text{g-air}/\text{m}^3$; ρ_s is the density of the bulk porous solid, g/m^3 ; C is the gas-phase concentration, g-species/g-air ; and C_s is the sorbed-phase concentration, $\text{g-species/g-bulk solid}$.

The above equation simply states that the total accumulation of the compounds (gas-phase plus the sorbed-phase) in a control volume is equal to that transferred by porous gas-phase diffusion and that by the distributed generation.

While the mass transfer equations are readily available, their applications to building materials are hindered by the lack of data on the diffusion coefficients for various materials. Methods for experimentally determining the diffusion coefficients are therefore necessary.

Other Mass Transfer Related Models

1. A Model for VOCs Emissions from Manufactured Wood Products:

$$E(t) = E(0) - K C \quad (19)$$

where K is the proportionality coefficient.

This model assumes that the source has a maximum (constant) emission factor when the ambient concentration is zero and decreases linearly with the increase of the concentration in air (Hoetjer and Koerts 1986; Mathews et al. 1987). This model is essentially equivalent to the constant vapor pressure model if one assumes that the surface concentration is constant and equal to $E(0)/K$.

2. A Model for Pollutant Emissions from Treated Wood Products:

$$E(t) = E(0)[1 - C(t)/C_v][M(t)/M_0] \quad (20)$$

where C_v is the saturated vapor concentration of the pollutant in air, mg/m³; $M(t)$ is the amount of pollutant remaining in the source at time t , mg/m²; and M_0 is the total emittable amount of pollutant in the source, mg/m².

This model assumes that the emission factor at any given time is proportional to the amount of pollutant remaining in the source and the difference between the pollutant concentration in air and the saturation vapor concentration. Jaycock et al. (1995) showed that this model could describe the emissions of biocides from isothiazolone-treated wood products.

In summary, statistical models are available for analyzing and reporting emission test results. Since these models are derived from relatively short-term test data (mostly up to 1-week period), their validity for predicting the emissions beyond the test period has yet to be evaluated with some long-term emission test data.

The trend in predicting the rates of VOC emissions from building materials/furnishings is to use mechanistic models that are based on fundamental mass transfer theory (i.e., the so-called mass transfer models). For “wet” coating materials applied on a realistic substrate (such as wood stains on an oak wood, paints on a gypsum board, etc.), the existing interfacial mass transfer model for evaporative sources appears to be adequate only for the initial emission period that is dominated by evaporation (about first 12 h). A more complete model that describes both the evaporative mass transfer and the internal diffusion (that becomes the controlling factor for the emission process after the initial emission period) is needed for “wet” coating materials. For “wet” installation materials (such as adhesives, caulk, and sealants), effective mass transfer models are yet to be developed. For dry materials (such as carpets, vinyl floorings, wood-based panels, gypsum wallboards, etc.), the 1-D internal diffusion mass transfer models have shown promising results, but comprehensive evaluations are necessary. The applications of mass transfer models are also hindered by the lack of data on the model parameters such as the in-material diffusion coefficients of VOCs for various building materials.

Therefore, there is a need to develop mass transfer models that can better describe the emission process and thus for predicting the emission rates beyond the standard testing period and testing conditions. Models for material systems (assemblies) and data for validating such models are especially needed.

Influential Factors of VOCs Emission

As the emission mechanism of VOCs is the same as formaldehyde (a high volatility organic compound, VVOC), the impact of influencing factors (temperature and relative humidity) on VOCs emission is similar with the impact on formaldehyde as described in the previous chapter. The emission characteristic parameters C_0 and D_m are functions of temperature (T) and relative humidity (RH). The equations are as follows (Xiong et al. 2016):

$$C_0 = \frac{C_1}{\sqrt{T}} \exp \left(C_2 \cdot RH - \frac{C_3}{T} \right) \quad (21)$$

where C_1 , C_2 , and C_3 are only related to the physical and chemical properties of the material-pollutant combinations.

$$D_m = D_1 T^{1.25} \exp \left(-\frac{D_2}{T} \right) \quad (22)$$

where D_1 and D_2 are only related to the physical and chemical properties of the material-pollutant combinations.

For formaldehyde and VOC emissions from building materials, Qian (2007) obtained a series of correlations between the emission rate and dimensionless emission time, or the mass transfer Fourier number (Fo_m , defined as $D_m t / \delta^2$). When the emission process reaches steady state (it means the conditions for which the emission rate change slowly), the Fo_m is no less than 0.2 (Qian 2007; Yao 2011), and the emission rate can be expressed as (Xiong et al. 2013):

$$E(t) = 2.1 \frac{D_m C_0}{\delta} \exp(-2.36 Fo_m) \quad (23)$$

The emission rate (E) is a function of emission characteristic parameters, C_0 , D_m and K . Therefore, E is a function of T and RH .

Substituting Eqs. (21) and (22) into Eq. (23), it yields:

$$E(t) = E_1 T^{0.75} \exp \left(E_2 \cdot RH - \frac{E_3}{T} - 2.36 Fo_m \right) \quad (24)$$

where E_1 , E_2 , and E_3 are only related with the physical and chemical properties of the material-pollutant combinations, $E_1 = 2.1 C_1 D_1 / \delta$, $E_2 = C_2$, $E_3 = C_3 + D_2$.

The parameter $E_3 (= C_3 + D_2)$ in Eq. (24) is generally of the order of 10^4 for commonly used building materials (Huang et al. 2015; Deng et al. 2009). Considering that Fo_m is approximately equal to or larger than 0.2 when the emission reaches steady state, the term($-2.36 Fo_m$) is relatively small compared with other terms in Eq. (24) (e.g., E_3/T is about 30 at room temperature) and can thus be ignored. Therefore, Eq. (24) can be simplified into the following:

$$E(t) = E_1 T^{0.75} \exp\left(E_2 \cdot RH - \frac{E_3}{T}\right) \quad (25)$$

This equation explicitly characterizes the relationship between the steady-state emission rate with T and RH . Further analysis indicates that, with the increase of T or RH , E increases accordingly. Once E for a given material-pollutant combination is

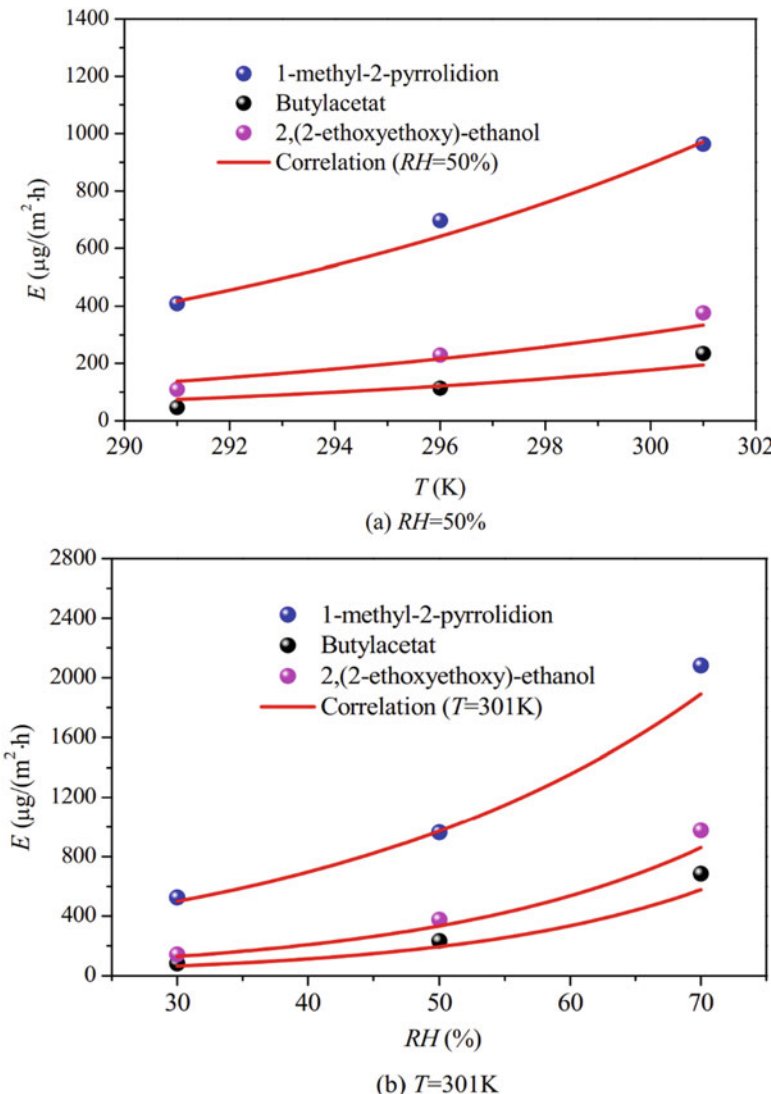


Fig. 4 The regression results by virtue of correlation (25) for three VOCs (1-methyl-2-pyrrolidinone, butyl acetate, and 2,(2-ethoxyethoxy)-ethanol). (Figure taken from Xiong et al. (2016))

measured at three or more sets of environmental conditions, the three parameters E_1 , E_2 , and E_3 can be determined from nonlinear curve fitting, the derived correlation (Eq. (25)) can then be applied to predict E at T and RH values different from the test conditions, which will be very helpful for engineering applications as well as for scientific studies.

The steady-state emission rate will change very slowly with Fo_m or emission time according to Eq. (24). Therefore, when using correlation (25) to predict E at different T and RH , the emission time corresponding to E should not differ substantially.

The regression results by virtue of correlation (25) for three VOCs (1-methyl-2-pyrrolidion, butyl acetate, and 2,(2-ethoxyethoxy)-ethanol) are shown in Fig. 4. Figure 4a presents the relationship of emission rate and temperature at a given relative humidity ($RH = 50\%$), and Fig. 4b shows the relationship of emission rate and relative humidity at a certain temperature ($T = 298$ K). The time point for the emission rate at steady state in this figure is 1 week. The R^2 for the three VOCs are all over 0.90, implying correlation (25) is also applicable for these pollutants. Further analysis based on the correlation indicates that the ratios of E in summer (with air conditioner, $T = 24$ °C, $RH = 50\%$) to that in winter (with air conditioner, $T = 20$ °C, $RH = 45\%$) in Beijing for 1-methyl-2-pyrrolidion, butyl acetate, and 2,(2-ethoxyethoxy)-ethanol from floor vanish are 1.66, 2.07, and 1.79, respectively (Xiong et al. 2016).

Conclusions

Reducing the concentration of VOCs indoors is an important indoor environment and health goal. The indoor building materials are the main indoor sources of VOCs pollutants. In order to control the indoor emissions, it is important to understand the VOCs emission characteristics of indoor building materials. Most studies about VOCs emission focused on dry materials and found that the three emission characteristic parameters, i.e., initial emission concentration (C_0), diffusion coefficient (D_m), and partition coefficient (K), are related to the building material, temperature, and relative humidity. More attention to the mechanism of VOCs emission, especially for wet materials, is needed in the future.

Cross-References

- [Epidemiology for Indoor Air Quality Problems](#)
- [Source/Sink Characteristics of VVOCs and VOCs](#)
- [Very Volatile Organic Compounds \(VVOCs\)](#)

References

- Agency for Toxic Substances and Disease Registry (ATSDR) (2007) Toxicological profile for xylene
Anand SS, Philip BK, Mehendale HM (2014) Volatile organic compounds. In: Encyclopedia of toxicology, 3rd edn, pp 967–970

- Andersen I, Lundqvist GR, Molhave L (1983) Human response to controlled levels of toluene in six-hour exposures. *Scand J Work Environ Health* 9:405–418
- ASTM D 3960-05 (98) (2018) Standard practice for determining volatile organic compound (VOC) content of paints and related coatings
- ASTM D-5226-90 (1990) Standard guide for small scale environmental chamber determinations of organic emissions from indoor Materidd~roducts. American Society for Testing and Materials, Philadelphia, PA
- Axley JW (1995) New Mass Transuort Elements and Comuonents for the NIST IAO Model. Research Report. NIST GCR 95-676. Building and Fire Research Laboratory, NIST, Gaithersburg, MD 20899.
- Baelum J, Lundqvist GR, Molhave L, Trolle Andersen N (1990) Human response to varying concentrations of toluene. *Int Arch Occup Environ Health* 62:65–71
- Boey KW, Foo SC, Jeyaratnam J (1997) Effects of occupational exposure to toluene: a neuropsychological study on workers in Singapore. *Ann Acad Med Singap* 26:184–187
- Cannella WJ (2000) Xylenes and ethylbenzene. In: Kirk-othmer encyclopedia of chemical technology. <https://doi.org/10.1002/0471238961.2425120503011414.a01.pub2>
- Centers for Disease Control and Prevention (CDC) (2017) Biomonitoring summary-xylenes
- Chang JCS, Guo Z (1992) Modeling of the fast organic emission from a wood finishing product – floor wax. *Atmos Environ* 26:V2365–V2370
- Chang JCS, Krebs KA (1992) Evaluation of para-dichlorobenzene emissions from solid moth repellant as a source of indoor air pollution. *J Air Waste Manag Assoc* 42:1214–1217
- Christiansson J, Yu TW, Neretnieks I (1993) Emission of VOCs from PVC-floorings – models for predicting the time dependent emission rates and resulting concentrations in the indoor air. In: Indoor air 93, proceedings of the 6th international conference on indoor air quality and climate, 2, pp 389–394
- Ciccolella A (2008) Volatile Organic Compounds (VOC): definition, classification and properties. *Rev Mal Respir* 25:155–163
- Clausen PA, Laursen B, Wolkoff E, Rasmussen E, Nielsen PA (1993) Emission of volatile organic compounds from a vinyl floor covering. In: Nagda NL (ed) Modeline of indoor air quality and exposure, ASTM STP 1205. American Society for Testing and Materials, pp 3–13
- Colombo A, Bortoli MD, Pecchio E, Schauenburg H, Schiltt H, Vissers H (1991) Small Chamber test and headspace analysis of volatile organic compounds emitted from household products. *Indoor Air* 1:13–21
- Crump KS (1994) Risk of benzene-induced leukaemia. A sensitivity analysis of the pliofilm cohort with additional follow-up and new exposure estimates. *J Toxicol Environ Health* 42: 219–242
- Deng QQ, Yang XD, Zhang JS (2009) Study on a new correlation between diffusion coefficient and temperature in porous building materials. *Atmos Environ* 43:2080–2083
- Dewulf J, Van Langenhove H, Wittmann G (2002) Analysis of volatile organic compounds using gas chromatography. *TrAC Trends Anal Chem* 21:637–646
- Eller N, Netterstrom B, Laursen P (1999) Risk of chronic effects on the central nervous system at low toluene exposure. *Occup Med* 49:389–395
- Environmental Protection Agency (EPA) (2012) Inhalation Health Effect Reference Values for Xylene – All Isomers
- Environmental Protection Agency (EPA) (1992) Respiratory health effects of passive smoking: lung cancer and other disorders
- Environmental Protection Agency (EPA) (2002) Toxicological review of benzene (noncancer effects) (CAS No. 71-43-2)
- Fabri J, Graeser U, Simo TA (2000) Xylenes. In: Ullmann's encyclopedia of industrial chemistry. https://doi.org/10.1002/14356007.a28_433. ISBN 978-3527306732
- Foo SC, Jeyaratnam J, Koh D (1990) Chronic neurobehavioural effects of toluene. *Br J Ind Med* 47: 480–484
- Foo SC, Phoon WO, Lee J (1988) Neurobehavioural symptoms among workersoccupationally exposed to toluene. *Asia Pac J Public Health* 2:192–197

- Fukuoka S (1975) Photochemical smog phenomena and plant damage due to them in Tokyo. Part I. Present state of photochemical smog in Japan. *Kankyo Hoken Rep (Japan)* 34:3–11
- GB 18582-2008 (2008) Indoor decorating and refurbishing materials: limit of harmful substances of interior architectural coatings
- Guo Z, Sparks LE, Tichenor BA, Chang JCS (1998) Predicting the emissions of individual VOCs from petroleum-based indoor coatings. *Atmos Environ* 32:231–237
- Guo Z, Tichenor BA (1992) Fundamental mass transfer models applied to evaluating the emissions of vapor-phase organics from interior architectural coatings. EPAIAWMA Symposium, Durham, NC
- Guo Z, Tichenor BA, Krebs KA, Roache NF (1996) Considerations on revisions of emission testing protocols
- Guo M, Yu W, Zhang S, Wang H, Wei S (2020) A numerical model predicting indoor volatile organic compound Volatile Organic Compounds emissions from multiple building materials. *Environ Sci Pollut Res* 27:587–596
- Hayes RB et al (1997) Benzene and the dose-related incidence of hematologic neoplasms in China. *J Natl Cancer Inst* 89:1065–1071
- Health Effects Institute (HEI) (2007) Mobile-source air toxics: a critical review of the literature on exposure and health effects, Boston, MA
- Health Canada (2011) Residential indoor air quality guideline-toluene
- Héroux MÈ, Gauvin D, Gilbert NL, Guay M, Dupuis G, Legris M, Lévesque B (2008) Housing characteristics and indoor concentrations of selected volatile organic compounds (VOCs) in Quebec City, Canada. *Indoor Built Environ* 17:128–137
- Huang SD, Xiong JY, Zhang YP (2015) Impact of temperature on the ratio of initial emittable concentration to total concentration for formaldehyde in building materials: theoretical correlation and validation. *Environ Sci Technol* 49:1537–1544
- Hoetjer JJ, Koerts F (1986) A model for formaldehyde release from particleboard. Formaldehyde Release from Wood Products. American Chemical Society, pp 125–144
- IARC Working Group on the Evaluation of Carcinogenic Risks to Humans (2012) Chemical Agents and Related Occupations. International Agency for Research on Cancer, Lyon. (IARC Monographs on the Evaluation of Carcinogenic Risks to Humans, No. 100F.) Occupational exposure as a painter. Available from: <https://www.ncbi.nlm.nih.gov/books/NBK304433/>
- Institute for Environment and Health (1999) IEH report on the benzene in the environment. MRC Institute for Environment and Health (Report R12), Leicester
- International Union of Pure and Applied Chemistry (IUPAC) (2008a) Subcommittee on gas kinetic data evaluation – data sheet HOx_AROM1. Research Triangle Park, NC
- International Union of Pure and Applied Chemistry (IUPAC) (2008b) Subcommittee on gas kinetic data evaluation – data sheet NO3_AROM1. Research Triangle Park, NC
- International Union of Pure and Applied Chemistry (IUPAC) (2008c) Subcommittee on gas kinetic data evaluation – data sheet O3_AROM1. Research Triangle Park, NC
- Jaycock MA, Doshi DR, Nungesser EH, Shade WD (1995) Development and evaluation of a source/sink model of indoor air concentrations from isothiazoline-treated wood used indoors. *Am Ind Hyg Assoc J* 56:546–557
- Kandyala R, Raghavendra SPC, Rajasekharan ST (2010) Xylene: an overview of its health hazards and preventive measures. *J Oral Maxillofac Pathol* 14(1):1–5
- Kang SK, Rohlman DS, Lee MY, Lee HS, Chung SY, Anger WK (2005) Neurobehavioral performance in workers exposed to toluene. *Environ Toxicol Pharmacol* 19:645–650
- Kays, Crawford (1981) Convective Heat and Mass Transfer, 2d edition. McGraw-Hill Book Company. New York.
- Levin H, Hodgson AT (1996) Screening and selecting building materials and products based on their emissions of volatile organic compounds (VOCs). Characterizing Source of Indoor Air Pollution and Related Sink Effects, ASTM STP, 1287, B.A. Tichenor, Ed., American Society for Testing and Materials, pp. 376–391.
- Little JC, Hodgson AT, Gadgil AJ (1994) Modeling emissions of volatile organic compounds from new carpets. *Atmos Environ* 28:227–234

- Marlowe IT, Bone CM, Byfield S et al (1995) The categorisation of volatile organic compounds. Environment Agency
- Mathews TG, Wilson DL, Thomson AJ, Mason MA, Balley SN, Nelms LH (1987) Interlaboratory comparison of formaldehyde emissions from particleboard underlayment in small scale environmental chambers. JAFCA 37:1320–1326
- McHale CM, Zhang LP, Smith MT (2012) Current understanding of the mechanism of benzene-induced leukemia in humans: implications for risk assessment. Carcinogenesis 33:240–252
- National Institute for Occupational Safety & Health (NIOSH) (1978) Occupational health guideline for xylene
- National Institute of Standards and Technology (NIST) (2005) Chemistry WebBook. NIST Standard Reference Database Number 69
- Qian K (2007) Study of the correlations and key parameters for VOC emissions from dry building materials (Master Thesis). Tsinghua University, Beijing
- Seeber A, Demes P, Kiesswetter E, Schaper M, Van Thriel C, Zupanic M (2005) Changes of neurobehavioral and sensory functions due to toluene exposure below 50 ppm? Environ Toxicol Pharmacol 19:635–643
- Seeber A, Schaper M, Zupanic M, Blaszkewicz M, Demes P, Kiesswetter E, Van Thriel C (2004) Toluene exposure below 50 ppm and cognitive function: a follow-up study with four repeated measurements in rotogravure printing plants. Int Arch Occup Environ Health 77:1–9
- Solomon S, Mills M, Heidt LE, Pollock WH, Tuck AF (1992) On the evaluation of ozone depletion potentials. J Geophys Res. <https://doi.org/10.1029/91JD02613>
- Streicher HZ, Gabow PA, Moss AH, Kono D, Kaehny WD (1981) Syndromes of toluene sniffing in adults. Ann Intern Med 94:758–762
- Salameh T, Sauvage S, Gaudion V, Léonardis T, Fronval I, Locoge N (2018) DNPH cartridge/ HPLC analysis – a still relevant method for OVOC monitoring: a contribution to the assessment of uncertainty in current atmospheric VOC measurements. 20th EGU General Assembly, EGU2018, Proceedings from the conference, Vienna, Austria, p. 14845
- Song S, Gao M, Xu W, Sun Y, Worsnop DR, Jayne JT, Zhang Y, Zhu L, Li M, Zhou Z, Cheng C, Lv Y, Wang Y, Peng W, Xu X, Lin N, Wang Y, Wang S, Munger JW, Jacob DJ, McElroy MB (2019) Possible heterogeneous chemistry of hydroxymethanesulfonate (HMS) in northern China winter haze. Atmospheric Chemistry and Physics 19(2):1357–1371. <https://doi.org/10.5194/acp-19-1357-2019>
- Tichenor BA, Guo Z (1991) The effect of ventilation on emission rates of wood finishing materials. Environ Int 17:317–323
- Tichenor BA, Guo Z, Dunn JE, Sparks LR, Mason MA (1991) The interaction of vapor phase organic compounds with indoor sinks. Indoor Air 1:23–35
- Soni V, Singh P, Shree V, Goel V (2018) Effects of VOCs on human health. In: Air pollution and control. Energy, environment, and sustainability. Springer, Singapore
- U.S. Federal Environmental Protection Agency (U.S. EPA) (1992) 40 CFR 51.100 – Definitions
- World Health Organization (WHO) (1989) Indoor air quality: organic pollutants
- World Health Organization (WHO) (2000) Air quality guidelines for Europe, 2nd edn
- World Health Organization (2010) WHO guidelines for indoor air quality. WHO, Geneva
- Xiong JY, Wei WJ, Huang SD, Zhang YP (2013) Association between the emission rate and temperature for chemical pollutants in building materials: general correlation and understanding. Environ Sci Technol 47:8540–8547
- Xiong JY, Zhang PP, Huang SD, Zhang YP (2016) Comprehensive influence of environmental factors on the emission rate of formaldehyde and VOCs in building materials: correlation development and exposure assessment. Environ Res 151:734–741
- Yao Y (2011) Research on some key problems of furniture VOC emission labeling system (Ph.D. thesis). Tsinghua University, Beijing
- Yuan B, Shao M, de Gouw J et al (2012) Volatile organic compounds (VOCs) in urban air: how chemistry affects the interpretation of positive matrix factorization (PMF) analysis. J Geophys Res. <https://doi.org/10.1029/2012JD018236>
- Zhang JS, Wang JM, Shaw CY (1997) A theoretical examination of a simplified procedure for data analysis in small chamber testing of material emissions. Internal Report No. (IRC-IR-733)

Zhang JS, Shaw CY, Kanabus-Kaminska JM, MacDonald RA, Magee RJ, Lusztyk E, Weichert HJ (1996) Study of air velocity and turbulence effects on organic compound emissions from building materials/furnishings using a new small test chamber. In: Tichenor BA (ed) Characterizing source of Indoor air pollution and related sink effects, ASTM STP 1287. American Society for Testing and Materials, pp 184–199



Semi-volatile Organic Compounds (SVOCs)

4

Jianping Cao

Contents

Introduction	100
Phthalate Esters (PAEs) and Their Alternatives	102
Brominated Flame Retardants (BFRs)	109
Polybrominated Diphenyl Ethers (PBDEs)	110
Hexabromocyclododecanes (HBCDs)	111
Organophosphorus Flame Retardants (OPFRs)	112
Per- and Polyfluorinated Alkyl Substances (PFAS)	117
Conclusions	122
Cross-References	123
References	123

Abstract

In modern buildings, abundant synthetic materials and products are used to meet various demands of occupants. A vast of semi-volatile organic compounds (SVOCs) are added as additives or solvents to facilitate the production of, or enhance the performance of, these materials and products, leading to the ubiquity of SVOCs in indoor environments. SVOCs can be slowly emitted from these sources and then be partitioned among gas phase and various indoor surfaces. Due to their strong partitioning between air and surfaces, SVOCs have long indoor persistence (days to years, or even more). Human exposure to some SVOCs have been proved to be associated with diverse health risks, which have led to product reformulations in some cases. However, few knowledges about the indoor fate, human exposure, and the associated health risks are currently available for many other widely used SVOCs as well as the increasing number of emerging SVOCs. This chapter provides an overview on the usage, basic physicochemical properties, and adverse health effects of four classes of

J. Cao (✉)

School of Environmental Science and Engineering, Sun Yat-sen University, Guangzhou, China
e-mail: caojp3@mail.sysu.edu.cn

SVOCs that have been frequently/newly investigated in the past 20 years, including (1) phthalate esters (PAEs) and their alternatives, (2) brominated flame retardants (BFRs), (3) organophosphate flame retardants (OPFRs), and (4) per- and polyfluoroalkyl substances (PFAS). Overall, this chapter aims to emphasize the importance of investigating SVOC pollution in indoor environments.

Keywords

Indoor air quality (IAQ) · Phthalate esters · Brominated flame retardants · Organophosphate flame retardants · Per- and polyfluoroalkyl substances

Introduction

At present, plastic products, composite wood, synthetic carpets, foam cushioning, scented detergent, and electronic equipment (e.g., computers, televisions, and washer/dryers) have become ubiquitous indoors (Weschler 2009). Lots of chemical substances are added as additives or solvents to facilitate the production of, or enhance the performance of, these materials and products. Many of these chemicals (such as formaldehyde, benzene series, phthalates, and flame retardants) that are potentially harmful to human body will be emitted into the indoor air, resulting in the deterioration of indoor air quality (IAQ) (Destaillets et al. 2008; Weschler 2009; Xu and Little 2006; Zhang et al. 2013). Among these indoor air pollutants, volatile organic compounds (VOCs) have been widely concerned and studied in the past decades (Ohura et al. 2009; Wang et al. 2010; Zhang et al. 2016). Taking China as the example, substantial projects of related research have been launched and a series of standards related to the control of indoor VOC pollution have been promulgated since 2000 (Wang et al. 2010). Due to the changes in materials/products, building ventilation, occupant behaviors, public awareness, and government actions, levels of many indoor pollutants (including formaldehyde, aromatic and chlorinated solvents, and chlorinated pesticides) were found to increase and then decrease since 1950s (Weschler 2009). However, levels of other indoor pollutants were found to increase and remain high (e.g., phthalate esters, brominated flame retardants, bisphenol A, and nonylphenol). As shown in Table 2 of Weschler (2009), most of indoor pollutants with increasing levels belonged to semi-volatile organic compounds (SVOCs).

SVOCs are generally defined as organic compounds with vapor pressures between 10^{-14} and 10^{-4} atm (10^{-9} to 10 Pa) at environmental temperature (Weschler and Nazaroff 2008) or with boiling points between 240/260 °C and 380/400 °C at ambient pressure (WHO 1989). Due to their low vapor pressures, it is thermodynamically favorable for SVOCs to partition from gas phase into condensed phases. Especially for some SVOCs with high molecular weight, over 90% of their total mass indoors may be sorbed on indoor surfaces. Consequently, organic compounds that have meaningful abundances in both the gas phase and condensed phases can also be referred to as SVOCs (Weschler and Nazaroff 2008). Different from volatile organic compounds (VOCs, boiling point between 50/100 °C and

240/260 °C) and very volatile organic compounds (VVOCs, boiling point between <0 °C and 50/100 °C), SVOCs are more stable, are difficult to degrade, and tend to persist for years in indoor environments (Van Loy et al. 1997; Wang et al. 2010). Figure 1 illustrates the fate and transport of SVOCs in indoor environments.

As shown in Fig. 1, the indoor fate and transport of SVOCs mainly comprise of three processes: (1) emission: SVOCs are emitted into the indoor air from products or materials containing SVOCs (designated as SVOC source) that enter the indoor environments; (2) sorption: SVOCs in the air are easily sorbed by interior surfaces (including airborne particles, settled dust, exposed inanimate surfaces, and skin surfaces); and (3) exposure: SVOC in multiphases enter the human body via three pathways (inhalation of air and airborne particles, nondietary ingestion of dust, and dermal absorption from air, deposited particles, or contacted surfaces) (Eichler et al. 2021; Little et al. 2012; Xu et al. 2010). If the SVOC source is removed or fresh air (free of SVOCs) is introduced, the SVOC concentrations in indoor air will decrease. Meanwhile, the condensed-phase SVOCs may be released from the interior surfaces to the indoor air (i.e., desorption process shown in Fig. 1), impeding the decrease of gas-phase SVOC concentrations (Weschler and Nazaroff 2008). The frequent sorption-desorption transition is the key reason that makes the indoor fate and transport of SVOCs, as well as the control of indoor SVOCs, much more complex than those of VVOCs and VOCs. Taking the USA as an example, the US EPA suggests several guidelines to preserve the indoor air quality, however a specific indoor air quality index for SVOCs does not exist (Lucattini et al. 2018). The occurrence, fate and transport, health effects, and/or toxicity of SVOCs in indoor environments have become hot research topics in the past decades (Xu and Zhang 2011). Mechanistic models for describing the indoor fate and transport of SVOCs can be found in other chapters of this handbook, including Chap. ▶ 23, “Source/Sink Characteristics of SVOCs,” ▶ 25, “Predicting VOC and SVOC Concentrations in

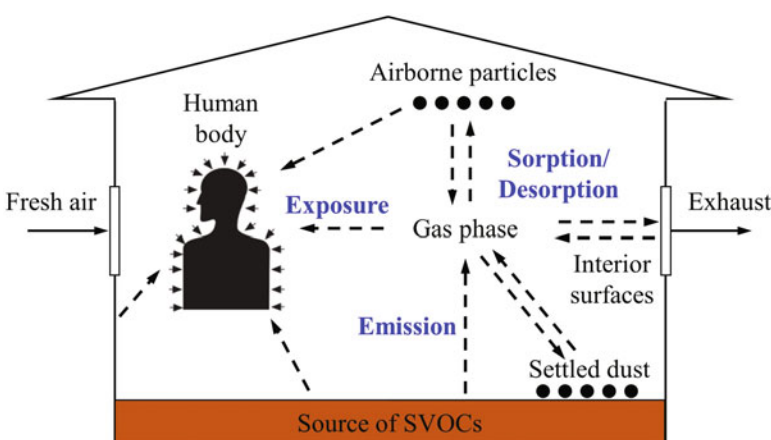


Fig. 1 Schematic of the fate and transport of SVOCs in indoor environments

Complex Indoor Environments,” and ► 38, “A Modular Mechanistic Framework for Assessing Human Exposure to Indoor Chemicals.”

Abundant studies have been attempted to measure the concentrations (or contents) of SVOCs in indoor air, dust, materials, and products (Bu et al. 2016; Lucattini et al. 2018; Melymuk et al. 2016; Raffy et al. 2017; Rudel and Perovich 2009; Shi et al. 2018; Wang et al. 2014; Wei et al. 2021). Lucattini et al. (2018) gave a relatively comprehensive review for the reported data of SVOCs in multiple indoor media (air, dust, and consumer products). The following classes of compounds were included: polychlorinated biphenyls (PCBs), polycyclic aromatic hydrocarbons (PAHs), polyfluorinated alkyl substances, polybrominated diphenyl ethers (PBDEs), brominated flame retardants (BFRs), emerging brominated flame retardants (EBFRs), organophosphate flame retardants (OPFRs), phthalate esters (PAEs), musks/fragrances, organochlorine pesticides, and pyrethroids. Based on this, the general information of the following classes of SVOCs are introduced in this chapter: (1) PAEs and their alternatives, (2) BFRs, (3) OPFRs, and (4) per- and polyfluoroalkyl substances (PFAS). They are the classes of SVOCs that are mainly released from indoor materials/products to the indoor air and have been frequently/ newly investigated in the field of IAQ, to the author’s best knowledge, since 2000.

Phthalate Esters (PAEs) and Their Alternatives

Phthalate esters (or phthalates, PAEs) are esters of phthalic acid (1,2-benzenedicarboxylic acid) with different alcohols. The general structure of PAEs is a diester of 1,2-dicarboxy-benzene, as shown in Fig. 2.

PAEs are hydrophobic compounds with low vapor pressures and viscous liquids with high boiling points and low melting points (like oil). The physicochemical properties of some commonly used PAEs are listed in Table 1.

PAEs can be divided into two groups according to their carbon chain length (i.e., R and R' in Fig. 2): high molecular weight (HMW) phthalates (7–13 carbon atoms) and low molecular weight (LMW) phthalates (3–6 carbon atoms) (Kashyap and Agarwal 2018). They are mainly used as plasticizers in the production of plastics, primarily polyvinyl chloride (PVC), to improve the product performance (e.g., flexibility and durability). Plastics are widely used in numerous indoor products, such as flooring, carpets, wall papers, synthetic leather, packaging, and toys. Di (2-ethylhexyl) phthalate (DEHP), followed by diisononyl phthalate (DINP), are the most commonly used PAEs. Additionally, PAEs with <3 carbon atoms (such as dimethyl phthalate [DMP] and diethyl phthalate [DEP]) are not used as plasticizers.

Fig. 2 General chemical structure of phthalate esters

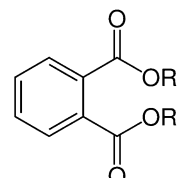


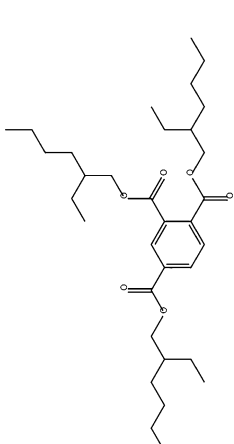
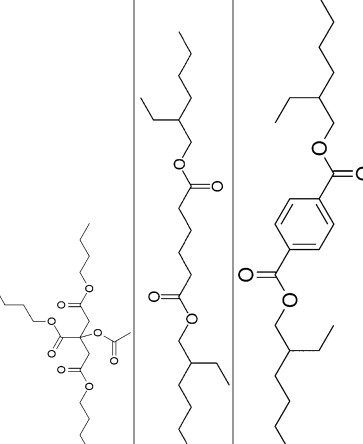
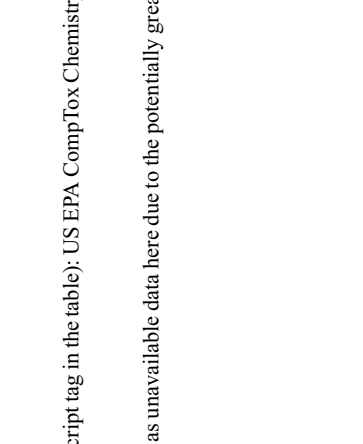
Table 1 Physicochemical properties of selected phthalate esters (PAEs) and their alternatives

PAEs and their alternatives	Formula	CAS	MW	Chain length	Vapor pressure ^a	Log K_{ow} ^b	Log K_{ow} ^c	Structure
Dimethyl phthalate (DMP)	C ₁₀ H ₁₀ O ₄	131-11-3	194.2	1	3.08 × 10 ⁻³ ~ 6.27 × 10 ⁻³	5.72	1.58-1.88	
Diethyl phthalate (DEP)	C ₁₂ H ₁₄ O ₄	84-66-2	222.2	2	9.16 × 10 ⁻⁴ ~ 2.10 × 10 ⁻³	6.75	2.44-2.71	
Di-n-butyl phthalate (DnBP)	C ₆ H ₂₂ O ₄	84-74-2	278.3	4	2.02 × 10 ⁻⁵ ~ 1.08 × 10 ⁻⁴	8.84	4.61-4.83	
Diisobutyl phthalate (DiBP)	C ₆ H ₂₂ O ₄	84-69-5	278.3	3	3.18 × 10 ⁻⁵ ~ 1.54 × 10 ⁻³	8.21	4.11-4.46	
Butyl benzyl phthalate (BBzP)	C ₁₉ H ₂₀ O ₄	85-68-7	312.4	4, 6	7.09 × 10 ⁻⁷ ~ 8.18 × 10 ⁻⁶	9.83	4.67-5.00	
Di(2-ethylhexyl) phthalate (DEHP)	C ₂₄ H ₃₈ O ₄	117-81-7	390.6	6	1.43 × 10 ⁻⁷ ~ 3.95 × 10 ⁻⁶	12.89-13.12 ^d	7.52-8.71	

(continued)

Table 1 (continued)

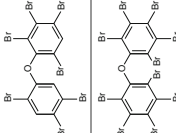
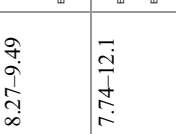
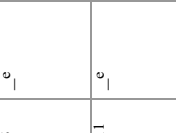
PAEs and their alternatives	Formula	CAS	MW	Chain length	Vapor pressure ^a	Log K_{ow}^b	Log K_{ow}^c	Structure
Di- <i>n</i> -octyl phthalate (DnOP)	C ₂₄ H ₃₈ O ₄	117-84-0	390.6	8	1.01 × 10 ⁻⁷ ~ 3.96 × 10 ⁻⁶	— ^c	8.10–9.08	
Diisomyonyl phthalate (DINP)	C ₂₆ H ₄₂ O ₄	68515-48-0	418.6	8–9	4.5 × 10 ⁻⁷ ^f	— ^c	8.8 ^f	
Diisodecyl phthalate (DIDP)	C ₂₈ H ₄₆ O ₄	89-16-7	446.7	9–10	8.89 × 10 ⁻⁸ ~ 5.28 × 10 ⁻⁷	— ^e	8.90–10.8	
Di(2-ethylhexyl) terphthalate (DEHTP)	C ₂₄ H ₃₈ O ₄	6422-86-2	390.6		4.31 × 10 ⁻⁷ ~ 1.31 × 10 ⁻⁶	12.52–13.45 ^d	7.55–9.54	
Di-isomyonyl cyclohexane-1,2-dicarboxylate (DINCH)	C ₂₆ H ₄₈ O ₄	166412-78-8	424.7		9.75 × 10 ⁻¹⁰ ~ 6.90 × 10 ^{-8g}	12.88–14.53 ^d	—	

	C ₃₃ H ₅₄ O ₆	3319-31-1	546.8	3.98 × 10 ⁻⁹ ~ 4.60 × 10 ⁻⁷	17.89-18.78 ^d	7.97-12.8
	C ₂₀ H ₃₄ O ₈	77-90-7	402.5	3.35 × 10 ⁻⁷ ~ 1.60 × 10 ⁻⁶	10.3	4.29-6.92
	C ₂₂ H ₄₂ O ₄	103-23-1	370.6	8.25 × 10 ⁻⁷ ~ 8.35 × 10 ⁻⁶	11.29-12.51 ^d	6.85-8.12
	C ₂₄ H ₃₈ O ₄	6422-86-2	390.6	4.31 × 10 ⁻⁷ ~ 1.31 × 10 ⁻⁶	12.56-13.45 ^d	7.55-9.54

^aVapor pressure at 25 °C, torr (1 torr = 133.3224 Pa)^b K_{oa} is the octanol-air partition coefficient at 25 °C^c K_{ow} is the octanol-water partition coefficient at 25 °C. Data source of a, b, and c (if there is no specific superscript tag in the table): US EPA CompTox Chemistry Dashboard ([USEPA](#))^dData source: Salthammer and Goss ([2019](#))^e $K_{oa} = 11.7$ is presented in US EPA CompTox Chemistry Dashboard for all these chemicals, which is treated as unavailable data here due to the potentially great uncertainties^fData source: CPSC ([2010](#))
^gData source: Wu et al. ([2016a](#))

Table 2 Physicochemical properties of individual PBDE congeners

PBDE congeners	Formula	CAS	MW	Vapor pressure ^a	$\log K_{ow}^b$	$\log K_{ow}^c$	Structure
2,2',4,4'-tetra-bromodiphenyl ether (BDE-47)	$C_{12}H_6Br_4O$	5436-43-1	485.8	$7.04 \times 10^{-8} \sim 4.19 \times 10^{-6}$	10.5	6.59-7.39	
2,2',3,4,4'-penta-bromodiphenyl ether (BDE-85)	$C_{12}H_5Br_5O$	182346-21-0	564.7	$7.29 \times 10^{-9} \sim 1.67 \times 10^{-7}$	11.6	7.16-8.02	
2,2',4,4',5-penta-bromodiphenyl ether (BDE-99)	$C_{12}H_5Br_5O$	60348-60-9	564.7	$1.92 \times 10^{-8} \sim 2.46 \times 10^{-7}$	11.3	7.18-8.19	
2,2',4,4',6-penta-bromodiphenyl ether (BDE-100)	$C_{12}H_5Br_5O$	189084-64-8	564.7	$2.94 \times 10^{-8} \sim 9.57 \times 10^{-7}$	11.5	7.08-8.03	
2,2',4,4',5,5'-hexa-bromodiphenyl ether (BDE-153)	$C_{12}H_4Br_6O$	68631-49-2	643.6	$4.51 \times 10^{-9} \sim 6.38 \times 10^{-8}$	12.2 ^d	7.77-8.98	
2,2',4,4',5,6'-hexa-bromodiphenyl ether (BDE-154)	$C_{12}H_4Br_6O$	207122-15-4	643.6	$4.97 \times 10^{-9} \sim 6.36 \times 10^{-8}$	13.2 ^d	7.75-8.83	

	$C_{12}H_3Br_7O$	207122-16-5	722.5	$1.26 \times 10^{-9} \sim 3.83 \times 10^{-8}$	- ^c	
	$C_{12}Br_{10}O$	1163-19-5	959.2	$1.64 \times 10^{-12} \sim 8.47 \times 10^{-11}$	- ^e	

^aVapor pressure at 25 °C, torr (1 torr = 133.3224 Pa)^b K_{Oa} is the octanol-air partition coefficient at 25 °C^c K_{ow} is the octanol-water partition coefficient at 25 °C. Data source of a, b, and c (if there is no specific superscript tag in the table): US EPA CompTox Chemistry Dashboard ([USEPA](#))^dData source: Okeme et al. ([2018](#))^e $K_{ow} = 11.7$ is presented in US EPA CompTox Chemistry Dashboard for all these chemicals, which is treated as unavailable data here due to the potentially great uncertainties

and not classified in any group. These PAEs are used as solvents and fixatives in fragrances, additives in cosmetics, medical devices, and personal care and cleaning products (Kashyap and Agarwal 2018). Some LMW phthalates (such as di-*n*-butyl phthalate [DnBP] and di-iso-butyl phthalate [DiBP]) also have applications similar to PAEs with <3 carbon atoms, i.e., used as solvents (Ait Bamai 2020). Overall, PAEs are widely used in indoor materials and products. For example, PAEs are presented in all classes of indoor products investigated by Lucattini et al. (2018): electronics, building materials, textiles, furniture, health care/personal/cleaning products, and cosmetics. Because PAEs are not chemically bound to PVC and other materials, they may migrate out to the surrounding environments, e.g., emission to the indoor air, during their usage (Clausen et al. 2004), and subsequently lead to the deterioration of indoor air quality.

Compared to the long duration of usage in the plasticizer industry (since 1930s), concerns over the possible adverse health risks of PAEs are relatively recent (since 1970s) (Mayer et al. 1972). Currently, PAEs are known to be reproductive and developmental toxicants (Kashyap and Agarwal 2018). Based on human biomonitoring studies, human exposure to PAEs may cause several adverse health outcomes, such as fertility problems, respiratory diseases, childhood obesity, and neuropsychological disorders (Katsikantami et al. 2016). Consequently, authoritative regulations on PAE use have been implemented in some countries and regions. Six PAEs, including DMP, DEP, DnBP, BBzP, DEHP, and DnOP (all included in Table 1), have been identified as priority pollutants by the US EPA and the European Union (EU) (Kashyap and Agarwal 2018). Mass fractions of DnBP, BBzP, DEHP, and DnOP have been limited to $\leq 0.1\%$ in toys and childcare articles by EU (Directive 2005/84/EC), the USA (Consumer Product Safety Improvement Act of 2008 (CPSIA, 2008), China (China National Standard GB 6675, 2014), and Japan (Japan Toy Safety Standard ST-2002 Part 3, 2011) (Kashyap and Agarwal 2018). Furthermore, since 2015, DnBP, BBzP, and DEHP have been classified as reproductive toxicant category 1B and completely banned for any application without a specific authorization from EU (Eichler et al. 2019). The chemical risk management regulations and activities of PAEs in EU, the USA, Canada, and Australia were comprehensively summarized in Eichler et al. (2019).

Because of the strict regulations on the use of PAEs, there has been a reduction in their production. Higher molecular weight phthalates are being manufactured and employed by the plastic industry. Taking the most commonly used PAE, namely DEHP, as an example, the market share of DEHP in EU decreased from 42% in 1999 to 10% in 2014 (Nagorka and Koschorreck 2020). It was replaced mainly by DINP and DIDP. However, the EU also sets a restriction of 0.1% by weight for DINP and DIDP for toys and childcare products that might be placed in the mouth (Eichler et al. 2019), due to the increasing concerns on the potentially adverse health effects of these higher molecular weight PAEs. Except for higher molecular weight PAEs, manufacturers of PAE plasticizers have switched to non-PAE plasticizers such as adipates or citrates, which accounted for 40% of the EU plasticizer market until 2019 (Nagorka and Koschorreck 2020). Terephthalates and cyclohexane dicarboxylic acid esters were firstly introduced to the alternative plasticizer market, with di-

(2-ethylhexyl) terephthalate (DEHTP) and di-isobutyl cyclohexane-1,2-dicarboxylate (DINCH) as the most widely used phthalate alternatives (Deng et al. 2021). Subsequently, trimellitates, citrates, and adipates, including tris(2-ethylhexyl) trimellitate (TOTM), tributyl-O-acetyl citrate (ATBC), and di(2-ethylhexyl) adipate (DEHA), were applied as phthalate alternatives in electronics, apparels, and building materials. Furthermore, isophthalate esters, cyclohexene dicarboxylic acid esters, and new cyclohexane dicarboxylic acid esters were developed as the newest phthalate alternatives, including di(2-ethylhexyl) isophthalate (DEHIP), di(2-ethylhexyl) tetrahydrophthalate (DEHTH), di(2-ethylhexyl) cyclohexane-1,4-dicarboxylate (1,4-DEHCH), and di(2-ethylhexyl) cyclohexane-1,2-dicarboxylate (1,2-DEHCH). The physicochemical properties of some commonly used phthalate alternatives are also listed in Table 1. Although most manufacturers declare that these non-PAE plasticizers have no adverse health and environmental effects, mounting evidence implies that they may exhibit various toxic effects, e.g., endocrine-disrupting activity, reproductive and developmental toxicity, and carcinogenicity (Deng et al. 2021).

Due to their ubiquity in indoor environments and high concerns to their health risks, comprehensive data on levels of traditional PAEs (such as DMP, DEP, DnBP, BBzP, DEHP, and DnOP) in indoor air and dust are available in the literature (Ait Bamai 2020; Kashyap and Agarwal 2018; Lucattini et al. 2018). Abundant studies have focused on the emissions of PAEs from PVC floorings since 2003 (Afshari et al. 2004; Benning et al. 2013; Cao et al. 2017; Clausen et al. 2004; Eichler et al. 2018; Ekelund et al. 2010; Fujii et al. 2003; Hsu et al. 2017; Jeon et al. 2016; Liang and Xu 2014; Liu and Zhang 2016; Noguchi and Yamasaki 2016; Pei et al. 2017; Shi et al. 2018; Wu et al. 2016b; Xu and Little 2006; Xu et al. 2012). However, much less data have been reported for higher molecular weight PAEs and phthalate alternatives. More concerns are required for the pollution problems related to the emerging PAEs and non-PAE plasticizers in indoor environments.

Brominated Flame Retardants (BFRs)

Flame retardants (FRs) are substances used in plastics, textiles, electrical equipment, and other materials (or products) to make them less flammable. The FRs that have been/are in use can generally divided into six main categories: halogenated FRs (brominated and/or chlorinated), phosphorous FRs, nitrogen, intumescence systems (e.g., expanded foam), mineral (containing aluminum or magnesium), and others, e.g., antimony trioxide and nanocomposites (Rauert 2014). The brominated flame retardants (BFRs) are one of the most widely used flame retardants in consumer products since the 1970s. BFRs inhibit or slow down the growth of fire by releasing free radical bromine atoms into the air, before the material can reach its ignition temperature, which reduces heat generation, slows the burning process, and prevents the fire cycle from establishing and sustaining itself. BFRs are added to the material/product either through additive or reactive processes. The mass fraction of BFRs in products can be up to 30%. Similar to PAEs, BFRs can migrate from source materials

to indoor air through volatilization or transfer to indoor dust via abrasion of the source material and direct source-dust contact (Rauert and Harrad 2015).

There are around 75 different commercial BFRs used in electrical equipment (e.g., TV casings and computer monitors), accounting for more than 50% of their usage. Polybrominated diphenyl ethers (PBDEs) and hexabromocyclododecanes (HBCDs) are the two most commonly used BFRs. The general chemical structures of PBDEs and HBCDs are shown in Fig. 3. Products containing PBDEs and HBCDs are ubiquitous in indoor environments with considerable concentrations in indoor air and dust (Harrad et al. 2010).

Polybrominated Diphenyl Ethers (PBDEs)

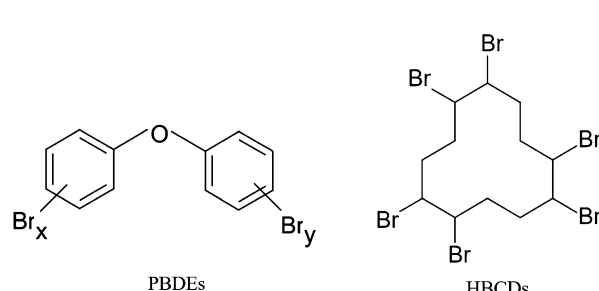
Penta-BDE, octa-BDE, and deca-BDE are the three PBDE formulations that are commonly produced and used. All formulations are comprised of congeners of different bromination levels and used as additives in products (Harrad et al. 2008; La Guardia et al. 2006):

1. Penta-BDE: mixture of BDE-47 (tetra-BDE), BDE-99 (penta-BDE), and some other tri- to hepta-BDEs; widely used in polyurethane foam (PUF) of carpets, furniture, and bedding, as well as in printed circuit boards and microprocessor packaging of computers
2. Octa-BDE: mixture of hexa- to deca-BDEs; used in thermoplastics, such as high impact polystyrene and acrylonitrile-butadiene-styrene copolymers
3. Deca-BDE: mixture of BDE-209 (deca-BDE) and low levels of nona- and octa-BDEs; used in thermoplastics applied in plastic housings for electrical good and textiles

Generally, the primary constituents of the three formulations are: tetra-BDE (BDE-47), penta-BDEs (BDEs –85, –99, –100), hexa-BDEs (BDE-153 and BDE-154), hepta-BDE (BDE-183), and deca-BDE (BDE-209). Therefore, these congeners are the predominant PBDEs found in indoor environments (La Guardia et al. 2006). Table 2 lists the selected physicochemical properties of these congeners.

Numerous evidences have indicated that PBDEs exert extensive toxicity and pose a great threat to human health. Human exposure to PBDEs has been found to be

Fig. 3 The general chemical structures of polybrominated diphenyl ethers (PBDEs) and hexabromocyclododecanes (HBCDs)



associated with endocrine dysfunction, developmental neurotoxicity, reproductive disorders, endocrine disruption, metabolism disruption, neurotoxicity, and carcinogenicity (Wu et al. 2020). Due to the concerns about potential human health effects of PBDEs, measures have been implemented to reduce or even stop their manufacture. For example, penta- and octa-BDEs were phased out in the EU and the USA in 2004. Deca-BDE was phased out in the USA in 2009 and eventually added to the Stockholm Convention without recycling exemptions in 2017. The ban of penta- and octa-BDEs was announced in China in 2014 (Li et al. 2021). Consequently, the use of PBDEs is declining, e.g., deca-BDE production in the USA decreased from 23,000 t in 2012 to <11 t in 2015 (Blum et al. 2019). Abundant data are available for the occurrence of PBDEs in indoor air, dust, and other environmental media (Ait Bamai 2020; Rauert 2014; Yu et al. 2016).

Hexabromocyclododecanes (HBCDs)

HBCDs are produced by bromination of cyclododecane in a batch process. HBCDs have a molecular formula of $C_{12}H_{18}Br_6$ (molecular weight 641.7), consisting of a ring of 12 carbon atoms to which 18 hydrogen and six bromine atoms are bound (as shown in Fig. 3). Due to the varying orientations of the bromine-carbon bonds, there are 16 stereoisomers of HBCDs, including six pairs of enantiomers and four meso configurations. The commercially available HBCDs are mainly (> 95%) comprised of three diastereomers, namely γ -HBCDs (75–89%), α -HBCD (10–13%), and β -HBCD (0.5–12%) (Szabo 2014). These HBCDs are mainly used as additive FRs in foams and expanded polystyrene that are used in numerous products, including upholstered furniture, interior textiles, car cushions, insulation blocks in building materials (e.g., walls, cellars, and roofs), packaging, and electric equipment (De Wit 2002). HBCDs are effective at low concentrations, e.g., 0.5% by weight in expanded polystyrene foams. However, they can also be present in fabrics, textiles, rubber, and plastics from 1–30% by weight (Rauert 2014). Table 3 lists the selected physicochemical properties of α -, β , and γ -HBCDs.

Compared to PBDEs, the available data on the health effects of HBCDs is still limited. According to the limited data, HBCDs are thought to affect the thyroid system via hepatic enzyme induction; and in cell culture, HBCDs were found to exert antagonistic effects on progesterone, androgen, and oestrogen receptors (Rauert 2014). Due to the environmental persistence and the potential toxicity of HBCDs, measures have also been implemented to reduce their production/use. In 2011, HBCD was included in the ECHA (European Chemicals Agency) list of substances subject to authorization under the Registration, Evaluation, Authorization, and Restriction of Chemicals (REACH) framework, with HBCD use not permitted without authorization after 2015 (UNEP 2011).

Compared to PAEs and PBDEs, much less studies have reported the concentrations of HBCDs in indoor air and dust. Nevertheless, relative higher levels of HBCDs were observed in indoor air (in Tokyo) and in indoor dust (in the UK and Belgium) among BFRs (Lucattini et al. 2018). The limited data on the toxicity and

Table 3 Physicochemical properties of α -, β , and γ -HBCDs

HBCDs	α -HBCD	β -HBCD	γ -HBCD
Vapor pressure (Pa at 25 °C) ^a	1.1×10^{-8}	5.8×10^{-9}	8.4×10^{-11}
Log K_{ow}^a	5.1	5.1	5.5
CAS	134237-50-6	134237-51-7	134237-52-8
Formula	$C_{12}H_{18}Br_6$	$C_{12}H_{18}Br_6$	$C_{12}H_{18}Br_6$
Structure			

^a K_{ow} is the octanol-water partition coefficient at 25 °C, the data source of both vapor pressure and K_{ow} is Rauert (2014)

indoor occurrence of HBCDs suggests that more concerns are required for the HBCD pollution in indoor environments.

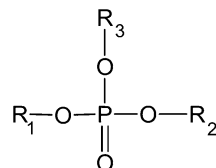
Despite the bans and phaseouts, products and materials in use or reuse will release the regulated BFRs. Meanwhile, the production and use of popular alternative FRs, such as organophosphate esters (OPEs), have increased sharply in recent decades, which results in their ubiquitous existence in the environment and human tissues worldwide.

Organophosphorus Flame Retardants (OPFRs)

Due to the environmental and health concerns about BFRs, organophosphorus flame retardants (OPFRs) were developed. Different groups of organophosphorus compounds, such as esters, phosphonates, and phosphites, are used in different applications (mostly as additives). These compounds are frequently used in plastics, textiles, and building materials as a replacement for BFRs (especially PBDEs) to maintain fire safety standards after their phaseouts (Marklund et al. 2003). Additionally, they are also widely used as plasticizers, stabilizers, and antifoaming, and as additives in lubricants and hydraulic fluids. Because OPFRs are always not chemically bound to the products, they may escape the products by volatilization, leaching, or abrasion, and subsequently reach different environmental compartments throughout the entire lifetime of the products (Marklund et al. 2003). Note “OPFRs” was also used as the abbreviation of “organophosphate flame retardants” in existing articles that only concerned about organophosphate flame retardants (the most commonly used organophosphorus flame retardants). In this chapter, the term “OPFRs” is treated as the short for “organophosphorus flame retardants.”

The most commonly used OPFRs are organophosphate esters, i.e., organic esters of phosphoric acid (Blum et al. 2019). The general structure of organophosphate flame retardants is shown in Fig. 4. R_1 , R_2 , and R_3 can be either alkyl chains or aryl

Fig. 4 General structure of organophosphate esters (most commonly used OPFRs)



groups, and they may be halogenated or nonhalogenated. Halogenated organophosphate esters are mainly used as additive FRs in furniture, textiles, building materials, polyurethane foam, and electronics, while nonhalogenated esters are also used as plasticizers in consumer products, textiles, and construction materials (Chupeau et al. 2020).

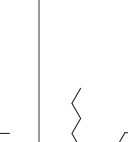
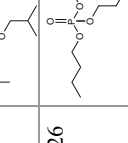
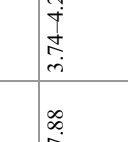
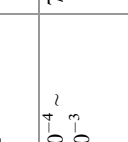
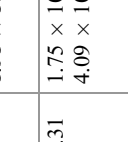
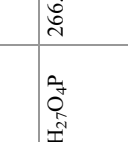
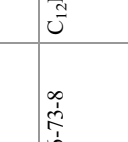
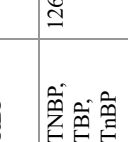
The global production and consumption of OPFRs were steadily increasing in recent decades. For example, the world production and consumption of organophosphate esters have sharply increased from 102,000 t in 1992 to 680,000 t in 2015 (Li et al. 2019). In Europe, the total consumption of OPFRs was 89,640 t in 2015, which was 18% of the total consumption of FRs and was twice as much as BFRs. Currently, OPFRs have become the second-largest flame retardants used in Europe, after aluminum hydroxide (Al(OH)_3) (Chupeau et al. 2020).

Most of OPFRs are liquid under room temperature. And compared with PBDEs, OPFRs tend to have higher vapor pressures and water solubility, and subsequently are expected to be less persistent in the environments (Blum et al. 2019). The selected physicochemical properties of some common OPFRs are listed in Table 4.

Similar to PAEs, OPFRs are also presented in all classes of indoor products investigated by Lucattini et al. (2018): electronics, building materials, textiles, furniture, health care/personal/cleaning products, and cosmetics. OPFRs can be detected in diverse environmental media, such as indoor dust, air, water, soil, sediment, and marine compartments. In summary, OPFRs are currently ubiquitous in both indoor and outdoor environments. Since the early 2000s, numerical studies have been conducted to investigate the levels of OPFRs in indoor dust and air. The detailed data have been well summarized in some recently published articles, such as Blum et al. (2019), Du et al. (2019), Li et al. (2019), and Chupeau et al. (2020).

Because the vapor pressures of OPFRs tend to be higher than those of PBDEs (comparing the data listed in Tables 2 and 4), it would be reasonable to assume that OPFR dust concentrations would be lower than PBDE dust concentrations. However, various studies have indicated that OPFR concentrations in indoor dust tended to be higher than PBDE concentrations in indoor dust from the early 2000s, mainly due to the increasing production and consumption of OPFRs (Blum et al. 2019). For example, Chen et al. (2020) found that PBDEs in Chinese indoor dust decreased gradually, while the concentrations of OPFRs increased gradually. Among all the kinds of OPFRs detected in indoor dust, TBOEP, TCPP, and TDCPP are the most concentrated in Europe (Chupeau et al. 2020). In China, chlorinated OPFRs (Cl-OPFRs, including TCEP, TCPP, and TDCPP) are the main OPFRs in indoor dust samples, and the OPFR concentrations in indoor dust was higher in

Table 4 Physicochemical properties of commonly used OPFRs

OPFRs	Acronyms	CAS	Formula	MW	Vapor pressure ^a	$\log K_{ow}$ ^b	$\log K_{oa}$	Structure
Tris (chloroethyl) phosphate	TCEP	115-96-8	$C_6H_{12}Cl_3O_4P$	285.49	$1.08 \times 10^{-4} \sim 6.09 \times 10^{-2}$	8.41	0.484-1.63	
Tris (2-chloroisopropyl) phosphate	TCPP, TCIPP	13674-84-5	$C_9H_{18}Cl_3O_4P$	327.57	$5.25 \times 10^{-5} \sim 3.74 \times 10^{-3}$	8.85	1.53-2.89	
Tris (1,3-dichloro-2-propyl) phosphate	TDCPP, TDClCPP	13674-87-8	$C_9H_{15}Cl_6O_4P$	430.90	$4.07 \times 10^{-8} \sim 1.64 \times 10^{-5}$	10.3	1.79-3.65	
Trimethyl phosphate	TMP, TMPA, TMPO	512-56-1	$C_3H_9O_4P$	140.07	0.539 ~ 0.848	4.14	-0.649 ~ -0.151	
Triethyl phosphate	TEP	78-40-0	$C_6H_{15}O_4P$	182.15	$8.89 \times 10^{-2} \sim 0.391$	5.79	0.800-1.08	
Tripropyl phosphate	TPP, TPRP	513-08-06	$C_9H_{21}O_4P$	224.23	$2.69 \times 10^{-3} \sim 2.88 \times 10^{-2}$	7.26	1.87-2.67	
Tris (isobutyl) phosphate	TIBP, TiBP	126-71-6	$C_{12}H_{27}O_4P$	266.31	$7.73 \times 10^{-4} \sim 1.91 \times 10^{-2}$	7.38	3.15-3.71	
Tri- <i>n</i> -butyl phosphate	TNBP, TBP, TbBP	126-73-8	$C_{12}H_{27}O_4P$	266.31	$1.75 \times 10^{-4} \sim 4.09 \times 10^{-3}$	7.88	3.74-4.26	

Tris (2-butoxyethyl) phosphate	TBOEP, TBEP, TBXP	78-51-3	$C_{18}H_{39}O_7P$	398.47 1.11×10^{-6} ~ 1.71×10^{-5}	-d	3.00-4.29
Tris (2-ethylhexyl) phosphate	TEHP, TOF, TOP	78-42-2	$C_{24}H_{51}O_4P$	434.63 8.28×10^{-8} ~ 2.80×10^{-6}	-d	8.95-10.1
Tris (phenyl) phosphate	TPHP	115-86-6	$C_{18}H_{15}O_4P$	326.28 1.26×10^{-6} ~ 6.28×10^{-6}	10.8	4.10-4.70
2-Ethylhexyl diphenyl phosphate	EHDPP, EDP, EHDP	1241-94-7	$C_{20}H_{27}O_4P$	362.4 6.49×10^{-7} ~ 4.98×10^{-5}	-d	5.68-6.63
Tris (methylphenyl) phosphate (or Tricresyl phosphate)	TMPP, TCP	1330-78-5	$C_{21}H_{29}O_4P$	368.36 1.1×10^{-7} e	-d	6.34e

a Vapor pressure at 25 °C, torr (1 torr = 133.3224 Pa)

b K_{Oa} is the octanol-air partition coefficient at 25 °C

c K_{ow} is the octanol-water partition coefficient at 25 °C. Data source of a, b, and c (if there is no specific superscript tag in the table): US EPA CompTox Chemistry Dashboard ([USEPA](#))

d $K_{Oa} = 11.7$ is presented in US EPA CompTox Chemistry Dashboard for all these chemicals, which is treated as unavailable data here due to the potentially great uncertainties

e Data source: Pantelaki and Voutsas ([2019](#))

economically developed areas of China such as Beijing, Shanghai, and Guangzhou (Chen et al. 2020). Similar conclusions were obtained by Li et al. (2019), a global-scale investigation. They measured 20 organophosphate esters in 341 house dust samples collected from 12 countries during 2010–2014. Cl-OPFRs were found to be the predominant compounds (51% of total OPFRs) in indoor dust samples, followed by alkyl-OPFRs (31%, including TMP, TEP, TNBP, TIBP, TBOEP, TEHP, and tripropyl phosphate), aryl-OPFRs (17%, including TPHP, TMPP, EHDPP, and three others), and three oligomeric organophosphate esters (1%). Total OPFR concentrations in house dust from more industrialized countries (South Korea, Japan, and the USA) were one or even two orders of magnitude higher than those from less industrialized countries (Greece, Saudi Arabia, Kuwait, Romania, Vietnam, China, Colombia, India, and Pakistan).

The ubiquity of OPFRs in the environments indicate ubiquitous human exposure to OPFRs. People can be exposed to OPFRs through skin contact, ingestion of dust, inhalation, and dietary intake. The adverse effects of human exposure to OPFRs have not been studied to the same extent as for the phased-out PBDEs, and are relatively less well known. Nevertheless, available data from toxicologic and epidemiological studies and risk assessments all imply that there are health concerns at current exposure levels for OPFRs (Blum et al. 2019). In 2017, the US Consumer Product Safety Commission (CPSC) initiated efforts to assess and issue a report on the risks to consumer health and safety from the use of additive OPFRs in certain consumer products (USCPSC 2017). Recently, some studies have shown that some OPFRs may be carcinogenic, neurotoxic, and endocrine disruptors, and there are particular concerns on Cl-OPFRs (Pantelaki and Voutsas 2019). For example, animal and/or epidemiologic studies have indicated that TCEP and TCPP had elicited moderate acute toxicity, TCEP and TDCPP were suspected to be carcinogenic, and TDCPP had neurotoxic properties and has been associated with altered hormone levels and the reduction of semen quality (Chen et al. 2020; Li et al. 2019). Some nonhalogenated OPFRs may also be associated with adverse health effects, e.g., animal studies had indicated that TNBP and TPHP had neurotoxic properties, TBOEP had developmental toxicity, and TNBP might be carcinogenic (Chen et al. 2020; Li et al. 2019). Due to their adverse health effects, some authoritative organizations are now addressing the problem related with the OPFR pollution. For example, US EPA released a problem formulation for Cl-OPFRs used in furniture foams and textiles on August 13, 2015 (USEPA 2015). Additionally, US EPA designated TCEP as one of the 20 high-priority substances for risk evaluation under the Toxic Substances Control Act in December 2019 (USEPA 2019). Furthermore, the European Commission proposed to prohibit the entire class of organohalogen chemicals (including Cl-OPFRs) in electronic display enclosures and stands by April 1, 2021 (Blum et al. 2019). The timeline of some major regulatory milestones for both PBDEs and OPFRs (mainly from the USA, EU, and Canada) can be found in Fig. 1 of Blum et al. (2019).

In summary, the available evidences have shown that the replacement of PBDEs with OPFRs may be a regrettable substitution (Blum et al. 2019). Since 2016, a group from US EPA (led by Dr. Xiaoyu Liu) had conducted a series of studies to

develop methods and collect data for characterizing and understanding the fate and transport of OPFRs in indoor environments (Liang et al. 2018a; Liang et al. 2018b; Liang et al. 2019; Liu et al. 2016; Liu and Folk 2021). It is foreseeable that the OPFR pollution in indoor environments would become a hot research topic in the field of IAQ.

Per- and Polyfluorinated Alkyl Substances (PFAS)

Per- and polyfluorinated alkyl substances (typically referred to as PFAS) are a class of over 4700 synthetic chemicals in which hydrocarbons of one or more C atoms have their H substituents partially or fully replaced by F (Morales-McDevitt 2021; NIH 2019). The C-F bond is strong, thermally and chemically stable, highly hydrophobic, lipophobic, and resistant to oxidation (Buck et al. 2011). Therefore, PFAS have been widely used in commercial products and industrial applications since the 1940s for their water-resistant, stain-resistant, fire-resistant, and anti-stick properties (DeLuca et al. 2021). According to Glüge et al. (2020), PFAS are currently used in almost all industry branches and many consumer products, and more than 200 use categories and subcategories are identified for more than 1400 individual PFAS. For example, PFAS are widely used as water- and stain-resistant coatings for cookware, food packaging, personal care products, carpet, upholstery, and outdoor textiles – they are all ubiquitous indoors (Eichler and Little 2020).

According to the Organization for Economic Cooperation and Development (OECD), PFAS are categorized as nonpolymeric or polymeric (OECD 2013). Nonpolymeric PFAS are comprised of four families: (1) perfluoroalkyl acids (PFAAs), which mainly include perfluoroalkyl carboxylic acids (PFCAs) and perfluoroalkane sulfonic acids (PFSAs); (2) compounds derived from perfluoroalkane sulfonyl fluoride (PASF); (3) fluorotelomer (FT)-based compounds; and (4) per- and polyfluoroalkyl ether (PFPE)-based compounds. Both PASF- and FT-derived or based products have the potential to degrade to long-chain PFSAs and PFCAs. The term “long-chain” PFAS refers to (1) PFCAs with 7 and more perfluoroalkyl carbons; (2) PFSAs with 6 and more perfluoroalkyl carbons; and (3) substances that have the potential to degrade to long-chain PFCAs or PFSAs. Polymeric PFAS are comprised of three groups: (1) fluoropolymers, e.g., polytetrafluoroethylene (PTFE); (2) side-chain fluorinated polymers that are composed of nonfluorinated backbones with per- and polyfluoroalkyl side chains (they are potential precursors of PFSAs and PFCAs); and (3) perfluoropolyethers that consist of backbones containing carbon and oxygen with fluorines directly attached to carbon. Table 5 lists the selected physicochemical properties of over 40 PFAS. Note, most of PFAS properties listed in Table 5 are predicted values, which should be associated with huge uncertainties and should be used with caution. For example, the vapor pressure of 10:2 FTOH (CAS 865-86-1) was measured to be 140 Pa while predicted to be 3.2 Pa at 25 °C according to Eichler and Little (2020). Generally, the huge number (still increasing rapidly) and diverse physicochemical properties of

Table 5 Physicochemical properties of selected PFAS

Compounds		Acronyms	CAS	Formula	MW	Vapor pressure ^a	$\log K_{ow}^b$	$\log K_{ow}^c$
PFAA precursors	Fluorotelomer iodides	6:2 FTI	2043-57-4	$C_8H_4F_{13}I$	474.0	1.3E+02	3.46	6.33
		10:2 FTI	2043-54-1	$C_{12}H_4F_{21}I$	674.0	1.1E+03	4.32	8.70
	Fluorotelomer olefins	18:2 FTI	65104-63-4	$C_{20}H_4F_{57}I$	1074.1	6.9E-04	6.83	13.90
		6:2 FTO	25291-17-2	$C_8H_3F_{13}$	346.1	9.2E+03	2.13	5.28
Fluorotelomer alcohols	10:2 FTO	30389-25-4	$C_{12}H_3F_{21}$	546.1	1.4E+03	3.26	8.15	
	12:2 FTO	67103-05-3	$C_{14}H_3F_{25}$	646.1	6.4E+02	3.6	8.58	
	4:2 FTOH	2043-47-2	$C_6H_5F_9O$	264.1	1.2E+03 ^d	3.82	3.30 ^d	
	6:2 FTOH	647-42-7	$C_8H_5F_{13}O$	364.1	3.7E+02 ^d	4.1	4.54 ^d	
	8:2 FTOH	678-39-7	$C_{10}H_5F_{17}O$	464.1	1.6E+00 ^d	4.22	5.58 ^d	
	10:2 FTOH	865-86-1	$C_{12}H_5F_{21}O$	564.1	1.4E+02 ^d	4.76	7.49	
	18:2 FTOH	65104-65-6	$C_{20}H_5F_{57}O$	964.2	4.6E-04	7.72	12.00	
	FOSE	10116-92-4	$C_{10}H_6F_{17}NO_3S$	543.2	1.6E-01	7.6	3.59	
<i>N</i> -Ethyl perfluoroctane sulfonamide sulfonamidoethanol	FOSA	754-91-6	$C_8H_2F_{17}NO_2S$	499.1	3.3E+01 ^d	4.3	5.95	
	EFOSE	1691-99-2	$C_{12}H_{10}F_{17}NO_3S$	571.3	2.7E+00	7.78 ^d	6.31	
	EFOSA	4151-50-2	$C_{10}H_6F_{17}NO_2S$	527.2	5.7E-05 ^d	4.92	6.25	
	MEFOSE	24448-09-7	$C_{11}H_8F_{17}NO_3S$	557.2	2.0E-03 ^d	7.70 ^d	5.94	
<i>N</i> -Methyl perfluoroctane sulfonamide sulfonamidoethanol	MefOSA	31506-32-8	$C_9H_4F_{17}NO_2S$	513.2	3.2E+01	4.56	6.07	
	monoPAP	57678-01-0	$C_8H_6F_{13}O_4P$	444.1	4.7E-02	7.84	3.24	
	10:2 monoPAP	57678-05-4	$C_{12}H_6F_{21}O_4P$	644.1	2.7E-03	7.96	6.02	
	12:2 monoPAP	57678-07-6	$C_{14}H_6F_{25}O_4P$	744.1	1.2E-01	8.11	5.20	

PFCA s	Polyfluoroalkyl phosphoric acid diesters	6:2 diPAP	57677-95-9	$C_{16}H_9E_{26}O_4P$	790.2	6.9E-04	9.08	7.30
		10:2 diPAP	1895-26-7	$C_{24}H_9F_{42}O_4P$	1190.2	1.3E-07	10.6	13.20
		12:2 diPAP	57677-99-3	$C_{28}H_9F_{50}O_4P$	1390.3	8.0E-08	11.3	15.80
	Fluorotelomer acrylates	6:2 FTAC	17527-29-6	$C_{11}H_7F_{13}O_2$	418.15	4.4E+01 ^d	3.87	5.20 ^d
		10:2 FTAC	17741-60-5	$C_{15}H_7F_{21}O_2$	618.2	2.7E+01	4.75	7.99
		18:2 FTAC	65104-64-5	$C_{23}H_7F_{37}O_2$	1018.2	3.7E-04	6.87	13.20
	Fluorotelomer methacrylates	6:2 FTMAC	2144-53-8	$C_{12}H_9F_{13}O_2$	432.2	1.9E+01	4.56	5.99
		10:2 FTMAC	2144-54-9	$C_{16}H_9F_{21}O_2$	632.2	4.5E+00	5.09	8.50
		18:2 FTMAC	65104-66-7	$C_{24}H_9F_{37}O_2$	1032.3	1.3E-04	7.44	13.70
	Perfluorobutanoic acid	PFBA	375-22-4	$C_4HF_7O_2$	214.0	8.5E+02 ^d	3.46	1.43 ^d
PFSAs	Perfluorohexanoic acid	PFHxA	307-24-4	$C_6HF_{11}O_2$	314.1	1.2E+02 ^d	3.83	2.51 ^d
	Perfluoroheptanoic acid	PFHpA	375-85-9	$C_7HF_{13}O_2$	364.1	7.3E+01 ^d	4.09	4.49
	Perfluoroctanoic acid	PFOA	335-67-1	$C_8HF_{15}O_2$	414.1	3.0E+02 ^d	4.16	3.60 ^d
	Perfluorononanoic acid	PFNA	375-95-1	$C_9HF_{17}O_2$	464.1	1.0E+01	4.20	6.18
	Perfluorodecanoic acid	PFDA	335-76-2	$C_{10}HF_{19}O_2$	514.1	4.1E+00	4.28	6.89
	Perfluorohexadecanoic acid	PFHxDA	67905-19-5	$C_{16}HF_{31}O_2$	814.1	6.7E-01	6.29	10.80
	Perfluorobutane sulfonic acid	PFBS	375-73-5; 59933-66-3	$C_4HF_9O_3S$	300.1	3.2E+01	4.16	1.98
	Perfluorohexane sulfonic acid	PFHxS	355-46-4	$C_6HF_{13}O_3S$	400.1	1.1E-06 ^d	4.27	2.20 ^d
	Perfluorohexapeptide sulfonic acid	PFHpS	375-92-8	$C_7HF_{15}O_3S$	450.1	1.5E+00	4.71	4.06
	Perfluorooctane sulfonic acid	PFOS	1763-23-1	$C_8HF_{17}O_3S$	500.1	3.3E-04 ^d	4.75	4.05
	Perfluorononane sulfonic acid	PFNS	474511-07-4	$C_9HF_{19}O_3S$	549.1	1.5E+00	4.97	1.68

(continued)

Table 5 (continued)

Compounds	Acronyms	CAS	Formula	MW	Vapor pressure ^a	$\log K_{oa}^b$	$\log K_{ow}^c$
Perfluorodecane sulfonic acid	PFDS	335-77-3	$C_{10}HF_{21}O_3S$	600.1	6.3E-01	5.76	5.81
Perfluorododecane sulfonic acid	PFDsDS	79/80-39-5	$C_{12}HF_{25}O_3S$	700.2	1.3E+00	6.30	4.58
Ammonium perfluoro-2-methyl-3-oxahexanoate	GenX	62037-80-3	$C_6H_4F_{11}NO_3$	347.0	5.52E-02	3.74	1.98

^aVapor pressure at 25 °C, torr (1 torr = 133.3224 Pa)^b K_{oa} is the octanol-air partition coefficient at 25 °C^c K_{ow} is the octanol-water partition coefficient at 25 °C. Data source of a, b, and c is Eichler and Little (2020)

d Both experimental and predicted data were provided by Eichler and Little (2020), the data with a superscript d is the measured value, otherwise the predicted values are presented in this table (because the measured value is not available)

PFAS make the research about the environmental transport, human exposure, and health risks of PFAS extremely challenging (Nakayama et al. 2019).

The most consistent feature of all PFAS is that their perfluorocarbon moieties break down very slowly (or even do not) under environmental conditions (Wang et al. 2018; Wang et al. 2017). Existing studies have estimated that PFAS such as perfluoroalkanes have lifetimes up to thousands of years (Ivy et al. 2012). Therefore, PFAS can be present in the environment for centuries or longer, even if the PFAS productions, applications, and environmental releases cease immediately. As such, PFAS have often been nicknamed “forever chemicals” (Kwiatkowski et al. 2020). The extreme persistence of PFAS, combined with their propensity for accumulation and mobility, has resulted in PFAS being ubiquitous globally, even in remote regions like the Arctic (Kwiatkowski et al. 2020). Concerns about the adverse effects of PFAS on human and environments have been raised since the 1990s (Morales-McDevitt 2021). PFAS have been proven to be linked to adverse effects for flora and fauna (including humans), e.g., developmental toxicity, neurotoxicity, immunotoxicity, carcinogenicity, thyroid malfunction, low birthweight, infertility, early menopause, elevated cholesterol, and fatty liver disease (Arvaniti and Stasinakis 2015; Buck et al. 2011; Morales-McDevitt 2021; Venkatesan and Halden 2013). In addition, precursors such as perfluoroctane sulfonamides (FOSAs) and perfluoroctane sulfonamide ethanol (FOSEs) have been found to have estrogenic effects (*in vitro*) and can be transformed to more stable compounds under natural conditions (Fromme et al. 2015).

Due to their longer usage, longer persistence in the environments, and potential higher health risks, perfluoroctanoic acid (PFOA) and perfluoroctane sulfonic acid (PFOS) are the two most well-studied PFAS (Kwiatkowski et al. 2020). They are also termed “long-chain” PFAS (OECD 2013). In 2008, PFOS, PFOA, and their salts were included in the Annex B of the Stockholm Convention. As a result, PFOA and PFOS have been largely replaced by shorter-chain PFAS, branched PFAS, and perfluoroether compounds (Eichler and Little 2020). However, short-chain PFAS may not be safe alternatives. Several studies have demonstrated that short-chain PFAS can be equally environmentally persistent, even more mobile in the environment, and more difficult to be removed than long-chain PFAS. Increasing evidences suggest that they are associated with similar adverse toxicological effects as long-chain PFAS (Kwiatkowski et al. 2020).

Given their ubiquitous presence, it should be important to understand the fate and transport of PFAS, especially in indoor environments where people spend most of their time and abundant PFAS-contained products are used. However, most focus has been on outdoor exposure and contaminated sites. Limited knowledge about PFAS behavior indoors and the contribution of specific exposure pathways is available, although some studies have investigated PFAS levels in indoor air and dust (which usually exceed those in outdoor media) (Eichler and Little 2020; Harrad et al. 2010; Shoeib et al. 2005). According to the traditional definition of SVOCs (vapor pressures between 10^{-9} and 10 Pa at environmental temperature), Eichler and Little (2020) concluded that many PFAS, especially long-chain, ionizable PFAAs, could be treated as SVOCs. They subsequently

proposed a framework to model human exposure to PFAS in indoor environments based on the current knowledge of (relatively) well-studied indoor SVOCs, especially PAEs. Nevertheless, the framework is currently infeasible due to the lack of thermodynamic and transport parameters that are necessary to describe PFAS behavior indoors. Overall, much more attentions should be paid for the ubiquitous, persistent, complex, and increasing PFAS pollution in indoor environments.

Conclusions

Due to the increasing demands for more comfortable and convenient homes and workplaces, lots of synthetic materials and products have been manufactured and subsequently used indoors. A vast of semi-volatile organic compounds (SVOCs) is added as additive or solvent to facilitate the production or enhance the performance of these materials and products, leading to the ubiquity of SVOCs in indoor environments. SVOCs can be slowly emitted from source materials/products and, depending on their physicochemical properties, can be partitioned among gas phase, airborne particles, settled dust, and other indoor surfaces. Human exposure to indoor SVOCs can occur via inhalation, ingestion, or dermal uptake. Some SVOCs have been proved to be associated with diverse health risks, which have led to product reformulations in some cases. Specific SVOCs have physicochemical properties that span vast ranges, e.g., vapor pressures and octanol-air partition coefficients can vary over ten orders of magnitude. Additionally, SVOCs have long indoor persistence (e.g., years) even after the primary source is removed. Therefore, it is relatively challenging to understand and characterize the fate, transport, and human exposure of SVOCs in indoor environments. Recent studies on these topics are summarized in several other chapters of this handbook, including ► Chaps. 23, “Source/Sink Characteristics of SVOCs,” ► 25, “Predicting VOC and SVOC Concentrations in Complex Indoor Environments,” ► 13, “Interaction Between Gas-Phase Pollutants and Particles,” ► 16, “Sampling and Analysis of Semi-volatile Organic Compounds (SVOCs) in Indoor Environment,” and ► 38, “A Modular Mechanistic Framework for Assessing Human Exposure to Indoor Chemicals.” However, existing studies have mainly focused on several classes of SVOCs, such as phthalates and flame retardants (PBDEs and OPFRs). Insufficient knowledge is presently for available many other SVOCs (e.g., phthalate alternatives and PFAS). In addition, different classes of SVOCs have always been investigated separately, with relatively little cross-communication. Due to the limited information and understanding, guideline values for SVOCs in air and other indoor media are rare (except for some PAHs). The above issues warrant further study. Certainly, except for SVOCs released from indoor materials and products (discussed in this chapter), attention should also be paid to indoor SVOCs related to other sources/processes, e.g., processes that occur indoors (combustion) and intrusion from outdoor air.

Cross-References

- A Modular Mechanistic Framework for Assessing Human Exposure to Indoor Chemicals
- Interaction Between Gas-Phase Pollutants and Particles
- Predicting VOC and SVOC Concentrations in Complex Indoor Environments
- Sampling and Analysis of Semi-volatile Organic Compounds (SVOCs) in Indoor Environments
- Source/Sink Characteristics of SVOCs

Acknowledgments The author acknowledges the Natural Science Foundation of China (No. 51908563), Guangdong Basic and Applied Basic Research Foundation (No. 2019A1515011179), Science and Technology Program of Guangzhou (No. 202102020990), and the special fund of Beijing Key Laboratory of Indoor Air Quality Evaluation and Control (No. BZ0344KF20-11) for financial support.

References

- Afshari A, Gunnarsen L, Clausen PA, Hansen V (2004) Emission of phthalates from PVC and other materials. *Indoor Air* 14(2):120–128
- Ait Bamai Y (2020) Semi-volatile organic compounds (SVOCs): phthalates and phosphorous flame retardants and health risks. In: Kishi R, Norbäck D, Araki A (eds) *Indoor environmental quality and health risk toward healthier environment for all*. Springer Singapore, Singapore, pp 159–178
- Arvaniti OS, Stasinakis AS (2015) Review on the occurrence, fate and removal of perfluorinated compounds during wastewater treatment. *Sci Total Environ* 524–525:81–92
- Benning JL, Liu Z, Tiwari A, Little JC, Marr LC (2013) Characterizing gas-particle interactions of phthalate plasticizer emitted from vinyl flooring. *Environ Sci Technol* 47(6):2696–2703
- Blum A, Behl M, Birnbaum LS, Diamond ML, Phillips A, Singla V, Sipes NS, Stapleton HM, Venier M (2019) Organophosphate ester flame retardants: are they a regrettable substitution for polybrominated diphenyl ethers? *Environ Sci Technol Lett* 6(11):638–649
- Bu Z, Zhang Y, Mmereki D, Yu W, Li B (2016) Indoor phthalate concentration in residential apartments in Chongqing, China: implications for preschool children's exposure and risk assessment. *Atmos Environ* 127:34–45
- Buck RC, Franklin J, Berger U, Conder JM, Cousins IT, de Voogt P, Jensen AA, Kannan K, Mabury SA, van Leeuwen SP (2011) Perfluoroalkyl and polyfluoroalkyl substances in the environment: terminology, classification, and origins. *Integr Environ Assess Manage* 7(4):513–541
- Cao J, Zhang X, Little JC, Zhang Y (2017) A SPME-based method for rapidly and accurately measuring the characteristic parameter for DEHP emitted from PVC floorings. *Indoor Air* 27(2): 417–426
- Chen Y, Liu Q, Ma J, Yang S, Wu Y, An Y (2020) A review on organophosphate flame retardants in indoor dust from China: implications for human exposure. *Chemosphere* 260:127633
- Chupeau Z, Bonvallot N, Mercier F, Le Bot B, Chevrier C, Glorennec P (2020) Organophosphorus flame retardants: a global review of indoor contamination and human exposure in Europe and epidemiological evidence. *Int J Environ Res Public Health* 17(18):6713
- Clausen PA, Hansen V, Gunnarsen L, Afshari A, Wolkoff P (2004) Emission of di-2-ethylhexyl phthalate from PVC flooring into air and uptake in dust: emission and sorption experiments in FLEC and CLIMPAQ. *Environ Sci Technol* 38(9):2531–2537

- CPSC (2010) Overview of dialkyl o-phthalates toxicity. <https://www.cpsc.gov/s3fs-public/phthalover.pdf>
- De Wit CA (2002) An overview of brominated flame retardants in the environment. *Chemosphere* 46(5):583–624
- DeLuca NM, Angrish M, Wilkins A, Thayer K, Cohen Hubal EA (2021) Human exposure pathways to poly- and perfluoroalkyl substances (PFAS) from indoor media: a systematic review protocol. *Environ Int* 146:106308
- Deng M, Liang X, Du B, Luo D, Chen H, Zhu C, Zeng L (2021) Beyond classic phthalates: occurrence of multiple emerging phthalate alternatives and their metabolites in human milk and implications for combined exposure in infants. *Environ Sci Technol Lett* 8(8):705–712
- Destaillets H, Maddalena RL, Singer BC, Hodgson AT, McKone TE (2008) Indoor pollutants emitted by office equipment: a review of reported data and information needs. *Atmos Environ* 42(7):1371–1388
- Du J, Li H, Xu S, Zhou Q, Jin M, Tang J (2019) A review of organophosphorus flame retardants (OPFRs): occurrence, bioaccumulation, toxicity, and organism exposure. *Environ Sci Pollut Res* 26(22):22126–22136
- Eichler CMA, Little JC (2020) A framework to model exposure to per- and polyfluoroalkyl substances in indoor environments. *Environ Sci Process Impacts* 22(3):500–511
- Eichler CMA, Wu Y, Cao J, Shi S, Little JC (2018) Equilibrium relationship between SVOCs in PVC products and the air in contact with the product. *Environ Sci Technol* 52(5):2918–2925
- Eichler CMA, Cohen Hubal EA, Little JC (2019) Assessing human exposure to chemicals in materials, products and articles: the international risk management landscape for phthalates. *Environ Sci Technol* 53(23):13583–13597
- Eichler CMA, Hubal EAC, Xu Y, Cao J, Bi C, Weschler CJ, Salthammer T, Morrison GC, Koivisto AJ, Zhang Y, Mandin C, Wei W, Blondeau P, Poppendieck D, Liu X, Delmaar CJE, Fantke P, Jolliet O, Shin H-M, Diamond ML, Shiraiwa M, Zuend A, Hopke PK, von Goetz N, Kulmala M, Little JC (2021) Assessing human exposure to SVOCs in materials, products, and articles: a modular mechanistic framework. *Environ Sci Technol* 55(1):25–43
- Ekelund M, Azhdar B, Gedde UW (2010) Evaporative loss kinetics of di(2-ethylhexyl)phthalate (DEHP) from pristine DEHP and plasticized PVC. *Polym Degrad Stab* 95(9):1789–1793
- Fromme H, Dreyer A, Dietrich S, Fembacher L, Lahrz T, Völkel W (2015) Neutral polyfluorinated compounds in indoor air in Germany – the LUPE 4 study. *Chemosphere* 139:572–578
- Fujii M, Shinohara N, Lim A, Otake T, Kumagai K, Yanagisawa Y (2003) A study on emission of phthalate esters from plastic materials using a passive flux sampler. *Atmos Environ* 37(39–40): 5495–5504
- Glüge J, Scheringer M, Cousins IT, DeWitt JC, Goldenman G, Herzke D, Lohmann R, Ng CA, Trier X, Wang Z (2020) An overview of the uses of per- and polyfluoroalkyl substances (PFAS). *Environ Sci Process Impacts* 22(12):2345–2373
- Harrad S, Ibarra C, Diamond M, Melymuk L, Robson M, Douwes J, Roosens L, Dirtu AC, Covaci A (2008) Polybrominated diphenyl ethers in domestic indoor dust from Canada, New Zealand, United Kingdom and United States. *Environ Int* 34(2):232–238
- Harrad S, de Wit CA, Abdallah MA-E, Bergh C, Björklund JA, Covaci A, Darnerud PO, de Boer J, Diamond M, Huber S, Leonards P, Mandalakis M, Östman C, Haug LS, Thomsen C, Webster TF (2010) Indoor contamination with hexabromocyclododecanes, polybrominated diphenyl ethers, and perfluoroalkyl compounds: an important exposure pathway for people? *Environ Sci Technol* 44(9):3221–3231
- Hsu NY, Liu YC, Lee CW, Lee CC, Su HJ (2017) Higher moisture content is associated with greater emissions of DEHP from PVC wallpaper. *Environ Res* 152:1–6
- Ivy DJ, Rigby M, Baasandorj M, Burkholder JB, Prinn RG (2012) Global emission estimates and radiative impact of C_4F_{10} , C_5F_{12} , C_6F_{14} , C_7F_{16} and C_8F_{18} . *Atmos Chem Phys* 12(16):7635–7645
- Jeon S, Kim KT, Choi K (2016) Migration of DEHP and DINP into dust from PVC flooring products at different surface temperature. *Sci Total Environ* 547:441–446

- Kashyap D, Agarwal T (2018) Concentration and factors affecting the distribution of phthalates in the air and dust: a global scenario. *Sci Total Environ* 635:817–827
- Katsikantami I, Sifakis S, Tzatzarakis MN, Vakonaki E, Kalantzi O-I, Tsatsakis AM, Rizos AK (2016) A global assessment of phthalates burden and related links to health effects. *Environ Int* 97:212–236
- Kwiatkowski CF, Andrews DQ, Birnbaum LS, Bruton TA, DeWitt JC, Knappe DRU, Maffini MV, Miller MF, Pelch KE, Reade A, Soehl A, Trier X, Venier M, Wagner CC, Wang Z, Blum A (2020) Scientific basis for managing PFAS as a chemical class. *Environ Sci Technol Lett* 7(8): 532–543
- La Guardia MJ, Hale RC, Harvey E (2006) Detailed polybrominated diphenyl ether (PBDE) congener composition of the widely used penta-, octa-, and deca-PBDE technical flame-retardant mixtures. *Environ Sci Technol* 40(20):6247–6254
- Li W, Wang Y, Asimakopoulos AG, Covaci A, Gevao B, Johnson-Restrepo B, Kumosani TA, Malarvannan G, Moon H-B, Nakata H, Sinha RK, Tran TM, Kannan K (2019) Organophosphate esters in indoor dust from 12 countries: concentrations, composition profiles, and human exposure. *Environ Int* 133:105178
- Li Z, Zhu Y, Wang D, Zhang X, Jones KC, Ma J, Wang P, Yang R, Li Y, Pei Z, Zhang Q, Jiang G (2021) Modeling of flame retardants in typical urban indoor environments in China during 2010–2030: influence of policy and decoration and implications for human exposure. *Environ Sci Technol* 55:11745–11755
- Liang Y, Xu Y (2014) Improved method for measuring and characterizing phthalate emissions from building materials and its application to exposure assessment. *Environ Sci Technol* 48(8):4475–4484
- Liang Y, Liu X, Allen MR (2018a) Measurements of parameters controlling the emissions of organophosphate flame retardants in indoor environments. *Environ Sci Technol* 52(10):5821–5829
- Liang Y, Liu X, Allen MR (2018b) Measuring and modeling surface sorption dynamics of organophosphate flame retardants on impervious surfaces. *Chemosphere* 193:754–762
- Liang Y, Liu X, Allen MR (2019) The influence of temperature on the emissions of organophosphate ester flame retardants from polyisocyanurate foam: measurement and modeling. *Chemosphere* 233:347–354
- Little JC, Weschler CJ, Nazaroff WW, Liu Z, Cohen Hubal EA (2012) Rapid methods to estimate potential exposure to semivolatile organic compounds in the indoor environment. *Environ Sci Technol* 46(20):11171–11178
- Liu X, Folk E (2021) Sorption and migration of organophosphate flame retardants between sources and settled dust. *Chemosphere* 278:130415
- Liu C, Zhang Y (2016) Characterizing the equilibrium relationship between DEHP in PVC flooring and air using a closed-chamber SPME method. *Build Environ* 95:283–290
- Liu X, Allen MR, Roache NF (2016) Characterization of organophosphorus flame retardants' sorption on building materials and consumer products. *Atmos Environ* 140:333–341
- Lucattini L, Poma G, Covaci A, de Boer J, Lamoree M, Leonards P (2018) A review of semi-volatile organic compounds (SVOCs) in the indoor environment: occurrence in consumer products, indoor air and dust. *Chemosphere* 201:466–482
- Marklund A, Andersson B, Haglund P (2003) Screening of organophosphorus compounds and their distribution in various indoor environments. *Chemosphere* 53(9):1137–1146
- Mayer FL, Stalling DL, Johnson JL (1972) Phthalate esters as environmental contaminants. *Nature* 238(5364):411–413
- Melymuk L, Bohlin-Nizzetto P, Vojta S, Kratka M, Kukucka P, Audy O, Pribylova P, Klanova J (2016) Distribution of legacy and emerging semivolatile organic compounds in five indoor matrices in a residential environment. *Chemosphere* 153:179–186
- Morales-McDevitt ME (2021) The air that we breathe: neutral PFAS in indoor and outdoor air. Open Access Master's Theses. Paper 1950. <https://digitalcommons.uri.edu/theses/1950>

- Nagorka R, Koschorreck J (2020) Trends for plasticizers in German freshwater environments – evidence for the substitution of DEHP with emerging phthalate and non-phthalate alternatives. *Environ Pollut* 262:114237
- Nakayama SF, Yoshikane M, Onoda Y, Nishihama Y, Iwai-Shimada M, Takagi M, Kobayashi Y, Isobe T (2019) Worldwide trends in tracing poly- and perfluoroalkyl substances (PFAS) in the environment. *TrAC Trends Anal Chem* 121:115410
- NIH (2019) Perfluoroalkyl and polyfluoroalkyl substances (PFAS). Accessed 21 Sept 2021
- Noguchi M, Yamasaki A (2016) Passive flux sampler measurements of emission rates of phthalates from poly(vinyl chloride) sheets. *Build Environ* 100:197–202
- OECD (2013) Synthesis paper on per- and polyfluorinated chemicals (PFCs). Accessed 21 Sept 2021
- Ohura T, Amagai T, Shen X, Li S, Zhang P, Zhu L (2009) Comparative study on indoor air quality in Japan and China: characteristics of residential indoor and outdoor VOCs. *Atmos Environ* 43 (40):6352–6359
- Okeme JO, Rodgers TFM, Jantunen LM, Diamond ML (2018) Examining the gas-particle partitioning of organophosphate esters: how reliable are air measurements? *Environ Sci Technol* 52(23):13834–13844
- Pantelaki I, Voutsas D (2019) Organophosphate flame retardants (OPFRs): a review on analytical methods and occurrence in wastewater and aquatic environment. *Sci Total Environ* 649:247–263
- Pei J, Yin Y, Cao J, Sun Y, Liu J, Zhang Y (2017) Time dependence of characteristic parameter for semi-volatile organic compounds (SVOCs) emitted from indoor materials. *Build Environ* 125: 339–347
- Raffy G, Mercier F, Blanchard O, Derbez M, Dassonville C, Bonvallot N, Glorenne P, Le Bot B (2017) Semi-volatile organic compounds in the air and dust of 30 French schools: a pilot study. *Indoor Air* 27(1):114–127
- Rauert CB (2014) Brominated flame retardant migration into indoor dust. University of Birmingham, Birmingham
- Rauert C, Harrad S (2015) Mass transfer of PBDEs from plastic TV casing to indoor dust via three migration pathways – a test chamber investigation. *Sci Total Environ* 536:568–574
- Rudel RA, Perovich LJ (2009) Endocrine disrupting chemicals in indoor and outdoor air. *Atmos Environ* 43(1):170–181
- Salthammer T, Goss KU (2019) Predicting the gas/particle distribution of SVOCs in the indoor environment using poly parameter linear free energy relationships. *Environ Sci Technol* 53(5): 2491–2499
- Shi S, Cao J, Zhang Y, Zhao B (2018) Emissions of phthalates from indoor flat materials in Chinese residences. *Environ Sci Technol* 52:13166–13173
- Shoeib M, Harner T, Wilford BH, Jones KC, Zhu J (2005) Perfluorinated sulfonamides in indoor and outdoor air and indoor dust: occurrence, partitioning, and human exposure. *Environ Sci Technol* 39(17):6599–6606
- Szabo DT (2014) Hexabromocyclododecane. In: Wexler P (ed) Encyclopedia of toxicology, 3rd edn. Academic, Oxford, pp 864–868
- UNEP (2011) Report of the persistent organic pollutants review committee on the work of its seventh meeting-Addendum: Risk management evaluation on hexabromocyclododecane (document: UNEP/POPS/POPRC.7/5). Available at: <https://www.informeia.org/en/risk-management-evaluation-hexabromocyclododecane> (accessed on March 9, 2022)
- USCPSC (2017) Guidance for hazardous additive, non-polymeric organohalogen flame retardants in certain consumer products. <https://www.cpsc.gov/Business%2D%2DManufacturing/Business-Education/Business-Guidance/flame-retardants>. Accessed 19 Sept 2021
- USEPA (2015) Assessments conducted on TSCA work plan chemicals prior to June 22, 2016. <https://www.epa.gov/assessing-and-managing-chemicals-under-tsca/assessments-conducted-tsca-work-plan-chemicals-prior#process>. Accessed 19 Sept 2021

- USEPA (2019) EPA finalizes list of next 20 chemicals to undergo risk evaluation under TSCA. <https://www.epa.gov/newsreleases/epa-finalizes-list-next-20-chemicals-undergo-risk-evaluation-under-tasca>. Accessed 19 Sept 2021
- USEPA CompTox Chemicals Dashboard. <https://comptox.epa.gov/dashboard>. Accessed 21 Sept 2021
- Van Loy MD, Lee VC, Gundel LA, Daisey JM, Sextro RG, Nazaroff WW (1997) Dynamic behavior of semivolatile organic compounds in indoor air. 1. Nicotine in a stainless steel chamber. *Environ Sci Technol* 31(9):2554–2561
- Venkatesan AK, Halden RU (2013) National inventory of perfluoroalkyl substances in archived U.S. biosolids from the 2001 EPA National Sewage Sludge Survey. *J Hazard Mater* 252–253: 413–418
- Wang L, Zhao B, Liu C, Lin H, Yang X, Zhang Y (2010) Indoor SVOC pollution in China: a review. *Chin Sci Bull* 55(15):1469–1478
- Wang X, Tao W, Xu Y, Feng J, Wang F (2014) Indoor phthalate concentration and exposure in residential and office buildings in Xi'an, China. *Atmos Environ* 87:146–152
- Wang Z, DeWitt JC, Higgins CP, Cousins IT (2017) A never-ending story of per- and poly-fluoroalkyl substances (PFASs)? *Environ Sci Technol* 51(5):2508–2518
- Wang Z, DeWitt J, Higgins CP, Cousins IT (2018) Correction to “A never-ending story of per- and polyfluoroalkyl substances (PFASs)?”. *Environ Sci Technol* 52(5):3325–3325
- Wei W, Dassonville C, Sivanantham S, Gregoire A, Mercier F, Le Bot B, Malingre L, Ramalho O, Derbez M, Mandin C (2021) Semivolatile organic compounds in French schools: partitioning between the gas phase, airborne particles and settled dust. *Indoor Air* 31(1):156–169
- Weschler CJ (2009) Changes in indoor pollutants since the 1950s. *Atmos Environ* 43(1):153–169
- Weschler CJ, Nazaroff WW (2008) Semivolatile organic compounds in indoor environments. *Atmos Environ* 42(40):9018–9040
- WHO (1989) Indoor air quality: organic pollutants. World Health Organization, Copenhagen
- Wu Y, Eichler CM, Chen S, Little JC (2016a) Simple method to measure the vapor pressure of phthalates and their alternatives. *Environ Sci Technol* 50(18):10082–10088
- Wu Y, Xie M, Cox SS, Marr LC, Little JC (2016b) A simple method to measure the gas-phase SVOC concentration adjacent to a material surface. *Indoor Air* 26(6):903–912
- Wu Z, He C, Han W, Song J, Li H, Zhang Y, Jing X, Wu W (2020) Exposure pathways, levels and toxicity of polybrominated diphenyl ethers in humans: a review. *Environ Res* 187:109531
- Xu Y, Little JC (2006) Predicting emissions of SVOCs from polymeric materials and their interaction with airborne particles. *Environ Sci Technol* 40(2):456–461
- Xu Y, Zhang J (2011) Understanding SVOCs. *ASHRAE J* 53(12):121–126
- Xu Y, Cohen HEA, Little JC (2010) Predicting residential exposure to phthalate plasticizer emitted from vinyl flooring: sensitivity, uncertainty, and implications for biomonitoring. *Environ Health Perspect* 118(2):253–258
- Xu Y, Liu Z, Park J, Clausen PA, Benning JL, Little JC (2012) Measuring and predicting the emission rate of phthalate plasticizer from vinyl flooring in a specially-designed chamber. *Environ Sci Technol* 46(22):12534–12541
- Yu G, Bu Q, Cao Z, Du X, Xia J, Wu M, Huang J (2016) Brominated flame retardants (BFRs): a review on environmental contamination in China. *Chemosphere* 150:479–490
- Zhang Y, Mo J, Weschler CJ (2013) Reducing health risks from indoor exposures in rapidly developing urban China. *Environ Health Perspect* 121(7):751–755
- Zhang Y, Xiong J, Mo J, Gong M, Cao J (2016) Understanding and controlling airborne organic compounds in the indoor environment: mass transfer analysis and applications. *Indoor Air* 26 (1):39–60



Fragranced Consumer Products as Sources

5

Nigel Goodman and Neda Nematollahi

Contents

Introduction	130
Measurement Methods and Techniques	132
Measurement of VOCs Emitted from Consumer Products	132
Measurement of VOCs in Chamber Studies	133
Measurement of VOCs Within Indoor Environments	135
Product Ingredients, Emissions, and Disclosure	139
Volatile Ingredients and Disclosure	139
Emissions Evaluated in Chamber Studies	145
VOCs from Product Use Indoors	146
Improving Indoor Air Environments	152
Fragrance-Free Policies and Practices	152
Preferences for Fragrance-free Environments	157
Conclusions	158
Cross-References	158
References	158

Abstract

Fragrance is used in consumer products around the world. However, fragrance has been associated with adverse effects on indoor and outdoor air quality and human health. Fragranced consumer products can emit and generate potentially hazardous compounds including formaldehyde and fine particulate matter. This chapter focuses on the volatile compounds emitted from fragranced consumer

N. Goodman (✉)

School of Property, Construction and Project Management, RMIT University, Melbourne, VIC, Australia

e-mail: nigel.goodman@rmit.edu.au

N. Nematollahi

Department of Infrastructure Engineering, Melbourne School of Engineering, The University of Melbourne, Parkville, VIC, Australia

e-mail: neda.nematollahi@unimelb.edu.au

products as reported in laboratory headspace analysis, environmental chambers experiments, and measurements of volatile compounds within indoor environments. First, the chapter provides information on the methods for measurement of volatile organic compounds (VOCs) emitted from products, the volatile compounds (i.e., VOCs and aldehydes) detected in environmental chamber studies, and the volatile compounds detected within indoor environments. Second, it analyzes and synthesizes data findings and research findings on product ingredients, emissions, and indoor air quality. Third, the chapter offer strategies and methods to improve indoor air quality. Key findings and results from the synthesis are as follows. Headspace analysis of fragrance consumer products revealed that terpenes were present in all fragranced products tested, but absent in all fragrance-free products tested. Environmental chamber experiments demonstrated that terpenes are among the most prevalent (and reactive) ingredients in fragranced consumer products, and that they readily react with other chemicals (e.g., ozone) to generate a range of secondary and potentially hazardous pollutants, including formaldehyde. Indoor air quality surveys (i.e., large population-based studies and targeted studies) revealed the terpenes were among the most frequently detected VOCs in offices, homes, and other everyday environments. These findings suggest that exposure to primary and secondary pollutants from fragranced consumer products is ongoing, and that risk assessment and management would be advantageous. Studies also demonstrated that approaches to improve indoor air quality can be relatively straightforward and effective. For instance, fragranced products can be removed or replaced by fragrance-free alternatives, almost entirely reducing terpene emissions. Finally, fragrance-free policies offer a beneficial, longer-term, and larger-scale solution to improve indoor air quality.

Keywords

Fragranced consumer products · Volatile organic compounds · Formaldehyde · Emissions · Health effects · Fragrance-free · Indoor air quality · Fragrance-free policy · Methods

Introduction

Everyday consumer products, especially those containing a fragrance, have emerged as a major source of indoor air pollutants. This chapter explores the emissions and effects of fragranced consumer products and the implications for indoor air quality. Special emphasis is given to methods to measure volatile emissions from products and within indoor environments.

“Fragranced consumer products,” as termed in this chapter, is a product that “contains an added fragrance or that is largely comprised of fragrance” (Steinemann 2019a). Fragranced products cover hundreds of everyday items, such as air fresheners, deodorizers, cleaning supplies, laundry detergents, fabric softeners, essential oils, candles, soaps, personal care products, colognes, and hand sanitizers.

A “fragrance” in a consumer product is a scent and, despite its singular name, it is a formulation of dozens of chemicals, such as volatile organic compounds (VOCs). Nearly 4,000 ingredients have been documented for use in the composition of a fragrance (IFRA 2020). A fragrance is generally intended to “provide an aroma, to mask an odor, or both” (Steinemann 2019a).

Fragranced consumer products are an interesting and important dimension of indoor air quality for several reasons:

First, in studies around the world, volatile chemicals, such as terpenes, from fragranced consumer products are among the most abundant pollutant indoors (e.g., Wang et al. 2017; Mandin et al. 2017). A reason is that fragranced consumer products are pervasive in society – used in homes, workplaces, schools, public buildings, health care facilities, transportation, and other indoor environments. Consequently, exposure has become almost unavoidable. For instance, in large-scale population studies across four countries (United States, Australia, United Kingdom, and Sweden), an estimated 99.1% of adults are exposed to fragranced products, at least once a week, from their own use (98.3%), from others’ use (90.6%), or from either or both (Steinemann 2021).

Second, adverse health effects from exposure to fragranced products are also pervasive and can be severe. In the aforementioned international studies, 32.2% of adults report health problems, such as breathing difficulties and migraine headaches, when exposed to one or more types of fragranced products, such as air fresheners, laundry products, and cleaning supplies. Further, 9.5% of adults report the effects can be disabling. Among vulnerable subpopulations, the prevalence of adverse effects is higher. For instance, 57.8% of asthmatic individuals and 75.8% of autistic individuals report adverse effects from fragranced products (Steinemann 2019c).

Third, relatively little is known about the actual ingredients in these products. No law in any country requires the disclosure of all specific ingredients in a consumer product (apart from foods, drugs, and cosmetics). Moreover, no law requires the disclosure of all specific ingredients in the fragrance mixture added to any product. However, studies found that typically fewer than 4% of all volatile ingredients, and 5% of all potentially hazardous air pollutants, are actually disclosed on product labels or safety data sheets. Thus, and paradoxically, an important source of exposure to pollutants indoors, fragranced consumer products, is exempt from full disclosure of the ingredients that contribute to the pollutants (Steinemann 2021).

Fourth, economic and societal consequences are compelling. In the international studies, 9.0% of adults have lost workdays or a job, within a past year, due to exposure to fragranced products in their workplace. Direct personal costs from exposure exceeded \$132 billion USD (Steinemann 2019b). Fragranced product exposures can also restrict access in society. For instance, 13.3% of the public report they are unable or reluctant to use the restrooms in a public place because of the presence of an air freshener, deodorizer, or scented product (Steinemann 2019b).

Fifth, and optimistically, improvements to indoor air quality can be readily and effectively achieved – with fragrance-free policies, practices, and products. Across four countries, a strong majority of the general public would prefer that workplaces, health care facilities, health care professionals, hotels, and airplanes were

fragrance-free rather than fragranced. Fragranced products can be removed entirely (such as with air fresheners) or replaced with fragrance-free versions (such as with laundry products). The result can be mutually beneficial to indoor air quality, human health and well-being, and the environment (Steinemann 2019a, 2021).

The specific aims of this chapter are to (1) provide information on the methods for measurement of VOCs emitted from products, VOCs in chamber studies, and VOCs within indoor environments, (2) analyze and synthesize data findings and research findings on product ingredients, emissions, and indoor air quality, and (3) offer strategies and methods to improve indoor air quality. This chapter will focus on VOCs, while recognizing that products can emit additional types of pollutants.

Measurement Methods and Techniques

This section provides background information and details of the methods and techniques used to analyze and quantify volatile compounds emitted from products, in environmental chamber studies, and within indoor environments. It includes details of the sampling strategies, sampling media, as well as techniques to analyze and quantify volatile compound data. The methods selected for this chapter include headspace GC/MS analysis, environmental chamber experiments, and measurement of volatile compounds within indoor environments.

Measurement of VOCs Emitted from Consumer Products

Overview

Gas chromatography-mass spectrometry (GC/MS) is an analytical method widely used to analyze and identify the chemical components in samples. When GC/MS is equipped with a column (e.g., coated capillary) for VOCs, it can be used for separation, analysis, and characterization of VOCs from samples. Among the different sampling techniques for GC/MS (e.g., direct injection, headspace sampling, automated thermal desorption), headspace sampling is used for the analysis of volatile chemicals in solid, liquid, and gaseous samples. A benefit of headspace sampling is that direct liquid or solid injection to the GC/MS is avoided. This approach means that the complex sample matrix in a liquid or solid sample can be simplified to the gas phase (EPA 1997; EPA Method 5021A 2014; Bicchi 2000).

For analyses using static headspace gas chromatography, liquid or solid samples are placed in a closed vial where an equilibration between the sample and the gas phase is established. This allows the capture and injection of the headspace gas into the GC/MS using a gas-tight syringe. A wide range of organic compounds can be detected using this method (provided they have sufficient volatility). The method is designed for analysis of samples containing low concentrations of VOCs. This procedure can be applied to solid samples with high concentrations of VOCs or to oily materials that may not be appropriate for the low-concentration technique (EPA 1997; EPA Method 5021A 2014).

GC/MS analysis of volatile organic compounds using headspace gas chromatography measurements generally follow the guidelines found in US EPA Compendium Method TO-15 (EPA 1999) and EPA Method 5021A (EPA 2014).

This section provides detailed information on headspace GC/MS measurements for analysis of fragranced consumer products, as used in our prior studies (e.g., Nematollahi et al. 2018a, b, 2019).

Details of Headspace Analysis Techniques

Headspace GC/MS measurements of products were performed using a Shimadzu GC/MS-QP2010 Plus instrument coupled to an automated Shimadzu AOC-5000 sample injection system. Approximately 2 g of each product were weighed into a 10 mL amber vial. Each vial was then tightly sealed with a magnetic screw cap with a PTFE/silicone septum. Samples were incubated at 40 °C for 1 h immediately prior to injection of 2.5 mL of the headspace into the injection port heated at 240 °C (split ratio 25). Separation was performed on a BPX-VOL capillary column (30 m × 0.25 mm, 1.4 µm film thickness) using helium as the carrier gas (flow rate 30 cm/s). The oven temperature was kept at 35 °C for 3 min, then increased by 5 °C/min to 220 °C and held at this temperature for 5 min. The total run time was 45 min. The mass spectrometer ion source and interface temperatures were maintained at 200 °C and 240 °C, respectively. The mass spectrometer was operated in full scan mode between 25 and 400 m/z. Blanks were analyzed periodically each day to account for any background impurities (Nematollahi et al. 2018a). The volatile sample components were identified based on the mass spectral library of the National Institute of Standards and Technology NIST Version 2.0 (Stein 2008).

This analysis focused on the VOC emissions emitted from products, even though other chemical classes (such as semi-volatile or nonvolatile organic compounds) could also be presented in the products. Moreover, this analysis focused on the primary VOC emissions emitted from products, even though secondary pollutants (such as formaldehyde) could also be generated. This leads to the need for chamber studies to understand the effects of interactions with other chemicals such as ozone.

Measurement of VOCs in Chamber Studies

Overview

Over the past 30–40 years, environmental chamber studies have been used to investigate the volatile emissions from consumer products and other materials. Environmental test chambers provide a precisely controlled environment that can be used to investigate the types and concentrations of emissions as well as the influence of environmental factors such as temperature, relative humidity, and air flow (Salthammer 2009).

Typically, a product (or sample) is placed in the chamber and the emissions of VOCs and other compounds are monitored by extracting air samples from the chamber. Air samples are collected onto sampling media (e.g., Tenax sorbent tubes) for subsequent analysis by thermal desorption (TD)/gas chromatography

(GC)/mass spectrometry (MS) (Destaillets et al. 2006). Controlled chamber experiments allow a more realistic understanding of the volatile emissions from products. In some experiments, oxidants such as OH radical or ozone are introduced into the chamber to investigate chemical reactivity of product emissions and simulate real world air pollutant interactions. Such experiments allow an understanding of the primary and secondary pollutants generated upon interaction with other gaseous pollutants in the chamber.

Details of chamber methods are included in the ISO 16000 series. For example, ISO 16000-6 (2021) provides methods for determination of VOCs in indoor and test chamber air (ISO 2021). The American Society for Testing and Materials (ASTM) also provides several emission chamber test methods, such as small-scale environmental chamber determinations of organic emissions from indoor materials/products (ASTM 2017).

Details of Chamber Study Techniques

Several authors have investigated VOCs emissions from fragranced consumer products in environmental chambers. Studies have focused on primary emissions from air fresheners and cleaning products (e.g., Singer et al. 2006a), and secondary organic aerosol (e.g., fine particles) generated from ozone-initiated reactions with fragranced products (Singer et al. 2006b; Coleman et al. 2008; Destaillats et al. 2006). This section will briefly summarize some of the methods used in chamber studies of air fresheners, with focus on the methods used to evaluate primary emissions and secondary reaction products (e.g., formaldehyde, PM_{2.5}).

First, we will focus on the methods used to evaluate primary volatile emissions from an air freshener in a large chamber (50 m³) as reported by Singer et al. (2006a). The chamber was made with conventional construction materials (e.g., wood, plywood, gypsum wall board) and included the following items: a small laminated table (surface area: 1.16 m²) positioned in the middle of the room and a series of air mixing fans in each corner. It was mechanically ventilated at approximately 0.5 h⁻¹ with an outdoor air supply that passed over a bed of activated carbon to remove ozone and organic compounds. Temperature was controlled but relative humidity was not. In the study, five readily available cleaning products and one plug-in air freshener were evaluated in the chamber under a series of product usage scenarios.

The air freshener was a “plug-in” type that contained unsaturated terpenoids (scented oil) dispersed by a heated dispenser. During the tests, the device was operated at the highest of three possible settings achieving an emission rate of 1.5 g per day. Air samples were collected on to Tenax sorbent tubes at pump flow rates of between 1.8 and 5.5 cm³/min for between 2 and 5 min (Singer et al. 2006a).

Samples were analyzed by thermal desorption gas chromatography/mass spectrometry (TD-GC/MS) in accordance with USEPA Method TO-1 (USEPA 1984). For details, see Singer et al. (2004).

Next, we will consider studies that evaluated primary and secondary emissions from air fresheners, including secondary organic aerosols (SOAs) from chemical interactions with oxidants. Destaillats et al. (2006) studied the reaction of ozone with terpene emissions from air fresheners and cleaning product in a 198 L stainless-

steel chamber lined with a Teflon film. (Teflon was used to reduce surface-related interactions and ozone decomposition.) The chamber had two inlet ports, one outlet port, and was operated under constant flow and positive pressure. Product gas-phase components (e.g., an air freshener) was introduced into one port, and an air stream containing ozone was admitted at the second inlet. Ozone was produced by UV irradiation of an airstream and measured using a calibrated ozone sensor; before and after each run, and at the outlet of the chamber. The temperature and relative humidity (RH) in the chamber were logged continuously. Airflow into the chamber was “zero quality” compressed air adjusted to obtain a RH between 40% and 60%. The chamber was located in a temperature controlled (23 ± 0.5 °C) room with volume of 20 m³ (Destaillets et al. 2006). Key variables explored in the study were ACH (between 1 and 3 h⁻¹), reaction time, and ozone concentration (high: 120–130 ppb, moderate: 60 ppb).

Sampling of VOCs followed similar methods reported in Singer et al. (2006b). To monitor levels of secondary pollutants, the study also detailed methods to determine the concentrations of aldehydes, fine particulate matter, and OH radicals. Many of these methods are covered in other sections of this chapter, book. For further details, please see Destaillats et al. (2006).

Measurement of VOCs Within Indoor Environments

Overview

A review of the methods used for sampling and analysis of indoor VOCs found that there is no standard (global) approach for IAQ sampling or VOC reporting (Goodman et al. 2017). Among the most widely recognized sampling and analytical methods are the protocols published by the International Organization for Standardization (e.g., 16,000 series) and the US EPA (e.g., Compendium Methods TO17 for VOCs and TO11A for carbonyls and formaldehyde) (US EPA 1999a, b). Sampling methods can vary by approach, media, time, volume, and active or passive techniques (Goodman et al. 2017). Active sampling requires a pump or evacuated canisters whereas passive sampling is diffusion controlled. Active sampling approaches include SUMMA canisters, sorbent tubes, and multisorbent tubes. Passive sampling generally requires only a single sorbent due to the lower diffusion controlled adsorption rates. These are often in the form of a disc, radial, or tape monitors.

The sampling methods chosen are critical as they influence the reliability of data and determine whether the findings can be compared to other studies and to health-based guidelines. For example, to evaluate levels of formaldehyde for comparison to the WHO guidelines (i.e., WHO 2010), active sampling for 30 min is recommended.

Details of VOC Sampling Techniques

Large Population-Based IAQ Studies

There have been significant research efforts that aim to understand levels of VOCs and aldehydes within homes, schools, and offices across Europe (Mandin et al. 2017;

Trantallidi et al. 2015), homes in Canada (Zhu et al. 2013), and offices and homes in the UK and the USA (i.e., Wang et al. 2017; Girman et al. 1999). This section summarizes the methods used in three of these studies.

First is the OFFICAIR study, which evaluated the levels of VOCs and aldehydes in 37 new or recently renovated office buildings across Europe, during the summer and winter seasons of 2012–2013 (Mandin et al. 2017). A key objective of the study was to develop a framework and tools to support health-based risk assessments of IAQ in new or recently renovated office buildings. In each office building, 4 rooms were investigated (148 rooms in total) from 8 European countries (i.e., Greece, Portugal, Spain, France, Italy, Hungary, the Netherlands, Finland, Belgium, the UK, and Denmark). None of the rooms were naturally ventilated and almost all rooms were equipped with a ventilation system (92%) and a cooling system (95%). Tests were performed for targeted pollutants including 12 VOCs, 7 aldehydes, ozone, and nitrogen dioxide. VOC samples were collected using Radiello® passive samplers (120-2 diffusive body, 145 cartridge) for 5 days. The VOCs were analyzed using thermal desorption coupled with capillary GC/MS in accordance with the methods described in ISO 16017–2. The thermal desorption was performed by heating the sampling tubes to 300 °C for 10 min using helium with flow rate of 50 mL min⁻¹. The desorbed VOCs were injected onto the GC/MS via a heated transfer line at 200 °C and separated using a capillary column (60 m × 250 µm × 1.4 µm) (GsTEK-624). Helium was used as the carrier gas with a flow rate of 6 mL min⁻¹. The oven temperature was kept at 40 °C for 5 min, then increased by 6 °C·min⁻¹ to 230 °C, and kept there for 5 min. The mass spectrometer was operated in full scan mode between 35 and 300 amu. Aldehydes were collected using Radiello® DNPH passive samplers (120-1 diffusive body, 165 cartridge) for 5 days. The aldehydes were analyzed using high-performance liquid chromatography coupled with UV detection in accordance with the methods described in the ISO 16000–4 standard. For additional details, see Mandin et al. (2017).

Second is the Canadian population-based national indoor air quality survey conducted in 2009–2011 within 3,857 households, including 3218 houses, 546 apartments, and 93 other dwellings, across Canada (Zhu et al. 2013). In this study, there were almost twice as many older dwellings (>50 years) than the newer dwellings (<10 years). The tests were performed for 84 targeted VOCs. Samples were collected using passive sampling techniques that were deployed by study participants in their homes using sampling tubes (Carbopack B 60/80 sorbent media) for a period of 7 days. The tubes were made from stainless steel (ID 5 mm × 90 mm long) and packed with Carbopack B 60/80 sorbent media. Deployment included switching a protective brass end cap with a Teflon diffusion cap during sampling, replacing the protective cap at the end of the sampling period, and finally shipping the sample in a prepaid Canada Post envelope to the analytical laboratory. The VOCs were analyzed using thermal desorption (model ATD650, Perkin-Elmer) coupled with capillary GC/MS (Agilent). Thermal desorption was performed by heating the sampling tubes to 330 °C for 12 min using helium with flow rate of 60 mL/min. The desorbed VOCs were injected onto the GC/MS via a heated transfer line at 300 °C and separated using a capillary column (60 m × 250 µm × 1.4 µm) (GsTEK-624). The oven

temperature was kept at 45 °C for 3 min, then increased by 6 °C·min⁻¹ to 180 °C, then 30 °C·min⁻¹ to 250 °C and kept there for 10 min. The mass spectrometer was operated in full scan mode between 33 and 400 amu. For more details, see Zhu et al. (2013).

Third is the United States Environmental Protection Agency's Building Assessment Survey and Evaluation study (BASE), a major cross-sectional study of indoor air quality at 56 public and private office buildings across the USA, conducted during summer and winter of 1995–1998 (Girman et al. 1999). Samples collected included VOCs, aldehydes, particulate matter, radon, microbiological contaminants, carbon monoxide, carbon dioxide, temperature, relative humidity, as well occupant perceptions of IAQ. For VOCs, the analysis was performed for 46 targeted compounds, many of which were selected based on their potential to be irritants, carcinogens, and systemic toxicants (Girman et al. 1999). Samples were collected at three indoor locations and at one outdoor location during times of normal building occupancy. Active sampling (requiring low flow pumps) was used in the study and different higher flow rates were used: for the indoor samples, flow rates were 5 ml/minute, and for the outdoor samples, flow rates were 6–8 ml/min (due to expected lower outdoor concentrations). Samples were collected using multisorbent sampling media (Tenax-TA, Ambersorb XE-340, and activated charcoal) for 8–10 h. The VOCs were analyzed using thermal desorption coupled with GC/MS using a modified version of EPA Method TO-1 (Berkeley Analytical Laboratories, Berkeley, CA). Formaldehyde and acetaldehyde were also sampled (although the detailed method are not described here). For additional details, see Girman et al. (1999).

A strength of population-based studies is that a large set of data is collected from a large number of buildings, and this provides more meaningful information. These data are potentially more representative of the levels of indoor pollutants and exposures of the wider population. One limitation of these studies is that they are based on a brief window or “snapshot” in time and may not reflect the long-term levels of pollutants. Also, short-term (i.e., 30 min) exposure data are needed to assess acute health effects (e.g., for formaldehyde) and cannot be easily assessed in such large studies.

VOCs Within Indoor Environments

This section summarizes the methods used in a study that investigated VOCs at a large Australian university. Several categories of indoor environment were evaluated in the study including locations of campus services, restrooms, renovated offices, a green building, meeting areas, and classrooms. Analysis of 41 VOCs across 20 locations observed indoor concentrations higher than outdoor concentrations for 97% of all VOC measurements (493 unique comparisons). Because this chapter focuses on fragranced consumer products as sources, we will concentrate our analysis on three indoor categories where levels of volatile emissions were among the most prevalent compounds. These are campus services, restrooms, and classrooms. The sampling methods used in the study are described below.

Indoor air samples were collected and analyzed in accordance with USEPA compendium methods TO-17 and TO-11A (US EPA 1999a, b). In all cases, outdoor

air samples were collected within close proximity to, and simultaneously with, indoor air samples.

Further details of the methods used in this study are as follows. For VOCs (other than carbonyl compounds), two multi-adsorbent tubes in series (Markes Carbograph 1TD/Carbopack X) were connected to a SKC Pocket Pump 210-1002 (Eighty Four PA, USA) at a flow rate of approximately 35 mL per minute for 2.5 h (5 L). For carbonyl compounds, a single low pressure drop dinitrophenylhydrazine LpDNPH S10 cartridge (Supelco Cat No 21014) was connected to TSI Incorporated SidePak SP730 (Shoreview, MN, USA) at a flow rate of approximately 1200 mL per minute for 7 h (500 L). An ozone scrubber (Supelco Cat No 505285) was placed in front of the S10 cartridge to prevent ozone interference with the carbonyls. According to established methods, 10% of samples were reserved as blanks (Wallace et al. 1991). Temperature and relative humidity were measured using a portable weather station (Holman, WS5052B).

A total of 47 VOC tubes and 35 carbonyl cartridges (indoor and outdoor) were analyzed. Analysis of VOCs used a PerkinElmer TurboMatrix™ 650 automated thermal desorber (ATD) and a Hewlett Packard 6890A gas chromatography (GC)/mass spectrometry (MS)/flame ionization detector (FID) in accordance with US EPA method TO-17. An Agilent (DB5-MS) capillary column (60 m × 0.32 mm × 1 µm) was used for compound separation. Certified gas standards were used for calibration; these included a benzene, toluene, ethylbenzene, and xylenes (BTEX) standard (Air Liquide–Scott Specialty Gases, Longmont, CO, SA), and a BTEX plus isoprene standard (National Physical Laboratory, Middlesex, UK). Where a gas standard was not available, quantification of VOCs was done using the FID response factor of toluene. Only VOCs with concentrations greater than the method detection limit (MDL) of the analytical instrument were reported. For VOCs, the MDL was between 0.01 and 0.04 µg/m³ determined as the 95th percentile of the response from 7 field blanks.

Analysis of carbonyl compounds (such as formaldehyde) is important as they can be both primary and secondary emissions from fragranced consumer products. In the study, analysis of carbonyls used ultra-high performance liquid chromatography (UHPLC) consisting of a Thermo Scientific Dionex Ultimate 3000 RS system with diode array detector (DAD) and mass spectrometry (MS) detector in accordance with US EPA Method TO-11A. A rapid separation liquid chromatography (RSLC) Acclaim™ (No. 077973) carbonyl column (150 mm × 2.1 mm, particle size: 2.2 µm) was used for compound separation. The chromatographic conditions included a flow rate of 0.4 mL/min and an injection volume of 3.0 µL. The DAD was operated in the 220–520 nm wavelength range with 360 nm used for mono-carbonyl quantification. The peaks were separated by gradient elution with an initial mobile phase of 52% acetonitrile and 48% deionized water (18.2 ΩM cm, Millipore Milli-Q Advantage) for 8.3 min, followed by a linear gradient to 100% acetonitrile for 8 min, with a column temperature of 30 °C. A certified liquid standard (Supelco Carb Method 1004 DNPH mix 2 C/N 47651-U) containing 30 µg/mL of each derivatized carbonyl was diluted 1:25 in a volumetric flask. This prepared standard was then used to perform a four-point calibration (0.15, 0.30, 0.6, and 1.2 µg/mL).

For carbonyl compounds, the MDL was between 0.01 and 0.07 $\mu\text{g}/\text{m}^3$, determined as the 95th percentile of the response from 8 field blanks. All original concentrations were blank corrected.

As with many experimental protocols, the methods used in this study had several limitations. First, the durations for sampling (e.g., 2.5 h, 7 h), required to collect sufficient volume to meet MDLs, differed from the durations for health-based guidelines (e.g., 30 min), thus preventing direct comparisons. Second, ethanol concentrations are semiquantitative due to possible sample breakthrough of multi-sorbent tubes. Third, sampling was conducted during summer and autumn, which may not represent VOC levels during all seasons.

It is useful to know that the sampling duration and volume collected during VOC and carbonyl sampling can be adapted for situations that require compliance with acute exposure guidelines (e.g., formaldehyde, 30 min) or to capture peak concentrations of pollutants during short-term activities such as cleaning or use of a fragranced consumer product. For instance, in a study of volatile emissions from dryer vents, a single multi-adsorbent tube (Markes Carbograph 1TD/Carbopack X) was connected to an SKC sampling pump (AirChek 220-5000TC) at a flow rate of approximately 150 mL per minute for 1 h (9 L) (Goodman et al. 2018).

Product Ingredients, Emissions, and Disclosure

Volatile Ingredients and Disclosure

Volatile Ingredients Emitted

This section provides results from the analysis of 289 products including air fresheners, laundry products, cleaning supplies, personal care products, hand sanitizers, air disinfectants, sunscreens, baby products, essential oils, and car air fresheners, both green and regular products. (In these studies, “green products” are considered as products with the claim of “green,” or a related term such as “organic,” “natural,” “no petrochemicals,” “certified green,” “certified organic,” or “essential oils” for the entire product or specific ingredients. “Regular products” are the products other than those in the “green” category.)

Notwithstanding the regulatory protections on full ingredient disclosure, products can be chemically analyzed to determine their constituents. (Although some companies have taken voluntary steps to disclose ingredients used in their fragranced products, this information is often a consolidated list of chemicals, rather than specific chemicals in a specific product. In cases where specific product information is provided, the general term “fragrance” is listed rather than the individual and specific chemicals in that fragrance mixture. Thus, consumers still lack information about complete and specific ingredients and potential exposures from any particular product.) A set of studies analyzed volatile organic compounds (VOCs) emitted from common consumer products, both fragranced and fragrance-free versions, and green and regular versions (Steinemann 2015; Nematollahi et al. 2018a, b, 2019, 2021; Steinemann et al. 2020, 2021). Products were randomly selected from stores in

the USA and Australia (AU), although the same or similar products are also available internationally.

The studies used gas chromatography/mass spectrometry (GC/MS) headspace analysis to identify the VOCs emitted directly from each product as described in the section on “[Details of Headspace Analysis Techniques](#).” The top 20 peaks (highest concentration compounds) for each product were identified from the sample chromatogram using mass spectral library matches.

Some definitions for these studies are as follows:

“VOC occurrences” refers to the collective number of individual VOCs or ingredients emitted from the products.

“VOC identities” refers to the number of distinctly named VOCs emitted from one or more of the products.

Main results of seven studies (Steinemann [2015](#); Nematollahi et al. [2018a, b, 2019, 2021](#); Steinemann et al. [2020, 2021](#)) are provided below. A summary of these results are provided in Table 1.

1. Study of 37 common consumer products: air fresheners, laundry products, cleaning supplies, and personal care products. The GC/MS analyses found 559 VOC occurrences, representing 156 VOC identities. Among these VOCs, 230 VOC occurrences, representing 42 VOC identities, are classified as potentially hazardous. All products emitted potentially hazardous VOCs.

The most common fragranced product VOCs (> 80% of products) were limonene and beta-pinene. The most common fragrance-free product VOC (100% of products) was ethanol, which was also in fragranced products. The most common potentially hazardous VOCs (>75% of products) were ethanol and limonene. No significant difference was found in the emissions of hazardous air pollutants between green fragranced products and regular fragranced products.

Fewer than 3% of the VOCs and fewer than 6% of potentially hazardous VOCs were disclosed on the product labels, safety data sheets, or website. Further, among the fragranced consumer products (other than cosmetics), 91% did not disclose the presence of a “fragrance” on the label or safety data sheet. Among the fragranced cosmetics, 89% did not disclose “fragrance” on the safety data sheet, but all disclosed “fragrance” on the label, as required.

2. Study of 134 common consumer products: air fresheners, laundry products, cleaning supplies, personal care products, and sunscreens. The GC/MS analyses found 1,538 VOC occurrences, representing 338 VOC identities. Among these VOCs, 517 VOC occurrences, representing 69 VOC identities, are classified as potentially hazardous. Nearly all products (99%) emitted potentially hazardous VOCs.

The most common fragranced product VOC (77% of products) was limonene. The most common fragrance-free product VOC (40% of products) was ethanol. The most common potentially hazardous VOCs (> 40% of products) were limonene and ethanol. No significant difference was found in emissions of the most prevalent potentially hazardous VOCs between green fragranced products and regular fragranced products.

Table 1 Summary of top 10 prevalent compounds emitted from the products across 7 studies

Compound	CAS #	Prevalence (# of products)		
		Total	Regular	Green
<i>Study of 37 common consumer products</i>				
Ethanol ^a	64-17-5	29	18	11
Limonene ^a	138-86-3	28	14	14
beta-Pinene	127-91-3	25	13	12
alpha-Pinene	80-56-8	23	12	11
Acetone ^a	67-64-1	20	7	13
Acetaldehyde ^a	75-07-0	15	11	4
2,4-Dimethyl-3-cyclohexene-1-carboxaldehyde (Triplal 1)	68039-49-6	14	6	8
Carene isomer	e.g., 13466-78-9	13	5	8
o-, m-, or p-Cymene	527-84-4, 535-77-3, or 99-87-6	13	5	8
Benzyl acetate	140-11-4	12	5	7
<i>Study of 134 common consumer products</i>				
Limonene ^a	138-86-3	82	40	42
Ethanol ^a	64-17-5	56	27	29
Acetaldehyde ^a	75-07-0	50	23	27
beta-trans-Ocimene	3779-61-1	49	12	37
Linalool	78-70-6	45	23	22
beta-Myrcene	123-35-3	42	11	31
Eucalyptol	470-82-6	42	17	25
gamma-Terpinene	99-85-4	35		
beta-Pinene	127-91-3	32		
alpha-Pinene	80-56-8	29		
<i>Study of 42 fragranced baby products</i>				
Limonene ^a	138-86-3	28	11	17
Acetaldehyde ^a	75-07-0	23	10	13
Ethanol ^a	64-17-5	23	14	9
alpha-Pinene	80-56-8	21	8	13
Linalool	78-70-6	20	4	16
beta-Myrcene	123-35-3	19	6	13
Acetone ^a	67-64-1	17	5	12
beta-Pinene	127-91-3	17	7	10
Eucalyptol	470-82-6	14	4	10
Ethyl butyrate	105-54-4	13	8	5
<i>Study of 24 commercial essential oils</i>				
alpha-Pinene	80-56-8	20	8	12
Limonene ^a	138-86-3	19	8	11

(continued)

Table 1 (continued)

Acetone ^a	67-64-1	17	8	9
Linalool	78-70-6	16	9	7
alpha-Phellandrene	99-83-2	16	4	12
beta-Myrcene	123-35-3	15	5	10
Camphene	79-92-5	15	5	10
Ethanol ^a	64-17-5	15	8	7
beta-Pinene	127-91-3	15	3	12
3-Carene	13466-78-9	14	3	11

Study of 12 car air fresheners

		(n = 12)	(n = 8)	(n = 4)
Limonene	138-86-3	10	8	2
Benzyl acetate	140-11-4	9	5	4
Acetone	67-64-1	9	7	2
Ethanol	64-17-5	9	6	3
Linalool	78-70-6	8	6	2
2-Methylbutyl acetate	624-41-9	8	4	4
Acetaldehyde ^a	75-07-0	8	7	1
Methanol ^a	67-56-1	8	5	3
3-Penten-2-one, 4-(2,6,6-trimethyl-2-cyclohexen-1-yl)	114933-28-7	7	4	3
beta-Myrcene ^a	123-35-3	7	5	2

Study of 14 commercial essential oils with therapeutic claims

		(n = 14)		
Acetaldehyde ^a	75-07-0	14		
alpha-Phellandrene	99-83-2	14		
alpha-Pinene	80-56-8	14		
Camphene	79-92-5	14		
Limonene ^a	138-86-3	14		
Methanol ^a	67-56-1	14		
Terpinolene	586-62-9	14		
3-Carene ^a	13466-78-9	13		
Acetone ^a	67-64-1	13		
beta-Phellandrene	555-10-2	13		

Study of 26 commonly used pandemic products

		(n = 26)	(n = 13)	(n = 13)
Limonene ^a	138-86-3	21	10	11
Ethanol ^a	64-17-5	17	7	10
alpha-Pinene	80-56-8	13	7	6
beta-Pinene	127-91-3	12	8	4
Acetaldehyde ^a	75-07-0	11	4	7
Eucalyptol	470-82-6	11	4	7
gamma-Terpinene	99-85-4	11	5	6

(continued)

Table 1 (continued)

beta-Myrcene	123-35-3	10	1	9
beta-trans-Ocimene	3779-61-1	10	3	7
Camphene	79-92-5	10	5	5

^aClassified as potentially hazardous under Safe Work Australia, Hazardous Chemical Information System (SWA 2020)

Fewer than 10% of VOCs, and fewer than 4% of potentially hazardous VOCs, were disclosed on the product labels, safety data sheets, or website.

3. Study of 42 fragranced baby products: shampoos, lotions, hair sprays, and fragrance. The GC/MS analyses found 684 VOC occurrences, representing 228 VOC identities. Among these VOCs, 207 VOC occurrences, representing 43 VOC identities, are classified as potentially hazardous.

The most common fragranced baby product VOC (67% of products) was limonene. The most common potentially hazardous VOCs (>55% of products) were limonene, acetaldehyde, and ethanol. No significant difference was found in the emissions of the most prevalent potentially hazardous VOCs between green fragranced baby products and regular fragranced baby products.

Fewer than 5% of VOCs, and fewer than 13% of potentially hazardous VOCs, were disclosed on the product labels, safety data sheets, or website.

4. Study of 24 commercial essential oils. The GC/MS analyses found 589 VOC occurrences, representing 188 VOC identities. Among these VOCs, 124 VOC occurrences, representing 33 VOC identities, are classified as potentially hazardous.

The most common essential oil VOCs (> 70% of oils) were alpha-pinene, limonene, and acetone. The most common potentially hazardous VOCs (> 70% of oils) were limonene and acetone. No significant difference was found in the emissions of the most prevalent potentially hazardous VOCs between natural and regular essential oils. No ingredients were disclosed on any of the essential oil labels.

5. Study of 12 car air fresheners. The GC/MS analyses found 546 VOC occurrences, representing 275 VOC identities. Among these VOCs, 30 VOC occurrences, representing 9 VOC identities, are classified as potentially hazardous.

The most common car air freshener VOCs (>70% of products) were limonene, benzyl acetate, acetone, and ethanol. The most common potentially hazardous VOCs (67% of products) were acetaldehyde and methanol. No significant difference was found in the emissions of the most prevalent potentially hazardous VOCs between green and regular car air fresheners. Fewer than 2% of VOCs, and none of the potentially hazardous VOCs, were disclosed on the product labels, safety data sheets, or website.

6. Study of 14 commercial essential oils with therapeutic claims. The GC/MS analyses found 1,034 VOC occurrences, representing 378 VOC identities. Among these VOCs, 251 VOC occurrences, representing 60 VOC identities, are classified as potentially hazardous.

The most common essential oil VOCs (> 90% of oils) were acetaldehyde, alpha-phellandrene, alpha-pinene, camphene, limonene, methanol, terpinolene, 3-carene, acetone, beta-phellandrene, ethanol, and gamma-terpinene. The most common potentially hazardous VOCs (> 90% of oils) were acetaldehyde, limonene, methanol, acetone, ethanol, and 3-carene.

Fewer than 1% of VOCs, and fewer than 1% of potentially hazardous VOCs, were disclosed on the product labels, safety data sheets, or website.

7. Study of 26 commonly used pandemic products: hand sanitizers, air disinfectants, multipurpose cleaners, and handwashing soap. The GC/MS analyses found 399 VOC occurrences, representing 172 VOC identities. Among these VOCs, 127 VOC occurrences, representing 46 VOC identities, are classified as potentially hazardous. Nearly all products (99%) emitted potentially hazardous VOCs.

The most common fragranced product VOC (40% of products) were limonene, ethanol, alpha-pinene, beta-pinene, and acetaldehyde. The most common potentially hazardous VOCs (25% of products) were limonene, ethanol, acetaldehyde, 3-carene, and methanol. No significant difference was found in emissions of the most prevalent potentially hazardous VOCs between green fragranced products and regular fragranced products.

Fewer than 4% of VOCs, and fewer than 11% of potentially hazardous VOCs, were disclosed on the product labels, safety data sheets, or website.

Across the 7 studies, the 289 products emitted collectively 5,349 VOC occurrences, representing 981 VOC identities. The most prevalent compounds in fragranced products were terpenes (limonene, alpha-pinene, beta-pinene), which were not found in fragrance-free products. The most prevalent compound in fragrance-free products was ethanol, which was also a common compound in fragranced products. Across the studies, the 289 products emitted collectively 1,486 potentially hazardous VOC occurrences, representing 130 VOC identities, which represents 28% of all VOC occurrences.

Relations Between Emissions and Listed Ingredients

Across the studies, on average, fewer than 4% of all VOCs, and fewer than 5% of potentially hazardous VOCs, were disclosed on any product label, safety data sheet, or website.

Ingredients in fragranced consumer products are not required to be specifically and fully disclosed, in any country (Lunny et al. 2017; Steinemann 2015; Steinemann et al. 2011). Main components of the regulations are as follows:

No law in any country requires the full disclosure of all ingredients in a chemical mixture termed “fragrance,” not on the product label, safety data sheet, or website. Instead, a product may list the general term “fragrance” (or another legally approved term, such as “perfume” or “parfum”) instead of listing all individual ingredients in that fragrance.

No law requires that consumer products (other than foods, drugs, and cosmetics) disclose all specific ingredients on the label, safety data sheet, or website. Further,

these products are typically not required to even list the general term “fragrance,” so consumers may not be aware that a product actually contains a fragrance mixture.

For the other classes of consumer products (i.e., foods, drugs, and cosmetics), while they do need to list all ingredients on the label (although not on the safety data sheet), the general term “fragrance” may be used instead of the complete and specific ingredients in that fragrance mixture.

Thus, and paradoxically, a major source of exposure to pollutants, fragranced consumer products, is exempt from full disclosure of the ingredients that contribute to the pollutants. Consequently, the public, professionals, and agencies lack information to understand the links between emissions, exposures, and effects on air quality and health.

Emissions Evaluated in Chamber Studies

This section summarizes results from chamber studies with focus on the primary and secondary emissions from fragranced consumer products including air fresheners. Key findings from each of studies (i.e., Singer et al. 2006a; Destaillats et al. 2006) are provided below.

In a chamber study of primary VOC emissions from an air freshener, among the most prevalent VOCs detected were unsaturated ozone reactive terpenes (e.g., d-limonene), and terpenoids (e.g., linalool, beta-Citronellol), the concentrations of these compounds ranged between 7 and 160 µg/m³ (Singer et al. 2006a). Several other VOCs were also prominent, including benzyl acetate and bornyl acetate and detected at concentrations between 280 µg/m³ and 410 µg/m³, respectively. The emission rates for selected VOCs from the air freshener were 7.7 mg/day for alpha-Citral, 39 mg/day for d-limonene, and 460 mg/day for bornyl acetate (Singer et al. 2006a). The study revealed the emission of terpenes and terpenoids from air fresheners can reach levels of tens to hundreds µg/m³.

Destaillats et al. (2006) focused on the secondary pollutants generated when emissions from fragranced products (such as an air freshener) reacted in the presence of ozone found that the production of secondary pollutants such as aldehydes and particles was mainly dependent on ozone concentration, but also influenced by parameters such as the air change rate. The air freshener in the study had more than 30 components including the following five compounds which exhibited significant reactivity to ozone: d-limonene, linalool, linalyl acetate, dihydromyrcenol, and β-citronellol. Table 2 summarizes results from chamber studies conducted with focus on this group of five compounds as well as the volatile oxidation products generated after interaction with different levels of ozone. When the reactive components of the air freshener were in the chamber with high ozone levels (3ACH), the resulting concentrations of volatile oxidation products were detected: formaldehyde (41 ± 0.4 ppb), acetone (41 ± 5), glycolaldehyde (13 ± 0.3), formic acid (24 ± 6), and acetic acid (36 ± 23). Experiments conducted at moderate ozone concentrations (approximately half) notably reduced the levels of volatile oxidation products detected (Table 2). A scanning mobility particle sizer

Table 2 VOCs and reaction products of an air freshener with ozone

	High ozone (3ACH)	Moderate ozone (3ACH)
Species	Concentration (ppb)	Concentration (ppb)
Ozone	126 ± 6	63 ± 0.5
<i>VOC components</i>		
d-limonene	121 ± 2	108 ± 3
Linalool	176 ± 3	170 ± 4
Linalyl acetate	66 ± 7	57 ± 3
Dihydromyrcenol	241 ± 3	242 ± 6
β-citronellol	19 ± 1	19 ± 1
<i>Volatile oxidation products</i>		
Formaldehyde	41 ± 0.4	16 ± 2
Acetaldehyde	ND	ND
Acetone	41 ± 5	14 ± 0.6
Glycolaldehyde	13 ± 0.3	7 ± 0.3
Formic acid	24 ± 6	14 ± 6
Acetic acid	36 ± 23	ND

ND = not detected

Data in this table was adapted from Destaillats et al. (2006)

(SMPS) (3071A, TSI Inc) detected particle nucleation events immediately after reactants (i.e., air freshener VOCs and ozone) were mixed in the chamber. Nucleation events were followed by a significant degree of secondary particle growth (Destaillats et al. 2006).

This environmental chamber study demonstrates the potential impact of ozone-initiated chemistry on the formation of secondary volatile pollutants and particles from air fresheners. Given the everyday and widespread use fragranced consumer products such as air fresheners, and the close proximity of humans, use of air fresheners may contribute to indoor exposure to certain secondary air pollutants, including formaldehyde (Destaillats et al. 2006).

VOCs from Product Use Indoors

This section will summarize results from several population-based studies across Europe, Canada, and the USA, as well as a study that investigated indoor levels of VOCs and carbonyl compounds at a large Australian university. In all of the studies in this section, the focus will be on the levels of volatile compounds associated with emissions from fragranced consumer products.

Population-Based Studies

This section provides results of volatile compounds within indoor environments from four population-based studies across Europe, Canada, the UK, and the USA. Main results of the three studies (Mandin et al. 2017; Zhu et al. 2013; Girman et al. 1999) are provided below.

1. *Study of 148 rooms in 37 office buildings across 8 European countries.*

Among the 19 targeted pollutants in this study, all were detected in at least 75% of the offices in both summer and winter seasons. Among the VOCs detected, the highest average concentration was measured for toluene in summer ($4.7 \mu\text{g m}^{-3}$) and for d-limonene in winter ($13 \mu\text{g m}^{-3}$). Compared to other studies of indoor air quality in office buildings, concentrations of benzene, toluene, ethylbenzene, and xylene were lower; and concentrations of α -pinene and d-limonene were higher in the OFFICEAIR buildings. In terms of the potential adverse health effects of volatile compounds, the 5 day average indoor concentrations for formaldehyde and ozone were lower than WHO indoor and ambient air quality guidelines; and for acrolein, α -pinene, and d-limonene, levels were lower than the estimated thresholds for irritative and respiratory effects (Mandin et al. 2017).

2. *Study of 3,857 households, including 3,218 houses, 546 apartments, and 93 other dwellings, across Canada.*

Among the 84 targeted VOCs, 47 were detected in more than 50% of Canadian homes. Among the 47 VOCs detected, 33 of them were higher in houses than in apartments, while only 4 were lower in houses than in apartments. The detection frequencies ranged from 51.62% for 1-propanol to 99.95% for toluene, ethylbenzene, and o-xylene. Compared to previous Canadian population-based studies, the arithmetic means of VOCs in this study were 2–5 times lower than those VOCs in the 1992 study, and the geometric means of VOCs were comparable to those reported in Europe. The VOCs detected within the indoor environments could be emitted from a number of possible common sources, including consumer products (Zhu et al. 2013). Further analysis of the data from this study, including levels of VOCs and associated health effects of the participants, has revealed that exposure to limonene may increase asthma prevalence (Dales and Cakmak 2019).

3. *Study of 56 public and private office buildings across the USA.*

Forty-eight VOCs were measured indoors at quantifiable concentrations. Eight VOCs, including acetone, toluene, m- and p-xlyenes, o-xylene, n-decane, n-undecane, n-dodecane, and nonanal, were detected in all samples. Further, 26 VOCs were found in 81–99% of the samples. Seven, VOCs, including acetone, toluene, d-limonene, m- and p-xlyenes, 2-butoxyethanol, and n-undecane, had the largest average indoor concentrations. Finally, 12 VOCs, including acetone, toluene, d-limonene, m- and p-xlyenes, 2-butoxyethanol, n-undecane, benzene, 1,1,1-trichloroethane, n-dodecane, hexanal, nonanal, and n-hexane, showed highest concentration frequency distributions compared to average indoor concentrations (Girman et al. 1999).

These studies showed that the VOCs within indoor environment can be emitted from several common sources, including fragranced consumer products. These findings can be used to inform risk assessment and risk management of exposure to VOCs within indoor environments. For example, in the OFFICEAIR Study, the use of consumer products (e.g., cleaning and personal care products) was found to be an important determinant of aldehyde and VOC levels in the

buildings. Strategies for reducing emissions included replacement with lower emitting alternative products (Mandin et al. 2017).

Indoor Air Environments at a University

We include selected results from this study as they provide a useful example of emissions associated with fragranced consumer products in everyday indoor locations, namely restrooms, classrooms, and campus services.

Among the 41 compounds analyzed, 17 were detected in all indoor and outdoor locations (i.e., 100% of measurements were above MDL). The concentrations of VOCs in outdoor (ambient) air were also evaluated in the study. These compounds were isobutane, n-butane, ethanol, 2-methylbutane, benzene, toluene, ethylbenzene, o-, m-, p-xylene, α -pinene, d-limonene, formaldehyde, acetaldehyde, acetone, methyl glyoxal, and hexaldehyde (Goodman et al. 2018). Notably, the hazardous air pollutants formaldehyde, benzene, toluene, and o-, m-, p-xylene were detected in all indoor and outdoor locations. In addition to these 17 compounds, 5 compounds (i.e., styrene, β -pinene, eucalyptol, naphthalene, and glyoxal) were detected in all indoor locations, and in up to 75% of outdoor locations. Benzothiazole was the only compound present in all indoor locations, but not at all outdoors.

Table 3 provides the ratios of indoor concentrations to corresponding outdoor concentrations (I/O ratios) for campus services, restrooms, and classrooms (i.e., three of the six indoor categories). Indoor concentrations were higher than outdoor concentrations for nearly all VOCs measured (above MDL).

Within each environment, the compounds with the highest I/O ratios were as follows: d-limonene (331) and ethanol (168) in campus services; ethanol (290) and d-limonene (123) in restrooms; and hexaldehyde (214) and styrene (84) in classrooms (Table 2). For terpenes and terpenoids, the highest I/O ratios were for d-limonene, measured in campus services and restrooms, and for α -pinene and β -pinene, measured classrooms (Fig. 1).

Table 4 shows the 12 most prevalent compounds in each category of indoor environment, ranked by concentration. Across all three environments, the most prevalent compounds at the highest GM concentrations were ethanol, formaldehyde, acetaldehyde, acetone, toluene, n-butane, 2-methylbutane, and d-limonene.

Explanations for higher levels indoors can be explored using the distinguishing features of each indoor environment.

In campus services, ethanol, d-limonene, n-butane, acetone, 2-methylbutane, and formaldehyde were among the most prevalent compounds at the highest concentrations. Many of the compounds identified in campus services have been associated with consumer products and cleaning supplies in previous studies (Steinemann 2015; Nazaroff and Weschler 2004).

In restrooms, ethanol, isobutane, d-limonene, acetone, and formaldehyde were among the most prevalent compounds at the highest concentrations. These compounds are frequently detected in studies of air freshener emissions and cleaning products (Steinemann 2015; Kim et al. 2015; Uhde and Schultz 2015). Yurdakul et al. (2017) identified cleaning agents and air fresheners as sources of VOCs in university offices. In another study, regular morning peaks in the concentration of

Table 3 Concentration range (minimum–maximum), geometric mean (GM), geometric standard deviation (GSD), and median indoor to outdoor concentration ratios for VOCs measured in all indoor environments

Compound	Method detection limit (MDL) ^a (µg/m ³)	Indoors % below MDL	Campus services (n = 4)			Restrooms (n = 2)			Classrooms (n = 3)			Outdoors (n = 8)			
			%	Range (µg/m ³)	GM (µg/m ³)	I/O	Range (µg/m ³)	GM (µg/m ³)	GSD	I/O	Range (µg/m ³)	GM (µg/m ³)	GSD	I/O	
<i>Isobutane</i>	0.03	0	0	1.7–11.6	4.8	2.0	5	5.2–312	40.4	7.7	100	2.6–3	2.9	1.1	3
<i>n-Butane</i>	0.04	0	0	3.4–17	8.2	1.8	5	4.4–170	27.5	6.2	33	5–7.8	5.9	1.2	3
<i>Ethanol^b</i>	0.03	0	0	9.8–462	61.3	5.4	168	16.3–628	101	6.2	290	25.5–50.7	34.1	1.3	8
<i>2-Methylbutane</i>	0.03	0	0	3.1–23	7.5	2.2	5	1.9–6.5	3.6	1.8	4	4.7–6.1	5.2	1.1	3
<i>Benzene</i>	0.02	0	0	0.2–1	0.5	1.8	3	0.4–0.5	0.4	1.0	2	0.7–1	0.9	1.1	3
<i>Trichloroethylene</i>	0.03	25	50	MDL–0.4	0.2	1.7	–	0.1–0.3	0.2	1.2	1	1.6–1.8	1.7	1.1	13
<i>Methyl methacrylate</i>	0.03	93.75	100	MDL	–	–	–	MDL	–	–	–	MDL	–	–	MDL
<i>Toluene</i>	0.02	0	0	1.4–7.3	2.8	2.0	3	5.1–5.7	5.4	1.0	4	13.1–81.9	25.5	2.3	6
<i>Tetrachloroethene</i>	0.03	6.25	12.5	MDL–0.7	0.2	3.6	3	0.1–0.2	0.2	1.2	3	0.2–0.3	0.2	1.1	1
<i>Ethylbenzene</i>	0.01	0	0	0.3–1.3	0.6	1.6	4	0.5–0.7	0.6	1.1	2	1.3–2.8	1.8	1.3	3
<i>p-Xylene</i>	0.02	0	0	0.6–2.4	1.2	1.6	3	1.1–1.3	1.2	1.1	3	3.2–5.5	4.1	1.2	4
<i>m-Xylene</i>	0.01	0	0	0.2–1	0.5	1.8	3	0.3–0.5	0.42	1.1	2	1–1.9	1.3	1.2	3
<i>Styrene</i>	0.03	0	50	0.1–1.6	0.4	2.3	–	2.1–3.8	2.9	1.3	–	4–9.9	5.9	1.5	84
<i>o-Xylene</i>	0.04	0	0	0.4–1.6	0.8	1.6	5	0.5–0.8	0.7	1.1	–	2.5–3.5	2.9	1.1	5
<i>R(-)3,7-Dimethyl-1,6-octadiene</i>	0.03	62.5	100	0.1–2.3	0.61	3.3	–	MDL–25.0	0.9	28.7	–	MDL	–	–	MDL
<i>a-Pinene</i>	0.03	0	0	0.5–1.7	1.0	1.5	18	0.6–2	1.0	1.8	30	10.4–35.8	17.3	1.7	53

(continued)

Table 3 (continued)

Compound	Method detection limit (MDL) ^a	Indoors % below MDL	Outdoors % below MDL	Campus services (<i>n</i> = 4)				Restrooms (<i>n</i> = 2)				Classrooms (<i>n</i> = 3)				Outdoors (<i>n</i> = 8)			
				($\mu\text{g}/\text{m}^3$)	($\mu\text{g}/\text{m}^3$)	($\mu\text{g}/\text{m}^3$)	($\mu\text{g}/\text{m}^3$)	($\mu\text{g}/\text{m}^3$)	($\mu\text{g}/\text{m}^3$)	($\mu\text{g}/\text{m}^3$)	($\mu\text{g}/\text{m}^3$)	($\mu\text{g}/\text{m}^3$)	($\mu\text{g}/\text{m}^3$)	($\mu\text{g}/\text{m}^3$)	($\mu\text{g}/\text{m}^3$)	($\mu\text{g}/\text{m}^3$)	($\mu\text{g}/\text{m}^3$)		
<i>β-Pinene</i>	0.03	0	75	0.2–1.3	0.5	1.8	—	0.5–1.7	0.9	1.8	—	6.8–9.5	7.8	1.2	52	MDL–0.2	0.04	1.9	
<i>d-Limonene</i>	0.03	0	0	5.7–30.6	12.6	1.9	33.1	30.6–41.1	35.5	1.2	123	4.8–14.9	7.4	1.6	53	MDL–0.3	0.07	2.2	
<i>Eucalyptol</i>	0.03	0	37.5	0.4–1.9	1.1	1.7	18	2.8–5.1	3.8	1.3	—	0.6–1.2	0.8	1.3	16	MDL–0.2	0.05	1.7	
<i>2-Methyl-6-methylene-2-octanol</i>	0.03	68.75	100	MDL–3.6	0.2	7.5	—	MDL–56.5	1.3	43.4	—	MDL	—	—	MDL	—	—	—	
<i>Phenylethyl alcohol</i>	0.03	93.75	100	MDL	—	—	—	MDL–17.7	0.7	24.3	—	MDL	—	—	—	MDL	—	—	
<i>Phenylmethyl acetate</i>	0.03	43.75	100	MDL–0.5	0.2	2.2	—	0.2–10.0	1.7	6.0	—	MDL	—	—	—	MDL	—	—	
<i>α-Methylbenzyl acetate</i>	0.03	87.5	100	MDL–0.1	0.03	1.0	—	1.8–15.8	5.5	2.9	—	MDL	—	—	—	MDL	—	—	
<i>Naphthalene</i>	0.03	0	75	0.1–0.3	0.2	1.2	—	0.1–0.3	0.2	1.3	—	1–1.5	1.3	1.2	35	MDL–0.04	0.03	1.1	
<i>Benzothiazole</i>	0.03	0	100	0.1–0.6	0.3	1.7	—	0.5–0.8	0.7	1.2	—	3.3–5.8	4.4	1.2	—	MDL	—	—	
<i>4-tert-Butylcyclohexyl acetate</i>	0.03	87.5	100	MDL–3.2	0.2	8.3	—	MDL	—	—	—	MDL	—	—	—	MDL	—	—	
<i>Formaldehyde</i>	0.03	0	0	3.9–18.9	7.2	1.9	3	3.8–9.9	6.2	1.6	4	13.5–26	16.9	1.4	12	0.5–2.4	1.1	1.7	
<i>Acetaldehyde</i>	0.04	0	0	1.7–9.2	3.2	1.9	4	2.7–3.8	3.2	1.2	5	6.5–18.9	9.4	1.6	11	0.1–0.8	0.44	1.9	

<i>Acetone</i>	0.07	0	0	6.1–10.7	8.1	1.2	3	6.7–10.8	8.5	1.3	5	36.4–86.3	48.6	1.5	22	0.5–3.8	1.4	1.8
<i>Acrolein</i>	0.01	100	100	MDL	—	—	—	MDL	—	—	—	MDL	—	—	—	MDL	—	—
<i>Propionaldehyde</i>	0.02	25	100	MDL–2.2	0.14	8.9	—	0.3–0.7	0.5	1.4	—	1.1–7.8	2.3	2.4	—	MDL	—	—
<i>Crotonaldehyde</i>	0.02	100	100	MDL	—	—	—	MDL	—	—	—	MDL	—	—	—	MDL	—	—
<i>MEK</i>	0.10	12.5	62.5	0.3–0.9	0.54	1.6	—	0.5–1.1	0.8	1.4	4	2.2–3.7	2.7	1.24	16	0.1–0.6	0.14	1.9
<i>Methacrolein</i>	0.02	68.75	100	MDL–0.4	0.03	3.7	—	MDL	—	—	—	MDL	0.1	3.9	—	MDL	—	—
<i>Butyraldehyde</i>	0.02	25	100	MDL–1.5	0.2	4.9	—	0.2–0.4	0.3	1.1	5	1–2.6	1.4	1.5	—	MDL–0.06	0.02	1.5
<i>Benzaldehyde</i>	0.04	12.5	87.5	MDL–1	0.3	3.4	—	0.4–0.7	0.5	1.3	—	1.6–2.6	1.9	1.2	38	MDL–0.04	0.04	1.4
<i>Valeraiddehyde</i>	0.03	25	100	MDL–1.3	0.1	5.5	—	0.1–0.3	0.2	1.3	—	2.2–7.5	3.4	1.7	—	MDL	—	—
<i>Glyoxal</i>	0.01	0	12.5	0.1–0.5	0.3	1.7	—	MDL–0.2	0.1	1.6	—	0.1–0.3	0.2	1.1	2	MDL–0.5	0.09	3.6
<i>m-Tolualdehyde</i>	0.03	93.75	100	MDL	—	—	—	MDL	—	—	—	MDL	—	—	—	MDL	—	—
<i>Methyl glyoxal</i>	0.02	0	0	1.8–4.8	2.4	1.5	1	0.3–0.6	0.4	1.3	1	0.8–1.4	1.1	1.2	2	0.1–1.7	0.45	2.5
<i>Hexaldehyde</i>	0.04	0	0	0.1–4.6	0.8	4.1	—	0.4–1	0.6	1.5	—	8.9–27.6	13.2	1.7	214	MDL–0.2	0.05	1.6

a Compounds reported are all above MDL in >50% of locations with corresponding ambient levels above MDL.

b Ethanol concentrations are semi-quantitative due to possible sample breakthrough.

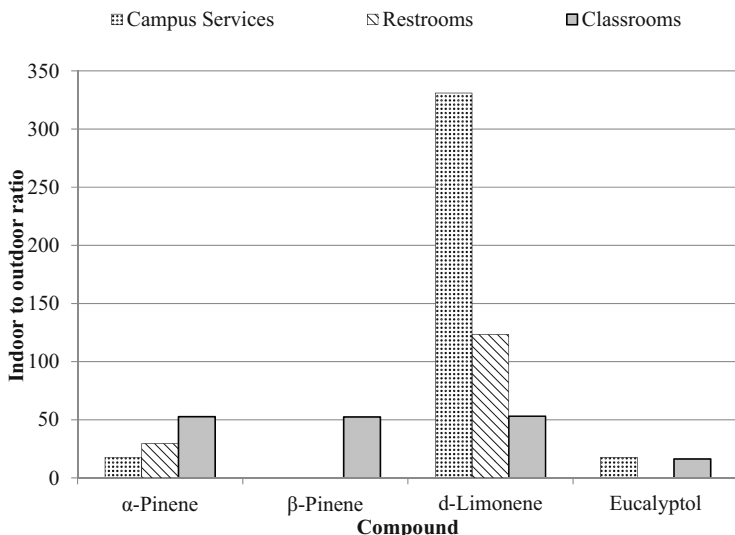


Fig. 1 Indoor to outdoor concentration ratios for terpenes and terpenoids

monoterpenes (range 5–17 ppb) were associated with cleaning activities (Solomon et al. 2008). By comparison, the highest combined concentration of monoterpenes (i.e., d-limonene, α -pinene, and β -pinene) in this study was $60.2 \mu\text{g}/\text{m}^3$ (10.81 ppb) measured in classrooms.

In classrooms, acetone, ethanol, toluene, formaldehyde, and α -pinene were among the most prevalent compounds at the highest concentrations.

Strategies to improve IAQ at a university can be relatively straightforward. For instance, where the primary sources are consumer products such as air fresheners and cleaning supplies, the university has successfully implemented a fragrance-free cleaning policy (in one building). Air fresheners are removed from restrooms, and fragranced cleaning products are used sparingly, if at all. An interesting extension of this study would be the comparison of indoor air quality levels before and after the implementation of fragrance-free policies, or a comparison of similar university environments with and without fragrance-free policies.

Improving Indoor Air Environments

Fragrance-Free Policies and Practices

A fragrance-free policy is a protocol, principle, or plan that is implemented to promote an environment without fragrance. Fragrance-free policies can be implemented by and can apply to a range of different groups and individuals, such as government agencies, industries, organizations, institutions, members, and employees. Fragrance-free policies can apply to a range of physical environments,

Table 4 The 12 most prevalent compounds based on geometric mean concentration

Compound	($\mu\text{g}/\text{m}^3$)	Compound	($\mu\text{g}/\text{m}^3$)
Campus services		Restrooms	
Ethanol	61.3	Ethanol	101
<i>d</i> -Limonene	12.6	Isobutane	40.4
<i>n</i> -Butane	8.2	<i>d</i> -Limonene	35.5
Acetone	8.1	<i>n</i> -Butane	27.5
2-Methylbutane	7.5	Acetone	8.5
Formaldehyde	7.2	Formaldehyde	6.2
Isobutane	4.8	α -MBA*	5.5
Acetaldehyde	3.2	Toluene	5.4
Toluene	2.8	Eucalyptol	3.8
Methyl glyoxal	2.4	2-Methylbutane	3.6
<i>p</i> -Xylene	1.2	Acetaldehyde	3.2
Eucalyptol	1.1	Styrene	2.9
Classrooms		Ambient	
Acetone	48.6	<i>n</i> -Butane	1.5
Ethanol	34.1	Acetone	1.4
Toluene	25.5	Formaldehyde	1.1
α -Pinene	17.3	Toluene	1.1
Formaldehyde	16.9	2-Methylbutane	1.1
Hexaldehyde	13.2	Ethanol	1.0
Acetaldehyde	9.4	Isobutane	0.90
β -Pinene	7.8	Methyl glyoxal	0.45
<i>d</i> -Limonene	7.4	Acetaldehyde	0.44
<i>n</i> -Butane	5.9	<i>p</i> -Xylene	0.43
Styrene	5.9	α -Xylene	0.24
2-Methylbutane	5.2	Ethylbenzene	0.19

such as an individual building, a specific area or floor in a building, a campus with a collection of buildings, or all buildings and facilities of an organization.

A fragrance-free practice is a practical step or action to reduce or avoid emissions, exposures, and effects from fragranced products. A common practice is the use of fragrance-free products. Fragrance-free products can offer similar functionality but without the potential issues associated with fragranced products. For instance, a cleaning or disinfection product may be similarly effective at its primary function without the added fragrance. Further, changes from fragranced to fragrance-free products can reduce terpenes emissions in a relatively short time period.

“Fragrance-free” products are considered as products with the claim of “fragrance-free” or “no fragrance.” To note, “unscented” products are not included in this category, because they may actually contain a fragrance to cover the scent.

Changing from fragranced to fragrance-free laundry products can reduce concentrations of fragrance chemicals (i.e., limonene) emitted from dryer vents by up to 99% within 4 weeks (Goodman et al. 2019). While the term “fragrance-free

products” is not intended to imply emissions-free products, they do offer an option for consumer product functionality without the fragrance compounds.

In addition, removing or discontinuing use of fragrance products can also reduce emissions and exposures. For instance, removing or turning off air fresheners in a restroom can reduce concentrations of fragrance chemicals within indoor environments by up to 96% within 2 weeks (Goodman et al. 2020). Because fragrance molecules can adhere to surfaces during product use, and be reemitted later even without the product in use, reduction may not be 100% immediately, but fragrance compound concentrations can decrease with time.

Moreover, the fact that fragranced products can constitute a barrier to participation in society can come under the auspices of disability legislation. The change to a fragrance-free product, the removal of the fragranced product, or a modification in facilities or operations to mitigate fragrance exposure, for instance, could be considered forms of reasonable accommodation. To this end, fragrance-free practices and policies have been implemented across the countries to accommodate sensitive and vulnerable individuals, as well as to reduce potential health risks and create a more healthful indoor air environment (Steinemann 2019a).

Switching to Fragrance-Free Products

This section presents the results from a study of the volatile emission from residential dryer vents. The study follows the sampling and analytical methods (as described in the section on “[Measurement of VOCs Within Indoor Environments](#)”) and further details can be found in Goodman et al. (2018). Concentrations of d-limonene at each phase of sampling and in each household are provided in Table 5.

In households using fragranced laundry detergent, the highest concentration of d-limonene from a dryer vent was $118 \mu\text{g}/\text{m}^3$ (mean $33.34 \mu\text{g}/\text{m}^3$). By contrast, in households using only fragrance-free detergent, the highest concentration of d-limonene from a dryer vent was $0.26 \mu\text{g}/\text{m}^3$ (mean $0.25 \mu\text{g}/\text{m}^3$). After households using fragranced detergent switched to using fragrance-free detergent, the concentrations of d-limonene in dryer vent emissions were reduced by up to 99.7% (mean 79.1%).

A strength of this study is the participation of households that use the products in everyday life, demonstrating the practicably achievable reductions in concentrations by switching products. Yet this strength has a corresponding limitation in that the households continued to wash clothing as normal, which may have subjected the machines to track-in fragrances from clothing during the 4-week period of using fragrance-free products. In addition, while reductions in d-limonene approached levels of fragrance-free households, it is conceivable that using fragrance-free products for a longer period of time would result in even further reductions, as the residual fragrance chemicals are removed from the machines and clothing. For instance, residual fragrance chemicals in machines could help explain the anomalous value for household #3 for sample (e) showing an increase in d-limonene.

This study demonstrated the improvements to air quality after switching from fragranced to fragrance-free products. It found that, by a change to fragrance-free laundry products, concentrations of d-limonene can be almost completely eliminated from the dryer vent emissions. This strategy may also reduce the formation and

Table 5 Concentration of d-limonene ($\mu\text{g}/\text{m}^3$) in fragranced households, before and after switch from fragranced to fragrance-free laundry product, and in fragrance-free households^a

Household number and type ^b	Laundry room background air				Dryer vent samples, no products				Dryer vent samples, with detergent			
	Before switching from fragranced		After switching from fragranced		Before switching from fragranced		After switching from fragranced		Before switching from fragranced		After switching from fragranced	
	Percentage reduction in d-limonene ($\mu\text{g}/\text{m}^3$)	Sample (a)	Percentage reduction in d-limonene (%)	Sample (d)/(a)	Fragrance-free ($\mu\text{g}/\text{m}^3$)	Sample (g)	Fragrance-free ($\mu\text{g}/\text{m}^3$)	Sample (b)	Fragrance-free ($\mu\text{g}/\text{m}^3$)	Sample (e)	Fragrance-free ($\mu\text{g}/\text{m}^3$)	Sample (f)
#1 (F)	0.70	0.59	15.7	—	1.13	1.02	9.7	—	2.35	1.50	36.2	—
#2 (F)	0.23	0.12	47.8	—	0.13	0.13	89.5	—	10.52	0.13	98.8	—
#3 (F)	0.47	0.25	46.8	—	0.37	0.63	(−70.3)	—	2.51	0.46	81.7	—
#4 (F)	1.28	0.35	72.7	—	0.61	0.26	57.4	—	118	0.36	99.7	—
#5 (FF)	—	—	0.24	—	—	—	0.40	—	—	—	0.26	—
#6 (FF)	—	—	0.35	—	—	—	0.49	—	—	—	0.24	—

^a Sample letters in parentheses refer to protocol in Goodman et al. (2018)

^b (F) = fragranced household; (FF) = fragrance-free household

concentrations of secondary pollutants such as formaldehyde, acetaldehyde, and ultrafine particles. Findings from this study can provide an important foundation for future research, and for demonstrating cost-effective strategies to reduce VOC emissions and personal exposures.

Removing Fragranced Products

This section presents the results from a study of indoor air quality emissions from air fresheners. It demonstrates how air quality within every day indoor environments can be improved by a relatively straightforward approach of switching off or removing the source of VOCs.

Concentrations of d-limonene at each phase of sampling and at each restroom are provided in Table 6.

In restrooms that used air fresheners (#1–4), the concentrations of d-limonene ranged from 5.15 µg/m³ to 9.68 µg/m³ (mean 6.78 µg/m³) on Day 1. After discontinuing use of air fresheners in those same restrooms, the concentrations of d-limonene ranged from (a) 0.23 µg/m³ to 0.72 µg/m³ on Day 3, (b) 0.35 µg/m³ to 1.31 µg/m³ on Day 7, and (c) 0.24 µg/m³ to 2.99 µg/m³ (mean 1.17 µg/m³) on Day 14.

In restrooms that did not use air fresheners (#5–8), the concentrations of d-limonene ranged from 0.23 µg/m³ to 2.29 µg/m³ (mean 0.84 µg/m³) on Day 1, and from 0.60 µg/m³ to 1.34 µg/m³ (mean 1.29 µg/m³) on Day 14.

Table 6 Concentrations and reductions of d-limonene during use, discontinued use, and no use of air fresheners

<i>Restrooms with air freshener used and discontinued</i>					
Restroom #	Air freshener used (Day 1) (µg/m ³)	Air freshener discontinued (Day 3) (µg/m ³)	Air freshener discontinued (Day 7) (µg/m ³)	Air freshener discontinued (Day 14) (µg/m ³)	Reduction in d-limonene on Day 14 (Day 1-Day 14)/(Day 1) (%)
#1	9.68	0.72	0.74	0.72	93%
#2	5.87	0.24	0.95	2.99	49%
#3	5.15	0.83	1.31	0.72	86%
#4	6.43	0.23	0.35	0.24	96%
mean	6.78	0.51	0.83	1.17	81%

Restrooms with no use of air fresheners

Restroom #	No air freshener used (Day 1) (µg/m ³)			No air freshener used (Day 14) (µg/m ³)	
#5	2.29	—	—	1.34	—
#6	0.48	—	—	0.71	—
#7	0.23	—	—	0.60	—
#8	0.36	—	—	2.50	—
mean	0.84	—	—	1.29	—

Key findings are as follows: (1) After air fresheners were discontinued from use, concentrations of d-limonene decreased up to 96% (average 81%) over 2 weeks, and major reductions (i.e., 92%) were accomplished by Day 3. (2) For all samples in all restrooms after air fresheners were discontinued or were not used, d-limonene concentrations were lower than any of the initial samples when air fresheners were in use. (3) After air fresheners were discontinued from use, concentrations of d-limonene approached the lower levels of restrooms that had not used any air fresheners (Goodman et al. 2020).

Thus, these findings suggest that discontinuing the use of air fresheners can have an almost immediate benefit for air quality by reducing d-limonene concentrations. These findings are supported by a prior study of dryer vent emissions (Goodman et al. 2019), which found d-limonene concentrations up to 118 µg/m³ during use of fragranced laundry products, and less than 1 µg/m³ during use of fragrance-free laundry products. After switching from fragranced to fragrance-free products for 4 weeks, concentrations of d-limonene decreased as much as 99.7% (mean 79.1%).

Preferences for Fragrance-free Environments

Nationally representative population surveys, across the four countries (The USA, AU, The UK, SE), found that more people, at least twice as many, prefer fragrance-free environments to fragranced environments, such as workplaces, health care facilities and professionals, hotels, and airplanes. Among vulnerable subpopulations, preferences for fragrance-free environments are even higher. Interestingly, even among individuals who do not report fragrance sensitivity, a majority of these non-fragrance sensitive individuals would nonetheless prefer fragrance-free environments. Specific results are presented by Steinemann (2018a, b, 2019a, b).

For example, for workplaces: 47.8% (53.1%, 42.8%, 44.7%, 50.7%) of the general population would support a fragrance-free policy in the workplace, compared to 20.4% (19.7%, 22.2%, 23.3%, 6.4%) that would not. Also, 56.7% of asthmatic individuals would support fragrance-free workplace policies, compared to 17.7% that would not; 65.5% of autistic individuals would support fragrance-free workplace policies, compared to 24.0% that would not; and 40.4% of non-fragrance sensitive individuals would support fragrance-free workplace policies, compared to 23.4% that would not. Thus, more than twice as many individuals would support (than would not) fragrance-free policies in workplaces.

In summary, across all settings (workplaces, health care facilities and health care professionals, hotels, and airplanes), more than twice as people prefer fragrance-free to fragranced environments. Even a majority of individuals who do not report fragrance sensitivity would nonetheless prefer fragrance-free environments. These findings are juxtaposed with trends of putting fragranced air through indoor environments, even at potential risks to individuals who can experience severe health effects from exposure.

Conclusions

This chapter presented sampling and analytical methods for evaluating the types and concentrations of VOCs and aldehydes associated with emissions from fragranced consumer products. It analyzed and synthesized findings from studies conducted using headspace analysis, in environmental test chambers, and within indoor environments. Fragranced consumer products are ubiquitous in society and emit numerous volatile organic compounds including hazardous air pollutants. However, improvements can be readily made to indoor air quality. Fragranced products can be replaced by fragrance-free versions. Also, fragranced products can be removed entirely with a greater reliance on other approaches such as adequate ventilation. Finally, fragrance-free policies offer a beneficial and broader scale approach to improve indoor air quality.

Cross-References

- Analytical Tools in Indoor Chemistry
 - History and Perspective on Indoor Air Quality Research
 - Indoor Air Quality in Offices
 - Indoor Air Quality in Schools
 - Sampling and Analysis of VVOCs and VOCs in Indoor Air
 - Testing and Reducing VOC Emissions from Building Materials and Furniture
 - The Health Effects of Indoor Air Pollution
 - Very Volatile Organic Compounds (VVOCs)
 - Volatile Organic Compounds (VOCs)
-

References

- ASTM (2017) ASTM D5116-17, standard guide for small-scale environmental chamber determinations of organic emissions from indoor materials/products, ASTM International, West Conshohocken. <http://www.astm.org>
- Bicchi C (2000) Essential oils | gas chromatography. In: Wilson ID (ed) Encyclopedia of separation science. Academic, San Diego, pp 2744–2755
- Coleman BK, Lunden MM, Destaillats H, Nazaroff WW (2008) Secondary organic aerosol from ozone-initiated reactions with terpene-rich household products. *Atmospheric Environment* 42 (35):8234–8245
- Dales RE, Cakmak S (2019) Is residential ambient air limonene associated with asthma? Findings from the Canadian Health Measures Survey. *Environ Pollut* 244:966–970
- Destaillats H, Lunden MM, Singer BC, Coleman BK, Hodgson AT, Weschler CJ, Nazaroff WW (2006) Indoor secondary pollutants from household product emissions in the presence of ozone: a bench-scale chamber study. *Environ Sci Technol* 40(14):4421–4428
- EPA (1997) Determination of gaseous organic compounds by direct interface gas chromatography-mass spectrometry. <https://www.epa.gov/sites/default/files/2020-08/documents/ctm-028.pdf>. Accessed 15 Oct 2021

- EPA (1999) Compendium of methods for the determination of toxic organic compounds in ambient air. Compendium Method TO-15. Determination of volatile organic compounds (VOCs) in air collected in specially-prepared canisters and analyzed by gas chromatography/mass spectrometry (GC/MS). <https://www3.epa.gov/ttnamti1/files/ambient/airtox/to-15r.pdf>. Accessed 02 Feb 2022
- EPA (2014) Method 5021A, Volatile organic compounds in various sample matrices using equilibrium headspace analysis. <https://www.epa.gov/sites/default/files/2015-12/documents/5021a.pdf>. Accessed 15 Oct 2021
- Girman JR, Hadwen GE, Burton LE, Womble SE, McCarthy JF (1999) Individual volatile organic compound prevalence and concentrations in 56 buildings of the building assessment survey and evaluation (BASE) study. *Indoor Air* 99:460–465
- Goodman NB, Steinemann A, Wheeler AJ, Paevere PJ, Cheng M, Brown SK (2017) Volatile organic compounds within indoor environments in Australia. *Build Environ* 122:116–125
- Goodman NB, Wheeler AJ, Paevere PJ, Selleck PW, Cheng M, Steinemann A (2018) Indoor volatile organic compounds at an Australian university. *Build Environ* 135:344–351
- Goodman NB, Wheeler AJ, Paevere PJ, Agosti G, Nematollahi N, Steinemann A (2019) Emissions from dryer vents during use of fragranced and fragrance-free laundry products. *Air Qual Atmos Health* 12(3):289–295
- Goodman N, Nematollahi N, Agosti G, Steinemann A (2020) Evaluating air quality with and without air fresheners. *Air Qual Atmos Health* 13(1):1–4
- IFRA (International Fragrance Association) (2020) IFRA transparency list. <https://ifrafragrance.org/initiatives/ifra-transparency-list>. Accessed 27 Aug 2020
- ISO (2021) 16000-6: Indoor air – Part 6: determination of volatile organic compounds in indoor and test chamber air by active sampling on Tenax TA sorbent, thermal desorption and gas chromatography using MS. FID (ISO/DIS 16000-6)
- Kim S, Hong SH, Bong CK, Cho MH (2015) Characterization of air freshener emission: the potential health effects. *J Toxicol Sci* 40(5):535–550
- Lunny S, Nelson R, Steinemann A (2017) Something in the air but not on the label: a call for increased regulatory ingredient disclosure for fragranced consumer products. *Univ NSW Law J* 40(4):1366–1391
- Mandin C, Trantallidi M, Cattaneo A, Canha N, Mihucz VG, Szigeti T, Mabilia R, Perreca E, Spinazzè A, Fossati S, De Kluijzenaar Y (2017) Assessment of indoor air quality in office buildings across Europe – the OFFICAIR study. *Sci Total Environ* 579:169–178
- Nazaroff WW, Weschler CJ (2004) Cleaning products and air fresheners: exposure to primary and secondary air pollutants. *Atmos Environ* 38(18):2841–2865
- Nematollahi N, Doronila A, Mornane P, Duan A, Kolev SD, Steinemann A (2018a) Volatile chemical emissions from fragranced baby products. *Air Qual Atmos Health* 11(7): 785–790
- Nematollahi N, Kolev SD, Steinemann A (2018b) Volatile chemical emissions from essential oils. *Air Qual Atmos Health* 11(8):949–954
- Nematollahi N, Kolev S, Steinemann A (2019) Volatile chemical emissions from 134 common consumer products. *Air Qual Atmos Health* 12(11):1259–1265
- Nematollahi N, Weinberg JL, Flattery J, Goodman N, Kolev SD, Steinemann A (2021) Volatile chemical emissions from essential oils with therapeutic claims. *Air Qual Atmos Health* 3: 365–369
- Safe Work Australia (SWA) (2020) Hazardous chemical information system (HCIS). Search Hazardous Chemicals. <http://hcis.safeworkaustralia.gov.au/HazardousChemical>. Accessed Oct 2020
- Salthammer T (2009) Environmental test chambers and cells. In: *Organic indoor air pollutants: occurrence, measurement, evaluation*. WILEY-VCH Verlag, Weinheim, pp 101–115
- Singer BC, Revzan KL, Hotchi T, Hodgson AT, Brown NJ (2004) Sorption of organic gases in a furnished room. *Atmos Environ* 38(16):2483–2494

- Singer BC, Destaillat H, Hodgson AT, Nazaroff WW (2006a) Cleaning products and air fresheners: emissions and resulting concentrations of glycol ethers and terpenoids. *Indoor air* 16(LBNL-58250)
- Singer BC, Coleman BK, Destaillats H, Hodgson AT, Lunden MM, Weschler CJ, Nazaroff WW (2006b) Indoor secondary pollutants from cleaning product and air freshener use in the presence of ozone. *Atmos Environ* 40(35):6696–6710
- Solomon SJ, Schade GW, Kuttippurath J, Ladstätter-Weissenmayer A, Burrows JP (2008) VOC concentrations in an indoor workplace environment of a university building. *Indoor and Built Environment* 17(3):260–268
- Stein SE (2008) NIST standard reference database 1A. The National Institute of Standards and Technology NIST, Gaithersburg, pp 1–49
- Steinemann A (2015) Volatile emissions from common consumer products. *Air Qual Atmos Health* 8(3):273–281
- Steinemann A (2018a) Fragranced consumer products: effects on asthmatics. *Air Qual Atmos Health* 11(1):3–9
- Steinemann A (2018b) Fragranced consumer products: effects on autistic adults in the United States, Australia, and United Kingdom. *Air Qual Atmos Health* 11(10):1137–1142
- Steinemann A (2019a) Ten questions concerning fragrance-free policies and indoor environments. *Build Environ* 159:106054
- Steinemann A (2019b) International prevalence of fragrance sensitivity. *Air Qual Atmos Health* 12(8):891–897
- Steinemann A (2019c) International prevalence of chemical sensitivity, co-prevalences with asthma and autism, and effects from fragranced consumer products. *Air Qual Atmos Health* 12(5):519–527
- Steinemann A (2021) The fragranced products phenomenon: air quality and health, science and policy. *Air Qual Atmos Health* 14(2):235–243
- Steinemann AC, MacGregor IC, Gordon SM, Gallagher LG, Davis AL, Ribeiro DS, Wallace LA (2011) Fragranced consumer products: chemicals emitted, ingredients unlisted. *Environ Impact Assess Rev* 31(3):328–333
- Steinemann A, Nematollahi N, Weinberg JL, Flattery J, Goodman N, Kolev SD (2020) Volatile chemical emissions from car air fresheners. *Air Qual Atmos Health* 11:1329–1334
- Steinemann A, Nematollahi N, Rismanchi B, Goodman N, Kolev SD (2021) Pandemic products and volatile chemical emissions. *Air Qual Atmos Health* 1:47–53
- Trantallidi M, Dimitroulopoulou C, Wolkoff P, Kephalopoulos S, Carrer EP (2015) EPHECT III: health risk assessment of exposure to household consumer products. *Sci Total Environ* 536:903–913
- Uhde E, Schulz N (2015) Impact of room fragrance products on indoor air quality. *Atmos Environ* 106:492–502
- USEPA (1984) Method for the determination of volatile organic compounds in ambient air using Tenax adsorption and gas chromatography/ mass spectrometry (GC/MS). Method TO-1, Revision 1.0. United States Environmental Protection Agency. <https://www3.epa.gov/ttnamtl/files/ambient/airtox/to-1.pdf>. Accessed 02 Feb 2022
- US EPA (1999a) Compendium method for the determination of toxic organic compounds in ambient air. Compendium Method TO-17, 2nd edn. Center for Environmental Research Information Office of Research and Development U.S. Environmental Protection Agency, Cincinnati
- US EPA (1999b) Compendium method TO-11A: determination of formaldehyde in ambient air using adsorbent cartridge followed by high performance liquid chromatography. Center for Environmental Research Information Office of Research and Development U.S. Environmental Protection Agency, Cincinnati
- Wallace L, Nelson WI, Ziegenfus R, Pellizzari E, Michael L, Whitmore R, Zelon H, Hartwell T, Perritt R, Westerdahl D (1991) The Los Angeles TEAM Study: personal exposures, indoor-

- outdoor air concentrations, and breath concentrations of 25 volatile organic compounds. *J Expo Anal Environ Epidemiol* 1(2):157–192
- Wang CM, Barratt B, Carslaw N, Doutsi A, Dunmore RE, Ward MW, Lewis AC (2017) Unexpectedly high concentrations of monoterpenes in a study of UK homes. *Environ Sci Process Impacts* 19(4):528–537
- WHO (2010) Guidelines for indoor air quality: selected pollutants WHO, 2010 WHO Regional Office for Europe
- Yurdakul S, Civan M, Özden Ö, Gaga E, Döğeroğlu T, Tuncel G (2017) Spatial variation of VOCs and inorganic pollutants in a university building. *Atmos Pollut Res* 8(1):1–2
- Zhu J, Wong SL, Cakmak S (2013) Nationally representative levels of selected volatile organic compounds in Canadian residential indoor air: population-based survey. *Environ Sci Technol* 47(23):13276–13283



Appliances for Cooking, Heating, and Other Energy Services

6

Tami C. Bond and Zachary Merrin

Contents

Introduction	164
Energy Sources and Energy Services	165
Fuels	165
Energy Services	167
Energy and End Use Data	169
Physical Appliances	170
Cooking Appliances	170
Space Heating Appliances	173
Water Heating Appliances	176
Lighting Appliances	176
Other Appliances	177
Appliance Performance Affecting Indoor Air	178
Efficiency and Energy Intensity	179
Emission Factors and Emission Rates	179
Capture and Unintended Releases	180
Characteristics of Emissions	181
Emission Factors	182
Particle Size Distributions	182
Chemical Composition of Particles	185
Prospects for Reducing Exposure	186
Improved Combustion and Appliances	187
Venting and Ventilation	188
Fuel Processing	189
Fuel Switching	190
Alternative Service Provision	190

T. C. Bond (✉)

Department of Mechanical Engineering, Colorado State University, Fort Collins, CO, USA
e-mail: Tami.Bond@colostate.edu

Z. Merrin

Indoor Climate Research and Training, University of Illinois at Urbana-Champaign, Urbana, IL,
USA
e-mail: zmerrin@illinois.edu

Conclusions	191
Cross-References	191
References	191

Abstract

Appliances employ energy to provide services such as cooking, space heating, water heating, and lighting. Available energy is delivered either by a carrier such as electricity or by combustion of a wide range of fuels ranging from natural gas to liquid fuels to solid coal, wood, or waste. When combustion occurs indoors without direct venting, occupants are exposed to effluents, as they have been throughout human history. Cooktops and cooking stoves have a multitude of forms depending on the fuel and the type of food, and are the most likely appliances to release effluents to occupied space. Devices that provide space heat and water heat are often enclosed, vented, and isolated from the living space, although fugitive emissions can still occur. Lighting has mostly transitioned to electricity although some regions use liquid fuels with high emissions. The nature of combustion alters the mass, particle size distributions, and chemical composition of emissions, with gaseous and liquid fuels yielding lower emissions. Strategies for separating humans from combustion emissions include improving combustion and ventilation, processing fuel, using cleaner fuels, and altering the ways in which energy services are provided. Appliances form part of a complex system that includes humans, infrastructure, and expectations in addition to fuels and devices.

Keywords

Combustion · Energy services · Emissions · Solid fuel · Household air pollution

Introduction

Control of fire is the one event that indisputably brands humans and human society. Anthropologists use indicators of fire control to mark the beginning of humanity (Eiseley 1954; Rolland 2004), and some theorists suggest that the use of controlled heat to degrade food allowed humans to redirect their digestive energy into brain power (Wrangham 2009). Humans' reliance on fire inevitably resulted in proximity to combustion, and inhaling combustion products has been ingrained with human existence. Many of the transitions associated with a modern society were driven by a desire for convenience and progress, and they also distanced humans from fire. Hearth fire migrated from the center of the living space, to enclosure in fireboxes, to sequestration in boilers housed in basements or closets (Pyne 1995). Eventually, combustion left many buildings entirely, relegated to distant steam plants to produce electricity. Now, even those fires are starting to be replaced with energy sources other than combustion. As infrastructure to deliver electricity, water, and natural gas became commonplace, women and men spent less time on collecting fuel, tending

fires, and transporting water. In tasks such as laundering and heating water, energy from combustion supplanted human work, and automation replaced attention. Over time, the combination of devices, energy sources, energy-delivering infrastructure, and human practice and expectations has become an integrated, stable system that may resist replacement of individual elements (Shove 2003; Geels 2005).

Key players in this evolution have been appliances: devices that perform a specific task or set of tasks. This chapter reviews the appliances, both traditional and modern, that play essential roles in delivering energy services. The word “appliance” often refers to devices that are marketed. This chapter uses the term to encompass all devices that fulfill a desired service. Devices that incorporate combustion are emphasized because they are most likely to affect indoor air quality. Appliances in residential buildings appear prominently because they perpetuate the juxtaposition between humans and combustion. The chapter first discusses the energy services that appliances provide and the fuels they use, followed by descriptions of their physical form and function. Performance measures that quantify how appliances affect indoor air appear next, followed by some tabulations of those measures to compare different fuel and device combinations. The chapter closes with a summary of motivations and possible actions to reduce indoor exposure from appliance emissions.

Energy Sources and Energy Services

Fuels

Fuels that power appliances vary by end use and by location (Table 1). Natural gas, primarily composed of methane, has low cost and relatively low emissions. These features make the fuel popular in developed urban areas where distribution

Table 1 Fuels used for combustion that occurs in buildings

Fuel name (other names)	Supply chain
Natural gas	Piping infrastructure
Propane (liquefied petroleum gas, LPG)	Commercial delivery, purchase at outlets
Kerosene (heating oil, paraffin)	Commercial delivery, purchase at outlets
Heating oil	Commercial delivery
Wood	Self-collection, commercial delivery
Charcoal (coal)	Commercial sale, usually from production in rural areas
Coal	Commercial delivery, self-collection
Animal waste (dung)	Self-collection, often involving drying and shaping
Agricultural residue	Self-collection, often involving storage following harvest season
Biomass pellets	Commercial sale, usually from local production
Biomass or coal briquettes	Commercial sale, usually from local production



Fig. 1 Various forms of solid fuel for combustion in homes. Clockwise from top left: firewood and large stored wood, mid-hills, Nepal; large coal chunks and hand-formed flat coal bricks intended for household combustion, China; charcoal made in rural areas to be sold in urban areas, Liberia; corn cobs for igniting fires, China; formed charcoal “honeycomb” briquettes sold by a small commercial enterprise, Nepal; two sizes of firewood and kindling, Shaanxi, China. (Photos courtesy: T. C. Bond except charcoal, E. Floess)

infrastructure is available. Propane is a common fuel choice in rural areas where it is typically delivered via trucks and stored on-site in pressurized tanks. Kerosene is transported and stored as a liquid. Heating oil, which is compositionally similar to diesel fuel, is delivered via truck as a liquid and is most often used to fuel space heating appliances.

Use of solid fuel is common in rural areas and in regions with little infrastructure for electricity and natural gas (Fig. 1). Because solid fuels are often considered inferior energy sources, they often do not have high value and therefore are used locally to meet the needs of homes or small industrial installations. Solid fuels require more user effort and attention compared to other fuels, as the fuel may need processing (e.g., splitting wood) and loading (e.g., filling a pellet hopper), and the appliance requires more frequent and additional cleaning. The most widely used solid fuel is wood from the trunks or branches of trees and bushes. Use of agricultural waste, such as corn stalks and cobs, or rice straw and husks, is extensive where farms exist. Animal waste can also burn when dried. It tends to be used as fuel only in specific cultures, such as in South Asia and the Tibetan Plateau. Fossil-fuel coal is burned in homes and commercial enterprises when it is abundant due to regional coal deposits. Coal use is widespread in East Asia, South Africa, and formerly throughout the United Kingdom and the Northeastern United States. Gathered fuel may also include urban, construction, or household waste to augment the fuel supply and

promote ignition. Self-collected fuels are common when consumers cannot afford delivery of energy sources or when they prefer not to rely on commercially generated energy.

There is an extra challenge in achieving clean and complete combustion of solid fuels because breakdown of the parent fuel and mixing with air occurs simultaneously with oxidation of the combustible fuel products. Quality and repeatability of solid-fuel combustion depends on the dimensions, shape, moisture content, and heating value of solid fuel. Thus, solid fuels may be thermally or physically processed to improve uniformity. Charcoal is the solid residue of wood that has been pyrolyzed in the absence of air, and it burns more uniformly and steadily than wood does because the volatile matter, which causes fluctuating combustion, has already been removed. There is a robust trade between rural areas where charcoal is generated and demand in urban areas, particularly in Africa and South Asia (Mwampamba et al. 2013a). Pellets or briquettes made from biomass or coal can increase physical consistency and improve combustion performance. They are usually made from the original fuel ground to small sizes and constituted into regular shapes, using a binding agent (Whittaker and Shield 2017) or heat in conjunction with high pressure. Such intermediate fuels can create entrepreneurial opportunities, yet they have never become as extensive as the charcoal trade.

Energy Services

Discussion of energy use in buildings often focuses on appliances or broad categories known as end uses: cooking, space conditioning, water heating, and lighting. However, the immutable outcome of interest is neither the end use nor the energy source powering it, but the services provided: hot meals, thermal comfort, enjoyable bathing, and illumination (Fig. 2) (Fouquet 2008; Fell 2017; Brand-Correa et al. 2018). Table 2 summarizes some energy services, associated appliances, and the energy sources that provide power. Because food types and styles are numerous, cooking itself is not a single service; the heat needed may be rapid and targeted or gentle, slow, and thorough. Small farms and agricultural businesses need heat for food drying and processing, preparing animal food, or heating greenhouses.

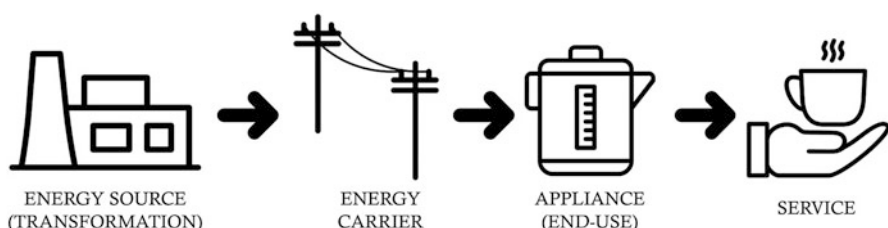


Fig. 2 Appliances fill the demand for energy services, powered by a variety of energy sources. Direct exposure to combustion effluents occurs when fuel combustion provides the source of usable energy and occurs within the appliance and indoor space

Table 2 Energy services and characteristics of appliances that provide them

Service (end use)	Appliance	Typical fuels	Venting
Fried, boiled, steamed food (cooking)	Stovetop burner	NG, LPG, kerosene (E)	Indoors
	Cooking stove	Charcoal, wood, AGR, animal waste, coal, biogas, pellets, briquettes	Indoors
Simmered or slow-cooked food (cooking)	Stovetop burner	NG, LPG (E)	Indoors
	Cooking stove	Kerosene, wood, charcoal, AGR, animal waste, coal, pellets, briquettes	Indoors
Bread (cooking)	Oven	NG, LPG, wood, AGR, animal waste, coal, briquettes (E)	Indoors
Grilled meat (cooking)	Grill	LPG, charcoal, wood, briquettes	Occurs outdoors
Safe food (food drying and preserving)	Food dryer	LPG, charcoal, wood, coal, briquettes (E)	Flue
Thermal comfort (space heating)	Central furnace or boiler	NG, heating oil, wood, coal (E)	Flue
	Wood stove	Wood	Flue (fugit)
	Fireplace	Wood	Flue (fugit)
	Gas fireplace	NG, propane	Flue or indoors
	Space heater	NG, propane (E)	Flue or indoors
Cleaning and bathing (water heating)	Storage water heater	NG, LPG (E)	Flue
	Tankless heater	NG, LPG (E)	Flue
	Cooking stove	Wood, AGR	Indoors
Convenient laundering	Clothes dryer	NG, LPG (E)	Flue
Illumination (lighting)	Hurricane lamp	Kerosene	Indoors
	Wick lamp	Kerosene	Indoors
Aesthetics	Fireplace	NG, wood (E)	Flue (fugit)
	Wood stove	Wood	Flue (fugit)

Fuels: *NG* natural gas, *LPG* liquefied petroleum gas or propane, *AGR* agricultural residue, *E* electric option is available that does not require indoor combustion. Venting: Indoors indicates frequent location, although portable appliances may be used or even installed outdoors. *Fugit* fugitive emissions to the indoor space may occur during door openings or in cases of poor installation

Commercial buildings and schools provide space conditioning and lighting, and some, such as hospitals and prisons, cook for large numbers of people. In some regions, recreational uses such as saunas are popular.

Fire and smoke also provide services beyond those typically associated with energy. Smoke yields distinct food tastes, and in some regions, it is used to preserve building materials or prevent pest infestation. People enjoy observing fire, and wood fireplaces or wood stoves with glass doors are often desirable. Fireplaces fueled by natural gas are more convenient and cleaner burning than wood fireplaces, but to achieve luminous flames and an appearance similar to prototypical fires, their combustion is deliberately imperfect. The desire for secondary services can be a justification to continue use of combustion-based devices in homes.

Energy and End Use Data

Energy carriers delivered via infrastructure, electricity and natural gas, are well metered except for losses and theft. Sales records exist for commercially refined and delivered fuels, such as LPG, heating oil, and kerosene. However, fuels that are collected or traded are not easily monitored. National agencies might report annual consumption data, but this information is often extrapolated from surveys of a limited part of the population in a specific timeframe, and then scaled to population for the relevant year. These reports are shared by national agencies such as the Energy Information Administration in the United States and The Energy and Resources Institute in India. The International Energy Agency, the United Nations, the Food and Agriculture Organization, and British Petroleum gather international energy consumption data. However, traceability of energy data sources is low, and data are shared among agencies; agreement between two data sets usually means they have originated with the same source, rather than providing independent confirmation.

Despite the governing role of the desired service in choosing fuels and appliances, data describing the contribution of each end use to residential and commercial consumption are scarce. Many national surveys inquire about households' primary fuel source but not about end uses. Even when detailed information on specific appliance use exists, quantities of energy used by each appliance are not recorded. Sales of appliances are reported, but disposal is not, so the number and type of appliances in use is not well constrained. This lack of data means that information about combustion appliances that affect indoor air is not known for any individual home without direct observation.

Figure 3 summarizes estimated energy supply for various household end uses in three large regions. Because of the paucity of data, different methods produced the percentage attributions: device surveys in the United States (Energy Information Administration 2015); household surveys in China (Zheng et al. 2014); and reported national fuel consumption combined with proxies in Africa (Winijkul et al. 2016). In all regions, lighting and appliances rely on electricity, while cooking is supplied by electricity and natural gas in the United States, by a diverse mix of sources in China, and dominated by solid fuel in Africa. Space heating, when required, uses more energy than cooking and is more likely to be supplied with cheaper solid fuels. Past government policies in China have favored district heat, which is often supplied by coal but not produced in the home.

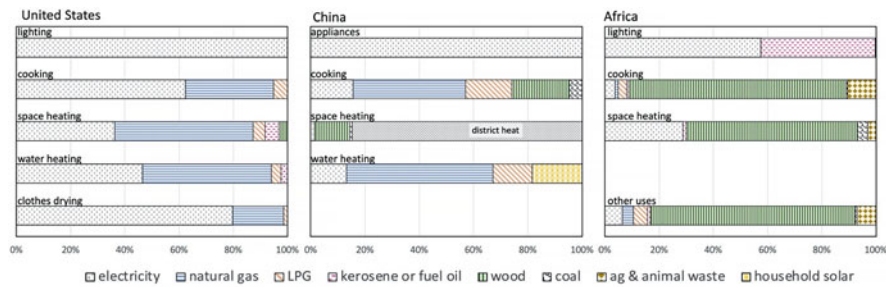


Fig. 3 Main energy sources or carriers providing household end uses. (Left) The United States, 2015; percentages based on number of devices reported in homes (Energy Information Administration 2015). (Center) China, 2012; apportioned energy among end uses based on surveys (Zheng et al. 2014). (Right) Africa, 2010: estimated apportionment among end uses using population and use proxies (Winijkul et al. 2016)

Physical Appliances

This section reviews the diverse forms and functions of combustion appliances that are likely to affect indoor air. Of greatest concern are fuels which are likely to yield products of incomplete combustion (PICs) in large quantities. Even with relatively clean-burning fuels such as natural gas, perfect combustion does not occur in real-world settings, and some pollutants like carbon monoxide (CO) and oxides of nitrogen (NO_x) are generated. These imperfections are more pronounced when the fuels contain impurities, or the appliance is insufficiently cleaned or maintained. Even when combustion is complete, if combustion is not vented, oxygen is depleted and carbon dioxide (CO₂) is elevated in indoor air. Combustion also generates water vapor, which can damage building materials and promote mold growth; in turn, those issues can result in health conditions such as asthma (Mudarri and Fisk 2007).

Cooking Appliances

The most common indoor cooking combustion appliances are stovetop burners, cooking stoves, and ovens. Other appliances not discussed here include outdoor grills, smokers, oil fryers, and butane torches. The most commonly used indoor cooking appliances (cooktops and ovens) are unvented, meaning that they emit all combustion emissions to the indoors. It is generally advisable to use local ventilation when cooking to exhaust combustion emissions and other contaminants generated by the cooking process, which include particulate matter and organic compounds.

Cooktops powered by combustion generate flames that are directly applied to cooking vessels, such as pots, pans, griddles, and woks. The vessel is heated by convection from the flames or exhaust gasses, and by radiation if hot solid fuels or surfaces are present. Household cooktops (Fig. 4) consist of two to five burners,



Fig. 4 Various forms of gas burners. Left to right: single burner connected to an outdoor biogas digester (Nepal, courtesy T. C. Bond); dual-burner cooking appliance supplied by a liquefied petroleum gas cylinder (Tonga, courtesy E. Floess); four-burner gas cooktop connected to natural-gas piping infrastructure (Europe, licensed)

usually of differing sizes, and high-end residential, restaurant, or commercial cooktops can contain many more. Single- or dual-burner appliances are common when households use delivered fuel. Liquid and gaseous fuels are delivered above atmospheric pressure, so the burner power can be modulated with a valve that alters the rate of fuel supply, changing the flame's size and heat release rate.

Cooking stoves are differentiated from cooktops because they have combustion chambers, usually for burning solid fuels. Solid-fuel combustion occurs in several steps, beginning with heating of unburned fuel before ignition, so retaining heat in the chamber is an essential part of continuous combustion. The combustion chamber may be partly enclosed with the flames contacting the pot directly, or it may be fully enclosed, with the heat transferred across a heat-conducting material (Fig. 5). There is a wide variety of strategies to heat pots (Fig. 6), and a similarly great diversity of stove forms depending on the fuel and the food (Westhoff and German 1995). In the simplest cooking “device,” the three-stone fire, the fuel structure itself serves as a combustion chamber. Cooking stoves include supports for either cooking vessels or foods. Controlling the rate of combustion is more difficult and less precise when burning solid fuel, which usually does not have a regular feeding mechanism. Heat release rates can be controlled by the speed of adding new fuel or by limiting airflow for oxidation.

Programs that redesign cooking stoves to improve efficiency and reduce exposure have been numerous. People have sought to improve combustion and reduce smoke for over 200 years (Franklin 1786; Rosin 1939). Widespread sharing of cooking-stove improvements for resource-constrained areas that rely on solid fuel is a more recent phenomenon. Partial enclosure of the combustion chamber with a C-shaped ridge of mud or clay is one of the simplest improvements. Some early “improved” mud stoves were found to worsen the combustion (Smith et al. 2000a) as the thermal mass drew heat away from the reaction. There has been more attention to assessing performance in the intervening years. Insulating combustion chambers is one improvement strategy, found in stoves such as the charcoal-burning Ceramic



Fig. 5 Three Central American stoves with similar cooking functions. (Left) Stove has a partly enclosed combustion chamber and no venting to outdoors. (Center) Stove built in local factory with enclosed, insulated combustion chamber, plancha (flat-top grill) and chimney. (Right) Site-built “Justa” stove with insulated combustion chamber, plancha, chimney, and décor. In this region, the plancha design serves to cook tortillas as well as to heat cooking pots. (Photos courtesy: T. C. Bond)

Jiko (Kinyanjui and Childers 1983) and “Rocket”-type wood stoves (Bryden et al. 2005). Adding chimneys to remove smoke from the living space and increase draft is another possible modification. However, chimneys increase both cost and maintenance requirements.

Combustion improvement in solid-fuel cooking stoves is also an area of active design and development (Reed and Larson 1997; Urban et al. 2002; Shan et al. 2017; Still et al. 2018; Pundle et al. 2019). Modifications include separate control of primary air introduced below the firebox, and secondary air supplied above the combustion. Mechanical fans can create mixing either above or below the fire, and thermoelectric generators can power them when electricity is not available. Separating fuel devolatilization from gas-phase combustion can yield cleaner combustion when stable; this strategy is sometimes called “gasification” by stove designers (Reed and Larson 1997; Mukunda et al. 2010; Clark et al. 2017). Cooking stoves have also been designed to optimize combustion with more reliably performing processed fuels like pellets and briquettes.

Gas ovens usually have one main burner beneath the floor to heat air, which in turn heats the food or other contents. These burners are not adjustable and operate at a fixed fuel consumption rate. During normal operation, the main burner ignites until the oven reaches the set temperature. Temperature is maintained by extinguishing and reigniting the burner, and is determined by the percentage of on-time and the ambient temperature. Ovens may have a second burner for broiling, which provides high and directed heat at the top of the main oven cavity, used for crisping or charring foods such as meats. Some ovens have a lower drawer for broiling that uses the main burner as the heat source. Burners for broiling typically operate continuously, only turning off if the oven overheats. Some older electric ovens required having the oven door partly open during broiling; this practice is outdated and was never applicable to gas broilers.



Fig. 6 Strategies for pot heating when burning solid fuel. Clockwise from top left: three-rock fire (Liberia, courtesy E. Floess); mud-constructed stove with iron bars to hold pot (Tonga, courtesy E. Floess); ceramic-lined, metal-clad insulated charcoal stove (Thailand, courtesy L. Childers); factory-manufactured metal coal stove with primary and secondary air provision (Eswatini, courtesy C. Pemberton-Pigott); multi-pot mud and clay stove with sunken pot holders to improve heat transfer (Nepal, courtesy T. C. Bond); masonry coal cooking stove that also heats water (China, courtesy T. C. Bond). Some of the photographs are taken outdoors, but all of the stove types are used indoors

Space Heating Appliances

Combustion devices for space heating produce heat from combustion and transfer it to the living space. Compared with cooking services, heat for comfort has fewer requirements for heating rates and characteristics. The primary requirement is that most of the heat reaches the air and structure of the living area, instead of escaping in the exhaust gas. Heating appliances include central warm-air furnaces, central hot-water and steam boilers, heating stoves that are free-standing or installed in a wall unit, masonry stoves, and fireplaces. Many climates do not require space heating at all, and people in some regions, instead of using a separate device to heat the space, operate the cooking appliance longer during cooler weather.

Central heating (Fig. 7) is popular because it is convenient and automated. The most common primary heating appliances in the United States homes are central



Fig. 7 Two versions of central heating appliances. (Left) Natural-gas furnace that distributes warm air throughout a building (the United States, licensed). (Right) Multifunctional coal stove that provides space heat by circulating hot water throughout a building and includes a surface for cooking (China, courtesy T. C. Bond). Both devices are vented to outdoors

forced-air furnaces (59% of all households, including electrically heated homes). These devices heat air either through combustion of natural gas or LPG, through electrical resistance, or with electric heat pumps, and distribute the warm air to all indoor spaces through ducts in wall cavities. In addition to space heating, these systems also provide air filtration and can accomplish space cooling and dehumidification. Boilers, or hydronic heating devices, are more common in the rest of the world. They heat water and circulate it around the living area through piping, transferring heat to indoor spaces via radiators. “Combi” boilers, paired with an indirectly heated tank, produce hot water both for space conditioning and for washing and bathing. Central-heating appliances are often housed in basements, closets, garages, or even outdoors in the case of wood boilers. They are almost always vented to outdoors with integral flues. Special cases of central heating include ducting hot exhaust under sleeping surfaces (*kangs* in China) or liquid-based heating of floors and walls (radian heat).

Free-standing heating stoves that burn solid fuels include combustion chambers, similar to cooking stoves. These devices have a similar general form in many regions (Fig. 8). Most often, the combustion chamber is fueled by hand, and the heating rate is controlled by the rate of air supply. The combustion chamber and chimney transfer heat to the living space through radiation and convection, and some stoves include fans to increase convection. Most of these stoves have flues to vent combustion products outdoors, so their main influence on indoor air quality is through leaks in



Fig. 8 Free-standing heating stoves, which have similar form around the world. From left to right: wood stove, Alaska, USA (courtesy P. W. Francisco); wood stove with viewing door, Germany (courtesy E. Floess); coal stove, China (courtesy T. C. Bond)

the flue or its connection to the stove, or through fugitive emissions when doors are open for feeding.

There are two general methods for limiting emissions below minimum certification levels in wood heating stoves: catalytic and secondary combustion (non-catalytic). Both methods allow the stoves to achieve more complete combustion, reducing pollutant emissions and generating additional heat. Some “hybrid” stoves utilize both methods. In catalytic stoves, the exhaust gasses are channeled through a ceramic element inside the stove. This element is coated with precious metals and enables additional chemical reactions, increasing the overall combustion completeness. Effectiveness depends on sufficient contact time between the smoke and the catalytic element. At high burn rates, the smoke may move too quickly through the catalyst for effective pollutant conversion. The catalyst does not work well at low temperatures, and it can become overloaded when emissions are very high during starting and reloading. At these times, the exhaust flow must bypass the catalyst to avoid fouling. The catalyst is a consumable component and must be replaced periodically at intervals determined by stove use, fuel quality, and user behavior.

Combustion improvements without catalysts involve control and preheating of air (Brunner et al. 2009). Air is preheated with a heat exchanger in the exhaust and supplied to the firebox after the primary combustion zone, where it is mixed with the combustion gasses to facilitate additional combustion. Non-catalytic stoves require higher temperatures than catalytic stoves, and those temperatures can hasten degradation of internal components.

Fireplaces and masonry heaters serve a decorative purpose in addition to providing space heat, and they are often located in the main living space. These devices usually have large thermal mass that draws heat from the combustion until it comes to equilibrium, so they provide the most effective space heat when they are operated

continuously. Similar to heating stoves, exhaust products are drawn away from the living space by the draft induced by buoyancy, and fugitive emissions are the main source of indoor air contaminants.

Free-standing or wall-mounted propane, kerosene, or natural-gas burners also provide space heating. Exhaust products can be either vented to outdoors or to indoors; the latter are sometimes advertised as “vent-free” or “ventless.” Ventless space heaters and fireplaces emit all combustion byproducts indoors and are nominally 100% efficient because no heat is lost through a flue. The relatively clean burning of natural gas or propane is the argument for allowing unvented combustion, yet these devices have high exhaust flows and allowing indoor emissions can be controversial. Appliance manufacturers usually recommend opening a window or using mechanical ventilation to avoid negative results, but this guidance relies on user compliance.

Water Heating Appliances

Hot water is used directly for bathing, cleaning, and washing clothes in addition to its application as a working fluid to circulate heat. Both storage water heaters and tankless or on-demand water heaters can be powered by natural gas, liquid fuel, or electricity. Boilers similar to those used for space heating are employed with solid fuel (see previous section). A simple but time-intensive method of obtaining warm water is heating a large pot on a stove used for cooking.

Common storage water heaters rely on natural draft to exhaust the combustion gasses, which rise due to buoyancy through the appliance and the flue. A draft hood, located between the top of the appliance and the bottom of the flue, allows ambient air to mix with the combustion gasses, relieving negative pressure around the burner and preventing downdrafts from extinguishing the flame. This opening in the combustion path also poses a potential hazard if there is a negative pressure in the building, which might be caused by an exhaust fan or improperly balanced conditioning system. In such a case, the buoyancy force might be insufficient to overcome the pressure difference, and the warm exhaust gasses can enter the living space. Some “power vent” water heaters use electric fans to propel exhaust gasses through the flue. Although these appliances reduce the risk of combustion gasses getting into the indoor air, they are more expensive to purchase and operate, and they do not work without electrical power.

Lighting Appliances

Lighting appliances generate illumination so that people can conduct activity when daylight is not available. In regions with electrical infrastructure, lighting is almost wholly electrical; some combustion-powered appliances such as street lighting are maintained for historical or aesthetic reasons, but it occurs outdoors. Because lighting is a small fraction of the total household energy demand in

resource-constrained regions, it is feasible to supply it even with limited electrical services or with solar power.

When lighting cannot be supported by electricity, illumination occurs through combustion that is deliberately not ideal (Fig. 9). The glow of an orange flame is caused by carbon particles that are the product of incomplete combustion, so that the sooty burning of kerosene or paraffin in simple wick lamps provides illumination. Emissions from this type of lighting can be extremely high. “Hurricane” lamps can enclose a glowing flame before burning out carbon particles, reducing emissions. Open flames in cooking stoves are also used for illumination.

Other Appliances

When electrical service is unreliable, households and businesses maintain backup generators powered by natural gas, propane, gasoline, or diesel fuel, with either two-stroke or four-stroke construction. In some world regions, regular, targeted power cuts occur to balance loads on central electrical plants, a practice known as



Fig. 9 Two fuel-powered lighting appliances. (Left) Kerosene wick lamp showing characteristic smoke. (Courtesy: N. Lam and A. Pillarsetti). (Right) Enclosed hurricane lamp (licensed)

“load shedding” (Koirala and Acharya 2022). Although generators are kept outdoors, they may be operated in close proximity to the living space, such as in courtyards.

Space cooling and refrigeration are consequential in energy consumption, but are almost completely supplied by electricity, and thus do not affect indoor air quality except for managing moisture content. An exception is combustion of natural gas or propane in absorption pumps, which can drive cooling cycles.

Clothes drying appliances are used extensively in some parts of the world, like the United States, and very little in other regions. Most clothes dryers are electric, but some are powered by gas or propane combustion. In combustion appliances, a large airflow vents the combustion gasses and moisture from the clothes to outdoors. Buildup of lint or other obstructions can impede this flow and allow harmful gasses to enter the living space.

Some recreational appliances are not discussed extensively here because they have limited application or because they often have little direct input to indoor concentrations. These include heaters for pools, spas, and saunas; cooking devices such as fire pits, smokers, and charcoal grills; and torches for lighting common spaces.

Appliance Performance Affecting Indoor Air

Appliance characteristics that affect indoor air are: (i) efficiency of converting energy sources to provide energy services; (ii) contaminants produced during energy conversion, which is often a matter of combustion quality; and (iii) escape of contaminants from the device within the indoor environment (Fig. 10).

National and international methods and standards are in force for many appliances. For example, cooking stoves have national or regional standards (AEPC 2016; ANSI 2016; Standards Administration of China 2017) as well as international test procedures and guidelines (ISO 2018a, b). Heating stoves and water-heating devices also have national or regional efficiency and emission standards. Method guidance specifies procedures for operating the device during a test, for measuring contaminant concentrations and other operational characteristics, and for interpreting the data to determine a performance metric. Standards provide maximum or minimum benchmarks for the measured performance metric. These benchmarks may tighten over time as design innovations improve performance.

When performance is sensitive to operational parameters, as it is in biomass stoves or small combustion devices, specifying methods and setting performance standards becomes more challenging. Some of the features responsible for variability may be tightly constrained during compliance testing to achieve reproducibility, so that performance during standardized testing may differ from the in-use performance that affects true indoor and outdoor concentrations (Johnson et al. 2008; Roden et al. 2009). Caution is advised in translating compliance-testing results to infer the influence of appliances on contaminant concentrations.

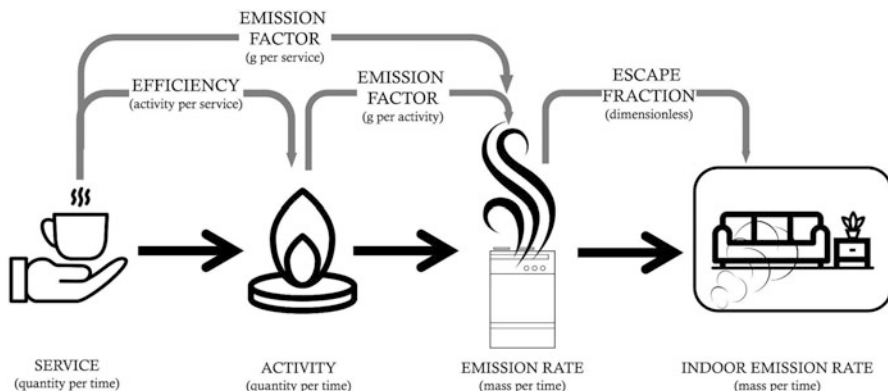


Fig. 10 Relationship between performance measures (upper row) and physical behavior relevant to indoor air quality. Device emission rate has also been used as a performance measure. The emission rate to the indoor environment is needed for models of indoor concentration

Even when contaminants are completely discharged outside the building shell, the exhaust can create a *neighborhood effect*; that is, elevated contaminant levels localized around groups of emitters, which may be returned to the indoor space through re-infiltration. This influence is not further discussed in this chapter, but in areas of high population density, its contribution to indoor air pollution should be recognized.

Efficiency and Energy Intensity

The term *efficiency* refers to a ratio between the quantity of energy used for the desired purpose and the quantity of energy supplied to the device. Efficiency affects indoor air quality because a more efficient device achieves the same service with less energy and less conversion. Appliance performance is often reported in terms of the service, rather than the quantity of energy used. For example, the amount of energy needed to transform the dough of baguette or chapati into the baked product does not appear even in technical discussions about appliances. A common measure related to efficiency is *energy intensity*, or the amount of energy required to perform a service. Another simple performance measure is the rate of energy consumption of a device of a certain size. This measure is appropriate for appliances, such as ovens, that provide many services.

Emission Factors and Emission Rates

An *emission factor* is the ratio between the mass of an emitted contaminant and a defined measure that quantifies the activity emitting the contaminant. The activity in the denominator may be the mass of fuel burned or the service achieved, such as

energy delivered to a cooking pot or lumens of light provided. Emission factors presented as mass of contaminant per mass of fuel burned ($\text{g}_{\text{contam}}/\text{kg}_{\text{fuel}}$) are closely related to the quality of combustion. Emission factors normalized to the service provided (e.g., $\text{g}_{\text{contam}}/\text{MJ}_{\text{service}}$) inherently incorporate the device efficiency as well; a less efficient device produces more contaminants to deliver the same service. Service-based emission factors communicate the causal relationship between service demand and contaminant release, but they can obscure the separate contributions of energy efficiency and of transformation quality.

Emission rates ($\text{g}_{\text{contam}}/\text{s}$) are needed for models of contaminant concentration (Fig. 10). Emission rates are the product of emission factors, which characterizes the device, and the rate of activity, which depends on the user and the situation.

Measured contaminant *concentrations* (g/m^3) are relevant to human exposure, but they alone do not provide emission factors that characterize device performance, or emission rates that are useful for modeling, because the amount of dilution with clean air after combustion is unknown. Determining emission rates requires measurement of the device exhaust flow in addition to concentrations, and then emission factors can be quantified if activity rates are also known. Alternatively, emission factors from carbon-based fuels can be determined by relating the carbon dioxide concentration to the carbon in the original fuel, and then emission rates can be found by applying activity rates. The latter method, known as the *carbon-balance method* or *ratio method*, is somewhat less accurate for fluctuating combustion because it does not account for covariation between emission factors and activity rates. In some measurement methods, either oxygen or carbon dioxide are used to adjust contaminant concentrations to those that would be measured at a certain percentage of excess air supplied to the combustion, and emission factors can be determined from these reports.

Capture and Unintended Releases

Combustion products become indoor contaminants unless they are removed from the environment. The most effective removal occurs by enclosing the entire reaction chamber and exhausting it through a pipe or chimney. Buoyancy, created by the heat of the reaction, is often the driving force expelling the products. The expulsion may also be assisted by a fan. Ventilation devices such as fans or exhaust hoods capture exhaust after it escapes from the appliance. Removal after release is less effective because spillage into the indoor space can occur and cool air entrained into the exhaust products reduces buoyancy. Some appliances, such as cooking stoves and unvented natural-gas fireplaces, have no design for removing combustion products from the indoor space. Some cooktops appear to have ventilation, but the exhaust is returned directly to the living space. For example, microwaves positioned over cooktops contain fans, but these recirculate air rather than exhausting it. Some appliances are designed to remove combustion products but release a small fraction of the generated products through backdrafting (Rapp et al. 2013), poorly sealed joints, or intentional breaches such as door openings during fuel feeding. These leakage or fugitive fractions are not well quantified.

Leaks can occur in fuel delivery systems such as connections, pipes, and pressure cylinders (Merrin and Francisco 2019). Although the device itself is not responsible for these releases, they can be attributed to the presence of the appliance.

Characteristics of Emissions

This section reviews numeric values for some of the performance metrics listed in the previous section. Study results summarized here are representative and not comprehensive; new measurements are reported frequently for highly variable devices like solid-fuel cooking stoves. The tabulation presented here provides a general comparison among devices and fuels. It is useful to identify when performance differs significantly by appliance; under those conditions, mitigation may occur by switching to better fuels or appliances. Recognizing appliances with variable performance also shows where reducing fluctuations and achieving robust performance can produce improvements in indoor and outdoor air quality.

Combustion processes govern emission magnitudes and characteristics. Complete combustion transforms fuel carbon into CO₂, and hydrogen into water. Flame temperature, fuel quality, combustion air quantity, and fuel-air mixing can affect combustion completeness and generate pollutants. PICs range from droplets of the fuel itself to incompletely oxidized compounds such as methane and CO. Flames' orange glow is caused by radiation of soot or black carbon particles (Saito et al. 1987). Light emission during oxidation of certain hydrocarbons is responsible for the appearance of blue flames (Gaydon et al. 1955). Products of incomplete combustion can be eliminated from the exhaust by giving them time to oxidize, by keeping them at elevated temperatures where oxidation reactions are favored, and by ensuring they are mixed with air. These principles are summarized in the aphorism "time, temperature, and turbulence." Emission of PICs is favored when air-fuel mixing is poor and when air entrained into combustion exhaust reduces the temperature. In contrast to PICs, nitrogen oxides, which originate from nitrogen in either air or fuel, form more easily at high temperatures. Appliances with exposed combustion chambers, such as cooktops, cookstoves, or fireplaces, have less control over the factors dictating combustion completeness and are more likely to produce pollutants.

Emissions from solid-fuel combustion are highly variable because of the complexity and diversity of processes. Combustion of large, unprocessed solid-fuel pieces involves a succession of processes: drying, pyrolysis, and release of volatile matter, gas-phase combustion of that volatile matter, and then oxidation of the remaining solid char. These steps occur sequentially, and the release rate of combustible organic matter varies as the pyrolysis front penetrates into the fuel. Imperfect mixing between gas-phase fuel and air causes flickering flames and escape of pollutants. The evolution of these processes depends on interaction between the fuel and the heat available within the combustion chamber, which in turn depends on loading practice. In addition to process fluctuation, the parent fuel has a variety of sizes, moisture contents, densities, and compositions, and may be heterogeneous even within a single piece of fuel. Initiating combustion requires additional material

that is more amenable to ignition, which can add substantial fuel mass (Thompson et al. 2019) and emissions of varying composition (Fedak et al. 2018).

Emission Factors

Mass emission factor, or mass of contaminant emitted per kilogram of fuel burned, is the characteristic that is easiest to measure, and thus, the most often reported. Emission performance can vary even among devices that are apparently similar. Performance differences originate in fuel quality, operator practice, and transient behavior caused by duty cycles (on-off switching). Specifically for solid-fuel stoves, comparative measurements of many devices (Jetter and Kariher 2009; MacCarty et al. 2010) and varying fuel types (Chen et al. 2006) have been reported, and meta-analyses have summarized performance across many studies (Shen et al. 2021). Despite this extensive work, variability among similar solid-fuel burning devices is not predictable.

Table 3 summarizes emission factors of fine particulate matter, carbon monoxide, and nitrogen oxides from some devices for the purpose of contrasting fuel and device combinations. For solid fuels, variability in CO and PM_{2.5} emissions is high, ranging over about a factor of 10 for each fuel-device combination. Carbon monoxide is a substantial part of the emission, representing about 10% of the fuel carbon. Gaseous, liquid, and pellet fuels emit much lower and less variable CO and PM_{2.5}. NOx emission factors have less variability and are similar among all fuel-device combinations.

Particle Size Distributions

Combustion produces mainly fine particles, less than 2.5 μm, by nucleation of gases to form new particles and by condensation of cooling gasses onto existing particles. Peaks of particle-number distributions mainly appear around 0.1–0.2 μm, known as the *accumulation mode*, or around 0.01–0.03 μm, known as the *nucleation* or Aitken mode. When particle precursors have similar chemical composition and temperature histories, all condensable material forms simultaneously and nucleation occurs, so that large numbers of nucleation-mode particles are formed. Initial particle sizes are determined within the highly reactive combustion zone, and as the plume cools through heat loss and entrainment of fresh air, condensation of semi-volatile material and coagulation among particles increases particle sizes (Chang et al. 2004). When particle precursors have similar chemical composition and temperature histories, all condensable material forms simultaneously and nucleation occurs, so that large numbers of nucleation-mode particles are emitted. This phenomenon occurs in combustion of gaseous fuels and sometimes liquid fuels. Combustion that produces high concentrations of precursors with varying volatility is more likely to yield nucleation early in the plume evolution that provides sites for later condensation of material, as is the case with solid-fuel combustion. In combustion without flues, most

Table 3 Emission factors for appliances commonly found in homes. Data are given for relative comparison of fuels and appliances, and are representative but not comprehensive. (#) indicates no data found. Data from laboratory studies are excluded when in-use data are available

Fuel	Appliance	Emission factor (g/kg fuel)			Data sources
		NOx	CO	PM _{2.5}	
Natural gas ^a	Water heater	0.76	0.248	#	Traynor et al. (1996)
	Furnace	0.6–2.1	0.6–0.9	0.0006–0.0032 ^b	Traynor et al. (1996), U.S. EPA (1998a), and McDonald (2009)
	Boiler	2.4	#	0.0009–0.003	McDonald (2009) and Aste et al. (2009)
	Condensing boiler	#	#	0.002	McDonald (2009)
	Cooktop	0.47–1.1	4	#	Traynor et al. (1996) and Lebel et al. (2022)
Heating oil	Oven	0.48–1.2	2.2	#	Traynor et al. (1996) and Lebel et al. (2022)
	Boiler	#	#	0.05–0.06	McDonald (2009)
	Condensing boiler	#	#	0.11	McDonald (2009)
Liquefied petroleum gas	Furnace	#	#	0.96	McDonald (2009)
	Space heater	0.03–0.9	0.7–3.0	0–0.002	Traynor et al. (1990)
	Cooking stove	0.08–3.3	8–19	0.01–0.52	Zhang et al. (1999), Smith et al. (2000a), MacCarty et al. (2010), and Shen et al. (2018)
Kerosene	Lamp (wick)	#	9–16	70–110	Lam et al. (2012)
	Lamp (pressure)	#	3	6–14	Lam et al. (2012)
	Cooking stove (wick)	0.6	8–16	0.1–0.52	Zhang et al. (1999) and Smith et al. (2000a)
	Cooking stove (prs)	1.5	7–62	0.2–2	Zhang et al. (1999), Smith et al. (2000a), and MacCarty et al. (2010)
Wood (unprocessed)	Fireplace	1.2	58–180	1.5–20	Fine et al. (2001), McDonald et al. (2000), Houck and Tiegs (1998),

(continued)

Table 3 (continued)

Fuel	Appliance	Emission factor (g/kg fuel)			Data sources
		NOx	CO	PM _{2.5}	
	Space heating stove	0–6.2	26–140	2.4–24	Dasch (1982), and U.S. EPA (1998b)
	Cooking stove	0.5–0.8	20–220	1–20	U.S. EPA (1998b), Butcher and Ellenbecker (1982), Shen et al. (2013), and Venkataraman and Rao (2001)
	Boiler	0.5–2.4	9–310	0.3–41	Traynor et al. (1990), Roden et al. (2009), and Wathore et al. (2017) ^u
Wood (pellets)	Space heating stove	Nd-4.4	Nd-26	0.4–0.55	U.S. EPA (1996)
	Cooking stove	#	14	0.4	Champion and Grieshop (2019)
	Boiler	0.8–3.6	0.6–22	0.1–1.3	Johansson et al. (2004)
Agricultural waste	Cooking stove	0.2–1.4	27–77	1.7–8.4	Traynor et al. (1990), Li et al. (2007), and Shen et al. (2010)
Animal waste	Cooking stove	#	57–180	12–68	Traynor et al. (1990), Fleming et al. (2018), Jayaratne et al. (2018), and Weyant et al. (2019)
Coal	Heating stove	#	16–120	10–79	Butcher and Ellenbecker (1982) and Macumber and Jaasma (1982)
	Cooking stove	0.15	70–170	3.2–23	Traynor et al. (1990), Shen et al. (2013), and Thompson et al. (2019)

^aAssumptions for converting natural-gas emission factors: non-condensing appliances, LHV = 34.6 MJ/m³; Condensing appliances, HHV = 38.3 MJ/m³, density at standard conditions: 0.711 kg/m³

^bHigher values are for cycling

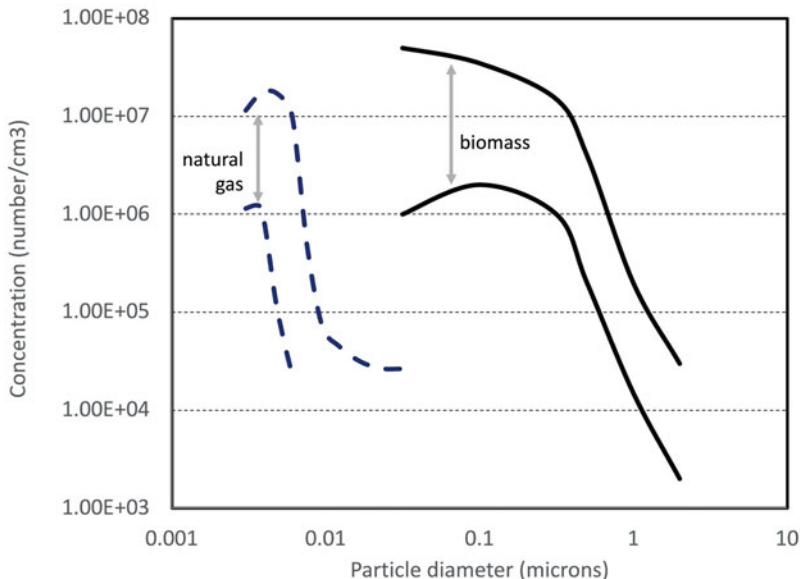


Fig. 11 Range of particle size distributions emitted from biomass (Li et al. 2007) and natural gas (Minutolo et al. 2008). Concentrations are normalized to 3% excess air

of this transformation takes place within the first few seconds, while temperatures and particle concentrations are high (Mena et al. 2017). Coarse particles, larger than $2.5\text{ }\mu\text{m}$, are usually emitted only when particles of ash or unburned fuel are present and when the exhaust air has enough draft to lift them.

Figure 11 compares particle sizes and concentrations from combustion of natural gas and of biomass. There have been many measurements of size distributions indoors or in plumes that are dominated by combustion products. These reports confirm that typical size distributions have number peaks in nucleation or accumulation modes; that particle sizes from gas, propane, and charcoal combustion are more likely to appear in the nucleation mode, and that unprocessed biomass fuels usually produce accumulation-mode particles (Ogulei et al. 2006; Tiwari et al. 2014; Shen et al. 2017; Xue et al. 2018). A few studies show that better combustion tends to make more, smaller particles that are less likely to be visible and that may have different health effects than larger ones (Masekameni et al. 2018). Most measured size distributions are not adjusted to a common dilution that allows comparison of the total number emitted from each fuel or service; Fig. 11 shows some exceptions.

Chemical Composition of Particles

Both the parent fuel and the combustion process affect the composition of emissions. When combustion yields only nucleation-mode particles with low mass, standard

chemical analysis may not be possible. Spectroscopic analysis has shown that very small particles from natural gas combustion may include molecules that contain only one or two aromatic rings (Minutolo et al. 2008).

The formation processes of accumulation-mode particles govern their overall composition. A special sequence of reactions very near flames builds graphitic structures through addition of carbon radicals to form soot or *black carbon* (Haynes and Wagner 1981; Frenklach 2002; Michelsen et al. 2020). Soot-forming reactions are favored when the parent fuel contains aromatic compounds (Han et al. 2021). Unburned fuel that is incompletely oxidized or completely unaltered is emitted in both particulate and gas phases (Simoneit et al. 1993; Schauer et al. 2001; Zhang et al. 2018). In atmospheric chemistry and source apportionment studies, this material is broadly termed *organic carbon*. Poor combustion can produce large quantities of organic carbon, with instantaneous emission factors ranging over four orders of magnitude; in contrast, black carbon emission factors have less variability (Weyant et al. 2019).

Fuels contain inorganic components such as metals, which are emitted either after vaporization, reaction, and condensation, or by mechanical release (Flagan and Friedlander 1978; Linak and Wendt 1998). Manufactured fuels contain ash-forming elements such as calcium and potassium, as well as heavy metals, depending on the origin of the feedstock (Chandrasekaran et al. 2012). These compounds appear in respirable particulate emissions (Kleeman et al. 1999; Johansson et al. 2003; Sanchis et al. 2014).

Sample treatment, especially dilution, affects the reported composition of emitted gases and particles, as well as mass emission factors for the separate phases. Many combustion emissions contain semi-volatile organic material (May et al. 2013) for which partitioning between gaseous and particle phases depends on concentration and temperature (Lipsky and Robinson 2006). This phenomenon can produce large differences in particulate emissions measured using heated sampling lines, compared with those measured after dilution or cooling.

Only a small percentage of the hundreds of organic compounds emitted from biomass combustion are amenable to quantification by gas chromatography. Levoglucosan is a primary constituent that is often used as a tracer (Simoneit et al. 1999; Weimer et al. 2008). Other identified components include polycyclic aromatic hydrocarbons, sugars other than levoglucosan, resin acids, substituted phenols, and substituted syringols (Evans and Milne 1987; Schauer et al. 2001; Fine et al. 2002; Bi et al. 2008).

Prospects for Reducing Exposure

Human exposure to indoor combustion products has decreased throughout history because of shifts associated with modernization. These changes provided cleaner and more convenient fuels or energy carriers through infrastructure or supply chains. They isolated fires in enclosed fireboxes and allowed their separation from the living space through automation. This societal and technological transformation continues.

When modern infrastructure has been developed, exposure to combustion products becomes a matter of preference and comparative cost. Some people prefer to heat with wood or to cook with natural gas even when other energy sources are available. Natural gas is often much cheaper than electricity, and unprocessed solid fuels can be cheaper still when they are self-collected.

Government, industry, and donor programs designed to improve indoor air quality through action on appliances have a variety of motivations. Although improved health may be one of the most obvious benefits, governments usually lack standing to regulate people's behavior in their own homes. Consumer safety and protection is a motivation for regulating appliance efficiency and emissions through standards. Combustion products travel outdoors and lead to deterioration of urban or regional air quality, so device emission limits may be imposed under ambient-air regulations. Governments enact national energy policy by imposing tariffs or taxes that favor certain fuels. Avoiding deforestation has sometimes been a driver for curtailing wood or charcoal use.

The desire to reduce climate change also leads to new perspectives on combustion. All carbon-based fuels generate the greenhouse gas carbon dioxide (CO₂) when burned, the largest contributor to anthropogenic climate change. In the context of reducing greenhouse-gas emissions, it is envisioned that most energy services in buildings will be provided by electricity generated without combustion – by solar photovoltaic panels, wind turbines, hydroelectric installations, or nuclear power plants. This scenario also assumes that indoor combustion will wane in popularity. A common assumption is that biomass fuels are preferred for climate protection over fossil fuels because they are “carbon-neutral” – that is, the emitted CO₂ is rapidly taken up by regrowth. This assumption is valid only when biomass is renewably harvested (Bailis et al. 2017) and when the products of incomplete combustion do not also have climate impacts (Smith et al. 2000b; Bond et al. 2004).

Improved Combustion and Appliances

Emissions from solid-fuel combustion are comparatively high and cooking emissions often occur indoors, so the effects of this combustion on human health are large (Soriano et al. 2020; Yun et al. 2020). Particular attention has been given to improving combustion in cooking stoves and disseminating those devices where solid-fuel use is common. Increased efficiency and reduced emissions can decrease exposure. Strategies such as retaining heat, increasing turbulence, or gasification (outlined in the section “Physical Appliances”) are deployed in factory-built cooking stoves or by programs that develop and implement improved-stove projects. Collaborations such as the Clean Cooking Alliance have gathered parties ranging from entrepreneurs to development organizations to public health professionals who share interest in affecting change.

Despite widespread agreement that modified combustion could improve indoor air quality, there are many challenges to displacing “traditional” combustion. Some cooking stove designers have neglected to consult with users or ensure good

performance, yielding poor products and a lack of market confidence. Manufacturers may respond to user demands to make stoves more marketable, and some of these changes may decrease combustion quality while increasing usability. An example is increased firebox dimensions to accommodate large fuel sizes, which require less feeding but produce smoke more easily. Users continue to employ traditional stoves if the replacements do not fulfill all the services required, a phenomenon known as “stacking” (Ruiz-Mercado and Masera 2015; Shankar et al. 2020). Household resources are often directed to achieve convenience, income generation, or added services such as mobile communications, instead of improved health. This low priority for health can be exacerbated when women, the predominant cooks and stove users, do not have strong voices in household decisions (Lindgren 2020). For these reasons, adoption and persistence of improved cooking stoves can be poor (Mobarak et al. 2012; Ramanathan et al. 2017). This apparently daunting set of obstacles reflects the insufficiency of effecting change in a complex system through simple technological replacement.

In contrast to solid-fuel appliances, modern gas appliances have relatively complete combustion and generate low amounts of pollutants other than CO₂. Even in this relatively clean burning, perfectly complete combustion is unrealistic outside of controlled laboratory settings (Lebel et al. 2022). Appliances naturally generate small quantities of pollutants, which increase as the appliance ages, fouls, and degrades. Although the large number of appliances worldwide may produce meaningful amounts of pollutants in the aggregate, complete elimination of pollutants by addressing each individual unit may not be feasible or cost effective.

Preventative maintenance of appliances aids in extending life span and keeping their performance. This maintenance is usually initiated by individual consumers, although it may be implemented by heating, ventilation, and air conditioning professionals. Inspection of stoves and ovens includes cleaning and ensuring that all elements such as burner caps and bases are correctly positioned, and that flames are symmetrical, consistent, and not excessively luminous. Preventative maintenance visits for combustion heating appliances, sometimes referred to as “clean and tune,” can include a wide range of services depending on the equipment type and condition, client requests, and the technician themselves. Technicians inspect and clean burners, adjust burner firing rates, and examine the condition of mechanical components such as blowers, pumps, and valves. They inspect heat exchangers, exhaust pipes, and fuel supply lines for integrity. On central warm-air systems they measure static pressure or temperature rise between supply and return air to determine whether the furnace is moving the appropriate amount of air. They use measured flue gas temperature and composition to assess appliance efficiency and excess air, and diagnose combustion issues. When the service reveals problems, the technician completes minor repairs, or recommends upgrades or replacements.

Venting and Ventilation

Ventilation and venting strategies remove combustion effluents from indoor air with varying efficiency (Fig. 12). In spaces without mechanical ventilation, air exchange

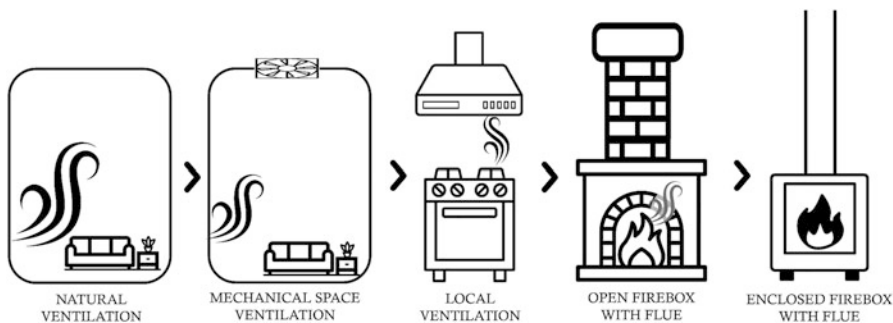


Fig. 12 Appliance ventilation and venting strategies for removal of combustion effluents, from least directed (left) to most directed (right)

is driven only by naturally occurring pressure differences. Air exchange rates can be very high in buildings where envelope sealing is limited; however, these “leaky” buildings are associated with resource-limited situations where emission rates may also be high.

Mechanical ventilation is incorporated into well-designed buildings, and as buildings have gotten more airtight to increase energy efficiency, intentional ventilation has become increasingly important to maintain adequate indoor air quality. Standards such as ASHRAE 62.2 in the United States (ASHRAE 2019) dictate minimum ventilation requirements for residential buildings to provide necessary fresh outdoor air. However, regardless of ventilation rates, exposure occurs if effluents are allowed to escape into the occupied space. Standards also specify local ventilation requirements in kitchens and bathrooms, removing contaminants generated from activities such as cooking and bathing before they completely disperse into the occupied space, and emission plumes may be incompletely captured by this local ventilation (Lunden et al. 2015). Exhaust hoods relying on natural draft have also been employed when electricity is unavailable (Bates 2008).

The most reliable venting strategy is the complete enclosure of combustion products within a firebox, attached to a flue with sufficient draft to expel pollutants. Openings between the firebox and the occupied space allow escape of combustion effluents, and also allow entrainment of fresh air, reduce exhaust temperatures, and diminish the buoyancy that creates draft.

Fuel Processing

Homogeneous fuels increase the reliability and predictability of combustion. Liquid and gaseous fuels have already undergone refinement, and it is in large part this isolation of fuel with specific volatility that enables clean and reliable combustion. Homogenizing solid fuels can also improve consistency, so that processed fuels are favored for their convenience; this transformation can also reduce emissions. The fuel is first broken down either thermally, or physically by grinding or pulverizing. The product of decomposition can either become pellets by forming it into small

pieces of consistent size and shape, or into briquettes by reconstituting the fuel with a binder. Processed, dried solid fuel may be advantageous in regions where residue from agricultural, forest, or mining activity is widespread (Zhi et al. 2009; Akowuah et al. 2012; Mwampamba et al. 2013b), although it is still more expensive than self-collected fuel.

Fuel Switching

An “energy ladder” of increasing fuel desirability, from waste to wood to gas and electricity, has been posited (Hosier and Dowd 1987; Leach 1992; Smith et al. 1994). Although this shift does describe aggregate transitions, the simple energy ladder does not account for the adaptive behavior exhibited by individuals (Masera et al. 2000; Hiemstra-van der Horst and Hovorka 2008), who use multiple fuels and devices to meet a variety of energy needs.

Countries including India and Indonesia have decades-long histories of subsidizing cleaner-burning fuels such as kerosene and liquefied petroleum gas, largely as measures to improve energy provision for impoverished people (Balachandra 2011; Thoday et al. 2018), although there is active discussion about which groups have benefited most from these subsidies (Rao 2012; Soile and Mu 2015). The consequences of indoor solid-fuel use for user health and ambient air quality have stimulated further action to examine and incentivize use of cleaner fuels, especially LPG (Gould and Urpelainen 2018; Thomas et al. 2022). Energy policy in China has emphasized banning residential coal in favor of LPG and electrified appliances, especially in the highly populated areas in the northeast (Liu et al. 2021). Some of these efforts have been tempered by supply limitations. Imported fuels like LPG are subject to price and supply volatility, especially during periods of political instability. Electrical grids that have supported only lighting and mobile phone charging may not have the capacity to transmit sufficient energy to handle peak heating or cooking loads.

Contrasting with efforts to adopt liquid or gas combustion and switch away from solid fuel, some high-income regions are beginning to move away from combustion entirely to avoid greenhouse-gas emissions (Nadel 2019). In 2019, the city of Berkeley, California, passed legislation to ban natural-gas connections to new, low-rise residential buildings. Within the next 2 years, 54 cities and counties in the United States, including New York City, passed similar legislation. These initiatives may have political consequences; in response to city-level initiatives, other states reacted by passing or proposing legislation that prohibited local bans.

Alternative Service Provision

Energy consumption and emissions can be greatly reduced by devices that provide similar services but deliver heat in a different way. Microwave ovens cook more rapidly by exciting water molecules inside food rather than relying on convective or

radiative heat transfer. Induction cooking also avoids heat transfer by heating the vessel directly through magnetic induction. Retained-heat cookers provide insulated compartments to keep heat from escaping a cooking vessel, avoiding the need to maintain its temperature with low-power combustion.

Some of the greatest shifts in reducing exposure are accomplished not by replacing devices or fuels, but by altering behavior so that people obtain desired services through completely different means. As people gain income and lose leisure time, they remove cooking from the home by purchasing prepared foods or eating in restaurants. Less space heating is required when people wear warmer clothing or use electric blankets, adaptations that are enabled by lightweight textiles and inexpensive manufacturing. Such societal transformations are rarely predicted, only observed.

Conclusions

Appliances are key elements of complex energy systems that may result in indoor exposures. Physical components of these systems include the appliances themselves and the fuels they employ, which govern the form of combustion through fuel release and air-fuel mixing. Combustion quality affects quantities, particle size distributions, and chemical composition of emissions, and solid-fuel emissions are usually much greater than those of liquid or gaseous fuels. The combination of emission and ventilation or venting affects indoor exposures. Other social and technical components of these systems include energy device users, occupants, and their expectations for obtaining energy services; infrastructure, supply chains, and markets; and local and national policies on energy, environment, and health. Any of these factors may play a role in promoting or inhibiting transitions to cleaner indoor air.

Cross-References

- ▶ [Cooking Aerosol](#)
 - ▶ [Household Air Pollution in Rural Area](#)
 - ▶ [Influence of Ventilation on Indoor Air Quality](#)
 - ▶ [The Health Effects of Indoor Air Pollution](#)
-

References

- AEPC (2016) Nepal Interim Benchmark for solid biomass Cookstoves. AEPC, Kathmandu
Akowuah JO, Kemausuor F, Mitchual SJ (2012) Physico-chemical characteristics and market potential of sawdust charcoal briquette. *Int J Energy Environ Eng* 3:1–6
ANSI (2016) ANSI standard Z21.1: household cooking gas appliances. ANSI, Washington, DC
ASHRAE (2019) ANSI/ASHRAE standard 62.2-2019: ventilation and acceptable indoor air quality in residential buildings. ASHRAE, Atlanta

- Aste N, Adhikari RS, Del Pero C (2009) Estimation of NO_x emissions associated with the natural gas consumption for residential heating in Italy. In: 2009 International conference on clean electrical power. IEEE, pp 202–206
- Bailis R, Wang Y, Drigo R et al (2017) Getting the numbers right: revisiting woodfuel sustainability in the developing world. Environ Res Lett 12:115002. <https://doi.org/10.1088/1748-9326/aa83ed>
- Balachandra P (2011) Dynamics of rural energy access in India: an assessment. Energy 36:5556–5567. <https://doi.org/10.1016/j.energy.2011.07.017>
- Bates E (2008) Chimney stoves and smoke hood. Appr Technol 35:50
- Bi X, Simoneit BRT, Sheng G, Fu J (2008) Characterization of molecular markers in smoke from residential coal combustion in China. Fuel 87:112–119. <https://doi.org/10.1016/j.fuel.2007.03.047>
- Bond T, Venkataraman C, Masera O (2004) Global atmospheric impacts of residential fuels. Energy Sustain Dev VIII:20–32
- Brand-Correa LI, Martin-Ortega J, Steinberger JK (2018) Human scale energy services: untangling a “golden thread”. Energy Res Soc Sci 38:178–187
- Brunner T, Obernberger I, Scharler R (2009) Primary measures for low-emission residential wood combustion—comparison of old with optimised modern systems. In: Proc. of the 17th European biomass conference, p 2009
- Bryden M, Still D, Scott P et al (2005) Design principles for wood burning cook stoves. Aprovecho Research Center, Cottage Grove
- Butcher SS, Ellenbecker MJ (1982) Particulate emission factors for small wood and coal stoves. J Air Pollut Control Assoc 32:380–384
- Champion WM, Grieshop AP (2019) Pellet-fed gasifier stoves approach gas-stove like performance during in-home use in Rwanda. Environ Sci Technol 53:6570–6579. <https://doi.org/10.1021/acs.est.9b00009>
- Chandrasekaran SR, Hopke PK, Rector L et al (2012) Chemical composition of wood chips and wood pellets. Energy Fuels 26:4932–4937
- Chang M-CO, Chow JC, Watson JG et al (2004) Measurement of ultrafine particle size distributions from coal-, oil-, and gas-fired stationary combustion sources. J Air Waste Manag Assoc 54: 1494–1505
- Chen Y, Zhi G, Feng Y et al (2006) Measurements of emission factors for primary carbonaceous particles from residential raw-coal combustion in China. Geophys Res Lett 33:L20815. <https://doi.org/10.1029/2006GL026966>
- Clark S, Carter E, Shan M et al (2017) Adoption and use of a semi-gasifier cooking and water heating stove and fuel intervention in the Tibetan Plateau, China. Environ Res Lett. <https://doi.org/10.1088/1748-9326/aa751e>
- Dasch JM (1982) Particulate and gaseous emissions from wood-burning fireplaces. Environ Sci Technol 16:639–645
- Eiseley LC (1954) Man the fire-maker. Sci Am 191:52–57
- Energy Information Administration (2015) Residential energy consumption survey. <https://www.eia.gov/consumption/residential/>. Accessed 30 Mar 2022
- Evans RJ, Milne TA (1987) Molecular characterization of the pyrolysis of biomass. I. Fundamentals. Energy Fuels 1:123–137
- Fedak KM, Good N, Dahlke J et al (2018) Chemical composition and emissions factors for cookstove startup (ignition) materials. Environ Sci Technol 52:9505–9513
- Fell MJ (2017) Energy services: a conceptual review. Energy Res Soc Sci 27:129–140. <https://doi.org/10.1016/j.erss.2017.02.010>
- Fine PM, Cass GR, Simoneit BRT (2001) Chemical characterization of fine particle emissions from fireplace combustion of woods grown in the northeastern United States. Environ Sci Technol 35: 2665–2675
- Fine PM, Cass GR, Simoneit BRT (2002) Organic compounds in biomass smoke from residential wood combustion: emissions characterization at a continental scale. J Geophys Res 107:8349. <https://doi.org/10.1029/2001JD000661>

- Flagan RC, Friedlander SK (1978) Particle formation in pulverized coal combustion – a review. In: Shaw DT (ed) Recent developments in aerosol science. Wiley, New York, pp 25–59
- Fleming LT, Lin P, Laskin A et al (2018) Molecular composition of particulate matter emissions from dung and brushwood burning household cookstoves in Haryana, India. *Atmos Chem Phys* 18:2461–2480. <https://doi.org/10.5194/acp-18-2461-2018>
- Fouquet R (2008) Heat, power and light: revolutions in energy services. Edward Elgar Publishing, Cheltenham
- Franklin B (1786) Description of a new stove for burning of pitcoal, and consuming all its smoke, by Dr. Franklin. *Trans Am Philos Soc* 2:57–74
- Frenklach M (2002) Reaction mechanism of soot formation in flames. *Phys Chem Chem Phys* 4: 2028–2037
- Gaydon AG, Moore NPW, Simonson JR (1955) Chemical and spectroscopic studies of blue flames in the auto-ignition of methane. *Proc R Soc A Math Phys Sci* 230:1–19
- Geels FW (2005) Processes and patterns in transitions and system innovations: refining the co-evolutionary multi-level perspective. *Technol Forecast Soc Change* 72:681–696. <https://doi.org/10.1016/j.techfore.2004.08.014>
- Gould CF, Urpelainen J (2018) LPG as a clean cooking fuel: adoption, use, and impact in rural India. *Energy Policy* 122:395–408
- Han Y, Chen Y, Feng Y et al (2021) Fuel aromaticity promotes low-temperature nucleation processes of elemental carbon from biomass and coal combustion. *Environ Sci Technol* 55: 2532–2540. <https://doi.org/10.1021/acs.est.0c06694>
- Haynes BS, Wagner HG (1981) Soot formation. *Prog Energy Combust Sci* 7:229–273
- Hiemstra-van der Horst G, Hovorka AJ (2008) Reassessing the “energy ladder”: household energy use in Maun, Botswana. *Energy Policy*. <https://doi.org/10.1016/j.enpol.2008.05.006>
- Hosier RH, Dowd J (1987) Household fuel choice in Zimbabwe: an empirical test of the energy ladder hypothesis. *Resour Energy* 9:347–361
- Houck JE, Tiegs PE (1998) Residential wood combustion technology review. Environmental Protection Agency, Washington, DC
- ISO (2018a) Clean cookstoves and clean cooking solutions – harmonized laboratory test protocols – part 1: standard test sequence for emissions and performance, safety and durability. International Organization for Standardization, Geneva
- ISO (2018b) ISO/TR 19867-3:2018: clean cookstoves and clean cooking solutions – harmonized laboratory test protocols – part 3: voluntary performance targets for cookstoves based on laboratory testing. International Organization for Standardization, Geneva
- Jayarathne T, Stockwell CE, Bhave PV et al (2018) Nepal Ambient Monitoring and Source Testing Experiment (NAMaSTE): emissions of particulate matter from wood-and dung-fueled cooking fires, garbage and crop residue burning, brick kilns, and other sources. *Atmos Chem Phys* 18: 2259–2286
- Jetter JJ, Kariher P (2009) Solid-fuel household cook stoves: characterization of performance and emissions. *Biomass Bioenergy* 33:294–305. <https://doi.org/10.1016/j.biombioe.2008.05.014>
- Johansson LS, Tullin C, Leckner B, Sjövall P (2003) Particle emissions from biomass combustion in small combustors. *Biomass Bioenergy* 25:435–446. [https://doi.org/10.1016/S0961-9534\(03\)00036-9](https://doi.org/10.1016/S0961-9534(03)00036-9)
- Johansson LS, Leckner B, Gustavsson L et al (2004) Emission characteristics of modern and old-type residential boilers fired with wood logs and wood pellets. *Atmos Environ* 38:4183–4195. <https://doi.org/10.1016/j.atmosenv.2004.04.020>
- Johnson M, Edwards R, Frenk CA, Masera O (2008) In-field greenhouse gas emissions from cookstoves in rural Mexican households. *Atmos Environ* 42:1206–1222
- Kinyanjui M, Childers L (1983) How to make the Kenyan Ceramic Jiko. Energy/Development International, Paris
- Kleeman MJ, Schauer JJ, Cass GR (1999) Size and composition distribution of fine particulate matter emitted from wood burning, meat charbroiling, and cigarettes. *Environ Sci Technol* 33: 3516–3523

- Koirala DP, Acharya B (2022) Households' fuel choices in the context of a decade-long load-shedding problem in Nepal. *Energy Policy* 162:112795. <https://doi.org/10.1016/j.enpol.2022.112795>
- Lam NL, Chen YJ, Weyant C et al (2012) Household light makes global heat: high black carbon emissions from kerosene wick lamps. *Environ Sci Technol* 46:13531–13538. <https://doi.org/10.1021/es302697h>
- Leach G (1992) The energy transition. *Energy Policy* 20:116–123
- Lebel ED, Finnegan CJ, Ouyang Z, Jackson RB (2022) Methane and NO_x emissions from natural gas stoves, cooktops, and ovens in residential homes. *Environ Sci Technol* 56:2529–2539. <https://doi.org/10.1021/acs.est.1c04707>
- Li X, Duan L, Wang S et al (2007) Emission characteristics of particulate matter from rural household biofuel combustion in China. *Energy Fuels* 21:845–851
- Linak WP, Wendt JOL (1998) Comparison of the particle size distributions and elemental partitioning from the combustion of pulverized coal and residual fuel oil. *Combust Sci Technol* 134:291–314
- Lindgren SA (2020) Clean cooking for all? A critical review of behavior, stakeholder engagement, and adoption for the global diffusion of improved cookstoves. *Energy Res Soc Sci* 68:101539. <https://doi.org/10.1016/j.erss.2020.101539>
- Lipsky EM, Robinson AM (2006) Effects of dilution on fine particle mass and partitioning of semivolatile organics in diesel exhaust and wood smoke. *Environ Sci Technol* 40:155–162
- Liu C, Zhu B, Ni J, Wei C (2021) Residential coal-switch policy in China: development, achievement, and challenge. *Energy Policy* 151:112165. <https://doi.org/10.1016/j.enpol.2021.112165>
- Lunden MM, Delp WW, Singer BC (2015) Capture efficiency of cooking-related fine and ultrafine particles by residential exhaust hoods. *Indoor Air* 25:45–58. <https://doi.org/10.1111/ina.12118>
- MacCarty N, Still D, Ogle D (2010) Fuel use and emissions performance of fifty cooking stoves in the laboratory and related benchmarks of performance. *Energy Sustain Dev* 14:161–171
- Macumber DW, Jaasma DR (1982) Efficiency and emissions of a hand-fired residential coalstove. In: Cooper JA, Malek D (eds) *Residential solid fuels*. Oregon Graduate Center, Portland, pp 313–332
- Masekameni DM, Brouwer D, Makonese T et al (2018) Size distribution of ultrafine particles generated from residential fixed-bed coal combustion in a typical brazier. *Aerosol Air Qual Res* 18:2618–2632
- Masera OR, Saatkamp BD, Kammen DM (2000) From linear fuel switching to multiple cooking strategies: a critique and alternative to the energy ladder model. *World Dev* 28:2083–2103
- May AA, Levin EJT, Hennigan CJ et al (2013) Gas-particle partitioning of primary organic aerosol emissions: 3. Biomass burning. *J Geophys Res Atmos* 118:11327–11338. <https://doi.org/10.1002/jgrd.50828>
- McDonald R (2009) Evaluation of gas, oil and wood pellet fueled residential heating system emissions characteristics. Brookhaven National Lab (BNL), Upton
- McDonald JD, Zielinska B, Fujita EM et al (2000) Fine particle and gaseous emission rates from residential wood combustion. *Environ Sci Technol* 34:2080–2091
- Mena F, Bond TC, Riemer N (2017) Plume-exit modeling to determine cloud condensation nuclei activity of aerosols from residential biofuel combustion. *Atmos Chem Phys* 17:9399–9415
- Merrin Z, Francisco PW (2019) Unburned methane emissions from residential natural gas appliances. *Environ Sci Technol* 53:5473–5482. <https://doi.org/10.1021/acs.est.8b05323>
- Michelsen HA, Colket MB, Bengtsson P-E et al (2020) A review of terminology used to describe soot formation and evolution under combustion and pyrolytic conditions. *ACS Nano* 14:12470–12490. <https://doi.org/10.1021/acsnano.0c06226>
- Minutolo P, D'Anna A, Commodo M et al (2008) Emission of ultrafine particles from natural gas domestic burners. *Environ Eng Sci* 25:1357–1364
- Mobarak AM, Dwivedi P, Bailis R et al (2012) Low demand for nontraditional cookstove technologies. *Proc Natl Acad Sci U S A* 109:10815–10820. <https://doi.org/10.1073/pnas.1115571109>

- Mudarri D, Fisk WJ (2007) Public health and economic impact of dampness and mold. *Indoor Air* 17:226–235
- Mukunda HS, Dasappa S, Paul PJ et al (2010) Gasifier stoves – science, technology and field outreach. *Curr Sci* 98:627–638
- Mwampamba TH, Ghilardi A, Sander K, Chaix KJ (2013a) Dispelling common misconceptions to improve attitudes and policy outlook on charcoal in developing countries. *Energy Sustain Dev* 17:75–85. <https://doi.org/10.1016/j.esd.2013.01.001>
- Mwampamba TH, Owen M, Pigat M (2013b) Opportunities, challenges and way forward for the charcoal briquette industry in sub-Saharan Africa. *Energy Sustain Dev* 17:158–170
- Nadel S (2019) Electrification in the transportation, buildings, and industrial sectors: a review of opportunities, barriers, and policies. *Curr Sustain Renew Energy Rep* 6:158–168
- Ogulei D, Hopke PK, Wallace LA (2006) Analysis of indoor particle size distributions in an occupied townhouse using positive matrix factorization. *Indoor Air* 16:204–215
- Pundle A, Sullivan B, Means P et al (2019) Predicting and analyzing the performance of biomass-burning natural draft rocket cookstoves using computational fluid dynamics. *Biomass Bioenergy* 131:105402
- Pyne SJ (1995) *World fire: the culture of fire on Earth*. Holt, New York
- Ramanathan T, Ramanathan N, Mohanty J et al (2017) Wireless sensors linked to climate financing for globally affordable clean cooking. *Nat Clim Change* 7:44. <https://doi.org/10.1038/nclimate3141>
- Rao ND (2012) Kerosene subsidies in India: when energy policy fails as social policy. *Energy Sustain Dev* 16:35–43
- Rapp VH, Pastor-Perez A, Singer BC, Wray CP (2013) Predicting backdrafting and spillage for natural-draft gas combustion appliances: a validation of VENT-II. *HVAC&R Res* 19:295–306
- Reed TB, Larson R (1997) A wood-gas stove for developing countries. In: *Developments in thermochemical biomass conversion*. Springer, Dordrecht, pp 985–993
- Roden CA, Bond TC, Conway S et al (2009) Laboratory and field investigations of particulate and carbon monoxide emissions from traditional and improved cookstoves. *Atmos Environ* 43: 1170–1181
- Rolland N (2004) Was the emergence of home bases and domestic fire a punctuated event? A review of the Middle Pleistocene record in Eurasia. *Asian Perspect* 43:248–280
- Rosin PO (1939) *The aerodynamics of domestic open fires*. Institute of fuel, London
- Ruiz-Mercado I, Masera O (2015) Patterns of stove use in the context of fuel-device stacking: rationale and implications. *EcoHealth* 12:42–56. <https://doi.org/10.1007/s10393-015-1009-4>
- Saito K, Williams FA, Gordon AS (1987) A study of the two-color soot zone for small hydrocarbon diffusion flames. *Combust Sci Technol* 51:285–305. <https://doi.org/10.1080/00102208708960326>
- Sanchis E, Ferrer M, Calvet S et al (2014) Gaseous and particulate emission profiles during controlled rice straw burning. *Atmos Environ* 98:25–31
- Schauer JJ, Kleeman MJ, Cass GR, Simoneit BRT (2001) Measurement of emissions from air pollution sources. 3. C1-C29 organic compounds from fireplace combustion of wood. *Environ Sci Technol* 35:1716–1728
- Shan M, Carter E, Baumgartner J et al (2017) A user-centered, iterative engineering approach for advanced biomass cookstove design and development. *Environ Res Lett* 12:95009
- Shankar AV, Quinn AK, Dickinson KL et al (2020) Everybody stacks: lessons from household energy case studies to inform design principles for clean energy transitions. *Energy Policy* 141: 111468
- Shen G, Yang Y, Wang W et al (2010) Emission factors of particulate matter and elemental carbon for crop residues and coals burned in typical household stoves in China. *Environ Sci Technol* 44: 7157–7162
- Shen G, Tao S, Wei S et al (2013) Field measurement of emission factors of PM, EC, OC, parent, nitro-, and oxy-polycyclic aromatic hydrocarbons for residential briquette, coal cake, and wood in rural Shanxi, China. *Environ Sci Technol* 47:2998–3005

- Shen G, Gaddam CK, Ebersviller SM et al (2017) A laboratory comparison of emission factors, number size distributions, and morphology of ultrafine particles from 11 different household cookstove-fuel systems. *Environ Sci Technol* 51:6522–6532. <https://doi.org/10.1021/acs.est.6b05928>
- Shen G, Hays MD, Smith KR et al (2018) Evaluating the performance of household liquefied petroleum gas cookstoves. *Environ Sci Technol* 52:904–915. <https://doi.org/10.1021/acs.est.7b05155>
- Shen H, Luo Z, Xiong R et al (2021) A critical review of pollutant emission factors from fuel combustion in home stoves. *Environ Int* 157:106841. <https://doi.org/10.1016/j.envint.2021.106841>
- Shove EA (2003) Comfort, cleanliness and convenience: the social organization of normality. Berg, Oxford, UK
- Simoneit BRT, Rogge WF, Mazurek MA et al (1993) Lignin pyrolysis products, lignans, and resin acids as specific tracers of plant classes in emissions from biomass combustion. *Environ Sci Technol* 27:2533–2541
- Simoneit BRT, Schauer JJ, Nolte CG et al (1999) Levoglucosan, a tracer for cellulose in biomass burning and atmospheric particles. *Atmos Environ* 33:173–182
- Smith KR, Apte MG, Ma Y et al (1994) Air pollution and the energy ladder in Asian cities. *Energy* 9:587–600
- Smith KR, Uma R, Kishore VVN et al (2000a) Greenhouse gases from small-scale combustion devices in developing countries: household stoves in India. Environmental Protection Agency, Research Triangle Park
- Smith KR, Uma R, Kishore VVN et al (2000b) Greenhouse implications of household stoves: an analysis for India. *Annu Rev Energy Environ* 25:741–763
- Soile I, Mu X (2015) Who benefit most from fuel subsidies? Evidence from Nigeria. *Energy Policy* 87:314–324. <https://doi.org/10.1016/j.enpol.2015.09.018>
- Soriano JB, Kendrick PJ, Paulson KR et al (2020) Prevalence and attributable health burden of chronic respiratory diseases, 1990–2017: a systematic analysis for the Global Burden of Disease Study 2017. *Lancet Respir Med* 8:585–596
- Standards Administration of China (2017) Clean biomass cookstove. Report No. GB/T 35564-2017.
- Still DK, Bentson S, Murray N et al (2018) Laboratory experiments regarding the use of filtration and retained heat to reduce particulate matter emissions from biomass cooking. *Energy Sustain Dev* 42:129–135
- Thoday K, Benjamin P, Gan M, Puzzolo E (2018) The Mega Conversion Program from kerosene to LPG in Indonesia: lessons learned and recommendations for future clean cooking energy expansion. *Energy Sustain Dev* 46:71–81
- Thomas C, William C, Peel JL et al (2022) Design and rationale of the HAPIN study: a multicountry randomized controlled trial to assess the effect of liquefied petroleum gas stove and continuous fuel distribution. *Environ Health Perspect* 128:47008. <https://doi.org/10.1289/EHP6407>
- Thompson RJ, Li J, Weyant CL et al (2019) Field emission measurements of solid fuel stoves in Yunnan, China demonstrate dominant causes of uncertainty in household emission inventories. *Environ Sci Technol*. <https://doi.org/10.1021/acs.est.8b07040>
- Tiwari M, Sahu SK, Bhangare RC et al (2014) Particle size distributions of ultrafine combustion aerosols generated from household fuels. *Atmos Pollut Res* 5:145–150. <https://doi.org/10.5094/APR.2014.018>
- Traynor GW, Apte MG, Sokol HA et al (1990) Selected organic pollutant emissions from unvented kerosene space heaters. *Environ Sci Technol* 24:1265–1270
- Traynor GW, Apte MG, Chang G-M (1996) Pollutant emission factors from residential natural gas appliances: a literature review. Lawrence Berkeley National Laboratory Report LBL-38123.
- U.S. EPA (1996) Chapter 1.10. Residential wood stoves. In: *Compilation of air pollutant emissions factors*. U.S. EPA, Washington, DC

- U.S. EPA (1998a) Chapter 1.4. Natural gas combustion. In: Compilation of air pollutant emissions factors. U.S. EPA, Washington, DC
- U.S. EPA (1998b) Chapter 1.1. Bituminous and subbituminous coal combustion. In: Compilation of air pollutant emissions factors. U.S. EPA, Washington, DC
- Urban GL, Bryden KM, Ashlock DA (2002) Engineering optimization of an improved plancha stove. *Energy Sustain Dev* 6:9–19
- Venkataraman C, Rao GUM (2001) Emission factors of carbon monoxide and size-resolved aerosols from biofuel combustion. *Environ Sci Technol* 35:2100–2107
- Wathore R, Mortimer K, Grieshop AP (2017) In-use emissions and estimated impacts of traditional, natural-and forced-draft cookstoves in rural Malawi. *Environ Sci Technol* 51:1929–1938
- Weimer S, Alfarra MR, Schreiber D et al (2008) Organic aerosol mass spectral signatures from wood-burning emissions: influence of burning conditions and wood type. *J Geophys Res Atmos* 113:10. <https://doi.org/10.1029/2007jd009309>
- Westhoff B, German D (1995) Stove images: a documentation of improved and traditional stoves in Africa, Asia and Latin America. Commission of the European Communities, Brussels
- Weyant CL, Chen P, Vaidya A et al (2019) Emission measurements from traditional biomass cookstoves in South Asia and Tibet. *Environ Sci Technol* 53:3306–3314. <https://doi.org/10.1021/acs.est.8b05199>
- Whittaker C, Shield I (2017) Factors affecting wood, energy grass and straw pellet durability – a review. *Renew Sust Energ Rev* 71:1–11
- Winijkul E, Fierce L, Bond TC (2016) Emissions from residential combustion considering end-uses and spatial constraints: part I, methods and spatial distribution. *Atmos Environ* 125:126–139. <https://doi.org/10.1016/j.atmosenv.2015.10.013>
- Wrangham R (2009) Catching fire: how cooking made us human. Basic Books, New York
- Xue J, Li Y, Peppers J et al (2018) Ultrafine particle emissions from natural gas, biogas, and biomethane combustion. *Environ Sci Technol* 52:13619–13628. <https://doi.org/10.1021/acs.est.8b04170>
- Yun X, Shen G, Shen H et al (2020) Residential solid fuel emissions contribute significantly to air pollution and associated health impacts in China. *Sci Adv* 6:eaba7621
- Zhang J, Smith KR, Uma R et al (1999) Carbon monoxide from cookstoves in developing countries: 1. Emission factors. *Chemos Glob Change Sci* 1:353–366
- Zhang Y, Yuan Q, Huang D et al (2018) Direct observations of fine primary particles from residential coal burning: insights into their morphology, composition, and hygroscopicity. *J Geophys Res Atmos* 123:12–964
- Zheng X, Wei C, Qin P et al (2014) Characteristics of residential energy consumption in China: findings from a household survey. *Energy Policy* 75:126–135
- Zhi GR, Peng CH, Chen YJ et al (2009) Deployment of coal briquettes and improved stoves: possibly an option for both environment and climate. *Environ Sci Technol* 43:5586–5591. <https://doi.org/10.1021/es802955d>



Vaping and Secondhand Exposure

7

Liqiao Li and Yifang Zhu

Contents

Introduction	200
Particulate Matter in E-Cig Aerosols	203
Particle Concentration and Size Distribution	203
Factors Affecting Indoor E-Cig Particle Concentrations	204
Effects of Proximity on SHV Aerosols	206
Vaping in a Laboratory Room	207
Vaping in Vape Shops	207
Transport of SHV Aerosols in Multiunit Indoor Environment	209
Laboratory Multiunit Setting	209
Vape Shops and Neighboring Indoor Spaces	210
Mitigation of SHV Aerosol Exposure in a Multiunit Setting	212
Chemical Composition of E-Cig Aerosols	214
Chemical Profiles of E-Cig Aerosols	214
Factors Affecting Chemical Compositions	217
Thirdhand Exposure	219
Health Effects	219
In Vivo and In Vitro Studies	219
Human Studies: Active Exposure to E-Cig Aerosols	220
Human Studies: Passive Exposure to SHV Aerosols	222
Conclusions	222
References	223

Abstract

Electronic cigarettes (e-cigs) use, which is also called vaping, has increased considerably in recent years. Although e-cig was initially designed as an alternative to tobacco cigarettes (t-cigs), there has been a high demand for flavored e-cig products among never-smoking adolescents and young adults. As a result, many

L. Li · Y. Zhu (✉)

Department of Environmental Health Sciences, Jonathan and Karin Fielding School of Public Health, University of California, Los Angeles, CA, USA
e-mail: liqiao93@ucla.edu; yifang@ucla.edu

bystanders are now at the risk of passive exposure to secondhand vaping (SHV) aerosols, which are spilled from the mouth before inhalation and exhaled by an e-cig user, especially in an indoor environment. This chapter summarizes the impacts of e-cigs on indoor air quality, chemical compositions of e-cig aerosols, factors affecting emissions, and associated respiratory and cardiovascular effects. The use of e-cigs in indoor environments leads to high levels of fine and ultrafine particles (UFPs) similar to t-cigs. Concentrations of chemical compounds in e-cig aerosols are generally lower than those in t-cig smoke, but a substantial amount of vaporized propylene glycol (PG), vegetable glycerin (VG), nicotine, and toxic substances, such as aldehydes and heavy metals, has been reported. Exposures to e-cig aerosols have biologic effects but only limited studies have focused on adverse respiratory and cardiovascular effects in humans. Nevertheless, the recent outbreak of the e-cig or vaping product use-associated lung injury (EVALI) that has been linked to cannabis products vaping raised serious public health concerns. Long-term studies are needed to better understand the health effects of exposures to e-cigs, especially SHV aerosols.

Keywords

Electronic cigarette · Particulate matter · Chemical composition · Indoor air · Health effects

Introduction

Electronic cigarettes (e-cigs), also known as vaping devices, are battery-powered nicotine delivery systems widely used as alternatives to traditional tobacco cigarettes (t-cig). For t-cigs, the combustion of tobacco leaves releases nicotine and substantial amounts of toxic by-products. In comparison, e-cigs generate aerosols by vaporizing e-liquids, which typically contain propylene glycol (PG), vegetable glycerin (VG), nicotine, and flavoring additives.

As shown in Fig. 1, there are several generations of e-cig devices since e-cig was first invented in 2003. E-cigs have evolved quickly over time from the cigalike type to the more advanced tank style with customizable voltage and e-liquids, and to the recent pod-based vaping systems such as JUUL pods. Although hundreds of different e-cig brands with various design features are currently available on the market, most e-cigs consist of a cartridge, tank, or pod with the e-liquid, a heating element (i.e., atomizer with heating coil), and a battery. In the meantime, thousands of flavors such as tobacco, menthol, fruit, candy, and sweets added in e-liquids have been widely adopted by e-cig users. Due to the high customizability of e-cig devices, many users are now even adding tetrahydrocannabinol (THC) or cannabidiol (CBD) oil into e-liquids for vaping marijuana.

E-cigs are marketed as a safer alternative to t-cigs because they are combustion free, yet their use has also increased greatly among never-smoking adolescents. Since 2011, the use of e-cigs or vaping has gained popularity among young adults

worldwide. The global e-cig market has grown rapidly, with more than 70% in North America and Europe. The number of e-cig users has also increased markedly, especially among adolescents, despite the Food and Drug Administration (FDA)'s prohibition of sales to persons under the age of 18. In the USA, although the rates of t-cig use among youth have declined over years, the current e-cig use among high school students has increased from 0.2 million in 2011 to 3.0 million in 2020 (CDC 2020) (Fig. 2). Similar increases among adolescents have been observed in other countries, such as the UK, Canada, South Korea, New Zealand, Finland, and Poland. E-cigs are popular among adolescents likely because of their appealing flavors. The newly introduced sleek and discreet JUUL pods which use nicotine salts to deliver higher levels of nicotine also provide a smoother and easier transition to vaping.

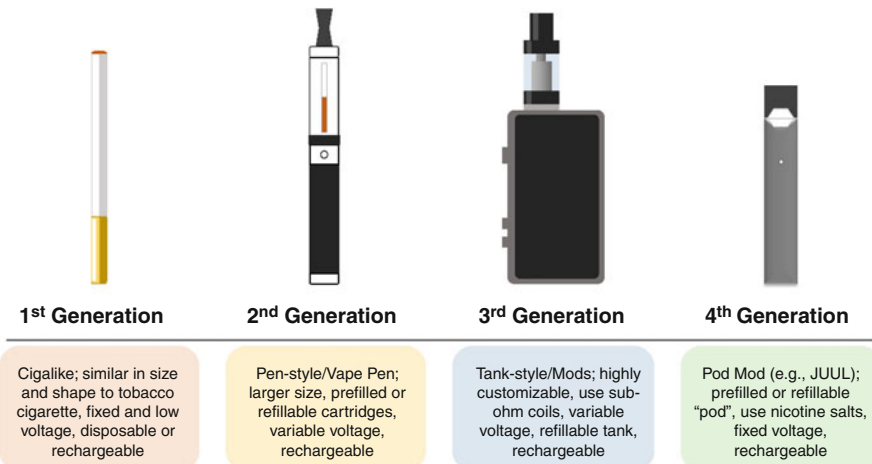
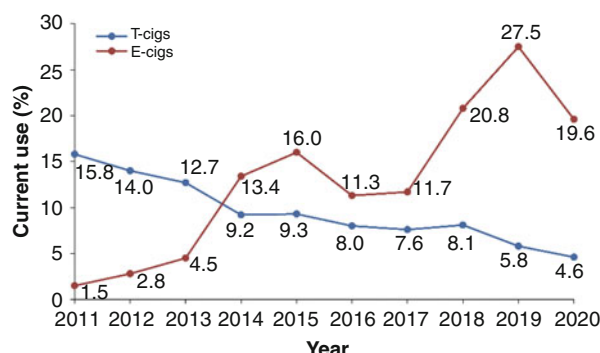


Fig. 1 Different generations of electronic cigarettes

Fig. 2 Percentage of high school students who currently use electronic cigarettes (e-cigs) and tobacco cigarettes (t-cigs) in the USA from 2011 to 2020. Based on data from the National Youth Tobacco Survey by the Centers for Disease Control and Prevention (CDC 2020)



Since 2019, many cases and deaths of e-cig or vaping product use–associated lung injury (EVALI) have been reported in the USA (Layden et al. 2019). E-cigs may not only pose health harms to active users but also bystanders. The majority of inhaled e-cig aerosols can be eventually exhaled, which may cause passive exposure to secondhand and even thirdhand vaping aerosols. E-cigs are commonly used in many places, such as homes, cars, restaurants, bars, and workplaces where vulnerable populations, such as children, adolescents, and pregnant women, might be exposed. The percentage of nonusers who were exposed to secondhand vaping (SHV) aerosols in an indoor environment ranged from 4% to 30% in Europe (Amalia et al. 2020). In the USA, more than half of middle and high school students were exposed to SHV aerosols (Gentzke et al. 2019). Exposure to SHV aerosols in indoor environments is of particular concern because people typically spend more than 80% of their time indoors, where emitted pollutants are not diluted as quickly or as extensively as outdoors. Yet, to what extent such secondhand exposures affect human health is poorly understood.

The process from e-cig emissions to passive exposures, and to potential health effects is presented schematically in Fig. 3 (Li et al. 2020b). The mainstream aerosols emitted from e-cigs are determined by many parameters related to e-cig devices and e-liquids. For an active user, the inhaled e-cig aerosols can be affected by puffing topography and related physiological factors. Due to e-cig use, SHV aerosols include a significant amount of particles that are exhaled by the e-cig user and a certain amount that are spilled from the mouth before inhalation (Logue et al. 2017). Once released into an indoor environment, e-cig aerosols are mainly affected by environmental parameters. The effects of such factors on e-cig particle concentrations and chemical compositions are discussed in later sections,

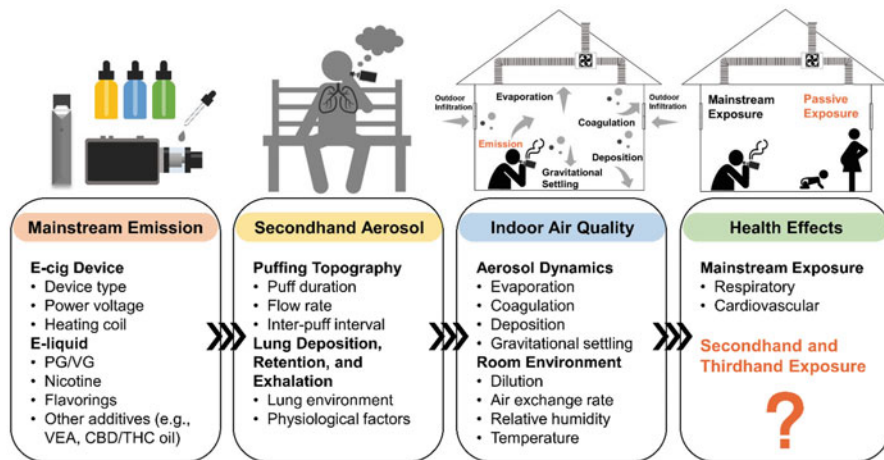


Fig. 3 Schematic process from e-cig emissions to passive exposures, and to potential health effects. (Adapted from Li et al. (2020b))

respectively. Both toxicological and epidemiological studies on health effects of e-cig aerosols are discussed in the “Health effects” section.

Particulate Matter in E-Cig Aerosols

Exposure to atmospheric particulate matter (PM) has been associated with mortality and morbidity in many epidemiological studies (Cohen et al. 2018; Burnett et al. 2018). Similar to t-cigs, high levels of fine particulate matter ($PM_{2.5}$, particles with aerodynamic diameters $\leq 2.5 \mu\text{m}$) and ultrafine particles (UFPs, particles with diameters $\leq 100 \text{ nm}$) have been observed in e-cig emissions (Li et al. 2020b). Exposure to outdoor $PM_{2.5}$ is a well-established risk factor for respiratory and cardiovascular diseases (Cohen et al. 2018). In addition, UFPs are also of great health concern because they have a greater surface area per unit mass than larger particles so that they can bind to more toxic chemicals (Terzano et al. 2010).

Particle Concentration and Size Distribution

Several indoor studies have reported high concentrations of $PM_{2.5}$ resulting from vaping (Fig. 4a), which could reach up to $1660 \mu\text{g}/\text{m}^3$ (Son et al. 2020), or ~66 times

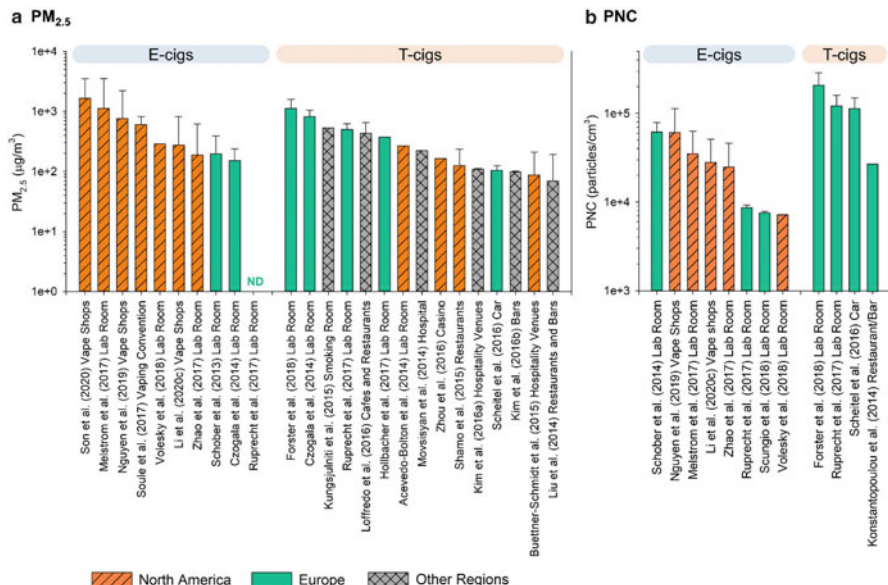


Fig. 4 Average concentrations of (a) $PM_{2.5}$ and (b) particle number concentration (PNC) from 13 studies on e-cigs and 16 studies on t-cigs in various indoor environments (i.e., laboratory settings and real-world public indoor spaces) by region. Abbreviation: ND not detectable. (Adapted from Li et al. (2020b) and references therein)

as high as the World Health Organization's recommended limit for 24-h outdoor concentrations of $25 \mu\text{g}/\text{m}^3$. In most cases, the reported indoor PM_{2.5} levels during vaping are above $150 \mu\text{g}/\text{m}^3$, which are similar to those produced by t-cigs. The impacts of e-cigs on indoor air quality are also similar to, if not greater than, other combustion-free nicotine delivery systems, such as waterpipe and "heat-not-burn" products (Forster et al. 2018; Fromme et al. 2009). The PM_{2.5} concentrations of $600\text{--}800 \mu\text{g}/\text{m}^3$, as reported in vape shops and vaping conventions, are about twice as high as those in hookah bars (Zhou et al. 2017). In comparison, the PM_{2.5} concentrations observed across a wide range of common indoor environments without e-cig use, such as homes, offices, schools, and day care, are from $8\text{--}52 \mu\text{g}/\text{m}^3$ (Morawska et al. 2017).

The indoor UFPs, which are approximately measured by the particle number concentration (PNC), can increase up to 20 times over the background during vaping ($0.7\text{--}6.2 \times 10^4 \text{ particles}/\text{cm}^3$; Fig. 4b) (Guo et al. 2010), but still lower than those from t-cigs ($7.0\text{--}21 \times 10^4 \text{ particles}/\text{cm}^3$) (Forster et al. 2018; Scheitel et al. 2016; Konstantopoulou et al. 2014) and other combustion-free nicotine delivery systems ($0.8\text{--}32 \times 10^4 \text{ particles}/\text{cm}^3$) (Fromme et al. 2009; Ruprecht et al. 2017; Forster et al. 2018). Similar to PM_{2.5}, indoor PNC from e-cig is also higher than other common indoor environments mentioned above (Morawska et al. 2017).

As shown in Fig. 4, studies on t-cig secondhand smoke (SHS) have been conducted worldwide, but studies on e-cigs are mainly from North America and Europe. The current prevalence of e-cig in other countries and regions is relatively low, but the e-cig market in many populous countries (e.g., China) is expanding rapidly. Thus, exposures to SHV aerosols will likely become a potential public health problem in those countries in the near future.

In addition to particle concentrations, particle size distribution is also important to respiratory health because smaller particles (especially UFPs) generally penetrate deeper into the lung. E-cig particles are primarily in the submicron size range, typically exhibiting a bimodal size distribution, with one mode located around 15–30 nm and the other around 85–100 nm (Schripp et al. 2013; Zhao et al. 2017; Scungio et al. 2018). Both particle concentration and particle size distribution can be affected by various factors as illustrated in Fig. 3 and discussed below.

Factors Affecting Indoor E-Cig Particle Concentrations

Changes in e-cig device, e-liquid, vaping topography, and indoor environment can all affect particle concentration and size distribution in e-cig aerosols, which may ultimately affect the lung deposition and exposure dose. Understanding the dynamics of e-cig particles in an indoor environment is important as it can guide exposure assessment and mitigation strategies.

E-Cig

E-cig device-related parameters: The heating element plays an important role in generating e-cig aerosols. Higher power voltage would transform more energy to

heat, resulting in higher heating coil temperature. More e-liquid can be vaporized at a higher voltage, thus the power level has been positively associated with both PNC and total PM mass concentration (Floyd et al. 2018; Gillman et al. 2016; Zhao et al. 2018). In addition, the particle sizes tend to be larger with an increasing voltage (Zhao et al. 2018; Lechasseur et al. 2019). The heating process is not consistent between brands and types of e-cigs due to the different design features, leading to large variations in e-cig emissions. For example, the tank style, which allows a higher voltage, can produce more particles than the cigalike type.

E-liquid compositions: Particle emissions from e-cigs are also influenced by the e-liquid compositions. More PG content in the e-liquid would produce a stronger “throat hit” feeling while more VG would generate thicker and larger visible “clouds.” Various volume combinations of PG and VG are available in the e-cig market to suit different e-cig users’ preferences. Higher PG/VG ratios tend to produce more particles (Baassiri et al. 2017; El-Hellani et al. 2018), while greater VG content increased the particle size (Lechasseur et al. 2019). Several studies reported that adding nicotine to e-liquids produces more particles (Fuoco et al. 2014; Manigrasso et al. 2015), while others did not (Zervas et al. 2018; Li et al. 2020a). The inconsistent results indicate how nicotine changes the e-cig emissions remains unclear, calling for future studies. In addition, e-cig aerosols are highly volatile. E-cig particles generated from nicotine-free e-liquid decay faster with increasing PG/VG ratios due to evaporation (Li et al. 2020a). However, this pattern was not observed with nicotine in the e-liquid. The recently introduced JUUL or other pod systems containing dissolved nicotine salts have raised even more health concerns due to their high nicotine content and popularity among adolescents, but have not been well studied (McKelvey et al. 2018).

Several studies have reported higher particle mass generated by tobacco flavor e-liquids than the menthol flavor (Zhao et al. 2018; Lee et al. 2017), while others observed little effects of flavors on particle emissions (Fuoco et al. 2014; Zervas et al. 2018; Manigrasso et al. 2015). Given the complexity of numerous flavoring additives, however, there is no conclusive evidence on the effects of flavors on particle emissions. Flavoring compounds in e-liquids have been largely linked to toxic chemicals which is discussed more later.

In recent years, the use of cannabis products such as THC or CBD in e-liquids as a method of delivering marijuana has emerged. The majority of the EVALI patients reported use of THC oil and a few reported use of CBD oil (Layden et al. 2019), suggesting the serious health risks of vaping cannabis products. A recent study (Wallace et al. 2020) characterized the emission from secondhand cannabis vaping, which had a higher $PM_{2.5}$ emission factor and lower particle removal rate than previous studies (Li et al. 2020a) found in e-cig aerosols without cannabis oil. Another study (Tang et al. 2021) reported that the presence of terpenoids in the e-liquid containing vaporizable cannabis concentrates resulted in significant levels of UFPs in the e-cig aerosol. Although the mechanisms of the EVALI outbreak has not been fully understood, the addition of vitamin E acetate used to dilute THC oil has been linked to it. The health effects of vaping cannabis products are discussed further below.

Vaping

Puffing topography (i.e., flow rate, puff duration, and inter-puff interval) and the process of inhalation and exhalation also affect e-cig aerosol emissions. In general, the particle concentration increases with higher puffing flow rates, longer puff durations, and greater puff frequencies (Gillman et al. 2016; Nguyen et al. 2019; Zhao et al. 2016). On the other hand, the particle size decreases with higher puffing flow rates and shorter puff durations (Zhao et al. 2016).

The inhaled e-cig particles tend to grow in human lungs under high humidity due to the hygroscopic effect, which is more prominent than t-cig smoke (Sosnowski and Kramek-Romanowska 2016). The initial particle size distribution plays an important role in the hygroscopic effect (Sosnowski and Odziomek 2018), where particles in the nanometer size range slightly increase their size, while particles greater than 0.5 μm become larger by more than 50%. These inhaled particles are deposited in the respiratory system, mainly through gravitational settling, impaction, and diffusion (Hinds 1999). Depending on the initial size, increasing particle size in the respiratory system may reduce the deposition due to diffusion but increase the deposition due to gravitational settling and impaction. Other physiological factors in the respiratory system, such as lung capacity, air flow, and breath pattern, might also affect e-cig aerosol dynamics.

Indoor Environment

A certain amount of aerosol can be spilled from the mouth before inhalation and the majority of droplets inhaled can be exhaled by an e-cig user. Once released into the room air, e-cig particles are subject to aerosol dynamics under various environmental conditions. In contrast to t-cig smoke, e-cig aerosols mainly consist of droplets that are more volatile because the e-liquid main ingredient, PG, has a relatively high saturation vapor pressure. E-cig particles have been observed to evaporate within seconds (Zhao et al. 2017). At high PNCs, coagulation is also an important particle removal mechanism that reduces the number of particles, but increases particle size (Floyd et al. 2018). In addition, e-cig particles can be removed from the room air by gravitational settling and surface deposition, leading to potential thirdhand exposures which also warrant future studies (Goniewicz and Lee 2015).

Increasing dilution or air exchange rate (AER) may enhance particle evaporation and reduce particle concentrations and particle sizes (Ingebrethsen et al. 2012; Floyd et al. 2018; Nguyen et al. 2019). Similarly, increasing temperature or decreasing relative humidity may also enhance evaporation and reduce particle size (Wright et al. 2016; Schripp et al. 2013). Because e-cig aerosols are dynamic, their concentrations decay rapidly over distances (>1.5 m) from the source (i.e., e-cig users), especially for PM_{2.5} mass concentrations (Zhao et al. 2017; Nguyen et al. 2019).

Effects of Proximity on SHV Aerosols

It has been shown that evaporation could occur to e-cig aerosol particles under a high dilution condition. After the SHV particles are released into indoor air, their spatial profiles provide information on how far e-cig particles can move in an indoor environment.

Vaping in a Laboratory Room

The PNC and $\text{PM}_{2.5}$ concentrations at different locations ranging from 0.8–2.5 m away from an e-cig user in an 80 m³ room are presented in Fig. 5 (Zhao et al. 2017). The mean PNCs were 1.7×10^4 , 3.4×10^3 , 2.1×10^3 , and 1.3×10^3 particles/cm³ at 0.8, 1.5, 2.0, and 2.5 m from the e-cig users, respectively, which indicate that PNC of SHV aerosols decreased quickly from the source (Fig. 5a). When the sampling location moved to 1.5, 2.0, and 2.5 m from the e-cig users, the PNC dropped to 20%, 12%, and 7% of what was measured at 0.8 m, respectively. Approximately, 80% of PNC dropped between 0.8 and 1.5 m, and only 7% of PNC remained beyond 2.5 m. Similarly, the mean $\text{PM}_{2.5}$ was 375, 15, 7, and 5 $\mu\text{g}/\text{m}^3$ at increasing distances (Fig. 5b). When the sampling location moved to 1.5, 2.0, and 2.5 m from the e-cig user, the $\text{PM}_{2.5}$ dropped to 4%, 2%, and 1% of what was measured at 0.8 m, respectively. About 96% of $\text{PM}_{2.5}$ reduction occurred between 0.8 and 1.5 m, which was greater than that of PNC. These data can be used to model the transport of e-cig particles in indoor environments and highlight the importance of proximity to e-cig users in secondhand exposure assessment.

Vaping in Vape Shops

In real world, vaping occurs in various indoor environments including vape shops, which are a new type of retailer, where customers can exclusively purchase e-cig products and sample e-liquids with a combination of flavors and varying levels of nicotine (Galstyan et al. 2019). In the USA, the growing vape shop industry accounts for 20% of the e-cig retail markets in 2019 and has proliferated globally over the past few years (Galstyan et al. 2019). While many states have established smoking bans in workplaces and public spaces, the use of e-cigs is unrestricted in vape shops. Nguyen et al. (2019) found that the PNC and $\text{PM}_{2.5}$ in vape shops fluctuated

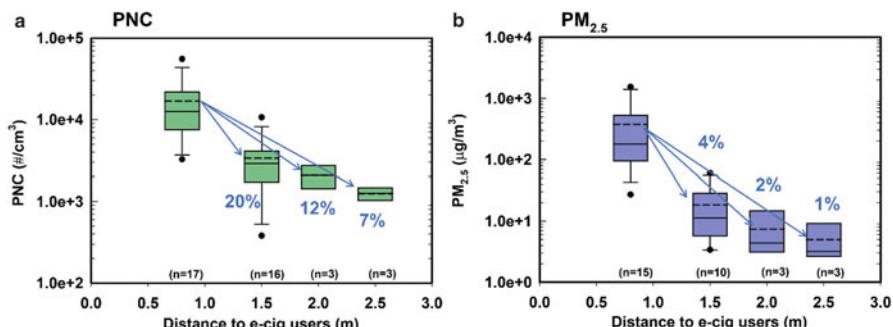


Fig. 5 (a) PNC and (b) $\text{PM}_{2.5}$ concentrations of secondhand vaping (SHV) aerosols at increasing distances from the e-cig users in an 80 m³ room. The dots above or below the boxes represent the outliers, which are beyond 1.5 IQR (interquartile range). The solid line in each box represents the median value, and the dash line in each box represents the mean value. (Adapted from Zhao et al. (2017))

dramatically and can even reach instantaneously up to 4.8×10^5 particles/cm³ and 37,500 µg/m³, respectively.

Figure 6 plots the mean PNC and PM_{2.5} concentrations measured over increasing distance from a vaping source in four vape shops (labeled as #1–4). Distances were designated based on the following degrees of proximity from the vaping source: (1) personal space (0.45 to <1.2 m); (2) social space (1.2 to <3.6 m); and (3) public space (3.6 m and beyond). Concentrations were compared at points within the personal space to public space except for vape shop #2, where concentrations were measured within the personal space to social space. Mean PNC and PM_{2.5} concentrations measured in the vape shops within the personal space of a vaping source were $2.0\text{--}12.6 \times 10^4$ particles/cm³ and 102–1858 µg/m³, respectively. From social space to public space, mean PNC and PM_{2.5} concentrations were $0.6\text{--}8.6 \times 10^4$ particles/cm³ and 34–1375 µg/m³, respectively. The observed decreasing concentration from the personal space to the social/public space suggests a proximity effect for SHV particle concentrations.

In contrast to the laboratory study (Zhao et al. 2017) that reported low indoor PM concentrations within the social space of an e-cig user (Fig. 5), high concentrations were still measured more than 4 m away from the vaping source in vape shops. As shown in Fig. 6, as much as 77% of PNC and 62% of PM_{2.5} measured within the personal space of a vaping source remained when measured at the public space. This is unlike the PNC and PM_{2.5} monitored in the laboratory room, where only 7% and 1% remained beyond the social space of the e-cig user. In the laboratory room, the AER was 4.1 h⁻¹ and spatial analysis was conducted after a short-term puffing by a single e-cig user. Even among the four vape shops, a greater percentage of remaining PM was observed in vape shops #1 and #4, where the AERs were lower and the average vaping frequency was higher than in shop #3 over a similar distance (~3 m).

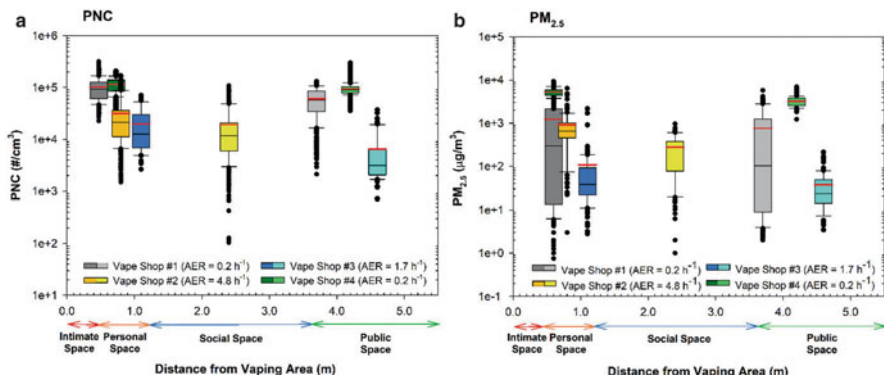


Fig. 6 (a) PNC and (b) PM_{2.5} concentrations at personal, social, and public distances away from vaping activity inside vape shops. From vaping activity, concentrations were measured at 0.6 and 3.7 m away in vape shop #1, 0.8 and 2.4 m away in vape shop #2, 1.1 and 4.6 m away in vape shop #3, and 0.6 and 4.2 m away in vape shop #4. (Adapted from Nguyen et al. (2019))

In general, factors contributing to the persistence and mixing of SHV aerosols in the vape shops include: (1) lower AERs, leading to exhaled e-cig vapor partial pressure buildup inside the shop and decrease in e-cig particle evaporation; (2) continuous puffing by multiple e-cig users, extending the proximity effect from aggregate emissions and leading to subsequent microplume transportation caused by turbulence; and (3) people moving around and the shop doors were usually closed. Overall, the high vaping density together with low AER in vape shops presents conditions that heighten the mixing potential of and sustained exposure to SHV aerosols unlike in laboratory or residential settings.

Transport of SHV Aerosols in Multiunit Indoor Environment

It has been well established that SHS can transfer from smoking units to smoke-free adjacent units through shared ventilation, open windows, holes in walls, hallways, and electric outlets in multiunit buildings. Analogous to SHS, these transfer mechanisms are also applicable to SHV aerosols.

Laboratory Multiunit Setting

The transport of SHV aerosols from a vaping room (Room V) to an adjacent nonvaping room (Room N) when the door connecting the two rooms was either open or closed is presented in Fig. 7 (Zhang et al. 2020). Door open condition represents a typical exposure scenario in a multizone indoor environment without any mitigation strategy. When the door was open, the PNC in Room V started to increase right after vaping began, peaked at the end of the vaping session, up to 2.7×10^4 particles/cm³, and returned to the background concentration within 40–50 min. Mean PNCs were measured at 2.0×10^4 particles/cm³ during vaping and 5.8×10^3 particles/cm³ during decay, respectively (Fig. 7a). In Room N, PNC started to increase 1 min after vaping began and increased up to 9.9×10^3 particles/cm³ about 3 min after vaping ended, suggesting a rapid transport of UFPs from Room V to Room N. The PNC returned to the background concentration about 40 min after vaping ended. Overall, mean PNCs were 5.7×10^3 particles cm⁻³ during vaping and 3.6×10^3 particles/cm³ during decay. Similarly, a smaller increase of PM_{2.5} concentrations was observed in Room N and less time was needed for it to return to the background concentration. In Room V, PM_{2.5} started to increase 1 min after vaping began, peaked coinciding with the end of the vaping session, up to 64 µg/m³, and then fell to near-background concentration in about 6 min. In Room N, after subtracting the background, the maximum PM_{2.5} concentration only reached 4 µg/m³ (Fig. 7c). When the door connecting the two rooms was closed, no spikes were observed in Room N for both PNC and PM_{2.5}, suggesting the effectiveness of door segregation (Figs. 7b, d).

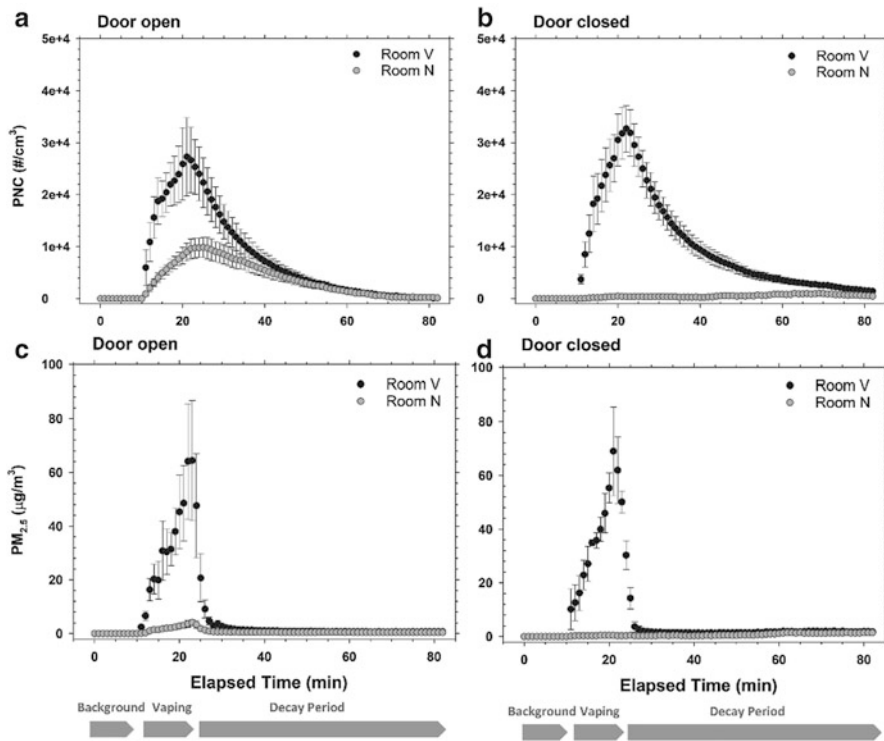


Fig. 7 The temporal trends of PNC and PM_{2.5} in the vaping room (Room V) and nonvaping room (Room N) when the door connecting the two rooms was open (**a** and **c**) and closed (**b** and **d**). Background concentration was subtracted. (Adapted from Zhang et al. (2020))

Vape Shops and Neighboring Indoor Spaces

Because vape shops are typically located in multiunit buildings with at least one neighboring business, such as an office, restaurant, retail store, or clinic, the SHV particles may also travel to these neighboring businesses. Exposure to the visible massive “clouds” produced in vape shops is an environmental and public health concern. A previous study (Li et al. 2020c) recruited six pairs of vape shops and their neighboring businesses in Southern California. The PNC and PM_{2.5} in the studied vape shops were significantly higher than their neighboring businesses. Out of the six studied pairs, PNCs in five vape shops and PM_{2.5} in two vape shops were significantly correlated with those in their neighboring businesses. A stronger correlation tends to be found in vape shops with higher vaping density (puffs/h/100 m³), defined as the total number of puffs per hour normalized by the shop volume. The weakest correlation was observed in the only pair that did not share the ventilation system. These results show that emissions from the vape shops can impact the indoor air quality in their neighboring indoor spaces.

Because no mechanical ventilation systems were actively in use for the studied vape shops and their neighboring businesses, natural ventilation through door opening was critical to reduce the exposure to SHV aerosols. The effects of door open and close on UFP transfer from a representative vape shop to its neighboring business are illustrated in Fig. 8. During the sampling period, the vape shop door was closed before 14:30 and open after 14:30. Following the PNC spikes in the vape shop, the PNC levels were also elevated in the nearby businesses. Shortly after the vape shop door was open, the PNC started to decay in the nearby businesses

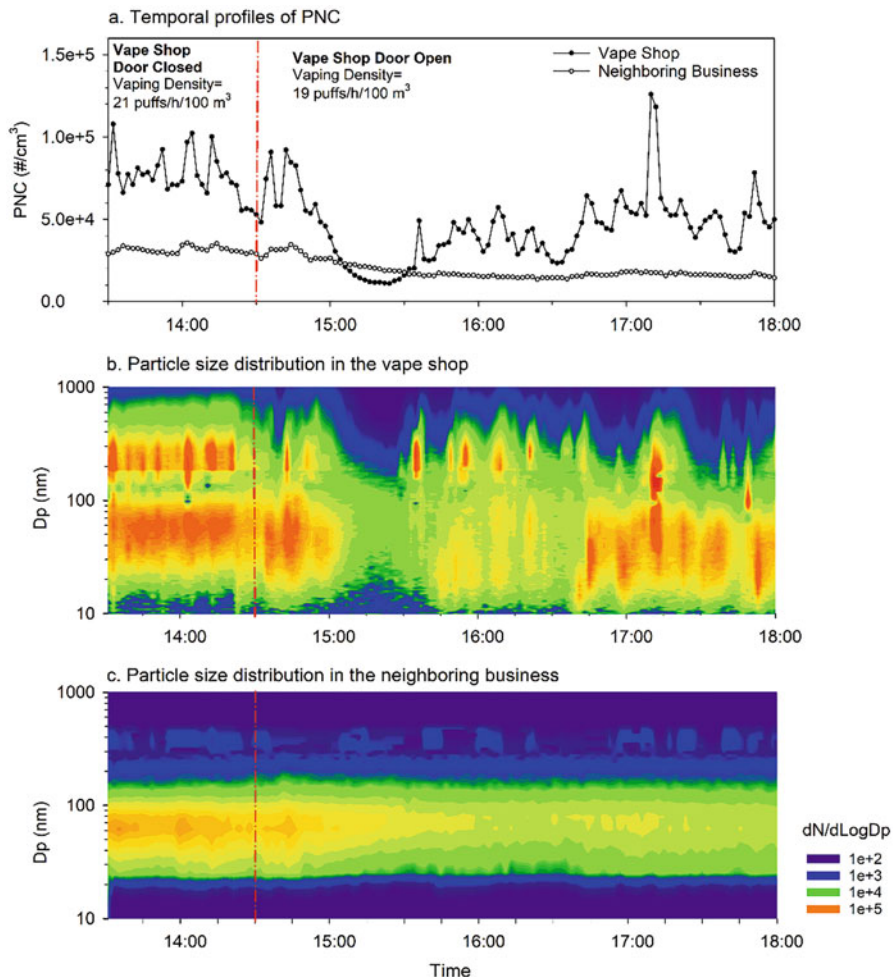


Fig. 8 Temporal profile of (a) PNC in a representative vape shop and its neighboring businesses as well as particle size distributions in (b) the vape shop and (c) neighboring businesses during overlapping business hours on a day with ventilation changes. Note: The door of vape shop was closed during 13:30–14:30 and the door was open during 14:30–18:00 (Li et al. 2020c)

(Fig. 8a). Consequently, the mean PNC decreased by 19% to 4.3×10^4 particles/cm³ in the vape shop and decreased by 33% to 1.8×10^4 particles/cm³ in nearby businesses.

Figure 8b, c present the contour plots of number-based particle size distribution for the vape shop and its neighboring businesses. The color intensity indicates the normalized PNC (dN/dLogD_p) for a given particle size at a given time. As demonstrated by Nguyen et al. (2019), the particles emitted in the vape shop was characterized by a bimodal particle number distribution of 60 nm and 250 nm when the shop door was closed. Meanwhile, UFPs largely penetrated into the neighboring businesses showing a single mode at 60 nm. Since UFPs may deposit deep into the human lung and induce greater adverse respiratory effects (Sturm 2016), the exposure to SHV related UFPs might bring more health concerns for employees and patrons in the neighboring businesses. After the door was open, PNC started to decrease immediately and the particle size distribution in the vape shop shifted to a single mode.

Opening and closing the vape shop doors changed the condition of ventilation in vape shops using natural ventilation. When the vape shop door was closed, an even stronger correlation in terms of PNC was observed. This was most likely a result of the enhanced particle concentration gradient between the vape shop and neighboring businesses because particles persisted and remained at high concentrations in the vape shop during door closed periods (Nguyen et al. 2019). However, no significant correlations between PNC in vape shops and that in neighboring businesses were observed when vape shop doors were open due to the enhanced dilution from outdoor air.

As a tracer compound, nicotine was detected in the air of all the studied vape shops and neighboring businesses. The mean concentration of the 24 h time-weighted average (TWA) nicotine measured in vape shops and neighboring businesses were $2.6 \mu\text{g}/\text{m}^3$ and $0.17 \mu\text{g}/\text{m}^3$, respectively. Assuming the nicotine measured in the neighboring businesses was all from its adjacent vape shop, the percentage of nicotine transfer ranged from 2.4% to 25%. The highest nicotine transfer rate (i.e., 25%) was observed in a pair likely because the neighboring businesses experienced significant impacts of both particle number and mass on their indoor air quality. Although the airborne nicotine levels varied depending on the level of nicotine in the e-liquids selected by e-cig users as well as the customer traffic, the identification of nicotine in all the studied vape shops and neighboring businesses confirmed that involuntary exposures to SHV aerosols occurred in those indoor environments.

Mitigation of SHV Aerosol Exposure in a Multiunit Setting

As discussed above, the effectiveness of mitigation strategies to reduce the transport of SHV aerosols from a vaping room (Room V) to its adjacent nonvaping room (Room N) in a multiunit laboratory setting has been investigated by Zhang et al. (2020). A total of six different experimental conditions were evaluated: (1) the

baseline scenario, in which the connecting door between the two rooms was open, the ventilation in both rooms was low, and no air purifier was operated; (2) the connecting door between the two rooms was closed; (3) the ventilation was enhanced in Room V; (4) the ventilation was enhanced in Room N; (5) an air purifier was operated in Room V; and (6) an air purifier was operated in Room N. Measurements were conducted for three sampling phases: a 10 min background measurement (Phase I), a 12 min vaping session (Phase II), and a 60 min decay period (Phase III).

Briefly, as shown in Fig. 9, when the door connecting Rooms V and N was closed (#2), mean PNC in Room N was significantly reduced by 87% to less than 1.0×10^3 particles cm^{-3} across Phase II and Phase III. It should be noted that mean PNC (1.0×10^4 particles cm^{-3}) in Room V was slightly higher relative to the baseline scenario (8.1×10^3 particles cm^{-3}) across both phases, likely because the dilution in Room N was inhibited. When ventilation was enhanced in Room V, mean PNC decreased by 42% in Room V and decreased by 46% in Room N during vaping and post-vaping sessions. Similarly, when ventilation was enhanced in Room N, mean PNC reduced from 8.1×10^3 to 6.4×10^3 particles cm^{-3} in Room V and significantly reduced from 3.9×10^3 to 1.2×10^3 particles cm^{-3} in Room N, respectively. When air filtration was increased in Room V, mean PNC slightly reduced by 17% in Room V and reduced by 23% in Room N across Phase II and Phase III. Similarly,

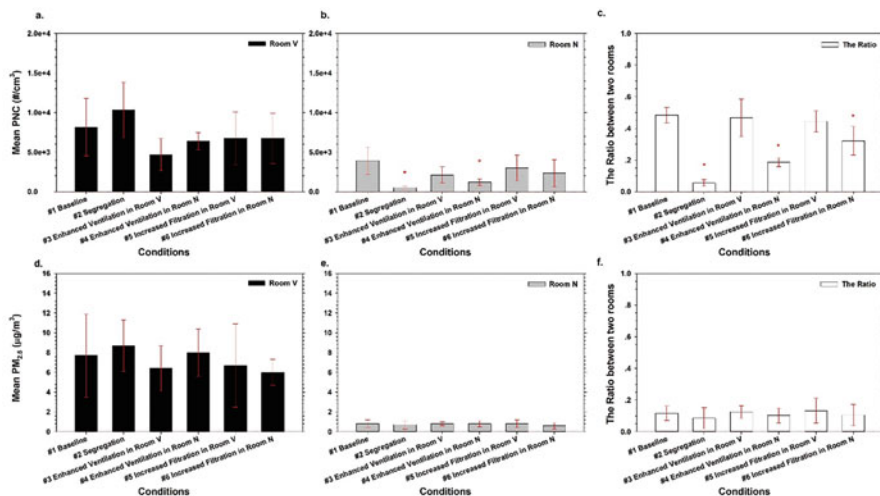


Fig. 9 Mean PNC due to e-cig use during vaping and post-vaping sessions in the (a) vaping room (Room V) and (b) its adjacent nonvaping room (Room N) and (c) the ratio between two rooms (i.e., Room N/Room V); mean PM_{2.5} due to e-cig use in (d) Room V and (e) Room N and (f) the ratio between two rooms; *indicates statistically significant ($p < 0.05$) based on the permutation test of the ratio between each condition and the baseline (#1). (Adapted from Zhang et al. (2020) under the terms of the Creative Commons Attribution 4.0 International License, <http://creativecommons.org/licenses/by/4.0/>)

when air filtration was increased in Room N, mean PNCs were reduced by 17% in Room V and by 40% in Room N across Phase II and Phase III.

As for PM_{2.5}, similar results were found under conditions #2–6 relative to the baseline scenario. In Room V, mean PM_{2.5} concentrations were measured at 6–9 µg m⁻³ across Phase II and Phase III under conditions #2–6. When the door connecting Room V and Room N was closed, peak PM_{2.5} concentrations increased from 64 to 69 µg m⁻³ in Room V. Peak value reduced by 38% to 40 µg m⁻³ when ventilation was enhanced in Room N. In Room N, under conditions #2–6, mean PM_{2.5} concentrations were about 1 µg m⁻³ and peak concentrations were less than 5 µg m⁻³ across Phase II and Phase III. Miller and Nazaroff (2001) have investigated the transport of SHS with a similar experimental design. The SHV particles (25–50 min) decayed much faster than SHS particles (120–240 min), presumably due to evaporation (Czogala et al., 2014).

To better understand the effects of tested mitigation strategies on the transport of SHV aerosols, the ratios of mean PNC and PM_{2.5} between two rooms are also presented in Fig. 9c, f. Segregation was the most effective method to reduce the transport of UFPs, in which the ratio was significantly reduced from 0.48 under the baseline condition to 0.06. Mitigation strategies applied in Room N, including enhancing ventilation (#4) and filtration (#6), significantly reduced the ratio to 0.19 and 0.32, respectively. However, when mitigations were applied in Room V, no significant differences were found. As for PM_{2.5}, the ratios were about 0.11 (0.09–0.13) with mitigations and no significant difference was found compared with the baseline (0.12). Overall, the transport of SHV aerosols could be effectively mitigated, especially by segregation. Other mitigations, including enhanced air ventilation and air filtration, could also increase particle removal.

Chemical Composition of E-Cig Aerosols

In addition to the physical characteristics, the effects of e-cig aerosols on health are largely determined by their chemical compositions. The most commonly reported chemicals in both mainstream and secondhand e-cig aerosols are PG, VG, nicotine, carbonyls, aromatic volatile organic compounds (VOCs), trace metals, and tobacco-specific nitrosamines (TSNAs) (Fig. 10) (Li et al. 2020b). Many chemicals are present in both gas and particulate phases. The partition between gas and particulate phases affects the concentration and fate of e-cig-emitted chemicals and warrants future study.

Chemical Profiles of E-Cig Aerosols

As shown in Fig. 10, the chemical profiles of mainstream and secondhand e-cig aerosols are similar, but as expected, the concentrations of most chemicals in the SHV are much lower than in the mainstream. Overall, the most abundant chemicals detected in the e-cig mainstream are PG and VG, followed by nicotine, carbonyls,

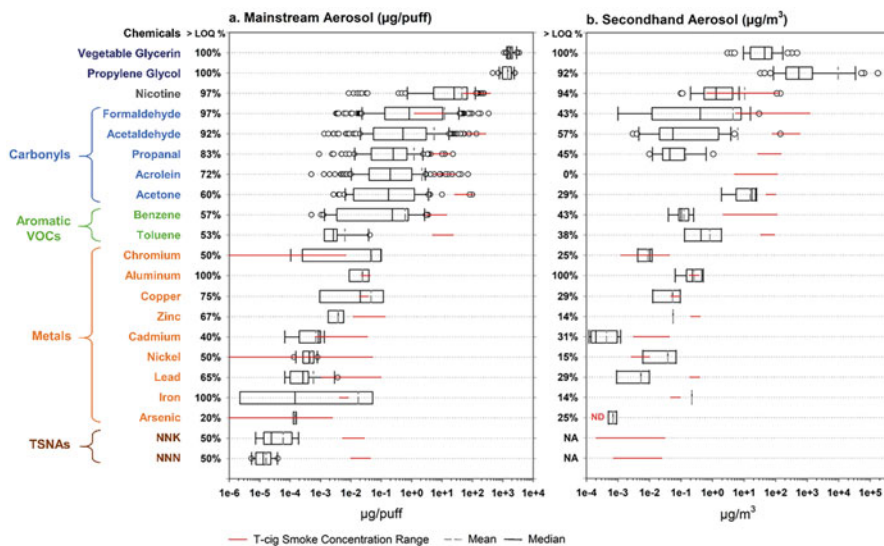


Fig. 10 Chemical compositions of e-cig aerosols including (a) emission rates of mainstream aerosols ($\mu\text{g}/\text{puff}$) from 37 studies and (b) concentration of secondhand aerosols ($\mu\text{g}/\text{m}^3$) from 11 indoor studies in which e-cig users vape in an indoor environment. Emission rates or concentrations of t-cig-emitted chemicals are presented in ranges (red line) as a reference group. All the data included are background-subtracted values, when applicable. “> LOQ%” indicates the percentage of available data points above the limit of quantification (LOQ). Abbreviations: VOCs = volatile organic compounds; TSNAAs = tobacco-specific nitrosamines; NNK = 4-(methylnitrosamino)-1-(3-pyridyl)-1-butanone; NNN=N'-Nitrosonornicotine (Li et al. 2020b and references therein)

aromatic VOCs, and trace metals. Most of the chemicals in the mainstream come from the major components of e-liquids: PG, VG, and nicotine. Although the FDA states that ingesting PG and VG in consumer and household products is safe, inhaling vaporized PG and VG at high concentrations could potentially irritate the lungs (Kienhuis et al. 2015), which is a unique health risk for e-cig aerosols (Liu et al. 2017). The significant amount of nicotine reported in the e-cig aerosols also poses several health risks. Existing evidence indicates that e-cig use can motivate youth to start smoking t-cig due to the highly addictive nature of nicotine (Glantz and Bareham 2018). In addition, nicotine contributes to adverse health effects on the cardiocirculatory, respiratory, and gastrointestinal systems (England et al. 2017; Benowitz and Burbank 2016; Mishra et al. 2015).

Other observed chemicals such as formaldehyde, acetaldehyde, propanal, acrolein, acetone, and benzene are likely produced by thermal degradation of PG and VG (Sleiman et al. 2016; Qu et al. 2019; Pankow et al. 2017). The detailed chemistry for the thermal degradation process of PG and VG is demonstrated in Fig. 11. E-cig-related aldehydes might also come from flavoring additives in the e-liquid (Khlystov and Samburova 2016). Aldehydes are cytotoxic and can have adverse respiratory effects. In addition, formaldehyde and acetaldehyde are classified by the

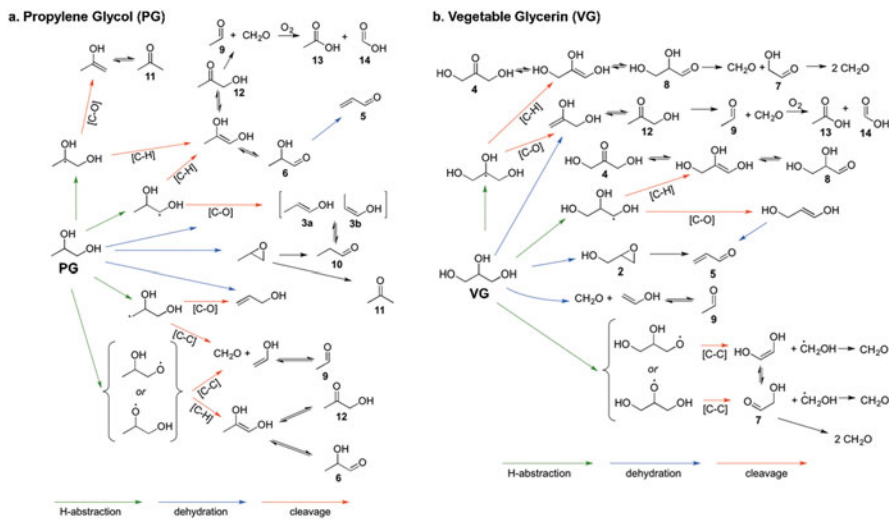


Fig. 11 Decomposition pathways of (a) propylene glycol (PG) and (b) vegetable glycerin (VG) in e-cig aerosols. The most prevalent reaction mechanisms involve oxidation and dehydration. Compound number definitions: 2, glycidol; 3a, b, propenol isomers; 4, dihydroxyacetone; 5, acrolein; 6, lactaldehyde; 7, glycolaldehyde; 8, glyceraldehyde; 9, acetaldehyde; 10, propanal; 11, acetone; 12, hydroxyacetone (acetol); 13, acetic acid; and 14, formic acid. (Adapted from Jensen et al. (2017) under the terms of the Creative Commons Attribution 4.0 International License, <http://creativecommons.org/licenses/by/4.0/>)

International Agency for Research on Cancer (IARC) as carcinogenic to humans (Group 1) and possibly carcinogenic to humans (Group 2B), respectively. In addition to the most commonly reported carbonyls, a few studies have also reported other compounds such as crotonaldehyde, methylglyoxal, glyoxal, dihydroxyacetone, butyraldehyde, benzaldehyde, isovaleraldehyde, valeraldehyde, and diacetyl in e-cig aerosols (Ward et al. 2020). Among the aromatic VOCs, the IARC lists benzene as a human carcinogen and toluene may be neurotoxic. One of the benzene formation mechanisms is decarboxylation of benzoic acid, suggesting the risk of using a large amount of benzoic acid in the pod system (Pankow et al. 2017). E-cig aerosols also contain a wide variety of VOCs at lower levels, such as acetonitrile, isoprene, ethanol, acetoin, and diacetyl, which likely originate from the flavoring additives (Lee et al. 2017; Klager et al. 2017).

The likely sources of trace metals, especially those with relatively higher concentrations (i.e., chromium, aluminum, and copper), are the metal-coated wires of the heating coils (Saffari et al. 2014; Williams et al. 2013). Inhaling trace metals might irritate the respiratory system and impair respiration (Williams et al. 2013). Cadmium, lead, chromium, arsenic, and nickel are also classified as human carcinogens. Many of these metals or metalloids were also identified in human biospecimens of e-cig users including urine, saliva, serum, and blood. Most metal or metalloid levels were comparable or higher than those identified in biospecimens of t-cig users (Zhao et al. 2020).

Although two studies found nicotine-derived nitrosamines, such as N'-Nitrosonornicotine (NNN) and 4-(methylnitrosamino)-1-(3-pyridyl)-1-butanone (NNK) (Goniewicz et al. 2014; Margham et al. 2016), which are strong carcinogens that may cause lung and oral cancers (Hecht et al. 2016), but whether these compounds are products of chemical reactions of nicotine or impurities of the e-liquid is not clear (Farsalinos et al. 2015). Less evidence exists in the literature on polycyclic aromatic hydrocarbons (PAHs) concentrations in e-cig aerosols which were reported either low or undetectable (Ward et al. 2020). On the other hand, reactive oxygen species (ROS) and free radicals in e-cig aerosols have also drawn some attention due to their potential to damage macromolecules and disrupt normal biological functions. ROS and free radicals were found in e-cig aerosols, although at lower levels than those found in t-cig smoke (Hasan et al. 2020; Son et al. 2019).

The concentrations of most chemicals in the e-cig mainstream aerosols are generally lower than those of t-cigs (Fig. 10). The only exceptions are PG and VG, which are major components of e-liquids and not present in t-cigs. Concentrations of trace metals in mainstream aerosols are similar in e-cigs and t-cigs. However, chromium, a carcinogenic and respiratory toxicant, is at higher concentrations in e-cigs, suggesting potential risks from chromium-coated wire in heating coils (Williams et al. 2013). The concentration of nicotine in e-cig mainstream aerosol is similar to or slightly lower than that in t-cig smoke. Of note, the nicotine content in a single JUUL pod with 5% nicotine strength is higher than that in 20 t-cigs which might lead to potential cytotoxicity and more significant addiction effects (Omaiye et al. 2019). The concentrations of carbonyls and aromatic VOCs are 10–1000 times higher in the mainstream emissions of t-cigs than in e-cigs. Because these compounds are highly toxic, the observed lower concentrations indicate that e-cig aerosols are likely less toxic than t-cig smoke (Cervellati et al. 2014). Alternatively, the mainstream emission rates of nicotine and degradation by-products such as formaldehyde, acetaldehyde, propanol, acrolein, acetone, and benzene in e-cig aerosols are at a similar level of “heat-not-burn” products (Cancelada et al. 2019), suggesting the impacts of combustion-free nicotine delivery systems on indoor air quality.

Factors Affecting Chemical Compositions

E-cig device: Chemical compositions in e-cig aerosols vary across different e-cig brands and types. The power levels and heating elements primarily determine the chemical emissions in e-cig aerosols. Extensive studies have investigated the relationship between the power and chemical concentrations in e-cig aerosols (Ward et al. 2020). When the power applied to the heating coil increases, carbonyl compounds (e.g., formaldehyde, acetaldehyde, propanal, acrolein, and acetone), aromatic VOCs (e.g., benzene and toluene), and trace metals in e-cig aerosols also increase (El-Hellani et al. 2018; Qu et al. 2019; Gillman et al. 2016; Pankow et al. 2017; Zhao et al. 2019). The types of atomizers in the tank-style systems can also affect the carbonyl emissions. For example, more carbonyls were produced using top-coil atomizers than bottom-coil atomizers, while sub-ohm coils with lower

resistance generated less carbonyls compared to supra-ohm tanks (Gillman et al. 2016). The tank-style systems with higher voltages were found to generate more toxic metals than cigalike or pod systems (Zhao et al. 2019). Similarly, nicotine yields were affected by the power outputs as well as the e-cig types and brands (Talih et al. 2015).

The first three generations of e-cig devices, ranging from cigalike to tank-style systems, use pure nicotine dissolved in the e-liquids. In contrast, the newest generation pod system (e.g., JUUL pod) uses a large amount of benzoic acid, as part of the nicotine salts formulation which brings more uncertainties on their health effects. The pod system was designed to have a lower power voltage but a higher nicotine dose to simulate t-cig smoking. As a result, higher levels of nicotine and lower levels of carbonyl compounds in the JUUL-generated aerosols were observed compared to other tank-style systems (Reilly et al. 2019).

E-liquid compositions: As previously discussed, the chemicals identified in e-cig aerosols are largely determined by the e-liquid compositions. The evidence in the literature suggests that the production of toxic chemicals, such as carbonyls and VOCs, has been associated with the flavoring compounds added to the e-liquid and the thermal degradation of PG and VG. Many chemical compounds such as acetaldehyde and acrolein were found in the e-cig aerosol but not in the e-liquid, suggesting the formation of toxicants during the heating process. Aldehydes formation was dependent on the PG/VG ratios. Certain chemicals, such as acetaldehyde, can be generated solely by PG degradation, while VG generates higher levels of formaldehyde and acrolein.

As to the flavoring additives, the aldehyde levels in e-cig aerosols from flavored e-liquids are significantly higher than those generated from pure PG or VG. Aldehydes concentrations increase as sucralose (an artificial sweetener) or diacetyl (a butter flavoring agent) concentration increases. Diacetyl and acetoin were found to be the most prevalent flavoring chemicals (Klager et al. 2017). Acetoin is a precursor to diacetyl in e-liquids, where diacetyl concentration was found proportional to acetoin. The inhalation of aerosols containing diacetyl may lead to the development of bronchiolitis obliterans or an irreversible respiratory disease, also known as “popcorn lung.” Another example is the formation of benzene in the e-cig aerosols. Benzene concentration increased with the addition of benzoic acid (an antimicrobial and flavoring agent) and benzaldehyde (an almond flavoring agent). Notably, the percentage of benzaldehyde transferred from e-liquid to e-cig aerosol is also higher with elevated PG content in the e-liquid. Higher nicotine delivery has also been associated with more PG content (El-Hellani et al. 2018). The reactions between PG and VG, together with nicotine and other flavoring additives, may have more complicated effects on the toxic emissions. Different from carbonyls and VOCs, e-liquid compositions have the minimal effects on the trace metals production.

Puffing topography: Similar to particle emissions, longer puff duration and greater puff frequency tend to generate more organic species (Zhao et al. 2018). Parameters such as puffing topography, e-cig type, and voltage sometimes interact with each other, resulting in combination effects on the chemical emissions (Beauval

et al. 2019). For example, increasing puff duration and frequency or decrease puff flow rate may result in higher heating coil temperature, where higher levels of carbonyls can be expected. However, varying degrees of these effects were observed depending on the wattage levels and e-cigs types. Interestingly, researchers found that conditions leading to formaldehyde formation tend to generate less acetaldehyde (Beauval et al. 2019). In general, the exhaled chemicals by the e-cig user can be quickly diluted in the environment, resulting in a low concentration. Nevertheless, little is known about the extent to which the inhalation and exhalation process affects the chemical compositions of the SHV aerosols.

Although a limited number of experimental studies focused on indoor chemical exposure, a modeling method has been successfully applied to predict the toxic intake and secondhand exposure levels (Logue et al. 2017). Logue et al. (2017) used the mass balance equation involving chemical emission rates, indoor volumes, air exchange rates, vaping patterns, and the leakage from the mouth before inhalation to evaluate the indoor pollutant levels in both home and bar scenarios. Key parameters, such as vaping patterns, type of atomizer, and the voltage which are linked to intake doses and indoor pollutant levels, need to be considered for future exposure assessment studies.

Thirdhand Exposure

Besides the secondhand exposure, the deposited residuals from vaping might be reemitted into the gas phase and serve as a potential source of thirdhand exposure (Khachatoorian et al. 2019; Goniewicz and Lee 2015). In a multiunit building, Khachatoorian et al. (2019) detected tobacco-specific residues, including nicotine, minor alkaloids, and TSNAs, on surfaces in an indoor space adjacent to a vape shop, suggesting potential thirdhand exposures to e-cig emissions. Given the limited data, thirdhand exposures to e-cig residues and associated health effects are poorly understood and warrant future study.

Health Effects

In Vivo and In Vitro Studies

In general, studies have shown that e-cig aerosols are less toxic than t-cig smoke (Oh and Kacker 2014). However, substantial evidence indicates that e-cig aerosols are not safe to cells in vitro or to animals in vivo. Results from in vitro studies have identified the biologic effects on various cell types such as normal human bronchial epithelial cells, vascular endothelial cells, and macrophages (Merecz-Sadowska et al. 2020). Associated with elevated ROS levels, e-cig aerosols may induce cytotoxicity and genotoxicity. Exposure to e-cig aerosols has been shown to decrease cell viability, increase pro-inflammatory cytokine production, and induce gene dysregulation, DNA damage, and alveolar macrophage apoptosis (Merecz-

Sadowska et al. 2020). Although PG and VG are generally considered safe if added to food, the inhalation of aerosolized PG and VG may promote asthmatic inflammation and elevate mucin expression in airway epithelia (Gotts et al. 2019). Regarding cytotoxicity and pro-inflammatory effects, PG was found to be more toxic than VG (Ma et al. 2020). Certain toxic effects have been linked to the addition of flavoring chemicals such as diacetyl, acetoin, and cinnamaldehyde, which may trigger inflammation and ROS production. In contrast, aerosols generated by flavorless e-liquids can also induce adverse effects such as dysregulation of gene expression and inflammatory protein secretion. Although the effect of nicotine on cells varies, adverse cellular responses of both nicotine-dependent and nicotine-independent effects have been found. Researchers also found that e-cig aerosols induce oxidative stress, inflammatory cytokine production, and cytotoxicity regardless of the addition of nicotine to the e-liquid (Ma et al. 2020).

Similarly, e-cig aerosols have been found to impair lung functions in animals, with inflammation and immune abnormalities as the likely underlying mechanisms (Dinakar and O'Connor 2016). Other acute effects include increased mucins and cytokines, and impaired autophagy. Chronic exposure induces elevated inflammation, weight loss, and emphysema (Gotts et al. 2019). A study has reported that the bronchoalveolar lavage fluid cellularity, mucin production, and lung oxidative stress marker associated with e-cig aerosols were at a comparable or even higher level than t-cig smoke (Glynnos et al. 2018). In addition to pulmonary effects, both short-term and chronic uses of e-cig aerosols were found to impair aortic endothelial function and perturb the cardiovascular system (Olfert et al. 2018). Moreover, e-cig aerosols also present marked carcinogenicity (Lee et al. 2018) and neurological toxicity (Nguyen et al. 2018) in animals. However, it remains controversial whether the dosages used in animal studies are relevant to human exposures, and whether the results are consistent across different species.

Human Studies: Active Exposure to E-Cig Aerosols

The respiratory and cardiovascular effects of e-cig aerosols were also examined in human studies, most of which have focused on the effects of active e-cig use with only a few studies on secondhand exposures. As indicated by circulating concentrations of cotinine, doses in active exposure studies are generally higher than those in secondhand studies. Overall, results of these studies suggest likely short-term effects of e-cig aerosols (≤ 2 h of exposure) on preclinical endpoints.

Respiratory Effects

Most human studies on the respiratory system examine the effects of short-term (≤ 1 h) exposure among a small number of healthy subjects. Lung function is one of the most commonly studied endpoints, but the results of different studies are inconsistent. Active e-cig use by healthy t-cig smokers over 5 min slightly but significantly reduced lung function measures (i.e., forced expiratory volume in 1 s [FEV1] and forced expiratory flow [FEF] 25%) in a randomized crossover trial

(Ferrari et al. 2015). However, similar effects were not observed in two crossover trials (one randomized and one nonrandomized), in which active vaping over 5 or 30 min did not change any lung function measures among healthy t-cig smokers (Flouris et al. 2013; Vardavas et al. 2012). In contrast, more consistent results were reported for airway resistance, which was significantly increased after active e-cig use or passive exposure in two clinical trials, as determined by impulse oscillometry (Vardavas et al. 2012; Tzortzi et al. 2018). In addition, a case-control study found substantially altered respiratory proteomic profiles among e-cig users indicative of impending airway obstruction (Dang et al. 2018). Nevertheless, the clinical importance of these early changes is not clear. It is still unclear whether increased airway resistance induced by e-cig aerosols will become worse over time and eventually contribute to decreased lung function.

Studies have also assessed the short-term effects (≤ 2 h) of e-cig aerosols on exhaled nitric oxide, a biomarker of airway inflammation associated with increased risk of asthma and bronchitis (Taylor et al. 2006). Several studies report no effect (Flouris et al. 2013; Ferrari et al. 2015), and other studies show either increased (Schober et al. 2014) or decreased exhaled nitric oxide concentrations after exposures (Vardavas et al. 2012; Tzortzi et al. 2018). In two cross-sectional studies of adolescents, e-cig use was significantly associated with a greater odds of asthma attacks (odds ratio [OR], 1.12; 95% CI, 1.01 to 1.26) (Kim et al. 2017) and chronic bronchitis symptoms (OR, 1.70; 95% CI, 1.11 to 2.59) (McConnell et al. 2017).

Between August 2019 and February 2020, the EVALI outbreak had resulted in 2807 cases and 68 deaths in the USA which underscored the acute health effects of vaping. Most patients have shown respiratory symptoms (i.e., cough, chest pain, and shortness of breath), constitutional symptoms (i.e., weight loss, fevers, and chills), and gastrointestinal symptoms (i.e., nausea, vomiting, diarrhea, and abdominal pain). EVALI has different pathologic findings, including acute fibrinous pneumonitis, diffuse alveolar damage, or organizing pneumonia (Butt et al. 2019). Investigations have found that THC, sometimes with vitamin E acetate, in most of the e-liquids is used by the EVALI patients. Vitamin E acetate has been considered as a possible agent that disrupts lung surfactant function and causes respiratory impairment. Although the development of EVALI has been associated with vaping, the cause of the lung injury has not been explicitly determined yet. Nevertheless, vaping cannabis products may pose a health risk of passive exposure to bystanders, where the associated health effects are largely unknown.

Cardiovascular Effects

The effects of active e-cig use on cardiovascular biomarkers have been documented. Both habitual and short-term e-cig use can cause a cardiac-autonomic imbalance, as indicated by heart rate variability. Nicotine has been suggested as a likely cause (Moheimani et al. 2017). The existing evidence also suggests that active e-cig use induces systemic oxidative stress and inflammation, and impairs endothelial function (Skotsimara et al. 2019). Although oxidative stress and inflammation are important in the pathogenesis of cardiovascular diseases, to what extent the observed cardiovascular effects of e-cigs are clinically relevant is unclear. The cross-sectional

National Health Interview Surveys of 2014 ($n = 37,000$) and 2016 ($n = 33,000$) found that daily e-cig use was associated with myocardial infarction (OR, 1.79; 95% CI, 1.20 to 2.66) (Alzahrani et al. 2018), but more evidence is needed, especially from long-term large cohort studies, before e-cig use can be linked to cardiovascular diseases.

Human Studies: Passive Exposure to SHV Aerosols

Evidence of passive exposures to SHV aerosols on respiratory and cardiovascular effects in humans is limited. Increased cotinine levels in biospecimens of nonsmokers due to passive exposure to SHV aerosols confirm that nonsmokers, including vulnerable populations, are at risks of exposures to nicotine and other toxicants exhaled by e-cig users (Flouris et al. 2013). In a nonrandomized crossover trial on SHV aerosols, a 1 h passive exposure did not significantly affect the lung function among healthy nonsmokers (Flouris et al. 2013). However, another study observed minor alterations in respiratory mechanics and exhaled biomarkers after a 30 min exposure to SHV aerosols, where an obstructive airway indicator (i.e., resonant frequency) was increased and fractional exhaled nitric oxide was reduced (Tzortzi et al. 2018). Similarly, a 30 min exposure to SHV aerosols also induced sensory irritations, including ocular, nasal, and throat-respiratory symptoms, which have been found positively associated with VOCs (Tzortzi et al. 2020). According to two cross-sectional surveys, exposures to SHV aerosols were associated with asthma exacerbations in the adolescent population (Bayly et al. 2019; Alnajem et al. 2020), suggesting potential adverse respiratory effects of passive exposures, at least among susceptible populations. Two studies that assessed the complete blood count and oxidative stress biomarkers, respectively, found no differences before and after the 1 h passive exposure among healthy nonsmokers (Flouris et al. 2012; Poulianiti et al. 2016). However, no cumulative or long-term cardiovascular effects were examined.

Conclusions

The evidence in the literature supports that use of e-cig degrades indoor air quality and bystanders are at risk of passive exposure. Indoor particle concentrations due to e-cigs are similar to those due to t-cigs. Similar to SHS, SHV aerosols can transfer from a vaping room to an adjacent vaping-free room in multiunit buildings. Indoor air pollution due to e-cigs could potentially be reduced by enhancing ventilation and air filtration. Unfortunately, studies on mitigation measures that may inform policy are still limited. Future studies also need to focus on identifying vulnerable populations and monitor places that may contribute to high levels of passive exposures, such as vape shops, vaping conventions, and other indoor environments with no restrictions on e-cig use.

Although studies of SHV aerosols are limited, their chemical composition profiles are similar to those of mainstream e-cig aerosols but at much lower concentrations.

E-cigs generate fewer carcinogenic and toxic compounds than t-cigs, but they still produce substantial amounts of PG, VG, and nicotine, as well as some toxic compounds such as aldehydes and heavy metals. Given the uncertainties of the chemical products of the heating process and the complexity of flavoring including cannabis additives, the e-cig design features and e-liquid compositions should be further studied to better understand their effects on e-cig aerosol toxicity to inform future regulations.

Evidence obtained from cell cultures and animal models has demonstrated the adverse health effects of e-cig use. Current human studies have focused on the acute effects and early biomarkers and have suggested potential respiratory and cardiovascular effects from e-cig aerosols. However, results from these studies are inconsistent, calling for large cohort and long-term studies that examine the linkage between e-cigs and clinical end points. In addition, the contribution of cannabis products and vitamin E acetate to EVALI and the associated passive exposure also warrant further research.

Although the effects of e-cigs on human health are not yet fully understood, the high levels of indoor air pollutants produced by e-cigs call for precautionary measures to protect public health. Many countries have taken steps to restrict e-cig use in public spaces. As of July 2021, 20 states and 990 municipalities in the USA have already expanded smoke-free laws to include e-cigs and have prohibited their use in smoke-free places. In certain places, such as casinos, bars, and other gaming venues where t-cigs are allowed, e-cig use can further worsen indoor air quality. Until the long-term health effects are fully established, we recommend restricting the use of e-cigs in public indoor spaces to protect bystanders from passive exposures to SHV aerosols.

References

- Alnajem A, Redha A, Alroumi D et al (2020) Use of electronic cigarettes and secondhand exposure to their aerosols are associated with asthma symptoms among adolescents: a cross-sectional study. *Respir Res* 21(1):300. <https://doi.org/10.1186/s12931-020-01569-9>
- Alzahrani T, Pena I, Temesgen N et al (2018) Association between electronic cigarette use and myocardial infarction. *Am J Prev Med* 55(4):455–461. <https://doi.org/10.1016/j.amepre.2018.05.004>
- Amalia B, Liu X, Lugo A et al (2020) Exposure to secondhand aerosol of electronic cigarettes in indoor settings in 12 European countries: data from the TackSHS survey. *Tobacco control: tobaccocontrol-2019-055376*. <https://doi.org/10.1136/tobaccocontrol-2019-055376>
- Baassiri M, Talih S, Salman R et al (2017) Clouds and “throat hit”: effects of liquid composition on nicotine emissions and physical characteristics of electronic cigarette aerosols. *Aerosol Sci Technol* 51(11):1231–1239. <https://doi.org/10.1080/0278626.2017.1341040>
- Bayly JE, Bernat D, Porter L et al (2019) Secondhand exposure to aerosols from electronic nicotine delivery systems and asthma exacerbations among youth with asthma. *Chest* 155(1):88–93. <https://doi.org/10.1016/j.chest.2018.10.005>
- Beauval N, Verrièle M, Garat A et al (2019) Influence of puffing conditions on the carbonyl composition of e-cigarette aerosols. *Int J Hyg Environ Health* 222(1):136–146. <https://doi.org/10.1016/j.ijheh.2018.08.015>

- Benowitz NL, Burbank AD (2016) Cardiovascular toxicity of nicotine: implications for electronic cigarette use. *Trends Cardiovasc Med* 26(6):515–523. <https://doi.org/10.1016/j.tcm.2016.03.001>
- Burnett R, Chen H, Szyszkowicz M et al (2018) Global estimates of mortality associated with long-term exposure to outdoor fine particulate matter. *Proc Natl Acad Sci* 115(38):9592. <https://doi.org/10.1073/pnas.1803222115>
- Butt YM, Smith ML, Tazelaar HD et al (2019) Pathology of vaping-associated lung injury. *N Engl J Med* 381(18):1780–1781. <https://doi.org/10.1056/NEJMcp1913069>
- Cancelada L, Sleiman M, Tang X et al (2019) Heated tobacco products: volatile emissions and their predicted impact on indoor air quality. *Environ Sci Technol* 53(13):7866–7876. <https://doi.org/10.1021/acs.est.9b02544>
- CDC (2020) Youth tobacco use: results from the National Youth Tobacco Survey. Centers for Disease Control and Prevention. <https://www.fda.gov/tobacco-products/youth-and-tobacco/youth-tobacco-use-results-national-youth-tobacco-survey>. Accessed 22 Dec 2020
- Cervellati F, Muresan XM, Sticcozzi C et al (2014) Comparative effects between electronic and cigarette smoke in human keratinocytes and epithelial lung cells. *Toxicol In Vitro* 28(5): 999–1005. <https://doi.org/10.1016/j.tiv.2014.04.012>
- Cohen AJ, Brauer M, Burnett R (2018) Estimates and 25-year trends of the global burden of disease attributable to ambient air pollution: an analysis of data from the Global Burden of Diseases Study 2015 (vol 389, pg 1907, 2017). *Lancet* 391(10130):1576–1576. [https://doi.org/10.1016/s0140-6736\(18\)30900-0](https://doi.org/10.1016/s0140-6736(18)30900-0)
- Dang H, Mascenik T, Graves LM et al (2018) Chronic E-cigarette exposure alters the human bronchial epithelial proteome. *Am J Respir Crit Care Med* 198(1):36–36. <https://doi.org/10.1164/rccm.201710-2033oc>
- Dinakar C, O'Connor GT (2016) The health effects of electronic cigarettes. *N Engl J Med* 375(14): 1372–1381. <https://doi.org/10.1056/NEJMra1502466>
- El-Hellani A, Salman R, El-Hage R et al (2018) Nicotine and carbonyl emissions from popular electronic cigarette products: correlation to liquid composition and design characteristics. *Nicotine Tob Res* 20(2):215–223. <https://doi.org/10.1093/ntr/ntw280>
- England LJ, Aagaard K, Bloch M et al (2017) Developmental toxicity of nicotine: a transdisciplinary synthesis and implications for emerging tobacco products. *Neurosci Biobehav Rev* 72: 176–189. <https://doi.org/10.1016/j.neubiorev.2016.11.013>
- Farsalinos KE, Gillman G, Poulas K et al (2015) Tobacco-specific nitrosamines in electronic cigarettes: comparison between liquid and aerosol levels. *Int J Environ Res Public Health* 12(8):9046–9053. <https://doi.org/10.3390/ijerph120809046>
- Ferrari M, Zanasi A, Nardi E et al (2015) Short-term effects of a nicotine-free e-cigarette compared to a traditional cigarette in smokers and non-smokers. *BMC Pulm Med* 15(1):1–9. <https://doi.org/10.1186/s12890-015-0106-z>
- Flouris AD, Chorti MS, Poulianiti KP et al (2013) Acute impact of active and passive electronic cigarette smoking on serum cotinine and lung function. *Inhal Toxicol* 25(2):91–101. <https://doi.org/10.3109/08958378.2012.758197>
- Flouris AD, Poulianiti KP, Chorti MS et al (2012) Acute effects of electronic and tobacco cigarette smoking on complete blood count. *Food Chem Toxicol* 50(10):3600–3603. <https://doi.org/10.1016/j.fct.2012.07.025>
- Floyd EL, Queimado L, Wang J et al (2018) Electronic cigarette power affects count concentration and particle size distribution of vaping aerosol. *PLoS One* 13(12). <https://doi.org/10.1371/journal.pone.0210147>
- Forster M, McAughey J, Prasad K et al (2018) Assessment of tobacco heating product THP1.0. Part 4: characterisation of indoor air quality and odour. *Regul Toxicol Pharmacol* 93:34–51. <https://doi.org/10.1016/j.yrtph.2017.09.017>
- Fromme H, Dietrich S, Heitmann D et al (2009) Indoor air contamination during a waterpipe (narghile) smoking session. *Food Chem Toxicol* 47(7):1636–1641. <https://doi.org/10.1016/j.fct.2009.04.017>

- Fuoco FC, Buonanno G, Stabile L et al (2014) Influential parameters on particle concentration and size distribution in the mainstream of e-cigarettes. *Environ Pollut* 184:523–529. <https://doi.org/10.1016/j.envpol.2013.10.010>
- Galstyan E, Galimov A, Sussman S (2019) Commentary: the emergence of pod mods at vape shops. *Eval Health Prof* 42(1):118–124. <https://doi.org/10.1177/0163278718812976>
- Gentzke AS, Wang TW, Marynak KL et al (2019) Exposure to secondhand smoke and secondhand E-cigarette aerosol among middle and high school students. *Prev Chronic Dis* 16:E42–E42. <https://doi.org/10.5888/pcd16.180531>
- Gillman IG, Kistler KA, Stewart EW et al (2016) Effect of variable power levels on the yield of total aerosol mass and formation of aldehydes in e-cigarette aerosols. *Regul Toxicol Pharmacol* 75: 58–65. <https://doi.org/10.1016/j.yrtph.2015.12.019>
- Glantz SA, Bareham DW (2018) E-cigarettes: use, effects on smoking, risks, and policy implications. In: Fielding JE, Brownson RC, Green LW (eds) Annual Review of Public Health, Vol 39, vol 39. Annual Review of Public Health. pp 215–235. <https://doi.org/10.1146/annurev-publhealth040617-013757>
- Glynos C, Bibli S-I, Katsaounou P et al (2018) Comparison of the effects of e-cigarette vapor with cigarette smoke on lung function and inflammation in mice. *Am J Phys Lung Cell Mol Phys* 315(5):L662–L672. <https://doi.org/10.1152/ajplung.00389.2017>
- Goniewicz ML, Knysak J, Gawron M et al (2014) Levels of selected carcinogens and toxicants in vapour from electronic cigarettes. *Tob Control* 23(2):133–139. <https://doi.org/10.1136/tobaccocontrol-2012-050859>
- Goniewicz ML, Lee L (2015) Electronic cigarettes are a source of thirdhand exposure to nicotine. *Nicotine Tob Res* 17(2):256–258. <https://doi.org/10.1093/ntr/ntu152>
- Gotts JE, Jordt SE, McConnell R et al (2019) What are the respiratory effects of e-cigarettes? *Brit Med J* 366:16. <https://doi.org/10.1136/bmj.l5275>
- Guo H, Morawska L, He CR et al (2010) Characterization of particle number concentrations and PM_{2.5} in a school: influence of outdoor air pollution on indoor air. *Environ Sci Pollut Res* 17(6): 1268–1278. <https://doi.org/10.1007/s11356-010-0306-2>
- Hasan F, Khachatryan L, Lomnicki S (2020) Comparative studies of environmentally persistent free radicals on Total particulate matter collected from electronic and tobacco cigarettes. *Environ Sci Technol* 54(9):5710–5718. <https://doi.org/10.1021/acs.est.0c00351>
- Hecht SS, Stepanov I, Carmella SG (2016) Exposure and metabolic activation biomarkers of carcinogenic tobacco-specific nitrosamines. *Acc Chem Res* 49(1):106–114. <https://doi.org/10.1021/acs.accounts.5b00472>
- Hinds WC (1999) Aerosol technology: properties, behavior, and measurement of airborne particles, 2nd edn. Wiley, New York
- Ingebretsen BJ, Cole SK, Alderman SL (2012) Electronic cigarette aerosol particle size distribution measurements. *Inhal Toxicol* 24(14):976–984. <https://doi.org/10.3109/08958378.2012.744781>
- Jensen RP, Strongin RM, Peyton DH (2017) Solvent chemistry in the electronic cigarette reaction vessel. *Sci Rep* 7. <https://doi.org/10.1038/srep42549>
- Khachatoorian C, Jacob P, Benowitz NL et al (2019) Electronic cigarette chemicals transfer from a vape shop to a nearby business in a multiple-tenant retail building. *Tob Control* 28(5):519–525. <https://doi.org/10.1136/tobaccocontrol-2018-054316>
- Khlystov A, Samburova V (2016) Flavoring compounds dominate toxic aldehyde production during E-cigarette vaping. *Environ Sci Technol* 50(23):13080–13085. <https://doi.org/10.1021/acs.est.6b05145>
- Kienhuis AS, Soeteman-Hernandez LG, Bos PMJ et al (2015) Potential harmful health effects of inhaling nicotine-free shisha-pen vapor: a chemical risk assessment of the main components propylene glycol and glycerol. *Tob Induc Dis* 13. <https://doi.org/10.1186/s12971-015-0038-7>
- Kim SY, Sim S, Choi HG (2017) Active, passive, and electronic cigarette smoking is associated with asthma in adolescents. *Sci Rep* 7(1):1–8. <https://doi.org/10.1038/s41598-017-17958-y>

- Klager S, Vallarino J, MacNaughton P et al (2017) Flavoring chemicals and aldehydes in E-cigarette emissions. *Environ Sci Technol* 51(18):10806–10813. <https://doi.org/10.1021/acs.est.7b02205>
- Konstantopoulou SS, Behrakis PK, Lazaris AC et al (2014) Indoor air quality in a bar/restaurant before and after the smoking ban in Athens, Greece. *Sci Total Environ* 476:136–143. <https://doi.org/10.1016/j.scitotenv.2013.11.129>
- Layden JE, Ghinai I, Pray I et al (2019) Pulmonary illness related to E-cigarette use in Illinois and Wisconsin — preliminary report. *N Engl J Med*. <https://doi.org/10.1056/NEJMoa1911614>
- Lechasseur A, Altmejd S, Turgeon N et al (2019) Variations in coil temperature/power and e-liquid constituents change size and lung deposition of particles emitted by an electronic cigarette. *Physiol Rep* 7(10):e14093. <https://doi.org/10.14814/phy2.14093>
- Lee H-W, Park S-H, M-w W et al (2018) E-cigarette smoke damages DNA and reduces repair activity in mouse lung, heart, and bladder as well as in human lung and bladder cells. *Proc Natl Acad Sci* 115(7):E1560–E1569. <https://doi.org/10.1073/pnas.1718185115>
- Lee MS, LeBouf RF, Son YS et al (2017) Nicotine, aerosol particles, carbonyls and volatile organic compounds in tobacco- and menthol-flavored e-cigarettes. *Environmental Health* 16. <https://doi.org/10.1186/s12940-017-0249-x>
- Li L, Lee ES, Nguyen C et al (2020a) Effects of propylene glycol, vegetable glycerin, and nicotine on emissions and dynamics of electronic cigarette aerosols. *Aerosol Sci Technol*:1–12. <https://doi.org/10.1080/02786826.2020.1771270>
- Li L, Lin Y, Xia T et al (2020b) Effects of electronic cigarettes on indoor air quality and health. *Annu Rev Public Health* 41:363–380. <https://doi.org/10.1146/annurev-publhealth-040119-094043>
- Li L, Nguyen C, Lin Y et al (2020c) Impacts of electronic cigarettes usage on air quality of vape shops and their nearby areas. *Science of the Total Environment*:143423. <https://doi.org/10.1016/j.scitotenv.2020.143423>
- Liu JM, Liang QW, Oldham MJ et al (2017) Determination of selected chemical levels in room air and on surfaces after the use of cartridge- and tank-based E-vapor products or conventional cigarettes. *Int J Environ Res Public Health* 14(9). <https://doi.org/10.3390/ijerph14090969>
- Logue JM, Sleiman M, Montesinos VN et al (2017) Emissions from electronic cigarettes: assessing vapers' intake of toxic compounds, secondhand exposures, and the associated health impacts. *Environ Sci Technol* 51(16):9271–9279. <https://doi.org/10.1021/acs.est.7b00710>
- Ma T, Wang X, Li L et al (2020) Electronic cigarette aerosols induce oxidative stress-dependent cell death and NF-κB mediated acute lung inflammation in mice. *Arch Toxicol*. <https://doi.org/10.1007/s00204-020-02920-1>
- Manigrasso M, Buonanno G, Fuoco FC et al (2015) Aerosol deposition doses in the human respiratory tree of electronic cigarette smokers. *Environ Pollut* 196:257–267. <https://doi.org/10.1016/j.envpol.2014.10.013>
- Margham J, McAdam K, Forster M et al (2016) Chemical composition of aerosol from an E-cigarette: a quantitative comparison with cigarette smoke. *Chem Res Toxicol* 29(10):1662–1678. <https://doi.org/10.1021/acs.chemrestox.6b00188>
- McConnell R, Barrington-Trimis JL, Wang K et al (2017) Electronic cigarette use and respiratory symptoms in adolescents. *Am J Respir Crit Care Med* 195(8):1043–1049. <https://doi.org/10.1164/rccm.201604-0804OC>
- McKelvey K, Baiocchi M, Halpern-Felsher B (2018) Adolescents' and young adults' use and perceptions of pod-based electronic cigarettes. *JAMA Netw Open* 1(6). <https://doi.org/10.1001/jamanetworkopen.2018.3535>
- Merecz-Sadowska A, Sitarek P, Zielinska-Blizniewska H et al (2020) A summary of in vitro and in vivo studies evaluating the impact of E-cigarette exposure on living organisms and the environment. *Int J Mol Sci* 21(2). <https://doi.org/10.3390/ijms21020652>
- Mishra A, Chaturvedi P, Datta S et al (2015) Harmful effects of nicotine. *Indian J Med Paediatr Oncol* 36(1):24–31. <https://doi.org/10.4103/0971-5851.151771>

- Moheimani RS, Bhetraratana M, Yin F et al (2017) Increased cardiac sympathetic activity and oxidative stress in habitual electronic cigarette users: implications for cardiovascular risk. *JAMA Cardiol* 2(3):278–285. <https://doi.org/10.1001/jamocardio.2016.5303>
- Morawska L, Ayoko GA, Bae GN et al (2017) Airborne particles in indoor environment of homes, schools, offices and aged care facilities: the main routes of exposure. *Environ Int* 108:75–83. <https://doi.org/10.1016/j.envint.2017.07.025>
- Nguyen C, Li L, Sen CA et al (2019) Fine and ultrafine particles concentrations in vape shops. *Atmos Environ* 211:159–169. <https://doi.org/10.1016/j.atmosenv.2019.05.015>
- Nguyen T, Li GE, Chen H et al (2018) Maternal E-cigarette exposure results in cognitive and epigenetic alterations in offspring in a mouse model. *Chem Res Toxicol* 31(7):601–611. <https://doi.org/10.1021/acs.chemrestox.8b00084>
- Oh AY, Kacker A (2014) Do electronic cigarettes impart a lower potential disease burden than conventional tobacco cigarettes?: review on E-cigarette vapor versus tobacco smoke. *Laryngoscope* 124(12):2702–2706. <https://doi.org/10.1002/lary.24750>
- Olfert IM, DeVallance E, Hoskinson H et al (2018) Chronic exposure to electronic cigarettes results in impaired cardiovascular function in mice. *J Appl Physiol* 124(3):573–582. <https://doi.org/10.1152/japplphysiol.00713.2017>
- Omaiye EE, McWhirter KJ, Luo W et al (2019) High-nicotine electronic cigarette products: toxicity of JUUL fluids and aerosols correlates strongly with nicotine and some flavor chemical concentrations. *Chem Res Toxicol*. <https://doi.org/10.1021/acs.chemrestox.8b00381>
- Pankow JF, Kim K, McWhirter KJ et al (2017) Benzene formation in electronic cigarettes. *PLoS One* 12(3). <https://doi.org/10.1371/journal.pone.0173055>
- Poulianiti K, Karatzafiri C, Flouris AD et al (2016) Antioxidant responses following active and passive smoking of tobacco and electronic cigarettes. *Toxicol Mech Methods* 26(6):455–461. <https://doi.org/10.1080/15376516.2016.1196281>
- Qu Y, Szulejko JE, Kim KH et al (2019) The effect of varying battery voltage output on the emission rate of carbonyls released from e-cigarette smoke. *Microchem J* 145:47–54. <https://doi.org/10.1016/j.microc.2018.10.019>
- Reilly SM, Bitzer ZT, Goel R et al (2019) Free radical, carbonyl, and nicotine levels produced by Juul electronic cigarettes. *Nicotine Tob Res* 21(9):1274–1278. <https://doi.org/10.1093/ntr/nty221>
- Ruprecht AA, De Marco C, Saffari A et al (2017) Environmental pollution and emission factors of electronic cigarettes, heat-not-burn tobacco products, and conventional cigarettes. *Aerosol Sci Technol* 51(6):674–684. <https://doi.org/10.1080/02786826.2017.1300231>
- Saffari A, Daher N, Ruprecht A et al (2014) Particulate metals and organic compounds from electronic and tobacco-containing cigarettes: comparison of emission rates and secondhand exposure. *Environ Sci Process Impacts* 16(10):2259–2267. <https://doi.org/10.1039/c4em00415a>
- Scheitel M, Stanic M, Neuberger M (2016) PM10, PM2.5, PM1, number and surface of particles at the child's seat when smoking a cigarette in a car. *AIMS Environ Sci* 3(4):582–591. <https://doi.org/10.3934/environsci.2016.4.582>
- Schober W, Szendrei K, Matzen W et al (2014) Use of electronic cigarettes (e-cigarettes) impairs indoor air quality and increases FeNO levels of e-cigarette consumers. *Int J Hyg Environ Health* 217(6):628–637. <https://doi.org/10.1016/j.ijheh.2013.11.003>
- Schripp T, Markewitz D, Uhde E et al (2013) Does e-cigarette consumption cause passive vaping? *Indoor Air* 23(1):25–31. <https://doi.org/10.1111/j.1600-0668.2012.00792.x>
- Scungio M, Stabile L, Buonanno G (2018) Measurements of electronic cigarette-generated particles for the evaluation of lung cancer risk of active and passive users. *J Aerosol Sci* 115:1–11. <https://doi.org/10.1016/j.jaerosci.2017.10.006>
- Skotsimara G, Antonopoulos AS, Oikonomou E et al (2019) Cardiovascular effects of electronic cigarettes: a systematic review and meta-analysis. *Eur J Prev Cardiol* 26(11):1219–1228. <https://doi.org/10.1177/2047487319832975>

- Sleiman M, Logue JM, Montesinos VN et al (2016) Emissions from electronic cigarettes: key parameters affecting the release of harmful chemicals. *Environ Sci Technol* 50(17):9644–9651. <https://doi.org/10.1021/acs.est.6b01741>
- Son Y, Giovenco DP, Delnevo C et al (2020) Indoor air quality and passive E-cigarette aerosol exposures in vape-shops. *Nicotine Tob Res.* <https://doi.org/10.1093/ntr/ntaa094>
- Son Y, Mishin V, Laskin JD et al (2019) Hydroxyl radicals in E-cigarette vapor and E-vapor oxidative potentials under different vaping patterns. *Chem Res Toxicol* 32(6):1087–1095. <https://doi.org/10.1021/acs.chemrestox.8b00400>
- Sosnowski TR, Kramek-Romanowska K (2016) Predicted deposition of E-cigarette aerosol in the human lungs. *J Aerosol Med Pulm Drug Deliv* 29(3):299–309. <https://doi.org/10.1089/jamp.2015.1268>
- Sosnowski TR, Odziomek M (2018) Particle size dynamics: toward a better understanding of electronic cigarette aerosol interactions with the respiratory system. *Front Physiol* 9. <https://doi.org/10.3389/fphys.2018.00853>
- Sturm R (2016) Total deposition of ultrafine particles in the lungs of healthy men and women: experimental and theoretical results. *Ann Transl Med* 4(12). <https://doi.org/10.21037/atm.2016.06.05>
- Talih S, Balhas Z, Eissenberg T et al (2015) Effects of user puff topography, device voltage, and liquid nicotine concentration on electronic cigarette nicotine yield: measurements and model predictions. *Nicotine Tob Res* 17(2):150–157. <https://doi.org/10.1093/ntr/ntu174>
- Tang X, Cancelada L, Rapp VH et al (2021) Emissions from heated terpenoids present in vaporizable cannabis concentrates. *Environ Sci Technol* 55(9):6160–6170. <https://doi.org/10.1021/acs.est.1c00351>
- Taylor DR, Pijnenburg MW, Smith AD et al (2006) Exhaled nitric oxide measurements: clinical application and interpretation. *Thorax* 61(9):817–827. <https://doi.org/10.1136/thx.2005.056093>
- Terzano C, Di Stefano F, Conti V et al (2010) Air pollution ultrafine particles: toxicity beyond the lung. *Eur Rev Med Pharmacol Sci* 14(10):809–821
- Tzortzi A, Teloniatis S, Matiampa G et al (2020) Passive exposure of non-smokers to E-cigarette aerosols: sensory irritation, timing and association with volatile organic compounds. *Environ Res* 182:108963. <https://doi.org/10.1016/j.envres.2019.108963>
- Tzortzi A, Teloniatis SI, Matiampa G et al (2018) Passive exposure to e-cigarette emissions: immediate respiratory effects. *Tob Prev Cessat* 4(May). <https://doi.org/10.18332/tpc/89977>
- Vardavas CI, Anagnostopoulos N, Koulias M et al (2012) Short-term pulmonary effects of using an electronic cigarette: impact on respiratory flow resistance, impedance, and exhaled nitric oxide. *Chest* 141(6):1400–1406. <https://doi.org/10.1378/chest.11-2443>
- Wallace L, Ott W, Zhao T et al (2020) Secondhand exposure from vaping marijuana: concentrations, emissions, and exposures determined using both research-grade and low-cost monitors. *Atmos Environ* 8:100093. <https://doi.org/10.1016/j.aeaoa.2020.100093>
- Ward AM, Yaman R, Ebbert JO (2020) Electronic nicotine delivery system design and aerosol toxicants: a systematic review. *PLoS One* 15(6). <https://doi.org/10.1371/journal.pone.0234189>
- Williams M, Villarreal A, Bozhilov K et al (2013) Metal and silicate particles including nanoparticles are present in electronic cigarette cartomizer fluid and aerosol. *PLoS One* 8(3):1–11. <https://doi.org/10.1371/journal.pone.0057987>
- Wright TP, Song C, Sears S et al (2016) Thermodynamic and kinetic behavior of glycerol aerosol. *Aerosol Sci Technol* 50(12):1385–1396. <https://doi.org/10.1080/02786826.2016.1245405>
- Zervas E, Litsiou E, Konstantopoulos K et al (2018) Physical characterization of the aerosol of an electronic cigarette: impact of refill liquids. *Inhal Toxicol* 30(6):218–223. <https://doi.org/10.1080/08958378.2018.1500662>
- Zhang L, Lin Y, Zhu Y (2020) Transport and mitigation of exhaled electronic cigarette aerosols in a multizone indoor environment. *Aerosol Air Qual Res* 20:2536–2547
- Zhao D, Aravindakshan A, Hilpert M et al (2020) Metal/metalloid levels in electronic cigarette liquids, aerosols, and human biosamples: a systematic review. *Environ Health Perspect* 128(3). <https://doi.org/10.1289/ehp5686>

- Zhao D, Navas-Acien A, Ilievski V et al (2019) Metal concentrations in electronic cigarette aerosol: effect of open-system and closed-system devices and power settings. Environ Res 174:125–134. <https://doi.org/10.1016/j.envres.2019.04.003>
- Zhao JY, Nelson J, Dada O et al (2018) Assessing electronic cigarette emissions: linking physico-chemical properties to product brand, e-liquid flavoring additives, operational voltage and user puffing patterns. Inhal Toxicol 30(2):78–88. <https://doi.org/10.1080/08958378.2018.1450462>
- Zhao T, Shu S, Guo Q et al. (2016) Effects of design parameters and puff topography on heating coil temperature and mainstream aerosols in electronic cigarettes. Atmospheric Environment 134: 61–69. <https://doi.org/10.1016/j.atmosenv.2016.03.027>
- Zhao TK, Nguyen C, Lin CH et al (2017) Characteristics of secondhand electronic cigarette aerosols from active human use. Aerosol Sci Technol 51(12):1368–1376. <https://doi.org/10.1080/02786826.2017.1355548>
- Zhou S, Behrooz L, Weitzman M et al (2017) Secondhand hookah smoke: an occupational hazard for hookah bar employees. Tob Control 26(1):40–45. <https://doi.org/10.1136/tobaccocontrol-2015-052505>

Part III

Indoor Air Particles



Introduction to Particles in Indoor Air

8

Philip K. Hopke and Cong Liu

Contents

Introduction	234
Sources	235
Primary	235
Secondary	238
Particle Compositions	238
Nonvolatile Species	239
Semi-Volatile Species	239
Indoor Particle Dynamics	240
Infiltration	240
Deposition	241
Resuspension	241
Conclusions	242
References	242

Abstract

This chapter provides an overview of the section on Indoor Air Particles. This section focuses on the physical processes that affect particle concentrations and some major sources. Penetration of particles from the ambient aerosol into the indoor environment is an important source of indoor particles. The particles depending on their size can then deposit and can be resuspended. Semi-volatile species partition into particles and the gaseous phase depending on factors such as vapor pressure at typical indoor temperatures and solubility into organic phases. The dynamics of these processes are presented in separate chapters that are

P. K. Hopke (✉)

Institute for a Sustainable Environment, Clarkson University, Potsdam, NY, USA

Department of Public Health Sciences, University of Rochester School of Medicine and Dentistry, Rochester, NY, USA

e-mail: phopke@clarkson.edu

C. Liu

School of Energy and Environment, Southeast University, Nanjing, China

outlined here. This chapter also introduces a number of major primary indoor sources such as cooking emissions and the use of personal care products. Different cooking styles can produce major differences in emission rates. Personal care products can directly emit particles and semi-volatile compounds, some of which can react with infiltrated ozone in chemistry described in the indoor air chemistry section.

Keywords

Particulate matter · Particles · Indoor sources · Ambient sources

Introduction

Particles have been an indoor air pollution problem from the time that humans first built fires in their caves. Fresh air was found in the ambient atmosphere. However, with increasing population and urbanization, particles in the ambient atmosphere became a problem. In 1157, unendurable air pollution from wood smoke led Eleanor of Aquitaine, wife of Henry II of England, to flee Tutbury Castle in Staffordshire, England. In 1257, Eleanor of Provence, Queen Consort of Henry III, had to leave Nottingham for Tutbury Castle because of the heavy coal smoke since coal had replaced wood due to deforestation (Brimblecombe 1976). The coal burning in London became such a problem that in 1306, Edward I banned coal burning when Parliament was in session.

In 1661, John Evelyn published “Fumifugium or the Inconvenience of the Aer, and Smoake of London Dissipated” and suggested moving industry out of London. Then in December 1930, there was a high haze episode in the Meuse Valley, Belgium resulting in 63 deaths in this industrialized river valley. In October 1948, in Donora, PA, there were 20 deaths while 6000 became sick in a 4.5-day inversion. Then in December 1952, there was the largest and most obvious of all modern air pollution events in London, England in which the government reported 4000 deaths, but recent work has suggested it was more likely between 10,000 and 12,000 deaths (Stone 2002; Bell et al. 2004). There continued to be episodes in the 1950s and 1960s including another London episode in 1962 leading to initial legislation in countries like the United Kingdom and the United States finally recognizing air pollution as a public health issue.

With the 1964 Report of the US Surgeon General on smoking and health that concluded that cigarette smoking caused cancer (US DHEW 1964), interest started to move toward indoor airborne particles. However, there were no large-scale studies of indoor particles until 1979 when the Harvard Six-City Study began indoor particulate matter (PM) measurements that extended until 1988 and included at least 1400 homes (Spengler et al. 1981, 1987). It was followed by the New York State ERDA study in 433 homes in two New York State counties in 1986 (Sheldon et al. 1989) and Particle Total Exposure Assessment Methodology (PTEAM) study of 178 homes in Riverside California in 1990 (Clayton et al. 1993). These studies

provided the initial indication that indoor airborne particles and indoor sources of particles also made significant contributions to peoples' exposures to airborne particulate matter and the indoor particles required appropriate assessment to fully understand the role of airborne particulate matter on human health.

This chapter provides an introduction to the nature and concentrations of particles to which people are exposed indoors.

Sources

Primary

Cooking

There are two sources of particulate emissions when cooking. One is from the source of heat (i.e., the stove and the pan) and the other is the cooking process itself. Both of these sources are covered in detail in their respective chapters in this handbook. Much of the world cooks with direct combustion-generated heat including natural gas, propane, liquid petroleum gas (LPG), kerosene, and solid fuels (wood and other biomass and coal) split about 50:50. Properly tuned natural gas combustion produces ultrafine particles with a geometric mean (GM) mobility diameter of 19.46 nm and a geometric standard deviation (GSD) of 1.36 while a propane flame aerosol had a GM of 26.51 nm and a GSD of 1.25 (Li and Hopke 1993). However, Wallace et al. (2008) found 4.2 nm from a single gas burner. Tiwari et al. (2014) reported that LPG produced particles with GM of 52 nm and a GSD of 1.23. Kerosene had a GM of 62 nm and a GSD of 1.41. For solid fuels, they reported GM (GSD) values of 1.23 nm (1.78), 48 nm (1.98), and 152 nm (1.89) for firewood, coal, and dung cake, respectively. Wang et al. (2020) report results for residential biomass and coal combustion and compares their results to a number of prior studies showing a wide variety of particle diameters depending on the exact nature of the fuel and combustion appliance. Depending on the nature of the appliance and how well it is vented to the outside atmosphere, there can be substantial input of particles into the cooking area resulting in high indoor particle number and PM concentrations. Even with chimneys, there can be short-circuiting back into the house if the chimney is not properly configured to produce good dispersion into the ambient surroundings. There can also be ultrafine particle emissions from electrical cooking surfaces (Wallace et al. 2008). They hypothesize that organic constituents that condense onto the heating elements volatilize and then nucleate to form <10 nm particles.

Cooking the food produces additional particles as reviewed by Amouei Torkmahalleh et al. (2017). Few people vent their stoves to outside of their homes. Thus, cooking represents a major short-term source of particle emissions. One of the main mechanisms occurs in frying in oils when water from the food vaporizes to form bubbles that burst and eject small oil droplets into the air. Just heating the oil or melted solid fats to above their smoke temperature will evolve particles. There are also the occasional issues of food burning and producing high short-term particle

concentrations. The size distributions of many specific cooking activities are reported by Ogulei et al. (2006) including emissions from frying, broiling, and boiling.

Heating

For many people, the same stove used for cooking is also used for room heating, particularly in those homes using solid fuels. Thus, similar sized particles would be emitted into the indoor space whether the stove is being used for cooking and/or heating. However, in more developed countries, central heating with the combustion appliance vented to the outside of the dwelling is more typical. Thus, similar fuels as for cooking may be burned but in more efficient and better vented appliances and thus delivering a much lower load of particles to the home's interior. It is possible that the central heating systems may have leaks and thus emit particles into the indoor air even with an efficient chimney (e.g., Li and Hopke 1991).

Cleaning

Although house cleaning is done to reduce the level of contamination in the indoor space, it also has the potential for adding particles to the indoor air in several ways. First, there is resuspension that will be presented in much greater detail in its specific chapter. Using sweeping tools like a broom will lift particles greater than 1 μm (Ji 2020) resulting in increased concentrations of PM_{2.5} and particularly PM₁₀. Vacuuming also increases the airborne PM concentrations, but their effectiveness in particle suspension depends on the nature of the floor covering (bare or carpet) and the nature of the filter in the cleaner (e.g., Corsi et al. 2008; Lewis et al. 2018). Older models typically used cloth bags that were very inefficient in collecting smaller particle size. Now many models have moved to HEPA filters with 99.97% efficiency that substantially reduced the suspended PM mass and particle number concentrations (Vicente et al. 2020).

Lifestyle

People do a number of things that introduce particles indoors including smoking, vaping, burning candles or incense, and using consumer spray products. Tobacco smoke and its airborne residuals (environmental tobacco smoke or ETS) were covered in detail by Samet and Wang (2001). However, since then there has been an exponential rise in vaping where a person uses a system to vaporize a solution of vegetable glycerin and polyethylene glycol (PEG) containing nicotine and typically some kind of flavoring agent. There is a chapter in this handbook devoted to vaping and its effects on indoor air quality. "Electronic" cigarettes were introduced in 2002, nominally as an aid to tobacco combustion smoking (Bhatnagar et al. 2014) and have grown exponentially in popularity (Rom et al. 2014) particularly among young people. They are most highly used in the United States and Europe (Rahman et al. 2014) and in China (Cai and Wang 2017) and are rising elsewhere as use of combustion cigarettes is stable or declining. Although the presence of the glycerin and PEG produce a visible plume, it largely evaporates and leaves a limited particulate residue.

Combustion in the form of candles and incense can produce high concentrations of particles and in some cases, PM. Candles can also include scents that add volatile and semi-volatile organic compounds in the air in addition to particles. Rasmussen et al. (2021) measured the emissions from candles made of five different materials, animal stearin, palm stearin, paraffin, including mixtures. Burning a candle also involves burning the wick and they examined several wick materials. They found modes in the particle size distributions in the range of 5.4–7.1 nm. Many candles have cored wicks made from cotton wrapped around a metal support. This design keeps the wick from falling into the wax and is especially useful for scented candles since the fragrant oils soften the wax resulting in noncored wicks to fall over. However, these wicks can then potentially add metallic particles to the indoor aerosol.

Several groups have characterized the emissions from burning incense (Jetter et al. 2002; Chang et al. 2007; Ji et al. 2010). The lower temperature of combustion produces a much larger diameter distribution with a peak size around 136 nm (Ji et al. 2010). The sizes measured in this study were comparable to similar measurements by Chang et al. (2007) on other types of incense. In many Asian countries, large quantities of incense are burned in various temples as part of the worship rituals (Lung and Kao 2003; Goel et al. 2017) resulting in PM concentrations ranging from 100s to 1000s of $\mu\text{g}/\text{m}^3$. Temples can represent a large enough source to affect ambient air quality. The impact of the Temple of the Tooth in Kandy Sri Lanka was observed by Seneviratne et al. (2017).

Various consumer products including air fresheners, spray cleaners, and personal care products aerosolize liquids or solids to provide their ingredients to serve their purpose. However, there is the likelihood of some of the material escaping into the indoor air. For example, there are spray oils to lubricate pans for cooking. Not all of the particle sprayed at the pan will stick to it. In cases where the active product is in solution, the particle is formed after the solvent has evaporated. Kim et al. (2020) showed that propellant-type products generated more particles than hand generated pressure. They found most of the particles were in sizes < 100 nm although some products produced an aerosol with a supermicron mode. More details are provided in ► Chap. 5, “Fragranced Consumer Products as Sources.”

Infiltration of Ambient Aerosol

Transport of ambient particles into indoor environment is a major long-term source. It occurs as a consequence of air exchange of indoor environment with outdoors. The exchange can occur deliberately, through ventilation (Liu and Zhang 2019), or by infiltration through gaps in the building envelope. Its intensity is determined by outdoor concentrations, air exchange rate, and any controls in the ventilation system if present. Buildings are ventilated via three modes: mechanical ventilation, natural ventilation, and infiltration. Mechanical ventilation uses mechanical equipment such as fans, while natural ventilation mainly occurs through open windows. Both modes are intentional ventilation. In contrast, infiltration is entry of outdoor air through unintentional openings in a building envelop such as window cracks. These ventilation methods can bring outdoor particle indoors. Its strength (in unit of mass/time)

is usually lower than the indoor sources described above. However, infiltration of ambient particles constantly occurs via any or all of the three ventilation modes while indoor sources are generally of limited durations. Thus, particles of ambient origin generally dominate the long-term exposure to indoor particles. The details of the infiltration mechanisms are described in ► Chap. 10, “Impact of Outdoor Particles on Indoor Air.”

Secondary

In addition to direct injection of particles into the indoor atmosphere from the sources summarized in the previous section, particles can also form indoors through chemical reactions. Indoor chemistry is described in the section devoted to this topic. Typically, light intensities indoors are insufficient to drive the same types of photochemical reactions observed in the ambient environment, there can be reactions between infiltrated ozone and reactive hydrocarbon compounds emitted into the indoor air. The presence of ozone in indoor air was reviewed by Weschler (2000) and many studies have been made on the reactions of olefinic compounds with ozone with the subsequent formation of hydroxyl radicals with its additional oxidizing capabilities. Another important aspect of the indoor environment is the presence of surfaces on which heterogeneous reactions can occur. The oxidation of hydrocarbon compounds adds oxygen to the molecule resulting in forming compounds that have lower vapor pressures. These compounds can then either condense on the existing particulate surface or nucleate to form new particles. Unlike the ambient atmosphere, the condensation sink, available surface area on which the material can condense, is typically low, thereby allowing new particle formation (McMurtry and Friedlander 1979). Thus, infiltrated ozone can react with the terpenes and terpenoids that are used as fragrances in cleaning and personal care products, air fresheners, and other products that produce a notable odor. These reactions can produce particles at concentrations observed in indoor air (Chen et al. 2011). This freshly formed secondary organic aerosol (SOA) also contains reactive oxygen species (ROS) (Chen et al. 2011) that can have direct human health effects (Hopke 2015).

Particle Compositions

Particulate matter (PM) is a complex mixture of chemical constituents. Chemical composition has been suggested to play a key role in health impacts with recent results showing differential effects from exposure to PM emitted by different sources (Rich et al. 2019; Croft et al. 2020; Hopke et al. 2020). Recently, an increasing body of evidence has suggested that oxidative stress induced by particle exposure is responsible for health risk, and attention should be paid to relevant species such as transition metals and organics (Hopke 2015). However, further work is needed to fully ascertain which compositions are more detrimental to health.

Particle composition is traditionally divided into three broad categories driven by measurement techniques: water-soluble ions, carbonaceous species, and elements other than carbon. Sampling and measurement methods are described in detail in Measuring Particle Concentration and Compositions in Indoor Air. Regarding their indoor fate, categorization based on volatility can be more useful to understand the outdoor-to-indoor transport and fate on particles from indoor sources. Then nonvolatile and semi-volatile species will be discussed. Semi-volatile species partition in both gas- and particle-phase, while nonvolatile species stay in particle-phase only.

Nonvolatile Species

Nonvolatile species in particles include sulfate, elemental carbon, and all the elements. They are in the condensed-phase and do not have gas-phase counterparts. Their movement follows bulk particles in transport processes. Knowledge about dynamics of indoor particles such as penetration and deposition is usually considered applicable for these species. Sulfate has been suggested as a useful surrogate to track ambient particles and other nonvolatile species in outdoor-to-indoor transport (Sarnat et al. 2002; Liu and Zhang 2019). Sulfate has negligible indoor sources, is chemically stable, typically has sufficient concentration to be accurately measured, and behaves similarly to particles composed of other nonvolatile species. The indoor/outdoor concentration ratio of sulfate can represent contribution of outdoor-origin particles/species to indoor concentrations.

Semi-Volatile Species

Semi-volatile species includes water-soluble ammonium nitrate, and a large fraction of organic carbon (OC) compounds. They establish partitioning relationships with their gaseous counterparts, i.e., ammonium nitrate-nitric acid and ammonia, and OC-semi-volatile organic compounds. Concentrations of these gaseous species differ between outdoors and indoors. Once semi-volatile species enter indoors as constituents of ambient particles, these partitioning relationships will be disturbed. These species will establish new relationships with their gaseous precursors indoors via re-partitioning. The new relationship will not necessarily reach equilibrium since there will also be differential deposition onto surfaces. This process has been called a phase change (Lunden et al. 2008) or volatilization effect (Sangiorgi et al. 2013). This phase shift makes indoor/outdoor relationship of the semi-volatile species more complex than the nonvolatile species. Efforts have been made to quantify this re-partitioning process for nitrate and ammonium (Liu et al. 2019).

OC is the most complex constituent of particles, since it represents multiple classes of compounds, instead of a single one with well-defined physical chemical properties. OC includes numerous compounds with largely unknown identities and a wide range of thermodynamic properties (Seinfeld and Pankow 2003). Outdoor SVOCs are mainly formed by oxidation of volatile organic compounds, and then

partition to particles as OC (Kroll and Seinfeld 2008; Glasius and Goldstein 2016). Once indoors, these semi-volatile particulate OC species volatilize (Johnson et al. 2016; Salthammer et al. 2018). Meanwhile, indoor SVOCs are emitted from chemical items such as plastics, electronics, and personal care products (Liu et al. 2013, 2015; Liu and Zhang 2016) and from cooking. They partition to the existing particles by adsorption and absorption (Pankow 1994, 2003). Based on mass transfer theory, the OC-SVOCs partition occurs on a compound-by-compound level, and gas-particle partitioning of OC is therefore bidirectional indoors. It is difficult to accurately describe and predict indoor OC of outdoor origin. Current analytical methods cannot characterize OC on a compound-by-compound level. Explicitly modeling indoor-outdoor transport of all individual organic compounds is not practical (Liu and Cao 2018). Hodas and Turpin (2014) applied a volatility basis set approach (Donahue et al. 2006) to examine shifts in partitioning of ambient OC when it transports from outdoors to indoors. They found that both temperature and indoor organic aerosol loading are important to describe this process. This behavior is presented in the section on Source/Sink Characteristics and the chapter in this section on Interaction of Gas Phase Pollutants and Particles.

Indoor Particle Dynamics

When the particles are suspended in the air, any force applied to them will be resisted by the air as they move with respect to it. Characterization of these applied and resistive forces is essential to understand particle movement on the macroscopic scale, termed as indoor particle dynamics. Because particles exhibit a wide range of particle sizes, particle dynamics cover issues from the continuum regime to transition regime to the molecular regime based on how air is considered as a fluid. In the continuum range, air is considered as a continuous fluid while in the molecular regime, the gas is considered in terms of the motion of individual molecules with the transition regime in between. Macroscopically, there are three major dynamic processes in an indoor environment of interest: infiltration, deposition, and resuspension. Basics about indoor particle dynamics are introduced in ► Chap. 9, “Introduction to Aerosol Dynamics.” Each of the three specific dynamic processes is detailed in the chapters that follow in this section.

Infiltration

Although we think of the outer shell of a building as a boundary separating the ambient atmosphere from the indoor air, particles and gases in the ambient air can penetrate through the walls into the interior of a building and contribute to the indoor air pollution. For particles, penetration is strongly dependent on particle size. For large particles, inertial behavior such as not being able to follow airflow streamlines when they are forced to deviate in direction leads to their impaction on the obstacle to the flow. Thus, as wind blows particles at a wall or window and air

flows into cracks, the larger particles ($> 1 \mu\text{m}$) can be removed by impaction onto the obstacle. Within the crack, flow rates are typically reduced and gravitational settling can occur leading to limitations in the penetrability of larger particle sizes. For smaller sized particle ($< 0.1 \mu\text{m}$), the diffusion coefficient increases with decreasing size so smaller particles can diffuse the surfaces of the cracks and be kept from the building interior. However, for sizes in between these limits, only gravitational settling is important and it is very slow so these particles have the greatest ability to penetrate into indoor spaces. Composition also matters since semi-volatile material may change phase given differences in temperature between the ambient and the interior environments. The details of these mechanisms are presented in ► Chap. 10, “Impact of Outdoor Particles on Indoor Air,” by Chen and Zhao.

Deposition

An important difference between indoor and outdoor air are the deposition rates given the much higher available surface area in indoor spaces due to walls and furniture. Particles settle to horizontal surfaces through gravitational setting depending on particle size. Deposition on other surfaces needs to be conceptualized in terms of multiple segment transport. The particles are transported to the boundary layer of a solid object like a wall through turbulent diffusion. The extent of the turbulence depends on the kinetic energy being deposited into the indoor air ranging from low values with just natural ventilation in a closed room to high when fans or forced air flow is used to move the air in a space. Typically, rooms will have dead spaces in places like corners or where air flows are blocked by furniture or other obstacles resulting in increased local deposition. Once the particle gets to the boundary layer, it must diffuse through it to the surface and stick to it. The thickness of the boundary layer also depends on the degree of turbulence in the room. The details of deposition are provided in ► Chap. 11, “Deposition,” by Benes and Holub.

Resuspension

Personal exposure studies like the PTEAM study (Wallace 1996) identified the effect of human activities like walking or sitting on furniture in terms of resuspending particulate matter (dust) and that such activities contribute to peoples’ “personal cloud” (Özkaynak et al. 1996). A few initial studies (Thatcher and Layton 1995; Brauer et al. 1999; Ferro et al. 1999; Long et al. 2000) examined the effects of a variety of specific activities on indoor PM concentrations and increases in the concentrations in the personal cloud of those involved in the activities. Subsequently, more detailed studies have been made on the effects of specific levels of activity on and the mechanisms of particle resuspension as described in ► Chap. 12, “Resuspension,” by Ferro.

Conclusions

At this time, much has been learned regarding particles in the indoor environment including sources, dynamics, transport within structures, control methods, and the effects of ambient concentrations. However, as lifestyles including furnishings, cleaning and personal care products, cooking styles, etc., energy usage, building construction, and related items continue to change, there will be a need for further study to elucidate what these changes will mean on the size, composition, concentrations, and resulting exposures resulting from particles in indoor air. This section provides an introduction to the basics of particle dynamic and many of the direct sources. Details of indoor air chemistry that can also form particles are presented in the Indoor Air Chemistry section. Thus, within this handbook, there is a broad introduction to the issues associated with the indoor aerosol.

References

- Amouei Torkmahalleh M, Gorjinezad S, Unluvecek HS, Hopke PK (2017) Review of factors impacting emission/concentration of cooking generated particulate matter. *Sci Total Environ* 586:1046–1056
- Bell ML, Davis DL, Fletcher T (2004) A retrospective assessment of mortality from the London Smog episode of 1952: the role of influenza and pollution. *Environ Health Perspect* 112:6–8
- Bhatnagar A, Whitsel LP, Ribisl KM, Bullen C, Chaloupka F, Piano MR, Robertson RM, McAuley T, Goff D, Benowitz N (2014) Electronic cigarettes: a policy statement from the American Heart Association. *Circulation* 130:1418–1436
- Brauer M, Hirtle RD, Hall AC, Yip TR (1999) Monitoring personal fine particle exposure with a particle counter. *J Expo Anal Environ Epidemiol* 9:228–236
- Brindlecombe P (1976) Attitudes and responses towards air pollution in medieval England. *J Air Pollution Control Assoc* 26(10):941–945
- Cai H, Wang C (2017) Graphical review: the redox dark side of e-cigarettes; exposure to oxidants and public health concerns. *Redox Biol* 13:402–406
- Chang YC, Lee HW, Tseng HH (2007) The formation of incense smoke. *J Aerosol Sci* 38:39–51
- Chen X, Hopke PK, Carter WPL (2011) Secondary organic aerosol from ozonolysis of biogenic volatile organic compounds: chamber studies of particle and reactive oxygen species formation. *Environ Sci Technol* 45:276–282
- Clayton CA, Perritt RL, Pellizzari ED, Thomas KW, Whitmore RW, Ozkaynak H, Spengler JD, Wallace LA (1993) Particle Total Exposure Assessment Methodology (PTEAM) study: distributions of aerosol and elemental concentrations in personal, indoor, and outdoor air samples in a Southern California community. *Expo Anal Environ Epidemiol* 3:227–250
- Corsi RL, Siegel JA, Chiang C (2008) Particle resuspension during the use of vacuum cleaners on residential carpet. *J Occup Environ Hyg* 5:232–238
- Croft DP, Zhang W, Lin S, Thurston SW, Hopke PK, van Wijngaarden E, Squizzato S, Masiol M, Utell MJ, Rich DQ (2020) The associations between source specific particulate matter and of respiratory infections in New York state adults. *Environ Sci Technol* 54:975–984
- Donahue NM, Robinson AL, Stanier CO, Pandis SN (2006) Coupled partitioning, dilution, and chemical aging of semivolatile organics. *Environ Sci Technol* 40(8):2635–2643
- Ferro AR, Hildemann LM, McBride SJ, Ott W, Switzer P (1999) Human exposure to particles due to indoor cleaning activities. In: Brebbia CA et al (eds) *Air pollution VII*. WIT Press, Southampton, pp. 487–496

- Glasius M, Goldstein AH (2016) Recent discoveries and future challenges in atmospheric organic chemistry. *Environ Sci Technol* 50(6):2754–2764. <https://doi.org/10.1021/acs.est.5b05105>
- Goel A, Wathore R, Chakraborty T, Agrawal M (2017) Characteristics of exposure to particles due to incense burning inside temples in Kanpur. *India Aerosol Air Qual Res* 17:608–615
- Hodas N, Turpin BJ (2014) Shifts in the gas-particle partitioning of ambient organics with transport into the indoor environment. *Aerosol Sci Technol* 48(3):271–281
- Hopke PK (2015) Reactive ambient particles. Chapter 1. In: Nadadur SS, Hollingsworth JW (eds) *Air pollution and health effects, molecular and integrative toxicology*. Springer-Verlag, London, pp 1–24
- Hopke PK, Croft D, Zhang W, Shao L, Masiol M, Squizzato S, Thurston SW, van Wijngaarden E, Utell MJ, Rich DQ (2020) Changes in the acute response of respiratory disease to PM_{2.5} in New York state from 2005 to 2016. *Sci Total Environ* 677:328–339
- Jetter JJ, Guo Z, McBriar JA, Flynn MR (2002) Characterization of emissions from burning incense. *Sci Total Environ* 295:51–67
- Ji JH (2020) Size distributions of suspended fine particles during cleaning in an office. *Aerosol Air Qual Res* 20:53–60
- Ji X, Le Bihan O, Ramalho O, Mandin C, D'Anna B, Martinon L, Nicolas M, Bard D, Pairon JC (2010) Characterization of particles emitted by incense burning in an experimental house. *Indoor Air* 20:147–158
- Johnson AM, Waring MS, DeCarlo PF (2016) Real-time transformation of outdoor aerosol components upon transport indoors measured with aerosol mass spectrometry. *Indoor Air* 27(1):230–240
- Kim T, Park J, Seo J, Yoon H, Lee B, Lim H, Lee D, Kim P, Yoon C, Lee K, Zoh K-D (2020) Behavioral characteristics to airborne particles generated from commercial spray products. *Environ Int* 140:105747
- Kroll JH, Seinfeld JH (2008) Chemistry of secondary organic aerosol: formation and evolution of low-volatility organics in the atmosphere. *Atmos Environ* 42(16):3593–3624. <https://doi.org/10.1016/j.atmosenv.2008.01.003>
- Lewis RD, Ong KH, Emo B, Kennedy J, Kesavan J, Elliot M (2018) Resuspension of house dust and allergens during walking and vacuum cleaning. *J Occup Environ Hyg* 15:235–245
- Li C-S, Hopke PK (1991) Characterization of Radon Decay products in a domestic environment. *Indoor Air* 4:539–561
- Li W, Hopke PK (1993) Initial size distributions and hygroscopicity of indoor combustion aerosol particles. *Aerosol Sci Technol* 19:305–316
- Liu C, Cao J (2018) Potential role of intraparticle diffusion in dynamic partitioning of secondary organic aerosols. *Atmospheric Pollut Res* 9(6):1131–1136
- Liu C, Zhang Y (2016) Characterizing the equilibrium relationship between DEHP in PVC flooring and air using a closed-chamber SPME method. *Build Environ* 95:283–290
- Liu C, Zhang Y (2019) Relations between indoor and outdoor PM2.5 and constituent concentrations. *Front Environ Sci Eng* 13(1). <https://doi.org/10.1007/s11783-019-1089-4>
- Liu C, Liu Z, Little JC, Zhang Y (2013) Convenient, rapid and accurate measurement of SVOC emission characteristics in experimental chambers. *PLoS One* 8(8):e72445
- Liu C, Zhang Y, Benning JL, Little JC (2015) The effect of ventilation on indoor exposure to semivolatile organic compounds. *Indoor Air* 25(3):285–296
- Liu C, Wang H, Guo H (2019) Redistribution of PM2.5-associated nitrate and ammonium during outdoor-to-indoor transport. *Indoor Air* 29(3):460–468
- Long CM, Suh HH, Koutrakis P (2000) Characterization of indoor particle sources using continuous mass and size monitors. *J Air Waste Manage Assoc* 50:1236–1250
- Lunden MM, Kirchstetter TW, Thatcher TL, Hering SV, Brown NJ (2008) Factors affecting the indoor concentrations of carbonaceous aerosols of outdoor origin. *Atmos Environ* 42(22):5660–5671
- Lung S-CC, Kao MC (2003) Worshippers' exposure to particulate matter in two temples in Taiwan. *J Air Waste Mange Assoc* 53:130–135

- McMurtry PH, Friedlander SK (1979) New particle formation in the presence of an aerosol. *Atmos Environ* 13:1635–1651
- Ogulei D, Hopke PK, Wallace LA (2006) Analysis of indoor particle size distributions in an occupied townhouse using positive matrix factorization. *Indoor Air* 16:204–215
- Özkaynak H, Xue J, Weker R, Butler D, Koutrakis P, Spengler J (1996) The Particle Team (PTEAM) study: analysis of the data. EPA Project Summary, EPA/600/SR-95/098, U.S. EPA: Research Triangle Park, NC.
- Pankow JF (1994) An absorption model of gas/particle partitioning of organic compounds in the atmosphere. *Atmos Environ* 28:185–188
- Pankow JF (2003) Gas/particle partitioning of neutral and ionizing compounds to single and multi-phase aerosol particles. 1. Unified modeling framework. *Atmos Environ* 37:3323–3333
- Rahman M, Hann N, Wilson A, Worrall-Carter L (2014) Electronic cigarettes: patterns of use, health effects, use in smoking cessation and regulatory issues. *Tob Induc Dis* 12:21
- Rasmussen BB, Wang K, Karstoft JG, Skov SN, Køcks M, Andersen C, Wierzbicka A, Pagels J, Pedersen PB, Glasius M, Bilde M (2021) Emissions of ultrafine particles from five types of candles during steady burn conditions. *Indoor Air*. <https://doi.org/10.1111/ina.12800>
- Rich DQ, Zhang W, Shao L, Squizzato S, Thurston SW, van Wijngaarden E, Croft D, Masiol M, Hopke PK (2019) Triggering of cardiovascular hospital admissions by source-specific fine particle concentrations in urban centers of New York State. *Environ Int* 126:387–394
- Rom O, Pecorelli A, Valacchi G, Reznick AZ (2014) Are E-cigarettes a safe and good alternative to cigarette smoking? *Ann N Y Acad Sci* 1340:65–74
- Salthammer T, Zhang Y, Mo J, Koch HM, Weschler CJ (2018) Assessing human exposure to organic pollutants in the indoor environment. *Angew Chem Int Ed* 57(38):12228–12263
- Samet JM, Wang SS (2001) Environmental tobacco smoke, Chapter 30. In: Spengler JD, Samet JM, McCarthy JF (eds) *Indoor air quality handbook*. McGraw Hill, New York, pp 30.1–30.30
- Sangiorgi G, Ferrero L, Ferrini BS, Lo Porto C, Perrone MG, Zangrando R, Gambaro A, Lazzati Z, Bolzacchini E (2013) Indoor airborne particle sources and semi-volatile partitioning effect of outdoor fine PM in offices. *Atmos Environ* 65:205–214
- Sarnat JA, Long CM, Koutrakis P, Coull BA, Schwartz J, Suh HH (2002) Using sulfur as a tracer of outdoor fine particulate matter. *Environ Sci Technol* 36(24):5305–5314
- Seinfeld JH, Pankow JF (2003) Organic atmospheric particulate material. *Annu Rev Phys Chem* 54(1):121–140
- Seneviratne S, Handagiripathira L, Sanjeevani S, Madusha D, Waduge VAA, Attanayake T, Bandara D, Hopke PK (2017) Identification of sources of fine particulate matter in Kandy, Sri Lanka. *Aerosol Air Qual Res* 17:476–484
- Sheldon LS, Hartwell TD, Cox BG, Sickles II JE, Pellizzari ED, Smith MX, Perritt RL, Jones SM (1989) An investigation of infiltration and indoor air quality. Final Report. NY State ERDA Contract No. 736-CON-BCS-85. New York State Energy Research and Development Authority, Albany, NY
- Spengler JD, Dockery DW, Turner WA, Wolfson JM, Ferris BG Jr (1981) Long-term measurements of respirable sulfates and particles inside and outside homes. *Atmos Environ* 15:23–30
- Spengler JD, Ware J, Speizer F, Ferris B, Dockery D, Lebret E, Brunekreef B (1987) Harvard's indoor air quality respiratory health study. In *Indoor Air '87: Proceedings of the 4th International Conference on Indoor Air Quality and Climate* (Seifert, B., ed.) Vol. 2, 742–746. Institute for water, soil, and air hygiene, W. Berlin.
- Stone R (2002) Counting the cost of London's Killer Smog. *Science* 298:2106–2107
- Thatcher TL, Layton DW (1995) Deposition, resuspension, and penetration of particles within a residence. *Atmos Environ* 29:1487–1497
- Tiwari M, Sahu SK, Bhangare RC, Yousaf A, Pandit GG (2014) Particle size distributions of ultrafine combustion aerosols generated from household fuels. *Atmos Pollut Res* 5:145–150
- US DHEW (U.S. Department of Health, Education, and Welfare) (1964) *Smoking and health: report of the advisory committee to the surgeon general of the public health service*. Department

- of Health, Education, and Welfare, Public Health Service, Center for Disease Control, Washington: U.S.. PHS Publication No. 1103
- Vicente ED, Vicente AM, Evtyugina M, Calvo AI, Oduber F, Alegre CB, Castro A, Fraile R, Nunes T, Lucarelli F, Calzolai G, Nava S, Alves CA (2020) Impact of vacuum cleaning on indoor air quality. *Build Environ* 180:107059
- Wallace L (1996) Indoor particles: a review. *J Air Waste Manage Assoc* 46:98–126
- Wallace L, Wang F, Howard-Reed C, Persily A (2008) Contribution of gas and electric stoves to residential ultrafine particle concentrations between 2 and 64 nm: size distributions and emission and coagulation remission and coagulation rates. *Environ Sci Technol* 42:8641–8647
- Wang D, Li Q, Shen G, Deng J, Zhou W, Hao J, Jiang J (2020) Significant ultrafine particle emissions from residential solid fuel combustion. *Sci Total Environ* 715:136992
- Weschler CJ (2000) Ozone in indoor environments: concentration and chemistry. *Indoor Air* 10: 269–288



Introduction to Aerosol Dynamics

9

Andrew Maynard and Philip K. Hopke

Contents

Introduction	248
Basics of Gas Behavior	248
Background	248
Properties of Gases	249
Kinetic Theory of Gases	249
Macroscopic Properties of Gases	256
Particle Motion in Air	261
Background	261
Drag	261
Stokes' Law	262
Particle Mobility	263
Slip Correction	263
Particle Shape	264
Tranquil and Stirred Settling	265
Definition of Particle Diameter: Aerodynamic Diameter	266
Particle Motion Under Acceleration	267
Brownian Motion	270
Conclusions	272
Nomenclature (Note that in some cases a symbol may be used to denote different values in different contexts. All equations listed should be evaluated using SI units (kg, m, s).)	
SI units for the values below are listed where appropriate)	273
References	274

A. Maynard (✉)

Arizona State University College of Global Futures, Arizona State University, Tempe, AZ, USA
e-mail: Andrew.Maynard@asu.edu

P. K. Hopke

Institute for a Sustainable Environment, Clarkson University, Potsdam, NY, USA

Department of Public Health Sciences, University of Rochester School of Medicine and Dentistry, Rochester, NY, USA

e-mail: phopke@clarkson.edu

Abstract

Aerosols play a substantial role in determining the quality and potential health impacts of indoor air. However, understanding how they are measured, monitored, and mitigated starts with a basic understanding of how they behave. The term “aerosol” refers to a collection of liquid and/or solid particles suspended in a gas. Aerosol behavior is determined by the physics of the suspending gas and the suspended particles and interactions between them. Starting from kinetic theory, this chapter develops an understanding of basic properties of gas behavior and how this is connected to aerosol behavior. Properties of gases from molecular mean free path and viscosity to boundary layers, Reynolds number, laminar and turbulent flow, and flow stagnation are described. Building on these, the chapter explores how interactions between particles and a surrounding gas affect behavior under different conditions. Concepts that are relevant to understanding aerosol behavior within indoor environments are addressed, including definitions of diameter (including aerodynamic diameter), linear and curvilinear motion, particle mobility, relaxation time, stopping distance, and diffusion. The chapter is designed to provide an introduction to aerosol dynamics that will be helpful in addressing the behavior and potential impacts of aerosols within indoor environments.

Keywords

Aerosol dynamics · Particles · Motion · Impaction · Diffusion · Inertia

Introduction

The purpose of this chapter is to provide an introduction to a number of physical processes that affect the behavior of particles in indoor environments. It is deliberately written at a level that allows people new to the field to get a grounding in the basics. It is not possible to provide a comprehensive and detailed introduction to aerosol dynamics here. For more information on the aerosol properties addressed in the chapter, the reader is referred to Hinds and Zhu (2022). For an advanced discussion of aerosol science topics, the reader is referred to Friedlander (2000).

Basics of Gas Behavior**Background**

Particles in the air move under a variety of forces. This chapter provides a basic understanding of the physical processes that govern the motion of particles and important behaviors such as settling, deposition, and resuspension. To begin, it is necessary to define the critical basic term: aerosol.

An aerosol is a collection of solid or liquid particles suspended in a gas. Here, it is important to recognize that the term “aerosol” refers to the two-phase system consisting of the particles and the gas, and not the suspended particles alone. The

term aerosol was coined around the 1920s as an analogy of hydrosols – suspensions of solid particles in a liquid. Aerosols are also referred to as suspended particulate matter, aero-colloidal systems, and disperse systems. However, particles and droplets are *not* aerosols. Rather, they are components of aerosols. Thus, in any given indoor space there is one and only one aerosol.

An aerosol may occur in many systems, either as a naturally occurring phenomenon or as man-made (anthropogenic) products. They are responsible for influencing processes and phenomena as diverse as cloud formation, global warming and cooling, visibility, rainbows, microchip fabrication, pigment formation, nanoscale material production, global material transport, the application of pesticides, asthma attacks, plant propagation, drug delivery, and various pulmonary, cardiovascular, and systemic diseases. Particle sizes range from the sub-nanometer (molecular clusters) to larger than several 100 μm . They may consist of biological material, including viruses and bacteria, solids, or liquids, and may be found in simple geometric forms such as spheres or highly complex morphologies. Each particle may consist of a single substance or may be a complex mixture of a number of substances. As a result, the study of aerosols is not only vital to the understanding of the environment in which we live and work, but it is a highly complex field that overlaps many other disciplines.

The first step to understanding the association between an aerosol and its effects on health (or its behavior in other systems) is to be able to appropriately characterize it. Likewise, the interpretation of aerosol measurements is dependent on an understanding of the assumptions and simplifications being made in the measurement process. This chapter is aimed at developing a sufficient comprehension of aerosol behavior to understand the basis of measurement methods, allow the correct methods to be selected for specific needs, and to allow a clear comprehension of the limitations and simplifications associated with any method used.

Properties of Gases

Since an aerosol is a two-phase system consisting of particles/droplets and gas, to fully understand aerosol behavior, it is also necessary to have a good understanding of how gases behave. Here, it is worth noting that with most aerosol concentrations encountered in indoor environments, the aerosol mass is sufficiently low to make the assumption that the presence of the particulate phase does not unduly influence the gas behavior. However, at high mass concentrations (typically where the aerosol density is greater than 1% different from the density of the gas alone), the presence of particles has a significant influence on gas properties.

Kinetic Theory of Gases

A good understanding of how gases behave can be gained from a very simple physical model that treats individual molecules as rigid spheres analogous to billiard balls (Fig. 1). This is referred to as the kinetic theory of gases (Loeb 1961), as it is

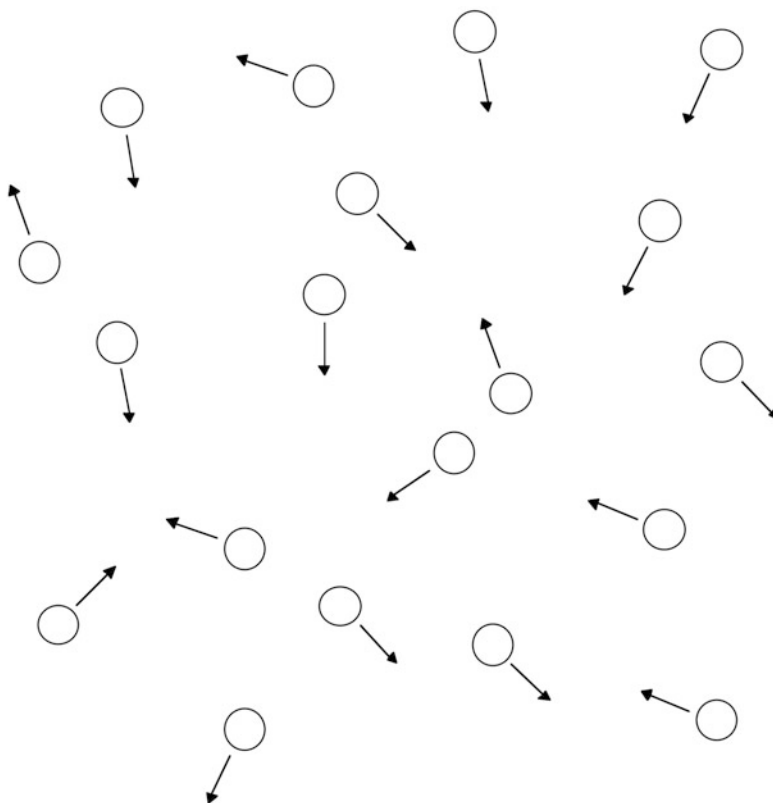


Fig. 1 Kinetic model of an ideal gas

based on the exchange of kinetic energy between molecules during collisions. Qualitatively understanding gas behavior using this model, while imperfect, provides a good foundation to understanding aerosol particle motion later on.

This model relies on a number of assumptions that, despite their simplicity, lead to a sophisticated understanding of gas behavior. These include:

- The gas consists of a great number of identical molecules.
- The physical dimensions of the molecules are much smaller than the distances between them.
- The molecules are rigid. Collisions between molecules are elastic (no energy is lost), and they travel in straight lines between collisions.

Starting from these assumptions, it is possible to describe properties such as temperature, pressure, viscosity, mean free path, diffusion, and thermal conductivity in terms of the number of molecules per unit volume N , the mass of individual molecules m , molecular diameter d_m , and mean molecule velocity c .

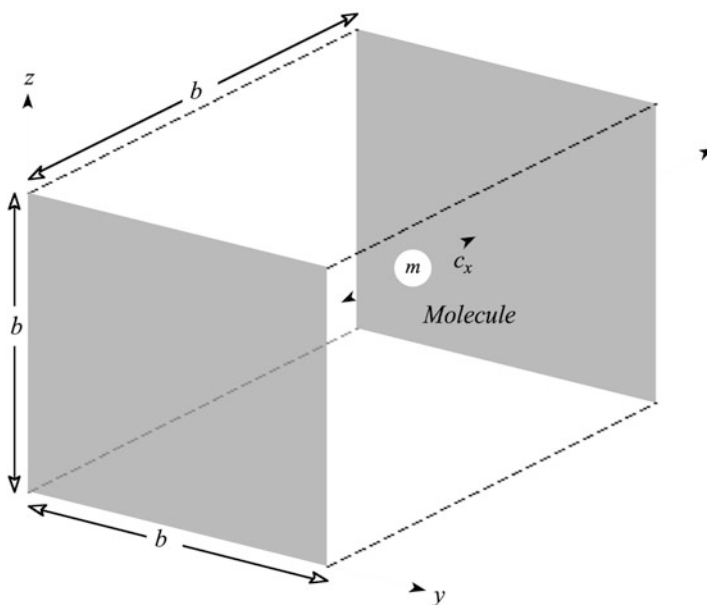


Fig. 2 Basis of describing pressure using kinetic gas theory

Pressure

Imagine a kinetic gas molecule enclosed in a cubic box. Each time the molecule collides with a wall of the box, it “pushes” the box away from it as it rebounds. As no energy is lost to the box wall, the molecule bounces back and forth between opposite walls indefinitely, giving the walls a little push with each collision. “Pressure” simply describes how much of the molecule’s effort goes into pushing the walls each second (i.e., the force) for each unit area of wall (Fig. 2).

The impulse of the molecule pushing against the wall is equal to the change in its momentum. Momentum is given by mass times velocity. We can assume that as the box is much more massive than the molecule, the molecule rebounds with an equal but opposite velocity to that with which it hit the wall. Thus, if the mean molecule velocity is c_x , the change in momentum is $2mc_x$. Here, the c_x notation denotes the molecule is bouncing back and forth in just one direction at any given moment.

The force applied to the box wall is simply the rate of change of momentum with time (Newton’s second law), which is given by the change in momentum for one collision, divided by the time between collisions. In our one-molecule-in-a-box model, the molecule has to travel from one side of the box to the other between collisions (remembering that we are looking at collisions with both of the end walls). Thus, if the length of the box is b , the time between collisions is simply distance divided by velocity or b/c . Therefore, the force exerted per collision is:

$$F = \frac{2mc}{b/c_x} = \frac{2mc^2}{b} \quad (1)$$

The force per unit area, or pressure, is simply F divided by the area of the box wall of interest. At this point, the molecule is just bouncing back and forth between two opposite walls, and so the area is the area of these two walls, or $2b^2$. And so pressure P is given by:

$$P = \frac{F}{2b^2} = \frac{c_x^2 m}{b^3} = \frac{c_x^2 m}{V} \quad (2)$$

where V is the volume of the box.

Equation (2) gives the pressure resulting from just 1 mol in a box. To extend this analysis to a box containing N molecules, we must do two things. First, if we assume that collisions between molecules within the box do not affect this analysis, then Eq. (2) can be multiplied by the total number of molecules (N) to derive the pressure from all molecules. However, these molecules will now be traveling in all directions, not just back and forth between the two opposite walls of the box.

In the more general case of molecules traveling in all directions, it can be shown that the mean square molecule velocity (c_x^2) in each direction (x , y , and z) is the same and that the overall mean square velocity of the particles is given by:

$$c^2 = c_x^2 + c_y^2 + c_z^2 \quad (3)$$

Thus, c_x^2 in Eq. (2) can be replaced by $c^2/3$.

From a set of simple assumptions based on a solid molecule trapped in a box, we therefore end up with pressure being defined as:

$$P = \frac{mNc^2}{3V} \quad (4)$$

or

$$PV = \frac{mNc^2}{3} \quad (5)$$

This equation is a statement of Boyle's law, which states that for an ideal gas $PV = \text{constant}$ for a fixed amount of gas at constant temperature.

Equation (5) is the microscopic form of the ideal gas law. It is more usually used in its macroscopic form of:

$$PV = nRT \quad (6)$$

where n is the number of moles of gas, R is the gas constant, and T is the gas temperature in Kelvin. For pressure in Newtons per square meter, or Pascals, and volume in m^3 (SI units), $R = 8.31 \text{ Pa m}^3/\text{K mol}$.

Mean Velocity

As can be seen from the above analysis, kinetic theory is powerful in that starting from very simple assumptions, a sophisticated understanding of gas behavior can be reached. For instance, Eqs. (5) and (6) can be used without much further work to derive an expression for the mean square velocity of particles in a gas. For 1 mole of gas, $PV = RT$ and $N = N_a$ (Avogadro's number, or the number of molecules in 1 mole of a substance [$N_a = 6.022 \times 10^{23}$ mol/mole]). Substituting these in Eq. (5),

$$c^2 = \frac{3RT}{mN_a} \quad (7)$$

A more useful quantity is the root of the mean square velocity or c_{rms} :

$$c_{rms} = \sqrt{c^2} = \sqrt{\frac{3RT}{mN_a}} \quad (8)$$

The root mean square velocity is the average velocity of molecules in a gas at temperature T . As the molecule velocity rises, so does the gas temperature, and vice versa. Remembering that the kinetic energy of the molecules is a function of their velocity, Eq. (8) shows us that the temperature of the gas is related to the kinetic energy of the individual molecules.

In practice, molecules in a gas will have a broad range of velocities. As a result, a number of different ways of calculating mean velocity exist, each leading to a slightly different result. The root mean square velocity is one such approach. A commonly used alternative is to calculate the arithmetic mean of particle velocity denoted by \bar{c} and calculated as:

$$\bar{c} = \sqrt{\frac{8RT}{\pi mN_a}} = \sqrt{\frac{8RT}{\pi M}} \quad (9)$$

where M is the molecular weight of the gas.

Mean Free Path

A key assumption in the analysis above is that molecules travel in straight lines between collisions. The distance between these collisions is important as it indicates whether assumptions about the molecule diameter being small compared to the distance between collisions are correct. It is even more important when particles are present in the gas. A particle that is much smaller than this collision distance will behave differently within the gas to one that is much larger than the mean collision distance. Here, the distance between collisions is referred to as the *free path*, and as there will be some variation in these distances in a gas, the quantity most usually used is the mean free path.

The mean free path of a molecule, λ , is calculated by dividing the mean velocity by the average number of collisions encountered per second (n_c):

$$\lambda = \frac{\bar{c}}{n_c} \quad (10)$$

n_c is calculated by making assumptions on the area that each molecule presents to others (the collision cross section) and the number of molecules per unit volume in the gas N . This leads to:

$$n_c = \sqrt{2N\pi d_m^2 \bar{c}} \quad (11)$$

where d_m is defined as the collision diameter of the molecule, usually considered to be the distance between molecule centers at the point of collision. For air, the approximate collision diameter is 3.7×10^{-10} m.

Combining Eqs. (10) and (11) yields:

$$\lambda = \frac{1}{\sqrt{2N\pi d_m^2}} \quad (12)$$

The mean free path for air at 101 kPa [1 atm] and 293 K is 0.066 μm.

Diffusion

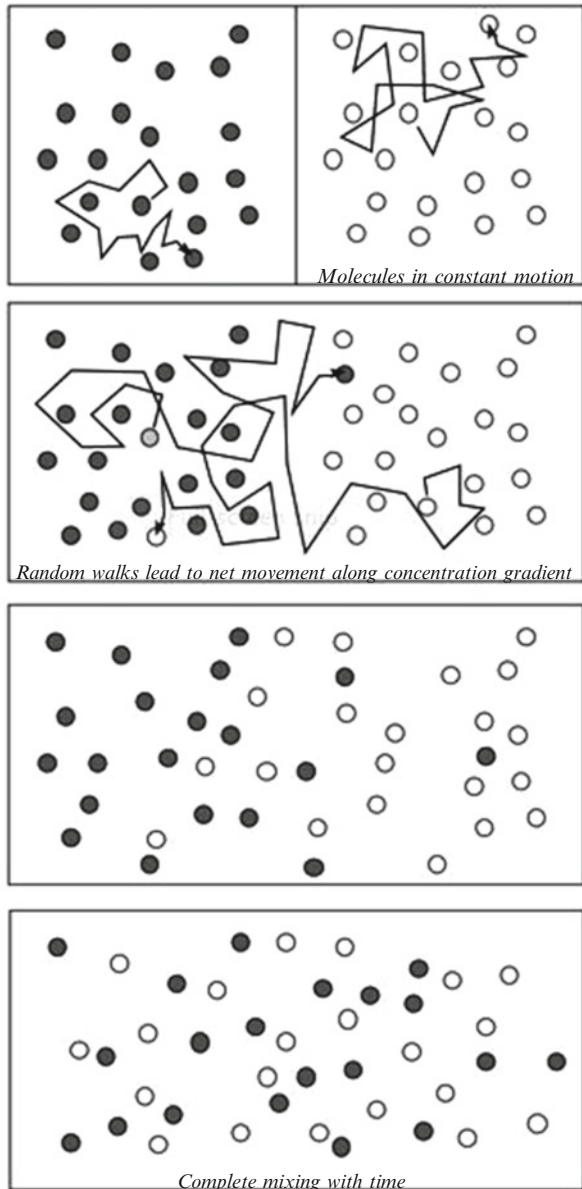
As the molecules in a gas are in constant motion, they will move from one place to another (migrate) within an enclosed space, even in the absence of a net flow of gas. If you were able to tag a single molecule and watch its progress with time, you would see it follow a series of jumps in random directions (associated with collisions with other molecules), gradually taking it further and further away from its original position. The molecules are said to take “random walks.” If all the molecules in an enclosure are identical, as one molecule moves away from its starting position, another one, indistinguishable from the first, takes its place. Thus, it is not apparent that there is continual movement within the gas. However, if you started with an enclosed volume with, say, red molecules on one side and white on the other, the red molecules would follow random walks that would take some of them over to the white side, and likewise, the white ones would follow random walks resulting in some ending up on the red side. The end result would be a uniform mixture of red and white molecules. This process of molecule migration is referred to as diffusion and is seen wherever there is a concentration gradient of a particular molecule type (Fig. 3).

The derivation of the equations determining diffusion is beyond this chapter. However, it is useful to be aware of the expression describing the quantity of a material diffusing per unit time through a unit area perpendicular to the direction of diffusion, J (Fick’s first law of diffusion):

$$J = -D \frac{dC}{dx} \quad (13)$$

J is the flux of material moving along the concentration gradient dC/dx . D is a constant of proportionality referred to as the diffusion coefficient.

Fig. 3 A simple model of molecular diffusion



Viscosity

The final gas property that it is useful to conceptualize in terms of kinetic theory is dynamic viscosity (usually simply referred to as viscosity). If two parallel plates with a gas between them move relative to each other, there will be a resisting force resulting from the intervening gas. From Newton's law of viscosity, the force that

must be applied to overcome this resisting force is proportional to the plate area A and the relative velocity U , and inversely proportional to the separation distance y . The constant of proportionality is the viscosity, η , giving

$$F = \frac{\eta A U}{y} \quad (14)$$

On a microscopic scale, molecules at the surface of either plate will have a net velocity in the same direction as the plate. A molecule traveling from one plate to the other through thermal motion will effectively remove a small amount of energy from the first plate and impart it to the other. The tendency in the absence of an external force will therefore be to reduce the relative motion between the plates. This is the source of the gas' viscosity. Using kinetic theory, it can be shown that η is a function of gas constants and temperature alone and that it increases with increasing temperature. It is independent of pressure.

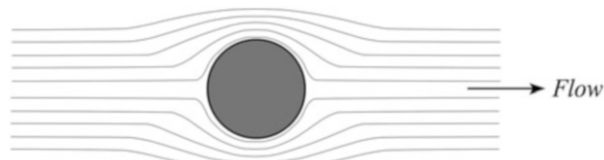
Macroscopic Properties of Gases

While kinetic theory provides a simple basis for understanding gas behavior, understanding the bulk motion and behavior of gases is not so straightforward. There are however fundamental properties of gas flow that need to be appreciated for an understanding of how aerosols behave. Bulk gas motion can be described using basic equations of motion and conservation known collectively as the Navier Stokes equations. While the underlying bases of these equations are relatively straightforward, solutions to the equations themselves are not. For simplicity, therefore, the main concepts and properties of gas flow will be introduced with little derivation of the underlying physics.

Streamlines

One important set of solutions to the Navier Stokes equations results in streamlines or patterns that graphically characterize flow. In simple terms, streamlines show the path that a tagged parcel of gas would take through a flow system. Introducing a thin stream of smoke into a flow is one common method of visualizing streamlines. The more densely packed the streamlines, the higher the gas velocity (Fig. 4).

Fig. 4 Illustration of flow streamlines around an object



Boundary Layers

One physical constraint applicable to real fluids (including gases) is that the velocity of the fluid must be zero at every point where the fluid connects with a solid boundary. This constraint means that there must exist a steep velocity gradient next to a surface across which a gas is moving. The boundary layer defines the layer within which the gas velocity differs significantly from the bulk gas velocity. Figure 5 illustrates the nature of typical boundary layers across a flat sheet and between a pair of plates. As can be seen, the boundary layer takes some time to fully develop. When the boundary layer is fully formed in a tube, the flow velocity has a parabolic profile across the tube diameter, with the velocity on the center-line being twice the average flow velocity (“Poiseuille flow”). A common rule of thumb is that it takes approximately 10 diameters for this equilibrium flow to be fully established.

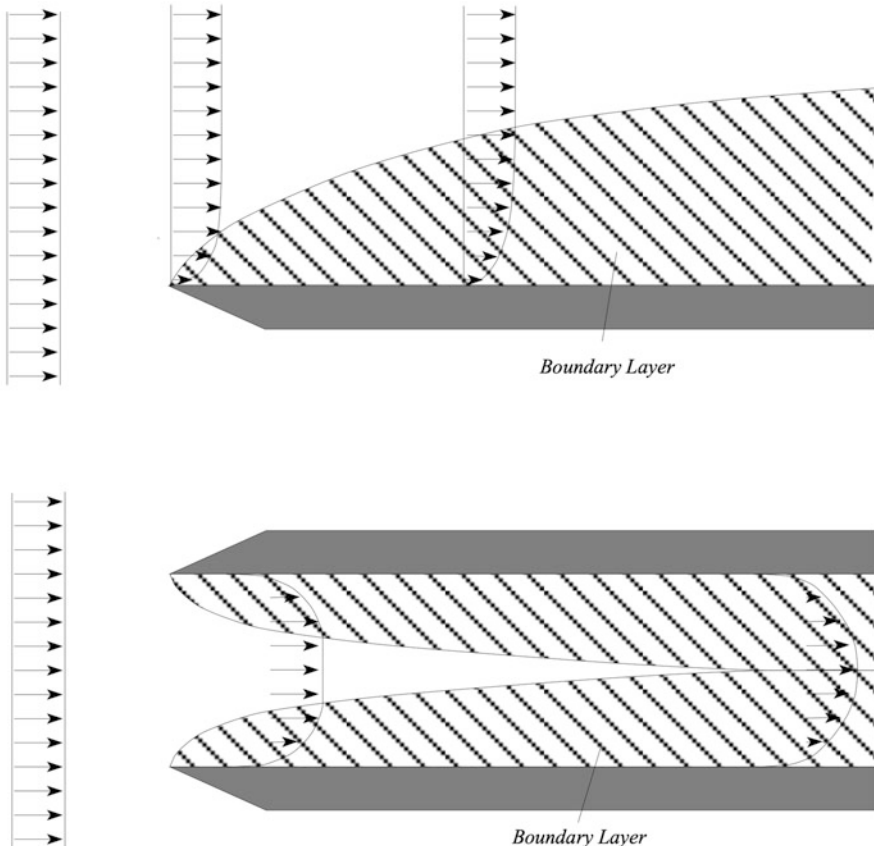


Fig. 5 Schematic of boundary layer formation on a surface and in a tube

Gas Flow Through a Tube

Two other characteristics of flow through a tube are worth noting as they are influential in how particles are transported. A constriction in the flow will force the gas to increase in velocity and be focused toward the center of the tube, leading to an effective tube diameter that is *smaller* than the actual diameter (Fig. 6). The contraction region is termed the “vena contracta.” Established tube flow round a bend in the tubing will result in secondary flow circulation within the tube (Fig. 7). In each case, the ten-diameters rule is a good rule of thumb for estimating the distance required to regain equilibrium flow after the disturbance.

Fig. 6 Flow in a *vena contracta*

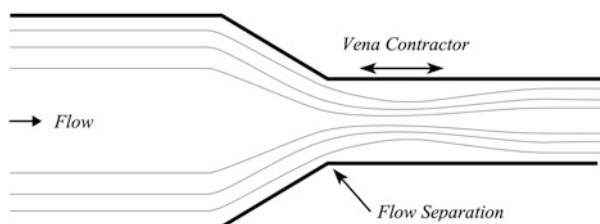
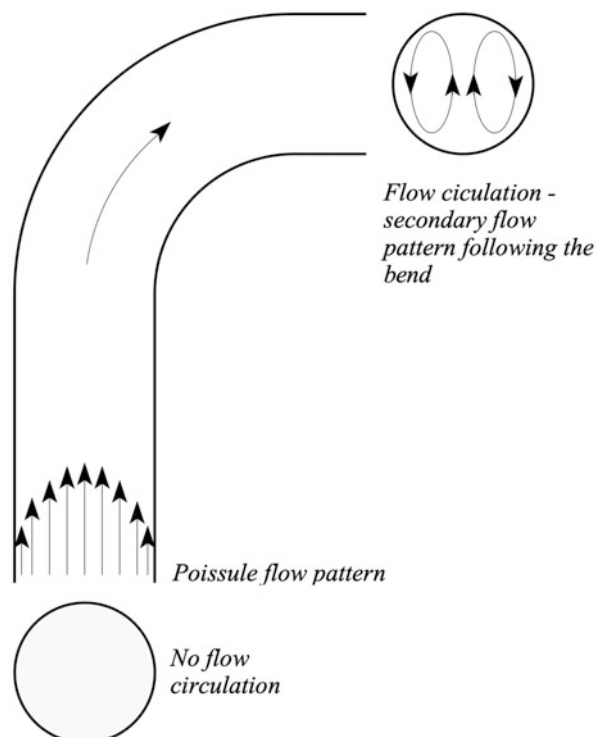


Fig. 7 Flow circulation around a 90° bend



Reynolds Number

An important aspect of understanding the flow of gases and the aerodynamic properties of aerosol particles is the Reynolds number (Re), a dimensionless number that characterizes fluid flow through a pipe or around an object. Dimensionless numbers are independent of scale and units and are widely used in engineering to characterize systems that exhibit similar properties at different scales. Aspect ratio is perhaps the simplest dimensionless number to understand. It has no dimension of its own and may be used to describe similarly shaped objects of any physical size. The Reynolds number has the following properties:

- It provides a benchmark to determine whether the flow is laminar or turbulent.
- It is proportional to the ratio of inertial forces to frictional forces acting on each element of the fluid.
- Geometrically similar flow will occur around geometrically similar objects at the same Reynolds number. Thus, for a given Re , the streamlines will be the same around objects of different size or flow of different fluids (or gas).

The Reynolds Number is defined as:

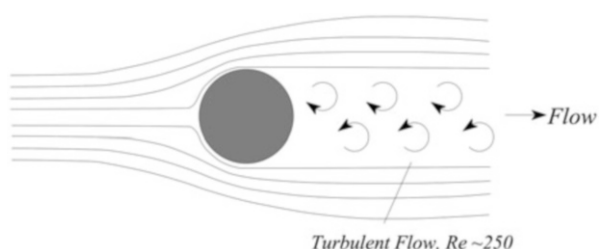
$$Re = \frac{\rho VL}{\eta} \quad (15)$$

where ρ is the gas density, V is the gas velocity, η is the gas viscosity, and L is a characteristic dimension. For instance, for flow through a tube, L is the tube diameter, and for flow around a particle, L is particle diameter. Re is dimensionless in any unit system, but obviously, all quantities need to be in the same system of units. Re depends only on the relative velocity between an object and the gas flow. It is aerodynamically equivalent for air to flow past a stationary object or for the object to move in stationary air.

Laminar and Turbulent Flow

Laminar flow around a particle occurs when $Re < 1$. Within this region, viscous forces are much greater than inertial forces. This type of flow is characterized by a smooth pattern of streamlines that are symmetrical on the upstream and downstream sides of the object (Fig. 8). At $Re \gg 1$ eddies form in the flow downstream of the

Fig. 8 Turbulent flow



object, breaking the smooth pattern of the streamlines and leading to random fluctuations in flow and velocity for small packets of gas. Flow within this regime is classed as turbulent flow. Turbulence is a complete topic in itself, and perhaps one of the least understood aspects of fluid flow. However, its influence on flow systems is highly significant. Generally, turbulence occurs when an obstruction or change in flow system leads to high localized flow velocities, and inertial forces dominating viscous forces. The result is randomly fluctuating gas motion superimposed on the mean flow. Two consequences are an increase in apparent viscosity and a sharp rise in the mixing properties of the gas. Flow through pipes is laminar for $Re < 2000$, and turbulent for $Re > 4000$. Whether the flow around a particle or through a flow channel is laminar or turbulent has a significant influence on particle motion and behavior within the flow.

Flow Stagnation

Where a streamline intercepts an object, the flow velocity falls to zero, resulting in a stagnation point. Stagnation points are particularly important when considering aerosol particle transportation, as particles approaching such a point run the risk of being trapped in a zone of very little air movement (Fig. 9).

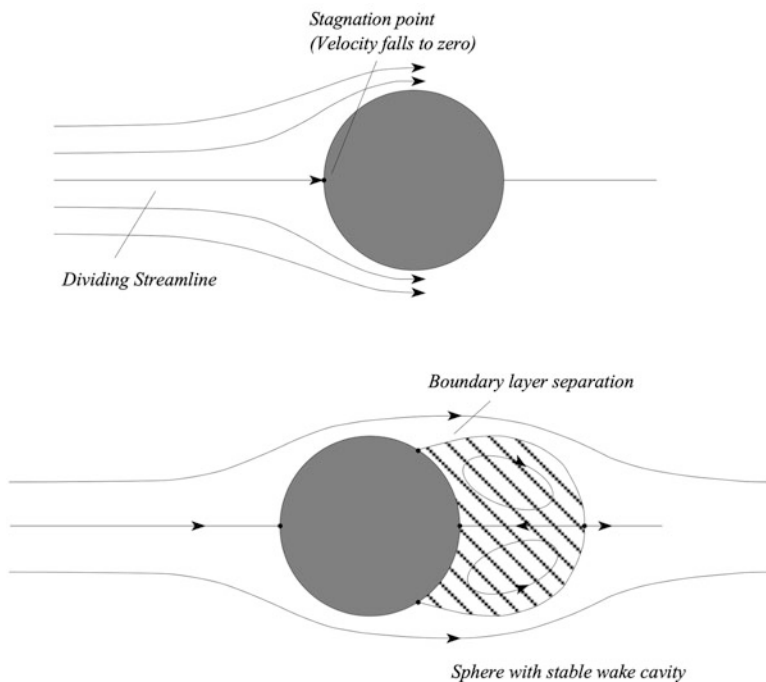


Fig. 9 Flow stagnation and separation

Flow Separation

For idealized inviscid frictionless flow, all streamlines impinging on an object would move around the object and continue in the object's wake. However, in the real world, where there is friction due to viscosity, some streamlines will lose sufficient energy to be "lost." The result is boundary layer separation – the fluid in the boundary layer close to the surface of the downstream side of the body comes to rest prematurely. When and where this occurs, the flow breaks away from the body, enclosing a negative-pressure recirculating region (this may or may not be turbulent). Formation of the vena contracta (Fig. 6) at a sharp change in flow channel is an example of flow separation. In a rapidly expanding flow channel, flow will separate from the channel walls. In general, the angle between the wall and the flow axis needs to be less than 7° to prevent separation. As in the case of stagnation points, aerosol particles run the risk of being trapped in regions of separated flow (Fig. 9). The mechanisms that determine whether a particle will enter such regions or not will be covered below.

Particle Motion in Air

Background

An understanding of how aerosol particles react in response to an applied force is fundamental to understanding many of the factors affecting their sampling, measurement, and characterization. As the particles are suspended in a gas, any external force applied to them will be resisted as they move with respect to the gas. A steady state will eventually be reached where the resistive forces equal the applied forces, leading to particles moving at a constant velocity (with respect to the gas). The resulting steady-state motion is often attained very rapidly, and an understanding of the relationship between an applied force (such as gravity, or an electrical field) and the resulting steady-state motion is a very useful tool in making sense of aerosol behavior. Once there is an understanding of the steady-state motion of aerosol particles, the basic concepts of motion under an applied force can be developed for the case where particles are under acceleration. *An understanding of both states is needed to understand many of the mechanisms leading to particle deposition and particle sampling.*

Drag

Drag is a force that opposes particle motion relative to the surrounding gas. It results from a number of mechanisms including gas viscosity (friction) and the energy required by the particle to displace gas as it moves (inertia). The applied force leading to particle motion with respect to the gas can be any force that acts differentially on the particles and the gas in an aerosol. For instance, an electrostatic

field will lead to a resultant force on charged particles but not on the carrier gas. And gravity will lead to a net force on suspended.

Newtonian Drag

Intuitively, drag is proportional to the projected area of a particle, and its velocity with respect to the gas. Newton derived the general equation for the drag force on a sphere while considering the motion of cannonballs through the air. He reasoned that the drag experienced by a cannonball results from the force required to remove the air from its path as it travels. The mass of air that has to be pushed aside each second by a sphere of diameter d is simply the projected area ($\pi d^2/4$) times the sphere's relative velocity (V) and the air's density (ρ_g). The force required to achieve this equals the change in momentum of the gas per unit time, which is simply equal to the mass of gas displaced times the relative velocity between the sphere and the gas.

This leads to the drag force F_D being given by:

$$F_D = \frac{\text{change of momentum}}{\text{unit time}} \propto \rho_g \frac{\pi}{4} d^2 V^2$$

$$F_D = \frac{C_D}{2} \rho_g \frac{\pi}{4} d^2 V^2 \quad (16)$$

where C_D is the drag coefficient. This is the general form of Newton's resistance equation and is valid for all sub-sonic particle motion, including that of aerosol particles. For situations where inertial forces dominate ($Re > 1000$), C_D is constant and is ~ 0.44 (for spheres). However, as viscous forces become significant at lower Re , C_D no longer remains constant but becomes dependent on Re . Below $Re \approx 1$, $C_D = 24/Re$, and in the transition region C_D can be approximated by an empirical expression:

$$C_D = \frac{24}{Re} (1 + 0.15 Re^{0.687}) \quad (17)$$

Stokes' Law

For aerosol particle motion, the particle Re is less than 1 in most cases and drag forces are dominated by viscous forces. The expression for the drag force on a particle in this regime was derived by George Stokes in 1851 and is given by:

$$F_D = 3\pi\eta Vd \quad (18)$$

where η is the gas viscosity, V the particle's relative motion, and d the particle diameter (spherical particles). In this regime, F_D is proportional to d and *not* d^2 . Comparing Stokes' law to Newton's law gives:

$$C_D = \frac{24\eta}{\rho_g V d} = \frac{24}{Re} \quad (19)$$

Particle Mobility

The drag on a particle is a function of its velocity. As a result, if a constant force is applied to a particle, it will eventually reach a velocity where the applied force matches the drag force. This is the maximum velocity attainable with the applied force and is referred to as the terminal velocity (or settling velocity when the force is gravity). Particles traveling at their terminal velocity are said to be in steady-state motion.

A useful concept when considering the steady-state motion of particles is their mobility. Mobility (usually denoted by the symbol B) is a measure of the relative ease of producing steady-state motion for an aerosol particle and is defined for spherical particles as:

$$B = \frac{V}{F_D} = \frac{1}{3\pi\eta d} \quad (20)$$

Using particle mobility, the terminal velocity of a particle, V_T , is expressed by:

$$V_T = FB \quad (21)$$

where F is the applied force.

An important application of Stokes' law is the derivation of the terminal velocity under gravity (particle settling velocity, V_{TS}). The gravitational force on a particle is given by mg where particle mass $m = \pi d^3 \rho / 6$. Thus, from Eq. (21), V_{TS} is given by:

$$V_{TS} = \frac{\pi d^3 \rho_p g}{6} \times \frac{1}{3\pi\eta d} = \frac{\pi d^2 \rho_p g}{18\eta} \quad (22)$$

This expression is valid for spherical particles $d > 1 \mu\text{m}$ and $Re < 1.0$.

Slip Correction

The derivation of Stokes' law assumes that particles are in the continuum regime (i.e., that the particle diameter is much larger than the gas mean free path and that the gas velocity at the particle's surface is zero). However, as particle diameter approaches and goes below the gas molecule mean free path, these assumptions begin to break down. The gas can no longer be treated as a continuous medium, and the assumption that gas velocity at the particle surface is zero becomes meaningless.

This phenomenon is sometimes visualized as the gas flow “slipping” across the particle surface. At the extreme, particles will behave like massive molecules, “slipping” between the gas molecules until a random collision takes place. For Stokes’ law to be used in this region – typically at particle diameters $< 1 \mu\text{m}$, a correction needs to be applied. This correction is usually referred to as the Slip Correction.

The first derivation of the correction factor was proposed by Cunningham (1910) and incorporated into the equation for the drag force on a particle as the Cunningham Slip Correction Factor C_C :

$$F_D = \frac{3\pi\eta Vd}{C_C} \quad (23)$$

where

$$C_C = 1 + \frac{2.52\lambda}{d} \quad (24)$$

Use of the Cunningham slip correction factor extends the applicable range of Stokes’ law to particles of diameter $0.1 \mu\text{m}$. A more generally applicable empirical form of the slip correction factor (developed by Davies 1945) is given by:

$$C_S = 1 + \frac{\lambda}{d} \left(2.34 + 1.05e^{-0.39\frac{d}{\lambda}} \right) \quad (25)$$

which is applicable for all particles smaller than $1 \mu\text{m}$ down to around 2 nm. A further extension to molecular sizes was presented by Ramamurthi and Hopke (1989).

Particle settling velocity for all particle sizes with $Re < 1$ becomes:

$$V_{TS} = \frac{\rho_p d^2 g C_S}{18\eta} \quad (26)$$

Particle Shape

The above expressions all assume that spherical particles are involved. If a particle is non-spherical, it will generally experience a different drag to a similarly sized sphere (Fig. 10). Generally, it is unusual to find spherical solid aerosol particles (unless they are manufactured specifically to be spheres), and so is particularly useful to know how particle shape affects drag, and therefore mobility and terminal velocity.

A correction factor, the Dynamic Shape Factor, is applied to Stokes’ law to account for the effect of shape on moving particles. The dynamic shape factor (χ) is defined by the ratio of the actual drag experienced by the particle to that experienced by an equivalent spherical particle. χ is given by:

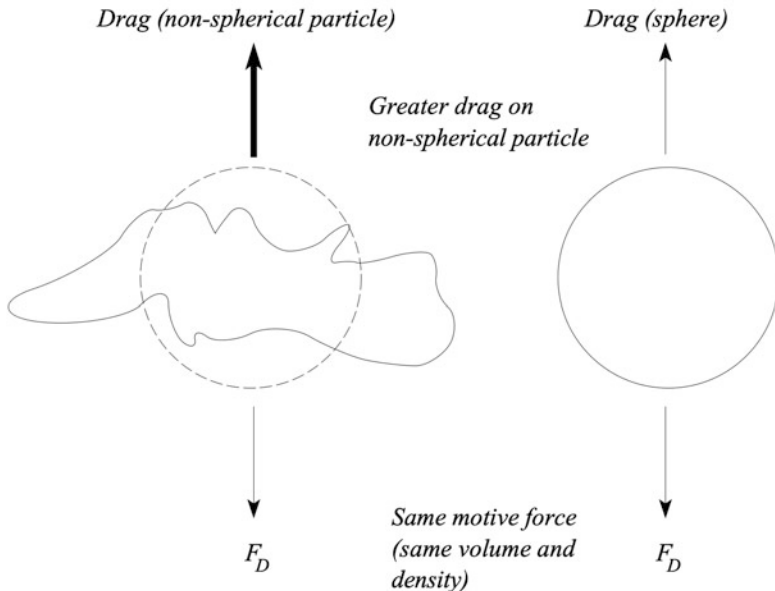


Fig. 10 Dynamic shape factor

$$\chi = \frac{F_D}{3\pi\eta V d_e} \quad (27)$$

where d_e is the equivalent volume diameter of the particle (i.e., the diameter of a spherical particle having the same volume). For a spherical particle, χ is 1.

Stokes' law including particle shape is given by:

$$F_D = \frac{3\pi\eta V d \chi}{C_S} \quad (28)$$

and particle terminal settling velocity becomes:

$$V_{TS} = \frac{\rho_p d^2 g C_S}{18\eta\chi} \quad (29)$$

Calculation of χ is complex, and for all but the simplest geometries, it must be measured experimentally. χ is always greater than 1. Compilations of shape factors are provided in Hinds and Zhu (2022).

Tranquil and Stirred Settling

Knowing V_{TS} allows an estimate to be made of how long it will take for a particle to settle from the air in an enclosed space. If there is no air motion within a room of

height h , it will simply take a time of $V_{TS} \times h$ for all particles to settle out. If the aerosol concentration N at a given point was measured, it would remain constant to a point and then abruptly fall to zero as the last particle settles past the reference point. However, air movement and activities in the room lead to different behaviors as described in ► Chaps. 11, “Deposition,” and ► 12, “Resuspension.”.

Definition of Particle Diameter: Aerodynamic Diameter

It is now possible to examine the concept of particle diameter. Previously in this chapter, it has been assumed that diameter d refers to a particle’s physical diameter, for instance, what might be seen and measured if examined under a microscope. However, the “diameter” of a particle depends strongly on the shape and composition of the particle and on the measurement method. Measuring particle diameter using microscopy, settling velocity, and light scattering, for instance, will all give different answers in many cases.

Here, there is a need for a measure of diameter that determines how a particle will behave in any given situation, and this may or may not be the same as its physical diameter. Differences in how particle diameter is characterized are particularly pertinent for non-spherical particles, where expressing particle size by a single parameter alone will always be an approximation. And here, understanding that the measured diameter of a particle is dependent on the way it is measured is particularly important when interpreting aerosol measurements (Fig. 11).

To a first approximation, particles being measured, characterized, or separated by inertial forces such as gravity or “centrifugal” force, are characterized by their settling velocity. Under inertial forces, two particles with the same settling velocity will behave in the same manner and be measured as being identical – even though they may have very different physical characteristics. It is common to define particles under these conditions by their aerodynamic diameter. Aerodynamic diameter is defined as the diameter of a sphere of density 1000 kg/m^3 with the same settling velocity as the particle of interest. A similar definition, used occasionally, is the Stokes’ diameter (d_s), which is the diameter of a sphere with the same density as the particle in question, and the same settling velocity. Re-arranging Eq. (29) and ignoring slip correction gives aerodynamic diameter (d_{ae}) as:

$$d_{ae} = d_e \left(\frac{\rho_p}{\rho_0 \chi} \right)^{\frac{1}{2}} = d_s \left(\frac{\rho_p}{\rho_0} \right)^{\frac{1}{2}} \quad (30)$$

where ρ_0 is 1000 kg/m^3 (“unit” density). For spheres, d_{ae} is simply

$$d_{ae} = d_p \left(\frac{\rho_p}{\rho_0} \right)^{\frac{1}{2}} \quad (31)$$

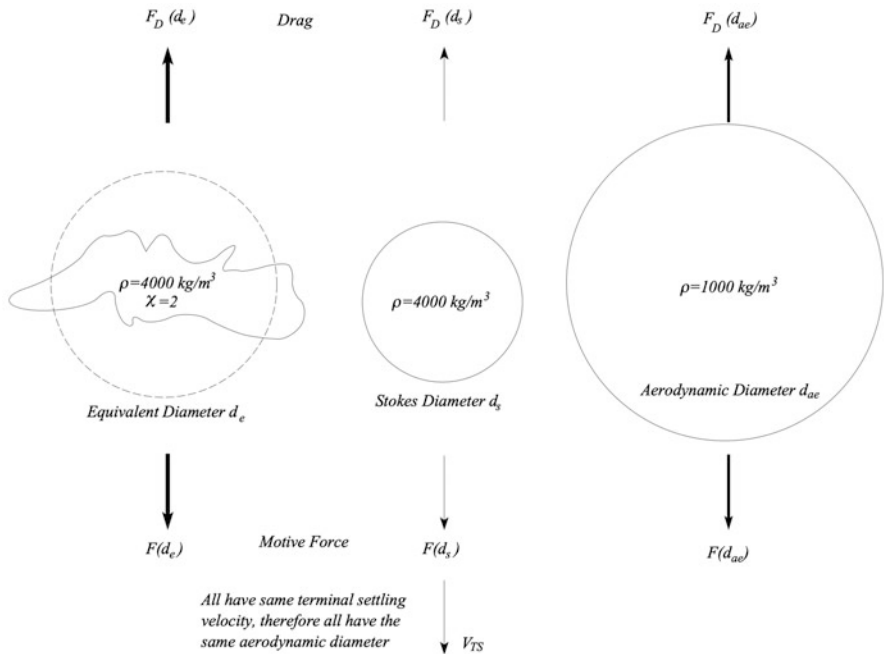


Fig. 11 Aerodynamic diameter. Despite variations in size and shape, all of these particles have the same aerodynamic diameter

For smaller particles where slip correction is important, Eqs. (30) and (31) need to be modified to include C_s for both d_p and d_e .

In general terms, it is common to speak of a particle's mobility diameter. Aerodynamic diameter is a special case where mechanical mobility is being considered. However, a similar approach is used for electrical mobility, diffusional mobility, thermophoretic mobility, etc. The important point to realize is that there is no absolute particle diameter. The diameter is defined by the method used to measure it.

Particle Motion Under Acceleration

A number of particle collection and measurement methods depend on the motion of particles under an accelerating force either leading to straight line acceleration or curvilinear motion (motion along a curved path). Here, three quantities are useful in understanding particles undergoing acceleration: particle relaxation time, stopping distance, and Stokes number. The concepts behind each quantity are described below, along with the necessary expressions to calculate them. However, a detailed derivation is beyond the scope of this chapter but can be found in Hinds and Zhu (2022).

Relaxation Time

We have already established that if you apply a steady force to a particle, it will eventually reach a steady velocity as the drag force matches the applied force. The assumption was made earlier that this steady state is reached relatively rapidly. However, knowing something about how long a particle takes to respond and “adjust” to a change in applied force is a useful tool for determining behavior under conditions of change.

Recall that under gravity, the terminal settling velocity is given by the mobility B multiplied by the applied force: in this case gravity (where $F = mg$). V_{TS} is written as:

$$V_{TS} = Bmg = \tau g \quad (32)$$

where τ has the units of time and is referred to the relaxation time. Relaxation time is a measure of how rapidly a particle will respond or “relax” to any changes in applied force. τ occurs in many instances within aerosol dynamics where a particle’s motion is governed by mechanical mobility. It is useful for understanding how rapidly different particles will respond to an applied force – for instance, if a group of particles with different diameters are moving under the influence of an electric field, it indicates which particles will continue to move for an appreciable amount of time when the field is switched off, and which will stop almost immediately. Re-arranging Eq. (32) and using the expression for mechanical mobility B gives:

$$\tau = \frac{\rho_p d^2 C_s}{18\eta} = \frac{\rho_0 d_a^2 C_s}{18\eta} \quad (33)$$

It takes 3τ for a particle to reach 95% of its new terminal velocity following a change in the applied force.

Stopping Distance

While relaxation time gives an indication of the time taken for a particle to adjust to a new set of forces, stopping distance is a measure of how far a particle will travel until it reaches a new steady state velocity under these forces. For instance, stopping distance S of a particle traveling at velocity V_0 will give the distance the particle will continue to travel after the applied force has been removed. Stopping distance is particularly important when it comes to determining the likelihood of particle deposition due to inertia.

Stopping distance for the situation where the motive force in the direction of travel is removed is given by:

$$S = V_0 \tau = Bm V_0 \quad (34)$$

where V_0 is the initial velocity. While τ gives the time taken to travel distance S , the actual time will be much longer since, as the particle slows down, the drag force will become smaller and the particle’s rate of deceleration will decrease, leading to the

distance traveled exponentially approaching the stopping distance S . In the absence of other forces, a particle will travel 95% of the distance toward S in a time of 3τ .

Curvilinear Motion

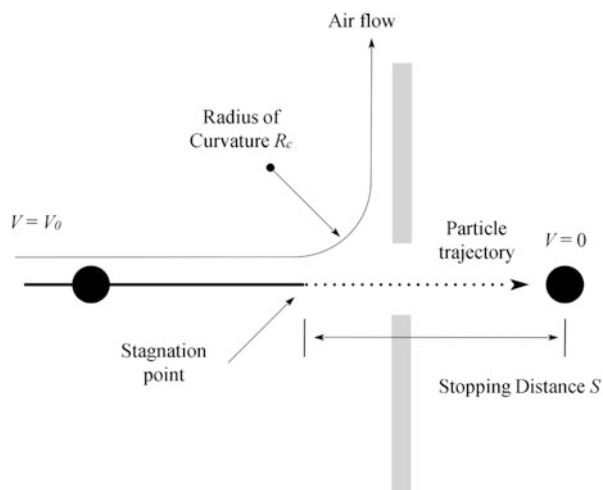
Curvilinear particle motion is an extension of straight-line motion and occurs when a particle experiences forces that are changing with respect to time and/or position. A good example is of particles in an aerosol flowing around an obstruction, or through a series of constrictions. The gas streamlines depicting flow in these situations will curve in response to the flow conditions. Particles entrained in the flow will also attempt to follow the streamlines as the varying flow direction exerts a force upon them. The degree to which particles will remain in the streamlines, or diverge from them, is characterized by the Stokes number Stk . Stk is the ratio of particle stopping distance to some measure of the size of the object causing the flow to diverge. In the illustrated example in Fig. 12, where R_C is the radius of curvature of the airflow as it deviates through a 90° bend, Stk is given by:

$$Stk = \frac{S}{R_C} = \frac{\tau V_0}{R_C}, Re_0 \leq 1 \quad (35)$$

Another example, if the particles are flowing in streamlines around a cylinder with its long axis oriented perpendicular to the flow, the characteristic dimension will be the cylinder's diameter, and Re_0 will be the initial particle Reynolds number ($V = V_0$).

Like Reynolds number, Stokes number is dimensionless. Stokes number can be understood as the “persistence” of a particle divided by the size of an obstruction. As Stk approaches zero, particles will follow the streamlines perfectly. As Stk increases,

Fig. 12 Illustration of stopping distance



a particle's resistance to any changes in direction will increase, resulting in increasingly more streamlines being crossed by the particle in regions of rapid flow direction change.

If a particle has the same values of Re and Stk for similar geometric conditions, the particle's motion will be the same. Equal Re ensures that the flow conditions are similar, while equality of Stk ensures that the particles motion in the flow fields are similar.

Brownian Motion

In 1827 the botanist Robert Brown first observed the random motion of pollen grains in water that is now called Brownian motion. Around 50 years later, similar behavior was noticed with smoke particles, and the connection was made between gas molecule motion and random particle motion. Molecules in a gas are in a continuous state of motion. Clearly, any aerosol particles present will be constantly bombarded by these molecules. If the particles are of similar mass to the gas molecules, they will move around in a similar way, and follow a similar random walk (Fig. 12). For particles very much larger than the gas mean free path, the collision rate with air molecules on all sides will be approximately equal, and there will be no net force leading to motion. However, in the transition region between these extremes, there is a finite probability of more collisions from one direction than the opposite direction, leading to a net force in that direction. The net direction, magnitude, and persistence of the force is itself random, leading to the random particle motions seen in Brownian motion. The motion is analogous to molecular motion, although it is important to remember that the particle motion is a result of many collisions with molecules and not in single collisions (Fig. 13).

Particle Brownian motion leads to three characteristics of particle behavior that are analogous or similar to molecular behavior in an ideal gas: diffusion, mean velocity, and mean free path.

Diffusion

The Brownian motion of aerosol particles leads to the bulk movement of particles through diffusion. As in the case of molecules, the flux of aerosol particles moving from a high to low concentration region through diffusion is given by Fick's first law of diffusion (Eq. 13). The diffusion coefficient D can be derived from equating the Stokes' drag force experienced by particles to the net force arising from molecular collisions. It is given by:

$$D = \frac{kTC_S}{3\pi\eta d} \quad (36)$$

k is the Boltzmann constant ($1.38 \times 10^{-23} \text{ J K}^{-1}$) and T the temperature of the gas in degrees Kelvin. The diffusion coefficient can be expressed in terms of particle mobility B :

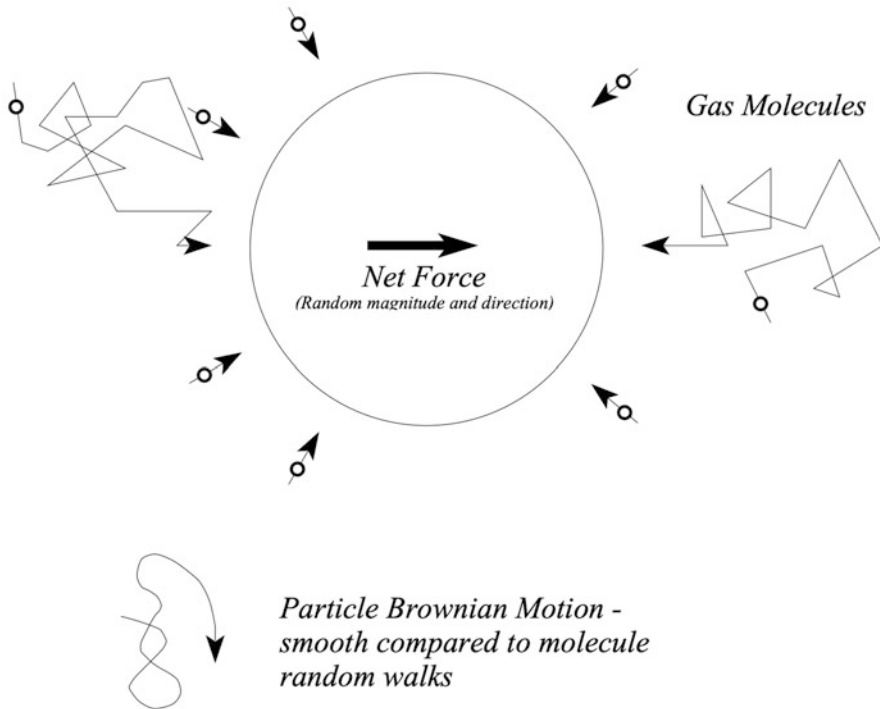


Fig. 13 Particle Brownian motion

$$D = kTB \quad (37)$$

D is proportional to temperature but inversely proportional to particle diameter. For small particles with high values of C_s , D is approximately proportional to $1/d^2$ since d^2 represents the cross-sectional area of a particle as it collides with gas molecules. However, the diffusion coefficient of a $0.01\text{ }\mu\text{m}$ particle is still three orders of magnitude smaller than that of a typical gas molecule.

The average distance a particle will travel from its starting position in a given time through diffusion is given by its displacement over time t . Brownian displacement is represented by the root mean square distance traveled, x_{rms} , and is given by:

$$x_{rms} = \sqrt{2Dt} \quad (38)$$

Mean Particle Velocity

As aerosol particles are constantly exchanging energy with the surrounding gas molecules, they have the same kinetic energy as these molecules. Therefore, in the same way that the root mean square and arithmetic mean velocities for gas molecules were derived, the same quantities can be derived for aerosol particles:

$$c_{rms} = \left(\frac{3kT}{m} \right)^{\frac{1}{2}} = \left(\frac{18kT}{\pi\rho_p d^3} \right)^{\frac{1}{2}} \quad (39)$$

$$\bar{c} = \left(\frac{8kT}{\pi m} \right)^{\frac{1}{2}} = \left(\frac{48kT}{\pi^2 \rho_p d^3} \right)^{\frac{1}{2}} \quad (40)$$

Mean Free Path

Particle mean free is not directly analogous to molecule mean free path. Since most aerosol particles are much more massive than gas molecules, it takes many collisions to lead to a change in direction of particle motion. However, the concepts are similar. Particle mean free path is defined as the distance traveled before molecular collisions have led to a complete (i.e., 90°) change in direction. This quantity is essentially the stopping distance of the particles under the influence of Brownian motion and is given by:

$$\lambda = \tau \bar{c} \quad (41)$$

The diffusion coefficient of an aerosol particle can be expressed in terms of particle mean free path and mean velocity:

$$D = \frac{\pi}{8} \lambda_p \bar{c} \quad (42)$$

Relative Deposition Velocities

In general, different deposition forces become dominant at different particle sizes. For large particles, gravitational deposition (or inertial deposition) is important. Electrostatic deposition becomes more important at smaller particle diameters, but for most aerosols the Boltzmann charge equilibrium (the distribution of positive and negative charges on a collection of aerosol particles at equilibrium) inhibits very small particles having sufficient charge for electrostatic deposition to be significant. In this region, diffusion rapidly becomes the dominant deposition mechanism.

Conclusions

This chapter provided an introduction to many of the concepts related to aerosol dynamics that will be helpful in understanding the other chapters in this section, such as deposition and resuspension. It is not meant to be comprehensive in covering all of the related topics, such as charged particle behavior in the presence of external electric fields or how to represent particle size distributions. Details on particle measurement methods are provided in the chapter on indoor particle concentrations, size distributions, and exposures. A comprehensive introduction to aerosol dynamics

is provided in a number of textbooks, including Hinds and Zhu (2022) and Friedlander (2000).

Nomenclature (Note that in some cases a symbol may be used to denote different values in different contexts. All equations listed should be evaluated using SI units (kg, m, s). SI units for the values below are listed where appropriate)

A	Area [m^2]
B	Particle mechanical mobility [$\text{m N}^{-1} \text{ s}^{-1}$]
c	Velocity [m/s]
c_x	Velocity in the x-direction [m]
c_{rms}	Root mean square velocity [m/s]
\bar{c}	Mean velocity [m/s]
C	Concentration (e.g., gas concentration) [concentration units/ m^3]
C_c	Cunningham slip correction [dimensionless]
C_s	Slip correction [dimensionless]
C_D	Drag coefficient [dimensionless]
D	Diffusion coefficient [m^2/s]
d	Particle diameter [m]
d_m	Collision diameter [m]
d_{ae}	Aerodynamic diameter [m]
d_e	Equivalent diameter (diameter of sphere with same volume) [m]
d_s	Stokes diameter [m]
F	Force [kg m/s^2 or N]
F_D	Drag force [kg m/s^2 or N]
g	Gravity [9.81 m/s^2]
J	Flux. Particles [$\#/ \text{m}^2/\text{s}$]
k	Boltzmann constant [$1.38 \times 10^{-23} \text{ J/K}$]
m	Mass. Often of a single particle or molecule. [kg]
N	Number of molecules per unit volume (gas kinetics) [$\#/ \text{m}^3$]
n	Number of moles of gas (gas kinetics) [mol]
N_a	Avogadro's number [$6.022 \times 10^{23} \text{ mol}^{-1}$]
n_c	Molecule collisions per second [$\#/ \text{s}$]
P	Pressure [N/m^2 or Pa]
R	Gas constant [$8.31 \text{ Pa m}^3/\text{K mol}$]
Re	Reynolds number [dimensionless]
R_c	Radius of curvature
S	Stopping distance [m]
Stk	Stokes number [dimensionless]
t	Time [s]
τ	Relaxation time [s]
T	Temperature [K]

U	Velocity. Usually free stream gas
V	Volume [m^3]
V_0	Initial velocity [m/s]
V_T	Terminal velocity [m/s]
V_{TS}	Settling velocity [m/s]
V_{th}	Thermophoretic deposition velocity [m]
x_{rms}	Root mean square distance traveled [m]
η	Viscosity [$\text{kg m}^{-1} \text{s}^{-1}$]
λ	Mean free path [m]
λ_p	Particle mean free path [m]
λ_g	Gas mean free path [m]
ρ	Density [kg/m^3]
ρ_g	Gas density [kg/m^3]
ρ_p	Particle density [kg/m^3]
ρ_0	Unit density [1000 kg/m ³]
χ	Dynamic shape correction factor

References

- Cunningham E (1910) On the velocity of steady fall of spherical particles through fluid medium. Proc Roy Soc London 83:357–365
- Davies CN (1945) Definitive equations for the fluid resistance of spheres. Proc Phys Soc 57: 259–270
- Friedlander SF (2000) Smoke, dust, and haze: fundamentals of aerosol dynamics, Topics in chemical engineering, 2nd edn. Oxford University Press, Oxford, UK
- Hinds WC, Zhu Y (2022) Aerosol technology: properties, behavior, and measurement of airborne particles, 3rd edn. Wiley, New York
- Loeb LB (1961) The kinetic theory of gases. Dover Publication, New York, p 326
- Ramamurthi M, Hopke PK (1989) On improving the validity of wire screen “unattached” fraction Rn daughter measurements. Health Phys 56:189–194



Impact of Outdoor Particles on Indoor Air 10

Chen Chen and Bin Zhao

Contents

Introduction	276
Penetration Factor	277
Measurement	277
Modeling	284
Infiltration Factor	285
Measurement Methods	285
Modeling Methods	287
Data Analysis	287
Conclusion	290
Cross-References	291
References	291

Abstract

Even people mostly stay indoors, they are constantly exposed to outdoor-originated particles. Outdoor particles can penetrate into indoor environments via the building envelope through ventilation and air infiltration. Penetration factor is the ratio of outdoor particles entering the indoor environments through the building's envelope, and infiltration factor is the equilibrium fraction of ambient particles that enter and remain suspended indoors. The penetration factor and infiltration factor are important parameters to understand the transport of particles from outdoors to indoors. Penetration factors can be measured according to regression approach, equilibrium concentration approach, or error analysis approach. The penetration factors are

C. Chen

Department of Building Science, School of Architecture, Tsinghua University, Beijing, China

B. Zhao (✉)

Department of Building Science, School of Architecture, Tsinghua University, Beijing, China

Beijing Key Laboratory of Indoor Air Quality Evaluation and Control, Tsinghua University, Beijing, China

e-mail: binzhao@tsinghua.edu.cn

0.78 ± 0.17 for accumulation-mode particles ($0.1\text{--}1\text{ }\mu\text{m}$ diameter). They decreased due to Brownian diffusion for smaller particles, or due to stronger gravitational settling and impaction for larger particles. In addition to particle sizes, penetration factors are determined by pressure differences, geometry and surface roughness of cracks, etc. Infiltration factors can be measured by regression approach, equilibrium concentration approach, or tracer element approach, and can also be simulated based on the air change rate, penetration factor and deposition rate. The infiltration factors of $\text{PM}_{2.5}$ are approximately 0.50, which are lower than ultrafine particles and higher than PM_{10} under the same conditions. Infiltration factors are also influenced by air change rates, window opening behaviors, ventilation systems, etc.

Keywords

Particulate matter · Indoor air · Penetration factor · Infiltration factor

Introduction

People spend 85–90% of their time indoors (Buonanno et al. 2014; Duan 2013; Klepeis et al. 2001; Lee and Lee 2017; Leech et al. 2002; Matz et al. 2014; Spalt et al. 2016). There are various sources of indoor particles. Ambient particles penetrate into indoor environments via the building envelope through ventilation and air infiltration (Chen and Zhao 2011; Nazaroff 2004). Indoor activities, for example, including cooking and smoking also lead to the generation of indoor particles (Chen et al. 2018a, b; Morawska et al. 2017; Nazaroff 2004). Besides, the indoor particle concentration is also determined by the deposition, coagulation and resuspension of particles. Assuming that air is well mixed indoors and the ambient concentration is steady, and the mass balance equation for particles can be expressed as (Rim et al. 2016; Thatcher and Layton 1995; Vu et al. 2017):

$$\frac{dC_{in}(d_p, t)}{dt} = aPC_{out}(d_p) - (a + k_d + k_c)C_{in}(d_p, t) + \frac{RL_f A_f}{V} + \frac{S(d_p, t)}{V} \quad (1)$$

$$k_d = \frac{A}{V} v_d \quad (2)$$

$$k_c = -\frac{\frac{1}{2} \sum_n \sum_m K_{m,n} C_{in}(m, t) C_{in}(n, t) - C_{in}(d_p, t) \sum_n K_{dp,n} C_{in}(n, t)}{C_{in}(d_p, t)} \quad (3)$$

where $C_{in}(d_p, t)$, $C_{in}(m, t)$, and $C_{in}(n, t)$ are the real-time indoor particle concentrations with diameter d_p , m , and n , respectively, at the measuring moment t , a is the air change rate, P is the penetration factor of outdoor particles entering the indoor environments through the building's envelope, k_d is the deposition rate, R is the particle resuspension rate, L_f is the mass loading of particles on accessible floor surfaces, A_f is the surface area of floors, S is the emission rate of particles generated from indoor sources, V is the volume of the room, k_c is the net rate of loss due to coagulation, and $K_{m,n}$ and $K_{dp,n}$ are the coagulation coefficients between particles

with diameter m and n , d_p and n , respectively. The numerator of equation for k_c represents the net loss of indoor concentration of particles with diameter d_p due to coagulation, which depends on the generation when particles with diameter m coagulate with particles with diameter n , and the reduction of the concentration when particles with diameter d_p coagulate with particles in all other size categories.

Ambient air pollution is still severe in a lot of areas, including India and China, which account for more than 30% of the world's population (Huang et al. 2018; Pant et al. 2016). Environmental events, such as Camp Fire (Li et al. 2020; Reid et al. 2015; Rooney et al. 2020), also increased ambient particle concentrations in those areas where ambient air pollution was well controlled before. Thus, assessing indoor exposure to outdoor-originated particles is important. **Penetration factor (P)** in Eq. (1) is one of important parameters to understand the transport of particles from outdoors to indoors. Besides, **infiltration factor (F_{inf})**, another important parameter, is defined as the **equilibrium** fraction of ambient particles that enter and remain suspended indoors (Ozkaynak et al. 1996; Wilson and Suh 1997). F_{inf} can be expressed as:

$$F_{\text{inf}} = \frac{C_{\text{in},os}(d_p, t_\infty)}{C_{\text{out}}(d_p, t_\infty)} \quad (4)$$

where $C_{\text{in},os}(d_p, t_\infty)$ is the indoor concentration of particle with diameter d_p originating from outdoor sources at steady state, and $C_{\text{out}}(d_p, t_\infty)$ is the outdoor concentration of particle with diameter d_p at steady state.

As outdoor particles contribute significantly to indoor aerosols, penetration factor and infiltration factor are discussed in this chapter as one of the most important indoor aerosol dynamics. And deposition, resuspension, and sources of particles will be explained in detail in next chapters of this section.

Penetration Factor

There are several experiments for penetration factors conducted in real buildings or laboratory. Nearly all studies neglected the effects of coagulation and resuspension based on mass balance equation as:

$$\frac{dC_{\text{in}}(d_p, t)}{dt} = aPC_{\text{out}}(d_p) - (a + k_d)C_{\text{in}}(d_p, t) + \frac{S(d_p, t)}{V} \quad (5)$$

Measurement

Methods in Real Buildings

Regression Approach

Koutrakis et al. (1992) sampled indoor and outdoor PM_{2.5} (fine particles whose aerodynamic diameters are not greater than 2.5 μm) in 187 residences and determined

the concentrations of elements in PM_{2.5}. Then, linear regression models between average indoor and outdoor concentration of PM_{2.5} and elements were developed as Eq. (6), which is the equilibrium solution. The penetration factor can be determined based on the slope of regression model, measured a and V , and estimated A/V and v_d .

$$C_{in} = \frac{aP}{a + \frac{A}{V}v_d} C_{out} + \frac{S}{V(a + \frac{A}{V}v_d)} \equiv \text{slope} \times C_{out} + \text{intercept} \quad (6)$$

Ozkaynak et al. (1994) modified this model as:

$$C_{in} = \frac{aPC_{out}}{a + k_d} + \frac{N_s S_s + T_c S_c}{(a + k_d)Vt} + \frac{Q_{other}}{(a + k_d)V} \quad (7)$$

where N_s is the number of cigarettes smoked, T_c is the duration of cooking, S_s and S_c are the mass of PM_{2.5}, PM₁₀ (coarse particles whose aerodynamic diameters are not greater than 10 μm), or elements generated per cigarette smoked and per hour of cooking, respectively, and Q_{other} is the mass flux of PM_{2.5}, PM₁₀ or elements from all other indoor sources. The C_{in} , C_{out} , N_s , T_c , V , and a were all measured or recorded in 293 residences. The penetration factor of PM_{2.5}, PM₁₀ and elements in PM_{2.5} and PM₁₀ can be determined using a nonlinear model as well as k_d , S_s , S_c , and Q_{other} (Ozkaynak et al. 1994, 1996).

Long et al. (2001) developed regression models of C_{out}/C_{in} as a function of $1/a$ based on nightly average data in 9 residences when the indoor sources can be neglected:

$$\frac{C_{out}}{C_{in}} = \frac{k_d}{P} \left(\frac{1}{a} \right) + \frac{1}{P} \equiv \text{slope} \times \left(\frac{1}{a} \right) + \text{intercept} \quad (8)$$

The values of P and K can be estimated from the intercept and slope.

This method is simple but the regression would be poor due to high variance of temporal contribution from specific indoor particle sources (Fonseca et al. 2014).

Equilibrium Concentration Approach

Tung et al. (1999) estimated the penetration factor of PM₁₀ in an office by measuring the equilibrium concentration as:

$$P = \frac{(a + k_d)C_{inf}}{aC_{out}} \quad (9)$$

where a and k_d were measured based on the natural decay curve of CO₂ and PM₁₀, respectively; C_{inf} was estimated as:

$$C_{in} - C_{inf} = \frac{1}{2} \left(C_{in,T_{1/2}} - C_{inf} \right) \quad (10)$$

where $C_{in,T_{1/2}}$ was the indoor concentration measured at the half-life, $T_{1/2}$; $T_{1/2}$ can be estimated as:

$$T_{1/2} = \frac{\ln 2}{a + k_d} \quad (11)$$

Numerous studies measured the equilibrium concentration for the penetration factor similarly (Chao et al. 2003; Chen et al. 2012b; Tran et al. 2017; Vette et al. 2001; Xie et al. 2020; Zhao et al. 2020). The decay curve of particle concentrations was monitored for 2–10 h until the steady state conditions were most likely achieved.

Zhou et al. (2019) turned off the ceiling cassette fan-coil unit in an office and monitored the indoor concentration of PM_{0.3–10} until it reached the equilibrium status. The penetration factor was calculated following Eq. (9) with the measured air change rate and the estimated deposition rate referring to previous studies. Vu et al. (2017) evaluated the penetration factor as the ratio of the downstream to upstream concentration through the mechanical ventilation system.

Peng et al. (2020) developed a method based on indoor PM_{2.5} removal by an air cleaner as Eq. (12). The average penetration factor is:

$$P = \left[\frac{1}{aC_{\text{out}}(d_p, t)} \frac{dC_{\text{in}}(d_p, t)}{dt} + \frac{(a + k_d + CAER)C_{\text{in}}(d_p, t)}{aC_{\text{out}}} \right] \quad (12)$$

where CAER is the ratio of the clean air delivery rate to the room volume.

Error Analysis Approach

Thatcher et al. (2003) developed a decay and rebound approach by measuring indoor and outdoor PM_{0.1–10} concentrations in two residences including three factors: (1) the particle loss rate following artificial elevation of indoor particle concentrations, (2) rapid reduction in particle concentration through induced ventilation by pressurization with HEPA-filtered air, and (3) the particle concentration rebound after house pressurization stopped. In such an experimental design, the indoor concentration varied over a wide range and the transient model in Eq. (13) was used to determine the combination of penetration factor and deposition rate that best fits the observed data, in other words, minimizes the sum of the square of differences between the measured and the modeled indoor concentration at each time step.

$$C_{\text{in}}(d_p, t + \Delta t) = C_{\text{in}}(d_p, t) + a(t)PC_{\text{out}}(d_p, t)\Delta t - [a(t) + k_d]C_{\text{in}}(d_p, t)\Delta t \quad (13)$$

where the time-varying air change rate, $a(t)$, is calculated using a transient mass balance of tracer gas (SF₆) approach that accounts for the injection rate and the time-dependent infiltration losses. Many studies monitored indoor and outdoor particle concentrations for hours or even days without invention and used such least-squares estimation for the penetration factor (Chatoutsidou et al. 2015; Mleczkowska et al. 2016; Rim et al. 2010, 2013). Bennett and Koutrakis (2006) simulated the indoor

concentration and employ least-squares estimation for the penetration factor as Eq. (14) similarly, which is also applied by Huang et al. (2017) and Wang et al. (2019):

$$C_{\text{in}}(d_p, t + \Delta t) = C_{\text{in}}(d_p, t) e^{-(a+k_d)\Delta t} + \frac{aPC_{\text{out}}(d_p, t)}{a + k_d} \left[1 - e^{-(a+k_d)\Delta t} \right] \quad (14)$$

Zhu et al. (2005) measured continuous concentrations of indoor and outdoor PM_{0.06-0.22} in four residences. The $\Delta C_{\text{in}}/\Delta t$ was used as a dependent variable in a linear regression while C_{in} and C_{out} were two independent variables in Eq. (15). Least-squares estimation was used to produce the best linear unbiased estimates for the penetration factor and deposition rate.

$$\frac{\Delta C_{\text{in}}(d_p, t)}{\Delta t} = aPC_{\text{out}}(d_p, t) - (a + k_d)C_{\text{in}}(d_p, t) \quad (15)$$

Stephens and Siegel (2012) and Zhao and Stephens (2017) modified the two-parameter error analysis approach. They measured the deposition rate by using a log-linear regression solution to the initial indoor decay portion of the data. With the earlier estimates of a and k_d , the penetration factor was then estimated using a one-parameter nonlinear least-squares regression following Eq. (13). The entire test period only lasted about 2–4 h, typically yielding relatively low uncertainties and high fitness for estimates of both P and k_d . Maskova et al. (2016, 2020) used the same approach for the penetration factor in historic buildings.

Hussein et al. (2006) and Chen et al. (2020b) modified the two-parameter error analysis approach in a different way. The three key parameters (the penetration factor, deposition rate and air change rate) were all estimated following Eq. (13) or Eq. (14) with the limitation of reasonable ranges.

Laboratory Methods

Different from measurements in real buildings, the pressure differences between inlet and outlet of the cracks can be maintained in laboratories to understand the factors influencing particle penetration.

Mosley et al. (2001) monitored particle concentrations in two compartments of a chamber as the particles are transported from the first compartment to the second one by advective flow via rectangular slits, simulating leakage paths. The penetration factor can be calculated based on the linear regression as following:

$$\frac{C_{\text{outlet}}(t)}{C_{\text{inlet}}(t)} \approx \frac{PQ}{V} t \equiv \text{slope} \times t \quad (16)$$

The penetration factor was also evaluated as the ratio of the downstream to upstream concentration through cracks or ventilation systems in many previous laboratory-based experiments (Jeng et al. 2006, 2007; Lai et al. 2012; Liu and

Nazaroff 2003; Lv et al. 2018; Stratigou et al. 2020; Wang et al. 2010; Xu et al. 2010).

Wang et al. (2020a, 2010) also applied the equilibrium concentration approach to their laboratory-based experiments. Lai et al. (2020) used the error analysis approach and developed a blower-door method giving higher precision. The penetration factor was measured based on the mass balance model of depressurization as Eq. (15) with the deposition rate estimated under pressurization.

Data Analysis

The penetration factor of UFPs (ultrafine particles, whose mobility diameters are not greater than $0.1 \mu\text{m}$), $\text{PM}_{2.5}$ and PM_{10} is in the range of 0.59–0.78, 0.72–1, and 0.69–0.86, respectively (Koutrakis et al. 1992; Ozkaynak et al. 1996; Tung et al. 1999; Williams et al. 2003; Zhao and Stephens 2017), which is consistent with the size-dependent results presented in Figs. 1 and 2. The size-dependent measured results in residences (A) and other real buildings (B) are presented in Fig. 1 (Chao et al. 2003; Chatoutsidou et al. 2015; Chen et al. 2020b; Hussein et al. 2006; Long et al. 2001; Maskova et al. 2016; Rim et al. 2010, 2013; Thatcher et al. 2003; Tran et al. 2017; Vette et al. 2001; Vu et al. 2017; Xie et al. 2020; Zhao and Stephens 2017; Zhao et al. 2020; Zhou et al. 2019; Zhu et al. 2005). The penetration factors are 0.78 ± 0.17 for accumulation-mode particles ($0.1\text{--}1 \mu\text{m}$ diameter). The penetration factors for UFPs

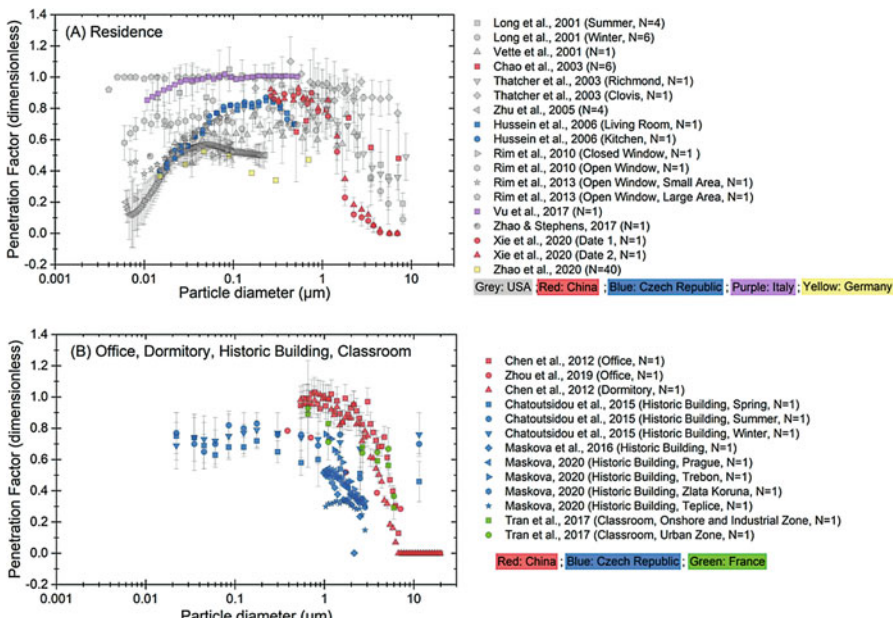


Fig. 1 Penetration factors measured in residences (a) and other buildings (b, including office, dormitory, historic building and classroom). Error bars represent standard errors

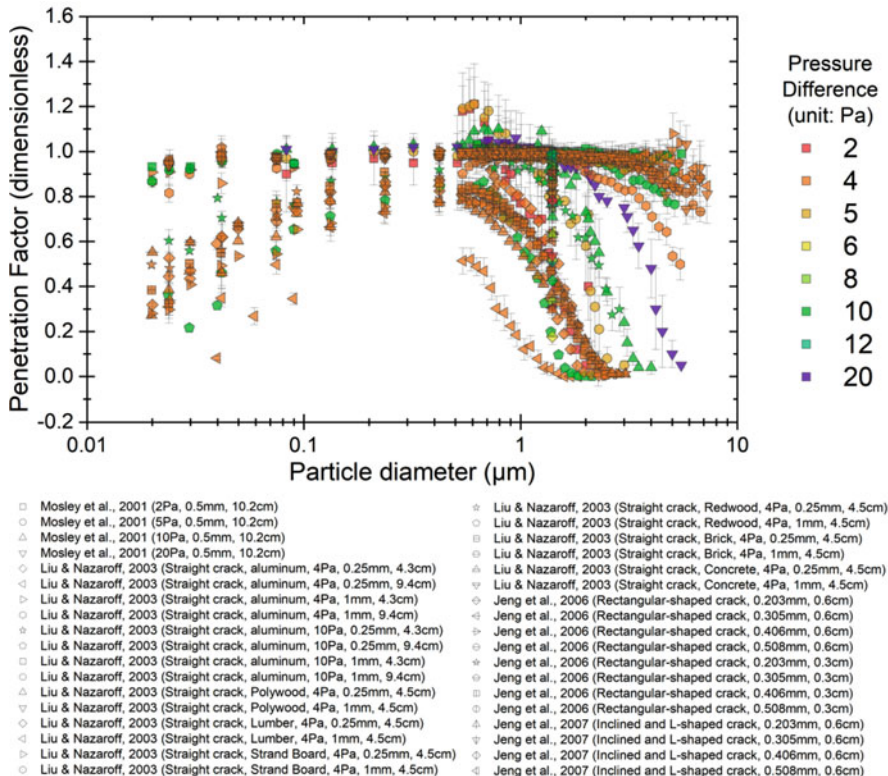


Fig. 2 Penetration factors measured in laboratories. Error bars represent standard errors (Adapted from Chen and Zhao (2011), Figure 7, with permission from Elsevier)

decreased to 0.61 ± 0.23 due to Brownian diffusion. The penetration factors for larger particles also decrease due to stronger gravitational settling and impaction with values of 0.48 ± 0.31 for particles greater than $1 \mu\text{m}$.

The penetration factors are influenced by air change rates and airtightness levels of building envelopes, which are determined by building types, seasons, window opening behaviors, years of construction, etc. (Chatoutsidou et al. 2015; Chen et al. 2020b; Long et al. 2001; Rim et al. 2010, 2013; Wang et al. 2019; Zhao and Stephens 2017). The measured results varied from building to building. Stephens and Siegel (2012) found that the penetration factor of PM_1 was significantly and negatively correlated with the years of construction of residences. In other words, higher fraction of outdoor PM_1 can enter leakier and older homes than those in tighter and newer homes. Stephens (2015) reanalyzed these results by Stephens and Siegel (2012) and the outdoor particle infiltration rates (aP) tended to be log-normally distributed with a geometric mean value of 0.16 h^{-1} and a geometric standard deviation of 2.33. Shi et al. (2017) collected measured data in real

buildings from previous studies (Chao et al. 2003; Chen et al. 2012b; Long et al. 2001; Thatcher et al. 2003; Vette et al. 2001; Zhu et al. 2005) and developed an empirical equation to estimate the penetration factors depending on particle diameter.

The measured data in laboratories in Fig. 2 showed the functions of penetration factors influencing by particle size, pressure differences, geometry and surface roughness of cracks (Jeng et al. 2006, 2007; Liu and Nazaroff 2003; Mosley et al. 2001). Penetration factors increase with larger pressure differences, larger crack height and smaller flow-path lengths (Jeng et al. 2006, 2007; Liu and Nazaroff 2003; Mosley et al. 2001). The effects of impaction and gravitation settling on large particles and Brownian diffusion on UFPs are similar to those in real buildings. Roughness appears to be relatively important for smaller particles because impaction and gravity begin to control deposition of larger particles in cracks. The roughness elements may be immersed within the particle concentration boundary layer for UFPs but extend well into the boundary layer for the case of 0.1–0.4 μm particles leading to a greater role in enhancing deposition for 0.1–0.4 μm particles than for UFPs (Liu and Nazaroff 2003). Based on the results of L-shape crack, Brownian diffusion is found to be the dominant particle deposition mechanism for a vertical crack while the gravitational sedimentation is the dominant deposition mechanism for a horizontal crack (Jeng et al. 2007). The penetration factors measured in laboratories are close to those measured in real buildings (Fig. 3).

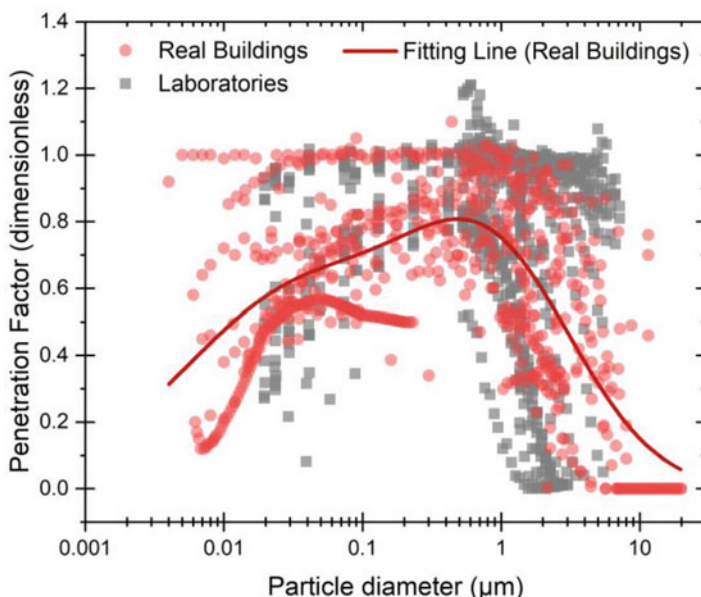


Fig. 3 Comparison of penetration factors measured in real buildings and laboratories

Modeling

Liu and Nazaroff (2001) developed a mathematical model to estimate the particle penetration factor through building cracks by considering the effects of three major particle deposition mechanisms: Brownian diffusion, gravitational settling, and impaction. Super-micron and ultrafine particles are significantly removed due to gravitational settling and Brownian diffusion, respectively. The penetration of accumulation-mode particles is also predicted to be approximately one when the crack height is larger than 0.25 mm, consistent with measurement results. The overall penetration is found to be influenced more by the largest cracks than by the smallest cracks in a building since airflow rates increase strongly as crack height increases. Especially, the modeled size-dependent penetration factors by Liu and Nazaroff (2001) when the crack is 1 mm high by 10 cm long at a fixed pressure drop of 4 Pa were summarized by Nazaroff (2004) and applied to further studies. For example, Ji and Zhao (2015) measured the size-dependent outdoor particle concentration and calculated the penetration factors of PM_{2.5} based on these modeled results and 69 groups of measured concentrations. The penetration factors of PM_{2.5} were found to be in the range of 0.90–0.97 with the mean value of 0.95.

Chen et al. (2012b) developed a methodology for predicting the penetration factor for actual engineering application. The geometries of the cracks in a building can be estimated according to the American Society of Heating, Refrigeration, American Society of Heating, Refrigeration, Air-Conditioning Engineers (ASHRAE) Handbook (ASHRAE 2001). The penetration of horizontal cracks can be calculated considering three major particle deposition mechanisms mentioned above, while the gravitational settling of particles in vertical cracks is negligible. The air change rate and effective air leakage area were found to be important factors influencing particle penetration through cracks in real buildings. The effect of inertial impaction cannot be neglected for coarse particles, especially when the air change rates are relatively large ($\sim 1 \text{ h}^{-1}$). However, the effect of the ratio of horizontal to vertical crack areas is negligible with such large air change rate.

Tian et al. (2009) and Lai et al. (2012) developed mathematical models to calculate particle penetration factor incorporating the influence of surface roughness. The penetration factor was found to be insensitive to roughness scales. The penetration factors through rough cracks are smaller than smooth crack at low pressure.

Zhao et al. (2010) developed and compared three models to model particle penetration factor through a single straight crack, including a mathematical model, an Eulerian model, and a Lagrangian model. It was found that the mathematical and the Eulerian model predicted the penetration factor reasonably while the Eulerian model showed the best agreement (Fig. 4). The Lagrangian model are less satisfied for UFPs and Chen and Zhao (2017) improved the accuracy by modifying the Brownian force in the model (Fig. 4).

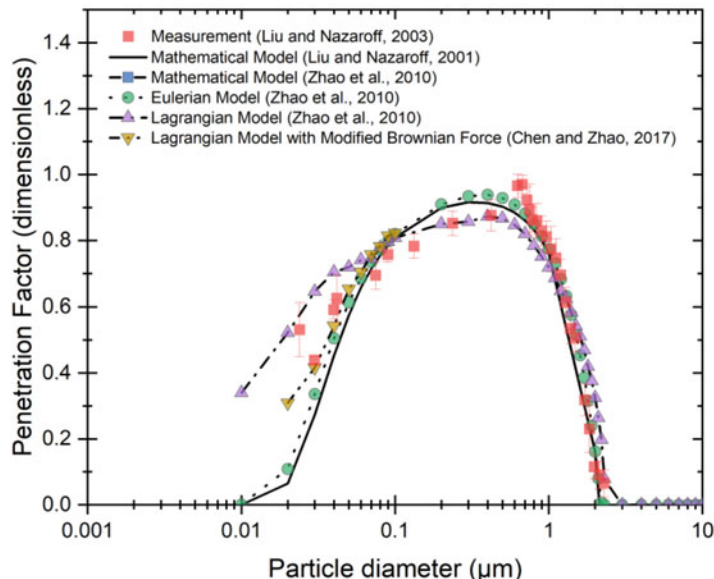


Fig. 4 Comparison of model predictions with experimental data for aluminum cracks when the crack is 0.25 mm high by 4.3 cm long at a fixed pressure drop of 4 Pa (Adapted from Chen and Zhao (2011), Figure 9, with permission from Elsevier)

Infiltration Factor

Measurement Methods

Regression Approach

After measuring the indoor and outdoor particle concentrations, the infiltration factor can be estimated the slope in Eq. (17), another form of Eq. (6):

$$C_{\text{in}} = F_{\text{inf}} C_{\text{out}} + C_{\text{is}} \equiv \text{slope} \times C_{\text{out}} + \text{intercept} \quad (17)$$

This approach was used in many previous studies (Barraza et al. 2014; Hoek et al. 2008; Hu et al. 2018; Lachenmyer and Hidy 2000; Landis et al. 2001; Meng et al. 2005, 2007; Ott et al. 2000; Rivas et al. 2015; Wallace et al. 2003; Williams et al. 2003; Wu et al. 2012).

According to section “[Methods in Real Buildings](#)”, the penetration factor and deposition rate can be determined by the nonlinear regression of Eq. (13) or (14). Then, the infiltration factor can be calculated based on their results as following (Allen et al. 2003; Chatoutsidou et al. 2015; Kearney et al. 2011; Rim et al. 2010, 2013):

$$F_{inf} = \frac{aP}{a + k_d} \quad (18)$$

The Eq. (14) can be expressed as the function of the changes of indoor concentrations in the indoor and outdoor concentrations as following:

$$\begin{aligned} \Delta C_{in}(d_p, t + \Delta t) &= \left[e^{-(a+k_d)\Delta t} - 1 \right] C_{in}(d_p, t) \\ &\quad + F_{inf} \left[1 - e^{-(a+k_d)\Delta t} \right] C_{out}(d_p, t) \\ &\equiv slope_1 C_{in}(d_p, t) + slope_2 C_{out}(d_p, t) \end{aligned} \quad (19)$$

The $slope_1$ and $slope_2$ can be solved using a linear regression forcing the intercept to zero. Thus, the infiltration factor can be calculated based on the regression results (Allen et al. 2003; Polidori et al. 2007).

Equilibrium Approach

The infiltration factors were calculated as the ratio of indoor to outdoor concentration with the absence of indoor sources, which were always measured during the overnight (Bhangar et al. 2011; Chen et al. 2011; Kearney et al. 2011, 2014; Long et al. 2001; MacNeill et al. 2012; Mullen et al. 2011a, b; Polidori et al. 2007; Rim et al. 2010, 2013; Sarnat et al. 2006; Wallace and Ott 2011; Wang et al. 2010; Zauli-Sajani et al. 2018; Zhao and Stephens 2017).

Tracer Element Approach

The tracer element should be selected based on the assumptions that (1) The tracer element must be present in both indoor and outdoor particle in sufficient quantities; (2) The tracer element should be primarily of outdoor origin, in other words, the indoor sources of the tracer element should be insignificant and the ratio of the indoor to outdoor tracer element concentrations shouldn't be larger than one; (3) The physical behaviors of the tracer element should be similar to those of outdoor particles, including deposition, penetration, and chemical stability (Ji et al. 2018; Long and Sarnat 2004; Sarnat et al. 2002).

Sulfur was always used as a tracer of outdoor PM_{2.5} (Allen et al. 2003; Chen et al. 2017, 2019; Cohen et al. 2009; Li et al. 2019; Meng et al. 2005; Miller et al. 2019; Sarnat et al. 2002; Wallace and Williams 2005; Zhou et al. 2018). Long and Sarnat (2004) found that nickel can serve as a strong tracer for total outdoor PM_{2.5}, especially particles with diameter of 0.04–0.5 μm, in the residences in the United State. However, Ji et al. (2018) found that there were indoor sources of sulfur in Chinese residences related to the sulfur-containing substances added to Chinese natural gas, and the indoor and outdoor concentrations of nickel were below the detection limit. Instead, iron is found to be more suitable as a tracer for outdoor PM_{2.5} in Beijing, China. The iron tracer approach was applied to the estimation of infiltration factor in Beijing to separate PM_{2.5} of outdoor and indoor origin (Chi et al. 2019). Wang et al. (2020b) confirmed the more stable effects of iron than sulfur on tracking outdoor PM_{2.5} in temporal and spatial scales in Nanjing, China.

The infiltration factors of PM_{2.5} can be calculated in the previous studies mentioned above as following:

$$F_{\text{inf}} = \frac{C_{\text{in,tracer}}}{C_{\text{out,tracer}}} \quad (20)$$

where $C_{\text{in,tracer}}$ and $C_{\text{out,tracer}}$ are the indoor and outdoor concentrations of the tracer elements in PM_{2.5}, respectively.

Hanninen et al. (2004) modified Eq. (20) and calculated the infiltration factors of PM_{2.5} as following:

$$F_{\text{inf}} = \frac{\text{slope}_{PM2.5}}{\text{slope}_{\text{tracer}}} \frac{C_{\text{in,tracer}}}{C_{\text{out,tracer}}} \quad (21)$$

where $\text{slope}_{PM2.5}$ and $\text{slope}_{\text{tracer}}$ are the indoor-outdoor regression slopes for PM_{2.5} and the tracer elements, respectively. The ratios of $\text{slope}_{PM2.5}$ to $\text{slope}_{\text{tracer}}$ are roughly equal to 1, with the range of 0.79 to 0.86.

Modeling Methods

Long-term or largescale measurements are challenging and costly to conduct. Thus, the infiltration factors can be predicted based on the mechanism shown in Eq. (18) considering the influence of the ventilation, particle penetration and deposition.

For instance, Chen et al. (2012a) calculated the seasonal infiltration factors of PM₁₀ for 83 cities in the United States and assessed their influence on the relationship between PM₁₀ and short-term mortality. El Orch et al. (2014) predicted statistical distribution of long-term size-resolved infiltration factors for typical single-family residential building stock in the United States. Shi et al. (2017) developed a Monte Carlo simulation model to simulated the probabilistic distributions of the PM_{2.5} and PM₁₀ infiltration factors for residences in Beijing, China. Xiang et al. (2019) estimated the infiltration factors of PM_{2.5} for 339 cities from 31 provinces in mainland China and Hu et al. (2020) comprehensively estimated the distribution of infiltration factors of PM_{2.5} and PM₁₀ across seasons, genders, and ages in 333 Chinese cities from 31 provinces.

Data Analysis

As Fig. 5 shown, the infiltration factors changed with particle diameters according to the measured results (Abt et al. 2000; Bennett and Koutrakis 2006; Chatoutsidou et al. 2015; Chen et al. 2011; Hu et al. 2018; Hussein et al. 2004, 2006; Lazaridis et al. 2017; Long et al. 2001; McAuley et al. 2010; Rim et al. 2010, 2013; Sarnat et al. 2006; Talbot et al. 2016; Wallace and Ott 2011; Zauli-Sajani et al. 2018; Zhao and Stephens 2017; Zhao et al. 2020; Zhu et al. 2005). Compared with penetration factor, the ranges of infiltration factors are larger. The infiltration factors are ranged from 0.20 to 1 with the mean value of 0.66 for accumulation-mode particles and

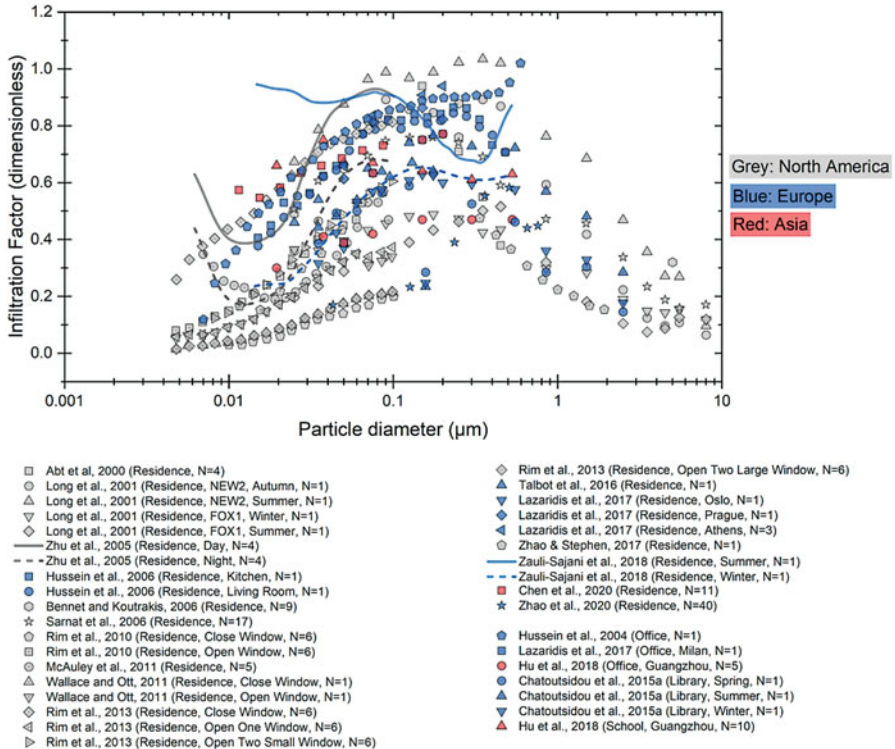


Fig. 5 Infiltration factors measured in residences and other buildings (including office, library and school)

standard deviation of 0.22. The infiltration factors of smaller and larger particles are less than accumulation-mode particles, which ranged from 0.40 ± 0.25 to 0.23 ± 0.14 , respectively. It's caused by the relatively high penetration and low deposition of accumulation-mode particles. Combining the effects of particle size distributions, the infiltration factors of UFPs, $\text{PM}_{2.5}$ and PM_{10} are shown in Fig. 6, which are 0.45 ± 0.19 (0.15 to 0.80), 0.51 ± 0.16 (0.16 to 0.78), and 0.40 ± 0.19 (0.17 to 0.70), respectively.

The large variation of infiltration factors is determined by air change rates (Zhao and Stephens 2017), window opening behaviors (Meier et al. 2015; Mullen et al. 2011b; Rim et al. 2010, 2013; Wallace and Ott 2011), ventilation systems (Bhangar et al. 2011; Meng et al. 2007, 2009; Mullen et al. 2011a; Quang et al. 2013; Saraga et al. 2017; Zhang and Zhu 2012), etc. Zhao and Stephens (2017) found that infiltration factors of UFPs generally increased with air change rate, but the infiltration factors for $\text{PM}_{2.5}$ were mostly influenced by deposition loss rate constants and/or envelope penetration factors.

The infiltration factors of UFPs are about 0.63 under window opening conditions and 0.32 under window closed conditions according to the measurements by Meier

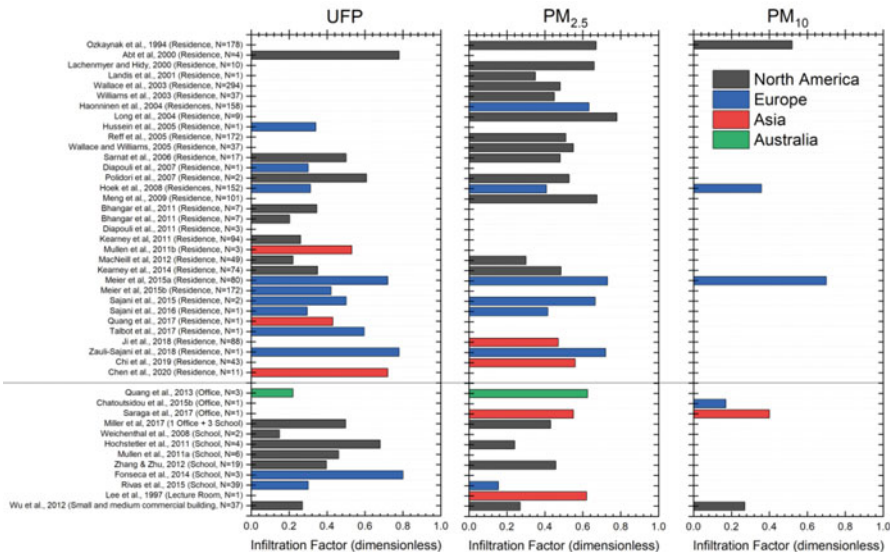


Fig. 6 Infiltration factors of UFP, PM_{2.5} and PM₁₀ measured in residences and other buildings (including office, school, lecture room and commercial building)

et al. (2015) and Mullen et al. (2011b). The infiltration factors of UFPs and PM_{2.5}, PM₁₀ are 0.26, 0.71 and 0.70 with mechanical ventilation systems on, respectively, and 0.29, 0.53 and 0.10 with mechanical ventilation systems off (Bhangar et al. 2011; Meng et al. 2009; Mullen et al. 2011a; Quang et al. 2013; Saraga et al. 2017). Zhang and Zhu (2012) compared five kinds of ventilation systems (old single duct system, new single duct system with one filter, new single duct system with two filters, window-mounted AC/fan and split system) and observed that the infiltration factors were lowest for UFPs (0.12) using old single duct system and for PM_{2.5} (0.35) using new single duct system with two filter, and largest for UFPs (0.66) and PM_{2.5} (0.59) using window-mounted AC/fan.

Different from PM_{2.5} and PM₁₀, the loss rates due to coagulation effects influenced the infiltration factors of UFPs (Chen et al. 2011; Franck et al. 2006; Vu et al. 2017). Chen et al. (2020) found the impacts of the factors on UFP infiltration factors exhibited the following ranking: a (air change rate) > A/V (ratio of the total deposition area to the room volume) > C_{out} (outdoor UFP concentration) > μ (geometric mean diameter of outdoor UFPs) > σ (geometric standard deviation of outdoor UFP diameters) > indoor temperature > indoor relative humidity > indoor ozone concentration. The effects of outdoor UFP concentrations due to coagulation were considerable. The infiltration factors of UFPs could be calculated as:

$$F_{inf} = 1.92 + 0.184 \ln a + 0.00178\mu - 0.0688\sigma - 0.273(A/V) - 0.0618 \ln C_{out} \quad (22)$$

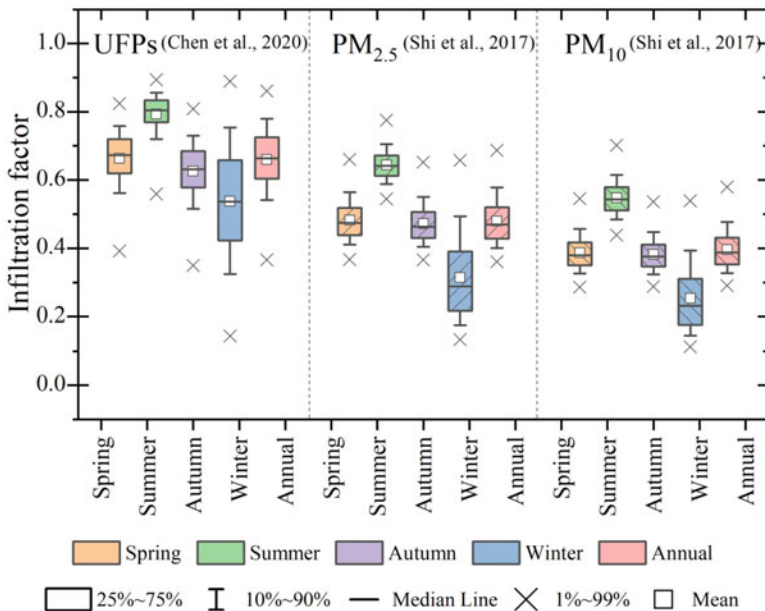


Fig. 7 The box-plots of seasonally-averaged and annually-averaged F_{inf} for residences in Beijing, China (Adapted from Chen et al. (2020a), Figure 3, with permission from Elsevier)

The simulated results are shown in Fig. 7 based on Eq. (22) for UFPs and Eq. (18) for $\text{PM}_{2.5}$ and PM_{10} using a Monte Carlo simulation model (Chen et al. 2011; Shi et al. 2017). The mean values of season-averaged infiltration factors of UFPs (annual-averaged value: 0.66 ± 0.10) were larger than those of $\text{PM}_{2.5}$ (annual-averaged value: 0.48 ± 0.07) and PM_{10} (annual-averaged value: 0.40 ± 0.06) in Beijing, China, indicating that residents would be exposed to higher fractions of outdoor-originated UFPs than $\text{PM}_{2.5}$ and PM_{10} . The simulated results of $\text{PM}_{2.5}$ showed good agreements with the measured results using tracer elements in Beijing (mean value: 0.49) by Ji et al. (2018), indicating the reasonability of results. The results using a Monte Carlo simulation model by Hu et al. (2020) showed that the annual average infiltration factors were higher in southern than in northern China. Hainan province had the highest infiltration factors, whereas Jilin had the lowest (Jilin–Hainan, annual average infiltration factor: PM_{10} , 0.19–0.45; $\text{PM}_{2.5}$, 0.49–0.76).

Conclusion

Measuring penetration factors or infiltration factors according to regression models is simple but the regression would be poor due to high variance of temporal contribution from specific indoor particle sources. Numerous studies obtained the penetration factors based on measured equilibrium concentrations and other known parameters, and obtained the infiltration factors directly. Such measurements always

require enough long time to reach the equilibrium status. The penetration factors can also be obtained by employing least-squares estimation to simulate indoor concentrations or their change rates. The infiltration factors can be also obtained according to tracer element approach. The tracer element is mainly from outdoor sources and shows similar physical behaviors as the focused particles. The ratio of indoor to outdoor tracer element concentrations is equal to the infiltration factor.

The penetration factor of UFPs, PM_{2.5} and PM₁₀ is in the range of 0.59–0.78, 0.72–1, and 0.69–0.86, respectively. The penetration factors are 0.78 ± 0.17 for accumulation-mode particles (0.1–1 μm diameter). They decreased due to Brownian diffusion for smaller particles, or due to stronger gravitational settling and impaction for larger particles. Penetration factors are determined by particle size, pressure differences, geometry and surface roughness of cracks, etc.

The infiltration factors of PM_{2.5} are approximately 0.50 according to measured and simulated results, which would be lower than ultrafine particles and higher than PM₁₀ under the same conditions. Infiltration factors are also influenced by air change rates, window opening behaviors, ventilation systems, etc. Additionally, the loss rates due to coagulation effects influenced the infiltration factors of UFPs, which is different from PM_{2.5} and PM₁₀.

Cross-References

- [Deposition](#)
 - [History and Perspective on Indoor Air Quality Research](#)
 - [Introduction to Aerosol Dynamics](#)
 - [Predicting VOC and SVOC Concentrations in Complex Indoor Environments](#)
-

References

- Abt E, Suh HH, Catalano P, Kourakis P (2000) Relative contribution of outdoor and indoor particle sources to indoor concentrations. *Environ Sci Technol* 34(17):3579–3587
- Allen R, Larson T, Sheppard L, Wallace L, Liu LJS (2003) Use of real-time light scattering data to estimate the contribution of infiltrated and indoor-generated particles to indoor air. *Environ Sci Technol* 37(16):3484–3492
- ASHRAE (2001) Chapter 26: ventilation and infiltration. In: ASHRAE 2001 HVAC fundamentals handbook. ASHRAE, Atlanta
- Barraza F, Jorquera H, Valdivia G, Montoya LD (2014) Indoor PM2.5 in Santiago, Chile, spring 2012: source apportionment and outdoor contributions. *Atmos Environ* 94:692–700
- Bennett DH, Kourakis P (2006) Determining the infiltration of outdoor particles in the indoor environment using a dynamic model. *J Aerosol Sci* 37(6):766–785
- Bhangar S, Mullen NA, Hering SV, Kreisberg NM, Nazaroff WW (2011) Ultrafine particle concentrations and exposures in seven residences in northern California. *Indoor Air* 21(2): 132–144
- Buonanno G, Stabile L, Morawska L (2014) Personal exposure to ultrafine particles: the influence of time-activity patterns. *Sci Total Environ* 468:903–907
- Chao CYH, Wan MP, Cheng ECK (2003) Penetration coefficient and deposition rate as a function of particle size in non-smoking naturally ventilated residences. *Atmos Environ* 37(30):4233–4241

- Chatoutsidou SE, Maskova L, Ondrackova L, Ondracek J, Lazaridis M, Smolik J (2015) Modeling of the aerosol infiltration characteristics in a cultural heritage building: the baroque library hall in Prague. *Build Environ* 89:253–263
- Chen C, Zhao B (2011) Review of relationship between indoor and outdoor particles: I/O ratio, infiltration factor and penetration factor. *Atmos Environ* 45(2):275–288
- Chen C, Zhao B (2017) A modified Brownian force for ultrafine particle penetration through building crack modeling. *Atmos Environ* 170:143–148
- Chen C, Zhao B, Weschler CJ (2012a) Indoor exposure to “outdoor PM10” assessing its influence on the relationship between PM10 and short-term mortality in US cities. *Epidemiology* 23(6): 870–878
- Chen C, Zhao B, Zhou WT, Jiang XY, Tan ZC (2012b) A methodology for predicting particle penetration factor through cracks of windows and doors for actual engineering application. *Build Environ* 47:339–348
- Chen XC, Jahn HJ, Engling G, Ward TJ, Kraemer A, Ho KF, Chan CY (2017) Characterization of ambient-generated exposure to fine particles using sulfate as a tracer in the Chinese megacity of Guangzhou. *Sci Total Environ* 580:347–357
- Chen C, Zhao YJ, Zhao B (2018a) Emission rates of multiple air pollutants generated from Chinese residential cooking. *Environ Sci Technol* 52(3):1081–1087
- Chen C, Zhao YJ, Zhao B (2018b) Emission rates of ultrafine and fine particles generated from human smoking of Chinese cigarettes. *Atmos Environ* 194:7–13
- Chen XC, Chow JC, Ward TJ, Cao JJ, Lee SC, Watson JG ... Ho KF (2019) Estimation of personal exposure to fine particles (PM2.5) of ambient origin for healthy adults in Hong Kong. *Sci Total Environ* 654:514–524
- Chen C, Yao M, Luo X, Zhu Y, Liu Z, Zhuo H, Zhao B (2020a) Outdoor-to-indoor transport of ultrafine particles: measurement and model development of infiltration factor. *Environ Pollut* 267:115402
- Chen ZG, Chen C, Wei S, Liu ZJ, Cao GQ, Du YW ... Wang YF (2020b) Determination of key parameters (air exchange rate, penetration factor and deposition rate) for selecting residential air cleaners under different window airtightness levels. *Sustain Cities Soc* 56:9
- Chi R, Chen C, Li HY, Pan L, Zhao B, Deng FR, Guo XB (2019) Different health effects of indoor- and outdoor-originated PM2.5 on cardiopulmonary function in COPD patients and healthy elderly adults. *Indoor Air* 29(2):192–201
- Cohen MA, Adar SD, Allen RW, Avol E, Curl CL, Gould T ... Kaufman JD (2009) Approach to estimating participant pollutant exposures in the multi-ethnic study of atherosclerosis and air pollution (MESA Air). *Environ Sci Technol* 43(13):4687–4693
- Duan XL (2013) Exposure factors handbook of Chinese population. China Environmental Press, Beijing
- El Orch Z, Stephens B, Waring MS (2014) Predictions and determinants of size-resolved particle infiltration factors in single-family homes in the US. *Build Environ* 74:106–118
- Fonseca J, Slezakova K, Morais S, Pereira MC (2014) Assessment of ultrafine particles in Portuguese preschools: levels and exposure doses. *Indoor Air* 24(6):618–628
- Franck U, Tuch T, Manjarrez M, Wiedensohler A, Herbarth O (2006) Indoor and outdoor sub-micrometer particles: exposure and epidemiologic relevance (“the 3 indoor Ls”). *Environ Toxicol* 21(6):606–613
- Hanninen OO, Lebret E, Ilacqua V, Katsouyanni K, Kunzli F, Sram RJ, Jantunen M (2004) Infiltration of ambient PM2.5 and levels of indoor generated non-ETS PM2.5 in residences of four European cities. *Atmos Environ* 38(37):6411–6423
- Hoek G, Kos G, Harrison RM, de Hartog J, Meliefste K, ten Brink H ... Hameri K (2008) Indoor-outdoor relationships of particle number and mass in four European cities. *Atmos Environ* 42(1):156–169
- Hu YJ, Bao LJ, Huang CL, Li SM, Liu P, Zeng EY (2018) Exposure to air particulate matter with a case study in Guangzhou: is indoor environment a safe haven in China? *Atmos Environ* 191:351–359
- Hu Y, Yao M, Liu Y, Zhao B (2020) Personal exposure to ambient PM2.5, PM10, O₃, NO₂, and SO₂ for different populations in 31 Chinese provinces. *Environ Int* 144:106018

- Huang WG, Xie XJ, Qi XQ, Huang JX, Li FJ (2017) Determination of particle penetration coefficient, particle deposition rate and air infiltration rate in classrooms based on monitored indoor and outdoor concentration levels of particle and carbon dioxide. In: Cui P, Liu J, Zhang W (eds) 10th international symposium on heating, ventilation and air conditioning, Ishvac2017, vol 205. Elsevier Science Bv, Amsterdam, pp 3117–3123
- Huang J, Pan X, Guo X, Li G (2018) Health impact of China's air pollution prevention and control action plan: an analysis of national air quality monitoring and mortality data. *Lancet Planet Health* 2(7):e313–e323
- Hussein T, Hameri K, Aaltonen P, Asmi A, Kakko L, Kulmala M (2004) Particle size characterization and the indoor-to-outdoor relationship of atmospheric aerosols in Helsinki. *Scand J Work Environ Health* 30:54–62
- Hussein T, Glytsos T, Ondracek J, Dohanyosova P, Zdimal V, Hameri K . . . Kulmala M (2006) Particle size characterization and emission rates during indoor activities in a house. *Atmos Environ* 40(23):4285–4307
- Jeng CJ, Kindzierski WB, Smith DW (2006) Particle penetration through rectangular-shaped cracks. *J Environ Eng Sci* 5:S111–S119
- Jeng CJ, Kindzierski WB, Smith DW (2007) Particle penetration through inclined and L-shaped cracks. *J Environ Eng ASCE* 133(3):331–339
- Ji WJ, Zhao B (2015) Contribution of outdoor-originating particles, indoor-emitted particles and indoor secondary organic aerosol (SOA) to residential indoor PM_{2.5} concentration: a model-based estimation. *Build Environ* 90:196–205
- Ji WJ, Li HY, Zhao B, Deng FR (2018) Tracer element for indoor PM_{2.5} in China migrated from outdoor. *Atmos Environ* 176:171–178
- Kearney J, Wallace L, MacNeill M, Xu X, VanRyswyk K, You H . . . Wheeler AJ (2011) Residential indoor and outdoor ultrafine particles in Windsor, Ontario. *Atmos Environ* 45(40):7583–7593
- Kearney J, Wallace L, MacNeill M, Heroux ME, Kindzierski W, Wheeler A (2014) Residential infiltration of fine and ultrafine particles in Edmonton. *Atmos Environ* 94:793–805
- Klepeis NE, Nelson WC, Ott WR, Robinson JP, Tsang AM, Switzer P . . . Engelmann WH (2001) The National Human Activity Pattern Survey (NHAPS): a resource for assessing exposure to environmental pollutants. *J Exposure Anal Environ Epidemiol* 11(3):231–252
- Koutrakis P, Briggs SLK, Leaderer BP (1992) Source apportionment of indoor aerosols in Suffolk and Onondaga counties, new-York. *Environ Sci Technol* 26(3):521–527
- Lachenmyer C, Hidy GM (2000) Urban measurements of outdoor-indoor PM25 concentrations and personal exposure in the deep south. Part I. Pilot study of mass concentrations for nonsmoking subjects. *Aerosol Sci Technol* 32(1):34–51
- Lai ACK, Fung JLS, Li M, Leung KY (2012) Penetration of fine particles through rough cracks. *Atmos Environ* 60:436–443
- Lai YH, Ridley I, Brimblecombe P (2020) Blower-door estimates of PM2.5 deposition rates and penetration factors in an idealized room. *Indoor Built Environ*. <https://doi.org/10.1177/1420326X20944427>
- Landis MS, Norris GA, Williams RW, Weinstein JP (2001) Personal exposures to PM2.5 mass and trace elements in Baltimore, MD, USA. *Atmos Environ* 35(36):6511–6524
- Lazaridis M, Eleftheriadis K, Zdimal V, Schwarz J, Wagner Z, Ondracek J . . . Smolik J (2017) Number concentrations and modal structure of indoor/outdoor fine particles in four European cities. *Aerosol Air Qual Res* 17(1):131–146
- Lee S, Lee K (2017) Seasonal differences in determinants of time location patterns in an urban population: a large population-based study in Korea. *Int J Environ Res Public Health* 14(7):672
- Leech JA, Nelson WC, Burnett RT, Aaron S, Raizenne ME (2002) It's about time: a comparison of Canadian and American time-activity patterns. *J Expo Anal Environ Epidemiol* 12(6):427–432
- Li N, Liu Z, Li YP, Li N, Chartier R, McWilliams A . . . Xe DQ (2019) Estimation of PM_{2.5} infiltration factors and personal exposure factors in two megacities, China. *Build Environ* 149: 297–304

- Li LF, Girguis M, Lurmann F, Pavlovic N, McClure C, Franklin M ... Habre R (2020) Ensemble-based deep learning for estimating PM_{2.5} over California with multisource big data including wildfire smoke. *Environ Int* 145:16
- Liu DL, Nazaroff WW (2001) Modeling pollutant penetration across building envelopes. *Atmos Environ* 35(26):4451–4462
- Liu DL, Nazaroff WW (2003) Particle penetration through building cracks. *Aerosol Sci Technol* 37(7):565–573
- Long CM, Sarnat JA (2004) Indoor-outdoor relationships and infiltration behavior of elemental components of outdoor PM_{2.5} for Boston-area homes. *Aerosol Sci Technol* 38:91–104
- Long CM, Suh HH, Catalano PJ, Koutrakis P (2001) Using time- and size-resolved particulate data to quantify indoor penetration and deposition behavior. *Environ Sci Technol* 35(10):2089–2099
- Lv Y, Wang HF, Wei SS, Wu TF, Liu T, Chen B (2018) The experimental study on indoor and outdoor penetration coefficient of atmospheric fine particles. *Build Environ* 132:70–82
- MacNeill M, Wallace L, Kearney J, Allen RW, Van Ryswyk K, Judek S ... Wheeler A (2012) Factors influencing variability in the infiltration of PM_{2.5} mass and its components. *Atmos Environ* 61:518–532
- Maskova L, Smolik J, Travnickova T, Havlica J, Ondrackova L, Ondracek J (2016) Contribution of visitors to the indoor PM in the National Library in Prague, Czech Republic. *Aerosol Air Qual Res* 16(7):1713–1721
- Maskova L, Smolik J, Ondracek J, Ondrackova L, Travnickova T, Havlica J (2020) Air quality in archives housed in historic buildings: assessment of concentration of indoor particles of outdoor origin. *Build Environ* 180:10
- Matz CJ, Stieb DM, Davis K, Egyed M, Rose A, Chou B, Brion O (2014) Effects of age, season, gender and urban-rural status on time-activity: Canadian human activity pattern survey 2 (CHAPS 2). *Int J Environ Res Public Health* 11(2):2108–2124
- McAuley TR, Fisher R, Zhou X, Jaques PA, Ferro AR (2010) Relationships of outdoor and indoor ultrafine particles at residences downwind of a major international border crossing in Buffalo, NY. *Indoor Air* 20(4):298–308
- Meier R, Schindler C, Eeftens M, Aguilera I, Ducret-Stich RE, Ineichen A ... Kunzli N (2015) Modeling indoor air pollution of outdoor origin in homes of SAPALDIA subjects in Switzerland. *Environ Int* 82:85–91
- Meng QY, Turpin BJ, Polidori A, Lee JH, Weisel C, Morandi M ... Zhang JF (2005) PM_{2.5} of ambient origin: estimates and exposure errors relevant to PM epidemiology. *Environ Sci Technol* 39(14):5105–5112
- Meng QY, Turpin BJ, Lee JH, Polidori A, Weisel CP, Morandi M ... Winer A (2007) How does infiltration behavior modify the composition of ambient PM_{2.5} in indoor spaces? An analysis of RIOPA data. *Environ Sci Technol* 41(21):7315–7321
- Meng QY, Spector D, Colome S, Turpin B (2009) Determinants of indoor and personal exposure to PM_{2.5} of indoor and outdoor origin during the RIOPA study. *Atmos Environ* 43(36):5750–5758
- Miller KA, Spalt EW, Gassett AJ, Curl CL, Larson TV, Avol E ... Kaufman JD (2019) Estimating ambient-origin PM_{2.5} exposure for epidemiology: observations, prediction, and validation using personal sampling in the Multi-Ethnic Study of Atherosclerosis. *J Exposure Sci Environ Epidemiol* 29(2):227–237
- Mleczkowska A, Strojecki M, Bratasz L, Kozlowski R (2016) Particle penetration and deposition inside historical churches. *Build Environ* 95:291–298
- Morawska L, Ayoko GA, Bae GN, Buonanno G, Chao CYH, Clifford S ... Wierzbicka A (2017) Airborne particles in indoor environment of homes, schools, offices and aged care facilities: the main routes of exposure. *Environ Int* 108:75–83
- Mosley RB, Greenwell DJ, Sparks LE, Guo Z, Tucker WG, Fortmann R, Whitfield C (2001) Penetration of ambient fine particles into the indoor environment. *Aerosol Sci Technol* 34(1):127–136
- Mullen NA, Bhangar S, Hering SV, Kreisberg NM, Nazaroff WW (2011a) Ultrafine particle concentrations and exposures in six elementary school classrooms in northern California. *Indoor Air* 21(1):77–87

- Mullen NA, Liu C, Zhang YP, Wang SX, Nazaroff WW (2011b) Ultrafine particle concentrations and exposures in four high-rise Beijing apartments. *Atmos Environ* 45(40):7574–7582
- Nazaroff WW (2004) Indoor particle dynamics. *Indoor Air* 14:175–183
- Ott W, Wallace L, Mage D (2000) Predicting particulate (PM10) personal exposure distributions using a random component superposition statistical model. *J Air Waste Manage Assoc* 50(8):1390–1406
- Ozkaynak H, Xue J, Weker R, Butler D, Koutrakis P, Spengler J (1994) The Particle Team (PTEAM) study: analysis of the data. Final report, vol III. Research Triangle Park: U.S. EPA
- Ozkaynak H, Xue J, Spengler J, Wallace L, Pellizzari E, Jenkins P (1996) Personal exposure to airborne particles and metals: results from the particle team study in Riverside, California. *J Expo Anal Environ Epidemiol* 6(1):57–78
- Pant P, Guttikunda SK, Peltier RE (2016) Exposure to particulate matter in India: a synthesis of findings and future directions. *Environ Res* 147:480–496
- Peng CH, Ni PY, Xi GN, Tian WG, Fan LJ, Zhou DC … Tang Y (2020) Evaluation of particle penetration factors based on indoor PM2.5 removal by an air cleaner. *Environ Sci Poll Res* 27(8):8395–8405
- Polidori A, Arhami M, Sioutas C, Delfino RJ, Allen R (2007) Indoor/outdoor relationships, trends, and carbonaceous content of fine particulate matter in retirement homes of the Los Angeles basin. *J Air Waste Manage Assoc* 57(3):366–379
- Quang TN, He CR, Morawska L, Knibbs LD (2013) Influence of ventilation and filtration on indoor particle concentrations in urban office buildings. *Atmos Environ* 79:41–52
- Reid CE, Jerrett M, Petersen ML, Pfister GG, Morefield PE, Tager IB … Balmes JR (2015) Spatiotemporal prediction of fine particulate matter during the 2008 Northern California wildfires using machine learning. *Environ Sci Technol* 49(6):3887–3896
- Rim D, Wallace L, Persily A (2010) Infiltration of outdoor ultrafine particles into a test house. *Environ Sci Technol* 44(15):5908–5913
- Rim D, Wallace LA, Persily AK (2013) Indoor ultrafine particles of outdoor origin: importance of window opening area and Fan operation condition. *Environ Sci Technol* 47(4):1922–1929
- Rim D, Choi JI, Wallace LA (2016) Size-resolved source emission rates of indoor ultrafine particles considering coagulation. *Environ Sci Technol* 50(18):10031–10038
- Rivas I, Viana M, Moreno T, Bouso L, Pandolfi M, Alvarez-Pedrerol M … Querol X (2015) Outdoor infiltration and indoor contribution of UFP and BC, OC, secondary inorganic ions and metals in PM2.5 in schools. *Atmos Environ* 106:129–138
- Rooney B, Wang Y, Jiang JH, Zhao B, Zeng ZC, Seinfeld JH (2020) Air quality impact of the northern California camp fire of November 2018. *Atmos Chem Phys* 20(23):14597–14616
- Saraga D, Maggos T, Sadoun E, Fthenou E, Hassan H, Tsiori V … Kakosimos K (2017) Chemical characterization of indoor and outdoor particulate matter (PM2.5, PM10) in Doha, Qatar. *Aerosol Air Qual Res* 17(5):1156–1168
- Sarnat JA, Long CM, Koutrakis P, Coull BA, Schwartz J, Suh HH (2002) Using sulfur as a tracer of outdoor fine particulate matter. *Environ Sci Technol* 36(24):5305–5314
- Sarnat SE, Coull BA, Ruiz PA, Koutrakis P, Suh HH (2006) The influences of ambient particle composition and size on particle infiltration in Los Angeles, CA, residences. *J Air Waste Manage Assoc* 56(2):186–196
- Shi SS, Chen C, Zhao B (2017) Modifications of exposure to ambient particulate matter: tackling bias in using ambient concentration as surrogate with particle infiltration factor and ambient exposure factor. *Environ Pollut* 220:337–347
- Spalt EW, Curl CL, Allen RW, Cohen M, Adar SD, Stukovsky KH … Kaufman JD (2016) Time-location patterns of a diverse population of older adults: the Multi-Ethnic Study of Atherosclerosis and Air Pollution (MESA Air). *J Exposure Sci Environ Epidemiol* 26(4):349–355
- Stephens B (2015) Building design and operational choices that impact indoor exposures to outdoor particulate matter inside residences. *Sci Technol Built Environ* 21(1):3–13
- Stephens B, Siegel JA (2012) Penetration of ambient submicron particles into single-family residences and associations with building characteristics. *Indoor Air* 22(6):501–513

- Stratigou E, Dusanter S, Brito J, Riffault V (2020) Investigation of PM10, PM2.5, PM1 in an unoccupied airflow-controlled room: how reliable to neglect resuspension and assume unreactive particles? *Build Environ* 186:8
- Talbot N, Kubelova L, Makes O, Cusack M, Ondracek J, Vodicka P ... Zdimal V (2016) Outdoor and indoor aerosol size, number, mass and compositional dynamics at an urban background site during warm season. *Atmos Environ* 131:171–184
- Thatcher TL, Layton DW (1995) Deposition, resuspension, and penetration of particles within a residence. *Atmos Environ* 29(13):1487–1497
- Thatcher TL, Lunden MM, Revzan KL, Sextro RG, Brown NJ (2003) A concentration rebound method for measuring particle penetration and deposition in the indoor environment. *Aerosol Sci Technol* 37(11):847–864
- Tian LW, Zhang GQ, Lin YL, Yu JH, Zhou J, Zhang Q (2009) Mathematical model of particle penetration through smooth/rough building envelop leakages. *Build Environ* 44(6):1144–1149
- Tran DT, Alleman LY, Coddeville P, Galloo JC (2017) Indoor particle dynamics in schools: determination of air exchange rate, size-resolved particle deposition rate and penetration factor in real-life conditions. *Indoor Built Environ* 26(10):1335–1350
- Tung TC, Chao CY, Burnett J (1999) A methodology to investigate the particulate penetration coefficient through building shell. *Atmos Environ* 33(6):881–893
- Vette AF, Rea AW, Lawless PA, Rodes CE, Evans G, Highsmith VR, Sheldon L (2001) Characterization of indoor-outdoor aerosol concentration relationships during the Fresno PM exposure studies. *Aerosol Sci Technol* 34(1):118–126
- Vu TV, Zauli-Sajani S, Poluzzi V, Delgado-Saborit JM, Harrison RM (2017) Loss processes affecting submicrometer particles in a house heavily affected by road traffic emissions. *Aerosol Sci Technol* 51(10):1201–1211
- Wallace L, Ott W (2011) Personal exposure to ultrafine particles. *J Exposure Sci Environ Epidemiol* 21(1):20–30
- Wallace L, Williams R (2005) Use of personal-indoor-outdoor sulfur concentrations to estimate the infiltration factor and outdoor exposure factor for individual homes and persons. *Environ Sci Technol* 39(6):1707–1714
- Wallace LA, Mitchell H, O'Connor GT, Neas L, Lippmann M, Kattan M ... Liu LJS (2003) Particle concentrations in inner-city homes of children with asthma: the effect of smoking, cooking, and outdoor pollution. *Environ Health Perspect* 111(9):1265–1272
- Wang YG, Hopke PK, Chalupa DC, Utell MJ (2010) Long-term characterization of indoor and outdoor ultrafine particles at a commercial building. *Environ Sci Technol* 44(15):5775–5780
- Wang XK, Gao Z, Yang JX, Yang XX (2019) In situ investigation on linkage between particle penetration and air exchange through building envelope. *Int J Vent* 18(4):233–245
- Wang WL, Kato N, Kimoto S, Matsui Y, Yoneda M (2020a) Simulation and evaluation of sheltering efficiency of houses equipped with ventilation systems. *Build Environ* 168:13
- Wang ZT, Liu C, Hua Q, Zheng XH, Ji WJ, Zhang XS (2020b) Effect of particulate iron on tracking indoor PM2.5 of outdoor origin: a case study in Nanjing, China. *Indoor Built Environ* 30(5):711–723
- Williams R, Suggs J, Rea A, Sheldon L, Rodes C, Thomburg J (2003) The Research Triangle Park particulate matter panel study: modeling ambient source contribution to personal and residential PM mass concentrations. *Atmos Environ* 37(38):5365–5378
- Wilson WE, Suh HH (1997) Fine particles and coarse particles: concentration relationships relevant to epidemiologic studies. *J Air Waste Manage Assoc* 47(12):1238–1249
- Wu XM, Apte MG, Bennett DH (2012) Indoor particle levels in small- and medium-sized commercial buildings in California. *Environ Sci Technol* 46(22):12355–12363
- Xiang JB, Weschler CJ, Wang QQ, Zhang L, Mo JH, Ma R ... Zhang YP (2019) Reducing Indoor levels of “outdoor PM2.5” in urban China: impact on mortalities. *Environ Sci Technol* 53(6):3119–3127

- Xie W, Fan YS, Zhang X, Tian GJ, Si PF (2020) A mathematical model for predicting indoor PM2.5 concentration under different ventilation methods in residential buildings. *Build Serv Eng Res Technol* 41(6):694–708
- Xu B, Liu SS, Zhu YF (2010) Ultrafine particle penetration through idealized vehicle cracks. *J Aerosol Sci* 41(9):859–868
- Zauli-Sajani S, Rovelli S, Trentini A, Bacco D, Marchesi S, Scotto F . . . Hanninen O (2018) Higher health effects of ambient particles during the warm season: the role of infiltration factors. *Sci Total Environ* 627:67–77
- Zhang Q, Zhu Y (2012) Characterizing ultrafine particles and other air pollutants at five schools in South Texas. *Indoor Air* 22(1):33–42
- Zhao H, Stephens B (2017) Using portable particle sizing instrumentation to rapidly measure the penetration of fine and ultrafine particles in unoccupied residences. *Indoor Air* 27(1):218–229
- Zhao B, Chen C, Yang XY, Lai ACK (2010) Comparison of three approaches to model particle penetration coefficient through a single straight crack in a building envelope. *Aerosol Sci Technol* 44(6):405–416
- Zhao JY, Birmili W, Wehner B, Daniels A, Weinhold K, Wang LN . . . Wiedensohler A (2020) Particle mass concentrations and number size distributions in 40 homes in Germany: indoor-to-outdoor relationships, diurnal and seasonal variation. *Aerosol Air Qual Res* 20(3):576–589
- Zhou XD, Cai J, Zhao Y, Chen RJ, Wang CC, Zhao A . . . Xu HH (2018) Estimation of residential fine particulate matter infiltration in Shanghai, China. *Environ Poll* 233:494–500
- Zhou B, Feng L, Shiu A, Hu SC, Wang Y, Li F . . . Xu Y (2019) Study on influencing mechanism of outdoor plant-related particles on indoor environment and its control measures during transitional period in Nanjing. *Aerosol Air Qual Res* 19(3):571–586
- Zhu YF, Hinds WC, Krudysz M, Kuhn T, Froines J, Sioutas C (2005) Penetration of freeway ultrafine particles into indoor environments. *J Aerosol Sci* 36(3):303–322



Deposition

11

Robert F. Holub and Michal Beneš

Contents

Introduction	300
Bulk Airflow and Interaction with Surfaces	301
Turbulent Nature of Indoor Air Flow	306
Recent Advances in Understanding Turbulence	308
Comparison of Brownian and Turbulent Diffusion by Means of Particle Approach	308
Analytic Solution of the Turbulent Wall Deposition	309
Improvements in the Wall Deposition Model	312
Dimensional Analysis in Deposition Rate Formulas	313
Fractal Nature of Turbulence	314
Applications	315
Boundary Layer Thickness	316
Eddy Diffusivity	317
Energy Dissipation	317
Comparison of Measured Data	318
Comparison of Experimental Configurations	319
Challenges in Understanding Principles of Particle: Surface Interaction	321
Fundamental Problems	322
Technical Problems	323
Advice	323
Conclusions	324
References	325

R. F. Holub

Center for Air and Aquatic Resources Engineering and Sciences, Clarkson University, Potsdam, NY, USA

M. Beneš (✉)

Department of Mathematics, Faculty of Nuclear Sciences and Physical Engineering, Czech Technical University in Prague, Prague, Czechia

e-mail: michal.benes@fjfi.cvut.cz

Abstract

Deposition of particles present in the air environment of enclosures and transported by its motion is a process that is important for the removal of particles from the enclosure volume. It can serve in cleaning the indoor air from unwanted impurities or, to the contrary, it can bring pollution to the surface that is the target of the deposition. The wall deposition (plateout), in particular, is the deposition applied to the surfaces surrounding the enclosure, a volume of a room, vessel, chamber, reactor, mine, or similar space. This process is at the end of the aerosol particle transport. It usually is a consequence of the interaction of the turbulent bulk motion with the diffusion near the wall and the wall attachment via van der Waals forces. Plateout has been widely studied experimentally and analytically using a variety of approaches and with many achievements. The aerosol chamber with an accurately controlled condensation nuclei, air flow and thermal properties together with a radioactive aerosol belong to the most advanced tools in deposition research. Despite advances in deposition research, the details of this process are not yet fully understood. This chapter aims to survey the achievements and formulate challenges motivating further research into aerosol particle deposition.

Keywords

Wall deposition · Plateout · Enclosed spaces · Fractal boundary · Turbulence

Introduction

Within the complexity of aerosol transport, deposition on surfaces is one of terminal phenomena contributing to the removal of aerosol particles from the bulk volume. It occurs whenever the aerosol particles lose their movement inside the volume because of a lack of forces exerted by the carrying gas phase. According to the literature, it may be due to lack of momentum in the proximity of a stagnant layer, due to gravitational forces, electrical field, thermal effects, etc. (see Fuchs 1964; Friedlander 2000; Seinfeld and Pandis 2016; Williams and Loyalka 1991 and others). The obvious importance of this phenomenon is underlined by the environmental concerns with industry, e.g., in mining, dusty fabrication procedures, nuclear industry, with the environment of urban and traffic areas as well as indoor building ventilation issues, air inhalation processes, or by the scientific applications such as cloud chambers in nuclear particle research.

Particle deposition in most situations is mostly a consequence of the interaction of the air flow with turbulent features with the Brownian diffusion. Both processes, being stochastic by their intrinsic nature, can be measured and described by deterministic models of fluid dynamics. However, bridging the experiments to models creates the need for using constitutive relations with unknown factors to be determined by processing the experimental data. Improvements in this area is subject of current research.

Wall deposition (plateout) is a removal process of particles to surfaces (of walls, ceilings and floors of rooms, vessels, propeller blades, and reactors). It differs from plateout in pipes, where there is a prevailing flow in one direction. Overall agreement

is that it depends on eddy diffusion and on the Brownian diffusion of the particles. The bottleneck is the diffusion through the stagnant layer on surfaces. The stagnant layer's thickness depends on the turbulence nature. The higher the turbulence, the thinner the layer the particles have to diffuse through, and therefore the higher the plateout. Brownian diffusion is dependent on the size of aerosols. Literature indicates various dependence of the eddy diffusivity on the power of distance from the wall allowing for the adjustment of the power exponent by the experiment but leaving the dimensionality of such modification mostly unresolved. This issue is addressed in this chapter as well.

The conventional treatment of wall deposition assumes that once particle hits the surface it sticks. However, it has been shown that VVOC, VOC, and SVOC (high/semi volatile compounds) can evaporate/sublimate from surfaces, and react with reactive oxygen species, or radiation to form new particles, starting from monomers, dimers, etc. It voids the assumption there is no source from the surfaces. Experimentally, it is very difficult to observe – unless one has a chamber that can attain an initial aerosol-free atmosphere.

Particle plateout can be studied using both inert and radioactive aerosols. The advantage of the latter is many orders of magnitude greater sensitivity. If radioactive aerosols from radon or thoron are used in an aerosol-free chamber, one gets monodispersed $\sim 1 \text{ nm}$ size aerosols. Unfortunately, very few people are taking advantage of this technique. What would be even more advantageous is to use standard radioactive isotope labeling techniques.

Recently, approaches based in the analytical treatment of simplified models of turbulent aerosol deposition were complemented by results of detailed numerical solution of equations of transport and fluid dynamics. It is shown later in this chapter that these results mutually agree and reproduce the experimental data. Such a robustness in modeling particle deposition allows consideration of even extreme situations such as experimental configurations when the air is not put into motion by propeller and its velocity becomes unmeasurable. On the other hand, intrinsic thermal oscillations and fluctuations give reason to believe that state of air still exhibits nature of turbulence.

Addressing these aspects of the aerosol transport toward surfaces, the chapter contains a summary of conservation laws governing the transport with an emphasis on the bulk-interface interaction. Due to the influence of the turbulent nature of the air flow and turbulent energy dissipation in enclosures, the corresponding models are complex. Simplifications that are useful for understanding the reported experimental results are summarized. This chapter also addresses issues arising in the research of aerosol wall deposition related both to the fundamental understanding of the processes involved as well as to the technical details of the underlying experimental work.

Bulk Airflow and Interaction with Surfaces

Essentially, deposition is a phenomenon of mass transfer from the bulk fluid consisting of the main carrier phase (air) and at least one dilute species (aerosol particles) in it. Respecting the experimental framework through which the models of aerosol

dynamics are validated, deposition is studied at medium scales (~ 1 m). Therefore, the aerosol as a collection of individual particles can be studied as part of continuum and represented by continuum quantities such as concentration, velocity, and temperature, and by size distribution if needed. Correspondingly, the dynamic model of deposition in a limited volume at least partially surrounded by solid boundary (wall) can be obtained by exploring the conservation laws for mass, momentum, and energy.

Assume that the indoor particle transport occurs in a spatial volume Ω over the time interval $(0, T)$. Respecting the purpose of the model, behavior of the indoor aerosol particles in bulk and on surfaces, and their volumic and mass contents and nature of interactions, we formulate the conservation laws of mass, momentum, and energy for the carrying main gaseous phase, aerosol particles, and additional passive components such as water vapor and condensation nuclei. We proceed in accordance with Slattery (1999), Kolev (2011), Gidaspow (1994), or Bauer et al. (2015) and Beneš et al. (2021).

The **mass balance** considers the air as the main gaseous component with density ρ_g [$\text{kg} \cdot \text{m}^{-3}$], \mathbf{v}_g the bulk velocity [$\text{m} \cdot \text{s}^{-1}$], and the volume fraction ε_g [1]. The aerosol particles essentially are condensed-phase small objects with the density ρ_a [$\text{kg} \cdot \text{m}^{-3}$], \mathbf{v}_a their bulk (macroscopic) velocity [$\text{m} \cdot \text{s}^{-1}$], and the volume fraction ε_a [1]. The solid condensation particles have the density ρ_s [$\text{kg} \cdot \text{m}^{-3}$], \mathbf{v}_s the bulk velocity [$\text{m} \cdot \text{s}^{-1}$], and the volume fraction ε_s [1]. The water vapor mass fraction is Y_w [1]. If no other phase or component is considered, the mass fraction filling the volume is

$$\varepsilon_g + \varepsilon_a + \varepsilon_s = 1. \quad (1)$$

Then the mass balances hold for gaseous phase without any volumetric source

$$\frac{\partial(\varepsilon_g \rho_g)}{\partial t} + \operatorname{div}(\varepsilon_g \rho_g \mathbf{v}_g) = 0, \quad (2)$$

the aerosol particles with the growth term $Q_a = Q_a(\varepsilon_a, \varepsilon_s, Y_w)$

$$\frac{\partial(\varepsilon_a \rho_a)}{\partial t} + \operatorname{div}(\varepsilon_a \rho_a \mathbf{v}_a) = Q_a(\varepsilon_a, \varepsilon_s, Y_w), \quad (3)$$

for the water vapor as a passive component of gas phase with the sink term

$$\frac{\partial(\varepsilon_g \rho_g Y_w)}{\partial t} + \operatorname{div}(\varepsilon_g \rho_g Y_w \mathbf{v}_g) = -Q_a(\varepsilon_g, \varepsilon_s, Y_w), \quad (4)$$

and for condensation nuclei with the source term $Q_s = Q_s(t, x)$

$$\frac{\partial(\varepsilon_s \rho_s)}{\partial t} + \operatorname{div}(\varepsilon_s \rho_s \mathbf{v}_s) = Q_s(t, x). \quad (5)$$

In what follows, we assume the proportion of particular components of the indoor particle transport, the solid and condensed phase densities are constant ($\rho_a = \text{const.}$, $\rho_s = \text{const.}$), the solid phase fraction negligible ($\varepsilon_g + \varepsilon_a \approx 1$), and the solid phase fully advected by the air flow ($\mathbf{v}_s \approx \mathbf{v}_g$). The mass balances then simplify to

$$\frac{\partial(\varepsilon_g \rho_g)}{\partial t} + \operatorname{div}(\varepsilon_g \rho_g \mathbf{v}_g) = 0, \quad (6)$$

$$\frac{\partial(\varepsilon_a)}{\partial t} + \operatorname{div}(\varepsilon_a \mathbf{v}_a) = \frac{1}{\rho_a} Q_a(\varepsilon_a, \varepsilon_s, Y_w), \quad (7)$$

$$\frac{\partial(\varepsilon_g \rho_g Y_w)}{\partial t} + \operatorname{div}(\varepsilon_g \rho_g Y_w \mathbf{v}_g) = -Q_a(\varepsilon_g, \varepsilon_s, Y_w), \quad (8)$$

and the condensation nuclei are decoupled having the gas velocity

$$\frac{\partial(\varepsilon_s)}{\partial t} + \operatorname{div}(\varepsilon_s \mathbf{v}_g) = \frac{1}{\rho_s} Q_s(t, x). \quad (9)$$

Within this framework, we formulate the **momentum conservation laws** for the gas phase

$$\frac{\partial(\varepsilon_g \rho_g \mathbf{v}_g)}{\partial t} + \operatorname{div}(\varepsilon_g \rho_g \mathbf{v}_g \mathbf{v}_g) = -\nabla P_g + \nabla \cdot (\varepsilon_g \mathbf{T}_g) + \beta(\mathbf{v}_a - \mathbf{v}_g) + \rho_g \mathbf{g}, \quad (10)$$

and for the aerosol particles

$$\begin{aligned} \frac{\partial(\varepsilon_a \rho_a \mathbf{v}_a)}{\partial t} + \operatorname{div}(\varepsilon_a \rho_a \mathbf{v}_a \mathbf{v}_a) &= -\nabla P_a + \nabla \cdot (\varepsilon_a \mathbf{T}_a) + \beta(\mathbf{v}_g - \mathbf{v}_a) \\ &\quad + (\rho_a - \rho_g) \varepsilon_a \mathbf{g}, \end{aligned} \quad (11)$$

where P_g , P_a are the pressures of gas and aerosol particles as phases, \mathbf{T}_g , \mathbf{T}_a the stress tensors of the gas and particles, and P_g is the drag coefficient between the gas and the particles. Due to nature of particles, we may further assume that the pressures are balanced through the interface conditions and there is no stress or friction between the aerosol particles themselves ($\mathbf{T}_a = 0$). The momentum balances then become

$$\frac{\partial(\varepsilon_g \rho_g \mathbf{v}_g)}{\partial t} + \operatorname{div}(\varepsilon_g \rho_g \mathbf{v}_g \mathbf{v}_g) = -\nabla P_g + \nabla \cdot (\varepsilon_g \mathbf{T}_g) + \beta(\mathbf{v}_a - \mathbf{v}_g) + \rho_g \mathbf{g}, \quad (12)$$

$$\frac{\partial(\varepsilon_a \rho_a \mathbf{v}_a)}{\partial t} + \operatorname{div}(\varepsilon_a \rho_a \mathbf{v}_a \mathbf{v}_a) = -\nabla P_g + \beta(\mathbf{v}_g - \mathbf{v}_a) + (\rho_a - \rho_g) \varepsilon_a \mathbf{g}. \quad (13)$$

The stress tensor for air as a Newtonian fluid is expressed as

$$\begin{aligned} \mathbf{T}_g &= -\lambda \operatorname{div} \mathbf{v} \mathbf{I} + 2\mu \mathbf{D}, \\ \mathbf{D} &= \frac{1}{2} \left(\nabla \mathbf{v} + (\nabla \mathbf{v})^T \right), \end{aligned} \quad (14)$$

where μ is the shear viscosity, λ is the bulk viscosity, and \mathbf{D} is the rate-of-deformation tensor.

The **energy conservation laws** in terms of internal energies U_g of the gas phase and U_a of the particles are

$$\frac{\partial(\varepsilon_g \rho_g U_g)}{\partial t} + \operatorname{div}(\varepsilon_g \rho_g U_g \mathbf{v}_g) = -P_g \nabla \cdot \mathbf{v}_g + \varepsilon_g \nabla \cdot (\mathbf{q}_g) + \rho_g \mathbf{g} \cdot \mathbf{v}_g, \quad (15)$$

$$\frac{\partial(\varepsilon_a \rho_a U_a)}{\partial t} + \operatorname{div}(\varepsilon_a \rho_a U_a \mathbf{v}_a) = -P_g \nabla \cdot \mathbf{v}_a + \varepsilon_a \nabla \cdot (\mathbf{q}_a) + (\rho_a - \rho_g) \mathbf{g} \cdot \mathbf{v}_a, \quad (16)$$

where \mathbf{q}_g , \mathbf{q}_a are the energy fluxes for the gas and the particles.

The system of eqs. (1–16) is closed by the state equation for the gas pressure,

$$P_g = P_g(\varepsilon_g, \varepsilon_a, \mathbf{v}_g, \mathbf{v}_a, \rho_g, \rho_a, U_g, U_a, Y_w), \quad (17)$$

by the initial conditions and the boundary conditions, among which, at the enclosure walls, the no-slip conditions for velocities

$$\mathbf{v}_g|_{\text{wall}} = 0, \mathbf{v}_a|_{\text{wall}} = 0 \quad (18)$$

and the zero volume fractions are set

$$\varepsilon_g|_{\text{wall}} = 0, \varepsilon_a|_{\text{wall}} = 0, \quad (19)$$

The inlet conditions (compare with Fig. 1) are crucial as they deliver both energy and mass into the enclosure.

$$\mathbf{v}_g|_{\text{inlet}} = \mathbf{v}_{\text{in}}, \varepsilon_g|_{\text{inlet}} = \varepsilon_{g,\text{in}}, \varepsilon_a|_{\text{inlet}} = \varepsilon_{a,\text{in}} \quad (20)$$

which eventually are dispersed into the volume by friction and lost by wall deposition.

Once this system of equations is resolved or approximated, the quantity of interest describing the wall loss of aerosol particles by the deposition is described by the **deposition rate** defined as

$$\beta_a = \frac{\int_{\text{wall}} \mathbf{j}_a \cdot \mathbf{n}_{\text{wall}}(x) dS}{\int_{\Omega} dx}, \quad (21)$$

where \mathbf{j}_a is the mass flux of the aerosol particles and \mathbf{n}_{wall} is the outward normal vector to the wall – the boundary of the domain Ω .

The deposition rate (Eq. 21) can be used to understand the process of removing aerosol particles from the entire volume of the enclosure described as

$$\frac{dN}{dt} = -\beta_a N, \quad (22)$$

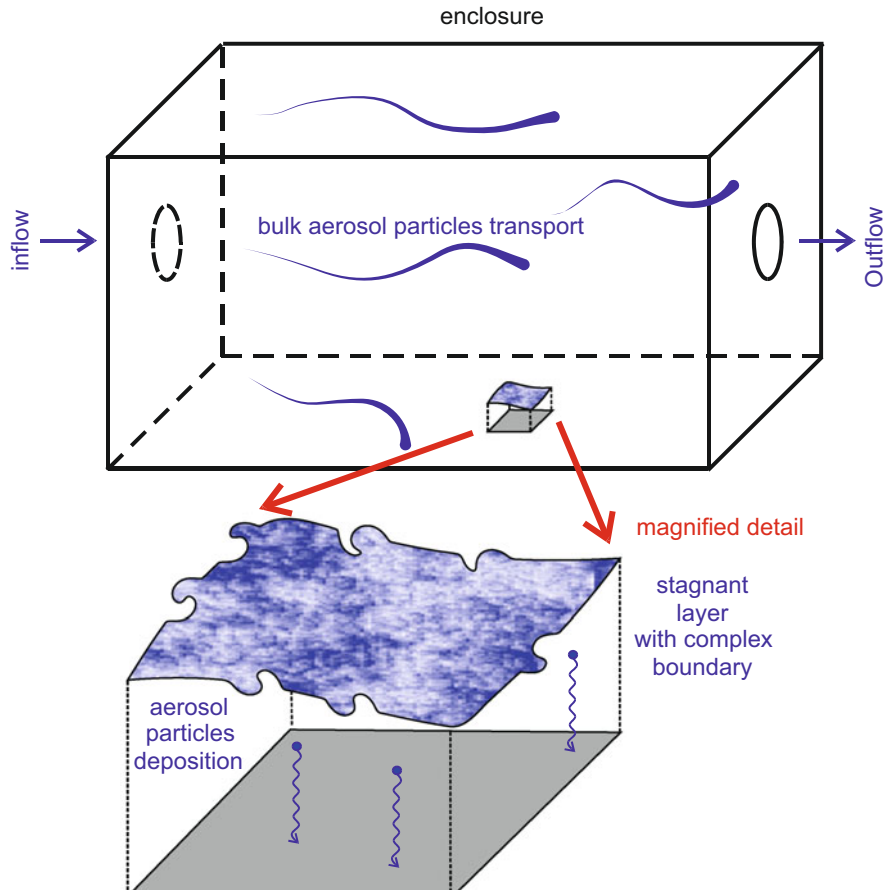


Fig. 1 Flow and transport of aerosol particles in an enclosure

where $N = N(t)$ is the number of aerosol particles in the enclosure, or its density, provided there is no additional source of particles in the volume.

We may further assume that the volume fraction of the aerosol particles is negligible ($\varepsilon_a \approx 0$), and therefore has no momentum contribution to the force balances. We rather work with the aerosol mass concentration c_a and replace corresponding quantities in Eq. (7) which makes the right side of the equation equal to Q_a (c_a, Y_w).

In the case that the aerosol bulk velocity is modified by the volumetric Brownian diffusion flux, the velocity is represented by:

$$\mathbf{v}_a = \mathbf{v}_g - \frac{1}{c_a} D_B \nabla c_a, \quad (23)$$

where $D_B = D_B(d_p)$ is the Brownian diffusion coefficient that depends on the particle diameter d_p . Eq. (7) becomes the advection-diffusion equation for the aerosol particle concentration

$$\frac{\partial c_a}{\partial t} + \operatorname{div}(c_a \mathbf{v}_g) = \nabla \cdot (D_B \nabla c_a) + Q_a(c_a, Y_w). \quad (24)$$

At the thermal equilibrium when the internal energies U_g , U_a do not change and no condensation or evaporation occurs ($Q_a(c_a, Y_w) = 0$), we have the following system of equations:

$$\frac{\partial \rho_g}{\partial t} + \operatorname{div}(\rho_g \mathbf{v}_g) = 0, \quad (25)$$

$$\frac{\partial(\rho_g \mathbf{v}_g)}{\partial t} + \operatorname{div}(\rho_g \mathbf{v}_g \mathbf{v}_g) = -\nabla P_g + \nabla \cdot \mathbf{T}_g + \rho_g \mathbf{g}, \quad (26)$$

$$\frac{\partial c_a}{\partial t} + \operatorname{div}(c_a \mathbf{v}_g) = \nabla \cdot (D_B \nabla c_a), \quad (27)$$

$$P_g = P_g(c_a, \mathbf{v}_g, \rho_g). \quad (28)$$

These equations are solved incorporating the boundary and initial conditions.

As indicated in Fig. 2, nature of such a convective diffusion process leads to stratification of the volume. The aerosol is being transported through the bulk volume inside the enclosure where shearless turbulence prevails. At the diffusion (laminar or stagnant) boundary layer close to the wall (boundary) of the enclosure, the Brownian diffusion competes with the eddy diffusion, prevails at the very proximity of surface and brings the particles to the wall.

Turbulent Nature of Indoor Air Flow

The motion of air and particles in an enclosure under usual conditions corresponding to living or commercial work spaces typically have moderate velocities and temperatures unlike the flow under industrial or transport conditions in turbines or around airplanes. However, when evaluating the Reynolds number for such flows, it might rise to values qualifying as being in the turbulent regime (see, e.g., Corner and Pendelbury 1951; Holub 1984; Holub et al. 1988; Cheng 1997, and others). Additionally, experimental evidence accompanying measurement of wall deposition in experimental chambers (Drouillard et al. 1984; Holub et al. 1991; Holub and Drouillard 1992; Nomura et al. 1997; Lahti-de Bruyne 1997; Cheng 1997; Okuyama et al. 1986; Linden et al. 2007; El Hamdani et al. 2008; Mishra and Mayya 2008; Mishra et al. 2009; De-Ling 2009) supports the understanding of this phenomenon as the one influenced by chaotic irregular motion of air. Therefore, it is useful to address aspects of turbulence description and describe quantities entering the evaluation of the deposition rate (Eq. 21)).

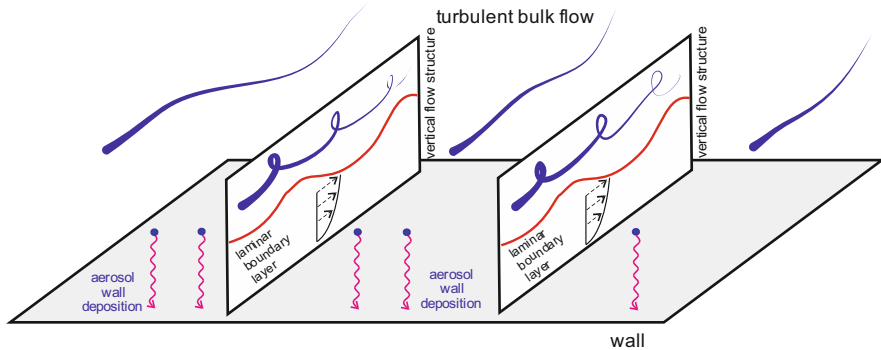


Fig. 2 Stratification of the deposition process

The computational complexity of the governing equations introduced in “Bulk Airflow and Interaction with Surfaces” section can be handled by accurate numerical methods used in the direct numerical simulation of the turbulent flow using contemporary high-performance computational tools (compare with, e.g., Parker et al. 2010, Liu et al. 2019), or a simplification of the model can be derived to obtain easily solvable model equations. The latter path has been explored in the past by variety of mathematical tools as described in Landau and Lifschitz (1959), Hinze (1975), Schlichting (1979), Bradshaw (1976), Monin and Yaglom (1975), Nelkin (1992), and summarized in modern textbooks (e.g., Pope 2000).

The derivation of the equations approximating turbulent flow at coarser spatial and temporal reference frames is based on averaging. Each quantity is decomposed to its mean value and associated fluctuations, e.g., gas density, gas volume fraction, gas velocity, and gas energy are expressed as

$$\begin{aligned} \varepsilon_g &= \bar{\varepsilon}_g + \varepsilon'_g, \\ \rho_g &= \bar{\rho}_g + \rho'_g, \\ \mathbf{v}_g &= \bar{\mathbf{v}}_g + \mathbf{v}'_g, \\ U_g &= \bar{U}_g + U'_g. \end{aligned} \quad (29)$$

Similarly, other quantities are treated in model (25–28). For example, Eq. (25) becomes

$$\begin{aligned} \frac{\partial \left(\bar{\varepsilon}_g \bar{\rho}_g + \bar{\varepsilon}_g \rho'_g + \varepsilon'_g \bar{\rho}_g + \varepsilon'_g \rho'_g \right)}{\partial t} \\ + \operatorname{div} \left(\bar{\varepsilon}_g \bar{\rho}_g \bar{\mathbf{v}}_g + \bar{\varepsilon}_g \bar{\rho}_g \mathbf{v}'_g + \bar{\varepsilon}_g \rho'_g \bar{\mathbf{v}}_g + \bar{\varepsilon}_g \rho'_g \mathbf{v}'_g + \varepsilon'_g \bar{\rho}_g \bar{\mathbf{v}}_g + \varepsilon'_g \bar{\rho}_g \mathbf{v}'_g + \varepsilon'_g \rho'_g \bar{\mathbf{v}}_g + \varepsilon'_g \rho'_g \mathbf{v}'_g \right) = 0 \end{aligned} \quad (30)$$

Repeated averaging removes terms linear in fluctuations and leaves others for further treatment

$$\frac{\partial \left(\bar{e}_g \bar{\rho}_g + \bar{e}'_g \bar{\rho}'_g \right)}{\partial t} + \text{div} \left(\bar{e}_g \bar{\rho}_g \bar{\mathbf{v}}_g + \bar{e}_g \bar{\rho}'_g \bar{\mathbf{v}}'_g + \bar{\rho}_g \bar{e}'_g \bar{\mathbf{v}}'_g + \bar{e}'_g \bar{\rho}'_g \bar{\mathbf{v}}_g + \bar{e}'_g \bar{\rho}'_g \bar{\mathbf{v}}'_g \right) = 0. \quad (31)$$

The terms such as $\bar{e}'_g \bar{\rho}'_g$, $\bar{\rho}'_g \bar{\mathbf{v}}'_g$, $\bar{e}'_g \bar{\mathbf{v}}'_g$, $\bar{e}'_g \bar{\mathbf{v}}'_g$ must be expressed by the averaged quantities in order to close the system of equations. For this purpose, various models of turbulence have been derived (e.g., algebraic or differential). For details, see Monin and Yaglom (1975), Pope (2000), or Graebel (2007).

With specific focus on the advection diffusion Eq. (27), the abovementioned decomposition is performed to obtain

$$\frac{\partial \bar{c}_a}{\partial t} + \nabla \cdot \left(\bar{c}_a \bar{\mathbf{v}}_g + \bar{c}'_a \bar{\mathbf{v}}'_g \right) = \nabla \cdot (D_B \nabla \bar{c}_a). \quad (32)$$

As described in Monin and Yaglom (1975), the term $\bar{c}'_a \bar{\mathbf{v}}'_g$ is expressed in terms of the mean quantity as

$$\bar{c}'_a \bar{\mathbf{v}}'_g = -\mathbf{K}_{\text{eddy}} \nabla \bar{c}_a, \quad (33)$$

where \mathbf{K}_{eddy} is the eddy diffusion tensor. This term is responsible for the diffusion transport produced the turbulent nature of the flow. Various attempts to express the tensor are discussed further in the text.

Recent Advances in Understanding Turbulence

The initial approach to describing the interaction of a turbulent flow with walls as boundaries of the flow region was based on the boundary layer theory (e.g., Schlichting 1979, Monin and Yaglom 1975). This layer was assumed to be flat and parallel to the surface having a predefined thickness usually entering important formulas evaluating the turbulent boundary layer flow. Some more recent advances in the research of turbulent flow showed that the eddy structures have very complex geometrical structures (see, e.g., Lesieur et al. 2002 or Gaißinski and Rovenski 2018 for reviews; Meneveau and Sreenivasan 1990, Evov et al. 1998, Kurien et al. 2000, Foias et al. 2001, and Biferale and Procaccia 2005 for related articles).

Comparison of Brownian and Turbulent Diffusion by Means of Particle Approach

The impact of the turbulent nature of the aerosol particles can be clearly seen in the experimental and theoretical analysis of the wall deposition. The turbulence term in transport Eq. (32) can be expressed using approximate formulas given by various turbulence models (see, e.g., von Kármán 1930; Monin and Yaglom 1975). Such models apply for the fully developed flow in external or internal aerodynamics (see, e.g., Anderson 2007). Their use for aerosol transport with small average velocities and nondeveloped turbulence deserves further investigation and comparison (for

more details and context, see Spiegel 1962; McCready and Hanratty 1984; Fotou and Pratsinis 1993; Jähne and Haußecker 1998; Nielsen 1998; Schimpf et al. 2000; Turney and Banerjee 2008; Li et al. 2012; and Goda 2014). This investigation can be done either by comparing various CFD strategies or using the particle approach following each aerosol element separately.

This particle or Lagrangian approach is presented by Ounis and Ahmadi (1990) and Ounis et al. (1991a, 1991b). The Brownian diffusion and the turbulent diffusion in the fully developed part of the turbulent flow far from the wall is compared. For this purpose, the Basset-Boussinesq-Oseen equation of motion in turbulent flow

$$m_p \frac{d\mathbf{v}^p}{dt} + \frac{3\pi\mu d_p}{C_c} (\mathbf{v}^p - \mathbf{v}^f) = \mathbf{N}(t) \quad (34)$$

is studied. Here m_p , \mathbf{v}^p , d_p is the particle mass, velocity, and diameter, μ is the viscosity, C_c the Cunningham correction to Stokes drag, $\mathbf{N}(t)$ the Brownian force, and \mathbf{v}^f the fluid velocity. The spectral method for stochastic linear systems is used to obtain a relationship for the total particle diffusivity depending on the turbulent diffusivity D_{eddy} as

$$D_{\text{eddy}} + \frac{1}{S_c Re_f}, \quad (35)$$

where $S_c = \frac{\nu}{D_B}$ is the Schmidt number, $Re_f = \frac{\rho_f V_0 l}{\mu}$ the Reynolds number of the fluid flow, ν the kinematic viscosity, ρ_f the fluid density, V_0 the fluid velocity scale, and l is the length scale. This comparison shows that for large Re_f , and/or for large S_c , the Brownian diffusion effect diminishes.

Analytic Solution of the Turbulent Wall Deposition

The aerosol deposition in the controlled experimental chambers has been studied in the past. For example, Langstroth and Gillespie (1947) experimentally analyzed the change in particle numbers in an enclosure due to coagulation and wall deposition. A theoretical basis for their results was established by Corner and Pendelbury (1951) who find the decay constants for the particle loss due to the both coagulation and wall deposition in the stirred and nonstirred environments in a chamber of rectangular geometry. For the case of the turbulent flow they have expressed the eddy diffusion flux as in Eq. (32) and used the following quadratic dependence of the eddy diffusion tensor on the distance from the wall denoted as ξ

$$\mathbf{K}_{\text{eddy}} = k_e \xi^2. \quad (36)$$

The coefficient k_e is in this relationship to describe the turbulent properties of the flow and is discussed later in this chapter.

A generalization of this approach and evaluation of Eq. (21) for the deposition rate has been presented in Crump and Seinfeld (1981) and used in subsequent papers

such as Crump and Seinfeld (1981). Similar to Corner and Pendelbury (1951), the stationary advection-diffusion problem is treated in a stagnant boundary layer within rotationally symmetric geometry. For this purpose, the equation

$$\frac{\partial \bar{c}_a}{\partial t} + \nabla \cdot (\bar{c}_a \bar{\mathbf{v}}_g + \bar{c}'_a \bar{\mathbf{v}}'_g) = \nabla \cdot (D_B \nabla \bar{c}_a), \quad (37)$$

is considered for the case of the incompressible advective medium ($\nabla \cdot \bar{\mathbf{v}}_g = 0$), the stationary solution ($\bar{c}_a = \bar{c}_a(x)$), and gravitational sedimentation ($\bar{\mathbf{v}}_g = V_s \mathbf{e}_{\text{vert}}$, V_s is the settling velocity, \mathbf{e}_{vert} the vertical direction). Using \mathbf{I} as the identity tensor, the equation becomes

$$\nabla \cdot ((D_B \mathbf{I} + \mathbf{K}_{\text{eddy}}) \nabla \bar{c}_a) + V_s \mathbf{e}_{\text{vert}} \cdot \nabla \bar{c}_a = 0, \quad (38)$$

and has the boundary conditions:

$$\bar{c}_a|_{\text{wall}} = 0, \bar{c}_a|_{r=\delta} = c_{\text{out}}, \quad (39)$$

where δ is the thickness of the boundary layer and c_{out} is the bulk aerosol concentration. Such a boundary condition is justified by Friedlander (2000), see Figs. 3 and 4.

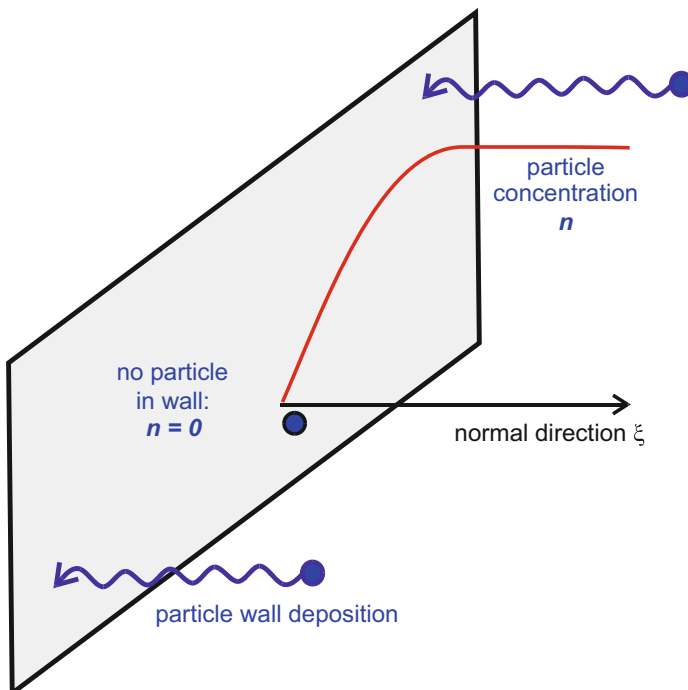


Fig. 3 Dirichlet boundary condition for the particle concentration at the wall as in Friedlander (2000)

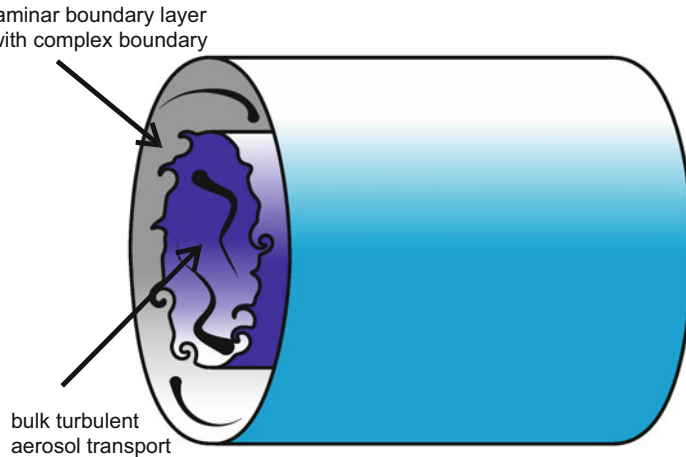


Fig. 4 Transport layers in a cylindrical enclosure

Crump and Seinfeld (1981) provide Eq. (21) for the combined turbulent and sedimentation wall deposition as

$$\beta_a = \frac{1}{\int dx} \int_{\text{wall}} \frac{V_s \mathbf{e}_{\text{vert}} \cdot \mathbf{n}_{\text{wall}}(x)}{\exp\left(\frac{\pi V_s \mathbf{e}_{\text{vert}} \cdot \mathbf{n}_{\text{wall}}(x)}{2\sqrt{k_e D_B}}\right) - 1} dS, \quad (40)$$

Equation (10) used for the cylindrical volume of radius R and area without bases gives

$$\beta_a = \frac{6\sqrt{k_e D_B}}{\pi R} F\left(\frac{\pi V_s}{2\sqrt{k_e D_B}}\right) + \frac{V_s}{\frac{4}{3}R}, \quad (41)$$

where $F(s) = \frac{1}{s} \int_0^s \frac{t}{e^t - 1} dt$.

For the cubic chamber it provides

$$\beta_a = \frac{1}{L} \left\{ \frac{8\sqrt{k_e D_B}}{\pi} + V_s \coth\left(\frac{\pi V_s}{4\sqrt{k_e D_B}}\right) \right\}, \quad (42)$$

in agreement with Corner and Pendelbury (1951).

According to Friedlander (2000), the settling velocity is expressed as

$$V_s = \frac{1}{18} \frac{(\rho_a - \rho_g)}{\mu} g d_p C_c, \quad (43)$$

where d_p is the particle diameter.

Crump and Seinfeld (1981) also extends the mentioned solution to the case when the eddy diffusivity has a general power-law form

$$\mathbf{K}_{\text{eddy}} = k_e \xi^n \quad (44)$$

with $n \geq 2$ is arbitrary. However, dimensionality of the quantity k_e fails to have its original meaning. The deposition rate becomes

$$\beta_a = \frac{1}{\int_{\Omega} dx} \int_{\text{wall}} \frac{v_s \mathbf{e}_{\text{vert}} \cdot \mathbf{n}_{\text{wall}}(x)}{\exp \left(\frac{\pi v_s \mathbf{e}_{\text{vert}} \cdot \mathbf{n}_{\text{wall}}(x)}{n \sin \left(\frac{\pi}{n} \right) \sqrt[n]{k_e D_B^{n-1}}} \right) - 1} dS. \quad (45)$$

This equation is also motivated by an alternative approach to the eddy diffusivity by Friedlander (2000) (originating in Lin et al. 1953) where $n = 3$.

$$\mathbf{K}_{\text{eddy}} = \nu \left(\frac{\xi^+}{14.5} \right)^3 \text{ with } \xi^+ = \frac{\xi V_0 (0.5f)^{0.5}}{\nu}, \quad (46)$$

where f is the Fanning friction factor.

Generalization to other values of n offers better fits to the experimental data as shown in Crump et al. (1982), Holub et al. (1988), Cheng (1997), and Lai and Nazaroff (2000). However, it creates problems with the dimensional analysis as indicated in Beneš and Holub (1996). This issue is addressed in the subsequent section.

Improvements in the Wall Deposition Model

Model adjustment motivated by experiments. The continuing experimental investigations of aerosol wall deposition in the context of the fine powder production in chemical reactors, radioactive aerosols in nuclear reactor safety, and atmospheric aerosol behavior led to the need of adjusting the model parameters according to the experimental data.

Okuyama et al. (1977) first studied the influence of turbulence on the bulk and surficial aerosol dynamics in a stirred tank, namely turbulent coagulation and deposition. In terms of the particle number concentration N , the aerosol stirred in a tank behaves according to equation

$$\frac{dN}{dt} = -K_a N^2 - \beta_a N, \quad (47)$$

where $K_a > 0$, $[m^3 s^{-1}]$ is the coagulation constant. Exploring the results of Corner and Pendelbury (1951) and Takahashi and Kasahara (1967), the deposition rate is evaluated for the vessel of cylindrical geometry (with diameter d_s and height h_s) as

$$\beta_a = \frac{8}{\pi d_s} \sqrt{k_e D_B} + \frac{V_s}{h_s} \coth \left(\frac{\pi V_s}{4\sqrt{k_e D_B}} \right). \quad (48)$$

where V_s is the settling velocity as in the section on turbulent wall deposition.

The particle deposition for aerosols up to 2 μm in turbulent chamber environment is analyzed in Okuyama et al. (1986). Here Eq. (44) is considered for the turbulent diffusion term. The best fit of particular experimental data suggested the value of the exponential factor $n = 2.7$ in deposition rate Eq. (45). This value has been used in the study of particle deposition onto rough surfaces by Shimada et al. (1987) that was based on Eq. (45) for the deposition rate applied to the regular geometry of rough surface.

The investigation of the rough surface deposition in the turbulent environment has been performed in various contexts as in Chamberlain (1967), Hahn et al. (1985), Hopke and Stukel (1993), Fan and Ahmadi (1993), (1995), Adhiwidjaja et al. (2000), Airaksinen et al. (2004), Hussein et al. (2009, 2012), and others.

Dimensional Analysis in Deposition Rate Formulas

The series of experimental results for ultrafine stirred aerosols deposited in an enclosure showed that Eq. (45) could have been used, provided the exponent n of the eddy diffusivity had values between 2 and 3. This fact is mentioned in Okuyama et al. (1986), Holub et al. (1988), and Van Dingenen (1989). Then, the eddy diffusivity is $D_{\text{eddy}} = k_e \xi^n [m^2 s^{-1}]$ while $\xi [m]$ that contradicts the dimensionality of k_e for arbitrary n . This discrepancy obviously propagates into Eq. (45) in the section on turbulent wall deposition.

$$\beta_a = \frac{1}{\int_{\Omega} dx} \int_{\text{wall}} \frac{V_s \mathbf{e}_{\text{vert}} \cdot \mathbf{n}_{\text{wall}}(x)}{\exp \left(\frac{\pi V_s \mathbf{e}_{\text{vert}} \cdot \mathbf{n}_{\text{wall}}(x)}{n \sin \left(\frac{\pi}{n} \right) \sqrt[n]{k_e D_B^{n-1}}} \right) - 1} dS. \quad (49)$$

This equation suddenly becomes questionable with unresolved dimensionality. This discrepancy can be removed as shown in Beneš and Holub (1996) by considering a dimensionally correct expression for the eddy diffusivity

$$D_{\text{eddy}} = k_e l_D^2 \left(\frac{\xi}{l_D} \right)^n, \quad (50)$$

where l_D is the turbulent diffusion layer thickness defined by Schlichting (1979) using the characteristic length L_{CH} of the flow (e.g., the enclosure dimension) as

$$l_D = \frac{L_{\text{CH}}}{\sqrt{\text{Re}}} \quad (51)$$

and $\xi \in [0, l_D]$ is the distance from the wall. Then, Eq. (45) becomes

$$\beta_a = \frac{1}{\int_{\Omega} dx} \int_{\text{wall}} \frac{V_s \mathbf{e}_{\text{vert}} \cdot \mathbf{n}_{\text{wall}}(x)}{\exp \left(\frac{\pi V_s \mathbf{e}_{\text{vert}} \cdot \mathbf{n}_{\text{wall}}(x)}{n \sin \left(\frac{\pi}{n} \right) \sqrt[n]{k_e l_D^{2-n} D_B^{n-1}}} \right) - 1} dS. \quad (52)$$

The deposition rate of the ultrafine particles in a chamber with the volume V and the wall area S , where the settling velocity can be neglected and after an asymptotic expansion, has the form

$$\beta_a = \frac{S}{V} \frac{n}{\pi} \sin \frac{\pi}{n} \sqrt[n]{k_e l_D^{2-n} D_B^{n-1}}, \quad (53)$$

and can be used for analyzing the experimental results as shown in Beneš and Holub (1996).

Fractal Nature of Turbulence

The agreement of Eq. (53) with experiments on ultrafine particle wall deposition given by the choice of $n \approx 2.7$ is not supported by any first principles analysis. An explanation supported by the nature of the flow occurring in enclosures can be sought in the geometric nature of turbulent air flow which can be explored. Geometric analyses of turbulent flow are provided by Schlichting (1960), Monin and Yaglom (1975), Meneveau and Sreenivasan (1990, 1991), and later by Lvov et al. (1998), Kurien (2000), Lesieur et al. (2002), Biferale and Procaccia (2005), and others. The complexity of turbulence implies that the turbulent diffusion boundary layer has a geometrically complex interface with the bulk of the flow. Geometric complexity can be described by fractal geometry (for a survey, see Peitgen et al. (2004), for mathematical background, see Edgar (2007)). As a consequence, the interface between the diffusion boundary layer and the turbulent bulk has an increased area allowing for greater mass transfer toward the wall. One may imagine such an increase from a two-dimensional projection where the length of this interface is increased. This expansion is shown schematically in Fig. 5. As shown by Beneš and Holub (1996), this approach led to agreement with the experimental data while keeping the original dimensionality of all quantities involved.

In particular, choosing a bounded domain Ω as a part of the boundary layer, we can consider the diffusion problem with Brownian and the turbulent terms as follows:

$$\nabla \cdot ((D_B \mathbf{I} + \mathbf{K}_{\text{eddy}}) \nabla \bar{c}_a) = 0, \quad (54)$$

with the boundary conditions.

$$\bar{c}_a|_{\partial\Omega_{\text{left}}} = \bar{c}_a|_{\partial\Omega_{\text{right}}}, \bar{c}_a|_{\partial\Omega_{\text{bottom}}} = 0, \bar{c}_a|_{\partial\Omega_{\text{top}}} = \bar{c}_{a,\text{bulk}}, \quad (55)$$

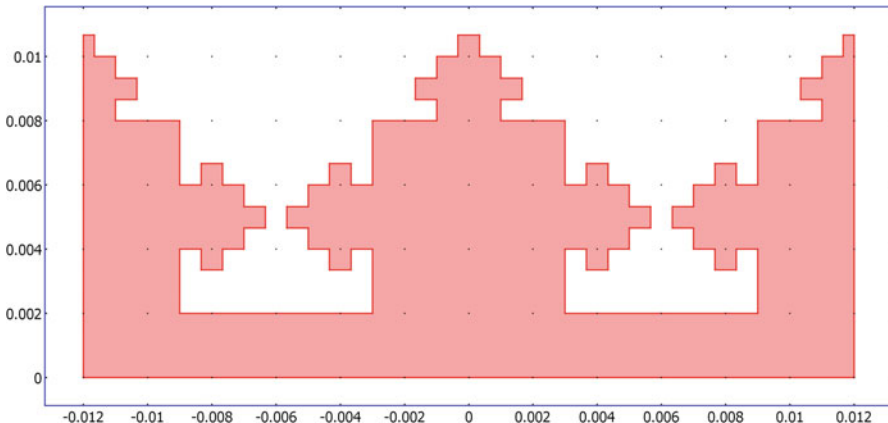


Fig. 5 Sketch of two-dimensional cross-section of the turbulent boundary layer with fractal-like interface with the bulk air volume

where c_{out} is the bulk aerosol concentration. Here, the eddy diffusion coefficient has quadratic dependence on the distance ξ from the wall

$$\mathbf{K}_{\text{eddy}} = k_e \xi^2. \quad (56)$$

The deposition rate is calculated by the formula

$$\beta_a = \frac{\int \mathbf{j}_a \cdot \mathbf{n}_{\text{wall}}(x) dS}{\int dx}, \quad (57)$$

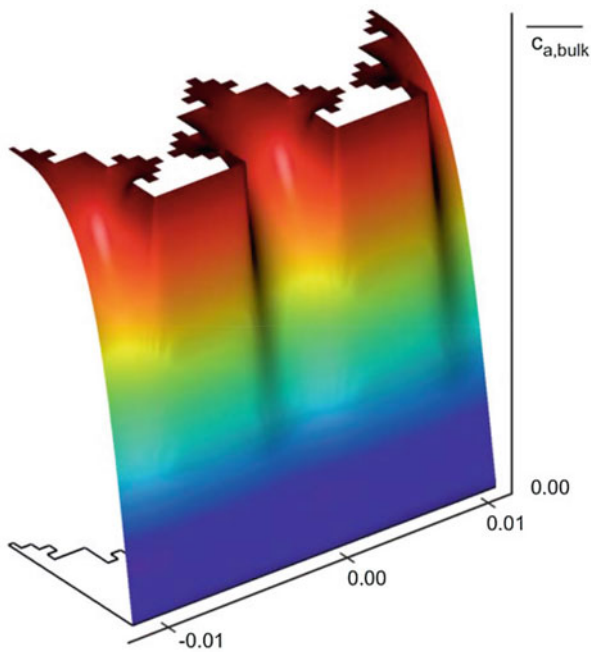
provided the solution of Eq. (54) is available (e.g., numerically, as indicated in Fig. 6). According to Beneš and Holub (1996), the agreement with the experimental data is achieved by this approach and has a similar effect as in Eq. (53).

This approach has been used and commented in a series of subsequent publications such as Cheng (1997), Nomura et al. (1997), Lai and Nazaroff (2000), Park and Lee (2002), Godoy et al. (2002), Wu et al. (2006), Schwarzenegger (2008), Rim et al. (2013), Wallace (2019), and others.

Applications

The description of the aerosol particle deposition on surfaces of an enclosure incorporates parameters of the flow, spatial environment, and particle properties. Such parameters are not always straightforward to obtain. This section is devoted to summarizing such parameters and some ways they can be determined. We also compare various experimental data presented in literature to the analytical modeling.

Fig. 6 Numerical solution of Eq. (54) in the turbulent boundary layer with geometrically complex interface to the bulk obtained by the finite element method



Boundary Layer Thickness

The flow of the gaseous phase carrying the aerosol particles under usual circumstances can always be understood as turbulent. The flow near surfaces forms several layers across which the flow conditions change from the bulk turbulence to the laminar flow and the boundary conditions at the surface (Monin and Yaglom 1975). One of these layers, the diffusion boundary layer, is important for the distribution of the aerosol particles near the wall that by its gradient determines the flux of particles toward the surface. As in Beneš and Holub (1996), the thickness of this layer l_D is determined as

$$l_D = \frac{L_{\text{CH}}}{\sqrt{\text{Re}}}, \quad (58)$$

where L_{CH} [m] is the characteristic length scale (for example, the chamber diameter, the distance an object perturbing the flow. Etc.) and Re [−] is the Reynolds number.

The value of l_D is of the order of centimeters in the experiments. The Reynolds number has its usual definition,

$$\text{Re} = \frac{\rho_g V_0 L_{\text{CH}}}{\mu_g}, \quad (59)$$

with ρ_g [$\text{kg} \cdot \text{m}^{-3}$] as the fluid density, V_0 [$\text{m} \cdot \text{s}^{-1}$] as the characteristic fluid velocity, and μ_g [$\text{kg} \cdot \text{m}^{-1} \cdot \text{s}^{-1}$] as the fluid viscosity that usually provides the information on its order of magnitude, not a precise value.

Using the parameters that are experimentally more accessible, one may, as in Cheng (1997), use:

$$\text{Re} = \frac{\rho_g \omega L_{\text{CH}}^2}{\mu_g}, \quad (60)$$

where ω [s^{-1}] is the fan rotational velocity. The value of Re is about 20000–30000 for experimental chambers. This approach, however, does not provide the information on the surface-to-volume ratio.

Eddy Diffusivity

The turbulent diffusion term described by Eq. (50) contains the coefficient k_e [s^{-1}] that according to Corner and Pendelbury (1951), Saffman and Turner (1956), and others is determined by:

$$k_e = \kappa_0^2 \left(\frac{2\varepsilon}{15\nu} \right)^{\frac{1}{2}}, \quad (61)$$

where ε [$\text{m}^2 \cdot \text{s}^{-3}$] is the average rate of energy dissipation per unit mass, $\nu = \frac{\mu_g}{\rho_g}$ is the kinematic viscosity, and κ_0 [–] is the von Kármán constant whose value is usually 0.4 but can range from 0.2 (Corner and Pendelbury 1951) to 7.9 (Okuyama et al. 1986). In some references, Eq. (62) has only the first power of κ_0 . This approach contains the energy dissipation, a phenomenon occurring near the wall whereas the bulk motion is essentially frictionless. The energy dissipation can be expressed in measurable quantities as well.

Energy Dissipation

The specific configuration of particle wall deposition in experimental chambers where the air flow is induced by a fan allows the consideration of the energy delivered by the fan to be fully dissipated by the friction of air at the chamber walls due to molecular viscosity.

Several formulas estimating the energy dissipation rate have been used in literature. In Friedlander (2000), p. 209, the equation for ε [$\text{m}^2 \cdot \text{s}^{-3}$] is

$$\varepsilon \approx \left(\frac{f}{2} \right)^{\frac{3}{2}} V_0^3 \frac{4}{L_{\text{CH}}}, \quad (62)$$

where f is the Fanning friction factor ($= 0.0025$).

Instrumentation for measurements of the pressure drop along the flow in a corridor or pipe has been greatly improved so that small portable instruments can measure as low-pressure differences as 0.1 Pa . (SETRA, Inc). Realizing that the energy dissipated must be proportional to the pressure loss due to wall friction, one can write

$$\varepsilon = \frac{\Delta P U}{\rho L} = \frac{\Delta P Q}{\rho V}, \quad (63)$$

where we provide example of experimental values observed while measuring the pressure drop along a corridor of an experimental mine as

ΔP = measured pressure drop along the pipe or adit [5 Pa]

Q = flow rate in pipe [$47.2 \text{ m}^3 \cdot \text{s}^{-1}$]

V = volume of the pipe ($= A_e L$) [m^3]

A = cross-section of the pipe [9.6 m^3]

$U = Q/A$ = air velocity [$0.6 \text{ m} \cdot \text{s}^{-1}$]

L = corridor length [314 m]

The eddy diffusivity coefficient in Eq. (62) then becomes

$$k_e = \kappa_0^2 \left(\frac{2\varepsilon}{15\nu} \right)^{1/2} = \kappa_0^2 \left(\frac{2\Delta P U}{15\rho L \nu} \right)^{1/2} = 1.53 \text{ s}^{-1}. \quad (64)$$

Comparison of Measured Data

In Fig. 7, the data presented in Holub and Drouillard (1992) (denoted as U and D), in Liu et al. (2019) (denoted as L), in Okuyama et al. (1986) (denoted as O), and in Holub et al. (1988) (denoted as G) are depicted. The data L have been obtained from computational studies presented in Liu et al. (2019) for two specific particle sizes.

To make these comparisons, it is assumed that most of the supplied kinetic energy is depleted along the walls in the stagnant layer. The rate of plateout is controlled by the diffusion across the stagnant layer. The thickness of the stagnant layer depends on the degree of turbulence. The kinetic energy removed at the outlet of the vessel is negligible and is not included in the subsequent calculation.

The inflowing air (F) is pumped into a chamber of volume V_{CH} through tubing of radius R , and length . Assuming that the kinetic energy injected into the system is the kinetic energy of the air in the inlet tubing, the equation for the energy dissipation can be written as:

$$\varepsilon = \frac{1}{2} \rho_g V_t U_t^2 \frac{1}{\rho_g V_{\text{ch}} \Delta t} \quad [\text{m}^2 \cdot \text{s}^{-3}], \quad (65)$$

where

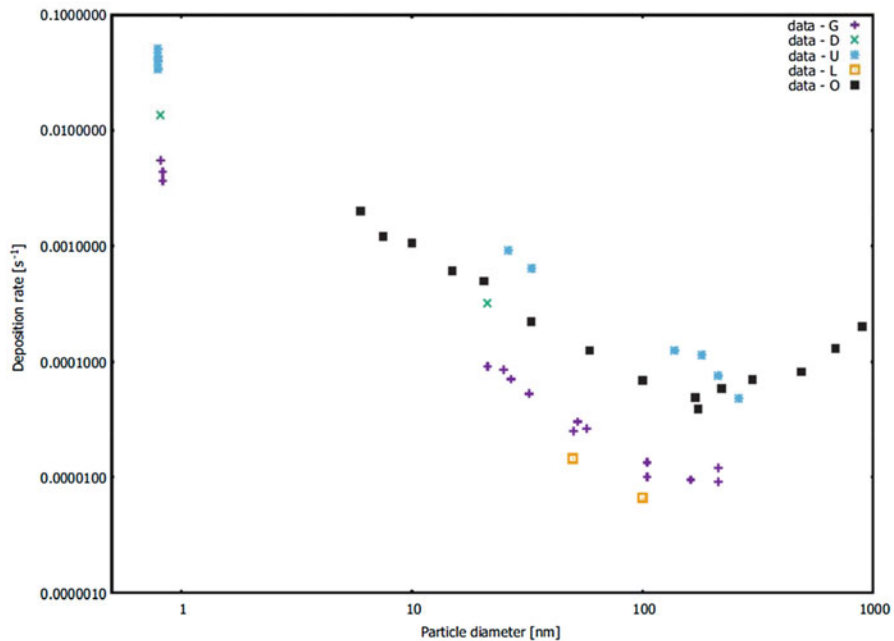


Fig. 7 Comparison of data from different aerosol chambers. (Data from Holub and Drouillard (1992) are denoted as U and D, from Liu et al. (2019) as L, from Okuyama et al. (1986) as O, from Holub et al. (1988) as G)

ρ_g is the air density [$\text{kg} \cdot \text{m}^{-3}$],
 $V_t = \pi R^2 L$ is the tubing volume [m^3],
 $U_t = \frac{F}{\pi R^2}$ is the air velocity [$\text{m} \cdot \text{s}^{-1}$],
 $\Delta t = \frac{L}{U_t}$ is the time it takes to empty the air from the tubing [s],

Consequently, the energy dissipation becomes

$$\varepsilon = \frac{1}{2} \frac{F^3}{\pi^2 R^4 V_{CH}} \quad [\text{m}^2 \cdot \text{s}^{-3}]. \quad (66)$$

Comparison of Experimental Configurations

Review of literature related to the measurement of aerosol wall deposition provides interesting details of measured data and explanations for the observed phenomena. Table 1 provides a summary with values used in the experiments. Table 2 explains the origin of particular data and provides comments to them.

Table 1 Comparison of various aerosol chamber measurements

Origin	Radius [m]	Height (cylinder)	Side	V/S	S/V	Beta [s^{-1}]	$\frac{v_{dep}}{cm.s^{-1}}$	Fan	Volume [m^3]	Surface [m^2]	k_e	n	Epsilon [$cm^2.s^{-3}$]	Condensation nuclei
[1] CLOUD	1.8400	3.0000		4.1700	0.2400	0.0018	0.1500	Yes	26.0000	6.2400				
[2] Cheng	0.3380			0.4950	2.0200	0.0018	0.0890	No	0.1610	0.3250	2.6-2.8	Not reported		
						0.0100	0.4900	1800 rpm			3.6500	2.6-2.8	Not reported	
[3] Holub	0.1600	2.1300		0.3400	2.9300	0.0220	0.7900	Yes	4.0000	11.7000	0.9650	2.6000	6.2400	Controlled
[4] SUJCHBO cubic chamber	2.1500	2.1500	0.3600	2.7800		0.04-0.08			10.0000	27.8000				Controlled
[5] SUG			0.1270	7.8600	0.0033	0.0420	No		0.2300	1.8100				
[6] PYLON	0.0280	0.0250	0.0140	71.5000	0.0028	0.0028	No		0.0000615	0.0044				
[7] HO	0.0540	6.0000	0.0270	37.0000	0.0900	0.2430			0.0550	2.0350				
[8] Liu	4.0000	2.0000	3.5000	1.7900	0.5600	0.0070	0.0120	No	39.0000	70.0000	2.4000	2.6000	0.4000	No
						0.0020	0.0360	No	39.0000	70.0000	2.4000	2.6000	0.4000	No
[9] Wonaschuetz	0.0500	0.0127	2.8000	0.3960		No	No	0.0010	0.0195					
[10] Takahashi													100/1000	
[11] Vämmarcke	1.0000	1.0000	1.0000	6.3500	0.1570				1.0000	6.3500		2.6000		

Table 2 References and comments to Table 1

Notation	References	Comment
[1] CLOUD	Dunnel et al. (2016)	CLOUD (cosmics leaving outdoor droplets) at CERN has apparently no concern for “wall deposition,” the role of fans in plateout of monomers is not considered (plateout rate on fans is much higher than on walls); HV sweep removes ions only; and no HEPA Bionaire air cleaner is used
[2] Cheng	Cheng (1997)	CN levels apparently controlled but not explicitly mentioned; performed the important experiment with “still air”
[3] Holub	Drouillard et al. (1984); Holub and Drouillard (1992)	Two chambers, CN controlled in both
[4] SUJCHBO	Otalal et al. (2017)	CN controlled best (=0); plateout rate not measured or calculated
[5] SUG	Van Dingenen (1989)	CN probably controlled; when $n > 2$ dimensionality mismatch
[6] PYLON	www.pylonelectronics.com	Small chamber, a Rn source, good for measuring plateout of Rn progeny; however, the company is not interested in pursuing it
[7] HO	Ho et al. (1982)	The chamber has been scrapped, as well as all related projects, in 1995. The very interesting data from that unique chamber are still not explained
[8] Liu	Liu et al. (2019)	This is not a chamber but a ventilated room. What is remarkable is that the plateout rate calculated using CFD agrees with our approach reported here. CN not reported
[9] Wonaschuetz	Wonaschuetz et al. (2017)	This small chamber experiment is not addressing plateout, nor radiation-induced unsticking from the surfaces
[10] Takahashi	Takahashi and Kasahara (1967)	This paper is not calculating epsilon from measured quantities
[11] Vanmarcke	Vanmarcke et al. (1991)	CN probably controlled but no epsilon calculated; k_e fitted; even when $n > 2$, dimensionality mismatch

Challenges in Understanding Principles of Particle: Surface Interaction

In this section we indicate problems remaining open for further investigation and challenges which should be met when attempting to understand subtle details of the phenomenon of aerosol particle wall deposition.

Fundamental Problems

Turbulent nature of the air flow. Experiments in aerosol chambers are performed under a variety of flow regimes. The usual velocities produced by the laboratory fans correspond to Reynolds numbers of the order of 10^4 corresponding to the fully developed turbulence that critically influences the diffusive transport in the boundary layer. Some other experiments (e.g., Cheng 1997) perform measurements with the fan turned off. However, the data obtained suggest that the framework of the eddy diffusivity is still applicable. We can hypothesize that despite of being unable to measure tiny fluctuations of the air flow and its temperature, there are still some irregular air motions exhibiting properties of turbulence, even though not fully developed. A decisive experiment to study this anomaly would require a thermally isolated chamber with temperature differences between the walls and the inside atmosphere being less than 0.05 K. Such systems, where the *stagnant layer* stretches across the whole chamber, have been used by Hirst and Harrison (1938), when measuring the diffusion coefficient of radon gas in air.

The challenges in understanding the diffusion limited phenomena could be presented by a particular example to roughly estimate the time it takes for a particle of a size about 1 nm to reach the surface of a chamber. Using the parameters of Cheng (1997) who had a spherical chamber of the radius 0.338 m, the deposition velocity given by $V_{\text{dep}} = \beta_a \frac{S}{V}$ is 0.025 cm s^{-1} . Therefore, the particle needs 1300 s or less to reach the wall if considering the deposition rate as the characteristic parameter. However, the one-dimensional diffusion equation (see Friedlander 2000, Eqs. [2.4, 2.7]) yield values of 3000–7000 s. Therefore, this discrepancy that is occurring when there is no apparent source of momentum in a laboratory-controlled enclosure needs to be understood.

Fractional dependence of the deposition rate on the particle size. The quadratic dependence of the eddy diffusivity on the distance from the wall originally suggested by the algebraic models of turbulence (see Crump and Seinfeld 1981) was soon challenged by experimental results (e.g., in Okuyama et al. 1986; Holub et al. 1988; Pandian and Friedlander 1988; Beneš and Holub 1996; Cheng 1997 up to Wallace et al. 2019), and a fractional power dependence was suggested. However, some results were accompanied by a dimensional discrepancy when using such a fractional power. This discrepancy was resolved by Beneš and Holub (1996) in two ways, suggesting a dimensionally correct fractional formula and, alternatively, matching the experimental data by considering the usual quadratic formula and a geometrically complex boundary between the diffusion layer and the turbulent bulk. For further studies of this phenomenon, it would be desirable to have a Rn/Tn aerosol chamber that produce condensation nuclei whenever needed and generate monodispersed aerosols at $\sim 1 \text{ nm}$ size. Such a chamber has to be sufficiently large ($4\text{--}10 \text{ m}^3$) to allow for taking samples without seriously disturbing the regime inside.

Understanding the reverse processes. Under some circumstances, the particles attached to the enclosure surface can be released back to the bulk volume. Although such effects have lower probability, their understanding still requires more knowledge coupling driving forces such as radioactive decay, thermal oscillations of air particles, strong diffusion flux toward the surface, or even quantum effects on surfaces (see Hsu et al. 1991 or Kong et al. 2020).

Arbitrariness of characteristic quantities. Some constitutive relations in the models of deposition contain dimensionless quantities obtained by the dimensional analysis (compare Ruzicka 2008; Szücs 1980). These quantities, e.g., the Reynolds number, are evaluated using a characteristic length or velocity, which typically provide orders of magnitude, not precise values. This uncertainty undermines the accuracy of the results of the modeling of the experiment.

Cunningham slip correction. Holub and Knutson (1987) first suggested that when the size of a particle approaches the size of air molecules, their size should be added into the denominator in the slip correction formula. Soon after Ramamurthi and Hopke (1989) did that by proposing an empirical correction. The unaddressed problem is that even this correction should be tailored to the specific shape of the molecules (not only to the diatomic air molecules) that are hitting the aerosol particle.

Technical Problems

Experimental data for ultrafine aerosols. Some authors did their measurements for such types of particles and anchored their data for sizes 1 nm using the radioactive Rn/Tn progeny producing monodispersed aerosols of 1 nm size in a condensation-nuclei-free chamber and modified the Cunningham slip correction at such sizes (see Cheng 1997; Holub and Knutson 1987; Ramamurthi and Hopke 1989; Rabajczyk et al. 2020 and others). In some other references, the ultrafine data have just been extrapolated.

Wall friction. In literature, the friction velocity as an adjustable parameter is used to fit data to the regression formulas. However, such a quantity is hardly measurable, even meaningful when there is no prevailing flow direction. As a measure of dissipation, the specific energy supplied to the volume is easier to be evaluated, usually by knowing the pressure drop or fan power delivered to the volume, as explained before.

Advice

As mentioned earlier, isotopic labels are recommended to be used. When embedded in the particles, the sensitivity would be orders of magnitude higher than the best aerosol instruments. Prior Rn/Tn work in a CN-free chamber produced ~1 nm particles that can be measured with incredible sensitivity. It gives invaluable data at smaller size aerosols (ultrafine particles, below 100 nm).

Test the assumption that plated out aerosols on surfaces do not become airborne (SVOCs, possibly even NVCs, nonvolatile compounds), all labelled by appropriate radioactive aerosols. If there is reentry, it would change the field of wall deposition.

Routinely use aerosol generators spiked with suitable radioactive isotopes and become familiar with standard radiochemical methods and their measurements.

As published in the past, and mentioned previously, Rn/Tn daughters in CN-free chambers create monodispersed ~1 nm aerosols. Because they have high specific radioactivity, they can be measured with orders of magnitude greater sensitivity, as mentioned before. When these get attached to larger particles, using graded screen array (GSA) methods (Holub and Knutson 1987; Cheng et al. 1992), one can get aerosol size distribution from 1 to ~500 nm. By combining data from an impactor with data from a GSA diffusion-based sampler, it was possible to cover the particle size range from 0.5 to 5000 nm; an unprecedented four orders of magnitude size span was demonstrated by Knutson and Tu (1996).

Extending this approach would be to label the particle sources with radioactive isotopes with suitable half-lives and chemical properties for concentrations that are too low to analyze by conventional means. For instance, surfaces are often covered with SVOCs and possibly NVCs (Wallace et al. 2013). When slightly heated, say 40–100 °C, generated particles can be measured. Usually their composition is unknown because standard analytical methods are not sensitive enough. If surfaces, exposed to heat, or stress, emit monomeric molecules, it would nullify the usual assumption that the surfaces do not emit anything. Also, composition could be determined.

Further extension of this idea would be to spike all aerosol generators, using different salts as a base (NaCl or Li_2SO_4), with radioactive isotopes and then measure their distribution using the GSA method. Each screen then would be measured using the deconvolution programs commonly used in deconvoluting radon and thoron progeny size spectra. It would require the full cooperation between two disparate subfields groups, or either one to learn the expertise of others.

To summarize this section, there are many unexplained anomalies, most at the molecular/nanometer sizes, that require measurements and explanations. They cannot be included here because it represents another entire chapter not directly relevant to indoor air quality. There is sufficient material to be summarized that a book would be needed to list all of them, and then suggest their potential explanations which is beyond the scope of this chapter.

Conclusions

The chapter summarizes the achievements in research on aerosol wall deposition. Based on the conservation laws related to the turbulent aerosol transport and the deposition on the surfaces, the deposition rates can be evaluated and used in experimental studies. The chapter formulates challenges in the detailed

understanding of the deposition processes. For their resolution, experimental enclosures with accurately controlled condensation nuclei, air flow and thermal properties together with a radioactive aerosol represent the most advanced tools in deposition research.

This work was partly supported by the Ministry of Education, Youth and Sports of the Czech Republic under the OP RDE grant number https://www.isvavai.cz/cep?s=jednoduche-vyhledavani&ss=detail&h=EF16_019%2F0000753 “Research center for low-carbon energy technologies,” and by the project number 21-09093S of the Czech Science Foundation “Multiphase <https://starfos.tacr.cz/en/project/GA21-09093S> flow, transport, and structural changes related to water freezing and thawing in the subsurface.”

References

- Adhiwidjaja I, Matsusaka S, Tanaka H, Masuda H (2000) Simultaneous phenomenon of particle deposition and Reentrainment: effects of surface roughness on deposition layer of striped pattern. *Aerosol Sci Technol* 33(4):323–333
- Airaksinen M, Kurnitski J, Pasanen P et al (2004) Fungal spore transport through a building structure. *Indoor Air* 14(2):92–104
- Anderson JD (2007) Fundamentals of aerodynamics, 4th edn. McGraw-Hill, New York
- Bauer P, Beneš M, Fučík R, Hoang HD, Klement V, Máca R, Mach J, Oberhuber T, Strachota P, Žabka V, Havlena V (2015) Numerical simulation of flow in fluidized beds. *Discrete Contin Dyn Syst* 8(5):833–846
- Beneš M, Eichler P, Klinkovský J, Kolář M, Solovský J, Strachota P, Žák A (2021) Numerical simulation of fluidization for application in oxyfuel combustion. *Discrete Contin Dyn Syst* 14(3):769–783
- Beneš M, Holub RF (1996) Aerosol Wall deposition in enclosures investigated by means of a stagnant layer. *Environ Int* 22(Suppl. 1):S883–S889
- Biferale L, Procaccia I (2005) Anisotropy in turbulent flows and in turbulent transport. *Phys Rep* 414(2–3):43–164
- Bradshaw P (1976) Turbulence. Springer-Verlag, Berlin
- Chamberlain AC (1967) Transport of lycopodium spores and other small particles to rough surfaces. *Proc R Soc Lond, A Math Phys. Sci* 296:45–70
- Cheng YS (1997) Wall deposition of radon progeny and particles in a spherical chamber. *Aerosol Sci Technol* 27:131–146
- Cheng YS, Su YF, Newton GJ, Yeh HC (1992) Use of a graded diffusion battery in measuring the radon activity size distribution. *J Aerosol Sci* 23:361–372
- Corner J, Pendelbury ED (1951) The coagulation and deposition of a stirred aerosol. *Proc Phys Soc Lond* B64:645–654
- Crump JG, Flagan RC, Seinfeld JH (1982) Particle wall loss rates in vessels. *Aerosol Sci Technol* 2(3):303–309
- Crump JG, Seinfeld JH (1981) Turbulent deposition and gravitational sedimentation of an aerosol in a vessel of arbitrary shape. *J Aerosol Sci* 12:405–415
- De-Ling L (2009) Particle deposition onto enclosure surfaces. Aerospace report no. TR-2009(8550)-2, Space Materials Laboratory, Physical Sciences Laboratories, Aerospace Corporation
- Drouillard RF, Davis TH, Smith EE, Holub RF (1984) Radiation hazard test facilities at Denver research center. Technical report Bureau of Mines IC 8965
- Dunne EM et al (2016) Global atmospheric particle formation from CERN CLOUD measurements. *Science* 354:1119–1124

- Edgar G (2007) Measure, topology and fractal geometry. Springer Verlag, Berlin
- El Hamdani S, Limam K, Abadie MO et al (2008) Deposition of fine particles on building internal surfaces. *Atmos Environ* 42:8893–8901
- Fan FG, Ahmadi G (1993) A sublayer model for turbulent deposition of particles in vertical ducts with smooth and rough surfaces. *J Aerosol Sci* 24(1):45–64
- Fan FG, Ahmadi G (1995) Analysis of particle motion in the near-wall shear layer vortices – application to the turbulent deposition processes. *J Colloid Interface Sci* 172:263–277
- Foias C, Manley O, Rosa R, Temam R (2001) Navier-stokes equations and turbulence, Encyclopedia of mathematics and its applications. Cambridge University Press, Cambridge. <https://doi.org/10.1017/CBO9780511546754>
- Fotou G, Pratsinis S (1993) A correlation for particle wall losses by diffusion in dilution chambers. *Aerosol Sci Technol* 18:213–218. <https://doi.org/10.1080/02786829308959596>
- Friedlander S (2000) Smoke, dust, and haze: fundamentals of aerosol dynamics. Oxford University Press
- Fuchs NA (1964) The mechanics of aerosols. Pergamon Press, Oxford, UK
- Gaissinski I, Rovenski V (2018) Modeling in fluid mechanics: instabilities and turbulence. CRC Press
- Gidaspow D (1994) Multiphase flow and fluidization: continuum and kinetic theory description. Academic Press
- Goda R (2014) Turbulence intensity and air velocity characteristics in a slot ventilated space. *Period Polytech Mech Eng* 58(1):1–6
- Godoy M, Hadler JC, Iunes PJ et al (2002) Effects of environmental conditions on the radon daughters spatial distribution. *Radiat Meas* 35(3):213–221
- Graebel W (2007) Advanced fluid mechanics. Academic Press, Cambridge, Massachusetts
- Hahn LA, Stukel JJ, Leong KH, Hopke PK (1985) Turbulent deposition of submicron particles on rough walls. *J Aerosol Sci* 16(1):81–86
- Hinze JO (1975) Turbulence, 2nd edn. McGraw-Hill, New York
- Hirst W, Harrison GE (1938) The diffusion of radon gas mixtures. *Proc R Soc Lond A* 169:573–586
- Ho W-L, Hopke PK, Stukel JJ (1982) The attachment of RaA (218Po) to monodisperse aerosol. *Atmos Environ* (1967) 16:825–836
- Holub RF (1984) Turbulent Plateout of radon daughters. *Rad Protec Dosi* 7:155–158
- Holub RF, Drouillard RF (1992) Two-filter radon detectors with aerosol chambers: a Progress report. In: The proceedings on international conference on radiation safety in uranium mining. Saskatoon
- Holub RF, Drouillard RF, Davis TH (1991) Orphan daughters at Denver radium site. In: Cross FT (ed) Indoor radon and lung cancer: reality or myth? Battelle Press, pp 467–475
- Holub RF, Knutson EO (1987) Chapter 25: Radon and its decay products, occurrence, properties, and health effects. In: Hopke PK (ed) Measuring polonium-218 diffusion-coefficient spectra using multiple wire screens, ACS symposium series, vol 331. American Chemical Society, pp 340–356
- Holub RF, Raes F, Van Dingenen R, Vanmarcke H (1988) Deposition of aerosols and unattached radon daughters in different chambers; theory and experiment. *Radiat Prot Dosim* 24:217–220
- Hopke PK, Stukel JJ (1993) Transport of particles to uranium mine walls. Mining research contract report H0292032. Bureau of Mines. U.S. Department of the Interior, Washington, D.C.
- Hsu C-H, Larson BE, El-Batanouny M, Willis CR, Martini KM (1991) Evidence of quantum motion of hydrogen on Pd(111) in helium-diffraction data. *Phys Rev Lett* 66(24):3164–3167
- Hussein T, Kubincová L, Džumbová L, Hruška A, Dohányosová P, Hemerka J, Smolík J (2009) Deposition of aerosol particles on rough surfaces inside a test chamber. *Build Environ* 44: 2056–2063
- Hussein T, Smolík J, Kerminen VM, Kulmala M (2012) Modeling dry deposition of aerosol particles onto rough surfaces. *Aerosol Sci Technol* 46:44–59. <https://doi.org/10.1080/02786826.2011.605814>
- Jähne B, Haußecker H (1998) Air-water gas exchange. *Annu Rev Fluid Mech* 30(1):443–468

- Knutson EO, Tu KW (1996) Size distribution of radon progeny aerosol in the working area of a dry uranium mine. *Environ Int* 22(1):S617–S632
- Kolev NI (2011) Multiphase flow dynamics 1. Springer-Verlag, Berlin
- Kong J, Jiménez-Martínez R, Troullinou C et al (2020) Measurement-induced, spatially-extended entanglement in a hot, strongly-interacting atomic system. *Nat Commun* 11:2415
- Kurien S, L'vov VS, Procaccia I, Sreenivasan KR (2000) The scaling structure of the velocity statistics in atmospheric boundary layer. *Phys Rev E* 61:407
- Lahti-DeBruyne ML (1997) The influence of fine particulate deposition and portable air cleaning devices on indoor air quality, master thesis, Colorado School of Mines, Environmental Science and Engineering
- Lai ACK, Nazaroff WW (2000) Modeling indoor particle deposition from turbulent flow onto smooth surfaces. *J Aerosol Sci* 31:463–476. [https://doi.org/10.1016/S0021-8502\(99\)00536-4](https://doi.org/10.1016/S0021-8502(99)00536-4)
- Landau LD, Lifshitz EM (1959) Fluid mechanics. Pergamon Press, London
- Langstroth GO, Gillespie T (1947) Coagulation and surface losses in disperse systems in still and turbulent air. *Can J Res* 25(5):455–471
- Lesieur M, Yaglom AM, David F (2002) New trends in turbulence. Turbulence: nouveaux aspects: les Houches session LXXIV 31 July–1 September 2000. Springer Science & Business Media
- Li C, Li X, Su Y, Zhu Y (2012) A new zero-equation turbulence model for micro-scale climate simulation. *Build Environ* 47:243–255
- Lin CS, Moulton RW, Putnam GL (1953) Mass transfer between solid wall and fluid streams. Mechanism and Eddy distribution relationships in turbulent flow. *Ind Eng Chem* 45(3): 636–640. <https://doi.org/10.1021/ie50519a048>
- Linden P, Bolster D, Buckley S (2007) Simplified models for particle dispersion in buildings, California energy commission, public interest energy research program, project report, March 2007 CEC-500-2007-XXX
- Liu X, Li F, Cai H et al (2019) A numerical investigation on the mixing factor and particle deposition velocity for enclosed spaces under natural ventilation. *Build Simul* 12:465–473
- Evov VS, Podivilov E, Pomyalov A, Procaccia I, Vandembroucq D (1998) Improved shell model of turbulence. *Phys Rev E* 58:1811–1822
- McCready MJ, Hanratty TJ (1984) A comparison of turbulent mass transfer at gas-liquid and solid-liquid interfaces. In: Brutsaert W, Jirka GH (eds) Gas transfer at water surfaces. Springer Netherlands, Dordrecht, pp 283–292
- Meneveau C, Sreenivasan KR (1990) Interface dimension in intermittent turbulence. *Phys Rev A* 41:2246–2248
- Meneveau C, Sreenivasan KR (1991) The multifractal nature of turbulent energy dissipation. *Fluid Mech* 224:429–484
- Mishra R, Mayya YS (2008) Study of a deposition-based direct thoron progeny sensor (DTPS) technique for estimating equilibrium equivalent thoron concentration (EETC) in indoor environment. *Radiat Meas* 43(8):1408–1416
- Mishra R, Mayya YS, Kushwaha HS (2009) Measurement of Rn-220/Rn-222 progeny deposition velocities on surfaces and their comparison with theoretical models. *J Aerosol Sci* 40(1):1–15
- Monin AS, Yaglom AM (1975) Statistical fluid mechanics. MIT Press, Cambridge, MA
- Nelkin M (1992) In what sense is turbulence an unsolved problem. *Science* 255:566–570
- Nielsen, P. V. (1998) The selection of turbulence models for prediction of room airflow. Department of building technology and structural engineering, indoor environmental engineering, vol R9828, no 86
- Nomura Y, Hopke PK, Fitzgerald B, Mesbah B (1997) Deposition of particles in a chamber as a function of ventilation rate. *Aerosol Sci Technol* 27:62–72
- Okuyama K, Kousaka Y, Kida Y, Yoshida T (1977) Turbulent coagulation of aerosols in a stirred tank. *J Chem Eng Japan* 10:142
- Okuyama K, Kousaka Y, Yamamoto S, Hosokawa T (1986) Particle loss of aerosols with particle diameters between 6 and 2000nm in stirred tank. *J Colloid Interface Sci* 110:214–223

- Otahal PPS, Burian I, Ondracek J, Zdimal V, Holub RF (2017) Simultaneous measurements of Nanoaerosols and radioactive aerosols containing the short-lived radon isotopes. *Radiat Prot Dosim* 177(1–2):53–56. <https://doi.org/10.1093/rpd/ncx157>. PMID: 29036690
- Ounis H, Ahmadi G (1990) A comparison of Brownian and turbulent diffusion. *Aerosol Sci Technol* 13(1):47–53
- Ounis H, Ahmadi G, McLaughlin JB (1991a) Brownian diffusion of submicrometer particles in the viscous sublayer. *J Colloid Interface Sci* 143(1):266–277
- Ounis H, Ahmadi G, McLaughlin JB (1991b) Dispersion and deposition of Brownian particles from point sources in a simulated turbulent channel flow. *J Colloid Interface Sci* 147(1):233–250
- Pandian MD, Friedlander SK (1988) Particle deposition to smooth and rough walls of stirred chambers: mechanisms and engineering correlations. *PCH Phys Chem Hydrodynam* 10: 639–645
- Park SH, Lee KW (2002) Analytical solution to change in size distribution of polydisperse particles in closed chamber due to diffusion and sedimentation. *Atmos Environ* 36(35):5459–5467
- Parker S, Nally J, Foat T, Preston S (2010) Refinement and testing of the drift-flux model for indoor aerosol dispersion and deposition modelling. *J Aerosol Sci* 41:921–934
- Peitgen H-O, Jurgens H, Saupe D (2004) Chaos and fractals: new frontiers of science, 2nd edn. Springer Verlag, New York
- Pope SB (2000) Turbulent flows. Cambridge University Press
- Rabajczyk A, Zielecka M, Porowski R, Hopke PK (2020) Metal nanoparticles in the air: state of the art and future perspectives. *Environ Sci Nano* 7:3233–3254
- Ramamurthi M, Hopke PK (1989) On improving the validity of wire screen “unattached” fraction Rn daughter measurements. *Health Phys* 56:189–194
- Rim D, Wallace L, Persily K, Andrew (2013) Indoor ultrafine particles of outdoor origin: importance of window opening area and Fan operation condition. *Environ Sci Technol* 47. <https://doi.org/10.1021/es303613e>
- Ruzicka MC (2008) On dimensionless numbers. *Chem Eng Res Des* 86(8):835–868
- Saffman P, Turner J (1956) On the collision of drops in turbulent clouds. *Journal of Fluid Mechanics* 1(1):16–30
- Schimpf, U., Haussecker, H., Jahne, B. (2000) On the investigations of micro turbulence at the water surface using infrared imaging, IGARSS 2000. IEEE 2000 international geoscience and remote sensing symposium. Taking the pulse of the planet: the role of remote sensing in managing the environment. Proceedings (Cat. No.00CH37120), vol. 3, pp. 1274–1276
- Schlichting H (1979) Boundary-layer theory, 7th edn. McGraw-Hill, New York
- Schwarzenegger A. Governor (2008) Simplified models for particulate dispersion in buildings, Pier final report, January 2008 CEC-500-2007-098, California energy commission, public interest research program
- Seinfeld JH, Pandis SN (2016) Atmospheric chemistry and physics (from air pollution to climate change), 3rd edn. John Wiley and Sons, New Jersey
- Shimada M, Okuyama K, Kousaka Y, Ohshima K (1987) Turbulent and Brownian diffusive deposition of aerosol particles onto a Rough Wall. *J Chem Engin of Japan* 20:67–64
- Slattery JC (1999) Advanced transport phenomena. Cambridge University Press, Cambridge
- Spiegel EA (1962) Thermal turbulence at very small Prandtl number. *J Geophys Res* 67(8): 3063–3070
- Szücs E (1980) Similitude and modelling. Akadémiai Kiadó, Budapest
- Takahashi K, Kasahara M (1967) A theoretical study of the equilibrium particle size distribution of aerosols. *Atmos Environ* 2(5):441–453
- Turney D, Banerjee S (2008) Transport phenomena at interfaces between turbulent fluids. *AICHE J* 54(2):344–349
- Van Dingenen R, Raes F, Vanmarcke H (1989) Molecule and aerosol particle wall losses in smog chambers made of glass. *J Aerosol Sci* 20:113–122

- Vanmarcke H, Landsheere C, Van Dingenen R, Poffijn A (1991) Influence of turbulence on the deposition rate constant of the unattached radon decay products. *Aerosol Sci Technol* 14: 257–265
- von Kármán Th. (1930) Mechanische Ähnlichkeit und Turbulenz, Nachrichten von der Gesellschaft der Wissenschaften zu Göttingen, Fachgruppe 1 (Mathematik) 5:58–76
- Wallace L, Jeong S, Rim D (2019) Dynamic behavior of indoor ultrafine particles (2.3–64 nm) due to burning candles in a residence. *Indoor Air* 29:1018–1027
- Wallace L, Kindzierski W, Kearney J, MacNeill M, Héroux ME, Wheeler AJ (2013) Fine and ultrafine particle decay rates in multiple homes. *Environ Sci Technol* 47(22):12929–12937
- Williams MMR, Loyalka SK (1991) *Aerosol science: theory and practice: with special applications to the nuclear industry*. Pergamon Press, Oxford
- Wonaschuetz A, Kallinger P, Szymanski W, Hitzenberger R (2017) Chemical composition of radiolytically formed particles using single-particle mass spectrometry. *J Aerosol Sci* 113: 242–249
- Wu CC, Lee GWM, Cheng PJ et al (2006) Effect of wall surface materials on deposition of particles with the aid of negative air ions. *J Aerosol Sci* 37:616–630



Resuspension

12

Andrea R. Ferro

Contents

Introduction	332
Definitions	333
Bulk Aerosol Resuspension Measurement and Modeling	334
Typical Bulk Aerosol Resuspension Experiments	334
Two-Compartment Material Balance Model	335
Resuspension Emission Rate Estimates	337
Resuspension Fraction Estimates	338
Particle Surface Loading	340
Dust Components of Concern	341
Human-Generated Particle Emissions	342
Resuspension by Crawling Infants	342
Uniform Mixing Assumption	343
Single-Particle Resuspension Measurement and Modeling	343
Conclusions	345
Cross-References	345
References	345

Abstract

Resuspension is an important source of indoor airborne particulate matter in occupied environments. Resuspension of settled particles from flooring, furnishings, clothing, and other surfaces can occur when the settled particles are disturbed via human activity, air currents, or other external forces. Resuspension models have been developed at multiple scales, from describing individual particle adhesion and detachment to estimating bulk effects from settled dust disturbance. Researchers have investigated the effects of many resuspension factors, including particle size, particle composition and morphology, particle

A. R. Ferro (✉)

Department of Civil and Environmental Engineering, Clarkson University, Potsdam, NY, USA

Institute for a Sustainable Environment, Clarkson University, Potsdam, NY, USA

e-mail: aferro@clarkson.edu

loading on surfaces, surface roughness, relative humidity, flooring type, walking style, and shoe type. Future work should address a better characterization of resuspension from clothing, improved incorporation of relative humidity and electrostatic effects into resuspension models, composition of size-resolved dust loading in various microenvironments, resuspension-related exposure in micro-environments of concern, such as hospitals and schools, and resuspension of specific dust components of concern such as nanoparticles, viruses, and per- and polyfluoroalkyl substances (PFAS) compounds.

Keywords

Adhesion · Detachment · Human activity · Particles · Particulate matter · Indoor dust

Introduction

Resuspension of particles from surfaces into the air is a major source of indoor particulate matter (PM) and its constituents (Kopperud et al. 2004). Human activities, such as walking, sitting on furniture, seated movements such as shuffling or stomping one's feet, vacuuming, sweeping, dusting, and folding clothes, result in measurable increased PM from resuspended particles (Ferro et al. 2004; Qian et al. 2014; Licina et al. 2017). Airflow from natural and mechanical ventilation can also resuspend dust from air ducts and indoor surfaces, although typical room air velocities are too low to initiate dust resuspension (Zhou et al. 2011; Nasr et al. 2019). The resuspension source has been characterized for many human activities, including walking, crawling, seated activities, and sleeping (Thatcher and Layton 1995; Wu et al. 2021; Licina et al. 2017; Boor et al. 2015). PM₁₀ mass emission rates for resuspension for human walking have been found to be on the order 1–10 mg/min, similar to emission rates for other major indoor PM sources including vacuuming, frying, candle burning, smoking, and incense burning (Qian et al. 2014). However, estimates for resuspension emission rates from human walking range over orders of magnitude, and, unlike combustion sources, the resuspended particle mass is dominated by supermicron particles (Qian et al. 2014; Thatcher and Layton 1995).

Indoor dust is a heterogeneous mix of particles generated from indoor sources, particles present in outdoor air that enter the indoor environment, and particles tracked in by humans and pets. Pollutants of concern in house dust include many organic pollutants, such as phthalates, flame retardants, pesticides, polycyclic aromatic hydrocarbons (PAHs) from combustion sources, and per- and polyfluoroalkyl substances (PFAS) compounds, heavy metals, allergens (e.g., mold spores, pollen, pet dander, and dust mite), and other biological particles (Lewis et al. 1999; Hytyäinen et al. 2018; Qian et al. 2012; Dodson et al. 2012; Morales-McDevitt et al. 2021; DeLuca et al. 2021; Raja et al. 2010).

Within the size range of inhalable particles (particle diameter D_p ≤ 10 µm), larger particles are easier to resuspend than smaller particles because the adhesion forces,

which include van der Waals, electrostatic, and capillary forces, are proportional to the particle diameter D_p , while the external forces exerted by air currents, such as those formed under the foot during human walking, are proportional to D_p^2 , and gravitational, vibrational, and centrifugal forces are proportional to D_p^3 (Hinds 1999). Thus, with increasing particle size, the magnitude of the removal forces to adhesion forces ratio increases for an applied external force. On the other hand, the resulting human inhalation exposure depends on the airborne concentration in the breathing zone and the length of time the person remains in the indoor space, which is discussed in ► Chap. 34, “Fundamentals of Exposure Science.” Thus, the lower deposition rates of, for example, 1 μm particles compared to 10 μm particles may result in higher exposures to the 1 μm particles even though they are more difficult to resuspend.

As an indoor source caused by occupant activity, resuspended dust has a relatively high intake fraction. Licina et al. (2017) estimated the particle intake fraction from human walking to be ~1/100, meaning an estimated 1 out of 100 particles resuspended are inhaled. This value is similar to the intake fraction for other indoor sources (Nazaroff 2008). As a comparison, outdoor sources have much lower intake fractions. For example, Taimisto et al. (2011) estimated the intake fraction for particles resuspended from vehicle traffic to be ~1/100,000. While the particle emission rate for moderate seated activities is less than half of that for walking, the intake fraction for resuspended particles from seated movements, estimated at ~1/10 to 1/20, is higher than that for human walking due to the fluid flow surrounding a seated person (Licina et al. 2017). Typically, a person’s body temperature is warmer than the indoor air temperature and buoyancy effects from the air warmed by the body result in a thermal plume that moves air up toward the breathing zone. The airflow pattern in the room is also strongly impacted by ventilation airflow, fans, temperature gradients from walls, windows and other objects, and wake effects from moving bodies in the room (Wu and Gao 2014).

Numerous studies have been undertaken to quantify resuspension and the factors affecting resuspension at the bulk and single-particle scales. Rather than provide an exhaustive review of the literature, the primary objective of this chapter is to describe the current state of knowledge and identify open scientific questions that have implications for indoor air and human exposure.

Definitions

Resuspension is the detachment and entrainment of particles from surfaces into the air. Particle resuspension in indoor, occupied environments has been reported in various ways. For bulk aerosol resuspension studies, resuspension has been reported as the:

- 1) Increase in airborne concentration (e.g., $\mu\text{g}/\text{m}^3$ or $#/ \text{m}^3$) above the background concentration resulting from a resuspension event (Serfozo et al. 2014).
- 2) Resuspension emission rate (e.g., $\mu\text{g}/\text{h}$, mg/min , $#/ \text{min}$) (Ferro et al. 2004; Lai et al. 2017; Benabed et al. 2019).

- 3) First-order resuspension rate coefficient (e.g., 1/h), which is multiplied by the settled dust loading on the surface and resuspension surface area to determine the particle mass or number emission rate (Thatcher and Layton 1995; Gomes et al. 2007; Qian et al. 2008; Qian and Ferro 2008; You and Wan 2015).
- 4) Resuspension fraction(–), which is the fraction of settled dust resuspended from one contact event. The resuspension fraction is multiplied by the frequency of contact events, the settled dust loading on the surface, and the contact area to estimate the resuspension emission rate (Tian et al. 2014; Lai et al. 2017; Benabed et al. 2020).
- 5) Resuspension emission factor (e.g., 1/m), which is the ratio of the airborne particle concentration in the volume and settled dust loading on the surface during a resuspension event (Rosati et al. 2008).
- 6) Dust-to-breathing zone transport efficiency(–), which is the probability of a settled particle being resuspended into the breathing zone (Wu et al. 2021).

For single-particle resuspension studies, resuspension is typically observed in a wind tunnel and defined as the detachment fraction(–), which is the fraction of particles on the surface that become detached for a given air velocity (e.g., Goldasteh et al. 2013).

Bulk Aerosol Resuspension Measurement and Modeling

Measurement and modeling studies have been conducted for experimental chambers, homes, commercial buildings, and mechanical foot apparatuses (Thatcher and Layton 1995; Tian et al. 2014; Wang et al., 2020). Figure 1 presents a typical PM concentration time series pattern due to human occupancy in an office building. The number concentration measurements were made with optical particle spectrometers located in an office area and conference room. Resuspension and infiltration of outdoor particles were the only particle sources at this location, and the influence of outdoor particles was minimal for the size range shown (5–10 μm) due to filtration in the heating, ventilation, and air conditioning (HVAC) system. The particle concentration was close to zero when the building was not occupied, and large peaks associated with human activity were observed during periods of occupancy. The concentration peaks in the conference room are higher than in the office area due to the relatively small volume of dilution air.

Typical Bulk Aerosol Resuspension Experiments

Typical bulk aerosol resuspension experiments include monitoring of airborne PM during background, resuspension, and decay periods in a chamber or room to quantify the resuspension source and the effect of various factors affecting particle resuspension, including:

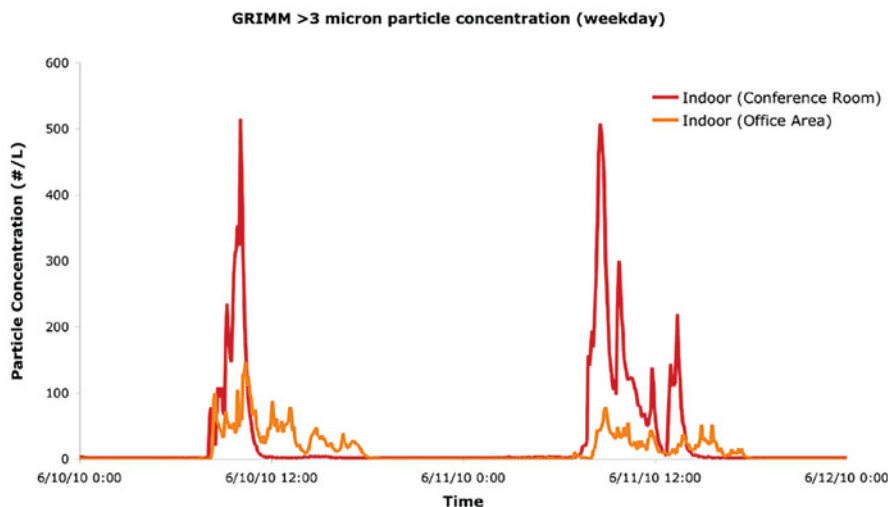


Fig. 1 Particle number concentration for particles greater than 5–10 μm in optical diameter measured with Grimm Technologies (Douglasville, GA, USA) model 1.108 portable laser aerosol spectrometer in an office area and conference room that were occupied during the work day

- Particle type
- Flooring type
- Shoe type
- Surface dust loading
- Relative humidity
- Electrostatic charge
- Individual walking style

During the experimental resuspension periods, particles are resuspended from surfaces via external forces resulting from actual human activity, simulated activity via mechanical apparatuses, air jets, or other mechanisms. Almost all experimental studies to date have employed semicontinuous optical and time-of-flight particle measurement techniques, which measure particles in the range of 0.3–20 μm in diameter, or integrated mass-based samples (e.g., Qian et al. 2008). More recently, particle resuspension for particles smaller than 0.3 μm have been reported (Benabed et al. 2020).

Two-Compartment Material Balance Model

For many bulk aerosol resuspension studies, experimental data are analyzed using a material balance approach. A two-compartment material balance model can be applied to quantify the resuspension rate and/or resuspension fraction (Schneider et al. 1999; Qian and Ferro 2008). The material balance for the air compartment is:

$$V \frac{dC_j}{dt} = E_{resusp,j} + E_{other,j} + C_{out,j}(Q) - C_j(\beta_j V + Q) \quad (1)$$

And the material balance for the surface compartment is:

$$A \frac{dL_j}{dt} = C_j(\beta_j V + Q) - E_{resusp,j} \quad (2)$$

Using units of meters (m), hours (h), and particle number (#), V is the volume of the air compartment (m^3), A is the area of the surface compartment (m^2), Q is the airflow rate into and out of the chamber (m^3/h), $C_{out,j}$ is the particle concentration of the air entering the compartment via the airflow rate for particle size bin j , C_j is the concentration in the compartment for particle size bin j ($\#/ \text{m}^3$), L_j is the surface dust loading for particle size bin j ($\#/ \text{m}^2$), $E_{resusp,j}$ is the size-dependent source emission rate ($\#/ \text{h}$) for resuspension, $E_{other,j}$ is the size-dependent source emission rate ($\#/ \text{h}$) for other indoor particle sources, and β_j is the size-dependent particle loss coefficient (1/h), which is dominated by particle deposition to surfaces following a resuspension source. The resuspension emission term is a source term for the air compartment and a sink, or loss, term for the surface compartment.

When the contribution of particles from outside the compartment and other indoor sources is negligible, the terms $E_{other,j}$ and $C_{out,j}$ can be ignored. Note that Eq. (1) does not include recirculation and filtration of air and Eq. (2) does not include track-in/track-out of particles to and from the surface compartment. Equations (1) and (2) also assume that particles remain in their original size bins throughout the resuspension/deposition process, and that the air and surface compartments are uniformly mixed. Because the fraction of particles removed from the surface is typically small, the surface dust loading is often assumed to be constant. This assumption is reasonable for experiments conducted over a large surface area with relatively short resuspension periods, but not when repetitive resuspension activity is targeted to a small surface area since the particle reservoir can become depleted.

The other parameters in Eqs. (1) and (2) can be either estimated or measured. The airflow rate is determined by the HVAC volumetric flowrate setting, face velocity measurements at the supply and/or return ducts, or via a tracer gas approach. The size-resolved particle loss rate can be determined by solving Eq. (1) during decay periods (periods following a particle source periods when indoor sources have been shut off or removed) with $E_{resusp,j}$ and $E_{other,j}$ set equal to zero. Thus, with known initial concentration/loading in the compartments and the measured time-resolved concentration C_j , the time-resolved resuspension emission rate can be determined by solving the two-compartment material balance. Alternatively, the average resuspension emission rate can be estimated by finding the best fit of the model to the concentration time series using $E_{resusp,j}$ as the fitting parameter.

Resuspension Emission Rate Estimates

Figure 2 provides resuspension emission rates estimates using the material balance approach. The reported resuspension emission rates are a function of particle size, and all studies show a general trend of increasing emission rate with increasing particle diameter, consistent with theoretical models for particle detachment. Most of these studies employed actual humans walking, although Wu et al. (2021) used a mechanical infant that mimicked crawling and Tian et al. (2014) used a mechanical foot that mimicked heel-toe walking. For the studies using human participants, the emission rates for $10 \mu\text{m}$ particles range from approximately 10^{-2} mg/min to 10^2 mg/min . The wide range of size-resolved estimates for resuspension emission rates is due to different experimental conditions. There are also differences in particle size binning from study to study. Note that Ferro et al. (2004) and Qian et al. (2008) reported cumulative mass concentrations of $\text{PM}_{2.5}$ and PM_5 , respectively.

One of the largest factors affecting resuspension rate is difference in surface dust loading. Because the resuspension rate is dependent on the amount of dust on the surface, variation in resuspension estimates can be reduced by separating the floor loading term from the resuspension rate and instead reporting the fraction of settled dust that is resuspended per footstep or unit of repeated activity. To account for the surface dust loading factor, the resuspension rate coefficient R_j is defined as:

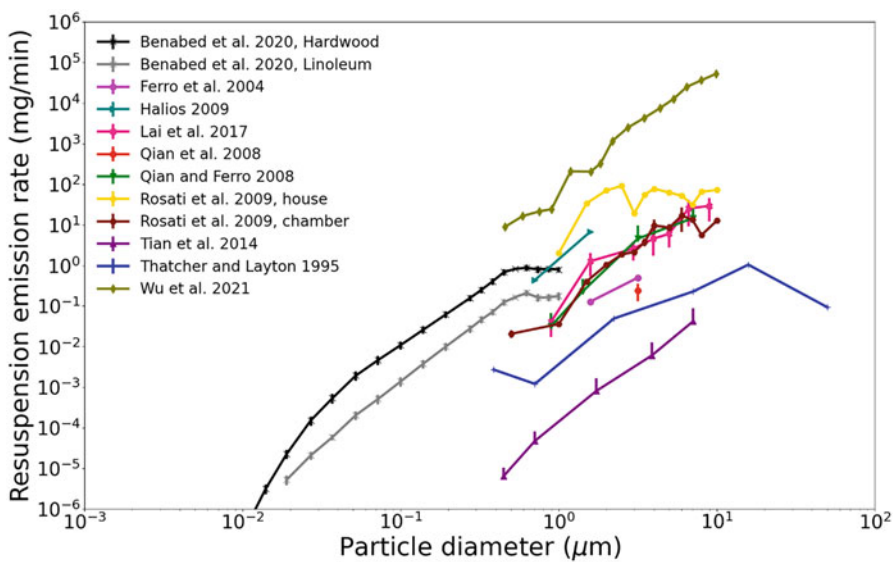


Fig. 2 Resuspension emission rate (mg/min) estimates by optical particle diameter and study. (Adapted and updated from Qian et al. 2014 for this publication by Jing Qian)

$$R_j = \frac{E_j}{AL_j} \quad (3)$$

Such that:

$$E_{resusp,j} = R_j AL_j \quad (4)$$

Using this form of the resuspension emission rate, the emission rate increases linearly with an increase in surface dust loading. This simplified linear relationship ignores the difference in the particle-to-particle adhesion force and the particle-to-surface adhesion force (Tian et al. 2014; Boor et al. 2013). Accordingly, previous studies have found that the resuspension rate increases with surface dust loading, but not linearly (Serfozo et al. 2014).

Because the entire surface area A (e.g., the floor area of a room) is typically not disturbed by human activity during the resuspension event, the surface area is not the same as the resuspension contact area, resulting in differences in resuspension rate coefficient estimates from this assumption alone. For repetitive activities, such as walking, with frequency f (steps/h), the resuspension fraction $r_j(-)$ is defined as the fraction of particles size j that are resuspended from the contact surface area A_s (m^2) per step:

$$r_j = \frac{E_{resusp,j}}{f A_s L_j} \quad (5)$$

Such that:

$$E_{resusp,j} = R_j AL_j = r_j f A_s L_j \quad (6)$$

Thus, resuspension rate coefficient or resuspension fraction can be incorporated into Eqs. (1) and (2) by substituting the corresponding expression for $E_{resusp,j}$.

Resuspension Fraction Estimates

The resuspension fraction accounts for both the surface dust loading and the contact area and therefore is more easily compared across different studies (Fig. 3). While the resuspension fraction estimates still vary widely, the variation is smaller than that for resuspension rates shown in Fig. 2. Additional factors that contribute to the wide range of results include the type of resuspension mechanism (e.g., mechanical device and walking style), material properties, and environmental conditions.

High person-to-person variability and even experiment-to-experiment variability with the same participant is a major challenge for the quantification of factors affecting resuspension, such as flooring type, dust loading, and environmental conditions (Qian et al. 2008). To address this variability, Tian et al. (2014) used a

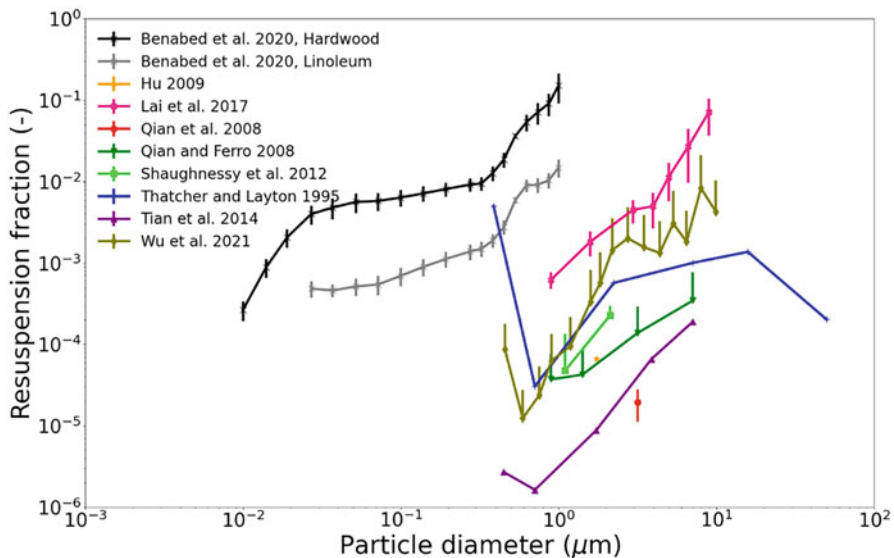


Fig. 3 Estimated size-resolved resuspension fraction by study (adapted and updated from Qian et al. 2014 for this publication by Jing Qian)

resuspension mechanism in a well-characterized and controlled experimental chamber on consistently seeded and conditioned flooring samples to characterize walking-induced particle resuspension as a function of flooring type, relative humidity, surface dust loading, and particle size. Similar to the results shown in Fig. 3, they found that the resuspension fraction r_j generally increases with particle size, with r_j values range from 10^{-6} for the smallest two size fractions to 10^{-4} – 10^{-3} for the largest size fraction. As described above, these values are lower than estimates for actual humans walking. However, the study design allowed for a direct comparison of the flooring effect. There were no statistical differences based on flooring for the smaller size fractions. However, for the coarse particles (3.0 – 5.0 μm and 5.0 – 10.0 μm), higher resuspension fractions were observed for carpets than for hard flooring, and higher resuspension fractions were observed for cut-pile carpets compared with closed-loop carpets of the same material. The low-density, cut-pile carpet resulted in the highest resuspension fractions of all the flooring types. Tian et al. (2014) also observed statistically significant differences for relative humidity and surface dust loading factors on the resuspension fraction, although these effects were smaller than for the flooring type, and multiple interaction effects between the factors were observed. The interaction effects, especially between flooring type, particle loading, and relative humidity, deserve further study.

The findings of higher resuspension from carpeted flooring than from hard flooring are consistent with most chambers and full-scale studies (e.g., Benabed et al. 2020; Qian and Ferro 2008; Ferro et al. 2004). One exception is Shaughnessy and Vu (2012), who reported that resuspension from hard flooring was higher than

for carpet for the particle size fraction of 0.8–1.5 μm and a relatively high surface dust loading of 18 g/m². This dust loading would have resulted in a multilayer of dust for which adhesion forces are primarily particle to particle, rather than a monolayer for which adhesion forces are particle to surface (Boor et al., 2013). Boor et al. (2013) found that the resuspension of particles that are deposited in multilayers can be enhanced compared to those in monolayers.

While almost all bulk aerosol resuspension studies have focused on particles >0.3 μm in diameter, Benabed et al. (2020) reported that particles ranging from 0.01–0.1 μm in diameter could be resuspended by human walking and estimated resuspension fractions for this size range an order of magnitude lower than those for 1 μm particles. Thus, while resuspension is not a major pathway of inhalation exposure for ultrafine particles, these particles could be resuspended singly or as agglomerates with larger particles. The formation of particle aggregates on surfaces would tend to enhance resuspension and result in the resuspension of particles that would not be predicted to detach as single particles. More studies are needed to quantify resuspension for ultrafine particles of concern, such as manufactured nanoparticles and pathogenic viruses.

Particle Surface Loading

As described above, two of the largest factors affecting bulk aerosol resuspension from human walking are flooring type and surface dust loading. Flooring type also influences the chemistry and microbiology of the dust settled on the flooring surface, acting as a reservoir for environmental contaminants and providing surfaces for chemical and biological transformations (Haines et al. 2020).

Surface dust loading estimates collected by Adgate et al. (1995) in more than 200 locations and Bramwell et al. (2015) in 20 locations show geometric mean mass loadings of dust on carpets were approximately 20 times higher than those on hard floorings. Few studies have characterized size-resolved surface loading in different microenvironments for particles in the inhalable range (<10 μm in diameter), and there are scant data for compositional characterization for <10 μm fraction of the house dust. Resuspension estimates to support inhalation exposure studies would greatly benefit from filling this knowledge gap.

Clearly, an effective mitigation strategy would be more regular cleaning of the flooring to reduce the surface dust loading. However, vacuuming carpets does not consistently reduce the particle resuspension due to human activity on the carpet, possibly because vacuuming can dislodge deep seeded particles and bring them closer to the surface or because studies often do not control for resuspension from other surfaces, such as clothing (Qian et al. 2008). Vacuuming has been shown to reduce the overall particle surface loading, although the remove is incomplete and depends on the efficiency of the vacuum cleaner, the velocity of the nozzle over the floor, and the number of passes made over the area (Reponen et al. 2002). Ong et al. (2014) found

that four passes moving the nozzle at 55 cm/s removed ~50% of the fungi, dust mites, and dust allergens from a carpet. Accordingly, Wu et al. (2021) found that airborne concentrations during resuspension events generally decreased after vacuuming the carpets.

Dust Components of Concern

Resuspended dust has a very different composition than ambient particulate matter. As described above, the intake fraction of resuspended dust is orders of magnitude higher than that of outdoor sources. Therefore, applying health-based ambient PM standards to indoor particle concentrations due to resuspension is not logical. However, levels of specific constituents of the resuspended dust can be compared with health-based standards.

Indoor surfaces act as reservoirs for environmental contaminants and provide sites for chemical and biological transformations (Haines et al. 2020). Thus, indoor dust has been found to be a reservoir of emerging and legacy pollutants (Morales-McDevitt et al. 2021; Dodson et al. 2012). As described above, pollutants of concern in house dust include many organic and inorganic pollutants, including PAHs, flame retardants, bisphenols and phthalates, heavy metals, allergens, and other biological particles. Many semi-volatile organic compounds (SVOCs) are also dust components of concern and the inhalation exposure estimates from resuspension are complicated by the partitioning between the dust and gas phases.

Resuspension of biological materials in indoor dust is an area of particular concern. Resuspension for bacterial and fungal species from human occupancy was reported by Qian et al. (2012) and Hospodsky et al. (2015) in both university classroom and children's classrooms, respectively. For these studies, resuspension was the primary source of the bacterial and fungal species in the indoor air (Qian et al. 2012; Hospodsky et al. 2015). Gomes et al. (2007) summarized studies reporting increases of roach, dog, cat, and dust mite allergens in indoor air due to dust disturbance, with the airborne concentration increasing 5–50 times after the floor dust was disturbed. Crawford et al. (2009) reported indoor and outdoor concentrations for fungal spores, pollen, and $(1 \rightarrow 3)$ - β -d-glucan for four single-family homes measured in four locations in the homes (living room, kitchen, bedroom, and basement). They found the highest fungi and pollen concentrations in living room samples where occupants are the most active, supporting the importance of human activity-induced resuspension as a major source of exposure for bioaerosols (Crawford et al. 2009). While there are no reported resuspension studies using live virus, there is some evidence that resuspension of SARS-CoV-2 from indoor surfaces and clothing may be an exposure pathway due to higher virus concentrations found in hospital changing rooms and bathrooms than in patient rooms (Liu et al. 2020). However, the importance of resuspension in viral transmission remains an open question.

Human-Generated Particle Emissions

Human-generated particle emissions include respiratory emissions as well as emissions from the human body, such as desquamation of skin flakes, fabric fragments, other particles that are intrinsic to clothing, and particles that are extrinsic to clothing. Like flooring, furnishings, and other objects, clothing acts as a reservoir for particles (Licina et al. 2017, 2019). Bhangar et al. (2016) compared airborne concentrations in a chamber with an exposed floor and covered floor and estimated that for both walking and seated activities conducted in a chamber, 30–40% of fluorescent biological particle emissions came from the clothing versus the floor. McDonagh and Byrne (2014) compared dust resuspension from different clothing materials and found the weave pattern had a larger effect than fiber type, with the highest concentration during the activity period resulting from loosely woven fleece material. They also found that high physical activity resulted in much higher airborne particle concentrations than low physical activity (McDonagh and Byrne 2014). Particle resuspension from the clothing is an important aspect of resuspension from human activity sources. However, the resuspension mechanism, particle composition, surface/fabric materials, temperature, and relative humidity, and other characteristics are different than those for floorings and require further investigation.

Resuspension by Crawling Infants

Most experimental resuspension studies have focused on human activity for adults; however, exposure from resuspended particles for children and crawling infants is of particular concern given their relatively high activity levels, the proximity of their breathing zone to the floor, and growing bodies. Hyytiäinen et al. (2018) reported that crawling (for a mechanical infant) resulted in a cloud of microbial content surrounding the infant, and they found average airborne levels of fungi and bacteria to be 8 to 21 times higher in the infant breathing zone than in the adult breathing zone. Wu et al. (2021) conducted bulk aerosol resuspension experiments using the same mechanical infant crawling on 12 carpets borrowed from residents in Helsinki, Finland, measuring the size-resolved aerosol and collecting integrated samples for later bioaerosol analysis in the near-floor zone and in the bulk air. The experimental protocol included background, activity, and decay periods, similar to the standard protocol described above, and the material balance model used is similar to that described in Eqs. (1–6), but with the air compartment divided into the two zones: a near-floor zone close to the robotic infant and a bulk air zone. They found resuspended particle concentrations in the near-floor zone ranged from 10^5 – 10^6 m³ during crawling activities, up to tenfold higher than those measured in the bulk air.

Application of the material balance resulted in estimated size-resolved resuspension fractions for crawling ranging from 10^6 – 10^1 . Wu et al. (2021) introduce the dust-to-breathing zone transport efficiency as the probability of a settled particle being resuspended into the breathing zone. Dust-to-breathing values ranged orders of magnitude from 0.1–200 per million, with expected increases with particle

size and strong dependence on carpet type. Resuspension emission rates from crawling ranged from $0.1\text{--}2 \times 10^4 \mu\text{g/h}$, the rate that increases increasing with increasing particle size, which are in the midrange of those reported for human walking.

Uniform Mixing Assumption

Illustrated by the difference in concentration in the near-floor zone and bulk air for the experiments conducted by Wu et al. (2021), the uniform mixing assumption is a source of error for the material balance results. For experimental studies, depending on the airflow in the room and proximity of the particle monitor to the source, this assumption may result in an overestimation or underestimation of the inhalation exposure. For modeling studies, this assumption tends to result in an underestimation of exposure in the breathing zone during a human activity resuspension event. Characteristic mixing times for indoor room air are on the order of minutes to tens of minutes, depending on the volume of the room, ventilation conditions, sunlight, and human activity (Mage and Ott 1996). Therefore, care should be taken when selecting the monitoring locations and averaging time used to represent the exposure (Klepeis 1999).

Single-Particle Resuspension Measurement and Modeling

Measurements and models for single-particle resuspension investigate the balance of adhesion and detachment forces at the particle scale. This is a rich area of research with landmark studies on particle adhesion dating back half a century or more (Hertz 1896; Johnson et al. 1971; Derjaguin et al. 1975). Single-particle resuspension studies investigate and incorporate intrinsic particle and surface properties, including particle size, morphology, surface roughness, surface chemistry, hygroscopicity, Young's modulus of elasticity (tensile or compressive stiffness of a solid material), as well as fluid mechanic structures of the applied airflow (Goldasteh et al. 2013).

For a single particle, particle detachment occurs when the external removal forces on the particle overcome the adhesion forces. For particle sizes of interest to human exposure, lift and gravity forces are typically neglected due to the relatively large van der Waals force between the particle and the substrate. Special cases include electrostatic, capillary, and vibrational forces. The capillary force adds to particle adhesion when the humidity is high enough for the meniscus to form between the particle and surface. The vibration could induce an external detachment force. The electrostatic force can increase the adhesion force if the particles and the surface carry opposite charges via triboelectric charging when the foot separates from the floor or act as an external detachment force when the particle and the surface carry similar charges.

For a spherical particle in the viscous sublayer exposed to turbulent fluid flow, the force required for rolling detachment is less than that for sliding or lifting detachment

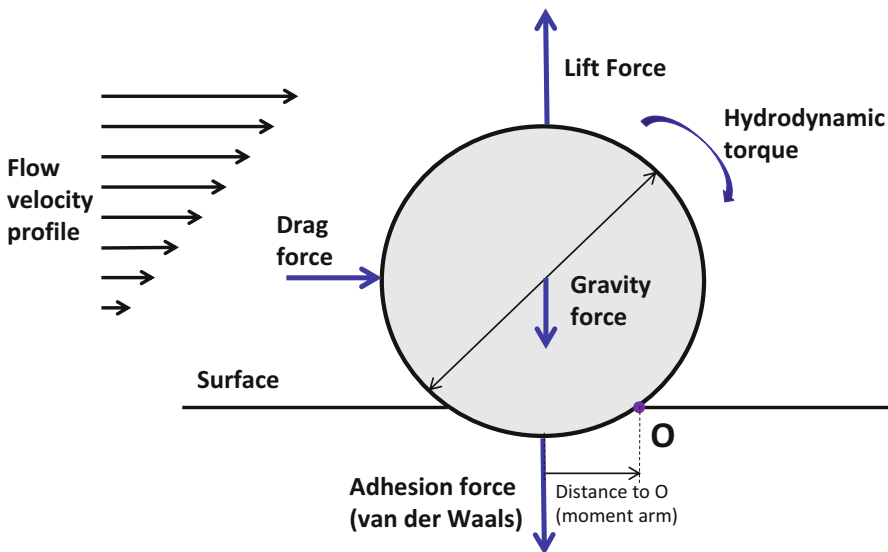


Fig. 4 Schematic force diagram showing rolling detachment of a particle from a substrate for an applied external airflow

(Soltani and Ahmadi 1994). Thus, detachment occurs when the external force moment around the point of contact O overcomes the resisting moment. As shown in Fig. 4, the external force moment for a particle in fluid flow includes the moment of the drag force and the hydrodynamic torque.

Because the particle is attached to the surface of the substrate, the flow surrounding the particle is characterized by the shear velocity. The shear velocity u^* (m/s) is defined as the square root of the wall shear stress τ_w divided by the fluid density ρ

$$u^* = \sqrt{\frac{\tau_w}{\rho}} \quad (7)$$

and can be estimated from the free-stream velocity based on the wind tunnel geometry. Multiple models exist to determine the adhesion force of a particle on a substrate and the pull-off force required to remove a spherical particle from a smooth substrate in the turbulent flow regime (Rumpf 1990; Johnson et al. 1971; Derjaguin et al. 1975; Tabor 1977; Rabinovich et al. 2000; Soltani et al. 1995).

Comparison of experiments with theory for spherical particles on smooth surfaces show that the particles detach at a critical shear velocity u_c^* (m/s) much lower than what is predicted by the theory, even for smooth materials such as glass beads on glass substrates (Nasr et al. 2019). This is because the materials have small-scale surface roughness that reduces the actual contact area with the substrate. The surface roughness can be modeled via surface asperities, each of which is in contact with the particle (Soltani and Ahmadi 1994). By incorporating the surface roughness effects via a roughness parameter and representing the nonsphericity of the particle with three bumps in contact with the rough surface, the models can reasonably predict

particle resuspension from most real substrates (Goldasteh et al. 2013; Nasr et al. 2019).

Single-particle detachment models are typically validated with wind tunnel experiments measuring particle detachment in turbulent flow regimes. However, due to the high velocity required to remove smaller particles from the surface, most experimental studies have investigated the resuspension of particles larger than 10 μm in diameter (Nasr et al. 2019). Thus, experimental validation of models for resuspension of particles less than 10 μm in diameter is limited and represents an important research need as many dust components of concern, such as microbial particles, are smaller than 10 μm .

Conclusions

Particle resuspension is a major source of indoor particulate matter. While the mechanisms for particle adhesion, detachment, and re-entrainment are well understood, there remain many open research questions. Most current estimates for resuspension are from human ambulation, either with human participants or with mechanical stepping or crawling devices. Even so, estimates for size-resolved resuspension emission rates and resuspension fractions per step range widely. Resuspension factors include walking style, flooring type, surface dust loading, relative humidity, and electrostatic charge. Of these factors, the electrostatic charge effect for resuspension from human walking is the least characterized. Resuspension of particles smaller than 0.3 μm is also an important area of research, especially for specific dust components of concern, such as manufactured nanoparticles and viruses. Finally, a better understanding of the size fractions associated with different pollutants would greatly improve human exposure models, as settled dust composition is often used as a proxy for chronic exposure to dust-related pollutants, and resuspension is a strong function of particle size and surface roughness.

Cross-References

- ▶ [Deposition](#)
- ▶ [Fundamentals of Exposure Science](#)
- ▶ [Introduction to Aerosol Dynamics](#)
- ▶ [Role of Clothing in Exposure to Indoor Pollutants](#)

References

- Adgate JL, Weisel C, Wang Y, Rhoads GG, Lioy PJ (1995) Lead in house dust: relationships between exposure metrics. Environ Res 70:134–147. <https://doi.org/10.1006/enrs.1995.1058>, ISSN 0013-9351
- Benabed A, Limam K, Janssens B, Bosschaerts W (2019) Human foot tapping-induced particle resuspension in indoor environments: flooring hardness effect. Indoor Built Environ 29: 230–239

- Benabed A, Boulbair A, Limam K (2020) Experimental study of the human walking-induced fine and ultrafine particle resuspension in a test chamber. *Build Environ* 171:106655. <https://doi.org/10.1016/j.buildenv.2020.106655>, ISSN 0360-1323
- Bhangar RI, Adams W, Pasut JA, Huffman EA, Arens JW, Taylor TD, Bruns WWN (2016) Chamber bioaerosol study: human emissions of size-resolved fluorescent biological aerosol particles. *Indoor Air* 26(2):193–206
- Boor BE, Spilak MP, Corsi RL, Novoselac A (2015) Characterizing particle resuspension from mattresses: chamber study. *Indoor Air* 25:441–456
- Boor BE, Siegel JA, Atila N (2013) Monolayer and multilayer particle deposits on hard surfaces: literature review and implications for particle resuspension in the indoor environment. *Aerosol Sci Technol* 47(8):831–847. <https://doi.org/10.1080/02786826.2013.794928>
- Bramwell L, Qian J, Howard-Reed C, Mondal S, Ferro AR (2015) An evaluation of the impact of flooring types on exposures to fine and coarse particles within the residential micro-environment using CONTAM. *J Exposure Sci Environ Epidemiol* 26:86–94. <https://doi.org/10.1038/jes.2015.31>
- Crawford C, Reponen T, Lee T, Iossifova Y, Levin L, Adhikari A, Grinshpun SA (2009) Temporal and spatial variation of indoor and outdoor airborne fungal spores, pollen, and (1→3)- β -D-glucan. *Aerobiologia* 25:147–158
- DeLuca NM, Angrish M, Wilkins A, Thayer K, Cohen Hubal EA (2021) Human exposure pathways to poly- and perfluoroalkyl substances (PFAS) from indoor media: a systematic review protocol. *Environ Int* 146:106308
- Derjaguin BV, Muller VM, Toporov YP (1975) Effect of contact deformations on the adhesion of particles. *J Colloid Interface Sci* 53:314–326
- Dodson RE, Perovich LJ, Covaci A, Van den Eede N, Ionas AC, Durtu AC, Brody JG, Rudel RA (2012) After the PBDE phase-out: a broad suite of flame retardants in repeat house dust samples from California. *Environ Sci Technol* 46:13056–13066
- Ferro AR, Kopperud RJ, Hildemann LM (2004) Source strengths for indoor human activities that resuspend particulate matter. *Environ Sci Technol* 38:1759–1764
- Goldasteh I, Ahmadi G, Ferro AR (2013) Wind tunnel study and numerical simulation of dust particle resuspension from indoor surfaces in turbulent flows. *J Adhes Sci Technol* 27(14): 1563–1579. <https://doi.org/10.1080/01694243.2012.747729>
- Gomes C, Freihaut J, Bahmfleth W (2007) Resuspension of allergen-containing particles under mechanical and aerodynamic disturbances from human walking. *Atmos Environ* 41(2007): 5257–5270. <https://doi.org/10.1016/j.atmosenv.2006.07.061>
- Haines SR, Adams RI, Boor BE, Bruton T, Downey J, Ferro AR, Gall E, Green BJ, Hegarty B, Horner E, Jacobs D, Lemieux P, Misztal PK, Morrison G, Perzanowski M, Reponen T, Rush R, Virgo T, Alkhayri C, Bope A, Cochran S, Cox J, Donohue A, May AA, Nastasi N, Nishioka M, Renninger N, Tian Y, Uebel-Niemeier C, Wilkinson D, Wu T, Zambrana J, Dannemiller KC (2020) Ten questions concerning the implications of carpet on indoor chemistry and microbiology. *Build Environ* 170:106589. <https://doi.org/10.1016/j.buildenv.2019.106589>
- Hertz H (1896) On the contact of rigid elastic solids. In: *Miscellaneous papers*. Jones and Schott, London
- Hinds WC (1999) *Aerosol technology: properties, behavior, and measurement of airborne particles*, 2nd Edition. Wiley
- Hospodsky D, Yamamoto N, Nazaroff WW, Miller D, Gorthala S, Peccia J (2015) Characterizing airborne fungal and bacterial concentrations and emission rates in six occupied children's classrooms. *Indoor Air* 25:641–652
- Hyytiäinen HK, Jayaprakash B, Kirjavainen PV, Saari SE, Holopainen R, Keskinen J, Hämeri K, Hyvärinen A, Boor BB, Täubel M (2018) Crawling-induced floor dust resuspension affects the microbiota of the infant breathing zone. *Microbiome* 6:25. <https://doi.org/10.1186/s40168-018-0405-8>
- Iman Goldasteh, Goodarz Ahmadi & Andrea R. Ferro (2013) Wind tunnel study and numerical simulation of dust particle resuspension from indoor surfaces in turbulent flows, *Journal of*

- Adhesion Science and Technology, 27:14, 1563–1579. <https://doi.org/10.1080/01694243.2012.747729>
- Johnson KL, Kendall K, Roberts AD (1971) Surface energy and the contact of elastic solids. *Proc R Soc A Math Phys Eng Sci.* 324:301–313
- Klepeis NE (1999) Validity of the uniform mixing assumption: determining human exposure to environmental tobacco smoke. *Environ Health Perspect* 107:357–363
- Kopperud RJ, Ferro AR, Hildemann LM (2004) Outdoor versus indoor contributions to indoor particulate matter (PM) determined by mass balance methods. *J Air Waste Manage Assoc* 54: 1188–1196
- Lai ACK, Tian Y, Tsoi JYL, Ferro AR (2017) Experimental study of the effect of shoes on particle resuspension from indoor flooring materials. *Build Environ* 118:251–258. <https://doi.org/10.1016/j.buildenv.2017.02.024>
- Lewis RG, Fortune CR, Willis RD, Camann DE, Antley JT (1999) Distribution of pesticides and polycyclic aromatic hydrocarbons in house dust as a function of particle size. *Environ Health Perspect* 107:721–726
- Licina D, Tian Y, Nazaroff WW (2017) Emission rates and the personal cloud effect associated with particle release from the perihuman environment. *Indoor Air* 27. <https://doi.org/10.1111/ina.12365>
- Licina D, Morrison GC, Bekö G, Weschler CJ, Nazaroff WW (2019) Clothing-mediated exposures to chemicals and particles. *Environ Sci Technol* 53:5559–5575. <https://doi.org/10.1021/acs.est.9b00272>
- Liu Y, Ning Z, Chen Y, Guo M, Liu Y, Gali NK, Sun L, Duan Y, Cai J, Westerdahl D, Liu X, Xu K, Ho K-f, Kan H, Fu Q, Lan K (2020) Aerodynamic analysis of SARS-CoV-2 in two Wuhan hospitals. *Nature* 582:557–560
- Mage DT, Ott WR (1996) Accounting for nonuniform mixing and human exposure in indoor environments. In: Tichenor BA (ed) Characterizing sources of indoor air pollution and related sink effects, ASTM STP 1287. American Society for Testing and Materials, pp 263–278. <https://www.astm.org/stp1287-eb.html>
- McDonagh A, Byrne MA (2014) The influence of human physical activity and contaminated clothing type on particle resuspension. *J Environ Radioact* 127:119e126
- Morales-McDevitt ME, Becanova J, Blum A, Bruton TA, Vojta S, Woodward M, Lohmann R (2021) The air that we breathe: neutral and volatile PFAS in indoor air. *Environ Sci Technol Lett.* <https://doi.org/10.1021/acs.estlett.1c00481>
- Nasr B, Ahmadi G, Ferro AR, Dhaniyala S (2019) Overview of mechanistic particle resuspension models: comparison with compilation of experimental data. *Adhes Sci Technol* 33:2631–2660. <https://doi.org/10.1080/01694243.2019.1650989>
- Nazaroff WW (2008) Inhalation intake fraction of pollutants from episodic indoor emissions. *Build Environ* 43:269–277
- Ong K-H, Lewis RD, Dixit A, MacDonald M, Yang M, Qian Z (2014) Inactivation of dust mites, dust mite allergen, and mold from carpet. *J Occup Environ Hyg* 11:519–527
- Qian J, Ferro AR (2008) Resuspension of dust particles in a chamber and associated environmental factors. *Aerosol Sci Technol* 42:566–578
- Qian J, Ferro AR, Fowler KR (2008) Estimating the resuspension rate and residence time of indoor particles. *J Air Waste Manage Assoc* 58:502–516
- Qian J, Hospodsky D, Yamamoto N, Nazaroff WW, Peccia J (2012) Size-resolved emission rates of airborne bacteria and fungi in an occupied classroom. *Indoor Air* 22:339–351
- Qian J, Peccia J, Ferro AR (2014) Walking-induced particle resuspension in indoor environments. *Atmos Environ* 89:464–481
- Rabinovich YI, Adler JJ, Ata A, Singh RK, Moudgil BM (2000) Adhesion between nanoscale rough surfaces. *J Colloid Interface Sci* 232:10–16
- Raja S, Xu Y, Ferro AR, Jaques PA, Hopke PK (2010) Resuspension of indoor aeroallergens and relationship to lung inflammation in asthmatic children. *Environ Int* 36:8–14

- Reponen T, Trakumas S, Willeke K, Grinshpun SA, Choe KT, Friedman W (2002) Dynamic monitoring of the dust pickup efficiency of vacuum cleaners. *AIHA J* 63:689–697
- Rosati JA, Thornburg J, Rodes C (2008) Resuspension of particulate matter from carpet due to human activity. *Aerosol Sci Technol* 42:472–482. <https://doi.org/10.1080/02786820802187069>
- Rumpf H (1990) Particle technology. Chapman & Hall, New York
- Schneider T, Kildesø J, Breum N (1999) A two compartment model for determining the contribution of sources, surface deposition and resuspension to air and surface dust concentration levels in occupied rooms. *Build Environ* 34:583–595
- Serfozo N, Chatoutsidou SE, Lazaridis M (2014) The effect of particle resuspension during walking activity to PM10 mass and number concentrations in an indoor microenvironment. *Build Environ* 82:180–189. <https://doi.org/10.1016/j.buildenv.2014.08.017>
- Shaughnessy R, Vu H (2012) Particle loadings and resuspension related to floor coverings in chamber and in occupied school environments. *Atmos Environ* 55:515–524
- Soltani M, Ahmadi G (1994) On particle adhesion and removal mechanisms in turbulent flows. *J Adhes Sci Technol* 8:763–785. <https://doi.org/10.1163/156856194X00799>
- Soltani M, Ahmadi G, Bayer RG, Gaynes MA (1995) Particle detachment mechanisms from rough surfaces under substrate acceleration. *J Adhes Sci Technol* 9:453–473
- Tabor D (1977) Surface forces and surface interactions. *J Colloid Interface Sci* 58:2–13
- Taimisto P, Tainio M, Karvosenoja N, et al (2011) Evaluation of intake fractions for different subpopulations due to primary fine particulate matter (PM2.5) emitted from domestic wood combustion and traffic in Finland. *Air Qual Atmos Health* 4:199–209. <https://doi.org/10.1007/s11869-011-0138-3>
- Thatcher TL, Layton DW (1995) Deposition, resuspension, and penetration of particles within a residence. *Atmos Environ* 29:1487–1497
- Tian Y, Sul K, Qian J, Mondal S, Ferro AR (2014) A comparative study of walking-induced dust resuspension using a consistent test mechanism. *Indoor Air* 24:592–603
- Wang K, Suyuan Y, Yingge W, Wei P (2020) Measurements and analysis of adhesive forces for micron particles on common indoor surfaces. *Indoor and Built Environment* 29(7):931–941. <https://doi.org/10.1177/1420326X19863830>
- Wu Y, Gao N (2014) The dynamics of the body motion induced wake flow and its effects on the contaminant dispersion. *Build Environ* 82:63–74
- Wu T, Fu M, Valkonen M, Täubel M, Xu Y, Boor BE (2021) Particle resuspension dynamics in the infant near-floor microenvironment. *Environ Sci Technol* 55:1864–1875
- You S, Wan MP (2015) Experimental investigation and modelling of human-walking-induced particle resuspension. *Indoor Built Environ* 24:564–576. <https://doi.org/10.1177/1420326X14526424>
- Zhou B, Zhao B, Tan Z (2011) How particle resuspension from inner surfaces of ventilation ducts affects indoor air quality – a modeling analysis. *Aerosol Sci Technol* 45:996–1009. <https://doi.org/10.1080/02786826.2011.576281>



Interaction Between Gas-Phase Pollutants and Particles

13

Jianping Cao

Contents

Introduction	350
Interaction Between Gas-Phase Pollutants and Airborne Particles	351
Overview	351
Equilibrium Models	352
Dynamic Models	358
Methods for Measuring/Estimating Key Parameters	367
Interaction Between Gas-Phase Pollutants and Settled Dust	372
Overall	372
Equilibrium Model	374
Dynamic Models	374
Conclusions	379
Cross-References	381
References	382

Abstract

Gas-phase chemicals can interact with and subsequently be retained by indoor particles, including both airborne particles and settled dust (particles deposited on indoor surfaces). Therefore, understanding the distribution and interactions between gas-phase chemicals and indoor particles is fundamental to exposure analysis and is especially important for semi-volatile organic compounds (SVOCs) with strong sorptivity. This chapter provides a summary of the available models for describing gas-particle interactions and the existing methods for estimating/measuring the key parameters involved in these models (especially the particle-gas partition coefficients). Due to the differences between mass transfer processes related to airborne particles and settled dust, this chapter is mainly divided into two parts, one for airborne particles and the other for settled dust.

J. Cao (✉)

School of Environmental Science and Engineering, Sun Yat-sen University, Guangzhou, China
e-mail: caojp3@mail.sysu.edu.cn

Keywords

Indoor air quality (IAQ) · Semi-volatile organic compounds (SVOCs) · Dynamic model · Partitioning · Airborne particles · Settled dust

Introduction

Gas-phase chemicals can interact with or partition to various indoor surfaces, e.g., walls, ceiling, window glass, clothing, human skin, and particles (including airborne particles and settled dusts), depending on their physicochemical properties (Salthammer et al. 2018). Therefore, indoor chemicals may enter human body via various pathways, e.g., inhalation of air and airborne particles, nondietary ingestion of dust, and dermal absorption from air, deposited particles, and contacted surfaces, as discussed in another chapter of this handbook ► [Chap. 35, “Exposure Routes and Types of Exposure”](#). Understanding the distribution of indoor chemicals is therefore fundamental to effective exposure analysis (Salthammer et al. 2018). Because airborne particles and settled dust can be either inhaled or ingested by people (especially children who frequently put their hands in mouths), it is important to investigate the interactions between gas-phase chemicals and indoor particles (Bi 2018).

Organic compounds in indoor environments are often categorized according to their volatility as very-volatile organic compounds (VVOCs, e.g., formaldehyde), volatile organic compounds (VOCs, e.g., benzene and toluene), and semi-volatile organic compounds (SVOCs, e.g., phthalate esters and organophosphate flame retardants) (Salthammer et al. 2018). The volatility (or vapor pressure) is one of the critical properties that determines the sorptivity of gas-phase chemicals on indoor surfaces, i.e., lower volatility corresponds to greater sorptivity (Weschler and Nazaroff 2008). For VVOCs and VOCs, most of their mass in the indoor environments tends to remain in the gas phase. Taking the interaction between gas phase and airborne particles as an example, Liu et al. (2013) found that the distribution into the particle phase can be neglected for VVOCs and VOCs due to their low sorptivity. While for SVOCs with higher sorptivity, distribution into the particle phase is dominant (Liu et al. 2013). For an SVOC with octanol-air partition coefficient (K_{OA}) > 13 , over 99% of its mass in the indoor air may be bound to airborne particles (with <1% presented in the gas phase) (Weschler and Nazaroff 2008). Note, K_{OA} is the ratio of a chemical’s concentration in octanol to its concentration in air at equilibrium, which is useful for predicting the partitioning behavior between air and environmental matrices such as particles, soil, and vegetation. Generally, lower volatility typically corresponds to greater K_{OA} ; K_{OA} of VVOCs and VOCs is often less than 10^8 , while K_{OA} of SVOCs with vapor pressures between 10^{-14} and 10^{-4} atm at indoor environmental temperatures is often greater than 10^8 (Weschler and Nazaroff 2008). Therefore, studies of the interaction between gaseous constituents and indoor particles have mainly focused on SVOCs.

This chapter provides a summary of studies about the interaction between gas-phase SVOCs and airborne particles or settled dust in indoor environments, especially summarizing the available models for describing gas-particle interactions and the existing methods for estimating/measuring key parameters that govern these interactions. Due to the differences between mass transfer processes related to airborne particles and settled dust, this chapter mainly comprises of two parts, one for airborne particles and the other for settled dust. The following SVOC-specific contents may also be practicable, in principle, for VVOCs and VOCs (and some inorganic chemicals) if the interactions between gas-phase VVOCs/VOCs and indoor particles are not negligible.

Interaction Between Gas-Phase Pollutants and Airborne Particles

Overview

Indoor airborne particles may strongly affect transport of, and human exposure to, indoor SVOCs, because SVOCs with low volatility partition strongly to airborne particles (Weschler et al. 2008). Apart from the aspects for human exposure mentioned above, several studies suggested that airborne particles may facilitate the transport of SVOCs from their source to the surrounding environments (Benning et al. 2013; Liu et al. 2012). For example, Lazarov et al. (2016) found that the presence of airborne particles might increase the emission rate of tris (1-chloroisopropyl) phosphate (TCPP, widely used as organophosphate flame retardant, a typical SVOC in indoor environments) by a factor of three, and subsequently increase human exposure to TCPP.

There have been many studies that have measured indoor airborne SVOC concentrations (Bu et al. 2016; Wang et al. 2014; Wei et al. 2017; Wensing et al. 2005; Weschler and Nazaroff 2010), most of which measured either the gas-phase concentration (C_g , $\mu\text{g}/\text{m}^3$) or the particle-phase concentration (C_{sp} , $\mu\text{g}/\text{m}^3$) (Bu et al. 2016; Wei et al. 2017; Weschler and Nazaroff 2010). In addition, some studies measured only the total airborne SVOC concentration (designated as C_{tot} , $C_{tot} = C_g + C_{sp}$) (Wensing et al. 2005). However, when assessing human exposure to indoor SVOCs, both C_g and C_{sp} are indispensable inputs (Eichler et al. 2021). For example, dermal exposure to gas-phase and particle-phase SVOCs have quite different transport processes, and hence assessment of exposure through these two pathways should be done separately (Shi and Zhao 2014). In existing studies on evaluating pollution levels or health risks of indoor SVOCs, C_g or C_{sp} was always predicted using a relationship between C_g and C_{sp} if the other was measured (Wei et al. 2016, 2017; Weschler et al. 2008). Therefore, understanding the relationship between gas- and particle-phase SVOCs is vital for accurately describing transport and fate, assessing human exposure, and determining effective control strategies for indoor SVOCs (Guo 2013; Salthammer et al. 2018; Xu and Little 2006).

Equilibrium Models

With the assumption of equilibrium interaction between gas phase and particles, the distribution of a gaseous substance and particle is defined both by the physical characteristics of this substance and by the laws of the adsorption and/or absorption processes (Salthammer and Goss 2019).

Gas-particle partitioning of organics in the air was first described quantitatively by Junge (1977), who developed an adsorption-based model for the transport of persistent compounds in the atmosphere. Based on the Brunauer-Emmett-Teller (BET) isotherm, Junge (1977) linked the fraction (Φ , dimensionless) of the substance adsorbed on solid airborne particles with its vapor pressure (P_s , Pa) and particle surface area concentration (C_{Ap} , m^2/m^3 , i.e., particle surface area per volume of air):

$$\Phi = \frac{\text{const} \cdot C_{Ap}}{P_s + \text{const} \cdot C_{Ap}} \quad (1)$$

where the constant (*const*, $\text{Pa}\cdot\text{m}$) depends on the molecular weight and heat of condensation of the sorbate.

Pankow (1987) showed that the BET isotherm assumed by Junge (1977) corresponds with the linear range of the Langmuir isotherm if the partial pressure (P , Pa) of the substance is significantly below the saturation vapor pressure ($P \ll P_s$). The expression for the Langmuir isotherm is:

$$\theta_L = \frac{b_L P}{1 + b_L P} \quad (2)$$

where θ_L (dimensionless) is the fraction of the sorption sites occupied by the sorbates, and b_L (Pa^{-1}) is the constant in the Langmuir isotherm. If the partial pressure of the sorbate is sufficiently low (i.e., $1 \gg b_L P$), Eq. (2) can be simplified as:

$$\theta_L = b_L P \quad (3)$$

Pankow (1987) further pointed out that the particulate-associated concentration of the adsorbing compound (C_{sp} , $\mu\text{g}/\text{m}^3$) for a Langmuirian sorption is:

$$C_{sp} = 10^6 M W_s \theta_L C_{Ap} N_s \quad (4)$$

where $M W_s$ (g/mol) is the molecular weight of the sorbate and N_s (mol/ m^2) is the moles of sorption sites per m^2 on particle surface. The factor of 10^6 converts 1 g to $10^6 \mu\text{g}$.

Using the ideal gas law, the gas-phase concentration (C_g , $\mu\text{g}/\text{m}^3$) and partial pressure (P , Pa) of the sorbate can be linked,

$$C_g = \frac{10^6 M W_s P}{R T} \quad (5)$$

where T (K) is the temperature and R (J/mol/K) is the ideal gas constant.

Combining Eqs. (3), (4), and (5), Pankow (1987) gave the following equation:

$$C_{sp} = b_L N_s R T C_{Ap} C_g = K_{pA} C_{Ap} C_g \quad (6)$$

where K_{pA} (m) is defined as the surface-area-normalized gas-particle partition coefficient, and $K_{pA} = b_L N_s R T$.

The fraction (Φ) of the substance adsorbed on particles is then

$$\Phi = \frac{C_{sp}}{C_g + C_{sp}} = \frac{K_{pA} \cdot C_{Ap}}{1 + K_{pA} \cdot C_{Ap}} \quad (7)$$

By assuming that the surface area concentration available for adsorption is proportional to the mass concentration of total suspended particles (TSP, $\mu\text{g}/\text{m}^3$), i.e., $C_{Ap} = A_{tsp} \cdot \text{TSP}$ (A_{tsp} [$\text{m}^2/\mu\text{g}$] is the specific surface area for total suspended particles), Yamasaki et al. (1982) first suggested the following approach for describing the equilibrium interaction between gas phase and particles:

$$C_{sp} = \text{TSP} \cdot K_p \cdot C_g \quad (8)$$

$$\Phi = \frac{\text{TSP} \cdot K_p}{1 + \text{TSP} \cdot K_p} \quad (9)$$

where K_p ($\text{m}^3/\mu\text{g}$) is defined as the particle-mass-normalized gas-particle partition coefficient. In this way, the particle-phase concentration (C_{sp}) is linearly related to the gas-phase concentration (C_g) and the mass concentration of total suspended particles (TSP, which is much easier to be obtained as compared to C_{Ap}). Comparing Eqs. (8) and (6), we can get $K_p = K_{pA} \cdot C_{pA} / \text{TSP} = K_{pA} \cdot A_{tsp}$ ($A_{tsp} = C_{pA} / \text{TSP}$).

Except for adsorptive partitioning, the gaseous substances can also absorb into liquid particles such as environmental tobacco smoke or liquid (organic and/or water) films on particles with solid cores. Gas-particle partitioning of organic pollutants in urban areas is better explained as absorption than adsorption (Pankow 1987). Junge (1977) also noted that the presences of “organic ether soluble matter may cause true absorption of some of the rather lipophilic compounds.” Since the 1990s, it has been postulated that SVOCs partition through an absorption process rather than by physical adsorption onto the surface of particles. SVOCs would “dissolve” in the amorphous organic matter (OM) in the atmosphere, which exists both as primary and as secondary organic aerosols (Lohmann and Lammel 2004). The absorptive partitioning of SVOCs into the OM in the particles is like a gas dissolving in a liquid, and the equations describing the absorptive partitioning between gas phase and particles takes the same form as Eqs. (8) and (9) (Pankow 1994).

Overall, Eqs. (8) and (9) have been commonly used for describing the equilibrium interaction between gaseous substance and airborne particles, regardless of the adsorptive partitioning or absorptive partitioning. The validity of Eqs. (8) and (9) has also been confirmed by experimental observations and theoretical considerations (Cousins and Mackay 2001). The particle-gas partition coefficient (K_p) is the only key parameter in the equilibrium model, which characterizes the sorption capacity of particles for the gas-phase substances. Various approaches have been proposed for predicting K_p of SVOCs.

Note, the equivalence between Eqs. (6) and (8) (or K_{pA} and K_p) for adsorptive interaction should be used with caution because the assumption made by Yamasaki et al. (1982) (the surface area concentration available for adsorption is proportional to the mass concentration of total suspended particles) may be invalid in some cases. For example, Wu et al. (2018) found that the K_p of di(2-ethylhexyl) phthalate (DEHP) adsorbed by $(\text{NH}_4)_2\text{SO}_4$ particles varied with particle size ($0.011 \text{ m}^3/\mu\text{g}$ for particles with media diameter of 70–80 nm versus $0.032 \text{ m}^3/\mu\text{g}$ for particles with median diameter of 40–50 nm). These two K_p were then converted into K_{pA} by Wu et al. (2018), and consistent results were obtained ($K_{pA} = 300 \text{ m}$ for 70–80 nm particles versus $K_{pA} = 360 \text{ m}$ for 40–50 nm particles). The reason is that the specific surface area of particles (A_{tsp}) varies with particle size distribution (particle surface area is proportional to the square of particle diameter, while particle mass is proportional to the cube of particle diameter). If the assumption of Yamasaki et al. (1982) fails for adsorptive interaction, the adsorption-specific model (Eq. (6)) and the surface-area-normalized gas-particle partition coefficient (K_{pA}) should be used instead of Eq. (8) and K_p . The following approaches for predicting K_p are all on the basis that the assumption of Yamasaki et al. (1982) is tenable. If not, the predicted K_p of adsorptive interaction should be converted to K_{pA} by $K_p = K_{pA} \cdot C_{pA}/\text{TSP} = K_{pA} \cdot A_{tsp}$.

Adsorption-Based Approach for Predicting K_p

In the case of adsorption, Pankow (1987) showed that K_p is inversely proportional to the saturation vapor pressure of the sorbates (P_s) at a specific temperature

$$K_p = \frac{N_s R T A_{tsp} e^{(Q_L - Q_V)/RT}}{P_s} \quad (10)$$

where Q_L and Q_V (kJ/mol) are the enthalpy of desorption from the surface and the enthalpy of vaporization of the adsorbed substance, respectively.

In other words, $\log K_p$ and $\log P_s$ are linearly related at a specific temperature (Cousins and Mackay 2001),

$$\log K_p = m \cdot \log P_s + b \quad (11)$$

where m and b are constants that are dependent on the properties of the corresponding chemicals and airborne particles. Regression of the measured $\log K_p$ against $\log P_s$ at similar temperature could yield the values of m and b for a class

of compounds. For chemicals that are solid in the observed temperature range, the vapor pressure of the subcooled liquid (P_L^0) is used instead of P_s . Theoretically, the value of m should be close to -1.0 but is typically in the range of -0.7 to -1.0 (Cousins and Mackay 2001). Possible reasons for this deviation are sampling artifacts, nonequilibrium partitioning, and the lack of constancy in Q_L and activities within a class of compounds (Cousins and Mackay 2001).

Absorption-Based Approach for Predicting K_p

Pankow (1987, 1998) demonstrated that K_p and the use of P_s as its descriptor was valid both for adsorption and absorption of SVOCs. In the case of absorptive partitioning, Pankow (1998) derived

$$K_p = \frac{f_{om}RT}{10^6 MW_{om}\zeta_{om}P_s} \quad (12)$$

where f_{om} is the fraction of OM in the particles, MW_{om} (g/mol) is the mean molecular weight of OM, and ζ_{om} is the activity coefficient of SVOCs in the OM on a mole fraction basis. ζ_{om} is a function of the properties of SVOCs and the composition of the particle, and characterizes the nonideality of the interaction between gaseous SVOCs and the OM of the particle. The factor of 10^6 accomplishes the unit conversion ($1 \text{ g} = 10^6 \mu\text{g}$).

Finizio et al. (1997) showed that P_s can be replaced with the octanol-air partition coefficient (K_{OA}) of SVOCs. Pankow (1994) and Harner and Bidleman (1998) replaced P_s in Eq. (12) by K_{OA} and obtained

$$K_p = f_{om} \frac{MW_{oct}\zeta_{oct}}{MW_{om}\zeta_{om}10^{12}\rho_{oct}} K_{OA} \quad (13)$$

where MW_{oct} (g/mol) is the molecular weight of octanal, ρ_{om} (g/cm³) is the density of octanol, and ζ_{oct} is the activity coefficient of SVOCs in octanol (*oct*). The factor of 10^{12} accomplishes the unit conversion ($1 \text{ g/cm}^3 = 10^{12} \mu\text{g/m}^3$). According to Eqs. (12) and (13), it can be seen that both K_p and K_{OA} are inversely proportional to P_s . The use of K_{OA} has the advantage that, unlike P_s , K_{OA} can be measured experimentally at ambient temperatures for solid solutes (Cousins and Mackay 2001).

Equation (13) was simplified by Harner and Bidleman (1998) with the assumption that both activity coefficients of SVOCs in octanol and OM and molecular weights of octanal and OM are similar and the octanol density is 0.82 g/cm^3 ,

$$\log K_p = \log K_{OA} + \log f_{om} - 11.91 \text{ or } K_p = 1.22 \times 10^{-12} f_{om} K_{OA} \quad (14)$$

Due to the differences of activity coefficients and molecular weights between octanol and OM, the constant(-11.91) may vary for different pairs of SVOCs and particle compositions and the slope of $\log K_{OA}$ may not be unity in some cases (Finizio et al. 1997; Wei et al. 2016). It also remains uncertain whether octanol can

adequately represent both polar and nonpolar classes of OM in particles (Cousins and Mackay 2001).

There is some debate whether the mechanism of gas-particle interaction is adsorption to active sites on the particle surface or absorption into organic matters in particles, or a combination of both. Pankow (1994) has shown that both absorptive and adsorptive partitioning mechanisms predict a fundamental inverse proportionality between K_p and P_s . Therefore, it is difficult to determine the mechanism of sorption based solely on the dependence of K_p on P_s (Cousins and Mackay 2001). In addition, the reported constants in Eqs. (11) and (14) may be significantly different among studies, and users may encounter difficulties in the selection of constants for the prediction of K_p (Wei et al. 2016). Based on the quantitative error analysis, Salthammer and Schripp (2015) demonstrated that the K_p values calculated on the basis of P_s and K_{OA} can be riddled with substantial error for indoor scenarios. The P_s - and K_{OA} -based approaches may cause high uncertainties for compounds with a K_p in the range of $0.01 \sim 0.1 \text{ m}^3/\mu\text{g}$ although such predictions yield quite reliable results for compounds of very high and very low volatility. However, it is clear that (1) particles of different origin have different sorptive properties, (2) humidity affects sorption, and (3) chemical-to-chemical differences and the effect of temperature can be described by both P_s and K_{OA} (Cousins and Mackay 2001).

Poly-Parameter Approach for Predicting K_p

Apart from the above two single-parameter approaches (P_s or K_{OA} as the single parameter), Salthammer and Goss (2019) applied a more complex approach, the poly-parameter linear free energy relationship (pp-LFER), to predict the gas-particle distribution of 14 SVOCs commonly found in indoor environments.

In contrast to the single-parameter approaches that ignore the intermolecular interactions, the pp-LFER approach uses a suite of five parameters to cover all relevant intermolecular interactions comprehensively. These five parameters are used to include interaction abilities like van der Walls, H-accepting (e-donating) and H-donating (e-accepting), the size of the sorbing compound, and the polarizability (which describes polar interactions that are not covered by the other parameters). Thus, the pp-LFER approach provides a more mechanistic understanding of the partition process, and Salthammer and Goss (2019) suggested that the pp-LFER approach would be a promising alternative for predicting K_p .

According to Goss (2005), the distribution of an organic compound between air and any condensed phase using the pp-LFER approach can be described by

$$K_p (\text{m}^3/\text{g}) = s \cdot S + a \cdot A + b \cdot B + l \cdot L + v \cdot V + c \quad (15)$$

where S , A , B , L , and V are compound-specific descriptors. S is the polarizability, A is the hydrogen bond acidity (donor), B is the hydrogen bond basicity (acceptor), V is the McGowan volume, and L is the logarithmic hexadecane-air partition coefficient ($\log K_{HdA}$). K_{HdA} is the equilibrium partition coefficient of chemicals between hexadecane and air, which is specifically used in the LFERs of Abraham (1993) and Goss (2005) because $\log K_{HdA}$ is proportional to their ability to interact by van

der Waals interactions for all compounds. The sorbent-specific parameters (here: particle-specific), i.e., s , a , b , l , and v , describe the complementary sorbent properties. Together with the fitting constant c , they need to be determined at the given relative humidity (RH) by multiple linear regression using experimental $\log K_p$ values, which is one of the drawbacks of the pp-LFER approach.

The McGowan volume V can be calculated from the molecular structure of the respective target compound following a procedure as described by Abraham and McGowan (1987). L can be determined experimentally by gas chromatography because the retention time of an organic substance is proportional to the stationary phase-gas partition coefficient in an isothermal gas chromatographic system with a suitable, completely nonpolar column (Salthammer and Goss 2019). For many compounds, S , A , and B are available via the UFZ-LSER database (Ulrich et al. 2017). For compounds with unknown descriptors, quantitative structure property relationships (QSPRs) based on structures provided as SMILES24 strings (simplified molecular-input line-entry system) have been developed for S , A , B , and L (Salthammer and Goss 2019). Among these descriptors, Salthammer and Goss (2019) found that the L -value is the single most influential molecular descriptor for the gas-particle interactions of SVOCs, and its accuracy is crucial for the predicted result. Therefore, they emphasized the necessity to determine the L -values of the target SVOCs experimentally although QSPR estimations are available.

According to the comparison results of Salthammer and Goss (2019), K_p 's estimated by the pp-LFER approach tend to be lower than those from the single-parameter approaches in most cases. The K_p value calculated from the pp-LFER approach agrees well with the experimental K_p for DEHP sorbed to pure organic particles (squalane and oleic acid). However, when considering uncertainties of the experimentally determined and calculated predictors as well as the heterogeneity of aerosols, it seems to be unlikely that precise estimates of K_p can be made. Finally, the direct comparison between K_p predicted by the pp-LFER approach (as well as the P_s - and K_{OA} -based approaches) and the measured K_p of SVOCs taken up by realistic indoor particles is still lacking.

Problems

The equilibrium model, i.e., Eq. (8), and the subsequent K_p -predicting approaches are helpful for understanding and describing the gas-particle interaction of indoor SVOCs. Several studies have used Eq. (8) to predict the interaction between gas-phase SVOCs and airborne particles in indoor environments by assuming that the gas-particle interaction has reached the equilibrium (Salthammer and Schripp 2015; Wei et al. 2016, 2017; Weschler et al. 2008). However, the equilibrium assumption should be interpreted with caution since significant deviations have been observed between measured data and predictions based on the equilibrium model (Cao et al. 2018; Shi and Zhao 2012). As predicted by Weschler and Nazaroff (2008) and Liu et al. (2013), the time required for mass transfer between gas-phase SVOCs and airborne particles to reach gas-particle equilibrium (i.e., the critical time for reaching equilibrium) falls in the range of seconds to days (which increases with increasing particle diameter or decreasing SVOC volatility), while the residence time

of indoor airborne particles is just on the order of 1 h (Guo 2013). Thus, the critical time for reaching gas-particle equilibrium can be longer than the residence time of indoor airborne particles. Consequently, the equilibrium between gas-phase SVOCs and airborne particles in the indoor environments is not a reasonable assumption for some cases, especially for less volatile compounds (or SVOCs with high K_{OA}), e.g., DEHP ($K_{OA} = 10^{12.9}$ at 25 °C (Weschler and Nazaroff 2010)). Thus, dynamic models considering the effects of particle residence time, instead of assuming equilibrium, have received increasing attention (Guo 2013; Liu et al. 2013; Shi and Zhao 2012).

Dynamic Models

Diffusion-Based Model

To describe the dynamic interactions between gas-phase SVOCs and airborne particle, Liu et al. (2013) developed a dynamic model involving the time period that airborne particles absorb (or adsorb) gas-phase SVOCs in the indoor air and the transient mass transfer between airborne particles and gas-phase SVOCs. Note, the following contents (the model developed by Liu et al. (2013) and other models derived from it) mainly focused on the organic layer of airborne particles. However, the surface of indoor particles can be either organic or aqueous (depending on the relative humidity [RH] of indoor air and the particle origin). Further study is required to involve the aqueous layer in the dynamic models and consider the effects of indoor RH on the dynamic interactions between gas-phase SVOCs and particles.

After summarizing the morphology observation and model description of airborne particles in the literature, Liu et al. (2013) concluded that the morphologies of various airborne particles may share a similar essential characteristic, i.e., a spherical particle consisting of an impermeable core and a homogenous outer layer that is capable for the adsorptive partitioning of gaseous compounds, as shown in Fig. 1. For SVOCs partitioning to particles, Liu et al. (2013) considered the outer layer as a liquid-like organic matter in the particles. Note, the adsorptive outer layer may not exist for some particles, such as the pure mineral particles. In this case, $R_1 = R_2$ in Fig. 1, the gas-phase SVOCs would be adsorbed on particle surfaces and an adsorption-based dynamic model should be used.

The transient mass transfer processes between gas-phase SVOCs and spherical particles are also shown in Fig. 1. Particles are exposed to air with a constant gas-phase SVOC concentration (C_g). The concentration of SVOCs absorbed in the particles (C_p , $\mu\text{g}/\text{m}^3$, mass of SVOCs per volume of particles) is initially equal to zero. The mass transfer process incorporates two stages, an external one (from bulk air and particle surface) and internal one (intraparticle diffusion between particle surface and inside). Assuming that the physical properties of particles are constant and there is no chemical reaction within particles, Liu et al. (2013) developed a model to describe the transient mass transfer absorption process, with the governing equation, boundary conditions, and initial condition listed below:

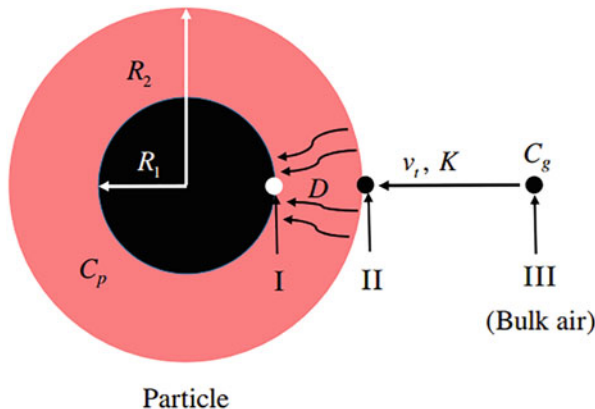


Fig. 1 Schematic of simplified morphology of airborne particles and the transient mass transfer between gas-phase SVOCs and airborne particles. The black region is impermeable for SVOCs. C_g is the SVOC concentration in the air, C_p is the SVOC concentration in a single particle, R_1 is radius of impermeable part, R_2 is radius of the whole particle, v_t is the mass transfer coefficient between air and particle, D is the diffusion coefficient of SVOCs within the particle, and K is the particle-gas partition coefficient (K_{part} in the following text). (Reprinted from Liu et al. (2016), Copyright (2021), with permission from Elsevier)

$$\begin{cases} \frac{\partial C_p}{\partial t} = D \left(\frac{\partial^2 C_p}{\partial r^2} + \frac{2}{r} \frac{\partial C_p}{\partial r} \right), & R_1 < r < R_2 \\ \frac{\partial C_p}{\partial r} = 0, & r = R_1 \\ -D \frac{\partial C_p}{\partial r} = v_t \left(\frac{C_p}{K_{part}} - C_g \right), & r = R_2 \\ C_p(r, t=0) = 0 \end{cases} \quad (16)$$

where t (s) is the time, D (m^2/s) is diffusion coefficient of SVOCs inside the particles, r (m) is radial distance, v_t (m/s) is mass transfer coefficient between gas-phase SVOCs and particles, K_{part} (dimensionless) is particle-gas partition coefficient of SVOCs, R_1 (m) is radius of impermeable part of the particle, and R_2 (m) is radius of the whole particle.

v_t characterizes the uptake rate of gas-phase SVOCs by airborne particles, which depends on the particle size relative to the mean free path of SVOC molecular in the air surrounding the particle. v_t is often estimated by (Cao et al. 2019; Seinfeld and Pandis 2016):

$$v_t = 2 \frac{D_g}{d_p} \cdot F = 2 \frac{D_g}{d_p} \cdot \frac{1 + Kn}{1 + 0.377Kn + 1.33Kn(1 + Kn)/\alpha} \quad (17)$$

where D_g (m^2/s) is the diffusion coefficient of SVOCs in the air; F is the Fuchs-Sutugin correction factor for noncontinuum effects (Seinfeld and Pandis 2016); α is the mass accommodation coefficient of SVOCs; Kn is Knudsen number, which is

determined by $Kn = \frac{3D_g}{d_p} \sqrt{\frac{2M}{2RT}}$; and M (kg/mol) is the SVOC molecular weight. Several other formulas are also available for estimating v_t as listed in Table 12.1 of Seinfeld and Pandis (2016), most of them exhibit the performance similar to Eq. (17). There are two unknown parameters in Eq. (17), D_g and α . D_g of SVOCs can be easily obtained by using experimental data or empirical correlations reported in the literature (Cao et al. 2017; Fuller et al. 1966). α was assumed to be unity ($\alpha = 1$) by Liu et al. (2013). Details about α are introduced in the next subsection “[Methods for Measuring/Estimating Key Parameters](#),” as well as the method for estimating D used by Liu et al. (2013).

Please note the difference between C_{sp} in Eq. (8) (mass of SVOCs per volume of air) and C_p in Eq. (16) (mass of SVOCs per volume of the liquid-like organic matter in a single particle). C_{sp} is a combination of C_p of different sizes of particles (Cao et al. 2018). Additionally, K_{part} is a dimensionless particle-gas partition coefficient of SVOCs, and K_{part} can be converted to K_p (particle-mass-normalized particle-gas partition coefficient) by $K_{part} = K_p \cdot \rho_p$ (ρ_p is the density of particles, $\mu\text{g}/\text{m}^3$).

The analytical solution for Eq. (16) were obtained by Liu et al. (2013):

$$C_p = K_{part} C_g \left(1 - \frac{\sum_{i=1}^{\infty} C_i X_i e^{-\beta_i^2 F_{O_m}}}{R_p} \right) \quad (18)$$

where

$$C_i = 2A \cdot B \quad (19)$$

$$X_i = \beta_i \cos [\beta_i (R_p - R_{12})] + H_1 \sin [\beta_i (R_p - R_{12})] \quad (20)$$

$$A = \left[(\beta_i^2 + H_1^2) \left(1 - R_{12} + \frac{H_2}{\beta_i^2 + H_2^2} \right) + H_1 \right]^{-1} \quad (21)$$

$$B = \left(1 + \frac{H_1}{\beta_i^2} \right) \sin [\beta_i (1 - R_{12})] + \frac{1 - H_1}{\beta_i} \cos [\beta_i (1 - R_{12})] \quad (22)$$

$$H_1 = \frac{1}{R_{12}}, \quad H_2 = \frac{Bi_m}{K_{part}} - 1 \quad (23)$$

$$R_p = \frac{r}{R_2}, \quad R_{12} = \frac{R_1}{R_2} \quad (24)$$

$$F_{O_m} = \frac{Dt}{R_2^2}, \quad Bi_m = \frac{v_t R_2}{D} \quad (25)$$

and β_i ($i = 1, 2, 3, \dots$) is the root of

$$\tan [\beta_i(1 - R_{12})] = \frac{\beta_i(H_1 + H_2)}{\beta_i^2 - H_1H_2}, \quad i = 1, 2, 3, \dots \quad (26)$$

The analytical solution of the diffusion-based dynamic model (Eq. 16) is quite complicated because an infinite series and a transcendental equation are involved in the solution. Additionally, if the gas-particle interaction reaches equilibrium, the equilibrium SVOC concentration in the particle will equal $K_{part}C_g$, i.e., $C_{p, equ} = K_{part}C_g$. Therefore, much more input parameters are required in the dynamic model as compared to the equilibrium model. According to Eqs. (18), (19), (20), (21), (22), (23), (24), (25), and (26), the SVOC concentration in the particle, C_p , takes the function form: $C_p = f(C_g, K_{part}, D, v_t, R_1, R_2, r, t)$. Therefore, six additional parameters are required to solve the diffusion-based dynamic model (except for K_{part} and C_g). Nevertheless, the diffusion-based dynamic model provides a clear mathematical description of the transient mass transfer between gas-phase SVOCs and airborne particles.

Simplified Model Based on Lumped Parameter Method

As indicated in Fig. 1, the mass transfer process between gas-phase SVOCs and airborne particles incorporates two parts, the external one from air to particle surface and the internal one via intraparticle diffusion. According to Eq. (16), it is the intraparticle diffusion that complicates the model. Therefore, the dynamic model may be greatly simplified if the intraparticle diffusion can be ignored. Weschler and Nazaroff (2008) compared the estimated timescales for the internal process to that for the external one for the organic constituents of airborne particles. They concluded that for airborne particles with a diameter smaller than 2 μm , it was the external process that dominated the partitioning process. Additionally, the kinetic evaporation of secondary organic aerosol and other organic aerosols in a thermodenuder was examined by including only the external mass transfer process (Cappa 2010).

In order to judge whether the internal or the external process dominates the dynamic gas-particle interaction, Liu et al. (2013) defined the following parameter:

$$\varepsilon = \frac{K_{part}C_g - C_p(R_2)}{K_{part}C_g - C_p(R_1)} \quad (27)$$

which represents the ratio of the concentration difference between particle surface and gas phase (external concentration difference) to the concentration difference between the innermost of the organic outer layer and gas phase (total concentration difference).

If ε is greater than 0.95, the external concentration difference accounts for more than 95% of the total concentration difference. Liu et al. (2013) considered that in such a situation, the external process was dominant, and the spatial concentration distribution inside the organic layer on this particle could be considered as uniform. Under such condition, the lumped parameter method (LPM), which lumps concentration

distribution inside the particle into one value, can be applied to address the gas-particle transient mass transfer problem.

The LPM is briefly introduced here. In mass transfer, the Biot number divided by the partition coefficient is defined as the ratio of internal mass transfer resistance to external mass transfer resistance, i.e., the Little number (Lt) (Zhang et al. 2016):

$$Lt = \frac{Bi_m}{K_{part}} = \frac{v_t L}{DK_{part}} < 0.1 \quad (28)$$

where Bi_m (dimensionless) is the Biot number for mass transfer and L (m) is the characteristic length (typically equals R_2 for a spherical particle). When this characteristic number (Lt) is smaller than 0.1 (Liu et al. 2013, 2016), the concentration difference between the surface of the particle (point II in Fig. 1) and the innermost of the organic layer of the particle (point I in Fig. 1) is less than 5% of the difference between gas phase (point III in Fig. 1) and the innermost of the organic layer of the particle (point I in Fig. 1). That is, the value of ϵ defined in Eq. (27) will be greater than 0.95 when $Lt < 0.1$. According to the analysis of Liu et al. (2013), Lt for SVOCs commonly found in the realistic environments (for particles in the size range of 0.01–10 μm) is significantly smaller than the critical value for the use of LPM ($Lt < 0.1$), as indicated in Fig. 2.

Overall, the above analysis indicates that the intraparticle mass transfer resistance can be neglected for gas-particle interaction of SVOCs, and the diffusion-based dynamic model (Eq. 16) can be simplified to only include the external mass transfer process:

$$V_p \frac{dC_p}{dt} = v_t A_p \left(C_g - \frac{C_p}{K_{part}} \right) \quad (29)$$

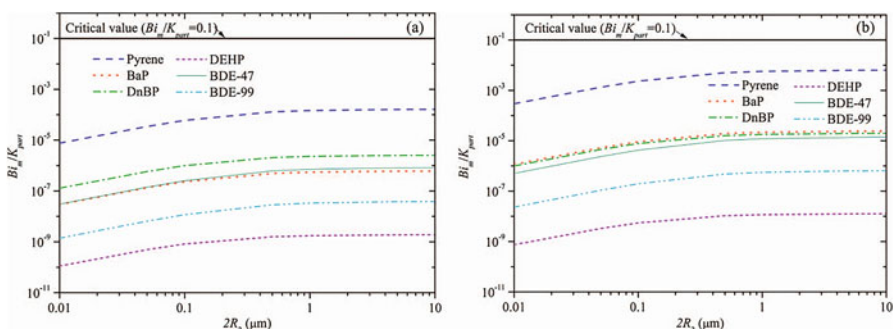


Fig. 2 For six commonly identified SVOCs indoors, comparison between calculated Bi_m/K_{part} and the critical value for neglecting the internal mass transfer resistance (0.1). X-axis: particle diameter. The fraction of absorptive volume in the particles equals 1 for both (a) and (b). (a) Nonporous particles, the volumetric fraction of organic materials equals 1. (b) Porous particles, the volumetric fraction of organic materials equals 0.3, and the volumetric fraction of elemental carbon equals 0.05. (Reprinted from Liu et al. (2013), Copyright (2021) @ The American Association for Aerosol Research, with permission from Taylor & Francis Ltd)

where V_p (m^3) and A_p (m^2) are the volume and surface area of a single particle. If the particle is treated as a sphere, $V_p = \frac{\pi}{6}d_p^3$ and $A_p = \frac{\pi}{4}d_p^2$ (where d_p [m] is the particle diameter, $d_p = 2R_2$ in Fig. 1).

Assuming that the SVOC concentration in the particle (C_p) is initially equal to zero, the analytical solution to Eq. (29) is:

$$C_p = K_{part}C_g(1 - e^{-\varphi t}) \quad \text{with} \quad \varphi = \frac{v_t A_p}{V_p K_{part}} = \frac{3v_t}{R_2 K_{part}} = \frac{6v_t}{d_p K_{part}} \quad (30)$$

where φ (s^{-1}) is the characteristic parameter that governs the timescale of SVOC gas-particle interactions. When C_p reaches 95% of the equilibrium concentration ($K_{part}C_g$), equilibrium can be considered to have been attained. Using this criterion, the critical time required for the attainment of equilibrium, t_c ($1 - e^{-\varphi t_c} = 0.95$, i.e., $\varphi t_c = -\ln 0.05 \approx 3$), is

$$t_c \approx 3\varphi^{-1} = \frac{d_p K_{part}}{2v_t} \quad (31)$$

Comparing Eq. (30) to Eq. (18), it can be seen that the analytical solution of LPM-based model is much simpler than that of the diffusion-based model. In addition, the number of input parameters of the LPM-based model decreases to 5 (C_g , K_{part} , v_t , R_2 , t) compared to that of the diffusion-based model (8 parameters). All these five parameters (C_g , K_{part} , v_t , R_2 , and t) can be directly measured or estimated. Due to the relatively simple function form and availability of parameters, the LPM-based model (Eq. 30) has been frequently used to describe the dynamic interaction between gas-phase SVOCs and airborne particles (Eichler et al. 2021). By comparing the experimental data (measured indoor gas-phase and particle-phase concentrations of polycyclic aromatic hydrocarbons) with model predictions, Shi and Zhao (2012) proved that the predictions of the LPM-based model agreed well with the experimental data.

It should be noted that C_p is the SVOC concentration within a single particle (mass of SVOCs per volume of a particle), while the particle-phase SVOC concentrations in the indoor air are always measured in the form of SVOC mass per volume of air (C_{sp}). Therefore, the prediction of Eq. (30) should be converted to C_{sp} by combining C_p of different sizes of particles (Cao et al. 2018),

$$C_{sp} = \int \frac{\partial \left(V_p \sum_{j=1}^{N_p} C_{pj} \right)}{\partial d_p} dd_p = \int \frac{\partial (N_p V_p \bar{C}_p)}{\partial d_p} dd_p = \frac{\text{TSP}}{\rho_p} \int \frac{\partial (\alpha_v \bar{C}_p)}{\partial d_p} dd_p \quad (32)$$

where N_p ($1/\text{m}^3$ (room volume)) is the number concentration of airborne particles with a specific diameter; the subscript j represents the j th particle ($j = 1 \sim N_p$) with a

specific diameter; α_V is the volume fraction of airborne particles with a specific diameter, $\alpha_V = N_p V_p / V_{tp}$; V_{tp} (m^3 (particle volume)/ m^3 (room volume)) is the total volume concentration of indoor airborne particles, $V_{tp} = \text{TSP}/\rho_p$; and \bar{C}_p is the mean C_p for all particles with a specific diameter; according to Eq. (30) we can get:

$$\bar{C}_p = \sum_{j=1}^{N_p} C_{p,j} / N_p = K_{part} C_g \sum_{j=1}^{N_p} \left(1 - \exp \left(-3 \frac{t_j}{t_{c,j}} \right) \right) / N_p \quad (33)$$

Note that, in most studies of dynamic models for indoor airborne SVOCs, t in Eq. (33) has always been regarded as the mean residence time of airborne particles in the indoor air (designated as $\bar{\tau}_r$), i.e., $\bar{C}_p = K_{part} C_g \sum_{j=1}^{N_p} \left(1 - \exp \left(-3 \frac{\bar{\tau}_{r,j}}{t_{c,j}} \right) \right) / N_p$ (Liuet al. 2013). If the indoor air is well mixed, $\bar{\tau}_r$ can be estimated by

$$\bar{\tau}_{r,j} = (ACH + \beta_j)^{-1} \quad (34)$$

where ACH (s^{-1}) is the air exchange rate of the room and β (s^{-1}) is the first-order deposition loss rate coefficient of airborne particles (which is size dependent).

Because the airborne particles can only be measured in several size bins, the integration in Eq. (32) can be replaced by the summation of different size bins, and noting that $K_{part} = K_p \cdot \rho_p$, we can get:

$$\begin{aligned} C_{sp} &= \frac{\text{TSP}}{\rho_p} \sum_{i=1}^n \alpha_{V,i} \bar{C}_{p,i} = K_p \cdot C_g \cdot \text{TSP} \sum_{i=1}^n \alpha_{V,i} \left(1 - \exp \left(-3 \frac{\bar{\tau}_{r,i}}{t_{c,i}} \right) \right) \\ &= \eta \cdot K_p \cdot C_g \cdot \text{TSP} \end{aligned} \quad (35)$$

where the subscript i represents the i th particle size bin ($i = 1 \sim n$, n is the number of particle size bins) and η is the ratio of C_{sp} estimated by the dynamic model to C_{sp} estimated by the equilibrium model. Because $\sum_i \alpha_{V,i} = 1$ and $1 - \exp \left(-3 \frac{\bar{\tau}_{r,i}}{t_{c,i}} \right) < 1$, it is easy to find that $\eta < 1$.

Dynamic Model Involving Intraparticle Reaction of SVOCs

The above models assume that there is no chemical reaction for SVOCs within the airborne particles. While in the diffusion process within the particles, several SVOCs (as well as other particle-associated compounds) may experience further chemical reactions (Liu and Cao 2018; Zhou et al. 2013). Therefore, Liu and Cao (2018) further provided a dynamic partitioning model of SVOCs by considering intraparticle diffusion, particle-phase reaction, and external mass transfer from bulk air to particle surfaces. Assuming that the intraparticle reaction follows the first-order chemical reactions and the whole particle is absorptive for SVOCs (i.e., $R_1 = 0$), the governing equations for SVOCs in airborne particles and boundary conditions and initial conditions are as follows (Liu and Cao 2018):

$$\begin{cases} \frac{\partial C_p}{\partial t} = D \left(\frac{\partial^2 C_p}{\partial r^2} + \frac{2}{r} \frac{\partial C_p}{\partial r} \right) - k_c C_p, & 0 < r < R_2 \\ \frac{\partial C_p}{\partial r} = 0, & r = 0 \\ -D \frac{\partial C_p}{\partial r} = v_t \left(\frac{C_p}{K_{part}} - C_g \right), & r = R_2 \\ C_p(r, t = 0) = 0 \end{cases} \quad (36)$$

where k_c (1/s) is a first-order rate constant and the term $-k_c C_p$ represents the rate of particle-phase chemical reaction.

The analytical solution for Eq. (36) were obtained as:

$$C_p = -\frac{K_{part} C_g}{R_p} \left[G_1 \left(e^{-R_p \sqrt{q}} - e^{-R_p \sqrt{q}} \right) + e^{-q F_{O_m}} \sum_{i=1}^{\infty} \left(e^{-\beta_i^2 F_{O_m}} C_i X_i \right) \right] \quad (37)$$

where

$$q = \frac{k_c R_2^2}{D} \quad (38)$$

$$G_1 = -\frac{1 + H}{\sqrt{q} e^{\sqrt{q}} + \sqrt{q} e^{-\sqrt{q}} + H e^{\sqrt{q}} - H e^{-\sqrt{q}}}, \quad H = \frac{Bi_m}{K_{part}} - 1 \quad (39)$$

$$\begin{aligned} C_i &= 2 A_i B_i, \quad A_i = \frac{\beta_i^2 + H^2}{\beta_i^2 + H^2 + H}, \quad B_i \\ &= -G_1 \frac{\frac{\sqrt{q} \sin \beta_i}{\beta_i^2} (e^{\sqrt{q}} + e^{-\sqrt{q}}) - \frac{\cos \beta_i}{\beta_i} (e^{\sqrt{q}} - e^{-\sqrt{q}})}{1 + q/\beta_i^2} \end{aligned} \quad (40)$$

$$X_i = \sin(\beta_i R_p) \quad (41)$$

and β_i ($i = 1, 2, 3, \dots$) is the root of

$$\beta_i \cot \beta_i = -H, \quad i = 1, 2, 3, \dots \quad (42)$$

The parameter, q , is designated as the dimensionless chemical term, which characterizes a ratio of diffusion timescale (R_2^2/D) to reaction timescale ($1/k_c$). Compared to the diffusion-based model for gas-particle interaction with the absence of chemical reactions, the above model (Eqs. 36, 37, 38, 39, 40, 41, and 42) is also very complicated. Furthermore, another parameter (k_c) is required for solving this model.

Similar to the simplification of Eq. (16) to Eq. (29), the above complicated diffusion-based model can also be simplified using the lumped parameter method. If ε defined in Eq. (27) is greater than 0.95, the above model (Eqs. 36, 37, 38, 39, 40, 41, and 42) can be simplified as:

$$V_p \frac{dC_p}{dt} = v_t A_p \left(C_g - \frac{C_p}{K_{part}} \right) - k_c V_p C_p \quad (43)$$

The analytical solution of Eq. (43) is:

$$\begin{aligned} C_p &= \frac{C_g}{M} (1 - e^{-MNt}), \text{ with } M = \frac{1}{K_{part}} + \frac{V_p k_c}{A_p} = \frac{1}{K_{part}} + \frac{k_c R_2}{3}, \text{ } N = \frac{v_t A_p}{V_p} \\ &= \frac{3v_t}{R_2} \end{aligned} \quad (44)$$

It can be seen that Eq. (44) can be converted into Eq. (30) in the absence of particle-phase reactions ($k_c = 0$). In addition, Liu and Cao (2018) found that the critical value of Lt for the use of the lumped parameter method ($(Lt)_{cr}$) can be greater with the presence of particle-phase reactions, i.e., $(Lt)_{cr}$ increases as q (or k_c) increases (chemical reaction gets more intense). Particularly, impact of chemical reactions on $(Lt)_{cr}$ becomes significant for q higher than 10. $(Lt)_{cr}$ changes little for q smaller than 10. $(Lt)_{cr}$ approaches 0.1 as q decreases. This is in sharp contrast with the case when chemical reaction is absent, for which $(Lt)_{cr}$ is a constant of 0.1 (see the above analysis related to Eq. (28)). Overall, the results of Liu and Cao (2018) indicate that taking particle-phase reaction into consideration allows a wider range to neglect intraparticle diffusion.

However, most of existing studies about the dynamic interactions between gas-phase SVOCs and indoor airborne particles ignores the particle-phase reactions, and the models involving chemical reactions (Eq. (36) and/or Eq. (43)) had not been applied for the gas-particle interactions in indoor environments, mainly due to the limited information about the particle-phase reaction rate constant (k_c). Further studies are therefore required for characterizing the particle-phase reactions of indoor SVOCs, especially quantifying the values of k_c .

Adsorption-Based Model

The above models all assume that the gas-particle interaction is dominated by absorption. However, the particles may be in semi-solid or solid states under some conditions, e.g., inorganic particles at low humidity (Shiraiwa et al. 2011), inorganic particles generated by laboratory apparatus (Cao et al. 2019; Wu et al. 2018), or organic particles at low temperature (Liu and Cao 2018). In these cases, SVOCs tend to accumulate on the particle surfaces, instead of diffusing into the particles, and the gas-particle interaction is more suitable to be described as surface adsorption (i.e., $R_1 = R_2$ in Fig. 1).

If the surface adsorption occurs, the corresponding dynamic model can be expressed as:

$$A_p \frac{dC_{pA}}{dt} = v_t A_p \left(C_g - \frac{C_{pA}}{K_{pA}} \right) \quad (45)$$

where C_{pA} ($\mu\text{g}/\text{m}^3$) is the SVOC concentration on the surface of a single particle.

The analytical solution to Eq. (45) is:

$$C_{pA} = K_{pA} C_g \left(1 - e^{-\frac{v_t t}{K_{pA}}} \right) \quad (46)$$

Methods for Measuring/Estimating Key Parameters

According to the above models, several parameters are required to be known before predicting the relationship between C_g and C_{sp} (or C_p) of indoor SVOCs with the absence of particle-phase reactions. They are the particle-gas partition coefficient (K_p or K_{par}) in both the equilibrium model and dynamic models, the mass transfer coefficient between bulk gas-phase SVOCs and particles (v_t) in the dynamic models, the diffusion coefficient of SVOCs inside the particles (D) in the diffusion-based dynamic model, the size distribution of airborne particles (α_V) for the dynamic models, the mass concentration of airborne particles (TSP) in all models, and the air exchange rate of the room (ACH) and the first-order deposition loss rate coefficient of airborne particles (β) to get the mean residence time of airborne particles. Among these parameters, α_V and TSP can be directly obtained by using particle sizers, such as the laser particle sizer and/or scanning electrical mobility sizer. ACH is always a routine parameter used for indicating the indoor air quality, which can be easily measured by releasing inert gases without indoor sources (e.g., SF₆ and CO₂ [without people in the room]) into the room and monitoring the decay rate of the released gases. v_t can be predicted using Eq. (17) if the mass accommodation coefficient (α) is known. The remained parameters, K_p , D , β , as well as α , should be adequately predicted or/and measured.

Particle-Gas Partition Coefficient (K_p)

Except for the estimation approaches introduced above (Eqs. 10, 11, 12, 13, 14, and 15), the values of K_p can also be obtained by measurements. In existing studies, the methods commonly used to measure K_p for indoor SVOCs are based on the equilibrium model, e.g., C_{sp} , C_g , and TSP in the realistic environments are measured simultaneously and K_p is calculated by $C_{sp}/(C_g \cdot \text{TSP})$ (Wang et al. 2014). According to Eq. (35), K_p measured in this way actually equals $\eta \cdot K_p$ ($\eta < 1$), which may significantly vary among homes with different ACH s since η tends to decrease as ACH increases (Cao et al. 2018).

Benning et al. (2013) was the first to quantify K_p of SVOCs after the interaction between gas-phase SVOCs and particles reaches equilibrium in a well-controlled chamber. However, the accuracy may be reduced by the complexity of the air velocity field within the chamber if the equilibrium cannot be attained at the chamber outlet, especially for SVOCs with greater K_p and airborne particles with larger diameters (as K_p or d_p increase, the critical time for equilibrium may be longer than the particle residence time in the chamber) (Cao et al. 2018; Wu et al. 2018).

To simplify the air velocity field and control the residence time of particles within the chamber, Wu et al. (2018) proposed a novel method for measuring K_p using a

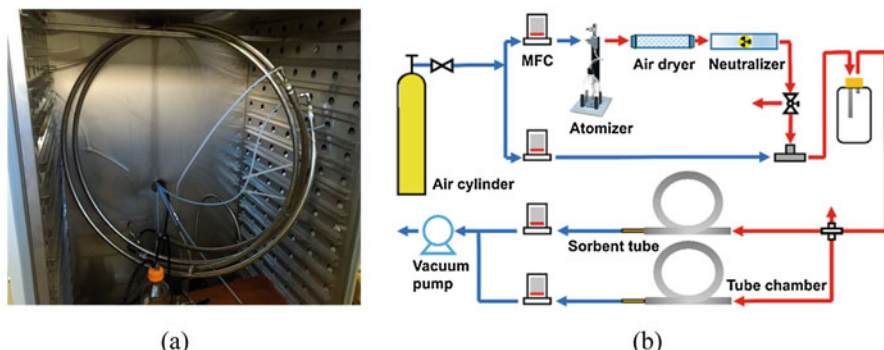


Fig. 3 The experimental setup for measuring K_p developed by Wu et al. (2018). (a) Photo and (b) schematic representation of the experimental setup with inorganic particle introduction. (Reused with permission from Wu et al. (2018). Copyright (2021) American Chemical Society)

laminar flow tube chamber (inner diameter: 1.72 cm, length: 3.60 m) coated with a thin layer of pure SVOC liquid on the inner surface as shown in Fig. 3.

Particle-laden air (polydisperse particles with median diameter in the ranges of 40–170 nm) at a controlled flow rate, which ensures air flow in the chamber is laminar, was introduced into the chamber. Two sorbent tubes were connected in parallel to the chamber outlet, one with a filter measuring the effluent C_g , the other without a filter measuring the sum of C_g and C_{sp} (i.e., $C_{tot} = C_g + C_{sp}$), with effluent C_{sp} obtained as $C_{tot} - C_g$. Given that the tube was sufficiently long, equilibrium between gas-phase SVOCs and particles was attained at the chamber outlet, and K_p was determined by $C_{sp}/(C_g \cdot TSP)$. However, for the cases of particles with larger diameters or SVOCs with higher K_p , significant uncertainty may be still introduced in the determined K_p because equilibrium might not be attained at the chamber outlet. In addition, integration of measurement errors of C_g and C_{sp} may also reduce the accuracy of K_p because separating C_g and C_{sp} experimentally is a challenge for SVOCs (Benning et al. 2013; Wang et al. 2015; Weschler and Nazaroff 2010). For example, measurement of C_g using sorbent tubes with a filter may be biased, with C_g underestimated due to sorption of gas-phase SVOCs to the filter or overestimated due to penetration of particles into the sorbent and the volatilization of SVOCs from the collected particles (Wang et al. 2015).

Cao et al. (2019) modified the method of Wu et al. (2018) by using a shorter tube (inner diameter: 1.72 cm, length: 0.30 m). A model (combining the above dynamic model for gas-particle interaction, Eq. (29), and the model describing the mass transfer of gaseous SVOCs in the chamber) was established to describe the dynamic mass transfer of SVOCs in the tube. The total airborne SVOC concentration (C_{tot}) was measured at the tube outlet. K_p was obtained by fitting the model to the measured C_{tot} (as well as particle size distribution and concentration). In this way, the requirements to reach equilibrium before the chamber outlet and to separate C_g and C_{sp} can be eliminated. However, the mass accommodation coefficient of SVOCs on particle surface

(α) should be known when applying this method to determine K_p , which would strongly limit its application for the cases where α is not available (as discussed below).

The above chamber methods have only been applied to measure K_p of DEHP sorbed by generated particles (inorganic: $(\text{NH}_4)_2\text{SO}_4$ particles, and organic: pure squalane and oleic acid particles). DEHP was selected as the target SVOC because it is ubiquitous in the indoor environment (Weschler and Nazaroff 2008) and because of the very low gas-phase concentration that means that the experiments are realistically challenging (Cao et al. 2017; Liang and Xu 2014). If accurate results can be obtained for DEHP, the proposed method should also be applicable to SVOCs with higher gas-phase concentrations because measurements are considered to be easier and more accurate (Xu et al. 2012). However, the K_p values measured in these studies exhibit relatively low reproducibility in parallel measurements and high inconsistency among different studies. For example, K_p of DEHP for the oleic acid particles was measured to be $0.23 \pm 0.13 \text{ m}^3/\mu\text{g}$ ($n = 8$) with a relative standard deviation of 57% by Wu et al. (2018). The situation was even worse for squalane particles ($K_p = 0.11 \pm 0.10 \text{ m}^3/\mu\text{g}$ [$n = 10$], with a relative standard deviation of 91%). The differences may be mainly caused by the unstable concentration and size distribution of the generated particles and the measurement uncertainty related to the SVOC concentrations. Therefore, further study is required to improve the method accuracy for measuring K_p and to measure K_p for more SVOC-particle pairs in the indoor environments.

Mass Accommodation Coefficient of SVOCs on Particle Surface (α)

When gas molecules strike the particle surface, the gas molecules can either be reflected (diffusely or specularly) or taken up at the surface (Davis 2006). The mass accommodation coefficient (α , also referred to as the evaporation coefficient at equilibrium) is defined as the probability that an SVOC molecule striking the particle surface is captured by the particle (Cao et al. 2019). Due to limited information about its value, α in Eq. (17) is always assumed to be unity in existing studies (Liu et al. 2013; Weschler and Nazaroff 2008). Under this condition, Eq. (17) can be simplified as:

$$v_t = 2 \frac{D_g}{d_p} \cdot \frac{1 + Kn}{1 + 1.71Kn + 1.33Kn^2} \quad (47)$$

However, some measurements of α have obtained values significantly smaller than unity (e.g., 0.28–0.46 (Saleh et al. 2012)). According to Eq. (17), the overall gas-particle transport rate (i.e., v_t) tends to decrease as α decreases (the decreasing tendency is more significant for smaller particles), as depicted in Fig. 4a. In addition, the value of η in Eq. (35) will increase as α increases, as shown in Fig. 4b for various K_p . This means that assuming α to be unity may lead to an overestimation of the particle-phase concentration (C_{sp}) estimated by Eq. (35) if the actual α is lower than unity. Taking DEHP as an example, C_{sp} will be overestimated by 20% if α equals 0.2 and K_p equals $0.1 \text{ m}^3/\mu\text{g}$ (for the interaction between DEHP and organic

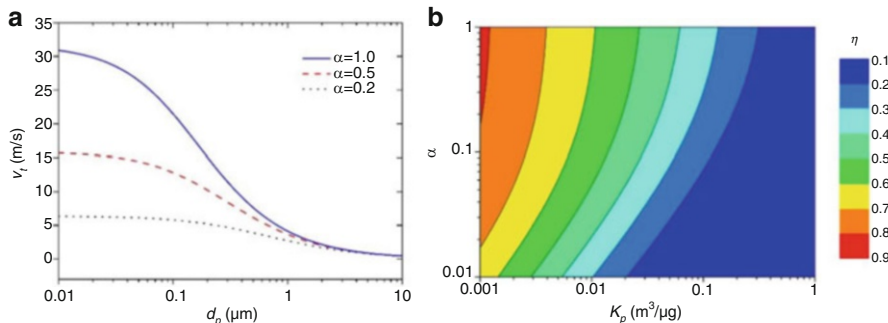


Fig. 4 (a) Gas-particle mass transfer coefficient of SVOCs (ν_t) as a function of particle diameter (d_p) for various mass accommodation coefficients (α). For the calculation, DEHP was selected as the target SVOC ($M = 391$ g/mol and $D_g = 2.64 \times 10^{-6}$ m²/s (Wu et al. 2018)), and temperature was set to 25 °C. (b) Value of η in Eq. (35) for various partition coefficients (K_p) and mass accommodation coefficients (α). The particle size distribution (α_s) measured by Yang et al. (2014) was used for the calculation. The air change rate of the room (ACH) was set as 0.5 h⁻¹. The particle deposition rate (β) was calculated from the empirical equation provided by Cao et al. (2018). (Reprinted from Cao et al. (2019), Copyright (2021) @ The American Association for Aerosol Research, with permission from Taylor & Francis Ltd)

particles (Wu et al. 2018)), i.e., $C_{sp} = 0.30K_p \cdot C_g \cdot \text{TSP}$ when $\alpha = 0.2$ vs. $C_{sp} = 0.36K_p \cdot C_g \cdot \text{TSP}$ if $\alpha = 1$. Consequently, selecting a correct α value in Eq. (17) may be helpful for accurately predicting the $C_g - C_{sp}$ relationship using the dynamic model, especially for particles with diameter less than 100 nm.

Two types of methods have generally been used to measure α . In both, α was obtained by fitting the corresponding models to the monitored dynamic response of d_p (particle diameter) or C_g of the target species to perturbations in the gas-particle equilibrium. The perturbations were achieved either by heating the particles generated in a cold environment (e.g., heated from 10 °C to 30 °C) (Cappa 2010; Saleh et al. 2012) or by injecting particles into an environment with a steady gas-phase concentration of the target species (Jefferson et al. 1997). One challenge associated with these methods is that the sorption of gas-phase species to the chamber walls is neglected. The wall loss may strongly affect the dynamic response to the perturbations and neglecting this effect may lead to uncertainty in the measured α (Cappa 2010; Ye et al. 2016). The wall loss effect may be even more significant for SVOCs which partition strongly to chamber walls such as DEHP (Xu and Little 2006), and thus may limit the applications of these methods to measure α for these SVOCs. The other challenge is that for some methods using a flow tube (also referred to as a thermodenuder) (Cappa 2010), gas-phase SVOCs were assumed to be uniformly distributed in the cross-section of the tube, which is not representative of actual conditions (Wu et al. 2016) and may lead to variations in the measured results.

Cao et al. (2019) proposed a tube chamber method for measuring α to overcome the limitations of these methods. Taking the interaction between DEHP and

$(\text{NH}_4)_2\text{SO}_4$ particles (with diameters in the range of 10–600 nm) as an example, the value of α was measured to be 0.20 ± 0.05 by Cao et al. (2019), preliminarily implying that assuming α to be unity may not be suitable for modeling the dynamic interaction between SVOCs and airborne particles. However, their method requires the knowledge of K_p , which may again limit the use of their method because K_p is also subject to considerable uncertainties as discussed above. Overall, further studies are required to quantify the uncertainty caused by assuming α as unity and to develop an accurate and simple method for measuring α of indoor SVOCs on airborne particles.

Intraparticle Diffusion Coefficient of SVOCs (D)

The method for estimating D used by Liu et al. (2013) is introduced here. For porous particles, D can be calculated with the following formula according to Weber and Digiano (1996):

$$D = \frac{D_l/\tau}{1 + \frac{(1-\alpha_p)K_{sl}}{\alpha_p}} \quad (48)$$

where D_l (m^2/s) is the diffusion coefficient in the free liquid, τ is tortuosity of particles, α_p is porosity of particles, and K_{sl} is the partition coefficient between the liquid in the pore and the pore material. Levin (1980) used the following correlation to estimate D_l :

$$D_l M^{0.5} = \text{constant} \quad (49)$$

Theis et al. (2001) experimentally determined the diffusion coefficient of benzene, toluene, ethylbenzene, and o-xylene in octanol at 25 °C. The constant in Eq. (49) from D_l and M of these chemicals is $(1.1 \pm 0.11) \times 10^{-10}$.

A common method to estimate the tortuosity of particles (τ) was provided by Wakao and Smith (1962):

$$\tau = \frac{1}{\alpha_p} \quad (50)$$

The value of porosity of particles (α_p) has been used as 0.5 in Eqs. (48) and (50) by Liu et al. (2013).

Assuming that the organic liquid and the pore material behave like octanol and elemental carbon (EC), respectively, K_{sl} can be calculated with the following formula (Liu et al. 2013):

$$K_{sl} = K_{EC_o} = \frac{K_{EC_w}}{K_{ow}} \quad (51)$$

where K_{EC_o} and K_{EC_w} are the partition coefficients between EC and octanol and water, respectively, and K_{ow} is the partition coefficient between octanol and water.

Table 1 Intraparticle diffusion coefficient of six typical SVOCs obtained by Liu et al. (2013)

SVOCs	Pyrene	BaP	DnBP	DEHP	BDE-47	BDE-99
$D \times 10^{11}$ (m ² /s)	0.0777	0.0350	9.08	8.39	2.24	2.40

BaP: benzo(a)pyrene; DnBP: di-n-butyl phthalate; DEHP: di(2-ethylhexyl) phthalate; BDE: brominated diphenyl ethers

With Eqs. (48), (49), (50), and (51), D 's of six SVOCs commonly found indoor were estimated to be in the range of $10^{-13} \sim 10^{-10}$ m²/s by Liu et al. (2013), as listed in Table 1.

Up to now, relatively few studies have been focused on the estimation and measurement of D . The above method for estimating D can be treated as a rough estimation and may be subject to huge uncertainty. Nevertheless, we may not necessarily need to know the accurate value of D for the gas-particle interaction of indoor SVOCs because the intraparticle diffusion can be reasonably neglected for both porous and nonporous particles with a diameter between 0.01 and 10 μm according to Liu et al. (2013), as discussed above.

Deposition Loss Rate Coefficient of Airborne Particles (β)

The deposition rate of airborne particles (β) is synthetically affected by particle size, gravitational settling, Brownian and turbulent diffusion, turbophoresis, thermophoresis (if there is a temperature difference), and diffusiophoresis (if there is a humidity difference). Several models have been established to predict β of indoor airborne particles under different conditions (Lai and Nazaroff 2000; Zhao and Wu 2006). ► Chap. 11, “Deposition,” of this handbook gives detailed discussions about deposition of airborne particles in indoor environments.

For the simplification of applications, Cao et al. (2018) provided a formula to estimate β by fitting the measured data from various studies (measured indoors) summarized by Riley et al. (2002):

$$\begin{aligned} \log \beta = & 0.00911(\log d_p)^6 + 0.0952(\log d_p)^5 + 0.0190(\log d_p)^4 - 0.536(\log d_p)^3 \\ & + 0.327(\log d_p)^2 + 1.53 \log d_p - 4.20 \end{aligned} \quad (52)$$

where the units of β and d_p are s⁻¹ and μm, respectively.

Interaction Between Gas-Phase Pollutants and Settled Dust

Overall

Settled dust are deposited particles on surfaces and always is a heterogeneous matrix. Indoor settled dust may incorporate harmful chemicals either by adsorption of gas phase, partitioning between dust and source material if dust is deposited on source

surface, or deterioration of indoor materials or consumer products (including microplastics in some cases). Due to its large specific area, settled dust is an important transfer and storage medium of indoor chemical pollutants (Bi 2018). The mixture of chemicals frequently detected in indoor settled dust include (Melymuk et al. 2020):

- Plastic additives: flame retardants (including polybrominated diphenyl ethers, hexabromocyclododecanes, and organophosphate ester flame retardants) and plasticizers (mainly phthalate esters and their alternatives)
- Polymer components such as bisphenols (bisphenol A, F, S, and AF) and alkylphenols
- Personal care and cleaning product components: parabens, synthetic fragrance compounds, triclosan, siloxanes, and UV filters
- Perfluorinated alkyl substances (PFASs) and related fluorinated compounds
- Pesticides: both banned “legacy” pesticides (like DDT and hexachlorocyclohexanes) and currently used pesticides (such as chlorpyrifos and permethrin)
- Industrial compounds, such as polychlorinated biphenyls (PCBs) and chlorinated paraffins
- Combustion by-products, e.g., polycyclic aromatic hydrocarbons, poly-chlorinated dibenzo-p-dioxins/dibenzofurans, and degradation products (e.g., polybrominated dibenzo-p-dioxins/dibenzofurans), and related compounds (e.g., nicotine)
- Heavy metals, particularly lead

According to the definition of SVOCs by Weschler and Nazaroff (2008), i.e., organic compounds with vapor pressures between 10^{-9} and 10 Pa, most of the above chemicals are SVOCs (except for heavy metals). This behavior can be expected because the relatively low volatility of SVOCs leads to their strong partitioning from gas phase to dust.

The highly contaminated dust may result in significant human exposure to chemicals by ingestion via hand-to-mouth or hand-to-object-to-mouth contact, inhalation of re-suspended particles, or dermal penetration by contact, as discussed in ► Chap. 35, “Exposure Routes and Types of Exposure” of this handbook. Particularly, Glorennec et al. (2021) pointed out that dust ingestion can be a strong contributor to total dust exposure for brominated flame retardants, certain phthalates, and polycyclic aromatic hydrocarbons. Therefore, Glorennec et al. (2021) further suggested to consider an indoor settled dust guideline as part of a policy to reduce exposure indoors to a given chemical or group of chemicals.

Settled dust that is sampled from floors, mattresses, moldings, and shelves has been widely used as an indicator for indoor pollutants (especially for SVOCs), due to its merits of low cost to collect and high concentrations of chemical pollutants (Melymuk et al. 2020). Indoor settled dust can often be regarded as a “passive sampler” for assessing the levels and human exposure of indoor pollutants. Therefore, it is of great importance to understand the transport of

SVOCs to settled dust, including the interaction between gas-phase SVOCs and settled dust.

Equilibrium Model

Similar to airborne particles, an equilibrium model was also often used to describe the interaction between gas-phase SVOCs and settled dust. Thus, SVOC concentration in settled dust is linearly correlated with gas-phase SVOC concentration by assuming that the gas-dust interaction reaches equilibrium immediately (Weschler and Nazaroff 2010),

$$X_{dust} = K_d C_g \quad (53)$$

where X_{dust} ($\mu\text{g/g}$) is the mass fraction of SVOCs in settled dust and K_d (m^3/g) is the dust-air partition coefficient of SVOCs.

Weschler and Nazaroff (2010) compared X_{dust} predicted by Eq. (53) to the measured median data reported in literature for 66 different SVOCs whose K_{OA} span more than five orders of magnitude. Even though the predictions correlated reasonably well with measurements ($R^2 = 0.76$), the authors also noted that the measured X_{dust} were systematically less than the predicted results for SVOCs with high K_{OA} , especially for SVOCs with K_{OA} larger than 10^{12} . The differences are mainly caused by the assumption of gas-dust equilibrium because X_{dust} may not have sufficient time to reach the equilibrium state as the value of K_{OA} increases (or K_d increases). Taking DEHP as an example, the time scale required to reach gas-dust equilibrium may be over 200 days according the model analysis of Kang et al. (2021) ($K_{OA} = 10^{11}$ for DEHP in their calculations), which may be significantly longer than the residence time of indoor settled dust (> 2000 hours if dust resuspension is the only removal mechanism according to Shi and Zhao (2015)). Thereafter, many studies have intended to model the dynamic interaction between SVOCs and indoor settled dust.

Dynamic Models

The migration of chemicals to settled dust mainly involves three pathways: (1) direct contact between the source surface and dust (direct contact), (2) volatilization from the source material and then accumulation in dust via the air (non-direct contact), and (3) abrasion of particles from product directly forming dust (Melymuk et al. 2020; Rauert and Harrad 2015; Sukiene et al. 2016). The dominant pathway depends on the source type as well as the compound's chemical properties (Sukiene et al. 2016). For example, Rauert and Harrad (2015) indicated that nondirect contact is minimal and abrasion/direct contact dominate for PBDEs from plastic TV casing, while Sukiene et al. (2016) postulated that the nondirect contact might be the dominant pathway (based on a small-scale field study for nine

SVOCs) and K_{OA} was a major determinant for the transfer of SVOCs into settled dust (SVOC with high K_{OA} is more likely to be found in dust than in air). To study the dynamic migration of SVOCs into settled dust, several models have been proposed.

Model Based on Aerosol Dynamics

With the assumption that indoor settled dust is a thin layer of particles on nonsource surfaces, Shi and Zhao (2015) developed a model to estimate X_{dust} of SVOCs by considering aerosol dynamics including particle deposition and resuspension. The particles were divided into n size bins. For i th size bin, they predicted the indoor mass load of settled dust on surface by the following equation:

$$\frac{dM_i}{dt} = v_{d,i}C_{mp,i} - R_{p,i}M_i \quad (54)$$

where M ($\mu\text{g}/\text{m}^2$) is the mass load of settled dust on surface, v_d (m/s) is the particle deposition velocity onto surface, and R_p (s^{-1}) is the particle resuspension rate. Details about v_d and R_p can be found in ► Chaps. 11, “Deposition,” and ► 12, “Resuspension,” of this handbook.

The indoor SVOCs associated with settled dust are affected by suspended particle deposition and settled dust resuspension. The concentration of SVOC in the settled dust in the i th size bin was then expressed as:

$$\frac{d(M_i X_{dust,i})}{dt} = h_{md} A_{dn,i} N_{dn,i} \left(C_g - \frac{X_{dust,i}}{K_d} \right) + v_{d,i} C_{sp,i} - R_{p,i} M_i X_{dust,i} \quad (55)$$

where h_{md} (m/s) is the mass transfer coefficient at the surface of settled dust, A_{dn} (m^2) is the surface area of a single dust particle, and N_{dn} (m^{-2}) is the number concentration of dust particles. The first term on the right-hand side represents the kinetic sorption between gas-phase SVOCs and settled dust. The second and third terms on the right-hand side represent the deposition of SVOCs associated with suspended particles and resuspension of SVOCs associated with settled dust, respectively. A_{dn} equals $\pi \cdot d_{dn}^2$ if dust particles are treated as a sphere, where d_{dn} is the diameter of dust particle. N_{dn} can be estimated by $M/(\rho_{dust} \cdot \pi \cdot d_{dn}^3 / 6)$, where ρ_{dust} is the density of dust particles. h_{md} was set to be the convective mass transfer coefficient of SVOCs onto flat surfaces, which may be biased because the surface of settled dust may be less smooth than flat surfaces.

Finally, the mass fraction of SVOCs in settled dust can be obtained by

$$X_{dust} = \sum_{i=1}^n X_{dust,i} \quad (56)$$

Shi and Zhao (2015) compared the predictions of Eqs. (54), (55), and (56) with the measured X_{dust} of 66 SVOCs reported in the literature (similar to the dataset of Weschler and Nazaroff (2010)). Compared to the equilibrium model, greater

consistency was observed between the predictions and measurements, demonstrating the good performance of their model.

The dust layer is a type of porous medium. The above model (Eqs. 54, 55, and 56) did not consider the influence of the structure of the dust layer on the concentration and change in the concentration gradient within the dust layer (Kang et al. 2021). Therefore, it is not possible to understand the mass transfer mechanism of phthalates in settled dust at the microlevel. More importantly, some of the published studies have demonstrated that the direct-contact pathway may play a much more extensive role than the nondirect contact pathway (Rauert and Harrad 2015; Schripp et al. 2010; Shinohara and Uchino 2020) that was not considered in the model. Therefore, Bi et al. (2021) proposed a diffusion-based model to estimate the direct transfer of SVOCs from the source surface to settled dust by considering the diffusion of gas-phase SVOCs in voids of dust layer. Soon afterward, Kang et al. (2021) extended the model to consider both the direct contact and nondirect contact pathways as well as solid-phase diffusion of SVOCs within the dust particles, which is introduced as follows.

Diffusion-Based Model

The transfer process of SVOCs from indoor sources to settled dust is shown schematically in Fig. 5. For simplification, the effects of the aerosol dynamics

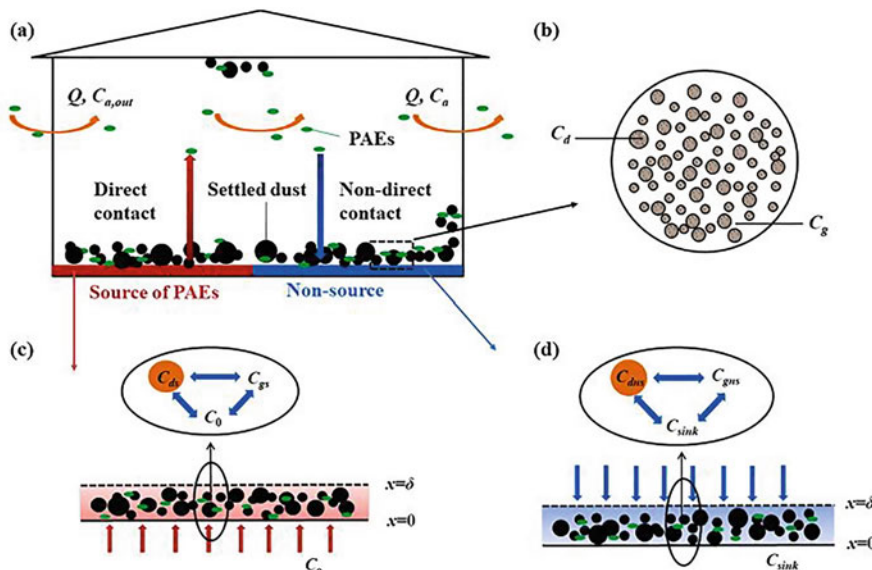


Fig. 5 Schematic representation of (a) migration of SVOCs from source to settled dust, (b) the equilibrium state in the dust layer, (c) the boundary condition of PAEs on the source surface, and (d) the boundary condition of PAEs on the nonsource surfaces. (Reprinted from Kang et al. (2021), Copyright (2021), with permission from Elsevier)

including particle deposition and dust resuspension are ignored. The change in the thickness and mass load of the settled dust is not considered in the model. Figure 5b is a downward view of the dust layer. As shown, the dust on the floor can be regarded as porous media, and an instantaneous equilibrium between gas-phase SVOCs in the pores and the sorption phase SVOCs in the matrix of the dust is assumed to be existed.

For a specific thickness of dust, the governing equations describing the migration of SVOCs between the source and nonsource surface with the dust on the surfaces can be expressed as:

$$(1 - \varepsilon)D_d \frac{\partial^2 X_{dust,s}}{\partial x^2} + \varepsilon D_g \frac{\partial^2 C_{g,d,s}}{\partial x^2} = (1 - \varepsilon) \frac{\partial X_{dust,s}}{\partial t} + \varepsilon \frac{\partial C_{g,d,s}}{\partial t}, \quad 0 < x < \delta \quad (57)$$

$$(1 - \varepsilon)D_d \frac{\partial^2 X_{dust,ns}}{\partial x^2} + \varepsilon D_g \frac{\partial^2 C_{g,d,ns}}{\partial x^2} = (1 - \varepsilon) \frac{\partial X_{dust,ns}}{\partial t} + \varepsilon \frac{\partial C_{g,d,ns}}{\partial t}, \quad 0 < x < \delta \quad (58)$$

where δ (m) is the thickness of the settled dust, x (m) is the distance to the surface, ε (dimensionless) is the porosity of the settled dust, D_d (m^2/s) is the diffusion coefficient of SVOCs in the dust matrix, $C_{g,d}$ ($\mu\text{g}/\text{m}^3$) is the gas-phase concentration of SVOCs in the voids of dust matrix, and the subscript s and ns represent the source surface and nonsource surface, respectively. The first and second terms on the left-hand side represent the solid-phase diffusion of SVOCs with the dust particles and the diffusion of gas-phase SVOCs in voids of dust matrix, respectively. The first and second terms on the right-hand side represent the temporal variation of dust- and gas-phase SVOC concentrations, respectively.

Within the dust matrix, a linear partition relationship between the gas-phase concentration and dust-phase concentration can be obtained due to the assumption of instantaneous equilibrium, i.e., Eq. (53). For settled dust on source surface, if there is an equilibrium state between the concentration in the source, dust-phase concentration, and gas-phase concentration at the interface on the source, as shown in Fig. 5c, the boundary condition at the interface between the source and settled dust can be expressed as:

$$X_{dust,s}|_{x=0} = \frac{K_d C_0}{K_{sg}} \quad (59)$$

$$C_{g,d,s}|_{x=0} = \frac{C_0}{K_{sg}} \quad (60)$$

where K_{sg} (dimensionless) is the partition coefficient between gas phase and the source and C_0 ($\mu\text{g}/\text{m}^3$) is the concentration of SVOCs in the source (which is always treated as a constant due to the slow loss of SVOCs from the source material (Xu and Little 2006)).

At the interface between the settled dust and gas phase, the convective mass transfer boundary for settled dust on source surfaces can be expressed as:

$$-(1 - \varepsilon)D_d \frac{\partial X_{dust,s}}{\partial x} \Big|_{x=\delta} - \varepsilon D_g \frac{\partial C_{g,d,s}}{\partial x} \Big|_{x=\delta} = h_{m,s}(C_{g,s} - C_g) \quad (61)$$

where C_g ($\mu\text{g}/\text{m}^3$) is the gas-phase concentration of SVOCs in the surrounding air.

For the nonsource surface, the boundary condition is similar to the boundary conditions for the source when $x = \delta$. Although the parameters for the dust on the source and nonsource surfaces may be different, the same properties and morphologies were assumed. When $x = 0$, the dynamic adsorption of gas-phase SVOCs onto the nonsource surface should be considered. If there is a state of equilibrium between the surface-phase concentration and gas-phase concentration, as shown in Fig. 5d, the boundary conditions for the nonsource can be described mathematically by the following equations:

$$-(1 - \varepsilon)D_d \frac{\partial X_{dust,ns}}{\partial x} \Big|_{x=0} - \varepsilon D_g \frac{\partial C_{g,d,ns}}{\partial x} \Big|_{x=0} = \frac{dC_{ns}}{dt} \quad (62)$$

$$-(1 - \varepsilon)D_d \frac{\partial X_{dust,ns}}{\partial x} \Big|_{x=\delta} - \varepsilon D_g \frac{\partial C_{g,d,ns}}{\partial x} \Big|_{x=\delta} = h_{m,ns}(C_{g,d,ns} - C_g) \quad (63)$$

$$C_{ns} = K_{ns} \cdot C_{g,d,ns} \Big|_{x=0} \quad (64)$$

where C_{ns} ($\mu\text{g}/\text{m}^2$) is the surface-phase concentration of SVOCs on nonsource surface and K_{ns} (m) is the partition coefficient between the gas and the sink (nonsource).

Assuming that the settled dust has no SVOCs initially, and the initial conditions are:

$$X_{dust,s} = X_{dust,ns} = 0, \quad C_{g,d,s} = C_{g,d,ns} = 0 \quad (65)$$

Based on Eqs. (57), (59), (60), (61), and (65), the dynamic transfer of SVOCs from the source into settled dust on the source surface can be estimated. Eqs. (58), (62), (63), (64), and (65) can be used to describe the corresponding process on nonsource surface.

For settled dust on source surface, good agreement between model predictions and measurements (experimental data of DEHP from Bi et al. (2021)) was obtained by Kang et al. (2021). However, the model performance has not been evaluated for nonsource surface. In addition, the effects of aerosol dynamics were ignored in the model of Kang et al. (2021), which may limit its application for realistic cases where airborne particles are continuously settled onto the surface.

None of the above models considered the source abrasion pathway, which may lead to underestimation of X_{dust} in realistic settled dust. In addition, the age (or residence time) of settled dust is another key parameter in the dynamic models, which is usually unknown and challenging to be obtained. Shi and Zhao (2015) set the residence time of settled dust to 7 days by assuming that settled dust was removed by cleaning activities once a week. While in the calculations of Kang

et al. (2021), the residence time of settled dust was well controlled because the measurements were obtained using chamber experiments that would be very different from the actual indoor conditions. Overall, further study is required for developing approaches for the accurate estimation of X_{dust} .

Dust-Gas Partition Coefficient (K_d)

K_d is always expected to be directly proportional to K_{OA} and the fraction of organic matter in the settled dust (f_{om_dust} , dimensionless), and inversely proportional to the dust density (ρ_{dust} , g/m³):

$$K_d = \frac{f_{om_dust} \cdot K_{OA}}{\rho_{dust}} \quad (66)$$

In existing studies using Eq. (66) to estimate K_d , f_{om_dust} and ρ_{dust} were often set to be 0.2 and 2.0×10^6 g/m³ (Weschler and Nazaroff 2010), respectively, if there are no measured results. As discussed above, acceptable agreement between measurements and estimations can be obtained using Eq. (66) and these values, especially for SVOCs with $K_{OA} < 10^8$. Additionally, the pp-LFER approach may also be applicable for estimating K_d . However, its performance has not yet been evaluated.

Studies have attempted to measure K_d of SVOCs by assuming that the interaction between gas-phase SVOCs and settled dust had reached equilibrium. According to the equilibrium model (i.e., Eq. 53), K_d can be calculated by X_{dust}/C_g by simultaneously measuring X_{dust} and C_g . Table 2 listed the results of K_d obtained from some published studies. It can be seen that K_d 's for similar SVOCs are inconsistent among the studies, e.g., K_d of DEHP varies from 258 m³/g to 1.1×10^5 m³/g. The inconsistencies may be due to the difference in the composition of the measured dust (mainly f_{om_dust}) and the migration pathways of SVOCs to dust (nondirect versus direct contact). Another potential reason may be the nonequilibrium interaction between SVOCs and settled dust, i.e., lower K_d values were measured in field tests (realistic indoor environments, the equilibrium state is not guaranteed), while the extremely high K_d values were measured in chamber studies (in which the equilibrium was observed in the experiments). Finally, significant deviations between the measured K_d and the predictions of Eq. (66) have also been noted, especially for SVOCs with larger K_{OA} (or K_d) (Bu et al. 2016). How to improve the accuracy of the estimation or measurement of K_d is worthy of further study.

Conclusions

Gas-phase pollutants can interact with or partition to indoor particles (including both airborne and settled particles) and subsequently influence the transport, fate, and human exposure of these pollutants in indoor environments. Several models including equilibrium and dynamic approaches have been proposed to describe the interactions between gas-phase pollutants and indoor particles. Methods have also been

Table 2 Measured results of dust-gas partition coefficient (K_d) obtained from the literature

SVOCs ^a	Dust type	Pathways	K_d (m ³ /g)	Temperature	References		
BBzP	House dust (field) ^b	Nondirect contact	962	21 °C	Bi et al. (2015)		
			202	30 °C			
			1970	21 °C			
			258	30 °C			
DiBP	House dust (field) ^b	No specific pathway	2.91 ~ 9.59	22 ~ 29 °C	Pei et al. (2018)		
DnBP			12.19 ~ 70.70				
DEHP			430 ~ 7690				
DEHP	House dust (chamber) ^c	Nondirect contact	1.4×10^5	28 °C	Shinohara and Uchino (2020)		
DnBP	House dust (chamber) ^c	Direct contact	7500 Low dust loading	25 °C	Bi et al. (2021)		
DEHP			5800 High dust loading				
			(0.23 ~ 1.1) × 10 ⁵ Low dust loading				
			(1.7 ~ 4.2) × 10 ⁴ High dust loading				
TCEP	House dust (chamber) ^c	Direct contact	20.75	20 ~ 23 °C	Liu and Folk (2021)		
TCPP	House dust (chamber) ^c	Nondirect contact	5.21				
	Arizona test dust (chamber) ^c	Direct contact	85.5				
TDCPP	House dust (chamber) ^c	Direct contact	14.8	(continued)			
	House dust (chamber) ^c	Nondirect contact	3.4				
	Arizona test dust (chamber) ^c	Direct contact	224.4				
TDCPP	House dust (chamber) ^c	Direct contact	273.8				
	House dust (chamber) ^c	Nondirect contact	42.8				
	Arizona test dust (chamber) ^c	Direct contact	13.7				

(continued)

Table 2 (continued)

SVOCs ^a	Dust type	Pathways	K_d (m ³ /g)	Temperature	References
PCB-8	House dust (chamber) ^c	Nondirect contact	$10^{0.2}$	Around 23 °C	Andersen and Frederiksen (2021)
PCB-18			$10^{0.3}$		
PCB-28			$10^{0.8}$		
PCB-31			$10^{0.8}$		
PCB-44			$10^{1.1}$		
PCB-52			$10^{1.0}$		
PCB-66			$10^{1.6}$		
PCB-74			$10^{1.4}$		
PCB-99			$10^{1.7}$		
PCB-101			$10^{1.6}$		

^aBBzP: Butyl benzyl phthalate; DiBP: Diisobutyl phthalate; DnBP: Di-n-butyl phthalate; DEHP: Di(2-ethylhexyl) phthalate; TCEP: Tris (chloroethyl) phosphate; TCPP: Tris (2-chloroisopropyl) phosphate; TDCPP: Tris (1,3-dichloro-2-propyl) phosphate; PCB: polychlorinated biphenyl

^b“Field” represents the measurements were conducted in realistic indoor environments

^c“Chamber” represents the results were obtained via a specially designed chamber

developed for measuring key parameters involved in these models, especially for the particle-gas partition coefficients (K_p for airborne particles and K_d for settled dust). These studies are helpful for understanding and describing the interactions between gas-phase pollutants and indoor particles. However, in many cases, equilibrium is not achieved and the parameter values needed in the models are not well known. Additionally, the surface of particles can be either organic or aqueous (depending on the RH of indoor air and the particle origin). RH should be a key factor that may significantly affect the gas-particle interactions of indoor pollutants (for both hydrophilic and hydrophobic species). However, the existing studies about the gas-particle interactions of indoor SVOCs have paid much less attention to the aqueous layers of particles and the effects of RH, especially in those studies that developed the dynamic models and the measurement methods for key parameters (both K_p and K_d). Thus, further study is required for comprehensively evaluating the performance of existing models (evaluating the agreement between model predictions and experimental measurements), improving the accuracy, stability, and practicability of the methods for measuring/predicting key parameters, and revealing the role of some key factors (such as the indoor temperature and RH, the organic and aqueous constituents of particles, and the physicochemical properties of SVOCs, e.g., the hydrophilic/hydrophobic property, the lipid solubility, and the volatility).

Cross-References

- [Deposition](#)
- [Exposure Routes and Types of Exposure](#)

- Resuspension
- Source/Sink Characteristics of SVOCs

Acknowledgments The author acknowledges the Natural Science Foundation of China (No. 51908563), Guangdong Basic and Applied Basic Research Foundation (No. 2019A1515011179), Science and Technology Program of Guangzhou (No. 202102020990), and the special fund of Beijing Key Laboratory of Indoor Air Quality Evaluation and Control (No. BZ0344KF20-11) for financial support.

References

- Abraham MH (1993) Scales of solute hydrogen-bonding: their construction and application to physicochemical and biochemical processes. *Chem Soc Rev* 22(2):73–83
- Abraham MH, McGowan JC (1987) The use of characteristic volumes to measure cavity terms in reversed phase liquid chromatography. *Chromatographia* 23(4):243–246
- Andersen HV, Frederiksen M (2021) Sorption of PCB from air to settled house dust in a contaminated indoor environment. *Chemosphere* 266:129139
- Benning JL, Liu Z, Tiwari A, Little JC, Marr LC (2013) Characterizing gas-particle interactions of phthalate plasticizer emitted from vinyl flooring. *Environ Sci Technol* 47(6):2696–2703
- Bi C (2018) Sorption of semi-volatile organic compounds to dust and other surfaces in indoor environments. The University of Texas at Austin
- Bi C, Liang Y, Xu Y (2015) Fate and transport of phthalates in indoor environments and the influence of temperature: a case study in a test house. *Environ Sci Technol* 49(16):9674–9681
- Bi C, Wang X, Li H, Li X, Xu Y (2021) Direct transfer of phthalate and alternative plasticizers from indoor source products to dust: laboratory measurements and predictive modeling. *Environ Sci Technol* 55(1):341–351
- Bu Z, Zhang Y, Mmereki D, Yu W, Li B (2016) Indoor phthalate concentration in residential apartments in Chongqing, China: implications for preschool children's exposure and risk assessment. *Atmos Environ* 127:34–45
- Cao J, Zhang X, Little JC, Zhang Y (2017) A SPME-based method for rapidly and accurately measuring the characteristic parameter for DEHP emitted from PVC floorings. *Indoor Air* 27(2): 417–426
- Cao J, Mo J, Sun Z, Zhang Y (2018) Indoor particle age, a new concept for improving the accuracy of estimating indoor airborne SVOC concentrations, and applications. *Build Environ* 136:88–97
- Cao J, Eichler CMA, Wu Y, Little JC (2019) Dynamic method to measure partition coefficient and mass accommodation coefficient for gas–particle interaction of phthalates. *Aerosol Sci Technol* 53(10):1158–1171
- Cappa C (2010) A model of aerosol evaporation kinetics in a thermodenuder. *Atmos Meas Tech* 3(3):579–592
- Cousins IT, Mackay D (2001) Gas–particle partitioning of organic compounds and its interpretation using relative solubilities. *Environ Sci Technol* 35(4):643–647
- Davis EJ (2006) A history and state-of-the-art of accommodation coefficients. *Atmos Res* 82(3–4): 561–578
- Eichler CMA, Hubal EAC, Xu Y, Cao J, Bi C, Weschler CJ, Salthammer T, Morrison GC, Koivisto AJ, Zhang Y, Mandin C, Wei W, Blondeau P, Poppendieck D, Liu X, Delmaar CJE, Fantke P, Jolliet O, Shin H-M, Diamond ML, Shiraiwa M, Zuend A, Hopke PK, von Goetz N, Kulmala M, Little JC (2021) Assessing human exposure to SVOCs in materials, products, and articles: a modular mechanistic framework. *Environ Sci Technol* 55(1):25–43
- Finizio A, Mackay D, Bidleman T, Harner T (1997) Octanol-air partition coefficient as a predictor of partitioning of semi-volatile organic chemicals to aerosols. *Atmos Environ* 31(15): 2289–2296

- Fuller EN, Schettler PD, Giddings JC (1966) New method for prediction of binary gas-phase diffusion coefficients. *Ind Eng Chem* 58(5):18–27
- Glorennec P, Shendell DG, Rasmussen PE, Waeber R, Egeghy P, Azuma K, Pelfrene A, Le Bot B, Esteve W, Perouel G, Pernelet Joly V, Noack Y, Delannoy M, Keirsbulck M, Mandin C (2021) Toward setting public health guidelines for chemicals in indoor settled dust? *Indoor Air* 31(1): 112–115
- Goss KU (2005) Predicting the equilibrium partitioning of organic compounds using just one linear solvation energy relationship (LSER). *Fluid Phase Equilib* 233(1):19–22
- Guo Z (2013) A framework for modelling non-steady-state concentrations of semivolatile organic compounds indoors – II. Interactions with particulate matter. *Indoor Built Environ* 23(1):26–43
- Harner T, Bidleman TF (1998) Octanol– air partition coefficient for describing particle/gas partitioning of aromatic compounds in urban air. *Environ Sci Technol* 32(10):1494–1502
- Jefferson A, Eisele F, Zieman P, Weber R, Marti J, McMurry P (1997) Measurements of the H₂SO₄ mass accommodation coefficient onto polydisperse aerosol. *J Geophys Res-Atmos* 102 (D15):19021–19028
- Junge C (1977) Basic considerations about trace constituents in the atmosphere as related to the fate of global pollutants. *Fate of pollutants in the air and water environments*. Wiley, New York
- Kang L, Wu S, Liu K, Wang X, Zhou X (2021) Direct and non-direct transfer of phthalate esters from indoor sources to settled dust: model analysis. *Build Environ* 202:108012
- Lai AC, Nazaroff WW (2000) Modeling indoor particle deposition from turbulent flow onto smooth surfaces. *J Aerosol Sci* 31(4):463–476
- Lazarov B, Swinnen R, Poelmans D, Spruyt M, Goelen E, Covaci A, Stranger M (2016) Influence of suspended particles on the emission of organophosphate flame retardant from insulation boards. *Environ Sci Pollut Res* 23(17):17183–17190
- Levin VA (1980) Relationship of octanol-water partition-coefficient and molecular-weight to rat-brain capillary-permeability. *J Med Chem* 23(6):682–684
- Liang Y, Xu Y (2014) Improved method for measuring and characterizing phthalate emissions from building materials and its application to exposure assessment. *Environ Sci Technol* 48(8): 4475–4484
- Liu C, Cao J (2018) Potential role of intraparticle diffusion in dynamic partitioning of secondary organic aerosols. *Atmos Pollut Res* 9(6):1131–1136
- Liu X, Folk E (2021) Sorption and migration of organophosphate flame retardants between sources and settled dust. *Chemosphere* 278:130415
- Liu C, Morrison GC, Zhang Y (2012) Role of aerosols in enhancing SVOC flux between air and indoor surfaces and its influence on exposure. *Atmos Environ* 55:347–356
- Liu C, Shi S, Weschler CJ, Zhao B, Zhang Y (2013) Analysis of the dynamic interaction between SVOCs and airborne particles. *Aerosol Sci Technol* 47(2):125–136
- Liu C, Cao J, Zhang Y (2016) Simplifying analysis of sorption of SVOCs to particles: lumped parameter method and application condition. *Int J Heat Mass Tran* 99:402–408
- Lohmann R, Lammel G (2004) Adsorptive and absorptive contributions to the gas-particle partitioning of polycyclic aromatic hydrocarbons: state of knowledge and recommended parametrization for modeling. *Environ Sci Technol* 38(14):3793–3803
- Melymuk L, Demirtepe H, Jílková SR (2020) Indoor dust and associated chemical exposures. *Curr Opin Environ Sci Health* 15:1–6
- Pankow JF (1987) Review and comparative-analysis of the theories on partitioning between the gas and aerosol particulate phases in the atmosphere. *Atmos Environ* 21:2275–2283
- Pankow JF (1994) An absorption model of gas/particle partitioning of organic compounds in the atmosphere. *Atmos Environ* 28(2):185–188
- Pankow JF (1998) Further discussion of the octanol/air partition coefficient K_{oa} as a correlating parameter for gas/particle partitioning coefficients. *Atmos Environ* 32(9):1493–1497
- Pei J, Sun Y, Yin Y (2018) The effect of air change rate and temperature on phthalate concentration in house dust. *Sci Total Environ* 639:760–768
- Rauert C, Harrad S (2015) Mass transfer of PBDEs from plastic TV casing to indoor dust via three migration pathways – a test chamber investigation. *Sci Total Environ* 536:568–574

- Riley WJ, McKone TE, Lai AC, Nazaroff WW (2002) Indoor particulate matter of outdoor origin: importance of size-dependent removal mechanisms. *Environ Sci Technol* 36(2):200–207
- Saleh R, Khlystov A, Shihadeh A (2012) Determination of evaporation coefficients of ambient and laboratory-generated semivolatile organic aerosols from phase equilibration kinetics in a thermodesnuder. *Aerosol Sci Technol* 46(1):22–30
- Salthammer T, Goss KU (2019) Predicting the gas/particle distribution of SVOCs in the indoor environment using poly parameter linear free energy relationships. *Environ Sci Technol* 53(5): 2491–2499
- Salthammer T, Schripp T (2015) Application of the Junge- and Pankow-equation for estimating indoor gas/particle distribution and exposure to SVOCs. *Atmos Environ* 106:467–476
- Salthammer T, Zhang Y, Mo J, Koch HM, Weschler CJ (2018) Assessing human exposure to organic pollutants in the indoor environment. *Angew Chem Int Edit* 57(38):12228–12263
- Schripp T, Fauck C, Salthammer T (2010) Chamber studies on mass-transfer of di(2-ethylhexyl) phthalate (DEHP) and di-n-butylphthalate (DnBP) from emission sources into house dust. *Atmos Environ* 44(24):2840–2845
- Seinfeld JH, Pandis SN (2016) Atmospheric chemistry and physics: from air pollution to climate change. Wiley
- Shi S, Zhao B (2012) Comparison of the predicted concentration of outdoor originated indoor polycyclic aromatic hydrocarbons between a kinetic partition model and a linear instantaneous model for gas–particle partition. *Atmos Environ* 59:93–101
- Shi S, Zhao B (2015) Estimating indoor semi-volatile organic compounds (SVOCs) associated with settled dust by an integrated kinetic model accounting for aerosol dynamics. *Atmos Environ* 107:52–61
- Shi S, Zhao B (2014) Modeled exposure assessment via inhalation and dermal pathways to airborne semivolatile organic compounds (SVOCs) in residences. *Environ Sci Technol* 48(10):5691–5699
- Shinohara N, Uchino K (2020) Diethylhexyl phthalate (DEHP) emission to indoor air and transfer to house dust from a PVC sheet. *Sci Total Environ* 711:134573
- Shiraiwa M, Ammann M, Koop T, Pöschl U (2011) Gas uptake and chemical aging of semisolid organic aerosol particles. *Proc Natl Acad Sci USA* 108(27):11003–11008
- Sukiene V, Gerecke AC, Park YM, Zennegg M, Bakker MI, Delmaar CJ, Hungerbuhler K, von Goetz N (2016) Tracking SVOCs' transfer from products to indoor air and settled dust with deuterium-labeled substances. *Environ Sci Technol* 50(8):4296–4303
- Theis AL, Waldack AJ, Hansen SM, Jeannot MA (2001) Headspace solvent microextraction. *Anal Chem* 73(23):5651–5654
- Ulrich N, Endo S, Brown TN, Watanabe N, Bronner G, Abraham MH, Goss KU (2017) UFZ-LSER database v 3.2.1 [Internet]. Leipzig
- Wakao N, Smith JM (1962) Diffusion in catalyst pellets. *Chem Eng Sci* 17(11):825–834
- Wang X, Tao W, Xu Y, Feng J, Wang F (2014) Indoor phthalate concentration and exposure in residential and office buildings in Xi'an, China. *Atmos Environ* 87:146–152
- Wang X, Bi C, Xu Y (2015) Modeling and analysis of sampling artifacts in measurements of gas-particle partitioning of semivolatile organic contaminants using filter-sorbent samplers. *Atmos Environ* 117:99–109
- Weber WJJ, Digiano FA (1996) Process dynamics in environmental systems. Wiley, New York
- Wei W, Mandin C, Blanchard O, Mercier F, Pelletier M, Le Bot B, Glorenne P, Ramalho O (2016) Distributions of the particle/gas and dust/gas partition coefficients for seventy-two semi-volatile organic compounds in indoor environment. *Chemosphere* 153:212–219
- Wei W, Mandin C, Blanchard O, Mercier F, Pelletier M, Le Bot B, Glorenne P, Ramalho O (2017) Predicting the gas-phase concentration of semi-volatile organic compounds from airborne particles: application to a French nationwide survey. *Sci Total Environ* 576:319–325
- Wensing M, Uhde E, Salthammer T (2005) Plastics additives in the indoor environment--flame retardants and plasticizers. *Sci Total Environ* 339(1–3):19–40

- Weschler CJ, Nazaroff WW (2008) Semivolatile organic compounds in indoor environments. *Atmos Environ* 42(40):9018–9040
- Weschler CJ, Nazaroff WW (2010) SVOC partitioning between the gas phase and settled dust indoors. *Atmos Environ* 44(30):3609–3620
- Weschler CJ, Salthammer T, Fromme H (2008) Partitioning of phthalates among the gas phase, airborne particles and settled dust in indoor environments. *Atmos Environ* 42(7):1449–1460
- Wu Y, Eichler CM, Chen S, Little JC (2016) Simple method to measure the vapor pressure of phthalates and their alternatives. *Environ Sci Technol* 50(18):10082–10088
- Wu Y, Eichler CMA, Cao J, Benning JL, Olson A, Chen S, Liu C, Vejerano EW, Marr LC, Little JC (2018) Particle/gas partitioning of phthalates to organic and inorganic airborne particles in the indoor environment. *Environ Sci Technol* 52(6):3583–3590
- Xu Y, Little JC (2006) Predicting emissions of SVOCs from polymeric materials and their interaction with airborne particles. *Environ Sci Technol* 40(2):456–461
- Xu Y, Liu Z, Park J, Clausen PA, Benning JL, Little JC (2012) Measuring and predicting the emission rate of phthalate plasticizer from vinyl flooring in a specially-designed chamber. *Environ Sci Technol* 46(22):12534–12541
- Yamasaki H, Kuwata K, Miyamoto H (1982) Effects of ambient temperature on aspects of airborne polycyclic aromatic hydrocarbons. *Environ Sci Technol* 16(4):189–194
- Yang F, Ding J, Huang W, Xie W, Liu W (2014) Particle size-specific distributions and preliminary exposure assessments of organophosphate flame retardants in office air particulate matter. *Environ Sci Technol* 48(1):63–70
- Ye P, Ding X, Hakala J, Hofbauer V, Robinson ES, Donahue NM (2016) Vapor wall loss of semi-volatile organic compounds in a Teflon chamber. *Aerosol Sci Technol* 50(8):822–834
- Zhang Y, Xiong J, Mo J, Gong M, Cao J (2016) Understanding and controlling airborne organic compounds in the indoor environment: mass transfer analysis and applications. *Indoor Air* 26(1):39–60
- Zhao B, Wu J (2006) Modeling particle deposition from fully developed turbulent flow in ventilation duct. *Atmos Environ* 40(3):457–466
- Zhou S, Shiraiwa M, McWhinney RD, Pöschl U, Abbatt JP (2013) Kinetic limitations in gas-particle reactions arising from slow diffusion in secondary organic aerosol. *Faraday Discuss* 165:391–406



Cooking Aerosol

14

Mehdi Amouei Torkmahalleh

Contents

Introduction	388
Methods	392
Frying Process	392
Hydrolysis	394
Oxidation	394
Thermal Alteration	395
Contribution of Food in the Frying Chemistry	395
Primary Organic Aerosol (POA)	395
Secondary Organic Aerosol (SOA)	396
Controlled Studies	397
Cooking Style/Method/Habit	397
Energy Source	398
Cooking Pan	409
Cooking Oil	411
Additives	413
Food	415
Temperature	415
Surface Area of the Pan/Position of the Pan on a Stove	416
Particle Loss (Coagulation, Ventilation, and Deposition)	417
Particle Morphology	418
Citizen Science	419
Conclusions	419
Cross-References	420
References	420

Previously, Department of Chemical and Materials Engineering, School of Engineering and Digital Sciences, Nazarbayev University, Nur-Sultan, Kazakhstan

M. Amouei Torkmahalleh (✉)

Division of Environmental and Occupational Health Sciences, School of Public Health, University of Illinois Chicago, Chicago, IL, USA

e-mail: memouei@gmail.com; mehdiat@uic.edu

Abstract

Among different indoor sources of aerosol, cooking has been well understood to be one of the major sources of indoor aerosol. This source contributes to indoor ultrafine particles (UFPs) even smaller than 3 nm. Over 700 articles have been published in the past 30 years that address the cooking aerosol. Still this area of research is open for scientists to uncover the underlying mechanisms of the cooking emissions and its health impact. Different areas of the publication have been recognized including emission/concentration/composition, exposure, health, physics/dynamics, and chemistry. We recommend current scientists to concentrate their research to the areas of cooking aerosol and health, and cooking aerosol chemistry and physics that have been given less attention with a particular attention to cluster mode particles (particles smaller than 3 nm). Factors that influence the emission of aerosol during cooking using gas and electric stoves have been reviewed in this chapter. Such factors include cooking method, burner size, type of stove (gas vs. electricity), fuel quality, cooking pan, position of the cooking pan on the stove, surface area of the pan, cooking oil, additives, food, cooking temperature, and ventilation. Changes to the cooking habit may result in significant reductions in the exposure of the cooks and indoor occupants to cooking aerosol.

Keywords

Cooking aerosol · Ultrafine particles · Secondary organic aerosol · Frying · Health

Introduction

People spend a vast majority of their time (up to 87% of their time) indoors (Klepeis et al. 2001). Exposure to indoor air pollution could be more important than exposure to ambient air pollution due to the factors such as higher exposure time and exposure within a confined environment. These differences result in higher exposure to indoor pollutants compared to outdoor pollutants.

Epidemiology, human exposure, and risk assessment studies confirmed the potential health effects associated to cooking emissions. Solid fuel (kerosene, biomass, and coal) cooking and heating in open fires and inefficient stoves have been practiced by three billion people worldwide, particularly in low- and middle-income countries. World Health Organization reported close to four million premature death every year due to household air pollution resulted from inefficient stoves operated by solid fuels and kerosene (WHO: <https://www.who.int/news-room/fact-sheets/detail/household-air-pollution-and-health>). Asthma showed to be positively associated with employing solid fuels cooking including wood, coal, and biomass through large population studies in India (Agrawal 2012) and the USA (Barry et al. 2010).

The contribution of solid fuels to cooking has decreased globally such that the highest reductions were observed in developed countries (Bonjour et al. 2013). In such countries, the indoor level of particulate matter (PM) has been reported to be significantly lower compared to the indoor PM concentration in developing countries (Abdullahi et al. 2013) including Uganda, Ghana, Gambia, Bangladesh, Pakistan, and India (Chowdhury et al. 2012; Hankey et al. 2015; Nasir et al. 2013; Singh 2014; Zhou et al. 2014). This difference is likely to be due to the type of the energy source such as gas or electric stoves used for cooking and heating. However, still there exist risks to human health due to the exposure to cooking particles when gas or electric stoves are used, particularly in poorly ventilated environments (Gorjinezad et al. 2017; Zhang et al. 2017; Sze-To et al. 2012). Category Group 2A, probably carcinogenic to human, was registered to high-temperature frying emissions by International Agency for Research on Cancer (IARC) (Anttila et al. 2006). Polycyclic aromatic hydrocarbons (PAHs) emitted during cooking are marked as potential carcinogenic and mutagenic compounds (Bekö et al. 2013; Jørgensen et al. 2013). A high potential of adverse health effects was reported for people exposed to emissions from Chinese cooking (See and Balasubramanian 2006a). Exposure to cooking emissions on a daily basis was reported to be a risk factor for lung cancer among nonsmoking Taiwanese women. This risk can be greater three times with the number of cooked meals per day (Ko et al. 2000).

Cooking has been proven to be a major source of indoor PM (Dennekamp et al. 2001; Wan et al. 2011). Exposure to cooking PM was found to be higher than the exposure to PM from most other everyday activities (Wallace and Howard-Reed 2002; Wallace and Ott 2011). PM_{2.5} and particle number emission rates during cooking in the kitchen can be higher than the particle emission rate during smoking in the living room (Nasir et al. 2013). Cooking was reported to be the major source of PM_{2.5} and submicron particle (7–808 nm) among 20 indoor activities in 15 houses in Australia (He et al. 2004).

Particles produced by about 1 min of cooking on gas are of similar number to the particles produced by 10 min of cigarette smoking or 1 min driving with heavy-duty vehicles (Kumar et al. 2013). A 3-year study in the USA that investigated particle emissions in indoor environments, including occupied homes, cars, and restaurants, found cooking using gas or electric stoves and toaster ovens to be the major sources of indoor ultrafine particles (UFP) (Wallace and Ott 2011). However, with advancements in aerosol instrumentation such studies deserve revisiting. For example, with the development of new Scanning Mobility Particle Sizer (SMPS), it is currently possible to measure the mobility diameter down to 1 nm.

Numerous studies have shown that several factors including energy sources (gas burners and electric burners) (Wallace et al. 2004b, 2008), cooking additives (Amouei Torkmahalleh et al. 2013a, 2017a), meat (Amouei Torkmahalleh et al. 2017b), cooking oil and cooking temperature (Amouei Torkmahalleh et al. 2012), and cooking pan (Broomandi et al. 2020; Amouei Torkmahalleh et al. 2018, 2019; Wallace et al. 2015) contributed to the particle production.

The particle mode diameter values (the diameter representing the highest particle concentration) during cooking for nine studies and 23 cooking episodes

were reviewed by Abdullahi et al. (2013) and reported to be between 20 and 100 nm. However, recent studies using advanced technologies such as a 1 nm SMPS (TSI, USA) or A11 Nano Condensation Nucleus Counter system (A11-nCNC, Airmodus Oy, Helsinki, Finland) revealed the production of copious numbers of particles smaller than 10 nm during cooking (up to an order of magnitude in count higher than particles larger than 10 nm) (Patel et al. 2020; Wallace et al. 2008). It was found that heating an electric stove or gas-stove burning itself without any cooking materials (such as pan, food, oils, and additives) could be a source of particles smaller than 10 nm with the peak diameter around 5 nm (Wallace et al. 2008).

The most important chemical properties of particles include inorganic ions, elemental composition, and carbonaceous compounds, including black carbon that is found in the cooking PM as well (Abdullahi et al. 2013; Gorjinezad et al. 2017; Zhang et al. 2010). Chronic exposure to cooking PM containing toxic trace elements such as Cu, Fe, and Zn and Polycyclic Aromatic Hydrocarbons (PAHs) could pose adverse health impacts (See and Balasubramanian, 2008). PAHs are among the carcinogenic and mutagenic compounds of cooking emissions that exist in the emitted gas phase as well as the particulate phase (Bekö et al. 2013; Jørgensen et al. 2013). Schauer et al. (2002) investigated the gas phase-emitted compounds during stir-frying in soybean oil, stir-frying in canola oil, and deep-frying potatoes in hydrogenated oil. Results showed carbonyls accounted for 84% of the mass of quantified gas-phase organic compound emitted during stir-frying vegetables in soybean oil. The next largest fraction of the emitted gases accounted for n-alkanoic acids (+25.2 mg/kg of vegetables cooked). Carbonyl emissions in the gas phase were 252 and 108 mg/kg of vegetables cooked during stir-frying in canola oil and deep-frying in hydrogenated soybean oil, respectively.

Naphthalene was the dominant PAH in all three kinds of oils. The emission rate was higher during stir-frying with soybean oil than canola oil and deep-frying. The PAH emission rate was reported to be 654 µg/kg of vegetable cooked, 588 µg/kg of vegetable cooked, and 338 µg/kg of potato cooked, during stir-frying in soybean oil, stir-frying in canola oil, and deep-frying potatoes in hydrogenated oil, respectively. Phenanthrene was the second abundant aromatic hydrocarbon with the emission rate of 138 µg/kg of vegetable cooked, 120 µg/kg of vegetable cooked, and 83 µg/kg of potato cooked, during stir-frying in soybean oil, stir-frying in canola oil, and deep-frying potatoes in hydrogenated oil, respectively.

Among all aliphatic aldehydes, acetaldehyde emission rate was higher for stir-frying in soybean oil (50,100 µg/kg of vegetable cooked) than canola oil (42,200 µg/kg of vegetable cooked) and more than twice bigger than deep-frying (20,900 µg/kg of potato cooked) when stir-frying in soybean oil, stir-frying in canola oil, and deep-frying potatoes in hydrogenated oil were conducted, respectively.

N-Alcanoic acid emission rate during stir-frying in soybean oil, stir-frying in canola oil, and deep-frying of potatoes was as the dominant fatty acid with the concentrations of 11,890 µg/kg of vegetable cooked, 12,200 µg/kg of vegetable cooked, and 3270 µg/kg of potato cooked, respectively. Katragadda et al. (2010) studied VOC emissions including aldehydes during the controlled heating of four

different cooking oils coconut, safflower, canola, and extra virgin olive oils. They reported increased VOC emissions with time such that these emissions increased considerably when the temperature exceeded the oils' smoke temperatures. The temperature at which the cooking oil continuously produces visible smoke is referred as smoke temperature. They found canola oil to emit the lowest amount of toxic compounds compared to other oils. It was concluded that coconut oil was inappropriate for cooking and frying given its low smoke temperature (175 °C). Even at temperatures as low as 180 °C, acrolein (2-propenal), a carcinogenic compound, was found in the cooking emissions (Katragadda et al. 2010).

Peng et al. (2017) examined aldehydes in fumes emitted during cooking using palm oil, rapeseed oil, sunflower oil, and soybean oil, and three cooking methods including stir-frying, panfrying, and deep-frying of two foods (potato and pork loin). The highest total aldehyde emissions were from deep-frying, followed by panfrying, and then stir-frying. Sunflower oil emitted the highest quantity of total aldehydes compared to the other two oils irrespective of cooking method and food type. Peng et al. (2017) suggested that stir-frying using oils structured with low unsaturated fatty acids such as palm oil or rapeseed oil can reduce the production of aldehydes in cooking oil fumes (COFs), in particular longer chain aldehydes such as hexanal and *t,t*-2,4-Decadienal. More information about composition of cooking PM and vapors emitted during cooking was presented by Abdullahi et al. (2013).

Animal studies demonstrated that inhaled insoluble UFPs may translocate to the secondary organs including heart, brain, kidney, and liver through alveolar deposition and the subsequent dissolution into the blood circulation. This translocation may impose subsequent toxicity (Bello and Warheit 2017). Cooking fumes produce a large number of small particles offering high surface area, which could be a crucial factor for particle toxicity. Such small ultrafine particles (UFPs) generated during cooking can be soluble and insoluble. However, the relative contribution of soluble and insoluble cooking particles in total particles has not been addressed in the literature. The insoluble cooking particles including liquid and solid particles may translocate into the blood circulation. However, the morphology of the cooking particles could be crucial for such a translocation. Soluble cooking particles are likely to dissolve into the blood and wash out through the kidney. The composition, size, and morphology of the cooking particles that could be critical factors from health point of view vary with the heating source such as gas burners, electric stoves, and solid fuels. It can also be correlated with the age and gender of the people exposed to the cooking fumes. Thus, studying the health effects of cooking aerosol is of the utmost importance, which has not been carefully explored in the literature so far.

Interest in publishing research articles sharing data on cooking PM has been increasing over past 30 years such that the cumulative number of articles in this field increased from 1 article in 1990 to 24 articles between 1990 and 2000, 153 articles between 1990 and 2010, and 785 articles between 1990 and 2020. The highest number of research articles published data on cooking PM was observed in 2020. From 2015 to 2020, an up to 100% increase in the number of published articles was observed (Fig. 1).

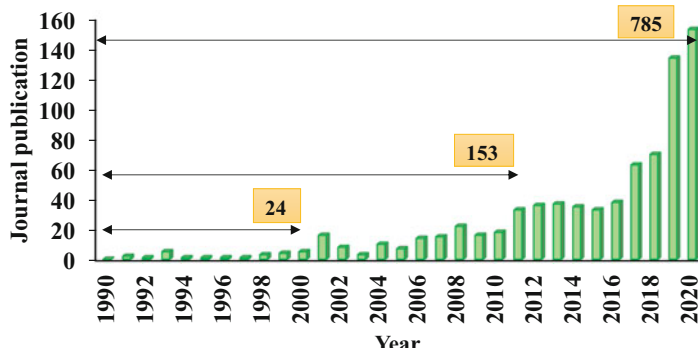


Fig. 1 The number of journal articles addressed cooking PM with time from 1990 to 2020 (all types of energy sources, including gas, electricity, and solid fuels). The numbers on the bars show the cumulative value

Methods

A comprehensive literature search using several keywords including “cooking,” “aerosol,” “particulate matter,” and combinations of these keywords was conducted to find the articles related to cooking emissions (with a focus on cooking PM). Studies on cooking using solid fuels were excluded from further review, and therefore, the focus of this chapter was on the emissions from cooking using gas and electric stoves.

Frying Process

Cooking oils undergo a dynamic and complex chemistry during the frying process. This chemistry is driven by the high temperature of the oil, the presence of the air, and moisture (Sebedio and Juaneda 2007). Fatty acids containing a chain of aliphatic carboxylic acid groups are abundant in vegetable oils (Scrimgeour 2005). Carboxyl and unsaturated groups found in the fatty acids that are among reactive components of the vegetable oils add to the complexity of the chemistry of the frying. Within this chemistry, there are three major chemical reactions during heating oils including hydrolysis, oxidation, and thermal alteration that result in a variety of products (Dobarganes and Márquez-Ruiz 2007).

The major constituents of the cooking oils are triglycerides. Triolein and trilinolein are the dominant triglycerides in cooking oils (Zambiazi et al. 2007). When the temperature of the cooking oils is sufficiently elevated during frying, the triglycerides decompose. As a result, fatty acids such as palmitic acid, linoleic acid, and oleic acid are produced (Crossley et al. 1962) and are likely to be found in the cooking emissions (Amouei Torkmahalleh et al. 2017a). Table 1 presents the composition of the vegetable oils (Zambiazi et al. 2007). As shown in Table 1, triolein and trilinolein are the major constituents of the vegetable oils.

Table 1 Mole fraction of different triglycerides in vegetable oils (Amouei Torkmahalleh et al. 2017a; Zamhiazi et al. 2007). C14:0 – trimyristin, C16:0 – tripalmitin, C16:1 – tripalmitolein, C18:0 – tristearin, C18:1 – triolein, C18:2 – trilinolein, C18:3 – trilinolenin, C20:1 – triarachidin, C20:0 – triarachidin, C22:1 – trierucin

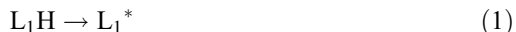
Oil	Trierucin	Trigadolein	Triarachidin	Trilinolenin	Trilinolein	Triolein	Tristearin	Triplamitolein	Triplamitin	Trimyristin
Sunflower	–	0.162	0.303	0.283	71.462	17.044	4.812	0.061	5.823	0.051
Peanut	0.126	1.504	1.451	0.242	32.667	51.241	2.787	0.063	9.886	0.032
Olive	–	0.322	0.503	0.664	7.053	76.014	3.612	0.926	10.906	–
Canola	–	1.556	0.647	8.457	20.329	63.06	1.889	0.212	3.789	0.061
Soybean	–	0.364	0.354	7.694	53.574	23.73	4.434	0.041	9.749	0.061
Safflower	–	–	–	0.15	79.031	11.505	2.401	0.08	6.733	0.1

Hydrolysis

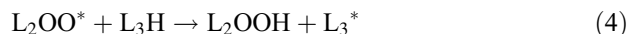
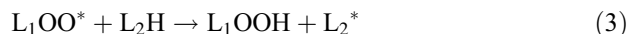
Fats undergo hydrolysis reactions (breakage of the ester bonds) in the presence of the moisture. This simple reaction produces diacylglycerides (DG) and free fatty acids (FFA). Further hydrolysis of DG leads to the formation of monoglycerol (MG), FFA, and glycerol. These chemicals are more polar and have lower molecular weights compared to the parent triglycerides (TG). The fatty acids formed as a result of hydrolysis are reactive and lead to the formation of the volatile organic compounds (VOCs) after the decomposition (Perkins 2007; Ericson 2007). Such VOCs influence the flavor of the fried food. For example, degradation of linoleic acid (C18:2) leads to the formation of acetaldehyde, 1-pentanol, pentanal, hexanal, 2-nonenal, 2-octanal, 2-heptanal, and 2,4-decadienal (Feron et al. 1991; Qu et al. 1992; Subramanian and Nakajima 1997; Wan et al. 1996). Similarly, degradation of oleic acid (C18:1) results in the formation of heptane, octane, heptanol, octanal, nonanal, decanal, 2-decanal, 1-undecen, and 2-undecenal (Feron et al. 1991; Qu et al. 1992; Subramanian and Nakajima 1997; Wan et al. 1996).

Oxidation

Lipid oxidation in air is defined as a classic set of free radical chain reactions involving initiation, propagation, and termination reactions (Schaich 2005). First, hydrogen abstraction occurs on an unsaturated fatty acid resulting in spontaneous free radical formation as presented in Reaction 1:



The resulting radical reacts with oxygen and other TGs (L_n) forming new radicals that propagate the chain reactions as shown below



Heating oil at high temperature triggers new chains producing alkoxyl and hydroxyl radicals as shown by Reaction 5.



Allylic hydroperoxides (LOOH) are the primary products of the FFA oxidation, which are unstable compounds. They decompose and recombine to terminate the radical reactions (Denisov and Afanas'ev 2005; Gunstone et al. 2007). Cyclization

of the alkoxy radical leads to the production of the epoxy, hydroxyl, and hydroperoxy acids located on one of the unsaturated fatty acids of the parent triglyceride. Therefore, oxidized monomers are formed that have at least one oxygenated group such as hydroxyl, epoxy, and keto (Dobarganes and Márquez-Ruiz 2007). Frying represented by high-temperature oil and air favors polymerization reactions that results in the formation of the oxidized dimers and oligomers.

Besides oxidized compounds with higher molecular weights compared to the parent triglycerides, lighter compounds are formed as well. Aldehydes, alkanes, carboxylic acids, esters, and ketones that constitute a major part of VOCs are formed as a result of the scission of peroxides, that is, the breakdown of LOOH products. The recombination of alkoxy radicals (LO^*) yields peroxides and ketones.

Thermal Alteration

High-temperature frying results in the formation of the cyclic fatty acids and nonpolar dimers. Under oxygen deficiency, isomerization and cyclization reactions in the presence of the unsaturated fatty acids take place. The products of such reactions include cis- and transfats with saturated and unsaturated cyclopentyl and cyclohexyl rings (Dobson 1998; Christie and Dobson 2000).

Contribution of Food in the Frying Chemistry

Carbohydrates or sugars in the food experience hydrolysis reactions in the presence of water during thermal cooking. Degradation of sugar molecules takes place during heating such that rings of sugar break and produce aldehydes and acids (Katragadda et al. 2010). As temperate increases sufficiently, the degradation products recombine to make chain-like molecules that can react with the amino acids resulting in the production of VOCs.

Primary Organic Aerosol (POA)

Cooking particles are classified into two groups including primary organic aerosol (POA) and secondary organic aerosol (SOA). However, the SOA is not directly emitted. Rather it is generated through reactions with the vapors emitted during cooking. This process is explained below.

During frying when cooking oil is heated at sufficiently high temperature, a variety of VOCs are generated through hydrolysis, oxidation, and thermal alteration. These VOCs immediately cool to room temperature and become supersaturated in the air above the cooking pan. As a result, the nucleation of these vapors takes place resulting in the production of a copious amount of POA (Amouei Torkmahalleh et al. 2017a).

Secondary Organic Aerosol (SOA)

Indoor SOA chemistry was reviewed by Weschler and Carslaw (2018) and in the section of this handbook on indoor air chemistry. Such chemistry takes place through reactions between ozone and variety of unsaturated indoor vapors such as terpenoid (Weschler and Carslaw 2018), limonene (Chen and Hopke 2010), α and β -pinene (Chen and Hopke 2009a), linalool (Chen and Hopke 2009b), and terpene mixtures (Fan et al. 2005). Typical indoor sources of such vapors could be consumer products (Corsi et al. 2007), building materials (Aoki and Tanabe 2007), and cleaning products (Destaillets et al. 2006). Formation of SOA during cooking has been reported in the literature (Liu et al. 2017b; Klein et al. 2019). Yet, we need more comprehensive and systematic studies to better understand the mechanisms of SOA formation during cooking, the fraction of SOA in total cooking particles (SOA+ Primary organic aerosol (POA)), and the contribution of cooking SOA to indoor SOA.

The main sources of vapor precursors during cooking were reported to be cooking oils (Liu et al. 2017a), additives, and condiments (Liu et al. 2017b). Liu et al. (2017b) studied VOCs from frying corn oil without and with some common Chinese additives including garlic, ginger, *Myrcia*, and *Zanthoxylum piperitum* (Sichuan pepper). Their experiments were conducted in two modes including with ozone and without ozone. To form SOA, cooking emissions were introduced into a continuous flow reactor where high-ozone concentrations oxidized the cooking-generated VOCs under dark conditions. While no VOCs and particles were observed during heating the pan itself, heated corn oil predominantly produced aldehydes (Liu et al. 2017a). However, during stir-frying the additives, other dominant vapors were produced including dihydrohydroxymaltol and diallyldisulfide (garlic), and monoterpenes and terpenoids (ginger, *Myrcia*, and *Zanthoxylum piperitum*). The SOA emission rates from stir-frying *Zanthoxylum piperitum* and *Myrcia* were $8.7 \mu\text{g min}^{-1} \text{ g}_{\text{spice}}^{-1}$ and $1.8 \mu\text{g min}^{-1} \text{ g}_{\text{spice}}^{-1}$ equivalent to 53% and 13.4% of their own POA emission rates, respectively. Stir-frying garlic and ginger emitted no SOA (Liu et al. 2017b). SOA formation through heating canola, corn, sunflower, peanut, and olive oils at 220°C in the presence of OH radicals (2.7×10^{10} to 1.7×10^{11} molecules $\text{cm}^{-3} \text{ s}$) was investigated by Liu et al. (2017a). The SOA production rate was ranked from the highest to the lowest as sunflower, corn, canola, olive, and peanut oil. A strong association ($R^2 = 0.97$) was reported between the SOA production rate and omega-6 fatty acids. The carbon-carbon double bond in the omega-6 n-6 position could react with the existing peroxy radicals producing long-chain aldehydes (Liu et al. 2017a) that have been reported to be the precursor of the SOA (Liu et al. 2017b).

Another interesting study (Klein et al. 2019) provided new insights into the formation of SOA during cooking. This study examined more than 100 cooking experiments including frying, deep-frying, charbroiling, and boiling at different temperature and using different oils (olive, canola, and sunflower oils); meat, vegetable, and condiments were employed as potential sources of vapor precursors for the SOA formation. The authors concluded that the cooking is a source of

unsaturated aldehydes while the production rate of terpenes is negligible during cooking. The major source of terpenes was found to be condiments (Klein et al. 2019).

In Chinese and Indian cooking styles, spices are heated before adding meat to the pan. Particularly, in Chinese style, spices are stir-fried at temperatures as high as 240 °C (Liu et al. 2017b) prior to the addition of the food to oils. Some spices such as ginger, *Myrcia*, and *Zanthoxylum piperitum* (Sichuan pepper) are widely used in Chinese cooking, and their essential oils contain monoterpenes (Singh et al. 2005). Thus, it is highly possible for such spices to emit monoterpenes during cooking at high temperature which can then react with indoor ozone and produce secondary organic aerosol (SOA) (Weschler and Carslaw 2018). Liu et al. (2017b) studied the SOA and primary organic aerosol (POA) formations during stir-frying garlic, ginger, *Myrcia*, and *Zanthoxylum piperitum* at 240 °C. They reported no production of SOA from garlic and ginger when they were stir-fried while stir-frying *Myrcia* and *Zanthoxylum piperitum* produced SOA. Nonetheless, this SOA production was much less than POA emission rates produced during the stir-frying of *Myrcia* and *Zanthoxylum piperitum* (13.4% and 53.1% of their own POA, respectively), and also it was 30% higher than the SOA produced from heated cooking oil (220 °C) under photooxidation (Liu et al. 2017a, 2018). This observation suggests that particles emitted during stir-frying spices are dominated by POA rather than SOA. However, it needs further investigation. Black pepper was also reported to produce SOA when it was added to the pan during frying beef using canola oil at 180 °C (Klein et al. 2016).

Controlled Studies

There are many factors such as oil, food, condiments, heating source, and pan affecting the cooking emissions, and understanding the contribution of each factor to overall cooking emission rate is a difficult task. However, through controlled studies such contributions have been uncovered. The following section discusses the impact of cooking components on the emission rates and concentrations of cooking PM.

Cooking Style/Method/Habit

A cooking style such as African, Asian, Western, or Middle Eastern can be defined based on the cooking habit and the cooking method (recipe) of the given nation. Cooking method is defined by the combination of different cooking components such as oil, food, vegetables, condiments (additives), sauces, and other elements that is a common recipe for a given nation. A cooking habit is the way a cook prefers to do the cooking. For example, some cooks prefer cooking at low temperature with a longer heating time while some others cook faster at high temperature. Some cooks add condiments to the food at the beginning of cooking while others do it at the end of cooking.

In Persian (Iranian) style cooking, there are variety of meals that are prepared using stewing and water-based cooking (cooking method) and the cooking may take up to several hours (cooking habit). This cooking style employs turmeric, black pepper, and salt in most of the meals as the three main additives used during the cooking while in Indian style cooking variety of vegetables are involved in cooking together with chilies, red pepper, and curry as main additives. Cooking in Eastern Asia such as Chinese and Taiwanese is mainly based on frying while in Western style cooking grilling and barbequing are practiced. Further information about cooking styles are available in (Abdullahi et al. 2013).

Cooking methods involve wet and dry cooking including but not limited to boiling, steaming, stewing, stir-frying, panfrying [sautéing], deep-frying, grilling, broiling, oven baking, toasting, air frying, and microwaving. Grilling and frying were reported to emit higher PM_{2.5} compared to other cooking methods (Olson and Burke 2006). Oil-based cooking such as frying produces higher concentrations of ultrafine particles (UFPs) and PM_{2.5} compared to water-based cooking such as boiling (See and Balasubramanian 2006b; Zhang et al. 2010). This result was also observed in other studies irrespective of the type of the food being cooked including meat and tofu (Alves et al. 2014; Lee et al. 2001; Huboyo et al. 2011; Zhou et al. 2014).

Some studies also showed higher UFPs and PM_{2.5} during frying compared to other types of cooking particularly grilling when a variety of food were cooked such as onions, eggplant, potato chips pork meat, bacon, and cheese (Buonanno et al. 2011; He et al. 2004; Nasir et al. 2013; See and Balasubramanian, 2008). The water in the cooking oils leads to the formation of the oil bubbles while heating. These bubbles burst at the surface of the oil resulting in the production of many small particles (Dua and Hopke 1996). This phenomenon is observed during frying that could be a reason for the observed increased emissions during frying compared to the grilling. Another reason for the differences in frying and grilling using a same food is the heating temperature. Typically, grilling beyond 100 °C is unpleasant and results in burnt food (Amouei Torkmahalleh et al. 2017b), but frying can be done at temperatures even higher than 200 C (Amouei Torkmahalleh et al. 2017c). This large difference can result in a significant difference in the particle emissions.

Table 2 presents the measured particle concentration and emission rates for different cooking methods reported in the literature.

Energy Source

► Chapter 6, “Appliances for Cooking, Heating, and Other Energy Services,” describes emissions from a variety of stoves including those using solid fuels. This chapter focusses on gas and electric stoves cooking. The gas flame or the heated electric coil itself produces a wide range of particles including UFPs with the major particle size range to be less than 10 nm (Wallace et al. 2008). However, the addition of food or oil to cooking enhances the particle mode diameter to larger than 10 nm.

The literature reports that cooking using gas stove produces higher level of UFPs and PM compared to the electric stove cooking (Buonanno et al. 2009; To and Yeung 2011;

Table 2 The particle concentration and emission rate values for different cooking methods (Amouei Torkmahalleh et al. 2017d)

Reference	Cooking method	Particle mass (Concentration/emission rate)		Particle number (Concentration/emission rate)	
		(mg.m ⁻³)	(mg.min ⁻¹)	(part.cm ⁻³)	(part.min ⁻¹)
Alves et al. 2014	Fried fish; seafood rice	0.097(PM _{2.5})			
	Roasted ribs	0.127			
	Grilled pork	0.107			
	Veal stroganoff stew	0.063			
	Chicken stew; Turkey stew with rice	0.055			
	Stewed pork chops with sausages	0.045			
	Boiled chicken with vegetables	0.041			
	Boiled pork meat with vegetables	0.027			
	Beef with rice; pork with boiled potatoes	0.029			
Amouei Torkmahalleh et al. 2017b, c	Grilling ground beef	13.8(PM _{2.5})			
	Heating corn oil	30.0			
Olson and Burke 2006	Grilling	679(PM _{2.5})	173 (PM _{2.5})		
	Frying	341	60		
	Oven	76	10		
	Toaster oven	72	51		
	Microwave	47	11		
Lee et al. 2001	Frying food in oil		1.4142 (PM ₁₀) 1.167 (PM _{2.5})		
	Streaming dim sum meal		0.0339 0.0287		
	Boiling food in soup		0.1053 0.0811		

(continued)

Table 2 (continued)

Reference	Cooking method	Particle mass (Concentration/emission rate)		Particle number (Concentration/emission rate)	
		(mg.m ⁻³)	(mg.min ⁻¹)	(part.cm ⁻³)	(part.min ⁻¹)
Huboyo et al. 2011	Tofu boiling	0.0229(PM _{2.5})			
	Tofu frying	0.04112			
	Chicken boiling	0.03086			
	Chicken frying	0.10164			
See and Balasubramanian 2008	Steaming	0.0657(PM _{2.5})			
	Boiling	0.0814			
	Stir-frying	0.12			
	Steaming	0.0657			
	Panfrying	0.13			
	Deep-frying	0.19			
To and Yeung 2011	Frying vermicelli with beef (domestic kitchen, gas cooking)	1.33 (PM ₁₀)			
	Panfrying of meat (domestic kitchen, gas cooking)	1.02			
	Deep-frying of chicken wings (domestic kitchen, gas cooking)	0.89			
	Frying vermicelli with beef (domestic kitchen, electric cooking)	1.03			
	Panfrying of meat (domestic kitchen, electric cooking)	0.52			
	Deep-frying of chicken wings	0.68			

(continued)

Table 2 (continued)

Reference	Cooking method	Particle mass (Concentration/emission rate)		Particle number (Concentration/emission rate)	
		(mg.m ⁻³)	(mg.min ⁻¹)	(part.cm ⁻³)	(part.min ⁻¹)
See and Balasubramanian 2006b	(domestic kitchen, electric cooking)				
	Deep-frying of tofu (commercial kitchen, gas cooking)	4.72			
	Griddle frying of meat (commercial kitchen, gas cooking)	2.26			
	Deep-frying of tofu (commercial kitchen, electric cooking)	3.98			
	Griddle frying of meat (commercial kitchen, electric cooking)	2.60			
Zhang et al. 2010	Grilling			2.5×10^4	
	Steaming tofu			6.9×10^4	
	Stir-frying tofu			9.3×10^4	
	Panfrying tofu			1.1×10^5	
	Deep-frying tofu			59.5×10^4	
Buonanno et al. 2011	Boiling pasta			1.34×10^4	
	Frying chickens			6.04×10^5	
	Frying chips			2.3×10^4	7.7×10^{12}
	Grilling chips			1.5×10^5	3.7×10^{12}

(continued)

Table 2 (continued)

Reference	Cooking method	Particle mass (Concentration/emission rate)		Particle number (Concentration/emission rate)	
		(mg.m ⁻³)	(mg.min ⁻¹)	(part.cm ⁻³)	(part.min ⁻¹)
Dennekamp et al. 2001	Frying onion			2.4×10^5	7.6×10^{12}
	Grilling onion			1.6×10^5	3.9×10^{12}
	Frying eggplant			2.3×10^5	7.2×10^{12}
	Grilling eggplant			1.6×10^5	3.6×10^{12}
	Frying cheese			2.8×10^5	8.5×10^{12}
	Grilling cheese			1.8×10^5	5.2×10^{12}
	Frying bacon			2.8×10^5	9.6×10^{12}
	Grilling bacon			2.0×10^5	5.6×10^{12}
	Frying pork meat			2.7×10^4	8.8×10^{12}
	Grilling pork			1.9×10^4	5.4×10^{12}
	Boiling water (gas stove)			13.3×10^4	
	Stir-frying vegetables (gas stove)			13.7×10^4	
	Stir-frying vegetables (electric stove)			1.1×10^4	
	Frying bacon (gas stove)			59.0×10^4	
	Frying bacon (electric stove)			15.9×10^4	
	Baking cake in gas oven			9.8×10^4	
	Baking cake in electric oven			3.0×10^4	
	Roasting meat in gas oven			12.4×10^4	
	Roasting meat in electric oven			2.4×10^4	
				12.5×10^4	

(continued)

Table 2 (continued)

Reference	Cooking method	Particle mass (Concentration/emission rate)		Particle number (Concentration/emission rate)	
		(mg.m ⁻³)	(mg.min ⁻¹)	(part.cm ⁻³)	(part.min ⁻¹)
Wu et al. 2012	Baking potatoes in gas oven				
	Baking potatoes in electric oven			1.6×10^4	
	Only grilling (gas)			10.3×10^4	
	Only grilling (electric)			7.7×10^4	
	Toasting bread (gas)			13.8×10^4	
	Toasting bread (electric)			13.4×10^4	
	Grilling bacon (gas)			41.3×10^4	
	Grilling bacon (electric)			53.0×10^4	
	Gas combustion			0.23×10^6	2.59×10^{11}
He et al. 2004	Heating an empty pan			4.0×10^6	58.36×10^{11}
	Boiling			0.47×10^6	5.33×10^{11}
	Steaming			0.36×10^6	4.70×10^{11}
	Panfrying			8.33×10^6	104.40×10^{11}
	Stir-frying			11.97×10^6	148.29×10^{11}
	Cooking	0.037(PM _{2.5})	0.11(PM _{2.5})	126.0×10^3	5.67×10^{11}
	Cooking pizza	0.735	1.59	137.3×10^3	1.65×10^{11}
	Frying	0.745	2.68	154.0×10^3	4.75×10^{11}
	Grilling	0.718	2.78	161.0×10^3	7.34×10^{11}
Chen et al. 2018	Kettle	0.013	0.03	15.6×10^3	0.35×10^{11}
	Microwave	0.016	0.03	16.3×10^3	0.55×10^{11}
	Oven	0.024	0.03	61.5×10^3	1.27×10^{11}
	Stove	0.057	0.24	179.0×10^3	7.33×10^{11}
	Toasting	0.035	0.11	114.0×10^3	6.75×10^{11}
	Boiling (fish, canola oil)	1	0.074 (PM _{2.5})		3.445×10^{12}
		2	0.420		9.036×10^{12}

(continued)

Table 2 (continued)

Reference	Cooking method	Particle mass (Concentration/emission rate)		Particle number (Concentration/emission rate)	
		(mg.m ⁻³)	(mg.min ⁻¹)	(part.cm ⁻³)	(part.min ⁻¹)
	Deep-frying (pork, soybean oil)				
	Boiling (pork, soybean oil)	3	0.189		1.409×10^{12}
	Steaming (mutton, sunflower oil)	4	0.208		1.508×10^{12}
	Boiling (chicken, peanut oil)	5	0.287		3.141×10^{12}
	Panfrying (chicken, canola oil)	6	10.018		20.211×10^{12}
	Deep-frying (mutton, peanut oil)	7	0.771		9.137×10^{12}
	Panfrying (mutton, soybean oil)	8	0.923		10.314×10^{12}
	Steaming (beef, canola oil)	9	0.0096		1.928×10^{12}
	Stir-frying (chicken, sunflower oil)	10	2.416		12.079×10^{12}
	Stir-frying (mutton, canola oil)	11	1.664		16.372×10^{12}
	Boiling (beef, sunflower oil)	12	0.031		1.387×10^{12}
	Panfrying (pork, sunflower oil)	13	3.942		14.086×10^{12}
	Deep-frying (fish,	14	0.640		9.269×10^{12}

(continued)

Table 2 (continued)

Reference	Cooking method	Particle mass (Concentration/emission rate)		Particle number (Concentration/emission rate)	
		(mg.m ⁻³)	(mg.min ⁻¹)	(part.cm ⁻³)	(part.min ⁻¹)
	sunflower oil)				
	Deep-frying (beef, blend oil)	15	1.030		9.636×10^{12}
	Panfrying (fish, blend oil)	16	5.416		16.507×10^{12}
	Steaming (chicken, blend oil)	17	0.031		1.371×10^{12}
	Deep-frying (chicken, soybean oil)	18	1.055		8.646×10^{12}
	Stir-frying (fish, peanut oil)	19	9.915		23.211×10^{12}
	Boiling (mutton, blend oil)	20	0.109		1.576×10^{12}
	Panfrying (beef, peanut oil)	21	2.461		17.370×10^{12}
	Stir-frying (pork, blend oil)	22	1.820		15.947×10^{12}
	Stir-frying (beef, soybean oil)	23	7.794		16.130×10^{12}
	Steaming (fish, soybean oil)	24	0.075		2.086×10^{12}
	Steaming (pork, peanut oil)	25	0.022		1.746×10^{12}

Dennekamp et al. 2001; Jørgensen et al. 2013; Wallace et al. 2008; Zhang et al. 2010). Patel et al. (2020) investigated the size distribution of particles down to 1 nm emitted from stir-frying using a gas (propane) stove and an electric hot plate. They

reported significantly higher (10 times) particle concentration during stir-frying using gas stove compared to the hot plate cooking.

Similarly, particle numbers from gas flame itself were higher (7 times) compared to the number of particles from the hot plate for sizes larger than 4 nm. Wallace et al. (2008) showed that over the size range of 2–64 nm, the average UFP emission rate from gas flame itself ($N = 22$) was 10.6×10^{12} part. min^{-1} while the corresponding value for the electric stove itself ($N = 30$) was 5.4×10^{12} part. min^{-1} .

Both gas and electric burners produce particles but by different mechanisms. The gas flame produces particles through the incomplete combustion (Li and Hopke 1993), the composition of the gas being combusted and the primary aeration affect the particle emission rate (Wagner et al. 2010). The electric coil generates particles through a different mechanism. Wallace et al. (2017) hypothesize that heated surfaces such as electric coils, cooking pans, empty beakers, etc. can produce particles during heating, and this particle emission can reach to zero after successive heating (Amouei Torkmahalleh et al. 2018; Wallace et al. 2015, 2017). The implementation of this hypothesis can be extended to indoor sources of particles such as heated iron, and hair dryer, toaster, etc. This hypothesis explains that a film of semivolatile organic compounds (SVOCs) deposits on the surface of the coil, stove, or pan during the noncooking period. During heating these surfaces, the SVOCs are desorbed from the heated surface, but then they immediately cool down to the ambient temperature resulting in supersaturation of the SVOCs and subsequent nucleation and particle formation. However, if the surface is heated continually, the SVOCs are completely desorbed and the emissions decline until zero emission is achieved. The particles generated through this mechanism contribute to the particle count but generally little to the particle mass. Thus, it was shown that PM mass concentration changes were negligible while UFP concentrations increased substantially (Wallace et al. 2015, 2017). Other possible sources of particles from the heated surfaces could be deposited dust (Glytsos et al. 2010), detergent residue formed on the surface after washing, and also skin oil transferred to the surfaces after touching (Wallace et al. 2015, 2017).

Figure 2 presents a contour plot showing three time intervals including indoor background (no particular sources), when a hotplate is heated at 320 °C and then when an empty beaker is heated on the hotplate at 320 °C. The background measurements started from 10:50 a.m. until 11:38 a.m. The background measurements showed the lack of particles larger than 3 nm with the presence of some particles smaller than 3 nm. At 11:38 a.m., the hotplate is switched on at 320 °C and nucleation of particles larger than 3 nm was observed such that particles between 3 and 10 nm dominate particle sizes <10 nm. As shown in Fig. 2, the number concentration decreases with time while the mode diameter increases creating a banana shape pattern suggesting coagulation over time. The concentration of particles generated by the heated hotplate continues to decrease until 13:50 p.m. when an empty beaker is placed on the hotplate. A copious amount of particles as small as 5 nm are produced. Additionally, particles smaller than 3 nm are produced. Again, a banana shape pattern is produced showing a decline in concentration over time because of continuously heating the beaker.

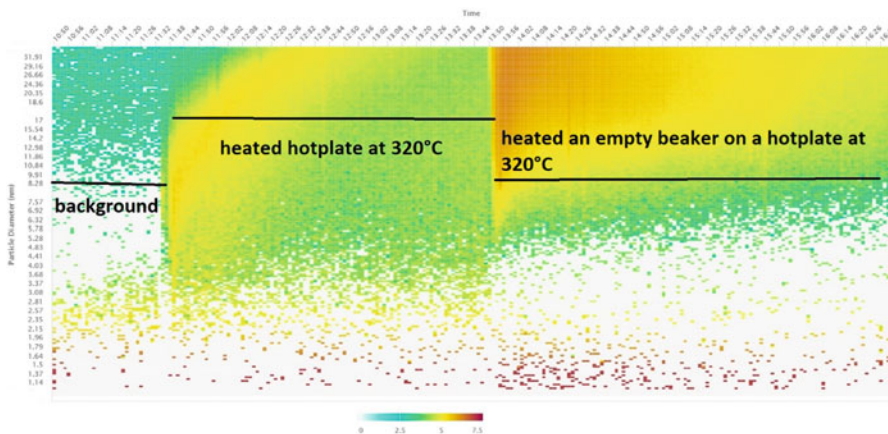


Fig. 2 Contour plot showing the particle size, concentration ($dN/d\log D_p$) and heating time for indoor background, heating hotplate, and heating an empty pan on a hotplate

Many studies showed that gas flames generate particles with higher mode diameters than heated electric stoves (Dennekamp et al. 2001; Wallace et al. 2008; Jørgensen et al. 2013). However, using advanced technologies such studies need to be revisited. For example, it would be interesting to study the differences in the particle mode diameter between gas flame and electric stove using a 1 nm SMPS. There exist studies that investigated size distribution of the particles from gas flame or electric stove itself down to 2 nm. Minutolo et al. (2010) and Wallace et al. (2008) reported average mode diameter for particles emitted from gas flame down to 2 and 5 nm, respectively. Patel et al. (2020) reported the mode diameter of particles generated from stir-frying using gas (propane) stove to be 1.6 nm. However, when an electric hot plate was used for the stir-frying, the mode diameter of the generated particles increased to 3 nm. The presence of the sub-3 nm particles in recent cooking studies as shown in Fig. 2 and also by Patel et al. (2020) and Laursen et al. (2021) needs further investigation to clearly understand the source of the sub-3 nm particles. The presence of such particles has been observed even in clean air (Laursen et al. 2021) or during background (no cooking) periods (Fig. 2) suggesting that these particles cannot be immediately registered for the cooking as possible measurement uncertainties exist. In addition to the cooking and its components including heated pan and stove as the source of sub-3 nm particles, the sub-3 nm particles found in the indoor background (baseline concentration) could be from ambient traffic emissions (Rönkkö et al. 2017) that penetrated indoors during cooking and noncooking periods. Alternatively, the source of uncertainty for counting sub-3 nm particles could be counting some ions instead of particles below 2 nm by the instrument (Patel et al. 2020). Another plausible reason could be uncertainties associated with the loss correction. When a few particles are counted at lower size limit of the instruments (with nano Differential Mobility Analyzer (DMA)), sharp spikes in the concentration typically at the lowest size are observed due to the loss correction (Laursen et al. 2021).

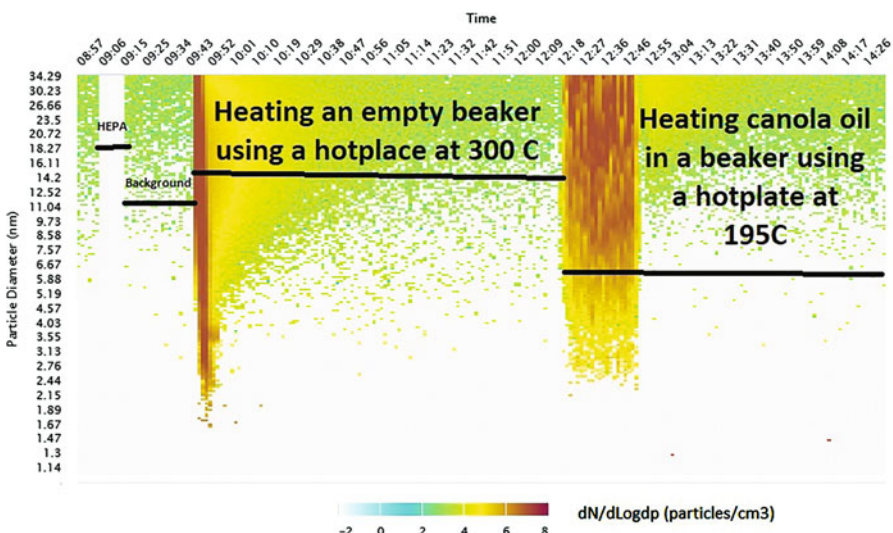


Fig. 3 A contour plot showing the particle size and concentrations ($dN/d\log D_p$) and heating time for indoor background, HEPA filter, Indoor background, heating empty beaker using a hotplate at $300\text{ }^{\circ}\text{C}$, and heating canola oil in the beaker using the hotplate at $195\text{ }^{\circ}\text{C}$

Such spikes may appear occasionally. However, if the particle emission is high in this size range, then the concentration spikes may disappear which was observed by Laursen et al. (2021) for candle burning. Figure 3 shows a contour plot presenting five different regions of particle size (1–35 nm), particle concentrations ($dN/d\log D_p$) and time including indoor background, HEPA filter, indoor background, heating empty beaker using a hotplate at $300\text{ }^{\circ}\text{C}$, and heating canola oil in the same beaker using the same hotplate at $195\text{ }^{\circ}\text{C}$. It is clear that when HEPA filter was connected to the instrument, it could remove all particles at all sizes. Heated beaker and hotplate were both sources of particles down to 1 nm and emitted high concentrations of particles which were about 4 orders of magnitude higher than the indoor background at all size ranges. However, heated canola oil produced particles larger than 2 nm. The concentrations of particles from the heated canola oil increased with the size of the particles such that the highest concentrations were observed for particles larger than 4 nm (four orders of magnitude higher than the indoor background). However, for particles between 3–4 nm and 2–3 nm, the concentrations of particles were almost 3 and 2 orders of magnitude higher than the indoor background concentrations, respectively. Figure 3 presents that continuously heating the beaker for 2 h (from 9:40 a.m. till 11:40 a.m.) using the hotplate at $300\text{ }^{\circ}\text{C}$ resulted in zero particle emissions from the beaker and hotplate collectively. At this time, when the background concentration was re-established, the oil was added to the hot beaker such that its temperature reached $195\text{ }^{\circ}\text{C}$, and the formation of the new particles from the heated oil itself was observed. Using this methodology, the particles from the heated oil itself can be quantified.

Cooking Pan

The literature review found that cooking pans can contribute to the UFP emissions and trace metal emissions (Broomandi et al. 2020). The mechanisms for the UFP emissions are the same as the SVOC mechanisms, explained for the hotplate, electric stove, or heated surfaces in the last section. Additionally, settled dust and detergent residue can contribute to the emissions. Since the SVOC film formation is hypothesized based on the surface adsorption, then the surface material of the pan, and the surface temperature of the pan that is established by its heat conductivity, could potentially influence the adsorption capacity of the SVOCs and thereby the particle emissions. Additionally, the duration of the exposure of the pan to indoor SVOCs is another factor that influences the adsorption loading. Little efforts were done to test this hypothesis (Amouei Torkmahalleh et al. 2019), and thus, it requires further investigations. Amouei Torkmahalleh et al. (2019) showed that the material of the pan can impact the UFPs (>10 nm) measured using the NanoTracer (Philips Aerasense, Netherlands). They reported that after approximately 24 hours of exposure of the all pans to indoor air, a ceramic pan emitted higher UFPs followed by granite, aluminum, and Teflon pans. Figure 4 shows the UFP concentrations in one of the experiments. The experiments were conducted for the four types of the pan that were exposed to indoor air at the same time for 24 hours. We heated during the same experimental day with a same heating level. However, the temperature of the pans might have been different given their heat conductivity. Although heating ceramic pan resulted in the higher UFP concentration (Fig. 4) and emission rate,

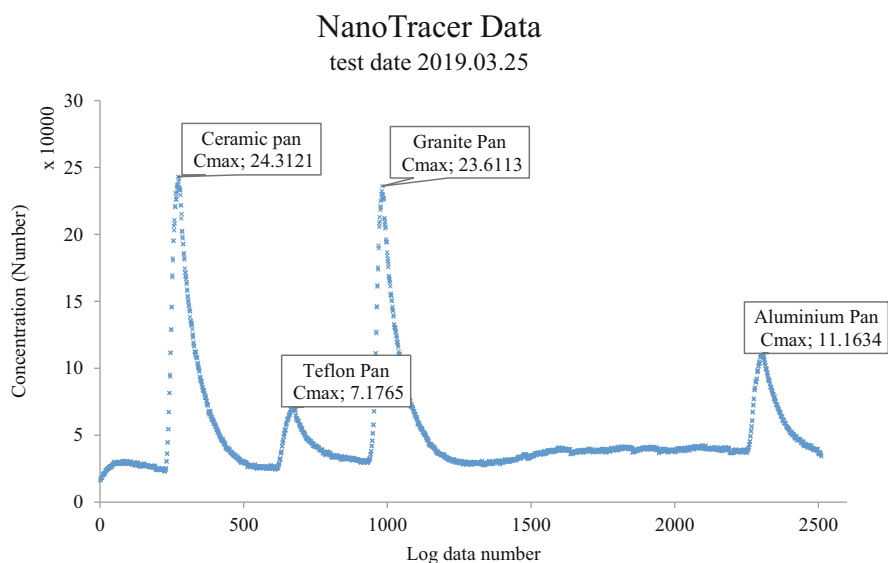


Fig. 4 Impact of the pan type on UFP emissions – X axis represents the time since the start of the experiments

the average temperature of the ceramic pan (185 °C) was less than that of granite pan (192 °C) and similar to the aluminum pan (182 °C) suggesting that pan material is a comparable factor to the pan temperature in particle production process.

A recent study examined the effect of cooking pan on PM_{2.5} emissions during frying (O'Leary et al. 2019). They studied the impact of a coated nonstick pan and stainless steel pan during frying chicken and potatoes in olive oil using a gas stove and reported that the emission rate increased up to 940% when the stainless steel pan was employed. The obvious reason for such a large increase was sticking the potato and chicken into the stainless steel pans. Thus, the material of the pan not only affects the adsorption of the SVOCs but also affects the interaction of the food with the pan, and both these factors influence particle emissions during cooking. The importance of this study was that it simulated a real cooking with three burners being involved in the cooking at the same time, for frying chicken, frying potatoes, and boiling vegetables.

The presence of the trace elements in the PM emitted during cooking has been identified in the literature (Gorjinezad et al. 2017; See and Balasubramanian 2006a, 2008). The source of the trace metals could be the oil, meat, or the pan. Previous studies demonstrated the presence of the trace elements such as Mn, Pb, Ba, Ag, Cu, As, Zn, and Cr in vegetable oils (He et al. 2014). Mendil et al. (2009) also reported the presence of the different trace elements in corn oil with Zn and Mn to be present at high concentrations. When cooking utensils are in contact with hot cooking oils and food during cooking, the dissolution of the trace elements from utensils to the oils is highly possible and the amount of the transferred elements depends on the type of food (Dan and Ebong 2013; Kumar et al. 1994). Trace metals such as Ni, Cr, Fe, Mn, and Al can be leached from different pans including stainless steel, cast iron, and PTFE-coated aluminum to heat oils (Dan and Ebong 2013; Kumar et al. 1994; Müller et al. 1993).

Dan and Ebong (2013) showed when stainless steel utensils were employed for cooking, the concentration of Fe (1.27–2.08 times), Ni (1.4–2.93 times), and Cr (1.34–2.64 times) in the food increased. Similarly, cooking in cast iron and PTFE-coated aluminum pans that are enriched in Fe and Al in their structure, respectively, resulted in leaching Fe (Kumar et al. 1994) and Al (Müller et al. 1993) into the cooked food and heated oils, respectively. Such studies demonstrated the impact of the cooking utensils, particularly cooking pan, on the trace element contents of the oil or food being cooked. However, the literature lacks strong evidence demonstrating the impact of the cooking utensils and pans on the trace element contents of the PM from cooked oil and food.

Four sets of experiments (three replications per experiment) were conducted to investigate the influence of the cooking pans on the concentrations of the trace elements in PM (Amouei Torkmahalleh et al. 2013b). Soybean and canola oils were heated individually in cast iron and ceramic pans. The results of soybean oil experiments were consistent with the results of the canola oil implying the impact of the pan on the trace element emissions. For example, heated cast iron pan in soybean and canola oils resulted in higher Fe concentrations in PM compared to stainless steel and ceramic pans.

Two different studies were conducted in the same apartment and under similar environmental conditions to quantify the trace elements during grilling (Amouei Torkmahalleh et al. 2017b) and heating corn oil (Amouei Torkmahalleh et al. 2017c). Although different cooking temperature (frying to be higher than grilling) and materials (oil vs meat) were employed in these studies, the measured trace element concentrations were statistically insignificant compared to each other suggesting the presence of a more influential source of trace elements compared to the meat or oil itself. This source could be potentially the cooking pan from which the trace elements are dissolved into the hot oil or blood of the meat during cooking. This observation triggered a recent study to better understand the contributions of the cooking pans to the trace element content of the emitted PM during cooking.

Broomandi et al. (2020) developed a hypothesis stating that the trace elements from cooking pan translocate to the cooking PM during cooking. They tried to show that trace elements are dissolved into the hot cooking oil and subsequently appear in the PM phase during the evaporation and the subsequent nucleation of the organic constituents of the cooking oils. This is rather a difficult hypothesis to investigate. To test this hypothesis, Broomandi et al. (2020) quantified the trace elements in PM when soybean oil was heated in three types of pans including cast iron, Teflon, and granitium pans under controlled experimental conditions. They argued that if they observe no statistically significant changes in the concentrations of all the trace elements in PM emitted from the heated soybean oil in three pans, then it is likely that the source of the trace elements is cooking oil. On the other hand, if the concentrations of one or more trace elements undergo statistically significant changes among the three types of the experiments, then the cooking pan is responsible for the emission of the trace elements. They reported that heating soybean oil in the cast iron pan resulted in higher Fe concentration in PM_1 ($8.49 \pm 3.35 \mu\text{g}/\text{m}^3$) compared to the Fe concentrations when Teflon ($8.05 \pm 2.27 \mu\text{g}/\text{m}^3$) and granitium ($7.45 \pm 1.38 \mu\text{g}/\text{m}^3$) pans were employed. Nevertheless, these differences were statistically insignificant. The Mn and Co emission rates were reported to be statistically significantly lower when cast iron was used compared to the granitium and Teflon pans. Thus, the study by Broomandi et al. (2020) with all of its limitations can support the hypothesis that trace elements translocate from cooking pan to PM during cooking. However, more controlled studies providing direct evidence are required to test this hypothesis.

Cooking Oil

Heating cooking oils is practiced during frying activities, and hence, studying the emissions from cooking oil itself is imperative for understanding the overall cooking emissions. Several controlled studies exist in the literature that investigated the impact of the cooking oils on particle emissions. At smoke temperature, the triglycerols of oil breakdown to glycerol and free-fatty acids. Further heating the oil results in the conversion of glycerol to acrolein that can be detected in the oil smokes (Katragadda et al. 2010). The content of the free-fatty acids of the oil influences the

smoke temperature. The smoke temperature of a cooking oil significantly depends on the chain length of the fatty acids rather than degree of unsaturation that is minimal factor. Oils that have higher content of short-chain fatty acids have lower smoke temperature (Katragadda et al. 2010).

The smoke temperature was reported to be the key factor influencing the particle emissions (Gao et al. 2013; Amouei Torkmahalleh et al. 2017d). High emitting cooking oils were reported to have typically low smoke temperature. That is, during cooking such oils are likely to be heated beyond their smoke temperature producing copious amount of particles. It is necessary to cook in oils with higher smoke temperature to reduce exposure to UFPs and PM. The smoke temperatures of the oils vary with the type of oils. Amouei Torkmahalleh et al. (2012) investigated the UFP and $PM_{2.5}$ concentrations and emission rates for seven different cooking oils including soybean, peanut, canola, olive, safflower, corn, and coconut oils. Each oil was heated to approximately 197 °C in a beaker on a hotplate. They characterized particle size distribution down to 10 nm. To separate the cooking particles from hotplate particles, they first heated the oils in the beaker and then transferred the beaker in a different chamber without the hotplate. The UFP and $PM_{2.5}$ concentrations were recorded while the oil temperature dropped below 197 °C. At the time of their study, the mechanisms for the particle emissions from heated surfaces such as hotplate or beaker were not known. Thus, it is likely that the study conducted by Amouei Torkmahalleh et al. (2012) did not exclude UFPs from the heated glass beaker while measuring the UFP emissions from the oils. However, this interference could have been ignored when the emission from the oils were compared assuming similar contribution of the beaker particles for all experiments. It is unlikely that heated beaker affected the $PM_{2.5}$ concentrations from the oil particles as it was demonstrated that particles from heated surfaces do not contribute to particle mass (Amouei Torkmahalleh et al. 2018; Wallace et al. 2015). Amouei Torkmahalleh et al. (2012) reported the particle mode diameter to be between 25 nm (peanut oil) and 80 nm (soybean oil). The lowest UFP and $PM_{2.5}$ emission rates were registered for soybean, canola, and safflower oils that had higher smoke temperature compared to the other tested oils (Amouei Torkmahalleh et al. 2012). Their study showed that selection of a low emitting oil for cooking could reduce the exposure to $PM_{2.5}$ and UFPs by over 90%. While their study showed a reverse association between the oil smoke temperature and the particle emissions, olive oil showed the different behavior. The highest PM emission was registered for olive oil compared to other oils even it was heated below its smoke temperature. This observation could be due to the presence of excess triolein with relatively high molecular weight (compared to other triglycerides) in olive oil compared to other oils (Amouei Torkmahalleh et al. 2017a). Another study by Gao et al. (2013) measured the PM mass emission rates in particles in the range of 0.1 to 10 μm and listed sunflower, soybean, and blended oils as low emitting oils while peanut and olive oil were reported to be high emitting oils consistent with Amouei Torkmahalleh et al. (2012) and Buonanno et al. (2009).

Four types of cooking oils including rapeseed, soybean, corn, and sunflower oils were compared to measure the $PM_{2.5}$ mass concentrations during heating to 265 °C using a pan and liquid petroleum gas as the fuel (Li et al. 2017). Rapeseed,

sunflower, soybean, and corn were ranked first, second, third, and fourth in PM emissions.

Selecting a low emitting cooking oil for frying is instrumental in reducing the exposure of the cooks to cooking fumes. The literature retorts that soybean oil is the least emitting oil while olive oil is among the most emitting oils. However, most of the previous studies compared different cooking oils using instruments only capable of monitoring particles down to 10 nm. Thus, such studies need to be revisited with instrumentation that detects particles below 10 nm and use revised experimental designs that separate the stove/hotplate and pan/beaker particles from oil particles.

Table 3 presents the particle concentration and emission rate values observed for different cooking oils.

Additives

Salt (sea salt and table salt) and black pepper are the most commonly used additives in different cooking styles. Some condiments are the major additives of a specific

Table 3 Influences of cooking oils on particle concentrations and emissions (Amouei Torkmahalleh et al. 2017d)

Reference	Oil (stove)	Particle mass (concentration/emission rate)		Particle number (concentration/emission rate)	
		(mg.m ⁻³)	(mg.min ⁻¹)	(part. cm ⁻³)	(part. min ⁻¹)
Gao et al. 2013	Olive		135(PM ₁₀)		
	Peanut		99		
	Rapeseed		66		
	Blend		42		
	Soybean		36		
	Sunflower		33		
Torkmahalleh et al. 2012	Olive		54(PM _{2.5})		1.6 × 10 ¹²
	Coconut		27		1.4 × 10 ¹²
	Corn		26		2.2 × 10 ¹²
	Soybean		5.7		3.3 × 10 ¹¹
	Canola		5.1		9.5 × 10 ¹¹
	Peanut		3.7		3.5 × 10 ¹²
	Safflower		2.8		8.1 × 10 ¹¹
Buonanno et al. 2009	Peanut (gas)				2.3 × 10 ¹²
	Olive (gas)				1.8 × 10 ¹²
	Sunflower (gas)				1.1 × 10 ¹²
	Peanut (electric)				2.7 × 10 ¹⁰
	Olive (electric)				1.2 × 10 ¹⁰
	Sunflower (electric)				1.1 × 10 ¹⁰
Sjaastad and Svendsen 2008	Margarine	11.6 (PM _{total})		595	
	Rapeseed	1		345	
	Soybean	1.4		227	
	Olive	1		223	

cooking style. For example, turmeric and curry are commonly used in Iranian and Indian recipes, respectively. Other condiments such as *Myrcia* and *Zanthoxylum piperitum* are employed in Chinese recipes. Additives or condiments may influence the emissions of cooking PM in two ways. Salts and pepper were found to reduce the particle emissions from canola and soybean oil (Amouei Torkmahalleh et al. 2013a). Five different additives including turmeric, garlic powder, black pepper, sea salt, and table salt were added to either canola oil or soybean oil while heating at 200 °C (below the smoke temperature) in a beaker, and the PM_{2.5} and particles number (10 nm to 10 µm) emission rates were quantified (Amouei Torkmahalleh et al. 2013a). When additives including black pepper, table salt, and sea salt were added to the canola oil at 200 °C, 85–90% and 45–53% reductions in PM_{2.5} and UFP emissions were observed, respectively, compared to the heated canola oil without additives. When soybean oil was used, table salt and sea salt reduced PM_{2.5} emissions by 47% and 77%, respectively, compared to the pure oil while black pepper showed no significant changes. Reductions in UFP emissions (51%, 61%, and 68%, respectively) compared to the pure soybean oil were also reported when black pepper, sea salt, and table salt were added to the heated soybean oil. Garlic and turmeric showed no changes in PM_{2.5} and UFPs in the presence of heated soybean and canola oils. This observation is consistent with Liu et al. (2017b) who observed no changes in the particle emissions when garlic and ginger were added to corn oil at 240 °C.

In a simulation study, Amouei Torkmahalleh et al. (2017a) showed that at 197 °C NaCl could reduce the emissions of triolein, trigadolein, and triarachidin from soybean oil by up to 48%. These results can explain the observed reductions in particle emissions when salt is added to the heated oil.

The addition of salt to the meat during grilling led to different observations compared to the heated salty oil. O'Leary et al. (2019) fried chicken and potatoes in olive oil using a coated nonstick pan on a gas stove. Then, they repeated the same experiment when salt was added to the chicken before frying. Although increases in the PM_{2.5} up to 47% were observed, this increase was not statistically significant. Similarly, Amouei Torkmahalleh et al. (2018) reported statistically insignificant increases when salty beef was grilled compared to the grilled unsalted beef. Further investigations are needed to improve our understanding of the underlying mechanisms of particle formation when salt and meat are present during grilling.

Spices may increase the particle emissions as reported by Liu et al. (2017b). They reported that the particle concentrations when *Myrcia* and *Zanthoxylum piperitum* were stir-fried in corn oil at 240 °C were approximately twice the concentrations of particles when the corn oil was heated in the absence of these spices. This increase could be potentially due to the primary particle emissions from heated spices themselves and due to the formation of secondary organic aerosol (SOA). The impact of four types of additives including white pepper, salt, garlic powder, and mixed spices on PM and VOCs during grilling pork was investigated. The meat was marinated with each type of additive before grilling. It was found that PM concentrations significantly decreased by 65.05%, 47.86%, 32.87%, and 56.01% when white pepper, salt, garlic, and mixed spices were employed during grilling. The

average concentrations of total carbonyl compounds (13 components) decreased when the grilling was conducted using the marinated meat with either of white pepper, salt, garlic powder, and mixed spices compared to the grilling with plain meat. Grilling salty meat showed statistically significant lower total VOC concentrations compared to the grilling plain meat, while other types of additives increased VOC concentrations.

Food

Particle emissions during cooking vegetables and meat were investigated in the literature. The current evidence in the literature shows that the frying and grilling meat result in higher particle emissions compared to the frying and grilling vegetables mainly due to the higher fat content. Buonanno et al. (2009) showed that grilling eggplant resulted in the lower particle number emission rates (2.6×10^{12} part. min^{-1}) compared to the grilling cheese, bacon, and wurstel sausage. The highest particle number emission rates were registered to grilling cheese (3.4×10^{12} part. min^{-1}). In another study, they also showed that frying and grilling cheese, bacon, and pork produce higher particles compared to the eggplants, potato chips, and onions using gas and electric stoves (Buonanno et al. 2011). Dennekamp et al. (2001) also showed that frying vegetables in vegetable oils resulted in reduced particle concentrations compared to the frying bacon. Frying tofu was found to produce less particles compared to the frying chicken (Huboyo et al. 2011). A study by Zhang et al. (2010) was in agreement with previous studies such that they also observed higher UFP and $\text{PM}_{2.5}$ concentrations during frying chicken and shrimp compared to the frying eggs, peppers, onions, and tomato.

Frying and grilling bacon emitted particles with larger mode diameter values compared to the frying or grilling eggplants, chips, and cheeses (Buonanno et al. 2011; Dennekamp et al. 2001).

Particle number and mass concentrations reported by the studies discussed in this section are presented in Table 4.

Temperature

Increased cooking temperature resulted in increased particle number and mass concentrations (Buonanno et al. 2009; Kumar et al. 2013; Amouei Torkmahalleh et al. 2012, 2013a; Zhang et al. 2010). The impact of temperature on cooking emissions was reported to be insignificant at the temperature range below the smoke temperature (Zhao et al. 2018). Nevertheless, exceptions may exist such as olive oil (Amouei Torkmahalleh et al. 2012). Buonanno et al. (2009) grilled 50 g bacon using a gas stove and observed 70% in particle number concentration and increase in particle mode diameter from 22 nm to 57 nm when grilling temperature changed from 82 to 114 °C. Amouei Torkmahalleh et al. (2012) showed that increase in particle emissions with temperature depends on the type of the oil. Low emitting

Table 4 The impacts of different food on particle mass and particle number concentrations (Amouei Torkmahalleh et al. 2017d)

Reference	Cooking method and food type (stove)	Number concentration (part.cm ⁻³)	Particle mass concentration (mg.m ⁻³)
Buonanno et al. 2009; Huboyo et al. 2011; To and Yeung 2011	Refer to Table 3		
	Refer to Table 2		
	Deep-frying of tofu		4.72
	Griddle frying of meat		2.26
	Frying vermicelli with beef		1.33
Zhang et al. 2010	Panfrying of meat		1.02
	Deep-frying of chicken wings		0.89
	Frying chicken and shrimp	1.99×10^5	0.2309
	Frying chicken and rice	1.13×10^5	0.0943
	Frying eggs and vegetable	0.92×10^5	0.0386
Jørgensen et al. 2013	Frying onions and tomato	0.99×10^5	0.0365
	Grilling fresh bacon	3.5×10^5	
Yeung and To 2008	Grilling smoked bacon	3.36×10^5	
	Panfrying steaks	8.53×10^5	
	Panfrying chicken fillets	8.58×10^5	
Dennekamp et al. 2001	Panfrying pork chops	8.83×10^5	
	Frying vegetable (gas)	1.37×10^5	
	Frying bacon (gas)	5.9×10^4	
	Frying vegetable (electric)	0.11×10^5	
	Frying bacon (electric)	0.159×10^5	

oils showed much less increase in particle concentration compared to the high emitting oils when the oil temperature increased from 130 to 197 °C. The PM_{2.5} emissions changed with temperature for all oils only beyond 150 °C. The increase in particle mode diameter with temperature was also reported by Amouei Torkmahalleh et al. (2012) such that the mode diameter increased on average from 30 nm to 47 nm for seven oils when the temperature increased from 178 °C to 197 °C. The reason for the observed increase in mode diameter with temperature could be due to the higher rate of coagulation at higher temperatures as higher temperatures increase the particle emissions and thereby concentrations. It could be also due to the increased concentrations of organic vapor at higher temperatures and thereby increased rate of condensation on the existing particles. Other studies also reported the increases in particle concentration and mode diameter with temperature during heating cooking oils (Gao et al. 2013), during panfrying of steak, chicken fillets, and pork chops (Yeung and To 2008), and during frying chicken (Zhang et al. 2010).

Surface Area of the Pan/Position of the Pan on a Stove

Amouei Torkmahalleh et al. (2012) demonstrated that the particle emissions increase with the surface area of the oil/pan. Thus, to reduce the particle emissions cooking in pans with smaller surface area is recommended.

Kitchen ventilation systems were found to be more efficient in filtering or venting out the particles during cooking on the rear burner compared to the front burner (Rim et al. 2012). The capture efficiency of a hood during stir-frying was reported to be 4–39% and 70–99% for front and back burners, respectively (Lunden et al. 2015). A similar observation was reported by Singer et al. (2012). However, O’Leary et al. (2019) observed a slight reduction in the concentration of frying particles when the back burner was used compared to the front burner such that this difference was statistically insignificant. They concluded that the observed insignificant difference could be attributed to the good coverage of the hood in their study over the front burner.

Particle Loss (Coagulation, Ventilation, and Deposition)

To reduce exposure of indoor occupants including the cooks to the cooking particles, two main approaches exist. The first approach is to reduce the particle emissions from the source by changing the cooking habit and employing cleaner energy while the second approach is to remove already produced particles from indoor air. The relative importance of these two approaches has not been addressed in the literature.

Factors affecting the emission of cooking particles have been addressed in the previous sections of this chapter. Here we discuss the factors affecting the removal of the cooking particles from indoor air. These factors include coagulation, deposition, and ventilation or air exchange.

The latter includes natural and forced ventilation. Coagulation was reported to be a dominant mechanism compared to the deposition and air exchange (Wallace et al. 2008). Wallace et al. (2008) estimated the coagulation, air change, and deposition rates of cooking particles in the size range of 2 to 64 nm in a test house to be +13 to -7 h^{-1} , $01\text{--}0.3 \text{ h}^{-1}$, and $< 0.5 \text{ h}^{-1}$, respectively. The highest rate of coagulation was registered for particles as small as 5 nm while coagulation rate for particles larger than 20 nm was found to be negligible. Coagulation was a dominant mechanism for concentrations as high as 30,000 particles/cm³. Using HR-TEM images, Cho et al. (2019) showed that ultrafine particles emitted from frying Atlantic salmon coagulated more rapidly than the accumulation mode particles (Rim et al. 2012).

Rim et al. (2012) showed that hood flow rate and particle size are the two factors in UFP removal such that the removal rate increased with particle size at 370 m³/h, while at 680 m³/h, the removal rate was almost the same over the size range of 4 nm to 20 nm.

Reductions in particles by a factor of 3–10 were reported due to ventilations during heating oils (Zhao et al. 2019). The capture efficiency of the ventilation system is a factor in reducing the indoor concentration of cooking particles, which varies with the type of the ventilation and fan speed (Lunden et al. 2015; Wallace et al. 2004a; Howard-Reed et al. 2003). It is possible to reduce the exposure of indoor occupants to cooking particles by using a proper ventilation system and a central fan and air conditioning (Howard-Reed et al. 2003). Particle deposition rates were examined in the presence of central heating and air conditioning (HAC) fan,

electrostatic precipitator (ESP), and fibrous mechanical filters (MECH). The ESP increased the particle deposition rates compared to the MECH and HAC fan (Wallace et al. 2004a; Howard-Reed et al. 2003). HAC fan alone and an in-duct ESP could reduce the indoor cooking particle concentrations by 25–50% and 55–85%, respectively. He et al. (2005) estimated the particle deposition rates in 14 residential houses in Brisbane. The lowest deposition rate was registered for particles in size range from 0.2 to 0.3 mm for both minimum (air exchange rate: $0.61 \pm 0.45 \text{ h}^{-1}$) and normal (air exchange rate $3.00 \pm 1.23 \text{ h}^{-1}$) ventilation conditions. Reductions in UFP concentrations are possible using increased flow rates of range hood. However, this reduction depends on the particle size (Rim et al. 2012). A flow rate of 95 l/s was reported to be necessary but not sufficient for range hoods to obtain a capture efficiency of 75% for the front burner (Singer et al. 2012). A similar observation in nine California homes was made by Singer et al. (2017) such that using a range hood (flow rate: 108 l/s), particle concentration reduced by 80–95%.

Particle Morphology

Understanding the morphology of the cooking particles will help us to estimate the particle transport and toxicity. Few data are available explaining the morphology of cooking emitted PM. The existing evidence suggest that aggregated branched chain-like structure PM accounted for the major morphology of gas and electric stoves frying (Buonanno et al. 2009) although individual nano-sized spheroid particles were observed. Combustion of solid fuel and gas stoves without food produced nano-size spherule primary particles that build submicron soot particles (Shen et al. 2017). Li et al. (2019) investigated the morphology of cooking particles ($\text{PM}_{2.5}$ and PM_{10}) collected in four Chinese restaurants that used different cooking styles, including Cantonese style (GD), Sichuan style (SC), Xibei style (XB), and Hunan style (HN). The cooking oil used in these restaurants was a blend of 94% soybean oil and 6% sunflower seed oil. PM morphology was categorized into six morphological classes in the study conducted by Li et al. (2019) including rectangular, flocculent, flat, irregular, spheroidal, and spherical shapes.

The most abundant particle morphology in PM_{10} was agglomerated rectangular (55%) shape. The flocculent shape accounted for 30% of the particles in PM_{10} . The percentage of flat particles was approximately 5%. Irregular particles showed the same percentages as flat particles. The spheroidal particles accounted for less than 2%.

The lowest of all the categories (~1.5%) was the regular spherical particle. $\text{PM}_{2.5}$ consisted of approximately 75% of rectangular particles. The next common shape was flocculent particles close to 20%.

Li et al. (2017) concluded that cooking style influenced the particle morphology such that rectangular particles were emitted largely from water-based cooking, while oil-based cooking and roasting produced abundantly spherical and spheroidal particles, respectively.

Citizen Science

Cooking is an inevitable activity in homes worldwide, and thus, exposure to cooking fumes in homes is unavoidable. However, the key question is how to cook while reducing the exposure to COFs. Employing ventilation has been demonstrated to be an approach to reduce exposure to cooking fumes. Nevertheless, not all homes are equipped with proper ventilation systems, and not all people use their ventilation systems during cooking. An alternative and novel opportunity to significantly reduce the exposure of home occupants to cooking fumes is to change the cooking habits and processes through controlling the factors influencing the cooking emissions, thereby reducing the emissions from the source as discussed in this chapter. For example, many people have misunderstood the suitability of olive oil in cooking. Olive oils are beneficial for eating as salad dressing or spreads on bread since they have high monounsaturated to polyunsaturated fatty acid ratio and contain powerful antioxidants such as polyphenols (Ktragadda et al. 2010; Velasco and Dobarganes 2002). However, olive oils are not among the best choices for thermal cooking in general and frying in particular with respect to the PM emissions.

It is important to transfer this knowledge and science to the general public using understandable language and popular communication tools. One way to publicize research outcomes in the area of cooking emissions is to involve people particularly women, commercial chefs, and young adults in research activities in this field that also promotes environmental equity. More importantly, social media such as Facebook, Instagram, Twitter, Clubhouse, WhatsApp, and Telegram are available to provide rapid and efficient communication with the public through different posts, lives, stories, and messages. Thus, researchers are encouraged to translate their research outcomes for public audience through such platforms. Existing examples are Instagram (addressed as *@aerosol_science_en* (English language) and *@aerosol_science* (Farsi Language)) and Clubhouse (addressed as *@profmehdi*) pages of the author of this chapter, Mehdi Amouei Torkmahalleh, to disseminate research findings related to the air quality in general and cooking emissions in particular.

Conclusions

While over 700 articles have been published over the past 30 years in the area of cooking aerosol, research on cooking aerosol deserves further attention in the area of health, chemistry, and physics. Few recent studies reported the production of particles smaller than 3 nm so-called “cluster mode particles.” However, doubt exists as to whether the cooking components are the source of these particles. Thus, future research should address the emission, dynamics, and exposure and health effects of sub-3 nm cooking particles. Frying cooking oils triggers the oil chemistry including hydrolysis, oxidation, and thermal alteration that result in the production of VOCs, PAH, and trace elements in the aerosol phases. In addition to the cooking oils, cooking pans could also be the source of the trace elements in the particulate phase.

What we have learned so far shows that opportunities exist to reduce exposure of cooks and indoor occupants to cooking aerosol by changing the cooking habits. Such cooking habits include employing low-emitting cooking oils, addition of salts to the oils at the beginning of cooking, using back burner on the stove, cooking in a low emitting pan, using a smaller pan, and cooking longer at lower temperature. Indoor air scientists particularly those studying cooking emissions are encouraged to include citizen science concepts and employ social media platforms in their research to increase public awareness and promote environmental equity with regard to indoor air quality and exposure to cooking fumes.

Cross-References

- [Appliances for Cooking, Heating, and Other Energy Services](#)
-

References

- Abdullahi KL, Delgado-Saborit JM, Harrison RM (2013) Emissions and indoor concentrations of particulate matter and its specific chemical components from cooking: a review. *Atmos Environ* 71:260–294
- Agrawal S (2012) Effect of indoor air pollution from biomass and solid fuel combustion on prevalence of self-reported asthma among adult men and women in India: findings from a nationwide large-scale cross-sectional survey. *J Asthma* 49(4):355–365
- Alves C, Duarte M, Nunes T, Moreira R, Rocha S (2014) Carbonaceous particles emitted from cooking activities in Portugal. *Glob Nest J* 16:412–420
- Amouei Torkmahalleh M, Goldasteh I, Zhao Y, Udochu NM, Rossner A, Hopke P, Ferro A (2012) PM_{2.5} and ultrafine particles emitted during heating of commercial cooking oils. *Indoor Air* 22 (6):483–491
- Amouei Torkmahalleh M, Zhao Y, Hopke P, Rossner A, Ferro A (2013a) Additive impacts on particle emissions from heating low emitting cooking oils. *Atmos Environ* 74:194–198
- Amouei Torkmahalleh M, Zhao Y, Hopke P, Rossner A, Ferro A (2013b) Influence of food surface area on PM_{2.5} and particle number concentration during frying. Paper presented at the Proceedings of the 2013 European aerosol conference, Prague, Czech Republic
- Amouei Torkmahalleh M, Kaibaldiyeva U, Kadyrbayeva A (2017a) A new computer model for the simulation of particulate matter formation from heated cooking oils using Aspen Plus. *Build. Simul.* 10, 535–550 (2017). <https://doi.org/10.1007/s12273-016-0341-0>
- Amouei Torkmahalleh M, Gorjinezad S, Keles M, Unluvcek HS, Azgin C, Cihan E, ... Ozturk F (2017b) A controlled study for the characterization of PM_{2.5} emitted during grilling ground beef meat. *J Aerosol Sci* 103:132–140
- Amouei Torkmahalleh M, Gorjinezad S, Keles M, Ozturk F, Hopke PK (2017c) Size segregated PM and its chemical composition emitted from heated corn oil. *Environ Res* 154:101–108
- Amouei Torkmahalleh M, Gorjinezad S, Unluvcek HS, Hopke PK (2017d) Review of factors impacting emission/concentration of cooking generated particulate matter. *Sci Total Environ* 586:1046–1056
- Amouei Torkmahalleh M, Ospanova S, Baibatyrova A, Nurbay S, Zhanakhmet G, Shah D (2018) Contributions of burner, pan, meat and salt to PM emission during grilling. *Environ Res* 164:11–17
- Amouei Torkmahalleh M, Sharifi H, Dareini M, Giorgio Buonanno G (2019) The impact of cooking pan material on ultrafine particle emission rates, 37th AAAR conference, Portland Oregon, October 14–18

- Anttila A, Apostoli P, Bond JA, Gerhardsson L, Gulson BL, Hartwig A, Hoet P, Ikeda M, Jaffe EK, Landrigan PJ, Levy L, Needelman HL, O'Flaherty EJ, Olin S, Olsen JH, Rossman TG, Sakai T, Shen X, Sorahan T, ... Waalkes MP (2006) IARC monographs on the evaluation of carcinogenic risks to humans: Inorganic and organic lead compounds. (IARC Monographs on the Evaluation of Carcinogenic Risks to Humans; Vol. 87.506p). World Health Organization International Agency for Research on Cancer
- Aoki T, Tanabe S (2007) Generation of sub-micron particles and secondary pollutants from building materials by ozone reaction. *Atmos Environ* 41:3139–3150
- Barry AC, Mannino DM, Hopenhayn C, Bush H (2010) Exposure to indoor biomass fuel pollutants and asthma prevalence in Southeastern Kentucky: results from the Burden of Lung Disease (BOLD) study. *J Asthma* 47(7):735–741
- Bekö G, Weschler CJ, Wierzbicka A, Karottki DG, Toftum J, Loft S, Clausen G (2013) Ultrafine particles: exposure and source apportionment in 56 Danish homes. *Environ Sci Technol* 47(18): 10240–10248
- Bello, Warheit (2017) Biokinetics of engineered nano-TiO₂ in rats administered by different exposure routes: implications for human health. *Nanotoxicology* 11(4):431–433
- Bonjour S, Adair-Rohani H, Wolf J, Bruce NG, Mehta S, Prüss-Ustün A, ... Smith KR (2013) Solid fuel use for household cooking: country and regional estimates for 1980–2010. *Environ Health Perspect* 121(7):784–790
- Broomandi P, Amouei Torkmahalleh M, Akturk M, Ngagine SH, Gorjinezad S, Ozturk F, ... Kim J (2020) A new exposure route to trace elements in indoor particulate matter. *Indoor Air* 30(3): 492–499
- Buonanno G, Morawska L, Stabile L (2009) Particle emission factors during cooking activities. *Atmos Environ* 43(20):3235–3242
- Buonanno G, Johnson G, Morawska L, Stabile L (2011) Volatility characterization of cooking-generated aerosol particles. *Aerosol Sci Technol* 45(9):1069–1077
- Chen X, Hopke PK (2009a) Secondary organic aerosol from alpha-pinene ozonolysis in dynamic chamber system. *Indoor Air* 19:335–345
- Chen X, Hopke PK (2009b) A chamber study of secondary organic aerosol formation by linalool ozonolysis. *Atmos Environ* 43:3935–3940
- Chen X, Hopke PK (2010) A chamber study of secondary organic aerosol formation by limonene ozonolysis. *Indoor Air* 20:320–328
- Chen C, Zhao Y, Zhao B (2018) Emission rates of multiple air pollutants generated from Chinese residential cooking. *Environ Sci Technol* 52(3):1081–1087
- Cho H, Youn JS, Oh I, Jung YW, Jeon KJ (2019) Determination of the emission rate for ultrafine and accumulation mode particles as a function of time during the pan-frying of fish. *Journal of environmental management* 236:75–80
- Chowdhury Z, Le LT, Al Masud A, Chang KC, Alauddin M, Hossain M, ... Hopke PK (2012) Quantification of indoor air pollution from using cookstoves and estimation of its health effects on adult women in northwest Bangladesh. *Aerosol Air Qual Res* 12(4):463–475
- Christie WW, Dobson G (2000) Formation of cyclic fatty acids during the frying process. *Eur J Lipid Sci Technol* 102:515–520. [https://doi.org/10.1002/1438-9312\(200009\)102:8/9<515::AID-EJLT515>3.0.CO;2-Z](https://doi.org/10.1002/1438-9312(200009)102:8/9<515::AID-EJLT515>3.0.CO;2-Z)
- Corsi RL, Siegel J, Karamalegos A, Simon H, Morrison GC (2007) Personal reactive clouds: introducing the concept of near-head chemistry. *Atmos Environ* 41:3161–3165
- Crossley A, Heyes T, Hudson B (1962) The effect of heat on pure triglycerides. *J Am Oil Chem Soc* 39(1):9–14
- Dan EU, Ebong GA (2013) Impact of cooking utensils on trace metal levels of processed food items. *Ann Food Sci Technol* 14(2):350–355
- Denisov ET, Afanas'ev IB (2005) Molecular products and thermochemistry of hydrocarbon oxidation. In: Denisov ET, Afanas'ev IB (eds) Oxidation and antioxidants in organic chemistry and biology. Taylor & Francis Group, pp 1–18
- Dennekamp M, Howarth S, Dick C, Cherrie JW, Donaldson K, Seaton A (2001) Ultrafine particles and nitrogen oxides generated by gas and electric cooking. *Occup Environ Med* 58(8):511–516

- Destaillets H, Lunden MM, Singer BC, Coleman BK, Hodgson AT, Weschler CJ, Nazaroff WW (2006) Indoor secondary pollutants from household product emissions in the presence of ozone: a bench-scale chamber study. *Environ Sci Technol* 40:4421–4428
- Dobarganes MC, Márquez-Ruiz G (2007) Formation and analysis of oxidized monomeric, dimeric, and higher oligomeric triglycerides. In: Erickson MD (ed) Deep frying: chemistry, nutrition, and practical applications, 2nd edn. pp 87–110
- Dobson G (1998) Cyclic fatty acids: qualitative and quantitative analysis. In: Hamilton RJ (ed) Lipid analysis in oils and fats. Blackie, London, pp 136–180
- Dua S, Hopke P (1996) Hygroscopic growth of assorted indoor aerosols. *Aerosol Sci Technol* 24(3): 151–160
- Ericson MD (ed) (2007) Deep frying: chemistry, nutrition, and practical applications, 2nd edn. pp 51–56
- Fan ZH, Weschler CJ, Han IK, Zhang JF (2005) Co-formation of hydroperoxides and ultra-fine particles during the reactions of ozone with a complex VOC mixture under simulated indoor conditions. *Atmos Environ* 39:5171–5182
- Feron VJ, Til HP, de Vrijer F, Woutersen RA, Cassee FR, van Bladeren PJ (1991) Aldehydes: occurrence, carcinogenic potential, mechanism of action and risk assessment. *Mutat Res* 259: 363–385
- Gao J, Cao C, Zhang X, Luo Z (2013) Volume-based size distribution of accumulation and coarse particles (PM0. 1–10) from cooking fume during oil heating. *Build Environ* 59:575–580
- Glytsos T, Ondráček J, Džumbová L, Kopanakis I, Lazaridis M (2010) Characterization of particulate matter concentrations during controlled indoor activities. *Atmos Environ* 44(12): 1539–1549
- Gorjinezad S, Kerimray A, Amouei Torkmahalleh M, Keleş M, Ozturk F, Hopke PK (2017) Quantifying trace elements in the emitted particulate matter during cooking and health risk assessment. *Environ Sci Pollut Res* 24(10):9515–9529
- Gunstone F, Knothe G, Kenar JA (2007) Chemical properties. In: Gunstone FG, Harwood JL, Dijkstra AJ (eds) The lipid handbook, 3rd edn. Taylor & Francis Group, Boca Raton, pp 535–589
- Hankey S, Sullivan K, Kinnick A, Koskey A, Grande K, Davidson JH, Marshall JD (2015) Using objective measures of stove use and indoor air quality to evaluate a cookstove intervention in rural Uganda. *Energy Sustain Dev* 25:67–74
- He C, Morawska L, Hitchins J, Gilbert D (2004) Contribution from indoor sources to particle number and mass concentrations in residential houses. *Atmos Environ* 38(21):3405–3415
- He C, Morawska L, Gilbert DL (2005) Particle deposition rates in residential houses. *Atmos Environ* 39(21):3891–3899
- He Y-M, Chen J-J, Zhou Y, Wang X-J, Liu X-Y (2014) Extraction induced by emulsion breaking for trace multi-element determination in edible vegetable oils by ICP-MS. *Anal Methods* 6(14): 5105–5111
- Howard-Reed C, Wallace LA, Emmerich SJ (2003) Effect of ventilation systems and air filters on decay rates of particles produced by indoor sources in an occupied townhouse. *Atmospheric Environment* 37(38):5295–5306
- Huboyo HS, Tohno S, Cao R (2011) Indoor PM_{2.5} characteristics and CO concentration related to water-based and oil-based cooking emissions using a gas stove. *Aerosol Air Qual Res* 11(4): 401–411
- Jørgensen RB, Strandberg B, Sjaastad AK, Johansen A, Svendsen K (2013) Simulated restaurant cook exposure to emissions of PAHs, mutagenic aldehydes, and particles from frying bacon. *J Occup Environ Hyg* 10(3):122–131
- Katragadda HR, Fullana A, Sidhu S, Barrachina A (2010) Emissions of volatile aldehydes from heated cooking oils. *Food Chem* 78(120):59–65
- Klein F, Farren NJ, Bozzetti C, Daellenbach KR, Kilic D, Kumar NK, ... Hamilton JF (2016) Indoor terpene emissions from cooking with herbs and pepper and their secondary organic aerosol production potential. *Sci Rep* 6(1):1–7

- Klein F, Baltensperger U, Prévôt, AS, El Haddad I (2019) Quantification of the impact of cooking processes on indoor concentrations of volatile organic species and primary and secondary organic aerosols. *Indoor air* 29(6):926–942
- Klepeis NE, Nelson WC, Ott WR, Robinson JP, Tsang AM, Switzer P, ... Engelmann WH (2001) The National Human Activity Pattern Survey (NHAPS): a resource for assessing exposure to environmental pollutants. *J Expo Sci Environ Epidemiol* 11(3):231–252
- Ko Y-C, Cheng LS-C, Lee C-H, Huang J-J, Huang M-S, Kao E-L, ... Lin H-J (2000) Chinese food cooking and lung cancer in women nonsmokers. *Am J Epidemiol*, 151(2):140–147
- Kumar R, Srivastava P, Srivastava S (1994) Leaching of heavy metals (Cr, Fe, and Ni) from stainless steel utensils in food simulants and food materials. *Bull Environ Contam Toxicol* 53 (2):259–266
- Kumar P, Pirjola L, Ketzel M, Harrison RM (2013) Nanoparticle emissions from 11 non-vehicle exhaust sources—a review. *Atmos Environ* 67:252–277
- Laursen, Rasmussen, Rosati, Gutzke, Østergaard, Ravn, Kjærgaard, Bilde, Glasius, Sigsgaard T (2021) Acute health effects from exposure to indoor ultrafine particles – a randomized controlled crossover study among young mild asthmatics. *Indoor Air*. <https://doi.org/10.1111/ina.12902>. See fewer authors first published: 07 July 2021
- Lee SC, Li W-M, Chan LY (2001) Indoor air quality at restaurants with different styles of cooking in metropolitan Hong Kong. *Sci Total Environ* 279(1–3):181–193
- Li W, Hopke P (1993) Initial size distributions and hygroscopicity of indoor combustion aerosol particles. *Aerosol Sci Technol* 19(3):305–316
- Li S, Gao J, He Y, Cao L, Li A, Mo S, ... Cao Y (2017) Determination of time-and size-dependent fine particle emission with varied oil heating in an experimental kitchen. *J Environ Sci* 51:157–164
- Li Y, Wu A, Wu Y, Xu J, Zhao Z, Tong M, Shengji L (2019) Morphological characterization and chemical composition of PM_{2.5} and PM₁₀ collected from four typical Chinese restaurants. *Aerosol Science and Technology* 53(10):1186–1196
- Liu T, Li Z, Chan M, Chan CK (2017a) Formation of secondary organic aerosols from gas-phase emissions of heated cooking oils. *Atmos Chem Phys* 17(12):7333–7344
- Liu T, Liu Q, Li Z, Huo L, Chan M, Li X, ... Chan CK (2017b) Emission of volatile organic compounds and production of secondary organic aerosol from stir-frying spices. *Sci Total Environ* 599:1614–1621
- Liu T, Wang Z, Huang DD, Wang X, Chan CK (2018) Significant production of secondary organic aerosol from emissions of heated cooking oils. *Environ Sci Technol Lett* 5(1):32–37
- Lunden MM, Delp WW, Singer BC (2015) Capture efficiency of cooking-related fine and ultrafine particles by residential exhaust hoods. *Indoor Air* 25(1):45–58
- Mendil D, Oluozlu OD, Tuzen M, Soylak M (2009) Investigation of the levels of some element in edible oil samples produced in Turkey by atomic absorption spectrometry. *J Hazard Mater* 165:724–728
- Minutolo et al. (2010) <https://www.aidic.it/aaas10/webpapers/47Minutolo.pdf>
- Müller JP, Steinegger A, Schlatter C (1993) Contribution of aluminium from packaging materials and cooking utensils to the daily aluminium intake. *Z Lebensm Unters Forsch* 197(4):332–341
- Nasir ZA, Colbeck I, Ali Z, Ahmad S (2013) Indoor particulate matter in developing countries: a case study in Pakistan and potential intervention strategies. *Environ Res Lett* 8(2):024002
- O'Leary C, de Kluijzenaar Y, Jacobs P, Borsboom W, Hall I, Jones B (2019) Investigating measurements of fine particle (PM 2.5) emissions from the cooking of meals and mitigating exposure using a cooker hood. *Indoor Air* 29(3):423–438
- Olson DA, Burke JM (2006) Distributions of PM_{2.5} source strengths for cooking from the Research Triangle Park particulate matter panel study. *Environ Sci Technol* 40(1):163–169
- Patel S, Sankhyan S, Boedicker EK, DeCarlo PF, Farmer DK, Goldstein AH, ... Vanhanen J (2020) Indoor particulate matter during HOMEChem: concentrations, size distributions, and exposures. *Environ Sci Technol* 54(12):7107–7116

- Peng CY, Lan CH, Lin PC, Kuo CY (2017) Effects of cooking method, cooking oil, and food type on aldehyde emissions in cooking oil fumes. *Hazard Mater* 324(Part B):160–167
- Perkins EG (2007) Volatile Odor and Flavor Components Formed in Deep Frying. In: Ericson, Michael D, editor. *Deep frying:chemistry, nutrition, and practical applications*. 2nd ed. 2007. p. 51–6
- Qu YH, Xu GX, Zhou JZ, Chen TD, Zhu LF, Shields PG et al (1992) Genotoxicity of heated cooked oil vapors. *Mutat Res* 298:105–111
- Rim D, Wallace L, Nabinger S, Persily A (2012) Reduction of exposure to ultrafine particles by kitchen exhaust hoods: the effects of exhaust flow rates, particle size, and burner position. *Sci Total Environ* 432:350–356
- Rönkkö T, Kuuluvainen H, Karjalainen P, Keskinen J, Hillamo R, Niemi JV, . . . Saukko E (2017) Traffic is a major source of atmospheric nanocluster aerosol. *Proc Natl Acad Sci* 114(29):7549–7554
- Schaich KM (2005) Lipid oxidation: theoretical aspects. In: Shahidi F (ed) *Bailey's industrial oil and fat products*, 6th edn. Wiley, pp 219–357
- Schauer JJ, Kleeman MJ, Cass GR, Simoneit BR (2002) Measurement of emissions from air pollution sources. 4. C1–C27 organic compounds from cooking with seed oils. *Environmental Science & Technology* 36(4):567–575
- Scrimgeour C (2005) Chemistry of fatty acids. In: Shahidi F (ed) *Bailey's industrial oil and fat products*, 6 vol ed. Wiley, pp 1–44
- Sebedlo J-L, Juaneda P (2007) Isomeric and Cyclic Fatty Acids as a Result of Frying. In: Erickson MD, editor. *Deep frying: chemistry, nutrition, and practical applications*. 2nd ed. 2007. p. 57–86
- See S, Balasubramanian R (2006a) Risk assessment of exposure to indoor aerosols associated with Chinese cooking. *Environ Res* 102(2):197–204
- See SW, Balasubramanian R (2006b) Physical characteristics of ultrafine particles emitted from different gas cooking methods. *Aerosol Air Qual Res* 6(1):82–92
- See SW, Balasubramanian R (2008) Chemical characteristics of fine particles emitted from different gas cooking methods. *Atmos Environ* 42(39):8852–8862
- Shen G, Gaddam C, Ebersviller S, Vander Wal R, Williams C, Faircloth J, Jetter J, Hays M (2017) A laboratory comparison of emission factors, number size distributions, and morphology of ultrafine particles from 11 different household cookstove-fuel systems. *Environ Sci Technol* 51(11):6522–6532. <https://doi.org/10.1021/acs.est.6b05928>. American Chemical Society, Washington, DC
- Singer BC, Delp WW, Price PN, Apte MG (2012) Performance of installed cooking exhaust devices. *Indoor Air* 22(3):224–234
- Singer BC, Pass RZ, Delp WW, Lorenzetti DM, Maddalena RL (2017) Pollutant concentrations and emission rates from natural gas cooking burners without and with range hood exhaust in nine California homes. *Build Environ* 122:215–229
- Singh S (2014) Comparative study of indoor air pollution using traditional and improved cooking stoves in rural households of northern India. *Energy Sustain Dev* 19:1–6
- Singh G, Maurya S, Catalan C, De Lampasona M (2005) Studies on essential oils, part 42: chemical, antifungal, antioxidant and sprout suppressant studies on ginger essential oil and its oleoresin. *Flavour Fragr J* 20(1):1–6
- Sjaastad AK, Svendsen K (2008) Exposure to mutagenic aldehydes and particulate matter during panfrying of beefsteak with margarine, rapeseed oil, olive oil or soybean oil. *Ann Occup Hyg* 52 (8):739–745
- Subramanian R, Nakajima M (1997) Membrane degumming of crude soybean and rapeseed oil. *J Am Oil Chem Soc* 74:971–975
- Sze-To GN, Wu CL, Chao CY, Wan MP, Chan TC (2012) Exposure and cancer risk toward cooking-generated ultrafine and coarse particles in Hong Kong homes. *HVAC&R Res* 18(1–2):204–216
- To W, Yeung LL (2011) Effect of fuels on cooking fume emissions. *Indoor Built Environ* 20(5): 555–563

- Torkmahalleh MA, Goldasteh I, Zhao Y, Udochu NM, Rossner A, Hopke PK, et al (2012) PM 2.5 and ultrafine particles emitted during heating of commercial cooking oils. *Indoor Air* 22(6):483–91
- Velasco J, Dobarganes C (2002) Oxidative stability of virgin olive oil. *Eur J Lipid Sci Technol* 104: 661–676
- Wagner AY, Livbjerg H, Kristensen PG, Glarborg P (2010) Particle emissions from domestic gas cookers. *Combust Sci Technol* 182(10):1511–1527
- Wallace L, Howard-Reed C (2002) Continuous monitoring of ultrafine, fine, and coarse particles in a residence for 18 months in 1999–2000. *J Air Waste Manage Assoc* 52(7):828–844
- Wallace L, Ott W (2011) Personal exposure to ultrafine particles. *J Expo Sci Environ Epidemiol* 21(1):20–30
- Wallace, Emmerich, Howard-Reed (2004a) Effect of central fans and in-duct filters on deposition rates of ultrafine and fine particles in an occupied townhouse. *Atmospheric Environment* 38:405–413
- Wallace LA, Emmerich SJ, Howard-Reed C (2004b) Source strengths of ultrafine and fine particles due to cooking with a gas stove. *Environ Sci Technol* 38(8):2304–2311
- Wallace L, Wang F, Howard-Reed C, Persily A (2008) Contribution of gas and electric stoves to residential ultrafine particle concentrations between 2 and 64 nm: size distributions and emission and coagulation rates. *Environ Sci Technol* 42(23):8641–8647
- Wallace LA, Ott WR, Weschler CJ (2015) Ultrafine particles from electric appliances and cooking pans: experiments suggesting desorption/nucleation of sorbed organics as the primary source. *Indoor Air* 25(5):536–546
- Wallace, Ott WR, Weschler CJ, Lai ACK (2017) Desorption of SVOCs from heated surfaces in the form of ultrafine particles. *Environ Sci Technol* 51(3):1140–1146. <https://doi.org/10.1021/acs.est.6b03248>
- Wan PJ, Pakarinen DR, Miscella RJ Sr (1996) Refining test for the determination of cottonseed oil color. *J Am Oil Chem Soc* 73:815–817
- Wan M-P, Wu C-L, To G-NS, Chan T-C, Chao CY (2011) Ultrafine particles, and PM2. 5 generated from cooking in homes. *Atmos Environ* 45(34):6141–6148
- Weschler CJ, Carslaw N (2018) Indoor chemistry. *Environ Sci Technol* 52(5):2419–2428
- Wu CL, Chao CY, Sze-To GN, Wan MP, Chan TC (2012) Ultrafine particle emissions from cigarette smouldering, incense burning, vacuum cleaner motor operation and cooking. *Indoor Built Environ* 21(6):782–796
- Yeung LL, To W (2008) Size distributions of the aerosols emitted from commercial cooking processes. *Indoor Built Environ* 17(3):220–229
- Zambiazi RC, Przybylski R, Zambiazi MW, Mendonça CB (2007) Fatty acid composition of vegetable oils and fats. *Boletim do Centro de Pesquisa de Processamento de Alimentos* 25(1)
- Zhang Q, Gangopamu RH, Ramirez D, Zhu Y (2010) Measurement of ultrafine particles and other air pollutants emitted by cooking activities. *Int J Environ Res Public Health* 7(4):1744–1759
- Zhang N, Han B, He F, Xu J, Zhao R, Zhang Y, Bai Z (2017) Chemical characteristic of PM2. 5 emission and inhalational carcinogenic risk of domestic Chinese cooking. *Environ Pollut* 227: 24–30
- Zhao YJ, Chen C, Zhao B (2018) Is oil temperature a key factor influencing air pollutant emissions from Chinese cooking? *Atmos Environ* 193:190–197
- Zhao Y, Zhang Z, Ji C, Liu L, Zhang B, Huan C (2019) Characterization of particulate matter from heating and cooling several edible oils. *Build Environ* 152:204–213
- Zhou Z, Dionisio KL, Verissimo TG, Kerr AS, Coull B, Howie S, ... Fornace K (2014) Chemical characterization and source apportionment of household fine particulate matter in rural, peri-urban, and urban West Africa. *Environ Sci Technol* 48(2):1343–1351

Part IV

Measurement and Evaluation



Sampling and Analysis of VVOCs and VOCs in Indoor Air 15

Jinhan Mo and Yingjun Liu

Contents

Introduction	430
Sampling and Analysis of VVOCs	430
Sampling	431
Sampling Treatment	431
Sample Analysis	432
Sampling and Analysis of VOCs	432
Sampling	432
Sampling Treatment	435
Sample Analysis	435
Conclusion	436
References	436

Abstract

Indoor air is a complicated matrix. There are various volatile organic compounds (VVOCs) such as formaldehyde and volatile organic compounds (VOCs) such as benzene, toluene, and xylene in indoor air. They are of low concentration and have different polarities. This chapter first introduces the sampling methods, sample treatment, and analysis of VVOCs (mainly carbonyls and ketones) in indoor air. The 2,4-dinitrophenyl-hydrazine (DNPH) derivatization – high-performance liquid chromatography (HPLC) method – is the most commonly used for the determination of VVOCs. Then four sampling methods for VOCs, including active sampling, passive sampling, whole-air sampling, and solid-phase microextraction (SPME), are introduced. Thermal desorption and solvent

J. Mo (✉)

Department of Building Science, School of Architecture, Tsinghua University, Beijing, China
e-mail: mojinhan@tsinghua.edu.cn

Y. Liu

Department of Environmental Health, College of Environmental Sciences and Engineering, Peking University, Beijing, China
e-mail: yingjun.liu@pku.edu.cn

extraction are two commonly used methods to pretreat the samples for further analysis. GC combined with MS, FID, ECD, or BID is frequently used for the VVOCs, VOCs, quantitation.

Keywords

Carbonyl · Concentration · Sampling · Treatment · Measurement

Introduction

Since the 1950s, many manufactured materials such as composite wood, polymeric flooring, plastics, etc. have been widely used as building materials. They may emit harmful organic compounds, including very volatile organic compounds (VVOCs) such as formaldehyde; volatile organic compounds (VOCs) such as benzene, toluene, and xylene; and semivolatile organic compounds (SVOCs) such as phthalate esters and brominated flame-retardants (Weschler 2009). These compounds can cause various adverse health effects, ranging from irritation of the eyes, skin, mucous membranes, and the respiratory tract (WHO 2010; Jones 1999; Billionnet et al. 2011) to the highly toxic effects of reactive organics, such as chronic asthma and cancer (WHO 2010; McGwin et al. 2010; Hulin et al. 2010).

There are different criteria for the classification of VVOCs and VOCs. The original classifications of the WHO (1989) for VVOCs and VOCs cover boiling points from $<0\text{ }^{\circ}\text{C}$ to $50\text{--}100\text{ }^{\circ}\text{C}$, from $50\text{--}100\text{ }^{\circ}\text{C}$ to $240\text{--}260\text{ }^{\circ}\text{C}$, respectively. The US EPA does not differentiate between VOCs and VVOCs and uses various definitions (<http://www.epa.gov/iaq/voc.html>): volatile organic compounds (VOC) mean any compound of carbon, excluding carbon monoxide, carbon dioxide, carbonic acid, metallic carbides or carbonates, and ammonium carbonate, which participates in atmospheric photochemical reactions, except those designated by EPA as having negligible photochemical reactivity. Salthammer (2016) summarized a list of VVOCs with relevance for the indoor environment.

Sampling and analysis of such indoor organic compounds are crucial for evaluating their exposure risks (Miller et al. 2022; Wang et al. 2020). There are two types of analytical methods for VVOCs and VOCs: real-time and off-line methods. The real-time monitoring of indoor organic compounds is introduced in ► Chap. 18, “Real-Time Monitoring of Indoor Organic Compounds.” In this chapter, the off-line sampling methods, sample treatment, and analysis of VVOCs and VOCs in indoor air will be introduced and discussed.

Sampling and Analysis of VVOCs

In organic chemistry, a carbonyl group is a functional group composed of a carbon atom double-bonded to an oxygen atom: C=O. VVOCs often contain a carbonyl group. Thus, most VVOCs are carbonyls. In the indoor environment, the dominant

VVOCs are aldehydes (such as formaldehyde, acetaldehyde, and ketones) (Salthammer 2016). The detailed description of VVOCs can be found in ► Chap. 22, “Source/Sink Characteristics of VVOCs and VOCs.”

Sampling

The sampling methods for airborne carbonyls often use a simultaneous sampling/derivatization process using sorbents or impregnated filters/cartridges coated with the derivatizing agent (Barro et al. 2009). The commonly used method used in indoor monitoring for VVOCs is 2,4-dinitrophenyl-hydrazine (DNPH) (Salthammer et al. 2010; Saito et al. 2006) to form colored dinitrophenylhydrazone suitable for UV detection. There are also other methods such as 5-dimethylaminonaphthalene-1-sulfohydrazide (dansylhydrazine, DNSH) (Pereira et al. 2002), pentafluorophenylhydrazine (PFBH) (Koziel et al. 2001), and 3-methyl-2-benzothiazolinone hydrazine (MBTH) (Xiao et al. 2018). The sampling methods can be used for both active and passive sampling.

For example, the DNPH method is frequently used in many standard methods for the determination of VVOCs. In acidic solution, hydrazone are formed from 2,4-dinitrophenylhydrazine (DNPH) by nucleophilic addition to the carbonyl group, followed by elimination of water (Salthammer et al. 2010). In the sampling process, ambient air is pulled by a pump through cartridges typically containing silica gel and coated with an acid solution of DNPH. After sampling, the cartridge is then eluted with acetonitrile. The eluate can be directly used for HPLC-UV analysis. Some studies improved the DNPH method for carbon isotope analysis of atmospheric acetone (Wen et al. 2006). Solid-phase microextraction (SPME) was used to monitor ten selected VVOCs in newly renovated rooms (Hippelein 2006). Koziel et al. (2001) developed a new sampling and analysis method combining solid-phase microextraction (SPME) and DNPH for formaldehyde in indoor air. To reduce sampling time, Saito et al. (2006) coated DNPH on the surface of a needle to simultaneously achieve the derivatization/collection process of indoor aldehydes and ketones.

The MBTH method is a nonselective colorimetric method for determining aliphatic aldehydes of low molecular weight. The MBTH method only quantifies total aldehydes in ambient air. Furthermore, strong reducing agents can interfere with the determination of aldehydes (Salthammer et al. 2010).

Sampling Treatment

The sampled VVOCs or carbonyls are usually eluted by solvent extraction, except for SPME-based or needle-based methods using direct thermal desorption in the injection port of gas chromatography (GC). Since most procedures for aldehyde analysis imply the use of high-performance liquid chromatography (HPLC), acetonitrile is often used as the solvent (Barro et al. 2009).

Sample Analysis

The ISO 16000-3 standard was developed to provide a method to determine formaldehyde and other carbonyl compounds (ISO 16000-3 2011). Generally, indoor aldehydes and other carbonyls are determined by detecting the fluorescent derivatives formed in the derivatization reactions. If only formaldehyde is the target, the MBTH method can be used and the absorbance of formaldehyde derivative is monitored at 628 nm with a UV spectrophotometer (Xiao et al. 2018). If there are various VVOCs in air, the sampled carbonyls are separated by HPLC, and absorbance or fluorescence changes are used for their detection (Barro et al. 2009). Analytical standard procedures for aldehydes and ketones in ambient air, such as TO-5 (US EPA 1984c) and TO-11A (US EPA 1999a) are often used. Even et al. (2021) adopted the ISO 16000-6 standard method (ISO 16000-6 2011) for VVOCs measurement by GC/MS.

Sampling and Analysis of VOCs

VOCs are emitted from various products and materials used indoors, such as paints, furniture, building materials, glues, and adhesives (Vallecillos et al. 2021). The detailed description of VOCs can be found in ► Chap. 22, “Source/Sink Characteristics of VVOCs and VOCs.”

Sampling

There are four types of sampling methods for VOCs, including active sampling, passive sampling, whole-air sampling, and solid-phase microextraction (SPME).

Active Sampling

Active sampling uses pumps to pull air through a single adsorbent or mixtures of adsorbents, where the airborne VOCs are captured and concentrated. Thus, the essential factors for active samplings are the selections of adsorbents, the amount of adsorbents, and the active pumping airflow rate. Many types of adsorbents have been used for indoor VOCs monitoring, such as silica gel (McGath et al. 2014), activated carbon (Sinha et al. 2006), Tenax (Fang et al. 2019), Carbotrap (De Bortoli et al. 1992), Carbopack (McClenney et al. 2006), Carbosieve (Pallau et al. 2007), and Carboxen (Su et al. 2007). Tenax has been extensively used in the active sampling of indoor VOCs, due to its hydrophobic nature, thermal stability, and rapid desorption kinetics (Fang et al. 2019; Norris et al. 2019; US EPA 1984a; ISO 16000-62,011).

Some studies combined several different adsorbents in one cartridge to capture VOCs of a wide volatility range. Pallau et al. (2007) studied the influence of relative humidity and ozone on the sampling of volatile organic compounds on carbotrap/carbon sieve adsorbents. Ribes et al. (2007) have developed a dynamic



Fig. 1 Schematic diagrams of the triple adsorbent cartridge

method to collect VOCs on multisorbent tubes filled with 70 mg Carbotrap, 100 mg CarbopackX, and 90 g Carboxen. Triple adsorbent cartridges were also utilized to capture VOCs from diluted sidestream tobacco smoke (Ueta et al. 2010). Usually, along with the pump flow, the packing order of different adsorbents in one cartridge should be weak adsorbent to strong adsorbent, as shown in Fig. 1.

Active sampling by pumps requires a trained person to set up air sampling. The sampling times are usually 30 min to 1 h, but low flow pumps can extend sampling times to 24 h (Crump 2001). Active sampling is likely to determine a relatively short-term concentration, such as the peak or worst-case. The pump flow rate will strongly influence the sampling volume of compounds. Before sampling, the pump flow must be calibrated. If using active sampling for relatively long time sampling, such as several hours, the pump flow rate should be examined before and after the sampling. A particle filter is also recommended at a long-term active sampling to avoid particle deposition into the sampling tubes. The reliable active sampling flow range is about 20 to 225 mL/min (Xian et al. 2011). It should be noted that the breakthrough problem must be considered in the active sampling.

Passive Sampling

In passive sampling, the transport of VOCs to the sampling medium is caused by diffusion. Compared with active sampling, passive sampling has increased attention due to its simplicity and has become a widely accepted method (Chandra et al. 2020; Cao et al. 2016a). Passive air sampling using sorbent tubes offers certain advantages over active sampling, including no need for electrical power, simplicity of use, reduction of operational costs, and suitability for personal exposure measurements (Brown et al. 1992; Du et al. 2014b; Ishizaka et al. 2019). However, the uptake rate (UR) of passive sampling needs to be obtained first to describe the equivalent

amount of ambient air collected during exposure, which is the challenge in using passive sampling (Jia and Fu 2017). More details about passive sampling can be found in ► Chap. 17, “Passive Samplers for Indoor Gaseous Pollutants.”

Whole-Air Sampling

Whole air sampling is a simple approach to directly collect air samples in field tests using sampling bags or canisters (Camel and Caude 1995). The collected air can be analyzed by GC, either by direct injection or through preconcentration processes (cold trap or a cryofocusing device) according to US EPA method TO-14A (US EPA 1999a) and TO-15 (US EPA 1999b).

The often-used sampling vessels are plastic bags and stainless-steel canisters. Plastic bags are usually made by Teflon, Tedlar, or aluminized Tedlar to avoid VOCs being adsorbed onto the inner surface. The inevitable problem of plastic-bag sampling is that filling the bags needs the air sample to be pumped in, which will add a potential source of contamination through the pumping system. Stainless-steel canisters such as Summa canisters (US EPA 1999b) have been frequently used in the sampling of indoor VOCs. The canister can be pumped out creating a vacuum before sampling and does not need a pumping system during the sampling. Similar to the plastic-bag method, the inner surface of stainless-steel canisters must be carefully pretreated to avoid VOC adsorption and carryover from prior samples. However, the Summa canister is much more expensive than the plastic bag. In general, it is not convenient to carry many stainless-steel canisters in the field-test studies, which limits the usage of the whole-air sampling.

Solid-Phase Microextraction

Solid-phase microextraction (SPME) was introduced in 1990 (Arthur and Pawliszyn 1990) and is based on solid-phase extraction (SPE). Although SPE method reduces the use of solvents and reduces laboratory costs, SPE cartridges are usually made by plastic, which will adsorb the other compounds and makes the SPE method often suffer from high blank values (Arthur and Pawliszyn 1990). In comparison, SPME is a solid-phase extraction sampling technique that involves the use of a fiber coated with an extracting phase, which extracts specific kinds of analytes from different kinds of media. The SPME method is a solvent-free process without sample preparation and then provides extremely fast chromatography. The coating on the fiber is important for the enrichment of the compounds of interest (Larroque et al. 2006).

SPME should be calibrated when measuring VOC concentrations. Calibration is the main obstacle for applying SPME to indoor air monitoring (Barro et al. 2009). Ouyang and Pawliszyn (2008) reported a detailed review of calibration methods for SPME. In the traditional calibration process, the sampling process ends when the equilibrium between the fiber coating and the target VOC has been reached (Ouyang and Pawliszyn 2008), and a linear relationship for the target VOC between the mass adsorbed by the coating and the concentration in the medium can be quantified (Cao et al. 2017). Cao et al. (2016b) further developed an analytical model to characterize SPME sampling for VOCs and SVOCs by considering the surface mass transfer process. The model can conveniently calculate the chemical concentrations in a

sample matrix. In addition, the model can be used to determine the characteristic parameters (partition coefficient and diffusion coefficient) for the kinetic calibration of SPME samplings. Sample volume plays an extremely important role in analysis by SPME (Górecki 1997). Its effect on the analysis results can be neglected only when it is much larger than the fiber capacity (Górecki et al. 1998). Hippelien (2006) was able to use SPME to measure VVOCs in rooms, such as acetone, methyl acetate, and 2-methylpentane.

Sampling Treatment

After the capture of target compounds by the above four types of sampling methods, it is necessary to release the compounds before the final chemical analysis. Thus, the treatment of samples is essential. Normally, the sampling method, treatment method, and analysis methods should match each other. For example, the Tenax sampling tubes can be treated by thermal desorption and then analyzed by GC or GC/MS (US EPA 1984a).

Thermal desorption techniques are widely used for treating samples collected by solid-phase adsorbents, such as activated carbon, Tenax, and Carbotrap. Usually the desorbed compounds can be directly injected into GC/MS system for further separation and quantification. For example, SPME samples can also be inserted in the injection port of GC and then thermally desorbed due to the high temperature in the injection port. VOCs have been widely extracted from adsorbents by thermal desorption (Kim et al. 2001; Fang et al. 2019; Du et al. 2014b; Du et al. 2014a). An automatic thermal desorption platform combined with a GC/MS system is often used to analyze large batches of samples.

When VOCs are too strongly adsorbed, thermal desorption may not completely desorb the compounds. Another alternative and commonly used treatment method is solvent extraction. Carbon disulfide is one of the most common solvents used for solvent desorption due to its good solubilization properties for many analytes (Barro et al. 2009). There are also other solvents used in the literature, such as methanol, toluene, hexane, or acetone. Chen et al. (2020) used hexane as the solvent to elute compounds from SPE columns.

Sample Analysis

The most commonly used method for determining indoor VOCs is gas chromatography/mass spectrometry combined with (automatic) thermal desorption, (A)TD-GC/MS. US EPA has published the standards for VOC measurement by GC or GC/MS (US EPA 1984a, b, 1999a, b). The standard methods cover the samples from different sampling and treatment methods. The basic function of GC is to separate compounds of a mixture, and then MS will qualitatively and quantitatively identify VOCs. As an alternative to MS, there are other methods to measure VOCs, such as flame ionization detector (FID) (ISO 16000-62,011), photoionization detector (PID)

(Soo et al. 2018), electron capture detector (ECD) (Sakai et al. 2004), and barrier discharge ionization detector (BID) (Antoniadou et al. 2019).

If the sample contains many compounds, it is hard to completely separate all compounds in one-dimensional GC. Liu and Phillips (1991) first developed a multidimensional gas chromatography technique, comprehensive two-dimensional gas chromatography (GCxGC). The GCxGC utilizes two different columns with two different stationary phases. In GCxGC, all of the effluent from the first dimension column is diverted to the second dimension column via a modulator. The modulator quickly traps, then “injects,” the effluent from the first dimension column onto the second dimension. Lewis et al. (2000) used GCxGC technique to successfully separate more than 500 chemical species of VOCs from urban air samples.

For more polar VOCs, the samples can be extracted by liquid solvents, and then the compounds can be determined by HPLC (Hong et al. 2001).

Conclusion

Indoor air is a complicated matrix. VVOCs and VOCs in indoor air are usually of very low concentrations. Thus, the sampling and analysis of VVOCs and VOCs in indoor air are crucial for identifying and evaluating their exposure risk. This chapter briefly summarizes the sampling methods, sample treatment, and analysis of VVOCs and VOCs in indoor air. The sampling method, treatment method, and analysis methods should match each other. Air samples are usually collected by active sampling, passive sampling, whole-air sampling, and solid-phase microextraction (SPME). Thermal desorption and solvent extraction are two commonly used methods to pretreat the samples for further analysis. GC combined with MS, FID, ECD, or BID is frequently used for the VVOCs, VOCs, quantitation. HPLC is often used for the detection of carbonyls and ketones.

References

- Antoniadou M, Zachariadis GA, Rosenberg E (2019) Investigating the performance characteristics of the barrier discharge ionization detector and comparison to the flame ionization detector for the gas chromatographic analysis of volatile and semivolatile organic compounds. *Anal Lett* 52(17):2822–2839. <https://doi.org/10.1080/00032719.2019.1628247>
- Arthur CL, Pawliszyn J (1990) Solid phase microextraction with thermal desorption using fused silica optical fibers. *Anal Chem* 62(19):2145–2148. <https://doi.org/10.1021/ac00218a019>
- Barro R, Regueiro J, Llompart M, Garcia-Jares C (2009) Analysis of industrial contaminants in indoor air: part 1. Volatile organic compounds, carbonyl compounds, polycyclic aromatic hydrocarbons and polychlorinated biphenyls. *J Chromatogr A* 1216(3):540–566. <https://doi.org/10.1016/j.chroma.2008.10.117>
- Billionnet C, Gay E, Kirchner S, Leynaert B, Annesi-Maesano I (2011) Quantitative assessments of indoor air pollution and respiratory health in a population-based sample of French dwellings. *Environ Res* 111(3):425–434. <https://doi.org/10.1016/j.envres.2011.02.008>

- Brown VM, Crump DR, Gardiner D (1992) Measurement of volatile organic compounds in indoor air by a passive technique. *Environ Technol* 13(4):367–375. <https://doi.org/10.1080/09593339209385164>
- Camel V, Caude M (1995) Trace enrichment methods for the determination of organic pollutants in ambient air. *J Chromatogr A* 710(1):3–19. [https://doi.org/10.1016/0021-9673\(95\)00080-7](https://doi.org/10.1016/0021-9673(95)00080-7)
- Cao J, Du Z, Mo J, Li X, Xu Q, Zhang Y (2016a) Inverse problem optimization method to design passive samplers for volatile organic compounds: principle and application. *Environ Sci Technol* 50(24):13477–13485. <https://doi.org/10.1021/acs.est.6b04872>
- Cao J, Xiong J, Wang L, Xu Y, Zhang Y (2016b) Transient method for determining indoor chemical concentrations based on SPME: model development and calibration. *Environ Sci Technol* 50(17):9452–9459. <https://doi.org/10.1021/acs.est.6b01328>
- Cao J, Zhang X, Little JC, Zhang Y (2017) A SPME-based method for rapidly and accurately measuring the characteristic parameter for DEHP emitted from PVC floorings. *Indoor Air* 27(2): 417–426. <https://doi.org/10.1111/ina.12312>
- Chandra BP, McClure CD, Mulligan J, Jaffe DA (2020) Optimization of a method for the detection of biomass-burning relevant VOCs in urban areas using thermal desorption gas chromatography mass spectrometry. *Atmos* 11(3):276. <https://doi.org/10.3390/atmos11030276>
- Chen Z, Afshari A, Mo J (2020) A method using porous media to deliver gas-phase phthalates rapidly and at a constant concentration: effects of temperature and media. *Environ Pollut* 262: 113823. <https://doi.org/10.1016/j.envpol.2019.113823>
- Crump D (2001) Strategies and protocols for indoor air monitoring of pollutants. *Indoor Built Environ* 10(3–4):125–131. <https://doi.org/10.1159/000049226>
- De Bortoli M, Knöppel H, Pecchio E, Schauenburg H, Visser H (1992) Comparison of Tenax and Carbotrap for VOC sampling in indoor air. *Indoor Air* 2(4):216–224. <https://doi.org/10.1111/j.1600-0668.1992.00004.x>
- Du Z, Mo J, Zhang Y, Xu Q (2014a) Benzene, toluene and xylenes in newly renovated homes and associated health risk in Guangzhou, China. *Build Environ* 72(0):75–81. <https://doi.org/10.1016/j.buildenv.2013.10.013>
- Du ZJ, Mo JH, Zhang YP (2014b) Risk assessment of population inhalation exposure to volatile organic compounds and carbonyls in urban China. *Environ Int* 73:33–45. <https://doi.org/10.1016/j.envint.2014.06.014>
- Even M, Juritsch E, Richter M (2021) Measurement of very volatile organic compounds (VVOCs) in indoor air by sorbent-based active sampling: identifying the gaps towards standardisation. *TrAC Trends Anal Chem* 140:116265. <https://doi.org/10.1016/j.trac.2021.116265>
- Fang L, Norris C, Johnson K, Cui XX, Sun JQ, Teng YB, Tian EZ, Xu W, Lig Z, Mo JH, Schauer JJ, Black M, Bergin M, Zhang J, Zhang YP (2019) Toxic volatile organic compounds in 20 homes in Shanghai: concentrations, inhalation health risks, and the impacts of household air cleaning. *Build Environ* 157:309–318. <https://doi.org/10.1016/j.buildenv.2019.04.047>
- Górecki T (1997) Effect of sample volume on quantitative analysis by solid-phase Micro-extractionPart 1. Theoretical considerations. *Analyst* 122(10):1079–1086. <https://doi.org/10.1039/A701303E>
- Górecki T, Khaled A, Pawliszyn J (1998) The effect of sample volume on quantitative analysis by solid phase microextraction part 2.† experimental verification. *Analyst* 123(12):2819–2824. <https://doi.org/10.1039/A806788K>
- Hippelein M (2006) Analysing selected VVOCs in indoor air with solid phase microextraction (SPME): a case study. *Chemosphere* 65(2):271–277. <https://doi.org/10.1016/j.chemosphere.2006.02.041>
- Hong J, Maguhn J, Freitag D, Kettrup A (2001) Detection of volatile organic peroxides in indoor air. *Fresenius J Anal Chem* 371(7):961–965. <https://doi.org/10.1007/s002160101085>
- Hulin M, Caillaud D, Annesi-Maesano I (2010) Indoor air pollution and childhood asthma: variations between urban and rural areas. *Indoor Air* 20(6):502–514. <https://doi.org/10.1111/j.1600-0668.2010.00673.x>

- Ishizaka TD, Kawashima A, Hishida N, Hamada N (2019) Measurement of total volatile organic compound (TVOC) in indoor air using passive solvent extraction method. *Air Qual Atmos Hlth* 12(2):173–187. <https://doi.org/10.1007/s11869-018-0639-4>
- ISO 16000-3 (2011) Indoor air – part 3: determination of formaldehyde and other carbonyl compounds in indoor air and test chamber air – active sampling method. Beuth Verlag, Berlin
- ISO 16000-6 (2011) Indoor air – part 6: determination of volatile organic compounds in indoor and test chamber air by active sampling on Tenax TA sorbent. Thermal Desorption and Gas Chromatography Using MS/FID
- Jia C, Fu X (2017) Diffusive uptake rates of volatile organic compounds on standard ATD tubes for environmental and workplace applications. *Environments* 4(4):87. <https://doi.org/10.3390/environments4040087>
- Jones AP (1999) Indoor air quality and health. *Atmos Environ* 33(28):4535–4564. [https://doi.org/10.1016/s1352-2310\(99\)00272-1](https://doi.org/10.1016/s1352-2310(99)00272-1)
- Kim YM, Harrad S, Harrison RM (2001) Concentrations and sources of VOCs in urban domestic and public microenvironments. *Environ Sci Technol* 35(6):997–1004. <https://doi.org/10.1021/es000192y>
- Koziel JA, Noah J, Pawliszyn J (2001) Field sampling and determination of formaldehyde in indoor air with solid-phase microextraction and on-fiber derivatization. *Environ Sci Technol* 35(7): 1481–1486. <https://doi.org/10.1021/es001653i>
- Larroque V, Desauziers V, Moch P (2006) Comparison of two solid-phase microextraction methods for the quantitative analysis of VOCs in indoor air. *Anal Bioanal Chem* 386(5): 1457–1464. <https://doi.org/10.1007/s00216-006-0714-9>
- Lewis AC, Carslaw N, Marriott PJ, Kinghorn RM, Morrison P, Lee AL, Bartle KD, Pilling MJ (2000) A larger pool of ozone-forming carbon compounds in urban atmospheres. *Nature* 405(6788):778–781. <https://doi.org/10.1038/35015540>
- Liu Z, Phillips JB (1991) Comprehensive two-dimensional gas chromatography using an on-column thermal modulator Interface. *J Chromatogr Sci* 29(6):227–231. <https://doi.org/10.1093/chromsci/29.6.227>
- McClenny WA, Jacumin HH Jr, Oliver KD, Daughtrey EH Jr, Whitaker DA (2006) Comparison of 24 h averaged VOC monitoring results for residential indoor and outdoor air using Carbopack X-filled diffusive samplers and active sampling—a pilot study. *J Environ Monit* 8(2):263–269. <https://doi.org/10.1039/b507850d>
- McGath M, McCarthy B, Bosworth J (2014) Environmental monitoring of volatile organic compounds using silica gel, zeolite and activated charcoal. *MRS Online Proceedings Library* 1656(1):199–209. <https://doi.org/10.1557/opl.2014.812>
- McGwin G, Lienert J, Kennedy JI (2010) Formaldehyde exposure and asthma in children: a systematic review. *Environ Health Persp* 118(3):313–317. <https://doi.org/10.1289/ehp.0901143>
- Miller DD, Bajracharya A, Dickinson GN, Durbin TA, McGarry JKP, Moser EP, Nunez LA, Pukkila EJ, Scott PS, Sutton PJ, Johnston NAC (2022) Diffusive uptake rates for passive air sampling: application to volatile organic compound exposure during FIREX-AQ campaign. *Chemosphere* 287(Pt 1):131808. <https://doi.org/10.1016/j.chemosphere.2021.131808>
- Norris C, Fang L, Barkjohn KK, Carlson D, Zhang YP, Mo JH, Li Z, Zhang JF, Cui XX, Schauer JJ, Davis A, Black M, Bergin MH (2019) Sources of volatile organic compounds in suburban homes in Shanghai, China, and the impact of air filtration on compound concentrations. *Chemosphere* 231:256–268. <https://doi.org/10.1016/j.chemosphere.2019.05.059>
- Ouyang G, Pawliszyn J (2008) A critical review in calibration methods for solid-phase micro-extraction. *Anal Chim Acta* 627(2):184–197. <https://doi.org/10.1016/j.aca.2008.08.015>
- Pallau F, Mirabel P, Millet M (2007) Influence of relative humidity and ozone on the sampling of volatile organic compounds on carbotrap/carbosieve adsorbents. *Environ Monit Assess* 127(1–3):177–187. <https://doi.org/10.1007/s10661-006-9272-z>
- Pereira EA, Carrilho E, Tavares MFM (2002) Laser-induced fluorescence and UV detection of derivatized aldehydes in air samples using capillary electrophoresis. *J Chromatogr A* 979(1): 409–416. [https://doi.org/10.1016/S0021-9673\(02\)01258-X](https://doi.org/10.1016/S0021-9673(02)01258-X)

- Ribes A, Carrera G, Gallego E, Roca X, Berenguer MJ, Guardino X (2007) Development and validation of a method for air-quality and nuisance odors monitoring of volatile organic compounds using multi-sorbent adsorption and gas chromatography/mass spectrometry thermal desorption system. *J Chromatogr A* 1140(1):44–55. <https://doi.org/10.1016/j.chroma.2006.11.062>
- Saito Y, Ueta I, Ogawa M, Jinno K (2006) Simultaneous derivatization/preconcentration of volatile aldehydes with a miniaturized fiber-packed sample preparation device designed for gas chromatographic analysis. *Anal Bioanal Chem* 386(3):725–732. <https://doi.org/10.1007/s00216-006-0509-z>
- Sakai K, Norbäck D, Mi Y, Shibata E, Kamijima M, Yamada T, Takeuchi Y (2004) A comparison of indoor air pollutants in Japan and Sweden: formaldehyde, nitrogen dioxide, and chlorinated volatile organic compounds. *Environ Res* 94(1):75–85. [https://doi.org/10.1016/S0013-9351\(03\)00140-3](https://doi.org/10.1016/S0013-9351(03)00140-3)
- Salthammer T (2016) Very volatile organic compounds: an understudied class of indoor air pollutants. *Indoor Air* 26(1):25–38. <https://doi.org/10.1111/ina.12173>
- Salthammer T, Mentese S, Marutzky R (2010) Formaldehyde in the indoor environment. *Chem Rev* 110(4):2536–2572. <https://doi.org/10.1021/cr800399g>
- Sinha SN, Kulkarni PK, Shah SH, Desai NM, Patel GM, Mansuri MM, Saiyed HN (2006) Environmental monitoring of benzene and toluene produced in indoor air due to combustion of solid biomass fuels. *Sci Total Environ* 357(1):280–287. <https://doi.org/10.1016/j.scitotenv.2005.08.011>
- Soo J-C, Lee EG, LeBouf RF, Kashon ML, Chisholm W, Harper M (2018) Evaluation of a portable gas chromatograph with photoionization detector under variations of VOC concentration, temperature, and relative humidity. *J Occup Environ Hyg* 15(4):351–360. <https://doi.org/10.1080/15459624.2018.1426860>
- Su H-J, Chao C-J, Chang H-Y, Wu P-C (2007) The effects of evaporating essential oils on indoor air quality. *Atmos Environ* 41(6):1230–1236. <https://doi.org/10.1016/j.atmosenv.2006.09.044>
- Ueta I, Saito Y, Teraoka K, Miura T, Jinno K (2010) Determination of volatile organic compounds for a systematic evaluation of third-hand smoking. *Anal Sci* 26(5):569–574. <https://doi.org/10.2116/analsci.26.569>
- US EPA (1984a) Compendium of methods for the determination of toxic organic compounds in ambient air, method TO-1: method for the determination of Volatile Organic Compounds (VOCs) in Ambient Air Using Tenax® Adsorption and Gas Chromatography/Mass Spectrometry (GC/MS)
- US EPA (1984b) Compendium of methods for the determination of Toxic organic compounds in Ambient Air, method TO-2: method for the determination of Volatile Organic Compounds (VOCs) in Ambient Air by Carbon Molecular Sieve Adsorption and Gas Chromatography/Mass Spectrometry (GC/MS)
- US EPA (1984c) Compendium of Methods for the Determination of Toxic Organic Compounds in Ambient Air, Method TO-5: Determination of Aldehydes and Ketones in Ambient Air Using High Performance Liquid Chromatography (HPLC)
- US EPA (1999a) Compendium of Methods for the Determination of Toxic Organic Compounds in Ambient Air, Method TO-14A: Determination Of Volatile Organic Compounds (VOCs) In Ambient Air Using Specially Prepared Canisters With Subsequent Analysis By Gas Chromatography
- US EPA (1999b) Compendium of Methods for the Determination of Toxic Organic Compounds in Ambient Air, Method TO-15: Determination of Volatile Organic Compounds (VOCs) In Air Collected In Specially-Prepared Canisters And Analyzed By Gas Chromatography Mass Spectrometry (GC/MS)
- Vallejos L, Borrull A, Marce RM, Borrull F (2021) Presence of emerging organic contaminants and solvents in schools using passive sampling. *Sci Total Environ* 764:142903. <https://doi.org/10.1016/j.scitotenv.2020.142903>

- Wang H, Zheng J, Yang T, He Z, Zhang P, Liu X, Zhang M, Sun L, Yu X, Zhao J, Liu X, Xu B, Tong L, Xiong J (2020) Predicting the emission characteristics of VOCs in a simulated vehicle cabin environment based on small-scale chamber tests: Parameter determination and validation. Environ Int:142. <https://doi.org/10.1016/j.envint.2020.105817>
- Wen S, Yu Y, Guo S, Feng Y, Sheng G, Wang X, Bi X, Fu J, Jia W (2006) Improvement of 2,4-dinitrophenylhydrazine derivatization method for carbon isotope analysis of atmospheric acetone. Rapid Commun Mass Spectrom 20(8):1322–1326. <https://doi.org/10.1002/rcm.2453>
- Weschler CJ (2009) Changes in indoor pollutants since the 1950s. Atmos Environ 43(1):153–169. <https://doi.org/10.1016/j.atmosenv.2008.09.044>
- WHO (1989) Indoor air quality: organic pollutants. EURO Reports and Studies No 111. World Health Organization Regional Office for Europe, Copenhagen
- WHO (2010) WHO guidelines for indoor air quality: selected pollutants. World Health Organization
- Xian Q, Y-I F, Chan CC, Zhu J (2011) Use of reference chemicals to determine passive uptake rates of common indoor air VOCs by collocation deployment of active and passive samplers. J Environ Monitor 13(9):2527–2534. <https://doi.org/10.1039/C1EM10278H>
- Xiao R, Mo JH, Zhang YP, Gao DW (2018) An in-situ thermally regenerated air purifier for indoor formaldehyde removal. Indoor Air 28(2):266–275. <https://doi.org/10.1111/ina.12441>



Sampling and Analysis of Semi-volatile Organic Compounds (SVOCs) in Indoor Environments

16

Zidong Song, Jianping Cao, and Ying Xu

Contents

Introduction	442
Sampling	443
Passive Air Sampling	443
Active Air Sampling	447
Dust and Surface Sampling	451
Sample Pretreatment	452
Solvent Extraction	452
Cleanup	457
Concentration	458
Thermal Desorption (TD)	458
Chemical Analysis	459
Chromatography	459
Mass Spectrometry (MS)	459
Conclusion	460
Cross-References	460
References	460

Z. Song

Department of Building Science, Tsinghua University, Beijing, China
e-mail: szd19@mails.tsinghua.edu.cn

J. Cao

School of Environmental Science and Engineering, Sun Yat-sen University, Guangzhou, China
e-mail: caojp3@mail.sysu.edu.cn

Y. Xu (✉)

Department of Building Science, Tsinghua University, Beijing, China

Department of Civil, Architectural and Environmental Engineering, The University of Texas at Austin, Austin, TX, USA

e-mail: xu-ying@mail.tsinghua.edu.cn

Abstract

Semi-volatile organic compounds (SVOCs) are ubiquitous indoor air pollutants and have adverse effects on human health. They partition strongly to interior surfaces, particles, and dust due to their physicochemical properties. This chapter provides an overview of the sampling and analytical methods of SVOCs in indoor environments, including sampling, sample pretreatment, and chemical analysis procedures. First, the general principles and techniques of gaseous and particulate SVOCs sampling, including passive air sampling, active air sampling, and dust sampling, are discussed. Second, common pretreatment methods are reviewed. Four different extraction methods, including Soxhlet extraction, accelerated solvent extraction, ultrasonication extraction, and microwave-assisted extraction, are compared. For cleanup and concentration, filtration, centrifugation, evaporation, and nitrogen blow are discussed. Finally, several widely used chemical analysis techniques are introduced. This chapter reviews the advantages and disadvantages of general methods for sampling and analysis of SVOCs in indoor environments and suggests future research needs.

Keywords

SVOCs · Sampling · Pretreatment · Chemical analysis

Introduction

Semi-volatile organic compounds (SVOCs) are defined as compounds with boiling points ranging from 240—260 °C to 380—400 °C with polar compounds in the high ends of the intervals (Clausen and Kofoed-Sørensen 2009). Another definition demonstrates SVOCs as compounds with saturation vapor pressures ranging from 10^{-2} kPa (10^{-1} torr) to 10^{-8} kPa (10^{-7} torr) (Clausen and Kofoed-Sørensen 2009). Therefore, SVOCs are likely to be distributed between the gas phase and the particle phase in indoor air. Indoor SVOCs include flame retardants, such as the polybrominated diphenyl ethers (PBDEs) and organophosphate esters (OPEs); pesticides, such as chlordane, chlorpyrifos, and diazinon; plasticizers, such as phthalates (PAEs); heat transfer fluids, such as the polychlorinated biphenyls (PCBs); and combustion byproducts, such as polycyclic aromatic hydrocarbons (PAHs), dioxins, and furans (Weschler and Nazaroff 2010). SVOCs are derived from a wide range of indoor sources, including building materials, consumer products, and furnishings, and they have been linked to serious adverse health effects. For example, Heudorf et al. (2007) found that exposure to some phthalates results in profound and irreversible changes in the development of the reproductive tract in males. Vonderheide et al. (2008) demonstrated that exposure to PBDEs may cause impairment of the brain and nerve tissues. As SVOCs are an important class of indoor pollutants that are of great health concern, sampling and analysis of SVOCs in indoor environments is essential to characterizing their concentration, fate, and transport mechanisms, and to avoid potential health effects. The aim of this chapter

is to review and compare different techniques of sampling, pretreatment, and chemical analysis of SVOCs in indoor environments, and to provide readers with recommendations for suitable methods in different situations.

Sampling

Semi-volatile organic compounds (SVOCs) are present not only in indoor air but also on suspended particles, dust, and interior surfaces (Clausen and Kofoed-Sørensen 2009). The objective of this section is to introduce the general principles and techniques regarding SVOC sampling from different environmental media.

Passive Air Sampling

SVOCs can be collected in two ways: passive air sampling and active air sampling. Passive air sampling does not use electrical power; instead, it captures SVOCs by sorbents via diffusion mechanisms. Typically, passive air samplers (PASs), such as a semipermeable membrane device (SPMD), polyurethane foam (PUF) disk, poly-dimethylsiloxane (PDMS), and XAD-2 resin-based passive air samplers (XAD-PASs), are installed at specified sampling sites. After a sampling period, usually several weeks or months for SVOCs, the PASs are collected, and SVOCs captured by the sorbents can be desorbed or extracted for further analysis.

To quantify the air concentration, the relationship between the sampled mass of the analyte in the PAS and its gas-phase concentration at the sampling location should be established. The mass transfer process of chemicals in a PAS can be described as (Bartkow et al. 2005):

$$V_s \frac{\partial C_s}{\partial t} = k_o A_s \left(C_g - \frac{C_s}{K_{sg}} \right) \quad (1)$$

$$\frac{1}{k_o} = \frac{1}{k_g} + \frac{1}{k_s K_{sg}} + \frac{1}{Q/A_s} \quad (2)$$

where V_s [L^3] is the volume of sorbent, C_s [ng/m^3] is the concentration of the analyte in the sorbent, t [s] is the sampling time, k_o [m/s] is the overall mass transfer coefficient from air to the sorbent, A_s [m^2] is the area of sorbent, C_g [ng/m^3] is the concentration of the analyte in gas phase, K_{sg} is the sorbent/air partition coefficient, k_g [m/s] is the mass transfer coefficient for the air-side boundary layer, k_s [m/s] is the mass transfer coefficient for the sorbent-side boundary layer, and Q [m^3/s] is the air flow rate on the surface of the sorbent. When $\frac{C_s}{K_{sg}}$ is much smaller than C_g (the captured amount is far from the equilibrium amount), Eq. (1) can be integrated and the amount of analyte in the PASs (N_s [ng]) can be calculated by:

$$N_s = k_o A_s C_g t = R C_g t \quad (3)$$

where R [m^3/h] is defined as the sampling rate of PASs, $R = k_o A_s$.

The air-side mass transfer coefficient can be expressed as $k_g = D/\delta$, where D [m^2/s] is the air diffusivity of a specific compound and δ [m] is the length of the diffusion path. For PAS sampling, if the mass transfer is air controlled (i.e., $k_o \approx k_g$), the sampling rate (R [m^3/h]) equals $D \cdot A_s/\delta$. The relationship suggests that when PASs are exposed to elevated wind speeds, the sampling rate increases due to the decreased thickness of air boundary layer (Bartkow et al. 2005), and when the flow field near the PAS is unstable during sampling, the thickness of air boundary layer (δ) may also change continuously. As a result, it is difficult to measure the boundary layer thickness and accurately quantify the sampling amount using PASs in field studies.

To obtain the sampling rate, depuration compounds (DCs) are commonly added to PASs prior to field measurements. DCs have similar properties to the analytes but do not exist in the environment. Typically, isotope-labeled compounds are used as DCs and they are added to the PAS before field sampling. Assuming that the mass transfer processes for the uptake of the analytes and loss of DCs are in opposite directions and air-side-controlled, the concentration of DCs is zero in the environment, and the mass transfer rate is not affected by chemicals, the sampling rate of PASs can be derived from Eq. (1) as follows (Moeckel et al. 2009):

$$R = \frac{-\ln \left(\frac{C_{DC}^{corr}}{C_{DC,0}} \right) \cdot K_{PAS-A} \cdot \rho_{PAS} \cdot V}{t} \quad (4)$$

$$C_{DC}^{corr} = \frac{C_{DC}}{C_{DC-stable}/C_{DC-stable,0}} \quad (5)$$

where $C_{DC,0}$ and C_{DC} [ng/sample] are the initial and final concentrations of the DC during the deployment period, respectively, K_{PAS-A} [m^3/g] is the DC's PAS-air partition coefficient, ρ_{PAS} [g/ m^3] is the PAS bulk density, V [m^3] is the volume of the PAS, and t [h] is the deployment period. In Eq. (5), $C_{DC-stable,0}$ and $C_{DC-stable}$ [ng/sample] are the initial and final concentrations of a stable DC during the deployment period, respectively. C_{DC} values are corrected by the recoveries of the stable DC during sampling using C_{DC}^{corr} [ng/sample]. The purpose is to reduce uncertainties associated with the loss of DCs during spiking, collection, and pre-treatment (Moeckel et al. 2009).

Many types of passive samplers have been adopted for SVOC sampling. Table 1 lists their applications in different studies. Details of passive sampler design and a model that allows the optimization of a passive sampling system are discussed in ► Chap. 17, “Passive Samplers for Indoor Gaseous Pollutants,” in this handbook.

Compared to conventional PASs, solid-phase microextraction (SPME) is a recently developed passive sampling device. The SPME sampler consists of a fiber holder and a fiber assembly that contains a 1-cm long SPME fiber. The SPME fiber consists of a thin fused-silica or metal core coated with a thin polymeric film, and the fiber diameter is less than 0.5 mm. For sampling, the fiber is exposed to the air and then quickly inserted into a gas chromatography (GC) injection port for direct analysis (Pawliszyn et al. 1997).

Table 1 Passive air sampling methods applied in different studies

Studies	Sampler type	Analytes	Sampling site	Sampling time (days)
Harner et al. (2004)	PUF disk, SPMD	PCBs, organochlorine pesticides (OCPs)	Urban rural transect	About 120
Choi et al. (2008)	XAD-PAS	PCBs, OCPs	Research station	365
He and Balasubramanian (2010)	PUF disk	PAHs, OCPs	Research station	68
Schuster et al. (2010)	SPMD	PCBs, polybrominated diphenyl ethers (PBDEs)	The UK-Norway transect	730
Zhu et al. (2013)	SPMD	PAHs	Rooftop of campus building	52, 90
Gawor et al. (2014)	XAD-PAS	Per- and polyfluoroalkyl substances (PFAS)	The Global Atmospheric Passive Sampling sites	365
Bennett et al. (2015)	PUF disk	PBDEs	Homes	26–42
Sun et al. (2016)	PUF disk	PBDEs	Homes and offices	90
Okeme et al. (2018)	PUF disk, PDMS	Phthalates, brominated flame retardants (BFRs), PBDEs, OPEs	Homes	About 21
Meng et al. (2020)	PUF disk	Phthalates	Computer rooms, offices, laboratories, classrooms and dormitories	31

A typical sampling profile for an SPME device consists of three parts: linear regime, kinetic regime, and near equilibrium, as shown in Fig. 1 (Ouyang and Pawliszyn 2007), in which t_{50} and t_{95} represent the time when the extracted amount reaches 50% and 95% of the equilibrium amount, respectively. To quantify the sampling amount of the analyte using an SPME, both equilibrium and nonequilibrium methods are used depending on the sampling time (Ouyang and Pawliszyn 2008).

The equilibrium method applies only if the analyte has reached a near equilibrium distribution between the sample matrix and fiber coating. At equilibrium conditions, the extracted amount of analyte (n [ng]) can be expressed as (Pawliszyn 2012):

$$n = \frac{K_{fs} V_f V_s C_0}{K_{fs} V_f + V_s} \quad (6)$$

where K_{fs} is the partition coefficient of analytes between the fiber coating and the sample matrix, V_f [L] is the fiber coating volume, V_s [L] is the volume of sample

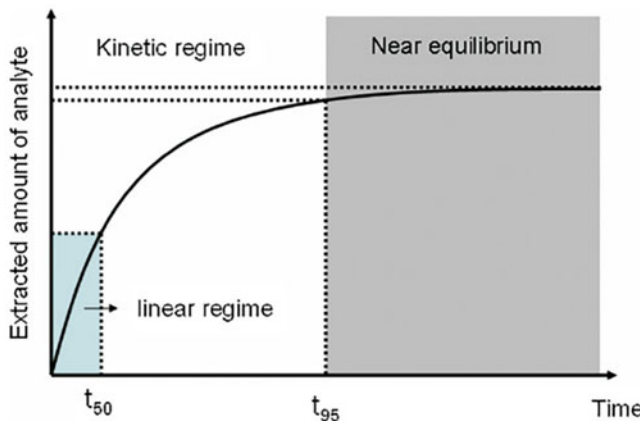


Fig. 1 Typical sampling profile for an SPME. (©With permission of Ouyang and Pawliszyn 2007)

matrix, and C_0 [ng/L] is the initial concentration of analyte in the sample matrix. When the volume of the sample matrix is much larger than the volume of the coating ($V_s \gg V_f$), Eq. (6) can be simplified to:

$$n = K_{fs}V_fC_0 \quad (7)$$

Equation (7) suggests that the amount of the extracted analyte is independent of V_s and the sampling time. As a result, the SPME fiber can be directly exposed to the sample matrix (e.g., air, water, blood) to obtain its concentration (C_0) when equilibrium is reached and K_{fs} is known (Ouyang and Pawliszyn 2008).

The equilibrium method has been used for on-site sampling of many organic pollutants like VOCs (Müller et al. 1999), but it may not be appropriate for SVOCs, since it takes a long time period to reach equilibrium due to the large K_{fs} value (Isetun et al. 2004). Therefore, a nonequilibrium SPME method was developed for SVOC sampling. This method assumes that the sampling rate remains constant throughout the sampling period. Therefore, the whole sampling period should be in the linear regime (i.e., the total sampling time is less than t_{50}). The extracted amount of analytes can then be quantified as $n = R \cdot C_0 \cdot t$, where R is estimated based on air diffusivity and the shape factor of SPME (Ouyang and Pawliszyn 2007). The concentration is then determined by linearly fitting the extracted amount (n) to different sampling times (t). However, the nonequilibrium method may only be suitable in a closed or stable chamber system because small changes of air flow in the field (indoor or outdoor environments) near an SPME may vary the sampling rate significantly. Cao et al. (2016) applied the non-equilibrium method and successfully measured the concentrations of dibutyl phthalate (DnBP) and di(2-ethylhexyl) phthalate (DEHP) in a sealed chamber system. The results were used to analyze the characteristics of phthalate emissions from vinyl flooring.

Active Air Sampling

Active air sampling usually needs three components: a pump, a sampling media, and a flow calibrator. During sampling, the pump generates a fixed flow rate and drives the air through the sampling media as shown in Fig. 2a. The average sampling flow rate is determined by a flow calibrator before, during, and after the sampling. Since the controlled flow rate is significantly higher than the sampling rate of the PAS, the time needed for active air sampling is shorter than passive air sampling, typically hours to days. The air concentration can then be calculated as:

$$C_a = \frac{M}{t \cdot R_s} \quad (8)$$

where C_a [$\mu\text{g}/\text{m}^3$] is the SVOC concentration, M [μg] is the sample mass collected by the sampling media, t [s] is the sampling time, and R_s [m^3/s] is the sampling flow rate. Several aspects should be optimized before sampling, including the type of sorbent used, the sampling time, and the sampling flow rate.

A combination of a filter and sorbent bed is typically used to collect particle- and gas-phase SVOCs (Tuduri et al. 2012). This method traps the particle phase on a quartz or glass fiber filter first (Fig. 2b). The gas phase is sampled downstream on a solid sorbent, such as polyurethane foam (PUF), XAD-2, or Tenax. Instead of a filter, a denuder/impactor can also be used for sampling particle-phase SVOCs (Mader et al. 2001), as depicted in Fig. 2b. In addition, a denuder system is also suitable for air sampling of SVOCs, in which annular denuder tubes (coated with appropriate adsorbents) trap the gas phase while particles pass through the tubes and are collected by the downstream filter. The filter may connect with a backup sorbent cartridge to capture any gas-phase SVOCs desorbed from the particles.

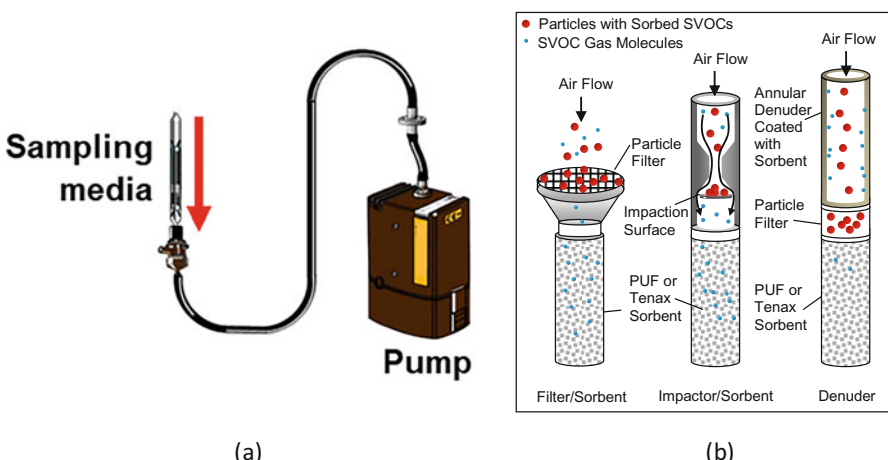


Fig. 2 (a) Active air sampling and (b) methods to measure gas- and particle-phase SVOCs

Generally, the concentration of total airborne SVOCs (the sum of gas- and particle- phase SVOCs) is determined through these methods. However, several studies have also used the results to calculate the partition coefficient between gas and particle phases for SVOCs (Cao et al. 2019; Zhou et al. 2021). However, these sampling systems may induce artifacts that disturb gas/particle partitioning. For example, for the filter/sorbent system, positive artifacts (overestimation of the particle phase) are mainly due to the sorption of gaseous species on the filter, while negative artifacts (underestimation of the particle phase) result from desorption of SVOCs from particles collected on the filter (Cheng et al. 2009). For the denuder system, several artifacts can also bias the measurement of the gas/particle partition coefficient, including incomplete gas phase removal, particle loss in the denuder tube, and SVOC off-gassing from particles when their corresponding gas phase components are removed in the denuder (Cheng et al. 2009).

In general, PUF, XAD, and Tenax are suitable sorbents for most SVOCs. Filters and sorbents such as PUF and XAD-2 are commonly extracted using solvents before GC analysis, while thermal desorption instruments are required to desorb Tenax. XAD-2 usually contains a lot of contaminants and needs extensive cleanup before use. In contrast, PUF and Tenax need to be cleaned up to a certain extent before use, but they may absorb vapors in the air during storage thereby increasing the background levels of blanks, so they must be stored carefully. Depending on method quantification limits, to obtain enough samples for analysis, PUF and XAD samplers must usually collect a larger sample volume than Tenax tubes, as listed in Table 2.

Compared to conventional methods, the needle trap device (NTD) method was recently developed for sampling of SVOCs. The NTD is prepared by packing a sorbent into a needle with a small hole on its side (Fig. 3). It combines the concept of active sampling and SPME (Asl-Hariri et al. 2014). For sampling, air is drawn through the needle by a sampling pump, and both gas- and particle-phase analytes are trapped by the sorbent. Desorption is performed by inserting the needle into a GC injection port with a carrier gas flowing into the needle through the side hole to aid the introduction of desorbed analytes into the GC column. Since the NTD technique integrates sampling, pre-concentration, and sample introduction into a single step, it is superior to conventional sampling techniques, being solvent-free, accurate, sensitive, and cost and time efficient. The NTD approach has been used for VOC and SVOC measurements in ambient air and water (Niri et al. 2009; Ueta et al. 2009). It has also been successfully applied to collect particle-free and particle-bound SVOCs for PAHs (Li et al. 2010) and insecticides (Niri et al. 2009) and has shown high efficiency in capturing particles with a size range of 0.01 μm to 100 μm . Recently, Li et al. (2020) developed a new NTD method for sampling SVOCs, such as phthalates, organophosphates, and polybrominated diphenyl ethers (PBDEs), in experimental chambers and fields. The NTD method shows high sensitivity and reproducibility, and better performance has been observed with the NTD method as compared to traditional methods. Their results indicated that the NTD method is a simple, sensitive, effective, reusable, and inexpensive technique for air sampling of SVOCs at a concentration level between 2 ng/m³ and 100 $\mu\text{g}/\text{m}^3$ (Li et al. 2020). Table 3 lists recent studies on NTD sampling of SVOCs.

Table 2 Active air sampling methods in different studies

Studies	Sorbent tube	Analytes	mean air concentration (mg/m ³)	Sampling time (h)	Flow rate (L/min)	Sampling volume (m ³)
Cessna et al. (1995)	PUF	Trifluralin	88–2517	1–2	25	1.5–3
Ré-Poppi and Santiago-Silva (2005)	XAD-2	PAHs	21–63	72	34	147
Tsapakis and Stephanou (2005)	PUF	PAHs	31–85	24	625	900
Xu et al. (2012)	Tenax-TA	DEHP	800–900	24	0.13	0.19
Aragón et al. (2013)	Tenax-TA	OPEs, phthalates	10–136,400	0.25	0.03–0.1	4.5×10^{-4} –1.5 × 10 ⁻³
Armstrong et al. (2013)	PUF/XAD-2	Chlopyrifos, chlopyrifos-oxon	2–2039	6	6	2.2
Liang and Xu (2014)	Tenax-TA	Phthalates	20–24,700	24	0.15	0.22
Xu et al. (2014)	Tenax-TA	Phthalates, PBDEs	2–5770	24	0.075–0.1	0.11–0.14
Xu et al. (2014)	PUF	Phthalates, PBDEs	2–5770	48	25	72
Das et al. (2020)	PUF/XAD-2	Chlopyrifos	24	6	220	79

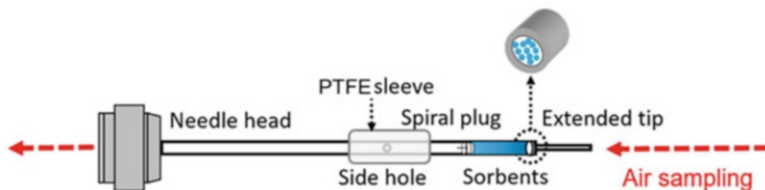


Fig. 3 Schematic of air sampling with an NTD. (©With permission of Li et al. 2020)

Table 3 NTD methods used in recent studies

Studies	NTD design	Analytes	Sampling time (h)	Flow rate (mL/min)
Ghalichi et al. (2019)	The needle was packed with the synthesized XAD-2/polyaniline sorbent, fixed by two layers of glass wool.	PAH	1–4	1
Soury et al. (2019)	The sorbent of this device was synthesized with Zn ₃ (BTC) ₂ metal-organic framework (Zn-MOF). To prevent the blocking of the NTD, each NTD mixed 1.5 mg of sorbent with 1 mg of glass particles.	PAH	0.5	3
Ghosh et al. (2020)	Tenax/Carboxen was used as the material for sorbent bed. A tee adapter was designed with one end fitted to the needle and the other end to the pump.	Butylated hydroxytoluene (BHT)	—	10
Li et al. (2020)	Divinylbenzene (DVB) particles (HayeSep® Q, mesh size 60/80 and surface area 582 m ² g ⁻¹) were chosen as the sorbent materials. Two spring plugs and a small amount of epoxy resin were used to hold the DVB particles inside the NTD.	Phthalates, PBDEs	—	15 ± 1

In summary, both passive and active air sampling methods have strengths and drawbacks. Compared to active sampling, in which a high known volume of air can be sampled within a short time period, passive sampling is time-consuming. In addition, uncertainty associated with quantification of the mass transfer rate reduces the accuracy of the measured SVOC air concentration using the passive method. However, the cost of active sampling is often higher than that of passive sampling due to the use of sampling pumps, electricity, and especially the associated labor. Therefore, active air sampling can be applied to accurately and rapidly quantify SVOC air concentrations (Liang and Xu 2014). In contrast, passive air sampling is suitable for measuring the average air concentration over a long period of time in field studies, especially for those with a large number of sampling sites, or for sampling sites requiring low noise levels or with no electrical output (Shen et al. 2005).

Dust and Surface Sampling

SVOCs partition strongly to household dust (Weschler and Nazaroff 2010). Inadvertent ingestion of house dust is reportedly the largest contributor to SVOC exposure for all life stages (Bamai et al. 2016). Because young children spend a considerable amount of time on the floor, where contaminated particles accumulate, and frequently put their hands and other objects in their mouths, the increased ingestion of dust can lead to significantly higher SVOC exposure than adults. Vacuuming has been commonly used as a sampling method for dust-phase SVOCs. To avoid contamination from the plastic parts of vacuum cleaners, a pre-cleaned cellulose thimble is usually inserted between the cleaner tube extender and the crevice tool. Dust samples are captured by the thimble during vacuuming and are then extracted for further chemical analysis (Stapleton et al. 2012b). Larsson et al. (2017) used filters instead of a thimble to collect dust samples in Swedish preschools. In their study, the filter was fixed in a styrene-acrylonitrile container inside a polypropylene holder that was installed on the nozzle of a vacuum cleaner (Larsson et al. 2017). Compared to thimbles, cellulose filters are thin and flexible, but they are commonly fragile and should be installed in a container with careful pretreatment procedures.

In addition to settled dust, building heating, ventilation and air conditioning (HVAC) filter dust has also become a useful sampling medium to measure SVOC concentrations in airborne particles. HVAC filters can be installed with minimal effort for a particular period of time and capture particles from large volumes of air, resulting in the collection of spatially and temporally integrated concentrations. The large volume of air that passes through the filters simply increases the sensitivity of sampling and analysis. This approach overcomes the limitation of traditional air sampling methods that only provide a “snapshot” of compound concentrations, which can vary significantly with time and within a building. When combined with HVAC system characterization, such as system run-times, volumetric flow rates, and mass of dust collected, HVAC filter dust sampling provides a novel filter forensics methodology to detect and quantify particulate SVOC concentrations in indoor air (Bi et al. 2018). However, HVAC filter dust sampling is limited to regions where centralized HVAC systems are installed in buildings. In addition, seasonal and environmental factors may affect the composition of SVOCs in HVAC filter dust. For example, the average runtime for HVAC systems in winter is 10%, which is much shorter than in summer (31%). This difference may result in lower dust loading and shorter dust age on winter filters (Bi et al. 2018). The impact of dust loading and age on the concentrations of SVOCs in HVAC filter dust remains unclear (Bi et al. 2018).

Available evidence on the accumulation of atmospheric SVOCs on urban surfaces (Liu et al. 2003) suggests that SVOC molecules may also be sorbed onto a wide range of indoor surfaces and even human occupants. For sampling SVOCs on interior surfaces, wiping is a simple and commonly used technique (Lu and Fenske 1999; Cohen Hubal et al. 2006; Persson et al. 2018). Surgical gauze pads soaked with a solvent are applied and wipe across an identified surface area several times (Lu and Fenske 1999). Cotton sponges and PUF foam rollers have also been used in some studies, but because the whole sponge may not be pressed uniformly during

wiping, it may reduce the sampling efficiency (Cohen Hubal et al. 2006). Additionally, surface-phase SVOCs can also be collected through surface press sampling. Cohen Hubal et al. (2006) measured pesticide residue on interior surfaces in classrooms of a child care center. C₁₈-impregnated Teflon extraction disks were used as the sampling medium in that study. During sampling, the sampler was pressed to the sampling surface for 2 min and then extracted for further chemical analysis (Cohen Hubal et al. 2006). However, surface press sampling is likely affected by the pressure on the samplers, which may lead to great uncertainties.

Sample Pretreatment

Collected samples typically require pretreatment before chemical analysis. Extraction, concentration, and cleanup are typical procedures used for pretreatment. In addition, thermal desorbers are a type of pretreatment instrument that can also complete these procedures. The aims of sample pretreatment are to ensure SVOC concentrations above the instrumental detection limit for chemical analysis and to remove impurities from the sample to protect analytical instruments. This section introduces the common sample pretreatment techniques.

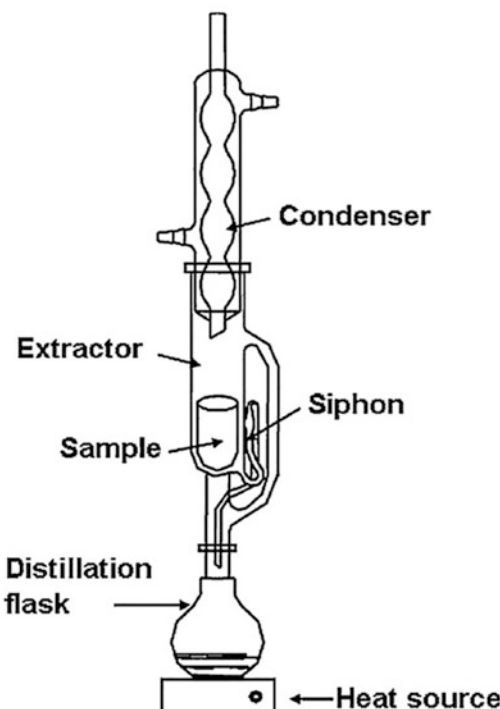
Solvent Extraction

Soxhlet Extraction

Soxhlet extraction has been a standard extraction technique for over a century (Luque de Castro and Priego-Capote 2010). In this system (Fig. 4), solid samples are extracted in a thimble holder filled with a flowing solvent that was continuously evaporated from a distillation flask at the bottom and condensed in a condenser on the top. During extraction, the combination of a heat source and condenser can circulate the solvent in the extractor. The sample is held by the thimble and the analytes are dissolved by the fresh solvent throughout the whole period. A siphon is designed to periodically empty the solvent in the thimble and carry the extracted analytes into the distillation flask. The temperature of the heat source should be set a little bit higher than the solvent's boiling point and significantly lower than the analytes' boiling point so that the solvent can remain circulating in the system while the extracted analytes can be retained in the flask.

The principle of this system is to keep the analytes dissolved in the circulated fresh solvent. It is a simple technique that has a relatively high extraction efficiency and requires inexpensive equipment and little manual work. However, compared to other extraction methods, Soxhlet extraction is particularly time-consuming and uses a large amount of solvents. Disposal of waste solvents is also expensive and is likely to cause environmental problems (Luque de Castro and García-Ayuso 1998). Table 4 lists several studies that used Soxhlet extraction to extract SVOCs from solid samples.

Fig. 4 Schematic of a classical Soxhlet extractor.
(©With permission of Luque de Castro and Priego-Capote 2010)



Accelerated Solvent Extraction (ASE)

Accelerated solvent extraction (ASE), also known as pressurized solvent extraction (PSE) or pressurized liquid extraction (PLE), is widely used as an alternative to Soxhlet extraction. ASE performs under high temperature and pressure. Samples are heated in an oven and are pressurized by a pump (Richter et al. 1996). In the ASE system, extraction occurs at a higher temperature than Soxhlet extraction or microwave-assisted extraction (MAE), because the solvent's boiling point is elevated in the pressurized extraction cell. As a result, the analytes' solubility is significantly improved due to decreased viscosity and superficial tension of the solvent (Mustafa and Turner 2011). This considerable improvement can also lead to less extraction time and lower solvent consumption. Table 5 lists several studies that applied the ASE method to extract SVOCs.

Ultrasonication Extraction (USE)

Ultrasonication extraction (USE) uses high frequency pulses to provide high shear stress and maintain high extraction efficiency. Ultrasonic baths are the most widely used USE system (e.g., Bi et al. 2018; Tang et al. 2020). As shown in Fig. 5, transducers are used as the source of ultrasound power (Chemal et al. 2017). Samples are placed in a container (e.g., a flask or a beaker) and submerged in

Table 4 Soxhlet extraction methods in different studies

Studies	Samples	Analytes	Extraction time	Solvent	Solvent volume (solvent flow rate)
Hwang and Cutright (2004)	2 g of soil	PAHs	15 h	Dichloromethane (DCM)	25 mL
Cai et al. (2012)	20 g of sewage sludge	PAHs, phthalates, chlorobenzenes, nitroaromatic compounds	24 h	Acetone/DCM (1/1, v/v)	100 mL
Klees et al. (2013)	1–2 g of street dust	PCBs	16 h	Toluene	300 mL
Sun et al. (2013)	20 g of sediments	Phthalates	48 h	DCM	(4–6 cycles/h)
Mi et al. (2019)	10 g of sediments	Phthalates	16 h	DCM	(5 mL/min)
Peng et al. (2020)	25 cm ² of play mat	PBDEs, OPEs	48 h	n-hexane/acetone (1/1, v/v)	200 mL

Table 5 ASE methods in different studies

Studies	Samples	Analytes	Extraction cycle	Solvent	Extraction condition
Stapleton et al. (2009)	0.2–0.5 g of furniture foam and indoor dust	OPEs	3 times	Hexane/DCM (1/1, v/v)	100 °C and 1500 psi
Kalachova et al. (2012)	0.5 g of household and car dust	BFRs	3 times	Hexane/DCM (1/1, v/v)	100 °C and 1500 psi
Klees et al. (2013)	1–2 g of sea sand	PCBs	1 time	Toluene	140 °C and 110 bar (optimized)
Celeiro et al. (2015)	1.5 g of clean sand	Fragrance allergens, musks, phthalates, and preservatives	1 time	Methanol	110 °C and 1500 psi (optimized)
Pil-Bala et al. (2019)	5 g of cheese	Endocrine-disrupting compounds	1 time	Acetone	70 °C and 1000 psi

solvent. During extraction, the container is immersed in pure water in the bath tank, with the water level in the tank higher than the level of solvent inside the container. USE can be operated at room temperature, but ice bags are

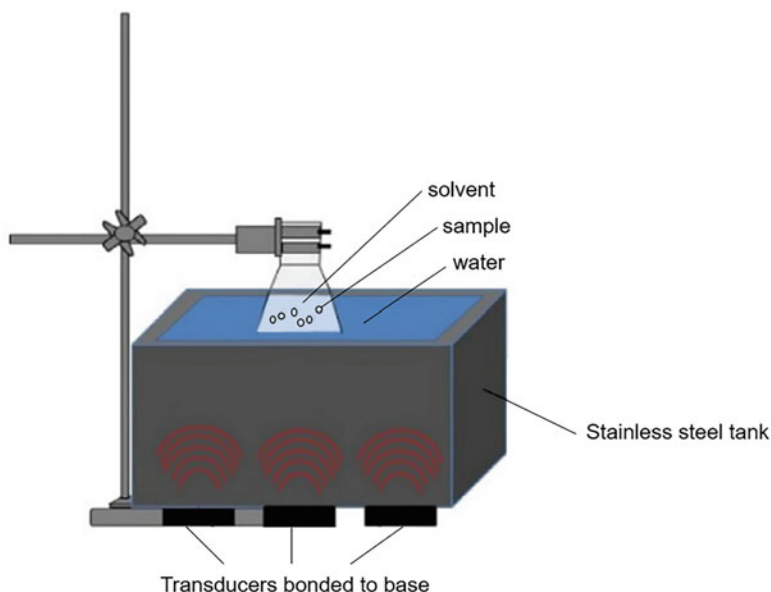


Fig. 5 Schematic of ultrasonic bath system. (©With permission of Chemat et al. 2017)

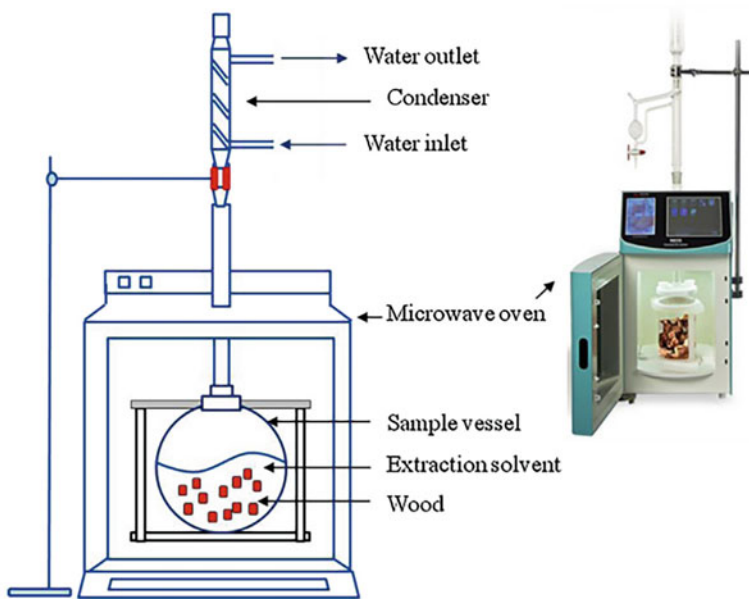
recommended to maintain a low water temperature to prevent unexpected solvent loss (Chemat et al. 2017). Fragile samples such as C₁₈ disks may break under ultrasound power, and therefore a mild extraction technique such as Soxhlet extraction may be more suitable. Similar to Soxhlet extraction, the USE system utilizes a large amount of solvents, but it is inexpensive, time efficient, and easy to operate. It has a very high extraction efficiency and can extract a number of samples in parallel. However, ultrasonication may produce oxidative free radicals that can degrade the sample and produce underreporting of the actual concentrations (Riesz et al. 1985). Therefore, surrogate compounds and recovery checks are strongly suggested. Table 6 lists several studies that have used USE to extract SVOCs from different samples.

Microwave-Assisted Extraction (MAE)

MAE uses microwaves as auxiliary energy for extraction (Bouras et al. 2015). In the system (Fig. 6), a sample vessel containing a solvent and samples is placed in microwave-producing equipment (typically a microwave oven). The mass transfer between the sample and solvent is significantly enhanced due to the high temperature in the vessel (Bouras et al. 2015). Thus, a cooling system is needed for condensation and circulation of the evaporated solvent. The use of microwaves shortens the extraction time and increases the extraction efficiency without extra solvent or cost (Bouras et al. 2015). However, MAE also has several restrictions. Cleanup procedures are needed for solid impurities after the extraction. Additionally, for heat-sensitive bioactive compounds, the use of microwave

Table 6 USE methods in different studies

Studies	Samples	Analytes	Extraction time	Solvent	Solvent volume
Shen et al. (2007)	1 g of cosmetic products	Phthalates and parabens	30 min	Methanol	10 mL
Stapleton et al. (2012a)	0.05 g of foam pieces	Flame retardant additives	15 min	DCM	1 mL
Bi et al. (2018)	HVAC filter and settled dust	Phthalates and OPEs	30 min, repeated 3 times	n-hexane	Not mentioned
Persson et al. (2018)	Indoor dust and window wipes	Phthalates	10 min	n-hexane/acetone (3/1, v/v)	2 mL
Tang et al. (2020)	0.5 g of preschool children's clothing	Phthalates	30 min (the first time), 20 min (the second time)	n-hexane/acetone (1/1, v/v)	40 mL (the first time), 30 mL (the second time)

**Fig. 6** Schematic of the MAE system. (©With permission of Bouras et al. 2015)

will lead to degradation of some target compounds (Bouras et al. 2015). Table 7 lists several studies that have utilized the MAE method. Finally, the advantages and disadvantages of different extraction techniques are summarized in Table 8.

Table 7 MAE methods used in different studies

Studies	Samples	Analytes	Extraction time	Solvent	Extraction temperature
Purcaro et al. (2009)	1/2/3 g of smoked meat	PAHs	5/15/ 30 min	n-hexane, n-hexane/ acetone (3/1, v/v)	60/90/ 115 °C
Liang et al. (2010)	1 g of soil	Phthalates	30 min	5 mL of acetonitrile	100 °C
Sun et al. (2012)	0.5 g of edible vegetable oil	Phthalates	20 min	5 mL of methanol	100 °C
Salazar-Beltrán et al. (2018)	0.5 g of polyethylene terephthalate bottles	Phthalates	30 min	5 mL of acetonitrile	140 °C

Table 8 Comparison of different extraction methods (Eskilsson and Björklund 2000)

	Advantages	Drawbacks
Soxhlet	Low cost No filtration requirement	Low extraction speed Large solvent volume Laborious cleaning work, which typically results in relatively frequent breakage
ASE	Fast extraction speed Low solvent volume High temperature No filtration requirement	High capital cost, but savings in solvent costs, breakage, throughput, and labor
USE	Low cost Fast extraction speed Available for multiple extractions	Large solvent volume Large manual work (repeated extractions are usually needed) Filtration requirement May degrade the sample and produce underreporting of the actual concentrations
MAE	Fast extraction speed Low solvent volume High temperature Available for multiple extractions	Extraction solvent must be able to absorb microwaves Only suitable for polar compounds Filtration requirement

Cleanup

After solvent extraction, the extracted solution normally contains solid impurities. Cleanup procedures are required to remove them and protect analytical instruments. Centrifugation and filtration are the two typical cleanup methods. In a centrifugation process, liquid samples are placed in a centrifuge tube, which spins at a constant speed and temperature for several minutes. Under centrifugal force, suspended

particles in the solution will be separated from the supernatant. In the filtration process, the samples are pushed through a filter. Particles larger than the filter's pore size are trapped on the filter and separated from the solution.

Filtration and centrifugation both have advantages and disadvantages. Only the supernatant of the extracts can be used after centrifugation, while all the extracted solution can be collected after filtration. However, during filtration, particles may form a cake on the filter and block the rest of the solution from passing through the filter, which is called blinding (Soerensen et al. 1997). Therefore, to achieve good filtration efficiency, filters with different pore sizes are used, and the process is usually carried out level by level. Considering the sample loss that occurs during multiple steps, filtration is more complicated than centrifugation and is not suitable for removing large amounts of particles. To achieve a good recovery rate, cleanup was typically carried out before the concentration step (e.g., Bohlin et al. 2014).

Concentration

Concentration is necessary to ensure that the analytes in the extracts can be detected and quantified by analytical instruments, considering that the use of a large amount of solvent may significantly dilute the extracts. Evaporation and nitrogen blowdown are typical methods to reduce solvent volume. Rotary evaporation is commonly used, in which the solvent is evaporated in a vessel partially immersed in hot water and continuously rotated to maintain a large heated area (Erickson et al. 1981). Since it reduces solvent volume very rapidly, rotary evaporation is typically used to remove a large portion of solvent. In contrast, nitrogen blowdown is a gentle and slow concentration method. During the process, the solvent is volatilized by a stream of high purity nitrogen blowing across the surface of the solution. Due to its low concentration speed, it is recommended to perform nitrogen blowdown after rotary evaporation as a further concentration step. Cheng (2003) reported that if only rotary evaporation was used to concentrate the solution to a final volume of less than 1 mL, a large amount of analyte would be lost. Therefore, the combination of rotary evaporation and nitrogen blowdown can provide acceptable recovery ratios and is recommended.

Thermal Desorption (TD)

Thermal desorption (TD) is a technique that extracts SVOCs from sorbents or a solid matrix by heating the sample in a stream of inert gas. The extracted SVOCs are subsequently captured by an electrically cooled cold trap and concentrated there prior to transfer to a GC column for chemical analysis through a heated transfer line. TD is applicable to a wide range of sample types including solids, liquids, and gases. Sorbent tubes are generally used to collect gas samples up to several hundreds of liters. Since the two-stage desorption process (tube desorption and trap desorption) mentioned above focuses the analytes into a narrow band of gas and ensures the

analytes being transferred to the GC quickly by heating the cold trap rapidly, greater sensitivity than that of solvent extraction can be achieved (Clausen and Kofoed-Sørensen 2009). In addition, TD instruments can be programmed to run a series of tubes automatically, and it is more environmentally friendly than solvent extraction. However, compared with other sample pretreatment methods, the cost of TD instruments is normally high. Additionally, the sorbent tubes can only be thermally desorbed once, while the samples from solvent extraction can be stored at low temperature for repeat analysis.

Chemical Analysis

Chromatography

Gas chromatography (GC) and high-performance liquid chromatography (HPLC) are two of the most commonly used chromatography techniques for analyzing indoor SVOCs. Compared to HPLC, GC is easier to operate and has low running expenses, but it is only suitable for SVOCs that are stable at the temperatures used in GCs (generally less than 350 °C) (Clausen and Kofoed-Sørensen 2009). Many SVOCs in indoor environments can be analyzed by GC, including polycyclic aromatic hydrocarbons (Possanzini et al. 2004), phthalates (Babu-Rajendran et al. 2018), polychlorinated biphenyls (Dmitrovic et al. 2002), polybrominated diphenyl ethers (Sapozhnikova et al. 2015), dichlorodiphenyltrichloroethane (DDT) (Sapozhnikova et al. 2015), organophosphate esters (Mihajlović et al. 2011), and per- and polyfluoroalkyl substances (Scott et al. 2006).

HPLC is a more complex and expensive method than GC. There are many parameters that need to be optimized, and solvent consumption is large. It is a widely used method for analyzing less volatile, strongly polar or thermally unstable SVOCs that are not suitable for GC (Clausen and Kofoed-Sørensen 2009). HPLC is often used to quantify human metabolites due to exposure to phthalates, OPEs, parabens, phenols, antibacterial agents, and per- and PFASs (Blount et al. 2000; Hoffman et al. 2018). Other SVOCs such as PAHs, pesticides, PBDEs, polychlorinated dibenzodioxins (PCDDs), and polychlorinated dibenzofurans (PCDFs) can also be analyzed by HPLC (Król et al. 2011; Petry et al. 2014).

Mass Spectrometry (MS)

The most commonly used SVOC detection method in conjunction with chromatography is mass spectrometry (MS). Unlike conventional detectors, such as flame ionization detectors (FID), that can only identify compounds with the aid of standard solutions, MS determines compounds by comparing fragment ions with available commercial mass spectral libraries. Applications of MS are generally divided into targeted and non-targeted analysis. At present, single quadrupole is still the most widely used mass analyzer for targeted approaches because of its low cost, easy

maintenance, and simple operation (Gruber et al. 2020). Recently, triple quadrupole has taken the lead in targeted analysis. In the multi-reaction monitoring (MRM) mode of triple quadrupole, the sensitivity and selectivity are higher than that in single quadrupole's selected ion monitoring (SIM) mode (Gruber et al. 2020).

With the development of high-resolution MS analyzers such as time-of-flight (TOF) and Orbitrap, non-target screening of SVOCs has attracted increasing attention from researchers. Both TOF and Orbitrap can provide high sensitivity, resolution, and mass accuracy to meet the needs of non-targeted analysis (Gómez-Ramos et al. 2019). Compared to Orbitrap, TOF costs less and has a higher acquisition speed, and it is thereby widely applied in environmental research as a non-targeted analysis technique (Chung et al. 2017; Phillips et al. 2018). However, Orbitrap has a higher mass spectral resolution than TOF with advantages of high resolving power (up to 120 K at m/z 200) and mass accuracy lower than 1 ppm (Gómez-Ramos et al. 2019). It is a more powerful but more costly tool for non-targeted analysis of SVOCs (Wang et al. 2019; Phatthalung et al. 2021).

Conclusion

The current review provides information on several techniques for the sampling, pretreatment, and chemical analysis of SVOCs in indoor environments. Understanding the advantages and disadvantages of different methods is important for the selection of suitable techniques for different analytes and situations. However, as existing methods still have some limitations, it is necessary to further optimize the process parameters to improve the performance and efficiency of different methods and develop new technologies.

Cross-References

- [Passive Samplers for Indoor Gaseous Pollutants](#)
-

References

- Aragón M, Borrull F, Marcé RM (2013) Thermal desorption-gas chromatography – mass spectrometry method to determine phthalate and organophosphate esters from air. *J Chromatogr A* 1303:76–82
- Armstrong JL, Fenske RA, Yost MG, Tchong-french M, Yu J (2013) Chemosphere comparison of polyurethane foam and XAD-2 sampling matrices to measure airborne organophosphorus pesticides and their oxygen analogs in an agricultural community. *Chemosphere* 92(4):451–457
- Asl-Hariri S, Gómez-Ríos GA, Gionfriddo E, Dawes P, Pawliszyn J (2014) Development of needle trap technology for on-site determinations: active and passive sampling. *Anal Chem* 86(12): 5889–5897
- Babu-Rajendran R, Preethi G, Poopal RK, Nikhil NP, Vimalkumar K, Subramanian A, Krishna-Kumar S (2018) GC–MS determination of phthalate esters in human urine: a potential

- biomarker for phthalate bio-monitoring. *J Chromatogr B Anal Technol Biomed Life Sci* 1079: 15–24
- Bamai YA, Araki A, Kawai T, Tsuboi T, Saito I, Yoshioka E, ... Kishi R (2016) Exposure to phthalates in house dust and associated allergies in children aged 6–12 years. *Environ Int* 96:16–23
- Bartkow ME, Booij K, Kennedy KE, Müller JF, Hawker DW (2005) Passive air sampling theory for semivolatile organic compounds. *Chemosphere* 60(2):170–176
- Bennett DH, Moran RE, Wu X (May), Tulve NS, Clifton MS, Colón M, ... Hertz-Pannier I (2015) Polybrominated diphenyl ether (PBDE) concentrations and resulting exposure in homes in California: relationships among passive air, surface wipe and dust concentrations, and temporal variability. *Indoor Air* 25(2):220–229
- Bi C, Maestre JP, Li H, Zhang G, Givehchi R, Mahdavi A, ... Xu Y (2018) Phthalates and organophosphates in settled dust and HVAC filter dust of U.S. low-income homes: association with season, building characteristics, and childhood asthma. *Environ Int* 121:916–930
- Blount BC, Milgram KE, Silva MJ, Malek NA, Reidy JA, Needham LL, Brock JW (2000) Quantitative detection of eight phthalate metabolites in human urine using HPLC-APCI-MS/MS. *Anal Chem* 72(17):4127–4134
- Bohlin P, Audy O, Škrdlíková L, Kukučka P, Přibylová P, Prokeš R, ... Klánová J (2014) Outdoor passive air monitoring of semi volatile organic compounds (SVOCs): a critical evaluation of performance and limitations of polyurethane foam (PUF) disks. *Environ Sci Process Impacts* 16(3):433–444
- Bouras M, Chadni M, Barba FJ, Grimi N, Bals O (2015) Optimization of microwave-assisted extraction of polyphenols from Quercus bark. *Indus Crops Prod* 77:590–601
- Cai Q, Mo C, Lü H, Zeng Q, Wu Q, Li Y (2012) Bioresource technology effect of composting on the removal of semivolatile organic chemicals (SVOCs) from sewage sludge. *Bioresour Technol* 126:453–457
- Cao J, Xiong J, Wang L, Xu Y, Zhang Y (2016) Transient method for determining indoor chemical concentrations based on SPME: model development and calibration. *Environ Sci Technol* 50(17):9452–9459
- Cao J, Eichler CMA, Wu Y, Little JC (2019) Dynamic method to measure partition coefficient and mass accommodation coefficient for gas–particle interaction of phthalates. *Aerosol Sci Technol* 53(10):1158–1171
- Celeiro M, Lamas JP, Garcia-Jares C, Llompart M (2015) Pressurized liquid extraction-gas chromatography-mass spectrometry analysis of fragrance allergens, musks, phthalates and preservatives in baby wipes. *J Chromatogr A* 1384:9–21
- Cessna AJ, Kerr LA, Pattey E, Zhu T, Desjardins RL (1995) Field comparison of polyurethane foam plugs and mini-tubes containing Tenax-TA resin as trapping media for the aerodynamic gradient measurement of trifluralin vapour fluxes. *J Chromatogr A* 710(1):251–257
- Chemat F, Rombaut N, Sicaire AG, Meullemiestre A, Fabiano-Tixier AS, Abert-Vian M (2017) Ultrasound assisted extraction of food and natural products. Mechanisms, techniques, combinations, protocols and applications. A review. *Ultrason Sonochem* 34:540–560
- Cheng CC (2003) Recovery of polycyclic aromatic hydrocarbons during solvent evaporation with a rotary evaporator. *Polycycl Aromat Compd* 23(3):315–325
- Cheng Y, He KB, Duan FK, Zheng M, Ma YL, Tan JH (2009) Measurement of semivolatile carbonaceous aerosols and its implications: a review. *Environ Int* 35(3):674–681
- Choi SD, Baek SY, Chang YS, Wania F, Ikonomou MG, Yoon YJ, ... Hong S (2008) Passive air sampling of polychlorinated biphenyls and organochlorine pesticides at the Korean Arctic and Antarctic Research Stations: implications for long-range transport and local pollution. *Environ Sci Technol* 42(19):7125–7131
- Chung IY, Park YM, Lee HJ, Kim H, Kim DH, Kim IG, ... Kwon JH (2017) Nontarget screening using passive air and water sampling with a level II fugacity model to identify unregulated environmental contaminants. *J Environ Sci (China)* 62:84–91
- Clausen PA, Kofoed-Sørensen V (2009) Sampling and analysis of SVOCs and POMs in indoor air. *Organic Indoor Air Pollutants* 1:19–42

- Cohen Hubal EA, Egeghy PP, Leovic KW, Akland GG (2006) Measuring potential dermal transfer of a pesticide to children in a child care center. *Environ Health Perspect* 114(2):264–269
- Das S, Hageman KJ, Taylor M, Michelsen-Heath S, Stewart I (2020) Fate of the organophosphate insecticide, chlorpyrifos, in leaves, soil, and air following application. *Chemosphere* 243:125194
- Dmitrovic J, Chan SC, Chan SHY (2002) Analysis of pesticides and PCB congeners in serum by GC/MS with SPE sample cleanup. *Toxicol Lett* 134(1–3):253–258
- Erickson MD, Giguere MT, Whitaker DA (1981) Comparison of common solvent evaporation techniques in organic analysis. *Anal Lett* 14(11):841–857
- Eskilsson CS, Björklund E (2000) Analytical-scale microwave-assisted extraction. *J Chromatogr A* 902:227–250
- Gawor A, Shunthirasingham C, Hayward SJ, Lei YD, Gouin T, Mmereki BT, ... Wania F (2014) Neutral polyfluoroalkyl substances in the global atmosphere. *Environ Sci Process Impacts* 16(3):404–413
- Ghalichi Z, Bahrami A, Ghorbani F (2019) Application of a needle trap device packed with XAD-2 polyaniline composite for sampling naphthalene and phenanthrene in air. *J Chromatogr A* 1602: 74–82
- Ghosh C, Singh V, Grandy J, Pawliszyn J (2020) Development and validation of a headspace needle-trap method for rapid quantitative estimation of butylated hydroxytoluene from cosmetics by hand-portable GC-MS. *RSC Adv* 10(11):6671–6677
- Gómez-Ramos MM, Ucles S, Ferrer C, Fernández-Alba AR, Hernando MD (2019) Exploration of environmental contaminants in honeybees using GC-TOF-MS and GC-Orbitrap-MS. *Sci Total Environ* 647:232–244
- Gruber B, David F, Sandra P (2020) Capillary gas chromatography-mass spectrometry: current trends and perspectives. *TrAC – Trends Anal Chem* 124:115475
- Harner T, Shoeib M, Diamond M, Stern G, Rosenberg B (2004) Using passive air samplers to assess urban-rural trends for persistent organic pollutants. 1. Polychlorinated biphenyls and organochlorine pesticides. *Environ Sci Technol* 38(17):4474–4483
- He J, Balasubramanian R (2010) A comparative evaluation of passive and active samplers for measurements of gaseous semi-volatile organic compounds in the tropical atmosphere. *Atmos Environ* 44(7):884–891
- Heudorf U, Mersch-Sundermann V, Angerer J (2007) Phthalates: toxicology and exposure. *Int J Hyg Environ Health* 210(5):623–634
- Hoffman K, Hammel SC, Phillips AL, Lorenzo AM, Chen A, Calafat AM, ... Stapleton HM (2018) Biomarkers of exposure to SVOCs in children and their demographic associations: the TESIE study. *Environ Int* 119:26–36
- Hwang S, Cutright TJ (2004) Preliminary evaluation of PAH sorptive changes in soil by Soxhlet extraction. *Environ Int* 30(2):151–158
- Isetun S, Nilsson U, Colmsjö A, Johansson R (2004) Air sampling of organophosphate triesters using SPME under non-equilibrium conditions. *Anal Bioanal Chem* 378(7):1847–1853
- Kalachova K, Hradkova P, Lankova D, Hajslava J, Pulkabrova J (2012) Occurrence of brominated flame retardants in household and car dust from the Czech Republic. *Sci Total Environ* 441: 182–193
- Klees M, Hiester E, Bruckmann P, Schmidt TC (2013) Determination of polychlorinated biphenyls and polychlorinated dibenzo-p-dioxins and dibenzofurans by pressurized liquid extraction and gas chromatography coupled to mass spectrometry in street dust samples. *J Chromatogr A* 1300: 17–23
- Król S, Zabiegała B, Namieśnik J (2011) Monitoring and analytics of semivolatile organic compounds (SVOCs) in indoor air. *Anal Bioanal Chem* 400(6):1751–1769
- Larsson K, Lindh CH, Jönsson BA, Giovanoulis G, Bibi M, Bottai M, ... Berglund M (2017) Phthalates, non-phthalate plasticizers and bisphenols in Swedish preschool dust in relation to children's exposure. *Environ Int* 102:114–124
- Li XA, Ouyang GF, Lord H, Pawliszyn J (2010) Theory and validation of solid-phase micro-extraction and needle trap devices for aerosol sample. *Anal Chem* 82(22):9521–9527

- Li H, Bi C, Li X, Xu Y (2020) A needle trap device method for sampling and analysis of semi-volatile organic compounds in air. *Chemosphere* 250:126284
- Liang Y, Xu Y (2014) An improved method for measuring and characterizing phthalate emissions from building materials and its application to exposure assessment. *Indoor air 2014 – 13th international conference on indoor air quality and climate*, no 3, pp 102–109
- Liang P, Zhang L, Peng L, Li Q, Zhao E (2010) Determination of phthalate esters in soil samples by microwave assisted extraction and high performance liquid chromatography. *Bull Environ Contam Toxicol* 85(2):147–151
- Liu QT, Diamond ML, Gingrich SE, Ondov JM, Maciejczyk P, Stern GA (2003) Accumulation of metals, trace elements and semi-volatile organic compounds on exterior window surfaces in Baltimore. *Environ Pollut* 122(1):51–61
- Lu C, Fenske RA (1999) Dermal transfer of chlorpyrifos residues from residential surfaces: comparison of hand press, hand drag, wipe, and polyurethane foam roller measurements after broadcast and aerosol pesticide applications. *Environ Health Perspect* 107(6):463–467
- Luque de Castro MD, García-Ayuso LE (1998) Soxhlet extraction of solid materials: an outdated technique with a promising innovative future. *Anal Chim Acta* 369(1–2):1–10
- Luque de Castro MD, Priego-Capote F (2010) Soxhlet extraction: past and present panacea. *J Chromatogr A* 1217(16):2383–2389
- Mader BT, Flagan RC, Seinfeld JH (2001) Sampling atmospheric carbonaceous aerosols using a particle trap impactor/denuder sampler. *Environ Sci Technol* 35(24):4857–4867
- Meng Z, Wang L, Cao B, Huang Z, Liu F, Zhang J (2020) Indoor airborne phthalates in university campuses and exposure assessment. *Build Environ* 180:107002
- Mi L, Xie Z, Zhao Z, Zhong M, Mi W, Ebinghaus R, Tang J (2019) Occurrence and spatial distribution of phthalate esters in sediments of the Bohai and Yellow seas. *Sci Total Environ* 653:792–800
- Mihajlović I, Miloradov MV, Fries E (2011) Application of twisselmann extraction, SPME, and GC-MS to assess input sources for organophosphate esters into soil. *Environ Sci Technol* 45(6): 2264–2269
- Moeckel C, Harner T, Nizzetto L, Strandberg B, Lindroth A, Jones KC (2009) Use of depuration compounds in passive air samplers: results from active sampling-supported field deployment, potential uses, and recommendations. *Environ Sci Technol* 43(9):3227–3232
- Müller L, Górecki T, Pawliszyn J (1999) Optimization of the SPME device design for field applications. *Fresenius J Anal Chem* 364(7):610–616
- Mustafa A, Turner C (2011) Pressurized liquid extraction as a green approach in food and herbal plants extraction: a review. *Anal Chim Acta* 703(1):8–18
- Niri VH, Eom I-Y, Kermani FR, Pawliszyn J (2009) Sampling free and particle-bound chemicals using solid-phase microextraction and needle trap device simultaneously. *J Sep Sci* 32(7): 1075–1080
- Okeme JO, Yang C, Abdollahi A, Dhal S, Harris SA, Jantunen LM, ... Diamond ML (2018) Passive air sampling of flame retardants and plasticizers in Canadian homes using PDMS, XAD-coated PDMS and PUF samplers. *Environ Pollut* 239:109–117
- Ouyang G, Pawliszyn J (2007) Configurations and calibration methods for passive sampling techniques. *J Chromatogr A* 1168(1–2):226–235
- Ouyang G, Pawliszyn J (2008) A critical review in calibration methods for solid-phase micro-extraction. *Anal Chim Acta* 627(2):184–197
- Pawliszyn J (2012) Theory of solid-phase microextraction. In: *Handbook of solid phase micro-extraction*. Elsevier, pp 13–59
- Pawliszyn J, Pawliszyn B, Pawliszyn M (1997) Solid phase microextraction (SPME). *Chem Educ* 2:1–7
- Peng B, Yu ZM, Wu CC, Liu LY, Zeng L, Zeng EY (2020) Polybrominated diphenyl ethers and organophosphate esters flame retardants in play mats from China and the exposure risks for children. *Environ Int* 135:105348
- Persson J, Wang T, Hagberg J (2018) Organophosphate flame retardants and plasticizers in indoor dust, air and window wipes in newly built low-energy preschools. *Sci Total Environ* 628–629: 159–168

- Petry T, Vitale D, Joachim FJ, Smith B, Cruse L, Mascarenhas R, ... Singal M (2014) Human health risk evaluation of selected VOC, SVOC and particulate emissions from scented candles. *Regul Toxicol Pharmacol* 69(1):55–70
- Phatthalung WN, Suttinun O, Phungsai P, Kasuga I, Kurisu F, Furumai H, Musikavong C (2021) Non-target screening of dissolved organic matter in raw water, coagulated water, and chlorinated water by Orbitrap mass spectrometry. *Chemosphere* 264:128437
- Phillips KA, Yau A, Favela KA, Isaacs KK, McEachran A, Grulke C, ... Wambaugh JF (2018) Suspect screening analysis of chemicals in consumer products. *Environ Sci Technol* 52(5): 3125–3135
- Pil-Bala B, Khandaghi J, Afshar Mogaddam MR (2019) Analysis of endocrine-disrupting compounds from cheese samples using pressurized liquid extraction combined with dispersive liquid–liquid microextraction followed by high-performance liquid chromatography. *Food Anal Methods* 12(7):1604–1611
- Possanzini M, Di Palo V, Gigliucci P, Tomasi Scianò MC, Cecinato A (2004) Determination of phase-distributed PAH in Rome ambient air by denuder/GC-MS method. *Atmos Environ* 38(12):1727–1734
- Purcaro G, Moret S, Conte LS (2009) Optimisation of microwave assisted extraction (MAE) for polycyclic aromatic hydrocarbon (PAH) determination in smoked meat. *Meat Sci* 81(1): 275–280
- Ré-Poppi N, Santiago-Silva M (2005) Polycyclic aromatic hydrocarbons and other selected organic compounds in ambient air of Campo Grande City, Brazil. *Atmos Environ* 39(16):2839–2850
- Richter BE, Jones BA, Ezzell JL, Porter NL, Avdalovic N, Pohl C (1996) Accelerated solvent extraction: a technique for sample preparation. *Anal Chem* 68(6):1033–1039
- Riesz P, Berdahl D, Christman CL (1985) Free radical generation by ultrasound in aqueous and nonaqueous solutions. *Environ Health Perspect* 64:233–252
- Salazar-Beltrán D, Hinojosa-Reyes L, Palomino-Cabello C, Turnes-Palomino G, Hernández-Ramírez A, Guzmán-Mar JL (2018) Determination of phthalate acid esters plasticizers in polyethylene terephthalate bottles and its correlation with some physicochemical properties. *Polym Test* 68:87–94
- Sapozhnikova Y, Simons T, Lehotay SJ (2015) Evaluation of a fast and simple sample preparation method for polybrominated diphenyl ether (PBDE) flame retardants and dichlorodiphenyltrichloroethane (DDT) pesticides in fish for analysis by ELISA compared with GC-MS/MS. *J Agric Food Chem* 63(18):4429–4434
- Schuster JK, Gioia R, Breivik K, Steinnes E, Scheringer M, Jones KC (2010) Trends in European background air reflect reductions in primary emissions of PCBs and PBDEs. *Environ Sci Technol* 44(17):6760–6766
- Scott BF, Moody CA, Spencer C, Small JM, Muir DCG, Mabury SA (2006) Analysis for perfluorocarboxylic acids/anions in surface waters and precipitation using GC-MS and analysis of PFOA from large-volume samples. *Environ Sci Technol* 40(20):6405–6410
- Shen L, Wania F, Lei YD, Teixeira C, Muir DCG, Bidleman TF (2005) Atmospheric distribution and long-range transport behavior of organochlorine pesticides in North America. *Environ Sci Technol* 39:409–420
- Shen HY, Jiang HL, Mao HL, Pan G, Zhou L, Cao YF (2007) Simultaneous determination of seven phthalates and four parabens in cosmetic products using HPLC-DAD and GC-MS methods. *J Sep Sci* 30(1):48–54
- Soerensen BL, Keiding K, Lauritzen SL (1997) A theoretical model for blinding in cake filtration. *Water Environ Res* 69(2):168–173
- Soury S, Bahrami A, Alizadeh S, Ghorbani F (2019) Development of a needle trap device packed with zinc based metal-organic framework sorbent for the sampling and analysis of polycyclic aromatic hydrocarbons in the air. *Microchem J* 148:346–354
- Stapleton HM, Klosterhaus S, Eagle S, Fuh J, Meeker JD, Blum A, Webster TF (2009) Detection of organophosphate flame retardants in furniture foam and U.S. house dust. *Environ Sci Technol* 43(19):7490–7495

- Stapleton HM, Sharma S, Getzinger G, Ferguson PL, Gabriel M, Webster TF, Blum A (2012a) Novel and high volume use flame retardants in US couches reflective of the 2005 PentaBDE phase out. *Environ Sci Technol* 46(24):13432–13439
- Stapleton HM, Eagle S, Sjödin A, Webster TF (2012b) Serum PBDEs in a North Carolina toddler cohort: associations with handwipes, house dust, and socioeconomic variables. *Environ Health Perspect* 120(7):1049–1054
- Sun H, Yang Y, Li H, Zhang J, Sun N (2012) Development of multiresidue analysis for twenty phthalate esters in edible vegetable oils by microwave-assisted extraction-gel permeation chromatography-solid phase extraction-gas chromatography-tandem mass spectrometry. *J Agric Food Chem* 60(22):5532–5539
- Sun J, Huang J, Zhang A, Liu W, Cheng W (2013) Occurrence of phthalate esters in sediments in Qiantang River, China and inference with urbanization and river flow regime. *J Hazard Mater* 248–249(1):142–149
- Sun J, Wang Q, Zhuang S, Zhang A (2016) Occurrence of polybrominated diphenyl ethers in indoor air and dust in Hangzhou, China: level, role of electric appliances, and human exposure. *Environ Pollut* 218:942–949
- Tang Z, Chai M, Wang Y, Cheng J (2020) Phthalates in preschool children's clothing manufactured in seven Asian countries: occurrence, profiles and potential health risks. *J Hazard Mater* 387: 121–161
- Tsapakis M, Stephanou EG (2005) Occurrence of gaseous and particulate polycyclic aromatic hydrocarbons in the urban atmosphere: study of sources and ambient temperature effect on the gas/particle concentration and distribution. *Environ Pollut* 133(1):147–156
- Tuduri L, Millet M, Briand O, Montury M (2012) Passive air sampling of semi-volatile organic compounds. *TrAC – Trends Anal Chem* 31(2):38–49
- Ueta I, Saito Y, Hosoe M, Okamoto M, Ohkita H, Shirai S, Tamura H, Jinno K (2009) Breath acetone analysis with miniaturized sample preparation device: in-needle preconcentration and subsequent determination by gas chromatography-mass spectroscopy. *J Chromatogr B* 877(24): 2551–2556
- Vonderheide AP, Mueller KE, Meija J, Welsh GL (2008) Polybrominated diphenyl ethers: causes for concern and knowledge gaps regarding environmental distribution, fate and toxicity. *Sci Total Environ* 400(1–3):425–436
- Wang J, Chow W, Wong JW, Leung D, Chang J, Li M (2019) Non-target data acquisition for target analysis (nDATA) of 845 pesticide residues in fruits and vegetables using UHPLC/ESI Q-Orbitrap. *Anal Bioanal Chem* 411(7):1421–1431
- Weschler CJ, Nazaroff WW (2010) SVOC partitioning between the gas phase and settled dust indoors. *Atmos Environ* 44(30):3609–3620
- Xu Y, Liu Z, Park J, Clausen PA, Benning JL, Little JC (2012) Measuring and predicting the emission rate of phthalate plasticizer from vinyl flooring in a specially-designed chamber. *Environ Sci Technol* 46(22):12534–12541
- Xu Y, Liang Y, Urquidi JR, Siegel JA (2014) Phthalates and polybrominated diphenyl ethers in retail stores. *Atmos Environ* 87:53–64
- Zhou X, Lian J, Cheng Y, Wang X (2021) The gas/particle partitioning behavior of phthalate esters in indoor environment: effects of temperature and humidity. *Environ Res* 194:110681
- Zhu X, Zhou C, Henkelmann B, Wang Z, Ma X, Pfister G, ... Mu J (2013) Monitoring of PAHs profiles in the urban air of alian, China with active high-volume sampler and semipermeable membrane devices. *Polycycl Aromat Compd* 33(3):265–288



Passive Samplers for Indoor Gaseous Pollutants

17

Jianping Cao

Contents

Introduction	468
Overview of Passive Samplers	469
Representative Passive Samplers	469
Passive Sampling Theory	473
Optimal Design of Passive Samplers	479
Method Principle	480
Illustration of Optimization Outputs	484
Application and Discussions	486
Conclusions	488
Cross-References	488
References	489

Abstract

A passive sampler is a device which is capable of preconcentrating an analyte without the help of a pump. Due to its advantages of simple operation, easy portability, and no external power, passive sampling is a promising method for multi-point sampling, remote-area sampling, long-term sampling, and personal sampling compared to active sampling. Over the past decades, numerous passive samplers have been developed and successfully applied for monitoring concentrations of indoor gaseous pollutants, especially volatile organic compounds (VOCs). This chapter provides an overview of the evolution of passive samplers and passive sampling theories since 1970s, and introduces an inverse-problem-based method for the optimal design of passive samplers with the goal of minimal sampling errors.

J. Cao (✉)

School of Environmental Science and Engineering, Sun Yat-sen University, Guangzhou, China
e-mail: caojp3@mail.sysu.edu.cn

Keywords

Indoor air quality (IAQ) · Passive air sampling (PAS) · Volatile organic compounds (VOCs) · Mass transfer · Inverse problem optimization method

Introduction

Nowadays man-made chemicals are abundant in various indoor environments (Weschler 2009). Exposure to some of these chemicals, especially certain volatile organic compounds (VOCs), are related with sick building syndrome (e.g., mucous membrane irritation, headache and fatigue) (Destaillets et al. 2008; Kim et al. 2001; Wolkoff 1995), other morbidities (WHO 1983), and even cancer (WHO 2000). Therefore, monitoring VOC concentrations in various environments is essential for the evaluation of their exposure concentrations and the potential associated health risks. Concentrations of VOCs are often quite low in the air (below or around magnitude of $100 \mu\text{g}/\text{m}^3$). Thus, enrichment of the sample is a very important step for their quantitative determination (Du et al. 2013). Generally, two sorbent enrichment technologies are frequently used: active sampling and passive sampling (Du et al. 2013). Passive sampling is defined as any sampling technique based on free mass transfer of analyte molecules from the sampled medium to a collecting medium (due to the difference in chemical potentials of analyte between these two media) (Gorecki and Namiesnik 2002). As a result, a pump and its power supply are eliminated. Because of its simplicity and low cost (both for manufacture and sample analysis), passive sampling is a promising method for multi-point sampling, remote-area sampling, long-term sampling, and personal sampling compared to active sampling (Du et al. 2013; Kot-Wasik et al. 2007).

Over the past several decades, there has been growing demand for environmental monitoring and exposure evaluation. Thus, the design and application of passive sampling have been extensively developed (Brown et al. 1981; Cocheo et al. 1996; Du et al. 2014; Namieśnik et al. 2005). Passive samplers have been successfully applied for monitoring concentrations of pollutants in indoor air, workplace air, ambient air, and other matrixes (Kot-Wasik et al. 2007; Partyka et al. 2007). Passive sampling has been shown to have the same accuracy as active sampling (Bohlin et al. 2014; Du et al. 2013). Nevertheless, the performance of the existing passive samplers for monitoring VOC concentrations still varies among different sampling environments, suggesting the need for improving the sampling stability of passive samplers (Cao et al. 2016a). Thus, this chapter starts with a summary of the representative passive samplers and passive sampling theory reported in the literature since 1970s, and then introduces a method for the optimal design of passive samplers with the goal of minimal sampling error.

Overview of Passive Samplers

Representative Passive Samplers

The start of passive sampling methods dates to 1853 when Swiss chemist Schonbein employed a strip of filter paper saturated with potassium iodide to detect the presence of O₃ in the atmosphere (Namieśnik et al. 2005). The first true passive samplers, which enabled the quantitative determination of analytes, were designed in 1973 producing two different types, (1) tube-type passive sampler for detecting NO₂ concentration in outdoor air, in which the analyte diffused from the sampled air to the sorbent through a static layer of gas (Palmes and Gunnison 1973); and (2) a permeation device for detecting SO₂ concentration in workplace air, in which the analyte permeated from the sampled air to the sorbent through a polymer membrane (Reiszner and West 1973). Since then, different designs of passive samplers have been proposed as prototypes or have been commercially available. Generally speaking, three types of passive samplers can be identified based on their geometry: tube-type samplers, badge-type samplers, and radial samplers as shown in Figs. 1 and 2. Details of representative passive samplers are summarized in Table 1 with an emphasis on the geometry type, barrier type, sorbents, and analytes. Although the radial type samplers were developed more recently, they combined the features of tube and badge samplers, and they tended to be the most appealing passive samplers in common applications (Zabiegala et al. 2010).

Although the details of the implementations varied widely among the different types of passive samplers, most passive samplers include two main parts, the sorbent, and the barrier covering the sorbent as shown in Fig. 3. When a passive sampler is exposed to the measured matrix, the analyte will transfer through the boundary layer around the barrier surface, then diffuse through the barrier, and finally be adsorbed by the sorbent and diffuse in the sorbent (Cao et al. 2016a).



Tube-type sampler (Perkin-Elmer,
Brown et al. (1981))



Badge-type sampler (OVM 3500,
Namieśnik et al. (2005))



Radial sampler (Radiello,
Cocheo et al. (1996))

Fig. 1 Three types of representative passive samplers. (a) Tube-type sampler (Perkin-Elmer, Brown et al. (1981)). (b) Badge-type sampler (OVM 3500, Namieśnik et al. (2005)). (c) Radial sampler (Radiello, Cocheo et al. (1996)). (Adapted with permission from Cao et al. (2016a). Copyright (2021) American Chemical Society)

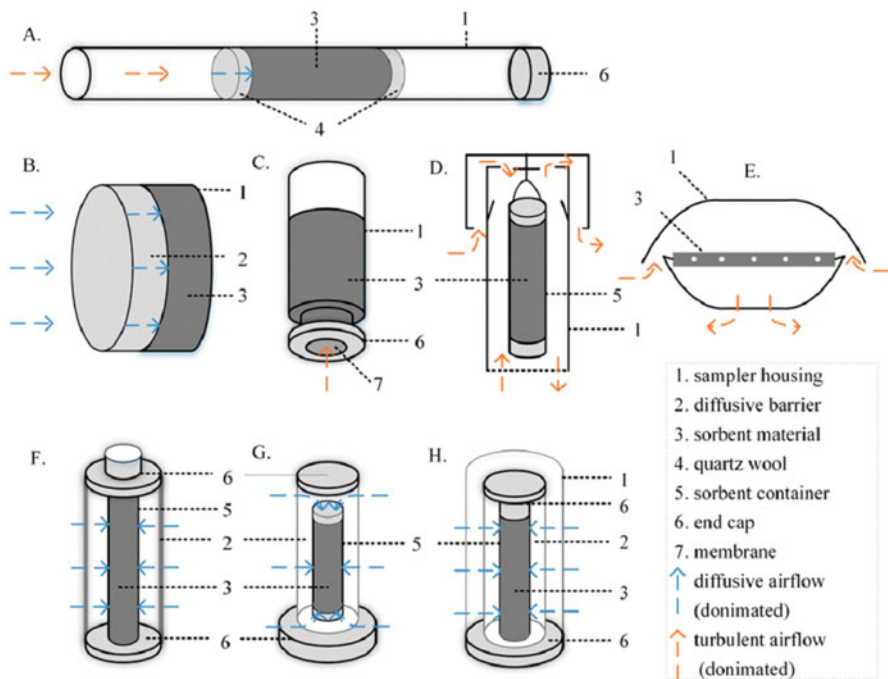


Fig. 2 Schematics of different types of passive samplers. (a) basic tube-type. (b) basic badge-type sampler. (c) modified badge-type WMSTM™ sampler. (d) radial-type XAD-PAS. (e) two-bowl type PUF-PAS. (f) radial-type Radiello® sampler. (g) modified axial-type combined radial-type POD sampler. (h) modified radial-type THPDS sampler. (Reprinted with permission from Huang et al. (2018))

The barrier helps to define a relatively steady sampling rate by eliminating or minimizing effects of environmental factors (especially the fluctuating velocity of the sampled air), which is crucial for quantitative analysis. According to the type of the barrier, most passive samplers can be classified into two main categories: diffusion-based passive sampler (the analyte diffuses through a static layer of air or a porous medium from the sampled air to the sorbent) and permeation-based passive sampler (the analyte permeates through a polymer membrane from the sampled air to the sorbent) (Huang et al. 2018).

For the diffusion-based passive samplers, static air was used as the first type of barriers (Brown et al. 1981; Namieśnik et al. 2005; Palmes and Gunnison 1973), while tiny air tunnels or porous polymer layer were more frequently used as barriers in the newer generation of passive samplers (Cocheo et al. 1996; Kourakis et al. 1993; Olansandan. et al. 1999). This change is because the mass transfer of analyte through the tiny air tunnels or porous polymer is much less responsive to the fluctuation of air velocity. For the permeation-based passive samplers, a dimethyl silicone polymer was firstly employed as the permeation membrane by Reiszner and West (1973). Since then, multiple non-porous polymers were used in the passive

Table 1 Changes of the design of passive samplers

Year	Passive sampler	Geometry	Barrier types	Sorbents	Analytes	References
1973	Palmes Tube	Tube	Static air (Diffusion)	Stainless steel mesh impregnated with trichloroamine	NO ₂	Palmes and Gunnison (1973)
1973	Reiszner-West sampler	Badge	Silicone membrane (Permeation)	Sodium tetrachloromercurate	SO ₂	Reiszner and West (1973)
1979, 2000	Fern Dosimeter	Badge	Static air with stainless steel mesh Teflon filter (1 μm pores) (Diffusion)	Impregnated filter, various chemicals depending on analyte	NH ₃ , Formaldehyde	Fenn (1979), Gillett et al. (2000)
1980	OVM 3500	Badge	Static air (Diffusion)	Single or double adsorbent depending on analytes	VOCs	Namieśnik et al. (2005)
1981	Perkin-Elmer tube	Tube	Static air (Diffusion)	Thermally desorbable sorbent	VOCs	Brown et al. (1981)
1985	ORSA-5	Tube	Static air (Diffusion)	Active carbon	VOCs	Stockton and Underhill (1985)
1985	Sampler designed by Lewis	Badge	200-mesh wire screens and perforated plates (Diffusion)	Tenax GC	VOCs	Lewis et al. (1985)
1990	SPME	Tube	Static air (Diffusion)	Fibers coated by sorption solutions	VOCs	Arthur and Pawliszyn (1990)
1992	SKC 575	Badge	Channels in plastic body (Diffusion)	Activated charcoal	VOCs	Guild et al. (1992)
1992, 2002	Sampler designed by Namieśnik	Badge	Commercial polyethylene films, silicone membranes (Permeation)	Active charcoal	VOCs	Namieśnik et al. (1992); Zabiegala et al. (2002)
1993, 2002	SPMD designed by Huckins	Tube	Low density polyethylene (Permeation)	Synthetic lipid triolein	lipophilic organic, SVOCs	Huckins et al. (2002), Petty et al. (1993)

(continued)

Table 1 (continued)

Year	Passive sampler	Geometry	Barrier types	Sorbents	Analytes	References
1993, 1999	Ogawa sampler	Badge	Air channels in plastic at both sides (Diffusion)	Pre-coated filter	O ₃ , NO _x , SO ₂	Kourtrakis et al. (1993), Liard et al. (1999)
1996	Radiello	Radial	Microporous polyethylene film and air (Diffusion)	Thermally desortable sorbents	VOCs	Coecheo et al. (1996)
1999	Shibata gas-tube sampler	Radial	Porous PTFE membrane (Diffusion)	Granular activated carbon	VOCs	Olausandan et al. (1999)
2000, 2001	Analyst, Analyst 2	Badge	Removable stainless-steel mesh grid and air cavity (Diffusion)	Active carbon, Carbopack C	VOCs, SVOC	Bertoni et al. (2000), Bertoni et al. (2001)
2001	GABIE sampler	Badge	Porous PUF windscreens and static air (Diffusion)	Active carbon	VOCs	Delcourt and Sandino (2001)
2002	Sampler by Yanamoto et al.	Badge	Porous PTFE membrane (Diffusion)	Carbopack B	VOCs	Yamamoto et al. (2002)
2010	Sampler by Seethapathy et al.	Glass vial	PDMS/PDMS-polycarbonate copolymer (Permeation)	Active carbon	VOCs	Seethapathy and Gorecki (2010)
2013	THPDS	Radial	Stainless-steel powder sintered porous cylinder (Diffusion)	Silica zeolite	BTX	Du et al. (2013)

Adapted with permission from Cao et al. (2016a). Copyright (2021) American Chemical Society

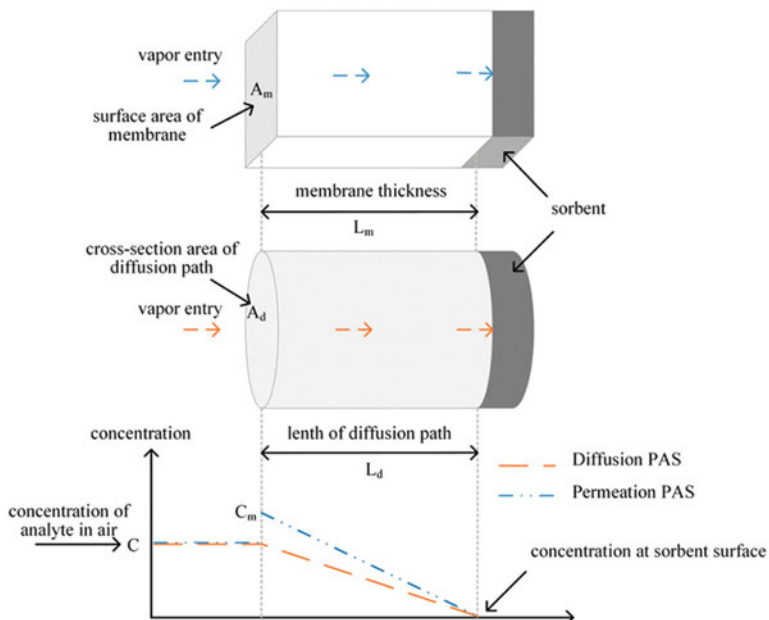


Fig. 3 Concentration profiles for diffusion and permeation passive samplers. (Reprinted with permission from Huang et al. (2018))

samplers, including semi-permeable membrane devices (SPMD), low-density polyethylene (LDPE) tubes, trimethylpentane containing passive samplers (TRIMPS), ionic liquid SPMD (IL-SPMD), and triolein-embedded cellulose acetate membrane (TECAM) as summarized by Esteve-Turrillas et al. (2007). Because the thin non-porous membrane tends to be rather fragile and contains pinholes that allow the direct penetration of air flow, permeation-based passive samplers are generally of badge type.

Analytes are retained in different sorbents by physical or chemical sorption (Harper 2000). For analysis, the analytes retained in sorbents are liberated by thermal desorption or solvent extraction depending on the type and the properties of the sorbents and the analytes.

Passive Sampling Theory

As shown in Fig. 3, the transport of the analyte from the sampled air to the passive samplers can be divided into four steps: (1) transfer through the boundary layer around the barrier surface (from the ambient air to the barrier surface), (2) diffuse/penetrate through the barrier (from the barrier surface to the sorbent-barrier interface), (3) be adsorbed by the sorbent, and (4) diffuse in the sorbent (Huang et al. 2018).

Early in 1973, Palmes and Gunnison (1973) described the mass transfer through the stagnant air gap in Palmes tube by Fick's First Law,

$$\frac{dm}{dt} = D_s A \frac{C_a - C_s}{L} \quad (1)$$

where m (μg) is the mass collected by the sampler, t (s) is the time, dm/dt ($\mu\text{g}/\text{s}$) is the sampling flux, D_s (m^2/s) is the diffusion coefficient of the analyte in the barrier, A (m^2) is the cross-sectional area of the sampler, C_a ($\mu\text{g}/\text{m}^3$) is the concentration of chemical in bulk air, C_s ($\mu\text{g}/\text{m}^3$) is the concentration at the air side of the air-sorbent interface, and L (m) is the diffusion distance (i.e., the length of the stagnant air gap between the sorbent and the ambient air).

Palmes and Gunnison (1973) assumed that the sorbent was an ideal sink for the analyte, and thus, the analyte concentration adjacent to the air-sorbent interface (i.e., C_s) was equal to zero throughout the whole sampling process. Consequently, the mass collected by the sampler (m) can be estimated by,

$$m = SR \cdot C_a \cdot t_s \quad (2)$$

where t_s (s) is the sampling time, and SR (m^3/s) represents the sampling rate of the sampler, which equals $D_s A / L$ according to Eq. (1), i.e.,

$$SR = \frac{D_s A}{L} \quad (3)$$

The diffusion-based model (Eq. (2)) has been widely used for describing the relationship between the sampled mass of the analyte in the diffusion-based passive samplers and C_a .

For permeation passive samplers, permeation is the principal process involving the dissolution of the analyte at the outer surface of the membrane, diffusion of the analyte through the membrane (analogous to diffusion through a liquid) and evaporation of the analyte at the other side of the membrane. In 1973, the permeation of the analyte through a polymer film was firstly mathematically described by Reiszner and West (1973) as,

$$\frac{dm}{dt} = \frac{D_s A (p_1 - p_2)}{S} \quad (4)$$

where p_1 and p_2 (Pa) are the partial pressures of the analyte near the external and internal surfaces of the membrane, respectively; and S (m) is the membrane thickness.

Supposing the partial pressure gradient is linear within the membrane and the collection efficiency of the sorbent is 100% (i.e., the sorbent is an ideal sink for the analyte, $p_2 = 0$), the mass of the analyte collected in the sorbent can be described:

$$m = \frac{D_s A}{S} p_1 t_s \quad (5)$$

Furthermore, the partial pressure of the analyte at a given temperature can be easily converted to its mass concentration in the air using the idea gas law equation,

$$p_1 = cRT \Rightarrow p_1M = (cM)RT = C_aRT \Rightarrow p_1 = \frac{RT}{M}C_a = HC_a \quad (6)$$

where R (J/(mol·K)) is the universal gas constant, T (K) is the temperature, c (mol/m³) is the molar concentration of the analyte, M (μg/mol) is the molecular weight of the analyte, and $H (= RT/M)$ is a constant.

Substituting Eq. (6) into Eq. (5),

$$m = SR \cdot C_a \cdot t \quad (7)$$

where SR is the sampling rate, $SR = \frac{D_s H A}{S}$. Generally, the product of D_s and H is usually called the permeation coefficient P , i.e., $P = D_s H$, and $SR = PA/S$.

According to these two models (Eq. (3) for diffusion-based sampler and Eq. (7) for permeation-based sampler), the sampling rates of both the diffusion-based and permeation-based passive samplers can be easily obtained. That is, the sampling rate is proportional to the diffusion/permeation area and diffusion/permeation coefficient, and inversely proportional to the diffusion/permeation distance. For a passive sampler with a defined geometry and used at a constant temperature, its sampling rate should be a constant for a given analyte. Given these prevailing theories for passive samplers, many passive samplers have been designed and evaluated using these two models (Batterman et al. 2002; Bertoni et al. 2004; Hardy et al. 1979; Pennequin-Cardinal et al. 2005b).

However, the key assumption of these two models (ideal sink) is just satisfied for the uptake of chemicals in strong sorbents. Sampling rates of passive samplers were often observed to decrease as sampling time increased in either laboratory or field experiments (Ballach et al. 1999; Kilic and Ballantine 1998; Pennequin-Cardinal et al. 2005a; Tolnai et al. 2001; Walgraeve et al. 2011). Furthermore, convective mass transfer on the barrier surface was shown to significantly affect sampling rates (Cao et al. 2016b; Gair and Penkett 1995; Plaisance 2011; Soderstrom and Bergqvist 2004). However, this mass transfer is excluded in Eqs. (2) and (7). Therefore, the models based on Eqs. (2) and (7) may not fully describe the uptake of analyte from air, through the barrier, and into sorbents. As summarized in Table 2, several models have been modified to describe the uptake of analytes by passive samplers. However, none of these models fully considered the three steps of analyte transport from ambient air to the sorbent, i.e., transfer through the boundary layer around the barrier surface, diffuse/penetrate through the barrier, and diffuse in the sorbent (and be captured by the sorbent).

Recently, Cao et al. (2016a) developed a transient model that fully considered the mass transfer processes in passive samplers. As illustrated in Fig. 4, the model was developed on the basis of the radial-type diffusion sampler (e.g., Radiello sampler in Fig. 1c) because it had better performance and was commonly used (Du et al. 2013). Several assumption were made in the model: (1) the barrier and sorbent were both made of porous media, (2) the mass transfer of analyte in passive sampler was one-dimensional, i.e., only mass transfer in the radial direction was considered; (3) the analyte in the porous air was assumed to be in equilibrium with the sorbent

Table 2 Evolution of the passive air sampling theory

	Across air boundary	Mass transfer through barrier	Diffusion within sorbent	Sorption/Desorption equilibrium within sorbent	Type of model
Palmes and Gunnison (1973)	×	√	×	×	Steady
Hearl and Manning (1980)	×	×	√	×	Unsteady
Coutant et al. (1985)	×	√ (Diffusion)	√	×	Unsteady
Tolnai et al. (2001)	×	√	√	×	Unsteady
Gorecki and Namiesnik (2002)	×	√	×	×	Steady
Bartkow et al. (2005)	√	×	×	×	Steady
Seethapathy and Gorecki (2010)	×	√ (Permeation)	×	×	Steady
Zhang and Wania (2012)	√	×	√	√	Unsteady

“×” means the item is not included in that model; “√” means the item is included in that model
Adapted with permission from Cao et al. (2016a). Copyright (2021) American Chemical Society

at each point; (4) the sorption isotherm was linear over the concentration range of interest (Lee et al. 2005; Lewis and Mulik 1985); (5) mass transfer in the barrier was pseudo-steady state (due to the diffusion coefficient in the barrier being significantly larger than that in the sorbent, e.g., 10^{-6} m²/s compared to 10^{-11} m²/s (Lewis and Mulik 1985)); and (6) analyte sorption to the barrier was assumed to be negligible.

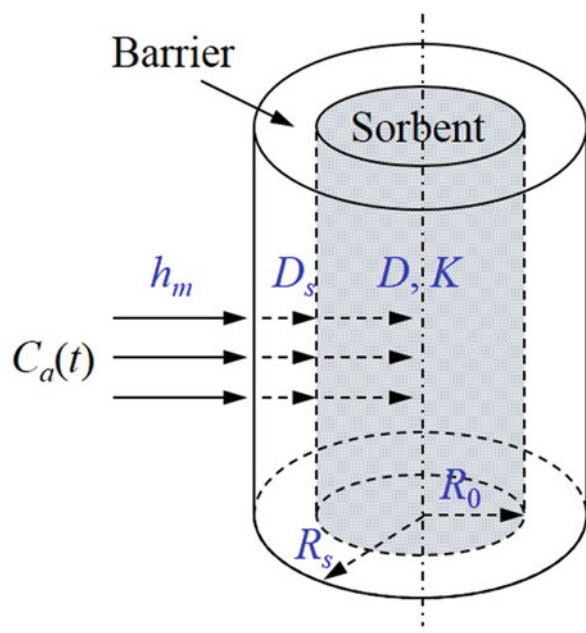
The mass transport of the analyte within the radial sorbent can be treated as the sorption of chemicals by porous media (Lee et al. 2005). The governing equation is expressed as,

$$\frac{\partial C}{\partial t} = D \left(\frac{\partial^2 C}{\partial r^2} + \frac{1}{r} \frac{\partial C}{\partial r} \right) (0 < r < R_0) \quad (8)$$

where C (μg/m³) is the VOC concentration in the sorbent, D (m²/s) is the “effective” diffusivity of the analyte in the sorbent, r (m) is the distance to the cylinder axis of the sorbent, and R_0 (m) is the radius of sorbent cylinder (also the inner radius of the barrier). Here, the surface diffusion of the analyte is negligible as the surface diffusion coefficient is several orders of magnitude lower than the diffusion coefficient in the porous air (Blondeau et al. 2003; Satterfield 1981).

At the cylinder axis of the sorbent (there is no mass flux here), the boundary condition is:

Fig. 4 Schematic of mass transfer of the analyte from ambient air to the sorbent for radial sampler. (Adapted with permission from Cao et al. (2016a). Copyright (2021) American Chemical Society)



$$\left. \frac{\partial C}{\partial r} \right|_{r=0} = 0 \quad (9)$$

At the interface between the sorbent and the barrier, the boundary condition is expressed as:

$$D \left. \frac{\partial C}{\partial r} \right|_{r=R_0} = h_{me} \left(C_a(t) - \frac{C}{K} \right) \quad (10)$$

where K (dimensionless) is the equilibrium partition coefficient of the analyte between the sorbent and the air, and h_{me} (m/s) is the “effective” convective mass transfer coefficient of the analyte from the bulk air to the sorbent-barrier interface. According to the above assumption (5), h_{me} can be calculated as:

$$\frac{1}{h_{me}} = \frac{1}{h_m} + \frac{1}{h_m'} = \frac{1}{h_m} + \frac{\ln(R_s/R_0)}{D_s} \quad (11)$$

where h_m (m/s) is the convective mass transfer coefficient of the analyte above the barrier, which can be calculated by empirical formulas (Bergman et al. 2011), R_s (m) is the outer radius of the barrier, D_s (m^2/s) is the effective diffusion coefficient of the analyte in the barrier, and h_m' (m/s) is the effective mass transfer coefficient, which is obtained by the mass transfer resistance for cylindrical system (one-dimensional diffusion) (Bergman et al. 2011). The parameter, h_{me} , involves

the information of barrier material (D_s), sampler geometry (R_s and R_0), and external condition of the sampling matrix (h_m).

Before sampling, the analyte remained in the passive sampler should be eliminated. Therefore, the initial condition is:

$$t = 0 : C = 0 \quad (0 < r < R_0) \quad (12)$$

The mass of analyte collected by the sampler (m) after t_s can be estimated by,

$$m(t_s) = 2\pi h \int_0^{R_0} r C(r, t_s) dr \quad (13)$$

where t_s (s) is the sampling period, h (m) is the height of the sorbent.

Eqs. 8, 9, 10, 11, and 12 provide the complete model that describes the mass transfer of the analyte from the bulk air to the sorbent of passive sampler. Comparisons between experimental data from the literature (benzene and toluene sampled by Radiello sampler (Oury et al. 2006)) and model outputs have been conducted by Cao et al. (2016a). Good agreement between model predictions and measured data both for benzene and toluene were obtained, implying high accuracy of Eqs. 8, 9, 10, 11, and 12.

Cao et al. (2016a) also developed a similar model for the tube-type diffusion sampler (e.g., Perkin-Elmer sampler in Fig. 1a). As shown in Fig. 5, with the same assumptions made above, the governing equation of mass transfer of the analyte within the sorbent is expressed as,

$$\frac{\partial C}{\partial t} = D \frac{\partial^2 C}{\partial x^2}, \quad (0 < x < L_s) \quad (14)$$

where x (m) is the distance to the end of the sorbent and L_s (m) is the thickness of the sorbent material.

At the end of the sorbent, the boundary condition is:

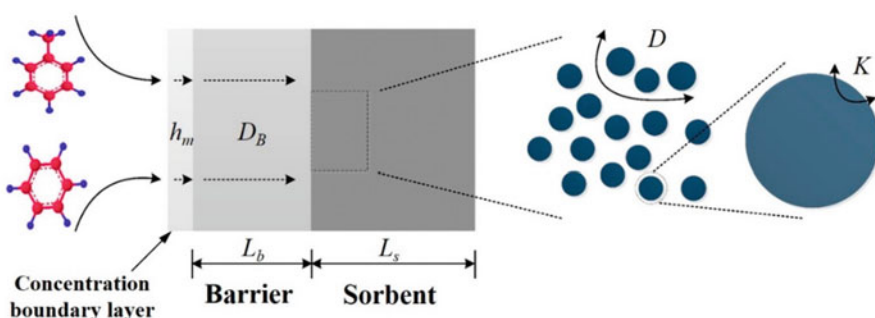


Fig. 5 Schematic of mass transfer process of the analyte in tube-type diffusion sampler. (Reprinted with permission from Cao et al. (2016a). Copyright (2021) American Chemical Society)

$$\left. \frac{\partial C}{\partial x} \right|_{x=0} = 0 \quad (15)$$

At the interface between the sorbent and the barrier, the boundary condition is:

$$D \left. \frac{\partial C}{\partial x} \right|_{x=L_s} = h_{m,e} \left(C_a(t) - \frac{C}{K} \right) \quad (16)$$

where $h_{m,e}$ is also the “equivalent” convective mass transfer coefficient of the analyte from the bulk air to the sorbent-barrier interface, which can be calculated by:

$$\frac{1}{h_{m,e}} = \frac{1}{h_m} + \frac{1}{h_m'} = \frac{1}{h_m} + \frac{L_b}{D_s} \quad (17)$$

where h_m' ($= D_s/L_b$) is the equivalent mass transfer coefficient for analyte diffusion through the barrier, which is obtained by the mass transfer resistance for diffusion through a flat plate (one-dimensional steady-state diffusion) (Bergman et al. 2011). h_m (m/s) is the convective mass transfer coefficient of the analyte at the external surface of the barrier, which also can be calculated using the empirical formula (Bergman et al. 2011).

The initial condition is:

$$t = 0 : C = 0 \quad (0 < x < L_s) \quad (18)$$

Eqs. 14, 15, 16, 17, and 18 form the complete model that describes the mass transfer of the analyte from the bulk air to the sorbent of a tube-type diffusion passive sampler. Comparing Eqs. 14, 15, 16, 17, and 18 to Eqs. 8, 9, 10, 11, and 12, it is easy to show that these two models are very similar.

Optimal Design of Passive Samplers

As mention above, the performance of the existing passive samplers for monitoring VOC concentrations still varies among different sampling environments. For example, significant uncertainties were observed when employing OVM badge samplers to measure concentrations of benzene, toluene and xylenes (BTX) (Du et al. 2013; Pratt et al. 2005). The sampling rates of Perkin-Elmer tube samplers deviated by up to 300% (for benzene) in some studies (Tolnai et al. 2001). Based on experiments, Plaisance et al. (2008) concluded that sampling rate is the main factor influencing the performance (accuracy) of passive samplers, e.g., variation of sampling rate contributes more than 80% of the sampling uncertainty (benzene measured by Radiello sampler).

In general, the traditional method for improving passive samplers employs the idea of “trial and error,” i.e., testing the performance of passive samplers with different combination of sorbent and barrier materials as well as different sizes, and selecting the optimized one with minimum testing error. In this case, abundant test experiments are required resulting in long development periods and high costs. Thus, it can be inconvenient to develop a fully optimized passive sampler that meets the requirements of field test (especially for a wide range of target pollutants). Zhang et al. (2015) proposed an inverse-problem-based method for solving building energy and environment problems. As they have noted, “the objective of an inverse problem is to find the most suitable model parameters to obtain model results that are the most expected (those that tend to be maximal or minimal).” With the principle of Zhang et al.’s method, Cao et al. (2016a) proposed a method for optimizing radial passive samplers by combining the mass transfer model in passive samplers with the goal of minimal sampling error. In this way, substantial time and cost required in the traditional approach can be eliminated.

Method Principle

In the design of passive samplers, the key parameters to be determined are the sorption properties of materials of passive sampler (both barrier and sorbent materials) and geometry of passive sampler. Since the objective of passive sampler is to determine gas-phase concentration of the analyte based on the measured mass of analyte collected by the sampler (m), the expected result of optimizing passive samplers is to minimize the error in the estimated value of m . Prior studies suggested that the error in m originate primarily from three aspects (if the temperature keeps constant): the fluctuation of analyte concentration in the measured environment, the variation of wind velocity in the measured environment, and the error of m introduced by chemical analysis (Pennequin-Cardinal et al. 2005b; Plaisance et al. 2008).

The relative error attributed to the fluctuation of analyte concentration of the measured environment, $\varepsilon(C)$, can be defined as,

$$\varepsilon(C) = \frac{|m - m_C|}{m_C} \quad (19)$$

where m is the mass of the analyte collected by the sampler in time t_s during which the concentration varies (in a real environment, the concentration is C_a), m_C is the mass of the analyte collected by the sampler in time t_s during which the concentration keeps constant (in controlled chamber, the concentration is C_C , $\mu\text{g}/\text{m}^3$). Noting, $\int_0^{t_s} C_C dt$ should be equal to $\int_0^{t_s} C_a dt$.

The relative error caused by the variation of wind velocity in the measured environment, $\varepsilon(V)$, can be defined as:

$$\varepsilon(V) = \max \left(\frac{m_{v,\max}}{m_C} - 1, 1 - \frac{m_{v,\min}}{m_C} \right) \quad (20)$$

where $m_{v,\max}$ is the mass of the analyte collected by the sampler at the maximum wind velocity, $m_{v,\min}$ is the mass of the analyte collected by the sampler at the minimum wind velocity.

The relative error of m from the chemical analysis is related with the method detection limit (MDL), i.e.,

$$\varepsilon(MDL) = MDL/m_C \quad (21)$$

Taking these three factors into consideration, the function of relative error of m (ε) can be defined as:

$$\varepsilon = \sqrt{\varepsilon(C)^2 + \varepsilon(V)^2 + \varepsilon(MDL)^2} \quad (22)$$

As mentioned above, the principle of inverse problem optimization method for passive sampler is to determine the sorption properties of sorbent and barrier materials as well as geometry of passive sampler with minimum ε , based on the mass transfer model in passive samplers, i.e., Eqs. 8, 9, 10, 11, 12, and 13 for the radical-type diffusion sampler.

Eqs. 8, 9, 10, 11, 12, and 13 and 19, 20, 21, and 22 indicate that ε is of the following function form:

$$\varepsilon = f(D, K, h_m', R_0, h, C_a(t), \varepsilon(V), MDL, t_s) \quad (23)$$

Sampling of the VOC concentrations in normal indoor environments was the target case in Cao et al. (2016a). When calculating, a combined standard condition was set at temperature of 20 °C, wind velocity of 0.2 m/s, VOC concentration of 0.05 mg/m³ (common indoor average level of benzene or toluene (Kim et al. 2001; Liu et al. 2013; Sarigiannis et al. 2011; Son et al. 2003)), $R_0 = 2.4$ mm and $h = 6.0$ cm (commonly used for radial-type passive sampler, e.g., Radiello (Cocheo et al. 1996)), and t_s of 24 h. Note: the effects of relative humidity were not considered in Cao et al. (2016a) despite competitive sorption in the sorbents may exist between VOCs and water vapor. The fluctuant VOC concentration in the measured environment was supposed to be:

$$C_a(t) = C_{AVE} + 0.5 \cdot C_{AVE} \cdot \sin \left(\frac{2\pi}{t_T} t + 160^\circ \right) \quad (24)$$

where t_T is the period of concentration change, 24 h; C_{AVE} is the time-weighted average concentration, which is assigned to be 0.05 mg/m³, representative of

common indoor level (Kim et al. 2001; Liu et al. 2013; Sarigiannis et al. 2011; Son et al. 2003). Values in Eq. (24) were determined by fitting the results of a field test in a residential bedroom (more than 3 months after adding decorations, measured by Cao et al. (2016a)). Thus, Eq. (24) was expected to reflect the real characteristic of indoor concentration fluctuations.

The wind velocity covered a wide range of $0.1 \sim 3$ m/s, covering the range of typical indoor common wind speeds and the normal speed of people walking (Baldwin and Maynard 1998; Bao et al. 2000; GB/T 18883 2002). The *MDLs* of benzene, toluene and ethylbenzene analyzed using gas chromatograph-thermal desorption complying with standard method GB 11737-89 (in Chinese) are 50 ng, 100 ng, and 200 ng, respectively, while the *MDL* of toluene (VOCs) for the same method is 5 ng (MDHS 80 1995). Cao et al. (2016a) selected 50 ng as a conservative estimate of the *MDL* for the analysis of VOCs. To numerically solve the model (Eqs. 8, 9, 10, 11, 12, and 13), the sorbent was divided into 30 slices and the barrier was divided into 100 slices. Then the partial differential equations can be discretized into a system of ordinary differential equations.

Considering the above conditions, D , K and h_m' were unknown and were the parameters that required optimization. The properties of sorbent material (determined by D and K) and the barrier material (determined by D_s involved in h_m' according to Eq. (11)) as well as the size of passive sampler can then be determined (determined by R_s involved in h_m' according to Eq. (11)). The effects of some of the model parameters (D , K , and h_m') on the error of M were analyzed by performing sensitivity analysis with the parameterized mass transfer model. The ranges of D , K and h_m' were selected as $1 \times 10^{-15} - 1 \times 10^{-7}$ m²/s, $1 \times 10^2 - 1 \times 10^8$ and $2 \times 10^{-5} - 1 \times 10^{-2}$ m/s, respectively, to cover a broad range of possible cases. The results of sensitivity analysis of D , K , and h_m' are shown in Fig. 6.

Figure 6a shows the variation of the relative errors of m attributed to the fluctuations of VOC concentrations ($\varepsilon(C)$), the variations of wind velocity ($\varepsilon(V)$) and chemical analysis ($\varepsilon(MDL)$) as well as the composite error of m (ε) for various D (when $K = 2.0 \times 10^6$ and $h_m' = 3.6 \times 10^{-4}$, typical values for benzene series (Cao et al. 2016a)). These analyses indicated that as D increases: (1) $\varepsilon(C)$ is decreasing, i.e., the effect of the fluctuation of concentration is weakening; (2) $\varepsilon(V)$ will increase since the effect of external mass transfer resistance (associated with wind velocity) will be more significant for larger D (reducing the internal mass transfer resistance); (3) $\varepsilon(MDL)$ will decrease since the sorption amount of VOC in the sorbent with the same sampling time (i.e., m) will increase for larger D (which reduces the mass transfer resistance of the whole process). This figure also indicates the composite error, ε , will decrease to a constant value as D increases; meanwhile, ε is insensitive to the variation of D .

Figure 6b shows sensitivity analysis results of K (when $D = 9.0 \times 10^{-12}$ and $h_m' = 3.6 \times 10^{-4}$). Similarly to results of D , $\varepsilon(V)$ will increase as K increases, while $\varepsilon(C)$ and $\varepsilon(MDL)$ will decrease. The composite error, ε , will decrease to a constant as K increases, and the effect of K on ε is quite significant for K with small values. Figure 6c shows that ε is very sensitive to changes in h_m' , the value

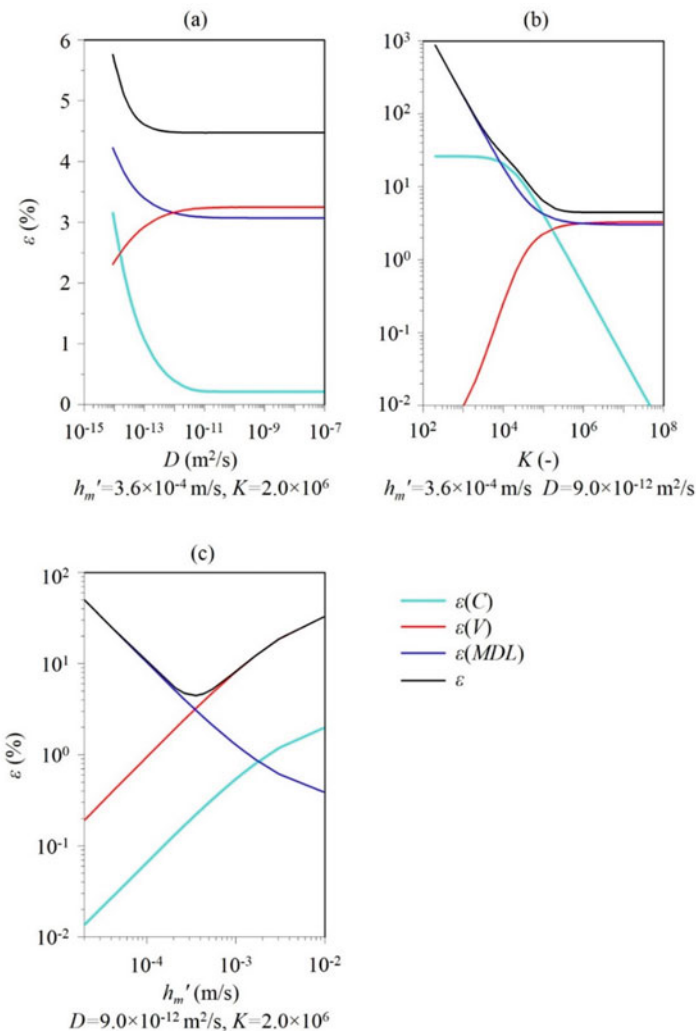


Fig. 6 Sensitivity analysis of model parameters for the relative error of m (ε). (a) D ; (b) K ; and (c) h_m' . (Reprinted with permission from Cao et al. (2016a). Copyright (2021) American Chemical Society)

of ε will decrease firstly and then increase as h_m' increases. The sensitivity analysis results have significance for determining the optimized parameters of passive sampler with the minimum ε . Thus, when searching for the optimized parameters, we can increase the values of D , K and h_m' from certain values (i.e., lower boundary of the range of each parameter), and then stop the calculation when ε approached the minimum value (constant for D and K , while beginning to increase h_m').

Table 3 Optimized parameters of radial passive samplers for benzene and formaldehyde in a normal indoor environment

Chemicals	$D (\times 10^{12} \text{ m}^2/\text{s})$	$K (\times 10^7)$	$h_m' (\times 10^{-4} \text{ m/s})$	$\varepsilon (\%)$
Benzene	0.70	0.60	3.6	4.5
Formaldehyde	6.0	3.0	4.4	3.7

Reprinted with permission from Cao et al. (2016a). Copyright (2021) American Chemical Society

Illustration of Optimization Outputs

In the analysis of Cao et al. (2016a), optimization of radial passive samplers for benzene and formaldehyde in a normal indoor environment was conducted based on the above method, the optimized parameters and minimum values of ε are listed in Table 3. It can be seen that the minimum ε are just 4.5% and 3.7% for sampling of benzene and formaldehyde, respectively. Figure 7 shows the calculated results of ε for various D and K when h_m' is equal to the value listed in Table 3, which indicates that the value of ε is decreasing as K and D increases (in consistent with the above sensitivity analysis results).

Due to the limitation of existing sorbents (i.e., unlikely to find the sorbent meeting the optimized values of D and K), Fig. 7 is useful for selecting the appropriate sorbent by plotting ε of existing sorbents in the figure. Fig. 7 compares the calculated ε of six commonly used sorbents, i.e., Carbograph 4 (used by Radiello sampler), active alumina, active carbon, active manganese oxide, silica gel, and silica zeolite. The results show that for passive sampling of benzene, active alumina, active carbon, Carbograph 4, and silica zeolite are the appropriate sorbents with minimum ε (calculated); while for formaldehyde, active alumina and active manganese oxide are most suitable. However, Carbograph 4, silica gel, and silica zeolite are also acceptable. Although the calculated ε should not be interpreted as the measurement uncertainty in field test, the modeled results are expected to reflect the uncertainty and the performance of passive samplers to a reasonable extent.

In the practical selection of sorbent, the physical and chemical properties of the sorbent need to be considered. Since active manganese oxide may react with VOCs when the temperature is sufficiently high, it is not suitable to be selected as the sorbent if the samples are to be analyzed by thermal desorption-GC-MS. Due to abundant pores in active carbon, desorption of VOCs from this sorbent requires a long period of time and the desorption efficiency is relatively low leading to low throughput because of long analysis times (Du et al. 2013). Water vapor is easily adsorbed by silica gel, which may result in uncertain sampling of VOCs (e.g., formaldehyde). Furthermore, when optimizing passive samplers, the cost should also be considered, and Carbograph 4 is much more expensive than silica zeolite (Du et al. 2013). Therefore, silica zeolite, which is low cost, hydrophobic, and having good desorption efficiency was suggested to be the most appropriate sorbent among the aforementioned sorbents for sampling of benzene (the modeled $\varepsilon < 5\%$) and formaldehyde (the modeled $\varepsilon < 15\%$) by Cao et al. (2016a).

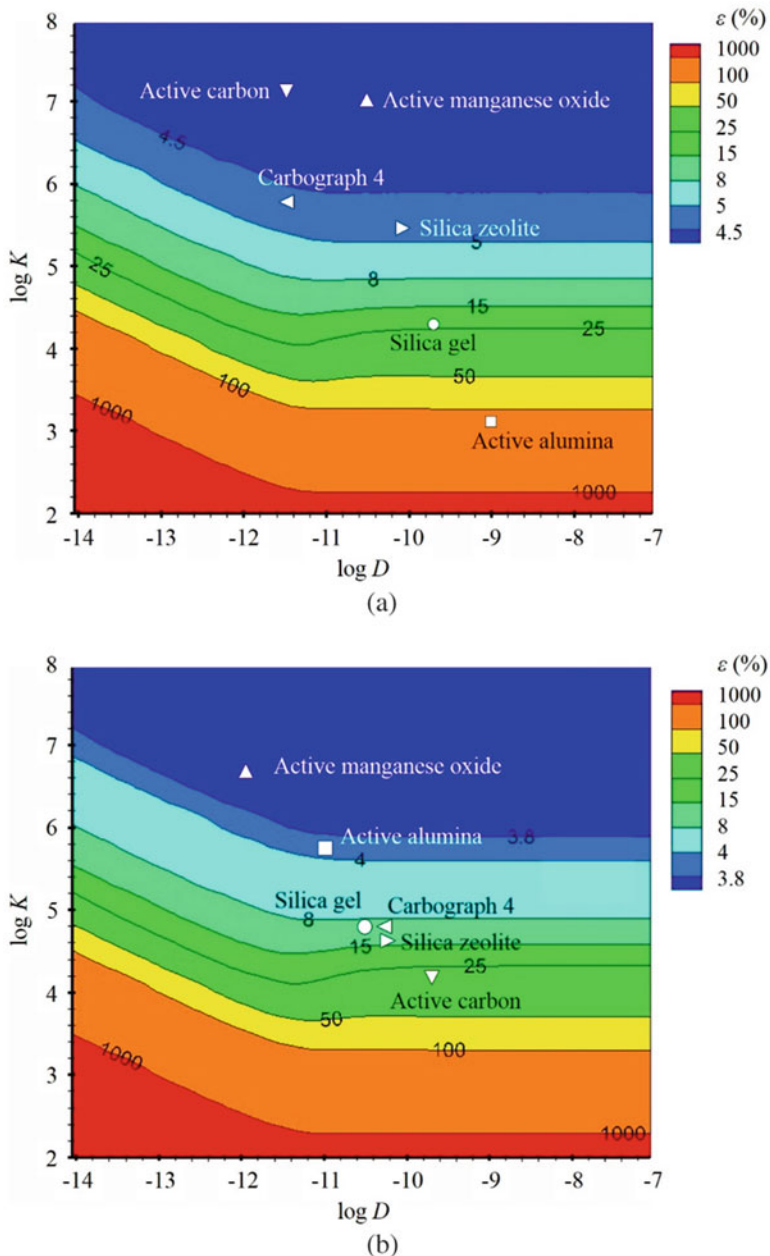


Fig. 7 Variation of ε for various D (m^2/s) and K when: (a) $h_m' = 3.6 \times 10^{-4} \text{ m/s}$ for benzene, (b) $h_m' = 4.4 \times 10^{-4} \text{ m/s}$ for formaldehyde. (Reprinted with permission from Cao et al. (2016a). Copyright (2021) American Chemical Society)

The radius of the sorbent, R_0 , was assumed to be 2.4 mm in the above analysis. The radius can be optimized after selecting the suitable sorbent, i.e., silica zeolite. According to Eq. (23), if D and K of silica zeolite are measured, h_m' and R_0 are the two remaining parameters requiring to be optimized for sampling of VOC concentration in a normal indoor environment. By referring to the method and experimental system developed by Xu et al. (2011), D and K of silica zeolite were measured to be 7.5×10^{-11} m²/s and 3.1×10^5 for benzene by Cao et al. (2016a). Similarly to the method (just mentioned above) for determining D , K and h_m' , the optimized h_m' and R_0 are determined to be 2.45×10^{-4} m/s and 2.15 mm, respectively, for sampling of benzene in a normal indoor environment with the minimum ε to be 4.8%, while the value of ε for a commonly used sampler (i.e., Radiello (Cocheo et al. 1996)) under the same condition is calculated to be 28%.

Application and Discussions

Benzene has been identified as the predominant risk compound in the indoor air compared with other VOCs (e.g., formaldehyde) (Loh et al. 2007). Therefore, a novel radial diffusive sampler, named Tsinghua Passive Diffusive Sampler (THPDS), for indoor benzene measurement was developed according to the above optimization results. Specifically, silica zeolite (FX-2021, Shanghai Fuxu Molecular Sieve Ltd.) was selected as the sorbent with a radius of 2.15 mm (the mass is about 60 mg), the effective mass transfer coefficient (h_m') was set as 2.45×10^{-4} m/s (which is determined by the size and material of the barrier). In design of THPDS, a stainless-steel powder sintered porous cylinder, which is low cost and with weak sorption capacity of benzene (Du et al. 2013), was selected as the barrier with the length of 30 mm, inner diameter of 4.3 mm (i.e., $2R_0$), external diameter of 10.3 mm

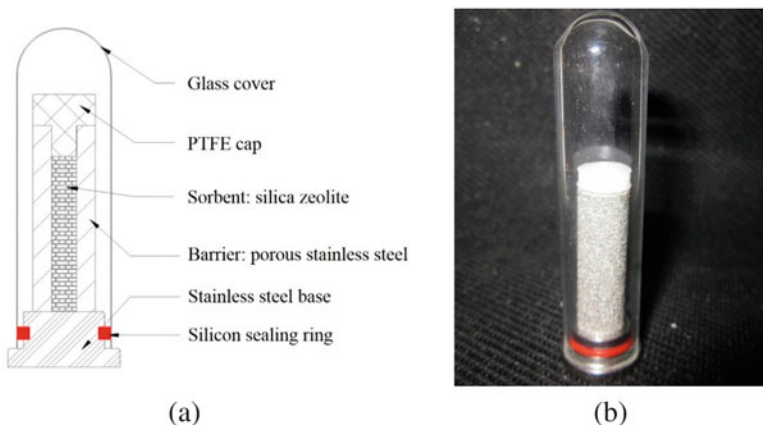


Fig. 8 Tsinghua passive diffusive sampler (THPDS): (a) structure illustration; (b) photo. (Reprinted with permission from Cao et al. (2016a). Copyright (2021) American Chemical Society)

(i.e., $2R_s$), and porosity of 37–38%. Other components and structure of THPDS are illustrated in Fig. 8. As assumed above that sorption of VOC to the barrier should be ignored, the adsorptivity of porous stainless-steel for benzene was tested by exposing the THPDS without sorbent (i.e., just the porous stainless-steel) to $10 \mu\text{g}/\text{m}^3$ gas-phase benzene for 30 days. After that, the sorption amount of benzene in the barrier was lower than the detection limit of the corresponding chemical analysis method (which is the same method for analyzing THPDS, see detailed in Du et al. (2013)), implying that it is reasonable to neglect the sorption of benzene to the barrier. Similar results were obtained for benzene series compounds, i.e., toluene and xylene.

The performance of newly designed THPDS was then evaluated through experimental measurement. The detailed experimental setup and testing results has been reported by Du et al. (2013), including evaluation of the desorption efficiency, background, effect of wind velocity, effects of temperature and relative humidity, and comparison with other sampling methods. According to their evaluation, the uncertainties (at 95% confidence) of THPDS for benzene, toluene, and xylene were 22%, 23%, and 17%, respectively. Compared to several commercial passive samplers, the uncertainties of THPDS were lower than most cases as illustrated in Fig. 9.

However, it should be noted that the measured ε (22%) is quite larger than the modeled ε (4.8%) for benzene, possibly because the errors introduced by other

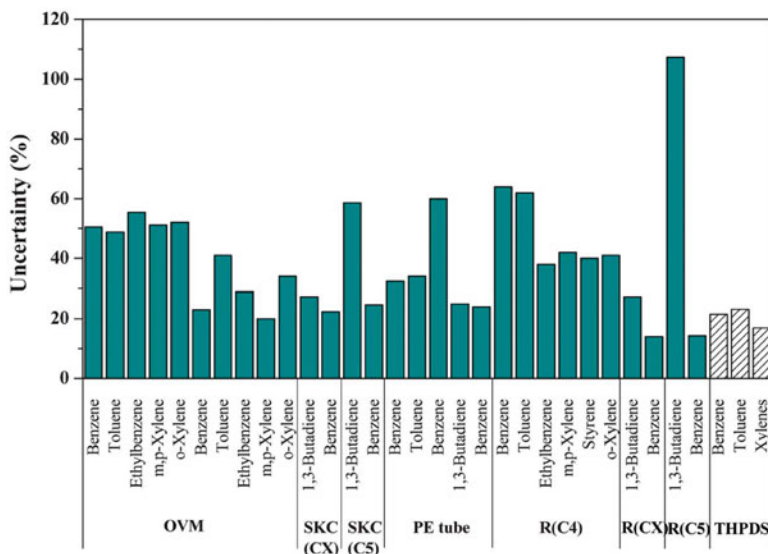


Fig. 9 Uncertainties of VOC determinations by different diffusive samplers against a reference method under field tests. SKC (CX): SKC samplers filled with Carbopack X, SKC (C5): SKC samplers filled with Carbograph 5, R (C4): Radiello samplers filled with Carbograph 4, R (CX): Radiello samplers filled with Carbopack X, R (C5): Radiello samplers filled with Carbograph 5. (Reprinted with permission from Du et al. (2013))

factors, such as temperature variation, humidity, desorption efficiency and storage time of samplers are not considered when modeling the composite error (i.e., Eq. (22)). Further study considering these factors when optimizing and designing passive samplers is requisite. Application of the above method to other series of VOCs, e.g., aldehydes and hydrochloric ethers, also warrants further investigation. In addition, assumption 3) of the above model may not suitable for sorption of formaldehyde (chemical reaction may occur), applicability of this assumption or errors introduced by it for modelling of formaldehyde in passive samplers require more extensive research. Furthermore, the optimized results are focused on one specific compound (e.g., benzene or formaldehyde), optimization of passive samplers that can simultaneously monitor the concentrations of different VOCs can be very challenging. As mentioned above, it is unlikely to find the sorbent that meets the optimized values of D and K , development of new sorbents may be helpful for the optimization of passive samplers. Finally, further study focusing on the optimization of passive sampler of semi-volatile organic compounds (SVOCs) is valuable (Zhang and Wania 2012), which may require to eliminate the barrier layer due to low volatility of SVOCs (Weschler and Nazaroff 2008). Several studies demonstrated that solid-phase micro-extraction (SPME) can be used as passive sampler of SVOCs in laboratory experiments (Cao et al. 2016b, 2017); however, further study is needed to evaluate whether it is applicable in the field test. Details about the passive sampling of SVOCs can be found in another chapter of this handbook (► Chap. 16, “Sampling and Analysis of Semi-volatile Organic Compounds (SVOCs) in Indoor Environments”) and a recent critical review by Wania and Shunthirasingham (2020).

Conclusions

Over the decades, numerous efforts have focused on the development of reliable passive samplers. Tube-type samplers, badge-type samplers, and radial samplers appeared in succession. Meanwhile, many passive sampling theories have been investigated. This chapter provided a brief summary of representative passive samplers and passive sampling theories reported in the literature, with emphasis on the passive sampling of indoor VOCs. Then, an optimization method (for minimizing the sampling error) based on a relatively comprehensive passive sampling model was introduced in this chapter. However, the actual performance of the designed sampler was found to be considerably deviated from the designed performance, indicating the requirement for further investigation of passive sampling models and optimized design of passive samplers.

Cross-References

- [Sampling and Analysis of Semi-volatile Organic Compounds \(SVOCs\) in Indoor Environments](#)

Acknowledgments The author acknowledges the Natural Science Foundation of China (No. 51908563), Guangdong Basic and Applied Basic Research Foundation (No. 2019A1515011179), Science and Technology Program of Guangzhou (No. 202102020990), and the special fund of Beijing Key Laboratory of Indoor Air Quality Evaluation and Control (No. BZ0344KF20-11) for financial support.

References

- Arthur CL, Pawliszyn J (1990) Solid-phase microextraction with thermal-desorption using fused-silica optical fibers. *Anal Chem* 62(19):2145–2148
- Baldwin PEJ, Maynard AD (1998) A survey of wind speeds in indoor workplaces. *Ann Occup Hyg* 42(5):303–313
- Ballach J, Greuter B, Schultz E, Jaeschke W (1999) Variations of uptake rates in benzene diffusive sampling as a function of ambient conditions. *Sci Total Environ* 244:203–217
- Bao Z, Ma P, Tong J, Wang C (2000) Research on the velocity characteristic of human walking. *Lab Res Explor* 19(6):39–42
- Bartkow ME, Booij K, Kennedy KE, Muller JF, Hawker DW (2005) Passive air sampling theory for semivolatile organic compounds. *Chemosphere* 60(2):170–176
- Batterman S, Metts T, Kalliokoski P (2002) Diffusive uptake in passive and active adsorbent sampling using thermal desorption tubes. *J Environ Monit* 4(6):870–878
- Bergman TL, Incropera FP, Lavine AS (2011) Fundamentals of heat and mass transfer. John Wiley & Sons, New York.
- Bertoni G, Tappa R, Allegrini I (2000) Assessment of a new passive device for the monitoring of benzene and other volatile aromatic compounds in the atmosphere. *Ann Chim-Rome* 90(3–4):249–263
- Bertoni G, Tappa R, Cecinato A (2001) Environmental monitoring of semi volatile polycyclic aromatic hydrocarbons by means of diffusive sampling devices and GC-MS analysis. *Chromatographia* 53:S312–S316
- Bertoni G, Ciuchini C, Tappa R (2004) Long-term diffusive samplers for the indoor air quality evaluation. *Ann Chim-Rome* 94(9–10):637–646
- Blondeau P, Tiffonnet A, Damian A, Amiri O, Molina J (2003) Assessment of contaminant diffusivities in building materials from porosimetry tests. *Indoor Air* 13(3):310–318
- Bohlin P, Audy O, Škrdlíková L, Kukučka P, Přibylová P, Prokeš R, Vojta Š, Klánová J (2014) Outdoor passive air monitoring of semi volatile organic compounds (SVOCs): a critical evaluation of performance and limitations of polyurethane foam (PUF) disks. *Environ Sci Process Impacts* 16(3):433–444
- Brown R, Charlton J, Saunders K (1981) The development of an improved diffusive sampler. *Am Indust Hygiene Assoc J* 42(12):865–869
- Cao J, Du Z, Mo J, Li X, Xu Q, Zhang Y (2016a) Inverse problem optimization method to design passive samplers for volatile organic compounds: principle and application. *Environ Sci Technol* 50(24):13477–13485
- Cao J, Xiong J, Wang L, Xu Y, Zhang Y (2016b) Transient method for determining indoor chemical concentrations based on SPME: model development and calibration. *Environ Sci Technol* 50(17):9452–9459
- Cao J, Zhang X, Little JC, Zhang Y (2017) A SPME-based method for rapidly and accurately measuring the characteristic parameter for DEHP emitted from PVC floorings. *Indoor Air* 27 (2):417–426
- Cocheo V, Boaretto C, Sacco P (1996) High uptake rate radial diffusive sampler suitable for both solvent and thermal desorption. *Am Ind Hyg Assoc J* 57(10):897–904
- Coutant RW, Lewis RG, Mulik J (1985) Passive sampling devices with reversible adsorption. *Anal Chem* 57(1):219–223

- Delcourt J, Sandino JP (2001) Performance assessment of a passive sampler in industrial atmospheres. *Int Arch Occup Environ Health* 74(1):49–54
- Destaillets H, Maddalena RL, Singer BC, Hodgson AT, McKone TE (2008) Indoor pollutants emitted by office equipment: a review of reported data and information needs. *Atmos Environ* 42(7):1371–1388
- Du Z, Mo J, Zhang Y, Li X, Xu Q (2013) Evaluation of a new passive sampler using hydrophobic zeolites as adsorbents for exposure measurement of indoor BTX. *Anal Methods* 5(14): 3463–3472
- Du ZJ, Mo JH, Zhang YP, Xu QJ (2014) Benzene, toluene and xylenes in newly renovated homes and associated health risk in Guangzhou, China. *Build Environ* 72:75–81
- Esteve-Turrillas FA, Pastor A, Yusa V, de la Guardia M (2007) Using semi-permeable membrane devices as passive samplers. *Trac-Trend Anal Chem* 26(7):703–712
- Ferm M (1979) Method for determination of atmospheric ammonia. *Atmos Environ* 13(10): 1385–1393
- Gair AJ, Penkett SA (1995) The effects of wind-speed and turbulence on the performance of diffusion tube samplers. *Atmos Environ* 29(18):2529–2533
- GB/T 18883 (2002) Standards for indoor air quality (in Chinese)
- Gillet RW, Kreibich H, Ayers GP (2000) Measurement of indoor formaldehyde concentrations with a passive sampler. *Environ Sci Technol* 34(10):2051–2056
- Gorecki T, Namiesnik J (2002) Passive sampling. *Trac-Trend Anal Chem* 21(4):276–291
- Guild LV, Myrmel KH, Myers G, Dietrich DG (1992) Bi-level passive monitor validation: a reliable way of assuring sampling accuracy for a larger number of related chemical hazards. *Appl Occup Environ Hyg* 7(5):310–317
- Hardy JK, Dasgupta PK, Reiszner KD, West PW (1979) Personal chlorine monitor utilizing permeation sampling. *Environ Sci Technol* 13(9):1090–1093
- Harper M (2000) Sorbent trapping of volatile organic compounds from air. *J Chromatogr A* 885(1–2):129–151
- Hearl FJ, Manning MP (1980) Transient-response of diffusion dosimeters. *Am Ind Hyg Assoc J* 41(11):778–783
- Huang C, Shan W, Xiao H (2018) Recent advances in passive air sampling of volatile organic compounds. *Aerosol Air Qual Res* 18(3):602–622
- Huckins JN, Petty JD, Lebo JA, Almeida FV, Booij K, Alvarez DA, Clark RC, Mogensen BB (2002) Development of the permeability/performance reference compound approach for in situ calibration of semipermeable membrane devices. *Environ Sci Technol* 36(1):85–91
- Kilic N, Ballantine JA (1998) Comparison of various adsorbents for long-term diffusive sampling of volatile organic compounds. *Analyst* 123(9):1795–1797
- Kim YM, Harrad S, Harrison RM (2001) Concentrations and sources of VOCs in urban domestic and public microenvironments. *Environ Sci Technol* 35(6):997–1004
- Kot-Wasik A, Zabiegala B, Urbanowicz M, Dominiak E, Wasik A, Namieśnik J (2007) Advances in passive sampling in environmental studies. *Anal Chim Acta* 602(2):141–163
- Kourakis P, Wolfson JM, Bunyaviroch A, Froehlich SE, Hirano K, Mulik JD (1993) Measurement of ambient ozone using a nitrite-coated filter. *Anal Chem* 65(3):209–214
- Lee CS, Haghhighat F, Ghaly WS (2005) A study on VOC source and sink behavior in porous building materials - analytical model development and assessment. *Indoor Air* 15(3):183–196
- Lewis RG, Mulik J (1985) Passive sampling devices with reversible adsorption. *Anal Chem* 57(1): 219–223
- Lewis RG, Mulik JD, Coutant RW, Wooten GW, McMinn CR (1985) Thermally desorbable passive sampling device for volatile organic-chemicals in ambient air. *Anal Chem* 57(1): 214–219
- Liard R, Zureik M, Le Moullec Y, Soussan D, Glorian M, Grimfeld A, Neukirch F (1999) Use of personal passive samplers for measurement of NO₂, NO, and O₃ levels in panel studies. *Environ Res* 81(4):339–348
- Liu Q, Liu Y, Zhang M (2013) Personal exposure and source characteristics of carbonyl compounds and BTEXs within homes in Beijing, China. *Build Environ* 61:210–216

- Loh MM, Levy JI, Spengler JD, Houseman EA, Bennett DH (2007) Ranking cancer risks of organic hazardous air pollutants in the United States. *Environ Health Perspect* 115(8):1160–1168
- MDHS 80 (1995) Volatile organic compounds in air – laboratory method using diffusive solid sorbent tubes, thermal desorption and gas chromatography. Health & Safety Laboratory, Derbyshire
- Namieśnik J, Górecki T, Zabiegala B, Janicki W (1992) Investigations on the applicability of some commercial polyethylene films to permeation-type passive samplers for organic vapours. *Indoor Air* 2:115–120
- Namieśnik J, Zabiegala B, Kot-Wasik A, Partyka M, Wasik A (2005) Passive sampling and/or extraction techniques in environmental analysis: a review. *Anal Bioanal Chem* 381(2): 279–301
- Olansandan, Amagai T, Matsushita H (1999) A passive sampler-GC/ECD method for analyzing 18 volatile organohalogen compounds in indoor and outdoor air and its application to a survey on indoor pollution in Shizuoka, Japan. *Talanta* 50(4):851–863
- Oury B, Lhuillier F, Protois J-C, Moréle Y (2006) Behavior of the GABIE, 3M 3500, PerkinElmer Tenax TA, and RADIELLO 145 diffusive samplers exposed over a long time to a low concentration of VOCs. *J Occup Environ Hyg* 3(10):547–557
- Palmes ED, Gunnison AF (1973) Personal monitoring device for gaseous contaminants. *Am Ind Hyg Assoc J* 34(2):78–81
- Partyka M, Zabiegala B, Namieśnik J, Przyjazny A (2007) Application of passive samplers in monitoring of organic constituents of air. *Crit Rev Anal Chem* 37(1):51–78
- Pennequin-Cardinal A, Plaisance H, Locoge N, Ramalho O, Kirchner S, Galloo JC (2005a) Dependence on sampling rates of Radiello(R)) diffusion sampler for BTEX measurements with the concentration level and exposure time. *Talanta* 65(5):1233–1240
- Pennequin-Cardinal A, Plaisance H, Locoge N, Ramalho O, Kirchner S, Galloo JC (2005b) Performances of the Radiello(R)) diffusion sampler for BTEX measurements: influence of environmental conditions and determination of modelled sampling rates. *Atmos Environ* 39(14):2535–2544
- Petty JD, Huckins JN, Zajicek JL (1993) Application of semipermeable-membrane devices (SPMDS) as passive air samplers. *Chemosphere* 27(9):1609–1624
- Plaisance H (2011) The effect of the wind velocity on the uptake rates of various diffusive samplers. *Int J Environ an Ch* 91(14):1341–1352
- Plaisance H, Leonards T, Gerboles M (2008) Assessment of uncertainty of benzene measurements by Radiello diffusive sampler. *Atmos Environ* 42(10):2555–2568
- Pratt GC, Bock D, Stock TH, Morandi M, Adgate JL, Ramachandran G, Mongin SJ, Sexton K (2005) A field comparison of volatile organic compound measurements using passive organic vapor monitors and stainless steel canisters. *Environ Sci Technol* 39(9):3261–3268
- Reiszner KD, West PW (1973) Collection and determination of sulfur-dioxide incorporating permeation and West-Gaeke procedure. *Environ Sci Technol* 7(6):526–532
- Sarigiannis DA, Karakitsios SP, Gotti A, Liakos IL, Katsogiannis A (2011) Exposure to major volatile organic compounds and carbonyls in European indoor environments and associated health risk. *Environ Int* 37(4):743–765
- Satterfield CN (1981) Mass transfer in heterogeneous catalysis. RE Krieger Publishing Company, Florida
- Seethapathy S, Górecki T (2010) Polydimethylsiloxane-based permeation passive air sampler. Part II: effect of temperature and humidity on the calibration constants. *J Chromatogr A* 1217(50): 7907–7913
- Soderstrom HS, Bergqvist PA (2004) Passive air sampling using semipermeable membrane devices at different wind-speeds in situ calibrated by performance reference compounds. *Environ Sci Technol* 38(18):4828–4834
- Son B, Breyses P, Yang W (2003) Volatile organic compounds concentrations in residential indoor and outdoor and its personal exposure in Korea. *Environ Int* 29(1):79–85
- Stockton SD, Underhill DW (1985) Field-evaluation of passive organic vapor samplers. *Am Ind Hyg Assoc J* 46(9):526–531

- Tolnai B, Gelencsér A, Hlavay J (2001) Theoretical approach to non-constant uptake rates for tube-type diffusive samplers. *Talanta* 54(4):703–713
- Walgraeve C, Demeestere K, Dewulf J, Van Huffel K, Van Langenhove H (2011) Uptake rate behavior of tube-type passive samplers for volatile organic compounds under controlled atmospheric conditions. *Atmos Environ* 45(32):5872–5879
- Wania F, Shunthirasingham C (2020) Passive air sampling for semi-volatile organic chemicals. *Environ Sci Process Impacts* 22(10):1925–2002
- Weschler CJ (2009) Changes in indoor pollutants since the 1950s. *Atmos Environ* 43(1):153–169
- Weschler CJ, Nazaroff WW (2008) Semivolatile organic compounds in indoor environments. *Atmos Environ* 42(40):9018–9040
- WHO (1983) Indoor air pollutants: exposure and health effects. *EURO Rep Stud* 78:1–42
- WHO (2000) Air quality guidelines for Europe, 2nd edn. WHO Regional Office for Europe, Copenhagen
- Wolkoff P (1995) Volatile organic compounds – sources, measurements, emissions, and the impact on indoor air quality. *Indoor Air* 5(S3):5–73
- Xu Q, Li X, Mo J, Zhang Y (2011) Study on the performance evaluation of indoor VOC removal adsorbents (in Chinese). *J Eng Thermophys* 32(2):311–313
- Yamamoto N, Matsubasa T, Kumagai N, Mori S, Suzuki K (2002) A diffusive badge sampler for volatile organic compounds in ambient air and determination using a thermal desorption-GC/MS system. *Anal Chem* 74(2):484–487
- Zabiegala B, Gorecki T, Przyk E, Namiesnik J (2002) Permeation passive sampling as a tool for the evaluation of indoor air quality. *Atmos Environ* 36(17):2907–2916
- Zabiegala B, Krol S, Namiesnik J (2010) Monitoring VOCs in atmospheric air II. Sample collection and preparation. *Trac-Trend Anal Chem* 29(9):1101–1112
- Zhang X, Wania F (2012) Modeling the uptake of semivolatile organic compounds by passive air samplers: importance of mass transfer processes within the porous sampling media. *Environ Sci Technol* 46(17):9563–9570
- Zhang Y, Zhang Y, Shi W, Shang R, Cheng R, Wang X (2015) A new approach, based on the inverse problem and variation method, for solving building energy and environment problems: preliminary study and illustrative examples. *Build Environ* 91:204–218



Real-Time Monitoring of Indoor Organic Compounds

18

Yingjun Liu and Jinhan Mo

Contents

Introduction	494
Real-Time Monitoring of Formaldehyde	495
Formaldehyde Multimode Monitor	496
MIRA Pico Formaldehyde Analyzer	497
Proton-Transfer-Reaction Mass Spectrometry and Other CIMS	497
Basics of PTR-MS and Other CIMS	498
Application on Real-Time Monitoring of Indoor Air	500
Automated GC	510
Conclusions	513
References	513

Abstract

Online measurement techniques of airborne organic compounds have been greatly improved over the past several decades, and they are increasingly applied to indoor air research. Some instruments are designed to accurately measure a specific organic pollutant. Herein we review online measurement techniques for formaldehyde and highlight two recently developed portable devices that are accurate enough for indoor applications. Other instruments can measure many organic compounds simultaneously. The available techniques can be classified into two categories: chemical ionization mass spectrometry (CIMS) and automated gas chromatography (GC) systems. CIMS has high sensitivity and fast response, but often has limited chemical specificity. There are about ten types of

Y. Liu (✉)

Department of Environmental Health, College of Environmental Sciences and Engineering, Peking University, Beijing, China
e-mail: yingjun.liu@pku.edu.cn

J. Mo

Department of Building Science, School of Architecture, Tsinghua University, Beijing, China
e-mail: mojinhan@tsinghua.edu.cn

CIMS available, among which proton transfer reaction mass spectrometry (PTR-MS) is most widely used and can measure a large variety of volatile organic compounds. GC-based instruments can have better chemical specificity than CIMS, but the time resolution is lower. Herein we describe operation principles of common CIMS and GC-based instruments, and summarize how these instruments have been applied for indoor air monitoring to gain new insights about the dynamics, emission, chemistry, and exposure of indoor organic compounds. The limited number of indoor applications using these online instruments already demonstrate the great potential of these new tools to advance our understanding of indoor organic chemicals.

Keywords

Online · VOC · SVOC · CIMS · PTR-MS

Introduction

Organic compounds constituent an important class of indoor air pollutants. The indoor air concentrations of many organic compounds are often a few times or several orders of magnitude higher than the outdoor levels, due to direct emission and secondary formation from building and furnishing materials, from occupants, as well as from occupant activities. Indoor exposure to some organic pollutants has been associated to adverse health effects, while for many other organic compounds, the health risks are still being understood. It is thus important to understand the speciation, exposure level, source characteristics, and dynamic behavior of indoor organic compounds.

Concentrations of organic compounds in any given indoor space can vary with the source characteristics, ventilation rates, and temperature among other factors (Parts 2, “Indoor Air Chemicals,” and 5, “Source/Sink Characteristics”). Real-time monitoring of organic compounds can directly characterize their dynamic behavior and time-resolved exposure patterns. Combining the dynamic behavior of organic compounds and simultaneous measurements of environmental parameters, we can better understand the underlying processes controlling the concentrations. Making real-time measurements of organic compounds is, however, nontrivial. First of all, the instruments need to be highly sensitive. The indoor air concentrations of organic compounds, although often higher than outdoors, are typically in the range of tens of ng/m^3 to a few hundred $\mu\text{g}/\text{m}^3$. Secondly, it is challenging to separately measure the large variety of organic compounds present in the indoor air. There are alkanes, alkenes, aromatics, alcohols, aldehydes, ketones, organic acids, peroxides, furans, siloxanes, furanoids, chlorides among others, as well as compounds with multiple functional groups. Some airborne organic compounds are volatile and only present in the gas phase, some others partition between gas phase and particle phase, and the other low-volatility compounds predominantly reside on the particles. The differing phase state requires different sampling methods.

Despite of the challenges, great progress has been made on online measurement techniques for airborne organic compounds over the past several decades. Some real-time instruments are designed to accurately measure a specific organic pollutant. In indoor air research, a particular focus is formaldehyde ([► Chap. 2, “Very Volatile Organic Compounds \(VVOCs\)”\). In the next section, the available online techniques for formaldehyde measurement are summarized and two recently developed portable devices are highlighted. Other instruments aim to measure many organic compounds simultaneously. For measurements of organic compounds at least partially present in the gas phase, including volatile organic compounds \(VOCs\) and semi-volatile organic compounds \(SVOCs\), the available techniques can be classified into two categories: \(1\) chemical ionization mass spectrometry \(CIMS\) and \(2\) automated gas-chromatography \(GC\) systems. The following two sections review the operation principles and indoor applications of these two categories of techniques, respectively. In the section about CIMS, the proton transfer reaction mass spectrometry \(PTR-MS\), which has been widely used for online VOC measurements, is the major focus. In the section about GC-based techniques, two types of instruments respectively designed for the measurement of VOCs and SVOCs are introduced. There are also specialized online techniques to measure particle-bound organic compounds. These techniques are not discussed in this chapter since they are presented in the chapter about particle composition measurement \(\[► Chap. 19, “Measuring Particle Concentrations and Composition in Indoor Air”\]\(#\)\).](#)

Real-Time Monitoring of Formaldehyde

Formaldehyde (HCHO) is one of the most pervasive pollutants in the indoor environment. Airborne formaldehyde concentrations range from tens to hundreds of ppb indoors, while the ambient levels are in the range of hundreds of ppt to several tens of ppb (Salthammer et al. [2010](#)). The common procedure for analyzing formaldehyde in the indoor air is trapping formaldehyde in absorbers or on impregnated cartridges through reaction with derivative agents and then analyzing the resulting chromophore offline by chromatography and/or spectroscopy. The most widely used two derivation methods are the 2,4-dinitrophenylhydrazine (DNPH) method and the acetylacetone method (also called Hantzsch method), which are followed by HPLC analysis and UV/vis spectroscopy or fluorimetry, respectively. These offline methods are reliable and accepted as international or national standards, but can only provide time-integrated or snap-shot formaldehyde concentration.

Sophisticated chemical, spectrometric, and spectroscopic methods have been developed for in situ measurements of gas-phase formaldehyde. Traditional real-time measurement technology employs Hantzsch fluorimetry. This wet-chemistry-based technique is accurate but labor and resource intensive. PTR-MS, which will be discussed in detail in the next section, can also detect formaldehyde. The formaldehyde response in PTR-MS is, however, sensitive to humidity and subject to interference from many other organic compounds which fragment as CH_3O^+ . Highly sensitive spectroscopic techniques have been developed for ambient HCHO measurement, such as laser-

induced fluorescence (LIF) and quantum cascade laser spectroscopy (QCLS). These instruments can provide high-quality scientific data with high time resolution (in seconds). All the abovementioned instruments are bulky, expensive, and often difficult to operate and to maintain. They have been used for outdoor formaldehyde measurements, but their indoor application is limited (Huangfu et al. 2019).

Alternatively, small, cheap formaldehyde sensors using either electrochemical or photoelectric photometry technologies are also available. These sensors often have poor detection limits or are subject to interferences from many other common species in the indoor air. They are mainly used for commercial purposes (e.g., home air quality monitor) and rarely for scientific research.

Here we highlight two recently developed and commercially available HCHO measurement devices, which have sufficient detection limits for indoor measurements, yet are portable and easy to operate. These techniques fall between the two extremes of measurement techniques described earlier, in term of measurement accuracy, cost, and ease of use. They are promising for monitoring formaldehyde concentrations in real time in normally occupied indoor spaces.

Formaldehyde Multimode Monitor

The formaldehyde multimode monitor (FM-801, Graywolf Sensing Solution) measures formaldehyde through colorimetric reaction. The sensor element is made of porous glass impregnated with both β -diketone and ammonium ions, which is initially colorless, turns yellow after reaction with formaldehyde (Maruo et al. 2008). The yellowing is proportional to the formaldehyde concentration and the duration of exposure, and is measured via photoelectric photometry. This device utilizes passive diffusion sampling and is normally operated at 30-min exposure times. The size is small, just slightly bigger and thicker than a smartphone.

The stated measurement accuracy of this formaldehyde monitor is ± 4 ppb for <40 ppb and $\pm 10\%$ of reading for ≥ 40 ppb for 30-min exposures. By re-zeroing between readings, the sensor cartridge is reusable within certain HCHO exposure (approximately 150×30 min tests at 80 ppb HCHO and 1000 tests at <10 ppb HCHO) and can be used for continuous monitoring for several days in normal indoor environments. The standard software for this device reports readings below 10 ppb as “ $<\text{LOD}$,” but the actual limit of detection (LOD) is down to <5 ppb. Carter et al. (2014) determined that the LOD (2σ) was 2 ppb through tests conducted in a controlled environment. As a related note, modified software is available to access readings below the nominal detection limit of 10 ppb (Singer et al. 2020).

Cross-sensitivity of this formaldehyde monitor to many other common indoor air pollutants has been systematically evaluated (Maruo et al. 2010). Interferences from most of the compounds are negligible at concentration levels well above the typical concentrations anticipated in the residential settings. The only exception is the presence of high NO₂ from use of gas cooking burner (Singer et al. 2020).

Online formaldehyde measurements using this portal device were compared with offline measurements using the DNPH methods in the laboratory settings (Carter et al. 2014), as well as in real indoor environments (Maruo et al. 2010; Nirlo et al. 2015). The reported concentrations agree within the stated accuracy in all the studies, and the correlation coefficients (R^2) were within 0.94–0.99.

MIRA Pico Formaldehyde Analyzer

MIRA Pico formaldehyde analyzer (Aries Technologies, USA) utilizes laser absorption spectroscopy to measure formaldehyde. Quantification is based on a distinct, mid-infrared “fingerprint” of formaldehyde at 2831.64 cm^{-1} . The device employs a two-inlet design and three-way valve system that allows for the measurement and subtraction of a zero during data collection. For zero measurement, the air flow is directed into the zero inlet containing an inline DNPH cartridge that filters out more than 99% HCHO. Utilizing an Aeris miniature laser-based sensor engine, the analyzer is only $30\text{ cm} \times 20\text{ cm} \times 10\text{ cm}$ in size, including a built-in pump and battery.

The stated LOD (1σ) of the device is 1 ppb for 1-s integration time. Shutter et al. (2019) evaluated its performance in reference to more established LIF instrumentation. The Aeris device displays linear behavior ($R^2 > 0.940$) when compared with both the LIF instrument from Harvard and that of NASA Goddard. The 3σ LOD for 2, 15, and 60 min integration time are 2.2, 0.7, and 0.4 ppbv HCHO, respectively. The accuracy was found to be $\pm(10\% + 0.3)$ ppbv when compared against LIF instrumentation.

Shutter et al. (2019) collocated this device and a Harvard LIF instrument in Cambridge, MA, to sample outdoor air for several days via a shared inlet line. Formaldehyde concentrations were within 1–8 ppb. The readings of the two instruments differed by less than 10%, which is consistent with the laboratory test. So far, the Aeris device has not been evaluated for indoor formaldehyde measurements yet.

Proton-Transfer-Reaction Mass Spectrometry and Other CIMS

Chemical ionization mass spectrometry (CIMS) ionizes a sample of molecules by gas-phase ion/molecular reactions and then detects the formed ions using mass spectrometry. Chemical ionization is relatively “soft,” leading to limited fragmentation. The exact masses of the product ions thus preserve the molecular composition of their parent compounds to some extent. CIMS allows for measurements of organic compounds in the air with high time response (seconds to minutes) and high sensitivity (sub-ppt to tens of ppt) and without the need for sample treatment. The specific organic species detectable by CIMS mainly depends on the reagent ion used.

Proton-transfer-reaction mass spectrometry (PTR-MS), which ionizes molecules through proton transfer reactions with the hydronium ions (H_3O^+), is the most widely used CIMS for real-time measurement of VOCs in the atmosphere. In recent

years, PTR-MS has been increasingly applied to indoor air research. This section provides a brief introduction of the PTR-MS technique and other CIMS and discusses how the CIMS technique has been used to gain new insights of the speciation, sources, chemistry, emission characteristics, and dynamic behaviors of indoor VOCs. More technical information about PTR-MS can be found in some comprehensive review articles (de Gouw and Warneke 2007; Yuan et al. 2017).

Basics of PTR-MS and Other CIMS

As illustrated in Fig. 1, the PTR-MS instrument consists of three parts: ion source, drift tube, and mass analyzer. Hydronium ions are continuously produced in the ion source and ionize organic molecules (R) in the sample air in the drift tube via proton transfer reaction:



The product ion RH^+ is then detected using a mass analyzer at the end of drift tube. Three features of Reaction (R1) make PTR-MS the most widely used CIMS technique for VOC measurements. Firstly, the reaction is thermodynamically spontaneous for any organic molecules having proton affinity greater than water (691 kJ/mol), allowing for detection of a broad range of VOCs including unsaturated hydrocarbons (except ethene) and VOCs containing oxygen, nitrogen, sulfur, halogens, and silicon, among others. Secondly, the exothermicity of the proton transfer reactions is low enough that the extent of product ion fragmentation is limited. Thus, it is possible to recognize the parent molecular species from the measured product ions. Thirdly, for most VOCs, the reaction proceeds at a rate close to the collision rate, allowing for estimating the mixing ratio of parent species from measured

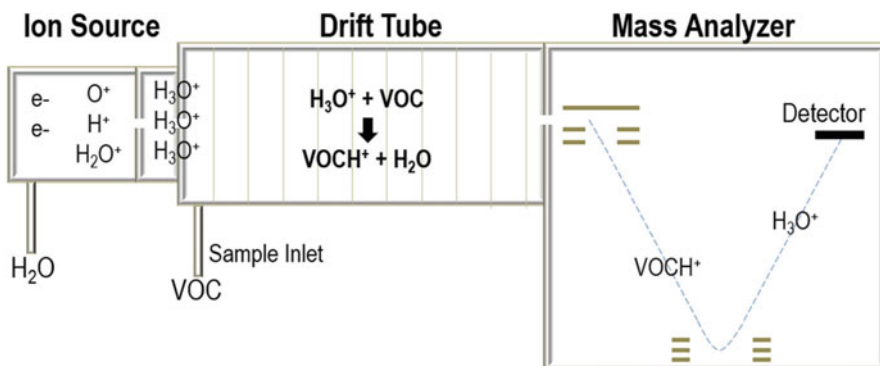


Fig. 1 Schematics of a proton transfer reaction mass spectrometer (PTR-MS) equipped with a time-of-flight detector

product ions even in the absence of standards. In PTR-MS, the reagent ions are generally present in much greater abundance than the analyte, so that we can assume the signal of produced ions is proportional to the mixing ratio of the parent compound in the sampled air.

PTR-MS was initially developed in late 1990s by Lindinger and co-workers at the University of Innsbruck in Austria, and its performance has been gradually improved over the years. There are more than ten models of PTR-MS available from several manufactures, with differing sensitivity, mass resolution, and price. One major difference among these models is the included mass spectrometer. The first-generation PTR-MS uses quadrupole mass analyzer (Lindinger et al. 1998). It only determines the mass of product ion at unit mass resolution and is thus unable to distinguish isobaric compounds (such as $\text{C}_2\text{H}_6\text{O}$ and CH_2O_2). In the late 2000s, time-of-flight (TOF) detectors, which has much higher mass resolution ($m/\Delta m > 4000$), were applied to PTR-MS, enabling resolving molecules with the same nominal mass but containing different elements (Jordan et al. 2009). More recently, long TOF detectors with even higher mass resolution ($m/\Delta m$ can reach $\sim 10,000$) are used in some advanced models (Breitenlechner et al. 2017; Krechmer et al. 2018), further improving the separation of isobaric ions. Another major improvement occurred to ion transmission efficiency from the drift tube to the mass analyzer. Ion transmission in this part strongly affects the sensitivity of the instrument. For example, the PTR-QiTof (Ionicon) using quadrupole ion guide enabled an average increase of sensitivity by a factor of 25, compared to the PTR-TOF 8000 (Ionicon) using the conventional lens system (Sulzer et al. 2014). As another improvement, new designs of the gas inlet and reaction chamber with less wall interaction have recently emerged, extending the measurable compounds from VOCs to SVOCs (Breitenlechner et al. 2017; Krechmer et al. 2018).

PTR-MS is a powerful instrument for VOC measurements, but also have some limitations. PTR-MS only obtains the mass-to-charge ratio (m/z) of the product ions. Although the combination of TOF detector and high-resolution fitting can help translate strong peaks in the mass spectra to chemical formulas without ambiguity, the chemical formula alone is a useful but by no means a unique indicator of the VOC's identity. Moreover, the interpretation of mass spectra can be further complicated by fragmentation of the product ions and formation of cluster ions. It is typically a steep learning curve to grasp data processing and interpretation of high-resolution PTR-MS spectra.

Some other CIMS instruments are also available for online measurements of organic species in the air. The positive reagent ions in addition to H_3O^+ include NH_4^+ , NO^+ , and O_2^+ . The commonly used negative reagent ions include nitrate (NO_3^-), iodide (I^-), and acetate (CH_3COO^-). Compared with H_3O^+ , most of the other reagent ions are more selective and can only ionize a subset of organic compounds with certain functional groups. O_2^+ is more energetic than H_3O^+ , but also leads to more fragmentation. Table 1 lists the analyte compound classes of individual reagent ions and references in which they are applied for real-time monitoring of indoor air.

Table 1 Common types of CIMS and compounds

Reagent ion	Analyte compound classes	Indoor application
H_3O^+	Small oxygenated compounds, polar molecules, alkenes, aromatics	See the main text
NO^+	Alcohols, substituted aromatics, cyclic and branched alkanes, long-chain semi-volatile alkanes, aldehydes and ketone (differentiating the isomers)	N.A.
O_2^+	Alkanes, carbon disulfide, ammonia, halogenated compounds	N.A.
NH_4^+	Highly functionalized VOCs, oxygenated compounds, peroxides	N.A.
NO_3^-	Polar low-volatility oxygenated compounds, strong acids (e.g., H_2SO_4)	See footnote ^a
CH_3COO^-	Carboxylic acids (except acetic acid), nitrophenols, peroxy acids, and benzoyl peroxide	See footnote ^b
I^-	Polar VOC (such as organic acid, peroxides), inorganic chlorinated compounds	See footnote ^c

^aPrice et al. (2019)^bLiu et al. (2017), Farmer et al. (2019), and Wang et al. (2020)^cWong et al. (2017), Farmer et al. (2019), Price et al. (2019), Wang et al. (2020), and Finewax et al. (2021)

Application on Real-Time Monitoring of Indoor Air

PTR-MS has been applied for time-resolved observations of speciated VOCs in a variety of indoor environments in the past 10 years. The majority of the reported observations were conducted in normally occupied public indoor spaces including a football stadium (Veres et al. 2013), a cinema (Williams et al. 2016; Stönnér et al. 2018), two classrooms (Tang et al. 2015, 2016; Liu et al. 2016), a museum (Pagonis et al. 2019; Price et al. 2019), and an athletic center (Finewax et al. 2021). Some other work extended to residential environments where people often spend most of their time. Multi-week observation campaigns were conducted in two normally occupied houses in California, USA, in 2016–2018 (Liu et al. 2019, 2021; Lunderberg et al. 2021b). More recently, similar observations were performed in two new apartment buildings in Beijing, China, for five apartments in each (Qiu et al. 2021). Moreover, extensive field experiments with scripted occupant activities were conducted in a test house in Texas, USA (Farmer et al. 2019), as well as in a rented apartment in Hong Kong, China (Lyu et al. 2021). The former study, called the House Observations of Microbial and Environmental Chemistry (HOMEChem) study, involves a large collaborative research team and an unprecedentedly large suite of online instruments.

Application of CIMS other than PTR-MS to indoor air monitoring is less. Liu et al. (2017) monitored gas-phase carboxylic acids in a university classroom using an acetate-CIMS in addition to a PTR-MS. Wong et al. (2017) and Finewax et al. (2021) observed the chemistry of chlorine-containing compounds associated with cleaning activities using iodide-CIMS in a lab and in an athletic center, respectively. In HOMEChem, several types of CIMS were deployed. These

existing studies demonstrate the feasibility and potential of using CIMS techniques for real-time monitoring in the indoor environment. On the ground of these studies, we will first summarize key technical consideration of deploying PTR-MS or other CIMS in the real indoor environment, and then discuss how the data obtained by CIMS have been analyzed to expand our understanding of organic compounds in the indoor air.

Technical Considerations of CIMS Deployment in the Indoor Environment

Space is often a key limiting factor when deploying a PTR-MS and other CIMS in the real indoor environments. A CIMS instrument and its associated gas-handling/calibration system typically occupy an area of a few square meters. The instrument often has high power consumption and generates a considerable amount of heat and its pumping system is constantly making noise. Researchers need to access the instruments periodically for calibration and maintenance. The place to house the instrument needs, therefore, to be sheltered, with stable power supply and thermal comfort for the instrument, reasonably close to the studied indoor space, and accessible by the operators without intervening the monitored indoor environment from its normal operational state. To find such an instrument location is often not easy and requires some special arrangement as well as great supports from the owner and occupants of the properties. For example, the UC Berkeley team deployed their PTR-TOF in an uncoupled garage of the first house H1 they studied (Liu et al. 2019), and then built an air-conditioned instrument shed next to the second house H2 (Lunderberg et al. 2021b). The Peking University team deployed PTR-QiTof in an unoccupied apartment to study the indoor air of some other apartments on the same building (Qiu et al. 2021). For HOMEChem, four instrument trailers were set up outside of the test house.

Depending on where the instrument locates, long sampling tubes of tens of meters are sometimes needed to draw air from the studied indoor space to the instrument. In these cases, the tubing wall effects have to be considered. For common VOCs, the degree of delay through a chemically inert PFA tube varies proportionally with tubing length and inversely with flow rate and its saturation concentration (Pagonis et al. 2017). Taking the medium-volatility VOC nonanal ($C_9H_{18}O$; with saturation concentration $C^* = 3 \times 10^6 \mu\text{g}/\text{m}^3$ at 25°C) for example, the delay through a 30-m sampling tube (1/4" OD) is estimated to be 2.4 min at flow rate of 1 L/min. Note that the tubing delay is defined as the amount of time required for the signal to achieve 90% of the total change through a tube in response to a step-function change in sample concentration. One commonly adopted approach to minimize the tubing wall effect is increasing the total flow rate through the tube. For example, air was constantly drawn through each inlet tube at a controlled flow rate of 2 L/min in addition to the sampling flow rates by the instruments (Liu et al. 2019; Qiu et al. 2021). In the case that the sampling tubing runs from the studied indoor space to outdoors then to the indoor space housing the instrument, we also need to consider temperature gradient the sample air might experience and the associated problems. For example, large temperature drop outdoors at night might lead to

enhanced wall effects and even condensation. Heating and insulating the outdoor sections of the sampling tubes can help to avoid these issues.

A useful sampling strategy of PTR-MS in indoor air research is partially transforming its strength of fast time response to gain information of spatial variability. This can be achieved by setting up multiple inlets to differing locations and automatically switching between them. The most widely used is two-inlet setup, i.e., alternatively sampling from room air and supply/outdoor air. Six-inlet setup is also reported. In the study of California houses, PTR-TOF sequentially sampled from the kitchen, bedroom area, basement, crawl space, attic, and outdoors in 30-min cycles, with each location for 5 min (Liu et al. 2019). In the study of apartments in Beijing, air was sequentially sampled from 4 to 5 apartments (1 or 2 locations in each apartment) of the same building and outdoors in 30-min cycles (Qiu et al. 2021). In these cases, the time resolution at each measurement location dropped to 30 min, but the number of measured places greatly expanded.

Data Analysis Providing New Scientific Understanding

The data obtained by PTR-MS are featured of good chemical specificity and high time resolution. They can also be spatially resolved depending on the experimental design. The data set from a single instrument is often already 2- or 3-dimensional “big data.” There can be many different ways to extract new scientific understandings from the big data. Below we will present some directions to explore the data based on the existing literature.

VOC speciation. The high-resolution PTR-MS spectra using TOF detector or long TOF detector contain rich information of VOC speciation. From the hundreds of VOC signals detected simultaneously, it is possible to identify some important VOC species that are not normally considered. For example, Tang et al. (2015) noticed clusters of ions present at high intensity in the range of 300–500 m/z on their PTR-TOF spectra measured in a university classroom (abundant ions were not expected to appear in this mass range based on prior outdoor VOC measurements). They eventually attributed these ions to cyclic volatile methylsiloxanes. Their finding that siloxanes were the most abundant VOCs emitted from engineering students in the classroom aroused wide attention to chemical emissions from personal care products. More recently, Qiu et al. (2021) observed unexpected high signals of $C_xH_{2x-1}O_4^+$ and $C_xH_{2x-3}O_3^+$ ions ($x = 6–9$) in three out of ten new apartments in Beijing (note that organic compounds containing three or four oxygen typically fragment extensively in PTR-MS). By trial and error, the authors eventually attributed these signals to dimethyl esters (DBEs), a solvent mixture of dimethyl esters of succinic, glutaric, and adipic acids ($C_xH_{2x-2}O_4$, where $x = 6–9$). DBEs have been increasingly used in the coating industry, but are rarely known for their occurrence in the indoor air. In the study, the measured indoor DBE concentrations in all three apartments exceeded the screening level recommended by the Michigan Department of Environmental Quality, USA, suggesting that DBEs might emerge as potential indoor pollutants that merit further attention.

While most existing analyses of PTR-MS data focus on selected abundant ions (compounds), some work tried to perform full-spectrum, non-targeted analyses to

make maximum use of obtained VOC speciation information (Tang et al. 2016; Liu et al. 2019; Lunderberg et al. 2021b). Liu et al. (2019) reported that 656 mass peaks were detected in the PTR-TOF spectra of normally occupied house H1 in California in the summer campaign and 661 in the winter campaign. They eventually extracted 218 VOC signals (organic ion formulas) to represent measured VOC speciation in the summer and 171 in the winter after extensive quality control procedures. These procedures included removing background ions predominantly arising from the instrument and from tubing, assigning chemical formulas based on exact masses of the ions, combining isotopic ions and identified fragment ions, removing interference ions, tracer ions, sticky ions, and inorganic ions, and applying an abundance threshold of >5 ppt. Although substantial amount of time and effort is needed to do this kind of full spectra analysis, the obtained VOC speciation information, in addition to their temporal and spatial variation, forms basis of comprehensive analysis of overall feature of VOC emission and exposure which have never been conducted before (Liu et al. 2019; Lunderberg et al. 2021a, b).

Temporal variation of observed VOC signals. High time resolution is a key advantage of PTR-MS and other CIMS instruments. Temporal variation of the mixing ratios of organic species is often indicative of their emission sources. The first few studies using PTR-MS for real-time monitoring were conducted in built environments regularly occupied by large numbers of people, such as football stadiums, cinema, and classrooms. These studies highlight the magnitude of various impacts human beings have on the VOC composition in their immediate environment. Veres et al. (2013) reported that the mixing ratios of many VOCs increased by more than two times inside Coface Arena in Mainz, Germany, during a football match in the presence of $\sim 31,000$ attendees. The temporal pattern of these VOCs generally followed enhancement of CO₂ concentration attributable to human exhaled breath. Based on the detailed temporal pattern, several distinct source categories were identified, including human respiration, ozonolysis of skin oils, and cigarette smoke/combustion. Liu et al. (2016) applied positive matrix factorization to the unit-resolution mass spectral data of PTR-MS observed in a university classroom, and detected a “human influence” component that varied with level of occupancy and with ventilation in a manner analogous to CO₂. They found that this factor contributed to 40% of the measured daytime VOC concentration in the classroom. Williams et al. (2016) carefully examined the high time resolution (30 s) data measured in a cinema, found that many VOCs in cinema air varied distinctively and reproducibly with time for a particular film, suggesting that the chemical composition of breath emission of cinema audience vary in response to audiovisual cues.

In the non-targeted VOC analysis in normally occupied residence H1, Liu et al. (2019) summarized that the time series of observed VOCs in the living zone was generally characterized by clear short-term enhancements (spikes) on top of more slowly varying baseline levels. The short-term spikes were associated with occupants and their activities. Figure 2 illustrates the time series of kitchen concentrations for selected compounds on one particular day along with recorded occupant activities. Different VOC species spiked as the occupants toasted bread and made coffee

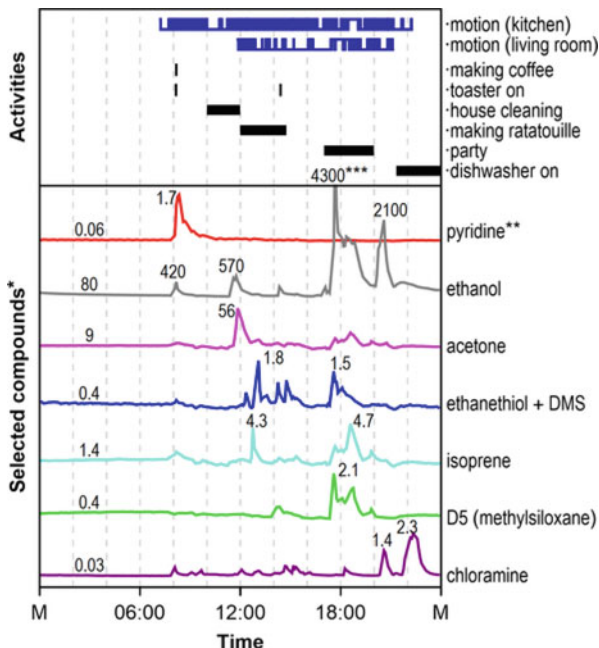


Fig. 2 Time series on a selected day of (top) activities recorded by sensors and occupants and (bottom) kitchen concentrations of selected compounds. Selected compounds (associated major ions) include pyridine ($C_5H_5N^+$), ethanol ($C_2H_5O^+$), acetone ($C_3H_7O^+$), ethanethiol + dimethyl sulfide (DMS; $C_2H_7S^+$), isoprene ($C_5H_9^+$), methylsiloxane D5 ($C_{10}H_{31}O_5Si_5^+$), and chloramine (H_3NCl^+). *Background and peak concentrations (in ppb) of each compound are noted. **Pyridine appeared sticky in our inlet system and consequently the peak signal represents a lowerbound estimate. ***Peak value out of plot range. (Adopted from Liu et al. 2019)

for breakfast, cleaned the floor and made ratatouille during the day, hosted a party in the evening, and then washed the dishes at night. Based on these features, the authors developed further statistical analysis to identify prominent VOC-emitting activities as well as VOC species dominantly contributed by activity emissions. They counted the number of spiked VOC signals in each hour and examined the averaged diel variation during the summer and winter campaigns, respectively. The number of spiked signals peaked at breakfast and at dinner time in both campaigns and the diel pattern resembles remarkably that of stove burner use, which serves as a proxy indicator for cooking activities. This spike analysis strongly suggests that cooking activities made a major contribution to occupant-associated intermittent VOC emissions at least in the studied house. Based on the observation that the presence of spikes in a concentration time series can increase the mean across the whole observational period, but has less effect on the median, the authors took the mean-to-median concentration ratio as a quantitative indicator of the relative importance of occupant-related emissions for a given compound. The analysis identified a range of

compounds with major (dominant) contributions from occupant activities, such as ethanol (beer and wine, toasting bread and other cooking, cleaning), monoterpenes (citrus fruits, cooking, cleaning), pyrrole (making coffee, cooking), D5 and D6 (use of personal care products). More importantly, the analysis suggests that for the majority of VOCs, intermittent event emissions were not their major source. Based on supplementary spatial distribution of VOC signals, the dominant sources were instead continuous emissions into the living space from building material and furnishing.

In addition to the observational studies in normally occupied spaces, experimental studies were also conducted to directly examine how various scripted occupant activities impact indoor VOC composition in a test house in the USA and a rented apartment in Hong Kong (Farmer et al. 2019; Lyu et al. 2021). Investigated activities include cooking, cleaning, incense/candle burning, smoking, painting, and enhanced ventilation. A particularly noteworthy finding is regarding the dynamic gas-surface partitioning of organic species. As a part of HOMEChem, Wang et al. (2020) explored the dynamic response of 19 common indoor air contaminants in sequential enhanced-ventilation experiments using PTR-TOF and some other CIMS. Figure 3 shows the observed time series of selected compounds. By fitting exponential growth curves to the time series data, they determined for each compound the dynamic response time length needed to reestablish steady-state conditions after ventilation perturbations. The derived time constants for all small acids and for phenol were similar, on average, between 700 and 1000 s, much smaller than the reciprocal of air exchange rate (~ 3600 s). This observation, combined with the consistently high response signals, for the first time suggests that there are large weakly polar and polar absorptive surface reservoirs in the studied indoor environment.

Spatial variation of observed VOC signals. When PTR-MS was used to alternatively measure indoor and outdoor/supply air, we can tell directly from the indoor-to-outdoor (I/O) ratio whether an organic species is mainly of indoor or outdoor origin. For >75% of the ~200 measured VOC signals in a house in northern California, the average living-zone concentrations were more than 5 times higher than outdoors ($I/O > 5$) (Liu et al. 2019). For about half of the VOC signals, the difference was at least one order of magnitude ($I/O > 10$). The implication is that the major sources of VOCs in the living zone were emissions directly into the living zone.

More detailed spatial information of VOC species might help better constrain the sources. For the abovementioned house, the authors found that the I/O ratio of some VOC signals in the attic can be 4–10 times higher than the transport-focused predictions, suggesting strong direct emission sources into the attic (Liu et al. 2019). Given that the attic was unoccupied and unfinished, the emission was attributed to emission from wooden building materials. Based on the chemical speciation information of VOCs featured of elevated attic I/O ratio, the authors further hypothesized that these compounds are at least partly volatile products from wood decomposition.

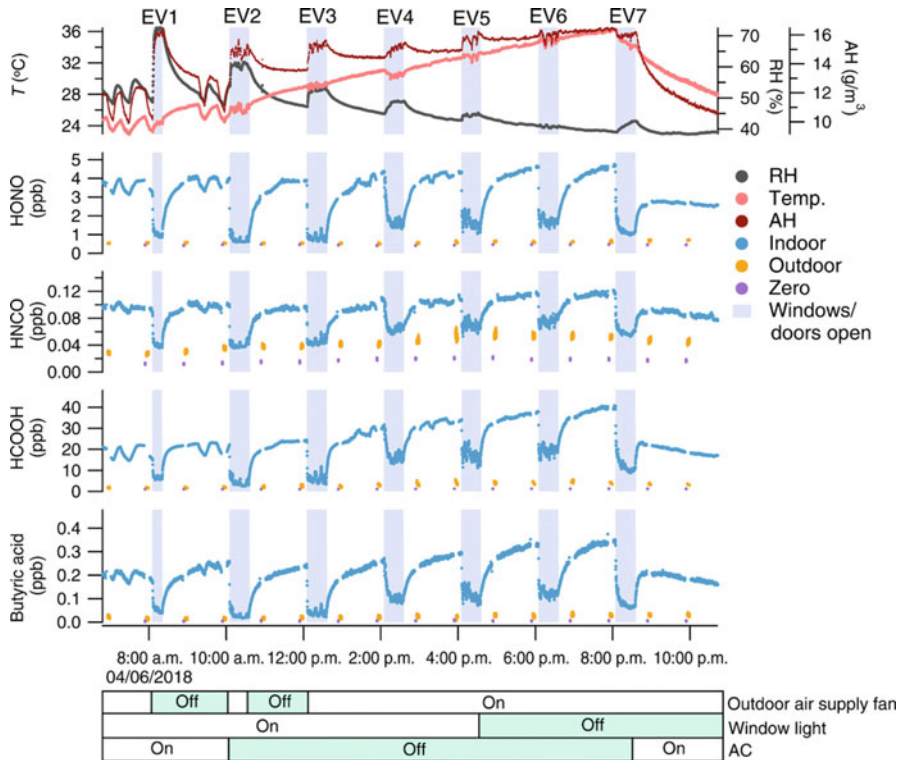


Fig. 3 Indoor mixing ratios of several acids during extensive ventilation experiments during HOMEChem campaigns. The top panel shows the measured house temperature (T ; left axis), relative humidity (RH; right axis), and absolute humidity (AH; second right axis). The shaded areas indicate when doors and windows were open to increase the ventilation rate of the house. The hourly 2-min background measurement (measuring zero air) is shown with purple dots, followed by a 5-min outdoor measurement (orange dots). The average air exchange rate (AER) when the house is closed was about 0.5 h. The color bars at the bottom of the plot show the state of outdoor air supply fan (on/off), window light (with/without), and air conditioning (AC) (on/off) during the experiment, with the green shaded periods showing when the fan, window light, and AC were off. (Adopted from Wang et al. 2020)

Temporal variation of indoor source rate of VOCs. Temporal variation of VOC concentrations reflects the dynamic behavior of its source strength, but is also subject to variation of the air exchange rate among other factors. To obtain more quantitative understanding of VOC source characteristics, we can determine time-resolved indoor source strength from measured time evolution of indoor and outdoor concentrations based on a mass balance analysis. Assuming that the internal volume of an indoor space can be effectively considered as well-mixed, the indoor mass balance of a VOC can be represented by the following equation

$$\frac{dC_{in}}{dt} V = \frac{E}{\rho} - A \cdot (C_{in} - C_{out}) \cdot V \quad (1)$$

where $C_{\text{in}} = C_{\text{in}}(t)$ and $C_{\text{out}} = C_{\text{out}}(t)$ are the concentrations indoors and outdoors (ppb; part per billion by volume); V is the volume of the living zone (m^3); $E = E(t)$ is the net indoor source rate (mg/h); ρ is the gas density for the compound (mg/mm^3); and $A = A(t)$ is the air exchange rate (h^{-1}). Treating $A(t)$ and $E(t)$ as constant over each interval of Δt [$t, t + \Delta t$], we obtain the following approximation for E by integrating Eq. (1):

$$E = \rho V \left(\frac{C_{\text{in}}(t + \Delta t) - C_{\text{in}}(t)}{\Delta t} + A \cdot (\overline{C_{\text{in}}} - \overline{C_{\text{out}}}) \right), \quad (2)$$

where $\overline{C_{\text{in}}}$ and $\overline{C_{\text{out}}}$ are the time averages over $[t, t + \Delta t]$ of C_{in} and C_{out} , respectively. Note that this equation is a simplified representation, the determined E is a net value, incorporating not only indoor emissions and chemical production but also indoor wall interactions and possible indoor losses from chemical reactions.

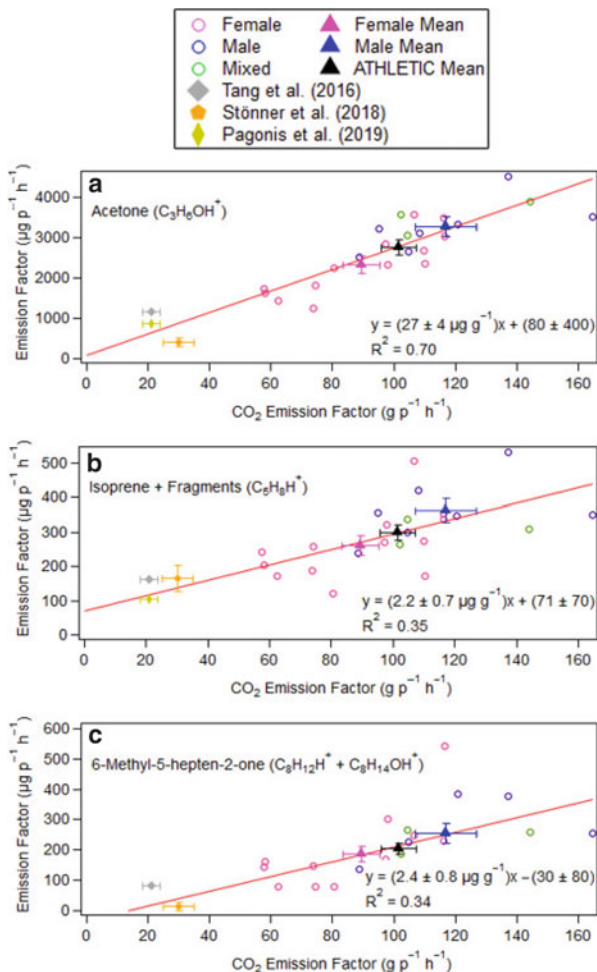
In use of Eq. (2), we need to take a Δt value at least a few times larger than the time resolution of C_{in} and C_{out} measurements. We also need to know $A(t)$. A constant value can be assumed for air exchange rate in the case of public indoor space with dominant mechanical ventilation. In naturally ventilated space, air exchange rates can vary greatly with time and have been to be determined in real time. In this regard, a tracer methods based on selected deuterated alkenes, which are measurable by PTR-TOF, has been developed to quantify air exchange rate in normally occupied indoor spaces (Liu et al. 2018).

For indoor spaces that are intermittently occupied by a large number of people, per-person emission factors ($\mu\text{g}/\text{p/h}$) for human-derived VOCs can be estimated by taking the difference of emission rate when occupied (E_{occ}) and that when vacant (E_{vac}) and then dividing by the occupancy level. Per-person emission factors for a range of VOCs such as isoprene, acetone, and 6-methyl-5-hepen-2-one (6-MHO) have been calculated in this way in a classroom, a cinema, a museum, and an athletic center (Tang et al. 2016; Stönnér et al. 2018; Pagonis et al. 2019; Finewax et al. 2021). As shown in Fig. 4, Finewax et al. found that the emission factors of many compounds increase with the level of physical exercise, indicated by the emission factor of CO_2 . The obtained emission factors can be useful parameters to model occupants' influence to indoor air quality.

The observation-derived source rate has also been used to quantitatively understand indoor ozone chemistry (Liu et al. 2021). As shown in Fig. 5, source strength of the featured skin oil oxidation product 6-MHO exhibited a high correlation with indoor ozone concentration in a house normally occupied by a couple, the fitted intercept (baseline emission) was small compared with the range of fitted slope times indoor ozone (ozone-dependent production), confirming that ozone reaction was indeed the major source of 6-MHO. In addition, the source strength in the episodic presence of a larger number of occupants appeared above the trend line, consistent with the expectation that human skin oil is the precursor. An unexpected observation in this study presents ozone chemistry during vacancy. The author analyzed a subset of data from Fig. 5a with indoor ozone concentration restricted to a small range of 2–4 ppb, as shown in Fig. 5b. They found that the source strength did not exhibit

Fig. 4 VOC vs. CO₂ emission factors for individual exercise sessions (open circles) in an athletic center. From top to bottom shows acetone (C₃H₆OH⁺) and 6-methyl-5-hepten-2-one (6-MHO, C₈H₁₂H⁺ + C₈H₁₄OH⁺), respectively. Open circle markers in pink represent exercise events with at least 75% females, blue open circle markers were exercise events with at least 75% males, and green data points contain less than 75% females or males. The ATHLETIC mean is the mean for all campaign data points. Error bars are standard errors for each dataset.

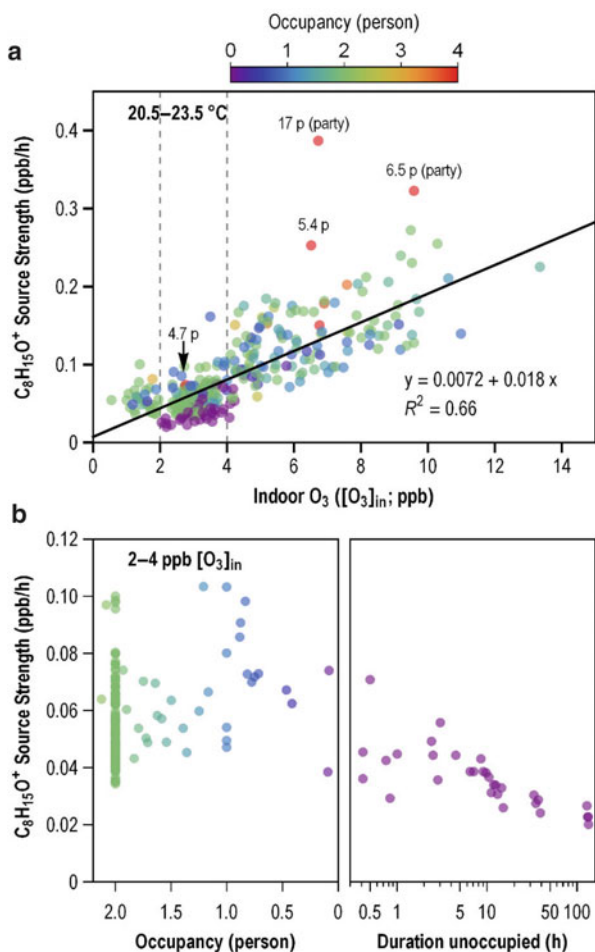
(Adopted from Finewax et al. 2021)



discernable change with the occupancy level ($0 < \text{occupancy} \leq 2$ persons), and diminished only by about half from when the house was unoccupied for ~ 130 h. Given that the reaction between ozone and 6-MHO is fast and there are low baseline emissions (i.e., small intercept in Fig. 5a), it is unlikely that surface reservoirs were a substantial source of 6-MHO during the unoccupied period. Instead the more probable explanation is that ozone reacted with squalene in skin flakes and skin oils that had accumulated on exposed surfaces in the home. The inferred contribution of off-body skin oil/flakes to 6-MHO source strength during normal occupancy (0.045 ppb/h) was substantially larger than the contribution from the body envelopes of the occupants (~ 0.011 ppb/h).

As a further note, based on the same set of data, Liu et al. (2019) found that the emission rates of VOC species that have a dominant contribution from building-related

Fig. 5 Dependence of $C_8H_{15}O^+$ (6-MHO) source strength on (a) indoor ozone concentration and (b) occupancy. (a) Shows all available data using 2-h resolution and restricted to an indoor temperature range of 20.5–23.5 °C. (b) Uses a subset of data in a (bounded by dashed lines, with indoor ozone of 2–4 ppb) and plots $C_8H_{15}O^+$ source strength versus occupancy for $2 \geq \text{occupancy} > 0$ (Left) and versus unoccupied time duration for occupancy = 0 (Right), respectively. In a, the black line shows a linear fit of data after excluding outliers of $C_8H_{15}O^+$ source strength (greater than upper quartile plus $3 \times$ interquartile range); exact occupancy level was labeled for occupancy > 4 . Occupancy level represents the average for the 2-h integration period and so can be a noninteger value when occupants are present for only part of the interval. (Adapted from Liu et al. 2021)



sources exhibited strong temperature dependence. The summed emission rate of all the species increased with temperature in each season as well as across the two seasons. The value at 23 °C was about twice of that at 16 °C. Similar temperature dependencies were evident for most individual ions/groups of ions, such as acetic acid.

Exposure assessment. Human exposure to VOCs has been difficult to characterize, because both VOC concentrations and indoor occupancy vary rapidly. The CIMS instruments make high-resolution exposure assessment of VOCs possible. Lunderberg et al. (2021b) report time-resolved exposures from multi-season sampling of more than 200 VOCs in two California residences. Chemical-specific source apportionment revealed that time-averaged exposures for most VOCs were mainly attributable to continuous indoor emissions from buildings and their static contents.

Also contributing to exposures were occupant-related activities, such as cooking, and outdoor-to-indoor transport. Health risk assessments are possible for a subset of the observed VOCs. Acrolein, acetaldehyde, and acrylic acid concentrations were above chronic advisory health guidelines, whereas exposures for other assessable species were typically well below the guideline levels. In a separate paper, Lunderberg et al. (2021a) evaluated residential intake fractions (iF, mass inhaled by an individual per unit mass emitted) for indoor VOC releases. Despite that emission patterns varied between compounds, all VOC-specific iF estimates were clustered near the values of the living space tracer gases ($iF \sim 0.3\% = 3000 \text{ ppm}$). These experimental observations substantiate the theoretical expectation that iF values are largely independent of analyte characteristics, a useful simplification for exposure assessments.

Automated GC

Automated gas-chromatography systems are also available for real-time measurements of organic species. The analysis typically begins with a sample collection and pre-concentration step, followed by rapid heating of the sample, and detection by standard gas chromatographic methods. Limited by the time length required for gas chromatography analysis, the time resolution of these instruments ranges typically from 30 min to 1 h. Compared with CIMS, the time resolution of GC-based online instruments is much lower, but the chemical specificity can be better.

Many research groups have assembled their own automated GC systems for VOC measurements, and a variety of such systems are also commercially available. Major differences among the various automated GC systems lie in the pre-concentration techniques and the columns and detectors. The commonly used pre-concentration techniques include cryogenic trapping, sorbent enrichment, and a combination of these two methods. Solid adsorbents have been proven reliable for concentrating certain compounds, but for some other compounds, there can be substantial artifact formation and compound losses during the sample enrichment and desorption processes (Apel et al. 2003). Liquid nitrogen is often used for cryogenic trapping in the laboratory setting, but its application is limited in field studies by the use and availability of large volumes of liquid nitrogen. Cryogen-free cooling devices that can create liquid-nitrogen equivalent trapping condition have also been developed for pre-concentration (Sive et al. 2005; Wang et al. 2014). These devices utilize multicomponent mixed refrigerant in a cascade refrigeration cycle, which is closely related to the refrigeration system of a home refrigerator. Many automated GC systems employ multiple sets of separation columns and detectors to expand the range of compounds measurable by the instrument. For example, Sive et al. (2005) used two flame ionization detectors (FID), one electron capture detector (ECD), and one mass spectrometers to measure C3–C7 and C5–C10 nonmethane hydrocarbons, halocarbons, alkyl nitrates, and oxygenated VOCs in 40-min time resolution. Each detector was connected to a separate column optimized for measurements of a set of compounds. The four columns were housed in the same GC oven and ran in parallel.

Abeleira et al. (2017) employed 3 FIDs and 1 ECD to measure 46 individual VOCs including C₂–C₈ nonmethane hydrocarbons, C₁–C₂ halocarbons, C₁–C₅ alkyl nitrates, and several OVOCs with hourly time resolution. These online GC systems have been widely used in atmospheric research, but their application in the indoor air study is limited. To our knowledge, the only reported deployment is during HOMEChem (Farmer et al. 2019).

An automatic GC system for SVOC measurements, semi-volatile thermal desorption aerosol gas chromatograph (SV-TAG), has also been developed (Zhao et al. 2013). The key component of SV-TAG is a high-surface-area passivated stainless steel fiber filter that quantitatively collects both gas- and particle-phase organic compounds less volatile than tetradecane (C₁₄H₃₀). A separation between gas- and particle-phase collection can be determined through a difference method by periodically sampling ambient air through a multichannel charcoal denuder that efficiently removes gas-phase compounds. Samples collected on the filter are desorbed with a ramped temperature into helium saturated with a trimethylsilylation agent *N*-methyl-*N*-(trimethylsilyl) trifluoroacetamide (MSTFA), allowing for online derivatization of the otherwise non-elutable organic chemicals with hydroxyl groups (Isaacman et al. 2014). SV-TAG employs an automatic injection system which can introduce liquid stands to the collection cell reproducibly and thereby achieve in situ calibration (Isaacman et al. 2011). Moreover, in SV-TAG, a valveless sample introduction interface replaces the traditional multiport valve, offering the advantage of long-term reliability and stable sample transfer efficiency under high operation temperature (Kreisberg et al. 2014). Although SV-TAG is more recently developed compared with the GC system for VOC measurements, it has been applied to the observation campaign in a single-family house H2 in north California (Kristensen et al. 2019), as well as to the HOMEChem campaign (Lunderberg et al. 2020).

Kristensen et al. (2019) provides an overview of SV-TAG measurements in H2. Figure 6 shows TIC chromatograms from typical SV-TAG gas-plus-particle sample analyses for several representative cases: outdoor air, indoor air during normal occupancy with no activity, indoor air during cleaning, and indoor air during a cooking event. A large difference both in chemical complexity and in the abundance of SVOCs is consistently observed between indoor and outdoor air, even without contributions from occupant activities. In addition, relative to the baseline indoor condition, both cleaning and cooking activities enhanced the signal intensity. The enhancement is more substantial during cooking, with many new compounds appearing at longer retention time (i.e., with lower volatility), such as straight-chained saturated and unsaturated fatty acids, monoglycerides, and sterols. In comparison, cleaning activities is featured of more volatile compounds such as nonanal and terpineol.

Kristensen also explored the overall features of SVOC dynamics and gas/particle partitioning in the studied house. For the majority of the campaign, gas-phase SVOCs accounted for more than 90% of the total airborne (gas-plus-particle) SVOC concentrations in this residence. However, measurement of the SVOC gas/particle distributions revealed higher contributions of low volatility particle-bound organics during

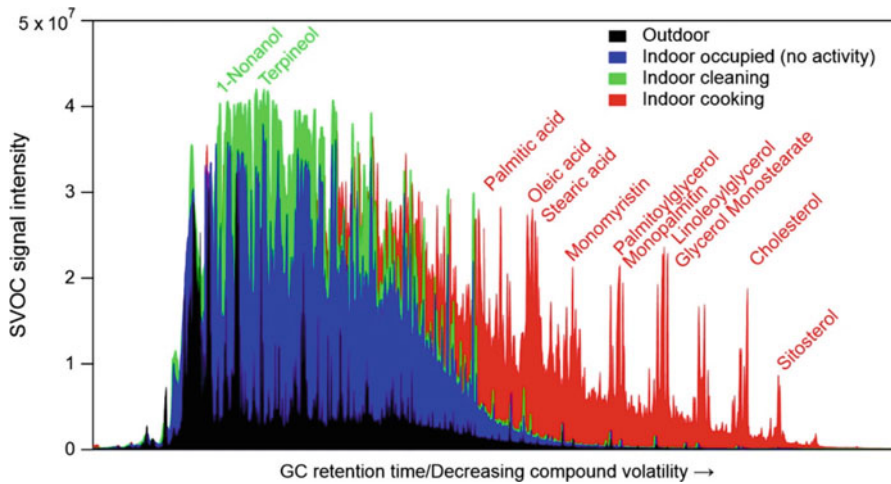


Fig. 6 Total ion chromatograms from SV-TAG analysis of gas-plus-particle samples from outdoor (black), indoor occupied (no activity, blue), cleaning (green), and cooking (red). Compounds associated with the biweekly cleaning (1-nonanol, terpineol) are labeled as well as carboxylic acids (palmitic acid, oleic acid, steric acid), glycerols (linoleoyl glycerol, palmitoyl glycerol, monomyristin, monopalmitin, monostearin), and sterols (cholesterol and sitosterol) identified in the indoor air during cooking activities. (Adopted from Kristensen et al. 2019)

cooking events along with evidence of cooking-associated enhancement of the partitioning into the particle phase of many semi-volatile species responding to the increased indoor particle mass concentrations. The total airborne SVOC concentration shows a positive temperature dependence during both occupied and vacant periods, suggesting that temperature-modulated emissions and/or partitioning with indoor surfaces is a key component of indoor SVOC dynamics.

Based on the same data set, Lunderberg et al. (2019) looked into the dynamic behavior of a specific class of SVOCs, phthalate diesters. They found that concentrations of higher vapor pressure phthalates correlated well with indoor temperature, with little discernible influence from direct occupant activity. Conversely, occupant activities substantially influenced the concentrations and dynamics of a lower vapor pressure compound, diethylhexyl phthalate (DEHP), mainly through production of particulate matter during cooking events.

Lunderberg et al. (2020) further combined the data set from the H2 campaign and that from HOMEChem campaign to show that surface emissions modulate indoor SVOC concentrations through volatility-dependent partitioning. For SVOCs with vapor pressures in the range of C13–C23 alkanes, airborne concentrations in H2 were observed to be correlated with indoor air temperature. Observed temperature dependencies were quantitatively similar to theoretical predictions that assumed a surface-air boundary layer with equilibrium partitioning maintained at the air-surface interface. For SVOCs with vapor pressures corresponding to C25–C31 alkanes, airborne concentrations correlated with airborne particle mass concentration. During

HOMEChem, lower-volatility siloxanes exhibited ongoing emissions after a high emission event associated with oven use in the “Thanksgiving” experiment. In particular, the airborne concentration siloxanes became elevated during the cooking events without oven use on the next day. The suggestion is that the siloxanes emitted from a primary source can be deposited throughout a residence and then reemitted during subsequent particle loading events.

Conclusions

In summary, research-grade online instruments are now available to realize real-time monitoring of volatile and semi-volatile organic compounds in the indoor environment. The pioneering efforts towards this direction in the past decade have demonstrated that the time-resolved measurement data are very useful for investigating the dynamic behaviors of organic compounds in the indoor air and the underlying mechanisms. There is still much more we can learn from the real-time measurements and the resultant big data. Meanwhile, since the available online instruments are expensive, there is also a need for more cost-effective instruments that would permit more widespread measurements to be made.

References

- Abeleira A, Pollack IB, Sive B et al (2017) Source characterization of volatile organic compounds in the Colorado Northern Front Range Metropolitan Area during spring and summer 2015. *J Geophys Res Atmos* 122:3595–3613. <https://doi.org/10.1002/2016JD026227>
- Apel EC, Calvert JG, Gilpin TM et al (2003) Nonmethane hydrocarbon intercomparison experiment (NOMHICE): task 4, ambient air. *J Geophys Res Atmos* 108:4300. <https://doi.org/10.1029/2002JD002936>
- Breitenlechner M, Fischer L, Hainer M et al (2017) PTR3: an instrument for studying the lifecycle of reactive organic carbon in the atmosphere. *Anal Chem* 89:5824–5831. <https://doi.org/10.1021/acs.analchem.6b05110>
- Carter EM, Jackson MC, Katz LE, Speitel GE (2014) A coupled sensor-spectrophotometric device for continuous measurement of formaldehyde in indoor environments. *J Expo Sci Environ Epidemiol* 24:305–310. <https://doi.org/10.1038/jes.2013.61>
- de Gouw J, Warneke C (2007) Measurements of volatile organic compounds in the Earth’s atmosphere using proton-transfer-reaction mass spectrometry. *Mass Spectrom Rev* 26:223–257. <https://doi.org/10.1002/mas.20119>
- Farmer DK, Vance ME, Abbatt JPD et al (2019) Overview of HOMEChem: house observations of microbial and environmental chemistry. *Environ Sci Process Impacts* 21:1280–1300. <https://doi.org/10.1039/C9EM00228F>
- Finewax Z, Pagonis D, Clafin MS, et al (2021) Quantification and source characterization of volatile organic compounds from exercising and application of chlorine-based cleaning products in a university athletic center. *Indoor Air* 31:1323–1339. <https://doi.org/10.1111/ina.12781>
- Huangfu Y, Lima NM, O’Keeffe PT et al (2019) Diel variation of formaldehyde levels and other VOCs in homes driven by temperature dependent infiltration and emission rates. *Build Environ* 159:106153. <https://doi.org/10.1016/j.buildenv.2019.05.031>

- Isaacman G, Kreisberg NM, Worton DR et al (2011) A versatile and reproducible automatic injection system for liquid standard introduction: application to in-situ calibration. *Atmos Meas Tech* 4:1937–1942. <https://doi.org/10.5194/amt-4-1937-2011>
- Isaacman G, Kreisberg NM, Yee LD et al (2014) Online derivatization for hourly measurements of gas- and particle-phase semi-volatile oxygenated organic compounds by thermal desorption aerosol gas chromatography (SV-TAG). *Atmos Meas Tech* 7:4417–4429. <https://doi.org/10.5194/amt-7-4417-2014>
- Jordan A, Haidacher S, Hanel G et al (2009) An online ultra-high sensitivity proton-transfer-reaction mass-spectrometer combined with switchable reagent ion capability (PTR+SRI-MS). *Int J Mass Spectrom* 286:32–38. <https://doi.org/10.1016/j.ijms.2009.06.006>
- Krechmer J, Lopez-Hilfiker F, Koss A et al (2018) Evaluation of a new reagent-ion source and focusing ion-molecule reactor for use in proton-transfer-reaction mass spectrometry. *Anal Chem* 90:12011–12018. <https://doi.org/10.1021/acs.analchem.8b02641>
- Kreisberg NM, Worton DR, Zhao Y et al (2014) Development of an automated high-temperature valveless injection system for online gas chromatography. *Atmos Meas Tech* 7:4431–4444. <https://doi.org/10.5194/amt-7-4431-2014>
- Kristensen K, Lunderberg DM, Liu Y et al (2019) Sources and dynamics of semivolatile organic compounds in a single-family residence in northern California. *Indoor Air* 29:645–655. <https://doi.org/10.1111/ina.12561>
- Lindinger W, Hansel A, Jordan A (1998) On-line monitoring of volatile organic compounds at pptv levels by means of proton-transfer-reaction mass spectrometry (PTR-MS) - medical applications, food control and environmental research. *Int J Mass Spectrom* 173:191–241
- Liu S, Li R, Wild RJ et al (2016) Contribution of human-related sources to indoor volatile organic compounds in a university classroom. *Indoor Air* 26:925–938. <https://doi.org/10.1111/ina.12272>
- Liu S, Thompson SL, Stark H et al (2017) Gas-phase carboxylic acids in a university classroom: abundance, variability, and sources. *Environ Sci Technol* 51:5454–5463. <https://doi.org/10.1021/acs.est.7b01358>
- Liu Y, Misztal PK, Xiong J et al (2018) Detailed investigation of ventilation rates and airflow patterns in a northern California residence. *Indoor Air* 28:572–584. <https://doi.org/10.1111/ina.12462>
- Liu Y, Misztal PK, Xiong J et al (2019) Characterizing sources and emissions of volatile organic compounds in a northern California residence using space- and time-resolved measurements. *Indoor Air* 29:630–644. <https://doi.org/10.1111/ina.12562>
- Liu Y, Misztal PK, Arata C et al (2021) Observing ozone chemistry in an occupied residence. *Proc Natl Acad Sci U S A* 118:e2018140118. <https://doi.org/10.1073/pnas.2018140118>
- Lunderberg DM, Kristensen K, Liu Y et al (2019) Characterizing airborne phthalate concentrations and dynamics in a normally occupied residence. *Environ Sci Technol* 53:7337–7346. <https://doi.org/10.1021/acs.est.9b02123>
- Lunderberg DM, Kristensen K, Tian Y et al (2020) Surface emissions modulate indoor SVOC concentrations through volatility-dependent partitioning. *Environ Sci Technol* 54:6751–6760. <https://doi.org/10.1021/acs.est.0c00966>
- Lunderberg DM, Liu Y, Misztal PK et al (2021a) Intake fractions for volatile organic compounds in two occupied California residences. *Environ Sci Technol Lett* 8:386–391. <https://doi.org/10.1021/acs.estlett.1c00265>
- Lunderberg DM, Misztal PK, Liu Y et al (2021b) High-resolution exposure assessment for volatile organic compounds in two California residences. *Environ Sci Technol* 55:6740–6751. <https://doi.org/10.1021/acs.est.0c08304>
- Lyu X, Huo Y, Yang J et al (2021) Real-time molecular characterization of air pollutants in a Hong Kong residence: implication of indoor source emissions and heterogeneous chemistry. *Indoor Air*. <https://doi.org/10.1111/ina.12826>

- Maruo YY, Nakamura J, Uchiyama M (2008) Development of formaldehyde sensing element using porous glass impregnated with β -diketone. *Talanta* 74:1141–1147. <https://doi.org/10.1016/j.talanta.2007.08.017>
- Maruo YY, Yamada T, Nakamura J et al (2010) Formaldehyde measurements in residential indoor air using a developed sensor element in the Kanto area of Japan. *Indoor Air* 20:486–493. <https://doi.org/10.1111/j.1600-0668.2010.00670.x>
- Nirlo EL, Crain N, Corsi RL, Siegel JA (2015) Field evaluation of five volatile organic compound measurement techniques: implications for green building decision making. *Sci Technol Built Environ* 21:67–79. <https://doi.org/10.1080/10789669.2014.969172>
- Pagonis D, Krechmer JE, de Gouw J et al (2017) Effects of gas-wall partitioning in Teflon tubing and instrumentation on time-resolved measurements of gas-phase organic compounds. *Atmos Meas Tech* 10:4687–4696. <https://doi.org/10.5194/amt-10-4687-2017>
- Pagonis D, Price DJ, Algrim LB et al (2019) Time-resolved measurements of indoor chemical emissions, deposition, and reactions in a university art museum. *Environ Sci Technol* 53:4794–4802. <https://doi.org/10.1021/acs.est.9b00276>
- Price DJ, Day DA, Pagonis D et al (2019) Budgets of organic carbon composition and oxidation in indoor air. *Environ Sci Technol* 53:13053–13063. <https://doi.org/10.1021/acs.est.9b04689>
- Qiu J, Xie D, Li Y et al (2021) Dibasic esters observed as potential emerging indoor air pollutants in new apartments in Beijing, China. *Environ Sci Technol Lett* 8:445–450. <https://doi.org/10.1021/acs.estlett.1c00198>
- Salthammer T, Mentese S, Marutzky R (2010) Formaldehyde in the indoor environment. *Chem Rev* 110:2536–2572. <https://doi.org/10.1021/cr800399g>
- Shutter JD, Allen NT, Hanisco TF et al (2019) A new laser-based and ultra-portable gas sensor for indoor and outdoor formaldehyde (HCHO) monitoring. *Atmos Meas Tech* 12:6079–6089. <https://doi.org/10.5194/amt-12-6079-2019>
- Singer BC, Chan WR, Kim Y-S et al (2020) Indoor air quality in California homes with code-required mechanical ventilation. *Indoor Air* 30:885–899. <https://doi.org/10.1111/ina.12676>
- Sive BC, Zhou Y, Troop D et al (2005) Development of a cryogen-free concentration system for measurements of volatile organic compounds. *Anal Chem* 77:6989–6998. <https://doi.org/10.1021/ac0506231>
- Stönnér C, Edtbauer A, Williams J (2018) Real-world volatile organic compound emission rates from seated adults and children for use in indoor air studies. *Indoor Air* 28:164–172. <https://doi.org/10.1111/ina.12405>
- Sulzer P, Hartungen E, Hanel G et al (2014) A proton transfer reaction-quadrupole interface time-of-flight mass spectrometer (PTR-QiTof): high speed due to extreme sensitivity. *Int J Mass Spectrom* 368:1–5. <https://doi.org/10.1016/j.ijms.2014.05.004>
- Tang X, Misztal PK, Nazaroff WW, Goldstein AH (2015) Siloxanes are the most abundant volatile organic compound emitted from engineering students in a classroom. *Environ Sci Technol Lett* 2:303–307. <https://doi.org/10.1021/acs.estlett.5b00256>
- Tang X, Misztal PK, Nazaroff WW, Goldstein AH (2016) Volatile organic compound emissions from humans indoors. *Environ Sci Technol* 50:12686–12694. <https://doi.org/10.1021/acs.est.6b04415>
- Veres PR, Faber P, Drewnick F et al (2013) Anthropogenic sources of VOC in a football stadium: assessing human emissions in the atmosphere. *Atmos Environ* 77:1052–1059. <https://doi.org/10.1016/j.atmosenv.2013.05.076>
- Wang M, Zeng L, Lu S et al (2014) Development and validation of a cryogen-free automatic gas chromatograph system (GC-MS/FID) for online measurements of volatile organic compounds. *Anal Methods* 6:9424–9434. <https://doi.org/10.1039/C4AY01855A>
- Wang C, Collins DB, Arata C et al (2020) Surface reservoirs dominate dynamic gas-surface partitioning of many indoor air constituents. *Sci Adv* 6:eaay8973. <https://doi.org/10.1126/sciadv.aay8973>

- Williams J, Stönnér C, Wicker J et al (2016) Cinema audiences reproducibly vary the chemical composition of air during films, by broadcasting scene specific emissions on breath. *Sci Rep* 6: 25464
- Wong JPS, Carslaw N, Zhao R et al (2017) Observations and impacts of bleach washing on indoor chlorine chemistry. *Indoor Air* 27:1082–1090. <https://doi.org/10.1111/ina.12402>
- Yuan B, Koss AR, Warneke C et al (2017) Proton-transfer-reaction mass spectrometry: applications in atmospheric sciences. *Chem Rev* 117:13187–13229. <https://doi.org/10.1021/acs.chemrev.7b00325>
- Zhao Y, Kreisberg NM, Worton DR et al (2013) Development of an in situ thermal desorption gas chromatography instrument for quantifying atmospheric semi-volatile organic compounds. *Aerosol Sci Technol* 47:258–266. <https://doi.org/10.1080/02786826.2012.747673>



Measuring Particle Concentrations and Composition in Indoor Air

19

Lance Wallace and Philip K. Hopke

Contents

Introduction	518
Particles Mass Measurements	519
Measurement Methods	519
Fixed Location Samplers	521
Portable and/or Personal Samplers	521
PM Composition Measurements	522
Analytical Strategy	522
PM Source Identification and Apportionment	526
Continuous PM Monitors	527
Particle Monitors	527
Ultrafine Particles	531
Health Effects	531
Measurement Methods	531
UFP Emission Sources	538
Concluding Note	556
Cross-References	556
References	556

L. Wallace

United States Environmental Protection Agency (Retired), Santa Rosa, CA, USA

P. K. Hopke (✉)

Institute for a Sustainable Environment, Clarkson University, Potsdam, NY, USA

Department of Public Health Sciences, University of Rochester School of Medicine and Dentistry,
Rochester, NY, USA

e-mail: phopke@clarkson.edu

Abstract

This chapter focuses on methods to measure the mass concentrations of airborne particulate matter, its chemical composition, and the particle number concentrations and the size distributions in indoor air. Particulate matter (PM) is a complex mixture of inorganic and organic compounds with semivolatile components making accurate determinations of its properties difficult. Many of the methods are derived from measurements in the ambient air, but with the simplification that the indoor environment is protected from precipitation and generally from large variations in temperature and relative humidity. PM measurements first collected integral filters that were weighed to obtain the mass of material separated from a known volume of air to obtain the PM mass concentration typically in units of $\mu\text{g}/\text{m}^3$. These samples can be subjected to separation and analysis methods to determine its chemical constituents including elements, ions, collective carbonaceous species, and individual organic compounds. Continuous PM mass measurement systems have been developed based on beta attenuation, oscillating microbalances, and light scattering. There have been major recent developments of low-cost light scattering monitors that permit the use of multiple monitors to simultaneously obtain more detailed data from multiple locations. Particle counting methods date to the late nineteenth century, but have been refined to permit detection of particles as small as 1 nm. These units can be combined with electrical mobility separation to provide particle size distributions. Particle size is important since it determines the penetration and deposition into the human respiratory and the aerosol dynamics in the indoor space. A number of studies employing these methods have been summarized to provide access to the literature to determine the details of how individual studies were conducted. Such information will help in the design of future studies of particle in indoor air.

Keywords

Particulate matter · Particles · Particle number concentration · Particulate compositions · Measurement methods

Introduction

The largest environmental cause of morbidity and mortality is small particles, $\leq 2.5 \mu\text{m}$ in aerodynamic diameter (PM_{2.5}). Ambient particles are emitted by industrial processes, vehicles, and fires and formed through atmospheric oxidative processes of emitted gases like SO₂, NO_x, and volatile organic compounds (VOCs). Indoors they are emitted mainly by combustion (smoking, cooking, heating, candle burning). The Global Burden of Disease (2020) estimated 6.67 million deaths in 2019 from “air pollution,” which includes both outdoor and indoor fine particles. For indoor air pollution only, other sources estimate 1.6 million or 1.8 million deaths in 2017 (Ritchie 2013; Lee et al. 2020). The toll from fine particles indoors is mainly

from using biomass for both cooking and heating in poor countries without access to an electric grid or clean cooking fuels. Although there is overall improvement, the number of children under 5 dying from household air pollution is still very high at about 200,000. The health impacts from indoor particulate matter are presented in ► “The Health Effects of Indoor Air Pollution” of this Handbook.

Particles Mass Measurements

Measurement Methods

The leading textbook for particle measurement methods is *Aerosol Measurement* (third edition) (Kulkarni et al. 2011). The following discussion highlights a limited number of measurement methods and instruments that have been widely used in indoor studies.

The recognized gold standard for measuring particle mass is to collect the particles on a weighed filter and weigh it after sampling and conditioning to remove particle-bound water. The conditioning process is performed before and after sampling. The basic approach is to equilibrate the filters for at least 24 h at a fixed temperature and relative humidity to remove water from filter and the particulate deposit on the exposed filter. Any particle with water soluble constituents will be hygroscopic meaning it will absorb water vapor from the air at a relative humidity below 100%. The US EPA method uses $23 \pm 1^\circ\text{C}$ and $35 \pm 5\%$ RH. More often higher RH values (40–50%) are employed. However, prior work has shown that most particles require RH to be below 30% to fully dry the particles (Khlystov et al. 2005).

Initially, ambient air sampling focused on total suspended particles (TSP). An open face filter housed in a rain shelter was connected to a vacuum cleaner motor so that TSP could be collected. Subsequently, it was recognized that larger particles were not typically inhalable except under heavier working conditions and ambient PM samplers shifted to having size selective inlets. The first of these were designed to have a 50% collection efficiency (cutpoint) at $10 \mu\text{m}$ aerodynamic diameter to accompany the 1987 US National Ambient Air Quality Standard (NAAQS) for PM_{10} . In 1997, the US Environmental Protection Agency promulgated a NAAQS for PM with aerodynamic diameters $\leq 2.5 \mu\text{m}$ ($\text{PM}_{2.5}$). The size selection comes from the use of impactors (Le et al. 2019) or cyclones (Kenny et al. 2000, 2004). Standard PM samplers for ambient PM typically operate at flow rates of 16.7 LPM or greater. Thus, PM ambient sampling is conducted for TSP, PM_{10} , and/or $\text{PM}_{2.5}$ depending on the exposure assessment that is to be done.

However, different size definitions are employed for PM sampling in occupational settings. Because when working hard and needing more air flow into the lungs, people switch from nose breathing to mouth breathing. Inhalation through the oral cavity allows larger particles into the respiratory tract. Thus, industrial hygienists define “inhalable particles” with aerodynamic diameters up to $100 \mu\text{m}$. Particles that can penetrate into the tracheobronchial tree are terms “thoracic particles.”

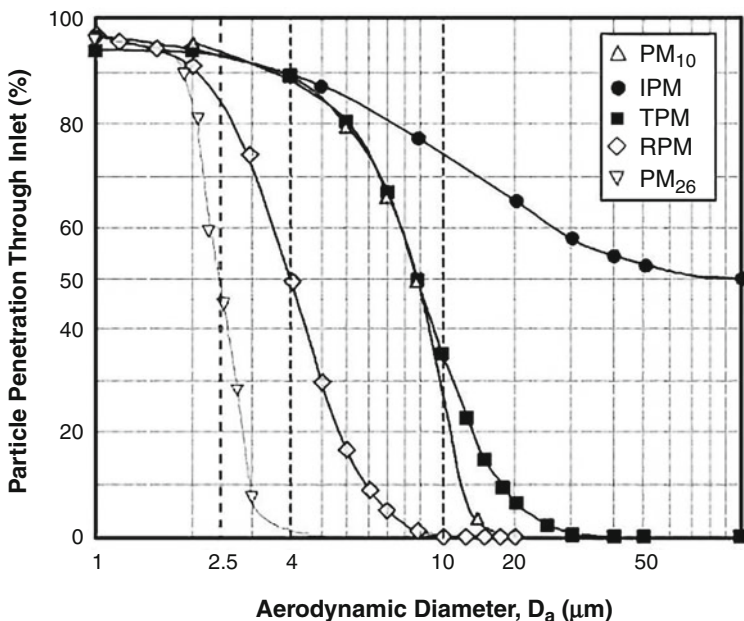


Fig. 1 Comparison of penetration curves for ambient and industrial hygiene sampling of airborne PM. (Figure taken from (USEPA 2004))

This particle size range is very similar to that of PM_{10} . Finally, particles that can penetrate further into the respiratory tract are termed “respirable particles” that have a cutpoint at $4 \mu\text{m}$, or somewhat larger than $\text{PM}_{2.5}$. These size definitions were formalized as the international workplace sampling conventions (ISO 1995). These two sets of collection efficiency curves are compared in Fig. 1.

There is no corresponding network for measuring indoor concentrations although people spend 87% of their time indoors (Klepeis et al. 1996, 2001). Multiple studies have compared outdoor and indoor measurements to try to estimate the total exposure of residents to indoor and outdoor particles. Measurement methods available for indoor particles include gravimetric methods employing portable pumps to collect particles on filters that are usually weighed in a laboratory off site. However, sampling PM indoors creates additional challenges compared to ambient PM sampling because of the limited volume of air in an indoor environment. If the flow rate through the sampler is too high, the sampler becomes an air filtration system substantially changing the concentration in the monitored space. Thus, the volumetric flows cannot be as high as in ambient sampler and are typically $\leq 10 \text{ LPM}$ and generally of the order of 4 or 5 LPM. The total mass flux into the sampler is of the order of 25% of a low volume ambient sampler, thereby making the measurement of the chemical composition of the collected PM sample more difficult. Thus, an integrated sampling/analysis protocol needs to be developed for any particular indoor PM compositional measurement program.

Fixed Location Samplers

Sampling can be at fixed locations or it can move with the individual by using a personal sampler and portable pump. Fixed site samplers usually use line power and can then operate for extended time periods. There are several samplers that can be used for this purpose. Marple et al. (1987) developed the MS&T Area Sampler. This sampler is widely referred to as the Harvard Impactor (HI) that is capable of collecting either PM_{2.5} or PM₁₀ particles on a filter over a time period ranging from 8 h to a week (Turner et al. 2000). Flow rates of 4, 10, and 20 LPM and size cuts of 1, 2.5, and 10 microns (μm) were laboratory tested and penetration curves were determined. For the past 20 years, HIs have been employed in many studies of indoor airborne particles.

A widely used, commercially available, low volume sampler is the MiniVol (Airmetrics, Inc. Springfield, OR, USA). The sampler was jointly patented by the US Environmental Protection Agency (USEPA) and the Lane Oregon Regional Air Pollution Authority (Lane et al. 2001). It operates at 5 LPM and comes with either a PM_{2.5} or PM₁₀ inlet. It is relatively portable and can be either battery or line powered so it has flexibility in where it can be placed.

Another commercially available system is the Ecotech MicroVol 1100 Low Volume Air Sampler. It operates at flow rates between 1.0 and 4.5 LPM through TSP/PM₁₀ size selective inlets and has an optional PM_{2.5} inlet. It operates on line power, battery, or a solar panel with battery. Catrambone et al. (2019) developed a Very Low Volume Sampler (VLVS) using the Smart Sampler (FAI Instruments, Fonte Nuova, Rome, IT) (<http://www.fai-instruments.com/>). Other studies have made use of locally constructed PM samplers (e.g., (Kim et al. 2004; Zhu et al. 2011)) using commercially available inlet cyclones, an inline filter holder, and a small pump.

A subclass of the gravimetric methods is the cascade impactor (Dzubay et al. 1976). In these samplers, multiple samples are collected on stages that represent different size fractions. The substrate from each stage is weighed to determine the contributions of the different size fractions to the total PM mass. Size is important in determining the deposition in the various lung regions, since large particles penetrate only to the thoracic region, whereas small particles can go deeper, reaching the alveolar region where they can be transferred to the blood. The Personal Cascade Impactor Sampler (PCIS), a 5-stage, 9 LPM cascade impactor was developed by Misra et al. (2002) and tested by Singh et al. (2003). It has been commercialized as the Sioutas Personal Cascade Impactor (<https://www.skcltd.com/products2/sampling-heads/sioutas-personal-cascade-impactor.html>). A 10-stage, 2 LPM personal cascade impactor has been reported by Chen et al. (2018). The commercial version of this sampler is mini-MOUDI impactor (<https://tsi.com/products/cascade-impactors/moudi-non-rotating-impactors/mini-moudi-impactors/>) and comes in 6-, 8-, and 10-stage models.

Portable and/or Personal Samplers

Other research personal samples have been developed such as the Harvard School of Public Health Personal Exposure Monitor (H-PEM) (Demokritou et al. 2001) and

commercialized by BGI, Inc (bgi-mesalabs.com). These samplers use an impactor and is similar to the Personal Environmental Monitor (PEM) developed at the University of Minnesota (Marple et al. 1987) that is available from SKC, Inc. (<https://www.skcltd.com>). Both of these designs can have different particle size cuts (2.5, 4, 5, or 10 μm) operating at 2,4, or 10 LPM depending on the model. With an impactor, the sample can be collected on a variety of substrates including filters or thin solid surfaces. Impactors have the additional value of having lower losses of semivolatile species.

RTI International has also developed a portable monitor/sampler called the microPEM (Du et al. 2019) (<https://www.rti.org/impact/micropem-sensor-measuring-exposure-air-pollution>). This unit provides a direct real-time measurement of PM₁₀ and PM_{2.5} and collects the particles on a filter that can then be weighed to provide data for the calibration of the real-time sensor and for subsequent chemical characterization.

Besides PM mass measurements, PM chemical components, such as elements (e.g., sulfur, lead), black carbon (BC), organic carbon (OC), chemical constituents (sulfates, nitrates, ammonia, acidity, secondary organic aerosols (SOA) are sometimes included. The next section of this chapter provides more information on composition measurement methods.

PM Composition Measurements

Analytical Strategy

The commonly applied approach to ambient aerosol chemical characterization typically relies on sample collection on three different types of filters (Solomon et al. 2014). A Teflon filter is analyzed for mass and elemental analysis. A nylon filter behind a diffusion denuder is analyzed for ions and a quartz filter is analyzed for organic and elemental carbon. Indoor air and personal sampling generally only provides a single filter so a strategy needs to be developed to provide the chemical speciation information required to meet the project objectives. The most commonly used filter is a Teflon filter to permit good mass measurements. Quartz filters have also been used, but care must be taken with them since quartz fibers can break resulting in mass loss from the sample.

Light Absorption

Light absorption is an old method and was the basis for the PM concentrations measured during the December 1952 London Fog episode and was reported as “black smoke” or “British smoke.” It is the carbonaceous matter in PM that will often absorb light and provide information that can be used in source identification and apportionment studies. The most commonly measured feature is “black carbon” (BC). There is no uniformly agreed upon definition of “black carbon.” Atmospheric BC often called “soot” is formed via high temperature combustion where it is formed near the flame as the material moves into a cooler area. It has a

low hydrogen to carbon ratio, but is not pure graphite. The measurements based on light absorption do not determine the amount of light absorbing carbonaceous matter. The BC mass is estimated based on a mass absorption coefficient that provides an estimate of the mass of carbon per unit light absorption at some given wavelength.

Its absorptivity varies by wavelength by roughly λ^{-1} with a range of $\lambda^{-0.8}$ to $\lambda^{-1.1}$ (Schnaiter et al. 2003, 2005). Alternatively, compounds with multiple fused aromatic ring structures will more strongly absorb light in the ultraviolet and lower end of the visible light wavelength range (350–470 nm). The particulate carbonaceous material with this type of light absorption is typically termed “brown carbon” (BrC). It is formed in lower temperature combustion that produces humic-like substances (HULIS) (Li et al. 2019). BC and BrC are discussed in detail by Andreae and Gelencsér (2006). Major sources of BrC are solid fuel (biomass and coal) burning and to a lesser extent, secondary aerosol formation. BC is non-volatile while BrC is semi-volatile. Thus, it is important to store samples under refrigeration and better to freeze them prior to analysis to avoid the loss of the more volatile components.

Black smoke was measured by white light reflection (Coulson and Ellison 1963; Davies and Aylward 1951) and systems to make these measurements are still available as the EEL Model 43D smoke stain reflectometer (Diffusion Systems, Ltd. London). The presence of “graphitic” carbon in urban aerosol samples was extensively studied by Hansen et al. (1982) using transmission of 630 nm light. Ultimately, 880 nm light has become the standard wavelength at which BC is measured since at that wavelength, the particulate absorption is dominated by the BC component because light absorbed by other particulate components is significantly less (Sandradewi et al. 2008). However, Sandradewi et al. (2008) use 950 nm absorption in their analytical scheme. Light absorption at 370 and 470 nm has been used to estimate the relative amounts of BC and BrC (Sandradewi et al. 2008; Wang et al. 2011).

BC is typically associated with vehicular emissions while the BrC is assigned to biomass burning. Wang et al. (2011) determined that the difference between BrC (370 nm) and BC (880 nm) that they termed Delta-C was highly correlated with levoglucosan ($r^2 = 0.89$ in winter), a well-known tracer of biomass burning particles (Simoneit et al. 1999). Delta-C has been used to provide a better source separation of biomass burning aerosol in ambient samples (Wang et al. 2012). It could also be useful in identifying cigarette smoke in indoor air (Lawless et al. 2004). To make these measurements, commercially available systems like the Magee OT21 can provide transmission measurements at 2 wavelengths comparable to those made in an aethalometer. Another transmission through a filter system is the Particle Soot Absorption Photometer (PSAP; Radiance Research, Seattle, WA). It is really designed to be a semicontinuous instrument similar to an aethalometer, but it can be used for individual filter measurements. Originally it used a 567 nm LED as the light source (Bond et al. 1999). A 3-wavelength PSAP operates with 467, 530 and 660 nm light sources. Diffusions Systems Ltd. continues to sell the ELL Model 43D.

Elemental Analyses

A commonly used approach for elemental analyses on Teflon filters is x-ray fluorescence (XRF) (Landsberger and Creatchman 1999) that measures the areal density (ng/cm^2) of each measurable element. Thus, sensitivity can be increased by using a smaller diameter filter. XRF requires the sample to be a uniform thin layer and thus, sampling on Teflon or other membrane filters provide appropriate samples. It has a nominal range of detectable elements from Na to U, but realistically, around 15 can be adequately detected. It has good sensitivity for the major crustal elements (Al, Si, Ca, Fe) and several other major elements like S. XRF has the advantage of being “non-destructive.” For most elements, the analysis does not disturb the sample composition. However, since many XRF systems operate in a vacuum, any semi-volatile material will be lost from the filter such as organic compounds and ammonium nitrate. Thus, it is important to perform the light absorption analysis first in order to properly determine the BrC components.

It is not feasible to do quantitative XRF analyses on quartz filter since the particles penetrate into the matte of the quartz fibers with losses of the fluoresced x-rays as they move toward the detector. To analyze elements in the PM on quartz filters, it is necessary to use inductively coupled plasma (ICP) with an appropriate detector after acid digestion of the sample. However, acid-digestion should be conducted after water leaching of the filter for ion analyses if those species are of interest. More details on ICP based methods are presented below.

Analysis of Water-Soluble Ions

It is possible to analyze water soluble ions using ion chromatography (IC). To obtain the samples for analysis, the filter is leached with high purity ($18 \text{ M}\Omega$) water. Teflon filters require wetting with a small amount of high purity ethanol. Both cations and anions can be determined but they require different separation columns and thus, multiple runs are required after modifying the instrument are needed. Cations typically determined include NH_4^+ , Na^+ , Mg_2^+ , K^+ and Ca_2^+ . The commonly determined anions include NO_3^- , SO_4^{2-} , Cl^- , and PO_4^{3-} . These are typically measured using commonly employed column and eluants. By changing the chromatographic conditions, short chain organic mono- and di-acidic ions (formate, acetate, propionate, oxalate, and malonate) can also be determined (Sunder Raman and Hopke 2006). If a quartz filter was used, then aliquots of the water leachate need to be analyzed for elements using the ICP-based analysis.

Inductively Coupled Plasma Methods

Inductively coupled plasma methods employ radiofrequency radiation to convert a flowing stream of argon gas into a plasma at high temperatures (5500 to 6500°K) in a quartz vessel. The water solution containing the elements to be ionized is introduced into the plasma with a nebulizer that breaks the stream into droplets that evaporate to provide the solid material that is vaporized and ionized. The amount of the elements present can be determined by measuring the atomic radiation coming from the excited atoms called atomic emission spectroscopy (ICP/AES) or by extracting the

elemental ions into a mass spectrometer (ICP/MS). For most elements, ICP/MS is more sensitive and is more commonly employed.

To provide the solution of analytes, the filter is acid digested. There are various approaches to the choice of acid(s) depending on how thoroughly the filter is to be digested. Some groups use ultrapure HNO₃ followed by HF (Querol et al. 1996) to obtain a total digestion including the quartz filter if they were used to collect the sample. This procedure produces a sample with significant quantities of Si that are corrected by subtraction of blank filter values. It is more typical to use just ultrapure HNO₃. This procedure will not dissolve Si and several other elements such as Ti. Other procedures may include HCl. However, Cl can combine with Ar to form an ion called an isobaric interference that has the same mass as As. Although the addition of HCl would improve the dissolution of some elements, it should not be used if the analysis is being done using ICP/MS. It would not affect ICP/AES analyses. ICP-based analyses can typically provide a wider array of elemental concentrations ranging from Li to U. However, it is a destructive and more expensive analysis. Thus, the choice of analytical method for elements depends on the elements needed for the subsequent data analyses and the availability of resources to perform the necessary procedures.

Organic and Elemental Carbon

Light absorption does not measure the mass of carbonaceous species. It is estimated based on known or estimated mass absorption coefficients. To directly measure the mass of carbon on a filter, thermal-optical methods are typically used (Birch and Cary 1996). These methods provide an empirical separation between “organic” and “elemental” carbon. The underlying assumption is that the organic compounds that comprise the organic carbon (OC) have some degree of volatility and thus, can be separated from the filter by heating it. Alternatively, the elemental carbon (EC) is thermally refractory and will remain on the filter until removed by oxidation. Thus, instruments have been developed that use a sequence of increasing temperatures to heat a small portion of the filter. To avoid oxidizing the material, a helium atmosphere is used. Because some of the larger carbon molecules and molecules with a number of oxygens have low vapor pressures, relative high temperatures (>500 °C) are required. These steps provide the measurement of OC. Given the use of high temperatures, samples need to be collected on quartz filters or high melting point metal impactor foils (not Al). The evolved organic compounds are catalytically oxidized to CO₂. The CO₂ measured so the system provides measurement of carbon and not carbonaceous material mass. Once the initial sequence of temperatures has been completed, the atmosphere is changed to helium containing a few percent of oxygen to oxidize the carbon remaining on the filter and a second sequence of increasing temperatures is applied to the sample to measure the EC.

There is no standard protocol that defines the temperatures and time-at-temperature for each step. The major protocols are NIOSH (Birch and Cary 1996), IMPROVE-A (Chow et al. 2007), and EUSAAR-2 (Cavalli et al. 2010). Each protocol produces different measures of OC and EC. Only the total amount of carbon is reproducible among the protocols. Thus, these quantities are defined by

the method used to make the measurements. There are typically relationships between EC and BC, but they can vary depending on the source of the carbonaceous particles (Salako et al. 2012).

Organic Compound Analysis

Generally, the determination of organic compounds in indoor air samples is difficult because of the relatively small mass of PM that is collected. The basic approach is to separate and identify the compounds using gas chromatography coupled with mass spectrometry (GC/MS). To transfer the organic material into the GC, there are two approaches: extraction and thermal desorption.

The remaining portion of the quartz filter after using the punch for the OC/EC analysis are then extracted for the analysis of polar and non-polar compounds. These compounds include source tracers termed molecular markers that include species like levoglucosan (biomass burning), cholesterol (meat cooking), etc. Prior to extraction, the filter is spiked with a set of perdeuterated surrogate standard compounds covering a wide range of a molecular weights, volatility and functional groups to quantify the extraction efficiency. The substrates are extracted using as Soxhlet extractor or instruments like the Dionex Accelerated Solvent Extractor (ASE350). Extracts are concentrated and then split into two aliquots. One aliquot is directly analyzed for non-polar species by GC/MS. The second fraction is derivatized to reduce the polarity with a material such as bis (trimethylsilyl) tri-fluoroacetamide (BSTFA) plus 1% trimethylchlorosilane (TMCS) as a catalyst (Pashynska et al. 2002). Using procedures like that described by Edney et al. (2005), the derivatized samples are then analyzed by GC/MS.

In thermal desorption/gas chromatography/mass spectrometry (TD/GC/MS), the filter is heated and evolved gas is directly introduced in the GC and then analyzed (Falkovich and Rudich 2001). Sheesley et al. (2015) subsequently developed a modified TD/GC/MS system that employs an in-situ derivatization that adds tri-methylsilyl groups to alcohol functional groups on simple carbohydrates, like levoglucosan and sterols. Thus, both non-polar and polar compounds can be analyzed directly without extraction and concentration. Both approaches have been used to determine organic compounds in airborne particle samples (Meng et al. 2005).

PM Source Identification and Apportionment

The PM compositional data can then be used in source apportionment studies using tools like the chemical mass balance (CMB) or positive matrix factorization (PMF) (Hopke 2016). There have been studies where measurements have been made in multiple environments (indoor, outdoor, and personal) and the data used to determine the indoor and ambient sources of PM. The first major study of personal exposure to PM was the 1991 Particle Total Exposure Assessment Methodology (PTEAM) study in Riverside, CA (Özkaynak et al. 1996). Personal exposure monitors were worn by the study subjects with 2 samples per person and 178 individual participants. The filters were weighed and elemental concentrations were

determined using X-ray fluorescence (XRF). In addition, indoor and outdoor samples were collected separately and analyzed in a similar manner. Yakovleva et al. (1999) performed a 3-way analysis using a trilinear model and identified 7 source types. Three soil factors with similar profiles, but different time dependence and distribution between indoor, outdoor, and personal samples were determined. Particles from the third soil source only appeared in personal samples leading to the assumption that those particles were resuspended by various personal activities. A “Personal Activities” source appeared in the indoor and personal samples. The “Personal Activities” contribution showed an excellent correlation with number of smokers in the house and smoking during the monitoring period. Those particles were associated with everyday indoor personal activities, such as cooking, smoking, using personal hygiene sprays, etc. Other sources included oil combustion, sea-salt, secondary sulfate, motor vehicle exhaust contributed to the outdoor PM. Cooking and vacuuming were also associated with “Indoor Soil” and “Personal Activities.”

Subsequently, other studies of multiple source types (indoor, outdoor, and personal) were reported by Hopke et al. (2003) and Zhao et al. (2006, 2007). In these studies, a model was developed to explicitly separate indoor and outdoor source types. This model provide a better separation of indoor and outdoor sources than simply applying the normal bilinear model to a combined indoor/outdoor data set that is done in a number of studies.

Continuous PM Monitors

It is desirable to have highly time resolved measurements given short duration, high emission events like cooking, smoking, and other particle generating activities. Mechanisms for continuous PM monitoring used for ambient PM monitoring have been adapted to indoor systems including light scattering, beta attenuation monitors (BAMs), and tapered element oscillating microbalance (TEOM) that can provide highly accurate measurement but at relatively high cost per unit. There are portable BAM (e-BAM) (Kim et al. 2016; Schweizer et al. 2016) and TEOM (Cantrell et al. 1996, 1997). The e-BAM has been used in field studies of indoor spaces such as subway stations (Kim et al. 2016). The portable TEOM was designed to be a continuous personal dust monitor for the exposure assessment of miners (Kissell et al. 2002) and has not been reported as being used in indoor air monitoring.

Particle Monitors

Aerodynamic Particle Sizers

Since the size of a particle is such an important consideration, determining for example how quickly it can be removed from the indoor air by striking a surface such as the floor or ceiling, techniques to measure the particle size are required. Aerodynamic particle sizers use an accelerated flow to separate particles according to their inertia. The time of flight between two sensors can then determine the inertia

and ultimately the size. An example is the APS 3321 model (TSI, Shoreview, MN) which can differentiate between about 52 sizes between 0.5 and 20 μm .

Optical Particle Monitors

A large class of instruments widely used in indoor particle studies are optical particle monitors. These monitors employ a light source to scatter light from particles passing through a sensing chamber. The light source may be visible or infrared and often use lasers or LEDs. The scattered light is collected by detectors surrounding the sensing chamber and can be analyzed using Mie theory to determine particle size. Pulse height or other measure can provide a count of the number of particles. The particle mass (e.g., PM_{2.5}) can then be estimated by calculating the total volume (assuming spherical particles) and assigning an average density. Optical monitors are often calibrated by the manufacturer to a particle mixture of known density such as Arizona Road Dust (specific gravity 2.6). A drawback of all optical particle monitors is that they must be recalibrated to whatever particle mixture is being studied. The recalibration is done using gravimetric sampling.

One widely used research-grade optical monitor is the SidePak (TSI, Shoreview, MN). The SidePak is a small portable sampler with a flow rate of around 1 LPM (0.7–1.8 LPM). It is calibrated to Arizona Road Dust or a related test aerosol, including secondhand tobacco smoke (Jiang et al. 2011). A more recent example of recalibrating the SidePak to an aerosol mixture created by combusting or vaping marijuana is provided by Zhao et al. (2020). The calibration factors (CF) for four types of marijuana sources (glass pipe, joint, bong, and vaping pen) were 0.31 (SE = 0.02), 0.39 (SE = 0.02), 0.40 (SE = 0.01), and 0.44 (SE = 0.03), respectively. These CF values were then used in subsequent studies to determine emission rates of the four sources (Ott et al. 2021) and estimates of exposure from vaping marijuana (Wallace et al. 2020).

A second widely-used optical monitor is the DustTrak (TSI, Shoreview, MN). Several of these optical instruments were compared with gravimetric mass measurements by Wang et al. (2016). Often the data from these instruments need to be adjusted with a correction factor (CF) (Susz et al. 2020). The DustTrak has the advantage of provision of a place for a filter to be installed for later weighing in the laboratory allowing direct determination of the CF as well as analysis of the composition. In Wang et al. study, the bias of a TSI DustTrak relative to gravimetric measurements of environmental tobacco smoke (ETS) ranged from 2% to 15% when a photometric calibration factor (PCF) of 0.38 was applied. Li and Hopke (1993) reported that side stream cigarette smoke generated with a smoking machine was unimodal and lognormally distributed with a geometric mean diameter of 140.7 nm and a geometric standard deviation of 1.53 so the DustTrak would be useful for ETS type measurements with proper correction. Rivas et al. (2017) reported other issues with the DustTrak DRX in which sudden artifact jumps in PM concentration occurred. They suggest that the measured data should be handled with care and meticulously reviewed and revised before being considered valid.

Wallace et al. (2011) compared DustTrak (Model 8520) and personal DataRAM (pDR) (ThermoScientific, Waltham, MA, USA) for PM_{2.5} against each other and

against simultaneously collected gravimetric samples (Wheeler et al. 2011). The DustTrak and pDR were in reasonable agreement ($R^2 = 0.90$ and 0.70, respectively) with the gravimetric PM_{2.5} values. The instrumental limits of detection were approximately 5 µg/m³. Both units had multiplicative biases of about 2.5 and 1.6, respectively, relative to the gravimetric samples. However, proper correction provided values with an average bias-corrected precision of ~10%. Thus, appropriate bias corrections provided very good agreement with standard gravimetric methods. Some instruments such as the Grimm model 1.108 (Cheng, 2008) have a built-in filter holder to permit collection of an integrated gravimetric sample over the course of the measurement period.

In general, calibration work for such devices by taking some parallel gravimetric measurements of the PM that is to be monitored is advised. Li et al. (2019) provides a useful framework for in-field calibrations to provide more accurate use of such devices. They suggest collocation with reference quality instruments to provide a number of data points to build the model. Since particle hygroscopicity is an important factor in changing the amount of scattered light because the absorption of water vapor increases the particle size and modifies the refractive index. Thus, they suggest developing regression models that include relative humidity (RH).

Semicontinuous Composition Measurements

Over the past 20 years, there has been an extensive development of instruments for the semicontinuous characterization of the composition of airborne PM. most of these instruments are available for compositional measurements, but they have generally been designed to sample the ambient aerosol and typically are quite expensive. There have been only a few instances of their use to characterize indoor PM (Ji et al. 2010; Patel et al. 2020). However, one of the measured earliest species was black carbon (BC) or light absorbing carbon (LAC) using an aethalometer whose principle was presented by Hansen et al. (1984). Subsequently, an instrument was developed in which PM is collected on a filter tape and the light transmission is determined. Initially a single wavelength of 990 nm was used, but now multiple wavelength units are available. Portable units are now available for personal or indoor BC monitoring (Cai et al. 2014). Multiple wavelength units could be useful in measuring the emissions from various source types that produce black or brown carbon particles.

Low-Cost Monitors

However, these better-quality light scattering systems still cost thousands of dollars so using many of them for exposure studies is not always feasible. Thus, in recent years, there has been a substantial growth in the use of low-cost PM monitors. This development has exciting implications for investigators of particle exposures near or even inside homes and also epidemiological studies. Epidemiology has long had only one source of particle measurements (the regulatory ambient monitoring carried out by governments). In studying health effects in large populations, epidemiologists are forced to use the regulatory data as their only input in estimating human exposure. Yet we know that most exposure occurs indoors or at work. We also know that indoor exposures are not simply a multiple of outdoor concentrations.

Therefore, obtaining direct continuous long-term records of individual home concentrations will be a great boon to epidemiology.

These monitors evolved from the light scattering sensors originally developed for use in smoke detectors to eliminate the use of radioactivity that had been the basis for the earlier designs. Litton (2002a, b) recognized that these sensors could be used to measure particle concentrations in occupational setting with a low cost device that could be replicated to monitor in multiple locations. Litton et al. (2004) then developed these detectors into a monitor that was used for monitoring cooking emissions in developing countries (e.g., (Smith et al. 2007)). A variety of low-cost sensors for consumers have been developed over the past decade to permit people to monitor air quality in their own home environments. The initial units continued to use the sensors from smoke detectors that typically use an LED with a wavelength of $\sim 1 \mu\text{m}$ and thus, the lower cutoff size that can be efficiently detected was around 500 nm.

Evaluations of these early units found a wide range of performance when compared to higher quality light scattering or reference devices (Williams et al. 2014). An early comparison of four monitor types (Speck, Dylos, Air Assure, and UB AirSense) was performed at Clarkson University using cigarette smoke and Arizona Test Dust (Manikonda et al. 2016). All four types were found adequate for indoor use. Subsequently, there has been development of more sophisticated sensors using lower wavelength lasers that increased the light intensity and reduced the lower size cut-off. These units also require careful analysis of the accuracy and precision of the monitors. There has been sufficient interest in these monitors that the South Coast Air Quality Management District of California has established a testing facility to permit uniform, high quality evaluation of the available monitors (AQ-SPEC 2016). Calibration systems have been developed for these monitors (Holstius et al. 2014; Sayahi et al. 2019a). Other tests for accuracy and precision have been made (Delp and Singer 2020; Williams et al. 2014). These systems generally provide particle counts as the individual particle scatter light and produce a pulse. The count data then need to be converted into mass concentrations. Brattich et al. (2020) provide information on these conversions although the details for any specific commercial monitor are proprietary. A variety of methods have been used to develop calibrations of low-cost monitors (e.g., (Si et al. 2020)). The US EPA (2017) has developed a guidance document for using these monitors.

A few models have performed well, some within a factor of two accuracy with research grade instruments depending on the nature of the aerosol. Monitors cost between \$100 and several thousand dollars. There are currently several $\sim \$200$ monitors based on Plantower PMS5003 laser-based sensors. It has a 50% counting efficiency for 300 nm particles and uses a $\sim 650 \text{ nm}$ wavelength. In the United States, a popular low-cost monitor is provided to buyers by PurpleAir.com, a Utah-based company. The company offers to register the monitors so that the data are continuously uploaded to the Web. At present, more than 16,000 monitors are operating worldwide and their data are freely available to anyone. Most are used outdoors near homes. However, a fair number are being used indoors (about 2000 monitors in California alone). The Plantower sensor is used in the PurpleAir and other monitors

(Chen et al. 2017; Gupta et al. 2018; Jiao et al. 2016; Kelly et al. 2017; Morawska et al. 2018; Ardon-Dryer et al. 2020; Badura et al. 2018, 2019; Barkjohn et al. 2020; Becnel et al. 2019; Bi et al. 2020; Bulot et al. 2019; Delp and Singer 2020; Feenstra et al. 2019; Francis et al. 2019; He et al. 2020; Holder et al. 2020; Kaduwela et al. 2019; Karagulian et al. 2019; Kim et al. 2019; Kuula et al. 2017, 2020; Levy Zamora et al. 2018; Li et al. 2020; Magi et al. 2020; Masic et al. 2019; Masic A et al. 2020; Sayahi et al. 2019b; Singer and Delp 2018; Stavroulas et al. 2020; Tryner et al. 2019a, b, 2020; Wang et al. 2019, 2020; Zheng et al. 2018; Zou et al. 2020, 2021). Findings of these studies are highlighted in Table 1. However, monitor technology has been changing rapidly and newer, more accurate systems are likely to come onto the market (AQ-SPEC 2016).

The difference between estimated exposure using only ambient measurements and true exposure (the sum of outdoor-penetrated and indoor-generated exposure) is *exposure error*. Recently a study has estimated the extent of exposure error for a group of 91 California homes near 91 outdoor monitors (Bi et al. 2021). The error is largest at low outdoor concentrations, due to the increased relative importance of indoor-generated concentrations at these low (but much more common) outdoor concentrations (Fig. 2).

Ultrafine Particles

Health Effects

Ultrafine particles (UFP) are defined as particles below 100 nm or 0.1 μm in diameter. They may cause health effects, including mortality (Bräuner et al. 2007, 2008; HEI 2013; Ohlwein et al. 2019; Stölzel et al. 2007; Utell and Frampton 2000; Wichmann et al. 2000). These effects are not likely due to the particulate mass, since they contribute a tiny fraction of the mass of almost any aerosol. However, they are known to be able to cross cell membranes, and often accumulate near the cell's ATP energy producers. Their toxicity may be more related to their surface area and chemistry rather than other physical parameters (Oberdörster et al. 2005). They may also cross the blood-brain barrier (Oberdörster et al. 2005). Multiple toxicological studies have found effects on cell lines and animal models (Donaldson et al. 2005). Interestingly, effects are not strong for respiratory function, but effects on the heart (e.g., heart rate variability) are more pronounced (Ohlrein 2019). Thus, measurement of this size range is important to provide more complete particulate exposure estimates.

Measurement Methods

Condensation Particle Counters

Neither gravitational nor optical methods are applicable to UFP, since they do not contribute to mass and they are too small to effectively scatter light. The most widely

Table 1 Studies using low-cost monitors

Reference	Year	Model PMS-	Number monitors	Location	Time span	Comment
Manikonda et al. (2016)	2016	N/A	1–3 each of four types	Clarkson Univ test chamber	N/A	Four monitors (Speck, Dylos, TSI AirAssure, UB AirSense) tested using cigarette smoke & Arizona Test Dust. All found adequate for indoor use.
Chen et al. (2017)	2017	3003 5003	N/A	Taiwan	N/A	General outline of system with data archiving. Two short-term case studies.
Kelly et al. (2017)	2017	1003 3003	Utah			ambient and wind tunnel expts comparing to research-grade and FEM/FRM monitors Linear difference between 200 and 85 $\mu\text{g}/\text{m}^3$. Correlating with gravimetric 0.88
Gupta et al. (2018)	2018	5003		California	October 2017	Focus on wildfires. Comparisons with research-grade instruments showed 35% overestimate of PM2.5.
Wang et al. (2019)	2019	7003	17	Shanghai, China	7 days	Compared with TEOM: Outdoor R^2 0.72–0.78, mean RSD 21%; indoor R^2 0.95–0.96, mean RSD 16%.
Singer and Delp (2018)	2018	5003	2–3	Berkeley		Tested 7 monitor types with 16 particle sources.
Zheng et al. (2018)	2018	3003	7	Durham NC; Kanpur, India	NC: 90 days; India 45 days	1-h mean errors of 200% in Durham, but 35–46% in India, indicating improved performance at high concentrations. Following empirical RH correction, estimates are within ~10%.
Beenel et al. (2019)	2019	3003	50	Salt Lake County, Utah	6 months	Individual calibration improved RMSE by 1.8 times. Good agreement (88% R^2) with reference monitors
Bulot et al. (2019)	2019	5003 7003	6	Southampton, UK	1 year	Moderate to good correlation: $0.61 < r < 0.88$.
Feenstra et al. (2019)	2019	5003	3	Southern California	8 weeks	compared to research-grade AND FEM monitor

Francis et al. (2019)	2019	5003	N/A	Sabah, Malaysia	1 week	Use of particle number to estimate mass. PM_1 & $\text{PM}_{2.5}$, $R^2 = 0.82$ & 0.88. PM_{10} unreliable.
He et al. (2020)	2020	5003	6	Clarkson Univ. NY		Theoretical analysis of transfer function. All size channels include response to sizes outside their boundaries.
Kaduwela et al. (2019)	2019	7003	1	Albany, CA	2 weeks	School study including wildfire days (15X increase in particle number indoors).
Levy Zamora et al. (2018)	2018	A003	3	Baltimore, MD	1 month, 10 days	Accuracy 87-96%, precision 9-10% for incense, cooking, and residential indoor. Underestimates with precision 10-24% for NaCl, talcum powder, oleic acid. Overestimate of ambient data by 1.6-2.4X, reduced to 0.9-1.4X after correction for RH.
Magi et al. (2020)	2020	5003	1	Charlotte, NC	16 months	Multiple linear regression with T, RH, and BAM improved accuracy by 27-57%. 15% of data < LOD of $5 \mu\text{g}/\text{m}^3$.
Malings et al. (2020)	2020	5003	20	Pittsburgh, PA	17 months	Multiple segmented linear regression with T and RH (10 parameters). Median correlation with BAM of 0.73; mean absolute error $2.5 \mu\text{g}/\text{m}^3$, bias $-0.14 \mu\text{g}/\text{m}^3$
Masic et al. (2019, 2020)	2019, 2020	5003	2	Sarajevo, Bosnia	16 months	R^2 93% and 96%. Bias 37% and 31%
Kim et al. (2019)	2019	5003		South Korea	5 days	pork barbecuing, secondhand smoke correlations of 0.97, 0.86 vs. GRIMM, urban air near traffic 0.88 vs. BAM
Sayahi et al. (2019b)	2019b	1003 5003	4	Utah	320 days	One PMS 5003 overestimated PM2.5 compared to TEOM by factor of 1.47 but the other agreed well. Correlations >0.87 in winter, lower in spring and wildfire season

(continued)

Table 1 (continued)

Kuula et al. (2020)	2020	5003	3	Finland		Testing with monodisperse size fractions showed the 5003 valid detection range is <0.8 um. Thus it cannot be used for particles >2.5 um
Tryner et al. (2019a, b)	2019	5003	8	Fort Collins, CO	1 week	Gravimetric correction reduced bias and RSD. CF1 values 50% higher than ATM values at high PM _{2.5} concentrations
Ardon-Dryer et al. (2020)	2020	5003	>28	Denver, Salt Lake City San Francisco, Vallejo	2 years (2017 & 2018 of data	Four regions with 7 PA monitors compared to nearby AQS FEM monitors. 75% of comparisons exceeded 0.8 correlation coeff.
Barkjohn et al. (2020)	2020	5003	50	39 sites in 16 states across the United states	9/28/2017- 1/13/ 2020	Nationwide model: $PM2.5 = 0.524 * PA_{CF1} - 0.0852 RH + 5.72$
Bi et al. (2020)	2020	5003	2090	California	1 year	Overestimate of 13/11.1 = 17%, based on 137,000 1-h measurements. Calibration reduced bias to ~0. Most important parameter in estimating PM _{2.5} was the PM _{2.5} /PM ₁₀ ratio.
Delp and Singer (2020)	2020	1003 5003	53	Camp Fire area in California	November 2018	Calibration factor for Purple Air during 14 smoky days was 0.48, reducing residual error from 102% (IQR 74–133%) to 0% ($\pm 15\%$).
Holder et al. (2020)	2020	5003		Several wildfires in western and eastern US	8/8/18 to 6/30/ 19 at RTP	PA sensors well correlated with reference monitor and linear up to 200 ug/m ³ . CF1 mean bias was 2.03, ATM was 1.37
Stavroulas et al. (2020)	2020	5003		Athens, Ioannina (Greece)	winter spring 2020 summer 2019	R2 0.98 vs. optical research-grade inst, 0.87 vs. BAM. Bias was easily correctible and mean absolute error was reduced to 0.18 and 0.12 for Athens and Ioannina

Wallace et al. (2020)	2020	5003	4	Santa Rosa, CA Redwood city, CA	14 months (124 experiments)	Indoor measurements of aerosol from vaping marijuana liquids. Purple Air monitors were collocated with research-grade monitors. Precision and COV were comparable across all monitor types. Calibration factor estimate was about 3.0.
Wang et al. (2020)	2020	1003 3003 5003	9	Berkeley, CA	1 month	3 different monitors incorporating the three models listed. All performed reasonably well (within a factor of two) with multiple different aerosols containing particles $>0.25\text{ }\mu\text{m}$.
Zou et al. (2020)	2020	N/A		Ohio		Chamber study. 8 brands investigated. No effect of temperature. RH accounted for about 11% of residual error but could be corrected for
Zusman et al. (2020)	2020	A003	80	Seattle, 6 other cities	30-95 weeks	PM _{2.5} precision $r = 0.99$, accuracy $R^2 = 0.96$, RMSE $1.15\text{ }\mu\text{g/m}^3$. Region-specific models in 6 other cities $R^2 = 0.74\text{-}0.95$, RMSE $0.84\text{-}2.46\text{ }\mu\text{g/m}^3$. Seattle model applied to other 6 cities: $R^2 = 0.67\text{-}0.84$, RMSE $1.67\text{-}3.41\text{ }\mu\text{g/m}^3$.
Wallace et al. (2021)	2021	5003	33	California	November 2018 to June 30 2020	A new method of calculating PM1 and PM2.5 that does not depend on the hidden Plantower algorithm was developed and applied to determine a calibration factor based on 33 outdoor Purple air monitors near 27 EPA FEM outdoor monitors.

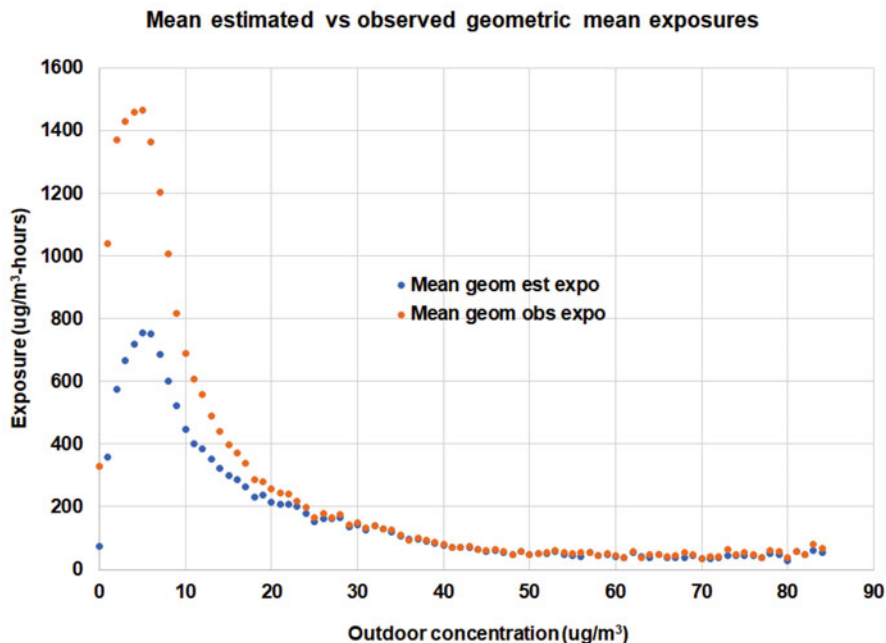


Fig. 2 Exposure error is the difference between the measured indoor exposure (orange) and that calculated from outdoor-penetrated air (blue). (Data source Ref. (Bi et al., 2021))

used method of measuring UFP is the condensation particle counter (CPC). CPCs were originally developed by Aitken (Aitken 1888) and developed into a portable system (Aitken 1892). A model of this device has been recently calibrated (Leigh-Manuell et al. 2020). The history of the development of the CPC is presented by McMurry (McMurry 2000). Current continuous devices employ two regions held at widely different temperatures. In one region is a supersaturated vapor. The particles enter this region and moving in to a cooler region, the vapor condenses around them, increasing their diameter to about 10 micrometers (μm). At this size, they scatter light from a laser beam and are counted. The lower size limit of detection for these devices were typically around 5–10 nm.

For many years, the supersaturated vapor consisted of an alcohol such as butanol. Later, a water-based CPC was developed that operates in a reverse approach (Hering et al. 2005) with the particles first passes through a cold dry region followed by a warm moist region. Water has some advantages over butanol, including non-flammability, lack of odor, and no toxicity. Also, for hydrophilic particles, the water-based CPC (commercially available from TSI) has an improved lower limit of detection approaching 2.5 nm.

The upper limit of detection for CPCs is typically 1–3 μm . However, since UFP typically form 90–95% of all particles $<1 \mu\text{m}$, the counts returned by a CPC are generally considered to be reasonable estimates of UFP number concentrations.

Two portable CPCs have been used in some of the studies reviewed below: the P-Trak, and the Model 3007, both manufactured by TSI. The P-Trak counts particles >20 nm with an upper number concentration limit of $500,000 \text{ cm}^{-3}$. The Model 3007 can “see” smaller particles (10 nm) but with a nominal upper limit of $100,000 \text{ cm}^{-3}$. The term “nominal” is used because although particle coincidence does begin to occur at $100,000 \text{ cm}^{-3}$, it is possible to correct the Model 3007 to obtain reasonable readings up to about $300,000 \text{ cm}^{-3}$ (Hameri et al. 2002). The Model 3007 is the more precise instrument (to within 20%), with a sensor to regulate airflow that is lacking in the P-Trak.

Particle Size Distributions

To obtain the size distribution of the UFP instead just the total number concentrations, a differential mobility analyzer (DMA) is typically employed in conjunction with a CPC. This instrument takes advantage of the electrical mobility of particles by charging the particles with either a radioactive source or soft x-rays and then subjecting them to an electric field. In the most commonly used DMA, the particles enter between two concentric cylinders held at different electric potential. The particles then bend toward the cylinder at the lower potential. Smaller particles will bend more rapidly and strike the cylinder at a different point along the axis than larger particles. A gap in the cylinder allows particles of a given diameter to escape, where they are typically directed into a CPC and counted. By varying the voltage, particles of any given diameter can be selected. To obtain a full size distribution of the particles, the voltage can be varied in a systematic manner. The instrument using this approach combines a DMA and a CPC; the most common commercial version is called a Scanning Mobility Particle Sizer (SMPS) (TSI, Shoreview, MN). A typical scan may take 2.5–5 min to produce a range of about 100 sizes, equally spaced on a logarithmic scale.

Until about 2000, commercial versions of the SMPS had a lower limit of detection of about 10 nm. Then, Chen et al. (Chen et al. 1998) developed an instrument capable of measuring down to about 2.5 nm. This instrument (Model 3908, TSI) employs a nano-DMA with a range of about 3.2–105 nm, or 2.6–65 nm when modified to reach the smallest possible size. Scan time has been reduced to about 1 min. An extensive review of ultrafine particles (measurement methods and observed indoor size distributions) was produced for Environment Canada (Wallace 2009).

“1-nm” Instruments

The history of particle instrumentation has been toward being able to measure smaller and smaller yet particles. Optical particle monitors could only go down to 0.3 μm (300 nm). Early differential mobility instruments could measure down to about 10 nm. Around 2000, Chen et al. (1998) developed a new design that could reach 2.5 nm. Although this does not sound like such a large improvement, in fact early users of the instrument discovered that for some sources such as gas and electric stoves and power tools 90% of the particles produced were between 2.5 and 10 nm.

Although not driven by considerations of indoor particles, a more recent development has succeeded in pushing the lower bound down close to 1 nm (Kangasluoma et al. 2015). This size is approximately the size of a large molecule or atomic cluster. The development has been driven by considerations of chemical reactions, which are important in causing gas-to-particle nucleation. Nucleation “bursts” creating UFPs over hundreds of square kilometers have been noted. The reactions leading to nucleation require instruments capable of observing the growth of the particles from their inception as molecular clusters.

UFP Emission Sources

Gas Burning Appliance Emissions

Wallace et al. (2004) provided initial studies of the size distribution of particles from a gas stove. Wallace et al. (2008) extended the earlier studies of gas stoves using the nano-DMA to investigate particles between 2 and 10 nm. It was found that 95% of the particles produced by the gas stovetop burners lie in this previously unstudied region (Fig. 3). The particle sizes are centered around 5–6 nm, and had an average peak concentration in the bedroom of $200,000 \text{ cm}^{-3}$. For comparison, this is 10 times the typical urban outdoor UFP concentration of about $20,000 \text{ cm}^{-3}$. Gas dryers also emit ultrafine particles (Wallace 2005).

Electric Stove Emissions

Electric stoves, present in 60% of US homes, may be the most important source of UFP. Dennekamp et al. (2001) performed several cooking tests on electric stoves, finding an increase of $90,000\text{--}110,000 \text{ cm}^{-3}$ for heating 1–4 rings to maximum temperature. However, they found that boiling water or stir-frying did not increase the number of particles. Frying bacon produced an increase of $159,000 \text{ cm}^{-3}$. Grilling toast produced an increase of $130,000 \text{ cm}^{-3}$, and grilling bacon produced

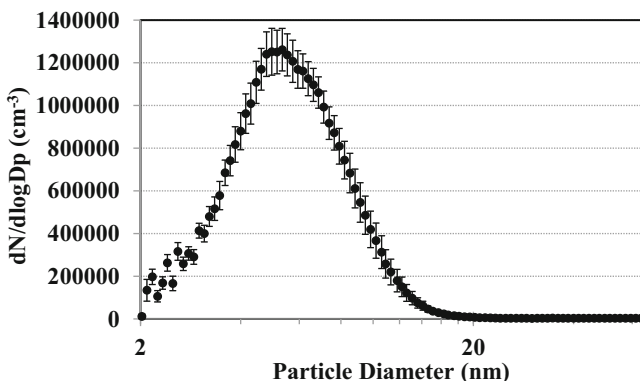


Fig. 3 Particle size distribution observed in bedroom of NIST test house due to use of gas stovetop burner in kitchen for 10 min ($N = 11$ experiments)

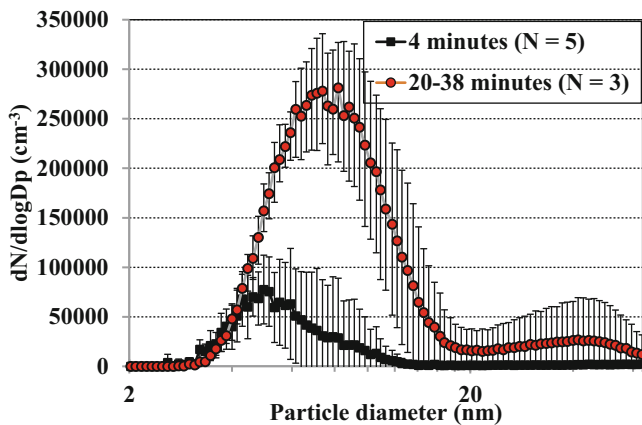


Fig. 4 Particle size distributions observed in bedroom of NIST test house due to use of electric stovetop for short and long periods

an increase of 530,000 cm⁻³. These results were extended to smaller particles (down to 2 nm) by Wallace et al. (2008). As with gas stoves, it was found that electric stovetop coils also emit mostly small particles <10 nm (Fig. 4).

Electric Motors

Appliances with electric motors are widespread, including blenders, mixers, shavers, power tools, etc. Again, not many tests have been done, but they show that all those named can produce UFP, sometimes in large quantities. In this case, the process for producing UFP occurs in the brushes and armature of the electric motor (Smczak et al. 2007). The particle composition may include graphite from the brushes or copper from the wiring.

Other Electric Appliances

However, many common appliances make use of electric heating: hair dryers, electric toasters and toaster ovens, coffee makers, etc. Hair dryers, toasters and toaster ovens do in fact produce copious quantities of UFP, but coffee makers have not been shown to produce UFP. The process of producing UFP from electric appliances is now known to be due to material (probably SVOCs) accumulating over time on the burners (Wallace et al. 2015, 2017).

Candle Burning

A third major indoor source of UFP is candle burning. Bekö et al. (2013) studied 56 homes in Denmark and concluded that candle burning was about as strong a source as cooking.

Source Identification and Apportionment

Given the differences in the emitted size distributions, it is possible to use particle size distributions to conduct source identification and apportionment

studies. Ogulei et al. (2006) used particle size measurements made using an SMPS and an APS. Using positive matrix factorization, they identified nine particle sources including two sources associated with gas burner use: boiling water and frying tortillas. Boiling water for tea or coffee was found to be associated only with the smallest particles, with a number mode close to the detection limit of the SMPS (i.e., 10 nm). Frying tortillas produced particles with a number mode at about 90 nm while broiling fish produced particles with a number mode at about 50 nm. A citronella candle was often burned during the study period, and this practice was found to produce a 200 nm modal number distribution. Other indoor particle sources identified included sweeping/vacuuming (volume mode at 2 μm); use of the electric toaster oven (number mode at 30 nm); and pouring of kitty litter (volume mode $>10 \mu\text{m}$). Two outdoor sources were also resolved: traffic (number mode at about 150 nm) and wood smoke (major number mode at about 70 nm).

Emission Rates

A study of multiple sources of UFP involving either combustion or heating elements was carried out by Wallace and Ott (2010). A Model 3007 CPC (TSI, Shoreview, MN) was used to measure such sources as gas stoves, electric stoves, electric toaster ovens, steam irons, gas clothes dryers, and more than a dozen more common appliances.

Only a few field studies have attempted to estimate UFP emission rates of indoor sources. Emission rates of $0.35\text{--}7.34 \times 10^{11} \text{ min}^{-1}$ were reported for multiple types of cooking in 15 homes in Brisbane, for UFP $>15 \text{ nm}$ (He et al. 2020). Wallace et al. (2004) found a mean emission rate of UFP $>10 \text{ nm}$ for 24 cooking episodes of $3.3 \times 10^{12} \text{ min}^{-1}$. This rate is sufficient to attain a peak concentration of about $100,000 \text{ cm}^{-3}$ in a typical home of 350 m^3 (1500 sq ft.)

Using the nano-DMA, Wallace et al. (2008) extended measurement of emission rates of indoor sources down to 2 nm. For both gas stovetop burners and electric stovetop coils, large quantities of UFP were produced in the previously unstudied region between 2 and 10 nm. Both sources produced particles that peaked at about 5–7 nm, and often 90% of all UFP produced were $<10 \text{ nm}$. Emission rates sometimes exceeded 10^{13} min^{-1} , and worst-case concentrations exceeding 10^6 cm^{-3} were observed. This finding suggests that previous reports of UFP concentrations produced by indoor sources may have been substantially underestimated. However, these sources of $<10 \text{ nm}$ particles were limited to the stovetops; ovens in both types of stoves and also toaster ovens produced mainly particles $>10 \text{ nm}$. Since the fundamental source (gas and electricity) is the same in the ovens as in the stovetops, it is probable that many particles $<10 \text{ nm}$ are being created but coagulate rapidly in the enclosed spaces and thus are not observed in the kitchen or household. A third major indoor source of UFP is candle burning. Wallace et al. (2019) studied the dynamic behavior (UFP number emission rate and deposition rate) of burning candles in a residence. A number of the studies that measured UFP indoors are listed in Tables 2 and 3.

Table 2 Ultrafine particle emission rates from indoor sources

Appliance	Event	N	Range of emission rates ($\times 10^{12}$) (particles min $^{-1}$)	Mean emission rate ($\times 10^{12}$) (particles min $^{-1}$)	SD ($\times 10^{12}$) (particles min $^{-1}$)	SE ($\times 10^{12}$) (particles min $^{-1}$)	Range of 1-h averages ($\times 10^3$) (particles cm $^{-3}$)
Gas stove & toaster oven	Cooking	23	1.1–11.6	5.11	3.04	0.63	6–94
Gas clothes dryer	Drying clothes	6	2.2–5.6	4.40	1.60	0.65	16–50
Air popper	Popping corn	4	1.4–6.0	4.26	2.03	1.01	19–55
Electric toaster	Toasting	1		3.8		99	
Match	Lighting candles	3	2.3–5.0	3.65	1.91	1.10	4.4–26
Spray cleaner	Housecleaning	6	1.5–3.2	2.60	0.61	0.25	33–162
Electric toaster oven	Cooking	54	0.19–6.9	2.11	1.34	0.18	7–144
Gas stove	Cooking	95	0.37–6.9	1.89	1.71	0.18	8–223
Electric stove	Cooking	21	0.24–4.4	1.25	1.08	0.24	6–145
Cigarette	Smoking	4	0.38–1	0.58	0.29	0.15	4–14
Electric mixer	Preparing food	5	0.02–1.5	0.57	0.72	0.32	0.004–61
Candles	Burning candles	10	0.13–1.0	0.56	0.25	0.08	9–139
Curling irons	Grooming	3	0.14–0.4	0.29	0.13	0.07	0.005–193
Steam iron	Ironing	6	0.04–0.35	0.24	0.11	0.04	10–81
Hair dryers	Grooming	8	0.0007–0.7	0.23	0.22	0.08	-0.01–137
Space heater	Heating	3	0.03–0.29	0.13	0.13	0.08	3.6–57
Hair straightener	Grooming	1		0.11			16
Laser printer	Printing 10 pages	3	0.03–0.10	0.06	0.04	0.02	0.068–4.2
Vacuums	Housecleaning	2	0.02–0.10	0.06	0.06	0.04	0.31–3.5
Fireplace	Fire lit	1		0.003		0.14	

Wallace LA, Ott WR (2010) Personal exposure to ultrafine particles. *J Expos Sci Environ Epidemiol* 21:20–30

Table 3 Studies of indoor concentrations, sources, and emission rates of ultrafine particles

Study	Pub year	Objective	Building type	Number of builds	Period of sampling	Meas method	Particle size (nm)	Results, concentrations (cm^{-3}), conclusions, comments
Li and Hopke (1993)	1993	Apartment	Apt. building	1	12	DMPS	17–886	First to study UFP from cooking: soup, scrambled eggs, fried chicken, with modes of 30, 40, 50 nm, respectively. Outdoor mode was 70 nm. Background UFP levels in kitchen averaged 13,000; cooking peaks reached 150,000.
Abt et al. (2000a)	2000a	Indoor sources	Homes	3	6–12 days per home	SMPS	20–500	First to use SMPS to study indoor-outdoor relationships. Cooking the most important indoor source of UFP.
Abt et al. (2000b)	2000b	Penetration	Homes	3	6–12 days per home	SMPS	20–500	Unable to calculate P and k for individual homes. For six cooking events, direct measures of $k = 1.07 \pm 0.23 \text{ h}^{-1}$
Long et al. (2001)	2001	Indoor sources	Homes	9	6–12 days per home	SMPS	20–500	Main sources: cooking and burning candles. Also 5 cleaning events with Pine-Sol (reaction of ozone with terpenes). Data generally presented in volume rather than number concentrations.

Wallace et al. (2020)	2000	Indoor sources	Home	1	18 mo	SMPS	10–950	Candles, matches, incense, and frying, sauteeing, broiling, deep-frying, and stir-frying important indoor sources of UFP. The gas oven, gas burners, and electric toaster oven were all important sources. A source-proximity effect was noted, with the kitchen monitor reading two to five times higher than the upstairs monitor.
Dennekamp et al. (2001)	2001	Cooking emission rates	Lab (70 m ³)	1	11 types of cooking on both gas and electric stoves. 89 experiments	SMPS	10–500	Probably first study to show electric stoves emit UFP. Range of concentrations (in cm ⁻³): Stovetop (gas): 3000–60,000; (elec) 9000–16,000. Oven (gas): 10,000–12,000; (elec): 2000–3000. Grill (gas): 10,000–41,000; (elec) 8,000–53,000.
Koponen et al. (2001)	2001	Indoor-outdoor	Office bldg	1 room	3 weeks	SMPS	7–500 nm	I/O ratios: ~0.1 (8–25 nm); 0.15 (25–90 nm); 0.3 (90–500 nm) (est. from Fig. 4)
Long et al. (2001)	2001	Penetration	Homes	9	6–12 days per home	SMPS	20–500	Unable (with 1 exception) to calculate P and k for individual homes. Pooled estimates of P : 0.90–1.05; k : 0.59–0.29 h ⁻¹

(continued)

Table 3 (continued)

Morawska et al. (2001)	2001	Indoor-outdoor	Homes	16		SMPS, CPC >7	15–685, >7	Median I/O was 0.97. Range 0.44–2.46. Rather high values due to open windows, indoor sources. Under minimum ventilation, median I/O (CPC) = 0.56, range = 0.21–1.99
Levy et al. (2002)	2002	Levels	Non-residential	6	29	P-Trak	20– 1000	UFP in the apt., coffee shop, hospital, library, and mall = 0.6, 0.3, 0.1, 0.2, and 0.1 × outdoors, resp. Food court 150,000 indoors compared to 40,000 out.
Sarnat et al. (2002)	2002	Sulfur as a marker for infiltration	HOmes	6	36	SMPS	20–500	I/O ratios for S well correlated with those for particles in the 60–500 nm range, supporting use of S as marker for PM2.5 infiltration.
Wallace (2000)	2000	Indoor sources	Home	1	18 mo	SMPS	10–950	Indoor sources were active 22% of the time. Fraction of indoor concentration due to indoor sources was 0.82 for the 10–18 nm category; 0.68 for 18–50 nm, and 0.5 for 50–100 nm

Franck et al. (2003)	2003	Penetration	Laboratory, gatehouse	Room	1500 I/O samples	DMPS	15–800	Simultaneous indoor-outdoor sampling in two rooms-indoor activities low. I/O ratios 0.01 at 17 nm, increasing to 0.6 at 150 nm, dropping to 0.2 at 600 nm
Rundell (2003)	2003	Effect of ice resurfacing machines	Ice arena	10 arenas	28 days total	P-Trak	20–1000	104,000 indoors; 4000 outdoors. Pre-resurfacing: 35000–45,000. Post-resurfacing: 120,000–160,000.
Cyrys (Stözel et al. 2007)	2004	Indoor-outdoor	Hospital	two rooms	two 8-week periods summer & winter	CPC	7–3000	Median I/O ratio 0.42. Windows closed: 0.33; open: 0.78
Hameri et al. (2004)	2004	Fine and UFP	Helsinki locations					
He et al. (2004)	2004	Emission rates, penetration	Homes	15	2 days per home	SMPS, CPC	15–685; 7–808	Standardized 10-min cooking test (frying in oil) emitted median value of 10^{12} min^{-1} . Normal cooking ($N = 106$) emitted $1–7 \times 10^{11} \text{ min}^{-1}$. Smoking ($N = 6$) emitted $1.9 \times 10^{11} \text{ min}^{-1}$.
Wallace et al. (2004)	2004	Cooking emission rates	Home	1	44	SMPS	10–450	Cooking with gas stove created about 10 times as many UFP as observed in noncooking periods. Emission rates on the order of 10^{14} h^{-1} .

(continued)

Table 3 (continued)

Wallace et al. (2004)	2004	Effect of filters on deposition rates	Home	1	18 mo	SMPS	10–950	Deposition rates calculated for four conditions: fan off, fan on, fibrous filter, electrostatic precipitator.
Afshari et al. (2005)	2005	Indoor sources	Laboratory	Room-size chamber	NR (137)	P-Trak	20–1000	"U"-shaped distribution with the minimum occurring near 0.1 μm , as predicted by theory. Central fan with no filter or with a standard furnace filter increased deposition rates by amounts on the order of 0.1–0.5 h^{-1} . The fibrous filter increased deposition rates by up to 2 h^{-1} for UFP. The ESP increased deposition rates by 2–3 h^{-1} . However, the ESP lost efficiency after several weeks and needed regular cleaning to maintain its effectiveness. A reduction of particle levels by 50% or more could be achieved by use of the ESP when operating properly.

Hussein et al. (2002, 2004)	2002, 2004	Indoor-outdoor	Home	1	21	nano-DMA & DMPS	electric stove, steam iron, operating propane gas camping stove, electric air heater, electric radiators studied. Emission rates about 10^{11} min $^{-1}$ for many activities.
Hussein et al. (2005)	2005	Evaluate model	Office room, home	1 each	45 days (office); 21 (home)	DMPS	Loss rate ($a + k$) varied from about 1 h^{-1} for 10-nm particles to about 0.4 h^{-1} for 100-nm particles. UFP indoor-outdoor ratio with no indoor sources was about 0.36.
Matson (2005)	2005	Indoor sources	Homes, offices	5 offices, 3 homes	33	Model 3007, P-Trak	The home here is the same one as above. Emission rates were estimated for four activities in the home. Offices had I/O ratios < 1 , suggesting few indoor sources. Homes had strong indoor sources including cooking and candle burning
Wallace (2005)	2005	Gas clothes dryer as UFP source	Home	1	150 h over 18 months	SMPS	Vented gas clothes dryer produced UFP concentrations $> 100,000$, with estimated emission rate of 6×10^{12} particles per drying cycle.

(continued)

Table 3 (continued)

Zhu et al. (2005)	2005	Penetration	Apt. building	4	6 days/apt. Then 2 apts sampled at night only	SMPS P-Trak	6–220 20– 1000	Indoor: 7000–12,000; outdoor: 14,000–20,000. I/O ratios appeared to increase below 20 nm for unknown reasons. Estimated penetration coefficient appeared to reach asymptote of 0.6, well below theoretical expectations. Air exchange measurements may be biased high in apartments
Hussein et al. (2006)	2006	Indoor sources	Apartment	1	14	SMPS	14–552	Cooking was the main source, producing values as high as 180,000 in the kitchen. Living room was typically about 1/3 of kitchen values. Smoking produced values of 36,000 from baseline of 6000.
Jeong et al. (2006)	2006	Particle number	Rochester and Toronto					
Murr et al. (2006)	2006	Composition	Residences	10	10	thermal precipitator	>10 nm	Thermal precipitator collects particles on TEM grids for elemental analysis. Gas particles contain primary 30-nm spheres and carbon nanotubes about 100 nm long by 10 in diameter.

See and Balasubramanian (2006)	2006	Emission rates of cooking	Home	1	1 h		SMPS	10–500	Five cooking methods tested on gas stove, with samples taken at nose height of cook. Concentrations increased from 54,000 (steaming) to 110,000 (frying) to 595,000 (deep-frying)
Wallace et al. (2006)	2006	Indoor sources, emission rates	Home	1	3 years		SMPS	10–950	18 activities analyzed, including cooking with gas stove, toasting, burning candles and incense, etc. Peak modes were near 10 nm for gas stovetop burners, around 30 nm for electric toaster and toaster oven, 60 nm for burning candles and incense, and near 70 nm for penetration of outdoor particles. The highest mean number concentrations were due to complex cooking, producing average number concentrations of $35,000\text{--}50,000\text{ cm}^{-3}$, compared to $12,000\text{ cm}^{-3}$ outdoors and 3500 cm^{-3} indoors when no sources were observed.

(continued)

Table 3 (continued)

Diapouli et al. (2007)	2007	Indoor-outdoor	7 schools, 1 home	2–5 days per school	Model 3007	10–1000	Outdoor levels of 14,000–39,000 in Athens in winter, 5000–8000 in summer.
							Indoor mean in schools of 17,000–outdoor 27,000.
							Indoor mean in non-smoking homes 14,000.
Fromme et al. (2007)	2007	Levels	Schools	64	5 h/classroom	SMPS	10–487 Median (mean) 5660 (6509).
Mitsakou et al. (2007)	2007	Lung deposition during cooking	Apt. building	1	one 15-min cooking event, one overnight	SMPS	10–300 Lung deposition from a 15-min cooking episode >10 × total deposition over 8-h sleeping period.
Valente et al. (2007)	2007	Effect of banning smoking	Public places	40	20 min	P-Trak	20–1000 UFP reduced from 76,000 to 38,000 after smoking ban
Weichenthal et al. (2007)	2007	Effect of home heating systems	Homes	36	1 per home	P-Trak	20–1000 No increase due to home heating systems; strong increases from smoking, cooking with electric stove
Gehin et al. (2008)	2008	Size distribution emission rates					
Hoek et al. (2008)	2008	Indoor-outdoor	Homes in 4 cities	152	1 week/home	CPC	7–3000 Four cities:: Helsinki, Athens, Amsterdam, Birmingham. Regressed indoor on outdoor values to obtain average infiltration factor for central site (0.06,

					0.25, 0.43, and 0.15, respectively) and for just outside home (0.42, 0.42, 0.19, 0.22). Mean indoor-generated particles ranged from 3000–6000 from central-site regressions, 2000–7000 from outdoor regressions. Using sulfate, infiltration factor was 0.59, 0.61, 0.78, and 0.61, resp.
Stieb et al. (2008)	2008	Effect of air quality advice	Home, office, car	Variable	13 days P-Trak 20–1000
Wallace et al. (2008)	2008	Cooking emission rates	Test house	1 ~150 SMPS 2–64	First study to look at indoor sources in the 2–10 nm region. Both gas and electric stovetop burners/coils produced UFP peaks around 5 nm; 90% of total UFP <10 nm. Coagulation dominates deposition and air exchange rates in determining fate of UFP in first hour. Emission rates about 10^{13} min^{-1} .

(continued)

Table 3 (continued)

Weichenthal et al. (2008)	2008	Levels	Schools	2	60 (37 classrooms)	P-Trak	20– 1000	Outdoor levels of 14,000 exceeded indoor levels of 5000, indicating few sources of UFP in classrooms
Wensing et al. (2008)	2008	Laser printers	Chamber, office room	1	Multiple (12 in office room)	FMPS, SMPS, P-Trak	5.6– 560, 10– 1000, 20– 1000	Source may be fuser, not toner particles. 45-min average concentrations in office room (72 m^3) ranged from 4600–14,000 cm^{-3}
Wallace (2009)	2009	Indoor sources	Homes	2	~100	Model 3007	10– 1000	20 sources tested, including cooking, candles, steam iron, hair dryers, fireplace, laser printer, air popper.. Emission rates calculated for all sources
Rim et al. (2013)	2010	infiltration	test house	1	29 60-h weekends from August 2008– Sept 2009	SMPS	2– 64 nm, 3– 100 nm	Penetration P was near zero for particles < 10 nm, went from 0.2 at 10 nm to an asymptote of 0.6 for particles >30 nm. Finf ranged from 0–0.3 with windows closed and from 0 to 0.6 with one window open
Sultan et al. (2011)	2011	air cleaner UFP effectiveness	Test room	1		SMPS		12 portable air cleaners tested. HEPA and ESP were best performers.

Kearney et al. (2011)	2011	all except smoking	Homes	94	5 days	P-Trak	45 homes of adults one season; 49 homes with asthmatic children: 2 seasons
Wheeler et al. (2011)	2011	all except smoking	Homes	95	5 days	P-Trak	personal, indoor and outdoor concentrations measured using continuous monitors
Wallace and Ott (2010)	2010	stoves, driving, eating out	Homes, restaurants, autos		3 years	SMPS, Model 3007	Major sources included restaurants, cooking on gas or electric stoves, use of toaster ovens- emission rates $>10^{12}/\text{min}$
Rim et al. (2012)	2012	coagulation model	Test house			SMPS	10–400 nm 18–960 nm $>10 \text{ nm}$
Rim et al. (2012)	2012	Kitchen exhaust fans	Test house	2	2 fans tested at four flow rates	SMPS	2.5–100 nm Coagulation a significant contributor to particle loss/gain at concentrations $>20,000 \text{ cm}^{-3}$.
Zhang and Zhu (2012)	2012	UFP, other	Schools	5			
Beko et al. (2013)	2013		Homes	56			Candle burning and cooking the major indoor source of PM and UFP
Buonanno et al. (2013)	2013						
Rim et al. (2013)	2013	outdoor penetration	test building				

(continued)

Table 3 (continued)

Azimi and Stephens (2013)	2014	HVAC filter removal efficacy				194 outdoor particle size distributions used to estimate single-pass removal for PM2.5 and UFP
Buonanno et al. (2014)	2014	time-activity patterns	24 couples	48 h		Exposures higher for women due to cooking
Fonseca et al. (2014)	2014	UFP in pre-schools	Preschools			Exposure in Asian cities about 4 times that in European cities
Kumar et al. (2014)	2014	Modeled exposure from Outdoor sources	Outdoor	UFP size distributions from 42 cities		
Kearney et al. (2014)	2014	Measure concentrations and exposures	Homes	74		Dust Trak, P-Trak
Soppa et al. (2017)	2017	Effect on blood pressure	Test room	54		50 homes in Edmonton each season. Finf estimates for both fine particles (FP) and UFP.
Spilak et al. (2014)	2014	Homes		27		Toast affected BP—Grilling and candle burning did not
Beko et al. (2015)	2015		59 persons	48 h		home was 50% of exposure, other indoor 40%; in transit or outdoors <5%. But highest concentrations in transit.
Issaxson et al. (2015)	2015		22 homes			cooking and candle burning the major sources

Meier et al. (2015)	2015	Homes		80	1–2 weeks		
Wallace et al. (2015)	2015					compared indoor to outdoor UFP. Mean indoor conc = 7800 cm^{-3} .	
Zauli Sejani et al. (2015)	2015						
Singer et al. (2017)	2017						
Wallace et al. (2017)	2017						
Slezakova et al. (2018)	2018	Fitness centers	4			Surface chemistry and secondary organic aerosols	
Weschler and Carslaw (2018)	2018	Review article on indoor chemistry					
Nguyen et al. (2019)	2019	marijuana	Vape shops				
Slezakova et al. (2019)	2019	all	schools	73		Highest levels at canteens	
Garcia-Hernandez et al. (2020)	2019	Children				Review of children (under 18) exposure to UFP; 32 studies, 10 personal exposure, 22 indoor	
Wallace et al. (2019)	2019	candles	Home	1		High emissions $10^{13}/\text{min}$; mode about 5 nm	
Chen et al. (2020)	2020	cooking with oil					

Concluding Note

In this chapter, we have presented an introduction to sampling and measurement instruments. This survey is not meant to be comprehensive and there are many similar tools available from other manufacturers. The mention of specific products was not meant to endorse them but to alert the reader to instruments that have been widely used and results published in the literature. The field is constantly advancing and thus, there may be alternative instruments that will be a better match to specific project goals and a wide search of what is available will be useful in allowing each investigator to find the best approach for their specific needs.

Cross-References

- [Disease Burden of Indoor Air Pollution](#)
-

References

- Abt E, Suh HH, Catalano P, Koutrakis P (2000a) Relative contribution of outdoor and indoor particle sources to indoor concentrations. *Environ Sci Technol* 34:3579–3587
- Abt E, Suh HH, Allen G, Koutrakis P (2000b) Characterization of indoor particle sources: a study conducted in the metropolitan Boston area. *Environ Health Perspect* 108(1):35–44
- Afshari A, Matson U, Ekberg LE (2005) Characterization of indoor sources of fine and ultrafine particles: a study conducted in a full-scale chamber. *Indoor Air* 15:141–150
- Aitken J (1888) On the number of dust particles in the atmosphere. *Nature* 37(957):428–430
- Aitken J (1892) On a simple pocket dust-counter. *Proc R Soc Edinb* 18:39–52
- Andreae MO, Gelencsér A (2006) Black carbon or brown carbon? The nature of light-absorbing carbonaceous aerosols. *Atmos Chem Phys* 6:3131–3148
- AQ-SPEC (2016). <http://www.aqmd.gov/docs/default-source/aq-spec/field-evaluations/purpleair%20field-evaluation.pdf>. Accessed 19 Dec 2020
- Ardon-Dryer K, Dryer Y, Williams JN, Moghimi N (2020) Measurements of PM_{2.5} with PurpleAir under atmospheric conditions. *Atmos Meas Tech* 13:5441–5458
- Azimi P, Stephens B (2013) HVAC filtration for controlling infectious airborne disease transmission in indoor environments: predicting risk reductions and operational costs. *Build Environ* 70:150–160. <https://doi.org/10.1016/j.buildenv.2013.08.025>
- Badura M, Batog P, Drzeniecka-Osiadacz A, Modzel P (2018) Evaluation of low-cost sensors for ambient PM_{2.5} monitoring. *Sensors* 2018:1–16
- Badura M, Batog P, Drzeniecka-Osiadacz A, Modzel P (2019) Regression methods in the calibration of low-cost sensors for ambient particulate matter measurements. *SN Appl Sci* 1:622
- Barkjohn KK, Gantt B, Clements AL (2020) Development and application of a United States wide correction for PM2.5 data collected with the PurpleAir sensor. *Atmos Meas Tech Discuss*. <https://doi.org/10.5194/amt-2020-413>
- Becnel T, Tingey K, Whitaker J, Sayahi T, Le K, Goffin P, Butterfield A, Kelly K, Gaillardon PE (2019) A distributed low-cost pollution monitoring platform. *IEEE Internet Things J* 6: 10738–10748
- Bekö G, Kjeldsen BU, Olsen Y, Schipperijn J, Wierzbicka A, Karottki DG, … Clausen G (2015) Contribution of various microenvironments to the daily personal exposure to ultrafine particles: personal monitoring coupled with Gps tracking. *Atmos Environ* 110:122–129

- Bekö G, Weschler CJ, Wierzbicka A, Karottki DG, Toftum J, Loft S, Clausen G (2013) Ultrafine particles: exposure and source apportionment in 56 Danish homes. *Environ Sci Technol* 47: 10240–10248
- Bi J, Wildani A, Chang HH, Liu Y (2020) Incorporating low-cost sensor measurements into high-resolution PM_{2.5} modeling at a large spatial scale. *Environ Sci Technol* 54:2152–2162
- Bi J, Wallace LA, Sarnat JA, Liu Y (2021) Characterizing outdoor infiltration and indoor contribution of PM_{2.5} with citizen-based low-cost monitoring data. *Environ Pollut* 276: 116763
- Birch ME, Cary RA (1996) Elemental carbon-based method for monitoring occupational exposures to particulate diesel exhaust. *Aerosol Sci Technol* 25:221–241
- Bond TC, Anderson TL, Campbell D (1999) Calibration and intercomparison of filter-based measurements of visible light absorption by aerosols. *Aerosol Sci Technol* 30:582–600
- Brattich E, Bracci A, Zappi A, Morozzi P, Di Sabatino S, Porcù F, Di Nicola F, Tositti L (2020) How to get the best from low-cost particulate matter sensors: guidelines and practical recommendations. *Sensors* 20:3073
- Bräuner EV, Forchhammer L, Møller P, Simonsen J, Glasius M, Wählén P, Raaschou-Nielsen O, Loft S (2007) Exposure to ultrafine particles from ambient air and oxidative stress-induced DNA damage. *Environ Health Perspect* 115:1177–1182
- Bräuner EV, Forchhammer L, Møller P, Barregard L, Gunnarsen L, Afshari A, Wählén P, Glasius M, Dragsted LO, Basu S, Raaschou-Nielsen O, Loft S (2008) Indoor particles affect vascular function in the aged: an air filtration-based intervention study. *Am J Resp Crit Care Med* 177: 419–425
- Bulot FMJ, Johnston SJ, Basford PJ, Easton NHC, Apetroaie-Cristea M, Foster GL, Morris AKR, Cox SJ, Loxham M (2019) Long-term field comparison of multiple low-cost particulate matter sensors in an outdoor urban environment. *Sci Rep* 9:7497
- Buonanno G, Marks GB, Morawska L (2013) Health effects of daily airborne particle dose in children: direct association between personal dose and respiratory health effects. *Environ Pollut* 180:246–250
- Buonanno G, Stabile L, Morawska L (2014) Personal exposure to ultrafine particles: the influence of time-activity patterns. *Sci Total Environ* 468–469:903–907
- Cai J, Yan B, Ross J, Zhang D, Kinney PL, Perzanowski MS, Jung K, Miller R, Chillrud SN (2014) Validation of MicroAeth® as a black carbon monitor for fixed-site measurement and optimization for personal exposure characterization. *Aerosol Air Qual Res* 14:1–9
- Cantrell BK, Stein SW, Patashnick H, Hassel D (1996) Status of a tapered element, oscillating microbalance-based continuous respirable coal mine dust monitor. *Appl Occup Environ Hyg* 11: 624–629
- Cantrell BK, Williams KL, Stein SW, Hassel O, Patashnick H (1997) Continuous respirable dust monitor development. In: Proceedings of the 6th international mine ventilation congress. Society of Mining Engineers, Littleton
- Catrambone M, Canepari S, Cerasa M, Sargolini T, Perrino C (2019) Performance evaluation of a very-low-volume sampler for atmospheric particulate matter. *Aerosol Air Qual Res* 19: 2160–2172
- Cavalli F, Viana M, Yttri KE, Genberg J, Putaud JP (2010) Toward a standardised thermal-optical protocol for measuring atmospheric organic and elemental carbon: the EUSAAR protocol. *Atmos Meas Tech* 3:79–89
- Chen D-R, Pui D, Hummes D, Fissan H, Quant FR, Sem GJ (1998) Design and evaluation of a nanometer aerosol differential mobility analyzer (Nano-DMA). *J Aerosol Sci* 29:497–509
- Chen LJ, Ho Y-H, Lee H-C, Wu H-C, Liu H-M, Hsieh H-H, Huang Y-T, Lung S-CC (2017) An open framework for participatory PM_{2.5} monitoring in smart cities. *IEEE Access* 5: 14441–14454
- Chen M, Romay FJ, Marple VA (2018) Design and evaluation of a low flow personal cascade impactor. *Aerosol Sci Technol* 52:192–197
- Chen W, Wang P, Zhang D, Liu J, Dai X (2020) The impact of water on particle emissions from heated cooking oil. *Aerosol Air Qual Res* 20:533–543

- Cheng Y-H (2008) Comparison of the TSI model 8520 and Grimm series 1.108 portable aerosol instruments used to monitor particulate matter in an iron foundry. *J Occup Environ Hyg* 5: 157–168
- Chow JC, Watson JG, Chen LWA, Chang MCO, Robinson NF, Trimble D, Kohl S (2007) The IMPROVE_a temperature protocol for thermal/optical carbon analysis: maintaining consistency with a long-term database. *J Air Waste Manage Assoc* 57:1014–1023
- Coulson J, Ellison JK (1963) A calibration of the filter-paper method of estimation of smoke. *Br J Appl Phys* 14:899–903
- Davies CN, Aylward M (1951) The photoelectric measurement of coal dust stains on filter paper. *Br J Appl Phys* 2:352–359
- Delp WW, Singer BC (2020) Wildfire smoke adjustment factors for low-cost and professional PM_{2.5} monitors with optical sensors. *Sensors* 20:3685
- Demokritou P, Kavouras IG, Ferguson ST, Koutrakis P (2001) Development and laboratory performance evaluation of a personal multipollutant sampler for simultaneous measurements of particulate and gaseous pollutants. *Aerosol Sci Technol* 35:741–752
- Dennekamp M, Howarth S, Dick C, Cherrie JW, Donaldson K, Seaton A (2001) Ultrafine particles and nitrogen oxides generated by gas and electric cooking. *Occup Environ Med* 58:511–516
- Diapouli E, Chaloulakou A, Spyrellis N (2007) Levels of ultrafine particles in different microenvironments – implications to children exposure. *Sci Total Environ* 388:128–136
- Donaldson K, Tran L, Jimenez LA, Duffin R, Newby DE, Mills N, MacNee W, Stone V (2005) Combustion-derived nanoparticles: a review of their toxicology following inhalation exposure. *Part Fibre Toxicol* 2:10
- Donghyun Rim , Michal Green , Lance Wallace , Andrew Persily & Jung-Il Choi (2012) Evolution of Ultrafine Particle Size Distributions Following Indoor Episodic Releases: Relative Importance of Coagulation, Deposition and Ventilation, *Aerosol Science and Technology*, 46:5, 494–503
- Du Y, Wang Q, Sun Q, Zhang T, Li T, Yan B (2019) Assessment of PM_{2.5} monitoring using MicroPEM: a validation study in a city with elevated PM_{2.5} levels. *Ecotoxicol Environ Safety* 171:518–522
- Dzubay TG, Hines LE, Stevens RK (1976) Particle bounce errors in cascade impactors. *Atmos Environ* 19:229–234
- Edney EO, Kleindienst TE, Jaoui M, Levandowski M, Offenberg JH, Wang W, Claeys M (2005) Formation of 2-methyltetrosols and 2-methylglyceric acid in secondary organic aerosol from laboratory irradiated isoprene/NOx/SO2/air mixtures and their detection in ambient PM2.5 samples collected in the Eastern United States. *Atmos Environ* 39:5281–5289
- Fonseca J, Slezakova K, Morais S, Pereira MC (2014) Assessment of ultrafine particles in Portuguese preschools: levels and exposure doses. *Indoor Air* 24:618–628
- Falkovich AH, Rudich Y (2001) Analysis of semivolatile organic compounds in atmospheric aerosols by direct sample introduction thermal desorption GC/MS. *Environ Sci Technol* 35: 2326–2333
- Feenstra B, Papastolou V, Hasheminassab S, Zhang H, Boghossian BD, Cocker D, Polidori A (2019) Performance evaluation of twelve low-cost PM2.5 sensors at an ambient air monitoring site. *Atmos Environ* 216:116946
- Francis AS, Chee FP, Chang JHW, Sentian J, Dayou J, Payus CM (2019) Parametric model for estimation of mass concentration based on particle count distribution for ambient air monitoring. *J Phys Conf Ser* 1358:012042
- Franck U, Herbarth O, Wehner B, Wiedensohler A, Manjarrez M (2003) How do the indoor size distributions of airborne submicron and ultrafine particles in the absence of significant indoor sources depend on outdoor distributions? *Indoor Air* 13:174–181
- Fromme H, Twardella D, Dietrich S, Heitmann D, Schierl R, Liebl B, Ruden H (2007) Particulate matter in the indoor air of classrooms – exploratory results from Munich and surrounding area. *Atmos Environ* 41:854–866

- García-Hernandez C, Ferrero A, Estarlich M, Ballester F (2020) Exposure to ultrafine particles in children until 18 years of age: a systematic review. *Indoor Air* 30(1):7–23
- Gehin E, Ramalho O, Kirchner S (2008) Size distribution and emission rate measurement of fine and ultrafine particle from indoor human activities. *Atmos Environ* 42:8341–8352
- Global Burden of Disease (2020) Global burden of 87 risk factors in 204 countries and territories, 1990–2019: a systematic analysis for the Global Burden of Disease Study 2019. *Lancet* 396: 1135–1159
- Gupta P, Doralswamy P, Levy R, Pikelnaya O, Maibach J, Feenstra B, Polidori A, Kiros F, Mills KC (2018) Impact of California fires on local and regional air quality: the role of a low-cost sensor network and satellite observations. *GeoHealth* 2:172–181
- Ritchie H, Roser M (2013) Indoor air pollution. Published online at OurWorldInData.org. Retrieved from: <https://ourworldindata.org/indoor-air-pollution> [Online Resource]
- Hameri K, Koponen IK, Aalto PP, Kulmala M (2002) The particle detection efficiency of the TSI-3007 condensation particle counter. *J Aerosol Sci* 33:1463–1469
- Hameri K, Hussein T, Kulmala M, Aalto P (2004) Measurements of fine and ultrafine particles in Helsinki: connection between outdoor and indoor air quality. *Boreal Environ Res* 9:459–467
- Hansen ADA, Rosen H, Novakov T (1982) Real-time measurement of the absorption coefficient of aerosol particles. *Appl Opt* 21:3060
- Hansen ADA, Rosen H, Novakov T (1984) The Aethalometer: an instrument for the real-time measurement of optical absorption by aerosol particles. *Sci Total Environ* 36:191–196
- He M, Kuerbanjiang N, Dhaniyala S (2020) Performance characteristics of the low-cost Plantower PMS optical sensor. *Aerosol Sci Technol* 54(2):232–241. <https://doi.org/10.1080/02786826.2019.1696015>
- HEI (2013) Understanding the health effects of ambient ultrafine particles. Report by the HEI review panel on ultrafine particles. Health Effects Institute, Boston. <https://www.healtheffects.org/publication/understanding-health-effects-ambient-ultrafine-particles>. Accessed 22 Jan 2021
- Hering SV, Stolzenburg MR, Quant FR, O’Berreit DR, Keady PB (2005) A laminar-flow, water-based condensation particle counter (WCPC). *Aerosol Sci Technol* 39:659–672
- He C, Morawska L, Hitchins J, Gilbert D (2004) Contribution from indoor sources to particle number and mass concentrations in residential houses. *Atmos Environ* 38:3405–3415
- Hoek G, Kos G, Harrison R, de Hartog J, Meliefste K, ten Brink H, Katsouyanni K, Karakatsani A, Lianou M, Kotronarou A, Kavouras I, Pekkanen J, Vallius M, Kulmala M, Puustinen A, Thomas S, Meddings C, Ayres J, van Wijnen J, Hameri K (2008) Indoor-outdoor relationships of particle number and mass in four European cities. *Atmos Environ* 42:156–169
- Holder AL, Mebus AK, Maghran LA, McGown MR, Stewart KE, Vallano DM, Elleman RA, Baker KR (2020) Field evaluation of low-cost particulate matter sensors for measuring wildfire smoke. *Sensors* 20:4796
- Holstius DM, Pillarisetti A, Smith KR, Seto E (2014) Field calibrations of a low-cost aerosol sensor at a regulatory monitoring site in California. *Atmos Meas Tech* 7:1121–1131
- Hopke PK (2016) Review of receptor modeling methods for source apportionment. *J Air Waste Manag Assoc* 66:237–259
- Hopke PK, Ramadan Z, Paatero P, Norris GA, Landis MS, Williams RW, Lewis CW (2003) Receptor modeling of ambient and personal exposure samples: 1998 Baltimore particulate matter epidemiology-exposure study. *Atmos Environ* 37:3289–3302
- Hussein T, Glytsos T, Ondracek J, Dohanyosova P, Zdimal V, Hämeri K, Lazaridis M, Smolik J, Kulmala M (2006) Particle size characterization and emission rates during indoor activities in a house. *Atmos Environ* 40:4285–4307
- Hussein T, Hameri K, Kulmala M (2002) Long-term indoor-outdoor aerosol measurement in Helsinki, Finland. *Boreal Environ Res* 7:141–150
- Hussein T, Hämeri K, Aalto P, Asmi A, Kakko L, Kulmala M (2004) Particle size characterization and the indoor-to-outdoor relationship of atmospheric aerosols in Helsinki. *Scand J Work Environ Health* 30(Suppl. 2):54–62

- Hussein T, Korhonen H, Herrmann E, Hämeri K, Lehtinen KEJ, Kulmala M (2005) Emission rates due to indoor activities: indoor aerosol model development, evaluation, and applications. *Aerosol Sci Technol* 39:1111–1127
- Isaxon C, Gudmundsson A, Nordin EZ, Lönnblad L, Dahl A, Wieslander G, Bohgard M, Wierzbicka A (2015) Contribution of indoor-generated particles to residential exposure. *Atmos Environ* 106:458–466
- ISO (1995) Air quality-particle size fraction definitions for health-related sampling, ISO standard 7708. International Standards Organisation, Geneva
- Jeong CH, Evans GJ, Hopke PK, Chalupa D, Utell MJ (2006) Influence of atmospheric dispersion and new particle formation events on ambient particle number concentration in Rochester, United States, and Toronto, Canada. *J Air Waste Manage Assoc* 56:431–443
- Ji X, Le Bihan O, Ramalho O, Mandin C, D'Anna B, Martinon L, Nicolas M, Bard D, Pairon JC (2010) Characterisation of particles emitted by incense burning in an experimental house. *Indoor Air* 20:147–158
- Jiang RT, Acevedo-Bolton V, Cheng KC, Klepeis NE, Ott WR, Hildemann LM (2011) Determination of response of real-time SidePak AM510 monitor to secondhand smoke, other common indoor aerosols, and outdoor aerosol. *J Environ Monit* 1:1695–1702
- Jiao W, Hagler G, Williams R, Sharpe R, Brown R, Garver D, Judge R, Caudill M, Rickard J, Davis M, Weinstock L, Zimmer-Dauphinee S, Buckley K (2016) Community Air Sensor Network (CAIRSENSE) project: evaluation of low-cost sensor performance in a suburban environment in the southeastern United States. *Atmos Meas Tech* 9:5281–5292
- Kaduwela AP, Kaduwela AP, Jrade E, Brusseau M, Morris S, Morris J, Risk V (2019) Development of a low-cost air sensor package and indoor air quality monitoring in a California middle school: detection of a distant wildfire. *J Air Waste Manage Assoc* 69:1015–1022
- Kangasluoma K, Ahonen L, Attoui M, Vuollekoski H, Kulmala M, Petäjä T (2015) Sub-3 nm particle detection with commercial TSI 3772 and Airmodus A20 fine condensation particle counters. *Aerosol Sci Technol* 49:674–681
- Karagulian F, Barbiere M, Kotsev A, Spinelle L, Gerboles M, Lagler F, Redon N, Crunaire S, Borowiak A (2019) Review of the performance of low-cost sensors for air quality monitoring. *Atmos* 10:506
- Kearney J, Wallace L, MacNeill M, Xu X, Vanryswyk K, You H, Kulka R, Wheeler AJ (2011) Residential indoor and outdoor ultrafine particles in Windsor, Ontario. *Atmos Environ* 45: 7583–7593
- Kearney J, Wallace L, MacNeill M, Héroux ME, Kindzierski W, Wheeler A (2014) Residential infiltration of fine and ultrafine particles in Edmonton. *Atmos Environ* 94:793–805
- Kelly KE, Whitaker J, Petty A, Widmer C, Dybwad A, Sleeth D, Martin R, Butterfield A (2017) Ambient and laboratory evaluation of a low-cost particulate matter sensor. *Environ Pollut* 221: 491–500
- Kenny LC, Gussman R, Meyer M (2000) Development of a sharp-cut cyclone for ambient aerosol monitoring applications. *aerosol Sci. Aerosol Sci Technol* 32:338–358
- Kenny LC, Merrifield T, Mark D, Gussman R, Thorpe A (2004) The development and designation testing of a new USEPA-approved fine particle inlet: a study of the USEPA designation process. *Aerosol Sci Technol* 38(S2):15–22
- Khlystov A, Stanier CO, Takahama S, Pandis SN (2005) Water content of ambient aerosol during the Pittsburgh air quality study. *J Geophys Res-Atmos* 110(D7):715–737
- Kim JY, Magari SR, Herrick RF, Smith TJ, Christiani DC (2004) Comparison of fine particle measurements from a direct-reading instrument and a gravimetric sampling method. *J Occup Environ Hyg* 1:707–715
- Kim G-S, Son Y-S, Lee J-H, Kim I-W, Kim J-C, Oh J-T, Kim H (2016) Air pollution monitoring and control system for Subway stations using environmental sensors. *J Sens* 2016:1–10
- Kim S, Park S, Lee J (2019) Evaluation of performance of inexpensive laser based PM2.5 sensor monitors for typical indoor and outdoor hotspots of South Korea. *Appl Sci* 9:1947

- Kissell FN, Volkwein JC, Kohler J (2002) Historical perspective of personal dust sampling in coal mines. In: Proceedings of the mine ventilation conference. Balkema, Lisse, pp 619–623
- Klepeis NE, Tsang AM, Behar JV (1996) Analysis of the National Human Activity Pattern Survey (NHAPS) respondents from a standpoint of exposure assessment. Final EPA report, EPA/600/R96-074. EPA, Washington, DC
- Klepeis NE, Neilson WC, Ott WR, Robinson JP, Tsang AM, Switzer P, Behar JV, Hern SC, Englemann WH (2001) The national human activity pattern survey (NHAPS): a resource for assessing exposure to environmental pollutants. *J Exp Anal Environ Epidemiol* 11:231–252
- Koponen IK, Asmi A, Keronen P, Puhto K, Kulmala M (2001) Indoor air measurement campaign in Helsinki, Finland 1999 and the effect of outdoor air pollution on indoor air. *Atmos Environ* 35: 1465–1477
- Kuan Ken Lee, Rong Bing, Joanne Kiang, Sophia Bashir, Nicholas Spath, Dominik Stelzle, Kevin Mortimer, Anda Bularga, Dimitrios Doudesis, Shruti S Joshi, Fiona Strachan, Sophie Gumy, Heather Adair-Rohani, Engi F Attia, Michael H Chung, Mark R Miller, David E Newby, Nicholas L Mills, David A McAllister, Anoop S V Shah, Adverse health effects associated with household air pollution: a systematic review, meta-analysis, and burden estimation study, *The Lancet Global Health*, Volume 8, Issue 11, 2020, Pages e1427-e1434, ISSN 2214-109X, [https://doi.org/10.1016/S2214-109X\(20\)30343-0](https://doi.org/10.1016/S2214-109X(20)30343-0). (<https://www.sciencedirect.com/science/article/pii/S2214109X20303430>)
- Kulkarni P, Baron PA, Willeke K (eds) (2011) Aerosol measurement: principles, techniques, and applications, 3rd edn. Wiley. ISBN: 978-0-470-38741-2
- Kumar P, Morawska L, Birmili W, Paasonen P, Hu M, Kulmala M, Harrison RM, Norford L, Britter R (2014) Ultrafine particles in cities. *Environ Int* 66:1–10
- Kuula J, Mäkelä T, Hillamo R, Timonen H (2017) Response characterization of an inexpensive aerosol sensor. *Sensors* 17:2915
- Kuula J, Mäkelä T, Aurela M, Teiniälä K, Varjonen S, González Ó, Timonen H (2020) Laboratory evaluation of particle-size selectivity of optical low-cost particulate matter sensors. *Atmos Meas Tech* 13:2413–2423
- Landsberger S, Creactchman M (eds) (1999) Elemental analysis of airborne particles, 1st edn. Gordon and Breach Science Publisher, Amsterdam
- Lane DD, Baldauf RW, Marotz GA (2001) Performance characterization of the portable miniVOL particulate matter sampler. *Trans Ecol Environ* 47:659–670
- Lawless PA, Rodes CE, Ensor DS (2004) Multiwavelength absorbance of filter deposits for determination of environmental tobacco smoke and black carbon. *Atmos Environ* 38: 3373–3383
- Le T-C, Shukla KK, Sung J-C, Li Z, Yeh H, Huang W, Tsai CJ (2019) Sampling efficiency of low-volume PM₁₀ inlets with different impaction substrates. *Aerosol Sci Technol* 53:295–308
- Lee KK, Bing R, Kiang J, Bashir S, Spath N, Stelzle D, Mortimer K, Bularga A, Doudesis D, Joshi SS, Strachan F, Gumy S, Adair-Rohani H, Attia EF, Chung MH, Miller MR, Newby DE, Mills NL, McAllister DA, Shah ASV (2020) Adverse health effects associated with household air pollution: a systematic review, meta-analysis, and burden estimation study. *Lancet Global Health* 8(11):e1427–e1434
- Leigh-Manuell D, Hopke PK, Dhaniyal S (2020) The Aitken counter: revisiting its design and performance characteristics. *Aerosol Sci Technol* 54:999–1006
- Levy Zamora M, Xiong F, Gentner D, Kerkez B, Kohrman-Glaser J, Koehler K (2018) Field and laboratory evaluations of the low-cost Plantower particulate matter sensor. *Environ Sci Technol* 53:838–849
- Levy JI, Dumyahn T, Spengler JD (2002) Particulate matter and polycyclic aromatic hydrocarbon concentrations in indoor and outdoor microenvironments in Boston, Massachusetts. *J Expo Anal Environ Epidemiol* 12:104–114
- Li W, Hopke PK (1993) Initial size distribution and hygroscopicity of indoor combustion aerosol particles. *Aerosol Sci Technol* 19:305–316

- Li ZY, Che W, Lau AK, Fung JC, Lin C, Lu X (2019) A feasible experimental framework for field calibration of portable light-scattering aerosol monitors: case of TSI DustTrak. *Environ Pollut* 255:113136
- Li JY, Mattewal SK, Patel S, Biswas P (2020) Evaluation of nine low-cost-sensor-based particulate matter monitors. *Aerosol Air Qual Res* 20:254–270
- Litton CD (2002a) The use of light scattering and ion chamber responses for the detection of fires in diesel contaminated atmospheres. *Fire Safety J* 37:409–425
- Litton CD (2002b) Studies of the measurement of respirable coal dusts and diesel particulate matter. *Meas Sci Technol* 13:365–374
- Litton CD, Smith KR, Edwards R, Allen T (2004) Combined optical and ionization measurement techniques for inexpensive characterization of micrometer and submicrometer aerosols. *Aerosol Sci Technol* 38:1054–1062
- Long CM, Suh HH, Catalano P, Koutrakis P (2001) Using time- and size-resolved particulate data to quantify indoor penetration and deposition behavior. *Environ Sci Tech* 35:2089–2099
- Magi BI, Cupini C, Francis J, Green M, Hauser C (2020) Evaluation of PM_{2.5} measured in an urban setting using a low-cost optical particle counter and a Federal Equivalent Method. Beta attenuation monitor. *Aerosol Sci Technol* 54:147–159
- Malings C, Tanzer R, Hauryliuk A, Saha PK, Robinson AL, Presto AA, Subramanian R (2020) Fine particle mass monitoring with low-cost sensors: corrections and long-term performance evaluation. *Aerosol Sci Technol* 54:160–174
- Manikonda A, Zikova N, Hopke PK, Ferro AR (2016) Laboratory assessment of low-cost PM monitors. *J Aerosol Sci* 102:29–40
- Marple V, Rubow KL, Turner W, Spengler J (1987) Low flow rate sharp cut impactors for indoor air sampling: design and calibration. *J Air & Waste Manage Assoc* 37:1303–1307
- Masic A, Bibic D, Pikula B, Dzaferovic-Masic E, Musemic R (2019) Experimental study of temperature inversions above urban area using unmanned aerial vehicle. *Therm Sci* 23: 3327–3338
- Masic A, Bibic D, Pikula B, Blazevic A, Huremovic J, Zero S (2020) Evaluation of optical particulate matter sensors under realistic conditions of strong and mild urban pollution. *Atmos Meas Tech* 13:6427–6443
- Matson U (2005) Comparison of the modelling and the experimental results on concentrations of ultra-fine particles indoors. *Build Environ* 40:996–1002
- McMurtry PH (2000) The history of condensation nucleus counters. *Aerosol Sci Technol* 33: 297–322
- Meng QY, Turpin BJ, Korn L, Weisel CP, Morandi M, Colome S, Zhang JFJ, Stock T, Spektor D, Winer A, Zhang L, Lee JH, Giovanetti R, Cui W, Kwon J, Alimokhtari S, Shendell D, Jones J, Farrar C, Maberti S (2005) Influence of ambient (outdoor) sources on residential indoor and personal PM_{2.5} concentrations: analyses of RIOPA data. *J Exp Anal Environ Epidemiol* 15: 17–28
- Meier R, Eeftens M, Phuleria HC, Ineichen A, Corradi E, Davey M, Fierz M, Ducret-Stich RE, Aguilera I, Schindler C, Rochat T, Probst-Hensch N, Tsai MY, Künzli N (2015) Differences in indoor versus outdoor concentrations of ultrafine particles, PM_{2.5}, PMabsorbance and NO₂ in Swiss homes. *J Expo Sci Environ Epidemiol* 25(5):499–505
- Misra C, Singh M, Shen S, Hall PM, Sioutas C (2002) Development and evaluation of a personal cascade impactor sampler (PCIS). *J Aerosol Sci* 33:1027–1047
- Morawska L, He C, Hitchins J, Gilbert D, Parappukkaran S (2001) The relationship between indoor and outdoor airborne particles in the residential environment. *Atmos Environ* 35:3463–3473
- Morawska L, Thai PK, Liu X, Asumadu-Sakyi A, Ayoko G, Bartonova A, Bedini A, Chai F, Christensen B, Dunbabin M, Gao J, Hagler GSW, Jayaratne R, Kumar P, Lau AKH, Louie PKK, Mazaheri M, Ning Z, Motta N, Mullins B, Rahman MM, Ristovski Z, Shafiei M, Tjondronegoro D, Westerdahl D, Williams R (2018) Applications of low-cost sensing technologies for air quality monitoring and exposure assessment: how far have they gone? *Environ Int* 116:286–299

- Mitsakou C, Housiadas C, Eleftheriadis K, Vratolis S, Helmis C, Asimakopoulos D (2007) Lung deposition of fine and ultrafine particles outdoors and indoors during a cooking event and a no activity period. *Indoor Air* 17(2):143–152
- Murr LE, Soto KF, Garza KM, Guerrero PA, Martinez F, Esquivel EV, Ramirez DA, Shi Y, Bang JJ, Venzor J 3rd. (2006) Combustion-generated nanoparticulates in the El Paso, TX, USA/Juarez, Mexico Metroplex: their comparative characterization and potential for adverse health effects. *Int J Environ Res Public Health* 3(1):48–66
- Nguyen C, Li L, Sen CA, Ronquillo E, Zhu Y (2019) Fine and ultrafine particles concentrations in vape shops. *Atmos Environ* 211:159–169
- Oberdörster G, Oberdörster E, Oberdörster J (2005) Nanotoxicology: an emerging discipline evolving from studies of ultrafine particles. *Environ Health Perspect* 113:823–839
- Ogulei D, Hopke PK, Wallace LA (2006) Analysis of indoor particle size distributions from an occupied townhouse using positive matrix factorization. *Indoor Air* 16:204–215
- Ohlwein S, Kappeler R, Kutlar Joss M et al (2019) Health effects of ultrafine particles: a systematic literature review update of epidemiological evidence. *Int J Public Health* 64:547–559. <https://doi.org/10.1007/s00038-019-01202-7>
- Ott WR, Zhao T, Cheng K-C, Wallace LA, Hildemann LM (2021) Measuring indoor fine particle concentrations, emission rates, and decay rates from cannabis use in a residence. *Atmos Environ* 10:100106. <https://doi.org/10.1016/j.aeaoa.2021.100106>
- Ohlwein S, Kappeler R, Jos MJ, Künzli N, Hoffmann B (2019) Health effects of ultrafine particles: a systematic literature review update of epidemiological evidence. *Int J Public Health* 64: 547–559
- Özkaynak H, Xue J, Spengler JD, Wallace LA, Pellizzari ED, Jenkins P (1996) Personal exposure to airborne particles and metals: results from the particle TEAM study in Riverside, CA. *J Expo Anal Environ Epidemiol* 6:57–78
- Patel S, Sankhyan S, Boedicker EK, DeCarlo PF, Farmer DK, Goldstein AH, Katz EF, Nazaroff WW, Tian Y, Vanhanen J, Vance ME (2020) Indoor particulate matter during HOMEChem: concentrations, size distributions, and exposures. *Environ Sci Technol* 54:7107–7116
- Pashynska V, Vermeylen R, Vas G, Maenhaut W, Claeys M (2002) Development of a gas chromatographic/ion trap mass spectrometric method for the determination of levoglucosan and saccharide compounds in atmospheric aerosols. Application to urban aerosols. *J Mass Spectrom* 37:1249–1257
- Querol X, Alastuey A, Lopez-Soler A, Mantilla E, Plana F (1996) Mineralogy of atmospheric particulates around a large coal-fired power station. *Atmos Environ* 30:3557–3572
- Rim D, Wallace L, Nabinger S, Persily A. Reduction of exposure to ultrafine particles by kitchen exhaust hoods: the effects of exhaust flow rates, particle size, and burner position. *Sci Total Environ.* 2012 Aug 15;432:350–6.
- Rim D, Green M, Wallace L, Persily A, Choi JI (2012a) Evolution of ultrafine particle size distributions following indoor episodic releases: relative importance of coagulation, deposition and ventilation. *Aerosol Sci Technol* 46(5):494–503
- Rim D, Wallace L, Nabinger S, Persily A (2012b) Reduction of exposure to ultrafine particles by kitchen exhaust hoods: the effects of exhaust flow rates, particle size, and burner position. *Sci Total Environ* 15(432):350–356
- Rim D, Wallace LA, Persily AK (2013) Indoor ultrafine particles of outdoor origin: importance of window opening area and fan operation condition. *Environ Sci Technol* 47:1922–1929
- Rivas I, Mazaheri M, Viana M, Moreno T, Clifford S, He C, Bischof OF, Martins V, Reche C, Alastuey A, Alvarez-Pedrerol M, Sunyer J, Morawska L, Querol X (2017) Identification of technical problems affecting performance of DustTrak DRX aerosol monitors. *Sci Total Environ* 584–585:849–855
- Rundell KW (2003) High levels of airborne ultrafine and fine particulate matter in indoor ice arenas. *Inhal Tox* 15:237–250
- Salako GO, Hopke PK, Cohen DD, Begum BA, Biswas SK, Pandit GG, Chung YS, Rahman SA, Hamzah MS, Davy P, Markowitz A, Shagijamma D, Lodoysamba S, Wimolwattanapun W,

- Bunrapob S (2012) Exploring the variation between EC and BC in a variety of locations exploring the variation between EC and BC in a variety of locations. *Aerosol Air Qual Res* 12: 1–7
- Sandradewi J, Prévôt AS, Szidat S, Perron N, Alfarra MR, Lanz VA, Weingartner E, Baltensperger U (2008) Using aerosol light absorption measurements for the quantitative determination of wood burning and traffic emission contributions to particulate matter. *Environ Sci Technol* 42: 3316–3323
- Sarnat JA, Long CM, Koutrakis P, Coull BA, Schwartz J, Suh HH (2002) Using Sulfur as a tracer of outdoor fine particulate matter. *Environ Sci Technol* 36:5305–5314
- Sayahi T, Kaufman D, Becnel TK, K, Butterfield AE, Collingwood S, Zhang, Y Gaillardon P-E, Kelly, KE. (2019a) Development of a calibration chamber to evaluate the performance of low-cost particulate matter sensors. *Environ Pollut* 255:113131
- Sayahi T, Butterfield A, Kelly KE (2019b) Long-term field evaluation of the Plantower PMS low-cost particulate matter sensors. *Environ Poll* 245:932–940
- Schnaiter M, Horvath H, Möhlter O, Naumann K-H, Saafhoff H, Schöck OW (2003) UV-VIS-NIR spectral optical properties of soot and soot-containing aerosols. *J Aerosol Sci* 34:1421–1444
- Schnaiter M, Linke C, Möhler O, Naumann K-H, Saathoff H, Wagner R, Schurath U (2005) Absorption amplification of black carbon internally mixed with secondary organic aerosols. *J Geophys Res* 110:D19204
- Schweizer D, Cisneros R, Shaw G (2016) A comparative analysis of temporary and permanent beta attenuation monitors: the importance of understanding data and equipment limitations when creating PM_{2.5} air quality health advisories. *Atmos Pollut Res* 7:865–875
- See SW, Balasubramanian R (2006) Physical characteristics of ultrafine particles emitted from different gas cooking methods. *Aerosol Air Qual Res* 6:82–96
- Sheesley RJ, Mark M, Jeff T, De M, Brandon R, Shelton JJS (2015) Development of an in situ derivatization technique for rapid analysis of levoglucosan and polar compounds in atmospheric organic aerosol. *Atmos Environ* 123:251–255
- Slezakova K, de Oliveira Fernandes E, Pereira M do C (2019) Assessment of ultrafine particles in primary schools: emphasis on different indoor microenvironments. *Environ Pollut* 246:885–895
- Slezakova K, Peixoto C, Oliveira M, Delerue-Matos C, Pereira MDC, Morais S (2018) Indoor particulate pollution in fitness centres with emphasis on ultrafine particles. *Environ Pollut* 233:180–193
- Si M, Xiong Y, Du S, Du K (2020) Evaluation and calibration of a low-cost particle sensor in ambient conditions using machine-learning methods. *Atmos Meas Tech* 13:1693–1707
- Simoneit BRT, Schauer JJ, Nolte CG, Oros DR, Elias VO, Fraser MP, Rogge WF, Cass GR (1999) Levoglucosan, a tracer for cellulose in biomass burning and atmospheric particles. *Atmos Environ* 33:173–182
- Singer BC, Delp WW (2018) Response of consumer and research grade indoor air quality monitors to residential sources of fine particles. *Indoor Air* 28:624–639
- Singer BC, Pass RZ, Delp WW, Lorenzetti DM, Maddalena RL (2017) Pollutant concentrations and emission rates from natural gas cooking burners without and with range hood exhaust in nine California homes. *Build Environ* 122:215–229
- Singh M, Misra C, Sioutas C (2003) Field evaluation of a personal cascade impactor sampler (PCIS). *Atmos Environ* 37:4781–4793
- Smczak W, Menzel N, Keck L (2007) Emission of ultrafine copper particles by universal motors controlled by phase angle. *J Aerosol Sci* 38:520–531
- Smith KR, Dutta K, Chengappa C, Gusain PPS, Masera O, Berrueta V, Edwards R, Bailis R, Naumoff Shields K (2007) Monitoring and evaluation of improved biomass cookstove programs for indoor air quality and stove performance: conclusions from the Household Energy and Health Project. *Energy Sustain Dev* XI:5–18
- Solomon PA, Crumpler D, Flanagan JB, Jayanty RKM, Rickman EE, McDade CE (2014) US national PM2.5 chemical speciation monitoring networks – CSN and IMPROVE: description of networks. *J Air Waste Manag Assoc* 64:1410–1438

- Soppa VJ, Schins RPF, Hennig F, Nieuwenhuijsen MJ, Hellack B, Quass U, Kaminski H, Sasse B, Shinnawi S, Kuhlbusch TAJ, Hoffmann B (2017) Arterial blood pressure responses to short-term exposure to fine and ultrafine particles from indoor sources – a randomized sham-controlled exposure study of healthy volunteers. *Environ Res* 158:225–232
- Spilak MP, Frederiksen M, Kolarik B, Gunnarsen L (2014) Exposure to ultrafine particles in relation to indoor events and dwelling characteristics. *Build Environ* 74:65–74
- Stieb DM, Burnett RT, Smith-Doiron M, Brion O, Hyun Shin H, Economou V (2008) A new multipollutant, no-threshold air quality health index based on short-term associations observed in daily time-series analyses. *J Air Waste Manag Assoc* 58(3):435–450. <https://doi.org/10.3155/1047-3289.58.3.435>
- Stavroulas I, Grivas G, Michalopoulos P, Liakakou E, Bougiatioti A, Kalkavouras P, Fameli KM, Hatzianastassiou N, Mihalopoulos N, Gerasopoulos D (2020) Field evaluation of low-cost PM sensors (purple air PA-II) under variable urban air quality conditions in Greece. *Atmos* 11:926
- Stölzel M, Breitner S, Cyrys J, Pitz M, Wölke G, Kreyling W, Heinrich J, Wichmann HE, Peters A (2007) Daily mortality and particulate matter in different size classes in Erfurt Germany. *J Expo Sci Environ Epi* 17:458–467
- Sultan ZM, Nilsson GJ, Magee RJ (2011) Removal of ultrafine particles in indoor air: performance of various portable air cleaner technologies. *HVAC&R Res* 17:513–525
- Sunder Raman R, Hopke PK (2006) An ion chromatographic analysis of water-soluble, short-chain organic acids in ambient particulate matter. *Int J Environ Anal Chem* 86:767–777
- Susz A, Pratte P, Goujon-Ginglinger C (2020) Real-time monitoring of suspended particulate matter in indoor air: validation and application of a light-scattering sensor. *Aerosol Air Qual Res* 20: 2384–2395
- Tryner J, Quinn C, Windom BC, Volckens J (2019a) Design and evaluation of a portable PM_{2.5} monitor featuring a low-cost sensor in line with an active filter sampler. *Environ Sci Process Impacts* 21:1403–1415
- Tryner J, Good N, Wilson A, Clark ML, Peel JL, Volckens J (2019b) Variation in gravimetric correction factors for nephelometer-derived estimates of personal exposure to PM_{2.5}. *Environ Pollut* 250:251–261
- Tryner J, L'Orange C, Mehaffy J, Miller-Lionberg D, Hofstetter JC, Wilson A, Volckens J (2020) Laboratory evaluation of low-cost PurpleAir PM monitors and in-field correction using co-located portable filter samplers. *Atmos Environ* 220:117067
- Turner WA, Olson BA, Allen GA (2000) Calibration of sharp cut impactors for indoor and outdoor particle sampling. *J Air Waste Manag Assoc* 50:484–487
- USEPA (2004) Air quality criteria for particulate matter, report no. EPA/600/P-99/002aF. Available from <https://cfpub.epa.gov/ncea/risk/recordisplay.cfm?deid=87903>
- USEPA (2017) How to use air sensors: air sensor guidebook. Available from <https://www.epa.gov/air-sensor-toolbox/how-use-air-sensors-air-sensor-guidebook>
- Utell MJ, Frampton MW (2000) Acute health effects of ambient air pollution: the ultrafine particle hypothesis. *J Aerosol Med* 13:355–359
- Valente P, Forastiere F, Bacosi A, Cattani G, Di Carlo S, Ferri M, Figa-Talamanca I, Marconi A, Paoletti L, Perucci C, Zuccaro P (2007) Exposure to fine and ultrafine particles from secondhand smoke in public places before and after the smoking ban, Italy 2005. *Tob Control* 16:312–317
- Wallace, L. A. (2000). Real-Time Monitoring of Particles, PAH, and CO in An Occupied Townhouse, *Applied Occup. Environ. Hygiene* 15(1):39–47.
- Wallace LA (2005) Ultrafine particles from a vented gas clothes dryer. *Atmos Environ* 39: 5777–5786
- Wallace LA (2009) Ultrafine particles: a review. Prepared for Environment Canada. https://www.researchgate.net/publication/236004182_Ultrafine_Particles_A_Review. Accessed 22 Jan 2021
- Wallace LA, Ott WR (2010) Personal exposure to ultrafine particles. *J Expos Sci Environ Epidemiol* 21:20–30
- Wallace LA, Emmerich SJ, Howard-Reed C (2004) Source strengths of ultrafine and fine particles due to cooking with a gas stove. *Environ Sci Technol* 38:2304–2311

- Wallace LA, Wang F, Howard-Reed C, Persily A (2008) Contribution of gas and electric stoves to residential ultrafine particle concentrations between 2 and 64 nm: size distributions and emission and coagulation rates. *Environ Sci Technol* 42:8641–8647
- Wallace LA, Wheeler AJ, Kearney J, Van Ryswyk K, You H, Kulka RH, Rasmussen PE, Brook JR, Xu X (2011) Validation of continuous particle monitors for personal, indoor and outdoor exposures. *J Expo Anal Environ Epidemiol* 21:49–64
- Wallace LA, Ott WR, Weschler CJ (2015) Ultrafine particles from electric appliances and cooking pans: experiments suggesting desorption/nucleation of sorbed organics as the primary source. *Indoor Air* 25:536–546
- Wallace LA, Ott WR, Weschler CJ, Lai ACK (2017) Desorption of SVOCs from heated surfaces in the form of ultrafine particles. *Environ Sci Technol* 51(3):1140–1146
- Wallace L, Jeong S-G, Rim D (2019) Dynamic behavior of indoor ultrafine particles (2.3–64 nm) due to burning candles in a residence. *Indoor Air* 29:1018–1027
- Wallace LA, Ott WR, Zhao T, Cheng K-C, Hildemann L (2020) Secondhand exposure from vaping marijuana: concentrations, emissions, and exposures determined using both research-grade and low-cost monitors. *Atmos Environ X* 8:100093
- Wallace L, Bi J, Ott WR, Sarnat JA, Liu Y (2021) Calibration of low-cost PurpleAir outdoor monitors using an improved method of calculating PM2.5. *Atmos Environ* 256:118432. <https://doi.org/10.1016/j.atmosenvir.2021.118432>
- Wallace L, Emmerich S, Howard-Reed C (2004) Effect of central fans and in-duct filters on deposition rates of ultrafine and fine particles in an occupied townhouse. *Atmos Environ* 38:405–413
- Wallace L, Williams R, Rea A, Croghan C (2006) Continuous weeklong measurements of personal exposures and indoor concentrations of fine particles for 37 health-impaired North Carolina residents for up to four seasons. *Atmos Environ* 40:399–414
- Wang Y, Hopke PK, Rattigan OV, Xia X (2011) Characterization of residential wood combustion particles using the two-wavelength aethalometer. *Environ Sci Technol* 45:7387–7393
- Wang Y, Hopke PK, Rattigan OV, Chalupa DC, Utell MJ (2012) Multiple-year black carbon measurements and source apportionment using Delta-C in Rochester, New York. *J Air Waste Manag Assoc* 62:880–887
- Wang Z, Calderón L, Patton AP, Sorensen Allacci MA, Senick J, Wener R, Andrews CJ, Mainelis G (2016) Comparison of real-time instruments and gravimetric method when measuring particulate matter in a residential building. *J Air Waste Manage Assoc* 66:1109–1120
- Wang K, Chen FE, Au W, Zhao Z, Xia Z-L (2019) Evaluating the feasibility of a personal particle exposure monitor in outdoor and indoor microenvironments in Shanghai, China. *Int J Environ Health Res* 29:209–220
- Wang Z, Delp WW, Singer BC (2020) Performance of low-cost indoor air quality monitors for PM2.5 and PM10 from residential sources. *Build Environ* 171:106654
- Weichenthal S, Dufresne A, Infante-Rivard C, Joseph L (2007) Indoor ultrafine particle exposures and home heating systems: a cross-sectional survey of Canadian homes during the winter months. *J Expo Sci Environ Epidemiol* 17:288–297
- Weichenthal S, Dufresne A, Infante-Rivard C, Joseph L (2008) Characterizing and predicting ultrafine particle counts in Canadian classrooms during the winter months: model development and evaluation. *Environ Res* 106:349–360
- Wensing M, Schripp T, Uhdea E, Salthammer T (2008) Ultra-fine particles release from hardcopy devices: sources, real-room measurements and efficiency of filter accessories. *Sci Tot Environ* 407:418–427
- Weschler CJ, Carslaw N (2018) Indoor chemistry. *Environ Sci Technol* 52(5):2419–2428
- Wheeler A, Wallace LA, Kearney J, Van Ryswyk K, You H, Kulka R (2011) Personal, indoor, and outdoor concentrations of fine and ultrafine particles using continuous monitors in multiple residences. *Aerosol Sci Technol* 45:1078–1089

- Wichmann HE, Spix C, Tuch T, Wolke G, Peters A, Heinrich J, Kreyling WG, Heyder J (2000) Daily mortality and fine and ultrafine particles in Erfurt Germany part I: role of particle number and particle mass. *Res Rep Health Eff Inst* 98:5–86. discussion 87–94
- Williams R, Kaufman A, Hanley T, Rice J, Garvey S (2014) Evaluation of field-deployed low cost pm sensors. EPA/600/R-14/464 (NTIS PB 2015-102104). U.S. Environmental Protection Agency, Washington, DC. https://cfpub.epa.gov/si/si_public_record_report.cfm?dirEntryId=297517
- Yakovleva E, Hopke PK, Wallace LA (1999) Receptor Modeling assessment of particle Total exposure assessment methodology data. *Environ Sci Technol* 33:3645–3652
- Zauli Sajani S, Ricciardelli I, Trentini A, Bacco D, Maccone C, Castellazzi S, Lauriola P, Poluzzi V, Harrison RM (2015) Spatial and indoor/outdoor gradients in urban concentrations of ultrafine particles and PM_{2.5} mass and chemical components. *Atmos Environ* 103:307–320
- Zhao W, Hopke PK, Norris G, Williams R, Paatero P (2006) Source apportionment and analysis on ambient and personal exposure samples with a combined receptor model and an adaptive blank estimation strategy. *Atmos Environ* 40:3788–3801
- Zhao W, Hopke PK, Gelfand EW, Rabinovitch N (2007) Use of an expanded receptor model for personal exposure analysis in schoolchildren with asthma. *Atmos Environ* 41:4084–4096
- Zhao T, Cheng K-C, Ott WR, Wallace LA, Hildemann LM (2020) Characteristics of secondhand cannabis smoke from common smoking methods: calibration factor, emission rate, and particle removal rate. *Atmos Environ* 242:117731
- Zhang Q, Zhu Y (2012) Characterizing ultrafine particles and other air pollutants at five schools in South Texas. *Indoor Air* 22(1):33–42
- Zheng T, Bergin MH, Johnson KK, Tripathi SN, Shirodkar S, Landis MS, Sutaria R, Carlson DE (2018) Field evaluation of low-cost particulate matter sensors in high- and low-concentration environments. *Atmos Meas Technol* 11:4823–4846
- Zhu Y, Hinds WC, Krudysz M, Kuhn T, Froines J, Sioutas C (2005) Penetration of freeway ultrafine particles into indoor environments. *J Aerosol Sci* 36(3):303–322
- Zhu Y, Smith TJ, Davis ME, Levy JI, Herrick R, Jiang H (2011) Comparing gravimetric and real-time sampling of PM(2.5) concentrations inside truck cabins. *J Occup Environ Hyg* 8:662–672
- Zou Y, Young M, Chen J, Liu J, May A, Clark JD (2020) Examining the functional range of commercially available low-cost airborne particle sensors and consequences for monitoring of indoor air quality in residences. *Indoor Air* 30:213–234
- Zou Y, Clark JD, May AA (2021) A systematic investigation on the effects of temperature and relative humidity on the performance of eight low-cost particle sensors and devices. *J Aerosol Sci* 152:105715
- Zusman M, Schumacher CS, Gassett AJ, Spalt EW, Austin E, Larson TV, Arvin GC, Seto E, Kaufman JD, Sheppard L (2020) Calibration of low-cost particulate matter sensors: model development for a multi-city epidemiological study. *Environ Int* 134:105329



Visualization and Measurement of Indoor Airflow by Color Sequence Enhanced Particle Streak Velocimetry

20

Huan Wang and Xianting Li

Contents

Introduction	570
Theory and Limitations of Traditional PSV	574
Theory of Traditional PSV	575
Limitations of Traditional PSV	576
Theory and Implementation of CSPSV	577
Color Sequence Illumination System	577
Operational Procedure of CSPSV	579
Quad-View CSPSV	579
Image Processing and Stereo Correspondence Algorithm	582
Digital Image Processing	582
Rectification-Based Sparse Stereo Correspondence	584
Accuracy Verification	585
Experimental Setup of Rotating Board Test	586
Accuracy Verification on Rotating Board	586
Experimental Setup in the Wind Tunnel	588
Verification with HWA	588
Applications and Results	591
Vortex Flow Test	591
Airflow Pattern Induced by Ceiling Fan	592
Airflow Pattern Induced by Mixing Ventilation and AFN	602
Conclusions	605
References	606

Abstract

Airflow measurement plays a crucially important role for studying the indoor environment. Two primary nonintrusive airflow approaches that use bubbles as seeds to visualize and track the airflow are particle tracking velocimetry (PTV)

H. Wang · X. Li (✉)

Department of Building Science, Beijing Key Laboratory of Indoor Air Quality Evaluation and Control, Tsinghua University, Beijing, China
e-mail: xtngli@tsinghua.edu.cn

and particle streak velocimetry (PSV). The major advantage of PTV and PSV is the limited disturbance they impart to the tested airflow. However, the drawback is that they are not capable of room-scale measurements. Therefore, a new approach, i.e., color sequence enhanced particle streak velocimetry (CSPSV), is introduced. The core component of CSPSV is the color sequence illumination system (CSIS), which consists of three controlled lights of different colors and one of white light. The concept is to change the illumination color of the test zone in a given sequence during the exposure time. Then the color-coded time sequence information is inputted into an algorithm for both three-dimensional (3D) reconstruction and stereo pair matching. The theory and composition, image-processing and pair-matching algorithms, verification and applications of CSPSV are introduced in the chapter. The relative magnitude error of CSPSV is mostly below 5% within $0.12 \sim 2.45$ m/s, and the results from CSPSV are in consist with a hot-wire anemometer. CSPSV can be used in different indoor airflows such as vortex flow, airflows induced by the ceiling fan and adjustable fan networks, etc. CSPSV combines the advantages of PTV and PSV, reduces the requirement for high-speed cameras, and can be easily extended to measure the airflow in a large space.

Keywords

Nonintrusive measurement · Particle streak velocimetry · Indoor airflow · Digital image process · Color sequence illumination

Introduction

The airflow pattern in a room is one of the key factors that affects indoor thermal comfort, energy efficiency, and air quality. Therefore, test and measurement technology for indoor airflows has been an important research area and is drawing increasing attention with latest technology developments. Because the range of indoor airflow velocities is large, normally from 0.5 to 10 m/s near an inlet or outlet to several centimeters per second near a corner or in an occupied zone, and indoor airflow is commonly highly turbulent and unsteady (Sandberg 2007), accurate measurement of indoor airflows in large spaces has been challenging for an extended period of time.

Historically, releasing smoke or colored gases to the target zone is one of the most easily conducted airflow visualization approaches. The drawback of this approach is that the phenomenon can only be visible for a short time period and provides almost little quantifiable airflow information. With the need for the development of flow measurement technologies, methods have been developed, such as ultrasonic anemometry (UA) (Knowles and Athelstan 1953), laser Doppler anemometry (LDA) (Cummins et al. 1964), and particle image velocimetry (PIV) (Adrian 1984; Pickering and Halliwell 1985). Both UA and LDA are point-wise solutions that provide precise three-component velocity information at one point or on a grid with a mobile

system. However, the test is time consuming, and it is difficult to guarantee that the indoor airflow field will be stable during the test. Thus, they are only suitable for stationary laboratory tests. PIV is currently the most widely used and commercially available nonintrusive airflow measurement system and has been used in indoor air tests. Given the potential danger of exposure to the laser slice and high cost for high-power laser generators, the measurement space of PIV is limited to dozens of square centimeters in a plane (Li et al. 2015) or even smaller zones.

Compared with PIV, particle tracking velocimetry (PTV) takes images at a higher speed and directly tracks each visible seeding particle instead of the image characteristics in PIV, by connecting the images taken at two or more given time intervals. Since the scale of indoor airflows is normally in meters, PTV selects bubbles as seeding particles for lower light intensity requirement. Its typical setup includes a bubble generator for air visualization, an illumination system to make the seeding bubbles more distinguishable from the background particles, and multiple cameras that can simultaneously record the test zone from different angles as shown in Fig. 1. The cameras and lights are operated at a typical sequence as shown in Fig. 2a, and a typical image (Fig. 2b) is obtained (Ohmi and Li 2000). Basically, similar to our eyes, a pair of cameras can perform stereo vision and calculate the three-dimensional (3D) position of each target based on the position, orientation, and settings of the cameras. By introducing more cameras, the 3D reconstructed results of PTV can be further checked and improved. Hence, PTV can provide 3D flow data with a relatively high spatial and temporal resolution (Maas et al. 1993). However, the tracking and 3D matching algorithm require the displacement of individual particles between each successive image to be no more than several pixels, which forces the image acquisition rate for each camera to be increased to 100 Hz (Biwole et al. 2009). The large amount of image data from

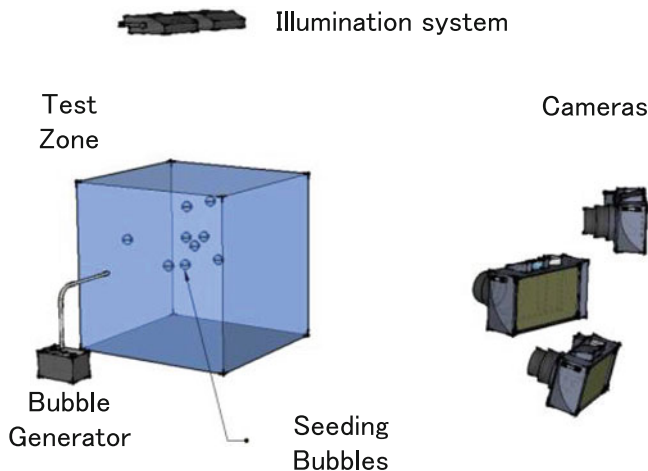


Fig. 1 Typical experimental setup for PTV measurements. (Reprinted from Wang et al. (2017), with permission from Elsevier)

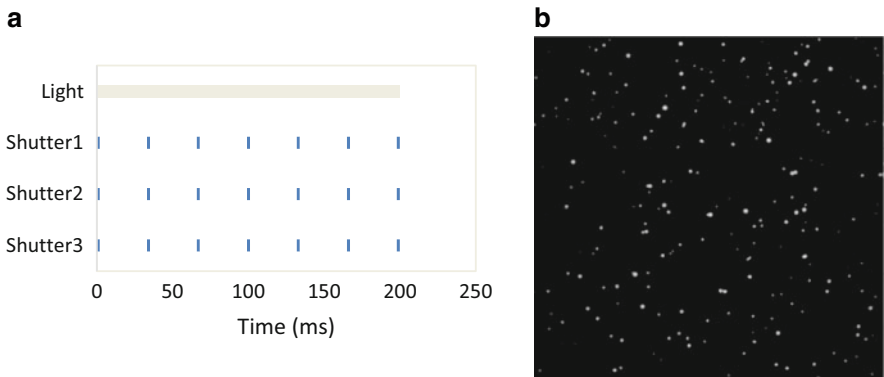


Fig. 2 Sequence of operation and typical image of PTV. (a) Typical sequence of operation of PTV. (b) Typical image of PTV (Ohmi and Li 2000). (Reprinted from Wang et al. (2017), with permission from Elsevier)

each camera exerts extreme pressure on the subsequent data-processing system and often requires a supercomputer to process the data (Li et al. 2008) while limiting individual sample times to be several seconds (Biwole et al. 2009; Fu et al. 2015). The development of parallel computation (Barker et al. 2012), new processing algorithms (Ohmi et al. 2010), and smart cameras (Kreizer and Liberzon 2010) can help to solve these problems to some extent. However, such new technologies may also make the measurement system much more complicated and difficult to design and operate for actual room-scale measurements. Another important drawback for the application of PTV is its illumination system. To obtain a clear image of each individual spot, the exposure time for each frame is usually within several microseconds. The illumination system has to be notably powerful, which delivers additional heat to the test zone and makes it difficult to extend the measurement domain. Since the frame rate and resolution are trade-off parameters for cameras, the low resolution of high-speed cameras also limits the extension of test zone for PTV. Limited by the image acquisition and analysis speed and the illumination system, the reported test zone of PTV is commonly approximately one cubic meter (Fu et al. 2015), which is still not sufficiently large for room ventilation tests.

In actual indoor environment, the airflow can be affected by many factors such as indoor partitions, heat sources, movement of objects and radiation, which make it difficult or even impossible to be totally simulated in a small-scale model. In addition, the velocity of indoor airflows covers a wide range. Hence, the normal intrusive measurement method cannot be sufficiently accurate for both normal and low-speed flows (Popielek et al. 2007). Therefore, a room-scale, high-dynamic-range, and nonintrusive airflow measurement system is crucial for the laboratory study of thermal comfort (Voelker et al. 2014), pollution transport (Kato et al. 2003; Mao and Gao 2015), and the field test of diffuser design (Elvsén and Sandberg 2009) and airflow pattern design (Rosenstiel and Grigat 2010).

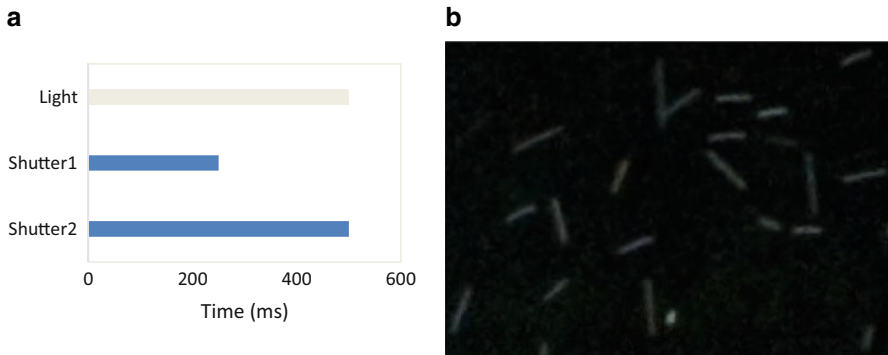


Fig. 3 Sequence of operation and typical image of PSV. (a) Typical sequence of operation of PSV. (b) Typical image of PSV. (Reprinted from Wang et al. (2017), with permission from Elsevier)

As another nonintrusive flow measurement method, particle streak velocimetry (PSV) operates with a longer exposure time and shares the typical setup of PTV in Fig. 1. However, PSV employs a much longer exposure time than PTV and records the bubble's trajectory as shown in Fig. 3. Because pair matching in PSV is conducted for streaks with two connected end points instead of individual points in PTV, PSV can function well with only two cameras. The three-component velocity is calculated based on the length of each streak and the exposure period (Fage and Townend 1932; Adamczyk and Rimal 1988). A longer exposure time enables both easier capture of the seeding particles and decreases the requirement of camera frame rate. Because two cameras capture the targets at the identical start time from different angles, the 3D position of these streaks could be reconstructed based on the calibration data of two cameras. Since the exposure time is preset, the velocity can be obtained by dividing the trajectory length by time.

Nevertheless, as shown in Fig. 3b, streaks on images cannot indicate the flow direction of seeding, which is the major drawback of PSV and attracted the attention of many researchers. One solution was to set the exposure time of one camera at half that of the other camera (Sun 2007) as shown in Fig. 3a. Because the indoor airflow is highly turbulent, the mathematical middle point of a long streak does not always denote the same end point of a short streak. Another widely used method is to compare the displacement in two consecutive images and assign the displacement by their similar geometrical characteristics (area and length) (Malavasi et al. 2011). The requirement of this method is that the time duration between two successive images is notably short and the density of particles is low. Another useful approach is using a multi-pulse laser or shutting down the illumination system for a short period during exposure to mark a blank space near the head or rear of the streak (Müller et al. 2001). These technologies enable the flow direction to be determined by adding temporal information to regular streaks and may be effective when the airflow is stable and the seeding density is relatively low. However, because the indoor airflow is three-dimensional and turbulent, the streaks could be highly twisted, which makes the recognition extremely difficult, especially for complex airflows.

As analyzed above, the study of indoor airflow patterns requires a room-sized, 3D airflow measurement system, and PTV and PSV both have their advantages and drawbacks. Photographic images captured by the camera can be affected by different aspects such as the light source, reflection properties of the object surface, and camera optics (Szelski 2011). Normally, PTV and PSV mainly focus on the image acquisition and process section. Using multiple light pulses to add more information onto one single frame was proposed (Adrian 1991; Ding et al. 2013) and proven to be efficient and effective (Voss et al. 2012; Westerweel et al. 2013). For small solid tracers, different color-dyed particles can help the search for homologous points in different frames much easier, and dramatically decreased the number of ambiguities (Tarlet et al. 2009; Bendicks1 et al. 2011). These studies provided hints to improve the performance of seeding particle tracking through specially designed optical imaging systems.

In room-scale airflow measurement, helium-filled soap bubbles (HFSB) are widely used seeding particles that provide a great potential for color-coded imaging methods. As the HFSBs are transparent and can reflect light notably well (Tropea 2011), changing the color of light source can change the bubbles' appearance on the imaging sensor that could provide more information than individual white spots. Investigators (McGregor et al. 2007; Pick and Lehmann 2009; Watamura et al. 2013) utilized this capability by marking the measurement space with different color layers of light to distinguish the distance in the depth direction. If a color sequence illumination system (CSIS) is involved to change the light color in the test zone in a given sequence, the path and flow direction of the bubbles can be simultaneously recorded in one frame. Therefore, particle path extrapolation (used in PTV) and streak direction trials (used in PSV) are no longer needed, which improves the measurement accuracy and decreases the calculation load. Since CSIS can be easily extended and the required frame rate of the camera is low allowing higher resolution cameras can be involved, the test space of such kind of velocimetry measurements can be extended to several cubic meters.

In this chapter, a new approach called color sequence particle streak velocimetry (CSPSV) is introduced by adding time sequence information into one single frame using CSIS (Wang et al. 2017). The basic principle and algorithm of CSPSV are introduced by utilizing digital image processing and multiple view geometry. The accuracy of CSPSV is verified by both the movement of white dots on a rotating target and in a wind tunnel comparison with hot-wire anemometer (HWA). Finally, three cases in actual indoor airflow studies are presented to demonstrate the capability and reliability of the CSPSV method including a vortex in a scale tunnel, and the airflow patterns induced by the ceiling fan and adjustable fan network.

Theory and Limitations of Traditional PSV

PSV partially fulfils the requirement of a room-scale ventilation measurement with its large test space and relatively low data acquisition rate but suffers from the streak direction ambiguities.

Theory of Traditional PSV

A brief introduction to the traditional PSV will provide a general view of how image-based multi-view velocimetry works. As previously mentioned, the setup of traditional PSV is similar to that of PTV as shown in Fig. 1 with a typical operation of sequence in Fig. 3a. For PSV, the most fundamental part is the matching and reconstruction of the 3D position of seeding bubbles based on the images captured from different angles. The basic model of binocular stereo vision for PSV is demonstrated in Fig. 4. The image coordinate frames of the left and right cameras are $o_1u_1v_1$ and $o_2u_2v_2$, where O_1 and O_2 are the optical centers, f_1 and f_2 are the focal lengths, and O_1n_1 and O_2n_2 are the optical axes of the cameras, which are perpendicular to the imaging sensors. Assuming that A is a seeding bubble in the test zone at (X, Y, Z) of the world coordinate, on two camera imaging planes, it is recorded as spots $a_1(U_1, V_1)$ and $a_2(U_2, V_2)$ in each image coordinate. In the camera calibration process, matrix C can be determined, which contains the positions of O_1 and O_2 and the orientation of camera optical axes O_1n_1 and O_2n_2 . Then, the camera model can be built as in Eq. 1 (Heikkila and Silven 1997), where i refers to different camera numbers, and matrix C contains the camera calibration information. Basically, by back-projecting lines O_1a_1 and O_2a_2 and calculating whether they have a conjugate point, we can determine whether a_1 and a_2 correspond to point A in 3D space. In detail, the matching criterion indicator δ can be written as in Eq. 2 (Sun 2007), where the point information indicators S_{11} , S_{21} , S_{31} , S_{12} , S_{22} , and S_{32} are defined in Eq. 3,

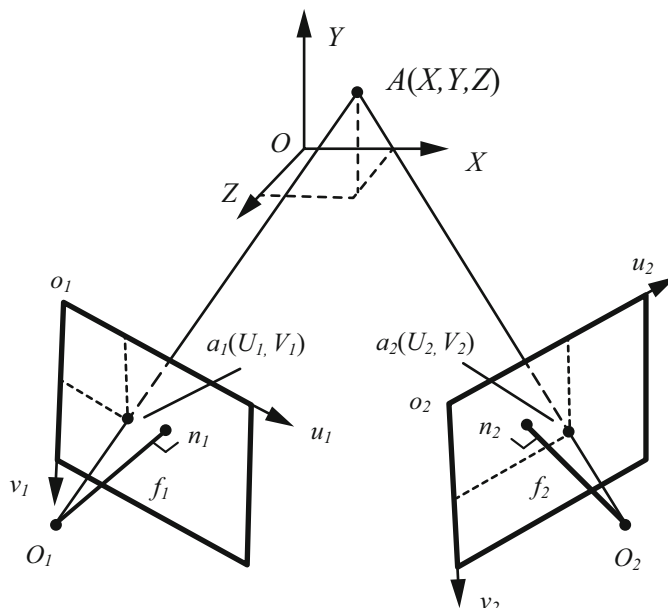


Fig. 4 Model of a binocular stereo vision. (Reprinted from Wang et al. (2017), with permission from Elsevier)

and c_{jkn} are the elements of matrix C with j as the row index, k as the column index and n as the camera number index. If δ for a pair of points from separate images is below a threshold, this pair of points corresponds to one bubble, and its position in the world coordinate system can be calculated using Eq. 4.

$$\begin{Bmatrix} U_i W_i \\ V_i W_i \\ W_i \\ 1 \end{Bmatrix} = \begin{bmatrix} c_{11i} & c_{12i} & c_{13i} & c_{14i} \\ c_{21i} & c_{22i} & c_{23i} & c_{24i} \\ c_{31i} & c_{32i} & c_{33i} & c_{34i} \\ 0 & 0 & 0 & 1 \end{bmatrix} \begin{Bmatrix} X \\ Y \\ Z \\ 1 \end{Bmatrix} = C \begin{Bmatrix} X \\ Y \\ Z \\ 1 \end{Bmatrix} \quad (1)$$

$$\begin{aligned} \delta \equiv & (S_{21}S_{32} - S_{31}S_{22})(c_{142} - c_{141}) + (S_{31}S_{12} - S_{11}S_{32})(c_{242} - c_{241}) \\ & + (S_{11}S_{22} - S_{21}S_{12})(c_{342} - c_{341}) \end{aligned} \quad (2)$$

$$\left. \begin{array}{l} S_{11} = c_{111}U_1 + c_{121}V_1 + c_{131} \\ S_{21} = c_{211}U_1 + c_{221}V_1 + c_{231} \\ S_{32} = c_{311}U_1 + c_{321}V_1 + c_{331} \\ S_{12} = c_{112}U_2 + c_{122}V_2 + c_{132} \\ S_{22} = c_{212}U_2 + c_{222}V_2 + c_{232} \\ S_{32} = c_{312}U_2 + c_{322}V_2 + c_{332} \end{array} \right\} \quad (3)$$

$$\begin{pmatrix} x \\ y \\ z \end{pmatrix} = \frac{S_{11}(c_{242} - c_{241}) - S_{21}(c_{142} - c_{141})}{S_{12}S_{21} - S_{11}S_{22}} \begin{pmatrix} S_{12} \\ S_{22} \\ S_{32} \end{pmatrix} + \begin{pmatrix} c_{142} \\ c_{242} \\ c_{342} \end{pmatrix} \quad (4)$$

Limitations of Traditional PSV

In PSV, the two end points of a streak extracted by morphology analyses are used as key points. However, the streak direction is unknown from individual images. A common solution (Sun 2007) is to set the exposure time of one camera (image 2) to be only half of that of the other camera (image 1) to obtain a long streak AB and a short streak CD as shown in Fig. 5. Then, the streak with a longer exposure time AB is cut into two halves at the mathematical middle point marked M. With different initial assumptions of the streak direction, four pairs of streaks AM-CD, MB-CD and AM-DC, MB-DC are formed and calculated for their match criterion. If the pair-matching criterion of the two ends $|\delta_{start}| + |\delta_{end}|$ is less than a threshold implies that both end points match and the corresponding initial assumed direction is correct. Then this pair of streaks captured by different cameras belongs to one bubble and the 3D displacement of the bubbles in a given time duration can be calculated. Because the time interval is known, the velocity components can be reconstructed in 3D space (Sun et al. 2004). However, the mathematical middle point M is not the actual middle path point of the streak M', and the displacement between them produces serious errors when the bubble's path is curved. Because indoor airflow is commonly highly

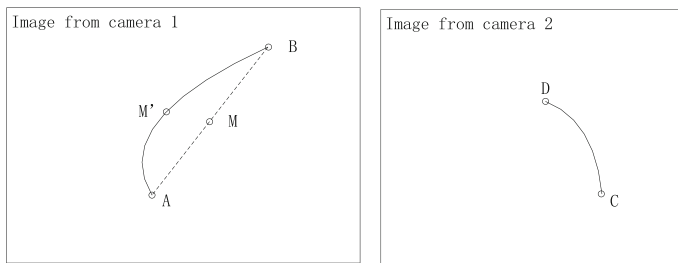


Fig. 5 3D reconstruction for PSV. (Reprinted from Wang et al. (2017), with permission from Elsevier)

turbulent, this drawback introduces ambiguities to pair matching and affects the accuracy of PSV.

Theory and Implementation of CSPSV

Based on the fundamental principles of CSPSV, the system setup and operation procedure for 3D velocity reconstruction are introduced in the following sections, including the components and function of CSIS, extracting streak and spot information from images, reconstructing the bubbles' trajectory, and determining the 3D velocity in the test zone.

Color Sequence Illumination System

The task of the illumination system in regular PSV and PTV is only to illuminate the seeding particles, whereas in CSPSV, CSIS is introduced primarily as a time sequence marker, which codes the test zone with different color of light and helps to capture more time sequence information with the color cameras.

In detail, CSIS has three color lights (red, green, and blue) and a white light, typically functioning in the pattern presented in Fig. 6a. When the shutters open, the light color of the test zone is first changed to red and a red spot is marked on the camera sensor. After that, the white light is immediately switched on to help to record the streaks of the bubbles after the red spots. The white streaks are designed to link together the color spots of one bubble and differentiate them from the other spots. When half of the exposure time has been reached, the green light is switched on to mark a green spot on the sensor. During the exposure time, the white light is switched off when colored light pulses to improve the contrast. Then, the white light is turned on until the blue pulse is initiated. Such a design for CSIS can increase the signal-to-noise ratio of color spots, especially for the low-speed spots.

With CSIS and operating at a longer exposure time, the color cameras can capture the sequence of color spots on the bubble's white path, as shown in Fig. 6b. The white light is used to link the color spots produced by one single bubble. Since the

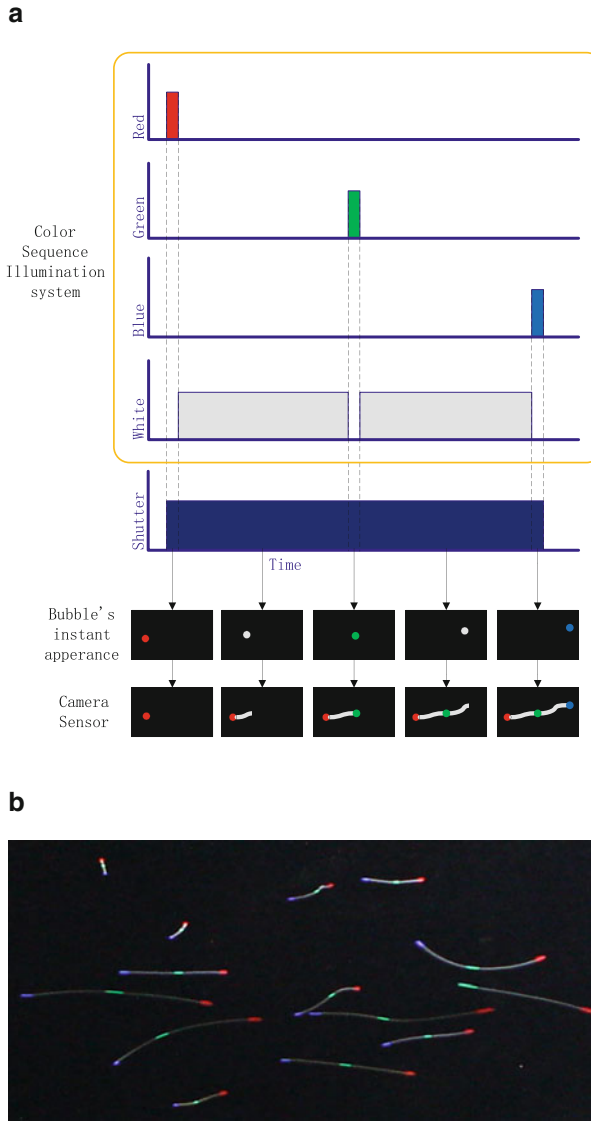


Fig. 6 Sequence of operation and a typical image of CSPSV. (a) Illumination sequence of CSPSV. (b) Typical image of CSPSV. (Reprinted with permission from Wang et al. (2018), © The Optical Society)

three different colors are introduced within one camera frame, both the path and direction of each bubble are simultaneously recorded. With the white streak linking the start, middle, and end points of a bubble, it becomes much easier and reliable to track the seeding bubbles. With this information, stereo pair matching can be more

accurately processed, and hence, the 3D information of the flow field can be obtained more reliably.

The CSIS also plays a crucial role in extending the measuring space. The CSPSV method records the bubbles' path with direction instead of individual spots (in PTV) and addresses the ambiguous direction problem of PSV. Thus, the frame rate requirement of CSPSV is reduced from 100 Hz (typical PTV) to 10 Hz (typical PSV). Further, there are at least two time intervals recorded by the camera in a single frame. The lower frame rate requirement enables higher-resolution cameras to be feasible for CSPSV, covering a wider space and extending the test zone to a larger space, potentially including whole-room ventilation tests.

In CSPSV, because the start and end points of a streak have been clearly marked with CSIS, the direction matching trials are no longer required. Thus, the pair-matching calculation for each streak can be four times faster than that in normal PSV (Sun 2007). Moreover, CSPSV uses the same sequence of operation for each camera, i.e., each key point is simultaneously taken. This character helps to reduce pair-matching ambiguities and results in a significantly improved pair-matching success rate than PSV. Compared with PTV, CSPSV utilizes the white streaks to link the color key spots, which makes bubble tracking notably easy with no need for extrapolation and reduces the camera frame rate from 100 Hz to several Hz.

Operational Procedure of CSPSV

The operational procedure of a CSPSV system is shown in Fig. 7. First, the bubbles are released into the test zone as tracers, to check the view of each camera. Then, the CSIS should be synchronized with the cameras to ensure the time sequence of each frame. After the cameras are set, the camera calibration should be performed to obtain the information of stereo cameras for 3D reconstruction. During the recording images, the cameras and CSIS should be simultaneously operated. Subsequently, the digital image processing and 3D reconstruction algorithm can rebuild the 3D vector for captured bubbles. Finally, data post-processing and visualization tools are utilized to achieve a better illustration of the airflow field.

Quad-View CSPSV

The primary drawback of CSPSV with two cameras or a stereo CSPSV is the blind zone as illustrated in Fig. 8. To illuminate the whole test space with little effect, a light source is placed both on the top of the ceiling and under the transparent glass floor, projecting toward each other. This type of setup causes a blind zone for each camera orientation, and the blind zone varies with the direction of the camera's orientations. As in Fig. 8, the blind zone of upper cameras is marked blue and that of the lower cameras orange. The zone that can be captured by both cameras is in green. The view angles are presented with a dashed line to mark the limitations of overexposure caused by placement of the CSIS modules.

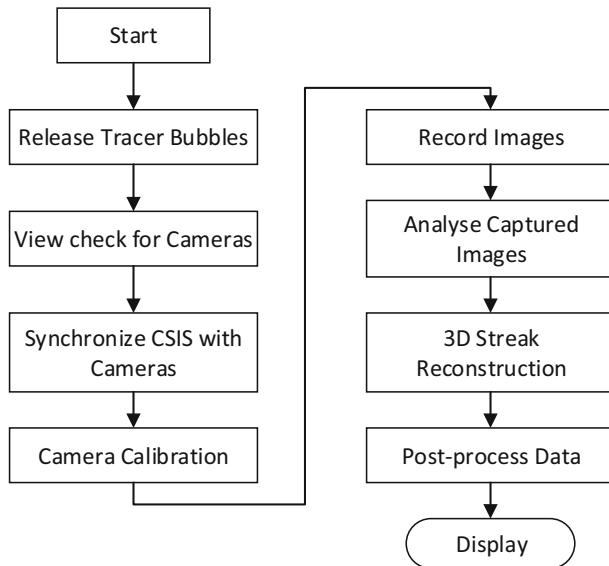


Fig. 7 Operation process for CSPSV

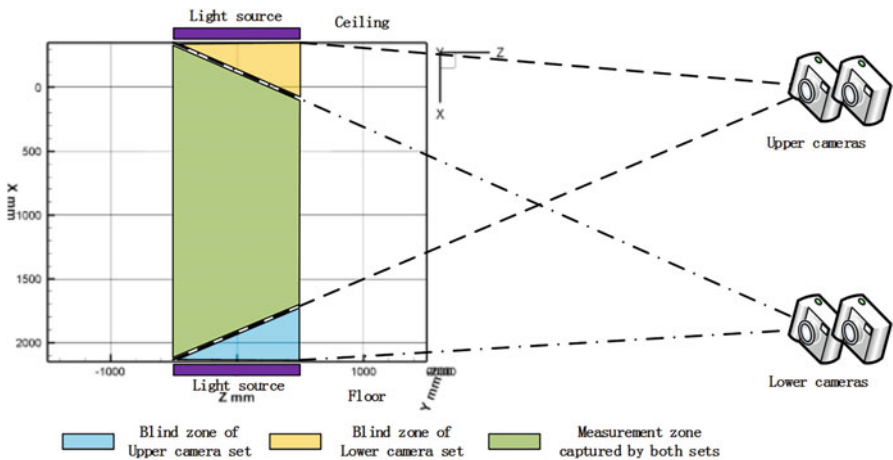


Fig. 8 Comparison for blind zone captured by two pair of cameras. (Reprinted from Wang et al. (2019), with permission from Elsevier)

As mentioned above, the measurement zone of a stereo CSPSV is always affected by overexposed regions. When the flow measurements could be crucial near light sources, one method to increase the measurement space is to add more cameras to capture the movement from different angles and merge the measurement data together. In this section, a new quad-view CSPSV is introduced with four cameras that are deployed in two groups and operated synchronously. The upper cameras are

primarily used to capture the air movements near the ceiling while the lower cameras primarily target the air movements near the floor, as shown in Fig. 8.

With these settings, both camera sets can capture the airflow in the middle of the room as marked in green. If the results are simply added together, some vectors will be duplicated. To solve this problem, a data merge algorithm was designed as described in Fig. 9. The 3D streak reconstructions for each pair of cameras are conducted separately. Subsequently, the distance between each pair of 3D vectors in 3D spaces is calculated, which consists of two vectors from the same frame but in different pair-sets, as in Eq. 5.

$$D = \sqrt{(X_{1s} - X_{2s})^2 + (Y_{1s} - Y_{2s})^2 + (Z_{1s} - Z_{2s})^2 + (X_{1e} - X_{2e})^2 + (Y_{1e} - Y_{2e})^2 + (Z_{1e} - Z_{2e})^2} \quad (5)$$

where X , Y , and Z are the components of the vector in the 3D space. The subscripts s and e represent the start and end points of the vector. Subscripts 1 and 2 are for the vectors from the upper cameras and the lower cameras, respectively.

When the distance between two streaks are extremely close, the streak with a larger epipolar error is rejected. The distance threshold is set at 20 mm in most cases. With this algorithm, the vectors captured by two camera sets can be merged together for a wider measurement space.

The quad-view CSPSV combined the measurement results of two normal stereo CSPSV systems. Therefore, the measurement region is expanded, the blind zone is minimized, and the high accuracy of each stereo CSPSV is preserved. Since there are a lot of buildings with even larger spaces that cannot be covered by a pair of cameras, this system is designed to accommodate more cameras to create the multiple-view

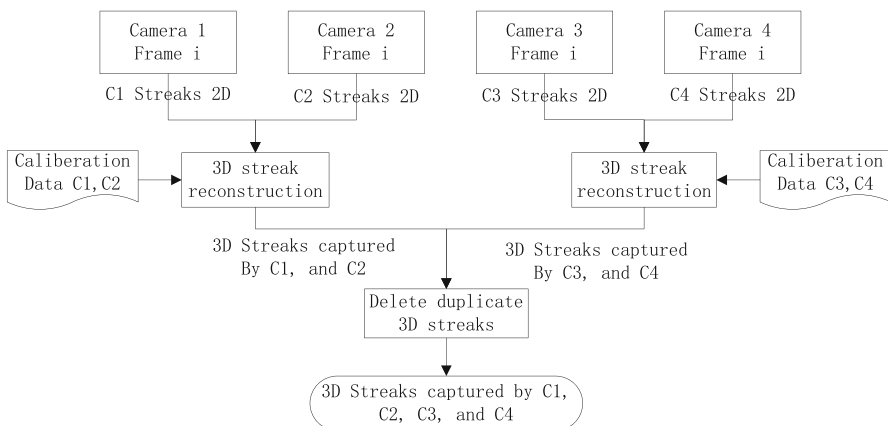


Fig. 9 Algorithm for quad-view CSPSV. (Reprinted from Wang et al. (2019), with permission from Elsevier)

CSPSV and will further support three-dimensional three-component (3D3C) airflow pattern measurements in large spaces like stadiums.

Image Processing and Stereo Correspondence Algorithm

With CSIS, the information on individual image is significantly richer. Specific digital image-processing algorithm and pair-matching algorithm are designed to extract the information and make full use of these advantages.

Digital Image Processing

After the acquisition of these informative images, the segmentation algorithm and information-handling process must be carefully designed. Unlike in PSV, where only the measured end points are employed, CSPSV images have multiple types of information that is collected: spot color, spot location, streak location, and number of pixels that each streak covers as shown in Fig. 6b. The spot and streak locations are of fundamental importance. Although humans can easily distinguish spots and streaks from the background, the computer has difficulty doing so. By changing the color image into grayscale and expressing its level on the z axis, the light intensity of pixel can be better displayed as shown in Fig. 10. The streaks and spots appear like ridges of different heights and mountain peaks, respectively. For spots, the light that is scattered and transmitted from seeding bubbles obeys a Gaussian distribution (Nobach and Honkanen 2005), and the streak can be considered as a series of spots along the given path. Therefore, the segmentation and enhancement can be based on a Gaussian distribution.

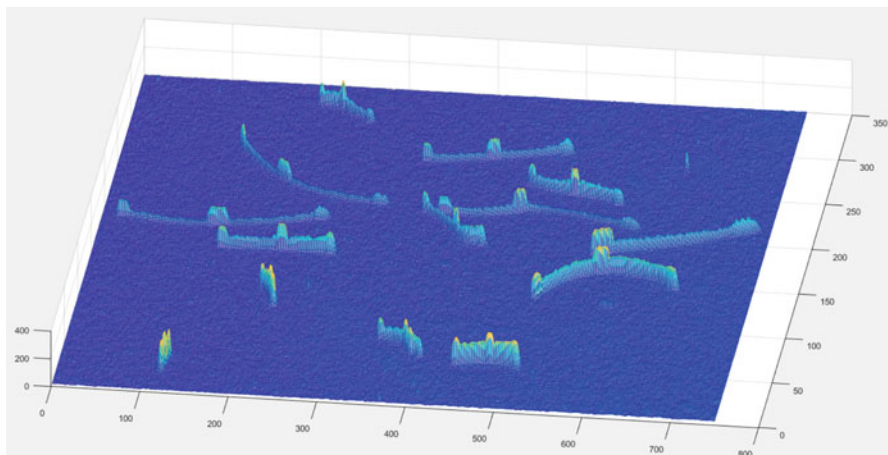


Fig. 10 Grayscale mesh of Fig. 6b

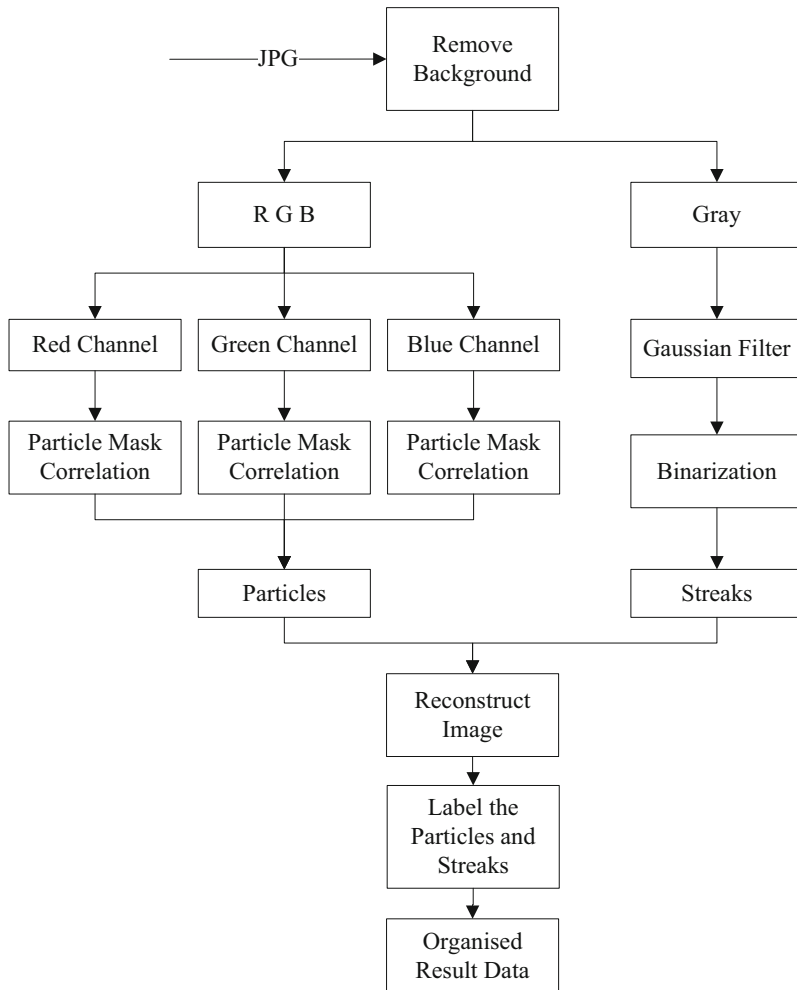


Fig. 11 Flowchart for image processing. (Reprinted from Wang et al. (2017), with permission from Elsevier)

The flowchart for image processing is shown in Fig. 11. Because the background remains bright, removing the background is essential to enhance the distinction between streaks and background. Since spots and streaks have different characteristics, they are handled with two separate procedures. For spot detection of the three different colors, i.e., red, green, and blue, dividing the original image into the respective RGB channels can reduce the effect of the white streak. Next, the particle mask correlation (PMC) method (Takehara and Etoh 1999) based on a Gaussian distribution is used to identify the spots in different color channels. For streak recognition, the total signal recorded in all channels is summed and converted into a grayscale image. Because the streaks can be considered as gathered spots, a

Gaussian filter can also help to suppress the background noise and enhance the signal from the bubbles. Then, the OTSU algorithm (Otsu 1979) is applied to enhance the binarization of images.

In CSPSV, the colored spots provide the key points for the start, middle, and end time of bubbles. Therefore, image information extraction is conducted to link the spots of the same seeding bubbles. If images are taken using the sequence in Fig. 6a, three vectors can be extracted from the image: from the red spot to the green spot, from the green spot to the blue spot with one time duration, and from the red spot to the blue spot with two time durations. Using this digital image-processing scheme, the bubble trajectory information of these images is collected and automatically arranged for 3D streak pair matching with high precision.

Rectification-Based Sparse Stereo Correspondence

After image processing, the 3D stereo reconstruction algorithm is designed to evaluate the 2D vectors from two cameras to produce the 3D vector results. Unlike traditional stereo correspondence, the information gathered from the raw CSPSV image is a series of sparse vectors, invalidating the smoothness assumptions for regular stereo correspondence (Szeliski 2011). As a sparse stereo correspondence problem, the traditional matching algorithm for neighboring pixels (Shi et al. 2015) also becomes ineffective. Pair matching based on the end points (Sun 2007) is also not enough for complex flow phenomenon. However, the start, middle, and end points of a streak together can be used for pair-matching judgment, which can improve the system accuracy.

Since the epipolar constraint alone is not adequate for pair-matching judgment (Maas 1992), rectified images from two cameras are adopted as important criteria. With the calibration data of the cameras, the streaks on the rectified images of the same bubble can be adjusted along the same horizontal line (Fusiello et al. 2000) as shown in Fig. 12. The pixel difference, Delta, of the corresponding color spots from two cameras in Y-axis after rectification can be calculated in Eq. 6:

$$\Delta = Y_1^{\text{rectified}} - Y_2^{\text{rectified}} \quad (6)$$

By adding the absolute number of pixels between the corresponding spots of each streak from different cameras in the rectified Y-axis, a new criterion, $C_{\text{Rectified } Y}$, between each streak from different cameras is defined in Eq. 7.

$$C_{\text{Rectified } Y} = |\Delta_{\text{start}}| + |\Delta_{\text{middle}}| + |\Delta_{\text{end}}| \quad (7)$$

If two streaks captured by different cameras are from the same bubble, $C_{\text{Rectified } Y}$ should be very close to zero and can be used as a prefilter to expedite the search for candidate matching streak pairs and, at the same time, improve the accuracy of pair matching.

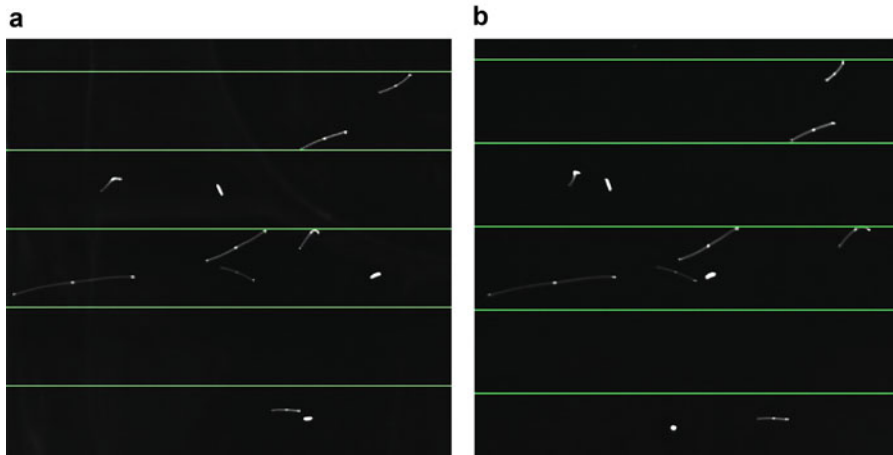


Fig. 12 Rectified image from cameras. (a) Left camera. (b) Right camera. (Reprinted with permission from Wang et al. (2018), © The Optical Society)

After finding the candidate matching streak pairs, the epipolar constraint residual is calculated for three spots:

$$\mathbf{R}_{\text{spot}} = \mathbf{P}_1^T \mathbf{F}_{12} \mathbf{P}_2 \quad (8)$$

where \mathbf{P}_1 and \mathbf{P}_2 are the normalized pixel coordinates in cameras 1 and 2, respectively, and \mathbf{F}_{12} is the fundamental matrix based on the calibration data (Fu et al. 2015),

$$\mathbf{F}_{12} = [\mathbf{T}_1 - \mathbf{R}_1 \cdot \mathbf{R}_2^T \cdot \mathbf{T}_2] \times \mathbf{R}_1 \cdot \mathbf{R}_2^T \quad (9)$$

Matrixes \mathbf{R}_1 , \mathbf{T}_1 , \mathbf{R}_2 , and \mathbf{T}_2 are extrinsic parameters from calibration. By adding the residuals together for the whole streak pair, C_{Epipolar} is calculated in Eq. 10.

$$C_{\text{Epipolar}} = \mathbf{R}_{\text{start}} + \mathbf{R}_{\text{middle}} + \mathbf{R}_{\text{end}} \quad (10)$$

C_{Epipolar} can be used to evaluate the entire streak matching performance. Finally, the geometry bounds are evaluated for gross errors.

With these specific designed digital image-processing algorithm and pair-matching algorithm, the color-coded sequence information can be accurately extracted and made full use of, which lay the solid foundation for the accuracy of CSPSV system.

Accuracy Verification

The accuracy of the CSPSV measurement system was verified before further application. Two different targets were employed: a rotating board test for detailed three-component velocity verification and a wind tunnel test for the comparison with regular instruments HWA.

Experimental Setup of Rotating Board Test

Because the airflow speed is notably difficult to be precisely measured and used as a known speed, image-based velocimeters commonly use rotating white dots of a known track and speed instead. The dots are usually indicated on a rotating black board or a needle to simulate the particle motion (Sun 2007; Barker 2012; Zappa et al. 2013). The rotating board here is made of black PVC reinforced with an aluminum support. Along its longitudinal axis, dots are placed at 10, 15, 20, 30, 35, and 40 cm from the center of rotation. The board is driven by a closed-loop step motor with a 1:50 harmonic wave reducer that increased the torque and smoothed the rotation. By sending different pulse frequencies to the motor, the rotation speed can be adjusted from 0 to 1.6 rev/s. In this experiment, the rotation speed was selected as 0.2 rev/s and 0.6 rev/s, which corresponds to the speed magnitude of these dots of 0.12–2.45 m/s, respectively. To verify the velocity of each dot in three directions, the position of the rotating board was also monitored and shown on a LED lattice board. Therefore, from a single image, the velocity of the dots and the position of the board can be determined.

Because CSPSV reduces the requirement for a high-speed camera, regular single-lens reflex cameras can handle the task. In this test, two common single-lens reflex cameras (model: Cannon 70D) with 24 mm focal length lens are utilized. During the test, the exposure time for the two cameras is 200 ms, and they are synchronized with CSIS. As in Fig. 6b, the color sequence of CSIS is from red to green and blue with a pulse width of 3 ms and a flashing frequency of 10 Hz. The raw image is shown in Fig. 13, from which we can clearly determine the color spots and white streaks. With images taken by two cameras from different angles, the tracks of each dot can be reconstructed in 3D space using the aforementioned algorithm. Given the location and rotation speed of the board, the speed of these dots in three directions can be calculated and treated as the known speed.

Accuracy Verification on Rotating Board

For a stereotypical 3D imaging system, the measurement error varies with different directions. Comparisons of each component velocity between the measured and known speeds are shown in Figs. 14 and 15. The U, V, and W directions represent the velocity vector directions in the X, Y, and Z axes, respectively. The red and green bars represent the real and measured speed of the dots, respectively.

In the low-speed test, the rotating speed was set to 0.2 rev/s, which made the velocity of the dots so low it is difficult to be precisely measured. In Fig. 14a and b, the displacement between the actual speed and the measurement in the U and V directions is small (generally below 5%). Although the relative error is larger at some points, it is mainly because the actual speed is so small. Figure 14c shows that the relative error of CSPSV in the W direction is higher than those in the U and V directions because there were only two cameras in the tested system. Thus, the information gathered in the Z direction was insufficient. Despite this systematic

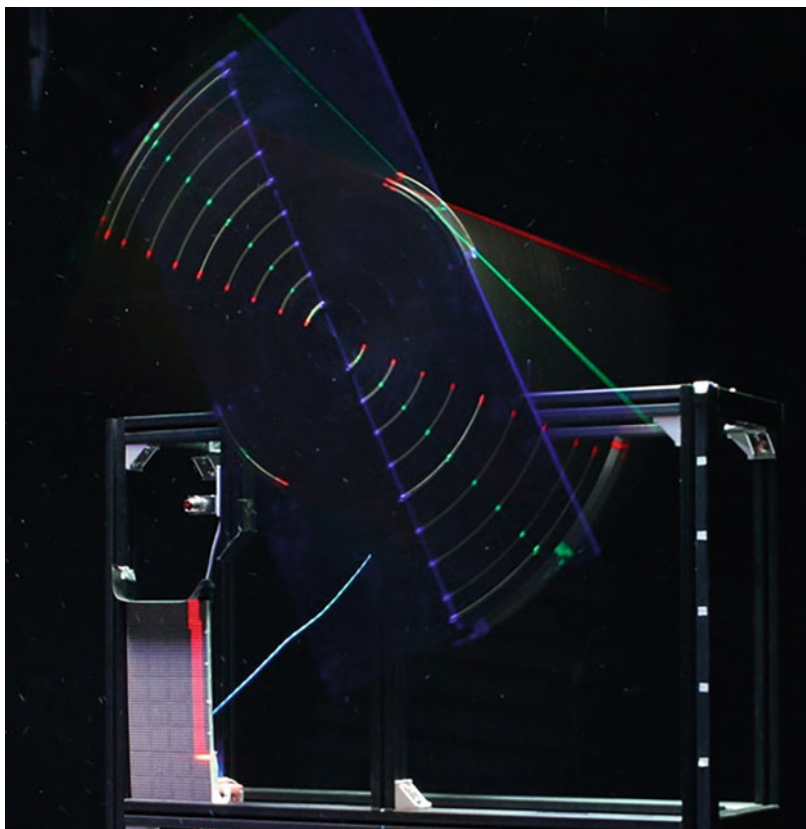


Fig. 13 Image of a rotating board for verification. (Reprinted from Wang et al. (2017), with permission from Elsevier)

drawback, the result for the W direction remained acceptable, particularly for the low-speed airflow measurement. The magnitude accuracy is notably satisfactory as shown in Fig. 14d.

In the high-speed test, the rotational speed increases to 0.6 rev/s, and the tangential speed of the outer dots increases to 2.5 m/s. In Fig. 15a, b, c, and d, the relative error in all directions decreases when the real speed increases. In most cases, the relative error is less than 5%, which is satisfactory for room ventilation measurement.

The verification range of $0.12 \sim 2.45$ m/s covers the primary testing speed in normal room airflow speed measurement. The CSPSV system showed an excellent precision in this range. In addition, all the streaks were successfully matched with a much lower magnitude of relative error than that in a previous study, where only half of the pair matching was successful and the relative error was 20% (Sun 2007). The rotating-board experiment confirms that CSPSV can perform highly accurate speed measurements.

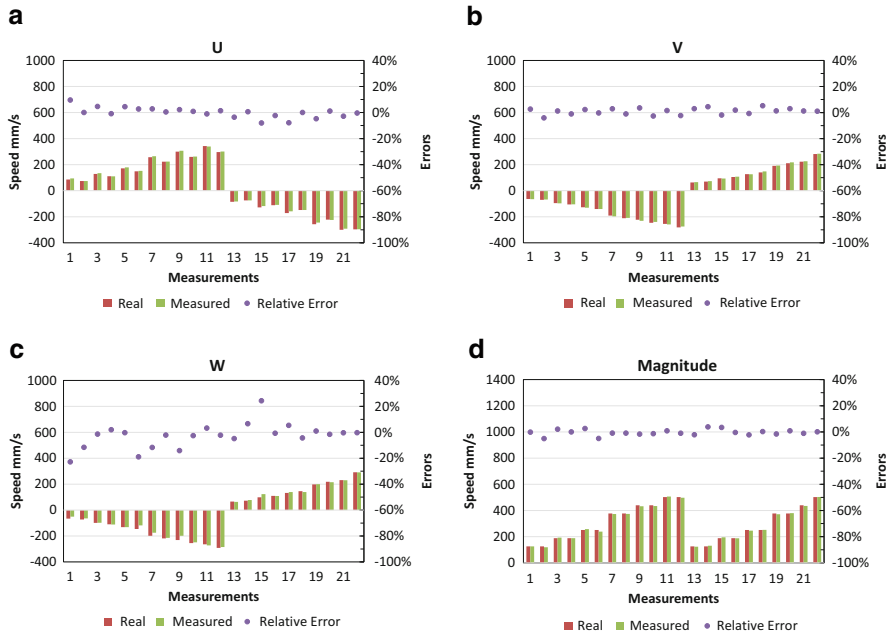


Fig. 14 Verification results for a low rotation speed. (a) U direction and relative error. (b) V direction and relative error. (c) W direction and relative error. (d) Magnitude and relative error. (Reprinted from Wang et al. (2017), with permission from Elsevier)

Experimental Setup in the Wind Tunnel

The CSPSV system is further verified in a wind tunnel to test the parallel flow for verification with regular airflow measurement instrument HWA. As shown in Fig. 16, the wind tunnel is 4.5 m long. The main fan with an inverter blows airflow into the plenum chamber at one side of the main tunnel to provide a steady airflow into the tunnel. The section of the tunnel is 20 cm high and 54 cm wide. A bypass tunnel and a recirculation fan are set beside the main tunnel.

During parallel flow verification, only the main fan is operating to offer a steady and smooth airflow of different speeds within the main tunnel.

The test zone is located near the middle of the tunnel marked with an orange dashed line. During the experiments, two cameras (sp-20000c, JAI) with a 35-mm lens (F1.4, Zeiss) are set above the test zone. The CSIS is set beside the test zone, projecting color-coded light into the test zone. Buoyancy-neutral helium-filled soap bubbles are released at the outlet of the fans marked with yellow dots.

Verification with HWA

The verification experiment was between the high-accuracy HWA and CSPSV to evaluate the accuracy of CSPSV in real airflow measurement. The HWA was the

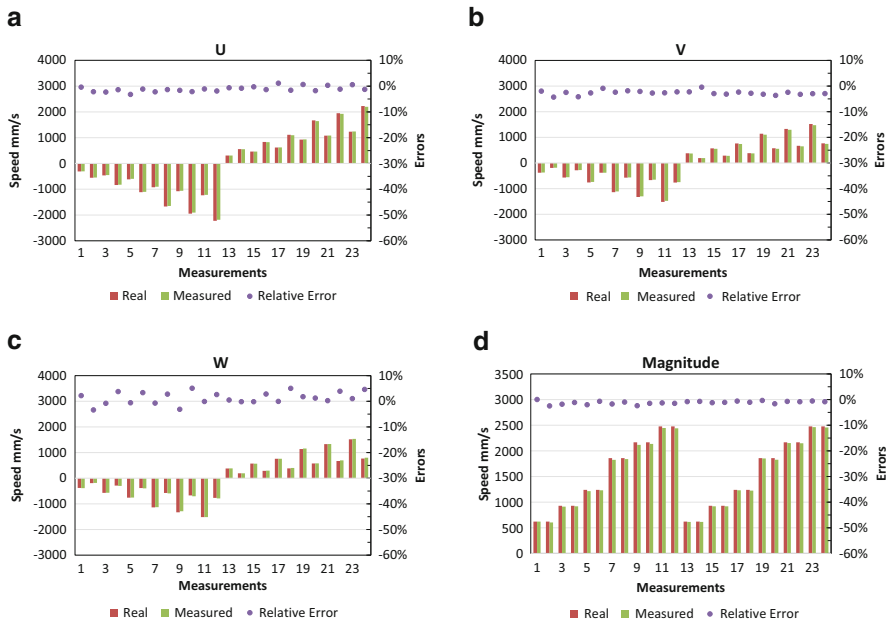


Fig. 15 Verification results for a high rotation speed. (a) U direction and relative error. (b) V direction and relative error. (c) W direction and relative error. (d) Magnitude and relative error. (Reprinted from Wang et al. (2017), with permission from Elsevier)

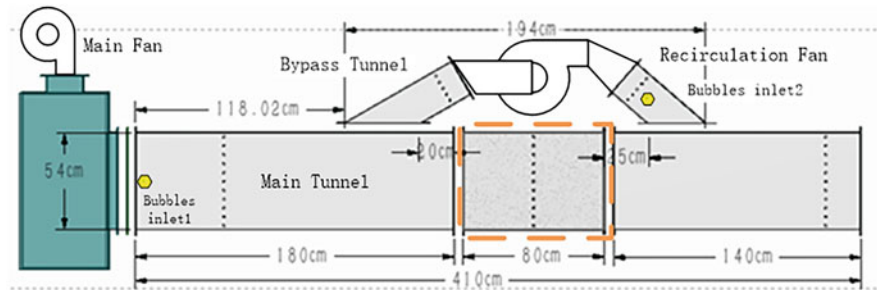


Fig. 16 Experimental setup of wind tunnel. (Reprinted with permission from Wang et al. (2018), © The Optical Society)

principal research tool for most turbulent flow studies and always used for verification. The HWA tests the heat release rate from the hot wire to calculate the airflow speed. It is more sensitive to flows perpendicular to its hot wire (Bruun 1995). Therefore, parallel flow, which is easy to produce and can be measured precisely by both the normal HWA and CSPSV, is selected as the flow pattern for verification. By changing the inverter frequency of the main fan, three cases are tested for different airflow speeds. In this test, the flash time period of the CSIS is set to 30 ms, while the exposure time for the two cameras is set to 60 ms. The HWA is from KANOMAX

(model 0963-00), which can provide an accuracy of ± 0.1 m/s within the range of 0.1–4.9 m/s.

The test results are presented in Fig. 17a when the main fan is running at 10 Hz. It can be seen that most vectors are parallel and the velocity is somewhat equal. A detailed comparison of the measurement from the HWA and CSPSV is presented in Fig. 17b, c, and d. Three different airflow speeds were tested: 0.67, 1.0, and 1.36 m/s. The average speeds measured by the HWA at different locations on the X-axis are marked by orange triangles with error bars. The magnitudes of the vectors measured by CSPSV under different wind speeds are marked with blue dots. When the wind speed of the tunnel is high, it was not easy for the bubbles to spread along its path within a short distance. Therefore, the resulting vectors are more highly clustered at the higher speed as shown in Fig. 17c and d.

From Fig. 17b, c, and d, the average speeds of both instruments were very similar, and the scatter of the CSPSV results was near the average level. Overall, the speed provided by CSPSV was slightly higher than that of the HWA. One possible reason could be that the sensor wire of the HWA is more sensitive to the perpendicular flow than the parallel flow. Although most of the airflow in the wind

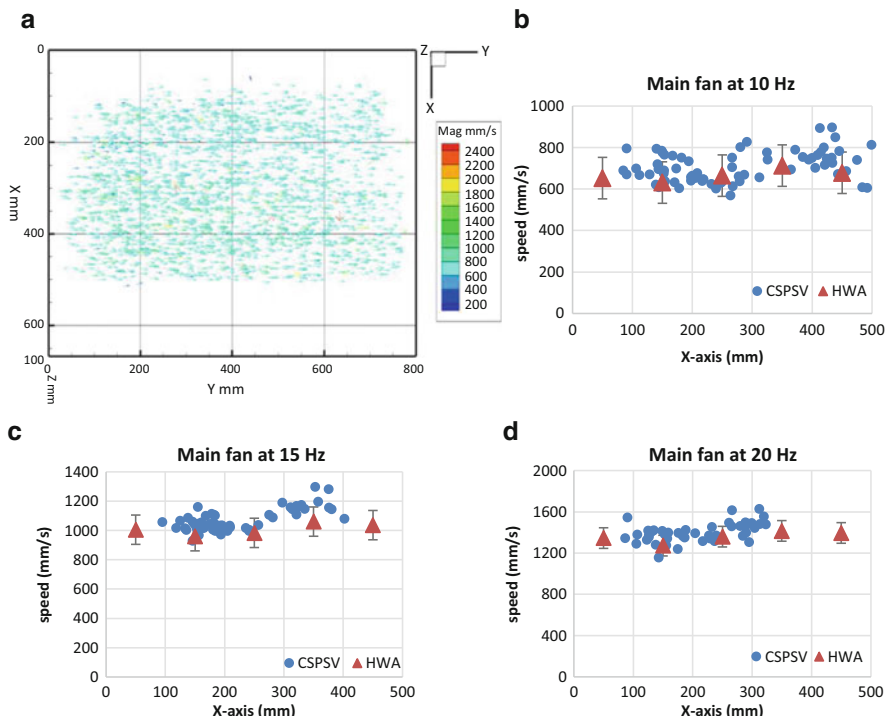


Fig. 17 CSPSV results and comparison with HWA. (a) Vectors results at 10 Hz. (b) Magnitude at 10 Hz. (c) Magnitude at 15 Hz. (d) Magnitude at 20 Hz. (Reprinted with permission from Wang et al. (2018), © The Optical Society)

tunnel is perpendicular to the sensor wire, there is still some turbulent flow that cannot be measured precisely by the HWA, whereas it can be captured by CSPSV. This verification with the normal instrument has proven the accuracy of CSPSV for airflow measurements in a moderately large zone.

Applications and Results

In this part, three cases have been measured to demonstrate the capability and reliability of the CSPSV method in actual tests including the vortex in a scale tunnel, and the airflow patterns induced by a ceiling fan and an adjustable fan network (AFN).

Vortex Flow Test

Theoretically, a vortex is very sensitive to the disturbance from invasive sensors and difficult to measure with regular instruments (such as a HWA). Hence, CSPSV is utilized for the vortex flow test for its nonintrusive advantage. The test is conducted in the scale tunnel with the recirculation fan set on the bypass tunnel opened as shown in Fig. 16. This setting can produce a large vortex in the main tunnel. During the experiment, the main tunnel fan supplies $260 \text{ m}^3/\text{h}$ of air into the tunnel, while the circulation fan circulates $523 \text{ m}^3/\text{h}$ of air within the tunnel. Hence, there will be a large vortex within the test zone, which is a much more complicated airflow phenomenon and difficult to measure with normal instruments, especially at this large scale. Since the target air speed is faster in this experiment, the exposure time was set shorter. The flash rate of the CSIS is set to 25 ms, and the camera exposure time is 50 ms. The 3D vectors are presented in Fig. 18a and b.

Since the vectors are the 3D3Cs distributed in the space, they are interpolated into grid for further calculation and analysis. In this test, uniform 50 mm grids were used to investigate the turbulence intensity (TI). The turbulent velocity fluctuation is calculated using Eq. 11.

$$v' = \sqrt{\bar{v}^2} \quad (11)$$

where v' is the root-mean-square of the turbulent velocity fluctuations. Subsequently, the TI can be calculated using Eq. 12.

$$TI = \frac{v'}{\bar{V}} \quad (12)$$

where \bar{V} is the mean velocity. The averaged results and TI results are presented in Fig. 18c and d. From vector field as in Fig. 18b, the gradient of the flow is very large and the flow is chaotic. The region of the vortex core can be captured and illustrated very well for this large space and shows a good consistency with the flow dynamics

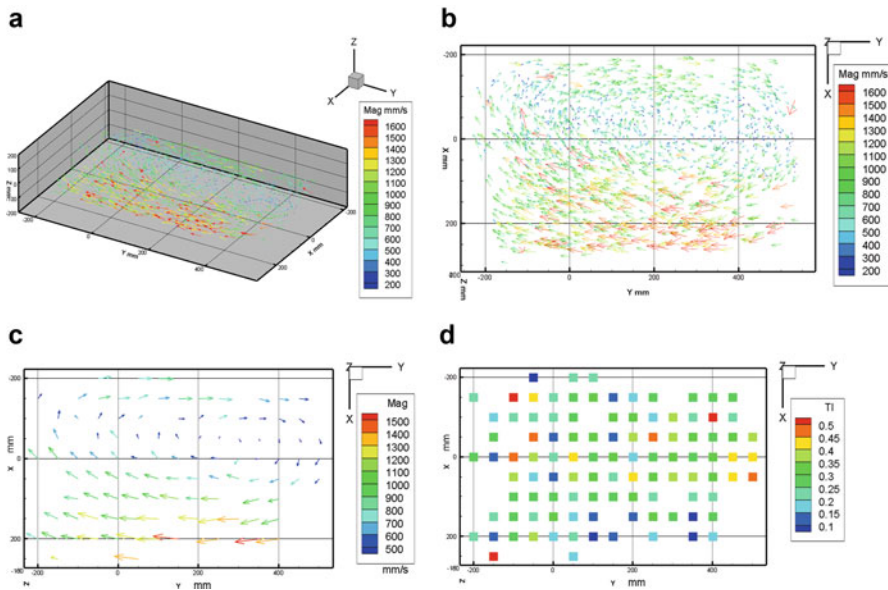


Fig. 18 Test results of CSPSV. (a) 3D view. (b) Vortex top view. (c) Averaged vectors. (d) TI. (Reprinted with permission from Wang et al. (2018), © The Optical Society)

analysis. This test proves the capability of CSPSV to capture and measure the complex airflow with a moderately large measuring space.

Airflow Pattern Induced by Ceiling Fan

This test is designed to measure the airflow pattern induced by ceiling fan, which is of high gradient and fast velocity.

Chamber Setup

The experiment is conducted in the airflow visualization and measurement platform located at Tsinghua University. The platform consists of a sealed chamber, four cameras, and illumination systems. The chamber is $4\text{ m} \times 2.5\text{ m} \times 3\text{ m}$ in width, height, and depth. Three surfaces (e.g., the ceiling, roof, and front-side wall) of the chamber are made of high-transparency glass. To avoid the airflow field in the chamber from being blocked, the cameras and illumination systems are placed outside the chamber. In total, 40 CSIS modules are located above the ceiling and under the floor. They are placed on the length direction of the chamber from left to right, creating an illumination zone that is also the airflow measurement zone sizes: $4\text{ m} \times 2.5\text{ m} \times 0.8\text{ m}$ in the middle of the chamber. As the CSIS modules are isolated from the chamber, the heat produced from them affects little on the airflow field.

A normal ceiling fan with three plastic blades of diameter 60 cm is utilized. It rotates at a constant speed of 330 rounds per min (rpm). The power supply is 220 V AC, with a constant power consumption of 6.34 W. The fan is fixed at 2.15 m above the floor, 0.35 m away from the ceiling, and in the middle of the test chamber.

The seeding particles used are HFSBs produced by a commercially available bubble generator SAI Model 5. The diameter of the HFSB ranges from 1 to 3 mm and filled with helium, thus rendering the Stokes' number less than 0.1. These bubbles are released from the top center of the ceiling over the fan, and a complement diffuser is utilized to decelerate the bubble speed to 0.15 m/s, such that its effect on disturbing the primary airflow field can be ignored.

The typical image with 50 ms exposure time during experiment is shown in Fig. 19. Some regions are partially enlarged in the image for a better illustration. From Fig. 19, the streaks with different length and direction can demonstrate the dramatic changes of airflow pattern between these regions as well as the effectiveness of CSIS.

Imaging Settings

To capture the airflow characteristic near the ceiling and floor, four high-resolution cameras (sp-20000c, JAI) with 35-mm lens (F1.4, Zeiss) are utilized for different view angles, as shown in Fig. 8. The four cameras are located on the transparent side and out of the chamber. As mentioned in a previous study (Liu et al. 2018), a fan-induced airflow demonstrates a large gradient between the jet core and surrounding entrainment flow. In this test, two types of cases are set for different exposure times, as shown in Table 1. A long-exposure-time case aims at the low-speed entrainment airflow, while a short-exposure-time case aims at the high-speed jet

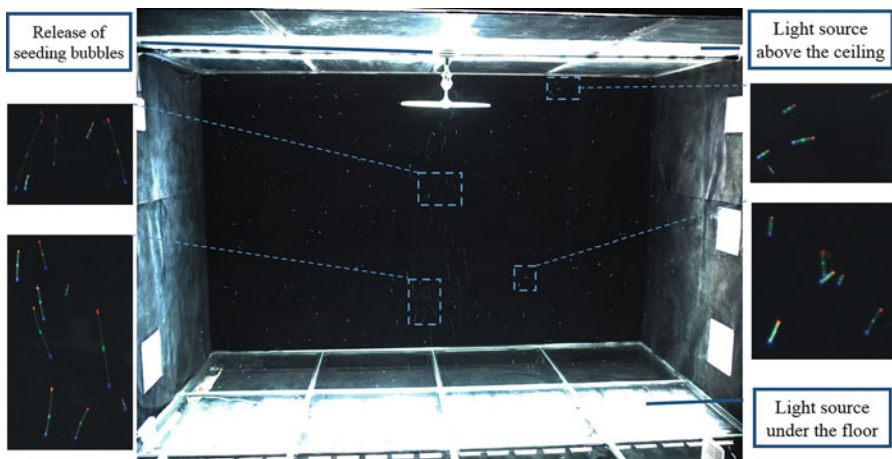
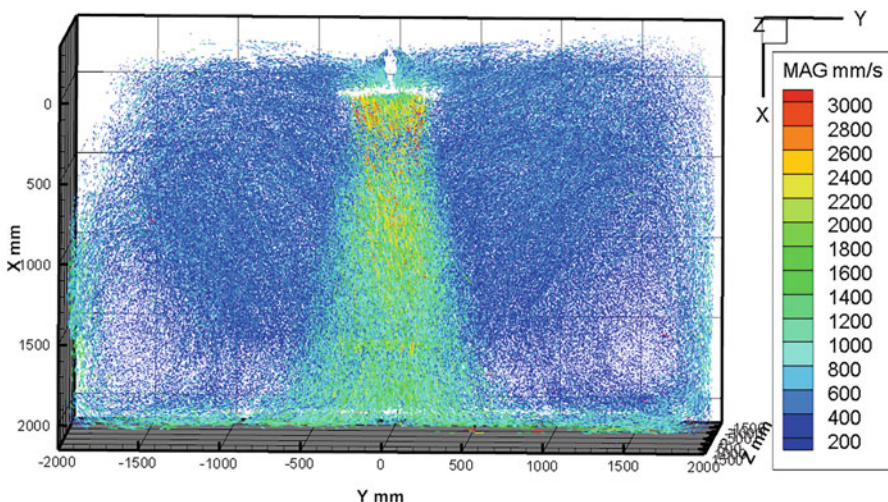


Fig. 19 Experimental setup and typical image of fan test. (Reprinted from Wang et al. (2019), with permission from Elsevier)

Table 1 Case setting

Case name	Exposure time	Target zone	Sample frequency	Sample frames	Time interval between two color flashes
Short exposure	50 ms	Jet Core	10 Hz	2700	25 ms
Long exposure	200 ms	Entrainment	4 Hz	3300	50 ms

**Fig. 20** Vectors induced by ceiling fan. (Reprinted from Wang et al. (2019), with permission from Elsevier)

core region. In total, each camera captures 6000 frames of the bubble's time sequence image. During experiments, the CSIS is synchronized with camera.

Results

After the images are captured, the time sequence information on the images is processed with the algorithms mentioned above. Quad-view CSPSV can provide detailed 3D velocity vectors field within the test space and can be illustrated as air velocity vectors similar to the CFD simulation results. In this test, 417,671 vectors are reconstructed and are presented in Fig. 20. For the convenience of calibration and image processing, the height of chamber is presented as X axis, the width of chamber is presented as Y axis, and the depth of chamber is presented as Z axis.

In addition to the vector field, the raw images can also provide considerable information about the flow pattern. Figure 21 demonstrates the accumulated color streaks of 200 images in the measurement zone with short exposure time. It is obtained by subtracting the raw image with the background to get the streaks in each image and then adding them together. Figure 21 shows the continuous trajectory of seeding bubbles during 20 s, and from the movements, two big vortices can

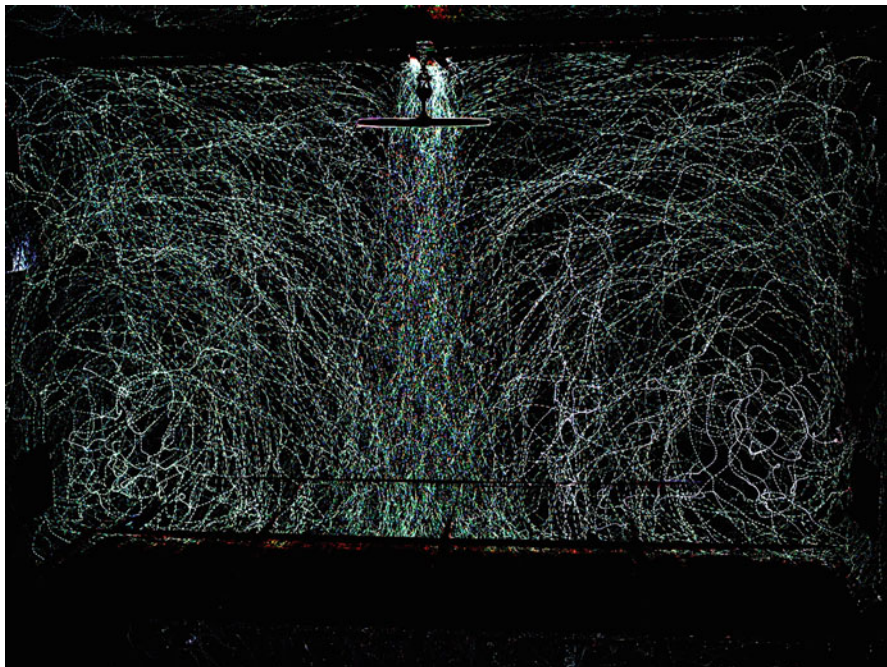


Fig. 21 Accumulated traces of 200 images in the measurement zone. (Reprinted from Wang et al. (2019), with permission from Elsevier)

be observed located in the lower part of the room, and the main part of the room is influenced by the fan jet.

To streamline the vector data interpretation, the results are interpolated with 20 mm grids with inverse-distance interpolation method (Tecplot 2018) to investigate the detailed airflow characteristics in different regions. Figure 22 shows the middle section from the front view of the chamber. As shown, the airflow induced by the ceiling fan can be divided into six zones based on the airflow patterns.

The jet core zone is located immediately under three fan blades, and the fast jet flow is the primary momentum of chamber circulation. The jet has the highest speed at its boundary and expand slowly along its path. **The spreading zone** is near the floor where the jet core impinges the floor; this layer is relatively thin while the speed is higher than 1 m/s. When the spreading airflow reaches the wall, the flow direction changes to vertical upward and decelerates gradually. Between the spreading zone and wall zone, **the recirculation zones** are marked with triangular frames on both sides. The recirculation flow zones are surrounded by the entrainment flow, recirculation flow, and wall flow, while the vortex flow follows the change in direction of these flows. **The entrainment zone** is primarily induced by the jet core. The entrainment zone occupies the largest space in the chamber with an evenly low air speed, and the boundary between the jet core and entrainment flow is sharp and clear. **The suction zone** is located above the fan blades. As the fan is located

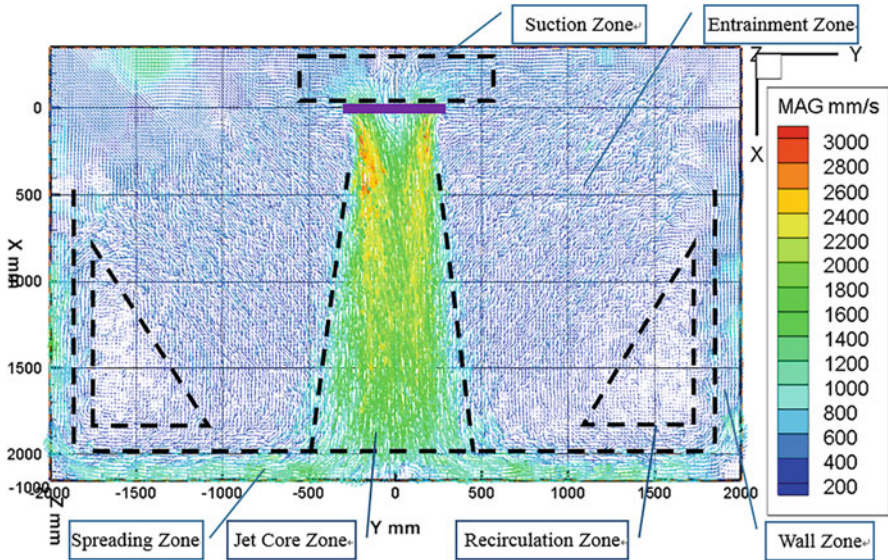


Fig. 22 Velocity distribution on the middle section of fan-induced airflow (Reprinted from Wang et al. (2019), with permission from Elsevier)

sufficiently far from the ceiling and the speed of the convergent flow decays rapidly, the suction zone is not large and appears symmetrical. These characters convey the complexity of the flow pattern induced by the ceiling fan and can facilitate in the better understanding and utilization of ceiling fans in an indoor environment.

The raw data can be further mapped into a grid of size 100 mm × 100 mm × 100 mm to calculate the TI level. As shown in Fig. 23, the zone under the fan blade tip has a much higher TI values, while the center of the fan has relatively lower TI values. The edge of the jet core zone has TI levels of 50–75%, but the TI level in the center part of the core zone are between 15% and 35%. From the view of the entire space, the TI levels are higher in the bottom part but lower the in upper part especially when close to the ceiling and walls. The overall averaged TI is approximately 40% and is much larger than that in regular rooms.

As the result vector field is of high density and 3D3C, the vorticity can be calculated for the better understanding of the swirling character of airflows, which can hardly be achieved with regular measurement instruments especially in this scale. The vorticity on different directions is calculated respectively for a better understanding of this flow pattern. The equation is as follows:

$$\omega_z = \frac{\partial v}{\partial x} - \frac{\partial u}{\partial y} \quad (13)$$

$$\omega_x = \frac{\partial w}{\partial y} - \frac{\partial v}{\partial z} \quad (14)$$

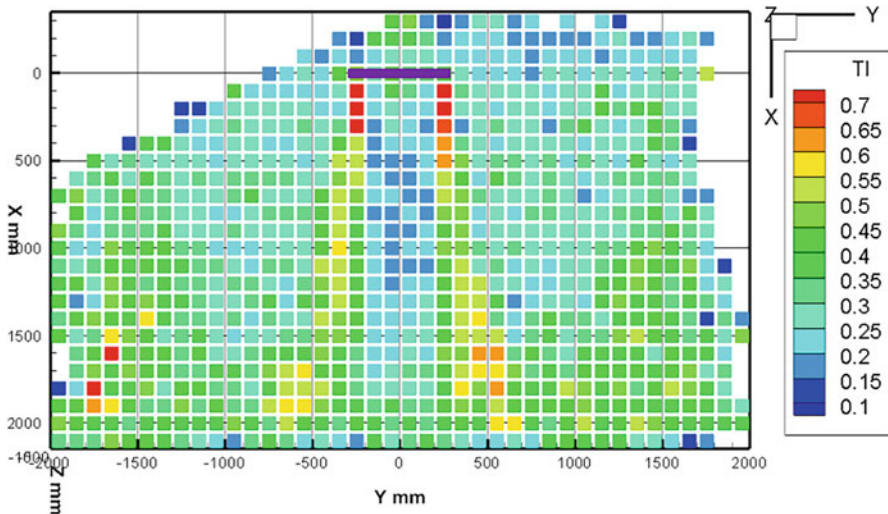


Fig. 23 TI distribution in the middle section. (Reprinted from Wang et al. (2019), with permission from Elsevier)

where u is the velocity component in the X direction, v is the velocity component in the Y direction, and w is the velocity component in the Z direction. ω_z can illustrate the swirling direction of flow in the XY plane, and ω_x can illustrate the swirling direction of flow in the horizontal plane. Figure 24a presents the vorticity ω_z calculated with Eq. 11 in the middle section of the chamber and illustrates the swirling direction of flow on the XY plane. The color legend on the right side represents the swirling direction of the airflow on the XY plane. Red means the airflow swirls in the counterclockwise direction, while blue means the airflow swirls in the clockwise direction. It can be seen that the airflow under the fan blades swirls in different directions. The two edges of the jet core zone exhibit higher but opposite directions of ω_z vorticity, thus demonstrating the highest speed airflow caused by the fan blade on each side swirl to opposite directions. Meanwhile, in the center region of the fan, counter direction swirling flows exist that may be caused by the difference in rotation speed along the radii of the fan blades.

Figure 24b demonstrates the vorticity ω_x calculated with Eq. 12 illustrate the swirling direction of the airflow in the horizontal plane. The almost continuous blue region means the airflow swirl with the same direction of the fan blade. This phenomenon becomes gradually inconspicuous beyond a three diameter length from the fan blade. However, in other regions, the swirling phenomenon is not evident.

Unlike the normal jet promoted by pressure difference, a fan jet is propelled by the rotation of fan blades, which produces its own characteristics. The detailed velocity field is further illustrated and studied below. As shown in Fig. 25, the peak air speed occurred at one-third of the fan blade radius below the fan. The highest speed regions only constitute a small portion of the jet core, and the gradient

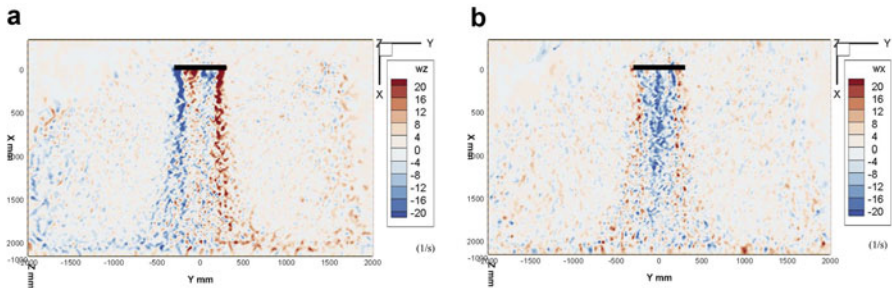


Fig. 24 Vorticity in the middle section of the fan-induced airflow. (a) Vorticity ω_z , (b) Vorticity ω_x . (Reprinted from Wang et al. (2019), with permission from Elsevier)

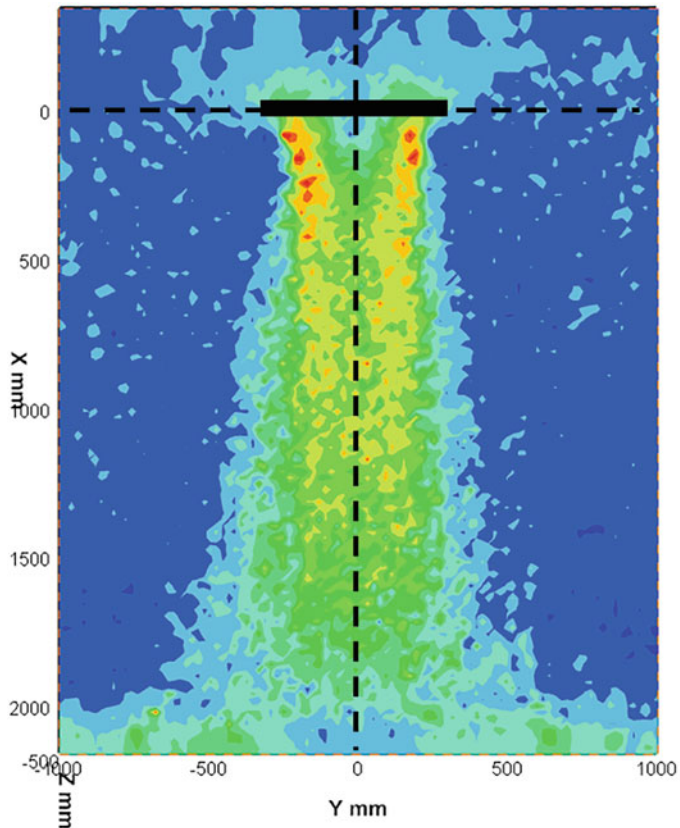


Fig. 25 Velocity contour through fan's center (Reprinted from Wang et al. (2019), with permission from Elsevier)

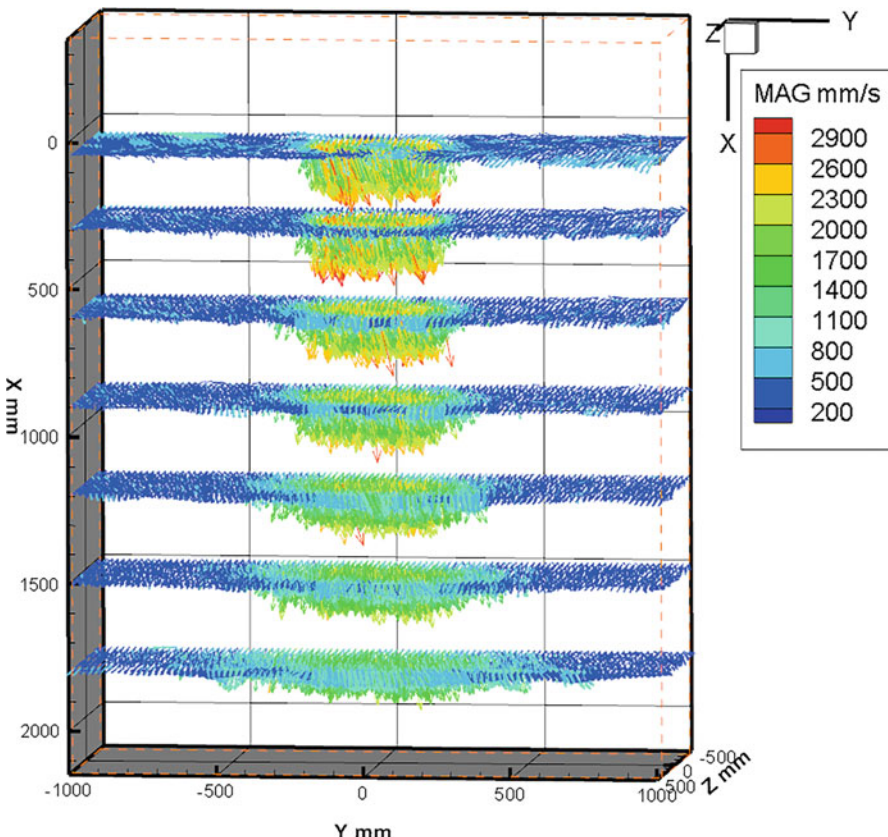


Fig. 26 Vectors on different horizontal planes (Reprinted from Wang et al. (2019), with permission from Elsevier)

of the speed difference is large and becomes diluted along its path. The diameter of the jet flow narrows slightly at first and subsequently expands gradually. The jet flow also swirls in the same rotation direction with the fan blades as shown in Fig. 26. The vertical planes are at 5 cm, 30 cm, 60 cm, 90 cm, 120 cm, 150 cm, and 180 cm from the fan's blades. From the vectors' direction, it can be found that the rotation speed along the jet path decreases while the jet expands in a larger space.

To better illustrate the changes of the airflow induced by the jet, slices of a velocity vector field are plotted at different heights as shown in Fig. 27 and discussed below. Figure 27a demonstrates the airflow 10 cm above the fan. It can be found that within the suction zone, when the air gathers from the surrounding to the fan blade while at the center of the fan, the air speed is low. Figure 27b more clearly illustrates the high-speed swirling ring produced by the fan blades. A clear high-speed vector ring can be seen that has a narrower diameter than the fan blades and rotates in the same direction. Around the jet core, the surrounding air is drawn towards the center. Unlike a normal circular jet with the highest speed jet core located in the center of the

flow, a fan jet exhibits the highest speed region near the outer boundary of the jet. As shown in Fig. 27b, c, d, and e, within a 30 cm distance (semidiameter of the fan blade) from the fan blades, the flow characteristic does not change significantly thereby proving the stability of this unique jet flow pattern. When comparing Fig. 27e and f, the high-speed region becomes diluted and the core region expands as the distance goes further downward. At an even longer distance from the fan blades, the highest speed decreases. The diameter of the jet core extends to the same diameter of the fan blade below 60 cm as shown in Fig. 27h.

The high-speed ring was further diluted at longer distances as shown in Fig. 27i, j, k, and l. When the fan jet reaches two times its diameter as shown in Fig. 27m, the high-speed ring almost disappeared. The jet center also has the highest speed

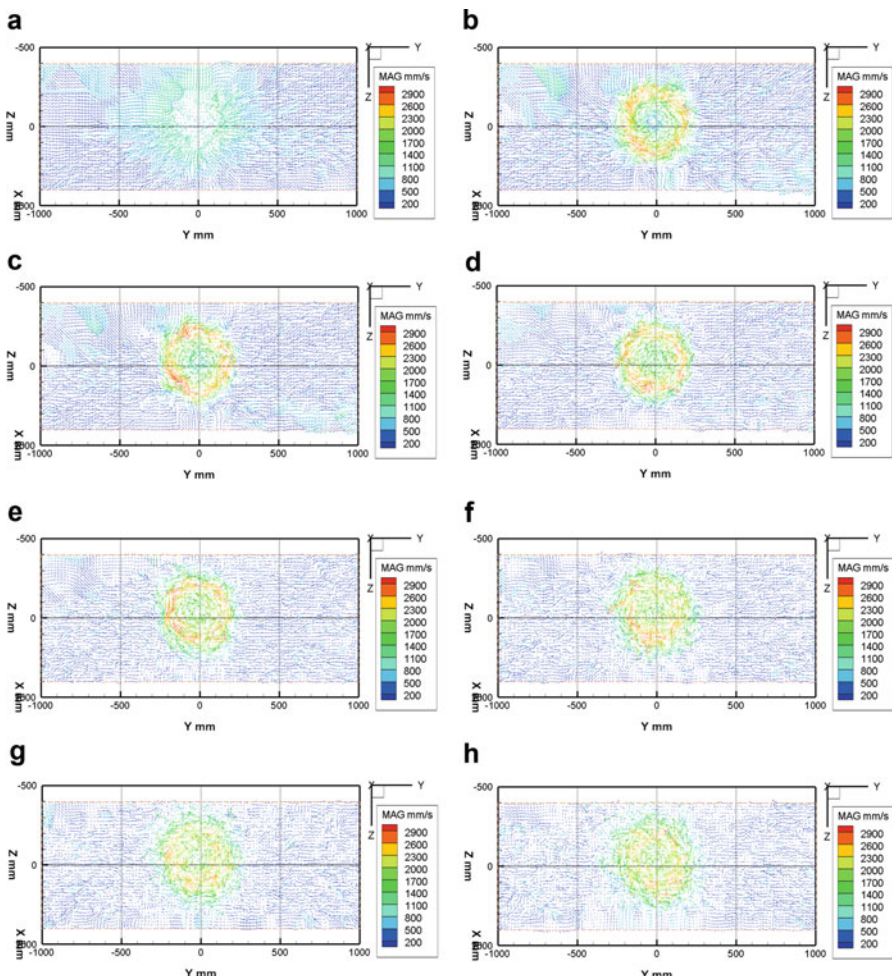


Fig. 27 (continued)

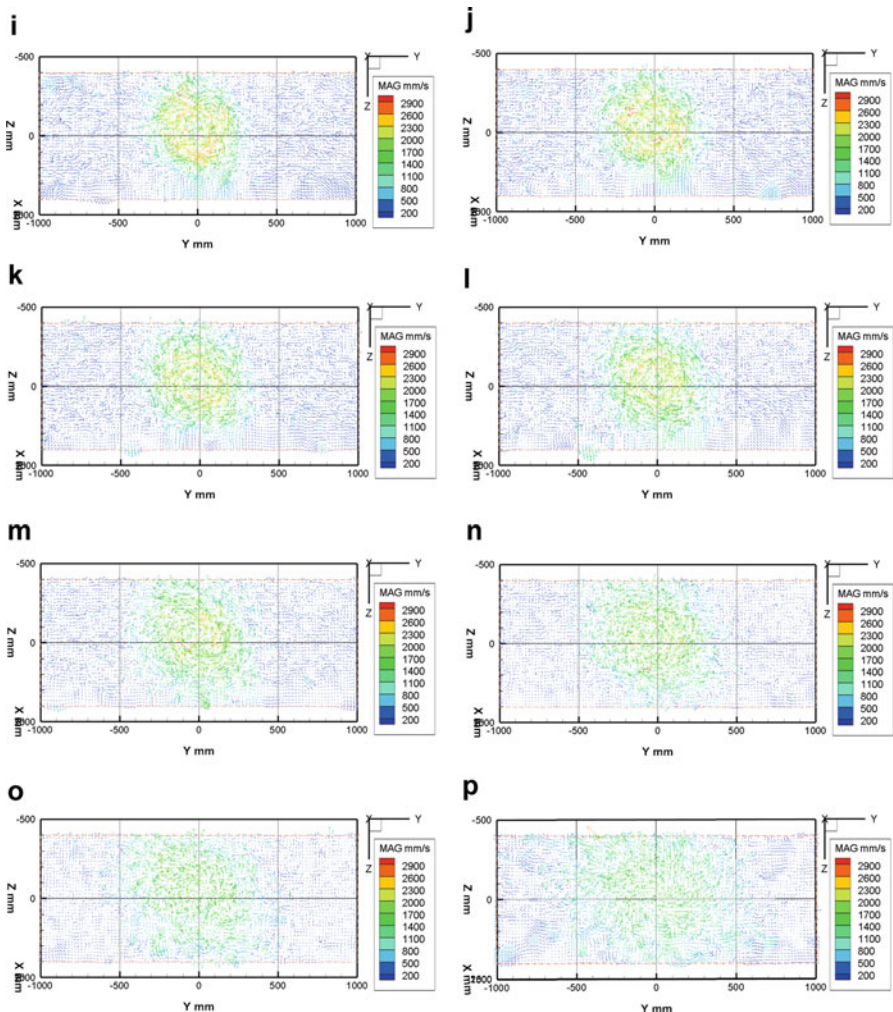


Fig. 27 Vector field at different heights. (a) 10 cm above the fan blades. (b) 5 cm below the fan blades. (c) 10 cm below the fan blades. (d) 20 cm below the fan blades. (e) 30 cm below the fan blades. (f) 40 cm below the fan blades. (g) 50 cm below the fan blades. (h) 60 cm below the fan blades. (i) 70 cm below the fan blades. (j) 80 cm below the fan blades. (k) 90 cm below the fan blades. (l) 100 cm below the fan blades. (m) 120 cm below the fan blades. (n) 140 cm below the fan blades. (o) 160 cm below the fan blades. (p) 180 cm below the fan blades. (Reprinted from Wang et al. (2019), with permission from Elsevier)

and the entire jet region is swirling as shown in Fig. 27n. When the jet travels even further as shown in Fig. 27o, the jet velocity becomes almost uniform. However, swirling phenomenon still exists even when it is three-times-diameter away from the fan blades and the speed is lower than 1.5 m/s as shown in Fig. 27p.

Based on the results above, CSPSV can be a more promising method for complicated indoor airflow measurements.

Airflow Pattern Induced by Mixing Ventilation and AFN

Traditional heating, ventilation, and air conditioning systems are predesigned and operated using a fixed airflow pattern like mixing ventilation (MV). However, the indoor occupancy and heat sources always vary, making the fixed airflow pattern may not always be efficient. Therefore an adjustable fan network (AFN) (Wang et al. 2020) was proposed for improving airflow pattern flexibility and tested with CSPSV.

Flow Pattern of MV

The airflow patterns of MV with different air exchange rate per hour (ACH) are measured as a comparison baseline. With the seeding bubbles released and mixed in the supply air, the trace of the supplied air can be recorded and compared with the baseline MV cases to illustrate the airflow pattern and evaluate the effects of the AFN.

(a) CASE-A (ACH = 1)

The continuous trace of seeding bubbles within the 20 s is shown in Fig. 28a. The supplied air-jet spread diagonally across the room and produces a large vortex located at the lower-left part of the room. The vector fields were calculated as shown in Fig. 28b. Based on the vector field, the penetration length of the supplied air is also short, and the entire indoor air movement is overly slow. Therefore, the main function of AFN for this case is set to extend the penetration length.

(b) CASE-B (ACH = 3)

The accumulated traces of seeding bubbles within 20 s for CASE-B is shown in Fig. 29a. The vector fields are shown in Fig. 29b. The supplied air flows across the upper part of the room and hits the opposite wall at high speed, as opposed to flowing into the occupied zone. The main target of AFN would, therefore, be diffusing the air more directly into the occupied zone.

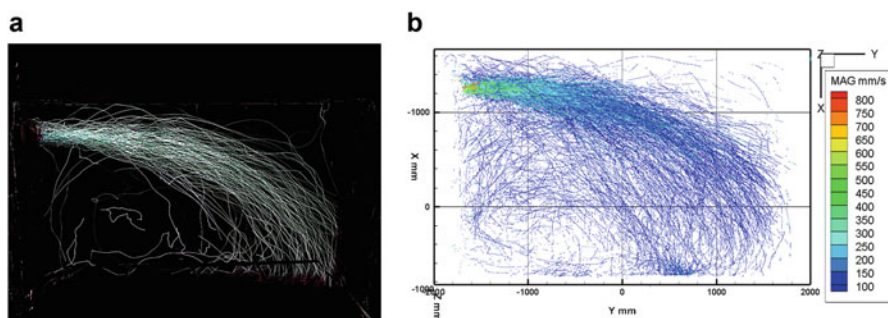


Fig. 28 Accumulated traces and vector field result of MV (ACH = 1) (Wang et al. 2020). (a) Accumulated traces. (b) Vector field

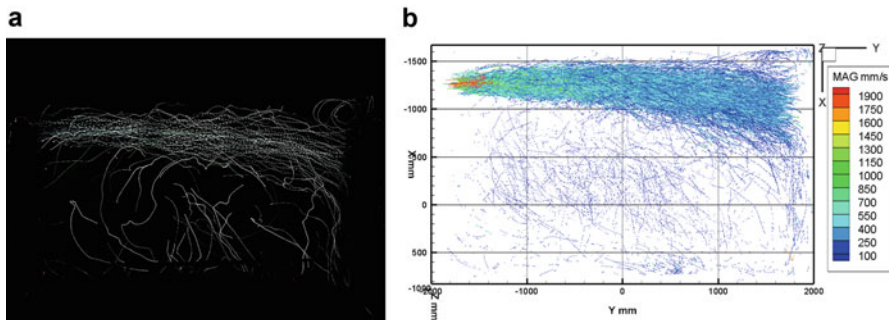


Fig. 29 Accumulated traces and vector field result of MV ($ACH = 3$) (Wang et al. 2020). (a) Accumulated traces. (b) Vector field

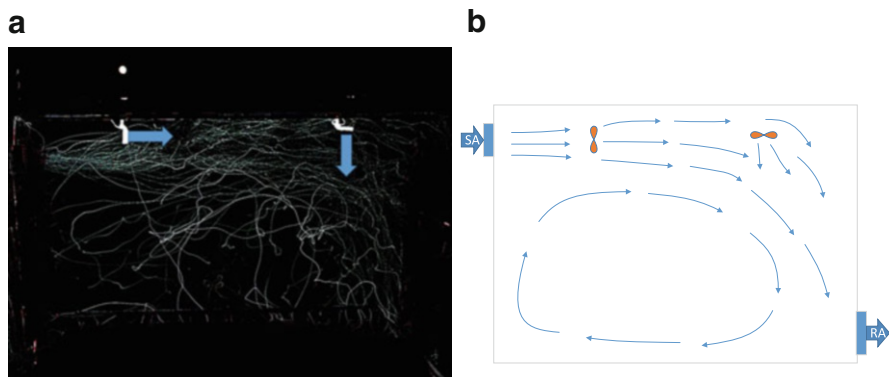


Fig. 30 Accumulated traces and schematic diagram of CASE-A1 (Wang et al. 2020). (a) Accumulated traces. (b) Schematic diagram

Flow Pattern of Cases with AFN

The measurement results presented above indicate that the ventilation effects of MV vary significantly with the air exchange rate, which is difficult to manipulate for the different indoor scenarios. The main limitations of CASE-A are the low ventilation rate and short penetration length. Therefore, two cases are tested to extend the spread region of the supplied air with AFN.

For CASE-A1, the operation of vector air-driven modules (VADM) (Wang et al. 2020) and the accumulated traces are shown in Fig. 30a. The VADM on the left propels the supplied air up to the right corner like a relay. Next, the VADM on the right pushes the supplied air downward into the occupied zone. A schematic diagram of this airflow pattern is shown Fig. 30b. With AFN, the indoor airflow pattern can efficiently transport the supplied air for a longer range.

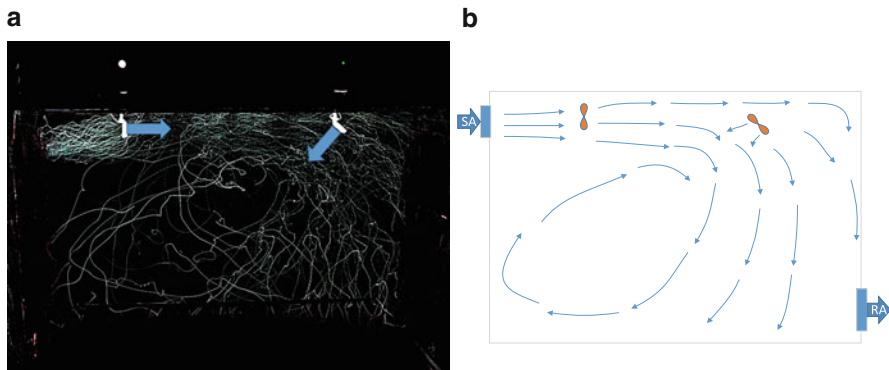


Fig. 31 Accumulated traces and schematic diagram of CASE-A2 (Wang et al. 2020). (a) Accumulated traces. (b) Schematic diagram

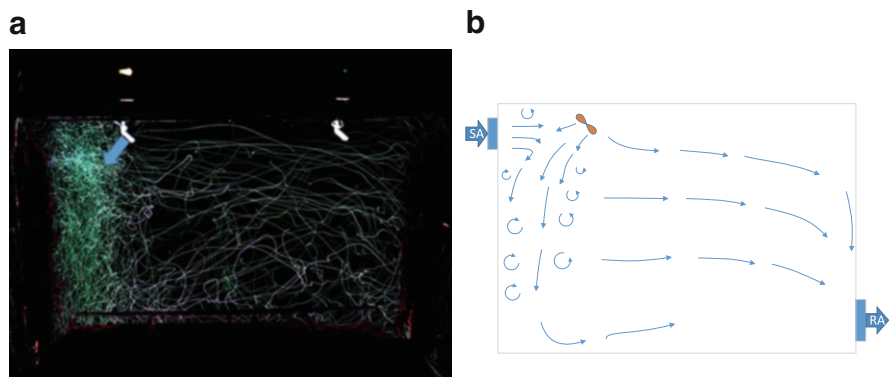


Fig. 32 Accumulated traces and schematic diagram of CASE-B1 (Wang et al. 2020). (a) Accumulated traces. (b) Schematic diagram

For better diffusion of the supplied air into the right-side occupied zone in CASE-A2, the right side VADM reverted to backward blowing. As shown in Fig. 31a, the supplied air is more evenly distributed into the right-side occupied zone. A schematic diagram of this airflow pattern is shown Fig. 31b.

For CASE-B, the increased ventilation rate results in a large increase in the penetration length, and the supplied air-jet mainly remains in the upper zone of the room as opposed to being in the occupied zone. Therefore, the main target of CASE-B1 is to enhance the ventilation in the left section of the room. Elsewhere, the left VADM is turned backward and blew downward against the inlet airflow. As shown in Fig. 32a, the left VADM pushes the inlet airflow into the left occupied zone. A schematic diagram of this airflow pattern is shown Fig. 32b. This leads to improved ventilation in the left part of the room according to the accumulated traces.

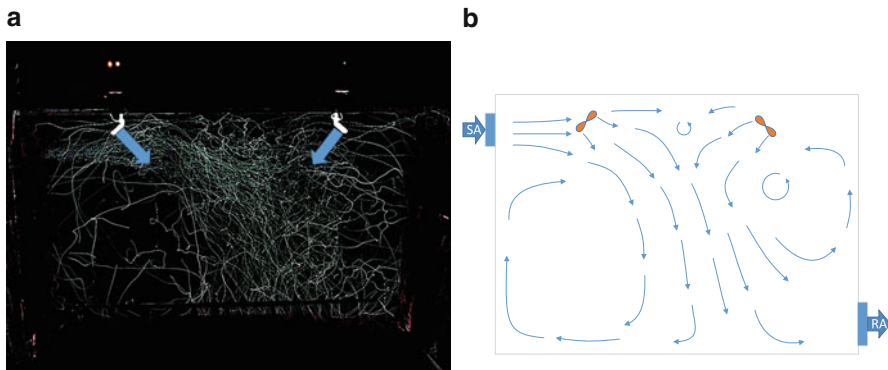


Fig. 33 Accumulated traces and schematic diagram of CASE-B2 (Wang et al. 2020). (a) Accumulated traces. (b) Schematic diagram

When multiple people are evenly distributed in the occupied zone, a well-mixing flow pattern offers the best solution. In CASE-B2, the two VADMs are set to blow towards the middle section of the room. As shown in Fig. 33a and b, this resulted in improved mixing ventilation in the entire room.

As demonstrated in the six cases, VADMs can operate as a network that enhances its maneuverability compared to the traditional air distribution systems. With an AFN, the indoor airflow pattern can be easily adjusted based on the real-time position of occupants and other sources.

Conclusions

In this chapter, CSPSV is introduced as a method to combine the advantages of the PTV and PSV with a new bubble-information-gathering scheme. Some conclusions can be drawn as follows:

1. By coding the test zone using the CSIS, more information was added to one single streak (including the time interval and time sequence). CSPSV made the tracking and 3D trajectory reconstruction of bubbles' tracks much easier and more reliable.
2. Through verification with different targets, it was observed that in the verification range of $0.12 \sim 2.45$ m/s, the relative error of the CSPSV results were mostly below 5%, and the results from CSPSV were consistent with the traditional instrument, HWA.
3. Applications in multiple cases showed that CSPSV was capable of effectively measuring complex airflows.

Acknowledgments The author(s) disclose receipt of the following financial support for the research, authorship, and publication of this chapter: the National Natural Science Foundation of China (Grant No. 51521005, 51908313).

References

- Adamczyk AA, Rimai L (1988) 2-Dimensional particle tracking, velocimetry (PTV): technique and image processing algorithms. *Exp Fluids* 6:373–380. <https://doi.org/10.1007/BF00206543>
- Adrian RJ (1984) Scattering particle characteristics and their effect on pulsed laser measurements of fluid flow: speckle velocimetry vs particle image velocimetry. *Appl Opt* 23:1690–1691. <https://doi.org/10.1364/AO.23.001690>
- Adrian R (1991) Particle imaging techniques for experimental fluid mechanics. *Annu Rev Fluid Mech* 23:261–304
- Barker DE (2012) Development of a scalable real-time Lagrangian particle tracking system for volumetric flow field characterization. University of Illinois at Urbana-Champaign, Urbana
- Barker D, Lifflander J, Arya A, Zhang Y (2012) A parallel algorithm for 3D particle tracking and Lagrangian trajectory reconstruction. *Meas Sci Technol* 23. <https://doi.org/10.1088/0957-0233/23/2/025301>
- Bendicks C, Tarlet D, Roloff C et al (2011) Improved 3-D particle tracking velocimetry with colored particles. *J Signal Inf Process* 02:59–71. <https://doi.org/10.4236/jsip.2011.22009>
- Biwole PH, Yan W, Zhang Y, Roux JJ (2009) A complete 3D particle tracking algorithm and its applications to the indoor airflow study. *Meas Sci Technol* 20:115403. <https://doi.org/10.1088/0957-0233/20/11/115403>
- Bruun HH (1995) Hot wire anemometry : principles and signal analysis. Oxford Universtiy Press, Oxford
- Cummins HZ, Knable N, Yeh Y (1964) Observation of diffusion broadening of rayleigh scattered light. *Phys Rev Lett* 12:150–153. <https://doi.org/10.1103/PhysRevLett.12.150>
- Ding L, Discetti S, Adrian RJ, Gogineni S (2013) Multiple-pulse PIV: numerical evaluation and experimental validation. 10th Int symp part image Velocim - PIV 13, Delft, Netherlands, July 1–3, 2013
- Elvsén PA, Sandberg M (2009) Buoyant jet in a ventilated room: velocity field, temperature field and airflow patterns analysed with three different whole-field methods. *Build Environ* 44: 137–145
- Fage A, Townend H (1932) Turbulent motion near a wall. *Proc R Soc A*:657–677
- Fu S, Biwole PH, Mathis C (2015) Particle tracking velocimetry for indoor airflow field: a review. *Build Environ* 87:34–44. <https://doi.org/10.1016/j.buildenv.2015.01.014>
- Fusiello A, Trucco E, Verri A (2000) Compact algorithm for rectification of stereo pairs. *Mach Vis Appl* 12:16–22. <https://doi.org/10.1007/s001380050120>
- Heikkila J, Silven O (1997) A four-step camera calibration procedure with implicit image correction. In: Proceedings of IEEE computer society conference on computer vision and pattern recognition, pp 1106–1112
- Kato S, Ito K, Murakami S (2003) Analysis of visitation frequency through particle tracking method based on LES and model experiment. *Indoor Air* 13:182–193
- Knowles EMW, Athelstan FS (1953) Meteorological instruments, 3rd edn. University of Toronto Press, Toronto
- Kreizer M, Liberzon A (2010) Three-dimensional particle tracking method using FPGA-based real-time image processing and four-view image splitter. *Exp Fluids* 50:613–620. <https://doi.org/10.1007/s00348-010-0964-3>
- Li D, Zhang Y, Sun Y, Yan W (2008) A multi-frame particle tracking algorithm robust against input noise. *Meas Sci Technol* 19:105401. <https://doi.org/10.1088/0957-0233/19/10/105401>
- Li J, Cao X, Liu J et al (2015) Global air flow field distribution in a cabin mock-up measured via large-scale 2D-PIV. *Build Environ Part 2* 93:234–244. <https://doi.org/10.1016/j.buildenv.2015.06.030>
- Liu S, Lipczynska A, Schiavon S, Arens E (2018) Detailed experimental investigation of air speed field induced by ceiling fans. *Build Environ* 142:342–360. <https://doi.org/10.1016/j.buildenv.2018.06.037>

- Maas H-G (1992) Complexity analysis for the establishment of image correspondences of dense spatial target fields. *Int Arch Photogramm Remote Sens* 29:102–107
- Maas HG, Gruen A, Papantoniou D (1993) Particle tracking velocimetry in three-dimensional flows Part 1. Photogrammetric determination of particle coordinates. *Exp Fluids* 146:133–146
- Malavasi S, Corretto R, Fossati F (2011) PSV and marker detection techniques for investigating the wake of an oscillating cylinder in a large wind tunnel. *Flow Meas Instrum* 22:428–437. <https://doi.org/10.1016/j.flowmeasinst.2011.06.007>
- Mao J, Gao N (2015) The airborne transmission of infection between flats in high-rise residential buildings: a review. *Build Environ* 94:516–531
- McGregor TJ, Spence DJ, Coutts DW (2007) Laser-based volumetric color-coded three-dimensional particle velocimetry. *Opt Lasers Eng* 45:882–889. <https://doi.org/10.1016/j.optlaseng.2007.01.009>
- Müller D, Müller B, Renz U (2001) Three-dimensional particle-streak tracking (PST) velocity measurements of a heat exchanger inlet flow. *Exp Fluids* 30:645–656. <https://doi.org/10.1007/s003480000242>
- Nobach H, Honkanen M (2005) Two-dimensional Gaussian regression for sub-pixel displacement estimation in particle image velocimetry or particle position estimation in particle tracking velocimetry. *Exp Fluids* 38:511–515. <https://doi.org/10.1007/s00348-005-0942-3>
- Ohmi K, Li H (2000) Particle-tracking velocimetry with new algorithms. *Meas Sci Technol* 11: 603–616. <https://doi.org/10.1088/0957-0233/11/6/303>
- Ohmi K, Panday S, Sapkota A (2010) Particle tracking velocimetry with an ant colony optimization algorithm. *Exp Fluids* 48:2010. <https://doi.org/10.1007/s00348-009-0815-2>
- Otsu N (1979) A threshold selection method from gray level histograms. *IEEE Trans Syst Man Cybern* 9:62–66. <https://doi.org/10.1109/TSMC.1979.4310076>
- Pick S, Lehmann FO (2009) Stereoscopic PIV on multiple color-coded light sheets and its application to axial flow in flapping robotic insect wings. *Exp Fluids* 47:1009–1023. <https://doi.org/10.1007/s00348-009-0687-5>
- Pickering CJD, Halliwell NA (1985) Particle image velocimetry: fringe visibility and pedestal removal. *Appl Opt* 24:2474–2476. <https://doi.org/10.1364/AO.24.002474>
- Popolek Z, Jørgensen FE, Melikov AK et al (2007) Assessment of uncertainty in measurements with low velocity thermal anemometers. *Int J Vent* 6:113–128
- Rosenstiel M, Grigat R-R (2010) Segmentation and classification of streaks in a large-scale particle streak tracking system. *Flow Meas Instrum* 21:1–7. <https://doi.org/10.1016/j.flowmeasinst.2009.10.001>
- Sandberg M (2007) Whole-field measuring methods in ventilated rooms. *HVAC&R Res* 13: 951–970. <https://doi.org/10.1080/10789669.2007.10391464>
- Shi C, Wang G, Yin X et al (2015) High-accuracy stereo matching based on adaptive ground control points. *IEEE Trans Image Process* 24:1412–1423. <https://doi.org/10.1109/TIP.2015.2393054>
- Sun Y (2007) Volumetric particle streak-tracking velocimetry and its application in indoor airflow measurements. University of Illinois at Urbana-Champaign, Urbana
- Sun Y, Zhang Y, Zhao L, Wang X (2004) An algorithm of stereoscopic particle image velocimetry for full-scale room airflow studies. In: ASHRAE transactions. pp 75–80
- Szeliski R (2011) Computer vision: algorithms and applications. Springer, London
- Takehara K, Etoh T (1999) A study on particle identification in PTV particle mask correlation method. *J Vis* 1:313–323. <https://doi.org/10.1007/BF03181412>
- Tarlet D, Bendicks C, Bordás R et al (2009) Colored tracer particles employed for 3-D particle tracking velocimetry (PTV) in gas flows. *Notes Numer Fluid Mech Multidiscip Des* 106: 93–102. https://doi.org/10.1007/978-3-642-01106-1_10
- Tecplot (2018) User's Manual. http://download.tecplot.com/360/current/360_users_manual.pdf
- Tropea C (2011) Optical particle characterization in flows. *Annu Rev Fluid Mech* 43:399–426. <https://doi.org/10.1146/annurev-fluid-122109-160721>
- Voelker C, Maempel S, Kornadt O (2014) Measuring the human body's microclimate using a thermal manikin. *Indoor Air* 1–13. <https://doi.org/10.1111/ina.12112>

- Voss B, Stapf J, Berthe A, Garbe CS (2012) Bichromatic particle streak velocimetry bPSV interfacial, volumetric three-component velocimetry using a single camera. *Exp Fluids* 53: 1405–1420. <https://doi.org/10.1007/s00348-012-1355-8>
- Wang H, Li X, Shao X et al (2017) A colour-sequence enhanced particle streak velocimetry method for air flow measurement in a ventilated space. *Build Environ* 112:77–87. <https://doi.org/10.1016/j.buildenv.2016.11.015>
- Wang H, Wang G, Li X (2018) High-performance color sequence particle streak velocimetry for 3D airflow measurement. *Appl Opt* 57:1518–1523. <https://doi.org/10.1364/AO.57.001518>
- Wang H, Zhang H, Hu X et al (2019) Measurement of airflow pattern induced by ceiling fan with quad-view colour sequence particle streak velocimetry. *Build Environ* 152:122–134. <https://doi.org/10.1016/j.buildenv.2019.02.015>
- Wang H, Wang G, Li X (2020) Implementation of demand-oriented ventilation with adjustable fan network. *Indoor Built Environ* 29:621–635. <https://doi.org/10.1177/1420326X19897114>
- Watamura T, Tasaka Y, Murai Y (2013) LCD-projector-based 3D color PTV. *Exp Thermal Fluid Sci* 47:68–80. <https://doi.org/10.1016/j.expthermflusci.2012.12.019>
- Westerweel J, Elsinga GE, Adrian RJ (2013) Particle image velocimetry for complex and turbulent flows. *Annu Rev Fluid Mech* 45:409–436. <https://doi.org/10.1146/annurev-fluid-120710-101204>
- Zappa E, Malavasi S, Negri M (2013) Uncertainty budget in PSV technique measurements. *Flow Meas Instrum* 30:144–153. <https://doi.org/10.1016/j.flowmeasinst.2013.02.002>



Measurements of Perceived Indoor Air Quality

21

Pawel Wargocki and Krystyna Kostyrko

Contents

Introduction	610
Measurements of Perceived Air Quality (PAQ)	612
Untrained Panels and Acceptability Scale	613
Trained Panels and Decipol Scale	615
Comparison of Assessments Made by Trained and Untrained Panels	616
Applications – Estimation of Sensory Pollution Load	617
Measurements of Odor Intensity	618
Applications – Odor Persistency	621
Procedural Aspects of Sensory Measurements of Perceived Air Quality	622
Selection of Human Observers (Panelists) for Sensory Measurements	622
Adaptation	623
Impact of Temperature and Relative Humidity	624
Quantification of Odor Pollution Sources in Buildings	628
Nonsensory Analysis of Odorant Concentration in the Air	628
Gas Chromatography-Olfactometry-Mass Spectrometry (GC-O-MS)	629
Olfactometry	630
Olfactometry Analysis for Determining the Odorant Detection Threshold (Test D)	631
Dynamic Olfactometry – Analysis of Odor Concentration	631
Calibration of an Olfactometer	633
Selection of Panelists for Performing Measurements Using Dynamic Olfactometry	633
Indirect Olfactometry	635

P. Wargocki ()

International Centre for Indoor Environment and Energy, Department of Civil Engineering,
Technical University of Denmark, Kongens Lyngby, Denmark

e-mail: pawar@dtu.dk; paw@byg.dtu.dk

K. Kostyrko

Building Research Institute, Department of Thermal Physics, Acoustics and Environment, Warsaw,
Poland

e-mail: k.kostyrko@upcpoczta.pl

Direct Olfactometry	636
Conclusions	637
References	638

Abstract

Chemical analysis of the composition of indoor air characterizes exposures, but sometimes this analysis may be insufficient to describe the effects of these exposures on building occupants, especially to characterize sensory effects caused by exposures to pollutants in buildings. The present chapter presents the methods used to characterize these effects. The methods using olfactometers and gas chromatography-olfactometry-mass spectroscopy (GC-O-MS) are described together with the methods using sensory panels and subjective evaluations. The latter provides direct information on how indoor air quality is perceived by building occupants, and includes assessments of acceptability of air quality and the perceived odor intensity; the assessments of acceptability can be used to determine the percentage of people dissatisfied with air quality. The limitations of methods are described together with the factors influencing the measurements using human subjects, including physical factors such as temperature and relative humidity, psychological factors such as adaptation, and procedural factors such as the number of inhalations before the assessment is completed. Possible applications of the results of measurements are shown, including characterization of emissions from building products and determination of ventilation requirements to reach a specific level of air quality characterized by the percentage of dissatisfied occupants. It is concluded that the methods presented should be considered supplementary to the chemical measurements as none of both methods can provide complete characterization of indoor air quality. When used together, they provide a more comprehensive characterization of indoor air and its quality. It is subsequently recommended that sensory evaluations of air quality and olfactometry methods (also using GC-O-MS) become part of protocols used for characterizing indoor air quality because they can capture the effects and potential consequences that other methods for measuring indoor air quality are not fully capable of measuring.

Keywords

Indoor air quality · Perceived air quality · Sensory assessments · Olfactometry

Introduction

Humans are constantly exposed indoors to varying concentrations of chemical compounds. The compounds originate from outdoor sources, e.g., urban traffic, and indoor sources such as people, tobacco smoking, and the building (building materials and furnishing, electronic equipment, and the heating, ventilation, and air-conditioning systems) (Wargocki 2004). A typical mixture of chemical compounds indoors may contain several hundred or more compounds. These compounds can affect indoor air quality thereby the well-being and health of occupants.

Despite significant progress in analytical chemistry, a complex compound-by-compound approach employing detailed chemical analysis may not always provide an adequate basis for modeling the effects of indoor air quality on humans. This limitation is, among others, due to complicated indoor air chemistry, interactions between compounds, and mainly insufficient sensory and toxicological information regarding single compounds and particularly their mixtures. Considering additionally that various physiological and psychological variables play an essential role when humans evaluate air quality, it seems reasonable to use the human response to measure indoor air quality supplementing chemical analysis.

Different methods have been used to measure the effects of indoor air quality on humans (e.g., ECA 1991, 1999; Rohr 2001; Wyon and Wargocki 2005). These measurements can be used to set the limiting criteria regarding indoor air quality. The present chapter focuses on the methods used for evaluating the sensory effects on humans caused by exposure to air indoors.

Sensory effects are caused by stimulation of the olfactory sense situated in a small area of the nasal cavity and sensitive to around half a million odors, the general chemical sense situated all over the mucous membrane of the nose and sensitive to more than one hundred thousand irritants, and the thermal sense located in the nasal cavity and sensitive to varying levels of air temperature and relative humidity, providing that the air temperature is different from the mucosal temperature which is about 30–32 °C (Fig. 1). Some harmful pollutants such as radon or carbon monoxide cannot be sensed and quantified using sensory evaluations. Still, in majority of cases, the sensory effects may provide the first indication of possible adverse effects of exposures since the human senses have an important warning function against danger in the environment (Sowa 2020).

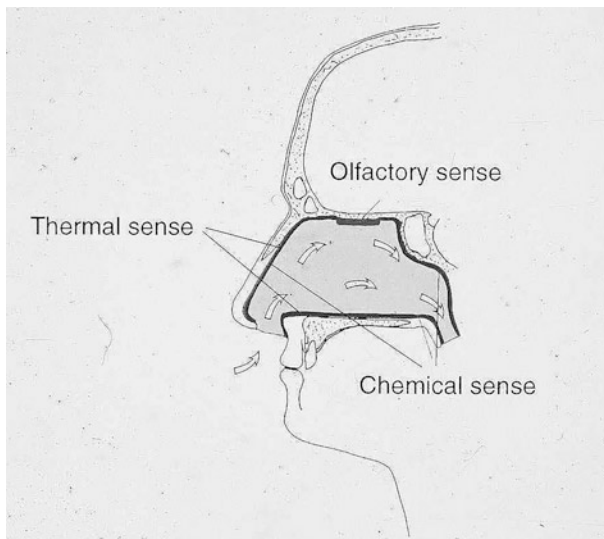


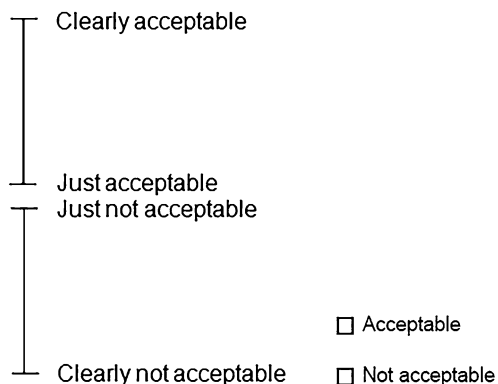
Fig. 1 Human nose

Sensory measurements of air quality using humans to assess air quality have been routinely used in air quality investigations since the 1990s. They have been used in laboratory experiments (Knudsen et al. 1998) and during field evaluations in existing buildings (Wargocki et al. 2004). Among many applications, sensory assessments have been used to characterize the emissions from building materials (ISO 16000-28 2012) and consequently have become a part of some labeling schemes defining requirements for emissions from building products (ECA 2005; Daumling et al. 2008). They have also been used when prescribing ventilation requirements indoors by specifying the maximum proportion of dissatisfied people with indoor air quality (ASHRAE Standard 62.1 2019; EN16798-1 2019). Recently, the developments have been in progress to use these methods to rate the air cleaners' performance as well (Olesen et al. 2021). Additionally, they are essential parameters when discussing the morphology of the models describing indoor air quality and indoor environmental quality (Licina and Langer 2021; Wargocki et al. 2021; Wei et al. 2020; Altomonte et al. 2020; Piasecki and Kostyrko 2019), and when the interactions between the parameters describing indoor air quality are described for the purpose of deriving the weighting coefficients depicting their importance when the overall indoor air quality and indoor environmental quality are determined (Frontczak and Wargocki 2011; Piasecki and Kostyrko 2020).

Measurements of Perceived Air Quality (PAQ)

Assessments of acceptability of air quality have been used to determine air quality as is perceived by building occupants and expressed by the percentage of satisfied or dissatisfied building occupants. Initially, in the case of assessments of acceptability of air quality, the dichotomous yes/no scale was used (Fanger and Berg-Munch 1983), Fig. 2. Later, it became more common to use a continuous acceptability scale (Gunnarsen and Fanger 1992) or its slightly modified version (Clausen 2000), Fig. 2. In addition to the methods described above in which people performing evaluations are not specially trained and only taught how to use the scales (and called

Fig. 2 The dichotomous (left) and continuous (right) scale used to assess the acceptability of air quality



subsequently untrained observers, subjects and panelists while their group untrained panel), it was common for a period to use specially trained people to perform sensory evaluations (a so-called trained observers, subjects and panelists and their group trained panel) using a well-defined reference exposure created from different levels of acetone (2-propanone) in the air (Bluyssen et al. 1989), Fig. 4.

Untrained Panels and Acceptability Scale

To assess the acceptability of air quality, a continuous visual analog scale is typically used by untrained human observers (Fig. 2). Observers are instructed to indicate whether the quality of air to which they are exposed is acceptable or not, and the degree of acceptability. To create the proper context for evaluations, the scale is usually preceded by the following sentence: "Imagine that you are exposed to this air during your daily work. How do you assess the air quality?". If the quality is assessed as acceptable, the observers mark the degree of acceptability on the upper part of the scale. If it is not acceptable, they mark the lower part of the scale. No additional instructions or training are given to the observers regarding the use of the scale; this is why they are called untrained observers (subjects) or untrained panelists. Observers usually receive written instructions concerning measurements and there should be at least one practice session before the actual measurements so that the observers become familiar with the measuring procedure. Assessments of acceptability of air quality are made immediately upon exposure to pollutants as the number of inhalations may cause olfactory fatigue (adaptation) and thus affect the sensory evaluations. Prior to the subsequent evaluation, observers take several inhalations of unpolluted air. Also, the temperature and relative humidity of the exposure can influence acceptability ratings. These parameters and other procedural aspects that can disturb sensory evaluations are discussed later.

The exposure can be partial (e.g., only nose or face being exposed to the air under evaluation) or full (when whole body is exposed to the air being assessed). The former is usually used in laboratory evaluations in which the assessments are typically made after just one inhalation of the air being evaluated, while the latter in the field measurements where observers render acceptability votes after entering a space and usually inhale more than once the air being evaluated. The described types of exposure may also affect the sensory evaluations and is discussed later.

All votes are rendered independently of other observers and without influence from a person conducting the measurements to avoid bias. The assessments are balanced for order of presentation and randomized to avoid systematic errors.

Using sensory assessments of the same exposure in a given environment made by a group of observers (a panel), mean votes of acceptability of air quality are usually calculated after the ratings made on the paper questionnaire are digitized at least twice in order to avoid gross errors; sometimes medians are used as well. Before doing so, the continuous acceptability scale is coded as follows: Clearly acceptable = 1; Just acceptable/Just not acceptable = 0; Clearly not

acceptable = -1 (Fig. 2). In the case dichotomous acceptability scale is used, it is coded as follows: Acceptable = 1; Not acceptable = 0 (Fig. 2).

Single ratings made by each observer in a group are used for calculating the group mean vote of acceptability characterizing indoor air quality in a given environment as shown in Eq. (1):

$$\text{ACC} = \frac{\sum_{i=1}^{i=N} (\text{ACC})_i}{N} \quad (1)$$

where

ACC = average vote of acceptability of air quality

ACC_i = acceptability vote by the observer

N = number of observers

The accuracy of evaluations is expressed by an experimental standard deviation (or standard error, SE) of the average of the N votes of acceptability (Eq. 2):

$$\text{SE} = \frac{\text{SD}_{\text{average}}}{\sqrt{N}} \quad (2)$$

where

SE = experimental standard deviation of the average of the N votes of acceptability scores

$\text{SD}_{\text{average}}$ = experimental standard deviation of individual observations

N = number of observers

Using mean acceptability ratings, the percentage dissatisfied with the air quality can be calculated (Gunnarsen and Fanger 1992) as follows:

$$\text{PD} = \frac{\exp(-0.18 - 5.28 \cdot \text{ACC})}{1 + \exp(-0.18 - 5.28 \cdot \text{ACC})} \cdot 100 \quad (3)$$

where

PD = percentage dissatisfied with the indoor air quality, %

ACC = average vote of acceptability

The relationship presented in Eq. (3) is typically used to determine the percentage of people dissatisfied with air quality; Figure 3 presents also other attempts, where the relationships between the ratings of acceptability of air quality and the percentage of dissatisfied were created. They deviate slightly especially at the levels below 50-60% dissatisfied.

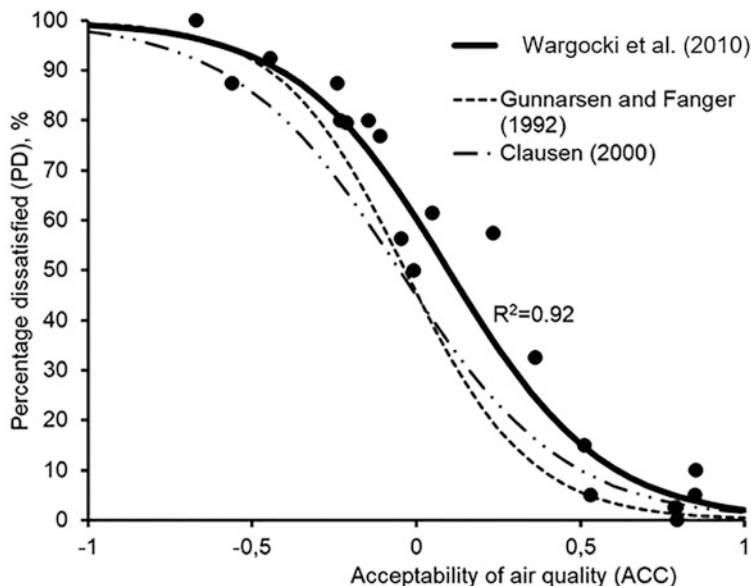


Fig. 3 Percentage of dissatisfied with air quality as a function of acceptability of air quality. To determine PD, the assessments of acceptability on a dichotomous scale (Fig. 2) were collected, while to determine acceptability levels the continuous acceptability scale was used to ensure that the votes on both axes are independent. Dashed line shows the relationship of Gunnarsen and Fanger (1992) (equation (3)), dashed-dotted line of Clausen (2000) and the thick continuous line show the relationship developed by Wargocki et al. (2009, 2010)

Trained Panels and Decipol Scale

To reduce the number of observers and, at the same time, the cost of the measurements without reducing accuracy of sensory evaluations, the measurements of perceived air quality with trained observers (panelists) have been proposed and adopted. Usually, 10–15 trained observers (panelists) are selected to perform these measurements. Unlike untrained observers rendering the assessments on an acceptability scale, as described above, trained observers assess the air quality directly in decipol. Decipol is a unit describing the perceived air quality as defined by Fanger et al. (1988): One decipol is the pollution caused by one standard person (one olf), ventilated by 10 l/s of unpolluted air. The relationship between decipol and the percentage of dissatisfied is expressed by the following equation:

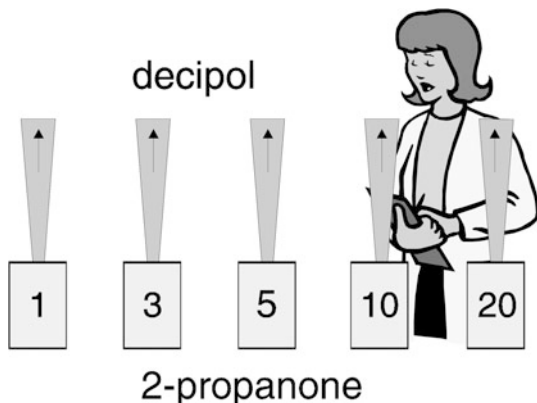
$$\text{PAQ} = 112 \cdot [\ln(\text{PD}) - 5.98]^{-4} \quad (4)$$

where

PAQ = perceived air quality, decipol

PD = percentage dissatisfied with the air quality, %

Fig. 4 The principle of measurement of perceived air quality using trained observers (panelists)



Trained panels performing sensory evaluations in decipol use the reference exposures of 2-propanone (acetone). The different levels of 2-propanone are used to reproduce perceived air quality levels in decipol (Fig. 4) according to the relationship of Bluysen et al. (1989), as shown in the following equation (5). Usually, five reference levels are used corresponding to 1, 3, 5, 10 and 20 decipols (see Fig. 4):

$$\text{PAQ} = 0.84 + 0.22 \cdot C \quad (5)$$

where

PAQ = perceived air quality, decipol

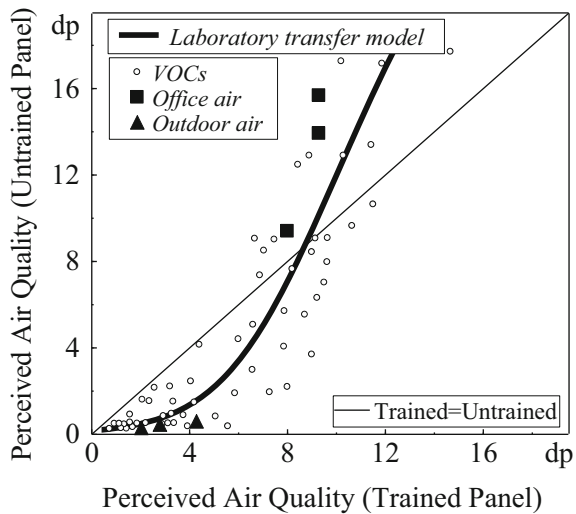
C = concentration of 2-propanone (acetone) over background level, ppm

The method using trained observers (panelists) to assess air quality is similar to the odor equal-intensity matching described later.

Comparison of Assessments Made by Trained and Untrained Panels

In theory, the ratings using the acceptability scale and decipol should not be different because they use the same underlying theory (Fanger 1988). However, deviations between the two measuring methods have been observed (Spiess and Fitzner 1999; Wargocki and Fanger 1999). To accommodate these differences, the relationship was developed between the sensory ratings performed by the trained subjects in decipol using the reference scale made of 2-propanone (acetone) and untrained observers (panelists) using the acceptability scale after they were converted to decipol. Figure 5 shows this relationship indicating that at low decipol levels corresponding to low concentrations of air pollutants, when untrained observers (panelists) assess the air quality to be good, their trained counterparts rate the quality of the same air to be worse; the reverse is observed at high concentrations of air pollutants.

Fig. 5 Panelists' reliability characteristics in the sensory analysis showing the ratings of perceived air quality made by trained and untrained subjects (Wargocki and Fanger 1999)



To adjust for this systematic difference, the transfer function (equation 6) was developed by Wargocki and Fanger (1999); the function is valid at levels below 16 decipols:

$$ACC = 2.7 - 2.3 \cdot \log(PAQ_{TR} + 7.4) \quad (6)$$

where

ACC = mean vote of acceptability of air quality by untrained observers

PAQ_{TR} = perceived air quality in decipol assessed by trained observers, using 2-propanone (acetone) as a reference gas

Applications – Estimation of Sensory Pollution Load

Measurements of perceived air quality can be used to estimate a sensory pollution load defined as the equivalent number of standard persons (called olfs) required to cause the same percentage of dissatisfied observers with the air quality as is the percentage dissatisfied caused by the actual pollution source (Fanger 1988):

$$G = 0.1 \cdot (PAQ_i - PAQ_o) \cdot Q \cdot \varepsilon_V \quad (7)$$

where

G = sensory pollution load (expressed as pollution caused by the equivalent number of standard persons), olf

Q = outdoor air supply rate (ventilation rate), L/s

PAQ_i = perceived indoor air quality, decipol

PAQ_o = perceived outdoor air quality, decipol

ε_v = ventilation effectiveness

Measurements of Odor Intensity

The Weber-Fechner law states that the change in a stimulus (perceived intensity of an odor) that will be just noticeable is a constant ratio of the original stimulus (perceived intensity of an threshold odor). Therefore intensity as a measure of the strength of the odor stimulus can be related to odor concentration.

Odor intensity can be measured using different scales. Figure 6 shows two examples of such scales: the category odor intensity scale used by Yaglou et al. (1936) and the category ratio scale CR10 developed by Borg and Borg (2001). The two scales use very similar descriptors of odor intensity. The difference is that the CR10 scale follows the psychophysical function that describes the relationship between the strength of the stimulus and the response.

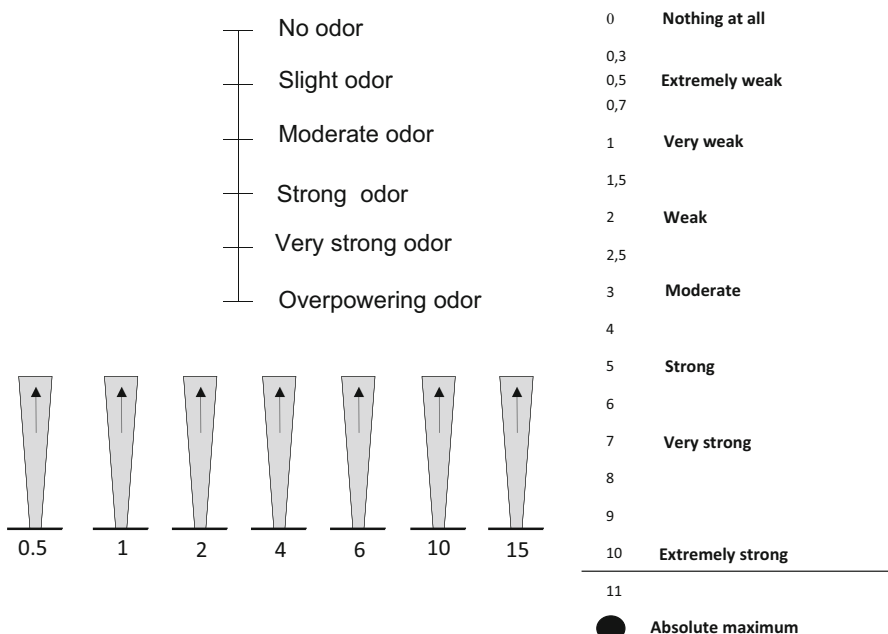


Fig. 6 Three different scales used to assess odor intensity. Top left – category odor intensity scale (Yaglou et al. 1936); the ratings on the scale are coded as follows: No odor = 0; Slight odor = 1; Moderate odor = 2; Strong odor = 3; Very strong odor = 4; Overpowering odor = 5. Right: Category–ratio scale, CR10 scale (Borg and Borg 2001). Bottom left – equal-intensity matching scale with acetone as a reference (Müller et al. 2005) where 0 corresponds to an odor intensity produced by acetone at a concentration of 20 mg/m^3 (odor detection threshold of acetone), 1 corresponds to an odor intensity produced by acetone at 40 mg/m^3 , 2 corresponds to an odor intensity produced by acetone at 60 mg/m^3 , and so on

Another method for assessing odor intensity being an extension of trained panel assessments is the method of equal-intensity matching with acetone as a reference proposed by Müller et al. (2005) (Fig. 6). The method uses the same approach as in the case of measurements with trained panels but uses the unit PI, perceived intensity, (Π) to express the sensory impact. According to the PI definition, the lower limit of the equal-intensity matching acetone scale, i.e., its zero value, is determined by the odor detection threshold of acetone (2-propanone). The tests performed with the dynamic and static olfactometer have shown that the average value of the acetone detection threshold in the air is approximately 20 mg/m^3 (it is in the range of $15\text{--}35 \text{ mg/m}^3$ in the so-called standardized olfactory thresholds, e.g., Devos et al. (1990)). The equal-intensity matching with acetone and PI unit are included in the ISO Standard 16000-28 (2012) and are the part of building material emission testing in Germany (AgBB 2005).

Figure 7 shows the relationship between different odor intensity scales indicating strong correlations between different odor intensity scales suggesting that they can be used interchangeably.

The relationship between the sensory ratings made using the acceptability scale and different odor intensity scales is shown in Fig. 8 (Wargocki et al. 2009, 2010). The figure shows that acceptability ratings of air quality are strongly linearly correlated with the ratings of odor intensity regardless of the type of scale and independently of the type of exposure (the dots represent air polluted by different building materials at different exposure/concentration levels).

As a result of the relationship presented in Fig. 8, Fig. 9 was developed (Wargocki et al. 2009, 2010). It shows the relationship between perceived air quality expressed as the percentage of dissatisfied and odor intensity (on the category scale). It can be observed that moderate odor intensity ($OI = 2$) corresponds to about 50% dissatisfied; moderate odor intensity level was used by Yaglou et al. (1936) to determine ventilation requirements in spaces occupied by people. It should be noted that the relationship

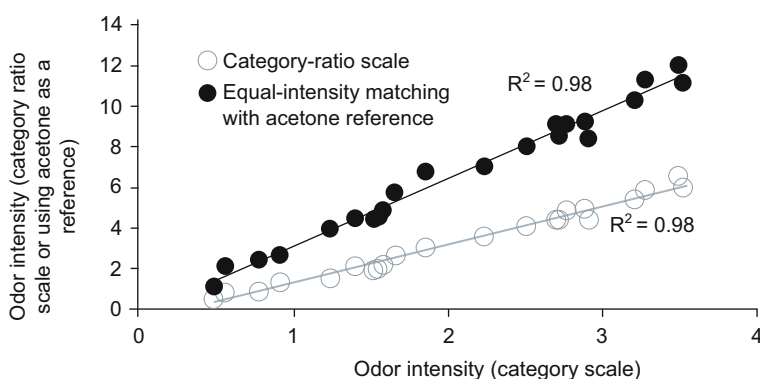


Fig. 7 Odor intensity assessed using a category-ratio scale and equal-intensity matching with a reference gas of acetone as a function of odor intensity assessed using a category scale (Wargocki et al. 2009, 2010). The coding of the scales is presented in Fig. 6

presented in Fig. 9 was developed by exposing people to emissions from building materials, whereas Yaglou et al. (1936) exposed people to emissions from humans (bioeffluents).

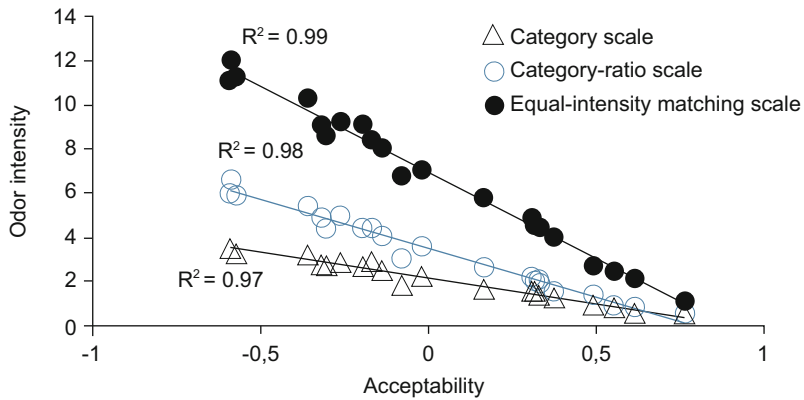


Fig. 8 Odor intensity assessed using a category scale, category-ratio scale, and equal-intensity matching scale with a reference gas of acetone as a function of the assessments of the acceptability of air quality (Wargocki et al. 2009, 2010). The coding of the scales is shown in Fig. 6

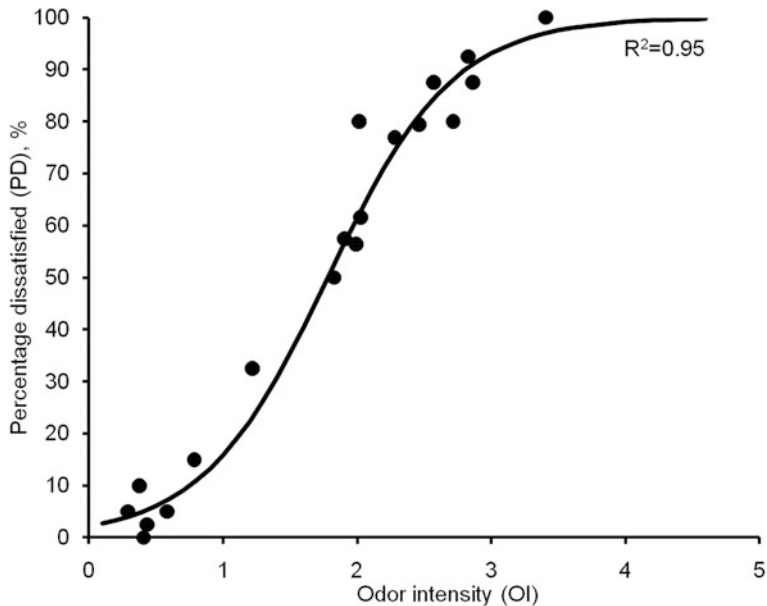


Fig. 9 Percentage of dissatisfied with air quality (estimated using assessments of acceptability on a dichotomous scale) as a function of odor intensity (Wargocki et al. 2009, 2010). The coding of the scale is shown in Fig. 6

Applications – Odor Persistency

Odor persistency was proposed to define how easy it is to remove the odor by reducing its concentration when, e.g., ventilation is applied. It is assumed that the less persistent the smell, the easier it is to remove it from the room. Dravnieks and Jarke (1980) developed the method of determining odor persistency using n-butanol as the standard; the method is recommended by the ASTM E544-99(2004) standard.

Odor persistency (m) describes how odor intensity decreases as the odorous pollutants are diluted (Fig. 10). Odor intensity is related to the odor concentration (dilution ratio) by the power law (Steven's law):

$$I = kC^n \quad (8)$$

where

I is the odor intensity

C is the dilution ratio

k and n are constants for each odor sample

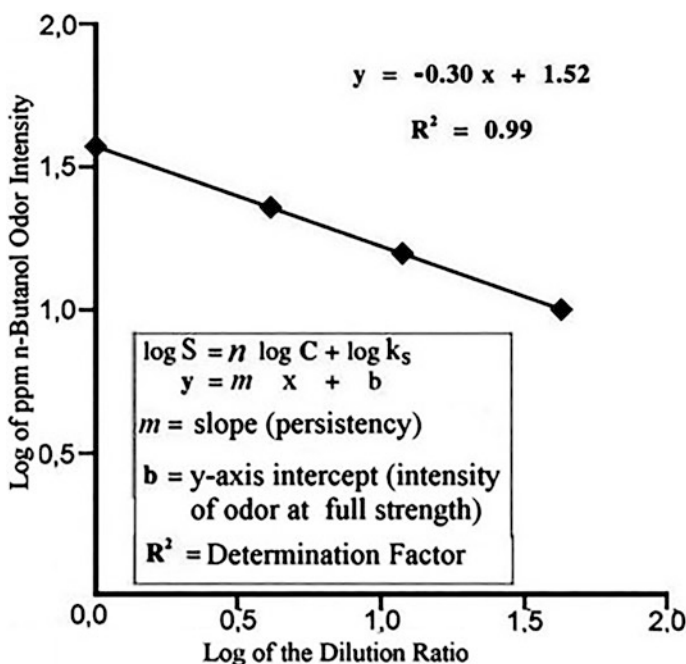


Fig. 10 An example showing how odor persistency in a room can be calculated. With an initial dilution factor of an odorant in the air equal to 0 (characterized by the logarithm of the odor intensity S and expressed in the mixing ratio of n-butanol in air in ppm equal to 1.52), the odorant had to be diluted 1.7 times (by ventilation), yielding the mixing ratio of n-butanol in air at 1.01 ppm as a result. The odor persistency was determined from the slope (m) of the curve. The example is taken from (McGinley and McGinley 2000)

The logarithmic transformation can transform the power law into a straight line as is indicated in Fig. 10:

$$\log I = n \log C + \log k \quad (9)$$

Procedural Aspects of Sensory Measurements of Perceived Air Quality

Many procedural details need to be considered during sensory measurements because many factors can influence sensory ratings. Some of these factors include temperature and relative humidity of inhaled (sniffed) air (Fang et al. 1998a), adaptation (Gunnarsen and Fanger 1992; Clausen 2000; Knudsen et al. 2004), the air speed in the facial region (Melikov and Kaczmarczyk 2008), and whether only face (facial exposure) or the entire body (the whole-body exposure) are exposed to the air that is being assessed (Knudsen et al. 1993; Fang et al. 1998b; Clausen 2000). Procedural details involve, among others, how many inhalations (sniffs) of the assessed air should be taken before the assessment is rendered and whether observers (panelists) are aware of the exposure being assessed, i.e. whether information about the exposure is given. The latter was investigated by Wilkins et al. (2007); they informed the subjects about exposures by placing a written label where the assessments were performed. It was also examined by Moschandreas and Relwani's (1992) where, the subjects could or could not see the cigarettes' smoking during sensory assessments. Besides, no studies have been conducted to examine whether sensory ratings are affected when subjects can see sources creating the exposure so no firm conclusions on this aspect can be drawn. Finally, an important methodological aspect is how many persons are selected and using which selection (inclusion) criteria when the persons are selected for the sensory panels to perform the ratings of perceived air quality.

Selection of Human Observers (Panelists) for Sensory Measurements

The selection of human observers performing sensory evaluations of air quality can bias the results of measurements of perceived air quality and therefore must follow the specific rules. At best, the observers from the relevant population for which the measurements are addressed should be selected. This approach may however be difficult to achieve in practice. A rational compromise is to select observers of a similar age, as age has been shown to have a considerable impact on olfaction. Selection criteria should additionally ensure the inclusion of nonsmokers, subjects with no asthma, allergy, or other hypersensitivities, no sensory handicaps (e.g., hearing impairment), and generally people in a good health condition (taking no regular medication or not suffering from the upper airway or respiratory infections); people with asthma and allergy could be included but their number should reflect the

proportion in the population, it must though be ensured that the sensory evaluations do not elicit allergic symptoms. The information necessary during the selection process can be collected by interviewing the potential subjects or through self-reports on the specially prepared questionnaires. In a short interview prior to selection, the attitude of people who are being selected toward the measurements, their motivation, and personal hygiene should be evaluated. Those whose personal hygiene could influence the measurements and whose motivation is poor should be excluded.

The olfactory sensitivity of observers should be documented. This, for example, can be done by exposing the observers to reference stimuli. In such case, the observers can take olfactory tests comprising a ranking test with n-butanol at four concentrations: 10, 80, 320, and 1280 ppm (vol./vol.) and a matching test with n-butanol, 2-butoxyethanol, and 2-butanone, each compound being at a concentration of 640 ppm (vol./vol.) and a “blank” exposure with no chemical compound according to ISO 8587 (1988) and ISO 8586-1 (1993). The former evaluates the ability of people to classify different odor intensities of the same substance, and the latter the capacity of people to identify several odorous stimuli. A questionnaire with a chemical sensitivity scale (CSS) can additionally be used to characterize further the sensory panel; it examines the experience with and exposure to odors and sensory irritants, and compares with the data for general population (Nordin et al. 2003, 2004). Other methods can be found later in the present chapter (EN 13725 2003; Kosmider, 2008).

The number of observers evaluating the air quality considerably affects the accuracy of measurements. This is because of considerable variation in ratings of acceptability of air quality among individuals due to variation in chemosensory sensitivity and an influence of other variables such as personality, preference, mood, and prior experience with different odors and exposures to pollutants. The standard deviation of the acceptability ratings is usually between 0.3 and 0.6 (Gunnarsen and Bluyssen 1994; Knudsen et al. 1998). Increasing the number of observers above 30–50 people has consequently a small effect on accuracy (Fig. 11). At the same time, increasing the number of observers causes logistic problems and increases the cost of the measurements, especially when they are conducted in the field. Considering the above reasoning, 30–40 observers are usually selected (Wargocki, 2004).

Adaptation

Human senses exhibit a reduction in sensitivity with the duration of exposure when the air is polluted by odors (adaptation), while the increase in the intensity of response with the duration of exposure when the air is polluted by irritants. Gunnarsen and Fanger (1992) observed considerable adaptation when human bioeffluents were the pollution source, probably due to bioeffluents comprising mainly odors, moderate adaptation when tobacco smoke was the source, and almost no adaptation when the air was polluted by building materials, as the last two sources probably also included many irritants. They observed that adaptation occurred within the first 6 minutes of exposure, while in the work of Jørgensen and

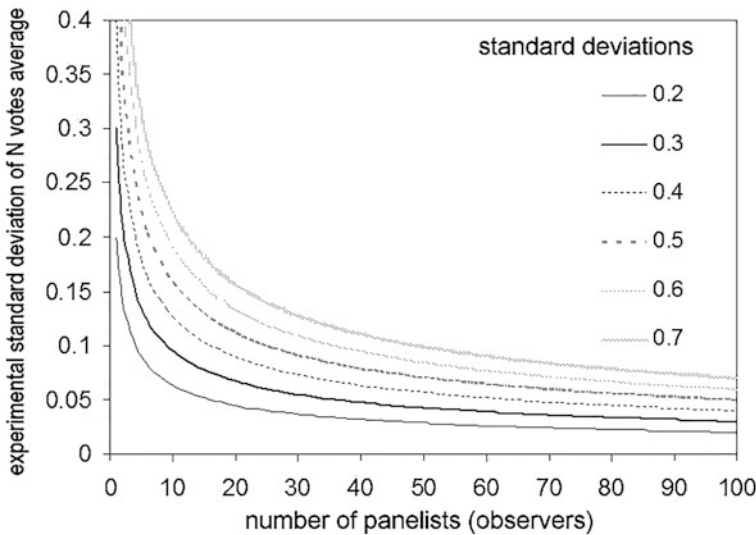


Fig. 11 The relationship between the size of the panel assessing air quality using the continuous acceptability scale and the experimental standard deviation of the average vote made by the observers (panelists); the dependence was calculated for different values of the standard deviation of individual assessments of the observers. As indicated in the text, increasing the number of observers above 40 has very little effect on the experimental standard deviation independently of standard deviation. The relationship is from (Berglund et al. 2010)

Vestergaard (1998) cited by Clausen (2000), the strong adaptation to indoor air polluted by typical building materials occurred already in the course of the first seven inspirations, corresponding to an exposure of about 24 seconds (Fig. 12).

Since it is often challenging to conduct measurements in which observers take only one breath when rendering the air quality assessment, especially in field measurements, some sensory adaptation would always be present when the measurements of perceived air quality are made. Consequently, to make it possible to compare the results of different indoor air quality measurements, the exposure time during assessment should be standardized. It can be done in the laboratory measurements by allowing subjects always to take the same number of inhalations of polluted air (preferably one) when assessing the air quality. In the case of field measurements, the exposure time can be standardized by having the subjects walk a similar distance prior to assessing air quality after preferably one inhalation. To further reduce systematic errors, the assessments can be repeated.

Impact of Temperature and Relative Humidity

Assessments of perceived air quality using an acceptability scale are strongly affected by the air's temperature and relative humidity, while their impact on the assessments of

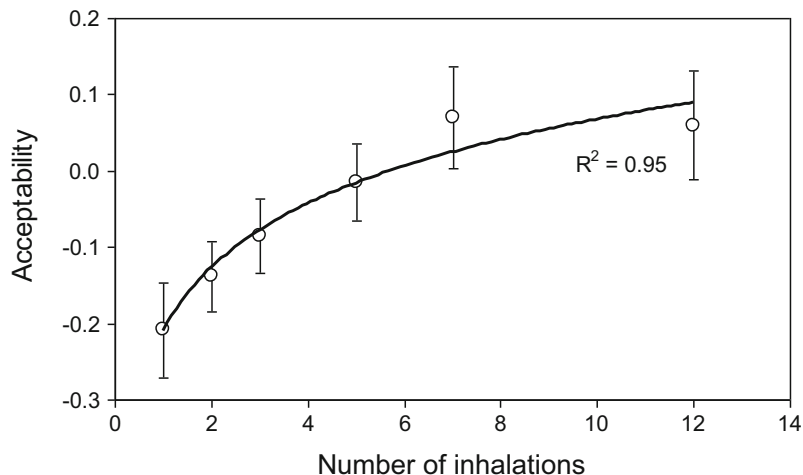


Fig. 12 Assessment of indoor air quality as a function of the number of inhalations; error bars indicate the standard deviation of individual assessments of the observer (Clausen 2000). The coding of the scale is shown in Fig. 2

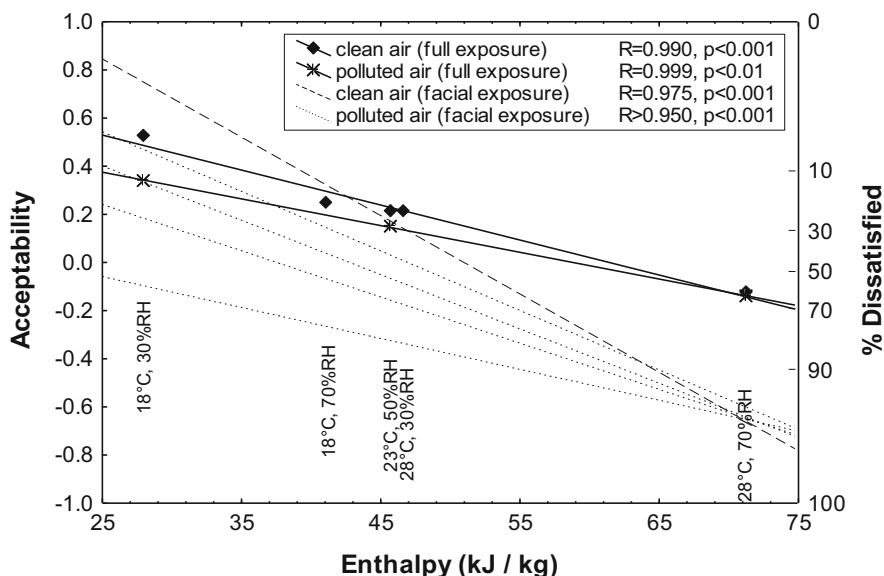


Fig. 13 The impact of temperature and relative humidity on perceived air quality evaluated using acceptability scale; the figure is from Fang et al. (1998a, b)

odor intensity is less pronounced (Berglund and Cain 1989; Fang et al. 1998a; Toftum et al. 1998). Figure 13 illustrates the effects of temperature and relative humidity on acceptability ratings (Fang et al., 1998a, b) where temperature and relative humidity

are expressed as enthalpy of air Fig. 13 shows that the effect depends on the type of exposure - facial (when the only face is exposed) and whole body (when the assessments are made by entering the space); the effect is stronger for the former.

It should be noted that the relationships presented in Fig. 13 intersect at the same enthalpy for either the facial or whole-body exposure. This result may suggest the underlying mechanism which is surmised to be the cooling of the nasal mucosa (see Fig. 1) decreasing with increasing enthalpy of air.

Fang et al. (1998a, b) developed models allowing conversion of the acceptability assessments at different temperatures and relative humidities of air (expressed as enthalpy) performed using facial (Eq. 10) and whole-body (Eq. 11) exposures to the reference conditions of 23 °C and 50% RH (enthalpy of 45.39 kJ/kg):

$$\text{ACC} = \text{ACC}_0 - 0.0247 \cdot (E - E_0) - 0.0416 \cdot \text{ACC}_0 \cdot (E - E_0) \quad (10)$$

$$\text{ACC} = \text{ACC}_0 - 0.00416 \cdot (E - E_0) - 0.0416 \cdot \text{ACC}_0 \cdot (E - E_0) \quad (11)$$

where

ACC = acceptability of air quality at any enthalpy in the range between 18°C/30% RH to 28°C/70%RH

ACC_0 = acceptability of air quality at the reference condition (enthalpy E_0)

E = enthalpy (kJ/kg) of the air at which the assessments of acceptability (ACC) were made

E_0 = enthalpy of air at the reference conditions set to 23 °C and 50%RH and thus the resulting enthalpy of 45.39 kJ/kg

Equation (10) can only be applied for the assessments of acceptability higher than -0.6 , and Eq. (11) for the ratings higher than -0.1 . Other reference conditions than 23°C and 45%RH can be selected; in such the case, the coefficients in Eqs. (10) and (11) need to be recalculated (Bluyssen et al. 1996; Spiess and Fitzner 1999).

Piasecki et al. (2020) studied the impact on sensory discomfort (expressed as percentage of dissatisfied with air quality, PD) at air humidity from 60% to 90%RH and temperature from 26°C to 28°C (Fig. 14). They observed that the impact of humidity on the dissatisfaction in a warm and humid indoor environment is higher than that indicated in the thermal comfort model (Fanger 1970). They proposed an experimental relationship to be used in environments with a high enthalpy of humid air in which Fanger's comfort model begins to show lower dissatisfaction than the experimental results, thus suggesting that a separate element should be included in the model to describe dissatisfaction.

Roelofsen (2016) analyzed the impact of the air temperature and relative humidity on perceived air quality and proposed the relationship between the freshness of the air polluted by human bioeffluents and its temperature and humidity. Similarly to the study of Piasecki et al. (2020) and Fang et al. (1998a, b), he strongly emphasized the need to account for dissatisfaction caused by reduced perceived air quality due to

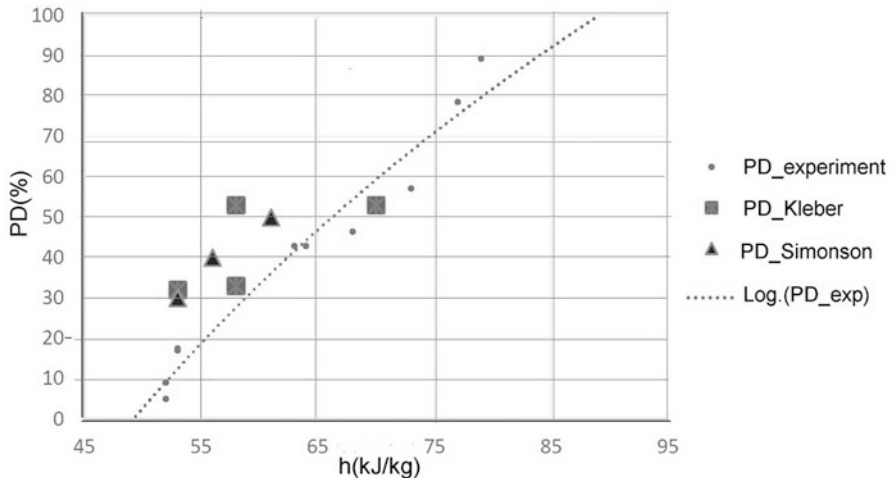


Fig. 14 Comparison of the experimental results of Piasecki et al. (2020) with the former similar research by Kleber and Wagner (2018) and Simonson (2000) showing the percentage of dissatisfied (PD) in hot and humid environments; PD is percentage dissatisfied and h is enthalpy of hot and humid air.

increased temperature and relative humidity of air when designing buildings and indoor space, rather than using the requirements only to avoid thermal discomfort.

To account for moisture balance of the nasal mucosa in sensory ratings, Roelofsen (2018), based on the published results, proposed the following model where freshness of air is expressed on a seven-point scale from 0 to 6 (Fanger et al., 1988; Berglund and Cain, 1989); the model accounts for the heat transfer in the nose:

$$F = a + b \cdot (\text{ta}_{\text{nasal mucosa}} - \text{ta}) + c \cdot (\text{pa}_{\text{nasal mucosa}} - 0.01 \cdot \text{pa}) + d \cdot 10 \cdot G / (V \cdot \varepsilon_v) \quad (12)$$

where

F = freshness of the air, according to a seven-point continuous linear scale

ta = air temperature ($^{\circ}\text{C}$)

$\text{ta}_{\text{nasal mucosa}}$ = mean temperature of the nasal mucosa surface ($^{\circ}\text{C}$)

$\text{pa}_{\text{nasal mucosa}}$ = mean vapor pressure at the nasal mucosa surface (Pa)

pa = vapor pressure of the air (Pa)

G = sensory pollution load (olf) at different metabolism expressed as

$$G = 0.985 \cdot M^{1.299} \quad (13)$$

M = metabolic rate (met)

V = outdoor air supply rate (L/s)

ε_v = ventilation-effectiveness, according to CR 1752 (1998)

$a - d$: regression coefficients(–)

Quantification of Odor Pollution Sources in Buildings

Nonsensory Analysis of Odorant Concentration in the Air

Nonsensory analysis methods are described in EPA Method TO-17 (1999), and a scientific monograph by Kostyrko and Wargocki (2014), as well as other chapters in the present Handbook. In these methods, a known volume of air (a sample for subsequent analysis) is taken from the room by aspiration through one (or several) sorption tubes containing, e.g., Tenax® TA sorbent, placed in the air of the volume where IAQ is tested. Volatile organic compounds (VOCs) are retained on the sorbent filling of the sorption tube connected to the suction pump. After sampling, the tubes are transported to the laboratory for analysis where they are analyzed. If possible, the analysis is made within 4 weeks; more extended storage is possible if properly conditioned (EN ISO 16000-5 2007). Further description of the measurements of VOCs can be found in the present Handbook in ► Chap. 3, “[Volatile Organic Compounds \(VOCs\)](#),” by Huang (2022). The GC-MS analysis method is also described in detail in ISO 16000-6 (2004). The sampling and analysis strategy described in EN ISO 16017-1 (2002) and EN ISO 16017-2 (2003) cover a wide range of VOC including aromatic hydrocarbons, chlorinated hydrocarbons, esters and ethers, glycols, ketones, and alcohols, among which there are many aromatic compounds (Massold et al. 2005).

Measured concentrations of organic pollutants can be compared against their odor thresholds (if available) by dividing the concentration by the odor threshold. Such derived ratios are summed up to determine whether their sum is below one; if higher it is likely that the mixture can produce perceptible odor (Salis et al. 2017). However, the VOCs (e.g., mVOCs derived from metabolic transformations of biological impurities (Kostyrko and Kozicki 2018; Liu et al. 2018) having exceptionally low odor thresholds can be overlooked in this method. Generally, past experience shows that it is a good approximation that VOCs having extremely low odor thresholds will dominate the odor perception, thus even when the sum of derived ratios is lower than one the mixture can be perceptible.

With regard to odor detection thresholds, the newest published measurements should be used, e.g., Nagata and Takeuchi (2003), since older work such as those by Devos et al. (1990) and therein may not provide an accurate estimation of the detection threshold - they can provide odor detection thresholds a few orders of magnitudes higher. The work of Abraham et al. (2002) and Cain and Cometto-Muniz (1995) can also be considered when determining odor thresholds of individual compounds and their mixtures (Cometto-Muñiz et al. 1997, 2004). Methods of analysis of air pollution with odorants should be further developed considering more precise analyses and a broader range of odorants.

Gas Chromatography-Olfactometry-Mass Spectrometry (GC-O-MS)

Gas chromatography-olfactometry-mass spectrometry (GC-O-MS) is a combination of gas chromatography-olfactometry (GC-O) and gas chromatography-mass spectrometry (GC-MS). Gas chromatography-olfactometry (GC-O) is a method combining the information supplied by chemical characterization and by odor perception. A panelist (an observer) sniffs the gas, and every time he/she sniffs an odorous substance, a sensorial response in terms of presence and type of odor is marked on the chromatogram.

In the environmental analysis, particularly in the analysis of air content odorants, the most important advantages of the GC-O-MS include much better-resolving power and higher sensitivity than the classical chromatography.

The primary device in the method is a modified gas chromatograph so that the “Y” divider is located at the end of the chromatography column to which the detector is connected (e.g., FID) on the one end of the “Y” divider and the olfactometer with the odor port on the other one (Fig. 15). A sample of the odorous gas is split into two streams, one of which is directed to the olfactometer. Before presenting it to a panelist, it is first mixed with moist air (to avoid discomfort during assessments) and then passes through a heated pipe. During analysis, a panelist indicates when the odor is perceived. At the same time the compound can be detected with the detector included in the GC. As a result of the analysis, an aromagram is obtained presenting olfactory peaks (Fig. 15).

In the measurement system where mixtures are analyzed with a GC chromatograph, substances, including odorants, leave the GC column separately. As the entire mixture is not analyzed at any given moment as a whole, individual chemical compounds can be detected, which allows the detection of odorants individually (Cai et al. 2007; Kozicki 2022) but not the entire mixture as a whole.

GC-O-MS was used in applications regarding pollution sources in buildings, e.g., to detect pollutants emitted from linoleum (Jensen et al. 1995).

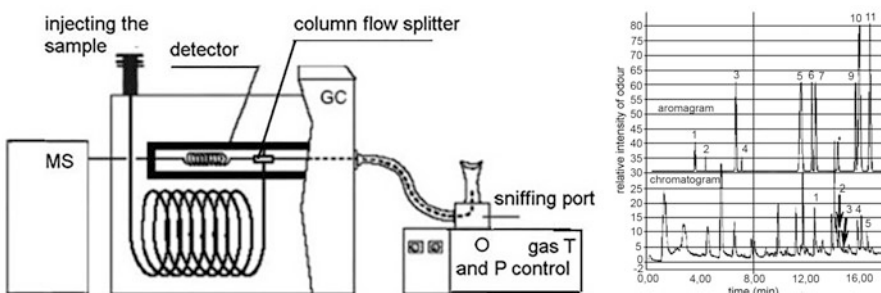


Fig. 15 GC-O-MS: apparatus (left) and the method of presenting the results on a mass spectrometer-chromatogram-aromagram (from Zhang et al. 2010) (right)

Olfactometry

Olfactometry is the principal tool for measuring odor characteristics. An olfactometer is designed to dilute the odorous gas samples and present these dilutions to the sensory panel. After obtaining their responses, a statistical treatment of the data permits the olfactometric result to be calculated.

The olfactometry method was born in the 1960s in the USA but developed and introduced into the regulations as dynamic olfactometry only in 1979 when described in the ASTM E 679-79 (1979) standard replaced by the ASTM E 544-2004 (2004). In Europe, due to the economic importance of odor nuisance, the international research program on Interlaboratory Comparison of Olfactometry (ICO) was carried out in 2002–2003 to compare the results obtained in various research laboratories, and run continuously ever since (Maxeiner 2005). As a result of this undertaking, the EN13725 (2003) standard was created concerning the determination of the odor concentration by the dynamic olfactometry method. The standard was established to provide a common basis for assessing odorant emissions in the European Union Member States and is used to evaluate odorant emissions released from point and surface sources.

The physical quantity measured by olfactometry is the odor concentration c_{od} , which defines the “distance” of c , the odorant concentration in air, from the odorant threshold concentration c_{th} . It is a dimensionless number determining the physical intensity of the odor. The odor concentration c_{od} expresses the ratio of $c[\mu\text{g}_{\text{odorant}}/\text{m}^3_{\text{air}}]$, the actual odorant concentration in the air, to $c_{\text{th}}[\mu\text{g}_{\text{odorant}}/\text{m}^3_{\text{air}}]$, the concentration at the level of the odor threshold, and denotes the degree to which the odorant had to be diluted (in fragrant gas) to reach the threshold when it can be perceived:

$$c_{\text{od}} = c/c_{\text{th}} \quad (14)$$

For convenience, both concerning single odorants and their mixtures, the concept of the odor unit (ou) was introduced with the following definition:

The odor concentration is the number of units of odors in 1 m^3 of gas under standard conditions.

One ou/m^3 equals 40 ppbv n-butanol. Odor concentration, c_{od} in ou_E/m^3 , expressed as the number of European odor units in 1 m^3 of gas under standard conditions, is determined by the **EROM** reference standard (European Reference Odor Mass). The dilution factor at the panel threshold $\bar{Z}_{\text{ITE,pan}}$ denotes the dilution factor (degree) at the 50% detection threshold and is multiplied by the unit $1 \text{ ou}_E/\text{m}^3$

$$c_{\text{od}} = \bar{Z}_{\text{ITE,pan}} \times 1 \text{ ou}_E/\text{m}^3 \quad (15)$$

where $\bar{Z}_{\text{ITE,pan}}$ is the geometric mean of dilution ratio values Z_{ITE} of all valid panel members in one measurement after the retrospective screening. It is also the

numerical result of odor concentration measurement with the dynamic olfactometer according to EN 13725-03 (2003).

The dilution factor at the panel threshold $\bar{Z}_{ITE,pan}$ is the dilution factor applied to the sample to arrive at the physiological response of the panel that is equivalent to that for 1 ou_E/m³. This dilution factor is the nominal value of the odor concentration of the examined sample c_{od} in ou_E/m³.

Olfactometric analyses are tested in the laboratory (EN 13725-03 2003 and ASTM E544-04 2004) or in the field, during which the odor samples are gathered and then exposed to the target population in the study area. The main advantage of olfactometry is the direct correlation between the odor and the detector's sensitivity where the detector is human nose.

Olfactometry Analysis for Determining the Odorant Detection Threshold (Test D)

The “triangle” differential test described in the standard ISO 13301 (2002) is the widely used classical method to determine the odor detection threshold. Standard ISO 13301 (2002) describes the “triangle test” method in the forced-choice version, which is called the “three-alternative forced-choice (3-AFC) procedure.” In the terminology of psychophysical tests (Lötsch et al. 2008), the method is called a sensory discrimination test (Test D – Discrimination).

The triangle bag method is often used (Ueno et al. 2008), involving a specific order of presenting the samples with odors:

- Creating a selected assessment team (panel) of at least six people (panelists)
- Presenting to each panel three bags, including two with a different gas (e.g., clean air) and one with a diluted sample of the tested odorant with a known odorant concentration; each of the panelists judges in which bag the smell differs from the other two bags; the presentation of samples of the tested odor is continued, increasingly diluted with a dilution step of three, until the panelists give erroneous answers
- Calculating the individual odor detection threshold for each panelist as the geometric mean of the two values – the sample dilution value that was correctly recognized last and the dilution value of the sample that was misidentified first
- Calculating the detection threshold of the tested odorant as the geometric mean value of the individual detection thresholds of all panelists

Dynamic Olfactometry – Analysis of Odor Concentration

A dynamic olfactometer is an apparatus in which a sample of an odoriferous gas (fragrant air) is gradually diluted with an odorless gas in a specific Z ratio and presented to a team of odor panelists for assessment through the outlet delivering successively streams of odorous and odorless gas, i.e., clean air (Fig. 16). Dynamic

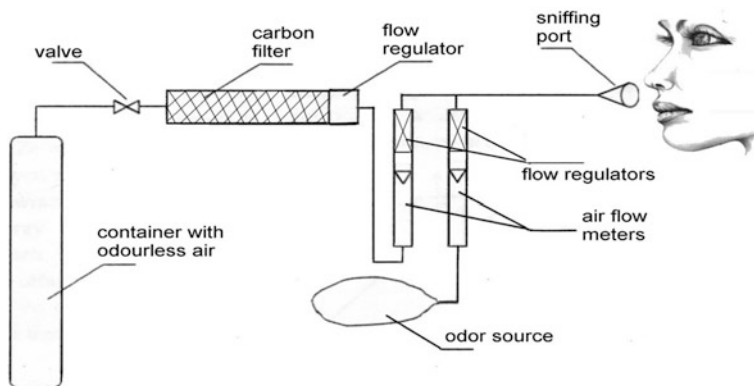


Fig. 16 Principle of diluting a sample of an odoriferous gas with odorless air for the determination of the odor concentration in a dynamic olfactometer

olfactometry includes the analysis of the olfactory stimulus using panelists' ratings against the setting of the Z dilution rate on a dynamic olfactometer.

In the method, samples are diluted with clean air and then connected to an olfactometer. A panel (composed of trained people, see selection procedure below) sniffs the diluted odor through the olfactometer. The level of dilution is gradually reduced until a panelist first perceives the odor and presses a button providing the signal for the odor concentration. The panelists are selected by examining their individual detection thresholds (at least in three sessions) according to the requirements specified in EN 13725 (2003).

In the standardized dynamic olfactometry method (EN 13725 2003), two methods of collecting responses from panelists are used:

- A forced selection method – panelists are presented with gases from two, three, or more ports, one for odorous gas and the other two for inert gases. The order of changes in odorant concentration and the location of the odorant gas nozzle is random, with the evaluation time <15 s.
- A simplified “yes/no” method – the procedure of estimating the test result does not consider the level of certainty of the answers; there is no question whether the answer is certain, guessed, or just a guess.

The average degree of dilution is expressed by the geometric mean of the individual Z values (dilution ratios) indicated by the panelists (Z_{ITE}). The result of an olfactometer measurement is numerically equal to the odor concentration c_{od} value expressed in European odor units [ou_E/m^3]. According to Van Harreveld et al. (2008) and Maxeiner (2005), the inaccuracy of the result of the odor concentration measurement is 10–20%.

The dynamic olfactometry method is used to measure the odor concentration of odorants when evaluating odor nuisance (with restrictions for toxic gases) both in open spaces and in ventilated indoor spaces (EN 13725: 2003). The uncertainty

analysis given in the standard does not consider the findings of the BIPM-ISO, “guide on the expression of uncertainty in measurements” (JCGM100 2008).

Calibration of an Olfactometer

The olfactometer should perform a dilution at the specified step ranging from 2 to at least 2^{14} . With the introduction of the European odor unit $1 \text{ ou}_E/\text{m}^3$, the typical dynamic olfactometer measuring range should be $1^1 \text{ ou}_E/\text{m}^3 - 10^7 \text{ ou}_E/\text{m}^3$ (including predilution).

Calibration is performed using a tracer gas – the recommended gases are CO₂ and CO. During calibration, an analytical gas dilution control method is used, most often using an NDIR, a nondispersive infrared (NDIR) analyzer. Following the standard’s requirements (Ueno et al. 2008), two metrological parameters of the dynamic olfactometer are checked by precise measurement of the mass streams of mixed gases after setting each successive dilution value of the tested gas stream on the olfactometer.

Performance quality requirements are:

- Accuracy of setting the dilution ratio for each dilution step <0.20 (20%)
- Instability of the set dilution ratio over time for each dilution step <0.05 (5%)

This olfactometer calibration technique has metrological traceability if the mass flow meters are calibrated using the primary calibration standard. As a result of the performance testing, the measured dilution ratios are calculated for each dilution step. These ratios, not theoretical values, are used in the final measurement calculation.

The European Standard EN 13725 (2003) describes the calibration procedure. Five test results shall be collected for every dilution setting. Between measurements of each test result, the controls of the dilution instrument are set to another setting, if applicable. Accuracy and operative speed at high dilutions have been examined by Cozzutto et al. (2018). Based on the studies by Jiang (2002) and standard AS/NZS 4323.3 (2001), determination of the accuracy of the dynamic olfactometer requires taking readings every 10 seconds. This repetition is relevant for the determination of instability. At least ten panelists’ observations shall be recorded. Thus, metrological testing of the olfactometer should be done before the sensory performance and should not be replaced by sensory performance. Figure 17 shows an example of calibration results.

A dynamic olfactometer should be calibrated at least once a year.

Selection of Panelists for Performing Measurements Using Dynamic Olfactometry

The selection of panelists is based on at least ten assessments of individual variability and sensitivity of smell to the smell of n-butanol (Kośmider 2008). A measure of odor sensitivity is the *individual threshold estimate (ITE)* value of n-butanol in

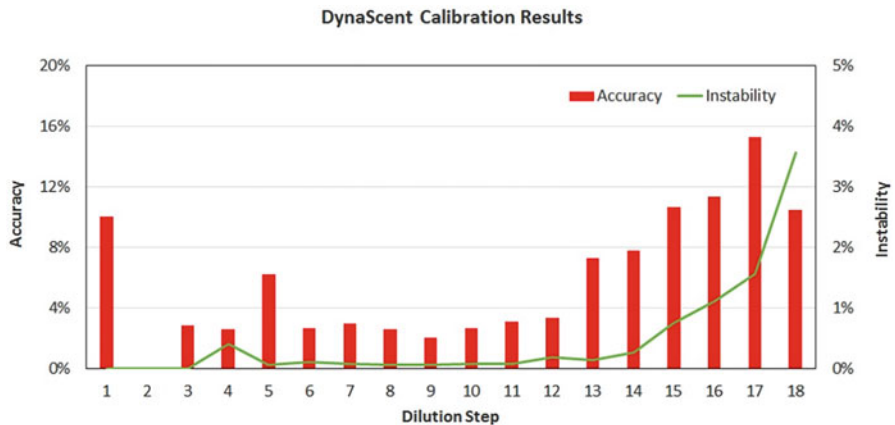


Fig. 17 An example of the stationary olfactometer calibration results. The bars represent the accuracy (left) and the curve shows instability (right) (source: <https://environodor.com.au/products/dynascent-digital-olfactometer/instrument-calibration>)

nitrogen ITE_{butanol}. ITEs should be collected over a minimum of three dilution series presentation sessions on separate days with an interval of 1 day between sessions. The individual standard deviation (SD_{ITE}) is calculated for each panelist from the logarithms of these individually obtained threshold values.

The requirements for panelists are defined by odor sensitivity within a specific tolerance limit when evaluating odor concentration c_{od}

$$c_{\text{od}} = \bar{Z}_{\text{ITE,pan}} \times 1 \quad [\text{ou}_E/\text{m}^3] \quad (16)$$

where $\bar{Z}_{\text{ITE,pan}}$ is the average value of the dilution numbers using the votes of panel members.

The panelist is selected when the geometric mean of the n-butanol sensing threshold ITE_{butanol} is between 0.5 and 2 times the concentration of the EROM standard, i.e., in the range from 62 to 246 $\mu\text{g}/\text{m}^3$. Additionally, the panelist is selected when the standard deviation SD_{ITE} antilog is less than 2.3. To check the latter, the standard deviation of the individual threshold sensing SD_{ITE} is calculated for each panelist and compared with the entire panel's antilog value.

As a result, these panelists are excluded whose individual ITE_{butanol} sensing threshold scores differ by more than five times the geometric mean for the entire panel calculated from the individual Z_{ITE} scores of all panelists. A panelist is also excluded if during a test in which a series of dynamic dilutions of gas streams from several odor samples are presented, including blank samples, more than 20% TRUE responses to the blank samples are given.

The sense of smell of each panelist should be systematically tested at least once every 12 measurements in which the panel has participated. Not meeting the above criteria results in temporary exclusion (EN 13725 2003).

Indirect Olfactometry

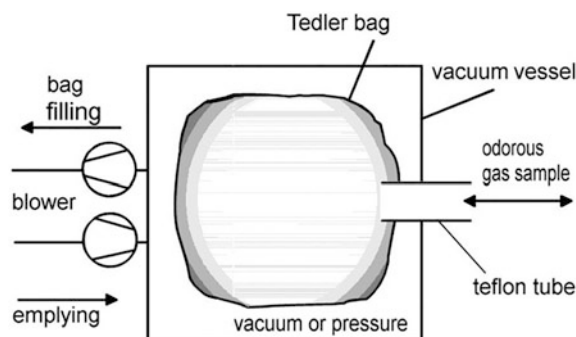
In the case of the indirect olfactometry (delayed measurement), the odorous gas samples are collected into foil bags and transported to a fixed or mobile olfactometric laboratory for analysis with a dynamic olfactometer. When the extracted odorous gas is hot or humid, it should be initially diluted with a dry, odorless, and chemically inert gas to prevent condensation.

If the concentration of odorants in the room is considered constant, it is recommended to determine the average odor concentration based on three samples taken at random during 1 day. With fluctuating odor emissions, instantaneous samples should be taken several times. The general rules for determining the number of samples follow the metrological rule of achieving maximum precision in odor measurement. Theoretical models making measurement precision dependent on the sampling point densities related to the area of the tested room in m^2 are somewhat unreliable (Mui et al. 2008).

The sampling technique differs substantially according to the type of odor emission source. From point sources, such as the ventilation outlets, samples are collected either directly into bags or a sampling line consisting of a sampling probe, a guide tube, and a particulate filter (see also ISO 10396 2007). Contact surfaces of the sample with construction materials should be limited, as far as possible, and in practice conditioning (rinsing) of containers (Fig. 18). The storage time of the sample prior to analysis should not exceed 30 hours. The sampling method for assessing the quality of air contaminated by building materials using bags is described by Müller et al. (2003, 2005).

The bags for odorous gas samples are made of a foil of nalophan, Tedlar, hard polyethylene, and polycarbonate, or fluorinated ethylene propylene (FEP). The feed tube is made of quartz glass or Teflon; the pipes are made of Teflon, stainless steel, or other odorless and practically nonabsorbent materials. Due to the low price and advertised chemical resistance, the most popular in the USA and European laboratories are DuPont™ bags called Tedlar Bags or Tedlar® made of PVF (polyvinyl fluoride) foil. Three US laboratories (Lötsch et al. 2008) carried out tests to check how the parameters of the samples change when stored in the bags: The chemical

Fig. 18 Principle of the design of vacuum vessels for taking gas samples into sealed bags



composition of the standard changed linearly due to the adsorption and chemical reactions of the ingredients, and the odor concentration dropped sharply after the third day. Various ways of conditioning Tedlar® bags (e.g., for 24 h in an oven at 100 °C) have been examined as well.

Materials for containers (bags) for odorous air samples are described in the EN 13725 standard (2003). According to Kouichi Tatsu et al. (2008), the most suitable sample material for the odorous gas containing volatile VOC odorants is FEP, a copolymer of tetrafluoroethylene and hexafluoropropylene.

In some measuring conditions, samples of odorous gas for olfactometer testing are taken using syringes, e.g., Hamilton syringes, canisters, or other equipment.

Direct Olfactometry

In the case of direct olfactometry, the measurements are performed online without delay. In this mode, the fragrant gas stream directly enters the dilution apparatus and is diluted therein with the odorless, inert gas stream before being fed to the port, where it is assessed as one stream using the sense of smell. The device used for direct olfactometry is illustrated in Fig. 19.

The field olfactometer carries out a series of dilutions by mixing a stream of fragrant air $V_{\text{fragrant air}}$, with a clean air V_{cleanair} filtered through a carbon filter and thus free of any odorants (McGinley and McGinley 2003). In the case of field olfactometry, the measurement result is the degree of odor gas dilution set by the panelist when the odor in the gas is at the perceptible threshold. This result is recorded as the value of the ratio of the mixed gas streams D/T (*dilution-to-threshold*):

$$D/T = \frac{V_{\text{clean air}}}{V_{\text{fragrant air}}} \quad (17)$$

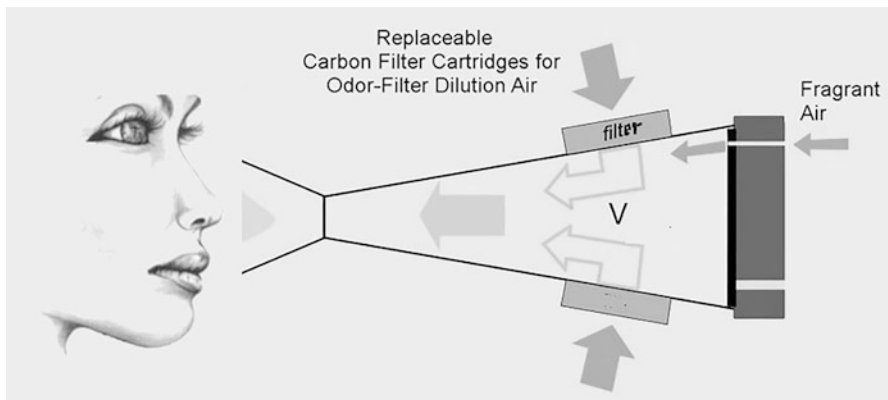


Fig. 19 The field olfactometer (Nasal Ranger® Field Olfactometer)

During the measurement, as in dynamic laboratory olfactometers, the panelists themselves increase by changing the set D/T value and the proportion of the odorous (unfiltered) air stream until an individual odor perception threshold is reached. Based on the D/T value, the preliminary individually estimated odor concentration Z is calculated as:

$$Z = \frac{V_{\text{clean air}} + V_{\text{fragrant air}}}{V_{\text{clean air}}} = \frac{V_{\text{clean air}}}{V_{\text{fragrant air}}} + 1 = \frac{D}{T} + 1 \quad (18)$$

However, considering the large jump in the D/T settings value, it is safer to calculate the Z_{ITE} value from the YES setting (Z_{n+1}) and the previous setting (smell not yet felt), i.e., Z_n (Sheffield et al. 2004). Then the estimation of the individual Z_{ITE} detection threshold is expressed as the geometric mean of the values of Z_{n+1} and Z_n

$$D/T_{\text{average}} = 10^{\frac{\log D/T_n + \log D/T_{n+1}}{2}} \quad (19)$$

If the panelists take the measurements, a series of field olfactometer measurements with the team members can be performed. The odor panel value can be calculated from the set of individual Z_{ITE} detection threshold results obtained by panelists (assuming a certain constancy of odor conditions in the environment in a given place and a given period). The geometric mean formula is used for the calculations:

$$c_{\text{od}} \ [\text{ou}/\text{m}^3] = \sqrt[n]{\prod^n Z_{ITE}} \quad (20)$$

where c_{od} is the odor concentration and n is the number of Z_{ITE} scores obtained by the members of the assessment team (panelists).

The field direct olfactometer equipment includes a set of 15 scented pencils saturated with n-butanol at various concentrations (*n-butanol Odor Pen Test Kit*) (Lay et al. 2004) intended for use in the selection and screening of members of the sensory panel (evaluation team).

Conclusions

Sensory evaluations of indoor air quality provide information on the effects of air pollutants in buildings on indoor air quality as it is perceived by building occupants. They can be performed in situ (in actual buildings) and the laboratory. They are supplementary to chemical measurements, which may not capture all pollutants that cause sensory discomfort. Therefore, they should always be considered for inclusion in protocols for characterizing indoor air quality in buildings.

Sensory evaluations of indoor air quality can be used for estimating the percentage of occupants dissatisfied with indoor air quality and, subsequently, ventilation

requirements to improve air quality as occupants perceive it. This approach has been used to define ventilation requirements included as prescriptive requirements in ASHRAE Standard 62-1 (2019) and CEN Standard EN-16798-1 (2019).

Sensory evaluations can also be used to characterize the emissions from building materials and products. This method is used in the Danish labeling scheme (Witterseh 2002; Daumling et al. 2008) and Germany (AgBB 2005). The method for using sensory panels to characterize emissions from building products is described in ISO 16000-28 (2012).

Sensory evaluations of indoor air quality can also be used to characterize other effects on building occupants. For example, Wargocki et al. (1999, 2000) showed the relationship between perceived air quality and the performance of office work, while Wang et al. (2013) and Kim et al. (2019) related the perception of indoor air quality with the sick building syndrome (SBS) symptoms.

References

- Abraham MH, Gola JM, Cometto-Muniz JE, Cain WS (2002) A model for odor thresholds. *Chem Senses* 27(2):95–104
- AgBB (AusschusszurgesundheitlichenBewertung von Bauprodukten) (2005) Vorgehens-weisebei der gesundheitlichenBewertung der Emissionen von flüchtigenorganischen Verbindungen (VOC) ausbauprodukten. Zuletzt aufgerufen am 7.05.21. <http://www.umweltbundesamt.de/themen/gesundheit/kommissionen-arbeitsgruppen/ausschuss-zur-gesundheitlichen-bewertung-von> [the newer version is Ausschuss zur gesundheitlichen Bewertung von Bauprodukten (AgBB –2021). Anforderungen an die Innenraumluftqualität in Gebäuden: Gesundheitliche Bewertung der Emissionen von flüchtigen organischen Verbindungen (VVOC, VOC und SVOC) aus Bauprodukten Aktualisierte NIK-Werte-Liste 2020 im Anhang. <http://www.umweltbundesamt.de/themen/gesundheit/kommissionen-arbeitsgruppen/ausschuss-zur-gesundheitlichen-bewertung-von>]
- Altomonte S, Allen J, Bluysen PM, Brager G, Heschong L, Loder A, Schiavon S, Veitch JA, Wang L, Wargocki P (2020) Ten questions concerning well-being in the built environment. *Build Environ* 180:106949
- AS/NZS 4323.3:2001 Stationary source emissions – determination of odor concentration by dynamic olfactometry. Australian Standard
- ASHRAE Standard 62-2019 (2019) Ventilation for acceptable indoor air quality. American Society of Heating and Air-Conditioning Engineers Inc., Atlanta
- ASTM International E544-04 (2004) Standard practice for referencing suprathreshold odor intensity. ASTM International, Philadelphia
- Berglund LS, Cain WS (1989) Perceived air quality and the thermal environment. In: Proceedings of the ASHRAE/SOEH conference I.A.Q '89- the human equation: health and comfort
- Berglund B, Zheng L, Wargocki P, Knudsen N, Asfhari A, Müller D, Dahlms A, Müller B (2010) Method of member selection for a defined panel and testing of panel performance. SysPAQ Project no. 23936, Deliverable No. 4 Update. Berlin
- Bluyssen PM, Kondo H, Pejtersen J, Gunnarsen L, Clausen G, Fanger PO (1989) A trained panel to evaluate perceived air quality. In: Kulić E, Todorović B, Novak P (eds) Proceedings of CLIMA 2000, vol 3, pp 25–30
- Bluyssen PM, de Oliveira Fernandes E, Groes L, Clausen G, Fanger PO, Valbjørn O, Bernhard CA, Roulet CA (1996) European indoor air quality audit project in 56 office buildings. *Indoor Air* 6: 221–238

- Borg G, Borg E (2001) A new generation of scaling methods: level-anchored ratio scaling. *Psychologica* 28:15–45
- Cai L, Koziel JA, Davis J, Lo YC, Xin H (2007) Characterization of volatile organic compounds and odors by in vivo sampling of beef cattle rumen gas using solid phase microextraction and gas chromatography-mass spectrometry-olfactometry, Iowa State University, and Iowa Beef Center. A.S. Leaflet R2209, Report 2007
- Cain WS, Cometto-Muniz JE (1995) Irritation and odor as indicators of indoor pollution. *Occup Med State Art Rev* 10(1):133–145
- CEN (1998) Technical report CR 1752: ventilation for buildings: design criteria for the indoor environment. European Committee for Standardization, Brussels
- Clausen G (2000) Sensory evaluation of emissions and indoor air quality. In: Proceedings of healthy buildings 2000, vol 1, Espoo, pp 53–62
- Cometto-Muñiz JE, Cain WS, Hudnell HK (1997) Agonistic sensory effects of airborne chemicals in mixtures: odor, nasal pungency, and eye irritation. *Perception and Psychophysics* 59(5): 665–674
- Cometto-Muñiz JE, Cain WS, Abraham MH (2004) Detection of single and mixed VOCs by smell and by sensory irritation. *Indoor Air* 14:108–117
- Cozzutto S, Pettarin N, Barbieri G, Licen S, Barbieri P (2018) Testing performances of a newly designer olfactometer. *Chem Eng Trans* 68:325–330. <https://doi.org/10.3303/CET1868055>
- Daumling C, Brenske K, Crump D, Funch L, Hansen K, Horn W, Kephalaopoulos S, Maupetit F, Saarela K, Tirkkonen T, Witterseh T (2008) Harmonisation of material labellingschemes in the EU. In: Proceedings of indoor air
- Devos M, Patte F, Rouault J, Laffort P, van Gemert LJ (1990) Standardized human olfactory thresholds. IRL Press, Oxford
- Dravnieks A, Jarke F (1980) Odor threshold measurement by dynamic Olfactometry: significant operational variables. *J Air Pollut Control Assoc* 30(12):1284–1289
- ECA (European Concerted Action “Indoor Air Quality and Its Impact on Man”) (1991) Effects of indoor air pollution on human health, Report no. 10, EUR 14086 EN, Luxembourg: Office for Publications of the European Communities
- ECA (1999) Sensory evaluation of indoor air quality, Report no. 20, EUR 18676 EN. Office for Publications of the European Communities, Luxembourg
- ECA (2005) Harmonisation of indoor material emissions labeling systems in the EU inventory of existing schemes, Report no 24. EUR 21891 EN, Luxembourg
- EN 13725 (2003) Air quality – determination of odor concentration by dynamic olfactometry
- EN 16798-1 (2019) Energy performance of buildings – ventilation for buildings – Part 1: indoor environmental input parameters for design and assessment of energy performance of buildings addressing indoor air quality, thermal environment, lighting, and acoustics – module M1-6
- EN ISO 16000-5 (2007) Indoor air – Part 5: sampling strategy for volatile organic compounds (VOCs)
- EN ISO 16017-1 (2002) Indoor, ambient and workplace air — Sampling and analysis of volatile organic compounds by sorbent tube/thermal desorption/capillary gas chromatography – Part 1: Pumped sampling
- EN ISO 16017-2 (2003) Indoor, ambient, and workplace air – Sampling and analysis of volatile organic compounds by sorbent tube/thermal desorption/capillary gas chromatography – Part 2: diffusive sampling
- EPA Method TO-17 (1999) Determination of volatile organic compounds in ambient air using active sampling onto sorbent tubes. Compendium of method for toxic organic air pollutants. January 1999
- Fang L, Clausen G, Fanger PO (1998a) Impact of temperature and humidity on the perception of indoor air quality. *Indoor Air* 8:80–90
- Fang L, Clausen G, Fanger PO (1998b) Impact of temperature and humidity on the perception of indoor air quality during immediate and more extended whole-body exposures. *Indoor Air* 8: 276–284

- Fanger PO (1970) Thermal comfort. Analysis and applications in environmental engineering. Danish Technical Press, Copenhagen
- Fanger PO (1988) Introduction of the olf and the decipol units to quantify air pollution perceived by humans indoors and outdoors. *Energ Buildings* 12:1–6
- Fanger PO, Berg-Munch B (1983) Ventilation and body odor. In: Proc. of an engineering foundation conf. on management of atmospheres in tightly enclosed spaces. ASHRAE, Atlanta, pp 45–50
- Fanger PO, Lauridsen J, Bluyssen P, Clausen G (1988) Air pollution sources in offices and assembly halls quantified by the olf unit. *Energ Buildings* 12:7–19
- Frontczak M, Wargocki P (2011) Literature survey on how different factors influence human comfort in indoor environments. *Building and Environment* 46(4):922–937
- Gunnarsen L, Bluyssen PM (1994) Sensory measurements using trained and untrained panel. In: Proceedings of healthy buildings '94, vol 2. Technical University of Budapest, Budapest, Hungary, pp 533–538
- Gunnarsen L, Fanger PO (1992) Adaptation to indoor air pollution. *Energ Buildings* 18:43–54
- ISO 10396 (2007) Stationary source emissions; sampling for the automated determination of gas concentration
- ISO 13301 (2002) Sensory analysis – methodology – general guidance for measuring odor, flavor, and taste detection thresholds by a three alternative forced-choice (3-AFC) procedure
- ISO 16000-28 (2012) Indoor air — Part 28: determination of odor emissions from building products using test chambers
- ISO 16000-6 (2004) Indoor Air – Part 6. Determination of volatile organic compounds in indoor and test chamber by active sampling on Tenax TA® sorbent, thermal desorption, and gas chromatography Rusing MS/FID
- ISO 8586-1 (1993) Sensory analysis – general guidance for the selection, training, and monitoring of assessors – Part 1: selected assessors
- ISO 8587 (1988) Sensory analysis – methodology – ranking test
- JCGM 100:2008 (GUM 1995 with minor corrections). Evaluation of measurement data — guide to the expression of uncertainty in measurement
- Jensen B, Wolkoff P, Wilkins CK (1995) Characterization of linoleum. Part 2: preliminary odor evaluation. *Indoor Air* 5(1):44–49
- Jiang J (2002) Development of the next generation olfactometer-dynascent, odor management review. Ministry of the Environment, Japan, Beppu City
- Jørgensen M, Vestergaard L (1998) Sensory characterization of emission from building materials. Selection of low-emitting materials and evaluation of the method. Lyngby, Laboratory of Indoor Environment and Energy, Department of Energy Engineering, the Technical University of Denmark (in Danish with English summary)
- Kim J, Jang M, Choi K, Kim K (2019) Perception of indoor air quality (IAQ) by workers in underground shopping centers in relation to sick-building syndrome (SBS) and store type: a cross-sectional study in Korea. *BMC Public Health* 19(1):1–9
- Kleber M, Wagner A (2018) Investigation of indoor thermal comfort in warm-humid conditions at a German climate test facility. *Build Environ* 128:216–224
- Knudsen HN, Clausen G, Fanger PO (1993) Prediction of perceived air quality in a space-based on small scale experiments. In: Proceedings of the 6th international conference on indoor air quality and climate – indoor air '93, vol 2, Helsinki – Indoor air '93, pp 585–590
- Knudsen HN, Valbjørn O, Nielsen PA (1998) Determination of exposure-response relationships for emissions from building products. *Indoor Air* 8:264–275
- Knudsen HN, Clausen PA, Shibuya H, Wilkins K, Wolkoff P (2004) Evaluation of products containing linseed oil, By-og Byg Document 54, Danish Building Research Institute (SBI). (In Danish), 75 p
- Kośmider J (2008) Prezentacja technik pomiarów odometrycznych. Część 2. Kontrola wrażliwości węchu. Materiały Seminarium RTP 26398: Ograniczanie uciążliwości odorowych w Polsce. Międzyzdroje, marzec 2008
- Kostyrko K, Kozicki M (2018) Trends in odor measurements and determining mVOC content in the interiors of buildings. The Scientific Papers of Faculty of Electrical and Control Engineering,

- Gdańsk University of Technology (in Polish). L Inter-University Conference on Metrology MKM 2018 Szczecin – Kopenhagen, September 2018
- Kostyrko K, Wargocki P (2014) Measurement of odors and perceived indoor air quality in buildings. Building Research Institute, Warszawa. (in Polish)
- Kozicki M (2022) Identification of olfactory nuisance of floor products containing bitumens with the TD–GC–MS/O method. Materials 15:959. <https://doi.org/10.3390/ma1503095>
- Lay AM, McGinley CM, Nasal A (2004) Chemosensory performance test for odor inspectors. In: Proceedings of the Water Environment Federation/Air & Waste Management Association International Specialty Conference: Odors and Air Emissions. Water Environment Federation, Washington, Bellevue, April 2004
- Licina D, Langer S (2021) Indoor air quality investigation before and after relocation to WELL-certified office buildings. *Build Environ* 204:108182
- Liu Z, Ma S, Cao G, Meng C, He B (2018) Distribution characteristics, growth, reproduction and transmission modes and control strategies for microbial contamination in HVAC systems: a literature review. *Energy & Buildings* 177:77–95
- Lötsch J, Reichmann H, Hummel T (2008) Different odor tests contribute differently to the evaluation of olfactory loss. *Chem Senses* 33:17–21
- Massold E, Bähr C, Salthammer T, Brown SK (2005) Determination of VOC and TVOC in air using desorption GC-MS – practical implications for test chamber experiments. *Chromatographia* 62(1/2)
- Maxeiner B (2005) Olfactometric Interlaboratory Comparisons Test 2005. WFF/AWWA odors and air emissions 2006. Water Environment Federation, p 688
- McGinley CM, McGinley MA (2000) Odor intensity scales for enforcement, monitoring and testing. In: Air and Waste Management Association, 2000 Annual Conference. Session No: EE-6, Session Title: Odor Management and Regulation. Salt Lake City, UT. June 19_21
- McGinley MA, McGinley CM (2003) Comparison of field olfactometers in a controlled chamber using hydrogen sulfide as the test odorant. In: Proceedings of International Water Association 2nd international conference on odor and VOCs: measurement, regulation, and control techniques. Singapore, September 2003
- Melikov A, Kaczmarczyk J (2008) Impact of air movement on perceived air quality at different pollution level and temperature. In: Proceedings of indoor air 2008, on CD ROM
- Moschandreas DJ, Relwani SM (1992) Perception of environmental tobacco smoke odors. An olfactory and visual response. *Atmos Environ* 26B(3):263–269
- Mui KW, Wong LT, Hui PS (2008) Choices of sampling locations for assessment of air pollutant exposure concentration in an Open-Plan Office of Hong-Kong. In: Proceedings of indoor air 2008, Paper ID. 19. Denmark, Copenhagen, August 2008
- Müller B (2003) 11. VDI-TGA Jahrestagung-Gerät zur Entnahme und Darbietung von Luftproben. HLH-Heizung Luftung Klima Haustechnik 54(10):43–45
- Müller B, Müller D, Horn W, Jann O (2005) The use of gas sampling bags for evaluating the odors of building materials. In: Indoor air 2005, 10th international conference on indoor air quality and climate, China, Beijing, September 2005
- Nagata Y, Takeuchi N (2003) Measurement of odor threshold by triangle odor bag method. *Odor Meas Rev* 118:118–127
- Nordin S, Millqvist E, Lowhagen O, Bende M (2003) The chemical sensitivity scale: psychometric properties and comparison with the noise sensitivity scale. *J Environ Psychol* 23:359–367
- Nordin S, Bende M, Millqvist E (2004) Normative data for the chemical sensitivity scale. *J Environ Psychol* 24:399–403
- Olesen BW, Sekhar C, Wargocki P (2021) VIP 42: the concept for substituting ventilation by gas-phase air cleaning. AIVC
- Piasecki M, Kostyrko KB (2019) Combined model for IAQ assessment: part 1—morphology of the model and selection of substantial air quality impact sub-models. *Appl Sci* 9:918. <https://doi.org/10.3390/app9183918>
- Piasecki M, Kostyrko K (2020) Development of weighting scheme for indoor air quality model using a multi-attribute decision making method. *Energies* 13:3120. <https://doi.org/10.3390/en13123120>

- Piasecki M, Kostyrko K, Fedorczak-Cisak M, Nowak K (2020) Air enthalpy as an IAQ indicator in hot and humid environment—experimental evaluation. *Energies* 13:1481. <https://doi.org/10.3390/en13061481>
- Roelofsen P (2016) Modelling relationships between a comfortable indoor environment, perception and performance change. Ph.D. thesis. Delft University of Technology, Industrial Design Engineering, Delft
- Roelofsen P (2018) A new methodology for the evaluation of the perceived air quality depending on the air pollution caused by human bioeffluents, the temperature, the humidity as well as air velocity. *Intell Build Int* 10(3):154–161. <https://doi.org/10.1080/17508975.2018.1434475>
- Rohr AC (2001) Chapter 26: Methods for assessing irritation effects in IAQ field and laboratory studies. In: Spengler JD (ed) Indoor air quality handbook. McGraw-Hill, New York
- Salis LCR, Abadie M, Wargocki P, Rode C (2017) Towards the definition of indicators for assessment of indoor air quality and energy performance in low-energy residential buildings. *Energ Buildings* 152:492–502
- Sheffield R, Thompson M, Dye B, Parker D (2004) Evaluation of field-based odor assessment methods. The University of Idaho. Water Environment Federation/A&WMA Odors and Air Emissions
- Simonson CJ (2000) Moisture, thermal and ventilation performance of Tapanila ecological house. In: VTT Tiedotteita – Meddelanden – Research Notes, by VTT Technical Research Centre of Finland, Espoo, Finland
- Sowa J (2020) Creation of the indoor environment in office buildings. *ASHRAE J* 62(7):64–68
- Spiess T, Fitzner K (1999) New developments in assessing perceived air quality in the laboratory with trained and untrained panels. In: Raw G, Aizlewood C, Warren P (eds) Proceedings of indoor air '99, Edinburgh, the 8th international conference on indoor air quality and climate, Vol, vol 2, pp 567–575
- Tatsu K, Tanabe S-I, Hoshino K, Sato K (2008) Proceedings of indoor air '08, Paper ID. 166. Denmark, Copenhagen, August 2008
- Toftum J, Jørgensen AS, Fanger PO (1998) Effect of humidity and temperature of inspired air on perceived comfort. *Energ Buildings* 28:15–23
- Ueno H, Amano S, Merecka B, Kośmider J (2008) Difference of the odor concentrations measured by the triangle odor bag method and the dynamic olfactometry. In: 3rd IWA International conference on odor and VOCs, Barcelona, October 2008
- Van Harreveld AP, Mannebeck D, Maxeiner B (2008) Proficiency testing as the key element of implementing EN 13725 olfactometry. In: 3rd IWA international conference on odor and VOCs, Barcelona, October 2008
- VOC Method Update (2005) SKC appendices to EPA method TO-17. Determination of volatile organic compounds (VOCs) in ambient or indoor air. SKC Inc. Publication 1667
- Wang J, Li B, Yang Q, Yu W, Wang H, Norback D, Sundell J (2013) Odors and sensations of humidity and dryness in relation to sick building syndrome and home environment in Chongqing, China. *PLoS One* 8(8):e72385
- Wargocki P (2004) Sensory pollution sources in buildings. *Indoor Air* 14(Suppl 7):82–91
- Wargocki P, Fanger PO (1999) A transfer model between perceived air quality judged by a trained panel and by an untrained panel. In: Proceedings of indoor air '99, vol 2, pp 594–599
- Wargocki P, Wyon DP, Baik YK, Clausen G, Fanger PO (1999) Perceived air quality, Sick Building Syndrome (SBS) symptoms, and productivity in an office with two different pollution loads. *Indoor Air* 9:165–179
- Wargocki P, Wyon DP, Fanger PO (2000) Productivity is affected by the air quality in offices. In Proceedings of healthy buildings 1, 1, pp 635–640
- Wargocki P, Fanger PO, Krupicz P, Szczecinski A (2004) Sensory pollution loads in six office buildings and a department store. *Energ Buildings* 36:995–1001
- Wargocki P, Knudsen HN, Rabstajn A, Afshari A (2009) Measurement of perceived air quality: correlation between odor intensity, acceptability, and characteristics of air. In: Proceedings of Healthy Buildings 2009, Paper103. Syracuse

- Wargocki P, Knudsen HN, Krzyzanowska J (2010) Some methodological aspects of sensory testing of indoor air quality. In: Clima 2010, 9–12 May, Antalya: 10th REHVA World Congress: sustainable energy use in buildings clima 2010: 10th REHVA World Congress
- Wargocki P, Wei W, Bendžalová J, Espigares-Correa C, Gerard C, Greslou O, Rivallain M, Sesana MM, Olesen BW, Zirngibl J, Mandin C (2021) TAIL, a new scheme for rating indoor environmental quality in Office and hotels undergoing deep energy renovation (EU ALDREN project). *Energy & Buildings* 244:111029
- Wei W, Wargocki P, Zirngibl J, Bendžalová J, Mandin C (2020) Review of parameters used to assess the quality of the indoor environment in Green Building certification schemes for offices and hotels. *Energy & Buildings* 209:109683
- Wilkins K, Wolkoff P, Knudsen HN, Clausen PA (2007) The impact of information on perceived air quality – 'organic' vs. 'synthetic' building materials. *Indoor Air* 17:130–134
- Witterseh T (2002) Status of the indoor climate labeling scheme in Denmark. In: Proceedings of indoor air, vol 2002, pp 612–614
- Wyon DP, Wargocki P (2005) Indoor air quality effects on office work. In: Croome D (ed) Creating productive environment, in press
- Yaglou CP, Riley EC, Coggins DI (1936) Ventilation requirements. *ASHVE Trans* 42:133–162
- Zhang S, Cai L, Koziel JA, Hoff SJ, Schmidt DR, Clanton CJ, Jacobson LD, Parker DB, Heber AJ (2010) Field air sampling and simultaneous chemical and sensory analysis of livestock odorants with sorbent tubes and GC–MS/olfactometry. *Sensors Actuators B. Chemical* 146:437–432

Part V

Source/Sink Characteristics



Source/Sink Characteristics of VVOCs and VOCs

22

Tao Yang, Ningrui Liu, Xiaojun Zhou, John C. Little, and
Yinping Zhang

Contents

Introduction	648
Model Development for Describing Source/Sink Processes	649
Empirical Models	650
Mass-Transfer Models	651
Measurement Methods for VVOC/VOC Characteristic Parameters	667
Experimental Techniques for Measuring Model Parameters	668
Correlations Between Model Parameters and Physical/Chemical Properties	679
Dimensionless Analysis of Characteristic Parameters	683
Source Control to Reduce the VVOC/VOC Emissions	684
Influencing Factors on VVOC/VOC Characteristic Parameters	685
The Initial Emittable Concentration, C_0	685
The Diffusion Coefficient, D	687
The Partition Coefficient, K	687

T. Yang

Department of Building Science, Tsinghua University, Beijing, China

Beijing Key Laboratory of Indoor Air Quality Evaluation and Control, Beijing, China

e-mail: yangtao1991@mail.tsinghua.edu.cn

N. Liu · Y. Zhang (✉)

Department of Building Science, School of Architecture, Tsinghua University, Beijing, China

Beijing Key Laboratory of Indoor Air Quality Evaluation and Control, Beijing, China

e-mail: liunr18@mails.tsinghua.edu.cn; zhangyp@mail.tsinghua.edu.cn;

zhangyp@tsinghua.edu.cn

X. Zhou

School of Human Settlements and Civil Engineering, Xi'an Jiaotong University, Xi'an, China
e-mail: zhouxiaojun@xjtu.edu.cn

J. C. Little (✉)

Department of Civil and Environmental Engineering, Virginia Tech, Blacksburg, VA, USA
e-mail: jcl@vt.edu

Conclusions	688
Cross-References	688
References	690

Abstract

Quantitative knowledge of indoor source and sink characteristics is fundamental to understanding mass-transfer behavior of indoor organic chemicals, e.g., very volatile organic compounds (VVOCs) and volatile organic compounds (VOCs), and reducing human exposures to those contaminants. The key to acquiring source and sink characteristics of VVOCs and VOCs is to establish accurate physically based models with rational parameters to describe the mass-transfer process and to reliably obtain the key parameters involved in models. In this chapter, we therefore introduce representative research on the topic of “source/sink characteristics,” spanning mass-transfer analysis at the micro-, meso-, and macroscales. This research covers: (i) modeling the emissions from indoor sources, (ii) measuring the characteristic parameters used in source/sink models, and (iii) dimensionless analysis and influencing factors of the characteristic parameters. A general introduction of modeling and key parameters is presented for researchers to comprehensively understand the emission mechanism and mass-transfer principles, as well as to develop engineering applications. Additional details can be obtained from the original papers. The research summary presented in this chapter provides a foundation for future investigation in the broader area of “indoor air quality control.”

Keywords

Mass transfer · Source/sink · Model · Characteristic parameters · Dimensionless analysis

Introduction

Many new man-made materials (including composite wood, vinyl flooring, and plastic products) have been developed and widely used in indoor environments in the past few decades. These materials may emit a range of potentially hazardous airborne pollutants including very volatile organic compounds (VVOCs, specified as compounds with a boiling point of less than 50 °C, such as formaldehyde, acetaldehyde) and volatile organic compounds (VOCs, specified as compounds with a boiling point in a range of 50–240 °C, such as benzene, toluene, xylene) (Weschler 2009; Weschler and Nazaroff 2008). Exposure to these chemicals, sometimes referred to as “modern exposure,” is associated with certain health concerns (such as headaches, asthma, lung cancer) (Wolkoff and Nielsen 2001; Boeglin et al. 2006; Jie et al. 2011; Zhang et al. 2013), and has the potential to significantly degrade indoor air quality, work efficiency, and individual health. To effectively assess and reduce such health risks, it is necessary to comprehensively understand the mechanistic pathway of airborne pollutants from source to exposure.

In the past three decades, research on mass-transfer phenomena and exposure control of airborne organic compounds in indoor environments has greatly increased. Chronologically, the focus of research is linked to the requirements of the time. In the early stage, more attention was paid to whether the properties of the target building material would meet consumer requirements. Thus, European and American labeling procedures focused on the resulting concentration or emission rate from a single building material in a test chamber, and specified a threshold concentration for the target compound within a specific time period as the quality standard for the building material. The limitation is that some knowledge about the test material was obtained, but the test results could not be used to predict or explain indoor transport and exposure. For example, when several such test materials are placed in a room simultaneously, the resulting pollutant concentration cannot be easily assessed. As a result, there was a need to understand the mechanistic mass-transfer behavior (i.e., source/sink characteristics) of VVOCs and VOCs. To meet this need, research was directed at the development of mass-transfer models and the determination of model parameters. Further, with the development of green and healthy buildings, the traditional indoor air-quality assessment performed after building completion was costly and seldom met consumer expectation. With the growing demand for resource conservation and pollution reduction, there was a need to evaluate the possible impact on indoor concentrations before building construction. In general, it was this continuous improvement in engineering requirements that deepened the understanding of mass-transfer mechanisms and the resulting ability to control indoor air quality.

To effectively control hazardous organic compounds in indoor air and reduce their potentially adverse effects on human health, it is necessary to quantitatively understand the transport of the pollutants from sources to the occupants. As shown in Fig. 1, this primarily includes understanding of (1) the source, that is, target pollutants being emitted from indoor sources or entering from outdoors to indoors (steps 1.1 and 1.2 in Fig. 1); (2) transport, that is, pollutants from indoor or outdoor sources will transfer and distribute between various indoor media, and affect indoor chemical concentrations (step 2); (3) exposure, that is, occupants can be exposed to indoor pollutants via multiple pathways with associated health risks (steps 3 and 4); and (4) feedback, that is, control strategies that can be applied to the preceding steps (step 5).

Thus, the objectives of this chapter are to: (1) review representative research on source/sink characteristics; (2) identify problems or tasks worthy of further study; and (3) attract more researchers to address the so-called “modern exposure” issues.

It should be noted that although VVOCs and VOCs are handled differently when sampling due to their different physical properties, the mechanisms affecting emissions and transport within the indoor environment are similar. Thus, the research reviewed in this chapter is applicable to mass transfer of both VVOCs and VOCs.

Model Development for Describing Source/Sink Processes

To characterize VVOC/VOC mass transfer from building materials to occupants for risk assessment purposes and source emission control, emission chamber tests are often performed. Although valuable results for specific test conditions can be

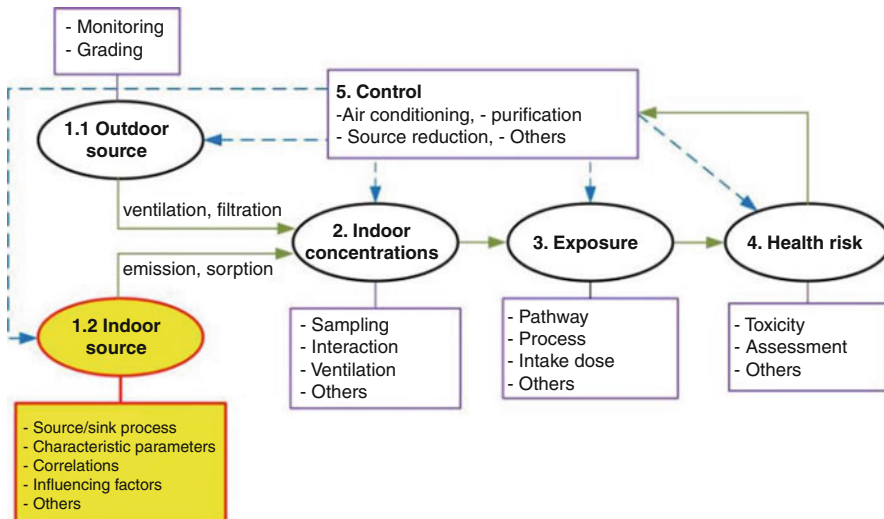


Fig. 1 Schematic showing transport and potential control of indoor chemicals as they move between their sources and the occupants in a building (Zhang et al. 2016)

obtained by direct measurements, they are frequently not applicable to other conditions. In addition, chamber experiments are often expensive, time-consuming, and difficult. Many predictive models have therefore been developed to understand the mechanisms governing VVOC/VOC emissions and transport in the indoor environment. Generally, these models can be categorized into two groups: empirical models and physically based (or mechanistic) mass-transfer models.

Empirical Models

Early models were constructed using statistical analysis of emission chamber test data. Although these models were simple and easy to use, they lacked a physical basis and could not reveal mass-transfer mechanisms and influencing factors, and therefore could not be extended from the test conditions to other conditions.

Dunn (1987) and Clausen (1993) proposed two widely used first-order decay models. The two models assumed that a climatic chamber consists of four (hypothetical) compartments, including source, chamber air, an exit, and a sink, and introduced several first-order rate constants to describe the flows among these compartments as illustrated in Fig. 2. First-order decay models often fit the short-term emissions data very well, but almost always underestimate the long-term emissions. To overcome this problem, higher-order decay models were developed by taking both short- and long-term emissions into account. Clausen et al. (1993) proposed a second-order decay model, and Tichenor et al. (1991a) proposed a more complex model. This model has been applied to many sources that feature rapid

Fig. 2 Schematic showing how two first-order decay models (Dunn 1987; Clausen 1993) are established

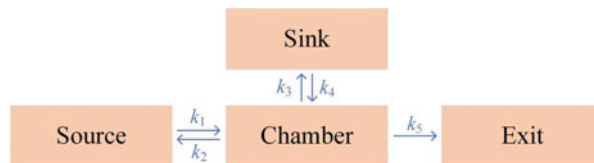


Table 1 List of several empirical models developed by early IAQ modelers

Description	Expression	References
First-order decay model	$E = E_0 e^{-kt}$ $E = M_0 k e^{-kt}$	Dunn (1987) Clausen (1993)
Second-order decay	$E = \frac{E_0}{1 + k_2 t E_0}$	Clausen et al. (1993)
n th-order decay	$E = \frac{E_0}{n-1 \sqrt{1 + (n-1) k_n t E_0^{n-1}}}$	Tichenor et al. (1991a)
Formaldehyde from building materials	$E = E_0 - k_m C$	Mathews et al. (1987)

emissions in the early stage, followed by long-lasting, low-level emissions. In general, it fits long-term data better than the first-order models. On the other hand, higher-order models can sometimes be misused. For example, they allow an infinite amount of pollutant to be emitted from the source, which is physically impossible. Thus, these models may overestimate total emissions.

Building materials have been identified as important indoor pollution sources. For a long time, modelers had to rely on statistical and empirical models. Mathews et al. (1987) developed an empirical model for formaldehyde emissions from particle-board and other engineered wood. Similar to other empirical models, this model lacks a physical basis and provides no insight into the controlling mechanisms. This and the previously mentioned empirical models are summarized in Table 1.

In a useful review, Guo (2002a, b) compiled 52 indoor emission source models found in the literature, which represented the achievements that modelers made in the early years. The review consists of two parts. Part 1 provides an overview of the 52 models, briefly discussing their validity, usefulness, limitations, and flaws. Part 2 focuses on parameter estimation and reviews 48 measurement methods.

Mass-Transfer Models

Compared with empirical models, mass-transfer models are based on valid mass-transfer mechanisms with model parameters that have a clear physical meaning, and therefore can predict emissions for different conditions if the relevant model parameters are known. In this section, we review the development of source/sink models to illustrate the application of mass transfer in addressing problems outlined in Fig. 1: (1) revealing the emission mechanism (or process) of airborne organic compounds released from indoor materials; (2) predicting the concentration of target VVOC/

VOC in indoor air during the emission period; (3) assessing the human exposure and risk to certain airborne chemicals; (4) controlling the source emissions and optimizing the performance of air cleaning equipment/techniques.

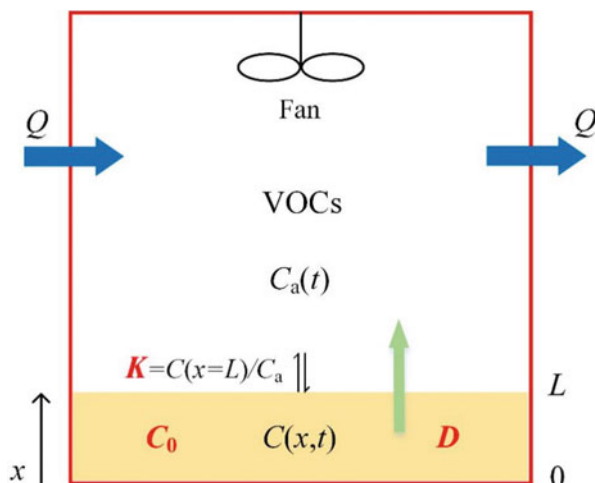
Source/Sink Models for Dry Building Materials

To develop valid source/sink models for dry building materials (e.g., wallboard, wood-based boards, vinyl flooring, etc.), it is necessary to (1) understand the emission mechanisms and behavior of VVOCs/VOCs from indoor materials or products; (2) describe the mass-transfer process using the associated mass-transfer laws or equations (where necessary, rational assumptions can be made to simplify the mass-transfer process); (3) obtain the mathematical solution to the models by various analytical methods; and (4) validate the models and test the applicability of the results.

Considering internal diffusion in the source material and equilibrium partitioning at the material surface, Little et al. (1994) developed a model (Fig. 3) to account for observed emissions of VOCs from new carpets. To simplify the problem, Little et al. assumed that (1) the initial emittable concentration of target pollutant, C_0 , is uniform in the polymer slab; (2) the mass-transfer resistance between the polymer surface and the bulk chamber air is small in comparison to the resistance within the polymer layer itself; (3) the inlet and initial VOC concentrations in the chamber are zero; (4) diffusion inside the polymer slab is one dimensional; (5) the diffusion coefficient D and partition coefficient K are constant and independent of material-phase concentration within low concentration range; (6) the chamber or room air is well mixed; and (7) possible sorption of the VOC to the stainless-steel chamber surface can be neglected.

With these assumptions, the governing equation for internal diffusion based on Fick's second law becomes:

Fig. 3 Schematic of mechanisms governing emissions from a material slab in a chamber or room



$$\frac{\partial C}{\partial t} = D \cdot \frac{\partial^2 C}{\partial x^2} \quad (1)$$

where C is the concentration of the contaminant in the material slab, $\mu\text{g}/\text{m}^3$; D is the diffusion coefficient, m^2/s , assumed to be independent of concentration; t is the emission time, s ; and x is linear distance, m .

Since the material layer is resting on the stainless-steel floor of the chamber, the first boundary condition assumes that there is no flux out of the base of the material slab. Moreover, equilibrium is assumed to exist between the contaminant concentrations in the surface layer of the polymer and the chamber air. Thus, the boundary conditions for Eq. (1) are:

$$\left. \frac{\partial C}{\partial x} \right|_{x=0} = 0, \quad t > 0 \quad (2)$$

$$K = \frac{C|_{x=L}}{C_a}, \quad t > 0 \quad (3)$$

where K is the material/air partition coefficient; C_a is the VOC concentration in the chamber air, $\mu\text{g}/\text{m}^3$; and L is the thickness of the material layer, m .

The initial condition assumes that the compound of interest is uniformly distributed throughout the material layer, or:

$$C(x, t) = C_0, \quad t = 0, \quad 0 \leq x \leq L \quad (4)$$

A second flux boundary condition is imposed through a mass balance on the VOC in the chamber air:

$$V \frac{dC_a(t)}{dt} = -DA \left. \frac{\partial C(x, t)}{\partial x} \right|_{x=L} - QC_a(t), \quad t > 0 \quad (5)$$

where V is the volume of air in the chamber, m^3 ; A is the area covered by the carpet, m^2 ; and Q is the volumetric flow rate of air through the chamber, m^3/s .

The solution to Eqs. (1), (2), (3), (4), and (5) is obtained from an analogous heat-transfer solution, which is first transformed into mass-transfer terms and then adjusted to account for equilibrium partitioning, yielding:

$$C(x, t) = 2C_0 \sum_{n=1}^{\infty} \left\{ \frac{\exp(-Dq_n^2 t)(h - kq_n^2) \cos(q_n x)}{[L(h - kq_n^2)^2 + q_n^2(L + k) + h] \cos(q_n L)} \right\} \quad (6)$$

with

$$h = \frac{Q}{A \cdot D \cdot K} \quad (7)$$

$$k = \frac{V}{A \cdot K} \quad (8)$$

and the q_n are the positive roots of

$$q_n \tan(q_n L) = h - kq_n^2, \quad (n = 1, 2, \dots) \quad (9)$$

Equation (6) gives the contaminant concentration in the polymer slab as a function of linear distance (x) and emission time (t). The concentration of contaminant in the chamber air is obtained by first finding the concentration at the surface of the polymer slab and then substituting this value into Eq. (3).

Analysis reveals that the physical properties D and K and the initial VOC concentration in the material C_0 are the three key parameters, referred to as “emission characteristic parameters,” which collectively characterize the emission behavior of VOCs in indoor environments. Little et al.’s model provides the foundation for the subsequent mechanistic studies of the source/sink characteristics of VVOC/VOCs.

Assumptions (1), (2), and (3) of Little et al.’s model are not always valid in real situations. How can the model be improved when the assumptions do not match the actual situation? How to describe the sorption process with the model? What about a comprehensive prediction for a material with multiple layers? The following research addresses these questions by extending and improving Little et al.’s model.

Single-Layer Source Models. A numerical approach was presented by Yang et al. (2001a) for the simulation of VOC emissions from solid materials. They combined a three-dimensional (3-D) numerical mass-transfer analysis to calculate the external convective mass transfer in chamber air, with the one-dimensional (1-D) approach used in Little et al.’s model for internal diffusion. Because this approach is quite complicated due to the 3-D numerical computation, Huang and Haghighe (2002) developed a numerical and an analytical model to predict the VOC emission rate from dry building materials. Both models consider the mass-diffusion process within the material and the mass-convection and -diffusion processes in the boundary layer. The mass-diffusion process within the material is still described by Eqs. (1) and (2) in Little et al.’s model, while the mass-convection and -diffusion processes in the boundary layer, Eq. (3), is replaced by:

$$-D \cdot \frac{\partial C(x, t)}{\partial x} \Big|_{x=L} = h_m \left(\frac{C(x, t)|_{x=L}}{K} - C_a(t) \right) \quad (10)$$

where C_a is the VOC concentration in the chamber air, $\mu\text{g}/\text{m}^3$, h_m is the convective mass transfer coefficient, m/s . Equation (10) shows how external convective mass transfer is taken into account. Numerical solutions for $C(x, t)$, and $C_a(t)$ were analyzed based on a finite difference method. Under the condition that $C_a(t) \ll C(x = L, t)/K$, which is reasonable for many scenarios, a full analytical solution for $C(x, t)$, and $C_a(t)$ is derived. Because it is assumed that C_a is negligible compared to the VOC concentration adjacent to the material surface, this means that it is not applicable for closed chambers.

Kumar and Little (2003a) validated the strategy to characterize the rate of absorption and desorption of VOCs by diffusion-controlled building materials. An

analytical model for a single-layer homogeneous material with one surface that emits/absorbs a VOC to/from well-mixed air is set up and a fully analytical solution of $C(x, t)$ and $C_a(t)$ is also obtained. This model neglects convective mass-transfer resistance, but considers nonuniform C_0 and included a time-dependent y_{in} . Xu and Zhang (2003) developed an improved generally applicable model for calculating the surface VOC emissions from building materials and instantaneous VOC distributions in materials. They also introduced h_m (estimated from available empirical correlations) instead of the assumptions (2) and (3) of Little et al.'s model. Thus, a semi-analytical (but not fully explicit) solution is analyzed by the variable separation method and computation from the initial condition. The results of using the model were validated with experiments reported in the literature, as shown in Fig. 4.

Deng and Kim (2004) obtained fully analytical solutions of $C_a(t)$, $C(t)$ and $E(t)$ using the Laplace transform, which provides a useful approach to the analytical solution. Compared to other models capable of accounting for those two mechanisms, this model is fully analytical and can be conveniently applied. The analytical solution of $C_a(t)$ derived by Deng and Kim (2004) can be expressed as:

$$C_a(t) = 2C_0\beta \sum_{n=1}^{\infty} \frac{q_n \sin q_n}{G_n} e^{-DL^{-2}q_n^2 t} \quad (11)$$

with

$$Bi_m = h_m L / D \quad (12)$$

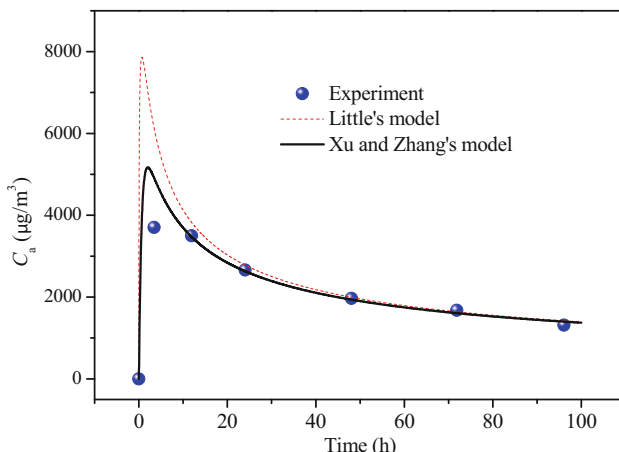


Fig. 4 Comparison of experimental results with emission prediction by Little's model and Xu and Zhang's model. (Reprinted from Xu and Zhang (2003), Copyright 2003, with permission from Elsevier)

$$\alpha = QL^2/VD \quad (13)$$

$$\beta = AL/V \quad (14)$$

$$G_n = \frac{[K\beta + (\alpha - q_n^2)KBi_m^{-1} + 2]q_n^2 \cos q_n + q_n \sin q_n \times}{[K\beta + (\alpha - 3q_n^2)KBi_m^{-1} + \alpha - q_n^2]} \quad (15)$$

and the q_n are the positive roots of

$$q_n \tan q_n = \frac{\alpha - q_n^2}{K\beta + (\alpha - q_n^2)KBi_m^{-1}}, \quad (n = 1, 2, \dots) \quad (16)$$

where C_a is the VOC concentration in the chamber air, $\mu\text{g}/\text{m}^3$, A is the source emission area of the material, m^2 , L is the half thickness of the building material, m , V is the volume of chamber, m^3 , Bi_m is the Biot number for heat transfer, h_m is the convective mass transfer coefficient, m/s , and Q is the volumetric flow rate of chamber air, m^3/s .

However, its application is relatively limited because it is based on assumption (3) of Little et al.'s model.

Taking the external convective mass transfer into account as well as a nonuniform initial material-phase concentration, Xu and Zhang (2004) developed a semi-analytical model focusing on emission behavior of building materials, an extension of their earlier work (Xu and Zhang 2003), and a semi-analytical solution is provided for this model. For the specific case that C_0 is uniform, the proposed model is validated with experimental data. Wang et al. (2006) set up a semi-analytical model for VOC emissions from both surfaces of dry, flat-plate building materials. Based on the analytic model, the influence of several factors on source emission was discussed. In addition, the conditions for simplifying double surface emission into single surface emission were also discussed. Deng and Kim (2007) investigated VOC emission from new carpet and its transport in an aged apartment by using a three-dimensional computational fluid dynamics (CFD) model. A numerical solution for single-layer homogeneous material with one surface emitting is obtained. Compared with the prior studies, this model considers the condition of non-well-mixed air, which is different from assumption (6) of Little et al.'s model. Xiong et al. (2012) further proposed a general fully analytical model to characterize VOC emission/sorption processes under different conditions (airtight or ventilated). These predictive models above generally consider the physical emission process only, but neglect the chemical reaction process, which may cause discrepancy in predicting long-term formaldehyde emissions for the cases where chemical reaction (i.e., hydrolysis) occurs over time. By combining the chemical-reaction process with a physical mass-transfer process, an improved mechanistic model was developed by He et al. (2019) to more accurately predict long-term emission behavior. In this method, a first-order chemical reaction is applied to describe the hydrolysis process between urea-formaldehyde (UF) resin and water vapor inside the material. Thus, the internal diffusion governing Eq. (1) can be rewritten as:

$$\frac{\partial C}{\partial t} = D \cdot \frac{\partial^2 C}{\partial x^2} + R_c \cdot C \quad (17)$$

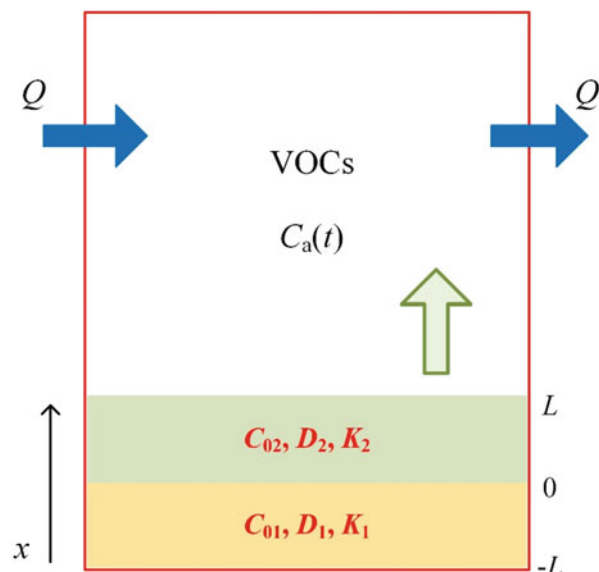
where, R_c is the first-order reaction rate constant, 1/s.

By virtue of the Laplace transform, an analytical solution is derived including four parameters, i.e., C_0 , D , K , and R_c , which comprehensively considers the effect of physical and chemical processes. Chamber experiments under controlled temperature and relative humidity for a laminate flooring product made with high-emitting composite wood core were performed for nearly 1.5 years to examine the long-term formaldehyde emission behavior. The good agreement between mechanistic model prediction and test data validates the effectiveness of the developed model.

Multilayer Source Models. Prior models usually considered the target building material as a single layer. In practice, many indoor furnishings and building structures are comprised of layers of different materials, which may alternatively act as VOC sources or sinks depending on their emission and sorption potentials and the indoor environmental conditions as well. Further model prediction for multilayer emission can be developed building on the well-established single-layer source framework.

Employing the homologous mass-transfer principle as for the single-layer models, a model was developed by Kumar and Little (2003b) to predict the rate of mass transfer between a double-layer material and indoor air, considering diffusion-controlled emissions from the composite material (Fig. 5). The model allows non-uniform initial material-phase concentrations in each of the two layers, while external convective mass transfer was again ignored. An analytical solution to the double-layer model was obtained and a parametric analysis was performed

Fig. 5 Schematic representation of a double-layer model



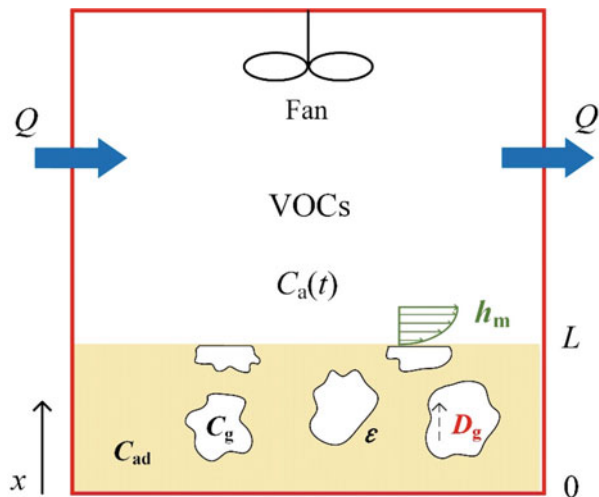
illustrating the behavior of the model as a function of the primary model parameters. In addition, it is a generalized sink/source model, meaning that it is also capable of predicting sorption.

Haghish and Huang (2003) included external convective mass transfer in their numerical integrated IAQ model, which is applied to predict the VOC emission rate of a multilayer material, the VOC sink rate of a material, and the room air VOC concentration with both source and sink materials. Hu et al. (2007) built an analytical mass-transfer model with a semi-analytical solution for predicting emissions of VOCs from multilayer building materials and a nonuniform initial material-phase concentration is included. With the consideration of convective surfaces on both sides, this model does not neglect the mass-transfer resistance through the gas-phase boundary layer. Based upon the model and the dimensionless analysis, the applicable conditions of Kumar and Little (2003b) double-layer model were discussed, but the model is practically limited by the many parameters and complicated forms of semi-analytical solution. Li and Niu (2007) derived a numerical solution of $C_a(t)$ using single-zone method for a whole room IAQ model consisting of multi-phase emission/sorption for wall materials. This model can successfully handle different building scenarios. Deng et al. (2008) presented a fully analytical solution of $C_a(t)$ to describe the emission/sorption of VOCs from/on multiple single-layer materials coexisting in buildings. The study revealed that the coexistence of multiple materials may decrease the emission rate of VOCs from each material. One obstacle to a numerical solution for multilayer composite materials arises from the difficulty in solving sharply discontinuous concentration profiles at the interface of two adjacent materials. Therefore, by considering the flaws existing in the analytical model and conventional numerical methods, the state-space method, widely used in the heat-transfer field, was applied by Yan et al. (2009) to simulate VOC emissions from building materials. Their model assumes that building material is composed of a number of finite layers, in each of which the instantaneous VOC concentration is homogeneous during the entire emission process. Based on this assumption, the method is generally applied to simulate VOC emissions from arbitrary layers of building materials, and the solution is explicit and simple. Wang and Zhang (2011) developed a general mass-transfer model for analyzing VOC emissions from dry multilayer building materials with two emission surfaces. This model adds to an earlier multilayer model by considering chemical reactions within the materials. Consequently, it can be used to analyze the effect of these chemical reactions on removing VOCs, and for characterizing secondary VOC emissions from the building material.

Source Models for Porous Materials. Physical models have been developed to predict VOC source (emission) and sink (sorption) behavior of building materials. Porous building materials (e.g., gypsum, concrete, wood-based products, carpet, wallpaper, etc.) are not only sources of indoor air pollutants such as VOC but they are also strong sinks of these pollutants. The knowledge of VOC transfer mechanisms in these materials is an important step for controlling the indoor VOC concentration levels, and for determining the optimum ventilation requirements for acceptable IAQ.

Generally, a porous building material can be modeled if it consists of pores and solid parts. A VOC in a pore is in the gas phase and/or adsorbed phase on the pore

Fig. 6 Schematic representation of VOC emission from a porous material



surface, as shown in Fig. 6. VOC transport within the building material is mainly by gas-phase diffusion through the pores, and the adsorbed-phase diffusion, or diffusion through the solid part is assumed to be negligible (Tiffonnet et al. 2000; Murakami et al. 2000). Murakami et al. (2003) presented physical models for numerically analyzing the transport of VOCs from porous building material by CFD simulation. Lee (2003) further developed the multi-phase approach, including surface diffusion (adsorbed-phase diffusion) as well as gas-phase diffusion in the pores. Equation (18) is usually used to describe the one-dimensional problem considering only gas-phase diffusion and sorption:

$$\varepsilon \frac{\partial C_g}{\partial t} = D_g \frac{\partial^2 C_g}{\partial x^2} - \frac{\partial C_{ad}}{\partial t} \quad (18)$$

where ε is the porosity of porous media; C_g is the gas-phase concentration of VOC in porous media, $\mu\text{g}/\text{m}^3$; C_{ad} is the adsorbed-phase concentration of VOC in porous media, $\mu\text{g}/\text{m}^3$; D_g is the effective gas-phase diffusion coefficient of VOC within porous media, m^2/s ; and D_{ad} is the diffusion coefficient of adsorbed phase VOC in porous media, m^2/s .

Considering both primary and secondary source/sink behaviors for the first time, a new analytical model was developed by Lee et al. (2005) to predict emission/sorption behaviors of VOCs in porous building materials. The governing equation of one-dimensional gas-phase and surface diffusion within the porous material including physical adsorption/desorption and generation or elimination of VOC due to secondary source or sink behavior is given by:

$$\varepsilon \frac{\partial C_g}{\partial t} + \frac{\partial C_{ad}}{\partial t} = D_g \frac{\partial^2 C_g}{\partial x^2} + D_{ad} \frac{\partial^2 C_{ad}}{\partial x^2} + g(x, t) \quad (19)$$

where D_{ad} is the adsorbed-phase diffusion coefficient of VOC in porous media, m^2/s , and $g(x,t)$ are time and space-dependent VOC generation/elimination due to secondary source/sink behavior, $\mu\text{g}/(\text{m}^3 \cdot \text{s})$. The positive sign (+) for $g(x,t)$ is for the secondary source behavior and the negative (-) is for the secondary sink behavior.

Not fully explicit analytical solutions of $C(x, t)$, $E(t)$, and $C_a(t)$ have been derived, which may require a finite difference method to calculate from initial conditions. Coupled with CFD analysis using the conventional convection approach, the porous emission model can be extended to a more detailed numerical conjugate mass-transfer model developed by Lee et al. (2006), with a numerical solution solved by a combination of 2-D laminar forced convection and unsteady 1-D diffusion and sorption using CFD.

The equations for the porous material are analogous to those described for the single-phase materials. Although some additional parameters are needed for the porous models, it has been shown that these models could be converted from one form to another as long as the linear sorption isotherm is used in both approaches. (Haghighe et al. 2005).

Sink Models. Building materials may act as both sources of and sinks for VOCs in indoor air. Generally, sorption is the reverse process of emission. Almost all existing sink models assume that sorption is fully reversible, and thus, several source models (Kumar and Little 2003a, b; Haghighe and Huang 2003; Li and Niu 2007; Deng et al. 2008; Yan et al. 2009; Xiong et al. 2012) can be used as sink models. Other models, focusing on sink phenomena, have also been proposed.

Based on the linear Langmuir adsorption isotherm (Langmuir 1916), Tichenor et al. (1991b) developed a widely used sorption model to characterize the adsorption/desorption behaviors existing at the material/air interface:

$$V \frac{dC_a}{dt} = k_d A M - k_a A C_a - Q C_a \quad (20)$$

$$\frac{dM}{dt} = k_a A - k_d M \quad (21)$$

where C_a is the concentration in the chamber or room air, $\mu\text{g}/\text{m}^3$; M is the mass on the sink surface, $\mu\text{g}/\text{m}$; k_a is the adsorption rate constant, $1/\text{s}$; and k_d is the desorption rate constant, m/s , A is the sink surface area of the material.

For the Langmuir model, only the adsorption/desorption process at the interface is considered, while internal diffusion is neglected, which is not applicable for long-term prediction. To overcome this, certain physical models have been proposed which not only account for the adsorption and desorption process at the interface, but also include the internal diffusion process.

Little and Hodgson (1996) presented a physical model to characterize and predict the source and sink behavior of homogeneous, diffusion-controlled building materials, but ignored the convective mass-transfer processes outside materials. To extend the prior work, a sink-diffusion model to describe the interaction between material surfaces and VOCs in indoor air was developed by Jørgensen et al. (2000), based on adsorption/desorption on the material surfaces and diffusion into the

materials. In this model, an embedded sink (E) is introduced to represent the diffusion effect inside the materials, so that Eq. (20) is replaced by the following equations:

$$\frac{dM}{dt} = k_a C_a - k_d M - k_{\text{diff}}(M - E) \quad (22)$$

$$\frac{dE}{dt} = k_{\text{diff}}(M - E) \quad (23)$$

The sink-diffusion model gives a better description of the desorption curve than the Langmuir model, especially for prediction with stronger sorption effects. As the adsorption, desorption, and diffusion processes occur simultaneously, it is difficult to propose a method to measure the parameters k_a , k_d , and k_{diff} directly. These parameters are usually determined by nonlinear fitting to experimental data rather than by independent experiments.

Yang et al. (2001b) developed a model to predict the VOC sorption rate into materials, which can be used as a “wall function” in combination with more complex gas-phase models that account for nonuniform mixing to predict the sorption process. The model, however, is inherently complicated due to the CFD approach used to calculate external mass transfer. Deng et al. (2010) introduced a tool called sorption saturation degree (SSD), which can be characterized by dimensionless correlations and parameters to evaluate sorption capacity of building materials. Furthermore, numerical models considering simultaneous source and sink behavior of multilayer materials have been developed, which more closely approximate to the real indoor environment. Yu and Kim (2013) reviewed the state-of-the-art knowledge on characterization of emission behavior of VOCs and formaldehyde from building materials and emphasized the need to consider diffusion and sink effects as an overall strategy for modeling VOC emissions from materials, so as to develop evaluation tools for estimating or predicting VOC concentrations in the indoor environment. The aforementioned VOC emission models for dry building materials with a brief description of their characteristics are listed in Table 2, as well as the model solution approach.

Source/Sink Models for Wet Coating Materials

In addition to the reviewed models for VOC emission/sorption from dry materials, a variety of “wet” products, mostly coatings such as wood stains, varnishes, and paints, are also frequently used indoors (Liu et al. 2013). As suggested in several chamber experiments, VVOC/VOC emission from wet coating materials consist of two stages: (1) the wet stage, in which the material is initially quite wet and characterized by high emission rates and fast decay due to liquid evaporation at the material surface; and (2) the dry stage, in which much of the liquid has evaporated, and the material releases contaminants at a much lower rate, dominated by internal diffusion. A transition phase usually exists between the two stages, which makes the prediction of VOC emissions from wet coating materials more complicated.

Early mass-transfer models for wet coating materials considered emissions as a pure evaporative process. Examples include the vapor pressure and boundary layer

Table 2 VOC emission models developed for dry building materials

Types	Features, limitations, and comments	References
Single-layer source models	<ul style="list-style-type: none"> Giving governing equation, boundary conditions, and initial condition Full analytical solution of $C(x, t)$, and $C_a(t)$ Three “emission parameters,” C_0, D, and K, introduced Convective mass transfer process neglected 	Little et al. (1994)
	<ul style="list-style-type: none"> A 3-D numerical analysis for external convective mass transfer combined with 1-D analytical analysis for internal diffusion Too complicated 	Yang et al. (2001a)
	<ul style="list-style-type: none"> 1-D mass-transfer analysis for both external convection and internal diffusion Numerical solutions by a finite difference method Not applicable for a closed chamber 	Huang and Haghigat (2002)
	<ul style="list-style-type: none"> A generalized sink/source model with full analytical solution of $C_a(t)$ Neglecting convective mass transfer resistance Considering nonuniform C_0 and including time-dependent y_{in} 	Kumar and Little (2003a)
	<ul style="list-style-type: none"> Introducing h_m for the convective mass transfer process Semi-analytical solution Describing the application condition for assumption (2) of Little’s model 	Xu and Zhang (2003)
	<ul style="list-style-type: none"> Full analytical solutions of $C_a(t)$, $C(t)$, and $E(t)$ using Laplace transform Suitable for a ventilated chamber 	Deng and Kim (2004)
	<ul style="list-style-type: none"> Model with any initial emittable concentration and nonuniform distribution of C_0 Semi-analytical solution 	Xu and Zhang (2004)
	<ul style="list-style-type: none"> A double surface emission model with semi-analytical solution Analysis of conditions for simplifying double surface emission into single surface 	Wang et al. (2006)
	<ul style="list-style-type: none"> Considering non-well-mixed air Numerical solution using CFD 	Deng and Kim (2007)
	<ul style="list-style-type: none"> A general analytical model for characterizing emission/sorption in the material Applicable for emission/sorption behavior in ventilated or closed chamber 	Xiong et al. (2012)
	<ul style="list-style-type: none"> Considering a first-order chemical reaction (i.e., hydrolysis) Applicable for long-term formaldehyde emission 	He et al. (2019)
Multilayer source models	<ul style="list-style-type: none"> A double-layer emission model with full analytical solution of $C(x, t)$ Nonuniform initial concentration in material phase considered Ignoring convective mass transfer process 	Kumar and Little (2003b)

(continued)

Table 2 (continued)

Types	Features, limitations, and comments	References
	<ul style="list-style-type: none"> External convective mass transfer included A numerical solution Integrated IAQ model for source/sink behavior of single- or multilayer material 	Haghhighat and Huang (2003)
	<ul style="list-style-type: none"> Multilayer double surface emission model with a semi-analytical solution <ul style="list-style-type: none"> Nonuniform C_0 and mass transfer resistance considered Many parameters and complicated forms of solution 	Hu et al. (2007)
	<ul style="list-style-type: none"> Multiple materials coexisting Numerical solution using single-zone method 	Li and Niu (2007)
	<ul style="list-style-type: none"> Full analytical solution of $C_a(t)$ and $E(t)$ for each layer obtained <ul style="list-style-type: none"> Coexistence of multiple materials may decrease VOC emission rate from each material 	Deng et al. (2008)
	<ul style="list-style-type: none"> State-space method for multilayer emissions Explicit and simple numerical solution Suitable for cases where a reaction is producing or removing VOC 	Yan et al. (2009)
	<ul style="list-style-type: none"> Chemical reaction inside material considered Capable for characterizing secondary VOC emissions Generalized and complicated analytical solution 	Wang and Zhang (2011)
Porous models	<ul style="list-style-type: none"> Porous material with one surface that emits/absorbs VOC to/from the room air Numerical solution using CFD 	Murakami et al. (2003)
	<ul style="list-style-type: none"> Including adsorbed-phase diffusion as well as gas-phase diffusion in the pores One-dimensional diffusion Analytical solution 	Lee (2003)
	<ul style="list-style-type: none"> Primary and secondary source/sink effect first considered Not fully explicit analytical solution 	Lee et al. (2005)
	<ul style="list-style-type: none"> Conjugate mass transfer model Considering unsteady two-dimensional laminar forced convection Numerical solution obtained using CFD 	Lee et al. (2006)
Sink models	<ul style="list-style-type: none"> Langmuir model Neglecting diffusion inside material Unable to actually predict long-term sorption 	Tichenor et al. (1991b)
	<ul style="list-style-type: none"> Based on linear Langmuir sorption isotherm Neglecting surface convective mass transfer 	Little and Hodgson (1996)
	<ul style="list-style-type: none"> A sink-diffusion model with an embedded sink (E) is introduced Difficult to measure sink parameters 	Jørgensen et al. (2000)
	<ul style="list-style-type: none"> Similar equations to source model, with different initial and boundary conditions Complicated calculation and analysis with CFD simulation 	Yang et al. (2001b)

(continued)

Table 2 (continued)

Types	Features, limitations, and comments	References
	<ul style="list-style-type: none"> Numerical models with similar source/sink behavior of multilayer materials Closer to real indoor environment 	Deng et al. (2010)
	<ul style="list-style-type: none"> A review on VOC emission/sorption Providing a realistic route to impact assessment of VOC in indoor environment 	Yu and Kim (2013)

(VB) model (Tichenor et al. 1993) for total volatile organic compounds (TVOCs) and the subsequent VBX model (Guo et al. 1998) employing the same mass-transfer principle. The VB and VBX models assume that the liquid on the substrate is a uniform mixture of VOCs, which evaporate into air and do not penetrate into the substrate. The VB and VBX models ignore the mass transfer between the coating film and the substrate and the diffusion within the film itself, both of which may be negligible at the wet stage when evaporation and external convective mass transfer dominate, but may become important when the film is dry. Thus, the two models can predict short-term emissions with relatively good accuracy, but are not suitable for the dry stage.

Considering the internal diffusion of the liquid film, Sparks et al. (1999) developed a semi-analytical model for evaluating the impact of latex paint emission on IAQ, although it does not have a sound mass-transfer basis. To examine the entire emission process, Yang et al. (2001c) proposed a numerical model to simulate VOC emissions from wet coating materials, with the consideration of the VOC mass-transfer process in the air and at the material/air interface, and diffusion in the material film and also in the substrate. In this model, the material is divided into two separate layers: the upper layer (liquid film) is the substrate infused with liquid, while the lower layer is the substrate (shown in Fig. 7) with both layers treated as a continuum. Fick's law can be used to describe transient diffusion within the liquid film and the substrate, or:

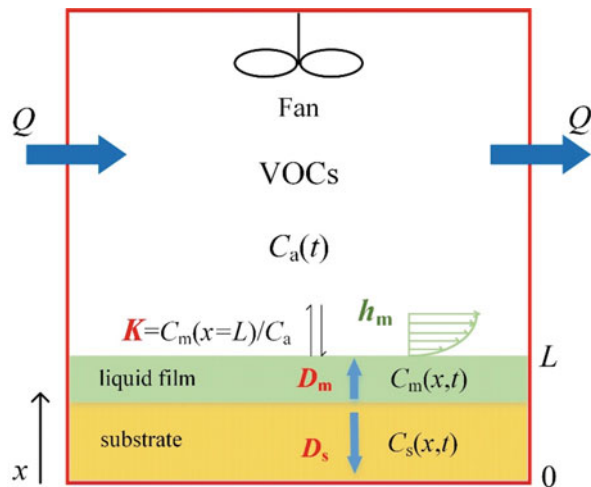
$$\frac{\partial C_m}{\partial t} = \frac{\partial}{\partial x} \left(D_m \frac{\partial C_m}{\partial x} \right) \quad (24)$$

$$\frac{\partial C_s}{\partial t} = \frac{\partial}{\partial x} \left(D_s \frac{\partial C_s}{\partial x} \right) = D_s \frac{\partial^2 C_s}{\partial x^2} \quad (25)$$

where C_m is the material-phase VOC concentration in the liquid film, $\mu\text{g}/\text{m}^3$; C_s is the material-phase VOC concentration in the substance, $\mu\text{g}/\text{m}^3$; D_m is the effective diffusion coefficient in the liquid film, m^2/s ; and D_s is the diffusion coefficient in the substance, m^2/s .

At the film/substrate interface, the flux and the concentration should be continuous:

Fig. 7 Schematic describing the VOC emission from a wet coating material



$$-D_m \frac{\partial C_m}{\partial x} = -D_s \frac{\partial C_s}{\partial x} \quad (26)$$

$$C_m = C_s \quad (27)$$

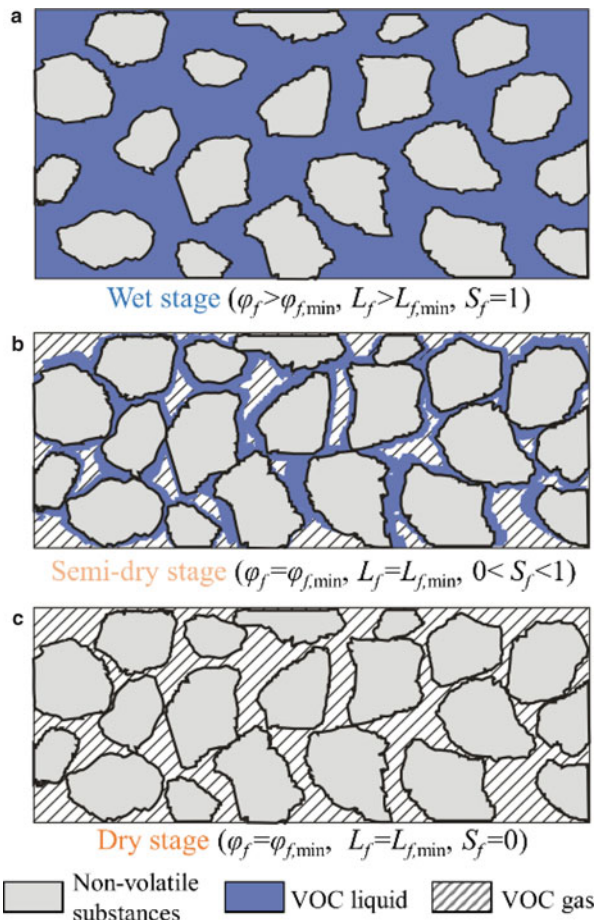
At the bottom of the substrate, zero-flux, or $C_s = 0$, can be taken as the boundary condition. At the material/air interface, an instantaneously reversible equilibrium is assumed, or:

$$C_m|_{x=L} = KC_a \quad (28)$$

Combining Eqs. (24), (25), (26), (27), and (28), a numerical solution is obtained using the CFD calculation of mass transfer in the chamber air. It should be noted that the D_m will change with the decreasing C_m , requiring empirical correlations to quantify the dependence of D_m on C_m , which complicates the process.

The numerical model developed by Haghigat and Huang (2003) is not only used for the emission/sorption behavior of VOCs from dry building material, but also is applicable for the dry/wet or wet/dry material assembly, also under consideration of the dependence of D_m on C_m . To eliminate the complexity due to the concentration dependence, Li et al. (2006) proposed a simplification of the previous model by assuming that the VOC concentration in the material film is always uniform so that diffusion within the film can be ignored. The simplified model should agree well with the cases of thin liquid film, but needs caution in the late emission stage as diffusion inside the liquid film becomes dominant. Altinkaya (2009) developed a mathematical model to describe the emission characteristics of VOCs from homogeneous wet coating materials deposited on impermeable substrates. The model considers mass transfer in the material and in air, boundary layer resistance, and the change in the coating thickness with time

Fig. 8 Schematic of the paint film during drying process (φ_f is the porosity of paint film; L_f is the paint film thickness; S_f is the VOC liquid saturation of the paint film porosity) subscript min. (Reprinted from Zhou et al. (2020), Copyright 2020, with permission from Elsevier)



due to emission of VOCs. However, there is difficulty to obtain most of the model parameters, and the introduction of a moving boundary in the numerical calculation means that the model is inherently more complicated to use. Zhou et al. (2020) proposed a mathematical model for characterizing the full process of VOC emissions from paint film coating on porous substrates. By introducing the saturation of VOC liquid in the pores of the paint film (S_f), this model can give quantitative definitions for three states of the paint film including wet, semi-dry, and dry (Fig. 8). VOC mass transfer in the air, at the air-paint interface, in the paint film, at the paint-substrate interface, and in the porous substrate is mathematically described.

The aforementioned VOC emission models for wet coating materials are listed in Table 3 in chronological order, with a brief introduction of the model characteristics.

Table 3 VOC emission models developed for wet coating materials

Works	Features, limitations, and comments
VB model (Tichenor et al. 1993) and VBX model (Guo et al. 1998)	<ul style="list-style-type: none"> • Considers emission as a pure evaporative process • Assumes that the liquid on substrate is a uniform mixture of VOCs • Neglects the mass transfer between the liquid film and substrate, not applicable in the dry stage
Sparks et al. (1999)	<ul style="list-style-type: none"> • Internal diffusion of the liquid film is considered • Semi-analytical solution
Yang et al. (2001c)	<ul style="list-style-type: none"> • A numerical model • Two layers divided with the upper liquid film and the lower substrate • Including multiple mass transfer processes between liquid film, substrate, and chamber air
Haghishat and Huang (2003)	<ul style="list-style-type: none"> • Dry/wet or wet/dry building material assembly acting as a source • Numerical solution using finite difference method
Li et al. (2006)	<ul style="list-style-type: none"> • Diffusion process in liquid film is ignored, suitable for case of thin liquid film, but not applicable in the dry stage • Numerical solution using implicit finite-volume method
Altinkaya (2009)	<ul style="list-style-type: none"> • Assumes that the substrate is impermeable • Both internal and external mass transfer resistances considered • Numerical solution • Complicated to use
Zhou et al. (2020)	<ul style="list-style-type: none"> • Transitions of the paint film from wet to dry are defined quantitatively • VOC emission characteristics of different drying stages can be depicted • Numerical solution • Some model parameters are difficult to obtain

Measurement Methods for VVOC/VOC Characteristic Parameters

An important issue for the validation and application of mass-transfer models is the estimation of model parameters. In addition to the easily obtained parameters such as V , Q , A , and L , the key parameters in the solid VOC models primarily include C_0 , D , and K . Besides the inherent errors caused by the assumptions of the models, the accuracy of prediction is greatly dependent on the reliability of model parameters. Therefore, the measurement of model parameters is a prerequisite to apply the models and has resulted in a range of studies. Characterization of model parameters can be specified into two categories: experimental techniques, and correlations between model parameters and physical/chemical properties of target pollutants/materials or the environmental conditions. Therefore, this section will review the developed methods for measuring the source/sink characteristic parameters in

these two categories. Furthermore, the dimensionless analysis of key parameters is also discussed.

Experimental Techniques for Measuring Model Parameters

The Initial Emittable Concentration, C_0

Traditional methods for measuring VOC concentrations in dry materials have used solvents or heat to extract target compounds. Cox et al. (2001a) proposed a fluidized-bed desorption (FBD) method for the determination of initial emittable VOC content (or concentration) in vinyl flooring. Due to the shortening of the mass-transfer path and increasing of the emission area, the experimental time is no more than 7 days. However, there are still some limitations in the FBD method due to the complex experimental system and the fact that the material has to be ground into powder.

Smith et al. (2009) proposed a multi-flushing extraction method for determining C_0 . In this method, material specimens were also ground into powder and then allowed to emit in a recirculation loop. The emission involves multiple equilibrium cycles by multi-flushing the chamber, and continues until the equilibrium VOC concentration in chamber air of the last cycle is less than 10% of the first cycle. Therefore, the initial emittable mass, M_0 , can be calculated as:

$$M_0 = \sum_{i=1}^n VC_{\text{equ},i} + \frac{VC_{\text{equ},n}}{C_{\text{equ},n-1}/C_{\text{equ},n} - 1} \quad (29)$$

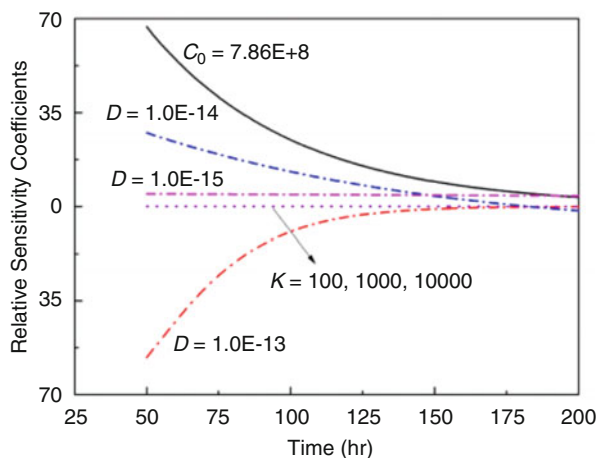
where M_0 is the initial emittable contaminant mass, μg ; V is the volume of the airtight chamber, m^3 ; $C_{\text{equ},i}$ is the equilibrium concentration of VOC in the airtight chamber during the i th period, $\mu\text{g}/\text{m}^3$; and n is the total number of cycles of the experiment. C_0 can be calculated as the ratio of M_0 to the material volume (V_m). Except for grinding, the main drawback is the required time since it may need many cycles to reach the appropriate condition.

Li (2013) presented a novel procedure for estimating C_0 and D in building materials. This new method determines these two parameters by two observations from a chamber test in a non-fitting and sequential way, which defines a well-posed problem and requires no iterative procedure. The most outstanding feature of this method is that multiple estimates of the parameters can be obtained when more than two experimental data points are available. However, the method cannot provide an estimation for K , due to the insensitivity of C_a (air-phase concentration) to K (see Fig. 9).

The Diffusion Coefficient, D

Cup Method. The cup method is one of the simplest techniques to measure D presented by Kirchner et al. (1999). The building material is fixed on the top of a cup containing pure VOC liquid, the system is placed on the electronic balance,

Fig. 9 Sensitivity analysis of C_a to C_0 , D , and K . (Reprinted from Li (2013), Copyright 2013, with permission from American Chemical Society)



and its mass change is recorded with time. According to Fick's diffusion law, D can be calculated as:

$$D = \frac{m}{A} \frac{L}{C_{\text{sat}}} \quad (30)$$

where m is the steady-state mass flux of the VOC through the material, $\mu\text{g/s}$, A is the source emission area of the material, m^2 , L is the thickness of the material, m , and C_{sat} is the saturation concentration of VOC at given temperature, $\mu\text{g/m}^3$.

As D has been shown to be concentration dependent at high concentration levels, the result of the cup method will overestimate D for the saturated concentration of VOC in the cup, which is much higher than the indoor concentration. Furthermore, due to the use of pure VOC liquid, one experiment can only measure the diffusion coefficient of one VOC.

CLIMPAQ Method. To overcome the flaw of cup method, which measures only one VOC at a time, Meininghaus et al. (2000) used the CLIMPAQ method (Chamber for Laboratory Investigations of Materials, Pollution and Air Quality) to determine D of several VOCs simultaneously. The test material is placed between two CLIMPAQs, referred to as the primary and secondary chambers. Air with a constant concentration of VOCs is introduced into the primary chamber while the secondary chamber is ventilated with clean air. The steady-state VOC concentrations in the two chambers are recorded, and D can be calculated as:

$$D = -\frac{m}{A} \frac{\Delta x}{\Delta C} = \frac{Q L}{A} \frac{C_2}{C_1 - C_2} \quad (31)$$

where m is the steady-state mass flux of the VOC through the material, $\mu\text{g/s}$, A is the source emission area of the material, m^2 , Q is the volumetric flow rate of air through the CLIMPAQs, m^3/s , L is the thickness of the material, m , C_1 and C_2 are

the equilibrium VOC concentrations in the primary and secondary chamber, respectively.

The main drawback of this method is that it neglects the external convective mass-transfer resistance at the material surfaces, which may result in an underestimation of D .

Two-Chamber Method. Employing a two-airtight-chamber test, Bodalal et al. (2000) proposed a method to determine D and K simultaneously. The test material, which is free of VOCs, separates two airtight chambers, referred to as a high-concentration chamber and a low-concentration chamber. During the experiment, the target VOCs diffuse from the high-concentration chamber through the test material into the low-concentration chamber. Assuming both chambers are well mixed, an analytical solution is derived as:

$$\ln \left(\frac{y_1 - y_2}{y} \right) = \ln \left[\frac{4K \cdot A \cdot L/V}{q_1^2 + (K \cdot A \cdot L/V)(2 + K \cdot A \cdot L/V)} \right] - \frac{q_1^2 D}{L^2} t \quad (32)$$

where y_1 and y_2 are the VOC concentrations in the high-concentration chamber and in low-concentration chamber, respectively, $\mu\text{g}/\text{m}^3$, and y is the initial VOC concentration in the high-concentration chamber, $\mu\text{g}/\text{m}^3$, A is the source emission area of the material, m^2 , L is the thickness of the material, m , V is the volume of environmental chamber, m^3 .

D and K can be obtained by linear regression of the experimental data. This method also neglects the effect of the external convective mass-transfer process and may have similar limitations as the CLIMPAQ method.

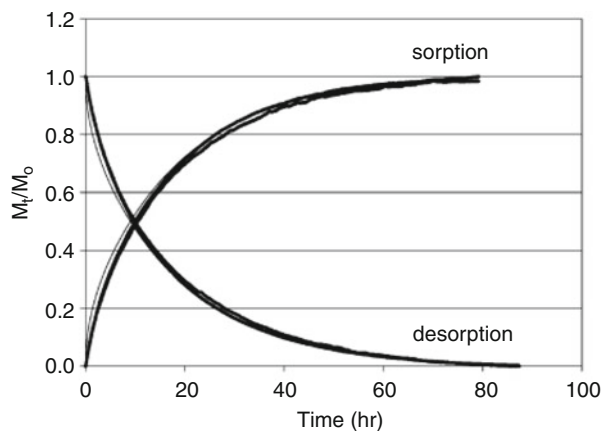
Microbalance Method. A microbalance method was developed by Cox et al. (2001b) to measure D and K separately for vinyl flooring. A thin slab-shaped sample is cut from test material and put into a small glass chamber attached to a high-resolution microbalance. During the experiment, carrier gas with a known concentration of VOC is introduced for sorption until equilibrium, then the desorption test is conducted. The D is determined by fitting Fick's diffusion model to the sorption and desorption curve (see Fig. 10). The samples used for this method are quite small and thin so that it is only applicable to uniform materials.

Inverse Method. Based on Deng and Kim's model (2004), an inverse method was developed by Li and Niu (2005) to estimate the constants D and K of VOCs in the building material. With the use of simulated measurements as input data for the inverse analysis, the parameter-estimation problem was solved by using the Levenberg-Marquardt method (1963) of minimization of the least-squares norm. However, this method cannot solve three key parameters at the same time, and it is necessary to measure at least one key parameter in advance.

The Partition Coefficient, K

Headspace Method. The headspace method developed by Tiffonnet et al. (2002) is a simple and direct method to determine K by measuring both the material-phase concentration and gas-phase concentration at equilibrium. In this method, building materials containing no VOCs are placed in an airtight environmental chamber and

Fig. 10 Fitting transient sorption/desorption data (symbols) to a diffusion model (lines) for determination of D . (Reprinted from Cox et al. (2001b), Copyright 2001, with permission from Elsevier)



then injected with a certain mass of acetone, M_s . When the adsorption equilibrium is reached, K can be calculated by the following equation:

$$K = \frac{C_m}{C_a} = \frac{M_s - C_{\text{equ}}V}{C_{\text{equ}}V} \quad (33)$$

where M_s is the known mass of VOC injected in headspace method, μg , C_{equ} is the gas-phase concentration of acetone in equilibrium, $\mu\text{g}/\text{m}^3$, V is the volume of environmental chamber, m^3 .

Several sensitive methods (e.g., Xiong et al. 2009, 2011a; Wang and Zhang 2009; Wang et al. 2008), which employ the basic idea of the headspace method to measure K and C_0 simultaneously, have been developed.

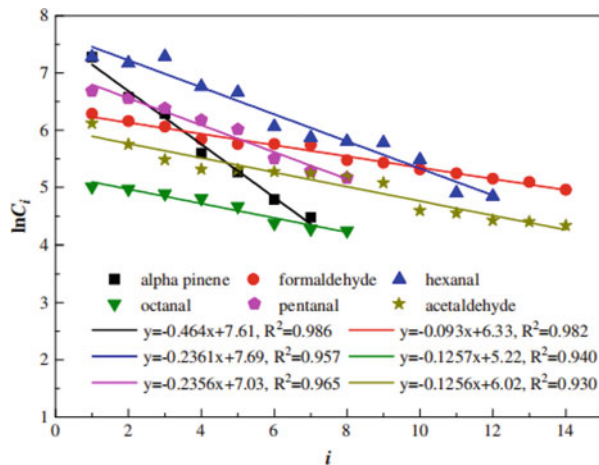
Multi-emission/Flush Regression Method (MEFR). Based on the extraction method presented by Smith et al. (2009), an improved method, the multi-emission/flush regression method, was proposed by Xiong et al. (2009) to simultaneously determine K and C_0 . In this method, a piece of particle board is placed in the closed chamber where it freely emits until equilibrium is established. Then multiple equilibria are formed by duplicate emission/flushing cycles, and the gas-phase concentration in the chamber air at equilibrium is noted. Based on mass conservation and Henry's linear sorption law, for the i th equilibrium state, we get:

$$\ln C_{\text{equ},i} = \ln \frac{K}{R_v + K} \cdot i + \ln \frac{C_0}{K}, \quad (i = 1, 2, \dots) \quad (34)$$

where $C_{\text{equ},i}$ is the equilibrium VOC concentration in the chamber during the i th period, $\mu\text{g}/\text{m}^3$, R_v ($= V/V_m$) is the ratio of chamber volume (V) to material volume (V_m).

Then, C_0 and K can be simultaneously obtained through linear regression of the experimental data (see Fig. 11). Compared to the extraction method, this method has

Fig. 11 Regression for six VOCs in the tested particle board. (Reprinted from Xiong et al. (2009), Copyright 2009, with permission from Elsevier)



the following advantages: (1) it is unnecessary to emit completely from the material, thus greatly reducing experimental time; (2) it can avoid the measurement uncertainties at low VOC concentrations; and (3) it does not require grinding the building material and is thus more convenient to use. However, the proposed method is also somewhat time-consuming due to several emission/flushing cycles.

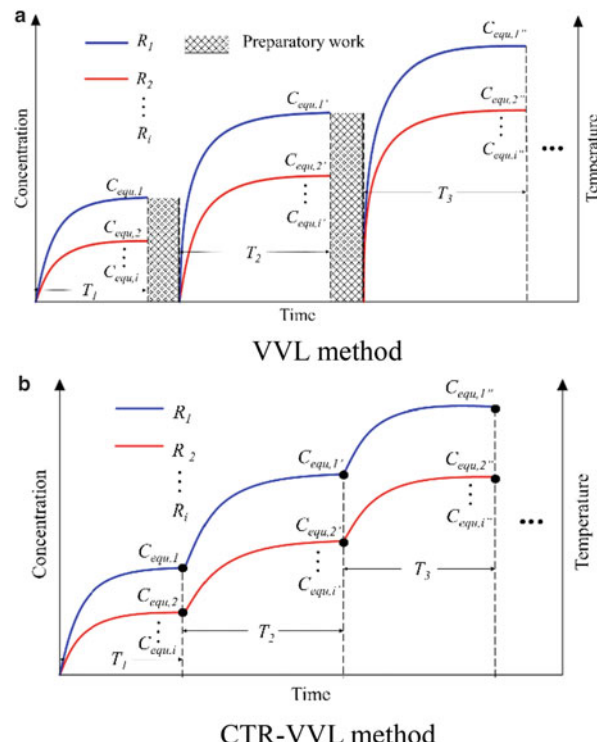
Variable Volume Loading Method (VVL). Xiong et al. (2011a) developed a convenient and rapid method for simultaneously measuring C_0 and K of formaldehyde and other aldehydes in building materials. In this method, the building material is placed in the closed chamber where it freely emits until equilibrium is reached, as shown in Fig. 12a. Then multiple equilibria are formed by changing the volumetric air/material phase ratio, and the gas-phase concentration in the chamber air at equilibrium is measured. A regression method can be applied by using more than two sets of experiments with different volumetric air/material phase ratios (designated as R_i , $i = 1, 2, \dots$). The regression formula is:

$$\frac{1}{C_{\text{equ},i}} = \frac{1}{C_0}R_i + \frac{K}{C_0}, \quad (i = 1, 2, \dots) \quad (35)$$

where $C_{\text{equ},i}$ is the equilibrium VOC concentration in the chamber during the i th period, $\mu\text{g}/\text{m}^3$, $R_i (= V/V_m)$ is the different ratio of chamber volume (V) to material volume (V_m).

Thus, C_0 and K can be obtained from the slope and intercept of the regression line by applying Eq. (35) to the experimental data. This method has the following features: (1) it requires a relatively short experimental time (less than 24 h for the cases studied); and (2) is convenient for routine measurement. It should be pointed out that the proposed method does not consider the chemical state of the formaldehyde and VOCs in the building material. In addition, it is also only applicable for homogeneous building materials.

Fig. 12 Schematic diagrams of the (a) VVL and (b) CTR-VVL methods.
 (Reprinted from Liu et al. (2015a), Copyright 2015, with permission from Elsevier)



CTR-VVL Method. Based on the VVL method, a CTR-VVL method was proposed by Liu et al. (2015a) to simultaneously measure K and C_0 . By linearly fitting $C_{equi,i}$ and R_i using Eq. (35), C_0 and K can be obtained from the slope and intercept. In an airtight space, the equilibrium VOC concentrations of the same material are distinct at different temperatures. Based on the emission characteristics of formaldehyde, for an identical piece of material and corresponding to a fixed R_i , continuous measurements of the equilibrium concentrations of formaldehyde were made at temperature ranging from low to high. The environmental chamber was not opened until all measurements of one R_i were completed under multiple sets of temperatures. The measurements of another R_i began when the background concentration fell below the limit. This experimental method is known as the CTR-VVL method, with a schematic diagram shown in Fig. 12b. There are several advantages compared with the VVL method: (1) An identical piece of material is tested under multiple working conditions to reduce the measuring error as well as the material consumption; and (2) CTR-VVL method sets the previous equilibrium concentration as the initial environmental concentration of the following temperature condition, which accelerates the process to reach the equilibrium concentration.

Rapid and Accurate Measurement Method

The aforementioned measurement methods are used for the determination of one or two emission parameter(s), but are not able to measure three key parameters simultaneously. Based on the work performed by Xu and Zhang (2003, 2004) and Deng and Kim (2004), a series of rapid and accurate methods to simultaneously measure the three key parameters have been developed, and are introduced as follows:

A Simple Method to Measure C_0 , K , and D Simultaneously. This method was developed by Wang and Zhang (2009) to determine C_0 under conditions similar to those in common indoor environments, together with K and D . The tested materials are placed in an airtight environmental chamber where the air is well mixed. A water-bath jacket is used to control the air temperature in the chamber. The materials undergo a multi-sorption/emission process and the instantaneous formaldehyde concentration in the chamber is recorded. At equilibrium, after the emission or sorption process, the following equation can be derived:

$$(C_{a,0} - C_{\text{equ}}) \cdot V/V_m = K \cdot C_{\text{equ}} - C_0 \quad (36)$$

where $C_{a,0}$ is the initial formaldehyde concentration in the chamber, $\mu\text{g}/\text{m}^3$, and C_{equ} is the equilibrium formaldehyde concentration in the chamber after an emission or sorption process, $\mu\text{g}/\text{m}^3$, V is the volume of environmental chamber, m^3 , V_m is the volume of tested material, m^3 .

If a series of $C_{a,0}$ and C_{equ} are measured, the parameters K and C_0 can be obtained by linear regression. Then D can be obtained by fitting the concentration at the emission stage into a mass-transfer-based model developed by Xu and Zhang (2003). Thus, all three key emission characteristic parameters, C_0 , K , and D , can be determined in one experiment. Because only D is determined by nonlinear least-squares regression, the relative error of regression can be decreased.

This study indicated that the room temperature sorption/emission method is practical to measure C_0 , D , and K with the important advantages of the experimental system and the measuring procedure being simple. Also, the method simultaneously determines the three key parameters of dry building materials in a short time (about 7 days). However, as the peak concentration after injection is hard to detect, the measurement accuracy will be affected.

C-History Method. This method focuses on the emission process of VOCs from some building materials in a closed chamber. Because of the shortcomings for the aforementioned methods, Xiong et al. (2011b) developed a novel method to rapidly and simultaneously determine C_0 , D , and K of formaldehyde and VOCs in building materials.

Based on several assumptions widely adopted in previous studies, the analytical solution describing VOC emission is:

$$C_a(t) = \frac{C_0\beta}{K\beta + 1} + 2C_0\beta \sum_{n=1}^{\infty} \frac{\sin q_n}{q_n A_n} e^{-DL^{-2}q_n^2 t} \quad (37)$$

with

$$A_n = (K\beta - q_n^2 K B_i m^{-1} + 1) \cos q_n - (1 + 2 K B_i m^{-1}) q_n \sin q_n, \quad (n = 1, 2, \dots) \quad (38)$$

where C_a is the formaldehyde concentration in chamber air, $\mu\text{g}/\text{m}^3$, $\beta = AL/V$, A is the source emission area of the material, m^2 , L is the half thickness of the building material, m , V is the volume of chamber, m^3 , $B_i m$ is the Biot number for heat transfer ($= h_m L/D$); h_m is the convective mass transfer coefficient, m/s , and q_n are the positive roots of

$$\frac{\tan q_n}{q_n} = \frac{1}{q_n^2 K B_i m^{-1} - K \beta}, \quad (n = 1, 2, \dots) \quad (39)$$

When the emission process reaches the equilibrium state, the equilibrium chamber VOC concentration, C_{equ} , can be represented as:

$$C_{\text{equ}} = \frac{C_0 \beta}{K \beta + 1} \quad (40)$$

For the infinite exponential series of Eq. (37), the terms decay very fast. Therefore, for a sufficiently long emission time, t , only the first term ($n = 1$) is significant, meaning that:

$$\ln \left(\frac{C_{\text{equ}} - C_a(t)}{C_{\text{equ}}} \right) = -DL^{-2} q_1^2 t + \ln \left(-\frac{2(K\beta + 1) \sin q_1}{q_1 A_1} \right) \quad (41)$$

where q_1 is the first root of Eq. (39), and A_1 is the first term of A_n .

If we denote the slope and intercept of Eq. (41) as SL and INT, this equation can be rewritten as:

$$\ln \left(\frac{C_{\text{equ}} - C_a(t)}{C_{\text{equ}}} \right) = -SL \cdot t + INT \quad (42)$$

where SL and INT are both functions of D and K .

Therefore, if the VOC concentration in the chamber versus time is treated as the form of Eq. (42), the SL and INT can be obtained by linear curve fitting. The two parameters D and K can be obtained directly because they are functions of SL and INT, and we have two equations with two unknown parameters. Combining Eq. (40) and the known value of K , C_0 can be calculated. Since the main characteristic of this method is to apply the concentration history of VOCs in a closed chamber, it is called the C-history method.

Compared to the available methods of determining the three parameters described in the literature, this approach has the following salient features: (1) The three parameters can be simultaneously obtained; (2) it is time-saving, generally taking

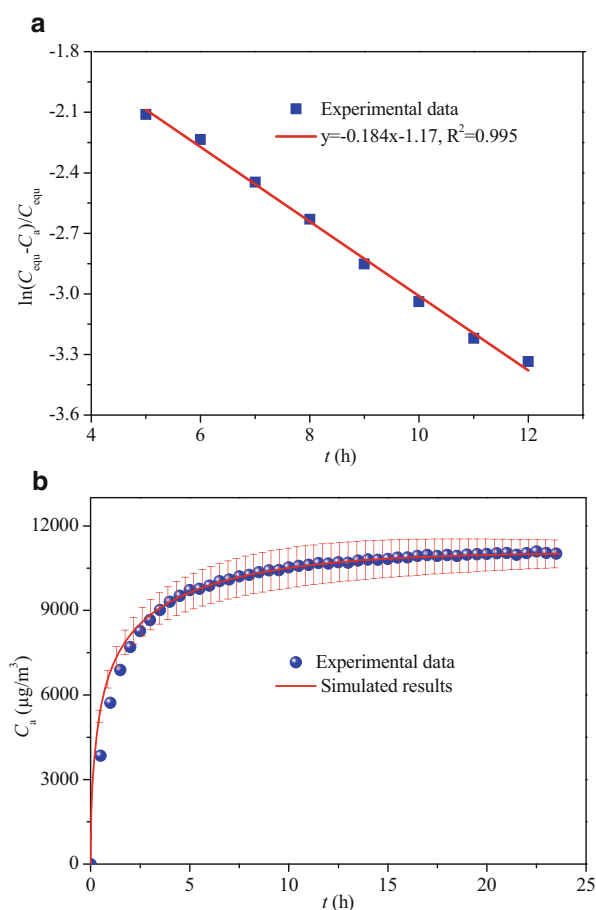
less than 3 days for the cases studied; and (3) the maximum relative standard deviations of the measured C_0 , D , and K are all less than 10%, which are acceptable for engineering applications.

The results using C-history method to chamber formaldehyde concentration data are shown in Fig. 13.

In the application of the proposed C-history method, the choice of time interval by using Eq. (42) to fit experimental data is very important. Further analysis reveals that when the test period is within the linear region (i.e., $t_1 < t < t_2$, $t_1 = 0.125 L^2/D$, $t_2 = 1.50 L^2/D$), then Eq. (42) can be rationally applied.

In this method, considering the VOC concentration in a closed chamber should be sampled multiple times, it is required that chamber volume should be not too small, otherwise multiple sampling might destroy the formaldehyde/VOC mass conservation in the closed chamber, which would result in deviations of measured parameters.

Fig. 13 Results of (a) linear fitting applying Eq. (42) for MDF1, and (b) comparison between simulated results and closed chamber experimental data for formaldehyde of MDF1. (Reprinted from Xiong et al. (2011b), Copyright 2011, with permission from American Chemical Society)



Ventilated-Chamber C-History Method. In order to overcome the problems in C-history method, Huang et al. (2013) developed a novel method, the ventilated-chamber C-history method, to rapidly and accurately measure the three emission characteristic parameters.

This method involves two physical processes: the building material first emits formaldehyde/VOCs in a chamber under airtight conditions until equilibrium is reached; then, clean air is introduced into the chamber, causing the decrease of the concentration in the chamber. The latter process is regarded as emission in a ventilated chamber ($N > 0$). The concentration curve versus time of the chamber formaldehyde/VOC concentration (C_a) during the two processes is shown in Fig. 14.

Based on mass-transfer analysis presented by Deng and Kim (2004) and Xiong et al. (2011b), an analytical solution to the whole physical process can be derived as:

$$\ln \frac{C_a(t)}{C_{\text{equ}}} = \text{SL} \cdot t^* + \text{INT} \quad (43)$$

$$\text{SL} = -DL^{-2}q_1^2 \quad (44)$$

$$\text{INT} = \ln \left(2\alpha \cdot \frac{\cos q_1 - KBi_m^{-1}q_1 \sin q_1}{G_1} \right) \quad (45)$$

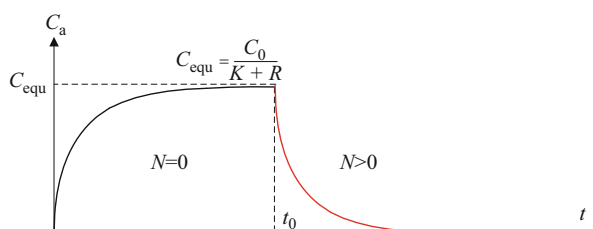
with the mass conservation relationship:

$$C_{\text{equ}} = \frac{C_0}{K + R_v} \quad (46)$$

where t^* is defined as $t-t_0$, representing the emission time under ventilated conditions, C_a is the formaldehyde/VOC concentration in chamber air, $\mu\text{g}/\text{m}^3$, C_{equ} is the equilibrium concentration in the chamber air, $\mu\text{g}/\text{m}^3$, Bi_m is the Biot number ($= h_m L/D$); L is the thickness of the tested material, m, h_m is the convective mass transfer coefficient, m/s , R_v ($= V/V_m$) is the ratio of chamber volume (V) to material volume (V_m).

The SL and INT can be obtained by linear curve fitting once the chamber formaldehyde/VOC concentration is treated as the form of Eq. (43). After that, the D and K can be determined directly because there are two Eqs. (44) and (45) containing the two unknown parameters (D and K). Combining the determined K and Eq. (46), C_0 can be calculated.

Fig. 14 Formaldehyde/VOC concentration in chamber air in two process steps.
(Reprinted from Huang et al. (2013), Copyright 2013, with permission from Elsevier)



For small chamber tests, the ventilated-chamber C-history method is more suitable than the C-history method, and some commonly used measurement instruments (e.g., GC/MS, HPLC) can be applied. In addition, the proposed method can be very time-saving and accurate, with an experimental time of less than 12 h and R^2 ranging from 0.96 to 0.99 for the cases studied, because it is not necessary to reach emission equilibrium in the ventilated chamber for linear regression.

Improved C-History Method. Both types of C-history methods (using either closed or ventilated chambers) mentioned above require the emission time (t) within a specific range, which may prolong experimental time and reduce method accuracy. In order to overcome this limitation, Zhang et al. (2018) propose an improved C-history method based on the full analytical solution of the mass-transfer model describing the VOC emission process.

For the ventilated chamber C-history method, the analytical solution of the mass-transfer model describing emission process of the targeted compound during the ventilated chamber emission process is

$$\frac{C_a(t)}{C_{\text{equ}}} = 2\alpha \sum_{n=1}^{\infty} \frac{\cos q_n - KBi_m^{-1} q_n \sin q_n}{G_n} e^{-DL^{-2}q_n^2 t} \quad (47)$$

and q_n are the positive roots of

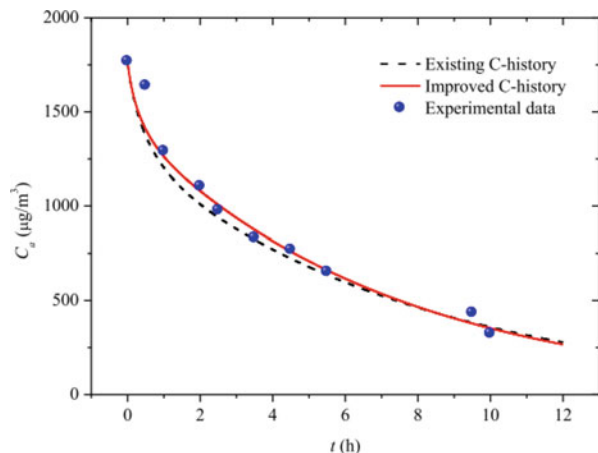
$$q_n \tan q_n = \frac{\alpha - q_n^2}{K\beta + (\alpha - q_n^2)KBi_m^{-1}}, \quad (n = 1, 2, \dots) \quad (48)$$

where C_a is the VOC concentration in chamber air, $\mu\text{g}/\text{m}^3$, C_{equ} is the equilibria concentration in the chamber air, $\mu\text{g}/\text{m}^3$, Bi_m is the Biot number ($= h_m L/D$); L is the thickness of the tested material, m, h_m is the convective mass transfer coefficient, m/s.

As C_{equ} can be directly measured in the closed chamber and h_m can be determined using empirical correlations, the remaining unknown parameters in Eq. (47) are D and K . The Levenberg-Marquardt algorithm is chosen for the nonlinear fitting in MATLAB. Then, C_0 can be obtained by using Eq. (46). To summarize, this method uses a ventilated chamber to measure a C-history series, and then simultaneously determines C_0 , D , and K . Instead of the simplified solution used in existing methods, the full analytical solution is adopted for determining parameters, meaning that the measured data matching the time interval discussed in previous C-history methods ($t > 0.125 L^2/D$) are also applicable.

Figure 15 shows the comparison between experimental data and simulated results (which are obtained by substituting the emission parameters determined by both methods into Eq. (47)). The simulated results agree well with experiment data, implying both methods are likely accurate enough. Furthermore, results have shown that the improved method is more rapid and accurate than the existing methods.

Fig. 15 Comparison between the experimental data and simulated results obtained using the improved C-history method. (Reprinted from Zhang et al. (2018), Copyright 2018, with permission from Elsevier)



Measurement methods for the three key emission parameters are listed in Table 4, with a brief introduction to the characteristics of each method.

Correlations Between Model Parameters and Physical/Chemical Properties

The Initial Emittable Concentration, C_0

The initial emittable concentration of formaldehyde (C_0) in building material has been found to be much lower than the concentration measured by the perforator method (C_{total}) at room temperature (Wang and Zhang 2009). Xiong and Zhang (2010) found that the C_0 at room temperature is far less than the value measured by the perforator method recommended by the Chinese National Standard GB/T 17657-1999, which measures the total concentration of formaldehyde in medium density board. This means most of formaldehyde in the building material cannot be emitted at room temperature.

Heterogeneous adsorption theory of porous media is applied to explain the above phenomena by statistical physics (Huang et al. 2015). The emission of formaldehyde and VOCs from building materials is mainly a physical process for short-term emissions. From the microscopic perspective, the formaldehyde and VOC molecules are bonded to the material surface by adsorption, and a molecule is emittable only when the kinetic energy of this molecule is high enough to overcome the bonding forces, that is, to overcome an energy barrier, the adsorption energy. The sum of these molecules constitutes the initial emittable concentration (C_0), which is clearly lower than the total concentration (C_{total}). Zhou et al. (2016) systematically analyzed the multi-scale desorption mechanism of VOCs, and then proposed the mathematical characterization of the distribution law of adsorption potential in porous building materials. An analytical formula for the distribution of multiple initial emittable concentrations was derived based on the nonuniform desorption criterion.

Table 4 Measurement methods developed for three key emission parameters

Parameter(s) to obtain	Description	Features, limitations, and comments	References
C_0	Fluidized-bed desorption method (FBD)	<ul style="list-style-type: none"> • Only several hours were required • Complicated experimental system and changed material structure 	Cox et al. (2001a)
	Multi-flushing extraction method	<ul style="list-style-type: none"> • Simple experimental system • Long experimental time and changed material structure 	Smith et al. (2009)
	Non-fitting method	<ul style="list-style-type: none"> • Determining parameters C_0 and D • Standard deviation can be estimated without any assumption on distribution of experimental errors • K is not determined 	Li (2013)
D_m	Cup method	<ul style="list-style-type: none"> • D is overestimated and only one VOC can be measured at one time 	Kirchner et al. (1999)
	CLIMPAQ method	<ul style="list-style-type: none"> • Several VOCs can be tested at a time • External convective mass transfer resistance is ignored 	Meininghaus et al. (2000)
	Two-chamber method	<ul style="list-style-type: none"> • Determines D and K simultaneously • The external convective mass transfer resistance is ignored, causing an underestimation of D 	Bodalal et al. (2000)
	Microbalance method	<ul style="list-style-type: none"> • D_m and K simultaneously obtained • Suitable for relatively uniform material • Also neglects the external convective mass transfer process 	Cox et al. (2001b)
	Inverse method	<ul style="list-style-type: none"> • Based on Deng and Kim's model (2004) • Cannot solve three key parameters at the same time 	Li and Niu (2005)
K	Headspace method	<ul style="list-style-type: none"> • Necessary to remove the VOC in building material prior to experiment 	Tiffonnet et al. (2002)
	Multi-emission/flush regression method (MEFR)	<ul style="list-style-type: none"> • Two parameters (C_0, K) are measured simultaneously • Simple experimental system, easy to perform, high precision • Rather time-consuming due to several emission/flushing cycles 	Xiong et al. (2009)
	Variable volume loading method (VVL)	<ul style="list-style-type: none"> • Short experimental time, high precision, two parameters (C_0, K) simultaneous measured 	Xiong et al. (2011a)
	CTR-VVL method	<ul style="list-style-type: none"> • Short experimental time (less than 24 h), convenient for routine measurement • Only applicable for homogeneous building materials. 	Liu et al. (2015a)
Rapid for all three	Multi-sorption/emission regression method	<ul style="list-style-type: none"> • Measuring the parameters C_0, D_m, and K • Experiments take about 7 days • Hard to detect the peak concentration after injection, affecting the accuracy 	Wang and Zhang (2009)

(continued)

Table 4 (continued)

Parameter(s) to obtain	Description	Features, limitations, and comments	References
	C-history method	<ul style="list-style-type: none"> • Obtaining C_0, D_m, and K simultaneously by linear regression • Time-saving, three parameters simultaneously obtained, high precision • Large chamber volume is required due to multiple sampling 	Xiong et al. (2011b)
	Ventilated-chamber C-history method	<ul style="list-style-type: none"> • Two emission processes (closed and ventilated) • Three parameters simultaneously obtained, relatively high precision, without the limit of chamber volume • Rather time-consuming due to two emission stages 	Huang et al. (2013)
	Improved C-history method	<ul style="list-style-type: none"> • Three key parameters obtained simultaneously, high measurement precision without emission time interval limitation 	Zhang et al. (2018)

The Diffusion Coefficient, D

From the mesoscale perspective, most building materials are porous media. Therefore, the mesoscale structure plays an important role in the diffusion coefficient of VOC inside the pores of the material.

Treybal (1981) found that surface diffusion is several orders of magnitude smaller than molecular diffusion and Knudsen diffusion, and the contribution of surface diffusion to mass transfer can be ignored under this condition. Carniglia (1986) proposed a model to calculate the effective diffusion coefficient (D_e) by simultaneously considering the contribution of molecular and Knudsen diffusion and the microstructure parameters. The parameters ε and τ can be directly calculated using the data from mercury intrusion porosimetry (MIP) experiments:

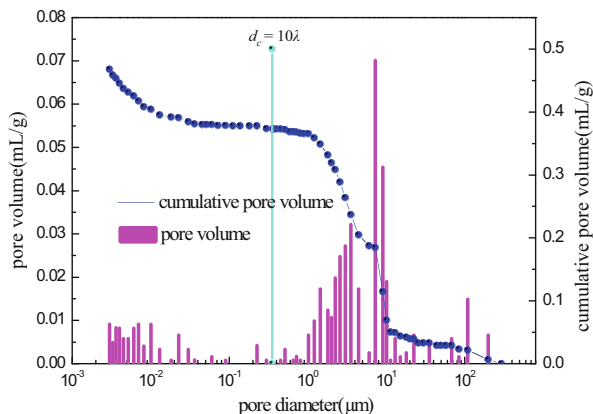
$$D_e = D_r \frac{\varepsilon}{\tau} \quad (49)$$

where ε is the porosity; τ is the tortuosity factor; and D_r is the mean (reference) diffusion coefficient in the porous material, m^2/s .

Blondeau et al. (2003) developed a parallel pore model to calculate D_r by assuming that the pores involve many parallel connections. Seo et al. (2005) used a mean pore model to calculate D_r by simplifying all types of pores as an average pore with equivalent diameter.

In many cases, neither treatment characterizes the features of diffusion paths in porous materials very well, resulting in large errors. By virtue of an MIP experiment, a side face image of REV (representative elementary volume) in a piece of fiberboard is observed by scanning electron microscope (shown in Fig. 16); it was found that

Fig. 16 Pore size distribution of a medium-density fiberboard. (Reprinted from Xiong et al. (2008), Copyright 2008, with permission from Elsevier)



the connection between the macro- and mesopores in a REV is in series. The pore size distribution of porous building materials shows that its internal structure conforms to the fractal theory, which was proposed by Mandelbrot in 1967. The pore size distribution of several kinds of fiberboard and particleboard was observed by mercury porosimetry, showing that their fractal dimension conforms to the fractal criterion. Based on the fractal theory and mercury porosimetry, a macro-meso two-scale model was proposed by Xiong et al. (2008) to determine D_r assuming that the macro- and mesopores are connected physically, thus the D_r can be derived as:

$$\frac{1}{\varepsilon D_r} = \frac{\alpha^2}{\varepsilon_1 D_1} + \frac{(1 - \alpha)^2}{\varepsilon_2 D_2} \quad (50)$$

where ε is the total porosity of the material; ε_1 , ε_2 are the porosities of the macro- and mesopores, respectively; d_1 and d_2 are average diameters of the macro- and mesopores, respectively, m; α is defined as $\alpha = \varepsilon_1 d_2^2 / (\varepsilon_1 d_2^2 + \varepsilon_2 d_1^2)$; D_1 is Fick's diffusion coefficient, m^2/s ; and D_2 is transitional diffusion coefficient, m^2/s .

Equation (50) establishes the relationship between mesoscale structure parameters and the macroscale diffusion coefficient. The diffusion process of the VOC inside the pores can be controlled by changing the mesoscale structure. The effective coefficients calculated using this model come within 20% of the values obtained by Qian et al. (2007) from experimental data using the same material.

Zheng et al. (2012) developed a capillary bundle model for gas diffusion through fractal porous media based on fractal characteristics of porous media and rarefied gas effect of small-size pores/capillaries. It is found that the proposed gas-diffusivity model is expressed as a function of micro-structural parameters (the pore area fractal dimension, the tortuosity fractal dimension, porosity, and pore sizes) of porous media.

Liu et al. (2015b) proposed a multistage series-connection fractal capillary-bundle (MSFC) model, which assumed that the variable-diameter capillaries formed by macropores connected in series as the main mass-transfer paths in porous building materials. An analytical solution of D_e was deduced from the MSFC model, which included a detailed description of the fractal structures in porous building materials.

The Partition Coefficient, K

It has been reported that the characteristic parameters D and K are related to the chemical and physical properties of a VOC, for example, the molecular weight (M) and the vapor pressure (P). Based on the experimental data, correlations between diffusion coefficient and molecular weight, partition coefficient and vapor pressure, were separately derived by Bodalal et al. (2001):

$$D = a/M^{n_1} \quad (51)$$

$$K = b/P^{n_2} \quad (52)$$

where, a , b , n_1 , and n_2 are constants for a specific chemical class in target material.

The results indicate that the diffusion coefficient is inversely proportional to the molecular weight. Also, the partition coefficient is inversely proportional to vapor pressure at a given temperature.

Wang et al. (2008) derived a correlation between K and the VOC liquid molar volume based on the theory of adsorption potential, expressed as follows:

$$\ln K = c_1 v_l + c_2 \quad (53)$$

where v_l is the VOC liquid molar volume, and c_1 and c_2 are constants for a specific chemical class in the material.

Liu et al. (2015a) deduced that a dual-scale calculation model of K based on the Dubinin-Radushkevich and Freundlich adsorption theory (Freundlich and Hatfield 1926), respectively, corresponded with micropores and macro-mesopores in porous materials. The model considers several factors that affect the partition coefficient, such as pore scale, porosity, temperature, VOC properties, and other parameters.

Dimensionless Analysis of Characteristic Parameters

Dimensionless analysis is a powerful approach to solving the two aforementioned problems. Xu and Zhang (2003) normalized the equations in Little et al.'s model by using dimensionless analysis without the assumption that h_m is infinitely large. They found that the dimensionless emission rate of VOCs is a function of Bi_m/K and Fo_m , where Bi_m is the Biot number for mass transfer, and Fo_m is the Fourier number for mass transfer. The result reveals general emission characteristics of VOCs from building materials. Based upon their dimensionless analysis, the applicable

condition of Little et al.'s model was derived as: $Fo_m > 10^{-4}$, and $Lt > 35$. Using this condition, the relative error of the emission rate calculated is less than 5%. To simplify the analysis, Bi_m/K , is suggested as the Little number, Lt . The physical meaning of Lt is the ratio of diffusion mass-transfer resistance in material to convective mass-transfer resistance in air with mass transfer expressed as chemical potential or fugacity. This study is the first approach using dimensionless analysis to obtain generalized VOC emission correlations for building materials by fitting the experimental data. For VOC emissions from building materials, the material/air partition coefficient is generally in the range of 10^2 – 10^5 , which results in Lt greater than 10. This means that the emission characteristics are mainly controlled by internal diffusion, and that external convection only occurs during the initial period of the emission process (Xu and Zhang 2003).

Qian et al. (2007) presented a detailed dimensionless analysis of VOC emissions. Based on the associated mass-transfer model, they obtained dimensionless correlations between VOC emission rate and total VOC emission quantity and found that the dimensionless emission rate and total emission quantity are functions of just four dimensionless parameters, Bi_m/K or Lt , Fo_m , the dimensionless air exchange rate (NL^2/D), and the ratio of building material volume to chamber or room volume (AL/V). Using the correlations, the VOC emission rate from dry building materials can be conveniently calculated without having to solve the complicated mass-transfer equations. Thus, it is very simple to estimate VOC emissions for a given condition. The relationship also explicitly explains the impacts of air velocity, load ratio, and air exchange rate on the VOC emission rate.

It should be noted that the correlations of Qian et al. (2007) are applicable only to ventilated conditions. To obtain dimensionless correlations for airtight conditions, Xiong et al. (2011c) derived empirical correlations to predict the dimensionless rate, $E(t)$, based on dimensionless parameters, βK , Fo_m , and Bi_m/K . The predicted correlation is in quite good agreement with the experimental results. Based on the model presented by Little and Hodgson (1996), empirical correlations are derived by Deng et al. (2010) to predict the sorption behavior of VOC in solid material, associated with the dimensionless parameters α , βK , and Fo_m .

Source Control to Reduce the VVOC/VOC Emissions

Compared with other common VOC reduction measures (e.g., ventilation dilution, air purification), source control is a more straightforward and better approach to reduce indoor VOC emission rates or concentrations. Considering that the emission rate or concentration is a function of the three emission parameters C_0 , D , and K , methods for source control are focused on restraining one or more characteristic parameters, as the following examples show:

Yuan et al. (2007) proposed a low diffusive barrier layer (clay/polyurethane composite layer) to reduce emissions. The existence of nanoparticles results in a highly tortuous diffusion path, which greatly reduces D , thus decreases the emission rate. Using a low diffusion-coefficient film as a decorative layer in flooring material,

VOC emissions from flooring material were greatly reduced by He et al. (2010). By lowering the ratio of formaldehyde to urea in the resin, and adding formaldehyde scavengers during the panel manufacturing process, formaldehyde emissions have also been reduced by Roffael (2006).

Influencing Factors on VVOC/VOC Characteristic Parameters

The Initial Emittable Concentration, C_0

Temperature and relative humidity can simultaneously change in indoor environment, which significantly affects the emission rate of formaldehyde and VOCs from building materials. Xiong and Zhang (2010) found that C_0 of formaldehyde in building material changes with environmental conditions, in particular with temperature. A similar phenomenon was investigated by Crawford and Lungu (2011), i.e., that C_0 of styrene from a vinyl ester resin thermoset composite material changed with temperature. To quantify the relationship between the C_0 and environmental temperature, theoretical correlations between the proportion of emittable amount to the total amount ($P = C_0/C_{\text{total}}$) and temperature was obtained by Huang et al. (2015):

$$\ln P \sqrt{T} = -\frac{H_1}{T} + H_2 \quad (54)$$

$$C_0 = \frac{H_3}{\sqrt{T}} \exp\left(-\frac{H_1}{T}\right) \quad (55)$$

where P is the proportion of emittable amount (C_0) to the total amount (C_{total}), T is the temperature, K, $H_3 = C_{\text{total}} \exp(H_2)$, H_1 and H_2 are constants independent of temperature and are related to the physical properties of the material-formaldehyde combinations.

The derived correlations (Eqs. (54) and (55)) quantitatively establish the relationship between P , C_0 , and T for formaldehyde emissions from building materials. When the parameters H_1 and H_2 (or H_3) are obtained from available results, the derived correlations can be used to predict P and C_0 at other temperatures. This is very helpful and should be useful for engineering applications.

Linear curve fitting by applying Eq. (54) to the experimental data of formaldehyde emissions at different temperatures, as well as data from previous research (Huang et al. 2013) is shown in Fig. 17. The results indicate that both R^2 are about 0.97, demonstrating a high accuracy.

Prior studies generally focused on the single effect of temperature or relative humidity, and the combined effect was not considered. Xiong et al. (2016) investigated the comprehensive influence of temperature and relative humidity on the C_0 and on the emission rate of pollutants from building materials, and derived correlations between C_0 and combined environmental factors theoretically, or:

Fig. 17 Comparison of theoretical correlations and experimental data. (Reprinted from Huang et al. (2015), Copyright 2015, with permission from American Chemical Society)

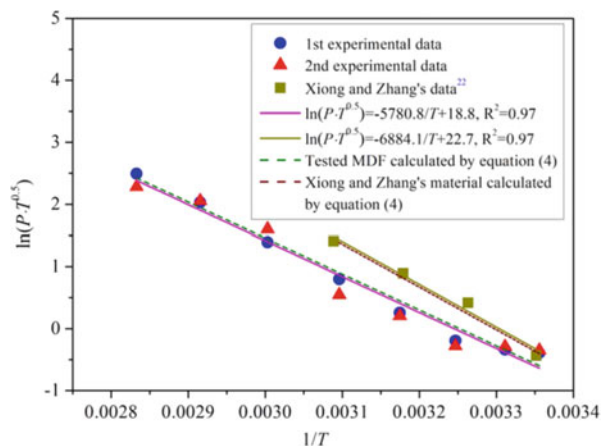
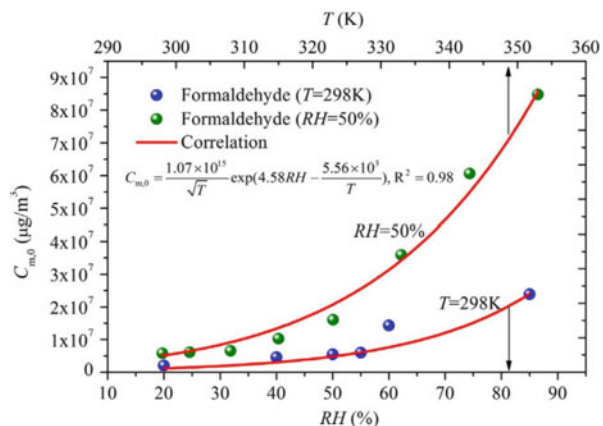


Fig. 18 The correlation between C_0 and T , RH for formaldehyde emissions from medium density fiberboard. (Reprinted from Xiong et al. (2016), Copyright 2016, with permission from Elsevier)



$$C_0 = \frac{H_1}{\sqrt{T}} \exp \left(H_2 \cdot RH - \frac{H_3}{T} \right) \quad (56)$$

where T is the environmental temperature, K ; RH is the relative humidity; and H_1 , H_2 , and H_3 are positive constants, which do not change with temperature and relative humidity, but are only related to the physical and chemical properties of the material-pollutant combinations.

Regression results of the correlation between C_0 and the comprehensive effect are shown in Fig. 18. The fitting degree (R^2) is 0.98, indicating acceptable regression accuracy.

The Diffusion Coefficient, D

Diffusion of VOCs in building materials is a function of molecular motion, so the diffusion coefficient is strongly dependent on temperature. For VOC diffusion in porous materials, when molecular diffusion is dominant, Deng et al. (2009) derived a theoretical correlation to characterize the influence of temperature on D :

$$D = H_1 T^{1.25} \exp\left(-\frac{H_2}{T}\right) \quad (57)$$

where H_1 and H_2 are positive constants, which are not related to temperature, but are only related to the physical and chemical properties of the material-pollutant combinations.

Calculations using Eq. (57) agree well with experimental data for four types of building materials. Huang et al. (2015) measured the C_0 , D , and K of formaldehyde from a medium density fiberboard (MDF) at eight different temperatures, and found that if the temperature is below 50 °C, the D increases with increasing T , while if the temperature is above 50 °C, the D may decrease with the increase of T . The possible explanation given by Huang et al. (2015) is that when the temperature is relatively high, the diffusion may change from Fickian diffusion to transition diffusion or Knudsen diffusion, resulting in the decrease of D .

The Partition Coefficient, K

The Arrhenius relation is used for some sorption transport phenomena (e.g., chemical engineering sorption separation) to characterize the impact of temperature on the partition coefficient (Ruthven et al. 1984):

$$K = K_0 \exp\left(-\frac{U}{RT}\right) \quad (58)$$

where U is internal energy of desorption; R is the universal gas constant, and K_0 is a constant independent of temperature.

Based on the Langmuir equation, Zhang et al. (2007) derived a correlation between partitioning coefficient and temperature as follow:

$$K = H_1 T^{0.5} \exp\left(-\frac{H_2}{T}\right) \quad (59)$$

where H_1 and H_2 are positive constants, which are not dependent on temperature, but are only related to the physical and chemical properties of the material-pollutant combinations.

The correlation derived by Zhang et al. (2007) is similar to the Arrhenius equation. However, the correlation derived in this study has one more term, $T^{0.5}$. Experiments for formaldehyde emissions from four types of building materials at

different temperatures ranging from 18 °C to 50 °C were performed by Zhang et al. (2007), and the results validated the reliability of the temperature correlation. For the experiments conducted by Huang et al. (2015), it was found that if the temperature is below 50 °C, the K decreases with a decrease of T , while if the temperature is above 50 °C, K may increase with an increase of T . The mechanistic reason for explaining this phenomenon requires further study.

Conclusions

Investigating the source/sink characteristics of VVOCs and VOCs in building materials is a prerequisite for understanding emission mechanisms to achieve improved source control of indoor pollutants. This chapter reviewed research on predictive models for VVOC/VOC source/sink characteristics and highlighted methods for measuring the source emission parameters of indoor materials, providing the foundation for comprehending the mass-transfer principle and improving indoor air quality.

There remain many issues that require further investigation, including: (1) When multiple source or sink materials exist simultaneously in indoor environments, the emission/sorption behaviors from/to materials become more complicated, which requires more complex models to describe the mass-transfer process; (2) more attention should be paid to long-term contaminant emission behaviors and relevant modeling; (3) the emission characteristics of VOCs from human skin due to the use of personal care products or chemical reactions with chemicals in ambient air; and (4) the mechanisms underlying the influence of temperature, humidity, and timing on key emission characteristic parameters, especially factors varying in a wide range.

Besides the building materials, residents also contribute to indoor air pollution. The metabolic products of the human body are generally released into ambient air through the skin or breath, and may react with oxidized media in the environment to generate new pollutants (e.g., VOCs). The impact of human occupancy on the indoor environment is far more important than initially imagined and further investigations are likely to uncover additional impacts. Research on the reaction between the human body and the ambient air may significantly enrich the knowledge of VOC mass transfer behavior in the indoor environment.

Cross-References

- [Very Volatile Organic Compounds \(VVOCs\)](#)

Nomenclature

A	Source emission area, m ²
Bi_m	Biot number for mass transfer
C	Material-phase contaminant concentration, µg/m ³

C_0	Initial emittable contaminant concentration, $\mu\text{g}/\text{m}^3$
C_1	Equilibrium contaminant concentration in the primary chamber, $\mu\text{g}/\text{m}^3$
C_2	Equilibrium contaminant concentration in the secondary chamber, $\mu\text{g}/\text{m}^3$
C_a	Contaminant concentration in chamber air, $\mu\text{g}/\text{m}^3$
$C_{a,0}$	Initial chamber contaminant concentration, $\mu\text{g}/\text{m}^3$
C_{ad}	Adsorbed-phase concentration of VOC in porous media, $\mu\text{g}/\text{m}^3$
C_{equ}	Equilibrium contaminant concentration in the chamber, $\mu\text{g}/\text{m}^3$
$C_{equ,i}$	Equilibrium contaminant concentration in the chamber during the i th period, $\mu\text{g}/\text{m}^3$
C_g	Gas-phase concentration of VOC in porous media, $\mu\text{g}/\text{m}^3$
C_{in}	Inlet contaminant concentration, $\mu\text{g}/\text{m}^3$
C_m	Material-phase contaminant concentration in the liquid film, $\mu\text{g}/\text{m}^3$
C_s	Material-phase contaminant concentration in the substrate, $\mu\text{g}/\text{m}^3$
C_{sat}	Saturation concentration of contaminant at given temperature, $\mu\text{g}/\text{m}^3$
C_{total}	The total contaminant concentration in the material, $\mu\text{g}/\text{m}^3$
D	Diffusion coefficient, m^2/s
D_1	Fick's diffusion coefficient, m^2/s
D_2	Transitional diffusion coefficient, m^2/s
d_1	Average diameter of macropores, m
d_2	Average diameter of mesopores, m
D_{ad}	Adsorbed-phase diffusion coefficient of VOC in porous media, m^2/s
D_e	Effective diffusion coefficient in the porous material, m^2/s
D_g	Effective gas-phase diffusion coefficient of VOC within porous media, m^2/s
D_m	Effective diffusion coefficient in the liquid film, m^2/s
D_r	Mean (reference) diffusion coefficient in the porous material, m^2/s
D_s	Diffusion coefficient in the substrate, m^2/s
Fo_m	Mass transfer Fourier number
$g(x,t)$	Time and space dependent VOC generation/elimination due secondary source/sink behavior, $\mu\text{g}/(\text{m}^3 \cdot \text{s})$
h_m	Convective mass transfer coefficient, m/s
K	Partition coefficient
k_a	Adsorption rate constant, $1/\text{s}$
k_d	Desorption rate constant, m/s
L	Thickness of the material, m
L_f	Paint film thickness
m	Steady-state mass flux of contaminant through the material, $\mu\text{g}/\text{s}$
M	Contaminant mass on sink surface, $\mu\text{g}/\text{m}$
M_0	Initial emittable contaminant mass, μg
M_s	Certain mass of contaminant injected in headspace method, μg
n	Total number of emission cycles
P	Proportion of emittable contaminant amount in the total amount
Q	Ventilation rate, m^3/s
R	Universal gas constant
R_c	Reaction rate constant, $1/\text{s}$

R_v	Ratio of chamber volume to the material volume
S_f	Saturation of VOC liquid in the pores of paint film
T	Temperature, K
t	Emission time (s)
U	Internal energy of desorption
v_l	Contaminant liquid molar volume
V	Volume of environmental chamber, m^3
x	Linear distance, m
y	Initial contaminant concentration in the high-concentration chamber, $\mu\text{g}/\text{m}^3$
y_1	Concentration in the high-concentration chamber, $\mu\text{g}/\text{m}^3$
y_2	Concentration in the high-concentration chamber, $\mu\text{g}/\text{m}^3$

Greek Letters

α	Dimensionless air exchange rate
β	Ratio of material volume to chamber volume
ε	Porosity of porous media
ε_1	Porosity of the macropores
ε_2	Porosity of the mesopores
τ	Tortuosity factor
φ_f	Porosity of the paint film

References

- Altinkaya SA (2009) Predicting emission characteristics of volatile organic compounds from wet surface coatings. *Chem Eng J* 155:586–593
- Blondeau P, Tiffonnet AL, Damiani A et al (2003) Assessment of contaminant diffusivities in building materials from porosimetry tests. *Indoor Air* 13:302–310
- Bodalal A, Zhang JS, Plett EG (2000) A method for measuring internal diffusion and equilibrium partition coefficients of volatile organic compounds for building materials. *Build Environ* 35: 101–110
- Bodalal A, Zhang J, Plett E et al (2001) Correlations between the internal diffusion and equilibrium partition coefficients of volatile organic compounds (VOCs) in building materials and the VOC properties. *ASHRAE Trans* 107:789–800
- Boeglin ML, Wessels D, Henshel D (2006) An investigation of the relationship between air emissions of volatile organic compounds and the incidence of cancer in Indiana counties. *Environ Res* 100:242–254
- Carniglia SC (1986) Construction of the tortuosity factor from porosimetry. *J Catal* 102:401–418
- Clausen PA (1993) Emission of volatile and semivolatile organic compounds from waterborne paints—the effect of the film thickness. *Indoor Air* 3:269–275
- Clausen PA, Laursen B, Wolkoff P et al (1993) Emission of volatile organic compounds from a vinyl floor covering. In: Nagda NL (ed) *Modeling of indoor air quality and exposure*, ASTM STP 1205. American Society for Testing and Materials, Philadelphia, pp 3–13
- Cox SS, Little JC, Hodgson AT (2001a) Measuring concentrations of volatile organic compounds in vinyl flooring. *J Air Waste Manag Assoc* 51:1195–1201
- Cox SS, Zhao D, Little JC (2001b) Measuring partition and diffusion coefficients for volatile organic compounds in vinyl flooring. *Atmos Environ* 35:3823–3830

- Crawford S, Lungu CT (2011) Influence of temperature on styrene emission from a vinyl ester resin thermoset composite material. *Sci Total Environ* 409:3403–3408
- Deng B, Kim CN (2004) An analytical model for VOCs emission from dry building materials. *Atmos Environ* 38:1173–1180
- Deng B, Kim CN (2007) CFD simulation of VOCs concentrations in a resident building with new carpet under different ventilation strategies. *Build Environ* 42:297–303
- Deng B, Yu B, Kim C (2008) An analytical solution for VOCs emission from multiple sources/sinks in buildings. *Chin Sci Bull* 53:1100–1106
- Deng Q, Yang X, Zhang J (2009) Study on a new correlation between diffusion coefficient and temperature in porous building materials. *Atmos Environ* 43:2080–2083
- Deng Q, Yang X, Zhang J (2010) New indices to evaluate volatile organic compound sorption capacity of building materials. *HVAC&R Res* 16:95–105
- Dunn LE (1987) Models and statistical methods for gaseous emission testing of finite sources in well-mixed chambers. *Atmos Environ* 21:425–430
- Freundlich H, Hatfield H (1926) Colloid and capillary chemistry. Methuen & Co, London
- Guo Z (2002a) Review of indoor emission source models. Part 1. Overview. *Environ Pollut* 120: 533–549
- Guo Z (2002b) Review of indoor emission source models. Part 2. Parameter estimation. *Environ Pollut* 120:551–564
- Guo Z, Sparks LE, Tichenor BA et al (1998) Predicting the emissions of individual VOCs from petroleum-based indoor coatings. *Atmos Environ* 32:231–237
- Haghghat F, Huang H (2003) Integrated IAQ model for prediction of VOC emissions from building material. *Build Environ* 38:1007–1017
- Haghghat F, Huang H, Lee C (2005) Modeling approaches for indoor air VOC emissions from dry building materials - a review. *ASHRAE Trans* 111:635–645
- He Z, Wei W, Zhang Y (2010) Dynamic-static chamber method for simultaneous measurement of the diffusion and partition coefficients of VOCs in barrier layers of building materials. *Indoor Built Environ* 19:465–475
- He Z, Xiong J, Kumagai K et al (2019) An improved mechanism-based model for predicting the long-term formaldehyde emissions from composite wood products with exposed edges and seams. *Environ Int* 132:105086
- Hu H, Zhang Y, Wang X et al (2007) An analytical mass transfer model for predicting VOC emissions from multi-layered building materials with convective surfaces on both sides. *Int J Heat Mass Transf* 50:2069–2077
- Huang H, Haghghat F (2002) Modelling of volatile organic compounds emission from dry building materials. *Build Environ* 37:1349–1360
- Huang S, Xiong J, Zhang Y (2013) A rapid and accurate method, ventilated chamber C-history method of measuring the emission characteristic parameters of formaldehyde/VOCs in building materials. *J Hazard Mater* 261:542–549
- Huang S, Xiong J, Zhang Y (2015) Impact of temperature on the ratio of initial emittable concentration to total concentration for formaldehyde in building materials: theoretical correlation and validation. *Environ Sci Technol* 49:1537–1544
- Jie Y, Ismail NH, Isa ZM (2011) Do indoor environments influence asthma and asthma-related symptoms among adults in homes? A review of the literature. *J Formos Med Assoc* 110:555–563
- Jørgensen RB, Dokka TH, Bjørseth O (2000) Introduction of a sink-diffusion model to describe the interaction between volatile organic compounds (VOCs) and material surfaces. *Indoor Air* 10: 27–38
- Kirchner S, Badey JR, Knudsen HN et al (1999) Sorption capacities and diffusion coefficients of indoor surface materials exposed to VOCs: proposal of new test procedures. In: Proceedings of the 8th international conference of indoor air 1999, Edinburg, pp 430–435
- Kumar D, Little JC (2003a) Single-layer model to predict the source/sink behavior of diffusion-controlled building materials. *Environ Sci Technol* 37:3821–3827
- Kumar D, Little JC (2003b) Characterizing the source/sink behavior of double-layer building materials. *Atmos Environ* 37:5529–5537

- Langmuir I (1916) The constitution and fundamental properties of drys and wets. Part I. *J Am Chem Soc* 38:2221–2295
- Lee CS (2003) A theoretical study on VOC source and sink behavior of porous building material. Ph.D. thesis, Concordia University
- Lee CS, Haghigat F, Ghaly WS (2005) A study on VOC source and sink behavior in porous building materials - analytical model development and assessment. *Indoor Air* 15:183–196
- Lee CS, Haghigat F, Ghaly WS (2006) Conjugate mass transfer modeling for VOC source and sink behavior of porous building materials: when to apply it? *J Build Phys* 30:91–111
- Li M (2013) Robust nonfitting way to determine mass diffusivity and initial concentration for VOCs in building materials with accuracy estimation. *Environ Sci Technol* 47:9086–9092
- Li F, Niu J (2005) Simultaneous estimation of VOCs diffusion and partition coefficients in building materials via inverse analysis. *Build Environ* 40:1366–1374
- Li F, Niu J (2007) Control of volatile organic compounds indoorsd development of an integrated mass-transfer-based model and its application. *Atmos Environ* 41:2344–2354
- Li F, Niu J, Zhang L (2006) A physically-based model for prediction of VOCs emissions from paint applied to an absorptive substrate. *Build Environ* 41:1317–1325
- Little JC, Hodgson AT (1996) A strategy for characterizing homogeneous, diffusion-controlled, indoor sources and sinks. In: Characterizing sources of indoor air pollution and related sink effects, ASTM STP 1287. American Society for Testing and Materials, Philadelphia, pp 294–304
- Little JC, Hodgson AT, Gadgil AJ (1994) Modeling emissions of volatile organic compounds from new carpets. *Atmos Environ* 28(2):227–234
- Liu Z, Ye W, Little JC (2013) Predicting emissions of volatile and semivolatile organic compounds from building materials: a review. *Build Environ* 64:7–25
- Liu Y, Zhou X, Wang D et al (2015a) A prediction model of VOC partition coefficient in porous building materials based on adsorption potential theory. *Build Environ* 93:221–233
- Liu Y, Zhou X, Wang D et al (2015b) A diffusivity model for predicting VOC diffusion in porous building materials based on fractal theory. *J Hazard Mater* 299:685–695
- Marquardt DW (1963) An algorithm for least-squares estimation of nonlinear parameters. *J Soc Ind Appl Math* 11:431–441
- Mathews TJ, Hawthorne AR, Thompson CV (1987) Formaldehyde sorption and desorption characteristics of gypsum wallboard. *Environ Sci Technol* 21:629–634
- Meininghaus R, Gunnarsen L, Knudsen HN (2000) Diffusion and sorption of volatile organic compounds in building materialsimpact on indoor air quality. *Environ Sci Technol* 34: 3101–3108
- Murakami S, Kato S, Kondo Y et al (2000) VOC distribution in a room based on CFD simulation coupled with emission/sorption analysis. In: Proceedings of the 7th international conference on air distribution in rooms, Reading, vol 1, pp 473–478
- Murakami S, Kato S, Ito K et al (2003) Modeling and CFD prediction for diffusion and adsorption within room with various adsorption isotherms. *Indoor Air* 13:20–27
- Qian K, Zhang Y, Little JC et al (2007) Dimensionless correlations to predict VOC emissions from dry building materials. *Atmos Environ* 41:352–359
- Roffael E (2006) Volatile organic compounds and formaldehyde in nature, wood and wood based panels. *Holz Roh Werkst* 64:144–149
- Ruthven DM et al (1984) Principles of adsorption and adsorption processes. Wiley, New York, pp 68–69
- Seo J, Kato S, Ataka Y et al (2005) Evaluation of effective diffusion coefficient in various building materials and absorbents by mercury intrusion porosimetry. In: Proceedings of indoor air, Beijing, pp 1854–1859
- Smith JF, Gao Z, Zhang J et al (2009) A new experimental method for the determination of emittable initial VOC concentrations in building materials and sorption isotherms for IVOCs. *Clean Soil Air Water* 37:454–458
- Sparks LE, Guo Z, Chang JC (1999) Volatile organic compound emissions from latex paint – part 1. Chamber experiments and source model development. *Indoor Air* 9:10–17

- Tichenor BA, Guo Z, Dorsey JA (1991a) Emission rates of mercury from latex paints. In: IAQ 91-healthy buildings, American Society of Heating, Refrigerating and Air-Conditioning Engineers, Atlanta, pp 276–279
- Tichenor BA, Guo Z, Dunn JE et al (1991b) The interaction of vapour phase organic compounds with indoor sinks. *Indoor Air* 1:23–35
- Tichenor BA, Guo Z, Sparks LE (1993) Fundamental mass transfer model for indoor air emissions from surface coatings. *Indoor Air* 3:263–268
- Tiffonnet AL, Blondeau P, Amiri O et al (2000) Assessment of contaminant diffusivities in building materials from porosity tests. In: Proceedings of healthy buildings 2000, Espoo, vol 4, pp 199–203
- Tiffonnet AL, Blondeau P, Allard F et al (2002) Sorption isotherms of acetone on various building materials. *Indoor Built Environ* 11:95–104
- Treybal RE (1981) Mass Transfer Operations, 3rd edn. McGraw-Hill Book Company, New York
- Wang X, Zhang Y (2009) A new method for determining the initial mobile formaldehyde concentrations, partition coefficients and diffusion coefficients of dry building materials. *J Air Waste Manage Assoc* 59:819–825
- Wang X, Zhang Y (2011) General analytical mass transfer model for VOC emissions from multi-layer dry building materials with internal chemical reactions. *Chin Sci Bull* 56:222–228
- Wang X, Zhang Y, Zhao R (2006) Study on characteristics of double surface VOC emissions from dry flat-plate building materials. *Chin Sci Bull* 51:2287–2293
- Wang X, Zhang Y, Xiong J (2008) Correlation between the solid/air partition coefficient and liquid molar volume for VOCs in building materials. *Atmos Environ* 42:7768–7774
- Weschler CJ (2009) Changes in indoor pollutants since the 1950s. *Atmos Environ* 43:153–169
- Weschler CJ, Nazaroff WW (2008) Semivolatile organic compounds in indoor environments. *Atmos Environ* 42:9018–9040
- Wolkoff P, Nielsen GD (2001) Organic compounds in indoor air-their relevance for perceived indoor air quality? *Atmos Environ* 35:4407–4417
- Xiong J, Zhang Y (2010) Impact of temperature on the initial emittable concentration of formaldehyde in building materials: experimental observation. *Indoor Air* 20:523–529
- Xiong J, Zhang Y, Wang X et al (2008) Macro-meso two-scale model for predicting the VOC diffusion coefficients and emission characteristics of porous building materials. *Atmos Environ* 42:5278–5290
- Xiong J, Chen W, Smith JF et al (2009) An improved extraction method to determine the initial emittable concentration and the partition coefficient of VOCs in dry building materials. *Atmos Environ* 43:4102–4107
- Xiong J, Yan W, Zhang Y (2011a) Variable volume loading method: a convenient and rapid method for measuring the initial emittable concentration and partition coefficient of formaldehyde and other aldehydes in building materials. *Environ Sci Technol* 45:10111–10116
- Xiong J, Yao Y, Zhang Y (2011b) C-history method: rapid measurement of the initial emittable concentration, diffusion and partition coefficients for formaldehyde and VOCs in building materials. *Environ Sci Technol* 45:3584–3590
- Xiong J, Zhang Y, Huang S (2011c) Characterisation of VOC and formaldehyde emission from building materials in a static environmental chamber: model development and application. *Indoor Built Environ* 20:217–225
- Xiong J, Huang S, Zhang Y (2012) A novel method for measuring the diffusion, partition and convective mass transfer coefficients of formaldehyde and VOC in building materials. *PLoS One* 7:e49342
- Xiong J, Zhang P, Huang S et al (2016) Comprehensive influence of environmental factors on the emission rate of formaldehyde and VOCs in building materials: correlation development and exposure assessment. *Environ Res* 151:734–741
- Xu Y, Zhang Y (2003) An improved mass transfer based model for analyzing VOC emissions from building materials. *Atmos Environ* 37:2497–2505
- Xu Y, Zhang Y (2004) A general model for analyzing single surface VOC emission characteristics from building materials and its application. *Atmos Environ* 38:113–119

- Yan W, Zhang Y, Wang X (2009) Simulation of VOC emissions from building materials by using the state-space method. *Build Environ* 44:471–478
- Yang X, Chen Q, Zhang J et al (2001a) Numerical simulation of VOC emissions from dry materials. *Build Environ* 36:1099–1107
- Yang X, Chen Q, Zhang J et al (2001b) A mass transfer model for simulating VOC sorption on building materials. *Atmos Environ* 35:1291–1299
- Yang X, Chen Q, Zeng J et al (2001c) A mass transfer model for simulating volatile organic compound emissions from “wet” coating materials applied to absorptive substrates. *Int J Heat Mass Transf* 44:1803–1815
- Yu CWF, Kim JT (2013) Material emissions and indoor simulation. *Indoor Built Environ* 22:21–29
- Yuan H, Little JC, Marand E et al (2007) Using fugacity to predict volatile emissions from layered materials with a clay/polymer diffusion barrier. *Atmos Environ* 41:9300–9308
- Zhang Y, Luo X, Wang X et al (2007) Influence of temperature on formaldehyde emission parameters of dry building materials. *Atmos Environ* 41:3203–3216
- Zhang Y, Mo J, Weschler CJ (2013) Reducing health risks from indoor exposures in rapidly developing urban China. *Environ Health Perspect* 121:751–755
- Zhang Y, Xiong J, Mo J et al (2016) Understanding and controlling airborne organic compounds in the indoor environment: mass transfer analysis and applications. *Indoor Air* 26:39–60
- Zhang X, Cao J, Wei J et al (2018) Improved C-history method for rapidly and accurately measuring the characteristic parameters of formaldehyde/VOCs emitted from building materials. *Build Environ* 143:570–578
- Zheng Q, Yu B, Wang S et al (2012) A diffusivity model for gas diffusion through fractal porous media. *Chem Eng Sci* 68(1):650–655
- Zhou X, Liu Y, Song C et al (2016) A study on the formaldehyde emission parameters of porous building materials based on adsorption potential theory. *Build Environ* 106:254–264
- Zhou X, Gao Z, Wang X et al (2020) Mathematical model for characterizing the full process of volatile organic compound emissions from paint film coating on porous substrates. *Build Environ* 182:107062



Source/Sink Characteristics of SVOCs

23

Yili Wu, Jianping Cao, John C. Little, and Ying Xu

Contents

Introduction	696
SVOC Emissions from Source Materials	697
Emission Model	697
Existing Methods for Measuring Key Emission Parameter (y_0)	699
Equilibrium Relationship Between Source Materials and Air	709
Sorption by Sink Materials	713
Sorption Processes and Models	713
Existing Methods for Measuring Key Sorption Parameters (K_s and D)	716
Prediction of the Key Sorption Parameters	720
Sorption to Particles/Dust	726
Interaction Between Gas-Phase SVOCs and Suspended Particles	726
Existing Methods for Measuring Key Sorption Parameter (K_p)	730
Prediction of the Key Sorption Parameter (K_p)	732
Conclusion	735
Cross-References	735
References	735

Y. Wu

Department of Building Science, Tsinghua University, Beijing, China

J. Cao

School of Environmental Science and Engineering, Sun Yat-sen University, Guangzhou, China

J. C. Little

Department of Civil and Environmental Engineering, Virginia Tech, Blacksburg, VA, USA

Y. Xu (✉)

Department of Building Science, Tsinghua University, Beijing, China

Department of Civil, Architectural and Environmental Engineering, The University of Texas at Austin, Austin, TX, USA

e-mail: xu-ying@mail.tsinghua.edu.cn

Abstract

Semivolatile organic compounds (SVOCs) are ubiquitous and persistent in indoor environments. It is important to understand the mechanisms governing their emission, sorption, and transport. This article reviews the source and sink characteristics of SVOCs, including their emission from source materials, sorption to sink surfaces, and sorption to particles or dust, as well as the experimental and modeling methods to determine key parameters that control these processes.

Keywords

SVOC · Emission · Sorption · Modeling, Chamber test

Introduction

Semivolatile organic compounds (SVOCs) are a group of organic compounds with vapor pressures ranging from 10^{-9} Pa to ~ 10 Pa (Weschler and Nazaroff, 2008) and boiling points ranging from 240 °C to 400 °C (WHO 2010). They are extensively used as additives in building materials and consumer products to enhance product performance. For example, polybrominated diphenyl ethers (PBDEs) and phthalate esters are the most typical flame retardants and plasticizers, respectively. Since they are not chemically bound to the polymer matrix, they can slowly emit from source materials to the surrounding environment (Kemmlein et al. 2003; Xu and Little 2006; Xu et al. 2009, 2010). In addition, combustion by-products, such as nicotine and polycyclic aromatic hydrocarbons (PAHs), as well as pesticides and biocides, such as organophosphates, carbamates, and pyrethroids, are also SVOCs.

SVOCs are ubiquitous and persistent in the indoor environment. Because of their low vapor pressure, they tend to partition/sorb onto airborne particles, dust, and interior surfaces, including windows, mirrors, dishware, furniture, clothes, and even human skin (Weschler and Nazaroff 2008; Wang et al. 2010; Nazaroff and Goldstein 2015). Weschler and Nazaroff (2008) showed that if ventilation serves as the only removal mechanism, SVOCs with a moderate sorption capacity can remain indoors for hundreds to thousands of hours, while those with strong sorption capacity can persist for years, so that sinks such as furniture may even become secondary sources.

The presence of SVOCs in indoor environments may lead to significant human exposure through inhalation, ingestion, and dermal uptake. Airborne SVOCs including gas-phase and particle-phase SVOCs are inhaled by residents. Ingestion may occur with intake of dust and food contaminated by SVOCs. Children are the main target for this exposure pathway due to frequent hand-to-mouth contact. Dermal uptake usually results from direct contact with SVOCs on sink surfaces and as a result of SVOC transport from contaminated air directly to skin. Some studies have suggested that longtime exposure to SVOCs will lead to adverse health effects (Shelby 2006). For example, many studies reported that exposure to several kinds

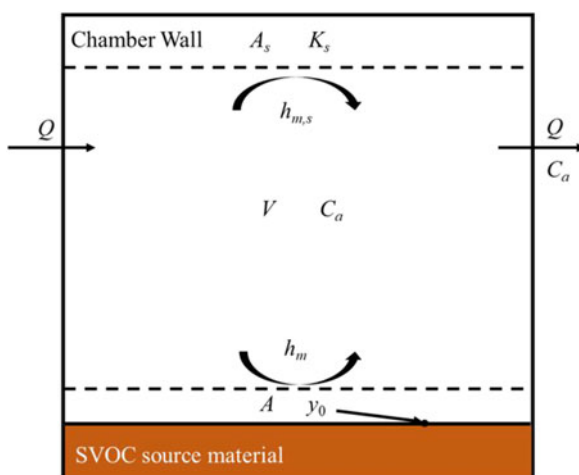
of phthalates including butyl benzyl phthalate (BBzP), di-n-butyl phthalate (DnBP), and di-(2-ethylhexyl) phthalate (DEHP) is associated with irreversible changes in reproductive tract development (Kay et al. 2013, 2014; Zarean et al. 2016; Hoyer et al. 2018). Other serious health concerns such as autism spectrum disorders, disruption of hormones, prenatal mortality, reduced growth and birth weight, allergy and childhood asthma, thyroid function alteration, decreased semen quality, and permanent learning and memory impairment were also found to be associated with phthalate and organophosphate exposure (Meeker and Stapleton 2010; Dishaw et al. 2014; Miodovnik et al. 2014; Ferguson et al. 2016; Hoffman et al. 2017; Zhao et al. 2017). Therefore, it is of great necessity to investigate the emission/sorption behavior (source/sink characteristics) of SVOCs and evaluate the potential human exposure levels and risks.

SVOC Emissions from Source Materials

Emission Model

Similar to (Volatile organic compounds) VOCs, the emission of SVOCs from building materials, consumer products, and articles consist of two processes: molecular diffusion in the source material and surface convective mass transfer to the surrounding air. These processes are illustrated in Fig. 1, with an SVOC source material slab placed in a chamber. Xu and Little (2006) proposed a mathematical model that describes these processes and predicts the emission rate of SVOCs from polymeric materials. In the model, the transient diffusion of SVOCs in the source material is expressed by Fick's second law:

Fig. 1 Schematic of SVOC mass transfer in a chamber (in the absence of suspended particles). (©With permission of Cao et al. 2017)



$$\frac{\partial C(x, t)}{\partial t} = D \frac{\partial^2 C(x, t)}{\partial x^2} \quad (1)$$

where $C(x, t)$ ($\mu\text{g}/\text{m}^3$) is the SVOC material-phase concentration, D (m^2/s) is the material-phase diffusion coefficient, x (m) is the vertical distance from the bottom of the slab, and t (s) is elapsed time. At the beginning, the SVOC concentration is assumed to be uniform throughout the material, which leads to the initial condition:

$$C(x, t) = C_0 \text{ for } t = 0, 0 \leq x \leq L \quad (2)$$

where C_0 ($\mu\text{g}/\text{m}^3$) is the initial material-phase concentration and L (m) is the vertical length of the slab. The boundary condition at the base of the slab is

$$\frac{\partial C(x, t)}{\partial t} = 0 \text{ for } t > 0, x = 0 \quad (3)$$

The boundary condition of the top of the slab is

$$-D \frac{\partial C(x, t)}{\partial x} = h_m(y_0(t) - y(t)) \text{ for } t > 0, x = L \quad (4)$$

where y_0 ($\mu\text{g}/\text{m}^3$) is the SVOC gas-phase concentration in equilibrium with the material phase and immediately adjacent to the slab surface, y ($\mu\text{g}/\text{m}^3$) is the SVOC gas-phase concentration in the chamber air, and h_m (m/s) is the external convective mass-transfer coefficient. An instant partition equilibrium is assumed to exist between the material surface and the air near the surface, or

$$C(x, t) = K_{ma}y_0(t) \text{ for } t > 0, x = L \quad (5)$$

where K_{ma} is the source surface/air partition coefficient.

After emission from the source material, gas-phase SVOCs will sorb to the chamber surfaces, with sorption potentially expressed by Langmuir or Freundlich isotherms, both of which are characterized by the sink surface/air partition coefficient, or

$$q(t) = K_s y(t) \quad (6)$$

$$q(t) = K_s y(t)^n \quad (7)$$

where q ($\mu\text{g}/\text{m}^2$) is the sink surface-phase concentration of SVOC, K_s (m) is the sink surface/air partition coefficient, and n is the Freundlich isotherm parameter.

The SVOC accumulated in a chamber obeys the following mass balance:

$$\frac{dy(t)}{dt}V = Qy_{in}(t) + A\dot{m}(t) - A_s \frac{dq(t)}{dt} - Qy(t) \quad (8)$$

$$\dot{m}(t) = h_m(y_0(t) - y(t)) \quad (9)$$

where V (m^3) is the chamber volume, Q (m^3/s) is the air flow rate, y_{in} ($\mu\text{g}/\text{m}^3$) is the gas-phase concentration of SVOC at the inlet, A (m^2) is the source surface area, \dot{m} ($\mu\text{g}/(\text{m}^2\text{s})$) is the emission rate, and A_s (m^2) is the sink surface area.

The above model clearly shows that the emission rate of SVOCs is influenced by the partition and sorption behavior. Based on the model, Xu and Little (2006) conducted sensitivity analysis to identify the most important parameters that influence SVOC emission. They found that emissions of SVOCs are subject to “external” control (partitioning from the material into the gas phase, convective mass transfer through the boundary layer, and strong sorption onto interior surfaces including airborne particles). The main difference between VOC and SVOC emissions is mainly due to their different physicochemical properties. Compared to VOCs, the vapor pressures of SVOCs are much lower, which results in their strong sorption to surfaces. Therefore, external gas-phase resistance and exterior sinks dominate the emission behavior of SVOCs. Moreover, the initial material-phase concentration C_0 of SVOCs is usually much higher than that of VOCs, making the material-phase concentration effectively constant, meaning that diffusion is not an important mechanism.

Existing Methods for Measuring Key Emission Parameter (y_0)

CLIMPAQ and FLEC Chamber Methods

Clausen et al. (2004) applied CLIMPAQ (Chamber for Laboratory Investigations of Materials, Pollution, and Air Quality) and FLEC (Field and Laboratory Emission Cell) to investigate the emission of DEHP from PVC flooring. Air in both chambers was sampled at the outlet and analyzed to obtain the DEHP concentration ($\mu\text{g}/\text{m}^3$). The entire emission experiment lasted for almost 400 days. At the beginning of the experiment, the gas-phase concentration increased over time, but after 150 days, the concentration tended to remain stable, which indicated that the emission process had reached steady state. To characterize the emission behavior, the specific emission rate (SER , $\mu\text{g m}^{-2} \text{h}^{-1}$) was calculated using the steady-state data:

$$SER = C \cdot N / L \quad (10)$$

where C ($\mu\text{g}/\text{m}^3$) is gas-phase concentration at steady state, N (h^{-1}) is the air exchange rate, and L (m^2/m^3) is the test pieces loading factor. The $SERs$ in CLIMPAQ are in the range of 0.2–0.4 $\mu\text{g}/\text{m}^2/\text{h}^1$, approximately 5–10 times lower than that in FLEC, with 1–1.6 $\mu\text{g}/\text{m}^2/\text{h}^1$. The inconsistency may be explained by the five times higher L/N ratio in CLIMPAQ. Therefore, SER changes with the design of

the chamber, which means it is not an ideal parameter to characterize emission of SVOCs from various materials.

As mentioned earlier, the emission rate of SVOCs from a material is calculated by Eq. (9) using the mass-transfer coefficient and the concentration difference between indoor (bulk) air and y_0 . Therefore, y_0 has to be considered as the key parameter that characterizes SVOC emission. In recent years, most experimental studies and efforts were directed toward the determination of y_0 values for different SVOC/material combinations. The following sections summarize the existing methods for measuring y_0 .

Sandwich-like Chamber Method

The emission of SVOCs in CLIMPAQ and FLEC requires extremely longtime periods of time (almost 150 days) to reach steady state because of the strong sink effect of SVOCs on internal chamber walls, which demonstrates that CLIMPAQ and FLEC may not be suitable for the measurement of characteristic parameters of SVOCs. For this reason, Xu et al. (2012) developed a “sandwich-like” chamber to characterize SVOC emissions. The chamber is composed of two pieces of test material and a thin stainless steel chamber “ring,” which forms a cylindrical chamber cavity by placing the “ring” in between the two test material pieces and then pressing them tightly together (Fig. 2). In this way, the emission area is maximized, and the sorption area is minimized to reduce the impact of SVOC sorption to the chamber surfaces. Using this chamber to test the emission of DEHP from PVC flooring, the time for gas-phase DEHP to reach steady state is considerably reduced to about 20 days, which is a significant improvement compared to the CLIMPAQ and FLEC chambers.

Based on this sandwich-like chamber, Liang and Xu (2014a, b) further improved the performance of the chamber by changing the chamber shape from cylindrical to half-cylindrical (Fig. 3), with three inlets and six outlets to increase air flow mixing

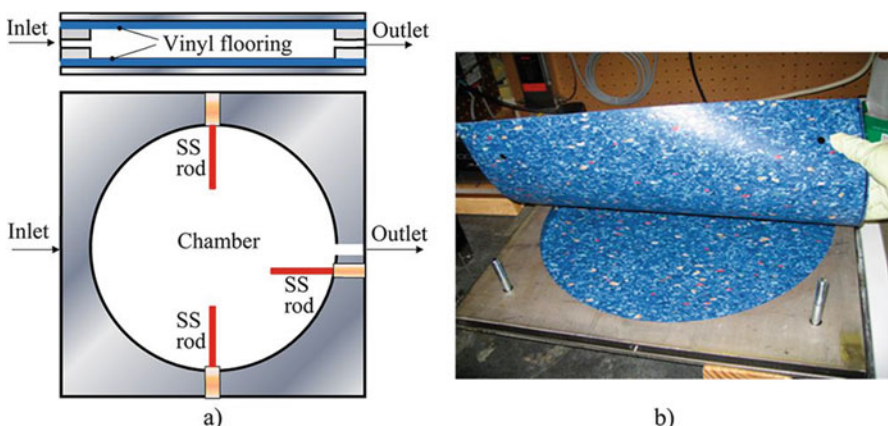
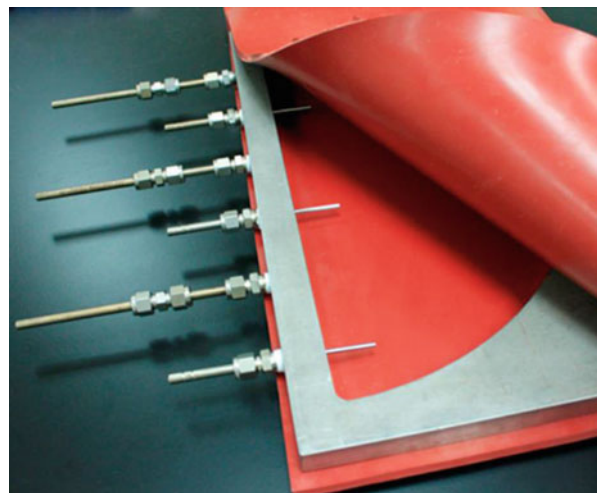


Fig. 2 Configuration of the chamber; (a) side and top view, (b) photo. (©With permission of Xu et al. 2012. Copyright 2021 American Chemical Society)

Fig. 3 The specially designed sandwich-like chamber. (©With permission of Liang and Xu 2014a. Copyright 2021 American Chemical Society)



and to increase the air flow rate. With the improved method, the time to reach steady state was shortened to less than 5 days. In addition, they measured the y_0 values of a range of phthalates from various vinyl floorings based on the following equation, which is obtained by applying the steady-state condition to Eq. (8):

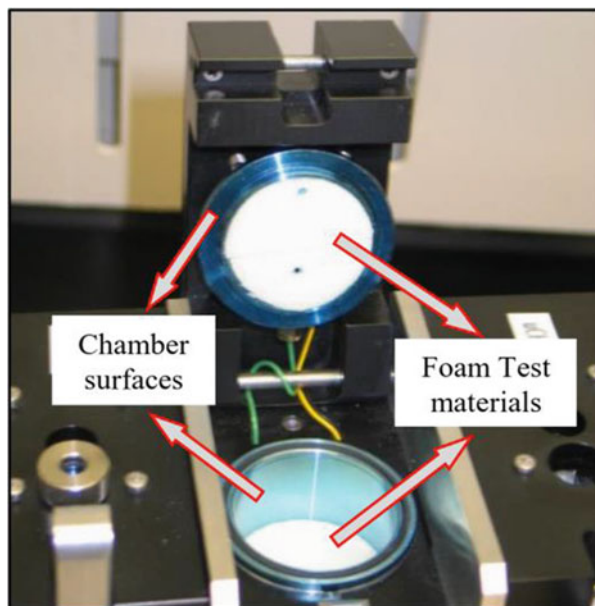
$$y_0 = \frac{y_{ss} \cdot Q}{h_m \cdot A} + y_{ss} \quad (11)$$

where y_{ss} is the gas-phase concentration of SVOC at steady state. Although this specially designed chamber is a significant improvement from the earlier SVOC emission tests, it still has some limitations. For example, since the gas tightness is formed by the test material itself, it is required to be flat, impervious, and flexible, which limits the applicability of this emission chamber to certain materials.

To overcome the abovementioned limitation, Liang et al. (2018a, b) developed a material-air-material (M-A-M) open-ended cylinder microchamber to measure y_0 of organophosphate flame retardants (OPRFs) from a polyisocyanurate rigid foam. When conducting emission experiments, two pieces of foam are attached to the bottom and the top of the chamber using double-sided tape. As shown in Fig. 4, unlike the sandwich-like chamber developed by Xu et al. (2012), the M-A-M emission chamber is self-sealed rather than being sealed by the test materials. Therefore, it broadens the scope of application to pervious materials.

Furthermore, it is also “sandwich-like,” so that the ratio of emission to sorption surface area is also large. Using this chamber, the gas-phase concentration of OPRFs (TCEP and TCPP) reaches steady state within 40 h. However, the common drawback of the sandwich-like methods is that the convective mass-transfer coefficient h_m at the source surface is required to be measured independently, which results in additional experiments and brings potential errors to the measured y_0 .

Fig. 4 The M-A-M microchamber with source materials. (©With permission of Liang et al. 2018b. Copyright 2021 American Chemical Society)



Yang et al. (2019) applied the sandwich-like emission chamber developed by Xu et al. (2012) to simultaneously determined y_0 and h_m values of DEHP emission from vehicle cabin materials. Yang et al. (2019) used different calculation methods to obtain y_0 . Equation (11) is still used in the determination of y_0 , but it is transformed into:

$$\frac{1}{y_{ss}} = \frac{Q}{h_m A y_0} + \frac{1}{y_0} \quad (12)$$

Since h_m can be expressed as a function of Q , or $h_m = C_1 Q^{0.5}$, Eq. (12) can be rewritten as:

$$\frac{1}{y_{ss}} = \frac{Q^{0.5}}{C_1 A y_0} + \frac{1}{y_0} \quad (13)$$

where C_1 is a constant related to the size of the test material and the physical properties of SVOCs. A series of experiments were conducted at different ventilation rates and the respective y_{ss} values were measured to obtain the slope and intercept by linear curve fitting (varied ventilation rate [VVR] method). By this means, C_1 , y_0 , and h_m were derived simultaneously, and the potential errors of y_0 caused by h_m can be avoided. Solid-phase microextraction (SPME) was used for steady-state chamber air sampling instead of Tenax thermal desorption (TD) tubes. SPME possesses the virtue of nonexhaustive and small-volume sampling, leading to shorter extraction

time compared with other methods. However, because this is a passive sampling method, the amount of SVOC extracted by SPME cannot reflect the gas-phase SVOC concentration directly, and calibration is needed, which may result in further experiments and errors. In addition, there are some other limitations in Yang's method. The determination of one y_0 value requires at least four different flow rate experiments, and for each flow rate experiment, the SPME method needs to be calibrated again, because the extraction amount of SPME at equilibrium varies with ventilation rate. Therefore, the test process is complicated, and the experimental time is hardly reduced. Moreover, the regression method has a risk of multiple solutions since more than one parameter is determined simultaneously (He and Yang 2005).

A microemission cell (μ EC) chamber (Fig. 5), which can be easily held in one hand, was developed by Li et al. (2022, *in preparation*) to characterize the emission of multiple SVOCs from various consumer products. Combined with a novel active air sampling technique, the needle trap device (NTD), the time for gas-phase SVOCs in the μ EC to reach steady state was significantly reduced. For example, DEHP emitted from car interior can be characterized within 10 min. This is attributed to the high ratio of emission to sorption surface area, no loss of SVOCs in sampling pathways, the high mass transfer enhanced by using a fan, and the improvement of the sensitivity of the sampling device.

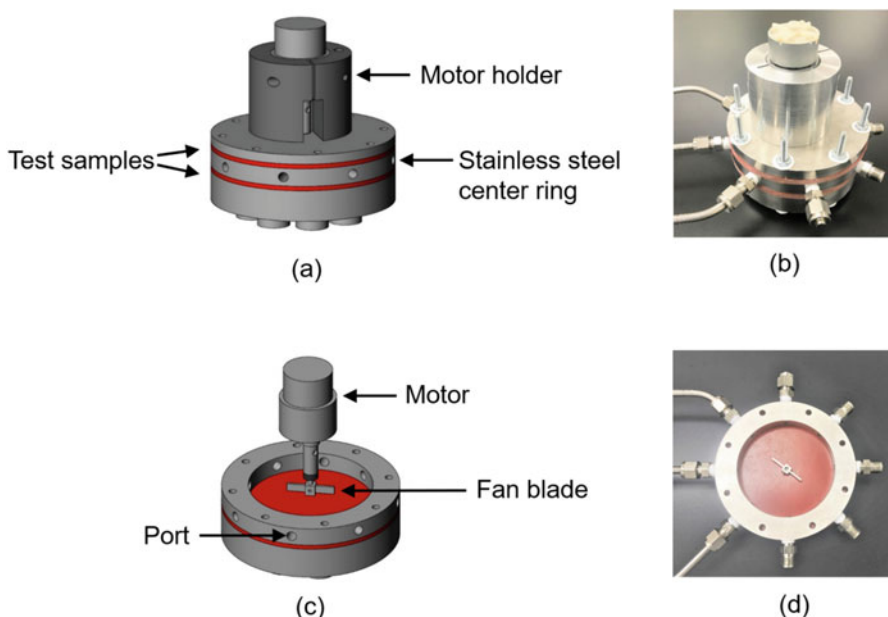


Fig. 5 (a) Configuration of microemission cell; (b) photo of microemission cell; (c) configuration of open microemission cell; and (d) photo of top view of open microemission cell. (Li et al. 2022, *in preparation*)

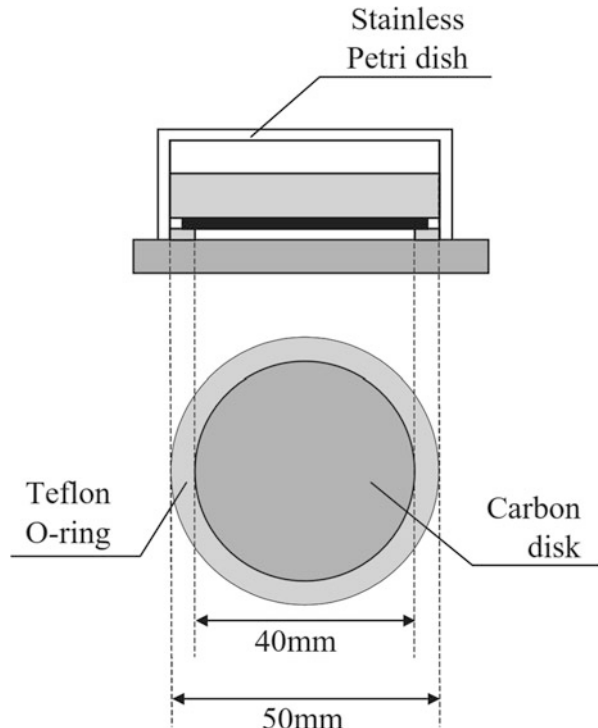
Passive Flux Sampler (PFS) Method

A diffusion-based passive flux sampler for measuring the emission flux of phthalate esters was first developed by Fujii et al. (2003). The configuration of the sampler is displayed in Fig. 6. The phthalate esters emitted from the test materials diffuse through the O-ring and adsorb directly onto the carbon disk. After several days of exposure, the carbon disk is removed for chemical analysis, and the flux can be calculated by Fick's law.

Based on the PFS developed by Fujii et al. (2003), a series of investigations (Ni et al. 2007; Noguchi and Yamasaki 2016) concerning SVOC emissions under different temperature conditions was conducted. Moreover, the relationship between emission flux and chemical content in the materials was examined.

Wu et al. (2016) also proposed a simple diffusion-based passive flux sampler method to measure y_0 . Standard stainless steel thermal desorption tubes (Tenax TA tubes) are employed in this method. As shown in Fig. 7, the test material that is perpendicular to and placed at the opening of the Tenax TA tube serves as the SVOC source. Tenax TA packed in the upper section of the tube serves as a perfect and instantaneous SVOC sink. A large and a small cylinder are used to hold the tube in place. Corresponding to this method, a mechanistic model was developed to describe the transport of gas-phase SVOCs in the tube (Fig. 8). Gas-phase SVOC transient

Fig. 6 A vertical and cross-sectional diagram of the passive flux sampler. (©With permission of Fujii et al. 2003)



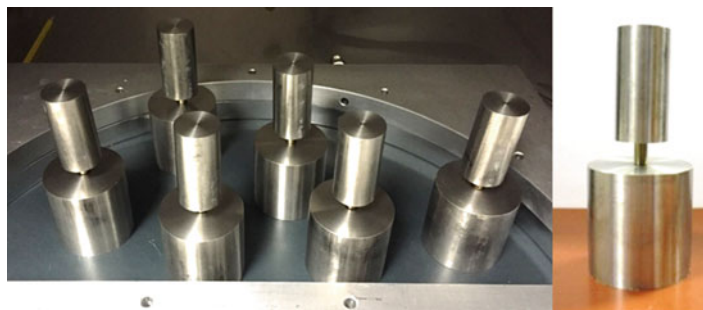
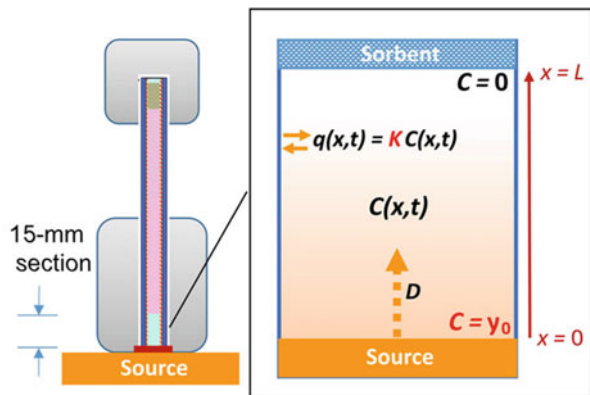


Fig. 7 Diffusive passive sampling method. (©With permission of Wu et al. 2016)

Fig. 8 Schematic representation of the diffusive sampler and diffusion model.
©With permission of Wu et al. 2016)



diffusion in the tube is characterized by Fick's second law, and the analytical solution is derived as:

$$C(x, t) = y_0 \left(1 - \frac{x}{L}\right) + \frac{2}{\pi} \sum_{n=1}^{\infty} \left(-\frac{y_0}{n}\right) \cdot \sin\left(\frac{n\pi x}{L}\right) \cdot \exp\left(-\frac{D_a n^2 \pi^2 t}{RL^2}\right) \quad (14)$$

where $C(x, t)$ ($\mu\text{g}/\text{m}^3$) is the SVOC gas-phase concentration in desorption tube at location x and time t , D_a (m^2/s) is the SVOC diffusion coefficient in air, R is a retardation factor caused by tube surface adsorption, and L (m) is the length of the air diffusion path.

This mathematical model assumes that SVOC gas-phase concentration is evenly distributed at the cross-section of the desorption tube. However, while SVOCs diffuse in the tube, they will be adsorbed by the inner tube surface, and this process is described by an instantaneous linear partition equilibrium:

$$q(x, t) = K_s C(x, t) \quad (15)$$

where $q(x, t)$ is the surface-phase concentration of SVOC and K_s (m) is the surface/air partition coefficient. By integrating $q(x, t)$ over distance x , the adsorbed amount of SVOCs on the tube surface versus time can be expressed as:

$$M_q(t) = \int_0^x q(x, t) \pi d dx \quad (16)$$

For the perfect sink at the top of the tube ($x = L$), the mass flux diffused into it can be represented by:

$$J(t)|_{x=L} = \frac{D_a y_0}{L} \left(1 + 2 \sum_{n=1}^{\infty} \cos(n\pi) \cdot \exp\left(-\frac{D_a n^2 \pi^2 t}{RL^2}\right) \right) \quad (17)$$

By integrating $J(t)|_{x=L}$ over time t , the amount of SVOCs absorbed by the perfect sink M_j versus time is:

$$M_j(t) = \int_0^t J(t) dt \Big|_{x=L} \quad (18)$$

The total amount of SVOC emitted from source material is equal to the sum of M_q and M_j :

$$M(t) = M_q(t) + M_j(t) \quad (19)$$

By fitting the model to experimental data $M(t)$, y_0 and K_s can be simultaneously derived.

When applying the model, there is an assumption that the gas-phase concentration of SVOCs is uniform on the transversal surface of the tube. However, it may not be applicable to those SVOCs with large K_s , since the tube surface is a strong sink for these SVOCs. To this end, the authors developed a two-dimensional (2-D) model based on cylindrical coordinate to characterize these cases:

$$\frac{\partial C(r, z, t)}{\partial t} = \frac{1}{r} \frac{\partial}{\partial r} \left(r D_a \frac{\partial C(r, z, t)}{\partial r} \right) + D_a \frac{\partial^2 C(r, z, t)}{\partial z^2} \quad (20)$$

where r and z are the radius and height of the tube, respectively. The numerical solution of the 2-D model can be derived by finite difference methods, and y_0 and K_s can therefore be obtained. Wu et al. (2016b) found that for SVOCs with K_s larger than 1000 m, the 2-D model is more reliable.

Applying this method, emissions of DEHP, DnBP, and DiBP from PVC flooring were tested, and the results are comparable to those reported in the previous study (Liang and Xu 2014a). The experimental time of this diffusion-based PFS method is approximately 180 h. This method is much simpler compared with the aforementioned ventilated chamber methods, and because it is a sealed chamber, it does not need to consider the mass-transfer coefficient of the tube surfaces. However, there

are still some limitations. The 2-D mass-transfer model is complicated, and there are possibilities of multiple solutions when fitting two parameters simultaneously via nonlinear regression (Liang et al. 2018b). Liang et al. (2018a, b) used this method to determine the y_0 values of organophosphate flame retardants (TCEP, TCPP, and TDCPP) from PIR foam material, and found that the y_0 values obtained by PFS method are 48–54% lower compared with those obtained using the M-A-M method. For the limitation of complicated 2-D mass-transfer model, Eichler et al. (2018) modified the diffusive sampler by changing the thermal desorption tubes to a circular stainless steel washer with thickness of 0.254 mm. Because the diffusion distance of SVOCs was extremely short (0.254 mm), the sorption of SVOCs on inner surfaces of the washer was negligible and therefore the 1-D mass-transfer model is enough to characterize the transport of SVOCs.

SPME-Based Sealed Chamber Method

Cao et al. (2017) developed a SPME-based sealed chamber (Fig. 9) method to measure y_0 . A SPME fiber is inserted into the chamber to sample air through the holes drilled in the side of the stainless steel ring separating the two pieces of source

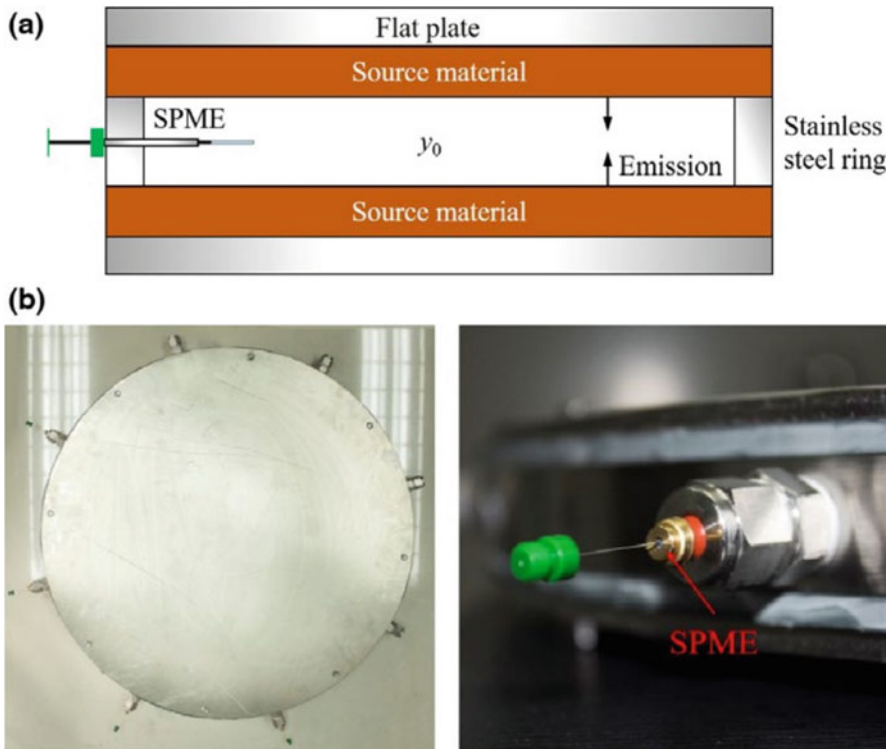


Fig. 9 (a) Schematic of the experimental system and (b) photographs. (©With permission of Cao et al. 2017)

material (Fig. 9b). The steady-state SVOC concentration in the chamber air is considered as y_0 when $Q = 0$ in Eq. (11) and it is determined by the following procedure. Ouyang and Pawliszyn (2008) recognize that the adsorption rate of SVOCs on SPME coating is constant in a short enough sampling duration (it is defined as the early stage where the adsorbed mass is less than 50% of the equilibrium mass):

$$M = D_a S C_g t \quad (21)$$

where M (μg) is the SVOC mass adsorbed on the coating, D_a (m^2/s) is the SVOC diffusion coefficient in the air, and S is the shape factor related to the length and external diameter of SPME coating. Assuming that steady state can be achieved quickly, C_g , SVOC concentration in the chamber air is substituted by y_0 :

$$M = D_a S y_0 t \quad (22)$$

Therefore, by monitoring the adsorbed mass of SVOC on the SPME coating with respect to time, y_0 can be obtained by linear curve fitting.

Cao et al. (2017) used this method to determine the y_0 of DEHP emitted from PVC floorings and the duration of the experiment was about 1 day (26 h), which is a great improvement compared to previous methods (several days or even several months). In addition, this sealed chamber method also overcomes the liability that the h_m on the source surface will cause inaccuracy in y_0 because it is often estimated. Although this method is rapid and accurate, it still has some limitations. First, it is restricted to flat and relatively soft materials. Second, the adsorption rate of SPME coating defined as $D_a S$ (Eq. 22) is irrelevant to the properties of target SVOCs, which may not hold true for all the SVOCs. For example, for SVOCs with relatively low vapor pressures, the adsorption rate of SPME coating should be smaller than for those with higher vapor pressures. Third, because the sampling must be conducted before reaching sorption equilibrium, and different SVOCs may have different sorption characteristics with respect to the SPME coating, it is necessary to investigate the sampling time in advance. Last, calibration of SPME may be time consuming and could result in substantial uncertainty.

Other Methods

Xiong et al. (Xiong et al. 2016) solved the mass-transfer model of SVOC emission (Eqs. 8 and 9) in a much simpler way compared with traditional partial differential equation-based analytical or numerical solutions. With this approach, an exponential relationship between the gas-phase SVOC concentration and elapsed time was established, by which y_0 and h_m can be derived simultaneously. Moreover, unlike most of the sandwich-like methods applying the steady-state gas-phase concentration to obtain y_0 (Eq. 11), this method does not require that steady state has been reached, but utilizes the data of the early stage of the experiment, which means the experimental duration can be shortened, and therefore it is called the “early stage C-history method.”

So far, the abovementioned methods were mainly used to measure the y_0 values of phthalates. Chemicals like flame retardants (e.g., organophosphates and PBDEs) were rarely tested due to their strong affinity to chamber surfaces and the difficulties associated with determining low concentrations. Only a few studies (Kemmlein et al. 2003; Salthammer et al. 2003; Bakó-Biro et al. 2004; Ni et al. 2007) focused on developing experimental chamber methods to measure their specific emission rates from a broad range of consumer goods (e.g., insulating materials, foams, TVs, computers, printed circuit boards, etc.). Glass tubes packed with PUF plugs and Tenax tubes were used to sample gas-phase flame retardants in a chamber (Kemmlein et al. 2003; Salthammer et al. 2003). However, as previously mentioned, these chemicals have an extremely strong sink effect, which results in very low concentrations that are difficult to be accurately detected. Therefore, it is of great importance to develop more sensitive and reliable sampling techniques for these chemicals. The NTD-GC/MS sampling and analysis technique developed by Li et al. (2022, *in preparation*) may be a potential method.

All the experimentally determined y_0 values of a variety of SVOCs emitted from different materials are summarized in Table 1.

Equilibrium Relationship Between Source Materials and Air

Relationship Between y_0 and Temperature

Several studies have found that y_0 increases rapidly with increasing temperature (Clausen et al. 2012; Liang and Xu 2014b; Bi et al. 2015; Wu et al. 2016). The relationship between temperature and the ratio of C_0 ($\mu\text{g}/\text{m}^3$) (the material-phase concentration of SVOCs in the source material) to y_0 can be characterized by the van't Hoff equation (Cao et al. 2017):

$$\ln \left(\frac{C_0}{y_0} \right) = \frac{\Delta H_p}{RT} + Y \quad (23)$$

where ΔH_p (J/mol) is the enthalpy of SVOC phase change from source material phase to gas phase, R (J/(mol · K)) is the universal gas constant, T (K) is the temperature, and Y is a constant. Because C_0 is constant for many SVOCs, Eq. (23) can be transformed into:

$$\ln y_0 = -\frac{\Delta H_p}{RT} + \ln C_0 - Y \quad (24)$$

where ΔH_p is relatively constant within a range of temperature, and in this case it can be seen from Eq. (24) that y_0 increases with increasing temperature.

Relationship Between y_0 , SVOC Weight Fraction, and Vapor Pressure

Liu and Zhang (2016) found that for DEHP emitted from PVC floorings, when the DEHP weight fraction of source material increases from 13% to 23% at 23 °C, the

Table 1 Key parameter (y_0) of SVOC emission

Sample ID	Chemical	Source material	y_0 ($\mu\text{g}/\text{m}^3$)	Testing method	Temperature ($^\circ\text{C}$)	References
	DEHP	PVC flooring	0.82 ^a	FLEC	20.1–23.6	(Clausen et al. 2004)
	DEHP	PVC flooring	1.1	Sandwich-like chamber	22 ± 0.2	(Xu et al. 2012)
Sample 1	DEHP	PVC flooring	2.3	Half-sandwich-like chamber	25	(Liang and Xu 2014b)
Sample 2	DEHP		2.37			
Sample 3	DINP		0.42			
	DEHP		0.02			
Sample 4	BBP		8.47			
	Iso-DEHP		0.12			
Sample5	DnBP		24.7			
	DEHP		1.54			
	TCEP	Polyisocyanurate rigid foam	8.43 ^b	M-A-M micro chamber	23 ± 1	(Liang et al. 2018b)
	TCPP		3.64 ^b			
	DEHP	Seat cushion	0.35	VVR method	25	(Yang et al. 2019)
			3.03		35	
			30.3		50	
		Car mat	0.88		25	
			5.21		35	

Sample 1	DEHP	PVC flooring	45.5	Diffusion-based PFS method	50	
Sample 2	DEHP		2.8 ± 5%		25 ± 0.3	(Wu et al. 2016)
	DnBP		0.9			
	DnBP		25			
	DiBP		49.8			
	TCEP	Polyisocyanurate rigid foam	4.33 ^c	Diffusion-based PFS method	23 ± 1	(Liang et al. 2018b)
	TCPP		1.67 ^c			
	TDCPP		4.4 ^c			
Sample 1	DEHP	PVC flooring	0.43	SPME-based sealed chamber	15	(Cao et al. 2017)
			1.0		20	
			1.9		25	
			3.8		30	
			0.16		15	
Sample 2	DEHP		0.16		15	
			0.35		20	
			0.70		25	
			1.4		30	

^aThis γ_0 value is calculated using the air flow, air velocity at test piece surface, area of test piece, and the final gas-phase concentration of DEHP provided in the article

^bMean value of two tests

^cMean value of the results of three positions on the test sample

ratio of y_0 to saturated gas-phase concentration of pure DEHP, y_{sat} , increases from 69% to 74%. y_{sat} is calculated as $y_{sat} = \frac{P_{sat} \cdot MW}{RT}$, where P_{sat} is the saturated vapor pressure, and MW is molecular weight. Cao et al. (2017a) observed a similar result, and derived a mathematical expression of the relationship:

$$\frac{y_0}{y_{sat,DEHP}} = 1.00 - e^{-0.0860m} \quad (25)$$

where m is the DEHP weight fraction of source material. Moreover, the relationship between $y_{sat,DEHP}$ and temperature was measured using their SPME-based sealed chamber:

$$\ln y_{sat,DEHP} = -1.00 \times 10^3 \times \frac{103.67}{RT} + 42.80 \quad (26)$$

By combining Eqs. (25 and 26), the relationship between y_0 and weight fraction can be represented as:

$$\ln y_0 = -\frac{104}{RT} + \ln(1.00 - e^{-0.0860m}) + 42.80 \quad (27)$$

It should be noted that Eq. (27) only holds true for chemicals whose enthalpy of phase change from material phase to air is approximately equal to enthalpy of vaporization for its pure liquid. Otherwise, the temperature effect on $\frac{y_0}{y_{sat,DEHP}}$ should be incorporated in Eq. (25).

The abovementioned equilibrium relationship between y_0 , y_{sat} , and m is for DEHP and PVC floorings, and whether the relationship can be applied to other chemical/material combinations remains uncertain. Eichler et al. (2018) investigated the equilibrium relationship for phthalates and their alternatives and different source materials including backpack, toys, vinyl flooring, table cloth, wall paper, and crib mattress cover. Distinct from Cao's result (2017a, b) (Eq. 25), the ratio of y_0 to y_{sat} is positively proportional to weight fraction at 25 °C:

$$\frac{y_0}{y_{ss}} = 5.12 \cdot m \quad (28)$$

Furthermore, Liang et al. (2018a, 2018b) explored the relationship for phthalates, organophosphates flame retardants, and various source materials (e.g., PVC flooring, polyisocyanurate rigid foam) with relatively low weight fraction (<15%). The result at temperature ranging from 23 °C to 25 °C is:

$$\frac{y_0}{y_{ss}} = 3.40 \cdot m \quad (29)$$

Similar to the results of Eichler (2018) and Liang et al. (2018a, b), Li et al. (2022, in preparation) also found a linear relationship between $\frac{y_0}{y_{ss}}$ and m for additional

chemical/material combinations (phthalates and their alternatives from crib mattress covers, wall covering, infant changing pads, children's backpack, etc.; organophosphates from portable crib foam, insulation board, and foam spray; dihydroxy alcohol from paints, etc.). The slope is 4.87 in Li et al. (2022, *in preparation*). The slopes obtained from these three studies are slightly different, this may be due to experimental uncertainties and variations in chemical/material combinations used in data processing. Both the structure of materials (e.g., porous or impermeable) and the type of SVOC influence the emission process because of different chemical bond interactions.

Sorption by Sink Materials

Sorption Processes and Models

Impermeable Surfaces

Because of their extremely low vapor pressure, many SVOCs prefer to sorb to the surface phase rather than remain in the gas phase, and for this reason it is important to investigate the sorption behavior of SVOCs. In ventilated environments, a boundary layer is assumed to exist between the sink material surface and bulk air. The sorption process consists of two stages: mass transfer of SVOCs from bulk air to the boundary layer and partitioning between boundary layer and sink material surface. For the first stage of mass transfer, we have:

$$\frac{dq_s(t)}{dt} = h_{m,s}(y(t) - y_s(t)) \quad (30)$$

where q_s ($\mu\text{g}/\text{m}^2$) is the sink surface-phase concentration, $h_{m,s}$ (m/s) is the convective mass-transfer coefficient near sink surface, y ($\mu\text{g}/\text{m}^3$) is the bulk air concentration, and y_s is gas-phase concentration in the boundary layer. As the mass transfer proceeds, y_s will gradually increase to y , which means that sorption equilibrium has been reached. In a quiescent environment without ventilation, there is no boundary layer and there is no difference between gas-phase concentration near the sink surface (y_s) and bulk air (y).

As for the second stage of partitioning, various models have been developed to represent the relationship between y_s and q_s . In the simplest case, a linear isotherm can be established under the following two assumptions (Schwarzenbach et al. 2016). First, the attraction of the sorption sites on surfaces to molecules remains constant throughout the entire concentration range; second, the sorption sites are far from saturated with regard to the low gas-phase concentration of chemicals (Schwarzenbach et al. 2016). The linear isotherm can be presented as:

$$q_s = K_s y_s \quad (31)$$

where q_s is the equilibrium concentration of chemical on solid surface ($\mu\text{g}/\text{m}^2$), or in the solid phase ($\mu\text{g}/\text{m}^3$), and K_s (m or dimensionless) is the partition coefficient.

However, if the sorption sites are limited and can gradually become saturated as the amount of gas-phase chemicals increases, there should be a maximum value of q_s . The linear isotherm is no longer applicable in these cases and a Langmuir isotherm (Langmuir 1916) should be adopted, expressed as (Nazaroff and Alvarez-Cohen 2001):

$$q_e = q_{max} \frac{K_L y_e}{1 + K_L y_e} \quad (32)$$

where q_{max} ($\mu\text{g}/\text{m}^2$) is the maximum equilibrium surface-phase concentration, and K_L ($\text{m}^3/\mu\text{g}$) is the equilibrium Langmuir isotherm constant. There are some assumptions that should be satisfied when applying this isotherm. First, all the sorption sites on a homogeneous surface are equally likely to be occupied by any molecules, which means each site has the same sorption-free energy. Second, the likelihood of a molecule being attached to a sorption site is independent of whether the adjacent site has been occupied by other molecules. Third, sorption is a monolayer process, with no other molecules overlaying. However, for air contaminants whose partial pressure in the air is extremely low, the sorption sites for the chemical are rarely saturated, in this case, the Langmuir isotherm can be simplified to a linear isotherm (Liang et al. 2018a).

The two abovementioned isotherms are used to describe linear sorption processes. Compared to these two, an empirical relationship referred to as the Freundlich isotherm (Freundlich 1906) is widely applied as the mathematical model for nonlinear, heterogeneous, and multilayer sorption. In these cases, the sorption sites are of different types and possess different sorption-free energies. The equation of Freundlich isotherm is:

$$q_s = K_F y_s^n \quad (33)$$

where K_F ($\text{m}^{3n-2} \times \mu\text{g}^{1-n}$) is the Freundlich constant, and n is the Freundlich exponent, which serves as an indicator of free energy potential (Weber Jr and DiGiano 1996). When $n = 1$, the equation transforms into a linear isotherm and the free energies of different sorption sites are considered as constant over the chemical concentration range. When $n > 1$, as the chemical concentration increases, the free energies increase for further sorption. Last, when $n < 1$, in contrast to the previous situation, the free energies are weakened with enhanced sorbate amount.

Linear, Langmuir, and Freundlich isotherms are the earliest, most classic, and commonly used models for the characterization of sorption. However, there exist some cases where none of these three isotherms are sufficient to describe the sorption process. To improve the effectiveness and reliability of data fitting, different combinations of these three isotherms can be developed, e.g., the Sips model (Sips 1948) and the Koble-Corrigan model (Koble and Corrigan 1952). In general, the

development of these models paved the way for establishing models specifically for SVOC sorption.

For the sorption of SVOCs, Xu and Little (2006) first proposed the use of the Freundlich equation to characterize SVOC sorption between chamber air and stainless steel chamber surfaces, while for sorption from chamber air to airborne particles, a linear relationship was adopted (Xu and Little 2006). These equations are incorporated in the SVOC emission model they developed. Later, they simplified the emission model and in this updated model, the Freundlich equation was replaced by a linear isotherm to clarify the sorption relationship of SVOCs between gases and chamber surfaces (Xu et al. 2012). Since then, the linear equilibrium relationship gained its popularity in being used to depict the partition behavior of SVOCs in either surface/air or particle/air. For example, Bi et al. (2015) adopted a linear equilibrium partition coefficient to investigate the sorption strength of phthalates on indoor surfaces such as windows, dish plates, mirrors, fabric cloths, etc. However, the author also found that a thin organic film developed at the interface between impervious surfaces and indoor air (Bi et al. 2015). This was verified by the approximation between dimensionless partition coefficients and phthalates' octanol-air partition coefficients, K_{oa} . In addition to this study, many other studies of SVOC surface sorption have demonstrated the growth and existence of organic films (Diamond et al. 2000; Liu et al. 2003; Butt et al. 2004; Wu et al. 2008). The organic films developed on impervious surfaces are formed by the dry deposition of airborne particles and the partitioning between gas-phase chemicals and film (Liu et al. 2003; Butt et al. 2004). The films comprise of condensed organic matter, inorganic molecules and ions, moisture and settled particles, and generally have a thickness of 5–20 nm (Liu et al. 2003) and grow at a rate of 0.11–0.31 nm/day (Wu et al. 2008). The surfaces coated with organic films can continuously accumulate SVOCs (Wu et al. 2017), which means that no longer a monolayer of SVOCs can be assumed, and the widely used linear model cannot reasonably explain the development of and SVOC partitioning to organic films. Therefore, the Freundlich model should be adopted in these cases. Wallace et al. (2017) quantitatively measured the amount of organic matter accumulated on petri dishes or foils, which also illustrates the necessity of applying multilayer models when organic films exit on the sorption surfaces.

Weschler and Nazaroff (2017) proposed a model accounting for the film growth contribution of SVOCs across a wide range of $\log K_{oa}$ values. The model characterizes the dynamic process, the surface/volumetric concentration changes of SVOCs sorbed to the film, and the increase of film thickness:

$$\frac{dM_{fi}}{dt} = v_{di} \left(C_{gi} - \frac{M_{fi}}{XK_{oai}} \right) \quad (34)$$

where M_{fi} is the surface concentration of sorbed SVOCs of group i (the sorbed SVOCs in the organic film are divided into several groups according to $\log K_{oa}$), v_{di} is the deposition velocity of SVOCs of group i , C_{gi} is the gas-phase concentration of

SVOCs of group i , and X is film thickness, which is coupled with the SVOC concentration in the film:

$$X = X_0 + \sum_{i=1}^n \frac{M_{fi}}{\rho_i} \quad (35)$$

where X_0 is the initial film thickness, and ρ_i is the density of the sorbed SVOCs of group i . Based on the model simulation, the authors found that at the beginning of the buildup of organic film, SVOCs adsorbed to the surface at the maximum rate and SVOCs with lower $\log K_{oa}$ ($\log K_{oa} \approx 8\text{--}10$) contribute more to film growth. However, from the perspective of film thickness, these SVOCs are not dominant. After they equilibrate with the surface film, SVOCs with $\log K_{oa} \approx 11\text{--}13$ dominate film growth and make up the majority of film components. SVOCs with $\log K_{oa} > 13$ tend to remain in the gas phase and scarcely contribute to film growth.

Permeable Surfaces

For permeable materials, an instantaneous linear isotherm is used to describe SVOC partitioning behavior:

$$C_m = K_s y_s \quad (36)$$

where C_m is the equilibrium concentration of the chemical in the solid material ($\mu\text{g}/\text{m}^3$), and K_s (dimensionless) is the partition coefficient. Fick's second law is applied to describe the diffusion of a chemical into the solid phase:

$$\frac{\partial C_m(x)}{\partial t} = D \frac{\partial^2 C_m(x)}{\partial x^2}, 0 < x < \delta \quad (37)$$

where D (m^2/s) is the diffusion coefficient of SVOCs in material phase and δ (m) is the thickness of material.

Existing Methods for Measuring Key Sorption Parameters (K_s and D)

Ventilated Chamber Method

As previously mentioned, all the sorption models involve critical parameters, which characterize sorption capacity, such as K_s and D . The usefulness of the sorption models depends on the reliability and availability of the model parameters. For this reason, it is important to develop techniques to measure key model parameters. The most common approach is to measure the absorbed mass of SVOCs in materials at different exposure times, then fit the sorption model to the experimental data to obtain K_s and D .

Liu et al. (2014) developed a ventilated dual chamber method (Fig. 10) to determine K_s and D of five PCB congeners in eight materials including polypropylene, polyether ether ketone, glass, and stainless steel. The dual chambers were divided as source and test chambers, and throughout the experiment, the gas-phase

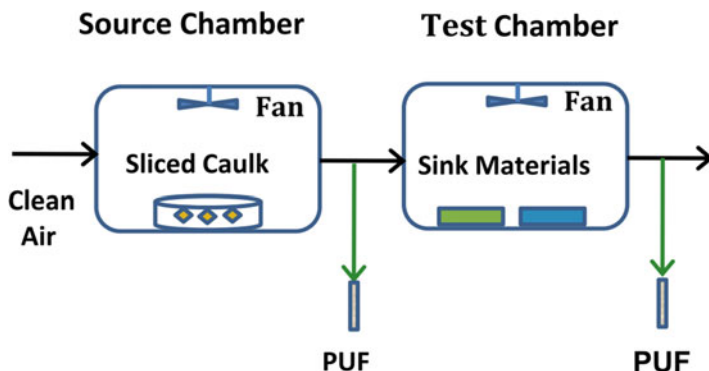


Fig. 10 Schematic of the dual chamber. (©With permission of Liu et al. 2014)

concentration at the outlet of the two chambers was monitored using polyurethane foam (PUF), and test materials were taken out from the test chamber at different time intervals to measure the amount of sorbed PCBs. The entire test lasted for at least 18 days. These data were fitted with the mathematical sorption model. There are some limitations in this method. For example, K_s and D were determined simultaneously with one dataset, which may lead to the risk of multiple solutions. Moreover, it is hard to guarantee that the air in the test chamber is fully mixed since the chamber size is relatively large, which may result in potential errors.

Liang and Xu (2014a) applied the specially designed sandwich-like chamber (Fig. 3 in “SVOC Emissions from Source Materials”) to characterize surface sorption of DEHP, DINP, DnBP, BBP, and Iso-DEHP. Unlike Liu’s method (2014), the partition and diffusion coefficients were determined by linear isotherm and Fick’s law, respectively, which avoids the multisolution problem since K_s and D were obtained independently. However, because K_s was obtained based on the equilibrium surface concentration and the steady-state gas-phase concentration, a longer test duration (more than 30 days) was needed for SVOCs to reach equilibrium.

As mentioned earlier, the linear isotherm is not capable of explaining the partition effects of multilayer sorption, and Liang et al. (2018a) adopted both linear isotherm (simplified Langmuir isotherm) and Freundlich isotherm models to investigate the sorption dynamics of organophosphate flame retardants (OPFRs) on impervious surfaces using similar chambers to Liu’s study (2014). The model parameters K_L , K_F , and n were fitted in desorption stage. Although both the isotherms provided similar fitting results for the gas-phase OPFR concentrations, the Freundlich isotherm was more advantageous in describing surface-phase OPFR concentrations, which suggest the possibility of an organic film forming on the chamber surfaces, thus leading to multilayer adsorption.

All the abovementioned methods applied ventilated chambers and the test materials must be taken out at different times to measure the accumulated mass of SVOCs. This interrupts the fate and transport of SVOCs in the chamber and introduces uncertainty in the results. To overcome this problem, Yang et al. (2020)

developed a sandwich-like chamber based on Liang and Xu's design (2014a). However, unlike the previous ventilated methods, the gas-phase SVOCs concentration instead of test material-phase concentration were measured versus time to avoid interference. In addition, this method not only simultaneously determines K_s and D , but also another important parameter, y_0 , which is the gas-phase concentration immediately adjacent to the source material surface. Nevertheless, there still exists the drawback of a nonunique solution.

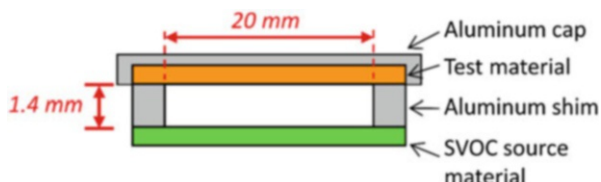
Sealed Chamber Method

Apart from ventilated chambers, sealed chambers using passive sampling techniques are also widely used in the determination of K_s and D . The sealed chamber is often designed with the source material serving as the base and test (or sink) material serving as the top of the chamber. A circular shim/ring is placed between these two materials and determines the diffusion distance (Wu et al. 2017). According to this design, molecular diffusion of SVOCs driven by the concentration gradient between source materials and chamber air is the only mechanism that governs the mass flux (Wu et al. 2017). Therefore, Fick's law can be employed to describe the transport of SVOCs, and the sorption linear isotherm is used in the boundary condition of the model. Multiple sets of this kind of small chamber are prepared and the mass of SVOCs collected on the test materials are periodically measured. Using the sealed chamber method can avoid the effects of not knowing the accurate values of convective mass-transfer coefficients of different surfaces and air flow rates (Cao et al. 2016a), and also shortens the experimental time because the kinetic stage of sorption process is often used to obtain key parameters. Wu et al. (2017) modified their diffusion-based PFS chamber (Fig. 11) to measure the K_s values of DEHP on impervious surfaces (aluminum, glass, etc.) and explore the effects of surface roughness on the sorption process.

Cao et al. (2016) designed a symmetrical sealed chamber (Fig. 12) to determine the y_0 values of three phthalates in PVC floorings and their K_s values on pure cotton shirts. In this method, the test period is substantially shortened because it only uses the early-stage concentration of the sorption process. However, it is hard to examine the impact of environmental conditions since the chamber is sealed. Additionally, the test materials need to be of regular shape, which constrains the applicability of the method.

Cao et al. (2017) developed a SPME-based C_a -history method to measure D of DiBP, DnBP, and TCPP in clothing. The chamber used in this method is the same as that used for y_0 measurements (Cao et al. 2017), with a slight difference in the configuration of source and sink materials. For this method, source and sink

Fig. 11 Schematic of the diffusive sampler. (©With permission of Wu et al. 2017. Copyright 2021 American Chemical Society)



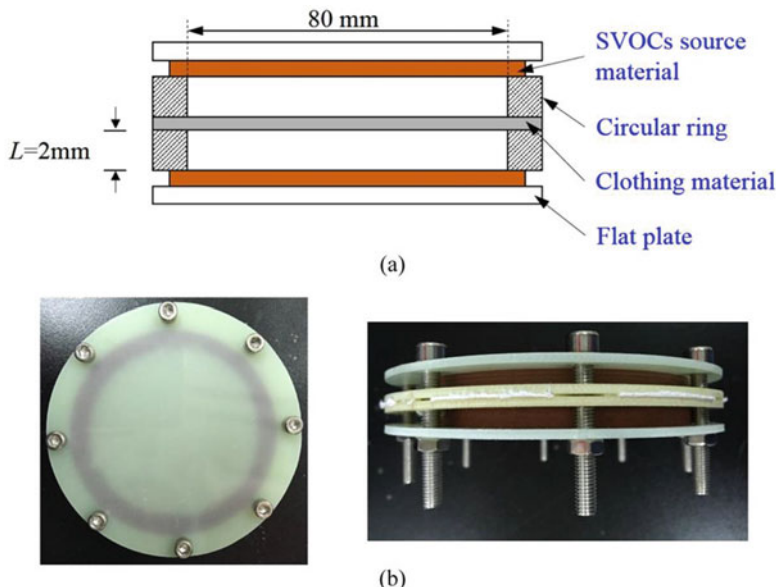


Fig. 12 (a) Schematic of the symmetrical diffusion chamber; (b) photo of the symmetrical diffusion chamber. (©With permission of Cao et al. 2016a. Copyright 2021 American Chemical Society)

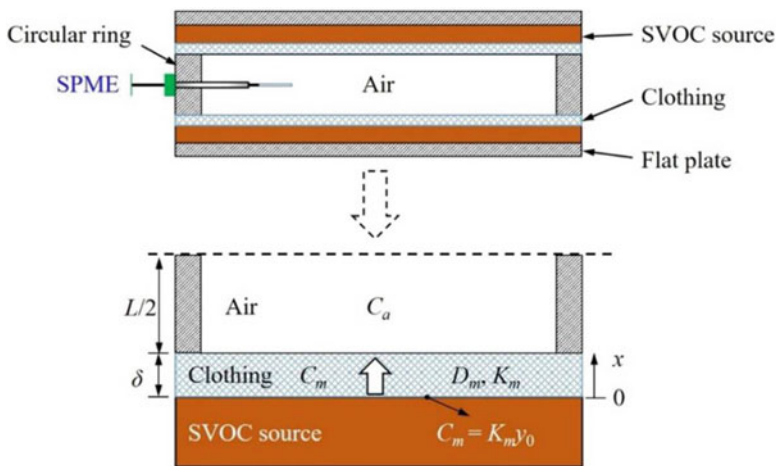


Fig. 13 Schematic diagram of SVOC mass transfer in the chamber. (©With permission of Cao et al. 2017. Copyright 2021 American Chemical Society). (Here D_m refers to D noted in this article)

materials are pressed together tightly (Fig. 13). In this way, the mass-transfer process from source to sink materials is markedly improved and the experimental duration can be shortened.

If the gas-phase SVOC concentration versus time is measured during the experiment, D can be obtained by linear fitting within 16 days. However, the experimental time will be longer for chemicals with smaller D and for thick sink materials (Cao et al. 2017).

All the experimentally determined K_s and D values of a variety of SVOCs and materials combinations are summarized in Table 2.

Prediction of the Key Sorption Parameters

Gas/Surface Partition Coefficient (K_s)

The binding forces that cause sorption behavior originating from intermolecular attraction consist of nonspecific van der Waals interactions and specific electron donor–acceptor (EDA) interactions (Goss 2004). For polar SVOCs such as nicotine, they undergo both van der Waals interactions and EDA interactions (Petrick et al. 2010), while for nonpolar SVOCs, which comprise the majority of SVOCs, their molecular interactions are mainly governed by van der Waals forces. These intermolecular interactions and the molecules' freedom of orientation, configuration, and translation constitute the free energy of transfer, which defines the potential of sorption (Schwarzenbach et al. 2016). The sorption behavior is correlated with free energy of transfer. Therefore, the partition coefficients can be estimated using substance descriptors representing molecular properties (Stenzel et al. 2013). Poly-parameter linear free energy relationships (pp-LFERs) developed by Goss (2005) and based on Abraham's two linear solvation energy relationship (LSER) can be applied to various environmental systems, if the system constants and the values of substance descriptors are accessible. The form of the pp-LFERs is:

$$\log K = sS + aA + bB + vV + lL + c \quad (38)$$

where the capital letters on the right side of the equation are the substance descriptors, and the small letters are the system constants that describe the properties of the two partition phases. S represents the dipolarity/polarizability of the substance, A and B denote the hydrogen bond donor and acceptor properties, respectively. These three descriptors are the measures of molecular specific interactions. V refers to the McGowan volume of the substance, and L is the logarithmic hexadecane-air partition coefficient. V and L are the measures of the cavity energy and nonspecific van der Waals interactions. As long as the substance and system descriptors are established, the partition coefficient can be predicted with high reliability. Stenzel et al. (2013) determined the substance descriptors of 40 flame retardants by measuring the gas-chromatographic retention times and liquid/liquid partition coefficients with multiple linear regression analysis. The pp-LFERs were also used to evaluate the partition coefficients of polyurethane foams (PUFs) under different temperature and humidity conditions for a wide range of organic compounds (Kamprad and Goss 2007).

Table 2 Key parameters of SVOC surface sorption (K_s)

Sample ID	Chemical	Sink material	K_s (m/dimensionless)	D (m ² /h)	Testing method	Temperature (°C)	References
PCB-52	Glass		6.75×10^5	1.20×10^{-17}	Ventilated dual chamber method	23	Liu et al. (2014)
PCB-66			3.66×10^5	1.20×10^{-17}			
PCB-101			6.29×10^6	5.83×10^{-18}			
PCB-110			1.40×10^7	5.83×10^{-18}			
PCB-118			3.64×10^7	5.83×10^{-18}			
PCB-52	Stainless steel		5.59×10^6	1.19×10^{-16}			
PCB-66			2.26×10^7	1.19×10^{-16}			
PCB-101			3.50×10^7	5.78×10^{-17}			
PCB-110			6.80×10^7	5.78×10^{-17}			
PCB-118			1.50×10^8	5.78×10^{-17}			
PCB-52	PTFE		6.18×10^6	1.17×10^{-15}			
PCB-66			2.35×10^7	1.17×10^{-15}			
PCB-101			3.60×10^7	5.65×10^{-16}			
PCB-110			6.76×10^7	5.65×10^{-16}			
PCB-118			1.44×10^8	5.65×10^{-16}			
PCB-52	Ketron PEEK		2.93×10^7	1.78×10^{-16}			
PCB-66			1.07×10^8	1.78×10^{-16}			
PCB-101			1.61×10^8	8.61×10^{-17}			
PCB-110			2.971×10^8	8.61×10^{-17}			
PCB-118			6.16×10^8	8.61×10^{-17}			
PCB-52	Polypropylene stress relief sheet		9.14×10^6	1.33×10^{-10}			
PCB-66			2.49×10^7	1.33×10^{-10}			
PCB-101			3.44×10^7	6.46×10^{-11}			

(continued)

Table 2 (continued)

Sample ID	Chemical	Sink material	K_s (m/dimensionless)	D (m ² /h)	Testing method	Temperature (°C)	References
PCB-110			5.52×10^7	6.46×10^{-11}			
PCB-118			9.73×10^7	6.46×10^{-11}			
PCB-52	HDPE polyethylene sheet		1.28×10^7	1.34×10^{-10}			
PCB-66			3.13×10^7	1.34×10^{-10}			
PCB-101			4.16×10^7	6.47×10^{-11}			
PCB-110			6.34×10^7	6.47×10^{-11}			
PCB-118			1.05×10^8	6.47×10^{-11}			
PCB-52	LDPE polyethylene sheet		1.66×10^7	3.18×10^{-10}			
PCB-66			2.98×10^7	3.18×10^{-10}			
PCB-101			3.60×10^7	1.54×10^{-10}			
PCB-110			4.75×10^7	1.54×10^{-10}			
PCB-118			6.62×10^7	1.54×10^{-10}			
PCB-52	Concrete disks		1.29×10^7	1.26×10^{-11}			
PCB-66			3.47×10^7	1.26×10^{-11}			
PCB-101			4.76×10^7	6.12×10^{-12}			
PCB-110			7.60×10^7	6.12×10^{-12}			
PCB-118			1.33×10^8	6.12×10^{-12}			
Sample 2	DEHP	Stainless steel	1500 (m)	\	Sandwich-like chamber	25 ± 0.5	(Liang and Xu 2014b)
Sample 3	DEHP	Stainless steel	2200 (m)				
	DINP		2100 (m)	\			

Sample 4	BBP	Stainless steel	620 (m)	/		
	Iso-DEHP		3060 (m)	/		
Sample 5	DnBP	Stainless steel	63 (m)	/		
	DEHP		930 (m)	/		
DEHP	Pure cotton T-shirts	6.02 × 10 ⁶	2.79 × 10 ⁻¹⁰	Modified sandwich-like chamber	25 ± 0.5	(Yang et al. 2020)
	DnBP		1.28 × 10 ⁶	1.16 × 10 ⁻⁹		
DiBP			4.32 × 10 ⁵	1.79 × 10 ⁻⁹		
	DINP		7.21 × 10 ⁶	2.15 × 10 ⁻¹⁰		
Sample 1	DEHP	Pure cotton T-shirts	2.8 × 10 ⁷	Cm-history method	32 ± 0.5	(Cao et al. 2016)
	DEHP	Pure cotton T-shirts	2.9 × 10 ⁷			
Sample 2	DiBP		2.0 × 10 ⁵			
	DnBP		3.8 × 10 ⁵			
Sample 1	DEHP	Pure cotton T-shirts	6.6 × 10 ⁷	/		
	DEHP	Pure cotton T-shirts	6.9 × 10 ⁷	/		
Sample 2	DiBP		5.1 × 10 ⁵		25 ± 0.5	
	DnBP		1.1 × 10 ⁶			
DEHP	Aluminum	600 (m)	/	Diffusion-based PFS	25	(Wu et al. 2017)
	Stainless steel #1	1200 (m)	/			
	Stainless steel #2	1300 (m)	/			
	Steel	10,000 (m)	/			

(continued)

Table 2 (continued)

Sample ID	Chemical	Sink material	K_s (m/dimensionless)	D (m ² /h)	Testing method	Temperature (°C)	References
DiBP	Polished glass	600 (m)	\	\	SPME-based C_a -history method	25 ± 0.5	(Cao et al. 2017)
	Ground glass	4200 (m)					
	Acrylic	500 (m)					
DnBP	Pure cotton T-shirts	\	1.83×10^{-9}	1.01×10^{-9} 8.64×10^{-10}			
TCPP		\	\				

Diffusion Coefficient (D)

The diffusion coefficient in the sink material, D , is influenced by several factors, e.g., temperature and porosity. D can be estimated by the following equation (Morrison et al. 2017):

$$D = D_a \varepsilon^n / K_m \quad (39)$$

where D_a (m^2/s) is the diffusion coefficient in air, ε is the porosity of the sink material, and n is a constant always assigned as 3/2 or 4/3 (Armitage et al. 2013; Cao et al. 2016a, 2016b). Furthermore, D_a is dependent on temperature and pressure according to the semi-empirical relation established by Fuller et al. (1966):

$$D_a = 10^{-3} \frac{T^{1.75} \left[\left(\frac{1}{M_{air}} \right) + (1/M) \right]^{1/2}}{p \left[\bar{V}_{air}^{1/3} + \bar{V}^{1/3} \right]^2} \quad (\text{cm}^2 \text{s}^{-1}) \quad (40)$$

where T (K) is temperature, p (atm) is the gas-phase pressure, M_{air} (28.97 g/mol) is the average molar mass of air, M (g/mol) is the molar mass of the target SVOC, \bar{V}_{air} ($\approx 20.1 \text{ cm}^3/\text{mol}$) is the average molar volume of the gases in air, and \bar{V} (cm^3/mol) is the molar volume of the target SVOC. Therefore, D is dependent on temperature and gas-phase pressure, in which case D is positively proportional to $T^{1.75}$ and inversely proportional to p . However, several studies on volatile organic compounds (VOCs) have found that D estimated using this empirical formula are vastly different from those experimentally measured (Blondeau et al. 2003; Cao et al. 2017). Xiong et al. (2008) explored the reason for this inconsistency and pointed out that researchers' different understanding of material pore structure leads to the inconsistency. If the macropores (pores with diameter larger than 10λ , where λ is the mean free path of the VOC molecule) and mesopores (pores with diameter less than 10λ) are treated as in series connection, the mesopores play a more important role in the determination of diffusion rate of chemicals. On the contrary, if the macro- and mesopores are treated as in parallel connection, the macropores dominate, and D will be overestimated. Based on these findings, Xiong et al. (2008) established a macro-meso two-scale model to predict the diffusion coefficient of VOCs in porous materials. However, its suitability to estimate diffusion coefficients of SVOCs has not been evaluated.

Relationship Between K_s and Temperature, Surface Roughness, Vapor Pressure, and Other Potential Impact Factors

Apart from the pp-LFERs, K_s can also be estimated by other physical or chemical properties of substances. Wu et al. (2017) revealed that surface roughness has a significant effect on the adsorption process of DEHP. K_s is linearly correlated with the roughness factor of material surfaces. In this case, Wu et al. (2017) proposed the possibility that the K_s values of some SVOCs can be easily determined by measuring the surface roughness rather than conducting time-consuming experiments. Xu et al. (2009) pointed out that K_s of phthalates on various surfaces are related to vapor

pressures. The relationship was derived for BBP, DBP, and BPA. Although only three chemicals were applied to obtain the relationship, which cannot yield a definite conclusion, with more datasets used to validate the relationship, it will also serve as a convenient method to estimate K_s . Linear relationships between the logarithm of vapor pressures and partition coefficients of DEHP, DINP, and DnBP on stainless steel were also found (Liang and Xu 2014a).

Sorption to Particles/Dust

SVOCs emitted from source materials not only sorb to common surfaces indoors, but also partition to settled dust and suspended particles (Bi et al. 2018). Considering the potential toxicity of SVOCs to human health and the fact that particles and dust can be ingested by people, especially children who frequently put their hands in mouths, it is important to investigate SVOC sorption by particles and dust.

Interaction Between Gas-Phase SVOCs and Suspended Particles

The Equilibrium Model

There are both equilibrium models and dynamic models to describe the mass-transfer process of gas-phase SVOCs sorbing to particles. For equilibrium model, an instant partition equilibrium is assumed between gas phase and particle surface (Yamasaki et al. 1982; Finizio et al. 1997):

$$F = K_p \cdot C_a \cdot TSP \quad (41)$$

where F ($\mu\text{g}/\text{m}^3$) is the particle-phase concentration of SVOCs, K_p ($\text{m}^3/\mu\text{g}$) is the gas/particle partition coefficient, C_a ($\mu\text{g}/\text{m}^3$) is the gas-phase concentration of SVOCs, and TSP ($\mu\text{g}/\text{m}^3$) is the total suspended particle mass concentration.

The Dynamic Model

In real indoor environments, the partitioning process seldom reaches equilibrium due to the nearly constant removal of suspended particles through ventilation and deposition. In addition, the instant equilibrium model is more appropriate for relatively volatile chemicals such as pyrene, and particles with relatively small diameter (0.01–10 μm), but is not reasonable for less volatile chemicals such as DEHP, and particles with a diameter larger than 2.5 μm (Liu et al. 2013). Otherwise, pronounced deviation (a two orders of magnitude error in gas-phase concentration and a factor of two error in particle-phase concentration) will be generated if the equilibrium model is used (Liu et al. 2013). For this reason, it is necessary to use dynamic models to characterize the gas/particle partitioning of SVOCs.

An important point for accurately establishing the dynamic model is to determine what the rate limiting process regarding the mass transfer is, either external (mass transfer from bulk air to particle surface) or internal (diffusion in and out of the

particle). Typically, this is determined by comparing the timescale of each process (Strommen and Kamens 1997).

For the description of particles, Liu et al. (2013) proposed a physically based model of a particle, which possesses the essential feature of typical particles containing organic components. The representative particle consists of an impermeable core and a permeable homogenous outer layer (Fig. 14). Corresponding to this physical model, a mathematical model to describe the diffusion in the particle was developed:

$$\frac{\partial F}{\partial t} = D_{sp} \left(\frac{\partial^2 F}{\partial r^2} + \frac{2}{r} \frac{\partial F}{\partial r} \right), R_1 < r < R_2 \quad (42)$$

where F ($\mu\text{g}/\text{m}^3$, mass of SVOC per volume of particle) is the particle-phase SVOC concentration, D_{sp} (m^2/s) is the intraparticle diffusion coefficient of SVOC, and r (m) is the diffusive distance. The boundary conditions are:

$$\frac{\partial F}{\partial r} = 0, r = R_1 \quad (43)$$

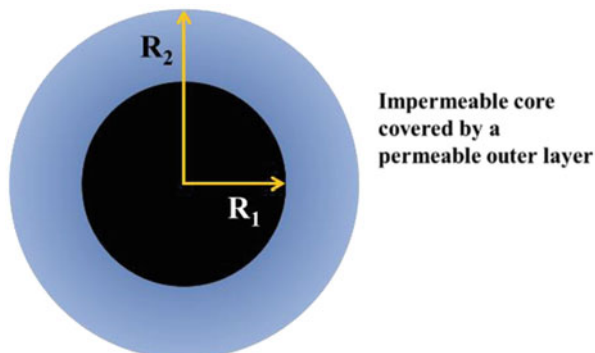
$$D_{sp} \frac{\partial F}{\partial r} = v_t \left(C_a - \frac{F}{K_p} \right), r = R_2 \quad (44)$$

where v_t (m/s) is the mass-transfer coefficient at gas/particle interface, C_a ($\mu\text{g}/\text{m}^3$, mass of SVOC per volume of air) is the gas-phase concentration of SVOCs in bulk air, and K_p is the gas/particle partition coefficient. The initial condition is:

$$F(r, t = 0) = 0 \quad (45)$$

To determine the rate-limiting process of mass transfer, the above model (Eqs. 42–45) is normalized by defining the following dimensionless parameters:

Fig. 14 The physically based model of particles with organic matter. (©With permission of Liu et al. 2013)



$$F^* = \frac{(K_p C_a - F)}{(K_p C_a)}, R_p = \frac{r}{R_2}, R_{12} = \frac{R_1}{R_2}, Fo_m = \frac{(D_s p t)}{(R_2^2)}, Bi_m = \frac{(v_t R_2)}{D_s p}$$

In this way, the dimensionless particle-phase concentration, F^* , is a function of:

$$F^* = f\left(\frac{Bi_m}{K_p}, Fo_m, R_p, R_{12}\right) \quad (46)$$

where $\frac{Bi_m}{K_p}$ indicates a ratio of internal mass-transfer resistance to external mass-transfer resistance. As $\frac{Bi_m}{K_p}$ increases, the internal mass-transfer resistance is stronger. To evaluate which resistance is more significant for the gas/particle dynamic interaction, a parameter, ε , is established:

$$\varepsilon = \frac{F^*(R_p = 1)}{F^*(R_p = R_{12})} \quad (47)$$

As $\frac{Bi_m}{K_p}$ decreases, which means external resistance plays a more important role in the mass-transfer resistance, ε increases. When $\frac{Bi_m}{K_p}$ decreases to a critical value, ε increases to 95% and the internal resistance can be neglected; the complicated intraparticle diffusion process (Eqs. 42–45) is not necessary for describing the gas/particle interaction. Instead, the lumped-parameter method is sufficient to describe the interaction between gas-phase SVOCs and particles. In addition, ε is also subject to the fraction of impermeable volume of the particle, f_v :

$$f_v = 1 - R_{12}^3 \quad (48)$$

Therefore, f_v and $\frac{Bi_m}{K_p}$ together determine whether the internal mass-transfer resistance can be ignored. The critical $\frac{Bi_m}{K_p}$ decreases with increasing f_v . With the commonly identified SVOCs (Pyrene, DEHP, DnBP, BaP, BDE-47, and BDE-99) and porous and nonporous particles with diameter varying from 0.01 to 10 μm , their $\frac{Bi_m}{K_p}$'s are smaller than the critical $\frac{Bi_m}{K_p}$, in which case the concentration gradient within the particle can be ignored, and for convenience, the lumped-parameter method may be applied for the characterization of gas/particle partition process.

Another important point for dynamic gas/particle modeling is to determine the time required to attain partition equilibrium. Based on the above analysis, the lumped parameter method is used:

$$V_p \frac{dF}{dt} = v_t A_p \left(C_a - \frac{F}{K_p} \right) \quad (49)$$

where V_p is the volume of the particle and A_p is the surface area of the particle. The analytical solution of Eq. (49) is:

$$F = K_p C_a (1 - e^{-\varphi t}) \quad (50)$$

$$\varphi = \frac{v_t A_p}{V_p K_p} = \frac{6 v_t}{d_p K_p} \quad (51)$$

where φ is the characteristic parameter concerning the timescales of gas/particle partitioning of SVOCs. If it is assumed that the partition equilibrium is achieved when the particle concentration F reaches 95% of the equilibrium concentration $K_p C_a$, then the critical time for attaining gas/particle partition equilibrium is:

$$t_c = 3\varphi^{-1} \quad (52)$$

The criterion, which establishes whether the gas/particle interaction can be described as instantaneous partition equilibrium, is based on a comparison between equilibrium timescales and the residence time of particle indoors (which is mainly controlled by air exchange rate [on the order of 1 h^{-1}]). If the equilibrium timescale is one order shorter than the residence time, then the instant partition equilibrium is reasonable for the modeling (Eq. 41). Otherwise, it is necessary to adopt a dynamic model to characterize gas/particle interaction:

$$\frac{dF}{dt} = \frac{TSP \cdot A_p}{V_p} v_t \left(C_a - \frac{F}{TSP \cdot K_p} \right) - \frac{Q}{V} F \quad (53)$$

It can be seen from Eq. (51) that the critical time for attaining partition equilibrium is a function of the mass-transfer coefficient on the particle surface, v_t , the particle diameter, d_p , and the gas/particle partition coefficient K_p . v_t varies with SVOCs and the composition of particles, but the variation can be neglected compared to that in K_p , which varies by several orders of magnitude (Liu et al. 2013). Therefore, t_c is mainly governed by K_p and d_p .

Role of Aerosols in Enhancing SVOC Flux Between Air and Indoor Surfaces

Xu and Little (2006) investigated the impact of particles on SVOC emission and they found that because of the presence of particles, the bulk gas-phase concentration of SVOCs will decrease, leading to a larger concentration gradient between surface boundary layer and bulk air, and therefore enhancing the SVOC emission rate. Through conducting experiments, Benning et al. (2013) reached a similar conclusion that particles can enhance DEHP flux from a material surface.

For SVOC sorption to surfaces, Liu et al. (2012) found that SVOC transport in the boundary layer between air and surfaces is significantly enhanced in the presence of particles, and the sorption rate is thereby increased. This is because particles transport SVOCs to surfaces through eddy and Brownian diffusion, and in the boundary layer, particles can release SVOCs and decrease the mass-

transfer resistance between air and surfaces (Weschler and Nazaroff 2008). The flux enhancement is influenced by particle diameter (d_p), gas/particle partition coefficient (K_p), and air velocity near surfaces (Liu et al. 2012). As d_p decreases, flux enhancement is inclined to increase. However, for particles with extremely small diameters (e.g., $d_p < 0.05 \mu\text{m}$) and SVOCs with $\log K_p = 13$, the enhancement will drop somewhat. The flux enhancement is more pronounced for chemicals with lower volatility; it is not significant if the $\log K_p$ value of SVOCs is lower than 10, but as the K_p value increases, the flux enhancement increases.

Existing Methods for Measuring Key Sorption Parameter (K_p)

Existing Methods Used in Atmospheric Field (Equilibrium Model)

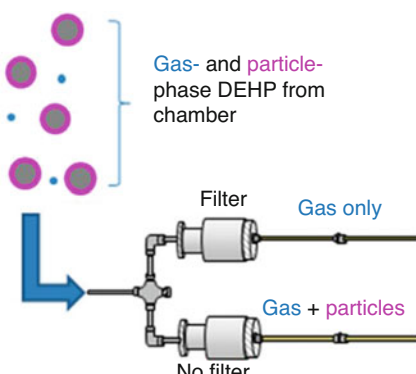
In field test, Eq. (41) was first proposed by Yamasaki (1982) to depict the partition behavior of PAHs on particles in ambient air, and now it is widely applied to determine K_p by monitoring the particle- and gas-phase concentration of SVOCs and the total suspended particle mass concentration.

Sandwich-like Chamber Method

Benning et al. (2013) applied the sandwich-like chamber method developed by Xu et al. (2012) to measure K_p of DEHP to ammonium sulfate particles. The airborne (particle- and gas-phase) concentration and gas-phase concentration of DEHP at the outlet of the chamber were measured together by controlling the loading of polytetrafluoroethylene (PTFE) membrane filter on different sampling trains of the chamber outlet (Fig. 15). In this way, the particle-phase concentration of DEHP can be calculated as the concentration difference between the two sampling trains, and the gas/particle partition coefficient can be derived as:

$$K_p = \frac{F}{C_a \cdot TSP} \quad (54)$$

Fig. 15 Experimental sampling setup for the measurement of gas-phase and airborne DEHP. (©With permission of Benning et al. 2013. Copyright 2021 American Chemical Society)



where C_a ($\mu\text{g}/\text{m}^3$) is the long-term average steady-state gas-phase concentration of DEHP, and TSP is the average measured total suspended particle mass concentration of both before and after passing through the chamber.

Using this method, K_p of DEHP on ammonium sulfate particles was determined to be $0.032 \pm 0.003 \text{ m}^3/\mu\text{g}$. The K_p of DEHP can also be estimated by empirical relationship based on vapor pressure (Pankow 1987, 1994; Naumova et al. 2003) or the octanol-air partition coefficient (Finizio et al. 1997; Harner and Bidleman 1998; Cousins and Mackay 2001). The result obtained by Benning et al. (2013) is one order of magnitude lower than that obtained based on the vapor pressure, i.e., $0.25 \text{ m}^3/\mu\text{g}$. However, it is only a factor of two lower than that obtained based on the octanol-air partition coefficient, i.e., $0.64 \text{ m}^3/\mu\text{g}$. This discrepancy may be due to the difference of particle composition (organic/inorganic), particle mass concentration, particle size, and the uncertainties of DEHP's vapor pressure. Benning's method (2013) was the first chamber experiment to quantify K_p .

Tube Chamber

Wu et al. (2018) developed a long tube chamber (Fig. 16) method to determine the K_p of DEHP on one inorganic particle (ammonium sulfate) and two organic particles (oleic acid and squalane). Similar to the sandwich-like chamber, the tube chamber is designed to maximize the ratio of SVOC source area to sink area. A thin layer of pure DEHP liquid was coated on the internal surface of the tube to serve as the emission source. Air mixed with particles at a specific concentration was introduced into the tube at a controlled flow rate to guarantee a laminar flow in the tube, avoiding inaccuracy caused by complex flow field in the chamber. The K_p value of DEHP on inorganic particles reported by Wu et al. (2018) is $0.011 \pm 0.10 \text{ m}^3/\mu\text{g}$, which is slightly lower than that reported by Benning et al. (2013). For organic particles, the measured K_p value is $0.23 \pm 0.13 \text{ m}^3/\mu\text{g}$ for oleic acid and $0.11 \pm 0.10 \text{ m}^3/\mu\text{g}$ for squalane.

Fig. 16 Photo of experimental setup of the long tube chamber method.
(© With permission of Wu et al. 2018. Copyright 2021 American Chemical Society)



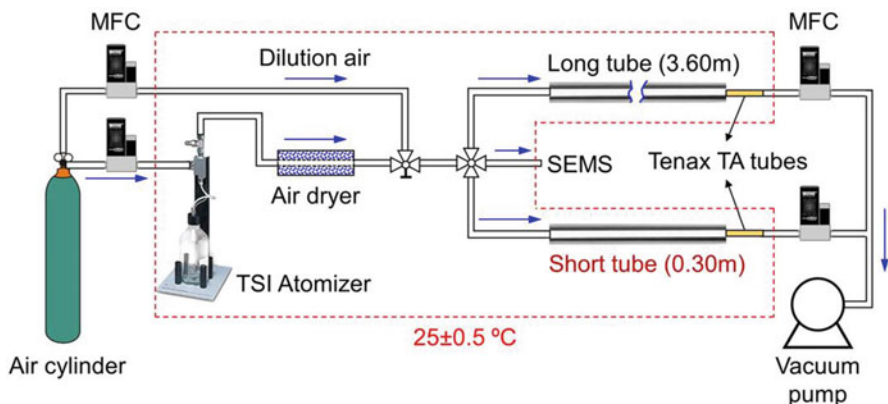


Fig. 17 Experimental system. (© With permission of Cao et al. 2019)

The two abovementioned chamber methods require that the sorption equilibrium between gas-phase SVOCs and particles has to be attained, which may increase inaccuracy and uncertainty, especially for SVOCs with larger K_p and particles with larger diameter. Furthermore, the gas-phase concentration of SVOCs may be underestimated because they are inclined to sorb to the filter during sampling (Fig. 15), and measurement errors are generated. To overcome these two problems, Cao et al. (2019) improved the method of Wu et al. (2018) and determined the K_p of DEHP on ammonium sulfate. The tube chamber method was modified from one tube to two tubes of different lengths (3.60 and 0.30 m) in parallel (to both conducted equilibrium and dynamic methods) (Fig. 17). A mass-transfer model of SVOCs in the tube chamber was established, and unlike the previous methods (Benning et al. 2013; Wu et al. 2018), only the total airborne SVOC concentration needed to be measured by Tenax tubes and gas-phase and particle-phase DEHP were not separated. K_p values were derived by fitting the mass-transfer model to the measured total airborne SVOC concentration, which agreed well with the previous studies (Benning et al. 2013; Wu et al. 2018).

All the experimentally determined K_p values of SVOCs are summarized in Table 3.

Prediction of the Key Sorption Parameter (K_p)

Junge-Pankow Method: K_p - P_s Relationship and K_p - K_{OA} Relationship

Apart from using experimental methods to quantify K_p , empirical relationships are also widely used to predict K_p for SVOCs. The Junge-Pankow model (Junge 1977; Pankow 1987) and the K_{oa} absorption model (Finizio et al. 1997; Harner and Bidleman 1998; Weschler and Nazaroff 2010) are most frequently applied. In the Junge-Pankow model, the particle fraction of chemical, φ , which is calculated as the

Table 3 Key parameters of SVOC particle sorption (K_p)

Chemical	Particle	Median particle diameter (nm)	K_p	Testing method	Temperature (°C)	References
DEHP	Ammonium sulfate	40–50	0.032 ± 0.003 (m ³ /μg)	Modified sandwich-like chamber	22 ± 0.3	(Benning et al. 2013)
	Ammonium sulfate	70–80	0.011 ± 0.004 (m ³ /μg)	Long tube chamber	25 ± 0.5	
Oleic	40–130	0.23 ± 0.13 (m ³ /μg)				(Wu et al. 2018)
	110–170	0.11 ± 0.10 (m ³ /μg)				
DEHP	Ammonium sulfate	50–60	260 ± 80 (m) (surface-area-normalized partition coefficient)	Dynamic long tube chamber	25	(Cao et al. 2019)

particle-phase concentration over the total airborne concentration, is correlated with the subcooled liquid vapor pressure of chemical, P_s (Junge 1977; Pankow 1987):

$$\varphi = \frac{c\theta}{P_s + c\theta} \quad (55)$$

where c is a constant related with the desorption heat of particle surface, vaporization heat of the chemical, and the number of adsorption sites on the particle, and θ is the surface area of the particle.

According to the definition of φ , it can be derived as:

$$\varphi = \frac{F}{F + C_a} \quad (56)$$

Substituting Eqs. (54 and 56) into (55) gives an equation of the following form:

$$\log K_p = -\log P_s + b \quad (57)$$

The intercept ($b = \log \frac{c\theta}{TSP}$) is dependent on the inherent properties of the particles, and the slope is required to be close to -1 for true equilibrium partitioning as described in Pankow (1994). However, this may not be satisfied for all regression cases of different SVOCs. The possible reasons are the artificial errors in sampling and kinetic effects. However, the slope may still not be -1 , even if the above two problems are avoided, due to the thermodynamic effect, which means that the difference between desorption heat and vaporization heat does not remain constant within a class of chemicals (Pankow and Bidleman 1992). Wei et al. (2016) reviewed the empirical equations of K_p and P_s for a wide range of SVOCs and they used all the published equations to derive the K_p distribution of numerous SVOCs. This way, the deviation related to the selection of a particular equation can be diminished.

Another generally used empirical correlation for K_p prediction is the K_{oa} absorption model, which indicates that K_{oa} and P_s are most relevant (Cousins and Mackay 2001). Finizio et al. (1997) first proposed K_{oa} to be a predictor for K_p of SVOCs in two forms:

$$\log K_p = a + b \log K_{oa} \quad (58)$$

where a and b are constants and a is related to the inherent properties of the chemical and b . When b is assigned to be 1.0, Eq. (58) is transformed to be:

$$\frac{K_p}{K_{oa}} = B$$

where B is within the order of 10^{-12} and decreases with increasing K_{oa} , which may be due to the kinetic effect (Finizio et al. 1997).

Following Finizio et al. (1997), other researchers began to investigate the relationship between K_p and K_{oa} , and empirical equations for PAHs (Weschler et al. 2008),

PCBs (Harner and Bidleman 1998; Kaupp and McLachlan 1999), organochlorine pesticides (Kaupp and McLachlan 1999), and PCNs (Harner and Bidleman 1998) were established.

Pp-LFER Method

Both the estimation from P_s and K_{oa} are single parameter approaches. It is unclear whether one descriptor is enough to characterize the comprehensive chemical diversity due to van der Waals and H-bond interactions (Salthammer and Goss 2019). As mentioned in the section of “Prediction of the Key Sorption Parameters” the poly-parameter linear free energy relationship (pp-LFER) may overcome this limitation and can be adopted to estimate K_p . Using this method, Salthammer and Goss (2019) determined the K_p values of 14 SVOCs (mostly phthalates) on water-insoluble organic matter (WIOM), for which the dominant mechanism is absorption. The results derived from pp-LFERs are significantly lower than those based on P_s and K_{oa} in most cases (Salthammer and Goss 2019). Although pp-LFER appears to be a more comprehensive method for K_p estimation, it is challenging to obtain the precise values of multiple descriptors (e.g., van der Waals interactions, L ; polarizability, S ; hydrogen bond acidity, A ; and hydrogen bond basicity, B). Therefore, the uncertainties arising from parameterization should be carefully taken into account.

Conclusion

Many efforts have focused on exploring the mechanisms governing SVOC source and sink behavior (i.e., emission, sorption, and partitioning) and developing methods to determine the key parameters that control these processes. The substantial achievements have been reviewed in this chapter. However, there still are many topics that require further investigation to improve our understanding of SVOC fate and transport in indoor environments and their impacts on human health, such as standard methods to determine key parameters, insight into the SVOC source and sink processes at the molecular level, the influence of environmental conditions, and different mechanisms that may occur in new source and sink materials.

Cross-References

- [Indoor Gas-Phase Chemistry](#)
- [Indoor Surface Chemistry](#)

References

- Armitage JM, Hayward SJ, Wania F (2013) Modeling the uptake of neutral organic chemicals on XAD passive air samplers under variable temperatures, external wind speeds and ambient air concentrations (PAS-SIM). Environ Sci Technol 47:13546–13554

- Bako-Biro Z, Wargocki P, Weschler CJ, Fanger PO (2004) Effects of pollution from personal computers on perceived air quality, SBS symptoms and productivity in offices. *Indoor Air* 14: 178–187
- Benning JL, Liu Z, Tiwari A et al (2013) Characterizing gas-particle interactions of phthalate plasticizer emitted from vinyl flooring. *Environ Sci Technol* 47:2696–2703. <https://doi.org/10.1021/es304725b>
- Bi C, Liang Y, Xu Y (2015) Fate and transport of phthalates in indoor environments and the influence of temperature: a case study in a test house. *Environ Sci Technol* 49:9674–9681. <https://doi.org/10.1021/acs.est.5b02787>
- Bi C, Maestre JP, Li H et al (2018) Phthalates and organophosphates in settled dust and HVAC filter dust of US low-income homes: association with season, building characteristics, and childhood asthma. *Environ Int* 121:916–930
- Blondeau P, Tiffonnet A, Damian A et al (2003) Assessment of contaminant diffusivities in building materials from porosimetry tests. *Indoor Air* 13:310–318
- Butt CM, Diamond ML, Truong J et al (2004) Spatial distribution of polybrominated diphenyl ethers in southern Ontario as measured in indoor and outdoor window organic films. *Environ Sci Technol* 38:724–731
- Cao J, Du Z, Mo J et al (2016b) Inverse problem optimization method to design passive samplers for volatile organic compounds: principle and application. *Environ Sci Technol* 50: 13477–13485
- Cao J, Eichler CM, Wu Y, Little JC (2019) Dynamic method to measure partition coefficient and mass accommodation coefficient for gas–particle interaction of phthalates. *Aerosol Sci Technol* 53:1158–1171
- Cao J, Liu N, Zhang Y (2017b) SPME-based C_a -history method for measuring SVOC diffusion coefficients in clothing material. *Environ Sci Technol* 51:9137–9145. <https://doi.org/10.1021/acs.est.7b02540>
- Cao J, Weschler CJ, Luo J, Zhang Y (2016a) C_m -history method, a novel approach to simultaneously measure source and sink parameters important for estimating indoor exposures to phthalates. *Environ Sci Technol* 50:825–834. <https://doi.org/10.1021/acs.est.5b04404>
- Cao J, Zhang X, Little JC, Zhang Y (2017a) A SPME-based method for rapidly and accurately measuring the characteristic parameter for DEHP emitted from PVC floorings. *Indoor Air* 27: 417–426. <https://doi.org/10.1111/ina.12312>
- Clausen PA, Hansen V, Gunnarsen L et al (2004) Emission of Di-2-ethylhexyl phthalate from PVC flooring into air and uptake in dust: emission and sorption experiments in FLEC and CLIMPAQ. *Environ Sci Technol* 38:2531–2537. <https://doi.org/10.1021/es0347944>
- Clausen PA, Liu Z, Kofoed-Sørensen V et al (2012) Influence of temperature on the emission of Di-(2-ethylhexyl)phthalate (DEHP) from PVC flooring in the emission cell FLEC. *Environ Sci Technol* 46:909–915. <https://doi.org/10.1021/es2035625>
- Cousins IT, Mackay D (2001) Gas–particle partitioning of organic compounds and its interpretation using relative solubilities. *Environ Sci Technol* 35:643–647
- Diamond ML, Gingrich SE, Fertuck K et al (2000) Evidence for organic film on an impervious urban surface: characterization and potential teratogenic effects. *Environ Sci Technol* 34: 2900–2908
- Dishaw L, Macaulay L, Roberts SC, Stapleton HM (2014) Exposures, mechanisms, and impacts of endocrine-active flame retardants. *Gastrointest • Endocr Metab Dis* 19:125–133. <https://doi.org/10.1016/j.coph.2014.09.018>
- Eichler CMA, Wu Y, Cao J et al (2018) Equilibrium relationship between SVOCs in PVC products and the air in contact with the product. *Environ Sci Technol* 52:2918–2925. <https://doi.org/10.1021/acs.est.7b06253>
- Ferguson KK, Meeker JD, Cantonwine DE et al (2016) Urinary phthalate metabolite and bisphenol a associations with ultrasound and delivery indices of fetal growth. *Environ Int* 94:531–537. <https://doi.org/10.1016/j.envint.2016.06.013>

- Finizio A, Mackay D, Bidleman T, Harner T (1997) Octanol-air partition coefficient as a predictor of partitioning of semi-volatile organic chemicals to aerosols. *Atmos Environ* 31: 2289–2296
- Freundlich H (1906) Over the adsorption in solution. *J Phys Chem* 57:1100–1107
- Fujii M, Shinohara N, Lim A et al (2003) A study on emission of phthalate esters from plastic materials using a passive flux sampler. *Atmos Environ* 37:5495–5504
- Fuller EN, Schettler PD, Giddings JC (1966) New method for prediction of binary gas-phase diffusion coefficients. *Ind Eng Chem* 58:18–27
- Goss K-U (2004) The air/surface adsorption equilibrium of organic compounds under ambient conditions. *Crit Rev Environ Sci Technol* 34:339–389
- Goss K-U (2005) Predicting the equilibrium partitioning of organic compounds using just one linear solvation energy relationship (LSER). *Fluid Phase Equilib* 233:19–22. <https://doi.org/10.1016/j.fluid.2005.04.006>
- Harner T, Bidleman TF (1998) Octanol-air partition coefficient for describing particle/gas partitioning of aromatic compounds in urban air. *Environ Sci Technol* 32:1494–1502
- He G, Yang X (2005) On regression method to obtain emission parameters of building materials. *Build Environ* 40:1282–1287. <https://doi.org/10.1016/j.buildenv.2004.11.002>
- Hoffman K, Sosa JA, Stapleton HM (2017) Do flame retardant chemicals increase the risk for thyroid dysregulation and cancer? *Current Opinion in Oncology* 29(1):7–13. <https://doi.org/10.1097/CCO.0000000000000335>
- Høyér BB, Lelters V, Giwercman A et al (2018) Impact of Di-2-Ethylhexyl phthalate metabolites on male reproductive function: a systematic review of human evidence. *Curr Environ Health Rep* 5:20–33. <https://doi.org/10.1007/s40572-018-0174-3>
- Junge CE (1977) Basic consideration about trace constituents in the atmosphere as related to the fate of global pollutants. In *Fate of Pollutants in Air and Water Environmerits*, ed. I. H. Suffett, Part I, pp. 7–26. Wiley, New York
- Kamprad I, Goss K-U (2007) Systematic investigation of the sorption properties of polyurethane foams for organic vapors. *Anal Chem* 79:4222–4227
- Kaupp H, McLachlan MS (1999) Gas/particle partitioning of PCDD/fs, PCBs, PCNs and PAHs. *Chemosphere* 38:3411–3421
- Kay VR, Bloom MS, Foster WG (2014) Reproductive and developmental effects of phthalate diesters in males. *Crit Rev Toxicol* 44:467–498. <https://doi.org/10.3109/10408444.2013.875983>
- Kay VR, Chambers C, Foster WG (2013) Reproductive and developmental effects of phthalate diesters in females. *Crit Rev Toxicol* 43:200–219. <https://doi.org/10.3109/10408444.2013.766149>
- Kemmlein S, Hahn O, Jann O (2003) Emissions of organophosphate and brominated flame retardants from selected consumer products and building materials. *Indoor Air Chem Phys Pap Indoor Air* 37:5485–5493. <https://doi.org/10.1016/j.atmosenv.2003.09.025>
- Koble RA, Corrigan TE (1952) Adsorption isotherms for pure hydrocarbons. *Ind Eng Chem* 44: 383–387
- Langmuir I (1916) The constitution and fundamental properties of solids and liquids. Part I Solids J Am Chem Soc 38:2221–2295. <https://doi.org/10.1021/ja02268a002>
- Li H, Wu Y, Bi C, Eichler CMA, Little J, Xu Y (2022, in preparation) Endocrine Disrupting Compounds in Consumer Products: A Novel Method toward Risk-based High-throughput Prioritization, In preparation
- Liang Y, Liu X, Allen MR (2018a) Measuring and modeling surface sorption dynamics of organophosphate flame retardants on impervious surfaces. *Chemosphere* 193:754–762. <https://doi.org/10.1016/j.chemosphere.2017.11.080>
- Liang Y, Liu X, Allen MR (2018b) Measurements of parameters controlling the emissions of organophosphate flame retardants in indoor environments. *Environ Sci Technol* 52:5821–5829. <https://doi.org/10.1021/acs.est.8b00224>

- Liang Y, Xu Y (2014a) Improved method for measuring and characterizing phthalate emissions from building materials and its application to exposure assessment. *Environ Sci Technol* 48: 4475–4484. <https://doi.org/10.1021/es405809r>
- Liang Y, Xu Y (2014b) Emission of phthalates and phthalate alternatives from vinyl flooring and crib mattress covers: the influence of temperature. *Environ Sci Technol* 48:14228–14237. <https://doi.org/10.1021/es504801x>
- Liu Q-T, Chen R, McCarry BE et al (2003) Characterization of polar organic compounds in the organic film on indoor and outdoor glass windows. *Environ Sci Technol* 37:2340–2349
- Liu X, Guo Z, Roache NF (2014) Experimental method development for estimating solid-phase diffusion coefficients and material/air partition coefficients of SVOCs. *Atmos Environ* 89:76–84. <https://doi.org/10.1016/j.atmosenv.2014.02.021>
- Liu C, Morrison GC, Zhang Y (2012) Role of aerosols in enhancing SVOC flux between air and indoor surfaces and its influence on exposure. *Atmos Environ* 55:347–356. <https://doi.org/10.1016/j.atmosenv.2012.03.030>
- Liu C, Shi S, Weschler C et al (2013) Analysis of the dynamic interaction between SVOCs and airborne particles. *Aerosol Sci Technol* 47:125–136
- Liu C, Zhang Y (2016) Characterizing the equilibrium relationship between DEHP in PVC flooring and air using a closed-chamber SPME method. *Build Environ* 95:283–290. <https://doi.org/10.1016/j.buildenv.2015.09.028>
- Meeker JD, Stapleton HM (2010) House dust concentrations of organophosphate flame retardants in relation to hormone levels and semen quality parameters. *Environ Health Perspect* 118:318–323. <https://doi.org/10.1289/ehp.0901332>
- Miodovnik A, Edwards A, Bellinger DC, Hauser R (2014) Developmental neurotoxicity of orthophthalate diesters: review of human and experimental evidence. *Neurotoxicology* 41:112–122. <https://doi.org/10.1016/j.neuro.2014.01.007>
- Morrison G, Weschler CJ, Bekö G (2017) Dermal uptake of phthalates from clothing: comparison of model to human participant results. *Indoor Air* 27:642–649
- Naumova YY, Offenberg JH, Eisenreich SJ et al (2003) Gas/particle distribution of polycyclic aromatic hydrocarbons in coupled outdoor/indoor atmospheres. *Atmos Environ* 37:703–719
- Nazaroff W, Alvarez-Cohen L (2001) Environmental engineering science, John Wiley & Sons
- Nazaroff WW, Goldstein AH (2015) Indoor chemistry: research opportunities and challenges. *Indoor Air* 25:357–361. <https://doi.org/10.1111/ina.12219>
- Ni Y, Kumagai K, Yanagisawa Y (2007) Measuring emissions of organophosphate flame retardants using a passive flux sampler. *Atmos Environ* 41:3235–3240
- Noguchi M, Yamasaki A (2016) Passive flux sampler measurements of emission rates of phthalates from poly (vinyl chloride) sheets. *Build Environ* 100:197–202
- Ouyang G, Pawliszyn J (2008) A critical review in calibration methods for solid-phase micro-extraction. *Anal Chim Acta* 627:184–197. <https://doi.org/10.1016/j.aca.2008.08.015>
- Pankow JF (1987) Review and comparative analysis of the theories on partitioning between the gas and aerosol particulate phases in the atmosphere. *Atmospheric Environ* 1967 21:2275–2283
- Pankow JF (1994) An absorption model of gas/particle partitioning of organic compounds in the atmosphere. *Atmos Environ* 28:185–188
- Pankow JF, Bidleman TF (1992) Interdependence of the slopes and intercepts from log-log correlations of measured gas-particle partitioning and vapor pressure—I. theory and analysis of available data. *Atmospheric Environ Part Gen Top* 26:1071–1080
- Patrick L, Destaillats H, Zouev I et al (2010) Sorption, desorption, and surface oxidative fate of nicotine. *Phys Chem Chem Phys* 12:10356. <https://doi.org/10.1039/c002643c>
- Salthammer T, Fuhrmann F, Uhde E (2003) Flame retardants in the indoor environment – part II: release of VOCs (triethylphosphosphate and halogenated degradation products) from polyurethane. *Indoor Air* 13:49–52
- Salthammer T, Goss K-U (2019) Predicting the gas/particle distribution of SVOCs in the indoor environment using poly parameter linear free energy relationships. *Environ Sci Technol* 53: 2491–2499. <https://doi.org/10.1021/acs.est.8b06585>

- Schwarzenbach RP, Gschwend PM, Imboden DM (2016) Environmental organic chemistry. Wiley
- Shelby MD (2006) NTP-CERHR monograph on the potential human reproductive and developmental effects of di (2-ethylhexyl) phthalate (DEHP). NTP CERHR MON v, vii–7, II-iii-xiii passim
- Sips R (1948) On the structure of a catalyst surface. *J Chem Phys* 16:490–495
- Stenzel A, Goss K-U, Endo S (2013) Determination of Polyparameter linear free energy relationship (pp-LFER) substance descriptors for established and alternative flame retardants. *Environ Sci Technol* 130125075250002. <https://doi.org/10.1021/es304780a>
- Strommen MR, Kamens RM (1997) Development and application of a dual-impedance radial diffusion model to simulate the partitioning of semivolatile organic compounds in combustion aerosols. *Environ Sci Technol* 31:2983–2990
- Wallace LA, Ott WR, Weschler CJ, Lai ACK (2017) Desorption of SVOCs from heated surfaces in the form of ultrafine particles. *Environ Sci Technol* 51:1140–1146. <https://doi.org/10.1021/acs.est.6b03248>
- Wang L, Zhao B, Liu C et al (2010) Indoor SVOC pollution in China: a review. *Chin Sci Bull* 55: 1469–1478. <https://doi.org/10.1007/s11434-010-3094-7>
- Weber WJ Jr, DiGiano FA (1996) Process dynamics in environmental systems. JOHN WILEY SONS INC, New York
- Wei W, Mandin C, Blanchard O et al (2016) Distributions of the particle/gas and dust/gas partition coefficients for seventy-two semi-volatile organic compounds in indoor environment. *Chemosphere* 153:212–219
- Weschler CJ, Nazaroff WW (2008) Semivolatile organic compounds in indoor environments. *Atmos Environ* 42:9018–9040. <https://doi.org/10.1016/j.atmosenv.2008.09.052>
- Weschler CJ, Nazaroff WW (2010) SVOC partitioning between the gas phase and settled dust indoors. *Atmos Environ* 44:3609–3620. <https://doi.org/10.1016/j.atmosenv.2010.06.029>
- Weschler CJ, Nazaroff WW (2017) Growth of organic films on indoor surfaces. *Indoor Air* 27: 1101–1112. <https://doi.org/10.1111/ina.12396>
- Weschler CJ, Salthammer T, Fromme H (2008) Partitioning of phthalates among the gas phase, airborne particles and settled dust in indoor environments. *Atmos Environ* 42:1449–1460
- WHO (2010) World health organization regional office for europe selected pollutants
- Wu Y, Cox SS, Xu Y et al (2016b) A reference method for measuring emissions of SVOCs in small chambers. *Build Environ* 95:126–132. <https://doi.org/10.1016/j.buildenv.2015.08.025>
- Wu Y, Eichler CMA, Cao J et al (2018) Particle/gas partitioning of phthalates to organic and inorganic airborne particles in the indoor environment. *Environ Sci Technol* 52:3583–3590. <https://doi.org/10.1021/acs.est.7b05982>
- Wu Y, Eichler CMA, Leng W et al (2017) Adsorption of phthalates on impervious indoor surfaces. *Environ Sci Technol* 51:2907–2913. <https://doi.org/10.1021/acs.est.6b05853>
- Wu RW, Harner T, Diamond ML (2008) Evolution rates and PCB content of surface films that develop on impervious urban surfaces. *Atmos Environ* 42:6131–6143
- Wu Y, Xie M, Cox SS et al (2016a) A simple method to measure the gas-phase SVOC concentration adjacent to a material surface. *Indoor Air* 26:903–912. <https://doi.org/10.1111/ina.12270>
- Xiong J, Cao J, Zhang Y (2016) Early stage C-history method: rapid and accurate determination of the key SVOC emission or sorption parameters of indoor materials. *Build Environ* 95:314–321
- Xiong J, Zhang Y, Wang X, Chang D (2008) Macro–meso two-scale model for predicting the VOC diffusion coefficients and emission characteristics of porous building materials. *Atmos Environ* 42:5278–5290
- Xu Y, Cohen Hubal EA, Clausen PA, Little JC (2009) Predicting residential exposure to phthalate plasticizer emitted from vinyl flooring: a mechanistic analysis. *Environ Sci Technol* 43:2374–2380. <https://doi.org/10.1021/es801354f>
- Xu Y, Cohen Hubal EA, Little JC (2010) Predicting residential exposure to phthalate plasticizer emitted from vinyl flooring: sensitivity, uncertainty, and implications for biomonitoring. *Environ Health Perspect* 118:253–258. <https://doi.org/10.1289/ehp.0900559>

- Xu Y, Little JC (2006) Predicting emissions of SVOCs from polymeric materials and their interaction with airborne particles. Environ Sci Technol 40:456–461. <https://doi.org/10.1021/es051517j>
- Xu Y, Liu Z, Park J et al (2012) Measuring and predicting the emission rate of phthalate plasticizer from vinyl flooring in a specially-designed chamber. Environ Sci Technol 46:12534–12541. <https://doi.org/10.1021/es302319m>
- Yamasaki H, Kuwata K, Miyamoto H (1982) Effects of ambient temperature on aspects of airborne polycyclic aromatic hydrocarbons. Environ Sci Technol 16:189–194
- Yang T, He Z, Zhang S, et al (2019) Emissions of DEHP from vehicle cabin materials: parameter determination, impact factors and exposure analysis. Environ Sci Process Impacts 21: 1323–1333. <https://doi.org/10.1039/C9EM00200F>
- Yang T, Wang H, Zhang X, et al (2020) Characterization of phthalates in sink and source materials: measurement methods and the impact on exposure assessment. J Hazard Mater 396: 122689. <https://doi.org/https://doi.org/10.1016/j.jhazmat.2020.122689>
- Zarean M, Keikha M, Poursafa P et al (2016) A systematic review on the adverse health effects of di-2-ethylhexyl phthalate. Environ Sci Pollut Res 23:24642–24693. <https://doi.org/10.1007/s11356-016-7648-3>
- Zhao F, Chen M, Gao F et al (2017) Organophosphorus flame retardants in pregnant women and their transfer to chorionic villi. Environ Sci Technol 51:6489–6497. <https://doi.org/10.1021/acs.est.7b01122>



Reference Materials for Building Product Emission Characterization

24

Dustin Poppendieck, Wenjuan Wei, and Mengyan Gong

Contents

Introduction	742
Why Test Material Emissions?	742
What Chemicals are Analyzed in Emission Testing?	743
How Does Emission Testing Work?	746
Reference Materials	748
Definitions	748
Building Product Reference Materials Used in Emission Testing	750
Designed Reference Materials Used in Emission Testing	751
Inter-laboratory Proficiency Testing Studies of Reference Materials	759
Uncertainties in Emission Testing When Using Reference Materials	763
Reference Material Variability	763
Emission Test System Variability	765
Analytical Measurement Variability	767
Inter-laboratory Study Procedure Variability	768
Conclusions	769
References	769

Abstract

Building products contain volatile organic compounds (VOCs), which can be emitted into indoor air and result in human exposures in the indoor environment. The emission rate, commonly measured in environmental chambers, is a key parameter to characterize the emission of a chemical of interest from materials in

D. Poppendieck · M. Gong

National Institute of Standards and Technology (NIST), Engineering Lab, Gaithersburg, MD, USA
e-mail: Dustin.Poppendieck@nist.gov

W. Wei (✉)

Scientific and Technical Centre for Building (CSTB), Health and Comfort Department, French Indoor Air Quality Observatory (OQAI), University of Paris-Est, Champs-sur-Marne, France
e-mail: Wenjuan.Wei@cstb.fr

© This is a U.S. Government work and not under copyright protection in the U.S.;
foreign copyright protection may apply 2022

741

Y. Zhang et al. (eds.), *Handbook of Indoor Air Quality*,
https://doi.org/10.1007/978-981-16-7680-2_25

a building. Reference materials with known emission rates can be used to characterize the uncertainty associated with building product emission testing. This chapter describes VOC emission testing and explores the types of reference materials that have been used to validate product emission testing. Detailed descriptions of five types of reference materials are presented, addressing their emission mechanisms, production methods, application protocols, and use in inter-laboratory emission tests. This chapter also describes some of the causes of uncertainty associated with reference materials, emission testing systems, analytical measurement methods, and inter-laboratory study procedures.

Keywords

Volatile organic compounds · Formaldehyde · Chamber · Inter-laboratory · Concentration

Introduction

Airborne emission testing is the quantification of the migration of chemicals from a building material or product into the gas phase. In general, a building material or product is placed in an environment at a controlled temperature, relative humidity, airflow rate, and pressure. The gas phase concentration of the chemical of interest is measured after certain conditions are met (e.g., the concentration of the chemical reaches steady state in the controlled environment). Some regulations or product labeling schemes define emission limits from tested materials as steady state gas-phase concentrations (mass per volume) under specified conditions. Under steady-state conditions the emission rate is the mass of chemical (concentration multiplied by the sample volume) emitted during the sampling period.

Why Test Material Emissions?

The concentration of most chemicals in indoor air is higher than outdoor air (Weschler 2006). The source of elevated indoor airborne chemical concentrations can be building materials, consumer products, occupants, and occupant activities, along with chemical reactions in the air. Quantifying the emissions of chemicals from building materials and consumer products into indoor spaces can increase the accuracy of indoor chemical concentration and exposure modeling. This improved exposure modeling may provide opportunities to reduce indoor chemical exposures.

There are two primary drivers for airborne emission testing of materials and products. First, some countries set regulatory maximum emission limits for chemicals or classes of chemicals from specific products (e.g., formaldehyde from wood products; Table 1). Second, voluntary product labeling schemes, or product certifications, and industry consensus standards can encourage producers to test products to gain market advantages. Product certification programs can be regulatory or voluntary.

Table 1 Examples of Emission Regulations

Country	Identification	Regulation Name
United States (USEPA)	Title VI TSCA	Formaldehyde Emission Standards for Composite Wood Products Rule (Title VI of the Toxic Substances Control Act (TSCA))
United States (CARB)	CWP ATCM	Composite Wood Products Airborne Toxic Control Measure (ATCM)
China	GB 18580-2017	Indoor Decorating and Refurbishing Materials – Limit of Formaldehyde Emission of Wood-Based Panels and Finishing Products
Germany	ChemVerbotsV	German Chemicals Prohibition Ordinance
France	Décret n°2011-321	Labeling of Construction and Decoration Products Regarding VOC Emissions
Japan	JIS A 5905	Fiberboards
Japan	JIS A 5908	Particleboards

Each regulation or certification label scheme requires a test protocol to determine emission rates from a specific product (Table 2). Many of the test methods have been developed and maintained by nongovernmental consensus-based organizations (e.g., the International Organization for Standardization (ISO) and ASTM International). The methods have varying degrees of parameter and measurement specificity (e.g., ASTM guides give information or series of options, while ASTM test methods require specific steps that produce a result). Some methods are specific to a product type (e.g., ANSI/BIFMA M7.1 focuses on furniture). Many methods are based in part on or refer to ISO 16000-9 (Indoor air – Part 9: Determination of the emission of volatile organic compounds from building products and furnishing – Emission test chamber method), for example, EN 16516. As described below methods can be either static (sealed chamber) or dynamic (flow-through chamber).

What Chemicals are Analyzed in Emission Testing?

Emission testing is used to quantify emission of an individual chemical, a group of chemicals or both. Due to regulatory requirements (e.g., USEPA Formaldehyde Emission Standards for Composite Wood Products Rule) formaldehyde is the most often targeted individual chemical for emission testing. Emissions of other volatile organic compounds (VOCs) are often covered by product emission labeling programs. There are many different definitions for VOCs and semi-volatile organic compounds (SVOCs) (ASTM 2017), with definitions using chemical boiling point, vapor pressure, and/or retention time on a gas chromatogram (GC) analytical column or combinations of these three. The total emitted mass of VOCs can be quantified in multiple ways: (1) as the sum of individually quantified chemicals within a range of boiling points, vapor pressures, and/or retention times, or (2) as an approximate quantification of components by integrating peaks using toluene equivalents (Oppel et al. 2020).

Table 2 Examples of Testing Standards

Test Method ID	Region	Type	Method Name	Chemicals
ISO 16000-9	International	Dynamic	Indoor air – Part 9: Determination of the Emission of Volatile Organic Compounds from Building Products and Furnishing – Emission Test Chamber Method	VOCs
ISO 16000-10	International	Dynamic	Indoor Air – Part 10: Determination of the Emission of Volatile Organic Compounds from Building Products and Furnishing – Emission Test Cell Method	VOCs
ASTM D5116	US	Dynamic	Standard Guide for Small-Scale Environmental Chamber Determinations of Organic Emissions from Indoor Materials/Products	VOCs
ASTM D6670	US	Dynamic	Standard Practice for Full-Scale Chamber Determination of Volatile Organic Emissions from Indoor Materials/Products Emission Rate	VOCs
ASTM D7706	US	Dynamic	Standard Practice for Rapid Screening of VOC Emissions from Products Using Micro-Scale Chambers	VOCs
ASTM D6007	US	Dynamic	Standard Test Method for Determining Formaldehyde Concentrations in Air from Wood Products Using a Small-Scale Chamber	Formaldehyde
ASTM E1333	US	Dynamic	Standard Test Method for Determining Formaldehyde Concentrations in Air and Emission Rates from Wood Products Using a Large Chamber	Formaldehyde
ASTM D5582	US	Static	Standard Test Method for Determining Formaldehyde Levels from Wood Products Using a Desiccator	Formaldehyde
CDPH Standard Method V1.2	US	Dynamic	Standard Method for the Testing & Evaluation of VOC Emissions from Indoor Sources Using Environmental Chambers	VOCs
ANSI/BIFMA M7.1	US	Dynamic	Testing for VOC Emissions from Office Furniture and Seating	VOCs and Formaldehyde

(continued)

Table 2 (continued)

Test Method ID	Region	Type	Method Name	Chemicals
UL 2821	US	Dynamic	GREENGUARD Standard for Building Materials, Finishes and Furnishings	VOCs and Formaldehyde
EN 16516	EU	Dynamic	Construction Products: Assessment of Release of Dangerous Substances – Determination of Emissions into Indoor Air	VOCs
EN 717-1	EU	Dynamic	Wood-based Panels – Determination of Formaldehyde Release – Formaldehyde Emission by the Chamber Method	Formaldehyde
EN 717-3	EU	Static	Wood-based panels – Determination of formaldehyde Release – Formaldehyde Release by the Flask Method	Formaldehyde
GEV	EU	Dynamic	GEV – Testing Method Determination of Volatile Organic Compounds for Evaluation of Emissions Controlled Products for Flooring Installation, Adhesives, Construction Products, as well as Lacquers, Finishes and Oils for Parquet, for Mineral Floorings and for Resilient Floorings	VOCs
GB/T 17657-2013	China	Dynamic	Test Methods of Evaluating the Properties of Wood-based Panels and Surface Decorated Wood-based Panels	Formaldehyde
JIS A 1911: 2015	Japan	Dynamic	Determination of the Emission of Formaldehyde by Building Materials and Building Related Products – Large Chamber Method	Formaldehyde
JIS A 1901: 2015	Japan	Dynamic	Determination of the Emission of Volatile Organic Compounds and Aldehydes by Building Products – Small Chamber Method	VOCs
JIS A 1460	Japan	Static	Determination of the emission of Formaldehyde from Building Boards – Desiccator Method	Formaldehyde

Formaldehyde and other VOC emission rates are quantified by determining the mass of the chemical in the air per time (chemical concentration multiplied by flow rate). The VOC emission rate is often controlled by the chemical diffusion through a material. In contrast, the SVOC emission rate is usually determined by the

convective mass transfer above the surface of the material, which is dependent on the airflow rate and the SVOC concentration in the bulk air. Since these two parameters can vary with time, with variations between different chambers and built environments, mass per time emission rates are not useful parameters for quantifying SVOC emissions from indoor materials. For SVOCs, a mass transfer approach as described in ASTM D8141 (ASTM 2017) needs to be used to quantify emissions from products indoors. For this reason, there are few SVOC test standards, regulations, labeling programs, or reference materials. The remainder of this document will focus on VOC emission testing (both individual and total) and reference materials.

How Does Emission Testing Work?

There are a variety of approaches to measure VOCs emissions from materials. Broadly, they can be broken down into three types: extractor methods, static methods, and dynamic methods.

Extractor or perforator methods directly quantify the amount of chemical present in the product. For example, formaldehyde perforator methods (e.g., EN 120: Wood-based panels; determination of formaldehyde content) involve boiling a wood product sample in toluene to remove formaldehyde (Risholm-Sundman et al. 2007; Roffael et al. 2010). The collected formaldehyde is then transferred to water for optical analysis.

Static methods often involve placing wood products in closed systems in the presence of water at a constant temperature. The formaldehyde migrates through the air phase from the test specimen into the water. After a defined time, the water is analyzed for the presence of formaldehyde. Static methods include flask (EN 717-3) and desiccator methods (JIS A 1460). The relative humidity in these methods is high due to the presence of liquid water in the system. The high humidity may impact the measured emission rate.

The reference materials reviewed for this document have not been tested using static or extractor methods. Rather, most reference materials to date highlighted in academic publications have been used with dynamic chamber methods. In these methods, a test specimen is placed in a chamber held at a constant temperature and relative humidity. Pre-humidified air is supplied to chamber at a defined airflow rate. The concentration of the chemical(s) of interest is measured in the chamber exhaust air. Some methods are performed at elevated temperatures and/or at a low relative humidity. There is a wide range of dynamic testing methods (Table 2) that vary in requirements, including chamber volume, temperature, relative humidity, air velocity, air change rate, loading rate, exposed edges, pre-chamber conditioning, duration of exposure of the test specimen in the chamber, and sample time (Poppendieck and Gong 2020).

Dynamic Emission Test System Components

Dynamic emission chamber test systems consist of a chamber, a temperature control system, an airflow control system, and a relative humidity control system (Fig. 1). In addition, temperature, airflow, pressure, and relative humidity are monitored.

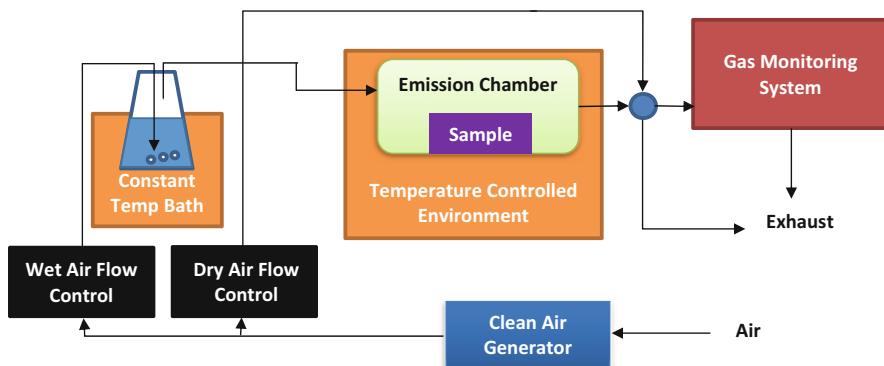


Fig. 1 Example schematic for an emission test system

There is a wide range of chamber sizes used depending on the purpose of the test method. Chamber sizes can vary from 0.00003 m^3 for screening emission testing of a portion of a product (ASTM D7706) to 30 m^3 for testing a complete product (e.g., full sheet of plywood, ASTM E1333 or ASTM 6670). Smaller chambers can be enclosed in external temperature control systems (e.g., incubators). Larger chambers can have dedicated heating, ventilation, and air conditioning systems to control temperature and relative humidity.

Since dynamic emission chambers use concentration measurements and airflow rates to determine the emitted mass, dynamic chamber systems employ mass flow controllers or mass flow meters to accurately measure the airflow rates. To control relative humidity, many chamber systems smaller than 1 m^3 split the incoming chamber airflow between a dry line and wet line (Fig. 1). The wet line is bubbled through water to increase the relative humidity. The two lines are then mixed in a controlled manner prior to entering the chamber to achieve the desired relative humidity. Most dynamic emission methods specify a maximum pressure in the chamber, which can be controlled with the exhaust system.

Dynamic Emission Testing Variability

Given the potential for systematic errors (e.g., an incorrectly calibrated temperature probe) to influence the reported emission rates, inter-laboratory (among laboratories) comparison studies can be performed to ensure the accuracy of emission testing systems. The California Composite Wood Products Airborne Toxic Control Measure (ATCM) requires third-party emission certification laboratories to participate in inter-laboratory studies for at a minimum of every 2 years. The uncertainty of measured concentrations or emission rates in dynamic emission testing is a function of three factors: (1) sample variation of the material being tested, (2) the emission testing system, and (3) the analytical concentration measurement.

The analytical concentration measurements have been historically performed in dynamic emission chambers by either trapping the analyte on a sorbent followed by thermal desorption and quantification in a thermal desorption gas chromatograph (TD-GC) or derivatization followed by extraction and analysis with high-performance

liquid chromatography (HP-LC) system. The uncertainty associated with these analytical measurements can be determined by conducting inter-laboratory studies using spiked sorbent tubes or extraction liquids. Kirchner (2007) demonstrated that for 10 out of 11 chemicals analyzed on spiked Tenax tubes, the relative standard deviations (RSDs) were less than 4% ($n = 6$), demonstrating small analytical uncertainty in inter-laboratory studies is possible.

It is difficult to distinguish emission testing system uncertainty from sample variation and analytical uncertainty. The tested sample (either a building material or designed reference material) can be heterogeneous at the scale tested. In addition, shipping, storage, and handling issues can influence the emission rate of a sample. Each emission test system design can also vary. Finally, the airflow rate, temperature, relative humidity, and pressure can all impact the actual chemical concentration in a chamber. These contributions to uncertainty are described in more detail in the section “Uncertainties in Emission Testing when Using Reference Materials.”

Reference Materials

The development of emission testing reference materials is intended to reduce uncertainty related to sample variation of the material being tested, specifically sample heterogeneity and handling issues. An ideal emission testing reference material emits the target compound at a predictable rate in quantities sufficient for detection and quantification over the required period of time while being independent of age and handling of the material (Cox et al. 2010; Uhde and Aksteiner 2018; ISO 2015).

Definitions

According to the International Bureau of Weights and Measures (BIPM) international vocabulary of metrology, a reference material is defined as a “material sufficiently homogeneous and stable with reference to specified properties, which has been established to be fit for its intended use in measurement” or in examination of nominal properties (ISO 2015). There are many kinds of reference materials created for specific uses.

For example, the US National Institute of Standards and Technology (NIST) has six different categories of reference materials that are intended for different specified purposes, for example, primary standards (PSs), standard reference materials (SRMs), research gas mixtures (RGMs), NIST traceable reference materials (NTRMs), reference materials (RMs), and research-grade test materials (RGTM) (Beauchamp et al. 2021). The reference values assigned to PSs, SRMs, and RGMs are metrologically traceable to internationally recognized higher-order reference systems, for example, the International System of Units (SI). The reference values assigned to NTRMs are traceable to existing PSs and SRMs. The reference values assigned to RMs are determined following

between-method harmonization, within-method precision assessment, and process stability assessment. RGTMs are a subset of the exploratory materials undergoing the first step of development towards reference materials and are prepared to be fit-for-purpose, homogeneous, and stable.

Types of Reference Materials

A certified reference material (CRM) is a reference material that has been characterized by a “metrologically valid procedure” to determine the “associated uncertainty” and includes a statement of metrological traceability (Beauchamp et al. 2021; ISO 2015, 2016). CRMs are metrologically traceable and produced by a responsible reference material producer (ISO 2016). All CRMs are reference materials, but not all reference materials are CRMs. For example, four of the six NIST reference material types are CRMs (PSs, SRMs, RGMs, and NTRMs). Reference materials need only to be homogeneous, stable, and fit for use; they do not need to be traceable. Traditionally, reference materials used for emission testing have not been certified (CRMs) or traceable.

True Values, Traceability and Consensus Approaches

There are multiple means that can be used to establish the mass value emitted from an emission testing reference material. The true mass value is the mass that would be the emitted mass if there was no measurement error (Beauchamp et al. 2021), but the exact true mass value is impossible to measure. CRM certificates report estimates of the true mass value with a specified uncertainty and stated confidence.

Ideally, measurement results from CRMs are traceable to the SI reference system using two or more independent methods (Beauchamp et al. 2021). This makes the stated CRM reported value method independent. In other words, chamber flow measurements would be directly traceable to the primary and secondary values. A certificate attached to a CRM would account for all uncertainty in that traceability train to estimate the true emission value.

Alternatively, consensus values can be used to estimate the emitted mass true value for reference materials that are not CRMs through inter-laboratory studies with enough participants (Beauchamp et al. 2021). Reference materials whose true values are estimated via consensus efforts do not need to be traceable. However, consensus values can only be established during inter-laboratory studies that have enough participants. The required number of participants is a function of spread in the results, the data analysis methods, and if a control material was used. To date, all emission testing reference materials have used a consensus value to estimate the true value. This means there are no commercial emission testing products that can be used independently of an inter-laboratory study campaign that could be used to evaluate the performance of an emission testing system.

Types of Emission Testing Reference Materials

To date, there is a limited number of published inter-laboratory studies for the measurement of VOCs emissions from materials in emission test chambers (De Bortoli et al. 1999; Risholm-Sundman et al. 2007; Wilke et al. 2009; Yrieix

et al. 2010; Howard-Reed et al. 2011; Wilke et al. 2011; Howard-Reed et al. 2014; Horn et al. 2018; Oppl et al. 2020).

Historically, inter-laboratory studies used building material samples as the reference material (De Bortoli et al. 1999; Kirchner 2007; Risholm-Sundman et al. 2007; Wilke et al. 2009; Yrieix et al. 2010). For this discussion, building product reference materials are defined as any emission testing material typically used as a building product that has not been spiked with compounds (described in section “Building Product Reference Materials Used in Emission Testing”). More recently, reference materials have been designed specifically for emission testing purposes. These systems (described in section “Designed Reference Materials Used in Emission Testing”) either spike chemicals of interest into various materials or they emit chemicals of interest from a designed liquid source.

Building Product Reference Materials Used in Emission Testing

Inter-laboratory studies that have used building product reference materials have included carpet, carpet cushion, paint, particleboard, polyvinyl chloride (PVC) flooring, rubber flooring, and sealants. Summaries of these studies follow.

De Bortoli et al. (1999) conducted an inter-laboratory study with 18 laboratories from 10 European countries. Five VOCs (*n*-decane, *n*-undecane, *n*-dodecane, 2-phenoxy ethanol, *n*-tridecane) from carpet, eight VOCs (phenol, 2-(2-butoxyethoxy)ethanol, C7 benzene, C8 benzene-1, C8 benzene-2, *n*-tetradecane, C9 benzene and 2,2,4-trimethyl-1,3-pentanediol diisobutyrate) from PVC cushion, and two VOCs (2-(2-ethoxyethoxy)ethanol and Texanol) from paint were evaluated. The RSDs of area-specific emission rates for carpet, PVC cushion, and paint ranged from 25% to 91%, 27% to 83%, and 21% to 69%, respectively. The intra-laboratory (same lab) variance (range 0% to 38%, mean 2.3% to 10% depending on the chemical) was smaller than the inter-laboratory variance. Analytical errors, losses of the heaviest compounds due to sorption on the chamber wall and non-homogeneity of the materials were suggested as the main reasons for inter-laboratory discrepancies.

Risholm-Sundman et al. (2007) conducted an inter-laboratory study with six laboratories. Formaldehyde emission from particleboards was tested with three replicate samples in each laboratory. The 16% variation in inter-laboratory tests was larger than the 6% intra-laboratory variation. Edge sealing, conditioning of the sample before the test, and test temperature were cited as potential reasons for the discrepancies.

Kirchner (2007) conducted an inter-laboratory study with 11 laboratories. Three VOCs emitted from PVC flooring (cyclohexanone, 2-methoxy-1-methylethylacetate, and diethylene glycol monobutyl ether) and five VOCs from rubber flooring (styrene, cyclohexanone, benzaldehyde, benzothiazole, and 2,6-di-*t*-butyl-4-methylphenol) were evaluated. RSDs ranged from 64% to 87% for PVC flooring and from 22% to 43% for rubber flooring. The variability in the PVC emissions was attributed to damage of the material in packaging for shipping.

The intra-laboratory variation for spiked VOCs on sorbent tubes was between 2% to 10% for the PVC flooring chemicals and 6% and 15% for the rubber flooring chemicals. Hence, the inter-laboratory variation was not limited to the analytical discrepancies.

Wilke et al. (2009) conducted an inter-laboratory study with 37 laboratories from Europe. Seven VOCs (butanol, butyl acetate, dibutylether and butyl acrylate, ethandiol, propanoic acid butyl ester, and butanoic acid butyl ester) emitted from a sealant were evaluated. Test chamber volumes ranged between 0.02 m³ and 1.0 m³. RSDs ranged from 17% to 61%. The 61% RSD for ethanediol was attributed to poor adsorption onto Tenax and a poor peak shape influencing quantification with gas chromatography.

Yrieix et al. (2010) conducted an inter-laboratory study with six European laboratories. Six VOCs (formaldehyde, acetaldehyde, pentanal, hexanal, alpha-pinene, and beta-pinene) emitted from urea-formaldehyde particleboard were measured. RSDs ranged from 17% to 45%. The lower RSD for formaldehyde emissions (17%) compared to other non-aldehyde emissions (27% to 45%) was attributed to the higher heterogeneity of natural wood compounds than of the urea formaldehyde resin of the tested product.

Combined these historical studies on building materials indicate that the uncertainty attributed to analytical concentration measurement (Kirchner 2007) and sample variation of the material being tested (Risholm-Sundman et al. 2007) are likely lower than uncertainty related to the emission testing system. However, the range of uncertainty related to emission testing using building materials for inter-laboratory studies (conducted between 1999 and 2010, RSD 16% to 91%) indicated that improvements to all three factors impacting emission testing (sample variation of the material being tested, the emission testing system, and the analytical concentration measurement) were needed.

Designed Reference Materials Used in Emission Testing

A range of emission testing reference materials have been developed since 2010. Unlike the previously described building product reference materials, these specifically designed materials either spike chemicals of interest into materials or involve evaporation of the chemicals from a liquid solution. These materials include lacquers, films, molded thermoplastic polyurethane plates, liquid-diffusion-film-emissions systems, and temperature-controlled diffusive evaporators.

To use these materials as a reference material in a chamber test, the material is placed inside the chamber under specified temperature, relative humidity, and airflow rate conditions. The concentration profile of the target compound in the chamber air is measured after sealing the chamber for a specified duration. For intra-laboratory and inter-laboratory comparisons, material samples of the same batch are used in the different chambers, so that the measured concentration profiles of the target compounds among the different chambers are comparable.

Drying or Curing Reference Material

Examples of drying or curing reference materials have used lacquer or adhesive as the carrier substrate of the target compounds. The reference material is comprised of a Petri dish and a layer of the cured mixture and target compounds (Fig. 2). The reference material can be designed for emission of the mixture of several target compounds if the compounds are compatible with the lacquer or adhesive solvent and form a uniform mixture.

Nohr et al. (2014a, b) prepared lacquer reference materials using the following steps:

1. The selected lacquer product is decanted into a screw-cap bottle to serve as the carrier substrate of the reference material.
2. Defined amounts of the target compounds in pure liquid form are added to the lacquer using gas-tight syringes. The lacquer is stirred magnetically to form the mixture. The compounds existing in the solid form under room temperatures, such as lindane, are dissolved in methanol before being added to the lacquer.
3. The bottle is then sealed. The mixture of the lacquer and the target compounds is agitated for 1 h to ensure a mixed solution.
4. Based on the expected emission rates of the target compounds, specified amounts of the lacquer mixture are spread on Petri dishes.
5. After the preparation of a batch, the Petri dishes are immediately placed into an environmental controlled chamber for 1 day to 3 days for the lacquer mixture to cure.
6. Then the Petri dishes are capped, moved out of the environmental chamber, sealed with aluminum-coated polyethylene composite foils, and shipped to users.

Since lacquer or adhesive is used as the carrier substrate of the reference material and also emits certain solvents, the selected lacquer should account for the following requirements.

Fig. 2 Photo of a batch of lacquer reference materials. Used with permission from Bundesanstalt für Materialforschung und -prüfung, Berlin (BAM)



1. The target compounds of the reference material should not be contained in the original lacquer or adhesive. This ensures that the emission rates of the target compounds are designable and controllable.
2. The signals of the solvents emitted from the lacquer or adhesive should not overlap with the signals of the target compounds for the analytical system. This ensures quantification of the target compounds.
3. The lacquer or adhesive should have low emission rates of solvents. This ensures that the analytical system is not overloaded, and the signals of the solvents do not mask the signals of the target compounds.

Nohr et al. (2014b) examined 12 lacquers for use as a reference materials (6 acrylic-based and 6 alkyd-based) made by the same manufacturer and purchased from the same local building supply store. The acrylic lacquers contained water, a dispersion of acrylate and polyurethane, glycols, additives, preservatives (methyl-, benzyl-, and chlor-isothiazolinone), and pigments (for colored lacquers). The alkyd lacquers contained alkyd resin, additives, white spirit, and pigments (for colored lacquers). The lacquers were mixed with the target compounds following the preparation protocols of the lacquer reference materials listed above. After being cured, the samples were placed in an environmental chamber. Solvents were detected in the air of the chambers loaded with the alkyd lacquers. The signals of the alkyd lacquers masked the signals of some target compounds, such as *n*-methyl- α -pyrrolidone and 2-ethyl-1-hexanol. The high solvent concentrations remained in the chambers for more than 3 days, and the high solvent signals resulted in significant carryover in the analytical system. Compared to the alkyd lacquers, the acrylic lacquers had lower emission rates of solvents, which allowed the emission rate profiles of the target compounds to be more accurately quantified.

For intra-laboratory and inter-laboratory measurements, the chamber air should be sampled at a specific time after loading the reference materials into the environment chambers to reduce the measurement errors associated with the emission rate decay of the reference materials. Moreover, to ensure homogeneity of the material samples, the sample preparation requires large chamber capacities for curing the liquid lacquer mixture of the same batch at the same time.

Film Reference Material

Film reference materials use a solid film as substrate, and the target compound is adsorbed into the film (Fig. 3). The reference material is designed for single-compound emission to avoid competitive diffusion and adsorption of multiple compounds in the diffusion film.

The reference material samples can be prepared by the following steps (Howard-Reed et al. 2011, 2014; Liu et al. 2013, 2014; Cox et al. 2010):

1. A single film sheet is cut into a batch of film samples with the same size.
2. The film samples are placed in loading vessels. Each film is exposed on both sides to the air in the vessel. The air outlet of the last vessel is connected to a

microbalance system. A film sample is hanging inside the microbalance system to monitor its mass during the loading process.

3. According to the mass of the target compound expected to be loaded in each film, the gas-phase target compound at a certain concentration is passed continuously through the vessels and the microbalance system.
4. The mass increase of the single film inside the microbalance is monitored continuously until it reaches steady state. It is assumed the films in vessels upstream of the microbalance are at the same steady-state value. The loading of the target compound is then complete.
5. The film samples are taken out of the vessels, sealed, packed, and are ready to be shipped to the users.

The emission rate of the reference material depends on the mass of the target compound adsorbed in the film and the material properties of the film. The important material properties include thickness, surface area, and the diffusion and partition coefficients of the film. After loading the reference material with the target compound and placing it in a clean environmental chamber, the concentration profile of the target compound in the chamber air should be similar to that generated by a typical homogeneous dry building material.

Significant variation in the emission rate among different material samples of the same batch has been observed after loading. This suggests that loading optimization is needed for the film reference material to improve the measurement reproducibility of its emission rate.

For emission of toluene, a polymethyl pentene (PMP) polymer film (Fig. 3) was selected as a substrate (Cox et al. 2010). The PMP film does not contain organic additives such as plasticizers or stabilizers that could complicate emission rates. For emission of formaldehyde, the PMP film and a polycarbonate (PC) film were both evaluated in terms of their adsorption and desorption properties. Since PC is polar



Fig. 3 Film reference material in loading vessel and last film attached to a microbalance

and PMP is non-polar, the PC film had a much greater formaldehyde solubility than the PMP film (Liu et al. 2013).

The emission rate of the target compound from the reference material and the concentration of the compound in the chamber air can be well-characterized by the mechanistic emission model (Cox et al. 2010). The model considers the reference material as a single-layer porous material with a uniform initial concentration of the target compound. This model is frequently used to characterize the emission of VOCs from dry surface materials. Therefore, the emission profile of the film reference material should be representative of that of dry surface materials.

TPU Reference Material

Thermoplastic polyurethane (TPU) reference materials use molded TPU plates as substrates. The target compounds are impregnated into the TPU plates using high-pressure liquid carbon dioxide (CO_2 , Fig. 4). The reference material can be designed for emission of the mixture of several target compounds. A uniform mixture of the target compounds and liquid CO_2 can be injected into the TPU plates.

The TPU reference material samples can be prepared by the following steps (Richter et al. 2017):

1. A batch of molded TPU plates with designed dimensions is produced. The TPU samples are then stored in a dehydrator for 24 h.
2. The TPU sample masses are measured and placed in a high-pressure view cell. After sealing the cell, certain amounts of the target compounds are injected into the cell using syringes.
3. Liquid CO_2 is added to the cell using a regulating valve until the liquid CO_2 and the target compounds combine into one phase. This typically occurs above a pressure of 60 bar and at a temperature of 20 °C.
4. The high pressure is maintained in the cell for a designated time to allow the target compounds to permeate the TPU plates. A magnetic stirrer is used inside the cell to increase the mass transport during the permeation process.
5. The chamber is then slowly depressurized to allow the CO_2 to leave the TPU samples.
6. The TPU samples are stored in a dehydrator for 4 h, then shrink-wrapped in aluminum-coated polyethylene foil.



Fig. 4 Schematic of the TPU reference material. Used with permission from Bundesanstalt für Materialforschung und -prüfung, Berlin (BAM)

The emission test of a TPU reference material impregnated with styrene measured in an environmental chamber for 25 days showed that the emission rate of the styrene reference material decreased with time (Richter et al. 2017). Significant variation in the emission rate among different material samples of the same batch was observed within 10 days after their fabrication. This suggests that sample storage and hominization may be needed for the TPU reference material to improve the measurement reproducibility of its emission rate. Moreover, studies of the emission mechanism of the TPU reference material are also needed. An emission mechanism study will allow a better understanding of the emission characteristics of the reference material and determining the theoretical emission rates for future development.

LiFE Reference Material

A liquid diffusion-film-emission (LiFE) reference material is comprised of a polytetrafluoroethylene (PTFE) or stainless-steel bottle containing pure liquid VOC as the emission source, a thin diffusion film to cover the opening of the bottle to control the emission rate and fastening pieces to hold the bottle and film in place (Fig. 5). The bottle and all the fastening pieces are made of PTFE or stainless steel. Due to low diffusivity of VOCs through PTFE and stainless steel, VOC diffusion through the bottle container can be neglected compared to that through the diffusion film at room temperatures (Wei et al. 2012a, b, 2013; Poppendieck et al. 2018).

The reference material is designed for single-compound emission to avoid competitive diffusion and adsorption of multiple compounds in the diffusion film. The film material is chosen based on the properties of the chemical. An aluminum oxide melamine-impregnated paper was selected to be the diffusion film for the toluene reference material (Wei et al. 2012a, b, 2013), and a polydimethylsiloxane film was selected to be the diffusion film for the formaldehyde reference material (Wei et al. 2013).

The reference material samples can be prepared by the following steps (Wei et al. 2012a, b, 2013).

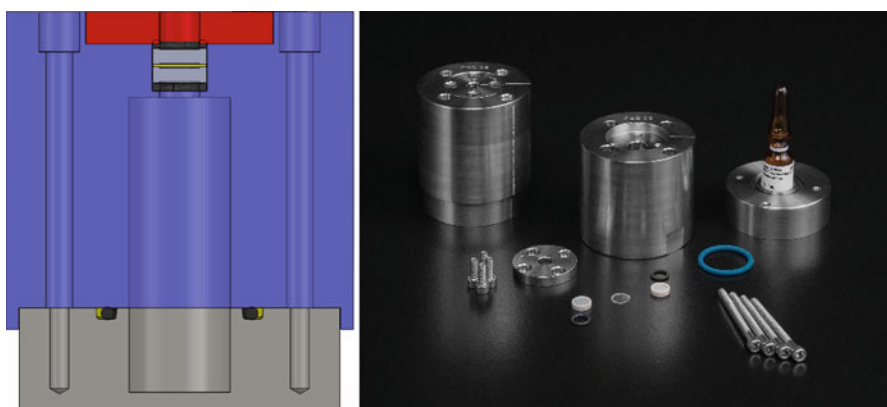


Fig. 5 LiFE reference material assembly and components. Photo Credit Dan Greb, 2021

1. Based on the expected emission rate of the target compound, and the diffusion and partition coefficients of the selected diffusion film, the diameter of the film is calculated, and the bottle and fastening pieces are chosen according to the size of the diffusion film.
2. The target compound in liquid form is placed into the bottle. Pure VOC liquid at room temperatures is used as the emission source of the reference material. Formaldehyde exists in the gas phase under room temperatures; thus, formalin solution (formaldehyde in water) is used as the emission source.
3. The diffusion film is then fixed on top of the bottle using fastening pieces. These can include screws, stainless steel frits, and o-rings.

During the use of the reference material, the concentration of the target compound at the lower surface of the diffusion film is its saturation concentration. Volatile compounds, such as formaldehyde, benzene and toluene, can diffuse through the film within a few hours (Wei et al. 2012a, b, 2013; Poppendieck et al. 2018). The reference material has a constant emission rate of the target compound under constant temperature and relative humidity. The emission rate of the reference material should be representative of the emission levels of building materials. To reach a desired emission rate, the diameter of the film increases with decreasing diffusion coefficient of the film. Therefore, the mass transfer and geometric parameters of the film need to be optimized. Reference materials with large diameters may be difficult to load in small environmental chambers. Reference materials with small diameters may have higher uncertainties in the emission rate.

The constant emission rate can be described as a function of the diffusion and partition coefficients as well as the diameter and thickness of the film. Figure 6 shows the geometry-diffusion relation of the film for different emission levels. The zone in the dashed line is optimized with regard to the mass transfer and geometric parameters.

The variability in LiFE reference materials is directly tied to the film. Film thickness, flatness, seals, and handling of films can all lead to varying emission rates from otherwise identical LiFE bottles. Films specifically produced for uniform thickness, placed between stainless steel frits, and held together with a constant pressure using o-rings have been employed to reduce variability between LiFE reference materials (Poppendieck et al. 2018).

Temperature-Controlled Diffusive Evaporator

The temperature-controlled diffusive evaporator reference material is comprised of a stainless steel bottle containing pure liquid VOC as the emission source, a thin diffusive capillary acting as an emission restrictor, and a temperature control system to heat the bottle to a set temperature (Fig. 7) (Uhde and Aksteiner 2018). The battery-powered, electronic control system is contained within the sealed bottle. The reference material allows for multiple-compound emission depending on the liquid reservoir. The bottle is sized so ampules of liquid source fluid can be directly placed within the bottle. The temperature of the bottle can be adjusted from 30 °C to 55 °C.

Fig. 6 Geometry-diffusion relation of the diffusion film (A : surface area, L : thickness, D_m : diffusion coefficient, K : partition coefficient)

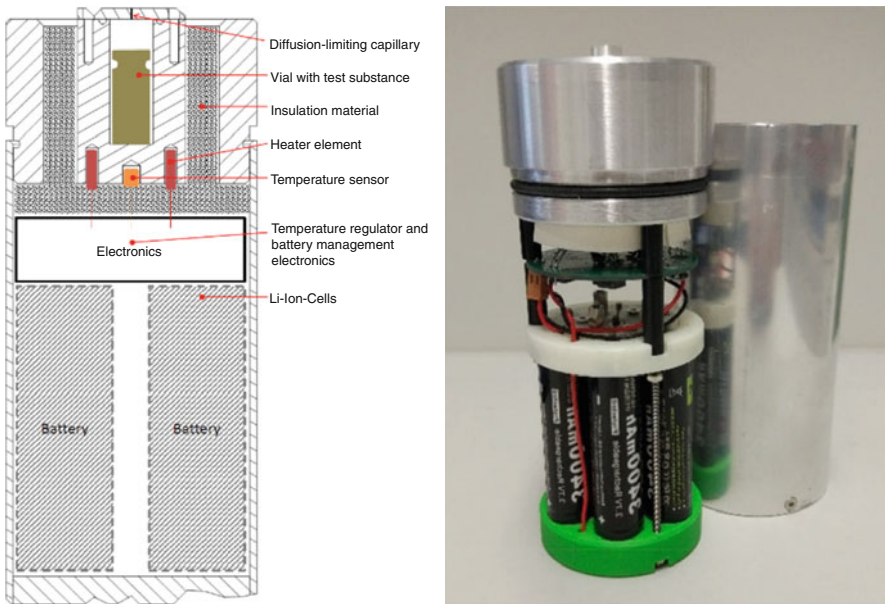
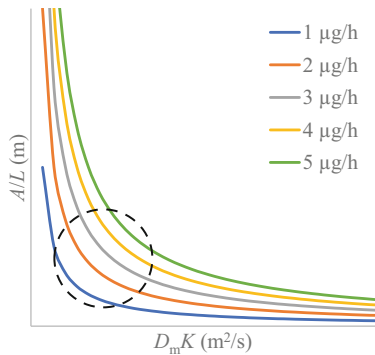


Fig. 7 Diagram of temperature-controlled diffusive evaporator (Illustration and Photo used with permission from creator Erik Uhde)

The reference material samples can be prepared by the following steps (Uhde and Aksteiner 2018).

1. The target compound in liquid form is placed into the bottle.
2. Based on the volatility of the target compound the bottle temperature is set.
3. The bottle is sealed and place in the chamber.

The elevated temperature of the system allows the quantification of less volatile chemicals like dodecane. Long-term performance and inter-laboratory tests have not been performed on temperature controlled diffusive evaporator reference materials.

Inter-laboratory Proficiency Testing Studies of Reference Materials

Between 2009 and 2018 a total of eight inter-laboratory studies using designed reference materials were reported in the literature (Table 3). These studies used films, lacquer, adhesives, and LiFE reference materials with 4 to 55 participating laboratories. A variety of chamber sizes, analyses, and chamber methods were used. Reported RSDs quantify the combined uncertainty from: (1) sample variation of the material being tested, (2) the emission testing system, (3) the analytical concentration measurement, and (4) procedure variability.

Reference Material Studies

Each of the eight reference materials studies had unique challenges and drew varying conclusions.

Film. There have been two inter-laboratory studies using film reference materials conducted by the same group. Howard-Reed et al. (2011) conducted a pilot inter-laboratory study with four laboratories using a film loaded with toluene as the reference material. Average RSDs of toluene emission rates determined by different laboratories were 9% to 15%. Generally, RSDs were lower for samples taken at later times. Analysis of between-batch and within-batch variance indicated that the film sample age (time between produced and tested) may be a more important variable than differences between the batches or among samples within a batch. This study highlights the challenge of storage for commercial reference materials prior to sale.

Howard-Reed et al. (2014) conducted a follow-up inter-laboratory study to evaluate a toluene film in chambers of various sizes in 14 laboratories in seven countries. Each laboratory was provided duplicate specimens, standard analytical solutions, and a test protocol. Based on chamber size used in the study, ten laboratories were grouped as small chambers and the remaining four were considered large chambers. RSDs range from 19% to 23% for laboratories using a small chamber and meeting all the test method criteria. RSDs for laboratories using a large chamber were higher (55–57%). Keeping the film at a subzero Celsius temperature until tested proved difficult for international shipping. This study highlights how challenging shipping and storage temperature can be for reference material distribution.

Lacquer. The Bundesanstalt für Materialforschung und -prüfung (BAM, Federal Institute for Materials Research and Testing) has conducted four international proficiency tests (2009, 2014, 2016, 2018) using lacquer reference materials (Wilke et al. 2021). A separate group (Oppl et al. 2020) also conducted an independent lacquer and adhesive study.

In 2009, Wilke et al. (2011) from BAM conducted a study that involved 37 international laboratories. A lacquer standard reference material containing nine chemicals was used as the testing material. Of the nine chemicals diethyl phthalate

Table 3 Summary of inter-laboratory studies of designed reference materials for chamber testing of chemical emissions.

Reference	Test Year	Test material	Chemicals	Chamber method	Chamber	Inter-laboratory RSDs
Howard-Reed et al. (2011)	2009	film	Toluene	ASTM 5116	0.05 m ³ to 0.086 m ³	9% to 15% (n = 4)
Howard-Reed et al. (2014)	2012	film	Toluene	ASTM 5116	0.024 m ³ to 0.12 m ³ 0.225 m ³ to 1.0 m ³	19% to 23% (n = 10) 55% to 57% (n = 4)
Wilke et al. (2011)	2009	lacquer	9 VOCs (styrene, diethyl glycol dimethyl ether, phenol, limonene, tridecane, benzene, hexanal, diethyl phthalate and D4-siloxane)	ISO 16000-9	N = 32 < 0.1 m ³ 0.1 m ³ < n = 34 < 1 m ³ N = 34 > 1 m ³	28% to 69% (n = 37)
Horn et al. (2018)	2014	lacquer	9 VOCs (hexanal, styrene, n-decane, limonene, 2-ethyl-1-hexanol, N-methyl- <i>o</i> -pyrrolidone, 2-ethylhexyl acrylate, dimethyl phthalate, and n-hexadecane)	ISO 16000-9	0.02 m ³ to 3 m ³	29% to 63% (n = 55)
Wilke et al. (2021)	2016	lacquer	8 VOCs (Butyl acetate, Styrene, Decane, 1,3,5-Trimethylbenzene, 3-Carene, Dodecane, Texanol, 2-Propoxyethanol)	ISO 16000-9	n = 13 < 0.1 m ³ 0.1 m ³ < n = 51 < 1 m ³ n = 36 > 1 m ³	22% to 48% (n = 49)
Oppl et al. (2020)	2017	adhesive and lacquer	7 VOCs (2-Ethyl-1-hexanol, Acetic acid, 1-Butanol, Propylene glycol, Triethylamine, Dipropylene glycol mono methyl ether, and Butylhydroxy- toloul)	GEV / EN 16516	—	30% to 41% (n = 33); 21% - 64% (n = 25)
Wilke et al. (2021)	2018	lacquer	12 VOCs (Styrene, Toluene, Decane, 2-Propoxyethanol, Triethylamin, Cyclohexanone, Camphene, Octanal, p-Cymene, Butylglycol acetate, Dimethyl adipate, Butyl hydroxy toluene)	EN 16516	n = 7 < 0.1 m ³ 0.1 m ³ < n = 66 < 1 m ³ n = 27 > 1 m ³	22% to 39% (n = 50)
Poppendieck et al. (2018)	2017	LiFE	Formaldehyde	ASTM 6007	0.02 m ³ to 0.086 m ³	14% (n = 4)

and D4-siloxane were not detected by most of the laboratories. Benzene, the most volatile compound, had the highest RSD of 69%. The authors hypothesized this may be due to varying air velocities over the lacquer surface during the drying process of the lacquer causing different evaporation rates among samples. The RSDs for the other six chemicals ranged from 28% to 50%. This study highlights the difficulties in manufacturing consistent reference materials.

In 2014, the BAM group (Horn et al. 2018) challenged 55 laboratories with a lacquer standard reference material. Nine VOCs were tested in chambers ranging in size from 0.02 m³ to 3 m³. Generally, both the inter-laboratory and intra-laboratory variations for *n*-methyl- α -pyrrolidone, 1,2-dimethyl phthalate, and *n*-hexadecane were higher than the other chemicals. The authors attribute this to analytical issues. The overall results show that the inter-laboratory RSDs ranged from 29% to 63% for all 55 participants, while the intra-laboratory RSDs ranged from 5% to 19%. This study highlights the need for precise reference materials to allow for determination of causes of inter-laboratory variations.

In 2016, the BAM group (Wilke et al. 2021) challenged 49 laboratories with a lacquer reference material spiked with eight VOCs. In 2018, they repeated the study with 50 laboratories with a lacquer reference material spiked with 12 VOCs. In these studies, VOCs with higher boiling points (dimethyl adipate, 227 °C; butyl hydroxy toluene, 265 °C; texanol, 244 °C) had similar magnitude RSDs as those with lower boiling points. All sampling was conducted within 7 days of drying of the lacquer. There may be a challenge to store commercial lacquer reference materials for longer periods prior to sale.

Oppel et al. (2020) conducted an inter-laboratory study with 33 laboratories from 12 countries. Two spiked flooring adhesives and one spiked parquet lacquer were tested using the GEV testing method for emission testing of products for flooring installation, adhesives, and building materials. The testing included the preparation of the test materials by the participants, rather than a central manufacturer. Participants were not informed of the VOCs to be analyzed. This resulted in variations in which chemicals were analyzed with substance specific calibration versus toluene equivalents. A total of 15 laboratories quantified the concentrations of 2-methyl-4-isothiazolin-3-one with substance-specific calibration (mean 27 mg m⁻³), while 19 laboratories reported 2-methyl-4-isothiazolin-3-one concentrations using toluene equivalents with a mean concentration of 10 mg m⁻³. Non-identified VOCs were reported by 15–20 of the laboratories for the three reference materials. RSDs for individual target VOCs ranged from 21% to 64%. This study highlights how analytical challenges can affect the reported concentrations for emission reference materials, especially when the chemicals are unknown to the user.

LiFE. Poppendieck et al. (2018) conducted an inter-laboratory study with four laboratories. Formalin was placed in stainless steel bottles, and formaldehyde diffused through a polydimethylsiloxane (PDMS) film at the top. Intra-laboratory RSD of six bottle systems was 5%. Inter-laboratory RSD between four laboratories was 14%. Testing laboratories had slightly different temperatures, relative humidities and chamber air change rates. The authors theorized that variability in commercially purchased film thickness effected the results. This study highlights the potential

difficulty in producing commercially viable reference materials due to material component challenges.

Inter-laboratory Summary

The RSDs for inter-laboratory tests have varied with year of the study, the type of reference material and the chemicals studied.

Wilke et al. (2021) notes a decrease in RSD over the last 20 years for European inter-laboratory testing. A review by Oppl (2008) in which six published and several unpublished inter-laboratory tests with 10–20 participants were summarized showed that the included studies using building materials had similar RSDs of $\pm 50\%$. The study by De Bortoli et al. (1999), which also used building product reference materials, had a mean RSD of 51%, while the most recent lacquer study by Wilke et al. (2021) in 2018 had a mean RSD of 28%.

This trend coincides with the transition away from building material reference materials to designed reference materials for use in inter-laboratory studies (Fig. 8). In addition, studies using multiple chemical lacquer reference materials (Table 3) have had higher RSD than those using single chemical film or LiFE reference materials. However, the studies using film or LiFE reference materials have had far fewer participants than the Lacquer studies.

Wilke et al. (2021) examined trends in four lacquer reference material studies from 2009 to 2018 (Table 3) in the context of chemical properties. There was a relationship between a chemical's RSD and Log K_{ow} (octanol-water partition coefficient) values. For chemicals with a Log K_{ow} less than 0, the RSD values were between 38% and 58%, while for chemicals with a Log K_{ow} greater than 4 the RSD

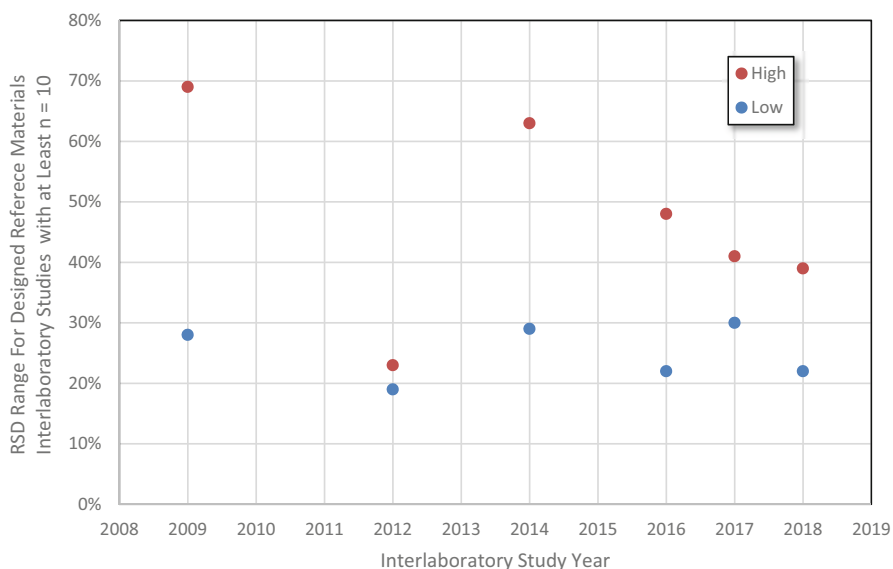


Fig. 8 RSD values for designed reference material inter-laboratory studies

values were between 20% and 32%. However, Wilke et al. (2021) showed that the boiling point was a poor predictor of the inter-laboratory RSD for chemicals with boiling points below 270 °C.

Generally, several factors have been controlled or examined to reduce variability in the inter-laboratory testing. These factors include preliminary testing to check the heterogeneity of testing materials, packaging and shipping. However, few studies discussed the influence of different factors on the variability in detail. Chemical analysis of the samples of the chamber air has been considered as the main factor for variation in the emission testing results Oppl (2008), but no quantitative analysis has been given for this conclusion. Identification of important influencing factors and quantification of the degree of influence of each factor on the observed discrepancies would be helpful for better control of the factors and thus reduction of the variability of inter-laboratory study results. In addition, as test materials and analytical techniques are evolving, it is important to evaluate testing procedures regularly.

Uncertainties in Emission Testing When Using Reference Materials

Uncertainty quantified in inter-laboratory studies using reference materials can be attributed to four major components:

1. Reference material variability
2. Emission testing system variability
3. Analytical measurement variability
4. Inter-laboratory study procedure variability

These issues are discussed in detail below.

Reference Material Variability

There are three major issues that are of concern and can affect reference material variability: producibility, homogeneity, and stability.

Producibility

Emission reference materials need to be able to be produced safely in a large enough batch to be useful for comparison purposes. To produce the emission reference materials, target compounds at high concentrations are often used. These concentrations potentially can be dangerous to the manufacturer or user of the reference material. For drying or curing reference materials, neat compounds are added to the lacquer or adhesive. For the LiFE reference material, pure liquid compounds and formalin solution are used to be the emission source. For the film and TPU reference materials, high concentrations of target compounds are adsorbed or impregnated into the substrate materials to be the emission source. The target compound, such as

formaldehyde and toluene, or the source solution like formalin, can have hazardous effects if improperly handled.

To produce a batch of reference materials for inter-laboratory comparisons, all the material samples should be produced at the same time for homogeneity. Designing a production method to make sufficient emission materials in one batch can be challenging. For the film and TPU reference materials, the number of reference materials produced in one batch is limited by the volume of the vessels for the target compounds to be adsorbed or impregnated into the substrate materials. Larger volumes may have mixing issues that can lead to homogeneity issues between samples. For lacquer reference materials, the lacquer mixture is poured into Petri dishes under a certain time limit to ensure the homogeneity among the samples, and the number of Petri dishes in one batch is limited by the volume of the environmental chamber for the lacquer mixture to cure.

User operation also needs to be considered to ensure that varying user techniques do not affect the emission rate. For instance, for the LiFE and temperature-controlled evaporator reference materials, the bottle filled with the liquid compound should always be moved in a slow, level manner to avoid contact of the liquid compound with the diffusion film.

Homogeneity

Homogeneous reference materials are needed for intra-laboratory test results to be reproducible and for the inter-laboratory test results to be comparable (Horn et al. 2018). Homogeneous reference materials ideally have an identical emission rate profile among different material samples for the target compound. The homogeneity of the reference materials is associated with the nature of the materials and their production methods. Historically, challenges associated with acquiring or producing homogenous reference materials (De Bortoli et al. 1999) have been one of the largest barriers to commercially viable certified reference materials.

For the lacquer and adhesive reference material, adequate stirring is essential to form a uniform mixture of the target compounds. For the TPU reference material, stirring also allows formation of a uniform mixture of the liquid CO₂ and target compounds, so that the target compounds can be impregnated homogeneously into the TPU substrate. Richter et al. (2017) noted that TPU emission variability between batches persisted for up to ten days after production. After ten days the emission profiles between batches homogenized.

For the LiFE and film reference materials, the emission rate of the reference material is controlled by the diffusion films. Varying film thickness was identified as one reason for variation in emission rates for LiFE systems (Poppendieck et al. 2018). The selected films should be as homogeneous as possible, with film thickness of each sample measured.

Stability

Time is required for shipment of the reference materials and storage at the laboratory prior to chamber testing. For inter-laboratory comparisons, the time needed for shipments ranges often from 2 days to 14 days, depending on if the shipment is

local or international (Horn et al. 2018; Howard-Reed et al. 2011, 2014). Reference materials containing hazardous materials can be delayed further, especially when transported through international borders. In addition, for commercially viable products the reference material may need to be stored prior to sale for months or years prior to use.

The environmental conditions, for example, temperature and relative humidity, during shipment and storage may influence the stability of the reference materials, and the target compounds may emit from the reference material and be lost through the packaging (Horn et al. 2018; Howard-Reed et al. 2014). To reduce loss of the target compounds, the film reference material has been shipped on dry ice to reduce the temperature in the package (Howard-Reed et al. 2011, 2014). However, the environmental conditions during shipment can be altered due to unexpected delays or other problems. Therefore, losses of target compounds may occur during shipment and storage, especially of high volatility compounds. To evaluate the stability of the lacquer reference materials, two material samples were wrapped in aluminum-coated polyethylene composite-foils and stored at 23 °C and 50% RH. A total of 14 days was the estimated maximum time for shipment and storage (Horn et al. 2018). Among the nine compounds emitted by the lacquer reference material, the emission rates of hexanal, styrene and *n*-decane decreased by 10% to 30% after 14 days, while the emission rates of limonene, 2-ethyl-1-hexanol, *n*-methyl- α -pyrrolidone, 2-ethylhexyl acrylate, dimethyl phthalate, and *n*-hexadecane were consistent with the freshly produced samples (Horn et al. 2018).

Storage test results suggest that (1) the environmental conditions for storage and shipment need to be verified prior to usage of the reference materials; (2) emission rate decay needs to be verified for certain compounds prior to chamber testing; and (3) to ensure the comparability of the inter-laboratory test results, reference materials with short storage lives should be from the same batch and loaded in the environmental chambers at the same time.

Emission Test System Variability

The emission rate of the reference material can be influenced by the experimental condition of the environmental chamber, for example, temperature, relative humidity, and air change rate (Howard-Reed et al. 2014; Nohr et al. 2014a, b; Wei et al. 2012a, 2013). Systematic bias in these parameters can result in bias in the measured emission rate of the reference material. This is one reason intra-laboratory variability is typically lower than inter-laboratory variability (Risholm-Sundman et al. 2007; Horn et al. 2018; Wilke et al. 2021; De Bortoli et al. 1999; ISO 2015; Richter et al. 2017).

Temperature

Emission rates often increase with increasing chamber temperature. Wei et al. (2013) noted that formaldehyde emitted from the LiFE bottle is controlled by the Henry's law constant, the film diffusion coefficient, and the air-membrane

partition coefficient, all of which are temperature dependent. Liu et al. (2014) highlighted for a film reference material that as temperature increases the diffusion coefficient for the target chemical in the film decreases and the partition coefficient between the air and film increases. The results by Liu et al. (2014) demonstrate these impacts as toluene concentrations more than tripled as temperatures increased from 10 °C to 30 °C in a chamber with a film reference material. Wei et al. (2012a) found an R² (square of correlation coefficient) value of 0.97 for the correlation between the emission rate and temperature for toluene emitted from a LiFE bottle between 10 °C and 30 °C.

Hence, chamber temperature control or measurement issues could be a significant contributor to elevated inter-laboratory RSD values. To address temperature uncertainty, temperature should be measured in each individual chamber, as temperature can vary in large temperature-controlled enclosures. In addition, temperature measurements should be checked to traceable standards on a regular basis.

Relative Humidity

The influence of relative humidity on the emission rate may depend on the target compound and reference material (Liu et al. 2014). Wei et al. (2013) note that mechanistically relative humidity affects a chemical's film diffusion coefficient and partition coefficient for a LiFE system, but to a lesser degree than the temperature. Wei et al. (2012a) found toluene emitted from a LiFE bottle decreased when relative humidity increased from 33% to 50%, but the impact was mixed at 70%. Overall, Wei et al. (2012a) found the impact of changes in relative humidity on toluene emissions was less than those of temperature. Liu et al. (2014) showed the changes in the relative humidity did not significantly influence the diffusion coefficient and partition coefficient for a film system at tested temperatures.

Air Change Rate

The air change rate, λ (1/time), will directly affect the concentration in the chamber. When steady state is achieved the chamber mass balance takes the form in Eq. 1:

$$C = \frac{E}{\lambda V} = \frac{E}{Q} \quad (1)$$

where E is the emission rate (mass/time), C is concentration in the chamber (mass/sample volume), and V is chamber volume (volume). The air change rate is defined as the chamber flow rate, Q (volume/time) divided by the chamber volume V. Hence, if the actual airflow rate is greater than intended, the measured concentration will be lower than intended for the same emission rate. This is important for regulations that rely on chamber concentrations rather than emission rates (e.g., USEPA Formaldehyde Emission Standards for Composite Wood Products Rule).

In addition, under certain conditions the emission rate can be dependent upon the air speed above the material. Wei et al. (2012a) noted that the influence of the airflow speed on the emission rate is less than 1% if

$$\frac{1}{h_m} < 0.01 \frac{L}{D} \quad (2)$$

where L is the material thickness (length), D is the material diffusion coefficient (length squared/time), and h_m is the convective mass transfer coefficient (length/time). Typically, the airflow speed over the material can be ignored for most VOCs if it is higher than 0.014 m/s, while it can be an important factor for SVOCs. To address uncertainties due to airflow, flow measurements should be validated to traceable standards on a regular basis.

Chamber Impacts

Less volatile chemicals can sorb to the chamber walls to various degrees depending on the chamber material and chamber loading rate (Horn et al. 2018; De Bortoli et al. 1999). This sorption can complicate the calculation of the emission rate for these chemicals.

Summary

To reduce the uncertainty in the emission rate of reference materials, mass-transfer parameters, for example, diffusion and partition coefficients of the target compounds in the reference material, should not vary significantly with the temperature, relative humidity, and airflow.

Analytical Measurement Variability

Analytical measurements to quantify chamber concentrations can also lead to uncertainty in quantified chamber emission rates. In most cases, over half of the combined standard uncertainty of inter-laboratory studies has been attributed to the calibration and precision of analytical equipment (Howard-Reed et al. 2014). Contributors to uncertainty can include analytical equipment type, sampling uncertainty, and standard bias.

Analytical Equipment

One issue in comparing chamber concentrations for inter-laboratory studies is that each lab could quantify the chemical using a different method. For instance, there now exist a wide range of commercial means to quantify formaldehyde concentrations in chambers, including chromotropic acid, 2,4-Dinitrophenylhydrazine (DNPH) derivatization, Hantzsch reaction derivatization, electrochemical cell, photoacoustic, cavity ringdown, FTIR spectrometry, chemical ionization mass spectrometer, and laser adsorption spectrometer. Sample times for the varying methods can be every second or last an hour, and the sensitivity can vary for each technique.

Sampling Uncertainty

Each sample pump or flow controller will also introduce uncertainty in the final emission rate measurement. Derivatization and sorbent methods will be affected by the stability of the derivatization or sorbent under the storage conditions used after sampling but prior to analysis. Wet chemistry methods introduce uncertainty related to acid strength, solvent volumes, and other reagents.

Gas chromatograph columns, co-eluting peaks, unresolved baselines, and method of peak integration can all impact quantification analysis of chemicals using gas chromatographic methods (De Bortoli et al. 1999; Oppl 2008).

Standards Bias

Use of toluene equivalence analysis for quantification will result in different values than when using specific calibrants (Oppl 2008). Oppl et al. (2020) reported that for a 33-participant inter-laboratory study the RSDs of total volatile organic compounds (TVOC) (the sum of VOC concentrations) quantified using toluene equivalence were between 30% and 38%. In the same study, the RSD for TVOC values determined from specific calibrants ranged from 36% to 41%. The same study showed that the TVOC values determined from specific calibrants were 1 to 2.5 times larger than those determined from toluene equivalents.

Inter-laboratory Study Procedure Variability

Inter-laboratory study participants are often given a set of procedures and parameters under which to run the experiment (e.g., ASTM E691 Standard Practice for Conducting an Inter-laboratory Study to Determine the Precision of a Test Method) (ATSM 2020). For instance, the inter-laboratory study may specify the chamber volume, airflow rate, temperature and relative humidity, air speed above the material, the sampling time(s) along with the sampling device, tubes, columns, internal standards, thermal desorption, and GC operation (Horn et al. 2018). Some inter-laboratory studies create data entry spreadsheets to ensure uniform data collection (Howard-Reed et al. 2014).

However, the instructions may not always be followed exactly. De Bortoli et al. (1999) and Howard-Reed et al. (2014) had issues with participants using the correct chamber airflow rates and storage temperature. Some inter-laboratory studies notify the participants of the target chemicals (Poppendieck et al. 2018) while others do not (Horn et al. 2018). A study by Oppl et al. (2020), which did not notify participants of the target chemicals, showed between 4 and 8 of the 33 participants were unable to quantify the target chemical depending on the matrix. Some inter-laboratory studies send a liquid calibration solution to separately assess the laboratory performance. However, not all laboratories used it in the Howard-Reed et al. (2014) study. Finally, studies need to have enough participants to evaluate statistical significance. Some preliminary studies (e.g., (Howard-Reed et al. 2011; Poppendieck et al. 2018) only involved four laboratories.

Conclusions

Regulators and emission certification programs are implementing emission test systems in an ever-increasing frequency to reduce or at least monitor the impacts of materials on indoor air quality. Validation of these testing platforms has relied on inter-laboratory testing for the last 30 years. Over that period, emission testing performance has improved (Fig. 8), as measured by reduced relative standard deviations of inter-laboratory studies. Over the last 15 years inter-laboratory studies have moved away from using existing building materials to specifically designed materials for emission testing. However, use of these designed materials still requires a time-consuming inter-laboratory effort, as currently there are no certified reference materials available on the market. This is due to the challenges associated with determining the uncertainty associated with the material (as opposed to the emission testing and analytical systems) and determining the metrological traceability of the measurements. However, it is hoped that in the future designed reference materials can be certified and manufactured that are fit-for-purpose, homogeneous, and stable.

Disclaimer Certain commercial equipment, instruments, or materials are identified in this chapter in order to specify the procedures adequately. Such identification is not intended to imply recommendation or endorsement by NIST, nor is it intended to imply that the materials or equipment identified are necessarily the best available for the purpose.

References

- ASTM (2017) D8141-17 standard Guide for selecting volatile organic compounds (VOCs) and semi-volatile organic compounds (SVOCs) emission testing methods to determine emission parameters for modeling of indoor environments. ASTM International
- ATSM (2020) E691 standard practice for conducting an Interlaboratory study to determine the precision of a test method. ASTM International
- Beauchamp CR, Camara JE, Carney J, Choquette SJ, Cole KD, DeRose PC, Duewer DL, Epstein MS, Kline MC, Lippa, KA, Lucon E, Molloy J, Nelson MA, Phinney KW, Polakoski M, Possolo A, Sander LC, Schiel JE, Sharpless KE, Toman B, Winchester MR, Windover D. 2021 NIST Special Publication 260–136 2021 edition: metrological tools for the reference materials and reference instruments of the NIST Material Measurement Laboratory
- Cox SS, Liu Z, Little JC, Howard-Reed C, Nabinger SJ, Persily A (2010) Diffusion-controlled reference material for VOC emissions testing: proof of concept. Indoor Air 20:424–433
- Bortoli D, Maurizio SK, Kirchner S, Schauenburg H, Vissers H (1999) State-of-the-Art in the measurement of volatile organic compounds emitted from building products: results of European Interlaboratory comparison. Indoor Air 9:103–116
- Horn W, Richter M, Nohr M, Wilke O, Jann O (2018) Application of a novel reference material in an international round robin test on material emissions testing. Indoor Air 28:181–187
- Howard-Reed C, Liu Z, Benning J, Cox S, Samarov D, Leber D, Hodgson AT, Mason S, Won D, Little JC (2011) Diffusion-controlled reference material for volatile organic compound emissions testing: pilot inter-laboratory study. Build Environ 46:1504–1511
- Howard-Reed C, Liu Z, Cox S, Leber D, Samarov D, Little JC (2014) Diffusion-controlled toluene reference material for VOC emissions testing: international interlaboratory study. J Air Waste Manage Assoc 64:468–480
- ISO (2015) Guide 30: reference materials – selected terms and definitions. In ISO GUIDE 30:2015(E)

- ISO (2016) General requirements for the competence of reference material producers. In ISO 17034:2016
- Kirchner D (2007) Emissionsmessungen auf dem Prüfstand. DIBt Mitteilungen 38:77–85
- Liu Z, Howard-Reed C, Cox SS, Ye W, Little JC (2014) Diffusion-controlled reference material for VOC emissions testing: effect of temperature and humidity. Indoor Air 24:283–291
- Liu Z, Liu X, Zhao X, Cox SS, Little JC (2013) Developing a reference material for diffusion-controlled formaldehyde emissions testing. Environ Sci Technol 47:12946–12951
- Nohr M, Horn W, Jann O, Richter M, Lorenz W (2014a) Development of a multi-VOC reference material for quality assurance in materials emission testing. Anal Bioanal Chem 407:3231–3237
- Nohr M, Horn W, Wiegner K, Richter M, Lorenz W (2014b) Development of a material with reproducible emission of selected volatile organic compounds – mu-Chamber study. Chemosphere 107:224–229
- Oppl R (2008) Reliability of VOC emission chamber testing – progress and remaining challenges. Gefahrstoffe Reinhalt Luft 68:83–86
- Oppl R, Broege M, Kuebart F, Neuhaus T, Wensing M (2020) Reliability of VOC emission chamber testing – a round-robin test with flooring adhesives and a parquet lacquer. Gefahrstoffe 80:141–150
- Poppendieck D, Gong M (2020) Demystifying regulations and dynamic standard testing methods for formaldehyde emissions from wood products. In: Indoor Air 2020 Conference. Souel, South Korea
- Poppendieck D, Li N, Chen W (2018) Evaluation of a formaldehyde reference material for small chamber emission testing. In: Indoor Air 2018 Conference. Philadelphia, PA
- Richter M, Mull B, Horn W, Brödner D, Mölders N, Renner M (2017) Reproducibly emitting reference material on thermoplastic polyurethane basis for quality assurance/quality control of emission test chamber measurements. Build Environ 122:230–236
- Risholm-Sundman M, Larsen A, Vestin E, Weibull A (2007) Formaldehyde emission – comparison of different standard methods. Atmos Environ 41:3193–3202
- Roffael E, Johnsson B, Engström B (2010) On the measurement of formaldehyde release from low-emission wood-based panels using the perforator method. Wood Sci Technol 44:369–377
- Uhde E, Aksteiner N (2018) Autonomous diffusive source for the validation of chamber testing. In: Indoor Air 2018 Conference. Philadelphia, PA
- Wei W, Howard-Reed C, Persily A, Zhang Y (2013) Standard formaldehyde source for chamber testing of material emissions: model development, experimental evaluation, and impacts of environmental factors. Environ Sci Technol 47:7848–7854
- Wei W, Greer S, Howard-Reed C, Persily A, Zhang Y (2012a) VOC emissions from a LIFE reference: small chamber tests and factorial studies. Build Environ 57:282–289
- Wei W, Zhang Y, Xiong J, Li M (2012b) A standard reference for chamber testing of material VOC emissions: design principle and performance. Atmos Environ 47:381–388
- Weschler CJ (2006) Ozone's impact on public health: contributions from indoor exposures to ozone and products of ozone-initiated chemistry. Environ Health Perspect 114:1489–1496
- Wilke O, Horn W, Jann O (2009) European interlaboratory study for sampling VOC emissions – step 3 – emission test chamber measurements. Paper no 343. In: Proceedings of the healthy buildings conference. Syracuse, NY, USA
- Wilke O, Horn W, Richter M, Jann O (2021) Volatile organic compounds from building products - results from six round robin tests with emission test chambers conducted between 2008 and 2018. Indoor Air 31:2049–2057
- Wilke O, Horn W, Wiegner K (2011) Interlaboratory study to check the performance of test chamber measurements for product emission testing. In: Indoor air 2011 Conference. Austin, TX
- Yrieix C, Dulaurent A, Laffargue C, Maupetit F, Pacary T, Uhde E (2010) Characterization of VOC and formaldehyde emissions from a wood based panel: results from an inter-laboratory comparison. Chemosphere 79:414–419



Predicting VOC and SVOC Concentrations in Complex Indoor Environments

25

Jianyin Xiong, Xinke Wang, and Yinping Zhang

Contents

Introduction	772
Predicting VOC Concentrations in Real Indoor Environments	774
VOC Emission/Sorption from Multiple Sources/Sinks in Different Indoor Settings	774
VOC Emission from Occupants Due to the Use of Personal Care Products	778
Reactions of Ozone with Squalene in Realistic Indoor Environments	783
Predicting SVOC Concentrations in Complex Indoor Environments	788
Two Types of Models for Predicting the Fate and Transport of SVOCs in Real Indoor Environments	792
Estimating Partition Coefficients of SVOCs Between the Gas Phase, Airborne Particles, Settled Dust, and Surfaces	796
Challenge to Accurate Prediction of Indoor SVOC Concentration in Complex Indoor Environment	801
Conclusion	803
Cross-References	804
References	804

Abstract

In this chapter, recent developments in the prediction of VOC and SVOC concentrations in complex indoor environment are reviewed. The fate and transport of VOCs and SVOCs in indoor settings is more complicated than in

J. Xiong

School of Mechanical Engineering, Beijing Institute of Technology, Beijing, China
e-mail: xiongyj@bit.edu.cn

X. Wang (✉)

School of Human Settlements and Civil Engineering, Xi'an Jiaotong University, Xi'an, China
e-mail: wangxinke@mail.xjtu.edu.cn

Y. Zhang

Department of Building Science, School of Architecture, Tsinghua University, Beijing, China
Beijing Key Laboratory of Indoor Air Quality Evaluation and Control, Beijing, China
e-mail: zhangyp@mail.tsinghua.edu.cn

chambers, and the presence of occupants can greatly affect indoor air quality. First, this chapter addresses multiple VOC emission/sorption of building materials in different indoor settings. Then, VOC emissions from occupants due to the use of personal care products in university classroom are introduced. Following that, the indoor chemistry of VOCs related to ozone/squalene reactions in real residence is given. Aside from VOCs, it is also of concern to predict concentrations and fate of indoor SVOCs to further assess human exposure to these ubiquitous chemicals and their potential health effects. Based on the source emission characteristics of SVOCs, emission models are described as well as critical differences between modeling VOCs and SVOCs. Due to the substantial partitioning of SVOCs among the gas, particle, dust, and surface, partitioning models and correlations for estimating partition coefficients are reviewed. Lastly, the dynamics of SVOCs in different phases are described using fugacity-based and mass-transfer-based models.

Keywords

Volatile organic compounds (VOCs) · Semi-volatile organic compounds (SVOCs) · Personal care products · Indoor chemistry · Complex indoor environments

Introduction

Due to the ubiquitous use of a wide range of consumer products and articles such as building materials, decorative items, furniture, personal care products, and baby care products in real indoor environments, it is important to assess human exposure to volatile organic compounds (VOCs) and semi-volatile organic compounds (SVOCs) emitted from these products and articles. For this purpose, data on the concentration of VOCs and SVOCs in indoor environments is needed. Predicting VOC and SVOC concentrations with models can provide detailed information, for example, about concentration changes over time, chemical distribution among indoor compartments, and the influence of certain activities, which may help implement measures to improve indoor air quality. In this chapter, models that focus on VOC and SVOC emission, transport, and fate in real indoor environments are reviewed.

According to definition, VOCs are classified as a class of organic compounds with a boiling point ranging from 50 °C to 240 °C, while SVOCs with a boiling point ranging from 240 °C to 400 °C. Compared with VOCs, SVOCs have higher boiling points and lower saturated vapor pressures. Since the chemical properties of VOCs and SVOCs are different, it leads to that the described models and key parameters are also different. Therefore, the predictions on VOCs and SVOCs in real indoor environment are introduced separately, by different sections in this chapter.

As far as the VOCs are concerned, in contrast to controlled chamber studies, the mass transport of VOCs occurred in real indoor environments owns several characteristics: (1) Multiple sources, sinks, and surfaces coexist (Wang et al. 2020), and the

ventilation conditions vary with time and space (Liu et al. 2019), which complicates VOC emission and transport behaviors. The emissions from one material may interact with emissions from other materials, which means that a simple summation of emissions from individual materials may not represent reality. (2) In addition to the emissions from indoor materials and products, the presence of occupants contributes significantly to indoor air composition (Weschler and Carslaw 2018), especially in densely occupied indoor settings, e.g., classroom, meeting room. The impact of occupancy includes two aspects. On one hand, the use of personal care products and cleaning products will affect the concentration of chemicals indoors. On the other hand, there are many sources of reactive chemicals in real indoor air, including outdoor air. Pollutants such as ozone can enter with the ventilation air or air that infiltrates through window frames, doors, and other openings in the building envelope. The reactions between ozone and squalene, which is abundant in human skin oil, will generate a variety of oxidation products, which may further have an adverse effect on indoor air quality. Therefore, the introduction on the prediction of VOCs in real indoor settings will include three sections: section “[VOC Emission/Sorption from Multiple Sources/Sinks in Different Indoor Settings](#)”; section “[VOC Emission from Occupants Due to the Use of Personal Care Products](#)”; section “[Reactions of Ozone with Squalene in Realistic Indoor Environments](#).“ These sections represent the VOC transport in different indoor settings (including in-cabin environment, classroom and residence) on different levels (including physical transport, chemical reaction, and physical-chemical combined transport). Since much work has been done, we just introduce some typical work in these three aspects. It should be noted that, field observations in realistic indoor settings under normal occupancy are important complements to laboratory investigations. The application of highly accurate online equipment for time- and space-resolved measurements provides the dataset for modeling input (Liu et al. 2019).

Similar to VOCs, SVOCs also include various kinds of compounds such as phthalate esters (PAEs), polycyclic aromatic compounds (PAHs), polybrominated diphenyl ethers (PBDEs), and polychlorinated biphenyls (PCBs) (Weschler and Nazaroff 2008). Field measurements show that SVOCs are ubiquitous in various consumer products and articles used in real indoor environment (Xu and Zhang 2011; Lucattini et al. 2018).

Carpets, textiles, and clothing became important emission sources of polyester and polypropylene, since woven carpets made of cotton and wool have been widely replaced by tufted carpets made of synthetic fibers such as nylon, rayon, and acrylics in the 1950s (Weschler 2009). Some additives including flame retardants (FRs) and surfactants are added to these materials, so FRs (organophosphate and brominated flame retardants (OPFRs and BRFs)) and per- and polyfluoroalkyl substances (PFASs) are commonly found in fiber carpets and other textile products. The use of electronic equipment is resulting in increased emission of some SVOCs including OPFRs and BFRs into indoor environments (Weschler 2009). One study from China (Chen et al. 2010) showed that PBDEs derived from penta-, octa-, and deca-mixtures were detected in 83.3%, 58.3%, and 83.3% of the television casings, respectively. Concentrations of PBDEs in computer monitor casings were generally <50 ng/g,

except for one sample which contained 13,304 ng/g. The concentrations of PBDEs were higher in computer components (mean value 279,965 ng/g) than in television and computer casings. Besides FRs, plasticizers, TBBPA, PBDEs, 1,2-Bis(2,4,6-tribromophenoxy)ethane (BTBPE), tris(phenyl)phosphate (TPhP), tris (2-chloroisopropyl) phosphate (TCIPP), and tris(methylphenyl) phosphate (TMPP) were also found at relatively high concentrations (ranging from $\mu\text{g}/\text{g}$ to mg/g) (Ballesteros-Gómez et al. 2013; Brandsma et al. 2014). In furniture, soft foam in cushioning for bedding, sofas, and chairs may emit some kind of FRs (Lucattini et al. 2018). Building materials such as insulating foams, flooring, facades, paints, varnishes, sealants, and adhesives mainly comprise of FRs, perfluorocarboxylic acids (PFCAs), PAEs, and PCBs (Lucattini et al. 2018). Interestingly, also products intended to improve hygiene, such as personal care, health care, and cleaning products, may emit SVOCs that can negatively affect people's health. Investigations showed at least one polyfluorinated compound (PFC) existed in any given household cleaning product or spray (Danish Environmental Protection Agency 2006). Some phthalates including diethyl phthalate (DEP) and dibutyl phthalate (DBP) were found in moisturizers and nail polish samples (Chen et al. 2005). Thus, it can be concluded that indoor SVOC sources are ubiquitous and various, and that the emissions are complicated, which makes the prediction of SVOC concentrations in indoor environments difficult.

Predicting VOC Concentrations in Real Indoor Environments

VOC Emission/Sorption from Multiple Sources/Sinks in Different Indoor Settings

Sink-Diffusion Model in Multi-Sink Residential Rooms

Due to the complexity of real indoor settings, many mass transfer processes may happen concurrently, e.g., emission or sorption from or to different materials and products. Singer and some co-authors (Singer et al. 2007) have done much work on the sorption behaviors of VOCs in residence. They conducted a series of experiments to characterize VOC sorption in residential rooms with furnishings and material surfaces unaltered and in a furnished chamber designed to simulate a residential room (Singer et al. 2007). For the tested ten rooms, multiple sinks coexisted, which can be grouped into four categories: (1) fleecy/padded (e.g., carpet, upholstery, bedding, other fabrics); (2) painted wallboard/plaster; (3) hard/porous (e.g., wood, plastic, laminate, paper); (4) hard nonporous (e.g., glass, metal, tile, porcelain). During the test, a VOC mixture was rapidly volatized into the room, which generated a net movement of VOC mass from the gas phase to the room materials. The sorption processes lasted for 5 h until quasi steady state was reached. Singer et al. (2007) applied the following sink-diffusion model to simulate the VOC mass balance in the residential room:

$$\frac{dC}{dt} = -(\lambda + \lambda_a)C + \lambda_d M \quad (1)$$

$$\frac{dM}{dt} = \lambda_a C - (\lambda_d + k_1)M + k_2 E \quad (2)$$

$$\frac{dE}{dt} = -k_2 E + k_1 M \quad (3)$$

where, C is the VOC concentration in the room air; M is the VOC mass in the exposed surface sink; E is the potentially embedded sink in contact with the surface but not directly with room air; λ_a , λ_d , k_1 , k_2 are coefficients describing rates of mass transfer among compartments.

Figure 1 shows the predictions of the sink-diffusion model for some tested VOCs, and the comparison with experimental data. The good agreement demonstrates the effectiveness of the sink-diffusion model in predicting multi-sorption scenarios. The main drawback of this model lies in that, the parameters (λ_a , λ_d , k_1 , k_2) in the model are fitting coefficients, which lack of clear physical meanings. Therefore, physics-based model is required.

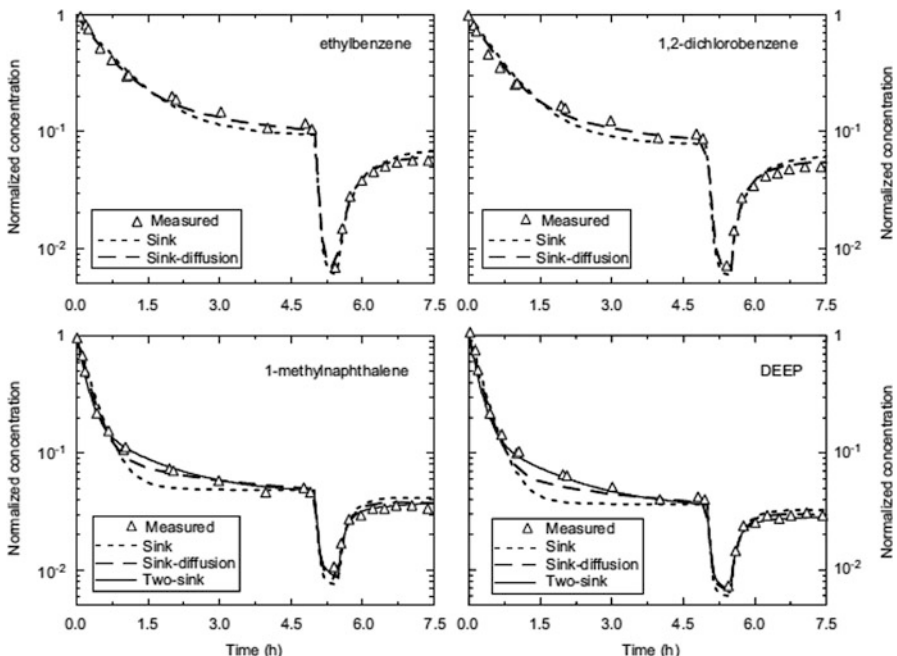


Fig. 1 Comparison of sink-diffusion model predictions with experimental data in multiple sink residential rooms (Singer et al. 2007)

Physics-Based Emission Model in Multi-Source In-Cabin Environments

In addition to the common built environment (residence, office, classroom, etc.), in-cabin environment is also regarded as a generalized indoor environment, in which people spend 6.5% of their time per day, with much longer times for taxi drivers, for example. The VOC concentrations in vehicle cabins are often very high, and the emission rate and concentrations of VOCs can increase dramatically when the vehicle is exposed to sun in the hot summer season, so more attention should be paid to this micro environment. In real in-cabin environments, multiple source materials (e.g., upholstery, carpet, seat, flooring materials) coexist. This generates a multi-source emission process, and these emissions may interact with each other, as shown in Fig. 2. By examining multiple VOC emissions in indoor environments, Deng et al. (2008) derived a physics-based analytical model to describe the multi-source emission behaviors by virtue of Laplace transformation. This model implicitly indicates the relationship between the gas-phase VOC concentrations and emission time. Since the derivation process and the analytical solutions are complicated, they are not given here.

By investigating the emissions of VOCs in in-cabin environments, Wang et al. (2020) applied a physics-based multi-source emission model to predict VOC emissions from multiple vehicle cabin materials. The emission rate from each material E_i can be calculated by Eq. (4):

$$E_i(t) = D_{m,i} \sum_{n=1}^{\infty} \frac{2(q_{n,i}^2 + Bi_{m,i}^2/K_i^2) \sin^2 q_{n,i}}{L_i(q_{n,i}^2 + Bi_{m,i}^2/K_i^2 + Bi_{m,i}/K_i)} \left[C_{0,i} e^{-D_{m,i}L_i^{-2}q_{n,i}^2 t} + \int_0^t e^{-D_{m,i}L_i^{-2}q_{n,i}^2(t-\tau)} K_i dC_a(\tau) \right] \quad (4)$$

where subscript i stands for the different vehicle cabin materials; C_0 is the initial emittable concentration, $\mu\text{g}/\text{m}^3$; D_m is the diffusion coefficient, m^2/s ; K is the partition coefficient; L is the thickness of the material; $q_{n,i}$ are the positive roots of

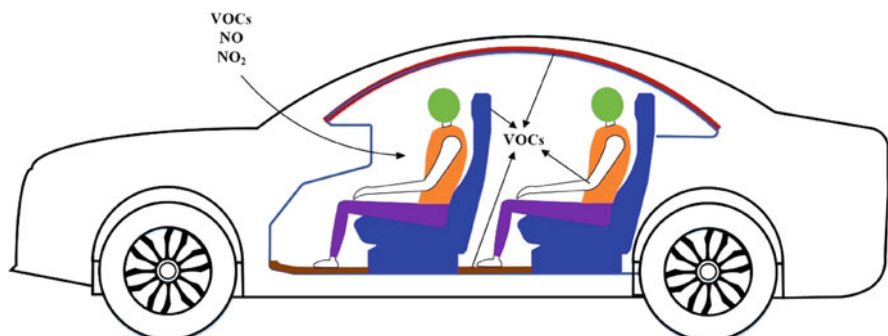


Fig. 2 Schematic of multi-source emissions in real in-cabin environment

$$q_{n,i} \tan q_{n,i} = \frac{Bi_{m,i}}{K_i} \quad (n = 1, 2, 3, \dots) \quad (5)$$

According to mass conservation, the gas-phase VOC concentration in the in-cabin environment conforms to the following equation:

$$V \frac{dC_a(t)}{dt} = QC_{in} - \sum_i A_i E_i(t) - QC_a(t) \quad (6)$$

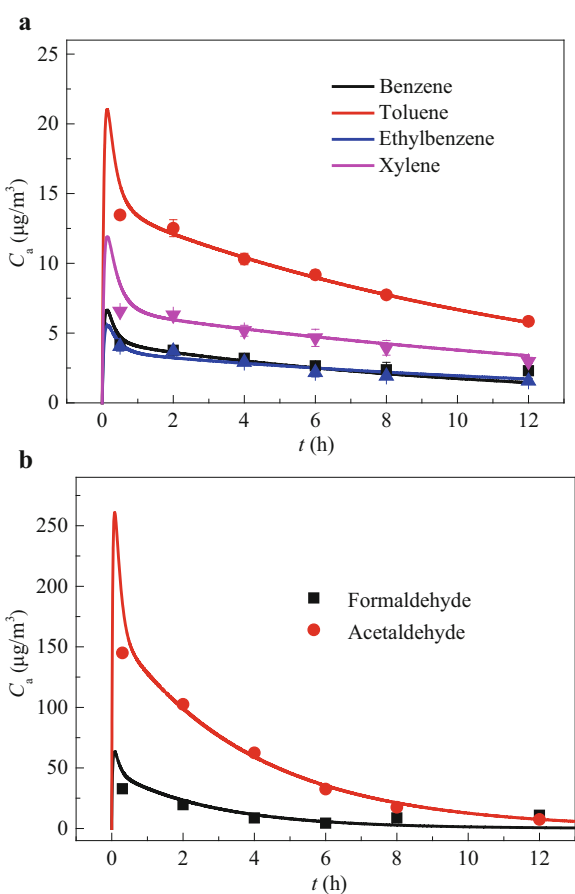
where A_i is the surface area of the vehicle cabin material i , m^2 ; Q is the ventilation rate, m^3/s ; V is the volume of the environment, m^3 ; and C_{in} is the inlet concentration, $\mu\text{g}/\text{m}^3$. The initial condition is:

$$C_a(t) = 0, \quad t = 0 \quad (7)$$

The gas-phase VOC concentration C_a in the in-cabin environment for multi-source emissions can be solved by combining the above Eqs. (4), (5), (6), and (7).

The above model can be regarded as a physics-based semi-analytical model. The key parameters for each vehicle cabin material in the multi-source model can be determined using a ventilated-chamber C-history method (Huang et al. 2013). To validate the multi-source emission model, Wang et al. (2020) built a simulated in-cabin environment with similar volume and materials as a realistic vehicle cabin. The testing system is comprised of a 3 m^3 environmental chamber with controlled temperature, relative humidity, and air exchange rate. Prior to the experiment, the gas-phase VOC concentrations in the environmental chamber were sampled to obtain the background concentration. The temperature was set at 25°C , and the humidity was maintained at 50%. One type of car roof upholstery, one carpet, and two seats were positioned in a typical vehicle cabin arrangement in the test chamber. During the experiment, a constant flow of 99.9% clean air (air exchange rate: 1 h^{-1}) was introduced into the 3 m^3 environmental chamber, and the VOCs were sampled at regular intervals using thermal desorption (TD) sampling tubes (Tenax-TA and DNPH were used as sorbents), which were then analyzed using GC-MS or HPLC to obtain the gas-phase VOC concentrations in the chamber. The key parameters determined by the ventilated-chamber C-history method in a small-scale chamber were used to predict the emission behaviors in the simulated vehicle cabin using the multi-source emission model. The comparison between model predictions and experimental data for the different VOCs is shown in Fig. 3. From this figure, we can see that most of experimental data are located on or near the curve predicted by the model. This good agreement ($R^2 = 0.82\text{--}0.99$) not only verifies the reliability of the multi-source model, but more importantly demonstrates the feasibility of applying key parameters determined in small-scale chamber tests to predict multiple emission scenarios in large-scale vehicle cabin environments. This means that the measured key parameters for different vehicle cabin materials are helpful for predicting pollution levels and for assessing exposure in realistic vehicle cabins, thus

Fig. 3 Comparison between the model prediction and experimental data for multi-source emissions in a simulated vehicle cabin (Wang et al. 2020)



providing a technical means to theoretically evaluate in-cabin air quality when designing a new vehicle.

VOC Emission from Occupants Due to the Use of Personal Care Products

Background

The emission of cyclic volatile methylsiloxanes (cVMS) due to the use of personal care products is regarded as an important contributor to indoor air pollution (Tang et al. 2015). cVMS are organic chemicals used in a wide range of personal care products due to their high thermal stability and smooth texture. Products containing cVMS include antiperspirants, skin and hair care formulations, sunscreen, and cosmetics (Montemayor et al. 2013). Octamethylcyclotetrasiloxane (D4), decamethylcyclopentasiloxane (D5), and dodecamethylcyclohexasiloxane

(D6) are three widely used cVMS. These cVMS are of particular concern, because they are potentially persistent, bioaccumulative and toxic, and have been shown to be associated with connective tissue disorders, adverse immunologic responses, and fatal liver and lung damage (Lieberman et al. 1999). cVMS can be emitted from the original sources and then partition into the indoor air due to their high Henry's law constants. The concentrations of cVMS in indoor air may differ based on regional regulations and regional preferences for different types of personal care products and compounds. The analysis of 91 samples from different sites in the United Kingdom (UK) and Italy indicated that the D4, D5, and D6 concentrations in indoor air were in the range of 19–270 $\mu\text{g m}^{-3}$, 2.4–440 $\mu\text{g m}^{-3}$, and 0.47–79 $\mu\text{g m}^{-3}$, respectively (Pieri et al. 2013). Based on 3857 samples of Canadian residential indoor air, Zhu et al. (2013) reported that the representative levels of indoor D4 and D5 concentrations were within the range of 5.45–7.94 $\mu\text{g m}^{-3}$ and 35.47–47.18 $\mu\text{g m}^{-3}$, respectively. In Chicago, the indoor air concentrations of D4, D5, and D6 were measured to be 0.03–0.5 $\mu\text{g m}^{-3}$, 0.97–56 $\mu\text{g m}^{-3}$, and 0–2.8 $\mu\text{g m}^{-3}$, respectively (Yucuis et al. 2013). Therefore, modeling and prediction of cVMS due to the frequent use of personal care products in indoor environment is very important.

Model for Predicting cVMS Emissions

Most experimental studies indicated that D5 is the dominant cVMS, both in personal care products and in indoor air, even comprising more than 90% of total cVMS (Tang et al. 2015; Yucuis et al. 2013). The modeling of D5 concentrations in the outdoor atmosphere is well developed. However, very little research has been done to model D5 emissions in indoor environments, especially from human skin after the use of personal care products. Up to now, three kinds of models have been proposed, including the multi-pathway exposure model (Ernstoff et al. 2016), the adsorption/desorption model (Xiong et al. 2016), and the physics-based model (Yang et al. 2018).

In the multi-pathway exposure model, the mass transfer of D5 through the skin lipids and the indoor air can be described by the following two equations (Ernstoff et al. 2016):

$$\frac{dm_c(t)}{dt} = -k_{p,a} \cdot m_c(t) - k_{p,s} \cdot m_c(t) \quad (8)$$

$$V \frac{dC_a}{dt} = Q \cdot C_{in} - Q \cdot C_a + k_{p,a} \cdot m_c(t) \quad (9)$$

where, $m_c(t)$ is the remaining mass of D5 in the skin lipids at time t (μg) and $k_{p,a}$ and $k_{p,s}$ are the product-to-air rate constant and the product-to-skin (dermal uptake) rate constant, respectively, (h^{-1}), which can be calculated by the following equations:

$$k_{p,s} = 1 / \left(L / K_p^{\text{aq}} + L / \varphi_w \right) \quad (10)$$

$$k_{p,a} = 1 / (L / \varphi_a + L / \varphi_w) \quad (11)$$

where, K_p^{aq} is the skin-permeation coefficient (m/h); φ_w is the mass-transfer coefficient through the aqueous film (m/h); $k_{p,a}$ is the mass-transfer coefficient from the aqueous film to the air (m/h); and L is the thickness of the skin lipids (m).

Detailed calculation indicates that the ratio of $k_{p,a}$ to $k_{p,s}$ for D5 is about 27, meaning that most of D5 is volatilized from the skin lipid surface. Therefore, dermal uptake can be neglected. Based on this analysis, the solution of Eqs. (8) and (9) can be derived as:

$$C_a(t) = C_{\text{in}} + \frac{M_0 \cdot k_{p,a}}{Q - k_{p,a} \cdot V} \left(\exp(-k_{p,a}t) - \exp\left(-\frac{Q}{V}t\right) \right) \quad (12)$$

where, $M_0 = C_0 \times A \times L$ is the initial mass of D5 inside the skin lipids, μg ; C_0 is the initial emittable concentration of D5, $\mu\text{g}/\text{m}^3$.

For the adsorption/desorption model, by neglecting the internal diffusion process, the indoor gas-phase D5 concentration emitted from skin lipids can be described as (Xiong et al. 2016):

$$C_a(t) = \frac{M_0 \cdot A \cdot h_m \cdot LF}{K_e \cdot (r_2 - r_1)} [\exp(-r_1 t) - \exp(-r_2 t)] \quad (13)$$

where r_1 and r_2 are the two roots of the following equation:

$$r^2 - (h_m/K_e + N + h_m L)r + N h_m / K_e = 0 \quad (14)$$

where $K_e = K \times L$ is the skin/air partition coefficient (m); $LF = A/V$ is the loading factor (m^2/m^3); and $N = Q/V$ is the air-exchange rate (h^{-1}).

A recent study found that the physics-based model agrees better with experimental data than the multi-pathway exposure model and the adsorption/desorption model (Yang et al. 2018). Therefore, the physics-based model will be introduced in more detail here, including model development, determination of key parameters in the model, and validation.

When personal care products are applied, the ingredients are initially present in a separate layer on top of the skin lipids, and some of the ingredients will partition into the skin lipids from this separate layer. The following assumptions are introduced to obtain the physics-based model: (1) The diffusion of D5 through the skin-lipid layer is represented as one-dimensional; (2) the skin forms an impermeable barrier with regard to D5 penetration, which is consistent with earlier dermal absorption studies (Montemayor et al. 2013); (3) adsorption/absorption of D5 to interior surfaces is negligible (this assumption needs further validation); and (4) the D5 level indoors is well mixed. With these assumptions, emission can be described as shown in Fig. 4.

The analytical solution of the indoor D5 concentration can be derived as (Xiong et al. 2012):

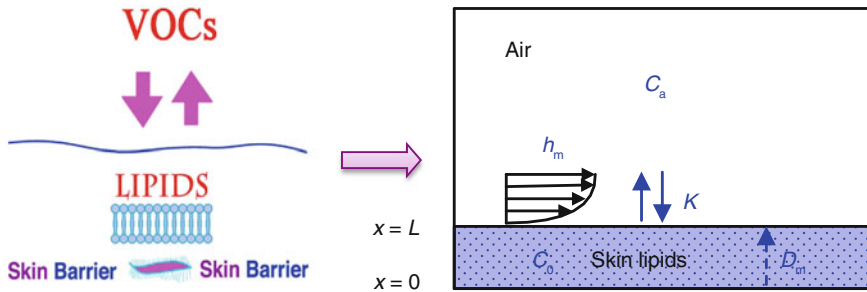


Fig. 4 Schematic of D5 emission from skin lipids

$$C_a(t) = A_1 + 2A_2 \cdot \sum_{n=1}^{\infty} \frac{A_3 \cdot q_n \sin q_n - A_4 \cdot \cos q_n}{G_n} e^{-D_m L^{-2} q_n^2 t} \quad (15)$$

where $G_n = [K\beta + (\alpha - q_n^2)KBi_m^{-1} + 2]q_n^2 \cos q_n + [K\beta + (\alpha - 3q_n^2)KBi_m^{-1} + \alpha - q_n^2]q_n \sin q_n$; $A_1 = C_{in}$; $A_2 = C_0$; $A_3 = \beta$; $A_4 = 0$; $\alpha = QL^2/D_m V$; $\beta = AL/V$; $Bi_m = h_m L/D_m$; and q_n are the positive roots of

$$q_n \tan q_n = \frac{\alpha - q_n^2}{K\beta + (\alpha - q_n^2)KBi_m^{-1}} \quad (n = 1, 2, \dots) \quad (16)$$

For real occupant emission tests, the volume of the environment is often very large (room or full-scale chamber) and the convective mass-transfer coefficient is very small (natural convection in many scenarios). Under this condition, the term $K\beta$ will be much smaller than $\alpha K/Bi_m$ (generally by two to four orders of magnitude smaller) in Eq. (16), and thus can be ignored. Equation (16) can then be simplified:

$$q_n \tan q_n = \frac{Bi_m}{K} \quad (n = 1, 2, \dots) \quad (17)$$

With Eq. (13) and the condition $K\beta \ll \alpha K/Bi_m$, the analytical solution (Eq. (15)) can be further reduced to:

$$C_a(t) = C_{in} + \sum_{n=1}^{\infty} \frac{2\beta C_0}{(\alpha - q_n^2)(1 + K/Bi_m + q_n^2 K^2/Bi_m^2)} e^{-D_m L^{-2} q_n^2 t} \quad (18)$$

Determination of Key Parameters in the Model

To calculate the indoor D5 concentration, the three key parameters (C_0 , D_m , K) for the model need to be known. The key parameters C_0 and D_m can be determined using a C-history method based on the analytical solution (Yang et al. 2017). During the mid-term emission period (i.e., when the mass-transfer Fourier number, Fo_m , is larger than 0.125), the following equation exists:

$$\ln [C_a(t) - C_{in}] = SL \cdot t + INT \quad (19)$$

with

$$SL = -D_m L^{-2} q_1^2 \quad (20)$$

$$INT = \frac{2\beta C_0}{(\alpha - q_1^2)(1 + K/Bi_m + q_1^2 K^2 / Bi_m^2)} \quad (21)$$

where q_1 is the first positive root of Eq. (17), which is in the range of $0-\pi/2$.

Equations (19), (20), and (21) indicate that the logarithm of $C_a(t)-C_{in}$ correlates linearly to the emission time t , and the slope (SL) and intercept (INT) are functions of the two key parameters C_0 and D_m . Therefore, if linear curve fitting is performed with the experimental data of $C_a(t)-C_{in}$ against t , SL and INT can be obtained, following which C_0 and D_m can be determined by solving two equations with these two key parameters. For D5 emission from skin lipids, the initial K can be approximately predicted by the following correlation:

$$\log K = \log K_{ow} + \log (HRT) \quad (22)$$

where K_{ow} is the octanol-water partition coefficient; H is the Henry constant; R is the gas constant; and T is the temperature.

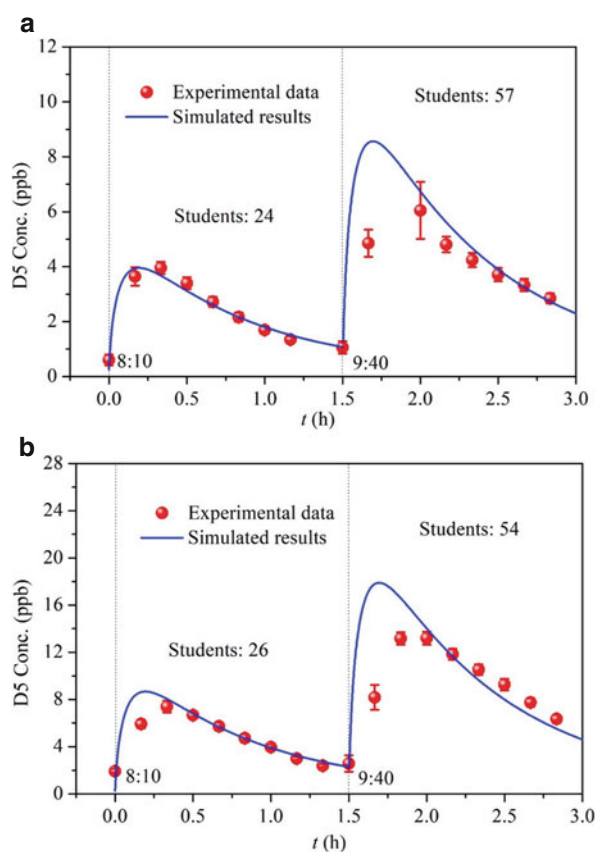
The thickness of the skin lipid layer is an important parameter for D5 emission models and varies for different persons and different regions of the body. It is generally in the range of 0.5–1.3 μm . To simplify the analysis, the thickness of skin lipid layer is assumed to be 1 μm throughout the entire body.

A field campaign was conducted in 2014 during several class sessions in a university classroom to examine the emission characteristics of D5 from skin lipids (Tang et al. 2015). Based on the SL and INT by using Eq. (19) with the experimental data, values determined for C_0 and D_m during class session 1 on Nov 6 (number of students: 24) are $C_0 = (8.80 \pm 0.62) \times 10^{10} \mu\text{g}/\text{m}^3$ and $D_m = (1.46 \pm 0.08) \times 10^{-16} \text{ m}^2/\text{s}$, while the values for class session 1 on Nov 13 (number of students: 26) are $C_0 = (1.93 \pm 0.16) \times 10^{11} \mu\text{g}/\text{m}^3$ and $D_m = (1.35 \pm 0.07) \times 10^{-16} \text{ m}^2/\text{s}$. These results indicate that the relative standard deviation for C_0 and D_m is less than 10%, which is relatively small. By comparing the determined key parameters from different test days, it can be concluded that the range of values for D_m is very narrow, while C_0 differs by about one order of magnitude. The reason needs further investigation.

Validation of the Physics-Based Model

With the above key parameters, the D5 concentration for other class sessions can be predicted. Figure 5a shows the comparison between model prediction and experimental data for class session 1 and class session 2 (number of students: 57) on Nov 6, while Fig. 5b shows the comparison for class session 1 and class session 2 (number of students: 54) on Nov 13. The agreement for the mid- and long-term emissions in Fig. 5 is good, demonstrating the effectiveness of the emission model as well as of the parameter estimation method. In the field test, class session 1 and 2 have different

Fig. 5 Comparison between model predictions and experimental data for D5 concentrations for different class sessions on (a) Nov 6 and (b) Nov 13 (Yang et al. 2018)



numbers of students (both on Nov 6 and Nov 13), and thus can be regarded as independent experiments. The good agreement between model predictions and experimental data for class session 2 can be taken as independent validation, which speaks for the accuracy of the physics-based model.

Reactions of Ozone with Squalene in Realistic Indoor Environments

Background

In addition to VOC sorption and emission, ozone-initiated chemistry is also important for indoor air quality (Weschler and Carslaw 2018). Most previous studies were performed in unoccupied indoor settings, and only a few studies refer to the influence of occupants on indoor chemistry. In densely occupied settings, people can be the dominant sink for indoor ozone. Studies in a simulated aircraft cabin confirmed that the reactions between ozone and occupants were responsible for more than 50% of the total ozone removal (Weschler et al. 2007). Measurements of the

ozone concentration in a real classroom indicated that the ozone removal caused by 25 occupants was approximately 2.6 times larger than that caused by the available surfaces in the classroom including its furniture (Fischer et al. 2013). The presence of human occupants can substantially reduce indoor ozone concentrations and increase the levels of byproducts (Weschler 2016). This is because ozone can react with the constituents of skin lipids on the exposed body parts, worn clothing fabrics, and human hair to generate a series of oxidation products (Wisthaler and Weschler 2010). Squalene has been reported to be the single-most abundant ozone-reactive constituent of skin lipids (Fu et al. 2013). Ozone reacts with squalene to generate a range of VOCs, such as acetone, geranyl acetone (GA), 6-methyl-5-hepten-2-one (6-MHO), and 4-oxopentanal (4-OPA) (Wisthaler and Weschler 2010). Some of these volatile products have been characterized as sensitizers and asthma triggers (Anderson et al. 2012). Additional low volatility products that accumulate in the lipids may be skin irritants and could also diffuse into the bloodstream over time to cause more adverse health effects. Hence, understanding the heterogeneous reaction between squalene and ozone and transport characteristics of the products is very important.

Models for Predicting Ozone/Squalene Reactions

The kinetic characteristics of heterogeneous reactions between ozone and squalene including the reaction rate constants as well as products have been investigated in various studies (Fu et al. 2013; Zhou et al. 2016). At present, the most common and effective way to explore dermal exposure to gas-phase chemicals is through mathematical models (Gong et al. 2014; Morrison et al. 2016). Gong et al. (2014) proposed a transient-state mass transfer model to predict air-to-skin-to-blood absorption of six phthalate esters for varying exposure conditions. Morrison et al. (2016) improved Gong et al.'s model by including a layer of skin surface lipids and the effect of clothing. However, these models describe only the physical transport of a chemical from the air into the blood stream without taking chemical reactions into account.

Incorporating both mass transport and chemical reactions, Lakey et al. (2017) developed a kinetic multilayer (KM-SUB-Skin) model to estimate the concentrations of squalene ozonolysis products in the gas phase and in the skin. This model includes different layers: a gas phase, a near-surface gas phase, a sorption layer, a skin oil layer, a number of bulk layers in the stratum corneum and the viable epidermis. The concentration of the various reactants and products in the gas phase ($[Z]_g$), the sorption layer ($[Z]_s$), the skin oil layer ($[Z]_{oil}$), the stratum corneum layers ($[Z]_{sc}$), the viable epidermis layers ($[Z]_{ve}$) in the KM-SUB-Skin model were determined over time through a set of differential equations describing the mass balance of each molecule for gas, surface, and skin bulk layers, which have been adapted from Shiraiwa et al. (2010). For the $[Z]_g$, $[Z]_s$, $[Z]_{oil}$, the differential equations are given below:

$$\frac{d[Z]_g}{dt} = (J_{\text{des},Z} - J_{\text{ads},Z}) \frac{S}{V_{\text{room}}} + P_{g,Z} \quad (23)$$

$$\frac{d[Z]_s}{dt} = J_{\text{ads},Z} - J_{\text{des},Z} + J_{s_oil,Z} - J_{oil_s,Z} \quad (24)$$

$$\frac{d[Z]_{\text{oil}}}{dt} = (J_{s_oil,Z} - J_{oil_s,Z}) \frac{A}{V_{\text{oil}}} + (J_{sc1_oil,Z} - J_{oil_sc1,Z}) \frac{A}{V_{\text{oil}}} + P_{oil,Z} \quad (25)$$

where J represents various different types of mass transport fluxes such as adsorption and desorption (shown by the subscripts ads and des, respectively) and mass transport between different layers; P is a production or loss term in a given layer due to reactions; S is the total surface area of the people in the room; A is the surface area of a layer; and V_{room} is the volume of the room.

This model neglects the convective mass-transfer resistance from air to skin and the partitioning (adsorption/desorption) processes on indoor surfaces, which will cause some deviations for realistic indoor setting simulations. Later, Lakey et al. (2019) improved the KM-SUB-Skin model by taking into account the convective effect from the gas phase to the human surface and clothes (called KM-SUB-Skin-Clothing model), while the effect of indoor-surface partitioning was still not included. Xiong et al. (2019) developed a kinetic model by considering the adsorption/desorption of products on indoor surfaces to predict the concentration of squalene/ozone reaction products in a classroom. However, this model does not consider the transport of products inside the skin, and thus cannot further evaluate the exposure via dermal uptake. Recently, Zhang et al. (2021) developed a physical-chemical coupling model to more accurately predict the characteristics of squalene/ozone reaction products in the gas phase and in the skin, by considering the external convection along the skin lipid surface, internal diffusion inside the skin, indoor surface uptake (including surface partitioning, and diffusion inside the wall). Considering that the concept of KM-SUB-Skin-Clothing model is very similar to the model described by Eqs. (23), (24), and (25), we just briefly introduce the physical-chemical coupling model here.

The physical-chemical coupling model is based on the transient-state mass-transfer models described by Gong et al. (2014) and Morrison et al. (2016). As shown in Fig. 6, during the uptake of chemicals from the gas phase to the dermal capillaries, the chemical will pass through three layers: skin surface lipids (SSL), stratum corneum (SC), and viable epidermis (VE). SSL, a thin layer consisting of sebum secreted by sebaceous glands and a small amount of lipids from SC, is assumed to be $\sim 0.5 \mu\text{m}$ in this model (Lakey et al. 2017). SC, which consists of about 15–20 layers of dead cells, is the outermost part of the epidermis and its thickness is $\sim 25 \mu\text{m}$. VE, consisting of some living cells, is between the SC and dermis, with a thickness of $\sim 100 \mu\text{m}$. Squalene in the SSL can be oxidized by ozone to produce some primary and secondary products. Among them, 6-MHO and 4-OPA are the most abundant, thus are selected as the analysis targets. The absorption process of 6-MHO and 4-OPA from air to dermal capillaries mainly includes

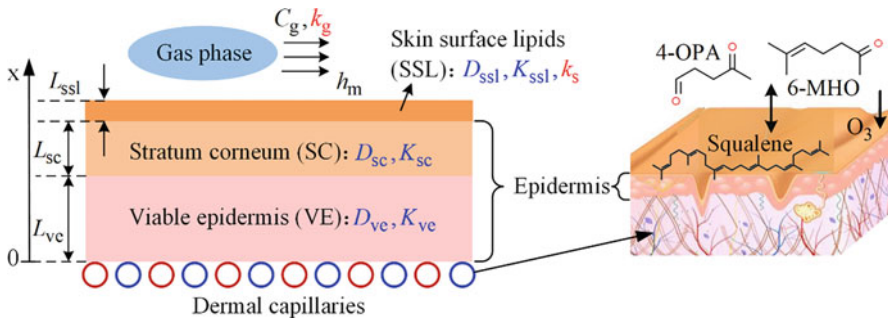
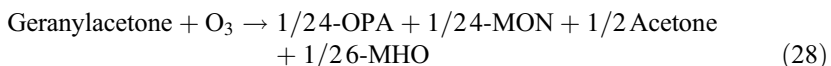


Fig. 6 Schematic illustrating layers and parameters involved in dermal exposure processes. The blue parameters describe the physical diffusion and partitioning; the red parameters indicate chemical reactions; the remaining parameters are defined in the context (Zhang et al. 2021)

chemical reactions in the gas phase and in the SSL; convective mass transfer at the air-SSL boundary layer; diffusion inside the SSL, SC, and VE; and indoor surface uptake (i.e., surface partitioning and internal diffusion of permeable material). Relevant chemical reactions are given by Eqs. (26), (27), and (28):



Here, Eqs. (26), (27), and (28) are simplified to focus only on the dominant stable products, while the moderately lived intermediate products (e.g., secondary ozonides) and other products such as organic acids, hydroxyl acetone, 4-MON, 4-MOD, and various organic hydroperoxides are not included.

Several assumptions are made to derive the physical-chemical coupling model: (1) The three layers (SSL, SC, VE) of the skin are homogeneous, and the mass transfer through each layer is assumed to follow one-dimensional diffusion; (2) the concentration of all products in the blood at the VE-dermis interface is assumed to be zero because of the abundant capillaries at VE-dermis interface and fast blood flow; (3) equilibrium exists at the interfaces between two contiguous layers and the flux is conserved; and (4) the squalene concentration in SSL is regarded as constant since it can be produced by the human body naturally and continually. With these assumptions, the governing equations of the oxidation products Y (6-MHO, 4-OPA, and GA) can be described as follows (Zhang et al. 2021):

$$\frac{\partial C_{ve_Y}}{\partial t} = D_{ve_Y} \frac{\partial^2 C_{ve_Y}}{\partial x^2} \quad \text{for } 0 < x < L_{ve} \quad (29)$$

$$\frac{\partial C_{sc_Y}}{\partial t} = D_{sc_Y} \frac{\partial^2 C_{sc_Y}}{\partial x^2} \quad \text{for } L_{ve} < x < L_{ve} + L_{sc} \quad (30)$$

$$\frac{\partial C_{ssl_Y}}{\partial t} = D_{ssl_Y} \frac{\partial^2 C_{ssl_Y}}{\partial x^2} + P_{ssl_Y} \quad \text{for } L_{ve} + L_{sc} < x < L_{ve} + L_{sc} + L_{ssl} \quad (31)$$

$$\begin{aligned} \frac{\partial C_{g_Y}}{\partial t} = & N(C_{out_Y} - C_{g_Y}) - \frac{A_h}{V_r} D_{ssl_Y} \frac{\partial C_{ssl_Y}}{\partial x} \Big|_{x=L_{sc}+L_{ve}+L_{ssl}} + P_{g_Y} \\ & + q_{ob_Y} C_{in_O_3} - \frac{A_r}{V_r} E_Y \quad \text{for } x \\ & > L_{ve} + L_{sc} + L_{ssl} \end{aligned} \quad (32)$$

where the subscripts ve, sc, ssl, and g represent the layers of VE, SC, SSL, and the gas phase, respectively; C_{ve_Y} , C_{sc_Y} , C_{ssl_Y} , and C_{g_Y} are the concentrations of Y in the corresponding layers (ppb); D_{ve_Y} , D_{sc_Y} , and D_{ssl_Y} are the diffusion coefficients of Y in the corresponding layers ($\text{cm}^2 \text{ s}^{-1}$); L_{ve} , L_{sc} , L_{ssl} are the thicknesses of the corresponding layers (cm); t is time (s); x is the distance vertical to the VE-dermis interface (cm); N is the air exchange rate (h^{-1}); C_{out_Y} is the concentration of Y in the supply air from outdoors (ppb); A_h and A_r are the surface areas of human skin and room, respectively (cm^2); V_r is the volume of indoor space (cm^3); P_{ssl_Y} and P_{g_Y} are the production or loss term in the SSL and gas phase due to chemical reactions (ppb s^{-1}); q_{ob_Y} is the production rate of Y from off-body squalene in indoor environment (e.g., furnishings, worn clothing), which is determined by curve fitting (s^{-1}); $C_{in_O_3}$ is the concentrations of ozone in indoor air (ppb); and E_Y represents the convective mass-transfer flux on the indoor surface, which can be written as

$$E_Y = h_{ms}(C_{g_Y} - C_{gi_Y}) \quad (33)$$

where h_{ms} is the convective mass-transfer coefficient across the indoor surface (cm s^{-1}); C_{g_Y} is the concentration of Y in indoor air (ppb); and C_{gi_Y} is the gas-phase concentration of Y at the surface (ppb).

Since indoor surfaces are generally permeable, the internal diffusion of products in the materials should be considered. A sink model proposed by Jorgensen et al. (2000) is applied to reflect this effect. The time-dependent concentrations of ozone in the SSL and gas phase can be represented by the following equations:

$$\begin{aligned} \frac{\partial C_{ssl_O_3}}{\partial t} = & D_{ssl_O_3} \frac{\partial^2 C_{ssl_O_3}}{\partial x^2} - k_{1s} C_{ssl_O_3} C_{sq} - k_{2s} C_{ssl_O_3} C_{ssl_6MHO} \\ & - k_{3s} C_{ssl_O_3} C_{ssl_GA} - k_{4s} C_{ssl_O_3} C_{others} \quad \text{for } L_{ve} + L_{sc} \\ & < x < L_{ve} + L_{sc} + L_{ssl} \end{aligned} \quad (34)$$

$$\frac{\partial C_{\text{in_O}_3}}{\partial t} = N(C_{\text{out_O}_3} - C_{\text{in_O}_3}) - \frac{A_h}{V_r} D_{\text{ssl_O}_3} \frac{\partial C_{\text{ssl_O}_3}}{\partial x} \Big|_{x=L_{\text{sc}}+L_{\text{ve}}+L_{\text{ssl}}} \\ - k_{2g} C_{\text{in_O}_3} C_{\text{g_6MHO}} - k_{3g} C_{\text{in_O}_3} C_{\text{g_GA}} - k_r C_{\text{in_O}_3} \quad \text{for } x \\ > L_{\text{ve}} + L_{\text{sc}} + L_{\text{ssl}} \quad (35)$$

where $C_{\text{ssl_O}_3}$ is the concentrations of ozone in the SSL (ppb); $D_{\text{ssl_O}_3}$ is the diffusion coefficient of ozone in the SSL ($\text{cm}^2 \text{s}^{-1}$); k_{1s} , k_{2s} , and k_{3s} are the second-order rate constants occurring in the SSL ($\text{ppb}^{-1} \text{s}^{-1}$); k_{4s} is the second-order rate constants for reactions of ozone with other double bonds in the SSL ($\text{ppb}^{-1} \text{s}^{-1}$); C_{others} is the concentration of other unsaturated reactants in the SSL (ppb); C_{sq} is the concentration of squalene in the SSL (ppb); k_{2g} and k_{3g} are the second-order rate constants occurring in the gas phase ($\text{ppb}^{-1} \text{s}^{-1}$); $C_{\text{out_O}_3}$ is the ozone concentration in the supply air from outdoors (ppb); and k_r is the removal rate of ozone caused by other indoor reactions (s^{-1}).

Validation of the Chemical-Physical Model with Test Data in a House

Experiments were conducted in a single-family house to validate the accuracy of the model (Liu et al. 2019), by using PTR-TOF-MS. To find a common parameter set that could explain both occupied and unoccupied scenarios, a global optimization based on the Multi-objective optimization using Genetic Algorithm and Monte Carlo search is applied for parameters determination. With the determined parameters, the concentrations of ozone, 6-MHO, and 4-OPA in the house on other test days can be predicted using the physical-chemical coupling model. Figure 7 provides the scatter plots at 30 min time resolution of all the model predictions and measurements for ozone, 6-MHO, and 4-OPA, including 9 days (13–19 August, and 22–26 August) in the single-family house (about 350 data points). The data points are evenly distributed around the 1:1 line ($y = x$). For 6-MHO and 4-OPA, more than 90% of the points are within $\pm 15\%$ fluctuation (uncertainty). For ozone, more than 80% of the points are within $\pm 20\%$ fluctuation. The R^2 for the three modeled compounds are above 0.82, indicating good accuracy of the developed model. To examine the applicability of the model to different indoor settings, the model was used to predict the concentrations of ozone, 6-MHO, and 4-OPA in a simulated occupied office in the study of Wisthaler and Weschler (2010). The comparison of model prediction with experimental data, as shown in Fig. 8, indicates that predictions based on the physical-chemical coupling model agree well with the experimental data, with R^2 above 0.9, demonstrating the generalizability of the model for different indoor settings.

Predicting SVOC Concentrations in Complex Indoor Environments

Due to low vapor pressure, SVOCs tend to adhere to indoor surfaces including walls, floors, ceilings, airborne particles, dust, and so forth. Therefore, the fate of indoor SVOCs is much more complex than VOCs due to dynamic interaction between

Fig. 7 Scatter plots of model prediction with measured data for (a) 6-MHO and 4-OPA, (b) ozone (Zhang et al. 2021)

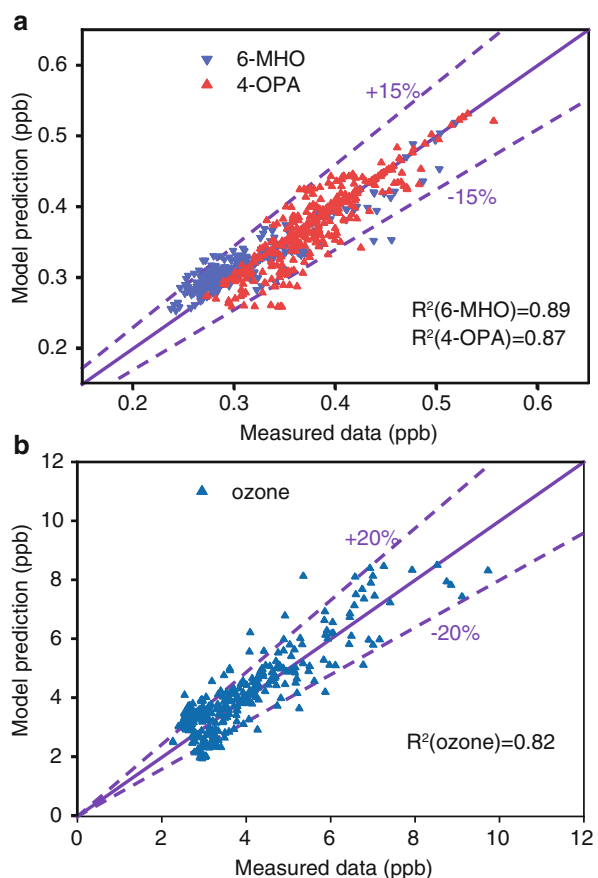
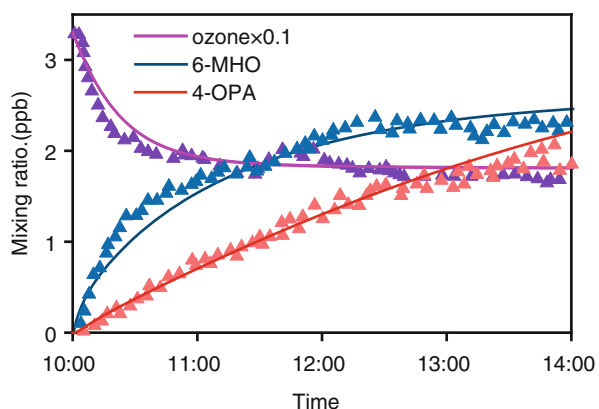


Fig. 8 Comparison of model prediction with experimental data for ozone, 6-MHO, and 4-OPA in the simulated office published by Wisthaler and Weschler (2010)



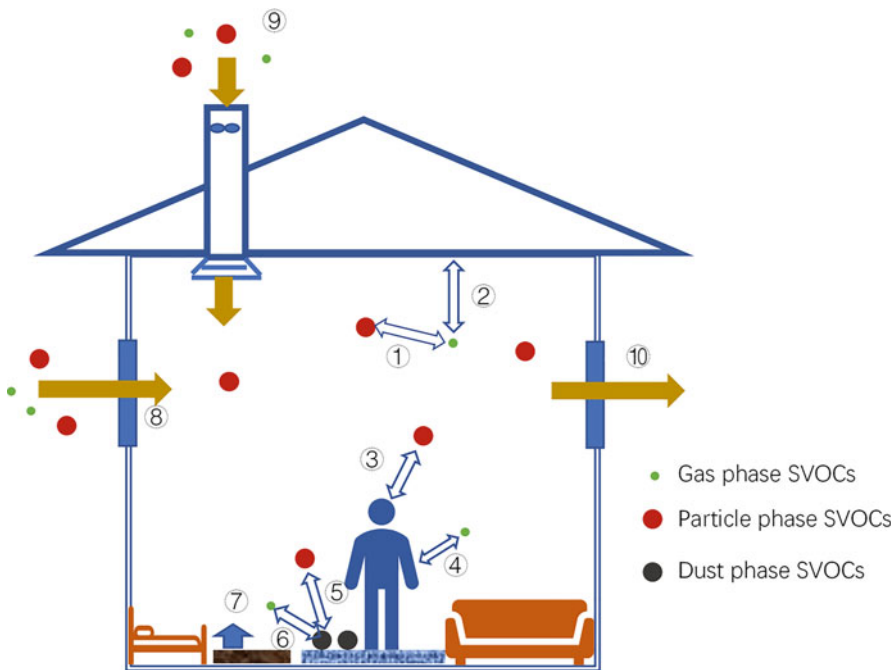


Fig. 9 Schematic shows for indoor SVOC fate. ① Interaction between gas and particle phase SVOCs; ② Interaction between gas and surface phase SVOCs; ③ and ④ Interaction between particle phase SVOCs and human body; ⑤ Interaction between particle and dust phase SVOCs; ⑥ Interaction between gas and dust phase SVOCs; ⑦ Emission from the source; ⑧ Natural ventilation; ⑨ Mechanic ventilation; ⑩ Exhaust out of the buildings

SVOCs and various indoor sinks, as shown in Fig. 9. Indoor concentrations of SVOCs in different phases are affected by many factors including source and sink characteristics, dynamic partitioning between different phases, natural and mechanical ventilation, behavior of residents such as house cleaning, cooking activities, and so forth as shown in Fig. 10. The fate and transport of indoor SVOCs is a very complex process and it is a great challenge to accurately simulate indoor SVOCs dynamics. To predict SVOC concentrations in real indoor environments accurately, reasonable physical models to reveal how these factors affect indoor SVOC fate are the foundation together with the determination methods for the parameters in the models as shown in Fig. 11. The mechanism methods for predicting the fate and transport of SVOCs fall into three categories: mass transfer-based methods, fugacity theory methods, and data-driven models. Due to scarce measured data, especially instantaneous data with time for indoor SVOC concentrations, there is no data-driven model for predicting indoor SVOC concentrations (Wei et al. 2019a). For the other two kinds of methods, the framework as illustrated in Fig. 12 should be followed. Knowledge of the mechanisms and characteristics of SVOC emission and partitioning in indoor environments is essential for predicting SVOC

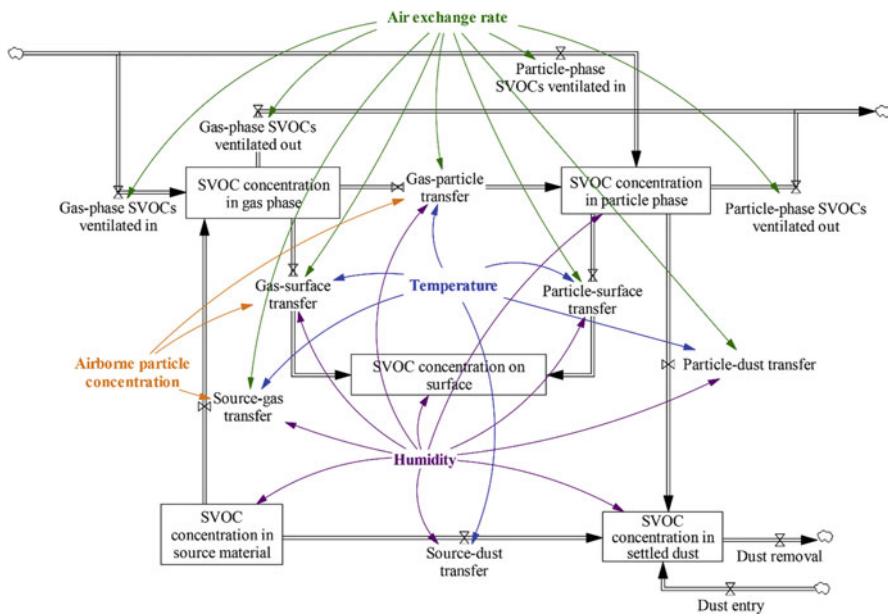
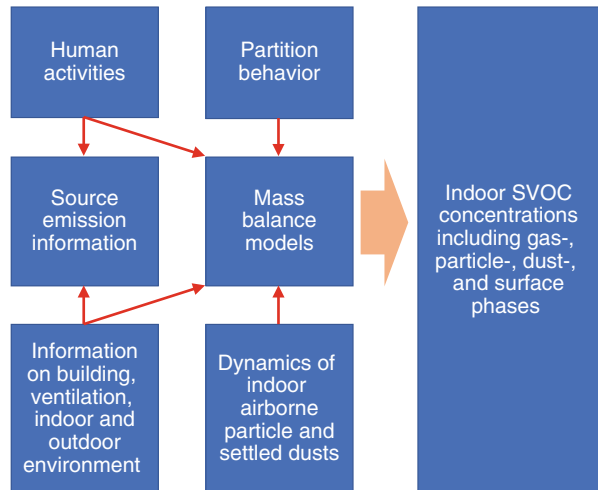


Fig. 10 Influence of environmental factors on indoor SVOCs. (Reprinted from Wei et al. (2019a), Copyright 2021, with permission from Elsevier)

Fig. 11 A modular framework for predicting indoor SVOC concentrations in complex indoor environments



concentrations. These models are described in detail in ▶ Chap. 23, “Source/Sink Characteristics of SVOCs.” As the focus, the mass transfer models will be introduced in section “Two Types of Models for Predicting the Fate and Transport of SVOCs in Real Indoor Environments.” Besides, the estimation methods on the

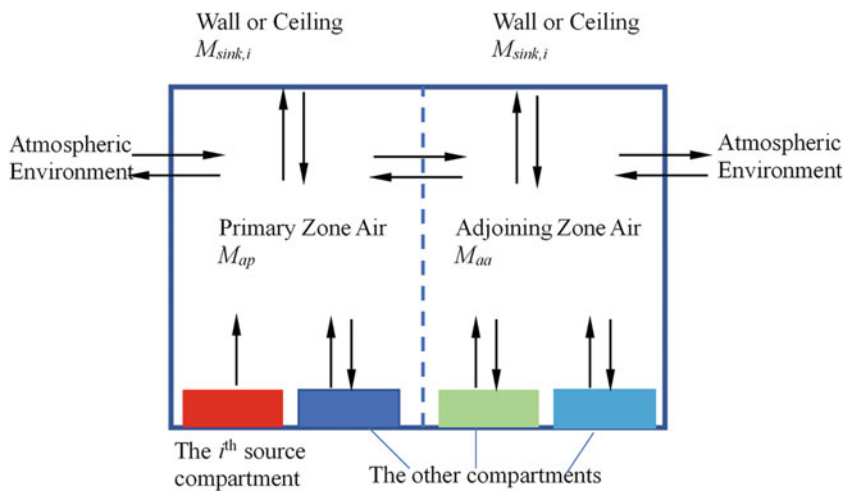


Fig. 12 Model framework for the indoor fugacity models. (Reprinted from Bennett and Furtaw (2004), Copyright 2021, with permission from American Chemical Society)

partition coefficients of SVOCs between different compartments in the models will also be described as key factors in section “[Estimating Partition Coefficients of SVOCs Between the Gas Phase, Airborne Particles, Settled Dust, and Surfaces](#).” Finally, the challenge to prediction accuracy will be discussed in section “[Challenge to Accurate Prediction of Indoor SVOC Concentration in Complex Indoor Environment](#).”

Two Types of Models for Predicting the Fate and Transport of SVOCs in Real Indoor Environments

Both mass transfer models and fugacity models are based on mass balance. Fugacity models are a kind of models early and widely used for indoor fate modeling (Bennett and Furtaw 2004) to describe the dynamic mass balance of indoor chemicals with different compartments based on the concept of fugacity (Shin et al. 2012). The models are applied for predicting indoor fate of pesticides (Bennett and Furtaw 2004) and PBDEs (Zhang et al. 2009). In the models, some typical compartments including floorings, walls, furniture, and other media are considered as shown in Fig. 12 (Zhang et al. 2009; Shin et al. 2012).

In the fugacity models, the mass of the compound in the compartment (g) can be expressed in terms of fugacity (Bennett and Furtaw 2004). The governing equation for the change of mass in the *i*th compartment over time can be written as Eq. (36-1) (Bennett and Furtaw 2004):

$$\frac{dM_i}{dt} = -L_i M_i + \sum_{j=1}^N T_j M_j \quad (36-1)$$

Table 1 The expression of fugacity capacities of SVOCs with different phases in different compartments

Compartments	Phase	Equations	Remarks
Air	Gas	$Z_a = \frac{1}{RT}$	R is the ideal gas constant, T is the absolute temperature of air
	Particle	$Z_p = K_{pg} TSP Z_p$	K_{pg} is the particle-gas partition coefficient; TSP is the particle concentration
Source	Source	$Z_{source} = KZ_a$	K is the source-air partition coefficient
Sink(walls)	Surface	$Z_{sink} = K_{sg} Z_a$	All non-source surface can be regarded as sink
Dust	Dust	$Z_{dust} = K_{dg} Z_a$	

where L_i is the loss rate constant for the i^{th} compartment (g/d) and M_j is mass of the j^{th} compartment connected with compartment i and T_j is the transfer factor (1/d). For different compartments, T_j and L_i have different meanings. For example, if i represents surface compartment, L_i is the desorption coefficient and T_i is the adsorption coefficient. Hence, the governing equation for the surface can be expressed as shown in Eq. (36-2):

$$\frac{dM_{surface}}{dt} = -k_d M_{surface} + k_s \frac{M_{air}}{V} \quad (36-2)$$

M_i can be expressed in terms of fugacity through Eq. (37):

$$M_i = f_i Z_i V_i \quad (37)$$

where f_i is the fugacity of the chemical in the i^{th} compartment, Z_i is the fugacity capacity to characterize the holding capacity of the i^{th} compartment for a chemical substance based on the properties of both the material and the chemical. Obviously, Z_i is a key parameter to determine fugacity of SVOCs in media and the values of Z_i in different media are listed in Table 1 (Zhang et al. 2009).

Recently, Liang et al. (2019) developed a general mass transfer-based model for predicting the fate and transport of phthalates in indoor environments. In this model, the indoor fate of phthalates including emission from indoor sources, indoor transport in the air, interaction with particle and dusts, uptake by impermeable surfaces (e.g., wood floors, furniture, ceilings, tiles, glass, or windows), and accumulation of phthalates within porous materials (e.g., carpet) with consideration of particle penetration is shown in Fig. 13. Based on the mass balance, the variation of phthalates in well-mixed environments obeys the following equation:

$$\begin{aligned} V \frac{dC_g}{dt} + V \frac{dC_{part}}{dt} &= Q(C_{g,in} + C_{part,in}) - Q(C_g + C_{part}) + h_{m,s} A_s (y_0 - C_g) \\ &\quad - h_{m,ns} A_{ns} (C_g - C_{ns}) - v_d (A_s + A_{ns}) C_{part} \\ &\quad + R M_s A_s P_{dust,s} + R M_{ns} A_{ns} P_{dust,ns} \end{aligned} \quad (38)$$

where V is the volume of the room, m³; t is time (h); C_g and C_{part} are the phthalate concentrations in the gas and particle phases in indoor air, respectively ($\mu\text{g}/\text{m}^3$); Q is

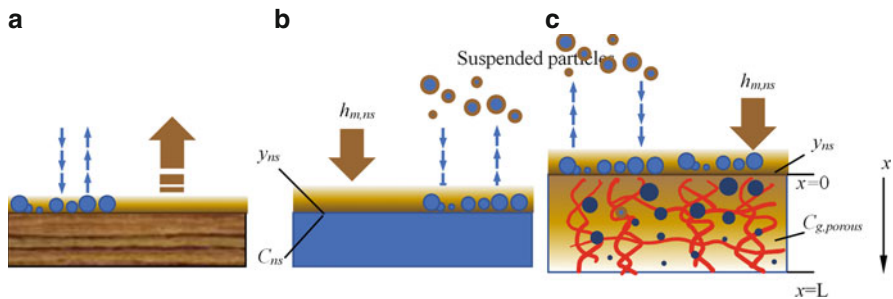


Fig. 13 SVOCs dynamics on the surface. (a) The source surface; (b) the non-source impermeable surface; (c) the non-source porous surface

flow rate of outdoor air (m^3/h); $C_{g,in}$ and $C_{part,in}$ are the phthalate concentrations in gas and particle phases in the outdoor air ($\mu\text{g}/\text{m}^3$); $h_{m,s}$ and $h_{m,ns}$ are the convective mass-transfer coefficients on the source and non-source surfaces, respectively, (m/h); A_s and A_{ns} are the areas of indoor source and non-source surfaces, respectively, (m^2); y_0 is the gas-phase concentration in the air adjacent to the source ($\mu\text{g}/\text{m}^3$); v_d is the deposition rate of particles onto indoor surfaces (m/h); R is the resuspension rate (h^{-1}); M_s and M_{ns} are the mass loadings of settled dust on source and non-source surfaces, respectively ($\mu\text{g}/\text{m}^2$); and $P_{dust,s}$ and $P_{dust,ns}$ are the concentrations of phthalates in the dust settled on source and non-source surfaces, respectively ($\mu\text{g}/\text{g}$).

Diffusion of SVOCs inside particles can be ignored (Liu et al. 2013), that is, the phase concentration can be regarded as a uniformly lumped concentration in particle. Thus, the adsorption rate of SVOCs by particles can be described by Eq. (39):

$$\dot{m}_{p,s} = h_{m,p} A_p N_p \left(C_g - \frac{C_{part}}{K_p TSP} \right) \quad (39)$$

where $h_{m,p}$ is the convective mass transfer coefficient (m/s); A_p is the area of a single particle (m^2), and N_p is the particle number per m^3 air ($1/\text{m}^3$).

Considering the dynamics of particle-phase phthalates, its concentration can be determined by Eq. (40):

$$V \frac{dC_{part}}{dt} = Q(C_{part,in} - C_{part}) + \dot{m}_{p,s} - v_d(A_s + A_{ns})C_{part} + RM_s A_s P_{dust,s} + RM_{ns} A_{ns} P_{dust,ns} \quad (40)$$

If fine particles with diameters smaller than $2.5 \mu\text{m}$ dominate in indoor air, the other terms except $\dot{m}_{p,s}$ on the right side of Eq. (40) can be ignored. For SVOCs with vapor pressures in the range between pyrene and DEHP (not including DEHP), equilibrium can be reached within a short time. Thus, Eq. (40) can be further simplified by replacing $C_{part} = K_p TSP C_g$.

The dynamics of indoor particles can be described as:

$$V \frac{dTSP}{dt} = QP_p TSP_{in} - QP_p TSP - v_d(A_s + A_{ns})TSP + RM_s A_s + RM_{ns} A_{ns} + S \quad (41)$$

where P_p is the penetration coefficient of particles from outdoors to indoors and S is the source density of indoor particles (mg/h).

Equation (42) describes that the dust loading of the settled dust on the source or non-source surfaces changes with time due to the particle deposition and the dust resuspension as shown in Fig. 13.

$$\frac{dM_s}{dt} = -v_d TSP + RM_s A_s \text{ and } \frac{dM_{ns}}{dt} = -v_d TSP + RM_{ns} A_{ns} \quad (42)$$

In Liang et al. (2019), a simple equilibrium between $P_{dust,s}$ and y_0 on the source surface is assumed, that is, $P_{dust,s} = K_{dust,s} y_0$ as shown in Fig. 13a. Similarly, a simple equilibrium between $P_{dust,ns}$ and C_{ns} on the non-source surface as $P_{dust,ns} = K_{dust,ns} C_{ns}$ is assumed. Different from the source surface, the accumulation of phthalates on the non-source surface should be considered. For those impermeable surfaces such as wood floors, glass mirrors, and windows, Eq. (43) can be used to describe the variation of phthalate concentrations on the surface as shown in Fig. 13b.

$$\frac{d(C_{ns} + M_{ns} P_{dust,ns})}{dt} = h_{m,ns} (C_g - C_{ns}) + v_d C_{part} - RM_{ns} P_{dust,ns} \quad (43)$$

For the porous surfaces such as carpet, diffusion into the inside of the surfaces cannot be ignored, as shown in Fig. 13c. In the model, multi-phase mass-diffusion theory in porous media is employed to describe the process with the governing equation and initial and boundary conditions as follows:

$$(\varepsilon + (1 - \varepsilon)K_{ns} + K_{dust,ns} m_x) \frac{\partial C_{g,porous}}{\partial t} = \varepsilon D_g \frac{\partial^2 C_{g,porous}}{\partial x^2} \quad (44-1)$$

$$C_{g,porous} = 0, \text{ for } t = 0, 0 \leq x \leq L \quad (44-2)$$

$$\frac{\partial C_{g,porous}}{\partial x} = 0, \text{ for } t > 0, x = L \quad (44-3)$$

$$C_g = y_{ns}, \text{ for } t > 0, x = 0 \quad (44-4)$$

where ε is the porosity of the material; x is the coordinate along the depth (m); m_x is the dust mass concentration at the depth x ($\mu\text{g}/\text{m}^3$), and m_x distributes with x as $m_x = \frac{m_{x=0}}{e^x}$, m_x can be obtained by solving $\int_0^L m_x dx = M_{ns}$; $C_{g,porous}$ is the gas concentration of SVOCs in the pore of the material ($\mu\text{g}/\text{m}^3$); and L is the thickness of the material (m).

Thus, the fate and concentrations of SVOCs in the different phases in indoor environments can be described by Eqs. (38), (39), (40), (41), (42), (43), and (44). To predict the fate and transport of SVOCs in real indoor environments using the model, the parameters for describing building characteristics, ventilation, atmospheric environmental conditions (particle concentration, particle- and gas-phase SVOC concentration in ambient air), indoor temperature, source characteristics parameters, surface characteristics parameters have to be provided at first, then the partition coefficients between different phases can be estimated by the method described in section “[Estimating Partition Coefficients of SVOCs Between the Gas Phase, Airborne Particles, Settled Dust, and Surfaces](#).” Based on the determined or estimated parameters, by numerically solving Eqs. (38), (39), (40), (41), (42), (43), and (44) in coupled mode, the instantaneous concentration of SVOCs in the different phases in the media will be obtained. The details on the methods of numerical solution can refer to Patankar’s classic book (Partankar 1980). Besides this model, some similar models (Wei et al. 2019a; Shi and Zhao 2015) with some special considerations were proposed to predict indoor concentrations of SVOCs and the solution method is similar.

Though there are some measurements for indoor SVOCs concentration, only one complete experiment in a real indoor environment was found in the literature to obtain the dynamic concentrations in different phases including gas, particle, dusts, and surfaces. The experiment was conducted in a test house located at the University of Texas at Austin as shown in Fig. 14a (Bi et al. 2015), which is a three-bedroom, two-bathroom, 110 m² residential building built in 2008. In the house, 2-month periodical measurements of total airborne (i.e., gas and particle phase) and dust phase BBzP (benzyl butyl phthalate) were taken together with the concentrations on various surfaces including stoneware dish plates and mirrors in the test house at the controlled temperature (21 ± 0.8 °C). Then, based on the estimated or experimentally measured parameters used in the model presented above, the SVOC concentrations were predicted and compared to the measured concentrations as shown in Fig. 14b–e. The model is able to predict the dynamic variation of indoor BBzP concentration in different media with acceptable uncertainty.

Estimating Partition Coefficients of SVOCs Between the Gas Phase, Airborne Particles, Settled Dust, and Surfaces

Due to low vapor pressure, SVOCs tend to adhere to indoor surfaces including airborne particles, settled dusts and walls, which is very different from VOCs and is substantial to indoor SVOC concentrations. In common, the equilibrium partitioning between different compartments is characterized by partition coefficients defined by Eqs. (45), (46), and (47) (Weschler and Nazaroff 2010; Liang et al. 2019).

$$K_p = \frac{C_{part}}{TSP C_{gas}} \quad (45)$$

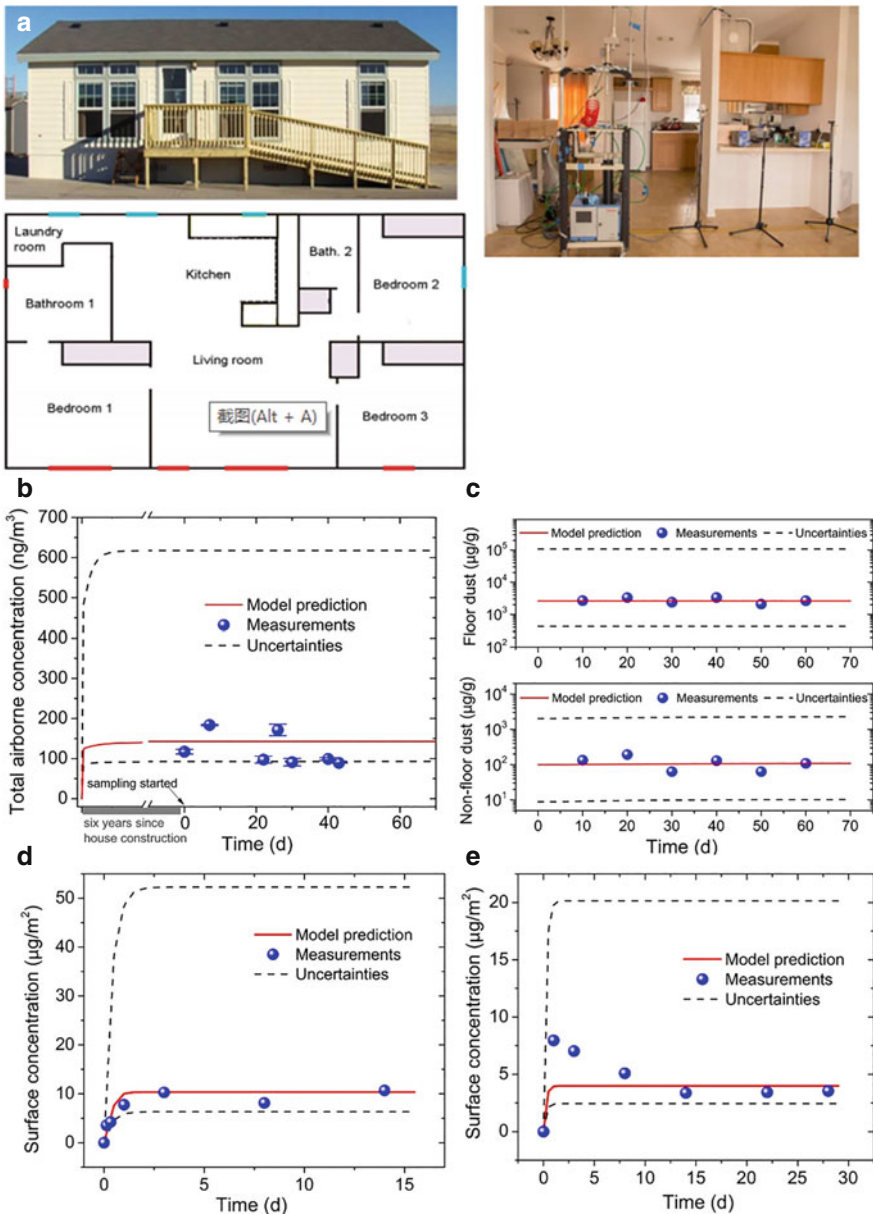


Fig. 14 Predicted results by the model and comparison with experimental data. (a) UT test house at University of Texas at Austin. (Reprinted from Bi et al. (2015) Copyright 2021 with permission from American Chemical Society); (b) suspended airborne BBzP concentration; (c) settled dust phase BBzP concentration; (d) plate surface phase BBzP concentration; and (e) mirror surface BBzP concentration. (Reprinted from Liang et al. (2019) Copyright 2021, with permission John Wiley and Sons)

$$K_{dg} = \frac{C_{dust}}{C_{gas}} \quad (46)$$

$$K_{sg} = \frac{C_{surface}}{C_{gas}} \quad (47)$$

where C_{part} is the particle phase concentration in the air ($\mu\text{g}/\text{m}^3$); TSP is the average particle concentration in the air ($\mu\text{g}/\text{m}^3$); C_{gas} is the gas phase concentration in the air ($\mu\text{g}/\text{m}^3$); C_{dust} is the dust phase concentration in the settled dusts ($\mu\text{g}/\text{mg}$); $C_{surface}$ is the surface phase concentration ($\mu\text{g}/\text{m}^2$). Thus K_p , K_{dg} , and K_{sg} are not dimensionless and their units are $\text{m}^3/\mu\text{g}$, m^3/mg and m , respectively.

Based on the assumption that the affinity of an SVOC for sorbed organic matter is similar to its affinity for octanol, Weschler and Nazaroff (2010) estimated partition coefficients by Eq. (48).

$$K_{SVOC,m} = f_{om,m} K_{oa} \quad (48)$$

where $K_{SVOC,m}$ is the medium-air partition coefficient in the respective compartment, $f_{om,m}$ is the fraction of organic matter in the medium, and K_{oa} is the octanal-air partition coefficient of the SVOC. On indoor impermeable surfaces, similar organic films are likely to be ubiquitous on indoor surfaces (Weschler and Nazaroff 2017), $f_{om,m}$ can be approximated to 1. Further information on organic films on impermeable surfaces can be found in Weschler and Nazaroff's paper (2017).

Considering the difference between octanal and organic matter, K_{part} can be estimated by the following equation (Finizio et al. 1997).

$$\log(K_p) = \log(K_{oa}) + \log\left(1.22 \times 10^{-12} \times f_{om} \times \frac{M_o}{M_{om}} \times \frac{\gamma_o}{\gamma_{om}}\right) \quad (49)$$

where M_o (g/mol) and M_{om} (g/mol) are the molecular weights of octanol and the mean molecular weight of the organic matter phase, respectively, and γ_o and γ_{om} are the activity coefficients of the chemical in octanol and in the organic matter phase, respectively. The model expressed as Eq. (49) is called single parameter model because it considers only the sorption of SVOCs by organic matter in particles.

K_p can also be estimated based on the vapor pressure of the SVOC of interest at different temperature, as shown in Eq. (50) based on Pankow's partitioning theory (Pankow 1994; Wei et al. 2019b).

$$K_p = \frac{f_{om}RT}{10^6 M_{om} \gamma_{om} p_b T_b^{(1-\frac{T_b}{T})} e^{\frac{\beta}{R}(1-\frac{T_b}{T})}} \quad (50)$$

where p_b is the SVOC vapor pressure at the boiling point (Pa); T is the absolute temperature (K); T_b is the absolute temperature at the boiling point (K); and β is a constant. From Eq. (50), the effect of the temperature on partition coefficients may

be found and can also be simplified as shown in Eq. (51) (Wei et al. 2016), which was validated with experimental data (Wei et al. 2016; Zhou et al. 2021).

$$\log(K_{p,T}) = \frac{A}{T} + B \quad (51)$$

Because some of the parameters in the theoretical models are difficult to obtain, the following empirical correlations with the sub-cooled vapor pressure p_L and the octanol-air partition coefficient K_{oa} are often used to estimate particle-gas partition coefficients.

$$\log(K_p) = m_p \log p_L + b_p \quad (52)$$

$$\log(K_p) = m_o \log K_{oa} + b_o \quad (53)$$

where m and b are the empirical parameters that were obtained by fitting the measured data into Eqs. (52) and (53). m and p also correlate with the air temperature t , $\log(K_{oa})$, and $\log(p_L)$ (Qiao et al. 2021).

$$m_o = -m_p = 0.011t + 0.263 \quad (54)$$

$$b_o = -(0.135t + 5.006) \quad (55)$$

$$b_p = -(0.054t + 3.101) \quad (56)$$

$$m_o = \frac{1}{a-b} [\log(1 + 2.4f_{om}^{-1}10^{10-b}) - \log(1 + 2.4f_{om}^{-1}10^{10-a})] \quad (57)$$

$$b_o = -11.38m_o - 1.53 \quad (58)$$

$$m_p = 1 - \frac{1}{c-d} [\log(1 + 1.20f_{om}^{-1}10^{-d-4}) - \log(1 + 1.20f_{om}^{-1}10^{-c-4})] \quad (59)$$

$$b_p = 4.92m_p - 1.53 \quad (60)$$

where a and b are the maximum and minimum values of $\log(K_{oa})$ of SVOCs for the sampling event/events, respectively, and c and d are the maximum and minimum values of $\log(p_L)$ of SVOCs for the sampling event/events, respectively. The above equations are applicable in the range from -40°C to 38°C .

In most models, only the organic fraction of particles is assumed to sorb SVOCs. Dachs and Eisenreich (2000) indicated that elemental carbon fraction of particles should also be considered as potentially adsorbing SVOCs. Therefore, the following two-parameter model was proposed:

$$K_p = f_{om} \times \frac{M_o}{M_{om}\rho_{oc}} \times \frac{\gamma_o}{\gamma_{om}} K_{oa} + f_{ec} \times \frac{a_{ec}}{a_p\rho_{ec}} \times K_{sa} \quad (61)$$

where ρ_{oc} and ρ_{ec} are the density of the organic matter and elemental carbon, respectively ($\mu\text{g}/\text{m}^3$); f_{ec} is the mass fraction of elemental carbon; a_{ec} and a_p are the specific areas of elemental carbon and the aerosol particles, respectively (m^2/g); and K_{sa} is the elemental carbon-air partition coefficient.

Under consideration of the sorption to the inorganic fraction of the particles, the two-parameter model was improved and a three-parameter model was developed (Zhou et al. 2020):

$$K_p = f_{om} \times \frac{M_o}{M_{om}\rho_{oc}} \times \frac{\gamma_o}{\gamma_{om}} K_{oa} + f_{ec} \times \frac{a_{ec}}{a_p\rho_{ec}} \times K_{sa} + f_N \frac{K_N}{\rho_{ec}} \quad (62)$$

where f_N is the mass fraction of the inorganic material in the particle ($1-f_{om}-f_{ec}$); K_N is the inorganic material-gas partition coefficient, and ρ_N is the density of the inorganic material ($\mu\text{g}/\text{m}^3$).

All of the above models originated from Junge and Pankow's partitioning theory (Pankow 1987 1994) and the estimation of K_p was based on K_{oa} or p_L . After applying the Junge-Pankow equation for estimating indoor gas/particle distribution, Salthammer and Schripp (2015) found that the K_p values estimated by the models can result in substantial error for indoor scenarios. Therefore, the method of pp-LFER (Poly Parameter-Linear Free Energy Relationships) was applied to estimate the partition coefficients of SVOCs between different phases as a promising alternative. In the method, particle/gas partition coefficient K_p can be predicted using Eq. (63) (Goss 2005).

$$\log(K_p) = s \cdot S + a \cdot A + b \cdot B + l \cdot L + v \cdot V + c \quad (63)$$

where S , A , B , and V are compound-specific Abraham descriptors. S is the polarizability/dipolarizability, A is the hydrogen bound acidity (donor), B is the hydrogen bond basicity (acceptor), L is the logarithmic hexadecane/air partition coefficient (a surrogate for van der Waals term) and V is the McGowan volume. These parameters can be obtained from databases (Ulrich et al. 2017) or QSPRs (Quantitative Structure Property Relationships) (Huang and Jolliet 2019). s , a , b , l , and v are particle-specific parameters, which together with constant c are obtained by multiple-linear regression using experimental $\log(K_p)$ values.

Based on theoretical analysis, Weschler et al. suggested for SVOCs with high K_{oa} values that SVOCs sorbed to airborne particles and settled dust may not have sufficient time to equilibrate with the gas phase (Weschler and Nazaroff 2008, 2010). Liu et al. (2013) performed a further analysis on the dynamic mass transfer of SVOCs from the gas phase into airborne particles based on a normalized mass-transfer model. It is found that for SVOCs with a lower vapor pressure, it may take more than several hours to reach equilibrium between gas and particle phase. Comparing with the residence time of particles in the indoor environment, the assumption of instantaneous equilibrium between gas-phase and airborne particle-phase SVOCs in the indoor environments is not a feasible, especially for SVOCs with lower vapor pressure. Thus, the particle-gas partition coefficient measured from

particle- and gas-phase SVOC concentrations may not be the actual partition coefficient, but may instead vary with time and can be designated as apparent partition coefficient, $K_{p,a}$. It is correlated with K_p as Eq. (64) and will reach to K_p for enough time (Liu et al. 2013).

$$K_{p,a} = K_p \left(1 - e^{-\frac{6v_t t}{d_p TSP K_p}} \right) \quad (64)$$

v_t is the effective gas/particle mass-transfer coefficient (m/s); d_p is the diameter of the particles (m); t is time (s); TSP is the concentration of total suspended particles ($\mu\text{g}/\text{m}^3$). Based on Eq. (64), the concept of particle age was proposed to consider the effect of nonequilibrium partitioning (Cao et al. 2018).

In contrast to K_p , SVOC partitioning between impervious surfaces and air has received little attention to date. Weschler et al. (2008) proposed that SVOC partitioning to surfaces is affected by a thin organic film covering indoor surfaces and that the film will grow over time (Weschler and Nazaroff 2017). Hence, surface-air partition coefficients are often approximated using K_{oa} and thus different surfaces have identical K_s value close to K_{oa} , which was verified in experiments (Wu et al. 2017). In the only existing models, equilibrium partitioning was assumed and experiments showed that the roughness of indoor surfaces plays an important role for partitioning between surface and gas phase SVOCs, but further research needs to be done (Wu et al. 2017).

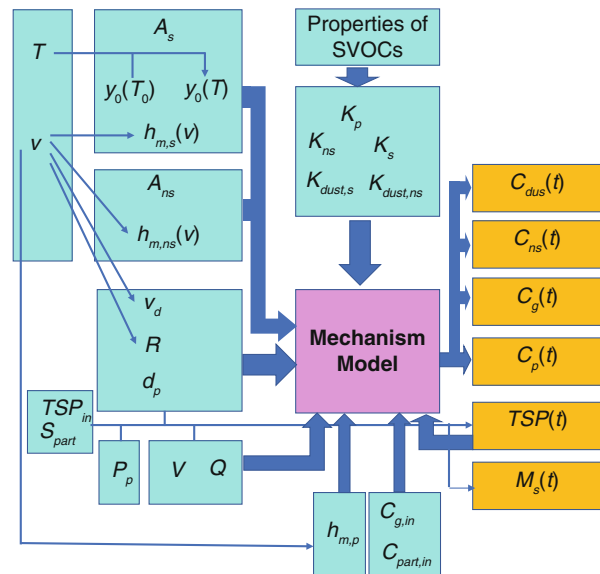
Challenge to Accurate Prediction of Indoor SVOC Concentration in Complex Indoor Environment

Figure 15 shows the flow chart for employing the models with some determined parameters to predict indoor SVOC concentrations in complex indoor environment accurately. Accuracy of the prediction may be affected by each step. Hence, it is a challenging task to predict indoor SVOC concentrations with small uncertainty.

Firstly, because emissions of SVOCs from the source and adsorption by some sinks are both sensitive to indoor environmental parameters including temperature and velocity of indoor air (Xu and Zhang 2011), variation of indoor environmental parameters can greatly affect emission rates of SVOCs so that accurate prediction of emission rates must be based on accurate prediction of indoor thermal environment. Due to all kinds of random factors such as meteorological conditions, it is difficult to predict indoor thermal environment accurately. Prediction bias of indoor thermal environment may lead to large uncertainty for prediction of indoor SVOC concentrations. In common, indoor temperature is not predicted in most of simulation cases and is often set as one constant or several constants for different period. Thus, large uncertainty will be brought in.

Secondly, ventilation is a key factor influencing indoor SVOC concentrations by exchanging indoor and outdoor air and also affects emission rate of SVOC from the sources (Lyng et al. 2015). Air exchange rate of mechanical ventilation is easy to

Fig. 15 Flow chart to predict indoor SVOC concentrations



obtain but that of natural ventilation is much more random depending on meteorological conditions. Because of random of natural ventilation, the unchanged ventilation rate or estimated average ventilation rate is set as an inputting parameter, which may result in some bias from practical concentrations. In addition, for some SVOCs originating mainly from indoor articles, outdoor concentration may be regarded as zero and it will not bring in large effect on indoor concentration prediction. But the sources of some SVOCs such as PAHs may also lie outdoors and the concentrations of outdoor SVOCs may greatly affect indoor SVOCs. Accurate inputting of outdoor SVOC concentrations will be key to predict indoor SVOC concentrations. It will be a challenging issue to obtain accurate outdoor SVOC concentrations.

Thirdly, partitioning plays an important role for indoor fate and transportation of SVOCs; accurate determination of partition coefficients is key to prediction uncertainty. It is difficult to measure these coefficients and must rely on theoretical estimation. However, because theoretical estimations are often based on some assumptions or empirical parameters, large deviation from the practical values may be produced, which depends on the theoretical models. Accurate estimation of partition coefficients is a challenge by itself.

Last but not least, the models mentioned in section “[Two Types of Models for Predicting the Fate and Transport of SVOCs in Real Indoor Environments](#)” are also based on some assumptions, which may also result in some uncertainty. The assumption of well mixing is a general assumption for both VOCs and SVOCs.

Because the fate and transport of SVOCs are often sensitive to local environmental factors, the deviation deriving from the well mixing for SVOCs may be larger than for VOCs. Field investigation showed different dust-phase phthalate concentration in different position in a house (Liu et al. 2020) and revealed large deviation of well mixing from practical conditions. Up to now, there is no measurement to validate the assumption of well mixing for indoor airborne SVOCs. The non-uniform distribution of indoor SVOCs may challenge the accurate predictions by the existing models.

Conclusion

The fates of VOCs/SVOCs are very complex due to various dynamic emission sources, interactions between different surfaces and potential chemical reactions. The prediction of VOC/SVOC concentrations in complex indoor environments must rely on some known information such as emission characteristics from the sources, ventilation scheme, kinetic physical parameters for physical adsorption or absorption by surfaces, and chemical parameters for indoor chemistry. With determined or estimated parameters, the physical models in the literature can predict VOC concentrations with an acceptable accuracy. However, the emission profiles from various indoor sources are often absent and need to be measured in chamber experiments. The mentioned methods in previous chapters can help to determine the key parameters for VOC emissions from the sources rapidly. Another challenge is the existence of indoor ozone originated from outdoor air or indoor sources, which may increase the complexity of the prediction due to chemical reactions between some VOCs and ozone. The recently developed physical-chemical model in literature was introduced to characterize the indoor ozone-initiated chemistry, which made the prediction of indoor VOC concentrations with indoor secondary reactions possible. In contrast to VOCs, it is more difficult to predict indoor SVOC concentrations. As emerging indoor pollutants, emission characteristics for SVOC emissions from indoor sources have been studied only for less than 20 years and study on the fate of indoor SVOCs is much less than VOCs. And some mechanism on the interactions between different SVOC phases is still being studied. In addition, not enough continuous measurement of indoor SVOC concentrations in practical indoor environment provided support for developing the models to predict indoor SVOC concentrations. These factors may affect the effectiveness for the accurate prediction of the indoor SVOC concentrations. Nevertheless, the study is still in progress. This chapter introduces a general model in literature with understanding indoor SVOC fate and also reviews some methods to estimate the key partition coefficients between different phases of SVOCs. The model seems to be successful to predict SVOC concentration in a test house with an acceptable agreement with the measured data. Certainly, more research are still needed to develop some simpler methods suitable for engineering applications.

Cross-References

► Source/Sink Characteristics of SVOCs

References

- Anderson SE, Franko JF, Jackson LG, Wells JR, Ham JE, Meade BJ (2012) Irritancy and allergic responses induced by exposure to the indoor air chemical 4-oxopentanal. *Toxicol Sci* 127:371–381
- Ballesteros-Gómez A, Boer J, Leonards P (2013) Novel analytical methods for flame retardants and plasticizers based on gas chromatography, comprehensive two-dimensional gas chromatography, and direct probe coupled to atmospheric pressure chemical ionization-high resolution time-of-flight-mass spectrometry. *Anal Chem* 85:9572–9580
- Bennett DH, Furtaw EJ (2004) Fugacity-based indoor residential pesticide fate model. *Environ Sci Technol* 38(7):2142–2152
- Bi C, Liang Y, Xu Y (2015) Fate and transport of phthalates in indoor environments and the influence of temperature: a case study in a test house. *Environ Sci Technol* 49(16):9674–9681
- Brandsma SH, Boer J, Velzen MJM, Leonards PEG (2014) Organophosphorus flame retardants (PFRs) and plasticizers in house and car dust and the influence of electronic equipment. *Chemosphere* 116:3–9
- Cao J, Mo J, Sun Z, Zhang Y (2018) Indoor particle age, a new concept for improving the accuracy of estimating indoor airborne SVOC concentrations, and applications. *Build Environ* 136:88–97
- Chen H, Wang C, Wang X, Hao N, Liu J (2005) Determination of phthalate esters in cosmetics by gas chromatography with flame ionization detection and mass spectrometric detection. *Int J Cosmet Sci* 27:205–210
- Chen SJ, Ma YJ, Wang J, Tian M, Luo YJ, Chen D, Mai BX (2010) Measurement and human exposure assessment of brominated flame retardants in household products from South China. *J Hazard Mater* 176:979–984
- Dachs J, Eisenreich SJ (2000) Adsorption onto aerosol soot carbon dominates gas-particle partitioning of polycyclic aromatic hydrocarbons. *Environ Sci Technol* 34(17):3690–3697
- Danish Environmental Protection Agency (2006) Total health assessment of chemicals in indoor climate from various consumer products. Survey of Chemical Substances in Consumer Products. Paper no. 75 2006
- Deng BQ, Bo Y, Kim CN (2008) An analytical solution for VOCs emission from multiple sources/sinks in buildings. *Chin Sci Bull* 53:1100–1106
- Ernstoff AS, Fantke P, Csiszar SA, Henderson AD, Chung S, Jolliet O (2016) Multi-pathway exposure modeling of chemicals in cosmetics with application to shampoo. *Environ Int* 92–93:87–96
- Finizio A, Mackay D, Bidleman T, Harner T (1997) Octanol-air partition coefficient as a predictor of partitioning of semi-volatile organic chemicals to aerosols. *Atmos Environ* 31(15):2289–2296
- Fischer A, Ljungström E, Langer S (2013) Ozone removal by occupants in a classroom. *Atmos Environ* 81:11–17
- Fu D, Leng CB, Kelley J, Zeng G, Zhang YH, Liu Y (2013) ATR-IR study of ozone initiated heterogeneous oxidation of squalene in an indoor environment. *Environ Sci Technol* 47:10611–10618
- Gong M, Zhang Y, Weschler CJ (2014) Predicting dermal absorption of gas-phase chemicals: transient model development, evaluation, and application. *Indoor Air* 24:292–306
- Goss KU (2005) Predicting the equilibrium partitioning of organic compounds using just one linear solvation energy relationship (LSER). *Fluid Phase Equilib* 233(1):19–22
- Huang L, Jolliet O (2019) A quantitative structure-property relationship (QSPR) for estimating solid material-air partition coefficients of organic compounds. *Indoor Air* 29(1):79–88

- Huang SD, Xiong JY, Zhang YP (2013) A rapid and accurate method, ventilated chamber C-history method, of measuring the emission characteristic parameters of formaldehyde/VOCs in building materials. *J Hazard Mater* 261:542–549
- Jorgensen RB, Dokka TH, Bjørseth O (2000) Introduction of a sink-diffusion model to describe the interaction between volatile organic compounds (VOCs) and material surfaces. *Indoor Air* 10: 27–38
- Lakey PSJ, Wisthaler A, Berkemeier T, Mikoviny T, Poschl U, Shiraiwa M (2017) Chemical kinetics of multiphase reactions between ozone and human skin lipids: implications for indoor air quality and health effects. *Indoor Air* 27:816–828
- Lakey PSJ, Morrison GC, Won Y, Parry KM, von Domaros M, Tobias DJ, Rim D, Shiraiwa M (2019) The impact of clothing on ozone and squalene ozonolysis products in indoor environments. *Commun Chem* 2:56
- Liang Y, Bi C, Wang X, Xu Y (2019) A general mechanistic model for predicting the fate and transport of phthalates in indoor environments. *Indoor Air* 29(1):55–69
- Lieberman MW, Lykissa ED, Barrios R, Qu CN, Kala G, Kala SV (1999) Cyclosiloxanes produce fatal liver and lung damage in mice. *Environ Health Perspect* 107:161–165
- Liu C, Shi S, Weschler C, Zhao B, Zhang Y (2013) Analysis of the dynamic interaction between SVOCs and airborne particles. *Aerosol Sci Technol* 47(2):125–136
- Liu YJ, Misztal PK, Xiong JY, Tian YL, Arata C, Weber RJ, Nazaroff WW, Goldstein AH (2019) Characterizing sources and emissions of volatile organic compounds in a northern California residence using space- and time-resolved measurements. *Indoor Air* 29:630–644
- Liu K, Kang L, Li A, Zheng J, Wang X, Zhou X, Wang F (2020) Field investigation on phthalates in settled dust from five different surfaces in residential apartments. *Building and Environment* 177:106856
- Lucattini L, Poma G, Covaci A, Boer J, Lamoree M, Leonards P (2018) A review of semi-volatile organic compounds (SVOCs) in the indoor environment: occurrence in consumer products, indoor air and dust. *Chemosphere* 201:466–482
- Lyng N, Gunnarsen L, Andersen H (2015) The effect of ventilation on the indoor air concentration of PCB: an intervention study. *Build Environ* 94(1):305–312
- Montemayor BP, Price BB, van Egmond RA (2013) Accounting for intended use application in characterizing the contributions of cyclopentasiloxane (D5) to aquatic loadings following personal care product use: antiperspirants, skin care products and hair care products. *Chemosphere* 93:735–740
- Morrison GC, Weschler CJ, Bekö G (2016) Dermal uptake directly from air under transient conditions: advances in modeling and comparisons with experimental results for human subjects. *Indoor Air* 26:913–924
- Pankow JF (1987) Review and comparative analysis of the theories on partitioning between the gas and aerosol particulate phases in the atmosphere. *Atmos Environ* 21(11):2275–2283
- Pankow JF (1994) An absorption model of gas/particle partitioning of organic compounds in the atmosphere. *Atmos Environ* 28(2):185–188
- Partapkar S (1980) Numerical heat transfer and fluid flow. McGraw-Hill, New York
- Pieri F, Katsoyiannis A, Martellini T, Hughes D, Jones KC, Cincinelli A (2013) Occurrence of linear and cyclic volatile methyl siloxanes in indoor air samples (UK and Italy) and their isotopic characterization. *Environ Int* 59:363–371
- Qiao LN, Ma WL, Zhang ZF, Liu LY, Song WW, Jia HL, Zhu HN, Li WL, Macdonald RW, Nikolaev A, Li YF (2021) Slopes and intercepts from log-log correlations of gas/particle quotient and octanol-air partition coefficient (vapor-pressure) for semi-volatile organic compounds: II. Theoretical predictions vs. monitoring. *Chemosphere* 273:128860
- Salthammer T, Schripp T (2015) Application of the Junge- and Pankow-equation for estimating indoor gas/particle distribution and exposure to SVOCs. *Atmos Environ* 106:467–476
- Shi S, Zhao B (2015) Estimating indoor semi-volatile organic compounds (SVOCs) associated with settled dust by an integrated kinetic model accounting for aerosol dynamics. *Atmos Environ* 107:52–61

- Shin HM, McKone TE, Bennett DH (2012) Intake fraction for the indoor environment: a tool for prioritizing indoor chemical sources. *Environ Sci Technol* 46(18):10063–10072
- Shiraiwa M, Pfrang C, Pöschl U (2010) Kinetic multi-layer model of aerosol surface and bulk chemistry (KM-SUB): the influence of interfacial transport and bulk diffusion on the oxidation of oleic acid by ozone. *Atmos Chem Phys* 10:3673–3691
- Singer BC, Hodgson AT, Hotchi T, Ming KY, Sextro RG, Wood EE, Brown NJ (2007) Sorption of organic gases in residential rooms. *Atmos Environ* 41:3251–3265
- Tang X, Misztal PK, Nazaroff WW, Goldstein AH (2015) Siloxanes are the most abundant volatile organic compound emitted from engineering students in a classroom. *Environ Sci Technol Lett* 2:303–307
- Ulrich N, Endo S, Brown T, Watanabe N, Bronner G, Abraham M, Goss K (2017) UFZ-LSER Database v 3.2. 1 [Internet]. Helmholtz Centre for Environmental Research – UFZ, Leipzig
- Wang HM, Zheng JH, Yang T, He ZC, Zhang P, Liu YF, Zhang MX, Sun LH, Yu XF, Zhao J, Liu XY, Xu BP, Tong LP, Xiong JY (2020) Predicting the emission characteristics of VOCs in a simulated vehicle cabin environment based on small-scale chamber tests: parameter determination and validation. *Environ Int* 142:105817
- Wei W, Mandin C, Blanchard O, Mercier F, Pelletier M, Le Bot B, Glorennec P, Ramalho O (2016) Temperature dependence of the particle/gas partition coefficient: an application to predict indoor gas-phase concentrations of semi-volatile organic compounds. *Sci Total Environ* 563–564:506–512
- Wei W, Ramalho O, Mandin C (2019a) A long-term dynamic model for predicting the concentration of semivolatile organic compounds in indoor environments: application to phthalates. *Build Environ* 148:11–19
- Wei W, Mandin C, Blanchard O, Mercier F, Pelletier M, Le Bot B, Glorennec P, Ramalho O (2019b) Semi-volatile organic compounds in French dwellings: an estimation of concentrations in the gas phase and particulate phase from settled dust. *Sci Total Environ* 650:2742–2750
- Weschler CJ (2009) Changes in indoor pollutants since the 1950s. *Atmos Environ* 43(1):153–169
- Weschler CJ (2016) Roles of the human occupant in indoor chemistry. *Indoor Air* 26:6–24
- Weschler CJ, Carslaw N (2018) Indoor chemistry. *Environ Sci Technol* 52:2419–2428
- Weschler CJ, Nazaroff WW (2008) Semivolatile organic compounds in indoor environments. *Atmos Environ* 42(40):9018–9040
- Weschler CJ, Nazaroff WW (2010) SVOC partitioning between the gas phase and settled dust indoors. *Atmos Environ* 44(30):3609–3620
- Weschler CJ, Nazaroff WW (2017) Growth of organic films on indoor surfaces. *Indoor Air* 27(6): 1101–1112
- Weschler CJ, Wisthaler A, Cowlin S, Tamás G, Strøm-Tejsen P, Hodgson AT, Destaillats H, Herrington J, Zhang J, Nazaroff WW (2007) Ozone-initiated chemistry in an occupied simulated aircraft cabin. *Environ Sci Technol* 41:6177–6184
- Weschler CJ, Saltherammer T, Fromme H (2008) Partitioning of phthalates among the gas phase, airborne particles and settled dust in indoor environments. *Atmos Environ* 42(7):1449–1460
- Wisthaler A, Weschler CJ (2010) Reactions of ozone with human skin lipids: sources of carbonyls, di carbonyls, and hydroxyl carbonyls in indoor air. *Proc Natl Acad Sci U S A* 107:6568–6575
- Wu Y, Eichler CMA, Leng W, Cox SS, Marr LC, Little JC (2017) Adsorption of phthalates on impervious indoor surfaces. *Environ Sci Technol* 51(5):2907–2913
- Xiong JY, Liu C, Zhang YP (2012) A general analytical model for formaldehyde and VOC emission/sorption in single-layer building materials and its application in determining the characteristic parameters. *Atmos Environ* 47:288–294
- Xiong JY, Cao JP, Zhang YP (2016) Early stage C-history method: rapid and accurate determination of the key SVOC emission or sorption parameters of indoor materials. *Build Environ* 95:314–321
- Xiong JY, He ZC, Tang XC, Misztal PK, Goldstein AH (2019) Modeling the time-dependent concentrations of primary and secondary reaction products of ozone with squalene in a university classroom. *Environ Sci Technol* 53:8262–8270

- Yang T, Zhang PP, Xu BP, Xiong JY (2017) Predicting VOC emissions from materials in vehicle cabins: determination of the key parameters and the influence of environmental factors. *Int J Heat Mass Transf* 110:671–679
- Yang T, Xiong JY, Tang XC, Misztal PK (2018) Predicting indoor emissions of cyclic volatile methylsiloxanes from the use of personal care products by university students. *Environ Sci Technol* 52:14208–14215
- Yucuis RA, Stanier CO, Hornbuckle KC (2013) Cyclic siloxanes in air, including identification of high levels in Chicago and distinct diurnal variation. *Chemosphere* 92:905–910
- Zhang X, Diamond ML, Ibarra C, Harrad S (2009) Multimedia modeling of polybrominated diphenyl ether emissions and fate indoors. *Environ Sci Technol* 43(8):2845–2850
- Zhang MX, Xiong JY, Liu YJ, Misztal PK, Goldstein AH (2021) Physical–chemical coupling model for characterizing the reaction of ozone with squalene in realistic indoor environments. *Environ Sci Technol* 55:1690–1698
- Zhou SM, Forbes MW, Abbatt JPD (2016) Kinetics and products from heterogeneous oxidation of squalene with ozone. *Environ Sci Technol* 50:11688–11697
- Zhou X, Luo C, Liu K, Wang X (2020) A novel model for predicting the semivolatile organic compound partition coefficient of multicomponent airborne particles. *Build Environ* 167: 106446
- Zhou X, Lian J, Cheng Y, Wang X (2021) The gas/particle partitioning behavior of phthalate esters in indoor environment: effects of temperature and humidity. *Environ Res* 194:110681
- Zhu JP, Wong SL, Cakmak S (2013) Nationally representative levels of selected volatile organic compounds in Canadian residential indoor air: population-based survey. *Environ Sci Technol* 47:13276–13283
- Xu Y, Zhang JS (2011) Understanding SVOCs. *ASHRAE Journal* 53(12):121–125

Part VI

Indoor Chemistry



Framing Indoor Chemistry Topics

26

Michael S. Waring and Glenn C. Morrison

Contents

Introduction	812
Comparing Chemistry Occurring Indoors and Outdoors	812
Indoor Gas-Phase Chemistry	812
Indoor Photochemistry	813
Indoor Surface Chemistry	814
Occupant Emissions and Chemistry	815
Analytical Tools in Indoor Chemistry	815
Indoor Chemistry Modeling of Gas-, Particle-, and Surface-Phase Processes	816
Conclusion	817

Abstract

Indoor chemistry is a complex topic that has received much research attention in recent years. This section offers chapters that cover the following topics: comparing chemistry occurring indoors and outdoors; indoor gas-phase chemistry; indoor photochemistry; indoor surface chemistry; occupant emissions and chemistry; analytical tools in indoor chemistry; and indoor chemistry modeling. After reading this section, those interested in indoor chemistry research will have a strong grounding in indoor chemistry fundaments and the current state of the field, and they should be able to identify future directions for fruitful research.

Keywords

Overview · Indoor chemistry · Gas-phase · Surface-phase · Aerosol · Modeling

M. S. Waring (✉)

Drexel University, Philadelphia, PA, USA

e-mail: msw59@drexel.edu

G. C. Morrison

Environmental Sciences and Engineering, University of North Carolina, Chapel Hill, NC, USA

e-mail: glenn.morrison@unc.edu

Introduction

This indoor chemistry section offers chapters related to the study of indoor chemical transformations and processes. This topic is very broad in scope including research that spans from fundamental to application-based scale. It is a growing field that is continuously accommodating new researchers. In this introductory chapter, we outline and offer a brief description of the chapters in this section. Supporting references are not included here but are available in the individual chapters themselves.

Comparing Chemistry Occurring Indoors and Outdoors

The chemical reactions occurring indoors are largely the same as those occurring outdoors but differ in their extent due to the availability and intensity of sources, surfaces, and driving forces such as sunlight. The contemporary study of indoor chemistry, therefore, benefits from the accumulated knowledge and techniques developed as the result of nearly a century of research on outdoor atmospheric processes. Indeed, recent intensive application of experimental methods, technology, and modeling have rapidly advanced the field of indoor chemistry.

Like outdoor air, indoor environments are subject to complex sources and drivers. To understand this complexity, the authors suggest drawing parallels with outdoor processes and identifying simplifying characteristics where possible. For example, what has been learned about the biogeochemical processes occurring within the Sea Surface MicroLayer may be valuable in understanding thin films, complete with their own unique microbiome, on indoor surfaces. Similarly, outdoor “dark chemistry” is more relevant to indoor spaces due to limited input of strong UV light. Unlike the ambient atmosphere, indoor environments are much easier to control and perturb to unravel processes including source strengths, interactions of chemicals with indoor compartments, particle formation, and so forth. Recent perturbation experiments have revealed the presence of surface reservoirs that store acids and SVOCs as strong buffers against efforts to reduce air concentrations by controls such as increased outdoor air exchange. Introduction of controlled trace species reveals the path air takes when passing through homes, knowledge key to understanding its chemical history. In all, collaboration among experts in atmospheric physics and chemistry, building science, surface science, microbiology, and related modeling will be necessary to advance the science of indoor air chemistry in the face of 50 years of regulatory neglect.

Indoor Gas-Phase Chemistry

The indoor environment is rich in volatile organic compounds (VOC) that are emitted from building materials and activities such as cleaning, cooking, or using personal care products. These VOCs can undergo oxidation reactions in the

gas-phase. The primary drivers of indoor VOC oxidation are reactions with ozone (O_3) and the hydroxyl radical (OH), though VOC reactions with nitrate radicals (NO_3) and chlorine radicals can sometimes be important. Whether a particular gas phase reaction is important indoors depends on whether it occurs on a timescale that is competitive with the residence time of indoor air, which is set by the outdoor air exchange rate of the building (also called the ventilation air exchange rate).

This chapter reviews that state of knowledge of indoor air gas phase chemistry, with a strong focus on oxidation reactions with VOCs. Indoor ozone is typically due to outdoor-to-indoor transport, with indoor concentrations often at a factor of 0.2–0.7 of outdoor concentrations. Most indoor oxidation is initiated by reactions of ozone with one or more double bonds in alkenes, including compounds such as terpenoids and squalene. Ozone reactions with alkenes follow the well-established Criegee mechanism. First, ozone adds to the double bond forming a primary ozonide that rapidly decomposes to form stable carbonyls as well as Criegee Intermediate (CI) radicals and hydroxyl radicals (OH). These ozone-alkene reactions are often the dominate source of OH indoors, although photolysis of nitrous acid (HONO) has recently emerged as a second important source. While ozone reacts only with double bonds in alkenes, OH has the potential to react with almost any VOC at a fast enough rate to affect product concentrations. Reactions of VOCs with ozone and OH also generate peroxy radicals (RO_2), which can undergo further reactions to yield peroxydes, organic nitrates, peroxyacetyl nitrates, carboxylic acids, alcohols, and carbonyls. Oxidation of VOCs by the nitrate or chlorine radical can also generate peroxy radicals that behave similarly to those produced by ozone or OH reactions. The products generated by VOC oxidation have a large range of volatilities from very volatile to weakly volatile in nature. Products with low to semivolatility can partition to the organic aerosol phase, acting as a meaningful source of secondary organic aerosol (SOA) in indoor environments. This process is especially important for ozone-terpene reactions indoors.

Indoor Photochemistry

Outdoors, light from the sun initiates much of the chemistry that is responsible for ambient air pollution. Although light levels are generally much lower indoors, photochemistry still occurs and can meaningfully drive chemistry in special situations and locations where light is intense enough and of the right wavelength.

This chapter provides a detailed description of the range of chemistry and chemical products resulting from photochemistry. Photochemistry begins when a molecule absorbs light, then reacts. Energetic radicals that are common products of photolysis can then go on to react with other nearby molecules. Major reactions discussed include photolysis of nitrous acid that generates the hydroxyl radical (OH) that can then initiate oxidation of organics and other species. Other species of interest include photolabile aldehydes, hydrogen peroxide, chlorine dioxide (used in fumigation), and hypochlorous acid (a product of bleach cleaning). The intensity and spectrum of light near windows and near certain artificial light sources are

sufficient to raise radical concentrations significantly above indoor background levels. Heterogenous photochemistry has been observed to take place on indoor surfaces. For example, light-induced generation of nitrous acid on paint has been ascribed to photocatalysis of nitrogen dioxide. Some researchers have proposed that photochemistry over long time periods may expose occupants to small congener photolysis products of brominated flame retardants. Advanced models that combine computational fluid dynamics (CFD) with photochemistry predict that chemical concentrations can vary by one or more orders of magnitude throughout indoor environments subject to spatially nonuniform light flux. Although historically neglected in indoor air research, photochemistry deserves more attention especially in identifying chemicals and conditions where photochemistry meaningfully alters occupant exposure to harmful products. Understanding the impact of this chemistry has become even more important as more photo-reactive precursors are added to indoor environments (disinfectants and fumigants), as photocatalysts are included building materials, and as we increase our use of ultraviolet light for air and surface disinfection.

Indoor Surface Chemistry

Buildings are rich in surfaces available for chemical interactions. Considering only the geometrically projected area of building surfaces and furnishings, the surface area-to-volume ratio of the indoor air volume is much greater than outdoor air. The internal surfaces, such as the surface of textile fibers or pores within drywall, can increase the available surface area by one or more orders of magnitude. Early researchers recognized that surfaces were responsible for the observation that the concentrations of ozone indoors were much lower than outdoors. Over time, other chemical reactions and interactions were identified that were supported by indoor surfaces.

Indoor surfaces can act as chemical reservoir, extending the time to interact and react with other chemical species. For example, indoor materials and the films that coat their surfaces can hold onto very large amounts of semivolatile organic compounds as well as volatile acids and bases. These surface reservoirs act to stabilize air concentrations, limiting the effectiveness of controls such as periodic “airing out” by opening windows. Fragrance compounds, oils, and many other unsaturated organic compounds can be adsorbed to (or absorbed within) indoor materials for sufficient time to allow ozone to collide and subsequently react with their double bonds, forming aldehydes, ketones, carboxylic acids, and other volatile and semivolatile oxidized species. Surfaces support the formation of nitrous acid from nitrogen dioxide, conversion of amines to carcinogenic nitrosamines, hydrolysis of phthalates, and many other chemical processes. Not only does surface chemistry alter the composition of the air we breathe, but also it alters the composition of the surfaces themselves. Therefore, indoor surface chemistry influences our intake of pollutants by both air and surface-mediated exposure pathways.

Occupant Emissions and Chemistry

Human malodor is among the earliest drivers of active building ventilation. Occupants are a major source of indoor chemicals that can lower air quality directly or through their subsequent chemical transformations. Breath, skin, and intestinal gases contribute meaningfully to the total volatile organic compound concentration in an occupied building (by mass). While generally considered nontoxic, occupant emissions may affect cognitive performance or be respiratory irritants.

In addition to CO₂, breath contains numerous products of metabolism including acetone, isoprene, nitric oxide, and products of oxidative stress. The composition of breath can be influenced by intake of exogenous chemical from exposure to smoke, solvents, and other nonnatural species present indoors. Skin emissions include glandular secretions, often quite malodorous, as well as products of the metabolism of microflora on skin. The skin is a major sink for the photochemical pollutant ozone. While lowering indoor air levels of ozone, this chemistry generates a host of notable products that themselves can participate in chemistry to form irritants and contribute to aerosol mass. Skin flakes, skin oil, and other secretions are also deposited on indoor surfaces and can act as a further sink for oxidants and source of emissions to indoor air. Personal factors, including age, sex, physical activity, metabolism, menstruation, diet, clothing, and use of personal care products can influence emissions. As a building factor, ventilation not only dilutes occupant emissions but also introduces outdoor pollutants that can increase the production rate of some reaction products with skin and breath compounds. Temperature and relative humidity can also alter the yields of ozonolysis products from skin and clothing.

Analytical Tools in Indoor Chemistry

The indoor environment contains meaningful concentrations of many organic and inorganic species that exist in the gas, aerosol, or surface phases. Due to their sheer number and chemical complexity, identifying and quantifying these compounds is a great challenge. Moreover, these compounds often must be measured at high time resolution, since building-relevant timescales such as residence time are short, and sources and sinks often vary over orders of minutes or even seconds. Current and emerging analytical instruments that were originally intended for outdoor air quality measurements have recently been brought indoors. This chapter discusses chemical measurement principles, addressing issues such as selectivity to measure target compounds and sensitivity to measure changes in concentration. Different strategies for measuring indoor compounds are reviewed, including bulk versus compound-specific; offline versus online; chemical versus physical analysis; low-cost sensors versus research instrumentation; and analytical chemistry approaches for different types of measurements.

Inert gases like carbon dioxide are relatively easy to measure, while reactive gases range from relatively easy (like ozone) to very difficult to the point of only a few labs having the capability (like hydroxyl or nitrate radicals). Volatile organic compounds

(VOC) and semivolatile organic compounds (SVOC) were traditionally measured in an offline manner using combinations of gas-chromatographs and detectors. Newer instrument methods such as proton-transfer reaction mass spectrometry (PTR-MS) and chemical ionization mass spectrometry (CIMS) have enabled fast detection and quantification of a multitude of indoor VOCs. When these instruments are equipped with time-of-flight (TOF) mass analyzers, their resolving power is orders of magnitude higher than quadrupole-based predecessors. For particles, scanning mobility particle sizers (SMPS) allow precise quantification of size distributions, while aerosol mass spectrometers (AMS) and aerosol chemical speciation monitors (ACSM) have been used in indoor experiments to detect changes in bulk chemical composition. Although the AMS-type instruments fragment aerosol components, soft ionization techniques that minimize fragmentation and provide molecular level information are also available.

Indoor Chemistry Modeling of Gas-, Particle-, and Surface-Phase Processes

Modeling of indoor chemical processes can be used to effectively predict indoor concentrations and exposure as well as to investigate certain processes not practical experimentally or to test the completeness of our understanding of process. Early indoor model development came in the 1980s when Nazaroff and Cass used concentration balances to predict the fate of chemically reactive pollutants in a museum setting, considering effects of ventilation, filtration, surface reaction, emission, and chemical reactions. A few years later, the same authors offered a similarly robust, size-resolved particle model. In the decades afterward, a host of indoor models and techniques were developed, some of which are as follows.

Early gas-phase reaction models used limited chemistry schemes, for example, to indicate the importance of ozone-alkene reactions on indoor hydroxyl radical (OH) concentrations, which were previously thought to be negligible indoors. Subsequently, indoor gas-phase reaction models were developed that incorporated detailed reaction mechanism, and they later included gas-to-particle partitioning based on vapor pressures of predicted compounds to predict formation of indoor secondary organic aerosol (SOA) from ozone or OH reactions with volatile organic compounds (VOC). A second class of models was also developed to predict indoor SOA using a mass yield framework within the volatility basis set (VBS), which organizes numerous SOA forming compounds generated by VOC oxidation into bins separated by volatility and then predicts partitioning. The two-dimensional VBS has also been used to further allow tracking of later generation oxidation reactions and organic aerosol density, water uptake, and phase state. The transformation of ammonium nitrate upon transport indoors has also been simulated. Finally, surface reactions have been modeled using the parameter of the deposition velocity, which is a mass transfer coefficient that includes information on reactive uptake and boundary layer transport. The deposition velocity can be used with surface yields to predict indoor air concentrations. Kinetic models have also been used to simulate

ozone reactions with human skin, and computational fluid dynamics have predicted heterogeneous concentrations of indoor byproducts due to ozone reactions with skin and also indoor OH concentrations.

Conclusion

As this introductory chapter demonstrates, indoor chemistry topics are widely variable in their scope. They include a range of issues such as outdoor to indoor transport, indoor chemical transformations among different phases indoors, and building and mechanical system processes. Researchers that study indoor chemistry utilize both sophisticated instruments as well as consumer grade sensors in lab and field campaigns and also develop detailed models to understand and inform observations.



Indoor Air Quality Through the Lens of Outdoor Atmospheric Chemistry

27

Jonathan P. D. Abbatt and Douglas B. Collins

Contents

Introduction	820
Primary Chemical Sources	821
Reactivity	824
Partitioning	826
Impact of Dynamics on Chemistry	828
Working Toward Solutions	829
Cross-References	830
References	831

Abstract

Outdoor atmospheric chemistry and air quality have been the topic of research that intensified in earnest around the mid-twentieth century, while indoor air quality research has only been a key focus of chemical researchers over the last 30 years. Examining practices and approaches employed in the outdoor atmospheric chemistry research enterprise provides an additional viewpoint from which we can chart new paths to increase scientific understanding of indoor chemistry. This chapter explores our understanding of primary chemical sources, homogeneous and multiphase reactivity, gas-surface partitioning, and the coupling between the chemistry and dynamics of indoor air through the lens of

Jonathan P. D. Abbatt and Douglas B. Collins contributed equally.

J. P. D. Abbatt (✉)

Department of Chemistry, University of Toronto, Toronto, ON, Canada
e-mail: jonathan.abbatt@utoronto.ca

D. B. Collins

Department of Chemistry, Bucknell University, Lewisburg, PA, USA
e-mail: d.collins@bucknell.edu

outdoor atmospheric chemistry. The means to mitigate degraded air quality outdoors are heavily rooted in public policy actions, while the commercial sector mainly promulgates solutions for indoor air quality, making practical and actionable outcomes to research essential for prompt improvements to indoor environments. Indoor and outdoor environments have many important scientific distinctions, but a shared vision for healthy environments motivates both research communities in the same way.

Keywords

Multiphase chemistry · Partitioning · Trace gas sources · Dynamics · Environmental inequality

Introduction

Air quality has been of general public awareness for centuries but only became clearly codified over approximately the last 150 years. In the late nineteenth century, actions to address public health during intense urbanization were based, at least in part, on the human sense of smell in the waning years of adherence to the miasma theory (Kiechle 2017). The notion that exposure to “bad air” was a risk for contracting disease was broadly replaced by the germ theory. Modern understanding of infectious disease, indeed, includes the possibility that a subset of known infectious diseases can be spread through exposure to airborne biological particles. However, a general sense of healthfulness continues to be connected with our sense of smell as a detector of air quality, both indoors and outdoors. Important health effects of poor air quality are also associated with exposure to *chemical* agents, rather than just biological ones; poor air quality is associated with various noncommunicable diseases and is a leading global health risk factor (Murray et al. 2020).

Scientific understanding of outdoor air quality has grown significantly since the mid-twentieth century. Tracking radiogenic isotopes released from atomic bomb detonations allowed for new insights on long range transport (Burton and Stewart 1960). Around the same period, smog formation represented an intense health and safety problem in major cities like Los Angeles and London; similar air quality problems persist to varying degrees to this day in urban environments around the globe. Arie Haagen-Smit’s discovery of the photochemical processes that created smog and recognition that ozone played a central role in urban air pollution (Haagen-Smit and Fox 1956) were critical achievements in establishing the importance of chemistry in atmospheric phenomena that degraded air quality. Following growing scientific understanding, along with dedicated efforts to communicate these findings, government regulations and public policy have been used to address outdoor air quality problems to impressive effect (Hand et al. 2020). Key advancements in chemical analysis technology continue to allow for an ever-increasing level of detail in our understanding of atmospheric chemistry through increases in sensitivity, portability, spatial/temporal coverage, and chemical specificity to target measures that will help to mitigate poor air quality.

Building science and indoor air quality have also advanced dramatically since the mid-twentieth century. Specific studies of indoor chemistry began in the 1970s and have been accelerating especially since the mid-1990s (Weschler 2011). In the same period, however, improvements to building technology and energy efficiency have advanced more rapidly than methods to thoroughly understand and address indoor air quality from a chemical perspective. It remains critical to increase our understanding of indoor chemistry and clearly communicate new knowledge to the public. Significant progress has been made in elucidating the chemistry that occurs in both the gas phase and on surfaces indoors. More recent applications of highly sensitive, specific, and rapid online chemical measurements of the gas phase, aerosol particles, and surfaces have continued to enhance our depth of understanding (Farmer 2019). Since improvements in indoor air quality are promulgated by the building industry, researchers need to continue to develop a clear and predictive understanding of the processes that lead to degraded air quality along with solutions for practitioners to implement. Therefore, the outcomes and goals of indoor chemistry studies differ slightly from outdoor air, where changes in public policy are often a more crucial element of effective solutions.

In this chapter, we seek to unpack the approaches of outdoor atmospheric chemistry research with an eye toward their application to future studies of indoor air chemistry. The objective within each topical section is to explore several ways in which outdoor atmospheric chemistry has been conducted; examples have been chosen such that they shed light on the way that indoor chemistry is currently studied or could be studied in the future.

Primary Chemical Sources

Introduction of outdoor air is an important chemical source for indoor air. At the same time, mounting evidence shows the growing importance of indoor activities and emissions of volatile chemical products on outdoor air quality (McDonald et al. 2018). Processes that add chemical constituents to the air are important controlling factors in atmospheric chemistry and often represent the most viable opportunity for mitigating poor air quality. Considering only primary (i.e., direct) emissions, sources are often categorized as “natural” or “anthropogenic,” although the line can be blurred in some cases, like agriculture, wildfires, or land-use change. Each source has its own chemical signature, including but not limited to: a wide variety of volatile and semi-volatile organic compounds (VOCs and SVOCs: hydrocarbons, carbonyl compounds, organic acids, amines), including compounds that are considered to be persistent organic pollutants; oxides and/or oxoacids of sulfur (SO_2 , H_2SO_4), nitrogen (NO , NO_2 , HNO_2 , HNO_3 , organic nitrates), or carbon (CO , CO_2); inorganic acids (HCl , H_2S , HCN) and bases (NH_3); and aerosol particles of organic, inorganic, biological, mineral, or mixed composition (Finlayson-Pitts and Pitts 2000). The source signatures of many types of anthropogenic sources can be replicated in laboratory settings if they are associated with engineered systems (e.g., combustion engines). However, deviations in emission strengths or chemical composition

between controlled laboratory operating conditions and less-controlled field operation can be important (Frey et al. 2003; Gentner et al. 2017). Natural sources of aerosols and gases to the outdoor environment can be more challenging to simulate and study in a controlled manner. Emission processes can be the result of nuanced couplings between physical, chemical, and biological processes, along with a wide variety of spatial (nanometer to kilometer) and temporal (second to year) scales.

To account for couplings between ambient environmental conditions and emission source signatures, field experiments are targeted for strategic or opportunistic sampling of the atmosphere. Anthropogenic sources can be probed over timescales in which variations in activity are either predictable or known externally, such as weekday/weekend studies or episodic shutdowns/reductions of source activity, like the public response to the COVID-19 global pandemic (Kroll et al. 2020). Field experiments, in some cases, yield less specific chemical information than is achievable in laboratory studies due to various confounding environmental factors but provide key constraints and guidance for more fundamental study and continued model development. Improvements in transportable and field-deployable chemical measurement technology have enabled major advances, allowing for online measurement approaches to field campaigns that were previously restricted to laboratory studies or offline operation (Laskin et al. 2018). Supplementing field observations with controlled laboratory experimentation using emission source simulators can yield a greater depth of fundamental understanding but are often subject to a variety of their own caveats. However, coordinated combinations of field measurements, laboratory studies, and modeling have provided significant insight on complex atmospheric chemistry topics (Burkholder et al. 2017; Ault et al. 2020).

It is possible for indoor air quality to bridge the gap between field and laboratory studies more readily than outdoors as perturbations to the indoor environment can be made deliberately. Two key approaches to perturbing indoor air composition are available: enhanced ventilation or air cleaning to rapidly reduce concentrations of compounds that are more abundant indoors than outdoors, and source modulation that can provide episodic additions of chemical constituents to indoor air. Each of these approaches can yield important insights about emission rates and rapid post-emission processes like chemical reactions or phase partitioning that act as sinks for aerosol particles or traces gases of interest. At the same time, care must be taken to understand the realism of the perturbation strength. Comparison of deliberate perturbations to indoor air composition and chemical processes should be compared against measurements of opportunistic perturbations due to non-prescribed occupant activity or normal building system operations. Modulation of HVAC operating status (cooling and heating cycles), window opening, day/night temperature and light cycles, and occupant cooking or cleaning activities are key opportunities for study.

The concept that source emission and physicochemical processes near to the chemical source can respond to the environment has been noted indoors in the context of relative humidity (RH) and temperature (T) for some gases (Parthasarathy et al. 2011) and aerosol particles (Xie et al. 2007; Salimifard et al. 2017). Emission source behavior studies in realistic environments are important to perform, despite being subject to complication by interfering chemical signals or poorly constrained

sink processes that influence airborne constituent concentrations. Complementary use of controlled source characterization studies in the laboratory environment using smaller or more controllable chambers allows for deeper inspection of fundamental principles, while implementation of similar experiments in more complex, realistic indoor environments allows for an accounting of rapid interactions between the source and/or freshly emitted material with the realistic surroundings, providing an “effective” source strength.

Additional complexity beyond varying RH and T are possible. Studies of biosphere-atmosphere coupling in the outdoor environment require careful accounting for biogeochemical processes in terrestrial or marine environments. For instance, chamber studies of biogenic VOC production from plants may constrain emission rates, which can then be juxtaposed with emission estimates derived from ambient measurements of the same VOCs in or near a forest canopy outdoors. The field studies of ambient air may, for instance, make clear that measurements that account for stress responses, including those arising from herbivory or disease, are necessary (Faiola and Taipale 2020). In addition, meteorological conditions can influence the behavior of biological systems that drive emissions, and atmospheric conditions also influence the chemistry that may occur. For some biological systems, atmospheric deposition of limiting nutrients can drive productivity, which affects the fluxes and/or compositions of gases and particles emitted to the atmosphere (Mahowald et al. 2009).

One approach to understanding biosphere-atmosphere interactions is to make a large suite of measurements near to (or within) a major biogenic source of emissions, such as the Amazon rainforest. This permits source signature characterization and studies of the reactivity as emissions are transported away from the source or interact with other atmospheric constituents (see section “Reactivity”). The GoAmazon project involved a multi-platform field campaign that built upon a longer time series of chemical measurements from a tall tower in the Amazon (Martin et al. 2017). The study sampled a “clean” biogenic signature from the highly productive rainforest and juxtaposed those biogenic emissions with episodic influence from a major urban area (Manaus, Brazil). The indoor environment bears perhaps unexpected similarity to the GoAmazon study and other forested regions: the building and its contents are major sources of VOCs with their own emissions behavior. Indoor air composition is influenced by the “natural background” of the building, with occupant activity or other time-dependent source behavior (e.g., cooking, cleaning, changes in outdoor air composition and introduction rate) superimposed on top. It becomes clear that a broad view of the building, its behaviors, and chemical signatures is important to gain a more holistic understanding of indoor air quality.

A different approach to understanding a highly complex and coupled system is exemplified by approaches to understanding ocean-atmosphere exchange. The ocean is home to a large and diverse biomass that participates in chemical exchange with the atmosphere. Deposition of inorganic material (e.g., iron, nitrate, phosphate) and uptake of CO₂ provide nutrients for primary production and carbon fixation by microalgae (Emerson and Hedges 2008; Mahowald et al. 2009), but changes in microbiological activity of the near-surface ocean can drive major changes in the

water-to-air fluxes of both particles and gases (Wurl et al. 2017; Collins and Grassian 2018). Recognizing the effects of microbial succession on the organic composition of the surface ocean (Prather et al. 2013) has provided key insights into the aerosols and gases that arise from differences in biological activity (Wang et al. 2015; Mayer et al. 2020) that naturally occur on month-long and kilometer scales (Dall’Osto et al. 2019). At the same time, the physical processes that control material fluxes across the air-sea interface occur on the micrometer length scale and involve nuanced (bio)chemistry that occurs in a thin gelatinous film on the ocean surface called the sea surface microlayer (SSML) (Cunliffe and Murrell 2009). Biogeochemical processes occurring within the SSML can be sources of trace gases, but the physical properties of the SSML also physically mediate air-sea gas transfer in both directions (Frew 1997; Wurl et al. 2017). In addition, the air-exposed film may participate in multiphase chemistry, leading to the reactive uptake and/or production of various trace gases (Wurl et al. 2017; Collins and Grassian 2018; Schneider et al. 2019). In the indoor environment, significant effort on the microbiology of the built environment has been initiated (Gilbert and Stephens 2018). Treating the indoor microbiome in a manner analogous to the microbiome of the surface ocean could yield important new insights. It could be important to treat the bidirectional exchange of material on microbially colonized indoor surfaces with care, as a recent study has shown that the gut microbiome can respond to the chemical environment to which a person is exposed (Gardner et al. 2020). Do bidirectional feedbacks and/or important couplings exist between the microbial communities and the chemistry of the air within a building?

Reactivity

The strength and nature of the sources that supply reactive compounds to the atmosphere impart an important control on the overall amount and type of reactivity observed in the air. Most gaseous and aerosol reactions in the outdoor atmosphere are driven by a cascade of energy from ultraviolet (UV) light in the Sun’s spectrum. Although the most energetic photons are removed in the stratosphere, sunlight with wavelengths in the near UV range penetrates to the ground. Through photochemistry, OH radicals are formed, which then oxidize VOCs and lead to the formation of O₃ when NO_x is present. This flow of energy from the Sun also drives nocturnal chemistry, with O₃ formed during the day reacting in the dark with alkenes, also forming radicals (Finlayson-Pitts and Pitts 2000). The implicit approach in atmospheric chemistry is to attempt to define the dispersal of photochemical energy: Which oxidants form? What are their sinks? What oxidation products arise? Large field campaigns are organized around simultaneous, *in situ* measurement of short-lived radicals and their precursors along with assessments of radical loss mechanisms (Carlton et al. 2018). Photochemical models, which include representations of fundamental gas-phase chemistry and are constrained by observations from field studies, embody our understanding of the energy cascade from sunlight into more oxidized species.

The same questions arise with the chemistry of aerosol particles and cloud droplets, requiring detailed chemical characterization of the condensed-phase component of the atmosphere. Such multiphase chemistry involves the coupled chemical and mass transfer interactions of atmospheric gases with the surfaces and interior of aerosols, cloud droplets, and ground materials (Ravishankara 1997). In particular, the gaseous products of oxidation reactions may partition to aerosol particles (see section “[Partitioning](#)”), giving rise to secondary aerosol formation. In aqueous aerosol particles and cloud droplets, it is important to evaluate the degree to which condensed-phase oxidants such as H₂O₂ react with dissolved constituents, giving rise to more oxidized and water-soluble species. This is how one important component of acid rain, sulfuric acid, forms.

We can also track the Sun’s input, along with generated oxidants and their impacts, to the indoor environment. Although sunlight penetrates windows, the shortest, most photochemically active wavelengths are attenuated by glass and the total indoor volume illuminated by direct sunlight is generally low. As well, most indoor lighting is a weak source of UV light (Kowal et al. 2017). As a result, less photochemical energy is available indoors than outdoors and OH radical concentrations are generally low, largely generated by ozone/alkene reactions. Coupled with short indoor air residence times (on the order of hours) (Murray and Burmaster 1995), conditions are not conducive for gaseous reactions to be the primary chemical sink for most indoor contaminants. Ozone is an important low-light oxidant, but it is not generated *in situ* to a significant degree (Young et al. 2019). While secondary organic aerosol formation can occur in specific situations with high organic precursor and oxidant levels (Waring 2014), the relative contribution of indoor secondary aerosol formation is smaller than the importance of secondary aerosol formation to the total outdoor aerosol mass. Rather, a characteristic feature of indoor environments is that the major flux of photochemically generated secondary pollutants, such as O₃, NO₂, and organic- and sulfate-containing aerosol, is usually associated with introduction of outdoor air. As described above, tracking outdoor-to-indoor transport is a major focus of indoor chemistry and represents a key connection point to outdoor air quality.

With oxidant mixing ratios considerably lower than in outdoor environments, a common misconception is that little oxidation chemistry occurs indoors. In specific situations, gas-phase reactions of ozone with high mixing ratios of terpenes and photolysis of HONO in direct sunlight are important sources of indoor OH (Finlayson-Pitts and Pitts 2000; Gómez Alvarez et al. 2013). As well, ozone mixing ratios are low indoors because *so much* oxidation chemistry is occurring. Just as in outdoor environments, where ozone dry deposits onto reactive surfaces like vegetation, ozone experiences efficient deposition to indoor surfaces with high surface-area-to-volume ratios and which can be coated by reactive surface-sorbed molecules (Morrison 2008), such as unsaturated oils from humans or cooking (Zhou et al. 2019b), or products of incomplete combustion, such as polycyclic aromatic hydrocarbons (Zhou et al. 2019a). Whereas the approach of outdoor air pollution research is to focus on the exposure to airborne pollutants by inhalation, it is important to consider indoor exposures based also on human contact with contaminated surfaces,

like dermal uptake or ingestion. The broader spectrum of exposure routes relevant to indoor environments lends importance to understanding the nature of gas-surface multiphase processes.

In the gas phase, an exciting recent finding is the significance for organic molecules of auto-oxidation processes driven by rapid intramolecular isomerizations, giving rise to the formation of highly oxygenated organic molecules (HOMs) (Crounse et al. 2013). Although studied to understand rapid oxidation processes in outdoor environments, even low indoor OH radical and ozone concentrations have the potential to drive the formation of secondary organic aerosol (Kruza et al. 2020). As well, surface-sorbed molecules can react via OH-surface collisions, leading to gradual modification of surface composition over long periods (Alwarda et al. 2018; Morrison et al. 2019).

A distinct and important set of indoor chemical reactions occurs via the use of cleaning agents. The oxidizing capacity of the indoor environment can be amplified significantly in a manner not applicable to outdoor air. Cleaning agents like chlorine bleach and hydrogen peroxide, which are excellent nonspecific biological oxidizing agents, are used in large quantities, especially during the COVID-19 pandemic. HOCl, which exists in both the aqueous and gaseous phases during chlorine bleach use, reacts with a wide variety of organic functional groups, including amines, thiols, and carbon-carbon double bonds to form organochlorine products. In addition, HOCl can drive the formation of volatile chloramines and other reactive species when bleach washing is used (Wong et al. 2017; Mattila et al. 2020). H₂O₂ is also an effective biocide that can photochemically release gas-phase OH when used in large quantities and can also decompose to generate condensed-phase OH radicals on surfaces in the presence of iron.

A challenge to both indoor and outdoor communities is the study of reactions between closed-shell molecules without direct photochemical involvement. High molecular weight organic species form within aerosol particles via condensation reactions between oxygenated organic precursors (Jang et al. 2002). They are likely to also form in highly concentrated organic films like the sea-surface microlayer and are important on indoor surfaces where reaction times are long and reactant surface concentrations can be high. As well, it is known that the ester linkages in surface-bound phthalates can hydrolyze if the pH conditions of the substrates are appropriate (Bope et al. 2019). Such reactions are generally neglected outdoors, given that they are the fastest under alkaline conditions.

Partitioning

Determining whether a molecule resides in the gas phase or in an aerosol particle, or is part of a surface reservoir, is of central importance to assessments of human chemical exposure, both indoors and out. Gases can be inhaled but soluble species are scavenged from the breath high in the respiratory tract. Molecules residing in fine particulate matter can reach deep into the lungs before being deposited. Dermal

exposure can occur via touching contaminated surfaces or through interactions with contaminants that have partitioned to clothing.

In the outdoor environment, the recent focus on phase partitioning has centered around secondary organic aerosol: the oxidation of VOC precursors leads to the formation of semi-volatile species that can partition to aerosol particles. The HOMs that arise from auto-oxidation processes (see section “[Reactivity](#)”) are frequently of such low volatility that they either undergo one-way condensation to preexisting particles or to help nucleate new particles (Bianchi et al. 2019). On the other hand, some emissions from the tail pipe of an internal-combustion-engine car are initially part of the particulate exhaust from the car, but then evaporate as dilution occurs downwind of the emission source (Robinson et al. 2007). It is important to describe this highly dynamic environment, with molecules readily moving from the gas phase to aerosol particles and back again.

Recent indoor studies also attempt to capture that dynamic partitioning, illustrated nicely by the impact of third-hand tobacco smoke on indoor air quality. Semi-volatile smoking emissions deposited to indoor walls, furniture, and clothing re-volatilize from these surfaces long after, or far away, from the smoking event (DeCarlo et al. 2018). A striking example is the impact of tobacco smoking on the air quality in a nonsmoking movie theater, where high levels of smoke-derived VOCs are observed in the theater having been carried inside on the clothing of occupants who previously smoked outside (Sheu et al. 2020). These VOCs can partition to aerosol particles, changing their composition to partly reflect the composition of the third-hand smoke (Collins et al. 2018b).

Gas-surface partitioning behavior is also apparent in indoor spaces when they are ventilated, by opening windows for example. The mixing ratios of most gases, ozone and NO_x being notable exceptions in most cases, decline because the indoor air is diluted with cleaner air from outside. When the windows are closed, the mixing ratios reestablish steady state levels, reflecting the flux of molecules from indoor surface reservoirs to the gas phase (Collins et al. 2018a; Wang et al. 2020). On the other hand, when excess HONO is added to a house, for example, from a gas stove, it is readily taken up by the indoor surface reservoirs (Collins et al. 2018a). Valuable insights into chemical mechanisms can be readily conducted indoors by such perturbation experiments.

A perturbation also arises from the partitioning-dependence of acidic and basic molecules when acidic (i.e., vinegar) or basic (i.e., ammonia) cleaning solutions are used (Wang et al. 2020). Acidic gases that dissociate upon partitioning into polar indoor surface reservoirs are released to a room when vinegar washing proceeds, that is, the additional acidity shifts the equilibrium state in the surface toward the more volatile, non-dissociated form of the acid. Less water-soluble molecules do not behave in this manner, likely because they are either partitioned into a less polar, more organic-rich surface reservoir or because pH does not affect their volatility.

Outdoor, forced system perturbations are not possible, and we rely instead on the natural variability of the environment to provide such information. For example, the flux of ammonia to and from the Earth’s surface is dependent on the gas-phase ammonia mixing ratio, the pH of the water in the ground, and the pH of the aerosol in

the overlying atmosphere. Such bidirectional flux behavior is only now being incorporated into chemical transport models of the outdoor atmosphere (Whaley et al. 2018; Pleim et al. 2019).

Finally, partitioning to liquid water is a well-known phenomenon in outdoor environments, where water-soluble gases are readily scavenged to cloud water. This is one of the major atmospheric cleansing processes. These lessons are being applied indoors when considering the impact of air conditioning systems on the behavior of water-soluble molecules (Duncan et al. 2019; Wang et al. 2020). Liquid water condenses on the cold coils of the air conditioning unit, leading to partitioning of soluble gases. This process is manifest as oscillatory water-soluble gas mixing ratio behavior in the indoor space, as the air conditioning unit that recycles the air turns off and on. There is a direct analogy to clouds: when it rains, water-soluble gases are removed from the atmosphere, but cloud droplet evaporation leads to their release back to the gas phase. Likewise, with air conditioning, if sufficient water builds up on the cooling coils that it drains from the unit, then the air inside the house is cleaned somewhat of those species. If the water evaporates instead, those species are returned to the gas phase. In addition to impacts on gas-phase composition, control of indoor environmental conditions also affects aerosol phase state and water content (Cummings et al. 2020).

Impact of Dynamics on Chemistry

Simultaneous production, consumption, phase partitioning, and transport of chemicals in the environment necessitates a broad and multifaceted approach to realizing an understanding of the system as a whole. Advances in atmospheric chemistry often come through the interplay of field measurements, laboratory studies, and modeling due to the complex nature of atmospheric chemical processes and their interplay with environmental conditions and the dynamics and structure of the atmosphere (Burkholder et al. 2017).

The atmosphere, while a seemingly continuous fluid medium, has a variety of structural features that control chemistry. Atmospheric boundaries, like zonal boundaries in a building, limit mixing between two parcels of air but are penetrable on relatively long timescales. Certain chemical processes that may be rapid in one region of the atmosphere, such as catalytic ozone destruction in the stratosphere, are unimportant in other regions. The so-called ozone hole in Earth's stratosphere is a seasonal feature that only becomes apparent when cloud particles are abundant during polar sunrise (Molina et al. 1987; Tolbert et al. 1987) and when a distinct fluid dynamical zone, the polar vortex, restricts mixing with air at lower latitudes (Schoeberl and Hartmann 1991). Still, the halocarbon compounds that lead to catalytic ozone depletion (Molina and Rowland 1974) are emitted at Earth's surface and are only capable of reaching the stratosphere because they have atmospheric lifetimes that are much longer than the characteristic mixing time across the tropopause (the boundary that separates the troposphere from the overlying stratosphere). This classic atmospheric chemistry example illustrates

the importance of characterizing the chemical environments of different indoor zones by carefully taking into account the sources, chemistry, transport, and the importance of different phases to a given phenomenon.

Recent studies using real-time measurements of trace gases have illustrated the level of control that transport dynamics and the boundary structure within buildings have on the composition of indoor air. Space- and time-resolved measurements of inhabited buildings (e.g., residences, schools, and offices) require sophisticated instrumentation, broad access to the building for scientists, and careful collection of metadata but can yield important results and information about the impact of indoor activities and building structure on indoor air quality. A notable study using a residence across multiple seasons employed a chemical tracer approach to understand and quantify transport between zones (Liu et al. 2018). The *route* of air exchange between the indoors and outdoors may be important to consider and may include a variety of parallel paths including transit through other zones of the building. Such behavior may have important implications for the chemicals that can be lost from, or entrained within, the air as it moves from outdoors to indoors; physical and chemical aspects of the building itself may have important and non-intuitive impacts on the chemistry that drives indoor air quality.

Modeling the interplay of chemistry and dynamics in the outdoor atmosphere is often performed on a variety of spatial scales: from full global simulations down detailed regional models, and then even further down to simulate the detailed physics of single clouds, for instance. The level of detail in a large-scale model is necessarily coarse and becomes generally more sophisticated as the model scale becomes smaller. Gas phase chemistry can be simulated in roughly any pixel or grid cell size with the assumption that the grid cell is homogeneously mixed. Using this “well mixed” assumption, box modeling has proven useful for a variety of indoor chemistry scenarios for the last few decades. Exciting results from computational fluid dynamics (CFD) models that include chemical mechanisms are beginning to show interesting and important chemical gradients within a single building zone (Won et al. 2019, 2020). Spatially resolved chemical measurements of air within a room could be designed to couple with CFD modeling. Process-level chemical models may be nested within the CFD simulations or could be parameterized to reduce computational expense. Efforts to reduce computational cost have enabled major advancements in atmospheric and chemical modeling. Collaboration between computational scientists (Shiraiwa et al. 2019) will help to translate indoor measurements and process-level studies into actionable outcomes and should strive to produce new computational tools to advance the practice of producing and maintaining healthy environments within buildings.

Working Toward Solutions

Collaboration among experts in diverse fields of engineering, chemistry, biology, public policy, building science, public health, and others will be required to grasp the breadth of interactions that influence indoor air quality and to devise methods for

optimizing the living and working environment where many people spend the majority of their lives. Outdoor atmospheric chemistry issues that represent degraded environmental conditions (e.g., acid rain, stratospheric ozone depletion, urban pollution) have been addressed through broad public policy actions such as the international Montreal Protocol on Substances that Deplete the Ozone Layer or the Clean Air Act in the United States. Indoor air quality, however, is subject to weaker government regulation and has been mostly addressed by concerned homeowners or private institutions. A commercial indoor air quality industry has thus emerged to enable private mitigation actions to take place. Outdoor air quality issues include important aspects of environmental justice, as poor air quality disproportionately affects impoverished and non-white communities (Mikati et al. 2018). Health risks due to ambient airborne particulate matter pollution exposure are decreasing in wealthier regions and increasing in poorer regions worldwide (Murray et al. 2020). Since people spend a dominant fraction of their time indoors (Klepeis et al. 2001), a large portion of unhealthy outdoor air is actually breathed while inside the home. Housing quality has also been shown to have a relationship with rates of asthma and other chronic diseases, specifically among urban public housing inhabitants (Digenis-Bury et al. 2008; Northridge et al. 2010), where poor indoor environmental quality can compound negative effects of outdoor air quality. The comparatively weak ability of poorer groups living in nations with highly developed economies, along with large swaths of people in nations with still developing economies, to implement adaptations to our changing climate will exacerbate inequalities in housing and indoor air quality (Islam and Winkel 2017). The commercialization and private-responsibility that has been built into improving indoor air quality has the potential to multiply existing environmental inequalities as groups of people with low access to financial resources may not have the means or the opportunity to implement engineering solutions or retrofits that mitigate degraded indoor air quality (Northridge et al. 2010). As experts and practitioners of air quality studies and solutions, we must acknowledge and work against structural inequality from our own perspectives and positions of power.

Cross-References

- ▶ [Analytical Tools in Indoor Chemistry](#)
- ▶ [History and Perspective on Indoor Air Quality Research](#)
- ▶ [Impact of Outdoor Particles on Indoor Air](#)
- ▶ [Indoor Gas-Phase Chemistry](#)
- ▶ [Indoor Photochemistry](#)
- ▶ [Indoor Surface Chemistry](#)
- ▶ [Measuring Particle Concentrations and Composition in Indoor Air](#)
- ▶ [Occupant Emissions and Chemistry](#)
- ▶ [Predicting VOC and SVOC Concentrations in Complex Indoor Environments](#)
- ▶ [Real-Time Monitoring of Indoor Organic Compounds](#)

- ▶ Sampling and Analysis of Semi-volatile Organic Compounds (SVOCs) in Indoor Environments
- ▶ Sampling and Analysis of VVOCs and VOCs in Indoor Air
- ▶ Semi-Volatile Organic Compounds (SVOCs)
- ▶ Source/Sink Characteristics of SVOCs
- ▶ Source/Sink Characteristics of VVOCs and VOCs
- ▶ Very Volatile Organic Compounds (VVOCs)
- ▶ Volatile Organic Compounds (VOCs)

Acknowledgments This work was supported by the Chemistry of Indoor Environments program of the Alfred P. Sloan Foundation. JPDA was supported by grant G-2019-11404. DBC was supported by the Surface Consortium for the Chemistry of Indoor Environments (SURF-CIE) from the Alfred P. Sloan Foundation (G-2019-12365) via the University of California, San Diego.

References

- Alwarda R, Zhou S, Abbatt JPD (2018) Heterogeneous oxidation of indoor surfaces by gas-phase hydroxyl radicals. *Indoor Air* 28:655–664. <https://doi.org/10.1111/ina.12476>
- Ault AP, Grassian VH, Carslaw N et al (2020) Indoor surface chemistry: developing a molecular picture of reactions on indoor interfaces. *Chem* 6:3203–3218. <https://doi.org/10.1016/j.chempr.2020.08.023>
- Bianchi F, Kurtén T, Riva M et al (2019) Highly oxygenated organic molecules (HOM) from gas-phase autoxidation involving peroxy radicals: a key contributor to atmospheric aerosol. *Chem Rev* 119:3472–3509. <https://doi.org/10.1021/acs.chemrev.8b00395>
- Bope A, Haines SR, Hegarty B et al (2019) Degradation of phthalate esters in floor dust at elevated relative humidity. *Environ Sci:Process Impacts* 21:1268–1279. <https://doi.org/10.1039/C9EM00050J>
- Burkholder JB, Abbatt JPD, Barnes I et al (2017) The essential role for laboratory studies in atmospheric chemistry. *Environ Sci Technol* 51:2519–2528. <https://doi.org/10.1021/acs.est.6b04947>
- Burton WM, Stewart NG (1960) Use of long-lived natural radioactivity as an atmospheric tracer. *Nature* 186:584–589. <https://doi.org/10.1038/186584a0>
- Carlton AG, de Gouw J, Jimenez JL et al (2018) Synthesis of the southeast atmosphere studies: investigating fundamental atmospheric chemistry questions. *Bull Am Met Soc* 99:547–567. <https://doi.org/10.1175/BAMS-D-16-0048.1>
- Collins DB, Grassian VH (2018) Gas-liquid interfaces in the atmosphere: impacts, complexity, and challenges. In: *Physical chemistry of gas-liquid interfaces*. Elsevier, pp 271–313
- Collins DB, Hems RF, Zhou S et al (2018a) Evidence for gas–surface equilibrium control of indoor nitrous acid. *Environ Sci Technol* 52:12419–12427. <https://doi.org/10.1021/acs.est.8b04512>
- Collins DB, Wang C, Abbatt JPD (2018b) Selective uptake of third-hand tobacco smoke components to inorganic and organic aerosol particles. *Environ Sci Technol* 52:13195–13201. <https://doi.org/10.1021/acs.est.8b03880>
- Crounse JD, Nielsen LB, Jorgensen S et al (2013) Autoxidation of organic compounds in the atmosphere. *J Phys Chem Lett* 4:3513–3520. <https://doi.org/10.1021/jz4019207>
- Cummings BE, Li Y, DeCarlo PF et al (2020) Indoor aerosol water content and phase state in U.S. residences: impacts of relative humidity, aerosol mass and composition, and mechanical system operation. *Environ Sci Process Impacts* 22:2031–2057. <https://doi.org/10.1039/D0EM00122H>
- Cunliffe M, Murrell JC (2009) The sea-surface microlayer is a gelatinous biofilm. *ISME J* 3:1001–1003. <https://doi.org/10.1038/ismej.2009.69>

- Dall’Osto M, Airs RL, Beale R et al (2019) Simultaneous detection of alkylamines in the surface ocean and atmosphere of the antarctic sympagic environment. *ACS Earth Space Chem.* <https://doi.org/10.1021/acsearthspacechem.9b00028>
- DeCarlo PF, Avery AM, Waring MS (2018) Thirdhand smoke uptake to aerosol particles in the indoor environment. *Science Adv* 4:eaap8368. <https://doi.org/10.1126/sciadv.aap8368>
- Digenis-Bury EC, Brooks DR, Chen L et al (2008) Use of a population-based survey to describe the health of Boston public housing residents. *Am J Public Health* 98:85–91. <https://doi.org/10.2105/AJPH.2006.094912>
- Duncan SM, Tomaz S, Morrison G et al (2019) Dynamics of residential water-soluble organic gases: insights into sources and sinks. *Environ Sci Technol* 53:1812–1821. <https://doi.org/10.1021/acs.est.8b05852>
- Emerson SR, Hedges JI (2008) Chemical oceanography and the marine carbon cycle. Cambridge University Press, Cambridge
- Faiola C, Taipale D (2020) Impact of insect herbivory on plant stress volatile emissions from trees: a synthesis of quantitative measurements and recommendations for future research. *Atmos Environ X* 5:100060. <https://doi.org/10.1016/j.aeaoa.2019.100060>
- Farmer DK (2019) Analytical challenges and opportunities for indoor air chemistry field studies. *Anal Chem* 91:3761–3767. <https://doi.org/10.1021/acs.analchem.9b00277>
- Finlayson-Pitts BJ, Pitts JN (2000) Chemistry of the upper and lower atmosphere: theory, experiments, and applications. Academic Press, San Diego
- Frew NM (1997) The role of organic films in air–sea gas exchange. In: Liss PS, Duce RA (eds) The sea surface and global change. Cambridge University Press, Cambridge, pp 121–172
- Frey HC, Unal A, Rouphail NM, Colyar JD (2003) On-road measurement of vehicle tailpipe emissions using a portable instrument. *J Air Waste Manage Assoc* 53:992–1002. <https://doi.org/10.1080/10473289.2003.10466245>
- Gardner CM, Hoffman K, Stapleton HM, Gunsch CK (2020) Exposures to Semivolatile organic compounds in indoor environments and associations with the gut microbiomes of children. *Environ Sci Technol Lett Article ASAP*. <https://doi.org/10.1021/acs.estlett.0c00776>
- Gentner DR, Jathar SH, Gordon TD et al (2017) Review of urban secondary organic aerosol formation from gasoline and diesel motor vehicle emissions. *Environ Sci Technol* 51: 1074–1093. <https://doi.org/10.1021/acs.est.6b04509>
- Gilbert JA, Stephens B (2018) Microbiology of the built environment. *Nat Rev Microbiol* 16: 661–670. <http://dx.doi.org.ezproxy.bucknell.edu/10.1038/s41579-018-0065-5>
- Gómez Alvarez E, Amedro D, Afif C et al (2013) Unexpectedly high indoor hydroxyl radical concentrations associated with nitrous acid. *Proc Natl Acad Sci U S A* 110:13294–13299. <https://doi.org/10.1073/pnas.1308310110>
- Haagen-Smit AJ, Fox MM (1956) Ozone formation in photochemical oxidation of organic substances. *Ind Eng Chem* 48:1484–1487. <https://doi.org/10.1021/ie51400a033>
- Hand JL, Prenni AJ, Copeland S et al (2020) Thirty years of the Clean Air Act Amendments: impacts on haze in remote regions of the United States (1990–2018). *Atmos Environ* 243: 117865. <https://doi.org/10.1016/j.atmosenv.2020.117865>
- Islam SN, Winkel J (2017) Climate change and social inequality. United Nations Department of Economic and Social Affairs
- Jang M, Czoschke NM, Lee S, Kamens RM (2002) Heterogeneous atmospheric aerosol production by acid-catalyzed particle-phase reactions. *Science* 298:814–817. <https://doi.org/10.1126/science.1075798>
- Kiechle MA (2017) Smell detectives: an olfactory history of nineteenth-century urban America. University of Washington Press, Seattle
- Kleppeis NE, Nelson WC, Ott WR et al (2001) The National Human Activity Pattern Survey (NHAPS): a resource for assessing exposure to environmental pollutants. *J Expo Sci Env Epidemiol* 11:231–252. <https://doi.org/10.1038/sj.jea.7500165>

- Kowal SF, Allen SR, Kahan TF (2017) Wavelength-resolved photon fluxes of indoor light sources: implications for HO_x production. *Environ Sci Technol* 51:10423–10430. <https://doi.org/10.1021/acs.est.7b02015>
- Kroll JH, Heald CL, Cappa CD et al (2020) The complex chemical effects of COVID-19 shutdowns on air quality. *Nat Chem* 12:777–779. <https://doi.org/10.1038/s41557-020-0535-z>
- Kruza M, McFiggans G, Waring MS et al (2020) Indoor secondary organic aerosols: towards an improved representation of their formation and composition in models. *Atmos Environ* 240: 117784. <https://doi.org/10.1016/j.atmosenv.2020.117784>
- Laskin J, Laskin A, Nizkorodov SA (2018) Mass spectrometry analysis in atmospheric chemistry. *Anal Chem* 90:166–189. <https://doi.org/10.1021/acs.analchem.7b04249>
- Liu Y, Misztal PK, Xiong J et al (2018) Detailed investigation of ventilation rates and airflow patterns in a northern California residence. *Indoor Air* 28:572–584. <https://doi.org/10.1111/ina.12462>
- Mahowald NM, Engelstaedter S, Luo C et al (2009) Atmospheric iron deposition: global distribution, variability, and human perturbations. *Annu Rev Mar Sci* 1:245–278. <https://doi.org/10.1146/annurev.marine.010908.163727>
- Martin ST, Artaxo P, Machado L et al (2017) The Green Ocean Amazon Experiment (GoAmazon2014/5) observes pollution affecting gases, aerosols, clouds, and rainfall over the rain Forest. *Bull Am Met Soc* 98:981–997. <https://doi.org/10.1175/BAMS-D-15-00221.1>
- Mattila JM, Lakey PSJ, Shiraiwa M et al (2020) Multiphase chemistry controls inorganic chlorinated and nitrogenated compounds in indoor air during bleach cleaning. *Environ Sci Technol* 54:1730–1739. <https://doi.org/10.1021/acs.est.9b05767>
- Mayer KJ, Wang X, Santander MV et al (2020) Secondary marine aerosol plays a dominant role over primary sea spray aerosol in cloud formation. *ACS Cent Sci Article ASAP*. <https://doi.org/10.1021/acscentsci.0c00793>
- McDonald BC, de Gouw JA, Gilman JB et al (2018) Volatile chemical products emerging as largest petrochemical source of urban organic emissions. *Science* 359:760–764. <https://doi.org/10.1126/science.aaoq524>
- Mikati I, Benson AF, Luben TJ et al (2018) Disparities in distribution of particulate matter emission sources by race and poverty status. *Am J Public Health* 108:480–485. <https://doi.org/10.2105/AJPH.2017.304297>
- Molina MJ, Rowland FS (1974) Stratospheric sink for chlorofluoromethanes: chlorine atom-catalysed destruction of ozone. *Nature* 249:810–812. <https://doi.org/10.1038/249810a0>
- Molina MJ, Tso T-L, Molina LT, Wang FC-Y (1987) Antarctic stratospheric chemistry of chlorine nitrate, hydrogen chloride, and ice: release of active chlorine. *Science* 238:1253–1257. <https://doi.org/10.1126/science.238.4831.1253>
- Morrison G (2008) Interfacial chemistry in indoor environments. *Environ Sci Technol* 42: 3495–3499. <https://doi.org/10.1021/es087114b>
- Morrison G, Lakey PSJ, Abbatt J, Shiraiwa M (2019) Indoor boundary layer chemistry modeling. *Indoor Air* 29:956–967. <https://doi.org/10.1111/ina.12601>
- Murray DM, Burmaster DE (1995) Residential air exchange rates in the United States: empirical and estimated parametric distributions by season and climatic region. *Risk Anal* 15:459–465. <https://doi.org/10.1111/j.1539-6924.1995.tb00338.x>
- Murray CJL, Aravkin AY, Zheng P et al (2020) Global burden of 87 risk factors in 204 countries and territories, 1990–2019: a systematic analysis for the global burden of disease study 2019. *Lancet* 396:1223–1249. [https://doi.org/10.1016/S0140-6736\(20\)30752-2](https://doi.org/10.1016/S0140-6736(20)30752-2)
- Northridge J, Ramirez OF, Stingone JA, Claudio L (2010) The role of housing type and housing quality in urban children with asthma. *J Urban Health* 87:211–224. <https://doi.org/10.1007/s11524-009-9404-1>
- Parthasarathy S, Maddalena RL, Russell ML, Apte MG (2011) Effect of temperature and humidity on formaldehyde emissions in temporary housing units. *J Air Waste Manage Assoc* 61:689–695. <https://doi.org/10.3155/1047-3289.61.6.689>

- Pleim JE, Ran L, Appel W et al (2019) New bidirectional ammonia flux model in an air quality model coupled with an agricultural model. *J Adv Model Earth Sy* 11:2934–2957. <https://doi.org/10.1029/2019MS001728>
- Prather KA, Bertram TH, Grassian VH et al (2013) Bringing the ocean into the laboratory to probe the chemical complexity of sea spray aerosol. *Proc Natl Acad Sci U S A* 110:7550–7555. <https://doi.org/10.1073/pnas.1300262110>
- Ravishankara AR (1997) Heterogeneous and multiphase chemistry in the troposphere. *Science* 276: 1058–1065. <https://doi.org/10.1126/science.276.5315.1058>
- Robinson AL, Donahue NM, Shrivastava MK et al (2007) Rethinking organic aerosols: Semi-volatile emissions and photochemical aging. *Science* 315:1259–1262. <https://doi.org/10.1126/science.1133061>
- Salimifard P, Rim D, Gomes C et al (2017) Resuspension of biological particles from indoor surfaces: effects of humidity and air swirl. *Sci Total Environ* 583:241–247. <https://doi.org/10.1016/j.scitotenv.2017.01.058>
- Schneider SR, Collins DB, Lim CY et al (2019) Formation of secondary organic aerosol from the heterogeneous oxidation by ozone of a phytoplankton culture. *ACS Earth Space Chem* 3: 2298–2306. <https://doi.org/10.1021/acsearthspacechem.9b00201>
- Schoeberl MR, Hartmann DL (1991) The dynamics of the stratospheric polar vortex and its relation to springtime ozone depletions. *Science* 251:46–52. <https://doi.org/10.1126/science.251.4989.46>
- Sheu R, Stönnér C, Ditto JC et al (2020) Human transport of thirdhand tobacco smoke: a prominent source of hazardous air pollutants into indoor nonsmoking environments. *Science Adv* 6: eaay4109. <https://doi.org/10.1126/sciadv.aay4109>
- Shiraiwa M, Carslaw N, Tobias DJ et al (2019) Modelling consortium for chemistry of indoor environments (MOCCIE): integrating chemical processes from molecular to room scales. *Environ Sci Process Impacts* 21:1240–1254. <https://doi.org/10.1039/C9EM00123A>
- Tolbert MA, Rossi MJ, Malhotra R, Golden DM (1987) Reaction of chlorine nitrate with hydrogen chloride and water at antarctic stratospheric temperatures. *Science* 238:1258–1260. <https://doi.org/10.1126/science.238.4831.1258>
- Wang X, Sultana CM, Trueblood J et al (2015) Microbial control of sea spray aerosol composition: a tale of two blooms. *ACS Cent Sci* 1:124–131. <https://doi.org/10.1021/acscentsci.5b00148>
- Wang C, Collins DB, Arata C et al (2020) Surface reservoirs dominate dynamic gas-surface partitioning of many indoor air constituents. *Science Adv* 6:eaay8973. <https://doi.org/10.1126/sciadv.aay8973>
- Waring MS (2014) Secondary organic aerosol in residences: predicting its fraction of fine particle mass and determinants of formation strength. *Indoor Air* 24:376–389. <https://doi.org/10.1111/ina.12092>
- Weschler CJ (2011) Chemistry in indoor environments: 20 years of research. *Indoor Air* 21:205–218. <https://doi.org/10.1111/j.1600-0668.2011.00713.x>
- Whaley CH, Makar PA, Shephard MW et al (2018) Contributions of natural and anthropogenic sources to ambient ammonia in the Athabasca Oil Sands and north-western Canada. *Atmos Chem Phys* 18:2011–2034. <https://doi.org/10.5194/acp-18-2011-2018>
- Won Y, Waring M, Rim D (2019) Understanding the spatial heterogeneity of indoor OH and HO₂ due to photolysis of HONO using computational fluid dynamics simulation. *Environ Sci Technol* 53:14470–14478. <https://doi.org/10.1021/acs.est.9b06315>
- Won Y, Lakey PSJ, Morrison G et al (2020) Spatial distributions of ozonolysis products from human surfaces in ventilated rooms. *Indoor Air* 30:1229–1240. <https://doi.org/10.1111/ina.12700>
- Wong JPS, Carslaw N, Zhao R et al (2017) Observations and impacts of bleach washing on indoor chlorine chemistry. *Indoor Air* 27:1082–1090. <https://doi.org/10.1111/ina.12402>
- Wurl O, Ekau W, Landing WM et al (2017) Sea surface microlayer in a changing ocean – a perspective. *Elementa Sci Anthrop* 5:31. <https://doi.org/10.1525/elementa.228>

- Xie X, Li Y, Chwang ATY et al (2007) How far droplets can move in indoor environments – revisiting the Wells evaporation-falling curve. *Indoor Air* 17:211–225. <https://doi.org/10.1111/j.1600-0668.2007.00469.x>
- Young CJ, Zhou S, Siegel JA, Kahan TF (2019) Illuminating the dark side of indoor oxidants. *Environ Sci Process Impacts* 21:1229–1239. <https://doi.org/10.1039/C9EM0011E>
- Zhou S, Hwang BCH, Lakey PSJ et al (2019a) Multiphase reactivity of polycyclic aromatic hydrocarbons is driven by phase separation and diffusion limitations. *PNAS* 116:11658–11663. <https://doi.org/10.1073/pnas.1902517116>
- Zhou Z, Zhou S, Abbatt J (2019b) Kinetics and condensed-phase products in multiphase Ozonolysis of an unsaturated triglyceride. *Environ Sci Technol* 53:12467–12475. <https://doi.org/10.1021/acs.est.9b04460>



Indoor Gas-Phase Chemistry

28

Nicola Carslaw

Contents

Introduction	838
Gas-Phase Chemistry	839
Reactions of Ozone	839
Reactions of the Hydroxyl Radical	842
Reactions of the Nitrate Radical	846
Reactions of the Chlorine Radical	848
Comparing Indoor Oxidants	850
Role of Gas-Phase Chemistry in Particle Formation	850
Conclusion	851
Cross-References	852
References	852

Abstract

There are many similarities between indoor and outdoor air chemistry, not least the richness of the oxidation chemistry. Indoors, oxidation is driven to a large extent by ozone and the hydroxyl radical, with nitrate and chlorine radicals also making a contribution depending on the conditions. These reactions can lead to a variety of products, many of which are multifunctional and relatively long-lived. Some of them can then take part in further reactions indoors. This chapter summarizes the main gas-phase reactions indoors and also highlights the interconnectedness between some of the oxidation reactions, particularly between ozone and the hydroxyl radical. Oxidation of common indoor species such as monoterpenes by ozone leads to the formation of hydroxyl and peroxy radicals. There is then a range of radical-radical reactions possible that further transform the gas-phase composition indoors. Oxidation of terpenes and other volatile organic compounds by the hydroxyl radical can also produce ozone if there is

N. Carslaw (✉)

Department of Environment and Geography, University of York, York, UK
e-mail: nicola.carslaw@york.ac.uk

sufficient light indoors, so that these two oxidants are likely to coexist for many conditions typically experienced in buildings.

Keywords

Hydroxyl radical · Peroxy radical · Ozone · Nitrate radical · Chlorine radical

Introduction

Sources of air pollution are diverse indoors, with pollutants generated through activities such as cooking (particulate matter (PM), carbon monoxide (CO), nitrogen oxides (NO_x)), cleaning (mainly volatile organic compounds (VOCs) such as monoterpene, but also chlorinated compounds), and smoking (CO, PM, NO_x , and VOCs). Air pollutants can also be emitted from furnishing and building materials, home decoration products, and personal care products (Nazaroff and Weschler 2004). Consequently, many air pollutants are ubiquitous in typical buildings, and indoor VOC concentrations are often higher than those observed outdoors (Sarwar et al. 2002; Saarela et al. 2003), particularly during activities such as cleaning (Singer et al. 2006).

What is perhaps more surprising is that despite the low light levels indoors compared to outdoors, there is a vast array of gas-phase chemistry that can happen under typical indoor conditions, with many of these reactions familiar to those readers who have studied the chemistry of the ambient atmosphere. Of course, differences between conditions indoors and outdoors mean that indoor reactions can be more or less important than their outdoor counterparts. However, just like outdoors, much of the indoor gas-phase chemistry is driven by oxidation reactions, particularly with ozone (O_3) and hydroxyl radicals (OH) and to a lesser extent by nitrate radicals (NO_3^-) and chlorine (Cl) radicals.

The key requirement for a gas-phase reaction to be important indoors is that it can occur on a competitive time scale with ventilation (Weschler and Shields 2000). What does this mean in practice? Typical air exchange rates with outdoors can range from perhaps 0.2 h^{-1} for an airtight house to 2.0 h^{-1} for a leakier construction (Weschler 2000). So taking the value of 0.2 h^{-1} , for a gas-phase reaction to compete with removal via ventilation, its loss rate would need to exceed 0.2 h^{-1} . If we take the example of ozone, the loss rate ($\text{molecule cm}^{-3} \text{ s}^{-1}$) due to ventilation can be expressed simply as:

$$\text{Loss rate of ozone due to ventilation} = 0.2 / 3600 \times [\text{ozone}]$$

Note that the square brackets denote concentration (molecule cm^{-3}), and the ventilation rate has been converted to units of per second. Now, if we consider gas-phase loss of ozone, such as through reaction with limonene, then:

$$\text{Loss rate of ozone due to reaction with limonene} = k \times [\text{ozone}] \times [\text{limonene}]$$

where k is the rate coefficient for the reaction of ozone with limonene ($2.2 \times 10^{-16} \text{ cm}^{-3} \text{ molecule}^{-1} \text{ s}^{-1}$ Table 2). So we can now compare the losses. The ozone concentration can be ignored as it would be the same for each loss:

$$0.2/3600 = 2.2 \times 10^{-12} * [\text{Limonene}]$$

By rearranging this equation, we find that gas-phase loss will dominate ventilation loss when the limonene concentration exceeds $\sim 2.5 \times 10^{11} \text{ molecule cm}^{-3}$ (approximately 10 ppb), a situation that is frequently encountered indoors such as during cleaning (Singer et al. 2006). A similar calculation for the hydroxyl and nitrate radicals using the rate coefficients in Table 2 shows that limonene concentrations need to exceed less than 1 ppt for gas-phase loss to dominate removal of these species by ventilation. For limonene at least, oxidation by these species competes with, or significantly exceeds, removal by dilution from air exchange.

This chapter provides a summary of the key gas-phase reactions that occur indoors, the main reaction pathways for these reactions, and the species that can be formed through the resulting indoor air chemistry.

Gas-Phase Chemistry

Reactions of Ozone

Ozone (O_3) is a powerful oxidizing agent and will readily attack any molecule that contains a carbon-carbon double bond, such as alkenes and monoterpenes (Atkinson and Arey 2003). Unlike outdoors, where the hydroxyl radical (OH) tends to dominate oxidation of VOCs, the lower light levels indoors mean that the photochemical reactions that lead to OH production are less favored, and VOC oxidation by ozone becomes relatively more important. Ozone concentrations indoors are much lower than outdoors, as it rapidly deposits on indoor surfaces and also reacts with nitric oxide (NO). Consequently, indoor ozone concentrations tend to be 0.2–0.7 of those outdoors (Weschler 2000).

One group of indoor reactions that has received significant attention to date has been ozone-monoterpene reactions (Weschler and Carslaw 2018). These reactions have been studied in detail for several reasons: (i) monoterpenes are ubiquitous indoors given they are used in large quantities in personal care and cleaning products (Nazaroff and Weschler 2004); (ii) ozone is also ubiquitous indoors, gaining access from outdoors via windows, doors, and cracks in the building envelope as well as from indoor sources such as photocopiers and laser printers where they exist (Weschler 2000); and (iii) ozone-monoterpene reactions are fast enough to compete with typical air exchange rates indoors (Weschler and Carslaw 2018) and can produce a range of short-lived (e.g., radicals) and longer-lived complex multi-functional species in both the gas and condensed phases (Walser et al. 2007).

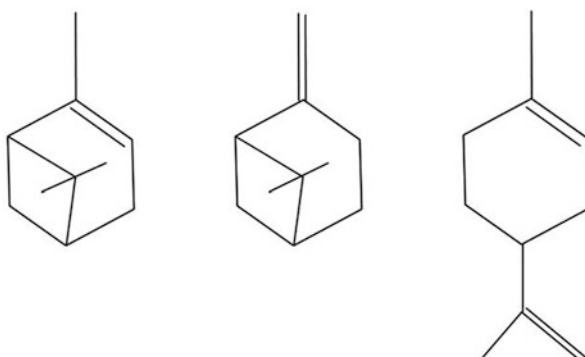
These reactions have also been widely studied by the atmospheric chemistry community, as monoterpenes are emitted in vast quantities from vegetation and their high reactivity and propensity to form secondary organic aerosol have implications for chemistry and climate (Steiner 2020).

Just like outdoors, there are seasonal and latitudinal implications for the importance of ozone concentrations and hence ozone chemistry indoors (Weschler 2000). High NO_x concentrations reduce those of ozone and tend to peak in the winter months outdoors when NO_x emissions are higher. Outdoor ozone concentrations therefore tend to peak in spring/summer, coinciding with the time of year when windows are typically open more often. Given the major contribution of outdoor ozone to indoor ozone concentrations, the location, time of year, and air exchange rate with outdoors are all vitally important in determining the indoor ozone concentration.

The monoterpenes are a group of species that have the formula C₁₀H₁₆ and are derived from two isoprene (C₅H₈) units. Figure 1 shows the structures of three common monoterpenes: α -pinene, β -pinene, and limonene. The presence of monoterpenes in numerous products and materials used indoors gives them an easy route into indoor environments (Nazarioff and Weschler 2004; Singer et al. 2006). Despite a common chemical formula, different monoterpenes have very different distributions of atoms within their complex ring structures, and the location of their one or two double bonds can be external and/or internal. The position of this double bond can have an impact on the resulting reactivity of these species, as well as the products that are formed when they are oxidized (Youssefi and Waring 2015).

The first step in the reactions between ozone and double-bonded species, such as monoterpenes, involves the addition of ozone across the double bond to form an ozonide. As ozonide species are energy-rich and very unstable, they quickly disintegrate to form stable carbonyl products, hydroxyl radicals, and Criegee Intermediate (CI) radical species (Aschmann et al. 2002). Figure 2 shows the first few steps of limonene ozonolysis as an example. Note that the ozonide is not shown here given it rapidly disintegrates, so the two products shown after the preliminary oxidation step of limonene by ozone in Fig. 2 are the CI radical species.

Fig. 1 The structures of three monoterpenes, common in indoor products such as cleaning products and fragrances: from the left are shown α -pinene, β -pinene, and δ -limonene



There are several implications of these reactions for indoor air chemistry. The formation of the hydroxyl radical (Fig. 2) allows the potential for even more oxidation chemistry (see next section). Hydroxyl radicals participate in similar reactions indoors to those they are involved in outdoors, including oxidizing numerous VOCs. Second, it is important to note that as well as forming OH radicals, ozone-monoterpene/alkene reactions also produce peroxy radicals (Fig. 2). This radical production then opens up the possibility of even more reactions indoors.

Given that ozone-monoterpene reactions produce OH radicals (Fig. 2) and that OH radicals can also react with monoterpenes (see next section), this raises the question about whether the monoterpenes act as a source or sink of OH. That depends on the rates of reaction of the individual monoterpene with OH and ozone, as well as the yield of OH formation from the ozone-monoterpene reaction (i.e., how many OH radicals are formed each time ozone reacts with a monoterpene). Table 1 illustrates this point for a selection of common monoterpenes.

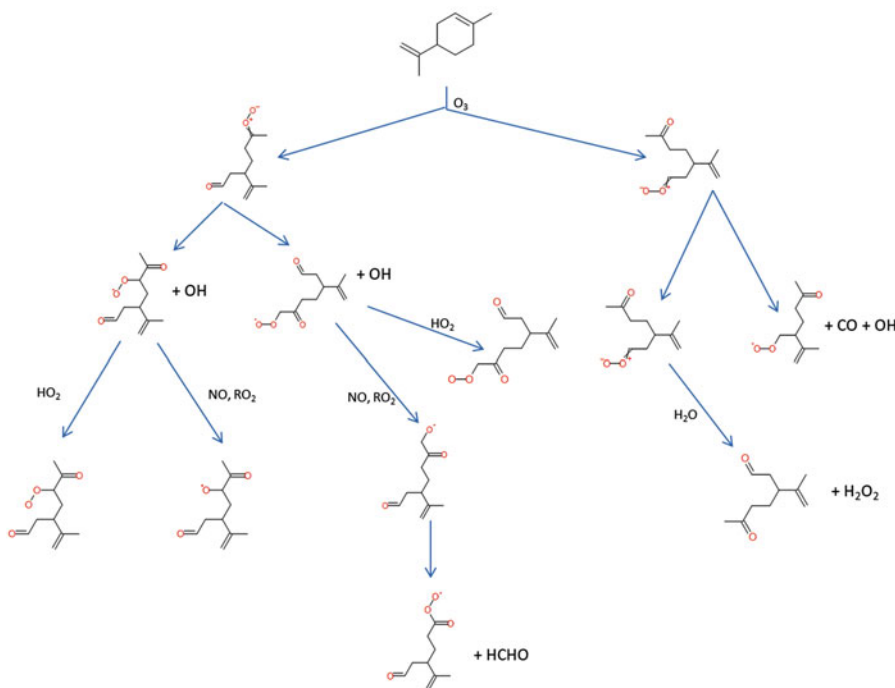


Fig. 2 The first three oxidation steps of limonene by ozone according to the master chemical mechanism, MCM (MCM n.d.). The blue arrows denote the dominant reaction pathways during cleaning with a limonene-based cleaner (based on results from Carslaw 2013) with the reactant that drives each reaction alongside the arrow. Absence of a reactant alongside an arrow means that the molecule decomposes/is collisionally stabilized to form the new species (e.g., the subsequent reactions of the CI radicals formed in the first step). Also shown are places where an OH radical is formed

Table 1 The OH yield following reaction between various monoterpenes and ozone, the rate coefficients for the reaction of each monoterpene with ozone and OH ($\text{cm}^3 \text{ molecule}^{-1} \text{ s}^{-1}$) (Atkinson et al. 2004; IUPAC Task Group n.d.) and the ozone concentration in ppb (O_3 switch) at which the VOC switches from being an OH sink to an OH source, assuming a background OH concentration of $3.4 \times 10^5 \text{ molecule cm}^{-3}$ (~0.01 ppt) (Carslaw 2007)

	OH yield	$k(\text{O}_3)$	$k(\text{OH})$	O_3 switch /ppb
Limonene	0.66	2.20×10^{-16}	1.65×10^{-10}	15
α -Pinene	0.8	9.60×10^{-17}	5.30×10^{-11}	9
β -Pinene	0.3	1.90×10^{-17}	7.60×10^{-11}	181
α -Terpinene	0.38	1.90×10^{-14}	3.50×10^{-10}	0.7
α -Terpinolene	0.7	1.60×10^{-15}	2.20×10^{-10}	3

The first point to notice from Table 1 is that the rate coefficients for reaction of monoterpenes with ozone are much slower than for OH. However, the indoor ozone concentration is often 5 to 6 orders of magnitude larger than that of OH indoors, which compensates somewhat. Table 1 also shows that there is a large variation in the OH yields for the different monoterpenes. Again, these variations relate to the structural differences as discussed earlier. The final column in Table 1 shows the ozone concentration at which a monoterpene will switch from being an OH sink to an OH source, assuming a background OH concentration of $3.4 \times 10^5 \text{ molecule cm}^{-3}$ (~0.01 ppt) as estimated in a modeling study by Carslaw (2007). It is likely that most of these monoterpenes act as net radical sources given typical indoor ozone concentrations (Weschler 2000), though β -pinene will always be an OH sink indoors. Note also that given ozonolysis of monoterpenes produces peroxy radicals and that these can be recycled to OH (see next section), these ozone concentrations are likely to be an upper limit for where monoterpenes become OH sources indoors.

Reactions of the Hydroxyl Radical

Once the hydroxyl radical is formed indoors such as through the ozonolysis reactions discussed in the previous section (Fig. 2), or indeed via indoor photolysis, it can initiate oxidation reactions just as for the outdoor environment, leading to more oxidative chemistry indoors than might otherwise have been expected. Reaction rates for the hydroxyl radical with VOCs are much faster than both its deposition onto indoor surfaces and exchange with outdoor air, which are negligible for OH indoors (Weschler and Shields 1996). Modeling studies since the 1990s typically predicted concentrations of the order of $1\text{--}4 \times 10^5 \text{ molecule cm}^{-3}$ (Weschler and Shields 1996; Sarwar et al. 2002; Carslaw 2007) and that the most important source of OH indoors was through the reaction of ozone with monoterpenes (Sarwar et al. 2002; Carslaw 2007; Mendez et al. 2017). These predicted indoor OH concentrations are about a factor of 5–10 less than outdoors in summer and comparable to outdoor concentrations at nighttime (Faloona et al. 2001) and during the daytime in winter (Heard et al. 2004).

These predicted background concentrations have been confirmed through recent measurement studies, which have also demonstrated that concentrations of OH can be substantially higher indoors. Gomez-Alvarez et al. (Gomez Alvarez et al. 2013) found that OH concentrations were elevated (1.8×10^6 molecule cm^{-3}) near windows owing to the photolysis of HONO (nitrous acid). Carslaw et al. (2017) measured elevated concentrations of OH radicals (4×10^6 molecule cm^{-3}) during surface cleaning with a limonene-based cleaner in a University PC classroom. In the same study, they operated an air-cleaning device which elevated OH concentrations even more, peaking at 2×10^7 molecule cm^{-3} . Background OH concentrations in this study were determined to be 6.5×10^5 molecule cm^{-3} . The enhanced indoor OH concentrations during cleaning are similar to, or even greater than ambient concentrations. Clearly then, OH formation and subsequent OH-driven oxidation is possible for a range of indoor conditions and could be particularly important depending on the activities that are taking place within a building.

Just like outdoors, OH is a powerful oxidant and very reactive indoors, able to react with NO_2 and NO, as well as a range of VOCs. It is less selective than ozone and reacts with single-bonded VOC species too, though the fastest reactions tend to be with the species that ozone preferentially reacts with, such as alkenes and monoterpenes (Atkinson et al. 2004). When OH reacts with VOCs, it can abstract an H atom to form an alkyl and then a peroxy radical. As an example, the initial net step for oxidation of ethane to form ethyl peroxy radicals is shown in R1:



Note that reaction R1 really encapsulates two steps (R1a and R1b):



However, given the ethyl alkyl radical formed in reaction R1a is so reactive, and that the quantity of oxygen in the atmosphere is so high, it is reasonable to write these two as one step (R1) and this convention will be adopted throughout the rest of this chapter. OH reactions with other VOCs follow the same general mechanism as in R1.

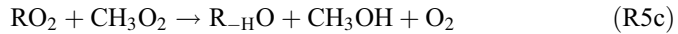
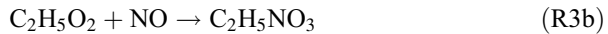
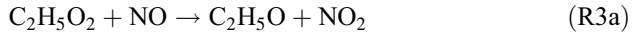
For alkenes (and other double-bonded species), OH can initially add to the double bond to form a peroxy radical, as shown for ethene in R2:



Oxidation by the OH radical is much more complicated for aromatic species. Toluene is a relatively common indoor VOC (Wang et al. 2017), and following reaction with OH can produce a number of different products with various yields (Jenkin et al. 2003; Bloss et al. 2005). The main oxidation pathway (~65%) leads to the production of a rather complex peroxy radical that involves breaking the original aromatic ring. The reaction also produces a second peroxy radical that maintains the

aromatic ring structure but at a lower yield (7%), as well as cresol (18%) and 2, 3-epoxy-6-oxo-4-heptenal (10%).

Once the peroxy radicals are formed, they either react with nitric oxide, NO (R3), or with other peroxy radicals (R4 and R5):



RO_2 is used here to denote peroxy radicals in general (where R denotes an alkyl group). The importance of the different pathways in R5 depends on the parent hydrocarbon. Indeed, whether a peroxy radical reacts with NO or another peroxy radical is determined by the particular conditions. If there is a source of NO_x indoors (e.g., a gas cooker), reactions such as R3 would be the most likely fate of the peroxy radicals. However, in the absence of NO_x sources indoors, or any from outdoors (e.g., if the building in question is not next to a busy road where pollutants are able to ingress), radical propagation reactions such as those represented by R4 and R5 would be more important. Note that R3b shows the minor (<1%) pathway for R3, to form ethyl nitrate. For the equivalent peroxy radical for dodecane (12 carbon atoms), the organic nitrate pathway is 44% of the total (Jenkin et al. 1997). The minor route represented by R3b becomes more important as the hydrocarbon gets bigger.

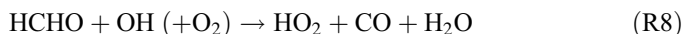
The $\text{C}_2\text{H}_5\text{O}$ radical produced in R3a can react further as shown in R6, in this case, to form acetaldehyde and the hydroperoxy radical (HO_2):



Depending on the indoor conditions, the hydroperoxy radical can then be rapidly recycled to OH as shown in R7, or react with other peroxy radicals, such as through reactions like R4:

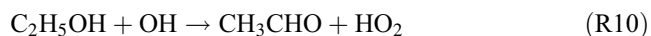


Reactions R5 and R6 also produce aldehyde species, with the generic structure RCHO (where R can be H or an alkyl group). Once formed, aldehydes can react with OH, or to be photolyzed as shown in R8 and R9 respectively for formaldehyde (HCHO):

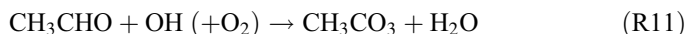


although deposition to surfaces and ventilation are likely to be more important removal mechanisms (Mendez et al. 2015). Reactions R7 and R8 are examples of propagation reactions between OH and HO₂ radicals. Just like outdoors, where one exists, so does the other, and so rapid regeneration of OH becomes possible through these cycles, opening up the possibility of further VOC oxidation reactions.

As well as aldehydes, these reactions lead to the production of other oxygenated VOCs such as peroxides (R4) and alcohols (R5b, R5c). The main fate of peroxides indoors is likely to be deposition onto surfaces and air exchange with outdoors (Fan et al. 2005), though partitioning to form secondary organic aerosol (SOA) is also likely to be significant for the larger peroxides (Carslaw 2013). This means that reactions such as R4 represent a radical termination reaction, effectively removing radicals from the system. The alcohols will likely react with OH to form HO₂ and an aldehyde, such as shown for ethanol in R10 to form acetaldehyde, another example of propagation of OH to HO₂ radicals:



It is worth noting that aldehydes from C₂ (acetaldehyde) and bigger can react with the OH radical to form acetyl peroxy radicals (RCO₃, where R is an alkyl group), which themselves react with NO₂ to form PAN (peroxyacetyl nitrate)-type species, as shown in reactions R11 and R12 for acetaldehyde:



There have been very few studies of PAN-type species indoors. One such study showed that the simplest PAN-type species as shown in R12 was formed indoors through chemistry rather than transported from outdoors and that concentrations were enhanced when the ozone concentration was higher (Fischer et al. 2014). PAN species are thermally labile, and so the indoor temperature will also determine where the equilibrium lies in R12.

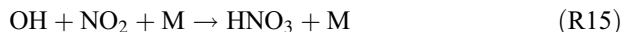
Another interesting aspect of this indoor chemistry is the ability of peroxy radicals to convert NO to NO₂ (nitrogen dioxide), as shown in reactions R3a and R7. This opens up the possibility of forming ozone indoors through photolysis, as shown in reactions R13, R14:



where “M” represents a molecule (typically nitrogen or oxygen molecules in air) that acquires excess energy from the reaction without affecting the chemistry. Clearly, reaction R13 happens much more slowly indoors compared to outdoors, but it is still possible under some indoor conditions, particularly next to a window or with strong indoor lighting such as compact fluorescent lights (Kowal et al. 2017).

The last two sections have shown that the chemistry of ozone and the hydroxyl radical indoors are intimately linked. VOC oxidation by ozone can make OH (and other radicals), but OH oxidation of VOCs can produce ozone indoors if there is sufficient lighting to drive R13. Therefore, if you have one of these oxidants indoors, you are likely to have the other. These connections are summarized in Fig. 3. Many of these reactions look similar to those observed outdoors. Apart from the photolysis rates, many of the rates of reaction indoors are comparable to outdoors and some can even exceed those typically observed outdoors, such as the reactions of ozone and the hydroxyl radical with monoterpenes (Carslaw 2007).

Finally, in the presence of NO_x , the major termination route for OH radicals is with NO_2 as shown in R15 to form nitric acid vapor (HNO_3):



As well as representing a loss of radicals from the system, this reaction also removes NO_x from indoor air. The major fate of HNO_3 indoors depends on the conditions. Deposition onto indoor surfaces and exchange with outdoors are likely to be important (Weschler et al. 1992), although partitioning to the aerosol phase to form ammonium nitrate could be important if ammonia concentrations are high indoors (Ampollini et al. 2019).

Reactions of the Nitrate Radical

The nitrate (NO_3) radical is another important oxidant outdoors, participating in various oxidation reactions. Outdoors, it only becomes important at night-time as it is photolyzed rapidly during the day (lifetime of ~ 5 s), and can also react rapidly with NO (Carslaw et al. 1997). Given the lower light levels indoors, it might be assumed that the nitrate radical could reach appreciable concentrations within buildings.

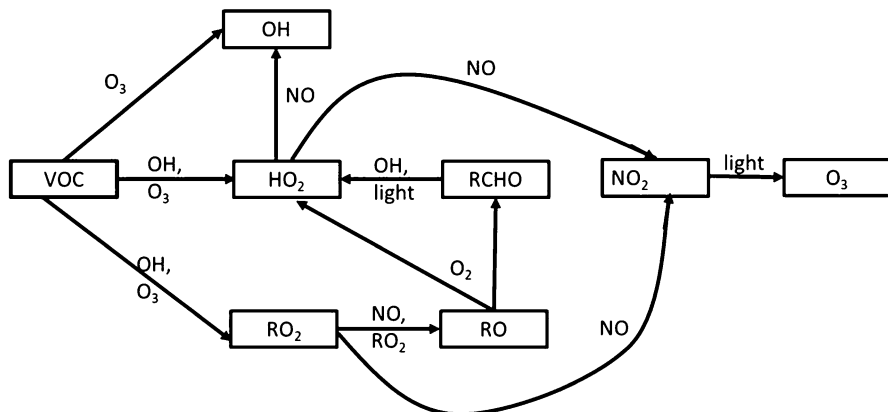


Fig. 3 Summary of the main connections between hydroxyl radical and ozone reactions indoors

Nitrate radicals are formed from the reaction of NO₂ with ozone, as shown in R16:



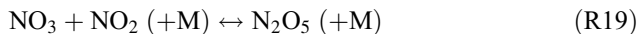
Once formed, the NO₃ radical can react rapidly with NO to reform NO₂ (R17):



So, you would only expect to find NO₃ indoors in the absence of indoor sources of NO (e.g., no combustion sources present). Indeed, high NO concentrations would also remove indoor ozone through R18, making it unlikely that the conditions would be favorable for NO₃ formation in the first place:



The nitrate radical can also react with NO₂ to form dinitrogen pentoxide (N₂O₅), with which it exists in equilibrium as shown in R19:

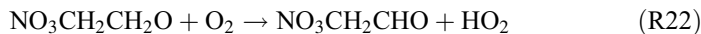


Outdoors, the accommodation coefficients of both NO₃ and N₂O₅ suggest that they may undergo deposition to moist particle surfaces (Carslaw et al. 1997). Such reactions would effectively remove NO₃ (and NO₂) from the system, but this chemistry has not been investigated indoors to date.

The NO₃ radical can undergo a series of oxidation reactions, more rapidly with species with a double bond. For instance, the reaction with ethene is shown in R20, which forms a nitrated peroxy radical:

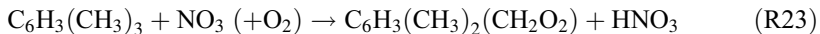


The peroxy radicals so formed can then partake in reactions such as those described in the previous section. The difference with the peroxy radicals formed through NO₃ oxidation is that at some point, NO₂ is likely to be formed, or a nitrated product that is analogous to the hydroxyl radical route equivalent. For instance, for the nitrated peroxy radical formed in R20, it will most likely react with NO or RO₂ to form the respective alkoxy radical, NO₃CH₂CH₂O. This radical in turn can then go through one of two pathways as shown by reactions R21 and R22:



With the rate of R22 being approximately seven times faster than R21 at 293 K (Jenkin et al. 1997). Reaction R22 can be considered to be analogous to R6 for OH: both reactions produce an aldehyde and HO₂ as products, but the aldehyde produced in R22 contains a nitrate rather than a hydroxyl group.

The nitrate radical can also react with some species to form HNO_3 , such as the reaction with 1,3,5-trimethylbenzene, as shown in reaction R23:



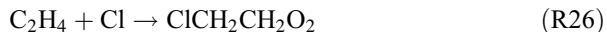
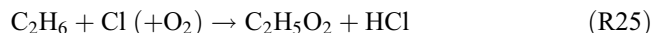
And similarly for the reaction with aldehydes, as shown in R24 for formaldehyde:



The NO_3 radical had not been directly measured indoors until a recent study confirmed its presence for the first time with an experiment that manipulated indoor concentrations (Arata et al. 2018). A portable butane stove was used to provide NO_x emissions in a residential kitchen which removed indoor ozone and consequently, no NO_3 was observed. However, when an ozone generator was used to enhance the indoor ozone concentration to ~40 ppb, there was sufficient NO_2 formed through reaction R18 to produce NO_3 at mixing ratios of ~3–4 ppt. Although these concentrations are low, they can still have significant impacts on indoor chemical processing. For instance, for a simulated UK residence under typical conditions, the indoor NO_3 concentration was predicted to never exceed 0.03 ppt, but NO_3 -monoterpene reactions were still responsible for ~17% of the RO_2 formation through initiation reactions under these conditions (Carslaw 2007). Further research is needed to more fully understand the impact of the nitrate radical on indoor gas-phase chemistry.

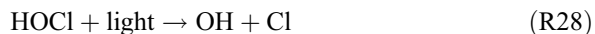
Reactions of the Chlorine Radical

Reactions of the chlorine (Cl) radical are analogous with those of the OH radical. They are generally faster than with OH, and there is also the potential to make chlorinated products through oxidation reactions. The reactions of the chlorine radical with ethane and ethene are shown in R25 and R26 and are analogous to R1 and R2 respectively for the equivalent hydroxyl radical reactions:



It can be seen from reaction R25 that the same peroxy radical is made as for oxidation by OH in R1, but HCl is made instead of H_2O as a byproduct.

Chlorine radical formation indoors is possible following cleaning activities that liberate various chlorine compounds. For instance, significant concentrations of both chlorine molecules and hypochlorous acid (HOCl) were shown to be formed in the 10s–100s of ppb range following floor mopping with a bleach cleaner (Wong et al. 2017). Both of these species can be photolyzed to liberate chlorine radicals as shown in R27 and R28 for chlorine and hypochlorous acid, respectively, the latter reaction also producing OH radicals:



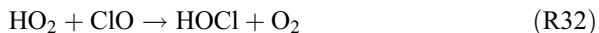
The level of light indoors is therefore critical in determining the importance of these sources of chlorine radicals. For instance, predicted indoor concentrations of chlorine radicals varied from near zero in the dark to approximately 3×10^5 molecule cm⁻³ if it was assumed that 3% of outdoor UV light and 10% of outdoor visible light were able to penetrate indoors (Wong et al. 2017).

As well as undergoing reactions with VOCs, chlorine radicals can react with HO₂ (R29), NO₃ (R30), and ozone (R31):



Out of these four reactions, the reaction with ozone (R31) dominates for typical indoor conditions. Although the rate coefficient for R31 (1.2×10^{-11} cm³ molecule⁻¹ s⁻¹) is a factor of 2 lower than that for R30 (2.4×10^{-11} cm³ molecule⁻¹ s⁻¹) and three times lower than R29b (3.5×10^{-11} cm³ molecule⁻¹ s⁻¹) at 293 K (Xue et al. 2015), the ozone concentration indoors is typically 1000 times higher than the concentrations of HO₂ and NO₃. The rate coefficient for R29a (9.0×10^{-12} cm³ molecule⁻¹ s⁻¹) is actually lower than that for R31 at 293 K.

The chlorine monoxide (ClO) formed in reactions R29a, R30, and R31 can then react with HO₂ (R32), OH (R33), NO (R34), and NO₂ (R35):



Given typical indoor conditions, reaction with NO and NO₂ is to be the most likely fate of chlorine monoxide. The rate coefficient for the reaction with NO₂ (R35) is approximately four times faster than that for NO (R34). Therefore, the ratio of NO to NO₂ will determine which of these two reactions controls the removal of chlorine monoxide. The fate of ClONO₂ is to undergo photolysis through one of two routes shown in R36 and R37, with R37 approximately ten times faster for typical indoor conditions (e.g., with halogen or incandescent lighting):



The chlorine and ClO chlorine monoxide radicals so produced can then cycle back through the reactions already described.

Comparing Indoor Oxidants

This chapter has demonstrated that there is a range of oxidants that can exist indoors, all contributing to the chemistry in the gas-phase and competing, in particular, to oxidize VOCs. Although hydroxyl, chlorine, and nitrate radical reactions tend to be faster than those of ozone, the latter typically exists at much higher concentrations than the radical species. Table 2 compares the rate coefficients of the four oxidative species with limonene, a ubiquitous VOC indoors. It then shows what the comparable radical concentrations would need to be to compete with oxidation for different concentrations of ozone.

Table 2 shows that even for higher indoor concentrations of ozone, the concentrations of NO_3 and OH that are required to oxidize equivalent limonene have been observed under some conditions as described in previous sections (Gómez Alvarez et al., 2013; Carslaw et al. 2017; Arata et al. 2018). Although chlorine radicals have not been measured directly indoors to date, their indoor concentration has been simulated using a model, to be in the range of values shown in Table 2, particularly with sufficient indoor light (Wong et al. 2017). Also, as discussed throughout this chapter, cycling between these oxidants means that once one of them is formed, there is potential for all of them to be produced and to take part in further indoor air chemistry.

Role of Gas-Phase Chemistry in Particle Formation

This chapter has focused on gas-phase reactions, but it is important to note that such reactions can also produce products which are sufficiently involatile to promote

Table 2 Rate coefficients for reaction of different oxidants with limonene ($\text{cm}^3 \text{ molecule}^{-1} \text{ s}^{-1}$) at 293 K. Values for NO_3 , ozone, and OH from Atkinson et al. (2004) and the IUPAC Task Group (n.d.) and those for Cl from Dash and Rajakumar (2014). Also included are the concentrations of NO_3 , OH and, Cl that are needed to oxidize an equivalent amount of limonene as the stated mixing ratio of ozone

	NO_3	O_3	OH	Cl
Rate coefficient	1.22×10^{-11}	2.2×10^{-16}	1.65×10^{-10}	9.12×10^{-10}
Equivalent concentration of oxidant (molecule cm^{-3}) for different ozone mixing ratios				
5 ppb	2.1×10^6		1.7×10^5	2.8×10^4
10 ppb	4.1×10^6		3.3×10^5	5.6×10^4
20 ppb	8.3×10^6		6.7×10^5	1.1×10^5
40 ppb	1.7×10^7		1.3×10^6	2.2×10^5

particle formation and growth, often referred to as secondary organic aerosol (SOA). The monoterpenes are an important group of SOA-forming VOCs, given the ubiquity of their sources indoors (Nazaroff and Weschler 2004). Following oxidation, they can produce a wide range of multifunctional species, including alcohol, aldehyde, ketone, and carboxylic acid groups: such groups tend to have lower vapor pressures than their parent terpene and can condense to form SOA (Walser et al. 2007).

The composition of particles formed in this way changes depending on indoor conditions. For instance, Carslaw et al. (2012) found from a modeling study that for typical background conditions in a UK residence, the simulated concentration of SOA was around $1 \mu\text{g}/\text{m}^3$ out of a total indoor particle concentration of $10.7 \mu\text{g}/\text{m}^3$, with the composition mainly comprised (85%) of organic nitrates and PAN-type species, with a smaller contribution from peroxide species (12%). However, during cleaning, the SOA concentration increased to $20 \mu\text{g}/\text{m}^3$ for a total indoor particle concentration of $30 \mu\text{g}/\text{m}^3$, with the composition now dominated by peroxide species (73%) and a much smaller contribution from nitrated organic species (21%). Clearly then, it is possible for gas-phase chemistry to lead to particles indoors, with the composition of these particles being dependent on indoor conditions. This in turn will have an impact on the volatility of the indoor air mixture.

Conclusion

This chapter has shown that there can be a wealth of gas-phase chemistry indoors, with the dominant reactions determined by the indoor conditions, such as light levels, oxidant, and NO_x concentrations, building location, occupant activities, and ventilation rates. The numerous controlling factors mean that two identical buildings could have very different indoor pollutant concentrations. So, a building next to a busy road where vehicle-emitted pollutants were able to infiltrate could have very different indoor air concentrations to one in a rural setting with higher outdoor ozone concentrations. Even the same building could have very different indoor air pollutant concentrations depending on the time of year, as ozone concentration and window opening frequency vary with season. Indoor VOC concentrations have also been shown to vary enormously in identical houses in the same street, depending on the behavior of the occupants (Wang et al. 2017).

Nevertheless, the gas-phase chemistry of indoor air is typically driven by ozone reactions with terpenes, which are reactions that can produce radical species, stable species such as carbonyl compounds, and also fine particles in the sub-micron range. An important product of such reactions is the OH radical, which can proceed to initiate further oxidation processes in an analogous manner to outdoors. This chapter has also shown that peroxy radicals are likely to be present wherever the OH radical exists, and there are also interactions between these radicals and chlorine radicals if there is a source of the latter indoors.

It is likely that indoor chemical processing indoors has become more important in recent years through a combination of increased outdoor ozone concentrations,

greater use indoors of terpenes in cleaning products and fragrances, and decreased ventilation rates (Weschler et al. 2006). The international lockdowns accompanying the 2020 COVID-19 pandemic have also allowed a glimpse of how indoor air chemistry might change in the future. The decreased NO_x emissions in urban areas that accompanied various lockdowns could be viewed as a proxy for future improvements in vehicle technologies that aim to decrease NO_x emissions outdoors. For instance, in the UK, the main lockdown in spring 2020 led to decreases in ambient NO_x concentrations of about 30–40% and a corresponding ozone increase of about the same amount (AQEG 2020). Model simulations showed that this increase in outdoor ozone led to an increase in indoor ozone concentrations of around 50% for typical residential conditions, with an accompanying 30% increase in HCHO caused by additional chemical reactions indoors. Further, the expected improvements in future vehicle emissions technologies also means that VOCs from use of personal care products indoors are likely to be responsible for an increasing proportion of fossil fuel VOC emissions in industrial areas outdoors, with a recent study estimating this proportion approached half of the total (McDonald et al. 2018). Coupled with climate change impacts that are likely to lead to more heatwaves and associated higher outdoor pollutant (e.g., ozone, PM) concentrations that can impact indoors (Terry et al. 2014), the gas-phase reactions described in this chapter are only likely to increase in importance.

Cross-References

- [Indoor Air Quality in the Context of Climate Change](#)
- [Indoor Photochemistry](#)
- [Influence of Ventilation on Indoor Air Quality](#)
- [Occupant Emissions and Chemistry](#)
- [Volatile Organic Compounds \(VOCs\)](#)

References

- Ampollini L, Katz EF, Bourne S, Tian Y, Novoselac A, Goldstein AH, Lucic G, Waring MS, DeCarlo PF (2019) Observations and contributions of real-time indoor ammonia concentrations during HOMEChem. Environ Sci Technol 53:8591–8598
- AQEG (Air Quality Expert Group) (2020) Estimation of changes in air pollution emissions, concentrations and exposure during the COVID-19 outbreak in the UK. Rapid evidence review – June 2020. https://uk-air.defra.gov.uk/library/reports.php?report_id=1005. Accessed 6 Jan 2021
- Arata C, Zarzana KJ, Misztal PK, Liu Y, Brown SS, Nazaroff WW, Goldstein AH (2018) Measurement of NO₃ and N₂O₅ in a residential kitchen. Environ Sci Technol Lett 5:595
- Aschmann SM, Arey J, Atkinson R (2002) OH radical formation from the gas-phase reactions of O₃ with a series of terpenes. Atmos Environ 36:4347
- Atkinson R, Arey J (2003) Gas-phase tropospheric chemistry of biogenic volatile organic compounds: a review. Atmos Environ 37(Suppl 2):S197–S219

- Atkinson R, Baulch DL, Cox RA, Crowley JN, Hampson RF, Hynes RG, Jenkin ME, Rossi MJ, Troe J (2004) Evaluated kinetic and photochemical data for atmospheric chemistry: Volume I – gas phase reactions of Ox, HOx, NOx and SOx species. *Atmos Chem Phys* 4:1461–1738
- Bloss C, Wagner V, Jenkin ME, Volkamer R, Bloss WJ, Lee JD, Heard DE, Wirtz K, Martin-Reviejo M, Rea G, Wenger JC, Pilling MJ (2005) Development of a detailed chemical mechanism (MCMv3.1) for the atmospheric oxidation of aromatic hydrocarbons. *Atmos Chem Phys* 5:641–664
- Carslaw N (2007) A new detailed chemical model for indoor air pollution. *Atmos Environ* 41(6): 1164–1179
- Carslaw N (2013) A mechanistic study of limonene oxidation products and pathways following cleaning activities. *Atmos Environ* 80:507–513
- Carslaw N, Coe H, Plane JMC, Cuevas EC (1997) Observations of the nitrate radical in the free troposphere at Izaña de Tenerife. *J Geophys Res* 102:10613–10622
- Carslaw N, Fletcher L, Heard D, Ingham T, Walker H (2017) Significant OH production under surface cleaning and air cleaning conditions: impact on indoor air quality. *Indoor Air* 27:1091–1100
- Dash MR, Rajakumar B (2014) Reaction kinetics of Cl atoms with limonene: an experimental and theoretical study. *Atmos Environ* 99:183–195
- Faloona I, Tan D, Brune W, Hurst J, Barket D, Couch TL, Shepson P, Apel E, Riemer D, Thornberry T, Carroll MA, Sillman S, Keeler GJ, Sagady J, Hooper D, Paterson K (2001) Nighttime observations of anomalously high levels of hydroxyl radicals above a deciduous forest canopy. *J Geophys Res* 106:24315–24333
- Fan ZH, Weschler CJ, Han IK, Zhang JF (2005) Co-formation of hydroperoxides and ultra-fine particles during the reactions of ozone with a complex VOC mixture under simulated indoor conditions. *Atmos Environ* 39:5171–5182
- Fischer A, Langer S, Ljungstrom E (2014) Chemistry and indoor air quality in a multi-storey wooden passive (low energy) building: formation of peroxyacetyl nitrate. *Indoor Built Environ* 23:485–496
- Gomez Alvarez E, Amedro D, Afif C, Gligorovski S, Schoemaecker C, Fittschen C, Doussin JF, Wortham H (2013) Unexpectedly high indoor hydroxyl radical concentrations associated with nitrous acid. *PNAS* 110:13294–13299
- Heard DE, Carpenter LJ, Creasey DJ, Hopkins JR, Lee JD, Lewis AC, Pilling MJ, Seakins PW, Carslaw N, Emmerson KM (2004) High levels of the hydroxyl radical in the winter urban troposphere. *Geophys Res Lett* 31(18):Art. No. L18112
- IUPAC Task Group on Atmospheric Chemical Kinetic Data Evaluation, (<http://iupac.pole-ether.fr>) Volume 2 (n.d.). Accessed 6 Jan 2021
- Jenkin ME, Saunders SM, Pilling MJ (1997) Construction and application of a master chemical mechanism (MCM) for modelling tropospheric chemistry. *Atmos Environ* 31:81–104
- Jenkin ME, Saunders SM, Wagner V, Pilling MJ (2003) Protocol for the development of the Master Chemical Mechanism, MCM v3 (Part B): tropospheric degradation of aromatic volatile organic compounds. *Atmos Chem Phys* 3:181–193
- Kowal SF, Allen SR, Kahan TF (2017) Wavelength-resolved photon fluxes of indoor light sources: implications for HOx production. *Environ Sci Technol* 51:10423–10430
- Master Chemical Mechanism (MCM) web site: <http://mcm.leeds.ac.uk/MCM/> (n.d.). Accessed 6 Jan 2021
- McDonald BC, de Gouw JA, Gilman JB, Jathar SH, Akherati A, Cappa CD, Jimenez JL, Lee-Taylor J, Hayes PL, McKeen SA, Cui YY, Kim S-W, Gentner DR, Isaacman-VanWert G, Goldstein AH, Harley RA, Frost GJ, Roberts JM, Ryerson TB, Trainer M (2018) Volatile chemical products emerging as largest petrochemical source of urban organic emissions. *Science* 359:760–764
- Mendez M, Blond N, Blondeau P, Schoemaecker C, Hauglustaine DA (2015) Assessment of the impact of oxidation processes on indoor air pollution using the new timeresolved INCA-Indoor model. *Atmos Environ* 122:521–530

- Mendez M, Blond N, Amedro D, Haugulstaine DA, Blondeau P, Afif C, Fittschen C, Schoemaecker C (2017) Identification of the major HO_x radical pathways in an indoor air environment. *Indoor Air* 27:443–451
- Nazaroff WW, Weschler CJ (2004) Cleaning products and air fresheners: exposure to primary and secondary air pollutants. *Atmos Environ* 38:2841–2865
- Saarela K, Tirkkonene T, Laine-Ylijoki J, Jurvelin J, Nieuwenhuijsen MJ, Jantunen M (2003) Exposure of population and microenvironmental distributions of volatile organic compound concentrations in the EXPOLIS study. *Atmos Environ* 37:5563
- Sarwar G, Corsi R, Kimura Y, Allen D, Weschler CJ (2002) Hydroxyl radicals in indoor environments. *Atmos Environ* 36:3973–3988
- Singer BC, Coleman BK, Destaillats H, Hodgson AT, Lunden MM, Weschler CJ, Nazaroff WW (2006) Indoor secondary pollutants from cleaning product and air freshener use in the presence of ozone. *Atmos Environ* 40(35):6696–6710
- Steiner AL (2020) Role of the terrestrial biosphere in atmospheric chemistry and climate. *Acc Chem Res* 53:1260–1268
- Terry AC, Carslaw N, Ashmore M, Dimitrulopoulou S, Carslaw DC (2014) Occupant exposure to indoor air pollutants in modern European offices: an integrated modelling approach. *Atmos Environ* 82:9–16
- Walser ML, Park J, Gomez AL, Russell AR, Nizkorodov SA (2007) Photochemical aging of secondary organic aerosol particles generated from the oxidation of d-limonene. *J Phys Chem A* 111:1907–1913
- Wang CM, Barratt B, Carslaw N, Doutsi A, Dunmore RE, Ward MW, Lewis AC (2017) Unexpectedly high concentrations of monoterpenes in a study of UK homes. *Environ Sci Process Impacts* 19:528–537
- Weschler CJ (2000) Ozone in indoor environments: concentration and chemistry. *Indoor Air* 10: 269–288
- Weschler CJ, Carslaw N (2018) Indoor chemistry, Invited feature article for *Environ Sci Technol* 52: 2419–2428
- Weschler CJ, Shields HC (1996) Production of the hydroxyl radical in indoor air. *Environ Sci Technol* 30:3250–3253
- Weschler CJ, Shields HC (2000) The influence of ventilation on reactions among indoor pollutants: modeling and experimental observations. *Indoor Air* 10(2):92–100
- Weschler CJ, Brauer M, Koutrakis P (1992) Indoor ozone and nitrogen dioxide – a potential pathway to the generation of nitrate radicals, dinitrogen pentoxide, and nitric-acid indoors. *Environ Sci Technol* 26(1):179–184
- Weschler CJ, Wells JR, Poppnick D, Hubbard H, Pearce TA (2006) Workgroup report: indoor chemistry and health. *Environ Health Perspect* 114:442–446
- Wong JPS, Carslaw N, Zhao R, Zhou S, Abbatt JPD (2017) Observations and impacts of bleach washing on indoor chlorine chemistry. *Indoor Air* 27:1082–1090
- Xue LK, Saunders SM, Wang T, Gao R, Wang XF, Zhang QZ, Wang WX (2015) Development of a chlorine chemistry module for the Master Chemical Mechanism. *Geosci Model Dev* 8:3151–3162
- Youssefi SF, Waring MS (2015) Indoor transient SOA formation from ozone + α -pinene reactions: impacts of air exchange and initial product concentrations, and comparison to limonene ozonolysis. *Atmos Environ* 112:106–115



Indoor Photochemistry

29

Tara F. Kahan, Cora J. Young, and Shan Zhou

Contents

Introduction to Photochemistry	856
Absorption Cross Section and Photolysis Quantum Yield	857
Photon Flux	859
Different Considerations for Condensed Phase and Heterogeneous Photochemistry	860
Concentration and Steady-State Concentration	861
Outdoor Photochemistry	862
Overview of Indoor Photochemistry	863
Important Gas Phase Photochemical Reactions Indoors	864
Factors Controlling Gas Phase Indoor Photochemistry	866
Solar Photon Flux	867
Photon Flux from Light Bulbs	868
Indoor Reactant Concentrations and Oxidant Steady-State Concentrations	870
Condensed Phase and Heterogeneous Indoor Photochemistry	871
Photochemical Formation of Oxidants on Painted Surfaces	872
Photochemistry in Dust and on Indoor Surface Films	873
Photochemistry in Indoor Aqueous Phases	874
Current Research	874
Measurements of Photochemically Generated Species	874
Photon Flux Measurements and Predictions	875
Models	876
Conclusions and Future Directions	878
References	880

T. F. Kahan (✉)

Department of Chemistry, University of Saskatchewan, Saskatoon, SK, Canada
e-mail: tara.kahan@usask.ca

C. J. Young

Department of Chemistry, York University, Toronto, ON, Canada

S. Zhou

Department of Civil and Environmental Engineering, Rice University, Houston, TX, USA

Abstract

Photochemistry is a rapidly growing research area in the field of indoor chemistry. Advances in measurement techniques and predictive models have altered our understanding of the effects of light on the composition of indoor atmospheres. Large knowledge gaps remain, however, including the question, “does photochemistry matter indoors?”. This chapter introduces readers to basic principles of photochemistry; provides context to indoor photochemistry using examples from better-understood outdoor atmospheric photochemical reactions; discusses our current understanding of the processes that control indoor photochemical reactions; outlines experimental and theoretical techniques commonly used to study indoor photochemistry; and provides some thoughts for the future.

Keywords

Photolysis · Kinetics · Radicals · Photon flux · Light source · Indoor photolabile species

Introduction to Photochemistry

Photochemistry describes chemical reactions initiated by the absorption of a photon. Photochemical reactions can be classified as “direct” or “indirect.” Direct photochemical reactions occur when the compound of interest (the “analyte”) absorbs a photon and reacts. A common form of direct photochemical reaction in the atmosphere is photolysis (the breaking of bonds following absorption of a photon). Direct photolysis can also involve other molecules. For example, the analyte can absorb a photon and then react with O₃ or another species in the air (or other reaction matrix, such as water). Indirect photochemistry occurs when a molecule other than the analyte absorbs a photon, and then causes the analyte to undergo a chemical transformation. In the gas phase, indirect photochemistry almost always refers to radical reactions. Radicals such as hydroxyl radicals (OH) and chlorine atoms (Cl) are formed from photolysis of (among other things) O₃ and Cl₂. These radicals go on to react with a wide range of atmospheric species. The reaction of radicals with atmospheric gases is often referred to as “photolysis,” despite the fact that only the radical was formed photochemically (i.e., the reaction between the radical and the analyte does not involve the absorption of photons). These types of reactions are more appropriately termed indirect photochemistry.

To understand indoor photochemistry, and how it differs from outdoor photochemistry, we must understand what factors determine the speed (or rate) at which photochemical reactions occur (and whether they occur at all). Full discussions of the fundamentals of photochemical reactions are available in textbooks such as Turro et al. (2009), and introductions to photochemistry from an atmospheric science perspective are provided in textbooks such as Jacob (1999), Finlayson-Pitts and

Pitts (2000), and Seinfeld and Pandis (2016). Here we give a brief overview of the fundamentals of photochemistry that are most relevant to indoor chemistry.

Photochemical reaction rates are generally given by the rate law (Eq. 1):

$$\text{Rate} = J[\text{analyte}] \quad (1)$$

Where J is the photolysis rate constant and $[\text{analyte}]$ is the analyte concentration. For a given analyte concentration, the larger the rate constant, the faster the reaction. Photochemical rate constants (J) depend on three factors, as shown in Eq. 2:

$$J = \sigma\phi F \quad (2)$$

Where σ is the absorption cross section of the analyte (in units of $\text{cm}^2 \text{molecule}^{-1}$), Φ is the photolysis quantum yield (unitless), and F is the photon flux ($\text{photons cm}^{-2} \text{s}^{-1}$). We discuss each of these variables in detail below. Note that Eq. 2 is for a single wavelength of light. In atmospheric chemistry (including indoor chemistry) light sources often span a broad range of wavelengths, and the appropriate equation becomes:

$$J = \int_{\lambda_i}^{\lambda_f} \sigma(\lambda)\phi(\lambda)F_\lambda d\lambda \quad (3)$$

In this equation, photolysis rate constants are integrated across the range of wavelengths of interest ($\lambda_i - \lambda_f$). The notation of $\sigma(\lambda)$ and $\Phi(\lambda)$ indicate that absorption cross sections and photolysis quantum yields are wavelength dependent. F_λ denotes the photon flux at a specific wavelength, and $d\lambda$ is the interval between wavelengths used in the calculation. The magnitude of the rate constant, and therefore on the reaction rate (as given by Eq. 1) depends on the magnitudes of σ , Φ , and λ . If one or more variable is zero or extremely low, reaction will not occur, regardless of the magnitude of other variables.

Absorption Cross Section and Photolysis Quantum Yield

While photon flux (F) depends on the light source, absorption cross section (σ) and photolysis quantum yield (Φ) are characteristic of individual analytes. Their magnitudes can depend on external factors such as temperature, pressure, and “solvent” (in either the gas or condensed phase). Since indoor chemistry generally occurs within a fairly narrow range of temperatures and pressures, we will not discuss these variables here. For now, we will focus on a solvent of air (i.e., gas phase reactions).

Several requirements must be met in order for photolysis to occur. First, the energy of the absorbed photon must be high enough to promote an electron into a higher electronic energy level. Such transitions are generally only achieved with ultraviolet (UV) (and occasionally visible) light. This is illustrated by Process (a) in Fig. 1. Once an electron is promoted to a higher electronic energy level, photolysis

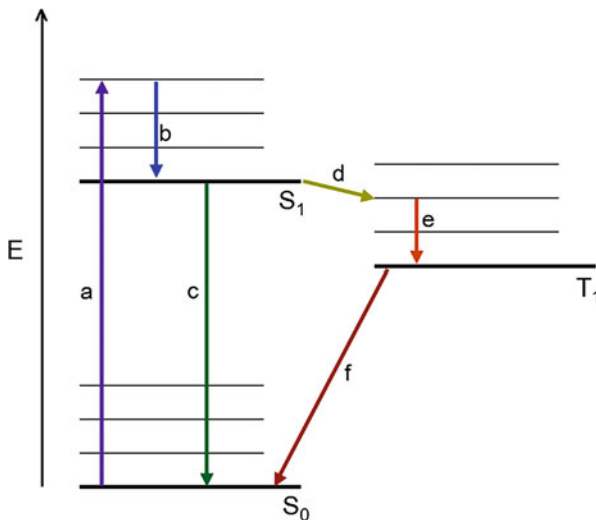


Fig. 1 Simplified Jablonski diagram showing energies (not to scale) of potential electronic and vibrational transitions following absorption of a photon. S_0 represents the ground state of the analyte, S_1 represents the first electronically excited singlet state, and T_1 represents the first excited triplet state. Thin horizontal lines denote vibrationally excited states of each electronic state (S_0 , S_1 , T_1). Arrows denote some possible processes: (a) electronic excitation from S_0 to a vibrationally excited level of S_1 ; (b) vibrational relaxation to S_1 ; (c) transition from S_1 to S_0 ; (d) intersystem crossing from S_1 to a vibrationally excited level of T_1 ; (e) vibrational relaxation to T_1 ; (f) transition from T_1 to S_0 . This schematic is an incomplete representation of possible processes, and does not include chemical reactions

will only occur if (1) the energy is sufficient to initiate a reaction (e.g., by breaking a bond), and (2) the reaction occurs rapidly enough to compete with other processes.

The photolysis quantum yield (Φ) describes the probability that the absorption of a photon will lead to a photochemical reaction. It is generally a fraction between 0 and 1. After absorbing a photon, molecules can release excess energy in various ways. Chemical reaction is one possibility, but nonchemical (i.e., physical) methods include vibrational relaxation, intersystem crossing, physical quenching, and radiative and non-radiative decay (represented by Processes (c), (d), and (f) in Fig. 1). The magnitude of Φ depends on the kinetics of photolysis relative to other competing processes.

$$\Phi = \frac{k_{react}}{\sum k_i} \quad (4)$$

Where k_{react} is the rate constant for chemical reaction and $\sum k_i$ is the sum of rate constants for all possible pathways of the excited species. If k_{react} is much larger than all other terms, the equation will simplify to

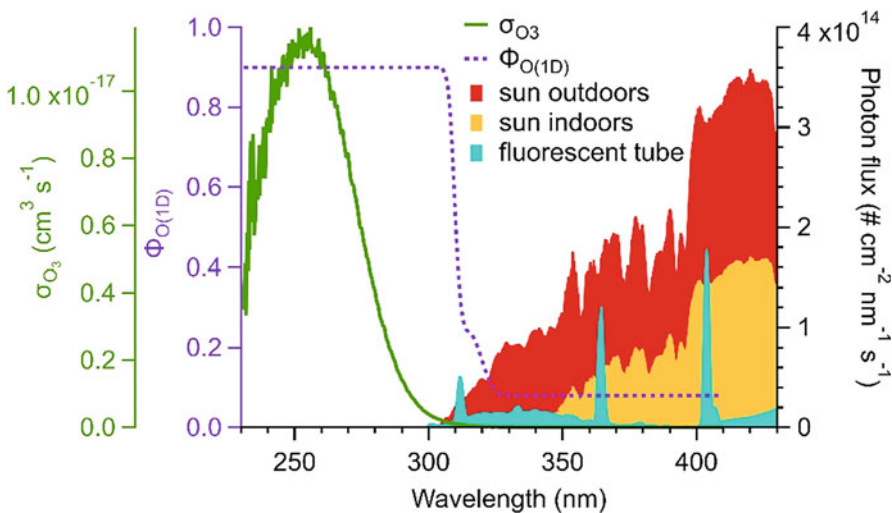


Fig. 2 Wavelength-resolved absorption cross sections and photolysis quantum yields for photochemical OH production from O_3 photolysis (left y axes), and wavelength-resolved photon fluxes from sunlight outdoors and indoors at a house in Austin, Texas around 11 am, June 23, 2018 and from a bare fluorescent tube at 2 mm from the tube center (right y axis; from data used in Zhou et al. (2020a))

$$\Phi = \frac{k_{react}}{k_{react}} \quad (5)$$

and the quantum yield will be 1, meaning that all absorbed photons lead to photochemistry. On the other hand, if k_{react} is very small compared to other processes, Φ will be very small. The product of σ and Φ determines the speed with which a reactant will undergo photolysis when irradiated with light at a given wavelength. As shown in Fig. 2, the photolysis quantum yield for $O(^1D)$ from O_3 photolysis drops to near-zero at wavelengths longer than ~ 320 nm. Thus, OH formation is generally negligible under irradiation at longer wavelengths.

Photon Flux

Photon flux describes the intensity of light available to analytes. In atmospheric chemistry, this includes direct light (from the sun or a lightbulb) as well as scattered and reflected light. A related term is “irradiance,” which describes the rate at which photons cross a unit area of a plane (from a hemisphere of directions). This is what many instruments measure; very few instruments capture photons from a full 360° . Measurement of irradiance and photon flux is discussed in section “[Photon Flux Measurements and Predictions](#).” Irradiance and photon flux differ only by the factor $\cos(\theta)$, where θ is the deviation of the direction of incoming photons from the

vertical to the plane of detection (i.e., light impinging directly on the real or imaginary plane will have $\theta = 0^\circ$, while light that travels parallel to the plane will have $\theta = 90^\circ$). When $\theta = 0^\circ$, $\cos(\theta) = 1$, and irradiance and photon flux are equal. This occurs when light is unidirectional, such as collimated outdoor sunlight on a clear day. Indoors, the contribution of light from different directions to total photon flux is poorly constrained, although research in this area is evolving rapidly. This is discussed in section “[Photon Flux Measurements and Predictions](#).”

Different Considerations for Condensed Phase and Heterogeneous Photochemistry

The above discussion focused on gas-phase photochemistry. Photochemical reactions also occur in condensed phases (such as aqueous solutions) and at atmospheric surfaces. The same principles apply, and the photochemical rate constant is still given by J . In liquids, σ is generally replaced by molar absorptivity (ε). The only difference between σ and ε is the units. Absorption cross sections ($\text{cm}^2 \text{molecule}^{-1}$) work well with common units for gas phase concentrations of molecule cm^{-3} , while $\varepsilon (\text{L mol}^{-1} \text{cm}^{-1})$ works well with molar concentrations commonly used in condensed phases (mol L^{-1}). The resulting photolysis rate constant is still in units of s^{-1} , and reaction rates are often in units of $\text{mol L}^{-1} \text{s}^{-1}$, since condensed-phase concentrations are generally given in terms of molarity rather than number density. For heterogeneous reactions, J is calculated as for gas phase reactions, but reaction rates have units of $\text{molecule cm}^{-2} \text{s}^{-1}$, since we use surface coverages (or surface densities) that represent a 2D coverage, rather than 3D concentration terms.

Analyte absorbance spectra are often different in the gas phase, condensed phase, and at surfaces. In condensed phases, interactions with solvent molecules lead to band broadening, so spectra are generally “smeared” across a range of wavelengths, whereas gas-phase absorbance spectra of small molecules often feature sharp, discrete peaks. Absorbance spectra on surfaces can be different from both the gas phase and the liquid phase. Spectra may be shifted to higher energies (“blue shifts”) or lower energies (“red shifts”) in liquids or at surfaces compared to in the gas phase due to interactions with surrounding molecules, and the magnitude of σ and Φ at a given wavelength may change.

The speciation of analytes may also be different in the different phases. For example, nitric acid (HNO_3) is in its molecular form in the gas phase, but in its ionic form (NO_3^-) in aqueous solution. These are distinct chemical species with different wavelength-resolved absorption spectra. At surfaces, nitric acid may exist in a mixture of ionic and molecular forms, depending on the availability of water molecules (Moussa et al. 2013; Riikonen et al. 2013; Marcotte et al. 2013; Morenz and Donaldson 2017). Photon fluxes at surfaces may also be very different than those in the nearby air. For example, light scattering within aqueous aerosols and ice granules has been reported to increase the effective photon flux by ~50–70% compared to in bulk aqueous solution (Nissenson et al. 2006; McFall and Anastasio 2016; Malley et al. 2017). Reflective surfaces can also increase effective photon fluxes. Little is currently known about surface and condensed phase photochemistry

indoors; we will summarize what is known in section “[Condensed Phase and Heterogeneous Indoor Photochemistry](#).”

Concentration and Steady-State Concentration

The above sections discuss what goes into a photochemical rate constant. We are often interested in photochemical *rates*, which depend on both the photochemical rate constant and the concentration of the reactant. A reaction rate describes the amount of change that occurs in some set time period, and has units of amount/time. The rate for a photochemical reaction is given by Eq. 1. Photochemical reaction rates depend linearly on reactant concentration. So even if a reaction has a large photolysis rate constant, the reaction will be slow if reactant concentration is very low. Conversely, high reactant concentrations can offset small rate constants, leading to nonnegligible reaction rates despite small J (see, for example, Wang et al. (2020) with respect to indoor ozone photochemistry).

Much of the chemistry of interest indoors is indirect photochemistry. Specifically, we often want to know how quickly species such as volatile organic compounds (VOCs) react with photochemically formed oxidants such as OH or Cl. The rate of reaction in this situation will be given by:

$$\text{Rate} = k[\text{analyte}][\text{oxidant}] \quad (6)$$

Where k is the second-order rate constant for the reaction between the analyte and the oxidant. Oxidant concentrations will be determined by their formation and loss rates (note: there may be multiple formation and loss mechanisms for a single oxidant).

$$\frac{d[\text{oxidant}]}{dt} = \sum \text{Rate}_f - \sum \text{Rate}_l \quad (7)$$

where $d[\text{oxidant}]/dt$ is the rate of change of the oxidant concentration with time and $\sum \text{Rate}_f$ and $\sum \text{Rate}_l$ are the total formation rates and total loss rates, respectively. When the total loss rate is much larger than the total formation rate, the oxidant will be consumed more rapidly than it is formed, and will be present at a constant low concentration referred to as a steady-state concentration, denoted by $[\text{oxidant}]_{ss}$. Under these conditions, we can assume that the rate of change of the oxidant is approximately zero (“the steady-state assumption”), which allows us to replace $d[\text{oxidant}]/dt$ in Eq. 7 with 0 and solve for oxidant concentration:

$$[\text{oxidant}]_{ss} = \frac{\sum \text{Rate}_f}{\sum k'_l} \quad (8)$$

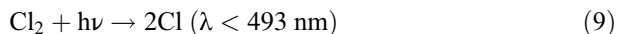
where k'_l is the first-order or pseudo-first-order rate constant for a loss process. This is given by the rate constant for the reaction multiplied by the concentrations of any reactants involved in the process *other than* the oxidant. The steady-state concentration calculated from Eq. 8 can be substituted into Eq. 6 to calculate the analyte

oxidation rate. The steady-state approximation is an important tool for calculating kinetics in atmospheric chemistry, both outdoors and indoors. We discuss steady-state approximations for various radicals in detail in section “[Indoor Reactant Concentrations and Oxidant Steady-State Concentrations](#).”

Outdoor Photochemistry

To provide context to our discussion of indoor photochemistry, we will provide a brief overview of key concepts in outdoor photochemistry. Photolysis reactions in the outdoor environment occur in the gas and condensed phases. Here we will focus primarily on gas-phase chemistry, but will discuss condensed phase and heterogeneous indoor chemistry in section “[Condensed Phase and Heterogeneous Indoor Photochemistry](#).” The dominant source of light outdoors is the sun, although limited photolysis can be initiated by artificial lights at night (Stark et al. 2011). The intensity and energy of sunlight are affected by two major factors: (i) the location of the sun, and (ii) the amount of light absorbing or scattering materials between the point of interest and the sun. The first factor, the location of the sun, is measured using the solar zenith angle (SZA), which is the angle between the position of the sun and a vertical line from the point of interest. Thus, an SZA of zero occurs when the sun is directly overhead. Several factors affect the SZA, including time of day, latitude, and time of year. For example, an SZA of zero occurs at the equator around noon on the solar equinoxes. Solar irradiance is inversely proportional to SZA, such that a higher angle results in less light reaching the surface. This occurs because at higher SZAs, light from the sun travels a longer distance through the atmosphere. Gas molecules that make up our atmosphere absorb and scatter light emitted from the sun, changing the light that reaches the surface of the Earth. This effect is more prevalent at shorter wavelengths, so fewer high-energy photons reach the surface of the Earth at high SZAs. The second factor, the presence of absorbing/scattering materials, is determined primarily by altitude, which determines how much of the atmosphere is between the point of interest and the sun. At the Earth’s surface, the second factor is determined mainly by the presence or absence of clouds, which reduce the light reaching the surface. The abundance of suspended aerosols that can absorb and scatter light also plays a role. On cloud-free days with little aerosol pollution, the shortest wavelengths that reach the surface of the Earth are approximately 290 nm. The intensity of this high-energy light reaching the surface is highly dependent on SZA (Fig. 3). Higher quantities of lower-energy (longer wavelength) photons reach the surface of the Earth, with less dependence on SZA.

As an example of gas-phase photolysis outdoors, we will examine three molecules: Cl₂ (Burkholder et al. 2015), HONO (Stutz et al. 2000), and O₃ (Burkholder et al. 2015):



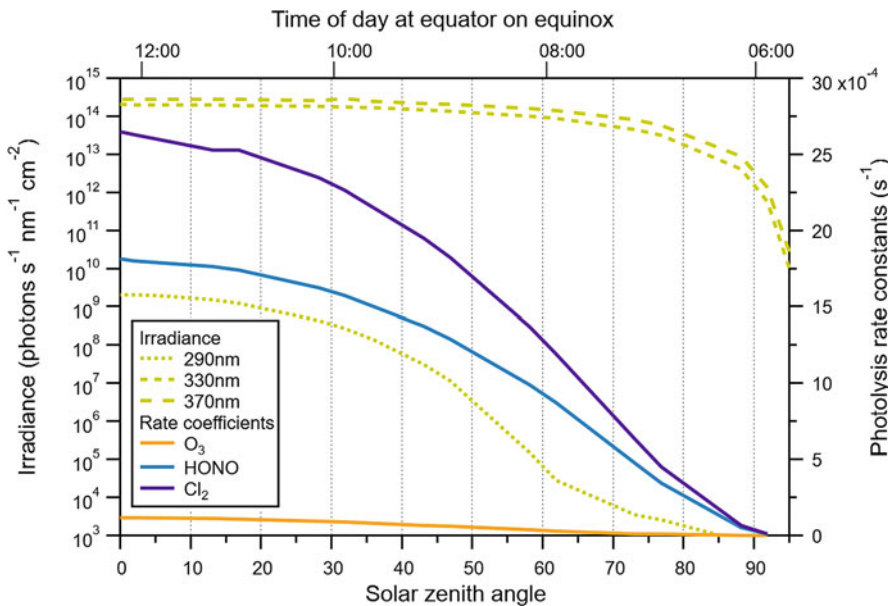
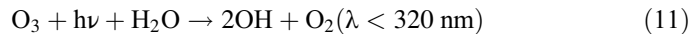
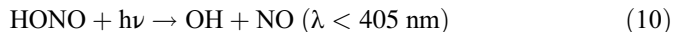


Fig. 3 Irradiance at 290, 330, and 370 nm shown with photolysis rate constants for O_3 , HONO, and Cl_2 as a function of solar zenith angle (SZA). Irradiance and rate constants were calculated using Tropospheric UV model for clear-sky conditions at sea level (Madronich and Flocke 1999)



While Cl_2 and HONO photolyze with visible light, O_3 photolysis requires UV light. Figure 3 shows that Cl_2 and HONO photolysis rate constants are much larger than O_3 photolysis rate constants at all times of the day. Despite this, ozone photolysis remains the dominant radical source over most daylight hours because of its high concentrations. At low SZAs, however, Cl_2 and HONO photolysis rates can exceed O_3 photolysis rates, and photolysis of HONO has been observed to be a much more important radical source than O_3 early in the morning (Young et al. 2012), as well as in the wintertime (Kim et al. 2014). Indoor environments have low UV light availability and are expected to have conditions similar to low-light outdoor conditions.

Overview of Indoor Photochemistry

While photochemistry drives atmospheric composition outdoors, its role indoors is less clear. The high energy photons ($\lambda < 320 \text{ nm}$) responsible for OH production from O_3 photolysis are attenuated by walls, roofs, and windows indoors. This shuts

down the primary source of atmospheric radicals outdoors, and leads to a chemical environment that may be similar to outdoor low-light conditions (with no light, such as at night, or with low light levels, especially at short wavelengths, such as at dawn and dusk). This means that radical levels will generally be lower indoors than outdoors, and that indoor photochemistry will be dominated by species that photolyze at longer wavelengths (>330 nm). While the possibility of indoor photochemistry has been suggested for decades (e.g., Nazaroff and Cass 1986; Carslaw 2007; Gligorovski and Weschler 2013), the first direct evidence of its importance was published in 2013, when measurements in a sunlit classroom demonstrated the formation of OH due to HONO photolysis (Gomez Alvarez et al. 2013), with measured OH concentrations reaching levels on the order of 10^6 molec cm^{-3} , similar to those outdoors. Since then, several studies have confirmed the importance of this reaction, and have identified other photochemical reactions as possible sources of indoor radicals (e.g., Young et al. 2019 and references therein; Carslaw et al. 2017; Farmer et al. 2019; Wang et al. 2020; Zhou et al. 2020b).

Although we know that photochemical reactions can occur indoors, we do not yet have enough information to reliably predict photochemical reaction rates under common indoor conditions, and to constrain the effects of photochemistry on indoor air composition. Knowledge from outdoor photochemical reactions, which have been widely studied, is very helpful to our understanding of indoor photochemistry, but indoor environments differ from outdoor environments in terms of photon fluxes and concentrations of photolabile analytes. Happily, research on indoor photochemistry is progressing rapidly on several fronts. Here we provide an overview of the current state of indoor photochemistry.

Important Gas Phase Photochemical Reactions Indoors

The photolysis of HONO to form OH (Eq. 10) is currently believed to be the most important photochemical source of indoor oxidants (Gligorovski and Weschler 2013; Gligorovski 2016; Gligorovski and Abbatt 2018; Young et al. 2019; Abbatt and Wang 2020). Nitrous acid has large absorption cross sections at wavelengths as long as 400 nm, and its photolysis quantum yield is 1 at all relevant wavelengths. This means that photons at wavelengths commonly present indoors (> 330 nm) can induce photolysis. This is similar to low-light environments outdoors (e.g., early morning and late evening) where HONO replaces O₃ as the dominant OH source, as discussed in section “[Outdoor Photochemistry](#).“ Hydroxyl radicals have been experimentally detected in sunlit rooms containing HONO (Gomez Alvarez et al. 2013), and OH has been predicted to form from HONO photolysis under a variety of light sources indoors including sunlight and indoor electric lights (Gandolfo et al. 2016; Kowal et al. 2017; Zhou et al. 2018, 2020a, 2020b). Particulate matter formation has been reported from HONO photolysis induced by fluorescent tubes (Wang et al. 2019). Other species such as formaldehyde (HCHO) and acetaldehyde (CH₃CHO) have been predicted to photolyze to form HO₂ under illumination from fluorescent tubes due to emission at ~ 318 nm, although this has not been experimentally verified

(Kowal et al. 2017). Nitrogen dioxide (NO_2) photolysis has been predicted to increase indoor O_3 levels under sunlit conditions (Kowal et al. 2017; Farmer et al. 2019). Photolysis has been suggested to be an important sink for nitrate radicals (NO_3), but calculations and experiments suggest that under common conditions in residential buildings, NO_3 steady-state concentrations will be negligible (Zhou et al. 2018; Arata et al. 2018; Young et al. 2019). Nitrate levels may be higher – and photochemistry an important sink – in non-residential buildings (Nøjgaard 2010). Nitrate steady-state concentrations are discussed in section “[Indoor Reactant Concentrations and Oxidant Steady-State Concentrations](#).”

While HONO, HCHO, and CH_3CHO are generally present indoors at fairly constant levels, some photolabile species have large temporal variability. The major class of compounds for which this is an issue is cleaning products. The use of chlorine bleach (NaOCl) can release photolabile species such as HOCl and Cl_2 into the air, which photolyze to produce OH and Cl radicals. Gas-phase products formed from the reaction of Cl_2 and HOCl with limonene, a common indoor VOC, formed high loadings of particulate matter under illumination by sunlight or a fluorescent tube (Wang et al. 2019). A combined measurement-model study reported high OH and HO_2 levels in a classroom following surface cleaning with a lemon-scented (i.e., limonene-containing) cleaner, and predicted that HO_2 was primarily formed by photolysis of volatile precursors emitted from the cleaning solution (Carslaw et al. 2017). Hydrogen peroxide (H_2O_2) emitted by H_2O_2 -based household cleaners has been predicted to photolyze under indoor sunlit conditions to form OH, although photolysis of ambient HONO is predicted to remain the major indoor OH source even during the use of H_2O_2 cleaners (Zhou et al. 2020b).

Cleaning in households and most commercial buildings is limited to the physical application of cleaning solutions to surfaces (e.g., mopping, spraying). In buildings where surface disinfection is extremely important, such as hospitals and food-processing plants, “no-touch devices” (NTDs) are increasingly used to decontaminate surfaces. These devices emit high concentrations of gas-phase disinfectants (or in some cases aerosolized disinfectant) into a sealed room or chamber. After emission, the disinfectant molecules settle on surfaces where they efficiently deactivate viruses and bacteria (e.g., ASHRAE; Davies et al. 2011). After some period of time (often ranging from 1 to 12 h), emission ceases and ventilation is resumed. People are allowed to enter the room after disinfectant levels have reached safe levels. Several disinfectants commonly used in NTDs (e.g., chlorine dioxide (OCIO), H_2O_2 , O_3) are photolabile. A modeling study predicted that the presence of photons from either room lights or sunlight during NTD use may greatly increase indoor oxidant levels (Wang et al. 2020). During OCIO fumigation, Cl radicals were predicted to reach peak levels greater than 2×10^8 molec cm^{-3} , and modeled O_3 (formed by reactions of photo-produced O atoms with O_2) reached peak levels of ~1500 ppm. This is 3 orders of magnitude larger than background O_3 levels, and 2 orders of magnitude larger than O_3 levels commonly used for fumigation. Under some conditions, predicted oxidant levels remained elevated after modeled fumigant levels decreased to safe levels. In the case of OCIO fumigation, Cl levels remained above 10^6 molec cm^{-3} after OCIO decreased to background levels (Wang et al.

2020). This means that people entering the room could be exposed to very high oxidant levels, as well as to oxidation products of species such as VOCs.

Ultraviolet light is sometimes used to disinfect indoor air and surfaces (e.g., ASHRAE). Germicidal UV disinfection often uses mercury lamps with emission centered at 254 nm. In some heating, ventilation, and air conditioning (HVAC) systems, UV-C lights are used to disinfect surfaces such as cooling coils and well pans, or to disinfect air as it passes by. Upper room or near-ceiling UV-C disinfection involves placing UV-C lamps facing the ceiling. UV-C portable room decontamination involves a bank of UV-C lights on wheels that is programmed to roll around an enclosed space. These are often used to disinfect surfaces in hospital rooms (e.g., ASHRAE). Additional uses of UV-C light such as handheld lights designed to disinfect small surfaces (e.g., door handles) and as components of portable air purifiers have gained popularity recently. Light at \sim 254 nm is very effective at deactivating bacteria and viruses. However, it can also photolyze a wide range of atmospheric species such as VOCs and small inorganic molecules, and exposure to UV-C light may cause skin and eye damage. The use of UV-C for HVAC and upper room disinfection is well-established and has clear benefits. As long as lightbulbs are purchased from reputable manufacturers (to ensure that only a narrow range of wavelengths is emitted) and installed properly (for example, with proper airflow), UV-C is a useful tool to improve IAQ and decontaminate surfaces, and unintended photochemical reactions should not affect the composition of indoor air apart from very near the light source. UV-C portable room decontamination is effective at decontaminating surfaces, and these units are not used when occupants are present, so air quality issues should be minimal (ASHRAE). On the other hand, UV-C in handheld units and in air purifiers is not necessarily effective at decontaminating air or surfaces, and the lack of regulation and standardization of these devices may lead to the formation of O₃ or other pollutants indoors (EPA 2018).

Factors Controlling Gas Phase Indoor Photochemistry

Photochemical reaction rates indoors can differ greatly from those outdoors due to differences in variables such as photon fluxes, analyte concentrations, and competing analyte sinks. Analyte concentrations and sinks are discussed in detail in other chapters. Here we will focus on photon fluxes. Indoor photon fluxes depend on the type of light source(s) present indoors, as wavelength-resolved emission profiles vary greatly between light sources. Common indoor light sources include sunlight entering buildings through windows and electric lights including light emitting diodes (LEDs), incandescents, halogens, compact fluorescent lights (CFL), and fluorescent tubes. While LED bulbs emit only within the visible spectrum, filtered indoor sunlight, incandescent light bulbs, and halogens all have substantial continuous emissions at wavelengths shorter than 400 nm (Kowal et al. 2017). Fluorescent lamps, including CFLs and fluorescent tubes, additionally feature strong discrete line emissions in the UV (Kowal et al. 2017;

Zhou et al. 2020a). Thus, the type of reactions – and their rates – that occur indoors will depend on the illumination source.

Solar Photon Flux

During the day, the dominant source of light indoors is sunlight entering the room through glass windows and/or doors. However, window glass acts as a filter, so the intensity and energy profile of sunlight indoors is altered from that outdoors. The optical properties of windows (due to factors such as composition, thickness, and coatings) and the presence of insect screens determine the transmission profile of sunlight (Hong Soo Lim and Kim 2010; Blocquet et al. 2018; Zhou et al. 2020a). Wavelength-resolved transmission varies greatly between individual windows; a recent comparison of UV transmittance of 77 windows and window glass samples suggested that J_{HONO} (and therefore OH_{ss}) could vary by up to a factor of 50 between individual windows (Zhou et al. 2020a). Despite the large variability between individual windows, transmittance profiles appear to be generally similar for windows in residential and nonresidential buildings (Zhou et al. 2020a), with the exception of windows coated with UV-reflecting films used in some energy-saving (“green”) buildings (Blocquet et al. 2018; Zhou et al. 2020a). Figure 4 shows average wavelength-resolved light transmittance, the distribution of total transmittance between 330 nm and 400 nm, and the distribution of cutoff wavelengths for windows and window glass samples reported by Zhou et al. (2020a). In general, most windows completely attenuate light at wavelengths shorter than 320 nm. Considering the overlap between the absorption band of photolabile molecules and window transmittance spectra, this suggests that O_3 will not photolyze from indoor sunlight, and that photolysis of HCHO will be very weak. If present at sufficiently high concentrations, other gas species such as H_2O_2 , NO_2 , NO_3 , HONO , Cl_2 , and HOCl could photolyze indoors under solar illumination and contribute to indoor oxidation chemistry in most buildings, regardless of window type.

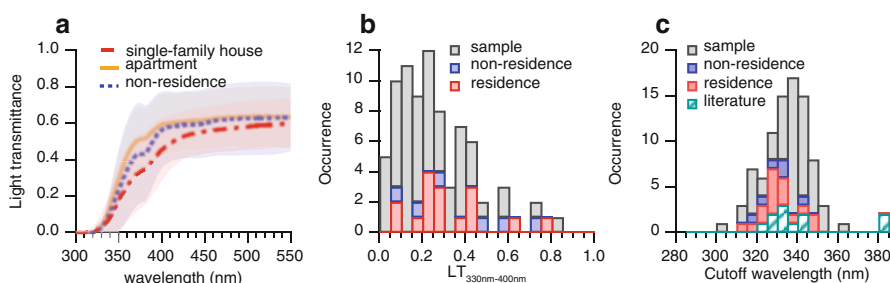


Fig. 4 (a) Average light transmittance spectra for windows in three types of buildings in the USA. Shaded bounds the standard deviations. (b) Histogram of average light transmittance (LT) between 330 nm and 400 nm for 77 windows or window glass samples. (c) Histogram of the cutoff wavelength of 88 windows or window glass samples. Copyright (2020) John Wiley & Sons A/S. Reproduced from Zhou et al. (2020a) with permission from Wiley

Window transmittance is a key factor in controlling indoor photon fluxes from sunlight, but a number of other variables are also important.

Direct vs. diffuse sunlight When a window is fully illuminated by direct sunlight, sunlight indoors will be direct within the volume described by the window shape and the angle of the incoming sunlight relative to the window, while all other light in the room will be diffuse. Conversely, when the window is not oriented toward the sun or it is overcast outdoors, light entering the building will be diffuse. Indoor diffuse sunlight has a similar spectral profile as indoor direct sunlight, but its intensity in the UV range is substantially lower and irradiances are less than 10 % of direct sunlight indoors (Gandolfo et al. 2016; Blocquet et al. 2018; Zhou et al. 2020a).

Distance from window Indoor UV solar fluxes from direct sunlight decrease linearly with increasing distance from the window (Hong Soo Lim and Kim 2010; Kowal et al. 2017; Blocquet et al. 2018; Zhou et al. 2020a). The rate of decrease depends primarily on SZA, with a weak distance dependences reported at low SZA (near noon), and strong dependences at high SZA (e.g., near sunrise and sunset) (Zhou et al. 2020a). Indoor diffuse solar UV irradiance decreases more rapidly with distance, with an exponential distance dependence (Zhou et al. 2020a).

Incident angle of sunlight on windows Most transmittance information about windows assumes an incident angle of 0° (i.e., a light path perpendicular to the plane of the window). However, sunlight rarely enters buildings at an incident angle of 0°. Model simulations and laboratory measurements have shown that window transmittance of UV light remains generally unchanged at incident angles lower than 20°–50°, but decreases rapidly at larger incident angles; at an incident angle of 80°, UV transmittance decreases to 13%–60% of the transmittance at normal incidence (Karlsson et al. 2001; Blocquet et al. 2018; Zhou et al. 2020a). The effect of solar incident angle on window transmittance could vary with individual windows, depending on many factors such as glass thickness, number of panes, infilling gas type, and composition.

Temporal variations Indoor UV fluxes can vary greatly over the course of the day, driven largely by the diurnal profile of outdoor solar irradiance and the orientation of the window relative to the sun (Zhou and Kahan 2021). Changes in outdoor cloud cover and the presence of objects blocking the sun outdoors or indoors can cause abrupt changes in indoor solar intensity. As a result, maximum indoor photon flux, and therefore indoor photolysis rates, will often occur at different times from that outdoors, and individual rooms within a building will have maximum photochemical reactivity at different times of the day (Zhou and Kahan 2021).

Photon Flux from Light Bulbs

Multiple factors affect the ability of electric light bulbs to initiate photochemistry indoors. As mentioned earlier, LEDs will not photolyze most indoor gas species, as

they do not emit at wavelengths shorter than 400 nm. Incandescent, halogen, and CFL bulbs emit UV radiation. As a result, these light sources could initiate photochemistry of many indoor species and may create elevated local oxidant and radical concentrations in the vicinity of the light source. However, emissions from these light sources depend strongly on the distance from the lamp. It has been estimated that they will generally only initiate photochemistry indoors within ~30 cm from the source (Kowal et al. 2017). Fluorescent tubes emit at wavelengths as short as 300 nm. Because they do not act as point sources, their intensity depends less strongly on distance than that of compact light bulbs. Photon fluxes from fluorescent tubes remain above 10% of original intensity within a distance of ~1.3 m from the source, which is sufficient intensity in the UV to initiate photochemistry (Kowal et al. 2017). In the absence of direct sunlight, fluorescent tubes may be important sources of photochemically generated radicals. They may also drive photolysis of analytes that only photolyze at wavelengths shorter than ~340 nm, such as formaldehyde (Kowal et al. 2017; Young et al. 2019). The effect of distance on photolysis is illustrated in Table 1, which provides a summary of the illumination conditions under which several indoor gas-phase species might be important photochemical radical precursors. While most light sources will initiate photochemistry near the source, only direct indoor sunlight and fluorescent tubes are expected to initiate radical production 1 m from the source.

Table 1 Common indoor light sources with their shortest emission wavelengths (λ_{\min}) and photolabile molecules that may be important radical precursors indoors under different lighting conditions as indicated by shaded cells

		λ_{\min} (nm)						
		Direct sunlight	Diffuse sunlight	Fluorescent tube	Halogen	Incandescent	CFL	LED
		325 – 350	325 – 350	300	300	300	360	400
O ₃	Near source							
HONO								
HCHO								
H ₂ O ₂ ^a								
NO ₂								
HOCl ^a								
Cl ₂ ^a								
ClNO ₂ ^a								
O ₃	1 m							
HONO								
HCHO								
H ₂ O ₂ ^a								
NO ₂								
HOCl ^a								
Cl ₂ ^a								
ClNO ₂ ^a								

^aPhotolysis of these analytes is too slow to generate significant radical levels at background concentrations. They are only expected to be important radical precursors when present at high concentrations, such as following the use of bleach (for HOCl, Cl₂, and ClNO₂) or H₂O₂-based (for H₂O₂) cleaners

Besides emission profiles, one of the largest factors affecting UV irradiance from electric lights is the presence of shades. Plastic shades covering fluorescent tubes were reported to attenuate UV light almost completely, effectively shutting off all indoor photolysis (Kowal et al. 2017). It is likely that different types of covers attenuate UV emission to different degrees, but this has not been investigated.

UV intensity increases with radiant power for halogens and CFLs (Kowal et al. 2017), and likely for other lamp types as well. Color temperature of light bulbs also affects UV emission intensities. Warmer color temperature has been shown to be associated with lower UV emissions for fluorescent tubes and CFLs; photochemical HO₂ production rates from HCHO photolysis is predicted to be 12 times greater under illumination from a warm white fluorescent tube (3000 K) than under illumination from a daylight tube (6500 K) (Zhou et al. 2020a).

Indoor Reactant Concentrations and Oxidant Steady-State Concentrations

Concentrations of gas-phase species are often very different indoors compared to outdoors. While many photolabile gas reactants have lower concentrations indoors, some – such as HONO – have much higher concentrations. Sources and sinks of reactants and photochemical products are also different indoors compared to outdoors. A major consideration is the air change rate (ACR). For a chemical reaction (photochemical or otherwise) to be important to the fate of a molecule, it must be rapid enough to compete with removal to the outdoors. Since ACRs can vary greatly, the contribution of indoor photochemistry to analyte fate and radical production will also vary. Measured indoor concentrations of a number of photochemical oxidant precursors are summarized in Young et al. (2019).

A major goal of constraining indoor photolysis rate constants is to better quantify indoor oxidant concentrations. Most indoor oxidants have large loss terms, so their concentrations are determined by the steady-state approximation (section “Concentration and Steady-State Concentration”). Equations 12 and 13 present simplified expressions for steady-state concentrations of OH ($[OH]_{ss}$) and NO₃ ($[NO_3]_{ss}$).

$$[OH]_{ss} = \frac{J_{HONO}[HONO] + k_{O3-alkene}[O_3][alkene]}{ACR + k_{OH-NO}[NO] + k_{OH-NO2}[NO_2]} \quad (12)$$

$$[NO_3]_{ss} = \frac{k_{O3-NO2}[O_3][NO_2]}{ACR + J_{NO3} + k_{NO3-VOC}[VOC] + k_{NO3-NO}[NO]} \quad (13)$$

J_{HONO} is the HONO photolysis rate constant. $k_{O3-alkene}$ is the second order rate constant for OH formation from ozone-alkene reactions. This calculation generally includes several alkene species thought to be important indoors. See for example Weschler and Shields (1996). k_{OH-NO} and k_{OH-NO2} are the second order rate constants of OH with NO and NO₂, respectively, k_{O3-NO2} is the second order rate constant for

O_3 with NO_2 , J_{NO_3} is the NO_3 photolysis rate constant, and k_{NO_3-VOC} and k_{NO_3-NO} are the second order rate constants for NO_3 with VOCs and NO. Other sources and sinks of OH and NO_3 exist indoors; Eqs. 12 and 13 include only the processes expected to dominate steady-state concentrations under common indoor conditions. These equations can be modified to include additional processes.

The primary known indoor OH sources are HONO photolysis and ozone-alkene reactions. In the dark, the ozone-alkene reaction becomes the only source term. Steady-state OH levels in the dark have been estimated to be on the order of 10^5 molecule cm^{-3} in the presence of 20 ppb O_3 and ~ 11 ppb alkenes (Weschler and Shields 1996). These O_3 levels are consistent with measurements in nonresidential buildings, but in residential buildings much lower O_3 levels (often less than 5 ppb) are commonly reported (Young et al. 2019). Steady-state OH levels in residences in the dark are therefore likely closer to 5×10^4 molecule cm^{-3} . Under direct sunlight, indoor $[OH]_{ss}$ can exceed 10^6 molecule cm^{-3} , making HONO photolysis the dominant OH source. We note that this applies primarily to areas illuminated by direct sunlight. Steady-state OH levels from HONO photolysis in volumes of air illuminated by diffuse sunlight have been predicted to range from $\sim 10^5$ – 10^6 molecule cm^{-3} within 1 m of an illuminated window (Zhou et al. 2020a). Illumination by fluorescent tubes can photolyze HONO, leading to predicted $[OH]_{ss}$ of $\sim 3 \times 10^6$ molecule cm^{-3} directly adjacent to the bulb, but this decreases by a factor of 10 at a distance of 1 m. Depending on the color temperature of the fluorescent tube and the presence of a shade, OH levels may be much lower (Zhou et al. 2020a).

Nitrate radical levels will likely be negligible in residences due to low source concentrations (especially O_3) and high sink concentrations (especially NO) (e.g., Young et al. 2019). Nitrate radical levels of up to ~ 20 pptv were reported in a conference room (Nøjgaard 2010); NO_3 levels may generally be higher in non-residential buildings, since larger ACR leads to higher O_3 concentrations and lower NO concentrations. Nitrate photolysis may therefore be important in some indoor locations.

Condensed Phase and Heterogeneous Indoor Photochemistry

One of the unique aspects of indoor environments is the high surface area to volume ratio (S/V). Many reactions can occur on these surfaces, as discussed in detail in Chap. VII.6. Here, we briefly discuss photochemical reactions on indoor surfaces and within condensed phases.

Few studies have directly investigated heterogeneous and condensed phase photochemical reactions indoors. These have primarily focused on two topics: photochemical formation of oxidants on painted surfaces, and photochemical transformations of pollutants associated with flame retardants in dust. These will be discussed below. Other photochemical processes may be important indoors, but there is a lack of literature on this. We discuss some potentially important areas of study in section “Future Directions.”

With respect to common indoor surfaces, photon fluxes within 1 cm of walls, floors, and metal counters were reported to be ~10% greater than those 1 m away due to reflections (Zhou et al. 2020a). While this enhancement will not significantly affect volume-averaged photon fluxes, it could increase heterogeneous photolysis rates as well as reaction rates very near the surfaces. If water or surface films are present, they may also alter the local photon flux through light scattering or competitive absorption (absorption of light by species other than the reactant of interest, also referred to as the inner filter effect).

Photochemical Formation of Oxidants on Painted Surfaces

Titanium dioxide (TiO_2) is a well-known catalyst both in manufactured materials and in the atmosphere (as a component of mineral dust). It has been incorporated into outdoor surfaces (e.g., buildings, roads) to reduce local NO_x and VOC levels, and to coatings applied to windows and high-touch surfaces to make the surfaces “self-cleaning.” Indoor paints containing TiO_2 nanoparticles are marketed as photocatalytic paints that remove NO_x and VOCs from the air; these have been shown to improve occupants’ assessment of indoor air quality under illuminated conditions (Kolarik and Toftum 2012). Indoor photocatalytic paints have been shown to reduce NO_2 levels under illumination at wavelengths relevant to indoors (e.g., Saltherammer and Fuhrmann 2007; Gandolfo et al. 2015, 2017), but gas-phase NO and HONO have been detected following NO_2 photocatalysis (Gandolfo et al. 2015, 2017). It has been suggested that HONO formed via NO_2 photocatalysis could double local OH levels (due to subsequent HONO photolysis) (Gandolfo et al. 2017), and high levels of gas-phase formaldehyde and acetaldehyde have been reported, likely caused by reactions of photocatalytically formed OH with components of the paint binder (Gandolfo et al. 2018).

Paint that is not designed with photocatalysis in mind may still contain TiO_2 as a brightener. Photocatalytic uptake of NO_2 to white interior paint resulting in gas-phase HONO formation has been reported (Bartolomei et al. 2014), and irradiation of nitrate-doped white house paint by artificial bulbs resulted in the production of gas-phase NO (Schwartz-Narbonne et al. 2019). The uptake of NO to surfaces coated with white, red, and green interior paints has also been investigated (Jones et al. 2020). Uptake was observed in the dark, and re-release of NO to the gas phase was observed under illumination by artificial bulbs. This behavior was attributed to physical uptake in the dark, including adsorption and diffusion through the paint, followed by photooxidation of NO to HONO, which photolyzes rapidly to produce NO as the primary gas-phase product (Jones et al. 2020). Interestingly, this result is different from observations when TiO_2 powder was the substrate, rather than paint containing TiO_2 . Under the same experimental conditions, the authors observed photo-enhanced NO uptake to TiO_2 resulting in the formation of gas-phase $\text{NO}_2 + \text{HONO}$ (NO_2 and HONO were not speciated in this study) (Jones et al. 2020).

Photochemistry in Dust and on Indoor Surface Films

Dust presents a complex indoor matrix. Its role in indoor chemistry (photochemical or otherwise) is poorly understood, but there is some evidence that photochemical reactions in dust could affect indoor exposure risks. An area of research that has received some interest in recent years is photochemical transformations of brominated flame retardants such as PBDEs (polybrominated diphenyl ethers). Several studies have reported that brominated flame retardants in dust collected from houses and vehicles undergo chemical transformation when exposed to outdoor sunlight or simulated sunlight (Stapleton and Dodder 2008; Lagalante et al. 2011). Smaller brominated species appear to be common products; photodegradation may therefore increase human exposure to smaller brominated congeners (Stapleton and Dodder 2008). We note that the studies performed to date have used illumination conditions relevant to outdoor environments; the kinetics and products of brominated flame retardants in dust irradiated at wavelengths relevant to indoor environments have not been reported.

Species other than brominated flame retardants may also undergo photochemical reactions in house dust. A number of aromatic pollutants such as polycyclic aromatic hydrocarbons (PAHs) have been detected in house dust (e.g., Salthammer 2020 and references therein). Many of these species absorb light at wavelengths relevant to indoor conditions, and photodegradation products can pose greater exposure risk than parent compounds. Azo dyes, which absorb visible light, have been identified as the dominant brominated species in house dust (Peng et al. 2016), and photosensitizers including benzophenones have been detected in house dust (Liu et al. 2016; Liu and Mabury 2019). Photodegradation of these photosensitizers has been reported in laboratory studies (Liu and Mabury 2019), although as with brominated flame retardants, these studies used illumination sources representative of outdoor sunlight.

Another complex matrix that may be important to indoor photochemistry is indoor surface films (Weschler and Nazaroff 2017; Lim and Abbatt 2020; Ault et al. 2020; Liu et al. 2020). Increased photo-enhanced conversion of NO₂ to HONO on glass was reported when surface films were present (Liu et al. 2020). At NO₂ levels of 50 ppb (relevant to levels reported during the use of gas stoves (Zhou et al. 2018; Liu et al. 2019b)), HONO levels in a 30 m³ kitchen were predicted to increase by ~4 ppb under illuminated conditions compared to in the dark. While photochemistry on indoor surface films remains largely unexplored, existing knowledge of photochemistry on outdoor surface films, or “urban grime,” may provide insight. Surface films can alter analyte partitioning coefficients; outdoors, surface films have been reported to enhance surface partitioning of a range of pollutants (e.g., Diamond et al. 2000; Wu et al. 2008). Surface films can also alter the chemical environment experienced by adsorbed analytes. For example, an indoor surface film coating an interior painted wall might shield analytes from TiO₂ in the paint and suppress photocatalytic reactions. Indoor surface films may alter local photon fluxes. Outdoor and indoor surface films have been reported to consist at least partially of particulate matter (as opposed to homogeneous films) (Grant et al. 2019; Kroptavich et al. 2020; Liu et al. 2020). This heterogeneous morphology could increase local photon fluxes via scattering (Kroptavich et al. 2020; Liu et al. 2020). Both indoor

and outdoor surface films have also recently been reported to absorb photons as long as 400 nm (Kroptavich et al. 2020; Liu et al. 2020). This overlaps with photons available indoors ($>\sim 330$ nm) and could reduce the number of photons available to analytes (competitive photon absorption). Absorbance of photons by surface films could also enable them to participate in photochemistry, for example, by forming reactive species or acting as photosensitizers (Kroptavich et al. 2020; Liu et al. 2020). In addition to the photo-enhanced NO₂ uptake reported on indoor surface films (Liu et al. 2020), photo-enhanced NO₂ uptake and nitric acid photolysis have been reported to occur more rapidly on outdoor surface films than on glass (Baergen and Donaldson 2016; Liu et al. 2019a). These enhancements have not been directly linked to absorptive properties of the surface films; further study is recommended.

Photochemistry in Indoor Aqueous Phases

Aqueous phase chemistry is not generally associated with indoor environments, but water is present indoors. Even at a relative humidity (RH) of 20%, which is on the low end of common indoor RHs, a thin film of water is present on most surfaces (Sumner et al. 2004). This water film appears to increase uptake of water-soluble organic compounds (WSOC) to indoor surfaces such as walls (Duncan et al. 2018). The effects of surficial water on heterogeneous indoor reactions have not been studied, but they may be important. For example, many atmospheric (outdoor) heterogeneous reactions show RH dependencies, and the uptake and reemission of NO to painted surfaces is different at 0 and 50% RH (Jones et al. 2020). Effects of water at surfaces could include competition for reactive surface sites, participation in photochemistry (e.g., photochemical heterogeneous transformation of NO₂ to HONO), or by affecting the speciation of analytes. As noted in section “[Different Considerations for Condensed Phase and Heterogeneous Photochemistry](#),” ionic species such as HNO₃ on indoor surfaces may be present in either the molecular form or the ionic form (NO₃⁻), or as a combination of both. Uptake of water vapor to indoor surface films has been reported to be substantially larger than to films of silicone vacuum grease used as a control at RHs relevant to indoor environments (Schwartz-Narbonne and Donaldson 2019). Those authors suggested that this uptake may be spatially heterogeneous; “pools” of water may exist at indoor surfaces.

Liquid water is present on “hidden” indoor surfaces such as condensate on cooling coils in HVAC systems. The composition of this water may be very different than that on visible indoor surfaces, and a wide range of photochemical reactions could occur when UV disinfection is used in HVAC systems.

Current Research

Measurements of Photochemically Generated Species

Photochemically generated species are often radicals. These are extremely difficult to detect and quantify. Photochemically produced OH and HO₂ indoors have been detected using laser-induced fluorescence – fluorescence assay through gas

expansion (LIF-FAGE) (Gomez Alvarez et al. 2013; Carslaw et al. 2017). While most researchers will not be able to detect radicals indoors, secondary products that are more easily detected may help to constrain the role of indoor photochemistry under different illumination conditions. For example, the formation of particulate matter was observed in an atmospheric chamber containing HONO when fluorescent lights were on, but not in the dark (Wang et al. 2019). This particle formation was attributed to secondary and tertiary reactions involving photochemically generated OH.

A number of field observations have reported results that may point to the influence of photochemistry. It is becoming increasingly common for studies to incorporate calculations of photolysis rate constants in manuscripts to provide some context about the possible role of photochemistry. These rate constants can be taken from the literature or calculated using photon fluxes that are either measured during the field campaign or reported in the literature, as discussed below.

Photon Flux Measurements and Predictions

Wavelength-resolved photon fluxes are key to predicting photochemical reaction kinetics, and, therefore, indoor air composition under illuminated conditions. Despite increasing attention to this area, there are no generalizable models of indoor UV photon fluxes. As discussed above, this is nontrivial, since photon fluxes depend strongly on location (both geographically and even within a single room) and time (both over the course of day and seasonally).

A range of techniques have been used to measure indoor photon fluxes. The gold standard for measuring outdoor photon fluxes is spectroradiometers that capture photons from 180 degrees. Some models combine two such instruments to capture a full 360°, and therefore true spherically integrated photon fluxes. Such radiometers have been used occasionally indoors (Gomez Alvarez et al. 2013; Gandolfo et al. 2016; Blocquet et al. 2018), but they are cost-prohibitive for most researchers and require significant training and calibration, so they are unlikely to be widely used for indoor measurements. Hand-held spectrometers are an attractive alternative, as they are easy to use and cost less than 10% of spectroradiometers that capture 180 or 360°. Their portability is another advantage; they can be rapidly moved throughout an indoor space to investigate the spatial distribution of photon fluxes, as demonstrated in Kowal et al. (2017), Blocquet et al. (2018), Zhou et al. (2020a), and Zhou et al. (2021). The main drawback of these instruments is that they collect photons from a limited range of angles. As discussed in section “[Different Considerations for Condensed Phase and Heterogeneous Photochemistry](#),” irradiance is related to photon flux by $\cos(\theta)$. So if all incoming light is unidirectional (e.g., collimated sunlight) and impinges directly on the detector surface, the irradiance measured by a handheld spectrometer should be roughly equal to total photon flux. However, if photons do not directly impinge on the detector surface, irradiance will need to be converted to photon flux. A more complicated scenario is when light is not unidirectional (e.g., a combination of direct, diffuse, and reflected light). In this case, photons that do not impinge directly on the surface will be undercounted. The

magnitude of the uncertainty in photon fluxes and predicted photolysis kinetics due to this undercounting has not been quantified, though some studies suggest that diffuse and scattered sunlight indoors will not significantly contribute to HONO photolysis (Gandolfo et al. 2016; Zhou et al. 2020a). If this observation is generalizable, accounting for the angle of incoming direct sunlight may be sufficient to quantify indoor UV photon fluxes using handheld spectrometers, but further characterization and validation of these devices for indoor use is suggested.

Another inexpensive option for indoor light measurements is photosynthetically active radiation (PAR) sensors, which provide total irradiance over a wavelength range (commonly 400–700 nm, although extended wavelength ranges of 340–1040 nm are available). These have been used to investigate spatial distributions of indoor photon fluxes (Blocquet et al. 2018). These are useful in conjunction with wavelength-resolved sensors, but are not well-suited for quantifying UV photon fluxes. The lack of wavelength resolution can also be an issue since analyte absorption cross sections and photolysis quantum yields can have strong wavelength dependences. Even with photon flux measurements that extend into the UV, the spectral dependence to that light can be extremely important. For analytes such as HONO, which absorb strongly throughout the UV, this is not an issue, but for analytes such as O₃, H₂O₂, and HCHO, which have strong wavelength dependences to either σ or Φ , knowing the wavelength dependence of F is crucial for predicting photolysis rate constants. Recent studies have provided comparisons of visible and UV light intensity indoors (Blocquet et al. 2018; Zhou et al. 2020a). If generalizable equations relating measured visible photon fluxes to UV photon fluxes indoors can be established, PAR sensors may become powerful tools for indoor photon flux measurements due to their portability and low cost. The issue of wavelength dependence mentioned above will still be a factor, however, so measurements with PAR sensors should be complemented by wavelength-resolved measurements whenever possible.

Models

Predictive models applied to indoor chemistry are discussed in detail in Chap. VII.10. Here, we focus on the way different models address indoor photochemical reactions. Box models use rate constants for sources and sinks to predict temporal evolutions of analyte concentrations under a range of atmospheric conditions. Commonly used for the study of reactions outdoors, box models designed specifically to study indoor chemistry have been developed. The INDCM (INdoor Detailed Chemistry Model) (Carslaw 2007) includes explicit chemical reactions for approximately 5000 chemical species. Photochemical rate constants are calculated using Eq. 3. Generally, a total, wavelength-independent photon flux of 2.3×10^{13} photons cm⁻² s⁻¹ is assumed between 300 and 400 nm. The INDCM can be modified to account for wavelength-resolved photon fluxes for specific

species by inputting values of J for each analyte. This feature has been used to calculate indoor radical levels under different lighting conditions (e.g., sunlight, fluorescent tubes) (Wang et al. 2020; Zhou et al. 2020b). The INteraction with Chemistry and Aerosols (INCA)-Indoor model (Mendez et al. 2015) serves a similar purpose as the INDCM. This model includes 1400 reactions and 640 VOCs, with some simplifications to reduce computation time. These simplifications make it a “semi-explicit” model, compared to the INDCM, which is an “explicit” model. Detailed comparisons of the two models are provided by the developers of the INCA-Indoor model (Mendez et al. 2015). Photolysis rate constants are calculated using literature values of σ and Φ , and photon fluxes are computed using the Total UltraViolet (TUV) model ((Madronich and Flocke 1999), described below) and attenuation factors for indoor light from Nazaroff and Cass (1986). INCA-Indoor has been used to investigate the importance of photon fluxes, ventilation rates, and cooking on indoor OH levels in the presence and absence of HONO (Mendez et al. 2015).

Box models are powerful predictive tools for indoor chemistry. A limitation of existing models is that they assume spatial homogeneity in terms of gas-phase composition. Sources and sinks of analytes can be spatially heterogeneous (e.g., due to emission from point source such as a gas stove). As discussed in section “[Factors Controlling Gas Phase Indoor Photochemistry](#),” indoor photon fluxes are often very spatially variable, so radical levels may differ by orders of magnitude in two locations within the same room, simply due to different lighting conditions. Computational flow dynamics (CFD) models have long been used to predict spatial distributions of analytes in various environments. A CFD model has recently been used to investigate the spatial distribution of radicals in a room due to photolysis of HONO generated from a gas stove (Won et al. 2019). This work reported that increased radical levels (compared to indoor background levels) were confined to directly sunlit volumes of air, but that oxidation products were distributed throughout the room. Figure 5 shows the predicted spatially resolved indoor OH levels in a room illuminated by sunlight entering the window from different angles, and Fig. 6 shows OH concentrations under illumination by various artificial light sources. This type of model is an important complement to indoor box models such as the INDCM and INCA-Indoor.

Finally, the TUV model bears mentioning, despite the fact that it is not designed for indoor chemistry (Madronich and Flocke 1999). This freely available and user-friendly model allows the calculation of irradiance and J values for more than one hundred common atmospheric gases under a variety of user-specified conditions (e.g., SZA, altitude, cloud, and aerosol prevalence). The TUV is widely used to calculate J values in models that describe outdoor chemistry (e.g., Gressent et al. 2016). It is already used in at least one indoor chemistry model (INCA-Indoor) (Mendez et al. 2015), and as further information about the relationship between outdoor and indoor solar photon fluxes emerges from studies such as those described in section “[Photon Flux Measurements and Predictions](#),” it will likely become an even more powerful tool for indoor chemistry research.

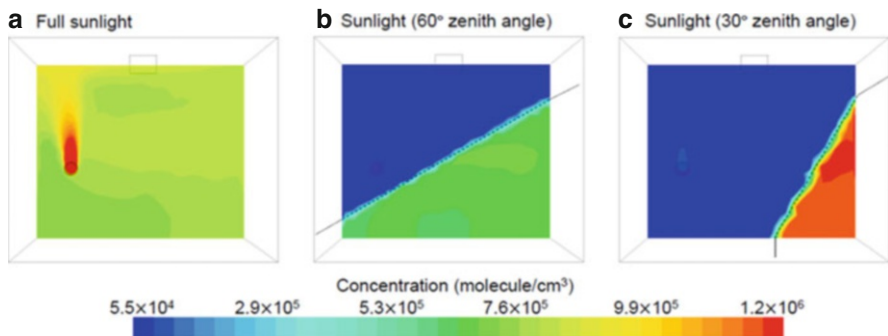


Fig. 5 Predicted spatially resolved indoor OH concentrations at different solar zenith angles. Reprinted with permission from Won et al. (2019). Copyright 2019 American Chemical Society

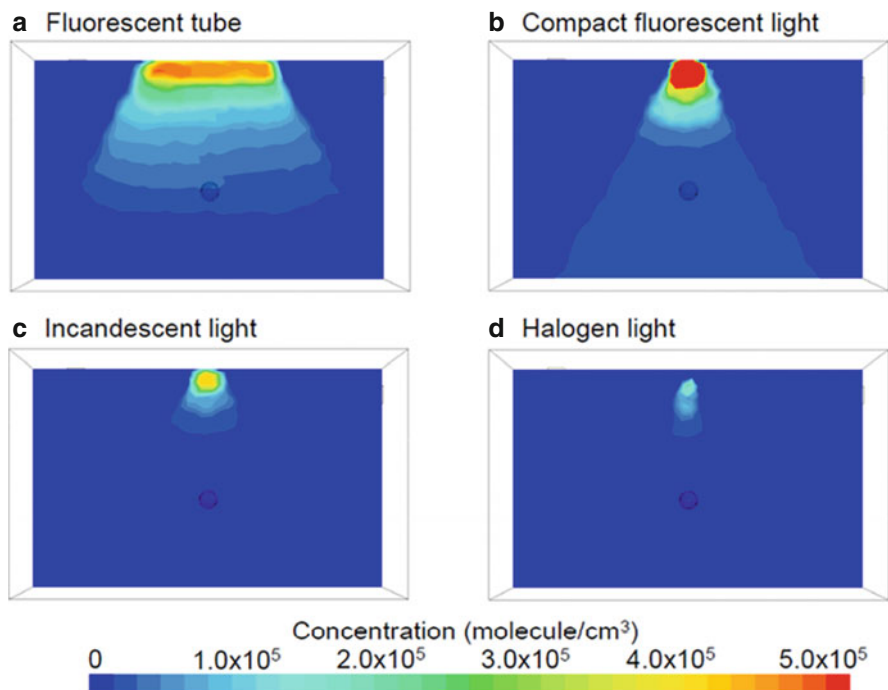


Fig. 6 Predicted spatially resolved OH concentrations under different artificial lighting conditions. Reprinted with permission from Won et al. (2019). Copyright 2019 American Chemical Society

Conclusions and Future Directions

The study of indoor photochemistry has made rapid bounds in recent years, but it remains an area ripe for discovery. The most pressing issue is constraining the role of photochemistry on the composition of the air indoors. We know that photochemistry

can occur indoors, and that it can greatly increase local radical levels. But under what conditions will it influence average radical levels throughout an indoor space? Can local regions of increased radical levels affect air quality? And what role does photochemistry on indoor surfaces play in determining indoor air composition? Given the rapid progress in indoor photochemistry research in recent years, we may have at least partial answers to these questions before long.

Indoor photochemistry can cause large spatial variability in indoor air composition within a single room due to the spatial heterogeneity of indoor photon fluxes, as illustrated in Figs. 5 and 6 (Won et al. 2019). The geometry of illuminated areas can change dramatically over the course of a day. This spatial and temporal variability makes it difficult to constrain the effects of photochemistry on indoor air composition. Box models, CFD models, and even architectural models that predict the spatial distribution of visible light intensity within a building will be powerful tools to predict the impact of photochemistry in indoor spaces. These models could be used for sensitivity tests on air composition under different lighting conditions, and to visualize the spatial distribution of analytes throughout an indoor environment over time. Existing box models could be modified to include multiple compartments with different photon fluxes, such as directly illuminated air volumes, diffusely illuminated air volumes, dark air volumes, and near-surface volumes. This practice is employed in many (outdoor) atmospheric models to account for different regions of the atmosphere that have different conditions (e.g., emissions, light availability, etc.). For example, GEOS-Chem, one of the most widely used chemical transport models, includes numerous air compartments to represent conditions in different surface locations and altitudes (Bey et al. 2001). The Multimedia Urban Model (MUM) is a box model that includes compartments for air, water, soil, and urban surfaces coated with urban grime (Diamond et al. 2001). The creators of MUM recently developed the Activity-Based Indoor Chemical Assessment Model (ABICAM) to investigate human exposure to semi-volatile pollutants such as phthalates (Kvasnicka et al. 2020). This model includes nine compartments relevant to indoor environments, including air, human skin lipids, various types of flooring, and indoor surface films, but does not include explicit chemical reactions. Employing these types of approaches to explicit and semi-explicit indoor box models could improve our ability to predict and understand photochemistry indoors.

Characterizing the temporal and spatial variations of indoor UV photon fluxes will also further our understanding of indoor photochemistry. Existing knowledge of indoor light intensity, including spatial and temporal variations, is almost entirely based on visible light. As discussed above, UV photon fluxes often do not scale linearly with visible photon fluxes indoors. Further measurements will lead to more robust relationships between UV photon fluxes and variables that are more widely measured such as visible photon fluxes indoors and outdoors. This information can be used to estimate the impact of photochemistry on measured indoor air composition and can provide models with useful input and parameterization information.

With improved characterization of inexpensive sensors such as handheld spectrometers and PARS, widespread indoor photon flux measurements may become possible. Measuring photon fluxes concurrently with photolabile species will be especially important to constraining the role of photochemistry on indoor air

composition. This has been done in a few experiments (e.g., Gomez Alvarez et al. 2013; Bartolomei et al. 2014; Blocquet et al. 2018; Zhou et al. 2018; Farmer et al. 2019; Liu et al. 2019b; Schwartz-Narbonne et al. 2019; Gandolfo et al. 2020; Mattila et al. 2020), but it is not currently standard practice.

Surface chemistry is likely very important indoors, but indoor surface photochemistry remains largely unexplored. Early results suggest that various surfaces such as painted walls (with and without photocatalytic coatings) and indoor surface films may contribute to NO_x cycling via photocatalyzed NO and NO₂ uptake (e.g., Bartolomei et al. 2014; Gandolfo et al. 2015; Schwartz-Narbonne et al. 2019; Jones et al. 2020; Liu et al. 2020), and photodegradation in dust may affect the exposure risks posed by aromatic pollutants (e.g., Stapleton and Dodder 2008; Lagalante et al. 2011; Liu and Mabury 2019). The field of indoor surface photochemistry is currently wide open.

Photochemistry initiated by UV disinfection may become increasingly important as this technology becomes more widely used. Unwanted photochemical reactions of UV-C disinfection are minimal when properly installed and operated. However, “off-label” uses of UV disinfection may adversely affect indoor air quality via photochemistry. The magnitude of these effects has not been widely studied. Further, UV disinfection in HVAC systems could also affect air composition, but photochemistry within HVAC systems remains unexplored.

Indoor photochemistry is a relatively new research field. The importance of indoor photochemistry to indoor air composition and air quality remains unclear, and will certainly depend greatly on local illumination conditions. Although many large questions remain, research in this area is progressing rapidly, and great strides toward answering key questions will likely be made in coming years.

Acknowledgments The authors thank the Alfred P. Sloan Foundation Chemistry of Indoor Environments grant G-2018-11062 for support. TFK holds a Canada Research Chair in Environmental Analytical Chemistry; this work was supported in part by the Canada Research Chairs program.

References

- Abbatt JPD, Wang C (2020) The atmospheric chemistry of indoor environments. *Environ Sci Process Impacts* 22:25–48. <https://doi.org/10.1039/C9EM00386J>
- Arata C, Zarzana KJ, Misztal PK et al (2018) Measurement of NO₃ and N₂O₅ in a residential kitchen. *Environ Sci Technol Lett* 5:595–599. <https://doi.org/10.1021/acs.estlett.8b00415>
- Ashrae Ashrae technical resources: filtration/disinfection. In: ASHRAE. <https://www.ashrae.org/technical-resources/filtration-disinfection>. Accessed 28 Jan 2021
- Ault AP, Grassian VH, Carslaw N et al (2020) Indoor surface chemistry: developing a molecular picture of reactions on indoor interfaces. *Chem* 6:3203–3218. <https://doi.org/10.1016/j.chempr.2020.08.023>
- Baergen AM, Donaldson DJ (2016) Formation of reactive nitrogen oxides from urban grime photochemistry. *Atmos Chem Phys* 16:6355–6363. <https://doi.org/10.5194/acp-16-6355-2016>

- Bartolomei V, Sörgel M, Gligorovski S et al (2014) Formation of indoor nitrous acid (HONO) by light-induced NO₂ heterogeneous reactions with white wall paint. Environ Sci Pollut Res 21: 9259–9269. <https://doi.org/10.1007/s11356-014-2836-5>
- Bey I, Jacob DJ, Yantosca RM et al (2001) Global modeling of tropospheric chemistry with assimilated meteorology: model description and evaluation. J Geophys Res Atmos 106: 23073–23095. <https://doi.org/10.1029/2001JD000807>
- Blocquet M, Guo F, Mendez M et al (2018) Impact of the spectral and spatial properties of natural light on indoor gas-phase chemistry: experimental and modeling study. Indoor Air 28:426–440. <https://doi.org/10.1111/ina.12450>
- Burkholder JB, Sander SP, Abbatt J, et al (2015) Chemical kinetics and photochemical data for use in atmospheric studies evaluation No.18. JPL Publ. 15-10 1–153
- Carslaw N (2007) A new detailed chemical model for indoor air pollution. Atmos Environ 41: 1164–1179. <https://doi.org/10.1016/j.atmosenv.2006.09.038>
- Carslaw N, Fletcher L, Heard D et al (2017) Significant OH production under surface cleaning and air cleaning conditions: impact on indoor air quality. Indoor Air 27:1091–1100. <https://doi.org/10.1111/ina.12394>
- Davies A, Pottage T, Bennett A, Walker J (2011) Gaseous and air decontamination technologies for Clostridium difficile in the healthcare environment. J Hosp Infect 77:199–203. <https://doi.org/10.1016/j.jhin.2010.08.012>
- Diamond ML, Gingrich SE, Fertuck K et al (2000) Evidence for organic film on an impervious urban surface: characterization and potential teratogenic effects. Environ Sci Technol 34:2900–2908. <https://doi.org/10.1021/es9906406>
- Diamond ML, Priemer DA, Law NL (2001) Developing a multimedia model of chemical dynamics in an urban area. Chemosphere 44:1655–1667. [https://doi.org/10.1016/S0045-6535\(00\)00509-9](https://doi.org/10.1016/S0045-6535(00)00509-9)
- Duncan SM, Sexton KG, Turpin BJ (2018) Oxygenated VOCs, aqueous chemistry, and potential impacts on residential indoor air composition. Indoor Air 28:198–212. <https://doi.org/10.1111/ina.12422>
- EPA (2018) Guide to air cleaners in the home 2nd edition
- Farmer DK, Vance ME, Abbatt JPD et al (2019) Overview of HOMEChem: house observations of microbial and environmental chemistry. Environ Sci Process Impacts 21:1280–1300. <https://doi.org/10.1039/C9EM00228F>
- Finlayson-Pitts BJ, Pitts JN (2000) Chemistry of the upper and lower atmosphere: theory, experiments, and applications. Academic Press, San Diego
- Gandolfo A, Bartolomei V, Gomez Alvarez E et al (2015) The effectiveness of indoor photocatalytic paints on NO_x and HONO levels. Appl Catal B Environ 166–167:84–90. <https://doi.org/10.1016/j.apcatb.2014.11.011>
- Gandolfo A, Gligorovski V, Bartolomei V et al (2016) Spectrally resolved actinic flux and photolysis frequencies of key species within an indoor environment. Build Environ 109: 50–57. <https://doi.org/10.1016/j.buildenv.2016.08.026>
- Gandolfo A, Rouyer L, Wortham H, Gligorovski S (2017) The influence of wall temperature on NO₂ removal and HONO levels released by indoor photocatalytic paints. Appl Catal B Environ 209:429–436. <https://doi.org/10.1016/j.apcatb.2017.03.021>
- Gandolfo A, Marque S, Temime-Roussel B et al (2018) Unexpectedly high levels of organic compounds released by indoor photocatalytic paints. Environ Sci Technol 52:11328–11337. <https://doi.org/10.1021/acs.est.8b03865>
- Gandolfo A, Bartolomei V, Truffier-Boutry D et al (2020) The impact of photocatalytic paint porosity on indoor NO_x and HONO levels. Phys Chem Chem Phys 22:589–598. <https://doi.org/10.1039/C9CP05477D>
- Gligorovski S (2016) Nitrous acid (HONO): an emerging indoor pollutant. J Photochem Photobiol A Chem 314:1–5. <https://doi.org/10.1016/j.jphotochem.2015.06.008>
- Gligorovski S, Abbatt JPD (2018) An indoor chemical cocktail. Science 359:632–633. <https://doi.org/10.1126/science.aar6837>

- Gligorovski S, Weschler CJ (2013) The oxidative capacity of indoor atmospheres. *Environ Sci Technol* 47:13905–13906. <https://doi.org/10.1021/es404928t>
- Gomez Alvarez E, Amedro D, Afif C et al (2013) Unexpectedly high indoor hydroxyl radical concentrations associated with nitrous acid. *Proc Natl Acad Sci* 110:13294–13299. <https://doi.org/10.1073/pnas.1308310110>
- Grant JS, Zhu Z, Anderton CR, Shaw SK (2019) Physical and chemical morphology of passively sampled environmental films. *ACS Earth Space Chem* 3:305–313. <https://doi.org/10.1021/acsearthspacechem.8b00158>
- Gressent A, Sauvage B, Cariolle D et al (2016) Modeling lightning-NO_x chemistry on a sub-grid scale in a global chemical transport model. *Atmos Chem Phys* 16:5867–5889. <https://doi.org/10.5194/acp-16-5867-2016>
- Jacob DJ (1999) Introduction to atmospheric chemistry. Princeton University Press, Princeton
- Jacob K., Nojgaard (2010) Indoor measurements of the sum of the nitrate radical NO₃ and nitrogen pentoxide N₂O₅ in Denmark. *Chemosphere* 79(8):898–904. <https://doi.org/10.1016/j.chemosphere.2010.02.025>
- Jones SH, Hosse FPR, Yang X, Donaldson DJ (2020) Loss of NO(g) to painted surfaces and its re-emission with indoor illumination. *Indoor Air* ina.12741. <https://doi.org/10.1111/ina.12741>
- Karlsson J, Rubin M, Roos A (2001) Evaluation of predictive models for the angle-dependent total solar energy transmittance of glazing materials. *Sol Energy* 71:23–31. [https://doi.org/10.1016/S0038-092X\(01\)00024-X](https://doi.org/10.1016/S0038-092X(01)00024-X)
- Kim S, Vandenboer TC, Young CJ et al (2014) The primary and recycling sources of OH during the NACHTT-2011 campaign: HONO as an important OH primary source in the wintertime. *J Geophys Res* 119. <https://doi.org/10.1002/2013JD019784>
- Kolarik J, Toftum J (2012) The impact of a photocatalytic paint on indoor air pollutants: sensory assessments. *Build Environ* 57:396–402. <https://doi.org/10.1016/j.buildenv.2012.06.010>
- Kowal SF, Allen SR, Kahan TF (2017) Wavelength-resolved photon fluxes of indoor light sources: implications for HO_x production. *Environ Sci Technol* 51:10423–10430. <https://doi.org/10.1021/acs.est.7b02015>
- Kroptavich CR, Zhou S, Kowal SF, Kahan TF (2020) Physical and chemical characterization of urban grime sampled from two cities. *ACS Earth Space Chem* 4:1813–1822. <https://doi.org/10.1021/acsearthspacechem.0c00192>
- Kvasnicka J, Cohen Hubal E, Ladan J et al (2020) Transient multimedia model for investigating the influence of indoor human activities on exposure to SVOCs. *Environ Sci Technol* 54: 10772–10782. <https://doi.org/10.1021/acs.est.0c03268>
- Lagalante AF, Shedd CS, Greenbacker PW (2011) Levels of polybrominated diphenyl ethers (PBDEs) in dust from personal automobiles in conjunction with studies on the photochemical degradation of decabromodiphenyl ether (BDE-209). *Environ Int* 37:899–906. <https://doi.org/10.1016/j.envint.2011.03.007>
- Lim CY, Abbott JP (2020) Chemical composition, spatial homogeneity, and growth of indoor surface films. *Environ Sci Technol* 54:14372–14379. <https://doi.org/10.1021/acs.est.0c04163>
- Lim HS, Kim G (2010) Spectral characteristics of UV light existing in indoor visual environment. *Indoor Built Environ* 19:586–591. <https://doi.org/10.1177/1420326X10380123>
- Liu R, Mabury SA (2019) Identification of photoinitiators, including novel phosphine oxides, and their transformation products in food packaging materials and indoor dust in Canada. *Environ Sci Technol* 53:4109–4118. <https://doi.org/10.1021/acs.est.9b00045>
- Liu R, Lin Y, Hu F et al (2016) Observation of emerging photoinitiator additives in household environment and sewage sludge in China. *Environ Sci Technol* 50:97–104. <https://doi.org/10.1021/acs.est.5b04977>
- Liu J, Li S, Mekic M et al (2019a) Photoenhanced uptake of NO₂ and HONO formation on real urban grime. *Environ Sci Technol Lett* 6:413–417. <https://doi.org/10.1021/acs.estlett.9b00308>
- Liu J, Li S, Zeng J et al (2019b) Assessing indoor gas phase oxidation capacity through real-time measurements of HONO and NO_x in Guangzhou, China. *Environ Sci Process Impacts* 21:1393–1402. <https://doi.org/10.1039/C9EM00194H>

- Liu J, Deng H, Lakey PSJ et al (2020) Unexpectedly high indoor HONO concentrations associated with photochemical NO₂ transformation on glass windows. Environ Sci Technol 54:15680–15688. <https://doi.org/10.1021/acs.est.0c05624>
- Madronich S, Flocke S (1999) The role of solar radiation in atmospheric chemistry. In: Boule P (ed) Environmental Photochemistry. Springer, Berlin Heidelberg, pp 1–26
- Malley PPA, Grossman JN, Kahan TF (2017) Effects of chromophoric dissolved organic matter on anthracene photolysis kinetics in aqueous solution and ice. J Phys Chem A 121:7619–7626. <https://doi.org/10.1021/acs.jpca.7b05199>
- Marcotte G, Ayotte P, Bendounan A et al (2013) Dissociative adsorption of nitric acid at the surface of amorphous solid water revealed by X-ray absorption spectroscopy. J Phys Chem Lett 4:2643–2648. <https://doi.org/10.1021/jz401310j>
- Mattila JM, Lakey PSJ, Shiraiwa M et al (2020) Multiphase chemistry controls inorganic chlorinated and nitrogenated compounds in indoor air during bleach cleaning. Environ Sci Technol 54:1730–1739. <https://doi.org/10.1021/acs.est.9b05767>
- McFall AS, Anastasio C (2016) Photon flux dependence on solute environment in water ices. Environ Chem 13:682. <https://doi.org/10.1071/EN15199>
- Mendez M, Blond N, Blondeau P et al (2015) Assessment of the impact of oxidation processes on indoor air pollution using the new time-resolved INCA-Indoor model. Atmos Environ 122:521–530. <https://doi.org/10.1016/j.atmosenv.2015.10.025>
- Morenz KJ, Donaldson DJ (2017) Chemical morphology of frozen mixed nitrate–salt solutions. J Phys Chem A 121:2166–2171. <https://doi.org/10.1021/acs.jpca.6b12608>
- Moussa SG, Stern AC, Raff JD et al (2013) Experimental and theoretical studies of the interaction of gas phase nitric acid and water with a self-assembled monolayer. Phys Chem Chem Phys 15: 448–458. <https://doi.org/10.1039/C2CP42405C>
- Nazaroff WW, Cass GR (1986) Mathematical modeling of chemically reactive pollutants in indoor air. Environ Sci Technol 20:924–934. <https://doi.org/10.1021/es00151a012>
- Nissenson P, Knox CJH, Finlayson-Pitts BJ et al (2006) Enhanced photolysis in aerosols: evidence for important surface effects. Phys Chem Chem Phys 8:4700. <https://doi.org/10.1039/b609219e>
- Peng H, Saunders DMV, Sun J et al (2016) Mutagenic Azo Dyes, rather than flame retardants, are the predominant brominated compounds in house dust. Environ Sci Technol 50:12669–12677. <https://doi.org/10.1021/acs.est.6b03954>
- Riikonen S, Parkkinen P, Halonen L, Gerber RB (2013) Ionization of nitric acid on crystalline ice: the role of defects and collective proton movement. J Phys Chem Lett 4:1850–1855. <https://doi.org/10.1021/jz400531q>
- Salthammer T (2020) Emerging indoor pollutants. Int J Hyg Environ Health 224:113423. <https://doi.org/10.1016/j.ijheh.2019.113423>
- Salthammer T, Fuhrmann F (2007) Photocatalytic surface reactions on indoor wall paint. Environ Sci Technol 41:6573–6578. <https://doi.org/10.1021/es070057m>
- Schwartz-Narbonne H, Donaldson DJ (2019) Water uptake by indoor surface films. Sci Rep 9: 11089. <https://doi.org/10.1038/s41598-019-47590-x>
- Schwartz-Narbonne H, Jones SH, Donaldson DJ (2019) Indoor lighting releases gas phase nitrogen oxides from indoor painted surfaces. Environ Sci Technol Lett 6:92–97. <https://doi.org/10.1021/acs.estlett.8b00685>
- Seinfeld JH, Pandis SN (2016) Atmospheric chemistry and physics: from air pollution to climate change, 3rd edn. John Wiley & Sons, Hoboken
- Stapleton HM, Dodder NG (2008) Photodegradation of decabromodiphenyl ether in house dust by natural sunlight. Environ Toxicol Chem 27:306. <https://doi.org/10.1897/07-301R.1>
- Stark H, Brown SS, Wong KW et al (2011) City lights and urban air. Nat Geosci 4:730–731. <https://doi.org/10.1038/ngeo1300>
- Stutz J, Kim ES, Platt U et al (2000) UV-visible absorption cross sections of nitrous acid. J Geophys Res-Atmospheres 105:14585–14592. <https://doi.org/10.1029/2000JD900003>
- Sumner AL, Menke EJ, Dubowski Y et al (2004) The nature of water on surfaces of laboratory systems and implications for heterogeneous chemistry in the troposphere. Phys Chem Chem Phys 6:604. <https://doi.org/10.1039/b308125g>

- Turro NJ, Ramamurthy V, Scaiano JC (2009) Principles of molecular photochemistry: an introduction. University Science Books, Sausalito
- Wang C, Collins DB, Abbatt JPD (2019) Indoor illumination of terpenes and bleach emissions leads to particle formation and growth. Environ Sci Technol 53:11792–11800. <https://doi.org/10.1021/acs.est.9b04261>
- Wang Z, Kowal SF, Carslaw N, Kahan TF (2020) Photolysis-driven indoor air chemistry following cleaning of hospital wards. Indoor Air 30:1241–1255. <https://doi.org/10.1111/ina.12702>
- Weschler CJ, Nazaroff WW (2017) Growth of organic films on indoor surfaces. Indoor Air 27: 1101–1112. <https://doi.org/10.1111/ina.12396>
- Weschler CJ, Shields HC (1996) Production of the hydroxyl radical in indoor air. Environ Sci Technol 30:3250–3258. <https://doi.org/10.1021/es960032f>
- Won Y, Waring M, Rim D (2019) Understanding the spatial heterogeneity of indoor OH and HO₂ due to photolysis of HONO using computational fluid dynamics simulation. Environ Sci Technol 53:14470–14478. <https://doi.org/10.1021/acs.est.9b06315>
- Wu RW, Harner T, Diamond ML, Wilford B (2008) Partitioning characteristics of PCBs in urban surface films. Atmos Environ 42:5696–5705. <https://doi.org/10.1016/j.atmosenv.2008.03.009>
- Young CJ, Washenfelder RA, Roberts JM et al (2012) Vertically resolved measurements of nighttime radical reservoirs in los angeles and their contribution to the urban radical budget. Environ Sci Technol:46. <https://doi.org/10.1021/es302206a>
- Young CJ, Zhou S, Siegel JA, Kahan TF (2019) Illuminating the dark side of indoor oxidants. Environ Sci Process Impacts 21:1229–1239. <https://doi.org/10.1039/C9EM0011E>
- Zhou S, Kahan TF (2021). Spatiotemporal characterization of irradiance and photolysis rate constants of indoor gas-phase species in the UTest house during HOMEChem. Indoor Air. 00: 1– 11. <https://doi.org/10.1111/ina.12966>
- Zhou S, Young CJ, VandenBoer TC et al (2018) Time-resolved measurements of nitric oxide, nitrogen dioxide, and nitrous acid in an occupied New York home. Environ Sci Technol 52: 8355–8364. <https://doi.org/10.1021/acs.est.8b01792>
- Zhou S, Kowal SF, Cregan AR, Kahan TF (2020a) Factors affecting wavelength-resolved ultraviolet irradiance indoors and their impacts on indoor photochemistry. Indoor Air. ina.12784. <https://doi.org/10.1111/ina.12784>
- Zhou S, Liu Z, Wang Z et al (2020b) Hydrogen peroxide emission and fate indoors during non-bleach cleaning: a chamber and modeling study. Environ Sci Technol 54:15643–15651. <https://doi.org/10.1021/acs.est.0c04702>



Indoor Surface Chemistry

30

Glenn C. Morrison

Contents

Introduction	886
Surfaces and Chemical Transformations	886
Indoor Surfaces	886
Ozone Initiated Chemistry	888
Nitrogen Oxides	891
Chlorine Chemistry	893
Acid-Base Chemistry	893
Hydrolysis	895
Conclusion	896
Cross-References	896
References	896

Abstract

Indoor surfaces support a wide variety of chemical transformations that can both reduce and increase the concentrations of indoor air pollutants. Building materials, furnishings, and occupants contribute to the large amount and very wide variety of exposed surfaces. Chemistry can take place directly at the interface between surface and air or in films that coat these surfaces. Important transformations include ozone reactions with surface oils like triglycerides and squalene; these lower indoor air concentrations of ozone but consequently increase the air concentrations of aldehydes, acids, and particles. Nitrogen oxides can react at surfaces to generate nitrous acid which then participates in the conversion of amines to potentially carcinogenic nitrosamines. Hydrolysis of phthalate plasticizers increases levels of odorous chemicals and acid-base chemistry controls the rate of some reactions while serving to store vast amounts of otherwise volatile molecules in surface reservoirs. To better understand and control indoor

G. C. Morrison (✉)

Environmental Sciences and Engineering, University of North Carolina, Chapel Hill, NC, USA
e-mail: Glenn.morrison@unc.edu

chemistry, research is now seeking a more fundamental understanding of the composition and morphology of surfaces as well as the mechanisms and rates of surface chemistry that degrade our indoor air quality.

Keywords

Surfaces · Furnishings · Condensed phase · Oxidation · Chemistry

Introduction

To alter the concentration of airborne pollutants in buildings, sources and sinks must be present and active. As a generalization, sources increase concentrations, while sinks reduce concentrations. Indoor surfaces act as both source and sink. Primary emissions of volatile organic compounds are a well-known source. But chemical transformations taking place on surfaces also play an important role. These transformations can consume some chemicals like ozone. This is why indoor ozone concentrations are so much lower than outdoor concentrations in most buildings. Reactions also generate products. If sufficiently volatile, these products can be released from surfaces, thereby making that surface a source of newly generated chemicals that increases their concentrations in indoor air. Indoor surfaces are particularly important because so much surface area is accessible to indoor air. These surfaces, including building surfaces, furnishings, and people, have an outsized impact on the composition of indoor air relative to chemistry taking place in air alone.

Until very recently, research into indoor surface chemistry has been sporadic, empirical, and often occurring as a secondary outcome of other research. Now more focused, fundamental, and theoretical studies are underway that are revealing in much greater detail the processes taking place on indoor surfaces. This chapter surveys the past several decades of indoor surface chemistry studies with a focus on several specific chemicals and phenomena. This chapter begins with a description of indoor surfaces and important characteristics of those surfaces that influence the chemistry. Then specific chemical species, classes, or phenomena are discussed including the chemistry of ozone, nitrogen oxides, chlorine, as well as acid-base chemistry and hydrolysis.

Surfaces and Chemical Transformations

Indoor Surfaces

The materials that make up our indoor environments include structural components, furnishings, decorations, and other functional elements. For this chapter, surfaces are broadly defined as the areas of materials or their coatings that are exposed to indoor air. This includes the two-dimensional interface between air and the solid/condensed

material and perhaps some three-dimensional thickness of material beneath that interface. It is at these surfaces where deposition, emission, and much indoor chemistry take place, thereby altering indoor air quality. The surface area available in buildings is quite large relative to the volume, providing ample area for chemical processes to occur. The geometrically projected (i.e., ignoring surface roughness and porosity) surface area to volume ratio has been estimated to range from $<2\text{ m}^2/\text{m}^3$ for empty rooms to $>5\text{ m}^2/\text{m}^3$ for small rooms with furnishings (Hodgson et al. 2005; Manuja et al. 2019). Surface area increases considerably when roughness and porosity are considered (Gall et al. 2015). For reactive gases depositing on surfaces at transport limited rates, removal rates can be greater than $20/\text{h}$ which is much higher than the rate of air change ($\sim 1/\text{h}$) in most buildings.

Indoor surfaces can influence chemistry from molecular scales to whole building scales (Shiraiwa et al. 2019). Indoor surfaces are neither clean nor smooth. For example, paint may look uniform and smooth to eye but is rough and porous under microscopy. Each building surface can be characterized by the substrate composition (e.g., polyvinylchloride of some flooring materials), the morphology (including surface area and porosity), and soiling (e.g., accumulation of particles and low-volatility chemicals).

The underlying compositions of building materials and furnishings (aka substrates) can be complex and wide-ranging. However, they can be generalized to two broad categories: organic and inorganic substances. Organic substances are often polymers such as cellulose (wood and paper), polyvinyl chloride (PVC flooring), latex (paint), and polyethylene terephthalate and nylon (carpet fibers). Low-volatility non-polymeric organic compounds that comprise building materials include plasticizers such as phthalates. Mineral-based inorganic substances include gypsum wallboard, concrete, and glass. Most building materials are composites of these categories. For example, drywall is usually composed of gypsum mixed with organic binders and faced with paper adhered by an organic adhesive. Ault et al. (2020) developed a list of building surfaces that include most of these substrate materials for laboratory studies of molecular scale indoor chemistry.

It has become well established that all indoor surfaces (absent recent cleaning) are coated with a film of “grime” that develops over time (Liu et al. 2003; Wallace et al. 2004, 2017; Weschler and Nazaroff 2017; Eichler et al. 2019; Or et al. 2020; Lim and Abbatt 2020). The coating is composed of deposited particles as well as organic and inorganic compounds including water. This film is thought to be responsible for much of observations of surface-related chemical phenomena including chemical partitioning and reactive deposition. Surface cleaning removes or alters the coating, changing surface characteristics (such as pH) and reducing exposure to accumulated chemicals.

Water present on surfaces can alter surface properties such as polarity, act as necessary reactants for some chemical transformations, or provide an aqueous environment for absorption and acid-based chemistry. Nazaroff and Weschler (2020) assign water indoors to three overlapping domains: bulk (such as present in a glass of water), sorbed, and surface films. For indoor chemistry, sorbed water and surface films of water are of most interest as they are more accessible (lower

transport barriers) and spread across large areas, including the internal pores of materials. For a typical residence, Nazaroff and Weschler predict sorbed or condensed water to be present on the order of tens of liters, thereby providing ample volume for sorption of polar molecules. At 50% RH, water covers most surfaces with the equivalent of approximately a monolayer, ensuring that chemistry can proceed if that reaction requires the presence of a water molecule.

Relative to indoor air, surfaces can enhance chemistry in buildings by increasing the time that the chemicals are retained indoors or altering the chemical environment. Processes such as adsorption and absorption allow chemicals to accumulate on surfaces and increase their average time spent indoors before being removed by ventilation or surface cleaning (Weschler and Nazaroff 2008). Even slow reactions may become relevant if this time increases from the timescale of air exchange (~ 1 h) to months or years (Morrison 2008). Surfaces may also alter the rates and mechanisms of reactions relative to the gas phase; for example, acid-catalyzed reactions may be slow or negligible in the gas phase but proceed at meaningful rates in an acidic surface film.

Ozone Initiated Chemistry

Indoor ozone concentrations are usually much lower than outdoor concentrations when no indoor ozone sources are present (Weschler 2000). This is because ozone that enters the building by ventilation or infiltration is consumed by reactions taking place in the gas phase and on surfaces. Early studies quantified this removal in buildings by reporting an ozone decay rate coefficient (a.k.a. loss-rate coefficient), k_{loss} (1/h), or a deposition velocity, v_d (m/h). The decay rate coefficient accounts for all losses, excluding outdoor-to-indoor air exchange, without ascribing the removal to a particular mechanism or sink. For a well-mixed building volume at steady state with no indoor ozone source,

$$k_{loss} = \lambda \left(\frac{C_{out}}{C_{in}} - 1 \right) \quad (1)$$

where λ is the air exchange rate (defined as the outdoor air flow rate entering the volume, Q , divided by the volume, V), C_{out} is the outdoor concentration of ozone, and C_{in} is the indoor concentration of ozone. The deposition velocity, on the other hand, is defined by assuming that ozone is lost primarily by deposition and conversion to other products on indoor surfaces. The deposition area is usually defined as the geometrically projected area, A . For a well-mixed building volume at steady state with no indoor ozone source or appreciable gas phase reactive loss of ozone,

$$v_d = \lambda \left(\frac{V}{A} \right) \left(\frac{C_{out}}{C_{in}} - 1 \right) \quad (2)$$

Both parameters can be influenced by air mixing. Higher air velocities and more intense turbulence both reduce the fluid-mechanical resistance for transport of gases from bulk room air to surfaces. Loss rate coefficients and deposition velocities have been reported for buildings and specific materials and reviewed in several sources (Nazaroff et al. 1993; Grontoft and Raychaudhuri 2004; Lamble et al. 2011). In general, clean smooth glassy or polymer-coated surfaces tend to have lower ozone deposition velocities. Surfaces that are rough and have a higher surface area, are porous and/or fleecy (e.g., textiles), are soiled or coated with reactive oils (e.g., skin), and masonry surfaces tend to have high ozone deposition velocities. These observations are consistent with ozone converting to other products on surface sites. When surface reactivity and uptake is relatively low, the conversion rate and therefore the deposition velocity increase with increasing surface area (both geometrically projected and internal) and a greater density of reactive sites (Morrison and Nazaroff 2002a; Gall et al. 2015). For a higher reactivity surface, the deposition velocity approaches an asymptote that is more influenced by air mixing (Cano-Ruiz et al. 1993). At the building level, the deposition velocities (and ozone decay rates) fall within a much narrower range than observed for individual materials; Nazaroff et al. (1993) speculated that this may be due to a net “averaging” of indoor surface reactivity and uniform soiling of accessible indoor surfaces.

In the absence of strong emissions of volatile alkenes, the primary loss mechanism for ozone on indoor surfaces is its reaction with carbon-carbon double bonds present in organic compounds present on the surfaces. There are many sources of double-bonded chemicals that replenish surfaces including natural fats, skin lipids, and terpenes (Deming and Ziemann 2020). A generalized reaction scheme is shown in Fig. 1.

Ozone reacts at a double-bond, forming a primary ozonide (not shown). This then can form a number of higher and lower volatility products. Carbonyl compounds are the most volatile, followed by acids, then other species such as secondary ozonides, peroxy species, and oligomer. Evidence for this chemistry became apparent in early studies that observed an increase in the air concentrations of aldehydes when indoor materials were exposed to ozone (Weschler et al. 1992b; Reiss et al. 1995; Morrison and Nazaroff 2002b). From building materials and indoor surfaces, nonanal and other aldehydes are dominant products of this reaction (Wisthaler et al. 2005; Wang and Morrison 2006, 2010; Nicolas et al. 2007; Weschler et al. 2007; Coleman et al. 2008; Lamble et al. 2011; Abbass et al. 2017). This points to the presence of one or more forms of an oleate and other unsaturated fatty acids or esters which are common in natural oils, but are also present in manufactured products.

The reactions of ozone with occupants, their clothing, and their skin lipids have been shown to be an important loss mechanism for ozone and contributor to products in indoor air (Wisthaler et al. 2005; Weschler et al. 2007; Coleman et al. 2008; Pandrangi and Morrison 2008; Wisthaler and Weschler 2010). The chemistry behind these observations has now been well documented (Thornberry and Abbatt 2003; Wisthaler and Weschler 2010; Zhou et al. 2016a, b). Squalene comprises about 12–15% (Nicolaides 1974) of skin oil but is responsible for approximately half of the

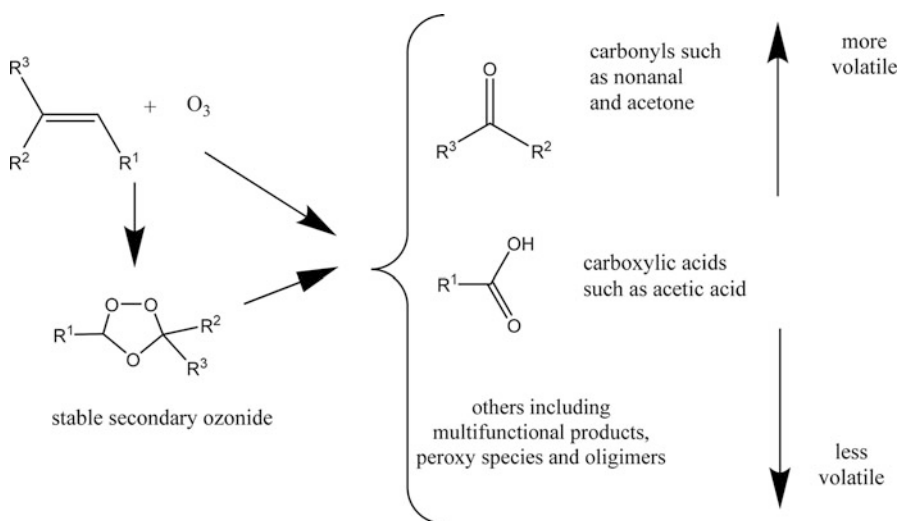


Fig. 1 Ozone reacts with a double bond present in a generalized chemical present on an indoor surface. This reaction results in multiple products that may remain on the surface or volatilize, increasing the air concentration

double bonds present (Pandangi and Morrison 2008). The other double bonds are distributed mostly among unsaturated fatty acids, their esters, ceramides, and cholesterol. Major unique products of ozone reactions with fresh skin lipids include 6-methyl-2-heptenone and geranyl acetone; these can volatilize and further participate in gas-phase chemistry. These ozone-human signature chemicals have been observed in occupied aircraft studies (Wisthaler et al. 2005; Weschler et al. 2007), classrooms and offices (Wisthaler and Weschler 2010; Liu et al. 2016; Tang et al. 2016), museums (Pagonis et al. 2019), a football stadium (Veres et al. 2013), a theater (Stönnér et al. 2018), and in controlled chamber experiments with people and or their clothing (Coleman et al. 2008; Rai et al. 2014; Salvador et al. 2019). Yields of products from skin lipid ozonolysis (the yield is defined as the molar generation rate of a product divided by the molar consumption rate of ozone) vary among individuals and may be influenced by the presence of exogenous fats (Morrison et al. 2020). The rates of product emissions from surfaces can be influenced by the intermediate formation of ozonides that store volatile products until the ozone decomposes (Zhou et al. 2019). Humidity can in turn influence the stability of ozonides and the proportion of products generated (Zhou et al. 2016a, 2019; Arata et al. 2019).

Consumer products contain fragrance compounds, terpenes, and terpene alcohols that contain double bonds that react with ozone. Most research has focused on the gas-phase chemistry of these species; despite their volatility, however, they do react with ozone when sorbed onto surfaces. Singer et al. (2006) observed enhanced ozone uptake at surfaces after they had been exposed to the gas-phase emissions of a fragranced air freshener. Ham and Wells (2011) observed products consistent with

oxidation of terpineol in pine-oil scented cleaners that had been applied to vinyl flooring and exposed to ozone. Adsorbed dihydromyrcenol, α -pinene, limonene, and terpineol have been observed to increase ozone uptake to model (glass/PVC) and real (paint) surfaces (Ham and Wells 2008; Springs and Morrison 2008; Shu and Morrison 2011, 2012).

Airborne particles can also be generated when ozone reacts with indoor surfaces and their coatings. Production of particles has been observed upon ozone exposure of building materials, filters, and terpenes adsorbed to solid substrates (Aoki and Tanabe 2007; Beko et al. 2007; Rai et al. 2013; Waring and Siegel 2013; Wang and Waring 2014; Avery et al. 2019).

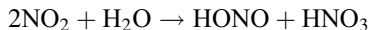
Ozone reaction kinetics, and possibly mechanisms, may be enhanced relative to gas-phase reactions. For example, reactions of ozone with condensed compounds can occur much faster than that in the gas phase (e.g., benzo[a]pyrene (Kwamena et al. 2004)). Several terpene compounds have been shown to react with ozone at much higher rates when sorbed to glass, polyvinylchloride, and painted surfaces (Springs and Morrison 2008; Shu and Morrison 2011, 2012). In some cases, the surface rate of ozone with adsorbed terpenes exceeds that in air, due to the high indoor surface area and enhanced reaction rates. Ham and Wells (2008, 2011) observed that yields of ozone-terpene reaction products are altered on surfaces, relative to gas-phase reactions. Stable secondary ozonides may also form in condensed materials and their stability influenced by the presence of water (Zhou et al. 2019). Humidity also influences the products formed when ozone reacts with squalene (Zhou et al. 2016a; Arata et al. 2019).

Nitrogen Oxides

Nitrogen oxides (NO , NO_2 , NO_3 , HNO_3 , HONO , N_2O_5) present in buildings are derived from outdoor air, indoor chemistry, or indoor combustion sources. With the exception of NO , most nitrogen oxides measurably partition, deposit, or react at indoor surfaces. The spatially averaged deposition velocity of NO_2 to indoor surfaces has been estimated to range between 0.007 and 0.4 m/h (Nazaroff et al. 1993), which is smaller than for ozone. Wainman et al. (2001) measured an NO_2 deposition velocity of ~1.2 m/h for carpet. There are few field measurements of gas phase NO_3 (Nøjgaard 2010), but as yet no field deposition measurements. Given the similarity to ozone (chemical rates and mechanisms), it is anticipated that NO_3 would deposit at rates similar to ozone. Deposition of HONO and HNO_3 is thought to be driven by gas-surface partitioning and acid-base chemistry (Weschler et al. 1992a; Wainman et al. 2001; Wang et al. 2020).

Important to the indoor chemistry of nitrogen oxides is the formation of nitrous acid (HONO) on indoor surfaces. Pitts et al. (1985) showed that NO_2 will deposit on indoor surfaces and form volatile HONO . With an indoor source of NO_2 (gas burners), the resulting concentration of HONO in indoor air can exceed outdoor concentrations (Pitts et al. 1989; Febo and Perrino 1991; Spicer et al. 1993). As long as some water is available, most surfaces can support this chemistry. For surfaces

that have been conditioned, that is, accumulated a thin layer of organic and inorganic “grime,” the chemistry is insensitive to the composition of the underlying surface, including Teflon and glass (Pitts et al. 1984). The reaction is first order in water and NO₂ (Finlayson-Pitts et al. 2003). The primary mechanism appears to be reactive dissolution into adsorbed water (Spicer et al. 1993), which also produces HNO₃ and other species (Finlayson-Pitts et al. 2003).



Light can also influence the surface chemistry of nitrogen oxides. Several studies have shown enhanced HONO production upon exposing indoor-relevant surfaces to light including paint, lacquer, glass-coated with cleaners, etc. Gómez Alvarez et al. (2014) suggested that coatings of organic compounds on indoor surfaces may act as photo-sensitizers, similar to photo-induced production of HONO on humic acid (Stemmler et al. 2007). Illuminated by some light sources, NO₂ uptake and release of HONO can be enhanced on white paint (Bartolomei et al. 2014) and on photo-catalytic paint (Gandolfo et al. 2015, 2017). Painted surfaces, coated with a nitrate salt, released NO, NO₂, and HONO when exposed to some light sources (Schwartz-Narbonne et al. 2019).

Surfaces and surface films may act as long-lasting reservoirs for HONO. Febo and Perrino (1991) and Spicer et al. (1993) observed that HONO concentrations will rebound quickly after airing out the building. This suggested that indoor surfaces have stored a substantial amount of HONO that can be released over an extended period of time. Wainman et al. (2001) observed similar behavior in a laboratory reactor and showed that this storage effect was enhanced at higher humidity and for materials with higher surface areas. They proposed that HONO will reversibly dissociate to the nitrite ion (NO₂⁻) in surface water (see also section “[Acid Base Chemistry](#)”); the accumulated NO₂⁻ acts as a future HONO source. For a pH above the pK_a of HONO (3.3), NO₂⁻ can dominate, and over time, a large nitrite reservoir can develop. This behavior has been observed in the HOMECHM experiments (Farmer et al. 2019; Wang et al. 2020) and successfully modeled (Collins et al. 2018a). During HOMECHM, bleaching surfaces resulted in a lowering of indoor HONO concentrations which was ascribed to an increase in surface film pH (shifting aqueous equilibrium from HONO to NO₂⁻) and formation of ClONO.

Nitrogen oxides also participate in organic chemistry on surfaces. Upon observing HONO formation indoors, Pitts suggested that this could lead to the *in vivo* formation of carcinogenic nitrosamines. *Ex vivo* formation was later observed by Sleiman et al. in their “third-hand smoke” studies (Sleiman et al. 2010, 2011). They observed conversion of nicotine (sorbed to a cellulose substrate) to multiple nitrosamines in a flow reactor. They also measured nicotine-specific nitrosamines on surfaces of a household, a vehicle, and skin, all of which were frequently exposed to cigarette smoke. Upon application of chlorine bleach, ClNO₂ is observed and ascribed to the chemistry of hypochlorous acid with NO₂⁻ (Wong et al. 2017; Mattila et al. 2020a, b).

Chlorine Chemistry

Chlorine-based chemical oxidants have been used for cleaning and disinfection indoors for over a century but have only recently been the subject of indoor chemistry investigations. To investigate the impact of gaseous oxidants, used for biological decontamination in buildings, Corsi and associates exposed a variety of surface materials to a high concentration of chlorine dioxide (ClO_2); they observed substantial uptake of ClO_2 to wallboard, carpet, paper, textiles, and dust with initial deposition velocities similar to ozone (Hubbard et al. 2009). The uptake rate decayed relatively rapidly, but the exposure concentrations were very high, hinting at chemistry that oxidized reactive sites on these materials. They also observed persistent emissions of carbonyl compounds as well as chlorinated by-products, long after exposure (Corsi et al. 2006).

Chlorine bleach can also contribute to chemical transformations on surfaces; several groups have observed increased emissions of nitrogen and chlorine containing compounds (Wong et al. 2017; Mattila et al. 2020a, b). Mattila et al. (2020a) proposed that amide absorption into the aqueous bleach film resulted in their observed emissions of isocyanates. The reaction of HOCl with amino acids was thought to be responsible for observed production of cyanogen chloride. Other compounds generated, presumably by reactions taking place in this aqueous surface film, included isocyanic acid, chloramines, trichloromethane, and tetrachloroethylene. In a modeling analysis of HOMEChem data, they ascribed observed emissions of chloramines and nitrilechloride to reactions of HOCl with ammonia and the nitrite ion (Mattila et al. 2020b). In a study of bleach cleaning of athletic gym equipment, Finewax et al. (2020) observed formation of chloraldimines, presumably from the reaction of HOCl with amino acids.

Acid-Base Chemistry

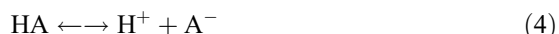
Many indoor chemicals have acid-base functionality such that reaction kinetics, mechanisms, and their affinity for a surface or a condensed phase may be influenced by the effective acidity of that phase. Examples include ammonia, organic bases (e.g., nicotine), inorganic acids (CO_2 , HNO_3 , HONO , HOCl), and organic acids (formic acid, acetic acid). What follows is a brief overview that draws greatly on the critical review of this chemistry by Nazaroff and Weschler (2020), which focused on chemicals that have a tendency to donate or accept protons (Brønsted-Lowry acids and bases).

Some gaseous acids and bases such as CO_2 , formic acid, acetic acid, NH_3 , and nicotine can be present at concentrations that meaningfully influence the pH of condensed water. Nazaroff and Weschler (2020) estimate that, in the absence of other ions, condensed water will be at a near-neutral pH (7) when in equilibrium with typical indoor concentrations of CO_2 and NH_3 . When considering other acids and bases, they tentatively conclude that condensed water indoors will be slightly acidic ($\text{pH} < 7$).

Where an aqueous phase is present and accessible, volatile acids and bases will partition to that phase. At equilibrium, the concentration of an acid in the aqueous phase is given by Henry's law:

$$[\text{HA}] = k_H P_{\text{HA}} \quad (3)$$

where, k_H is the Henry's law constant and P_{HA} is the partial pressure of the acid in air. The acid can dissociate



and the equilibrium constant for dissociation is given by

$$K_a = \frac{[\text{H}^+][\text{A}^-]}{[\text{HA}]} \quad (5)$$

By Eq. (3), at a given gas phase partial pressure, $[\text{HA}]$ is a constant and uninfluenced by pH. However, by Eq. (5), the concentration of the conjugate base, $[\text{A}^-]$, is strongly influenced by pH. Where $\text{pH} > \text{pK}_a$, $[\text{A}^-] > [\text{HA}]$; conversely, where $\text{pH} < \text{pK}_a$, $[\text{A}^-] < [\text{HA}]$. Similar expressions can be developed for bases that accept protons. The total molar concentration of the acid and its conjugate base ($[\text{HA}] + [\text{A}^-]$) is therefore dependent on both gas-aqueous partitioning and pH. A high pH will drive more of the acid to $[\text{A}^-]$, thereby increasing the total of "A" in solution.

Since $[\text{H}^+]$ can vary over many orders of magnitude, exposed condensed water can act as a large aqueous reservoir of volatile acids and bases. During real-time measurements of airborne organics in a residence, Duncan et al. (2019) observed that the concentrations of formic and acetic acids decreased dramatically when the central air conditioner (AC) was running, then increased when it was turned off. This behavior suggested that the acids absorbed into water that condensed on the AC coils. During an intensive investigation of chemistry in a test house (a.k.a. HOMEChem), Wang et al. (2020) observed a drop in the gas phase concentration of acids (including HONO, formic acid, and butyric acid) when windows were opened, but then a rapid rise upon window closure. They ascribe some of this behavior to the presence of partitioning to, and subsequent acid dissociation within, surface water reservoirs.

In more acidic solutions, the dominant form of amines can be the protonated conjugate acid (i.e., (amine) H^+); therefore one would also expect condensed water to act as an important reservoir. For example, the pK_a of the conjugate acid of nicotine is 7.9. In an aqueous solution with a pH lower than 7.9, the protonated form of nicotine will be dominant. The capacity of the surface water reservoir will increase by approximately a factor of 10 for each unit decrease in pH; therefore at a neutral pH, the aqueous concentration of protonated nicotine is expected to be ~10 times that of the neutral form. Other amines such as aniline have much lower pK_a values for their conjugate acid, suggesting that surface reservoirs will be less influential. Reservoir behavior for amines has been observed for particles (DeCarlo et al. 2018;

Collins et al. 2018b), building surfaces (Ongwandee et al. 2005; Ongwandee and Morrison 2008), people, skin, and textiles (Morrison et al. 2015; Sheu et al. 2020). A review of amines, amino acids, and other nitrogen-containing compounds found indoors can be found in Nazaroff and Weschler (2020).

The form of the species can also influence reaction mechanisms and kinetics. For example, the form of nitrite determines how rapidly it will become oxidized by ozone. HONO that has partitioned to an aqueous phase will dissociate,



Ozone can also partition to the solution. Ozone reacts rapidly with NO_2^- to form NO_3^- but much more slowly with HONO (Liu et al. 2001). Therefore, little reaction will take place if HONO dominates in the solution (when the $\text{pH} < \text{p}k_a$). Since the $\text{p}k_a$ for HONO is 3.16, NO_2^- will dominate in a neutral solution and the conversion to nitrate will proceed readily in the presence of ozone. Similarly, most of the chlorine chemistry discussed in the previous section is initiated by HOCl and less so by the conjugate base OCl^- . The neutral form of nicotine is known to react on surfaces with ozone (Destaillass et al. 2006; Petrick et al. 2010). However, Nazaroff and Weschler (2020) note that, “Given that pH plays a significant role in nicotine’s sorption to surfaces, related issue for future study is how the reactivity of non-ionized nicotine compares to that of monoprotonated nicotine.”

Acids are also responsible for material corrosion. This is particularly of concern for cultural artifacts. For example, acetic acid aggressively corrodes artifacts made of lead, nitric acid corrodes copper, and so forth. In efforts to slow the degradation of artwork and other artifacts, museums often focus on acid controls.

Hydrolysis

Hydrolysis, literally to “split apart with water,” cleaves parent molecules to form smaller, possibly more volatile and polar products. As the name implies, hydrolysis is influenced by the presence of water, but also by pH and temperature. In general, hydrolysis is slow under typical indoor conditions and neutral pH. However, given the large amount of building materials, and therefore large total mass of esters present, volatile reaction product emissions can be significant. Emissions resulting from hydrolysis do not decay over time in the same way as emissions of residual volatile species present in newly manufactured materials. Because the esters are degraded slowly but relatively continuously, meaningful emissions of degradation products can occur during the entire useful life of the product.

Esters that are prone to hydrolysis in indoor environments include some plasticizers and flame retardants. Protonated water can catalyze the hydrolysis of esters to form a carboxylic acid and an alcohol. Under basic conditions, the hydroxyl ion acts as a reactant that cleaves the ester to from a carboxylate salt and an alcohol.

For example, odor nuisance products such as 2-ethyl hexanol and 2-butanol are observed where plasticized materials are present, including polyvinylchloride (PVC)

flooring (Uhde and Salthammer 2007). Hydrolysis products of organophosphate esters have also been observed (Salthammer et al. 2003). Tri(chloropropyl)phosphate (TCP) hydrolyzes to odorous 2-chloro-1-propanol and tri(dichloropropyl)phosphate (TCCP) hydrolyzes to 1,3-dichloro-2-propanol, a suspected carcinogen. Urea-formaldehyde resins, which have been used as adhesives and as insulation foam, hydrolyze forming volatile formaldehyde.

Conclusion

There are many reactions taking place on indoor surfaces. These reactions alter surfaces, remove some chemicals from indoor air while generating volatile products that increase indoor concentrations of mainly oxidized compounds like aldehydes, alcohols, and acids. Our current understanding of this chemistry has improved substantially in the last decade but remains somewhat fragmentary. Key questions still to be addressed include

- What is the composition of real surface films?
- How are surface films organized? Are they homogenous or are they characterized by semi-separate aqueous and organic phases, as is sometimes observed in aerosols.
- What is the water content of indoor surfaces, where is it, and how much of the water can support aqueous solution chemistry?
- What is the pH of water on indoor surfaces, and how should this be defined?
- How important are substrate characteristics in controlling surface chemistry?
- What are the morphologies of indoor surfaces? Which surfaces and how much of that surface area is relevant to indoor chemistry and air quality.

These questions and more are the subject of contemporary indoor chemistry research; expect to see actionable answers soon.

Cross-References

- [Indoor Photochemistry](#)
- [Source/Sink Characteristics of SVOCs](#)
- [Source/Sink Characteristics of VVOCs and VOCs](#)

References

- Abbass OA, Sailor DJ, Gall ET (2017) Effect of fiber material on ozone removal and carbonyl production from carpets. *Atmos Environ* 148:42–48. <https://doi.org/10.1016/j.atmosenv.2016.10.034>
- Aoki T, Tanabe S (2007) Generation of sub-micron particles and secondary pollutants from building materials by ozone reaction. *Atmos Environ* 41:3139–3150

- Arata C, Heine N, Wang N et al (2019) Heterogeneous ozonolysis of squalene: gas-phase products depend on water vapor concentration. *Environ Sci Technol* 53:14441–14448. <https://doi.org/10.1021/acs.est.9b05957>
- Ault AP, Grassian VH, Carslaw N, et al (2020) Indoor surface chemistry: developing a molecular picture of reactions on indoor interfaces. *Chem.* <https://doi.org/10.1016/j.chempr.2020.08.023>
- Avery AM, Waring MS, DeCarlo PF (2019) Human occupant contribution to secondary aerosol mass in the indoor environment. *Environ Sci Process Impacts* 21:1301–1312. <https://doi.org/10.1039/c9em00097f>
- Bartolomei V, Sörgel M, Gligorovski S et al (2014) Formation of indoor nitrous acid (HONO) by light-induced NO₂ heterogeneous reactions with white wall paint. *Environ Sci Pollut Res* 21:9259–9269
- Beko G, Clausen G, Weschler CJ (2007) Further studies of oxidation processes on filter surfaces: evidence for oxidation products and the influence of time in service. *Atmos Environ* 41: 5202–5212
- Cano-Ruiz JA, Kong D, Balas RB, Nazaroff WW (1993) Removal of reactive gases at indoor surfaces: combining mass transport and surface kinetics. *Atmos Environ A* 27(A):2039–2050
- Coleman BK, Destaillats H, Hodgson AT, Nazaroff WW (2008) Ozone consumption and volatile byproduct formation from surface reactions with aircraft cabin materials and clothing fabrics. *Atmos Environ* 42:642–654. <https://doi.org/10.1016/j.atmosenv.2007.10.001>
- Collins DB, Hems RF, Zhou S et al (2018a) Evidence for gas–surface equilibrium control of indoor nitrous acid. *Environ Sci Technol* 52:12419–12427
- Collins DB, Wang C, Abbatt JPD (2018b) Selective uptake of third-hand tobacco smoke components to inorganic and organic aerosol particles. *Environ Sci Technol* 52:13195–13201. <https://doi.org/10.1021/acs.est.8b03880>
- Corsi RL, Hubbard H, Poppendieck D, et al (2006) Chlorine dioxide as a building disinfectant: surface consumption and by-product generation. pp 115–120
- DeCarlo PF, Avery AM, Waring MS (2018) Thirdhand smoke uptake to aerosol particles in the indoor environment. *Sci Adv* 4:eaap8368. <https://doi.org/10.1126/sciadv.aap8368>
- Deming BL, Ziemann PJ (2020) Quantification of alkenes on indoor surfaces and implications for chemical sources and sinks. *Indoor Air*. <https://doi.org/10.1111/ina.12662>
- Destaillats H, Singer BC, Lee SK, Gundel LA (2006) The effect of ozone on nicotine desorption from model surfaces: evidence for heterogeneous chemistry. *Environ Sci Technol* 40:1799–1805
- Duncan SM, Tomaz S, Morrison G, et al (2019) Dynamics of residential water-soluble organic gases: insights into sources and sinks. *Environ Sci Technol*. <https://doi.org/10.1021/acs.est.8b05852>
- Eichler CMA, Cao J, Isaacman-VanWertz G, Little JC (2019) Modeling the formation and growth of organic films on indoor surfaces. *Indoor Air* 29:17–29. <https://doi.org/10.1111/ina.12518>
- Febo A, Perrino C (1991) Prediction and experimental evidence for high air concentration of nitrous acid in indoor environments. *Atmos Environ A Gen Top* 25:1055–1061. [https://doi.org/10.1016/0960-1686\(91\)90147-Y](https://doi.org/10.1016/0960-1686(91)90147-Y)
- Finewax Z, Pagonis D, Clafin MS et al (2020) Quantification and source characterization of volatile organic compounds from exercising and application of chlorine-based cleaning products in a university athletic center. *Indoor Air*. <https://doi.org/10.1111/ina.12781>
- Finlayson-Pitts BJ, Wingen LM, Sumner AL et al (2003) The heterogeneous hydrolysis of NO₂ in laboratory systems and in outdoor and indoor atmospheres: an integrated mechanism. *Phys Chem Chem Phys* 5:223–242
- Gall ET, Siegel JA, Corsi RL (2015) Modeling ozone removal to indoor materials, including the effects of porosity, pore diameter, and thickness. *Environ Sci Technol* 49:4398–4406. <https://doi.org/10.1021/acs.est.5b00023>
- Gandolfo A, Bartolomei V, Gomez Alvarez E et al (2015) The effectiveness of indoor photocatalytic paints on NO_x and HONO levels. *Appl Catal B Environ* 166–167:84–90
- Gandolfo A, Rouyer L, Wortham H, Gligorovski S (2017) The influence of wall temperature on NO₂ removal and HONO levels released by indoor photocatalytic paints. *Appl Catal B Environ* 209:429–436. <https://doi.org/10.1016/j.apcatb.2017.03.021>

- Gómez Alvarez E, Sörgel M, Gligorovski S et al (2014) Light-induced nitrous acid (HONO) production from NO₂ heterogeneous reactions on household chemicals. *Atmos Environ* 95: 391–399. <https://doi.org/10.1016/j.atmosenv.2014.06.034>
- Grontoft T, Raychaudhuri MR (2004) Compilation of tables of surface deposition velocities for O₃, NO₂ and SO₂ to a range of indoor surfaces. *Atmos Environ* 38:533–544
- Ham JE, Wells JR (2008) Surface chemistry reactions of alpha-terpineol [(R)-2-(4-methyl-3-cyclohexenyl)isopropanol] with ozone and air on a glass and a vinyl tile. *Indoor Air* 18: 394–407
- Ham JE, Wells JR (2011) Surface chemistry of a pine-oil cleaner and other terpene mixtures with ozone on vinyl flooring tiles. *Chemosphere* 83:327–333
- Hodgson AT, Ming KY, Singer BC (2005) Quantifying object and material surface areas in residences. Ernest Orlando Lawrence Berkeley National Laboratory, Berkeley
- Hubbard H, Poppendieck D, Corsi RL (2009) Chlorine dioxide reactions with indoor materials during building disinfection: surface uptake. *Environ Sci Technol* 43:1329–1335
- Farmer DK, Vance ME, Abbatt JPD et al (2019) Overview of HOMEChem: house observations of microbial and environmental chemistry. *Environ Sci Process Impacts* 21:1280–1300. <https://doi.org/10.1039/C9EM00228F>
- Kwamena N-OA, Thornton JA, Abbatt JPD (2004) Kinetics of surface-bound benzo[a]pyrene and ozone on solid organic and salt aerosols. *J Phys Chem A* 108:11626–11634
- Lamble SP, Corsi RL, Morrison GC (2011) Ozone deposition velocities, reaction probabilities and product yields for green building materials. *Atmos Environ* 45:6965–6972
- Lim CY, Abbatt JP (2020) Chemical composition, spatial homogeneity, and growth of indoor surface films. *Environ Sci Technol* 54:14372–14379. <https://doi.org/10.1021/acs.est.0c04163>
- Liu Q, Schurter LM, Muller CE et al (2001) Kinetics and mechanisms of aqueous ozone reactions with bromide, sulfite, hydrogen sulfite, iodide, and nitrite ions. *Inorg Chem* 40:4436–4442. <https://doi.org/10.1021/ic000919j>
- Liu QT, Chen R, McCarry BE et al (2003) Characterization of polar organic compounds in the organic film on indoor and outdoor glass windows. *Environ Sci Technol* 37:2340–2349
- Liu S, Li R, Wild RJ et al (2016) Contribution of human-related sources to indoor volatile organic compounds in a university classroom. *Indoor Air* 26:925–938. <https://doi.org/10.1111/ina.12272>
- Manuja A, Ritchie J, Buch K et al (2019) Total surface area in indoor environments. *Environ Sci Process Impacts* 21:1384–1392. <https://doi.org/10.1039/C9EM00157C>
- Mattila JM, Arata C, Wang C et al (2020a) Dark chemistry during bleach cleaning enhances oxidation of organics and secondary organic aerosol production indoors. *Environ Sci Technol Lett* 7:795–801. <https://doi.org/10.1021/acs.estlett.0c00573>
- Mattila JM, Lakey PSJ, Shiraiwa M et al (2020b) Multiphase chemistry controls inorganic chlorinated and nitrogenated compounds in indoor air during bleach cleaning. *Environ Sci Technol* 54:1730–1739. <https://doi.org/10.1021/acs.est.9b05767>
- Morrison G (2008) Interfacial chemistry in indoor environments. *Environ Sci Technol* 42: 3494–3499
- Morrison G, Shakila NV, Parker K (2015) Accumulation of gas-phase methamphetamine on clothing, toy fabrics, and skin oil. *Indoor Air* 25:405–414. <https://doi.org/10.1111/ina.12159>
- Morrison GC, Eftekhari A, Majluf F, Krechmer JE (2020) Yields and variability of ozone reaction products from human skin. *Environ Sci Technol*. <https://doi.org/10.1021/acs.est.0c05262>
- Morrison GC, Nazaroff WW (2002a) The rate of ozone uptake on carpet: mathematical modeling. *Atmos Environ* 36:1749–1756
- Morrison GC, Nazaroff WW (2002b) Ozone interactions with carpet: secondary emissions of aldehydes. *Environ Sci Technol* 36:2185–2192
- Nazaroff WW, Gadgil AJ, Weschler CJ (1993) Critique of the use of deposition velocity in modeling indoor air quality. pp 81–104
- Nazaroff WW, Weschler CJ (2020) Indoor acids and bases. *Indoor Air* 30:559–644. <https://doi.org/10.1111/ina.12670>
- Nicolaides N (1974) Skin lipids: their biochemical uniqueness. *Science* 186:19–26

- Nicolas M, Ramalho O, Maupetit F (2007) Reactions between ozone and building products: impact on primary and secondary emissions. *Atmos Environ* 41:3129–3138
- Nøjgaard JK (2010) Indoor measurements of the sum of the nitrate radical, NO_3 , and nitrogen pentoxide, N_2O_5 in Denmark. *Chemosphere* 79:898–904
- Ongwande M, Bettinger SS, Morrison GC (2005) The influence of ammonia and carbon dioxide on the sorption of a basic organic pollutant to a mineral surface. *Indoor Air* 15:408–419
- Ongwande M, Morrison GC (2008) Influence of ammonia and carbon dioxide on the sorption of a basic organic pollutant to carpet and latex-painted gypsum board. *Environ Sci Technol* 42:5415–5420
- Pagonis D, Price DJ, Algrim LB et al (2019) Time-resolved measurements of indoor chemical emissions, deposition, and reactions in a university art Museum. *Environ Sci Technol* 53: 4794–4802. <https://doi.org/10.1021/acs.est.9b00276>
- Pandrangi LS, Morrison GC (2008) Ozone interactions with human hair: ozone uptake rates and product formation. *Atmos Environ* 42:5079–5089
- Petrick L, Destaillats H, Zouev I et al (2010) Sorption, desorption, and surface oxidative fate of nicotine. *Phys Chem Chem Phys* 12:10356–10364
- Pitts J, Biermann H, Tuazon E et al (1989) Time-resolved identification and measurement of indoor air pollutants by spectroscopic techniques: gaseous nitrous acid, methanol, formaldehyde and formic acid. *JAPCA* 39:1344–1347
- Pitts JN, Sanhueza E, Atkinson R et al (1984) An investigation of the dark formation of nitrous acid in environmental chambers. *Int J Chem Kinet* 16:919–939. <https://doi.org/10.1002/kin.550160712>
- Pitts JN Jr, Wallington TJ, Biermann HW, Winer AM (1985) Identification and measurement of nitrous acid in an indoor environment. *Atmos Environ A* 19:763–767
- Rai AC, Guo B, Lin C-H et al (2014) Ozone reaction with clothing and its initiated VOC emissions in an environmental chamber. *Indoor Air* 24:49–58
- Rai AC, Guo B, Lin C-H et al (2013) Ozone reaction with clothing and its initiated particle generation in an environmental chamber. *Atmos Environ* 77:885–892
- Reiss R, Ryan PB, Tibbetts S, Koutrakis P (1995) Measurement of organic acids, aldehydes, and ketones in residential environments and their relation to ozone. *J Air Waste Manag Assoc* 45:811–822
- Salthammer T, Fuhrmann F, Uhde E (2003) Flame retardants in the indoor environment – part II: release of VOCs (triethylphosphate and halogenated degradation products) from polyurethane. *Indoor Air* 13:49–52
- Salvador CM, Bekö G, Weschler CJ et al (2019) Indoor ozone/human chemistry and ventilation strategies. *Indoor Air* 29:913–925. <https://doi.org/10.1111/ina.12594>
- Schwartz-Narbonne H, Jones SH, Donaldson DJ (2019) Indoor lighting releases gas phase nitrogen oxides from indoor painted surfaces. *Environ Sci Technol Lett* 6:92–97. <https://doi.org/10.1021/acs.estlett.8b00685>
- Sheu R, Stönnér C, Ditto JC et al (2020) Human transport of thirdhand tobacco smoke: a prominent source of hazardous air pollutants into indoor nonsmoking environments. *Sci Adv* 6:eaay4109. <https://doi.org/10.1126/sciadv.aay4109>
- Shiraiwa M, Carslaw NJ, Tobias D et al (2019) Modelling consortium for chemistry of indoor environments (MOCCIE): integrating chemical processes from molecular to room scales. *Environ Sci Process Impacts* 21:1240–1254. <https://doi.org/10.1039/C9EM00123A>
- Shu S, Morrison GC (2012) Rate and reaction probability of the surface reaction between ozone and dihydromyrcenol measured in a bench scale reactor and a room-sized chamber. *Atmos Environ* 47:421–427
- Shu S, Morrison GC (2011) Surface reaction rate and probability of ozone and alpha-terpineol on glass, polyvinyl chloried and latex paint surfaces. *Environ Sci Technol*. <https://doi.org/10.1021/es2001194e>
- Singer BC, Coleman BK, Destaillats H et al (2006) Indoor secondary pollutants from cleaning product and air freshener use in the presence of ozone. *Atmos Environ* 40:6696–6710
- Sleiman M, Gundel LA, Pankow JF et al (2010) Formation of carcinogens indoors by surface-mediated reactions of nicotine with nitrous acid, leading to potential thirdhand smokehazards. *Proc Natl Acad Sci U S A* 107:6576–6581

- Sleiman M, Jacob P, Smith E, et al (2011) After the smoke clears: indoor chemistry of thirdhand smoke. pp 3065–3071
- Spicer CW, Kenny DV, Ward GF, Billick IH (1993) Transformations, lifetimes, and sources of NO₂, HONO, and HNO₃ in indoor environments. *J Air Waste Manag Assoc* 43:1479–1485
- Springs M, Morrison GC (2008) Reaction probability between terpenes and ozone on model indoor surfaces
- Stemmler K, Ndour M, Elshorbany Y et al (2007) Light induced conversion of nitrogen dioxide into nitrous acid on submicron humic acid aerosol. *Atmos Chem Phys* 7:4237–4248. <https://doi-org.libproxy.lib.unc.edu/10.5194/acp-7-4237-2007>
- Stönnér C, Edtbauer A, Williams J (2018) Real-world volatile organic compound emission rates from seated adults and children for use in indoor air studies. *Indoor Air* 28:164–172. <https://doi.org/10.1111/ina.12405>
- Tang X, Misztal PK, Nazaroff WW, Goldstein AH (2016) Volatile organic compound emissions from humans indoors. *Environ Sci Technol* 50:12686–12694. <https://doi.org/10.1021/acs.est.6b04415>
- Thornberry T, Abbott JPD (2003) Heterogeneous reaction of ozone with liquid unsaturated fatty acids: detailed kinetics and gas-phase product studies. *Phys Chem Chem Phys* 6:84–93
- Uhde E, Salthammer T (2007) Impact of reaction products from building materials and furnishings on indoor air quality—a review of recent advances in indoor chemistry. *Atmos Environ* 41:3111–3128
- Veres PR, Faber P, Drewnick F et al (2013) Anthropogenic sources of VOC in a football stadium: assessing human emissions in the atmosphere. *Atmos Environ* 77:1052–1059. <https://doi.org/10.1016/j.atmosenv.2013.05.076>
- Wainman T, Weschler CJ, Lioy PJ, Zhang J (2001) Effects of surface type and relative humidity on the production and concentration of nitrous acid in a model indoor environment. *Environ Sci Technol* 35:2200–2206
- Wallace LA, Emmerich SJ, Howard-Reed C (2004) Source strengths of ultrafine and fine particles due to cooking with a gas stove. *Environ Sci Technol* 38:2304–2311
- Wallace LA, Ott WR, Weschler CJ, Lai ACK (2017) Desorption of SVOCs from heated surfaces in the form of ultrafine particles. *Environ Sci Technol* 51:1140–1146. <https://doi.org/10.1021/acs.est.6b03248>
- Wang C, Collins DB, Arata C et al (2020) Surface reservoirs dominate dynamic gas-surface partitioning of many indoor air constituents. *Sci Adv* 6:eaay8973
- Wang C, Waring MS (2014) Secondary organic aerosol formation initiated from reactions between ozone and surface-sorbed squalene. *Atmos Environ* 84:222–229
- Wang H, Morrison G (2010) Ozone-surface reactions in five homes: surface reaction probabilities, aldehyde yields, and trends. *Indoor Air* 20:224–234
- Wang H, Morrison GC (2006) Ozone-initiated secondary emission rates of aldehydes from indoor surfaces in four homes. *Environ Sci Technol* 40:5263–5268
- Waring MS, Siegel JA (2013) Indoor secondary organic aerosol formation initiated from reactions between ozone and surface-sorbed d-limonene. *Environ Sci Technol* 47:6341–6348. <https://doi.org/10.1021/es400846d>
- Weschler CJ (2000) Ozone in indoor environments: concentration and chemistry. *Indoor Air* 10: 269–288
- Weschler CJ, Brauer M, Koutrakis P (1992a) Indoor ozone and nitrogen dioxide: a potential pathway to the generation of nitrate radicals, dinitrogen pentoxide, and nitric acid indoors. *Environ Sci Technol* 26:179–184
- Weschler CJ, Hodgson AT, Wooley JD (1992b) Indoor chemistry: ozone volatile organic compounds, and carpets. *Environ Sci Technol* 26:2371–2377
- Weschler CJ, Nazaroff WW (2017) Growth of organic films on indoor surfaces. *Indoor Air* 27: 1101–1112. <https://doi.org/10.1111/ina.12396>
- Weschler CJ, Nazaroff WW (2008) Semivolatile organic compounds in indoor environments. *Atmos Environ* 42:9018–9040

- Weschler CJ, Wisthaler A, Cowlin S et al (2007) Ozone-initiated chemistry in an occupied simulated aircraft cabin. *Environ Sci Technol* 41:6177–6184
- Wisthaler A, Tamas G, Wyon DP et al (2005) Products of ozone-initiated chemistry in a simulated aircraft environment. *Environ Sci Technol* 39:4823–4832. <https://doi.org/10.1021/es047992j>
- Wisthaler A, Weschler CJ (2010) Reactions of ozone with human skin lipids: sources of carbonyls, dicarbonyls, and hydroxycarbonyls in indoor air. *Proc Natl Acad Sci U S A* 107:6568–6575
- Wong JPS, Carslaw N, Zhao R et al (2017) Observations and impacts of bleach washing on indoor chlorine chemistry. *Indoor Air* 27:1082–1090. <https://doi.org/10.1111/ina.12402>
- Or VW, Wade M, Patel S et al (2020) Glass surface evolution following gas adsorption and particle deposition from indoor cooking events as probed by microspectroscopic analysis. *Environ Sci Process Impacts* 22:1698–1709. <https://doi.org/10.1039/D0EM00156B>
- Zhou S, Forbes MW, Abbatt JPD (2016a) Kinetics and products from heterogeneous oxidation of squalene with ozone. *Environ Sci Technol* 50:11688–11697. <https://doi.org/10.1021/acs.est.6b03270>
- Zhou S, Forbes MW, Katrib Y, Abbatt JPD (2016b) Rapid oxidation of skin oil by ozone. *Environ Sci Technol Lett* 3:170–174. <https://doi.org/10.1021/acs.estlett.6b00086>
- Zhou Z, Zhou S, Abbatt JPD (2019) Kinetics and condensed-phase products in multiphase ozonolysis of an unsaturated triglyceride. *Environ Sci Technol* 53:12467–12475. <https://doi.org/10.1021/acs.est.9b04460>



Occupant Emissions and Chemistry

31

Gabriel Bekö, Paweł Wargocki , and Emer Duffy

Contents

Introduction	904
Primary Emissions from Humans	907
Breath Emissions	907
Skin Emissions	908
Occupant-Related Chemical Transformations	911
Secondary Organic Aerosols	916
Modifying Factors	917
Role of Microbial Population	920
Effects on Perceived Air Quality	921
Health Effects of Human Emissions	922
Conclusions	923
Cross-References	924
References	924

G. Bekö · P. Wargocki

International Centre for Indoor Environment and Energy, Department of Civil Engineering,
Technical University of Denmark, Kongens Lyngby, Denmark

e-mail: gab@byg.dtu.dk; paw@byg.dtu.dk

E. Duffy

Insight SFI Research Centre for Data Analytics, School of Chemical Sciences, Dublin City
University, Dublin, Ireland

e-mail: emer.duffy25@mail.dcu.ie

Abstract

Humans are a major source of indoor chemicals. Breath and skin Occupant-Related Chemical Transformations in emissions meaningfully contribute to the chemical composition of indoor air. Volatile organic compounds emitted by humans originate from endogenous sources (metabolic processes), and from exogenous sources (environmental exposure, diet, and personal care products). They can result from microbial activity and can lead to odor nuisance and decreased perceived air quality. The emitted compounds can undergo chemical transformations, such as ozone-initiated reactions, which produce a range of new compounds. The reactions of ozone with squalene and other constituents of skin oils have been shown to significantly alter the composition of indoor air and alter its OH reactivity. Dermal emissions may impact perceived air quality more than emissions via breath. The understanding of the effects of various environmental and personal factors (e.g., temperature, humidity, personal hygiene, diet, clothing, personal care products, age, sex, emotional state) on human emissions, their chemical transformations, and their consequences for indoor air quality, comfort, and health is limited. This chapter presents an overview of occupant emissions and the indoor air chemistry associated with them. Personal and environmental factors that may influence human emissions are discussed. Emerging research on the potential impacts of occupant emissions on perceived indoor air quality and human health is presented, and key research questions to advance our understanding of occupant-related indoor air chemistry are highlighted.

Keywords

Human emissions · Breath · Skin · Chemical transformations · Organic compounds

Introduction

In the past, building materials and furnishing were considered the dominant sources of indoor air pollution. As emissions from building products were gradually reduced, the role of human emissions in indoor air quality began to be increasingly recognized. The presence of people indoors leads to chemical changes occurring both in the gas phase and on indoor surfaces. It has been reported that the compounds associated with the presence of humans contribute up to 40% of the measured daytime volatile organic compounds (VOC) concentration in indoor spaces (Liu et al. 2016). In another study, human-emitted VOCs were the dominant source during occupied periods in a well-ventilated classroom (57%) together with ventilation supply air, which was the second most important source of pollution (35%) (Tang et al. 2016). Indoor non-occupant emissions constituted 8% of the pollutant

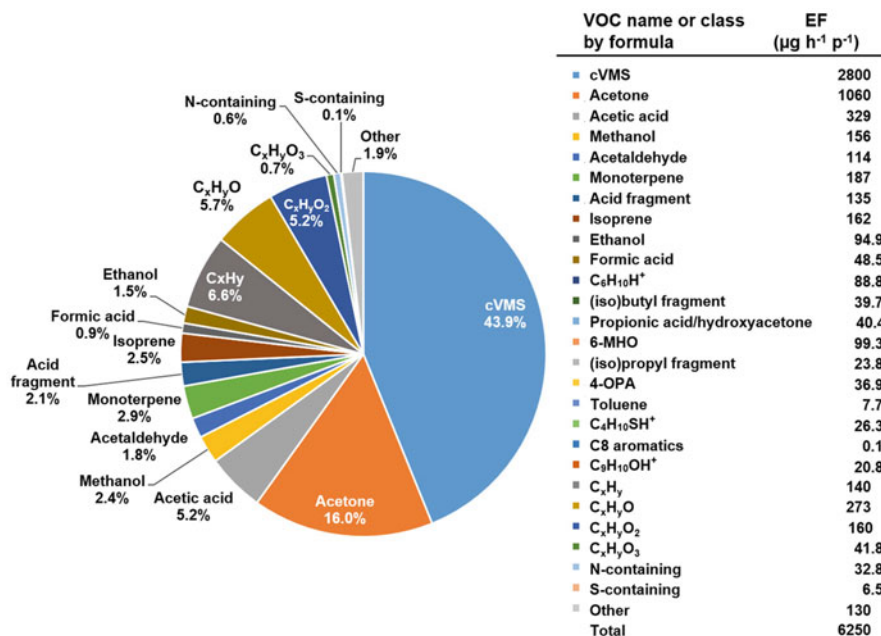


Fig. 1 Human occupant emission factors (EF, $\mu\text{g p}^{-1} \text{ h}^{-1}$) for chemical species shown as relative contributions to the total. (Reprinted with permission from “Tang et al. (2016) Volatile organic compound emissions from humans indoors. Environ Sci Technol 50:12686–12694,” Copyright (2016) American Chemical Society)

mass. The total occupant-associated VOC emission factor was 6.3 mg h^{-1} per person (Fig. 1).

Hundreds of VOCs are released from the human body via the breath, skin, and intestinal gases. These compounds are derived from endogenous metabolic processes in and on the human body and from exogenous sources such as airborne VOCs from environmental or occupational exposures, foods, and personal care products (Kwak and Preti 2011). They can influence indoor air chemistry and indoor air quality. Odorous compounds released in breath have been linked to oral microbial populations (Phillips et al. 1999). Body odor is also associated with decomposition of sweat and sebum by microbial activity (Barzantny et al. 2012; James et al. 2013).

The sebaceous glands across the body secrete oils to lubricate the skin. Many of the constituents of skin oils contain unsaturated carbon bonds that can undergo chemical transformations in the presence of ozone to produce a suite of new compounds in indoor air. These primary and secondary reactions can occur in the presence of humans and in previously occupied environments where skin oils are transferred to surfaces via touching and shedding of skin flakes. Ozonolysis of skin lipids is a sink for ozone present in indoor air, and an important source of indoor VOCs (Weschler et al. 2007; Wisthaler and Weschler 2010).

Changes in environmental conditions can influence the composition and rate of occupant emissions and their chemical transformations. Temperature affects occupant metabolic rates, sebum secretion and volatilization, and the rate of oxidation reactions. Higher temperatures have been shown to lead to higher emission rates of ammonia (Li et al. 2020). Humidity can affect emission of chemicals, their sorption to surfaces as well as chemical reactions occurring in indoor air. Ventilation can act as a source of reactive species such as ozone, reduce the concentration of reaction products, and reduce the time available for gas-phase reactions. Increasing ventilation rates will reduce the impact of occupants on indoor chemistry. Human occupancy itself can also reduce the air concentrations of some volatile and semi-volatile organic compounds (Weschler 2016).

Human skin and breath emissions vary over the course of day, as the influencing environmental and personal factors change. For example, emissions of siloxanes from personal care products depend on the time of their application. The factors that have been shown to influence breath and skin emissions include personal hygiene, diet, clothing, personal care products, but also health status (Shirasu and Touhara 2011), age and sex (Lechner et al. 2006; Sun et al. 2017), genetics (Preti and Leyden 2010), ethnicity (Prokop-Prigge et al. 2016), menstrual cycle (Sukul et al. 2018), and emotional state (Stönner et al. 2018; Williams et al. 2016).

Recent studies have highlighted the potential for human emissions to affect cognitive performance and cause neurobehavioral symptoms in people (Maddalena et al. 2015; Zhang et al. 2017a). Some ozonolysis products are suspected respiratory irritants (Jarvis et al. 2005; Anderson et al. 2007) or have previously been shown to cause skin irritation (Chiba et al. 2000). This chapter describes in greater detail the sources and underlying factors of human emissions as well as their chemical transformations and potential effects.

Table 1 Summary of major organic pollutants associated with various human body parts (Tsushima et al. 2018a, b)

Body part	Organic pollutant
Whole-body	acetic acid, acetone, butanol, butyric acid, ethanol, isoprene, lactic acid, methanol, pyruvic acid, toluene
Exhaled	acetone, dimethyl sulfide, ethanol, hydrogen sulfide, isoprene, methanol, methyl mercaptan
Dermally emitted:	
• Skin except head	• decanal, geranyl acetone, heptanal, nonanal, octanal, 6-MHO
• Axillae	• androstanol, androstenone, isovaleric acid, 3-hydroxy-3-methylhexanoic acid, 3-methyl-2-hexenoic acid
• Scalp	• γ -decalactone
• Hand, forearm	• decanal, dimethyl hexanedioate, geranyl acetone, lilia, nonanal, octanoic acid, pentadecane, phenol, 2-furancarboxaldehyde, 2-furanmethanol, 6-MHO
• Feet	• hydrogen sulfide, isovaleric acid, methanethiol
Intestines	ammonia, hydrogen sulfide

Primary Emissions from Humans

Humans emit many different organic compounds originating from breath, skin (sweat and sebaceous secretions), and intestinal gases (flatulence). Some studies measured whole-body bioeffluents, others analyzed bioeffluents emitted through breathing (exhaled bioeffluents) and skin (dermally emitted bioeffluents), or bioeffluents from a particular part of the body, for example, the oral cavity, axillae, scalp, hand, feet, and intestines (Table 1).

Compounds identified in breath and skin emissions mainly include hydrocarbons, acids, esters, alcohols, alkanes, aldehydes, ketones, furans, ethers, sulfur, nitrogen and halogen-containing compounds, and chlorinated biphenyls (de Lacy Costello et al. 2014; Filipiak et al. 2012). Five major compounds that represent 99% of bowel gas are nitrogen, oxygen, carbon dioxide (CO_2), hydrogen, and methane, though these do not necessarily lead to odor nuisance. However, intestinal gas contains a wide variety of gases in low concentrations, such as ammonia, hydrogen sulfide, volatile amino acids, short chain fatty acids, as well as other sulfur and nitrogen-containing compounds, organic acids, aldehydes, and ketones (Sato et al. 2001; Garner et al. 2007). Some of these compounds have a low odor threshold.

Breath Emissions

Human breath is a significant source of pollutants emitted indoors. Exhaled breath is largely composed of nitrogen, oxygen, carbon dioxide, water, and inert gases, in addition to trace components (VOCs). Breath VOCs are typically present at ppb (or lower) concentrations and include compounds that are generated in the body and taken up from the environment. Endogenous VOCs are primarily blood-borne compounds released via the lungs. Exogenous VOCs include compounds inhaled from the external environment or absorbed through the skin, in addition to compounds produced following oral ingestion of food, and those derived from smoking cigarettes (Shirasu and Touhara 2011).

Typical exhaled gases (e.g., CO_2 , nitrogen) are found in percent concentrations. Concentrations of exhaled CO_2 are used as an indicator of occupancy/human bioeffluents and ventilation in buildings. Constituents present at ppb concentrations or less include VOCs associated with normal metabolism (e.g., ethanol, isoprene, propanone, methanethiol, and nitric oxide (NO)), products of oxidative stress (e.g., propanedial, pentane) and compounds associated with food and environmental or occupational exposure (e.g., trichloromethane, benzene) (Wallace 1987). Breath analysis can be applied to examine exposure to environmental agents, from those in the typical home to domestic exposures influenced by nearby businesses and exposures outside the home (Vereb et al. 2011).

The chemical composition of human breath differs from person to person. Phillips et al. (1999) examined the breath VOCs of 50 humans and identified about 3500 compounds. About half of these had a positive alveolar gradient (abundance in breath minus abundance in air; positive when *in vivo* synthesis is greater than

clearance). However, the total number of breath VOCs did not vary between individuals widely within a fairly narrow range (a breath sample contained on average about 200 VOCs). Despite the large total number of different VOCs observed, there was a small group of 27 VOCs present in all subjects. These were suggested to be products of common metabolic processes.

Human breath contains the following compounds attributable to metabolic processes and observed at levels averaging 10 ppb or above: acetaldehyde, acetone, butanone, 1-butene, dimethyl sulfide, ethanol, ethyl acetate, ethylene, furan, hexanal, isoprene, isopropanol, methanol, methyl ethyl ketone, pentane, 1-pentene, and n-propanol. Compounds present from 1 to 10 ppb in breath include 1,1,1-trichloroethane, butane, cis- and trans-2-butene, 2-hexene, n-butyl alcohol, isobutyl alcohol, capryl alcohol, methyl isobutyl ketone, butyl acetate, ethyl benzene, indene, pentanal, and propanal (Fenske and Paulson 1999).

Sun et al. (2017) measured higher concentrations of endogenous VOCs than of exogenous VOCs in exhaled breath. However, the composition of exhaled breath can be considerably influenced by exposure to pollution, indoor-air contaminants, and particularly by smoking (Filipiak et al. 2012). Compounds that can be found in indoor and outdoor air as well as in exhaled breath include benzene, toluene, ethylbenzene, xylene (o-xylene, p-xylene), aldehydes (building materials and furnishing), benzaldehyde (combustion), acrolein, methacrolein, oleic acid and linoleic acids, propanal, and alcohols such as isomers of propanol (solvents, disinfectants). Constituents of consumer products such as siloxanes, d-limonene, camphor, plasticizers, Texanol, and its related compounds are also among the environmental volatiles possibly present in breath. Branched-chain alkanes in breath have been attributed to exposure in industrial and/or automotive emissions (Kwak and Preti 2011). In the study by Filipiak et al. (2012), most aldehydes had higher concentrations in indoor air than breath, indicating exogenous origin. More than 80 organic compounds were found to be significantly related to smoking, the largest group comprising unsaturated hydrocarbons (29 dienes, 27 alkenes, and 3 alkynes). VOCs with high concentrations in expired air were also often found in indoor air samples. Table 2 summarizes the major compounds reported in exhaled breath and compared to levels in indoor air.

Skin Emissions

Skin emissions are primarily derived from skin gland secretions and the resident microflora. Gland distribution at the skin surface varies across the body, and this is partially reflected in the regional diversity of emissions from the skin. The eccrine glands are distributed across the body and secrete water and electrolytes. The apocrine glands are localized in a few regions of the skin, and they secrete sweat (a fluid containing water, lipids, proteins, and odor precursors). Apocrine glands contribute greatly to VOC emissions produced from the underarm (axillary) regions. Malodor generation on axillary skin has been associated with biotransformation of

Table 2 Summary of major compounds measured in exhaled breath and indoor air by Filipiak et al. (2012)

Species	Compounds	Notes (corresponding to compounds)
Ketones	• 2-butanone, 2-pentanone	• both higher in breath than indoor air
Aldehydes	• acetaldehyde, propanal, acrolein, crotonaldehyde	• higher in exhaled breath of smokers • all aldehydes mostly significantly lower in breath than in indoor air; correlation found for few aldehydes
	• butanal, formaldehyde	
Alcohols	• methanol	• same in exhaled breath as indoor air
	• ethanol	• 3 times higher in breath than indoor air
Acids and esters	• acetic acid, propionic acid	• higher in breath than indoor air; higher in active smokers
	• methyl acetate	• found in nearly all breath samples, not in all indoor air samples (endogenous), higher level in expired than inspired air
Furans	• furfural	• lower in breath of smokers
	• furan; 2-methylfuran; 3-methylfuran; 2,4-dimethylfuran; 2,5-dimethylfuran; 2-ethyl-5-methylfuran; 2,3,5-trimethylfuran	• significant differences between smoker and non-smoker groups • all except 3-methylfuran and 2-ethyl-5-methylfuran found at nearly the same level in exhaled breath and indoor air samples for non-smokers • over fivefold higher level in breath of smokers compared to non-smokers
Aromatics	• toluene, benzene, ethyl benzene, phenol, styrene, o-xylene, p-xylene	• mostly higher in smokers; apart from toluene, all measured aromatics show lower levels in exhaled breath than indoor air for non-smokers
Saturated hydrocarbons	• propane, n-butane, n-pentane, n-hexane, n-decane, n-undecane, n-octane, n-nonane, n-heptane	• n-butane higher in inspired air than expired (in non-smokers) • n-heptane in breath only when also in inspired air; n-decane similar in air and breath • no straight-chained saturated hydrocarbons significantly related to smoking habit • methylated saturated hydrocarbons: significant difference between smokers and non-smokers
Unsaturated hydrocarbons	• alkenes: propene, 3-octene	• in breath similar to indoor air; higher in smokers
	• dienes	• almost never found in non-smokers (except pentadiene and hexadiene)
	• alkynes: propyne, 2-butyne, 1-butene-3-yne	• all especially in smokers, only propyne measured in non-smokers

(continued)

Table 2 (continued)

Species	Compounds	Notes (corresponding to compounds)
Sulfur compounds	• methanethiol	• same in breath and inspired air
	• dimethyl sulfide (DMS), methyl propyl sulfide, allyl methyl sulfide, 3-methylthiophene, 1-(methylthio)-1-propene	• elevated in breath compared to air; allyl methyl sulfide: only in breath, not air
	• ethyl methyl sulfide	• higher in smokers
Nitrogen-containing compounds	• acetonitrile; N,N-dimethylformamide; N,N-diethylformamide	• especially smokers' breath
	• 2-cyano-1-propene; N-methylpyrrole	• higher for smokers
	• (dimethylamino)-acetonitrile	• lower for smokers
	• 4-Propanenitrile	• lower for smokers, similar in breath as in indoor air

gland secretions into volatile odorous molecules by members of the skin microflora (James et al. 2013).

Emissions from the axillary region also contribute to poor indoor air quality. These compounds include androstenol, androstenone (ketone with a urine-like smell), and isovaleric acid (Bird and Gower 1981; Leyden et al. 1981). Axillary sweat contains marker compounds characteristic of individuals and sex. Among these, the following have been measured on skin: 2-phenylethanol, 1-tridecanol, undecanal, lilial, diphenyl ether (all characteristic of individual), pentadecanoic acid, hexadecanoic acid and heptadecanoic acid, methylhexadecanoic acid, and docosane (all characteristic of sex) (Bernier et al. 2000; Penn et al. 2007). C6 to C11 straight-chain, branched and unsaturated acids (3-methyl-2-hexenoic acid, 3-hydroxy-3-methylhexanoic acid) were the odorous compounds released in this region. Terminaly unsaturated acids, the 2-methyl-C6 to -C10 acids and the 4-ethyl-C5 to -C11 acids were also reported to be odor contributors (Zeng et al. 1996; Natsch et al. 2006). Short-chain fatty acid emissions from feet have been linked to foot odor (Marshall et al. 1988). VOCs emanating from palms include aromatics, amides, amines, halides, sulfides, and sulfonyls (Bernier et al. 1999, 2000). Alkenes and carboxylic acids have been shown to be emitted from the forearm (Ostrovskaya et al. 2001), 2-furancarboxaldehyde, 2-furanmethanol, decanal, dimethyl hexanedioate, nonanal, phenol, and carboxylic acid-methyl esters from hands (Curran et al. 2010; Prada et al. 2011). Tsushima et al. (2018b) contain a detailed summary of this literature.

The sebaceous glands secrete oils (sebum) to lubricate the skin. Sebum is composed of squalene, triglycerides, wax esters, and free fatty acids. The sebaceous glands are distributed across the body (except the palms of hands and soles of feet) and are found in the highest density on the face and scalp. Many of the constituents of skin oils contain unsaturated carbon bonds (C=C) which react readily with ozone. Humans are recognized as a sink for ozone in the environment and the reaction of

skin oil components with ozone produces a wide range of secondary products (further discussed in the “[Occupant-Related Chemical Transformations](#)” section below).

Skin oils contain pyroglutamic acid, a natural moisturizing substance present at 1% level in the human epidermis. Pyroglutamic acid does not react with gas-phase ozone, since it does not contain a carbon–carbon double bond. This chemical may be a convenient tracer of human skin oil contamination in indoor environments, given its relatively high abundance and low reactivity with the ozone (Zhou et al. 2016a). Liu et al. (2017) measured 12 carboxylic acids that correlated with CO₂ concentrations in a classroom. These have possible associations with human sources. A major component of human perspiration is lactic acid, although it is also used in commercial health-care products. Other human-related acids include saturated monoacids (octanoic, nonanoic, decanoic, undecanoic, and dodecanoic acid), unsaturated monoacids (hexenoic and nonenoic acid), and a carbonyl acid (pyruvic acid).

Emission rates of some VOC, for example, 1-butanol, acetic acid and 1,3-pentadiene, can be higher from skin than from breath. Aldehydes (e.g., 3-methyl-2-butenal, benzaldehyde, octanal, nonanal, and decanal) and ketones (e.g., 6-methyl-5-en-2-one) can be emitted through skin at volume fractions in the low parts per billion range (Ruzsanyi et al. 2012). 2-Ethylhexanol is often reported among skin emissions, but its endogenous nature is in fact not supported in the literature (Dormont et al. 2013). Ammonia is emitted from occupants’ skin as well as breath. Ammonia originates from the bacterial breakdown of proteins. It is transported by blood to the liver. Ammonia remaining in the blood can diffuse through the skin, in sweat, or breath. Li et al. (2020) summarized the limited research on ammonia emission rates from humans. Most research has focused on breath ammonia concentrations, despite the fact that dermal emissions tend to be substantially higher than breath emissions. Furukawa et al. (2017) measured dermal emissions from 13 locations on five males and five females. Higher ammonia emissions were measured on the feet, back, and lumbar region, and lower emissions were measured on upper arms, buttocks, thighs, and lower legs. This ranking roughly corresponds to the density of sweat glands at the different body locations. Li et al. (2020) isolated dermally emitted ammonia from exhaled ammonia in a climate chamber experiment, in which volunteers sat in one chamber with breathing masks covering their mouth and nose and exhaled into an adjacent twin chamber. Breath emission rates were estimated to be 15 to 50 times smaller than dermal emission rates. The difference between dermal-only and whole-body emission rates was relatively small, indicating the dominance of human ammonia emissions via the dermal route. Moreover, emission rates significantly increase with larger area of exposed (uncovered) skin area.

Occupant-Related Chemical Transformations

Human emissions can undergo chemical transformation and result in a suite of new compounds in indoor air. These reactions occur in the presence of humans and in previously occupied spaces, as skin oils are transferred to surfaces through touching,

and via skin flakes (squames) and their constituents shed by people in a process called desquamation contribute to the organic films on indoor surfaces. Squames contain skin surface lipids, and the squalene content of skin flakes is ~1% by weight (Clark and Shirley 1973). Settled dust in occupied settings also contains skin flakes and their associated skin oils, resulting in reactions between dust and ozone.

Approximately 80–90% (by weight) of skin oils contain long-chain acyl groups as free fatty acids, glycerides, wax esters, cholesterol esters, ceramides, and other species. Squalene is responsible for most of the remaining fraction (~10%) of skin surface lipids. The primary reaction is that between squalene and ozone. Reactions of unsaturated fatty acids are also meaningful. Squalene is responsible for about 50% of the unsaturated carbon bonds in skin surface lipids. Ozonolysis of skin lipids is an important source of indoor VOCs and a sink for indoor ozone. Acetone, geranyl acetone, 6-methyl-5-heptene-2-one (6-MHO; from squalene), aldehydes, especially decanal, undecanal, dodecanal, nonanal, hexanal, and octanal (from unsaturated fatty acids) are the major products (Weschler et al. 2007; Wisthaler and Weschler 2010; Fischer et al. 2013).

Other squalene-ozone reaction products include 4-oxopentanal, hydroxyacetone (also product of oxidation of isoprene), 1-hydroxy-6-methyl-5-hepten-1-one, as well as a number of secondary products, including, 5-hydroxy-4-oxopentanal (5-OH-4-OPA), 1,4-butanedial (succinic dialdehyde), 4-methyl-8-oxo-4-nonenal (4-MON), 4-methyl-4-octene-1,8-dial (4-MOD), 4-oxopentanoic acid, and 4-oxobutanoic acid. Additional less volatile products of ozonation of squalene include a number of long-chained polyunsaturated aldehydes and carboxylic acids, such as C27-pentaenal, C22-tetraenal, C17-trienal, C27-pentaenoic acid, C22-tetraenoic acid, and C17-trienoic acid, that remain bound to the surfaces as skin, hair, clothing, and particles. Ozone's reaction with squalene on these surfaces is fast and ozone removal is transport limited.

Some products (e.g., acetone, geranyl acetone, 6-MHO, and 4-oxopentanal (4-OPA)) are produced through secondary surface reactions between ozone and some of the primary squalene reaction products. For example, squalene and its ozonolysis product geranyl acetone are the major precursors for acetone and 6-MHO. 4-OPA is the major secondary reaction products as 6-MHO and geranyl acetone further react with ozone. Acetone can also be formed by 2-methyl-2-docosene (Yang et al. 2016). Salvador et al. (2019) applied a series of mass balance models to account for formation and removal of geranyl acetone, 6-MHO, and 4-OPA measured in a climate chamber with simulated occupancy using soiled t-shirts at two air change rates (1 h^{-1} and 3 h^{-1}) and two initial ozone mixing ratios (30 ppb and 60 ppb). Geranyl acetone was entirely produced in surface reactions on the t-shirts and removed almost equally by ventilation and further reaction with ozone. About 70% of gas-phase 6-MHO was produced in surface reactions on the t-shirts, the remainder in secondary gas-phase reactions of ozone with geranyl acetone. It was primarily removed by ventilation; reaction with ozone was responsible for about a third of its removal. 4-OPA was formed primarily on the surfaces of the shirts; gas-phase reactions of ozone with geranyl acetone and 6-MHO accounted

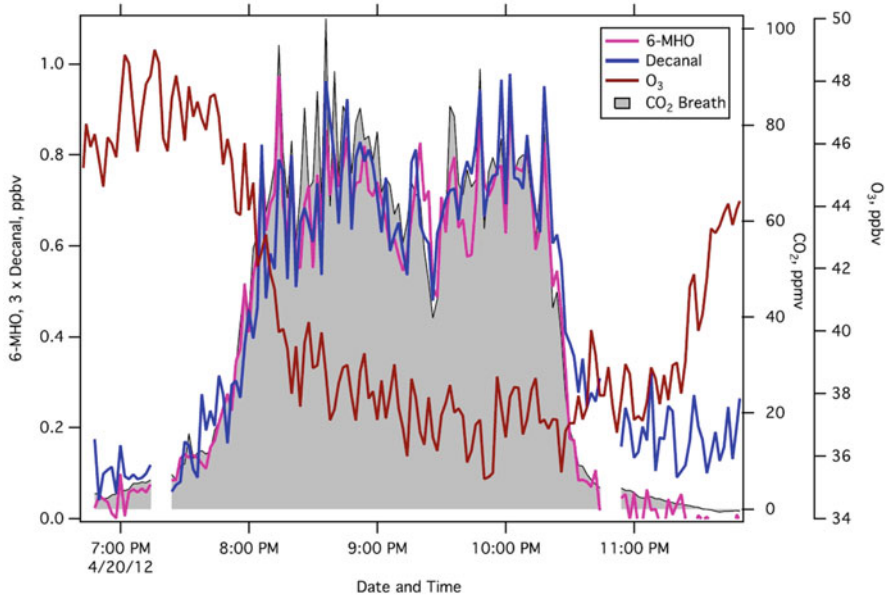


Fig. 2 Ozone (red), decanal (blue), and 6-MHO (green) measured in an occupied football stadium. The grey shading shows the CO₂ mixing ratios above background levels. (Reprinted from “Veres et al. (2013) Anthropogenic sources of VOC in a football stadium: Assessing human emissions in the atmosphere, Atmos Environ 77:1052–1059,” Copyright (2013), with permission from Elsevier)

for ~30% and ~10%, respectively. 4-OPA does not react with ozone and was therefore removed entirely by ventilation.

The removal of ozone and the production of ozonolysis reaction products such as 6-MHO and decanal has been observed upon the arrival of spectators in a football stadium (Fig. 2) (Veres et al. 2013). Ozonolysis reactions with VOCs and skin oils, combined with increased surface deposition during a match, were suggested to be responsible for titrating observed ozone by approximately 20%. A clear relationship between ozone and CO₂ was observed in occupied and unoccupied classrooms (Fischer et al. 2013). When students left the classroom, carbon dioxide levels decreased and ozone levels increased. When they returned, carbon dioxide levels increased and ozone levels decreased. First- and second-generation skin lipid ozonolysis products were found to correlate with CO₂ and anticorrelate with O₃ (Liu et al. 2016). These observations suggest a large impact that humans have on ozone levels in densely occupied rooms. Moreover, surface reactions of aged skin lipids (during unoccupied periods) transferred to indoor surfaces may be minor compared to the surface reactions on humans and on other indoor surfaces that contain freshly transferred skin oils during occupied periods.

Ozonolysis of skin lipids via the Criegee mechanism can produce hydrogen peroxide, organic peroxides, and short-lived highly reactive products including hydroxyl, hydroperoxyl, and alkyl peroxy radicals. The reactions of these radicals

with squalene and its reaction products, producing additional carbonyls, dicarbonyls, and hydroxycarbonyls. Some of the products of ozone/unsaturated fatty acid reactions include nonanoic acid, 9-oxononanoic acid, 9-oxooctadecanoic acid, and azelaic acid (from oleic acid), while in the case of linoleic acid, they include acrolein and α -acyloxyalkyl hydroperoxid (Weschler 2016). Dicarboxylic acids including adipic acid and suberic acid, arising from oxidation of the most common unsaturated acids, cis-hexadec-6-enoic acid and cis-octadec-8-enoic acid, respectively, were observed after exposing skin oil to ozone (Zhou et al. 2016a). Triolein, a high-MW compound present in skin oil, yields lower-MW ozonolysis products upon reaction with ozone, for example, nonanoic acid.

Levulinic acid, succinic acid, adipic acid, suberic acid, and 4-oxobutanoic acid are the major condensed phase products remaining on the skin, clothes, and other surfaces from heterogeneous ozonolysis of squalene (Zhou et al. 2016a, b). Some of these acids can partition into the gas phase. They were identified in the gas phase with their indoor concentration substantially higher than outdoors (Liu et al. 2017). 6-Oxohexanoic acid and levulinic acid were observed to correlate with CO₂ (Liu et al. 2017). Aromatic acids including benzoic and benzeneacetic acid (human skin secretions) have been reported by the authors but did not correlate with CO₂. Benzylsuccinic acid increased with increasing CO₂, but its human source has not been reported.

Some of the more important reactive species present in exhaled breath include isoprene, 1-ethene, 1-butene, 1-pentene, limonene, nitric oxide, and dimethyl sulfide. Exhaled isoprene reacts slowly with ozone, but reacts more quickly with hydroxyl and nitrate radicals (Weschler 2016). Tsushima et al. (2018b) measured the ozone-initiated transformation of organic compounds emitted from the human body in a unique stainless-steel twin-chamber that enabled the separation of dermal and exhaled emissions. Human subjects were sitting in a climate chamber wearing breathing masks. One-way valves ensured that they inhaled air from the chamber where they were sitting and exhaled into the adjacent chamber. Generally, larger concentration differences were observed between the two chambers when ozone was present. With ozone present, higher levels of reaction products were seen in the chamber with dermal bioeffluents. In a similar study performed in the same chambers, whole-body and dermal-only emissions removed around 75% of the ozone dosed into the chamber, while breath-only emission removed less than 10% (Bekö et al. 2020).

In addition to ozone, other major indoor oxidants include hydroxyl radicals (OH) and nitrate radicals (NO₃). The presence of occupants reduces oxidant concentrations and affects the formation of new products, including radicals (hydroxyl radicals (OH), hydroperoxy radicals (HO₂), and peroxy radicals (RO₂)) and nitrated organic compounds (Kruza and Carslaw 2019). Concentrations of OH and NO₃ are not meaningfully affected by reactions with squalene and unsaturated fatty acids on human surfaces. However, ozone/skin lipid chemistry produces species that affect the levels of free radical oxidants in the indoor environment. The reaction of ozone with 6-MHO produces hydroxyl radicals (OH), but 6-MHO rapidly consumes OH. It also reacts at a fast rate with nitrate radicals (produced by ozone reaction with NO₂). However, if humans are present in an indoor setting, ozone levels are lower, resulting in lower NO₃ levels. Geranyl acetone is expected to react rapidly with OH and NO₃,

producing additional 6-MHO. 4-OPA reacts with both OH and NO_3 radicals, although the effect of these reactions is small on OH levels and negligible on NO_3 levels. Exhaled isoprene reacts moderately with ozone, but reacts faster with hydroxyl and nitrate radicals, forming formaldehyde, methacrolein, and methyl-vinyl ketone among other products (Atkinson and Arey 2003). Moreover, when isoprene reacts with OH, alkyl peroxy radicals are formed, which can then react with NO to form organic nitrates. NO reacts rapidly with ozone, generating nitrogen dioxide, but its contribution to indoor NO_2 levels is small. NO also reacts rapidly with NO_3 .

Measurements of total OH reactivity (total oxidation capacity) account for all reactive organic species in the air. Comparing it to the summed reactivity, anticipated from known individual trace gases reveals whether all relevant species are being measured. Wang et al. (2021) applied this method in a stainless-steel climate chamber occupied by four volunteers, along with measurements using a PTR-ToF-MS and fast GC-MS. Whole-body, exhaled, and dermal emissions were assessed separately, in a fashion described above (Li et al. 2020; Tsushima et al. 2018b). The directly measured OH reactivity was compared with the estimated sum of the OH reactivity of the individually measured species with and without ozone added to the chamber. The average total OH reactivity of the chamber increased with the presence of four persons by 14 s^{-1} under ozone-free environment and by 33 s^{-1} with ozone present. The calculated OH reactivity was 16 s^{-1} without ozone and 33 s^{-1} with ozone. Under ozone-free conditions hydrocarbons (HC), dominated by isoprene from breath, contributed with the largest fraction to the total OH reactivity. After ozone was added, carbonyl compounds especially from dermal emissions constituted the largest fraction of the doubled total OH reactivity (Fig. 3). The reactivity

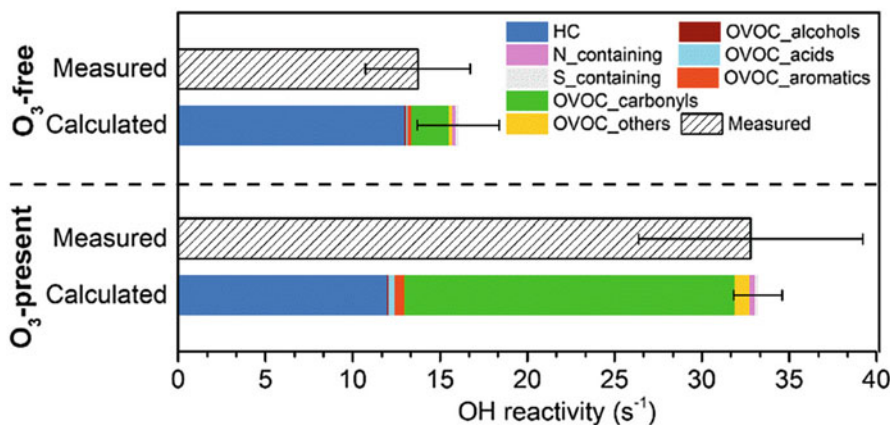


Fig. 3 Calculated and measured OH reactivity of adult whole-body emissions under ozone-free and ozone-present conditions. Error bars represent the standard deviation derived from the data of four identical experiments with three different groups of volunteers. (Reprinted with permission from “Wang et al. (2021) Total OH reactivity of emissions from humans: In situ measurement and budget analysis. Environ Sci Technol 55:149–159, <https://pubs.acs.org/doi/10.1021/acs.est.0c04206>,” Copyright (2020) American Chemical Society)

attributed to carbonyl compounds increased by almost an order of magnitude, with 6-MHO alone accounting for the largest fraction. For breath emissions alone, the total OH reactivity without ozone was similar to that with ozone present. For dermal emissions alone, the total OH reactivity without ozone was low. It increased significantly when ozone was present.

Human occupancy can also meaningfully alter the air concentrations of some volatile and semi-volatile organic compounds, for example, by removal via dust ingestion, inhalation, and dermal absorption. Some chemicals removed by the presence of occupants are known to participate in indoor chemistry, and their removal by occupancy therefore reduces product concentrations. Occupancy may reduce indoor concentrations of certain chemicals by up to 60% (Weschler 2016). He et al. (2019) recruited 98 healthy, non-smoking subjects and measured the concentrations of a range of organic compounds in their inhaled and exhaled breath at various locations including well-ventilated offices, classrooms, gas stations, and laundry rooms. Correlation coefficients between inhaled and exhaled breath concentrations varied between -0.03 and 0.96. Human breath was shown to be a source for some compounds and a sink for others. The authors observed that with increasing toluene concentrations, human breath turned from source to sink. It has been suggested that humans act as sinks for toluene when at sufficiently high ambient concentration toluene molecules diffuse from alveolus into the capillary and pulmonary veins driven by the partial pressure gradient. They can then reach all organs, while some may be stored in the periphery of the human body. The stored toluene can then be excreted via breath or other pathways when the external concentration is relatively low.

Secondary Organic Aerosols

Occupant related chemical reactions may contribute to indoor concentrations of ultrafine particles, as the reaction products condense on existing particles or nucleate to form new particles. Fadeyi et al. (2013) observed higher concentrations of secondary organic aerosols (SOA) from ozone-terpene reactions when a space was unoccupied, compared to when it was occupied. When occupants are present, less ozone is available for SOA generation. As semivolatile organic compounds (SVOCs) partition between the gas-phase and airborne particles, these changes in SOA levels caused by the presence of occupants alter the ratio of particle-phase to gas-phase SVOC, which has consequences for indoor air chemistry.

Although skin oil-ozone reactions can themselves be a source of SOA (Wang and Waring 2014), SOA produced from ozone-initiated reactions with limonene outweighs any SOA produced by ozone reacting with the surfaces of the human occupants. Humans may, however, meaningfully contribute to indoor SOA concentrations in indoor environments with low levels of terpenoids and other ozone-reactive pollutants. Submicron particles were also shown to be generated during ozone reactions with skin-oil-soiled t-shirts; higher particle production occurs at higher ozone levels and when the T-shirts are worn for a longer period of time (Rai

et al. 2013). In the outdoor environment, large isoprene emissions have been shown to significantly inhibit new particle formation correlated to the monoterpene emissions from vegetation. This may be due to the high reactivity of isoprene with the hydroxyl radical (OH). It is currently unclear if isoprene emissions from breath could suppress new particle formation in indoor air.

Modifying Factors

The types of pollutants and their emissions vary with differences in nutrition, health condition, menstrual cycle, age, sex, hygienic standards, environmental exposure, and even addiction to alcohol and cigarette smoking (Wallace 1987; Kuukasjarvi et al. 2004; Penn et al. 2007; Havlicek and Saxton 2009; Schwarz et al. 2009). For example, Sukul et al. (2018) examined the exhaled VOCs throughout menstrual cycles in 24 young and healthy women using high-resolution real-time mass-spectrometry. The changes in exhaled VOC concentrations were pronounced throughout all cycles. Intra-individual variations were low. The largest changes were observed at the ovulation phase. Ammonia and acetone concentrations decreased, while isoprene concentrations significantly increased compared to initial menstruation. Some menstrual effects on exhaled VOCs disappeared with the use of oral contraception. Natural menstrual cycle and contraceptive therapy may affect metabolic processes, some of which regulate or produce endogenous VOCs.

Evidence of genetic influences on axillary emissions has been reported. Variants in the ABCC11 gene are thought to play a key role. The study used GC-MS to study axillary odorant VOCs from 30 individuals of African-American, East Asian, and Caucasian descent and found that characteristic odorants varied quantitatively with respect to genetic origin (Preti and Leyden 2010; Prokop-Prigge et al. 2016). The odor produced in the axillae has also been shown to differ under stressful conditions compared to normally produced axillary odor (Chan and Haviland-Jones 2000).

Sun et al. (2017) found that age influenced the breath emissions of most measured VOCs. The emissions of, for example, acetone, isoprene, decanal, benzene depended on sex, while smoking status influenced the emissions of, among others, nonanal, toluene, benzene, 1-(methylthio)-propane, and cyclopentane. Isoprene, which is a major VOC constituent of exhaled breath, exhibits large variability with age and sex. Concentrations may become reasonably stable after reaching adulthood (Lechner et al. 2006; Sun et al. 2017; Taucher et al. 1997). Cardiac output, breathing pattern, sleep/wakefulness, physical activity as well as clinical conditions can further influence isoprene emission rates (Taucher et al. 1997; King et al. 2010). Levels of exhaled NO increase with upper respiratory tract infections, asthma, and certain other conditions. Changes in metabolism affect VOC breath and sweat composition (Pereira et al. 2015; Shirasu and Touhara 2011). Dimethylsulphone, benzothiazole, nonanal, and 2-nonenal were suggested to be biomarkers of increased age (Gallagher et al. 2008; Haze et al. 2001). Proposed gender markers from skin include pentadecanoic acid, hexadecenoic acid, heptadecanoic acid, nonadecane, and docosane (Penn et al. 2007).

No significant difference in OH reactivity could be identified between teenagers, young adults, and seniors (Wang et al. 2021). However, a possible trend of decreasing OH reactivity with increasing age in the presence of ozone has been observed. The OH reactivity of carbonyls was slightly lower for seniors. The OH reactivity of alcohols was lower for the senior group than for young adults, which was lower than for teenagers. The OH reactivity contribution from the nitrogen-containing species (dominated by ammonia) was highest for the teenager group. The senior group demonstrated the highest fractional reactivity for sulfur-containing species. The emission rates of skin lipids (primarily responsible for increased OH reactivity when ozone is present) tend to decrease with age (Waller and Maibach 2006). The proportion of different skin lipids is, however, similar regardless of age. In line with this, the top ten species contributing to the total OH reactivity were consistent across the three age groups.

Changes in environmental conditions such as temperature and relative humidity can affect the types of bioeffluents emitted as well as their emission rates. Metabolic rate and clothing change with temperature, and this can consequently affect human emissions. Moreover, higher temperatures may increase sebum secretion and consistency, increasing volatilization and consequently the emission and reaction rate of squalene. The number of resident skin flora can also increase with temperature. Moreover, temperature increases the rate of oxidation reactions. Tsushima et al. (2018b) measured dermal emissions and exhaled breath emissions from human subjects at chamber temperatures 23 °C and 28 °C. Higher concentrations of squalene and an unknown hexanedioic acid ester were observed at 28 °C. Acetic acid level was higher in the chamber when the temperature was 23 °C. Higher temperatures were shown to be strongly correlated also with higher emission rates of ammonia from people (Li et al. 2020). Ammonia concentrations in a climate chamber with no other sources were approximately three to four times higher at higher temperatures (~32 °C) than at lower temperatures (~28 °C).

Humidity is an important factor that can influence VOC emissions and compete with VOCs for sorptive uptake. It affects squalene ozonolysis. The reactions between ozone and squalene and between ozone and skin oils present on soiled t-shirts have been shown to be humidity dependent (Arata et al. 2019). The concentrations of some reaction products followed the variations in relative humidity deliberately changed in a climate chamber in a series of steps. In another study, increasing RH from 10% to 50% doubled the emissions of most ozonolysis by-products from a cotton surface. Nonanal and decanal emissions increased by a factor of five (Coleman et al. 2008). Humidity may also affect the distribution of squalene-ozone reaction products that are generated on indoor surfaces. This may be due to different pathways from the Criegee intermediates. Zhou et al. (2016b) found that at RH below 5%, the major condensed-phase products were levulinic acid and succinic acid. Under humid conditions (50% RH), the major products were 4-OPA, 4-oxobutanoic acid, and levulinic acid. High-molecular weight products were observed under dry conditions with indications that levulinic acid was involved in their formation. Higher RH also increases secondary organic aerosol formation from the ozonolysis of surface-film squalene (Wang and Waring 2014).

Ventilation can act as a source of reactive species (e.g., ozone), lower the concentration of reaction products, and reduce the time available for gas-phase reactions. Higher ventilation rates will thus result in a smaller impact of occupants on indoor chemistry. Intermittent ventilation (e.g., turning ventilation off overnight or on weekends) may lead to the accumulation of indoor-generated pollutants, but also to lower indoor ozone concentrations, delayed generation of ozone-initiated reaction products when the ventilation is turned back on again, and lower product concentrations compared to continuous ventilation. On the other hand, ozone removal rates by humans are mass transport limited, and ventilation strategies will have a marginal effect on them (Salvador et al. 2019).

The external environment contributes significantly to the skin's chemical composition. Molecular features of the skin can be matched with hygiene, diet, clothing, beauty products, plasticizers (e.g., o-formylbenzoic acid) or food constituents (e.g., sinapinic acid and oxidized polyethylene). Molecular families that include constituents of personal care products (PCPs) (e.g., C12 lauryl ether sulfate surfactant, cocoamidopropylbetaine (shampoo), avobenzone, and octocrylene (sunscreens)) were found on skin (Bouslimani et al. 2015). Constituents of personal care products used by occupants can contribute to occupant-related gaseous indoor pollutants. These include, for example, monoterpenes, linalool, and cyclic volatile siloxanes. Limonene has been shown to be one of the most abundant compounds in the breath and skin, presumably originating from diet (flavoring agents) and scented personal care products (Sanchez and Sacks 2006; Mochalski et al. 2014). Cyclic volatile methylsiloxanes (especially decamethylcyclopentasiloxane (D5)) are abundant in PCPs (such as antiperspirants) and have been reported as dominating VOC emissions in an occupied classroom, but the emission rate declined over the course of the day as the products off-gassed (Tang et al. 2015).

Human skin and breath emissions strongly vary over the course of a day. For example, emissions of exogenous compounds like terpenes or siloxanes from personal care products depend on the time of their application. Emotional state can also influence emissions. Small scale variances in emission rates were found to occur reproducibly over multiple screenings of the same film in a cinema. The peaks occurring in the time series of a compound during the screening of the film were induced by the physiological response of the audience to audio-visual stimuli (Stönnér et al. 2018; Williams et al. 2016). Crowd-based breath analyses may in the future assess group-based behaviors, exposures, and perhaps opinions and changes in mood (Williams and Pleil 2016).

Clothing acquires skin oils, which can be altered via microbial activity or react with ozone. The reaction products can desorb into indoor air. Squalene, for example, reacts with ozone on T-shirts, producing the above-mentioned ozonolysis products (Coleman et al. 2008; Rai et al. 2014; Salvador et al. 2019). The formation of nonanal on skin-oiled clothing can be mainly attributed to reactions between ozone and unsaturated fatty acids such as 9-octadecenoic acid and (Z)-7-hexadecenoic acid and their derivatives, such as (Z)-13-docosenamide. 6-Hexadecenoic acid (the most abundant unsaturated fatty acid of skin-oiled clothing) and 8-octadecenoic acid are the main reagents that contribute to the generation of decanal

(Yang et al. 2016). Wax esters and triglycerides also contribute to the formation of nonanal and decanal. Ozone reactions with terpenes or sesquiterpenes transferred to clothing from PCPs produce low volatility oxidation products (carbonyls and carboxylic acids). Reactions that occur on clothing can also generate nonylphenol, from the degradation of nonylphenol ethoxylate detergent residues (Antal et al. 2016) and formaldehyde from constituents of anti-wrinkling agents (De Groot et al. 2010). C6–C10 straight-chain saturated aldehydes were the major by-products of the ozone reaction with unsoiled cotton T-shirt fabric. The secondary emissions from soiled fabrics can be higher than from laundered fabrics (Coleman et al. 2008; Rai et al. 2014). Ozone consumption and by-product formation on clothes are affected by various environmental factors. Ozone-initiated VOC emissions were generally higher at higher ozone, humidity, soiling of T-shirt, and air change rate (Coleman et al. 2008; Rai et al. 2014).

Clothing contains a variety of chemicals acquired during manufacturing processes, as a consequence of packaging, transport, and storage, or deliberately added, such as anti-wrinkling agents, flame retardants, and antimicrobial agents. Clothing also acquires chemicals from the air during use, or via contact with surfaces, personal care products, and laundry detergents. Under favorable conditions, some of these chemicals can be emitted into indoor air or can chemically transform to other species. A detailed description of chemical emissions from clothing falls outside the scope of this chapter. We refer to Licina et al. (2019) and to ► Chap. 36, “Role of Clothing in Exposure to Indoor Pollutants,” of this Handbook for a comprehensive summary of the literature on the role of clothing in chemical emissions and exposures.

Role of Microbial Population

Apart from odorous human emissions of fecal nature, odorous compounds in breath are attributable to the microbial population in the mouth, producing volatile sulfur compounds (thiols, sulfides), skatol, organic acids, ammonia, and amines (Phillips et al. 1999). Body odor is further generated when the microbial activity decomposes the sebum and sweat (lipid peroxidation). *Staphylococcus epidermidis* and lipophilic corynebacteria that dominate bacterial community in the axillary region of the skin degrade precursor compounds found in odorless apocrine gland secretions into volatile fatty acids and thiolalcohols that are associated with malodor (Barzantny et al. 2012; James et al. 2013). The yeast *Pityrosporum ovale* metabolizes lipid substances on the scalp to fatty acids and glycerol, which undergo ring closure to the volatile and odorous γ -lactones. γ -Decalactone was reported to be responsible for the smell of unwashed hair (Inaba and Inaba 1992). Foot odor is primarily attributable to methanethiol produced by *Brevibacterium epidermidis* present on the skin and to isovaleric acid produced by the degradation of leucine found in sweat by *Staphylococcus epidermidis* (Kusano et al. 2012; Ara et al. 2006).

Molecular signatures can be correlated with the local microbial community, indicating molecular interrelations among the microbiota, human skin, and the

environment. Bouslimani et al. (2015) visualized the chemical composition and microbiological community composition of human skin surface. Of human origin, members of the molecular families of phosphatidylcholine, phosphatidylserine, and sphingosine lipid, a sterol family that includes a match to cholesterol, were found on skin. Bile acids, glycocholic acid, and taurocholic acid were also detected. Tryptamine from the skin was identical to the molecular feature collected from the cultured microbe *Staphylococcus*. Components of acyl glycerols that make up membranes of human cells (lipids such as oleic acid, palmitic acid, and monoacylated glycerols monoolein and monopalmitin) were found in larger amounts on the head, face, hands, chest, and back. The localization of oleic acid, palmitic acid, mono-oleic, and palmitic acylated glycerols matched the localization of the genus *Propionibacterium*. Some of these products might result from hydrolysis of triacylglycerides or diacylglycerides mediated by *Propionibacterium*. *Propionibacterium acnes* and *staphylococcus epidermidis* indeed hydrolyze tri-glyceride to fatty acids.

Effects on Perceived Air Quality

The perception of body odor was first investigated systematically by Yaglou et al. (1936), who used human subjects to judge the odor intensity and the freshness of air polluted by bioeffluents. The results have been the basis of ventilation standards and guidelines for decades to come. Later studies of similar characters with a greater number of subjects used the acceptability of air judged by a sensory panel to measure the perceived air quality. The newly developed unit “olf” described the sensory pollution load from a standard sedentary adult person (Fanger 1988).

Tsushima et al. (2018b) separated the dermal and exhaled human emissions from five male subjects wearing a breathing mask in a twin chamber. Another 23 subjects were recruited to perform sensory evaluations of the air from the two chambers. This was done while ozone was present or absent in the chambers containing the emissions, as well as at temperatures 23 °C and 28 °C in the chambers. The perceived air quality of the unoccupied chambers was also assessed. No significant difference was observed between the acceptability and odor intensity of the empty chamber and those with exhaled bioeffluents. The odor intensity was higher and the acceptability of the air lower with dermally emitted bioeffluents than with no bioeffluents or exhaled bioeffluents. Similar air quality was observed with whole-body emissions (dermal and breath) as with dermal emissions alone. It was concluded that dermally emitted bioeffluents play a major role in the occupant-related sensory nuisance experienced in indoor environments. The presence of ozone did not affect the results significantly. However, the air quality was consistently perceived poorer at higher temperature. Dermal secretions and the number of resident skin flora increase at elevated temperatures. This may lead to increased production of odorous substances.

Burdack-Freitag et al. (2011) used gas chromatography-olfactometry to identify significant human-induced odorants in densely occupied rooms. Six such

compounds were correlated with poor indoor air quality. Hexanal and (Z)-4-heptanal originate from lipid peroxidation, 2,3-butanedione from glucose metabolism and enzymatic oxidation of pyruvate, and 3-(methylthio)-propanal is an enzymatic degradation product from protein metabolism. 3-methyl-2-butene-1-thiol, an off-odor of beer with very low odor threshold, was identified in spaces with adults, but not in classrooms with small children. Finally, 6-MHO may be among the compounds responsible for the attraction of mosquitoes (Meijerink et al. 2000).

Wysocki et al. (2009) studied odor perception with the aim of reducing the odor threshold of axillary emissions using structurally similar compounds to “cross-adapt” the olfactory system. They found that exposing volunteers to pleasant-smelling ethyl esters of the axillary odorant 3-methyl-2-hexenoic acid resulted in reduced sensitivity to the esters over time, and sensitivity to 3-methyl-2-hexenoic acid was subsequently reduced (i.e., cross-adapted by the esters). The authors concluded that some potential cross-adapting agents could reduce the impact of human stress-related odors; however, the same chemicals may not necessarily be effective for male and female odors. A gender-specific response to both the odor-stimuli and the fragrance chemicals used to cross-adapt it was suggested.

Health Effects of Human Emissions

The literature available on the health effects of emissions from humans and their reaction products is limited. Emissions from humans, and particularly body odor, have been considered nontoxic. A recent study showed, however, that bioeffluent levels with CO₂ of 3000 ppm can cause increased intensities of some acute health symptoms (sleepiness, headache, fatigue, and other neurobehavioral symptoms) (Zhang et al. 2017a). Diastolic blood pressure, end-tidal CO₂ level, and concentration of salivary a-amylase increased after exposure to a higher level of bioeffluents (Zhang et al. 2017b). Exposure to bioeffluents was also shown to reduce cognitive performance (Maddalena et al. 2015; Zhang et al. 2017a, b).

Some products of ozone reactions with skin oil constituents have low odor and sensory irritation threshold (Devos et al. 1990; Wolkoff 2013). In a simulated aircraft cabin, human subjects judged the air quality and 12 symptoms, including eye and nasal irritation, lip and skin dryness, headache, dizziness, and mental tension, to be significantly worse when ozone was present in the air, compared to when it was absent (Strøm-Tejsen et al. 2008). Although the air pollution in the simulated aircraft was not limited to human emissions, most products of ozone-initiated chemistry in the cabin were derived from surface reactions with occupants and their clothing (Weschler et al. 2007). When inhaled, some of the products of these reactions, especially dicarbonyls, may be respiratory irritants (Jarvis et al. 2005; Anderson et al. 2007). It can be assumed that secondary products of human-ozone chemistry may be more irritating than primary products, given their multiple oxygen-containing functional groups (Weschler 2016). Some of the less volatile products may be skin irritants (Thiele et al. 1997; Weber et al. 1999). Anderson et al. (2012) have reported that both dermal and pulmonary exposure to 4-OPA may give rise to

allergic responses in mice. Wolkoff et al. (2013) determined human reference values for airflow limitation due to inflammation in the airways, accumulation of mucus, and bronchial constriction (0.03 ppm and 0.5 ppm for 4-OPA and 6-MHO, respectively) and for sensory irritation for some of the ozone-skin lipid reaction products (0.3 ppm for 6-MHO). Moreover, squalene ozonolysis products may cause other health problems related to oxidative stress. Fu et al. (2013) observed that squalene's interaction with ozone considerably enhanced its hydrophilicity and redox activity. The authors speculated that this could affect the ability of condensed phase reaction products to penetrate through the skin and cell membranes, posing an increased health risk in indoor environments. Enhanced redox activity in cells can damage cellular components such as proteins, lipids, and DNA. It is associated with increased levels of reactive oxygen species and oxidative stress, which has been linked to various human diseases.

Experimental animal studies show that skin exposure to ozone results in signs of oxidative stress, including depletion of antioxidants and the appearance of lipid peroxidation products in the epidermis (Weber et al. 1999). Squalene oxidation products have been shown to be comedogenic and to cause skin irritation in rabbit models (Chiba et al. 2000). More recently, squalene ozonolysis products have been shown to accumulate in human skin oil that has been exposed to ozone (Zhou et al. 2016a). These reaction products can diffuse through the skin and enter the blood where they have potential to cause adverse health effects (Lakey et al. 2017).

Conclusions

Primary emissions from humans, especially via exhaled breath, have been studied for a long time with the purpose to identify disease biomarkers and advance disease diagnostics. This has been largely done with limited success for clinical applications. It is only recently that the scientific community began to appreciate the significant role occupants play in indoor air chemistry. Our understanding of this field of science is now rapidly improving with the development and availability of novel measurement techniques and instrumentation. New methodologies allow us to revisit some of the research questions that have been puzzling scientists for decades, such as the personal and environmental factors that may influence human emission (e.g., diet, stress level, hygiene habits, age, sex, health condition, activity level, personal care products, clothing, and its laundering and storage). The inter- and intrapersonal variability of emissions, as well as the influence of prior exposure on human emissions, will likely receive increasing attention. New research questions are also being generated. It is, for example, currently unclear whether indoor air quality affects the dermal and oral emissions. Real-time measurements of OH, NO₃, Criegee intermediates, and other short-lived, highly reactive species in occupied and unoccupied indoor environments will significantly advance our understanding of indoor air chemistry in the near future (Gligorovski and Weschler 2013; Weschler 2016).

Occupants remove chemicals from the air via inhalation, dust ingestion, and dermal absorption. Occupant presence can thus significantly reduce the

concentrations of volatile chemicals and compete with other removal mechanisms, reducing the reactive capacity and therefore decreasing the concentrations of reaction products. Whether this removal can outweigh the production of new species caused by the presence of occupants warrants further attention. Quantifying how indoor environments change with occupancy is generally not well established. Occupancy leads to changes occurring not only in the gas phase, but also on indoor surfaces. Little is known, however, about the accumulation on indoor surfaces of the less volatile products of ozone/skin oil chemistry. Aerosol mass spectrometry can be used to investigate the influence of occupancy on the composition of airborne particles. Additionally, some of the mentioned measurements have yet to be performed in parallel under both occupied and unoccupied conditions, in order to reveal potential connections between various species. Experimental studies should then be coupled to modeling studies in order to improve the models, which can then in return help design better experiments.

Cross-References

► Role of Clothing in Exposure to Indoor Pollutants

Acknowledgments Part of the work on this chapter was done within the activities of the INDOor AIR POLLution NETwork (INDAIRPOLLNET) supported by the European Cooperation in Science and Technology (COST). We thank Nicola Carslaw for her comments to an earlier version of the text.

References

- Anderson SE, Wells JR, Fedorowicz A, Butterworth LF, Meade BJ, Munson AE (2007) Evaluation of the contact and respiratory sensitization potential of volatile organic compounds generated by simulated indoor air chemistry. *Toxicol Sci* 97:355–363
- Anderson SE, Franko J, Jackson LG, Wells JR, Ham JE, Meade BJ (2012) Irritancy and allergic responses induced by exposure to the indoor air chemical 4-oxopentanal. *Toxicol Sci* 127:371–381
- Antal B, Kuki Á, Nagy L, Nagy T, Zsuga M, Kéki S (2016) Rapid detection of hazardous chemicals in textiles by direct analysis in real-time mass spectrometry (DART-MS). *Anal Bioanal Chem* 408:5189–5198
- Ara K, Hama M, Akiba S, Koike K, Okiska K, Hagura T, Kamiya T, Tomita F (2006) Foot odor due to microbial metabolism and its control. *Can J Microbiol* 52:357–364
- Arata C, Heine N, Wang N, Misztal PK, Wargozi P, Bekö G, Williams J, Nazaroff WW, Wilson KR, Goldstein AH (2019) Heterogeneous ozonolysis of squalene: gas-phase products depend on water vapor concentration. *Environ Sci Technol* 53:14441–14448
- Atkinson R, Arey J (2003) Gas-phase tropospheric chemistry of biogenic volatile organic compounds: a review. *Atmos Environ* 37:S197–S219
- Barzantny H, Brune I, Tauch A (2012) Molecular basis of human body odour formation: insights deduced from corynebacterial genome sequences. *Int J Cosmet Sci* 34:2–11
- Bekö G, Wargozi P, Wang N, Li M, Weschler CJ, Morrison G, Langer S, Ernle L, Licina D, Yang S, Zannoni N, Williams J (2020) The indoor chemical human emissions and reactivity project (ICHEAR): overview of experimental methodology and preliminary results. *Indoor Air* 30(6):1213–1228

- Bernier UR, Booth MM, Yost RA (1999) Analysis of human skin emanations by gas chromatography/mass spectrometry. 1. Thermal desorption of attractants for the yellow fever mosquito (*Aedes aegypti*) from handled glass beads. *Anal Chem* 71:1–7
- Bernier UR, Kline DL, Barnard DR, Schreck CE, Yost RA (2000) Analysis of human skin emanations by gas chromatography/mass spectrometry. 2. Identification of volatile compounds that are candidate attractants for the yellow fever mosquito (*Aedes aegypti*). *Anal Chem* 72:747–756
- Bird S, Gower DB (1981) The validation and use of radioimmunoassay for 5-alpha-androste-16-en-3-one in human axillary collections. *J Steroid Biochem* 14:213–219
- Bouslimani A, Porto C, Rath CM, Wang M, Guo Y, Gonzalez A, Berg-Lyon D, Ackermann G, Christense GJM, Nakatsuji T, Zhang L, Borkowski AW, Meehan MJ, Dorrestain K, Gallo RL, Bandeira N, Knight R, Alexandrov T, Dorrestein PC (2015) Molecular cartography of the human skin surface in 3D. *Proc Nat Acad Sci U S A* 112(17):E2120–E2129
- Burdack-Freitag A, Mayer F, Breuer K (2011) Identification of anthropogenic odor active compounds causing bad air quality in highly occupied rooms. In: Proceedings of Indoor Air 2011, Paper ID 507, Austin, TX, USA
- Chan D, Haviland-Jones J (2000) Human olfactory communication of emotion. *Percept Mot Skills* 91:771–781
- Chiba K, Yoshizawa K, Makino I, Kawakami K, Onoue M (2000) Comedogenicity of squalene monohydroperoxide in the skin after topical application. *J Toxicol Sci* 25:77–83
- Clark RP, Shirley SG (1973) Identification of skin in airborne particulate matter. *Nature* 246:39–40
- Coleman BK, Destaillats H, Hodgson AT, Nazaroff WW (2008) Ozone consumption and volatile byproduct formation from surface reactions with aircraft cabin materials and clothing fabrics. *Atmos Environ* 42:642–654
- Curran AM, Prada PA, Furton KG (2010) The differentiation of the volatile organic signatures of individuals through SPME-GC/MS of characteristic human scent compounds. *J Forensic Sci* 55: 50–57
- De Groot AC, Le Coz CJ, Lensen GJ, Flyvholm M-A, Maibach HI, Coenraads P-J (2010) Formaldehyde-releasers: relationship to formaldehyde contact allergy. Formaldehyde-releasers in clothes: durable press chemical finishes. Part 1. *Contact Dermatitis* 62:259–271
- de Lacy Costello B, Amann A, Al-Kateb H, Flynn C, Filipiak W, Khalid T, Osborne D, Ratcliffe NM (2014) A review of the volatiles from the healthy human body. *J Breath Res* 8:014001
- Devos M, Patte F, Rouault J, Laffort P, Van Gemert LJ (1990) Standardized human olfactory thresholds. IRL Press, Oxford
- Dormont L, Bessière JM, Cohuet A (2013) Human skin volatiles: a review. *J Chem Ecol* 39:569–578
- Fadeyi MO, Weschler CJ, Tham KW, Wu WY, Sultan ZM (2013) Impact of human presence on secondary organic aerosols derived from ozone-initiated chemistry in a simulated office environment. *Environ Sci Technol* 47:3933–3941
- Fanger PO (1988) Introduction of the olf and the decipol units to quantify air pollution perceived by humans indoors and outdoors. *Energ Buildings* 12:1–6
- Fenske JD, Paulson SE (1999) Human breath emissions of VOCs. *J Air Waste Manag Assoc* 49: 594–598
- Filipiak W, Ruzsanyi V, Mochalski P, Filipiak A, Bajtarevic A, Ager C, Denz H, Hilbe W, Jamnig H, Hackls M, Dzien A, Amann A (2012) Dependence of exhaled breath composition on exogenous factors, smoking habits and exposure to air pollutants. *J Breath Res* 6:036008
- Fischer A, Ljunfström E, Langer S (2013) Ozone removal by occupants in a classroom. *Atmos Environ* 81:11–17
- Fu D, Leng CB, Kelley J, Zeng G, Zhang YH, Liu Y (2013) ATR-IR study of ozone initiated heterogeneous oxidation of squalene in an indoor environment. *Environ Sci Technol* 47:10611–10618
- Furukawa S, Sekine Y, Kimura K, Umezawa K, Asai S, Miyachi H (2017) Simultaneous and multi-point measurement of ammonia emanating from human skin surface for the estimation of whole body dermal emission rate. *J Chromatogr B* 1053:60–64

- Gallagher M, Wysocki CJ, Leyden JJ, Spielman AI, Sun X, Preti G (2008) Analyses of volatile organic compounds from human skin. *Br J Dermatol* 159:780–791
- Garner CE, Smith S, de Lacy CB, White P, Spencer R, Probert CSJ, Ratcliffem NM (2007) Volatile organic compounds from feces and their potential for diagnosis of gastrointestinal disease. *FASEB J* 21:1675–1688
- Gligorovski S, Weschler CJ (2013) The oxidative capacity of indoor atmospheres. *Environ Sci Technol* 47:13905–13906
- Havlicek J, Saxton T (2009) The effect of diet on human bodily odors, Chapter 3. In: Hasegawa K, Takahashi H (eds) New research on food habits. Nova Science Publishers. ISBN: 978-1-60456-864-6
- Haze S, Gozu Y, Nakamura S, Kohno Y, Sawano K, Ohta H, Yamazaki K (2001) 2-Nonenal newly found in human body odor tends to increase with aging. *J Invest Dermatol* 116:520–524
- He J, Sun X, Yang X (2019) Human respiratory system as sink for volatile organic compounds: evidence from field measurements. *Indoor Air* 29:968–978
- Inaba M, Inaba Y (1992) Human body odor: etiology, treatment and related factors. Springer
- James AG, Austin CJ, Cox DS, Taylor D, Calvert R (2013) Microbiological and biochemical origins of human axillary odour. *FEMS Microbiol Ecol* 83:527–540
- Jarvis J, Seed MJ, Elton R, Sawyer L, Agius R (2005) Relationship between chemical structure and the occupational asthma hazard of low molecular weight organic compounds. *Occup Environ Med* 62:243–250
- King J, Koc H, Unterkoferl K, Mochalski P, Kupferthaler A, Teschl G, Teschl S, Hinterhuber H, Amann A (2010) Physiological modeling of isoprene dynamics in exhaled breath. *J Theor Biol* 267:626–637
- Kruza M, Carslaw N (2019) How do breath and skin emissions impact indoor air chemistry? *Indoor Air* 29:369–379
- Kusano M, Mendez E, Furton KG (2012) Comparison of the volatile organic compounds from different biological specimens for profiling potential. *J Forensic Sci* 58:29–39
- Kuukasjarvi S, Eriksson CJP, Koskela E, Mappes T, Nissinen K, Rantala MJ (2004) Attractiveness of women's body odors over the menstrual cycle: the role of oral contraceptives and receiver sex. *Behav Ecol* 15:579–584
- Kwak J, Preti G (2011) Volatile disease biomarkers in breath: a critique. *Curr Pharm Biotechnol* 12: 1067–1074
- Lakey PSJ, Wisthaler A, Berkemeier T, Mikoviny T, Poschl U, Shiraiwa M (2017) Chemical kinetics of multiphase reactions between oxone and human skin lipids: implications for indoor air quality and health effects. *Indoor Air* 27:816–828
- Lechner M, Moser B, Niederseer D, Karlseder A, Holzknecht B, Fuchs M, Colvin S, Tilg H, Rieder J (2006) Gender and age specific differences in exhaled isoprene levels. *Respir Physiol Neurobiol* 154:478–483
- Leyden JJ, McGinley KJ, Hoelzle E, Labows JN, Kligman AM (1981) The microbiology of the human axillae and its relation to axillary odors. *J Invest Dermatol* 77:413–416
- Li M, Weschler CJ, Bekö G, Wargoocki P, Lucic G, Williams J (2020) Human ammonia emissions under various indoor environmental conditions. *Environ Sci Technol* 54:5419–5428
- Licina D, Morrison G, Bekö G, Weschler CJ, Nazaroff WW (2019) Clothing-mediated exposure to chemicals and particles. *Environ Sci Technol* 53:5559–5575
- Liu S, Li R, Wild RJ, Warneke C, de Gouw JA, Brown SS, Miller SL, Luongo JC, Jimenez JL, Ziemann PJ (2016) Contribution of human-related sources to indoor volatile organic compounds in a university classroom. *Indoor Air* 26:925–938
- Liu S, Thompson SL, Stark H, Ziemann PJ, Jimenez JL (2017) Gas-phase carboxylic acids in a university classroom: abundance, variability, and sources. *Environ Sci Technol* 51:5454–5463
- Maddalena R, Mendell MJ, Eliseeva K, Chan WR, Sullivan DP, Russell M, Satish U, Fisk WJ (2015) Effects of ventilation rate per person and per floor area on perceived air quality, sick building syndrome symptoms, and decision-making. *Indoor Air* 25:362–370

- Marshall J, Holland KT, Gribbon EM (1988) A comparative study of the cutaneous microflora of normal feet with low and high levels of odour. *J Appl Bacteriol* 65:61–68
- Meijerink J, Braks MAH, Brack AA, Adam W, Dekker T, Posthumus MA, Van Beek TA, Van Loon JJA (2000) Identification of olfactory stimulants for *Anopheles gambiae* from human sweat samples. *J Chem Ecol* 26(6):1367–1382
- Mochalski P, Unterkofler K, Hinterhuber H, Amann A (2014) Monitoring of selected skin-borne volatile markers of entrapped humans by selective reagent ionization time of flight mass spectrometry in NO⁺ mode. *Anal Chem* 86:3915–3923
- Natsch A, Derrer S, Flachsmann F, Schmidt J (2006) A broad diversity of volatile carboxylic acids, released by a bacterial aminoacylase from axilla secretions, as candidate molecules for the determination of human-body odor type. *Chem Biodivers* 3:1–20
- Ostrovskaya A, Landa PA, Sokolinsky M, Rosalia AD, Maes D (2001) Study and identification of volatile compounds from human skin. *J Cosmet Sci* 53:147–148
- Penn DJ, Oberzaucher E, Grammer K, Fischer G, Soini HA, Wiesler D, Novotny MV, Dixon SJ, Xu Y, Brereton RG (2007) Individual and gender fingerprints in human body odour. *J R Soc Interface* 4:331–340
- Pereira J, Porto-Figueira P, Cavaco C, Taunk K, Rapole S, Dhakne R, Nagarajaram H, Camara JS (2015) Breath analysis as a potential and non-invasive frontier in disease diagnosis: an overview. *Meta* 5:3–55
- Phillips M, Herrera J, Krishnan S, Zain M, Greenberg J, Cataneo RN (1999) Variation in volatile organic compounds in the breath of normal humans. *J Chromatogr B Biomed Sci Appl* 729:75–88
- Prada PA, Curran AM, Furton KG (2011) The evaluation of human hand odor volatiles on various textiles: a comparison between contact and noncontact sampling methods. *J Forensic Sci* 56: 866–881
- Preti G, Leyden JJ (2010) Genetic influences on human body odor: from genes to the axillae. *J Investig Dermatol* 130:344–346
- Prokop-Prigge KA, Greene K, Varallo L, Wysocki CJ, Preti G (2016) The effect of ethnicity on human axillary odorant production. *J Chem Ecol* 42:33–39
- Rai AC, Guo B, Lin CH, Zhang J, Pei J, Chen Q (2013) Ozone reaction with clothing and its initiated particle generation in an environmental chamber. *Atmos Environ* 77:885–892
- Rai AC, Guo B, Lin CH, Zhang J, Pei J, Chen Q (2014) Ozone reaction with clothing and its initiated VOC emissions in an environmental chamber. *Indoor Air* 24:49–58
- Ruzsanyi V, Mochalski P, Schmid A, Wiesenhofer H, Klieber M, Hinterhuber H, Amann A (2012) Ion mobility spectrometry for detection of skin volatiles. *J Chromatogr B* 911:84–92
- Salvador CM, Bekö G, Weschler CJ, Morrison G, Le Breton M, Hallquist M, Ekberg L, Langer S (2019) Indoor ozone/human chemistry and ventilation strategies. *Indoor Air* 29:913–925
- Sanchez JM, Sacks RD (2006) Development of a multibed sorption trap, comprehensive two dimensional gas chromatography, and time-of-flight mass spectrometry system for the analysis of volatile organic compounds in human breath. *Anal Chem* 78:3046–3054
- Sato H, Hirose T, Kimura T, Moriyama Y, Nakashima Y (2001) Analysis of malodorous volatile substances of human waste: feces and urine. *J Health Sci* 47(5):483–490
- Schwarz K, Pizzini A, Arendacka B, Zerlauth K, Filipiak W, Schmid A, Dzien A, Neuner S, Lechleitner M, Scholl-Burgi S, Miekisch W, Schubert J, Unterkofler K, Witkovsky V, Gastl G, Amann A (2009) Breath acetone-aspects of normal physiology related to age and gender as determined in a PTR-MS study. *J Breath Res* 3:027003
- Shirasu M, Touhara K (2011) The scent of disease: volatile organic compounds of the human body related to disease and disorder. *J Biochem* 150:257–266
- Stönnér C, Edtbauer A, Derstroff B, Bourtsoukidis E, Klüpfel T, Wicker J, Williams J (2018) Proof of concept study: testing human volatile organic compounds as tools for age classification of films. *PLoS One* 13(10):e0203044
- Strøm-Tejsen P, Weschler CJ, Wargozi P, Myskow D, Zarzycka J (2008) The influence of ozone on self-evaluation of symptoms in a simulated aircraft cabin. *J Expo Sci Environ Epidemiol* 18: 272–281

- Sukul P, Schubert JK, Trefz P, Miekosch W (2018) Natural menstrual rhythm and oral contraception diversely affect exhaled breath compositions. *Sci Rep* 8:10838
- Sun X, He J, Yang X (2017) Human breath as a source of VOCs in the built environment, Part II: concentration levels, emission rates and factor analysis. *Build Environ* 123:437–445
- Tang X, Misztal PK, Nazaroff WW, Goldstein AH (2015) Siloxanes are the most abundant volatile organic compound emitted from engineering students in a classroom. *Environ Sci Technol* 2: 303–307
- Tang X, Misztal PK, Nazaroff WW, Goldstein AH (2016) Volatile organic compound emissions from humans indoors. *Environ Sci Technol* 50:12686–12694
- Taucher J, Hansel A, Jordan A, Fall R, Futrell JH, Lindinger W (1997) Detection of isoprene in expired air from human subjects using proton-transfer-reaction mass spectrometry. *Rapid Commun Mass Spectrom* 11:1230–1234
- Thiele JJ, Podda M, Packer L (1997) Tropospheric ozone: an emerging environmental stress to skin. *Biol Chem* 378:1299–1305
- Tsushima S, Wargozi P, Tanabe S (2018a) Human bioeffluents: are exhaled and dermally-emitted bioeffluents different? In: Proceedings of indoor air 2018, Paper no 200, Philadelphia
- Tsushima S, Wargozi P, Tanabe S (2018b) Sensory evaluation and chemical analysis of exhaled and dermally emitted bioeffluents. *Indoor Air* 28:146–163
- Vereb H, Dietrich AM, Alfeeli B, Agah M (2011) The possibilities will take your breath away: breath analysis for assessing environmental exposure. *Environ Sci Technol* 45:8167–8175
- Veres PR, Faber P, Drewnick F, Lelieveld J, Williams J (2013) Anthropogenic sources of VOC in a football stadium: assessing human emissions in the atmosphere. *Atmos Environ* 77:1052–1059
- Wallace LA (1987) The TEAM study: summary and analysis: volume I. EPA 600/6-87/002a. NTIS PB 88-10006, US EPA, Washington, DC
- Waller JM, Maibach HI (2006) Age and skin structure and function, a quantitative approach (ii): protein, glycosaminoglycan, water, and lipid content and structure. *Skin Res Technol* 12(3): 145–154
- Wang CY, Waring MS (2014) Secondary organic aerosol formation initiated from reactions between ozone and surface-sorbed squalene. *Atmos Environ* 84:222–229
- Wang N, Zannoni N, Ernle L, Bekö G, Wargozi P, Li M, Weschler CJ, Williams J (2021) Total OH reactivity of emissions from humans: in situ measurement and budget analysis. *Environ Sci Technol* 55:149–159
- Weber SU, Thiele JJ, Cross CE, Packer L (1999) Vitamin C, uric acid, and glutathione gradients in murine stratum corneum and their susceptibility to ozone exposure. *J Invest Dermatol* 113: 1128–1132
- Weschler CJ (2016) Roles of the human occupant in indoor chemistry. *Indoor Air* 26:6–24
- Weschler CJ, Wisthaler A, Cowlin S, Tamas G, Ström-Tejsen P, Hodgson AT, Destaillats H, Herrington J, Zhang J, Nazaroff WW (2007) Ozone-initiated chemistry in an occupied simulated aircraft cabin. *Environ Sci Technol* 41:6177–6184
- Williams J, Pleil J (2016) Crowd-based breath analysis: assessing behavior, activity, exposures, and emotional response of people in groups. *J Breath Res* 10:032001
- Williams J, Stönnér C, Wicker J, Krauter N, Dersstroff B, Bourtsoukidis E, Klüpfel T, Kramer S (2016) Cinema audiences reproducibly vary the chemical composition of air during films, by broadcasting scene specific emissions on breath. *Sci Rep* 6:25464
- Wisthaler A, Weschler CJ (2010) Reactions of ozone with human skin lipids: sources of carbonyls, dicarbonyls, and hydroxycarbonyls in indoor air. *Proc Natl Acad Sci U S A* 107:6568–6575
- Wolkoff P (2013) Indoor air pollutants in office environments: assessment of comfort, health, and performance. *Int J Hyg Environ Health* 216:371–394
- Wolkoff P, Larsen ST, Hammer M, Kofoed-Sorensen V, Clausen PA, Nielsen GD (2013) Human reference values for acute airway effects of five common ozone-initiated terpene reaction products in indoor air. *Toxicol Lett* 216:54–64

- Wysocki CJ, Louie J, Leyden JJ, Blank D, Gill M, Smith L, McDermott K, Preti G (2009) Cross-adaptation of a model human stress-related odour with fragrance chemicals and ethyl esters of axillary odorants: gender specific effects. *Flavour Fragr J* 24:209–218
- Yaglou CP, Riley EC, Coggins DI (1936) Ventilation requirements. *ASHRAE Trans* 42:133–162
- Yang S, Gao K, Yang X (2016) Volatile organic compounds (VOCs) formation due to interactions between ozone and skin-oiled clothing: measurements by extraction analysis-reaction method. *Build Environ* 103:146–154
- Zeng XN, Leyden JJ, Spielman AI, Preti G (1996) Analysis of characteristic human female axillary odors: qualitative comparison to males. *J Chem Ecol* 22:237–257
- Zhang XJ, Wargocki P, Lian ZW, Thyregod C (2017a) Effects of exposure to carbon dioxide and bioeffluents on perceived air quality, self-assessed acute health symptoms, and cognitive performance. *Indoor Air* 27:47–64
- Zhang XJ, Wargocki P, Lian ZW (2017b) Physiological responses during exposure to carbon dioxide and bioeffluents at levels typically occurring indoors. *Indoor Air* 27:65–77
- Zhou S, Forbes MW, Katrib Y, Abbatt JPD (2016a) Rapid oxidation of skin oil by ozone. *Environ Sci Technol Lett* 3(4):170–174
- Zhou S, Forbes MW, Abbatt JPD (2016b) Kinetics and products from heterogeneous oxidation of squalene with ozone. *Environ Sci Technol* 50:11688–11697



Analytical Tools in Indoor Chemistry

32

Delphine K. Farmer, Matson Pothier, and James M. Mattila

Contents

Introduction	932
Measurement Principles	933
Instrumental Analysis	933
Measurement Strategies	934
On-Line Measurement of Gases	937
Inert Gases	937
Reactive Gases	937
Oxidants	937
Inorganic Trace Gases	938
Volatile Organic Compounds (VOCs)	939
On-Line Measurement of Particles	942
Particle Size Distributions	942
Chemical Measurement Techniques	945
Bulk Aerosol Composition Measurements	946
Speciated Aerosol Composition Measurements	947
Black Carbon	947
Other Particle Measurements	948
New Frontiers	948
Conclusion	949
References	949

Abstract

The chemical complexity of indoor surfaces and air creates challenges for quantitative analysis. The air includes inert trace gases, reactive trace gases, oxidants and radicals in the gas-phase, as well as particles across many orders of magnitude in size distribution. Measurements techniques must be able to

D. K. Farmer (✉) · M. Pothier · J. M. Mattila
Department of Chemistry, Colorado State University, Fort Collins, CO, USA
e-mail: delphine.farmer@colostate.edu; matson.pothier@colostate.edu;
James.Mattila@colostate.edu

© This is a U.S. Government work and not under copyright protection in the U.S.;
foreign copyright protection may apply 2022

931

Y. Zhang et al. (eds.), *Handbook of Indoor Air Quality*,
https://doi.org/10.1007/978-981-16-7680-2_35

capture the dynamic range and rapidly changing nature of indoor concentrations. Both passive and active sampling approaches are available, and chemical measurements may focus on speciated or bulk composition. The outdoor atmospheric chemistry community has established numerous on-line techniques for detecting trace gases and particles, and many of these techniques have been successfully applied to indoor environments. However, some of these techniques are subject to interferences in the indoor environment, requiring careful intercomparison. New frontiers in indoor analytical chemistry include development of new surface chemistry measurements, application of *in situ* chemical kinetics studies, development of low cost sensors, and closer linkage between health-relevant measurements and composition.

Keywords

Analytical chemistry · Indoor chemistry · Aerosol mass spectrometry · Chemical ionization · Chemiluminescence · On-line measurement

Introduction

The indoor environment is chemically complex. Relative to the outdoor environment, the indoor environment contains high concentrations of a myriad of organic and inorganic compounds that exist in multiple phases (Abbatt and Wang 2020). Cataloguing these compounds presents an analytical measurement challenge due to the sheer number of distinct molecules, as well as the breadth of unknown, as-yet-unmeasured compounds (Farmer 2019). Quantifying the compounds presents an even greater challenge, as this requires standards that can be challenging to obtain.

Not only must researchers identify and separate a vast number of compounds to investigate indoor chemistry, but they must do this rapidly. The built environment can change quickly in terms of sources and parameters. People can walk into a room and act as immediate sources of exhaled compounds – or sinks of ozone (Wisthaler and Weschler 2010). The cycling of an air conditioning system causes changes in not only relative humidity, but also air composition on the timescale of seconds to minutes (Duncan et al. 2019). From an instrument’s perspective, these rapid changes of concentration can occur over a large dynamic range. A single cooking event can cause gas and particle concentrations to change by over two orders of magnitude on the timescale of seconds (Boedicker et al. 2021)! In addition, buildings possess multiple surfaces, each with its own distinct chemical and physical properties. These surfaces play an important role in the chemistry of indoor environments, but present a new analytical challenge for the environmental chemistry community (Ault et al. 2020).

This chapter outlines the principles of chemical measurement as they relate to the indoor environment, before diving into specific measurement types used to detect gases, particles, and surfaces – before highlighting open questions and new frontiers.

Measurement Principles

Instrumental Analysis

Modern analytical chemistry uses instruments that are built around fundamental principles of physical chemistry to detect and (ideally) quantify molecules of interest. The two underlying criteria for practical use of instruments are their *selectivity* and their *sensitivity*. Selectivity refers to the capacity of an instrument to measure one compound (or suite of compounds) in a well-known manner, free of interferences from other molecules (or groups of molecules). These target compound(s) of interest are “analytes,” and selectivity is typically determined through a combination of laboratory tests and field experiments.

Sensitivity refers to how well an instrument can detect a given analyte, typically in terms of the change in instrument signal per change in concentration. Sensitivity defines an instrument’s capacity to quantify analytes, with a higher sensitivity meaning that an instrument can more easily detect small changes in concentration. Sensitivity is typically determined by calibration – whether by external standards, internal standards, or standard additions. Both external standard and standard addition approaches require true standards of the analyte of known purity and delivered to the instrument in a quantifiable manner. In contrast, internal standard approaches require a proxy standard, such as an isotopically labeled version of the analyte or other substance of similar physical and chemical properties. While standards of some compounds may be commercially available, other compounds, such as isoprene oxidation products, require elaborate laboratory synthesis (Zhang et al. 2012). Even when purchased, many substances that are relevant to the indoor environment exist in solid or liquid phases when pure, so must be quantitatively volatilized and transmitted to instrumentation.

The sensitivity of a measurement can be used to calculate a limit of detection (LOD), which corresponds to the smallest detectable concentration above a defined threshold. For many chemical applications, the LOD is taken as the concentration corresponding to a signal that is three times the noise above the background (i.e. $S/N = 3$) although higher or lower thresholds are sometimes used. The pursuit of lower LODs often manifests itself in substantial instrument development to reduce background measurements, whether through cooling optical detectors, cleaning internal components, or isolating electronics from signal interference.

As noted elsewhere in this handbook, indoor environments are marked by highly concentrated, complex mixtures of molecules in multiple phases. This chemical system challenges analytical measurements by providing an array of potential interferences to different detection techniques (Farmer et al. 2019a). Several approaches have emerged to investigate whether interferences are impacting measurements. Standard additions enable small quantities of analyte standards to be added to the real sample during sampling, thus accounting for matrix effects; comparing sensitivities from standard additions relative to external standards generated in a synthetic, clean background directly probes whether interferences exist (Brophy and Farmer 2015). Intercomparisons across different instruments, all measuring the same analyte in the

same matrix, also often reveal interferences. For example, during the House Observations of Microbial and Environmental Chemistry (HOMEChem) study in 2018, two separate detectors of nitrogen dioxide (NO_2), a common air toxic, occasionally diverged during cooking events. One instrument used differential optical absorption spectroscopy to directly detect NO_2 , while the other used a photolytic converter to transform NO_2 to NO, which was then detected by chemiluminescence upon reaction with O_3 . Unfortunately, the complex mixture of trace gases produced during cooking events included photolabile oxidized organic compounds that were photolyzed in the chemiluminescence instrument converter to reactive RO_2 radicals, which were capable of reacting with the NO and thus interfering with the measurement (Farmer et al. 2019a). This case highlights the challenges of bringing instrumentation that is frequently used in outdoor air quality into the indoor environment: the complex mixture of indoor gases can create strong, unexpected interferences that are impossible to account for in post-acquisition data analysis.

One key feature in selecting instrumentation to measure indoor air quality is the time response of competing measurements. As noted earlier, indoor concentrations of trace gases or particles change over the timescale of seconds or minutes when a candle is lit or a window is opened. If one is interested in capturing those rapid changes, detectors must operate on even faster timescales. However, for many studies, slower time resolution is adequate to capture average conditions, and avoids challenges of data storage and management. The timescale of measurements must consider not only the speed of processes under investigation, but also the short- and long-term precision of the measurements. Some instruments are capable of making fast measurements, but their sensitivity or background also changes frequently and requires frequent maintenance and attention. Ozone sensors provide good examples of this challenge: many techniques for ozone detection are available (Clifton et al. 2020). For example, one particularly fast sensor is a dry chemiluminescence measurement using titration of ozone by a solid dye, such as coumarin. Unfortunately, these techniques require frequent maintenance as the dye degrades with time, and the sensitivity can change on the timescale of days. Ultraviolet absorption is a less expensive, lower maintenance approach to measuring ozone, but is subject to interference from high levels of ultrafine particles, which can occur during cooking events.

Measurement Strategies

Several strategies exist for measuring indoor air, all with different benefits and disadvantages. A few paired strategies are described below.

Bulk Versus Compound-Specific Measurement

While some measurements target specific molecules (e.g., NO radical concentrations), bulk measurements detect a suite of compounds without specific differentiation (e.g., NO_y , which is the sum of all nitrogen oxides including NO, NO_2 , nitric acid, and all organic nitrates and peroxy nitrates). This bulk approach is particularly common in aerosol composition studies, in which bulk components like “total

“organic aerosol” and “bulk oxygen to carbon ratios of organic aerosol” provide insight on particle sources in the indoor environment, but require less targeted instrumentation than measurements that quantify different molecules that contribute to organic aerosol. Bulk composition measurements are typically more complete in terms of capturing a given suite of compounds or mass in phases, but have lower chemical resolution than compound-specific measurement (Hallquist et al. 2009). Within compound-specific measurements that have higher chemical resolution, typically at the expense of measurement completeness for a class of compounds, many mass spectrometry systems are capable of identifying compounds by elemental composition (i.e., the number of carbon, oxygen, hydrogen, or other atoms in a molecule) (Farmer and Jimenez 2010; Hallquist et al. 2009). However, the arrangement of those molecules into different structural isomers can impact the reaction rates or properties of the molecule, and separation of these isomers creates additional analytical challenges. For example, during the HOMEChem study, aerosol mass spectrometers measured bulk sub-micron aerosol composition well (Katz et al. 2021), while softer ionization mass spectrometry techniques (e.g., extractive electrospray ionization mass spectrometry and iodide adduct chemical ionization mass spectrometry) enabled adequate molecular specificity to quantify siloxane and phthalate aerosol components (Brown et al. 2021).

Off-Line Versus On-Line Measurements

Off-line measurements involve sample collection followed by analysis by a separate instrument in a separate location, and thus separated in time. On-line measurements involve sample collection and analysis at the same time with one instrument system. Off-line sample collection is typically simpler to operate than on-line instrumentation, and can be less intrusive to a building or home in terms of space and noise, while on-line measurements provide faster data, both in terms of time resolution (less time between data points) and in terms of less time between sample collection and a numerical result (discussed in detail for surfaces by Liu et al. 2020). Sample collection for off-line analysis can use passive or active approaches. Passive samplers allow analytes to accumulate on a sampler with time, with no active or moving parts, while active samplers physically move air or sample into a collection system. Passive samplers are discussed in more detail in ► [Chap. 17, “Passive Samplers for Indoor Gaseous Pollutants.”](#)

Chemical Versus Physical Analysis

While many of the measurements described in this chapter focus on chemical measurement and quantitation, numerous methods exist to measure chemical or physical properties of gases or particles in the indoor environment. For example, while mass spectrometry, chromatography, and spectroscopy measurements exist for detection of different chemical components of indoor air, additional instruments can enable detection of the volatility of different components (e.g., thermal denuders coupled to aerosol detectors), or the reactivity of the system to oxidants (e.g., OH reactivity measurements). Detection systems that measure chemical properties, rather than just composition, have not been widely applied to indoor environments,

but results consistently provide new insights on indoor systems. For example, Wang et al. (2021) measured OH reactivity of human emissions, demonstrating significant increases in the presence of ambient ozone, which reacts with skin oils to produce a diverse array of reactive, gas-phase oxidation products.

Low Cost Sensors Versus Research Instrumentation

Numerous research-grade detection techniques exist to quantify gas and particle components of indoor air. However, despite being commercially available, many of these techniques are (i) expensive (thousands of dollars for simple infrared absorption CO₂ measurements to hundreds of thousands of dollars for high resolution mass spectrometers capable of differentiating organic aerosol and gases), (ii) challenging to run (requiring highly trained operators to maintain the instruments and analyze data), and (iii) noisy (using loud pumps to actively pull air into the instruments). Despite the fast time resolution and wealth of data, these features have inhibited widespread use of advanced chemical techniques to study the indoor environment. Low cost sensors are thus popular for indoor air quality studies. Low cost sensors (typically on the order of hundreds of dollars) provide lower time and chemical resolution, but are cheaper and easier to operate. Numerous “indoor air quality” sensors are commercially available, but can have limited accuracy and reproducibility thus providing caveats for research applications (Li et al. 2020; Wang et al. 2020c). However, recent publications have highlighted the research potential of low cost sensors when combined with extensive data analysis (Liang et al. 2021).

Analytical Chemistry Approaches

Instruments for measuring the quality of indoor air take advantage of different chemical principles.

- Spectroscopic measurements take advantage of the way light interacts with different molecules through absorption, fluorescence, or chemiluminescence. Infrared absorption is a well-established approach for measuring greenhouse gases, including CO₂ and CH₄, while other wavelengths are used for detection of trace gases like SO₂ or NO₂. Fluorescence and chemiluminescence use the light emitted from molecules following either absorption or chemical reaction, respectively, to detect and quantify compounds. Other optical techniques take advantage of light scattering to detect particles.
- Mass spectrometry uses electric or magnetic fields to separate gaseous molecules after charging them based on the resulting mass-to-charge ratio. Different ionization techniques target different types of molecules, with hard ionization approaches (e.g. electron ionization or laser absorption) fragmenting molecules and enabling bulk analysis (in the absence of pre-separation) or structural determination (when coupled to pre-separation via gas or liquid chromatography). Soft ionization approaches incorporating electrospray or chemical ionization are becoming widely used for compound-specific analysis.
- Chromatography systems enable separation based on chemical interactions between samples and either solid or liquid instrument components. These

separations are commonly used prior to analysis by another approach (e.g. mass spectrometry, flame ionization, or photoionization detectors), and enhance the specificity of the detection system.

- Devices based on electrochemistry often provide advantages of size and cost, with small and portable commercial sensors. However, these detectors are often subject to interferences and have not been extensively used in indoor chemistry studies.
- Off-line samples can take advantage of more complex microscopy approaches, including scanning electron microscopy or transmission electron microscopy.

All of these approaches provide different benefits and disadvantages – and different ways to compare and contrast sensors. The sections below provide more detailed discussion of measurement approaches by gases, particles, and surfaces.

On-Line Measurement of Gases

Inert Gases

Historically, indoor air quality has focused on radon, carbon monoxide (CO), and carbon dioxide (CO₂), with a plethora of low-cost commercial sensors available for measurements. However, these low-cost techniques are typically aimed at determining whether air concentrations are above or below a threshold, or what the time-integrated values may be. Infrared absorption spectroscopy offers a particularly sensitive and selective measurement of CO and CO₂, as well as methane (CH₄).

Reactive Gases

Reactive gases can be categorized by several methods, one of which is to consider measurements as being oxidants, reactive inorganic trace gases, or reactive organic trace gases.

Oxidants

In the indoor environment, ozone is often considered the dominant oxidant, and is typically detected by commercial ultraviolet absorption spectroscopy measurements, although other techniques are available (see Clifton et al. 2020 for a recent review). One challenge with ultraviolet absorption measurements of ozone is the potential for interference from ultrafine particles, which can scatter light and generate a false positive signal. However, the use of filters on inlets can remove this problem. However, ozone is not the only indoor oxidant, with various modeling and measurement studies indicating that hydroxyl radicals (OH·), nitrate radicals (NO₃·), and peroxy radicals (HO₂·, RO₂·) are also potential indoor oxidants (Young et al. 2019).

OH^{\cdot} and peroxy radicals can be measured by either laser-induced fluorescence, or chemical ionization mass spectrometry; however, these measurements require sophisticated, home-built instrumentation and are thus limited (e.g., Alvarez et al. 2013; Carslaw et al. 2017). These radical measurements are prone to interferences, which have been noted in outdoor atmospheric field measurements, but the paucity of indoor measurements creates the potential for unexplored indoor interferences. Nitrate radicals can be directly measured by sophisticated cavity ring-down spectroscopy, but few groups have the instrumental capability to conduct those measurements. One indoor field measurement in a home suggested a very low level of nitrate radicals under typical residential conditions, below the detection limits of most instruments (Arata et al. 2018). Substantial input of ozone combined with NO radicals from combustion sources were required to elevate NO_3 substantially.

Inorganic Trace Gases

Inorganic trace gases include oxidized nitrogen (NO_x , HNO_3 , HONO , etc), reduced nitrogen (e.g. NH_3), sulfur-containing compounds (e.g., SO_2), and halogenated species (e.g., HCl , Cl_2). Commercial spectroscopic instruments are available for many of these compounds, including NO and NO_2 , NH_3 , SO_2 , and HCl . However, these commercial instruments are typically designed for outdoor air quality applications. As described above, surprising interferences can be present in indoor environments. Further, while some of these compounds are relatively easy to transfer through inlets from room air to instrument, others are more challenging. For example, NH_3 and HCl are “sticky” compounds that rapidly partition to surfaces, including Teflon inlet lines; as a result of this potential loss mechanism, indoor measurements must use very short inlets with the instrument physically located in the desired sampling location (Dawe et al. 2019; Ampollini et al. 2019). One approach to preventing compounds from partitioning to Teflon lines includes adding passivants to inlet air, which occupy adsorption spaces and reduce line losses. However, these passivants are often fluorinated organic compounds (e.g., Pollack et al. 2019 describes using a perfluoroctylamine to minimize inlet losses of ammonia). However, one important challenge with using fluorinated organic compounds is their potential to be oxidized to perfluorinated acids, which are long-lived environmental contaminants (Young et al. 2007).

Commercial instrumentation is not readily available for many inorganic trace gas species. Chemical ionization mass spectrometry with various reagent ions is an increasingly common technique for measuring halogenated gases in indoor environments, as well as nitrous acid (Mattila et al. 2020a; Mattila et al. 2020b; Collins et al. 2018; Wang et al. 2019; Wang et al. 2020a). However, chemical ionization mass spectrometers are expensive, relatively large ($1\text{--}2\text{ m}^3$), require careful calibration, and frequent maintenance and monitoring to ensure high quality data.

Volatile Organic Compounds (VOCs)

Organic trace gases typically include both volatile organic compounds (VOCs) that are exclusively considered present in the gas phase, and semi-volatile organic compounds (SVOCs) that are considered to be present in both gas and solid/liquid phases due to equilibrium partitioning. However, recent work has shown that even high volatile organic compounds like formic acid maintain a surface-air equilibrium in indoor environments due to the high surface area to volume ratio inside buildings. This section thus considers gaseous indoor organic compounds collectively.

Indoor VOC measurements have historically been performed using offline sampling techniques, such as VOC canisters and thermal desorption methods with adsorptive materials (e.g., Schlink et al. 2004). These techniques allow for quantification of numerous non-methane aromatic hydrocarbons (e.g., benzene, toluene, xylene), chlorocarbons (chloroform, carbon tetrachloride), and simple oxygenates (alcohols, carbonyls, esters). These offline measurements offer users a snapshot of VOC concentrations experienced indoors, and are particularly useful for projects aiming to sample multiple buildings and locations due to their relatively low cost, ease of use, and portability. However, the prolonged sampling times associated with these methods usually result in relatively slow time resolution (typically tens of minutes to hours or days) that do not capture dynamic temporal trends associated with perturbations to the indoor environment (i.e., cooking a meal or opening a window). These methods rely on external analysis of samples in a separate laboratory, typically involving gas chromatography instrumentation.

Formaldehyde is a VOC of particular interest due to its potential toxicity coupled to potentially high concentrations in buildings (Salthammer et al. 2010). Formaldehyde has thus been the focus of much instrument development for indoor analytical chemistry (e.g., Maruo et al. 2010; Gillett et al. 2000; Van den Broek et al. 2020). Formaldehyde is challenging to measure in indoor environments due to its dynamic range (1–1000 ppb); highly volatile nature, which inhibits collection via passive sampling; and potential interferences in online measurements. For example, proton transfer reaction mass spectrometry can measure formaldehyde on-line with high sensitivity and in real-time, but is subject to interferences from relative humidity that can be challenging to correct (Vlasenko et al. 2010). Emerging instrumentation using cavity ring-down spectroscopy is one particularly promising method for formaldehyde measurement in indoor environments. Formaldehyde and other “very volatile” organic compounds are discussed in Chapter “Source/Sink Characteristics.”

Due to the vast number of volatile organic compounds present in indoor air, techniques that measure multiple compounds at once are particularly useful. Gas chromatography coupled to flame ionization or photoionization detectors are one approach to measuring hydrocarbons and small oxidized VOCs although this method can be challenging to operate and time-consuming to analyze data (Abeleira et al. 2017). Alternately, collection of water soluble organic gases using mist chambers followed by off-line mass spectrometry analysis also provides potentially vast datasets of water soluble organic gases (WSOG), but requires extensive post-sampling sample analysis with access to sophisticated instrumentation (Duncan et al. 2019).

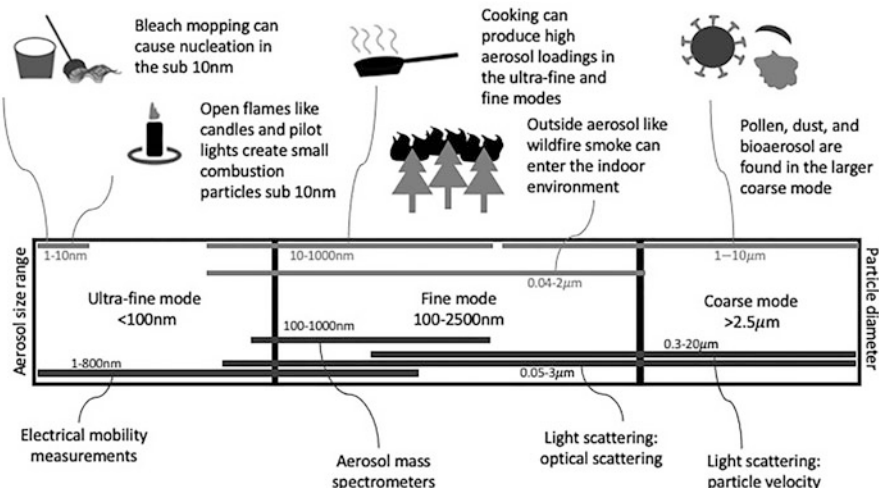


Fig. 1 Summary of particle size distributions and measurement approaches

Proton-transfer reaction mass spectrometry (PTR-MS) is a fast, field-deployable method for detecting and quantifying a multitude of indoor VOCs. This method accomplishes chemical ionization of analytes via proton-transfer from protonated water cluster reagent ions, allowing for subsequent detection via mass spectrometry. This method is sensitive and selective toward various reduced or lightly oxidized VOCs. A recent indoor field campaign in a California residence employed this instrumental method to probe background VOC emissions from building materials (formic acid, acetic acid, methanol), emissions from occupants (isoprene, siloxanes), and cooking (monoterpenes, ethanol, various O-, N-, or S-containing VOCs) (Liu et al. 2019). Other indoor field studies have used PTR-MS to measure chlorinated VOCs produced from bleach cleaning, including N-chloraldimines ($C_XH_YCl_N$), and toxic cyanogen chloride (ClCN) (Mattila et al. 2020a; Finewax et al. 2021).

In addition to PTR-MS, other chemical ionization mass spectrometry (CIMS) techniques have been successfully applied toward indoor air measurements. CIMS paired to iodide (I-) reagent ionization is sensitive and selective toward various oxygenated and nitrogenated VOCs, and inorganic chlorinated trace gases. Here, analyte ionization is accomplished via iodide-adduct formation driven by intermolecular forces between iodide and electropositive regions on the analyte (Lee et al. 2014). Iodide CIMS a powerful tool for studying indoor emissions from cooking (various O- and N-VOCs), bleach cleaning (HOCl, Cl₂, chloramines), and other WSOGs (Mattila et al. 2020b; Wang et al. 2020a; Wong et al. 2017; Duncan et al. 2019). Acetate (C₂H₃O₂⁻) reagent ions are effective for ionizing many gas-phase acids found indoors, including nitrous acid (HONO), isocyanic acid (HNCO), and various organic acids (Farmer et al. 2019a; Wang et al. 2020a; Wang et al. 2020b). Ionization with acetate CIMS occurs via proton-transfer, resulting in deprotonation of the gas-phase analyte (Brophy and Farmer 2016). Nitrate (NO₃⁻)

reagent ions have been utilized to detect low-volatility, highly volatilized gas-phase organics (Price et al. 2019), although the majority of these species likely reside in surface reservoirs and other condensed phases indoors, rather than indoor air. Combining CIMS measurements utilizing multiple reagent ion schemes allows users to capture a large fraction of indoor VOCs (Price et al. 2019). For instance, combining PTR-MS and iodide CIMS techniques likely captures a majority of the volatility space of atmospheric VOCs (Isaacman-VanWertz et al. 2017).

Modern field-deployable CIMS instruments used for atmospheric measurements are typically equipped with time-of-flight (TOF) mass analyzers, enabling mass resolutions orders of magnitude higher than quadrupole-based predecessors. The resolving power achieved by TOF instruments is crucial for fully characterizing complex atmospheric matrices, such as indoor air. Incorporating TOF mass analyzers in CIMS instruments also allows for collection of entire mass spectra at high (1 Hz) time resolutions, especially important for indoor environments where analyte mixing ratios can be highly dynamic on the order of minutes to seconds. These high sampling frequencies result in mass spectral ranges on the order of 500–1000 Da, which are usually sufficient for atmospheric trace gas applications.

Individual compounds detected by CIMS techniques can number in the hundreds to thousands. Many of these analytes may be calibrated using authentic gas-phase standards (i.e., VOC standard cylinders, permeation devices), but direct calibration of most compounds comprising CIMS spectra is infeasible. Bulk sensitivity estimations have been applied to CIMS field measurements, wherein instrumental sensitivity is parameterized to one or more controlling variable. For instance, PTR-MS sensitivities are routinely estimated based on the reaction rate coefficient between H₃O⁺ and the VOC of interest (Holzinger et al. 2019). Iodide CIMS sensitivity may be parameterized by the binding enthalpy of the iodide-analyte adduct (Lopez-Hilfiker et al. 2016; Mattila et al. 2020b). However, these methods have considerable uncertainty, and often yield order-of-magnitude sensitivity estimations at best.

CIMS instrumentation does not enable isomeric differentiation of detected chemical formulas, due to the inherent lack of sample pre-separation. Users will often have to rely on some a priori chemical knowledge of their sample to assume the structural identity of a detected chemical formula, i.e., if that compound is expected to be a prominent component of the sampled air. In most cases, the assigned empirical formula of a CIMS peak is some combination of different isomers. Some CIMS users have employed an in-line gas chromatography (GC) system for analyte pre-separation (GC-CIMS), although this invariably results in the loss of valuable time resolution due to extensive separation times.

The measurement of “total volatile organic compounds” remains an aspiration to indoor chemists. Such a measurement would provide useful context for even the most comprehensive measurements suites and determine the extent to which current measurements capture indoor organic carbon. “Total organic carbon” measurements are widely used in solid and liquid phases, and operate on the principle of combusting samples to CO₂. However, the gas phase has complications of a high CO₂ background (hundreds to thousands of parts per million CO₂ by volume), as well as methane and carbon monoxide. Thus any atmospheric total carbon

measurement requires subtraction of a very large and variable background signal to quantify the organic, non-methane component. Electrochemical sensors or other detection techniques may be useful. Alternative methods to constraining the extent to which air measurements capture the entire organic carbon budget include measuring the reactivity of air to OH radicals or ozone, and comparing model calculations of the lifetime of reactive components to measurements.

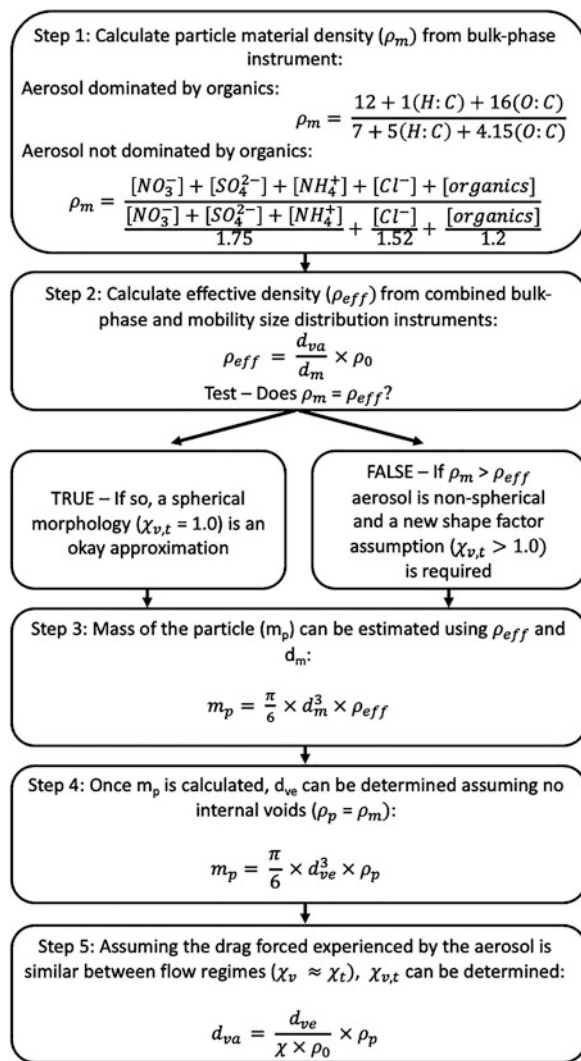
A substantial challenge of many of the techniques described above is the high cost. Many of the instruments described above are expensive and high-maintenance, and can require substantial electrical power and safety hazards (e.g., compressed gases, sealed radiation sources, calibration standards that include hazardous materials, etc.). These limitations prevent widespread application of detailed chemical assessment of indoor air across numerous buildings. Most detailed indoor chemistry studies are limited to laboratory environments, test houses, or single residences that are often occupied by individuals related to the study. To achieve a more widespread and long-term understanding of indoor air, lower cost and lower maintenance instruments that maintain the high quality data for at least a subset of measurements are essential. Low cost sensors are not the subject of this chapter, but are potentially exciting tools for understanding indoor air quality and chemistry.

On-Line Measurement of Particles

Particle Size Distributions

Indoor aerosols cover a range of sizes that include ultra-fine (particles 1–10 nm in diameter), fine (100–2500 nm in diameter), and coarse mode (>2,500 nm in diameter) (Fig. 1). Different subfields in aerosol science may have slightly different definitions of these modes, and are discussed in detail elsewhere in this book. Each mode has different sources in the indoor environment. For example, ultrafine particle sources include nucleation processes in which gas-phase molecules cluster to form new particles, as well as combustion sources (e.g., candle burning). Recent measurements show that bleach mopping can induce new particle formation, corresponding to increases in the ultrafine mode (Patel et al. 2020). Ultrafine particles typically experience substantial losses during transmission from outdoor air through engineered ventilation systems, but may enter indoor environments through open windows and doors. Sources of indoor fine mode aerosol include cooking and combustion sources, as well as infiltration of outdoor air. Coagulation and condensation processes can be substantial, and impact mass and composition of this mode. For example, ozonolysis of limonene can form fine mode secondary organic aerosol (Youssefi and Waring 2012). Coarse mode aerosol can include larger particles, such as oil droplets from cooking, skin flakes, and dust, which may be resuspended into the air from walking or vacuuming. Because the diameter of indoor particles spans orders of magnitude, no single instrument measures all particles. Instead, specific instruments focus on different aerosol modes, often measuring particle size distributions by number, which can then be converted to total mass

Fig. 2 Summary of approach for comparing size distributions derived from an aerosol mass spectrometer (d_{va}) and an SMPS (d_m). Note that this method systematically overestimates particle mass when effective density (ρ_{eff}) is used to determine particle mass. For smaller aerosol ($d_p < 80 \text{ nm}$) of mostly spherical shape ($\Sigma < 1.3$), the error is typically small and uncertainty in m_p will be accurate within 10%. However, for larger and more irregularly shaped aerosol, the uncertainty in m_p can be as large by up to a factor of 2



assuming density. Using multiple instruments with overlapping windows for size measurement can provide a more complete picture of aerosol size distribution, but measurements must be carefully seamed when instruments follow different measurement principles, which often results in slightly different definitions of particle diameter.

Aerosol counting and sizing instruments typically take advantage of light scattering of some form. For example, some instruments use light scattering to simply count particles, either irrespective of size or with a pre-measurement size selection, while others use scattering angles to derive size distributions. There are four

approaches to measuring and defining aerosol diameter, all of which make assumptions about the shape of sampled particles:

- Direct optical measurements detect size distributions as a function of *optical diameter* (d_o) uses light scattering and Mie theory to determine the size of the particle. Beyond assumptions about the shape of sampled particles, this approach also relies on assumptions about the refractive index. The refractive index of indoor aerosol can vary substantially from common calibration standards (Boedicker et al. 2021).
- Measurements that initially size select, and then count the resulting number of particles typically use differential mobility analyzers that define size distributions as a function of *electrical mobility diameter* (d_m). These separation techniques operate under atmospheric pressure, inducing the particle with a charge before moving the particle through a constant electric field. The size of particles that meet the criteria to pass through the electric field is determined from the force balance experienced by the charged particle between the constant electric field and the drag coefficient, which are dependent on particle shape (but not density). These techniques also typically assume that particles are only singly charged in the ionization system.
- Instruments that use the terminal falling speed (maximum velocity under atmospheric pressure) of particles provide size distributions based on *aerodynamic diameter* (d_a), which is a function of particle shape, size, and density. These distributions are derived from the time taken by individual particles to pass between two points, typically detected by light scattering by a pair of lasers. Measurements of aerodynamic diameter take place in a “continuum flow regime,” which is particularly effective for studying super-micron particles.
- Several newer instruments use the velocity of aerosol in a low pressure environment and thus provide distributions as a function of *vacuum aerodynamic diameter* (d_{va}). Size distributions in vacuum aerodynamic diameter are slightly different from aerodynamic diameter because the particles are in a transition or free molecular regime, rather than a continuum flow regime. These instruments have particle focusing lenses that dictate the size range and flow regime measured by the instrument. Aerodynamic measurements are functions of both density and particle shape.

It is important to remember that aerosol instruments are typically calibrated with spherical particles with a constant and known density. However, ambient aerosol can range from being simple spherical particles to large aggregates that are more challenging to define in physical diameter terminology. The physical particle diameter (d_p) is far simpler to define for a spherical particle than a nonspherical aggregate. More consistent definitions of particle size may be considered by the volume-equivalent particle diameter (d_{ve}), which represents the diameter of an irregular particle that is melted down to form a spherical particle while maintaining any internal voids, or the mass-equivalent diameter (d_{me}), which represents the mass but includes those internal voids (i.e., a particle with no internal voids would have a $d_{ve} = d_{me}$).

However, while d_{me} or d_{ve} may be more consistent across the irregularly shaped particles present in ambient air, these definitions do not correspond to direct measurements. For spherical particles $d_m = d_p = d_{ve}$; for irregularly shaped particles, d_m will always be biased to larger diameters ($d_m > d_{ve}$). Few studies test the underlying assumption that ambient aerosols are of consistent density and spherical shape, particularly in the indoor environment.

In considering how aerodynamic or vacuum aerodynamic diameter relates to volume equivalent particle diameter, one must consider both shape and density. Spherical particles have a proportional relationship between density and particle diameter:

$$d_a, d_{va} > d_{ve} \text{ for spherical aerosol with density greater than } 1.0 \text{ g/cm}^3$$

$$d_a, d_{va} < d_{ve} \text{ for spherical aerosol with density less than } 1.0 \text{ g/cm}^3$$

Increasing irregularity in particle shape (i.e., deviation from a spherical morphology) decreases both aerodynamic diameters:

$$d_a, d_{va} < d_{ve} \text{ for aerosol of unit density or lower with irregular particle shape}$$

$$d_a, d_{va} < \text{ or } > d_{ve} \text{ for aerosol of higher than unit density with irregular particle shape}$$

When density and shape assumptions are incorrect, datasets taken from different measurement approaches must be carefully considered to achieve self-consistent size distributions. DeCarlo, Slowik, and colleagues provide exceptional descriptions of the theory and application behind these comparisons (DeCarlo et al. 2004; Slowik et al. 2004). Figure 2 provides a flowchart to summarize steps in compare vacuum aerodynamic diameter to mobility diameter for two common instruments: the aerosol mass spectrometer (AMS), which measures vacuum aerodynamic diameter, and the scanning mobility particle sizer (SMPS), which measures electrical mobility diameter.

Overall, numerous instruments are capable of making particle size distribution measurements within different aerosol modes, although instruments typically only measure within about two decades of size range. However, care must be taken to understand the assumptions inherent in each measurement approach, particularly when synthesizing data into a single dataset or comparing size distributions of the same mode taken by different measurement approaches. Much of our understanding of these relationships and the importance of assumptions in influencing particle size measurements is driven by outdoor atmospheric chemistry studies. There is clearly great need to further test assumptions of particle shape and density in the indoor environment.

Chemical Measurement Techniques

Indoor aerosol composition is of emerging interest. While there is a strong history of particle collection for off-line measurements, real-time measurements of indoor

aerosol chemistry have emerged over the past decade. These measurements are typically grounded in techniques developed for outdoor atmospheric chemistry, and are summarized elsewhere (e.g., Farmer and Jimenez 2010; Pratt and Prather 2012). Most on-line aerosol composition measurements use mass spectrometry detection, although notable exceptions exist; for example, detection of oxidized nitrogen in particles by laser induced fluorescence (Rollins et al. 2012) following volatilization and thermal decomposition. This chapter focuses on the on-line aerosol composition techniques that have been applied to the indoor environment to illustrate principles of measurement. These instruments have typically measured aerosol composition for the entire population of particles within a given size range; single particle measurement techniques such as the aerosol time-of-flight mass spectrometer (ATOFMS) exist (Gard et al. 1997), but have yet to be applied to the built environment. This discussion is not an exhaustive compendium of techniques, in part because aerosol composition measurements are an active area of instrument development.

Aerosol composition measurements carry important restrictions; no on-line measurement detects the entire size range of ambient aerosol; inlet transmission and focusing lenses typically restrict the size window for analysis. Some techniques are further restricted by the method in which particles are transmitted into mass spectrometry detectors. Mass spectrometry requires analytes to be charged and in the gas phase. These requirements are particularly challenging for refractory material, including black carbon. Thus measurements that thermally volatilize aerosol to the gas-phase are usually considered non-refractory measures of aerosol composition, and separate measurements of refractory black carbon are required.

Bulk Aerosol Composition Measurements

Bulk composition measurements often use hard ionization coupled to mass spectrometry. These measurements are non-selective – that is, specific molecules are not identified because of the high degree of fragmentation induced by hard ionization. However, these techniques are typically considered quantitative, and provide an accurate mass of non-refractory aerosol. The Aerodyne Aerosol Mass Spectrometers and Aerosol Chemical Speciation Monitors have been widely used in indoor experiments (Avery et al. 2019; DeCarlo et al. 2018; Farmer et al. 2019b; Johnson et al. 2017; Dall’Osto et al. 2007; Klein et al. 2016; Joo et al. 2021). All of these instruments operate similarly, pulling air into the instrument through an aerodynamic particle lens, which focuses sub-micron aerosol ($d_{va} \sim 100\text{--}1000\text{ nm}$). This concentrated beam of aerosol passes through a differential pumping region; depending on the instrument, this pumping region can act as a particle time-of-flight tube that provides particle size information as the vacuum aerodynamic diameter. Particles then enter a vaporizer, where the non-refractory components are volatilized and ionized by electron ionization (70 eV). The resulting ions are dominated by fragments of the parent analytes,

and are detected by either a time-of-flight or quadrupole mass analyzer. The resolving power of the mass spectrometer depends on the instrument design; high resolution aerosol mass spectrometers usually have sufficient mass resolution ($m/\Delta m$ of ~ 4000) for elemental analysis of the peaks to directly determine the carbon, hydrogen, oxygen, and other heteroatoms in the aerosol. However, one specific challenge of applying aerosol mass spectrometry to indoor environments is establishing the relative ionization efficiency of indoor aerosol; indoor cooking organic aerosol shows an intriguingly high – but consistent – relative ionization efficiency (Katz et al. 2021).

Speciated Aerosol Composition Measurements

Where aerosol mass spectrometers use hard ionization and thus fragment aerosol components, soft ionization techniques minimize fragmentation and can provide molecular level information. For example, three instruments that have been used in indoor studies include: the semivolatile thermal desorption aerosol gas chromatography (SV-TAG) system (e.g., Lunderberg et al. 2020; Fortenberry et al. 2019), an extractive electrospray ionization mass spectrometer (EESI-MS) (Brown et al. 2021), and a high resolution time-of-flight chemical ionization mass spectrometer coupled to a filter inlet for gases and aerosols (FIGAERO-CIMS) (Brown et al. 2021). While instrument details are beyond the scope of this chapter, a few common principles are apparent. These measurements share the calibration challenges of the soft ionization systems used for gas phase measurements, and require careful consideration of instrument sensitivities for the range of analyte types being studied. The particle size range observed by these instruments is not as clear as the aerosol mass spectrometers with their aerosol lenses, so transmission efficiency and loss must be investigated based on inlet setups. These instruments are unable to provide size-resolved composition, but do provide molecular specification and, in the case of the FIGAERO-CIMS, profiles of volatility for each analyte.

Black Carbon

Black carbon measurements are typically optical in nature, and can include continuous filter measurements, laser-induced incandescence measurements, or thermal optical transmittance (Kondo et al. 2011). Each technique has advantages and disadvantages. For example, filter measurements can be subject to loading effects and humidity interferences in indoor environments (Sankhyan et al. 2021), although recent advances and careful operation may minimize these problems (Drinovec et al. 2015; Cai et al. 2013). Laser-induced incandescence measurements provide low detection limits with few interferences, and are capable of quantifying coatings on the black carbon particles but can have high maintenance needs.

Other Particle Measurements

Low cost sensors are not typically available for particle composition, but are available for PM_{2.5} mass and with some sizing information. While these measurements are becoming more widely used, care must be taken to account for different sensitivities to different types of aerosol, and there is need for addition work to validate measurement sensitivities for indoor air (Tryner et al. 2020; Wang et al. 2020d).

Instrument development for real-time, on-line measurement of coarse mode aerosol is a clear need for indoor chemistry. On-line bioaerosol measurements are scarce in indoor environments, but typically take advantage of fluorescent properties of biological particles combined with aerodynamic particle sizers (e.g., Tian et al. 2021).

Outdoor atmospheric chemists frequently couple on-line particle measurements with assessment of chemical or physical properties. For example, coupling measurements of aerosol size distribution and composition with thermal denuders enables measurements of particle volatility, while measurements of particle size distributions with and without dryers can provide aerosol liquid water content metrics. However, such measurements have not yet been widely deployed in indoor environments.

New Frontiers

Decades of instrument development for atmospheric chemistry research has provided an excellent opportunity for the field of indoor chemistry. These techniques enable not only quantitative, real-time measurements of indoor air gases and particles, but also intensive properties of those gases and particles. Emerging frontiers in analytical indoor chemistry include:

- Surface measurements. Surfaces play an integral role in the chemistry of the built environment: as mediators of gas concentrations through partitioning, as reservoirs for chemical compounds, and as sites for reactions. However, these surfaces are poorly characterized. Most existing techniques typically require surface sample collection for off-line analysis, but on-line measurement techniques would be exceptionally useful for improving our understanding of indoor chemistry.
- In situ chemical kinetics experiments that directly explore the rate constants of gases with oxidants (e.g., OH reactivity) have been useful in outdoor atmospheric chemistry to provide bounds on reactive carbon budgets. Such measurements would quantitatively describe the scope of indoor air composition, as well as the potential for indoor oxidation reactions and secondary organic aerosol formation. However, deployment of these measurements to indoor environments warrants caution as the substantial complexity and high concentrations present in indoor environments produce potential interferences. For example, OH reactivity measurements must account for interferences from NOx species, which rapidly change during cooking events.

- Low cost sensors have become more widely available and are essential for capturing spatial heterogeneity; both within single buildings and across multiple buildings and regions. However, these sensors are often subject to interferences and nuances that may be considered before widespread application to indoor chemistry research.
- The desire to link indoor chemistry to human health requires development of oxidative stress measurements. While such measurements have been used effectively in outdoor environments, they have not been extensively deployed in indoor environments, but present a unique opportunity.

Conclusion

The indoor environment is ripe for detailed chemical analysis. Most research to date has involved careful sample collection and off-line analysis, but recent work has increasingly transferred on-line measurements designed for outdoor atmospheric chemistry to indoor air. Due to the chemical complexity of indoor air, all indoor chemistry measurements require careful consideration of interferences and calibration sensitivity. There are many on-line, real-time instruments available to deploy in indoor environments from the field of atmospheric chemistry, and their successful implementation and careful consideration of analytical challenges will ensure new insights into the field of indoor chemistry.

Acknowledgments The authors thank the Alfred P. Sloan Foundation (Grant G-2018-11130) for funding.

References

- Abbatt JPD, Wang C (2020) The atmospheric chemistry of indoor environments. *Environ Sci Process Impacts* 22(1):25–48. <https://doi.org/10.1039/C9EM00386J>
- Abeleira A, Pollack IB, Sive B, Zhou Y, Fischer EV, Farmer DK (2017) Source characterization of volatile organic compounds in the Colorado Northern Front Range Metropolitan Area during spring and summer 2015. *J Geophys Res-Atmos* 122(6):3595–3613. <https://doi.org/10.1002/2016jd026227>
- Alvarez EG, Amedro D, Afif C, Gligorovski S, Schoemaecker C, Fittschen C, Doussin JF, Wortham H (2013) Unexpectedly high indoor hydroxyl radical concentrations associated with nitrous acid (vol 110, pg 13294, 2013). *Proc Natl Acad Sci USA* 110(39):15848–15848. <https://doi.org/10.1073/pnas.1314629110>
- Ampollini L, Katz EF, Bourne S, Tian Y, Novoselac A, Goldstein AH, Lucic G, Waring MS, DeCarlo PF (2019) Observations and contributions of real-time indoor ammonia concentrations during HOMEChem. *Environ Sci Technol* 53(15):8591–8598
- Arata C, Zarzana KJ, Misztal PK, Liu Y, Brown SS, Nazaroff WW, Goldstein AH (2018) Measurement of NO₃ and N₂O₅ in a residential kitchen. *Environ Sci Tech Let* 5(10): 595–599. <https://doi.org/10.1021/acs.estlett.8b00415>
- Ault AP, Grassian VH, Carslaw N, Collins DB, Destaillats H, Donaldson DJ, Farmer DK, Jimenez JL, McNeill VF, Morrison GC, O'Brien RE, Shiraiwa M, Vance ME, Wells JR, Xiong W (2020)

- Indoor surface chemistry: developing a molecular picture of reactions on indoor interfaces. *Chem* 6(12):3203–3218. <https://doi.org/10.1016/j.chempr.2020.08.023>
- Avery AM, Waring MS, DeCarlo PF (2019) Human occupant contribution to secondary aerosol mass in the indoor environment. *Environ Sci Process Impacts*. <https://doi.org/10.1039/C9EM00097F>
- Boedicker EK, Emerson EW, McMeeking GR, Patel S, Vance ME, Farmer DK (2021) Fates and spatial variations of accumulation mode particles in a multi-zone indoor environment during the HOMEChem campaign. *Environ Sci Process Impacts* 23(7):1029–1039. <https://doi.org/10.1039/D1EM00087J>
- Brophy P, Farmer D (2015) A switchable reagent ion high resolution time-of-flight chemical ionization mass spectrometer for real-time measurement of gas phase oxidized species: characterization from the 2013 southern oxidant and aerosol study. *Atmos Meas Tech* 8(7):2945–2959
- Brophy P, Farmer DK (2016) Clustering, methodology, and mechanistic insights into acetate chemical ionization using high-resolution time-of-flight mass spectrometry. *Atmos Meas Tech* 9(8):3969–3986. <https://doi.org/10.5194/amt-9-3969-2016>
- Brown WL, Day DA, Stark H, Pagonis D, Krechmer JE, Liu X, Price DJ, Katz EF, DeCarlo PF, Masoud CG, Wang DS, Hildebrandt Ruiz L, Arata C, Lunderberg DM, Goldstein AH, Farmer DK, Vance ME, Jimenez JL (2021) Real-time organic aerosol chemical speciation in the indoor environment using extractive electrospray ionization mass spectrometry. *Indoor Air* 31(1): 141–155. <https://doi.org/10.1111/ina.12721>
- Cai J, Yan B, Kinney PL, Perzanowski MS, Jung K-H, Li T, Xiu G, Zhang D, Olivo C, Ross J, Miller RL, Chillrud SN (2013) Optimization approaches to ameliorate humidity and vibration related issues using the MicroAeth black carbon monitor for personal exposure measurement. *Aerosol Sci Technol* 47(11):1196–1204. <https://doi.org/10.1080/02786826.2013.829551>
- Carslaw N, Fletcher L, Heard D, Ingham T, Walker H (2017) Significant OH production under surface cleaning and air cleaning conditions: impact on indoor air quality. *Indoor Air* 27(6): 1091–1100. <https://doi.org/10.1111/ina.12394>
- Clifton OE, Fiore AM, Massman WJ, Baublitz CB, Coyle M, Emberson L, Fares S, Farmer DK, Gentine P, Gerosa G, Guenther AB, Helmig D, Lombardozzi DL, Munger JW, Patton EG, Pusede SE, Schwede DB, Silva SJ, Sörgel M, Steiner AL, Tai APK (2020) Dry deposition of ozone over land: processes, measurement, and modeling. *Rev Geophys* 58(1):e2019RG000670. <https://doi.org/10.1029/2019RG000670>
- Collins DB, Hems RF, Zhou S, Wang C, Grignon E, Alavy M, Siegel JA, Abbatt JP (2018) Evidence for gas–surface equilibrium control of indoor nitrous acid. *Environ Sci Technol* 52 (21):12419–12427
- Dall’Osto M, Harrison RM, Charapidou E, Loupa G, Rapsomanikis S (2007) Characterisation of indoor airborne particles by using real-time aerosol mass spectrometry. *Sci Total Environ* 384(1–3):120–133
- Dawe KER, Furlani TC, Kowal SF, Kahan TF, VandenBoer TC, Young CJ (2019) Formation and emission of hydrogen chloride in indoor air. *Indoor Air* 29(1):70–78. <https://doi.org/10.1111/ina.12509>
- DeCarlo PF, Slowik JG, Worsnop DR, Davidovits P, Jimenez JL (2004) Particle morphology and density characterization by combined mobility and aerodynamic diameter measurements. Part 1: theory. *Aerosol Sci Technol* 38(12):1185–1205
- DeCarlo PF, Avery AM, Waring MS (2018) Thirdhand smoke uptake to aerosol particles in the indoor environment. *Sci Adv* 4 (5). ARTN eaap8368. <https://doi.org/10.1126/sciadv.aap8368>
- Drinovec L, Močnik G, Zotter P, Prévôt A, Ruckstuhl C, Coz E, Rupakheti M, Sciare J, Müller T, Wiedensohler A (2015) The “dual-spot” Aethalometer: an improved measurement of aerosol black carbon with real-time loading compensation. *Atmos Meas Tech* 8(5):1965–1979
- Duncan SM, Tomaz S, Morrison G, Webb M, Atkin JM, Surratt JD, Turpin BJ (2019) Dynamics of residential water-soluble organic gases: insights into sources and sinks. *Environ Sci Technol* 53: 1812–1821. <https://doi.org/10.1021/acs.est.8b05852>

- Farmer DK (2019) Analytical challenges and opportunities for indoor air chemistry field studies. *Anal Chem* 91(6):3761–3767. <https://doi.org/10.1021/acs.analchem.9b00277>
- Farmer DK, Jimenez JL (2010) Real-time atmospheric chemistry field instrumentation. *Anal Chem* 82:7879–7884. <https://doi.org/10.1021/ac1010603>
- Farmer DK, Vance ME, Abbatt JP, Abeleira A, Alves MR, Arata C, Boedicker E, Bourne S, Cardoso-Saldaña F, Corsi R (2019a) Overview of HOMEChem: house observations of microbial and environmental chemistry. *Environ Sci Process Impacts* 21(8):1280–1300
- Farmer DK, Vance ME, Abbatt JPD, Abeleira A, Alves MR, Arata C, Boedicker E, Bourne S, Cardoso-Saldaña F, Corsi R, DeCarlo PF, Goldstein AH, Grassian VH, Hildebrandt Ruiz L, Jimenez JL, Kahan TF, Katz EF, Mattila JM, Nazaroff WW, Novoselac A, O'Brien RE, Or VW, Patel S, Sankhyan S, Stevens PS, Tian Y, Wade M, Wang C, Zhou S, Zhou Y (2019b) Overview of HOMEChem: house observations of microbial and environmental chemistry. *Environ Sci Process Impacts* 21(8):1280–1300. <https://doi.org/10.1039/C9EM00228F>
- Finewax Z, Pagonis D, Claflin MS, Handschy AV, Brown WL, Jenks O, Nault BA, Day DA, Lerner BM, Jimenez JL, Ziemann PJ, de Gouw JA (2021) Quantification and source characterization of volatile organic compounds from exercising and application of chlorine-based cleaning products in a university athletic center. *Indoor Air* 31(5):1323–1339. <https://doi.org/10.1111/ina.12781>
- Fortenberry C, Walker M, Dang A, Loka A, Date G, Cysneiros de Carvalho K, Morrison G, Williams B (2019) Analysis of indoor particles and gases and their evolution with natural ventilation. *Indoor Air* 29(5):761–779
- Gard E, Mayer JE, Morrical BD, Dienes T, Fergenson DP, Prather KA (1997) Real-time analysis of individual atmospheric aerosol particles: design and performance of a portable ATOFMS. *Anal Chem* 69(20):4083–4091
- Gillett R, Kreibich H, Ayers G (2000) Measurement of indoor formaldehyde concentrations with a passive sampler. *Environ Sci Technol* 34(10):2051–2056
- Hallquist M, Wenger JC, Baltensperger U, Rudich Y, Simpson D, Claeys M, Dommen J, Donahue NM, George C, Goldstein AH, Hamilton JF, Herrmann H, Hoffmann T, Iinuma Y, Jang M, Jenkin ME, Jimenez JL, Kiendler-Scharr A, Maenhaut W, McFiggans G, Mentel TF, Monod A, Prevot ASH, Seinfeld JH, Surratt JD, Szmiigelski R, Wildt J (2009) The formation, properties and impact of secondary organic aerosol: current and emerging issues. *Atmos Chem Phys* 9(14):5155–5236
- Holzinger R, Acton WJF, Bloss WJ, Breitenlechner M, Crilley LR, Dusanter S, Gonin M, Gros V, Keutsch FN, Kiendler-Scharr A, Kramer LJ, Krechmer JE, Languijle B, Locoge N, Lopez-Hilfiker F, Materić D, Moreno S, Nemitz E, Quéléver LLJ, Sarda Esteve R, Sauvage S, Schallhart S, Sommariva R, Tillmann R, Wedel S, Worton DR, Xu K, Zaytsev A (2019) Validity and limitations of simple reaction kinetics to calculate concentrations of organic compounds from ion counts in PTR-MS. *Atmos Meas Tech* 12(11):6193–6208. <https://doi.org/10.5194/amt-12-6193-2019>
- Isaacman-VanWertz G, Massoli P, O'Brien RE, Nowak JB, Canagaratna MR, Jayne JT, Worsnop DR, Su L, Knopf DA, Misztal PK, Arata C, Goldstein AH, Kroll JH (2017) Using advanced mass spectrometry techniques to fully characterize atmospheric organic carbon: current capabilities and remaining gaps. *Faraday Discuss* 200:579–598. <https://doi.org/10.1039/C7FD00021A>
- Johnson AM, Waring MS, DeCarlo PF (2017) Real-time transformation of outdoor aerosol components upon transport indoors measured with aerosol mass spectrometry. *Indoor Air* 27(1): 230–240
- Joo T, Rivera-Rios JC, Alvarado-Velez D, Westgate S, Ng NL (2021) Formation of oxidized gases and secondary organic aerosol from a commercial oxidant-generating electronic air cleaner. *Environ Sci Tech Let* 8(8):691–698. <https://doi.org/10.1021/acs.estlett.1c00416>
- Katz EF, Guo H, Campuzano-Jost P, Day DA, Brown WL, Boedicker E, Pothier M, Lunderberg DM, Patel S, Patel K, Hayes PL, Avery A, Hildebrandt Ruiz L, Goldstein AH, Vance ME, Farmer DK, Jimenez JL, DeCarlo PF (2021) Quantification of cooking organic aerosol in the indoor environment using aerodyne aerosol mass spectrometers. *Aerosol Sci Tech* 1–16 <https://doi.org/10.1080/02786826.2021.1931013>

- Klein F, Farren NJ, Bozzetti C, Daellenbach KR, Kilic D, Kumar NK, Pieber SM, Slowik JG, Tuthill RN, Hamilton JF (2016) Indoor terpene emissions from cooking with herbs and pepper and their secondary organic aerosol production potential. *Sci Rep-Uk* 6(1):1–7
- Kondo Y, Sahu L, Moteki N, Khan F, Takegawa N, Liu X, Koike M, Miyakawa T (2011) Consistency and traceability of black carbon measurements made by laser-induced incandescence, thermal-optical transmittance, and filter-based photo-absorption techniques. *Aerosol Sci Technol* 45(2):295–312. <https://doi.org/10.1080/02786826.2010.533215>
- Lee BH, Lopez-Hilfiker FD, Mohr C, Kurten T, Worsnop DR, Thornton JA (2014) An iodide-adduct high-resolution time of flight chemical ionization mass spectrometer: application to atmospheric inorganic and organic compounds. *Environ Sci Technol* 48(11):6309–6317
- Li J, Mattewal SK, Patel S, Biswas P (2020) Evaluation of nine low-cost-sensor-based particulate matter monitors. *Aerosol Air Qual Res* 20(2):254–270. <https://doi.org/10.4209/aaqr.2018.12.0485>
- Liang Y, Sengupta D, Campmier MJ, Lunderberg DM, Apte JS, Goldstein AH (2021) Wildfire smoke impacts on indoor air quality assessed using crowdsourced data in California. *Proc Natl Acad Sci* 118(36):e2106478118. <https://doi.org/10.1073/pnas.2106478118>
- Liu Y, Misztal PK, Xiong J, Tian Y, Arata C, Weber RJ, Nazaroff WW, Goldstein AH (2019) Characterizing sources and emissions of volatile organic compounds in a northern California residence using space-and time-resolved measurements. *Indoor Air* 29(4):630–644
- Liu Y, Bé AG, Or VW, Alves MR, Grassian VH, Geiger FM (2020) Challenges and opportunities in molecular-level indoor surface chemistry and physics. *Cell Rep Phys Sci* 1(11):100256. <https://doi.org/10.1016/j.xrpp.2020.100256>
- Lopez-Hilfiker FD, Iyer S, Mohr C, Lee BH, D'Ambro EL, Kurten T, Thornton JA (2016) Constraining the sensitivity of iodide adduct chemical ionization mass spectrometry to multi-functional organic molecules using the collision limit and thermodynamic stability of iodide ion adducts. *Atmos Meas Tech* 9(4):1505–1512. <https://doi.org/10.5194/amt-9-1505-2016>
- Lunderberg DM, Kristensen K, Tian Y, Arata C, Misztal PK, Liu Y, Kreisberg N, Katz EF, DeCarlo PF, Patel S, Vance ME, Nazaroff WW, Goldstein AH (2020) Surface emissions modulate indoor SVOC concentrations through volatility-dependent partitioning. *Environ Sci Technol* 54(11): 6751–6760. <https://doi.org/10.1021/acs.est.0c00966>
- Maruo Y, Yamada T, Nakamura J, Izumi K, Uchiyama M (2010) Formaldehyde measurements in residential indoor air using a developed sensor element in the Kanto area of Japan. *Indoor Air* 20 (6):486–493
- Mattila JM, Arata C, Wang C, Katz EF, Abeleira A, Zhou Y, Zhou S, Goldstein AH, Abbatt JPD, DeCarlo PF, Farmer DK (2020a) Dark chemistry during bleach cleaning enhances oxidation of organics and secondary organic aerosol production indoors. *Environ Sci Tech Let*. <https://doi.org/10.1021/acs.estlett.0c00573>
- Mattila JM, Lakey PS, Shiraiwa M, Wang C, Abbatt JP, Arata C, Goldstein AH, Ampollini L, Katz EF, DeCarlo PF (2020b) Multiphase chemistry controls inorganic chlorinated and nitrogenated compounds in indoor air during bleach cleaning. *Environ Sci Technol* 54(3):1730–1739
- Patel S, Sankhyan S, Boedicker EK, DeCarlo PF, Farmer DK, Goldstein AH, Katz EF, Nazaroff WW, Tian Y, Vanhanen J (2020) Indoor particulate matter during HOMEChem: concentrations, size distributions, and exposures. *Environ Sci Technol* 54(12):7107–7116
- Pollack IB, Lindaas J, Roscioli JR, Agnese M, Permar W, Hu L, Fischer EV (2019) Evaluation of ambient ammonia measurements from a research aircraft using a closed-path QC-TILDAS operated with active continuous passivation. *Atmos Meas Tech* 12(7):3717–3742. <https://doi.org/10.5194/amt-12-3717-2019>
- Pratt KA, Prather KA (2012) Mass spectrometry of atmospheric aerosols—recent developments and applications. Part II: on-line mass spectrometry techniques. *Mass Spectrom Rev* 31(1):17–48
- Price DJ, Day DA, Pagonis D, Stark H, Algrim LB, Handschy AV, Liu S, Krechmer JE, Miller SL, Hunter JF (2019) Budgets of organic carbon composition and oxidation in indoor air. *Environ Sci Technol* 53(22):13053–13063
- Rollins AW, Browne EC, Min KE, Pusede SE, Wooldridge PJ, Gentner DR, Goldstein AH, Liu S, Day DA, Russell LM, Cohen RC (2012) Evidence for NO_x control over nighttime SOA formation. *Science* 337(6099):1210–1212. <https://doi.org/10.1126/science.1221520>

- Salthammer T, Mentese S, Marutzky R (2010) Formaldehyde in the indoor environment. *Chem Rev* 110(4):2536–2572. <https://doi.org/10.1021/cr800399g>
- Sankhyan S, Patel S, Katz E, DeCarlo PF, Farmer D, Nazaroff WW, Vance ME (2021) Indoor black carbon and brown carbon concentrations from cooking and outdoor penetration: insights from the HOMEChem study. *Environ Sci Process Impacts*. <https://doi.org/10.1039/D1EM00283J>
- Schlink U, Rehwagen M, Damm M, Richter M, Borte M, Herbarth O (2004) Seasonal cycle of indoor-VOCs: comparison of apartments and cities. *Atmos Environ* 38(8):1181–1190. <https://doi.org/10.1016/j.atmosenv.2003.11.003>
- Slowik JG, Stainken K, Davidovits P, Williams L, Jayne J, Kolb C, Worsnop DR, Rudich Y, DeCarlo PF, Jimenez JL (2004) Particle morphology and density characterization by combined mobility and aerodynamic diameter measurements. Part 2: application to combustion-generated soot aerosols as a function of fuel equivalence ratio. *Aerosol Sci Technol* 38(12):1206–1222
- Tian Y, Arata C, Boedicker E, Lunderberg DM, Patel S, Sankhyan S, Kristensen K, Misztal PK, Farmer DK, Vance M (2021) Indoor emissions of total and fluorescent supermicron particles during HOMEChem. *Indoor Air* 31(1):88–98
- Tryner J, L'Orange C, Mehaffy J, Miller-Lionberg D, Hofstetter JC, Wilson A, Volckens J (2020) Laboratory evaluation of low-cost PurpleAir PM monitors and in-field correction using co-located portable filter samplers. *Atmos Environ* 220:117067. <https://doi.org/10.1016/j.atmosenv.2019.117067>
- Van den Broek J, Cerrejon DK, Pratsinis SE, Güntner AT (2020) Selective formaldehyde detection at ppb in indoor air with a portable sensor. *J Hazard Mater* 399:123052
- Vlasenko A, Macdonald AM, Sjostedt SJ, Abbatt JPD (2010) Formaldehyde measurements by proton transfer reaction – mass spectrometry (PTR-MS): correction for humidity effects. *Atmos Meas Tech* 3(4):1055–1062. <https://doi.org/10.5194/amt-3-1055-2010>
- Wang C, Collins DB, Abbatt JP (2019) Indoor illumination of terpenes and bleach emissions leads to particle formation and growth. *Environ Sci Technol* 53(20):11792–11800
- Wang C, Bottorff B, Reidy E, Rosales CMF, Collins DB, Novoselac A, Farmer DK, Vance ME, Stevens PS, Abbatt JP (2020a) Cooking, bleach cleaning, and air conditioning strongly impact levels of HONO in a house. *Environ Sci Technol* 54(21):13488–13497
- Wang C, Collins DB, Arata C, Goldstein AH, Mattila JM, Farmer DK, Ampollini L, DeCarlo PF, Novoselac A, Vance ME (2020b) Surface reservoirs dominate dynamic gas-surface partitioning of many indoor air constituents. *Sci Adv* 6(8):eaay8973
- Wang Z, Delp WW, Singer BC (2020c) Performance of low-cost indoor air quality monitors for PM_{2.5} and PM₁₀ from residential sources. *Build Environ* 171:106654. <https://doi.org/10.1016/j.buildenv.2020.106654>
- Wang Z, Delp WW, Singer BC (2020d) Performance of low-cost indoor air quality monitors for PM_{2.5} and PM₁₀ from residential sources. *Build Environ* 171:106654
- Wang N, Zannoni N, Ernle L, Bekö G, Wargocki P, Li M, Weschler CJ, Williams J (2021) Total OH reactivity of emissions from humans: in situ measurement and budget analysis. *Environ Sci Technol* 55(1):149–159. <https://doi.org/10.1021/acs.est.0c04206>
- Wisthaler A, Weschler CJ (2010) Reactions of ozone with human skin lipids: sources of carbonyls, dicarbonyls, and hydroxycarbonyls in indoor air. *Proc Natl Acad Sci* 107(15):6568–6575
- Wong JPS, Carslaw N, Zhao R, Zhou S, Abbatt JPD (2017) Observations and impacts of bleach washing on indoor chlorine chemistry. *Indoor Air* 27(6):1082–1090. <https://doi.org/10.1111/ina.12402>
- Young CJ, Furdui VI, Franklin J, Koerner RM, Muir DC, Mabury SA (2007) Perfluorinated acids in arctic snow: new evidence for atmospheric formation. *Environ Sci Technol* 41(10):3455–3461
- Young CJ, Zhou S, Siegel JA, Kahan TF (2019) Illuminating the dark side of indoor oxidants. *Environ Sci Process Impacts* 21(8):1229–1239. <https://doi.org/10.1039/C9EM00111E>
- Youssefi S, Waring M (2012) Predicting secondary organic aerosol formation from terpenoid ozonolysis with varying yields in indoor environments. *Indoor Air* 22(5):415–426
- Zhang Z, Lin YH, Zhang H, Surratt JD, Ball LM, Gold A (2012) Technical note: synthesis of isoprene atmospheric oxidation products: isomeric epoxides and the rearrangement products cis- and trans-3-methyl-3,4-dihydroxytetrahydrofuran. *Atmos Chem Phys* 12(18):8529–8535. <https://doi.org/10.5194/acp-12-8529-2012>



Indoor Chemistry Modeling of Gas-, Particle-, and Surface-Phase Processes

33

Michael S. Waring and Manabu Shiraiwa

Contents

Introduction	956
Box Model for Indoor Air Pollutants	956
Modeling Gas-Phase Chemistry	958
General Gas-Phase Chemistry Concentration Balance	958
Simulating Important Gas-Phase Chemical Reactions	960
Modeling Indoor Particulate Matter Concentrations	963
General Particulate Matter Concentration Balance	963
Simulating Indoor Secondary Organic Aerosol	964
Simulating Indoor Organic Aerosol	967
Simulating Indoor Inorganic Aerosol	969
Surface Chemistry Modeling	970
Simulating Surface Chemistry Byproduct Formation	970
Modeling Transport Within Boundary Layer	971
Modeling Surface Processes	973
Modeling Skin Chemistry Example	976
References	978

Abstract

Indoor chemical processes can be successfully modeled using a variety of techniques. At the center of much indoor chemical process modeling is the mass or concentration balance, which can be used in single- or multizonal well-mixed models to predict the transient evolution of gas- and particle-phase species. This chapter first outlines the basic framework to simulate gas-phase chemical reactions, with a focus on ozone-driven reactions and the subsequent formation of

M. S. Waring (✉)
Drexel University, Philadelphia, PA, USA
e-mail: msw59@drexel.edu

M. Shiraiwa
University of California—Irvine, Irvine, CA, USA
e-mail: m.shiraiwa@uci.edu

hydroxyl radicals (OH) indoors. Then, indoor particle chemical modeling is described, with a focus on predicting indoor secondary organic aerosol (SOA) formation. Finally, surface-phase reaction frameworks are presented, with a focus on modeling byproducts due to oxidant deposition and understanding surface reaction processes themselves. In each section, we also highlight relevant indoor air literature articles that provide richer detail.

Keywords

Indoor chemistry · Modeling · Simulation · Aerosol · Surface

Introduction

Previous chapters in this section have discussed the state of knowledge of various aspects of indoor chemistry, such as gas-phase chemistry, surface chemistry, aerosol chemistry, among others. The majority of the understanding in those chapters was the result of experimental or observational investigations. This chapter instead relays basic information on indoor chemistry modeling techniques. Modeling is an effective tool to further our understanding of indoor chemical processes (Shiraiwa et al. 2019). It can serve many functions, including investigating processes under a wide range of parameters not practical in experiments or testing the agreement between modeled and measured values so as to confirm process understanding.

This chapter on indoor chemistry modeling functions as a primer and is generally organized into the following categories: box model for indoor air pollutants, gas-phase chemistry modeling, particle-phase chemistry modeling, and surface-phase chemistry modeling (computational fluid dynamics (CFD) modeling example). In each section, typical methods of modeling are described, and important papers in the literature are highlighted.

Box Model for Indoor Air Pollutants

Indoor pollutant concentrations in the gas or particle phase may be computed with a box model, which assumes that the pollutants from outdoors or emitted indoors are uniformly mixed within a volume of indoor air (Nazaroff and Alvarez-Cohen 2001). Species concentrations are thus spatially homogeneous but can change in time. The box model framework is the most commonly used framework for indoor chemistry investigations since, in essence, a modeler must choose between modeling chemical complexity with a box model or spatial complexity with other methods. Lately, however, CFD has been used to simulate certain simple chemical situations which are likely to exhibit spatial variation, as discussed later in this chapter.

In the context of indoor air in a building, the box model framework can be applied to a single-zone or multi-zone paradigm. In a building, a zone is often defined as a space within the building that has different characteristics than other zones in the

buildings. For instance, zones can be due to physical separations in buildings, or zones are often dictated by heating, ventilation, and air-conditioning system (HVAC) design such that a zone is group of spaces that share common air distribution and thermal control settings.

For the case of indoor air in a single zone, the change in any generic concentration of gas-phase component i with time can be represented with a concentration balance for the change in concentration of any species, C (e.g., ppb, #/cm³, or µg/m³), with respect to time, t (h):

$$\frac{dC}{dt} = S - lC \quad (1)$$

where the resulting concentration is established by a combination of a total source, S (e.g., pph/h, #/cm³-h, or µg/m³-h), and total loss rate, l (h⁻¹), in the indoor environment (Nazaroff and Cass 1986, 1989).

Equation (1) can be solved in a transient manner in an analytical or numerical fashion, or at steady state. For the case with parameters that are set at constant values over time (except the concentration being computed), the analytical solution to Eq. (1) is:

$$C(t) = C_{(t=0)} e^{-lt} + \frac{S}{l} (1 - e^{-lt}) \quad (2)$$

where $C(t)$ is the species concentration of interest over time, and $C_{(t=0)}$ is the initial concentration at the time zero datum. In Eq. (2), the first term on the right-hand side represents the decay of any species concentration that is present at time zero when modeling commences, and the second term on the right-hand side represents the change in the species concentration indoors due to active sources from the onset of the time horizon of interest (with those additions also being acted on by current losses in the system).

For the case of parameters on the right-hand side of Eq. (2) not being constant and changing during the time horizon of interest, Eq. (2) can still be used, but one must conceive the time zero datum as changing throughout the time horizon with discrete time steps imposed so that the previous time step is effectively treated as the initial concentration, $C_{(t=0)}$. Otherwise, a more formal numerical solution to solving first-order ordinary differential equations (ODE) can be used, such as the Euler, midpoint, or Runge-Kutta methods.

When parameters in Eq. (1) are constant over a long enough time horizon, the solution approaches its steady-state value, meaning it reaches a constant value that does not change in time anymore. The steady-state solution can be determined by setting the differential term $dC/dt = 0$ in Eq. (1) and rearranging to solve for C , or by substituting $t = \infty$ in Eq. (2) and simplifying it. Either method yields the steady-state concentration, C_{ss} , as in Eq. (3):

$$C_{ss} = \frac{S}{l} \quad (3)$$

Whether a modeler should use time-varying or steady-state assumptions to predict the concentration of interest depends on the interplay between the total loss rate and the amount of elapsed time since the values for the source and loss conditions were at a constant condition. For instance, the time to reach any fraction of the steady-state concentration once constant conditions begin is given by Eq. (4):

$$t_{f,ss} = \frac{\ln(1-f)}{-l} \quad (4)$$

where f is a factor bounded between (0.1) and represents the fraction of which a concentration compares to the eventual steady-state value. As Eq. (4) demonstrates, $t_{f,ss}$ is a function of the total loss rate alone, so the time to approach to 0.95 or 0.99 of a steady-state concentration is $t_{0.95,ss} = 3.0/l$ or $t_{0.99,ss} = 4.6/l$. Consider an example in which source and loss conditions of ozone in a building were constant for 30 min (i.e., 0.5 h), and ozone had a total loss rate of 4 h^{-1} . In this case, the $t_{0.95,ss} = 0.75 \text{ h}$ and $t_{0.99,ss} = 1.15 \text{ h}$, so the ozone would not be at steady state and the transient solution should be used. However, if conditions had been constant for, say, 2 h then using a steady-state equation to compute the ozone concentration would be appropriate.

Furthermore, multizonal models are a group of single-zone models that have linkages between zones based on interzonal airflow rates. Modelers can write their own code to facilitate solutions or can use software meant for such purposes. For instance, a multizonal indoor air modeling program called CONTAM has been developed by NIST, which accounts for pressure-driven flow among zones (Dols and Polidoro 2020). This chapter does not discuss multizonal modeling explicitly. The following sections expand on using the single-zone box model for gas-, particle-, and surface-phase modeling.

Modeling Gas-Phase Chemistry

General Gas-Phase Chemistry Concentration Balance

Equation (1) can be cast in a form including relevant parameters for considering gas-phase modeling within a single zone. Let us discuss a few reactions so as to demonstrate the model framework, centered around simulating the fate of a generic molecule F. Consider F that can be generated indoors by a biomolecular reaction, such that:



In reaction R1, a molecule G reacts with a molecule H to yield a molecule F. The reaction R1 also contains a parameter y_F , called the molar yield of F, which is often unity or integer values for simple reactions but can be fractional if the reaction between G and H produces more than one molecular outcome from a branching

standpoint. Moreover, consider that F can be removed from the indoor air by reaction with another molecule J, such that:



In reactions R1 and R2, ellipses are shown as potential products because we are only concerned about the fate of F in this example, and not other products.

Considering R1 and R2, the concentration balance in Eq. (1) can be expanded into a framework accounting for those generic reactions to model the concentration of species F, C_F (ppb), with respect to time, t (h), as in Eq. (5) (Nazaroff and Cass 1986):

$$\frac{dC_F}{dt} = P_F + \lambda C_{F,out} + \frac{E_F}{V} - r_F C_F - \lambda C_F - v_{d,F} \frac{A}{V} C_F \quad (5)$$

where the terms in Eq. (5) that correspond to gas-phase chemistry are P_F (ppb/h), which is the formation rate of F due to gas-phase reactions of G + H (as in R1), and r_i (h^{-1}), which is the loss rate of F due to gas-phase reactions with J (as in R2). Also, $C_{F,out}$ (ppb) is the concentration of species F in outdoor air; λ (h^{-1}) is the air exchange rate of indoor with outdoor air, which is the volumetric air flow through the building, Q (m^3/h), normalized by volume, V (m^3); E_F/V (ppb/h) is the volume-normalized emission rate of species F; $v_{d,F}$ (m/h) is the deposition velocity of species F to indoor surfaces; and A (m^2) is the surface area indoors.

On the right-hand-side of Eq. (5), the first positive term is the source of formation rate of F by gas-phase reactions (P_F), and the first negative term is the loss of F by gas-phase reactions (r_F). Besides these processes, C_F may be influenced by other mechanisms. In Eq. (5), the other two sources of F are transport from outdoors to indoors and indoor emission, respectively; the other two losses are loss to outdoors with air exchange and irreversible reaction on indoor surfaces (this mechanism is discussed in detail below). Other processes could be included in Eq. (5), such as including sorptive effects of volatile compounds on building surfaces (Singer et al. 2004), or modeling different types of air exchange mechanisms, but these are omitted in this section for brevity (section on particle chemistry includes different air exchange mechanisms since particles have different losses in each type of air stream).

The specific formulation for the term in Eq. (5) of the gas-phase chemistry formation rate for the concentration C_F due to R1, P_F (ppb/h), is as in Eq. (6):

$$P_F = y_F k_{G-H} C_G C_H \quad (6)$$

where y_F is molar yield of F due to reactions between species G and H; k_{G-H} ($\text{ppb}^{-1} \text{h}^{-1}$) is the biomolecular reaction rate constant between species G and H; and C_G and C_H (ppb) are concentrations of species G and H. The reaction rate constant quantifies the rate and direction (positive or negative) of a chemical reaction, is typically first or second order for indoor air reactions, and is a strong function of temperature (Seinfeld and Pandis 2016).

The specific formulation for the term in Eq. (5) of the gas-phase chemistry loss rate for the concentration C_F due to R2, r_i (h^{-1}), is as in Eq. (7):

$$r_F = k_{F-J} C_J \quad (7)$$

where k_{F-J} ($\text{ppb}^{-1} \text{ h}^{-1}$) is the biomolecular reaction rate constant between F and J; and C_J (ppb) is the concentration of species J. Though this example focuses on only two reactions R1 and R2, multiple reactions can sometimes act on the same species indoors. In cases like this, the total formation rate and total loss rate can be modeled as the summation of the individual formation or loss rates, respectively. Moreover, sometimes modeling cases multiple differential equations that are joined by reaction parameters.

In Eqs. (5), (6), and (7), the concentrations, emissions, and rate constants are expressed in terms of mole fractions (e.g., ppb), but they may be expressed as alternative concentration units, such as molec/cm^3 or $\mu\text{g/m}^3$, where conversion between units requires the use of the ideal gas law with Avogadro's number and/or molecular weights. For different concentration units, the reaction rate constants must have their units translated as well, for example, $\text{cm}^3/\text{molec-s}$ and $\text{m}^3/\mu\text{g-h}$.

Simulating Important Gas-Phase Chemical Reactions

Indoor gas-phase chemistry is diverse and situation dependent, so this section discusses relevant reactions and parameters for modeling common situations, including the oxidation of volatile organic compounds (VOCs), the generation of hydroxyl radicals (OH), and reactions involving nitrogen oxides (NO_x). Primary oxidants indoors that react with VOCs are ozone (O_3), the hydroxyl radical (OH), and the nitrate radical (NO_3) under certain conditions.

Indoor ozone chemistry drives many chemical pathways, and indoor ozone concentrations are often at 20–70% of ambient values (Weschler 2000). Ozone reacts with alkenes, which are unsaturated organic molecules containing carbon–carbon double bonds. The most dominant indoor alkenes are terpenoids, which are unsaturated compounds consisting of two or more isoprene units. Reaction rates of ozone with many indoor-emitted terpenoids have been determined, such as those for d-limonene, α - and β -pinene, and α -terpineol (Atkinson 2000; Wells 2005). In situations with strong terpenoid emissions, such as with the use of cleaners or air fresheners (Nazaroff and Weschler 2004), a few terpenoids such as d-limonene or α -terpineol can dominate the indoor ozone total reactivity (Waring and Wells 2015).

When ozone reacts with alkenes, the Criegee mechanism commences, in which a primary ozonide is formed that cleaves to yield a carbonyl and an excited Criegee intermediate (CI^*) (Atkinson and Arey 2003; Criegee 1975). The CI^* can form a stabilized Criegee intermediate (SCI) that follows multiple reaction pathways (the “SCI channel”), or it can rearrange and decompose to form an alkyl radical ($\text{R}\cdot$) and OH (the “hydroperoxide channel”) (Kroll and Seinfeld 2008). Therefore, reactions of ozone and alkenes (and so especially of ozone and terpenoids) are often the most

dominant source of OH indoors, since OH is not meaningfully sourced from outdoors due to its short lifetimes (Weschler and Shields 1996).

For many years, ozone-alkene reactions were thought to be the only OH source indoors. However, another recently discovered indoor source of OH that can sometimes be meaningful is the photolysis of nitrous acid (HONO) by indoor light at wavelengths ≤ 405 nm (Gómez-Alvarez et al. 2013). HONO can be formed indoors from combustion processes or by nitrogen dioxide (NO_2) hydrolysis on indoor surfaces (Spicer et al. 1993). Indoor light at these wavelengths is due to the attenuation of sunlight through windows or due to the use of indoor light fixtures (J. Young et al. 2019; Kowal et al. 2017).

The source of the nitrate radical (NO_3) indoors is from ozone reactions with NO_2 to yield NO_3 and O_2 . Once NO_3 is formed, the NO_3 and remaining NO_2 coexist in equilibrium with dinitrogen pentoxide (N_2O_5) (Atkinson 2000; Weschler et al. 1994). NO_3 is quite difficult to measure. However, concentrations are estimated at an upper bound of ~ 1 ppt (Nøjgaard 2010), though it may be most often at $\sim 10^{-2}$ ppt indoors.

Ozone reactions with alkenes and also OH or NO_3 reactions with any VOC forms alkyl radicals ($\text{R}\cdot$) that will react with O_2 to yield hydroxy radicals ($\text{HO}_2\cdot$) and peroxy radicals ($\text{RO}_2\cdot$). These radicals react with other species to form alkoxy radicals ($\text{RO}\cdot$) or compounds such as alcohols, carbonyls, carboxylic acids, and hydroperoxides, or also organic or peroxy nitrates (Atkinson and Arey 2003; Kroll and Seinfeld 2008). The less functionalized and lower-molecular-weight compounds are more volatile and tend to exist in the gas, while the more functionalized and higher-molecular-weight ones are less volatile and tend to exist in the particle phase.

Other reactions involving oxides of nitrogen are important indoors. One very fast reaction is that of ozone with nitric oxide (NO) to yield NO_2 and O_2 , which dominates ozone reactions and also titrates all ozone if enough NO is present indoors. Also, if NO is present, it can react with $\text{HO}_2\cdot$ radicals to yield OH and NO_2 . This reaction serves to essentially “recycle” OH radicals, since OH reactions themselves can lead to the formation of $\text{HO}_2\cdot$ radicals. Additionally, OH reacts with NO to yield HONO, which can photolyze to reform OH and NO; OH reacts with NO_2 to yield the NO_3 radical and O_2 ; and OH reacts with HONO to yield NO_2 and water vapor.

These reactions, and all that have been discussed in this section, are summarized in Table 1, along with rate constants at a temperature of 298 K. Moreover, Table 2 shows a list of volatile alkenes from residences (Logue et al. 2011), along with rate constant data at 298 K and OH molar yields from ozone + alkene reactions. In Table 2, the alkenes are ranked from most reactive to least reactive with ozone. Many other reactions are important indoors. For seminal examples in the indoor chemistry literature of gas-phase modeling with detailed chemical mechanisms, see papers by Carslaw (2007) and Sarwar et al. (2002).

To conclude this section, we end with an example on modeling OH concentrations indoors, which was similarly performed by Weschler and Shields (1996) in a seminal paper that argued for the presence of OH indoors owing to ozone + alkene reactions. Following the basic gas-phase reaction framework in R1 and R2 above,

Table 1 Reactions discussed in this section and their rate constants at temperature of 298 K

No.	Reaction	Rate constant	Source
R3	$O_3 + \text{alkene}_i \rightarrow OH + \text{other radicals} + \text{stable products}$	Table 2	1
R4	$O_3 + NO \rightarrow NO_2 + O_2$	$k_{O_3-NO} = 1.6 \text{ ppb}^{-1} h^{-1}$	2
R5	$O_3 + NO_2 \rightarrow NO_3 + O_2$	$k_{O_3-NO_2} = 0.0028 \text{ ppb}^{-1} h^{-1}$	2
R6	$OH + VOC_i \rightarrow \text{other radicals} + \text{stable products}$	Table 2	1
R7	$OH + NO + M \rightarrow HONO + M$	$k_{OH-NO} = 2800 \text{ ppb}^{-1} h^{-1}$	2
R8	$OH + HONO \rightarrow H_2O + NO_2$	$k_{OH-HONO} = 430 \text{ ppb}^{-1} h^{-1}$	2
R9	$HONO + h\nu \rightarrow OH + NO$	Depends on light	3
R10	$HO_2 + NO \rightarrow OH + NO_2$	$k_{HO_2-NO} = 736 \text{ ppb}^{-1} h^{-1}$	1
R11	$NO_3 + VOC_i \rightarrow \text{other radicals} + \text{stable products}$	Table 2	1
R12	$NO_3 + NO_2 \rightarrow N_2O_5$	$k_{NO_3-NO_2} = 180 \text{ ppb}^{-1} h^{-1}$	2
R13	$N_2O_5 \rightarrow NO_3 + NO_2$	$k_{N_2O_5(d)} = 250 \text{ h}^{-1}$	2

Atkinson (2000) and Master Chemical Mechanism v3.2

Atkinson et al. (1992)

Gómez-Alvarez et al. (2013)

Table 2 Reaction rate constants of ozone, OH, and NO_3 with alkenes (alk), and OH molar yield from ozone + alkene reactions, for alkenes from Logue et al. (2011)

	$k_{O_3\text{-alk}}$ ($\text{ppb}^{-1} h^{-1}$)	$k_{OH\text{-alk}}$ ($\text{ppb}^{-1} h^{-1}$)	$k_{NO_3\text{-alk}}$ ($\text{ppb}^{-1} h^{-1}$)	y_{OH}
Alkenes ¹				(–)
2-Carene	2.04E-02	7.1E+03	1.7E+03	0.85
d-Limonene	1.83E-02	1.5E+04	1.1E+03	0.86
α -Pinene	7.71E-03	4.6E+03	5.5E+02	0.85
3-Carene	3.28E-03	7.8E+03	8.1E+02	0.85
Styrene	1.51E-03	5.1E+03	1.3E+02	0.37
b-Pinene	1.33E-03	6.8E+03	2.2E+02	0.35
Isoprene	1.13E-03	8.9E+03	6.2E+01	0.27
1,3-Butadiene	5.59E-04	5.9E+03	9.0E+00	0.08
Crotonaldehyde	1.40E-04	3.0E+03	5.3E-01	0.2
Acrolein	2.57E-05	1.8E+03	2.8E-01	0
1,2,4-Trimethylbenzene	8.87E-07	2.9E+03	1.6E-01	0
Benzene	8.87E-07	1.1E+02	2.7E-03	0
Xylene, m/p	8.87E-07	1.6E+03	3.2E-02	0

Oxidant + alkene reaction rates from Atkinson (2000) and Master Chemical Mechanism v3.2, and molar yields for OH from Weschler and Shields (1996), with some estimated

the Weschler and Shields (1996) paper estimated OH in a low NO_x environment and only considered reactions R3 and R6 in Table 1. Further, due to its short lifetime indoors of about 1/10 of a second, OH can be computed as achieving as pseudo

steady-state concentration using concepts in Eqs. (5), (6), and (7), resulting in Eq. (8):

$$C_{\text{OH,ss}} = \frac{\lambda C_{\text{OH,out}} + C_{\text{O}_3} \sum y_{\text{OH,alk}} k_{\text{O}_3-\text{alk}} C_{\text{alk}}}{\lambda + v_{d,\text{OH}} \frac{A}{V} + \sum k_{\text{OH-VOC}} C_{\text{VOC}}} \quad (8)$$

The steady-state formulation in Eq. (8) contains sources of OH in the numerator and losses in the denominator (with general form as in Eq. (3)). The source of OH from outdoor air is shown, but it is negligible compared with that due to the totality of reactions of ozone with all alkenes indoors. The losses of OH of air exchange and surface deposition are also shown, but they are also practically negligible as compared to the loss of OH with reactions of VOCs indoors. Using an expression like this one with typical indoor alkene and VOC concentrations, Weschler and Shields (1996) estimated indoor OH concentrations at $\sim 10^5$ – 10^6 molec/cm³.

Modeling Indoor Particulate Matter Concentrations

General Particulate Matter Concentration Balance

The next few sections focus on the modeling of physical and chemical processes pertaining to particles in indoor environments. Particles are composed of organic and inorganic constituents that exist in a state of dynamic equilibrium between gas and particle phases, so aerosol mass is impacted by gas- or particle-phase reactions that cause chemical evolution of the aerosol and/or changes in thermodynamic states (e.g., temperature). Before discussing chemical transformation of aerosols, this section first outlines the modeling of particles considered as static entities (i.e., no phase change), offering an initial framework for elaboration.

Similar to the gas-phase chemistry modeling section above, Eq. (1) can be cast in a form indicative of parameters for the modeling of a well-mixed, static particle concentration, C_P ($\mu\text{g}/\text{m}^3$), with respect to time in a single zone, as shown in Eq. (9) (Nazaroff and Cass 1989):

$$\frac{dC_P}{dt} = s_{P,\text{out}} C_{P,\text{out}} + \frac{E_P}{V} - l_{AE} C_P - v_{d,P} \frac{A}{V} C_P \quad (9)$$

where $s_{P,\text{out}}$ (h^{-1}) is the source rate of outdoor particles, l_{AE} (h^{-1}) is the total loss rate due to all air exchange rates, and other parameters are analogous to previous equations but for particle concentrations. The parameters $s_{P,\text{out}}$ and l_{AE} account for an expanded air exchange framework from that shown in the gas-phase chemistry concentration balance in Eq. (5), since particle loss rates differ by airflow type (and different building types have different airflow types).

The parameter $s_{P,\text{out}}$ accounts for the various outdoor particle introduction possibilities with outdoor air exchange mechanisms, as shown in Eq. (10):

$$s_{\text{P,out}} = (1 - \eta)\lambda_{\text{mv}} + p\lambda_i + \lambda_{\text{nv}} \quad (10)$$

where λ_{mv} , λ_i , and λ_{nv} (h^{-1}) are mechanical ventilation, infiltration, and natural ventilation air exchange rates, respectively; η is the filtration efficiency; and p is the penetration of particles through the building envelope. Similarly, the l_{AE} parameter accounts for various losses due to air exchange mechanisms, as shown in Eq. (11):

$$l_{\text{AE}} = \lambda_{\text{mv}} + \lambda_i + \lambda_{\text{nv}} + \eta\lambda_r \quad (11)$$

where λ_r (h^{-1}) is the recirculation air exchange rate, and the product of η and λ_r is the loss rate by filtration in the recirculation air. Equation (9) can be written in terms of concentration of bulk particle mass ($\mu\text{g}/\text{m}^3$) or in terms of particle number ($\#/ \text{cm}^3$) on a number- or size-resolved basis (El Orch et al. 2014; Nazaroff 2004; Riley et al. 2002).

Simulating Indoor Secondary Organic Aerosol

Equation (9) is written for static particles sourced from outdoors or indoor emissions that do not undergo phase transformations. However, this chapter focuses on indoor chemistry modeling, so we now discuss modeling secondary organic aerosol (SOA), which is the most studied aspect of indoor chemistry with respect to particles. Organic aerosol is a system of compounds, ranging in volatility over many orders of magnitude, that are in a state of dynamic equilibrium between gas and particle phases. SOA is formed following oxidation of VOCs, generated when functionalized, low-volatility products like acids or peroxides undergo net partitioning from the gas-to-particle phase, thereby increasing OA mass. Indoors, SOA is likely most often due to reactions of ozone and terpenoids (Waring 2014).

Considering a particle population of only indoor formed SOA, a concentration balance for SOA, C_{SOA} ($\mu\text{g}/\text{m}^3$), with respective to time, t (h), as in Eq. (12):

$$\frac{dC_{\text{SOA}}}{dt} = P_{\text{SOA}} - l_{\text{AE}}C_{\text{SOA}} - v_{\text{d,SOA}} \frac{A}{V} C_{\text{SOA}} \quad (12)$$

where P_{SOA} ($\mu\text{g}/\text{m}^3\text{-h}$) is the source of net formation of SOA, and all other variables are the same or analogous to that in Eq. (9). The indoor-SOA formation rate can be modeled at various levels of complexity. As an example, for the reaction between concentrations of ozone, C_{O_3} (ppb), and a terpenoid, C_{terp} (ppb), the simplest way to represent P_{SOA} is:

$$P_{\text{SOA}} = Y_{\text{SOA}} k_{\text{O}_3-\text{terp}} C_{\text{O}_3} C_{\text{terp}} \Gamma_{\text{terp}} \quad (13)$$

where Y_{SOA} (–) is the SOA yield, and Γ_{terp} ($(\mu\text{g}/\text{m}^3)/\text{ppb}$) is a temperature-dependent conversion factor change units of the terpenoid from units of mixing ratio to mass concentration (Waring 2014; Youssefi and Waring 2012). By knowing Y_{SOA} along

with the reactant concentrations and the reaction rate constant between them, SOA formation can be estimated.

However, using a correct SOA yield, Y_{SOA} , for SOA formation is less straightforward than using a molar yield for product formation due to a single chemical reaction (e.g., y_F in R6). The earliest version of the SOA yield follows a format presented in the seminal paper, Odum et al. (1996), which derived a framework that builds upon the concept of absorptive partitioning theory developed by Pankow (1994a, 1994b), as in Eq. (14):

$$Y_{\text{SOA}} = \frac{\Delta C_{\text{SOA}}}{\Delta \text{ROG}} = C_{\text{OA}} \sum_i \left(\frac{\alpha_i K_{\text{gp},i}}{1 + K_{\text{gp},i} C_{\text{OA}}} \right) \quad (14)$$

where Y_{SOA} is defined as in the first equality as the change in SOA concentration, ΔC_{SOA} ($\mu\text{g}/\text{m}^3$), divided by the change in the reactive organic gas concentration, ΔROG ($\mu\text{g}/\text{m}^3$). The second equality in Eq. (11) was derived by Odum et al. (1996) and demonstrates that Y_{SOA} can be expressed as the summed effect of gas-to-particle partitioning of a set of individual reaction products, i , resulting from any organic gas oxidation. In that equality, C_{OA} ($\mu\text{g}/\text{m}^3$) is the concentration of any organic aerosol (i.e., not only SOA); α_i is the fractional mass yield of product i of the total ROG reacted; and $K_{\text{gp},i}$ ($\text{m}^3/\mu\text{g}$) is the gas-to-particle partitioning coefficient of product i to the OA phase at equilibrium.

As shown in Eq. (14), Y_{SOA} increases with the total organic particle concentration (C_{OA}), which includes any background OA in addition to the formed SOA, so Y_{SOA} is not a constant value, and yield curves vary non-linearly when the SOA or OA concentration changes. Yield curves are fit to data from SOA formation chamber experiments. Early papers fit data to Eq. (14) by assuming formation was attributable to just two hypothetical products (Griffin et al. 1999; Hoffmann et al. 1997; Odum et al. 1996)—with one being an average of lower-vapor-pressure compounds and the other being an average of higher-vapor-pressure compounds. However, this “two-product” approach was problematic because its parameters have high covariance (Presto and Donahue 2006) and fitted parameters could vary widely for the same SOA formation dataset.

To overcome this issue, Donahue et al. (2006) developed the “volatility basis set” (VBS) approach, which allows more hypothetical products but sets the volatility parameters for those products (represented by the $K_{\text{pg},i}$ in Eq. (14)) based on spacing organic matter product bins in a logical, constrained manner. In the VBS, the volatility parameter of choice is the effective saturation concentration, c_i^* ($\mu\text{g}/\text{m}^3$), which is the concentration above which condensation will occur (where $c_i^* = 1/K_{\text{pg},i}$). In the VBS, the SOA yield is typically called the aerosol mass fraction, ξ or AMF, and so Eq. (14) can be recast as Eq. (15):

$$\xi = \frac{\Delta C_{\text{SOA}}}{\Delta \text{ROG}} = \sum_i \alpha_i \xi_i = \sum_i \alpha_i \left(1 + \frac{c_i^*}{C_{\text{OA}}} \right)^{-1} \quad (15)$$

Table 3 Mass yields (α_i) over four c_i^* bins for common terpenoids for use in Eq. (15)

	$\log_{10}c^*$			
Terpenoid ¹	0	1	2	3
d-Limonene UB	0.34	0.28	0.32	0.59
d-Limonene	0.096	0.039	0.096	0.18
α -Pinene	0.055	0.09	0.12	0.18
β -Pinene	0.044	0.072	0.12	0.22
Camphepane	0.032	0.052	0.12	0.2
α -Terpinene	0.045	0.073	0.12	0.21
$\Delta 3$ -Carene	0.04	0.066	0.1	0.16

Mass yields from Lane et al. (2008); Waring (2014, 2016)

The VBS constrains the c_i^* bins at logarithmic spacing, for example, $c_i^* = (0.01, 0.1, 1, 10, 100, 1000 \mu\text{g}/\text{m}^3)$, and the number of bins can change depending on the data or application. Now, SOA formation chamber data is parameterized by only fitting α_i for each c_i^* bin.

Table 3 shows VBS data for SOA formation due to ozonolysis of select terpenoids, including the mass-based yields (α_i) over four c^* bins spanning 1 to $10^3 \mu\text{g}/\text{m}^3$. Each terpenoid has one set of α_i , except for d-limonene because unlike the other terpenoids it has two double bonds instead of one double bond. So, d-limonene mass yields fall between an upper and a lower bound (UB, LB), dictated by whether the reaction is ozone or limonene limited. Waring (2016) developed a parameterization of the AMF for d-limonene using UB and LB AMF values as a function of the initial ozone/limonene ratio and air exchange rate (see that paper for further details).

Volatility is a function of temperature, since higher temperatures increase vapor pressures of organic compounds. The VBS allows the shifting of c_i^* bins to account for any temperature likely to be encountered indoors with the Clausius-Clapeyron equation, as in:

$$c_i^*(T_{298 \text{ K}}) = c_i^*(T) \frac{T_{298 \text{ K}}}{T} \exp \left(\frac{\Delta H_i}{R} \left(\frac{1}{T_{298 \text{ K}}} - \frac{1}{T} \right) \right) \quad (16)$$

where $c_i^*(T_{298 \text{ K}})$ is the c_i^* at a reference temperature of 298 K; ΔH_i (kJ/mol) is the enthalpy of vaporization for product bin i , which has been parameterized as $\Delta H_i = -11 \times \log_{10}(c_i^*) + 129$ (Epstein et al. 2010); and R (kJ/K-mol) is the ideal gas constant. AMF values are typically reported for an assumed density of 1 g/cm³, and this so-called unit-density (ρ_{unit}) AMF can account for an actual measured or modeled density (ρ) by scaling it by ρ/ρ_{unit} .

The AMF approach (and SOA yield before it) is by far the most common way to model SOA formation in the indoor (and outdoor) air literature. For more details on this method, please see the papers Youssefi and Waring (2012) and Waring (2014). However, another approach has been used in conjunction with models that explicitly model chemical mechanisms (Carslaw et al. 2012; Sarwar et al. 2003; Sarwar and Corsi 2007). These papers predict a large set of organic products yielded by VOC oxidation (e.g., 100 s) and then predict kinetic partitioning of each compound to the

organic particle phase using the equilibrium partitioning parameter, $K_{\text{pg},i}$, and expressions to convert $K_{\text{pg},i}$ to absorption and desorption kinetic partitioning parameters. See those referenced papers for more details on this alternative method.

Simulating Indoor Organic Aerosol

All organic aerosols (OAs), not just SOA, exist as a system of 100 s or 1000 s of compounds in a state of dynamic equilibrium, with relative fractions of each compound in the gas versus particle phase determined by their volatility, which span over ten orders of magnitude from semivolatile to extremely low-volatile compounds (Seinfeld and Pandis 2016). Changes in thermodynamic state variables such as the temperature and relative humidity (RH) can cause net re-partitioning to occur, and so the relative fractions in gas versus particle phase will redistribute.

The VBS approach was introduced in the previous section to model SOA formation indoors. However, the VBS framework can also be used to model any OA type by lumping the entirety of the available organic material (OM) that can partition, no matter the source of the OM, into the set of log-spaced volatility bins constrained at log-spaced intervals of c^* . With any OM VBS, the partitioning can be predicted with a more general form of Eq. (15), as in Eq. (17):

$$\xi_i = \left(1 + \frac{c_i^*}{C_{\text{OA}}} \right)^{-1} \quad C_{\text{OA}} = \sum_i \xi_i C_{\text{OM},i} \quad (17)$$

where $C_{\text{OM},i}$ ($\mu\text{g}/\text{m}^3$) is the indoor OM mass concentration at a particular c_i^* , considering the total OM in both gas and condensed OA phases (Donahue et al. 2006). Equation (17) must be solved iteratively for C_{OA} . The total indoor $C_{\text{OM},i}$ in each bin is the sum of any OM present due to all OA factors, which considered together yield a single AMF and absorbing OA mass indoors.

As stated, the VBS considers the presence of multiple OA factors indoors, where each OA factor is the result of a different source. OA factors can be resolved from measurements with aerosol mass spectrometry (AMS) using positive matrix factorization (Cappa and Jimenez 2010). For instance, ambient OA resolves into VBS factors of hydrocarbon-like OA (HOA, a surrogate for freshly emitted OA due to anthropogenic activity), biomass burning OA (BBOA, a surrogate for OA associated with combustion and woodsmoke), oxygenated OA (OOA, a surrogate for SOA formed by reactions in the atmosphere), among others. This OOA can be further resolved into semivolatile (SV-OOA, surrogate for OOA that is fresh due to recent reactions) and low-volatility (LV-OOA, surrogate for OOA that is older and aged) subsets. Furthermore, indoor VBS OA factors can include those from cooking OA (COA, surrogate for OA due to cooking activities) or indoor-SOA (SOA-in, surrogate for OA due to chemical reactions occurring indoors). VBS profiles for some of these OA factors are demonstrated in Fig. 1.

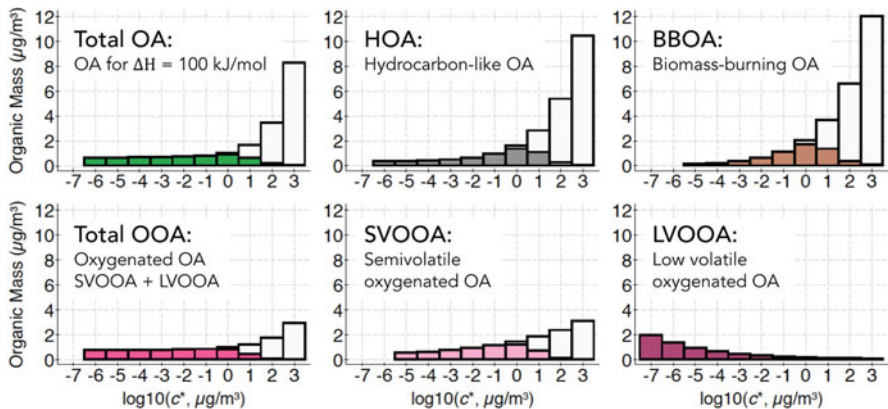


Fig. 1 Volatility basis set (VBS) profiles for organic material (OM) for six different OA factors, with each scaled to realize an OA concentration of $6 \mu\text{g}/\text{m}^3$ (from Cappa and Jimenez 2010)

Figure 1 was constructed using outdoor OM profiles determined from AMS measurements along with a thermodenuder during the MILAGRO outdoor air quality study in Mexico City (Cappa and Jimenez 2010). In Fig. 1, there are 11 c^* bins for OM that range in volatility \log_{10} spaced from 10^{-7} to $10^3 \mu\text{g}/\text{m}^3$. Cappa and Jimenez (2010) provided exponential fits that describe the VBS shapes of the OM distributions as a function of c^* , and those were used to scale the total OM such that the partitioning Eq. (9) yielded a COA for each VBS case of $6 \mu\text{g}/\text{m}^3$. As defined, the lower-volatility OM has an AMF of unity and resides totally in the particle phase, while the high-volatility OM is in the gas phase. When a bin's c^* equals the OA concentration, the OM is half in the gas and half in the particle phase.

The VBS approach outlined so far is also called the one-dimensional VBS (or 1D-VBS), since it organizes the OM into bins based on only one parameter, c^* . Therefore, all of the individual compounds comprising the OM with a particular volatility are lumped into the appropriate c^* bin without any information about the molecular properties or chemical composition. This approach is rather coarse, since, for example, OM in a higher-volatility c^* bin could comprise fresh, unoxidized HOA or low-molecular-weight, highly oxidized compounds.

To resolve this issue and provide more detail, a second-generation VBS framework was developed, called the two-dimensional VBS (or 2D-VBS), which allows tracking and accounting of the average chemical composition of OM in each c^* bin. In addition to organizing compounds by volatility (c^*) alone, the 2D-VBS adds a second organizing dimension of degree of oxygenation, which is parameterized by the ratio of oxygen atoms to carbon atoms (O:C) or average oxidation state (Donahue et al. 2011, 2012). Though the partitioning of the OM into the OA phase is still only a function of c^* alone in the 2D-VBS, the knowledge of the fractional amount of OM with a particular O:C in each c^* bin allows the calculation of other aerosol parameters, such as aerosol density, water content, or phase state

(Cummings et al. 2020). It also allows the computation of the evolution of bin-resolved OM as it reacts with OH indoors (Cummings and Waring 2019).

Under the VBS framework, rather than tracking the concentration of aerosol indoors, the concentration of OM due to different OA factors (e.g., HOM for HOA factor, BBOM for BBOA factor, OOM for OOA factor) is tracked using mass balance techniques, using modified forms of Eq. (1). Doing so requires resolving the OM into aerosol- and gas-phase constituents at each modeled time, since the aerosol portion of the OM (i.e., the OA) experiences different loss rates than the gas-phase OM portion. For instance, OA is lost irreversibly to surface deposition and filtration, while gaseous OM is not. See Cummings and Waring (2019) and Cummings et al. (2020) and the supplemental information within those articles for more detailed modeling of indoor OA using the 2D-VBS in indoor settings.

Simulating Indoor Inorganic Aerosol

Particulate matter broadly consists of a mix of organic compounds, inorganic compounds, and in most cases with appreciable humidity, aerosol associated water. While the previous sections discussed indoor organic aerosol treatments, this one discusses inorganic aerosol modeling. Inorganic aerosol components are fewer in number than organic ones, but with a mass often on the same order. The primary inorganic aerosol components are salts such as ammonium nitrate and ammonium sulfate (these are most common, but there are others), elemental carbon, and geologic minerals. Particle-phase ammonium nitrate (NH_4NO_3) is in thermodynamic equilibrium with its related gas-phase compounds of ammonia (NH_3) and nitric acid (HNO_3), and ammonium sulfate ($(\text{NH}_4)_2\text{SO}_4$) is in a similar condition with ammonium and sulfuric acid (H_2SO_4).

The inorganic salts may exist in the aerosol in a dry form in their crystalline phase, or they may exist in the aerosol as dissociated ions in aqueous solutions, where the state is determined by the relative humidity (RH) of the surrounding air, as the aerosol can take on water. Moreover, the mass of water associated with inorganic aerosols exposed to RH increases and decreases exhibits hysteresis. That is, dry salt aerosol takes up no water with increasing humidity until a critical RH is reached. At this point (i.e., at the deliquescence RH, DRH), the salt deliquesces and suddenly takes on a discrete amount of water. After the DRH, further RH increases incrementally enhance the aerosol water mass. However, with decreasing RH, an aqueous salt gradually loses water until crystallization occurs at an RH value lower the DRH, when its particular efflorescence RH (ERH) is reached. At this point below the ERH, the inorganic salt no longer attracts water, and the aerosol water mass approaches zero (Seinfeld and Pandis 2016).

Inorganic aerosol modeling indoors is less developed than organic aerosol modeling. The first models attempted to simulate ammonium nitrate behavior indoors, since ammonium nitrate partitioning between particle- and gas-phases exhibits a strong temperature dependence and indoor-outdoor temperature gradients are common in winter and summer seasons (Avery et al. 2019; Johnson et al. 2017).

For instance, Lunden et al. (2003) derived methods to describe the evaporation indoors of particle-phase ammonium nitrate to NH₃ and HNO₃ gases as a function of indoor temperature and relative humidity, and the developed model well recreated experimental data measured in a residence. Recently, Xie and Zhao (2020) adapted this method to account for size-resolved ammonium nitrate behavior.

Newer generation indoor inorganic models are likely to follow the frameworks used outdoors; that is, they may use the inorganic aerosol simulation tools of ISORROPIA and AIOMFAC. The first, ISORROPIA (Fountoukis and Nenes 2007; Nenes et al. 1998, 1999), is commonly used in outdoor chemical transport models. ISORROPIA considers inorganic aerosol components alone, by simulating thermodynamic equilibrium aerosol partitioning in the H₂SO₄, NH₃, HNO₃, HCl, Na⁺, H₂O system, and its newer version ISORROPIA-II additionally considers Ca²⁺, K⁺, and Mg²⁺ and their related salts. The second model, AIOMFAC (Zuend et al. 2008), is a more detailed benchmark style tool, and it considers inorganic and organic compound interactions in aqueous aerosol and allows determination of gas-liquid, solid-liquid, and liquid-liquid equilibria conditions in organic/inorganic multicomponent aerosol solutions.

Surface Chemistry Modeling

The remainder of this chapter largely focuses on the modeling of physical and chemical processes occurring on surfaces indoors. Due to high surface-to-volume ratios in buildings, interactions of gaseous species and indoor surfaces are abundant indoors. Gas-surface interactions consist of several physicochemical processes: turbulent and gas diffusion in the boundary layer, sorption to and desorption from the surface, surface-bulk exchange, bulk diffusion, as well as chemical reactions at the surface and in the bulk. For the description of heterogeneous and multiphase chemistry on indoor surfaces, a yield-based, surface byproduct chemistry modeling framework and also kinetic flux model framework with universally applicable rate equations and parameters for mass transport and chemical reactions can be applied (Pöschl et al. 2007).

Simulating Surface Chemistry Byproduct Formation

Let us again discuss a reaction so as to demonstrate the model framework, this time centered around simulating the fate of any reactant O and formed byproduct K. Consider that K that can be generated indoors by O reacting on a surface, such that R3 can be cast as:



In reaction R3, a molecule O reacts with molecules sorbed to an indoor surface or a molecule that is a constituent of the surface material itself, but R3 shows a

simplified representation as O reacting with a generic molecule on the surface, called Y_{surf} . R3 contains a parameter y_K , called the molar yield of K, which is typically fractional and is the molar ratio of the molar change of product to reactant in R3.

Similar to the gas-phase and particle-phase chemistry modeling sections above, Eq. (1) can be cast in a form indicative of parameters for the modeling of a well-mixed zone with byproduct K formation at values of concentration, C_K (ppb), this time due to surface reactions as in R3, with respect to time, as shown in Eq. (18):

$$\frac{dC_K}{dt} = P_{\text{surf},K} + \lambda C_{K,\text{out}} + \frac{E_K}{V} - r_K C_K - \lambda C_K \quad (18)$$

where the terms in Eq. (18) that correspond to surface-phase chemistry are $P_{\text{surf},K}$ (ppb/h), which is the formation rate of K due to occurrences as in R3. Other terms in Eq. (18) are analogous to those in Eq. (5), so they are not redefined.

The specific formulation for the term in Eq. (18) of the surface-phase chemistry formation rate for the concentration C_K due to R3, P_F (ppb/h), is as in Eq. (19):

$$P_{\text{surf},K} = y_K v_{d,O} \frac{A}{V} C_O \quad (19)$$

where the strength of the byproduct K formation is due to the combination of parameters of the concentration of O, C_O (ppb); the reaction rate of O on surfaces, which is the combination of the deposition velocity of O to surfaces, $v_{d,O}$ (m/h), and the surface-to-volume ratio, A/V ; and the molar yield of K due to that surface reaction of O, y_K . Therefore, the rate of overall byproduct K formation increases as the yield increases, as the deposition to the surface increases, or as the total amount of available surfaces increases.

This framework was primarily developed to accommodate treatment of ozone reactions on indoor surfaces and associated byproduct formation. As demonstrated above, ozone reacts in the gas phase with unsaturated VOCs (primarily terpenoids), but ozone also strongly reacts on surfaces indoors. Indeed, absence of large indoor VOC emissions, surface reactions are typically the dominant loss mechanism of ozone in buildings (Weschler 2000), and aldehydes are a common byproduct of this reaction. See Wang and Morrison (2006) for the measurement of molar yields of aldehydes due to ozone reactions on surfaces in real homes, and Waring and Siegel (2013) and Wang and Waring (2014) for chamber measurements of SOA formed by ozone surface reactions. This byproduct formation framework just offered is the simplest treatment of indoor surface reaction modeling, and the next sections explore other issues in more detail.

Modeling Transport Within Boundary Layer

To interact with surfaces, reactants must transport from the bulk air to surface through the fluid mechanical boundary layer, which is composed of a region of

slower-moving air adjacent to the surface that transitions to a region of higher-velocity air in the bulk phase. In the upper/outer region of the boundary layer, transport may be dominated by turbulent eddy dispersion or for laminar flow, shear dispersion, while transport of molecules is dominated by molecular diffusion in the quiescent region nearest the surface. The boundary layer theory simplifies the system by assuming that there is a well-mixed region outside the boundary layer, but the air within the boundary layer is quiescent and diffusion dominates transport (Morrison et al. 2019).

The governing equation of the fluid mechanics of the boundary layer with a gradient of turbulent eddy diffusion is described as follows (Lai and Nazaroff 2000):

$$\frac{d}{dy} \left((D_{g,X} + \varepsilon_p) \frac{d[X]}{dy} \right) + R_X = k_X [X] \quad (20)$$

where $[X]$ (cm^{-3}) is the concentration of a species X; k_X (s^{-1}) is the decay rate constant by all mechanisms of species X (s^{-1}); D_X (cm^2/s) is the gas-phase diffusivity of species X; and R_X ($\text{cm}^{-3} \text{s}^{-1}$) is the production rate of species X. Also, ε_p is the eddy diffusion coefficient, where it has the formulation of $\varepsilon_p = K_e y^m$ and K_e is the turbulence intensity, which may vary from ~ 0.1 to 10 s^{-1} indoors and m is in the range of 2 to 3 and is often valued at 2 (Lai and Nazaroff 2000).

In the absence of turbulence (e.g., $K_e = 0$) in a quiescent boundary layer, diffusion is the dominant transport mechanism, and net transport only occurs perpendicular to the surface. Equation (20) is simplified so the concentration $[X]$ is given by:

$$D_{g,X} \frac{d^2[X]}{dy^2} + R_X = k_X [X] \quad (21)$$

The concentration at the upper limit of the boundary layer is equal to the concentration in the well-mixed region of room air (e.g., bulk room air), as expressed in Eq. (22):

$$[X] = \frac{R_X}{k_X} \text{ at } y = \delta \quad (22)$$

The boundary layer thickness, δ (cm), is typically from 0.5 to > 2 cm, depending on the mixing conditions or temperature gradients between surface and room air (Cano-Ruiz et al. 1993). The concentration at the surface for a species with a very high uptake coefficient (e.g., hydroxyl radicals, OH) may be assumed to be equal to 0, so that:

$$[X] = 0 \text{ at } y = 0 \quad (23)$$

With these boundary conditions, Eq. (19) can be solved analytically to yield $[X]$ throughout the boundary layer, with the following solution in Eq. (24) (Morrison et al. 2019):

$$[X] = \frac{R_X}{k_X} \left(1 - e^{-\sqrt{\frac{k_X}{D_{g,X}}} y} \right) \quad (24)$$

In the presence of eddy turbulence and complex boundary conditions, Eq. (20) may need to be solved numerically. Additionally, instead of solving partial differential equations, recently a kinetic multilayer modeling approach has been used that allows to describe and simulate the system with multiple species and chemical reactions in the boundary layer (Morrison et al. 2019). The model treats gas-phase boundary layer with a number of layers, and the mass balance of species is described with a series of ordinary differential equations, which can be solved numerically. Depending on the complexity of the system of interest, unlimited numbers of species and chemical reactions can be flexibly added and treated.

Modeling Surface Processes

Once the gas molecules are transported through the boundary layer to the near-surface gas phase which is one mean free path away from the surface, they may collide to the surface. Based on kinetic theory and model framework (Pöschl et al. 2007), the gas kinetic flux of X colliding with the surface $J_{\text{coll},X}$ ($\text{cm}^{-2} \text{ s}^{-1}$) can be expressed as in Eq. (25):

$$J_{\text{coll},X} = \frac{[X]_{\text{gs}} \omega_X}{4} \quad (25)$$

where $[X]_{\text{gs}}$ (cm^{-3}) is the near-surface gas-phase concentration of X; and ω_X (cm/s) is the mean thermal velocity given by $\omega_X = (8 RT / (\pi M_X))^{1/2}$, where M_X (g/mol) is the molar mass of X; R is the gas constant; and T (K) is the absolute temperature. The flux of adsorption of gas molecules $J_{\text{ads},X}$ ($\text{cm}^{-2} \text{ s}^{-1}$) on the surface can be expressed as:

$$J_{\text{ads},X} = \alpha_{s,X} J_{\text{coll},X} \quad (26)$$

where $\alpha_{s,X}$ is surface accommodation coefficient, which represents the probability that X undergoes adsorption upon collision with the surface. The parameter $\alpha_{s,X}$ is determined by the surface accommodation coefficient on an adsorbate-free surface $\alpha_{s,0,X}$ and the sorption layer coverage θ , which is given by the sum of the fractional surface coverage of all adsorbate species:

$$\alpha_{s,X} = \alpha_{s,0,X} (1 - \theta) \quad (27)$$

The parameter $\alpha_{s,0,X}$ can be addressed by molecular dynamics simulations, and for instance, $\alpha_{s,0,X}$ is close to unity for indoor-relevant semivolatile compounds on skin lipids (von Domaros et al. 2020). For a single adsorbate system, $\theta = \sigma_{s,X} [X]_s$,

where $[X]_s$ (cm^{-2}) is the surface concentration of X; and $\sigma_{s,X}$ (cm^2) is the molecular cross section of X.

The adsorbed molecules can thermally desorb back into the gas phase. Desorption, the inverse of adsorption, can be described by a first-order rate coefficient. The flux of desorption of gas molecules, $J_{\text{des},X}$ ($\text{cm}^{-2} \text{ s}^{-1}$), can be expressed as in Eq. (28):

$$J_{\text{des},X} = k_{d,X}[X]_s \quad (28)$$

where $k_{d,X}$ (s^{-1}) is a first-order desorption rate coefficient. Since molecules are desorbed thermally, the parameter $k_{d,X}$ depends strongly on temperature, which can be described by an Arrhenius equation, as in Eq. (29):

$$k_{d,X} = A \cdot \exp \left(\frac{\Delta H_{\text{ads},X}}{RT} \right) \quad (29)$$

where A is a pre-exponential factor, which is approximately the vibrational frequency of a molecule bound to the surface (typically $\sim 10^{12}$ to 10^{14} s^{-1}); $\Delta H_{\text{ads},X}$ (kJ/mol) is adsorption enthalpy. The parameter $k_{d,X}$ is an inverse of the desorption lifetime $\tau_{d,X}$ ($= 1/k_{d,X}$), which is the mean residence time on the surface in the absence of surface reactions and surface-bulk transport processes. The parameter $\Delta H_{\text{ads},X}$ can be measured experimentally, and $\tau_{d,X}$ can be estimated by molecular dynamics simulations. For example, limonene adsorbs on a silica (SiO_2) surface with $\Delta H_{\text{ads},X} = 55 \text{ kJ/mol}$ and $\tau_{d,X} = \sim 25 \mu\text{s}$ (Fang et al. 2019).

In the presence of surface reaction with the loss rate of $L_{s,X}$ ($\text{cm}^{-2} \text{ s}^{-1}$), the surface mass balance and rate equation for surface concentration of X can be described as in Eq. (30):

$$\frac{d[X]_s}{dt} = J_{\text{ads},X} - J_{\text{des},X} - L_{s,X} \quad (30)$$

For a system with single adsorbate X under steady-state conditions ($d[X]_s/dt = 0$) in the absence of surface reactions ($L_{s,X} = 0$), the surface coverage θ can be described by combining Eqs. (23), (24), (25), and (26), with the result as in Eq. (31):

$$\theta = \frac{K_{\text{ads}}[X]_{\text{gs}}}{1 + K_{\text{ads}}[X]_{\text{gs}}} \quad (31)$$

where K_{ads} ($= \alpha_{s,0,X} \omega_X \sigma_{s,X} / (4 k_{d,X})$) is the Langmuir adsorption equilibrium constant. Equation (31) describes the Langmuir adsorption isotherm, which indicates that surface coverage saturates at high gas-phase concentration.

The uptake coefficient of X, a probability that a collision of X with the surface leads to net uptake of X, can be expressed as a ratio between the net flux of X from the gas phase to the condensed phase, $J_{\text{net},X}$ ($\text{cm}^{-2} \text{ s}^{-1}$), and $J_{\text{coll},X}$, as in Eq. (32):

$$\gamma_X = \frac{J_{\text{net},X}}{J_{\text{coll},X}} = \frac{J_{\text{ads},X} - J_{\text{des},X}}{J_{\text{coll},X}} \quad (32)$$

Bear in mind that the parameter γ_X is time dependent, and it reaches eventually zero for non-reactive uptake at equilibrium. For reactive uptake under steady-state conditions (e.g., $d[X]_s/dt = 0$), the parameter $\gamma_X = L_{s,X} / J_{\text{coll},X}$; hence, γ_X is also termed as reaction probability, which is often reported in experimental studies, and is a component in the deposition velocity theory.

The deposition velocity is a mass transfer coefficient used to describe irreversible removal of reactive gases at indoor surfaces. A conceptual model was developed by Cano-Ruiz et al. (1993), which combines mass transport and surface kinetics under three model airflow conditions: (1) forced laminar convection flow parallel to a flat plate, (2) laminar natural convection flow along an isothermal vertical plate, and (3) homogeneous turbulence in an enclosure. For the third case, the deposition velocity, $v_{d,X}$ (cm/s), of X can be described by a combination of the transport-limited deposition velocity, v_t (cm/s), and surface uptake deposition velocity, v_s (cm/s), as (Cano-Ruiz et al. 1993):

$$v_{d,X} = \left(\frac{1}{v_{t,X}} + \frac{1}{v_{s,X}} \right)^{-1} \quad (33)$$

where the transport-limited deposition velocity is:

$$v_{t,X} = D_{g,X}^{(1-1/m)} K_e^{(1/m)} \quad (34)$$

and the surface uptake deposition velocity is:

$$v_{s,X} = \frac{\gamma_X \omega_X}{4} \quad (35)$$

With above equations, the uptake coefficient and deposition velocity are shown to be related. Particularly, surface reaction rates are one of two rate-limiting aspects of the overall deposition velocity, with boundary layer transport being the other. At a particular transport condition, when the uptake coefficient is large and exceeds a certain threshold value, the deposition velocity reaches a constant value, with its overall rate being mainly controlled by transport through the boundary layer and thus depending on the flow conditions.

Finally, bulk diffusion is an important mechanism for species transport in bulk compartments such as in surface reservoirs or human skin, and it can be described with Fick's law of diffusion. Fick's first law indicates that the diffusion flux is proportional to the concentration gradient. The bulk diffusion flux of X, $J_{b,X}$ ($\text{cm}^{-2} \text{s}^{-1}$), can be expressed using a bulk diffusion coefficient, $D_{b,X}$ (cm^2/s), as in Eq. (36):

$$J_{b,X} = -D_{b,X} \frac{d[X]_b}{dx} \quad (36)$$

where $[X]_b$ (cm^{-3}) is the bulk concentration of X at any position x . Fick's second law describes the time evolution of $[X]_b$ with a partial differential equation, in the case of one-dimensional diffusion, as in Eq. (37):

$$\frac{\partial [X]_b}{\partial t} = -D_{b,X} \frac{\partial^2 [X]_b}{\partial x^2} \quad (37)$$

For the description of bulk diffusion within spherical particles, $[X]_b$ can be described as:

$$\frac{\partial [X]_b}{\partial t} = -\frac{D_{b,X}}{r^2} \frac{\partial}{\partial r} \left(r^2 \frac{\partial [X]_b}{\partial r} \right) \quad (38)$$

To solve these partial differential equations, the following boundary conditions are often employed: (1) the concentration at the surface (or near-surface bulk) is fixed over time at equilibrium value, as determined by vapor pressure, solubility, or partitioning coefficient; (2) the flux of X at the core is zero ($\partial[X]_b/\partial r|_{r=0} = 0$), and (3) the flux of X at both surface and core is zero ($\partial[X]_b/\partial r|_{r=r_p} = \partial[X]_b/\partial r|_{r=0} = 0$).

Modeling Skin Chemistry Example

As a good example for indoor surface chemistry modeling that integrates different modeling approaches with molecular to room scales, let us discuss ozone reactions with human skin lipids, which affect concentrations of ozone and organic compounds (byproducts) substantially (Wisthaler and Weschler 2010). The skin is covered by $\sim 0.45 \mu\text{m}$ thick skin oil, of which a large component is squalene (Kligman 1963). The stratum corneum is the outermost part of the skin and consists of 15–20 layers of dead flattened cells with a thickness of $\sim 25 \mu\text{m}$ (Egawa et al. 2007). The viable epidermis is the skin below the stratum corneum and consists of living cells with a thickness of $\sim 100 \mu\text{m}$ (Reddy et al. 2000).

Force field-based molecular dynamics simulations can be applied to simulate ozone interactions with squalene (proxy for skin oil), as in Fig. 2a (von Domaros et al. 2020). The surface mass accommodation coefficient can be calculated from the statistical fates of hundreds of ozone impingement trajectories, and the desorption lifetime from the statistics of the lifetime that ozone resides on the squalene surface before desorbing. Henry's law constant for ozone entering squalene can be calculated using an enhanced sampling method wherein external forces are used to pull the ozone molecule from the gas phase through the squalene-air interface and into the bulk squalene liquid.

The kinetic multilayer model of surface and bulk chemistry of the skin and clothing was developed, which explicitly resolves mass transport and chemical reactions in the gas phase, in clothing, in the gap between clothing and skin and in the skin, as in Fig. 2b (Lakey et al. 2019). The model includes different layers: a gas phase, a boundary layer, the clothing, the gap between the clothing and skin, a

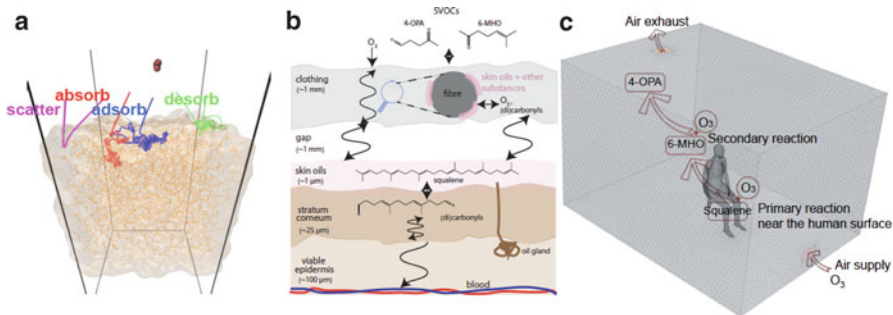


Fig. 2 Modeling skin ozonolysis with different approaches, bridging molecular to room scales. **(a)** Molecular dynamics simulations of ozone molecules in squalene, showing fates of trajectories of ozone molecules directed at the surface of a slab squalene from the gas. **(b)** A schematic of the kinetic multilayer model for interactions of O₃ with skin and clothing. Ozone can react with squalene forming volatile and semivolatile carbonyl products such as 4-OHA and 6-MHO. **(c)** Illustration of the geometry input to the computation fluid dynamics model for chemical reactions near and at the human surface. Reproduced from Shiraiwa et al. (2019) with permission from the Royal Society of Chemistry

sorption layer, the skin oil, the stratum corneum, the viable epidermis, and a layer of blood vessels (Lakey et al. 2017, 2019). It can simulate ozone reactions with human skin by treating chemical reactions and mass transport of ozone, skin lipid squalene, and oxidation products at the skin and in the gas phase (Lakey et al. 2017). It enables the spatial and temporal concentration profiles of species in the skin oil and underlying skin layers to be resolved. In the clothing, diffusion can be slowed down due to partitioning of chemical species to skin oils and other substances covering the fibers, as simulated by human envelope models by Morrison et al. (2016, 2017). Contact transfer between the upper layer of the skin and the clothing is also treated. Required kinetic parameters included surface accommodation coefficients, desorption lifetimes, gas-phase and bulk diffusion coefficients, partitioning coefficients, contact transfer rates, and reaction rate coefficients.

For examination of the spatial distributions of ozone and ozonolysis products, computational fluid dynamics (CFD) modeling can be applied to simulate surface reactions and gas-phase chain reactions in indoor environments. Outputs from the kinetic flux model including the ozone uptake coefficient and the product yields can be used as inputs in a CFD model, allowing analysis of spatial distribution of ozone, and primary and secondary carbonyl products throughout a room (Won et al. 2019, 2020). The CFD model solves time- and space-resolved concentrations iteratively based on heat, momentum, and mass balances in the discretized space with specific convergence criteria (Nielsen 2015; Rim et al. 2009; Sørensen and Weschler 2002). The model results reveal non-uniform indoor airflow distribution and transport of oxidants and reactants under different ventilation conditions (Rim et al. 2009). Figure 2c shows a CFD model that simulates the perihuman environment. The computational grids and the boundary conditions are treated to predict local velocity gradient near the human body and recirculating indoor airflow with reasonable

accuracy. Mass transport equations considering chemical reaction can be applied to each cell of the simulation domain (Launder and Spalding 1974), as in Eq. (39):

$$\frac{\partial}{\partial t}(\rho C_i) + \frac{\partial}{\partial x_j}(\rho u_j C_i) = \frac{\partial}{\partial x_j}\left(\rho D_i \frac{\partial C_i}{\partial x_j}\right) + R_i + S_i \quad (39)$$

where ρ is air density, u_j is air velocity, C_i is the mole fraction of chemical species, R_i is the reaction source term, D_i is molecular diffusion coefficient, and S_i is source term. The CFD solution calculates the effects of convection, diffusion (both molecular and turbulent), chemical reaction, and source emissions. The CFD modeling demonstrated that primary product concentrations are elevated in the breathing zone compared to the rest of the room (Lakey et al. 2019). Overall, the novel combination of MD simulations to constrain parameters, the kinetic model, and the CFD simulations resulted in insights into how to improve indoor air quality, reduce exposure, and design future experiments.

Acknowledgments This work was supported by the Chemistry of Indoor Environments program of the Alfred P. Sloan Foundation. MSW was supported by grant G-2017-10011. MSW and MS were supported by the Modelling Consortium for Chemistry of Indoor Environments (MOCCIE), under grant numbers G-2017-9796 and G-2019-12306.

References

- Atkinson R (2000) Atmospheric chemistry of VOCs and NOx. *Atmos Environ* 1994(34): 2063–2101. [https://doi.org/10.1016/S1352-2310\(99\)00460-4](https://doi.org/10.1016/S1352-2310(99)00460-4)
- Atkinson R, Arey J (2003) Gas-phase tropospheric chemistry of biogenic volatile organic compounds: a review. *Atmos Environ* 37:197–219. [https://doi.org/10.1016/S1352-2310\(03\)00391-1](https://doi.org/10.1016/S1352-2310(03)00391-1)
- Atkinson R, Baulch DL, Cox RA, Hampson RF, Kerr JA, Troe J (1992) Evaluated kinetic and photochemical data for atmospheric chemistry: supplement IV. IUPAC subcommittee on gas kinetic data evaluation for atmospheric chemistry. *J Phys Chem Ref Data* 21:1125–1568. <https://doi.org/10.1063/1.555918>
- Avery AM, Waring MS, DeCarlo PF (2019) Seasonal variation in aerosol composition and concentration upon transport from the outdoor to indoor environment. *Environ Sci Process Impacts* 21:528–547. <https://doi.org/10.1039/C8EM00471D>
- Cano-Ruiz JA, Kong D, Balas RB, Nazaroff WW (1993) Removal of reactive gases at indoor surfaces: combining mass transport and surface kinetics. *Atmos Environ Part Gen Top* 27: 2039–2050. [https://doi.org/10.1016/0960-1686\(93\)90276-5](https://doi.org/10.1016/0960-1686(93)90276-5)
- Cappa CD, Jimenez JL (2010) Quantitative estimates of the volatility of ambient organic aerosol. *Atmos Chem Phys* 10:5409–5424. <https://doi.org/10.5194/acp-10-5409-2010>
- Carslaw N (2007) A new detailed chemical model for indoor air pollution. *Atmos Environ* 41: 1164–1179. <https://doi.org/10.1016/j.atmosenv.2006.09.038>
- Carslaw N, Mota T, Jenkin ME, Barley MH, McFiggans G (2012) A significant role for nitrate and peroxide groups on indoor secondary organic aerosol. *Environ Sci Technol* 46:9290–9298. <https://doi.org/10.1021/es301350x>
- Criegee R (1975) Mechanism of ozonolysis. *Angew Chem Int Ed Engl* 14:745–752. <https://doi.org/10.1002/anie.197507451>
- Cummings B, Waring MS (2019) Predicting the importance of oxidative aging on indoor organic aerosol concentrations using the two-dimensional volatility basis set (2D-VBS). *Indoor Air* 29(4):616–629. <https://doi.org/10.1111/ina.12552>

- Cummings B, Li Y, DeCarlo P, Shiraiwa M, Waring M (2020) Indoor aerosol water content and phase state in U.S. residences: impacts of relative humidity, aerosol mass and composition, and mechanical system operation. *Environ Sci Process Impacts* 22:2031–2057. <https://doi.org/10.1039/D0EM00122H>
- Dols WS, Polidoro BJ, 2020. CONTAM user guide and program documentation version 3.4. National Institute of Standards and Technology. <https://doi.org/10.6028/NIST.TN.1887r1>
- Donahue NM, Robinson AL, Stanier CO, Pandis SN (2006) Coupled partitioning, dilution, and chemical aging of semivolatile organics. *Environ Sci Technol* 40:2635–2643. <https://doi.org/10.1021/es052297c>
- Donahue NM, Epstein SA, Pandis SN, Robinson AL (2011) A two-dimensional volatility basis set: 1. Organic-aerosol mixing thermodynamics. *Atmos Chem Phys* 11:3303–3318. <https://doi.org/10.5194/acp-11-3303-2011>
- Donahue NM, Kroll JH, Pandis SN, Robinson AL (2012) A two-dimensional volatility basis set – Part 2: diagnostics of organic-aerosol evolution. *Atmos Chem Phys* 12:615–634. <https://doi.org/10.5194/acp-12-615-2012>
- Egawa M, Hirao T, Takahashi M (2007) In vivo estimation of stratum corneum thickness from water concentration profiles obtained with Raman spectroscopy. *Acta Derm Venereol* 87:4–8. <https://doi.org/10.2340/00015555-0183>
- El Orch Z, Stephens B, Waring MS (2014) Predictions and determinants of size-resolved particle infiltration factors in single-family homes in the U.S. *Build Environ* 74:106–118. <https://doi.org/10.1016/j.buildenv.2014.01.006>
- Epstein SA, Riipinen I, Donahue NM (2010) A semiempirical correlation between enthalpy of vaporization and saturation concentration for organic aerosol. *Environ Sci Technol* 44:743–748. <https://doi.org/10.1021/es902497z>
- Fang Y, Lakey PS, Riahi S, AT MD, Shrestha M, Tobias DJ, Shiraiwa M, Grassian VH (2019) A molecular picture of surface interactions of organic compounds on prevalent indoor surfaces: limonene adsorption on SiO₂. *Chem Sci* 10:2906–2914. <https://doi.org/10.1039/C8SC05560B>
- Fountoukis C, Nenes A (2007) ISORROPIA II: a computationally efficient thermodynamic equilibrium model for K⁺–Ca²⁺–Mg²⁺–NH₄⁺–Na⁺–SO₄²⁻–NO₃⁻–Cl⁻–H₂O aerosols. *Atmos Chem Phys* 7:4639–4659. <https://doi.org/10.5194/acp-7-4639-2007>
- Gómez-Alvarez E, Amedro D, Afif C, Gligorovski S, Schoemaecker C, Fittschen C, Doussin J-F, Wortham H (2013) Unexpectedly high indoor hydroxyl radical concentrations associated with nitrous acid. *Proc Natl Acad Sci* 110:13294–13299. <https://doi.org/10.1073/pnas.1308310110>
- Griffin RJ, Cocker DR, Flagan RC, Seinfeld JH (1999) Organic aerosol formation from the oxidation of biogenic hydrocarbons. *J Geophys Res Atmos* 104:3555–3567. <https://doi.org/10.1029/1998JD100049>
- Hoffmann T, Odum JR, Bowman F, Collins D, Klockow D, Flagan RC, Seinfeld JH (1997) Formation of organic aerosols from the oxidation of biogenic hydrocarbons. *J Atmos Chem* 26:189–222. <https://doi.org/10.1023/A:1005734301837>
- Johnson AM, Waring MS, DeCarlo PF (2017) Real-time transformation of outdoor aerosol components upon transport indoors measured with aerosol mass spectrometry. *Indoor Air* 27: 230–240. <https://doi.org/10.1111/ina.12299>
- Kligman AM (1963) The uses of sebum. *Br J Dermatol* 75:307–319. <https://doi.org/10.1111/j.1365-2133.1963.tb13567.x>
- Kowal SF, Allen SR, Kahan TF (2017) Wavelength-resolved photon fluxes of indoor light sources: implications for HO_x production. *Environ Sci Technol* 51:10423–10430. <https://doi.org/10.1021/acs.est.7b02015>
- Kroll JH, Seinfeld JH (2008) Chemistry of secondary organic aerosol: formation and evolution of low-volatility organics in the atmosphere. *Atmos Environ* 42:3593–3624. <https://doi.org/10.1016/j.atmosenv.2008.01.003>
- Lai AC, Nazaroff WW (2000) Modeling indoor particle deposition from turbulent flow onto smooth surfaces. *J Aerosol Sci* 31:463–476. [https://doi.org/10.1016/S0021-8502\(99\)00536-4](https://doi.org/10.1016/S0021-8502(99)00536-4)
- Lakey PSJ, Wisthaler A, Berkemeier T, Mikoviny T, Pöschl U, Shiraiwa M (2017) Chemical kinetics of multiphase reactions between ozone and human skin lipids: implications for indoor air quality and health effects. *Indoor Air* 27:816–828. <https://doi.org/10.1111/ina.12360>

- Lakey PSJ, Morrison GC, Won Y, Parry KM, von Domaros M, Tobias DJ, Rim D, Shiraiwa M (2019) The impact of clothing on ozone and squalene ozonolysis products in indoor environments. *Commun Chem* 2:1–8. <https://doi.org/10.1038/s42004-019-0159-7>
- Lane TE, Donahue NM, Pandis SN (2008) Simulating secondary organic aerosol formation using the volatility basis-set approach in a chemical transport model. *Atmos Environ* 42:7439–7451. <https://doi.org/10.1016/j.atmosenv.2008.06.026>
- Lauder BE, Spalding DB (1974) The numerical computation of turbulent flows. *Comput Methods Appl Mech Eng* 3:269–289. [https://doi.org/10.1016/0045-7825\(74\)90029-2](https://doi.org/10.1016/0045-7825(74)90029-2)
- Logue JM, McKone TE, Sherman MH, Singer BC (2011) Hazard assessment of chemical air contaminants measured in residences. *Indoor Air* 21:92–109. <https://doi.org/10.1111/j.1600-0668.2010.00683.x>
- Lunden MM, Revzan KL, Fischer ML, Thatcher TL, Littlejohn D, Hering SV, Brown NJ (2003) The transformation of outdoor ammonium nitrate aerosols in the indoor environment. *Atmos Environ* 37:5633–5644. <https://doi.org/10.1016/j.atmosenv.2003.09.035>
- Morrison GC, Weschler CJ, Bekö G (2016) Dermal uptake directly from air under transient conditions: advances in modeling and comparisons with experimental results for human subjects. *Indoor Air* 26:913–924. <https://doi.org/10.1111/ina.12277>
- Morrison GC, Weschler CJ, Bekö G (2017) Dermal uptake of phthalates from clothing: Comparison of model to human participant results. *Indoor Air* 27:642–649. <https://doi.org/10.1111/ina.12354>
- Morrison G, Lakey PSJ, Abbatt J, Shiraiwa M (2019) Indoor boundary layer chemistry modeling. *Indoor Air* 29:956–967. <https://doi.org/10.1111/ina.12601>
- Nazaroff WW (2004) Indoor particle dynamics. *Indoor Air* 14:175–183. <https://doi.org/10.1111/j.1600-0668.2004.00286.x>
- Nazaroff WW, Alvarez-Cohen L (2001) Environmental engineering science. Wiley, New York
- Nazaroff WW, Cass GR (1986) Mathematical modeling of chemically reactive pollutants in indoor air. *Environ Sci Technol* 20:924–934. <https://doi.org/10.1021/es00151a012>
- Nazaroff WW, Cass GR (1989) Mathematical modeling of indoor aerosol dynamics. *Environ Sci Technol* 23:157–166. <https://doi.org/10.1021/es00179a003>
- Nazaroff WW, Weschler CJ (2004) Cleaning products and air fresheners: exposure to primary and secondary air pollutants. *Atmos Environ* 38:2841–2865. <https://doi.org/10.1016/j.atmosenv.2004.02.040>
- Nenes A, Pandis SN, Pilinis C (1998) ISORROPIA: a new thermodynamic equilibrium model for multiphase multicomponent inorganic aerosols. *Aquat Geochem* 4:123–152. <https://doi.org/10.1023/A:1009604003981>
- Nenes A, Pandis SN, Pilinis C (1999) Continued development and testing of a new thermodynamic aerosol module for urban and regional air quality models. *Atmos Environ* 33:1553–1560. [https://doi.org/10.1016/S1352-2310\(98\)00352-5](https://doi.org/10.1016/S1352-2310(98)00352-5)
- Nielsen PV (2015) Fifty years of CFD for room air distribution. *Build Environ* 91:78–90. <https://doi.org/10.1016/j.buildenv.2015.02.035>
- Nøjgaard JK (2010) Indoor measurements of the sum of the nitrate radical, NO₃, and nitrogen pentoxide, N₂O₅ in Denmark. *Chemosphere Oxf* 79:898–904. <https://doi.org/10.1016/j.chemosphere.2010.02.025>
- Odum JR, Hoffmann T, Bowman F, Collins D, Flagan RC, Seinfeld JH (1996) Gas/particle partitioning and secondary organic aerosol yields. *Environ Sci Technol* 30:2580–2585. <https://doi.org/10.1021/es950943+>
- Pankow JF (1994a) An absorption model of gas/particle partitioning of organic compounds in the atmosphere. *Atmos Environ* 28:185–188. [https://doi.org/10.1016/1352-2310\(94\)90093-0](https://doi.org/10.1016/1352-2310(94)90093-0)
- Pankow JF (1994b) An absorption model of the gas/aerosol partitioning involved in the formation of secondary organic aerosol. *Atmos Environ* 28:189–193. [https://doi.org/10.1016/1352-2310\(94\)90094-9](https://doi.org/10.1016/1352-2310(94)90094-9)
- Pöschl U, Rudich Y, Ammann M (2007) Kinetic model framework for aerosol and cloud surface chemistry and gas-particle interactions – Part 1: general equations, parameters, and terminology. *Atmos Chem Phys* 7:5989–6023. <https://doi.org/10.5194/acp-7-5989-2007>

- Presto AA, Donahue NM (2006) Investigation of α -pinene + ozone secondary organic aerosol formation at low total aerosol mass. *Environ Sci Technol* 40:3536–3543. <https://doi.org/10.1021/es052203z>
- Reddy MB, Guy RH, Bunge AL (2000) Does epidermal turnover reduce percutaneous penetration? *Pharm Res* 17:1414–1419. <https://doi.org/10.1023/A:1007522200422>
- Riley WJ, McKone TE, Lai ACK, Nazaroff WW (2002) Indoor particulate matter of outdoor origin: importance of size-dependent removal mechanisms. *Environ Sci Technol* 36:200–207. <https://doi.org/10.1021/es010723y>
- Rim D, Novoselec A, Morrison G (2009) The influence of chemical interactions at the human surface on breathing zone levels of reactants and products. *Indoor Air* 19:324–334. <https://doi.org/10.1111/j.1600-0668.2009.00595.x>
- Sarwar G, Corsi R (2007) The effects of ozone/limonene reactions on indoor secondary organic aerosols. *Atmos Environ* 41:959–973. <https://doi.org/10.1016/j.atmosenv.2006.09.032>
- Sarwar G, Corsi R, Kimura Y, Allen D, Weschler CJ (2002) Hydroxyl radicals in indoor environments. *Atmos Environ* 36:3973–3988. [https://doi.org/10.1016/S1352-2310\(02\)00278-9](https://doi.org/10.1016/S1352-2310(02)00278-9)
- Sarwar G, Corsi R, Allen D, Weschler C (2003) The significance of secondary organic aerosol formation and growth in buildings: experimental and computational evidence. *Atmos Environ* 37:1365–1381. [https://doi.org/10.1016/S1352-2310\(02\)01013-0](https://doi.org/10.1016/S1352-2310(02)01013-0)
- Seinfeld JH, Pandis SN (2016) Atmospheric chemistry and physics: from air pollution to climate change. John Wiley & Sons, Incorporated, Wiley-Blackwell, New York
- Shiraiwa M, Carslaw N, Tobias DJ, Waring MS, Rim D, Morrison G, Lakey PS, Kruza M, Von Domaros M, Cummings BE, Won Y (2019) Modelling consortium for chemistry of indoor environments (MOCCIE): integrating chemical processes from molecular to room scales. *Environ Sci Process Impacts* 21:1240–1254. <https://doi.org/10.1039/C9EM00123A>
- Singer BC, Revzan KL, Hotchi T, Hodgson AT, Brown NJ (2004) Sorption of organic gases in a furnished room. *Atmos Environ* 1994(38):2483–2494. <https://doi.org/10.1016/j.atmosenv.2004.02.003>
- Sørensen DN, Weschler CJ (2002) Modeling-gas phase reactions in indoor environments using computational fluid dynamics. *Atmos Environ* 1994(36):9–18. [https://doi.org/10.1016/S1352-2310\(01\)00479-4](https://doi.org/10.1016/S1352-2310(01)00479-4)
- Spicer CW, Kenny DV, Ward GF, Billick IH (1993) Transformations, lifetimes, and sources of NO₂, HONO, and HNO₃ in indoor environments. *Air Waste* 43:1479–1485. <https://doi.org/10.1080/1073161X.1993.10467221>
- von Domaros M, Lakey PSJ, Shiraiwa M, Tobias DJ (2020) Multiscale modeling of human skin oil-induced indoor air chemistry: combining kinetic models and molecular dynamics. *J Phys Chem B* 124:3836–3843. <https://doi.org/10.1021/acs.jpcb.0c02818>
- Wang H, Morrison GC (2006) Ozone-initiated secondary emission rates of aldehydes from indoor surfaces in four homes. *Environ Sci Technol* 40:5263–5268. <https://doi.org/10.1021/es060080s>
- Wang C, Waring MS (2014) Secondary organic aerosol formation initiated from reactions between ozone and surface-sorbed squalene. *Atmos Environ* 84:222–229. <https://doi.org/10.1016/j.atmosenv.2013.11.009>
- Waring MS (2014) Secondary organic aerosol in residences: predicting its fraction of fine particle mass and determinants of formation strength. *Indoor Air* 24:376–389. <https://doi.org/10.1111/ina.12092>
- Waring MS (2016) Secondary organic aerosol formation by limonene ozonolysis: parameterizing multi-generational chemistry in ozone- and residence time-limited indoor environments. *Atmos Environ* 144:79–86. <https://doi.org/10.1016/j.atmosenv.2016.08.051>
- Waring MS, Siegel JA (2013) Indoor secondary organic aerosol formation initiated from reactions between ozone and surface-sorbed d-limonene. *Environ Sci Technol* 47:6341–6348. <https://doi.org/10.1021/es400846d>
- Waring MS, Wells JR (2015) Volatile organic compound conversion by ozone, hydroxyl radicals, and nitrate radicals in residential indoor air: magnitudes and impacts of oxidant sources. *Atmos Environ* 106:382–391. <https://doi.org/10.1016/j.atmosenv.2014.06.062>

- Wells JR (2005) Gas-phase chemistry of α -terpineol with ozone and OH radical: rate constants and products. *Environ Sci Technol* 39:6937–6943. <https://doi.org/10.1021/es0481676>
- Weschler CJ (2000) Ozone in indoor environments: concentration and chemistry. *Indoor Air* 10: 269–288. <https://doi.org/10.1034/j.1600-0668.2000.010004269.x>
- Weschler CJ, Shields HC (1996) Production of the hydroxyl radical in indoor air. *Environ Sci Technol* 30:3250–3258. <https://doi.org/10.1021/es960032f>
- Weschler CJ, Shields HC, Naik DV (1994) Indoor chemistry involving O₃, NO, and NO₂ as evidenced by 14 months of measurements at a site in Southern California. *Environ Sci Technol* 28:2120–2132. <https://doi.org/10.1021/es00061a021>
- Wisthaler A, Weschler CJ (2010) Reactions of ozone with human skin lipids: Sources of carbonyls, dicarbonyls, and hydroxycarbonyls in indoor air. *Proc Natl Acad Sci* 107:6568–6575. <https://doi.org/10.1073/pnas.0904498106>
- Won Y, Waring M, Rim D (2019) Understanding the spatial heterogeneity of indoor OH and HO₂ due to photolysis of HONO using computational fluid dynamics simulation. *Environ Sci Technol*. <https://doi.org/10.1021/acs.est.9b06315>
- Won Y, Lakey PSJ, Morrison G, Shiraiwa M, Rim D (2020) Spatial distributions of ozonolysis products from human surfaces in ventilated rooms. *Indoor Air* 30:1229–1240. <https://doi.org/10.1111/ina.12700>
- Xie Y, Zhao B (2020) A chemical dynamic model for the infiltration of outdoor size-resolved ammonium nitrate aerosols to indoor environments. *Indoor Air* 30:275–283. <https://doi.org/10.1111/ina.12629>
- Young CJ, Zhou S, Siegel JA, Kahan TF (2019) Illuminating the dark side of indoor oxidants. *Environ Sci Process Impacts* 21:1229–1239. <https://doi.org/10.1039/C9EM00111E>
- Youssefi S, Waring MS (2012) Predicting secondary organic aerosol formation from terpenoid ozonolysis with varying yields in indoor environments. *Indoor Air* 22:415–426. <https://doi.org/10.1111/j.1600-0668.2012.00776.x>
- Zuend A, Marcolli C, Luo BP, Peter T (2008) A thermodynamic model of mixed organic-inorganic aerosols to predict activity coefficients. *Atmos Chem Phys* 8:4559–4593. <https://doi.org/10.5194/acp-8-4559-2008>

Part VII

Human Exposure to Indoor Pollutants



Fundamentals of Exposure Science

34

Andrea R. Ferro and Philip K. Hopke

Contents

Introduction	986
What Is Exposure Science?	986
Link Between Exposure Science and Indoor Air Quality, Toxicology, and Epidemiology	987
Exposure Definitions	988
Basic Exposure Model	989
Direct Versus Indirect Exposure Assessment	990
Direct Exposure Assessment (Measurement)	990
Indirect Exposure Assessment (Modeling)	995
Intake Fraction	997
Conclusions	998
References	998

Abstract

This chapter is an overview of exposure concepts related to indoor air pollutants and serves as an introduction to the other chapters in this section. Other sections of this handbook provide details on sampling, analysis, and/or monitoring of pollutants in the indoor environment. This chapter focuses on inhalation exposure, although the concepts can be applied to dermal and non-dietary ingestion exposure routes. To estimate inhalation exposure, it is necessary to combine

A. R. Ferro

Department of Civil and Environmental Engineering, Clarkson University, Potsdam, NY, USA

Institute for a Sustainable Environment, Clarkson University, Potsdam, NY, USA

e-mail: aferro@clarkson.edu

P. K. Hopke (✉)

Institute for a Sustainable Environment, Clarkson University, Potsdam, NY, USA

Department of Public Health Sciences, University of Rochester School of Medicine and Dentistry, Rochester, NY, USA

e-mail: phopke@clarkson.edu

pollutant concentrations with the time for which an individual or group of people are in contact with that concentration. The estimate of exposures allows the determination of the relationships between exposure to the pollutant and the potential adverse outcomes. Exposure is the link between the built environment and health effects due to the conditions within that built environment and the time-activity patterns of the occupants.

Keywords

Exposure · Concentration · Time-activity · Models · Measurements

Introduction

Quantifying human exposure is critical for many indoor air quality investigations, including supporting epidemiology studies, risk assessments, development of mitigation strategies, and sustainability efforts for cities and communities. Exposure science puts the target, or receptor, at the center of the investigation and enables the comparison of multiple exposure pathways for prioritizing pollutant sources, informing mitigation strategies, and outlining future research. The exposure science approach is especially important as we address emerging environmental contaminants (e.g., DeLuca et al. 2021). This chapter will define exposure science concepts and review current measurement and modeling methods for estimating inhalation exposure in nonindustrial indoor microenvironments, such as homes, schools, hospitals, and commercial buildings. We will discuss existing as well as promising future approaches for quantifying inhalation exposure.

What Is Exposure Science?

Exposure science is an interdisciplinary field investigating the contact between living organisms and chemical, physical, and biological stressors. Exposure science draws from the disciplines of biology, chemistry, ecology, toxicology, epidemiology, bioethics, medicine, behavioral science, environmental engineering, and others. In 1991, the US National Research Council (NRC) Committee on Advances in Assessing Human Exposure to Airborne Pollutants defined human exposure to a contaminant as “contact at a boundary between a human and the environment with a contaminant of a specific concentration for an interval of time” with units of exposure defined as concentration multiplied by time (NRC 1991). In 2012, the NRC Committee on Human and Environmental Exposure Science in the 21st Century defined exposure science as “the collection and analysis of quantitative and qualitative information needed to understand the nature of contact between receptors (such as people or ecosystems) and physical, chemical, or biologic stressors” (NRC 2012). The exposure science community, primarily led by the International Society for Exposure Science (ISES) and governmental related organizations such as the NRC and World Health

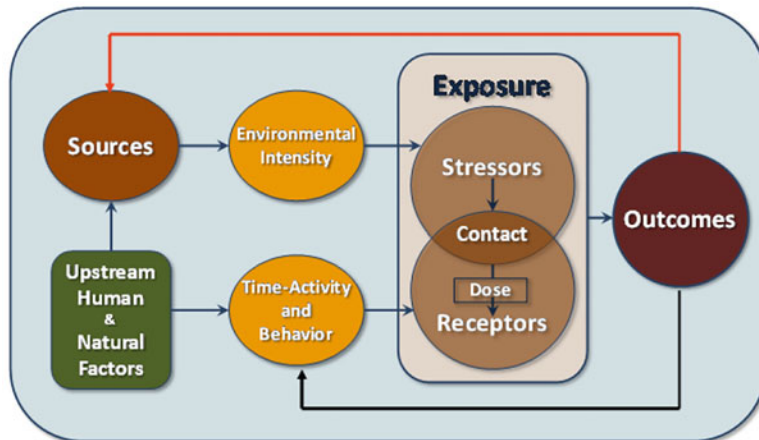


Fig. 1 Core elements of exposure science in conceptual framework. (Reproduced from NRC (2012) and used with permission)

Organization (WHO) International Programme on Chemical Safety (IPCS), have made efforts to identify priorities, enable progress, and standardize terms and definitions related to exposure science, and enable progress (NRC 2012; Zartarian et al. 2005; Environmental Protection Agency 2015).

The exposure science conceptual framework and its core elements are summarized in Fig. 1. Exposure occurs when the stressors are in contact (overlap in space and time) with the receptors. The earlier, classic version of the conceptual framework showed a linear continuum from source to health outcomes, without the feedback loops that impact both the stressors and receptors (NRC 2012). In this handbook, the stressors would be considered indoor chemical, biological, or physical agents that expose an individual. However, lifestyle, social conditions, and behavior are additional stressors that can affect health outcomes, and the study of these factors is an active area of exposure research (Lioy and Smith 2013).

Link Between Exposure Science and Indoor Air Quality, Toxicology, and Epidemiology

Exposure science is closely linked with indoor air quality (IAQ), toxicology, and epidemiology. IAQ links sources to environmental intensity (the top left two bubbles in Fig. 1), characterizing emissions, fate, and transport in the environment. For example, an IAQ study may model or measure the indoor concentration of particulate matter (PM) from an outdoor or indoor source, such as an operating cookstove. Exposure science adds the person or other living entity to determine the overlap between the stressor and receptor in time and space. The field of toxicology links the dose with health outcomes, while the field of epidemiology links the environmental intensity, exposure, or dose (either estimated or measured via

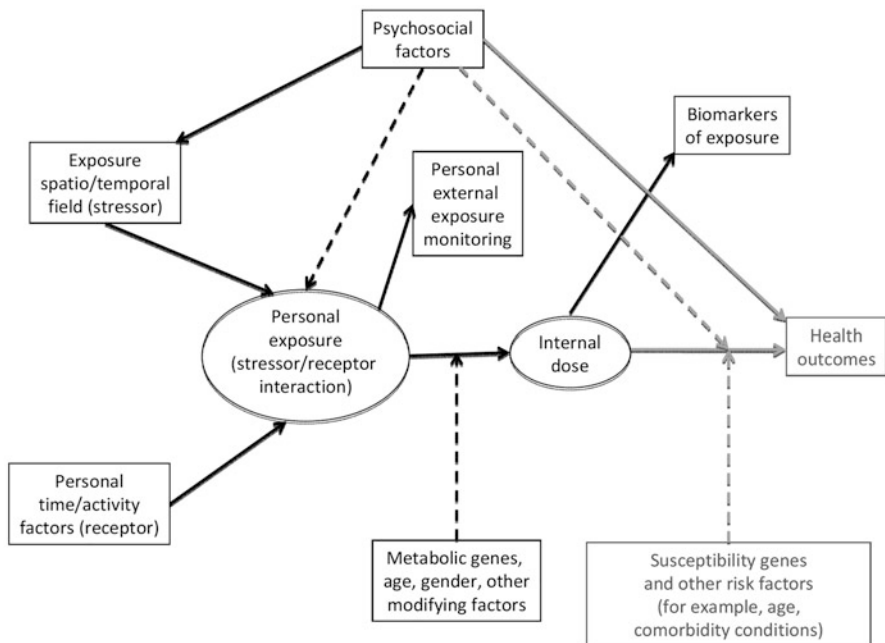


Fig. 2 General schema of exposure assessment in environmental epidemiology (Reproduced from NRC (2012) and used with permission). Items in gray related to health outcomes are considered to be outside the field of exposure science. “Boxes represent measurable quantities, and ovals denote hypothetical intermediate variables that can be assessed only indirectly. Solid arrows denote direct effects, and dashed arrows indicate modifying effects” (NRC 2012)

biomarkers) with health outcomes. As shown in Fig. 2, the conceptual framework from exposure to health effects also incorporates psychosocial and genetic factors. Accordingly, the “exposome” was defined as the “life-course environmental exposures (including lifestyle factors), from the prenatal period onwards” (Wild 2005). As sensor technology, biomonitoring, human genome mapping, geoinformatics, and data analysis techniques explode, big data is bringing these fields closer together.

Exposure Definitions

Efforts to standardize exposure terms and definitions have been ongoing (e.g., Zartarian et al. 1997, 2005; World Health Organization 2001; NRC 2012). Most recently, the US Exposure Science in the 21st Century (ES21) Federal Working Group compiled “The Glossary of Exposure Science Terms,” which is intended to be a living document (EPA 2015). Several exposure terms and definitions are included below (EPA 2015):

Exposure concentration: The exposure mass divided by the contact volume or the exposure mass divided by the mass of contact volume depending on the medium (Zartarian et al. 2005).

Exposure duration: The length of time over which continuous or intermittent contacts occur between an agent and a target. For example, if an individual is in contact with an agent for 10 min a day, for 300 days over a 1-year time period, the exposure duration is 1 year (Zartarian et al. 2005).

Exposure pathway: The course an agent takes from the source to the target (Zartarian et al. 2005).

Exposure route: The way an agent enters a target after contact (e.g., by ingestion, inhalation, or dermal absorption) (Zartarian et al. 2005).

Exposome: As a complementary approach to the genome, the totality of exposures over a lifetime, which predispose and predict health effects in an individual. This assumes that exposure begins in utero, encompasses environmental (including occupational) sources of injuries, irritations, and other stressors including lifestyle and diet, and is dependent upon characteristics of the individual. The exposome is the record of all exposures both internal and external that people receive throughout their lifetime.

Time-averaged exposure: The time-integrated exposure divided by the exposure duration. An example is the daily average exposure of an individual to carbon monoxide. (Also called time-weighted average exposure) (Zartarian et al. 2005).

Time-integrated exposure: The integral of instantaneous exposures over the exposure duration. An example is the area under a daily time profile of personal air monitor readings, with units of concentration multiplied by time (Zartarian et al. 2005).

Basic Exposure Model

Models provide estimates of personal or population exposures by estimating concentrations and by linking concentrations with activity patterns. The most basic exposure model is provided in Eq. (1), where the exposure for person i is calculated by summing the product of the concentration of the stressor in each microenvironment by the time spent by that person in the microenvironment over a designated period (Duan 1982):

$$E_i = \sum_{k=1}^K C_k t_{ik} \quad (1)$$

where:

E_i = total integrated exposure of person i

C_k = concentration of stressor in microenvironment k

t_{ik} = amount of time spent by i in k

K = total number of microenvironments

Direct Versus Indirect Exposure Assessment

There are two key elements to determining exposure to a pollutant: its concentration and the extent of contact by the individual with that specific concentration. Since the focus is on air exposures, the extent would typically be the length of time in a microenvironment in which the airborne pollutant concentration has been measured or modeled. The development of time-activity patterns that can be used to estimate the time duration spent in a specific microenvironment are described in ► [Chap. 37, “Time-Activity Patterns.”](#) This section deals with how the concentration that give rise to exposures can be determined or estimated.

Direct Exposure Assessment (Measurement)

Contributions from Indoor Sources

There are multiple chapters in this handbook describing a variety of indoor air pollution sources including cooking/heating appliances, cooking, consumer products, etc. The issue is then to convert the emissions rates from such sources into indoor air concentrations to which the room occupants are exposed. These models typically apply a mass balance model to estimate the effects of infiltration, exfiltration, sources, indoor chemistry, and sinks on the resulting pollutant concentrations. They can be single or multiple room models and have become more sophisticated as the interest in indoor air quality has increased. Various organization have developed models. The US National Institute of Standards and Technology (NIST) developed Fate and Transport of Indoor Microbial Aerosols (FaTIMA) (Dols et al. 2020) as a well-mixed, single zone simulation model. Another NIST model, CONTAM is a multizone indoor air quality and ventilation analysis program (<https://www.nist.gov/services-resources/software/contam>) described by Dols and Polidoro (2020). Analogous models have been developed for the European Union (MOEBIUS 2017).

The mass balance model (Nazaroff and Cass 1986) provides reasonable long-term simulations of indoor air pollutant concentrations. However, there are other models that attempt to deal with the issue of inhomogeneities and short-term variations in indoor air pollution. Near the source while emissions are occurring, the well-mixed assumption is clearly invalid. For example, Cheng et al. (2011, 2014) describe stochastic modeling of exposure near a source in a naturally ventilated room while Furtaw et al. (1996) modeled indoor air concentrations of a tracer gas at various distances from the source. The effect of the source could be modeled adequately using a two-compartment model. A tiered approach to modeling indoor air concentrations is provided by Keil (2000). The tiered approach begins with simpler models when they are sufficient and develops toward more complex models as needed for the purposes at hand.

Finally, more detailed concentration location information can be derived using computational fluid dynamics models. CFD can be used for detailed analysis that includes pollutant concentration distributions. It can simulate the shape of indoor

spaces and model pollutant diffusion (Murakami et al. 2003; Deng and Kim 2007). CFD can be calculated based on either steady- or unsteady-state behavior depending on the time being simulated. Unsteady CFD simulations are usually used to simulate the change of pollutant concentrations over time. Zhang et al. (2009) used it to analyze airflow and pollutant diffusion in passenger aircraft. Davardoost and Kahforoushan (2018) analyzed acetone, benzene, and toluene concentrations in a laboratory driven by temperature. These models are complex and computationally intensive to provide long-term exposure estimates, but they can provide detailed, time-varying concentration distributions that can be used in other types of models to provide distributions of exposures.

Contribution from Ambient Pollution

Although the focus of this handbook is on indoor air, the ambient (i.e., outdoor) air typically contributes substantially to indoor pollutant concentrations. Indoor concentrations of ambient air pollutants can roughly be predicted via ambient concentrations and the outdoor to indoor air infiltration rate. Infiltration rates are discussed in detail in ► Chap. 10, “Impact of Outdoor Particles on Indoor Air.” Other approaches to estimating outdoor contributions to indoor air are available (e.g., Tang et al. 2018; Taylor et al. 2019). Thus, to provide those ambient concentrations needed to estimate their contribution in indoor pollution, measurements are needed across a spatial domain for the time during which exposures are to be estimated. These data can be obtained in multiple ways.

Regulatory monitoring networks: The focus of almost all monitoring to enforce air quality regulations or guidelines is on ambient air concentrations. Many countries have established air quality monitoring networks to provide data on the concentrations typically of particulate matter (PM_{10} and $PM_{2.5}$), ozone, nitrogen oxides (NO_x), sulfur dioxide (SO_2), carbon monoxide (CO), and in some cases, specific toxic species in PM such as lead in total suspended particles (TSP). In most cases, these networks are maintained and operated by governmental agencies at the national or local levels. However, some jurisdictions contract the operations to private companies or nonprofit groups. An advantage of these networks is that they are generally operated over long periods so that it is possible to assess trends and examine long-term exposures.

Generally, there are well-defined protocols for operating the equipment including appropriate quality assurance/quality control processes and subsequent data validation that provides data with relatively well characterized uncertainties. However, there are also a number of networks where the quality efforts are limited or nonexistent, and thus, it is important to assess the data quality before utilizing it in any modeling on likely indoor air concentrations.

Nonregulatory networks: In the absence of regulatory networks or to supplement them given the expense on establishing and maintaining a regulatory quality network, other monitoring efforts can be mounted ranging from single monitors in a location of interest such as the regulatory quality monitors at many embassies of the United States to networks of low-cost sensors deployed across a large urban area. For example, the South Coast Air Quality Management District (SCAQMD)

that manages air quality in the Los Angeles California area has deployed a network of around 150 low-cost PM sensors. Many of these are deployed at the fence line of possible emission sources to assess the contribution of that facility to local air pollution. However, combining the data from these units with the regulatory monitoring stations can provide a more comprehensive assessment of pollutant concentrations across a complex urban area. The details of measurement methods in low-cost sensors are presented in ► Chap. 19, “Measuring Particle Concentrations and Composition in Indoor Air.” These monitors do not provide as accurate data as regulatory grade units, but their data can be useful if appropriate care is taken in maintaining and calibrating them. SCAQMD has developed a laboratory- and field-testing capability for low-cost monitors. Evaluations of monitors submitted to them for testing are provided at a website they established (<http://www.aqmd.gov/aq-spec>).

The United States Department of State identified air quality as an important issue for its personnel posted to embassies and consulates in cities with substantial air pollution. Their initial monitoring focused on particulate matter starting with a regulatory quality beta attenuation monitor (BAM) installed at its embassy in Beijing in 2008. The data are made publicly available through the US Environmental Protection Agency’s AirNow website (<https://www.airnow.gov/international/us-embassies-and-consulates/>). Although the website presents Air Quality Index (AQI) values, the actual hourly PM_{2.5} data are available for download. In 2021, there were over 60 locations with PM_{2.5} monitors with plans to continue to expand the network. Subsequently, they began adding regulatory ozone monitors at embassies that might have high values.

Satellite data: Another way to account for the spatial variation across an urban area that cannot be determined from a limited regulatory monitoring network is to utilize satellite observational data to estimate ground level PM concentrations. There are now multiple agencies that have launched satellites and provide observational products of airborne pollutants. The most commonly used products are aerosol optical depth (AOD) and gaseous pollutants (CO, O₃, and SO₂). These data are often column depth data meaning that they provide the total concentration per unit area integrated from the ground to the top of the atmosphere. For example, aerosol optical depth is a measure of the extinction of the solar beam by airborne particles that block sunlight by absorbing and/or scattering light. AOD is a measure of the extent to which direct sunlight is prevented from reaching the ground by the particles. There are also estimated surface concentrations. The data from the US National Aeronautics and Space Administration (NASA) can be freely downloaded (<https://search.earthdata.nasa.gov/search?fst0=Atmosphere>).

However, since the satellites are only over any given location typically one time per day, continuous data are not available. New geospatial satellites are being launched to provide continuous, higher resolution data. Generally, these results are processed further to provide higher spatial resolution data. There is an extensive literature on estimating ambient air concentrations from such data. For example, Shin et al. (2020) reviewed approaches to estimating ground-level PM concentrations from satellite data.

Direct Measurement Campaigns

Microenvironment (e.g., *indoor, in-cabin*): People spend their time in a series of microenvironments ranging from the places they sleep and eat to methods of transport to where they work and return to their dwelling. Thus, they may be indoors at home, in a vehicle, or in a workplace. “Indoors” may range from spaces well isolated from the ambient environment to open vehicles or work areas with only a roof to fend off rain. Microenvironments may need to be heated, cooled, and ventilated. Exposures only occur when these spaces are occupied, and the occupants modify the air quality by their emissions such as breathing and sweating as well as from the emissions they induce while there (emissions/chemical reactions on skin; resuspension from clothing and indoor surfaces, etc.) as well as other indoor sources. Thus, there are distributions of pollutant concentrations that need to be determined in all of the potentially inhabited microenvironments. Depending on the objectives of the exposure assessment being done, there can be measurement campaigns in a series of microenvironment using more complex and expensive systems that cannot be extensively replicated, networks of low-cost sensor monitors that can be deployed in multiple locations, or directly monitoring the exposure of specific individuals that can be aggregated to provide likely distributions of exposure for further analysis.

Field Campaigns

Field campaigns can be of relatively short duration or cover extended periods of time in a single location. As an example of short-term characterization of a specific microenvironment, Xu et al. (2010) measured the concentrations of PM₁₀, CO, CO₂, total volatile organic compounds (TVOCs), temperature, and relative humidity in the bedrooms of asthmatic children to test the effectiveness of an in-room air cleaner/ventilator over 6-week periods of the filter in place and another 6 weeks when the filter was removed and the vent blocked with a 2-week washout period in between. Thus, such short-term measurements coupled with physiological measurements allowed the determination of the efficacy of this treatment in reducing their symptoms.

Another example of short-term (several weeks to a few months), single location measurement campaigns is the measurement of the size distributions of the indoor radioactive aerosol produced by the decay of ²²²Rn. Using a unique monitoring system (Ramamurthi and Hopke 1991), measurements were made for 1–2 months) in six houses (Hopke et al. 1995) providing detailed size-dependent exposure data. These data were suitable to estimate the dose from the alpha particles deposited in the respiratory tract of the building occupants, the lung cancer risk, and the resulting uncertainties (Krewski et al. 1999).

An alternative approach is to instrument a building and make measurements in multiple locations over extended periods (several months or longer). Nazaroff and coworkers (Arata et al. 2018; Farmer et al. 2019; Kristensen et al. 2019; Liu et al. 2018, 2019; Lunderberg et al. 2019; Patel et al. 2020; Tian et al. 2018; Wang et al. 2020) made a comprehensive analysis of a single-family residence in Northern California from the ventilation system to the concentrations of various contaminants

(mostly organic) to assessing some of the reservoirs and physical processes that control the airborne concentrations. Thus, detailed exposure assessment to a variety of specific indoor air contaminants can be determined over a sufficient period to provide useful distributions of exposure that can then be part of statistical approaches to exposure and risk assessments.

Sensor Networks

The recent development of low-cost sensors for air pollutants like particulate matter have opened the opportunity for building networks of sensors throughout a building. More information about low-cost sensors is provided in ► Chap. 19, “[Measuring Particle Concentrations and Composition in Indoor Air](#).” Sensor networks can now be deployed to monitor a variety of gaseous pollutants and PM concentrations in multiple rooms with the data reported to a central database via WiFi connections. Commercial systems are being developed and marketed, but they are not yet in widespread use. These systems can be integrated with the building management system to adjust ventilation rates to reduce the pollutant concentrations below preset limits. The current primary use is to ensure CO₂ concentrations do not exceed control limits, but similar control strategies could be applied for PM or any of the other monitored gases including CO, VOCs, etc.

Hegde et al. (2020) describe their study in which a network of research-grade instruments and low-cost sensors were deployed in a home. They used this combination of tools to evaluate the low-cost sensor performance and then characterized the activities and conditions that increased the PM concentrations, and identified how these activities affected the PM levels in different rooms of a home. These data could then be used to estimate exposures if the time spent in each microenvironment during a given type of activity (cooking, cleaning, etc.) could be estimated.

Bi et al. (2021) report indoor/outdoor PM_{2.5} concentration relationships based on low-cost sensor data from 91 buildings (41 residential houses and 50 public/commercial buildings) that were publicly available from the sensor vendor. Thus, a “network” of monitors were available from which infiltration factors could be calculated and the distributions for specific buildings or across areas where multiple monitored buildings were present. Thus, additional spatial and temporal information on pollutant concentration may be available to support exposure assessments in areas being studied and where enough of the residents have installed their own low-cost monitors.

Personal (Breathing Zone)

In the studies described in the preceding section, the exposures would need to be estimated based on some type of measure of occupancy of the subject within given rooms at given times. Thus, these exposures would have some associated uncertainty, but could be extrapolated to multiple individuals. Personal monitoring provides direct measurements in breathing zone for specific environmental agents to provide the exposures to the subjects. These people would generally be enrolled in a cohort study of pollution and resulting health outcomes. This approach has been

used in many prior health effects studies, typically using a pump and instruments contained in a backpack or similar wearable housing. However, now new lighter and more portable systems are available that are more sensitive, able to detect a greater variety of chemical species, and provide geographical locations so that the concentrations of the species measured in specific environments can be determined. In addition, passive samplers for agents like VOCs can provide integrated exposure estimates although it would then not be possible to assign fractional exposures in the various microenvironments that the person occupied.

It is not feasible from a cost or logistical prospective to individually monitor large populations. Some information becomes available from publically available data such as that described by Bi et al. (2021). However, such measurements do not typically cover the entire range of microenvironments in which people may reside. However, if a personal monitoring campaign is properly planned with good information on the locations occupied and the duration of those microenvironmental stays are measured, a database of exposure concentrations for different microenvironments can be developed. Then, modeling of the likely exposures can be performed from the distributions of concentrations and occupancy durations as described in the next section.

Indirect Exposure Assessment (Modeling)

Exposure to an airborne pollutant is the sum of the product of the concentration in a microenvironment times the time spent in that microenvironment for all of the occupied microenvironments. If this information is available for a given individual, then the exposure can be fully assessed. Similarly, if personal monitoring has been done, then again the total exposure for that individual is known although the exposures in any given microenvironment cannot be determined. However, it is not normally possible to obtain such detailed exposures for a large population of individuals. Thus, to assess exposures to be able to relate exposure to health outcomes, it is necessary to model exposures.

Klepeis (2006) provides an introduction to modeling of human exposures to inhaled air pollutants. There needs to be estimates of air pollutant concentrations in the possibly occupied microenvironments and estimates of the time spent in those microenvironments. The time element is provided by time-activity data and is covered in ► [Chap. 37, “Time-Activity Patterns,”](#) of this handbook. To estimate the microenvironmental pollutant concentrations, several different modeling approaches may be needed.

Contribution of Ambient Pollution to Indoor Concentrations

The penetration of ambient pollutants indoors is dealt with in detail in ► [Chap. 10, “Impact of Outdoor Particles on Indoor Air.”](#) Ambient concentrations can be obtained through the measurement approaches described above. However, it is generally not possible to operate spatially detailed monitoring networks over a long time period since they are not part of a regulatory network with government

support to maintain them. To obtain the necessary concentration estimates, these data can be modeled using several types of models.

Land-Use Regression Modeling

Field measurements and detailed geographic information can be combined in land-use regression models to estimate concentrations at specific locations and times within a given spatial domain. These models have been increasingly used over the past 20 years becoming increasingly sophisticated in the amount of input data used and the mathematical tools used to build the models. Masiol et al. (2018) developed a land-use regression (LUR) model from low-cost PM monitor data that predict hourly PM_{2.5} values across Monroe County, New York, while Masiol et al. (2019) used low-cost ozone monitor data to develop a parallel LUR for ozone. Many other similar models have been developed such as for PM and a number of its components across Pittsburgh, PA, based on a network of low-cost monitors for PM and pollutant gases (Jain et al. 2021).

Air Quality Modeling

Alternatively, chemical transport models (Seinfeld and Pandis 2016) can be used to model ambient pollutant concentrations over a spatial domain for extensive periods. The commonly used models are the Community Multiscale Air Quality (CMAQ) model and the Comprehensive Air Quality Model with extensions (CAMx). These models are commonly used by regulatory agencies to assess the impacts of existing or planned new sources of air pollution. It can be used to estimate concentrations down to grid cell sizes of 4 × 4 km. The results have been used in a number of ambient health effects assessments (e.g., Rich et al. 2013). Although there is less spatial specificity than is available from LUR results, the models do not require any monitoring data other than for model evaluations.

Statistical Modeling

In many cases, the interest is in developing distributions of exposure from the distributions of concentrations in multiple microenvironments and the time spent in those environments. The basic concept of this modeling approach is to randomly select a concentration from the distribution of concentrations in a given microenvironment and multiply it by a randomly selected duration of occupancy obtained from the distribution of occupancy times from the time-activity data. These are then averaged over a number of possible occupancies to obtain a distribution of likely exposures. The distributions from multiple environments can be combined to obtain a distribution of total exposures. Clerc et al. (2015) reports the development of statistical models based on 19,000 measurements of 26 common chemical compounds. The model provides geometric means and standard deviations, and a software tool is described that provides rapid estimation of exposures. Keller et al. (2020) report a hierarchical model to estimate exposures to indoor stove emissions in Nepal based on temporally sparse, clustered longitudinal observations.

Intake Fraction

The intake fraction (iF) metric provides a source-to-intake relationship that allows prioritization of sources based on their relative contributions to the intake of a particular pollutant as well as a comparison of multiple exposure routes: inhalation, dermal, and non-dietary ingestion for the same pollutant. Bennett et al. (2002) defined the intake fraction (iF) as “the integrated incremental intake of a pollutant, summed over all exposed individuals, and occurring over a given exposure time, released from a specified source or source class, per unit of pollutant emitted” (Bennett et al. 2002). Here, intake is the crossing of the exposure contact boundary, for example, inhalation through the mouth or nose into the respiratory system (Zartarian et al. 2005). The calculated intake dose does not require diffusion through the subsequent resisting layer, for example, the pollutant may or may not diffuse through the pulmonary region of the respiratory system into the blood stream. For inhalation, iF can be calculated as shown in Eqs. (2) and (3):

$$IF = \frac{\int_{T_1}^{\infty} \left(\sum_{i=1}^P (C_i(t)Q_i(t)) \right) dt}{\int_{T_1}^{T_2} E(t) dt} \quad (2)$$

$$= \frac{COP}{E} \text{ for constant C} \quad (3)$$

where:

C_i = concentration (mass vol⁻¹)

Q_i = breathing rate (vol person⁻¹ time⁻¹)

P = population (persons)

E = emission rate (mass time⁻¹)

T_1 = start time for emission

T_2 = end time for emission

To estimate the health impact of the source, the iF is multiplied by the health impact per mass inhaled and the mass emitted (emission rate in mass per time multiplied by the amount of time the source was emitting). Thus, the change in health impact for various mitigation strategies can be calculated using the iF metric.

Since its introduction, iF has been estimated for many different indoor and outdoor sources with various modeling approaches. For example, Shin, McKone, and Bennett (2012) applied a fugacity-based approach to estimate indoor concentrations and compare iF for a suite of compounds released indoors. In their study, the iF values varied by chemical application mode, with iF values for air release of 10^{-3} , carpet application 10^{-5} to 10^{-3} , and vinyl application 10^{-5} to 10^{-2} . Gao et al. (2013) used real-time measurements and a dispersion modeling approach to calculate iF for different ventilation and found iF values ranging from 10^{-3} to 10^{-5} . Jolliet et al. (2015) used the iF approach to calculate and compare overall exposure to

consumer products. Licina et al. (2017) found a higher iF for seated versus walking persons.

The iF for a pollutant source released indoors is typically three orders of magnitude, or 1000 times, that of a pollutant source released outdoors due to the smaller mixing volume, slower air exchange rate, and large amount of time people spend indoors (Smith 1988; Lai et al. 2000; Nazaroff 2008). Thus, while both indoor and outdoor sources impact indoor air quality, indoor sources have much larger impacts on exposure per gram released.

Conclusions

This section includes chapters that provide more details on many of the topics needed to estimate the exposure of individuals and groups to indoor air contaminants. Details of measurement techniques, monitoring tools, and models are provided elsewhere in this handbook.

References

- Arata C, Zarzana KJ, Misztal PK, Liu Y, Brown SS, Nazaroff WW, Goldstein AH (2018) Measurement of NO_3 and N_2O_5 in a residential kitchen. *Environ Sci Technol Lett* 5:595–599
- Bennett DH, McKone TE, Evans JS, Nazaroff WW, Margni MD, Jolliet O, Smith KR (2002) Defining intake fraction. *Environ Sci Technol* 36:207A–211A
- Bi J, Wallace LA, Sarnat JA, Liu Y (2021) Characterizing outdoor infiltration and indoor contribution of $\text{PM}_{2.5}$ with citizen-based low-cost monitoring data. *Environ Pollut* 276:116763
- Cheng KC, Acevedo-Bolton V, Jiang RT, Klepeis NE, Ott WR, Fringer OB et al (2011) Modeling exposure close to air pollution sources in naturally ventilated residences: association of turbulent diffusion coefficient with air change rate. *Environ Sci Technol* 45:4016–4022
- Cheng KC, Acevedo-Bolton V, Jiang RT, Klepeis NE, Ott WR, Kitanidis PK, Hildemann LM (2014) Stochastic modeling of short-term exposure close to an air pollution source in a naturally-ventilated room: an autocorrelated random walk method. *J Expo Sci Environ Epidemiol* 24:311–318
- Clerc F, Bertrand N, Vincent R (2015) TEXAS: a Tool for EXposure ASsessment-Statistical models for estimating occupational exposure to chemical agents. *Ann Occup Hyg* 59:277–291
- Davardoost F, Kahforoushan D (2018) Health risk assessment of VOC emissions in laboratory rooms via a modeling approach. *Environ Sci Pollut Res* 25:17890–17900
- DeLuca NM, Angrish M, Wilkins A, Thayer K, Cohen Hubal EA (2021) Human exposure pathways to poly- and perfluoroalkyl substances (PFAS) from indoor media: a systematic review protocol. *Environ Int* 146:106308
- Deng B, Kim C (2007) CFD simulation of VOCs concentrations in a resident building with new carpet under different ventilation strategies. *Build Environ* 42:297–303
- Dols WS, Polidoro BJ (2020) CONTAM user guide and program documentation. NIST technical note 1887. Available from <https://www.nist.gov/el/energy-and-environment-division-73200/nist-multizone-modeling/software/contam/documentation>
- Dols WS, Polidoro BJ, Poppdeck D, Emmerich SJ (2020) A tool to model the Fate and Transport of Indoor Microbiological Aerosols (FaTIMA). National Institute of Standards and Technology, Gaithersburg. <https://doi.org/10.6028/nist.Tn.2095.TN2095>
- Duan N (1982) Microenvironment types: a model for human exposure to air pollution. *Environ Int* 8:305–309

- Environmental Protection Agency (2015) Glossary of exposure science terms. Compiled by the Exposure Science in the 21st Century (ES21) Federal Working Group. Retrieved on 22 July 2021. <https://www.epa.gov/innovation/exposure-science-21st-century-federal-working-group>
- Farmer DK, Vance ME, Abbatt JPD, Abeleira A, Alves MR, Arata C, Boedicker E, Bourne S, Cardoso-Saldaña F, Corsi R, DeCarlo PF, Goldstein AH, Grassian VH, Hildebrandt Ruiz L, Jimenez JL, Kahan TF, Katz EF, Mattila JM, Nazaroff WW, Novoselac A, O'Brien RE, Or VW, Patel S, Sankhyan S, Stevens PS, Tian Y, Wade M, Wang C, Zhou S, Zhou Y (2019) Overview of HOMEChem: House Observations of Microbial and Environmental Chemistry. *Environ Sci Processes Impacts* 21:1280–1300
- Furtaw EG, Pandian MD, Nelson DR (1996) Modeling indoor air concentrations in imperfectly mixed rooms. *J Air Waste Manag Assoc* 46:861–868
- Gao J, Cao C, Xiao Q, Xu B, Zhou X, Zhang X (2013) Determination of dynamic intake fraction of cooking-generated particles in the kitchen. *Build Environ* 65:146–153
- Hegde S, Min KT, Moore J, Lundrigan P, Patwari N, Collingwood S, Balch A, Kelly KE (2020) Indoor household particulate matter measurements using a network of low-cost sensors. *Aerosol Air Qual Res* 20:381–394
- Hopke PK, Jensen B, Li CS, Montassier N, Wasiolek P (1995) Assessment of the exposure to and dose from radon decay products in normally occupied homes. *Environ Sci Technol* 29: 1359–1364
- Jain S, Presto AA, Zimmerman N (2021) Spatial modeling of PM_{2.5}, NO₂, and CO concentrations measured by a low-cost sensor network: comparison of linear, machine learning, and hybrid land use models. *Environ Sci Technol*. <https://doi.org/10.1021/acs.est.1c02653>
- Jolliet O, Ernsthoff AS, Csiszar SA, Fantke P (2015) Defining product intake fraction to quantify and compare exposure to consumer products. *Environ Sci Technol* 49:8924–8931
- Keil CB (2000) A tiered approach to deterministic models for indoor air exposures. *Appl Occup Environ Hyg* 15:145–151
- Keller JP, Katz J, Pokhrel AK, Bates MN, Tielsch J, Zeger SL (2020) A hierarchical model for estimating the exposure-response curve by combining multiple studies of acute lower respiratory infections in children and household fine particulate matter air pollution. *Environ Epidemiol* 4:e119
- Kleppeis NE (2006) Modeling human exposure to air pollution, human exposure analysis. CRC Press, Stanford, pp 1–18. Available from https://www.researchgate.net/publication/242072856_Modeling_Human_Exposure_to_Air_Pollution
- Krewski D, Rai SN, Zielinski JM, Hopke PK (1999) Characterization of uncertainty and variability in residential radon cancer risks. *Ann N Y Acad Sci* 895:245–272
- Kristensen K, Lunderberg D, Liu Y, Misztal PK, Tian Y, Arata C, Nazaroff WW, Goldstein AH (2019) Sources and dynamics of semivolatile organic compounds in a single-family residence in northern California. *Indoor Air* 29:645–655
- Lai ACK, Thatcher TL, Nazaroff WW (2000) Inhalation transfer factors for air pollution health risk assessment. *J Air Waste Manage Assoc* 50(9):1688–1699. <https://doi.org/10.1080/10473289.2000.10464196>
- Licina D, Tian Y, Nazaroff WW (2017) Inhalation intake fraction of particulate matter from localized indoor emissions. *Build Environ* 123:14–22
- Lioy PJ, Smith KR (2013) A discussion of exposure science in the 21st century: a vision and a strategy. *Environ Health Perspect* 121:405–409
- Liu Y, Misztal PK, Xiong J, Tian Y, Arata C, Nazaroff WW, Goldstein AH (2018) Detailed investigation of ventilation rates and airflow patterns in a northern California residence. *Indoor Air* 28:572–584
- Liu Y, Misztal PK, Xiong J, Tian Y, Arata C, Weber RJ, Nazaroff WW, Goldstein AH (2019) Characterizing sources and emissions of volatile organic compounds in a northern California residence using space- and time-resolved measurements. *Indoor Air* 29:630–644
- Lunderberg DM, Kristensen K, Liu Y, Misztal PK, Tian Y, Arata C, Wernis R, Kreisberg N, Nazaroff WW, Goldstein AH (2019) Characterizing airborne phthalate concentrations and dynamics in a normally occupied residence. *Environ Sci Technol* 53:7337–7346

- Masiol M, Zíková N, Chalupa DC, Rich DQ, Ferro AR, Hopke PK (2018) Hourly land-use regression models based on low-cost PM monitor data. *Environ Res* 167:7–14
- Masiol M, Squizzato S, Chalupa D, Rich DQ, Hopke PK (2019) Spatial-temporal variations of summertime ozone concentrations across a metropolitan area using a network of low-cost monitors to develop 24 hourly land-use regression models. *Sci Total Environ* 654: 1167–1178. <https://doi.org/10.1016/j.scitotenv.2018.11.111>
- MOEEBIUS (2017) Modelling optimization of energy efficiency in buildings for urban sustainability. D3.5 MOEEBIUS Indoor Air Quality Assessment Models. Available from <http://www.moeebius.eu/>
- Murakami S, Kato S, Ito K, Zhu Q (2003) Modeling and CFD prediction for diffusion and adsorption within room with various adsorption isotherms. *Indoor Air* 13:20–27
- National Research Council (NRC) (1991) Human exposure assessment for airborne pollutants: advances and opportunities. National Academy Press, Washington, DC
- National Research Council (NRC) (2012) Exposure science in the 21st century: a vision and a strategy. The National Academies Press, Washington, DC. <https://doi.org/10.17226/13507>
- Nazaroff WW (2008) Inhalation intake fraction of pollutants from episodic indoor emissions. *Build Environ* 43:269–277
- Nazaroff WW, Cass GR (1986) Mathematical modeling of chemically reactive pollutants in indoor air. *Environ Sci Technol* 20:924–934
- Patel S, Sankhyan S, Boedicker EK, DeCarlo PF, Farmer DK, Goldstein AH, Katz EF, Nazaroff WW, Tian Y, Vanhanen J, Vance ME (2020) Indoor particulate matter during HOMEChem: concentrations, size distributions, and exposures. *Environ Sci Technol* 54:7107–7116
- Ramamurthi M, Hopke PK (1991) An automated, semi-continuous system for measuring indoor radon progeny activity-weighted size distributions, dp: 0.5–500 nm. *Aerosol Sci Technol* 14: 82–92
- Rich DQ, Ozkaynak H, Crooks J, Baxter L, Burke J, Ohman-Strickland P et al (2013) The triggering of myocardial infarction by fine particles is enhanced when particles are enriched in secondary species. *Environ Sci Technol* 47:9414–9423
- Seinfeld JH, Pandis SN (2016) Atmospheric chemistry and physics: from air pollution to climate change. Wiley, Hoboken
- Shin H-M, McKone TE, Bennett DH (2012) Intake fraction for the indoor environment: a tool for prioritizing indoor chemical sources. *Environ Sci Technol* 46:10063–10072. <https://doi.org/10.1021/es3018286>
- Shin M, Kang Y, Park S, Im J, Yoo C, Quackenbush LJ (2020) Estimating ground-level particulate matter concentrations using satellite-based data: a review. *GISci Remote Sens* 57:174–189
- Smith KR (1988) Air pollution: assessing total exposure in the United States. *Environment* 30(10–15):33–38
- Tang CH, Garshick E, Grady S, Coull B, Schwartz J, Koutrakis P (2018) Development of a modeling approach to estimate indoor-to-outdoor sulfur ratios and predict indoor PM_{2.5} and black carbon concentrations for Eastern Massachusetts households. *J Expo Sci Environ Epidemiol* 28:125–130
- Taylor J, Shrubsole C, Symonds P, Mackenzie I, Davies M (2019) Application of an indoor air pollution metamodel to a spatially-distributed housing stock. *Sci Total Environ* 667:390–399
- Tian Y, Liu Y, Misztal PK, Xiong J, Arata CM, Goldstein AH, Nazaroff WW (2018) Fluorescent biological aerosol particles: concentrations, emissions, and exposures in a northern California residence. *Indoor Air* 28:559–571
- Wang C, Collins DB, Arata C, Goldstein AH, Mattila JM, Farmer DK, Ampollini L, DeCarlo PF, Novoselac A, Vance ME, Nazaroff WW, Abbatt JPD (2020) Surface reservoirs dominate dynamic gas-surface partitioning of many indoor air constituents. *Sci Adv* 6:eaay8973
- Wild CP (2005) Complementing the genome with an “exposome”: the outstanding challenge of environmental exposure measurement in molecular epidemiology. *Cancer Epidemiol Biomark Prev* 14:1847–1850

- World Health Organization (2001) Glossary of exposure assessment-related terms: a compilation. Prepared by the Exposure Terminology Subcommittee of the IPCS Exposure Assessment Planning Workgroup for the International Programme on Chemical Safety Harmonization of Approaches to the Assessment of Risk from Exposure to Chemical. Retrieved on 22 July 2021. https://www.who.int/ipcs/publications/methods/harmonization/en/compilation_nov2001.pdf
- Xu MR, Raja S, Ferro AF, Jaques PJ, Hopke PK, Gressani C, Wetzel LE (2010) Effectiveness of heating, ventilation and air conditioning system with HEPA filter unit on indoor air quality and asthmatic children's health. *Build Environ* 45:330–337
- Zartarian VG, Ott W, Duan N (1997) A quantitative definition of exposure and related concepts. *J Expo Anal Environ Epidemiol* 7:411–437
- Zartarian V, Bahadori T, McKone T (2005) Adoption of an official ISEA glossary. *J Expo Sci Environ Epidemiol* 15:1–5. <https://doi.org/10.1038/sj.jea.7500411>
- Zhang Z, Chen X, Mazumdar S, Zhang T, Chen Q (2009) Experimental and numerical investigation of airflow and contaminant transport in an airliner cabin mockup. *Build Environ* 44:85–94



Exposure Routes and Types of Exposure

35

Elisabeth Feld-Cook and Clifford P. Weisel

Contents

Introduction	1004
Sources of Indoor Air Exposure	1006
Routes of Exposure	1007
Inhalation Exposure	1009
Dermal Exposure	1012
Non-dietary and Indirect Ingestion Exposure	1013
Biological Agents	1013
Examples of Common Toxicants in Indoor Air	1015
Penetrations of Vapors from Outside	1015
Volatile Organic Compounds (VOCs)	1015
Formaldehyde	1016
Radon	1016
Semi-volatile Organic Compounds (SVOCs)	1017
Role of House Dust	1018
Indoor Chemistry	1018
Consumer Goods and Personal Exposures	1019
Conclusions	1021
Cross-References	1022
References	1022

E. Feld-Cook

Chemical Terrorism, Biomonitoring Laboratory, Environmental and Chemical Laboratory Services,
Public Health and Environmental Laboratories, New Jersey Department of Health, Trenton, NJ,
USA

e-mail: Elisabeth.Cook@doh.nj.gov

C. P. Weisel (✉)

Environmental and Occupational Health Sciences Institute, Rutgers, The State University of New
Jersey, Piscataway, NJ, USA

e-mail: weisel@eohsi.rutgers.edu

© This is a U.S. Government work and not under copyright protection in the U.S.;
foreign copyright protection may apply 2022

1003

Y. Zhang et al. (eds.), *Handbook of Indoor Air Quality*,
https://doi.org/10.1007/978-981-16-7680-2_38

Abstract

Exposure to indoor air contaminants occurs not just through inhalation but also via dermal absorption of vapors or when touching surfaces that air contaminants deposit on, and by inadvertent ingestion of contaminated settled dust from hand to mouth behaviors, especially for children. Sources of indoor pollutants include penetration of outdoor air, emissions from indoor use of consumer and personal products, furnishing and building materials, resuspension of house dust, and indoor air chemistry. Multiple sources, limited ventilation, and finite volume of buildings results in higher air concentrations of many volatile and semi-volatile organic compounds within homes than outdoors. When personal products are used near the breathing zone, the concentration of the air breathed, and therefore the resulting inhalation exposure, can be higher than estimated from the indoor air concentrations. Semi-volatile organic compounds (SVOCs) partition between indoor air and surfaces, particularly into house dust which serves as a reservoir for many compounds. The partitioning of SVOCs between indoor air and surface/dust results in their having multiple exposure routes. This chapter presents examples of exposures that occur to various chemicals representative of broad categories of compounds, thereby providing general concepts that should be considered when evaluating potential exposures to indoor air pollutants. Since people spend, on average, more than 90% of their time indoors, indoor air is often the largest contributor to total exposures for volatile, semi-volatile, and particulate air contaminants.

Keywords

Inhalation exposure · VOCs · SVOCs · House dust · Indoor sources · Indoor chemistry

Introduction

During the average lifespan of a human of 79 years, an average of 69 years will be spent in an indoor environment, of which 54 years will be spent at their place of residence and 26 years will be spent sleeping, while only 6 years will be spent outdoors, and 4 years will be spent in a vehicle (calculated from the exposure factors handbook (U.S. Environmental Protection Agency 2011)). Since people spend a large percentage of their time (~90%) indoors (Brasche and Bischof 2005; Matz et al. 2014) and air concentrations of chemicals and biological agents indoors are often higher than outdoors (Azuma et al. 2016), characterization of exposures within the indoor environment is needed to protect public health. Penetration of chemical and biological agents from outdoor air to indoors provides the baseline levels present indoors, with the final outdoor contribution dependent upon losses for reactive or soluble volatile/semi-volatile compounds and for particles onto surfaces indoors or within the building's envelope. Higher indoor air concentrations compared to

outdoors can result when there are indoor or personal sources emitting pollutants or from chemical reactions indoors (Fig. 1). Unlike the outdoor environment, the indoor environment is a defined, finite space often with limited ventilation or air exchange and thus, the chemical or biological agents released or formed indoors do not dissipate as quickly as they do outdoors. This impact of indoor sources on air quality and exposure is particularly pronounced in buildings with insufficient air exchange rates to remove pollutants emitted or formed indoors. In 1981, the shift to lower air exchange rates to create more energy efficient buildings in the United States began (American Society of Heating, R. a. A.-C. E., Inc 1989). Lower air exchange rates can trap agents indoors leading to exposure to potentially harmful pollutants. There are numerous indoor sources of pollutants that can affect indoor air quality (Table 1). During the 1980s, the first comprehensive study comparing personal air to outdoor air was conducted by the US Environmental Protection Agency, as part of the Total Exposure Assessment Methodology (TEAM), initially examining a subset of volatile organic compounds (VOCs) and expanding to include particulate matter (PM) (Wallace et al. 1987, 2017). In subsequent years, studies comparing outdoor air to indoor and/or personal air have been carried out throughout the world. A consistent finding across these studies is that there is a stronger relationship between personal air, i.e., the levels in the breathing zone – air within 0.3 m of the nose and mouth, and indoor air concentration than between personal air and outdoor air, and that indoor and personal air levels for many air contaminants exceed their outdoor levels. Therefore, the indoor air levels have become

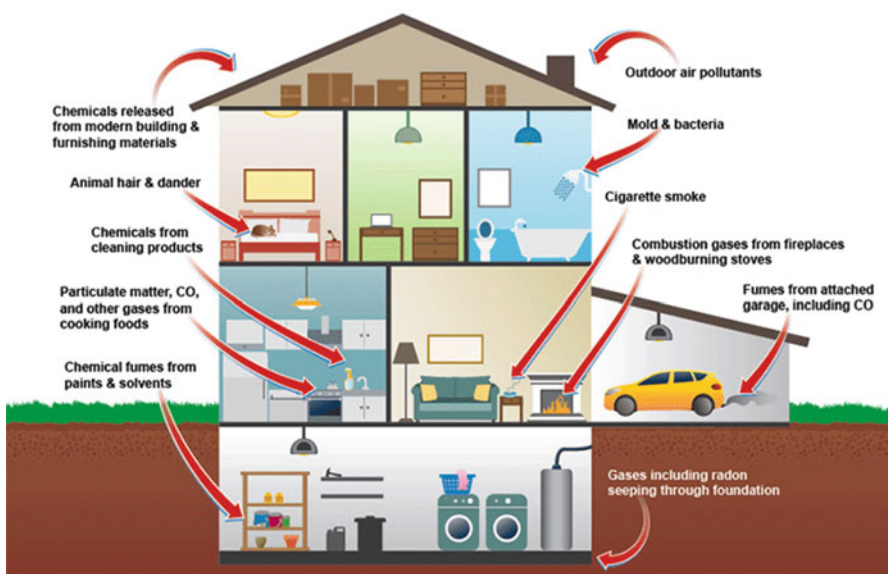


Fig. 1 Indoor and Outdoor Sources of Pollution affecting indoor air quality. (Source: <https://www.epa.gov/expobox/exposure-assessment-tools-media-air#indoorair>)

Table 1 Common sources of indoor air toxicants (Abdullahi et al. 2013; Destaillats et al. 2008; Liu et al. 2016, 2017; Nazaroff and Weschler 2004; Odabasi 2008; Schettler 2006; Seaman et al. 2009; Stönnér et al. 2018; Tang et al. 2015, 2016; Wang and Morrison 2006; Weschler 2009; Weschler and Carslaw 2018)

Source	Associated toxicant(s)
Building materials (i.e., paint, wood, PVC pipes, cable insulation)	Formaldehyde, Benzene, Toluene, Ethylbenzene, Xylenes (BTEX)
Cleaning agents and air fresheners	Terpenes, Ammonia, Chlorinated hydrocarbons, Disinfectants, Organic Solvents, Fragrances, Particulate Matter (PM)
Combustion appliances, cooking and heating	Polycyclic Aromatic Hydrocarbons (PAHs), Carbon Monoxide (CO), Nitric Oxides (NOx), Acrolein, PM
Disinfectants	Bleach, Quaternary Ammonium Compounds (QACs), Alcohols, Vinegar
Electric equipment (i.e., laser printers, photocopiers)	Ozone
Furniture, floor (i.e., carpets, vinyl) and wall coverings	Formaldehyde, Poly and Per-Fluorinated Alkyl Substances (PFAS)
Moist areas, uncleared areas	Microbial organics (Bacteria, Fungi, and Molds)
Personal care products (i.e., perfume, make up, lotion)	Phthalates, Parabens, Nanoparticles, Fragrances
Pesticides (Insecticides, fungicides, rodenticides)	Permethrins, Pyrethroids
Pets	Dander, Pollen, Tracked in Soil/dirt
Smoking	BTEX, PM, Formaldehyde, Furans

increasingly recognized as an, if not the most, important contributor to total exposure to air contaminants potentially affecting health.

Sources of Indoor Air Exposure

Many sources contribute to poor indoor air quality resulting in exposures to pollutants in the indoor environment. These include combustion processes (e.g., tobacco smoking, vaping, cooking, heating), off-gassing from building materials and furnishings, emissions from consumer products (e.g., household cleaners, cleaning activities, personal care items, solvents and glues used in hobbies, air fresheners), release of bioeffluents, evaporative releases from engines, solvents and paints stored in attached garages, contaminated soil gas, and penetration of outdoor air pollutants (Fig. 1). A listing of some common major sources with their associated toxicants are given in Table 1. Several of the chemicals indoors can react with oxidants present in the indoor air, such as ozone, which comes predominantly from outdoor air penetration, and with nitrogen dioxide, from outdoor air and combustion processes indoors, forming secondary chemical vapors and organic aerosols that can contribute further to the indoor air pollution. When considering exposure to indoor air pollutants, understanding both the relative contribution from different sources and

exposure routes are important. One approach to facilitate that comparison is to use an Intake Factor (*iF*). An *iF* describes the mass intake of a pollutant by individuals or population per mass unit of the pollutant released into the environment (Bennett et al. 2002). *iF* has been used in life cycle analysis assessments and risk assessments to identify the exposure pathways and design effective approaches to reduce exposure. *iF* values have identified pathways for chemicals that include those from consumer products and often result in greater exposure than industrial emissions for the same chemicals, even though the mass released into the air is orders of magnitude smaller. This is premised on the sources being “near field” rather than “far field” sources, i.e., indoor (“near field”) emissions have much higher *iF* than outdoor (“far field”) emissions, since the portion of a chemical emitted indoors resulting in an exposure will be much greater than from outdoor emissions (Jolliet et al. 2015). *iF* values can be calculated for individual exposure routes (inhalation, dermal, ingestion) and then summed to determine the total *iF* (Bennett et al. 2002; Jolliet et al. 2015). Based on the relationship between uses/properties of chemicals and their *iF*, the *iF* can be used to predict exposures to new chemicals that are to be introduced into the environment (Bennett et al. 2002).

Routes of Exposure

In a National Academy of Sciences report, exposure was defined “as a person’s contact with the concentration of a material before and after it crosses a boundary (nose, skin, mouth) between the human and the environment over an interval of time leading to a potential biological effective dose” (Lioy and Weisel 2014; National Research Council 2012). Exposure to agents in the air can occur through three routes: inhalation, dermal, and ingestion; since not only is the air directly breathed (inhalation) but air contaminants can be absorbed through the skin or deposited/absorbed onto dust or surfaces within a home that are touched (dermal) and hands or objects containing deposited or absorbed pollutants are placed in the mouth (inadvertent ingestion). The generic equation to calculate external inhalation exposure from pollutants in indoor air is to sum the time spent in different locations/activities multiplied by the average air concentration encountered in each locale, though this approach does not consider breathing rate which affects the amount of an agent that reaches the lungs (Eq. 1):

$$\text{External Inhalation Exposure} = \sum_{i=1}^n C_i \times \Delta t_i \quad (1)$$

where *i* is the location or activity (often referred to as the microenvironment) over *n* locations/activities, C_i is the air concentration in the *i*th microenvironment, and Δt_i is the time spent in the *i*th microenvironment. Different indoor locations or activities with different indoor air concentrations are represented as distinct microenvironments and the relative contribution of each to the exposure determined. Defining the

relevant microenvironments and sources of pollutants an individual or population are potentially exposed to can provide guidance in designing a questionnaire and time activity surveys, to assess the time spent in different microenvironments, the level of exertion which alters the breathing rate as described below, and where air concentrations should be measured – these elements are essential in calculating inhalation exposure across multiple indoor settings. Time activity patterns are discussed in detail in ► [Chap. 37, “Time-Activity Patterns,”](#) of this Handbook.

Equation 1 relates an estimate of inhalation exposures but does not fully account for multi-route exposures or the amount that enters the body.

External dermal exposure needs to consider there are different contacts at the skin depending upon the source as outlined in Eq. 2:

$$\text{External Dermal Exposure} = \sum_{i=1}^n (C_i \times SA_i \times EF_i \times \Delta t_i) \quad (2)$$

where C_i is the concentration in the medium contacting the skin, SA_i the surface area of the skin exposed, EF_i the frequency of exposure, and Δt_i is the duration of exposure for the i th dermal exposure event. For indoor air this will include a continuous exposure to contaminants in the air to exposed skin areas, in analogous fashion to inhalation exposure but also to contact with surfaces that have absorbed chemicals from the air and contact skin in a noncontinuous fashion.

External ingestion exposure is a noncontinuous exposure and has a mathematical construct similar to dermal exposure as shown in Eq. 3:

$$\text{External Ingestion Exposure} = \sum_{i=1}^n (C_i \times IR_i \times EF_i \times \Delta t_i) \quad (3)$$

where C_i is the concentration in the food or liquid consumed, IR_i the amount ingested, and EF_i the frequency of exposure, and Δt_i is the duration of exposure for the i th ingestion exposure event.

Calculating external dermal and ingestion exposure and combining the exposures among different exposure routes based on the contact at the body surface is not readily done since the units of external exposures vary by route. To better compare the exposures across routes and estimate total exposure, it has been proposed that the amount that enters the body (internal exposure or internal dose) be calculated (Lioy and Weisel 2014) or an iF be used. The internal exposure includes the external exposure, i.e., the amounts at the body boundary over time, and factors that depend on the exposure route: the breathing rate, deposition pattern in the lungs, and transport across the lung membrane for inhalation exposure, the parts of the body and surface area contacted and permeability coefficient across the skin for dermal exposure, and the bioavailability of the chemical in the media ingested and gastrointestinal absorption rate for ingestion exposure. The absorption rate varies with the lung > gastrointestinal tract > skin for most chemicals, though the form of the chemical (e.g., ionic vs non-charged) and matrix it is in can affect the rate. The

internal exposure can be expressed in the same units for the three exposure routes, typically as total mass (e.g., milligrams) absorbed during a set time period such as a day or as mass per body weight to facilitate comparison of potential impacts from exposure across individuals. Therefore, the total internal exposure can be calculated by summing the values across the three exposure routes.

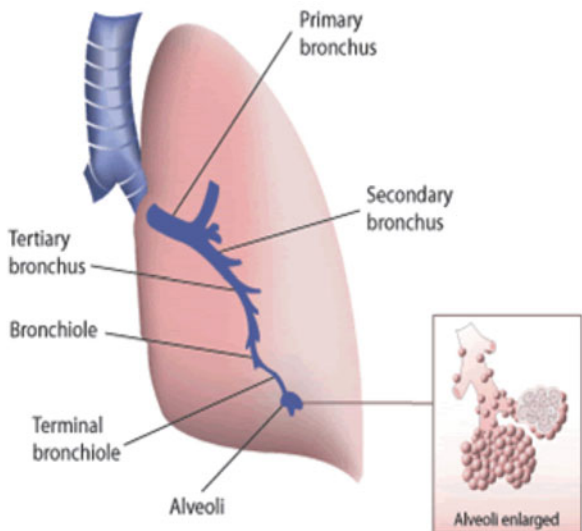
The *iF* includes the same parameters listed above for internal dose so the value from different routes can be summed after being normalized to the amount released from a source. *iF* values have been incorporated into multimedia, multi-pathway exposure models to assess the source-to-intake relationship (Bennett et al. 2002) and, for example, fine particulate matter ($PM_{2.5}$) from indoor air and outdoor indoor in urban and rural settings on a population basis (Fantke et al. 2016). The latter study found that the location, indoor air exchange rate, and level of occupancy affected the *iF* with indoor $PM_{2.5}$ exposure typically contributing “91–99% to effective intake fractions across indoor source environments.” A comprehensive review of factors that affect the *iF* for PM across different indoor environments was published by (Hodas et al. 2016).

As mentioned previously (Table 1), there are an abundance of indoor sources that can release chemicals into the air. Notable sources of indoor air pollution include off-gassing from furniture and building materials, personal care product use, pesticide applications, resuspension of dust, indoor air chemistry, and combustion sources (Biesterbos et al. 2013; Garcia-Hidalgo et al. 2017; Matt et al. 2004; U. S. Environmental Protection Agency 2018; Wu et al. 2010). An important, but avoidable combustion source leading to exposure to multiple pollutants is smoking indoors. Smoking is a major source of formaldehyde, benzene, and PM to name a few of the toxicants it releases into the air. Formaldehyde can also off-gas from furniture, building materials, and carpets. Personal care products including lotions, make-up, and perfumes, are sources of nanoparticles, phthalates, and parabens. Air fresheners and cleaning products contain multiple classes of potentially harmful chemicals including but not limited to PM, nanoparticles, disinfectants, chlorinated hydrocarbons, and various organic solvents that are released into the air during their use. Pesticides, such as insecticides, fungicides, and rodenticides, are a source of exposure for permethrins and pyrethroids. The following sections describe the routes these chemicals take to enter the human body.

Inhalation Exposure

Indoor inhalation exposure results from breathing an agent (chemical/physical/biological) while indoors (U.S. Environmental Protection Agency 2019). Indoor contaminants include: PM, vapors, VOCs, semi-volatile organic compounds (SVOCs), and biological agents. The size of the aerosols that comprises the PM affects its penetration indoors and whether/where it is deposited in the lungs. PM10, (particulate matter $<10\ \mu m$ in aerodynamic diameter) are inhalable, cross the mouth/nose barrier while smaller sized particles will penetrate more deeply in the lungs,

Fig. 2 Diagram of the lung.
(Source: <https://www3.epa.gov/region1/airquality/pm-human-health.html>)



into the alveoli (Figs. 2 and 3b). Changes in respiration rate can affect exposure, with people exercising having higher breathing rates leading to a larger intake of air and deeper penetration of the toxicants into the lungs. Elevated breathing rates likely occur in indoor gyms, recreational facilities, and schools. Besides exercise regimens done in those locations and in homes, higher ventilation rates compared to sedentary rates (Metabolic Equivalent (MET) <1.5) occur when performing many common activities (e.g., house cleaning, gardening, walking stairs) which results in breathing rates associated with light intensity activities (MET 1.5 to 3.0). Moderate intensity activities result in a further doubling of the breathing rate compared to light intensity activities (MET 3.0 to 6.0) and another doubling is associated with vigorous intensity activities (MET >6.0) (Lioy and Weisel 2014; U.S. Environmental Protection Agency 2011). Thus, the appropriate breathing or respiratory rate should be selected for the activity of the person being considered when estimating or comparing inhalation exposures.

Inhaled contaminants can reach different parts of the respiratory tract depending upon their physical form and chemical properties. Vapors that are highly soluble in aqueous solutions, (e.g., ammonia, acetone, formaldehyde) deposit into the mucus or thin layer of fluid covering the luminal surface of the airway toward the upper part of the respiratory tract. Non-polar VOCs and the vapor phase of SVOCs will penetrate to the alveoli where gas exchange occurs. The deposition of particles in the lung depends upon the breathing pattern, particle size and shape, flow dynamics, and the lung morphology. The respiratory tract is highly branched beginning at the bronchi which bifurcates to the two lungs. The respiratory tract has sequentially small diameter tubes (bronchioles) ending in the alveoli or air sacs where gas exchange occurs (Fig. 2). Particles deposit onto the walls of the respiratory tract via a number

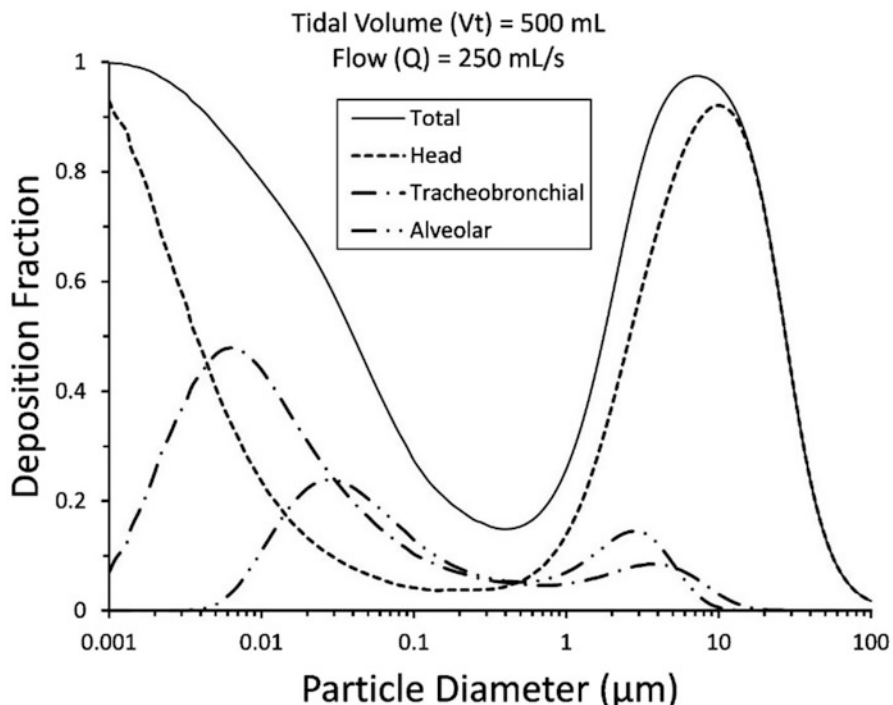


Fig. 3 Mathematical model of particle deposition via nasal breathing in the whole lung (Total), nose, naso-pharynx, and larynx (Head), tracheobronchial airways, and alveolar region in healthy adults. Tidal volume (V_t) is 500 mL, frequency of breathing is 15 bpm, and flow rate (Q) is 250 mL/s. Deposition was adjusted for particle inhalability, which is why particle deposition decreases for particles greater than 10 μm . Particles in the 0.3 to 0.5 μm range show the lowest deposition for any of the regions. (Above simulation conducted using the Multiple-Path Particle Dosimetry Model v3.01, Applied Research Associates © 2015). (Source: <https://www.epa.gov/pmcourse/particle-pollution-exposure>)

of processes: interception (by touching the wall surface – particularly important for fibers); impaction (particles that cannot stay within the air stream as it curves, $>10 \mu\text{m}$ in the nose and throat); sedimentation (when gravitational forces and air resistance exceed their buoyancy, particles $>0.5 \mu\text{m}$ in the bronchi); and diffusion (particles $<0.5 \mu\text{m}$ in the smaller bronchioles and alveoli) (Heyder 2004). Very small particles referred to as nanoparticles or ultrafines ($<100 \text{ nm}$) can be found in consumer products. Nanoparticles deposit mainly through diffusion and a portion can reach the alveolar sacs, though they also coagulate into larger agglomerates resulting in deposition in the upper section of the respiratory tract. A sharp particle size cutoff does not exist for deposition into different sections of the respiratory tract, rather particle properties such as hygroscopicity and particle shape, and physiological properties, lung morphology and minute ventilation, can affect their transport within the lungs (Oberdörster et al. 2005) (Fig. 3). The relatively high humidity and

temperature within the respiratory tract compared to the indoor environment can cause hydroscopic particles to grow, changing their effective size compared to their size in indoor air and therefore their lung deposition site (Azuma et al. 2018; Heyder 2004; Löndahl et al. 2014). Indoor air particles have sources of penetration from outdoors, resuspension of dust, human activities, and chemical formation.

Dermal Exposure

Indoor dermal exposure to air pollutants occurs via direct skin contact by vapors and by touching surfaces which particles have deposited or SVOCs have absorbed/adsorbed (Shi and Zhao 2014). Dermal exposure can result in skin irritation and/or absorption into the body through the epidermis. Dermal exposure can be determined from the duration/frequency of contact with surfaces/objects multiplied by the chemical's concentration on those surfaces/objects and the transfer rates from surfaces to the skin (Ott et al. 2006). For uptake of volatile compounds from the air, clothing can alter the surface area of exposed skin and therefore the dermal exposure. Some agents, with low gas-to-fabric partition coefficients, can penetrate through clothing, while others, with high gas-to-fabric partition coefficients, will adsorb to clothing and delay exposure to the skin. Agents with intermediate gas-to-fabric partition coefficients can accumulate on clothing prior to being worn, resulting in a higher dermal uptake (Liu et al. 2021; Morrison et al. 2016). If the clothing becomes wet, hydroscopic pollutants or particles may be absorbed or adhere to the clothing causing higher dermal exposure over a longer duration than would occur otherwise. The absorption of SVOCs into other fabrics that contact skin, such as bedding and furnishings can also result in dermal exposure. Transdermal absorption of the vapor phase of some SVOCs in the indoor air can exceed the dose associated with inhalation exposure. The compound's physiochemical properties, such as molecular weight and stratum corneum/air partition coefficient, influence the extent of vapor absorption (Weschler and Nazaroff 2014). Examples of the semi-volatile compound classes for which dermal absorption of vapors can exceed uptake from inhalation of vapors include parabens, low molecular weight phthalates, phenylphenols, and terpene alcohols.

Dermal exposure will also result when touching surfaces or settled dust that have absorbed/adsorbed volatile and semi-volatile compounds from the air. Transfer of SVOCs occurs from the dust and surfaces into the skin lipids. House dust has been shown to be a reservoir for many VOCs and SVOCs (Lioy et al. 2002). Surface films can absorb hydroscopic compounds (Duncan et al. 2018) or surfaces can become coated with a thin organic matter film which absorb SVOCs from the air based on its octanol-gas-phase partition coefficient and into skin oils (Weschler and Nazaroff 2014). These authors found a linear relationship between their predicted abundance of a range of SVOCs with levels measured in hand wipes for both children and adults, supporting the premise that SVOCs are transferred from indoor air-surface to film-skin and directly from air to skin through an equilibrium controlled pathway. This results in dermal exposure of SVOCs from indoor air. These processes can also

contribute to inadvertent ingestion. Intake fractions for SVOCs identified a number of indoor sources dominated the indoor air levels and provided estimates of the inhalation, dermal and non-dietary ingestion contributions which varied across compound (Shin et al. 2014).

Non-dietary and Indirect Ingestion Exposure

Ingestion exposure associated with indoor air contaminants ensues through the consumption of re-suspended contaminated soil and house dust and from large particles deposited in the respiratory tract that move with the mucous to the GI tract. Hand-to-mouth activities, especially for infants and children, can lead to inadvertent ingestion exposure (U.S. Environmental Protection Agency 2018). The activities that children engage in that can lead to non-dietary and indirect ingestion exposure include playing with toys or crawling on the floor then touching their mouths or eating with their hands. Infants and children are notorious for putting everyday items in their mouth including their own clothing and toys; and infants are given teething rings and pacifiers which are intended to be placed into the mouth, each of which may have absorbed SVOCs. It is estimated that hand-to-mouth activity and object-to-mouth activity occur at frequencies of 42–75 and 17–34 times/h, respectively (Kwong et al. 2020). Contaminants in the PM of indoor air settle and absorb onto multiple surfaces, including kitchen counters, which can be in contact with food, leading to ingestion exposure. Plastic toys and stuffed animals containing synthetic fibers are materials known to absorb semi-volatile and volatile organic compounds. When these items are placed in the mouth the saliva can extract the absorbed chemicals. Microorganisms can also deposit onto surfaces and then be ingested. These activities put children at a higher risk of exposure to harmful pollutants such as pesticides and house dust containing lead.

Biological Agents

While the focus of this chapter is on chemical agents that affect air quality, biological contaminants also contribute to poor air quality and can have multi-route exposures. Biological contaminants include bacteria, viruses, fungi, mold, dander, dust mites, pollen, and insect parts/dropping. These agents can elicit allergic and respiratory responses, such as exacerbation of asthma. They also move through the air within the indoor environment. Moist or wet materials and surfaces within a home composed of a matrix that can provide nutrients for growth (e.g., drywall, wallpaper, insulation, dust, fabric, upholstery), along with indoors having moderating temperature, can serve as a breeding ground for many biologics, particularly mold and fungi. Biologics that grow on surfaces can become airborne, (i.e., bioaerosols – aerosolized liquid droplets containing biological agents, microbes or cell fragments), from multiple sources. The pathways include: being released in or near the vents of an air handling system which blows air into the home; as part of resuspended house

dust; emitted from cold air or ultrasonic humidifiers; and from mechanical process that disturb growth surfaces. In addition, microbes and pollen can be blown indoors from outdoor sources. Bioaerosols are often small enough to be inhaled (inhalation exposure) and can be deposited on surfaces or in-house dust, resulting in dermal and ingestion exposure.

Since moisture is an important factor affecting the growth of mold and fungi in homes, exposures to mold and fungi can be reduced by keeping surfaces dry, through fixing water leakage problems, having adequate ventilation in areas where hot water or steam is produced, and by removing or cleaning water damaged carpets, furnishing, and building materials. Some biologics release spores ($\sim 10\text{--}100\ \mu\text{m}$ in size) into the indoor air which are distributed within homes and serve to seed new areas for growth. Human airborne transmission of viruses ($\sim 20\ \text{nm}$ to $400\ \text{nm}$ in size) and bacteria ($\sim 200\ \text{nm}$ to $100\ \mu\text{m}$ in size (Nazaroff 2016) between people can occur via coughing, sneezing, laughing, and even talking, particularly in crowded, inadequately ventilated rooms. These transmissions are more problematic indoors than outdoors, since indoor settings have limited volume and lower ventilation than outdoors. Taking steps to limit inter-individual transmissions and therefore the spread of infectious diseases, should rely on understanding of their exposure pathways which typically occur indoors. Exposure pathways include: airborne via micron or submicron particles which have different residence time in the air, dermal contact after viruses or bacteria are deposited on surfaces that are subsequently touched with hands that then touch eyes, nose, or the mouth providing an entry point into the body, or by depositing on food or dust that might be ingested. When the exposure pathways and routes for infectious agent transmission are identified, guidance on intervention steps can be provided.

Pollen and pollen grains, biologics with size ranges $<10\text{--}200\ \mu\text{m}$ (Miguel et al. 2006) have inhalation as their primary exposure route, affects the subpopulation sensitive or allergic to it. Pollen mainly has outdoor sources but can have indoor ones like flowering plants. Pollen types and levels vary seasonally, and exposure can be decreased by limiting window opening during periods of high pollen. It should be noted, though, that opening windows increases ventilation and decreases indoor air concentrations of agents released indoors. Thus, there needs to be an appropriate balance of when to open windows based on indoor air contaminant sources, outdoor biologic and chemical contaminants for a particular time and location, and how household residents may be exposed. Animal dander, insect parts, and dust mites have indoor sources with the exposure typically occurring by being in close proximity to the source. Sources often include bedding, mattresses, upholstered furnishing, carpeting, stuffed toys, etc. where people, often children, will generally have their face in close contact. Keeping these items clean by frequent washing can reduce exposures. Vacuums used to clean carpets and furnishing that have a High Efficiency Particulate Air (HEPA) filters trap small (<3 microns) particles with an $>99.9\%$ efficiency and can be effective to limit resuspension and exposure via an indoor air pathway. However, vacuums with low efficiency for small particles could result in resuspension of those particles, thereby potentially increasing inhalation exposure and spreading the dust to other parts of a home. In addition to direct exposure to the

biological agents, some mold, bacteria, and fungi emit VOCs which include mycotoxins, carbonyls, alcohols, terpenes, thiols, ethers, and esters, which can also be irritating or cause respiratory reactions.

Examples of Common Toxicants in Indoor Air

The following sections provide examples of compounds and their pathways that can lead to exposures within the indoor environment. It is not meant to be comprehensive but rather illustrative of pathways that could result in exposures to indoor air pollutants and the types of agents or activity scenarios that lead to those exposures.

Penetrations of Vapors from Outside

The outdoor air provides the baseline for indoor air concentrations for non-reactive, volatile pollutants. For reactive and water-soluble compounds losses occur during transport indoors as they react with or absorb onto surfaces within a building's interior or the building's envelope, the part of the structure separating the controlled inner environment from the ambient atmosphere. Volatile pollutants also enter buildings in soil gas that penetrates through cracks or openings in a building's foundation.

Volatile Organic Compounds (VOCs)

Mobile vehicles, commercial enterprises, and industries emit a plethora of VOCs into the air. These emissions result in ambient air having concentrations at the sub to tens and occasionally hundreds of $\mu\text{g}/\text{m}^3$ level, particularly in urban and suburban settings. Ambient pollutants enter buildings through ventilation systems (active and passive) and via natural air exchange processes, since buildings are not typically air-tight, and when windows are open. Common VOC pollutants in outdoor air include aromatic and aliphatic hydrocarbons, terpenes, chlorinated hydrocarbons, alcohols, ethers, nitriles, and carbonyls (See EPA Hazardous Air Pollutants (U.S. Environmental Protection Agency 2020)). Often, these compounds have indoor/outdoor (I/O) ratios in many homes exceeding unity (Dodson et al. 2009), indicative of indoor sources in addition to the contribution from the penetration of outdoor air. For VOCs that are banned in consumer products and therefore have no indoor sources, such as carbon tetrachloride, the I/O ratio is uniformly close to unity. Activities and materials that are sources of VOCs within buildings include: smoking (aromatic and aliphatic hydrocarbons, furans, nitriles, carbonyls, etc.), cleaning and air freshener products (terpenes, chlorinated hydrocarbons, hydrocarbon solvents, ethers, etc.), and chlorinated or contaminated tap water (disinfection by-products, volatile contaminants in water supply). Exposure to VOCs are typically governed by the indoor air concentrations encountered more than ambient outdoor air

concentrations since people spend most of their time indoors. However, for some VOCs, the indoor air concentrations could underestimate exposure. This occurs when the VOC is in a consumer product that is used in close proximity to the individual's breathing zone. The concentration of air breathed is higher than average room concentration, since as the compound diffuses and becomes mixed with room air its air concentration declines. Studies that have evaluated indoor and personal air often identify higher VOC air concentrations in the personal air that are associated with specific product use (Dawson and McAlary 2009; Weisel et al. 2008).

Formaldehyde

An example of a VOC with large indoor sources in some homes is formaldehyde. This single carbon carbonyl is present in many furnishings that contain foams, wood products, and combustion processes. It off-gasses from resins used in particle board, plywood, and fiber board, insulating materials that use urea formaldehyde foam, glues, adhesives, varnishes, etc. The emissions are particularly prevalent in new materials. While the emission rate decays with time, the emissions can continue for months to years and can fluctuate with relative humidity and indoor temperatures (Liu et al. 2006).

One example of a major incident involving an exposure to high concentrations of formaldehyde was during the clean-up of hurricane Katrina in New Orleans (ATSDR 2007). Temporary housing in the form of FEMA trailers was put up to shelter individuals whose homes were flooded. These trailers were off-gassing toxic levels of formaldehyde inside the trailers, which led to high exposures and adverse health outcomes (ATSDR 2007).

Radon

Radon is rarely a problem outdoors, but due to vapor intrusions into homes in areas with uranium geological features, radon levels can be problematic indoors (National Research Council 1999; Samet 2001). Radon penetrates through building foundations into basements and ground floor rooms as part of soil gas. If those spaces have poor ventilation, radon can increase to levels that have been linked to lung cancer (Alavanja et al. 1999; U.S. Environmental Protection Agency 2016). Radon and its progenies are particularly dangerous indoors because they can go undetected due to being odorless and colorless. The exposure of concern is the inhalation of radon decay products that adhere to particles which can be trapped in the lungs and further decay radioactively, providing a dose directly to lung tissue. The highest cancer rates associated with radon are when there is smoking in a home that also have elevated radon levels, as these hazards act synergistically.

VOCs vapor intrusion occurs in an analogous fashion to radon when a building is above an aquifer or soil contaminated with VOCs, e.g., from gasoline spills, leaking superfund sites and industrial spills. This can result in elevated VOC inhalation

exposures indoors. As with radon, the lowest floors in the home often have the highest air concentrations and are where the greatest exposure occurs, though VOCs will be distributed throughout a home more than radon since they do not radioactively decay and adhere to particles and surfaces as quickly as radon.

Semi-volatile Organic Compounds (SVOCs)

SVOCs include multiple classes of compounds. Exposures to SVOCs within indoor settings occur through inhalation, dermal, and ingestion routes due to the redistribution of the SVOCs between the air and surfaces. An important indoor reservoir for SVOCs is house dust. Some broad compound classes of SVOCs with indoor sources are pesticides, phthalates, flame retardants, poly and perfluoroalkyl substances (PFAS), polycyclic aromatic hydrocarbons (PAHs), and polychlorinated biphenyls (U.S. Environmental Protection Agency 2017a, b). SVOCs are often released into the indoor home environment during consumer product use. Following their initial release indoors, SVOCs have a dynamic lifecycle as they continually volatilize from and condense onto surfaces dependent upon their air concentration and the temperature of the air and room surfaces (Bi et al. 2015; Wallace et al. 2017; Weschler and Nazaroff 2014). House-dust serves as an important vector mediating this process due to its high surface area and organic content. Further, house dust can be resuspended within a home furthering the movement of SVOCs and providing additional exposure routes to the occupants, which includes inhalation of the dust, skin contact, and incidental ingestion after the dust adheres to hands, food, or objects placed in mouths (Little et al. 2012).

Pesticide applications are done indoors and outdoors immediately next to buildings by commercial applicators and residents, both on a scheduled and as-needed basis. The amount released into indoor air can vary greatly and is dependent upon the application method, ranging from minimal amounts for pesticides sprayed at small, localized areas, to levels that may cause health concern when released as a “fog”. Potentially hazardous exposures can occur if occupants are present during and/or shortly following the application when recommendations to avoid being indoors during those times are not followed. Redistribution of pesticides in a residential setting extends the time of exposure beyond the original application period and locations (Lioy et al. 2002). Health effects from pesticides and the susceptible populations vary, e.g., children and pregnant women. Thus, exposure pathways and routes for these groups need to be identified. When evaluating potential exposures to pesticides both historically available pesticides and new formulations should be considered, as well as application methodologies. In practice, actual application by untrained applicators or homeowners may differ from manufacturer’s recommended instructions or not understood, which can result in higher exposures (Grey et al. 2005).

Phthalates are incorporated into the plastics of many consumer products, home furnishings, vinyl flooring and wall coverings (Bornehag et al. 2005; Otake et al. 2004). The most common are: benzylbutylphthalate (BBP), dibutylphthalate

(DBP), di-(2-ethylhexyl)-phthalate (DEHP), di-isodecylphthalate (DIDP), and di-isonylphthalate (DINP) (Abb et al. 2009), though other phthalates have been detected in house dust (Kubwabo et al. 2016). They are present in house dust and air. Flame retardants have been incorporated into home furnishings, electronics and even clothing for babies to forestall the initiation or spreading of fires in homes beginning in 1975. These include brominated compounds, polybrominated diphenyl ethers (PBDEs), tetrabromobisphenol A, hexabromocyclododencane, and organophosphate flame retardants (OPFRs). Their use in the United States started to decline in 2015 when the adverse health outcomes of some chemical flame retardants were identified and their effectiveness for fire prevention was questioned. Since home furnishing continued to be used for years and these chemicals do not readily decompose, continued exposures occur as these compounds become continually incorporated into dust and have a vapor phase within buildings (Stapleton et al. 2008).

Role of House Dust

House dust can contain a wide array of toxicants that are present in the indoor air and absorbed onto the dust particles or have been tracked in from the outside on the bottom of shoes. Dust born toxicants include non-volatile metals and organic species, VOCs, and SVOCs. Multiple indoor surfaces accumulate dust including carpets, countertops, and floors. House dust exposure occurs via inhalation, dermal, and indirect/non-dietary ingestion. Carpeting has been demonstrated to be a reservoir for house dust (Lioy et al. 2002). Inhalation exposure to house dust can occur when it is resuspended into the air, such as through vacuuming or peoples' physical activities such as walking (Lewis et al. 2018; Pavilonis et al. 2015; Rasmussen et al. 2018; Shalat et al. 2011; Wang et al. 2012; Zhou et al. 2017, 2019). Depending upon the vacuum type, larger pieces of house dust are trapped by the vacuum filter but smaller ones can pass through the vacuum bag and become re-suspended into the air. While the particles will settle back down on surfaces over time, an individual within the indoor environment will still inhale the particles (U.S. Environmental Protection Agency 2018). The redistribution of house dust within an indoor setting can lead to inadvertent ingestion exposure and dermal exposure, especially to children who tend to put a lot of items into their mouths and have more contact with the floor than adults, where dust naturally accumulates (Kwong et al. 2020).

Indoor Chemistry

Reactions between ozone and unsaturated hydrocarbon-based compounds (having at least one double or triple carbon-carbon bond) are well known to occur outdoors forming secondary organic aerosols but also contribute to indoor chemistry (Weschler and Carslaw 2018). Nitrogen oxides (NO_x) from natural gas combustion and hypochlorite, from cleaning products, can also react with unsaturated

hydrocarbons. Short lived, intermediate species such as nitrous acids (HONO), and free radicals such as hydroxyl (OH), hydroperoxy (HO_2), organic peroxides (RO_2), as well as nitrate radicals formed from ozone and nitrogen oxides may play a role in indoor air chemistry. Ozone and nitrogen oxides penetrate from outdoors, with indoor sources existing (e.g., photocopies for ozone, combustion of gas for cooking and heating for nitrogen oxides). Unsaturated compounds have multiple sources indoors that include outdoor penetration, consumer and cleaning products (e.g., fragrances – terpenes, ammonia), building materials (e.g., wood-terpenes, plastics), cooking (e.g., oils and spices – terpenoids), and skin oils (e.g., squalene, unsaturated fatty acids, isoprene). Reactions with unsaturated hydrocarbons reduce indoor ozone air concentrations, which is a respiratory and ocular irritant, but the chemical reaction products may also be irritants or have other adverse health effects (Nazaroff and Weschler 2004). The extent that these reactions occur indoors is related to a home's air exchange rate. Higher air exchange rates bring more ambient ozone indoors while lower rates provide more time for the reaction to occur and the buildup of the unsaturated hydrocarbon precursors and reaction products.

Ozone-driven reactions incorporate an oxygen into the carbon structure forming aldehydes, ketones, and carboxylic acids of various carbon lengths and structure. Nitrogen containing moieties can be produced when nitrogen oxides are present. Both volatile and indoor secondary organic aerosols (SOA) are formed. Since skin oil compounds contain double bonds that react with ozone, the air concentration of their reaction products are higher surrounding an individual than elsewhere in the indoor environment, leading to higher inhalation exposure or dermal contact than might be estimated from room air measurements. Among the compounds observed from ozone-squalene reactions to which individuals are exposed are volatile species: 6-methyl-5-heptene-2-one (6MHO), geranyl acetone and 4-oxopental (4-OPA) (Wisthaler and Weschler 2010), and SOA containing levulinic, succinic, adipic, and suberic acids (Zhou et al. 2016).

Consumer Goods and Personal Exposures

According to the US EPA, consumer products contain more than 49,000 chemicals in 16,000 products (www.EPA.gov/chemical-research/chemical-and-products-data-base-cpdat accessed 1/20/21). While not all chemicals will be released into the air and some may be at very low concentrations and/or in a limited number of products, consumer products can be a source of multiple contaminants to the indoor air thereby exposing people via multiple routes. New furniture and building material which contain glues/adhesives, pressed wood, flame retardants, stains and sealers, dyes, stain treatment, etc. continuously release VOCs and SVOCs into the indoor air, with the amount emitted typically declining over time as the product ages and the amount of the agents present in the product declines. It is not unusual to smell chemicals emitted when new products are first brought into a home or after walls are painted, affecting air quality and leading to exposures. The amount released can vary over a day and seasonally due to temperature changes within a home, with more emissions

at higher temperatures. However, the temperature range indoors is not as great as outdoors so the cycling of emissions may be limited. Furniture containing polyurethane or other foams can absorb SVOCs from the air and subsequently release them, moderating and extending the time that SVOCs affect the indoor air concentration after the SVOCs are introduced into a home from a consumer product. The use of the plethora of personal, consumer products categorized as cosmetics and personal care products, cleaning and home maintenance products, pesticides, disinfectants, and scented candles and air fresheners, (e)-cigarettes, etc. contribute chemicals and particles, including nanoparticles, into the indoor air. The releases from consumer products typically occur sporadically, depending on how and when they are used. Some products are intentionally sprayed into or through the air. Others have evaporative emissions after the product is applied to the body or surfaces. Dust and particles containing residue from consumer product are resuspended from floors or surfaces when perturbed by physical movement.

Chemicals emitted from personal consumer products initially results in a non-uniform air concentration within a room and throughout a home. This is due to it having a localized source, i.e., product use, and incomplete mixing of air throughout a room and house, though over time a more uniform indoor air concentration is reached. Since many products are used in close proximity to people, the air concentration in the breathing zone resulting from that use is typically higher than in the “background” indoor air and drives the inhalation exposure. Studies that have examined both indoor and personal air concentration typically find that the daily average personal air concentrations are higher than the daily average indoor air concentrations (Turpin et al. 2007; Weisel et al. 2005). However, the ratio of the daily average personal to indoor air is smaller than the ratio that would be calculated for short-term peak exposures, as many products result in brief, large increases in breathing zone air concentration before the agents diffused throughout the room elevating the “background” indoor room air concentration by a smaller amount.

An evaluation of the impact of consumer products emissions on breathing zone air concentrations requires an understanding of the human activity patterns and actual product use. Some of the broad classes of agents in these products were given in Table 1, but that list represents only a portion of the agents released and to which people are exposed. Consumer product emissions can cause acute or chronic elevations of the breathing air concentrations and exposures depending upon the product and its use. Acute exposures can result from spraying of products such as hair and cosmetic products, pesticides, and cleaning products. Personal care products are typically sprayed toward the direction of a person presenting instantaneous, elevated inhalation exposures. Pesticides and cleaning products should be sprayed away from the face but create aerosols that drift toward the breathing zone prior to being dispersed throughout the room. For cleaning products, the person applying it often stays in close proximity to the area sprayed while cleaning the surface it was applied to, extending the time of elevated breathing zone air levels. Personal or breathing zone air samples have not been collected in many studies for some specific activities, such as showering and bathing, due to logistic issues. The activities can release contaminants into breathing zone air, such as disinfection by-products from

chlorinated water while showering, at levels much above the “background” indoor air, again presenting an exposure that is not captured from “background” indoor air concentration measurements. Smoking and vaping causes high exposures to many air contaminants, particularly to the individual smoking or vaping due to direct inhalation of the smoke and vapors and from the resulting contaminated breathing zone air. Other individuals who are in close proximity to the smoker or person who vapes will also encounter elevated breathing zone air levels compared to the “background” indoor air, prior to the smoke or vaping emissions being dispersed. Many indoor air studies have excluded homes with smokers from their target population because smoking often is the dominant indoor air source of particles and many gases.

Longer duration (subchronic and chronic) elevation of breathing zone air also occurs due to the proximity of people to some consumer product sources. These can include emission from products that are directly applied to the body, from clothing, and from furniture. Products applied to the skin can contain SVOCs that evaporate from the skin and will penetrate the breathing zone. Clothing can contain cleaning chemicals, fragrances, and surfactants present in detergents used to wash clothes and from dry cleaned clothes will off-gas the dry-cleaning chemicals, such tetra-chloroethene, for several days. Nanoparticles are being added to clothes to lessen odors by limiting bacterial growth (sliver nanoparticles) and to repel water and stains (silica nanoparticles), which can be released from mechanical abrasion. SVOCs and particulate emissions from furniture may also elevate breathing zone air since sitting on upholstered furniture or bedding often brings the face close to the source for extended times. These can include flame retardant chemicals (e.g., PBDEs), stain resistant chemicals (PFAS), dust mites, allergens, and SVOCs that were absorbed from the air by the material covering or foam padding in the furniture. These SVOCs can be released by the warmth provided by the body which shifts the equilibria from the absorbent surface to the air. The thermal properties of the body create an air boundary layer flow, with flow patterns around the body that move upwards since the body is typically warmer than the indoor air temperature. This upwards movement of air contaminants brings them into the breathing zone when they are emitted from lower sections of the front of the body and potentially from furniture being sat upon. Under conditions of low air mixing, these emissions close to the front of the body will impact the breathing zone concentrations (Licina et al. 2015).

Conclusions

Many indoor sources and low air exchange rates contribute to poor indoor air quality. Understanding the major routes of exposure: inhalation, dermal, and non-dietary and indirect ingestion is critical to identifying exposure pathways in the indoor environment to implement steps to reduce exposures and protect public health. As discussed in this chapter, these sources of exposures can originate indoors and near peoples, such as personal care products, building materials, house dust, or penetrate from outdoors or soil, such as radon, ozone, and VOCs. Indoor chemical reactions expose

the general population to additional compounds whose health effects are not completely known. Since people spend the majority of their time indoors during their lifetime, it is important to consider how these factors influence the quality of indoor air and exposures, and subsequently affect health.

Cross-References

- [Fundamentals of Exposure Science](#)
- [Household Air Pollution in Rural Area](#)
- [Occupant Emissions and Chemistry](#)
- [Role of Clothing in Exposure to Indoor Pollutants](#)
- [Time-Activity Patterns](#)
- [Very Volatile Organic Compounds \(VVOCs\)](#)

Acknowledgments Drs. Feld-Cook and Weisel are supported in part by NIEHS in part by the NIEHS training grant T32ES019854 and the NIEHS Center for Environmental Exposure and Disease NIEHS P30ES005022.

References

- Abb M, Heinrich T, Sorkau E, Lorenz W (2009) Phthalates in house dust. *Environ Int* 36(35): 965–970
- Abdullahi KL, Delgado-Saborit JM, Harrison RM (2013) Emissions and indoor concentrations of particulate matter and its specific chemical components from cooking: a review. *Atmos Environ* 71:260–294
- Alavanja MC, Lubin JH, Mahaffey JA, Brownson RC (1999) Residential radon exposure and risk of lung cancer in Missouri. *Am J Public Health* 89(7):1042–1048
- American Society of Heating, R. a. A.-C. E., Inc (1989) An American National Standard Ventilation for Acceptable Indoor Air Quality Standard 62.2. ANSI/ASHRAE 62–1989
- ATSDR (2007) Revised health consultation; formaldehyde sampling at FEMA temporary housing units. Baton Rouge, Louisiana
- Azuma K, Uchiyama I, Uchiyama S, Kunugita N (2016) Assessment of inhalation exposure to indoor air pollutants: screening for health risks of multiple pollutants in Japanese dwellings. *Environ Res* 145:39–49
- Azuma K, Ikeda K, Kagi N, Yanagi U, Osawa H (2018) Physicochemical risk factors for building-related symptoms in air-conditioned office buildings: ambient particles and combined exposure to indoor air pollutants. *Sci Total Environ* 616–617:1649–1655
- Bennett DH, Margni MD, McKone TE, Jolliet O (2002) Intake fraction for multimedia pollutants: a tool for life cycle analysis and comparative risk assessment. *Risk Anal* 22(5):905–918
- Bi C, Liang Y, Xu Y (2015) Fate and transport of phthalates in indoor environments and the influence of temperature: a case study in a test house. *Environ Sci Technol* 49(16):9674–9681
- Biesterbos JWH, Dudzina T, Delmaar CJE, Bakker MI, Russel FGM, von Goetz N, Scheepers PTJ, Roeleveld N (2013) Usage patterns of personal care products: important factors for exposure assessment. *Food Chem Toxicol* 55:8–17
- Bornehag C-G, Lundgren B, Weschler CJ, Sigsgaard T, Hagerhed-Engman L, Sundell J (2005) Phthalates in indoor dust and their association with building characteristics. *Environ Health Perspect* 113(10):1399–1404

- Brasche S, Bischof W (2005) Daily time spent indoors in German homes – baseline data for the assessment of indoor exposure of German occupants. *Int J Hyg Environ Health* 208(4):247–253
- Dawson HE, McAlary T (2009) A compilation of statistics for VOCs from post-1990 indoor air concentration studies in North American residences unaffected by subsurface vapor intrusion. *Groundw Monitor Remediat* 29(1):60–69
- Destaillets H, Maddalena RL, Singer BC, Hodgson AT, McKone TE (2008) Indoor pollutants emitted by office equipment: a review of reported data and information needs. *Atmos Environ* 42(7):1371–1388
- Dodson RE, Levy JI, Houseman EA, Spengler JD, Bennett DH (2009) Evaluating methods for predicting indoor residential volatile organic compound concentration distributions. *J Expo Sci Environ Epidemiol* 19(7):682–693
- Duncan SM, Sexton KG, Turpin BJ (2018) Oxygenated VOCs, aqueous chemistry, and potential impacts on residential indoor air composition. *Indoor Air* 28(1):198–212
- Fantke P, Ernstoff AS, Huang L, Csiszar SA, Jolliet O (2016) Coupled near-field and far-field exposure assessment framework for chemicals in consumer products. *Environ Int* 94:508–518
- Garcia-Hidalgo E, von Goetz N, Siegrist M, Hungerbühler K (2017) Use-patterns of personal care and household cleaning products in Switzerland. *Food Chem Toxicol* 99:24–39
- Grey CNB, Nieuwenhuijsen MJ, Golding J (2005) The use and disposal of household pesticides. *Environ Res* 97(1):109–115
- Heyder J (2004) Deposition of inhaled particles in the human respiratory tract and consequences for regional targeting in respiratory drug delivery. *Proc Am Thorac Soc* 1(4):315–320
- Hodas N, Loh M, Shin HM, Li D, Bennett D, McKone TE, Jolliet O, Weschler CJ, Jantunen M, Liou P, Fantke P (2016) Indoor inhalation intake fractions of fine particulate matter: review of influencing factors. *Indoor Air* 26(6):836–856
- Jolliet O, Ernstoff AS, Csiszar SA, Fantke P (2015) Defining product intake fraction to quantify and compare exposure to consumer products. *Environ Sci Technol* 49(15):8924–8931
- Kubwabo C, Fan X, Rasmussen PE, Wu F, Kosarac I (2016) Expanding the number of phthalates monitored in house dust. *Int J Environ Anal Chem* 96(7):667–681
- Kwong LH, Ercumen A, Pickering AJ, Unicomb L, Davis J, Luby SP (2020) Age-related changes to environmental exposure: variation in the frequency that young children place hands and objects in their mouths. *J Expo Sci Environ Epidemiol* 30:205–216
- Lewis RD, Ong KH, Emo B, Kennedy J, Kesavan J, Elliot M (2018) Resuspension of house dust and allergens during walking and vacuum cleaning. *J Occup Environ Hyg* 15(3):235–245
- Licina D, Melikov A, Sekhar C, Tham KW (2015) Human convective boundary layer and its interaction with room ventilation flow. *Indoor Air* 25(1):21–35
- Liou P, Weisel C (2014) *Exposure science: basic principles and applications*. Academic
- Liou PJ, Freeman NCG, Millette RJ (2002) Dust: a metric for use in residential and building exposure assessment and source characterization. *Environ Health Perspect* 110(10):969–983
- Little JC, Weschler CJ, Nazaroff WW, Liu Z, Cohen Hubal EA (2012) Rapid methods to estimate potential exposure to semivolatile organic compounds in the indoor environment. *Environ Sci Technol* 46(20):11171–11178
- Liu W, Zhang J, Zhang L, Turpin BJ, Weisel CP, Morandi MT, Stock TH, Colome S, Korn LR (2006) Estimating contributions of indoor and outdoor sources to indoor carbonyl concentrations in three urban areas of the United States. *Atmos Environ* 40(12):2202–2214
- Liu S, Li R, Wild RJ, Warneke C, de Gouw JA, Brown SS, Miller SL, Luongo JC, Jimenez JL, Zieman PJ (2016) Contribution of human-related sources to indoor volatile organic compounds in a university classroom. *Indoor Air* 26(6):925–938
- Liu S, Thompson SL, Stark H, Zieman PJ, Jimenez JL (2017) Gas-phase carboxylic acids in a university classroom: abundance, variability, and sources. *Environ Sci Technol* 51(10):5454–5463
- Liu N, Cao J, Huang J, Zhang Y (2021) Role of clothing in skin exposure to Di(n-butyl) phthalate and Tris(1-chloro-2-propyl) phosphate: experimental observations via skin wipes. *Environ Sci Technol Lett* 8(3):270–275

- Löndahl J, Möller W, Pagels JH, Kreyling WG, Swietlicki E, Schmid O (2014) Measurement techniques for respiratory tract deposition of airborne nanoparticles: a critical review. *J Aerosol Med Pulm Drug Deliv* 27(4):229–254
- Matt GE, Quintana PJE, Hovell MF, Bernert JT, Song S, Novianti N, Juarez T, Floro J, Gehrman C, Garcia M, Larson S (2004) Households contaminated by environmental tobacco smoke: sources of infant exposures. *Tob Control* 13(1):29–37
- Matz JC, Stieb MD, Davis K, Egyed M, Rose A, Chou B, Brion O (2014) Effects of age, season, gender and urban-rural status on time-activity: Canadian human activity pattern survey 2 (CHAPS 2). *Int J Environ Res Public Health* 11(2):2108
- Miguel et al (2006) Meteorological influences on respirable fragment release from chinese elm pollen aerosol science and technology. 40(9):690–696. <https://www.tandfonline.com/doi/full/10.1080/02786820600798869>
- Morrison GC, Weschler CJ, Bekö G, Koch HM, Saltherammer T, Schripp T, Toftum J, Clausen G (2016) Role of clothing in both accelerating and impeding dermal absorption of airborne SVOCs. *J Expo Sci Environ Epidemiol* 26(1):113–118
- National Research Council (1999) Health effects of exposure to radon: BEIR VI. The National Academies Press, Washington, DC
- National Research Council (2012) Exposure science in the 21st century: a vision and a strategy. The National Academies Press, Washington, DC
- Nazaroff WW (2016) Indoor bioaerosol dynamics. *Indoor Air* 26(1):61–78
- Nazaroff WW, Weschler CJ (2004) Cleaning products and air fresheners: exposure to primary and secondary air pollutants. *Atmos Environ* 38(18):2841–2865
- Oberdörster G, Oberdörster E, Oberdörster J (2005) Nanotoxicology: an emerging discipline evolving from studies of ultrafine particles. *Environ Health Perspect* 113(7):823–839
- Odabasi M (2008) Halogenated volatile organic compounds from the use of chlorine-bleach-containing household products. *Environ Sci Technol* 42(5):1445–1451
- Otake T, Yoshinaga J, Yanagisawa Y (2004) Exposure to phthalate esters from indoor environment. *J Expo Sci Environ Epidemiol* 14(7):524–528
- Ott WE, Steinemann A, Wallace L (eds) (2006) Exposure analysis. CRC Press, Taylor & Francis Group, Boca Raton
- Pavilonis BT, Lioy PJ, Guazzetti S, Bostick BC, Donna F, Peli M, Zimmerman NJ, Bertrand P, Lucas E, Smith DR, Georgopoulos PG, Mi Z, Royce SG, Lucchini RG (2015) Manganese concentrations in soil and settled dust in an area with historic ferroalloy production. *J Expo Sci Environ Epidemiol* 25(4):443–450
- Rasmussen PE, Levesque C, Chénier M, Gardner HD (2018) Contribution of metals in resuspended dust to indoor and personal inhalation exposures: relationships between PM10 and settled dust. *Build Environ* 143:513–522
- Samet J (2001) Radon. In: Spengler JD, Samet JM, McCarthy JF (eds) Indoor air quality handbook. McGraw-Hill Education, New York
- Schettler TED (2006) Human exposure to phthalates via consumer products. *Int J Androl* 29(1):134–139
- Seaman V, Bennett D, Cahill TM (2009) Indoor acrolein emission and decay rates resulting from domestic cooking events. *Atmos Environ* 43:6199–6204
- Shalat SL, Stambler AA, Wang Z, Mainelis G, Emoeokpere OH, Hernandez M, Lioy PJ, Black K (2011) Development and in-home testing of the Pretoddler inhalable particulate environmental robotic (PIPER Mk IV) sampler. *Environ Sci Technol* 45(7):2945–2950
- Shi S, Zhao B (2014) Modeled exposure assessment via inhalation and dermal pathways to airborne semivolatile organic compounds (SVOCs) in residences. *ES&T* 48:5791–5699. <https://pubs.acs.org/doi/10.1021/es500235q>
- Stapleton HM, Allen JG, Kelly SM, Konstantinov A, Klosterhaus S, Watkins D, McClean MD, Webster TF (2008) Alternate and new brominated flame retardants detected in U.S. House Dust. *Environ Sci Technol* 42(18):6910–6916
- Stönnér C, Edtbauer A, Williams J (2018) Real-world volatile organic compound emission rates from seated adults and children for use in indoor air studies. *Indoor Air* 28(1):164–172

- Tang X, Misztal PK, Nazaroff WW, Goldstein AH (2015) Siloxanes are the most abundant volatile organic compound emitted from engineering students in a classroom. *Environ Sci Technol Lett* 2(11):303–307
- Tang X, Misztal PK, Nazaroff WW, Goldstein AH (2016) Volatile organic compound emissions from humans indoors. *Environ Sci Technol* 50(23):12686–12694
- Turpin BJ, Weisel CP, Morandi M, Colome S, Stock T, Eisenreich S, Buckley B (2007) Relationships of Indoor, Outdoor, and Personal Air (RIOPA) Part II. Pollutants in Indoor, outdoor, and personal air: composition of particulate matter. Health Effect Institute and National Urban Air Toxics Research Center, Boston. 130 Part II: 110
- U. S. Environmental Protection Agency (2018) Introduction to indoor air quality: primary causes of indoor air problems. Retrieved 01-29-2021, 2021, from <https://www.epa.gov/indoor-air-quality-iaq/introduction-indoor-air-quality>
- U.S. Environmental Protection Agency (2011) Chapter 16. Activity factors. Exposure factors handbook 2011 edition. National Center for Environmental Assessment, Washington, DC. <https://www.epa.gov/expobox/about-exposure-factors-handbook>. Accessed 1/29/21
- U.S. Environmental Protection Agency (2016) A citizen's guide to Radon: the guide to protecting yourself and your family from Radon. EPA402/K-12/002. www.epa.gov/radon
- U.S. Environmental Protection Agency (2017a) Exposure levels for evaluating polychlorinated biphenyls (PCBs) in indoor school air. EPA/600/R-12/051. www.epa.gov/ord
- U.S. Environmental Protection Agency (2017b) Indoor Semi-volatile Organic Compounds (i-SVOC) Version 1.0. EPA/600/C-13/290 https://cfpub.epa.gov/si/si_public_record_report.cfm?Lab=NRMRL&dirEntryId=307451. Accessed 1/29/21
- U.S. Environmental Protection Agency (2018) ExpoBox: exposure assessment tools by routes-ingestion. EPA Office of Research and Development <https://www.epa.gov/expobox/exposure-assessment-tools-routes-ingestion>. Accessed 1/29/21
- U.S. Environmental Protection Agency (2019) Guidelines for exposure assessment. Washington, DC: 223pp, Oct 2019, EPA/100/B-1/001
- U.S. Environmental Protection Agency (2020) Initial list of hazardous air pollutants with modifications. <https://www.epa.gov/haps/initial-list-hazardous-air-pollutants-modifications>. Accessed 8/8/21
- Wallace LA, Pellizzari ED, Hartwell TD, Sparacino C, Whitmore R, Sheldon L, Zelon H, Perritt R (1987) The TEAM study: personal exposures to toxic substances in air, drinking water, and breath of 400 residents of New Jersey, North Carolina, and North Dakota. *Environ Res* 43(2):290–307
- Wallace LA, Ott WR, Weschler CJ, Lai ACK (2017) Desorption of SVOCs from heated surfaces in the form of ultrafine particles. *Environ Sci Technol* 51(3):1140–1146
- Wang H, Morrison GC (2006) Ozone-initiated secondary emission rates of aldehydes from indoor surfaces in four homes. *Environ Sci Technol* 40(17):5263–5268
- Wang Z, Shalat SL, Black K, Lioy PJ, Stambler AA, Emoekpere OH, Hernandez M, Han T, Ramagopal M, Mainelis G (2012) Use of a robotic sampling platform to assess young children's exposure to indoor bioaerosols. *Indoor Air* 22(2):159–169
- Weisel CP, Zhang JJ, Turpin BJ, Morandi MT, Colome S, Stock TH, Spektor DM (2005) Relationships of Indoor, Outdoor, and Personal Air (RIOPA). Part I. Collection methods and descriptive analyses. Health Effects Institute and National Urban Air Toxics Research Center, Boston, pp 130–131
- Weisel CP, Alimokhtari S, Sanders PF (2008) Indoor air VOC concentrations in suburban and rural New Jersey. *Environ Sci Technol* 42(22):8231–8238
- Weschler CJ (2009) Changes in indoor pollutants since the 1950s. *Atmos Environ* 43(1):153–169
- Weschler CJ, Carslaw N (2018) Indoor chemistry. *Environ Sci Technol* 52(5):2419–2428
- Weschler CJ, Nazaroff WW (2014) Dermal uptake of organic vapors commonly found in indoor air. *Environ Sci Technol* 48(2):1230–1237
- Wisthaler A, Weschler CJ (2010) Reactions of ozone with human skin lipids: sources of carbonyls, dicarbonyls, and hydroxycarbonyls in indoor air. *Proc Natl Acad Sci* 107(15):6568

- Wu X, Bennett DH, Ritz B, Cassady DL, Lee K, Hertz-Pannier I (2010) Usage pattern of personal care products in California households. *Food Chem Toxicol* 48(11):3109–3119
- Zhou S, Forbes MW, Katrib Y, Abbatt JPD (2016) Rapid oxidation of skin oil by ozone. *Environ Sci Technol Lett* 3(4):170–174
- Zhou J, Tierney NK, McCarthy TJ, Black KG, Hernandez M, Weisel CP (2017) Estimating infants' and toddlers' inhalation exposure to fragrance ingredients in baby personal care products. *Int J Occup Environ Health* 23(4):291–298
- Zhou J, Mainelis G, Weisel CP (2019) Pyrethroid levels in toddlers' breathing zone following a simulated indoor pesticide spray. *J Expo Sci Environ Epidemiol* 29(3):389–396



Role of Clothing in Exposure to Indoor Pollutants

36

Dusan Licina, Gabriel Bekö, and Jianping Cao

Contents

Introduction	1028
Exposures to Chemicals	1030
Evidence of Clothing-Associated Exposure to Chemicals	1030
Occurrence, Persistence, and Accumulation of Chemicals in Clothing	1033
Mechanisms, Quantification, and Prediction of Exposure and Transfer of Chemicals	1036
Exposures to Particles	1039
Clothing-Associated Exposures to Biotic and Abiotic Particles	1039
Toward Quantifying Clothing-Mediated Particle Exposures	1043
Factors Affecting Clothing-Mediated Particle Exposures	1046
Conclusions	1049
References	1051

Abstract

There is growing evidence that the clothing is an important source of exposure to various chemicals and particles on a daily basis. Emerging knowledge suggests that everyday clothing harbors various contaminants, which if inhaled, ingested, or dermally absorbed, could carry significant health risks. This chapter summarizes the state of the most recent knowledge regarding how clothing, during wear,

D. Licina (✉)

Human-Oriented Built Environment Lab, School of Architecture, Civil and Environmental Engineering, École polytechnique fédérale de Lausanne, Fribourg, Switzerland

e-mail: dusan.licina@epfl.ch

G. Bekö

International Centre for Indoor Environment and Energy, Department of Civil Engineering, Technical University of Denmark, Kongens Lyngby, Denmark

e-mail: gab@byg.dtu.dk

J. Cao

School of Environmental Science and Engineering, Sun Yat-sen University, Guangzhou, China
e-mail: caojp3@mail.sysu.edu.cn

influences exposure to molecular chemicals, abiotic particles, and biotic particles, including microbes and allergens. The underlying processes that govern the acquisition, retention, and transmission of clothing-associated contaminants and the consequences of these for subsequent exposures are explored. Chemicals of concern have been identified in clothing, including byproducts of their manufacture and chemicals that adhere to clothing during use and care. Analogously, clothing acts as a reservoir for biotic and abiotic particles acquired from occupational and environmental sources. Evidence suggests that while clothing can be protective by acting as a physical or chemical barrier, clothing-mediated exposures can be substantial in certain circumstances and may have adverse health consequences. This complex process is influenced by the type and history of the clothing, the nature of the contaminant, and by wear, care, and storage practices. This chapter also summarizes the most pressing knowledge gaps that are important for better quantification, prediction, and control of clothing-mediated exposures.

Keywords

Chemical exposures · Abiotic particles · Biological material · Exposure modelling · Health impacts

Introduction

Clothing harbors diverse chemicals, particles, and microbes. Some are present at the time clothing is purchased, and some are acquired during the care, storage, and use of garments. People spend most of their lives in intimate contact with clothing. They are exposed to the species found on and in their clothing via inhalation, ingestion, and dermal absorption (Fig. 1). More specifically, humans inhale species that desorb or are released from their clothing, ingest clothing-associated chemicals and particles when clothing materials enter their mouths, and acquire species on their skin from the clothing they wear. Clothing-mediated exposures are influenced by factors inherent to clothing, such as fiber type, weave, morphology, dyeing process, color, and chemical treatment (including incorporation of flame retardants, stain repellants, and anti-wrinkle agents). Exposures are also influenced by external factors such as washing, drying, storage, usage patterns, and environmental conditions. Once in the lungs, in the gastrointestinal system or on the skin, chemicals from clothing may be absorbed into the body. This exposure can further contribute to irritation, allergic reactions, and infections as well as risks for adverse health effects as diverse as cancer, birth defects, and heavy-metal poisoning (BfR 2012; KEMI 2014; Rovira and Domingo 2019).

This chapter, largely based on our earlier critical review of the topic (Licina et al. 2019), is organized in the following manner: We first present the role of clothing in exposure to chemicals, then to biotic and abiotic particles. In the part on chemical pollutants, we first present the recent evidence for the influence of clothing-mediated

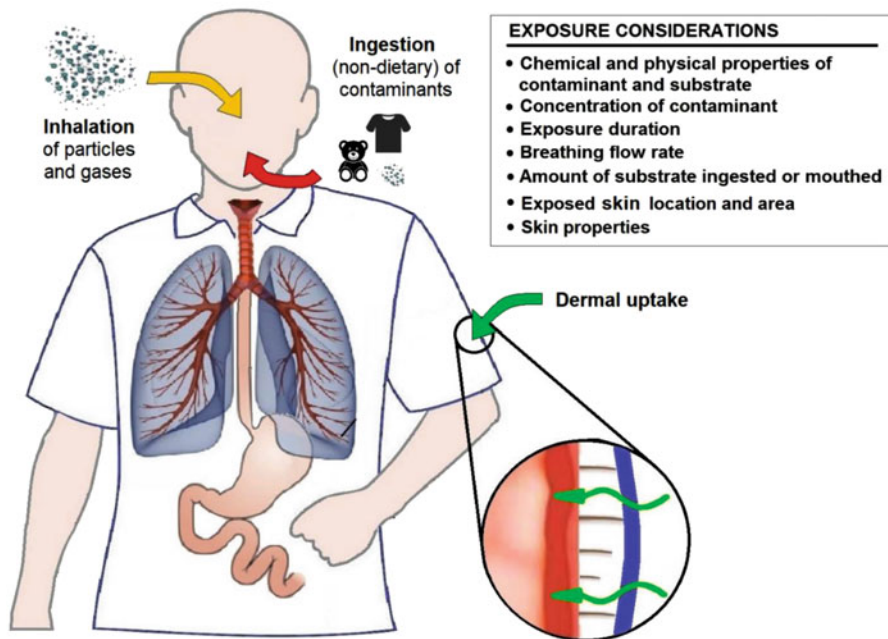


Fig. 1 Non-dietary routes of human exposure for contaminants of concern: Inhalation, ingestion and dermal absorption. (Reprinted with permission from D. Licina, G.C. Morrison, G. Beko, C.J. Weschler and W.W. Nazaroff, Clothing-mediated exposures to chemicals and particles, Environ. Sci. Technol., 2019, 53, 5559–5575, DOI: <https://doi.org/10.1021/acs.est.9b00272>. Copyright (2021) American Chemical Society)

exposure to chemicals. This is followed by a summary of the evidence of the occurrence and persistence of chemicals in clothing, and by discussion of the mechanisms of accumulation and transfer of chemicals. In the part on particles, we first present evidence for the influence of clothing-mediated exposure to biotic and abiotic particles. We then outline a framework for quantifying clothing-mediated particle exposures, and finally we review factors that influence clothing-associated exposures to particles. The chapter describes situations where the underlying factors influencing chemical and particle exposures are similar, while also recording fundamental ways that they differ. Whereas the potential influence on health risks is the key ultimate reason to improve understanding of clothing-mediated exposures, a detailed examination to quantify clothing-associated health risks is beyond the scope of this chapter. The concluding part examines several knowledge gaps that currently limit the ability to predict or mitigate clothing-related exposures to chemicals and particles. It also suggests some research directions that could reduce these limitations. Overall, the influence of clothing on environmental exposures is often substantial, but additional research efforts are warranted to better quantify, predict, and control clothing-related exposures, and ultimately understand how clothing influences human health and well-being.

Exposures to Chemicals

Evidence of Clothing-Associated Exposure to Chemicals

Clothing-Associated Chemicals in Skin, Blood, and Urine

Human exposure and uptake of organic compounds by means of transfer from treated fabrics has been investigated for several decades. For example, in the late 1970s, Blum et al. (1978) reported finding metabolites of the flame retardant tris (2,3-dibromopropyl)phosphate (tris) in the urine of children who had worn clothing treated with this chemical. Radiolabeled tris in treated and dried cloth was shown to penetrate the clipped skin of rabbits. Other studies showed that moistening the cloth with simulated sweat does not increase absorption. Earlier, Brown (1970) reported instances of infant poisoning attributable to use of phenolic disinfectants in improperly laundered hospital fabrics. More recently, forestry workers wearing permethrin-treated, tick-proof pants were shown to have significantly elevated levels of a permethrin metabolite in their urine (Rossbach et al. 2016). Moreover, absorption of ethylene oxide (a fumigant) and other pollutants such as glyphosate (an herbicide), malathion (an insecticide), and benzothiazole (used as dye, biocide, herbicide, and fungicide) from fabric into skin or a skin-mimicking membrane has been demonstrated in studies using an *in vitro* diffusion cell (Iadaresta et al. 2018).

In another study, measurements of polychlorinated dibenzo-p-dioxins and dibenzofurans (PCDD/F) in the stratum corneum, epidermis, and subcutis of eight volunteers as well as in a variety of new fabric swatches showed that some textiles are contaminated and can be an important source of exposure to these chemicals (Horstmann and McLachlan 1994). The PCDD/F species were shown to diffuse through the stratum corneum into the deeper layers of the skin. Stratum corneum concentrations were substantially higher after wearing contaminated shirts rather than uncontaminated shirts. Skin contamination was heterogeneous, both among individuals and among sites on the same individual. However, when identical, homogeneously contaminated T-shirts were used in a companion study, relatively little spatial and interpersonal variability was observed (Klasmeier et al. 1999). Uptake from polyester was found to be an order-of-magnitude lower than from cotton. Transfer of chemicals was found to increase for fabrics that were previously worn. Residual sweat and lipid compounds may have served as transfer vehicles, or possibly weakened the binding interaction between the fabric and PCDD/F. Heavy perspiration during intense physical activity also increased the migration rate of a textile dye, Dianix®, onto the skin of volunteer subjects, while contact time was found to be less important (Meinke et al. 2009).

As people perform their daily indoor (e.g., working, studying, playing, exercising) and outdoor routines (e.g., driving, cycling, walking), the clothes they wear can act as a means of transporting pollutants from one environment to another. This phenomenon has been studied in the context of health concerns related to “para-occupational” (or “take-home”) exposures. Certain hazardous chemicals, such as lead, beryllium, polychlorinated biphenyls (PCB), and pesticides, can be transferred

from a work site to the worker's home via clothing and thereby contribute to elevated levels in the blood and urine, or even to direct adverse health effects. For example, women who laundered agricultural work clothes had up to 42% higher serum levels of dichlorodiphenyltrichloroethane (DDT) and hexachlorobenzene compared to women who did not (Bradman et al. 2007). Similarly, women living in homes in which agricultural workers wore their work clothes had higher levels of most of the organochlorine pesticides that were being used (Bradman et al. 2007). Multivariate analyses by Park et al. (2015) indicated an association between serum levels of polybrominated diphenyl ethers in California firefighters and the storage and cleaning practices used for protective gear. Park et al. (2015) suggested that these flame retardants can be transported to fire stations via fireborne dust on soiled turnout gear and that good housekeeping practices can reduce subsequent exposure. Instances of para-occupational exposures for toxic and allelopathic particles will be discussed subsequently.

Influence of Clothing on Dermal Uptake of Airborne Chemicals

Until recently, the influence of clothing on dermal uptake of airborne organic compounds received relatively little attention. Initial studies examined a few chemicals, primarily volatile organic compounds in occupational settings. Recent efforts have addressed dermal exposures to semivolatile organic compounds common in everyday indoor settings. For example, Morrison et al. (2016) measured the uptake of two airborne phthalates, diethyl phthalate (DEP), and di-n-butyl phthalate (DnBP), by an individual wearing either clean clothes or clothes previously air-exposed in a chamber with elevated phthalate concentrations. When compared with dermal uptake for bare-skinned individuals under otherwise identical experimental conditions (Weschler et al. 2015), clean clothes decreased transdermal uptake by factors of 3–6, whereas previously exposed clothes increased dermal uptake by factors of 3 and 6 for DEP and DnBP, respectively. The same group of researchers subsequently obtained analogous results for nicotine (Bekö et al. 2018). Figure 2 metaphorically illustrates the role of clothing as either "protector" or "amplifier" of dermal uptake by using a tree and a rainstorm analogy. In another study, three subjects exhibited elevated urinary excretion rates of the UV filter benzophenone-3 (BP-3) and its metabolite benzophenone-1 shortly after donning T-shirts previously exposed to air with elevated BP-3 levels (Morrison et al. 2017a). The authors of that work suggested that dermal uptake of BP-3 from clothing could meaningfully contribute to overall body burdens.

The protective effect of uncontaminated clothing has also been indicated by reduced phthalate concentrations in skin wipe samples taken from body parts covered with clothing compared to uncovered skin (Gong et al. 2016). However, clothing did not provide total protection in these studies. In vitro experiments demonstrated reduced absorption of organophosphates through a cotton shirt as compared to unclothed skin (Moore et al. 2014). However, common clothing is reported to have little effect on dermal exposure to certain gases in hazardous material incidents, such as methyl bromide, sulfuryl fluoride, and chloropicrin (Gaskin et al. 2017).

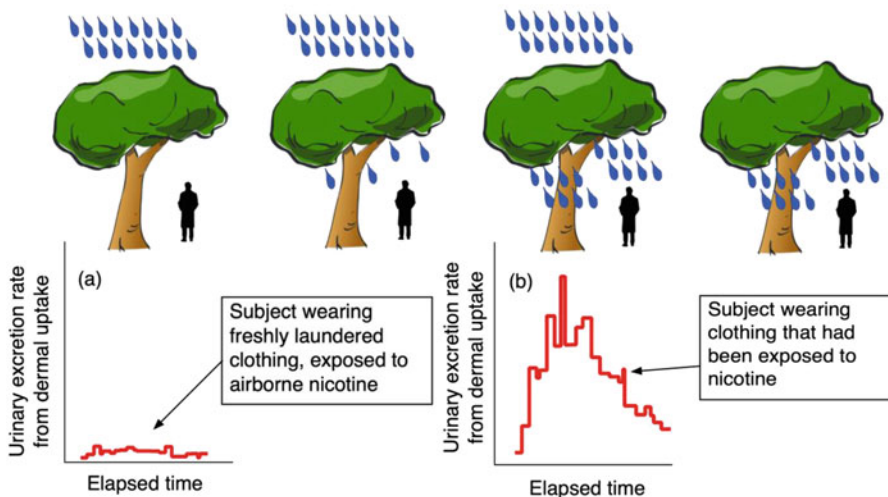


Fig. 2 Dynamic urinary excretion rates due to dermal uptake for nicotine and two urinary metabolites (summed) after exposing participants, who were wearing breathing hoods, to airborne nicotine (Bekö et al. 2018). (a) Freshly laundered clothing, unexposed to nicotine, is protective; this is analogous to a tree at the beginning of a rainstorm that protects a person from getting wet. (b) Clothing that has been previously exposed to airborne nicotine dramatically increases urinary excretion rate for days after wearing the clothing, just as standing under a tree after a long rainstorm is most certain to get the person wet. This exposure occurs while wearing the clothes in the environment containing the contaminant (third tree from left) and can continue after leaving this environment. (Reprinted with permission from D. Licina, G.C. Morrison, G. Beko, C.J. Weschler and W.W. Nazaroff, Clothing-mediated exposures to chemicals and particles, *Environ. Sci. Technol.*, 2019, 53, 5559–5575, <https://doi.org/10.1021/acs.est.9b00272>. Copyright (2021) American Chemical Society)

Numerical analysis of Cao et al. (2018) have shown that the skin-to-clothing contact (direct as opposed to indirect exposure via the air gap between skin and clothing) can significantly affect the skin exposure to chemicals. The effects of clothing on dermal exposure (i.e., accelerating effect of chemical-contaminated clothing and impeding effect of chemical-free clothing) can be stronger with increased skin-to-clothing contact (Liu et al. 2021). As a consequence, skin-to-clothing contact may be the primary pathway for chemicals from clothing to the skin surface. In the model by Cao et al. (2018) applied on the experimental scenarios described by Morrison et al. (2016), 62% and 87% of the total dermal exposure to DEP and DnBP was attributable to skin-to-clothing contact, respectively.

Health Effects as Evidence of Exposure

Studies of health effects related to hazardous substances in textiles further corroborates the significance of clothing-associated exposures. The existing studies have mainly focused on dermatitis caused by textile dyes and finishing resins. A limited literature also exists on carcinogenic, mutagenic, and reprotoxic substances in textile

articles. These effects have been suggested for certain dyes, especially azo dyes and for some antibacterial agents, such as triclosan. Brominated flame retardants, phthalates, and degradation products of highly fluorinated polymeric water repellents and stain repellents, which can be present in textile articles, have been associated with reproductive and developmental toxicity (Jurewicz and Hanke 2011). Evidence of direct health effects of such clothing-related exposures is lacking. Comprehensive reviews of textile-related health studies can be found in the report of the Swedish Chemicals Agency (KEMI 2014) and in the opinion statement of the German Federal Institute for Risk Assessment (BfR 2012).

Occurrence, Persistence, and Accumulation of Chemicals in Clothing

Figure 3 illustrates the typical clothing lifecycle from manufacturing and distribution to everyday use. The contaminants present in clothing are a mix of those present at the time of purchase (e.g., resulting from manufacturing processes; these possibly attenuate with time) and those acquired post-purchase. This mix changes with washing and drying practices, storage, and wear.

Chemicals Present at Time of Purchase

Most of the chemicals that have been measured in clothing at the time of purchase are a consequence of manufacturing processes (e.g., dyeing, bleaching, and finishing) or have been deliberately added and are intended to be retained during the life of the garment. The latter group, referred to as “auxiliaries,” includes antiwrinkling resins, flame retardants, antimicrobial agents, pesticides, surfactants,

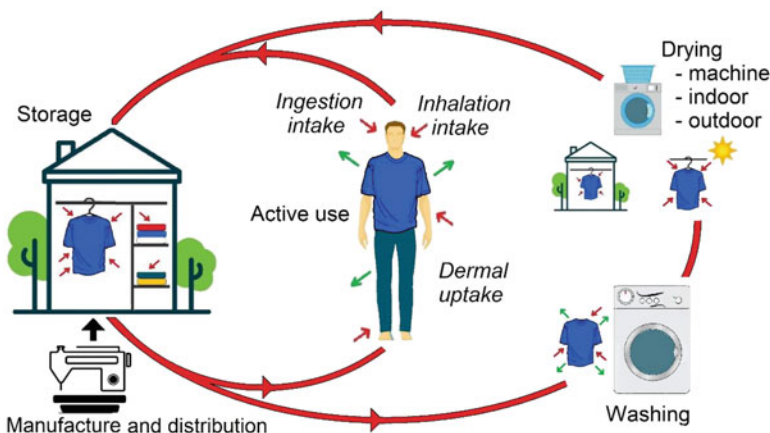


Fig. 3 Stages of clothing lifecycle that determine the rate of acquisition, retention and release of chemicals and particles. (Reprinted with permission from D. Licina, G.C. Morrison, G. Beko, C.J. Weschler and W.W. Nazaroff, Clothing-mediated exposures to chemicals and particles, Environ. Sci. Technol., 2019, 53, 5559–5575, DOI: <https://doi.org/10.1021/acs.est.9b00272>. Copyright (2021) American Chemical Society)

and other coating chemicals. Dyeing involves the largest range of chemicals, with an estimated 800 dyes currently in use (BfR 2012). A move towards more environmentally benign textile dyeing has been further altering the mix of chemicals used in dyeing. Some chemicals in clothing fabrics are present as a consequence of packaging, transport, storage, and other processes that occur between manufacture and purchase.

Chemicals that have been identified on newly purchased clothing include trace elements such as heavy metals (Rovira et al. 2017); residual aromatic amines associated with certain azo dyes (Kawakami et al. 2010); quinoline and substituted quinolines (Antal et al. 2016; Luongo et al. 2016); alkylphenol ethoxylates, alkylphenols, bisphenols, and benzophenones (Xue et al. 2017); benzothiazoles and benzotriazoles (Luongo et al. 2016), dioxins and furans (Horstmann and McLachlan 1994); PCBs, organo-phosphorous flame retardants and pesticides (Zhu et al. 2009); halogenated flame retardants (Blum et al. 1978); fluorinated surfactants (Liu et al. 2014); phthalate ester plasticizers (Schettler 2006); glycol solvents (Laursen et al. 2003); formaldehyde from antiwrinkle resins (De Groot and Maibach 2010); and common petrochemical fuel constituents such as linear and branched C₁₀–C₁₆ alkanes, C₃ alkylbenzenes, and straight-chained C₇–C₁₀ aldehydes (Lentini et al. 2000).

Relatively new chemical analysis techniques are being applied to assess chemicals in clothing. Antal et al. (2016) described the use of direct analysis in real-time (DART) mass spectrometry to measure more than 40 chemicals in 15 clothing items of different materials, types colors and origin. Identified compounds included alkylphenol ethoxylates, phthalate esters, alkyl amines, aniline, pyridine, quinoline, and substituted quinoline. In a recent review, Rovira and Domingo (2019) reported on chemicals that have a high probability of being detected on clothing, with a focus on the health risks posed by these species. These include various flame retardants, trace elements, and organic compounds (quinolines, bisphenol A, etc.). Of special note are extensive government reports from Denmark, Germany, The Netherlands, Sweden, and other countries that review and critically discuss chemicals found in clothing, especially the chemicals that may be present at the time of purchase (Licina et al. 2019).

Chemicals Acquired Post-Purchase

Chemicals present in air, especially indoor air, can also be present on clothing exposed to that air (Cao et al. 2016; Lao et al. 2018; Morrison et al. 2015, 2017b, 2018). A commonly encountered example of chemical uptake from air occurs when clothing is exposed to environmental tobacco smoke (ETS). Up to a milligram of nicotine can be sorbed by a square meter of cotton fabric during just a few hours of exposure (Piadé et al. 1999). Odors derived from ETS constituents can linger on clothing for hours to days. More generally, how much or how little of a chemical is transferred from air to clothing depends on several factors. One key factor is the partition coefficient between clothing and air (K_{ca}) for the fabric in question. As a rule of thumb, the more an airborne chemical resembles the chemical nature of the fabric that constitutes the clothing, the larger is the value of K_{ca} and consequently the

greater is the sorptive partitioning of that chemical to the clothing. The octanol/air partition coefficient (K_{oa}) is a good predictor of K_{ca} for cotton, since cotton is cellulosic, for which octanol is a reasonable surrogate (Morrison et al. 2015, 2018). Values of K_{ca} in relation to vapor pressure for several different fiber types have been reported (Morrison et al. 2018). Still needed are systematic investigations of K_{ca} for an array of environmental chemicals to a range of clothing fibers, including wool, polyester, nylon, rayon, and other synthetics, as well as to blends, to better estimate the sorption of airborne chemicals to these fiber types.

Clothing can also acquire chemicals while in closets, storage containers, and chests. A well-known example is sorption of the chemical agents used as moth repellants: naphthalene, camphor, and *p*-dichlorobenzene (Wang et al. 2011). Similarly, one would anticipate that phthalate esters or alternative plasticizers would be sorbed to clothing stored in polyvinyl chloride (PVC) storage boxes or bags.

Another route for transfer of chemicals to clothing is the contact with various surfaces. Such chemicals can migrate through clothing and become available for dermal uptake. Personal care products and fragrances applied to the skin or hair can also be transferred to clothing via contact. Clothing can retain certain chemicals transferred from personal care products, exposing the wearer, and, in principle, those sharing indoor spaces to such chemicals during storage and during repeat wearings until the item is effectively cleaned.

Laundering and dry-cleaning removes certain chemicals from clothing but can add others. The fraction of a chemical that is removed from clothing during cleaning varies with the nature of the chemical as well as with the cleaning practices, including the detergent or dry-cleaning solvent that is employed. Gong et al. (2016) found that the efficiency with which machine washing removed phthalates from cotton jeans increased with the octanol/water partition coefficient (K_{ow}) of the phthalate. During dry-cleaning, clothing can retain chemicals from cleaning solvents that subsequently contribute to personal exposures. During laundering, clothing may acquire scents (e.g., synthetic musks (BfR 2012)) and other detergent constituents (e.g., alkylphenol ethoxylates). Following the wash cycle, clothing is either air-dried or mechanically dried. When air-dried, the clothing can sorb chemicals from the air in which it is dried. When mechanically dried, some chemicals can be thermally desorbed while other chemicals (e.g., fabric softeners introduced using “dryer sheets”) may be sorbed by the clothing. Laundering also results in chemicals being transferred among the differing items that are washed or dried together. Cross-contamination of fabrics during laundering and storage has been reported for permethrin-treated garments (Faulde et al. 2006).

Chemicals on clothing can be chemically transformed to other species. Of longstanding concern are the abiotic and microbial reduction of azo dyes to carcinogenic aromatic amines such as aniline, benzidine, and 2-naphthylamine. For example, analysis of 86 textile products purchased in Japan detected aromatic amines at low concentrations in socks, undershorts, pants, and other garments (Kawakami et al. 2010). Oxidants can also degrade azo dyes, as shown by reactions initiated by the hydroxy radical, generating benzene and substituted benzenes (Spadaro et al. 1994). Photolytic debromination has been shown to produce low

levels of polybrominated dibenzofurans (Kajiwara et al. 2013) when clothing containing the flame retardant hexabromocyclododecane (HBCD) is dried in the sun.

Another significant source of chemicals in clothing is human skin. During wear for example, clothing acquires skin oils, whose constituents can be altered via microbial activity. Different fiber types promote the growth of different microbes, influencing malodor generation from microbial metabolism of apocrine and sebaceous secretions (Callewaert et al. 2014). Squalene, a major constituent of skin oil, has been shown to react with ozone on clothes generating products with a range of volatilities. The less volatile products remain on the apparel item, exposing the wearer to species such as C₂₇-pentaenal, C₂₂-tetraenal, C₁₇-trienal, and their carboxylic acid counterparts (Wisthaler and Weschler 2010). Squalene also reacts with HOCl, the active ingredient in chlorine bleach, to generate chlorinated squalene products. Three to four chlorine atoms become covalently incorporated into the squalene molecule during a 1-h exposure to 1 ppb HOCl (Schwartz-Narbonne et al. 2018). Such species may not be fully removed from clothing during washing. More generally, bleach oxidizes chemicals on clothing, increasing the water solubility of the contaminants but perhaps leaving behind oxidized and chlorinated residues. Numerous low volatility oxidation products, starting with primary carbonyls and carboxylic acids and evolving to products with high O to C ratios, result when ozone reacts with terpenes or sesquiterpenes transferred to clothing from personal care products. Other examples of chemicals generated via reactions that occur on clothing include nonylphenol, a known endocrine disruptor, from the degradation of nonylphenol ethoxylate detergent residues (Antal et al. 2016) and formaldehyde from urea-formaldehyde and melamine/formaldehyde resins used as antiwrinkling agents (De Groot and Maibach 2010). The potential for chemical transformations to occur on clothing is commonly overlooked during assessments of exposures to environmental chemicals.

Mechanisms, Quantification, and Prediction of Exposure and Transfer of Chemicals

Clothing influences chemical exposure by a variety of mechanisms, including some that are complex and poorly characterized. Organizations such as the US Environmental Protection Agency, the World Health Organization, and the European Chemicals Agency provide guidance on estimating exposure from consumer articles; however, such recommendations are based on a far-from-complete understanding and are therefore of limited utility in accurately characterizing complex chemical exposures mediated by clothing. Notwithstanding their limitations, these recommendations and models can be combined with stochastic representations of exposure factors and behaviors to estimate population distributions of exposure.

Dermal Transfer and Absorption

Most exposure models of skin contact transfer of chemicals from surfaces are conservative by design, i.e., they account, realistically, for the maximum potential

exposure for risk assessment and risk management purposes. Exposure is derived from factors including the skin area in contact; the concentration of the chemical in the material; the number, frequency, or duration of contact events; the type of contact; and a transfer efficiency. The transfer efficiency is the fraction of the chemical in the material that transfers during contact events. Experimental measurements of the transfer of pesticides and fluorescent tracers from carpet and of permethrin from military uniforms have been used to quantify transfer efficiency of residues from textiles. Some experimental results used to derive residue transfer efficiency are based on low-volatility chemicals directly applied to the side of the textile in contact with the skin. Therefore, the residue transfer model may inaccurately characterize exposure from clothing that has volatile or semivolatile chemicals distributed throughout the fabric. Recognizing that diffusive migration can occur within consumer materials, it has been proposed that a transfer efficiency can be derived from the amount that can diffuse from a thin “contact layer” of the material. The thickness of this layer can be specified for consumer products or can be estimated if diffusion coefficients are known for specific chemical-material combinations. These models generally do not account for the uptake resistance of skin itself.

Models of sweat-mediated transfer of chemicals from clothing also use a transfer efficiency approach. The leachable fraction is derived from experiments using artificial sweat to extract substances such as dyes (Meinke et al. 2009) and trace elements (Rovira et al. 2017). Often, the extracted fraction is assumed to be entirely transferred to the skin. Such an approach is likely to overestimate exposures, since only a fraction of the sweat will return to the skin from clothing. For example, Meinke et al. (2009) extracted fluorescent dyes from a polyester/cotton blend shirt using a sweat simulant and compared the predicted exposure (based on 100% transfer) to that observed in volunteers wearing the shirt during 30 min of exercise or for 12 h of normal activity. In these experiments, less than 1% of the estimated amount of a dye was transferred to volunteers during normal wear or sweating.

Indirect (non-contact) exposure to environmental contaminants can also be influenced by clothing. Clothing has been observed to reduce the transfer of airborne insecticides (Saleh et al. 1998), phthalate esters (Morrison et al. 2016), and organophosphate flame retardants (Moore et al. 2014) to skin. Some existing models of indirect dermal exposure to airborne contaminants have assumed that clothing is fully permeable. Other models assume that clothing is fully impermeable. For example, in estimating dermal uptake of polycyclic aromatic hydrocarbons from barbecue fumes to bare skin, Lao et al. (2018) assumed that areas covered by clothing were fully protected. Between these extremes, a mechanistic modeling approach has been introduced that accounts for the history of clothing, contaminant-transfer between clothing and the environment, sorptive partitioning of chemicals to clothing, diffusive and advective transfer through clothing and to skin lipids, as well as resistance to uptake through skin (Cao et al. 2018; Morrison et al. 2017a). The clothing component of these models is similar to that used to assess clothing for chemical protection and can account for uptake through clothing from air as well as exposure to contaminants present in clothing when donned.

Predictions using mechanistic models agree reasonably well with urinary excretion rate measurements for the limited number of human-subject studies in which adequate information is available to populate the model parameters (Cao et al. 2018; Morrison et al. 2017b). These models indicate that clothing can either reduce or increase dermal uptake relative to bare-skin uptake (Fig. 2). The extent of exposure is predicted to be sensitive to a chemical's partition coefficient between clothing and air (K_{ca}) (Cao et al. 2016; Morrison et al. 2018), the efficiency of chemical removal during laundering (Gong et al. 2016; Luongo et al. 2016), the air-gap between fabric and skin, laundering frequency, and the history of the clothing items prior to wear (Morrison et al. 2017a). Existing models could be further improved by an accurate measurement of the ratio of direct contact area to the total skin area, especially for chemicals with high values of K_{ca} , as well as by accounting for the transport of chemicals through the side openings of clothing. A key advantage of dynamic mechanistic models is that they can predict how clothing accumulates chemicals under non-equilibrium conditions. Such models can be used to derive simpler exposure heuristics for classes of chemicals, types of clothing, and exposure scenarios for risk assessment purposes.

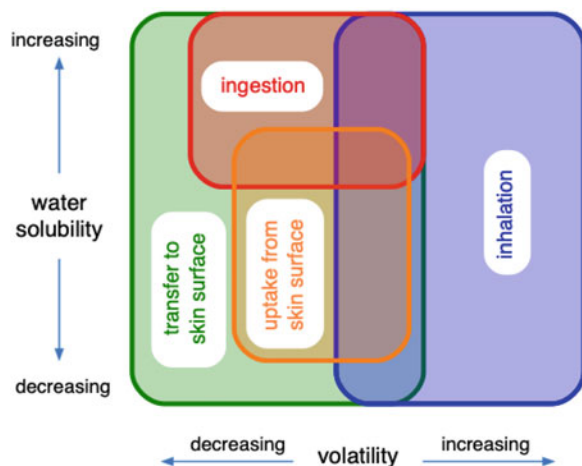
Inhalation

Inhalation exposures for clothing-associated chemicals can be modeled using methods similar to those used to estimate inhalation of chemicals emitted by consumer products. For example, the emission rate of dry-cleaning solvents from clothing hung in a closet can be combined with building air change rates to predict indoor air concentrations, which can then be used to assess inhalation exposures. Inhalation exposure from the emissions that are generated while wearing an article of clothing may be enhanced owing to the “personal cloud” effect, as described later for particles. For gaseous pollutants, personal-cloud type alterations have been illustrated in climate chamber experiments investigating transport and pollutant distribution in the breathing zone (Licina et al. 2015), as well as using computational fluid dynamics to predict breathing zone concentrations of volatile products that result from ozone reactions with the surface of the body and clothing (Rim et al. 2009). For a seated person under typical indoor conditions, inhalation exposure to volatile ozone reaction products with skin oils was predicted to be up to 2.5 times higher than the corresponding value for room-average concentrations. Predicted exposure to ozone itself was estimated to be 0.6 to 0.9 times the corresponding condition for room-average concentrations (Rim et al. 2009). Simulations are currently limited to simple scenarios, such as stationary seated or standing individuals. Experimental validation of personal cloud effects for clothing-associated chemical exposures are lacking.

Ingestion

Ingestion by mouthing of fabrics can be a significant exposure pathway, especially for young children. Exposure estimation requires information on the extractability of compounds in saliva, the frequency of mouthing clothing and the area of the fabric mouthed. Various studies quantified extractability using a broader set of

Fig. 4 The relative importance of clothing-associated exposure pathways based on a chemical's volatility and water solubility. (Reprinted with permission from D. Licina, G.C. Morrison, G. Beko, C.J. Weschler and W.W. Nazaroff, Clothing-mediated exposures to chemicals and particles, Environ. Sci. Technol., 2019, 53, 5559–5575, DOI: <https://doi.org/10.1021/acs.est.9b00272>. Copyright (2021) American Chemical Society)



in vitro bioavailability methods, which have been applied to determine extractability in saliva simulants of azo dyes and for silver from nanoparticles. For highly water-soluble species, upper bounds on exposure can be established by assuming that the chemical is completely extractable. In an evaluation of indirect exposure to environmental airborne methamphetamine in former residential methamphetamine labs, mouthing of cotton fabric by toddlers was predicted to generate intakes approximately 10 times greater than all other exposure pathways combined (Morrison et al. 2015).

A diagrammatic summary of these exposure pathways as influenced by physical-chemical properties is qualitatively shown in Fig. 4. Excepting particles and particle-associated chemicals, inhalation requires a chemical to be volatile enough to become airborne. Ingestion is important for more water-soluble chemicals. Most species can be transferred to skin by contact or transfer through the clothing-skin air gap. For both ingestion and transfer to the skin surface, the chemical must be of lower volatility to be present in clothing at meaningful concentrations. Transdermal uptake from the skin surface tends to be highest for chemicals with intermediate volatilities and relatively low water-solubilities.

Exposures to Particles

Clothing-Associated Exposures to Biotic and Abiotic Particles

A large number of environmental and occupational exposure studies indicate that clothing can act as an important source of particle-borne agents that contribute to human exposures. Clothing-associated exposures have been observed for biotic and abiotic particles, with varied acquisition, retention and release mechanisms,

exposure routes, and potential health outcomes. This subsection summarizes evidence from relevant empirical and field studies to provide an overview of exposure to biotic and abiotic particles associated with clothing.

Allergens

A substantial body of research related to clothing-associated exposures to particles has focused on the risk of allergenic exposures. Studies examining exposure to allergenic biological particles from clothing include cat allergen (*Fel d 1*), dog allergen (*Can d 1*), dust-mite allergen (*Der p1*, *Der f1*), and pollens including pollen fragments. Tovey et al. (1995) were among the first to identify clothing as a significant source of inhalable allergens. They showed that allergenic dust particles can become released into the air directly from clothing by body movement and can travel to the wearer's breathing zone by means of the buoyancy-driven thermal plume, thus causing increased allergenic exposures. Other researchers found that exposures to mite and cat allergens were strongly related to the quantity of particle-bound allergen found on wearer's clothing, suggesting that personal clothing could be an important factor influencing both mite and cat allergen exposure (D'Amato et al. 1997). Evidence of allergen exposure also has been reported for people that are not in direct contact or proximity to any allergenic source (D'Amato et al. 1997). These studies identified clothing as an important indirect exposure vector, transporting particle-borne allergens from one space to another.

Many studies investigating clothing-mediated exposures to pet allergens have focused on school environments. They have found that allergens can be transported on children's clothing from homes to schools, including both the cat allergen, *Fel d 1* (D'Amato et al. 1997), and the dog allergen, *Can f 1* (Berge et al. 1998). Several studies evidenced that children without pets can also acquire allergens while in school and subsequently bring them back to their homes and potentially expose their family members. A study focusing on exposure interventions found that the level of airborne cat allergens in schools could be effectively mitigated either by pet ownership prohibition or by using school uniforms (Karlsson et al. 2004). Additional evidence has shown that clothing can be a transport vector for the mite allergens, *Der f 1* and *Der p 1* (Berge et al. 1998), and for allergenic pollen (Jantunen and Saarinen 2011). In summary, this body of research persuasively documents that clothing can be an important secondary source of allergenic exposures in buildings. These exposures can also occur in environments in which there are no direct sources of allergens.

Pathogenic Microbes

Another category of clothing-related biological particles is pathogenic microorganisms that pose threats for the transmission of infectious diseases. Most research about clothing-associated pathogens has focused on health-care settings, owing to concern about hospital-acquired infections. Studies have identified pathogenic bacteria on physicians' white coats (Wiener-Well et al. 2011), on neckties (Lopez et al. 2009), on gloves (Snyder et al. 2008), on nurses' uniforms (Perry et al. 2001), and on the coats of medical students (Scott et al. 2015). A commonly detected pathogen on

health-care apparel is methicillin-resistant *Staphylococcus aureus* (MRSA) (Perry et al. 2001; Snyder et al. 2008; Wiener-Well et al. 2011). Other pathogenic bacteria found on healthcare workers' uniforms have included *Clostridium difficile* (Perry et al. 2001) and vancomycin-resistant *Enterococcus* (VRE) (Perry et al. 2001; Snyder et al. 2008; Wiener-Well et al. 2011). In addition to bacterial pathogens, analysis of clothing samples worn by caregivers and visitors has revealed the presence of respiratory syncytial virus, a major cause of respiratory infections among premature infants (Homaira et al. 2016).

Other studies have provided evidence that links bacterial occurrence in clothing with subsequent exposure. The direct dispersal of *Staphylococcus aureus* and other bacteria from clothing into air has been identified in operating theatres (Doig 1972), in isolation wards (Hambræus 1973), and in hospital storage rooms (Handorean et al. 2015). Early research indicates that pathogen liberation from clothing into air can occur by human movement that induces frictional interactions between clothing fibers and skin (Doig 1972; Duguid and Wallace 1948; Hill et al. 1974). A seminal study by Duguid and Wallace (1948) found that clothing can liberate pathogenic microbes by promoting skin shedding. That same study also showed that sterile, dust-proof fabrics can act as a barrier to the release of skin-associated microbes.

Nanomaterials Associated with Clothing Additives

During the past few decades, embedded nanomaterials have emerged as a class of technological innovations for improving certain features of clothing fabrics, such as reducing microbial growth and survival, protecting against ultraviolet radiation, and improving water repellency. To achieve specific targeted functions, prevalent nanostructured clothing additives have included titanium dioxide (TiO_2), silver, zinc oxide (ZnO), gold, copper, carbon nanotubes, and nanoclays (Dastjerdi and Montazer 2010). An emerging consensus indicates that excessive exposure to nanomaterials can contribute to detrimental health outcomes, including pulmonary inflammation, carcinogenicity, genotoxicity, and circulatory effects (Savolainen et al. 2010). However, the effects of nanomaterial additives in clothing on human exposure and consequent health effects remain a subject of debate. Such materials have the potential to be released from clothing fabrics and contribute to exposures of their wearers and others. The mechanisms of release from clothing are different for nanomaterials as compared with biological particles. For example, in addition to mechanical abrasion, nanoparticles can potentially be released from clothing by migrating into human sweat and saliva.

Majority of exposure-related studies performed to date have focused on the migration of silver nanoparticles from clothing into human sweat, their release during laundering, and their antimicrobial properties. Dermal exposure to clothing-embedded nanoparticles has not been rigorously investigated. One group of studies reported that TiO_2 and ZnO nanoparticles do not penetrate deeply into the skin (Nohynek et al. 2007). To the contrary, there is evidence of the increase of the ^{68}Zn isotope in the blood of a healthy adult after exposure to ^{68}ZnO nanoparticles in a sunscreen formulation (Gulson et al. 2012). One study reported that healthy skin is a more effective barrier for silver nanoparticles than damaged skin (Filon et al. 2015).

In summary, there is a need for more research to characterize the influence of antimicrobial agents, including nanoparticles, on microbial diversity in clothing, and on the development of microbial resistance over time. Whether the presence of nanomaterials on fabrics in contact with the skin could alter the local skin microbiota remains a key open question.

Para-occupational Exposures

Studies have reported instances of para-occupational (or “take-home”) exposures to hazardous particles encountered in workplaces. Most such studies have focused on asbestos. As reviewed by Donovan et al. (2012) and Goswami et al. (2013), there is abundant evidence for increased risks of mesothelioma and lung cancer owing to para-occupational exposure to asbestos fibers and asbestos-containing dust on workers’ clothing. However, relatively little research provides quantitative evidence that mechanistically links workplace encounters with subsequent household exposures. Sahmel et al. (2014) found that handling clothes contaminated with chrysotile asbestos resuspends 0.2–1.4% of the material. Similar to scenarios with allergenic exposures, other studies demonstrated that healthcare uniforms can act as a vector for pathogen transmission outside of hospitals. The recent COVID-19 pandemic has raised additional concern over this route of transmission of biological aerosols. Therefore, the take-home effect for particles and microbial exposure via clothing seems to be a plausible route of transmission worthy of increased attention.

Personal Cloud

Owing to proximity between clothing and breathing zone of a wearer, an enhancement of inhalation exposure to particles beyond the room-average levels may occur for clothing-associated particle emissions. This feature, defined as the “personal cloud,” was introduced previously for clothing-mediated chemical exposures.

There are multiple factors influencing the personal cloud effect associated with particle release from clothing. Key determinants involve size-dependent emission rates of particles from clothing, proximity of clothing to the breathing zone, and local air movement in relation to personal activities. Increasing evidence from controlled and field studies suggest that direct shedding from clothing surfaces may be a noteworthy source of coarse-mode particles and bioaerosols indoors (Bhangar et al. 2016; Licina et al. 2016; Yang et al. 2021; Zhou et al. 2017). However, none of these studies quantified clothing-associated contributions to the personal-cloud effect. A recent study by Licina et al. (2017) reported that clothing movement can release coarse particles into the perihuman space of a seated person, which can then be transported upwards by means of the buoyancy-induced human thermal plume. In that study, the contribution of such releases to the personal cloud was substantial – from 2 to 13 $\mu\text{g}/\text{m}^3$ in the particle diameter range 1–10 μm . The contribution of clothing-associated particle release to a personal cloud effect was observed only for seated occupants. During walking, occupants would strongly mix the room air and break away the thermal plume, which resulted in the absence of the personal cloud effect. The study suggests that the personal cloud is contingent on physical activities and that manipulating the metabolic thermal plume could alter exposure to

clothing-released particles. Additionally, during more intensive clothing manipulations, such as putting on and taking off a shirt, or folding and unfolding a shirt, sharp peaks in the breathing zone PM₁₀ mass concentration were detected, at times exceeding 40 µg/m³. Overall, the emerging evidence regarding the personal cloud combined with evidence that clothing can harbor allergens, potentially pathogenic microorganisms, and other harmful substances suggest that clothing surfaces may be an underappreciated factor influencing particle exposure, possibly with public-health relevance.

Toward Quantifying Clothing-Mediated Particle Exposures

The previous section summarized evidence that clothing-mediated exposures to biotic and abiotic particles are potentially meaningful in different circumstances. It is important to characterize exposures quantitatively and – in as far as it is possible – mechanistically, so that one is able to extract generalizable findings from relatively limited experimental evidence. This section outlines a framework that could guide and support systematic knowledge acquisition for better understanding how clothing influences inhalation exposures to biotic and abiotic particles.

The central element in this framework is the determination of size-resolved and composition-specific emission rates of particles associated with clothing. Such emission rates can be expressed in terms of particle mass per time (relevant to coarse particles) or particle number per time (relevant to submicron particles). Particle composition is another important characteristic in relation to health outcomes of concern: allergenic particles, infectious microbes, and abiotic particles each contribute to increased yet distinct adverse health risks.

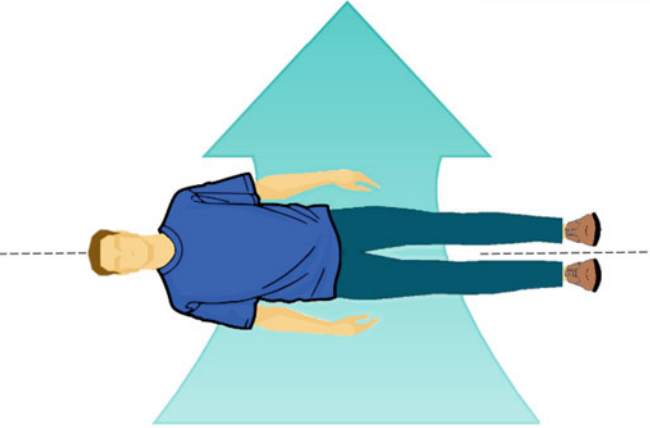
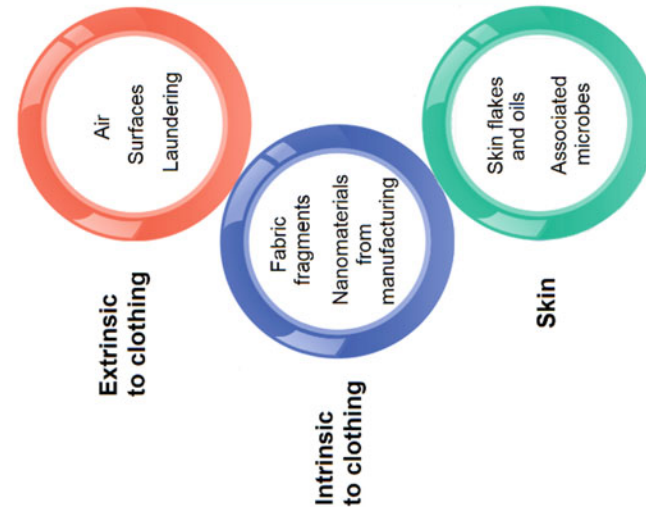
For known clothing-associated particle emission rates, contributions to exposures can be assessed. For example, particle emission rates from clothing can be incorporated into a single- or multi-compartment material balance model to estimate the component of exposure associated with increased indoor air concentrations. Alternatively, the intake fraction approach can be applied to estimate mass or particle number inhalation increments directly from emission rate information. Additional contributions to exposure from the personal-cloud effect can be assessed based on experimental evidence (Licina et al. 2017).

It is reasonable to expect that particle exposures associated with clothing occur mainly indoors. As with other indoor particle sources, emission rates can be inferred from measuring time- and size-resolved particle concentrations in chamber experiments with controlled environmental conditions (e.g., known ventilation rate, low particle backgrounds, and minimization of particle resuspension from flooring surfaces) and simulated activities (Bhangar et al. 2016; Licina et al. 2017; Yang et al. 2021). It is also plausible to infer emission rates from field observations; however, doing so for clothing-associated particle emissions poses the challenge of separately accounting for resuspension from flooring, commonly an important source of coarse particles indoors (Qian et al. 2014).

In assessing clothing-associated emissions, it is worthwhile to differentiate broadly among three particle source categories. As presented in Fig. 5, one category

PARTICLE SOURCE

PARTICLE RELEASE



Shedding - release of endogenous particles including skin flakes and associated microbes, and intrinsic fabric materials (clothing fragments and particles from manufacturing), as the result of skin-clothing frictional interactions

Resuspension - release and transport of exogenous particles that have previously settled onto clothing surfaces as the result of physical activity of a wearer or owing to a direct contact between clothing and other surfaces

Formation - release of ultrafine and nanocluster aerosols from ozone-skin oils chemistry
Migration - release of nanoparticles into human sweat and saliva

Resuspension characteristics

Dominant particle size mode:

- 3-5 μm diameter

Emission rate (skin-clothing frictional interactions):
 - 0.17 mg/h per sitting person (size range 1-10 μm)

- 0.45 mg/h per walking person (size range 1-10 μm)
 Clothing transport vector:
 - 0.3-3% of previous deposit (size range 1-10 μm)

Fig. 5 Particle source categories associated with clothing (left); and mechanisms of size dependent particle release and resuspension characteristics (right). Corresponding references: dominant particle size mode reported by Bhanger et al. (2016); size-resolved emission rates from sitting and walking person reported by Licina et al. (2017); release of previously deposited particles from clothing (transport vector effect) reported by Licina and Nazaroff (2018). (Reprinted with permission from D. Licina, G.C. Morrison, G. Beko, C.J. Weseloh and W.W. Nazaroff, Clothing-mediated exposures to chemicals and particles, Environ. Sci. Technol., 2019, 53, 5559–5575, DOI: <https://doi.org/10.1021/acs.est.9b00272>. Copyright (2021) American Chemical Society)

includes material that exists on human skin. For example, skin flakes (known as squames) are aerosolized through complex frictional interactions between clothing and skin. These squames consist of skin fragments with associated microbes, especially bacteria. Additionally, constituents of skin oils deposited on clothing (e.g., squalene, which is commonly present on clothing surfaces) rapidly react with ozone, producing ultrafine (Rai et al. 2013) and nanocluster aerosols (Bekö et al. 2020). A second category would be particles endogenous to the clothing fabric, such as fabric fragments and nanoparticle additives. These are typically acquired during manufacturing processes. A third category, the broadest, is exogenous particles that become associated with clothing articles by means of environmental transfer indoors and outdoors. The first category has been studied most carefully in connection with concerns about hospital-acquired infections. Knowledge on ultrafine and nanoparticle emissions generated by clothing surface chemistry is just beginning to emerge. Concern about the second category is increasing, in part due to the emerging use of nanoparticle fabric treatments. The third category would be relevant for concerns as diverse as allergen exposure, para-occupational exposure, and general enhancements of airborne particles via the personal cloud.

For squame emissions associated with clothing, key factors would include the state of the skin surface (dryness, for example), the nature and intensity of frictional interaction between fabric and skin, and the tightness of the weave. Variability in the emissions of skin-associated *Staphylococcus aureus* among individuals has been demonstrated to be large, and systematically higher for men than for women (Hill et al. 1974). Notwithstanding a long history of studies, the issue of what should be worn by medical staff in the operating theatre to minimize surgical site infections remains a subject of debate. For endogenous particle emissions (e.g., nanoparticle additives), one expects that important factors affecting emissions would include initial particle loading of the fabric, ability to remove particles by laundering, the nature of particle bonding with fibers, the nature and intensity of movement generating frictional forces, and the overall wear of the fabric.

For emissions of exogenous particles, one might envision clothing articles as environmental reservoirs and aim to account for the net movement of particles between these reservoirs and the surroundings. Consider an article of clothing, such as a T-shirt, passing through a cycle starting with laundering. The washing cycle might effectively remove previously deposited particles, but could conceivably add particles from dissolved salts in the wash water and from detergent residue. A tumble-dry cycle could effectively add some airborne exogenous particles filtered by the clothing items from the drying air that passes through the drum. The clothing article might then lose some of these particles, and contribute an increment of exposure, during the post-laundry handling of folding and placing in storage. When worn, the T-shirt can acquire exogenous particles by deposition from the air and by direct contact with particle-laden surfaces including the skin. Exogenous particles may also be acquired during storage intervals, especially if exposed in a manner that would be influenced by settling dust. The accumulation of particles during these processes could be quantified through deposition assessments, for example, through the multiplicative combination of exposure concentrations of

particles, a suitable deposition velocity, and duration of exposure. Knowing the size-resolved and composition-specific quantities of exogenous particles on a clothing article, one could assess the emission rate through the use of loss-rate coefficients. An analogous approach has been used to systematically investigate particle resuspension from walking (Qian et al. 2014).

Factors Affecting Clothing-Mediated Particle Exposures

The previous section outlined an approach that could be used to systematically assess clothing-associated exposures to particles. Specific information about relevant factors and processes is sparse. This section describes what is known from prior experimental investigations about the major factors that influence the size-dependent emissions of particles associated with clothing, emphasizing the relationship to inhalation exposures.

Early studies revealed important findings about clothing-skin surface interaction as a means of liberating bacteria-laden skin flakes (Doig 1972; Duguid and Wallace 1948; Hill et al. 1974). Recent advances in DNA-based measurements have enabled rapid progress in characterizing the human microbiome, including detailed descriptions of diverse communities of bacteria and fungi present on human skin. Different studies analyzed biological material from clothing surface samples or air exposed to clothing. They identified populations of pathogenic bacteria, respiratory syncytial virus, fungi, dust-mite and cat allergens, endotoxins, and allergenic pollen. Some quantitative evidence exists documenting microbial transfer to clothing from skin and by hands, although more studies are needed to quantify this phenomenon and to better characterize the process mechanistically.

Available evidence suggests that the rate of particle release from clothing fibers is influenced by a combination of three main factors: properties of clothing, environmental conditions, and human factors. A dominant factor influencing particle release from clothing is the intensity of movement. Up to an order of magnitude higher emission rates have been observed during vigorous bodily movement compared to slight activity, presumably owing to increased frictional interactions between clothing fibers and skin (Bhangar et al. 2016; Duguid and Wallace 1948; Licina et al. 2017; You et al. 2012). Men have been found to release significantly more particles compared to women (Hill et al. 1974). Another study found that application of skin lotion has been linked to reduced dispersal rate of biotic particles (Hall et al. 1986; Zhou et al. 2017). Some studies (Speers Jr et al. 1965), but not all (Hall et al. 1986), have found that the emission rate of biotic particles from clothing-skin interactions increases within an hour after showering. Transport of particles through clothing surfaces and subsequent dispersal can be reduced by wearing tightly-woven and non-woven fabrics (Whyte and Hejab 2007).

A few recent studies have applied a material-balance approach to infer size-resolved biotic particle emission rates associated with human occupancy. Qian et al. (2012) used quantitative PCR to infer that a single university classroom occupant contributes effective emissions of 37 million bacterial genomes per hour,

with a modal aerodynamic diameter of 3–5 µm. However, that study could not differentiate between emissions associated with clothing and those from other sources such as resuspension from a carpeted floor. Bhaggar et al. (2014) applied a laser-induced fluorescence technique to quantify the per person emission rate of fluorescent biological aerosol particles (FBAP) in the size range 1–15 µm diameter in an uncarpeted university classroom. Their work, which again did not isolate the contribution of clothing, yielded an average emission rate of 2 million FBAP per hour with modal diameters of 3–4 µm. In a subsequent chamber study, Bhaggar et al. (2016) found that at least 60–70% of occupancy-associated FBAP emissions originated from the floor. However, they also found that “*clothing, or its frictional interaction with human skin, was . . . a source of coarse particles, and especially of the highly fluorescent fraction.*” That study also revealed a dominant size mode for FBAP of 3–5 µm diameter. In another recent chamber study, Yang et al. (2021) found that occupants who wore long-sleeve shirts and pants produced 40% more fluorescent aerosol particles relative to occupants that wore t-shirts and shorts. The study found that the total and fluorescent particle emissions from young adults and teenagers were 50% higher compared to elderly people. This difference could be attributed to differences in skin conditions, as elderly replace their epidermis slower compared to younger people, which may result in lower particle shedding rate. Additional influencing factors could be increased skin roughness and wrinkle area of elderly, which may trap particles and reduce the physical contact with clothing.

When considering the specific issue of infectious disease transmission in relation to clothing, the persistence and survival of infectious agents on fabrics needs to be considered. Variation in building environmental conditions and properties of clothing fabrics produce various effects on microbial persistence and survival. Longitudinal assessment of bacteria survival across different studies showed a remarkably high persistence – from several days up to more than 90 days for isolates of VRE and MRSA (Neely and Maley 2000). Several studies suggest that survival and persistence of viruses and fungi on clothing fabrics has similar days- to months-long time scales (Neely and Orloff 2001). Among different factors influencing survival and persistence, relative humidity and fabric material have been explored. Increased relative humidity (from 35% to 78%) has been linked to reduced stability of both bacterial and viral strains in clothing (Sidwell et al. 1966). Survival and persistence of bacteria, virus, and fungi is higher on commonly used polyester and wool fabrics compared to cotton materials (Neely and Orloff 2001).

Another common theme in the literature concerning clothing-mediated exposure to pathogenic microbes considers the effectiveness of laundering practices such as washing, drying, and ironing. Mechanical removal includes fabric agitation assisted by surfactant properties of detergents, while inactivation processes can occur as a consequence of elevated water temperature combined with laundry additives such as sodium hypochlorite. Among relevant studies, Callewaert et al. (2015) documented microbial exchanges among clothing articles during washing. Nordstrom et al. (2012) found that home-washed hospital scrubs had increased prevalence of bacterial species compared to those laundered in hospitals, presumably due to low temperature washing. A 7-log reduction in bacterial load can be achieved by

10-min of washing with 60 °C water (Lakdawala et al. 2011). Adding sodium hypochlorite to a detergent is an effective way to eliminate bacteria and inactivate enteric and respiratory viruses (Gerba and Kennedy 2007); however, it might also lead to increases in the abundance of chlorinated organic compounds on clothing (Schwartz-Narbonne et al. 2018). Detergents free of bleach can reduce the prevalence of *Staphylococcus aureus* (Vikke and Giebner 2015), while adding bleach-enriched detergents completely eliminates the same. Recent adjustments in laundering procedures include addition of enzymes, reduced water use, lower water temperature, and bleach-free detergents.

Both biotic and abiotic material can be deposited onto clothing surfaces from various environmental sources including outdoor air and grassland (Jantunen and Saarinen 2011), residential air (Noble 2000), and public transport microenvironments (Liljegren et al. 2016). Physical contact with various indoor and outdoor surfaces and during the storage can be another pathway of particle acquisition (Clarke et al. 2015). The rate of deposition from air to clothing can be described using the deposition velocity concept. Studies have found that particle size and local air movement are dominant influencing factors (Liljegren et al. 2016).

Research has clearly documented that previously deposited material can be released into air from clothing (Licina and Nazaroff 2018; McDonagh and Byrne 2014b; Sahmel et al. 2014). For example, using a controlled chamber study approach, Licina and Nazaroff (2018) found that 0.3–3% of particles (size range 1–10 µm) deposited through settling could be released via fabric motion. In that work, the release fraction monotonically increased with particle size. Not surprisingly, they also found that the particle release fraction increased with the intensity of movement and with the amount of dust deposited onto the clothing fabrics. It was found that the majority of particle release from clothing occurs shortly after the onset of the movement.

The degree of particle binding to clothing fibers and the rate of resuspension may arise from a combined influence of different forces acting upon the fibers. The forces governing the release of clothing-embedded particles are abrasive actions between clothing surfaces – a consequence of physical activity of a wearer (Duguid and Wallace 1948; Hill et al. 1974). Forces influencing release are strongly linked to particle size. Because detachment forces increase more strongly with particle diameter than do adhesion forces, clothing-associated emissions are more discernible among coarse-mode than fine-mode particles (Bhangar et al. 2016; Licina et al. 2016, 2017; Yang et al. 2021; Zhou et al. 2017).

Common clothing fibers are wool, cotton, and polyester. Wool has been reported to have particle release rates up to 10 times higher than the other two materials (Yoon and Brimblecombe 2000); cotton exhibits higher emissions than polyester (You et al. 2012). The higher particle emissions from wool garments could be linked to different surface roughness and weave pattern (McDonagh and Byrne 2014a), but also to less frequent laundering as compared to cotton and polyester fabrics (Yoon and Brimblecombe 2000). Other clothing conditions found to increase particle release rate include increased clothing age (Cohen and Positano 1986) and reduced cleanliness (Yoon and Brimblecombe 2000). While it is generally understood that

adhesion forces acting on particles increase with relative humidity, we know of only three studies that have examined its effect on clothing-associated emissions. Yoon and Brimblecombe (2000) found an association between low relative humidity and increased particle emission rate. Similarly, particle emissions decreased by 30–60% when relative humidity increased from 34% to 62% (Yang et al. 2021). On the other hand, Zhou et al. (2017) reported an insignificant influence of relative humidity on particle emissions from clothing.

Conclusions

There is ample evidence that clothing influences human exposure to chemicals and particles. Yet, only a few studies have quantified clothing-mediated exposure by means of direct measurements (Bekö et al. 2018; Blum et al. 1978; Horstmann and McLachlan 1994; Licina et al. 2017; Morrison et al. 2016, 2017b; Rossbach et al. 2016).

We know surprisingly little about the occurrence of contaminants acquired by everyday clothing after purchase. For a relatively low cost, we could learn a large amount from simply assessing the occurrence, concentrations, and extractability (e.g., by sweat and saliva) of chemicals and particles in everyday clothing. Cross-sectional exposure studies would greatly benefit from the addition of clothing analyses, potentially identifying direct connections between clothing-associated exposure and health.

The diversity of clothing, environmental and human factors make predicting exposures challenging. Therefore, it will be important to reduce the many variables to those that are most influential. Progress can be achieved through models, laboratory, and field investigations of human exposure and uptake. In addition to chemical properties, important factors affecting exposures may include textile materials, weave, thickness, and permeability; wear, care, and storage practices; environmental conditions (e.g., relative humidity, ozone); intensity and types of activities; skin-oil transfer to clothing and its aging; human physiology (skin integrity, lipid generation, sweating) and personal hygiene habits. Simulated exposures with human subjects also should consider pollutant transfer from textiles other than clothing (e.g., pillows, quilts, bed linen). The sleeping environment is potentially of great importance in this matter given the large proportion of time spent in bed.

Predicting and controlling exposure rely on adequate understanding of underlying mechanisms. A robust literature describes transport mechanisms for chemicals among environmental reservoirs. Reasonable approaches have been proposed for assessing risk and exposure to chemicals in clothing. However, we have limited *in vivo* evaluations of such assessments. Compared with chemical transport, mechanisms of particle uptake and subsequent release from clothing are even less well understood. Further quantitative investigations of factors that drive acquisition, retention, and transmission of biotic and abiotic particles in clothing are needed to better link such processes to clothing associated exposures. In addition, enhancement of chemical and particle concentrations in the breathing zone compared to bulk air concentrations (“personal cloud” effect) should be taken into account when

considering emissions from clothing. We also need to better understand the extent to which clothing plays a role in the spread of infectious disease. Considerable research has focused on textile innovations and personal protective clothing designed to limit the spread of infectious agents in hospital environments. Researchers could usefully build upon lessons learned and consider the potential utility of incorporating such innovations in everyday clothing.

One should anticipate that future changes in clothing will influence exposure. The useful lifetime of some clothing has become shorter. High turnover (short ownership time) might yield greater exposure to chemicals that are present in newly purchased clothing, with proportionately less exposure to environmental chemicals that require a long period to equilibrate (e.g., high molecular weight phthalates). Similarly, increased use of antimicrobial agents as coatings on clothing articles may increase uptake of nanoparticles by the human body and lead to altered toxicological effects. Worth noting is that people in Western countries commonly have closets full of clothes that are rarely worn. These articles may have sufficient time to equilibrate with the chemicals present in their storage environment. Worldwide, demand for synthetic fabrics is increasing. Synthetics have chemical partitioning behaviors and moisture holding capacities that differ from those of natural fibers, altering the capacity to be reservoirs of contaminants. Advances in materials and adjustments in laundering procedures may also influence how clothing is cared for and how chemicals and particles are acquired and retained in clothing. Increased recycling and re-use of clothing can influence tertiary exposures.

It is also important to recognize that the new regulations for substances in clothing are beginning to emerge. As of November 2020, new EU-wide legislations were put in place, as amendment to the REACH regulation, to limit the use of 33 substances that are classified as carcinogenic, mutagenic, or toxic for reproduction (European Commission 2018). This regulation specifies maximum concentration limits for the use of the following group of substances in clothing and textiles: cadmium, chromium, arsenic, and lead compounds; chlorinated aromatic hydrocarbons; benzene and polycyclic aromatic hydrocarbons (PAHs); phthalates; formaldehyde; polar aprotic solvents; azo-dyes and acrylamides; and quinoline. Clothing products on the EU market that exceed these limits are banned. Moving forward, we need robust policies on a global level to eliminate hazardous substances and their anticipated replacements from clothing manufacturing processes. Together with requirements for manufacturers to fully disclose the material content and chemical makeup of clothing, these efforts could result in improved exposure management.

People spend nearly their entire lives in intimate contact with clothing and other textiles. The evidence reviewed in this chapter supports a view that this environmental compartment plays important roles in exposure and health risk. Consequently, clothing as a mediator of chemical and particle exposure deserves substantial attention from the environmental science research and regulatory communities.

Acknowledgments The authors acknowledge the substantial contribution of Glenn C. Morrison, Charles J. Weschler and William W Nazaroff to this chapter.

References

- Antal B, Kuki Á, Nagy L, Nagy T, Zsuga M, Kéki S (2016) Rapid detection of hazardous chemicals in textiles by direct analysis in real-time mass spectrometry (DART-MS). *Anal Bioanal Chem* 408(19):5189–5198
- Bekö G, Morrison G, Weschler CJ, Koch H, Pälmke C, Saltherammer T, Schripp T, Eftekhari A, Toftum J, Clausen G (2018) Dermal uptake of nicotine from air and clothing: experimental verification. *Indoor Air* 28(2):247–257
- Bekö G, Wargocki P, Wang N, Li M, Weschler CJ, Morrison G, Langer S, Ernle L, Licina D, Yang S (2020) The Indoor Chemical Human Emissions and Reactivity project (ICHEAR): overview of experimental methodology and preliminary results. *Indoor Air* 30(6):1213–1228
- Berge M, Munir A, Dreborg S (1998) Concentrations of cat (*Fel d 1*), dog (*Can f 1*) and mite (Der f 1 and Der p 1) allergens in the clothing and school environment of Swedish schoolchildren with and without pets at home. *Pediatr Allergy Immunol* 9(1):25–30
- BfR (2012) Introduction to the Problems Surrounding Garment Textiles. Updated BfR Opinion No. 041/2012, Bundesinstitut für Risikobewertung. <http://www.bfr.bund.de/cm/349/introduction-to-the-problems-surrounding-garment-textiles.pdf>. Accessed 20 Jan 2021
- Bhangar S, Huffman JA, Nazaroff W (2014) Size-resolved fluorescent biological aerosol particle concentrations and occupant emissions in a university classroom. *Indoor Air* 24(6):604–617
- Bhangar S, Adams RI, Pasut W, Huffman JA, Arens EA, Taylor JW, Bruns TD, Nazaroff WW (2016) Chamber bioaerosol study: human emissions of size-resolved fluorescent biological aerosol particles. *Indoor Air* 26(2):193–206
- Blum A, Gold M, Ames B, Jones F, Hett E, Dougherty R, Horning E, Dzidic I, Carroll D, Stillwell R (1978) Children absorb tris-BP flame retardant from sleepwear: urine contains the mutagenic metabolite, 2,3-dibromopropanol. *Science* 201(4360):1020–1023
- Bradman ASA, Schwartz JM, Fenster L, Barr DB, Holland NT, Eskenazi B (2007) Factors predicting organochlorine pesticide levels in pregnant Latina women living in a United States agricultural area. *J Expo Sci Environ Epidemiol* 17(4):388–399
- Brown BW (1970) Fatal phenol poisoning from improperly laundered diapers. *Am J Public Health Nations Health* 60(5):901–902
- Callewaert C, De Maeseneire E, Kerckhof F-M, Verliefde A, Van de Wiele T, Boon N (2014) Microbial odor profile of polyester and cotton clothes after a fitness session. *Appl Environ Microbiol* 80(21):6611–6619
- Callewaert C, Van Nevel S, Kerckhof F-M, Granitsiotis MS, Boon N (2015) Bacterial exchange in household washing machines. *Front Microbiol* 6:1381
- Cao J, Weschler CJ, Luo J, Zhang Y (2016) C m-history method, a novel approach to simultaneously measure source and sink parameters important for estimating indoor exposures to phthalates. *Environ Sci Technol* 50(2):825–834
- Cao J, Zhang X, Zhang Y (2018) Predicting dermal exposure to gas-phase semivolatile organic compounds (SVOCs): a further study of SVOC mass transfer between clothing and skin surface lipids. *Environ Sci Technol* 52(8):4676–4683
- Clarke D, Burke D, Gormally M, Byrne M (2015) Dynamics of house dust mite transfer in modern clothing fabrics. *Ann Allergy Asthma Immunol* 114(4):335–340
- Cohen BS, Positano R (1986) Resuspension of dust from work clothing as a source of inhalation exposure. *Am Ind Hyg Assoc J* 47(5):255–258
- D'Amato G, Liccardi G, Russo M, Barber D, D'Amato M, Carreira J (1997) Clothing is a carrier of cat allergens. *J Allergy Clin Immunol* 99(4):577–578
- Dastjerdi R, Montazer M (2010) A review on the application of inorganic nano-structured materials in the modification of textiles: focus on anti-microbial properties. *Colloids Surf B: Biointerfaces* 79(1):5–18
- De Groot AC, Maibach HI (2010) Does allergic contact dermatitis from formaldehyde in clothes treated with durable-press chemical finishes exist in the USA? *Contact Dermatitis* 62(3):127–136

- Doig CM (1972) The effect of clothing on the dissemination of bacteria in operating theatres. *Br J Surg* 59(11):878–881
- Donovan EP, Donovan BL, McKinley MA, Cowan DM, Paustenbach DJ (2012) Evaluation of take home (para-occupational) exposure to asbestos and disease: a review of the literature. *Crit Rev Toxicol* 42(9):703–731
- Duguid JP, Wallace AT (1948) Air infection with dust liberated from clothing. *Lancet* 252(6535): 845–849
- European Commission (2018) Commission Regulation (EU) 2018/1513 of 10 October 2018 amending Annex XVII to Regulation (EC) No 1907/2006 of the European Parliament and of the Council concerning the Registration, Evaluation, Authorisation and Restriction of Chemicals (REACH) as regards certain substances classified as carcinogenic, mutagenic or toxic for reproduction (CMR), category 1A or 1B (Text with EEA relevance). <https://eur-lex.europa.eu/legal-content/EN/TXT/PDF/?uri=CELEX:32018R1513>. Accessed 21 Jan 2021
- Faulde MK, Uedelhoven WM, Malerius M, Robbins RG (2006) Factory-based permethrin impregnation of uniforms: residual activity against *Aedes aegypti* and *Ixodes ricinus* in battle dress uniforms worn under field conditions, and cross-contamination during the laundering and storage process. *Mil Med* 171(6):472–477
- Filon FL, Mauro M, Adami G, Bovenzi M, Crosera M (2015) Nanoparticles skin absorption: new aspects for a safety profile evaluation. *Regul Toxicol Pharmacol* 72(2):310–322
- Gaskin S, Heath L, Pisaniello D, Edwards JW, Logan M, Baxter C (2017) Dermal absorption of fumigant gases during HAZMAT incident exposure scenarios – methyl bromide, sulfuryl fluoride, and chloropicrin. *Toxicol Ind Health* 33(7):547–554
- Gerba CP, Kennedy D (2007) Enteric virus survival during household laundering and impact of disinfection with sodium hypochlorite. *Appl Environ Microbiol* 73(14):4425–4428
- Gong M, Weschler CJ, Zhang Y (2016) Impact of clothing on dermal exposure to phthalates: observations and insights from sampling both skin and clothing. *Environ Sci Technol* 50(8): 4350–4357
- Goswami E, Craven V, Dahlstrom DL, Alexander D, Mowat F (2013) Domestic asbestos exposure: a review of epidemiologic and exposure data. *Int J Environ Res Public Health* 10(11): 5629–5670
- Gulson B, Wong H, Korsch M, Gomez L, Casey P, McCall M, McCulloch M, Trotter J, Stauber J, Greenoak G (2012) Comparison of dermal absorption of zinc from different sunscreen formulations and differing UV exposure based on stable isotope tracing. *Sci Total Environ* 420:313–318
- Hall G, Mackintosh C, Hoffman P (1986) The dispersal of bacteria and skin scales from the body after showering and after application of a skin lotion. *Epidemiol Infect* 97(2):289–298
- Hambraeus A (1973) Dispersal and transfer of *Staphylococcus aureus* in an isolation ward for burned patients. *Epidemiol Infect* 71(4):787–797
- Handorean A, Robertson CE, Harris JK, Frank D, Hull N, Kotter C, Stevens MJ, Baumgardner D, Pace NR, Hernandez M (2015) Microbial aerosol liberation from soiled textiles isolated during routine residuals handling in a modern health care setting. *Microbiome* 3(1):1–10
- Hill J, Howell A, Blowers R (1974) Effect of clothing on dispersal of *Staphylococcus aureus* by males and females. *Lancet* 304(7889):1131–1133
- Homaira N, Sheils J, Stelzer-Braid S, Lui K, Oie JL, Snelling T, Jaffe A, Rawlinson W (2016) Respiratory syncytial virus is present in the neonatal intensive care unit. *J Med Virol* 88(2): 196–201
- Horstmann M, McLachlan MS (1994) Textiles as a source of polychlorinated dibenz-p-dioxins and dibenzofurans (PCDD/F) in human skin and sewage sludge. *Environ Sci Pollut Res* 1(1):15–20
- Iadaresta F, Manniello MD, Östman C, Crescenzi C, Holmbäck J, Russo P (2018) Chemicals from textiles to skin: an in vitro permeation study of benzothiazole. *Environ Sci Pollut Res* 25(25): 24629–24638
- Jantunen J, Saarinen K (2011) Pollen transport by clothes. *Aerobiologia* 27(4):339–343
- Jurewicz J, Hanke W (2011) Exposure to phthalates: reproductive outcome and children health. A review of epidemiological studies. *Int J Occup Med Environ Health* 24(2):115–141

- Kajiwara N, Desborough J, Harrad S, Takigami H (2013) Photolysis of brominated flame retardants in textiles exposed to natural sunlight. *Environ Sci: Processes Impacts* 15(3):653–660
- Karlsson A-S, Andersson B, Renström A, Svedmyr J, Larsson K, Borres MP (2004) Airborne cat allergen reduction in classrooms that use special school clothing or ban pet ownership. *J Allergy Clin Immunol* 113(6):1172–1177
- Kawakami T, Isama K, Nakashima H, Tsuchiya T, Matsuoka A (2010) Analysis of primary aromatic amines originated from azo dyes in commercial textile products in Japan. *J Environ Sci Health A* 45(10):1281–1295
- KEMI (2014) Chemicals in textile – risks to human health and the environment. Report from a government assignment, REPORT 6/14, Swedish Chemicals Agency. <https://www.kemi.se/download/18.6df1d3df171c243fb23a98f3/1591454110491/rapport-6-14-chemicals-in-textiles.pdf>. Accessed 20 Jan 2021
- Klasmeier J, Mühlbach A, McLachlan MS (1999) PCDD/Fs in textiles – Part II: Transfer from clothing to human skin. *Chemosphere* 38(1):97–108
- Lakdawala N, Pham J, Shah M, Holton J (2011) Effectiveness of low-temperature domestic laundry on the decontamination of healthcare workers' uniforms. *Infect Control Hosp Epidemiol* 32(11):1103–1108
- Lao J-Y, Xie S-Y, Wu C-C, Bao L-J, Tao S, Zeng EY (2018) Importance of dermal absorption of polycyclic aromatic hydrocarbons derived from barbecue fumes. *Environ Sci Technol* 52(15):8330–8338
- Laursen S, Hansen J, Pommer K (2003) Survey of chemical compounds in textile fabrics. Danish Environmental Protection Agency, Copenhagen
- Lentini JJ, Dolan JA, Cherry C (2000) The petroleum-laced background. *J Forensic Sci* 45(5):968–989
- Licina D, Nazaroff W (2018) Clothing as a transport vector for airborne particles: chamber study. *Indoor Air* 28(3):404–414
- Licina D, Melikov A, Sekhar C, Tham KW (2015) Transport of gaseous pollutants by convective boundary layer around a human body. *Sci Technol Built Environ* 21(8):1175–1186
- Licina D, Bhangar S, Brooks B, Baker R, Firek B, Tang X, Morowitz MJ, Banfield JF, Nazaroff WW (2016) Concentrations and sources of airborne particles in a neonatal intensive care unit. *PLoS One* 11(5):e0154991
- Licina D, Tian Y, Nazaroff WW (2017) Emission rates and the personal cloud effect associated with particle release from the perihuman environment. *Indoor Air* 27(4):791–802
- Licina D, Morrison GC, Bekö G, Weschler CJ, Nazaroff WW (2019) Clothing-mediated exposures to chemicals and particles. *Environ Sci Technol* 53(10):5559–5575
- Liljegren JC, Brown DF, Lunden MM, Silcott D (2016) Particle deposition onto people in a transit venue. *Health Secur* 14(4):237–249
- Liu X, Guo Z, Krebs KA, Pope RH, Roache NF (2014) Concentrations and trends of perfluorinated chemicals in potential indoor sources from 2007 through 2011 in the US. *Chemosphere* 98:51–57
- Liu N, Cao J, Huang J, Zhang Y (2021) Role of clothing in skin exposure to di(*n*-butyl) phthalate and tris(1-chloro-2-propyl) phosphate: experimental observations via skin wipes. *Environ Sci Technol Lett.* Just accepted (January 20, 2021)
- Lopez P-J, Ron O, Parthasarathy P, Soothill J, Spitz L (2009) Bacterial counts from hospital doctors' ties are higher than those from shirts. *Am J Infect Control* 37(1):79–80
- Luongo G, Avagyan R, Hongyu R, Östman C (2016) The washout effect during laundry on benzothiazole, benzotriazole, quinoline, and their derivatives in clothing textiles. *Environ Sci Pollut Res* 23(3):2537–2548
- McDonagh A, Byrne M (2014a) The influence of human physical activity and contaminated clothing type on particle resuspension. *J Environ Radioact* 127:119–126
- McDonagh A, Byrne M (2014b) A study of the size distribution of aerosol particles resuspended from clothing surfaces. *J Aerosol Sci* 75:94–103
- Meinke M, Abdollahnia M, Ghr F, Platzek T, Lademann J (2009) Migration and penetration of a fluorescent textile dye into the skin – in vivo versus in vitro methods. *Exp Dermatol* 18(9):789–792

- Moore C, Wilkinson S, Blain P, Dunn M, Aust G, Williams F (2014) Use of a human skin in vitro model to investigate the influence of 'every-day' clothing and skin surface decontamination on the percutaneous penetration of organophosphates. *Toxicol Lett* 229(1):257–264
- Morrison G, Shakila N, Parker K (2015) Accumulation of gas-phase methamphetamine on clothing, toy fabrics, and skin oil. *Indoor Air* 25(4):405–414
- Morrison GC, Weschler CJ, Bekö G, Koch HM, Saltherammer T, Schripp T, Toftum J, Clausen G (2016) Role of clothing in both accelerating and impeding dermal absorption of airborne SVOCs. *J Expo Sci Environ Epidemiol* 26(1):113–118
- Morrison G, Weschler CJ, Bekö G (2017a) Dermal uptake of phthalates from clothing: comparison of model to human participant results. *Indoor Air* 27(3):642–649
- Morrison GC, Bekö G, Weschler CJ, Schripp T, Saltherammer T, Hill J, Andersson A-M, Toftum J, Clausen G, Frederiksen H (2017b) Dermal uptake of benzophenone-3 from clothing. *Environ Sci Technol* 51(19):11371–11379
- Morrison GC, Andersen HV, Gunnarsen L, Varol D, Uhde E, Kolarik B (2018) Partitioning of PCB s from air to clothing materials in a Danish apartment. *Indoor Air* 28(1):188–197
- Neely AN, Maley MP (2000) Survival of enterococci and staphylococci on hospital fabrics and plastic. *J Clin Microbiol* 38(2):724–726
- Neely AN, Orloff MM (2001) Survival of some medically important fungi on hospital fabrics and plastics. *J Clin Microbiol* 39(9):3360–3361
- Noble RE (2000) Environmental tobacco smoke uptake by clothing fabrics. *Sci Total Environ* 262(1–2):1–3
- Nohynek GJ, Lademann J, Ribaud C, Roberts MS (2007) Grey goo on the skin? Nanotechnology, cosmetic and sunscreen safety. *Crit Rev Toxicol* 37(3):251–277
- Nordstrom JM, Reynolds KA, Gerba CP (2012) Comparison of bacteria on new, disposable, laundered, and unlaundered hospital scrubs. *Am J Infect Control* 40(6):539–543
- Park J-S, Voss RW, McNeel S, Wu N, Guo T, Wang Y, Israel L, Das R, Petreas M (2015) High exposure of California firefighters to polybrominated diphenyl ethers. *Environ Sci Technol* 49(5):2948–2958
- Perry C, Marshall R, Jones E (2001) Bacterial contamination of uniforms. *J Hosp Infect* 48(3): 238–241
- Piadé JJ, D'André S, Sanders EB (1999) Sorption phenomena of nicotine and ethenylpyridine vapors on different materials in a test chamber. *Environ Sci Technol* 33(12):2046–2052
- Qian J, Hospodsky D, Yamamoto N, Nazaroff WW, Peccia J (2012) Size-resolved emission rates of airborne bacteria and fungi in an occupied classroom. *Indoor Air* 22(4):339–351
- Qian J, Peccia J, Ferro AR (2014) Walking-induced particle resuspension in indoor environments. *Atmos Environ* 89:464–481
- Rai AC, Guo B, Lin C-H, Zhang J, Pei J, Chen Q (2013) Ozone reaction with clothing and its initiated particle generation in an environmental chamber. *Atmos Environ* 77:885–892
- Rim D, Novoselec A, Morrison G (2009) The influence of chemical interactions at the human surface on breathing zone levels of reactants and products. *Indoor Air* 19(4):324
- Rossbach B, Kegel P, Süß H, Letzel S (2016) Biomonitoring and evaluation of permethrin uptake in forestry workers using permethrin-treated tick-proof pants. *J Expo Sci Environ Epidemiol* 26(1): 95–103
- Rovira J, Domingo JL (2019) Human health risks due to exposure to inorganic and organic chemicals from textiles: a review. *Environ Res* 168:62–69
- Rovira J, Nadal M, Schuhmacher M, Domingo JL (2017) Trace elements in skin-contact clothes and migration to artificial sweat: risk assessment of human dermal exposure. *Text Res J* 87(6):726–738
- Sahmel J, Barlow C, Simmons B, Gaffney S, Avens H, Madl A, Henshaw J, Lee R, Van Orden D, Sanchez M (2014) Evaluation of take-home exposure and risk associated with the handling of clothing contaminated with chrysotile asbestos. *Risk Anal* 34(8):1448–1468
- Saleh MA, Kamel A, El-Demerdash A, Jones J (1998) Penetration of household insecticides through different types of textile fabrics. *Chemosphere* 36(7):1543–1552

- Savolainen K, Pylkkänen L, Norppa H, Falck G, Lindberg H, Tuomi T, Vippola M, Alenius H, Hämeri K, Koivisto J (2010) Nanotechnologies, engineered nanomaterials and occupational health and safety—a review. *Saf Sci* 48(8):957–963
- Schettler T (2006) Human exposure to phthalates via consumer products. *Int J Androl* 29(1): 134–139
- Schwartz-Narbonne H, Wang C, Zhou S, Abbatt JP, Faust J (2018) Heterogeneous chlorination of squalene and oleic acid. *Environ Sci Technol* 53(3):1217–1224
- Scott E, Goodear N, Nicoloro JM, Marika DJ, Killion E, Duty SM (2015) Laundering habits of student nurses and correlation with the presence of *Staphylococcus aureus* on nursing scrub tops pre-and postlaundering. *Am J Infect Control* 43(9):1006–1008
- Sidwell RW, Dixon GJ, McNeil E (1966) Quantitative studies on fabrics as disseminators of viruses: I. Persistence of vaccinia virus on cotton and wool fabrics. *Appl Microbiol* 14(1):55–59
- Snyder GM, Thorn KA, Furuno JP, Perencevich EN, Roghmann M-C, Strauss SM, Netzer G, Harris AD (2008) Detection of methicillin-resistant *Staphylococcus aureus* and vancomycin-resistant enterococci on the gowns and gloves of healthcare workers. *Infect Control Hosp Epidemiol* 29(7):583–589
- Spadaro JT, Isabelle L, Renganathan V (1994) Hydroxyl radical mediated degradation of azo dyes: evidence for benzene generation. *Environ Sci Technol* 28(7):1389–1393
- Speers R Jr, Bernard H, O’Grady F, Shooter R (1965) Increased dispersal of skin bacteria into the air after shower-baths. *Lancet* 285(7383):478–480
- Tovey ER, Mahmic A, McDonald LG (1995) Clothing – an important source of mite allergen exposure. *J Allergy Clin Immunol* 96(6):999–1001
- Vikke HS, Giebner M (2015) UniStatus-a cross-sectional study on the contamination of uniforms in the Danish ambulance service. *BMC Res Notes* 8(1):95
- Wang Y, Zeng Z, Liu M (2011) Analysis of naphthalene residues in textile samples by GC-FID using sol-gel-derived SPME fiber. *J Chromatogr Sci* 49(1):29–34
- Weschler CJ, Bekö G, Koch HM, Salthammer T, Schripp T, Toftum J, Clausen G (2015) Transdermal uptake of diethyl phthalate and di(*n*-butyl) phthalate directly from air: experimental verification. *Environ Health Perspect* 123(10):928–934
- Whyte W, Hejab M (2007) Particle and microbial airborne dispersion from people. *Eur J Parenteral Pharm Sci* 12(2):39–46
- Wiener-Well Y, Galuty M, Rudensky B, Schlesinger Y, Attias D, Yinnon AM (2011) Nursing and physician attire as possible source of nosocomial infections. *Am J Infect Control* 39(7): 555–559
- Wisthaler A, Weschler CJ (2010) Reactions of ozone with human skin lipids: sources of carbonyls, dicarbonyls, and hydroxycarbonyls in indoor air. *Proc Natl Acad Sci* 107(15):6568–6575
- Xue J, Liu W, Kannan K (2017) Bisphenols, benzophenones, and bisphenol A diglycidyl ethers in textiles and infant clothing. *Environ Sci Technol* 51(9):5279–5286
- Yang S, Bekö G, Wargocki P, Williams J, Licina D (2021) Human emissions of size-resolved fluorescent aerosol particles: influence of personal and environmental factors. *Environ Sci Technol* 55(1):509–518
- Yoon YH, Brimblecombe P (2000) Clothing as a source of fibres within museums. *J Cult Herit* 1(4): 445–454
- You R, Cui W, Chen C, Zhao B (2012) Measuring the short-term emission rates of particles in the “personal cloud” with different clothes and activity intensities in a sealed chamber. *Aerosol Air Qual Res* 13(3):911–921
- Zhou J, Fang W, Cao Q, Yang L, Chang VC, Nazaroff WW (2017) Influence of moisturizer and relative humidity on human emissions of fluorescent biological aerosol particles. *Indoor Air* 27(3):587–598
- Zhu F, Ruan W, He M, Zeng F, Luan T, Tong Y, Lu T, Ouyang G (2009) Application of solid-phase microextraction for the determination of organophosphorus pesticides in textiles by gas chromatography with mass spectrometry. *Anal Chim Acta* 650(2):202–206



Time-Activity Patterns

37

Xiaoli Duan, Beibei Wang, and Suzhen Cao

Contents

Introduction	1058
Survey Method	1059
Questionnaire Method	1059
Global Positioning System Method	1061
Videotaping Method	1062
Sensors Method	1063
Mobile Phone Method	1064
Time-Activity Patterns Survey	1067
China	1067
USA	1076
Canada	1086
Korea	1096
Europe	1099
Africa	1106
Conclusion	1109
References	1110

Abstract

Time-activity pattern refers to the time and behavior of people at different locations. The knowledge of time-activity pattern is essential for indoor air pollution exposure assessment when direct personal exposure monitoring cannot be conducted. This chapter systematically reviewed the survey method of time-activity patterns and related large-scale surveys conducted in typical countries

X. Duan (✉)

School of Energy and Environmental Engineering, University of Science and Technology Beijing, Beijing, China

e-mail: jasmine@ustb.edu.cn

B. Wang · S. Cao

University of Science and Technology, Beijing, China

e-mail: wangbeibei723@163.com; love-lmd@163.com

worldwide. The survey method included both traditional and emerging survey methods, including questionnaire method, global positioning system method, videotaping method, sensors method, and mobile phone method. New technologies have great demand for data mining and analysis, so the data analysis technology is a great challenge and the focus of future research. Many countries like China, America, Canada, and Korea all carried out their national wide survey. Due to the discrepancy in culture, habits, and economical level, human time-activity patterns differed greatly among countries. Current surveys mainly adopt questionnaire survey method, with the development of exposure science, more accurate and detailed information, including location, time, duration, and activity patterns using new technologies that are necessary for future indoor air-related exposure assessment.

Keywords

Time-activity patterns · Human exposure · Exposure assessment · Survey method · Population survey

Introduction

Time-activity pattern refers to the time spent and behavior of people at different locations. It consists of three basic elements: location, duration, and activity. People may have different exposures to indoor air pollutant when they are in different indoor environments or engaged in different activities. There are differences in the concentrations of air pollutants in different indoor microenvironments. For instance, the concentrations of volatile organic compounds in gas stations and dry cleaners are higher than that in other indoor places (Cankaya et al. 2020). Additionally, individuals' inhalation rates vary under different activities, with the greater the activity intensity, the greater the inhalation rate. Time-activity patterns vary among individuals depending on culture, ethnicity, hobbies, location, sex, age, socioeconomic characteristics, and personal preferences (Duan et al. 2014). Therefore, the knowledge of time-activity patterns is essential for indoor air pollution exposure assessment when direct personal exposure monitoring cannot be conducted.

There are direct and indirect methods for assessing exposure to air pollution. Direct methods include in personal exposure monitoring and intraindividual exposure monitoring, i.e., exposure biomarker monitoring. Personal exposure monitoring requires the respondent to carry the monitoring instrument, with the implementation process complicated and costly, so it is not suitable for large-scale population. Additionally, instruments for monitoring some air pollutants with high sensitivity, portability, and sufficient time resolution are still lacking. In addition, since most air pollutants lack specific exposure markers, the applications of intraindividual exposure monitoring are very limited. The indirect assessment method assesses air pollutant exposure levels by integrating concentration monitoring data for air pollutants in different microenvironments and human time-activity pattern data using

time-weighted method. This method comprehensively considers the concentration of pollutants in various microenvironments and the duration and activity pattern of the subjects in different microenvironments, which could more comprehensively reflect the real situation of individual exposure. In addition, this method has the advantage of low cost and strong operability, and can be applied to exposure assessments for both small-scale fixed populations and a wide range of populations.

The use of indirect assessment methods to assess the exposure level to an air pollutant is generally calculated according to the formula (1):

$$\text{Exposure} = \sum C_i \times IR_j \times t_{ij} \quad (1)$$

Exposure – exposure dose to an air pollutant through inhalation route

C_i – concentration of an air pollutant in microenvironment i

IR_j – subject's inhalation rate under activity condition j

t_{ij} – subject's duration under activity condition j in microenvironment i

It can be observed that it is necessary to obtain the activity pattern and duration of the subject in different microenvironments in addition to the concentration of air pollutants in different microenvironments. Therefore, the time-activity pattern information of the subject is a key parameter to determine the accuracy of air pollutant exposure assessment. In the assessment of indoor air pollutant exposure, microenvironment classification can be divided into residential indoors, workplace indoors, school indoors, restaurants, shopping malls, bars, etc., but in many cases, more detailed classification is needed, such as residential interiors, subdivided into bedrooms, bathrooms, kitchens, garages, basements, laundry rooms, etc. In addition to directly using the time-activity pattern as an exposure parameter in the exposure assessment model, the specific activity itself can also indirectly reflect the exposure, such as whether it has been to a gas station or dry cleaner (volatile organic compound); whether it is with a smoker in the same room (environmental tobacco smoke) is a good indicator of the exposure to specific air pollutions for the respondents.

Survey Method

Time-activity data are generally obtained using recall questionnaires and diaries to record the person's activities in microenvironments. Other methods include the use of videotaping, global positioning system technology, and so on to provide information on individuals' locations.

Questionnaire Method

The questionnaire survey method collects time-activity pattern information of respondents by filling in a time-activity diary or questionnaire. This type of method

is currently most widely used, which is relatively simple, low cost, and can directly obtain the detailed activity information. However, it has the shortcomings of response error (recall bias), low temporal and spatial resolution, and large report burden of participants.

The questionnaire survey method can be divided into two categories according to the method of obtaining time-activity information, real-time diary recording method, and retrospective questionnaire survey method. The former requires the respondent to record the time, place, behavioral activities, and surrounding environment conditions of various microenvironments in real time, while the latter is to obtain the above information from the past (usually 24 h) or special time points through the investigation object. Although the method of real-time logging is relatively more accurate, the respondents are more burdened and usually only apply to small-sample individual monitoring studies, while retrospective survey methods are often used in large-scale population surveys.

In general, the questionnaire or the diary should include the cover of the questionnaire, the foreword of the questionnaire, and the content of the questionnaire.

- (a) The cover of the questionnaire should include the title of the questionnaire, the code of the questionnaire, the area of the respondent, and the information of the investigator.
 - 1. Questionnaire code: It is a unique identifier that distinguishes the questionnaire. It is generally composed of numbers and is located at the top right of the cover of the questionnaire.
 - 2. Questionnaire title: Used by respondents to understand the subject of the survey.
 - 3. Investigator information: Used to clarify the responsibilities and facilitate the inquiry and verification. It should include the name of the investigator, the date of the investigation, the name of the quality controller, the date of the quality control, and the length of the questionnaire.
- (b) Foreword to the questionnaire: Informed consent for obtaining the respondent should include the purpose and significance of the investigation, the commitment to confidentiality, the requirements for completing the questionnaire for the respondent, and the personal identity and organization name of the investigator.
- (c) Questionnaire content: It is the main body of the questionnaire, and should include test questions, answer methods, and instructions for answering.

The survey method includes telephone surveys, face-to-face surveys, and web surveys. Dialing by telephone is one of the most commonly used survey methods. For example, the National Human Activity Pattern Survey (NHAPS) was conducted by the US Environmental Protection Agency (EPA) in 1992–1994 to collect nationwide population exposures-related time-activity pattern information. University of Maryland Survey Center Computer-assisted telephone interview equipment was conducted to survey 9386 people in 48 states (Klepeis et al. 1996). The questionnaires used were divided into timetable for recording 24 h activity status and supplementary questionnaire. The former is the core of the questionnaire, and the

respondents were required to report all activities of the previous day in chronological order, the start and end time, detailed position (83 position codes), behavior (91 types), and whether someone is smoking.

In addition to the above telephone survey, face-to-face surveys was employed in a study on environmental exposure-related human activities patterns survey in the Chinese population, in which a multistage stratified cluster random sampling is used, and the respondents were investigated through a face-to-face questionnaire survey (Ministry of Ecology and Environment the People's Republic of China (MEE) 2013b, 2017c).

Global Positioning System Method

The global navigation satellite system (GNSS) refers broadly to all satellite navigation systems, such as GPS from the USA, Glonass from Russia, Galileo from the Europe, and BeiDou from China, that enables precise positioning of ground points. The methodology continuously records other information such as time, location, speed, and activity status of respondents in real time by wearing positioning devices, sometimes combined with accelerometers or other devices, and then parses the time-activity pattern status of respondents using tools such as geographic information systems (GIS) and specialized statistical packages. Among them, GNSS technology is increasingly used for time-activity pattern surveys, which have the advantages of good record continuity, high temporal resolution, and reduced subject burden compared to traditional time-activity survey methods (e.g., self-reported paper diaries and telephone interviews). However, barriers exist for accurately extracting time-activity patterns for human subjects from raw GNSS data because they are not consistently reliable due to errors caused by satellite or receiver issues, atmospheric and ionosphere disturbances, multiparty signal reflection, or signal loss or blocking. The multiparty problem occurs mainly in urban areas where tall buildings and structures reflect satellite signals many times before they reach a GNSS device, leading to GNSS coordinates errors.

In fact, few air pollution epidemiological studies have effectively used GNSS data to classify temporal activity patterns, possibly due to issues, including GNSS data quality, human subject compliance, and lack of reliable methods for mining raw GNSS data. GNSS data classification techniques have been largely documented in the field of travel behavior and physical activity research. Travel mode, activity location, and end-of-trip detections are the main applications of GNSS classification algorithms. Several studies have developed methods to classify travel activities using GNSS data or GNSS combined with body-worn sensors. Ellis et al. (2014) used body-worn sensors, such as accelerometers and SenseCam cameras, to classify physical activity into five modes (cycling, riding, sitting, standing, and walking/running) using a random forest classification model. Kohla et al. (2014) predicted eight modes of transportation based on a multivariate logistic regression model using GNSS and acceleration data. Combining GNSS, GIS, and accelerometer data, Brondeel et al. (2016) developed a trip-level traffic mode prediction model based

on a random forest approach and obtained a 90% correct prediction rate. However, the reliability of accelerometer data can be negatively affected by external factors, such as clothing and weather changes. Spatial data (e.g., roads and building roofs) have also been used to improve the accuracy of temporal activity classification. Nethery et al. (2014) manually mapped the boundaries of participants' homes and school buildings to help detect specific locations.

A tool that can be used to investigate time-activity patterns is presented here, MicroTrac, a model that uses global positioning system (GPS) data to estimate the time and duration people spend in different microenvironments (e.g., indoors and outdoors, work, and school) (USEPA). The model takes into account the time spent by individuals in specific locations and can improve air pollution exposure assessment for health research and risk assessment. MicroTrac addresses the limitations of time-activity diaries, including participant burden, diary returns, and inaccuracies due to reporting errors. MicroTrac is an automated classification model for estimating the time and duration spent by individuals in eight microenvironments (home, work, school, and car; other locations, indoors and outdoors). MicroTrac's inputs include GPS time course data (location, speed, and signal quality) and geocoded boundaries of respondents' homes, workplaces, and school building roofs. It has several novel features to classify GPS samples. First, MicroTrac uses a spatial buffer of building boundaries to account for spatial GPS inaccuracies. Second, MicroTrac uses a temporal buffer of GPS data to account for spatial errors that occur near structures that reflect GPS signals (e.g., high-rise buildings and dense tree cover). In addition, temporal filtering of GPS velocity samples is used to reduce misclassification within slow-moving or stopped vehicles (e.g., traffic congestion and traffic signals.) The performance characteristics of the MicroTrac model were evaluated in detail in a pilot study in central North Carolina by Breen et al. (2014).

Videotaping Method

Videotaping is a method in which trained videographers tape the subject's activities and subsequently extract the pertinent data manually or with computer software. Stanford's unique method of capturing children's microlevel activity time series (MLATS) lies in the use of a computer-based video extraction technique to extract children's activities from video footage. Results of this video-translation for a given subject yield the American Standard Code for Information Interchange (ASCII) files containing records of the following fields: an exposure boundary (e.g., left hand, right hand, and mouth), microenvironment (e.g., kitchen, garden, and bedroom), microactivity (e.g., playing, resting, repetitive action, and continuous action), object contacted (e.g., hard floor, upholstered furniture, soil, vegetation, and clothing), and duration in seconds. Each recorded line in the file corresponds to a unique time sequence of activity-related events (i.e., amount of time that body part spent touching that object in that microenvironment while performing that activity).

The process of collecting MLATS is labor-intensive. It requires the development of step-by-step methodologies suitable for the specific exposure scenarios as defined

by the needs of a particular project, and then the implementation of the methodologies to recruit and videotape subjects, train personnel, translate the videotaped activities into usable text files, and interpret the activity patterns. During the videotaping and video-translation process, steps must also be taken to ensure that quality MLATS data are collected and the data remains organized and protected.

Videotaping human activity for exposure assessment has become a more common practice over the past decade. In 1994, Stanford University's Exposure Research Group (ERG) conducted its first pilot study to collect MLATS data for young children. The pilot study involved videotaping four children of farmworkers in the Salinas Valley of California and converting their videotaped activities to valuable text files of contact behavior using video-translation techniques.

Sensors Method

The application of sensors has not been used for large-scale time-activity surveys. It has good application potential in the study of time-activity patterns. Currently, sensor-based time-activity research focuses on wireless sensor-based indoor positioning (Guo et al. 2017; Huang et al. 2019) and wearable device sensor-based activity recognition (Sprint et al. 2017).

In the past 10 years, due to the increasing demand for indoor positioning, the indoor positioning system (IPS) has been developed rapidly. Indoor positioning systems based on technologies such as LTE, WiFi, Bluetooth, wireless sensor network (WSN), or ultrawide band (UWB) have emerged. Such systems are often capable of (i) providing accurate location estimates to meet demand; (ii) facilitating the expansion; and (iii) inexpensive infrastructure inputs (Correa et al. 2017).

Another application for investigating time-activity patterns is to use sensor data to accurately identify the wearer's activity classification. Human activity recognition has become one of the hot topics in the field of artificial intelligence (AI) research in recent years, and many activity recognition methods have been proposed. Lukun Wang proposed continuous automatic encoder (CAE) as a new stochastic neural network model to improve the ability of model continuous data for wearable sensors to identify human activities (Wang 2016). Mary E. Rosenberger et al. compared the accuracy of the nine sensors in the 24 h activity measurement and found that no device was able to accurately capture the activity data for the entire 24 h workday. However, the future of activity measurement should aim at accurate 24 h measurements, and researchers should continue to select measurement devices based on the primary outcomes of the research objectives (Rosenberger et al. 2016). People have different breathing rates under different activities (such as sleeping, sitting, walking, etc.), so accurately identifying the active state helps to achieve reliable air pollution exposure assessment.

At present, sensor data mining methods are still one of the research hotspots because they cannot only provide accurate and continuous information on time activities, but also provide information on the physical activity of subjects, which has a very good application prospect in the investigation of exposure-related

activities. However, the mining and analysis of sensor data require some algorithm support. Ellis K et al. based on data obtained from 3D accelerators used a random forest model to predict five categories of physical activity (biking, cycling, sitting, standing, and walking/running) and hip accelerometers to predict four categories of physical activity (walking, and running); the average accuracy rate reached 92.3% (Ellis et al. 2014). When the accelerometer is combined with GPS data, the data can be analyzed to obtain the active activity of the wearer more related to environmental exposure.

Sensor methods typically require investigation and analysis to process measurement information from a subject's sensor rather than directly. A combination of multiple types of sensors or a comprehensive sensor-based survey framework with the ability to capture information such as location, time, duration, and activity patterns is used. The application of this sensor combination application in the study of time-activity patterns may be more desirable.

Mobile Phone Method

As the location-aware technologies grew and developed, scientists paid more and more attention to the feasibility of using them to observe urban mobility. Among these technologies, cellphone networks stand out as a more promising way of collecting data. Cellphone networks have a built-in capability of recording the location of their subscriber's cellphone without the need of any additional infrastructure. Massive and passive data such as cell phone traces provide samples of the whereabouts and movements of individuals. A method to reveal activity patterns is to emerge from cell phone data by analyzing relational signatures of activity time, duration, and land use.

There are some advantages for using cellphone data: advantages such as higher accuracy in comparison to traditional methods, all-daylong coverage of cellphone networks, reachability of data in all sorts of weather conditions, etc. Cellphone networks are capable of tracking a large portion of citizens for as long a period as required and for as many times as needed. The location updates are passive and the subscribers do not take any actions to make it happen. When we use the data obtained by cellphone networks to represent citizens movements the participant is unaware of being in the sample which increases the reliability of the data. On the other hand, some issues arise when we try to elicit traffic-related information from cellphones spatiotemporal data. The main challenge is that phone traces have low spatial precision and are sparsely sampled in time, which requires a precise set of techniques for mining hidden valuable information they contain.

Some people studied the trajectory of mining activity patterns and distributed activities in different parts of the network (Allahviranloo and Recker 2015). Although their data comes from GPS, the methods they propose can also be used for cell phone data. They attempted to infer the types of activities each person is engaged in at different locations by characteristics such as length of stay and distance from home. Later, they used the Markov chain of the conditional random field to

discover the relationship between the socioeconomic attributes of the individual and the sequence of activities and the temporal and spatial trajectories of the activity. Peter Widhalm and others worked to find patterns of urban activity in mobile phone data (Widhalm et al. 2015). To do this, they developed a dual approach. In the first phase, they detect stays and extract geocoded timestamps that form the travel chain. In the second phase, they combined the stay data with the land use data to cluster the activities. They model dependencies, activity types, trip scheduling, and land use types through a relational Markov network. They tested their approach using the Boston City CDR dataset and claimed that the results were consistent with the city survey. Yang Xu et al. tried to understand aggregate human mobility patters using passive mobile phone location dataset from Shenzhen, China (Xu et al. 2015). Their study presented a home-based approach to find human movements patterns that considered homes of individuals as anchor points and references to analyze those individuals' activities. Then they categorized people based on their approximate home locations to obtain aggregate mobility patterns for each BTS. Finally, they used a multilevel hierarchical clustering algorithm to classify regions that show similar mobility patterns.

Some study proposed a new method to distinguishing stays and activity locations from on-move points by considering factors other than duration of stop it is possible to robustly detect a stay (Zahedi and Shafahi 2016). Here are two conditions that if any of them is met, the point under consideration is highly likely to be a stay.

1. If a cellphone connects to a tower (or remains within a cluster of ping-ponging towers) for more than 20 min it can surely be stated that the user of that cellphone is purposefully staying near that tower, because the configuration of the city and the BTSs inside it are in a way that a moving cellphone is not likely to connect to one tower (or remains within the cluster of the towers with ping-pong handover) for more than 20 min. In other words, four consecutive repetitions of the same location in the time-stamped sequence indicates a stay.
2. For the points with two or three consecutive repetitions of the same location, if the cover range of the tower or towers representing that location is fairly small it can be assumed that the user has stopped in that location to perform some activity.

The general development of smartphones in recent years has provided convenient conditions for the monitoring of behavioral patterns. Smartphones mainly monitor behavior patterns based on GPS and motion sensors. The relevant working mechanisms and principles of GPS and sensors have been described in the above description. Activity recognition based on smartphone sensors is becoming an area of extensive research. Smartphones can collect important data from sensors. These sensors include acceleration sensors, position sensors, vision sensors, audio sensors, temperature sensors, and direction sensors. In addition, many applications are developed on smartphones using GPS and sensors. GPS and motion sensor-embedded smartphones provide a new platform for activity reasoning. Originally used for mobile phone enhancements, these sensors are now available for a variety of applications. Providing mobile phone users with information about their own

physical activity in an understandable format can enable users to make smarter and healthier lifestyle choices.

The National University of Science and Technology of Pakistan has developed an app (Arjum and Ilyas 2013). In this work, they built a smartphone app that tracks the user's physical activity and provides feedback, and in daily operations, the user is not required to lose the app to report estimates of calories burned by physical activity. This application differs from previous activity recognition work in that it: 1) it does not require user interaction settings, 2) it does not require additional sensing hardware, it only relies on the physical sensors of the low-end smartphone standard, 3) it does not require calibration, 4) it supports the detection of seven different physical activities, including walking, running, climbing stairs, going down the stairs, cycling, driving, and staying inactive, and 5) the decision tree classifier used by the activity diary app is accurate. Researchers are currently testing the "Activity Diary" application in the field and are working to open it to the public through the Google Android market. In 2018, Pratool B proposed a new system called "HuMAN" that fills this gap by identifying and classifying human complex family activities with wearable sensors (Bharti et al. 2018). Specifically, HuMAN achieves this classification by leveraging a selective multimodal sensor suite on wearable devices and enhances activity classification by carefully utilizing the placement of wearable devices in multiple locations on the human body. According to the richness of the perceived information, HuMAN's system consists of: (a) extracting a set of useful features from a selected multimodal sensor set; (b) a new two-level structure classification algorithm that uses multiple body position sensors to improve accuracy; and (c) improves the classification of complex activities with minimal external infrastructure support (for example, only a few Bluetooth beacons are used for location context). In a real home environment, the system was evaluated with ten users. The experimental results show that the system can detect 21 complex family activities with high precision. For the same user evaluation strategy, the average classification accuracy of all 21 activities was as high as 95%. Health Mate is also an application that can be used on Android and iOS systems to track human behavior and identify activities. It can manually record 30 different activities and automatically detect running, walking, and swimming. However, there is currently no relevant literature supporting the accuracy of this application.

On activities type recognition, Esfahani et al. introduced a new dataset, called position-aware multisensor (PAMS) (Esfahani and Malazi 2018). The dataset contains both accelerometer and gyroscope data. The gyroscope data boosts the accuracy of activity recognition methods as well as enables them to detect a wider range of activities. We also take the user information into account. Based on the biometric attributes of the participants, a separate learned model is generated to analyze their activities. We concentrate on several major activities, including sitting, standing, walking, running, ascending/descending stairs, and cycling.

In addition to the molded application, there is also a dataset on the smartphone for activity identification, among a group of 30 volunteers between the ages of 19 and 48 ongoing (Anguita et al. 2012). Everyone wears a smartphone on the waist (Samsung Galaxy S II) for six activities (walking, upstairs, downstairs, standing,

sitting, and laying). Using its embedded accelerometer and gyroscope, we capture three-axis acceleration and three-axis angular velocity at a constant rate of 50 Hz. Data has been manually tagged by video recording experiments. The obtained datasets were randomly divided into two groups, of which 70% of the volunteers were selected to generate training data and 30% of test data. The sensor signals (accelerometer and gyroscope) were preprocessed by applying a noise filter and then sampled in a fixed-width sliding window (128 readings/window) of 2.56 s and 50% overlap. The sensor acceleration signal has a gravity and body motion component that is separated into body acceleration and gravity using a Butterworth low pass filter. It is assumed that gravity has only a low-frequency component, so a filter having a cutoff frequency of 0.3 Hz is used. From each window, the feature vector is obtained by calculating variables from the time domain and the frequency domain.

Time-Activity Patterns Survey

China

Adults

The first Chinese Environmental Exposure-Related Human Activity Patterns Survey for adults (CEERHAPS-A) was carried out among 91,527 permanent residents aged 18 years and above in 159 counties/districts, 636 streets, and 1908 villages committees of 31 provinces, autonomous regions, and municipalities directly under the Central Government (excluding Hong Kong, Macao Special Administrative Region and Taiwan) in the People's Republic of China in 2011–2012. The multistage cluster random sampling method was used in this survey, with demographic characteristics, rural/urban status, and gender as stratified factors. Table 1 represents the distribution of interviewees by selected factors (Duan et al. 2014).

Face-to-face interviews were conducted to ask each interviewee about their basic information and time-activity patterns. All of the surveyors were trained to ensure they have the same understanding of each question. The contents of the survey included the basic situation of the respondents, the exposure characteristics related to environmental media, the exposure characteristics related to pollution sources, and the exposure behavior characteristics related to environmental health risk factors. Time-activity factors related to indoor air pollutant exposure mainly include time indoors. The mean and 5th ~ 95th percentile data of time indoor by gender, age, urban/rural, and region group are presented in Table 2.

Statistical analysis was completed using SAS. All results were weighted and adjusted as follows: first, the obtained data were weighted using factors calculated from the probabilities for adults in the household, resident groups in the village/community, village/community numbers in the town, and towns in the investigated site; the weighted results were then adjusted using poststratification weight analysis to normalize the population distributions of gender and age in our results with those in the Sixth China National Census (Ministry of Ecology and Environment the People's Republic of China (MEE) 2013a).

Table 1 Distribution of interviewees by selected factors

Category		Sample size	Proportion (%)
Total		91,121	100.0
Urban/Rural	Urban	41,826	45.9
	Rural	49,295	54.1
Gender	Male	41,296	45.3
	Female	49,825	54.7
Age	18 ~ 44	36,682	40.3
	45 ~ 59	32,374	35.5
	60 ~ 79	20,579	22.6
	80~	1486	1.6
Region	North	18,097	19.9
	East	22,965	25.2
	South	15,184	16.7
	Northwest	11,271	12.4
	Northeast	10,179	11.2
	Southwest	13,425	14.7
Province/Municipalities/Autonomous region	Beijing	1114	1.1
	Tianjin	1154	1.6
	Hebei	4409	5.2
	Shanxi	3441	2.8
	Neimenggu	3048	2.0
	Liaoning	3379	4.1
	Jilin	2738	2.4
	Heilongjiang	4062	3.1
	Shanghai	1161	1.2
	Jiangsu	3473	4.9
	Zhejiang	3428	3.5
	Anhui	3497	5.1
	Fujian	2898	4.3
	Jiangxi	2917	2.6
	Shandong	5591	7.4
	Henan	4931	6.9
	Hubei	3412	4.6
	Hunan	4059	5.7
	Guangdong	3250	5.3
	Guangxi	3380	3.6
	Hainan	1083	1.3
	Chongqing	969	2.5
	Sichuan	4581	5.7
	Guizhou	2855	2.5
	Yunnan	3491	3.7
	Xizang	1529	0.2
	Shaanxi	2868	1.2
	Gansu	2869	1.7

(continued)

Table 1 (continued)

Category		Sample size	Proportion (%)
	Qinghai	1592	0.7
	Ningxia	1138	0.8
	Xinjiang	2804	2.5

Table 2 Recommended values of time indoors

Category	Time indoors (min/day)					
	Mean	P5	P25	P50	P75	P95
Total	1167	876	1065	1200	1290	1373
Gender	Male	1152	855	1043	1185	1283
	Female	1183	900	1095	1215	1300
Age	18 ~ 44	1167	875	1065	1201	1292
	45 ~ 59	1157	866	1051	1185	1285
	60 ~ 79	1178	900	1086	1203	1295
	80~	1228	945	1164	1260	1331
Urban/Rural	Urban	1198	900	1120	1239	1313
	Rural	1142	865	1035	1165	1269
Region	North	1150	870	1045	1185	1275
	East	1197	900	1110	1239	1315
	South	1152	864	1060	1176	1273
	Northwest	1133	855	1036	1155	1251
	Northeast	1196	910	1103	1230	1310
	Southeast	1148	846	1030	1174	1290

The exchange of subjects in the sampling roll with other subjects was strictly monitored; less than a 5% exchange rate was allowed for each field site. To ensure uniformity, all surveyors were trained, tested, and deemed qualified, in their understanding of the questionnaire content and possible responses. Parallel questionnaires were performed among 5% of the participants. The subject response was 95% and the recovery rate of valid questionnaires was 99.6%. Ultimately, 91,121 households located in 9108 villages, 636 towns, and 159 counties were used in the analysis (Ministry of Ecology and Environment the People's Republic of China (MEE) 2013b).

Children

The Chinese Environmental Exposure-Related Human Activity Patterns Survey for Children (CEERHAPS-C) was the first national-scale survey of children's exposure factors conducted by Chinese Research Academy of Environmental Sciences from 2013–2014. It investigated the exposure characteristics of children under different conditions. In order to ensure the nationwide representativeness of the survey samples, the multistage stratified cluster random sampling design was adopted for the survey, with regions, rural/urban status, gender, and ages as stratified factors. The subjects in this survey included 75,519 children aged 0–17 years (children under 6 months need to be born in the place of investigation and other subjects need to live

in the place of investigation for more than 6 months) from 55 counties/districts, 165 townships/streets, and 316 schools in 30 provinces (districts and municipalities) of the People's Republic of China. The distribution of the survey respondents is presented in Table 3 (Ministry of Ecology and Environment the People's Republic of China (MEE) 2017a).

The field survey adopted the method of combining questionnaire survey and field measurement (semi-quantitative and quantitative). The questionnaire was designed by the self-designed questionnaire, which was conducted by one-to-one and face-to-face questionnaires by trained investigators. Children under 9 years old were answered by their caregivers; children over 9 years old were answered by the children themselves. The contents of the survey included the basic situation of the respondents, the exposure characteristics related to environmental media, the exposure characteristics related to pollution sources, and the exposure characteristics related to environmental health risk factors. Time-activity factors in this survey associated with exposure to indoor air pollutants mainly included time indoors, time exposure to cooking fumes, time exposure to secondhand smoke, and type of fuels used for cooking or heating in children's living indoor environment (Ministry of Ecology and Environment the People's Republic of China (MEE) 2017b).

Weighting of the survey data produced estimates representative of the Chinese child population. CEERHAPS-C sample weighting was carried out in two steps. The first step involved the computation of sampling weights of each stage, including district, school, and class. In the second step, the sample weights were poststratified by district, urbanicity, gender, and age to the 2010 Chinese child population. The final weight was the product of the base sample weight and the poststratification weight (Ministry of Ecology and Environment the People's Republic of China (MEE) 2017c). The recommended values of time indoors (min/day) are presented in Table 4.

The average time exposure to cooking fumes of children is presented in Table 5. The average daily exposure time of Chinese children to cooking oil fume was 11 min. In terms of age distribution, children aged 5 years had the shortest exposure time to cooking fume, which was 2 min/day, while children over 15 years old had the longest exposure time, which was 18 min/day. From the urban and rural distribution, children in rural areas had the highest exposure time to cooking fume than children in urban areas; from the regional distribution, children in Southwest China had the highest exposure time to cooking fume, while children in East China had the lowest exposure time.

The average time exposure to secondhand smoke of children is presented in Table 6. The average exposure time of children to secondhand smoke in China is 6 min per day. There was no significant difference in the age and sex distribution of children's exposure time to secondhand smoke. From the urban and rural distribution, rural children's exposure time to secondhand smoke was slightly higher than that of urban children; from the regional distribution, in general, children in Northeast China had the longest exposure time to secondhand smoke and the shortest exposure time in East China.

Table 3 Distribution of the survey respondents by selected factors

Category	Total	Urban/Rural		Regions				Southwest
		Urban	Rural	North	East	South	Northwest	
0 months ~	Total	75,490	38,503	36,987	15,113	19,618	13,410	9,523
	Male	37,675	19,024	18,651	7,555	9,797	6,694	4,780
	Female	37,815	19,479	18,336	7,558	9,821	6,716	4,743
	Total	2165	1077	1088	456	609	357	298
3 months ~	Male	1098	532	566	227	300	186	153
	Female	1067	545	522	229	309	171	145
	Total	2273	1264	1009	452	589	423	370
	Male	1168	653	515	239	321	200	140
6 months ~	Female	1105	611	494	213	268	223	130
	Total	2773	1514	1259	602	696	501	345
	Male	1439	762	677	327	370	253	171
	Female	1334	752	582	275	326	248	174
9 months ~	Total	1921	878	1043	385	520	342	252
	Male	957	438	519	189	271	168	115
	Female	964	440	524	196	249	174	137
	Total	5668	2701	2967	1069	1420	1084	759
1 year ~	Male	2969	1357	1612	579	725	582	387
	Female	2699	1344	1355	490	695	502	372
	Total	4777	2351	2426	993	1185	829	577
	Male	2503	1210	1293	513	599	434	317
2 years ~	Female	2274	1141	1133	480	586	395	260
	Total	4907	2463	2444	975	1203	924	681
	Male	2565	1258	1307	520	622	484	354
	Female	2242	1205	1137	455	581	440	327
3 years ~	Total	4807	2460	2347	972	1259	788	633
	Male							455
4 years ~	Total							700
	Male							

(continued)

Table 3 (continued)

Category		Total	Urban/Rural			Regions				Southwest
			Urban	Rural	North	East	South	Northwest	Northeast	
5 years ~	Male	2508	1289	1219	490	664	444	330	226	354
	Female	2299	1171	1128	482	595	344	303	229	346
	Total	4760	2468	2292	976	1242	816	646	422	658
6 years ~	Male	2452	1261	1191	500	642	413	348	222	327
	Female	2308	1207	1101	476	600	403	298	200	331
	Total	9622	5127	4495	2030	2614	1550	1107	905	1416
9 years ~	Male	4661	2475	2186	991	1280	747	541	418	684
	Female	4961	2652	2309	1039	1334	803	566	487	732
	Total	11,208	5915	5293	2296	2963	1977	1267	1097	1608
12 years ~	Male	5459	2908	2551	1054	1495	985	616	518	791
	Female	5749	3007	2742	1242	1468	992	651	579	817
	Total	10,751	5563	5188	2014	2864	2003	1325	1035	1510
15 ~ 17 years	Male	5197	2682	2515	984	1368	949	677	467	752
	Female	5554	2881	2673	1030	1496	1054	648	568	758
	Total	9858	4722	5136	1893	2454	1816	1363	814	1518
Male	Male	4699	2199	2500	942	1140	849	631	336	801
	Female	5159	2523	2636	951	1314	967	732	478	717

Table 4 Recommended values of time indoors (min/day)

Ages	Total	Gender		Urban/Rural		Regions					
		Male	Female	Urban	Rural	North	East	South	Northwest	Northeast	Southwest
0 month ~	1390	1392	1389	1399	1384	1408	1394	1365	1409	1438	1376
3 months ~	1350	1356	1344	1363	1338	1381	1351	1312	1361	1430	1361
6 months ~	1321	1323	1320	1327	1317	1333	1310	1285	1335	1420	1341
9 months ~	1303	1300	1306	1320	1291	1292	1310	1249	1319	1416	1334
1 year ~	1285	1283	1288	1299	1274	1261	1288	1259	1287	1377	1320
2 years ~	1279	1280	1277	1292	1268	1275	1283	1249	1259	1370	1291
3 years ~	1275	1274	1275	1290	1261	1279	1275	1252	1254	1367	1281
4 years ~	1284	1279	1289	1302	1269	1274	1288	1269	1254	1362	1288
5 years ~	1286	1285	1288	1298	1276	1279	1280	1289	1250	1349	1298
6 years ~	1297	1294	1299	1310	1291	1308	1265	1313	1280	1297	1291
9 years ~	1298	1296	1301	1309	1293	1309	1278	1308	1273	1307	1287
12 years ~	1300	1295	1306	1314	1291	1309	1309	1293	1274	1319	1294
15 ~ 17 years	1302	1296	1308	1301	1302	1308	1309	1298	1288	1310	1301

Table 5 The average time exposure to cooking fumes of children (min/day)

Ages	Total	Gender		Urban/Rural		Regions				Southwest
		Male	Female	Rural	Urban	North	East	South	Northwest	
Total	11	10	11	10	11	10	7	12	12	8
1 year ~	5	5	5	4	6	5	5	6	8	3
2 years ~	5	5	5	4	6	4	6	9	4	5
3 years ~	5	5	4	3	6	5	5	4	8	3
4 years ~	3	2	4	3	3	3	2	5	5	3
5 years ~	2	2	2	2	2	2	1	2	3	2
6 years ~	6	6	6	4	6	7	4	6	6	6
9 years ~	11	10	11	11	10	10	6	13	17	9
12 years ~	16	15	17	16	16	16	12	16	20	13
15 ~ 17 years	18	17	20	19	18	19	13	24	12	19

Table 6 The average time exposure to secondhand smoke of children (min/day)

Ages	Total	Gender		Urban/Rural		Regions					
		Male	Female	Urban	Rural	North	East	South	Northwest	Northeast	Southwest
Total	6	6	6	6	6	6	5	6	6	7	6
1 year ~	4	4	4	4	4	4	3	6	4	3	4
2 years ~	6	6	5	5	6	5	6	7	6	6	6
3 years ~	4	4	5	4	5	5	4	4	6	5	5
4 years ~	6	7	6	6	6	6	7	4	9	6	6
5 years ~	5	5	4	4	5	5	4	5	6	7	4
6 years ~	5	5	5	5	5	5	4	5	6	6	6
9 years ~	6	6	5	5	6	6	4	6	5	7	7
12 years ~	6	7	6	6	7	7	5	6	6	8	7
15~17 years	7	8	7	8	7	11	6	9	5	9	7

The proportion of children exposure to indoor environment with cooking or heating using solid fuels (%) is presented in Table 7. In China, 26.8% of children were exposed to indoor environments where solid fuels are used for cooking or heating, which was higher in rural areas than in urban areas. In terms of regional distribution, the number of children exposed in Northwest China was the highest, while the number of children exposed in East China was the lowest.

USA

California Activity Pattern Survey (1987–1988)

In California, 1762 residents aged 12 and older living in households containing a telephone were selected to participate in this survey. Interviews were conducted between 1987 and 1988 over four study periods by season: October–December, January–March, April–June, and July–September. The distribution of the sample by age and season of interview (October–December, January–March, April–June, and July–September) is shown in Table 8 (Wiley et al. 1991a).

During this research, interviewers collected some of the information related to four categories: a) personal background of the respondents, including age, education, area of residence, household income, and presence of children in the household; b) description of the respondent's living quarters, work conditions, and smoking behavior; c) a time diary of activities and locations, time spent outdoor and specific location like living room or kitchens in the home, or in automobiles or buses, as well as time spent in various activities such as cooking or playing sports; and d) time spent on one or more associated facets of daily activities that have implications for air pollution exposure (e.g., presence of smokers, cooking equipment, use of solvents, etc.).

Questionnaires and time diaries were conducted through computer-managed auxiliary telephone survey access (CATI) technology developed at the University of California at Berkeley. Interviewers asked respondents some time diary questions, with activities recorded in chronological order, along with the time each activity ended, where the activity occurred, and whether or not smokers were present during the activity. When respondents completed the diary, they were asked whether they spent time in potential exposures and other similar questions.

Indoor Activity Time of Various Microenvironments

Of the time spent indoors, 85% (1226 min per day) was spent in indoor location, and more than two-thirds (893 min per day) was inside the respondent's home, with the bedroom (524 min) and living room (196 min) being the main rooms of the house where time was spent. At the same time, of the time spent indoors away from home, about one-third of time was spent at places of work and other people's homes.

It could be seen that the most time-consuming activity was sleeping, namely the bedroom (524 min). About 328 min more time was spent there each day than in the next most time-intensive place, the living room (196 min). And almost three times as much time was spent in the living room as in the kitchen, the third most frequently

Table 7 The proportion of children exposure to indoor environment with cooking or heating using solid fuels (%)

Ages	Total	Urban/Rural		Regions				Southwest
		Urban	Rural	North	East	South	Northwest	
Total	26.8	18.0	32.1	26.4	17.7	27.7	66.2	31.2
0 month ~	17.1	7.5	24.9	17.6	12.5	18.8	25.3	56.7
3 years ~	22.0	11.3	30.9	28.6	15.6	21.2	41.2	64.7
6 years ~	20.4	13.2	23.6	19.4	17.4	20.2	42.9	10.8
12 ~ 17 years	38.2	30.0	43.1	39.8	23.2	40.2	82.4	35.2
								23.0

Solid fuels include coal and biomass, like firewood, charcoal, wood, animal waste, etc.

Table 8 Distribution of the sample by age and season of interview

Season of Interview	Adults 18 years ⁺	Adolescents 12–17 years	Total
Oct.–Dec. 1987	440	48	488
Jan.–Mar. 1988	418	55	473
Apr.–June 1988	265	25	290
July–Sept. 1988	456	55	511
Total	1579	183	1762

Table 9 Major of the data on respondent indoor location (number of valid observations = 1762)

Label	Reporting location (%)	Estimated population mean	Label	Reporting location (%)	Estimated population mean
In kitchen	75	73.9	At office	25	70.1
In living room	80	196.3	At plant	9	34.9
In dining room	29	21.1	At grocery store	22	12.4
In bathroom	74	32.9	At shopping mall	27	33.8
In bedroom	96	524.1	At school	15	40.4
In study	5	7.3	Other public place	8	13.2
In garage	9	9.1	At hospital	8	14.4
In basement	1	0.4	At restaurant	35	28.1
In utility room	5	2.6	At bar-nightclubs	5	8.0
Pool, spa	1	0.7	At church	5	6.3
Room to room	24	21.8	At indoor gym	4	4.2
Other HH Room	6	3.7	At other's home	30	60.6
Total at home	99	921.1	At auto repair/gas	12	10.5
			At hotel-motel	2	6.7
			At dry cleaners	1	0.4
			At beauty parlor	2	2.0
			At varying location	1	1.9
			Other indoor	9	11.7
			Total away	92	359.5

used room in the house (74 min). In general, less than half an hour per day on average was spent in the next set of at-home location – bathrooms, dining rooms, and “other” rooms. Garages, basements, utility rooms, and pool/spa areas took up less than 10 min per day when aggregated across the entire sample. The detailed data is shown in Table 9, 10, 11, 12, and 13.

Smoking and Secondhand Smoke Contact Time

Among the adult portion of the sample, about a fifth (22%) reported having smoking at least one cigarette on the diary, with about half of these smokers having smoked

Table 10 Mean time spent in various indoor locations by gender and employment station (Wiley et al. 1991a).

Location n=	Men			Women		
	Unemployed (249)	Employed (573)	Total (822)	Unemployed (430)	Employed (510)	Total (940)
Total at home	994	753	821	1092	863	965
Other Indoor Locations	226	451	389	223	419	231

Table 11 Mean time spent in various indoor locations by age and gender (Wiley et al. 1991a).

	Men						
	Age n=	12–17 (98)	18–24 (96)	25–34 (183)	35–44 (172)	45–54 (106)	55–64 (82)
Total at home	886	762	270	780	780	889	1098
Other indoor locations	369	411	416	407	383	270	152
Women							
Age n=	12–17 (85)	18–24 (96)	25–34 (223)	35–44 (179)	45–54 (110)	55–64 (112)	65+ (125)
Total at home	906	855	947	909	960	1079	1165
Other indoor locations	394	416	345	348	325	213	146

Table 12 Mean time spent in various indoor locations by region (Wiley et al. 1991a).

n=	South Coast region (328)	San Francisco Bay area (381)	Other areas of States (1053)
Total at home	842	907	923
Other indoor locations	383	361	327

Table 13 Mean time spent in various indoor locations by season (Wiley et al. 1991a).

n=	Fall (488)	Winter (473)	Spring (290)	Summer (511)
Total at home	915	927	864	869
Other indoor locations	351	349	384	346

more than ten cigarettes, and cigarette smoking was significantly higher among men. Smoking of cigars and pipes was highest among men aged 65 and over (6%), as well as men aged 45–54 (4%), but was almost nonexistent among younger men and among women of all age groups. According to the data, the place with the most smoking is at home. And other locations with the highest percentage of episodes with the presence of other smoking were bars and nightclubs (78%), restaurants (42%), plant/factories (37%), and other indoors (33%). Based on weighted data, about 62% of adults and adolescents of Californians would inhale secondhand smoke during the diary day. For such persons, the average duration of all activities with others smoking was 286 min per day. Over longer durations, say a week or more, the population prevalence of some degree of passive exposure to tobacco smoke must be quite high.

Kitchen Smoke Contact Time

Average time spent cooking was 38 min per day, with half of the sample (51%) engaging in some cooking activity on the diary day. Average cooking time per participant was 75 min, with one respondent reporting a high of 465 min cooking on the diary day. From the perspective of gender, women spent more time in cooking, and nonemployed women spent up to half again as much time as employed women in cooking. From the perspective of region, cooking time is the lowest in the South Coast Region. And from the perspective of season, time spent cooking was high in the spring.

Other Smoke Contact Time

In the research of CAPS, about 26% of respondents said they were at a gas station, parking garage, or auto repair shop, with 16% of all adult respondents saying they had pumped or poured gasoline. Also, 62% of the adult sample reported having an attached garage or carport at their dwelling unit. Some 37% reported that a motor vehicle had been parked in that attached garage or carport at their home. From the data point of view, men and employed persons reported being at auto repair shops/gas station/parking garage or pumping or pouring gas than women and unemployed persons, while differences in proximity to operating gas ovens and stoves were not significant across gender or employment status. From the perspective of age, spending time at auto repair shops/gas station/parking garage was higher among younger people, and the figures for pumping or pouring gasoline were also higher among younger people. From the perspective of region, having an attached garage was 11% higher in the San Francisco Bay area (70%) than in the South Coast region and other areas of the state (59%); however, the prevalence of being at auto repair shops/gas station/parking garages “yesterday” was higher in the South Coast region than in the other two areas of the state.

Heating Time

About 30% respondents reported that they were in a room heated by a gas furnace and the use of gas furnaces or any heat source was lower than average in the South Coast region. From the perspective of season, gas heat was the highest in winter

(52%) and the lowest in summer (2%), and the home heating reaches a peak in the winter months at 76% daily use and was only 4% during the summer months.

California Children's Activity Patterns Survey (1989–1990)

The California Children's Activity Patterns Survey (Wiley et al. 1991b) provided estimates of the time children spent in various activities and locations on a typical day. The target population for the children's survey consists of children 11 years old and younger living in California households at the time the survey was conducted. Households with no telephones were excluded, as were households in which there were no English-speaking adults.

The sample was stratified by region to provide a sufficient number of interviews to make comparisons among three major areas of the state: the Southern Coast (including Los Angeles, Orange, and Riverside counties and parts of San Bernardino and San Diego counties); the SF Bay area (including San Francisco, Alameda, Contra Costa, San Mateo, Napa, and parts of Solano, Sonoma, and Santa Clara counties); and counties not included above, i.e., "The Rest of State."

The questionnaire instrument for the California Children's Activity Patterns Survey was divided into three main parts: the adult sections, the children's section, and the daily time diary. When the randomly selected child was eight years old or less, the preferred respondent for all sections of the questionnaire was the parent or guardian who spent the most time with the child on the diary day. In most cases the preferred adult respondent was also the actual respondent. Approximately 92% the adult respondents were the parent or guardian who spent the most time with the selected child on the diary day. Nearly 98% of the adult respondents were either father, mother, step-father, or step-mother to the selected child. In fact, over three-quarters of the adult respondents were the children's mothers. When the selected child was 9–11 years old, he or she was the preferred respondent for the children's and diary sections of the questionnaire. This occurred in about 85% (269 of a total of 316) of such cases. The diary and children's sections were completed by the adult informant in 931 of the 1200 interviews. Most (about 58%) of these proxy interviews were conducted with adults who had spent at least eight waking hours with the child on the diary day. Less than 1% of the proxy interviews were with adults who had spent less than one waking hour with the child on the diary day.

The questionnaire was developed by staff of the Survey Research Center in consultation with the staff of the California Air Resources Board and a panel of scientific advisors. The content of the questionnaire is similar to that used for the 1987–1988 California survey of the activity patterns of adults and children aged 12–17 years (Wiley et al. 1991a). The majority of the substantive content of the questionnaire consists of three kinds of questions: a) direct questions about potential exposures to sources of air pollution on the diary day; b) the daily diary, an inventory of the child's activities and locations on the diary day, which includes beginning and ending times (i.e., durations in minutes); whether or not tobacco smoke was present, and a classification of each activity with respect to whether it occurred in an indoor or outdoor location; c) sociodemographic characteristics of the selected child (age, gender, race-ethnicity, and grade in school) and the adult respondent (marital

status, employment status, years of schooling, and household annual income). The direct questions about potential exposures were generally included the same as those used in the adult survey and items dealing with proximity to the following sources of air pollution, mainly on the diary day (i.e., the day before the interview): gasoline fumes from vehicles parked in attached garages or parking areas (on diary day), use of mothballs in the home (in general), use of toilet bowl deodorizers (in general), use of scented room fresheners (in general), gas heat on (on diary day) open windows (on diary day), use of a fan for ventilation (on diary day), use of air conditioners (on diary day), working vacuum cleaner (in general), child on floor and/or outside surface (on diary day), child around a humidifier or vaporizer (on diary day), child at gas station or auto repair shop (on diary day), child in room with gas oven on (on diary day), and potential exposure to paint products, solvents, pesticides, soaps or detergents, household cleaning agents, personal care aerosols, and hot showers or baths (all on diary day).

The questionnaires and the time diaries were administered via a computer-assisted telephone interviewing technology. The telephone interviews were conducted during April 1989 to February 1990 over four seasons: spring (April–June 1989), summer (July–September 1989), fall (October–December 1989), and winter (January–February 1990).

The data obtained from the survey interviews results in ten major activity categories (113 detailed activity code) and six major categories of locations (63 detailed code). The time respondents under 12 years of age spent in ten activity categories and six location categories are present in Table 14. For each of the categories, this table presents the mean duration for all survey participants. The activity category with the highest time expenditure was personal needs and care, with a mean of 794 min/day. Night sleep was the detailed activity that had the highest mean duration in that activity category. For all respondents, the largest mean amount of time spent was at home, with a mean of 1086 min/day. Table 15 shows the average time children spent in proximity to gasoline fumes and gas oven fumes. In general, the sampled children spent more time closer to gasoline fumes than to gas oven fumes.

Table 16 shows the mean time children under 12 years of age spent indoors by age and sex. Activities performed indoors were assumed to include household work, child care, personal needs and care, education, and communication/passive leisure. The average times spent in these indoor activities and half the time spent in each activity which could have occurred either indoors or outdoors (i.e., work related, goods/services, organizational activities, entertainment/social, do not know/not coded) were summed.

The National Human Activity Pattern Survey

The National Human Activity Pattern Survey (NHAPS), the first nationwide study, is a two-year nationwide telephone survey (9386 samples). The survey, supported by the US Environmental Protection Agency (EPA), aims to gather information about exposure patterns in human activity patterns.

The survey was conducted from late September 1992 to October 1993, and was followed up by the University of Maryland Research and Research Center using the

Table 14 Mean time (min/day) children under 12 years of age spent in ten major activity categories and six major location categories

Activity category	Mean duration	Location category	Mean duration
Work related	10	Home	1078
Household	53	School/Childcare	109
Childcare	<1	Friend's/Other's house	80
Good/Service	21	Stores, restaurants, shopping place	24
Personal needs and Care	794	In transit	69
Education	110	Other locations	79
Organizational activities	4		
Entertainment/Social	15		
Recreation	239		
Communication/Passive leisure	192		
Do not know/Not coded	2		
All activities	1440		

computer-assisted telephone follow-up system (CATI). Each survey time unit of the study consisted of independent, randomly sampled families. The NHAPS surveyed all of the families with telephone in 48 neighboring states, using a standard two-stage random digit dial (RDD) sample design to select the family.

In an adult-only family (e.g., respondents aged 18 or older), an adult is randomly selected. In families consisting of adults and children (respondents aged 17 or under), 60% of children are randomly selected from all children. Another 40% of adults are randomly selected from all adult residents. All data for adults is collected directly from selected respondents. For children under the age of 10, the family adult who knows the best about children's activities have completed an agent interview with the child. For children aged 10–17, adult respondents answered general family and demographic questions. Then, children between the ages of 10 and 17 answered questions about the time diary and diary of their own activities. Weekly and working day samples were sampled separately in the time unit of each sample collection. The study completed a survey of 9386 samples, and the statistical distribution of respondents is shown in Table 17.

During the survey, the interview time for each sample was controlled below 25 min. The questionnaire was set up in two different editions: Questionnaire A and Questionnaire B, both of which included demographic issues, a 24 h diary and a series of supplementary exposure issues. Among them, Questionnaire A emphasizes the exposure of potential pollutants in household air. NHAPS follows the method of past time diary research, which particularly enhances the accuracy of time estimates in microenvironment calls. The 24 h diary contains five main locations: own house, friends/other houses, travel, other indoors, and other outdoor locations. There are a total of 83 more specific location options, such as bedroom, kitchen, bars, restaurants, stadiums, shops, offices, trains, planes, etc. Fig. 1 shows a reported result of

Table 15 Mean time (min/day) children under 12 years of age spent in proximity to two potential sources of exposure by sex

		Boys						Girls					
Potential exposure		Birth to 1 Month	1 to <3 Months	3 to <6 Months	6 to <12 Months	1 to <2 Years	2 to <3 Years	3 to <6 Years	6 to <11 Years	11 Years	Birth to 11 years		
Gasoline fume	3	9	0	2	1	4	2	2	7	3			
Gas oven fume	0	0	2	2	1	3	0	1	0	1			
Potential exposure		Birth to 1 Month	1 to <3 Months	3 to <6 Months	6 to <12 Months	1 to <2 Years	2 to <3 Years	3 to <6 Years	6 to <11 Years	11 Years	Birth to 11 years		
Gasoline fume	0	3	0	3	1	2	1	2	1	1	2		
Gas oven fume	0	0	0	0	0	3	2	1	0	0	1		

Table 16 Mean time (min/day) children under 12 years of age spent indoors by age and sex

Age group	Boys		Girls	
	N	Indoor	N	Indoor
Birth to 1 month	3	1440	4	1440
1 to <3 months	7	1432	10	1431
3 to <6 months	15	1407	11	1421
6 to <12 months	31	1322	23	1280
1 to <2 years	54	1101	43	1164
2 to <3 years	62	1121	50	1102
3 to <6 years	151	1117	151	1140
6 to <11 years	239	1145	225	1183
11 years	62	1166	59	1215
Birth to 11 years	624	1181	576	1181

Table 17 Respondent distribution of NHAPS

Factor	Size	NHAPS (%)	Census (%)
Male	4294	46	49
Female	5088	54	51
<5 year	499	5	8
5 ~ 17 year	1292	14	19
18 ~ 64 year	6059	65	61
>64 year	1349	14	13
White	7591	81	83
Black	945	10	13
Asian	157	2	3
Hispanic	385	8	10
High School Grad	924	10	6
College Grad	1247	13	20
Postgrad	2612	28	32

Klepis et al. (1996)

time location associated with exposure to indoor air pollutants. Six of ten microenvironments and their respective durations are associated with exposure to indoor air pollution.

There are 91 different activity codes in the 24-h diary section of NHAPS, which are considered to be related to human exposure. The original NHAPS category was reclassified into eight categories, each of which contained multiple incidents such as cooking, laundry, housekeeping, bathing, sports, and more. Besides, whether or not someone else smokes in each microenvironment (excluding their own smoking) is also part of a diary that involves exposing specific activities. The content of the survey is related to the exposure level of indoor air pollution. The following two figures (Figs. 2 and 3) show that some of the findings from NHAPS were exposure-related activities and ETS exposure, respectively.

Human activity patterns are critical for identifying and determining human exposure to environmental contaminants, including of course indoor air pollutants exposure. The NHAPS survey covers a wide range of microenvironmental

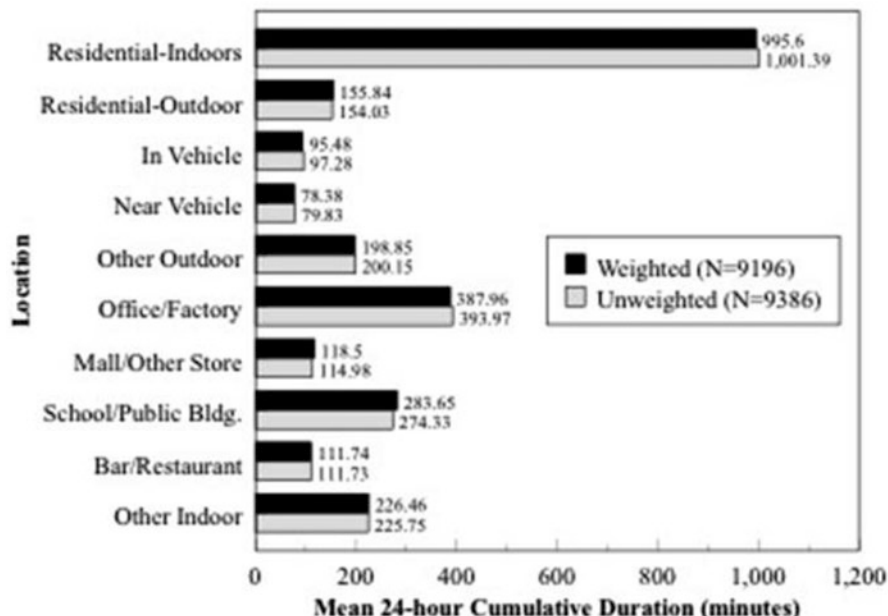


Fig. 1 The overall weighted and unweighted mean 24 h cumulative durations in each location. In the weighted analyses, 190 respondents with missing age or gender values were excluded (Kleppeis et al. 1996)

information related to human time-activity patterns. The NHAPS may provide useful information to indoor air pollution, but also provide experience and reference for the later investigation (Tables 18, 19, 20, and 21).

Canada

The Canadian Human Activity Pattern Survey II (CHAPS II) is the latest national time-activity pattern survey conducted in Canada from 2010–2011 to collect information on the time activities of Canadians of all ages. The survey was carried out taking into account the earlier Canadian Human Activity Model Survey (CHAPS I) conducted in 1994–1995 for the past 15 years, and changes in human activity patterns may have changed as the social situation changed. Moreover, the new survey compensates for some of the potential determinants of time-activity patterns that are not well captured in CHAPS I.

The target population for CHAPS II is the telephone resident who lived in the core area of the census metropolitan areas of: Vancouver, British Columbia; Edmonton, Alberta; Toronto, Ontario; Montreal, Quebec; and, Halifax, Nova Scotia, as well as those who lived in the rural portions of the Census Divisions of: Haldimand-Norfolk, Ontario, and Annapolis Valley-Kings County, Nova Scotia. The surveyed

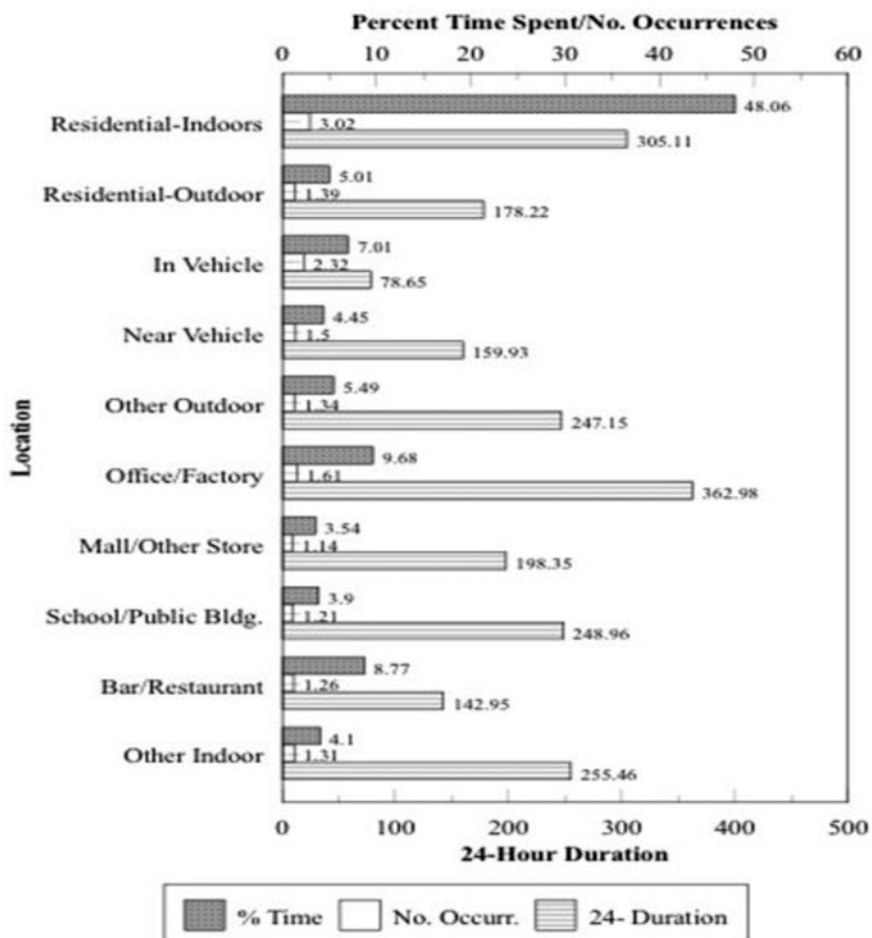


Fig. 2 The overall weighted ($N = 9196$) and unweighted ($N = 9386$) mean 24 h cumulative durations in each exposure activity. In the weighted analyses, 190 respondents with missing age or gender values were excluded (Klepeis et al. 1996)

areas include urban centers who account for 35% of Canada's total population, and two rural areas with more than 100,000 people. The residents in the survey included French residents, while CHAPS1 only English residents. The sample frame is divided into two sampling subframes for infants and noninfants.

CHAPS II included two survey periods from July to September 2010 (summer sampling) and January to January 2011 (season sampling). The survey conducted at each location is based on the sampling framework for the latest phone book listing information provided by ASDE Survey Sampler Inc and supplemented with random digit dialing (RDD) technology. The investigator obtains the zip code obtained from

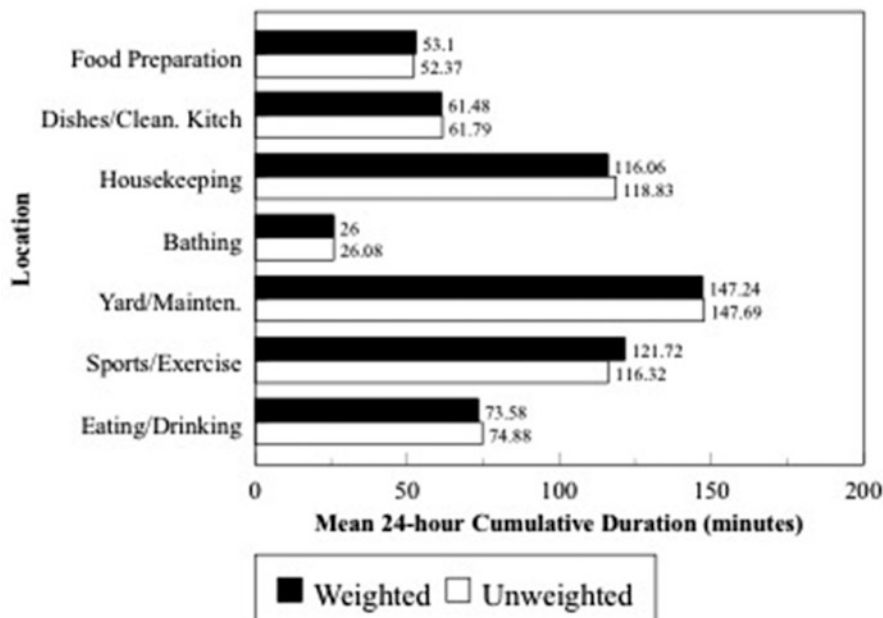


Fig. 3 The overall weighted percentage of time spent, mean number of occurrences, and mean 24 h cumulative durations (in minutes) of ETS exposure in each location (Klepeis et al. 1996)

the respondent and verifies the survey area of the respondent. In addition, different telephone number samples were drawn separately for noninfant and infant surveys as well as summer and winter sampling. The weighting includes several steps: initial calculation of basic weights; adjustment of nonresponse; adjustment of multiple telephone lines within the family; adjustment of over sampling of individuals under 18 years of age; deletion of records that are out of scope; and ensure that the population estimate is consistent with the region of the Canadian Census population-age-gender total.

The telephone survey consists of three main components: questions about the characteristics of the respondent and family composition; a 24 h memory diary; and a supplementary questionnaire on activities that are potentially exposed to specific pollutants, residential characteristics, and socioeconomic factors. Among the 24 h diaries, respondents were asked to describe what they did yesterday, from midnight the previous day to midnight last night, capturing the time, location, and amount of activity for each continuous event within 24 h. CHAPS II's main microenvironment survey was set under the two scenarios "At Home" (includes: indoors, outdoors, and indoors awake) and "Away from Home" (includes: indoors or in vehicle, outdoors, and other outdoor activities). The survey obtained possible potential factors affecting the time-activity pattern such as the age (Table 22), season, and urban-rural. Obviously, "Indoor Awake" is an important information that can be used for indoor air

Table 18 Time spent (min/day) in various rooms at home and in all rooms combined, doers only (Klepeis et al. 1996)

Category	Population group	N	Mean	N	Mean	N	Mean	N	Mean	N	Mean	N	Mean	indoors in a residence (all rooms)	
All	All	7063	92.6	6661	35	9151	563.1	274	142.2	193	117.8	458	73.2	9343	1001.4
Sex	Male	2988	75	3006	32.7	4157	549.6	132	160.4	120	144.1	70	78.4	4269	945.9
Sex	Female	4072	105.6	3653	36.9	4990	574.3	141	125.7	73	74.6	388	72.3	5070	1048.1
Sex	Refused	3	40	2	27.5	4	648.8	1	60					4	1060.0
Age (years)	—	144	102.7	122	43.9	184	525.1	3	171.7	1	20	6	65.8	187	1001.1
Age (years)	1–4	335	73.7	328	35.9	488	742	8	94.8	4	83.5	3	75	498	1211.6
Age (years)	5–11	477	60.5	490	31	689	669.1	25	135.4	6	63.3	3	105.7	700	1005.1
Age (years)	12–17	396	55	445	29.1	577	636.2	26	97.5	12	80.8	8	55.5	588	969.5
Age (years)	18–64	4531	90.3	4486	34.5	5891	532.7	170	151.3	130	134.5	362	73.6	6022	947.9
Age (years)	>64	1180	131.4	790	42.2	1322	550.8	42	143.8	40	88.6	76	72.6	1348	1174.6
Race	White	5827	95.1	5338	34.3	7403	553.4	248	133.8	165	109.5	400	69.2	7556	999.4
Race	Black	641	79.4	711	36.9	923	612.3	15	183.8	12	205	35	100.5	941	1016.0
Race	Asian	113	89.4	117	33.6	153	612.3	2	135	1	5	4	82.5	157	983.5
Race	Some others	119	69.1	134	47.3	174	590.7	3	468.7	6	186.3	6	86.7	181	996.1
Race	Hispanic	266	84.2	283	38.6	378	602.6	1	30	8	120	10	95.9	382	1009.4
Race	Refused	97	90.3	78	34.6	120	555.8	5	263.2	1	120	3	170	126	1019.7
Hispanic	No	6458	93.4	6067	34.5	8326	560.9	263	139	174	116.6	435	72.1	8498	1000.4
Hispanic	Yes	497	83.9	498	39.2	684	597.4	6	185	17	128.6	20	81.7	696	1009.8
Hispanic	DK	32	82.3	33	44.4	43	542.3	1	185		1	55	46	1097.9	
Hispanic	Refused	76	88.4	63	44.1	98	523.4	4	271.3	2	127.5	2	247.5	103	984.1
Employment	—	1200	62.3	1240	32	1736	679.5	57	115.6	21	79.7	12	76.8	1768	1053.3

(continued)

Table 18 (continued)

		Kitchen	Bathroom	Bedroom	Basement	Garage	Utility/ Laundry room	indoors in a residence (all rooms)
Category	Population group	N	Mean	N	Mean	N	Mean	N
Employment	Full time	2965	77.7	3130	33.4	3992	513.5	107
Employment	Part time	608	97.7	583	35.5	777	551.6	22
Employment	Not employed	2239	126.9	1661	40.2	2578	566.4	85
Employment	Refused	51	106.4	47	34.7	68	514	3
Education	-	1346	63.9	1386	32.2	1925	668.3	65
Education	< High school	678	108.1	522	40.9	807	554.8	15
Education	High school graduate	2043	107.2	1857	35.8	2549	534.1	78
Education	< College	1348	94.4	1305	36.1	1740	539.1	48
Education	College graduate	933	91.9	913	35	1223	526	39
Education	Postgraduate	715	88.2	678	32.1	907	525.2	29
Census region	Northeast	1645	99.6	1497	34.3	2037	561.5	90
Census region	Midwest	1601	96.1	1465	35.8	2045	552.4	123
Census region	South	2383	86.3	2340	35.1	3156	570	35
Census region	West	1434	91.4	1359	34.9	1913	564.9	26
Day of week	Weekday	4849	90.1	4613	33.9	6169	552.6	178

Day of week	Weekend	2214	98.3	2048	37.5	2982	584.9	96	154.8	77	101.4	136	84.1	3057	1074.8
Season	Winter	1938	96.6	1853	37	2475	576	80	144.5	51	115.6	145	75.2	2513	1034.9
Season	Spring	1780	89	1747	36.6	2365	559	65	174.2	59	136.8	89	81.9	2424	977.9
Season	Summer	1890	89.3	1772	32.8	2461	566.1	79	142.4	51	101.1	132	69.3	2522	980.5
Season	Fall	1455	96.2	1289	33	1850	547.2	50	96.4	32	112.9	92	67.3	1884	1014.8
Asthma	No	6510	92.4	6132	34.9	8420	560.8	253	143.1	184	118.6	432	73.8	8391	999.1
Asthma	Yes	503	94	493	35.2	671	593.8	20	124.7	9	101.1	26	64.2	689	1027.4
Asthma	DK	50	104.4	36	49.5	60	543.1	1	245					63	1025.7
Angina	No	6798	91.6	6473	34.6	8836	564.2	269	141.4	187	118.2	440	72.1	9019	997.8
Angina	Yes	207	122.5	145	51.9	244	535.5	3	201.7	6	104.2	16	103.1	249	1125.5
Angina	DK	58	105.9	43	44.9	71	522.1	2	152.5		2	72.5	75	1024.1	
Bronchitis/ Emphysema	No	6671	91.8	6327	34.8	8660	563.1	265	139	185	114.1	428	73.3	8840	997.7
Bronchitis/ Emphysema	Yes	338	104.8	296	36.8	423	570.1	8	233.8	8	201.9	30	72.4	432	1070.5
Bronchitis/ Emphysema	DK	54	117.9	38	54.6	68	524.8	1	245					71	1045.5

Klepeis et al. (1996)

— = Indicates missing data.

DK = The respondent replied "don't know".

Refused = Refused data.

N = Doer sample size.

Mean = Mean 24 h cumulative number of minutes for doers.

Blank = Not mentioned.

Table 19 Table time spent (min/day) at selected indoor locations, doers only (Klepeis et al. 1996)

			Restaurant	Indoors At Bar/Nightclub/ Bowling alley	indoors At school	office or factory	Schools, Churches, Hospitals, and Public Buildings	Malls, Grocery Stores, or Other Stores	Indoors at a Gym/Health Club
Category	Population group	N	Mean	N	Mean	N	Mean	N	Mean
All		2059	94.5	352	175.8	1224	343.4	1975	394
Sex	Male	986	87.5	213	174.3	581	358.6	1012	410.8
Sex	Female	1073	101	139	178.1	643	329.6	963	376.3
Age (years)	-	30	126.1	4	158.8	18	314.1	49	438.9
Age (years)	1 to 4	61	62.7		43	288.5	12	31.6	98
Age (years)	5 to 11	84	56.7	4	98.8	302	396.3	14	100.9
Age (years)	12 to 17	122	69.8	8	151.3	287	402.6	19	145.4
Age (years)	18 to 64	1503	101.2	313	180.2	550	295.4	1749	419
Age (years)	>64	259	83.6	23	141.2	24	187.7	132	145.8
Race	White	1747	91.7	297	173.6	928	348.5	1612	387.6
Race	Black	148	102.8	25	205.4	131	339.8	191	413.9
Race	Asian	37	81.3	8	169.9	39	332.4	42	428
Race	Some others	30	145.2	7	197.3	36	363.6	28	480.9
Race	Hispanic	78	123	10	121.3	76	294	74	394.5
Race	Refused	19	123.8	5	246.6	14	279.7	28	482.9
Hispanic	No	1911	92.9	327	177.1	1082	344.9	1805	393.5
Hispanic	Yes	129	116.7	20	144.9	127	333	138	393.6
Hispanic	DK	5	76	2	142.5	5	293	7	262.6
Hispanic	Refused	14	114.5	3	261	10	329.5	25	470
Employment	-	263	62.3	12	133.8	616	390.3	43	121.3

Employment	Full time	1063	105.5	223	182.4	275	331.3	1535	455.6	1029	300.3	1170	136.8	176	131.2
Employment	Part time	208	122.6	43	201.2	138	280.9	164	293	251.3	285	134.1	40	129.3	
Employment	Not employed	515	76.3	70	146.3	190	258.7	213	77.6	775	176.4	854	91.2	75	117.9
Employment	Refused	10	135	4	176.3	5	166	20	449.2	14	212.9	16	98.9	1	40
Education	-	299	72.2	13	146.5	679	388.9	80	225.1	917	340.3	420	88.3	81	136.9
Education	< High school	132	134.8	28	218	24	233.3	104	329.5	166	172.6	206	128.9	9	110.6
Education	High school	590	99.4	117	177.8	114	186.6	631	396.9	617	207.3	792	126.3	61	128.5
Education	> College	431	94.9	95	205.3	173	281.4	462	393.1	520	247.5	583	129.8	71	145.6
Education	College	359	89.5	55	141.8	93	300.4	415	437.2	351	261.6	411	117.9	81	122
Education	Graduate														
Education	Postgraduate	248	95	44	131.4	141	373.5	283	396.9	361	319.1	285	78.2	61	115.6
Census region	Northeast	409	94.4	83	179.3	261	345.7	465	399.1	645	272.7	622	110.2	83	140.5
Census region	Midwest	504	96.9	88	169.8	290	334.4	439	389.3	686	275.4	601	108.2	62	127
Census region	South	680	92.7	91	175.7	427	354	666	408.6	1036	278.4	871	127.9	118	125.7
Census region	West	466	94.9	90	178.5	246	332.8	405	369.1	565	267.4	603	107.9	101	127
Day Of week	Weekday	1291	97.3	192	167.5	1179	346.8	1759	406.8	2091	309.8	1721	117.5	281	121.3
Day Of week	Weekend	768	89.8	160	185.9	45	252	216	289.6	841	186	976	110.6	83	158.1
Season	Winter	524	97.7	93	182.7	392	369.3	531	390.7	847	296.6	683	111.7	127	139.8
Season	Spring	559	91.6	83	186.1	353	355.1	470	385.2	805	276.8	679	115.8	85	141.5
Season	Summer	556	95.1	99	160.3	207	316.8	550	393.5	667	254.1	759	113.1	81	109.9
Season	Fall	420	93.6	77	176.4	272	311	424	408.4	613	262.4	576	120.2	71	119.9

(continued)

Table 19 (continued)

			Restaurant	Indoors At Bar/Nightclub/ Bowling alley	indoors At school	office or factory	Schools, Churches, Hospitals, and Public Buildings	Malls, Grocery Stores, or Other Stores	Indoors at a Gym/Health Club
Category	Population group	N	Mean	N	Mean	N	Mean	N	Mean
Asthma	No	1903	94.1	331	176.3	1095	342.8	1845	395
Asthma	Yes	150	96.3	18	169.4	124	350.7	114	371.7
Asthma	DK	6	196.3	3	160	5	287	16	43.7
Angina	No	1998	94.9	345	177	1209	344.6	1931	395.7
Angina	Yes	50	69	5	82	9	205.8	26	265.5
Angina	DK	11	140.3	2	210	6	292.2	18	392.3
Bronchitis/ Emphysema	No	1945	93.7	333	177.3	1175	344.8	1873	395.6
Bronchitis/ Emphysema	Yes	104	96.1	17	148.6	42	306.7	86	356.4
Bronchitis/ Emphysema	DK	10	232.8	2	165	7	315.4	16	403.9

Klepeis et al. (1996)

— = Indicates missing data.

DK = The respondent replied "don't know".

Refused = Refused data.

N = Doer sample size.

Mean = Mean 24-h cumulative number of minutes for doers.

Blank = Not mentioned.

Table 20 Time spent (min/day) at selected indoor locations, doers only (Klepeis et al. 1996)

		Indoors At an auto repair shop/gas Station		Indoors At the Laundromat		Indoors At work (non-specific)		Indoors At dry cleaners	
Category	Population group	N	Mean	N	Mean	N	Mean	N	Mean
All		153	190.7	40	99.3	137	393.9	34	82
Gender	Male	105	241.5	9	150.2	96	435.3	11	105.5
Gender	Female	48	79.6	31	84.5	41	297.2	23	70.8
Age (years)	—	3	161.7			4	568.8	1	485
Age (years)	1–4	4	40			2	200	2	20
Age (years)	5–11	5	22	3	80.7	4	33.8		
Age (years)	12–17	7	153.9	33	101.2	2	207.5		
Age (years)	18–64	118	223.8	4	97.5	121	409.7	28	61
Age (years)	> 64	16	58.1			4	293.8	3	185
Race	White	130	195.5	31	102.2	113	397.9	25	70.7
Race	Black	12	149.7	6	75.7	13	379.2	7	131.4
Race	Asian	5	173						
Race	Some others	3	15			1	405	1	10
Race	Hispanic	3	350	3	116.7	9	314.8	1	91
Race	Refused					1	840		
Hispanic	No	148	188.9	37	97.9	121	388.7	31	83.8
Hispanic	Yes	5	243	3	116.7	12	361.1	3	63.7
Hispanic	DK					2	585		
Hispanic	Refused					2	717.5		
Employment	—	16	84.2	3	80.7	8	118.8	2	20
Employment	Full time	84	283.6	20	97.6	97	440.7	25	83.1
Employment	Part time	16	104.2	4	127.5	21	341.2	1	500
Employment	Not employed	35	65.9	13	97.4	9	250.6	6	28.5
Employment	Refused	2	17.5			2	425		
Education	—	18	95.1	3	80.7	11	234.1	2	20
Education	< High school	16	327.2	6	95	12	460.4	4	234
Education	High school graduate	51	233.4	17	101.4	50	409.6	8	84.1
Education	< College	32	253.5	6	91.5	29	368.9	6	146.3
Education	College graduate	19	72.9	7	126.4	22	405.7	12	13.5
Education	Postgraduate	17	49	1	2	13	443.7	2	50
Census region	Northeast	29	247.3	6	168.7	22	405.5	8	110
Census region	Midwest	48	230.9	8	94	26	418.6	10	19.1
Census region	South	43	165.7	18	85.9	58	379.7	8	197
Census region	West	33	115	8	82.5	31	391.7	8	17.8
Day Of week	Weekday	121	204.6	25	103.3	121	401.8	23	94

(continued)

Table 20 (continued)

		Indoors At an auto repair shop/gas Station		Indoors At the Laundromat		Indoors At work (non-specific)		Indoors At dry cleaners	
Category	Population group	N	Mean	N	Mean	N	Mean	N	Mean
Day Of week	Weekend	32	137.9	15	92.5	16	334.3	11	57.1
Season	Winter	28	177.1	11	86.5	42	390.8	12	74.6
Season	Spring	44	189.6	12	85.6	34	361.3	4	44.5
Season	Summer	52	171.7	12	118.7	41	400.9	8	20.3
Season	Fall	29	239.4	5	113.8	20	441.8	10	155.4
Asthma	No	145	191.3	37	95.5	124	393.2	32	86.7
Asthma	Yes	8	179.9	3	146.3	13	400.9	2	7.5
Angina	No	149	191	40	99.3	133	397.7	33	83.9
Angina	Yes	4	177.5			3	266.7	1	20
Angina	DK					1	280		
Bronchitis/Emphysema	No	146	189	35	92.3	131	397.1	33	84.1
Bronchitis/Emphysema	Yes	7	225	5	148	5	333.4	1	15
Bronchitis/Emphysema	DK					1	280		

Klepeis et al. (1996)

— = Indicates missing data.

DK = The respondent replied “don’t know”.

Refused = Refused data.

N = Doer sample size.

Mean = Mean 24 h cumulative number of minutes for doers.

Blank = Not mentioned.

pollution exposure assessment applications and extraction, which is inseparable from the exposure time-activity pattern of indoor air pollution.

Korea

The Time Use Survey

The Time Use Survey was conducted by the Korean National Statistical Office to calculate people’s time spent on various activities (Jang et al. 2014; Kim et al. 2006). The subjects were randomly sampled after designing a sample proportional to the population of 16 metropolitan cities across the nation, stratified by gender and age as of the autumn of 2007. Diaries were distributed to participants who volunteered to participate in advance so that they could record their time spent in various places every 10 min between 6:00 in the morning and 6:00 in the morning the next day. They wrote down their places of activity and how much time they spent in each

Table 21 NHAPS minutes spent with a smoker on the diary day for California (NHAPS – CA) versus the entire nation

Location with a smoker	n	Overall mean (min)	Doer%	Doer	Doer mean (min)
NHAPS-nation (17% of respondents reported being cigarette smokers; weighted)					
All locations	9196	163	43.8	3949	372
In a residence	9196	78	25.6	2331	305
Office – factory	9196	16	4.3	394	363
Bar – restaurant	9196	14	10	951	143
Other indoor	9196	19	7.6	725	247
In an enclosed vehicle	9196	11	14.5	1340	79
Outdoors	9196	24	11.4	1038	213
NHAPS-CA (14% of respondents reported being cigarette smokers; weighted)					
All locations	930	114	36.9	332	309
In a residence	930	45	16.5	164	270
Office – factory	930	9	3.4	26	280
Bar – restaurant	930	13	8	82	168
Other indoor	930	19	7.4	58	252
In an enclosed vehicle	930	5	8.3	82	58
Outdoors	930	23	11	108	209

Means and percentages have been calculated using sample weights, whereas the sample sizes n and doer n are raw counts. The time spent with a smoker does not include one's own smoking (Klepis et al. 1996).

throughout their 24 h routine, after which they entered the records into a web-based survey, which was designed to avoid repetition and overlapping of answers. The survey took place in the spring (March 21) and summer (July 4) of 2007 to reflect seasonal factors. The final number of participants was 2073 with 1001 in the spring survey and 1072 in the summer survey. After excluding the answers of 67 spring and 27 summer participants (who had clearly not recorded accurate information or had not responded to follow-up calls), data from 1980 respondents were used in the final analysis.

Locations were classified into the categories of indoor, outdoor, and transportation. Indoor locations were then further subdivided into homes and locations outside of the home. Outdoor locations were subdivided into the home, locations outside of the home, and movement, as well as various sub-subcategories for each of these three subcategories. Transportation was classified into the subcategories of the bus, taxi, subway, passenger car, truck, high-speed train, and airplane.

In order to estimate the amount of exposure to pollutants through the environment medium in the life of the individual, it is necessary to provide information about how much time has been active in some places. In particular, information on the ratio between indoor and outdoor activities and the time spent at home is an important variable in assessing exposure. In this handbook, it was proposed to separate the time and place by the location of the indoor and outdoor places, and transportation. In the development of the next-generation environmental technology development project, the Korean exposure index, and the cloud system, the research was conducted to

Table 22 Daily time spent in major locations by age group of the CHAPS II

Age Group	Location	Mean		Median		95th percentile	
		% of day	h: min	% of day	h: min	% of day	h: min
Infants (<1 year)	Indoors at home	89.2	21: 23	93.3	22: 22	99.9	23: 58
	Other indoor locations	4.8	1: 10	0	0:0	23.6	5: 39
Young Children (1–4 years)	Indoors at home	74	17: 44	71.6	17: 10	98	23: 30
	Other indoor locations	15.3	3: 40	9.6	2: 19	39.4	9: 23
Children (5–11 years)	Indoors at home	71.3	17: 07	70.1	16: 48	95.2	22: 50
	Other indoor locations	17.8	4: 16	18.1	4: 21	38.9	9: 20
Adolescents (12–19 years)	Indoors at home	69.5	16: 40	69.2	16: 36	98.3	23: 35
	Other indoor locations	20.8	4: 59	22.2	5: 19	44.8	10: 44
Adults (20–59 years)	Indoors at home	66.8	16: 02	64.5	15: 28	99.1	23: 45
	Other indoor locations	21.4	5: 08	16.9	4: 03	50.5	12: 06
Seniors (60+ years)	Indoors at home	77.7	18: 38	81.9	19: 38	100	24: 00
	Other indoor locations	12.5	2: 59	8	1: 55	40.6	9: 44

Matz et al. (2014)

evaluate the time spent in each activity's place for the purpose of exposure assessment. Indoor time is included in the interior of the house, offices, department stores, etc., where the respondent is home.

The time spent indoors during the day of the Korean adult is 1281.0 min (about 21 h and 30 min), which showed that most of the time were spent indoors. The outdoor travel time was 76.2 min and the transportation hours were 82.8 min.

The time of the day indoors was 1281.0 min. The women spent 1306.7 min indoor, higher than that of men with 1256.4 min. It tended to decrease in the time spent indoor, for example, the people aged 65 or older spent 1254.3 min indoor and was about 32 min shorter than that of people aged from 18 to 24 years old, who spent 1286.3 min indoor. Seasonal differences were shorter in the summer and about 8 min in the summer time compared to spring. From the time spent indoors, the longest detail place of the day was 440.0 min into the bedroom (about 7 h 20 min), the office 253.9 min, the living room/hallway 138.3 min. It was spent in the room for 8 h and 30 min except for bedtimes, which was for more than one-third of the day. The recommended values for indoor time are shown in Table 23.

Children's Time-Activity Patterns Survey

A study was conducted on 2080 male and female children under 9 years old in Korea (I) (2013) and (II) (2014) time-activity patterns. The selection of survey subjects was based on stratified sampling according to the square root proportional distribution for the whole country and based on the estimated population in 2013. The ratio of male to female was approximately 50:50, and 500 persons were surveyed by season (spring, summer, autumn, and winter). A time-activity logbook was developed to measure and investigate the time activities of children under the age of nine. The time unit of the time-activity logbook was 30 min, and the room was divided into indoor, school (kindergarten, day care, and elementary school) indoor, and other building indoor. The means of transportation were divided into walking, bicycle, taxi (or passenger car), bus, and train (or subway). Be sure to include the main act (study, play, watch TV, etc.) at the beginning, respectively. If there were more than two places during the time unit (30 min), all records were made and counted. The time-activity logbook allows one child's parents to record on behalf of the child.

The National Statistical Office Life Time Survey is an example of representative samples from all Koreans and is recorded 24 h a day at intervals of 10 min. Therefore, this data can be used as representative and reliable data for the time spent by the activities of the Korean people (10–18 years old). However, since this data is not the data that was examined for the purpose of exposure assessment, it does not provide information on the specific place where each activity occurred, and it does not distinguish whether the place is indoor or outdoor. Therefore, the National Statistical Office's Life Time Survey data was used to calculate the time required for specific activities among time-activity variables. Since the National Statistical Office (NSO) survey was not developed or classified according to the purpose of exposure assessment, the original data were reclassified and reworked according to the purpose of the exposure assessment.

The main exposure variables related to time activities are the time required by location, the time required by activity, and time spent on transportation. Among these exposure variables, the time required for each activity was from 0 to 9 years old, and the data from 10 years to 18 years old were reclassified and reanalyzed.

The indoor environment is divided into indoor, school, or kindergarten (day care center) indoor and other indoor. In Korea, only 16.86 h on weekdays, and 5.13 h on weekdays during daytime for children aged 0–9 years, and most of the time spent indoors. The average time spent living in a house during a day of a 10- to 18-year-old child was 12.11 h on a weekday, 9.84 h in school and other indoor environments (school, etc.), and 1.43 h on transportation (vehicle). The recommended values for indoor time are showed in Tables 24, 25, 26, and 27.

Europe

The EXPOLIS (Air Pollution Exposure Distributions of Adult Urban Populations in Europe) Study used uniform questionnaires and time-activity diaries in conjunction with personal monitoring of pollutant concentrations in several countries in Europe

Table 23 Time spent indoors (min/day)

Demographic group	N	Mean	SD	Min	Max	5th	25th	50th	75th	90th	95th	99th
Gender												
Male	1013	1256	137	370	1440	1010	1210	1290	1350	1390	1410	1440
Female	967	1307	107	500	1440	1140	1260	1320	1380	1420	1440	1440
Age												
18 ~ 24	270	1286	125	590	1440	1080	1240	1300	1380	1410	1430	1440
25 ~ 34	466	1287	108	720	1440	1100	1240	1310	1360	1400	1420	1440
35 ~ 44	480	1287	115	540	1440	1100	1240	1310	1360	1400	1430	1440
45 ~ 54	435	1278	126	370	1440	1070	1220	1300	1360	1400	1440	1440
55 ~ 64	285	1264	142	660	1440	980	1220	1290	1360	1400	1440	1440
≥65	44	1254	235	460	1440	650	1215	1305	1415	1440	1440	1440
Season												
Spring	934	1285	120	650	1440	1060	1230	1310	1370	1410	1440	1440
Summer	1046	1277	130	370	1440	1070	1230	1300	1360	1400	1430	1440
Area 1												
Seoul Kwang-gu City	958	1275	128	370	1440	1070	1230	1300	1360	1400	1430	1440
Degree	1022	1286	123	460	1440	1060	1240	1310	1370	1410	1440	1440
Area 2												
City	958	1275	128	370	1440	1070	1230	1300	1360	1400	1430	1440
Small city	797	1286	119	590	1440	1060	1230	1310	1370	1410	1440	1440
Eup	225	1289	133	460	1440	1030	1240	1320	1370	1410	1440	1440

Income level		1288	133	650	1440	1060	1230	1320	1380	1420	1440	1440
One million		288	1287	134	500	1440	1050	1230	1310	1380	1420	1440
2 million		318	1287	125	460	1440	1040	1230	1300	1370	1420	1440
Three million		447	1280	120	370	1440	1080	1230	1300	1350	1390	1410
More than 3 million		927	1277									
Level of education												
Elementary and middle school		74	1232	206	500	1440	820	1200	1290	1380	1430	1440
High sol		588	1288	134	590	1440	1050	1250	1320	1370	1420	1440
Daesol		1116	1281	116	370	1440	1090	1230	1300	1360	1400	1420
More than a graduate school		202	1278	107	800	1440	1090	1220	1300	1350	1400	1440
All		1980	1281	125	370	1440	1065	1230	1310	1360	1400	1440

Table 24 Time spent in house indoors by weekday by gender (h)

Age	N	Mean	S.D.	Boys				Girls			
				25%	50%	75%	95%	N	Mean	S.D.	25%
0 years	152	20.44	3.81	17.13	22.00	24.00	24.00	131	20.07	4.24	16.50
1 years	100	17.54	3.50	15.00	16.50	20.50	24.00	104	17.63	3.57	14.94
2 years	121	17.06	3.07	15.00	16.50	18.00	24.00	96	16.31	2.53	15.00
3 years	108	16.13	2.71	14.50	15.50	16.69	23.50	120	16.43	2.83	15.00
4 years	118	15.79	2.37	14.50	15.50	16.50	21.51	123	16.60	2.92	15.00
5 years	87	15.82	2.62	14.25	15.50	16.92	22.80	90	15.87	2.77	14.19
6 years	112	16.24	2.29	15.00	16.00	17.13	21.18	97	16.17	2.33	14.50
7 years	88	15.95	2.20	14.50	15.75	17.00	21.10	76	15.88	2.50	14.25
8 years	106	16.14	2.34	14.50	16.00	17.00	22.33	107	15.77	2.36	14.50
9 years	67	15.41	2.02	14.25	15.25	16.67	17.60	77	16.33	2.92	14.50
10 years	236	14.03	1.59	12.87	14.00	15.17	16.69	240	14.26	1.62	13.33
11 years	240	13.95	1.56	13.00	14.00	14.67	16.17	181	14.08	1.61	13.00
12 years	268	12.97	2.20	11.50	12.67	14.33	16.33	269	13.08	2.01	11.50
13 years	249	12.77	2.16	11.17	12.50	14.33	16.17	223	12.74	2.23	11.33
14 years	249	12.35	2.17	10.67	11.83	13.83	16.00	264	12.38	2.37	10.83
15 years	259	10.91	2.52	9.00	10.50	12.67	15.33	232	10.49	2.89	8.50
16 years	257	10.07	2.63	8.33	9.50	11.39	14.83	222	9.83	2.53	8.17
17 years	205	10.28	3.04	8.17	9.33	12.17	14.95	243	9.93	2.75	8.17
18 years	175	11.75	4.13	8.83	11.00	14.50	20.86	130	11.98	4.12	9.00

Table 25 Time spent in house indoors according to weekend by gender (h)

Age	N	Mean	S.D.	Boys				Girls			
				25%	50%	75%	95%	N	Mean	S.D.	25%
0 years	152	20.87	3.56	19.08	21.50	24.00	24.00	131	20.60	3.76	19.00
1 years	100	20.37	3.52	18.00	21.00	24.00	24.00	104	20.29	3.60	18.10
2 years	121	20.47	3.27	18.25	21.00	24.00	24.00	96	20.65	2.89	18.06
3 years	108	20.13	3.32	17.81	20.00	23.75	24.00	120	19.14	3.70	17.50
4 years	118	19.84	3.25	17.75	20.08	22.25	24.00	123	20.02	3.34	18.25
5 years	87	20.23	2.84	18.50	20.50	22.00	24.00	90	19.60	3.56	17.50
6 years	112	19.63	3.60	17.31	20.00	22.23	24.00	97	19.47	3.40	17.25
7 years	88	19.38	2.87	17.56	19.50	21.50	24.00	76	20.24	2.64	19.00
8 years	106	19.88	2.92	18.00	20.50	22.00	24.00	107	19.36	4.16	17.50
9 years	67	20.07	3.99	19.00	21.00	22.50	24.00	77	19.90	3.47	17.92
10 years	194	17.79	4.32	15.49	18.50	20.83	24.00	146	18.28	4.16	16.29
11 years	152	18.00	3.66	15.67	18.43	20.46	23.67	139	17.89	4.07	15.50
12 years	148	18.22	3.88	15.54	18.50	1.17	24.00	183	18.46	4.28	15.83
13 years	175	18.53	3.73	15.83	18.67	21.50	24.00	147	17.85	3.88	15.33
14 years	185	17.89	4.05	15.25	18.17	20.83	24.00	162	19.03	4.16	16.50
15 years	189	17.50	4.40	14.67	18.17	21.25	24.00	144	18.03	4.31	15.39
16 years	169	16.82	4.20	13.67	17.17	20.00	24.00	146	17.86	4.36	15.00
17 years	151	15.74	5.00	11.67	15.67	19.33	24.00	147	15.57	4.86	11.83
18 years	89	16.69	4.90	13.67	17.17	20.29	24.00	84	15.67	4.96	11.11

Table 26 Time spent in other indoor (school, nursery school) according to weekday by gender (h)

Age	N	Boys						Girls						
		Mean	S.D.	25%	50%	75%	95%	N	Mean	S.D.	25%	50%	75%	
0 years	152	2.38	3.40	0.00	5.63	9.62	131	3.07	3.98	0.00	0.75	6.50	9.70	
1 years	100	5.34	3.41	1.81	6.50	8.00	10.00	104	5.23	3.56	1.00	6.29	7.98	10.00
2 years	121	5.79	2.92	4.67	6.50	7.75	9.73	96	6.51	2.64	5.25	7.00	8.00	10.08
3 years	108	6.91	2.67	6.06	7.50	8.50	9.89	120	6.37	2.72	5.50	6.75	8.23	9.66
4 years	118	6.75	2.45	5.81	7.25	8.50	9.76	123	6.03	2.94	5.00	7.00	8.00	9.75
5 years	87	6.72	2.73	6.17	7.08	8.50	9.75	90	6.69	2.86	5.56	7.21	8.60	10.00
6 years	112	6.24	2.47	5.12	6.75	8.00	9.09	97	6.62	2.35	5.50	6.75	8.50	9.68
7 years	88	6.59	2.11	5.50	6.75	7.69	9.89	76	6.57	2.28	5.50	6.67	8.00	9.53
8 years	106	6.35	2.36	5.50	6.50	7.75	9.61	107	6.79	2.45	5.75	7.00	8.25	10.60
9 years	67	7.12	1.92	6.00	7.33	8.50	10.05	77	6.21	2.99	5.00	6.75	8.25	10.03
10 years	236	7.98	1.40	6.92	8.08	8.87	10.07	240	7.90	1.39	6.92	7.98	8.79	9.93
11 years	240	8.11	1.34	7.45	8.04	9.05	10.15	181	8.16	1.37	7.27	8.18	9.04	10.47
12 years	268	9.05	2.01	7.83	8.97	10.42	12.20	269	8.97	1.71	7.63	8.88	10.28	11.76
13 years	249	9.29	1.82	7.98	9.37	10.58	12.02	223	9.28	2.02	7.97	9.13	10.63	12.66
14 years	249	9.70	1.95	8.35	9.97	11.13	12.66	264	9.70	2.05	8.22	9.51	11.02	13.46
15 years	259	10.98	2.52	8.87	11.07	12.93	14.92	232	11.48	2.79	9.21	12.33	13.53	15.04
16 years	257	11.86	2.68	10.32	12.38	13.63	14.98	222	12.03	2.50	10.42	12.62	13.72	15.12
17 years	205	11.61	3.10	9.52	12.73	13.90	15.18	243	12.05	2.84	10.15	12.80	13.92	15.81
18 years	175	9.26	4.02	6.75	9.10	12.62	15.42	130	9.33	4.01	6.41	9.73	12.59	14.62

Table 27 Time spent in other indoor (school, nursery school) by weekend by gender (h)

Age	Gender		Boys						Girls					
	N	Mean	S.D.	25%	50%	75%	95%	N	Mean	S.D.	25%	50%	75%	95%
0 years	152	1.30	2.61	0.00	1.75	6.35	131	1.96	3.38	0.00	0.50	2.50	8.75	
1 years	100	1.50	2.60	0.00	0.00	2.25	6.50	104	1.67	2.90	0.00	0.50	2.21	6.06
2 years	121	1.53	2.24	0.00	0.25	2.50	6.48	96	1.44	2.05	0.00	0.17	2.50	6.04
3 years	108	1.97	2.59	0.00	0.92	3.25	7.79	120	2.50	2.99	0.00	2.00	4.00	8.33
4 years	118	1.92	2.67	0.00	0.58	3.00	8.29	123	1.91	2.58	0.00	0.67	3.08	8.47
5 years	87	1.55	1.95	0.00	1.00	2.50	6.43	90	2.39	2.93	0.00	1.00	4.00	8.31
6 years	112	2.17	3.10	0.00	1.00	3.19	8.40	97	2.09	2.37	0.00	1.50	3.33	6.73
7 years	88	2.14	2.33	0.00	1.50	3.88	6.50	76	1.61	1.98	0.00	1.17	2.50	6.11
8 years	106	2.09	2.36	0.00	1.50	3.19	7.00	107	2.78	3.96	0.00	1.33	3.75	10.50
9 years	67	1.67	3.69	0.00	0.00	2.08	6.93	77	2.02	2.19	0.00	1.50	3.29	6.55
10 years	194	3.86	3.25	1.49	3.50	5.56	9.17	146	3.68	2.99	1.34	3.58	5.22	9.08
11 years	152	3.59	2.73	1.50	3.26	5.34	8.04	139	3.98	3.11	1.35	3.73	5.58	8.70
12 years	148	3.50	2.87	1.07	3.04	5.38	8.58	183	3.79	3.50	1.13	3.03	5.73	10.56
13 years	175	3.46	2.84	1.00	3.00	5.23	9.24	147	4.11	3.03	1.83	3.78	6.00	9.27
14 years	185	4.14	3.26	1.60	3.98	6.05	9.59	162	3.40	3.23	0.41	2.97	5.28	8.75
15 years	189	4.50	3.67	1.35	3.95	7.06	11.50	144	4.19	3.61	1.17	3.68	6.35	11.05
16 years	169	4.87	3.50	1.84	4.52	7.31	11.43	146	4.20	3.28	1.04	4.42	6.52	10.05
17 years	151	6.19	4.43	2.63	5.42	9.57	13.77	147	6.47	4.31	3.07	6.63	9.97	14.19
18 years	89	4.83	3.95	1.85	3.62	7.25	12.89	84	5.87	4.34	1.77	5.34	9.81	12.40

(Hänninen et al. 2004). Within the framework of the EXPOLIS study, TMA (Time Microenvironment Activity) data of 1447 subjects in seven cities (Helsinki, Athens, Basel, Grenoble, Milan, Prague, and Oxford) had been collected between 1996 and 2000. In total, 543 subjects completed a diary during the period of personal exposure measurement, whereas 904 participated in a less demanding diary-only study (Schweizer et al. 2006).

The TMA diary was collected during working days only, for example, from Monday morning to Wednesday morning (from 06:00 to 06:00) or from Wednesday evening to Friday evening (from 18:00 to 18:00) for 48 h. Subjects were asked to record in the TMA diary every 15 min of the day in the appropriate microenvironment–activity category. Multiple entries were allowed for each 15 min segment (mE). We then calculated for each participant how much time he/she spent in each mE (each 15 min segment was divided evenly between all entries). They distinguish two aspects of an individual's TMA pattern during the sampling period: (1) whether the person enters a specific microenvironment at least once and therefore becomes what they call a “habitue” of the corresponding microenvironment (Graham and Mccurdy 2004; Mccurdy and Graham 2003), and (2) the total duration of time spent in specific microenvironments. To investigate TMA patterns across subgroups and cities, they present four criteria: (1) the percentage of people (habitue's) entering in each microenvironment, (2) the duration of participation by these habitues, (3) the determinants for becoming a habitue, and (4) the determinants for the duration of time spent in each microenvironment by the corresponding habitues (Eurostat 2010).

Table 28 presents the distribution of time spent in indoor locations (home, work, and other) by city. It only includes data of habitues. Home indoor dominated time spent in indoor locations with 100% habitues in all seven cities and with averages ranging from 13.5 h/day in Milan to 15.8 h/day in Oxford, or 56–66% of a day. The coefficient of variation was low with values between 19% in Milan and 28% in Grenoble.

Africa

Between January and June 2007, South Durban conducted a survey of 381 adults. The questionnaire included a set of questions on demographics, potential air pollution exposure sources, and a time-activity diary. The diary was divided into three microenvironments, namely indoor, outdoor, and in-vehicle. The first two microenvironments were subdivided into indoor at home, indoor other and indoor at work, and outdoor at home, outdoor other and outdoor at work, respectively (Matooane et al. 2011).

According to the results, data cleaning process resulted in 291 complete questionnaires which were analyzed using STATA 10. Robust regression with Huber-M estimation was used to determine drivers for time spent in microenvironments by the study population. Due to the limited number of weekend days, as a result of data

Table 28 Time spent in various indoor locations among people reporting time (habits)

	n	Min	Median	Max	Mean ^a	SD	Coefficient of variation (%)	Fraction of the study population (%)
Home indoors								
Helsinki	430	3.81	13.15	24.00	13.73	3.01	22	100
Athens	98	4.19	15.30	24.00	15.44	4.08	26	100
Basel	320	0.94	13.02	22.48	15.53	3.34	25	100
Grenoble	100	3.88	14.13	23.63	14.67	4.14	28	100
Milan	298	8.13	13.09	22.50	13.48	2.60	19	100
Prague	81	7.63	13.23	23.50	13.92	3.50	25	100
Oxford	100	2.75	15.19	24.00	15.76	3.17	20	100
All cities	1427	0.94	13.31	24.00	13.95	3.29	24	100
Work indoors								
Helsinki	370	0.07	7.48	11.04	6.83	2.15	31	86
Athens	67	1.19	6.13	13.06	5.90	2.34	40	68
Basel	266	0.13	7.38	13.31	6.67	2.50	37	83
Grenoble	79	0.38	7.00	13.25	6.73	2.62	39	79
Milan	267	0.25	7.50	12.19	7.09	2.14	30	90
Prague	71	0.75	7.50	10.50	6.52	2.68	41	88
Oxford	77	1.00	6.25	17.25	5.90	2.81	48	77
All cities	1197	0.07	7.29	16.63	6.71	2.37	35	84
Other indoors								
Helsinki	349	0.04	1.00	10.70	1.53	1.58	104	81
Athens	69	0.06	1.44	7.75	1.76	1.50	85	70
Basel	293	0.04	1.50	10.69	1.84	1.57	85	92
Grenoble	74	0.13	1.19	16.88	2.22	2.94	132	74
Milan	272	0.06	1.23	10.56	1.58	1.32	83	91
Prague	56	0.08	1.16	8.58	1.69	1.81	107	69
Oxford	69	0.13	0.81	6.25	1.30	1.31	101	69
All cities	1181	0.04	1.25	16.88	1.67	1.64	99	83
ETS indoors away from home, non-smokers only								
Helsinki	62	0.06	0.50	9.04	1.19	1.83	154	19
Athens	35	0.13	1.25	10.25	2.16	2.56	118	43
Basel	114	0.04	0.56	7.38	1.08	1.37	127	48
Grenoble	32	0.13	0.56	9.75	2.02	2.95	146	32
Milan	123	0.06	1.00	11.63	2.01	2.53	126	60
Prague	13	0.13	0.81	4.75	1.09	1.18	108	20
Oxford	6	0.13	0.13	1.38	0.41	0.51	124	7
All cities	385	0.42	0.75	11.63	1.56	2.16	139	35

Time expressed in hours per day

^aMeans for total population can be calculated by multiplying the means with the decimal habitue's fraction of the study population

collection constraints on weekend days, the analysis was confined to weekdays. On average participants spent approximately 21.2 ± 1.51 h/day in indoor environments, the home indoor microenvironment accounted for a large portion (82.5%) of time spent indoors. Table 29 indicates that significant gender, employment, educational, and family type differences in the distributions of the time spent in microenvironments were confined largely to “indoor at home” and “outdoor at home” microenvironments.

The statistically significant drivers for time spent indoors at home on weekdays were gender, occupational status, and temperature (Table 30). Time indoors at home increased significantly with being male and when temperatures were high. However, being employed resulted in participants spending significantly less time indoors at home. Only employment status remained a significant driver for time spent indoors at other locations. Of the many drivers for time spent in various microenvironments, our study found employment status, gender, and temperature to be the main drivers of time spent in various microenvironments in south Durban.

In Durban, South Africa studies have shown that more than seven out of ten households in low-income metropolitan areas rely on kerosene for domestic purposes, leading to widespread problems of poor indoor air quality (Muller et al. 2003). According to Statistics South Africa (SSA 2000), there are approximately five million households in South Africa currently using fossil fuels for domestic purposes. Of these, a fairly high proportion rely on kerosene, with 21% using it for cooking, 14% for heating, and 13% for lighting. And the residents of Cato Crest tend to live in smaller dwellings, often comprising only one room, which serves as a

Table 29 Time spent in indoor-home on weekdays

Factor	Mean (h)	Factor	Mean (h)
Female	18.86	<High school	16.66
Male	16.00	\geq High school	17.77
Unemployed	20.45	No child	17.60
Employed	13.45	<18 years old	16.75

Table 30 Determinants of time spent in microenvironments on weekdays

Variables	Home indoor (h)	Indoor other (h)
	Coefficient (95% CI)	Coefficient (95% CI)
Male ^a	0.32*(0.01–0.64)	-0.14(-0.33–0.04)
Age	-0.01(-0.02–0.003)	-0.01(-0.002–0.01)
\geq High school ^b	0.15(-0.19–0.48)	-0.07(-0.29–0.13)
Employed ^c	-8.16***(-8.51–7.80)	0.28**(-0.27–0.13)
Children ^d	0.24(-0.1–0.58)	-0.11(-0.31–0.09)
Summer ^e	0.38(-0.001–0.76)	-0.06(-0.28–0.16)
Temperature	0.07*(0.01–0.13)	-0.01(-0.04–0.02)
Precipitation	0.26(-0.17–0.69)	-0.05(-0.31–0.21)

Key: * = $p < 0.05$; ** = $p < 0.01$; *** = $p < 0.001$; a = female = 0; b = \leq primary school = 0; c = unemployed = 0; d = No children = 0; e = other season = 0

Table 31 Average hours spent per daily activity in summer and winter months

	Indoor, cooking	Indoor, other	Indoors, at work	Sleeping
Winter	2	2.6	8.2	10
Summer	2	2.4	8.3	9

multipurpose room in which most people slept and in which cooking was undertaken.

Air quality monitoring in 69 households took place over a 9-day period from 5 to 15 September 2000. This survey used the form of a questionnaire, and the questionnaire consisted of 48 closed-ended questions related to personal details, fuel use, building structure, cooking habits, and time-activity patterns. A multistage sampling method was used, in which the initial population was divided according to the eight recognized areas of Cato Crest. Within each area, transects were marked on aerial photographs along pathways that provided vehicular access at either end of a transect. The transects were also selected to ensure an even allocation of houses within areas. Thereafter, sampling along each transect was random, although certain difficulties were encountered. The haphazard and unplanned nature of the informal settlement made strict adherence to the sampling procedure difficult. In such cases the nearest dwelling to that designated on the aerial photograph was selected.

Women were targeted in the questionnaire as they were generally the only household members involved in cooking and other domestic activities. The questionnaires were administered by a group of ten trained students. All interviewers were fluent in isiZulu and English and conducted the interview in the language in which the respondent was most comfortable. The questionnaires were completed by the interviewers in English.

Of the 69 interviews conducted, 66 interviews were with female respondents. The average age of the interviewees was 34 years. Only ten respondents were employed full time, with 39 unemployed respondents. Two respondents were students.

In response to questions on the average time taken to cook meals, 45 respondents reported that it took between 1 and 2 h. Fifty respondents reported that there were people in their household that slept in the same room as the cooking was done in. Forty of these households had between 1 and 3 people sleeping in the “kitchen.” Table 31 shows the average number of hours spent conducting several different daily activities in summer and winter months.

Conclusion

So far, due to the advantages of simplicity of the method as well as low cost and direct access to detailed activity information, large-scale time-activity pattern surveys mainly adopt questionnaire survey method. However, the questionnaire survey method has the disadvantage of recall bias and low temporal and spatial resolution. In recent years, with the development of related technology, the application of GPS method is more and more popular. Compared with the traditional questionnaire

survey method, GPS method has the advantage of continuous recording, high spatial and temporal resolution, and less reporting burden of respondents. Meanwhile, with the development of wireless sensor technology, wearable sensor devices can accurately identify the activity state of the human body, and can be used to identify fine activity patterns in conjunction with GPS and other positioning devices. In addition, the widespread development of smart phones, mainly based on GPS and motion sensors, also provides convenience for monitoring time-activity patterns. However, the time-activity monitoring technology based on GPS, sensors, and smart phones has a great demand for data mining and analysis. In general, the data analysis technology of the new technology is a great challenge and the focus of future research. With the requirement of refined time-activity patterns information, new challenges are presented to the survey methods.

At present, the investigation of the time-activity pattern related to air exposure mainly focuses on the indoor and outdoor time. However, affected by various factors such as building decoration materials, HVAC systems, electronic office supplies, kitchen combustion products, and human activities (such as smoking), different microenvironment led to great differences in the types and intensity of air pollutants. Nowadays, with the development of air pollutant exposure assessment models, it is necessary to accurately match the air pollutants concentrations and human time-activity pattern both in time and space in the future. In addition to the survey of total indoor and outdoor time, more accurate and detailed time information is also needed to improve the precision of exposure assessment. In addition, previous time-activity pattern surveys paid less attention to activity intensity of the people, which could directly affect people's inhalation rate and indirectly affect their air pollution exposure levels. Therefore, collecting more accurate and detailed information, including location, time, duration, and activity patterns, is necessary.

References

- Allahviranloo M, Recker W (2015) Mining activity pattern trajectories and allocating activities in the network. *Transportation* 42(4):561–579
- Anguita D, Ghio A, Oneto L, Parra X, Reyes-Ortiz JL (2012) Human activity recognition on smartphones using a multiclass hardware-friendly support vector machine. Paper presented at the Proceedings of the 4th international conference on Ambient Assisted Living and Home Care
- Anjum A, Ilyas MU (2013) Activity recognition using smartphone sensors. Paper presented at the Consumer Communications and Networking Conference (CCNC), 2013 IEEE
- Bharti P, De D, Chellappan S, Das SK (2018) HuMAN: complex activity recognition with multi-modal multi-positional body sensing. *IEEE transactions on mobile computing*
- Breen MS, Long TC, Schultz BD, Crooks J, Breen M, Langstaff JE, ... Buckley TJ (2014) GPS-based microenvironment tracker (MicroTrac) model to estimate time-location of individuals for air pollution exposure assessments: model evaluation in central North Carolina. *J Expo Sci Environ Epidemiol* 24(4):412–420. <https://doi.org/10.1038/jes.2014.13>
- Brondeel R, Pannier B, Chaix B (2016) Associations of socioeconomic status with transport-related physical activity: combining a household travel survey and accelerometer data using random forests. *J Transp Health* 3(3):287–296. <https://doi.org/10.1016/j.jth.2016.06.002>
- Cankaya S, Pekey H, Pekey B, Aydin BO (2020) Volatile organic compound concentrations and their health risks in various workplace microenvironments. *Hum Ecol Risk Assess* 26(3):822–842

- Correa A, Barcelo M, Morell A, Vicario JL (2017) A review of pedestrian indoor positioning systems for mass market applications. *Sensors (Basel, Switzerland)* 17(8):1927. <https://doi.org/10.3390/s17081927>
- Duan X, Zhao X, Wang B, Chen Y, Cao S (2014) Highlights of the Chinese exposure factors handbook. Science Press, Beijing
- Ellis K, Kerr J, Godbole S, Lancikiet G, Wing D, Marshall S (2014) A random forest classifier for the prediction of energy expenditure and type of physical activity from wrist and hip accelerometers. *Physiol Meas* 35(11):2191–2203. <https://doi.org/10.1088/0967-3334/35/11/2191>
- Esfahani P, Malazi HT (2018) PAMS: a new position-aware multi-sensor dataset for human activity recognition using smartphones. Paper presented at the International Symposium on Computer Architecture & Digital Systems
- Eurostat (2010) Harmonised European time use survey: 2008 guidelines (methodologies and working papers). Reference materials for statistical research, 1–83, 81–82
- Graham SE, Mccurdy T (2004) Developing meaningful cohorts for human exposure models. *J Expos Anal Environ Epidemiol* 14(1):23–43
- Guo S, Xiong H, Zheng X, Zhou Y (2017) Activity recognition and semantic description for indoor mobile localization. *Sensors (Basel, Switzerland)* 17(3):649. <https://doi.org/10.3390/s17030649>
- Hänninen OO, Alm S, Katsouyanni K, Künzli N, Maroni M, Nieuwenhuijsen MJ et al (2004) The EXPOLIS study: implications for exposure research and environmental policy in Europe. *J Expo Sci Environ Epidemiol* 14(6):440–456. <https://doi.org/10.1038/sj.jea.7500342>
- Huang K, He K, Du X (2019) A hybrid method to improve the BLE-based indoor positioning in a dense bluetooth environment. *Sensors (Basel, Switzerland)* 19(2):424. <https://doi.org/10.3390/s19020424>
- Jang JY, Jo SN, Kim SY, Lee KE, Choi KH, Kim YH (2014) Activity factors of the Korean exposure factors handbook. *J Prev Med Public Health* 47(1):27–35
- Kim S, Cheong HK, Choi K, Yang JY, Kim SJ, Jo SN, Jang JY (2006) Development of Korean exposure factors handbook for exposure assessment. *Epidemiology* 17(Suppl):S460
- Klepeis N, Tsang A, Behar J (1996) Analysis of the National Human Activity Pattern Survey (NHAPS) Respondents from a standpoint of exposure assessment – Final EPA report
- Kohla B, Gerike R, Hössinger R, Meschik M, Sammer G, Unbehauen W (2014) A new algorithm for mode detection in travel surveys. In: Mobile technologies for activity-travel data collection and analysis. IGI Global, pp 134–151. <https://doi.org/10.4018/978-1-4666-6170-7.ch009>
- Matooane M, Naidoo R, Batterman S (2011) Time-activity patterns: a case of South Durban, South Africa. *Epidemiology* 22:S227
- Matz CJ, Stieb DM, Davis K, Egyed M, Rose A, Chou B, Brion O (2014) Effects of age, season, gender and urban-rural status on time-activity: Canadian Human Activity Pattern Survey 2 (CHAPS 2). *Int J Environ Res Public Health* 11(2):2108–2124. <https://doi.org/10.3390/ijerph110202108>
- Mccurdy T, Graham SE (2003) Using human activity data in exposure models: analysis of discriminating factors. *J Expos Anal Environ Epidemiol* 13(4):294–317
- Ministry of Ecology and Environment the People's Republic of China (MEE) (2013a) Exposure factors handbook of Chinese population (Adults). China Environmental Science Press, Beijing
- Ministry of Ecology and Environment the People's Republic of China (MEE) (2013b) Report of environmental exposure-related human activity pattern of Chinese population (Adults). China Environmental Science Press
- Ministry of Ecology and Environment the People's Republic of China (MEE) (2017a) Exposure factors handbook of Chinese population (children: 0 to 5 years). China Environmental Science Press, Beijing
- Ministry of Ecology and Environment the People's Republic of China (MEE) (2017b) Exposure factors handbook of Chinese population (children: 6 to 17 years). China Environmental Science Press, Beijing
- Ministry of Ecology and Environment the People's Republic of China (MEE) (2017c) Report of environmental exposure-related human activity patterns research of Chinese population (Children). China Environmental Science Press

- Muller E, Diab RD, Binedell M, Hounsome R (2003) Health risk assessment of kerosene usage in an informal settlement in Durban, South Africa. *Atmos Environ* 37(15):2015–2022
- Nethery E, Mallach G, Rainham D, Goldberg MS, Wheeler AJ (2014) Using Global Positioning Systems (GPS) and temperature data to generate time-activity classifications for estimating personal exposure in air monitoring studies: an automated method. *Environ Health* 13(1):33. <https://doi.org/10.1186/1476-069x-13-33>
- Rosenberger ME, Buman MP, Haskell WL, McConnell MV, Carstensen LL (2016) Twenty-four hours of sleep, sedentary behavior, and physical activity with nine wearable devices. *Med Sci Sports Exerc* 48(3):457–465. <https://doi.org/10.1249/MSS.0000000000000778>
- Schweizer C, Edwards RD, Bayer-Oglesby L, Gauderman WJ, Ilacqua V, Jantunen MJ, . . . Künzli N (2006) Indoor time–microenvironment–activity patterns in seven regions of Europe. *J Expo Sci Environ Epidemiol* 17:170
- Sprint G, Cook D, Weeks D, Dahmen J, La Fleur A (2017) Analyzing sensor-based time series data to track changes in physical activity during inpatient rehabilitation. *Sensors (Basel, Switzerland)* 17(10):2219. <https://doi.org/10.3390/s17102219>
- SSA (2000) Stats in brief. Statistics South Africa, Pretoria
- USEPA. <https://www.epa.gov/air-research/microenvironment-tracker-microtrac-model-helps-track-air-quality>
- Wang L (2016) Recognition of human activities using continuous autoencoders with wearable sensors. *Sensors (Basel, Switzerland)* 16(2):189–189. <https://doi.org/10.3390/s16020189>
- Widhalm P, Yang Y, Ulm M, Athavale S, González MC (2015) Discovering urban activity patterns in cell phone data. *Transportation* 42(4):597–623
- Wiley JA, Robinson JP, Piazza T, Garrett K, Cirksena K (1991a) Activity patterns of California residents. California Environmental Protection Agency, Air Resources Board, Research Division
- Wiley J, Robinson J, Cheng Y, Piazza T, Pladsen (1991b) Study of children's activity patterns. California Environmental Protection Agency, Air Resources Board, Research Division
- Xu Y, Shaw SL, Zhao Z, Yin L, Fang Z, Li Q (2015) Understanding aggregate human mobility patterns using passive mobile phone location data: a home-based approach. *Transportation* 42(4):625–646
- Zahedi S, Shafahi Y (2016) Estimating activity patterns using spatio-temporal data of cell phone networks. *Int J Urban Sci* 22:1–18



A Modular Mechanistic Framework for Assessing Human Exposure to Indoor Chemicals

38

Clara M. A. Eichler and John C. Little

Contents

Introduction	1114
A Modular Mechanistic Framework for Rapid Modeling of Indoor Exposure	1115
General Description of the Framework	1115
Assumptions	1117
Modeling and Parameterization	1118
Example 1: Di-n-Butyl Phthalate (DnBP) in Vinyl Flooring	1118
Example 2: Tris(2-Chloroethyl) Phosphate (TCEP) in Smartphone Casing	1130
Conclusions	1134
Cross-References	1135
References	1135

Abstract

A framework to predict human exposure to chemicals present in indoor environments is described with a focus on semivolatile organic compounds (SVOCs). The framework consists of six mechanistically consistent source emission categories (SECs), i.e., solid, soft, frequent contact, applied, sprayed, and high-temperature sources. Environmental compartments include the gas phase, airborne particles, settled dust, indoor surfaces, and clothing. Exposure may occur via contact with a source or via compartmentally mediated chemical uptake. To illustrate how the framework can be used to derive exposure estimates that can be used for rapid risk prioritization, two examples are described in detail. The first example focuses on

C. M. A. Eichler (✉)

Department of Civil and Environmental Engineering, Virginia Tech, Blacksburg, VA, USA

Department of Environmental Sciences and Engineering, University of North Carolina at Chapel Hill, Chapel Hill, NC, USA

e-mail: claramae@unc.edu

J. C. Little

Department of Civil and Environmental Engineering, Virginia Tech, Blacksburg, VA, USA

e-mail: jcl@vt.edu

di-n-butyl phthalate (DnBP) present in a vinyl flooring material, leading to mediated exposure to DnBP via different pathways. In the context of this example, the special role of clothing is also discussed. The second example explores contact exposure to tris(2-chloroethyl) phosphate (TCEP) in a smartphone casing. The two examples allow the identification of knowledge gaps, and fruitful directions for further research. In addition, next steps for further development and implementation of the framework as a community modeling tool are discussed.

Keywords

Model · Exposure · SVOCs · Scientific workflow · Open-source software

Introduction

One of the primary reasons to improve indoor air quality is to reduce exposure to potentially harmful chemicals present in various forms in the indoor environment. To effectively achieve this goal, exposure assessment strategies that focus on rapidly prioritizing sources of exposure and exposure pathways are needed. Furthermore, it is necessary to integrate our current understanding of the fundamental mechanisms that govern chemical emission and transport in these exposure assessments. For this purpose, Eichler et al. (2021) proposed a modular mechanistic modeling framework to assess human exposure to semivolatile organic compounds (SVOCs), which are introduced into indoor environments in materials, products, and articles. The focus of their work was on SVOCs because of the multimedia behavior of these chemicals, but the framework is designed to enable the integration of other volatile organic compounds (Liu et al. 2013; Salthammer et al. 2018; Zhang et al. 2016), as well as inorganic chemicals and airborne particles. Overall, the framework intends to provide an initial structure and guiding roadmap on which current and future exposure modeling efforts can build.

The framework currently integrates more than 15 years of research focusing on SVOCs (Bennett and Furtaw 2004; Li et al. 2018; Liang et al. 2019; Little et al. 2012; Weschler and Nazaroff 2008; Weschler et al. 2008; Xu and Little 2006) and is based on 16 points of consensus achieved among the international scientific community involved in the research (Eichler et al. 2021). One critical aspect is the focus on mechanistic (i.e., process-based) emission and transport models. Mechanistic models are robust, can be applied to different chemicals, and rely on well-established physicochemical processes such as diffusion, sorption, and equilibrium partitioning. Compared to empirical models, mechanistic models can be more easily scaled in complexity for different modeling purposes. However, mechanistic models may not yet be available for all relevant emission and transport processes, and in those cases, machine learning or statistical models (Wei et al. 2019) as well as expert opinion may need to be used.

Many of the models that this framework aims to integrate are discussed in detail in this handbook, in particular in ► Chap. 23, “Source/Sink Characteristics of SVOCs.”

This chapter therefore focuses on showing how the framework may be applied to assess exposure to chemicals, in particular SVOCs, in consumer products. Specifically, the objectives are to (1) briefly summarize the underlying principles of the modular mechanistic framework, (2) describe two exposure examples in detail, and (3) discuss current limitations, knowledge gaps, and next steps.

A Modular Mechanistic Framework for Rapid Modeling of Indoor Exposure

General Description of the Framework

The description of this framework is based on Eichler et al. (2021), who proposed it as a strategy to rapidly model indoor exposure to SVOCs. The framework can be expanded to assess exposure to other chemical classes, but the examples given here focus on SVOCs.

As shown in Fig. 1, the framework consists of three major elements. These are emission of a chemical from a source into an indoor compartment, transport of the chemical among compartments and any associated chemical transformations, and exposure of occupants to the chemical via contact or compartmentally mediated pathways. Any consumer product, article, or building material that contains the

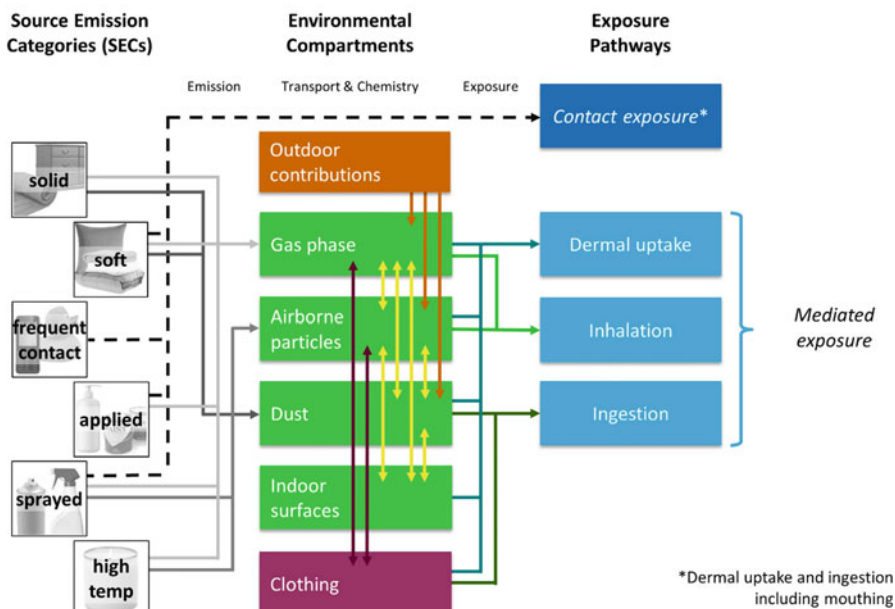


Fig. 1 The modular mechanistic framework for modeling indoor chemical emission, transport, chemistry, and exposure, as presented by Eichler et al. (2021) for SVOCs. (Reprinted with permission from Eichler et al. (2021). Copyright 2021 American Chemical Society)

chemical of interest, or a mixture of chemicals, and is present indoors can be considered as a source. To evaluate chemical emission into the compartments, each source is placed in mechanistically consistent source emission categories (SECs) that are potentially relevant for this particular type of chemical. For SVOCs such as phthalates and organophosphorus flame retardants (OPFRs), the following six SECs have been identified: solid sources, soft sources, applied liquid sources, sprayed liquid sources, high-temperature sources, and frequent contact sources. Exposure to a chemical in a source can be described for each SEC by mechanistically consistent models corresponding to a specific emission, transport, or exposure pathways. However, there is a continuum of sources present in indoor environments, and some sources cannot be clearly placed into one SEC. Instead, multiple SECs may be relevant, and in this case, all possible emission scenarios should be evaluated depending on the purpose of the assessment and the regulatory context.

From the source, emission occurs into different indoor compartments driven by the prevailing chemical activity (or fugacity) gradient. Key compartments in which a chemical can be present are the gas phase, airborne particles, settled dust, and indoor surfaces. Additionally, outdoor contributions and clothing are compartments that have to be considered separately. From sources categorized that are solid or soft, chemicals are emitted into the gas phase and also to dust settled onto the surface of the source, without entering the bulk gas phase. From applied sources, such as creams or paint, emission to the gas phase occurs. Sprayed (e.g., deodorants or air freshener) and high-temperature (e.g., candles or incense) sources emit chemicals into the gas phase and also into the airborne particles compartment. Once a chemical enters the indoor environment, transport among those compartments occurs to some extent for all chemicals. However, all compartments are not equally important for the various classes of chemicals, depending on their properties. Furthermore, chemical processing may occur in all compartments, depending on the chemical properties and the availability of reactants. Parameterizing models describing indoor chemistry remains challenging, but the potential relevance of these processes should be addressed at least qualitatively. Other chemical removal processes, e.g., microbial degradation and occupant activities such as cleaning, may have to be considered.

Some chemicals of interest indoors may also be present outdoors (e.g., polycyclic aromatic hydrocarbons (PAHs)) and may therefore contribute to the indoor mass balance. These chemicals can enter indoor environments with infiltrating air (gas and particle phase) and as dirt and dust carried in by occupants and pets. Chemicals present in the gas phase may partition from there to other compartments, which over time may become reservoirs from where a chemical can be reemitted, if the chemical activity gradient is reversed. Deposited airborne particles that accumulate in settled or resuspended dust may enter the airborne particle phase. Airborne particles and dust, and associated chemicals, also contribute to the potential buildup of organic films on indoor surfaces. Here, surfaces include all readily accessible interfacial regions (air-substrate interface and bulk substrate near the interface) of materials such as wood, painted walls, furnishings, glass, nonclothing fabrics, and upholstery. Uptake of chemicals by surfaces is strongly influenced by the presence of the thin organic films that develop on nearly all indoor surfaces over time.

For sources categorized as soft, applied, or sprayed, and especially for sources identified as frequent contact, contact exposure may play an important role. During contact exposure, the chemical in the source is in direct contact with the exposed individual by dermal uptake, ingestion of the source, or by mouthing of the source, instead of first entering an environmental compartment. The mediated exposure pathways are: (1) dermal uptake from air (gas and particle phases), dust, surfaces, and clothing; (2) inhalation of air (gas and particle phases); and (3) oral exposure, i.e., ingestion of dust or mouthing of clothing and other sink materials.

Figure 1 shows the generic mechanistic modeling framework developed by Eichler et al. (2021) for SVOCs. To adapt the framework for other classes of chemicals, such as volatile organic compounds (VOCs) or per- and polyfluoroalkyl substances (PFAS), additional SECs and indoor environmental compartments may have to be added. For example, some chemicals are present in food and beverages as additives or because of manufacturing, therefore the SEC “food contact materials (FCMs)” may be a useful addition in these cases. The corresponding indoor environmental compartment may then be “food and beverages,” from where additional ingestion exposure can occur. Currently, exposure to chemicals present in FCMs and partitioning into foodstuff is not considered in the framework. However, many FCMs (e.g., packaging, storage containers, and cookware) are often present indoors, and contact with food and other environmental compartments may increase exposure to some chemicals. It is an important task to expand the framework to include other, mechanistically consistent SECs and compartments that allow comprehensive exposure assessments of multiple classes of chemicals.

Assumptions

Emission, transport, chemistry, and exposure occurring in indoor environments are fundamentally dynamic processes. However, to simplify models, the following assumptions can be made in some cases.

1. *Equilibrium between environmental compartments.* Compartments with a large capacity for a chemical, e.g., due to a large available surface area, will take longer to reach equilibrium with other compartments. In this case, the assumption of equilibrium may no longer be applicable.
2. *Well-mixed indoor air.* Exceptions may apply for poorly ventilated spaces.
3. *Negligible outdoor contributions.* Not all chemicals found indoors have outdoor sources.

For SVOCs, it can usually be assumed that emission is externally controlled. The material-phase SVOC concentration C_0 is usually constant because source depletion occurs over a very long time period. These assumptions are not appropriate for VOCs, for which emissions are usually governed by diffusion within the material and depletion may occur within days to weeks (Xu and Little 2006; Liang and Xu 2014a).

Usually, normal conditions (i.e., a temperature of 20 °C and a pressure of 101.325 kPa) are implicitly assumed. Because many of the processes and their associated model parameters are temperature dependent, the parameter values must be appropriate for the assumed conditions. If parameters are available at other conditions (e.g., vapor pressure is often measured at 25 °C), they need to be adjusted.

Modeling and Parameterization

The arrows shown in Fig. 1 represent specific mechanistic models or submodels that can be used individually or combined to described the path of a chemical from a source via the indoor environment to an exposed individual. Many, but not all, models are available based on the current state of science. Many of those models are described within this handbook and can also be found in Eichler et al. (2021). The models used in the examples described below will be discussed in more detail, but different models may be applicable for other scenarios, depending on the goal of the assessment. Uncertainty and problems related to parameterization will be discussed as part of the examples and at the end of this chapter.

Example 1: Di-n-Butyl Phthalate (DnBP) in Vinyl Flooring

Source: For the first example, we estimate exposure of a young child to di-n-butyl phthalate (DnBP) emitted from vinyl flooring covering a room, for example, a kitchen. The initial step of any assessment using the framework is the characterization of the source, i.e., the identification of the relevant SEC (or SECs) and description of the chemical of interest in the source. DnBP is a plasticizer and an SVOC, thus we focus on the six SECs described for SVOCs in Eichler et al. (2021): solid, soft, frequent contact, applied, sprayed, and high temperature. For vinyl flooring, the SEC “solid” is most appropriate, because of the large emitting surface area and infrequent direct contact of the occupants with the source. This means that contact exposure is not considered and the focus is on mediated exposure.

For this example, it is assumed that the vinyl flooring contains 9 wt% DnBP. Using a density of polyvinyl chloride (PVC), the main component of vinyl flooring, of 1.5 g cm^{-3} (Eichler et al. 2018) corresponds to a C_0 of 0.135 g cm^{-3} . Additional information about DnBP of interest is its saturation vapor pressure p_s of $6.70 \times 10^{-3} \text{ Pa}$ at 25 °C (Wu et al. 2016) and its octanol-air partition coefficient (given as $\log(K_{\text{oa}})$) of 9.8 at 25 °C (Weschler and Nazaroff 2012). For the purpose of this example, we will also assume an indoor temperature of 25 °C, thus no further adjustment of these values will be necessary. The concentration of the chemical of interest is especially critical if the emission parameter y_0 , the gas-phase concentration immediately adjacent to the source material, is not known, because C_0 can be used to estimate y_0 . C_0 has to be either measured experimentally (using extraction procedures and chromatographic methods) or taken from product labels or

manufacturing data. C_0 is also important when evaluating certain contact exposure pathways.

Scenario: Next, the exposure scenario is defined in more detail, including the assumptions used in the model. As mentioned above, the DnBP-containing flooring is present in a kitchen, but for the purpose of this assessment, we estimate the concentrations in the environmental compartments throughout the entire house. The information about the house listed in Table 1 is assumed for this example; however, in many cases it is likely that a user has specific data available instead. The house parameterized here is a roughly standard, single-level US house. Basement, attic, and attached garage are not considered.

The following assumptions are made for modeling emission and transport of DnBP in this scenario:

1. Equilibrium among the indoor compartments has been achieved for DnBP.
2. Outdoor contributions of DnBP are negligible.
3. Interaction of DnBP with clothing is not considered.
4. Chemical and microbial reactions are not considered.
5. The flooring is the only source of DnBP in the house.
6. The concentration of total suspended particles (TSP) in the house is constant with no additional particles generated.
7. Dust removal (e.g., by vacuuming) takes place once per week.

These assumptions lead to a substantial simplification of the model, but they also introduce additional uncertainty.

Model selection: Following the framework (Fig. 1), emission occurs from the flooring into the gas phase, and also to dust settled on the source. Now it depends on the goal of the assessment if the emission rates are calculated independently, followed by modeling of each partitioning mechanism, or if a slightly broader,

Table 1 Parameters describing the indoor exposure scenario

Parameter	Symbol	Value	Reference
Total floor area of a US house	$A_{\text{floor},\text{total}}$	250 m ²	census.gov (2020)
Source surface area (kitchen)	A_{source}	19 m ²	Manuja et al. (2019)
Ceiling height of a US house	H_{ceiling}	2.4 m	Manuja et al. (2019)
Total volume of the house	$V_{\text{house},\text{total}}$	600 m ³	based on $A_{\text{floor},\text{total}}$ and H_{ceiling}
Surface area to volume ratio, with contents	S^*/V^*	3.2 m ⁻¹	Manuja et al. (2019)
Total surface area of the house	$A_{\text{house},\text{total}}$	1920 m ²	calculated, based on $V_{\text{house},\text{total}}$ and S^*/V^*
Air change rate	λ	0.4 h ⁻¹	Jaycock and Havics (2018)
Air flow rate through the house	Q	240 m ³ h ⁻¹	calculated, based on $V_{\text{house},\text{total}}$ and λ
Total suspended particle concentration	TSP	20 µg m ⁻³	Little et al. (2012)

mass balance–based approach is used that combines the relevant processes. Therefore, model selection is the next step. For this example, the mass balance approach is chosen to evaluate the concentrations of DnBP in the different environmental compartments after certain time periods. The mass balance reveals which additional parameters are needed. As described in Eichler et al. (2021), the general mass balance for describing transport of SVOCs in indoor environments is:

$$\begin{aligned} V \frac{dy}{dt} + V \frac{dF}{dt} = & Q \cdot (y_{\text{out}} + F_{\text{out}}) - Q \cdot (y + F) + h_m \cdot A_{\text{source}} \cdot (y_0 - y) \\ & - h_{m,s} \cdot A_{\text{sink}} \cdot (y - y_s) - v_d \cdot F \cdot (A_{\text{source}} + A_{\text{sink}}) + R_p \cdot M \cdot P_{\text{dust}} \cdot A_{\text{source}} \\ & + R_p \cdot M_s \cdot P_{\text{dust},s} \cdot A_{\text{sink}} \end{aligned} \quad (1)$$

where V is the volume of the indoor environment, y is the gas-phase SVOC concentration in the indoor environment, F is the particle-phase SVOC concentration in the indoor environment, t is time, Q is the air flow rate, y_{out} is the gas-phase SVOC concentration entering from outdoors, F_{out} is the particle-phase SVOC concentration entering from outdoors, h_m is the mass transfer coefficient for a source surface, A_{source} is the surface area of the source, y_0 is the gas-phase SVOC concentration in the boundary layer immediately adjacent to the source, $h_{m,s}$ is the mass transfer coefficient for a sink surface, A_{sink} is the sink surface area, y_s is the gas-phase SVOC concentration in the boundary layer immediately adjacent to the sink surface, v_d is the size-dependent particle deposition velocity, R_p is the size-dependent particle resuspension rate, M is the mass loading of settled dust on the source surface, P_{dust} is the concentration of SVOC in the dust settled on the source surface, M_s is the mass loading of settled dust on the sink surface, and $P_{\text{dust},s}$ is the concentration of SVOC in the dust settled on the sink surface.

Based on the first assumption, steady state has been achieved and the mass balance in Eq. 1 can be set equal to zero, thus eliminating the accumulation terms:

$$V \frac{dy}{dt} + V \frac{dF}{dt} = 0 \quad (2)$$

The first assumption also means that the gas-phase SVOC concentration in the boundary layer adjacent to the sink surfaces equals the bulk gas-phase concentration, i.e., no further loss to the surfaces occurs because equilibrium has been reached:

$$y_s = y \quad (3)$$

The second assumption yields:

$$Q \cdot (y_{\text{out}} + F_{\text{out}}) = 0 \quad (4)$$

F can be calculated as:

$$F = K_p \cdot TSP \cdot y \quad (5)$$

where K_p is the gas-particle partition coefficient. Similarly, P_{dust} and $P_{\text{dust},s}$ can be calculated using:

$$P_{\text{dust}} = K_{\text{dust}} \cdot y_0 \quad (6)$$

$$P_{\text{dust},s} = K_{\text{dust}} \cdot y_s \text{ (here : } P_{\text{dust},s} = K_{\text{dust}} \cdot y, \text{ see Eq. 3)} \quad (7)$$

where K_{dust} is the dust-gas partition coefficient.

Additional simplifications are made by assuming that $h_{m,s} = h_m$ and $M_s = M$. However, if measured data on mass transfer coefficients or mass loadings are available, they should be used. To explicitly calculate h_m or $h_{m,s}$, the correlation by Axley (1991) can be used, but see also Huang et al. (2004). Together with Eqs. 2–7, the simplifications result in the following mass balance, which can be rearranged to solve for y :

$$y = \frac{y_0 \cdot A_{\text{source}} \cdot (h_m + R_p \cdot M \cdot K_{\text{dust}})}{Q + Q \cdot TSP \cdot K_p + \nu_d \cdot TSP \cdot K_p \cdot (A_{\text{source}} + A_{\text{sink}}) - R_p \cdot M \cdot K_{\text{dust}} \cdot A_{\text{sink}}} \quad (8)$$

Having calculated y and further assuming solid sink surfaces with negligible porous surface area, the concentration of DnBP on the sink surfaces, C_s , at equilibrium can be calculated as:

$$C_s = K_s \cdot y_s \quad (9)$$

where K_s is the surface-gas partition coefficient. As stated in Eq. 3, we assume that $y_s = y$ for this scenario. K_s is specific to a material and a chemical, but has not been measured for many such combinations. If directly measured data cannot be used, K_s can be estimated based on different types of regressions established for specific scenarios. For example, Xu et al. (2009) established a regression model to estimate K_s for phthalates and for wooden floors, ceilings, and walls, or:

$$\log(K_s) = -0.779 \cdot \log(p_s) - 1.93 \quad (10)$$

where the vapor pressure p_s is given in mmHg. As this parameter depends directly on p_s and is also only valid for these material types, the resulting DnBP surface concentration is one of the more uncertain values.

K_p can be measured, but in most cases K_p is predicted based on either the K_{oa} of the chemical or on p_s (Salthammer and Goss 2019; Salthammer and Schripp 2015). Here, we will use the approach of Finizio et al. (1997):

$$K_p = \frac{f_{\text{om_part}} \cdot K_{\text{oa}}}{\rho_{\text{part}}} \quad (11)$$

where $f_{\text{om_part}}$ is the fraction of organic matter associated with airborne particles and ρ_{part} is the density of the airborne particles.

K_{dust} is defined as:

$$K_{\text{dust}} = \frac{f_{\text{om_dust}} \cdot K_{\text{oa}}}{\rho_{\text{dust}}} \quad (12)$$

where $f_{\text{om_dust}}$ is the fraction of organic matter in settled dust and ρ_{part} is the density of the settled dust.

To determine M , the following equation is used and solved for $t = 168$ h, based on assumption 7:

$$\frac{dM}{dt} = \nu_d \cdot TSP - R_p \cdot M \quad (13)$$

Parameterization: Now that all relevant equations to model SVOC transport indoors are known, the equations have to be parameterized. Accurately measured data for specific parameters should be used if available. Otherwise, literature values (and the associated uncertainties) have to be applied. For this example, the values shown in Table 2 have been used.

In this example, a measured value for y_0 is available. In many cases though y_0 may not be known. For those situations y_0 can be estimated based on C_0 , as described by Eichler et al. (2018), Liang et al. (2018), and Addington et al. (2020). The particle deposition velocity given here is at the lower bound of the range of deposition velocities for coarse mode particles (Weschler and Nazaroff 2017), which is assumed to make up the largest fraction of particles present in the indoor environment (Shi and Zhao 2012). If a more detailed description of the particle size distribution is

Table 2 Literature values used for parameterization of the transport models, SEC = solid

Parameter	Symbol	Value	Reference
Fraction of organic matter associated with airborne particles	$f_{\text{om_part}}$	0.4	Weschler and Nazaroff (2010)
Density of the airborne particles	ρ_{part}	1 g cm ⁻³	Weschler and Nazaroff (2010)
Fraction of organic matter in settled dust	$f_{\text{om_dust}}$	0.2	Weschler and Nazaroff (2010)
Density of the settled dust	ρ_{dust}	2 g cm ⁻³	Weschler and Nazaroff (2010)
Size-dependent particle deposition velocity	ν_d	4.9 m h ⁻¹	Shi and Zhao (2012) <i>Note:</i> for particle size fraction 2.5–10 µm
Size-dependent particle resuspension rate	R_p	7.2×10^{-5} h ⁻¹	Thatcher and Layton (1995)
Gas-phase concentration of the SVOC in the layer immediately adjacent to the source	y_0	24.7 µg m ⁻³	Liang and Xu (2014b) <i>Note:</i> y_0 measured at 25 °C
Mass transfer coefficient	h_m and $h_{m,s}$	1.44 m h ⁻¹	Xu et al. (2012)

available, the deposition velocity should be adapted accordingly, e.g., by using the size fraction weighted average.

Calculation of concentrations in indoor compartments: Using Eqs. 10–13, K_s , K_p , K_{dust} , and M can be calculated. The results are shown in Table 3. The calculated K_s value is relatively small, indicating that DnBP does not partition strongly to these surfaces. This corresponds with DnBP's relatively high vapor pressure, but the estimate for K_s has to be considered as highly uncertain because it is based on multiple simplifications. Thus, the K_s value reported in Table 3 is likely a lower bound for the given scenario.

Based on all the information gathered so far, F , P_{dust} , $P_{\text{dust,s}}$, y , and C_s can be calculated, as summarized in Table 4.

Exposure calculations: Now that the concentrations in the environmental compartments have been calculated, we can estimate the resulting exposure via the four pathways including dermal uptake from the gas phase, dermal uptake from sink surfaces, inhalation of air (gas and particle phases), and ingestion of dust. Dermal uptake of DnBP from airborne particles or dust is not considered in this example, but one approach to estimate exposure via this pathway is given in Eichler et al. (2021). Here, the following equations will be used to estimate exposure:

$$Ex_{\text{gas_b}} = y \cdot k_{p_s} \cdot A_{\text{exp}} \quad (14)$$

$$Ex_{\text{surf_d}} = C_s \cdot CR_s \cdot f_A \cdot A_{\text{hand}} \quad (15)$$

Table 3 Calculated model parameters, SEC = solid

Parameter	Symbol	Value	Reference
Surface-gas partition coefficient	K_s	26 m	Eq. 10
Gas-particle partition coefficient	K_p	$2.7 \times 10^{-3} \text{ m}^3 \mu\text{g}^{-1}$	Eq. 11
Dust-gas partition coefficient	K_{dust}	$680 \text{ m}^3 \text{ g}^{-1}$	Eq. 12
Mass loading of settled dust on the source and sink surfaces	M and M_s	$1.6 \times 10^4 \mu\text{g m}^{-2}$	Eq. 13

Table 4 Resulting DnBP concentrations in the indoor environmental compartments, SEC = solid

Parameter	Symbol	Value	Reference
DnBP concentration in the airborne particle phase	F	$0.010 \mu\text{g m}^{-3}$	Eq. 5
DnBP concentration in the dust settled on the source surface	P_{dust}	$16,700 \mu\text{g g}^{-1}$	Eq. 6
DnBP concentration in the dust settled on sink surfaces	$P_{\text{dust,s}}$	$130 \mu\text{g g}^{-1}$	Eq. 7
DnBP concentration in the bulk gas phase	y	$0.19 \mu\text{g m}^{-3}$	Eq. 8
DnBP concentration on sink surfaces	C_s	$5 \mu\text{g m}^{-2}$	Eq. 9

$$Ex_{inh} = (y + F) \cdot IR_{inh} \quad (16)$$

$$Ex_{dust_ing} = P_{dust} \cdot IR_{dust} \quad (17)$$

where Ex_{gas_b} is the transdermal exposure rate from the gas phase to the blood, $k_{p,g}$ is the transdermal permeability coefficient from the gas phase to the blood, A_{exp} is the exposed body surface area, Ex_{surf_d} is the dermal exposure rate for dermal contact with sink surfaces, CR_s is the rate of contact with sink surfaces, f_A is the fraction of chemical accessible for uptake or transfer efficiency, A_{hand} is the surface area of the hands in contact with the sink surface, Ex_{inh} is the inhalation exposure rate, IR_{inh} is the inhalation rate, Ex_{dust_ing} is the dust ingestion rate, and IR_{dust} is the dust intake rate.

The fraction of chemical accessible for uptake f_A , also described as transfer efficiency, has been studied using both chemicals (especially pesticides) and fluorescent tracers, as described in Chapter 7 of the EPA *Exposure Factors Handbook* (USEPA 2011). However, the *Handbook* does not provide explicit recommendations. Cohen Hubal et al. (2008) reported transfer efficiencies ranging from 0.8% to 45.5% for the first contact and 0.6–19.4% for the seventh contact, depending on skin condition (e.g., moist vs. dry skin) and surface loadings, among other factors. Based on the wide possible range, we select a transfer efficiency of 10%, acknowledging the high uncertain of this parameter.

It should be noted that, as given, the exposure rates Ex_{gas_b} and Ex_{surf_d} have different endpoints. Ex_{gas_b} is based on transfer from the gas phase through the skin to the blood stream (i.e., transdermal exposure), while Ex_{surf_d} describes the transfer of a chemical from a sink surface to the skin surface (i.e., dermal exposure). The reason for this inconsistency lies in the history of the equations and both have their relevance. Ex_{surf_d} is particularly relevant if mouthing of hands is considered as an additional exposure pathway, and it also provides an upper bound for the estimation of Ex_{surf_b} , the exposure rate from the skin-surface lipids into the blood stream, under steady state conditions. In this case, it is assumed that no other removal processes take place. In reality, skin permeability may be low and removal by evaporation or mechanical processes may occur, which decreases Ex_{surf_b} in comparison to Ex_{surf_d} . Ex_{surf_b} can be expressed as:

$$Ex_{surf_b} = C_{ssl} \cdot k_{p,ssl} \cdot A_{hand} \quad (18)$$

where C_{ssl} is the concentration of a chemical associated with skin-surface lipids, $k_{p,ssl}$ is the transdermal permeability coefficient from the skin-surface lipids to the blood, and δ_{ssl} is the thickness of the skin-surface lipid layer. C_{ssl} can be measured, e.g., with handwipes, or calculated by:

$$C_{ssl} = \frac{C_s \cdot f_A}{\delta_{ssl}} \quad (19)$$

Eq. 19 gives C_{ssl} after one contact with a sink surface.

Exposure rates can be converted to daily intake rates (DI , in $\mu\text{g kg}^{-1} \text{ day}^{-1}$) by using:

$$DI = Ex \cdot \frac{EF}{BW} \quad (20)$$

where Ex is the respective exposure rate or flux, EF is the exposure frequency in hours per day of a specific exposure route, and BW is the body weight of the exposed individual.

With the exception of $k_{p,g}$, $k_{p,ssl}$, and δ_{ssl} , all parameters needed for the exposure modeling equations can be found in or derived from information provided in the *Exposure Factors Handbook* by the US Environmental Protection Agency (EPA). $k_{p,g}$ is a combined permeability coefficient that describes SVOC transport from the bulk air through several layers of epidermis to the blood (Weschler and Nazaroff 2012). Similarly, $k_{p,ssl}$ describes SVOC transport from the skin lipid layer through the epidermis to the blood (Weschler and Nazaroff 2012). Weschler and Nazaroff (2012) provide an approach for calculating $k_{p,g}$ for different chemicals and give several examples, including for DnBP. $k_{p,g}$ and $k_{p,ssl}$ can vary by several orders of magnitude for different chemicals.

In this scenario, the exposed individual is a young child (2 to <3 years) living in the house. For exposure by dermal uptake from the gas phase, it is assumed that only the child's head, arms, and hands are exposed, while the rest of the body is covered by clean clothing. Here, the clothes that the child is wearing are considered a barrier that protects the clothed skin. As part of the scenario, we further assume that exposure only occurs during the time spent at home. All parameters used as model inputs are summarized in Table 5.

For the purpose of estimating exposure, an average dust concentration throughout the house can be calculated based on the fractions of source and sink floor surface area that is potentially available for a child to come in contact with dust. A child can potentially ingest dust from other locations than the floor, e.g., from a shelf, but it can be assumed that such horizontal surface areas correspond to the floor surface area on which a piece of furniture may be placed. The fractions f_{source} of source (floor) surface area and f_{sink} of sink (floor) surface area can be calculated as:

$$f_{\text{source}} = \frac{A_{\text{source}}}{A_{\text{total}}} \quad (21)$$

$$f_{\text{sink}} = \frac{(A_{\text{total}} - A_{\text{source}})}{A_{\text{total}}} \quad (22)$$

Then, the average DnBP concentration in the dust can be calculated as:

$$P_{\text{dust,avg}} = f_{\text{source}} \cdot P_{\text{dust}} + f_{\text{sink}} \cdot P_{\text{dust,s}} \quad (23)$$

For further calculation of exposure to DnBP by dust ingestion, P_{dust} in Eq. 17 is replaced by $P_{\text{dust,avg}}$. Table 6 summarizes the resulting exposure rates as well as the respective daily intake rates for the example scenario.

Table 6 shows that dermal uptake from sink surfaces and dust ingestion dominate exposure for this particular scenario, while transdermal uptake from the gas phase

Table 5 Parameters for exposure models from the literature

Parameter	Symbol	Value	Reference
Body weight (child, 2 to <3 years)	BW	13.8 kg	USEPA (2011)
Exposed skin surface area (child, 2 to <3 years; head, arms, and hands)	A_{exp}	0.167 m ²	USEPA (2011)
Hand surface area in contact with sink surfaces (child, 2 to <3 years, palms only)	A_{hand}	0.014 m ²	USEPA (2011)
Rate of contact with sink surfaces as indoor hand contact with objects/surfaces (child, 1–6 years)	CR_s	193 contacts h ⁻¹	USEPA (2011)
Fraction of chemical accessible for uptake from sink surfaces or transfer efficiency	f_A	0.1	estimated, see Cohen Hubal et al. (2008) and USEPA (2011)
Inhalation rate (child, 2 to <3 years)	IR_{inh}	8.9 m ³ d ⁻¹ = 0.37 m ³ h ⁻¹	USEPA (2011)
Dust ingestion rate (child, 2 to <6 years)	IR_{dust}	30 mg d ⁻¹ = 0.00125 g h ⁻¹	USEPA (2017)
Exposure frequency or time spent at residency/house (child, 2 to <6 years)	EF	979 min d ⁻¹ = 16.3 h d ⁻¹	USEPA (2011)
Transdermal permeability coefficient from the gas phase to the blood	k_{p_g}	4.8 m h ⁻¹	Weschler and Nazaroff (2012)
Transdermal permeability coefficient from the skin-surface lipids to the blood	k_{p_ssl}	0.095 × 10 ⁻⁶ m h ⁻¹	Weschler and Nazaroff (2012)
Thickness of the skin-surface lipid layer (children's hands)	δ_{ssl}	8.8 × 10 ⁻⁷ m ³ /m ²	Weschler and Nazaroff (2012)

and inhalation exposure are smaller contributors. Overall, the daily intake rate normalized by body weight for this child is 3.94 µg kg⁻¹ BW d⁻¹, excluding Ex_{surf_b} . This result could now be put in further context by comparison with the results for other products and/or chemicals, or by combining this exposure estimate with toxicity information. Another point of comparison is to estimate exposure for an adult under the same conditions, which yields a total daily intake rate of 1.29 µg kg⁻¹ BW d⁻¹, using the appropriate data from the EPA *Exposure Factors Handbook*. As discussed above, Ex_{surf_d} gives an upper bound for the amount of chemical potentially transported through the skin to the blood. Ex_{surf_b} provides a more conservative estimate. In addition, the uncertainty associated with (trans)dermal uptake of DnBP from sink surfaces is relatively high given that (1) K_s had to be estimated based on DnBP's vapor pressure and was averaged for the entire indoor sink surface area, (2) the transfer efficiency from the sink surfaces to the skin was assumed based on a very wide range of reported values, and (3) many other factors affect transdermal uptake that have not been included here. Several chapters of this handbook as well as Licina et al. (2019) provide a detailed discussion of this topic.

Table 6 Calculated exposure and daily intake rates for DnBP for a young child (2 to <3 years), SEC = solid

Parameter	Symbol	Value	Reference
Exposure by transdermal uptake from the gas phase	Ex_{gas_b}	0.15 $\mu\text{g h}^{-1}$	Eq. 14
Exposure by dermal uptake from sink surfaces	Ex_{surf_d}	1.37 $\mu\text{g h}^{-1}$	Eq. 15
Exposure by inhalation of air	Ex_{inh}	0.076 $\mu\text{g h}^{-1}$	Eq. 16
Exposure by ingestion of dust	Ex_{dust_ing}	1.74 $\mu\text{g h}^{-1}$	Eq. 17
Exposure by transdermal uptake from sink surfaces	Ex_{surf_b}	0.15 $\mu\text{g h}^{-1}$	Eq. 18
Daily intake rate via transdermal uptake from the gas phase	DI_{gas_b}	0.18 $\mu\text{g kg}^{-1} \text{BW d}^{-1}$	Eq. 20
Daily intake rate via dermal uptake from sink surfaces	DI_{surf_d}	1.62 $\mu\text{g kg}^{-1} \text{BW d}^{-1}$	Eq. 20
Daily intake rate via inhalation of air	DI_{inh}	0.089 $\mu\text{g kg}^{-1} \text{BW d}^{-1}$	Eq. 20
Daily intake rate via ingestion of dust	DI_{dust_ing}	2.05 $\mu\text{g kg}^{-1} \text{BW d}^{-1}$	Eq. 20
Daily intake rate via transdermal uptake from sink surfaces	DI_{surf_b}	0.17 $\mu\text{g kg}^{-1} \text{BW d}^{-1}$	Eq. 20

Uncertainty: Large uncertainties may have been introduced into the above calculations with the choice of data for the vapor pressure and the octanol-air partition coefficient. Both are important for estimating other parameters, such as the gas-particle partition coefficient. One way to address this problem is to include ranges and distributions into the model, using Monte-Carlo-based approaches. For example, a range of $p_s \pm 0.95 \cdot p_s$ following a normal distribution has been proposed for the vapor pressure (Salthammer and Schripp 2015). The choice of tools to predict chemical properties (e.g., SPARC, EpiSuite, COSMOTHERM, and others) can also influence the outcome of the calculation, and it is recommended to compare predictions and literature values to get a sense for the reliability of the chosen value. It further matters which predictive relationship is used to get certain model parameters, especially for partition coefficients. As discussed in Schossler et al. (2011), it makes a substantial difference if K_p is calculated based on K_{oa} or based on p_s . Furthermore, for compounds of intermediate volatility ($10^{-6} \text{ Pa} < p_s < 10^{-2} \text{ Pa}$) it is very difficult to predict the fraction of the compound present in the particle phase, because small variations in p_s or K_{oa} and in the particle-phase concentration yield substantial variations in the concentration ratio between gas and particle phases (Eichler et al. 2021). Variations of temperature and relative humidity on the parameters are not included in these models, but are expected to have an influence. For higher tier exposure assessments, more information should be included to address these factors, although our ability to include them remains limited. As will become more evident in the next example, gaps in the availability of exposure factors are an additional issue that introduces uncertainty in the exposure estimates.

Extension of Example 1: Considering the Impact of Clothing

The third assumption of the example described above stated that the impact of clothing (as environmental compartment and as mediator of exposure) was not considered. However, it is possible to include clothing based on the previous results. First, we can calculate the concentration of DnBP in the clothing material C_{cloth} that has equilibrated with the gas phase. The following equation can be applied if steady state has been reached:

$$K_{ca} = \frac{C_{\text{cloth}}}{y} \quad (24)$$

where K_{ca} is the clothing-air partition coefficient (either unitless or normalized by clothing mass or volume) and C_{cloth} is the concentration of a chemical in the cloth. For DnBP, K_{ca} has been determined experimentally by Morrison et al. (2015) for different types of cotton clothing. Here, we use the average values for K_{ca} and for the cloth density δ_{cloth} determined from those measurements (see Table 7). If K_{ca} is not known, $\log(K_{ca})$ can be roughly estimated based on $\log(K_{oa})$ (Morrison et al. 2018). For the calculation of the exposure estimate, both $C_{\text{cloth,vol}}$ and $C_{\text{cloth,area}}$ can be used, as discussed below.

Based on the cloth density, the mass fraction of the chemical in the clothing w_{cloth} can be determined:

$$w_{\text{cloth}} = \frac{C_{\text{cloth,vol}}}{\rho_{\text{cloth}}} \quad (25)$$

w_{cloth} is necessary to estimate exposure by mouthing, while in this example a simplified model based on the gas-phase concentration y is used to estimate exposure by transdermal uptake from the clothing material (Eq. 26).

The exposure calculations can now be expanded by considering transdermal uptake of DnBP from clothing worn by the child and mouthing of clothing that has accumulated DnBP. A simplified mechanistic model to estimate transdermal uptake of SVOCs from clothing has been proposed by Morrison (2020):

Table 7 Parameters for modeling clothing-air partitioning and model results, SEC = solid

Parameter	Symbol	Value	Reference
Clothing-air partition coefficient, normalized by volume	$K_{ca,\text{vol}}$	3,900,000	Morrison et al. (2015), average
Clothing-air partition coefficient, normalized by area	$K_{ca,\text{area}}$	4360 m	Morrison et al. (2015), average
Cloth density	ρ_{cloth}	$5.43 \times 10^{11} \mu\text{g m}^{-3}$	Morrison et al. (2015), average
Concentration of DnBP in the clothing, per clothing volume	$C_{\text{cloth,vol}}$	$754,000 \mu\text{g m}^{-3}$	Eq. 24
Concentration of DnBP in the clothing, per clothing surface area	$C_{\text{cloth,area}}$	$840 \mu\text{g m}^{-2}$	Eq. 24
Mass fraction of DnBP in the clothing	w_{cloth}	1.8×10^{-6}	Eq. 25

$$Ex_{cloth_b} = y \cdot \left(\frac{8.3 \cdot k_{p_b}}{8.3 + k_{p_b}} \right) \cdot A_{clothed} \quad (26)$$

where Ex_{cloth_b} is the exposure rate by transdermal uptake from clothing, k_{p_b} is the transdermal permeability coefficient for transport from the skin-surface boundary layer to the blood stream, and $A_{clothed}$ is the clothed body surface area. The factor 8.3 in m h^{-1} equals a normalized daily transdermal uptake of $0.2 \text{ mg m}^{-2} (\mu\text{g m}^{-3})^{-1} \text{ day}^{-1}$ and includes the assumption of a gap between skin and clothing of 2 mm. The factor further reflects clothing that is washed weekly, but removal of SVOCs is incomplete, and that had time to equilibrate with the indoor environment.

Exposure by mouthing of cloth can be estimated using:

$$Ex_{mouth} = w_{cloth} \cdot A_{moutherd} \cdot MR \cdot MF \quad (27)$$

where Ex_{mouth} is the exposure rate by mouthing, $A_{moutherd}$ is the mouthed area (here, of the cloth), MR is the migration rate of the chemical from the object or cloth, and MF is the mouthing frequency. The migration rate depends on the water solubility of the chemical, but also depends on the mass fraction of chemical in the mouthed object. For DnBP in PVC, Wormuth et al. (2006) reported a migration rate for a mass fraction of 11%, much higher than the mass fraction of DnBP in clothing considered here. In their 2014 report on phthalates and phthalate alternatives, the Chronic Hazard Advisory Panel (CHAP) was not able to identify other migration rates for DnBP, and more recent studies could also not be identified. Because of this limitation in the data availability, the following simplified equation is used to estimate exposure by mouthing:

$$Ex_{mouth} = C_{cloth,area} \cdot A_{moutherd} \cdot MF \cdot f_{soluble} \quad (28)$$

where $f_{soluble}$ is the fraction of chemical leached from the cloth during mouthing.

DnBP is not very water soluble ($K_H = 0.183 \text{ Pa m}^3 \text{ mol}^{-1}$ (USEPA 2021)), therefore the migration rates used for this example will be based on the assumption of leaching of 1% and of 100% of DnBP accumulated in the cloth. One percent may be considered the more likely value, while assuming 100% gives an upper bound.

Table 8 shows the parameters used for exposure estimation. To convert Ex_{cloth_b} to DI_{cloth_b} , it is assumed that the child is wearing clothes for 23 h per day. For the conversion of $Ex_{mouthing}$, 14 h per day of mouthing activity are assumed. This exposure frequencies differ from those for the other conversions, which were based on the time spent indoors. Table 9 summarizes the resulting exposure and daily intake rates.

The results show that exposure via mouthing can be an important contributor to the total daily intake rate, if a large fraction of the chemical is leaching from the cloth material. Furthermore, transdermal uptake from clothing can be a source of exposure that should not be neglected in the assessment, especially not for chemicals that have a relatively high skin permeability, such as DnBP.

Table 8 Parameters for modeling exposure mediated by clothing, SEC = solid

Parameter	Symbol	Value	Reference
Transdermal permeability coefficient for transport from the skin-surface boundary layer to the blood stream	k_{p_b}	23 m h ⁻¹	Weschler and Nazaroff (2012)
Body surface area covered by clothing, calculated as the difference between total body surface area (child, 2 to <3 years) and A_{exp}	$A_{clothed}$	0.443 m ²	USEPA (2011)
Mouthing cloth surface area	$A_{mouthed}$	0.001 m ²	CSPC (2014)
Mouthing frequency, mean value for cloth/towel	MF_{cloth}	5.4 contacts h ⁻¹	USEPA (2011)
Fraction of chemical leached during mouthing	$f_{soluble,1}$ $f_{soluble,2}$	0.01 1.0	Estimated
Exposure frequency to clothing	EF_{cloth}	23 h d ⁻¹	Estimated
Exposure frequency mouthing	$EF_{mouthing}$	14 h d ⁻¹	Estimated

Table 9 Estimated exposure and daily intake rates for DnBP for a young child (2 to <3 years), clothing mediated, SEC = solid

Parameter	Symbol	Value	Reference
Exposure by transdermal uptake from clothing	Ex_{cloth_b}	0.52 µg h ⁻¹	Eq. 26
Exposure by mouthing of cloth, based on 1% and 100% leaching of chemical	$Ex_{mouth,1}$ $Ex_{mouth,2}$	4.6 × 10 ⁻² µg h ⁻¹ 4.6 µg h ⁻¹	Eq. 28
Daily intake rate via transdermal uptake from clothing	DI_{cloth_b}	0.87 µg kg ⁻¹ BW d ⁻¹	Eq. 20
Daily intake rate via mouthing of cloth, based on 1% and 100% leaching of chemical	$DI_{mouth,1}$ $DI_{mouth,2}$	4.6 × 10 ⁻² µg kg ⁻¹ BW d ⁻¹ 4.6 µg kg ⁻¹ BW d ⁻¹	Eq. 20

As discussed above, substantial uncertainty is introduced into these calculations because of missing information to fully and robustly parameterize the exposure models. In addition, assuming that clothing does not contribute to overall exposure may lead to significant underestimation of total daily exposure. Further measurements are needed to provide more information on clothing-air partitioning and on the role of clothing in reducing or enhancing exposure.

Example 2: Tris(2-Chloroethyl) Phosphate (TCEP) in Smartphone Casing

Source: For this example, we assume a cell phone containing 5 wt% of tris (2-chloroethyl) phosphate (TCEP) in its casing. As in the first example, the initial step is to determine the applicable SEC. Here, the object has a small emitting surface area but is handled frequently, thus it can be considered a frequent contact source.

For frequent contact sources, the following contact exposure pathways may be of importance: (1) dermal uptake by direct contact with the source, (2) ingestion of the source, and (3) mouthing of the source. Here, the first and third pathway are likely to occur.

To further describe the source, information about the vapor pressure, K_{oa} , and the molecular weight of TCEP is needed. TCEP is an organophosphorus flame retardant (OPFR) and plasticizer that has been measured in a range of products and in indoor environments (see, for example, Liu et al. (2016), Liagkouridis et al. (2017), Vykoukalová et al. (2017)), and is considered an SVOC. Yang et al. (2019) determined concentrations of TCEP and other OPFRs in surface wipes of different products, including cell phones. This information is very useful, and the following calculations of exposure estimates could be based on these data (Table 10). Here, another approach is described to illustrate how the concentration of TCEP on the surface of the phone can be determined in a mechanistically sound way.

The relationship between C_0 and y_0 for SVOCs is based on a compound's vapor pressure and an activity coefficient (Eichler et al. 2018). Liang et al. (2018) investigated emission parameters of OPFRs and determined a relationship between C_0 and y_0 based on their findings and literature values for OPFRs and phthalates, where w_0 is the mass fraction based on C_0 :

$$\frac{y_0}{p_s} = 3.40 \cdot w_0 \quad (29)$$

Note that for use with Eq. 29, p_s has to be converted to $\mu\text{g m}^{-3}$, using the ideal gas law. Here, a temperature of 25 °C (298 K) was used for the conversion. Eq. 29 allows to calculate y_0 based on C_0 , if p_s is known. As shown in Table 10, the vapor pressure of TCEP has a relatively high uncertainty, because the values available in the literature span several orders of magnitude. Because Eq. 29 is based on the work by Liang et al. (2018), we are also using 0.00114 Pa in our calculations. However, as additional, more reliable measurements of p_s become available, Eq. 29 may have to be revised.

Scenario and model selection: Smartphones are often touched and likely to have developed a thin organic film on their surface. Here, we assume that the TCEP emitted from the phone casing is present in this film, and that the film has equilibrated with y_0 , i.e., the gas-phase concentration of TCEP immediately adjacent to the source material surface. To describe partitioning between y_0 and the concentration of TCEP in the film $C_{s,film}$, we assume that the surface film consists of predominantly organic material, and that K_{oa} can be used as partition coefficient (Weschler and Nazaroff 2017). Based on these considerations, Eq. 30 can be used to determine the TCEP concentration in the surface film on the phone:

$$C_{s,film} = y_0 \cdot K_{oa} \cdot \delta_{film} \quad (30)$$

where δ_{film} is the thickness of the organic surface film.

Table 10 Parameters used for estimating exposure to TCEP. If multiple values for a parameter were found, those printed in bold were selected for calculations. SEC = frequent contact

Parameter	Symbol	Value	Reference
Molecular weight of TCEP	MW_{TCEP}	285.48 g mol ⁻¹	USEPA (2021)
Vapor pressure of TCEP @ 25 °C	$p_{s,TCEP}$	0.00114 Pa 0.056 Pa 8.15 Pa	ECHA (2008), used in Liang et al. (2018) Okeme et al. (2020) USEPA (2021), experimental average
Octanol-air partition coefficient of TCEP @ 25 °C	$\log(K_{oa,TCEP})$	7.6 7.85 8.41	Yang et al. (2019) Okeme et al. (2020) USEPA (2021), predicted average
TCEP surface wipe concentration, cell phones (n = 31), geometric mean	$C_{s,wipe}$	10.2 µg m ⁻²	Yang et al. (2019)
Mass fraction of TCEP in smartphone casing	$w_{0,TCEP}$	0.05	Assumed for scenario
Thickness of organic film on smartphone	δ_{film}	1·10 ⁻⁹ m	Estimated, based on Weschler and Nazaroff (2017)
Gas-phase concentration of TCEP immediately adjacent to the source material surface	y_0	22.32 µg m ⁻³	Eq. 29
Concentration of TCEP in the organic surface film	$C_{s,film}$	15.80 µg m ⁻²	Eq. 30
Rate of contact with object	CR_{obj}	5 contacts h ⁻¹	Estimated, based on ca. 100 contacts with the phone per day
Transdermal permeability coefficient from the skin-surface lipids to the blood	$k_{p,ssl}$	9.0 × 10 ⁻⁸ m h ⁻¹	Calculated, based on Weschler and Nazaroff (2012) and data from SPARC online calculator
Mouthed object surface area	$A_{mouthed}$	0.001 m ²	CSPC (2014)
Mouthing frequency, mean value for object	MF_{obj}	4 contacts h ⁻¹	Estimated, based on USEPA (2011)
Exposure frequency mouthing and handling object	EF_{phone}	14 h d ⁻¹	Estimated

Exposure calculations: For frequent contact sources, no concentrations in indoor environmental compartments have to be calculated. Instead, for exposure by (trans) dermal uptake from the source and by mouthing, Eqs. 15, 18, and 27 or 28, respectively, can be used. Migration rates from a source to saliva could not be found for TCEP, therefore Eq. 28 will be used to estimate mouthing exposure in a similar way as for DnBP in the first example. Table 10 summarizes all parameters needed to estimate exposure to TCEP by touching and mouthing a frequent contact source. The exposed individual is again a young child (2 to <3 years) and the parameters used in Example 1 apply, unless stated otherwise.

The modeled concentration in the surface film $C_{s,\text{film}}$ is close to the concentration $C_{s,\text{wipe}}$ reported by Yang et al. (2019), giving overall confidence in the assumptions made in the model. However, as can be seen in Table 10, most values needed for the calculation of the exposure estimates had to be estimated because directly applicable information could not be found. As discussed above, p_s is a highly uncertain parameter in this example, and so is the film thickness δ_{film} , but because $C_{s,\text{film}}$ is supported by direct measurements, at least the order of magnitude of the result can be confirmed. Contact and mouthing frequencies as well as the exposure frequency have been estimated based on review of the EPA *Exposure Factors Handbook*, but may be under- or overestimating, and more observational data would be necessary to reduce uncertainty. The transfer efficiency f_A was assumed to be the same for DnBP and TCEP, which may not be the case, aside from the dependence of this parameter on many other factors. As migration rates of TCEP from an object into saliva were not available, the simplified version of the mouthing exposure model (Eq. 28) has to be used. TCEP is more water soluble than DnBP, but to explore this exposure, a range based on 1% and 100% leached chemical is applied again. These considerations should be kept in mind when evaluating the results (Table 11).

Based on $DI_{\text{surf_d}}$ in combination with $DI_{\text{mouth},1}$ and $DI_{\text{mouth},2}$, the daily intake rate based on contact exposure to this frequent contact source ranges from $0.11 \mu\text{g kg}^{-1} \text{BW d}^{-1}$ to $0.18 \mu\text{g kg}^{-1} \text{BW d}^{-1}$. $DI_{\text{surf_b}} = 0.011 \mu\text{g kg}^{-1} \text{BW d}^{-1}$ provides an additional lower bound. Contact rate (CR), transfer efficiency (f_A), and mouthing frequency (MF) are the most uncertain parameters of the exposure estimate, and variations can lead to a difference of about one order of magnitude. Further evaluation of these important exposure factors is necessary to allow more robust estimates. In addition, more information on migration rates (MR) is urgently needed to assess mouthing exposure more accurately.

Table 11 Estimated exposure and daily intake rates for TCEP for a young child (2 to <3 years), SEC = frequent contact

Parameter	Symbol	Value	Reference
Exposure by dermal contact with source surface	$Ex_{\text{surf_d}}$	$0.11 \mu\text{g h}^{-1}$	Eq. 15
Exposure by transdermal uptake from source surface	$Ex_{\text{surf_b}}$	$0.011 \mu\text{g h}^{-1}$	Eq. 18
Exposure by mouthing of source, based on 1% and 100% leaching of chemical	$Ex_{\text{mouth},1}$ $Ex_{\text{mouth},2}$	$6.3 \times 10^{-4} \mu\text{g h}^{-1}$ $0.063 \mu\text{g h}^{-1}$	Eq. 28
Daily intake rate via dermal contact with source surface	$DI_{\text{surf_d}}$	$0.11 \mu\text{g kg}^{-1} \text{BW d}^{-1}$	Eq. 20
Daily intake rate via transdermal uptake from source surface	$DI_{\text{surf_b}}$	$0.011 \mu\text{g kg}^{-1} \text{BW d}^{-1}$	Eq. 20
Daily intake rate via mouthing of source, based on 1% and 100% leaching of chemical	$DI_{\text{mouth},1}$ $DI_{\text{mouth},2}$	$6.4 \times 10^{-4} \mu\text{g kg}^{-1} \text{BW d}^{-1}$ $0.064 \mu\text{g kg}^{-1} \text{BW d}^{-1}$	Eq. 20

Conclusions

The previous examples were chosen to illustrate the application of the mechanistic framework to rapidly estimate exposure, but also to highlight some of the important considerations and existing gaps that need to be addressed. In addition to the knowledge gaps and sources of uncertainty, it is emphasized that many elements of the current version of the framework do not exist. In particular, the SECs “liquid applied,” “liquid sprayed,” and “high temperature” are missing mechanistically consistent models.

Some other important aspects are not yet included quantitatively in the framework, but should be considered as influencing factors and discussed qualitatively. In particular, these aspects include the influence of indoor chemistry and of occupancy and occupant characteristics on indoor environments and also on the exposure estimates derived using the framework. In general, additional research is necessary to not only improve our understanding of indoor chemistry, but also to include this understanding in the framework in a coherent way. Although these aspects still need to be addressed, the modular structure of the framework should facilitate the inclusion of new and improved knowledge as suitable models become available.

Currently identified compartments include the gas phase, airborne particles, dust, clothing, and surfaces. These compartments are all dynamic over quite different time scales, and this dynamic nature needs to be more completely represented in the framework. We also need to consider other potential SECs, other chemicals, other compartments and other exposure pathways, and whether or not these can all be coherently integrated within the current framework, both mechanistically and computationally. Indoor chemistry has already been mentioned, but we also need to include the effect of occupancy and occupant characteristics, as well as the way in which occupants interact with the various materials, products, and articles over their respective lifetimes in the indoor environment. Finally, in evaluating the generality of the proposed framework, we need to include potential variation of human exposure by location, demographics, and consumer practices.

The current version of the framework has been developed as part of a community, and we anticipate that the development can continue in the form of a community model, an approach which is increasingly being used in a range of knowledge domains (Barker et al. 2012; Byun and Schere 2006; Harri et al. 2009; Hipsey et al. 2019). Also, models organized according to scientific workflows (Jain et al. 2015; Talia 2013) are becoming increasingly popular. For specific decision contexts, including problem-driven and regulatory circumstances, opportunities to leverage extant data, algorithms, and models to analyze and visualize exposures need to be identified. Once the execution order of problem-solving steps to complete exposure analysis is identified, code can be developed as a processing workflow that can link data and computational algorithms published by different organizations. Overall, this would enable us to synthesize curated information and modeling methods to characterize human exposure, potentially fusing mechanistic and data-driven approaches in these scientific workflows. These flexible workflows could be used to analyze information, guide research, and inform decision-makers. Finally, it may be possible

to develop the computational framework as an open-source software platform, but this is not a simple task (see recent article in *Nature*, Nowogrodzki (2019)) and will probably require some form of long-term institutional support.

Cross-References

► Source/Sink Characteristics of SVOCs

Acknowledgments The authors acknowledge the Alfred P. Sloan Foundation (Modeling Consortium for Chemistry of Indoor Environments (MOCCIE) 2, No. G-2019-12306) and the National Toxicology Program (NTP) of the US Department of Health and Human Services for financial support.

References

- Addington CK, Phillips KA, Isaacs KK (2020) Estimation of the emission characteristics of SVOCs from household articles using group contribution methods. *Environ Sci Technol* 54:110–119
- Axley JW (1991) Adsorption modelling for building contaminant dispersal analysis. *Indoor Air* 2: 147–171
- Barker D, Huang X-Y, Liu Z, Auligné T, Zhang X, Rugg S, Ajjaji R, Bourgeois A, Bray J, Chen Y, Demirtas M, Guo Y-R, Henderson T, Huang W, Lin H-C, Michalakes J, Rizvi S, Zhang X (2012) The weather research and forecasting model's community variational/ensemble data assimilation system: WRFDA. *Bull Am Meteorol Soc* 93(6):831–843
- Bennett DH, Furtaw EJ (2004) Fugacity-based indoor residential pesticide fate model. *Environ Sci Technol* 38(7):2142–2152
- Byun D, Schere KL (2006) Review of the governing equations, computational algorithms, and other components of the Models-3 community multiscale air quality (CMAQ) modeling system. *Appl Mech Rev* 59(2):51–77
- census.gov (2020) Highlights of annual 2019 characteristics of new housing. [census.gov](https://www.census.gov)
- Cohen Hubal EA, Nishioka MG, Ivancic WA, Morara M, Egeghy PP (2008) Comparing surface residue transfer efficiencies to hands using polar and nonpolar fluorescent tracers. *Environ Sci Technol* 42(3):934–939
- CPSC (2014) Chronic Hazard advisory panel on phthalates and phthalate alternatives. U.S. Consumer Product Safety Commission, Bethesda
- ECHA (2008) Tris[2-chloro-1-(chloromethyl)ethyl] phosphate (TDCP) risk assessment. European Chemicals Agency
- Eichler CMA, Wu Y, Cao J, Shi S, Little JC (2018) Equilibrium relationship between SVOCs in PVC products and the air in contact with the product. *Environ Sci Technol* 52(5):2918–2925
- Eichler CMA, Cohen Hubal EA, Xu Y, Cao J, Bi C, Weschler CJ, Saltherammer T, Morrison GC, Koivisto AJ, Zhang Y, Mandin C, Wei W, Blondeau P, Poppendieck D, Liu X, Delmaar CJE, Fantke P, Jolliet O, Shin H-M, Diamond ML, Shiraiwa M, Zuend A, Hopke PK, von Goetz N, Kulmala M, Little JC (2021) Assessing human exposure to SVOCs in materials, products and articles: a modular mechanistic framework. *Environ Sci Technol* 55(1):25–43
- Finizio A, Mackay D, Bidleman T, Harner T (1997) Octanol-air partition coefficient as a predictor of partitioning of semi-volatile organic chemicals to aerosols. *Atmos Environ* 31(15):2289–2296
- Harri J, Filali F, Bonnet C (2009) Mobility models for vehicular ad hoc networks: a survey and taxonomy. *IEEE Commun Surv Tutor* 11(4):19–41

- Hipsey MR, Bruce LC, Boon C, Busch B, Carey CC, Hamilton DP, Hanson PC, Read JS, de Sousa E, Weber M, Winslow LA (2019) A General Lake model (GLM 3.0) for linking with high-frequency sensor data from the global Lake ecological observatory network (GLEON). *Geosci Model Dev* 12(1):473–523
- Huang JM, Chen Q, Ribot B, Rivoalen H (2004) Modelling contaminant exposure in a single-family house. *Indoor Built Environ* 13(1):5–19
- Jain A, Ong SP, Chen W, Medasani B, Qu X, Kocher M, Brafman M, Petretto G, Rignanese G-M, Hautier G, Gunter D, Persson KA (2015) FireWorks: a dynamic workflow system designed for high-throughput applications. *Concurr Comput Pract Exp* 27(17):5037–5059
- Jaycock M, Havics AA (2018) Residential inter-zonal ventilation rates for exposure modeling. *J Occup Env Hyg* 15(5):376–388
- Li L, Westgate JN, Hughes L, Zhang X, Givehchi B, Toose L, Armitage JM, Wania F, Egeghy P, Arnot JA (2018) A model for risk-based screening and prioritization of human exposure to chemicals from near-field sources. *Environ Sci Technol* 52(24):14235–14244
- Liagkouridis I, Lazarov B, Giovanoulis G, Cousins IT (2017) Mass transfer of an organophosphate flame retardant between product source and dust in direct contact. *Emerg Contam* 3:115–120
- Liang Y, Xu Y (2014a) Emission of phthalates and phthalate alternatives from vinyl flooring and crib mattress covers: the influence of temperature. *Environ Sci Technol* 48(24):14228–14237
- Liang Y, Xu Y (2014b) Improved method for measuring and characterizing phthalate emissions from building materials and its application to exposure assessment. *Environ Sci Technol* 48(8):4475–4484
- Liang Y, Liu X, Allen MR (2018) Measurements of parameters controlling the emissions of organophosphate flame retardants in indoor environments. *Environ Sci Technol* 52(10):5821–5829
- Liang Y, Bi C, Wang X, Xu Y (2019) A general mechanistic model for predicting the fate and transport of phthalates in indoor environments. *Indoor Air* 29:55–69
- Licina D, Morrison GC, Bekö G, Weschler CJ, Nazaroff WW (2019) Clothing-mediated exposures to chemicals and particles. *Environ Sci Technol* 53(10):5559–5575
- Little JC, Weschler CJ, Nazaroff WW, Liu Z, Cohen Hubal EA (2012) Rapid methods to estimate potential exposure to Semivolatile organic compounds in the indoor environment. *Environ Sci Technol* 46(20):11171–11178
- Liu Z, Ye W, Little JC (2013) Predicting emissions of volatile and semivolatile organic compounds from building materials: a review. *Build Environ* 64:7–25
- Liu X, Allen MR, Roache NF (2016) Characterization of organophosphorus flame retardants' sorption on building materials and consumer products. *Atmos. Environment* 140:333–341
- Manuja A, Ritchie J, Buch K, Wu Y, Eichler CMA, Little JC, Marr LC (2019) Total surface area in indoor environments. *Environ Sci Process Impacts* 21:1384–1392
- Morrison G (2020) SVOC MM framework: clothing mediated transdermal exposure. *Indoor Air* 2020, Seoul, South Korea
- Morrison GC, Li H, Mishra S, Buechlein M (2015) Airborne phthalate partitioning to cotton clothing. *Atmos Environ* 115:149–152
- Morrison G, Andersen HV, Gunnarsen L, Voral D, Uhde E, Kolarik B (2018) Partitioning of PCBs from air to clothing materials in a Danish apartment. *Indoor Air* 28(1):188–197
- Nowogrodzki A (2019) Tips for open-source software support. *Nature* 571:133–134
- Okeme JO, Rodgers TFM, Parnis JM, Diamond ML, Bidleman TF, Jantunen LM (2020) Gas chromatographic estimation of vapor pressures and octanol-air partition coefficients of semi-volatile organic compounds of emerging concern. *J Chem Eng Data* 65(5):2467–2675
- Salthammer T, Goss K-U (2019) Predicting the gas/particle distribution of SVOCs in the indoor environment using poly parameter linear free energy relationships. *Environ Sci Technol* 53: 2491–2499
- Salthammer T, Schripp T (2015) Application of the Junge- and Pankow-equation for estimating indoor gas/particle distribution and exposure to SVOCs. *Atmos Environ* 106:467–476

- Salthammer T, Zhang Y, Mo J, Koch HM, Weschler CJ (2018) Assessing human exposure to organic pollutants in the indoor environment. *Angew Chem Int Ed* 57(38):12228–12263
- Schlosser P, Schripp T, Salthammer T, Bahadir M (2011) Beyond phthalates: gas phase concentrations and modeled gas/particle distribution of modern plasticizers. *Sci Total Environ* 409(19): 4031–4038
- Shi S, Zhao B (2012) Comparison of the predicted concentration of outdoor originated indoor polycyclic aromatic hydrocarbons between a kinetic partition model and a linear instantaneous model for gas–particle partition. *Atmos Environ* 59:93–101
- Talia D (2013) Workflow systems for science: concepts and tools. *ISRN Softw Eng* 2013:404525
- Thatcher TL, Layton DW (1995) Deposition, resuspension, and penetration of particles within a residence. *Atmos. Environment* 29(13):1487–1497
- USEPA (2011) Exposure factors handbook. US Environmental Protection Agency
- USEPA (2017) Exposure factors handbook. US Environmental Protection Agency
- USEPA (2021) CompTox chemicals dashboard. US Environmental Protection Agency
- Vykoukalová M, Vernier M, Vojta S, Melymuk L, Bečanová J, Romanak K, Prokeš R, Okeme JO, Saini A, Diamond ML, Klánová J (2017) Organophosphate esters flame retardants in the indoor environment. *Environ Int* 106:97–104
- Wei W, Ramalho O, Malingre L, Sivanantham S, Little JC, Mandin C (2019) Machine learning and statistical models for predicting indoor air quality. *Indoor Air* 29(5):704–726
- Weschler CJ, Nazaroff WW (2008) Semivolatile organic compounds in indoor environments. *Atmos Environ* 42(40):9018–9040
- Weschler CJ, Nazaroff WW (2010) SVOC partitioning between the gas phase and settled dust indoors. *Atmos Environ* 44(30):3609–3620
- Weschler CJ, Nazaroff WW (2012) SVOC exposure indoors: fresh look at dermal pathways. *Indoor Air* 22(5):356–377
- Weschler CJ, Nazaroff WW (2017) Growth of organic films on indoor surfaces. *Indoor Air* 27(6): 1101–1112
- Weschler CJ, Salthammer T, Fromme H (2008) Partitioning of phthalates among the gas phase, airborne particles and settled dust in indoor environments. *Atmos Environ* 42:1449–1460
- Wormuth M, Scheringer M, Vollenweider M, Hungerbühler K (2006) What are the sources of exposure to eight frequently used phthalic acid esters in Europeans? *Risk Anal* 26(3):803–824
- Wu Y, Eichler CMA, Chen S, Little JC (2016) Simple method to measure the vapor pressure of phthalates and their alternatives. *Environ Sci Technol* 50:10082–10088
- Xu Y, Little JC (2006) Predicting emissions of SVOCs from polymeric materials and their interaction with airborne particles. *Environ Sci Technol* 40(2):456–461
- Xu Y, Cohen Hubal EA, Clausen PA, Little JC (2009) Predicting residential exposure to phthalate plasticizer emitted from vinyl flooring: a mechanistic analysis. *Environ Sci Technol* 43(7):2374–2380
- Xu Y, Liu Z, Park J, Clausen PA, Benning JL, Little JC (2012) Measuring and predicting the emission rate of phthalate plasticizer from vinyl flooring in a specially-designed chamber. *Environ Sci Technol* 46(22):12534–12541
- Yang C, Harris SA, Jantunen LM, Siddique S, Kubwabo C, Tsirlin D, Latifovic L, Fraser B, St-Jean M, De La Campa R, You H, Kulka R, Diamond ML (2019) Are cell phones an indicator of personal exposure to organophosphate flame retardants and plasticizers? *Environ Int* 122: 104–116
- Zhang Y, Xiong J, Mo J, Gong M, Cao J (2016) Understanding and controlling airborne organic compounds in the indoor environment: mass transfer analysis and applications. *Indoor Air* 26(1):39–60

Part VIII

Health Effects and Health Risk Assessment



The Health Effects of Indoor Air Pollution

39

Jonathan Samet, Fernando Holguin, and Meghan Buran

Contents

Introduction	1142
Indoor Exposures	1145
Secondhand Smoke Exposure	1145
Carbon Monoxide	1150
Household Air Pollution	1152
Radon	1157
Volatile and Semi-Volatile Compounds	1161
Bioaerosols	1164
Respiratory Infections	1167
Specific Diseases Associated with Indoor Air Quality	1171
Overview	1171
Multiple Chemical Sensitivity	1172
Sick Building Syndrome	1177
Conclusions	1179
References	1180

Abstract

This chapter brings a global clinical perspective to the health consequences of indoor air pollution. Its sections are provided in an order that is defined by exposures and by specific clinical entities. Indoor air pollution exposures discussed in this chapter include secondhand smoke, carbon monoxide, household air pollution, radon, volatile and semi-volatile compounds, bioaerosols, and respiratory infections. Background information is provided for each along with sources and exposures, risks, and mitigation/management. Specific clinical entities related to these exposures are also presented.

J. Samet (✉) · M. Buran
Colorado School of Public Health, Aurora, CO, USA
e-mail: Jon.Samet@cuanschutz.edu

F. Holguin
University of Colorado School of Medicine, Aurora, CO, USA

Keywords

Exposure · Secondhand smoke · Carbon monoxide · Household air pollution · Radon · Volatile compounds · Semi-volatile compounds · Bioaerosols · Respiratory infections · Sick building syndrome · Multiple chemical sensitivity

Introduction

The health effects of indoor air pollution reflect a broad array of exposures and circumstances that vary by place and that have changed over time, indeed across mankind's history. In higher-income countries, health concerns have varied as housing has changed and building design and maintenance have evolved, and some problems have been recognized and mitigated. In low- and some middle-income countries, indoor combustion of biomass fuels remains a potent source of indoor air pollution. The full health burden caused by indoor air pollution has not been addressed, but estimates from the Global Burden of Disease and the World Health Organization indicate a substantial contribution to morbidity and premature mortality (Table 1). The largest contribution to disease burden from indoor air pollution comes from household air pollution from biomass fuel combustion, reflecting the global and widespread persistence of this source and its potency in causing disease (World Health Organization 2018b).

In addressing the topic of this chapter – the health effects of indoor air pollution – a distinction needs to be made between those diseases that are linked to specific exposures, e.g., hypersensitivity pneumonitis; those multifactorial diseases that reflect the consequences of indoor air pollutants and other exposures; and those syndromic conditions, like multiple chemical sensitivity, that appear to result from a mix of specific and more general exposures. As addressed elsewhere in this volume, researchers using biomarkers have linked various injury processes, including inflammation and carcinogenesis, to indoor air pollution exposure. Plausibility considerations suggest that indoor air pollution could contribute to the causation and exacerbation of multiple acute and chronic diseases.

We spend much of our time indoors and consequently our perception of the quality of the indoor environment is a key contributor to general well-being. Construing health broadly as in the 1948 definition from the World Health

Table 1 Contribution of indoor air pollution sources to DALYs and Deaths, Global, Both Sexes, All Ages, 2019

Source	DALYs per 100,000	Deaths per 100,000
Household air pollution from solid fuels	1182.23	29.91
Residential radon	24.37	1.08
Secondhand smoke	478.22	16.86

Source: Institute for Health Metrics and Evaluation. GBD 2019. <https://vizhub.healthdata.org/gbd-compare/>

Organization – “Health is a state of complete physical, mental and social well-being and not merely the absence of disease” (World Health Organization 1948) – adverse effects on comfort and well-being from indoor air pollution are also relevant to this chapter. For example, the previous widespread contamination of indoor domestic, transportation, and work environments by tobacco smoke was a source of irritation and annoyance for nonsmokers.

This chapter brings a clinical perspective to the health consequences of indoor air pollution. Its sections are provided in an order that is defined by exposures and by specific clinical entities. Clinicians and other practitioners are not only likely to provide care for patients with specific clinical problems, e.g., multiple chemical sensitivity, but also to address questions related to particular exposures, e.g., secondhand smoke (SHS) or formaldehyde. The specific entities and the exposures, along with their interrelationships, are outlined in Table 2, which provides a matrix linking key clinical outcomes with causal exposures.

While there is a wide range of exposures from indoor air pollution, there are several common underlying mechanisms that lead to symptoms, organ damage, and disease. These include inflammation and irritation, allergic sensitization, chemical sensitization, asphyxiation, and carcinogenesis. As a result, the array of adverse health effects is broad. At the milder end, there may be eye and airway irritation, as with involuntary exposure to secondhand smoke (SHS), while at the more severe end, there may be increased risk for lung cancer, as with indoor radon exposure, and for death, as with acute carbon monoxide poisoning.

Given the length of time spent indoors, the burden of disease from indoor air pollution is substantial. Household air pollution from biomass fuel combustion is prevalent in low- and middle-income countries, leading to an estimated four million premature deaths annually (World Health Organization 2018). Secondhand smoke exposure’s burden of premature deaths is 1.2 million while radon is estimated to cause 84,000 deaths annually from lung cancer worldwide (World Health Organization 2021c). These figures emphasize the significance of indoor air pollution as a public health problem, while indoor air pollution also leads to health conditions and diseases needing attention by the health-care system.

This chapter provides broad, but necessarily incomplete, coverage of the health effects of indoor air pollution. Viewed against the status of the evidence at the time of the first edition of *Indoor Air Pollution: A Health Perspective* (Samet and Spengler 1991), there have been advances, but the fundamental health concerns remain. One exposure, secondhand smoke or SHS, persists, but exposures have been greatly diminished through regulation and a major shift in social norms in much of the world (World Health Organization 2021). For radon exposure and lung cancer, the characterization of risk has become more certain and proven approaches for mitigation of indoor radon are available. For biopathogens, such as molds, scientific methods have advanced providing new tools for research and best practices for their control have been strengthened, but the clinical picture is unchanged. Two multisystem syndromes – sick building

Table 2 Matrix of specific clinical entities and exposures related to indoor air pollution

Clinical entities	Exposures					Bioaerosols
	Secondhand smoke	Carbon monoxide	Household air pollution	Radon	Volatile and semi-volatile compounds	
Respiratory infections	X		X			
Multiple chemical sensitivity	X			X		X
Sick building syndrome	X	X		X		X
Hypersensitivity pneumonitis						X
Asthma	X		X		X	
Lung cancer	X		X	X		

syndrome and multiple chemical sensitivity or MCS – emerged across the latter decades of the twentieth century as particularly challenging problems. Sick building syndrome has waned, perhaps reflecting greater attention to building management, while MCS persists and is a focus of ongoing research. Indoor asbestos exposure coming from building materials was of high concern during the last decades of the twentieth century, as asbestos fibers were detected in indoor air from inadequately maintained building materials (Health Effects Institute, Asbestos Research Committee et al. 1991). That concern has largely dropped away as asbestos is no longer used in building construction in the USA and other high-income countries, and in-place materials are maintained or removed under regulation-required protocols (US EPA 2020a). Asbestos-containing cement is still used worldwide, but with declining frequency. Consequently, this chapter does not cover indoor asbestos, a material linked to several cancers and the nonmalignant respiratory disease asbestosis.

As this chapter is written, the pandemic of SARS-CoV-2 and the disease COVID-19 is in its second year, bringing urgent attention to indoor environments as a locus of transmission of viruses and other causes of respiratory infection. Finally, this chapter addresses the global problem of biomass fuel combustion, not included in the first edition.

Indoor Exposures

Secondhand Smoke Exposure

Introduction

Secondhand smoke (SHS), also referred to as environmental tobacco smoke (ETS), is the combination of sidestream smoke produced by a burning cigarette or other combustible tobacco product and the smoke components exhaled by a smoker (US DHHS 1986). Inhalation of SHS is generally termed passive or involuntary smoking. Being derived from the smoke generated by the burning cigarette, SHS contains numerous chemicals, many toxic and cancer-causing. Exposure to SHS is linked to multiple health problems in both children and adults with evidence showing that no level of exposure to SHS can be considered risk free (Centers for Disease Control and Prevention 2021).

Although active cigarette smoking had been established as a major preventable cause of morbidity and mortality in the USA with the publication of the 1964 Surgeon General Report on Smoking and Health (US Department of Health Education and Welfare 1964), SHS exposure was not extensively investigated until the 1970s. By the mid-1980s, the evidence was sufficient to causally associate SHS exposure with lung cancer in never smokers and with adverse effects on children, particularly related to smoking by parents. Since then, the evidence has continued to mount on the adverse effects caused by SHS exposure (Table 3).

Table 3 Increased disease and death associated with secondhand smoke exposure (source)

Disease	Increased risk of disease from SHS exposure	Deaths among nonsmokers per year from disease due to SHS exposure
Heart disease	25–30%	34,000
Stroke	20–30%	8,000
Lung cancer	20–30%	7,300

Source: CDC. 2020. Health Effects of Secondhand Smoke. Atlanta, GA: Centers for Disease Control and Prevention. https://www.cdc.gov/tobacco/data_statistics/fact_sheets/secondhand_smoke/health_effects/index.htm

Box 1 Health effects causally linked to secondhand smoke exposure in children and adults¹¹

Health effects in children	Health effects in adults
Middle ear disease	Cardiovascular disease
Respiratory symptoms, impaired lung function	Coronary heart disease
Lower respiratory illness	Stroke
Sudden infant death syndrome (SIDS)	Lung cancer
	Nasal irritation
	Reproductive effects in women: low birth weight

Source: U.S. DHHS. 2014. *The health consequences of smoking—50 years of progress: A report of the Surgeon General*, U.S. Department of Health and Human Services, Centers for Disease Control and Prevention, National Center for Chronic Disease Prevention and Health Promotion, Office on Smoking and Health, Atlanta, GA

Sources and Exposure

Tobacco smoke is a complex mixture of gases and particulate matter that contains a myriad of chemicals, perhaps 7,000 or more per the US Centers for Disease Control and Prevention (CDC). Tobacco combustion is a source of many volatile organic compounds (VOCs) and other toxins, including carbon monoxide, benzene, formaldehyde, and hydrogen cyanide, among many others (US Food and Drug Administration 2019). Secondhand smoke exposure occurs when a nonsmoker inhales the combination of both smoke from a burning cigarette (sidestream smoke) and the exhaled smoke from an active smoker. Smoke from other tobacco products and devices, including cigars, pipes, and water pipes, also leads to exposure to tobacco smoke. The scope of sources of exposure has been expanded as nonsmokers may also be exposed to the aerosols generated by the new vaping products, also referred to as electronic cigarettes and electronic nicotine delivery systems or ENDS

(US DHHS 2016). The exposure concentrations vary with the number of people smoking, and the characteristics of the indoor environment, including size and ventilation. Historically, when smoking was allowed without restriction, remarkably high concentrations of particles were measured in indoor environments with heavy smoking in progress (US DHHS 1986).

More recently, the concept of “thirdhand smoke” has been added to that of SHS (Jacob 3rd et al. 2017). Thirdhand smoke or THS refers to the SHS components that are deposited and adsorbed onto surfaces, some components revolatilizing and undergoing further transformations, e.g., through interactions with ozone. Non-smokers can be exposed to THS by contact with contaminated surfaces or inhaling components that have returned to the air. For some volatile components and nicotine specifically, exposure to THS may be a critical pathway. For example, nicotine exposures of infants and toddlers may be driven by contact with nicotine-contaminated surfaces, e.g., rugs and other furnishings, and the clothing of smoking parents.

Exposure to SHS can be assessed by measuring airborne nicotine concentration and also the concentration of smaller particles, particularly PM_{2.5} (particulate matter less than 2.5 microns in aerodynamic diameter), in indoor environments without other prominent sources of small particles (US DHHS 2006). Nicotine concentration has the advantage of being specific to tobacco smoke and it can be measured using passive or active sampling methods. Nicotine and its major metabolite, cotinine, are useful biomarkers for the same reason – specificity. Secondhand smoke exposure can be measured for nonsmokers in a variety of ways. While nicotine has a relatively brief half-life of several hours, cotinine has a half-life of 10–20 h in nonsmokers. Cotinine is used as a biomarker for exposure to tobacco smoke, whether from active or passive smoking, as it is only produced when nicotine is metabolized by the body and it stays in the body longer than nicotine (Baselt 2014). Cotinine concentration can be measured in blood serum, saliva, or urine; the concentration gives a useful internal dose estimate.

Environmental monitoring of SHS, characterized by taking air samples in indoor spaces, like bars or concert venues, is another method for exposure assessment. The approach is useful for documenting the presence of SHS and for providing a quantitative indication of the magnitude of exposure. It is also informative as to the impact of policy measures intended to reduce or eliminate SHS exposure. Finally, SHS exposure can be assessed via self-report on surveys. This method is readily used, although there is the potential for inaccuracy to arise. Nonetheless, self-report has been widely used in epidemiological research and studies using self-report have been critical in establishing the harms of SHS.

As assessed with the biomarker cotinine, SHS exposure has decreased in the USA from a high of 87.9% of nonsmokers having measurable levels of cotinine during 1988–1991 to only 25.2% during 2011–2014 (Tsai et al. 2018). This decline can be attributed to a combination of changing norms and policies, e.g., comprehensive smoke-free laws in public housing, affecting most public spaces, all airplanes, and most workplaces. National and local public health campaigns, e.g., CDC’s Tips from Former Smokers and the Truth Initiative, have contributed and smoking rates have

declined in the general population of the USA and other countries, making the source less widespread. However, globally, an estimated one-fifth of men and one-third of women are still regularly exposed to SHS (Drope et al. 2018), while almost half of the world's children are so exposed (World Health Organization 2021). Exposure to SHS is covered in the Framework Convention on Tobacco Control (FCTC), the World Health Organization's (WHO) treaty addressing tobacco.

While SHS exposure has decreased considerably over the last few decades, disparities in exposure remain in the USA and elsewhere. In the USA, groups with disparate, higher exposure to SHS include non-Hispanic Black Americans, children, people living below the poverty line, people who live in multiunit or public housing, and people who work in blue collar, service, or construction industries (Tsai et al. 2018). During 2011–2014, 50% of non-Hispanic Black Americans were exposed to SHS compared to 25.2% of the general population. Non-Hispanic Black children were also exposed at higher levels than their Hispanic and non-Hispanic counterparts (Walton et al. 2020). Overall, children aged 3–11 are disproportionately exposed to SHS in their homes and in vehicles, and those who live with a smoker or in multiunit housing are significantly more likely to be exposed to SHS (Tsai et al. 2018). Globally, the vast majority of tobacco smokers reside in low- and middle-income countries, placing an undue burden of SHS exposure on these countries' citizens (World Health Organization 2021).

Risk

The disease burden from SHS exposure is substantial in the USA and globally. According to the CDC, 2.5 million adult nonsmokers died from diseases caused by SHS exposure in the USA from the time of the 1964 Surgeon General Report until the 50th anniversary report (U.S. DHHS 2014). Globally, SHS exposure contributes to the deaths of 1.2 million nonsmokers per year (World Health Organization 2021). The burden of tobacco-related disease and mortality is highest in middle- and low-income countries where 80% of the world's smokers reside (World Health Organization 2021).

Exposure to SHS is causally associated with numerous adverse health effects in both children and adults. Infants exposed to secondhand smoke have an increased risk of death from sudden infant death syndrome (SIDS) (US DHHS 2006, 2014). Children have increased risk of asthma and asthma exacerbation, middle ear disease, upper respiratory illnesses, and possibly certain cancers (US DHHS 2006, 2014). Adults exposed to SHS have increased risk of heart attack, stroke, cardiovascular disease, COPD, lung cancer, and asthma as well as increased risk of death from these diseases (US DHHS 2006, 2014). Pregnant women also have an increased risk of fetal loss and having babies with fetal growth defects, and congenital malformations, particularly clefts (US DHHS 2006, 2014).

Infant and Childhood Adverse Health Effects Causally Linked to SHS Exposure

Smoking is estimated to be associated with 1,000 infant deaths per year in the USA as newborns exposed to tobacco in utero via maternal smoking are more likely to have a low birth weight, which increases the risk of health complications (US DHHS 2014). In infancy, those exposed to SHS have a significantly higher risk of sudden infant death syndrome (SIDS) (US DHHS 2006, 2010). When compared to infants

who died from other causes, infants who died from SIDS have higher concentrations of nicotine in their lungs (US DHHS 2006, 2010). It is posited that the chemicals in SHS interfere with the brain's ability to regulate breathing, resulting in the cessation of breathing and, ultimately, death. Secondhand smoke exposure in infancy and childhood is associated with additional health problems such as middle ear disease and increased ear infections, lower respiratory infections such as bronchitis and pneumonia, as well as asthma exacerbation (US DHHS 2006, 2010). Evidence also suggests that SHS is a risk factor for developing asthma as a child (US DHHS 2014).

Adult Adverse Health Effects Causally Linked to SHS Exposure

SHS interferes with normal functioning of the cardiovascular system, leading to increased risk of morbidity or death from cardiovascular diseases such as coronary heart disease and stroke. Even brief exposure to SHS can harm the lining of the blood vessels and make blood more viscous. The CDC estimates 2,194,000 premature deaths from coronary heart disease among nonsmokers exposed to SHS between 1964 and 2014 in the USA (US DHHS 2014). Secondhand smoke contributes to atherosclerosis, narrowing of the arteries by plaque, which restricts blood flow to and from the heart. Approximately 34,000 nonsmokers will die each year from SHS exposure-related heart disease and SHS exposure is associated with a 25–30% increased risk of developing heart disease for nonsmokers (US DHHS 2014). Strokes occur when blood supply to the brain is blocked or a blood vessel bursts in the brain (subarchnoid hemorrhage). Approximately 8,000 nonsmokers will die each year from SHS exposure-related stroke and SHS exposure among nonsmokers is associated with a 20–30% increased risk of suffering a stroke (US DHHS 2014).

Inhaling SHS, particularly over a long period, also damages the lining of the lungs. As the lung tissue is exposed over time, DNA in the cells of the epithelial lining of the lung may mutate irreparably, resulting in uncontrolled cell replication and lung cancer. Despite advances in treatment, lung cancer remains among the deadliest forms of cancer for both men and women. An estimated 7,330 nonsmokers will die each year from lung cancer related to SHS and 10–20% of lung cancer cases in the USA are among nonsmokers – approximately 20–40,000 cases per year (Centers for Disease Control and Prevention 2020, 2021a).

Mitigation/Management

Substantial evidence has supported the authoritative conclusion that no level of exposure to SHS is risk free for nonsmokers (US DHHS 2006, 2010; US Department of Health and Human Services, National Institutes of Health et al. 2014). Thus, the policy goal is to achieve public places and workplaces that are completely smoke free, along with encouraging policies for living spaces, e.g., homes, that limit SHS exposure. Greater exchange of outdoor with indoor air, i.e., ventilation, in areas where smoking is taking place does not assure healthy indoor air. In fact, the American Society of Heating, Refrigerating, and Air-Conditioning Engineers (ASHRAE), which provides guidelines for ventilation of indoor spaces, has concluded that healthy indoor air quality cannot be achieved if smoking is taking place (Samet et al. 2005). Neither increasing air exchange nor air cleaning are sufficient.

Prevention of exposures through government-level smoke-free policies is key to reducing SHS exposure. For example, smoking has long been banned in airplanes and is now banned in public housing by the US Department of Housing and Urban Development (US HUD 2017).

Comprehensive smoke-free policies and laws that prohibit smoking in public places protect the lives of both visitors and workers by reducing public smoking. Workers benefit further from a reduction in tobacco-related health problems when working in a smoke-free environment. Despite the benefits of such policies, only half of US states have laws banning smoking; much of the progress has been driven at the local level (American Nonsmokers' Rights Foundation 2021). While much progress has been made since SHS was determined to cause disease and death in nonsmokers, reduction of exposure has stalled at the US level with many states still not having comprehensive smoke-free laws requiring 100% smoke-free workplaces, restaurants, and bars. In order to reduce exposure to SHS and eliminate the remaining disparities in exposure, comprehensive smoke-free laws are essential.

Children are in a particularly vulnerable situation with regard to SHS exposure as they are typically unable to remove themselves from the offending environment. Children are disproportionately exposed to tobacco smoke in both homes and vehicles (Tsai et al. 2018). Voluntary and sufficiently strict smoke-free policies by parents and caregivers in their homes and vehicles would greatly reduce children's SHS exposure.

The WHO FCTC entered into force for ratifying countries in 2003 in response to the globalization of the tobacco epidemic through multinational tobacco companies. The FCTC's goal is to reduce tobacco smoking globally through establishing smoke-free environments, tobacco packaging, labeling, and education, appropriate taxation, curbs on the industry, as well as communications and public awareness programs (World Health Organization 2003). In the most recent WHO FCTC progress report, 165 of the 180 member countries reported implementing a complete or partial ban on tobacco smoking in indoor workplaces, public transport, indoor public places, and other locations (WHO Framework Convention on Tobacco Control 2018).

Smoke-free environments reduce nonsmokers' exposure to the harmful by-products of tobacco smoke. That understanding has changed social norms around smoking in homes as well. There is the possibility of completely eliminating exposure to SHS through smoke-free policies and changes in norms so that all environments become smoke free. The benefit is clear; communities will see a reduction in disease and death from SHS. The effectiveness of such interventions is well documented through measurements of nicotine in public environments and workplaces, declining biomarker levels, and associated changes in disease occurrence, particularly cardiovascular disease (National Research Council 2010).

Carbon Monoxide

Introduction

Carbon monoxide (CO) is a widespread indoor and outdoor pollutant generated by combustion (US EPA 2010a). It is a well-characterized pollutant as to the mechanism

of its health effects and its link to clinical outcomes, including death. Carbon monoxide has one straightforward mechanism of action in causing adverse health effects, binding firmly to hemoglobin, forming carboxyhemoglobin (COHb) (US EPA 2010a). Its affinity for the receptor molecule for oxygen exceeds that for oxygen, so that CO exposure reduces the oxygen-carrying capacity of the blood.

Carbon monoxide is endogenously produced and functions as a signaling molecule. Typically absent indoor or outdoor exposure to CO, about 1% of the body's hemoglobin is in the form of COHb in people who do not smoke tobacco products (US EPA 2010a). The level of COHb is a well-standardized assay that should be available in most clinical facilities.

Sources and Exposures

There are numerous sources of carbon monoxide in indoor environments, all related to combustion without adequate ventilation. For appliances that are vented by code, such as heating systems, hot water heaters, and stoves, failures of venting systems may result in elevated CO levels. Inappropriate use of unvented combustion sources indoors, e.g., charcoal-burning devices, may lead to very high and even lethal concentrations of CO. An additional source is vehicle emissions coming into a home from an attached garage. Cigarette smokers inhale high concentrations of CO in tobacco smoke and typically have an elevated, albeit generally nontoxic level of COHb. In less-developed countries where biomass fuels are used, carbon monoxide is an unavoidable indoor pollutant.

Risks

The most serious risk is asphyxiation coming from acute exposure to high levels of CO, generally unintentionally, but asphyxiation with CO is a still common cause of suicide. The asphyxiation occurs because the level of COHb reaches such high levels that insufficient oxygen is delivered to the brain and heart (O'Malley and O'Malley 2020). Chronic CO poisoning may also occur from ongoing exposure to elevated levels, coming, for example, from insufficiently ventilated gas-burning appliances, sometimes arising from maintenance failures. Common symptoms include lethargy, headache, difficulty concentrating, shortness of breath, and nausea and vomiting (O'Malley and O'Malley 2020). One characteristic feature of CO poisoning is improvement of the symptoms when away from the place of exposure, typically the home.

Clinically, a careful history is the starting point to making the diagnosis of CO poisoning. The nonspecificity of the clinical picture poses a challenge. Suspicion is needed to explore the timing of symptoms in relation to potential indoor exposure. In the case of acute, high-level exposure, one characteristic finding is a reddish hue to the skin and mucous membranes, often referred to as cherry red. The diagnosis is definitively established by measurement of the COHb level (O'Malley and O'Malley 2020).

Mitigation/Management

Prevention is critical for avoiding CO poisoning. Relatively inexpensive and accurate devices that detect CO and signal risky levels are now available and required by

code in homes in many states in the USA. Strategies for prevention include assuring that appliances are properly functioning and vented to the outside. Public education is needed, along with warnings not to use unvented combustion devices indoors, such as charcoal grills. In Houston, Texas, for example, there were multiple deaths ($N = 11$) during a prolonged electric power outage from carbon monoxide poisoning and more than 1400 visits for emergency care (Masson 2021). The exposure occurred as people sought to stay warm and to cook.

Household Air Pollution

Introduction

Globally, household air pollution (HAP) generated by combustion of biomass and other solid fuels are some of the leading causes of disease and premature mortality, particularly in low- and middle-income countries (LMICs). Approximately three billion people cook and heat by burning solid fuels in inefficient, simple stoves or open fires, routinely exposing themselves and household members to the smoke. For example, approximately one-third of Chinese households report cooking with coal (Duan et al. 2014). Each year, four million people die prematurely of illnesses attributable to HAP. People in low- and middle-income countries experience the overwhelming burden of disease and mortality from this exposure. Emissions from the burning of biomass fuels indoors are significant contributors to outdoor air pollution and also to greenhouse gases. Their control is essential to curbing climate change (Ramanathan 2020).

Sources and Exposure

Inefficient stoves and open fires are used for cooking across the world in millions of homes each day as covered in ► Chap. 6, “Appliances for Cooking, Heating, and Other Energy Services.” Pollutant-producing biomass fuels power these stoves and open fires: kerosene, dung, wood, and coal. These fuels and traditional cooking methods produce PM, methane, carbon monoxide, polycyclic aromatic hydrocarbons (PAHs), and volatile organic compounds (VOCs), all health-damaging pollutants.

Cooking stoves: There are many categories of cooking stoves that produce HAP, some more polluting than others: the three-stone fire, early “Improved Cook Stoves,” fuel-controlled stoves, micro-gasifiers, “fan-jet,” and nonbiomass. The three-stone fire is a traditional, cheap stove, requiring only three stones on which a cooking pot can be placed above a fire (Kshirsagar and Kalamkar 2014). While cheap, these stoves are inefficient, losing heat quickly and burning fuel inefficiently, and having no ventilation. Only one pot can be used at a time, increasing the amount of time that fuel sources are being burned, unventilated, within the home. Accidents are also prevalent ranging from burns to eye damage from flying embers.

Through the 1990s, early “Improved Cook Stoves” were developed to address some of the fuel usage and safety issues of the three-stone fire (Kshirsagar and Kalamkar 2014). These stoves were created using clay, ceramic, and buckets to enclose and insulate fuel combustion, decreasing the amount of fuel needed and

providing protection against children falling into open fires. Fuel-controlled stoves, mainly referred to as rocket stoves, are efficient and particularly hot burning (Kshirsagar and Kalamkar 2014). Small-diameter wood is burned in a combustion chamber with an insulated vertical chimney. Rocket stoves can be produced as portable, stationary (with a chimney), or with a forced air feature. They utilize far less fuel than their open flame counterparts and produce substantially less pollutants. Microgasifier cook stoves convert biomass into gas and are currently the cleanest burning option for solid biomass cooking (Roth 2011). These cook stoves convert biomass into gas and vapor, and provide better heat regulation and less fuel. This “gas burner” produces very little soot and other emissions. “Fan-jet” stoves introduce very strong air currents into the fuel source, significantly increasing the efficiency of combustion (Kshirsagar and Kalamkar 2014). However, these often rely on electricity and are expensive to produce; thus, they are not considered economically sustainable. Finally, there are nonbiomass stoves that utilize non-biomass fuel sources like alcohol, refined fossil fuels, biogas, coal, electricity, and solar power (Kshirsagar and Kalamkar 2014).

Fuel types: Wood fuel is the most commonly used biomass fuel (Kshirsagar and Kalamkar 2014). In many areas, wood fuel is plentiful and requires few tools or specialized knowledge to find and use. Wood can also be processed into pellets for use in certain types of cook stoves, particularly gasifier stoves.

Kerosene is a transparent liquid fossil fuel generated from crude oil refinement. While it is little used in developed countries, kerosene is still widely used as a cooking fuel in low- and middle-income countries (World Health Organization 2014). It is used in urban households where fuels need to be purchased rather than collected and utilities are either unreliable or cost-prohibitive.

Agricultural wastes – for example, rice straw, bagasse, and dried grass – and animal waste, or dung, are widely used fuel sources in low-income regions as they are free and widely accessible (Kshirsagar and Kalamkar 2014). It is primarily used in traditional stoves, such as the three-stone stove. Despite its commonplace use, dung is a particularly inefficient fuel source and produces more ash and smoke than its other biomass counterparts.

Coal is utilized most often in regions where cooking and heating are combined and availability is high, such as China and India, and rarely as a stand-alone cooking fuel (Kshirsagar and Kalamkar 2014). In parts of Eastern Europe, coal is still burned for space heating and is a major contributor to outdoor air pollution (Kshirsagar and Kalamkar 2014). Coal used for cooking and heating vary in composition and form: coal briquettes, coal cakes, coal ball, and raw coal.

Pollutants: HAP-producing cooking methods result in release of PM, methane, carbon monoxide, PAHs (including known carcinogens), and VOCs. Of particular concern is the production of PM by these cookstoves and fuels. Particulate matter from biomass fuel burning comprises a complex mixture of particles that can vary in size, shape, and composition. The health risks of PM have been extensively investigated as has the mechanistic basis by which they cause disease. PM exposure has been linked to eye, nose, and throat irritation; exacerbation of coronary and respiratory disease symptoms; cancer risk; and premature death, particularly in

susceptible people with cardiovascular or respiratory diseases (HEI Household Air Pollution Working Group 2018). Indoor PM levels are affected by many factors: outdoor levels, infiltration, ventilation, and filtration systems present in the home, indoor sources, and human activity (US EPA 2020b). Indoor biomass cooking in particular produces high levels of PM in homes that are well beyond guidelines for outdoor air (World Health Organization 2018b).

Risk

Health Effects Related to HAP

Understanding of the health risks of HAP has advanced greatly over the first two decades of the twenty-first century. Diverse adverse health consequences have been causally associated with HAP (Table 4) (Lee et al. 2020). Each year, an estimated four million people die prematurely of illnesses attributable to HAP with low- and middle-income countries experiencing the overwhelming burden of disease and mortality from this exposure (World Health Organization 2018b). While the global burden of cardiorespiratory, pediatric, and maternal diseases associated with HAP has declined in recent decades, it remains high in the world's poorest regions due to the continued need for and use of biomass fuel combustion for cooking. Women and children experience greater exposure as they assume responsibility for food preparation in these regions (World Health Organization 2018b).

Exposure to HAP increases the risk of acute lower respiratory infections in children, still a leading cause of death in young children (World Health Organization 2018a; Lee et al. 2020). HAP exposure increases risk for the development of pneumonia and other acute respiratory infections and accounts for half of all deaths from pneumonia in children under the age of five worldwide (World Health Organization 2018a; Lee et al. 2020). Evidence links HAP to tuberculosis, still a leading cause of death globally (World Health Organization 2018a; Lee et al. 2020). HAP

Table 4 Health effects attributable to household air pollution, 2017

Health effect	DALYs	Deaths
Communicable respiratory diseases (Acute respiratory infections and pulmonary tuberculosis)	27.4 million	–
Chronic respiratory diseases		
Asthma and COPD	18.4 million	–
Lung cancer	5.5 million	–
Cardiovascular diseases (Ischemic heart disease and cerebrovascular heart disease)	9.5 million	0.3 million
Under 5 mortality	–	0.78 million
Total DALYs	60.9 million	
Total deaths	1.8 million	

Source: Lee et al. (2020)

also increases the risk for development and exacerbation of asthma in children (World Health Organization 2018a; Lee et al. 2020). Finally, reflecting patterns of exposure in households, HAP is associated with increased risk of low birth weight and under age 5 mortality (World Health Organization 2018a; Lee et al. 2020).

Given the inhalation pathway of HAP, risk for chronic respiratory diseases is positively associated with HAP exposure (Lee et al. 2020). Chronic obstructive pulmonary disease (COPD) is a chronic inflammatory lung disease that leads to obstruction of airflow from the lungs. Symptoms include breathing difficulty, cough, mucus production, and wheezing. HAP exposure is possibly the most important risk factor for COPD among nonsmokers. Individuals exposed to HAP, which contains well-documented carcinogens, also have an increased risk of developing lung cancer (World Health Organization 2018b). Lung cancer is the leading cause of cancer death worldwide.

HAP is also associated with increased cardiovascular disease risk, likely through inflammatory mechanisms, possibly from the entry of very small particles into the circulation after translocation through the epithelial lining of the lung. HAP exposure is also linked to increased risk of death from cardiovascular disease and stroke (World Health Organization 2018b).

Finally, HAP is associated with the development of cataracts, the leading cause of blindness in adults in developing countries (World Health Organization 2018b). There is strong evidence linking HAP to cataract formation via inflammation and HAP exposure is estimated to be responsible for up to 25% of the global burden of cataract disease (HEI Household Air Pollution Working Group 2018).

Mitigation/Management

In order to reduce exposure to and disease resulting from HAP, lower emission, modern cookstoves, and fuel sources are needed to replace the open fires and inefficient cookstoves that are so widely used. Substantial improvements in health can be achieved through significant exposure reductions, necessitating the near-exclusive use of the lowest emission stoves and fuels. To be successful, solutions need to fit within cultural norms and practices, address affordability, and be implemented with communication about use and benefits of exclusive clean cooking stoves and fuels, particularly for child health.

These solutions reflect a four-decade story of characterizing the problem and seeking testing solutions. The story begins with the first measurements of PM during cooking with biomass fuels. These measurements were made in India by Kirk Smith, a pioneering researcher and tireless advocate for finding effective solutions for HAP (Smith et al. 1983). Moving from these measurements in the early 1980s, Smith championed further research to characterize HAP exposure and began to seek solutions, including carrying out a clinical trial in Guatemala (Smith et al. 2011). Over time, the global public health community and agencies awakened to the need to address HAP through research and interventions. Now, there is a substantial body of evidence from epidemiological and toxicological studies on HAP and from studies of interventions of lower-emitting stoves and fuels. Globally, a variety of clean cookstove initiatives have been in progress and are making a difference in reducing

the burden of HAP. Early on, emphasis was placed on replacing traditional cookstoves with more efficient low-emission devices. That effort is now complemented by substituting less polluting fuels for biomass fuels.

Thus, current efforts to reduce HAP include both less polluting stoves and fuels. Advanced biomass cookstoves can dramatically reduce HAP exposure. However, many households still employ “rocket stoves,” the design of which is relatively simple but not ideal for reducing HAP enough to reduce risk for adverse health outcomes. Cleaner, more efficient cookstoves are in production in many countries but they are not always easy to use, affordable, and long lasting. Clean fuels such as biogas, liquefied petroleum gas (LPG), ethanol, and solar sources have the potential to virtually eliminate cooking and heating emissions; however, these replacements are relatively costly and need to be implemented in a sustainable fashion.

Improved cookstove development has been attempted since the 1940s with increased scientific development in the 1970s and 1980s. Past initiatives include the Chinese National Improved Stove Program (CNISP) and the National Program on Improved Chulas. The CNISP took place from 1982–1992 and introduced 129 million cookstoves to rural Chinese areas (Smith et al. 1993). The National Program on Improved Chulas took place in India between 1985 and 2002 (Venkataraman et al. 2010). While the program resulted in 35 million units installed, stove quality issues, poor adoption rates due to government subsidy-based delivery mechanisms and lack of provisions for maintenance/repair, and little formal monitoring hampered the programs’ outcomes. These are lessons learned reflected in the initiatives that have followed.

Examples of current cleaner fuel distribution initiatives include Project Surya, the multicountry projects of Envirofit International, and the HAPIN trial, a multicountry research study (Project Surya 2009; Envirofit 2021; Household Air Pollution Intervention Network 2021). Project Surya in India focuses on women and addresses the product life cycle, considering the fuel supply chain, affordability, and maintenance access. The initiative is replacing 5,000 stoves each in pilot areas in the Himalayas, the Indo-Gangetic plain, and South India with solar stoves. Envirofit International is utilizing microloans with 6–8 month payback periods to create a lower entry cost to efficient cookstoves while also supporting cookstove technology innovation. Envirofit International currently serves over five million people with local production and distribution of clean cookstoves in East Africa, West Africa, Latin America, and Asia. The HAPIN Trial is a randomized controlled trial of LPG stoves and fuel distribution in 3200 households in four countries: Guatemala, India, Peru, and Rwanda. Personal exposure data as well as a variety of maternal and child health outcomes are being collected as part of this study to better inform the health benefits from switching to clean cookstoves. The trial’s findings should have global policy impact. These projects are reflective of the substantial scope of the global effort to find solutions to HAP.

Looking forward, the Clean Cooking Alliance and the National Biomass Cookstove Initiative are two major improved cookstove distribution initiatives (Clean Cooking Alliance 2021; Government of India and Energy 2021). The Clean Cooking Alliance has a goal of having 100 million homes adopt clean and efficient

cookstoves. Founded by members including the United Nations, the US Agency for International Development (USAID), the World Health Organization, the US Environmental Protection Agency, Shell, Morgan Stanley, and multiple national governments, this initiative aims to address barriers to uptake and to create local economic opportunities. The National Biomass Cookstove Initiative (India) aims to distribute 15 million clean biomass cookstoves over a decade, helping to reach the goal of 87% of Indian households utilizing the new cookstoves. Through this program, the government of India aims to reduce premature deaths from HAP exposure by 17%.

Adoption of clean cookstoves and fuels is not necessarily a one-step process – there are barriers to both their uptake and long-term use. First, there is often low awareness among low-income populations of the harms related to inefficient, high-emission cookstoves and fuels, and of the benefits of switching to the cleaner, low-/no-emission alternatives (Vigolo et al. 2018). Experience shows that successful introduction of these health-harming cookstoves requires consideration of cultural norms and practices. For instance, some culturally significant foods are traditionally made over three-stone fireplaces. A cleaner cookstove or fuel source may alter the resulting dish, changing traditional foods in unacceptable ways. There are also potential cost barriers to clean stoves and fuel (Vigolo et al. 2018). Populations using inefficient, health-damaging cookstoves are relatively poor and consequently purchasing a cleaner stove may be financially impossible. While some countries and organizations have established programs to address this issue, cost remains a barrier to uptake. In addition to initial cost barriers, there are also long-term cost barriers (Vigolo et al. 2018). Traditional biomass fuels are relatively cheap and, in some cases, free if available for gathering. Alternative, low-/no-emission fuels are more expensive, particularly for poor populations. While clean cookstove programs may initially cover these costs, long-term use of these cleaner fuels is dependent on affordability. Thus, in order to successfully transition populations to the cleanest cookstoves and fuels available, awareness of benefits and harms must be raised, cultural norms and practices must be considered and addressed, and both the initial and long-term costs must be managed.

Radon

Introduction

The gas radon is a ubiquitous indoor air pollutant that decays into a series of radioactive solid progeny, two emitting alpha particles that cause cancer-producing mutations in cells of the respiratory epithelium (National Research Council. Committee on Health Risks of Exposure to Radon 1999). Based on studies of radon-exposed underground miners and supporting mechanistic research, radon is a long-established occupational carcinogen, causing lung cancer. Epidemiological studies of multiple cohorts of miners show that risk increases with exposure and varies in a complex fashion with attained age, time since exposure, and smoking. Risk models have been developed for policy purposes that reflect these complexities and that provide risk estimates for establishing standards for occupational exposures and

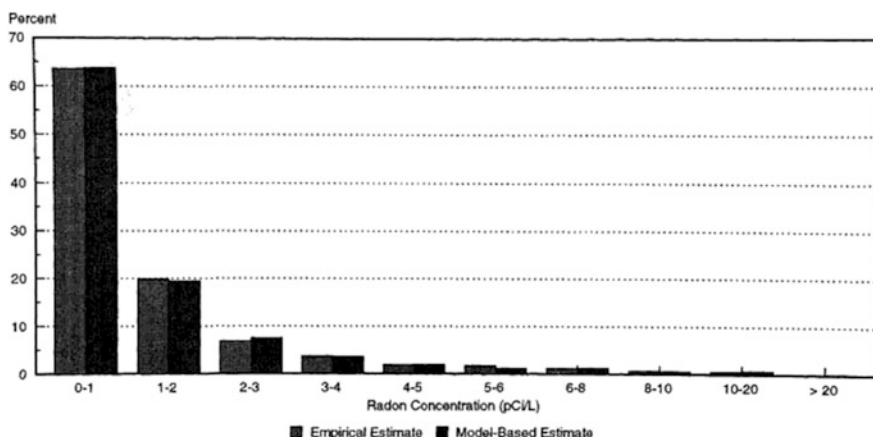
guidelines for exposures in homes and other indoor spaces. The most recent risk model, based on 11 epidemiological studies of underground miners, was developed by the Biological Effects of Ionizing Radiation (BEIR) VI Committee of the US National Research Council (National Research Council. Committee on Health Risks of Exposure to Radon 1999). Although the risk model dates to 1998, it continues to support policy (US EPA 2021c). With regard to the scientific basis for policy formulation, based on dosimetric considerations and mechanistic understanding, the BEIR VI Committee concluded that risk of lung cancer follows a no-threshold linear relationship at typical indoor exposures. This relationship implies that any exposure increases risk for lung cancer and that a no-risk level of radon indoors cannot be achieved. Hence, from the policy perspective, radon guidelines are aimed at achieving an acceptable level of risk.

The potential of radon to contaminate homes was reported as early as the 1950s (National Research Council. Committee on Health Risks of Exposure to Radon 1999). It received relatively little attention outside of Scandinavia, until the 1984 identification of a US home with concentrations equal to those in underground mines where miners had suffered excess lung cancer (Henderson 1989). The emergence of the indoor radon problem sparked epidemiological studies of the risks, mechanistic research, and applied research on mitigation approaches. Programs were launched in many countries to identify homes needing mitigation and guidelines were elaborated for acceptable concentrations. Numerous authoritative reports have now addressed the risks of radon, most recently that from the United Nations Scientific Committee on the Effects of Atomic Radiation (UNSCEAR) (2020).

Sources and Exposure

Radon is a naturally occurring pollutant generated in the decay series of uranium 238. Its immediate precursor is radium, which is present in rocks and sediments at concentrations that vary with geological characteristics. Radon, an inert gas, has a half-life of 3.8 days; thus, once formed, it has sufficient time to move through the soil and enter the atmosphere. Structures, including homes, create a pressure gradient across the soil that draws soil gas inside. Portals of entry include cracks in foundations and openings into basements. While soil gas is the dominant source, radon contamination of indoor environments may also occur in homes with high concentrations of radon in well water used in the home and in the unusual circumstance of radium-containing building materials, e.g., gypsum wallboard.

The radon concentration within a home reflects the microgeological circumstances of the home, the portals by which radon can enter the home, and the air exchange of the indoor of the home with outdoor air. The potential for a home to have a high radon concentration can be anticipated based on local and regional geology and also on prior testing in the area. However, the presence of homes with high concentrations is patchy; neighboring homes may have quite different concentrations. As shown in Fig. 1, the distribution of indoor concentrations in homes is lognormal with a substantial tail of high concentrations in homes (US EPA 1992).

EXHIBIT B-13**National Population Empirical Distribution With
the Lognormal Distribution Modeled Using the Median and
Best Range Estimator to Estimate the Lognormal Parameters**

Note: Actual values are presented in Exhibit B-12.

Fig. 1 National population empirical distribution with the lognormal distribution modeling using the median and best range estimator to estimate the lognormal parameters. (Source: U.S. Environmental Protection Agency 1992)

Risks

Radon and its progeny are a well-established cause of lung cancer. By the 1950s–1960s, the epidemiological evidence was strong and initial understanding of the dosimetry of the alpha particles emitted by radon progeny had been achieved (Harley 1953; Bale 1980). The epidemiological evidence causally links radon to increased lung cancer risk in both never smokers and smokers and documents synergism between the two exposures (National Research Council. Committee on Health Risks of Exposure to Radon 1999). Other health consequences of radon exposure have been investigated in the miner cohorts and in the general population, including cancers other than lung cancer, childhood leukemia, and respiratory and cardiovascular diseases. To date, the evidence is mixed for these other health outcomes (United Nations Scientific Committee on the Effects of Atomic Radiation 2020). In addition to the studies of underground miners, epidemiological studies have been carried out to directly estimate the risk of indoor radon (National Research Council and VI) 1999). Most of the studies are case-control in design, involving comparison of residential radon exposures of cases with those of controls of comparable demographics but without lung cancer. The findings from the studies of miners and these general population studies are convergent.

Analyses of the underground miner data have provided risk models that have been extended to indoor exposures of the general population to radon. The analyses show that risk increases with the cumulative exposure, diminishes with the time since exposure and chronological age, and increases at lower exposure rates. Lifetable methods have been used to estimate the risk of death from lung cancer with different patterns of exposure (National Research Council and Committee on the Biological Effects of Ionizing Radiation 1988).

Management

Strategies for reduction of the lung cancer risk associated with indoor radon exposure are now well worked out, involving measurement of indoor radon levels with devices that have been proven to be accurate, comparison of the measured level to guideline values, and implementation of mitigation if needed (US EPA 2021). These strategies have evolved over the three decades since the widespread nature of the indoor radon problem was noted. In general, indoor radon concentration in homes is not regulated and the guideline values are just that. In some jurisdictions, however, measurement of indoor radon is required at the time of purchase of a home, particularly in locations where there is a potential for high levels of radon in homes.

Fortunately, radon concentrations can be measured relatively cheaply and with sufficient accuracy to determine the need for mitigation (US EPA 2012). Devices are available that measure radon concentration in real time, that can provide concentration over several days, and that can measure radon concentration over longer periods of times, e.g., months. The continuous reading devices would generally not be needed for the indoor setting, except during installation of radon-reduction equipment. The guidelines for indoor concentration are generally based on annual or longer-term average, which is indicative of lung cancer risk. Track-etch detectors provide longer-term average values. However, such longer-term measurements are not compatible with the timing of home sales and are replaced by shorter-term measurements, which can be made with charcoal detectors. The US Environmental Protection Agency protocol for such measurements screens for the potential for higher concentrations, calling for closing the home to reduce ventilation and placing the detector in the lowest potentially habitable area of the home.

If a home or other property is shown to exceed guideline values, there is an array of mitigation approaches, depending on the home's characteristics. These include sealing cracks and other points of entry in basements and ventilating basements or the space beneath foundation concrete slabs. Prevention of higher concentrations of indoor radon is possible through construction approaches, particularly in areas known to have the potential for higher concentrations. Radon-resistant construction techniques have been developed and tested and are now widely used. The US Environmental Protection Agency offers recommendations (US EP 2021).

Volatile and Semi-Volatile Compounds

Introduction

Volatile organic compounds, generally referred to as VOCs, are a diverse group of compounds unified by having a high vapor pressure and hence are present as gases in indoor air. The US EPA offers a general definition of VOCs as follows: “Volatile organic compounds, or VOCs are organic chemical compounds whose composition makes it possible for them to evaporate under normal indoor atmospheric conditions of temperature and pressure” (US EPA 2021f). The sources are myriad in indoor environments (Table 5), first edition (Tucker 2001) and diverse VOCs may be present in indoor air. Because the VOCs are present in a mixture, concerns about health risks relate both to the total mixture and to some individual VOCs, e.g., formaldehyde, that have been specifically investigated. Semi-volatile

Table 5 Examples of hazardous VOCs that have been measured in indoor air, and their potential indoor sources

Compound	Categories of indoor sources with reported emissions data (Not all products in the category contain or emit the compound)
Acetaldehyde ^a	Floor materials, HVAC systems and components, machines, wood products
Benzene ^a	Furnishings, paints and coatings, wood products
Carbon tetrachloride ^a	Pesticides
Chloroform ^a	Furnishings, pesticides
Ethylbenzene	Floor materials, insulation products, machines, paints, and coatings
Formaldehyde ^a	Cabinetry, floor materials, furnishings, HVAC systems and components, indoor air reactions, insulation products, miscellaneous materials, paints and coatings, space heating and cooking equipment, wall and ceiling materials, wood products
Hexane	Floor materials, furnishings, paints and coatings, wood products
Methylene chloride ^a	Furnishings
Naphthalene	Pesticides (moth crystals)
Paradichlorobenzene ^a	Pesticides, floor materials
Styrene	Cabinetry, floor materials, insulation products, machines, miscellaneous materials, paints and coatings, wood products
Tetrachloroethylene ^a	Caulks and sealants, miscellaneous materials
Toluene	Adhesives, caulk and sealants, floor materials, furnishings, machines, paints and coatings, wall and ceiling materials, wood products
Trichloroethylene ^a	Furnishings
Xylenes (<i>o</i> , <i>m</i> , <i>p</i>)	Floor materials, furnishings, machines, paints and coatings, wall and ceiling materials

Sources: Tucker (2001), U.S. Environmental Protection Agency (1999)

^aIncluded in a list of 33 hazardous air pollutants proposed by the U.S. Environmental Protection Agency as urban air toxics, which are thought to pose the greatest health threat to people living in urban areas (US EPA 1999)

organic compounds, sometime abbreviated as SVOCs, may also be of concern with regard to health risks. Some of these compounds are quite well known because of their ubiquity and the concern for a wide range of health effects, e.g., formaldehyde.

There has been substantial work on emissions of VOCs from various materials along with efforts to reduce emissions through changes in manufacturing and composition of materials. Emissions testing of products and the then available data were covered in the first edition of this handbook (Tucker 2001).

The health consequences of exposure to these compounds are both specific to the toxicity of individual compounds and also general, reflecting the consequences of inhaling a mixture of VOCs, typically measured as total VOCs or TVOCs. The range of health effects is very broad, covering acute and chronic outcomes, including cancer and noncancer effects. Some are quite well studied, e.g., formaldehyde and benzene for which epidemiological and toxicological data are available, while for others toxicity is unstudied and potential risks are assessed based on structure and information from other compounds (Agency for Toxic Substances and Disease Registry 1999, 2007). One useful resource on toxicity is the Toxicological Profiles compiled by the Agency for Toxic Substances and Disease Registry (ATSDR) of the Centers for Disease Control and Prevention (2021). Some compounds are covered by the US EPA's Integrated Risk Information System (IRIS) program and have also been considered in specific reports from the US National Research Council, for example, arsenic and trichlorethylene (US EPA 2010b; National Research Council 2006; US EPA 2021e).

Sources and Exposure

Pioneering research from decades ago, the Total Exposure Assessment Methodology (TEAM) study (described in detail in the first edition) identified that indoor exposure to VOCs was ubiquitous and driven by widely used household products, furnishings, and common processes, such as dry-cleaning (Wallace 1987, 2001). At the time, tobacco smoking was a contributor for some VOCs, such as benzene. This study highlighted the importance of activities indoors as a source, e.g., hobbies involving use of solvents or other materials. Summarizing the key findings, concentrations of the various VOCs considered were far higher in indoor air than in comparison outdoor samples, reflecting the dominance of indoor sources for the VOCs; and outdoor sources were relatively minor contributors to personal exposures. Vapor intrusion, the entrainment of contaminated soil gas into homes, can be a prominent source of VOCs for homes built over contaminated ground (US EPA 2020c). Homes affected by vapor intrusion have been described with extremely high indoor levels of contaminants, leading to acute intoxication.

Risks

A lengthy array of adverse health effects has been linked to VOCs generally and to specific VOCs (US EPA 2021g). As summarized by the US Environmental Protection Agency, VOCs are linked to:

- “Eye, nose and throat irritation
- Headaches, loss of coordination and nausea
- Damage to liver, kidney and central nervous system
- Some organics can cause cancer in animals, some are suspected or known to cause cancer in humans.”

For some of the better-studied VOCs, the evidence is quite certain as to the causation of adverse effects, e.g., benzene is a known leukemogen based on epidemiological and toxicological evidence (Agency for Toxic Substances and Disease Registry 2007). Additionally, higher exposures to mixtures of VOCs have been linked to symptoms of irritation and impairment of neurocognitive functioning. Research on the risks to health of this diverse group of compounds has been complicated by their occurrence in mixtures that can be quite variable. For particular compounds, e.g., benzene, much of the evidence on risks comes from studies of exposed workers. Substantial effort has been directed at quantitative characterization of the risks of some of the regulated compounds: formaldehyde, benzene, and tetrachlorethylene (TCE). Further detail on these well-studied compounds follows.

Formaldehyde: With its many uses, formaldehyde is one of the world’s highest production volume chemicals. It is a simple molecule (HCHO) that exists as a gas at room temperature with an irritating and distinctive odor. Formaldehyde is widely used in commercial products, such as fiberboard, paneling, particleboard, various furnishing, and even clothing to make them easy to care for (US EPA 2021b). Formaldehyde is also used in the production of urea formaldehyde foam insulation (UFFI). Improperly cured UFFI led to widespread indoor air pollution with formaldehyde during the 1970s and 1980s and a ban on its use.

The risks of formaldehyde have been examined in toxicological and epidemiological studies, involving diverse populations with occupational exposure in particular. Both cancer and noncancer adverse effects have been identified and exposure to formaldehyde causes acute irritative effects and possibly exacerbates asthma. Because formaldehyde is widely used and regulated, its risks have been examined quantitatively in a number of major risk assessments, including by the EPA IRIS program. Risks for both cancer and noncancer outcomes have been quantified.

Benzene: Benzene is a widely used agent in manufacturing and as a solvent. Indoors, entrainment of gasoline vapor from an attached garage is a common source and it may be emitted by some household products, although use is declining. Homes with smokers tend to have higher concentrations in indoor air than homes where no smokers reside. Studies of workers exposed to benzene provide definitive evidence that affects the cells of the bone marrow and causes acute myelogenous leukemia (AML) (Agency for Toxic Substances and Disease Registry 2007). There is strong mechanistic understanding of the basis for these adverse effects. These findings have led to changes in product formulation intended to reduce benzene exposure.

Trichlorethylene (TCE): Trichlorethylene is another well-known VOC that has been widely used in various household products, including products for cleaning and

furniture care (US EPA 2021e). One of the intriguing findings from the TEAM study was the elevation of TCE levels in homes when dry-cleaned clothing was brought into the home. TCE is a carcinogen and there is concern about noncancer adverse effects (Agency for Toxic Substances and Disease Registry 2019).

Bioaerosols

Introduction

Bioaerosols are ubiquitous in indoor environments throughout the world, whether in high-, middle-, or low-income countries. The sources are myriad and include bacteria and the endotoxins that they produce, fungi and fungal toxins, allergens from insects, e.g., the house dust mite, and domestic animals, including pets and livestock, which may be kept within the living space, and also rodents. There are multiple mechanisms by which these agents can have adverse effects: primarily direct toxicity and immune mechanisms. They may cause specific diseases, e.g., hypersensitivity pneumonitis and exacerbate chronic diseases, particularly asthma. In the parts of the USA subject to high levels of indoor moisture and also to flooding, indoor mold growth is a major problem and one that leads to litigation.

Sources and Exposure

The prevalence of indoor mold has been 5–10% in cold climates and 10–30% in moderate and warm climates. Thus, a substantial proportion of the world's population is exposed to dampness-related exposures (Quansah et al. 2012). Indoor dampness and mold have been associated with increased upper and lower respiratory symptom prevalence and greater morbidity among those with underlying pulmonary diseases (King and Auger 2002; Kennedy and Grimes 2013; Hernberg et al. 2014). Molds can become airborne through single or aggregated spores, as well as mycelial and hyphal fragments and can affect human health through direct toxicity, production of mycotoxins, infection, or allergic sensitization (Holme et al. 2020). Given that exposure to fungi is ubiquitous, it is estimated that at least 10% of the population has allergic antibodies to fungal antigens, yet only a small percentage of those sensitive have clinical manifestations (Hardin et al. 2003). Most species are not pathogenic, yet some species can cause significant disease in immunocompromised patients or in healthy individuals when exposed to large concentrations (Hardin et al. 2003).

Risk

According to the World Health Organization's (WHO) guidelines on indoor pollution, there is sufficient epidemiological evidence to show that indoor exposure to damp or moldy areas, in both houses and public buildings, is associated with increased risk of increased respiratory symptoms, respiratory infections, and with greater risk for developing or exacerbating asthma (World Health Organization 2010). In a cross-sectional study of 46,000 participants from 20 countries in the International Study of Allergy and Asthma in Children (ISAAC), self-

reported dampness and visible mold were associated with increased odds of wheezing (OR 1.7 95%CI. 1.47, 1.99), rhinoconjunctivitis (OR 2.1; 95% CI 1.9, 2.5), and respiratory symptoms, such as cough and phlegm. Similar findings have been reported in other large cohort studies and meta-analyses (Fisk et al. 2007; Antova et al. 2008). In longitudinal and incident case-control studies, mold and dampness have been shown to increase the risk for developing asthma by as much as 50%, although the quantitative relationship of risk with cumulative exposure is uncertain (Quansah et al. 2012). It has been difficult to establish whether specific fungi are responsible for particular respiratory health effects associated with visible mold or dampness, given variations in sampling methodology, exposure misclassification, and confounding exposures (O'Connor et al. 2004). Yet the finding that ergosterol levels (as a measure of fungal biomass and a principal sterol of fungal membrane) and hydrophilic fungi have been associated with asthma and wheezing strengthens the potential for a causal relationship (Matheson et al. 2005; Park et al. 2008).

Several specific sources of bioaerosols are described below, including those generated by dust mites, cockroaches, and animals.

Dust mites: Dust mites are the source of widespread exposure to antigens that are excreted in their feces. There are multiple species with the most common in homes being those of the genus *Dermatophagoides*. The critical antigen from this species is Der p 1, which can be measured in house dust samples. Exposure to Der p 1 has been linked to respiratory allergic symptoms and particularly to asthma. Its presence in furnishings and beddings is driven by moisture so that dust mite allergy is particularly prominent in damp climates. Identifying that house dust mite antigens may be contributing to allergic symptoms and asthma in children, or less frequently in adults, requires awareness of the problem and potentially analysis of dust samples for Der p 1. Sensitization can be assessed with skin testing and measurement of antibody levels.

Proven strategies are available to control house dust mite growth and limit exposure (Wilson and Platts-Mills 2018). These strategies include: (1) careful selection of the materials used for pillow covers and mattresses so as to not provide a breeding ground; (2) humidity control to maintain humidity as low as possible, particularly in high-humidity circumstances; (3) room air cleaners, which have a limited role; (4) carpets, which should be limited in coverage and readily cleaned; and (5) vacuum cleaners, particularly if equipped with a HEPA filter. In clinical trials, interventions have been shown to reduce levels of Der p 1 antigen and to improve health outcomes.

Cockroaches: The presence of cockroaches and sensitization to proteins derived from them is well recognized and is problematic in inner-city housing, particularly if poorly maintained (Sheehan et al. 2010). The German cockroach, *Blattella Germanica*, is best studied. It produces multiple allergens that may contribute to allergy and to causation and exacerbation of asthma (Sohn and Kim 2012). These antigens can be detected in house dust samples. Cockroaches are important contributors to the problem termed “inner city asthma” (see below). Mitigation lies with identification of the problem and control of the infestation.

Pets and rodents: Household pets, particularly cats, can be a potent source of indoor allergen exposure. Cats shed the antigen Fel d 1, which is highly persistent in indoor environments. Dogs, while less allergenic, also shed sensitizing antigens. The relationship of pet dander with the development of sensitization, asthma, and allergic rhinitis is complex, and may ultimately depend on other factors such as atopy and other determinants of individual susceptibility, and the timing of exposure (Svanes et al. 2003). Finally, environments with infestation with rats and mice or where rats, mice, guinea pigs, and other small mammals are kept as pets may also be contaminated with allergens.

Asthma. Asthma, one of the most common diseases in children and adults, is characterized by chronic airway inflammation resulting in variable airway obstruction, which can be exacerbated by many triggers, including bioaerosols (National Asthma Education and Prevention Program Coordinating Committee Expert Panel Working Group 2020). This association with bioaerosols may explain why the severity is worse and the prevalence of this disease more common in urban and inner-city neighborhoods with poor housing conditions in which the exposure burden to indoor air pollutants is often substantial.

Indoor pollutants have been known to play an important role with the developing and worsening of asthma and other allergic diseases in urban or inner-city environments (Gergen and Togias 2015). These large urban areas often have a higher and more severe asthma prevalence and children living in such locations are more likely to be from minority and socioeconomically disadvantaged populations (Busse and Mitchell 2007). In the USA, inner-city African American and Hispanic children have nearly double the rates of allergic indoor sensitization compared with non-Hispanic Whites (Stevenson et al. 2001). The National Cooperative Inner-City Asthma Study (NCICAS), which is a network of investigators in multiple cities, found among 1528 children with asthma the following frequencies of skin reactivity: 36.8% for cockroach, 34.9% for house dust mite allergen, and 22.7% for cat dander (Kattan et al. 1997). The NCICAS showed that cockroach allergy, but not dust mite or cat allergies, is associated with increased hospitalizations, wheezing, and unscheduled medical visits. In a subsequent study, the National Cooperative Inner-City Study showed in a randomized study that educating caregivers on asthma management and environmental mitigation leads to substantial long-lasting reductions in morbidity (Evans 3rd et al. 1999). Pharmacological interventions can also be useful in reducing the disease burden associated with indoor allergens. Omalizumab, a monoclonal anti-IgE antibody substantially reduces asthma exacerbations and severity in inner-city asthmatic children. In subgroup analyses of NICAS participants who were sensitized and exposed to cockroach allergen, omalizumab reduced the rate of asthma exacerbations and inhaled corticosteroid dosage while increasing the number of asthma control days (Busse et al. 2011).

Mitigation/Management

Prevention through humidity control is critical for molds as is immediate attention to water leaks and floods. Pets are a known source of allergens and endotoxins and guidance should be offered as to their potential risks, particularly for people with

asthma and allergies. Home remediation interventions to eliminate dampness sources and visible mold improve asthma and upper airway allergy symptoms (Kercsmar et al. 2006; Burr et al. 2007). As such, the WHO's Indoor Air Pollution guidelines recommend that remediation should be given priority to prevent an additional contribution to poor health in populations who are already living with an increased burden (World Health Organization 2009). Both the WHO and the CDC acknowledge that the relations between dampness, microbial exposure, and health effects cannot be quantified precisely, and therefore argue against measuring molds in the environment, as no specific thresholds can be recommended for acceptable levels of contamination with microorganisms and standards for judging what is an acceptable, tolerable, or normal quantity of mold have not been established. Instead, both agencies recommend reducing exposure by focusing on removing contaminated structures and working to prevent subsequent mold growth.

Addressing health problems related to bioaerosols can be challenging. A health issue may be the triggering event for a search for its cause, possibly leading to the finding of mold and mildew, or there may be a clear indication that a home or other indoor environment has been affected by moisture. Problems that cannot be immediately diagnosed or that are refractory should be brought to the attention of an experienced indoor air quality specialist. See, for example, the several books by Jeffrey and Connie May (May and May 2008, 2020).

Respiratory Infections

Introduction

Indoor environments are a critical locus for transmission of respiratory infections. People mix indoors, inhale air that may be contaminated with infectious microbes, and touch surfaces (fomites) that may harbor viable organisms. Indoor transmission of airborne infection and its control have a long history that dates back nearly a century to the pioneering work of William Wells who proposed the theory of droplet transmission and explored related mechanisms for controlling transmission. From the pioneering work of Wells in the 1930s (Wells 1934) until the present, there was surprisingly little research on airborne transmission of respiratory pathogens until the twenty-first century when attention was given to influenza and SARS (severe acute respiratory syndrome), and more recently to SARS-CoV-2, the cause of COVID-19.

This section provides brief coverage of some of the major respiratory pathogens that are transmitted indoors and in association with the building environment. The material provides an overview of clinical and epidemiological features of these infections (Table 6); textbooks are available that provide full coverage (Nelson and Williams 2014).

There are several unifying concepts concerning airborne infectious agents. These relate to how agents are transmitted and their infectiousness as well as control strategies. For respiratory infections, there are four potential modes of transmission with two involving inhalation directly (Tang et al. 2021). Exhaled air from people

Table 6 Overview of clinical and epidemiological features of respiratory infections

Respiratory infection	Causes	Risk factors	Clinical characteristics	Prevention	Cases per year, the USA
Legionnaire's disease ^a	Bacteria of the Legionella type	Older age, smoking history, chronic lung disease, poor immune system	Cough, shortness of breath, fever, muscle pains, headaches	Good maintenance of water systems	10,000
Tuberculosis ^b	Mycobacterium tuberculosis	Smoking; HIV/AIDS	Chronic cough, fever, cough with bloody mucus, weight loss	Screening of those at high risk, vaccination	<200,000
Influenza ^c	Influenza A virus Influenza B virus Influenza C virus	Young children, older adults, pregnant women, people with chronic disease or weak immune systems	Fever, chills, muscle aches, cough, congestion, runny nose, headaches, fatigue	Handwashing, vaccination	>3 million
SARS ^d	SARS-associated coronavirus	Those in close contact with infected persons	Fever, dry cough, headaches, muscle aches, difficulty breathing	Handwashing, cough etiquette, avoiding close contact with those infected, avoid travel to affected areas	<1000*
SARS-CoV-2 ^e	SARS-associated coronavirus-2	Older adults, people with severe chronic underlying medical conditions	Fever or chills, cough, shortness of breath, difficulty breathing, fatigue, muscle or body aches, headache, new loss of taste or smell, sore throat, congestion or runny nose, nausea or vomiting, diarrhea	Handwashing, cough etiquette, masks, avoiding close contact with those infected, avoid travel to affected areas	Pandemic ongoing: >34 million cases

^aCDC. Legionella (Legionnaire's Disease and Pontiac Fever): Fast Facts. Centers for Disease Control and Prevention. March 5, 2021 (<https://www.cdc.gov/legionella/fastfacts.html>)

^bCDC. Tuberculosis. Centers for Disease Control and Prevention. December 31, 2018 (<https://www.cdc.gov/tb/default.htm>)

^cCDC. Influenza (flu). Centers for Disease Control and Prevention. July 30, 2021 (<https://www.cdc.gov/flu/index.htm>)

^dCDC. SARS Basics Fact Sheet. Centers for Disease Control and Prevention. December 6, 2017 (<https://www.cdc.gov/sars/about/fs-sars.html>)

^eCDC. COVID-19. Centers for Disease Control and Prevention. July 29, 2021 (<https://www.cdc.gov/coronavirus/2019-nCoV/index.html>)

with an active respiratory infection contains infectious particles in the form of larger particles (droplets) and smaller particles (aerosols) (Wang et al. 2021). The larger particles are typically generated by coughing and sneezing, sometimes referred to as “spray” transmission. The smaller particles are produced during exhalation and their numbers are increased by talking louder, singing, playing musical instruments, and other activities that increase the force of exhalation. Droplets and aerosols can contaminate the surfaces where they deposit, leading to fomite transmission. Transmission may be direct from person to person, e.g., by touching.

The characteristics of indoor environments have direct relevance to transmission of infection, particularly by the indoor aerosol, referring to particles less than 100 microns in aerodynamic diameter. Particularly at the smaller end of the size range of aerosols, the particles will remain airborne for hours and move widely across spaces. Thus, for aerosols, building ventilation is a determinant of concentration and air cleaning may also be a factor if designed to remove smaller airborne particles in the size range of aerosols.

Several other concepts extend to transmission of respiratory pathogens. In particular, the transmissibility of the infectiousness of the agent is a critical determinant of the course of an epidemic or outbreak (Van Sechteren and Hochberg 2017). The transmissibility is generally measured by the R_0 , which refers to the number of people becoming infected by contact with an infected individual at the start of an epidemic when all are susceptible. An epidemic propagates when the value of R_0 is greater than one such that the infection can spread and grow.

Risks

Discussions of several major, specific respiratory pathogens that are transmitted indoors follow.

Tuberculosis: At the start of the twentieth century, tuberculosis was the leading cause of death in the USA. Now, there are less than 10,000 new cases in the USA, but tuberculosis remains a leading cause of disease burden worldwide with an estimated 10,000,000 cases in 2019 (World Health Organization 2020a). Through the 1950s, the mode of transmission of tuberculosis was uncertain – fomites or airborne. Many campaigns to control tuberculosis had been based around the premise that transmission was by fomites, leading to campaigns to limit spitting, for example.

Riley and colleagues provided experimental proof of airborne transmission (Riley et al. 1962). They ducted the air from the tuberculosis ward at a Baltimore hotel through remotely placed cages holding guinea pigs. The animals developed tuberculosis. Analogous human exposure scenarios reaffirmed the findings. Airborne outbreaks have been reported on airplanes, in homeless shelters, and other indoor locations. Today’s measures to control tuberculosis build on the foundational work of Riley: isolation of the air from rooms containing people with infectious tuberculosis.

Legionnaires’ disease: Legionnaires’ disease was identified as the cause of a dramatic 1976 epidemic of severe and even fatal pneumonia among attendees at a Legionnaire’s convention in Philadelphia (Fraser et al. 1977). The outbreak was linked to a previously unknown genus of bacteria – the *Legionella*, which live in soil and

water. Infection occurs when water contaminated with *Legionella* is aerosolized. Documented outbreaks come from contaminated water systems and aerosolization by showers or other devices and from cooling towers, as with the index outbreak (World Health Organization 2007). Contaminated water within cooling towers may spread through the heating, ventilating, and air-conditioning system and also from spray released by the cooling tower. Cases have been reported among passersby near buildings with contaminated systems and contaminated aerosol may travel some distances and lead to infection. The problem of contaminated cooling towers with *Legionella* is well known and has led to the development of protocols for combatting contamination.

From the clinical perspective, Legionnaire's disease presents as a severe, acute respiratory infection, often with pneumonia. It can be fatal with a case fatality rate of 10% (25% for health care associated) (Centers for Disease Control and Prevention, National Center for Immunization and Respiratory Diseases et al. 2021b). Its diagnosis depends on the clinical picture and taking a history that may reveal potential locations for exposure to the responsible agent, e.g., a hotel stay, or the occurrence of other, similar cases.

SARS-CoV-2: As this chapter is written, the world is in its second year of a global pandemic with a coronavirus, SARS-CoV-2, which causes the disease COVID-19. To date (May, 2020), there have been an estimated 161,381,569 cases and 3,348,952 deaths globally (Center for Systems Science and Engineering [CSSE] at Johns Hopkins University 2021). The course of the pandemic is unknown for the short term and long term. Effective vaccines have been developed and are being delivered, but variants have been isolated worldwide, some having higher transmissibility and/or greater virulence than previously circulating strains.

The pandemic led to a notable acceleration in research on airborne transmission of respiratory infections and particularly of SARS-CoV-2. When SARS-CoV-2 emerged, severe acute respiratory syndrome (SARS) was known to be caused by the SARS-CoV-1 virus. Airborne transmission of that virus was well established, having been documented in airplanes, apartment blocks, and a hotel. Initially, transmission of SARS-CoV-2 was assumed to be transmitted by fomites and also via the airborne route (World Health Organization 2020b). However, there was uncertainty as to the mode of airborne transmission and the relative importance of larger droplets and smaller aerosols in transmission. The relative contributions of these different routes of transmission – fomites, larger droplets that travel only a few feet, and smaller aerosols that can remain suspended in indoor spaces, travel widely, and remain suspended for hours – are directly relevant to control strategies.

The shock of this pandemic exposed the many gaps in understanding of the transmission of respiratory viruses. Perhaps because of the implications for pandemic control, debate over the droplet vs aerosol transmission was strident. However, a consensus has been reached that gives emphasis to the critical role of aerosols.

Management

Prior to the COVID-19 pandemic, the role of the building environment in transmission of airborne pathogens was recognized but prevention of infection spread

indoors was not considered a primary design goal. Standard 61.1 of the American Society of Heating, Refrigerating, and Air Conditioning Engineers (ASHRAE) “...outlines minimum ventilation rates and other measures intended to provide IAQ that is acceptable to human occupants and that minimize adverse health effects” (ASHRAE 2019a, b). ASHRAE has commented on ventilation and air cleaning in limiting transmission of airborne infection in position papers (ASHRAE 2014, 2020). A 2020 document addresses infectious aerosols, acknowledging that infectious transmission by aerosols occurs through pathways involving the heating, ventilating, and air conditioning (HVAC) system (ASHRAE 2020). The document calls for attention to infection spread in the design and lists the following specific strategies for operations of HVAC systems, along with the strength of evidence:

- Enhanced filtration (higher minimum efficiency reporting value [MERV] filters over code minimums in occupant-dense and/or higher-risk spaces) (Evidence Level A – strongly recommend)
- Upper-room UVGI (with possible in-room fans) as a supplement to supply airflow (Evidence Level A)
- Local exhaust ventilation for source control (Evidence Level A)
- Personalized ventilation systems for certain high-risk tasks (Evidence Level B – recommend)
- Portable, free-standing high-efficiency particulate air (HEPA) filters (Evidence Level B)
- Temperature and humidity control (Evidence Level B)

During the course of the COVID-19 pandemic, the potential for transmission in poorly ventilated locations, particularly if crowded, has been recognized. The WHO has released an algorithm for assessing and improving ventilation (World Health Organization 2021). Responding to the pandemic, recommendations have also been made to incorporate infection-control measures into the design of buildings, a proposed paradigm shift that could come into play for users of this volume (Morawska et al. 2021).

Specific Diseases Associated with Indoor Air Quality

Overview

Given time-activity patterns, indoor environments are the predominant locus for inhaling diverse injurious pollutants. This topic is covered in depth in ► Chap. 37, “Time-Activity Patterns.” Additionally, outdoor air pollutants variably contribute to contamination of indoor environments. These exposures contribute to the exacerbation and causation of common diseases: asthma, chronic obstructive pulmonary disease (COPD), lung cancer, and cardiovascular disease. For lung cancer, for example, both radon and SHS are well-characterized causes (Table 2). Exposure to indoor air pollution may also reduce general well-being through irritation of mucous

membranes and other pathways. In addition to these contributions to the burden of morbidity and mortality from noncommunicable diseases, indoor air pollution is also linked to two specific clinical entities: multiple chemical sensitivity and sick building syndrome, both addressed subsequently. Antigens with indoor sources, e.g., from birds, cause the relatively uncommon disease of hypersensitivity pneumonitis.

With regard to noncommunicable diseases, exacerbation of asthma by indoor exposures is well described and consideration of indoor air pollution should be part of the clinical assessment, particularly for patients with more severe asthma. An extensive literature links SHS with exacerbation of asthma, particularly in children. Other irritants should also be queried clinically, including potential exposure to formaldehyde or other volatile organic compounds. Bioaerosols, covered elsewhere in this chapter, are also contributors to the burden of morbidity from asthma. For other noncommunicable diseases, radon is considered to be the second leading cause of lung cancer in the USA, following tobacco smoking, and indoor air pollution exacerbates COPD, in addition to asthma. Household air pollution is causally associated with COPD, particularly at the high exposure levels experienced in low-income countries.

The following sections address multiple chemical sensitivity, sick building syndrome, and hypersensitivity pneumonitis, all challenging problems for clinicians.

Multiple Chemical Sensitivity

Introduction

The syndrome of multiple chemical sensitivity, also referred to as MCS, has a long and controversial history. The underlying hypothesized mechanism dates to the 1950s and the allergist Theron Randolph ([1954](#), [1962](#)). He proposed that sensitization by one or more chemicals could lead to a more general sensitivity to additional chemicals, even at levels of exposure lower than those at which direct effects would not be anticipated. Since then, the concept of the MCS syndrome has been variably viewed from being considered as a valid clinical syndrome stemming from chemical-driven responses to a largely psychologically based phenomenon.

The first edition of the handbook described the history and manifestations of MCS in detail, and deeper background can be found in the second edition of *Chemical Exposures: Low Levels and High Stakes* by Ashford and Miller ([1998](#)). Randolph advanced the concept of *chemical susceptibility* in the 1950s, based on observation of a woman who sold cosmetics and seemed to have general responses to chemicals from products ([1954](#)). The subsequent history of the problem most often referred to as multiple chemical sensitivity is one of controversy with conflicting views of the underlying mechanisms and the “legitimacy” of MCS as a disease. Regardless of this controversy, patients do present with challenging clinical pictures that reflect sometimes debilitating symptoms in response to one or more chemicals, often with a generalization of symptom responses to a broader range of agents in a nonspecific fashion.

Various definitions have been offered; perhaps the most widely cited is that proposed by Cullen in 1987: “Multiple chemical sensitivity (MCS) is an acquired disorder characterized by recurrent symptoms, referable to multiple organ systems, occurring in response to demonstrable exposure to many chemically unrelated compounds at doses far below those established in the general population to cause harmful effects. No single widely accepted physiological function can be shown to correlate with these symptoms” (Cullen 1987). The definition speaks to the non-specificity of MCS and, there is still no single diagnostic test for the syndrome. Rather, the diagnosis rests on a skilled clinical evaluation and exclusion of alternative diagnoses before the diagnosis of MCS should be made.

A further broad and historical perspective is provided by the proceedings of workshop convened in 1988 by the National Research Council (National Research 1992). That workshop brought together a diverse group of participants, some with divergent views of MCS. It includes proposals for research that were not implemented in a comprehensive way and it provides individually authored chapters that set out the understanding at the time. Since then, there have been a substantial number of publications, although research funding has been limited. A 2018 systematic review, covering the period 1998–2015, identified 73 articles that met search criteria (Rossi and Pitidis 2018). Definitive conclusions were not reached and the authors called for more research.

Etiology

The name – multiple chemical sensitivity – speaks to the construct of etiology. Through one or more underlying mechanisms, exposure to one or more chemicals leads to sustained sensitivity to additional chemicals, triggering diverse symptoms that appear to reflect responses from different organs. Hence, viewed in this framework, the etiological agents are chemicals, although a single triggering mechanism has not been identified. Research has explored a variety of mechanisms but research has yet to point to a single mechanistic process that could underlie the broad manifestations of MCS. Miller, who has focused on MCS, proposed “toxicant induced loss of tolerance” (TILT) as an underlying and unifying mechanism. In this hypothesis, an initial high-level exposure or multiple lower-level exposures cause a loss of tolerance that leads to subsequent triggering by other agents at low levels. This hypothesis matches the clinical phenotype but leaves underlying mechanisms unspecified.

A range of research methods has been used to explore etiology: biomarkers of inflammation and imaging in particular. Etiological mechanisms remain unclear, however, beyond the broad mechanisms described previously, e.g., TILT, and there may be heterogeneity in the determinants of MCS that has yet to be identified.

Clinical and Epidemiological Picture

The clinical picture is well captured by Cullen’s definition: a broad array of manifestations and a history of triggering by chemical exposures, sometimes linked to a clear triggering event. In practice, the lack of specificity complicates, making a firm diagnosis and epidemiological investigation. In addition, while MCS is well known

among physicians who address environmental illness, it is obscure to many primary care physicians who are likely to be the first to see patients with MCS.

To facilitate research and care, two instruments have been developed for capturing the picture of MCS: the Environmental Exposure and Sensitivity Intolerance (EESI) instrument and the short version, the Quick Environmental Exposure and Sensitivity Intolerance (QEESI) instrument (Miller and Prihoda 1999a, b). Other instruments have been developed as well, but the most abundant data are based on the EESI and its variants.

The EESI is a standardized approach for identifying individuals with chemical sensitivities. A shorter version of the EESI, the Quick Environmental Exposure and Sensitivity Inventory (QEESI), is the most commonly used form of the inventory. Four scales are used in both the EESI and QEESI instruments: Symptom Severity, Chemical (Inhalant) Intolerance, Other Intolerance, and Life Impact, which measure features consistent with MCS. A fifth scale, the Masking Index, measures regular, ongoing exposures. The Symptom Severity, Chemical Intolerance, Other Intolerance, and Life Impact scales each have ten items rated from 0–10, while the Masking Index consists of 10 items answered “Yes” or “No.” The ten items in each scale are intended to cover a wide range of measures reflective of the causes, manifestations, and consequences of MCS.

A third inventory, the Brief Environmental Exposure and Sensitivity Inventory (BREESI), has been developed as a short, three-question, screener for chemical intolerance (Palmer et al. 2020). The BREESI compresses the Chemical Exposure and Other Intolerances scales into three, “Yes” or “No” questions. The Chemical Exposure scale is condensed into one question to assess the exposure to any of the chemical categories. The Other Intolerances scale is condensed into two questions, one related to food intolerances and one related to drug intolerances. Given the length of both the EESI and QEESI, the BREESI provides a simple way to determine if further investigation of an individual’s symptoms as MCS is warranted.

Surveys have been carried out in the USA and elsewhere to establish the prevalence of MCS. These surveys have used a variety of instruments, including the QEESI. Early surveys employed questions developed by the California Department of Health Services. Across the surveys, the reported prevalence figures for symptoms related to chemical exposures are around 10% with several percent reporting physician-diagnosed MCS.

The most recent survey in the USA was carried out in 2016 using a national sample of over 1,100 participants (Steinemann 2018). The instrument used covered a range of typical MCS symptoms and exposures linked to triggering. The results estimated the prevalence of medically diagnosed MCS as 12.8% among adults, self-reported chemical sensitivity as 25.9%, and either or both as 27.5%. The range of symptoms reported from exposure to fragranced consumer products is broad (Table 7) (Steinemann 2018). The multisystem nature of MCS is illustrated by the range of problems reported (Table 8). While the results of such surveys are subject to various types of bias, the prevalence rates indicate that substantial numbers of people experience chemical insensitivity.

Table 7 Health problems (frequency and type) reported from exposure to fragranced consumer products

	Gen Pop	MCS Diag	ChemSens	MCS/ ChemSens
Total (<i>N</i>) (% relative to general population)	1,137	145	294	313
	100.0%	12.8%	25.9%	27.5%
	<i>N</i> % of Column Total			
Total fragrance sensitive (<i>N</i>) (reporting one or more health problems) (% relative to Subpopulation)	394	125	238	247
	34.7%	86.2%	81.0%	78.9%
Type of health problem				
* <i>Migraine headaches</i>	179	68	124	128
	15.7%	46.9%	42.2%	40.9%
* <i>Asthma attacks</i>	91	46	75	75
	8.0%	31.7%	25.5%	24.0%
* <i>Neurological problems</i> (eg, dizziness, seizures, head pain, fainting, loss of coordination)	82	38	62	63
	7.2%	26.2%	21.1%	20.1%
* <i>Respiratory problems</i> (eg, difficulty breathing, coughing, shortness of breath)	211	73	147	148
	18.6%	50.3%	50.0%	47.3%
* <i>Skin problems</i> (eg, rashes, hives, red skin, tingling skin, dermatitis)	121	55	84	88
	10.6%	37.9%	28.6%	28.1%
* <i>Cognitive problems</i> (eg, difficulties thinking, concentrating, or remembering)	66	35	56	57
	5.8%	24.1%	19.0%	18.2%
* <i>Mucosal symptoms</i> (eg, watery or red eyes, nasal congestion, sneezing)	184	68	120	124
	16.2%	46.9%	40.8%	39.6%
* <i>Immune, system problems</i> (eg, swollen lymph glands, fever, fatigue)	45	31	39	39
	4.0%	21.4%	13.3%	12.5%
* <i>Gastrointestinal problems</i> (eg, nausea, bloating, cramping, diarrhea)	63	32	53	53
	5.5%	22.1%	18.0%	16.9%
* <i>Cardiovascular problems</i> (eg, fast or irregular heartbeat, jitteriness, chest discomfort)	50	28	37	38
	4.4%	19.3%	12.6%	12.1%
* <i>Musculoskeletal problems</i> (eg, muscle or joint pain, cramps, weakness)	43	28	35	36
	3.8%	19.3%	11.9%	11.5%
* <i>Other</i>	19	2	6	6
	1.7%	1.4%	2.0%	1.9%

Source: Steinemann (2018)

Management

Management of people with MCS poses complexities, given the nonspecificity of the syndrome and the lack of understanding of underlying mechanisms. An initial task for the clinician is to exclude specific disorders for which treatment may be

Table 8 Reported symptoms of multiple chemical sensitivity

Symptom	Source
Rapid heart rate Chest pain Sweating Shortness of breath Fatigue Flushing Dizziness Nausea Choking Trembling Numbness Coughing Hoarseness Difficulty concentrating	https://www.merckmanuals.com/home/special-subjects/idiopathic-environmental-intolerance/idiopathic-environmental-intolerance
Headaches Rashes Asthma Muscle and joint aches Memory loss Confusion	https://www.hopkinsmedicine.org/health/conditions-and-diseases/multiple-chemical-sensitivity
Burning, stinging eyes Wheezing, breathlessness Nausea Extreme fatigue/lethargy Headache/migraine/vertigo/dizziness Poor memory and concentration Runny nose (rhinitis) Sore throat, cough Sinus problems Skin rashes and/or itching skin Sensitivity to light and noise Sleeping problems Digestive upset Muscle and joint pain	https://www.multiplechemicalsensitivity.org/the-symptoms-of-multiple-chemical-sensitivity/

available, such as autoimmune disorders, e.g., polymyalgia rheumatica. From a patient's perspective, the path to a knowledgeable health-care provider may be long and frustrating. Often, the physicians seeing MCS patients initially may not have any knowledge of the syndrome and pursue extensive testing and alternative diagnoses, particularly psychiatric diagnoses. Patients may become distrustful of the health-care system, a barrier to further care and reaching a knowledgeable provider.

Exclusion of alternative diagnoses for which specific therapies are available is the first step clinically. The typical clinical picture will lead a knowledgeable provider to a diagnosis of MCS. Critical for management is the identification of triggers and

potential triggers and guidance on avoiding them. Ongoing supportive care is critical. The provider may also become involved in the broader dimensions of MCS, such as workplace accommodations and disability.

Sick Building Syndrome

Introduction

The syndrome of sick building syndrome or SBS received initial attention and definition in the late 1970s (Passarelli 2009). At that time, there were increasing reports of buildings where multiple occupants were experiencing symptoms that occurred in relationship to building occupancy. The manifestations were diverse and not specific. From clinical and epidemiological perspectives, the critical linkage was the timing of symptoms in relation to exposures to agents within the buildings and the occurrence of symptoms among multiple building occupants. SBS emerged at a time when tobacco smoking was still generally allowed in buildings and, by anecdote, building maintenance had not received sufficient attention as building aged. Additionally, the myriad sources of air pollution in work environments were not yet well recognized, including routine office products, furnishings, and building materials.

As SBS emerged, the tobacco industry made efforts to divert attention away from SHS as a cause of SBS, even though cigarette smoking was by then known to be a potent source of airborne particles and volatile and semi-volatile compounds, including nicotine (Proctor 2012). These efforts included influencing the findings of indoor air quality investigations and vigorous opposition to an attempt by the Occupational Safety and Health Administration (OSHA) to promulgate an indoor air quality standard that covered smoking in workplaces.

The first edition of the *Indoor Air Quality Handbook* included two chapters relevant to SBS, one on “occupant reactions to indoor air quality” and the other on “building-related illnesses.” The distinction remains useful with the first referring to symptoms and complexes of symptoms related to indoor environments and indoor air quality and the second referring to a range of specific and definable clinical entities for which medical treatment might be sought and lead to a diagnosis and therapeutic interventions. By contrast, SBS is nonspecific with the tautology of its name describing its origins and the nature of the symptoms.

Etiology

The syndrome’s name, sick building syndrome, inherently captures its etiology. People with SBS and buildings where SBS occurred have been an elusive target for systematic investigation using epidemiological approaches. Affected individuals have been largely cared for by individual clinicians who may or may not find the link to the responsible building environment. Numerous buildings have been investigated by the National Institute for Occupational Safety and Health (NIOSH) and by private consultant groups. The findings of NIOSH investigations through 1990, not subsequently updated, provide some insights with regard to causal factors at the time (OSHA 1999):

- Inadequate ventilation 52%
- Contamination from inside building 16%
- Contamination from outside building 10%
- Microbial contamination 5%
- Contamination from building fabric 4%
- Unknown sources 13%

Lacking, and complicating interpretation of these data, is the denominator: that is the underlying total population of buildings contributing those where sick building syndrome has occurred. In other words, these case investigations represent the numerator for an unclear denominator. Consequently, we lack a clear understanding of the epidemiology of SBS including its prevalence over time and how etiological drivers may have changed as the syndrome was recognized and preventive maintenance implemented. The relevance of these findings from three decades ago to today's buildings is uncertain, given the many changes in building design and operations and changes in sources, particularly smoking indoors.

Nonetheless, these data provide a broad understanding the etiology of SBS. Inadequate ventilation contributed to about half of the cases. By anecdote, many affected buildings had not been well maintained when the syndrome emerged. Unfortunately, in the USA and elsewhere, we lack a longitudinal data stream to define changing etiology, particularly with the banning of smoking indoors in most building environments around the world. Links to specific chemicals have not been made among the mixtures in indoor environments, but suspects include formaldehyde, various volatile organic compounds, and other agents that may have irritant, neuropsychological, or other effects.

Clinical Picture

People affected by SBS report a broad array of symptoms, often in relation to spending time in the building where exposure occurs. Typically prominent are symptoms related to the air-exposed mucous membranes of the eyes, nose, and throat, and upper airway. Commonly reported symptoms include irritation and burning of the eyes, nose, and throat, cough, and wheezing. Some reports also include symptoms of impaired neurocognition, such as confusion and also dizziness.

These symptoms are not specific and SBS is defined by their connection to the building environment. With such nonspecific symptoms, affected people are far more likely to have initial clinical contact with a generalist, rather than someone with training in environmental or occupational medicine who may make the connection to the building environment. Clinical history formats have been developed for that purpose. At times, people working in affected buildings have made the connection of their symptoms to their workplaces through discussions that have identified the commonality being in the building to the occurrence of symptoms in multiple people. One indicator of the link to the building is the lessening or disappearance of symptoms over the weekend or while on vacation followed by recurrence with return to work. The epidemiological context can affirm the link to

the building if there are multiple people working in the building who are affected or who work in the same place within the building.

Management

By definition, the occurrence of sick building syndrome reflects exposure(s) within the building as the causal agent(s). While specific symptoms may need clinical management, such as treatment of wheezing or eye irritation, resolution of the problems affecting building occupants requires finding the etiology within the building. The path to finding a solution may be complex as cooperation and collaboration with building owners and operators and business management may be needed. Litigation and labor relations may further cloud the course to a solution.

The general approach to patients with SBS remains making the clinical link to the building environment and assuring that the needed building survey and etiological investigations are made. For health-care providers, a first step is to connect a patient's symptoms to the problem building. To confirm the diagnosis and to initiate inquiry about the suspect building, referral to an experienced occupational/environmental medicine physician may prove valuable. The steps to resolution can be complicated, but necessarily involve actions that end with an assessment of the building to diagnose and correct the building's problems. The path to mitigation may flow through the patient, contact with the employer, an employee organization, the building owner, or other routes, sometimes including litigation. The health-care provider would typically be a source of information, but not be in the lead. An experienced building professional is needed.

Hypersensitivity Pneumonitis

Hypersensitivity pneumonitis, or allergic alveolitis, refers to a set of clinical disorders associated with inhaled antigens that cause lung injury via cell-mediated immunity. With sustained exposure, the underlying inflammatory process can lead to fibrosis with permanent lung injury. Among the antigens linked to hypersensitivity pneumonitis are those from pigeons (pigeon breeder's disease) and other birds, e.g., parakeets (bird fancier's disease), those from improperly maintained humidifiers, particularly thermophilic actinomycetes (humidifier lung), and those encountered by farmers, thermophilic actinomycetes and fungi (farmer's lung). These diseases are generally diagnosed by medical specialists, e.g., pulmonologists, and the relevant history will generally lead to an effort to mitigate exposures, if possible. In managing hypersensitivity pneumonitis, removal from exposure is essential; administration of glucocorticoids may be helpful. Questionnaires have been developed for patients diagnosed with hypersensitivity pneumonitis to survey for exposures to potential causal agents.

Conclusions

Indoor air pollution harms public health and causes symptoms and disease that bring people to the attention of health-care providers. Globally, HAP is now a well-established contributor to a substantial burden of morbidity and premature mortality.

It is one of several causes of acute respiratory infections in children and of chronic respiratory and cardiovascular diseases in adults. Solutions are in progress through national and global initiatives. One global indoor air pollution problem has been lessened, but not eliminated – exposure to SHS. A multi-pronged approach has reduced this once ubiquitous exposure: a decline in smoking, a change in social norms with nonsmokers claiming their right to smoke-free environments, legislation at local, state, and national levels, and WHO's global treaty, the FCTC. Public health approaches are also directed at emissions reductions from building materials and products, indoor radon mitigation, and airborne infection control, the last being accelerated greatly by the COVID-19 pandemic.

For people made ill by indoor air pollution and their health-care providers, establishing a link to indoor air pollution and finding a solution through eliminating exposure may be challenging. As covered in this review, indoor air pollution contributes to the causation and exacerbation of common diseases, such as asthma, but the links may not be readily discerned in particular individuals. Careful histories that cover environmental exposures may be helpful in identifying triggers, such as exposure to animal dander or the presence of a cockroach infestation. Consultation with a health-care provider skilled in management of environmental health problems may be needed as may services of an indoor air professional.

For patients and providers, the syndromes of MCS and sick building syndrome may be particularly challenging and frustrating. Specific diagnostic tests are not available and making the correct diagnosis demands a detailed history and exclusion of other conditions that may mimic symptoms of these entities. Affected individuals may become frustrated as a diagnosis and treatment are not offered. Additionally, the illness reflects external exposures that may not be subject to control in the instance of sick building syndrome nor to avoidance in the instance of MCS.

Looking to the future, indoor air quality will continue to affect health and well-being. Most importantly, as indoor environments and sources change, preserving and advancing health should remain an overarching consideration.

References

- Agency for Toxic Substances and Disease Registry (1999) Toxicological profile for formaldehyde. U.S. Department of Health and Human Services, Public Health Service, Agency for Toxic Substances and Disease Registry, Atlanta
- Agency for Toxic Substances and Disease Registry (2007). Toxicological profile for benzene. U.S. Department of Health and Human Services, Public Health Service, Agency for Toxic Substances and Disease Registry, Atlanta
- Agency for Toxic Substances and Disease Registry (2019) Toxicological profile for trichloroethylene. Department of Health and Human Services, Atlanta
- Agency for Toxic Substances and Disease Registry (2021, July 16, 2021) Toxicological profiles. Retrieved July 23, 2021, from <https://www.atsdr.cdc.gov/toxprofiledocs/index.html>
- American Nonsmokers' Rights Foundation (2021, January 1, 2021) Summary of 100% smokefree state laws and population protected by 100% U.S. smokefree laws. Retrieved April 10, 2021, from <http://www.no-smoke.org/pdf/SummaryUSPopList.pdf>

- Antova T, Pattenden S, Brunekreef B, Heinrich J, Rudnai P, Forastiere F, Luttmann-Gibson H, Grize L, Katsnelson B, Moshammer H, Nikiforov B, Slachtova H, Slotova K, Zlotkowska R, Fletcher T (2008) Exposure to indoor mould and children's respiratory health in the PATY study. *J Epidemiol Community Health* 62(8):708–714
- Ashford N, Miller C (1998) Chemical exposures: low levels and high stakes. Van Nostrand Reinhold, New York
- ASHRAE (2014) ASHRAE position document on airborne infectious diseases. ASHRAE, Atlanta
- ASHRAE (2019a) ANSI/ASHRAE standard 62.1-2019, ventilation for acceptable indoor air quality. ASHRAE, Atlanta
- ASHRAE (2019b) ANSI/ASHRAE standard 62.2-2019, ventilation and acceptable indoor air quality in residential buildings. ASHRAE, Atlanta
- ASHRAE (2020) ASHRAE position document on infectious aerosols. Atlanta, ASHRAE
- Bale WF (1980) Memorandum to the files, March 14, 1951: hazards associated with radon and thoron. *Health Phys* 38:1062–1066
- Baselt R (2014) Encyclopedia of toxicology. Oxford University Press, Oxford
- Burr ML, Matthews IP, Arthur RA, Watson HL, Gregory CJ, Dunstan FD, Palmer SR (2007) Effects on patients with asthma of eradicating visible indoor mould: a randomised controlled trial. *Thorax* 62(9):767–772
- Busse WW, Mitchell H (2007) Addressing issues of asthma in inner-city children. *J Allergy Clin Immunol* 119(1):43–49
- Busse WW, Morgan WJ, Gergen PJ, Mitchell HE, Gern JE, Liu AH, Gruchalla RS, Kattan M, Teach SJ, Pongracic JA, Chmiel JF, Steinbach SF, Calatroni A, Togias A, Thompson KM, Szefler SJ, Sorkness CA (2011) Randomized trial of omalizumab (anti-IgE) for asthma in inner-city children. *N Engl J Med* 364(11):1005–1015
- Center for Systems Science and Engineering (CSSE) at Johns Hopkins University (2021) COVID-19 dashboard. Retrieved May 14, 2021, from <https://www.coronavirus.jhu.edu/map.html>
- Centers for Disease Control and Prevention (2020, November 9, 2020). Lung cancer among people who never smoked. Retrieved April 10, 2021, from <https://www.cdc.gov/cancer/lung/nonsmokers/index.htm>
- Centers for Disease Control and Prevention (2021a, January 5, 2021) Secondhand smoke (SHS) facts. Retrieved March 23, 2021, from https://www.cdc.gov/tobacco/data_statistics/fact_sheets/secondhand_smoke/general_facts/index.htm
- Centers for Disease Control and Prevention, National Center for Immunization and Respiratory Diseases and D. o. B. Diseases (2021b, March 25, 2021) Legionella (Legionnaires' Disease and Pontiac Fever): Clinical Features. Retrieved May 14, 2021, from <https://www.cdc.gov/legionella/clinicians/clinical-features.html>
- Clean Cooking Alliance (2021) Homepage. Retrieved July 27, 2021, from <http://www.cleancookingalliance.org>
- Cullen MR (1987) Occupational medicine. Workers with multiple chemical sensitivities. State of the Art Reviews 2(4):655–806
- Drope J, Schluger N, Cahn Z, Drope J, Hamill S, Islami F, Liber A, Nargis N, Stoklosa M (2018) The tobacco atlas. American Cancer Society and Vital Strategies, Atlanta
- Duan X, Jiang Y, Wang B, Zhao X, Shen G, Cao S, Huang N, Qian Y, Chen Y, Wang L (2014) Household fuel use for cooking and heating in China: results from the first Chinese Environmental Exposure-Related Human Activity Patterns Survey (CEERHAPS). *Appl Energy* 136:692–703
- Envirofit (2021) Homepage. Retrieved July 27, 2021, from <https://www.envirofit.org>
- Evans R 3rd, Gergen PJ, Mitchell H, Kattan M, Kercsmar C, Crain E, Anderson J, Eggleston P, Malveaux FJ, Wedner HJ (1999) A randomized clinical trial to reduce asthma morbidity among inner-city children: results of the National Cooperative Inner-City Asthma Study. *J Pediatr* 135 (3):332–338
- Fisk WJ, Lei-Gomez Q, Mendell MJ (2007) Meta-analyses of the associations of respiratory health effects with dampness and mold in homes. *Indoor Air* 17(4):284–296

- Fraser DW, Tsai TR, Orenstein W, Parkin WE, Beecham HJ, Sharrar RG, Harris J, Mallison GF, Martin SM, McDade JE (1977) Legionnaires' disease: description of an epidemic of pneumonia. *N Engl J Med* 297(22):1189–1197
- Gergen PJ, Togias A (2015) Inner city asthma. *Immunol Allergy Clin N Am* 35(1):101–114
- Government of India and M. o. N. a. R. Energy (2021) National biomass cookstoves Programme." Retrieved July 27, 2021, from <http://164.100.94.214/national-biomass-cookstoves-programme>
- Hardin BD, Kelman BJ, Saxon A (2003) Adverse human health effects associated with molds in the indoor environment. *J Occup Environ Med* 45(5):470–478
- Harley JH (1953) Sampling and measurement of airborne daughter products of radon. *Nucleonics* 11:12–15
- Health Effects Institute, Asbestos Research Committee and Literature Review Panel (1991) Asbestos in public and commercial buildings: a literature review and synthesis of current knowledge. Health Effects Institute, Cambridge
- HEI Household Air Pollution Working Group (2018) Household air pollution and non-communicable disease. Communication 18. Health Effects Institute, Boston
- Henderson RF (1989) Symposium on lung cancer risk of exposure to radon. *Toxicol Sci* 13(4): 624–634
- Hernberg S, Sripaiboonkij P, Quansah R, Jaakkola JJ, Jaakkola MS (2014) Indoor molds and lung function in healthy adults. *Respir Med* 108(5):677–684
- Holme JA, Øya E, Afanou AKJ, Øvrevik J, Eduard W (2020) Characterization and pro-inflammatory potential of indoor mold particles. *Indoor Air* 30(4):662–681
- Household Air Pollution Intervention Network (2021) Homepage. Retrieved July 27, 2021, from <http://www.hapitrial.org>
- Jacob P 3rd, Benowitz NL, Destaillats H, Gundel L, Hang B, Martins-Green M, Matt GE, Quintana PJE, Samet JM, Schick SF, Talbot P, Aquilina NJ, Hovell MF, Mao J-H, Whitehead TP (2017) Thirdhand smoke: new evidence, challenges, and future directions. *Chem Res Toxicol* 30(1): 270–294
- Kattan M, Mitchell H, Eggleston P, Gergen P, Crain E, Redline S, Weiss K, Evans R 3rd, Kaslow R, Kercsmar C, Leckley F, Malveaux F, Wedner HJ (1997) Characteristics of inner-city children with asthma: the National Cooperative Inner-City Asthma Study. *Pediatr Pulmonol* 24(4):253–262
- Kennedy K, Grimes C (2013) Indoor water and dampness and the health effects on children: a review. *Curr Allergy Asthma Rep* 13(6):672–680
- Kercsmar CM, Dearborn DG, Schluchter M, Xue L, Kirchner HL, Sobolewski J, Greenberg SJ, Vesper SJ, Allan T (2006) Reduction in asthma morbidity in children as a result of home remediation aimed at moisture sources. *Environ Health Perspect* 114(10):1574–1580
- King N, Auger P (2002) Indoor air quality, fungi, and health. How do we stand? *Can Fam Physician* 48:298–302
- Kshirsagar MP, Kalamkar VR (2014) A comprehensive review on biomass cookstoves and a systematic approach for modern cookstove design. *Renew Sust Energ Rev* 30:580–603
- Lee KK, Bing R, Kiang J, Bashir S, Spath N, Stelzle D, Mortimer K, Bularga A, Doudesis D, Joshi SS (2020) Adverse health effects associated with household air pollution: a systematic review, meta-analysis, and burden estimation study. *Lancet Glob Health* 8(11):e1427–e1434
- Masson G (2021, April 30, 2021) 11 deaths, 1,400+ ED visits for carbon monoxide poisoning reported during Texas' winter power outage. Retrieved July 23, 2021, from <https://www.beckershospitalreview.com/public-health/11-deaths-1-400-ed-visits-for-carbon-monoxide-poisoning-reported-during-texas-winter-power-outage.html>
- Matheson MC, Abramson MJ, Dharmage SC, Forbes AB, Raven JM, Thien FC, Walters EH (2005) Changes in indoor allergen and fungal levels predict changes in asthma activity among young adults. *Clin Exp Allergy* 35(7):907–913
- May JC, May CL (2008) Jeff May's healthy home tips: a workbook for detecting, diagnosing, and eliminating pesky pests, stinky stenches, musty Mold, and other aggravating home problems. JHU Press, Baltimore

- May JC, May CL (2020) My house is killing me!: a complete guide to a healthier indoor environment. Johns Hopkins University Press, Baltimore
- Miller CS, Prihoda TJ (1999a) A controlled comparison of symptoms and chemical intolerances reported by Gulf War veterans, implant recipients and persons with multiple chemical sensitivity. *Toxicol Ind Health* 15(3–4):386–397
- Miller CS, Prihoda TJ (1999b) The Environmental Exposure and Sensitivity Inventory (EESI): a standardized approach for measuring chemical intolerances for research and clinical applications. *Toxicol Ind Health* 15(3–4):370–385
- Morawska L, Allen J, Bahnfleth W, Bluysen PM, Boerstra A, Buonanno G, Cao J, Dancer SJ, Floto A, Franchimont F (2021) A paradigm shift to combat indoor respiratory infection. *Science* 372(6543):689–691
- National Asthma Education and Prevention Program Coordinating Committee Expert Panel Working Group (2020) 2020 focused updates to the asthma management guidelines. U.S. Department of Health and Human Services, National Institutes of Health, National Heart, Lung, and Blood Institute, Bethesda
- National Research, C (1992) Multiple chemical sensitivities: a workshop. National Academies Press (US), Washington, DC. Copyright © National Academy of Sciences
- National Research Council (2006) Assessing the human health risks of trichloroethylene: key scientific issues. The National Academies Press, Washington, DC
- National Research Council (2010) Secondhand smoke exposure and cardiovascular effects: making sense of the evidence. National Academies Press, Washington, DC
- National Research Council and C. o. H. R. o. E. t. R. B. VI (1999) Health effects of exposure to radon: BEIR VI. Appendix G, epidemiologic studies in the indoor environment. National Academies Press, Washington, DC
- National Research Council and Committee on the Biological Effects of Ionizing Radiation (1988) Health risks of radon and other internally deposited alpha-emitters: BEIR IV. National Academy Press, Washington, DC
- National Research Council. Committee on Health Risks of Exposure to Radon (1999) Health effects of exposure to radon: BEIR VI. National Academy Press, Washington, DC
- Nelson KE, Williams CM (2014) Infectious disease epidemiology: theory and practice. Jones & Bartlett Publishers, Burlington
- O'Connor GT, Walter M, Mitchell H, Kattan M, Morgan WJ, Gruchalla RS, Pongracic JA, Smartt E, Stout JW, Evans R, Crain EF, Burge HA (2004) Airborne fungi in the homes of children with asthma in low-income urban communities: the Inner-City Asthma study. *J Allergy Clin Immunol* 114(3):599–606
- O'Malley GF, O'Malley R (2020, July 2020) Carbon monoxide poisoning. MERCK MANUAL Retrieved July 23, 2021, from <https://www.merckmanuals.com/home/injuries-and-poisoning/poisoning/carbon-monoxide-poisoning>
- OSHA (1999) OSHA technical manual (OTM), section III: chapter 2: indoor air quality investigation. United States Department of Labor, Occupational Safety and Health Administration, Washington, DC
- Palmer RF, Jaén CR, Perales RB, Rincon R, Forster JN, Miller CS (2020) Three questions for identifying chemically intolerant individuals in clinical and epidemiological populations: the brief environmental exposure and sensitivity inventory (BREESI). *PLoS One* 15(9):e0238296
- Park JH, Cox-Ganser JM, Kreiss K, White SK, Rao CY (2008) Hydrophilic fungi and ergosterol associated with respiratory illness in a water-damaged building. *Environ Health Perspect* 116(1): 45–50
- Passarelli GR (2009) Sick building syndrome: an overview to raise awareness. *J Build Apprais* 5(1): 55–66
- Proctor R (2012) Golden holocaust: origins of the cigarette catastrophe and the case for abolition. University of California Press, Berkeley
- Project Surya (2009) Project Surya: fighting climate change now. Retrieved July 27, 2021, from <http://www.projectsurya.org>

- Quansah R, Jaakkola MS, Hugg TT, Heikkinen SA, Jaakkola JJ (2012) Residential dampness and molds and the risk of developing asthma: a systematic review and meta-analysis. *PLoS One* 7(11):e47526
- Ramanathan V (2020) Climate change, air pollution, and health: common sources, similar impacts, and common solutions. In: Al-Delaimy WK, Ramanathan V, Sorondo MS (eds) *Health of people, health of planet and our responsibility: climate change, air pollution and health*. Springer International Publishing, Cham, pp 49–59
- Randolph TG (1954) Allergic type reactions to industrial solvents and liquid fuels. *J Lab Clin Med*, MOSBY-YEAR BOOK INC 11830 WESTLINE INDUSTRIAL DR, ST LOUIS, MO 63146-3318
- Randolph TG (1962) *Human ecology and susceptibility to the chemical environment*. Charles C. Thomas, Springfield, IL
- Riley RL, Mills CC, O'Grady F, Sultan LU, Wittstadt F, Shivpuri DN (1962) Infectiousness of air from a tuberculosis Ward. *Am Rev Respir Dis* 85(4):511–525
- Rossi S, Pitidis A (2018) Multiple chemical sensitivity: review of the state of the art in epidemiology, diagnosis, and future perspectives. *J Occup Environ Med* 60(2):138
- Roth C (2011) Micro gasification: cooking with gas from biomass. GIZ HERA - Poverty-oriented Basic Energy Service, Bonn
- Samet JM, Spengler JD (1991) Indoor air pollution. A health perspective. Johns Hopkins University Press, Baltimore
- Samet JM, Bohanon HR Jr, Coulter DB, Houston TP, Persily AK, Schoen LJ, Spengler J, Callaway CA, ASHRAE's Environmental Tobacco Smoke Position Document Committee (2005) ASHRAE position document on environmental tobacco smoke. American Society of Heating Refrigeration and Air Conditioning, Atlanta
- Sheehan WJ, Rangsithienchai PA, Wood RA, Rivard D, Chinratanapisit S, Perzanowski MS, Chew GL, Seltzer JM, Matsui EC, Phipatanakul W (2010) Pest and allergen exposure and abatement in inner-city asthma: a Work Group Report of the American Academy of Allergy, Asthma & Immunology Indoor Allergy/Air Pollution Committee. *J Allergy Clin Immunol* 125(3):575–581
- Smith KR, Aggarwal AL, Dave RM (1983) Air pollution and rural biomass fuels in developing countries: a pilot village study in India and implications for research and policy. *Atmos Environ* 17:2343–2362
- Smith KR, Shuhua G, Kun H, Daxiong Q (1993) One hundred million improved cookstoves in China: how was it done? *World Dev* 21(6):941–961
- Smith KR, McCracken JP, Weber MW, Hubbard A, Jenny A, Thompson LM, Balmes J, Diaz A, Arana B, Bruce N (2011) Effect of reduction in household air pollution on childhood pneumonia in Guatemala (RESPIRE): a randomised controlled trial. *Lancet* 378(9804):1717–1726
- Sohn MH, Kim K-E (2012) The cockroach and allergic diseases. *Allergy, Asthma Immunol Res* 4 (5):264–269
- Steinemann A (2018) National prevalence and effects of multiple chemical sensitivities. *J Occup Environ Med* 60(3):e152–e156
- Stevenson LA, Gergen PJ, Hoover DR, Rosenstreich D, Mannino DM, Matte TD (2001) Socio-demographic correlates of indoor allergen sensitivity among United States children. *J Allergy Clin Immunol* 108(5):747–752
- Svanes C, Heinrich J, Jarvis D, Chinn S, Omenaas E, Gulsvik A, Künzli N, Burney P (2003) Pet-keeping in childhood and adult asthma and hay fever: European community respiratory health survey. *J Allergy Clin Immunol* 112(2):289–300
- Tang JW, Bahnfleth WP, Bluyssen PM, Buonanno G, Jimenez JL, Kurnitski J, Li Y, Miller S, Sekhar C, Morawska L, Marr LC, Melikov AK, Nazaroff WW, Nielsen PV, Tellier R, Wargo P, Dancer SJ (2021) Dismantling myths on the airborne transmission of severe acute respiratory syndrome coronavirus-2 (SARS-CoV-2). *J Hosp Infect* 110:89–96
- Tsai J, Homa DM, Gentzke AS, Mahoney M, Sharapova SR, Sosnoff CS, Caron KT, Wang L, Melstrom PC, Trivers KF (2018) Exposure to secondhand smoke among nonsmokers—United States, 1988–2014. *Morb Mortal Wkly Rep* 67(48):1342

- Tucker WJ (2001) In: Spengler JD, Samet JM, McCarthy JF (eds) Volatile organic compounds. Indoor air quality handbook. McGraw-Hill Education, New York
- U.S. Department of Health and Human Services, National Institutes of Health and National Cancer Institute (2014) The health consequences of smoking—50 years of progress: a report of the Surgeon General. U.S. Department of Health and Human Services, Centers for Disease Control and Prevention, National Center for Chronic Disease Prevention and Health Promotion and Office on Smoking and Health, Atlanta
- U.S. Department of Health Education and Welfare (1964) Smoking and health: report of the Advisory Committee to the Surgeon General of the Public Health Service. U.S. Government Printing Office, Washington DC, 386
- U.S. DHHS (1986) The health consequences of involuntary smoking: a report of the Surgeon General. Department of Health and Human Services, public health service, Office on Smoking and Health, Washington, DC
- U.S. DHHS (2006) The health consequences of involuntary exposure to tobacco smoke. A report of the Surgeon General. U.S. Department of Health and Human Services, Centers for Disease Control and Prevention, coordinating Center for Health Promotion, National center for chronic disease prevention and health promotion, Office on Smoking and Health, Atlanta
- U.S. DHHS (2010) How tobacco smoke causes disease: the biology and behavioral basis for smoking-attributable disease. A report of the Surgeon General. U.S. Department of Health and Human Services, Centers for Disease Control and Prevention, National Center for Chronic Disease Prevention and Health Promotion, Office on Smoking and Health, Atlanta
- U.S. DHHS (2014) The health consequences of smoking—50 years of progress: a report of the Surgeon General. U.S. Department of Health and Human Services, Centers for Disease Control and Prevention, National Center for Chronic Disease Prevention and Health Promotion, Office on Smoking and Health, Atlanta
- U.S. DHHS (2016) Surgeon General's report: E-cigarette use among youth and young adults. Centers for Disease Control and Prevention, Atlanta
- U.S. Environmental Protection Agency (1999) National air toxics program: the integrated urban strategy. U.S. Environmental Protection Agency, pp 38706–40. Washington DC
- U.S. EPA (1992) National residential radon survey: summary report. Environmental Protection Agency, Washington, DC
- U.S. EPA (2010a) Integrated science assessment for carbon monoxide (final report). Environmental Protection Agency, Washington, DC
- U.S. EPA (2010b) IRIS toxicological review of inorganic arsenic (cancer) (external review draft, 2010). Environmental Protection Agency, Washington, DC
- U.S. EPA (2012) A citizen's guide to radon: the guide to protecting yourself and your family from radon. Environmental Protection Agency, Washington, DC
- U.S. EPA (2020a, September 25, 2020) Asbestos laws and regulations. Retrieved July 29, 2021, from <https://www.epa.gov/asbestos/asbestos-laws-and-regulations>
- U.S. EPA (2020b, October 13, 2020) Indoor particulate matter. Retrieved July 27, 2021, from <https://www.epa.gov/indoor-air-quality-iaq/indoor-particulate-matter>
- U.S. EPA (2020c, August 12, 2020) What is vapor intrusion? Retrieved July 23, 2021, from <https://www.epa.gov/vaporintrusion/what-vapor-intrusion>
- U.S. EPA (June 16, 2021a) Integrated risk information system (IRIS). Retrieved July 30, 2021, from <http://www.epa.gov/iris/>
- U.S. EPA (2021b, March 3, 2021) Facts about formaldehyde. Retrieved July 28, 2021, from <https://www.epa.gov/formaldehyde/facts-about-formaldehyde>
- U.S. EPA (2021c, April 1, 2021) Health risk of radon. Retrieved July 26, 2021, from <https://www.epa.gov/radon/health-risk-radon>
- U.S. EPA (2021d, July 13, 2021) Radon-resistant construction basics and techniques. Retrieved July 23, 2021, from <https://www.epa.gov/radon/radon-resistant-construction-basics-and-techniques>

- U.S. EPA (2021e, July 19, 2021) Risk management for trichloroethylene (TCE). Retrieved July 23, 2021, from <https://www.epa.gov/assessing-and-managing-chemicals-under-tsca/risk-management-trichloroethylene-tce>
- U.S. EPA (2021f, February 9, 2021) Technical overview of volatile organic compounds. Retrieved July 23, 2021, from <https://www.epa.gov/indoor-air-quality-iaq/technical-overview-volatile-organic-compounds#definition>
- U.S. EPA (2021g, February 10, 2021) Volatile organic compounds' impact on indoor air quality. Retrieved July 23, 2021, from <https://www.epa.gov/indoor-air-quality-iaq/volatile-organic-compounds-impact-indoor-air-quality>
- U.S. Food and Drug Administration (2019, October 7, 2019) Harmful and potentially harmful constituents in tobacco products and tobacco smoke: established list. Retrieved April 10, 2021, from <https://www.fda.gov/tobacco-products/rules-regulations-and-guidance/harmful-and-potentially-harmful-constituents-tobacco-products-and-tobacco-smoke-established-list>
- U.S. HUD (2017) Smoke-free public housing. Retrieved July 26, 2021, from <https://www.hud.gov/smokefreepublichousing>
- United Nations Scientific Committee on the Effects of Atomic Radiation (2020) UNSCEAR 2019 report—sources, effects and risks of ionizing radiation. Report to the General Assembly. New York
- Van Sechteren JM, Hochberg NS (2017) Principles of infectious diseases: transmission, diagnosis, prevention, and control. International encyclopedia of public health 22–39
- Venkataraman C, Sagar AD, Habib G, Lam N, Smith KR (2010) The Indian national initiative for advanced biomass cookstoves: the benefits of clean combustion. Energy Sustain Dev 14(2): 63–72
- Vigolo V, Sallaku R, Testa F (2018) Drivers and barriers to clean cooking: a systematic literature review from a consumer behavior perspective. Sustainability 10(11):4322
- Wallace LA (1987) Total exposure assessment methodology (TEAM) study: summary and analysis. Volume 1, Environmental Protection Agency, Office of Acid, Washington, DC
- Wallace LA (2001) Aldehydes. In: Spengler JD, Samet JM, McCarthy JF (eds) Indoor air quality handbook. McGraw-Hill Education, New York
- Walton K, Gentzke AS, Murphy-Hoefer R, Kenemer B, Neff LJ (2020) Peer reviewed: exposure to secondhand smoke in homes and vehicles among US Youths, United States, 2011–2019. Preventing Chronic Disease 17
- Wang CC, Prather KA, Sznitman J, Jimenez JL, Lakdawala SS, Tufekci Z, Marr LC (2021) Airborne transmission of respiratory viruses. Science 373(6558):eabd9149
- Wells WF (1934) On airborne infection. Study II. Droplets and droplet nuclei. Am J Hyg 20: 611–618
- WHO Framework Convention on Tobacco Control (2018) 2018 global progress report on implementation of the WHO framework convention on tobacco control. World Health Organization, Geneva
- Wilson JM, Platts-Mills TAE (2018) Home environmental interventions for house dust mite. J Allergy Clin Immunol In Practice 6(1):1–7
- World Health Organization (1948) Constitution of the World Health Organization. World Health Organization, Geneva
- World Health Organization (2003) WHO framework convention on tobacco control (FCTC). Retrieved July 1, 2015, from <http://www.who.int/fctc/en/>
- World Health Organization (2007) Legionella and the prevention of legionellosis. WHO Press, Geneva
- World Health Organization (2009) WHO guidelines for indoor air quality: dampness and mould. Switzerland, Geneva
- World Health Organization (2010) WHO guidelines for indoor air quality: selected pollutants. World Health Organization. Regional Office for Europe, Geneva

- World Health Organization (2014) WHO guidelines for indoor air quality: household fuel combustion. Review 9: summary of systematic review of household kerosene use. World Health Organization, Geneva
- World Health Organization (2018a) Child health: prescribing clean air. World Health Organization, Geneva
- World Health Organization (2018b, May 8, 2018) Household air pollution and health. Retrieved July 27, 2021, from <https://www.who.int/news-room/fact-sheets/detail/household-air-pollution-and-health>
- World Health Organization (2020a) Global tuberculosis report. 2020. World Health Organization, Geneva
- World Health Organization (2020b) Transmission of SARS-CoV-2: implications for infection prevention precautions. Scientific Brief, 9 July 2020. Retrieved July 30, 2021, from <https://www.who.int/news-room/commentaries/detail/transmission-of-sars-cov-2-implications-for-infection-prevention-precautions>
- World Health Organization (2021) Roadmap to improve and ensure good indoor ventilation in the context of COVID-19
- World Health Organization (2021a) More countries act against exposure to radon and associated cancer risks. Switzerland, Geneva
- World Health Organization (2021b, May 27, 2020) Tobacco. Fact sheets. Retrieved April 10, 2021, from <https://www.who.int/news-room/fact-sheets/detail/tobacco>
- World Health Organization (2021c) WHO report on the global tobacco epidemic, 2021. World Health Organization, Geneva



Epidemiology for Indoor Air Quality Problems

40

Shaodan Huang, Wenlou Zhang, Wanzhou Wang, and Furong Deng

Contents

Introduction	1190
Conventional Outcome Measures in Epidemiological Studies of Indoor Air Pollution	1190
Mortality, Morbidity, and Prevalence	1190
Subclinical Outcome Measures	1190
Classification of Adverse Health Effects of Indoor Air Pollution	1196
Short-Term Health Effects	1196
Long-Term Health Effects	1199
Specific Examples	1202
Environmental Tobacco Smoke	1202
Radon	1207
Nitrogen Dioxide (NO ₂)	1209
Formaldehyde and Volatile Organic Compounds (VOCs)	1211
Conclusions and Outlook	1213
References	1213

Abstract

People spend as much as 90% of their time in confined environments. A large number of previous environmental epidemiological studies have confirmed the association between indoor air pollution and population health, but there are still some limitations and deficiencies in the epidemiological studies on indoor air quality and population health. This chapter discusses the health effects of indoor air pollution on the cardiovascular system, respiratory system, and other systems from the perspective of short-term health effects and long-term health effects. The health outcome indexes commonly used in indoor air quality and population health research were summarized. The epidemiological studies on indoor smoking, nitrogen dioxide, TVOC, and radon were discussed as special

S. Huang · W. Zhang · W. Wang · F. Deng (✉)

Department of Occupational & Environmental Health Sciences, Peking University School of Public Health, Beijing, China

e-mail: frdeng@bjmu.edu.cn

examples in detail. This chapter also points out the problems existing in the current research on indoor air quality and population health and puts forward the prospect of future research.

Keywords

Indoor air · Epidemiology · Short-term health effects · Long-term health effects · Cardiovascular health · Respiratory health

Introduction

People spend as much as 90% of their time in confined environments, especially at home, and the concentrations of some air pollutants may be two- to five-fold higher indoors than outdoors (Marion et al. 2012). Poor indoor air quality poses a risk to the health of over half of the world's population, especially affecting poor people. Indoor air pollution is the eighth most important risk factor, being responsible for 2.7% of the global burden of disease (between 1.5 and two million deaths yearly) (Viegi et al. 2004). Therefore, concern over the health effects of indoor air pollution is increasing. Epidemiologic investigations on indoor air pollutants are of important practical significance for identifying countermeasures to control indoor air pollution, improve indoor air quality, and protect human health.

This chapter introduced the adverse health effects of indoor air pollution and reviews conventional outcome measures in epidemiological studies of indoor air pollution. We also took important indoor pollutants as examples and introduced the related epidemiology studies and guidelines.

Conventional Outcome Measures in Epidemiological Studies of Indoor Air Pollution

Mortality, Morbidity, and Prevalence

Mortality is the proportion of the total number of deaths in a given population in a given period of time. Morbidity (also called incidence rate) is defined as the number of new cases of disease (incident number) divided by the person-time over the period. Prevalence of a disease is the proportion of the population with the disease at the specified time. They are common outcome variables in cross-sectional studies and cohort studies and are usually used to assess the effect of long-term exposure to indoor air pollution.

Subclinical Outcome Measures

Outcome Measures for Respiratory System

Pulmonary function: Spirometry is the most common physiological test to measure the maximal inhales or exhales volumes of air of an individual with maximal effort

(Graham et al. 2019; Miller et al. 2005). In 1979, the American Thoracic Society (ATS) proposed the first statement on the standardization of spirometry. In 2005, a new document of standardization of spirometry bringing the views of the ATS and European Respiratory Society (ERS) was published and has been applied widely (Miller et al. 2005). This standard was updated again in 2019 (Graham et al. 2019). Through this test, some lung function indicators can be obtained, mainly including the forced vital capacity (FVC), forced expiratory volume in the first second (FEV₁, FEV₁/FVC, peak expiratory flow (PEF), and so on. FVC is the volume delivered during an expiration made as forcefully and completely as possible starting from full inspiration. FEV₁ is the volume delivered in the first second of an FVC maneuver. FEV₁/FVC is the ratio of FEV₁ to FVC and has been used to diagnose lung diseases such as chronic obstructive pulmonary disease (COPD). PEF is the largest flow during a forced expiration. Lung function has become one of the most commonly used outcome variables in assessing the respiratory health effects of indoor air pollution. Impaired lung function has been linked to short- and long-term exposure to indoor air pollution from fuel or incense burning and cooking oil fumes and certain indoor air pollutants including particulate matter among all kinds of people.

Airway inflammation: Airway inflammation is a central process in many lung diseases including asthma and COPD. Fractional exhaled nitric oxide (FeNO) and hydrogen sulfide (FeH₂S) have been developed as two noninvasive biomarkers of airway inflammation, reflecting eosinophilic and neutrophilic inflammation, respectively. In 2005, ATS and ERS recommended the standardized procedures for online and offline measurement of FeNO (American Thoracic Society; European Respiratory Society 2005). The FeNO is expressed in parts per billion, which is equivalent to nanoliters per liter. The exhalation flow rate used for a particular test can be expressed as a subscript of the flow rate in ml/s: for example, FeNO₅₀ at a flow rate of 50 ml/s. It's important to note that NO analysis should be performed before spirometry because spirometric maneuvers have been shown to transiently reduce exhaled NO levels. NO measurements can be performed using exhaled gas collected in a reservoir and subsequently analyzed for NO concentrations, which is called offline FeNO measurement. Other NO indicators have been developed to reflect the airway inflammation in different parts. For example, CaNO is the concentration of NO in the gas phase of the alveolar or acinar region (ppb), and CawNO is the tissue concentration of NO of the airway wall (ppb). FeNO and FeH₂S have been widely used in studies concerning respiratory health effects of ambient air pollutants. But in general, the evidence on the association of indoor air pollution with FeNO and FeH₂S is limited.

Induced sputum: In recent years, increasing evidence suggests that the respiratory microbiome is closely related to the occurrence and development of respiratory diseases, especially for some chronic lung diseases. Sputum induction has been recognized as the preferred sampling technique for assessing the respiratory microbiome. Sputum is an extracellular gel, including water, heavily glycosylated mucins, inhaled toxins and particulate matter, host cells, and bacteria and their associated products. Sputum may be induced through inhalation of saline solutions and it is noninvasive. Sputum inherently represents a variable mixture of upper and lower airway microbiota. Current knowledge of the respiratory microbiome still relies

mainly on the 16S rRNA gene sequencing approach. Other high-throughput techniques, such as metagenomics, metatranscriptomics, and metabolomics, can aid in both a broader investigation of microbial genomes and the examination of associated functional aspects and are increasingly used. Changes in the respiratory microbiome may also be involved in indoor air pollution-mediated pulmonary effects, which is worth investigating in the future.

Respiratory symptoms: Increased risks of some respiratory symptoms such as wheeze, cough, phlegm, rhinitis, and dyspnea have been associated with short- and long-term exposure to indoor air pollution. Some questionnaires have been developed to measure the symptoms of patients with chronic respiratory diseases. For example, the Modified British Medical Research Council (mMRC) questionnaire was used to assess the degree of dyspnea and it relates well to the prognosis of COPD. In addition, COPD Assessment Test (CAT) and the COPD Control Questionnaire (CCQ) have been developed to comprehensively assess the health status of COPD patients. CAT is an eight-item uni-dimensional measure of health status impairment in COPD. Another widely used questionnaire, St. George's Respiratory Questionnaire (SGRQ), can evaluate disease symptoms, patient's daily activity, and the impact of COPD on a patient's life, but it is too complex to use in routine practice.

Outcome Measures for Cardiovascular Health

Blood pressure: Blood pressure is defined as the pressure exerted by the blood upon the walls of the blood vessels. Elevated blood pressure, even under the threshold of hypertensive disorders, has been associated with increased cardiovascular diseases and mortality. The conventional indicators used is resting arterial blood pressure (ABP), mainly including systolic blood pressure (SBP), diastolic blood pressure (DBP), pulse pressure (PP), and also mean arterial blood pressure (MABP) calculated as the weighted average of SBP and DBP with weights of 1/3 and 2/3, respectively (Xia et al. 2021a). Recently, increasing studies show solicitude for ambulatory blood pressure allowing for repeated measurements of blood pressure. The ambulatory blood pressure can more sensitively capture the short-term associations of indoor air pollutants with blood pressure.

Cardiac function: Numerous studies have linked indoor air pollutants exposure to decreased cardiac autonomic function, as represented by heart rate variability (HRV). HRV is usually measured by an ambulatory electrocardiogram. The repeated measurements allow for capturing the cardiovascular effects of short-term indoor air pollutant exposures. The conventional measurements used are indicators for two major domains. The time-domain includes the standard deviation of normal-to-normal intervals (SDNN), and the frequency domain includes the very low-frequency (VLF) power (0.0033–0.04 Hz), the low-frequency (LF) power (0.04–0.15 Hz), the high-frequency (HF) power (0.15–0.40 Hz), and also LF/HF ratio, etc.

Other less used measures are cardiac structure indicators usually assessed by echocardiography. The outcomes are parameters describing the forms and structures of heart chambers, including left ventricular internal diameter in diastole, left

ventricular mass, left ventricular ejection fraction, left ventricular internal diameter in systole, left atrial anterior-posterior diameter, left atrial area (four- and two-chamber), lateral and septal E' velocity, lateral and septal A' velocity, lateral and septal S' velocity, E/A ratio, right ventricular width at the base and mid-cavity, right ventricular length, right ventricular systolic pressure, tricuspid annular plane systolic excursion, and right ventricular outflow tract time to peak velocity, etc. (Burroughs Peña et al. 2017). The cardiac structure is closely related to the blood-pumping functions of the heart.

Metabolic indicators: Traditionally used metabolic indicators are gluco-lipid parameters examined by clinical blood biochemistry tests, including fasting plasma glucose (FPG), total cholesterol (TC), high-density lipoprotein cholesterol (HDL-C), low-density lipoprotein cholesterol (LDL-C), triglycerides (TG), and very low-density lipoprotein cholesterol (VLDL-C). Meanwhile, hemoglobin A1C (HbA1C), fasting insulin, and C-peptide are also important circulating biomarkers for glucose metabolism. Noteworthily, C-peptide is the concurrent product of insulin derived from proinsulin, and secreted in equimolar dose. Emerging studies have found that C-peptide can more accurately characterize the real release amount of insulin, and also more sensitively predict the risks of multiple cardiovascular diseases.

Recent studies have also developed a series of novel indices based on these indicators, such as homoeostasis model assessment of insulin resistance index (HOMA-IR), homoeostasis model assessment of β -cell function (HOMA-B), non-high-density lipoprotein cholesterol (non-HDL-C), which is calculated as TC minus HDL-C, and TC/HDL-C, non-HDL-C/HDL-C, LDL-C/HDL-C, and TG/HDL-C. These indices have been found to be strong predictors for risks of cardiovascular diseases and mortality. In addition, further technologies have also been used to examine the apolipoprotein A1 (ApoA1), apolipoprotein B (ApoB), and ApoB/ApoA1 ratio. ApoA1 is an important apolipoprotein in HDL-C particles, and has potential protective effects for atherosclerosis. Meanwhile, ApoB is a major apolipoprotein in atherogenic lipoprotein particles, which may promote atherosclerosis. Increased ApoB/ApoA1 is associated with increased risks of cardiovascular diseases (He et al. 2021).

Inflammatory and oxidative indicators: Systematic inflammation and oxidative stress are two classic mechanisms for the adverse effects associated with indoor air pollution exposure. The widely used indicators of systematic inflammation are high-sensitivity C-reactive protein (hs-CRP) and fibrinogen. Hs-CRP is an acute-phase protein, which is considered as a robust predictor for cardiovascular diseases (Xia et al. 2021a). Meanwhile, fibrinogen is also a strong predictor for risks of coronary heart disease (CHD), and other vascular and nonvascular mortality. Other inflammatory indicators also include white blood cells (WBCs) and subgroups, including eosinophils, basophils, neutrophils, monocytes, and lymphocytes, as well as cytokines such as interleukin (IL)-6, IL-8, IL-1 β , IL-17, tumor necrosis factor- α (TNF- α), soluble intercellular cell adhesion molecule-1 (sICAM-1), monocyte chemotactic protein-1 (MCP-1), and macrophage inflammatory protein-1 α (MIP-1 α), etc. As for indicators for oxidative stress, superoxide dismutase (SOD), 8-hydroxy-2'-deoxyguanosine (8-OHdG), malondialdehyde (MDA), glutathione

peroxidase 1 (GPx-1), and oxidized low-density lipoprotein (Ox-LDL) are typical circulating biomarkers. SOD is an antioxidant enzyme preventing the potential adverse effects of oxidative stress. 8-OHdG is a sensitive biomarker to represent DNA damages. Meanwhile, MDA and Ox-LDL are also important indicators for lipid peroxidation.

Coagulation indicators: Increasing studies have identified the thrombosis-promoting effects of indoor air pollutants, which might be the underlying mechanisms for cardiovascular diseases such as stroke, CHD, and IHD (Chen et al. 2018). Typically used coagulation indicators include red blood cells (RBCs), platelets (PLT), plasminogen activator inhibitor-1 (PAI-1), soluble CD40 ligand (sCD40L), platelet aggregation rate (PAgT), P-selectin, tissue plasminogen activator (t-PA), d-dimer, etc. (Chen et al. 2015).

Metabolomics: Investigations on metabolomics aim at a systematic analysis of the metabolites produced by cells, tissues, or organisms. Metabolomics is a useful tool to identify the complex exposure biomarkers along with the changes in metabolic phenotypes related to adverse health outcomes, in order to elucidate the underlying mechanisms of health effects associated with indoor air pollutants exposure. Metabolomics methods can be divided into untargeted metabolomics and targeted metabolomics, both with the aim of identifying differentiated metabolites associated with exposures or health outcomes. To date, untargeted metabolomics has been more widely used, but current evidence on related biological pathways in human beings associated with indoor air pollution exposure is still limited.

Epigenetics: Studies on epigenetics focus on changes in gene functions and protein expressions that do not involve changes in DNA. MicroRNAs (miRNAs) are important factors in the epigenetic regulation of gene expressions. MiRNAs are composed of multiple small non-coding RNA molecules, which play a crucial role in messenger RNA (mRNA) silencing and gene expression regulation at the posttranscriptional level, and thus inhibit the process of protein synthesis (Chen et al. 2018; Vrijens et al. 2015). To date, miRNAs representative of miR-21, miR-34b, miR-125b, miR-146a, miR-223, and miR-340 associated with smoking, as well as miR-9, miR-10b, miR-21, miR-128, miR-143, miR-155, miR-222, miR-223, and miR-338 associated with air pollutants have been investigated (Vrijens et al. 2015). In addition, the associations of indoor air pollutants with mitochondrial DNA (mtDNA) methylation and DNA methylation have also received increasing attention. DNA methylation may induce the dysfunction of endothelium, which is firmly associated with cardiovascular diseases such as atherosclerosis and thrombosis.

Outcome Measures for Other Health Issues

Skin diseases and symptoms: Many indoor physical, chemical, and biological pollutants (e.g., cockroaches, rodents, pets, dust mites, fungus, air pollutants, endotoxin, tobacco, etc.) may be potential allergens leading to hypersensitivity reactions through inflammatory and other pathways. To date, most related studies centered around the effects on organs directly exposed to the indoor environment, such as skin and eyes. Air conditions have been associated with many allergic skin diseases and symptoms such as dermatitis, eczema, urticaria, and skin itching (Abolhasani et al. 2021).

However, to date, the outcome measures for clinical and subclinical skin conditions are still limited. Apart from self-reported disease history and physician diagnosis of skin diseases, there are few acknowledged indicators for skin issues. It deserves attention that recent studies found that interleukin-17 (IL-17), T-helper 17 (Th17) cell, and aryl hydrocarbon receptor (AhR) may be closely associated with several skin diseases such as atopic dermatitis, cellulitis, and psoriasis (Abolhasani et al. 2021). Further studies are still warranted to identify more sensitive outcome measures.

Eye diseases and symptoms: Studies have linked indoor air pollutants to eye diseases and symptoms, particularly dry eye symptoms and other eye irritations (Idarraga et al. 2020). Self-reported eye symptoms of a simple question (e.g., “Do you feel that your eyes are dry and uncomfortable?”) have widely been used in related studies. As for objective measures, the standardized questionnaires such as the Ocular Surface Disease Index (OSDI), the National Eye Institute Visual Functioning Questionnaire (NEI VFQ-25), the McMonnies Dry Eye Questionnaire, and the Short Form-12 (SF-12) Health Status Questionnaire are mostly used. The OSDI is a 12-item questionnaire composed of three major subscales including vision-related function, ocular symptoms, and environmental triggers (Schiffman et al. 2000). The main advantage of the OSDI is the capacity of capturing unique aspects of dry eye disease (Schiffman et al. 2000).

Mental health: Epidemiological studies have linked indoor air pollutants to mental disorders and subclinical mental health issues, such as anxiety, depression, and stress. Most of these studies used the results from standardized assessment tools as the primary outcome measures. Some widely used scales in related studies include the State-Trait Anxiety Inventory (STAI), the Beck Anxiety Inventory (BAI), the Hospital Anxiety and Depression Scale (HADS), the Center for Epidemiologic Studies Depression Scale (CES-D), the Beck Depression Inventory-II (BDI-II), the Geriatric Depression Scale (GDS), the Patient Health Questionnaire-9 (PHQ-9) for depression, and the Perceived Stress Scale (Liu et al. 2020a). In addition, the Depression Anxiety Stress Scales (DASS) has also been used to characterize the effects of indoor air pollutants on the mental health of the aforementioned three perspectives.

Cognitive health: Growing studies have found associations of indoor air pollutants with a variety of types of cognitive function including concentration, memory, perception, spatial orientation, and thinking. The outcome measures can be categorized into two major areas: brain function and work performance. Brain function refers to specific cognitive functions with dedicatedly designed tasks, while work performance involves links with real-world activities (Du et al. 2020). Comprehensive cognitive test batteries include the Behavioral Assessment and Research System (BARS), the Cognitive Drug Research (CDR), the Penn Computerized Neurocognitive Battery (CNB), and the CNS Vital Signs battery (CNS), etc.

Kidney health: The widely used outcome measures for kidney health for this topic are still limited to clinical indicators, representative of estimated glomerular filtration rate (eGFR), and urinary protein creatinine. The eGFR can be estimated based on age, gender, and serum creatinine concentrations. According to the National Kidney Foundation Kidney Disease Outcomes Quality Initiative

(NKF-K/DOQI), eGFR <60 ml/min/1.73 m² or urinary protein creatinine >30 mg/g is defined as chronic kidney disease (CKD) (Liang et al. 2021). However, some biomarkers associated with tubular injury, tubular function, kidney inflammation, and fibrosis used in clinical practice have still seldom been applied in studies on kidney effects of indoor air pollutants.

Classification of Adverse Health Effects of Indoor Air Pollution

Short-Term Health Effects

Effects on Respiratory System

The respiratory system is directly exposed to air pollutants, so it is the first to bear the brunt. People spend most of their time indoors, especially for susceptible populations like children, elderly, and patients with some chronic diseases. Therefore, it is imperative to explore the relationship between indoor air pollution and the respiratory health of the population.

Short-term exposure to indoor air pollution has been associated with some adverse respiratory outcomes, including lung function and respiratory symptoms. Particulate matter is one of the most widely investigated indoor air pollutants. It has been associated with impaired lung function among different populations. A panel study of 141 schoolchildren in Poland found that exposure to indoor PM₁ and PM_{2.5} was associated with the reduction of FEV₁ and PEF (Zwozdziaik et al. 2016). A study of 60 healthy adults found that increased PM_{2.5} in houses with houseplants was associated with a decreased percentage predicted peak expiratory flow rate (PEFR) (Chang et al. 2019). A panel study among healthy elderly women found outdoor-originated indoor PM_{2.5} was associated with decreased PEF in the non-heating season (Chi et al. 2019). Patients with respiratory problems may be more sensitive to indoor air pollution than healthy people. Chi et al. found that an inter-quartile range (IQR, 102.4 µg/m³) increase in indoor PM_{2.5} was associated with 1.7–2.3% reduction in FEV₁ of chronic obstructive pulmonary disease (COPD) patients during the heating season in Beijing, China (Chi et al. 2019). For respiratory symptoms, evidence from both developing and developed countries showed consistent associations between indoor particulate exposure and increased risks of wheeze symptoms and acute exacerbations in COPD patients (Hansel et al. 2013).

Particulate matter is a complex mixture consisting of various chemical components and comes from multiple sources. Compared with its mass concentration, some chemical constituents and sources may deserve more attention, but there is a limited literature for indoor PM_{2.5} components. It has been reported that indoor elemental carbon (EC) and primary organic carbon (POC) of PM_{2.5} were associated with decreased evening PEF of healthy young adults (Huang et al. 2019a). Indoor black carbon (BC), a marker of traffic-related PM_{2.5}, was reported to be associated with decreased FEV₁, FVC, and FEV₁/FVC of COPD patients (Hart et al. 2018). In addition, a panel study in Beijing found that indoor PM_{2.5} originated from indoor sources had stronger effects on lung function of COPD patients (Chi et al. 2019).

Some inorganic elements of indoor PM_{2.5} were observed to be negatively associated with FEV₁ and PEF of COPD patients (Zhang et al. 2021). However, the research evidence is still very limited, and the association of indoor particulate constituents and sources with respiratory health needs to be explored further.

Other indoor pollutants, such as ozone (O₃), carbon monoxide (CO), and total volatile organic compound (TVOC), may be also associated with poor respiratory outcomes in the population, but the literature is really limited.

Effects on the Cardiovascular System

The sample sizes in studies on the short-term health effects of indoor air pollutants are usually small. These studies make efforts to quantify the exposure-response associations for certain pollutants by utilizing real-time monitoring. Increasing attention has also been devoted to evaluate the health effects through a viewpoint of sources and constitutions, especially for indoor particulate matter (PM) pollution. Furthermore, the indoor condition provides an ideal opportunity to set a control group and take intervention measures. Accordingly, a wide range of studies also uses quasi-experimental and intervention designs to examine the protecting effects of reducing or controlling indoor air pollutants.

Evidence on this topic is generally limited, possibly due to the relatively small sample sizes and short study periods of related studies. However, studies found that indoor short-term exposures to outdoor air pollutants (PM and ozone) were significantly associated with increased mortality in the US cities (Chen et al. 2012).

Consistent evidence has reported the associations between short-term exposure to indoor air pollutants and elevation in blood pressure (Walzer et al. 2020; Xia et al. 2021a). A systematic review based on ten intervention studies focusing on non-smoking people in smoke-free homes demonstrated that, after using personal air cleaner at home over a median of 13.5 days, there was a significant decrease of 3.94 mmHg (95%CI: -7.00, -0.89) in mean systolic blood pressure (SBP) and an insignificant decrease trend of 0.95 mmHg (95% CI: -2.81, 0.91) in mean diastolic blood pressure (DBP), respectively (Walzer et al. 2020). Meanwhile, a meta-analysis based on 14 cross-over randomized controlled trials (RCTs) found that after utilizing indoor air purification interventions, there was a significant decrease of 2.28 mmHg (95% CI: -3.92, -0.64) in SBP, and a decrease of 0.35 mmHg (95% CI: -1.52, -0.83) in DBP and 0.86 mmHg (95% CI: -2.07, 0.34) in PP (Xia et al. 2021a).

Generally, increases in indoor air pollutants (size-fractionated PM, black carbon, O₃, etc.) are significantly associated with decreases in autonomic cardiac function indicators such as SDNN and HF (Huang et al. 2019b). In addition, a study even found reduced cardiac autonomic function among children under the background of relatively low-level ozone exposure (mean concentration of 8.7 ppb) (Huang et al. 2019b). Meanwhile, an intervention study found that lower household wood smoke exposure was associated with the occurrence of nonspecific ST-segment depression (McCracken et al. 2011).

Although not with consistent findings, most studies report that short-term exposure to indoor air pollutants are associated with activated systematic inflammatory and oxidative stress status representative of increased hs-CRP, IL-6, IL-8, TNF- α ,

fibrinogen, 8-OHdG, and MDA (Xia et al. 2021a). Summarizing the results of 14 RCTs found that utilizing indoor air purification interventions was associated with a 0.23 mg/L decrease (95% CI: -0.63, 0.18) in hs-CRP (Xia et al. 2021a). Furthermore, emerging evidence has reported benefits using biomarkers of coagulation and vasoconstriction (Chen et al. 2015) after filtration of indoor air for several days.

Genetics and omics are novel tools to explore the underlying mechanisms of the health effects associated with indoor air pollutants exposure. Increasing numbers of studies have linked indoor air pollutants to perturbation in metabolomics. Indicators of glucolipid metabolism, amino acid metabolism, and purine and urea cycles were identified as differentiated urinary metabolites in a series of studies indicating perturbations in energy metabolism, inflammation, and oxidative stress. The associations of indoor air pollutants with epigenetics have been increasingly investigated. Studies found that indoor air pollutants might be associated with DNA methylation in peripheral blood (Walker et al. 2020). In addition, PM_{2.5} may also affect micro RNAs (miRNAs) regulating the expression of systemic inflammation, coagulation, and vasoconstriction (Chen et al. 2018).

To date, no clear conclusions have been drawn for the cardiovascular hazards of sources and constitutions of indoor air pollutants due to the limited number of studies. However, combustion and road dust sources and related constituents have been considered important contributors to cardiovascular damages. Novel methods, such as exposomic approaches, and statistical methods like Bayesian Kernel Machine Regression (BKMR), weighted quantile sum (WQS) regression, and machine learning methods, have also been applied to further quantify the individual joint effects of certain sources and constitutions of indoor air pollutants on cardiovascular health.

It should be noted that a few studies have reported negative health effects after utilizing indoor air intervention facilities. A short-term intervention study among 44 children in Beijing, China reported that using an ionization air purifier was associated with negative alterations in cardiovascular health (Dong et al. 2019). The underlying mechanisms were explained to be the masking effects of massive production of negative air ions, which might shield the cardiovascular benefits of decreased indoor particles through lowering energy generation and anti-oxidation capacity with different metabolic pathways (Liu et al. 2020b). The findings stress the necessity of further evaluations on potential health hazards of indoor air intervention facilities, particularly among the susceptible subgroups.

Effects on Other Systems

Evidence for the effects of short-term exposure to indoor air pollution on other human systems is quite limited. A panel study conducted in 55 children with moderate-to-severe atopic dermatitis (AD) repeatedly measured indoor formaldehyde and their AD symptoms and found that a 10 ppb increase in formaldehyde increased AD symptoms by 79.2% (95% CI, 19.6–168.4%) in spring and by 39.9% (95% CI, 14.3–71.2%) in summer (Kim et al. 2021). Another prospective study of 30 children with AD in a day-care center found that indoor air pollutants including toluene increased the risk of AD aggravation (Kim et al. 2015b).

Long-Term Health Effects

Effects on the Respiratory System

Indoor air pollution is still severe in many regions and causes a heavy burden of the disease every year. Long-term exposure to indoor air pollution has been an important risk factor for many chronic non-communicable diseases such as COPD and asthma. Considering the cost and difficulty of long-term monitoring of indoor air pollutants with a large scale, solid fuel or biomass burning for cooking or heating is usually used as a measure of indoor air pollution. To date, indoor air pollution exposure has been linked to various respiratory diseases, including acute respiratory infections (ARIs), tuberculosis, asthma, chronic obstructive pulmonary disease, pneumoconiosis, and lung cancer. Current studies mainly focus on certain susceptible populations, including children, women, elderly people, and patients with chronic respiratory diseases, especially in developing countries.

Among the children, the analysis of data from the China Health and Nutrition Survey suggested that female children had an elevated risk of ARIs when exposed to solid fuel combustion emissions (Chen and Modrek 2018). When it comes to specific pollutants, evidence from birth cohort studies showed indoor particulate matter was associated with lower respiratory tract illness among children (Vanker et al. 2017). A panel study among 150 children found that increased in-home PM_{2.5} and PM_{2.5–10} concentrations were associated with significant increases in asthma symptoms and rescue medication use (McCormack et al. 2011). Additionally, a meta-analysis of the observational studies found that indoor formaldehyde was significantly associated with an increased risk of asthma in children (OR = 1.10, 95% CI: 1.00, 1.21, per 10 µg/m³) (Yu et al. 2020). These studies were mainly conducted in developing countries where household solid fuel was still widely used and indoor air pollution was severe. However, a meta-analysis of epidemiological studies from developed countries did not find significant association between indoor wood burning and respiratory outcomes in children including wheeze, cough, asthma, lower respiratory infection (LRI), and upper respiratory infection (URI) (Guercio et al. 2021).

Among the adults, previous studies also reported the significant association of indoor air pollution caused by wood or coal use for cooking and heating with increased risks of respiratory diseases, symptoms, such as cough, wheezing, dyspnea and phlegm, and lung function decline. A cohort study of 277,838 Chinese never-smokers found that compared with clean fuel users, solid fuel users had a higher risk for major respiratory diseases (HR = 1.36, 95% CI: 1.32, 1.40) including chronic lower respiratory disease (CLRD), COPD, and acute lower respiratory infection (ALRI) (Chan et al. 2019). Indoor air pollution has been also associated with the development of lung cancer. For example, a prospective cohort of never-smoking women in Shanghai ($N = 71,320$) found that indoor air pollution from poor ventilation of coal combustion could increase the risk of lung cancer (Kim et al. 2015a).

The elderly have shown higher sensitivity to particulate pollution and they tend to spend most of their time indoors. Therefore, the effect of indoor air pollution on the respiratory health of elderly people was also widely investigated. The evidence from

China Health and Retirement Longitudinal Study (CHARLS) suggested solid fuel use could significantly increase the possibility of chronic lung diseases and exacerbation of chronic lung diseases (Liu et al. 2018). A cohort study of 6,818 middle-aged and older adults found that solid fuel use in cooking and heating was associated with reduced PEF, especially in those aged >65 years, females, and smokers (Xia et al. 2021b). In general, indoor air pollution, especially those associated with solid fuel combustion, has been associated with multiple adverse respiratory outcomes in the population, and these effects should be of particular concern for certain susceptible populations.

Effects on the Cardiovascular System

A wide range of empirical investigations across different geographical regions and populations have been conducted to evaluate both pathogenic and subclinical effects on cardiovascular health associated with long-term cumulative exposure to indoor air pollutants. Meanwhile, the heterogeneity of exposure-health associations, particularly for the susceptible population subgroups have also received increasing attention.

It's difficult to perform long-term real-time indoor air pollutants monitoring in large population studies. Accordingly, most studies used qualitative variables as proxies for indoor pollutant exposures, representative of household fuels use, and passive smoking. Globally, polluting fuels and technologies were associated with excessive risks of 7% (95% CI: 4%, 11%) for cardiovascular mortality, as well as 9% (95% CI: 4%, 14%) for cerebrovascular diseases, 10% (95% CI: 9%, 11%) for ischaemic heart disease (IHD), and 13% (95% CI: 5%, 22%) for cardiovascular events (Lee et al. 2020). A meta-analysis based on 23 prospective and 17 case-control studies found that, compared to never smokers, exposure to second-hand smoking was significantly associated with increased risk of cardiovascular diseases (RR = 1.18, 95% CI: 1.10, 1.27) (Lv et al. 2015).

Interestingly, a cohort of 16,323 non-smoking women in Xuanwei, China, found that higher lifetime exposure intensity to smokeless coal was significantly associated with higher IHD mortality. However, the association between higher lifetime exposure to smoky coal and IHD mortality was much less significant (Bassig et al. 2020). The authors emphasized that, although smokeless coal was considered a cleaner fuel, it might be associated with excessive health risks (Bassig et al. 2020). From the ecological perspective, a cross-sectional study in England found that energy efficiency metrics (mean energy performance rating) were associated with a 0.5% increase in CVD hospital admissions, indicating that more energy efficiency improvements might result in higher admission rates for CVD (Sharpe et al. 2019).

Long-term associations of indoor air pollutants with subclinical outcomes are to a considerable extent beyond the debate of "adaptive theory," namely, the compensatory reactions to acute exposure to negative irritants in humans.

To date, evidence on associations of indoor air pollutants with blood pressure is still limited and also inconsistent. Based on 77,605 largely premenopausal women from 12 resource-poor countries, the Demographic and Health Surveys (DHS) found

that history of solid fuels use (vs clean fuels use) was associated with 0.58 mmHg higher SBP (95% CI: 0.23, 0.93), 0.30 mmHg higher DBP (95% CI: -0.12, 0.72), and 0.31 mmHg higher PP (95% CI: 0.14, 0.75) (Arku et al. 2018). However, with evidence on 43,313 rural participants in ten countries within the Prospective Urban and Rural Epidemiology (PURE) study, the authors found decreased SBP of 0.48 mmHg (95% CI: -0.95, -0.01) and decreased DBP of 0.44 mmHg (95% CI: -0.72, -0.15) among people using solid fuels compared to those using clean fuels (Arku et al. 2020). Chronic exposure to indoor biomass fuels was also associated with changes in biomarkers of oxidative stress and endothelial inflammation (Caravedo et al. 2016). As for cardiac function, daily biomass fuel has been linked to increased left ventricular internal diastolic diameter, left atrial diameter, and left atrial area, suggesting increased size and decreased systolic function of left ventricular (Burroughs Peña et al. 2017).

Trial methods, although not as widely as in short-term studies, have also been used to provide further evidence on this topic. A long-term randomized crossover intervention study based on 200 homemakers from Taiwan found that indoor air pollutants were significantly associated with increased BP, hs-CRP, and 8-OHDG. Meanwhile, compared to the control phase, those indicators were significantly better in the air filtration intervention phase, supporting the subclinical cardiovascular effects such as activated systematic inflammatory status when exposed to indoor air pollutants (Chuang et al. 2017). In addition, a real-world study found that, compared to women receiving energy packages (a facility promoted by the government of China as next-generation of clean technologies), those not receiving the packages had greater mean decreases in brachial SBP and DBP (Clark et al. 2019). This evidence implied the importance of further evaluations on the pros and cons of new measures (e.g., cleaner products) in the real-world context before formulating environmental policies at the population level.

Emerging studies on the health effects of indoor air pollutants are showing solicitude for the heterogeneity in exposure-response relations across regions in different urbanization stages. Urbanization profoundly shapes the environment, human settlements, lifestyles, and health behaviors, and thus posts mixed effects on population health (Liang et al. 2021). Areas with a lower social development index (SDI) were traditionally regarded as the susceptible regions of indoor air pollutants. One possible reason is the absence or delay of urbanization settings (e.g., cleaner technologies, which can effectively reduce the hazard composition of air pollution emissions) in less-developed areas. Meanwhile, regional age structures and sex proportions are also thought to be potential driving factors, but current evidence has still been unable to provide a clear conclusion (Lee et al. 2020; Lv et al. 2015).

There have also been several different findings. For instance, based on over 90,000 adults from 467 urban and rural communities in 11 low- to middle-income countries (LMIC), the aforementioned PURE study found stronger associations of the incidence of cardiovascular diseases with solid fuel use in people from urban areas, higher education levels, and with the highest home wealth index (Hystad et al. 2019), despite that the associations for all-cause mortality generally showed an inverse trend (Hystad et al. 2019). Apart from differences in disease characteristics,

further studies are still warranted to identify this susceptibility, particularly in terms of socio-economic factors associated with the regional urbanization process.

Effects on Other Systems

The health effect of long-term exposure to indoor air pollution has been also examined in other outcomes, mainly including mental health and abnormal development and physical function. An analysis of data from four visits of 7,005 middle- and old-age adults in the CHARLS found that long-term household air pollution exposure from solid fuel use was significantly associated with higher depression risk among Chinese older adults ($HR = 1.27$, 95% CI, 1.14–1.42 in heating; 1.26, 1.13–1.40 in cooking) (Li et al. 2021). This study also observed that longer durations of indoor air pollution exposure and the exposure from crop residue/wood burning were associated with higher depression risk. The evidence from CHARLS also found that solid fuel use for cooking and heating was significantly associated with a higher risk of cognitive impairment including episodic memory, orientation, and attention dimension, and the association was stronger among participants who were females, aged ≥ 65 years old, had low education level or had cardiovascular diseases (Luo et al. 2021). Indoor air pollution is also associated with abnormal growth and development in children and declined physical function of the elderly. A meta-analysis examined the association between indoor air pollution exposure and postnatal stunting and found that compared with cleaner fuels, exposure to indoor air pollution from solid fuel was significantly associated with a higher risk of stunting among children aged <5 years old ($OR = 1.19$, 95% CI, 1.10–1.29) (Pun et al. 2021). In addition, a study of 12,458 middle-aged and elder participants from CHARLS reported that solid fuel use in cooking was associated with the self-reported and performance-based physical functioning decline (Cao et al. 2021).

Specific Examples

Environmental Tobacco Smoke

Environmental tobacco smoke (ETS) itself is a complex mixture, representing the combination of side stream smoke with exhaled mainstream smoke. ETS is an irritant and significant indoor air pollutant. Active smoking exposes the smoker to approximately 16 times the ETS concentration, and 100- to 300-fold the total smoke dose experienced by a nonsmoker (Smith and Ogden 1998). Despite the much lower smoke exposure, it is known to cause lung cancer, heart disease, chronic obstructive pulmonary disease (COPD), emphysema, and other serious diseases in smokers and in non-smokers as well. According to EPA, ETS causes 3000 lung cancer deaths in adult nonsmokers (roughly 100 million never-smokers and long-term former smokers) in the United States each year; ETS is responsible for between 1,50,000 and 3,00,000 lower respiratory tract infections annually in the roughly 5.5 million children under 18 months of age, and that it exacerbates asthma in about 20% of asthmatic children (U.S.EPA 1992). WHO has estimated that 9–13% of all cancer

cases can be attributed to ETS in a nonsmoking population of which 50% are exposed to ETS (WHO 2009). The proportion of lower respiratory illness in infants attributed to ETS exposure can be estimated at 15–26% (WHO 2009).

Chemical Composition and Exposure Evaluation

ETS is a complex mixture of nearly 5,000 chemical compounds. This mixture contains 43 chemicals that have met the criteria of a known human or animal carcinogen established by the International Agency for Research on Cancer. Common carcinogens in ETS include arsenic, cadmium, benzo-pyrenes, nitrosamines, and vinyl chloride. Other chemical components that are likely to have detrimental effects on the cardio-respiratory system are carbon monoxide which causes the formation of carboxyhemoglobin, and polycyclic aromatic hydrocarbons which increase the size of spontaneous aortic lesions. Other toxicologically significant chemicals include aldehydes (acrolein, formaldehyde), hydrogen cyanide, nitrogen oxides, benzene, toluene, phenols (phenol, cresol), aromatic amines (nicotine, ABP (4-aminobiphenyl)), and harmala alkaloids (WHO 2009). The radioactive element polonium-210 is also known to occur in tobacco smoke (WHO 2009).

As ETS is a dynamic complex mixture of thousands of compounds in particulate and vapor phases, it cannot be measured directly as a whole. Instead, various marker compounds, such as nicotine and respirable suspended particles (RSPs), are used to quantify environmental exposure. In the United States, nicotine concentrations in homes where smoking occurs typically range from less than 1 $\mu\text{g}/\text{m}^3$ to over 10 $\mu\text{g}/\text{m}^3$ (U. S. EPA 1992). Concentrations in offices where people smoke typically range from near zero to over 30 $\mu\text{g}/\text{m}^3$. Levels in restaurants, and especially bars, tend to be even higher, and concentrations in confined spaces such as cars can be higher still. Measurements of ETS-associated RSPs in homes where people smoke range from a few $\mu\text{g}/\text{m}^3$ to over 500 $\mu\text{g}/\text{m}^3$, while levels in offices are generally less than 100 $\mu\text{g}/\text{m}^3$, and those in restaurants can exceed 1 mg/m³. ETS levels are directly related to smoker density; in countries with a higher smoking prevalence, average ETS levels could be higher (WHO 2000).

Health Effects

Experimental evidence has shown the presence of a tobacco-specific carcinogen in the urine of ETS-exposed nonsmokers (Hammond et al. 1993).

Lung cancer

Many health organizations concluded that exposure to ETS increases the risk of lung cancer. The U.S. Environmental protection Agency (EPA) has declared ETS as a known human lung carcinogen based on the following total weight of evidence: (1) chemical composition of ETS and MS, including over 40 known or suspected human carcinogens; (2) the known lung carcinogenicity of MS, with clear exposure-response relationships down to low levels and no evidence of a threshold; (3) supporting evidence from animal bioassays and genotoxicity tests; (4) measured exposure to, and bodily uptake of, ETS constituents; and (5) the consistent exposure-

related increases in risk seen in so many epidemiological studies from different countries using different designs.

The largest and best designed case-control study (Fontham et al. 1994), with 665 cases and a large percentage of direct case interviews, found statistically significant overall increases and exposure-response trends for never-smoking United States women exposed to spousal (30% excess risk), workplace (40% excess risk), and social (50% excess risk) ETS. Another study, the Dutch nested case-control study of de Waard et al. (1995), is noteworthy because although it consisted of only 212 nonsmoking females (23 cases and 191 controls), past nonsmoking status and ETS exposure were determined by biomarker measurements (cotinine level in a 12-h urine sample taken up to 15 years prior to case ascertainment) rather than on the basis of questionnaire responses as in the other ETS-lung cancer epidemiology studies. The results, although not statistically significant, yielded an odds ratio (OR) of about 2.6 for lung cancer from ETS exposure. A recent meta-analysis study (Hacksaw et al. 1997) used the data from 37 published epidemiological studies of nonsmokers who did and did not live with smokers. The excess risk of lung cancer was 24% (95% confidence interval (CI) 13–38%, $P < 0.001$) in nonsmokers who lived with a smoker. The excess risk-adjusted for the effects of bias and dietary confounding, was 26% (7–47%). The dose-response relationship for the risk of lung cancer with the number of cigarettes smoked by the spouse and with the duration of exposure were significant.

Other Cancers

The review by Tredaniel et al. (1994) evaluated the limited epidemiological evidence from studies of ETS and adult sinus, bladder, breast, and uterine cervix cancers, as well as possible cancers of other sites where the evidence is very scarce. They concluded that there was suggestive evidence of an association between ETS with sinus cancer. However, they found no association between ETS with bladder cancer, and equivocal evidence of associations with breast and cervical cancer.

The conclusion between ETS and sinus cancer was based on two positive studies on Japanese female never-smokers. Researchers found strong exposure-response relationships. However, the number of the total cases was only 60. A study in the United States has also reported a statistically significant increased risk for never-smoking men with wives who smoked ($OR = 3.0$, 95% CI = 1.0, 8.9), based on 28 cases (Zheng et al. 1994). Considering these consistent exposure-related responses and the strong supportive evidence, including the known causal association of active smoking and sinus cancer, the known causal association of ETS and lung cancer, and the fact that the nasal sinuses are generally the site of first contact of ETS. There is strong suggestive evidence that ETS is causally associated with sinus cancer.

It has been suggested that bladder cancer may be associated with exposure to ETS although the epidemiological evidence from the two studies reviewed by Tredaniel et al. (1994) and a study by Hirayama (1992) is equivocal. An association between ETS and cervical cancer has also been suggested, but few existing studies provide contradictory findings. The two studies of nonsmokers reviewed by Tredaniel et al.

are generally positive, and a third study found no consistent increases (Coker et al. 1992), while a Japanese cohort study reported a RR estimate of about 1.3 for nonsmoking wives of heavily smoking husbands (Hirayama 1992).

Wells (1991) reviewed data from two epidemiological studies and suggested that there may be an association between ETS exposure and breast cancer in nonsmokers. Two other studies have also found evidence of an association between EST and breast cancer (Smith et al. 1994; Morabia et al. 1994), with RR estimates ranging from about 1.3–2.4. However, no consistent association between active smoking and breast cancer has been established.

Non-cancer Respiratory Health Effects

ETS affects the developing respiratory system and causes an increased risk of the following health effects in children: (1) lower respiratory tract infections (e.g., bronchitis, bronchiolitis, and pneumonia) in infants and young children; (2) chronic middle-ear effusion in young children; (3) increased frequency and severity of asthma attacks in asthmatic children; (4) irritation of the upper respiratory tract; and (5) reduced lung function.

Adult nonsmokers exposed to ETS may experience small reductions in lung function and an increased frequency of respiratory symptoms. A review by Tredaniel et al. (1994) found no consistent evidence for an association between ETS and chronic respiratory symptoms or chronic obstructive pulmonary disease, including asthma, although decreased lung function from ETS exposure was noted. Symptoms of acute irritation of the eyes and respiratory tract were found to be associated with ETS exposure. Bascom et al. (1996) observed symptoms of eye and nose irritation, odor perception, and headache in subjects exposed to SS under controlled conditions. They also reported increased nasal congestion in the highest exposure group. Most of the field and laboratory studies of annoyance and acute irritation effects of ETS have focused on adults. However, these effects are likely to occur in children as well, since they are even more sensitive than adults to other non-cancer respiratory effects of ETS.

Cardiovascular Effects

According to the results of epidemiological and experimental studies, environmental tobacco smoke has significant harmful effects on the cardiovascular system. Epidemiological studies clearly show that active smoking has a causal relationship with cardiovascular disease. In addition, ETS also has an impact on cardiovascular disease in non-smokers. Studies of cardiovascular disease morbidity and mortality in ETS and non-smokers vary based on disease outcome (e.g., fatal and/or non-fatal events), gender, and alternative measures of ETS exposure (e.g., spouse smoking, cohabiting smoking, and work exposure). They also vary greatly in size and potential confounding factors for inspection. Steenland (1992) derived a quantitative risk estimate of 35,000–40,000 ETS-attributable deaths from heart disease per year among never-smokers and long-term smokers in the United States.

Mechanism studies have shown that acute ETS exposure will have cardiovascular effects on the human body. The main effects include decreased oxygen-carrying capacity leading to decreased exercise capacity and potential ischemia, as well as increased platelet activation, endothelial damage, changes in lipoprotein levels, and increased arterial wall thickness, which promotes atherosclerosis. In the case of platelet activation, ischemia, and atherosclerosis increase the risk of myocardial infarction and other serious cardiovascular diseases.

In different studies from different countries, the overall risk increase and exposure-response increase trends are consistent. The increased risk of these fatal and non-fatal cardiovascular events was observed from exposures to actual environmental levels of ETS. A large cohort study (Helsing et al. 1988) reported the estimated RR of death from arteriosclerosis caused by family ETS exposure, which was 1.31 for men and 1.24 for women, adjusted for a series of confounding factors. A significant exposure-response relationship was observed in women, but not in men. This study did not adjust for important cardiovascular disease risk factors, such as high blood pressure, diet, and serum cholesterol. The second large-scale study (Hirayama 1984, 1990) observed that women have a slightly increased risk of death from coronary heart disease due to their spouse smoking, and the exposure-response trend is significant. Both studies indicate that, as observed for active smoking, the relative risk increase in younger age groups may be greater. Smaller cohort studies reported that after adjusting for various confounding factors, marrying or cohabiting with a smoker resulted in an increased overall risk of many fatal and non-fatal cardiovascular disease endpoints (WHO 2000). Svendsen et al. (1987) reported an estimated adjusted RR of 2.23 (95% CI, 0.72–6.92) for deaths from coronary heart disease, and an estimated RR of 1.61 (95% CI, 0.96–2.71) for fatal or non-fatal coronary heart disease events caused by wife smoking and positive exposure. Case-control studies (He et al. 1989; La Vecchia et al. 1993; He et al. 1994) also examined a large number of risk factors for cardiovascular disease. The odds ratio of acute myocardial infarction resulting from a combination of marriage and current smoker is 1.21 (95% CI, 0.57–2.52); 1.50 (95% CI, 1.28–1.77) represents female coronary heart disease, 1.85 (95% CI, 0.86–4.00) represents women's non-fatal disease cases due to exposure at work, and 1.24 (95% CI, 0.56–2.72) from reports of husband smoking. In addition, positive contact trends were reported. In addition to cohort studies and case-control studies, there are also cross-sectional studies examining cardiovascular disease incidence and ETS. A statistically significant exposure-response relationship was observed. Serum cotinine is only closely related to diagnosed coronary heart disease.

Other Health Effects

Furthermore, as with active smoking, ETS reduces birth weight in the offspring of nonsmoking mothers. In infants, recent evidence suggests that ETS is a risk factor for sudden infant death syndrome (WHO 2000).

Guidelines

ETS has been found to be carcinogenic in humans and to produce a substantial amount of morbidity and mortality from other serious health effects at levels of 1–10 µg/m³ nicotine (taken as an indicator of ETS). Acute and chronic respiratory health effects on children have been demonstrated in homes with smokers (nicotine 1–10 µg/m³) and even in homes with occasional smoking (0.1–1 µg/m³). There is no evidence of a safe exposure level. The unit risk of cancer associated with lifetime ETS exposure in a home where one person smokes is approximately 1×10^{-3} (WHO 2000).

Radon

Radon is a radioactive gas that has no smell, color, or taste. Radon emanates from rocks and soils and tends to concentrate in enclosed spaces like underground mines or houses. Radon is a major contributor to the ionizing radiation dose received by the general population. The most important source of residential radon is soil gas infiltration. Other indoor sources are building materials.

Radon is the second cause of lung cancer in the general population, after smoking. The majority of radon-induced lung cancers are caused by low and moderate radon concentrations rather than by high radon concentrations, because in general less people are exposed to high indoor radon concentrations. Current estimates of the proportion of lung cancers attributable to radon range from 3% to 14%, depending on the average radon concentration in the country concerned and the calculation methods (WHO 2009). Most of the radon-induced lung cancer cases occur among smokers due to a strong combined effect of smoking and radon.

The World Health Organization first drew attention to the health effects from residential radon exposures in 1979, through a European working group on indoor air quality. Further, radon was classified as a human carcinogen in 1988 by International Agency for Research on Cancer (IARC), the WHO specialized cancer research agency.

Health Effects

Lung Cancer

There is overwhelming evidence that radon is acting as a cause of lung cancer in the general population at concentrations found in ordinary homes. In addition, the dose-response relationship appeared to be linear, with no evidence of a threshold, and there was substantial evidence of a risk increase even below 200 Bq/m³, the concentration at which action is currently advocated in many countries (WHO 2009).

According to Gray et al. (2009), 3.3% of deaths from lung cancer in the UK (one in 516 of all deaths) were caused by radon in the home in 2006 with an average Rn level of 21 Bq/m³. Overall, 48% of radon-related deaths occurred in adults aged 55–74. Most of the remainder occurred in those aged more than 75, with only 6% at ages less than 55, and virtually none below age 35. 58% of radon-related deaths were in

men. The risk for former smokers is substantially lower than for continuing smokers, even for those stopping as late as age 50, but it remains considerably above the risk for lifelong non-smokers.

Only an estimated 0.4% of homes in the UK would have measured radon concentrations of 200 (mean 304) Bq/m³ or higher. Although people living in such homes have a greater risk than those living in homes with lower measurements, few such people exist. The estimated percentage of deaths from radon-related lung cancer in homes with measurements of 200 Bq/m³ or more is 4%, with measurements of 100–199 Bq/m³ is 9%, and with measurements of 50–99 Bq/m³ is 17%. The remaining 70% of deaths from radon-related lung cancer are in homes where the measurement would be below 50 Bq/m³.

Surveys have been carried out to determine the distribution of residential radon concentrations in most of the 30 member countries of the Organization for Economic Co-operation and Development (OECD). The worldwide average indoor radon concentration has been estimated at 39 Bq/m³. Detailed calculations of the numbers of radon-induced lung cancers attributable to radon exposure have previously been published for a number of countries. The calculations are based on the estimated concentrations of indoor radon from the surveys and the indirect estimates of risk provided either by the studies of miners in the BEIR VI analysis or by the direct evidence provided by the European pooling studies (Table 1).

Other Diseases

Other diseases that can be induced by indoor radon include leukemia, and multiple sclerosis. Cardiovascular disease may be also associated with indoor radon.

Table 1 Estimates of the proportion of lung cancer attributable to radon in selected countries (WHO 2009)

Country	Mean indoor radon (Bq/m ³)	Percentage of lung cancer attributed to radon	Estimated no. of death due to radon-induced lung cancer each year
Canada (Brand et al. 2005)	28	7.8	1400
Germany (Menzler et al. 2008)	49	5	1896
Switzerland (Menzler et al. 2008)	78	8.3	132
United Kingdom (AGIR 2009)	21	3.3	1089
		6	2005
France (Catelinois et al. 2006)	89	5	1234
		12	2913
United States (BEIR VI 1999)	46	10–14	15,400–21,800

Rericha et al. (2006) evaluated the incidence of leukemia, lymphoma, and multiple myeloma in Czech uranium miners. They found a positive association between radon exposure and leukemia, including chronic lymphocytic leukemia. The relationship between radon exposure and cardiovascular disease has been examined in a number of cohorts of radon-exposed miners, but none has found evidence that radon could cause heart disease. A case-control study of stomach cancer in an area where there were high concentrations of natural uranium and other radionuclides in drinking water gave no indication of an increased risk (Auvinen et al. 2005).

About 20 ecological studies of exposure to radon in the general population and leukemia either in children or in adults have been carried out. Several of these, including a recent methodologically advanced study by Smith et al. (2007), have found associations between indoor radon concentration and the risk of leukemia (including chronic lymphocytic leukemia in the Smith et al. study) at the geographic level. An ecological study performed in Norway showed an association between multiple sclerosis and indoor radon concentration (Bolviken et al. 2003). Generally, these associations have been confirmed in a high-quality case-control or cohort study, either in radon-exposed miners or in the general population, although several such studies have been carried out (Laurier et al. 2001, Mohner et al. 2006). As with the studies of radon exposure and lung cancer, these ecological studies are prone to a number of biases. They are therefore likely to give misleading answers and should not be taken as evidence that radon is acting as a cause of these diseases.

Guidelines

Currently, no federal regulations govern acceptable radon levels for indoor residential and school environments. However, guidelines are available. The United States Environmental Protection Agency (US EPA) and the Surgeon General strongly recommend that all homes be tested for radon and, if levels are elevated, residents are urged to consider remediation. The US EPA's action guideline is 4 pCi/L (148 Bq/m³) for the indoor radon concentration (WHO 2009).

Nitrogen Dioxide (NO₂)

Nitrogen dioxide (NO₂) is a nitrogen oxide associated with combustion sources. It exists in the air in its gaseous form. NO₂ is volatile, reddish-brown in color, and heavier than air, and has a characteristic pungent odor perceptible from a concentration of 188 µg/m³ (0.1 ppm) (WHO 2010). Indoor levels of nitrogen dioxide are a function of both indoor and outdoor sources. The most important indoor sources of NO₂ include tobacco smoke and gas-, wood-, oil-, kerosene-, and coal-burning appliances such as stoves, ovens, space and water heaters, and fireplaces, particularly ones without chimneys or poorly maintained appliances. Outdoor NO₂ from natural and anthropogenic sources also influences indoor levels. Road traffic is the principal outdoor source of nitrogen dioxide.

Health Effects

There is evidence that NO₂ is associated with an increase in respiratory symptoms among the general population, particularly in children, in a range of epidemiological studies that the authors have previously reviewed. Results of longitudinal studies on asthmatic populations or subjects at risk of developing asthma are quite conclusive: an increase in NO₂ concentration was also associated with increased wheezing, breathing difficulty, chest tightness, shortness of breath, and cough. However, data at the general population level are more controversial. Few studies have found significantly increased risks of respiratory symptoms and asthma in association with a higher concentration of NO₂ at home or at school. Moreover, whether chronic exposure to indoor NO₂ contributes to the development of respiratory illness is unclear. Two longitudinal studies including children found a positive association between long-term exposure to indoor NO₂ and the risk of lower respiratory symptoms (U.S.EPA 2008; Brauer et al. 2006). In a Japanese cohort, exposure to NO₂ was associated with an increased risk of doctor-diagnosed asthma and bronchitis, but not with the incidence of these diseases (Morgenstern et al. 2008). Two birth cohort studies that followed 1,611 infants for one yr. and 1,205 for 18 months, and one cohort survey including 842 children enrolled at 9–10 yrs. of age did not confirm these results (Shima and Adachi 2000; Samet et al. 1993; Sunyer et al. 2004). Reasons for these conflicting results are unknown, but the difficulties in determining real exposure to indoor nitrogen dioxide could explain them in part. In homes, exposure can fluctuate depending mainly on the season of measurement in conjunction with the use of specific sources, such as gas appliances. Therefore, assessment over 1 week could not be representative of nitrogen dioxide exposure and, in particular, of peak concentrations during cooking or heating activities. Evidence of an association between exposure to indoor combustion, such as gas appliances, and asthma development and severity exists. In a randomized controlled trial, the replacement of unvented gas heaters with flued gas or electric heaters showed a decrease in nitrogen dioxide concentration (15.5 vs. 47.0 ppb, $p < 0.0001$) and a significantly reduced risk of breathing difficulty during the day and the night, chest tightness during the day and daytime asthma attacks in the intervention group (Linn et al. 1985). Finally, inconsistencies among studies may also be due to modification by other pollutants or higher susceptibility in some subgroups, such as female children (Morgenstern et al. 2008).

Guidelines

According to WHO, a one-hour indoor NO₂ guideline is 200 µg/m³; An annual average indoor nitrogen dioxide guideline is 40 µg/m³. Recent well-conducted epidemiological studies that have used measured indoor nitrogen dioxide levels support the occurrence of respiratory health effects at the level of the guideline (WHO 2010).

Formaldehyde and Volatile Organic Compounds (VOCs)

Formaldehyde and Volatile organic compounds (VOCs) are emitted as gases from certain solids or liquids. Concentrations of formaldehyde and many VOCs are consistently higher indoors (up to 10 times higher) than outdoors. Indoor sources of VOCs include building materials and furnishings, household products (paints, paint strippers and other solvents, wood preservatives, aerosol sprays, cleansers and disinfectants, moth repellents and air fresheners, stored fuels and automotive products, hobby supplies, dry-cleaned clothing, and pesticide), office equipment (such as copiers and printers, correction fluids, and carbonless copy paper), and graphics and craft materials (including glues and adhesives, permanent markers, and photographic solutions) (WHO 2010).

Health Effects

The health effects caused by formaldehyde and VOCs depend on the concentration and length of exposure to the chemicals. VOCs include a variety of chemicals that can cause eye, nose and throat irritation, shortness of breath, headaches, fatigue, nausea, dizziness, and skin problems. Higher concentrations may cause irritation of the lungs, as well as damage to the liver, kidney, or central nervous system. Long-term exposure may also cause damage to the liver, kidneys, or central nervous system. Some VOCs are suspected of causing cancer and some have been shown to cause cancer in humans.

Cancer

A number of the VOCs that are present in indoor air have been shown to cause cancer in animals exposed to high concentrations. The International Agency for Research on Cancer (IARC) has classified formaldehyde and benzene as carcinogens to humans. Estimates of the magnitudes of cancer risks posed by indoor air VOCs vary widely, with most estimates indicating that total excess individual risks for developing cancer with lifetime exposures for specific VOCs are between one in 10,000 and one in a million. Given the uncertainties in cancer risk assessment, particularly the uncertainties of extrapolating from high concentrations to typical lower indoor concentrations, or from animals to humans, as well as the limited available information on the effects of VOC mixtures, and the effects of VOCs on susceptible populations, the magnitude of the cancer risks posed by indoor VOCs will continue to have a high level of uncertainty.

Respiratory Health

Formaldehyde is one of the most studied pollutants in indoor air. Several cross-sectional studies showed an increased risk of asthma with high exposure to indoor formaldehyde, whereas some did not find any significant results (Marion et al. 2012). The first longitudinal study on the respiratory effects of indoor formaldehyde found a

significant positive association between formaldehyde concentration and incidence of asthma diagnosis (OR 1.7, 95% CI 1.1–2.6, for each formaldehyde increment of $10 \mu\text{g}\cdot\text{m}^{-3}$), but only among non-atopic children (U.S. EPA 2010). In a recent meta-analysis, McGwin et al. (2010) calculated a 17% increase in the risk of asthma (OR 1.17, 95% CI 1.01–1.36) for every $10 \mu\text{g}\cdot\text{m}^{-3}$ unit increase in formaldehyde concentration. Lastly, there is some convincing evidence of an effect of formaldehyde in asthma morbidities, such as respiratory symptoms or lung function (Marion et al. 2012).

Other indoor VOCs have been studied in relation to respiratory health. Significant associations between the indoor concentration of VOCs and asthma or asthma-like symptoms were found (Rumchev et al. 2004). This was confirmed by a survey using personal assessment of VOC exposure (Arif and Shah 2007), showing an increased risk of doctor-diagnosed asthma among those exposed to VOCs and, in particular, to aromatic compounds (OR 1.63, 95% CI 1.17–2.27). While existing studies suggest that exposure to VOC in utero could have an impact on the immune status of newborns (Baiz et al. 2011), no epidemiological study using objective measurements reports significant associations between exposure to formaldehyde and allergic sensitization.

Guidelines

For formaldehyde, the no-observed-adverse-effect-level (NOAEL) of $0.6 \text{ mg}/\text{m}^3$ for the eyeblink response is adjusted using an assessment factor of five derived from the standard deviation of nasal pungency (sensory irritation) thresholds, leading to a value of $0.12 \text{ mg}/\text{m}^3$, which has been rounded down to $0.1 \text{ mg}/\text{m}^3$. This threshold should not be exceeded at any 30-min interval during the day. The NOAEL for cell proliferation is $1.25 \text{ mg}/\text{m}^3$ for long-term exposures. An interspecies assessment factor of three is proposed because the effect is local (non-systemic) and directly due to formaldehyde itself; for inter-individual variation, an assessment factor as low as two is proposed because sensitivity differences are not seen among different populations (asthmatics, children, and older people). This process would lead to a proposed guideline of $0.21 \text{ mg}/\text{m}^3$ for the protection of health for long-term effects, including cancer (WHO 2010).

For benzene, there is no known exposure threshold for the risks of benzene exposure. The concentrations of airborne benzene associated with an excess lifetime risk of 1/10,000, 1/100,000, and 1/1,000,000 are 17, 1.7, and $0.17 \mu\text{g}/\text{m}^3$, respectively. Therefore, from a practical standpoint, it is expedient to reduce indoor exposure levels to as low as possible (WHO 2010).

For trichloroethylene (ACE), carcinogenicity (with the assumption of genotoxicity) is selected as the end-point for setting the guideline value. The unit risk estimate of $4.3 \times 10^{-7} (\mu\text{g}/\text{m}^3)^{-1}$, derived on the basis of increased Leydig cell tumors (testicular tumors) in rats, is proposed as the indoor air quality guideline. The concentrations of airborne TCE associated with an excess lifetime cancer risk of 1:10,000, 1:100,000, and 1:1,000,000 are respectively 230, 23, and $2.3 \mu\text{g}/\text{m}^3$ (WHO 2010).

For tetrachloroethylene (PERC), on the basis of the overall health risk evaluation, the recommended guideline for year-long exposure is $0.25 \text{ mg}/\text{m}^3$ (WHO 2010).

Conclusions and Outlook

In summary, the adverse health effect of indoor air pollution cannot be ignored. Even low-level exposure to indoor pollutants may have adverse health effects, especially for children, pregnant women, and people with chronic diseases. In general, the research on indoor air pollution and health has made some progress in the past 10 years, but there are still some shortcomings, and it is expected that in-depth systematic research will be carried out in the future.

1. Previous studies have mostly focused on indoor particulate matter and population health, and the population epidemiological research on indoor gaseous pollutants is relatively limited, especially in developing countries such as China where indoor pollution is more serious. Current researchers mostly focus on the short-term effects of pollutants. It is necessary to carry out more long-term research in the future to clarify the effect of indoor particulate matter on the cardiopulmonary health of patients with COPD.
2. Studies on the indoor environment and population health mostly focused on healthy people. Research evidence specifically for chronic disease patients, children, pregnant women, and other susceptible populations is relatively insufficient. The health outcomes are mostly cardiopulmonary health. In the future, the health effects of indoor air pollution on other organs and systems of the population need more attention.
3. There is insufficient evidence on the sources, characteristics, and health contributions of indoor air pollutants. In addition to outdoor penetration, the sources of indoor pollutants also include indoor cooking, human activities, smoking, and other important indoor sources, which may be more complex. In addition, the health threats of biological components of indoor particulate matter cannot be ignored.
4. So far, research on the biological mechanism of the human health hazards caused by different indoor pollutants is very limited: the population exposure and its biological mechanism are not very clear, and the relationship between the population's exposures to indoor pollutants has not been clearly established. Therefore, in-depth mechanism research is still needed. The rapid development of transcriptomics, proteomics, metabolomics, microbiome, and other omics technologies provides a good opportunity for mechanism research.
5. The intervention of indoor air pollution and its population health impact is also an emerging topic.

References

- Abolhasani R, Araghi F, Tabary M, Aryannejad A, Mashinchi B, Robati RM (2021) The impact of air pollution on skin and related disorders: a comprehensive review. Dermatol Ther 34:e14840
- Advisory Group on Ionising Radiation (AGIR) (2009) Radon and public health. radiation, Chemicals and environmental hazards. Health Protection Authority. (http://www.hpa.org.uk/web/HPAwebFile/HPAweb_C/1243838496865)

- American Thoracic Society; European Respiratory Society (2005) ATS/ERS recommendations for standardized procedures for the online and offline measurement of exhaled lower respiratory nitric oxide and nasal nitric oxide, 2005. *Am J Respir Crit Care Med* 171:912–930
- Arif AA, Shah SM (2007) Association between personal exposure to volatile organic compounds and asthma among US adult population. *Int Arch Occup Environ Health* 80:711–719
- Arku RE, Ezzati M, Baumgartner J, Fink G, Zhou B, Hystad P et al (2018) Elevated blood pressure and household solid fuel use in premenopausal women: analysis of 12 demographic and health surveys (dhs) from 10 countries. *Environ Res* 160:499–505
- Arku RE, Brauer M, Ahmed SH, AlHabib KF, Avezum Á, Bo J et al (2020) Long-term exposure to outdoor and household air pollution and blood pressure in the prospective urban and rural epidemiological (pure) study. *Environ Pollut* 262:114197
- Auvinen A et al (2005) Radon and other natural radionuclides in drinking water and risks of stomach cancer: a case-cohort study in Finland. *Int J Cancer* 10:109–113
- Baiz N, Slama R, Béné MC et al (2011) Exposure to air pollution before and during pregnancy can induce changes in newborn's cord blood lymphocytes involved in allergic response. *BMC Pregnancy Childbirth* 11:1–12
- Bascom R et al (1996) Tobacco smoke upper respiratory response relationships in healthy non-smokers. *Fundam Appl Toxicol* 29:86–93
- Bassig BA, Dean Hosgood H, Shu XO, Vermeulen R, Chen BE, Katki HA et al (2020) Ischaemic heart disease and stroke mortality by specific coal type among non-smoking women with substantial indoor air pollution exposure in China. *Int J Epidemiol* 49:56–68
- BEIR VI (1999) Health effects of exposure to radon. Washington, DC: The National Academies Press. <https://doi.org/10.17226/5499>.
- Bolviken B et al (2003) Radon: a possible risk factor in multiple sclerosis. *Neuroepidemiology* 22: 87–94
- Brand KP, Zielinski JM, Krewski D (2005) Residential radon in Canada: an uncertainty analysis of population and individual lung cancer risk. <https://doi.org/10.1111/j.1539-6924.2005.00587.x>
- Brauer M et al (2006) Traffic-related air pollution and otitis media. *Environ Health Perspect* 114: 1414–1418
- Burroughs Peña MS, Velazquez EJ, Rivera JD, Alenezi F, Wong C, Grigsby M et al (2017) Biomass fuel smoke exposure was associated with adverse cardiac remodeling and left ventricular dysfunction in Peru. *Indoor Air* 27:737–745
- Cao L, Gao J, Xia Y (2021) The effects of household solid fuel use on self-reported and performance-based physical functioning in middle-aged and older Chinese populations: a cross-sectional study. *Ecotoxicol Environ Saf* 213:112053
- Caravedo MA, Herrera PM, Mongilardi N, de Ferrari A, Davila-Roman VG, Gilman RH et al (2016) Chronic exposure to biomass fuel smoke and markers of endothelial inflammation. *Indoor Air* 26:768–775
- Catelinois O et al (2006) Lung cancer attributable to indoor radon exposure in France: impact of the risk models and uncertainty analysis. *Environ Health Perspect* 114(9):1361–1366
- Chan KH, Kurmi OP, Bennett DA, Yang L, Chen Y, Tan Y et al (2019) Solid fuel use and risks of respiratory diseases. A cohort study of 280,000 Chinese never-smokers. *Am J Respir Crit Care Med* 199:352–361
- Chang LT, Hong GB, Weng SP, Chuang HC, Chang TY, Liu CW et al (2019) Indoor ozone levels, houseplants and peak expiratory flow rates among healthy adults in Taipei, Taiwan. *Environ Int* 122:231–236
- Chen C, Modrek S (2018) Gendered impact of solid fuel use on acute respiratory infections in children in China. *BMC Public Health* 18:1170
- Chen C, Zhao B, Weschler CJ (2012) Indoor exposure to “outdoor PM10”: assessing its influence on the relationship between pm10 and short-term mortality in U.S. *Cities Epidemiol* 23:870–878
- Chen R, Zhao A, Chen H, Zhao Z, Cai J, Wang C et al (2015) Cardiopulmonary benefits of reducing indoor particles of outdoor origin: a randomized, double-blind crossover trial of air purifiers. *J Am Coll Cardiol* 65:2279–2287

- Chen R, Li H, Cai J, Wang C, Lin Z, Liu C et al (2018) Fine particulate air pollution and the expression of microRNAs and circulating cytokines relevant to inflammation, coagulation, and vasoconstriction. *Environ Health Perspect* 126:017007
- Chi R, Chen C, Li H, Pan L, Zhao B, Deng F et al (2019) Different health effects of indoor- and outdoor-originated PM2.5 on cardiopulmonary function in COPD patients and healthy elderly adults. *Indoor Air* 29:192–201
- Chuang HC, Ho KF, Lin LY, Chang TY, Hong GB, Ma CM et al (2017) Long-term indoor air conditioner filtration and cardiovascular health: a randomized crossover intervention study. *Environ Int* 106:91–96
- Clark SN, Schmidt AM, Carter EM, Schauer JJ, Yang X, Ezzati M et al (2019) Longitudinal evaluation of a household energy package on blood pressure, central hemodynamics, and arterial stiffness in China. *Environ Res* 177:108592
- Coker AL et al (1992) Active and passive cigarette smoke exposure and cervical intraepithelial neoplasia. *Cancer Epidemiol Biomark Prev* 1:349–356
- De Waard F et al (1995) Urinary cotinine and lung cancer risk in a female cohort. *Br J Cancer* 72: 784–787
- Dong W, Liu S, Chu M, Zhao B, Yang D, Chen C et al (2019) Different cardiorespiratory effects of indoor air pollution intervention with ionization air purifier: findings from a randomized, double-blind crossover study among school children in Beijing. *Environ Pollut* 254:113054
- Du B, Tandoc MC, Mack ML, Siegel JA (2020) Indoor CO₂ concentrations and cognitive function: a critical review. *Indoor Air* 30:1067–1082
- Fontham ETH et al (1994) Environmental tobacco smoke and lung cancer in non-smoking women: a multicenter study. *J Am Med Assoc* 271:1752–1759
- Graham BL, Steenbruggen I, Miller MR, Barjaktarevic IZ, Cooper BG, Hall GL et al (2019) Standardization of spirometry 2019 update. An official american thoracic society and european respiratory society technical statement. *Am J Respir Crit Care Med* 200:e70–e88
- Gray A, Read S, McGale P, Darby S (2009) Lung cancer deaths from indoor radon and the cost effectiveness and potential of policies to reduce them. *BMJ* 338:a3110
- Guercio V, Pojum IC, Leonardi GS, Shrubsole C, Gowers AM, Dimitroulopoulou S et al (2021) Exposure to indoor and outdoor air pollution from solid fuel combustion and respiratory outcomes in children in developed countries: a systematic review and meta-analysis. *Sci Total Environ* 755:142187
- Hacksaw AK et al (1997) The accumulated evidence on lung cancer and environmental tobacco smoke. *Br Med J* 315:980–988
- Hammond SK, Coglin J, Gann PH, Paul M, Taghizadeh K, Skipper PL, Tannenbaum SR (1993) *J Natl Cancer Inst* 85:474–478
- Hansel NN, McCormack MC, Belli AJ, Matsui EC, Peng RD, Aloe C et al (2013) In-home air pollution is linked to respiratory morbidity in former smokers with chronic obstructive pulmonary disease. *Am J Respir Crit Care Med* 187:1085–1090
- Hart JE, Grady ST, Laden F, Coull BA, Koutrakis P, Schwartz JD et al (2018) Effects of indoor and ambient black carbon and PM2.5 on pulmonary function among individuals with COPD. *Environ Health Persp* 126:127008
- He Y et al (1989) Women's passive smoking and coronary heart disease. *Chinese journal of preventive medicine* 23:19–22
- He Y et al (1994) Passive smoking at work as a risk factor for coronary heart disease in Chinese women who have never smoked. *Br Med J* 308:380–384
- He ZZ, Guo PY, Xu SL, Zhou Y, Jalaludin B, Leskinen A et al (2021) Associations of particulate matter sizes and chemical constituents with blood lipids: a panel study in Guangzhou, China. *Environ Sci Technol* 55:5065–5075
- Helsing KJ et al (1988) Heart disease mortality in non-smokers living with smokers. *Am J Epidemiol* 127:915–922
- Hirayama T (1984) Cancer mortality in nonsmoking women with smoking husbands based on a large-scale cohort study in Japan. *Prev Med* 13:680–690.

- Hirayama T (1990) Passive smoking (letter). *N Z Med J* 103:54
- Hirayama T (1992) Lung cancer and other diseases related to passive smoking: a large-scale cohort study. In: Gupta PC et al (eds) *Control of tobacco-related cancers and other diseases*. Oxford University Press, Bombay
- Huang S, Feng H, Zuo S, Liao J, He M, Shima M et al (2019a) Short-term effects of carbonaceous components in PM_{2.5} on pulmonary function: a panel study of 37 Chinese healthy adults. *Int J Environ Res Public Health* 16(13):2259
- Huang J, Song Y, Chu M, Dong W, Miller MR, Loh M et al (2019b) Cardiorespiratory responses to low-level ozone exposure: the indoor ozone study in children (dose). *Environ Int* 131:105021
- Hystad P, Duong M, Brauer M, Larkin A, Arku R, Kurmi OP et al (2019) Health effects of household solid fuel use: findings from 11 countries within the prospective urban and rural epidemiology study. *Environ Health Perspect* 127:57003
- Idarraga MA, Guerrero JS, Mosle SG, Miralles F, Galor A, Kumar N (2020) Relationships between short-term exposure to an indoor environment and dry eye (de) symptoms. *J Clin Med* 9(5):1316
- Kim C, Gao YT, Xiang YB, Barone-Adesi F, Zhang Y, Hosgood HD et al (2015a) Home kitchen ventilation, cooking fuels, and lung cancer risk in a prospective cohort of never smoking women in Shanghai, China. *Int J Cancer* 136:632–638
- Kim EH, Kim S, Lee JH, Kim J, Han Y, Kim YM et al (2015b) Indoor air pollution aggravates symptoms of atopic dermatitis in children. *PLoS One* 10:e0119501
- Kim YM, Kim J, Ha SC, Ahn K (2021) Harmful effect of indoor formaldehyde on atopic dermatitis in children: a longitudinal study. *Allergy, Asthma Immunol Res* 13:468–478
- La Vecchia CL et al (1993) Passive smoking and the risk of acute myocardial infarction (letter). *Lancet* 341:505–506
- Laurier D, Valenty M, Tirmarche M (2001) Radon exposure and the risk of leukemia: a review of epidemiological studies. *Health Phys* 81:272–288
- Lee KK, Bing R, Kiang J, Bashir S, Spath N, Stelzle D et al (2020) Adverse health effects associated with household air pollution: a systematic review, meta-analysis, and burden estimation study. *Lancet Glob Health* 8:e1427–e1434
- Li C, Zhou Y, Ding L (2021) Effects of long-term household air pollution exposure from solid fuel use on depression: evidence from national longitudinal surveys from 2011 to 2018. *Environ Pollut* 283:117350
- Liang Z, Wang W, Wang Y, Ma L, Liang C, Li P et al (2021) Urbanization, ambient air pollution, and prevalence of chronic kidney disease: a nationwide cross-sectional study. *Environ Int* 156:106752
- Linn WS et al (1985) Effects of exposure to 4-ppt nitrogen dioxide in healthy and asthmatic volunteers. *Arch Environ Health* 40:234–239
- Liu J, Hou B, Ma XW, Liao H (2018) Solid fuel use for cooking and its health effects on the elderly in rural China. *Environ Sci Pollut Res* 25:3669–3680
- Liu Y, Chen X, Yan Z (2020a) Depression in the house: the effects of household air pollution from solid fuel use among the middle-aged and older population in China. *Sci Total Environ* 703:134706
- Liu S, Huang Q, Wu Y, Song Y, Dong W, Chu M et al (2020b) Metabolic linkages between indoor negative air ions, particulate matter and cardiorespiratory function: a randomized, double-blind crossover study among children. *Environ Int* 138:105663
- Luo Y, Zhong Y, Pang L, Zhao Y, Liang R, Zheng X (2021) The effects of indoor air pollution from solid fuel use on cognitive function among middle-aged and older population in China. *Sci Total Environ* 754:142460
- Lv X, Sun J, Bi Y, Xu M, Lu J, Zhao L et al (2015) Risk of all-cause mortality and cardiovascular disease associated with secondhand smoke exposure: a systematic review and meta-analysis. *Int J Cardiol* 199:106–115
- Marion H, Marzia S, Giovanni V, Isabella AM (2012) Respiratory health and indoor air pollutants based on quantitative exposure assessments. *Eur Respir J* 40:1033–1045

- McCormack MC, Breysse PN, Matsui EC, Hansel NN, Peng RD, Curtin-Brosnan J et al (2011) Indoor particulate matter increases asthma morbidity in children with non-atopic and atopic asthma. *Ann Allergy Asthma Immunol* 106:308–315
- McCracken J, Smith KR, Stone P, Díaz A, Arana B, Schwartz J (2011) Intervention to lower household wood smoke exposure in Guatemala reduces st-segment depression on electrocardiograms. *Environ Health Perspect* 119:1562–1568
- McGwin G, Lienert J, Kennedy JI (2010) Formaldehyde exposure and asthma in children: a systematic review. *Environ Health Perspect* 118:313–317
- Menzler S et al (2008) Population attributable fraction for lung cancer due to residential radon in Switzerland and Germany. *Health Phys* 95:179–189
- Miller MR, Hankinson J, Brusasco V, Burgos F, Casaburi R, Coates A et al (2005) Standardisation of spirometry. *Eur Respir J* 26:319–338
- Mohner M et al (2006) Leukemia and exposure to ionizing radiation among German uranium miners. *Am J Ind Med* 49(4):238–248
- Morabia A et al (1994) A population-based case-control study of tobacco smoke and breast cancer (abstract). *Am J Epidemiol* 139:S28
- Morgenstern V et al (2008) Atopic diseases, allergic sensitization, and exposure to traffic-related air pollution in children. *American Journal of Respiratory & Critical Care Medicine* 177: 1331–1337
- Pun VC, Dowling R, Mehta S (2021) Ambient and household air pollution on early-life determinants of stunting—a systematic review and meta-analysis. *Environ Sci Pollut Res Int* 28:26404–26412
- Rericha V et al (2006) Incidence of leukemia, lymphoma, and multiple myeloma in Czech uranium miners: a case-cohort study. *Environ Health Perspect* 114(6):818–822
- Rumchev K, Spickett J, Bulsara M et al (2004) Association of domestic exposure to volatile organic compounds with asthma in young children. *Thorax* 59:746–751
- Samet JM, Lambert WE, Skipper BJ et al (1993) Nitrogen dioxide and respiratory illnesses in infants. *Am Rev Respir Dis* 148:1258–1265
- Schiffman RM, Christianson MD, Jacobsen G, Hirsch JD, Reis BL (2000) Reliability and validity of the ocular surface disease index. *Arch Ophthalmol* 118:615–621
- Sharpe RA, Machray KE, Fleming LE, Taylor T, Henley W, Chenore T et al (2019) Household energy efficiency and health: area-level analysis of hospital admissions in England. *Environ Int* 133:105164
- Shima M, Adachi M (2000) Effect of outdoor and indoor nitrogen dioxide on respiratory symptoms in schoolchildren. *Int J Epidemiol* 29:862–870.
- Smith CJ, Ogden MW (1998) Tobacco smoke and atherosclerosis progression. *JAMA* 280(1): 32–33
- Smith SJ et al (1994) Alcohol, smoking, passive smoking and caffeine in relation to breast cancer risk in young women. *Br J Cancer* 70:112–119
- Smith BJ, Zhang L, Field RW (2007) Iowa radon leukemia study: a hierarchical population risk model. *Stat Med* 10:26(25):4619–4642
- Steenland K (1992) Passive smoking and the risk of heart disease. *J Am Med Assoc* 267:94–99
- Sunyer J, Puig C, Torrent M et al (2004) Nitrogen dioxide is not associated with respiratory infection during the first year of life. *Int J Epidemiol* 33:116–120
- Svendsen KH et al (1987) Effects of passive smoking in the multiple risk factor intervention trial. *Am J Epidemiol* 126:783–795
- Tredaniel J et al (1994) Exposure to environmental tobacco smoke and adult non-neoplastic respiratory diseases. *Eur Respir J* 7:173–185
- U.S. Environmental Protection Agency. 1992. Respiratory health effects of passive smoking (also known as exposure to secondhand smoke or Environmental tobacco smoke ETS)
- U.S. Environmental Protection Agency (2008) Integrated science assessment for oxides of nitrogen – health criteria (final report), Washington, DC

- U.S. Environmental Protection Agency (U.S. EPA) (2010) IRIS toxicological review of formaldehyde. Washington, DC
- Vanker A, Barnett W, Workman L, Nduru PM, Sly PD, Gie RP et al (2017) Early-life exposure to indoor air pollution or tobacco smoke and lower respiratory tract illness and wheezing in african infants: a longitudinal birth cohort study. *The Lancet Planetary health* 1:e328–e336
- Viegi G, Simoni M, Scognamiglio A et al (2004) Indoor air pollution and airway disease. *Int J Tuberc Lung Dis* 8:1401–1415
- Vrijens K, Bollati V, Nawrot TS (2015) Micornas as potential signatures of environmental exposure or effect: a systematic review. *Environ Health Perspect* 123:399–411
- Walker ES, Fedak KM, Good N, Balmes J, Brook RD, Clark ML et al (2020) Acute differences in pulse wave velocity, augmentation index, and central pulse pressure following controlled exposures to cookstove air pollution in the subclinical tests of volunteers exposed to smoke (stoves) study. *Environ Res* 180:108831
- Walzer D, Gordon T, Thorpe L, Thurston G, Xia Y, Zhong H et al (2020) Effects of home particulate air filtration on blood pressure: a systematic review. *Hypertension* 76:44–50
- Wells AJ (1991) Breast cancer, cigarette smoking, and passive smoking (letter). *Am J Epidemiol* 133:208–210
- World Health Organization (2000) Air quality guidelines for Europe, 2nd edn. WHO, Geneva
- World Health Organization (2009) WHO handbook on indoor radon: a public health perspective. WHO, Geneva
- World Health Organization (2010) WHO guidelines for indoor air quality. WHO, Geneva
- Xia X, Chan KH, Lam KBH, Qiu H, Li Z, Yim SHL et al (2021a) Effectiveness of indoor air purification intervention in improving cardiovascular health: a systematic review and meta-analysis of randomized controlled trials. *Sci Total Environ* 789:147882
- Xia Y, Zhang H, Cao L, Zhao Y (2021b) Household solid fuel use and peak expiratory flow in middle-aged and older adults in China: a large cohort study (2011–2015). *Environ Res* 193: 110566
- Yu L, Wang B, Cheng M, Yang M, Gan S, Fan L et al (2020) Association between indoor formaldehyde exposure and asthma: a systematic review and meta-analysis of observational studies. *Indoor Air* 30:682–690
- Zhang W, Li H, Pan L, Xu J, Yang X, Dong W et al (2021) Chemical constituents and sources of indoor PM_{2.5} and cardiopulmonary function in patients with chronic obstructive pulmonary disease: estimation of individual and joint effects. *Environ Res* 197:111191
- Zheng W et al (1994) Risk factors for cancers of the nasal cavity and paranasal sinuses among white men in the United States. *Am J Epidemiol* 138:965–972
- Zwozdziak A, Sówka I, Willak-Janc E, Zwozdziak J, Kwiecińska K, Balińska-Miśkiewicz W (2016) Influence of pm(1) and pm(2.5) on lung function parameters in healthy schoolchildren-a panel study. *Environ Sci Pollut Res Int* 23:23892–23901



Animal Tests to Determine the Health Risks of Indoor Air Pollutants 41

Junfeng Zhang, Xu Yang, Xinyue Zheng, and Rui Li

Contents

Introduction	1220
Definition of Animal Test	1221
A Brief History of Animal Test	1221
Controversy and Principles	1221
Indoor Volatile Organic Compound (VOC) Pollution	1222
Formaldehyde and Toxic Effects	1223
Benzene and Toxic Effects	1227
Indoor Semi-Volatile Organic Compound (SVOC) Pollution	1228
Effects of PAEs on the Immune System	1229
Effects of PAEs on the Nervous System	1230
Effects of PAEs on the Reproductive System	1232
Effects of PAEs on Diabetes	1233
Radon and its Toxic Effects	1233
The Effects of Radon on the Respiratory System	1234
Other Health Effects of Radon	1234
Indoor Particulate Matter Pollution	1235
The Effect of PM _{2.5} on the Respiratory System	1236
Effect of PM _{2.5} on the Immune System	1237
Effects of PM _{2.5} on the Cardiovascular System	1238
Effects of PM _{2.5} on the Reproductive System	1239
Other Toxic Effects of PM _{2.5}	1239

J. Zhang

Nicholas School of the Environment, Duke University, Durham, NC, USA

Global Health Research Center, Duke Kunshan University, Kunshan, Jiangsu Province, China

Duke Global Health Institute, Durham, NC, USA

e-mail: junfeng.zhang@duke.edu

X. Yang · X. Zheng · R. Li (✉)

School of Life Sciences, Central China Normal University, Wuhan, China

e-mail: yangxu@mail.ccnu.edu.cn; zhengxy@mails.ccnu.edu.cn; ruili@ccnu.edu.cn

Limitations of and Alternatives to Animal Testing	1240
Conclusions	1242
Cross-References	1242
References	1242

Abstract

Public awareness of the importance of air quality in general, and of indoor air in particular, has grown over the past few decades. Sick building syndrome was an early indicator of this awareness, but harmful chemicals are still used in the manufacture of building materials, furniture, carpets, and other items used daily. Since people spend a significant amount of time indoors, extensive attention is being paid to health problems caused by indoor air pollutants. By examining changes in biomarker levels after an animal is exposed to indoor air pollutants, animal tests have been shown to be an effective way to evaluate health impacts, and to understand the underlying toxicological mechanisms, before examining the impacts on people. In this chapter, we discuss the fundamental principles of animal testing and describe the latest progress in the study of health impacts of indoor air pollutants. We review a number of experiments where laboratory animals are exposed to certain environmental pollutants and present their findings. Detailed descriptions of the toxicity mechanisms and the corresponding intervention measures are given, and strategies for the prevention and treatment of related diseases caused by indoor pollutants are also outlined.

Keywords

Toxicology study · Animal models · Health risks · Exposure · Molecular mechanism · Toxicity

Introduction

As has been noted in other chapters of this handbook, one of the reasons that so much research is focused on indoor air pollution is that people generally spend a significant portion of their time indoors, which makes indoor air quality extremely important to human health. Extensive research has shown that poor indoor air quality can induce or exacerbate a number of diseases such as allergic asthma and some types of cancers. To avoid these health impacts, it is indispensable to understand how and why these pollutants affect the body. Human epidemiological studies are limited, since it is impossible for us to conduct some biomedical analysis on human being, for example, the irreversible exposure and tissue slice analysis, and this has limited in-depth study. Thus, animal tests are needed to enable us to rigorously investigate the underlying mechanisms that result in negative health outcomes from being exposed to various pollutants.

Definition of Animal Test

Normally, animal test, also known as in vivo testing, refers to the use of nonhuman living organisms in experiments, in order to control the variables that could influence the behavior or biological system under study. On the one hand, animal testing is in contrast to studies of animals in their natural habitats (Franco et al. 2017), and on the other hand, animal testing is in contrast to in vitro studies that are conducted with microorganisms, cells, or biological molecules outside of their normal living environments (Barré-Sinoussi and Montagutelli 2015).

A Brief History of Animal Test

The origins of animal experiments can be traced back to the ancient Greek period in which written records from as early as the fourth century BC has been found. Writings by Aristotle and Erasistratus are among the earliest recorded accounts of experiments being performed on living animals (Cohen and Loew 2002). Animal testing has played a vital role in advancing scientific and medical research since its beginnings. In the twelfth century, an experimental method for testing surgical procedures on animals before using them on human patients was introduced by an Arabic physician named Avenzoar (Abdel-Halim 2005, 2006). The germ theory of medicine was convincingly demonstrated by introducing anthrax in sheep in the 1880s by Louis Pasteur, the famous French chemist and microbiologist (Mock and Fouet 2001). In the 1890s, Ivan Pavlov, a Russian physiologist, conducted a series of famous experiments on dogs to demonstrate what he called classical conditioning (Windholz 1987). In 1922, the first isolation of insulin from dogs was achieved, and thereafter the hormone has helped millions people who suffer from diabetes (Gorden 1997). The first transgenic mammal was created in 1974 by integrating simian DNA into the mouse genome, marking an important milestone in the genetic modification of animals (Jaenisch and Mintz 1974). Later, the birth of the first cloned sheep, Dolly, in 1996, demonstrated the possibility of producing cloned mammals from mature cells in specific body parts (Niemann et al. 2008).

Controversy and Principles

Although animal testing has contributed significantly to the advancement of human biomedicine, criticism and controversy have also followed. In 1655, the Irish physiologist Edmund O'Meara wrote that “the miserable torture of vivisection places the body in an unnatural state” (Maehle and Trohler 1987; Ryder 1989). O'Meara believed that vivisection caused so much pain to the animal, that it could affect the actual physiology during the process, leading to unreliable results. There were also ethical objections to the abuse of animals for the sole benefit of humans (Maehle and Trohler 1987). On the other side of the debate, people believed that animal testing was necessary to increase knowledge from both medical and biological perspectives. Claude Bernard, a renowned physiologist who considered

vivisection to be essential for physiological research (Lafollette and Shanks 1994), believed that “the science of life is a superb and dazzlingly lighted hall which may be reached only by passing through a long and ghastly kitchen” (Nurunnabi et al. 2012). Another physiologist, Dr. Walter B. Cannon said “The antivivisectionists are the second of the two types Theodore Roosevelt described when he said, ‘Common sense without conscience may lead to crime, but conscience without common sense may lead to folly, which is the handmaiden of crime.’” (Nicoll 1991).

Since it is really hard to determine whether or not humans should use animal testing for our own benefit, guiding principles for more ethical use of experimental animals (the 3Rs) must be taken seriously. First proposed by Russell and Burch in 1959 (Russell and Burch 1960), these principles are:

Replacement: the substitution for conscious living higher animals with insentient material.

Reduction: reducing the numbers of animals used to obtain sufficient information of a given precision.

Refinement: improvement in living conditions or experimental procedures to minimize pain and distress of the animals, and to enhance the welfare of these animals from birth to death.

The 3Rs are frequently presented as “the ways in which inhumanity can be and is being diminished or removed.” However, we can expand on this as follows (Tannenbaum and Bennett 2015): “Replacement minimizes research animal distress by substituting animals that can experience distress with insentient material that is incapable of feeling anything and therefore cannot experience distress. Reduction minimizes research animal distress by decreasing the number of animals that can experience distress. Refinement is, by definition, diminution or elimination of distress. This definition of refinement is not intended to suggest that replacement and reduction have a different aim. Refinement is presented as a distinct method of removing inhumanity because it focuses on the actual conduct of the research, and on how sentient research animals are treated.”

The 3Rs encourage researchers to find alternatives to animal testing, but in cases where this is not possible, animal welfare and scientific quality need to be prioritized. Globally, most researchers who are involved in animal testing implement the 3Rs, and these rules have even been incorporated into various regulations and laws (Liguori et al. 2017).

To more thoroughly implement the 3R principles, countries and organizations around the world have promulgated a set of ethical requirements for animal tests. In general, to ensure that animal experiments are performed only when necessary, any experiment that uses animals must first pass a rigorous set of ethical approvals before commencing.

Indoor Volatile Organic Compound (VOC) Pollution

VOCs are among the most important indoor air pollutants, because they are present in most building materials and can be continuously emitted over a long period, thus posing a greater health risk due to this long-term exposure (Rumchev et al. 2007).

Several hundred different VOCs have been identified in indoor air by both academic researchers and governmental organizations (Schlink et al. 2010; Zhu et al. 2013). VOCs can be divided into subgroups, including aromatic, aliphatic, chlorinated, and oxygenated hydrocarbons (Tsai 2019). The nature of indoor VOCs and their health effects are described in other chapters and will not be repeated here. There is increasing animal experimental evidence that some of these VOCs have toxic properties. In this chapter, we will introduce toxicological animal studies related to formaldehyde, benzene, and radon.

Formaldehyde and Toxic Effects

Formaldehyde (FA) is a colorless, pungent-smelling gas at room temperature, with a molecular mass of 30.03, and is easily soluble in water and ethanol (Dan et al. 2020). It is produced on a large scale and is very widely used in resins that go into a range of wood-based products including particle board and paper, plastics, and industrial chemicals. It is also used as a disinfectant and as a preservative (formalin) (Zhang et al. 2010). Due to the diversity of indoor formaldehyde sources as well as its characteristic of sustained release over a long period, indoor formaldehyde exposure is extremely common. ► [Chapter 2, “Very Volatile Organic Compounds \(VVOCs\),”](#) discusses formaldehyde in detail.

The impact of indoor formaldehyde pollution on human health can be wide ranging, quite severe, of long duration, and highly toxic. Different toxic effects on different tissues of the human body can be induced by formaldehyde, including irritation of the respiratory tract (asthma) (Neghab et al. 2011; Bono et al. 2016; Yu et al. 2020), neurotoxicity (Tang et al. 2013; Tulpule and Dringen 2013), reproductive toxicity (Merzoug and Toumi 2017), and immunotoxicity (Yu et al. 2014a; Jafari et al. 2015). High-dose formaldehyde exposure will increase the risk of acute poisoning, while low-dose formaldehyde exposure over a long period may result in chronic poisoning or even have carcinogenic effects.

In 2004, the International Agency for Research on Cancer (IARC) formed an expert working group to investigate the carcinogenicity of formaldehyde. Based on data from a systematic review of the literature, the group concluded that there was sufficient evidence that formaldehyde causes nasopharyngeal cancer in humans and classified it as a Category 1A carcinogen (WHO 2006). The group also concluded that there was “strong but not sufficient evidence for a causal association between leukemia and occupational exposure to formaldehyde” (Cogliano et al. 2005).

Health Impacts on the Respiratory System

Asthma is a complex pulmonary inflammatory disease, with typical symptoms including airway hyperresponsiveness, airflow obstruction, and airway inflammation. It is known that exposure to a number of chemicals including formaldehyde can induce asthma. To understand the underlying mechanism of FA exposure in asthma occurrence, especially when it is combined with allergen exposure, Liu et al. conducted a study with BALB/c mice, looking at the effects of combined exposure

to OVA and FA for 3 weeks, followed by a 1-week challenge with aerosolized OVA (Liu et al. 2011). Their results showed that mice exposed to both OVA and FA developed airway hyperresponsiveness and pulmonary tissue damage. There was also eosinophil infiltration, and increased levels of interleukin IL-4 and IL-6 in the lung tissue, suggesting that FA exposure can induce and aggravate asthma in BALB/c mice when it is combined with OVA immunization.

Indoor formaldehyde concentrations will vary according to changes in fresh air intake or air purification measures taken in the indoor environment. To study the effect of real daily indoor formaldehyde concentrations, Zhang et al. (2018) conducted a study exposing BALB/c mice to formaldehyde with fixed total concentrations but different exposure modes in an actual residence, and examined biomarkers related to the respiratory and the immune systems. After exposure, bronchoalveolar lavage fluid (BALF) and lung tissue homogenate were prepared and examined for oxidative stress, histopathological changes, and levels of typical inflammatory factors such as IL-4 and NF- κ B. It was found that intermittent exposure to fluctuating formaldehyde concentrations resulted in greater increases in BALF inflammatory cell numbers, and greater biological changes including apoptosis, and signs of more severe health damage compared to that seen when formaldehyde concentrations were constant. This study provides insights related to ventilation strategies that could be adopted to minimize the adverse health effects of indoor formaldehyde exposure. For example, a ventilation strategy that avoids higher peak concentrations will reduce health risks for the same average indoor formaldehyde concentration over the same time frame.

Health Impacts on the Nervous System

Individuals subjected to occupational FA exposure often exhibit abnormal behaviors such as sleep disorders, aggression, anxiety, depression, and especially, cognitive impairment. Coincidentally, patients suffering from a deficiency of melatonin (MT) also have cognitive problems such as those listed above. Mei et al. explored whether, and how, FA influences endogenous MT metabolism and induces cognitive decline by exposing healthy adult male mice to gaseous FA (3 mg/m^3) for 7 consecutive days (Mei et al. 2016). They found that FA exposure damaged spatial memory, which is linked to the death of hippocampal neurons. Biochemical analysis showed that FA exposure induced severe oxidative stress by decreasing systemic glutathione levels, especially, reducing MT levels in the brain. An intraperitoneal injection of MT obviously eased FA-induced hippocampal neuronal death, recovered MT levels in the brain, and attenuated memory decline. Injection of FA into the hippocampus markedly decreased brain MT concentrations at the tissue level. Moreover, FA was proved to directly inactivate MT in vitro and in vivo, at both cellular and molecular levels. These findings proposed that MT supplementation could be used to halt or reverse cognitive decline and can relieve mental disorders in occupationally FA-exposed populations. A recent study showed that pretreating mice with melatonin before exposing them to FA resulted in less inflammatory and oxidative impairment in the lung and liver tissues, and reduced micronuclei formation in bone marrow cells. The histological observation of lung tissue further confirmed the

parameters obtained in the biochemical studies, illustrating the possible beneficial effect of melatonin to reverse FA-induced damage (Bernardini et al. 2020).

Alzheimer's disease (AD) is a progressive neurological disorder. The number of AD cases is increasing every year, and patients are getting younger and younger. Exposure to FA occurs primarily indoors, with elderly people being more exposed because they spend more time indoors. To determine whether exposure to FA contributes to the development of AD, Liu et al. (2018) exposed C57BL/6 mice daily to FA (0, 0.155, 1.55, and 15.5 mg/kg/day) for 1 week and found that after FA exposure to high concentrations of FA (1.55 or 15.5 mg/kg/day), some early AD-like alterations, including cognitive deficits, pathological changes, accumulation of total β -amyloid plaques1-42 ($A\beta$ 1-42) and hyper-phosphorylation of tau (Tau-P) in the cerebral cortex, were found, while exposure to a low concentration of FA (0.155 mg/kg/day) had hardly any effect on the mouse brain. This study demonstrated that acute FA exposure at certain concentrations would elicit early AD-like alterations in the mouse brain. A recent study found that via upregulation of the Warburg effect, FA could induce ferroptosis in hippocampal neuronal cells (Li et al. 2021). The researchers explored the new mechanism of FA-induced neurotoxicity to help understand how to control damage to the central nervous system caused by environmental FA in normal daily life. Understanding the mechanism has provided new approaches for prevention and treatment of AD induced by FA.

Previous studies have found that the ionic receptor, N-methyl-D-aspartic acid receptor (NMDA2R), plays an important role in the development of the central nervous system and in cardiovascular regulation. Lu et al. (2008) exposed Kunming mice to formaldehyde, and then, using the Morris water maze (MWM), looked for any changes in their behavior. The forebrain tissue was examined showing that superoxide dismutase (SOD) activity and levels of glutathione (GSH) decreased remarkably in the 3 mg FA/m³ group ($P < 0.01$, compared with control group). The MWM results indicated that inhaled formaldehyde has a negative effect on learning and memory at 3 mg/m³ of gaseous formaldehyde but not at lower levels. Neuronal damage induced by oxidative stress may be the possible mechanism for these effects.

Health Impacts on the Hematopoietic System

To investigate whether formaldehyde adversely affects the bone marrow, Yu et al. (2014b) used SPF male ICR mice as the experimental animals for the study. After being exposed to formaldehyde at 20, 40, and 80 mg/m³, respectively, for 15 days in the isolated inhalation chambers, bone marrow cells were extracted. The number of WBCs and PLTs in the 40 and 80 mg/m³ groups were obviously reduced, but there was no change in the RBC numbers. There was also a reduction in the numbers of bone marrow cells and CFU-Fs in the 80 mg/m³ group. SOD activity was seen to decrease, and MDA levels increased. In addition, the researchers observed changes in cell cycling and found that there was an S phase arrest in the 80 mg/m³ group. The study proposed that formaldehyde, at a certain concentration, could induce hematopoietic toxicity by intensifying the oxidative stress. Using a similar animal experiment, this team also proved that changes in the expression of peroxidase 2 (Prx2)

(Yu et al. 2014a) and peroxidase 3 (prx3) (Yu et al. 2015) were involved in the hematopoietic toxicity of FA on bone marrow tissue.

Based on the findings that formaldehyde was considered to not directly damage hematopoietic stem/progenitor cells (HSC/HPC) in bone marrow, and that no one had previously explored whether FA had an effect on HSC/HPC cells in the mouse lung or rat nose, Zhao et al. (2021) investigated the effects of FA in this context. They hypothesized that FA inhalation could induce toxicity in the HSC/HPC cells present in the mouse lung and/or nose, rather than in the bone marrow. The researchers examined the cells of the lung, nose, bone marrow, and spleen of BALB/c mice after FA exposure. They found that in vivo exposure to FA at 3 mg/m³ or ex vivo exposure up to 400 μM FA reduced the formation of burst-forming unit-erythroid (BFU-E) cells, and colony-forming unit-granulocyte-macrophage (CFU-GM) colonies in the mouse lung and nose as well as in the bone marrow and spleen. Since these two colonies are formed by more stable myeloid progenitor cells, whether FA has a toxic effect on HSC/HPC can be judged from the quantitative changes in them. These findings were the first to empirically prove that FA exposure can damage mouse pulmonary and olfactory HSC/HPC, and provide potential biological plausibility for the induction of leukemia at the sites of entry rather than in the bone marrow.

Health Impacts on the Reproductive System

Previous studies have shown that FA exposure inhibits spermatogenesis and induces apoptosis of spermatogenic cells in testicular tissue of rodents (Zhou et al. 2006; Ozen et al. 2008). However, most of these studies involve the short-term effects from relatively high doses of FA exposure. Zhou et al. (2011) examined the more realistic situation where exposure is over a long period at a dose generally experienced indoors. They exposed 30 SD male rats to low doses of formaldehyde for 60 days. The results indicated that the reproductive toxicity of FA is dose-dependent. Sperm quantity and quality, testicular seminiferous tubular diameter, and the activities of superoxide dismutase and glutathione peroxidase were significantly decreased, while the level of malondialdehyde was significantly enhanced in rats from the 2.46 mg/m³ FA exposure group compared with those in the control group. They concluded that a level of 0.5 mg/m³ can be considered to be a safe level for FA exposure, but long-term FA exposure at a dose of 2.46 mg/m³ is harmful to the male reproductive system via inducing oxidative stress.

Merzoug and Toumi (2017) observed significant weight loss, blood immune system decline, reproductive failure, and other phenomena in young rats after exposing female Wistar rats to FA of 2 mg/kg/d during pregnancy. The phenomena of low fetal weight, fetal morphology measurement, and placental weight also appeared in the fetus. When the researchers administered the flavone hesperidin (HP), some hematological parameters improved, including reduced cortisol levels, and increased 17β-estradiol rates. This indicates that perinatal HP has a potentially preventive effect on FA toxicity.

Health Impact on Intestinal Microorganisms

After discovering that formaldehyde has toxic effects on lung tissues, neurons, and blood, Guo et al. (2018) wondered whether formaldehyde exposure could extend to the human intestinal system, and whether interactions between FA and the gut

microbiome may account for FA toxicity. This effect was confirmed by experimental animal research. Using BALB/c mice, the researchers determined through gene high-throughput sequencing, that the composition of intestinal microbiota in mice exposed to FA would change, and preliminarily explored the relevant potential metabolic processes that were behind these changes, such as α -linolenic acid metabolism and pathways in cancer. However, due to the small number of mice used in the experiment, the statistical analysis lacks certain reliability. In addition to changes in gate level, further confirmation is needed.

Benzene and Toxic Effects

Benzene, a toxic indoor ambient air pollutant, is a colorless and clear liquid at room temperature. It is volatile and soluble in water. In daily life, its main source is the combustion of wood and coal, as well as cigarettes and smoke (Loomis et al. 2017). Other indoor air sources of benzene include building materials, and furnishings, and as living standards improve, more sources of benzene have been introduced indoors. Indoor environmental pollution caused by volatile pollutants such as benzene has become more serious. Benzene is the chemical pollutant to which the human body is most frequently exposed. If it is not strictly controlled, benzene can cause strong irritation to human eyes, throat, and other parts, and poses a threat to human health (Williams et al. 2008). In 1974, the International Agency for Research on Cancer determined that benzene exposure can lead to hematopoietic toxic damage (IARC 1974). In 1982, scientists determined there was a significant correlation between benzene exposure and leukemia through a series of cohort studies (Tomatis 1982). Studies have shown that long-term exposure to benzene can cause obvious immunotoxicity in the human body, and can cause poisoning and reduce the number of red blood cells, total blood cells, and various types of white blood cells (Lan et al. 2004). In addition to leukemia, benzene exposure can increase the risk of other systemic tumors, such as lung cancer, non-Hodgkin's lymphoma, and multiple myeloma (Vlaanderen et al. 2012). The prevention and control of benzene pollution, and its influence on human health are still important indoor air pollution problems to be solved. The prevention, diagnosis, and treatment of benzene poisoning is still one of the hot issues in the field of public health.

To study the metabolic characteristics and hematopoietic toxicity mechanism of benzene poisoning, Sun et al. (2014) and others exposed C3H/HE mice by subcutaneous injection and successfully established a benzene poisoning mouse model. Histopathological examination showed that benzene inhibited the formation of hematopoietic cells in bone marrow and spleen, resulting in abnormal bone marrow morphology and differentiation. Metabolites of peripheral circulation and hematopoietic cells of the mice were obtained using the LC-MS method, and the expression levels of related protein pathways were compared. This showed that the fatty acid β oxidative metabolism pathway is a significant differential metabolic pathway. Therefore, it is of great practical significance to understand the key events in the occurrence of benzene hematopoietic toxicity and to explore the relevant mechanisms for the diagnosis, intervention, and early prevention of benzene poisoning.

To explore the immunological mechanisms of aplastic anemia, myelodysplastic syndrome, and acute myeloid leukemia, a benzene-induced hematopoietic toxicity BALB/c mouse model was established, and any changes in immune organs and T helper cell subsets (Th1, Th2, Th17, and Treg cells) were explored (Huang et al. 2021). After subcutaneous injection of 150 mg/kg benzene daily, for 28 days, the mice exhibited pancytopenia, and obvious pathological damage to bone marrow, spleen, and thymus. Flow cytometry demonstrated that the number of CD⁴⁺CD²⁵⁺Foxp³⁺ Treg cells in the spleen increased significantly. The level of IL-10 in the spleen, serum, and bone marrow increased, and levels of IL-17 in the spleen and serum decreased. These findings reveal that immunosuppression occurred in the benzene-induced hematopoietic toxicity model mice, and Treg cells and secreted IL-10 may play a key role in the process.

Formaldehyde and benzene (BZ) are both leukemic agents. Wei et al. (2017) exposed BALB/c mice to 3 mg/m³ of formaldehyde for 2 weeks, and then monitored the mice for 7 days after the exposure. The researchers included benzene (BZ) as a positive control, separately and together with FA because co-exposure occurs frequently. After 7 days of recovery, the CFU-transgenic and BFU-hepatitis E progenitor cell colonies and nucleated bone marrow cells in the mice exposed to FA were comparable to the control group, even though they were significantly reduced during the exposure period. In addition, although the increase in 8-hydroxydeoxyguanosine was not significant, the levels of reactive oxygen species (ROS) and 8-hydroxy-2'-deoxyguanosine (8-OHdG) in CFUGM and BFU-E from the mice exposed to FA did increase significantly. Levels of 8-OHdG were also higher than the controls, and levels of granulocyte-macrophage colony stimulating factor in the FA group were lower than that in the control group, while the receptor expression level was not upregulated. It is suggested that HSCs/HPCs of FA-exposed mice respond to a small amount of GM-CSF and proliferate rapidly, which may cause the possible risk of clonal expansion of abnormal stem/progenitor cells. In the postexposure period, co-exposure to FA and BZ is more effective in promoting the formation of CFU-GM and inducing the reactive oxygen species in 8-OHDG of BFU-E and CFU-GM. Compensation of myeloid progenitor cells with elevated ROS and 8-OHDG may lead to the risk of converting normal HSCs/HPCs into leukemia stem cells/progenitor cells. Therefore, co-exposure may bring a greater risk of leukemia.

Indoor Semi-Volatile Organic Compound (SVOC) Pollution

In addition to the common organic indoor air pollutants such as formaldehyde and benzene, the effect of semi-volatile organic compounds (SVOCs) on indoor air quality has attracted extensive attention. According to the World Health Organization (WHO 1989), SVOCs are a class of organic compounds with boiling points in the range of 240–400 °C and vapor pressures of $(0.1\text{--}10^{-7}) \times 133.322$ Pa, and include dioxins, polycyclic aromatic hydrocarbons (PAHs), organic pesticides, quinolines, nitrobenzenes, and phthalates. In indoor air, SVOCs are mainly found in gaseous and aerosol forms. Compared with VOCs, SVOCs have a higher boiling

point, a lower saturation vapor pressure, and stronger adsorption. Thus, it is more difficult to degrade and persists in air, water, soil, much like outdoor persistent organic compounds (Weschler and Nazaroff 2008).

The sources of SVOCs are widespread and complex, mostly man-made chemicals, including building and decorative materials, daily necessities, pollutants emitted during production and use (solvents, unreacted monomers and additives, etc.), such as plasticizers, flame retardants, monomeric raw materials, combustion products, and household insecticides (Pelletier et al. 2017). According to the research, indoor SVOCs are mainly plasticizer-like substances represented by phthalates, and high concentrations of these substances are found in some rooms which increases the risk to occupants' health (Mercier et al. 2012, 2014).

Studies have shown that SVOCs may induce multiple negative effects on the human respiratory system, endocrine system, and reproductive/genetic system through inhalation, or via oral or dermal routes, and these effects can lead to various diseases, including asthma, and allergies (Bornehag and Nanberg 2010). Using phthalates (PAEs) as an example, we analyze the relationship between indoor SVOCs and health effects.

There are currently more than 20 kinds of PAEs, that include diisononyl phthalate (DINP), di(2-ethylhexyl) phthalate (DEHP), and dibutyl phthalate (DNBP). Feng et al. (2020b) found that DIBP, DMEP, and DBP are the most common indoor PAEs. PAEs are semi-volatile, cumulative and highly toxic, are stable and long-lasting in the environment, and are common indoors. PAEs usually enter the body through breathing, the digestive tract, intravenous injection, and dermal contact. Although most PAEs are released by metabolic action, the small amount of residual PAEs may cause serious harm to humans (Latini et al. 2004; Koch et al. 2005, 2006). Several PAEs and their metabolites have been shown to have growth and developmental toxicity for animals, particularly for the reproductive development of males, with endocrine disrupting and modulating effects (Reynolds et al. 2004). Some PAEs are also carcinogenic for rodents, but their carcinogenicity has not been conclusively determined for humans (Latini et al. 2004).

Effects of PAEs on the Immune System

Epidemiological studies have suggested a possible association between exposure to DINP and the development of allergies. However, it is controversial to discuss the pathogenesis of allergic diseases caused by DINP because of a lack of sufficient scientific evidence of how or even whether DINP influences allergic immune responses. Kang et al. (2017) orally administered DINP for 3 weeks to BALB/c mice after they had been sensitized with fluorescein isothiocyanate (FITC). They found that oral administration of DINP exacerbated tissue damage in allergic dermatitis in the FITC-sensitized mice. This was accompanied by increased expression of TRPA1, IgG1, IL-6, and IL-13. The authors found that blocking TRPA1 using HC030031 effectively prevented the development of the allergic dermatitis induced by oral exposure to DINP, including downregulation of IgG1, IL-6, IL-13,

and a decrease of mast cell degranulation. Their findings also suggested that blocking NF- κ B inhibited TRPA1 expression, but that blocking TRPA1 has no significant effect on NF- κ B activation or TSLP expression. This study helped people understand the role of DINP in the development of allergic dermatitis and provides new insights into the mechanisms of adjuvant effects induced by DINP.

Similarly, Shen et al. (2017) found that oral administration of di-isodecyl phthalate (DIDP) exacerbated allergic dermatitis in mice. The combination of DIDP and FITC induces the synthesis of TSLP by activating the NF- κ B signaling pathway, which causes the activation of STATs and degranulation of skin mast cells, ultimately exacerbating allergic dermatitis. This study also showed that melatonin enhanced the expression of Nrf2, upregulated the antioxidant genes HO-1 and NQO1, decreased oxidative stress and TSLP levels, and thereby relieved allergic dermatitis. The results suggest that DIDP may exacerbate allergic dermatitis through oxidative stress and increased TSLP expression.

DEHP, a common plasticizer, was found to have an adjuvant effect in combination with ovalbumin (OVA). To further investigate the connection between thymic stromal lymphopoietin (TSLP) and the adjuvant effect of DEHP, You et al. (2016) sensitized BALB/c mice with OVA through daily oral administration, and neutralized the effect of TSLP with an anti-TSLP monoclonal antibody. The results showed a significant Th2 response in the DEHP-treatment group with upregulation of Th2-type cytokines such as interleukin 4 (IL-4), IL-5, and IL-13. In addition, eosinophil counts and pulmonary eosinophil cationic proteins (ECP) in the bronchoalveolar lavage fluid (BALF) were significantly increased. Neutralization of TSLP with an anti-TSLP monoclonal antibody reversed the adjuvant effect of DEHP on airway inflammation, airway wall structure, and airway hyper-responsiveness of acetylcholine, induced by OVA, indicating that TSLP is an effective target for inhibiting the adjuvant effect of OVA and DEHP exposure.

Exposing 5-week-old ICR male mice to vehicle saline, DEHP or DINP daily by oral administration, Gu et al. (2021) observed increased levels of reactive oxygen species and malondialdehyde, and decreased levels of glutathione, in the kidney, suggesting oxidative damage to the kidney. Elevated levels of renal inflammatory cytokines, tumor necrosis factor- α , and IL-6 further implied inflammation due to PAE exposure. Targeted lipidomics showed that a high dose of DEHP had a pronounced effect on the kidney, but DINP also caused significant changes in phosphatidylglycerol content, which is associated with glomerular podocyte lipid accumulation and inflammatory responses.

Effects of PAEs on the Nervous System

A lot is known about the characteristics of PAEs as endocrine disrupting chemicals; however, the effects and potential mechanisms of PAEs on neurotoxicity are still unclear. Tran et al. (2021) used zebrafish to investigate the effects of six phthalates, dimethyl phthalate (DMP), diethyl phthalate (DEP), benzyl butyl phthalate (BBZP), di(2-ethylhexyl) phthalate (DEHP), di-n-octyl phthalate (DNOP), and diisononyl

phthalate (DINP) on the motility of zebrafish embryos. After exposure to one of the six phthalates, the green fluorescent protein (GFP) transgenic (Tg) line was measured, and any changes to the expression profiles of genes related to the cholinergic and dopaminergic systems were assessed. The results prove that exposure to phthalates impairs development of the nervous system and neurochemicals in zebrafish embryos, although the specific mechanisms vary depending on the phthalate.

Poopal et al. (2020) studied the toxic effects of diheptyl phthalate (DHP) and diisodecyl phthalate (DIDP) on zebrafish at median lethal concentration (LC₅₀ 96-h). The intensity of swimming behavior and tissue biomarkers, including total antioxidant capacity (TAOC), aminotransferase, and acetylcholinesterase (ACHE), were evaluated after exposure. Zebrafish exposed to either of these phthalates for 15 days exhibited maladjusted swimming behavior and circadian rhythms. After the exposure period, the activity of aminotransferase in the liver and heart tissue was observed to have increased in both DHP and DIDP-treated zebrafish compared to the controls. TAOC and ACHE activity was reduced in the brain-, gill-, intestinal-, and muscle-tissues of the phthalate-treated zebrafish compared to the controls. The comparative study of swimming behavior and biomarkers makes it possible to determine whether the swimming response is mediated by external or internal stresses. Further research is needed to evaluate more molecular mechanisms and biomarkers to explore the toxicity of pollutants.

Feng et al. (2020a) investigated the neurotoxicity and mechanisms of di(2-ethylhexyl) phthalate (DEHP) exposure versus adolescent normal (P-normal) and adolescent type 2 diabetic (P-T2DM) ICR mice using typical neurobehavioral methods and transcriptome analysis. In open field experiments, DEHP exposure significantly increased the length of time spent in the central zone, and decreased the total distance covered and clockwise rotation. Morris water maze experiments showed that DEHP exposure significantly increased the time it took mice to locate the platform, and decreased the time spent in the target quadrant for both P-normal and P-T2DM mice. The results of transcriptome analysis demonstrated the effects of DEHP exposure on neural signaling pathways, including biogenic amines, neurotransmitters, neuroreceptors, and neurobiological processes. The analysis showed that P-T2DM mice were more sensitive than P-normal mice to the effects of DEHP. This study demonstrates the toxic effects of DEHP on the nervous system and suggests that potential neurotoxic mechanisms may be involved in synergy with cAMP-PKA-ERK1/2-CREB signaling pathways and Ca²⁺ signaling pathways.

Of all the phthalate esters, dibutyl phthalate (DBP) is second only to DEHP in terms of adverse health consequences, and its potential neurotoxicity has drawn extensive attention in recent years. To determine whether DBP induces neurotoxicity and anxiety-like behavior through oxidative stress, Yan et al. (2016a) used Kunming mice, and after exposure to DBP, used the elevated plus maze (EPM) and open field tests to observe any neurobehavioral changes, such as anxiety-like behavior. Oxidative stress levels were assessed by determining reactive oxygen species (ROS), glutathione (GSH), malondialdehyde (MDA), and DPC coefficients (DPC) to explore key upstream events. In addition, an antioxidant, monoacylglycerol

(MAG), was administered, to protect cells from antioxidant damage since it has been shown to improve memory and reduce learning impairment in rodents. The results showed a statistical association between oral exposure to DBP and anxiety-like effects in mice, as measured by EPM and the open field test. DBP exposure significantly increased the levels of ROS and MDA in the brain, and significantly reduced the levels of GSH in a dose-dependent manner, suggesting a correlation between oral exposure to DBP (25–125 mg/kg/day) and oxidative stress in the brain tissue of mice. MAG administration reduced the neurotoxicity and oxidative damage induced by oxidative stress.

Effects of PAEs on the Reproductive System

Di(2-ethylhexyl) phthalate (DEHP) is a typical endocrine disrupting chemical and is toxic to the reproductive system. Shi et al. (2019) found relatively few studies focusing on the effects of DEHP exposure on reproductive development in adolescence. The JAZF1/TR4 pathway plays a key role in male reproduction and includes the JAZF1, TR4, sperm 1, and cell cycle protein A1 genes. Therefore, Shi et al. examined testicular zinc and oxidative stress levels in SD rats exposed to increasing concentrations of DEHP by oral administration for 30 days. The results showed that DEHP exposure led to oxidative stress and a decrease in testicular zinc levels. In addition, hematoxylin and eosin staining, and terminal deoxynucleotidyl transferase-mediated notch and labeling assays showed significant morphological changes and apoptosis in the testicular tissue of the DEHP-exposed mice. Also, gene expression of JAZF1 increased, and expression of TR4, spermatozoa 1, and cell cycle protein A1 decreased. These results indicate that *in vivo* exposure to DEHP may induce reproductive toxicity in adolescent male rats through the JAZF1/TR4 pathway, and to oxidative stress.

To verify whether prenatal exposure to DEHP affects early onset gonadal dysfunction and subsequent reproductive aging in male mice, Barakat et al. (2017) administered DEHP orally to pregnant female CD-1 mice from day 11 of gestation to birth. The results showed that compared to control mice of the same age, all DEHP-exposed mice presented lower serum testosterone levels, higher serum estradiol levels, and higher luteinizing hormone (LH) levels. Histological evaluation showed that mice exposed prenatally to DEHP had apparent abnormalities of the gonad and epididymis, such as increasing germ cell apoptosis, degeneration of germinal tubules, oligospermia, hypospemia, and teratospermia. These observations confirm that prenatal exposure to DEHP may lead to premature reproductive aging in male mice.

Wang et al. (2017b) used SD female rats and exposed them to DEHP alone or in combination with vitamin E by daily oral administration from 12.5 days after gestation to 3 days postnatal. Results showed that vitamin E supplementation (200 mg/kg) reduced malformations, increased testicular weight, and prevented DEHP-induced maternal weight loss. Litter size, sex ratio, and live litter size were not affected, but the vitamin E supplementation had a protective effect on DEHP-induced testicular toxicity including reducing testicular apoptosis, decreasing PPAR expression, and maintaining testicular integrity.

Effects of PAEs on Diabetes

To explore the potential role of DEHP in diabetes-like symptoms, Wang et al. (2016) subjected BALB/c mice to streptozotocin (STZ) and a high-fat diet to establish a diabetes model. These mice were then exposed to DEHP, and their physiological indicators were monitored, including body weight and water consumption and blood biomarkers, including serum insulin and fasting blood sugar levels. At the end of the exposure regime, histopathological examinations of the pancreas and liver were performed. The level of oxidative stress was determined by assaying ROS and MDA in hepatocytes. As is commonly known, the most important histopathological changes in diabetes are increased blood sugar and decreased serum insulin. The results showed that DEHP did not directly induce diabetes at the treatment level but decreased serum insulin levels in DEHP-exposed nondiabetic animals. Histopathological observation showed there was dose-dependent impairment in the pancreatic tissue of the DEHP-exposed with STZ-treated group, accompanied by increased oxidative stress levels. It is hypothesized that oxidative stress may be involved in regulating this pathological process. This study contributes to elucidating the role of DEHP in the exacerbation of the disease in mice models of diabetes.

Radon and its Toxic Effects

Radon is a colorless, odorless, and chemically inert gas that can migrate from soil and rocks and accumulate in areas such as indoor houses and buildings. Indoor radon largely comes from indoor building materials such as brick, concrete, cement, ceramic tile, etc. Natural gas and domestic water are also important sources of indoor radon (Rozas et al. 2016).

Radon decay products are easily adsorbed onto particles, which can enter the human body through the respiratory tract, and be deposited in the lungs, causing damage to human health. Studies have shown that exposure to radon and radon daughters is closely related to lung cancer. Indoor radon pollution is the second largest risk factor for lung cancer after smoking, and about 10–30% of lung cancer deaths of nonsmokers are attributed to radon radiation (Gawełek et al. 2017; Casal-Mouriño et al. 2019; Lorenzo-González et al. 2019). The incidence rate of lung cancer caused by radon and radon decay products is estimated to be 10% of all lung cancer cases (Belpomme et al. 2007), of which 6–12% are in the UK, 7% in Germany, 10–14% in the USA, and the estimated value for China is 15%. Canada has investigated radon levels and the risk of lung cancer caused by radon in 19 cities since 1970, and in 2009, they reported that the indoor radon concentration was $4109 \pm 2.8 \text{ Bq/m}^3$, and the lung cancer caused by indoor radon exposure accounted for about 16% of the total lung cancer mortality (Chen et al. 2012).

The International Agency for Research on Cancer (IARC) has classified radon and daughters as Class I carcinogens, and the WHO also regards radon as one of the 19 known important human carcinogens. Lung cancer is included in the global burden of diseases list (IPCS 1999). It is generally believed that the risk of radon

to the human body is related to the indoor radon concentration, the age of the exposed person, and other factors (Pearce and Boyle 2005; Wichmann et al. 2005). The higher the indoor radon concentration is, the higher the risk of exposure to radon for people under the age of 55 (Pearce and Boyle 2005).

The Effects of Radon on the Respiratory System

Epithelial mesenchymal transition (EMT) plays an important role in tumorigenesis. However, the carcinogenic mechanism of EMT induced by chronic radon exposure is not clear. Chen et al. (2020) investigated the potential molecular mechanisms of EMT and lung cancer caused by repeated radon exposure. In animal experiments, BALB/c mice were exposed to radon gas at a cumulative dose of 60 and 120 working level months (WLM). Inhalation of radon gas caused lung damage and fibrosis in the mice, which was aggravated with increasing exposures. At the same time, a transformation similar to EMT occurred in the lung tissue of mice. Radon exposure increases p-PI3K, p-AKT, and p-mTOR in cells of mice. m-TOR and AKT inhibitors attenuate the EMT induced by radon exposure, by modulating the related biomarkers. These data demonstrate that radon exposure induces EMT through the PI3K/AKT/mTOR pathway in epithelial cells and lung tissue.

Wu et al. (2021) exposed male BALB/c mice to radon in an HD-3 radon chamber to determine the exact toxic effects that result from long-term radon exposure. Specific manifestations in the mouse lung were inflammatory responses and apoptosis, the severity of which were both dose-dependent and time-dependent. Furthermore, they found that melatonin treatment ameliorated mitochondrial dysfunction and attenuated the levels of oxidative stress and apoptosis caused by long-term radon exposure. This study provides a potential therapeutic application of melatonin for lung tissue injury caused by long-term radon exposure.

Nie et al. (2019) divided female BALB/c mice into two groups: a control group and a radon group (exposure to approximately 100,000 Bq/m³ which is equivalent to a maximum of 60 working months). Following exposure, it was discovered that about 1000 dysregulated lncRNA transcripts were found in the mice exposed to radon, and these lncRNAs may play an important role in the lung damage caused by radon exposure. Results from this study also indicate that the activation of ErbB2 and Notch pathways might be responsible for radon-induced pulmonary toxicity.

Other Health Effects of Radon

Radon and its decay products make a significant contribution to natural background radiation. Because of the complexity of radon exposure, the doses of radon exposures one experienced are difficult to quantify. Mirsch et al. (2020) has established a model with mice to assess tissue-specific radiation dose related to radon activity concentrations in order to propose a dependable means of evaluation for keeping from the harm by radon radiation. In their study, mice experienced radon exposure at

known concentrations while the number of 53BP1 foci consequently appeared was counted as an index of DNA damage induced by the exposure. This standard number was then compared with the number of foci induced by defined doses of other radiation as reference. Hence, the three-dimensional foci patterns were built based on image analysis, providing a way to assess the different types of radiation that caused DNA damage. It was demonstrated that α -particles induced two-thirds of the DNA damage in lung, while the other one-third in lung, as well as all in the kidney, heart, and liver were induced by β - and γ -rays. It is believed that biological dosimetry method proposed in this study can be used to calculate the risk level in application of the benchmark radiation protection guide.

To explore whether the oxidative damage caused may be involved in the carcinogenic process induced by radon, Nie et al. (2012) exposed Wistar rats to radon at a concentration of 100,000 Bq/m³. Levels of 8-OHDG, reactive oxygen species (ROS), and total antioxidants (T-AOC), and expression levels of some DNA repair enzymes were measured in rat urine and lungs. There was an increase in 8-OHDG and ROS levels, a decrease in T-AOC levels, and reduced OGG1 and MTH1 expression levels. The elevated levels of 8-OHDG in urine or lymphocytes was positively correlated with the cumulative exposure dose, whereas OGG1 and MHT1 expression levels in the lung were inversely correlated with cumulative exposure dose. Observations from this study have revealed that radon-induced carcinogenesis might originate with the induction of oxidative damage.

Kataoka et al. (2017) exposed BALB/c mice to different concentrations of radon for 24 h and then immediately analyzed SOD in brain tissue. The results showed that radon inhalation may cause SOD protein to pass through NF- κ B activation, causing DNA damage and oxidative stress.

Indoor Particulate Matter Pollution

Particulate matter pollution, especially PM_{2.5}, has been getting more attention as awareness of the health hazards has grown. In fact, particulate matter pollution is also one of the most significant indoor pollutants. The sources of particulate matter indoors include indoor sources such as particulate matter generation through metabolites such as dander (Yang et al. 2018), and several indoor activities such as smoking and cooking (Habre et al. 2014a; Pagel et al. 2016; Shao et al. 2017), and the ingress of outdoor particulate matter by gas exchange such as natural ventilation or wind seepage through walls (Ji and Zhao 2015). Other studies have shown that the use of indoor equipment such as vacuum cleaners and printers also generates indoor particulate matter pollution (Lioy et al. 1999). Indoor particulate matter varies depending on the building structure, ventilation methods, and particulate matter properties (Meng et al. 2005). Moreover, the composition of indoor particulate matter is higher in organic components than that found outdoors (Polidori et al. 2006).

PM_{2.5} is fine particulate matter with an aerodynamic diameter less than or equal to 2.5 μ m, which can be suspended in the air for a long time. PM_{2.5} is characterized by

small particle size, large surface area, strong activity, and the ability to easily adsorb a large number of harmful and toxic molecules. Studies have shown that the contribution of outdoor PM_{2.5} to indoor PM_{2.5} can be anywhere between 54% and 96% (Ji and Zhao 2015). Particles of this size, especially those below 0.1 μm, can penetrate deeply into the human respiratory system and even enter the circulatory system, thus causing various diseases (Pan et al. 2016).

The Effect of PM_{2.5} on the Respiratory System

Numerous epidemiological studies have shown that the increase in morbidity, hospitalization, and mortality of respiratory diseases is positively correlated with the increase in PM_{2.5} levels in the air, with a 1.13% increase in respiratory hospitalizations for every 10 μg/m³ increase in PM_{2.5} levels (Qiu et al. 2014). Roy et al. (2012) investigated the relationship between indoor air pollution indicators and lung function development in children aged 6–13 years ($n = 3273$) in four Chinese cities. Pulmonary function parameters (FVC and FEV1) were measured twice a year and the type of fuel used in the home was determined by questionnaire. The data showed that coal use in the home may contribute to impaired lung function development. Numerous studies have shown that high levels of PM_{2.5} results in airway inflammation (Davel et al. 2012; Wang et al. 2015), decreased lung function (Jacobson Lda et al. 2012; Wu et al. 2013), and the incidence and exacerbation of asthma and chronic obstructive pulmonary disease (COPD) (Nachman and Parker 2012; Gleason et al. 2014; Habre et al. 2014b).

Air pollution is linked to morbidity and mortality caused by respiratory diseases. However, the mechanisms involved have not been fully elucidated. Riva et al. (2011) investigated whether a single acute exposure to low doses of PM_{2.5} may lead to alterations in lung function and histology, and unleash inflammatory and oxidative stress processes, resulting in increased oxidative stress. They collected five samples from urban areas of São Paulo city and analyzed them for elemental and polycyclic aromatic hydrocarbon content. After intranasal drip administration of PM_{2.5} in male BALB/c mice, pulmonary function was determined, following which lung tissues were prepared for histological and biochemical analysis. Results revealed that this acute exposure to low doses of fine particulate matter led to lung inflammation, oxidative stress, and deterioration of lung impedance and histology in a dose-dependent manner.

To determine whether PM_{2.5} is involved in the exacerbation of asthma, Zhang et al. (2015) constructed an ovalbumin (OVA)-sensitized mouse model of asthma, and then subjected these mice to an airway drip of PM_{2.5}. PM_{2.5} was found to exacerbate inflammatory infiltration and structural lung damage in the asthmatic mice. The experiments demonstrated that acute exposure to PM_{2.5} may act synergistically with allergens to exacerbate asthma in sensitized mice, by promoting immune responses with Th2 imbalance.

Interleukin 17A (IL-17A), a representative member of the IL-17 family, is produced by secondary T lymphocytes and can be induced by IL-23. IL-17

cytokines can effectively recruit monocytes and neutrophils to sites of inflammation by increasing the production of chemokines in tissues, thereby delaying the inflammation. To explore the role of IL-17A in PM_{2.5}-induced lung injury, Cong et al. (2020) established a lung injury model by exposing C57BL/6J mice to PM_{2.5}. ELISA kits were used to examine the expression of inflammatory factors in the supernatant of alveolar lavage fluid. Primary bronchial epithelial cells (MBEC) were extracted and subjected to immunofluorescence analysis and Western blot assays. This study showed that PM_{2.5} promoted lung inflammation and fibrosis by inducing IL-17A secretion from $\gamma\delta$ T and Th17 cells, regulating the PI3K/Akt/mTOR signaling pathway, and inhibiting autophagy of bronchial epithelial cells. Exposure to PM_{2.5} can cause a variety of respiratory diseases. Since PM_{2.5} is ubiquitous in the environment, Zhang et al. (2021) explored the protective effect of IL-10 against PM_{2.5}-induced lung injury and its possible mechanisms. Wistar rats were exposed to PM_{2.5} and then treated with IL-10. Through these experiments, IL-10 treatment was found to ameliorate PM_{2.5}-induced acute lung injury, reduce mitochondrial damage, and inhibit inflammation, oxidative stress, and apoptosis in PM_{2.5}-treated rats.

Effect of PM_{2.5} on the Immune System

Yan et al. (2016b) explored whether indoor PM_{2.5} in the homes of children with allergic symptoms exacerbated their risk of allergy, not only compared with healthy children but also compared its toxicity with inflammatory response. The study collected indoor PM_{2.5} from the homes of allergic children and healthy children, and analyzed the composition of this indoor PM_{2.5}. Female Kunming mice were stimulated to produce large numbers of macrophages by intraperitoneal injection. After the mice were sacrificed, cell counts were performed and cells were cultured in a medium with two different PM_{2.5} suspensions. Based on the effect of PM_{2.5} on reactive oxygen species accumulation, lipid peroxidation, DNA damage, or cytokine production levels, PM_{2.5}-mediated oxidative damage and inflammatory responses in mouse peritoneal macrophages were evaluated. Oxidative stress may be associated with PM_{2.5}-induced toxicity, and PM_{2.5} in indoor environments housing allergic mice, led to more severe toxic effects and inflammatory responses in mouse peritoneal macrophages compared to effects in the non-allergic mice.

Chronic obstructive pulmonary disease (COPD) is associated with imbalances of T lymphocyte subsets (Th1/Th2, Th17/Treg). Gu et al. (2017) established a COPD mouse model through cigarette exposure with aerosol inhalation of PM_{2.5}. This study aimed to investigate whether PM_{2.5} could promote COPD development via Notch signaling pathways, leading to worsening immune disorders. The results showed that COPD mice had Th1- and Th17-mediated immune disorders and that the Notch signaling pathway was over-activated. The use of the inhibitor GSI partially inhibited activation of the Notch signaling pathway, and alleviated the immune disorders in the basal state and PM_{2.5}-induced immune disorders in COPD.

Ge et al. (2020) investigated the hematopoietic toxicity and associated molecular mechanisms in male BALB/c mice exposed to formaldehyde and PM_{2.5} alone or in

combination. The results showed that exposure to PM_{2.5} and formaldehyde may elicit hematopoietic toxicity by decreasing expression of hematopoietic growth factor, increasing oxidative stress and DNA damage, activating the “immune imbalance” pathway, and inhibiting the DNA repair-related mTOR pathway. DNA repair was significantly inhibited by deregulation of mammalian targets of the rapamycin (mTOR) pathway, while the researchers also found that treatment with vitamin E reduced these harmful effects.

Effects of PM_{2.5} on the Cardiovascular System

Numerous studies have shown that particulate matter (PM) in air pollution is associated with increased cardiovascular dysfunction, morbidity, and mortality (Dockery and Stone 2007). Ma et al. (2021) explored PM_{2.5} to induce myocardial inflammatory responses in Wistar rats by a new technique using a multifunctional aerosol concentration enrichment system. Histopathological examination of the left ventricular myocardial tissue was performed by direct oral and nasal exposure with hematoxylin-eosin (H&E) staining. Ultrastructural changes in cardiac specimens were observed by electron microscopy. Immunohistochemistry was used to detect CRP and ICAM-1 levels. The results showed that myocardial tissue in the exposed group was edematous, with widened myocardial gaps and inflammatory cell infiltration. The protein expression of CRP and ICAM-1 was increased in the exposed group. This experiment suggests that long-term exposure to PM_{2.5} inhalation promotes significant upregulation of ICAM-1 and CRP expression in myocardial tissues, ultrastructural changes in cardiomyocytes, and inward flow of inflammatory cells.

Zang et al. (2021) investigated the specific mechanism of PM_{2.5}-induced myocardial toxicity by drip injection of PM_{2.5} into the airway of SD male rats. Western blotting (WB) and real-time PCR (RT-PCR) were used to detect the expression of Ang II, ERK1/2, and TGF- β 1. The results indicated that the degree of myocardial fibrosis became more severe with increasing PM_{2.5} concentration, and the expression of Ang II, ERK1/2, and TGF- β 1 increased in the high-dose group, suggesting that activation of the renin-angiotensin system (RAS) may be involved in PM_{2.5}-induced myocardial fibrosis.

Duan et al. (2017) evaluated the multiple organ systems toxicity of PM_{2.5} in a zebrafish model. PM_{2.5}-induced embryotoxicity was dose- and time-dependent through mortality and hatching rate suppression. PM_{2.5} caused pericardial edema and decreased heart rate and cardiac output. The area of subintestinal vessels was significantly reduced in Tg(fli-1:EGFP) transgenic zebrafish strains, and morphological defects and yolk sac retention were associated with hepatocyte damage. In addition, PM_{2.5} disrupted axonal integrity in the Tg(NBT:EGFP) transgenic strain, altering axon length and pattern. Genes involved in cardiac function, angiogenesis, and neurological function were significantly downregulated, while genes related to liver metabolism were significantly upregulated. Their data suggest that PM_{2.5} causes cardiovascular toxicity, hepatotoxicity, and neurotoxicity in zebrafish.

Effects of PM_{2.5} on the Reproductive System

Liao et al. (2020) subjected female Kunming mice to PM_{2.5} exposure by airway drip for 28 days. They looked for apoptosis of mouse ovarian granulosa cells, oocytes, and quality of the embryos after insemination. The results showed that the number of apoptotic granulosa cells and oocytes increased after exposure to high concentrations of PM_{2.5}, indicating that PM_{2.5} induced apoptosis of mouse ovarian granulosa cells and oocytes and affected mouse embryo development.

There are only a limited number of toxicological studies of the effect of PM_{2.5} on the reproductive system and its potential mechanisms. In one study, Zhou et al. (2019) established a real-time whole-body PM_{2.5} exposure mouse model in C57BL/6 mice. PM_{2.5} exposure was found to lead to a significant increase in circulating leukocytes and lung inflammation, and also to testicular DNA damage and histopathological alterations, and a significant decrease in sperm density. PM_{2.5} exposure remarkably increased the expression of major components of NACHT, LRR, and PYD structure domains containing protein 3 (NALP3) inflammasomes, as well as increased expression of miR-183/96/182 targeting FOXO1 in testis. In addition, Yang et al. (2021) wondered whether the enzyme 1 (IRE1)/c-Jun NH 2-terminal kinase (JNK)/autophagy signaling pathway was activated by PM_{2.5} and whether this pathway mediates reproductive damage in male rats. After exposing male SD rats to PM_{2.5}, they found a loose structure of spermatogenic cells in the PM_{2.5} group and decreased numbers of both spermatogenic cells and mature spermatozoa. Structural damage of germ cells was ameliorated, and the number of exfoliative cells was reduced by intervention with the IRE1 inhibitor STF083010. Western blot analysis revealed significant upregulation of IRE1, phosphorylated JNK (p-JNK), beclin-1, and microtubule-associated protein 1 light chain 3 (LC3) II/LC3I protein expression, and downregulation of p62 protein. This study suggests that the activation of (IRE1)/c-Jun NH 2-terminal kinase (JNK)/autophagy signaling pathway may play a potential role in the mechanism of reproductive toxicity induced by PM_{2.5}.

Other Toxic Effects of PM_{2.5}

Ren et al. (2020) examined aromatic hydrocarbon receptor (AHR) activity and ROS levels in zebrafish embryo hearts, using fluorescence microscopy and qPCR. In addition, they looked for DNA damage and apoptosis by immunofluorescence. The results showed that inhibition of AHR, and elimination of ROS, significantly relieved PM_{2.5}-induced cardiac defects in the zebrafish embryos, suggesting that AHR mediates PM_{2.5} extractable organic matter (EOM)-induced oxidative stress, leading to DNA damage and apoptosis, which can be toxic to cardiac development.

Wang et al. (2017a) validated a Drosophila model for PM_{2.5} toxicity studies by the biological response of Drosophila exposed to high ambient concentrations of PM_{2.5}. Survival curves showed that exposure to PM_{2.5} significantly reduced the lifespan of Drosophila. This anti-longevity effect was observed in both male and female Drosophila, with males being more sensitive. Similar to the effects of human

exposure to concentrated ambient PM_{2.5}, exposure to PM_{2.5} may lead to premature death by inducing inflammation-related signals, oxidative stress, and metabolic abnormalities in the Drosophila, suggesting that Drosophila may also serve as a useful animal model for PM_{2.5} toxicity studies.

Limitations of and Alternatives to Animal Testing

Animal testing has contributed greatly to advancing understanding of the health risks that indoor air pollutants may cause, and an understanding of the underlying molecular mechanisms resulting in harm. Both, possible interventions to reverse harm, and suggestions for healthier living conditions and life-styles, have been proposed in this chapter, providing guidance for a healthier life. Increasingly researchers are using experimental animals to explore the toxicity of indoor air pollutants. Until recently, research using experimental animals was based on traditional anatomical technologies; however, the emergence of new technologies such as omics (Federico et al. 2020; Bode et al. 2021) and gene knockout (Chaix et al. 2019; Navabpour et al. 2020) provide new opportunities for the advancement of pollutant toxicity research. Seamless integrations of the traditional experimental animal exposure methods and some new research approaches, including transcriptomics (Ding et al. 2019; Wang et al. 2019), proteomics (Ma et al. 2018; Zhang et al. 2019), and metabolomics (Zhang et al. 1994; Costa et al. 2019), has provided an important platform for exploring the mechanisms responsible for the negative impact that ambient air pollutants have on human health.

However, the increased use of experimental animals has been controversial since conclusions drawn from animal research do not necessarily extrapolate to the human body (Robinson et al. 2019). In response, the use of experimental animals is restricted by ethics (Levy 2012), and the procedure for obtaining ethics approval in many countries around the world is quite strict. Secondly, different aspects of interspecies differences, including anatomy, metabolism, physiology, and genetics may greatly undermine the reliability of conducting animal experiments to explore underlying mechanisms of human disease or to foresee toxicity in humans induced by certain indoor pollutants (Langley 2009). People can partially improve the external validity by improving animal models. However, since the problem of interspecies differences cannot always be completely avoided, the external validity will always be weakened. Thus, the extrapolation of animal experimental results to humans will also be affected (Pound and Ritskes-Hoitinga 2018).

Therefore, there is an increasing trend to develop alternative (nonanimal) methods for toxicity testing, such as computer models (Knight et al. 2006), cultivated cells (Liu et al. 2013), and 3D cell cultures (Dutta et al. 2017).

1. 3D cell cultures, also known as organoids, have been substituted for animal models in certain types of research. Organoids can be grown *in vitro* on scaffolds (biological or synthetic hydrogels such as Matrigel) or in a culture medium (Corrò et al. 2020).

Embryonic pluripotent stem cells, adult stem cells, and induced pluripotent stem cells, three types of human or animal stem cells, are sources of organoids. Organoids grown in vitro can mimic the structure and function of different organs including the brain, liver, lung, kidney, and gut. Organoids are now being developed to study infectious diseases. Tumor 3D cell cultures from human patient biopsy cells can be applied to study the genomics and drug resistance of tumors in different organs. Organoids are also used to model genetic diseases such as cystic fibrosis (Artegiani and Clevers 2018), neurodegenerative diseases such as Alzheimer's and Parkinson's disease, infectious diseases such as MERS-COV and Norovirus, and parasitic infections such as *Toxoplasma gondii* (Corrò et al. 2020). Human and animal cell-derived organoids are also widely used in pharmacology and toxicology studies (Augustyniak et al. 2019; Steinberg et al. 2020).

2. Major alternatives to animal experiments also include the use of in vitro cell and tissue cultures. Cells and tissues from organs such as the liver, kidney, brain, and skin are removed from animals and can be stored in vitro in suitable growth media for days to months or even years. These methods are often used for preliminary screening of potential drug molecules/chemicals to examine their toxicity and efficacy (Shay and Wright 2000; Steinhoff et al. 2000). However, results obtained from in vitro experiments cannot generally be used directly to predict an organism's response to chemical exposure. Especially, due to the lack of interactions between different cell types, long-term and systemic responses cannot be modeled in vitro (Kim et al. 2019). Sometimes "human-on-a-chip" systems are applied to enhance the complexity of in vitro systems, where multiple cells can interact to mimic the cell-to-cell interactions that exist in human tissues (Sung et al. 2010), or numerically simulate the behavior of complex systems through mathematical modeling, using in vitro data to provide data for model development (Quignot and Bois 2013).
3. Various possible biological and toxic effects of chemicals or potential drug candidates can be predicted by computer-generated simulations, avoiding the use of animal testing. Only the most promising molecules from the initial screening will be tested in vivo. For example, in order to determine the receptor binding site of a drug, it is necessary to perform in vivo experiments. Computer-aided drug design (CADD) software can be used to predict receptor binding sites for potential drug molecules. CADD achieves the 3R goal by identifying possible binding sites and thus avoiding unnecessary animal testing of chemicals that are not biologically active, thus reducing the total number of experimental animals (Doke and Dhawale 2015). There are also objections, such as the National Academy of Sciences Institute for Laboratory Animal Research (National Research Council 2004), which argues that even sophisticated computer models cannot replace animal research and that computer models cannot handle the extremely complex interactions between molecules, cells, tissues, organs, organisms, and the environment.

Up to the present, use of animal testing to evaluate any health effect of indoor air pollutants remains the most effective, persuasive, and still irreplaceable research method, especially in explaining the molecular mechanism of pollutant

toxicity. Globally, in order to limit animal testing to those that fully consider all alternatives and minimize animal suffering, governmental and institutional review boards have developed legislative and ethical approval procedures (Festing and Wilkinson 2007). Those who use animal research in pursuit of academic goals must do so based on ethical principles and under regulated laboratory practices. Every researcher must make every effort to use animals in academic research in the most ethical and responsible manner, while contributing to the dissemination of knowledge without forgetting the ethical principles of legislation (Andersen and Winter 2019).

Conclusions

In order to have a deeper understanding of the health impacts of indoor air pollutants on humans, it is insufficient to rely only on epidemiological investigations and computer models. Through animal tests, the human body's response to exposure in the real environment can be simulated more comprehensively. Therefore, animal tests can help researchers gain effective insights into health impacts as well as the possible mechanisms, and potentially identify appropriate interventions in advance to prevent humans from being harmed by indoor air pollution. Although there are limitations to animal toxicology, it is still foreseeable that animal tests may be one of the most effective ways to understand the health effects of indoor pollution at present and in the future.

Cross-References

- [Application of Biomarkers in Assessing Health Risk of Indoor Air Pollutants](#)
- [Volatile Organic Compounds \(VOCs\)](#)

Acknowledgments The presented work was supported by the National Natural Science Foundation of China (42077403), the National Key Research and Development Program of China (2017YFC0702700), and Self-Determined Research Funds of CCNU from the Colleges' Basic Research and Operation of MOE (CCNU18JCXK07 and CCNU19TS066).

References

- Abdel-Halim RE (2005) Contributions of Ibn Zuhr (Avenzoar) to the progress of surgery: a study and translations from his book Al-Taisir. *Saudi Med J* 26(9):1333–1339
- Abdel-Halim RE (2006) Contributions of Muhadhdhab Al-Deen Al-Baghdadi to the progress of medicine and urology. A study and translations from his book Al-Mukhtar. *Saudi Med J* 27(11): 1631–1641
- Andersen ML, Winter LMF (2019) Animal models in biological and biomedical research – experimental and ethical concerns. *An Acad Bras Cienc* 91(suppl 1):e20170238
- Artegiani B, Clevers H (2018) Use and application of 3D-organoid technology. *Hum Mol Genet* 27 (R2):R99–R107

- Augustyniak J, Bertero A, Coccini T, Baderna D, Buzanska L, Caloni F (2019) Organoids are promising tools for species-specific in vitro toxicological studies. *J Appl Toxicol* 39(12):1610–1622
- Barakat R, Lin PP, Rattan S, Brehm E, Canisso IF, Abosalum ME, Flaws JA, Hess R, Ko C (2017) Prenatal exposure to DEHP induces premature reproductive senescence in male mice. *Toxicol Sci* 156(1):96–108
- Barré-Sinoussi F, Montagutelli X (2015) Animal models are essential to biological research: issues and perspectives. *Future Sci OA* 1(4):Fs063
- Belpomme D, Irigaray P, Hardell L, Clapp R, Montagnier L, Epstein S, Sasco AJ (2007) The multitude and diversity of environmental carcinogens. *Environ Res* 105(3):414–429
- Bernardini L, Barbosa E, Charão MF, Goethel G, Muller D, Bau C, Steffens NA, Santos Stein C, Moresco RN, Garcia SC, Souza Vencato M, Brucker N (2020) Oxidative damage, inflammation, genotoxic effect, and global DNA methylation caused by inhalation of formaldehyde and the purpose of melatonin. *Toxicol Res (Camb)* 9(6):778–789
- Bode D, Cull AH, Rubio-Lara JA, Kent DG (2021) Exploiting single-cell tools in gene and cell therapy. *Front Immunol* 12:702636
- Bono R, Munnia A, Romanazzi V, Bellisario V, Cellai F, Peluso MEM (2016) Formaldehyde-induced toxicity in the nasal epithelia of workers of a plastic laminate plant. *Toxicol Res (Camb)* 5(3):752–760
- Bornehag CG, Nanberg E (2010) Phthalate exposure and asthma in children. *Int J Androl* 33(2):333–345
- Casal-Mouriño A, Valdés L, Barros-Dios JM, Ruano-Ravina A (2019) Lung cancer survival among never smokers. *Cancer Lett* 451:142–149
- Chaix A, Lin T, Le HD, Chang MW, Panda S (2019) Time-restricted feeding prevents obesity and metabolic syndrome in mice lacking a circadian clock. *Cell Metab* 29(2):303–319
- Chen J, Moir D, Whyte J (2012) Canadian population risk of radon induced lung cancer: a re-assessment based on the recent cross-Canada radon survey. *Radiat Prot Dosim* 152(1–3):9–13
- Chen H, Chen N, Li F, Sun L, Du J, Chen Y, Cheng F, Li Y, Tian S, Jiang Q, Cui F, Tu Y (2020) Repeated radon exposure induced lung injury and epithelial-mesenchymal transition through the PI3K/AKT/mTOR pathway in human bronchial epithelial cells and mice. *Toxicol Lett* 334:4–13
- Cogliano VJ, Grosse Y, Baan RA, Straif K, Secretan MB, El Ghissassi F (2005) Meeting report: summary of IARC monographs on formaldehyde, 2-butoxyethanol, and 1-tert-butoxy-2-propanol. *Environ Health Perspect* 113(9):1205–1208
- Cohen B, Loew F (2002) Laboratory animal medicine: historical perspectives. *Lab Anim Med*:1–17
- Cong LH, Li T, Wang H, Wu YN, Wang SP, Zhao YY, Zhang GQ, Duan J (2020) IL-17A-producing T cells exacerbate fine particulate matter-induced lung inflammation and fibrosis by inhibiting PI3K/Akt/mTOR-mediated autophagy. *J Cell Mol Med* 24(15):8532–8544
- Corrò C, Novellasdemunt L, Li VSW (2020) A brief history of organoids. *Am J Phys Cell Phys* 319(1):C151–C165
- Costa LG, Cole TB, Dao K, Chang YC, Garrick JM (2019) Developmental impact of air pollution on brain function. *Neurochem Int* 131:104580
- Dan S, Pant M, Kaur T, Pant S (2020) Toxic effect of formaldehyde: a systematic review. *Int Res J Mod Eng Technol Sci* 2:179–189
- Davel AP, Lemos M, Pastro LM, Pedro SC, De André PA, Hebeda C, Farsky SH, Saldiva PH, Rossoni LV (2012) Endothelial dysfunction in the pulmonary artery induced by concentrated fine particulate matter exposure is associated with local but not systemic inflammation. *Toxicology* 295(1–3):39–46
- Ding Y, Gao K, Liu Y, Mao G, Chen K, Qiu X, Zhao T, Yang L, Feng W, Wu X (2019) Transcriptome analysis revealed the mechanism of the metabolic toxicity and susceptibility of di-(2-ethylhexyl)phthalate on adolescent male ICR mice with type 2 diabetes mellitus. *Arch Toxicol* 93(11):3183–3206
- Dockery DW, Stone PH (2007) Cardiovascular risks from fine particulate air pollution. *N Engl J Med* 356(5):511–513

- Doke SK, Dhawale SC (2015) Alternatives to animal testing: a review. *Saudi Pharm J* 23(3):223–229
- Duan J, Hu H, Zhang Y, Feng L, Shi Y, Miller MR, Sun Z (2017) Multi-organ toxicity induced by fine particulate matter PM(2.5) in zebrafish (*Danio rerio*) model. *Chemosphere* 180:24–32
- Dutta D, Heo I, Clevers H (2017) Disease modeling in stem cell-derived 3D organoid systems. *Trends Mol Med* 23(5):393–410
- Federico A, Serra A, Ha MK, Kohonen P, Choi J-S, Liampa I, Nymark P, Sanabria N, Cattelani L, Fratello M, Kinaret PAS, Jagiello K, Puzyn T, Melagraki G, Gulumian M, Afantitis A, Sarimveis H, Yoon T-H, Grafström R, Greco D (2020) Transcriptomics in toxicogenomics, part II: preprocessing and differential expression analysis for high quality data. *Nano* 10(5):903
- Feng W, Liu Y, Ding Y, Mao G, Zhao T, Chen K, Qiu X, Xu T, Zhao X, Wu X, Yang L (2020a) Typical neurobehavioral methods and transcriptome analysis reveal the neurotoxicity and mechanisms of di(2-ethylhexyl) phthalate on pubertal male ICR mice with type 2 diabetes mellitus. *Arch Toxicol* 94(4):1279–1302
- Feng YX, Feng NX, Zeng LJ, Chen X, Xiang L, Li YW, Cai QY, Mo CH (2020b) Occurrence and human health risks of phthalates in indoor air of laboratories. *Sci Total Environ* 707:135609
- Festing S, Wilkinson R (2007) The ethics of animal research. Talking point on the use of animals in scientific research. *EMBO Rep* 8(6):526–530
- Franco LS, Shanahan DF, Fuller RA (2017) A review of the benefits of nature experiences: more than meets the eye. *Int J Environ Res Public Health* 14(8):864
- Gawełek E, Drozdowska B, Fuchs A (2017) Radon as a risk factor of lung cancer. *Przegl Epidemiol* 71(1):90–98
- Ge J, Yang H, Lu X, Wang S, Zhao Y, Huang J, Xi Z, Zhang L, Li R (2020) Combined exposure to formaldehyde and PM2.5: hematopoietic toxicity and molecular mechanism in mice. *Environ Int* 144:106050
- Gleason JA, Bielory L, Fagliano JA (2014) Associations between ozone, PM2.5, and four pollen types on emergency department pediatric asthma events during the warm season in New Jersey: a case-crossover study. *Environ Res* 132:421–429
- Gorden P (1997) Non-insulin dependent diabetes--the past, present and future. *Ann Acad Med Singap* 26(3):326–330
- Gu XY, Chu X, Zeng XL, Bao HR, Liu XJ (2017) Effects of PM2.5 exposure on the Notch signaling pathway and immune imbalance in chronic obstructive pulmonary disease. *Environ Pollut* 226: 163–173
- Gu Y, Gao M, Zhang W, Yan L, Shao F, Zhou J (2021) Exposure to phthalates DEHP and DINP may lead to oxidative damage and lipidomic disruptions in mouse kidney. *Chemosphere* 271:129740
- Guo J, Zhao Y, Jiang X, Li R, Xie H, Ge L, Xie B, Yang X, Zhang L (2018) Exposure to formaldehyde perturbs the mouse gut microbiome. *Genes* 9(4):192
- Habre R, Coull B, Moshier E, Godbold J, Grunin A, Nath A, Castro W, Schachter N, Rohr A, Kattan M, Spengler J, Koutrakis P (2014a) Sources of indoor air pollution in New York City residences of asthmatic children. *J Expo Sci Environ Epidemiol* 24(3):269–278
- Habre R, Moshier E, Castro W, Nath A, Grunin A, Rohr A, Godbold J, Schachter N, Kattan M, Coull B, Koutrakis P (2014b) The effects of PM2.5 and its components from indoor and outdoor sources on cough and wheeze symptoms in asthmatic children. *J Expo Sci Environ Epidemiol* 24(4):380–387
- Huang J, Xu K, Yu L, Pu Y, Wang T, Sun R, Liang G, Yin L, Zhang J, Pu Y (2021) Immunosuppression characterized by increased Treg cell and IL-10 levels in benzene-induced hematopoietic toxicity mouse model. *Toxicology* 464:152990
- IARC (1974) Some anti-thyroid and related substances, nitrofurans and industrial chemicals. In: IARC monographs on the evaluation of the carcinogenic risk of chemicals to man, vol 7. IARC Scientific Publications, pp 111–140
- IPCS (1999) Environmental health criteria 211. World Health Organization Geneva, Switzerland
- Jacobson Lda S, Hacon Sde S, Castro HA, Ignotti E, Artaxo P, Ponce De Leon AC (2012) Association between fine particulate matter and the peak expiratory flow of schoolchildren in the Brazilian subequatorial Amazon: a panel study. *Environ Res* 117:27–35

- Jaenisch R, Mintz B (1974) Simian virus 40 DNA sequences in DNA of healthy adult mice derived from preimplantation blastocysts injected with viral DNA. *Proc Natl Acad Sci U S A* 71(4): 1250–1254
- Jafari MJ, Rahimi A, Omidi L, Behzadi MH, Rajabi MH (2015) Occupational exposure and health impairments of formaldehyde on employees of a wood industry. *Health Promot Perspect* 5(4): 296–303
- Ji W, Zhao B (2015) Contribution of outdoor-originating particles, indoor-emitted particles and indoor secondary organic aerosol (SOA) to residential indoor PM_{2.5} concentration: a model-based estimation. *Build Environ* 90:196–205
- Kang J, Ding Y, Li B, Liu H, Yang X, Chen M (2017) TRPA1 mediated aggravation of allergic contact dermatitis induced by DINP and regulated by NF-κB activation. *Sci Rep* 7(1):43586
- Kataoka T, Etani R, Kanzaki N, Kobashi Y, Yunoki Y, Ishida T, Sakoda A, Ishimori Y, Yamaoka K (2017) Radon inhalation induces manganese-superoxide dismutase in mouse brain via nuclear factor-κB activation. *J Radiat Res* 58(6):887–893
- Kim TW, Che JH, Yun JW (2019) Use of stem cells as alternative methods to animal experimentation in predictive toxicology. *Regul Toxicol Pharmacol* 105:15–29
- Knight A, Bailey J, Balcombe J (2006) Animal carcinogenicity studies: 3. Alternatives to the bioassay. *Altern Lab Anim* 34(1):39–48
- Koch HM, Bolt HM, Preuss R, Angerer J (2005) New metabolites of di(2-ethylhexyl)phthalate (DEHP) in human urine and serum after single oral doses of deuterium-labelled DEHP. *Arch Toxicol* 79(7):367–376
- Koch HM, Preuss R, Angerer J (2006) Di(2-ethylhexyl)phthalate (DEHP): human metabolism and internal exposure – an update and latest results1. *Int J Androl* 29(1):155–165
- Lafollette H, Shanks N (1994) Animal experimentation: the legacy of Claude Bernard. *Int Stud Philos Sci* 8(3):195–210
- Lan Q, Zhang L, Li G, Vermeulen R, Weinberg RS, Dosemeci M, Rappaport SM, Shen M, Alter BP, Wu Y, Kopp W, Waidyanatha S, Rabkin C, Guo W, Chanock S, Hayes RB, Linet M, Kim S, Yin S, Rothman N, Smith MT (2004) Hematotoxicity in workers exposed to low levels of benzene. *Science* 306(5702):1774–1776
- Langley G (2009) The validity of animal experiments in medical research. *RSDA* 1:161–168
- Latini G, Verrotti A, De Felice C (2004) Di-2-ethylhexyl phthalate and endocrine disruption: a review. *Curr Drug Targets Immune Endocr Metabol Disord* 4(1):37–40
- Levy N (2012) The use of animal as models: ethical considerations. *Int J Stroke* 7(5):440–442
- Li XN, Yang SQ, Li M, Li XS, Tian Q, Xiao F, Tang YY, Kang X, Wang CY, Zou W, Zhang P, Tang XQ (2021) Formaldehyde induces ferroptosis in hippocampal neuronal cells by upregulation of the Warburg effect. *Toxicology* 448:152650
- Liao BQ, Liu CB, Xie SJ, Liu Y, Deng YB, He SW, Fu BB, Wang YL, Chen MH, Lin YH, Li FP, Xie X, Hong XR, Wang HL (2020) Effects of fine particulate matter (PM(2.5)) on ovarian function and embryo quality in mice. *Environ Int* 135:105338
- Liguori GR, Jeronimus BF, De Aquinas Liguori TT, Moreira LFP, Harmsen MC (2017) Ethical issues in the use of animal models for tissue engineering: reflections on legal aspects, moral theory, three Rs strategies, and harm-benefit analysis. *Tissue Eng Part C Methods* 23(12):850–862
- Lioy PJ, Wainman T, Zhang J, Goldsmith S (1999) Typical household vacuum cleaners: the collection efficiency and emissions characteristics for fine particles. *J Air Waste Manag Assoc* 49(2):200–206
- Liu D, Zheng Y, Li B, Yao H, Li R, Zhang Y, Yang X (2011) Adjuvant effects of gaseous formaldehyde on the hyper-responsiveness and inflammation in a mouse asthma model immunized by ovalbumin. *J Immunotoxicol* 8(4):305–314
- Liu W, Deng Y, Liu Y, Gong W, Deng W (2013) Stem cell models for drug discovery and toxicology studies. *J Biochem Mol Toxicol* 27(1):17–27
- Liu X, Zhang Y, Wu R, Ye M, Zhao Y, Kang J, Ma P, Li J, Yang X (2018) Acute formaldehyde exposure induced early Alzheimer-like changes in mouse brain. *Toxicol Mech Methods* 28(2):95–104
- Loomis D, Guyton KZ, Grosse Y, El Ghissassi F, Bouvard V, Benbrahim-Tallaa L, Guha N, Vilahur N, Mattock H, Straif K (2017) Carcinogenicity of benzene. *Lancet Oncol* 18(12): 1574–1575

- Lorenzo-González M, Torres-Durán M, Barbosa-Lorenzo R, Provencio-Pulla M, Barros-Dios JM, Ruano-Ravina A (2019) Radon exposure: a major cause of lung cancer. *Expert Rev Respir Med* 13(9):839–850
- Lu Z, Li CM, Qiao Y, Yan Y, Yang X (2008) Effect of inhaled formaldehyde on learning and memory of mice. *Indoor Air* 18(2):77–83
- Ma S, Wang C, Zhao B, Ren X, Tian S, Wang J, Zhang C, Shao Y, Qiu M, Wang X (2018) Tandem mass tags labeled quantitative proteomics to study the effect of tobacco smoke exposure on the rat lung. *Biochim Biophys Acta Proteins Proteomics* 1866(3):496–506
- Ma XN, Li RQ, Xie JL, Li SH, Li JW, Yan XX (2021) PM2.5-induced inflammation and myocardial cell injury in rats. *Eur Rev Med Pharmacol Sci* 25(21):6670–6677
- Maehle A-H, Trohler U (1987) Animal experimentation: a student guide to balancing the issues. Monamy V (ed) Australian and New Zealand Council for the Care of Animals in Research and Teaching (ANZCCART), Glen Osmond, South Australia
- Mei Y, Duan C, Li X, Zhao Y, Cao F, Shang S, Ding S, Yue X, Gao G, Yang H, Shen L, Feng X, Jia J, Tong Z, Yang X (2016) Reduction of endogenous melatonin accelerates cognitive decline in mice in a simulated occupational formaldehyde exposure environment. *Int J Environ Res Public Health* 13(3):258
- Meng QY, Turpin BJ, Polidori A, Lee JH, Weisel C, Morandi M, Colome S, Stock T, Winer A, Zhang J (2005) PM2.5 of ambient origin: estimates and exposure errors relevant to PM epidemiology. *Environ Sci Technol* 39(14):5105–5112
- Mercier F, Glorenne P, Blanchard O, Le Bot B (2012) Analysis of semi-volatile organic compounds in indoor suspended particulate matter by thermal desorption coupled with gas chromatography/mass spectrometry. *J Chromatogr A* 1254:107–114
- Mercier F, Gilles E, Saramito G, Glorenne P, Le Bot B (2014) A multi-residue method for the simultaneous analysis in indoor dust of several classes of semi-volatile organic compounds by pressurized liquid extraction and gas chromatography/tandem mass spectrometry. *J Chromatogr A* 1336:101–111
- Merzoug S, Toumi ML (2017) Effects of hesperidin on formaldehyde-induced toxicity in pregnant rats. *EXCLI J* 16:400–413
- Mirsch J, Hintz L, Maier A, Fournier C, Lobrich M (2020) An assessment of radiation doses from radon exposures using a mouse model system. *Int J Radiat Oncol Biol Phys* 108(3):770–778
- Mock M, Fouet A (2001) Anthrax. *Annu Rev Microbiol* 55(1):647–671
- Nachman KE, Parker JD (2012) Exposures to fine particulate air pollution and respiratory outcomes in adults using two national datasets: a cross-sectional study. *Environ Health* 11(1):25
- National Research Council (2004) Science, medicine, and animals. National Academies Press, Washington, DC
- Navabpour S, Kwapis JL, Jarome TJ (2020) A neuroscientist's guide to transgenic mice and other genetic tools. *Neurosci Biobehav Rev* 108:732–748
- Neghab M, Soltanzadeh A, Choobineh A (2011) Respiratory morbidity induced by occupational inhalation exposure to formaldehyde. *Ind Health* 49(1):89–94
- Nicoll CS (1991) A physiologist's views on the animal rights/liberation movement. *Physiologist* 34 (6):303, 306–308, 315
- Nie JH, Chen ZH, Liu X, Wu YW, Li JX, Cao Y, Hei TK, Tong J (2012) Oxidative damage in various tissues of rats exposed to radon. *J Toxicol Environ Health A* 75(12):694–699
- Nie J, Wu J, Chen Z, Jiao Y, Zhang J, Tian H, Li J, Tong J (2019) Expression profiles of long non-coding RNA in mouse lung tissue exposed to radon. *J Toxicol Environ Health A* 82(15): 854–861
- Niemann H, Tian XC, King WA, Lee RS (2008) Epigenetic reprogramming in embryonic and foetal development upon somatic cell nuclear transfer cloning. *Reproduction* 135(2):151–163
- Nurunnabi ASM, Afroz R, Alam S (2012) Animal research in medical science: pros and cons. *Health Sci J PMC* 2:28–33
- Ozen OA, Kus MA, Kus I, Alkoc OA, Songur A (2008) Protective effects of melatonin against formaldehyde-induced oxidative damage and apoptosis in rat testes: an immunohistochemical and biochemical study. *Syst Biol Reprod Med* 54(4–5):169–176

- Pagel ÉC, Costa Reis N Jr, De Alvarez CE, Santos JM, Conti MM, Boldrini RS, Kerr AS (2016) Characterization of the indoor particles and their sources in an Antarctic research station. *Environ Monit Assess* 188(3):167
- Pan X, Gong YY, Martinelli I, Angelici L, Favero C, Bertazzi PA, Mannucci PM, Ariëns RA, Routledge MN (2016) Fibrin clot structure is affected by levels of particulate air pollution exposure in patients with venous thrombosis. *Environ Int* 92–93:70–76
- Pearce J, Boyle P (2005) Examining the relationship between lung cancer and radon in small areas across Scotland. *Health Place* 11(3):275–282
- Pelletier M, Bonvalot N, Glorennec P (2017) Aggregating exposures & cumulating risk for semivolatile organic compounds: a review. *Environ Res* 158:649–659
- Polidori A, Turpin B, Meng QY, Lee JH, Weisel C, Morandi M, Colome S, Stock T, Winer A, Zhang J, Kwon J, Alimokhtari S, Shendell D, Jones J, Farrar C, Maberti S (2006) Fine organic particulate matter dominates indoor-generated PM_{2.5} in RIOPA homes. *J Expo Sci Environ Epidemiol* 16(4):321–331
- Poopal RK, Zhang J, Zhao R, Ramesh M, Ren Z (2020) Biochemical and behavior effects induced by diheptyl phthalate (DHpP) and Diisodecyl phthalate (DIDP) exposed to zebrafish. *Chemosphere* 252:126498
- Pound P, Ritskes-Hoitinga M (2018) Is it possible to overcome issues of external validity in preclinical animal research? Why most animal models are bound to fail. *J Transl Med* 16(1):304
- Qiu H, Tian LW, Pun VC, Ho KF, Wong TW, Yu IT (2014) Coarse particulate matter associated with increased risk of emergency hospital admissions for pneumonia in Hong Kong. *Thorax* 69(11):1027–1033
- Quignot N, Bois FY (2013) A computational model to predict rat ovarian steroid secretion from in vitro experiments with endocrine disruptors. *PLoS One* 8(1):e53891
- Ren F, Ji C, Huang Y, Aniagu S, Jiang Y, Chen T (2020) AHR-mediated ROS production contributes to the cardiac developmental toxicity of PM_{2.5} in zebrafish embryos. *Sci Total Environ* 719:135097
- Reynolds P, Urayama KY, Von Behren J, Feusner J (2004) Birth characteristics and hepatoblastoma risk in young children. *Cancer* 100(5):1070–1076
- Riva DR, Magalhães CB, Lopes AA, Lanças T, Mauad T, Malm O, Valenca SS, Saldiva PH, Faffe DS, Zin WA (2011) Low dose of fine particulate matter (PM_{2.5}) can induce acute oxidative stress, inflammation and pulmonary impairment in healthy mice. *Inhal Toxicol* 23(5):257–267
- Robinson NB, Krieger K, Khan FM, Huffman W, Chang M, Naik A, Yongle R, Hameed I, Krieger K, Girardi LN, Gaudino M (2019) The current state of animal models in research: a review. *Int J Surg* 72:9–13
- Roy A, Chapman RS, Hu W, Wei F, Liu X, Zhang J (2012) Indoor air pollution and lung function growth among children in four Chinese cities. *Indoor Air* 22(1):3–11
- Rozas S, Idoeta R, Alegría N, Herranz M (2016) Radiological characterisation and radon equilibrium factor in the outdoor air of a post-industrial urban area. *J Environ Radioact* 151:126–135
- Rumchev K, Brown H, Spickett J (2007) Volatile organic compounds: do they present a risk to our health? *Rev Environ Health* 22(1):39–55
- Russell WMS, Burch RL (1960) The principles of humane experimental technique. Methuen and Co., Ltd., London
- Ryder RD (1989) Animal revolution: changing attitudes towards speciesism. Basil Blackwell Ltd, UK, Oxford
- Schlink U, Thiem A, Kohajda T, Richter M, Strebel K (2010) Quantile regression of indoor air concentrations of volatile organic compounds (VOC). *Sci Total Environ* 408(18):3840–3851
- Shao Z, Bi J, Ma Z, Wang J (2017) Seasonal trends of indoor fine particulate matter and its determinants in urban residences in Nanjing, China. *Build Environ* 125:319–325
- Shay JW, Wright WE (2000) The use of telomerized cells for tissue engineering. *Nat Biotechnol* 18 (1):22–23
- Shen S, Li J, You H, Wu Z, Wu Y, Zhao Y, Zhu Y, Guo Q, Li X, Li R, Ma P, Yang X, Chen M (2017) Oral exposure to diisodecyl phthalate aggravates allergic dermatitis by oxidative stress and enhancement of thymic stromal lymphopoietin. *Food Chem Toxicol* 99:60–69

- Shi YQ, Fu GQ, Zhao J, Cheng SZ, Li Y, Yi LN, Li Z, Zhang L, Zhang ZB, Dai J, Zhang DY (2019) Di(2-ethylhexyl)phthalate induces reproductive toxicity via JAZF1/TR4 pathway and oxidative stress in pubertal male rats. *Toxicol Ind Health* 35(3):228–238
- Steinberg N, Bertero A, Chiono V, Dell'era P, Di Angelantonio S, Hartung T, Perego S, Raimondi MT, Xinaris C, Caloni F, De Angelis I, Alloisio S, Baderna D (2020) iPS, organoids and 3D models as advanced tools for *in vitro* toxicology. *ALTEX* 37(1):136–140
- Steinhoff G, Stock U, Karim N, Mertsching H, Timke A, Meliss RR, Pethig K, Haverich A, Bader A (2000) Tissue engineering of pulmonary heart valves on allogenic acellular matrix conduits: *in vivo* restoration of valve tissue. *Circulation* 102(19 Suppl 3):Iii50–55
- Sun R, Zhang J, Yin L, Pu Y (2014) Investigation into variation of endogenous metabolites in bone marrow cells and plasma in C3H/He mice exposed to benzene. *Int J Mol Sci* 15(3):4994–5010
- Sung JH, Esch MB, Shuler ML (2010) Integration of *in silico* and *in vitro* platforms for pharmacokinetic-pharmacodynamic modeling. *Expert Opin Drug Metab Toxicol* 6(9):1063–1081
- Tang XQ, Fang HR, Zhou CF, Zhuang YY, Zhang P, Gu HF, Hu B (2013) A novel mechanism of formaldehyde neurotoxicity: inhibition of hydrogen sulfide generation by promoting over-production of nitric oxide. *PLoS One* 8(1):e54829
- Tannenbaum J, Bennett BT (2015) Russell and Burch's 3Rs then and now: the need for clarity in definition and purpose. *J Am Assoc Lab Anim Sci* 54(2):120–132
- Tomatis L (1982) IARC benzene report. *Science* 218(4569):214–214
- Tran CM, Do TN, Kim K-T (2021) Comparative analysis of neurotoxicity of six phthalates in zebrafish embryos. *Toxics* 9(1):5
- Tsai WT (2019) An overview of health hazards of volatile organic compounds regulated as indoor air pollutants. *Rev Environ Health* 34(1):81–89
- Tulpule K, Dringen R (2013) Formaldehyde in brain: an overlooked player in neurodegeneration? *J Neurochem* 127(1):7–21
- Vlaanderen J, Lan Q, Kromhout H, Rothman N, Vermeulen R (2012) Occupational benzene exposure and the risk of chronic myeloid leukemia: a meta-analysis of cohort studies incorporating study quality dimensions. *Am J Ind Med* 55(9):779–785
- Wang G, Zhao J, Jiang R, Song W (2015) Rat lung response to ozone and fine particulate matter (PM2.5) exposures. *Environ Toxicol* 30(3):343–356
- Wang J, Li J, Zahid KR, Wang K, Qian Y, Ma P, Ding S, Yang X, Wang X (2016) Adverse effect of DEHP exposure on the serum insulin level of Balb/c mice. *Mol Cell Toxicol* 12(1):83–91
- Wang X, Chen M, Zhong M, Hu Z, Qiu L, Rajagopalan S, Fossett NG, Chen LC, Ying Z (2017a) Exposure to concentrated ambient PM2.5 shortens lifespan and induces inflammation-associated signaling and oxidative stress in *Drosophila*. *Toxicol Sci* 156(1):199–207
- Wang Y, Chen B, Lin T, Wu S, Wei G (2017b) Protective effects of vitamin E against reproductive toxicity induced by di(2-ethylhexyl) phthalate via PPAR-dependent mechanisms. *Toxicol Mech Methods* 27(7):551–559
- Wang H, Shen X, Liu J, Wu C, Gao J, Zhang Z, Zhang F, Ding W, Lu Z (2019) The effect of exposure time and concentration of airborne PM2.5 on lung injury in mice: a transcriptome analysis. *Redox Biol* 26:101264
- Wei C, Chen M, You H, Qiu F, Wen H, Yuan J, Xiang S, Yang X (2017) Formaldehyde and co-exposure with benzene induce compensation of bone marrow and hematopoietic stem/progenitor cells in BALB/c mice during post-exposure period. *Toxicol Appl Pharmacol* 324: 36–44
- Weschler CJ, Nazaroff WW (2008) Semivolatile organic compounds in indoor environments. *Atmos Environ* 42(40):9018–9040
- WHO (1989) Indoor air quality: organic pollutants. *Environ Technol Lett* 10(9):855–858
- WHO (2006) Formaldehyde, 2-butoxyethanol and 1-tert-butoxypropan-2-ol. *IARC Monogr Eval Carcinog Risks Hum* 88:1–478
- Wichmann HE, Schaffrath Rosario A, Heid IM, Kreuzer M, Heinrich J, Kreienbrock L (2005) Lung cancer risk due to radon in dwellings—evaluation of the epidemiological knowledge. *Int Congr Ser* 1276:54–57

- Williams PR, Panko JM, Unice K, Brown JL, Paustenbach DJ (2008) Occupational exposures associated with petroleum-derived products containing trace levels of benzene. *J Occup Environ Hyg* 5(9):565–574
- Windholz G (1987) Pavlov as a psychologist. A reappraisal. *Pavlov J Biol Sci* 22(3):103–112
- Wu S, Deng F, Hao Y, Shima M, Wang X, Zheng C, Wei H, Lv H, Lu X, Huang J, Qin Y, Guo X (2013) Chemical constituents of fine particulate air pollution and pulmonary function in healthy adults: the Healthy Volunteer Natural Relocation study. *J Hazard Mater* 260:183–191
- Wu Q, Fang L, Yang Y, Wang A, Chen X, Sun J, Wan J, Hong C, Tong J, Tao S, Tian H (2021) Protection of melatonin against long-term radon exposure-caused lung injury. *Environ Toxicol* 36(4):472–483
- Yan B, Guo J, Liu X, Li J, Yang X, Ma P, Wu Y (2016a) Oxidative stress mediates dibutyl phthalate-induced anxiety-like behavior in Kunming mice. *Environ Toxicol Pharmacol* 45:45–51
- Yan B, Li J, Guo J, Ma P, Wu Z, Ling Z, Guo H, Hiroshi Y, Yanagi U, Yang X, Zhu S, Chen M (2016b) The toxic effects of indoor atmospheric fine particulate matter collected from allergic and non-allergic families in Wuhan on mouse peritoneal macrophages. *J Appl Toxicol* 36(4):596–608
- Yang Y, Liu L, Xu C, Li N, Liu Z, Wang Q, Xu D (2018) Source apportionment and influencing factor analysis of residential indoor PM_{2.5} in Beijing. *Int J Environ Res Public Health* 15(4):686
- Yang Y, Feng Y, Huang H, Cui L, Li F (2021) PM_{2.5} exposure induces reproductive injury through IRE1/JNK/autophagy signaling in male rats. *Ecotoxicol Environ Saf* 211:111924
- You H, Li R, Wei C, Chen S, Mao L, Zhang Z, Yang X (2016) Thymic stromal lymphopoietin neutralization inhibits the immune adjuvant effect of di-(2-ethylhexyl) phthalate in balb/c mouse asthma model. *PLoS One* 11(7):e0159479
- Yu G, Chen Q, Liu X, Guo C, Du H, Sun Z (2014a) Formaldehyde induces bone marrow toxicity in mice by inhibiting peroxiredoxin 2 expression. *Mol Med Rep* 10(4):1915–1920
- Yu GY, Song XF, Liu Y, Sun ZW (2014b) Inhaled formaldehyde induces bone marrow toxicity via oxidative stress in exposed mice. *Asian Pac J Cancer Prev* 15(13):5253–5257
- Yu GY, Song XF, Zhao SH, Liu Y, Sun ZW (2015) Formaldehyde induces the bone marrow toxicity in mice by regulating the expression of Prx3 protein. *J Huazhong Univ Sci Technolog Med Sci* 35(1):82–86
- Yu L, Wang B, Cheng M, Yang M, Gan S, Fan L, Wang D, Chen W (2020) Association between indoor formaldehyde exposure and asthma: a systematic review and meta-analysis of observational studies. *Indoor Air* 30(4):682–690
- Zang X, Zhao J, Lu C (2021) PM_{2.5} inducing myocardial fibrosis mediated by Ang II/ERK1/2/TGF-beta1 signaling pathway in mice model. *J Renin Angiotensin Aldosterone Syst* 22(1):14703203211003786
- Zhang J, Lioy PJ, He Q (1994) Characteristics of aldehydes: concentrations, sources, and exposures for indoor and outdoor residential microenvironments. *Environ Sci Technol* 28(1):146–152
- Zhang L, Freeman L, Nakamura J, Hecht S, Vandenberg J, Smith M, Sonawane B (2010) Formaldehyde and leukemia: epidemiology, potential mechanisms, and implications for risk assessment. *Environ Mol Mutagen* 51(3):181–191
- Zhang X, Zhong W, Meng Q, Lin Q, Fang C, Huang X, Li C, Huang Y, Tan J (2015) Ambient PM_{2.5} exposure exacerbates severity of allergic asthma in previously sensitized mice. *J Asthma* 52(8):785–794
- Zhang X, Zhao Y, Song J, Yang X, Zhang J, Zhang Y, Li R (2018) Differential health effects of constant versus intermittent exposure to formaldehyde in mice: implications for building ventilation strategies. *Environ Sci Technol* 52(3):1551–1560
- Zhang C, Jeong CB, Lee JS, Wang D, Wang M (2019) Transgenerational proteome plasticity in resilience of a marine copepod in response to environmentally relevant concentrations of microplastics. *Environ Sci Technol* 53(14):8426–8436
- Zhang N, Li P, Lin H, Shuo T, Ping F, Su L, Chen G (2021) IL-10 ameliorates PM_{2.5}-induced lung injury by activating the AMPK/SIRT1/PGC-1α pathway. *Environ Toxicol Pharmacol* 86:103659

- Zhao Y, Magana LC, Cui H, Huang J, Mchale CM, Yang X, Looney MR, Li R, Zhang L (2021) Formaldehyde-induced hematopoietic stem and progenitor cell toxicity in mouse lung and nose. *Arch Toxicol* 95(2):693–701
- Zhou DX, Qiu SD, Zhang J, Tian H, Wang HX (2006) The protective effect of vitamin E against oxidative damage caused by formaldehyde in the testes of adult rats. *Asian J Androl* 8(5):584–588
- Zhou D, Zhang J, Wang H (2011) Assessment of the potential reproductive toxicity of long-term exposure of adult male rats to low-dose formaldehyde. *Toxicol Ind Health* 27(7):591–598
- Zhou L, Su X, Li B, Chu C, Sun H, Zhang N, Han B, Li C, Zou B, Niu Y, Zhang R (2019) PM2.5 exposure impairs sperm quality through testicular damage dependent on NALP3 inflammasome and miR-183/96/182 cluster targeting FOXO1 in mouse. *Ecotoxicol Environ Saf* 169:551–563
- Zhu J, Wong SL, Cakmak S (2013) Nationally representative levels of selected volatile organic compounds in Canadian residential indoor air: population-based survey. *Environ Sci Technol* 47(23):13276–13283



Application of Biomarkers in Assessing Health Risk of Indoor Air Pollutants

42

Jing Huang, Jiawei Wang, Teng Yang, and Junfeng Zhang

Contents

Introduction	1252
Application of Biomarkers in Assessing Health Risks of the Respiratory System	1253
The Structure and Function of the Respiratory System	1253
Indoor Air Pollution Affects Respiratory Health	1253
Biomarkers of Respiratory Health Effects of Indoor Air Pollution	1254
Application of Biomarkers in Assessing Health Risks of the Cardiovascular System	1260
The Structure and Function of the Cardiovascular System	1260
Indoor Air Pollution Affects Cardiovascular Health	1261
Biomarkers of Cardiovascular Health Effects of Indoor Air Pollution	1261
Application of Biomarkers in Assessing Health Risks of the Hematologic System	1268
The Structure and Function of the Hematologic System	1268
Indoor Air Pollution Affects Hematologic Health	1268
Biomarkers of Hematologic Health Effects of Indoor Air Pollution	1268
Application of Biomarkers in Assessing Systemic Inflammation and Oxidative Stress	1273
Biomarkers of Systemic Inflammation of Indoor Air Pollution	1273
Biomarkers of Oxidative Stress in Relation to Indoor Air Pollution	1277
Application of Biomarkers in Assessing Health Risks of the Immune System	1279
Composition and Function of the Immune System	1279
Health Effect on the Immune System of Indoor Air Pollution	1279
Biomarkers in Assessing Health Risks of the Immune System	1280

J. Huang · J. Wang · T. Yang

Department of Occupational and Environmental Health Sciences, Peking University School of Public Health, Beijing, China

e-mail: jing_huang@bjmu.edu.cn; wangjiawei@bjmu.edu.cn; 1595952019@pku.edu.cn

J. Zhang (✉)

Nicholas School of the Environment, Duke University, Durham, NC, USA

Global Health Research Center, Duke Kunshan University, Kunshan, Jiangsu Province, China

Duke Global Health Institute, Durham, NC, USA

e-mail: junfeng.zhang@duke.edu

Application of Biomarkers in Assessing Health Risks of the Reproductive System	1284
The Structure and Function of the Reproductive System	1284
Health Effect on the Reproductive System of Indoor Air Pollution	1284
Biomarkers in Assessing Health Risks of the Reproductive System	1285
Application of Biomarkers in Assessing Health Risks of Other Physiologic Systems	1288
Kidneys	1288
Thyroid	1289
Metabolic System	1289
Cognitive Function	1290
Conclusion	1291
References	1293

Abstract

Increasing attention has been paid on health risks of indoor air pollution since most people spend up to 90% of their time indoors. The indoor air pollution mixture is mainly comprised of particulate matter (PM) and gaseous pollutants such as volatile organic compounds (VOCs), nitrogen dioxide (NO_2), ozone (O_3), carbon monoxide (CO), carbon dioxide (CO_2), and sulfur dioxide (SO_2) as well as emerging contaminants such as semivolatile organic compounds (SVOCs). Indoor air pollution from solid fuel combustion is among the ten largest contributors to global burden of disease. Pathophysiology-based biomarkers are useful in the identification of early adverse health effects and in surveillance or monitoring of health status or disease progression. To facilitate appropriate applications of biomarkers in assessing health risk of indoor air pollutants, this chapter summarized researches exploring the adverse effects of indoor air pollutants exposure on the respiratory system, cardiovascular system, hematologic system, immune system, reproductive system, and other systems using representative biomarkers. The summary intends to facilitate understanding of the potential biological mechanisms through which the major indoor air pollutants would affect human health.

Keywords

Indoor air pollutants · Biomarkers · Adverse health effects · Biological mechanisms

Introduction

Indoor environmental conditions significantly affect human health, given that most people spend around 90% of their time indoors, mainly at home or in the workplace (Leech et al. 2002). Indoor air pollution is characterized as a complex mixture of particulate matter (PM), gaseous pollutants, and semivolatile compounds that partition between the particulate and gaseous phases. PM contains inorganic substances (e.g., metals) and organic compounds (e.g., larger molecular weight polycyclic aromatic hydrocarbons [PAHs]). Commonly measured gaseous pollutants include volatile organic compounds (VOCs, e.g., formaldehyde, benzene), nitrogen dioxide (NO_2), ozone (O_3), carbon monoxide (CO), carbon dioxide (CO_2), and sulfur

dioxide (SO_2). The outdoor environment, human activities in buildings, and building materials are the primary sources of indoor air pollutants (Tran et al. 2020). In households that use solid fuels (e.g., wood and other biomass, coal) for cooking and/or space heating, women and young children are particularly exposed to high levels of PM and gaseous products of incomplete combustion (e.g., fine particles, CO, and PAHs) of solid fuels (Bruce et al. 2000). According to the systematic analysis for the Global Burden of Disease Study, indoor air pollution is one of the ten largest contributors to global disability-adjusted life years (DALYs) between 1990 and 2015 (GBD 2015 Risk Factors Collaborators 2016).

Most recognized diseases associated with indoor air pollution are those of the respiratory and cardiovascular systems. The respiratory health effects of the smoke from solid-fuel combustion include chronic obstructive pulmonary disease (COPD), asthma, acute respiratory infection, and pulmonary tuberculosis in low- and medium-income countries (Kurmi et al. 2012). Indoor PM exposure has been associated with premature death in people with heart, nonfatal heart attacks, and irregular heartbeat (Tran et al. 2020). In addition, exposure to phthalates, a class of common indoor air pollutants, has been associated with adverse reproductive outcomes such as decreased semen quality in males (Radke et al. 2018), and preterm birth in females (Radke et al. 2019).

Pathophysiology-based biomarkers are useful in identifying preclinical effects and understanding biological mechanisms through which indoor air pollutants adversely affect health. In this chapter, we aim to summarize the applications of representative biomarkers in assessing health risks associated with indoor air pollutants. This summary is organized by biomarker responses in physiologic systems including respiratory system, cardiovascular system, immune system, reproductive system, and other systems (Fig. 1).

Application of Biomarkers in Assessing Health Risks of the Respiratory System

The Structure and Function of the Respiratory System

The respiratory system is comprised of upper respiratory tract (nasal passages), conducting airways (larynx, trachea, bronchi, bronchioles, and terminal bronchioles), and lower respiratory tract (alveolar ducts and alveoli) (Greeley 2016). The primary function of the respiratory system is ventilation, facilitating the exchange of gases between the air and blood and between the blood and body tissues.

Indoor Air Pollution Affects Respiratory Health

There is a large body of literature reporting the association between indoor air pollution and adverse health effects on the respiratory system. The health effects of indoor air pollution have been clarified clearly in the Handbook chapter

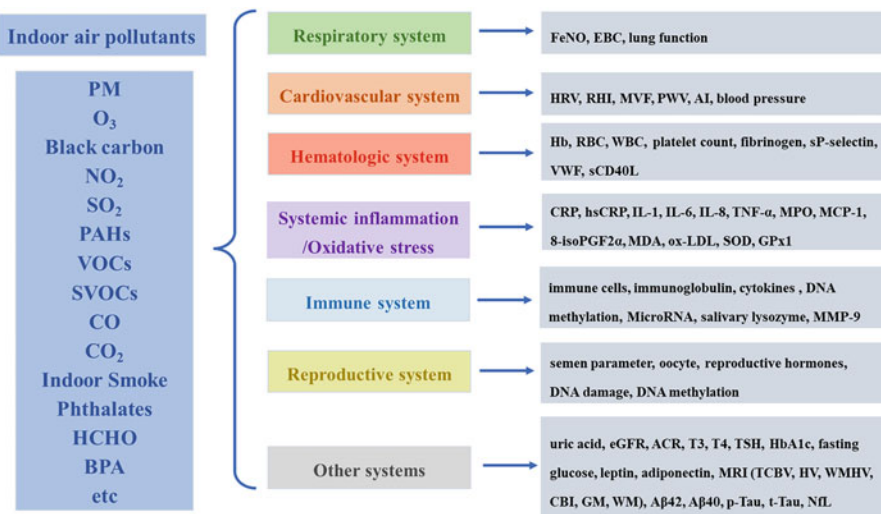


Fig. 1 Biomarkers used in assessing health risks of indoor air pollutants. PM: particulate matter, O₃: ozone, NO₂: nitrogen dioxide, SO₂: sulfur dioxide, PAHs: polycyclic aromatic hydrocarbons, TVOCs: total volatile organic compounds, CO: carbon monoxide, BPA: Bisphenol A, FeNO: fractional exhaled nitric oxide, EBC: exhaled breath condensate, HRV: heart rate variability, RHI: reactive hyperemia index, MVF: Microvascular function, PWV: Pulse wave velocity, AI: augmentation index, Hb: hemoglobin, RBC: red blood cell, WBC: white blood cell, sP-selectin: soluble P-selectin, VWF: Von Willebrand Factor, sCD40L: soluble CD40 ligand, CRP: C-reactive protein, hsCRP: high-sensitivity C-reactive protein, IL-1: interleukin-1, TNF- α : tumor necrosis factor- α , MPO: myeloperoxidase, MCP-1: monocyte chemoattractant protein-1, 8-isoPGF2 α : Iso-prostaglandin F2 α , MDA: malondialdehyde, ox-LDL: oxidized low-density lipoprotein, SOD: superoxide dismutase, GPx1: glutathione peroxidase, MMP-9: Matrix metalloproteinase 9, eGFR: estimated glomerular filtration rate, ACR: albumin to creatinine ratio, T3: triiodothyronine, T4: thyroxine, TSH: thyroid-stimulating hormone, HbA1c: glycated hemoglobin, TVBC: total cerebral brain volume, HV: hippocampal volume, WMHV: white matter hyperintensity volume, CBI: covert brain infarcts, GM: gray matter, WM: white matter, and NfL: neurofilament light

The Health Effects of Indoor Air Pollution by Jonathan Samet, Fernando Holguin, Meghan Buran. Indoor air pollution has been associated with incidence, prevalence, or exacerbation of respiratory diseases such as asthma, chronic bronchitis, and chronic obstructive pulmonary disease (COPD) as well (Hulin et al. 2012). To assess disease exacerbation or investigate biological mechanisms, biomarkers have been used to detect respiratory pathophysiological changes in human in response to indoor air pollution exposure, as described below and in Table 1.

Biomarkers of Respiratory Health Effects of Indoor Air Pollution

Fractional Exhaled Nitric Oxide (FeNO)

Fractional exhaled nitric oxide (FeNO) is derived from L-arginine with the action of inducible nitric oxide synthase (iNOS) in airway-epithelial cells. FeNO is a sensitive

Table 1 Biomarkers of the respiratory system used in assessing health risk of indoor air pollutants

Study site	Year	Study design	Pollutant	Participant, N	Biomarker	Reference
Shanghai	2015	Randomized double-blind crossover trial	PM _{2.5}	Healthy college student, 35	FeNO	Chen et al. (2015b)
Beijing	2020	Randomized crossover trial	PM _{2.5}	Healthy college student, 29	FeNO	Han et al. (2020)
Wuhan	2019	Pilot study	PM _{2.5} -bound PAHs	Postgraduate students, 20	FeNO	Li et al. (2019)
Changsha	2017	Longitudinal study	Ozone, PM _{2.5} , NO ₂ , and SO ₂	Healthy adults, 89	FeNO, EBC MDA, and EBC CNN	Day et al. (2017)
Honduran	2018	Cross-sectional study	PM _{2.5} , BC	Women, 139	FeNO	Benka-Coker et al. (2018)
Southern California	2016	Cohort study	NO	Schoolchildren, 1635	FeNO	Eckel et al. (2016)
Beijing	2019	Randomized double-blind crossover trial	PM _{0.5} , PM _{1.0} , PM _{2.5} , PM ₁₀ , and BC	Children, 44	FeNO, PEF, and FEV ₁	Dong et al. (2019)
Washington	2005	Panel study	BC	Patients with asthma or chronic obstructive pulmonary disease, 16	FeNO	Jansen et al. (2005)
Colorado	2019	Cross-sectional study	/	Residents, 253	FVC, FEV ₁ , and FEV ₁ /FVC	Humphrey et al. (2020)
Canada	2014	Cross-sectional study	VOC	Residents, 3857	FVC, FEV ₁ , and FEV ₁ /FVC	Cakmak et al. (2014)
Osaka and Hyogo prefectures	2020	Randomized crossover trial	PM _{2.5} , PM _{10-2.5} , and ozone	Healthy nonsmoking adults, 32	FVC, FEV ₁ , FEV ₁ /FVC, MMEF, and PEF	Yoda et al. (2020)

(continued)

Table 1 (continued)

Study site	Year	Study design	Pollutant	Participant, N	Biomarker	Reference
Manitoba	2013	Randomized double-blind crossover trial	PM _{2.5}	Residents, 37	FVC, FEV ₁ , and FEF _{25–75}	Weichenthal et al. (2013)
Eastern Massachusetts	2018	Panel study	PM _{2.5} , BC	Patients with COPD, 125	FVC, FEV ₁ , and FEV ₁ /FVC	Hart et al. (2018)
Seven European countries	2015	Multicenter study	PM ₁₀ , PM _{0.1} , formaldehyde, NO ₂ , and ozone	Elderly people, 600	FVC, FEV ₁ , and FEV ₁ /FVC	Bentayeb et al. (2015)
Cincinnati-Kentucky-Indiana tri-state area	2019	Randomized crossover trial	UVPM, PM _{2.5}	Asthmatic children aged 10–16 years, 44	FVC, FEV ₁ , FEV ₁ /FVC, and FEF _{25–75}	Isiugo et al. (2019)
Copenhagen	2014	Cross-sectional study	PNC (10–300 nm), PM _{2.5}	Residents, 78	FVC, FEV ₁ , and FEV ₁ /FVC	Karotki et al. (2014)

PM: particulate matter, PM_{2.5}: particulate matter with an aerodynamic diameter $\leq 2.5 \mu\text{m}$, PM_{0.5}: particulate matter with an aerodynamic diameter $\leq 0.5 \mu\text{m}$, PM₁₀: particulate matter with an aerodynamic diameter $\leq 10 \mu\text{m}$, PAHs: polycyclic aromatic hydrocarbons, NO₂: nitrogen dioxide, SO₂: sulfur dioxide, BC: black carbon, UVM: ultraviolet light-absorbing particulate matter, PNC: particle number concentration, FeNO: fractional exhaled nitric oxide, EBC: exhaled breath condensate, MDA: malondialdehyde, EBCNN: the sum of EBC nitrite and nitrate, FVC: forced vital capacity, FEV₁: forced expiratory volume in one second, MMEF: maximal midexpiratory flow, PEF: peak expiratory flow rate, and FEF_{25–75}: forced expiratory flow at 25–75% of vital capacity

and noninvasive marker reflecting airway inflammation, which measures the levels of inflammation objectively and quantitatively. It appears to be high variability across different individuals in their FeNO in response to increasing levels of indoor air pollutants.

In a randomized, double-blind crossover trial of air purifiers conducted among 35 healthy college students in Shanghai, China, the researchers reported that the FeNO geometric mean level was significantly decreased by 17% (95% confidence interval (CI): 3.6%, 32.5%) following the true-purified air scenario compared to following the sham-purified air scenario. Furthermore, an interquartile range (IQR) increase in indoor PM_{2.5} was associated with an increase in FeNO of 11.3% (95% CI: 0.6%, 23.0%) (Chen et al. 2015b). Another randomized crossover trial conducted on 29 healthy young adults in Beijing, China, found that indoor PM_{2.5} concentrations were significantly lower during the true air filtration period than during the sham purification period. An IQR (71.3 µg/m³) increase in 24-h personal PM_{2.5} was associated with an increase of 16.0% (95% CI: 3.7%, 28.4%) in FeNO (Zhao et al. 2020). A pilot study conducted among 20 postgraduate students found that a one-unit increase in inhaled dose of PM_{2.5}-bound polycyclic aromatic hydrocarbons (PAHs) or in urinary concentrations of \sum OH-PAHs was associated with a maximum FeNO increase of 13.5% (95% CI: 5.4%, 22.2%) at lag 2 day or of 6.8% (95% CI: 3.4%, 10.2%) at lag 1 day, respectively (Li et al. 2019). A longitudinal study in 89 healthy adult participants living in a work campus in Changsha City, China, found that a 10-ppb increase in 24-hour personal ozone exposure was associated with a mean increase of 18.1% (95% CI: 4.5%, 33.5%) in FeNO (Day et al. 2017). However, a cross-sectional study conducted among 139 women in rural Honduras reported a null association of FeNO with exposure to household air pollution (Benka-Coker et al. 2018).

Children, the elderly, and people with preexisting diseases are more susceptible in FeNO in response to indoor air pollution exposure. A study conducted among 1635 southern California schoolchildren reported that traffic-related air pollution (TRAP) indoors was associated with proximal and distal airway inflammation by relating indoor nitric oxide (NO), a marker of TRAP exposure in the indoor microenvironment, to airway and alveolar sources of exhaled nitric oxide. A 10 ppb higher indoor NO concentration was associated with 0.10 ppb higher average alveolar NO concentration ($C_{\text{A}}\text{NO}$) (95% CI: 0.04–0.16), 4.0% higher maximum airway wall NO flux ($J'_{\text{aw}}\text{NO}$ (95% CI: -2.8–11.3)), and 0.2% lower airway wall tissue diffusing capacity ($D_{\text{aw}}\text{NO}$) (95% CI: -4.8–4.6) (Eckel et al. 2016). A randomized, double-blind crossover study among 44 healthy school children found that indoor PM_{0.5}, PM_{2.5}, PM₁₀, and black carbon (BC) were decreased significantly by 48%, 44%, 34%, and 50% with a real ionization air purifier. The use of ionization air purifier can effectively decrease FeNO by 14.7% (Dong et al. 2019), and an IQR increase in PM_{1.0} (22.2 µg/m³) and BC (3.6 µg/m³) was associated with the increase in FeNO of 23.5% and 22.1%, respectively. A study conducted among 16 older subjects with asthma or chronic obstructive pulmonary disease (COPD) in Seattle, Washington, reported that for the seven subjects with asthma, a 1 µg/m³ increase in indoor and personal BC was associated with the increase in FeNO of 4.0 ppb (95% CI: 2.0, 5.9) and 1.2 ppb (95% CI: 0.2, 2.2), respectively (Jansen et al. 2005).

Exhaled Breath Condensate (EBC)

Exhaled breath condensate (EBC), thought of either as a body fluid or a condensate of exhaled gas, has emerged as a promising biospecimen that can be used to measure biomarkers reflecting respiratory health. EBC contains biomarkers, some of which can be assessed in a way equivalent to using other biospecimens such as blood, sweat, tears, urine, and saliva (Davis et al. 2012). EBC is a noninvasive mean of sampling the airways, allowing biomarkers of airway inflammation and oxidative stress to be directly measured using this specimen.

Malondialdehyde in Exhaled Breath Condensate

As a stable product of lipid peroxidation, malondialdehyde (MDA) has long been considered a biomarker of oxidative stress. Increased oxidative stress levels can result from increasing concentrations of reactive oxygen species (ROS) in cells and tissues. ROS react with lipids in the cell membrane and in body fluids, generating peroxidation products including MDA. A longitudinal study involving 89 healthy office workers living in a work campus in Changsha City, China, was conducted to examine the association between ozone exposure and cardiopulmonary pathophysiologic mechanisms (Day et al. 2017). In this study, with single-pollutant models, a 10-ppb increase in 24-hour personal O₃ exposure concentration (largely driven by indoor concentration) was associated with a significant decrease in EBC MDA of 26.3% (95% CI: -37.9%, -12.4%). For 2-week O₃ exposure concentration, a 10-ppb increase was associated with a significant decrease in EBC MDA level of 52.0% (95% CI: -67.0%, -30.4%). For other pollutants including PM_{2.5}, NO₂, and SO₂, each of these pollutants shared various positive associations with EBC MDA level, with only the 2-week NO₂ exposure concentration significantly associated with the increase in EBC MDA level of 29.9% (95% CI: 11.5%, 51.2%) as well as the 2-week SO₂ exposure concentration significantly associated with the increase in EBC MDA level of 258.9% (95% CI: 92.4%, 569.4%) after multiple testing correction.

The Sum of EBC Nitrite and Nitrate (EBCNN)

The EBCNN level reflects NO metabolism in the airways and is related to pulmonary inflammation, as airway tissue inflammation results in extra production of NO (NO measured in exhaled breath, FeNO, is another biomarker of pulmonary inflammation, as discussed above) The same study in the 89 office workers as described above found that in single-pollutant models, a 10-ppb increase in 24-hour O₃ exposure concentration was associated with the significant increase in EBCNN of 53.8% (95% CI: 23.6%, 91.5%). For 2-week O₃ exposure concentration, a 10-ppb increase was associated with the significant increase in EBCNN of 158.9% (95% CI: 61.2%, 315.8%) (Day et al. 2017).

Lung Function Parameters

Lung function parameters, including forced vital capacity (FVC), forced expiratory volume in the first second (FEV₁), FEV₁/FVC, peak expiratory flow (PEF), and FEF_{25–75%}, can reflect the early health effects of indoor air pollution on the

respiratory system. The Framingham Heart Study concluded that short-term exposure to PM_{2.5}, NO₂, and O₃ within US EPA standards was associated with lower lung function (Rice et al. 2013). Based on observed adverse effects on lung function caused by outdoor air pollution, studies have explored the associations between indoor air pollutants and lung function. A cross-sectional study from the Colorado Home Energy Efficiency and Respiratory health (CHEER) reported that annual average infiltration rate (AAIR) was positively associated with increased FEV₁/FVC z-scores, such as 1-unit change in AAIR was corresponded to a half of a standard deviation in lung function ($\beta = 0.51$, CI: 0.02–0.99). The results indicated that increased home ventilation, which may alter the composition of indoor air, was associated with improvement of respiratory health (Humphrey et al. 2020). A population-based cross-sectional survey designed to be representative of the Canadian population reported that increasing indoor concentrations of certain VOCs were associated with decreasing lung function (Cakmak et al. 2014). A randomized crossover intervention study conducted in 32 healthy adults reported that an IQR increase of 4.09 µg/m³ in indoor PM_{10–2.5} was associated with a significant decrease in the FEV₁/FVC of 0.52% (95% CI: 0.05%, 1.00%); an IQR increase of 2.81 ppb in indoor O₃ was associated with a significant decrease in maximal midexpiratory flow (MMEF) of 0.23 L/s (95% CI: 0.07, 0.40) (Yoda et al. 2020). A randomized, double-blind crossover study in 37 people living in 20 residences on a First Nations Reserve in Manitoba, Canada, reported that indoor PM_{2.5} decreased substantially during air filtration and that air filter use was associated with a 217 mL (95% CI: 23, 410) increase in FEV₁. This study also reported consistent inverse associations between PM_{2.5} exposure and lung function parameters including FEV₁, FVC, and PEF_{25%–75%} (Weichenthal et al. 2013).

Several studies have explored the association between indoor air pollution and lung function among vulnerable people such as children, the elderly, and individuals with preexisting diseases. A panel study conducted among 125 patients with COPD reported that increasing indoor exposures to black carbon particles (BC) were associated with decreases in prebronchodilator FEV₁, FVC, and FEV₁/FVC. Each IQR increase in indoor BC from the weekly integrated filter was associated with a 17.87 mL (95% CI: 1.98, 33.76) decrease in prebronchodilator FEV₁ (Hart et al. 2018). Another study investigated the association between indoor air quality and respiratory morbidity and lung function among elderly people residing in nursing homes in seven European countries. One of the main findings was that the subjects exposed to indoor concentrations above the median values of ultrafine particles (PM_{0.1}) and NO₂ were more likely (adjusted OR of 8.16 and 95% CI of 2.24–29.3 for PM_{0.1} and adjusted OR of 3.74 and 95% CI of 1.06–13.1 for NO₂) to have a low FEV₁/FVC ratio (<70%, indicative of airway obstruction, compared to the subjects exposed to indoor concentrations below the median values) (Bentayeb et al. 2015). A randomized crossover trial conducted among 44 asthmatic children of 10–16 years old found that one-unit increase in the first principal component variable representing indoor PM (predominantly composed of ultraviolet light absorbing particulate matter (UVM) and PM_{2.5}) was associated with a decrease in FEV₁/FVC ratio by 4.1% (99% CI: 1.4%, 6.9%), and that 17.7 µg/m³ increase in indoor

PM_{2.5} was associated with 6.1% (99% CI: 1.9%, 10.2%) decrease in percent-predicted FEV₁/FVC ratio and 12.9% (99% CI: 1.0%, 24.9%) decrease in FEF_{25–75}. This study also found that indoor PM was more strongly associated with lung function than outdoor PM (Isiugo et al. 2019). A cross-sectional study investigating the relationship between exposure to indoor PM and respiratory health in middle-aged subjects in Copenhagen, Denmark, reported that high levels of indoor particle number concentrations (PNC, 10–300 nm) were associated with significantly lower lung function. One IQR increase in indoor PNC was associated with a decrease in FEV₁/FVC of 2.1% (95% CI: 0.4%, 3.8%) (Karottki et al. 2014). A randomized, double-blind crossover study among 44 school children in Beijing, China, demonstrated that indoor air purification by PM filtration was associated with significantly higher FEV₁. This beneficial effect of the intervention was consistent with other findings of the study that increasing indoor concentrations of sized-fractional PM was associated with decreasing FEV₁. Particularly, the most significant reduction of FEV₁ was 6.5% per IQR increase in PM_{0.5} (17.9 µg/m³) and 7.0% per IQR increase in BC (3.6 µg/m³) (Dong et al. 2019).

However, not all studies have shown a significant association between indoor air pollution and lung function. A randomized, double-blind, crossover intervention study in 48 nonsmoking subjects (51 to 81 years) in 27 homes reported that the particle filters reduced the concentration of PM_{2.5} indoors significantly; however, no beneficial effect on lung function was found in this elderly population (Karottki et al. 2013). A randomized, double-blind crossover trial among 35 healthy college students also measured reduced indoor PM_{2.5} concentrations during the use of air filtration but failed to observe a statistically significant improvement in lung function in Shanghai, China (Chen et al. 2015b). The inconsistent findings on the lung function effect of indoor air pollution exposure and the lung function effect of indoor air purification can be attributed to differences in study design and sample size, study participants, exposure levels or the magnitude of exposure reduction in intervention studies, and timing of lung function measurement relevant to exposure, and potential confounding factors including temperature, relative humidity, and other indoor air pollutants. Nevertheless, lung function parameters, such as FVC, FEV₁, FEV₁/FVC, PEF, and FEF_{25–75%}, are useful biomarkers in assessing the health effects of indoor air pollution.

Application of Biomarkers in Assessing Health Risks of the Cardiovascular System

The Structure and Function of the Cardiovascular System

The cardiovascular system comprises heart and blood vessels including arteries, veins, and capillaries. Two circulation systems, including pulmonary circulation and somatic circulation, are involved in the cardiovascular system. In the pulmonary circulation, the deoxygenated blood is transported from the right ventricle into the lungs through the pulmonary artery. After enriching with oxygen in the lungs, it flows into the left atrium through pulmonary veins. In somatic circulation, blood is

pumped through the left ventricle and the aorta to supply all the body with oxygen-enriched blood. After ingesting by organs and cells, the blood low in oxygen and enriched in CO₂ turns back toward the heart through veins. Inhaled air pollutants can disrupt the normal circulation of blood through a number of pathologic processes as described below.

Indoor Air Pollution Affects Cardiovascular Health

Previous studies have demonstrated the associations between outdoor air pollution and adverse cardiovascular health effects, including acute myocardial infarction, coronary artery disease, stroke, peripheral artery disease, congestive heart failure, and cardiovascular mortality (Brook et al. 2010; Kaufman et al. 2012). Indoor air pollution is considered to cause similar or greater adverse effects on the cardiovascular system when considering that a large fraction of outdoor air pollutants can penetrate into the indoor environment and that the majority of the total exposure actually occurs indoors (Xiang et al. 2019). In addition to pollutant infiltrating from outdoors, pollutants can be directly emitted to the indoor environment from indoor sources such as cooking, tobacco smoking, consumer products, and building material off gassing. The biomarkers of cardiovascular health effects of indoor air pollution were shown as below and in Table 2.

Biomarkers of Cardiovascular Health Effects of Indoor Air Pollution

Cardiac Autonomic Function

Previous studies demonstrate that air pollution may cause adverse effects on autonomic function, including decreased heart rate variability (HRV) (Chuang et al. 2007; Schwartz et al. 2005). HRV provides a noninvasive measurement by assessing the activity of the cardiac autonomic system and has been used to evaluate the cardiac effects of environmental exposures.

A randomized crossover study evaluated the effects of short-term indoor air filtration intervention on cardiovascular health in 35 nonsmoking elderly participants living in Beijing. The study found a positive association between indoor air pollution exposure and impaired cardiac autonomic nervous system (Liu et al. 2018). In the study, households were randomly allocated to receive 2-week true or sham filtration with portable air filtration. The authors reported that indoor PM_{2.5} and indoor black carbon (BC) decreased 34.8% and 35.3%, respectively, during the true filtration period. The results also indicated that the standard deviation of normal-to-normal intervals (SDNN) decreased by -1.25% (95% CI: -2.06, -0.42) with a 10 µg/m³ increase in 8-h indoor PM_{2.5}-moving average, whereas the results for the square root of the mean of the squared differences between adjacent normal-to-normal intervals (RSDNN), low frequency (LF), high frequency (HF), and total power (TP) were similar to the effect of PM_{2.5} on SDNN. In addition, RSDNN decreased by -5.93% (95% CI: -9.37, -2.35) with a 1 µg/m³ increase in 8-h indoor BC-moving average.

Table 2 Biomarkers of the cardiovascular system used in assessing health risk of indoor air pollutants

Study site	Year	Study design	Pollutant	Participant, N	Biomarker	Reference
Beijing	2018	Randomized crossover trial	PM _{2.5} , BC	Nonsmoking elderly, 35	SDNN, RMSSD, LF, HF, TP, SBP, DBP, and MAP	Liu et al. (2018)
Taipei	2013	Panel study	PM _{2.5} , PM ₁₀ , TVOCs, and CO	Healthy adults, 300	SDNN, RMSSD	Lin et al. (2013)
Beijing	2018	Repeated-measure study	PM, BC	Patients with chronic obstructive pulmonary disease, 43	SDNN, RMSSD, SDANN, pNN50, HR, LF, HF, TP, and LF/FF	Pan et al. (2018)
Beijing	2019	Repeated-measure study	Ozone	Middle-school children	SDNN, RMSSD, SDANN, pNN50, HR, LF, HF, TP, and LF/FF	Huang et al. (2019)
Beijing	2020	Randomized double-blind crossover trial	PM	Healthy children, 44	SDNN, RMSSD, pNN50, HR, LF, HF, TP, and LF/FF	Liu et al. (2020)
Beijing	2019	Randomized double-blind crossover trial	PM _{0.5} , PM _{1.0} , PM _{2.5} , PM ₁₀ , and BC	Children, 44	SDNN, RMSSD, SDANN, pNN50, HR, LF, HF, TP, LF/FF, II_ST, V2_ST, and V5_ST	Dong et al. (2019)
British Columbia	2011	Randomized crossover trial	PM _{2.5}	Healthy adults, 45	HRI, SBP, DBP	Allen et al. (2011)
Copenhagen	2008	Randomized double-blind crossover trial	PM _{2.5} , PM _{10-2.5}	Healthy elderly, 42	MVF, SBP, DBP	Brauner et al. (2008)
Copenhagen	2013	Randomized double-blind crossover trial	PNC, PM _{2.5}	Healthy elderly, 51	MVF, SBP, and DBP	Karotki et al. (2013)
Chaurikharka	2019	Observational study	PM ₁₀ , PM _{2.5} , and BC	Residents, 78	PWV, SBP, and DBP	Pratali et al. (2019)
Duisburg	2019	Randomized crossover trial	PM ₁₀ , PM _{2.5} , and PNC	Healthy adults, 55	AI, PWV	Soppa et al. (2019)

Shanghai	2015	Randomized double-blind crossover trial	$\text{PM}_{2.5}$	Healthy college students, 35	SBP, DBP, and PP	Chen et al. (2015b)
Shanghai	2017	Randomized double-blind crossover trial	$\text{PM}_{2.5}$	Healthy college students, 55	SBP, DBP, and PP	Li et al. (2017)
Detroit	2018	Randomized double-blind crossover trial	$\text{PM}_{2.5}$	Residents, 40	SBP, DBP, PWV, SDNN, LF/HF, and AI	Morishita et al. (2018)
Peru	2020	Cross-sectional study	$\text{PM}_{2.5}$, CO	Residents, 902	SBP, DBP	Kephart et al. (2020)
Somerville	2015	Randomized crossover trial	PNC	Residents living near highways, 20	SBP, DBP	Padró-Martínez et al. (2015)
Manitoba	2013	Randomized double-blind crossover trial	$\text{PM}_{2.5}$	Residents, 37	RHI, SBP, and DBP	Weichenthal et al. (2013)
New Jersey	2014	Randomized crossover trial	$\text{PM}_{2.5}$, BC, CO, and NO_2	Healthy adults, 21	SDNN, rSDNN, LF, HF, and HR	Laumbach et al. (2014)

PM_i : particulate matter, $\text{PM}_{2.5}$: particulate matter with an aerodynamic diameter $\leq 2.5 \mu\text{m}$, $\text{PM}_{0.5}$: particulate matter with an aerodynamic diameter $\leq 0.5 \mu\text{m}$, PM_{10} : particulate matter with an aerodynamic diameter $\leq 10 \mu\text{m}$, CO: carbon monoxide, TVOCs: total volatile organic compounds, BC: black carbon, FNC: particle number concentration, SDNN: standard deviation of normal-to-normal intervals, RMSSD: the square root of the mean of the squared differences between adjacent normal-to-normal intervals, LF: low frequency, HF: high frequency, TP: total power, SBP: systolic blood pressure, DBP: diastolic blood pressure, MAP: ambulatory mean arterial pressure, SDANN: standard deviation of the averages of normal-to-normal intervals in all 5-min segments of the entire recording, HR: heart rate, pNN50: percentage of number of normal-to-normal interval with difference ≥ 50 ms, RHI: reactive hyperemia index, MVF: microvascular function, PWV: pulse wave velocity, AI: pulse wave velocity, AI: augmentation index, and PP: pulse pressure

A panel study of 300 healthy subjects living in Taipei was conducted to explore the relationship between indoor air pollution and cardiovascular health. In the study, three exposure conditions were investigated: Participants were required to keep their windows open during the first two visits and closed during the next two visits. The closed window conditions were coupled with the use of air conditioning (Lin et al. 2013). The results of the Taipei study demonstrated decreases in HRV were associated with increased levels of indoor particles and total volatile organic compounds (VOCs). In specific, an IQR increase in indoor PM_{2.5} was associated with decreases in SDNN of 4.6% (95% CI: -5.5%, -3.7%) and 1.5% (95% CI: -2.0%, -1.0%) during the period of keeping windows open and the period of window closing and air conditioning use, respectively; an IQR increase in indoor PM_{2.5} was also associated with the decrease in RSDNN of 3.5% (95% CI: -6.5%, -0.5%) and 2.4% (95% CI: -4.5%, -0.3%) during the period of keeping windows open and the period of window closing and AC use, respectively. In the same panel study, the similar associations between total VOCs and SDNN, RSDNN were also reported; the effects of indoor PM_{2.5} and total VOCs on SDNN were significantly stronger with windows open compared with the period of keeping windows closed.

A repeated-measure study in 43 COPD patients in Beijing monitored indoor concentrations of size-fractioned PM, including PM_{0.5}, PM_{1.0}, PM_{2.5}, PM_{5.0}, and PM₁₀, and 24-h-ambulatory electrocardiogram (ECG) (Pan et al. 2018). The study indicated that increasing levels of size-fractioned PM and BC were associated with decreased HRV indices and increased heart rate (HR). In specific, an IQR (3.14 µg/m³) increase in 8-h BC-moving average and an IQR (20.72 µg/m³) increase in 5-min PM_{0.5}-moving average concentrations were associated with declines of 7.45% (95% CI: -10.89%, -3.88%) and 16.40% (95% CI: -21.06%, -11.41%) in LF, respectively. The smaller the particles size, the greater effects on HRV indices and HR. Similar strong inverse associations were found for HF and SDNN with size-fractioned PM and BC, respectively.

In another study, 46 middle-school children in Beijing were measured longitudinally for their personal exposure to ozone, PM, and BC as well as ECG (Huang et al. 2019). The study found that per IQR increase in ozone at 2-hour moving average was associated with -7.8% (95% CI: -9.9%, -5.6%) reduction in SDNN and 2.6% (95% CI: 1.6%, 3.6%) increment in HR. The associations were stronger at high BC levels (BC ≥ 3.7 µg/m³).

A randomized, double-blind crossover study among 44 healthy children also reported that reduced PM improved HRV, showing percent reductions in HRV indices per IQR increases in size-fractionated PM and BC over different moving averages (Liu et al. 2020). The greatest decrease in HF was 16.1% per IQR increase in PM_{0.5} (17.9 µg/m³) at 5-min moving average. The smaller the PM size, the stronger the effect observed. The greatest decreases were observed at 5-min moving averages for PM_{0.5} and PM_{1.0}, but 2-h moving averages for PM_{2.5}, PM₅, and PM₁₀. For BC, the greatest decrease in HF was 18.8% per IQR increase (3.6 µg/m³) at 3-h moving average. The association patterns of other indices including LF and SDNN were similar with HF. In addition, significant increases in V5_ST elevation were

associated with PM_{0.5} and PM_{1.0}. The greatest increase in V5_ST elevation was 0.022 mV per IQR increase in PM_{1.0} (22.2 µg/m³) (Dong et al. 2019).

However, some studies have not observed an association between indoor air pollution and HRV (Laumbach et al. 2014). A randomized, double-blind crossover intervention study among 40 nonsmoking older adults in a low-income senior residential building in Detroit, Michigan, did not find significant changes in HRV indices by period (Morishita et al. 2018). Another randomized crossover intervention trial in a panel of 35 nonsmoking senior participants conducted in China found an inverse association, although not statistically significant, between the use of portable air purifiers and HRV parameters (Shao et al. 2017).

Vascular Function

Vascular function is essential to assess cardiovascular health, and previous studies explored the associations between indoor air pollution and vascular function.

Reactive Hyperemia Index (RHI)

Reactive hyperemia index (RHI) is a promising cardiovascular risk predictor. Previous studies have validated its value in assessing coronary microvascular endothelial function and in predicting cardiovascular outcome in patients at risk, including those with chronic kidney disease (Liu et al. 2017). In a randomized crossover intervention study of the impact of particle exposures on endothelial function, 45 healthy adult residents of British Columbia, Canada, were randomized to receive consecutive 7-day periods of filtered and nonfiltered indoor air intervention (Allen et al. 2011). The results showed that indoor air purification was associated with a 9.4% (95% CI: 0.9, 18%) increase in RHI, implying improved endothelial function. However, two other studies did not find a significant increase of RHI associated with an indoor air purification intervention (Kajbafzadeh et al. 2015; Weichenthal et al. 2013).

Microvascular Function (MVF)

Measures of MVF have emerged as potential surrogate markers of cardiovascular outcomes. An air filtration-based intervention study including 21 nonsmoking and healthy elderly couples was conducted to explore the effects of indoor particles on the vascular function. In this crossover trial, the subjects were randomized to receive consecutive 48-hour particle-filtered or unfiltered indoor air. The results demonstrated that reduction of particle concentration in indoor air by filtration significantly improves MVF (Brauner et al. 2008). Similarly, a randomized, double-blind, crossover intervention study with a consecutive 2-week period of with or without air purification also found a significant association between decreased PM_{2.5} and improved MVF (Karottki et al. 2013).

Pulse Wave Velocity (PWV)

PWV is a simple and noninvasive indicator to assess stiffness of the arteries. PWV measures the performance of the arteries and has been established as a reliable prognostic parameter for cardiovascular morbidity and mortality in a variety of

adult populations including older adults, patients with end-stage renal disease, diabetes, and hypertension. An observational study monitored indoor levels of PM₁₀, PM_{2.5}, and BC in a Himalayan village (Pratali et al. 2019). The study found that average BC was correlated with PWV ($R = 0.589$, $P < 0.001$) especially in subjects older than 30 years. In a multiple variable analysis, BC remained an independent predictor of PWV ($\beta = 0.556$, $P = 0.001$).

Augmentation Index (AI)

The augmentation index (AI) is another indicator of arterial stiffness and has been shown to be elevated in those with hypercholesterolemia (Wilkinson et al. 2002). It is considered an early sign of vascular damage. It has been suggested that an increase in arterial stiffness is associated with increased systolic blood pressure (SBP) and diastolic blood pressure (DBP). Arterial stiffness is one of the major risk factors of cardiovascular disease (CVD) (Greenwald 2007). A randomized sham-controlled exposure study in 55 healthy adults investigated the effect of short-term exposure to indoor fine and ultrafine particles (UFP) on AI (Soppa et al. 2019). The study analyzed the association of particle emissions from several indoor sources, including candle burning, toasting bread, and frying sausages, with changes in pulse wave analysis indices. The study found that during candle burning, UFP concentrations were substantially increased, which was associated with a 9.5% (95% CI: 3.1%, 15.9%) increase in AI. During toasting bread, PM₁₀ and PM_{2.5} concentrations were increased significantly and were associated with 5.8% (95% CI: 3.2%, 8.4%) increase in AI 2 hours following the peak PM₁₀ exposure and 8.1% (95% CI: 2.5%, 13.7%) increase in AI immediately after PM_{2.5} peak exposure.

Blood Pressure

Blood pressure (BP) is one of the most widely used noninvasive indicators to assess vascular function and is the most significant risk factor for cardiovascular disease. A recent systematic review and meta-analysis of 65 epidemiological studies covering 16 countries reported that short-term exposures to four (PM₁₀, PM_{2.5}, SO₂, NO₂), two (PM_{2.5} and SO₂), and four air pollutants (PM₁₀, PM_{2.5}, SO₂, and NO₂) were significantly associated with hypertension, systolic blood pressure (SBP), and diastole blood pressure (DBP), respectively. The overall meta-analysis showed significant associations of long-term exposures to PM_{2.5} with hypertension as well as significant associations of PM₁₀, PM_{2.5}, NO₂, with DBP (Yang et al. 2018). Numerous studies have investigated the associations between indoor air pollution and BP (Allen et al. 2011; Brauner et al. 2008; Karottki et al. 2013; Kephart et al. 2020; Morishita et al. 2018; Padró-Martínez et al. 2015; Pratali et al. 2019; Weichenthal et al. 2013).

A randomized, double-blind crossover trial was conducted among 40 nonsmoking older adults in Detroit, Michigan. The participants experienced in their bedrooms and living rooms the following three conditions, each of 3-day duration, separated by 1-week washout periods: unfiltered air (sham filtration), low-efficiency (LE) HEPA filtration, and high-efficiency (HE) HEPA filtration, respectively. The results showed that personal PM_{2.5} exposures were significantly reduced by HEPA filtration from a

mean (SD) of 15.5 (10.9) $\mu\text{g}/\text{m}^3$ under the sham filtration to 10.9 (7.4) $\mu\text{g}/\text{m}^3$ under the LE filtration and 7.4 (3.3) $\mu\text{g}/\text{m}^3$ under the HE filtration. Compared with sham filtration, any HEPA filtration decreased SBP and DBP by 3.2 mm Hg (95% CI: -6.1 to -0.2 mm Hg) and 1.5 mm Hg (95% CI: -3.3 to 0.2 mm Hg), respectively. A continuous decrease occurred in SBP and DBP during the 3-day period of the LE filtration, with a mean of 3.4 mm Hg (95% CI: -6.8 to -0.1 mm Hg) and 2.2 mm Hg (95% CI: -4.2 to -0.3 mm Hg), respectively. Similarly, for the HE filtration, SBP and DBP decreased by 2.9 mm Hg (95% CI: -6.2 to 0.5 mm Hg) and 0.8 mm Hg (95% CI: -2.8 to 1.2 mm Hg), respectively (Morishita et al. 2018).

Thirty-five healthy college students in Shanghai, China, were recruited into a randomized, double-blind crossover trial and alternated the use of true or sham air purifiers for 48 hours with a 2-week washout interval (Chen et al. 2015b). The results showed that air purification resulted in a 57% reduction in PM_{2.5} concentration from 96.2 to 41.3 $\mu\text{g}/\text{m}^3$ within hours of operation; SBP, DBP, and pulse pressure decreased 2.7% (95% CI: -5.1%, -0.4%), 4.8% (95% CI: -8.5%, -1.2%), and 0.1% (95% CI: -8.5%, 7.7%), respectively, compared to the sham-purification. In this intervention study, an IQR increase (64 $\mu\text{g}/\text{m}^3$) in continuous indoor PM_{2.5} concentration was associated with an increase of 4.0% (95%CI: 0.9%, 7.2%) in DBP. In another randomized, double-blind crossover trial in 55 healthy college students in Shanghai, China, true and sham air purifiers were placed in subjects' dormitories randomly for 9 days with a 12-day washout interval (Li et al. 2017). The use of air purifiers reduced personal PM_{2.5} significantly from 53.1 $\mu\text{g}/\text{m}^3$ during the sham purification to 24.3 $\mu\text{g}/\text{m}^3$ during the real purification. Concomitantly, SBP was 2.61% (95% CI: 0.39%, 4.79%) higher during the sham purification than during the true purification. A 10 $\mu\text{g}/\text{m}^3$ increase in PM_{2.5} exposure was associated with 0.86% (95% CI: 0.10%, 1.62%) increase in SBP. Similar changes, although without a statistically significance, were observed for DBP and pulse pressure. Additionally, significant decreases in both SBP and DBP were observed following true purification from the prepurification values, while no significant changes were seen following sham purification. In another randomized crossover intervention study of short-term indoor air filtration intervention on cardiovascular health among 35 nonsmoking elderly participants living in Beijing in the winter of 2013, portable air filtration units were randomly allocated to active filtration for 2 weeks and sham filtration for 2 weeks in the households (Liu et al. 2018). Twelve-hour daytime ambulatory blood pressure (ABP) was measured during active and sham filtration, and real-time indoor and outdoor PM_{2.5} and indoor BC concentrations were measured. The study found that indoor PM_{2.5} and indoor BC decreased by 34.8% and 35.3% during active filtration. Indoor PM_{2.5} and BC exposures were significantly associated with increased ABP indices. Each 10 $\mu\text{g}/\text{m}^3$ increase in 8-hour moving average exposure of indoor PM_{2.5} was associated with increases of 0.39% (95% CI: 0.03%, 0.75%), 0.57% (95% CI: 0.05%, 1.10%), and 0.49% (95% CI: 0.07%, 0.92%) in SBP, DBP, and mean arterial pressure, respectively.

The aforementioned studies provide scientific evidence on cardiovascular health benefits reflected by reduced blood pressure of using air purifiers. The associations between indoor air pollutants and blood pressure, observed in these studies, support

the usefulness of blood pressure measures (SBP, DBP, and/or pulse pressure) as biomarkers of cardiovascular health in indoor air health studies.

Application of Biomarkers in Assessing Health Risks of the Hematologic System

The Structure and Function of the Hematologic System

The hematologic system consists of cells, tissues, and organs responsible for producing and maintaining blood and blood cells. Blood consists of plasma and blood cells (red blood cells, white blood cells, platelets, etc.) and is connected with all tissues and organs through the circulation system, involved in various physiological activities and maintaining the normal metabolism and homeostasis.

Indoor Air Pollution Affects Hematologic Health

The updated American Heart Association scientific statement in 2010 postulated that thrombosis and coagulation are among the mechanisms to explain the biological actions responsible for the adverse cardiovascular effects of PM (Brook et al. 2010). Indoor air pollution is also associated with thrombosis and blood coagulation. For example, chronic indoor pollution exposure to biomass cooking in rural India was associated with elevated circulating markers of platelet activation (Ray et al. 2006). The biomarkers of hematologic health effects of indoor air pollution were shown as below and in Table 3.

Biomarkers of Hematologic Health Effects of Indoor Air Pollution

Blood-Related Parameters

Hemoglobin (Hb)

A total of 41 nonsmoking elderly volunteers participated in a randomized, double-blind, crossover study with two consecutive 48-hour exposure scenarios of either particle-filtered or nonfiltered in their homes (Brauner et al. 2008). The results showed that hemoglobin (Hb) concentration was significantly improved by 0.9% (95% CI: 0.1%, 1.8%) during air filtration, as assessed in the mixed-effects model with inclusion of filtration as a categorical variable. A study conducted in rural north-east India investigated the levels of PM_{2.5} and PM₁₀ released during cooking with fuelwood and subsequent changes in hematological parameters (Rabha et al. 2018). The results showed the reduction of Hb concentration was significantly associated with higher PM_{2.5} and PM₁₀, respectively, after adjusting for confounding factors (e.g., age, height, weight, cooking index, and monthly income) in multiple linear regressions. One percent increases in the levels of PM_{2.5} and PM₁₀ resulted in 0.62%

Table 3 Biomarkers of the hematologic system used in assessing health risk of indoor air pollutants

Study site	Year	Study design	Pollutant	Participant, N	Biomarker	Reference
Copenhagen	2008	Randomized double-blind crossover trial	PM _{2.5} , PM _{10-2.5} ,	Healthy elderly, 42	Hb, RBC count, platelet count, plasma-selectin, and fibrinogen	Brauner et al. (2008)
Assam	2018	Cross-sectional study	PM _{2.5} , PM ₁₀	Healthy rural women, 200	Hb, WBC count, RBC count, and platelet count	Rabha et al. (2018)
Hungarian	2003	Cross-sectional study	NO ₂ , formaldehyde, benzene, xylene, and toluene	Asthmatic children, 176	RBC count, WBC count, and platelet count	Erdei et al. (2003)
Tehran	2017	Panel study	PM ₁₀ , PM _{2.5} , and PM ₁	Nonsmoking elderly, 44 Nonsmoking male high school students, 40	WBC count, vWF	Hassanvand et al. (2017)
Taipei	2013	Panel study	PM _{2.5} , PM ₁₀ , TVOCs, and CO	Healthy adults, 300	Fibrinogen	Lin et al. (2013)
Beijing	2020	Randomized crossover trial	PM _{2.5}	Healthy college students, 29	sP-selectin, vWF	Han et al. (2020)
Los Angeles	2008	Panel study	PM _{0.25} , PM _{2.5-10}	Nonsmoking elderly with a history of coronary artery disease, 29	sP-selectin, fibrinogen	Delfino et al. (2008)
Somerville	2015	Randomized crossover trial	PNC	Residents living near highways, 20	Fibrinogen	Padró-Martínez et al. (2015)
Shanghai	2018	Randomized double-blind crossover trial	PM _{2.5} , PNC	Healthy adults, 70	vWF	Cui et al. (2018)

(continued)

Table 3 (continued)

Study site	Year	Study design	Pollutant	Participant, N	Biomarker	Reference
Shanghai	2015	Randomized double-blind crossover trial	PM _{2.5}	Healthy college students, 35	sCD40L	Chen et al. (2015b)
Beijing	2020	Randomized double-blind crossover trial	PM _{2.5}	Healthy college students, 29	sCD40L	Sun et al. (2020)

PM: particulate matter, PM_{2.5}: particulate matter with an aerodynamic diameter $\leq 2.5 \mu\text{m}$, PM_{0.5}: particulate matter with an aerodynamic diameter $\leq 0.5 \mu\text{m}$, PM₁: particulate matter with an aerodynamic diameter $\leq 1 \mu\text{m}$, PM₁₀: particulate matter with an aerodynamic diameter $\leq 10 \mu\text{m}$, NO₂: nitrogen dioxide, CO: carbon monoxide, TVOCs: total volatile organic compounds, PNC: particle number concentration, Hb: hemoglobin, RBC: red blood cell, WBC: white blood cell, vWF: von Willebrand factor, sP-selectin: soluble P-selectin, and sCD40L: soluble CD40 ligand

(95% CI: -0.057 , -0.003) and 0.54% (95% CI: -0.057 , -0.002) decrease in Hb concentration, respectively.

Red Blood Cells (RBC)

A cross-sectional study among Hungarian asthmatic school children aged 9–11 years reported a significant association between higher indoor nitrogen dioxide (NO_2) concentration and increased RBC count (Erdei et al. 2003). The authors speculated that the increase in RBC count associated with higher indoor NO_2 might have been a consequence of insufficient oxygen concentration indoors, because the indoor combustion source of NO_2 could have depleted oxygen indoors. Higher RBC levels may be used as a biomarker reflecting the negative effect of indoor air pollution on oxygenation in the blood.

White Blood Cells (WBC)

A study conducted in rural northeast India investigated the levels of $\text{PM}_{2.5}$ and PM_{10} released during cooking with fuelwood and subsequent changes in hematological parameters (Rabha et al. 2018). The study found that WBC had a positive and significant association with PM_{10} concentration, with 0.66% (95% CI: 0.019, 0.158) increase in WBC per 1% increase in PM_{10} concentration. A cross-sectional study among Hungarian asthmatic school children aged 9–11 years old also reported the significant association between high indoor NO_2 concentration and increased WBC count (Erdei et al. 2003).

A study involving a panel of 44 nonsmoking elderly subjects living in a retirement home and a panel of 40 healthy young adults living in a school dormitory in Tehran city, Iran, was conducted to clarify the effects of short-term exposure to size-fractionated PM (Hassanvand et al. 2017). The results showed that in the healthy young panel, exposure to PM_{10} , $\text{PM}_{2.5-10}$, and $\text{PM}_{1-2.5}$ was associated with increased WBC at different lag times, with the strongest association of 17.6% (95% CI: 10.5%, 25.2%) observed between WBC and $\text{PM}_{2.5}$ at lag 1. In the elderly population, exposure to PM_{10} , $\text{PM}_{2.5-10}$, $\text{PM}_{2.5}$, $\text{PM}_{1-2.5}$, and PM_1 was also strongly associated with increased WBC. Acute increases in WBC counts are associated with acute systemic inflammation.

Platelet Count

A study conducted in rural northeast India investigated the levels of $\text{PM}_{2.5}$ and PM_{10} released during cooking with wood and subsequent changes in hematological parameters (Rabha et al. 2018). The results showed that platelet counts were positively and significantly associated with both $\text{PM}_{2.5}$ and PM_{10} , with a 0.91% (95% CI: 0.105, 0.283) and 0.79% (95% CI: 0.095, 0.287) increase per 1% increase in the levels of $\text{PM}_{2.5}$ and PM_{10} , respectively. In a study of the health impacts of indoor air pollution from household cooking fuels, biomass fuel users were exposed to three times higher particulate pollution in kitchen and had significantly higher platelet aggregation than clean fuel users (23.2 versus 15.9 Ohm) (Dutta et al. 2011). An increase in platelet count is associated with an increased risk for blood coagulation or thrombosis.

Blood Coagulation Biomarkers

Fibrinogen

Fibrinogen, a soluble protein, is generated in the liver and mainly presents in the blood plasma. It is a key biomarker for blood coagulation. A panel of 300 healthy subjects from Taipei, aged 20 and over, were recruited to explore whether improving indoor air quality through air conditioning can improve cardiovascular health in human subjects (Lin et al. 2013). The results showed that the increase in fibrinogen was associated with increased levels of indoor particles and total VOCs in single-pollutant and two-pollutant models. In specific, in single-pollutant model, an IQR increase in PM_{2.5} and TVOC was associated with increases of 5.3% (95% CI: 1.5%, 15.2%) and 8.9% (95% CI: 4.2%, 13.6%) in fibrinogen concentration, respectively. In a two-pollutant models, an IQR increase in PM_{2.5} and TVOC was associated with increases of 3.4% (95% CI: 1.5%, 5.2%) and 1.6% (95% CI: 0.2%, 3.0%) in fibrinogen concentration, respectively.

Soluble P-Selectin (sP-Selectin)

The biomarker sP-selectin, also known as sCD62P, is derived predominantly from activated platelets and represents a circulating marker of platelet activation (De Pergola et al. 2008). Previous studies showed that elevated sP-selectin was observed in diseases associated with arterial thromboses, such as coronary artery disease and acute myocardial infarction (Ferroni et al. 2009; Polek et al. 2009).

A randomized crossover trial was conducted on 29 healthy young adults in Beijing, China. In the study, three waves of health measurements were conducted before, during, and after two typical PM_{2.5} pollution waves (PPWs), under filtered and sham indoor air purification with a washout interval of at least 2 weeks. The study found that sP-selectin concentration increased by 12.0% (95% CI: 3.8%, 20.8%) during-PPWs periods compared with pre-PPWs periods under sham purification, while the percentage change of 7.6% (95% CI: -1.9%, 18.1%) under the filtered condition was nonsignificant. The study further found that 24-h and 48-h personal PM_{2.5}-moving averages were significantly associated with sP-selectin, suggesting sP-selectin is a good biomarker for understanding the pathological process linking indoor air pollution and adverse health effects (Zhao et al. 2020). Consistently, in a panel study of 29 nonsmoking elderly subjects with a history of coronary artery disease, indoor PM_{0.25} and PM_{2.5–10} were positively and significantly associated with sP-selectin (Delfino et al. 2008).

Von Willebrand Factor (vWF)

Von Willebrand Factor (vWF) is a marker of blood coagulation process, an indicator of endothelial dysfunction, and has been linked to coronary events. A panel study of elderly subjects and healthy young adults was conducted to explore the short-term effects of size-fractionated PM on circulating biomarkers (Hassanvand et al. 2017). The results showed no associations between vWF and any PM size fractions in healthy young adults. However, vWF was positively

associated with PM_{1–2.5}, PM_{2.5}, PM_{2.5–10}, and PM₁₀ in the elderly subjects. In a double-blind, randomized crossover study among 70 healthy nonsmoking adults, compared to sham filtration, true HEPA filtration decreased indoor PM_{2.5} by 72.4% and particle number concentration by 59.2%, and concomitantly lowered vWF by 26.9% (95% CI: 7.3%, 46.4%) 24 h after the end of filtration, indicating reduced risk for thrombosis (Cui et al. 2018).

Soluble CD40 Ligand (sCD40L)

Soluble CD40 ligand (sCD40L) in blood is a surface adhesion molecule involved in both inflammatory and thrombogenic processes. A randomized, double-blind crossover trial among 35 healthy college students in Shanghai, China, reported that decreased in sCD40L of 64.9% (95% CI: -82.3%, 30.3%) was associated with the true-purification scenario compared to the sham-purification scenario (Chen et al. 2015b). The study also found that an IQR change (64 µg/m³) of continuous indoor PM_{2.5} concentration was associated with a 71.3% (95% CI: 29.8%, 126.1%) increase in sCD40L concentration. Similarly, another randomized, double-blind crossover trial of true or sham indoor air filtration among 29 healthy young adults in Beijing, China, reported that the increase in time-weighted personal PM_{2.5} was significantly associated with increased sCD40L (Sun et al. 2020).

Application of Biomarkers in Assessing Systemic Inflammation and Oxidative Stress

Inflammation and oxidative stress are common pathophysiological mechanisms underlying many diseases, including major chronic diseases such as cardiovascular diseases, cancer, chronic respiratory diseases, and diabetes. Air pollution exposure has been well linked to inflammatory and oxidative stress responses in both human and animal models. The biomarkers in assessing systemic inflammation and oxidative stress of indoor air pollution are shown below and in Table 4.

Biomarkers of Systemic Inflammation of Indoor Air Pollution

C-Reactive Protein (CRP) and High-Sensitivity CRP (hsCRP)

C-reactive protein (CRP) is a protein in the blood that signals acute inflammation. To determine the risk for heart disease, a more sensitive CRP test called high-sensitivity CRP (hsCRP) is available. A randomized crossover intervention study of 45 healthy adults exposed to consecutive 7-day periods of filtered and unfiltered air with portable air filters reported a 32.6% (95% CI: 4.4%, 60.9%) decrease in CRP associated with the filtration and a suggestive (without a statistical significance) association between indoor PM_{2.5} and CRP (Allen et al. 2011). A cross-sectional study assessed the relationship of indoor PM_{2.5} and CO with CRP, and the results showed that an IQR increase in PM_{2.5} and CO were associated with differences in CRP of -0.76 mg/L (95% CI: -1.64 to 0.11) and 0.36 mg/L (95% CI: -0.71 to

Table 4 Biomarkers of systemic inflammation and oxidative stress used in assessing health risk of indoor air pollutants

Study site	Year	Study design	Pollutant	Participant, N	Biomarker	Reference
West Bengal	2012	Case-control study	Indoor air pollution from biomass fuel use	142 women exposed to indoor air pollution from biomass burning and 126 age-matched control women	TNF- α , IL-6, IL-12, IL-8, MPO, and SOD	Banerjee et al. (2012)
Peru	2020	Cross-sectional study	PM _{2.5} , CO	Residents, 902	CRP	Kephart et al. (2020)
Peru	2021	Cross-sectional study	PM _{2.5} , BC, CO, and NO ₂	Adult women, 180	CRP, IL-6, IL-10, IL-1 β , and TNF- α	Fandino-Del-Rio et al. (2021)
Copenhagen	2008	Randomized double-blind crossover trial	PM _{2.5} , PM _{10-2.5}	Healthy elderly, 42	CRP, IL-6, TNF- α , and 8-isoPGF2 α	Brauner et al. (2008)
British Columbia	2011	Randomized crossover trial	PM _{2.5}	Healthy adults, 45	CRP, IL-6, MDA, and 8-isoprostanate	Allen et al. (2011)
Shanghai	2017	Randomized double-blind crossover trial	PM _{2.5}	Healthy college students, 55	8-OHDG, MDA, 8-isoPGF2 α , SOD, hsCRP, IL-1 β , and IL-6	Li et al. (2017)
Taipei	2017	Randomized crossover trial	PM _{2.5} , TVOCs	Homemakers, 200	hsCRP, 8-OHDG	Chuang et al. (2017)
Eastern Massachusetts	2018	Panel study	BC	Patients with COPD, 85	CRP, IL-6	Garsick et al. (2018)
Taipei	2013	Panel study	PM _{2.5} , PM ₁₀ , TVOCs, and CO	Healthy adults, 300	hsCRP, 8-OHDG	Lin et al. (2013)
Shanghai	2015	Randomized double-blind crossover trial	PM _{2.5}	Healthy college students, 35	CRP, MCP-1, IL-1 β , TNF- α , IL-6, and MPO	Chen et al. (2015b)
Shanghai	2018	Randomized double-blind crossover trial	PM _{2.5}	Healthy college students, 55	IL-1, IL-6, and TNF- α	Chen et al. (2018)

Beijing	2017	Randomized crossover trial	PM _{2.5} , BC	Nonsmoking elderly, 35	IL-6, IL-8, and CRP	Shao et al. (2017)
Beijing	2020	Randomized crossover trial	PM _{2.5}	Healthy college students, 29	8-isopGF2 α , MDA, ox-LDL, GPx1, and EC-SOD	Han et al. (2020)
Boston	2018	Panel study	BC	Patients with COPD, 82	MDA, 8-OHdG	Grady et al. (2018)
West Bengal	2011	Case-control study	PM _{2.5} , PM ₁₀ ,	244 women using biomass fuels and 236 age-matched women using LPG	ox-LDL, ROS, and SOD	Dutta et al. (2011)

PM: particulate matter, PM_{2.5}: particulate matter with an aerodynamic diameter $\leq 2.5 \mu\text{m}$, PM₁₀: particulate matter with an aerodynamic diameter $\leq 10 \mu\text{m}$, BC: black carbon, CO: carbon monoxide, TVOCs: total volatile organic compounds, CRP: C-reactive protein, IL-6: interleukin-6, MDA: malondialdehyde, 8-isopGF2 α : Iso-prostaglandin F2 α , 8-OHdG: 8-hydroxy-2'-deoxyguanosine, SOD: superoxide dismutase, hsCRP: high-sensitivity C-reactive protein, IL-1 β : interleukin-1 β , IL-6: interleukin-6, TNF- α : tumor necrosis factor- α , MCP-1: monocyte chemoattractant protein-1, MPO: myeloperoxidase, IL-1: interleukin-1, IL-8: interleukin-8, ox-LDL: oxidized low-density lipoprotein, GPx1: glutathione peroxidase, and EC-SOD: extracellular superoxide dismutase

1.42), respectively (Kephart et al. 2020). In another randomized, double-blind crossover trial conducted in 55 healthy college students in Shanghai, a significant difference in hsCRP was observed following the intervention compared to following the control (Li et al. 2017). A randomized crossover intervention study recruited 200 homemakers from Taipei and randomly assigned 100 of them to air filtration or control intervention to explore the effect of long-term indoor air conditioner filtration on the association between air pollution and cardiovascular health (Chuang et al. 2017). The results of this study showed that increased levels of PM_{2.5} and TVOCs were associated with increased hs-CRP. An IQR increase in PM_{2.5} and TVOCs were associated with increases of 6.23% (95% CI: 2.82%, 9.64%) and 2.41% (95% CI: 1.63%, 3.19%) in hsCRP, respectively. In a study among 85 COPD patients, there was a 10.9% increase in CRP (95% CI: 0.7%, 22.2%) for each IQR increase in indoor BC concentration (Garshick et al. 2018).

In a panel of 300 healthy subjects aged 20 years old and over in Taipei, China, the increase in hsCRP was associated with increased levels of indoor particles and total VOCs in single and two-pollutant models (Lin et al. 2013). Specially, in the single-pollutant model, an IQR increase in PM_{2.5} and TVOC was associated with increases of 13.0% (95% CI: 6.4%, 19.7%) and 19.7% (95% CI: 10.2%, 29.1%) in hs-CRP, respectively. In the two-pollutant model, an IQR increase in PM_{2.5} and TVOC was associated with increases of 15.0% (95% CI: 9.7%, 20.3%) and 13.7% (95% CI: 8.7%, 18.6%) in hsCRP, respectively.

Inflammatory Cytokines

Cytokines are small-molecule proteins that are acutely synthesized and secreted by immune cells and nonimmune cells (e.g., endothelial cells, epithelial cells) in response to a stimulus. Cytokines can have either pro- or anti-inflammatory effects, and these effects can be contextual. Cytokines have been most commonly analyzed using enzyme-linked immunosorbent assays (ELISA) individually. Multiple cytokines can be measured simultaneously using so-called multiplex assays on a flow cytometer (Sun et al. 2020).

In 142 premenopausal, never-smoking women chronically exposed to indoor air pollution from biomass burning and 126 age-matched control women who cooked with a cleaner fuel, namely liquefied petroleum gas (LPG), a panel study showed that biomass users had 72%, 67%, and 54% higher plasma levels of the proinflammatory cytokines including tumor necrosis factor- α (TNF- α), IL-6, and IL-12, respectively, and doubled neutrophil chemoattractant IL-8 (Banerjee et al. 2012). A cross-sectional study among adult women in rural Peru reported that kitchen area black carbon (BC) concentrations were positively associated with proinflammatory cytokine TNF- α , while negatively associated with anti-inflammatory cytokine IL-10 (Fandiño-Del-Rio et al. 2021). In a randomized double-blind crossover trial, 35 healthy college students in Shanghai were measured for levels of proinflammatory cytokines including interleukin-1 β (IL-1 β), IL-6, and TNF- α (Chen et al. 2015b). Compared with the sham purification scenario, the true purification was associated with 68.1% (95% CI: 44.3%, 81.7%) decrease of IL-1 β , and an IQR

increase ($64 \mu\text{g}/\text{m}^3$) of continuous indoor $\text{PM}_{2.5}$ concentration was significantly associated with 69.7% (95% CI: 30.6%, 120.3%) increase in IL-1 β . In another randomized, double-blind crossover trial using true versus sham filtration, biomarkers of systemic inflammation, including IL-1 β , IL-6, and TNF- α , were measured in 55 healthy college students in Shanghai (Li et al. 2017). The study reported a significant between-treatment difference in IL-1 β .

In a similar double-blind, randomized crossover study in 55 healthy young adults in Shanghai, China, higher $\text{PM}_{2.5}$ exposure (mainly driven by indoor exposure) was positively associated with the expression of IL-1, IL-6, and TNF- α (Chen et al. 2018). A randomized crossover intervention trial in seniors living in Beijing also reported significant decreases in IL-8 of 58.59% (95% CI: -76.31%, -27.64%) in the total participants and 70.04% (95% CI: -83.05, -47.05) in the subset of COPD patients during the active-mode filtration period compared to the sham-mode filtration period (Shao et al. 2017). Taken together, the evidence is strong to indicate that biomarkers of proinflammatory cytokines such as IL-1, IL-6, IL-8, and TNF- α in the blood were associated with indoor air pollution exposure.

Myeloperoxidase (MPO)

Myeloperoxidase (MPO) is a lysosomal enzyme which presents in granulocytic and monocytic cells, and it is an established biomarker of inflammation. It has been suggested that MPO plays a significant role in the development of the atherosclerotic lesion and in rendering plaques unstable. An increase in MPO concentration in biological fluids is indicative of tissue or systemic inflammation. A randomized double-blind crossover trial found that a significant decrease of -17.5% (95% CI: -30.8%, -5.5%) in the concentration of plasma MPO was associated with true air purification compared with sham purification in 35 healthy college students living in Shanghai (Chen et al. 2015b). However, the evidence is limited on MPO responses to indoor air pollution exposure.

Monocyte Chemoattractant Protein-1 (MCP-1)

Monocyte chemoattractant protein-1 (MCP-1) is one of the key chemokines that regulate migration and infiltration of monocytes and macrophages in response to inflammation. The same study described above concerning MPO also reported a significant decrease in blood MCP-1 by -32.8% (95% CI: -67.5%, -5.3%) following the true filtration. This MCP-1 decrease indicated a reduced level of systemic inflammation.

Biomarkers of Oxidative Stress in Relation to Indoor Air Pollution

The imbalance between the generation of reactive oxygen species (ROS) and endogenous antioxidant capacity leads to oxidative stress when the balance shifts towards more ROS generation. Oxidative stress is a risk factor for many diseases and for accelerating aging of cells, tissue, and human.

Iso-Prostaglandin F2 α (8-isoPGF2 α)

Iso-prostaglandin F2 α (8-isoPGF2 α) is a major metabolite from the peroxidation of arachidonic acid. This compound, often simply called 8-isoprostanate, is among most commonly used biomarkers of lipid peroxidation. This compound has been considered as a potent vasoconstrictor of lung and has been identified to be associated with asthma, lung diseases, and atherosclerosis. A study showed significant associations of both 24-h and 48-h personal PM_{2.5} moving averages with 8-isoPGF2 α in 29 healthy young adults living in Beijing (Zhao et al. 2020), indicating that increased indoor PM exposure was associated with increased oxidative stress measured as lipid peroxidation. When indoor PM levels were reduced via the use of air filtration, a significant reduction in 8-isoPGF2 α level was observed in 55 healthy college students living in Shanghai (Li et al. 2017). A randomized double-blind crossover trial among 21 couples reported a borderline significant association between number concentration of particles (10–700 nm) and 8-isoPGF2 α (Brauner et al. 2008).

Malondialdehyde (MDA)

Malondialdehyde (MDA) is generated by the peroxidation of polyunsaturated fatty acids in cell membranes. It is also produced in the process of prostaglandin synthesis. MDA is a frequently used biomarker of oxidative damage. MDA can be measured in biological fluids (e.g., urine, blood, nasal mucus, and exhaled breath condensate) in two forms: MDA free from conjugation and MDA conjugated with proteins or other biomolecules. A study recruiting 82 COPD patients assessed the relationships between indoor BC exposure and urinary oxidative stress biomarkers (Grady et al. 2018). The study found a positive association between BC exposure and MDA. Specifically, 0.8% (95% CI: -5.4%, 7.4%) increase in free MDA and 5.4% (95% CI: -2.4%, 14.0%) increase in total MDA (free and conjugated) were associated with per IQR increase in multiday-integrated BC. Additionally, effects on total MDA were statistically significant with averaged 1–4 days BC exposure before urine collection (8.3% increase; 95% CI: 0.03%, 17.3%). The previously mentioned intervention study in 55 healthy Shanghai college students reported significantly lowered MDA concentrations using true purification than sham filtration (Li et al. 2017).

Oxidized Low-Density Lipoprotein (Ox-LDL)

Reactive oxygen species (ROS) can oxidize low-density lipoprotein (LDL). The product (ox-LDL) is shown to cause proatherogenic effects through endothelial activation (Kattoor et al. 2019). In 29 healthy young adults in Beijing, a significant increase of 9.2% (95% CI: 0.3%, 18.0%) in ox-LDL was associated with an IQR increase in 24-h personal PM_{2.5} moving average, and the personal PM_{2.5} exposure was principally from indoor exposure in this air-purification intervention study (Zhao et al. 2020). A case-control study assessing the health impacts of indoor air pollution reported that women using biomass fuels had three times more particulate pollution in kitchen, as well as elevated ox-LDL (170.6 vs. 45.9 U/l; $P < 0.001$), compared to women using liquified petroleum gas (LPG) (Dutta et al. 2011).

Superoxide Dismutase (SOD) and Glutathione Peroxidase 1 (GPx1)

Superoxide dismutase (SOD) and glutathione peroxidase 1 (GPx1) are cellular antioxidant enzymes, which play a central role in the control of ROS. SOD is represented by three different ubiquitously expressed enzymes that convert superoxide anion to hydrogen peroxide. GPx1 is the ubiquitous intracellular form and a key antioxidant enzyme within most cells, including the endothelium (Blankenberg et al. 2003). These biomarkers of oxidative stress have been widely used in *in vitro* and in *vivo* animal studies of particle toxicity (Deng et al. 2013; Guan et al. 2019; Wang et al. 2019). Several studies have explored the associations between the two antioxidation enzymes and indoor air pollutants, but no significant associations were observed (Zhao et al. 2020). The aforementioned case-control study in biomass versus LPG users showed that women exposed to biomass smoke had a 13% lower SOD level than the controls (Dutta et al. 2011).

Application of Biomarkers in Assessing Health Risks of the Immune System

Composition and Function of the Immune System

The immune system is complex, consisting of cells, tissues, and molecules that mediate unique reactions resisting pathogens and noninfectious substances, including harmless environmental molecules, tumors, and unaltered host components. The most important physiologic function of the immune system is to prevent or eradicate infections. The immune system plays a vital role in defending against tumors, controlling tissue regeneration and scarring, injuring cells, and inducing pathologic inflammation, recognizing and responding to tissue grafts and newly introduced proteins.

The immune system is formed from two main parts: innate immunity and adaptive immunity. Innate immunity, also called natural immunity or native immunity, is always present in healthy individuals and provides immediate protection against microbial invasion. Adaptive immunity, also called specific immunity or acquired immunity, consists of two types of humoral immunity and cell-mediated immunity and requires proliferation and differentiation of lymphocytes in response to microbes before it can provide adequate defense, namely the complex mechanism allows it to perform comprehensive and powerful function compared with innate immunity that is the critical first barrier to outside harmful factors (Abbas et al. 2019). The human immune system is involved in responding and defending against the insult from air pollution exposure. Hence, immunological biomarkers are used in studying the health effects or assessing the health risk of air pollution exposure.

Health Effect on the Immune System of Indoor Air Pollution

Among the diseases that have been related to indoor air pollution, asthma may have the strongest link to immunologic responses to a variety of indoor pollutants

including dust mites, microbes, tobacco smoke, phthalates, endotoxin, and nitrogen dioxide (Kanchongkittiphon et al. 2014). Other diseases that have been linked to immunologic effects of indoor air pollutants include allergic diseases such as wheeze, rhinitis, and eczema, as well as other respiratory systems and illnesses (e.g., bronchitis, persistent cough, and chronic obstructive pulmonary disease) (Bolling et al. 2020; Braun et al. 2020).

Children are susceptible population to immunology diseases due to their developing immune systems. Recently, there has been an increasing interest in the potential role of prenatal exposure to indoor air pollution in the development of immunologic disorders. Taking the developing immune system may be especially susceptible to low-dose exposure to indoor air pollutants into consideration, early-life exposures are more likely to produce persistent, irreversible changes to immunological development, consequently increasing the risk for an allergic phenotype for the life time. The biomarkers in assessing immune system health of indoor air pollution were shown as below and in Table 5.

Biomarkers in Assessing Health Risks of the Immune System

Immune Cells

Lymphocytes

The development of lymphocytes, including T lymphocytes ($CD3^+$, $CD4^+$, and $CD8^+$), B lymphocytes ($CD19^+$, $CD20^+$, $CD21^+$, and $CD22^+$), and natural killer (NK) cells, starts during the earlier weeks of gestation. Significant associations have been observed between polycyclic aromatic hydrocarbons (PAH) or $PM_{2.5}$ during early gestation and increases in $CD3^+$ and $CD4^+$ lymphocytes percentages and decreases in $CD19^+$ and NK cells percentages in cord blood. In contrast, exposures during late gestation were associated with decreases in $CD3^+$ and $CD4^+$ fractions and increases in $CD19^+$ and NK cells fractions (Herr et al. 2010).

Dendritic Cells

Dendritic cells (DC) play a crucial role as antigen-presenting cells to initiate an appropriate immune response to inhaled antigens. Mature dendritic cells are differentiated from monocytes and can recognize antigens via different pathways. A study found that simultaneous exposure of crushed whole-body house dust mite (HDM) extract, instead of allergen Der p1 and hexabromocyclododecane (HBCD), can enhance the antigen presentation and maturation/activation of DC (Canbaz et al. 2016).

Immunoglobulin

Immunoglobulins (Igs) are bifunctional molecules, binding to antigens with high specificity and initiating other biologic functions. Ig binding directly neutralizes toxins. A main function of Igs is the opsonization, which is the promotion of the target (e.g., particle, spore, and microbe cell) to the phagocyte. IgG is the main effector

Table 5 Biomarkers of the immune system used in assessing health risk of indoor air pollutants

Study site	Year	Study design	Pollutant	Participant, N	Biomarker	Reference
Teplice and Prachatic, Czech Republic	2010	Cohort study	PAH, PM _{2.5}	Mother/infant pairs, 1397	CD3 ⁺ , CD4 ⁺ , and CD19 ⁺ lymphocytes, NK cells	Herr et al. (2010)
Amsterdam, Netherlands	2016	Experiments in vitro	HBCD, HDM	Healthy male volunteers, 7	DC	Canbaz et al. (2016)
Finland	2020	Case-control study	Streptomyces albus and Aspergillus versicolor	Workers, 159	IgG, IgG1, and IgG3 serum antibodies	Atosuo et al. (2020)
10 Canadian cities	2016	Cohort study	NO ₂ , PM _{2.5}	Pregnant women, 2001	IgE, IL-33, and TSLP	Ashley-Martin et al. (2016)
New York state, America	2017	Cohort study	Prenatal smoking	Children, 3459	IL-8	Chahal et al. (2017)
Warszawa /	2006	Case-control study	Environmental tobacco smoke	Atopic children with asthma 24; healthy control subjects 26	IL-13	Feleszko et al. (2006)
	2020	Review	Second-Hand Smoke and Prenatal Tobacco Smoke	/	DNA methylation	Braun et al. (2020)
Taipei, China	2015	Cross-sectional study	Phthalate	Children, 256	DNA methylation of TNF- α	Wang et al. (2015)
Leipzig, Germany	2014	Prospective study	Prenatal Tobacco Smoke	Mother-child pairs, 629	miR-223	Herberth et al. (2014)
Changchun, China	2019	Case-control study	HCHO, NO ₂ , and particles (PM ₁₀ , PM _{2.5} , and PM ₁)	Children with asthma and health subjects, 360	miR-155	Liu et al. (2019)

(continued)

Table 5 (continued)

Study site	Year	Study design	Pollutant	Participant, N	Biomarker	Reference
Shanghai, China	2019	Randomized crossover study	PM _{2.5}	Preschool children, 43	Salivary lysozyme	Gao et al. (2019)
Liverpool, England	2011	Prospective descriptive study	Passive smoking	Children, 39	MMP-9	De et al. (2011)

PAH: polycyclic aromatic hydrocarbons, PM_{2.5}: fine particles less than 2.5 microns in diameter, NK cells: natural killer cells, HBCD: hexabromocyclododecane, HDM: house dust mite, DC: dendritic cells, IgG: immunoglobulins G, NO₂: nitrogen dioxide, IL-33: interleukin-33, TSILP: thymic stromal lymphopoietin, TNF- α : tumor necrosis factor- α , miR: MicroRNA, MMP-9: Matrix metalloproteinase 9

in serum, and the IgA response is directed toward the mucosa. A published study found that compared to individuals living in the control reference buildings, those residing in microbe-dense buildings had higher levels of spore-specific IgG, IgG1, and IgG3 serum antibody (Atosuo et al. 2020). Immunoglobulin E (IgE) plays a vital role in the development of allergic diseases. Serum IgE are significant for the diagnosis of allergies. Cord blood IgE levels have been previously used to assess the immunotoxin effects of in utero environmental contaminant exposure (Ashley-Martin et al. 2016).

Cytokines

Inflammatory cytokines are described above under Biomarkers of Systemic Inflammation. Cytokines play an important role in immune responses to a stimulus, especially given that cytokines, including interleukins (ILs), interferons (IFNs), and tumor necrosis factor-alpha (TNF- α), are mainly produced by immune cells. Cytokines are a unique class of regulatory proteins that play an essential role in maintaining and regulating immune system functions. An imbalance in cytokines and/or cytokine receptors can lead to different pathological disorders, such as asthma, allergy, etc. (Ramani et al. 2015). Prenatal tobacco smoke exposure has been associated with an increase in IL-8 levels among neonates (Chahal et al. 2017). For children exposure to parental tobacco smoke, significant increases in IL-13 were observed compared with those nonexposed children (Feleszko et al. 2006).

IL-33 and thymic stromal lymphopoietin (TSLP) are two epithelial cell-derived cytokines that participate in allergic disease and type 2 inflammation. These mediators have a critical role in the etiology of atopic dermatitis, often the first manifestation of allergic disease in childhood. Ashley-Martin et al. (2016) reported elevated cord blood concentrations of IL-33 and TSLP were associated with maternal NO₂ exposure for newborn girls but not boys.

DNA Methylation as Epigenetic Biomarkers

Tobacco smoke is a potent environmental factor for DNA methylation. Parental tobacco smoke (PTS) exposure can induce epigenetic changes in the fetus with sequelae in later life, altering risks for allergic diseases. For example, PTS exposure can accelerate CpG methylation in the gene loci of FOXP3 and IFN γ , and lead to lower promoter methylation in the neuropeptide S receptor 1 (NPSR1) and higher expression of AXL gene methylation at birth (Braun et al. 2020). These abnormal DNA methylations were associated with the higher risk of asthma or bronchus symptoms. In addition, the increased risk of asthma caused by exposure to phthalate may also be mediated through alterations in DNA methylation of TNF- α (Wang et al. 2015).

MicroRNA

MicroRNAs (miRNAs) are small RNA molecules with about 22 nucleotides that regulate posttranscriptional gene expression. Placental miRNAs are coresponsible for the development of the maternal placenta and for the development of fetus. An upregulation of miR-223 in maternal and cord blood by PTS exposure has been associated with lower T regulatory cells (Treg) cell numbers in cord blood, subsequently increasing the risk for allergies (Herberth et al. 2014). A recent study showed

positive associations between higher serum levels of miR-155 and asthma in children exposed to indoor air pollution (Liu et al. 2019).

Salivary Lysozyme

Salivary lysozyme, an antibacterial protein, is part of the innate defensive mechanism. It is a noninvasive biomarker and activates immunity responses through the hydrolysis of β -1,4-glycosidic bonds of bacterial cell wall peptidoglycan. A recent study found that salivary lysozyme was significantly and inversely associated with indoor PM_{2.5} and that certain nasal bacteria might play critical roles in mediating PM_{2.5} exposure and children's lysozyme levels (Gao et al. 2019).

Matrix Metalloproteinase-9

Matrix metalloproteinase-9 (MMP-9) is thought to contribute partly to the pathogenesis of allergy, regulating the activity of certain soluble proteins and responsible for the degradation of extracellular matrix components. Increasing levels of MMP-9 has been reported to increase acute allergic responses in the nose, lung, and skin, respectively. In children exposed to secondhand smoke, the MMP-9 activity and concentrations in nasal secretions were higher than in children without secondhand smoke exposure (De et al. 2011).

Application of Biomarkers in Assessing Health Risks of the Reproductive System

The Structure and Function of the Reproductive System

The structure of the reproductive system is different between male and female. The reproductive system in male consists of a pair of testes, delivery channels, seminal vesicles, the prostate, the bulbourethral glands, and the penis. In female, this system includes the ovaries, fallopian tubes, uterus, vagina, accessory glands, and external genital organs. Within the context of producing offspring, the main function of the reproductive system includes producing eggs and sperm cells and secreting hormones, which are responsible by primary productive organs consisting of testes and ovaries; transporting and sustaining these cells; and nurturing the developing offspring (Abbas et al. 2019).

Health Effect on the Reproductive System of Indoor Air Pollution

Partial indoor air pollutants such as phthalates, bisphenol A, and flame retardants are endocrine disruptors chemicals (EDCs), which refer to compounds with the endocrine-disrupting mechanism of action that seriously affect human reproduction. In this context, indoor air pollution could lead to adverse health effects on the reproductive system including infertility, cryptorchidism, decreased semen quality, and hypospadias (Sifakis et al. 2017). Tobacco smoke with high exposure, occurring

mainly indoors, has been associated with reproductive hormone system dysfunction and impaired sperm development in males (Dai et al. 2015), and ovarian toxicity in females (Budani and Tiboni 2017). The biomarkers of reproductive health effects of indoor air pollution were shown as below and in Table 6.

Biomarkers in Assessing Health Risks of the Reproductive System

Semen Parameter

Male reproductive health is usually related to the process of spermatogenesis, and semen parameters are thought to be the most sensitive marker of adverse environmental exposures. The following 6 semen parameters are typically used to characterize semen quality: semen concentration, sperm volume, total sperm number, progressive motility, morphology, and acrosin activity. Acrosin activity levels are related to sperm morphology and in vitro fertilization rate. Pan et al. (2015) found that acrosin activity was negatively associated with mono-*n*-butyl phthalate (MBP), mono-isobutyl phthalate (MiBP), MEHP, and that %MEHP in total phthalates, MBP, and MiBP were also negatively associated with sperm morphology.

Oocyte

The oocyte is the primary determinant of embryo developmental competence in women and delivers half the chromosomal complement to the embryo. Mok-Lin et al. (2010) found that urinary bisphenol A (BPA) concentrations were inversely associated with the number of oocytes retrieved per cycle referring to female fertility, with an average decrease of 12% for each log unit increase in SG-BPA. BPA is a high-volume chemical that has been widely used to make hard plastic items such as baby bottles, food containers, and storage containers.

Reproductive Hormones

Reproductive hormones play an essential role in the development of the reproductive system. They consist of follicle-stimulating hormone (FSH), luteinizing hormone (LH), estradiol (E2), testosterone (TEST), prolactin (PROL), anti-Müllerian hormone (AMH), insulin like-factor 3 (INSL3), etc. Both males and females produce and secrete reproductive hormones, but the quantity and function of reproductive hormones are different for males and for females.

In the male, FSH usually reflects the status of spermatogenesis as a result of feedback between the testis and hypothalamus/pituitary glands. An elevated level of FSH indicates abnormal sperm production. LH is an essential hormone that stimulates TEST production by the Leydig cells, and, together with FSH, regulates spermatogenesis. Low TEST levels are associated with abnormal sexual differentiation and decreased fertility (Radke et al. 2018). INSL3, a primary secretory product of Leydig cells, plays a crucial role in testicular descent and germ cell survival and is associated with spermatogenesis and sperm morphology in adult men. In a study of the effect of phthalates on reproductive hormones in 599 men, urinary metabolites of phthalates were measured, including mono-isobutyl phthalate (MiBP), monomethyl phthalate

Table 6 Biomarkers of the reproductive system used in assessing health risk of indoor air pollutants

Study site	Year	Study design	Pollutant	Participant, N	Biomarker	Reference
Nanjing, China	2015	Cross-sectional study	Phthalate	Men of reproductive age, 1066	Acrosin activity, sperm morphology, and INSL3, DFI	Pan et al. (2015)
Massachusetts, America	2010	Prospective cohort study	BPA	Women undergoing in vitro fertilization, 84	Oocytes; E ₂	Moh-Lin et al. (2010)
Saudi Arabia	2019	Cross-sectional study	Phthalate	Men who were part of couples undergoing IVF or intracytoplasmic sperm injection, 599	TEST; PROL; E ₂ ; LH; FSH; and sperm concentration	Al-Saleh et al. (2019)
America	2016	Cross-sectional study	Tobacco smoke, indoor heating/cooking sources (wood, artificial firelogs)	Premenopausal women, 913	AMH	White et al. (2016)
Massachusetts, America	2007	Cross-sectional study	Phthalate	Men from an infertility clinic, 379	CE; tail%; TDM	Hauser et al. (2007)
Hungary	2005	Cohort study	Tobacco smoke	Females who had received in vitro fertilization, 40	Cumulus cells	Sinko et al. (2005)
Chongqing, China	2019	Cross-sectional study	Phthalate	Volunteers, 118	LINE-1 DNA methylation	Tian et al. (2019)
California, America	2017	Cohort study	Phthalate	Mother-child pairs, 336	DMRs	Solomon et al. (2017)

INSL3: insulin like-factor 3, DFI: DNA fragmentation index, BPA: Bisphenol A, E₂: estradiol, IVF: in vitro fertilization, TEST: testosterone, PROL: prolactin, LH: luteinizing hormone, FSH: follicle-stimulating hormone, AMH: anti-Müllerian hormone, CE: comet extent, Tail%: percentage of DNA in tail, TDM: tail distributed moment, LINE-1: long interspersed nuclear element-1, and DMRs: differentially methylated regions

(MEP), mono-(2-ethylhexyl) phthalate (MEHP), mono-(2-ethyl-5-hydroxyhexyl) phthalate (MEHHP), and mono-(2-ethyl-5-oxohexyl) phthalate (MEOHP); and % MEHP represents the urinary level of the primary metabolite MEHP as a proportion of total DEHP metabolites (Al-Saleh et al. 2019). This study found negative associations between TEST and MiBP, between FSH and MEHHP, and between PROL and MEOHP, respectively. The study also found positive associations between E₂ and MEP, %MEHP and LH, respectively. The study further found that FSH mediated significantly and up to 60% of the positive relationship between sperm concentration and MEHHP, while FSH and LH, respectively, mediated 15% and 12% of the negative association between sperm concentration and %MEHP (Al-Saleh et al. 2019). In another study, serum levels of INSL3 were negatively associated with urinary MEHP and %MEHP, respectively (Pan et al. 2015).

In the female, estrogens are female hormones responsible for the onset and progression of female reproductive cycles, of which E₂ is the most important hormone. Serum anti-Müllerian hormone (AMH) is a common biomarker of ovarian reserve, and lower AMH levels (e.g., <1 ng/mL) may indicate a woman with diminished ovarian reserve and, hence, with an increased risk for infertility. Mok-Lin et al. (2010) found that the number of oocytes retrieved was strongly correlated with peak serum E₂ concentrations, and both of oocyte count and serum E₂ were negatively associated with increasing urinary BPA concentrations. Serum AMH levels have been found to be lower in current heavy smokers and have been negatively associated with long-term exposure to environmental tobacco smoke (active and passive smoking) and indoor burning of wood or artificial fire logs, respectively (White et al. 2016). Therefore, serum AMH can serve as a biomarker of female reproductive effects (specifically ovarian reserve or infertility risk) of indoor air pollutants emitted from combusting biomass (tobacco and wood).

DNA Damage

Sperm DNA Fragmentation Index (DFI) represents sperm DNA damage levels. DFI has been positively associated with phthalate (MBP and MiBP) exposures (Pan et al. 2015). Sperm DNA damage levels can also be measured as comet extent (CE), percentage of DNA in tail (Tail%), and tail distributed moment (TDM). These biomarkers of sperm DNA damage are typically assayed using the neutral comet assay (Hauser et al. 2007).

In developing follicles, cumulus cells are coupled to the growing oocyte through gap junctions as a functional syncytium that facilitates the transfer of signals as well as nutrients into and out of the oocyte and between follicle cells. Thus, cumulus cells play a pivotal role in oocyte maturation and maintenance. Sinko et al. (2005) found that smoking was associated with significantly elevated DNA damage levels in cumulus cells in women who were scheduled for in vitro fertilization.

DNA Methylation

DNA methylation plays a vital role in sperm maturation. Abnormal epigenetic modification may result in impaired spermatogenesis and compromised sperm function. The global DNA methylation surrogate (long interspersed nuclear

element-1, LINE-1) hypermethylation has been related to decreased sperm motility, reduced sperm quality, and lower sperm morphology. Tian et al. (2019) reported sperm LINE-1 DNA methylation was negatively associated with exposure to total DEHP isomers and sperm quality, respectively. They further found that LINE-1 DNA methylation mediated 20.7% of the association between DEHP exposure and sperm motility.

Differentially methylated regions (DMRs) utilizing co-correlation patterns between nearby CpG sites, taking advantage of the epigenomic structure, may be more informative than methylation in individual CpG sites in predicting disease or health status. Solomon et al. (2017) examined the effects of prenatal (in utero) phthalate exposure and on cord blood DNA methylation. Concentrations of 11 phthalate metabolites were analyzed in maternal urine samples, and DNA methylation was assessed and adjusted for cord blood cell composition. They identified 27 DMRs, the majority of which were associated with multiple phthalate metabolites. Furthermore, 51% of the significant DMRs were associated with the di-(2-ethylhexyl) phthalate metabolites. In addition, five individual CpG sites, showing hypermethylation, were associated with phthalate metabolite concentrations. Solomon et al. (2017) also identified specific genes in the DMRs related to male fertility including IFT140, TESC, and PRDM8. This study provides a good example for DNA methylation at specific CpG sites and at specific regions of the epigenetic structure to serve as biomarkers of early-life (e.g., during fetal development) exposure to environmental chemicals such as phthalates.

Application of Biomarkers in Assessing Health Risks of Other Physiologic Systems

Kidneys

The kidney is the primary organ of the urinary system, filtering the blood, removing wastes, and excreting the urine. Serum uric acid, estimated glomerular filtration rate (eGFR) estimated with serum creatinine, and urinary albumin to creatinine ratio (ACR) are common measures of renal impairment. Farzan et al. (2016) found that PAH metabolites were positively associated with uric acid and negatively associated with eGFR in adolescents (each 100% increase in 2-hydroxyphenanthrene and 3-hydroxyphenanthrene was associated with a 3.36% increase (95% CI: 0.338–6.372; $p=0.032$) in uric acid and a 2.66% decrease (95% CI: –4.979 to –0.331; $p=0.028$) in eGFR, respectively). Kidney injury molecule-1 (KIM-1) and neutrophil gelatinase-associated lipocalin (NGAL) are biomarkers of proximal tubule injury and distal tubule damage. Jacobson et al. (2020) found that urinary concentrations of bisphenol A (BPA), phthalic acid, and phthalate metabolites, respectively, were associated with increased NGAL and KIM-1 concentrations over time, indicating that exposure to these chemicals (mostly occurring indoors) affected renal function biomarkers in the long term.

Thyroid

The thyroid is an essential organ of the endocrine system located in the neck. Thyroid hormones secretion is vital for fetal and child growth and brain development, for the control of metabolism and energy balance, and many aspects of normal physiology, including nervous, cardiovascular, pulmonary, and reproductive systems. About 95% of active thyroid hormones is thyroxine (T4), and most of the remaining 5% is triiodothyronine (T3). Thyroid hormone secretion is regulated by a negative feedback mechanism about thyrotropin (TSH) and itself. Thyroglobulin antibody and thyroid peroxidase antibody are common autoantibodies that could cause thyroid autoimmunity. Wang et al. (2013) found that smoking during pregnancy was associated with higher free T3 levels and lower free T4 levels in euthyroid women (Mannisto et al. 2012). Another study found associations of urinary BPA with thyroid measures and increased thyroid function were independent of thyroglobulin antibody and thyroid peroxidase antibodies in Chinese adults ().

Metabolic System

Two major metabolic disorders have been linked to indoor air pollution: diabetes and obesity.

Diabetes is a metabolic disease closely related to cardiovascular diseases. Fasting glucose and glycated hemoglobin (HbA1c) are common biomarkers of diabetes. HbA1c, reflecting average plasma glucose concentration over the past 3 months, has been used as one of the indicators for defining prediabetes (HbA1c between 5.7% and 6.4%) and diabetes (HbA1c >6.4%). A meta-analysis of prospective cohort studies showed that long-time exposure to high levels of PM_{2.5} and NO₂ was significantly associated with elevated risk of type 2 diabetes mellitus (Wang et al. 2014). Rajkumar et al. (2018) found a higher prevalence of prediabetes and diabetes in women with higher exposure to household air pollution and suggestive evidence for a stronger effect in women ≥40 years of age in Honduras. In a case-control study conducted in China, Duan et al. (2019) found a significant positive association between urinary mono (2-ethylhexyl) phthalate and fasting glucose (Duan et al. 2019).

Epigenetic regulation of miRNAs, specifically miR-9-5p, miR-16-5p, miR-29a-3p, and miR-330-3p, has been associated with gestational diabetes mellitus (GDM). For instance, miR-16-5p was mainly associated with MAPK, insulin, TGF-β, and Mtor-signaling pathways (Zhu et al. 2015). A study reported that adjusted urinary mono-benzyl phthalate (adjusted for dilution by urinary creatinine value) levels and adjusted MEHP concentrations were positively associated with miR-16-5p expression levels and miR-29a-3p expression levels, respectively, while MBP concentrations and unadjusted MiBP levels were negatively in relation to miR-29a-3p expression levels (Martinez-Ibarra et al. 2019).

The prevalence of overweight and obesity has increased steadily around the globe since 1980 (Stevens et al. 2012). A hypothesized contributor to the increasing prevalence is exposure to phthalates and BPA, as these compounds may operate through complex causal pathways starting from in utero development to childhood and adult obesity. Insight into the susceptibility of fetal development to the potential adverse effects of phthalates and BPA can be obtained by examining biomarkers of fetal metabolic function such as leptin and adiponectin. Elevated leptin levels are associated with increased body mass index (BMI) in adults and large for gestational age infants. High cord blood leptin levels have been positively correlated with birth weight and insulin resistance, whereas low cord blood leptin levels have been associated with small for gestational age. Ashley-Martin et al. (2014) found that BPA was negatively associated with adiponectin levels, and mono-(3-carboxypropyl) (MCPP) was associated with increased odds of high leptin among males. Metabolomics, using unbiased and data-driven approaches to measure the relative concentrations of endogenous low-molecular weight metabolites in biofluids, has been recently applied to explore in vivo pathologic alterations associated with phthalate exposure. For example, it was found that in Chinese children among the metabolic markers related to MnBP exposure, 1-methylhydantoin, pyrrole-2-carboxylic acid, and monostearin were positively associated with obesity indices (Xia et al. 2018). Simultaneously, hydroxyproline, l-ornithine, and lactate were negatively associated with overweight and obesity in children (Xia et al. 2018).

Cognitive Function

In recent years, several major epidemiologic studies have reported significant associations between air pollutants and cognitive function in cross-sectional and cohort studies. Cognitive function was assessed through direct clinical exams of study subjects or through the retrieval of a medical record database (Paul et al. 2019). Questionnaires, scales, and tests such as Mini-Mental State Examination (MMSE), immediate word recall, delayed word recall and verbal fluency, the Benton Visual Retention Test, and Trail Making Test were commonly used to assess cognitive function (Falck et al. 2017). In addition to these assessments, emerging biomarkers were also used in recent studies.

A series of studies have used magnetic resonance imaging (MRI) scans of brain to assess cognitive function. Using the MRI technique, for example, Wilker et al. measured total cerebral brain volume (TCBV), hippocampal volume (HV), white matter hyperintensity volume (WMHV), and covert brain infarcts (CBI) in subjects participating the Framingham Offspring Study. By associating these brain image measures with PM_{2.5} exposure, the authors reported that a 2 µg/m³ increase in PM_{2.5} exposure was associated with 0.32% (95%CI: 0.59, 0.05) smaller TCBV (Wilker et al. 2015). A prospective study of 1403 older women enrolled in the Women's Health Initiative

Memory Study (WHIMS) reported that for each IQR increment change ($3.49 \mu\text{g}/\text{m}^3$) of cumulative PM_{2.5} exposure, the average WM volume (95% CI) was 6.23 (3.72 – 8.74) cm³ lower in the total brain and 4.47 (2.27 – 6.67) cm³ lower in the association areas, equivalent to 1–2 years of brain aging (Chen et al. 2015a). Similar studies provide important evidence that air pollution influences brain function and brain structure (Casanova et al. 2016; Power et al. 2018; Wilker et al. 2016).

The pathological hallmarks of Alzheimer's disease (AD) include the extracellular accumulation of amyloid- β (A β) and intracellular aggregates of hyperphosphorylated tau (Frisoni et al. 2017). In a population of cognitively unimpaired adults, greater exposure to NO₂ and PM_{2.5} was associated with higher levels of brain A β deposition, while a greater exposure to PM₁₀ and PM_{2.5} was associated with higher levels of CSF NfL (Alemany et al. 2021). A cross-sectional study including 18,178 US participants with cognitive impairment who received an amyloid PET scan reported that greater PM_{2.5} exposures were significantly associated with brain A β plaques, after adjusting for demographic, lifestyle, and socioeconomic factors as well as medical comorbidities (Iaccarino et al. 2021). Although biomarkers of cognitive function related to ambient air pollution have been assessed recently, few studies apply these biomarkers in the assessment of cognitive function in relation to indoor air pollution. Considering personal exposure to air pollution can be dominated by indoor exposures, it is promising to use A β , tau, and MRI as early and sensitive biomarkers to assess cognitive function associated with indoor air pollution.

The biomarkers of other systems of indoor air pollution were summarized in Table 7.

Conclusion

This chapter provides a summary of biomarkers that can reflect changes in concentrations or expression levels in molecular patterns (e.g., DNA methylation) associated with exposure to indoor air pollutants. These biomarkers can be measured in bodily fluids (e.g., blood, urine, exhaled breath, saliva, and nasal mucus) from human participants. Given that these biomarkers are specific to the pathophysiology of the respiratory system, cardiovascular system, hematologic system, immune system, reproductive system, and other systems, application of these biomarkers would provide insight into the health risk of indoor air pollutants exposure. Furthermore, considering these biomarkers reflect subclinical or preclinical changes, and are typically more sensitive than clinical outcomes, they are particularly useful to understand the potential biological mechanisms through which indoor air pollutants would affect human health. The mechanistic insights would strengthen the causal inference of the health effects, thereby reducing the uncertainty in the estimation of health risks attributable to specific indoor air pollutants or sources.

Table 7 Biomarkers of other physiologic systems used in assessing health risk of indoor air pollutants

Study site	Year	Study design	Pollutant	Participant, N	Biomarker	Reference
America	2016	Cross-sectional study	PAH	Adolescents, 660	Uric acid, eGFR, and ACR	Farzan et al. (2016)
America and Canada	2020	Cohort study	BPA, phthalates	Children and adolescents, 618	KIM-1, NGAL	Jacobson et al. (2020)
Finland	2012	Cohort study	Tobacco smoke	Euthyroid mothers, 4837	T3, T4	Mannisto et al. (2012)
Shanghai, China	2013	Cross-sectional study	BPA	People age 40 years or older, 3394	T3, TSH	Wang et al. (2013)
Honduras	2018	Cross-sectional study	PM _{2.5} , BC	Women in rural, 142	HbA1c	Rajkumar et al. (2018)
Tianjin, China	2019	Case-control study	Phthalate	T2DM cases and controls, 500	Fasting glucose	Duan et al. (2019)
Mexico	2019	Case-control study	Phthalates	Women with GDM and nondiabetics, 40	miR-16-5p, miR-29a-3p	Martinez-Ibarra et al. (2019)
10 Canadian sites	2014	Cohort study	Phthalate, BPA	Pregnant women, 2001	Adiponectin, Leptin	Ashley-Martin et al. (2014)
China	2018	Case-control study	Phthalate	Overweight/obese children and normal weight children, 149	Metabolic markers	Xia et al. (2018)
New England Region	2015	Cross-sectional study	PM _{2.5}	Healthy elderly, 943	MRI (TCBV, HV, WMHV, and CBI)	Wilker et al. (2015)
United States	2015	Cohort study	PM _{2.5}	Older women, 1403	MRI (GM, WM)	Chen et al. (2015a)
Barcelona	2021	Cross-sectional study	NO ₂ , PM _{2.5} , and PM ₁₀	Cognitively unimpaired adults, 156	Aβ42, Aβ40, p-Tau, t-Tau, and NfL	Alemany et al. (2021)
United States	2020	Cross-sectional study	PM _{2.5} , O ₃	Cognitively impaired adults, 18,178	PET Aβ	Iaccarino et al. (2021)

PAH: polycyclic aromatic hydrocarbons, eGFR: estimated glomerular filtration rate, ACR: albumin to creatinine ratio, BPA: Bisphenol A, KIM-1: kidney injury molecule-1, NGAL: neutrophil gelatinase-associated lipocalin, T3: triiodothyronine, T4: thyroxine, TSH: thyroid-stimulating hormone, BC: black carbon, HbA1c: glycated hemoglobin, T2DM: type 2 diabetes mellitus, GDM: gestational diabetes mellitus, miR: MicroRNA, TVBC: total cerebral brain volume, HV: hippocampal volume, WMHV: white matter hyperintensity volume, CBI: covert brain infarcts, and NfL: neurofilament light

References

- Abbas AK, Lichtman AH, Pillai S (2019) Basic immunology E-book: functions and disorders of the immune system. Elsevier Health Sciences
- Alemany S et al (2021) Associations between air pollution and biomarkers of Alzheimer's disease in cognitively unimpaired individuals. Environ Int 157:106864. <https://doi.org/10.1016/j.envint.2021.106864>
- Allen RW et al (2011) An air filter intervention study of endothelial function among healthy adults in a woodsmoke-impacted community. Am J Respir Crit Care Med 183:1222–1230. <https://doi.org/10.1164/rccm.201010-1572OC>
- Al-Saleh I et al (2019) The relationships between urinary phthalate metabolites, reproductive hormones and semen parameters in men attending in vitro fertilization clinic. Sci Total Environ 658:982–995. <https://doi.org/10.1016/j.scitotenv.2018.12.261>
- Ashley-Martin J et al (2014) A birth cohort study to investigate the association between prenatal phthalate and bisphenol A exposures and fetal markers of metabolic dysfunction. Environ Health 13:84. <https://doi.org/10.1186/1476-069X-13-84>
- Ashley-Martin J et al (2016) Air pollution during pregnancy and cord blood immune system biomarkers. J Occup Environ Med 58:979–986. <https://doi.org/10.1097/JOM.0000000000000841>
- Atosuo J, Karhuvaara O, Suominen E, Vilen L, Nuutila J, Putus T (2020) Indoor exposure to Streptomyces albus and aspergillus versicolor elevates the levels of spore-specific IgG, IgG1 and IgG3 serum antibodies in building users – a new ELISA-based assay for exposure assessment. Sci Total Environ 698:134335. <https://doi.org/10.1016/j.scitotenv.2019.134335>
- Banerjee A, Mondal NK, Das D, Ray MR (2012) Neutrophilic inflammatory response and oxidative stress in premenopausal women chronically exposed to indoor air pollution from biomass burning. Inflammation 35:671–683. <https://doi.org/10.1007/s10753-011-9360-2>
- Benka-Coker ML et al (2018) Exposure to household air pollution from biomass Cookstoves and levels of Fractional Exhaled Nitric Oxide (FeNO) among Honduran women. Int J Environ Res Public Health 15. <https://doi.org/10.3390/ijerph15112544>
- Bentayeb M et al (2015) Indoor air quality, ventilation and respiratory health in elderly residents living in nursing homes in Europe. Eur Respir J 45:1228–1238. <https://doi.org/10.1183/09031936.00082414>
- Blankenberg S et al (2003) Glutathione peroxidase 1 activity and cardiovascular events in patients with coronary artery disease. N Engl J Med 349:1605–1613. <https://doi.org/10.1056/NEJMoa030535>
- Bolling AK, Sripada K, Becher R, Beko G (2020) Phthalate exposure and allergic diseases: review of epidemiological and experimental evidence. Environ Int 139:105706. <https://doi.org/10.1016/j.envint.2020.105706>
- Braun M, Klingelhofer D, Oremek GM, Quarcoo D, Groneberg DA (2020) Influence of second-hand smoke and prenatal tobacco smoke exposure on biomarkers, genetics and physiological processes in children—an overview in research insights of the last few years. Int J Environ Res Public Health 17. <https://doi.org/10.3390/ijerph17093212>
- Brauner EV et al (2008) Indoor particles affect vascular function in the aged: an air filtration-based intervention study. Am J Respir Crit Care Med 177:419–425. <https://doi.org/10.1164/rccm.200704-632OC>
- Brook RD et al (2010) Particulate matter air pollution and cardiovascular disease: an update to the scientific statement from the American Heart Association. Circulation 121:2331–2378. <https://doi.org/10.1161/CIR.0b013e3181dbece1>
- Bruce N, Perez-Padilla R, Albalak R (2000) Indoor air pollution in developing countries: a major environmental and public health challenge. Bull World Health Organ 78:1078–1092
- Budani MC, Tiboni GM (2017) Ovotoxicity of cigarette smoke: a systematic review of the literature. Reprod Toxicol 72:164–181. <https://doi.org/10.1016/j.reprotox.2017.06.184>
- Cakmak S, Dales RE, Liu L, Kauri LM, Lemieux CL, Hebborn C, Zhu J (2014) Residential exposure to volatile organic compounds and lung function: results from a population-based

- cross-sectional survey. *Environ Pollut* 194:145–151. <https://doi.org/10.1016/j.envpol.2014.07.020>
- Canbaz D, Lebre MC, Logiantara A, van Ree R, van Rijt LS (2016) Indoor pollutant hexabromocyclododecane enhances house dust mite-induced activation of human monocyte-derived dendritic cells. *J Immunotoxicol* 13:810–816. <https://doi.org/10.1080/1547691X.2016.1200224>
- Casanova R et al (2016) A voxel-based morphometry study reveals local brain structural alterations associated with ambient fine particles in older women. *Front Hum Neurosci* 10:495. <https://doi.org/10.3389/fnhum.2016.00495>
- Chahal N, McLain AC, Ghassabian A, Michels KA, Bell EM, Lawrence DA, Yeung EH (2017) Maternal smoking and newborn cytokine and immunoglobulin levels. *Nicotine Tob Res* 19: 789–796. <https://doi.org/10.1093/ntr/ntw324>
- Chen J-C et al (2015a) Ambient air pollution and neurotoxicity on brain structure: evidence from women's health initiative memory study. *Ann Neurol* 78:466–476. <https://doi.org/10.1002/ana.24460>
- Chen R et al (2015b) Cardiopulmonary benefits of reducing indoor particles of outdoor origin: a randomized, double-blind crossover trial of air purifiers. *J Am Coll Cardiol* 65:2279–2287. <https://doi.org/10.1016/j.jacc.2015.03.553>
- Chen R et al (2018) Fine particulate air pollution and the expression of microRNAs and circulating cytokines relevant to inflammation, coagulation, and vasoconstriction. *Environ Health Perspect* 126:017007. <https://doi.org/10.1289/EHP1447>
- Chuang KJ, Chan CC, Su TC, Lee CT, Tang CS (2007) The effect of urban air pollution on inflammation, oxidative stress, coagulation, and autonomic dysfunction in young adults. *Am J Respir Crit Care Med* 176:370–376. <https://doi.org/10.1164/rccm.200611-1627OC>
- Chuang HC et al (2017) Long-term indoor air conditioner filtration and cardiovascular health: a randomized crossover intervention study. *Environ Int* 106:91–96. <https://doi.org/10.1016/j.envint.2017.06.008>
- Cui X et al (2018) Cardiopulmonary effects of overnight indoor air filtration in healthy non-smoking adults: a double-blind randomized crossover study. *Environ Int* 114:27–36. <https://doi.org/10.1016/j.envint.2018.02.010>
- Dai JB, Wang ZX, Qiao ZD (2015) The hazardous effects of tobacco smoking on male fertility. *Asian J Androl* 17:954–960. <https://doi.org/10.4103/1008-682X.150847>
- Davis MD, Montpetit A, Hunt J (2012) Exhaled breath condensate: an overview. *Immunol Allergy Clin N Am* 32:363–375. <https://doi.org/10.1016/j.iac.2012.06.014>
- Day DB et al (2017) Association of Ozone Exposure with Cardiorespiratory Pathophysiologic Mechanisms in healthy adults. *JAMA Intern Med* 177:1344–1353. <https://doi.org/10.1001/jamainternmed.2017.2842>
- De Pergola G et al (2008) sP-selectin plasma levels in obesity: association with insulin resistance and related metabolic and prothrombotic factors. *Nutr Metab Cardiovasc Dis* 18:227–232. <https://doi.org/10.1016/j.numecd.2006.09.010>
- De S, Leong SC, Fenton JE, Carter SD, Clarke RW, Jones AS (2011) The effect of passive smoking on the levels of matrix metalloproteinase 9 in nasal secretions of children. *Am J Rhinol Allergy* 25:226–230. <https://doi.org/10.2500/ajra.2011.25.3623>
- Delfino RJ et al (2008) Circulating biomarkers of inflammation, antioxidant activity, and platelet activation are associated with primary combustion aerosols in subjects with coronary artery disease. *Environ Health Perspect* 116:898–906. <https://doi.org/10.1289/ehp.11189>
- Deng X et al (2013) PM2.5-induced oxidative stress triggers autophagy in human lung epithelial A549 cells. *Toxicol In Vitro* 27:1762–1770. <https://doi.org/10.1016/j.tiv.2013.05.004>
- Dong W et al (2019) Different cardiorespiratory effects of indoor air pollution intervention with ionization air purifier: findings from a randomized, double-blind crossover study among school children in Beijing. *Environ Pollut* 254:113054. <https://doi.org/10.1016/j.envpol.2019.113054>

- Duan Y, Sun H, Han L, Chen L (2019) Association between phthalate exposure and glycosylated hemoglobin, fasting glucose, and type 2 diabetes mellitus: a case-control study in China. *Sci Total Environ* 670:41–49. <https://doi.org/10.1016/j.scitotenv.2019.03.192>
- Dutta A, Mukherjee B, Das D, Banerjee A, Ray MR (2011) Hypertension with elevated levels of oxidized low-density lipoprotein and anticardiolipin antibody in the circulation of pre-menopausal Indian women chronically exposed to biomass smoke during cooking. *Indoor Air* 21:165–176. <https://doi.org/10.1111/j.1600-0668.2010.00694.x>
- Eckel SP et al (2016) Traffic-related air pollution and alveolar nitric oxide in southern California children. *Eur Respir J* 47:1348–1356. <https://doi.org/10.1183/13993003.01176-2015>
- Erdei E, Bobvos J, Brózik M, Páldy A, Farkas I, Vaskövi E, Rudnai P (2003) Indoor air pollutants and immune biomarkers among Hungarian asthmatic children. *Arch Environ Health* 58:337–347
- Falck RS, Davis JC, Liu-Ambrose T (2017) What is the association between sedentary behaviour and cognitive function? A systematic review. *Br J Sports Med* 51:800–811. <https://doi.org/10.1136/bjsports-2015-095551>
- Fandiño-Del-Rio M et al (2021) Household air pollution and blood markers of inflammation: a cross-sectional analysis. *Indoor Air* 31:1509–1521. <https://doi.org/10.1111/ina.12814>
- Farzan SF, Chen Y, Trachtman H, Trasande L (2016) Urinary polycyclic aromatic hydrocarbons and measures of oxidative stress, inflammation and renal function in adolescents: NHANES 2003–2008. *Environ Res* 144:149–157. <https://doi.org/10.1016/j.envres.2015.11.012>
- Feleszko W et al (2006) Parental tobacco smoking is associated with augmented IL-13 secretion in children with allergic asthma. *J Allergy Clin Immunol* 117:97–102. <https://doi.org/10.1016/j.jaci.2005.09.008>
- Ferroni P, Martini F, Riondino S, La Farina F, Magnapera A, Ciatti F, Guadagni F (2009) Soluble P-selectin as a marker of in vivo platelet activation. *Clin Chim Acta* 399:88–91. <https://doi.org/10.1016/j.cca.2008.09.018>
- Frisoni GB et al (2017) Strategic roadmap for an early diagnosis of Alzheimer's disease based on biomarkers. *Lancet Neurol* 16:661–676. [https://doi.org/10.1016/s1474-4422\(17\)30159-x](https://doi.org/10.1016/s1474-4422(17)30159-x)
- Gao X et al (2019) Effects of filtered fresh air ventilation on classroom indoor air and biomarkers in saliva and nasal samples: a randomized crossover intervention study in preschool children. *Environ Res* 179:108749. <https://doi.org/10.1016/j.envres.2019.108749>
- Garshick E et al (2018) Indoor black carbon and biomarkers of systemic inflammation and endothelial activation in COPD patients. *Environ Res* 165:358–364. <https://doi.org/10.1016/j.envres.2018.05.010>
- GBD 2015 Risk Factors Collaborators (2016) Global, regional, and national comparative risk assessment of 79 behavioural, environmental and occupational, and metabolic risks or clusters of risks, 1990–2015: a systematic analysis for the Global Burden of Disease Study 2015. *Lancet* 388:1659–1724. [https://doi.org/10.1016/S0140-6736\(16\)31679-8](https://doi.org/10.1016/S0140-6736(16)31679-8)
- Grady ST et al (2018) Indoor black carbon of outdoor origin and oxidative stress biomarkers in patients with chronic obstructive pulmonary disease. *Environ Int* 115:188–195. <https://doi.org/10.1016/j.envint.2018.02.040>
- Greeley MA (2016) Chapter 4 – Respiratory system. In: Parker GA, Picut CA (eds) *Atlas of histology of the juvenile rat*. Academic, Boston, pp 89–125. <https://doi.org/10.1016/B978-0-12-802682-3.00004-5>
- Greenwald SE (2007) Ageing of the conduit arteries. *J Pathol* 211:157–172. <https://doi.org/10.1002/path.2101>
- Guan L et al (2019) PM2.5 exposure induces systemic inflammation and oxidative stress in an intracranial atherosclerosis rat model. *Environ Toxicol* 34:530–538. <https://doi.org/10.1002/tox.22707>
- Han TT et al (2020) Human herpesvirus 6 reactivation in unmanipulated haploidentical hematopoietic stem cell transplantation predicts the occurrence of grade II to IV acute graft-versus-host disease. *Transpl Infect Dis*:e13544. <https://doi.org/10.1111/tid.13544>

- Hart JE et al (2018) Effects of indoor and ambient black carbon and [formula: see text] on pulmonary function among individuals with COPD. *Environ Health Perspect* 126:127008. <https://doi.org/10.1289/ehp3668>
- Hassanvand MS et al (2017) Short-term effects of particle size fractions on circulating biomarkers of inflammation in a panel of elderly subjects and healthy young adults. *Environ Pollut* 223: 695–704. <https://doi.org/10.1016/j.envpol.2017.02.005>
- Hauser R, Meeker JD, Singh NP, Silva MJ, Ryan L, Duty S, Calafat AM (2007) DNA damage in human sperm is related to urinary levels of phthalate monoester and oxidative metabolites. *Hum Reprod* 22:688–695. <https://doi.org/10.1093/humrep/dej428>
- Herberth G et al (2014) Maternal and cord blood miR-223 expression associates with prenatal tobacco smoke exposure and low regulatory T-cell numbers. *J Allergy Clin Immunol* 133: 543–550. <https://doi.org/10.1016/j.jaci.2013.06.036>
- Herr CE et al (2010) Air pollution exposure during critical time periods in gestation and alterations in cord blood lymphocyte distribution: a cohort of livebirths. *Environ Health* 9:46. <https://doi.org/10.1186/1476-069X-9-46>
- Huang J et al (2019) Cardiorespiratory responses to low-level ozone exposure: the inDoor Ozone Study in children (DOSE). *Environ Int* 131:105021. <https://doi.org/10.1016/j.envint.2019.105021>
- Hulin M, Simoni M, Viegi G, Annesi-Maesano I (2012) Respiratory health and indoor air pollutants based on quantitative exposure assessments. *Eur Respir J* 40:1033–1045. <https://doi.org/10.1183/09031936.00159011>
- Humphrey JL et al (2020) Air infiltration in low-income, urban homes and its relationship to lung function. *J Expo Sci Environ Epidemiol* 30:262–270. <https://doi.org/10.1038/s41370-019-0184-8>
- Iaccarino L et al (2021) Association between ambient air pollution and amyloid positron emission tomography positivity in older adults with cognitive impairment. *JAMA Neurol* 78:197–207. <https://doi.org/10.1001/jamaneurol.2020.3962>
- Isiugo K et al (2019) Indoor particulate matter and lung function in children. *Sci Total Environ* 663: 408–417. <https://doi.org/10.1016/j.scitotenv.2019.01.309>
- Jacobson MH et al (2020) Serially assessed bisphenol A and phthalate exposure and association with kidney function in children with chronic kidney disease in the US and Canada: a longitudinal cohort study. *PLoS Med* 17:e1003384. <https://doi.org/10.1371/journal.pmed.1003384>
- Jansen KL, Larson TV, Koenig JQ, Mar TF, Fields C, Stewart J, Lippmann M (2005) Associations between health effects and particulate matter and black carbon in subjects with respiratory disease. *Environ Health Perspect* 113:1741–1746. <https://doi.org/10.1289/ehp.8153>
- Kajbafzadeh M, Brauer M, Karlen B, Carlsten C, van Eeden S, Allen RW (2015) The impacts of traffic-related and woodsmoke particulate matter on measures of cardiovascular health: a HEPA filter intervention study. *Occup Environ Med* 72:394–400. <https://doi.org/10.1136/oemed-2014-102696>
- Kanchongkittiphon W, Gaffin JM, Phipatanakul W (2014) The indoor environment and inner-city childhood asthma. *Asian Pac J Allergy Immunol* 32:103–110
- Karottki DG et al (2013) An indoor air filtration study in homes of elderly: cardiovascular and respiratory effects of exposure to particulate matter. *Environ Health* 12:116. <https://doi.org/10.1186/1476-069X-12-116>
- Karottki DG et al (2014) Cardiovascular and lung function in relation to outdoor and indoor exposure to fine and ultrafine particulate matter in middle-aged subjects. *Environ Int* 73: 372–381. <https://doi.org/10.1016/j.envint.2014.08.019>
- Kattoor AJ, Kanuri SH, Mehta JL (2019) Role of Ox-LDL and LOX-1 in Atherogenesis. *Curr Med Chem* 26:1693–1700. <https://doi.org/10.2174/092986732566180508100950>
- Kaufman JD et al (2012) Prospective study of particulate air pollution exposures, subclinical atherosclerosis, and clinical cardiovascular disease: the multi-ethnic study of atherosclerosis

- and air pollution (MESA air). *Am J Epidemiol* 176:825–837. <https://doi.org/10.1093/aje/kws169>
- Kephart JL, Fandiño-Del-Rio M, Koehler K, Bernabe-Ortiz A, Miranda JJ, Gilman RH, Checkley W (2020) Indoor air pollution concentrations and cardiometabolic health across four diverse settings in Peru: a cross-sectional study. *Environ Health* 19:59. <https://doi.org/10.1186/s12940-020-00612-y>
- Kurmi OP, Lam KB, Ayres JG (2012) Indoor air pollution and the lung in low- and medium-income countries. *Eur Respir J* 40:239–254. <https://doi.org/10.1183/09031936.00190211>
- Laumbach RJ et al (2014) A controlled trial of acute effects of human exposure to traffic particles on pulmonary oxidative stress and heart rate variability. Part Fibre Toxicol 11:45. <https://doi.org/10.1186/s12989-014-0045-5>
- Leech JA, Nelson WC, Burnett RT, Aaron S, Raizenne ME (2002) It's about time: a comparison of Canadian and American time-activity patterns. *J Expo Anal Environ Epidemiol* 12:427–432. <https://doi.org/10.1038/sj.jea.7500244>
- Li H et al (2017) Particulate matter exposure and stress hormone levels: a randomized, double-blind, crossover trial of air purification. *Circulation* 136:618–627. <https://doi.org/10.1161/CIRCULATIONAHA.116.026796>
- Li T et al (2019) Associations between inhaled doses of PM2.5-bound polycyclic aromatic hydrocarbons and fractional exhaled nitric oxide. *Chemosphere* 218:992–1001. <https://doi.org/10.1016/j.chemosphere.2018.11.196>
- Lin LY, Chuang HC, Liu IJ, Chen HW, Chuang KJ (2013) Reducing indoor air pollution by air conditioning is associated with improvements in cardiovascular health among the general population. *Sci Total Environ* 463–464:176–181. <https://doi.org/10.1016/j.scitotenv.2013.05.093>
- Liu W et al (2017) Reactive hyperemia index in patients on maintenance hemodialysis: cross-sectional data from a cohort study. *Sci Rep* 7:45757. <https://doi.org/10.1038/srep45757>
- Liu S et al (2018) Cardiovascular benefits of short-term indoor air filtration intervention in elderly living in Beijing: an extended analysis of BIAPSY study. *Environ Res* 167:632–638. <https://doi.org/10.1016/j.envres.2018.08.026>
- Liu Q, Wang W, Jing W (2019) Indoor air pollution aggravates asthma in Chinese children and induces the changes in serum level of miR-155. *Int J Environ Health Res* 29:22–30. <https://doi.org/10.1080/09603123.2018.1506569>
- Liu S et al (2020) Metabolic linkages between indoor negative air ions, particulate matter and cardiorespiratory function: a randomized, double-blind crossover study among children. *Environ Int* 138:105663. <https://doi.org/10.1016/j.envint.2020.105663>
- Mannisto T et al (2012) Smoking and early pregnancy thyroid hormone and anti-thyroid antibody levels in euthyroid mothers of the Northern Finland Birth Cohort 1986. *Thyroid* 22:944–950. <https://doi.org/10.1089/thy.2011.0377>
- Martinez-Ibarra A et al (2019) Unhealthy levels of phthalates and bisphenol A in Mexican pregnant women with gestational diabetes and its association to altered expression of miRNAs involved with metabolic disease. *Int J Mol Sci*:20. <https://doi.org/10.3390/ijms20133343>
- Mok-Lin E et al (2010) Urinary bisphenol A concentrations and ovarian response among women undergoing IVF. *Int J Androl* 33:385–393. <https://doi.org/10.1111/j.1365-2605.2009.01014.x>
- Morishita M, Adar SD, D'Souza J, Ziembra RA, Bard RL, Spino C, Brook RD (2018) Effect of portable air filtration systems on personal exposure to fine particulate matter and blood pressure among residents in a low-income senior facility: a randomized clinical trial. *JAMA Intern Med* 178:1350–1357. <https://doi.org/10.1001/jamainternmed.2018.3308>
- Padró-Martínez LT et al (2015) A randomized cross-over air filtration intervention trial for reducing cardiovascular health risks in residents of public housing near a highway. *Int J Environ Res Public Health* 12:7814–7838. <https://doi.org/10.3390/ijerph120707814>
- Pan Y et al (2015) Association between phthalate metabolites and biomarkers of reproductive function in 1066 Chinese men of reproductive age. *J Hazard Mater* 300:729–736. <https://doi.org/10.1016/j.jhazmat.2015.08.011>

- Pan L et al (2018) The short-term effects of indoor size-fractionated particulate matter and black carbon on cardiac autonomic function in COPD patients. *Environ Int* 112:261–268. <https://doi.org/10.1016/j.envint.2017.12.037>
- Paul KC, Haan M, Mayeda ER, Ritz BR (2019) Ambient air pollution, noise, and late-life cognitive decline and dementia risk. *Annu Rev Public Health* 40:203–220. <https://doi.org/10.1146/annurev-publhealth-040218-044058>
- Polek A, Sobczewski W, Matowicka-Karna J (2009) P-selectin and its role in some diseases
- Power MC et al (2018) The Association of Long-Term Exposure to particulate matter air pollution with brain MRI findings: the ARIC study. *Environ Health Perspect* 126:027009. <https://doi.org/10.1289/ehp2152>
- Pratali L et al (2019) Indoor air pollution exposure effects on lung and cardiovascular health in the high Himalayas, Nepal: an observational study. *Eur J Intern Med* 61:81–87. <https://doi.org/10.1016/j.ejim.2018.10.023>
- Rabha R, Ghosh S, Padhy PK (2018) Indoor air pollution in rural north-east India: elemental compositions, changes in haematological indices, oxidative stress and health risks. *Ecotoxicol Environ Saf* 165:393–403. <https://doi.org/10.1016/j.ecoenv.2018.09.014>
- Radke EG, Braun JM, Meeker JD, Cooper GS (2018) Phthalate exposure and male reproductive outcomes: a systematic review of the human epidemiological evidence. *Environ Int* 121: 764–793. <https://doi.org/10.1016/j.envint.2018.07.029>
- Radke EG, Glenn BS, Braun JM, Cooper GS (2019) Phthalate exposure and female reproductive and developmental outcomes: a systematic review of the human epidemiological evidence. *Environ Int* 130:104580. <https://doi.org/10.1016/j.envint.2019.02.003>
- Rajkumar S et al (2018) Exposure to household air pollution from biomass-burning cookstoves and HbA1c and diabetic status among Honduran women. *Indoor Air*. <https://doi.org/10.1111/ina.12484>
- Ramani T, Auletta CS, Weinstock D, Mounho-Zamora B, Ryan PC, Salcedo TW, Bannish G (2015) Cytokines: the good, the bad, and the deadly. *Int J Toxicol* 34:355–365. <https://doi.org/10.1177/1091581815584918>
- Ray MR et al (2006) Platelet activation, upregulation of CD11b/CD18 expression on leukocytes and increase in circulating leukocyte-platelet aggregates in Indian women chronically exposed to biomass smoke. *Hum Exp Toxicol* 25:627–635. <https://doi.org/10.1177/0960327106074603>
- Rice MB et al (2013) Short-term exposure to air pollution and lung function in the Framingham Heart Study. *Am J Respir Crit Care Med* 188:1351–1357. <https://doi.org/10.1164/rccm.201308-1414OC>
- Schwartz J et al (2005) Traffic related pollution and heart rate variability in a panel of elderly subjects. *Thorax* 60:455–461. <https://doi.org/10.1136/thx.2004.024836>
- Shao D et al (2017) Cardiorespiratory responses of air filtration: a randomized crossover intervention trial in seniors living in Beijing: Beijing Indoor Air Purifier Study, BIAPSY. *Sci Total Environ* 603-604:541–549. <https://doi.org/10.1016/j.scitotenv.2017.06.095>
- Sifakis S, Androutsopoulos VP, Tsatsakis AM, Spandidos DA (2017) Human exposure to endocrine disrupting chemicals: effects on the male and female reproductive systems. *Environ Toxicol Pharmacol* 51:56–70. <https://doi.org/10.1016/j.etap.2017.02.024>
- Sinko I, Morocz M, Zadori J, Kokavszky K, Rasko I (2005) Effect of cigarette smoking on DNA damage of human cumulus cells analyzed by comet assay. *Reprod Toxicol* 20:65–71. <https://doi.org/10.1016/j.reprotox.2004.12.007>
- Solomon O et al (2017) Prenatal phthalate exposure and altered patterns of DNA methylation in cord blood. *Environ Mol Mutagen* 58:398–410. <https://doi.org/10.1002/em.22095>
- Soppa VJ et al (2019) Effects of short-term exposure to fine and ultrafine particles from indoor sources on arterial stiffness – a randomized sham-controlled exposure study. *Int J Hyg Environ Health* 222:1115–1132. <https://doi.org/10.1016/j.ijheh.2019.08.002>
- Stevens GA et al (2012) National, regional, and global trends in adult overweight and obesity prevalences. *Popul Health Metrics* 10:22. <https://doi.org/10.1186/1478-7954-10-22>

- Sun Y et al (2020) Inflammatory cytokines and DNA methylation in healthy young adults exposure to fine particulate matter: a randomized, double-blind crossover trial of air filtration. *J Hazard Mater* 398:122817. <https://doi.org/10.1016/j.jhazmat.2020.122817>
- Tian M, Liu L, Zhang J, Huang Q, Shen H (2019) Positive association of low-level environmental phthalate exposure with sperm motility was mediated by DNA methylation: a pilot study. *Chemosphere* 220:459–467. <https://doi.org/10.1016/j.chemosphere.2018.12.155>
- Tran VV, Park D, Lee YC (2020) Indoor air pollution, related human diseases, and recent trends in the control and improvement of indoor air quality. *Int J Environ Res Public Health* 17. <https://doi.org/10.3390/ijerph17082927>
- Wang T et al (2013) Urinary bisphenol a concentration and thyroid function in Chinese adults. *Epidemiology* 24:295–302. <https://doi.org/10.1097/EDE.0b013e318280e02f>
- Wang B, Xu D, Jing Z, Liu D, Yan S, Wang Y (2014) Effect of long-term exposure to air pollution on type 2 diabetes mellitus risk: a systemic review and meta-analysis of cohort studies. *Eur J Endocrinol* 171:R173–R182. <https://doi.org/10.1530/EJE-14-0365>
- Wang JJ, Karmaus WJ, Chen SL, Holloway JW, Ewart S (2015) Effects of phthalate exposure on asthma may be mediated through alterations in DNA methylation. *Clin Epigenetics* 7:27. <https://doi.org/10.1186/s13148-015-0060-x>
- Wang L, Xu J, Liu H, Li J, Hao H (2019) PM2.5 inhibits SOD1 expression by up-regulating microRNA-206 and promotes ROS accumulation and disease progression in asthmatic mice. *Int Immunopharmacol* 76:105871. <https://doi.org/10.1016/j.intimp.2019.105871>
- Weichenthal S et al (2013) A randomized double-blind crossover study of indoor air filtration and acute changes in cardiorespiratory health in a first nations community. *Indoor Air* 23:175–184. <https://doi.org/10.1111/ina.12019>
- White AJ, Sandler DP, D'Aloisio AA, Stanczyk F, Whitworth KW, Baird DD, Nichols HB (2016) Antimullerian hormone in relation to tobacco and marijuana use and sources of indoor heating/ cooking. *Fertil Steril* 106:723–730. <https://doi.org/10.1016/j.fertnstert.2016.05.015>
- Wilker EH et al (2015) Long-term exposure to fine particulate matter, residential proximity to major roads and measures of brain structure. *Stroke* 46:1161–1166. <https://doi.org/10.1161/strokeaha.114.008348>
- Wilker EH et al (2016) Fine particulate matter, residential proximity to major roads, and markers of small vessel disease in a memory study population. *J Alzheimers Dis* 53:1315–1323. <https://doi.org/10.3233/jad-151143>
- Wilkinson IB et al (2002) Increased central pulse pressure and augmentation index in subjects with hypercholesterolemia. *J Am Coll Cardiol* 39:1005–1011. [https://doi.org/10.1016/s0735-1097\(02\)01723-0](https://doi.org/10.1016/s0735-1097(02)01723-0)
- Xia B et al (2018) Phthalate exposure and childhood overweight and obesity: urinary metabolomic evidence. *Environ Int* 121:159–168. <https://doi.org/10.1016/j.envint.2018.09.001>
- Xiang J et al (2019) Reducing indoor levels of “Outdoor PM(2.5)” in urban China: impact on mortalities. *Environ Sci Technol* 53:3119–3127. <https://doi.org/10.1021/acs.est.8b06878>
- Yang BY, Qian Z, Howard SW, Vaughn MG, Fan SJ, Liu KK, Dong GH (2018) Global association between ambient air pollution and blood pressure: a systematic review and meta-analysis. *Environ Pollut* 235:576–588. <https://doi.org/10.1016/j.envpol.2018.01.001>
- Yoda Y, Tamura K, Adachi S, Otani N, Nakayama SF, Shima M (2020) Effects of the use of air purifier on indoor environment and respiratory system among healthy adults. *Int J Environ Res Public Health* 17. <https://doi.org/10.3390/ijerph17103687>
- Zhao Y et al (2020) Cardiorespiratory responses to fine particles during ambient PM2.5 pollution waves: findings from a randomized crossover trial in young healthy adults. *Environ Int* 139: 105590. <https://doi.org/10.1016/j.envint.2020.105590>
- Zhu Y, Tian F, Li H, Zhou Y, Lu J, Ge Q (2015) Profiling maternal plasma microRNA expression in early pregnancy to predict gestational diabetes mellitus. *Int J Gynaecol Obstet* 130:49–53. <https://doi.org/10.1016/j.ijo.2015.01.010>



The Full Chain Model: Linking Chemical Exposure from Indoor Sources to Human Health Effects

43

Anna-Sofia Preece, Huan Shu, and Carl-Gustaf Bornehag

Contents

Introduction	1302
The Full Chain Model	1303
The SELMA Study	1305
Chemical Exposure	1305
Airway Outcomes	1306
Applying SELMA Data to the Full Chain Model	1308
Environmental Exposure	1308
Human Exposure	1309
Health Effects	1313
Relevance of the Results	1316
Conclusions	1317
Cross-References	1317
References	1318

Abstract

There is an increasing concern for health risks from exposure to chemical emissions in indoor environments where we spend a lot of time. A chain of complex relationships connects emission sources, exposure, and health effects. For some indoor contaminants, we know a lot about the separate relationships. However, linking specific sources and environmental exposure pathways to

A.-S. Preece · H. Shu

Division of Public Health Sciences, Institution of Health Sciences, Karlstad University, Karlstad, Sweden

e-mail: anna-sofia.preece@kau.se; huan.shu@kau.se

C.-G. Bornehag (✉)

Division of Public Health Sciences, Institution of Health Sciences, Karlstad University, Karlstad, Sweden

Icahn School of Medicine at Mount Sinai, New York, NY, USA

e-mail: carl-gustaf.bornehag@kau.se

hazardous effects is challenging, with a lack of evidence that is needed for risk assessment as a result.

This chapter presents the full chain model that follows chemicals and maps the relationships from sources to potential health effects. It is a tool to establish relevant scientific knowledge regarding chemical exposure. The model consists of three overlapping sections: environmental exposure, human exposure, and health effects, and includes relationships between emission sources, environmental pathways, human uptake, and effects on health and development.

As a demonstration, results from the Swedish Environmental Longitudinal Mother and child Asthma and allergy (SELMA) study were applied to the full chain model. Phthalates, a group of abundant indoor contaminants, and airway disorders were used as an example. Starting with polyvinyl chloride (PVC) flooring as an emission source, connections were made between indoor dust levels, exposure and uptake among pregnant women, and airway symptoms in young children. By using the full chain model, not only separate relationships were identified. Butylbenzyl phthalate could be followed from a source to elevated environmental exposure and human uptake to associations with a higher risk for airway outcomes in children.

Keywords

Biomarkers · Dust · Human intake · Indoor exposure · Phthalates

Introduction

In modern society, we used to consider hazardous chemical exposure to mainly originate from industrial emissions and occupational environments. Increasingly, this framework has been replaced by concerns over the diffuse chemical emissions that we are all exposed to from our everyday activities and indoor spaces. In general, people spend 85% or more of their time indoors (Schweizer et al. 2007). A large number of chemicals can leach from building materials and consumer goods to indoor dust and air. This process means that we are almost continuously exposed to diffuse chemical mixtures in our homes, schools, offices, and hospitals (Salthammer et al. 2018).

To prevent hazardous exposure, we must determine the risk for effects on human health. Many scientific studies have investigated chemical exposure and its associations with adverse health effects. Their results provide valuable information. However, research tends to investigate separate relationships. Human exposure and resulting health effects depend on a chain of complex relationships, starting at the source from where the contaminant originated. Therefore, we lack evidence that allows us to predict what risk indoor sources and chemical emissions pose. Such information is vital for an adequate risk assessment.

This chapter presents the full chain model as an approach to establishing relevant scientific knowledge that addresses this knowledge gap. The model follows contaminants from source, over environmental exposure and human exposure, to health

effects (Preece 2021; Shu 2017). As a demonstration, results from the Swedish Environmental Longitudinal Mother and child Asthma and allergy (SELMA) study are applied to the full chain model. The example illustrates how phthalates can be followed from polyvinyl chloride (PVC) flooring through a chain of relationships connected to airway symptoms in young children.

The Full Chain Model

The full chain model (Fig. 1) depicts human chemical exposure by mapping relevant factors and their relationship. It can be employed to establish information on environmental contaminants that are needed for risk assessment (Preece 2021; Shu 2017) by facilitating the collection and evaluation of exposure data. It consists of three overlapping triangular sections that describe

- Environmental exposure
- Human exposure
- Health effects

The first section, environmental exposure is explained by the sources from where the contaminants originate and how they are released to the environment. Emitted contaminants can adhere to particles or evaporate into the air (Weschler et al. 2008). Indoor particles are either dust that is generally made up of particles that may become airborne but will eventually settle, or fine particles that remain airborne, so-called particulate matter (Weschler et al. 2008; WHO 1999). The emission

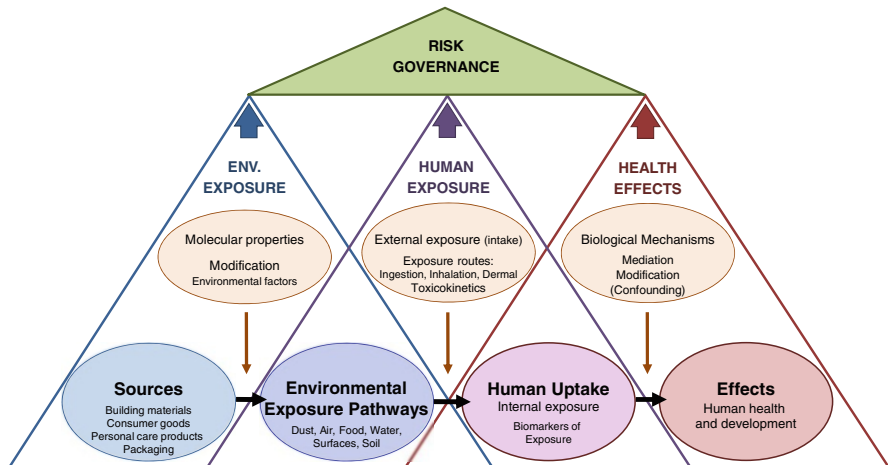


Fig. 1 The full chain model follows human chemical exposure from sources to potential health effects. The model is divided into three overlapping sections that describe relevant relationships for environmental exposure, human exposure, and health effects

process and environmental fate of a contaminant are affected by its molecular properties, such as molecular weight, volatility, and degree of water solubility (Weschler et al. 2008). Indoor physical conditions can also modify environmental exposure, such as temperature, humidity, and air exchange rate (Wei et al. 2018). The age and life cycle of the emission sources may also be relevant to consider. In the indoor environment, settled dust and air can become exposure pathways through which contaminants expose humans. Other exposure pathways include food, drink, personal care products, surfaces we touch, and soil.

The middle section of the full chain model is human exposure. It describes the interface between the environment and humans by linking environmental exposure to human uptake (internal exposure). Biomonitoring is frequently used to quantify chemical uptake in humans. It involves chemical analysis of biosamples such as blood or urine to detect the contaminant itself or markers of exposure (e.g., metabolites). These samples provide indirect information on the total uptake at a specific time point for the individual that provided the sample (Koch et al. 2012; Wittassek and Angerer 2008). The biomonitoring data represents the combined uptake from multiple sources and all pathways (such as diet, dust, air, and sometimes medical devices leaching directly to the blood) that the person was exposed to (Salthammer et al. 2018).

To understand how different sources and exposure pathways contribute to the total uptake of an indoor contaminant, we must have knowledge of the processes that result in human uptake. For uptake to occur, it must first have made contact with human tissue. In an indoor space, we are exposed through the routes of ingestion, inhalation, or dermal absorption, i.e., a person is exposed through the nose, mouth, or skin. This combination of processes is referred to as external exposure or intake (Zartarian et al. 2005). However, inhaling contaminated air or unintentionally ingesting contaminated dust may not always lead to absorption and uptake. Instead, a fraction of the contaminant is likely to be exhaled or excreted without being absorbed into the human tissue. Hence, external exposure (intake) may or may not result in the uptake of an indoor contaminant (Zartarian et al. 2005).

The processes that determine whether external exposure results in uptake depend on many parameters (Salthammer et al. 2018) that are summarized as exposure routes and toxicokinetics in the full chain model. Ingestion of dust particles is an exposure route that results in unintentional oral intake, where the contaminant is exposed to digestive processes and may be absorbed via the digestive tract. Inhalation results in the intake of contaminants in two forms, either in gas phase or adsorbed to airborne particles, i.e., the particulate phase. Gas-phase compounds and very small particles ($<5\text{ }\mu\text{m}$) can generally travel through the airways deep into the lung alveoli. There, contaminants may expose the lung tissue and contribute to uptake (Bølling et al. 2013; Salthammer et al. 2018). Our skin is in constant contact with the surrounding air, dust, and clothing and is permeable to various compounds. Toxicokinetics describes processes such as disposition, interactions, metabolism, and excretion of toxic compounds over time (Koch et al. 2012). A contaminant may be absorbed and distributed in tissues differently depending on whether the intake is oral, respiratory, or skin contact (Salthammer et al. 2018).

Bølling et al. (2013) suggest that tissues that serve as a barrier between environment and body, such as the airways, lungs, or skin, may be exposed to considerably higher concentrations of a contaminant than the exposure that can be detected in biomonitoring studies. Dust ingestion rates, inhalation rates, and dermal absorption rates can vary between infants, children, adults, pregnant women, and the elderly. Hence, individuals that spend the same time in the same indoor environment may be exposed differently to indoor contaminants (US Environmental Protection Agency [EPA] 2017).

The third section, health effects, associate chemical exposure to human health and developmental outcomes. Such relationships are generally deemed as noncausal because of the risk of confounding. However, if potential mediators or effect modifiers are included the observational data can be interpreted more toward causality.

The SELMA Study

The SELMA study is designed to investigate the importance of early life exposure to environmental factors during pregnancy and infancy, and their significance for health and development in children. The prospective pregnancy cohort follows approximately 2,000 mother-child pairs from early pregnancy over birth through childhood. Women were enrolled during early pregnancy (median tenth week of pregnancy) from 2007–2010. Data has been collected through questionnaires, environmental samples collected in the participant's homes, and biosampling of blood and urine from the participants. In brief, data on participant background information, home characteristics including flooring material, and health outcomes were acquired through self-administered questionnaires. Chemical exposure was assessed in dust samples collected in the participant's home and in blood and urine collected from the pregnant mothers and from the children. Serum was also analyzed for biomarkers of nicotine/tobacco use (cotinine) and urine for creatinine to allow for urine dilution adjustment. More details regarding the recruitment process, study design, and data collection can be found in Bornehag et al. (2012).

Chemical Exposure

Phthalates make up a group of inexpensive and versatile synthetic chemicals that are added to many building materials and large numbers of consumer goods. The leading use of phthalates is as plasticizers in plastic materials such as PVC, also known as vinyl (SCA 2015). Other uses include solvents, lubricants, thinners, and stabilizers (SCA 2015). Materials that may contain phthalates include plastics, rubber, synthetic leather, and textiles. The products include packaging, food containers, construction materials, sports and leisure equipment, toys, fabrics, footwear, clothes, carpets, electronics, paints, cleaning agents, personal care products, cosmetics, and fragrances (European Chemicals Agency [ECHA] 2021). Phthalates are

among the most well-studied group of semi-volatile indoor contaminants (Weschler et al. 2008). They do not bioaccumulate, instead phthalates are excreted and their half-lives in the human body range from a few hours to a few days, (Andersen et al. 2018; Koch et al. 2012). Still, the extensive use of phthalates results in continuous human exposure.

Concern for phthalate exposure to human health has been raised for over 40 years (Colborn et al. 1993). Experimental studies in cell and animal models and population-based epidemiological studies have provided evidence that links exposure to several phthalates to effects on human reproduction, neuro-development, and endocrine disruption (Bergman et al. 2013; Engel et al. 2021; Radke et al. 2018). Because of these concerns, restrictions have been imposed on several phthalates. However, not all use is regulated and new phthalates are continuously introduced as replacements (Bui et al. 2016). Environmental exposure to phthalates is mainly an indoor concern since the amounts in outdoor dust and air are magnitudes lower than indoors (Guo and Kannan 2011).

In SELMA, seven phthalates were analyzed in bedroom dust from 500 families. Dust samples collected twice; around week 25 of pregnancy (prenatally) and during infancy when the child was 6 months old (postnatally). Corresponding phthalate metabolites were quantified in urine samples collected from the pregnant mothers at enrolment. Phthalates and corresponding metabolites that were included in the chemical analysis are listed in Table 1.

Airway Outcomes

In the SELMA study we have studied wheeze and croup in the children. These outcomes were chosen as indicators of inflammatory responses in early age since asthma cannot be diagnosed in young children (Herzog and Cunningham-Rundles 2011). Wheeze is characterized by a high-pitched continuous sound caused by airway constriction. Wheeze is mainly caused by viral infections or asthma (Ducharme et al. 2014). Many children with early wheeze grow out of symptoms and have no further respiratory problems. However, early childhood wheeze is a risk factor for asthma development (Herzog and Cunningham-Rundles 2011). Croup (acute subglottic laryngitis) is characterized by airway inflammation and swelling of the upper airways that cause acute breathing difficulties and a barking cough. It mainly affects young children between 6 months and 3 years old (Mazurek et al. 2019). There may be a relationship between croup and asthma, but no clear link has been established (Bjornson and Johnson 2008; Mazurek et al. 2019; Pruijkken et al. 2009).

Environmental exposures including indoor contaminants and cleaning products have been suggested as contributing risk factors for respiratory outcomes such as asthma (Dallongeville et al. 2016; Parks and Takaro 2020; Stern et al. 2020). There are epidemiological reports of associations between phthalate exposure and asthma and other airway conditions. However, the results are not conclusive as reviewed by, e.g., Bølling et al. (2020) and Casas and Gascon (2020). Associations that separately link

Table 1 Names and CAS numbers of phthalates and corresponding metabolites included in chemical analysis of bedroom dust and pregnant mother's urine in the SELMA study

Dust analysis			Urine analysis		
Phthalate	Common name	CAS	Metabolite	Common name	CAS
DEP	Di-ethyl phthalate	84-66-2	MEP	Monoethyl phthalate	2306-33-4
DnBP	Di- <i>n</i> -butyl phthalate	84-74-2	MBP ^a	MnBP	Mono- <i>n</i> -butyl phthalate
DiBP	Di-iso-butyl phthalate	84-69-5		MiBP	Mono-iso-butyl phthalate
BBzP	Butylbenzyl phthalate	85-68-7	MBzP	Monobenzyl phthalate	2528-16-7
DEHP	Di-2-ethylhexyl phthalate	117-81-7	MEHP ^b	Mono-ethyl-hexyl phthalate	4376-20-9
			MEHHP	Mono-ethyl-hydroxyl-hexyl phthalate	40321-99-1
			MEOHP	Mono-ethyl-oxo-hexyl phthalate	40321-98-0
			MECPP	Mono-ethyl-carboxy-pentyl phthalate	40809-41-4
			MCMHP	Mono-carboxy-methyl-hexyl phthalate	82975-93-7
DiNP	Di-iso-nonyl phthalate	68515-48-0	MHINP ^b	Mono-hydroxy-iso-nonyl phthalate	936021-98-6
			MOiNP	Mono-oxo-iso-nonyl phthalate	936022-00-3
			MCiOP	Mono-carboxy-iso-octyl phthalate	936022-02-5
DiDP ^c	Di- <i>iso-decyl</i> phthalate	26761-40-0	MHiDP ^d	Mono-hydroxy-iso-decyl phthalate	31047-64-0
DPHP	Di-2-propylheptyl phthalate	53306-54-0	MCiNP ^d	Mono-carboxy-iso-nonyl phthalate	

^aMetabolites of DnBP and DiBP are difficult to distinguish in the chemical analysis. Therefore, their results are reported as MBP (Σ DBP)

^bSummary concentrations of DEHP and DiNP were calculated from the molar sum of the metabolites and the molecular weight of the corresponding parent phthalate (Σ DEHP and Σ DiNP, respectively)

^cNot included in chemical analysis of dust

^dMetabolite of both DiDP and DPHP

phthalate sources to environmental exposure, phthalates in dust and air to human uptake, or phthalates in dust and their metabolites in urine to airway outcomes are frequently reported. Despite this result, we still lack enough evidence to predict how phthalate exposure may affect children's airway health, and to what extent indoor phthalate sources and exposure contribute to the observed health effects.

Applying SELMA Data to the Full Chain Model

We now apply results from the SELMA study to the full chain model (Fig. 1). More specifically, we are demonstrating connections between PVC flooring as a source of indoor phthalate emission, exposure via dust, uptake, and the relationship to airway symptoms in young children.

Environmental Exposure

Sources of indoor phthalate emission include a great number of materials and consumer goods, where PVC plastics is dominant (SCA 2015). In the SELMA study, 25% of the families reported having PVC flooring in the parent's bedroom (Shu et al. 2019). Only wood and parquet were the more common flooring materials (43%), while laminate flooring was the third most common type of flooring (18%).

In the SELMA study, phthalates were analyzed in bedroom dust samples collected in 496 homes before and after birth of the child. Phthalates were abundant, with detection rates $\geq 90\%$. DEHP was dominant with geometric mean (GM) levels 102–131 $\mu\text{g/g}$ dust. Levels of diethyl phthalate (DEP) and di-2-propylheptyl phthalate (DPHP) were the lowest with GM levels between 1.3 and 1.9 $\mu\text{g/g}$ (Preece et al. 2022). The SELMA results are within the range of phthalate levels in residential indoor dust that have been reported by numerous other studies. DEHP is generally the most abundant phthalate detected in indoor dust from all countries, which reflects its domination of global plasticizer production and wide use in PVC plastic (Gao et al. 2018; SCA 2015). In dust collected in homes, median levels of DEHP ranged from around 100 $\mu\text{g/g}$ up to 1200 $\mu\text{g/g}$ as presented by a review of 94 studies that analyzed phthalate levels in indoor dust and/or air samples (Bu et al. 2020). For other phthalates, the results vary more between regions. For example, butylbenzyl phthalate (BBzP) is often the second most dominant phthalate in North American studies, while the abundance of BBzP varies in European countries, and the levels are low in most studies from Asia. Levels of DEP in dust are generally low in all countries, while it is more abundant in the air (Bu et al. 2020).

Dust is a frequently chosen matrix to estimate environmental contamination (Bu et al. 2020; Lucattini et al. 2018). Although it is a complex matrix, contaminants detected in dust provides an approximation of emissions to all available sources in a particular indoor space (Weschler et al. 2008). Phthalate concentrations in dust are strongly related to the available phthalate emission sources (Lucattini et al. 2018) and the total amount of emitted phthalates (Salthammer et al. 2018; Weschler et al. 2008). PVC flooring reported by the SELMA families was associated with higher levels of di-*n*-butyl phthalate (DnBP), BBzP, and diethylhexyl phthalate (DEHP) compared to other flooring materials (Fig. 2). Reports from other studies have linked PVC flooring to higher levels of several phthalates in homes, preschools, and offices (Bi et al. 2018; Christia et al. 2019; Larsson et al. 2017). The number of rooms with PVC flooring in a home has been reported to correlate with the levels of BBzP and DEHP in the dust (Bornehag et al. 2005).

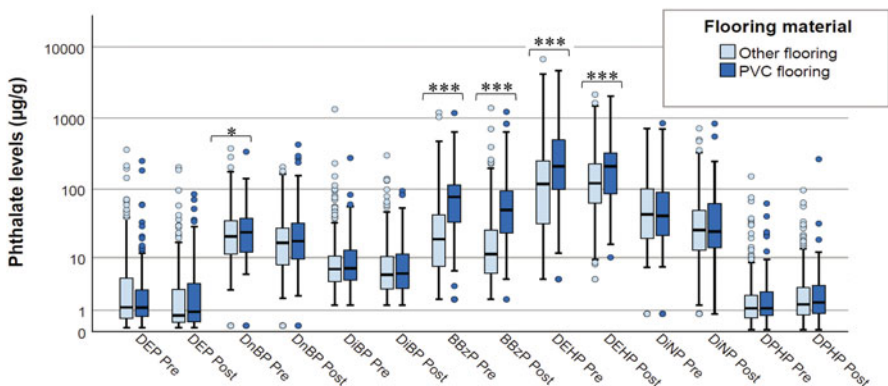


Fig. 2 Phthalate levels in dust ($\mu\text{g/g}$) collected during pregnancy (pre) or 6 months after birth (post) stratified for flooring material, shown on a \log_{10} scale. The flooring materials were categorized as “other than PVC” ($n = 378$) or “PVC” ($n = 118$). Levels below the limit of detection (LOD) were assigned a replacement value of $\text{LOD}/\sqrt{2}$. * $P < 0.05$, *** $P < 0.001$ for the difference between flooring materials

The results from the SELMA study show that phthalates are common contaminants in bedroom dust, and that PVC flooring acts as a source for phthalates in dust. Other published research results confirm these findings.

Human Exposure

Phthalates are metabolized fairly rapidly in the human body and measuring the resulting metabolites in urine serves as a method to quantify phthalate uptake (Wang et al. 2019; Wittassek and Angerer 2008). In SELMA, phthalate metabolite concentrations were also used to estimate the total phthalate intake followed by comparisons to phthalate intake from indoor dust.

Phthalate Metabolites in Urine

All pregnant SELMA mothers had detectable urinary levels of several phthalate metabolites, and in more than 98% of mothers all 13 analyzed metabolites were detectable (Shu et al. 2019). The DnBP and DiBP metabolites are difficult to distinguish in chemical analysis. Therefore, their results are reported as a sum denoted DBP. Crude- and creatinine-adjusted results revealed that GM concentrations of metabolites of DEP and DBP were dominant (37 and 33 nmol/mmol creatinine, respectively) and two orders of magnitude higher than two metabolites originating from either di-iso-decyl phthalate (DiDP) or DPHP which were the least abundant (0.41 and 0.21 nmol/mmol creatinine, respectively). In between, the GM concentration of the BBzP metabolite monobenzyl phthalate (MBzP) was 6.8 nmol/mmol creatinine (Shu et al. 2019). The data also reveals increasing or decreasing exposure trends over time, indicating that phthalate restrictions and replacement can make an impact on human uptake (Shu et al. 2018a).

A large number of biomonitoring studies reveal a ubiquitous phthalate exposure among all tested populations and age groups. However, exposure profiles vary a lot both within and between populations, as reviewed by, e.g., Lioy et al. (2015) and Wang et al. (2019). Pregnancy is a time when women might make changes to lifestyle and diet that could also affect their phthalate exposure. However, biomonitoring data suggest that exposure among pregnant women does not show any substantial difference compared to women in general (Lioy et al. 2015; Wang et al. 2019). The SELMA results are comparable to other studies that collected urine around the same time period (2007–2010). However, the concentration of BBzP in SELMA is higher than most other reports (Lioy et al. 2015; Preece et al. 2021a; Shu et al. 2019). One possible explanation is that PVC materials in the indoor environment may contribute to the BBzP exposure among these women.

Phthalate Metabolites in Urine and PVC Flooring

In the SELMA study, the relationship between urinary metabolite concentrations and PVC flooring was studied using general linear regression models adjusted for the mother's age, education, smoking, and urine creatinine (Shu et al. 2019). The results show that three metabolite concentrations from the parent compounds DBP ($P < 0.001$), BBzP ($P < 0.001$), and DEHP ($P < 0.05$) are higher in urine from women with PVC flooring in their homes when compared with women with other flooring materials. An increasing number of rooms with PVC flooring was associated with increasing concentrations of the metabolites. Hence, the results indicate that PVC flooring in the home makes a relevant contribution to BBzP uptake in pregnant women. Support for this finding can be found for pregnant women (Sugeng et al. 2020) and infants (Carlstedt et al. 2013).

Phthalates in Urine and Dust

When cross-sectional phthalate metabolites in urine and phthalate levels in dust were compared in SELMA ($n = 455$), a positive relationship was found for DEP, DnBP, di-iso-butyl phthalate (DiBP), and BBzP ($P < 0.001$). The relationship was strongest for BBzP (Pearson correlation coefficient $r = 0.37$). For DEHP, no significant correlation was found. The results indicate that dust and the home indoor environment is a relevant contributor to the total intake of phthalates, BBzP in particular. However, the intake of DEHP is more strongly influenced by other exposure routes (e.g., diet or other indoor environments than the home) (Preece et al. 2021b). Data on phthalates in urine and dust samples can be used further to estimate the total phthalate intake and the contribution to intake from the indoor environment.

Total Daily External Phthalate Exposure (Intake)

In SELMA, estimations of each woman's total daily external phthalate exposure (intake) were back-calculated from metabolite concentrations of five phthalates. Complete data on matched phthalates in dust, metabolites in urine, flooring material, and personal characteristics were available for 455 women (Preece et al. 2021b). The greatest total daily median intake was found for DEHP with 2.95 µg/kg body weight/day. It was of similar magnitude for DEP (2.16 µg/kg/day) and DBP (2.36 µg/kg/day).

For BBzP, it was an order of magnitude lower (0.54 µg/kg/day). For each phthalate, the total intake among the participants showed substantial variability (two to three orders of magnitude) although the interquartile range was within the same magnitude for all phthalates (Preece et al. 2021b). The SELMA intake estimations did not include di-isobutyl phthalate (DiNP) or DPHP due to less available experimental data to determine the parameters needed for intake modeling. The DPHP levels in dust were also very low which combined with its lower volatility would result in a low indoor-related intake.

Based on phthalate metabolite concentrations, several studies have estimated the total daily phthalate intake among adults in general and pregnant women (Wang et al. 2019). These estimations vary between different populations, as can be expected from the variation in phthalate metabolite concentrations. Reported total daily intakes of DEHP among women of reproductive age (including pregnant women) range between 1.5 and 4.1 µg/kg body weight/day (Ait Bamai et al. 2015; Liou et al. 2015; Sugeng et al. 2020). The result for the pregnant women in SELMA was within this range. The median total intakes are generally one or two orders of magnitude lower than authority guidance values (Wang et al. 2019). In the EU the tolerable daily intake (TDI) for DEHP is 50 µg/kg/day (Silano et al. 2019). However, individuals with exposure levels exceeding the 95th percentile of the population generally exceeded the tolerable daily phthalate intake (Wang et al. 2019). This exceedance was also the case in SELMA, where the TDI was exceeded for DBP and DEHP among the seven (1.5%) most highly exposed women (Preece et al. 2021b). The total phthalate intake can be compared to the intake explained by phthalates in the dust.

Intake from Dust and Contribution to Total Intake

Phthalate levels detected in the SELMA bedroom dust were used to estimate the phthalate intake through dust ingestion, inhalation, and dermal absorption at home using steady-state models based on the method described by Bekö et al. (2013). The SELMA study focused on phthalate intake over 13 h during which the pregnant women were expected to be at home (Schweizer et al. 2007). Phthalate intake from dust ingestion was estimated for 5 h only, during which the pregnant women were expected to be awake in their homes during the day. No dust ingestion was presumed to take place during sleep (EPA 2017). The results show that median indoor intake is the highest for DBP (640 ng/kg/day), followed by DEP (210 ng/kg/day), DEHP (200 ng/kg/day), and lowest for BBzP (12 ng/kg/day). Dermal absorption was the main indoor exposure route for DEP and DBP, dust ingestion and inhalation were most important for BBzP, and dust ingestion was the most relevant indoor exposure route for DEHP.

Compared to the total daily intakes (24 h), the indoor related intakes during 13 h at home are equivalent to relative contributions of 12% for DEP, 28% for DBP, 2.1% for BBzP, and 0.7% for DEHP (medians). For the most highly exposed that exceeded the TDI limit for DBP, the indoor-related intake in their homes made a meaningful contribution to this concerning intake (Preece et al. 2021b). The intake differences between women with PVC flooring or other flooring materials are shown in Fig. 3.

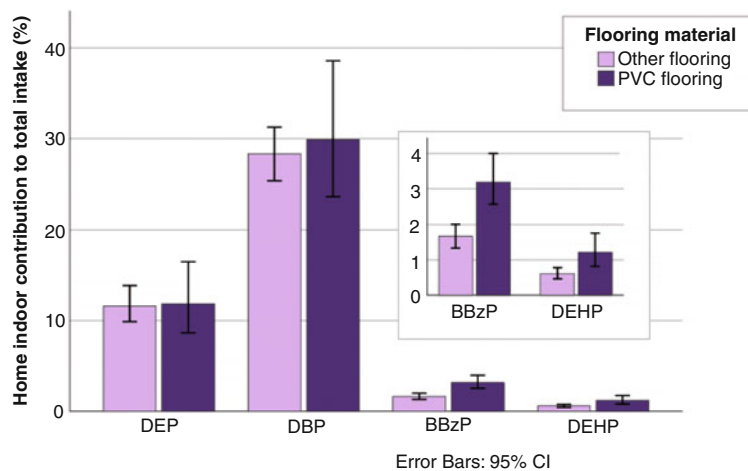


Fig. 3 Median intake contribution (%) to the total daily phthalate intake from dust ingestion, inhalation, and dermal absorption from the air during 13 h at home among 455 pregnant women with or without PVC flooring

For women with PVC bedroom flooring, the indoor contribution to intake of BBzP and DEHP was around twice as high compared to women with other flooring materials. However, the contribution to the total intake was marginal (1–2%). The flooring material had only minor effect on the intake contribution for DEP and ΣDBP (Preece et al. 2021b).

Previously, phthalate intake has been estimated from phthalate levels in residential dust, air, or both dust and air among adults in several studies. Phthalate intake from dust ingestion or air inhalation are generally estimated in these studies. A limited number of studies estimate dermal absorption of phthalates including Dodson et al. (2015); Li et al. (2021); Pelletier et al. (2017); Wang et al. (2014); and Zhu et al. (2019). Studies that estimate intake and include both measurements of environmental exposure and biomonitoring data are also limited. We identified four studies that estimated total daily phthalate intake and contributions from indoor exposure. One study included the exposure route dust ingestion only (Shi et al. 2021), while the other two also included inhalation and dermal absorption (Giovanoulis et al. 2018; Guo and Kannan 2011). Guo and Kannan (2011) compared the intake in China and the USA based on dust and urine measurements that were not collected from the same study populations (dust sample sizes were N = 33 and N = 75). The intake estimations were calculated from theoretical reference values for adults. Shi et al. (2021) compared dust ingestion to total daily intake based on dust, urine, and person-by-person data collected in the same study population of mothers to children aged 0–7 years (N = 47). Finally, Giovanoulis et al. (2018) used dust, air, urine, and person-by-person data that was collected in the same study population of adults (N = 61). A meta-analysis was conducted by Bu et al. (2020) where intake from the three exposure routes were estimated based on phthalate levels

in dust from 35 previous studies. SELMA is a relatively large cohort compared to other studies that analyze phthalate exposure in data from both dust and urine samples.

Generally, intakes are estimated over 24 h in other studies while the SELMA results are based on 13 h spent at home. Despite this, the SELMA results were generally close to or within the range of intakes reported elsewhere as results vary between one or two orders of magnitude for most phthalates and intake routes.

The current intake estimations performed in SELMA and other studies suggest that dermal absorption of DEP and DBP is dominant compared to dust ingestion and inhalation (Bu et al. 2020; Giovanoulis et al. 2018; Preece et al. 2021b). However, experimental studies on human subjects conclude that inhalation is comparable to or greater than the uptake from dermal absorption (Weschler et al. 2015; Andersen et al. 2018). Therefore, the dermal absorption of phthalates from the air might be overestimated and/or the inhalation intake underestimated by theoretical methods. Estimating intake requires knowledge of behavior in circulation, distribution in various tissues, metabolic pathways, and elimination/clearance processes (Koch et al. 2012; Salthammer et al. 2018). So far, the models are used to predict exposures as averages in larger populations, they are not precise enough to accurately predict intakes for individuals (Weschler et al. 2008). Increasing knowledge about these parameters will result in more precise estimations.

The results from the SELMA study show that dust can explain a relevant intake of DEP and DBP from the indoor environment. Analysis suggests that the indoor environment also makes a relevant contribution to the total uptake of some phthalates, particularly BBzP. Women with PVC flooring have a higher intake of BBzP and DEHP while analysis of uptake suggests DBP uptake can also be higher among women with PVC flooring. This result confirms the relationship between human exposure from indoor environment and human uptake. It also links a source of phthalate emission to human exposure.

Health Effects

Associations between phthalate exposure during pregnancy or phthalate levels in dust and two airway symptoms in young children were investigated in SELMA. The outcomes were wheeze or croup at 12 or 24 months of age.

Prenatal Phthalate Exposure

Three analyses explored associations between 13 metabolites from 8 parent phthalates (Table 1) in prenatal maternal urine and airway symptoms in their children. First, wheeze at 12 months of age was investigated. The prevalence of ever wheeze was 30% (23% of girls and 35% of boys). Some associations between metabolites of DiNP and ever wheeze were found, which were stronger among girls than boys (Shu et al. 2018b).

Second, one year later at 24 months of age, the prevalence of ever wheeze was 34% (27% of girls and 41% of boys). Associations and indications of a dose-

response relationships were found between metabolites of more high molecular weight DiDP and DPHP and wheeze (Preece et al. 2021a). No significant associations between DiNP metabolites and wheeze were found when the full study population was considered. In subgroup analyses, the associations between DiDP and DPHP metabolites and wheeze were stronger for boys than girls. Effects on wheeze among children whose parents reported not having (54%) or having (46%) asthma and/or rhinitis were also investigated. Wheeze was more common if parents did have asthma/rhinitis than if not (41% and 29%, respectively). Associations between metabolite concentrations and wheeze were stronger among the children whose parents did not suffer from asthma/rhinitis (Fig. 4). In this subgroup, there were further associations between wheeze and metabolites of BBzP and DiNP, with indications of dose-response relationships (Preece et al. 2021a).

Third, croup and associations with maternal metabolite concentrations were investigated at 12 months of age. The prevalence of ever croup was 10% (7% of girls and 12% of boys). Associations were found between ever croup and metabolites of BBzP and DEHP. The associations were stronger among boys (Shu et al. 2018b).

Other biomonitoring studies have also assessed associations between phthalate exposure of pregnant women and effects on children's health and development. Relating to airway conditions, metabolites of DBP, BBzP, and/or DEHP have been associated with asthma and wheeze in children aged 0–9 years in several studies with 145–1489 participants from Spain (Gascon et al. 2015), Germany (Jahreis et al. 2018), Taiwan (Ku et al. 2015), Poland (Podlecka et al. 2020), Ukraine, Greenland (Smit et al. 2015), and the USA (Whyatt et al. 2014). Adgent et al. (2020) found an adverse mixture effect among US children whose mothers did not have asthma, and Ait Bamai et al. (2018) found an association between DEHP and wheeze among Japanese girls but not boys. No effect on asthma was found among Danish children (Jøhnk et al. 2020). The number of reports including DiNP, DiDP, and DPHP in the

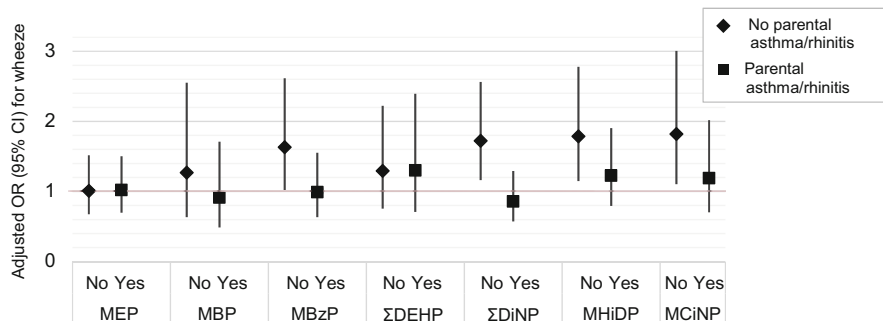


Fig. 4 Associations between prenatal phthalate exposure and infant wheeze (odds ratios with 95% CIs), stratified for parental asthma and/or rhinitis (N = 1148). Logistic regression models were adjusted for sex of the child, and mother's education, smoking, and creatinine in urine. Summary concentrations of DEHP and DiNP were calculated from the molar sum of the metabolites and the molecular weight of the corresponding parent phthalate

analysis were more limited. Prenatal concentrations of DiNP and DiDP metabolites were associated with decreasing lung function and increased risk of probable asthma among 5- to 7-year-olds (Berger et al. 2019; Vernet et al. 2017). However, contrasting results showing protective effects from higher concentrations of DiDP metabolites on asthma and wheeze among US children were reported by Adgent et al. (2020).

Differences in time points when prenatal exposure and the airway outcome were assessed may contribute to the contradictory results. Most studies analyzed urine collected during the third trimester of pregnancy. The first trimester of pregnancy represents the initial development of the fetal respiratory system and immune system, while the third trimester is characterized by tissue maturation (Nikolic et al. 2018; Pinkerton and Joad 2006). Today, our understanding of the distinct stages of early human development and possible critical exposure time windows is limited (Pinkerton and Joad 2006). The chosen outcome assessment time point is also relevant to consider. Effects from prenatal exposure combined with interaction from the postnatal environment and airway infections may influence the maturation of the airways that continue after birth (Driscoll et al. 2020; Nikolic et al. 2018; Pinkerton and Joad 2006). The effect of environmental phthalate exposure during early childhood is another question to investigate.

Phthalates in Dust

The relationship between environmental monitoring data and human health outcomes can be investigated; hence, linking the left and right sections of the full chain model. In SELMA, associations between seven phthalates in bedroom dust (Table 1) and the airway outcome croup were explored at 12 months of age. The prevalence of ever croup was 10% (6% of girls and 13% of boys). The results showed that higher levels of DEP and DEHP in dust were associated with croup. The associations were stronger for boys among which BBzP levels were also associated with croup (Preece et al. 2021c).

Phthalates in indoor dust and airway outcomes have been investigated in several other studies. Croup has not been used as an outcome, but wheeze and asthma have been associated with levels of DBP, BBzP, and/or DEHP among children aged 1–14 years in studies from North America and Europe (Bekö et al. 2015; Bornehag et al. 2004; Kolarik et al. 2008; Navaranjan et al. 2021). BBzP was associated with rhinitis and eczema but not asthma in children aged 3–9 years from Taiwan (Hsu et al. 2012). Two Japanese studies associated DnBP and DEHP with rhinoconjunctivitis, DiBP and BBzP with eczema, and DiBP and BBzP with atopic dermatitis but not to asthma in 0- to 14-year-old children (Ait Bamai et al. 2016; Ait Bamai et al. 2014). High molecular weight phthalates in the dust were associated with asthma and wheeze in Chinese children aged around 7 years (Zhang et al. 2021). Plastic wall materials or PVC flooring have been associated with wheeze and/or asthma in Finnish, Russian, and Swedish children aged 1–13 years (Jaakkola et al. 2004; Jaakkola et al. 2000; Larsson et al. 2010; Shu et al. 2014).

Hence, the associations between BBzP and DEHP in dust and an airway outcome in children found in SELMA have support in previous literature. However, an

association between DEP in dust and croup was also identified (Preece et al. 2021c). This finding has no substantial support since croup is not frequently used as an outcome to investigate phthalate exposure effects and associations between DEP and other airway conditions have not been reported by other studies.

Relevance of the Results

We have used the example of phthalates and airway symptoms, but we believe this model is a useful tool for collecting evidence of exposure from source to health effect for other indoor contaminants and health outcomes. There are many sources of other semi-volatile compounds in our indoor environments of relevance for human health, including brominated flame retardants, perfluorinated compounds, and organophosphates (Salthammer et al. 2018).

The SELMA results applied in the full chain model showed that an indoor source of phthalate emission, PVC flooring, makes a difference on the phthalate levels in the dust. In turn, this result has an effect on human uptake and children's airway symptoms. This approach allowed us to not only investigate separate associations, but to connect a number of relationships that are necessary to understand human exposure and its effects. One phthalate, BBzP, could be followed over the full chain of relationships, from source to association with airway outcomes in children. As previously described, support for these results of the separate links in the full chain model has been found in the scientific literature.

We analyzed one source, PVC flooring. This source was chosen as it has previously been linked to higher phthalate levels in indoor dust (Bornehag et al. 2005). PVC flooring materials are relevant to investigate since they are durable and may remain in use in people's homes for a considerable time, hence acting as a permanent emission source throughout their long use (Swedish Chemical Agency [SCA] 2015; Wormuth et al. 2006). The current results suggest that the indoor environment makes a relevant, but not dominating, contribution to the total phthalate intake among pregnant women. The intake is fairly low for the majority, but for the most highly exposed, the contribution was concerning. Introducing measures to reduce exposure for this group is particularly important. Collecting more data on parameters that modify environmental exposure will provide more robust results. They include temperature, phthalate degradation, relative humidity, air exchange rate, and composition of dust (Bope et al. 2019; Salthammer et al. 2018; Wei et al. 2018; Weiss et al. 2018; Weschler et al. 2008).

Assessing chemical exposure in early life is relevant, since early development modulation may persist and contribute to adverse health effects later in life (DeWitt and Patil 2018; Grandjean et al. 2019). We still need to learn more about how the observed early childhood effects relate to long-term airway health and asthma development. The airway outcomes wheeze, croup, and asthma can rarely be explained by one simple cause. Instead, genetic and environmental factors interact during disease development (Herzog and Cunningham-Rundles 2011). As there are no cures, prevention is vital to reduce suffering and societal cost (Mukherjee et al. 2016).

Identifying and reducing exposure to modifiable environmental risk factors could make a meaningful contribution to preventive strategies (Beasley et al. 2015). Factors to consider that are not explicitly mentioned in the full chain model include the time points of exposure and health outcome assessment. Also, chemical mixture effects can influence associations between exposure and outcomes.

Reducing airway disease is part of the work to ensure health and well-being for all, the third of the 17 sustainable development goals in Agenda 2030 of the United Nations (UN) (United Nations [UN] 2015). The results from SELMA suggest that the risk for airway conditions associated with phthalates in dust and air is quite low for the individual child. However, airway disease is common, so limiting indoor phthalate sources and exposure during early human development may reduce a harmful exposure and benefit overall public health. Gaining a more complete picture of chemical exposure, as proposed in the full chain model, will also contribute to achieve the 12th sustainable development goal on consumption and production patterns. Specifically, subgoal 12.4 states that we must achieve an environmentally sound management of chemicals and reduce release in order to minimize impacts on human health (UN 2015). Competence in various fields such as chemistry, engineering, toxicology, epidemiology, biostatistics, medicine, etc. is needed to understand human exposure to indoor contaminants (Salthammer et al. 2018). To provide relevant input for risk assessment, establishment of strong interdisciplinary approaches are necessary. The full chain model is a tool that can facilitate such work. It may also be used to connect existing results from different studies and to identify research gaps.

Conclusions

In this chapter, we applied results from one cohort study to the full chain model. This example allowed us to link indoor exposure from source to health effects. We found that one source, PVC flooring, made an impact on the levels of several phthalates in indoor dust, which was linked to a higher phthalate uptake among pregnant women, which was further associated with wheeze in young children. Phthalates in dust were also associated with croup during infancy.

These results are concordant with results from other studies. However, more knowledge and a better understanding of various environmental and biological modifying factors would make the results more robust. The full chain model approach can facilitate the acquiring of evidence that is necessary for adequate risk governance and the development of strategies to reduce hazardous chemical exposure in our indoor environments.

Cross-References

- ▶ [Application of Biomarkers in Assessing Health Risk of Indoor Air Pollutants](#)
- ▶ [Disease Burden of Indoor Air Pollution](#)

- Sampling and Analysis of Semi-volatile Organic Compounds (SVOCs) in Indoor Environments
- Semi-volatile Organic Compounds (SVOCs)
- Source/Sink Characteristics of SVOCs

References

- Adgent MA, Carroll KN, Hazlehurst MF, Loftus CT, Szpiro AA, Karr CJ, Barrett ES, LeWinn KZ, Bush NR, Tylavsky FA, Kannan K, Sathyarayana S (2020) A combined cohort analysis of prenatal exposure to phthalate mixtures and childhood asthma. *Environ Int* 143:105970. <https://doi.org/10.1016/j.envint.2020.105970>
- Ait Bamai Y, Araki A, Kawai T, Tsuboi T, Saito I, Yoshioka E, Kanazawa A, Tajima S, Shi C, Tamakoshi A, Kishi R (2014) Associations of phthalate concentrations in floor dust and multi-surface dust with the interior materials in Japanese dwellings. *Sci Total Environ* 468–469: 147–157. <https://doi.org/10.1016/j.scitotenv.2013.07.107>
- Ait Bamai Y, Araki A, Kawai T, Tsuboi T, Yoshioka E, Kanazawa A, Cong S, Kishi R (2015) Comparisons of urinary phthalate metabolites and daily phthalate intakes among Japanese families. *Int J Hyg Environ Health* 218(5):461–470. <https://doi.org/10.1016/j.ijheh.2015.03.013>
- Ait Bamai Y, Araki A, Kawai T, Tsuboi T, Saito I, Yoshioka E, Cong S, Kishi R (2016) Exposure to phthalates in house dust and associated allergies in children aged 6–12 years. *Environ Int* 96: 16–23. <https://doi.org/10.1016/j.envint.2016.08.025>
- Ait Bamai Y, Miyashita C, Araki A, Nakajima T, Sasaki S, Kishi R (2018) Effects of prenatal di (2-ethylhexyl) phthalate exposure on childhood allergies and infectious diseases: the Hokkaido study on environment and Children's health. *Sci Total Environ* 618:1408–1415. <https://doi.org/10.1016/j.scitotenv.2017.09.270>
- Andersen C, Krais AM, Eriksson AC, Jakobsson J, Londahl J, Nielsen J, Lindh CH, Pagels J, Gudmundsson A, Wierzbicka A (2018) Inhalation and dermal uptake of particle and gas-phase phthalates: a human exposure study. *Environ Sci Technol* 52(21):12792–12800. <https://doi.org/10.1021/acs.est.8b03761>
- Beasley R, Semprini A, Mitchell EA (2015) Risk factors for asthma: is prevention possible? *Lancet* 386(9998):1075–1085. [https://doi.org/10.1016/s0140-6736\(15\)00156-7](https://doi.org/10.1016/s0140-6736(15)00156-7)
- Bekö G, Weschler CJ, Langer S, Callesen M, Toftum J, Clausen G (2013) Children's phthalate intakes and resultant cumulative exposures estimated from urine compared with estimates from dust ingestion, inhalation and dermal absorption in their homes and daycare centers. *PLoS One* 8(4):e62442. <https://doi.org/10.1371/journal.pone.0062442>
- Bekö G, Callesen M, Weschler CJ, Toftum J, Langer S, Sigsgaard T, Host A, Kold Jensen T, Clausen G (2015) Phthalate exposure through different pathways and allergic sensitization in preschool children with asthma, allergic rhinoconjunctivitis and atopic dermatitis. *Environ Res* 137:432–439. <https://doi.org/10.1016/j.envres.2015.01.012>
- Berger K, Eskenazi B, Balmes J, Kogut K, Holland N, Calafat AM, Harley KG (2019) Prenatal high molecular weight phthalates and bisphenol A, and childhood respiratory and allergic outcomes. *Pediatr Allergy Immunol* 30(1):36–46. <https://doi.org/10.1111/pai.12992>
- Bergman Å, Heindel JJ, Jobling S, Kidd K, Zoeller TR (2013) State of the science of endocrine disrupting chemicals 2012: summary for decision-makers. World Health Organization, United Nations Environment Programme, Inter-Organization Programme for the Sound Management of Chemicals. <https://apps.who.int/iris/handle/10665/78102>
- Bi C, Maestre JP, Li H, Zhang G, Givehchi R, Mahdavi A, Kinney KA, Siegel J, Horner SD, Xu Y (2018) Phthalates and organophosphates in settled dust and HVAC filter dust of U.S. low-income homes: association with season, building characteristics, and childhood asthma. *Environ Int* 121(Pt 1):916–930. <https://doi.org/10.1016/j.envint.2018.09.013>

- Bjornson CL, Johnson DW (2008) Croup. Lancet 371(9609):329–339. [https://doi.org/10.1016/S0140-6736\(08\)60170-1](https://doi.org/10.1016/S0140-6736(08)60170-1)
- Bølling AK, Holme JK, Bornehag C-G, Nygaard UC, Bertelsen RJ, Nånerg E, Bodin J, Sakhi AK, Thomsen C, Becher R (2013) Pulmonary phthalate exposure and asthma—is PPAR a plausible mechanistic link? EXCLI J 12:733–759. <https://www.ncbi.nlm.nih.gov/pmc/articles/PMC4662182/?report=reader>
- Bølling AK, Sripada K, Becher R, Bekö G (2020) Phthalate exposure and allergic diseases: review of epidemiological and experimental evidence. Environ Int 139:105706. <https://doi.org/10.1016/j.envint.2020.105706>
- Bope A, Haines SR, Hegarty B, Weschler CJ, Peccia J, Dannemiller KC (2019) Degradation of phthalate esters in floor dust at elevated relative humidity. Environ Sci Process Impacts 21(8): 1268–1279. <https://doi.org/10.1039/c9em00050j>
- Bornehag CG, Sundell J, Weschler CJ, Sigsgaard T, Lundgren B, Hasselgren M, Hagerhed-Engman L (2004) The association between asthma and allergic symptoms in children and phthalates in house dust: a nested case-control study. Environ Health Perspect 112(14):1393–1397. <https://doi.org/10.1289/ehp.7187>
- Bornehag CG, Lundgren B, Weschler CJ, Sigsgaard T, Hagerhed-Engman L, Sundell J (2005) Phthalates in indoor dust and their association with building characteristics. Environ Health Perspect 113(10):1399–1404. <https://doi.org/10.1289/ehp.7809>
- Bornehag CG, Moniruzzaman S, Larsson M, Lindström CB, Hasselgren M, Bodin A, von Kobyletzkic LB, Carlstedt F, Lundin F, Nånerg E, Jönsson BA, Sigsgaard T, Janson S (2012) The SELMA study: a birth cohort study in Sweden following more than 2000 mother-child pairs. Paediatr Perinat Epidemiol 26(5):456–467. <https://doi.org/10.1111/j.1365-3016.2012.01314.x>
- Bu SB, Wang YL, Wang HY, Wang F, Tan YF (2020) Analysis of global commonly-used phthalates and non-dietary exposure assessment in indoor environment. Build Environ 177. <https://doi.org/10.1016/j.buildenv.2020.106853>
- Bui TT, Giovanoulis G, Cousins AP, Magner J, Cousins IT, de Wit CA (2016) Human exposure, hazard and risk of alternative plasticizers to phthalate esters. Sci Total Environ 541:451–467. <https://doi.org/10.1016/j.scitotenv.2015.09.036>
- Carlstedt F, Jönsson B, Bornehag CG (2013) PVC flooring is related to human uptake of phthalates in infants. Indoor Air 23(1):32–39. <https://doi.org/10.1111/j.1600-0668.2012.00788.x>
- Casas M, Gascon M (2020) Prenatal exposure to endocrine-disrupting chemicals and asthma and allergic diseases. J Investig Allergol Clin Immunol 30(4):215–228. <https://doi.org/10.18176/jiaci.0580>
- Christia C, Poma G, Harrad S, de Wit CA, Sjostrom Y, Leonards P, Lamoree M, Covaci A (2019) Occurrence of legacy and alternative plasticizers in indoor dust from various EU countries and implications for human exposure via dust ingestion and dermal absorption. Environ Res 171: 204–212. <https://doi.org/10.1016/j.envres.2018.11.034>
- Colborn T, vom Saal FS, Soto AM (1993) Developmental effects of endocrine-disrupting chemicals in wildlife and humans. Environ Health Perspect 101(5):378–384. <https://doi.org/10.1289/ehp.93101378>
- Dallongeville A, Costet N, Zmirou-Navier D, Le Bot B, Chevrier C, Deguen S, Annesi-Maesano I, Blanchard O (2016) Volatile and semi-volatile organic compounds of respiratory health relevance in French dwellings. Indoor Air 26(3):426–438. <https://doi.org/10.1111/ina.12225>
- DeWitt JC, Patasil HB (2018) Endocrine disruptors and the developing immune system. Curr Opin Toxicol 10:31–36. <https://doi.org/10.1016/j.cotox.2017.12.005>
- Dodson RE, Camann DE, Morello-Frosch R, Brody JG, Rudel RA (2015) Semivolatile organic compounds in homes: strategies for efficient and systematic exposure measurement based on empirical and theoretical factors. Environ Sci Technol 49(1):113–122. <https://doi.org/10.1021/es502988r>
- Driscoll AJ, Arshad SH, Bont L, Brunwasser SM, Cherian T, Englund JA, Fell DB, Hammitt LL, Hartert TV, Innis BL, Karron RA, Langley GE, Mulholland EK, Munywoki PK, Nair H, Ortiz JR, Savitz DA, Scheltema NM, Simoes EAF, Feikin DR (2020) Does respiratory syncytial virus

- lower respiratory illness in early life cause recurrent wheeze of early childhood and asthma? Critical review of the evidence and guidance for future studies from a World Health Organization-sponsored meeting. *Vaccine* 38(11):2435–2448. <https://doi.org/10.1016/j.vaccine.2020.01.020>
- Ducharme FM, Tse SM, Chauhan B (2014) Diagnosis, management, and prognosis of preschool wheeze. *Lancet* 383(9928):1593–1604. [https://doi.org/10.1016/S0140-6736\(14\)60615-2](https://doi.org/10.1016/S0140-6736(14)60615-2)
- Engel SM, Patisaul HB, Brody C, Hauser R, Zota AR, Bennet DH, Swanson M, Whyatt RM (2021) Neurotoxicity of ortho-phthalates: recommendations for critical policy reforms to protect brain development in children. *Am J Public Health* 111(4):687–695. <https://doi.org/10.2105/AJPH.2020.306014>
- European Chemicals Agency (ECHA) (2021) Substance Infocard – uses and formulation. <https://echa.europa.eu/substance-information/-/substanceinfo/100.001.409>
- Gao D, Li Z, Wang H, Liang H (2018) An overview of phthalate acid ester pollution in China over the last decade: environmental occurrence and human exposure. *Sci Total Environ* 645: 1400–1409. <https://doi.org/10.1016/j.scitotenv.2018.07.093>
- Gascon M, Casas M, Morales E, Valvi D, Ballesteros-Gomez A, Luque N, Rubio S, Monfort N, Ventura R, Martinez D, Sunyer J, Vrijheid M (2015) Prenatal exposure to bisphenol A and phthalates and childhood respiratory tract infections and allergy. *J Allergy Clin Immunol* 135(2): 370–378. <https://doi.org/10.1016/j.jaci.2014.09.030>
- Giovanoulis G, Bui T, Xu F, Papadopoulou E, Padilla-Sanchez JA, Covaci A, Haug LS, Cousins AP, Magner J, Cousins IT, de Wit CA (2018) Multi-pathway human exposure assessment of phthalate esters and DINCH. *Environ Int* 112:115–126. <https://doi.org/10.1016/j.envint.2017.12.016>
- Grandjean P, Abdennebi-Najar L, Barouki R, Cranor CF, Etzel RA, Gee D, Heindel JJ, Hougaard KS, Hunt P, Nawrot TS, Prins GS, Ritz B, Soffritti M, Sunyer J, Weihe P (2019) Timescales of developmental toxicity impacting on research and needs for intervention. *Basic Clin Pharmacol Toxicol* 125:70–80. <https://doi.org/10.1111/bcpt.13162>
- Guo Y, Kannan K (2011) Comparative assessment of human exposure to phthalate esters from house dust in China and the United States. *Environ Sci Technol* 45(8):3788–3794. <https://doi.org/10.1021/es2002106>
- Herzog R, Cunningham-Rundles S (2011) Pediatric asthma: natural history, assessment, and treatment. *Mt Sinai J Med* 78(5):645–660. <https://doi.org/10.1002/msj.20285>
- Hsu NY, Lee CC, Wang JY, Li YC, Chang HW, Chen CY, Bornehag CG, Wu PC, Sundell J, Su HJ (2012) Predicted risk of childhood allergy, asthma, and reported symptoms using measured phthalate exposure in dust and urine. *Indoor Air* 22(3):186–199. <https://doi.org/10.1111/j.1600-0668.2011.00753.x>
- Jaakkola JJ, Verkasalo PK, Jaakkola N (2000) Plastic wall materials in the home and respiratory health in young children. *Am J Public Health* 90(5):797–799. <https://doi.org/10.2105/ajph.90.5.797>
- Jaakkola JJ, Parise H, Kislitsin V, Lebedeva NI, Spengler JD (2004) Asthma, wheezing, and allergies in Russian schoolchildren in relation to new surface materials in the home. *Am J Public Health* 94(4):560–562. <https://doi.org/10.2105/ajph.94.4.560>
- Jahreis S, Trump S, Bauer M, Bauer T, Thurmann L, Feltens R, Wang Q, Gu L, Grutzmann K, Roder S, Averbeck M, Weichenhan D, Plass C, Sack U, Borte M, Dubourg V, Schuurmann G, Simon JC, von Bergen M, Polte T (2018) Maternal phthalate exposure promotes allergic airway inflammation over 2 generations through epigenetic modifications. *J Allergy Clin Immunol* 141(2):741–753. <https://doi.org/10.1016/j.jaci.2017.03.017>
- Jøhnk C, Host A, Husby S, Schoeters G, Timmermann CAG, Kyhl HB, Beck IH, Andersson AM, Frederiksen H, Jensen TK (2020) Maternal phthalate exposure and asthma, rhinitis and eczema in 552 children aged 5 years: a prospective cohort study. *Environ Health* 19(1):32. <https://doi.org/10.1186/s12940-020-00586-x>

- Koch HM, Christensen KLY, Harth V, Lorber M, Brüning T (2012) Di-n-butyl phthalate (DnBP) and diisobutyl phthalate (DiBP) metabolism in a human volunteer after single oral doses. *Arch Toxicol* 86(12):1829–1839. <https://doi.org/10.1007/s00204-012-0908-1>
- Kolarik B, Naydenov K, Larsson M, Bornehag CG, Sundell J (2008) The association between phthalates in dust and allergic diseases among Bulgarian children. *Environ Health Perspect* 116(1):98–103. <https://doi.org/10.1289/ehp.10498>
- Ku HY, Su PH, Wen HJ, Sun HL, Wang CJ, Chen HY, Jaakkola JJ, Wang SL, Tmics Group (2015) Prenatal and postnatal exposure to phthalate esters and asthma: a 9-year follow-up study of a Taiwanese birth cohort. *PLoS One* 10(4):e0123309. <https://doi.org/10.1371/journal.pone.0123309>
- Larsson M, Hagerhed-Engman L, Kolarik B, James P, Lundin F, Janson S, Sundell J, Bornehag CG (2010) PVC – as flooring material – and its association with incident asthma in a Swedish child cohort study. *Indoor Air* 20(6):494–501. <https://doi.org/10.1111/j.1600-0668.2010.00671.x>
- Larsson K, Lindh CH, Jönsson BA, Giovanoulis G, Bibi M, Bottai M, Bergstrom A, Berglund M (2017) Phthalates, non-phthalate plasticizers and bisphenols in Swedish preschool dust in relation to children's exposure. *Environ Int* 102:114–124. <https://doi.org/10.1016/j.envint.2017.02.006>
- Li X, Zhang WP, Lv JP, Liu WX, Sun SW, Guo CS, Xu J (2021) Distribution, source apportionment, and health risk assessment of phthalate esters in indoor dust samples across China. *Environ Sci Europe* 33(1). <https://doi.org/10.1186/s12302-021-00457-3>
- Lioy PJ, Hauser R, Gennings C, Koch HM, Mirkes PE, Schwetz BA, Kortenkamp A (2015) Assessment of phthalates/phthalate alternatives in children's toys and childcare articles: review of the report including conclusions and recommendation of the chronic hazard advisory panel of the consumer product safety commission. *J Expo Sci Environ Epidemiol* 25(4):343–353. <https://doi.org/10.1038/jes.2015.33>
- Lucattini L, Poma G, Covaci A, de Boer J, Lamoree MH, Leonards PEG (2018) A review of semi-volatile organic compounds (SVOCs) in the indoor environment: occurrence in consumer products, indoor air and dust. *Chemosphere* 201:466–482. <https://doi.org/10.1016/j.chemosphere.2018.02.161>
- Mazurek H, Breborowicz A, Doniec Z, Emeryk A, Krenke K, Kulus M, Zielnik-Jurkiewicz B (2019) Acute subglottic laryngitis: etiology, epidemiology, pathogenesis and clinical picture. *Adv Respir Med* 87(5):308–316. <https://doi.org/10.5603/ARM.2019.0056>
- Mukherjee M, Stoddart A, Gupta RP, Nwariu BI, Farr A, Heaven M, Fitzsimmons D, Bandyopadhyay A, Aftab C, Simpson CR, Lyons RA, Fischbacher C, Dibben C, Shields MD, Phillips CJ, Strachan DP, Davies GA, McKinstry B, Sheikh A (2016) The epidemiology, healthcare and societal burden and costs of asthma in the UK and its member nations: analyses of standalone and linked national databases. *BMC Med* 14(1):113. <https://doi.org/10.1186/s12916-016-0657-8>
- Navarajan G, Diamond ML, Harris SA, Jantunen LM, Bernstein S, Scott JA, Takaro TK, Dai R, Lefebvre DL, Azad MB, Becker AB, Mandhane PJ, Moraes TJ, Simons E, Turvey SE, Sears MR, Subbarao P, Brook JR (2021) Early life exposure to phthalates and the development of childhood asthma among Canadian children. *Environ Res* 197:110981. <https://doi.org/10.1016/j.envres.2021.110981>
- Nikolic MZ, Sun D, Rawlins EL (2018) Human lung development: recent progress and new challenges. *Development* 145(16):dev163485. <https://doi.org/10.1242/dev.163485>
- Parks J, Takaro TK (2020) Exposure to cleaning products and childhood asthma: more than just a link? *Expert Rev Respir Med* 14(12):1185–1188. <https://doi.org/10.1080/17476348.2020.1813572>
- Pelletier M, Bonvallot N, Ramalho O, Mandin C, Wei W, Raffy G, Mercier F, Blanchard O, Le Bot B, Glorenne P (2017) Indoor residential exposure to semivolatile organic compounds in France. *Environ Int* 109:81–88. <https://doi.org/10.1016/j.envint.2017.08.024>

- Pinkerton KE, Joad JP (2006) Influence of air pollution on respiratory health during perinatal development. *Clin Exp Pharmacol Physiol* 33(3):269–272. <https://doi.org/10.1111/j.1440-1681.2006.04357.x>
- Podlecka D, Gromadzinska J, Mikolajewska K, Fijalkowska B, Stelmach I, Jerzynska J (2020) Longitudinal effect of phthalates exposure on allergic diseases in children. *Ann Allergy Asthma Immunol* 125(1):84–89. <https://doi.org/10.1016/j.anai.2020.03.022>
- Preece A-S (2021) Phthalates: a full chain story: connecting phthalate sources, indoor dust, human intake, and airway symptoms in children (publication number 2021:29) Karlstad University, Sweden. <http://urn.kb.se/resolve?urn=urn:nbn:se:kau:diva-86337>
- Preece AS, Knutz M, Lindh CH, Bornehag CG, Shu H (2021a) Prenatal phthalate exposure and early childhood wheeze in the SELMA study. *J Expo Sci Environ Epidemiol*. <https://doi.org/10.1038/s41370-021-00382-w>
- Preece AS, Shu H, Knutz M, Krais AM, Bekö G, Bornehag CG (2021b) Indoor phthalate exposure and contributions to total intake among pregnant women in the SELMA study. *Indoor Air* 31(5): 1495–1508. <https://doi.org/10.1111/ina.12813>
- Preece AS, Shu H, Knutz M, Krais AM, Wikström S, Bornehag CG (2021c) Phthalate levels in indoor dust and associations to croup in the SELMA study. *J Expo Sci Environ Epidemiol* 31(2): 257–265. <https://doi.org/10.1038/s41370-020-00264-7>
- Preece AS, Shu H, Knutz M, Krais AM, Bornehag CG (2022) Phthalate levels in prenatal and postnatal bedroom dust in the SELMA study. *Environ Res* 113429. <https://doi.org/10.1016/j.envres.2022.113429>
- Pruikonen H, Dunder T, Renko M, Pokka T, Uhari M (2009) Risk factors for croup in children with recurrent respiratory infections: a case-control study. *Paediatr Perinat Epidemiol* 23(2): 153–159. <https://doi.org/10.1111/j.1365-3016.2008.00986.x>
- Radke EG, Braun JM, Meeker JD, Cooper GS (2018) Phthalate exposure and male reproductive outcomes: a systematic review of the human epidemiological evidence. *Environ Int* 121 (Pt 1):764–793. <https://doi.org/10.1016/j.envint.2018.07.029>
- Salthammer T, Zhang Y, Mo J, Koch HM, Weschler CJ (2018) Assessing human exposure to organic pollutants in the indoor environment. *Angew Chem Int Ed Engl* 57(38):12228–12263. <https://doi.org/10.1002/anie.201711023>
- Schweizer C, Edwards RD, Bayer-Oglesby L, Gauderman WJ, Ilacqua V, Jantunen MJ, Lai HK, Nieuwenhuijsen M, Kunzli N (2007) Indoor time-microenvironment-activity patterns in seven regions of Europe. *J Expo Sci Environ Epidemiol* 17(2):170–181. <https://doi.org/10.1038/sj.jes.7500490>
- Shi Y, Liu X, Xie Q, Pan XF, Mei Z (2021) Plastic additives and personal care products in South China house dust and exposure in child-mother pairs. *Environ Pollut* 281:116347. <https://doi.org/10.1016/j.envpol.2020.116347>
- Shu H (2017) Phthalates: on the issue of sources, human uptake, time trends and health effects. Karlstad University, Sweden. DiVA, id: diva2:1131172. Sweden. <http://urn.kb.se/resolve?urn=urn:nbn:se:kau:diva-62637>
- Shu H, Jönsson BA, Larsson M, Nänberg E, Bornehag CG (2014) PVC flooring at home and development of asthma among young children in Sweden, a 10-year follow-up. *Indoor Air* 24(3):227–235. <https://doi.org/10.1111/ina.12074>
- Shu H, Jönsson BA, Gennings C, Svensson A, Nänberg E, Lindh CH, Knutz M, Takaro TK, Bornehag CG (2018a) Temporal trends of phthalate exposures during 2007–2010 in Swedish pregnant women. *J Expo Sci Environ Epidemiol* 28(5):437–447. <https://doi.org/10.1038/s41370-018-0020-6>
- Shu H, Wikström S, Jönsson BAG, Lindh CH, Svensson A, Nänberg E, Bornehag CG (2018b) Prenatal phthalate exposure was associated with croup in Swedish infants. *Acta Paediatr* 107(6): 1011–1019. <https://doi.org/10.1111/apa.14245>
- Shu H, Jönsson BAG, Gennings C, Lindh CH, Nänberg E, Bornehag CG (2019) PVC flooring at home and uptake of phthalates in pregnant women. *Indoor Air* 29(1):43–54. <https://doi.org/10.1111/ina.12508>

- Silano V, Baviera JMB, Bolognesi C, Chesson A, Cocconcelli PS, Crebelli R, Gott DM, Grob K, Lampi E, Mortensen A, Riviere G, Steffensen IL, Tlustos C, Van Loveren H, Vernis L, Zorn H, Cravedi JP, Fortes C, Pocas MDT, Enzyme EPFCM (2019) Update of the risk assessment of di-butylphthalate (DBP), butyl-benzyl-phthalate (BBP), bis(2-ethylhexyl)phthalate (DEHP), di-isonylphthalate (DINP) and di-isodecylphthalate (DIDP) for use in food contact materials. *EFSA J* 17(12). <https://doi.org/10.2903/j.efsa.2019.5838>
- Smit LAM, Lengers V, Hoyer BB, Lindh CH, Pedersen HS, Liermontova I, Jonsson BAG, Piersma AH, Bonde JP, Toft G, Vermeulen R, Heederik D (2015) Prenatal exposure to environmental chemical contaminants and asthma and eczema in school-age children. *Allergy* 70(6):653–660. <https://doi.org/10.1111/all.12605>
- Stern J, Pier J, Litonjua AA (2020) Asthma epidemiology and risk factors. *Semin Immunopathol* 42(1):5–15. <https://doi.org/10.1007/s00281-020-00785-1>
- Sugeng EJ, Symeonides C, O'Hely M, Vuillermin P, Sly PD, Vijayasarathy S, Thompson K, Pezic A, Mueller JF, Ponsonby AL, Barwon Infant Study Investigator Group (2020) Predictors with regard to ingestion, inhalation and dermal absorption of estimated phthalate daily intakes in pregnant women: the Barwon infant study. *Environ Int* 139:105700. <https://doi.org/10.1016/j.envint.2020.105700>
- Swedish Chemical Agency (SCA) (2015) Phthalates which are toxic for reproduction and endocrine-disrupting: proposals for a phase-out in Sweden (Report 4/15). <https://www.kemi.se/publikationer/rapporter/2015/report-4-15-phthalates-which-are-toxic-for-reproduction-and-endocrine-disrupting%2D%2D-proposals-for-a-phase-out-in-sweden>
- United Nations (UN) (2015) Transforming our world: the 2030 agenda for sustainable development. <http://bit.ly/TransformAgendaSDG-pdf>
- US Environmental Protection Agency (EPA) (2017) Exposure factors handbook, chapter 5: soil and dust ingestion. National Center for Environmental Assessment. www.epa.gov/expobox/exposure-factors-handbook-chapter-5
- Vernet C, Pin I, Giorgis-Allemand L, Philippat C, Benmerad M, Quentin J, Calafat AM, Ye X, Annesi-Maesano I, Siroux V, Slama R, Eden Mother-Child Cohort Study Group (2017) *In utero* exposure to select phenols and phthalates and respiratory health in five-year-old boys: a prospective study. *Environ Health Perspect* 125(9):097006. <https://doi.org/10.1289/EHP1015>
- Wang XK, Tao W, Xu Y, Feng JT, Wang FH (2014) Indoor phthalate concentration and exposure in residential and office buildings in Xi'an, China. *Atmos Environ* 87:146–152. <https://doi.org/10.1016/j.atmosenv.2014.01.018>
- Wang Y, Zhu H, Kannan K (2019) A review of biomonitoring of phthalate exposures. *Toxics* 7(2): 21. <https://doi.org/10.3390/toxics7020021>
- Wei W, Mandin C, Ramalho O (2018) Influence of indoor environmental factors on mass transfer parameters and concentrations of semi-volatile organic compounds. *Chemosphere* 195: 223–235. <https://doi.org/10.1016/j.chemosphere.2017.12.072>
- Weiss JM, Gustafsson A, Gerde P, Bergman A, Lindh CH, Krais AM (2018) Daily intake of phthalates, MEHP, and DINCH by ingestion and inhalation. *Chemosphere* 208:40–49. <https://doi.org/10.1016/j.chemosphere.2018.05.094>
- Weschler CJ, Salthammer T, Fromme H (2008) Partitioning of phthalates among the gas phase, airborne particles and settled dust in indoor environments. *Atmos Environ* 42(7):1449–1460. <https://doi.org/10.1016/j.atmosenv.2007.11.014>
- Weschler CJ, Bekö G, Koch HM, Salthammer T, Schripp T, Toftum J, Clausen G (2015) Transdermal uptake of diethyl phthalate and di(n-butyl) phthalate directly from air: Experimental verification. *Environ Health Perspect* 23(10), 928–934. <https://doi.org/10.1289/ehp.1409151>
- Whyatt RM, Perzanowski MS, Just AC, Rundle AG, Donohue KM, Calafat AM, Hoepner LA, Perera FP, Miller RL (2014) Asthma in inner-city children at 5–11 years of age and prenatal exposure to phthalates: the Columbia Center for Children's environmental health cohort. *Environ Health Perspect* 122(10):1141–1146. <https://doi.org/10.1289/ehp.1307670>
- Wittassek M, Angerer J (2008) Phthalates: metabolism and exposure. *Int J Androl* 31(2):131–136. <https://doi.org/10.1111/j.1365-2605.2007.00837.x>

- World Health Organization (WHO) (1999) Hazard prevention and control in the work environment: airborne dust. WHO/SDE/OEH/99.14. <https://apps.who.int/iris/handle/10665/66147>
- Wormuth M, Scheringer M, Vollenweider M, Hungerbuhler K (2006) What are the sources of exposure to eight frequently used phthalic acid esters in Europeans? *Risk Anal* 26(3):803–824. <https://doi.org/10.1111/j.1539-6924.2006.00770.x>
- Zartarian V, Bahadri T, McKone T (2005) Adoption of an official ISEA glossary. *J Expo Anal Environ Epidemiol* 15(1):1–5. <https://doi.org/10.1038/sj.jea.7500411>
- Zhang J, Sun C, Lu R, Zou Z, Liu W, Huang C (2021) Associations between phthalic acid esters in household dust and childhood asthma in Shanghai, China. *Environ Res* 200:111760. <https://doi.org/10.1016/j.envres.2021.111760>
- Zhu Q, Jia J, Zhang K, Zhang H, Liao C, Jiang G (2019) Phthalate esters in indoor dust from several regions, China and their implications for human exposure. *Sci Total Environ* 652:1187–1194. <https://doi.org/10.1016/j.scitotenv.2018.10.326>



Disease Burden of Indoor Air Pollution

44

Otto Hänninen, Corinne Mandin, Wei Liu, Ningrui Liu,
Zhuohui Zhao, and Yiping Zhang

Contents

Introduction	1326
Global Burden of Disease Studies (GBD)	1327
Risk Assessment (RA)	1330
Environmental Burden of Disease (EBD)	1332
Health Impact Assessment (HIA)	1334
Methods	1335
Population Attributable Fraction (PAF)	1337
Linking with Toxicological Databases	1339

The original version of this chapter was revised. The correction to this chapter can be found at
https://doi.org/10.1007/978-981-16-7680-2_82

O. Hänninen (✉)

Finnish Institute for Health and Welfare, Environmental Epidemiology, Environmental Health, Health Security, Kuopio, Finland
e-mail: otto.hanninen@thl.fi

C. Mandin

Scientific and Technical Center for Building (CSTB), Marne-La-Vallée, France
e-mail: corinne.mandin@cstb.fr

W. Liu

Institute for Health and Environment, Chongqing University of Science and Technology, Chongqing, China

N. Liu · Y. Zhang

Department of Building Science, School of Architecture, Tsinghua University, Beijing, China
Beijing Key Laboratory of Indoor Air Quality Evaluation and Control, Beijing, China
e-mail: liunr18@mails.tsinghua.edu.cn; zhangyp@mail.tsinghua.edu.cn

Z. Zhao

Department of Environmental Health, School of Public Health, Fudan University, Shanghai, China
e-mail: zhzhao@fudan.edu.cn

© Springer Nature Singapore Pte Ltd. 2022, corrected publication 2022

1325

Y. Zhang et al. (eds.), *Handbook of Indoor Air Quality*,

https://doi.org/10.1007/978-981-16-7680-2_48

Current Estimates of Indoor Air Burden of Disease	1339
European EBoDE Study	1340
Indoor Specific Follow-Up in the HealthVent Study	1345
Indoor Air Pollution and Associated Socio-economic Costs in France	1351
Disease Burden of Indoor Air Pollutants in China	1356
Discussion	1362
Summary	1363
References	1363

Abstract

The highest environmentally related health benefits can be expected from policies that effectively target environmental exposures having high contributions to the population burden of disease (BoD). Such policies are demonstrated, for example, by the smoking bans in public places that have shown significant population health improvements in many countries. The health impacts of environmental exposures range from mild effects like annoyance to effects on chronic morbidity such as asthma, cardiovascular diseases, cancer, and even premature mortality, challenging the quantitative comparison of alternative policy options.

The environmental burden of disease provides a useful quantitative indicator of environmental health impacts, including chemical pollutants and noise. It allows quantitative comparisons of public health impacts associated with a wide range of environmental risk factors and targeting research and especially risk management to the major issues. This chapter gives an overview of the methods and presents five studies to demonstrate the use of the concepts.

Keywords

Burden of disease · Health risk characterization · Population attributable fraction (PAF) · Disability adjusted life years (DALY) · Incidence · Intake-daly

Introduction

The objectives of applying burden of disease tools to indoor air include (i) identification of pollutants and exposures relevant for indoor environments, (ii) demonstrating application of a harmonized environmental methodology on reducing burden of disease (EBD), and (iii) making the methods available for further applications and refinement. The factors to be considered for stressor selections should include (i) public health relevance, potential for (ii) high individual risks, (iii) public concerns, and (iv) large economic impacts.

Burden of disease methods have been widely accepted on global scale for assessing the health status of nations and identifying health losses caused by wide range of risk factors such as pollution, behavior, infectious diseases, nutrition, and violence (Fig. 1). The results highlight the global significance of environmental pollution, while indoor environments are largely missing as the air pollution component includes only unvented indoor use of solid fuels, typical of the developing countries.

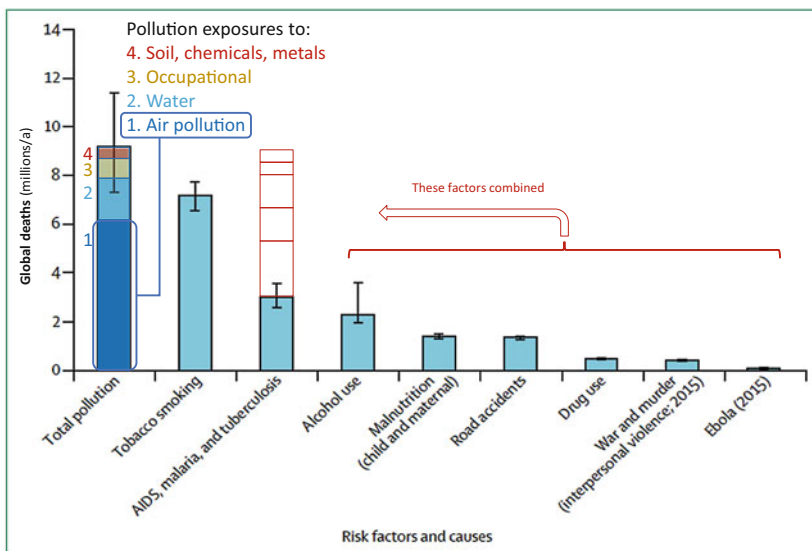


Fig. 1 Global estimated premature deaths by major risk factors and causes in 2015 using data from the GBD 2016 Study. (Modified from Landrigan et al. 2018)

Nevertheless, over the past decade there is emerging activity applying BoD methods focusing on indoor specific exposures (Table 1). This chapter introduces these methods and approaches.

Health risk characterization involves three nested assessment levels: (i) underlying health burden caused by diseases and corresponding causes (burden of disease, BoD); (ii) fractions of these burdens than can be attributed to risk factors (environmental burden of disease (EBD)); and (iii) impact of policies on these environmental burdens, assessed in the health impact assessment (HIA) process (Table 2).

The focus of most environmental risk assessments is on level (ii), overall impact associated with a given environmental exposure. However, a large part of the methodological literature quite correctly suggests that assessments should focus on the preventable fraction. This section introduces these approaches.

Global Burden of Disease Studies (GBD)

Burden of disease methods were proposed in 1990 by the collaborative work of World Bank, Harvard University, and World Health Organization (WHO) as an improvement to the earlier state of the art in characterizing health status of populations (Murray and Lopez 1996). A consistent and comparative description of the burden of diseases and injuries and the risk factors that cause them is an important input to health decision-making and planning processes. Information that is available on mortality, morbidity, and health status of populations in all regions of the world is fragmentary and sometimes inconsistent. Thus, a framework for integrating, validating, analyzing, and disseminating such information is needed to

Table 1 Characteristics of selected studies that have reported burden of disease results on indoor exposures and applying and demonstrating in some extent the methods covered in this chapter (Boulanger et al. 2017)

Selected studies:	EBoDE	HealthVent	Logue	Boulanger	CIAP	GBD
Notes			a		b	c
Countries	6, Europe	26, Europe	1, USA	1, France	1, China	204, Global
Pollutants (indoor sources/ total listed)	3/9	6/9	4/9	3/6	9/13	3/7
Additional non-criteria air pollutants			+62			
Additional risk factors						+81
Ambient air pollutants						
Fine particles (PM _{2.5})	PAF	PAF(inf)	IND	PAF	PAF (inf)	PAF
Ozone	PAF		IND		PAF (inf)	PAF
Nitrogen dioxide			IND		PAF (inf)	PAF
Volatile organic compounds (TVOC)		EJ-PAF				
Benzene	UR		ID	UR		
Sulphur dioxide			IND		PAF (inf)	
Bioaerosols (pollen)		EJ-PAF				
Indoor generated air pollutants						
Indoor-generated particles		PAF				d
Second-hand smoke	PAF*	PAF*	Literature +IND	Literature		PAF*
Dampness and mold		PAF				
Carbon monoxide		EJ-PAF	IND	Literature	PAF	
Indoor-generated volatiles		EJ-PAF				
Radon	PAF	PAF	Literature	Literature	PAF	PAF
Pollutants emitted from industrial products						

(continued)

Table 1 (continued)

Selected studies:	EBoDE	HealthVent	Logue	Boulanger	CIAP	GBD
Formaldehyde	PAF		ID		PAF	
Trichloroethylene				UR		

PAF = population attributable fraction; inf = infiltration of ambient pollution indoors; IND=Intake-incidence-daily method; ID=Intake-daily method; UR = Unit risk (exposure \times unit risk); EJ = expert judgment

^a Logue et al. (2012) study includes 69 + 2 pollutants not fully listed here

^b Chinese study on indoor air pollution, see the corresponding subchapter for more details

^c GBD study covers 87 risk factors including some pollutants and counting also groups and subgroups

^d GBD study accounts only for indoor generated exposures from household use of solid fuels

* Impact of active smoking removed first from population background disease burden

Table 2 Three nested levels related to burden of disease assessments

Level	Conceptual framework and elements	
i	Burden of disease (BoD)	
		Causes (diseases)
		Severity (disability weight)
		Duration (length)
		Incidence, prevalence
ii	Environmental burden of disease (EBD)	
		Risk factors (exposures)
		Attributable fraction
iii	Health impact assessment (HIA)	
		Policies
		Impact on exposures
		Expected change in EBD

assess the comparative importance of diseases, injuries and risk factors in causing premature death, loss of health and disability in different populations. Countries can combine this type of evidence along with information about policies and costs to decide how to set their health agenda.

The first GBD study quantified the health effects of more than 100 diseases and injuries for eight regions of the world in 1990. It generated comprehensive and internally consistent estimates of mortality and morbidity by age, sex and region. The study also introduced a new metric, the disability-adjusted life-year (DALY), as a single measure to quantify the burden of diseases, injuries and risk factors. The DALY estimate is based on years of life lost from premature death and years of life lived in less than full health. GBD 1990 study was subsequently updated by WHO for the target years 2000–2002–2004 and included a more extensive analysis of the mortality and burden of disease attributable to 26 global risk factors using a consistent analytic framework known as comparative risk factor assessment (CRA).

The burden of disease was originally calculated from estimated or registered incidence data of various diseases, using disease specific disability weights defined

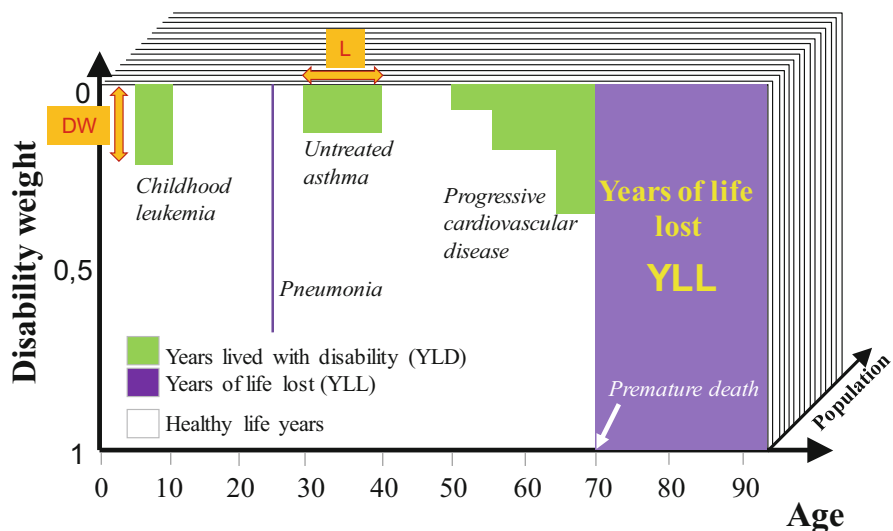


Fig. 2 Burden of disease concepts: premature mortality leads to years of life lost (YLL). Disability weight (DW) are used together with the disease duration (L) to calculate comparable estimate of years lived with disability (YLD). (Adopted from Hollander et al. 1999)

by expert panels, estimated disease specific durations, and accounting for years of life lost due to premature mortality (Fig. 2). The original studies used the longest living Japanese and South Korean populations for determining the life expectancy for calculation of years of life lost.

Since 2010 the Institute for Health Metrics and Evaluation (IHME), located at University of Washington, USA, and other academic partners have collaborated on the GBD 2010 global burden of disease study, published on 14 December 2012. Regional estimates of deaths and DALYs using a new method for calculation of DALYs for the years 1990, 2005, and 2010 were reported. Subsequently, over the past decade several updates and improvements were prepared and published. Most comprehensive global study – analyzing 286 causes of death, 369 diseases and injuries, and 87 risk factors in 204 countries and territories – until now is the GBD 2019 study (GBD 2021a; Vos et al. 2020).

National burden of disease estimates from both IHME and WHO are readily available and have been actively used as a key input to top-down assessment of indoor air burdens.

Risk Assessment (RA)

Health risk assessment (HRA) was largely developed prior to the GBD work by the US Environmental Protection Agency (US EPA) in the 1980s to quantitatively or semi-quantitatively inform decision-makers on the types and probability of environmental risks. As of today, it still remains the most comprehensive theoretical

framework for health risk assessments through the evolution of risk characterization and quantification, including the environmental burden of disease (Fig. 3).

The nature and probability of adverse potential health effects in humans who may be exposed to hazardous chemicals in contaminated environmental media in the past, now or in the future were characterized (US EPA 1989). HRA as defined by the US EPA consisted of three input elements, used to characterize the risk (Table 3). It is noteworthy, that the components do not include the target population characteristics such as age and health profiles that actually may substantially modify the risk characteristics.

The role of target population at risk with age, sex, and health characteristics has become obvious through the adaptation of the burden of disease methods and moving from hazard indexes and quotients toward more quantitative risk characterization based on epidemiological evidence from real human populations as will be presented below.

The risk characterization provided a useful and flexible framework for how in practice the risks should be presented. Based on the toxicological evidence in the 1980s, two major lines of analyses emerged (see Xiong et al. 2018 for a review),

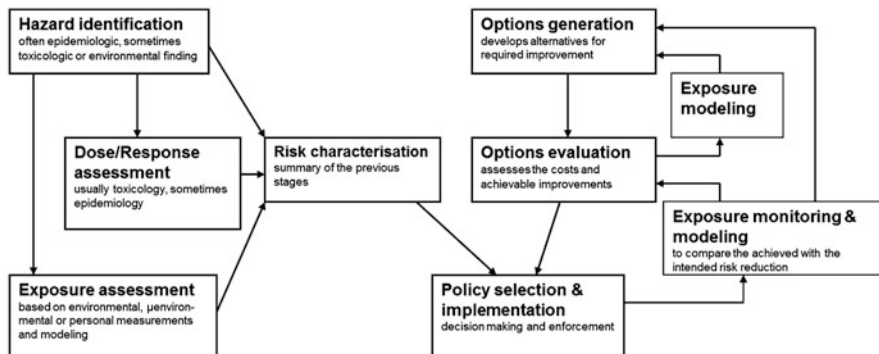


Fig. 3 Components of risk assessment and management processes (based on NRC 1983)

Table 3 Components of the US-EPA risk assessment process (based on NRC 1983)

Level	Assessment
I	Hazard Identification scientific information on the hazardous properties of environmental agents;
II	Dose-response quantitative relationship between exposure and effects
III	Exposures the extent of human exposure to those agents
IV	Risk characterization the product of the risk assessment is a statement regarding the probability and nature of harm in populations or exposed individuals

presented below shortly to provide the background on which burden of disease methods were developed for a good reason. The first approach focused on non-carcinogenic risks and health outcomes, remaining totally ignorant on the types of non-carcinogenic health outcome: the risk was quantified by comparing exposures (pollutant concentrations in the contact medium such as air) or doses (amount of substances entering the body or target organs) with the available health or toxicology based reference values for that chemical and presenting the single chemical or exposure value as hazard quotient:

$$HQ_i = \frac{E}{Rf} \quad (1)$$

where HQ : hazard quotient, E : exposure or dose, Rf : selected reference toxicological level (derived from, e.g., no observed effect level (NOEL)).

Further, regardless of the potentially widely varying differences in types of health outcomes and toxicological mechanisms associated with the exposure in question, aggregation of the hazard quotients was done by defining hazard index as a cumulative sum over hazard quotients:

$$HI = \sum_i HQ_i \quad (2)$$

where HI : hazard index, HQ : hazard quotient.

Thus the hazard index seemingly provided additivity, while remaining semi-quantitative at best as a characterization of risk.

Better quantification was already possible for carcinogenic risks at that time. The selected cancer model assumed linear no-threshold risk probabilities of developing cancer as function of the exposures:

$$p = E \times CSF \quad (3)$$

where p : probability, E : exposure or dose, CSF : cancer slope factor (ratio of cancer probability to dose).

At that time, no safe level was assumed for carcinogenic exposures and use of simple linear relationship allowed for estimation of the cancer slope from basically single-dose tests or ecological data sets. As can be seen from this short introduction, risks were estimated separately for two different types of complex disease groups and there was no possibility to quantitatively compare them for prioritization, setting the scene for the development of new approaches in the 1990s.

Environmental Burden of Disease (EBD)

Environmental exposures are associated with a large variety of human diseases ranging from milder effects like headaches and annoyance to severe diseases such as cancer, and premature deaths. Therefore, quantitative comparison of such risks

and prioritization of preventive measures cannot be based on merely incidence or prevalence rates. The environmental burden of disease methodology accounts for both years of life lost due to mortality as well as years lived with various disabilities. The latter are quantified using, besides the duration of the condition, condition specific severity weights. Such weights inherently contain a value component, but in practice, the resulting environmental burden of disease estimates have been found quite useful.

Improved population health registries and harmonization of disease codes together with statistical methods such as population attributable fraction that can be estimated from epidemiological data, allow for rapid and comparable international assessments.

In the first global burden of disease study by Murray and Lopez (1997), two environmental risk factor groups were considered: (i) poor water, sanitation, and hygiene and (ii) air pollution. In the updates of the global burden of disease project for 2002 and 2004, additional environmental risk factors were included: (iii) lead, (iv) indoor air pollution from solid fuel combustion, and (v) climate change.

One of the first more comprehensive analyses of environmental burden of diseases from a number of risk factors was conducted by de Hollander et al. (1999) in the Netherlands. A total of 19 environmental risk factors were covered.

The World Health Organization then took the lead to harmonize the EBD methods (Prüss-Ustün et al. 2003) and published a series of reports on environmental burden of disease quantifying the amount of disease caused by selected environmental risks factors including chemicals and mixtures as well as physical exposures such as noise and radiation.

Similar to the overall population health status, disease burden attributable to the environment can be expressed in deaths and in disability-adjusted life years (DALYs). The latter measure combines the burden due to death and disability in a single index. Using such an index permits the comparison of the burden due to various environmental risk factors with other risk factors or diseases.

The environmental burden of disease quantifies the amount of disease caused by environmental risks. In 2016, as much as 24% of all deaths worldwide were attributable to the environment (Prüss-Ustün et al. 2016). The realization of how much disease and ill health can be attributed to modifiable environmental risks may contribute to identifying prevention opportunities and should add impetus to global efforts encouraging sound preventive measures through available policies, strategies, interventions, technologies and knowledge.

Additional information required for the rational development of policies by the health sector and activities of other sectors which directly manage or influence the determinants of health includes the effectiveness and cost-effectiveness of interventions, the availability of resources, and the type of policy environment.

Due to background exposures from natural sources and practical limitations in removing anthropogenic pollution, the total attributable burden of disease cannot be directly interpreted as reduction potential. In many cases natural background prevents from completely removing the exposures, natural ionizing radiation or atmospheric particulate matter being examples. Nevertheless, EBD estimates can be used

to identify areas of high disease burden for more detailed analysis of the reduction potential by targeted policies. The use of quantitative methods like EBD and health impact assessment should be promoted to inform policymakers about the health benefits of specific policy measures.

Health Impact Assessment (HIA)

According to WHO, health impact assessment (HIA) is a practical approach used to judge the potential health effects of a policy, program or project on a population, particularly on vulnerable or disadvantaged groups. Recommendations are produced for decision-makers and stakeholders, with the aim of maximizing the proposal's positive health effects and minimizing its negative health effects. The approach can be applied in diverse economic sectors and uses quantitative, qualitative, and participatory techniques (WHO 2021).

HIA provides a way to engage with members of the public affected by a particular proposal. It also helps decision-makers make choices about alternatives and improvements to prevent disease or injury and to actively promote health. It is based on the four interlinked values of democracy (promoting stakeholder participation), equity (considering the impact on the whole population), sustainable development and the ethical use of evidence.

US Centers for Disease Control and Prevention (US-CDC 2021) has identified six steps in conducting an HIA:

1. Screening (identifying plan, project, or policy decisions for which an HIA would be useful).
2. Scoping (planning the HIA and identifying what health risks and benefits to consider).
3. Assessment (identifying affected populations and quantifying health impacts of the decision).
4. Recommendations (suggesting practical actions to promote positive health effects and minimize negative health effects).
5. Reporting (presenting results to decision-makers, affected communities, and other stakeholders).
6. Monitoring and evaluation (determining the HIA's impact on the decision and health status).

There is a significant conceptual difference between the overall environmental burden of disease associated with a selected exposure and the target of health impact assessment. While HIA may aggregate over several pollutants and exposures associated with the policy under scrutiny, the HIA, by definition, focuses on the change in health effects, i.e., the impact of the policy in question. Typically, the impact of a single policy is rather small on overall environmental exposures. Thus, it is critical to keep the overall burden attributable to a given exposure conceptually separate from the estimated health impact of a selected policy or decision.

Building on the previous concepts of BOD, RA (HRA; CRA), EBD, and HIA, details of applying burden of disease methodology on selected exposures are provided and discussed hereafter.

Methods

Burden of disease is a measure of sickness and death in a population. The burden of disease methodology is based on making years lived with a disability (*YLD*) comparable with years of life lost (*YLL*) due to premature mortality. Summing these two components produces disability adjusted life years (DALY) as the quantitative measure of burden of disease (Murray and Lopez 1997):

$$BoD = YLL + YLD \quad (4)$$

where years of life lost (*YLL*) in a case of premature mortality are calculated as the age-specific remaining life expectancy (*LE*) at the age at death (*AD*):

$$YLL = LE - AD \quad (5)$$

The value of the time lived in non-fatal health states, in comparison with life lost due to premature mortality, is estimated using health state weights reflecting social preferences for different states of health. Incidences of acute and chronic diseases and corresponding mean durations available in health registries are supplemented with disability weights to calculate corresponding estimate of years lived with disability (*YLD*) accounting for the duration of the disease (*L*) and the disease severity expressed as a disease specific disability weight (*DW*):

$$YLD = DW \times L \quad (6)$$

Some disability weights used in DALY calculations quantify societal preferences for different health states. Others are based on medical expert panel assessments of the conditions, taking into account for the potential need for hospitalization, medication, and differences in disease progression in patients. Both WHO and IHME have published their own disability weights.

It is noteworthy that the questionnaire-based weights do not typically represent the lived experience of a disability or health state. Neither do they imply any societal value for the person in a disability or health state. Nevertheless, they may quantify societal preferences for health states in relation to the societal ideal of good health. The term “disability” is used broadly to refer to departures from good or ideal health in any of the important domains of health. These include mobility, self-care, participation in usual activities, pain and discomfort, anxiety and depression, and cognitive impairment (Prüss-Ustün et al. 2003). Examples of disability weight values, collected from dedicated questionnaire panels, are shown in Table 4. Treatment of diseases further modifies the diseases and thus the disabilities. In many cases a

Table 4 Examples of early disability weights. (Adopted from Murray and Lopez 1996) compared with GBD 2019 sequelae. The early approach considered disabilities by disease treatment status. Since then several rounds of international and various national updates have been conducted. Here as an example the corresponding number of sequelae from the GBD 2019 study are shown for comparison. Details of the conditions can be found from the GBD documentation (GBD 2021a)

		Murray and Lopez (1996)			GBD 2019 Sequelae		
	Disease/sequelae containing	Type	DW	DW	n	DW	DW
			Untreated	Treated		min	max
1	AIDS ^a		0.50	0.50	24	0.078	0.642
2	Infertility		0.18	0.18	38	0.005	0.329
3	Diarrhoea	episodes	0.11	0.11	16	0.051	0.582
4	Measles	episodes	0.15	0.15	2	0.051	0.133
5	Tuberculosis		0.27	0.27	16	0	0.495
6	Malaria	episodes	0.20	0.20	28	0	0.625
7	Trachoma	blindness	0.60	0.49	3	0.031	0.187
8	Trachoma	low vision	0.24	0.24	3	0.031	0.187
9	Lower respiratory tract infection	episodes	0.28	0.28	3	0.051	0.296
10	Lower respiratory tract infection ^b	chronic	0.01	0.01	—	—	—
11	Cancers	terminal stage	0.81	0.81	74	0.049	0.631
12	Diabetes mellitus	uncomplicated	0.01	0.03	52	0	0.633
13	Unipolar major depression	episodes	0.60	0.30	—	—	—
14	Alcohol dependence syndrome		0.18	0.18	23	0	0.57
15	Parkinson disease		0.39	0.32	3	0.01	0.575
16	Alzheimer disease		0.64	0.64	3	0.069	0.449
17	Post-traumatic stress disorder		0.11	0.11	—	—	—
18	Angina pectoris		0.23	0.10	3	0.033	0.167
19	Congestive heart failure		0.32	0.17	308	0.011	0.512
20	Chronic obstructive lung disease (COPD)	symptomatic	0.43	0.39	61	0.019	0.512
21	Asthma, cases		0.10	0.06	4	0	0.133
22	Deafness		0.22	0.17	44	0.01	0.316
23	Benign prostatic hypertrophy		0.04	0.04	1	0.067	0.067
24	Osteoarthritis, symptomatic hip or knee		0.16	0.11	16	0	0.165
25	Brain injury, long-term sequelae		0.41	0.35	—	—	—
26	Spinal cord injury		0.73	0.73	6	0.296	0.296

(continued)

Table 4 (continued)

	Disease/sequelae containing	Murray and Lopez (1996)			GBD 2019 Sequelae		
		Type	DW	DW	n	DW	DW
			Untreated	Treated		min	max
27	Sprains		0.06	0.06	—	—	—
28	Burns (>60%) – long term		0.25	0.25	—	—	—

^a GBD values contain also HIV sequelae not included here

^b included in above row summary of GBD-values.

treated disease is substantially less disabling than a non-treated disease. These differences are highlighted in the table, too.

A unit risk model for attributable incidence (AI, or estimated number of cases) can be calculated using similar probability-based approach as was developed originally for the cancer slope method described earlier, supplemented merely by the population size (see, e.g., Xiong et al. 2018 for more details):

$$AI = E \times UR \times N \quad (7)$$

where AI : attributable incidence (No. of cases), E : exposure, UR : unit risk (e.g., cancer slope; probability of the outcome per exposure), N : population size (persons).

Excess risk approach has been applied also estimation of attributable incidence when epidemiological estimate of relative risk has been available (Xiong et al. 2018). This method is a simplification of the full population attributable fraction calculation that will be explained next:

$$AI = (RR_E - 1) \times B \quad (8)$$

where AI : attributable incidence, RR : relative risk to the exposed population, B : background incidence.

Equation (8) is the first equation introducing a key variable based on epidemiological methods. It has been suggested that human-based evidence from real populations represents the most relevant and reliable evidence on exposure-response relationships (e.g., Klaassen, 2008). Such data accounts for actual levels of exposure and avoids the use of extrapolation methods inherently typical for toxicological in vitro and in vivo estimates from cell and animal studies, and most importantly, the use of theoretical safety and sensitivity scaling factors.

Population Attributable Fraction (PAF)

The burden of disease estimates describe the overall burden in a population and generally only a small fraction of the adverse outcomes can be attributed to the given environmental and other risk factors.

The burden of disease can be estimated using a bottom-up approach described in Eqs. 4, 5, and 6. However, the mathematical properties of relative risks offer an operational way to estimate the fraction of disease burden associated with a given risk factor when epidemiological data are available. In 1953, Levin first proposed the concept of the population attributable fraction. Since then, the phrases “population attributable risk,” “population attributable risk proportion,” “excess fraction,” and “etiological fraction” have been used interchangeably to refer to the proportion of disease risk in a population that can be attributed to the causal effects of a risk factor or set of factors (Rockhill et al. 1998).

In this context, the environmental burden of disease associated with a given risk factor can be calculated simply from the overall population burden of a given disease by multiplying it by the epidemiological estimate of the population attributable fraction. National background burden of disease estimates are directly available from both the World Health Organization and Institute of Health Metrics and Evaluation.

Attributable burden EBD is calculated from background burden (BoD) using the population attributable fraction (PAF) as

$$EBD = PAF \times BoD \quad (9)$$

The population attributable fraction (PAF) can be derived from relative risk (*RR*) as described in more detail, e.g., in Hänninen and Knol (2011):

$$PAF = \frac{f \times (RR - 1)}{f \times (RR - 1) + 1} \quad (10)$$

where *f* is the fraction of population exposed to a given factor and *RR* is the relative risk of the exposed population.

In the case of environmental exposures, the relative risk is commonly expressed per a standard increment of exposures, e.g., $10 \mu\text{g m}^{-3}$ as in the case of fine particles. Simplified approaches for most practical purposes use linear scaling; in this case, exposure to, e.g., $15 \mu\text{g m}^{-3}$ would be expressed as $E = 1.5$. Also, many non-linear exposure response functions have been proposed and even becoming the standard approach. The log-linear association, simply derived mathematically from the group-level definition of relative risk, leads to supra exposure response relationship and relative risk at prevailing exposure level:

$$RR = e^{(E \ln RR^o)} = RR^o E \quad (11)$$

One of the early non-linear approaches for particulate matter was suggested by Ostro and applied, e.g., by WHO (Ostro 2004). More recently many empirical and parametric sublinear associations have been proposed based on meta-analysis of especially particulate matter exposures such as versions of integrated exposure response function (IER; Burnett et al. 2014; Cohen et al. 2017), global exposure mortality model (GEMM; Burnett et al. 2018) and GBD 2021b. Debate on linearity

versus supra- and sub-linearity and existence of a safe level (biological or toxicological threshold) versus use of uncertainty cut-off levels at low exposures continues. In the absence of solid evidence on deviance from linearity it would seem reasonable to use linear estimation as a simplification and including low-end extrapolation even in lack of observational data at extremely low concentrations. Nevertheless, there is no wide consensus on any preferred approach.

Linking with Toxicological Databases

Epidemiological data from large populations is currently available for population attributable fraction-based, top-down estimation of environmental burden of disease only for a relatively small number of risk factors (see, e.g., Table 1). In the context of life cycle assessments, Mark Huijbregts and colleagues proposed a human toxicological effect model for carcinogenic and non-carcinogenic chemicals (Huijbregts et al. 2005). They presented a methodology to derive human damage and effect factors of toxic pollutants, starting from a lognormal dose-response function and applied the method to calculate combined human damage and effect factors for a total of 1,192 substances, including a subdivision into carcinogenic and non-carcinogenic compounds. Uncertainties in the damage and effect factors were also estimated.

Logue et al. (2012) applied this method for 69 + 2 indoor air exposures in the United States. The strengths of the approach include (i) top-down approach from established estimates of non-communicable diseases; (ii) use of disability adjusted life years as a comparable and harmonized metric; and (iii) availability of the method for many chemical substances. On the uncertainties side, it must be taken into account that the toxicological evidence is extrapolated to burden of disease without any specific understanding or justification of biological mechanisms beyond processing carcinogens separately, or considerations of interspecies scaling, sensitive subpopulations, temporal exposure patterns over developmental stages, etc. Liu et al. continued with similar estimates for China to be discussed in more detail in corresponding section later in this chapter. and used the results of Logue et al. for comparison.

In the next subchapter, we look in detail how the presented methods have been applied in estimation of indoor air attributable burden of disease in selected international and national studies and give an overview of the results reported.

Current Estimates of Indoor Air Burden of Disease

This section presents the state of art in applying the burden of disease methods to indoor exposures by presenting the key elements of a few selected international and national studies. It is expected that the field of applying burden of disease concepts for estimating the health effects of indoor exposures will continue to rapidly expand

and the reader is advised to supplement the material here with new studies reported in the scientific literature.

European EBoDE Study

One of the first European projects applying burden of disease methodology for selected exposures also including indoor air characteristics was the multinational Environmental Burden of Disease in European Countries (EBoDE) study. Six countries, each with national funding and a research team, participated the project supported by World Health Organization. Several meetings were organized at the Bonn office of WHO European Centre of Environment and Health and representative from the Environmental Burden of Disease Programme, Geneva, actively took part in the work in 2010–2011. The results were first published as a project report (Hänninen and Knol 2011) and then the key results as a peer reviewed journal article (Hänninen et al. 2014). The report remains a useful source of the assessment methods that are partly reproduced in this handbook chapter.

EBoDE remains the only study that proposed the use of a lag time between exposures and effect, which is significant for, e.g., the initiation of a cancer but also for development of cardiovascular and other chronic diseases. EBoDE was also one of the first studies that compared discounting, the standard approach in 2010, with non-discounted estimates. Discounting downscals health effects, mortality in particular, of children and thus counteracted the strategical objectives of Children's Environment and Health Action Plan (CEHAPE). Since then both IHME and WHO have chosen to drop discounting.

Stressor Selection

Four criteria were defined for the selection of environmental stressors to be included in the study:

1. Public health impact
2. High individual risk
3. High political or public concern
4. Economic significance

In addition, the selection was affected by the feasibility of the calculation. Therefore, we also considered the availabilities of:

- Exposure data
- Evidence-based exposure response function(s)
- Baseline health statistics

A total of nine stressors were selected: benzene, dioxins, fine particulate matter ($PM_{2.5}$) formaldehyde, lead, radon, second-hand smoke (SHS), and traffic noise. Formaldehyde, radon and SHS directly represented indoor dominant exposures.

Transportation noise effects also dominantly occurs in indoor spaces such as bedrooms and offices. Fine particles have significant indoor sources, but in the EBoDE study, only outdoor concentrations were used (see follow-up improvements in this respect in the next section on HealthVent study).

Exposure Assessment

Exposure data were primarily collected from international harmonized and validated sources, supplemented with national studies data and from other sources. Population representative exposures were targeted, accounting for potential differences in the urban and rural exposures, different age groups, gender, and other relevant sub-groups.

International exposure data were available for SHS, transport noise, ozone, PM and radon. National data were used for benzene, dioxins, formaldehyde, and lead, with complementary information from (non-comprehensive) international data sources such as AirBase ambient data for benzene; several international multiple center studies for indoor concentrations of benzene and formaldehyde covering some of the participating countries, and WHO Mother's milk database for dioxins.

The study also attempted assessment of exposure trends, relevant for harmonizing the target year exposures, accounting for health effect lag, with limited success. For several stressors (e.g., lead, dioxins) not enough data were available to make sensible trend estimates. For other stressors (PM, ozone, benzene), temporal and/or spatial variability was so large that reliable evaluations of the trend on the basis of these data were not possible. In these cases, expert judgment was used to estimate trends and corresponding confidence intervals. Due to the large uncertainties, no national trend estimates were created.

Exposure-Response Relationship Modelling

For each combination of environmental stressors and health endpoint, exposure-response functions were selected from:

- Recent international meta-analyses or WHO guidelines
- If not available, then from individual high-quality studies

Recent active and unstable evolution of concentration-response relationships for ambient particles in the GBD studies effectively demonstrates the challenges even for PM_{2.5}, which represents the most studied exposures with epidemiological data from the largest cohorts. Particles were modelled in EBoDE study using relative risks from earlier studies (Pope et al. 2002, 2004).

Formaldehyde and lead response models included an estimated safe threshold level at 100 µg m⁻³ and 24 µg l⁻¹, respectively. Further, a lead model for lower intelligence quotient and hypertensive disease were quantified by step functions over the diagnostic threshold of 70 pt. and 140 mm Hg, respectively. Transportation noise modelling applied polynomial prevalence response for both sleep disturbance and annoyance. For all other exposures, a linear (unit risk models) or log-linear (relative risk models) were applied as summarized in Table 5.

Table 5 Summary of EBoDE health endpoints, exposure units and exposure/response-relationships for the indoor relevant exposures

Stressor	Health endpoint	Population	Exposure estimate	Unit of exposure	Type of ERF	Point estimate	LCL (95%)	UCL (95%)	Reference (s) for ERF	Method
SHS	Tracheas, bronchus and lung cancers ^{c)}	Adult non-smokers	% of people exposed (=yes)	yes/no	RR	1.21	1.13	1.30	US S.G. 2006	PAF
	Ischemic heart disease	Adult non-smokers		yes/no	RR	1.27	1.19	1.36	US S.G. 2006	PAF
	Asthma induction	Adult non-smokers		yes/no	RR	1.97	1.19	3.25	Jaakkola et al. 2003	PAF
	Asthma induction	Children (<14 yr)		parental y/n	RR	1.32	1.24	1.41	Cal-EPA 2005	PAF
	Lower respiratory infections	Infants (<2 yr)		parental y/n	RR	1.55	1.42	1.69	US S.G. 2006	PAF
	Otitis media	Toddlers (<3 yr)		parental y/n	RR	1.38	1.21	1.56	Eitzel et al. 1992; Cal-EPA 2005	PAF
Formaldehyde	Asthma aggravation (children) (morbidity only)	Toddlers (<3 yr)	Annual mean residential indoor concentration	$\mu\text{g m}^{-3}$	RR	1.017	1.004	1.025	Rumchev et al. 2002	PAF
Road traffic noise	High sleep disturbance (HSD) (morbidity only)	All	Persons exposed to predefined exposure categories	Lnight (dB)	UR	function	function	Miedema and Vos 2007	n × DW × L	
	Ischemic heart disease (IHD)	All		Lday16h (dB)	OR	function	function	Babisch 2006	PAF	

Railway noise	High sleep disturbance (HSD) (morbidity only)	All		Lnight (dB)	UR	function	function	Miedema and Vos 2007	n × DW × L
Aircraft noise	High sleep disturbance (HSD) (morbidity only)	All		Lnight (dB)	UR	function	function	Miedema and Vos 2007	n × DW × L
PM _{2.5} ^a	Cardiopulmonary disease	Adults (>30 yr)	Population weighted ambient level	µg m ⁻³	RR	1.0077	1.0020	Pope et al. 2002; WHO 2006	PAF
Lung cancer	Adults (>30 yr)			µg m ⁻³	RR	1.012	1.004	Pope et al. 2002; WHO 2006	PAF
Chronic bronchitis (new cases)	Adults (>27 yr)			µg m ⁻³	UR	5.33 × 10 ⁻⁵	1.70 × 10 ⁻⁶	Hurley et al. 2005; WHO 2006	n × DW × L
Restricted activity days (RAD)	15–64 yr			µg m ⁻³	UR	0.0902	0.0792	Hurley et al. 2005; WHO 2006	n × DW × L
Radon	Lung cancer	All	Residential mean level	Bq m ⁻³	RR	1.0016	1.0005	Darby et al. 2005	PAF

^a PM_{2.5} exposures were collected for ambient air and indoor sources not accounted for

^b Ozone mortality estimated with relative risk based PAF model, was set to cause loss of exactly 1 year of life

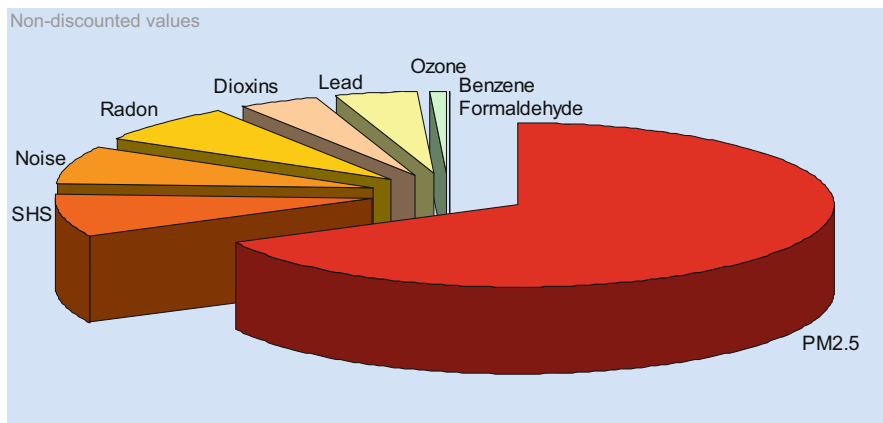


Fig. 4 EBoDE estimates of the relative burden attributable to the chosen nine stressors in six European countries (Hänninen and Knol 2011)

While the nine chosen stressors do not represent a comprehensive list of toxicants causing measurable public health impacts in European countries, the dominant role of ambient particles (PM_{2.5}) was obvious (Fig. 4). The health impacts of second-hand smoke, traffic noise, and radon were similar. Radon was more important in Finland than in the other participating countries due to the geological characteristics. The results suggested that 3–7% of the national burden of disease in the participating six countries is associated with the selected nine environmental stressors. Particulate matter (PM) is estimated to be associated with the highest disease burden (6.000 to 10.000 DALYs per million people), followed by traffic noise, second-hand smoke, and radon.

Ranking of environmental health impacts was elaborated with caution. However, even while “discounting” affected some of the estimates (especially radon, and SHS and particles) quite substantially, the ranking remained consistent. Only among the runner-up group of SHS, noise, and radon did the order change since noise effects are to a large extent immediate and not affected by discounting.

Long tradition prevails in assessing parametric uncertainties in environmental epidemiology and subsequent extrapolations in risk characterization. Exposure estimates already contain uncertainties that are difficult to be quantified. In an ideal world, unbiased random sampling could be used, reducing the exposure uncertainty to normal statistical uncertainty. In reality, exposure data is always available from geographically, socioeconomically, and temporally limited or chosen cohorts or panels, thus limiting and potentially, even likely to bias, representativity.

Further, it remains much more challenging to include model uncertainties in the overall uncertainty assessment. The EBoDE study applied expert judgment to categorize overall uncertainties in the estimates as presented in Fig. 5. It was suggested that the most reliable estimates were those for particles, second-hand smoke, radon, and benzene and the most uncertain ones were for dioxins and

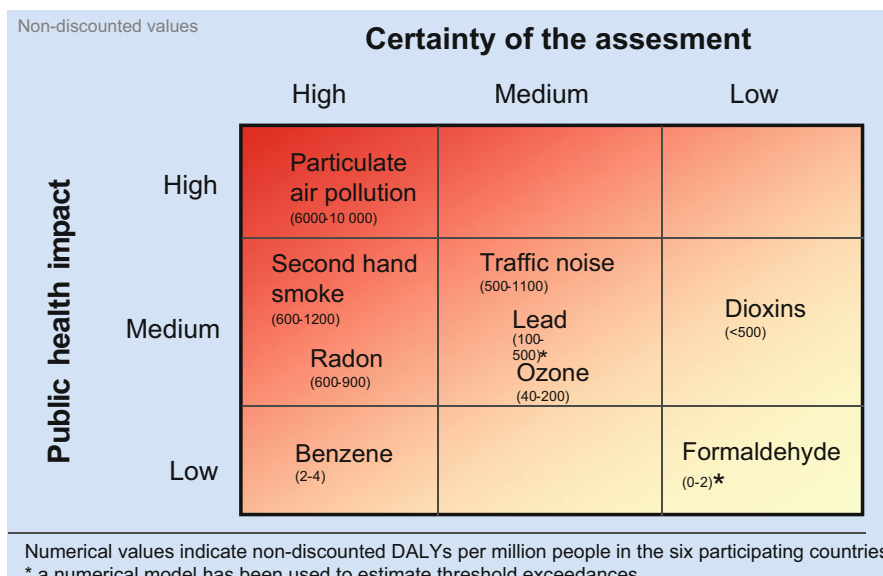


Fig. 5 Expert judgment estimates of relative uncertainty in the nine stressor estimates of environmental burden of disease in six European countries (Hänninen and Knol 2011)

formaldehyde. For the latter, even the types of endpoints and causality were considered uncertain.

The EBoDE estimates suggested that fine particles ($PM_{2.5}$) were the leading environmental health risk in European countries in 2010 by causing up to ten thousand non-discounted lost years of health per million people annually in the EU. The next most important public health impacts were associated with second-hand smoke and radon, both representing indoor exposures. The benzene estimate was also considered scientifically robust, but remained lower than 1% of the previous discussed stressors. Traffic noise, lead, and ozone estimates ranged from 40 to 1100 DALY/million, including relatively large uncertainties. The lowest certainties were warranted for dioxin and formaldehyde effects.

Indoor Specific Follow-Up in the HealthVent Study

While the earlier EBoDE study covered selected population exposures, it did not specifically consider indoor exposures. The EU-funded HealthVent project did that by adding physical exposure modelling related to infiltration of ambient air pollutants as part of building ventilation as well as estimates of indoor generated exposures to fine particles and volatile organic compounds. Further, mortality due to acute carbon monoxide poisoning and exposures to dampness and mold were added using register data and simplified yes/no exposure characterization,

respectively. Moreover, allergic reactions due to ambient bioaerosol exposures such as pollens was added by using expert judgment PAF.

While the EBoDE study covered only six selected countries, the HealthVent model was developed for 26 EU countries omitting only Malta of the member states at that time due to lack of national data from this small island state. On the other hand, while in EBoDE support from the World Health Organization made it possible to compare discounted and non-discounted approaches, in HealthVent, it was necessary to revert back to publicly available data sources, which meant that only discounted burden of disease models could be evaluated.

Stressor selection and indoor exposure modelling was conducted to exposures adjusted for their indoor air relevance:

- EBoDE pollutants included: ambient PM_{2.5}, radon, SHS
- Pollutants added to EBoDE: bioaerosols, CO, indoor generated PM_{2.5}, total VOCs
- Pollutants excluded: benzene, dioxins, formaldehyde, lead, ozone, traffic noise

The indoor and outdoor generated components of the indoor concentrations were derived using the single compartment, complete mixing, mass-balance model as suggested by Wilson et al. (2000) and applied later, e.g., by Hänninen et al. 2004, 2011, 2013 and Diapouli et al. 2013. Using the complete mass-balance equation (see Hänninen and Asikainen 2013, for more details):

$$\overline{C}_i = \frac{Pa}{a+k} \overline{C}_a + \frac{G}{V(a+k)} - \frac{\Delta C_i}{\Delta t(a+k)} \quad (12)$$

the ambient originated, i.e., infiltrated concentration was solved, after omitting the transient delta-component, as

$$C_{ai} = \frac{pa}{a+k} C_a = F_{INF} \times C_a \quad (13)$$

This equation was also used in ventilation scenarios, where the air exchange rate was adjusted. The simplified aerosol model parameters shown in Table 6 were used. Accordingly, the indoor generated concentration would then be

Table 6 Mass-balance parameters for the ambient air pollutants included in the model

Pollutant	Mass balance parameters				
	Dp(eff) μm	Penetration (P) [fraction]	Density g cm ⁻³	Decay (k) h ⁻¹	Finf [fraction]
PM _{2.5}	<2	90%	1.5	0.14	0.55
Pollen	10	80%	1.0	5.41	0.07
VOC	n/a	100%	n/a	0.10	0.69

Dp(eff) = effective particle diameter; Finf = resulting infiltration factor at a=0.22 h⁻¹; in the model the actual Finf values are calculated according to the used ventilation rates.

$$C_{ig} = \frac{G}{V} \times \frac{1}{(a \times k)} \quad (14)$$

but could also be calculated from the observed indoor concentration by subtracting the infiltrated component

$$C_{ig} = C_i - C_{ai} \quad (15)$$

Exposure-response relationship modelling and results

Fine particles, radon, and second-hand smoke were modelled using the same response models as in EBoDE. Also, dampness and mold estimates were calculated using the PAF approach, but the exposure indicator was merely a fraction of affected homes based on yes/no questionnaires. However, simplified exposure-response relationships were used for the remaining exposures. Carbon monoxide poisoning fatalities were obtained from national registers and WHO and a loss of 20 years was assumed for all cases. This approach may be an underestimation, certainly it is for children and teenagers. Pollen and VOC related allergies were estimated by expert judgment PAF values and concentration-ratio adjusted PAF, respectively.

In the baseline results, the main addition to the EBoDE outcome was the estimate for indoor generated fine particles, representing 16% of the disease burden of the included pollutants in 26 EU countries (Fig. 6). All HealthVent estimates were calculated using discounted values and thus, produced lower estimates for all significant sources of premature mortality, such as particles, carbon monoxide, radon, and second-hand smoke. Alternatively, for dampness and mold, bioaerosols, and VOCs the application of discounting played no significant role.

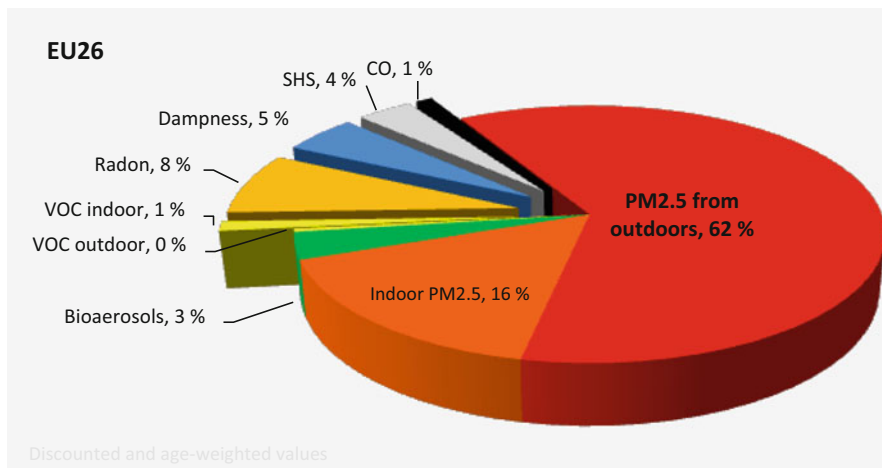


Fig. 6 Overall HealthVent results for the 26 EU countries in 2010. Total disease burden estimated at 2.1 million DALY (Hänninen and Asikainen 2013; Asikainen et al. 2016)

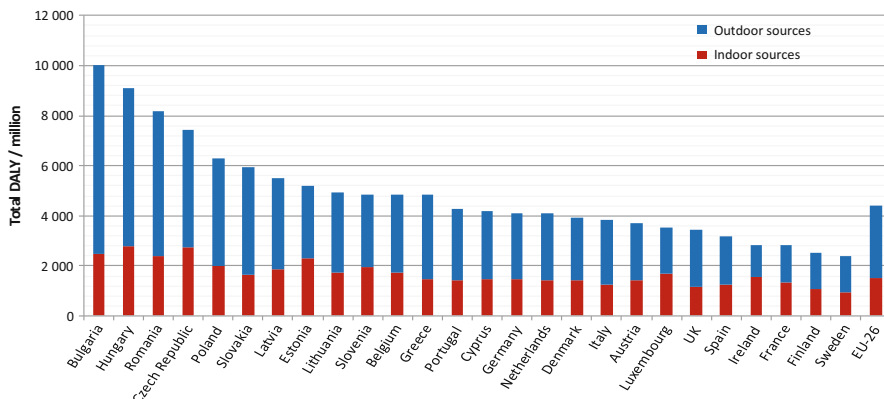


Fig. 7 National discounted disease burdens divided to indoor and outdoor source contributions (Hänninen and Asikainen 2013)

The HealthVent approach allowed to utilize high quality European Environmental Agency data for the population weighted ambient particle concentrations and thus comparing the disease burden of indoor and outdoor sources on national levels (Fig. 7). Differences between the indoor source burden are substantially more modest than the variability attributed to ambient component. Eastern European countries represented the worst ambient air quality in 2010.

Using estimates for Germany as an example, it can be shown that cardiovascular diseases are dominant, representing over 50% of the total burden (Fig. 8), followed by lung cancer, asthma, and COPD. Fine particles were the most significant exposures also in Germany in 2010.

HealthVent quantified the balance of indoor and outdoor air sources on the burden of disease for health optimization of ventilation rates as shown in Fig. 9. Interestingly the lowest burden occurs for ventilation rates of around 4 lps per person.

To date, HealthVent remains the only study that was able to conduct health impact assessment, i.e., calculate the quantitative health benefits that could be expected from implementation of defined ventilation guidelines. To support the development of European health-based ventilation guidelines, three scenarios were modelled (Fig. 10). Optimization of ventilation rates only or filtration of air intake only were less effective than targeted source control and optimized ventilation together.

The maximum reduction of the disease burden was almost 50%. Figure 11 shows the reduction potential of various diseases attributed to indoor (red) and outdoor (blue) sources. Cardiovascular diseases also dominated at the EU26 level. The largest reductions were projected for lung cancer from indoor sources and asthma from outdoor sources.

Indoor source concentrations of fine particles were estimated from relatively old EXPOLIS data, only available for four cities. While these cities (Athens, Basel, Prague, Helsinki) cover all the climatological regions of Europe, they do have limited geographical and national representativity, and thus, the exposure estimates

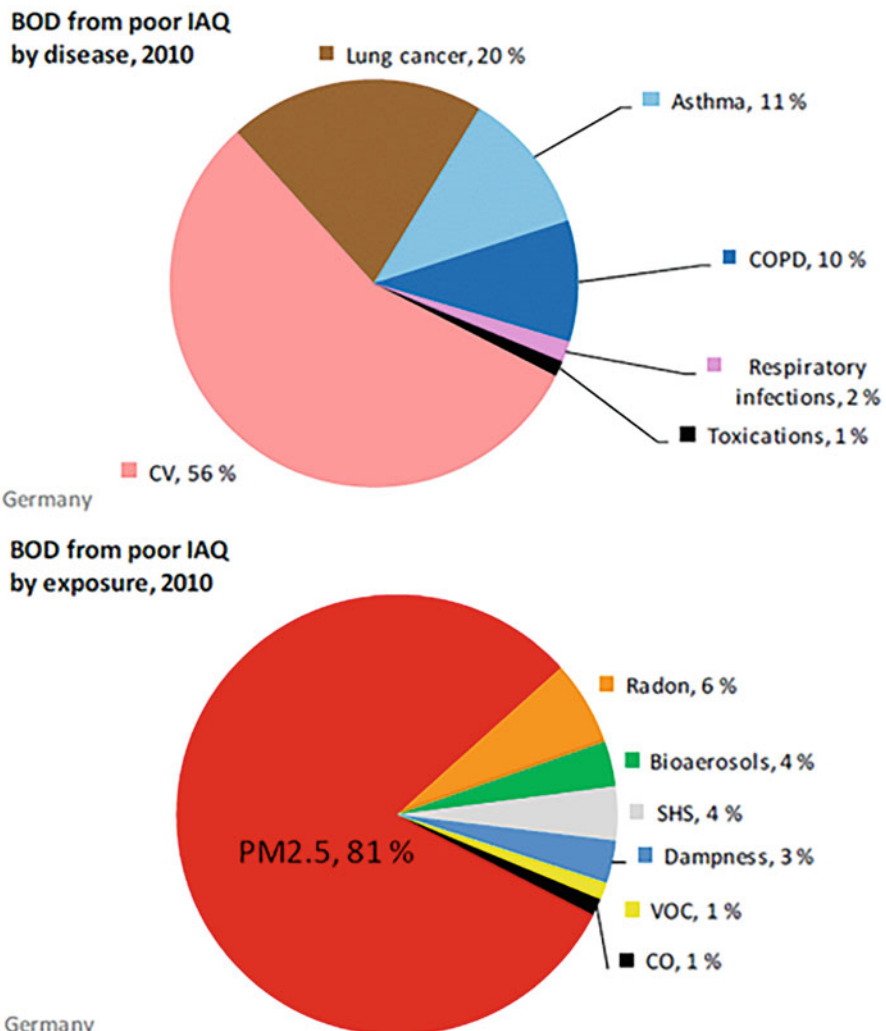


Fig. 8 Diseases attributed to indoor exposures in Germany in 2010 according to the HealthVent study (Hänninen and Asikainen 2013)

can be expected to be relatively uncertain. It remains a critical issue to update European estimates of population exposures to indoor generated particles as well as globally to consider methods to improve the corresponding concentration-response functions. Significant amounts of work have been conducted over the past decade for creating new models for ambient particles, but practically nothing has been proposed for the indoor generated ones.

The overall discounted health effect was substantially lower at 2.1 million DALY in EU26 (ca. 4200 DALY/million) than the non-discounted six-country estimates in

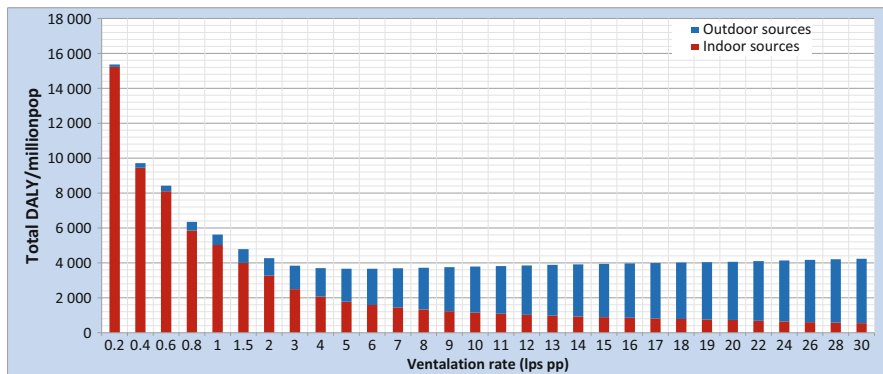


Fig. 9 Burden of diseases due to indoor air exposures as function of modified ventilation level. At low ventilation rates the indoor source contribution peak; as ventilation rate increases the indoor emissions are effectively diluted and the infiltration of ambient air pollution gradually increases (Hänninen and Asikainen 2013)

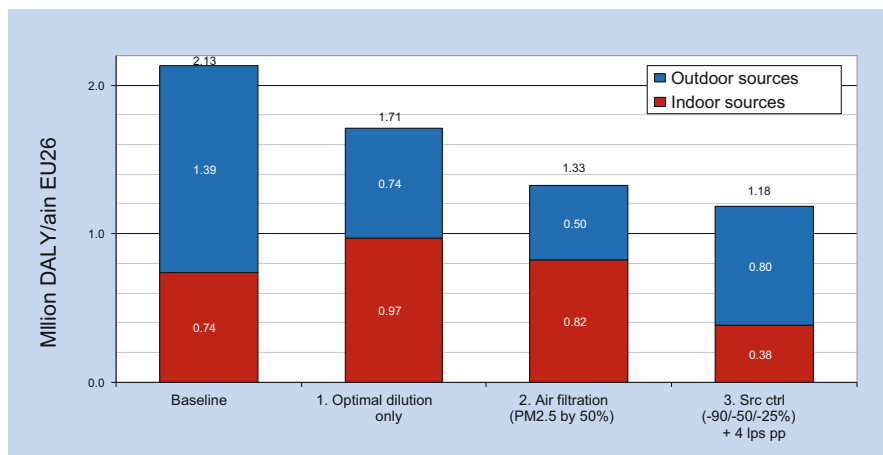


Fig. 10 Baseline burden was compared with three alternative reduction scenarios (Hänninen and Asikainen 2013; Carrer et al. 2018)

the EBoDE study (e.g., ca. 8000 DALY/million for ambient particles only), even though a relatively large component from indoor generated particles was added. Alternatively, traffic noise and other non-indoor pollution related exposures were excluded, but the main reasons for the reduction are that discounting was used, and the indoor exposure-related burden was calculated using the same exposure response relationship after accounting for the infiltration. Lack of personal exposure or even personal dose based health risk estimation remains a challenge.

The overall picture of the dominant role of fine particles was also confirmed in the HealthVent study. It was estimated that reduction of unnecessary ventilation could

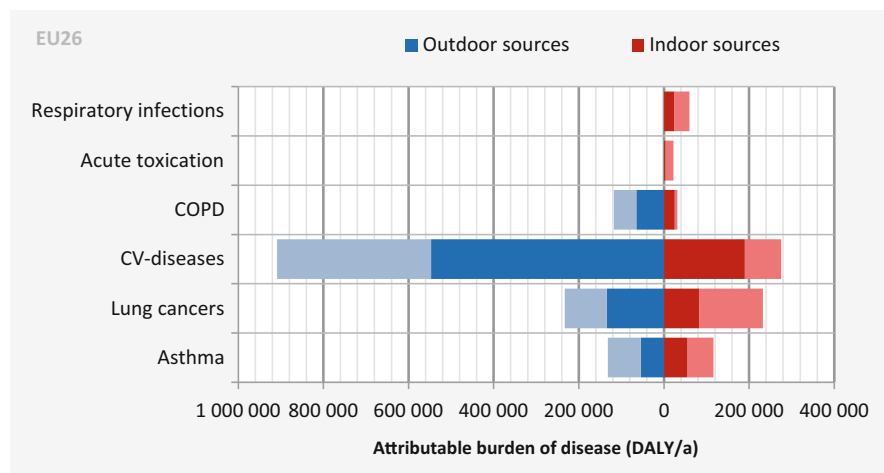


Fig. 11 Contribution of main disease categories to the burden of disease in EU26 caused by indoor air exposures to pollutants originating from outdoor (blue) and indoor (red) air (Hänninen and Asikainen 2013). The estimated maximum reduction is shown in the lighter shade by disease category. (COPD = chronic obstructive pulmonary disease, CV = cardiovascular diseases) (Hänninen and Asikainen 2013)

reduce disease burden by 15% and filtration of ambient intake air up to 30%, but most efficient controls involved a combination of indoor source control with optimized ventilation, allowing the annual saving of ca. 0.9 million DALYs in EU.

Indoor Air Pollution and Associated Socio-economic Costs in France

In 2001, the French government set in place a permanent research program on indoor air quality called the French Indoor Air Quality Observatory. Over time, with increasing knowledge on indoor pollution, i.e., increasing number of pollutants to be considered and rising evidence of health effects, it appeared necessary to the policymakers supporting the IAQ Observatory to have quantitative values expressing the impact of this environmental pollution at the national scale. Such evaluations of the socio-economic costs are useful to hierarchize the public health priorities and facilitate the development of appropriate policies. In 2014, the health impacts in terms of mortality and morbidity, as well as the economic impact, associated with indoor air pollution in France were assessed (Boulanger et al. 2017).

Pollutants Considered for the Evaluation

The target pollutants were selected based on: (i) existing data already documenting the health impact, i.e., attributable diseases and deaths, for the population in France, (ii) published dose-response relationships, and (iii) existing data on exposure in indoor environments at the national scale allowing for health impact calculations to be performed as needed.

Benzene, trichloroethylene, radon, carbon monoxide (CO), fine particles ($PM_{2.5}$), and second-hand smoke (SHS) were included:

- Annual deaths due to exposure to radon were already available (Catelinois et al. 2007)
- Mortality and hospitalization due to CO poisoning are monitored every year by the French Institute for Public Health Surveillance
- Number of deaths per year due to passive smoking was available (ERS 2006)
- For benzene, trichloroethylene, and $PM_{2.5}$, it was possible to calculate the yearly mortality associated with indoor exposure because both dose-response relationships and indoor concentrations in French dwellings were available.

Evaluation of Yearly Mortality

When not already available, i.e., for benzene, trichloroethylene, and $PM_{2.5}$, the yearly mortality was calculated through two approaches depending on the nature of the available data. The first method follows the principles of quantitative health risk assessment based on the NRC (1983) method, and the second is based on concepts and methods relating to the health impact assessment approach. For both of these approaches, toxicological data and indoor concentrations related to each target pollutant were needed:

- Toxicological data were retrieved from existing reviews and monographs. The health endpoints of each target pollutant are presented in Table 7;
- Indoor concentrations were those measured in dwellings at the national scale by the French Indoor Air Quality Observatory (Langer et al. 2016). Since the measurements were conducted between 2003 and 2005, the reference year for this evaluation was set at 2004. In the absence of monitoring surveys in other indoor environments in France at the time of the evaluation, the concentrations measured in the housing stock were considered to represent the indoor air concentrations in all indoor environments. The median indoor concentrations were considered to be the exposure concentration of the whole population for the target pollutants. The time spent indoors by the French population was considered to constitute 90% of the lifetime.

The excess collective risk resulting from benzene and trichloroethylene indoor exposure, respectively, was calculated based on the principles of quantitative health

Table 7 Summary of health endpoints considered for the six target pollutants

Radon	Second-hand smoke	Carbon monoxide	Benzene	Trichloroethylene	$PM_{2.5}$
Lung cancer	Lung cancer Heart attack Stroke COPD	Asphyxia	Leukemia	Kidney cancer	Lung cancer Cardiovascular disease COPD

COPD: Chronic Obstructive Pulmonary Disease

risk assessment, using Eq. (7) introduced in the Methods section of this chapter. The unit risk proposed by WHO (2000) for acute leukemia associated with benzene exposure through inhalation was used. For trichloroethylene, the inhalation unit risk proposed by the USSG (2006) for kidney cancer was used. PM_{2.5} health impacts were determined based on Eq. (10). To avoid any double counting since the impact of second-hand smoke, which includes particles emitted through smoking, is evaluated separately, the median concentration of PM_{2.5} was the one measured in non-smoker dwellings. The background concentration was the 5th percentile of the PM_{2.5} concentration distribution in non-smoker dwellings. The RR used were derived from Pope et al. (2002, 2004).

For each disease, the difference between the average age of death and the life expectancy of the general population, considered to be 80 years of age, was needed to determine the number of life-years lost. The average age of death for each studied disease was obtained from the French Center for Epidemiology on Medical Causes of Death.

The number of deaths of each disease in the reference year (2004) and the number of life-years lost used to calculate the external cost of mortality are presented in Table 8. For the target pollutants, indoor air pollution was estimated to be annually associated with about 20,000 deaths in France.

Evaluation of Yearly Morbidity

When not already available, the morbidity of each studied health effect, i.e., the new cases of the disease attributed to the indoor exposure, was estimated from the

Table 8 Estimates of the yearly health impacts associated with indoor exposure to each of the six target pollutants and external costs in France

	Radon	Second-hand smoke	Carbon monoxide	Benzene	Trichloroethylene	PM _{2.5}
Cases per year in France (2004)						
Number of deaths (n _d)	2,074	1,114	98	342	15	16,236
Number of life-years lost per death	11	15	47	15	15	15
Number of new cases (n _c)	2,388	2,836	—	385	41	22,784
Number of life-years with the disease per case	1.5	37.5	—	15	1.5	26.5
Costs (M€, 2004)						
Costs of premature deaths	2,089	322	237	453	19.6	5,760
Costs due to loss of life quality	309	837	0	383	6.7	7,350
Costs due to loss of productivity	282	85	72	38	1.5	1,102
Total external costs	2,680	1,244	309	874	27.8	14,212

mortality/morbidity ratio for this disease multiplied by the calculated (or available) mortality rate of the French population for the given disease. The mortality/morbidity ratio was obtained using data provided by the National Institute for Cancer, the French Ministry of Health and the French Institute for Public Health Surveillance. Moreover, the number of life-years with each studied disease was needed: data provided by the National Institute for Cancer and by WHO on the survival times for each studied disease were used.

The number of new cases of each disease in the reference year (2004) and the number of life-years with the disease used to calculate the external cost of morbidity are reported in Table 8. For the target pollutants, indoor air pollution was estimated to be annually associated with about 28,000 new cases of a disease in France.

Socio-economic Cost Evaluation

The socio-economic impacts of indoor air pollution were defined as the monetary value of the negative consequences of indoor air pollution, i.e., the quantity of resources lost by society as a result of exposure to this pollution. Since the objective was to assess the socio-economic costs to society, only public costs were calculated; costs supported by private companies or by individuals were not assessed. In this context, there are two types of socio-economic costs to be considered: external costs and impacts on public finances, whose respective calculation is described hereafter.

From an economic perspective, indoor air pollution is a negative externality, i.e., a consequence whereby no monetary compensation is initially planned, leading to external costs. To calculate these costs, the value of a statistical life year (VOLY) is needed. The VOLY is derived from the value of a statistical life (VSL). Different methods exist to assess the VSL, among them the “willingness to pay” approach. In France, following this approach, a VSL was set for all the socio-economic analyses and the VOLY was estimated to €115,000. Since the costs are increasing in the future relative to the reference year, an adjustment rate of 4% per year was applied in the calculations. For each pollutant and each disease associated with indoor exposure to this pollutant, the number of life years lost between the average age at death and the life expectancy was multiplied by the adjusted value of life year to calculate the total cost due to the premature deaths according to Eq. (16).

$$\text{External cost of premature deaths} = n_d \times \sum_i \frac{\text{VOLY}}{(1+r)^i} \quad (16)$$

where, n_d = number of premature deaths associated with a disease generated by one pollutant, VOLY = value of a statistical life year, €115,000, r = adjustment rate, 4%, and i = number of life – years lost because of the disease.

The external costs also include the costs associated with morbidity, i.e., quality of life loss and productivity loss. The socio-economic costs in terms of the loss of quality of life were derived from the calculated morbidity value and from the average disability weight defined by WHO for each disease. Similar to the costs of mortality, quality of life costs were adjusted over the number of years of life with a given disease prior to death, with the adjustment rate of 4% per year. Each adjusted cost

was then multiplied by the number of new cases for each disease associated with indoor exposure to a studied pollutant to obtain the total cost of quality of life loss for each disease according to Eq. (17).

$$\text{External cost of loss of quality of life} = n_c \times \sum_j \frac{\delta \times VOLY}{(1+r)^j} \quad (17)$$

where n_c = number of new cases associated with a disease generated by one pollutant, δ = loss of quality of life, i.e., average disability weight defined by the WHO for the disease, $VOLY$ = value of a statistical life year, €115,000, r = adjustment rate, 4%, j = number of years of life with a given disease prior to death.

Finally, to estimate production loss, the “discounted income stream” approach, proposed by the National Institute for Cancer, was used to assess the production value that an individual would have generated if he had not died from cancer or another disease.

Regarding public finances (i.e., the second type of costs to be considered), indoor air pollution involves expenses that are supported by public finances. First, the different diseases associated with indoor air pollution generate a demand for healthcare which represents a cost to public finances. Second, to reduce indoor air pollution, the State invests in public research. Lastly, when deaths occur between age 60, i.e., the start of retirement, and 80, the life expectancy, savings resulting from the non-payment of full or partial retirement pensions were calculated. The average annual retirement pension value in 2004 (€15,000) was adjusted by 4% over the number of years of retirement lost.

The external costs per pollutant and disease are reported in Table 8. Overall, the external costs were estimated to M€19,347 in the reference year (2004). Besides, the costs for public finances in the reference year were estimated to M€96. In total, for the target pollutants, indoor air pollution was estimated to cost M€19,443 in France in 2004.

The external costs represent nearly all of the total cost, and the impacts on public finances represent less than 1% of the total cost. Overall, mortality and morbidity have the same effect, i.e., 46% of the external costs. However, it varies depending on the pollutant. Particles contribute the most to the total cost (approximately €14 billion). Radon also has a significant health cost (€2.68 billion). The pollutants’ relative contributions to costs are ranked as follows: particles > radon > SHS > benzene > carbon monoxide > trichloroethylene.

Limitations and Conclusions

The limitations of this evaluation include the limited number of indoor pollutants, due to lack of dose-response relationships and/or to indoor exposures that are not comprehensively characterized in France compared, e.g., to China, as described in the next section. The indoor concentrations measured in dwellings were extrapolated to other indoor environments. The health effects identified for a given pollutant were not exhaustive. Moreover, health effects associated with exposure to mixtures of pollutants were not assessed. The health impact estimation method used was based

on quantitative health risk assessment and health impact calculation principles. Other approaches exist, such as the ones described in the other sections of this chapter based on the DALY. There are uncertainties regarding the average age at death or the ratio of morbidity to mortality. From an economic point of view, the valuation of €115,000 per year of life lost is debatable. The discount rate was considered to be the same regardless of the time horizon or the severity of the disease.

Despite these limitations, such an evaluation provides an order of magnitude of the impact of indoor air pollution and confirms that it is imperative for researchers and policymakers to continue addressing indoor air quality issues. Moreover, such figures can now serve as a baseline for cost-benefit analyses on possible strategies used to reduce indoor air pollution, with the objective to identify the most efficient strategy.

Disease Burden of Indoor Air Pollutants in China

To comprehensively have a good knowledge of health impacts of indoor air pollutants (IAPs) in different kinds of buildings in China, the Burden of Disease for Indoor Air Pollutants (IAP-BD) study was launched in China, using the updated methods from the GBD study (Murray et al., 2012) and studies for burden of diseases due to indoor pollutants in other countries or regions (Hänninen et al. 2014, Logue et al. 2012).

Indoor Exposure Assessment

The list of dominant indoor air pollutants in China was summarized based on the national standards for indoor air quality GB/T 18883 (National Health Commission of China 2002), WHO air quality guideline (WHO 2006, 2010), and the study on cancer risk of IAPs in China (Du et al. 2014). Additionally, several rounds of seminars were held and experts from multidisciplinary backgrounds provided advice on this list. The final list of IAPs in China in this study contained five types of pollutants, particulate matters, inorganic chemical pollutants, volatile organic compounds (VOCs), semi-volatile organic compounds (SVOCs), and microbial pollutants, and 31 IAPs in total.

For PM_{2.5}, SO₂, NO₂, and O₃, that predominantly come from outdoors, the infiltration factor method (Hu et al. 2020; Xiang et al. 2019) was applied to estimate the indoor exposure concentrations. For the other 27 indoor air pollutants that come primarily from indoor sources, systematic reviews were conducted to summarize and estimate the concentration distributions of these indoor air pollutants in China. (Zhang et al. 2021; Guo et al. 2020; Sun et al. 2021; Su et al. 2021) After the data collection, the Monte Carlo method was employed to estimate the concentration distributions of these 27 IAPs in China (Bu et al. 2019). Finally, the concentration distributions of each IAP across China were generated for residences, offices, and schools, weighted by population of all provinces in China. To differentiate the exposure concentrations of these IAPs in adults and children, the average concentration distributions were calculated for adults weighted by the time allocation in

residences and offices, and for children weighted by the time spent in residences and schools.

The PM_{2.5} concentrations and related inorganic chemical pollutants in China are shown in Fig. 12. The concentrations of nine kinds of VOCs are shown in Fig. 13. Additionally, Fig. 14 summarized the exposure values of microbial pollutants and dust-phase SVOCs in China. Clearly, most of the IAPs in China had higher concentrations than those in Europe and USA.

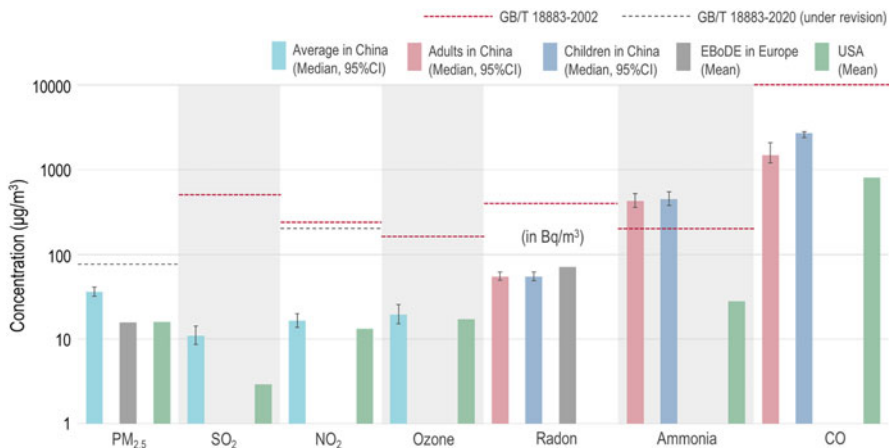


Fig. 12 The concentration of PM_{2.5} and inorganic chemical pollutants in China, Europe and USA. The colorful bar represents the point estimate, and the line represents the 95% confidence interval

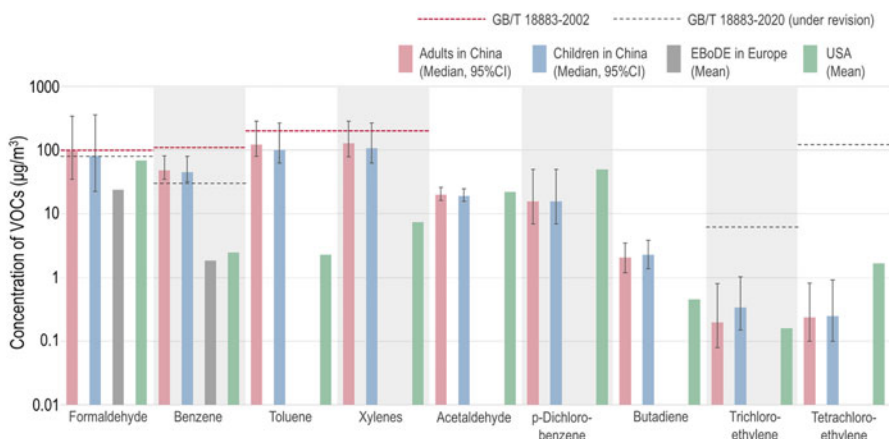


Fig. 13 The concentration of VOCs in China, Europe and USA. The column bars represent the point estimates, and the error bars the 95% confidence interval. Xylenes include m-, p-, o-xylenes



Fig. 14 The concentration of microbial pollutants and dust-phase SVOCs in China, Europe and USA. The column bars represent the point estimates, and the error bars the 95% confidence interval. In the 13 SVOCs, the first 5 pollutants belong to phthalates and the latter 8 pollutants belong to PAHs

Associations Between IAPs and Health Outcomes

For PM_{2.5}, the integrated exposure-response (IER) model was directly applied to describe the associations between the PM_{2.5} concentration and several health outcomes. (Burnett et al. 2014) For other indoor air pollutants, systematic reviews were conducted to summarize available concentration-response (C-R) relationships for various health outcomes from epidemiological studies. Finally, the information on location, year, sample size, study type, effect size, and exposure concentrations were collected from eligible studies for the meta-analysis. The results of the meta-analysis have been shown in Figs. 15, 16, and 17.

Disease Burden Attributable to Indoor Air Pollutants in China

Using concentrations and associations between IAPs and health outcomes, the disease burden attributable to IAPs can be estimated according to the PAF method mentioned in the section of methods above. In this section, only significant C-R relationships between IAPs and outcomes (underlined in Figs. 15, 16, and 17) were included. The insignificant C-R relationships were excluded in this analysis, such as the relationship between benzene and asthma, which required further evidence. When the concentration was higher than the maximum reported in the available epidemiological studies, the RR was assumed to behave as a horizontal level instead of a simple nonlinear extrapolation by the equation in the methods section.

Estimation of IAP-BD in China

The total DALY rate due to exposure to indoor air pollutants in China was ca. 33,000 per million, accounting for 12.5% of total DALY rate that rose to 263,000 per million in 2017 in China. (GBD 2021c) Among all the selected indoor air pollutants, PM_{2.5}, benzene, NO₂, butadiene, and ozone ranked in the top five DALY losses, all of which were all over 1000 per million (Fig. 18). In particular, PM_{2.5} led to 17,600 DALY

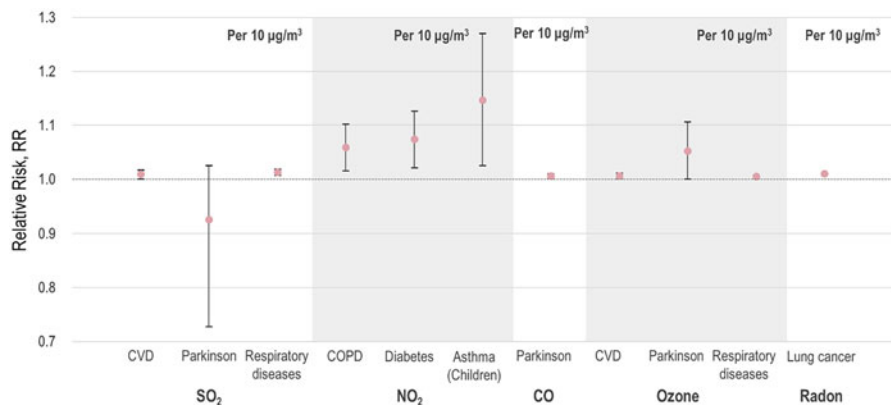


Fig. 15 The associations between health outcomes and inorganic chemical pollutants through meta-analysis (relative risk and 95% confidence interval)

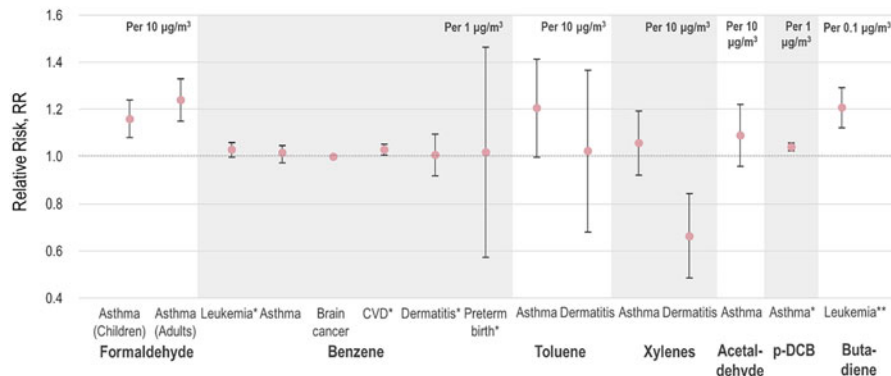


Fig. 16 The associations between health outcomes and VOCs through meta-analysis (relative risk and 95% confidence interval)

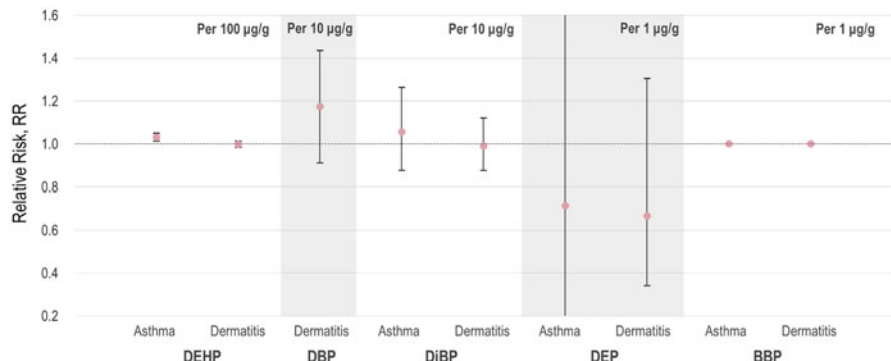


Fig. 17 The associations between health outcomes and SVOCs through meta-analysis (relative risk and 95% confidence interval)

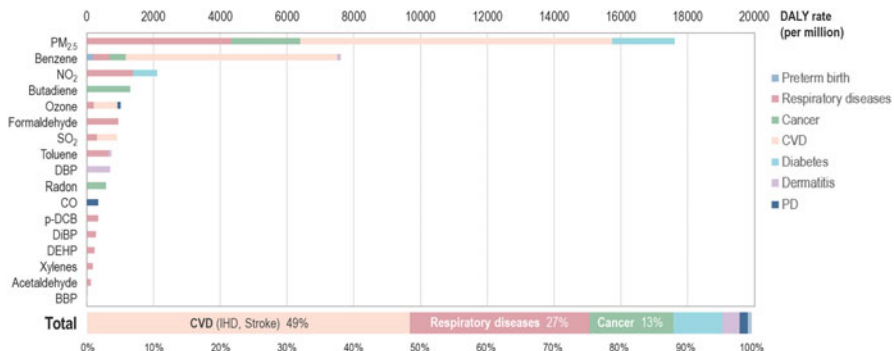


Fig. 18 The composition of DALY rate attributable to indoor air pollutants in China according to various health outcomes

losses per million, approximately 50% of the disease burden due to all indoor air pollutants. Additionally, butadiene exposure (1300 DALY losses per million) has not been considered in the related standard but ranked 4th, suggesting to requires greater attention given its importance. The other three pollutants, benzene, NO₂, and ozone, were controlled by the current national standard in China, but still contributed to over 30% of attributable DALY losses, suggesting that the standards in the future should be tightened to decrease the disease burden of these three IAPs. Formaldehyde, which ranked 6th, produced nearly the same disease burden as ozone, so formaldehyde is also worth focusing on. From the perspective of the type of IAPs, the disease burden of IAPs other than PM_{2.5} accounted for nearly 50% but had been previously neglected. Additionally, many VOCs and SVOCs did not have sufficient evidence to support associations with various health outcomes, suggesting that they may cause more disease burden in reality than the estimation in this study. All these results imply that the health effects caused by VOCs and SVOCs have to be the focal point in future studies. From Fig. 18, it can be also seen that cardiovascular diseases, COPD, respiratory diseases, lung cancer, and diabetes accounted for the majority ($\approx 90\%$) in the DALY losses attributable to IAPs. The largest proportion of disease burden owing to IAP exposure was concerned with cardiovascular diseases (including ischemic heart disease and stroke), which accounted for nearly 52%, followed by COPD.

Comparison of IAP-BD Among Countries

As previously mentioned, the concentrations of many indoor air pollutants in China were higher than those in Europe and USA, thus inducing higher disease burdens attributable to IAPs (Hänninen et al. 2014; Logue et al. 2012). To ensure fair and valid comparisons, the disease burden of IAPs in Europe and USA was estimated by combining the concentrations reported in the study of six European countries and USA (Hänninen et al. 2014; Logue et al. 2012) and the C-R relationship summarized in this study. The IAP-BD in China (32,900 DALY losses per million) is significantly



Fig. 19 The ranking of indoor air pollutants according to attributable disease burden in China, Europe (EBoDE, 6 countries), and USA

higher than that in USA (24,500 DALY losses per million), followed by the six European countries. The IAP-BD in the Netherlands was the smallest, only 16,300 DALY losses per million, nearly half of that in China. From the view of the proportion of IAP-BD, China also ranked the highest, where the IAP-BD reached 12.5% of the total DALY losses in 2017. Instead, the IAP-BD in European countries and USA ranged from 5.8% to 7.9%, suggesting that it is essential to address the problems of indoor air pollution in China in the near-term future. The ranking of IAPs in different regions is shown in Fig. 19. PM_{2.5} ranked first in China, Europe, and the USA according to attributable DALY losses, accounting for over 50% of the IAP-BD. Benzene, NO₂, and formaldehyde all ranked in the top of the lists in these countries, each of which contributed nearly or even more than 1000 DALY losses per million.

Limitations and Future Study

This IAP-BD study in China has some limitations. Considering the IAP concentrations, the precision of the exposure parameters and concentrations depends on the original field studies from which it is difficult to assess the accuracy of these original data from small-size samples. From 2000 to 2017, the concentrations of some IAPs may change a lot, but this issue has not yet been accounted for in this study. Similarly, as the first estimation in China, we have not considered the province-level IAP concentrations given the lack of field measurement data. Further studies can organize the field measurement of IAP concentrations in different provinces across China during each year to acquire more reliable concentration data. Considering the health effects of IAPs other than PM_{2.5}, many available associations between IAP exposure and health outcomes are primarily based on case-control studies or cross-sectional studies due to the lack of cohort study in this field, and are insignificant after meta-analysis. Therefore, the evidence is insufficient to support causal relationships between IAP exposure and these diseases. Moreover, currently available C-R relationships in the epidemiological literature have not taken the co-exposure of multiple IAPs (especially from similar pollution sources) into consideration. Further studies can focus on cohort studies of large Chinese populations exposed to multiple IAPs to obtain the reliable and accurate C-R relationships between IAP concentrations and various health outcomes.

Discussion

The burden of disease methods allow for comparability of largely differing health outcomes for prioritization of risk mitigation. Risk assessment is a critical input toward quantifying the reduction potential of health losses. The risk assessment paradigm introduced risk characterization, and finally, the burden of disease approach allows for comparative quantification of attributable fractions. Health impact assessment by definition attempts to look at non-health sector policies and their impact on health, which must be implemented via complex exposure and exposure-change analyses.

In practice the current burden of disease estimates are quite clearly dominated by the years of life lost (YLL) component while the morbidity (YLD) remains less important in quantitative terms. Partly the YLL dominance originate from the handling of life expectancy: the current approaches use life-table projections for 2050 of the healthiest populations globally, leading to life expectancies that clearly exceed most actual national values. Thus, the calculated YLL component also accounts for the expected improvements in life expectancies over the coming decades. On the other hand, the morbidity component is the one that affects productivity, academic performance, lost working and school days, and general wellbeing of the populations. It may be important to consider these factors separately for better visibility.

Risk estimates contain many uncertainties including population representativeness, measurement errors, modelling errors, statistical uncertainties in exposures, and exposure-response relationships. The risk assessment community is continuously improving the assessment of uncertainties and the epidemiological parameters routinely come with confidence intervals. Alternatively, air quality modelers and exposure scientists do not regularly provide confidence intervals for their estimates. It remains on the responsibility of the risk assessors then to combine these sources of uncertainties using statistical and probabilistic techniques.

The GBD studies are looking at the richest set of risk factors, including 87 components or groups. Still, they can only attribute half or less of the national burden on these factors. It remains an open but important question: From where does the remaining half of the disease burden come?

Millions of chemicals are produced worldwide by industries, combustion processes and other anthropogenic and natural sources. While toxicological data suggests much larger relevance, currently the EBD/BOD methods account for a very small fraction of all chemicals and their environmental degradation products. It may be that there are many missing pollutants that would warrant to be added into the assessments. While writing this text in early 2022, the continuing global COVID-19 pandemic demonstrates also the importance of infectious agents that are not covered here. However, their contribution to burden of disease as well as the importance of time-use in indoor spaces and role of ventilation is high.

Summary

The environmental burden of disease provides a useful quantitative indicator of the population level health impacts of environmental factors, including chemical pollutants and noise. It allows quantitative comparisons of public health impacts associated with a wide range of environmental risk factors and targeting research and especially risk management to the major issues.

Environmental burden of disease methods have been successfully applied to a number of indoor air settings in Europe, North America, and China, although a number of challenges remain. Especially exposure assessment is substantially more complicated for indoor spaces than for ambient air, but also the number of pollutants found in indoor spaces is large and suitable health response models are not yet available for many of them.

The environmental burden of disease cannot directly be interpreted as a reducible burden. In many cases, exposures to natural sources of pollution or the existence of overlapping risk factors lead to the fact that exposures cannot be completely eliminated. Examples of such factors are, e.g., atmospheric particles and radon, both originating also from natural sources.

Further analysis may also be applicable for the cost effectiveness of various risk management actions. In some cases, reduction in exposures may require complex and potentially expensive legislative changes, e.g., removing lead from fuels, water pipes, canned foods, paints, and so on, over the past decades. Currently, similar challenges are being experienced, e.g., controlling exposure to fine particles, which also present widely and have very heterogeneous sources. Combining environmental burden of disease estimates with cost-effectiveness methodologies allows societies to target their environmental control efforts as efficiently as possible.

Acknowledgments This text is based, among other cited sources, on work and materials produced in the EBoDE project (by intramural funding by the participating institutes); HEALTHVENT project (by EU Health Programme Grant Nr. 2009 12 08.). Indoor exposure dependency on aerosol sizes was developed in TRANSPHORM (by EU FP7) and PMSIZEX (by Academy of Finland). Parallel work on health risk assessment was supported by the COST Action IS1408. Collaborators in these projects are warmly thanked for their intellectual contributions. The French study was supported by the French Agency for Food, Environmental and Occupational Health and Safety (Anses; Grant n°CRD-2011-11) and the French Indoor Air Quality Observatory.

References

- Asikainen A, Carrer P, Kephalopoulos S, de Oliveira FE, Wargocki P, Hänninen O (2016) Reducing burden of disease from residential indoor air exposures in Europe (HEALTHVENT project). Special Issue on “Challenges and Opportunities for Urban Environmental Health and Sustainability”. Environ Health 15(S1):61–72. <https://doi.org/10.1186/s12940-016-0101-8>
- Babisch W (2006) Transportation noise and cardiovascular risk: Review and synthesis of epidemiological studies, exposure-response curve and risk estimation. WaBoLu-Hefte; 01/06, Umweltbundesamt, Berlin

- Boulanger G, Bayeux T, Mandin C, Kirchner S, Vergriette B, Pernelet-Joly V, Kopp P (2017) Socio-economic costs of indoor air pollution: A tentative estimation for some pollutants of health interest in France. *Environ Int* 104:14–24. <https://doi.org/10.1016/j.envint.2017.03.025>
- Bu ZM, Mmereki D, Wang JH, Dong C (2019) Exposure to commonly-used phthalates and the associated health risks in indoor environment of urban China. *Sci Total Environ* 658:843–853
- Burnett R, Pope C III, Ezzati M, Olives C, Lim S, Mehta S, Shin HH, Singh G, Hubbell B, Brauer M, Anderson H, Smith K, Balmes J, Bruce N, Kan H, Laden F, Prüss-Ustün A, Turner M, Gapstur S, Diver W, Cohen A (2014) An integrated risk function for estimating the global burden of disease attributable to ambient fine particulate matter exposure. *Environ Health Perspect* 122(4):397–404
- Burnett R, Chen H, Szyszkowicz M, Fann N, Hubbell B, Pope C III, Apté J, Brauer M, Cohen A, Weichenthal S, Coggins J, Di Q, Brunekreef B, Frostad J, Lim S, Kan H, Walker K, Thurston G, Hayes R, Lim C, Turner M, Jerrett M, Krewski D, Gapstur S, Diver W, Ostro B, Goldberg D, Crouse D, Martin R, Peters P, Pinault L, Tjepkem M, Donkelaar A, Villeneuve P, Miller A, Yin P, Zhou M, Wang L, Janssen N, Marra M, Atkinson R, Tsang H, Thach T, Cannon J, Allene R, Hart J, Laden F, Cesaroni G, Forastiere F, Weinmayr G, Jaensch A, Nagel G, Concin H, Spadaro J (2018) Global estimates of mortality associated with longterm exposure to outdoor fine particulate matter. *PNAS*. <https://doi.org/10.1073/pnas.1803222115>
- Californian EPA (2005) Proposed identification of environmental tobacco smoke as a toxic air contaminant. Sacramento, California, Californian Environmental Protection Agency.
- Carrer P, de Oliveira FE, Santos H, Hänninen O, Kephalaopoulos S, Wargocki P (2018) On the development of health-based ventilation guidelines: principles, approach and proposed framework. *Int J Environ Res Public Health* 15:1360. <http://www.mdpi.com/1660-4601/15/7/1360>
- Catelinois O, Rogel A, Laurier D, Billon S, Hémon D, Verger P, Tirmarche M (2007) Evaluation de l'impact sanitaire de l'exposition domestique au radon en France. *Bull Epidemiol Hebd* 18-19: 155–158
- Cohen A, Brauer M, Burnett R, Anderson H, Frostad J, Estep K, Balakrishnan K, Brunekreef B, Dandona L, Dandona R, Feigin V, Freedman G, Hubbell B, Jobling A, Kan H, Knibbs L, Liu Y, Martin R, Morawska L, III C, Shin H, Straif K, Shaddick G, Thomas M, Dingenen R, Donkelaar A, Vos T, Murray C, Forouzanfar M (2017) Estimates and 25-year trends of the global burden of disease attributable to ambient air pollution: an analysis of data from the Global Burden of Diseases Study 2015. *Lancet* 389:1907–1918. [https://doi.org/10.1016/S0140-6736\(17\)30505-6](https://doi.org/10.1016/S0140-6736(17)30505-6)
- Darby S, Hill D, Auvinen A, Barros-Dios JM, Baysson H, Bochicchio F, Deo H, Falk R, Forastiere F, Hakama M, Heid I, Kreienbrock L, Kreutzer M, Lagarde F, Mäkeläinen I, Muirhead C, Obereigner W, Pershagen G, Ruano-Ravina A, Ruosteenja E, Schaffrath-Rosario A, Tirmarche M, Tomasek L, Whitley E, Wichmann H-E, Doll R (2005) Radon in homes and lung cancer risk: collaborative analysis of individual data from 13 European casecontrol studies. *British Medical Journal* 330:223–226. <http://www.bmjjournals.org/cgi/reprint/330/7485/223> (accessed 2 July 2009)
- Diapouli E, Chaloulakou A, Koutrakis P (2013) Estimating the concentration of indoor particles of outdoor origin: A review. *J Air Waste Manage Assoc* 63:1113–1129
- Du ZJ, Mo JH, Zhang YP (2014) Risk assessment of population inhalation exposure to volatile organic compounds and carbonyls in urban China. *Environ Int* 73:33–45
- ERS (2006) Lifting the Smokescreen, 10 Reasons for a Smoke Free Europe. The Smoke Free Partnership. Brussels, European Respiratory Society. ISBN 1-904097-56-1. https://smokefreepartnership.eu/images/Reports-and-Position-Papers/Lifting_the_smokescreen.pdf. Accessed on January 17th, 2022
- Etzel RA, Pattishall EN, Haley NJ, Fletcher RH, Henderson FW (1992) Passive smoking and middle ear effusion among children in day care. *Pediatrics* 90:228–232
- GBD (2019) Global Burden of Disease Collaborative Network. Global Burden of Disease Study 2019 (GBD 2019) Disability Weights. Institute for Health Metrics and Evaluation (IHME), Seattle, 2020. <http://ghdx.healthdata.org/record/ihme-data/gbd-2019-disability-weights>. Accessed 2021-04-30

- GBD (2021a) Institute of Health Metrics and Evaluation (IHME). <http://www.healthdata.org/gbd/2019>
- GBD (2021b) Global Burden of Disease Collaborative Network. Global Burden of Disease Study 2019 (GBD 2019) Particulate Matter Risk Curves. Institute for Health Metrics and Evaluation (IHME), Seattle. <https://doi.org/10.6069/KHWH-2703>
- GBD (2021c) GBD compare. <https://vizhub.healthdata.org/gbd-compare>. Accessed 27 Apr 2021
- Guo K, Qian H, Zhao D, Ye J, Zheng X (2020) Indoor exposure levels of bacteria and fungi in residences, schools, and offices in China: a systematic review. *Indoor Air* 30(6):1147–1165
- Hänninen O, Asikainen A (eds.) (2013) Efficient reduction of indoor exposures: Health benefits from optimizing ventilation, filtration and indoor source controls. National Institute for Health and Welfare (THL). Report 2/2013. 92 pages. Helsinki 2013. ISBN 978-952-245-821-6 (printed) ISBN 978-952-245-822-3 (online publication) <http://urn.fi/URN:ISBN:978-952-245-822-3>. Accessed 2014-11-24
- Hänninen O, Knol A (eds.) (2011) European perspectives on Environmental Burden of Disease; Estimates for nine stressors in six countries. THL Reports 1/2011, Helsinki, Finland. 86 pp + 2 appendixes. ISBN 978-952-245-413-3. <http://www.thl.fi/thl-client/pdfs/b75f6999-e7c4-4550-a939-3bccb19e41c1>. Accessed 2011-03-23
- Hänninen OO, Lebret E, Ilacqua V, Katsouyanni K, Künzli N, Srám RJ, Jantunen MJ (2004) Infiltration of ambient PM_{2.5} and levels of indoor generated non-ETS PM_{2.5} in residences of four European cities. *Atmos Environ* 38(37):6411–6423
- Hänninen O, Hoek G, Mallone S, Chellini E, Katsouyanni K, Kuenzli N, Gariazzo C, Cattani G, Marconi A, Molnár P, Bellander T, Jantunen M (2011) Seasonal patterns of outdoor PM infiltration into indoor environments: review and meta-analysis of available studies from different climatological zones in Europe. *Air Qual Atmos Health* 4(3–4):221–233. <https://doi.org/10.1007/s11869-010-0076-5>. <http://www.springerlink.com/content/k26h4563110m373g/fulltext.pdf>. Accessed 2011-08-31
- Hänninen O, Sorjamaa R, Lippinen P, Cyrys J, Lanki T, Pekkanen J (2013) Aerosol-based modelling of infiltration of ambient PM_{2.5} and evaluation against population-based measurements in homes in Helsinki, Finland. *J Aerosol Sci* 66:111–122. <https://doi.org/10.1016/j.jaerosci.2013.08.004>. <http://www.sciencedirect.com/science/article/pii/S0021850213001754>
- Hänninen O, Knol A, Jantunen M, Lim T-A, Conrad A, Rappolder M, Carrer P, Fanetti A-C, Kim R, Buekers J, Torfs R, Iavarone I, Classen T, Hornberg C, Mekel O, the EBoDE Group (2014) Environmental burden of disease in Europe: estimates for nine stressors in six countries. *Environ Health Perspect*. <https://doi.org/10.1289/ehp.1206154>. <http://ehp.niehs.nih.gov/1206154/>
- Hollander de A, Melse J, Lebret E, Kramers P (1999) An aggregate public health indicator to represent the impact of multiple environmental exposures. *Epidemiology* 10(5):606–617
- Hu Y, Yao MY, Liu YM, Zhao B (2020) Personal exposure to ambient PM_{2.5}, PM₁₀, O₃, NO₂, and SO₂ for different populations in 31 Chinese provinces. *Environ Int* 144
- Huijbregts MAJ, Rombouts LJA, Ragas AMJ, van de Meent D (2005) Human-toxicological effect and damage factors of carcinogenic and non-carcinogenic chemicals for life cycle impact assessment. *Integr Environ Assess Manag* 1(3):181–244
- Hurley F, Hunt A, Cowie H, Holland M, Miller B, Pye S, Watkiss P (2005) Methodology Paper (Volume 2) for Service Contract for carrying out cost-benefit analysis of air quality related issues, in particular in the clean air for Europe (CAFE) programme. AEA Technology Environment, 133 pp. http://ec.europa.eu/environment/archives/air/cafe/pdf/cba_methodology_vol2.pdf (accessed 7 July 2009)
- Jaakkola MS, Piipari R, et al (2003) Environmental tobacco smoke and adult-onset asthma: a population-based incident case-control study. *Am J Public Health* 93(12):2055–60
- Klaassen CD (2008) Toxicology: the basic science of poisons. McGraw-hill, 7 edition, ISBN1601197837, 1310 pp.
- Landrigan PJ, Fuller R, Acosta NJR, Adeyi O, Arnold R, Basu NN, Baldé AB, Bertollini R, Bose-O'Reilly S, Boufford JI, Breysse PN, Chiles T, Mahidol C, Coll-Seck AM, Cropper ML, Fobil J, Fuster V, Greenstone M, Haines A, Hanrahan D, Hunter D, Khare M, Krupnick A, Lanphear B,

- Lohani B, Martin K, Mathiasen KV, McTeer MA, Murray CJL, Ndhimananjara JD, Perera F, Potočnik J, Preker AS, Ramesh J, Rockström J, Salinas C, Samson LD, Sandilya K, Sly PD, Smith KR, Steiner A, Stewart RB, Suk WA, van Schayck OCP, Yadama GN, Yumkella K, Zhong M (2018) The lancet commission on pollution and health. *Lancet* 391:462–512
- Langer S, Ramalho O, Derbez M, Ribéron J, Kirchner S, Mandin C (2016) Indoor environmental quality in French dwellings and building characteristics. *Atmos Environ* 128:82–91. <https://doi.org/10.1016/j.atmosenv.2015.12.060>
- Logue J, Price P, Sherman M, Singer B (2012) A method to estimate the chronic health impact of air pollutants in U.S. residences. *Environ Health Perspect* 120(2):2016–2222
- Miedema HME, Vos H (2007) Associations between self-reported sleep disturbance and transport noise based on reanalyses of pooled data from 24 studies. *Behavioural Sleep Medicine* 5(1):1–20
- Murray CJL, Lopez AD, (1996) The global burden of disease: a comprehensive assessment of mortality and disability from diseases, injuries and risk factors in 1990 and projected to 2020. Harvard School of Public Health on behalf of the World Health Organization and the World Bank. Cambridge
- Murray CJ, Lopez AD (1997) Global mortality, disability, and the contribution of risk factors: global burden of disease study. *Lancet* 349(9063):1436–1442
- Murray CJL, Ezzati M, Flaxman AD, Lim S, Lozano R, Michaud C, Naghavi M, Salomon JA, Shibuya K, Vos T et al (2012) GBD 2010: design, definitions, and metrics. *Lancet* 380(9859): 2063–2066
- Murray C, Aravkin A, Zheng P et al (2020) Global burden of 87 risk factors in 204 countries and territories, 1990–2019: a systematic analysis for the Global Burden of Disease Study 2019. *The Lancet* 17 October 2020. [https://doi.org/10.1016/S0140-6736\(20\)30752-2](https://doi.org/10.1016/S0140-6736(20)30752-2)
- National Health Commission of China (2002) GB/T 18883, Indoor air quality standard. <http://c.gb688.cn/bzgk/gb/showGb?type=online&hcno=59392CE8FD4422912D711459014EA4A7>. Accessed 20 April 2021
- NRC (1983) Risk assessment in the federal government: managing the process. National Research Council, The National Academies Press, Washington, DC. <https://doi.org/10.17226/366>. 205 pp.
- Ostro B (2004) Outdoor air pollution: assessing the environmental burden of disease at national and local levels. Environmental burden of disease series, no 5; World Health Organization, Geneva, Switzerland. Available online: https://www.who.int/quantifying_ehimpacts/publications/ebd5.pdf. Accessed on 15 Jan 2019
- Pope CA III, Burnett RT, Thun MJ, Calle EE, Krewski D, Ito K, Thurston GD (2002) Lung cancer, cardiopulmonary mortality, and long term exposure to fine particulate air pollution. *J Amer Med Assoc* 287(1132):1141
- Pope CA III, Burnett RT, Thurston GD, Thun MJ, Calle EE, Krewski D, Godleski J (2004) Cardiovascular mortality and long-term exposure to particulate air pollution epidemiological evidence of general pathophysiological pathways of disease. *Circulation* 2004:71–77
- Prüss-Üstün A, Mathers C, Corvalán C, Woodward A (2003) Environmental burden of disease series 1, introduction and methods. Assessing the environmental burden of disease at national and local levels. World Health Organization, protection of the human environment, Geneva. 71 pp.
- Prüss-Üstün A, Wolf J, Corvalán C, Bos R, Neira M. 2016. Preventing disease through healthy environments. A global assessment of the burden of disease from environmental risks. World Health Organization, Geneva, Switzerland. 147 pp. ISBN 978 92 4 156519 6
- Rockhill B, Newman B, Weinberg C (1998) Use and misuse of population attributable fractions. *Am J Public Health* 88(1):15–19
- Rumchev KB, Spickett JT, Bulsara MK, Phillips MR, Stick SM (2002) Domestic exposure to formaldehyde significantly increases the risk of asthma in young children. *Eur Respir J* 20:403–408
- Su C, Pan M, Zhang Y et al (2021) Indoor exposure levels of radon in dwellings, schools, and offices in China from 2000 to 2020: a systematic review. *Indoor Air* 00:1–14. <https://doi.org/10.1111/ina.12920>

- Sun C, Hong S, Cai G, Zhang Y, Kan H, Zhao Z et al (2021) Indoor exposure levels of ammonia in residences, schools, and offices in china from 1980 To 2019: a systematic review. *Indoor Air* 31(6):1691–1706
- US CDC (2021) Healthy places. <https://www.cdc.gov/healthyplaces/hia.htm>
- US EPA (1989) Risk assessment guidance for superfund human health evaluation manual. United States Environmental Protection Agency, Washington, DC
- US Surgeon General (2006) The health consequences of involuntary exposure to tobacco smoke: a report of the Surgeon General
- Vos T, Lim S, Murray C, et al (2020) Global burden of 369 diseases and injuries, 1990–2019: a systematic analysis for the Global Burden of Disease Study 2019. *The Lancet*. 17 October 2020. [https://doi.org/10.1016/S0140-6736\(20\)30925-9](https://doi.org/10.1016/S0140-6736(20)30925-9)
- WHO (2006) Air quality guidelines for particulate matter, ozone, nitrogen dioxide and sulfur dioxide – global update 2005. World Health Organization, WHO Press, Cham
- WHO (2010) Guidelines for indoor air quality - selected pollutants. World Health Organization, WHO Press, Cham
- WHO (2021) Health impact assessment. <https://www.who.int/health-topics/health-impact-assessment>
- Wilson WE, Mage DT, Grant LD (2000) Estimating separately personal exposure to ambient and nonambient particulate matter for epidemiology and risk assessment: why and how. *J Air Waste Manage Assoc* 50:1167–1183
- Xiang JB, Weschler CJ, Wang QQ, Zhang L, Mo JH, Ma R, Zhang JF, Zhang YP (2019) Reducing indoor levels of "outdoor PM2.5" in urban China: impact on mortalities. *Environ Sci Technol* 53(6):3119–3127
- Xiong K, Rumrich I, Kukec A, Rejc T, Pasetto R, Iavarone I, Hänninen O (2018) Methods of health risk and impact assessment at industrially contaminated sites: systematic review. *Epidemiologia & Prevenzione* 42(5–6) S1:49–58. http://www.epiprev.it/environmental-health-challenges-from-industrial-contamination_art4 (special issue online <http://www.epiprev.it/pubblicazione/epidemiol-prev-2018-42-5-6-suppl-1>). <http://urn.fi/URN:NBN:fi-fe2019111337830>
- Zhang A, Liu Y, Zhao B, Zhang Y, Zheng X (2021) Indoor pm2.5 concentrations in China: a concise review of the literature published in the past 40 years. *Build Environ* 198(4):107898

Part IX

Indoor Air Quality and Cognitive Performance



Metrics and Methods (Performance Indicators, Methods, and Measurement)

45

David P. Wyon

Contents

Introduction	1372
The Metrics That Might Predict Productivity	1373
Health	1373
Comfort	1374
Self-Estimated Productivity	1374
Component Skills	1374
Field Validation	1375
Research Strategy for Cost-Benefit Analysis of IEQ	1376
Experimental Strategy	1383
Strategy When Selecting Sample Size	1384
Significance of an Experiment	1384
Validity of an Experiment	1385
Interpretation in Terms of an Environmental Halo Effect	1386
The Ethics of Experimental Research on Human Subjects	1387
Health Risk, Pain, and Discomfort	1387
Invasion of Privacy	1388
Social Pressure to Participate	1388
Experiments That Do Not Require ERB Approval	1388
Documenting the Argument	1389
Strategy for Dealing with Missing Data	1389
Independent-Measures Designs	1390
Repeated-Measures Designs	1390
Experimental Protocols	1391
Protocol	1392
Conclusion	1395
References	1395

D. P. Wyon (✉)

International Centre for Indoor Environment & Energy (ICIEE), Department of Civil Engineering,
Technical University of Denmark (DTU), Kongens Lyngby, Denmark
e-mail: dpw@byg.dtu.dk

Abstract

This chapter sets out a rationale and some detailed recommendations for selecting the most efficient metrics and methods for applied research on how any factor that determines Indoor Environmental Quality (IEQ) – such as Indoor Air Quality (IAQ) – affects building occupants, with the specific purpose of obtaining a scientific basis for the economic and engineering decisions that must be made when constructing and operating buildings. These are decisions that affect a building's first cost, operating cost, energy-efficiency, environmental impact, and sustainability. The expense of meeting the goals in each of these areas must be justified in terms of how IEQ will affect the occupants of the building in terms of their health, comfort, and performance. There may be costs and benefits in each of these areas, and the IEQ effects on them must be quantified if they are to be used in cost-benefit analyses to justify the above expenses. The metrics and measures and the research strategy discussed in this chapter can be used for this applied purpose, to assess the effects of any environmental factor in the indoor environment, including those determining thermal conditions, air quality, acoustic conditions, and lighting.

Keywords

Cognitive performance · IEQ · IAQ · Research strategy · Metrics · Methods

Introduction

A great deal of published IEQ research cannot be used to justify costs and was not intended to be so used because it was motivated by a search for basic knowledge, such as how individuals differ, or the nature of the causative pathways by which IEQ affects occupants. These areas of IEQ research are outside the scope of the present chapter, because buildings and their heating, cooling, and ventilation systems are usually designed and operated for occupants as a group, with no knowledge of the requirements of the individual or of the mechanisms by which IEQ affects different individuals differently. In those few buildings where some control of local IEQ is delegated to the individual occupant's workstation, occupants must still endure the general conditions when they are elsewhere in the building and the control that is provided at each workplace averages out and has only a peripheral effect on energy use.

It is important to realize that all of the costs of constructing and operating a building, and even the cost of eventually demolishing and disposing of it, must be covered by the value added by the activities of its occupants. Not by the benefits the building provides for their health and comfort, as safeguarding these outcome variables often involves additional costs, but by the added value of what they do in the building. This comes down to their cognitive performance, as very little physical work is performed in modern buildings. In school and university buildings, the

added value will occur in the future when the students perform work in other buildings and perform it better as a consequence of the learning that took place at school and university, and learning requires effective cognitive performance. In buildings that house dwellings, the added value is that the rest and recuperation that a dwelling provides can improve productivity at work, for example, if bedroom IAQ affects sleep quality and through this, next-day performance, improving bedroom IAQ adds value. In buildings that house workplaces, such as offices, factories, workshops, and commercial premises, the added value is the improved productivity that good workplace IEQ can promote by ensuring effective cognitive performance. To assess how IEQ affects added value, research must therefore use methods and metrics that quantify how IEQ affects cognitive performance. It is worth noting here that the bottom line is determined by group average workplace productivity and that individual differences determine its variance but not its mean value. It is thus the size of group average effects that must be experimentally determined for use in cost-benefit analyses.

This chapter discusses in general terms the research strategy that should be used to assess IEQ effects on occupants. It is not a review of the literature, because an exhaustive review of such a general field would be far too long for a handbook chapter. However, a small number of published research reports are cited as examples to support some of the conclusions and recommendations.

The Metrics That Might Predict Productivity

The overall goal of applied IEQ research is to identify, reduce, and preferably eliminate all negative effects on metrics that characterize health, comfort, and cognitive performance, but they are not all equally able to predict and quantify IEQ effects on added value in terms of productivity improvements.

Health

Buildings provide shelter from the outdoor environment that safeguards the health of the occupants – shelter from excessive heat or cold and from wind and rain, and shade to eliminate the health risks of direct solar radiation. Preventing any residual negative effects on health is therefore the first priority of all IEQ research. If IEQ factors increase the risk of accidents or illnesses that cause absence from study or work, they clearly reduce productivity and the added value that good IEQ promotes. Real-world cross-sectional surveys can be conducted to identify such risks, and field-intervention experiments can even be used to demonstrate them, although it would be unethical to prolong the exposure of control groups to unimproved conditions solely for that purpose. Where no such risks have been demonstrated, negative IEQ effects on health can usually be avoided by ensuring that neither comfort nor performance is negatively affected, because these two categories of outcome variable are almost always more sensitive to IEQ than are health metrics.

Comfort

Buildings are constructed and operated to facilitate and promote the human activities they contain and achieving comfort is a secondary goal, basically because comfort can be achieved elsewhere. It should not be assumed without proof that the cognitive performance of occupants who do not complain of discomfort is optimal, because subjective comfort can often be preserved at the expense of performance – by working more slowly or by taking longer breaks from work, for example. This is especially true for thermal comfort under conditions warmer than group average neutrality, because the level of concentration required for efficient performance of cognitive tasks may result in postural changes (sitting up straight, leaning forward, etc.) and the involuntary tensing of opposing muscle groups that is associated with a higher level of activation, causing an increase in metabolic rate that contributes additionally to heat stress. There are several demonstrations in the literature that subjective thermal comfort does not necessarily lead to optimal performance, for example, Pepler and Warner (1968) as reinterpreted by Wyon (1970), Lan et al. (2020, 2021). Further demonstrations of this truism are clearly required to validate or correct the increasingly widespread tendency to equate thermal and other kinds of comfort with optimal performance.

Self-Estimated Productivity

Self-estimated productivity, in some publications also termed “IEQ productivity belief,” co-varies with other subjective estimates such as thermal, acoustic, and visual comfort, due to the “environmental halo effect” discussed in a later section of this chapter. While comfort ratings are personal and cannot be either disputed or validated, self-estimated productivity can and should be validated against measured productivity. In the few instances where this has been done, it has been found to provide very unreliable predictions, differing by up to 30% from objectively measured productivity (Kroner et al. 1992; Wargocki et al. 2000; Haneda et al. 2009; Lan et al. 2021) because what subjects are able to report is how hard they are working, and working hard is not the same as working efficiently. Under conditions that make it possible to work efficiently, it is possible to work well without the feeling that one is working hard. Self-estimated productivity can therefore be a very misleading outcome variable. There is no substitute for using measured task performance as the dependent variable in experiments whose purpose is to promote productivity by optimizing IEQ, because while improving subjective comfort and reducing subjective symptom intensity are valid and useful goals in themselves, these changes do not guarantee improved performance or productivity.

Component Skills

Real work always consists of performing a complex sequence of subtasks, which may each be differently affected by the working environment, obscuring any overall

effect. Simulated work can be used to examine the effects of the environment on the performance of each separate subtask, such as text typing, proofreading, mathematical calculation, logical thinking, and creative thinking, each of which requires the exercise of a different “component skill.” These tasks can be presented on paper, if this is appropriately realistic, or on a computer screen, in which case both remote presentation over the internet and automated analysis of performance is possible (Toftum et al. 2005). As all of these subtasks are involved in the performance of real office work, environmental effects on any one of them may become the metric on which the limiting criterion for a particular parameter of the working environment is set. While it would be valuable to determine which subtasks are critical in a given workplace, this has not yet been attempted and would not necessarily apply to all workplaces.

Field Validation

However realistic the IEQ simulation, experiments in which paid volunteers perform simulated work differ from real workplaces in terms of motivation, recruitment, and the consequences of poor performance, so their ability to predict productivity in the real world must be validated. It might be thought that they are more sensitive to changes in IEQ metrics, but in the case of both educational and office workplaces it has been found that they are less sensitive, probably because volunteer subjects are able to maintain a higher level of motivation and effort throughout the necessarily short duration of experimental exposures than is normal in the routine performance of daily work. End-of-year examination results as a function of classroom ventilation rates have been shown to be successfully predicted from laboratory exposures in which IAQ effects on tasks typical of school-work were quantified (e.g., Haverinen-Shaughnessy and Shaughnessy 2015), and talk-time at call centers has been successfully predicted from laboratory experiments in which IAQ effects on tasks typical of office work were quantified (e.g., Tham et al. 2003; Wargocki et al. 2004). Both of these outcome metrics are close to being “bottom-line” metrics of productivity – the learning that takes place in schools is assessed in terms of examination results, and call-center operators interact with their computer software to answer the enquiries of callers in what amounts to a paradigm of office work. More learning would be required to improve examination results, and more call-center operators would have to be employed if poor IEQ increased talk-time. Kroner et al. (1992 op. cit.) successfully used the time to resolution of insurance claims as a metric of the productivity of claims assessors over several weeks or months, and not only validated the extent to which individual control of thermal conditions at the workplace would improve productivity, as shown by Wyon (1996b), but also that self-estimated productivity failed completely to predict the loss of actual productivity following a move to new premises. Field-intervention experiments in which these and similar outcome variables are used to validate or refute self-estimated productivity as a predictor of actual productivity are long overdue

Research Strategy for Cost-Benefit Analysis of IEQ

To prove that IEQ affects occupants in an experiment it is necessary to demonstrate that an observed effect of IEQ could not have occurred by chance. To do this and to reliably estimate the size of the effect requires an experiment in which human subjects are exposed to two or more IEQ conditions. The design of the experiment must rule out alternative explanations. Experimental design is one of the most important methods to be considered in this chapter, more important than the choice of the metrics used to quantify the observed effects. The metrics determine the level of measurement (Nominal, Ordinal or Interval) and thus the choice of statistical methods, but the experimental design determines what assumptions must be made in the statistical analysis, as discussed below. The more assumptions that are involved in a statistical analysis, the lower the “face validity” of the conclusions. Face validity – how easily non-scientists can be convinced that the findings are valid and applicable – is what makes research of practical use for decision-makers who must justify the cost of constructing and operating a building.

The International Centre for Indoor Environment & Energy (ICIEE), referred to as “the Centre” in the following, was established at the end of the last millennium as part of the Department of Civil Engineering at the Technical University of Denmark. Its purpose was to develop the knowledge and insights necessary to resolve the conflict between improving the quality of indoor environments, to safeguard health and improve comfort and productivity, and the need to conserve energy in buildings. Research conducted at the Centre was to have the scientific goal of acquiring new knowledge and the practical goal of developing solutions that are acceptable to building occupants and shown to be economically viable for building owners and operators and for society at large. The human criteria by which solutions are judged are at three levels: health, comfort, and productivity. This chapter sets out the methodological choices that came to characterize research on human criteria for IEQ at the Centre, and the rationale behind these choices. The 25 basic choices set out in the paper, here expressed so that 17 of them are straight either/or choices, and 8 as multiple choices, for example where neither or both would each be a valid approach, define almost two billion different ways of conducting indoor environmental research (1,719,926,784 ways). Making a choice of method that differs from the one indicated by the rationale described in this chapter would radically alter the nature of an experiment and would thus affect its chances of serving a particular purpose. It is essential to identify where different methodological choices have been made when comparing findings obtained by different research strategies. Very few such different choices have so far been found to be appropriate in the search for limiting criteria for environmental factors such as temperature, air quality, outside air supply rate, lighting, or noise.

The 25 basic methodological choices that must be made.

1. *Field or laboratory studies?*

Both are essential, separately and combined in the form of realistic simulation experiments. Problems encountered and perhaps investigated initially in the

field can often be studied experimentally only in simplified form in the laboratory, while solutions that have been developed or discovered in the laboratory must be validated in the field. Even realistic simulation experiments require field validation, with real subjects performing real work, as opposed to paid subjects performing simulated work, as motivation and attitude to work may still differ. Only field experiments in which subjects need not be paid to participate can usually be of sufficient length for longer-term negative symptoms to develop.

2. *Field surveys or field intervention experiments?*

Surveys cannot distinguish between the effects of two factors that change in a related way, that is, when their effects are confounded. This is often the case in the field. Field intervention experiments in which one factor such as the outdoor air supply rate is changed while all other factors remain unchanged combine the realism of field studies with the power of the experimental approach. However, field surveys that are designed to determine the frequency of certain symptoms or complaints, the types of building in which they occur and the environmental conditions with which they are associated are often used to guide the focus of the experimental work. Field intervention experiments are the preferred approach to validating results obtained in laboratory studies, or hypotheses of causation derived from survey data. With smart buildings connected to the internet, new types of field intervention experiments are becoming possible: this was recently demonstrated in a remotely conducted experiment in over a hundred buildings, in each of which temperature set-points were being adjusted by occupants using their cellphones (Wyon and Ridenour 2018). Adjustment of a set-point up or down was taken to indicate that the temperature was considered to be too low or too high, respectively, by some member of the household and as these adjustments and measurements of the indoor temperature were available over the internet to the operator of the buildings' heating system, it was possible to determine which of two control regimes led to the least thermal discomfort and the smallest thermal excursions, without visiting any of the buildings. The experimental design included week-long repetitions and was balanced for order of presentation over a period of 4 weeks. This approach had the added advantages that the costs were negligible, as no additional equipment was installed, no interviews were conducted, and no questionnaires were distributed. As the experimenters did not need to visit any of the buildings or contact any of the subjects, this meant that the subjects were blind to the interventions and so could not bias the results due to their own expectations.

3. *Moderate or extreme levels of environmental stress?*

Environmental researchers and toxicologists have historically preferred to expose subjects to fairly extreme levels of a given environmental factor, assuming that human response will then be greater and thus easier to demonstrate, and that it is possible to interpolate the severity of effects between those occurring at extreme and neutral levels of the causative factor. This tradition began because of the high levels of stress encountered by military personnel and by workers in heavy industry. Research on the civilian population almost always exposes subjects to very moderate levels of environmental stress, for the following

reasons: (1) the results are intended to be applicable to the civilian population, light industry, office work, and dwellings; (2) the mechanisms by which moderate stress has an effect are different, involving psychological as well as physiological processes; and (3) it is thus not necessarily valid to assume that the magnitude of moderate stress effects will be predicted by interpolation from the effects of extreme stress.

4. *Subjects: male or female, old or young?*

Environmental researchers have traditionally studied the responses of young adult male subjects. Research should usually involve equal numbers of male and female subjects, but where Sick Building Syndrome (SBS) symptoms are expected to appear on the chain of causation, it may be an advantage to expose only female subjects, because female employees are found in field surveys to report more of such symptoms and are thus expected to be the more environmentally sensitive category. Young adults 20–35 are preferred because so many are available as volunteers for experiments, while older volunteers tend to be less representative of the underlying population who are engaged in paid work.

5. *Normally healthy subjects or especially sensitive sub-groups?*

Research should usually be conducted on randomly selected volunteer subjects, excluding only those suffering from colds or other forms of ill health, or using medication that is likely to have relevant side-effects. Subgroups expected to be especially sensitive may be studied when their requirements are likely to be critical in a workplace, for example, female subjects in the case of SBS and contact-lens wearers in the case of low humidity.

6. *Personality and IQ assessments?*

Many psychological laboratories engaged in the investigation of environmental stress begin by assessing the personality traits and intelligence of their subjects and may even select subjects according to the results of such tests. Research on the indoor environment has the practical goal of ensuring that they are acceptable to all building occupants and so the discovery of some unexpected bias due to personality or intelligence would be of merely academic interest.

7. *Naïve or fully informed subjects?*

Ethical considerations mandate full and informed consent. However, if possible, subjects should be kept “blind” to the interventions in field experiments, that is, they should not be informed of when each condition is established even if they must be told what each condition entails, and they should be randomly assigned to conditions in the laboratory without knowing which is which. In this way, not even the expectations of subjects who have given full and informed consent can bias the results.

8. *Repeated-measures or independent-measures experimental designs?*

Physiological measures are unaffected by prior exposure (unless acclimatization takes place). This is not true for subjective judgments and even less so for performance. Learning, increased familiarity, and over-familiarity (boredom leading to reduced motivation) can have as powerful effects as those of the environmental factors whose effects are being studied, and it is not always

possible, even theoretically, to devise parallel tasks of equal difficulty. Independent-measures designs, in which subjects are randomly assigned to conditions and each subject is exposed to only one condition, avoid all of these problems. However, it has been found empirically that repeated-measures designs with balanced order of presentation are a more efficient approach even when subjective and performance criteria are used.

9. *Health parameters – objective or subjective?*

Objective measures that cannot be affected by expectation are a valuable way of proving that mechanisms are real and not imagined. However, subjective ratings of symptom intensity are usually found to be the most sensitive to environmental influences and the most immediately relevant to human goals. They may often be the only available measure, for example, in the case of pain, soreness, difficulty in thinking clearly or headache.

10. *Subjective rating – category scales or visual-analogue (VA) scales?*

For a change to be reported on a category scale, the subject must believe that a change has taken place. The response obtained is thus a function of the subject's mental model of the underlying mechanism, which may be mistaken. Reports obtained by having subjects mark VA-scales can be unconsciously affected by environmental factors, independently of mental models, and can thus document changes in subjective response even when the subjects themselves do not think that a change has taken place.

11. *Graduated or ungraduated VA-scales?*

In repeated-measures designs in the field or laboratory, subjects must provide successive responses during or after each exposure to each of a set of experimental conditions. If the scales are graduated, it is too easy for them to remember where they marked the scale before. Their response then communicates only how they themselves think changes in the indoor environment affect them – and they may well be wrong.

12. *Acceptability – yes/no or reported on a continuous scale?*

Environmental research often obtains subjects' environmental perceptions on verbally defined scales, for example, of warmth, odor, or loudness. What is "acceptable" is later decided quite arbitrarily by the experimenter. There is no substitute for asking subjects directly whether conditions would be acceptable for daily occupation. It is more efficient to obtain judgments on a continuous scale that is divided between acceptable/unacceptable, to force subjects to make a clear choice, while asking them additionally to rate the degree of acceptability or unacceptability. The DTU Split Scale of Acceptability was developed for this purpose. The two "End-Labels" characterize one end of an ungraduated line as denoting "Completely Acceptable" and the other end as "Completely Unacceptable." The line has a gap in the middle whose two sides are labeled "Just acceptable" and "Just not acceptable." Subjects are asked to place a mark on the scale to indicate the acceptability of the conditions to which they are exposed for everyday occupation. Instead of the 1 Bit of information conveyed by a "Yes/No" rating of acceptability, each response contains much more than 1 bit of information, and responses obtained from a limited number of subjects can more

accurately predict population acceptability. Using Probit Analysis (Finney 1971), a sigmoidal relationship can be derived to estimate the proportion dissatisfied (PD) as a function of the average scale marking, pooling all scale markings across all experimental conditions. The average scale marking in each condition that is used to estimate the PD in that condition is then based on all the available data instead of on a tally of binary responses. This is particularly valuable when the number of subjects exposed to a given condition is low.

13. *Inactive or hard-working subjects?*

Subjects in physiological experiments are traditionally required to do nothing except endure the environmental stress. Following this tradition, subjects in subjective thermal comfort experiments were historically required to do nothing except express at intervals their degree of discomfort, reading or staring into space meanwhile. When asked “Is the temperature comfortable?”, their response should really have been “Comfortable for what? Reading? Doing nothing? Dozing off?” It is now known that performing even sedentary work can raise metabolic rate sufficiently to affect thermal comfort. Recent results suggest that air quality and background noise, by affecting alertness, can have a similar effect. To ensure realism, even subjects in experiments whose dependent variables are subjective should be required to perform simulated work even if it is thought unlikely that the environmental exposure will measurably affect performance.

14. *Highly motivated or unmotivated subjects?*

Environmental stress can have the effect of reducing motivation. This mechanism would not affect the performance of unmotivated subjects. On the other hand, unusually high motivation may be assumed to reduce environmental effects to unrealistically low levels. Volunteer subjects are often motivated by a desire to prove what they can do, both to oblige the experimenters and to justify to themselves the time they have spent attending the experiment. Only long exposures and repetitive work can bring motivation down to the levels that are characteristic of real workplaces.

15. *Diagnostic tests or performance tasks?*

Diagnostic tests attempt to assess a particular facility, usually a theoretical construct such as memory or spatial perception. Environmental researchers have often assumed that such tasks are more sensitive to environmental effects than performance tasks that involve using several facilities. This turns out to be untrue. Diagnostic tests should be used sparingly, for three main reasons: (1) they have repeatedly been found to be less sensitive than performance tasks to environmental effects; (2) they are unfamiliar so learning effects render them unsuitable for repeated-measures designs; and (3) results obtained with them have less face-validity than results obtained on tasks that are closely similar to actual work, because it would require an unrealistic amount of additional research to determine how important each facility is for the performance of each real-world task.

16. *Well-practiced or unfamiliar tasks?*

Unfamiliar tasks are more difficult for subjects to perform. Environmental researchers have historically assumed that the greater the level of difficulty of a

task, the more sensitive it will be to environmental effects. This turns out to be untrue. Well-practiced tasks such as typing, proofreading, and addition should be used in indoor environmental research, for three main reasons: (1) they have repeatedly been found to be more sensitive to environmental effects; (2) learning effects are minimized, which makes them suitable for repeated-measures designs; and (3) their similarity to normal work means that the results are immediately applicable to workplaces. Practice and familiarity determine the level of difficulty of a task under optimal IEQ conditions. Suboptimal IEQ conditions increase the level of difficulty, decreasing average performance. It is axiomatic that if the level of difficulty is sufficiently low, all subjects will be able to perform it efficiently, while if it is impossibly high, no subject will be able to do so. Performance, however assessed, asymptotically approaches zero as level of difficulty increases, and 100% as it decreases. There is in other words a sigmoidal relationship between performance and level of difficulty, with a point of inflection somewhere between the extremes. It is at this point that the slope of the relationship reaches its maximum value, that is, that a given change in the level of difficulty has its greatest effect on performance. The sensitivity of an experiment to changes in IEQ is maximized by ensuring that the level of task difficulty is at this point, providing always that it is a level of difficulty that is encountered in the daily activities of building occupants and is thus a realistic simulation of their daily work.

17. *Real work or component skills?*

Real work always consists of performing a complex sequence of subtasks, which may each be differently affected by the working environment, obscuring any overall effect. Simulated work should therefore be used to examine the effects of the environment on the performance of each separate subtask, such as text typing, proof-reading, mathematical calculation, logical thinking, and creative thinking, each of which requires the exercise of a different “component skill.” As all of the subtasks are involved in the performance of real office work, environmental effects on any one of them may become the basis on which the limiting criterion for a particular factor of the working environment is set.

18. *Speed or errors?*

In the performance of repetitive tasks, experimental subjects have been found to trade off speed against errors, that is, they reduce the rate at which they perform a task if they have the impression that errors would otherwise increase, even if no feedback on errors is provided. Recording only the rate of correct responses does not permit an examination of this trade-off, which may itself be affected by environmental stress. In real workplaces, the consequences of error determine the rate at which work can be performed. At one end of the scale, errors may be lethal or catastrophically expensive, while at the other extreme the consequences may be trivial. In simulated work, there are no real consequences of making an error, yet it is empirically observed that when environmental stress increases task difficulty, subjects still tend to adjust their rate of working to maintain a constant percentage error, although they do not always succeed in doing so. For these reasons, the performance of repetitive work should be evaluated by recording speed and percentage errors separately.

19. *Convergent thinking or divergent, open-ended thinking?*

Most repetitive tasks require convergent thinking – there is only one correct response, and the subject must employ rule-based logical thinking to find it. This is true of text-typing, proofreading, grammatical logic, and all mathematical tasks. Speed and errors are adequate criteria for such tasks. Computers perform or at least supervise an increasing proportion of such tasks but are unable to undertake or even supervise divergent and open-ended tasks. Creative thinking is no longer a preferred activity of the privileged few – it is the daily responsibility of the many. In open-ended tasks there are an unlimited number of correct answers, which are distinguished only by their utility and their originality. Speed is secondary and errors are tolerated, but originality is highly prized and rewarded. Simulated work should include an open-ended test of creative thinking, in which responses are first screened for utility, then numerically scored for originality. The score is obtained by using information theory to convert the probability of occurrence of each response into reduction of uncertainty, measured in bits. The probability that a randomly selected subject would have given a particular response is empirically estimated by determining the proportion of all the subjects in the experiment who did so. This approach, originally conceived to place individuals on a continuous scale of creativity that was found to be “orthogonal” to IQ (i.e., not predicted by an individual’s IQ score), is used as a paradigm of divergent thinking, to reveal environmental effects (Wyon 1996a). It is not claimed to be real creative work, but it is assumed to be subject to the same mechanisms of environmental influence.

20. *Number of subjects: $N = 15, 30, 60?$*

Published physiological studies have sometimes been carried out on a single subject (usually the author), and often on as few as five subjects. Fifteen would be a large number of subjects for such research, and even experiments on mental performance have used this few. It is usually unwise to expose fewer than 20 subjects to each condition in an independent-measures design intended to reveal environmental effects on performance. Research involving environmental effects on simulated office work in a closely controlled environment has successfully used 30 subjects in repeated-measures designs. In field experiments where there are many uncontrolled but still influential factors, only the availability of large amounts of existing performance data can justify running even a repeated-measures experiment with so few subjects. In all other cases, field experiments should aim to expose at least 60 subjects to each condition.

21. *Exposure times in laboratory experiments: 2, 4, 8 h?*

One- and 2-h exposures are the norm in performance experiments, corresponding to the length of time university students with a course requirement to participate in research as experimental subjects are able to attend. Employees currently work for about 8 h per day, but seldom for more than 4 h at a time. Environmental effects on simulated work are usually studied in exposures lasting from 3.5 to 5.5 h, depending on the latency of the mechanisms believed to be on the causal chain. Exposures of this length, particularly when

they are scheduled late in the day, allow a realistic degree of fatigue to develop. In field experiments, of course, exposure sessions continue throughout the working day, and in view of the inevitable break in exposure at each weekend, it is usually expedient to arrange interventions so that each condition is established for one whole working week. Repetitions are required to reduce chance confounding with external conditions such as weather.

22. *One or more independent variables?*

Although physiological responses usually show very little interaction between such factors as heat and noise, or light and air quality, subjective judgments of acceptability may do so, and performance may be affected in very complex and unexpected ways by combinations of stressors. Research should include a systematic examination of the nature of interactions between two and more environmental stress factors at these higher levels of environmental response.

23. *Reconnaissance or crucial test of a hypothesis?*

Experiments should always be designed to provide a crucial test of one or more hypotheses rather than as “fishing expeditions” into unknown territory.

24. *Physical and chemical measurements?*

Research on human criteria need include only those physical and chemical measurements that are necessary to document that experimental interventions have succeeded and that exposure conditions are sufficiently similar to conditions in the field for the findings to be applicable in practice. The emphasis is always on determining human response to the environmental changes that are experimentally induced, and the temptation to measure everything in sight should be resisted, as it can inflate costs well beyond what is justified.

25. *Physiological measurements?*

Research whose purpose is to optimize IEQ need to include only a very limited number of physiological measurements, as the environmental conditions of interest involve such low levels of physiological stress that such physiological responses would not provide a basis for setting limiting criteria. Limiting criteria are usually based on the more environmentally sensitive subjective and behavioral response measures.

Experimental Strategy

In general, the three main strands of applied experimental research that have been conducted with the above approach are:

1. Scientific experiments whose purpose is to discover and describe the mechanisms by which environmental factors affect building occupants.
2. Based on this understanding, engineering development of solutions to the conflict between energy conservation and improved indoor environmental conditions.
3. Field validation of laboratory findings and field determination of the acceptability and applicability of the proposed solutions.

Strategy When Selecting Sample Size

There are two main issues: (1) the number of subjects that must be studied to be able to prove that the effects observed could not have occurred by chance; and (2) the number of subjects that must be studied in order to be able to generalize the results to the entire population. These two issues are discussed below.

Significance of an Experiment

Inferential statistics are used to determine the probability that the observed result could have occurred by chance even if there were no effect of the environmental factor under study, that is, if the Null Hypothesis were true. If this probability is less than 0.05, it is conventional to regard the result as statistically significant, but the criterion for accepting that it is a real effect will always depend on the consequences of a decision based on the finding, which may be economic or human, trivial or severe. It may be appropriate to discount an apparent effect that would in any case occur in 5% of experiments by chance, and to select a lower probability, such as ($P < 0.01$) or even ($P < 0.001$), accepting the result as genuine only if these higher levels of statistical significance are reached. The frequency distribution of the observed dependent variable is always the basis for the statistical calculation, whether it conforms to a parametric distribution such as the Gaussian distribution, or not. A frequency distribution is the relative frequency with which different magnitudes of a variable, from the smallest to the largest possible, will be observed, all else being equal. If the Null Hypothesis is true, the two or more experimental conditions can be regarded as random samples and the measurements obtained under all conditions can be pooled when deriving the frequency distribution. This is therefore what is assumed in the calculation of probability of occurrence.

The main source of variability is to be found in the innumerable differences that exist between individual subjects in terms of their age, gender, size, weight, intelligence, personality, training, experience, and attitude, to name but a few. Two characteristics of the frequency distribution determine the probability that will be calculated by parametric or nonparametric statistical methods: (1) the size of the effect that appears to be due to a change in an environmental factor; and (2) the variability between the measurements obtained. The probability of obtaining a result by chance will be reduced if the apparent effect is large and/or the variability between measurements or between subjects is small. If these characteristics were known, it would be possible to determine in advance how many subjects should be studied for an effect of a given size to become statistically significant at the selected level. They are indeed known to the extent that the measure has been used before in similar experiments, but as research is the process of extending existing knowledge and one or more aspects of each experiment will usually differ from what has ever been tried before, it is logically impossible to predict either with 100% accuracy.

Best practice is then to make an educated guess as to the likely size of the environmental effect and to assume that the variability will be the same as in previous

experiments. Outcome variables used to assess health, comfort, and performance have been found to differ significantly between environmental conditions in which 5–10% of subjects are dissatisfied in the best or reference condition and 40–80% are dissatisfied in the worst condition if 30 subjects are used as their own controls in a repeated-measures design and balanced for order of presentation, while considerably more subject-exposures would be required in independent measures designs in which subjects are assigned at random to conditions (50–80 randomly selected subjects would have to be exposed to each condition to achieve the same statistical power).

Sample size can be determined empirically: enough subjects have been tested if the result can be shown to be statistically significant. Significance depends on the characteristics of the outcome variable and on how it is affected by the indoor environment, but it has nothing to do with having large subject numbers or with whether the subjects are representative of the general population.

Validity of an Experiment

The result of an experiment is valid if it predicts what happens in the real world. For this to happen, the probability that the observed result could have occurred by chance must be low, as discussed in the preceding subsection, but the subjects and the conditions to which they were exposed must also be representative of the real world. In order to be able to control certain environmental factors within narrow limits, experiments carried out in a laboratory may expose subjects to very unrealistic conditions, for example, in windowless climate chambers with stainless steel surfaces, so that the results cannot be assumed to be transferable to the real world without validation. Environmental research should preferably be carried out in a “field laboratory” that outwardly resembles a real office in terms of its dimensions, acoustics, lighting, surface finishes, windows, view out, furnishing, and decoration. This increases the “face validity” of the experiment, that is, it seems likely to most unbiased commentators that similar results would occur if the subjects were exposed to the same environmental conditions in the real world.

Validation may still be deemed necessary when experiments are carried out using paid subjects exposed for a limited time and performing simulated work. Attitude and motivation may be different in the real world, as may fatigue and the consequences of a mistake, so the effect of the environment may differ. Only validation studies in the field can eliminate this possibility. It has been demonstrated in several field experiments in call-centers, one in Denmark and the others in the Tropics, that the effects of air quality on the performance of office work that were first discovered by exposing 30 young Danish women for 5 h in a field laboratory really do occur in practice when call-center employees perform real work 8 h a day for 9 weeks. It would obviously be absurd to insist that such findings should be validated in every workplace, country, and climate of the world, and the onus is now on the skeptic to show that there is reason to believe that a different result would be observed if the gender, age, workplace, type of work, or national characteristics of the subjects were different. It is generally accepted that

clinical trials need not be repeated in different but generally similar populations, as physiology and disease are so universally the same. The physiological and psychological determinants of behavior in response to the indoor environment may well be as universal as those that determine pharmacological effects on patients suffering from the same disease.

It is therefore more important to perform validation experiments in the field than to increase the sample size in the laboratory, bearing in mind that differences between experimental situations may be as influential as differences between people.

Interpretation in Terms of an Environmental Halo Effect

When we consider a person good (or bad) in one category, we are likely to make a similar evaluation in other categories. It is as if we cannot easily separate categories. It may also be connected with dissonance avoidance, as making them good at one thing and bad at another would make an overall evaluation difficult. Thorndike (1920) found that when army officers were asked to rate their charges in terms of intelligence, physique, leadership, and character, there was a high cross-correlation. This was later confirmed by Asch (1946).

This has led to the halo effect being defined as the extension of an overall impression of a person (or of one particularly outstanding trait) to influence the total judgment of that person. The effect is to evaluate an individual high on many traits because of a belief that the individual is high on one trait. The halo effect occurs when you form an overall *positive* impression of someone because of one good characteristic. That positive judgment carries over into areas where that person might or might not have any competence. The halo effect is often cited as a major reason why interviews are so unreliable for evaluating potential employees, because the result is influenced by a person's strengths, weaknesses, physical appearance, behavior, or any other single factor. The halo effect is most often apparent in situations where one person is responsible for evaluating or assessing another in some way. Examples of such situations include assessment of applicants for jobs, scholarships, or awards; designating job or committee assignments based on perceived capabilities or past performance; and in evaluating academic, job, or athletic performance. The halo effect can undermine an individual's effort to be objective in making judgments because people respond to others in a variety of ways, making true objectivity nearly impossible. However, the halo effect causes one characteristic or quality of an individual to override all others. To counteract the halo effect, decision makers can break the evaluation process into specific steps, evaluating only one characteristic at a time, but human judgments can never be free of complex influences.

By extension, an "environmental halo effect" can be said to occur when one particular aspect of the environment that is judged very positively, such as air quality, has a positive influence on how other aspects, such as temperature, noise,

cleanliness, and lighting, are rated. Wargocki et al. (2002) seem to have been the first to invoke an environmental halo effect to explain why subjects in an experiment in which one factor was improved systematically rated other factors more positively even though they had not been improved, but it is not difficult to find further examples of this effect.

The Ethics of Experimental Research on Human Subjects

Not all research on human subjects must be approved by an Ethics Review Board (ERB). In this section the main reasons for seeking ERB approval are set out. ERBs were originally set up to protect the interests of patients undergoing medical treatment, balancing any health risk, pain, or discomfort involved against the possible benefits for them personally. In an imperfect world it cannot be assumed that researchers always act in the interests of their subjects. Instead, it must be assumed that the proposed experiment may bring some benefit to other interests, which might be commercial, political, military, or personal career advancement. ERBs take an impartial view of this. There is nothing wrong with advancing other interests, provided that the interests of the subjects are safeguarded.

Health Risk, Pain, and Discomfort

When experiments that increase the risk of illness or injury are undertaken it is obvious to all concerned that ERB approval must be obtained, for even if subjects are prepared to run the risk, their interests must be protected by weighing the risks for the subjects against any possible benefit for them personally. That there is benefit for other members of society is not a sufficient reason for allowing researchers to impose risks on the subjects in the sample. ERBs are prepared to allow subjects to take an informed risk provided that some genuine benefit for them personally may result and will allow volunteers to undergo considerable discomfort even if this is not the case. ERBs pay great attention to the detailed information on the risks and possible benefits of the experiment that is made available to subjects, and they insist that subjects are clearly informed that they may terminate their participation at any time. An important function of an ERB is to be able to make an expert assessment of the potential risks imposed in an experiment. The fact that researchers wish to conduct an experiment is no guarantee that they are sufficiently competent in the relevant area of expertise to be able to make a correct assessment of the risks. ERB members are experts in risk assessment, and their time is valuable. It is for this reason that it would be absurd if all planned research on human subjects should be obliged to obtain ERB approval, as ERBs would no longer have sufficient time for risk assessment in cases where subjects are exposed to unusual conditions.

Invasion of Privacy

ERB approval is always required when researchers wish to access personal medical files, or to obtain directly from subjects their medical or social history, including for example their medication, tax, social, or criminal records. Similarly, covert surveillance however conducted (by video camera with or without recording or even by systematic direct observation) is in most countries against the law in public places, and even in homes and workplaces, and ERB approval for it is very difficult to obtain even if subjects are first made aware of it and consent specifically to it. ERB approval must always be sought for both kinds of invasion of privacy.

Social Pressure to Participate

Subjects may feel an obligation to volunteer to participate in an experiment. This is certainly the case for patients who are or have been in medical care. One of the main reasons for requiring ERB approval for all experiments conducted by physicians is that their patients do feel this obligation, not only in gratitude for the care they have received but also out of the somewhat base suspicion that the standard of care they will receive in the future might be compromised if they do not volunteer. Nobody is exempt from some form of this pressure and medical journals therefore stipulate that they will not publish research unless ERB approval for it was granted. Scientific and engineering journals do not make this stipulation. The reason is that while altruism and respect for science as the search for truth may give rise to some residual social pressure to participate in scientific experiments, experience shows that few subjects nowadays volunteer altruistically. In engineering, which is the art of making things work even if the underlying processes are not fully understood, altruism would be misplaced so subjects make their decision based firmly on their own interests. The same is true for marketing surveys and opinion polls. Clinical practice and most pharmaceutical trials, in a way that is analogous to engineering, must be regarded as the art of helping patients to return to good health even if the underlying processes are not fully understood, so to apply the term science to all research conducted by physicians is misleading. However, as shown above, there are sufficient reasons for requiring ERB approval for all research conducted by physicians.

Experiments That Do Not Require ERB Approval

If there clearly are no risks, no pain or discomfort, no invasion of privacy, and no social pressure to participate, ERB approval is not required. This is the case for a very large proportion of research involving human subjects. There is never zero risk in any human activity, and in this connection the correct rule of thumb is that if the experiment is so designed that subjects will be exposed to conditions within the range that is normally experienced by members of the public, or if the subjects are members of a particular category, such as factory workers in a particular branch of

industry, within the range normally experienced by that category, the risks are acceptable and ERB approval is not required on the grounds of risk. The same yardstick may be used for pain and discomfort. It would clearly be a waste of everybody's time, not least of ERB time, if marketing surveys and opinion polls were obliged to obtain ERB approval. Similarly, if the engineer responsible for commissioning a heating and ventilation system by optimizing the temperature set point and the outside air intake dampers had to obtain ERB approval to do so and to ask occupants whether the resulting conditions were acceptable, most building systems would not be optimized and ERBs would be able to consider little else. Most IEQ research is much closer to the optimization of building systems than it is to medical research, and it is for this reason that ERB approval is seldom required.

Documenting the Argument

The above argument does not amount to a claim that IEQ research is exempt from obtaining ERB approval. On the contrary, every time a new study involving human subjects is planned, at the point where the detailed experimental protocol has been defined, active consideration must be given to the need for obtaining ERB approval. Point by point, the above reasons for requiring ERB approval must be evaluated. Only if they clearly can be dismissed should preparations continue without an application for ERB approval. The arguments behind a decision not to seek ERB approval should in every such case be formulated in writing and should become an explicit part of the protocol itself, just as ERB approval, if sought and obtained, would have become a part of the protocol. It may often be appropriate to include this section of the protocol in the covering letter when a manuscript reporting the study is submitted for peer-reviewed publication.

Strategy for Dealing with Missing Data

Missing data is a constantly recurring problem in the analysis of all experiments. In the physical sciences and in engineering it simply reduces the sample size, which can be remedied by running more experiments, but in research on human subjects this may not be possible, that is, due to the difficulty of recruiting more subjects at short notice. At the same time, missing data is much more likely to occur in research on human subjects than in the physical sciences, due to the many possible reasons for unplanned and unforeseeable absence of subjects from some of the exposures. Subjects may become ill, may unintentionally oversleep or fail to arrive in time for many other reasons, or may simply change their priorities and decide to do something else instead. Increasing the hourly amount paid to subjects can affect only the last of these reasons for absence, which in practice tends to be the least frequent. As the problems presented by missing data in independent-measures designs and repeated-measures designs are very different, and the remedies that can be recommended differ, they are treated separately in the following. Common to both

is that any report of the analysis must always state what data was missing from the intended design, for example, how many subjects were missing under each condition, and must also provide a detailed account of what was done about the problem in modifying the design of the experiment or of the analysis.

Independent-Measures Designs

Subjects who miss an exposure in an independent-measures design should ideally be replaced with other subjects. As subjects are randomized between conditions, the only bias introduced is that subjects recruited later may differ from those recruited originally. It may therefore be a good idea to run the same number of extra subjects in each condition, so that they can continue to be randomly assigned to all conditions instead of only to those in which missing data occurred. Exceeding the intended sample size is never a problem, while exposing too few subjects to one or more condition may unacceptably reduce the power of the available comparisons. Provided that the maximum number of subjects missing does not exceed the original group size for each exposure, the number of additional exposures required need not be greater than the number of conditions being compared.

If it is not possible to supplement subject numbers in this way, comparisons between conditions should always be made using all of the available data. Although here too subject numbers will differ between conditions, this does not present any problems in the statistical analysis. Similarly, diagrams showing how the group mean or median varied between conditions should be based on all the available data, not just on those subjects who were originally recruited.

Repeated-Measures Designs

In a repeated-measures design, subjects who miss even a single exposure cause major problems of analysis, because it will seldom be possible to replace individual subjects without either: (a) introducing bias to an otherwise balanced order of presentation of conditions; or (b) repeating the whole design to avoid this problem. The latter is usually not possible because of the cost, time, resources, and recruitment it would incur.

In any comparison across all conditions, an analysis omitting all subjects who were not exposed to all conditions should always be made so that the reader can better estimate the consequences of the various assumptions that are necessary in substituting for missing data in any supplementary analysis. As it is not usually legitimate to make pair-wise comparisons between conditions unless a test of the Null Hypothesis (NH) of no difference between any of the conditions approaches significance, this is a very important rule to obey even if the reduced number of subjects available results in a reduced level of significance. If it is reasonable to reject the NH, any pair-wise comparison between conditions should then be made using all of the data available, that is, data from all of the subjects who were exposed to both

those conditions. The result is that pair-wise comparisons between different pairs of conditions will be conducted on slightly different samples of subjects. This does not matter for the statistical test of the NH of no difference between the two conditions, as the subjects were in each case only a sample of the same underlying population from which they were recruited. However, in deriving mean or median values for each condition for the purpose of creating a diagram that enables the reader to visually compare each condition with all others, it is not advisable to use all available data, because some of the differences that will be apparent will be due to differences between subjects that were eliminated in the within-subjects statistical comparison. It is therefore better to derive the group means and medians used for this purpose only from subjects who were exposed to all conditions.

Reconstructing missing data so as to be able to use the genuine data that was obtained from all subjects is only worth undertaking if the overall NH of no difference between any of the conditions cannot be rejected without this arbitrary procedure. Researchers should bear in mind that readers will always cynically assume that they have adopted the strategy that best favors their preferred result and will be unimpressed by the rational arguments that can be advanced for it. Unless reconstruction of missing data results in formal significance that could not otherwise be achieved, it may thus be a waste of time.

Missing data can be reconstructed by assuming either: (a) that within-subject differences between conditions arose by chance; or (b) that between-subject differences arose by chance. Both these assumptions are more plausible than the many required to justify mathematical models of human response. Under assumption (a), missing data is replaced by the mean or median value (as appropriate) of data obtained from the same subject under the remaining conditions. Although this may seem like the most rational procedure, as (a) is the NH that underlies the within-subject comparison, it has the effect of altering the group mean or median values for any condition in which there was missing data, which may lead readers to assume that this was the reason that the strategy was adopted. Although no bias has been introduced to the within-subject comparison, reconstructed missing data should still not be used to derive the group means shown in diagrams, as explained above. Under assumption (b), missing data in each condition is replaced by the mean or median of all the subjects who were in fact exposed to it, or at least of those subjects in the same category, for example, of the same age or gender. It should be noted that although this does not change the group mean value for each condition, it is capable of introducing some bias into a within-subject comparison between conditions. In a genuine search for the truth, the relative validity of (a) or (b) must be based on a necessarily subjective assessment of the observed variability between and within subjects.

Experimental Protocols

Experiments that appear to address the same information requirement may differ in terms of apparently trivial details that nevertheless turn out to affect their findings. If an intended replication fails to validate a prior experiment, because some apparently

trivial change has been made, the advance of scientific knowledge is delayed. This may have very expensive consequences, not just in terms of the cost of further repeating the experiment, but also in terms of the consequential losses that may be caused by the need to base practical decisions on imperfect knowledge, pending the acquisition of firm knowledge. This section of the present chapter defines a formal document that describes a proposed experiment in such detail that any researchers who are qualified and experienced in the field of research and acting independently, would be able to perform the experiment in an identical manner without further briefing. This document, known as the “Protocol” for the experiment, sets out the hypotheses to be tested, summarizes prior knowledge, provides a rationale for the approach, describes the experimental design, the methodology, the data that will be acquired, and the statistical analysis and presentation of the findings, specifying in detail every aspect of the proposed experiment that might affect those findings.

The experimental protocol serves three main purposes: (1) it ensures that an experiment can be replicated exactly; (2) it documents what has been agreed and ensures that all those involved in the experiment know exactly how it will be carried out; and (3) its preparation ensures that the experimental process has been completely thought through from data acquisition to analysis to presentation of results in good time to make the necessary changes to the experimental design, that is, if more data would be needed for a given conclusion to be valid, or for certain tables or figures to be prepared.

Protocol

In order to serve the above purposes, all 30 of the following sections should be completed before the experiment can be considered as being ready to start:

1. Project title

Choose a brief title that describes the general nature of the experimental effort, and preferably also an acronym based on it, then prepare a subtitle that delimits the scope of the experiment.

Example: “Indoor Air Quality effects on self-estimated and objectively-measured Cognitive Performance (IAQCP)”

2. Project nature and purpose

Provide a single paragraph description of what is proposed and why.

Example: “Self-estimated performance as rated by office workers is often used as an outcome variable in experiments whose purpose is to optimize the working environment but may reflect effort rather than achievement. The proposed field-intervention experiment will obtain both of these measures over a period of several weeks in working call-centers, using routinely-recorded talk-time records as an objective indicator of cognitive performance. The intervention will be to covertly change the rate at which outdoor air is supplied to the call-center in a repeated-measures design balanced for order of presentation of conditions.”

3. Project leader

Designate the person responsible for running the project and provide contact details.

4. Team members

Designate team members, their contact details, their respective responsibilities, and the extent of their contribution to the project.

5. Funding agencies

List the funding agencies, their respective contributions to the total cost, and the dates by which progress, financial, and final reports must be provided to each of them.

6. Budget and facilities

State the total budget and the amount released each year, then list the experimental facilities that will be used, with their nominal leasing value per day.

7. Liaison with stakeholders

List the persons to whom progress reports must be submitted, any “milestones” (defined points in the process) by which they must receive a progress report and their due dates. List the confidentiality agreements that have been signed with any commercial funding sources. On a separate list, identify the target groups for the project findings, and specify which of them should receive one or more of the following forms of report: a heads-up notice that the project is on-going; preliminary confidential notification of the findings; reprints of any published articles; the final report.

8. Current knowledge

Summarize previous research findings that are relevant for the projected research, including papers reporting any use of the proposed methodology. List all references under Point 30 below for future use in the preparation, analysis, and reporting of the research. Distinguish between field and laboratory studies, and between experimental and observational (cross-sectional) surveys. Cut and paste to the protocol the most relevant sections of the reports cited, for example, how-to descriptions of the methodology and the reported mean and SD of the measurements that were obtained by using it (for use in a power analysis to determine sample size and experimental design). Include subjective knowledge based on experience or reasoned expectation but distinguish this kind of knowledge very clearly from knowledge based on scientific observation and inferential statistics (with stated *P*-values that quantify the probability that the observed results could have occurred by chance).

9. Knowledge requirement

State clearly the new knowledge that the project is being undertaken to provide, in the form of questions that it should be possible to answer once the project has been completed, for example (for the project instance above) “Does self-estimated performance reliably indicate actual performance of office work? Does improving IAQ significantly improve either (or both) of these outcome variables? If so, what is the shape of the dose-response curve?”

10. *Formal hypotheses*

Formally state the hypotheses to be tested in the proposed analysis of the data.

11. *Rationale*

Describe the rationale for the experiment and justify the expense.

12. *Scope and approach*

Delimit the scope of the experiment and justify the approach to be adopted.

13. *Experimental design*

Stipulate and justify the design of the experiment, for example, how it will eliminate confounding and any unintended bias due to the influence of uncontrolled factors.

14. *Measurements to be made*

List the measurements to be made and justify the omission of others.

15. *Methodology and equipment*

Stipulate the methods and equipment that will be used, including the manufacturer, model, range, accuracy, and calibration status of each instrument (for inclusion in the final report).

16. *Database to be acquired*

Define the database to be acquired and set up the data management software for storing and retrieving data. List who has access to it and whether it will be made public.

17. *Statistical methodology*

List and justify the statistical methods that will be used for analysis. List the non-parametric methods that will be used if the data is found not to be Normally distributed. Specify where 1-tail and 2-tail *P*-values will be appropriate.

18. *Tables and Figures*

Prepare blank versions of the Tables and Figures that will be used to present the results. It is very important to do this in advance because it often serves as a reminder to include measurements and observations without which such a presentation would be impossible, before it is too late to include them.

19. *Possible conclusions*

List what conclusions it might be possible to draw from the experimental results, including the Null Hypothesis of no significant effects.

20. *Possible publication*

List the journals to which it is intended to submit a report of the experiment.

21. *Other dissemination of findings*

List other ways by which the results will be disseminated, for example, papers to specified future conference, internal reports, lectures, press releases.

22. *Venue*

Stipulate the buildings and rooms in each building where the experiment will be conducted.

23. *Permissions required*

List the permissions required and where they will be obtained, for example, from employers, building operators, building owners, Ethics Review Board (if applicable), personal data protection authority. In Europe, ensure GDPR compliance (General Data Protection Regulation).

24. Cost estimates

List all the estimated costs, including salaries, leasing of premises and equipment, calibration of instruments, consumables, payment to subject, travel, accommodation, etc.

25. Recruitment required

State where, when, and how subjects and research assistants will be recruited, including the exclusion criteria to be applied.

26. Time schedule

Prepare a provisional time schedule for all preparations, set-up, data acquisition, analysis, and reporting.

27. Duty roster

Stipulate who will be responsible for what and when.

28. Contingency plans

Prepare contingency plans for dealing with delays, illness, absenteeism, and missing data.

29. Exit plan

Describe what will happen when the experiment ends – what will be dismantled and by whom, what equipment will be left in place, etc.

30. References

List all the references cited above for possible use in the final report.

Conclusion

In IEQ research whose purpose is to justify the cost of the construction and operation of the building concerned, the research strategy adopted must be very carefully considered. The design of the necessary experiments will usually differ from what is appropriate in basic research whose sole purpose is to advance scientific understanding. This chapter discusses in detail how to select appropriate metrics and methods for applied IEQ research and recommends the most effective approach.

References

- Asch SE (1946) Forming impressions of personality. *J Abnorm Soc Psychol* 41:258–290
- Finney DJ (1971) Probit analysis, 3rd edn. University Press, Cambridge
- Haneda M, Wargocki P, Delewski M, Tanabe S (2009) The effects of thermal discomfort on task performance, fatigue and mental workload examined in a subjective experiment. In: Proceedings of healthy buildings 2009, Syracuse, NY, USA
- Haverinen-Shaughnessy U, Shaughnessy RJ (2015) Effects of classroom ventilation rate and temperature on students' test scores. *PLoS One* 10(8):e0136165. <https://doi.org/10.1371/journal.pone.0136165>
- Kroner W, Stark-Martin JA, Willemain T (1992) Using advanced office technology to increase productivity: the impact of environmentally responsive workstations (ERWs) on productivity and worker attitude. Rensselaer Polytech Inst, Center for Architectural Research, Troy, NY

- Lan L, Xia L, Heijo R, Wyon DP, Wargocki P (2020) Perceived air quality and cognitive performance decrease at moderately raised indoor temperatures even when clothed for comfort. *Indoor Air* 30(5):841–859
- Lan L, Tang J, Wargocki P, Wyon DP, Lian Z (2021) Cognitive performance was reduced by higher air temperature even when thermal comfort was maintained over the 24–28°C range. *Indoor Air*. <https://doi.org/10.1111/ina.12916>
- Pepler RD, Warner RE (1968) Temperature and learning: an experimental study. *ASHRAE Trans* 74:211–219
- Tham KW, Willem HC, Sekhar SC, Wyon DP, Wargocki P, Fanger PO (2003) Temperature and ventilation effects on the work performance of office workers (study of a call centre in the tropics). In: *Proceedings of healthy buildings 2003*, Singapore, pp 280–286
- Thorndike EL (1920) A constant error in psychological ratings. *J Appl Psychol* 4:469–477
- Toftum J, Wyon DP, Svanekjær H, Lantner A (2005) Remote Performance measurement (RPM) – a new, internet-based method for the measurement of occupant performance in office buildings. In: *Proceedings of indoor air 2005*, Beijing, China, pp 357–361
- Wargocki P, Wyon DP, Sundell J, Clausen G, Fanger PO (2000) The effects of outdoor air supply rate in an office on perceived air quality, Sick Building Syndrome (SBS) symptoms and productivity. *Indoor Air* 10:222–236
- Wargocki P, Wyon DP, Nielsen JB, Fanger PO (2002) Call-centre occupant response to new and used filters at two outdoor air supply rates. In: *Proceedings of indoor air 2002*, Monterey, CA, USA, vol 3, pp 449–454
- Wargocki P, Wyon DP, Fanger PO (2004) The performance and subjective responses of call-centre operators with new and used supply air filters at two outside air supply rates. *Indoor Air* 14 (Suppl 8):7–16
- Wyon DP (1970) Studies of children under imposed noise and heat stress. *Ergonomics* 13(5): 598–612
- Wyon DP (1996a) Creative thinking as the dependent variable in six environmental experiments: a review. *Indoor Air* 96(1):419–422
- Wyon DP (1996b) Individual microclimate control: required range, probable benefits and current feasibility. *Indoor Air '96* 1:1067–1072
- Wyon DP, Ridenour JE (2018) A covert field-intervention experiment to determine how heating controls that conserve energy affect thermal comfort. *Indoor Air* 28:763–767



Postulated Pathways Between Environmental Exposures and Cognitive Performance

46

Kwok Wai Tham, Paweł Wargocki , and Shin-ichi Tanabe

Contents

Introduction	1398
Sensory Responses as Initiators of Pathways	1399
Physiological and Neurological Pathways	1399
Psychological Pathways	1402
Concluding Remarks	1403
Cross References	1404
References	1404

Abstract

Pathways exist between environmental exposure and cognitive performance. These include both sensory and nonsensory stimuli and moderation bodily condition, natural dispositions, and nurtured through experience, societal norms, and acclimation. Physiological and neurological mechanisms reflect natural homeostasis to stimuli. Physiological, psychological, and neurological responses are interrelated. Together, they impact the cognitive performances across the spectrum of indicators

K. W. Tham ()

Department of the Built Environment, College of Design and Engineering, National University of Singapore, Singapore, Singapore

e-mail: bdgkwt@nus.edu.sg

P. Wargocki

International Centre for Indoor Environment and Energy, Department of Civil Engineering, Technical University of Denmark, Kongens Lyngby, Denmark

e-mail: paw@byg.dtu.dk

S.-i. Tanabe

Department of Architecture, Waseda University, Tokyo, Japan

e-mail: tanabe@waseda.jp

such as attention, memory, language processing, reasoning, computation, and decision-making.

Keywords

Pathways · Cognitive performance · Homeostasis · Physiological · Neurological · Psychological · Exposure

Introduction

There is a complex set of relationships involving various stimuli and their pathways that affects cognitive performance (Fig. 1). Within any indoor environment, exposure presents the context in which human responses occur. Cognitive outcomes are the main interest as it is the main determinant of performance. Cognition is fundamental to the entire process of work. Cognition refers to “the mental action or process of acquiring knowledge and understanding through thought, experience, and the senses” (Stevenson 2010). It encompasses many aspects of intellectual functions and processes such as attention, the formation of knowledge, memory and working memory, judgment and evaluation, reasoning and “computation,” problem-solving and decision-making, comprehension, and production of language (Wolfe et al. 2006; Barsalou 2014). Cognitive processes act on assimilated knowledge to process and generate outcomes. In the office environment and knowledge-based work, cognitive processes are fundamental to productivity, and in schools, to learning.

Upon exposure, sensory stimulation invokes the initial reactions that spawn physiological and neurological mechanisms. Physiologically, the body seeks to restore the state of steady internal, physical, and chemical conditions maintained by various regulation systems for optimal functioning, through continual homeostasis (Cannon 1929; Davies 2016). Depending on the route and effect of stimuli, mechanisms are triggered which impact neurological adjustments that affect cognitive function. These effects may be direct and instantaneous if they directly engage and disrupt cognitive processes or may occur over time as a consequence of homeostasis.

Upon exposure, sensory stimulation can also invoke psychological responses. These perceptions lead to instantaneous interpretations of the environment which

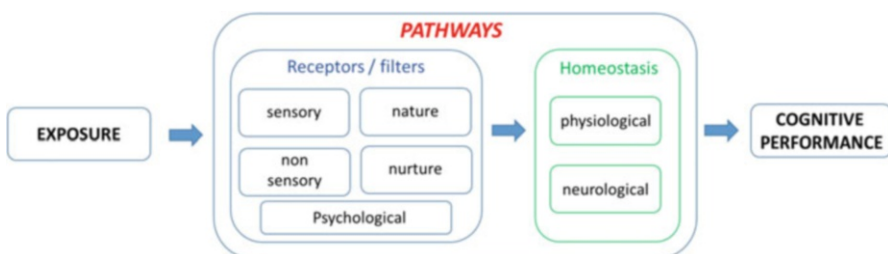


Fig. 1 Postulated pathways linking exposure to cognitive performance

influence the affective state (mood and emotions), and in turn attitude and inclinations toward work, and hence performance.

The effects and responses to stimuli are also moderated by individual diversity and personality (Røysamb et al. 2018). The “make-up” of each person is constituted by nature and molded by nurture via acclimation, culture, and societal practices. Exposure to the same set of indoor environmental conditions often results in differing responses and effects on performance for different individuals.

These interweave to provide a holistic set of pathways between exposure and performance outcomes. Active behavioral response is often resorted, at the individual level, to achieve immediate mitigation against undesirable sensory or physiological, and even neurological, effects. Such adaptive behavior is not included in this chapter. Seldom do indoor environmental conditions fall so far outside the thermal comfort zone that motor (muscular) control is affected; this will also not be addressed in this chapter.

Sensory Responses as Initiators of Pathways

Exposure may broadly be categorized as *environmental* (generally referred to as indoor environmental quality (IEQ)) or *nonenvironmental*. IEQ dimension is further categorized as indoor air quality (IAQ) or non-IAQ (thermal, noise, vibration, light, visual, and so on). Although thermal and IAQ are almost inextricably linked in most analyses, a distinguishable consideration is that IAQ results in contaminants entering the body (whether through inhalation, ingestion, or dermally), whereas thermal parameters act similarly to the non-IAQ parameters in that they impact the sensory or perceptive dimensions evoking responses that are not associated with contaminants uptake.

Heat, moisture, light, sound, and odorants constitute sensory inputs to the occupant picked up by a plethora of sensory receptors in the eye, ear, skin, nose, mouth, and mucous membranes. Most sensory receptors have a threshold of conscious detection, below which it remains subliminal. Whether subliminal or overt, these stimuli lead to *physiological*, *neurological*, and *psychological* responses that are direct or causative pathways that impact performance.

The responses are manifestations of the body’s systemic adjustment and stress which range from instantaneous through transients and eventually steady state where a new equilibrium is established via homeostasis. The detection of sensory input initiates these pathways leading to effects on performance.

Physiological and Neurological Pathways

Overt (conscious) sensations initiate physiological (homeostasis) responses, and some may invoke psychological reactions; neurological responses may also be affected. Subliminal exposures, though not invoking a conscious psychological perceptive response (which include instantaneous reactions), nonetheless lead to a

homeostasis response after a period of transience when the respective organs react to the pollutants conveyed by the circulatory system (Hutter et al. 2013). The body's sympathetic nervous system (SNS) governs all the organs as the body assembles a holistic and coordinated response to maintain homeostasis. Examples include constriction/dilation of the pupil of the eye in response to light intensity and blood flow regulation to thermal environments. In so doing, other organs are involved.

Reactive responses exhibit *transience* through which adaptation occurs, often reducing the impacts as adjustment occurs to mitigate or de-sensitize the effects of the stimuli, or *accumulation* of effects leading to a build-up of stress that progressively deteriorates cognitive performance. Reactive responses are associated with homeostasis as the body adjusts to minimize the effects of adverse sensory inputs as well as alleviation of stresses resulting from the accumulation of contaminants. The effects are usually bidirectional: When stimuli impose adverse stress, homeostasis may provide limited compensatory adaptation beyond which the deterioration of cognitive function and increase of biochemical stress accumulate, and subsequently, performance increasingly worsens. When the stimuli return toward optimal conditions, the homeostatic stress is relieved, returning cognitive function to the original levels.

Examples pertinent to pathways of performance include the following:

- Heart rate and heart rate variability, blood pressure as the heart optimizes blood regulation (Zhang et al. 2017; Azuma et al. 2018).
- Brain functions (tied intimately with cognitive function) modulate as manifested by the fluctuation of brainwaves of different frequency (as detected by electroencephalography (EEG) (Lang et al. 2022; Abbasi et al. 2020) and cerebral blood flow (Nishihara et al. 2014).
- Lung function reaction to odor and contaminant stimuli detected through end-tidal CO₂ concentration and volume, breathing rate (Mishra et al. 2021).

The intensity of the responses increases mostly disproportionately with the stimuli. The nonlinear effect is exemplified by the Predicted Mean Vote (PMV) thermal response (Fanger 1970), sound loudness (dBA) scale, glare, and olfactory perception (Fanger 1988) scales. Within *comfort* or *acceptable* levels, the responses do not impose significant physiological demands on the body. Less diversion of resources for homeostasis is required, enabling the capacity to maintain performance. As conditions move further away from the comfort or acceptable levels, several mechanisms result in deterioration of performance.

One important receptor which does not have a threshold of consciousness is the intrinsically photosensitive retinal ganglion cells (ipRGCs) which suppress melanopsin expression (Provencio et al. 1998; Hattar et al. 2002). Recently, melanopic light intensity for the workplace and living environment is widely discussed (Vetter et al. 2021).

Whether conscious or otherwise, these stimuli detection initiate bodily responses that subsequently affect cognitive performance, perception, and health. The exposure duration evokes transient responses which are the immediate (first) perception

and sensory reactions, followed by an adaptation where homeostasis effects adjust the physiological and neurological states toward an equilibrium state.

When homeostasis is insufficient to mitigate the adverse effects of pollutant accumulation or sensory discomfort, sick building symptoms (SBS) (called also non-clinical acute health symptoms or building-related symptoms) begin to manifest and have been demonstrated to adversely deteriorate cognitive performance (Tham and Willem 2005). Even the perception of inadequate air quality adversely affects cognitive performance (Wargocki and Wyon 2017; Lan et al. 2020).

Instantaneous effects result from overt (conscious) sensory inputs that directly affect cognitive function. The effect may be favorable or adverse. Adverse effects occur when:

- Compromising the effectiveness of the sensory signals is essential for conveying information for cognitive processes that precede the performance. Glare deteriorates visual acuity, hampering visual content. Loud sounds reduce the speech transmission index (efficiency of communication) by reducing the signal-to-noise ratio rendering it increasingly difficult to differentiate the intended auditory signals from competing disturbances. The tear film quality was reduced and the inter-blink interval was changed at very low RH (Wyon et al. 2006).
- Directly disrupting the primary cognitive processes (Jones et al. 2000; Macken et al. 2003; Sorqvist 2010). Noise, especially irrelevant sounds that contain semantics or rhythm, distracts and leads to the depletion of finite attentional resources that one can devote to focus and decipher the intended message. It also results in interference causing a momentary shift in attention from the focal task due to an unexpected change in the sound environment, which could contain either specific (e.g., their name being called) or generic cues (e.g., phone ringing) to the listeners.
- Sudden overpowering stimuli evoke acute responses and disrupt cognitive resource deployment. Sudden strong odor, a large increase in sound pressure level, or illuminance level are triggers of immediate cognitive disruption, though this is rare, and not usually considered in performance literature.

There are also favorable effects which are attributable to:

- Relief from fatigue that evokes attentional and stress recovery from focused work. Biophilia, or its digital and physical versions, have been demonstrated to affect attention and restoration (Kaplan 1995) and stress recovery (Ulrich et al. 1991).

Two most frequently alluded psychological models of reactive response to stimuli that impact cognitive performance are the arousal (*inverted U*) theory (Yerkes and Dodson 1908) and the *Extended U (Maximal Adaptability) model* (Hancock and Warm 2003).

The *arousal (inverted U)* theory (Yerkes and Dodson 1908) assumes that stimuli directly determine the task performer's cognitive efficiency regardless of other factors. This reduces to a dose-response relationship. Performance of a particular

task improves as arousal (activation, stress, and motivation) increases until reaching an optimal level, especially for cognitively challenging tasks. Beyond this optimum, performance starts to decline when the arousal level continues to rise, and likewise with a reduction below the optimal level of arousal. As an example, for thermal effects, this implies there is an optimal temperature or its subjective perception (thermal sensation, often characterized by the thermal sensation vote) for cognitive performance (e.g., Enander and Hygge 1990; Witterseh et al. 2004).

The alternative *Extended U (Maximal Adaptability) model* (Hancock and Warm 2003) posits that human performance remains relatively stable across a broad range of acceptable stimuli but rapidly deteriorates at the boundaries of stimuli acceptability. Within this range, the attentional resources, alternatively referred to as cognitive capacity, are being drawn upon to compensate for the adverse effects of increasing stimuli stress. When this is depleted, cognitive performance drops sharply. It is not difficult to assume that cognitive adjustments are easily accomplished within the stimuli's comfort zone to maintain near-optimum performance.

Not all stimuli are adverse, and the effects are dependent on the cognitive functions being engaged. Not all work is best suited for the same environment, and the nature of work is best supported by a corresponding combination of the environment to achieve the optimal outcomes. Creative work is better facilitated in slightly warmer environments as contrasted against mundane repetitive work which thrives better in slightly cooler environments.

There is a dichotomy of results of the effect of stimuli on performance: those showing statistically significant effect versus those that do not. Such a dose-response effect is either nullified by the individual diversity or the extended-U model whereby adaptation, or motivation, draws upon the cognitive capacity to sustain performance. For simpler tasks, the sustenance of performance is easily achieved, whereas the stress becomes increasingly difficult as task difficulty/complexity increases. The depletion of attentional resources is accompanied by secretions from the sympathetic nervous system (SNS) and manifested as measurable biomarkers (e.g., α -amylase) (Tham and Willem 2005) and could eventually lead to neurological symptoms of fatigue, headache, and difficulty concentrating and thinking clearly.

Psychological Pathways

Non-IEQ parameters encompass a wide spectrum of factors that influence perception, satisfaction, and affective state with a consequential impact on cognitive performance. Innate (health predispositions and sensitization, personality) and acquired (preferences, expectations, and stereotypes) factors influence the psychological evaluation; mismatch between the actual environment and these personal factors results in environmental stress.

Environmental stressors act indirectly on work performance by reducing state variables: motivation, alertness, and focus that support high-functioning work performance. Exposure to environmental stress appears to erode individuals' ability to compensate for environmental stress, reducing motivation and focus. These results

indicate that environmental stressors reduce not only the cognitive capacity for work but also the rate of work (i.e., motivation) (Lamb and Kwok 2016). Other parameters such as type of space, building design, and working conditions have an impact on the overall satisfaction of indoor occupants. Workspace design, conditions of the ambient environment, lighting, visual and acoustical privacy, status indicators, social relationships, and the availability of personal control are of critical importance to worker satisfaction and productivity (Wineman 2016).

Affective state or mood is susceptible to IEQ parameters. Light can affect mood in several ways: by directly modulating the availability of neurotransmitters such as serotonin, which is involved in mood regulation, and by entraining and stabilizing circadian rhythms, thereby addressing circadian de-synchronization and sleep disorders, which are rather common in people suffering from mental disorders (Blume et al. 2019). A positive mood is demonstrated to lead to better short-term memory and problem-solving.

Environmental and individual diversity coincides with an intrinsic desire for control over the workplace environment.

Concluding Remarks

Sensory receptors constitute the first gateway to pathways of impact. These are moderated by age, health, bodily build (Body mass index, size, and shape), and acclimation (that accounts for adaptation after a sufficient period of adjustment between climates). Genetic inheritance confers predisposition in physiological and neurological responses, asthma being a good example (Dold et al. 1992).

Personality strongly influences the individual's response and resilience to stimuli. It is also partly nature and partly nurture (Røysamb et al. 2018). Personality drives motivation and resilience in tackling and completing tasks, harnessing different degrees of persistence and effort. This often leads to different performance outcomes even when the stimuli are the same.

These pathways impact the response of a person.

Physiologically, homeostasis evokes responses from various organs as the body seeks to restore balance against adverse, or undesirable, states caused by the stimuli. The processes of such balancing may lead to the accumulation of stresses especially when the natural capacity to adapt is insufficient to restore the balance. This accumulation of stresses manifests as SBS symptoms (reduced well-being) in the short term; prolonged and sustained stress eventually impacts health.

In parallel, psychological reactions determined by mindset, values, and attitude express in terms of affective or mood manifestations and influence perception, satisfaction, and acceptability of the environment.

Behavioral adjustment is also relied upon through allostasis; these are actions external to the body including adjustment of clothing level, seeking visual relief through biophilia, and so forth.

As effort is deployed toward tasks, cognitive capacity is depleted and may cause mental fatigue, stress, change in concentration, and alertness; these have been

demonstrated by brain waves of various frequencies through, e.g., EEG measurements, near-infrared spectroscopy (NIRS), and functional magnetic resonance imaging (fMRI).

Physiological, psychological, and neurological responses are interrelated. Together, they impact the cognitive performances across the spectrum of indicators (such as attention, memory, language processing, reasoning, computation, and decision-making).

Cross References

- [A Modular Mechanistic Framework for Assessing Human Exposure to Indoor Chemicals](#)
 - [Exposure Routes and Types of Exposure](#)
 - [Fundamentals of Exposure Science](#)
-

References

- Abbasi AM, Motamedzade M, Aliabadi M, Golmohammadi R, Tapak L (2020) Combined effects of noise and air temperature on human neurophysiological responses in a simulated indoor environment. *Appl Ergon* 88:103189
- Azuma K, Kagi N, Yanagi U, Osawa H (2018) Effects of low-level inhalation exposure to carbon dioxide in indoor environments: a short review on human health and psychomotor performance. *Environ Int* 121(Pt 1):51–56
- Barsalou LW (2014) Cognitive psychology: Aaooverview for cognitive scientists
- Blume C, Garbazza C, Spitschan M (2019) Effects of light on human circadian rhythms, sleep and mood. *Somnologie (Berl)* 23(3):147–156
- Cannon WB (1929) Organization for physiological homeostasis. *Physiol Rev* 9(3):399–431
- Davies KJ (2016) Adaptive homeostasis. *Mol Asp Med* 49:1–7
- Dold S, Wjst M, Von Mutius E, Reitmeir P, Stiepel E (1992) Genetic risk for asthma, allergic rhinitis, and atopic dermatitis. *Arch Dis Child* 67(8):1018–1022
- Fanger PO (1970) Thermal comfort. Analysis and applications in environmental engineering. Thermal comfort. Analysis and applications in environmental engineering
- Enander AE, Hygge S (1990) Thermal stress and human performance. Scandinavian journal of work, environment & health, pp 44–50
- Fanger PO (1988) Introduction of the olf and the decipol units to quantify air pollution perceived by humans indoors and outdoors. *Energ Buildings* 12(1):1–6
- Hancock PA, Warm JS (2003) A dynamic model of stress and sustained attention. *J Human Perform Extreme Environ* 7(1):4
- Hattar S, Liao H-W, Takao M, Berson DM, Yau K-W (2002) Melanopsin-containing retinal ganglion cells: architecture, projections, and intrinsic photosensitivity. *Science* 295(5557): 1065–1070
- Hutter H-P, Haluza D, Pieglar K, Hohenblum P, Fröhlich M, Scharf S, Uhl M, Damberger B, Tappler P, Kundi M (2013) Semivolatile compounds in schools and their influence on cognitive performance of children. *Int J Occup Med Environ Health* 26(4):628–635
- Jones DM, Alford D, Macken WJ, Banbury SP, Tremblay S (2000) Interference from degraded auditory stimuli: linear effects of changing-state in the irrelevant sequence. *J Acoust Soc Am* 108(3):1082–1088

- Kaplan S (1995) The restorative benefits of nature: toward an integrative framework. *J Environ Psychol* 15(3):169–182
- Lamb S, Kwok KC (2016) A longitudinal investigation of work environment stressors on the performance and wellbeing of office workers. *Appl Ergon* 52:104–111
- Lan L, Xia L, Hejjo R, Wyon DP, Wargocki P (2020) Perceived air quality and cognitive performance decrease at moderately raised indoor temperatures even when clothed for comfort. *Indoor Air* 30(5):841–859
- Lang X, Wargocki P, Liu W (2022) Investigating the relation between electroencephalogram, thermal comfort, and cognitive performance in neutral to hot indoor environment. *Indoor air* 32(1): e12941
- Macken WJ, Tremblay S, Houghton RJ, Nicholls AP, Jones DM (2003) Does auditory streaming require attention? Evidence from attentional selectivity in short-term memory. *J Exp Psychol Hum Percept Perform* 29(1):43
- Mishra AK, Schiavon S, Wargocki P, Tham KW (2021) Respiratory performance of humans exposed to moderate levels of carbon dioxide. *Indoor Air* 31(5):1540–1552
- Nishihara N, Wargocki P, Tanabe S-I (2014) Cerebral blood flow, fatigue, mental effort, and task performance in offices with two different pollution loads. *Build Environ* 71:153–164
- Provencio I, Jiang G, Willem J, Hayes WP, Rollag MD (1998) Melanopsin: an opsin in melanophores, brain, and eye. *Proc Natl Acad Sci* 95(1):340–345
- Røysamb E, Nes RB, Czajkowski NO, Vassend O (2018) Genetics, personality and wellbeing. A twin study of traits, facets and life satisfaction. *Sci Rep* 8(1):1–13
- Sorqvist P (2010) High working memory capacity attenuates the deviation effect but not the changing-state effect: further support for the duplex-mechanism account of auditory distraction. *Mem Cogn* 38(5):651–658
- Stevenson A (2010) Oxford dictionary of English. Oxford University Press, Oxford
- Tham K, Willem H (2005) Temperature and ventilation effects on performance and neurobehavioral-related symptoms of tropically acclimatized call center operators near thermal neutrality. *ASHRAE Trans* 111(Pt 2):687–698
- Ulrich RS, Simons RF, Losito BD, Fiorito E, Miles MA, Zelson M (1991) Stress recovery during exposure to natural and urban environments. *J Environ Psychol* 11(3):201–230
- Vetter C, Pattison PM, Houser K, Herf M, Phillips AJ, Wright KP, Skene DJ, Brainard GC, Boivin DB, Glickman G (2021) A review of human physiological responses to light: implications for the development of integrative lighting solutions. *LEUKOS*:1–28
- Wargocki P, Wyon DP (2017) Ten questions concerning thermal and indoor air quality effects on the performance of office work and schoolwork. *Build Environ* 112:359–366
- Wineman JD (2016) Office design and evaluation. *Environ Behav* 14(3):271–298
- Witterseh T, Wyon DP, Clausen G (2004) The effects of moderate heat stress and open-plan office noise distraction on SBS symptoms and on the performance of office work. *Indoor air* 14:30–40
- Wolfe JM, Kluender KR, Levi DM, Bartoshuk LM, Herz RS, Klatzky RL, Lederman SJ, Merfeld D (2006) Sensation & perception. Sinauer, Sunderland
- Wyon DP, Fang L, Lagercrantz L, Fanger PO (2006) Experimental determination of the limiting criteria for human exposure to low winter humidity indoors (RP-1160). *Hvac&R Research* 12(2):201–213
- Yerkes RM, Dodson JD (1908) The relation of strength of stimulus to rapidity of habit-formation. *Journal of Comparative Neurology and Psychology* 18:459–482
- Zhang X, Wargocki P, Lian Z (2017) Physiological responses during exposure to carbon dioxide and bioeffluents at levels typically occurring indoors. *Indoor Air* 27(1):65–77



Effects from Exposures to Human Bioeffluents and Carbon Dioxide

47

Xiaojing Zhang, Asit Mishra, and Paweł Wargocki

Contents

Introduction	1408
Effect of Human Bioeffluents (with Carbon Dioxide) on Cognitive Performance	1408
Effect of (Pure) Carbon Dioxide on Cognitive Performance	1410
Effects at Carbon Dioxide Concentrations Typically Occurring Indoors	
($\text{CO}_2 < 5000 \text{ ppm}$)	1410
Effects at Carbon Dioxide Concentrations Higher than PEL ($\text{CO}_2 > 5000 \text{ ppm}$)	1411
Long-Term Exposures (>1 Day)	1412
Exploring the Possibility of Underlying Physiological Mechanisms	1412
Conclusions	1414
Cross-References	1415
References	1415

Abstract

This chapter summarizes information published to date on the effects of human bioeffluents and carbon dioxide (CO_2) on cognitive performance. Few studies have been carried out in this domain. They used simulated office tasks such as mathematical calculation and proof-reading and highly demanding cognitive tasks such as

X. Zhang (✉)

Beijing Key Laboratory of Green Built Environment and Energy Efficient Technology, College of Architecture and Civil Engineering, Beijing University of Technology, Beijing, China
e-mail: xjzhanger@bjut.edu.cn

A. Mishra

SinBerBEST, Berkeley Education Alliance for Research in Singapore, Singapore, Singapore
e-mail: asit.mishra@bears-berkeley.sg

P. Wargocki

International Centre for Indoor Environment and Energy, Department of Civil Engineering,
Technical University of Denmark, Kongens Lyngby, Denmark
e-mail: paw@byg.dtu.dk

decision-making tests and simulated flights to examine the effects on cognitive performance. Concerning the effects of bioeffluents, the literature shows that the performance of simulated office work was reduced at CO₂ levels above 3000 ppm; at CO₂ levels between 1600 ppm and 3000 ppm, the effects have been observed; below 1600 ppm, no effects were observed. For highly demanding tasks, the effects were seen at the CO₂ level of 950 ppm and over. Concerning the effects of pure CO₂, it was shown that highly demanding tasks were affected at the levels at and over 1000 ppm; however, the results were inconsistent in the published studies, some showing no effects above 1000 ppm; for the tasks simulating office work, incidental effects were seen at CO₂ level of 1200 ppm and 3000 ppm and no effects until 20,000 ppm, and even higher concentrations. These results require validation in future experiments, and mechanisms underlying the observed effects need to be delineated, especially since studies with human cells, *ex vivo*, indicate physiological impacts at the levels of 1000 ppm and higher, above the background level of CO₂. Potential confounders also need careful examination, and they include, among others, an accurate exposure control, quality of cognitive performance measures, population diversities, and the length of exposure.

Keywords

Human bioeffluents · Carbon dioxide · Cognitive performance · Physiological impacts

Introduction

Over the last three decades, the focus in the field of indoor air quality has been on the emissions from building and furnishing materials and equipment. Not much work was dedicated to studying the effects of emissions from humans (human bioeffluents). Because reduced emissions from building and furnishing materials result in human bioeffluents becoming the dominant indoor pollutants, their effects require attention and further studies. Also, they are dominant in densely occupied spaces such as school classrooms and conference rooms. Consequently, the focus has been turned on bioeffluents and carbon dioxide (CO₂), a primary human bioeffluent. Recent studies have documented that they may impair cognitive performance at levels typically occurring indoors (Fisk et al. 2019; Du et al. 2020).

This chapter summarizes the published evidence on the impact of human bioeffluents and CO₂ on cognitive performance and explores the possible mechanism underlying the observed effects.

Effect of Human Bioeffluents (with Carbon Dioxide) on Cognitive Performance

Very few experiments attempted isolating the effects of bioeffluents from the effects caused by exposures to other pollutants. In these studies, different concentrations of bioeffluents were established by varying ventilation rates.

Consequently, the concentrations of pollutants emitted by other sources also change unless reduced to a minimum and could, therefore, contribute to the observed effects (Du et al. 2020).

Only six studies provide information on cognitive performance during exposures to human bioeffluents alone. Four out of the six studies examined the effects using tasks representing real-world performance. Bakó-Biró (2004) exposed 23 subjects to two different levels of human bioeffluents for 2.8 hours. They observed no change in the performance of simulated office work, including the tasks such as text typing, addition, and multiplication when metabolically generated CO₂ levels, representing the exposure level to bioeffluents, increased from 650 ppm to 1100 ppm. Maula et al. (2017) created two bioeffluent exposures so that CO₂ levels were 540 ppm and 2260 ppm; the experiments were performed in a low-polluting office and different exposure levels by altering the ventilation rate. After 4-hour exposure, 36 subjects reported only a weak effect on their work memory performance at higher bioeffluent exposure level represented by the higher CO₂ concentration, while various other task types were unaffected. Zhang et al. (2017a, b) exposed 25 subjects in a climate chamber for 255 minutes to three levels of human bioeffluents with the corresponding CO₂ concentrations of 500 ppm, 1000 ppm, and 3000 ppm. They examined the effects of exposure to human bioeffluents on cognitive performance using multiple tasks similar to those used by Bakó-Biró and tests measuring different cognitive abilities and found a significant decrease in simulated office tasks and cue-utilization tests only when the CO₂ level was 3000 ppm. In a follow-up study, Zhang et al. (2017c) compared the responses of ten subjects at a bioeffluents level with CO₂ concentration at 1600 ppm with that at 500 ppm and did not observe any significant differences in performance of office-like tasks.

The remaining two studies examined the effects on highly demanding cognitive skills using the Strategic Management Simulation (SMS) test. Maddalena et al. (2015) showed that, when 16 subjects were exposed for 4 hours to bioeffluents when CO₂ was at the level of 1800 ppm, there was a significant reduction in their decision-making performance compared with 900 ppm, although there were no differences between the conditions in terms of subjectively reported perception of air quality or acute health symptoms. Allen et al. (2016) used SMS to examine the relationship between human bioeffluents exposure (by altering ventilation rate) and decision-making performance among 24 subjects. Their results show that during exposures to a moderate bioeffluents level with a CO₂ concentration of 950 ppm, subjects scored higher in eight of nine domains of the decision-making test than their performance at reference exposure with a CO₂ level of 500 ppm.

In summary, the short-term exposures to human bioeffluents (≤ 4.5 hours) at the levels corresponding to real life-exposures (CO₂ ≤ 3000 ppm) were shown to negatively affect the tasks simulating office work when CO₂ levels representing the levels of bioeffluents were above 1600 ppm, while highly demanding cognitive functions at the CO₂ level of 950 ppm. Further research on the discrepancy between different findings is necessary.

Effect of (Pure) Carbon Dioxide on Cognitive Performance

This section examines studies that investigated the effects of exposure to pure CO₂, independently of other bioeffluents.

CO₂ is classified as a central nervous system depressant by National Institute for Occupational Safety and Health (NIOSH). Chronic exposure to elevated levels of CO₂ (>8000 ppm) can lead to symptoms like headache, sleepiness, irritability, tremors, and enlarged retinal veins (NIOSH 1976). The Occupational Safety and Health Administration (OSHA) specifies a permissible exposure limit (PEL) as 5000 ppm, averaged over an 8 hours per day, 5 days working week (OSHA 2019); the ceiling level is 30,000 ppm for 15 minutes exposure.

The negative effects of exposure to elevated CO₂ can also be expressed by the increased partial pressure of CO₂ in arterial blood (PaCO₂). The effect is called hypercapnia, an excess of CO₂ in the human body, and is agreed to occur when PaCO₂ > 45 mmHg (Aida et al. 1998; Kawata et al. 2007).

Effects at Carbon Dioxide Concentrations Typically Occurring Indoors (CO₂ < 5000 ppm)

Studies in the past two decades since 2000 have focused on exposures to CO₂ levels under the OSHA's PEL of 5000 ppm; such exposures are relevant for nonindustrial environments. Some of these studies have reported that exposures to pure CO₂ reduced performance with complex decision-making (Strategic Management Simulation – SMS), at 1000 ppm, 1400 ppm, and 2500 ppm (Allen et al. 2016; Satish et al. 2012), and reduced successful completion of subjectively rated maneuvers in a flight simulator at 1500 ppm and 2500 ppm (Allen et al. 2019). However, the performance in SMS tests administered to trainee astronauts (Scully et al. 2019) and submariners (Rodeheffer et al. 2018) did not decline during exposures to pure CO₂ at 2500 ppm, 5000 ppm, and 15,000 ppm. However, Scully et al. (2019) observed a decline in performance, using SMS, at CO₂ of 1200 ppm compared to 600 ppm, but no effects at higher exposures to CO₂.

The tests conducted using office-like tasks and neurocognitive test batteries on the contrary have not found performance being affected at exposures to pure CO₂ between 500 ppm and 5000 ppm (Zhang et al. 2016, 2017a, b), at 3000 ppm (Liu et al. 2017) and 4000 ppm (Xia et al. 2020), and comparing 1500 ppm and 5000 ppm or 3500 ppm and 5000 ppm (Zhang et al. 2020). However, Kajtar and Herczeg (2012) observed reduced performance of proofreading at 3000 ppm, Snow et al. (2019) found an absence of learning effect with CO₂ exposure of 2700 ppm, and Zhang et al. (2020) reported a significant decline in performance of the Multi-attribute Task Battery (MATB) tasks when the CO₂ concentration increased from 1500 ppm to 3500 ppm; no significant differences were actually observed between 1500 ppm and 5000 ppm, or 3500 ppm and 5000 ppm. Scully et al. (2019) noted a declining trend in aggregate accuracy, speed, and efficiency scores at CO₂ exposure of 1200 ppm compared to the baseline of 600 ppm (similar

to the effects observed for SMS performance reported above), but no effects at higher levels of CO₂. Lee et al. (2022) proposed an integrated task performance measure, combining task performance and EEG signals, using which they found an impact on cognitive tasks related to working memory and simple reaction, for tasks undertaken at 500 ppm versus 1000 ppm, but no impact was found for 500 ppm versus 2500 ppm.

Using human neutrophils, an ex vivo study showed the elevated generation of microparticles with a high inflammatory cytokine content when incubated in a buffer equilibrated with 1000–4000 ppm additional CO₂, above background level (Thom et al. 2017). The enhanced production of these microparticles lasted for several hours after short-term exposure to elevated CO₂. An increase of the end-tidal CO₂ levels (ETCO₂) to hypercapnic levels of 47 mmHg while breathing through a mouthpiece did not affect cognitive performance or alertness (based on EEG) (Bloch-Salisbury et al. 2003). Zhang et al. (2021) noted greater effort expended, based on ECG and EEG signals, at CO₂ exposures of 3000 ppm and 5000 ppm, compared to 1500 ppm. These results indicate a possible mechanism of how elevated CO₂ levels may impact the functionality of human organs that needs careful further investigations.

Effects at Carbon Dioxide Concentrations Higher than PEL (CO₂ > 5000 ppm)

Though not found in typical buildings, levels of CO₂ higher than the PEL from OSHA (>5000 ppm) can be encountered in specialized circumstances like submarines, granaries, breweries, etc. Rodeheffer et al. (2018), even when using SMS with submariners, did not detect any impact on cognitive performance at exposure to 15,000 ppm of CO₂. In a sustained exposure to CO₂ at 20,000 ppm, over 4 hours, which included bouts of exercise, specific physiological parameters like blood pH and respiratory rate increased but remained within normal ranges, and task performance was not impacted, vis-à-vis exposure at 700 ppm (Maniscalco et al. 2021).

Divers, breathing air with 10,000 ppm and 20,000 ppm CO₂ over 60 minutes (Haran and Lovelace 2015) and 15,000 ppm and 30,000 ppm CO₂ over 30 minutes (Selkirk et al. 2010), did not show significant impact on cognitive and postural stability assessments. Some of the divers reported increased depth and rate of breathing, headaches, and labored breathing (Haran and Lovelace 2015), and long-term memory showed a slight adverse impact (Selkirk et al. 2010). Even at 30,000 ppm exposure, the divers' ETCO₂ had not reached hypercapnic levels.

For concentrations well above OSHA PEL, Sayers et al. (1987) found a threshold of 55,000 ppm CO₂ inhalation or 51 mm Hg for ETCO₂ for exposures of 20 minutes, beyond which the performance in reasoning tasks was reduced, but accuracy and short-term memory remained unaffected.

Breathing 75,000 ppm CO₂ showed an arousal effect, helping focus attention during simpler tasks, but increased respiratory rate during a complex task (Diaper

et al. 2012). In combination with physical strain, the inhalation of 40,000 ppm CO₂ showed an impact on stimulus encoding and response choice (Vercruyssen 2014), but the inhalation of CO₂ at 30,000 and 40,000 ppm (Vercruyssen et al. 2007) and 40,000 and 50,000 ppm (Sheehy et al. 1982) did not have any effect on the performance of psychomotor and cognitive tests.

Long-Term Exposures (>1 Day)

Most of the research reported above examined short-term exposures to pure CO₂ from minutes (inhalation experiments) to maximum of an office day – 8 hours (Allen et al. 2016). There have been a few studies examining exposures beyond 24 hours. Twenty-six days at CO₂ of 7000 ppm had a small effect and at 12,000 ppm had a significant effect on tracking performance (Manzey and Lorenz 1998), but the effect sizes of neither were such to consider that they had an operational significance. Head-down tilt bed rest (HDBR) is used as a space flight analog. A 26.5-hour HDBR in ambient air increased response speed and adversely affected accuracy while overall cognitive efficiency remained comparable; when HDBR was combined with exposure to 5000 ppm CO₂, response speed reduced and accuracy improved (Basner et al. 2017). Self-reports of mental fatigue and physical fatigue increased as more time was spent in the CO₂ exposure condition. Exposed to 5000 ppm CO₂, participants were less likely to report a headache, sleepier, and less bored. Examining cognitive tasks performance of nine astronauts, with exposures of up to 7 days, no clear association was found between CO₂ levels and performance though it was concluded that CO₂ levels of 2600–3300 ppm in the space stations could likely lead to a 1% risk of reported headaches (James et al. 2011). The anecdotal report had suggested that during space flights, crew ability with complex tasks reduces – compared to when on the ground – and analysis pointed to a level of 2000 ppm is the limit above which decision-making was affected (James 2013). A limitation of studies related to space flights concerning the effects of pure CO₂ is that the exposures confound the impact of just CO₂ with other pollutants, including bioeffluents.

Exploring the Possibility of Underlying Physiological Mechanisms

Figure 1 illustrates the plausible physiological pathways explaining the effects of exposures to CO₂ with and without other bioeffluents.

If required, the human body can store up to 120 liters of gaseous CO₂ (Adolph et al. 1929; Seed et al. 1970). It is difficult to ascertain a single value of CO₂ as a safe exposure limit due to wide inter-individual variations (Permentier et al. 2017). Hypercapnia can affect multiple bodily systems, including the brain and central

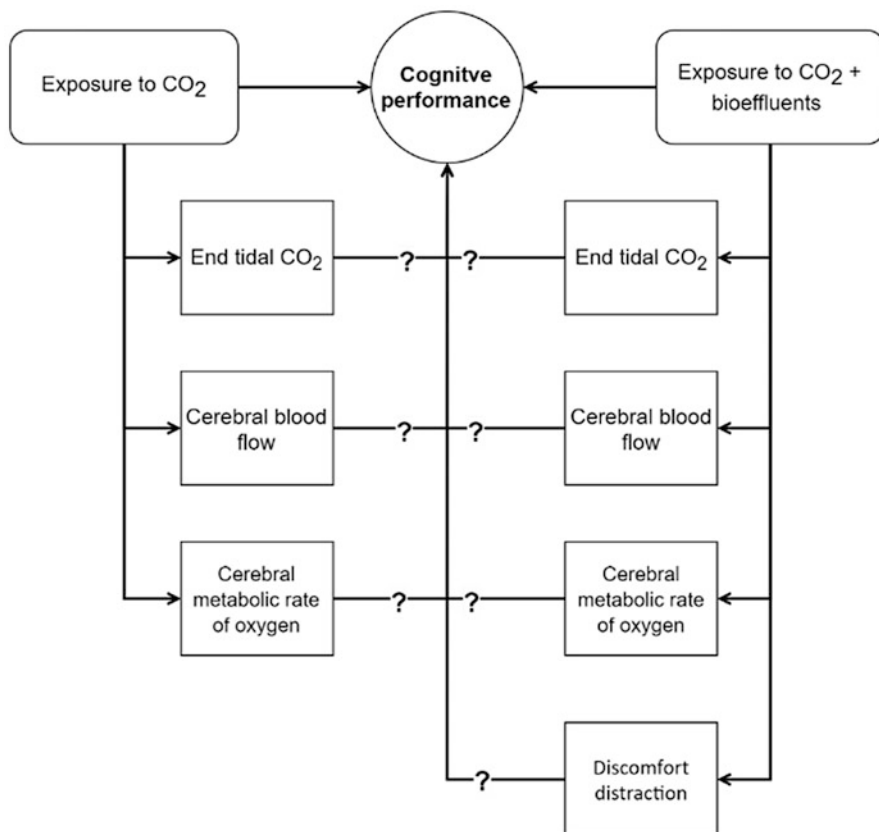


Fig. 1 An illustration of hypothesized modes of how exposures to CO₂ and bioeffluents could physiologically impact cognitive performance

nervous system (CNS) and the cardiorespiratory system. ETCO₂ relates closely to PaCO₂ and, thus, body CO₂ levels (McSwain 2010; Young et al. 1991).

While the impact on the cardiorespiratory system does not directly impact performance as the impact on CNS, an increase in heart rate and blood pressure and labored breathing could very well impact task performance. The likely mechanisms are explained below.

Physiological responses to increased levels of bioeffluents (at lowered ventilation) include increased cerebral blood flow (CBF) (Sliwka et al. 1998). PaCO₂ is the most influential regulator of CBF (Madden 1993). Increased CBF can cause headaches, thus impacting performance (Madden 1993; Nishihara et al. 2014). A minimal increase in PaCO₂ tension (4–6 mmHg) is probably required to initiate cerebral vasodilation (Battisti-Charbonney et al. 2011; Patterson et al. 1955; Wasserman et al.

1962), but this is an effect of breathing ~25,000 ppm CO₂ (Patterson et al. 1955). These levels are unlikely to occur indoors.

Change in cerebral metabolic rate of oxygen (CMRO₂) was found to be proportional to change in ETCO₂ (Xu et al. 2011). Without a significant change in ETCO₂, it is likely that CMRO₂ does not change either. Exposure to CO₂ with bioeffluents, and not just high levels of CO₂, can increase ETCO₂ (Schaefer et al. 1963; Vehviläinen et al. 2016; Zhang et al. 2017a, b; Garner et al. 2011), hence can impact CMRO₂. In a poorly ventilated meeting room with a mean CO₂ level of 2756 ppm, the PaCO₂ levels of occupants reached ~48 mmHg (Vehviläinen et al. 2016). Similar levels of PaCO₂ have been recorded at much higher exposures to just pure CO₂ (without bioeffluents); these levels were >15,000 ppm CO₂ (Reich and Rusinek 1989; Schaefer et al. 1963).

Another reason behind the cognitive effects of bioeffluents could be the symptoms that result from poor ventilation like odor dissatisfaction, tiredness, tightness in the chest, nose/sinus symptoms, etc. (Apte et al. 2000; Kim et al. 2018; Lu et al. 2015; Myhrvold et al. 1996). The human brain has limited capacity, and the cognitive load theory of performance (Sweller 2011) suggests that if it is distracted due to discomfort, performance would also be negatively impacted.

Research so far has not included vulnerable populations like children, the elderly, and people with respiratory issues (chronic obstructive pulmonary disease (COPD), asthma, and alike). It is known that age reduces sensitivity to hypoxia and hypercapnia, but that does not allow extrapolation regarding cognitive effects (Janssens et al. 1999; Permentier et al. 2017). Studies would also need to consider longer-term chronic and chronic-intermittent exposures. Since low ventilation levels lead to an increase in other pollutants along with bioeffluents, future studies would need to explicitly exclude the impacts of other pollutants when examining cognitive performance.

Conclusions

The evidence in the literature suggests that both human bioeffluents and CO₂ itself, at the level typically occurring indoors (CO₂ ≤ 5000 ppm), could impair cognitive performance. However, the effects could occur at different levels also depending on the type of cognitive tasks performed (Fig. 2).

It should also be underlined that there remain significant inconsistencies in the findings regarding the impact on performance, especially with the effects of pure CO₂. At the same time, there is an incomplete understanding of how exposure to bioeffluents affects cognitive performance. An aspect that needs careful consideration in future studies is accurate exposure control. Isolating the exposure to bioeffluents from other indoor pollutants is a much-needed step. Other potential confounders include duration of exposure, use of a standardized set of cognitive measures, and backgrounds of participants. One aspect that has not been investigated is the role of CO₂ in modifying the effects of other pollutants, i.e., an adjuvant effect of CO₂.

	CO_2	Human bioeffluents (with CO_2)	
Cognitive impacts	 Office-like tasks  Highly demanding tasks	No adverse effects until 20,000 ppm, possibly higher. Incidental effects at 1,200 ppm and 3,000 ppm. Adverse effects at and over 1,000 ppm, but inconsistent. Adverse effects over 1,600 ppm.	
Physiological impacts	 End-tidal CO_2  Human neutrophils- <i>ex vivo</i>	Hypercapnic levels reached between 15,000 to 25,000 ppm and over. Significant increase in inflammatory cytokines generation at 1,000 ppm and higher, above background levels.	Hypercapnic levels at 2,700 ppm. No data.

Fig. 2 A summary of observed effects, on different physiological and cognitive aspects, due to exposure to CO_2 and CO_2 with other bioeffluents

Cross-References

- [Indoor Air Quality in Offices](#)
- [Occupant Emissions and Chemistry](#)

References

- Adolph EF, Nance FD, Shiling MS (1929) The carbon dioxide capacity of the human body and the progressive effects of carbon dioxide upon the breathing. *Am J Physiol Leg Content* 87:532–541
- Aida A, Miyamoto K, Nishimura M, Aiba M, Kira S, Kawakami Y, the Respiratory Failure Research Group in Japan (1998) Prognostic value of hypercapnia in patients with chronic respiratory failure during long-term oxygen therapy. *Am J Respir Crit Care Med* 158:188–193

- Allen JG, MacNaughton P, Satish U, Santanam S, Vallarino J, Spengler JD (2016) Associations of cognitive function scores with carbon dioxide, ventilation, and volatile organic compound exposures in office workers: a controlled exposure study of green and conventional office environments. *Environ Health Perspect* 124(6):805–812
- Allen JG, MacNaughton P, Cedeno-Laurent JG, Cao XD, Flanigan S, Vallarino J, Rueda F, Donnelly-McLay D, Spengler JD (2019) Airplane pilot flight performance on 21 maneuvers in a flight simulator under varying carbon dioxide concentrations. *J Expo Sci Environ Epidemiol* 29(4):457–468
- Apte MG, Fisk WJ, Daisey JM (2000) Associations between indoor CO₂ concentrations and sick building syndrome symptoms in U.S. office buildings: an analysis of the 1994–1996 BASE study data. *Indoor Air* 10(4):246–257
- Bakó-Biró Z (2004) Human perception, SBS symptoms and performance of office work during exposure to air polluted by building materials and personal computers. Ph.D. dissertation. Technical University of Denmark, Copenhagen
- Basner M, Nasrini J, Hermosillo E, McGuire S, Dinges DF, Moore TM, Gur RC, Rittweger J, Mulder E, Wittkowski M, Donoviel D, Stevens B, Bershad EM (2017) Effects of -12° head-down tilt with and without elevated levels of CO₂ on cognitive performance: the SPACECOT study. *J Appl Physiol* 124(3):750–760
- Battisti-Charbonney A, Fisher J, Duffin J (2011) The cerebrovascular response to carbon dioxide in humans. *J Physiol* 589(12):3039–3048
- Bloch-Salisbury E, Lansing R, Shea SA (2003) Acute changes in carbon dioxide levels alter the electroencephalogram without affecting cognitive function. *Psychophysiology* 37(4):418–426
- Diaper A, Nutt DJ, Munafò MR, White JL, Farmer EW, Bailey JE (2012) The effects of 7.5% carbon dioxide inhalation on task performance in healthy volunteers. *J Psychopharmacol* 26(4):487–496
- Du B, Tandoc M, Mack ML, Siegel JA (2020) Indoor CO₂ concentrations and cognitive function: a critical review. *Indoor Air* 30(6):1067–1082
- Fisk W, Wargocki P, Zhang XJ (2019) Do indoor CO₂ levels directly affect perceived air quality, health, or work performance? *ASHRAE J* 61(9):70–77
- Garner M, Attwood A, Baldwin DS, James A, Munafò MR (2011) Inhalation of 7.5% carbon dioxide increases threat processing in humans. *Neuropsychopharmacology* 36(8):1557–1562
- Haran FJ, Lovelace A (2015) Effects of inspired CO₂ and breathing resistance on neurocognitive and postural stability in U.S. Navy divers. Defense Technical Information Center, Fort Belvoir. <https://doi.org/10.21236/AD1003579>
- James JT (2013) Surprising effects of CO₂ exposure on decision making. In: 43rd international conference on environmental systems. Presented at the 43rd international conference on environmental systems, American Institute of Aeronautics and Astronautics, Vail, CO. <https://doi.org/10.2514/6.2013-3463>
- James J, Matty C, Meyers V, Sipes W, Scully R (2011) Crew health and performance improvements with reduced carbon dioxide levels and the resource impact to accomplish those reductions. American Institute of Aeronautics and Astronautics. <https://doi.org/10.2514/6.2011-5047>
- Janssens JP, Pache JC, Nicod LP (1999) Physiological changes in respiratory function associated with aging. *Eur Respir J* 13:197–205
- Kajtar L, Herczeg L (2012) Influence of carbon-dioxide concentration on human well-being and intensity of mental work. *Q J Hung Meteorol Serv* 116:145–169
- Kawata N, Tatsumi K, Terada J, Tada Y, Tanabe N, Takiguchi Y, Kuriyama T (2007) Daytime hypercapnia in obstructive sleep apnea syndrome. *Chest* 132:1832–1838
- Kim J, Kong M, Hong T, Jeong K, Lee M (2018) Physiological response of building occupants based on their activity and the indoor environmental quality condition changes. *Build Environ* 145:96–103
- Lee J, Wan Kim T, Lee C, Koo C (2022) Integrated approach to evaluating the effect of indoor CO₂ concentration on human cognitive performance and neural responses in office environment. *J Manag Eng* 38:04021085. [https://doi.org/10.1061/\(ASCE\)ME.1943-5479.000099](https://doi.org/10.1061/(ASCE)ME.1943-5479.000099)

- Liu WW, Zhong WD, Wargocki P (2017) Performance, acute health symptoms, and physiological responses during exposure to high air temperature and carbon dioxide concentration. *Build Environ* 114:96–105
- Lu CY, Lin JM, Chen YY, Chen YC (2015) Building-related symptoms among office employees associated with indoor carbon dioxide and total volatile organic compounds. *Int J Environ Res Public Health* 12(6):5833–5845
- Maddalena R, Mendell MJ, Eliseeva K, Chan WR, Sullivan DP, Russell M, Satish U, Fisk WJ (2015) Effects of ventilation rate per person and per floor area on perceived air quality, sick building syndrome symptoms, and decision-making. *Indoor Air* 25(4):362–370
- Madden JA (1993) The effect of carbon dioxide on cerebral arteries. *Pharmacol Ther* 59(2): 229–250
- Maniscalco J, Hoffmeyer F, Monsé C, Jettkant B, Marek E, Brüning T, Bünger J, Sucker K (2021) Physiological responses, self-reported health effects, and cognitive performance during exposure to carbon dioxide at 20 000 ppm. *Indoor Air*. <https://doi.org/10.1111/ina.12939>
- Manzey D, Lorenz B (1998) Joint NASA-ESA-DARA study. Part three: effects of chronically elevated CO₂ on mental performance during 26 days of confinement. *Aviat Space Environ Med* 69(5):506–514
- Maula H, Hongisto V, Naatula V, Haapakangas A, Koskela H (2017) The effect of low ventilation rate with elevated bioeffluent concentration on work performance, perceived indoor air quality, and health symptoms. *Indoor Air* 27(6):1141–1153
- McSwain SD (2010) End-tidal and arterial carbon dioxide measurements correlate across all levels of physiologic dead space. *Respir Care* 55:6
- Myhrvold AN, Olsen E, Lauridsen Ø, (1996) Indoor environment in schools-pupils' health and performance in regard to CO₂ concentrations. In: Proceedings of Indoor Air '96, vol 1, pp 369–374
- NIOSH (1976) Criteria for a recommended standard: occupational exposure to carbon dioxide. <https://doi.org/10.26616/NIOSHPUB76194>
- Nishihara N, Wargocki P, Tanabe S (2014) Cerebral blood flow, fatigue, mental effort, and task performance in offices with two different pollution loads. *Build Environ* 71:153–164
- OSHA (2019) Permissible exposure limits – annotated tables. Occupational Safety and Health Administration (WWW document). <https://www.osha.gov/annotated-pels>. Accessed 13 May 2021
- Patterson JL, Heyman A, Battey LL, Ferguson RW (1955) Threshold of response of the cerebral vessels of man to increase in blood carbon dioxide. *J Clin Investig* 34(12):1857–1864
- Permentier K, Vercammen S, Soetaert S, Schellemans C (2017) Carbon dioxide poisoning: a literature review of an often forgotten cause of intoxication in the emergency department. *Int J Emerg Med* 10(1):14
- Reich T, Rusinek H (1989) Cerebral cortical and white matter reactivity to carbon dioxide. *Stroke* 20(4):453–457
- Rodeheffer CD, Sarah C, Clarke JM, Fothergill DM (2018) Acute exposure to low-to-moderate carbon dioxide levels and submariner decision-making. *Aerospace Med Hum Perform* 89(6): 520–525
- Satish U, Mendell MJ, Shekhar K, Hotchi T, Sullivan D, Streufert S, Fisk WJ (2012) Is CO₂ an indoor pollutant? Direct effects of low-to-moderate CO₂ concentrations on human decision-making performance. *Environ Health Perspect* 120(12):1671–1677
- Sayers JA, Smith RE, Holland RL, Keatinge WR (1987) Effects of carbon dioxide on mental performance. *J Appl Physiol* 63(1):25–30
- Schaefer KE, Hastings BJ, Carey CR, Nichols G (1963) Respiratory acclimatization to carbon dioxide. *J Appl Physiol* 18(6):1071–1078
- Scully RR, Basner M, Nasrini J, Lam CW, Hermosillo E, Gur RC, Moore T, Alexander DJ, Satish U, Ryder VE (2019) Effects of acute exposures to carbon dioxide on decision making and cognition in astronaut-like subjects. *NPJ Microgravity* 5:17
- Seed RF, Shakespeare TF, Muldoon MJ (1970) Carbon dioxide homeostasis during anaesthesia for laparoscopy. *Anaesthesia* 25:223–231

- Selkirk A, Shykoff B, Briggs J (2010) Cognitive effects of hypercapnia on immersed working divers. Defense Technical Information Center, Fort Belvoir. <https://doi.org/10.21236/ADA561029>
- Sheehy JB, Kamon E, Kiser D (1982) Effects of carbon dioxide inhalation on psychomotor and mental performance during exercise and recovery. *Hum Factors* 24:581–588
- Sliwka U, Krasney JA, Simon SG, Schmidt P, Noth J (1998) Effects of sustained low-level elevations of carbon dioxide on cerebral blood flow and autoregulation of the intracerebral arteries in humans. *Aviat Space Environ Med* 69:299–306
- Snow S, Boyson AS, Paas KHW, Gough H, King MF, Barlow J, Noakes CJ, Schraefel MC (2019) Exploring the physiological, neurophysiological, and cognitive performance effects of elevated carbon dioxide concentrations indoors. *Build Environ* 156:243–252
- Sweller J (2011) Cognitive load theory. In: *Psychology of learning and motivation*, vol 55. Elsevier, San Diego, pp 37–76
- Thom SR, Bhopale VM, Hu J, Yang M (2017) Increased carbon dioxide levels stimulate neutrophils to produce microparticles and activate the nucleotide-binding domain-like receptor 3 inflammasome. *Free Radic Biol Med* 106:406–416
- Vehviläinen T, Lindholm H, Rintamäki H, Pääkkönen R, Hirvonen A, Niemi O, Vinha J (2016) High indoor CO₂ concentrations in an office environment increases the transcutaneous CO₂ level and sleepiness during cognitive work. *J Occup Environ Hyg* 13:19–29
- Vercruyssen M (2014) Breathing carbon dioxide (4% for 1-hour) slows response selection, not stimulus encoding. *Proc Hum Factors Ergon Soc Annu Meet* 58(1):914–918
- Vercruyssen M, Kamon E, Hancock PA (2007) Effects of carbon dioxide inhalation on psychomotor and mental performance during exercise and recovery. *Int J Occup Saf Ergon* 13(1):15–27
- Wasserman AJ, Patterson JL, Hunter AR (1962) The cerebral vascular response to reduction in arterial carbon dioxide tension. *Surv Anesthesiol* 6(3):238–239
- Xia YL, Shikii S, Shimomura Y (2020) Determining how different levels of indoor carbon dioxide affect human monotonous task performance and their effects on human activation states using a lab experiment: a tracking task. *Ergonomics* 63(11):1350–1358
- Xu F, Uh J, Brier MR, Hart J, Yezhuvath US, Gu H, Yang Y, Lu H (2011) The influence of carbon dioxide on brain activity and metabolism in conscious humans. *J Cereb Blood Flow Metab* 31(1): 58–67
- Young WL, Prohovnik I, Ornstein E, Ostapkovich N, Matteo RS (1991) Cerebral blood flow reactivity to changes in carbon dioxide calculated using end-tidal versus arterial tensions. *J Cereb Blood Flow Metab* 11:1031–1035
- Zhang XJ, Wargocki P, Lian ZW (2016) Human responses to carbon dioxide, a follow-up study at recommended exposure limits in non-industrial environments. *Build Environ* 100:162–171
- Zhang XJ, Wargocki P, Lian ZW, Thyregod C (2017a) Effects of exposure to carbon dioxide and bioeffluents on perceived air quality, self-assessed acute health symptoms, and cognitive performance. *Indoor Air* 27(1):47–64
- Zhang XJ, Wargocki P, Lian ZW (2017b) Physiological responses during exposure to carbon dioxide and bioeffluents at levels typically occurring indoors. *Indoor Air* 27(1):65–77
- Zhang XJ, Wargocki P, Lian ZW, Xie JC, Liu JP (2017c) Responses to human bioeffluents at levels recommended by ventilation standards. *Procedia Eng* 205:609–614
- Zhang J, Pang LP, Cao XD, Wanyan XR, Wang X, Liang J, Zhang L (2020) The effects of elevated carbon dioxide concentration and mental workload on task performance in an enclosed environmental chamber. *Build Environ* 178:106938
- Zhang J, Cao XD, Wang X, Pang LP, Liang J, Zhang L (2021) Physiological responses to elevated carbon dioxide concentration and mental workload during performing MATB tasks. *Build Environ* 195:107752



Effects of IAQ on Office Work Performance

48

Jose Ali Porras-Salazar, Stefano Schiavon, and Kwok Wai Tham

Contents

Introduction	1420
Studies Examining the Effects of IAQ on Work Performance	1420
Studies Where Pollution Levels Were Altered by Modifying the Concentration of Specific Pollutants	1433
Studies Where Pollution Levels Were Altered by Modifying Ventilation Rates	1436
Studies Where Pollution Levels Were Altered by Adding or Removing a Pollution Source and/or Sink	1438
Limitations and Future Work	1439
Conclusions	1440
Cross-References	1442
References	1443

Abstract

We reviewed 32 studies published since 1980 that have examined the effects of indoor air quality (IAQ) on work performance in non-industrial and non-educational spaces. We found that (i) reduced ventilation rates (VR)—indicative of poor air quality—can affect some aspects of cognitive performance, hence the performance of office work; (ii) toluene effects on work performance

J. A. Porras-Salazar

Berkeley Education Alliance for Research in Singapore, Singapore, Singapore

e-mail: jose.porrassalazar@ucr.ac.cr

S. Schiavon (✉)

Center for the Built Environment, University of California, Berkeley, CA, USA

e-mail: schiavon@berkeley.edu

K. W. Tham

Department of the Built Environment, College of Design and Engineering, National University of Singapore, Singapore, Singapore

e-mail: bdgkwt@nus.edu.sg

were only found at high concentrations that are not common in office buildings; (iii) the effects of CO₂ – as a pollutant and not as a proxy for ventilation – were not consistent, as some studies found effects, others did not; (iv) similar inconsistencies as for CO₂ were found for the effects TVOCs. Plausible reasons explaining the discrepancies are differences in tested populations such as participants' age and occupation, sleep quality, experiment design, exposure time, task complexity, and uncertainty in pollution exposure. In addition to the research necessary to clarify the observed discrepancies, future investigations should focus on developing a shared understanding of the meaning of work performance and what are the methods and metrics to measure it, and estimating the magnitude and shape of the relationship between different variables that represent IAQ such as ventilation rate or CO₂ and performance.

Keywords

Indoor air quality · Ventilation · CO₂ concentration · VOC · Work performance · Productivity · Cognitive performance

Introduction

Humans spend more time living in enclosed spaces, such as buildings, than at any other time in their evolution (Kleppeis et al. 2001). Indoor air quality (IAQ) is different from outdoor air quality. It has received increasing attention from governments, political institutions, and the scientific community. In this subchapter, we aim to review publications that have examined the effects of IAQ on work performance in non-industrial and non-educational spaces and were published from 1980.

We proposed 1980 as the starting date because two documents were published around this year that highlighted the importance of IAQ and probably increased the scientific community's interest in the subject. The first document, titled *Health Aspects Related to Indoor Air Quality* (WHO 1979), created awareness about the possible health consequences of decreased ventilation rates (VR) in buildings due to the adoption of several energy-saving proposals to counteract the oil crisis of the 1970s. The second document, *Indoor Pollutants Field* (National Research Council 1981), requested by the US Environmental Protection Agency (EPA), noted that insufficient importance had been given to indoor air exposure despite IAQ potentially being more critical to human health and well-being than outdoor air.

Studies Examining the Effects of IAQ on Work Performance

We found 32 studies in 28 peer-reviewed journal articles published between 1983 and 2021; Table 1 provides the summary. The difference between the number of studies and articles is because Tham and Willem (2005), Kajtár and Herczeg

Table 1 Summary of studies examining the effect of indoor air quality on office work performance

Study	Journal	Location	Exposure place	No. of conditions ^a /Duration of exposure per condition	No. of participants ^b /Occupation	Performance assessment	Summary of results ^c	Classification ^d
Andersen et al. (1983)	Scandinavian Journal of Work, Environment and Health	Denmark	Chamber	4/ 360 min	16/ Students	Five-choice serial reaction, rotary pursuit, screw plate, Landolt's rings, Bourdon Wiersma, multiplication, sentence comprehension, and word memory	No statistically significant effects of the toluene exposure were found in any of the eight tests	A (Toluene)
Bælum et al. (1985)	Scandinavian Journal of Work Environment & Health	Denmark	Chamber	3/ 450 min	43/43 were printers, while for the other 43 the occupation was not provided	Peg board, Screw plate, Rotary pursuit, Track tracing errors, Simulated assembly line, Landolt's ring, color discrimination, multiplication, Five-choice, and vigilance	Significant effects were found on two of the perceptual tests – one measurement of Landolt's ring and two measurements of color discrimination – and one of the visuomotor tests – on the peg board	A (Toluene)
Molhave et al. (1986)	Environment International	Denmark	Chamber	2/ 165 min	62/ NA	Digit span and graphic continuous performance tests	Participants performed significantly worst on both digit span forwards and backwards when	A (VOCs)

(continued)

Table 1 (continued)

Study	Journal	Location	Exposure place	No. of conditions ^{a/} Duration of exposure per condition	No. of participants ^{b/} Occupation	Performance assessment	Summary of results ^c	Classification ^d
Bælum et al. (1990)	International Archives of Occupational and Environmental Health	Denmark	Chamber	3/ 420 min	24/ NA	Peg board test, color test, vigilance clock test with peripheral lights, five-choice serial reaction test	the concentration of a mixture of 22 VOCs was increased from 5 to 25 mg/m ³	A (Toluene)
Otto et al. (1992)	Archives of Environmental Health	US	NA	2/ 165 min	66/ NA	NES ^e	Just a marginal improvement was observed in the forward visual digit span when the concentration of a mixture of 22 VOCs was increased from 0 to 25 mg/m ³ . Finding was isolated and was considered a random occurrence	A (VOCs)

Wargocki et al. (1999)	Indoor Air	Denmark	Office-like controlled environment	2/ 265 min	30/ Students	PAB ^f and simulated office work	Participants typed 6.5% less text but performed better at math (added 3.8% more units) when the pollution load was present. No significant effects were reported for the psychological tests	C (Carpet)
Wargocki et al. (2000)	Indoor Air	Denmark	Office-like controlled environment	3/ 276 min	30/ Students	Simulated office work tasks: text typing, proofreading, addition and creative thinking	Participants typed 4% more characters per minute when VRs were increased from 3 to 30 L/s per person	C (Carpet)
Wargocki et al. (2002)	Indoor Air	Sweden	Office-like controlled environment	2/ 276 min	30/ Students	Typing, addition, proofreading	The speed and accuracy of text typing were 1.5% and 7% lower when the pollution load was present.	C (Carpet)
Balkó-Biró et al. (2004)	Indoor Air	Denmark	Office-like controlled environment	2/ 288 min	30/ Students	Text typing and proofreading	Text typing and reading speed decreased by 0.5% and 4% respectively, and errors increased by 20% with PCs present	C (Personal computers)

(continued)

Table 1 (continued)

Study	Journal	Location	Exposure place	No. of conditions ^a / Duration of exposure per condition	No. of participants ^b / Occupation	Performance assessment	Summary of results ^c	Classification ^d
Wargocki et al. (2004)	Indoor Air	Denmark	Call Centre	4/ 2 working weeks	26/ Call center agents	Talk time	Replacing the used B ^e filter with a clean filter reduced the talk-time by approximately 10% at 2.5 L/s per person, but had no significant effect at 2.5 L/s per person	B
Fang et al. (2004)	Indoor Air	Denmark	Office-like controlled environment	2/ 280 min	30/ NA	Simulated office work tasks: text typing, proofreading, addition and creative thinking	No significant changes in responses were observed	B
Tham (2004)	Indoor Air	Singapore	Call Centre	4/ 2 working weeks	56/ Call center agents	Talk time	Talk time was reduced significantly when the outdoor air supply rate was increased from 5 L/s per person to 10 L/s per person at 24.5 °C	B

Fedderspiel et al. (2004)	Indoor Air	US	Call Centre	3/ 19 days	NA/ Nurses	Talk time and average handle time	No significant changes were observed	B
Tham and Willem (2005)	ASHRAE Transactions	Singapore	Call Centre	4/ 2 working weeks	27/ Call center agents	Talk time	Doubling the outdoor air supply rate at 24.5 °C significantly reduced talk time by approximately 7% to 9%	B
Park and Yoon (2011)	Indoor Air	South Korea	Office-like controlled environment	3/ 480 min	24/ Students	Addition, Stroop, text typing, proofreading, searching, matching to sample, initiative memorization (8%) when VR was increased from 5 to 20 L/s per person	Participants performed better at text typing (5.2%), addition (4.7% above), and memorization (8%) when VR was increased from 5 to 20 L/s per person	B
Satish et al. (2012)	Environmental Health Perspectives	USA	Chamber	3/ 150 min	22/ NA	SMS ^h	Participants performed worst in six of the nine scales of SMS when CO ₂ was increased from 600 to 1000 ppm, and large and statistically significant	A (CO ₂)

(continued)

Table 1 (continued)

Study	Journal	Location	Exposure place	No. of conditions ^a / Duration of exposure per condition	No. of participants ^b / Occupation	Performance assessment	Summary of results ^c	Classification ^d
Kajtár and Herczeg (2014)	Quarterly Journal of the Hungarian Meteorological Service	Hungary	Chamber	4/ 140 min	10/ NA	Reading a manipulated text and search for typographic errors.	reductions occurred in seven of the SMS scales at 2500 ppm	A (CO ₂)
Maddalena et al. (2015)	Indoor Air	US	Office-like controlled environment	2/ 240 min	16/ Students and university staff	SMS ⁱ	No significant differences were observed	B
			Office-like controlled environment	2/ 240 min	16/ Students and university staff	SMS ⁱ		B

Allen et al. (2016)	Environmental Health Perspectives	US	Chamber	2/ 480 min	24/ Professional-grade employees	SMS ⁱ	Participants performed worst in seven of the nine SMS scales when CO ₂ was raised from 945 to 1400 ppm	B (CO ₂)
Zhang et al. (2016a)	Building and Environment	Denmark	Chamber	4/ 153 min	10/ Students	Simulated office work tasks: text typing and addition	Participants performed on average 61% higher on the “Green building” day (low concentration of VOCs) than under the normal condition	C (VOC _S)
Zhang et al. (2017)	Indoor Air	Denmark	Chamber	3/ 255 min	25/ Students	Psychological tests: redirection, grammatical reasoning, Stroop, and Stroop with feedback. Simulated office work tasks: text typing, arithmetical calculations, and proofreading	No significant differences were observed	A (CO ₂)
Liu et al. (2017)	Building and Environment	Denmark	Chamber	2/ 180 min	12/ Students	A battery of neurobehavioral tests	No significant differences were observed	A (CO ₂)

(continued)

Table 1 (continued)

Study	Journal	Location	Exposure place	No. of conditions ^a /Duration of exposure per condition	No. of participants ^b /Occupation	Performance assessment	Summary of results ^c	Classification ^d
Maula et al. (2017)	Indoor Air	Finland	Office-like controlled environment	2/ 120 min	36/ Students	Typing, star counting, operation span, N-back, information retrieval, creative thinking, and long-term memory tasks when VR was increased from 2.3 and	Significant differences were found at the information retrieval and operation span tasks when VR was increased from 2.3 and 28.2 L/s per person	B
Allen et al. (2018)	Journal of Exposure Science & Environmental Epidemiology	US	Flight simulator	3/ 180 min	30/ Pilots	FAA Designated Pilot Examiner	Aeroplane pilots performed better at 700 and 1500 ppm compared to 2500 ppm	A (CO ₂)
Rodeheffer et al. (2018)	Aerospace Medicine and Human Performance	US	Chamber	3/ 125 min	12/ Submarine-qualified sailors	SMS ^h	No significant differences were observed	A (CO ₂)
Scully et al. (2019)	npj Microgravity	US	Chamber	4/ 240 min	22/ Astronaut-like persons	SMS ⁱ and Cognition ^h	When CO ₂ was increased from 600 (baseline) to 600 (baseline) to	A (CO ₂)

Snow et al. (2019)	Building and Environment	UK	Naturally ventilated office	2/ 50 min	31/ Students and university staff	CNS Vital Signs ^j

(continued)

Table 1 (continued)

Study	Journal	Location	Exposure place	No. of conditions ^{a/} Duration of exposure per condition	No. of participants ^{b/} Occupation	Performance assessment	Summary of results ^{c/}	Classification ^{d/}
Cedeño Laurent et al. (2021) ^k	Environmental Research Letters	China, India, Mexico, Thailand, USA, and UK	NA	12 months (Longitudinal observational study)/ 15 min/ week	302/ Office workers	Stroop color-word test and two-digit, visual addition–subtraction test	Five cognitive performance metrics of office workers were significantly associated with real-time indoor concentrations of PM2.5 and CO ₂	C

^a Number of comparable IAQ conditions (e.g., indoor environmental parameters remained barely unchanged except for one of the proxies of the IAQ – CO₂, VOCs, VR)

^b Number of subjects per IAQ condition (The studies of Belum et al. (1985, 1990) and Rodeheffer et al. (2018) were a between-subjects experiment)

^c All experiments used a within-subjects intervention design except for Rodeheffer et al. (2018) and Belum et al. (1990), that used a between-subjects intervention design, and Cedeño Laurent et al. (2021) that was a longitudinal observational study

^d (A): Studies where IAQ was altered by modifying the concentration of specific pollutants (e.g., adding CO₂ or VOCs). (B): Studies where pollution levels were altered by modifying ventilation rates. (C) Studies where pollution levels were altered by adding or removing a pollution source and/or sink

^e Neurobehavioral Evaluation System (NESF): (1) Primary Behavioral Tests: Auditory Digit Span, Visual Digit Span, Finger Tapping, Continuous Performance Test, Symbol Digit Substitution, Serial Digit Learning Pattern, Pattern Memory, Switching attention, Mood scales. (2) Secondary Behavioral Tests: Associative Learning, Pattern Comparison, Simple Reaction Time, Grammatical Reasoning, Horizontal Addition

^f Walter Reed performance assessment battery (PAB): two-letter search, two-column addition, logical reasoning, serial addition/subtraction, Stroop 1, running memory, six-letter search, and code substitution. Simulated office work: Text typing, addition, knowledge test, and recall test.

^g Ventilation rates in combination with air filters

^h Cognition tasks: Motor Praxis (MPT), Visual Object Learning Task (VOLT), Fractal 2-Back (F2B), Abstract Matching (AM), Line Orientation (LOT), Digital Symbol Substitution (DSST), Balloon Analog Risk (BART), Psychomotor Vigilance Test (PVT), Matrix Reasoning (MR), Emotion Recognition Task (ERT)

ⁱ Strategic Management Simulation (SMS) measures: Basic Activity Level, Task Orientation, Breadth of Approach, Basic Strategy, Applied Activity, Level Focused Activity, Level Information Orientation, Information Utilization, and Initiative

^j CNS Vital signs: executive function, reaction time, working memory, complex attention, simple attention, sustained attention, and cognitive flexibility

^k Results are based on modeling rather than experimenting. Generalized additive mixed models were used to quantify the individual effects of PM2.5 and CO₂ on each of the five cognitive test metrics of interest:

Two environmental target levels were evaluated per environmental exposure of interest:

PM2.5	CO ₂
Low	High
Concentrations of below 50% (<6 $\mu\text{g m}^{-3}$) of the US National Ambient Air Quality Standard (NAAQS)	Concentrations of above 100% (>12 $\mu\text{g m}^{-3}$) of the US National Ambient Air Quality Standard (NAAQS)
	Low <600 ppm High >950 ppm

(2014), Maddalena et al. (2015), and Allen et al. (2016) reported two studies per publication each. In our literature search, we only looked for peer-reviewed journal articles that examined the effects of IAQ on office work performance. As independent variables representing IAQ (exposures), we used ventilation rates, CO₂ concentration, fine particles, and volatile organic compounds (VOC) but not odor exposure. The dependent variables (effects) were diagnostic tests, simulated office work tasks, and the existing work performance outcome metrics. Absence rates and self-estimated performance were not considered.

The reviewed studies were conducted in 12 countries with 1212 young adults and adults whose weighted mean age was 31 years. In the identified studies, 45% of the participants were college or university students (which we consider as young adults), 13% were call center agents, 19% had different professions such as nurses, pilots, university staff, submariners, and astronauts, while for the remaining 23%, the occupation was not reported. The median number of subjects per study was 27 persons, while the largest included 302 participants (Cedeño Laurent et al. 2021) and the smallest ten subjects (Kajtár and Herczeg 2014; Zhang et al. 2016a). The exposure time to each indoor quality condition examined ranged between 1 and 8 h (mean exposure time = 247 ± 113 min), except for the studies conducted in call centers and the study of Cedeño Laurent et al. (2021), which lasted longer than one day.

We classified – and summarized below – the studies into three groups according to which effects were examined and how the indoor air pollution load was altered. The classification was done as follows:

- A. Studies where IAQ was changed by modifying the concentration of specific pollutants (e.g., adding CO₂ or VOCs) while maintaining all other parameters unchanged: The exposure to the particular pollutant is changed.
- B. Studies where pollution levels were altered by modifying ventilation rates: At higher VRs, a decrease in the exposure level is expected due to the dilution of the contaminants.
- C. Studies where pollution levels were altered by adding or removing a pollution source and/or sink: An increase/decrease in the exposure level is expected, but the pollutants added or removed and the changes in their concentrations are not specified.

Figure 1 shows a timeline chart with the 28 articles ordered by the year of publication. It can be seen that while during the eighties, the focus was on examining the effects of toluene and other VOCs on work performance, attention shifted to ventilation rates at the beginning of this century and to CO₂ in the last decade. This latest shift is probably a consequence of the awareness among researchers of the increasing levels of CO₂ in outdoor air and how the subsequent increase in indoor concentrations could affect work performance in the future.

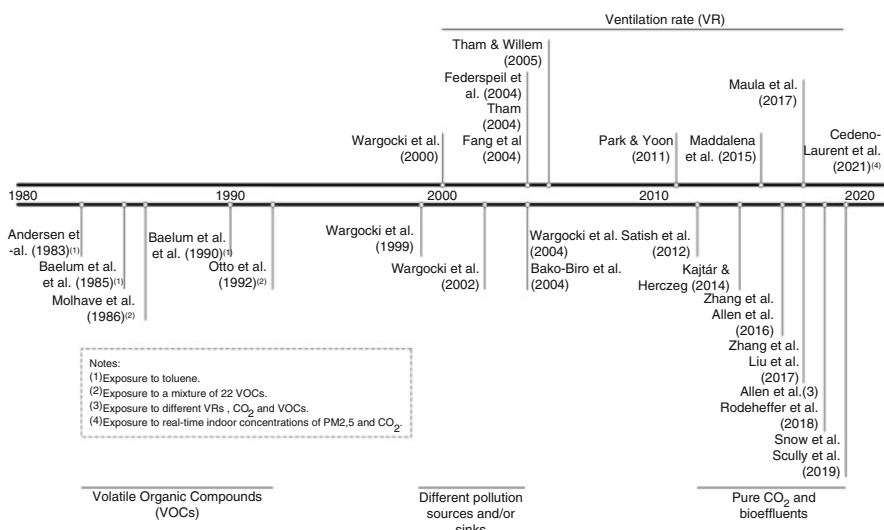


Fig. 1 Timeline chart showing the articles included in this review ordered by year of publication

Studies Where Pollution Levels Were Altered by Modifying the Concentration of Specific Pollutants

The Effects of CO₂ on Work Performance, Simulated Work Performance, and/or Cognitive Abilities

Before 2012, CO₂ was considered to have significant effects on human performance only at very high concentrations (>10,000 ppm) (e.g., Sayers et al. (1987)). Therefore, studies that, before this year, documented associations between indoor CO₂ and performance at the typical concentrations that occur in non-industrial buildings attributed them not to the presence of CO₂ but a change in the indoor air pollutant load indicated by a change in the levels of CO₂, i.e., CO₂ was considered a marker of other contaminants and not a pollutant itself. However, this way of thinking was challenged by the results of the experiment of Satish et al. (2012), which showed that when CO₂ concentration was increased from 600 to 1000 ppm by injection rather than emitted by humans, moderate and statistically significant decrements occurred in the performance of a computerized test called Strategic Management Simulation (SMS) – a decision-making performance test – while large reductions occurred at 2500 ppm.

The results of Kajtár and Herczeg (2014) and Allen et al. (2016), published a few years later, supported this statement. Kajtár and Herczeg (2014) conducted two studies. Although no significant differences were observed in the first experiment, the participants performed significantly worse at the high CO₂ levels (3000 and 4000 ppm) in the second one. For their part, Allen et al. (2016), who used the same testing battery as Satish et al. (2012), observed that the scores of seven of the nine SMS

decision-making measures decreased when the CO₂ concentration was raised from 945 ppm to 1400 ppm. However, Zhang et al.'s (2016a, 2017) and Liu et al.'s (2017) studies showed no significant effects of elevated artificially injected CO₂ exposures on cognitive performance. Zhang et al. (2017) hypothesized that a plausible explanation for the discrepancies found was the difference in the cognitive tasks applied and their difficulty – the tests included in the SMS battery were more complex than the "*simple cognitive tests and tasks resembling office work*" they applied. This may be further explained by the Maximal Adaptability Theory, which posits that subjects were able to draw upon their cognitive capacity to compensate against adverse effects of higher CO₂ exposures to maintain their performance under less cognitively demanding tasks.

Unlike previous studies that used SMS, Rodeheffer et al. (2018) did not observe significant differences for any of the nine SMS measures of decision-making between the CO₂ exposure conditions (600, 2500, and 15,000 ppm) and Scully et al. (2019) – who also used the Cognition test battery – observed them only at 1200 ppm, but not at 2500, or 5000 ppm; in Scully et al. (2019) the effects at 1200 ppm were seen both for the performance of SMS and other cognitive tasks. Rodeheffer et al. noted that the effect sizes in their experiments were very low, suggesting that any potential change in cognitive function attributed to CO₂ exposure is of little importance in practice. They also argued that differences in the results could be attributable to the acclimation of their participants – submarine sailors who were used to work in environments with high CO₂ concentrations. For their part, Scully et al. (2019) pointed out three possible explanations for the disagreements with previous studies. The first one refers to differences in population type – while in the studies of Satish et al. and Allen et al., the participants were university students, Scully et al. and Rodeheffer et al. used astronauts and submariners, who by their profession could have high performance and due to their rigorous training, could be better prepared to withstand the cognitive impairment/demand and could have developed compensatory responses. However, this does not explain the performance decline when the astronauts were exposed to 1200 ppm of CO₂. The second reason stated by Scully et al. was the age of the participants – they were older in the Scully et al. (mean age = 38.8 year) and Rodeheffer et al. (mean age = 30 year) studies, and according to Scully et al., there is abundant evidence that the way young and/or novice individuals make decisions differ from those who are older and/or more experienced. As proof of this, Scully et al. found that there is a more remarkable similarity in the most affected measures between the studies of Satish et al. and Allen et al. and their study and Rodeheffer et al. Finally, the third reason is related to the amount of sleep obtained by the subjects before the exposure to CO₂. According to the study by MacNaughton et al. (2017), who also used SMS, an increase in sleep hours by 25% was associated with improvements in cognitive functions by almost 3%. The difference in sleep time between the participants of Scully et al. and Satish et al. could not be carried out because the latter did not report this information.

Allen et al. (2018) – same research group as Allen et al. (2016) – conducted an experiment to examine the effects of elevated CO₂ on commercial airline pilots in a flight simulator, finding that performance was better at 700 ppm and 1500 ppm than at 2500 ppm.

Finally, Snow et al. (2019) experimented in a small naturally ventilated office, where participants were exposed to three conditions: baseline, normal CO₂ (830 ppm), and high CO₂ (2700 ppm). The results showed that performance did not decrease during the high CO₂ condition; however, the authors interpreted the absence of an expected learning effect in two tests to suggest that CO₂ might still have adversely affected performance. Self-reported sleepiness was significantly higher in the normal and high CO₂ conditions relative to baseline but was not correlated with the CO₂.

In summary, the discussion on whether CO₂ is in itself a pollutant that affects cognitive performance is not settled for now because there are substantial discrepancies between the results of the experiments. Five studies found effects ((Satish et al. 2012; Kajtár and Herczeg 2014; Allen et al. 2016, 2018; Snow et al. 2019), but another five did not (Kajtár and Herczeg 2014; Zhang et al. 2016a, 2017; Liu et al. 2017; Rodeheffer et al. 2018), and one found them at 1200 ppm, but not at 2500 and 5000 ppm (Scully et al. 2019). Moreover, a physiological mechanism has not been yet proved, and Mishra et al. (2021) showed that CO₂ found in buildings does not affect human respiration performance.

The Effects of Volatile Organic Compounds (VOCs) on Cognitive Abilities

Three studies examined the effects of toluene on cognitive performance (Andersen et al. 1983; Bælum et al. 1985, 1990); all of them were conducted by the same research group in Denmark. Participants were exposed to conditions that ranged from clean air to 377 mg/m³ (100 ppm) of toluene. Bælum et al. (1985) were the only ones who found significant effects on two perceptual and one visuo-motor tests; however, the impact occurred when the toluene concentration was 377 mg/m³ (100 ppm), which will only happen in workplaces where toluene is used industrially, so the results do not constitute evidence that this VOC will reduce work performance in non-industrial buildings, at least not at the levels indoors.

Mølhav et al. (1986) and Otto et al. (1992) investigated the effects of a low-level concentration combination of 22 VOCs – typical of those present in new buildings – on performance; both experiments exposed participants to concentrations of 0, 5, and 25 mg/m³ measured as a toluene equivalent concentration. These values were chosen to reflect pure (clean) air, typical new-home concentrations, and the highest concentration found in new Danish homes. While the first study results showed that the scores on both digit span forwards and backwards decreased significantly, in the second one only a marginal deterioration was observed in the forward visual digit span at 25 mg/m³. Because this finding was isolated and not expected, it was considered a random occurrence. According to Otto et al., the differences found between the results of both studies were because of two reasons: design problems in the experiment by Mølhav et al. that they attempted to amend (e.g., unlike Mølhav et al., all sessions were conducted at the same time and control and exposure sessions were separated by at least one week to reduce fatigue, carry-over effects and effects time of day), and differences in sample characteristics (e.g., Mølhav et al. used an equal number of men and women, the age range was wider, and the participants were selected because were chemically sensitive and had a documented history of indoor weather problems).

Studies Where Pollution Levels Were Altered by Modifying Ventilation Rates

Office-Like Controlled Environments

Wargocki et al. (2000) examined the effects on cognitive performance by changing ventilation rates (VRs) set to be 3, 10, and 30 L/s per person. A 20-year-old carpet equivalent to floor room size was placed behind a partition so the participants could not see it. The results show that the participants typed 4% more characters per minute when the VR was increased from 3 to 30 L/s per person. Fang et al. (2004) conducted a study that used the same space, carpet, sample size, office work tasks, and exposure time as Wargocki et al. (2000) but new subjects. Despite these similarities, increasing VR from 3.5 to 10 L/s per person did not cause significant effects on cognitive performance. The authors argued that their experiment was not specifically designed to look at the effect of VRs on performance – as Wargocki et al.’s did – which could explain the differences in the results.

With an experimental design similar to the previous ones – but without adding additional sources of indoor air pollution other than those generated by the participants (bioeffluents) – Park and Yoon (2011) and Maula et al. (2017) examined the effects of different VRs on cognitive performance: 5, 10 and 20, and 2.3 and 28.2 L/s per person, were used respectively. In Park and Yoon’s (2011) experiment, participants performed better on the tasks of text typing (5.2%), addition (4.7% above), and memorization (8%) at higher VRs, confirming Wargocki et al.’s (2000) findings and extending their results to other cognitive abilities. After analyzing indoor air during exposure, researchers found high concentrations of volatile organic compounds (VOCs) due to a recent renovation of the exposure chamber. For their part, Maula et al. (2017) found no differences in the text typing task as in previous experiments. In contrast, participants performed statistically significantly better at the information retrieval and operation span tasks. Because differences were only found in one task and as a trend in another, while performance was unaffected in five tasks, the authors categorized the effect of VR on cognitive work performance as “weak”.

Maddalena et al. (2015) carried out two experiments with a slightly different experimental procedure; the cognitive performance was measured with SMS. In the first one, ventilation rates of 2.6 and 8.5 L/s per person were provided while maintaining a ventilation rate of ≥ 5.6 L/s per m^2 ; while in the second, 5.5 and 0.8 L/s per m^2 were provided while maintaining a ventilation rate of ~ 8.4 L/s per person. The results of both studies showed that at low VRs, there was a moderate but statistically significant reduction in cognitive function of all performance metrics – except for Information Management – from the SMS battery test.

Call-Centers

Five studies have examined the effects of VR alone (Federspiel et al. 2004), or in combination with temperature (Tham 2004; Tham and Willem 2005), or air filters (Wargocki et al. 2004) on the work performance of call center agents. Tham (2004)

examined two levels of outdoor air supply rates (5 and 10 L/s per person) at two temperature settings (22.5 °C and 24.5 °C). The author found that talk time was reduced significantly when the outdoor air supply rate was increased from 5 L/s per person to 10 L/s per person at 24.5 °C.

Fedderspiel et al. (2004) studied the effects of ventilation as the only variable on performance; for this purpose, the difference between indoor and outdoor CO₂ concentrations (ΔCO_2) was increased from 13 to 610 ppm. However, the authors did not observe significant changes in wrap-up time, and even though the talk time was faster when the VR was higher, the relationship was not strong.

Wargocki et al. (2004) conducted a study in a call center where the participants were exposed to four different conditions by alternating a new air filter with one that had been in place for 6 months and by adjusting the outdoor air supply rate to 2.5 and 25 L/s per person. The results show that increasing the outdoor air supply rate reduced talk-time by 6% with a new filter in place but increased talk time by 8% with the used filter. Replacing the used filter with a clean filter reduced the talk-time by approximately 10% at the high ventilation rate but had no significant effect at the low rate. Ozone chemistry on the dirt accumulated in used filters is known to produce by-products with an adverse effect on the olfactory sense and likely affected performance (Bekö et al. 2007; Fadeyi et al. 2009).

Tham and Willem (2005) used a 2X2 intervention experiment design where supply rates and temperatures in two call centers were modified. In call center A, the VRs were 3 and 6 L/s per person, while in call center B, 9 and 18 L/s per person. The temperatures were the same at the two sites (22.5 °C and 24.5 °C). The authors found that at 24.5 °C, doubling the VR significantly reduced the talk time by 7% to 9%, while at 22.5 °C, the talk time increased in both call centers, but differences were not significant. As causal mechanisms, Tham and Willem (2005) suggested that a decrease in the VR could have increased symptoms related to neurological behavior and reduced self-perceived productivity, which in turn could have manifested itself through the observed increase in mean talk time.

In summary, except for the studies of Fang et al. (2004) and Fedderspiel et al. (2004), all other studies conducted in controlled office-like settings and call centers positively impacted cognitive performance by increasing ventilation rates. Improvements were found in (i) decision-making tasks – all the SMS battery tests except for the Information Management test, (ii) office work tasks, (iii) cognitive abilities tests (memory), and (iv) existing performance outcomes (talk time). Higher VRs could improve the IAQ by removing and/or diluting pollutants. The outdoor air was assumed to be clean but chemical characteristics were not always reported. This assumption does not hold in many parts of the world. As discussed by Maula et al. (2017), it is essential to underline that significant effects were found only in a subset of the tests and tasks applied and sometimes in only one of the metrics used to measure cognitive performance (i.e., speed or accuracy). Furthermore, it would be convenient to estimate the magnitude of the effect (the effect size) predicted by the research hypothesis to know if the difference found is large enough to be of practical importance (Lakens 2013).

Relationships Between Ventilation and Cognitive Performance

Using nine studies published between 1997 and 2004 in journals, conferences, and reports, Seppänen et al. (2006) developed a relationship between work performance and increased ventilation. Five studies were conducted in call centers (Wargocki et al. 2000; Heschong Mahone Group 2003; Federspiel et al. 2004; Tham 2004; Tham and Willem 2004), one in an office building (Heschong Mahone Group 2003), two in an office-like controlled environment (Wargocki et al. 1999; Bakó-Biró 2004), and one in a classroom with students aged 16 to 19-years (Myhrvold and Olsen 1997). According to the authors, the reviewed studies showed an improvement in the average performance – between 1 and 3% – when the ventilation with outdoor air increased by 10 L/s per person. In the proposed relationship, the authors estimated that performance improves in the ventilation range of 6.5 to 17 L/s per person with a 90% confidence interval (CI) and up to 15 L/s per person with a 95% CI. Ventilation rates above 45 L/s per person were not seen to improve the performance. Despite its wide use, some limitations should be considered before using Seppänen et al.'s relationship. The limitations of a relationship between temperature and work performance developed by the same authors following a similar approach, and which may thus be applied to this relationship, are discussed in detail by Porras-Salazar et al. (2021).

Studies Where Pollution Levels Were Altered by Adding or Removing a Pollution Source and/or Sink

Wargocki et al. (1999) carried out a study in Denmark in which the pollution levels were altered by introducing and removing a 20-year-old used carpet. The results show that when the pollution source was present, the participants typed 6.5% less text. Using a similar experimental methodology as Wargocki et al. (1999), Wargocki et al. (2002) carried out an experiment in Sweden where the speed and accuracy of text typing were 1.5% and 7% lower when the old carpet was present. When comparing both experiments – Danish and Swedish – the authors found that the agreement between them was moderate ($Kappa = 0.477$, $P = 0.0005$).

Bakó-Biró et al. (2004) performed a similar experiment but under the presence or absence of 3-month-old personal computers (PCs) with the cathode-ray tube (CRT) monitors. Throughout the exposure, the outdoor air supply was maintained at 10 L/s per person. Text typing and reading speed decreased by 0.5% and 4% respectively, and errors increased by 20% with the PCs present.

Allen et al. (2016) examined the effects of different IEQ conditions that were representative of “conventional” (higher concentrations of VOCs – between 500 and 666 $\mu\text{g}/\text{m}^3$) and “green” (low concentrations of VOCs – less than 50 $\mu\text{g}/\text{m}^3$) office buildings in the United States. Before the participants arrived, different sources were placed in the diffuser that provided air to the office cubicles to enhance the level of VOCs. Authors found that, on average, cognitive scores were 61% higher under “green” building conditions, their cognitive performance being measured using SMS.

The main limitation of the studies described above is that the use of an uncharacterized source of pollution makes it difficult to compare the results with other studies and/or generalize the findings.

Limitations and Future Work

Across the selected studies, various work performance assessment methods were used including simulated work tasks, cognitive tests, and existing work performance outcomes. However, some of them have shortcomings, such as that the tasks could be simple and could not capture the complexity of office work (Mishra et al. 2020), or the selection of task or test batteries was not always justified. An exception is the study of Scully et al. (2019), where the selection of the Cognition battery was based on the fact that it was explicitly designed to evaluate the cognitive performance of astronauts, and each of the included tasks is related to a cognitive domain and the areas of the brain that are primarily recruited to perform them. The increase in the use of physiological and biochemical evaluations in the indoor environmental quality (IEQ) field has opened the possibility of a better understanding of what the causal mechanisms involved in the relationship between IAQ and work performance could be; however, more research is required on the subject because so far few studies have used them (e.g., Zhang et al. 2016a, b).

There is a need to discuss how the results of the studies in which IAQ effects on performance were observed should be interpreted. The discussion should extend to how the results are reported so they can be used in meta-analyses. The debate should help answer some questions: Is a statistically significant effect on one or two tests reason enough to conclude a deterioration in overall work performance? Which type of tests are affected? Are the effects on some abilities more critical than others? Besides the statistical significance, should the magnitude of the effect be considered? Lack of shared agreement can lead to misinterpretations or opposing interpretations of similar findings. For example, Park and Yoon (2011) applied seven tests and found statistical significance in two of them. They concluded that increasing VRs would improve work performance. On the opposite, in the study of Maula et al. (2017), where a battery of seven tests was used to assess the performance, the authors concluded that the effect of VR on work performance was “weak” because statistically better results were obtained only in two out of the seven tests.

Regarding the magnitude of the effect, the null hypothesis significance test method (NHST) should be complemented with the estimation and notification of the effect size (ES) and its confidence interval (CI), as has been the case in other research fields among behavioral and social sciences (Nickerson 2000; Johnson 2016). ES is a quantity that directly measures the strength of the association or difference between variables and has the advantage that allows researchers to: (i) present the magnitude of the effects in a standardized manner, (ii) easily compare the results of different studies, and (iii) plan new studies (e.g., estimate sample sizes) (Lakens 2013). Across the included articles, only Rodeheffer et al. (2018) reported

the Eta-squared (η^2) – that as the r^2 describes the proportion of variance that is explained by group membership (Lakens 2013) – and its 95% CI. Another good practice that will allow the subsequent estimation of the ES – when not reported in the articles – and will ensure research can be reproduced and reanalyzed, is to provide raw data or data allowing the calculation of the effect size.

Ventilation rates are likely to affect work performance; however, an optimal VR has not yet been defined that, for example, allows adequate removal or dilution of pollutants without using excess energy, or can reduce the spread of airborne pathogens, or be efficient in controlling heating and cooling loads.

With the exception of the studies by Mølhave et al. (1986), Bælum et al. (1990), Allen et al. (2018), and Scully et al. (2019), the subjects who participated in the selected studies were generally healthy young adults between 20 and 35 years old, and there were no studies where the mean age of the subjects was greater than 40 years. This may be related to the difficulties of recruiting middle-aged subjects (36–64 years) to participate in the experiments; however, as life expectancy and retirement age increase, it is necessary to investigate the effects of IAQ in middle-aged workers and people with health problems.

Finally, the selected studies, regardless of whether they were carried out in a call center, a flight simulator, or in a climatic chamber, followed similar procedures in which the participants worked individually and in front of a screen where they had to complete a list of very specific tasks for a short time without real-life consequences if the work was not done correctly. Under these circumstances, essential performance dimensions like contextual, adaptive, and counterproductive performance could not be assessed. However, in most office workplaces today, employees are exposed to a complex and dynamic environment where, for example, prosocial and adaptive behaviors are highly desired by organizations because of the importance of skills such as leadership, communication, negotiation, teamwork, creativity, honesty, and self-management. Therefore, extrapolating overall work performance from these simple tasks is hard. Consequently, IAQ researchers have so far been able to examine the effects of IAQ on task performance primarily and laterally and sporadically capture contextual and prosocial performance indicators (e.g., attention to duty, creativity). It would be desirable to advance experimental designs and performance metrics further so that the effects of IAQ on overall job performance can be better described.

Conclusions

Table 2 presents our conclusions for each of the three categories we divided the 32 studies included in this literature review. The results show that (i) an increase in ventilation rates has a positive impact on cognitive performance – at least for some cognitive abilities – and therefore for the performance of office work; (ii) toluene effects on work performance were only found at high concentrations that are not common in office buildings. The results are inconsistent for the studies that examined the effects of pure CO₂ and TVOCs.

Table 2 Summary of conclusions

Categorisation	Subcategorisation	Number of studies	Main conclusion
How pollution load was altered	Type of space/ type of pollutant		
By modifying the concentration of specific pollutants	NA/ CO ₂	11	The results of the studies have substantial discrepancies. Five studies found effects ((Satish et al. 2012; Kajtár and Herczeg 2014; Allen et al. 2016, 2018) + Snow et al. (2019) who found no differences between conditions, but concluded that the absence of an expected learning effect suggested that CO ₂ may have affected performance), another five did not (Kajtár and Herczeg 2014; Zhang et al. 2016a, 2017; Liu et al. 2017; Rodeheffer et al. 2018), and one found them at 1200 ppm, but not at 2500 and 5000 ppm. (Scully et al. 2019). Four of the studies used a computer-based test of decision-making performance called the Strategic Management Simulation (SMS), half of them found effects, and the other half did not.
	NA/ TVOCs	3	Only three studies have been conducted, and the results are contradictory and difficult to compare due to the design of the experiments. Therefore, more research is needed to resolve the discrepancies found.
	NA/ Toluene	3	One of the three studies showed effects but at a toluene concentration rarely found in non-industrial spaces – 377 mg/m ³ (100 ppm). Consequently, it can be concluded that at the concentrations under which toluene is commonly found in office buildings, it does not affect workers' performance.
By modifying ventilation rates	Office-like controlled spaces/ NA	6	Increasing VRs improved participants' performance in all SMS battery tests except for Information Management, as well as on office tasks – typing and addition – and cognitive abilities tests — memorization. Higher VRs may have improved air quality by displacing and/or diluting pollutants.
	Call centres/ NA	5	Four of the five studies found effects; however, three of them belong to the same research group and were conducted in the same location.

(continued)

Table 2 (continued)

Categorisation	Subcategorisation	Number of studies	Main conclusion
How pollution load was altered	Type of space/ type of pollutant		
			Taking into account that an increase in VR had a positive effect on performance in office-like controlled spaces, it would be expected that it will also have it in office centers. New studies could strengthen this hypothesis and the findings so far.
By adding or removing a pollution source and/or sink.	NA/ NA	4	There are five studies and due to their characteristics are difficult to compare with other experiments.

Plausible reasons that may explain the discrepancies in the results include (i) differences in populations, i.e., age (Scully et al. 2019), occupation (Rodeheffer et al. 2018; Scully et al. 2019), and health status of the participants (Otto et al. 1992); (ii) differences in experimental designs, i.e., sample size, within or between subjects design (Rodeheffer et al. 2018); (iii) presence of uncharacterized contaminants (Maula et al. 2017); (iv) sleep status of the participants (Scully et al. 2019); (vi) exposure time (Kajtár and Herczeg 2014; Allen et al. 2018); (vii) task complexity (Zhang et al. 2016a); and (viii) uncertainty in pollution exposure. Additionally to the research needed to address the discrepancies observed in the studies examining the effects of CO₂ and TVOCs, future investigations should focus on: (i) developing a shared understanding of the meaning of work performance and the methods and metrics to measure it, (ii) estimating the magnitude and shape of the relationship between ventilation rates and performance, (iii) exploring the effects of IAQ on the performance for mid-age workers and people with compromised health conditions, and (iv) exploration of the causal mechanisms involved in the relationship between IAQ and work performance.

Cross-References

- [ASTM and ASHRAE Standards for the Assessment of Indoor Air Quality](#)
- [Economic Consequences](#)
- [Effects from Exposures to Human Bioeffluents and Carbon Dioxide](#)
- [Indoor Air Quality in Offices](#)
- [Influence of Ventilation on Indoor Air Quality](#)
- [Metrics and Methods \(Performance Indicators, Methods, and Measurement\)](#)
- [Postulated Pathways Between Environmental Exposures and Cognitive Performance](#)
- [Volatile Organic Compounds \(VOCs\)](#)

References

- Allen JG, Macnaughton P, Satish U et al (2016) Associations of cognitive function scores with carbon dioxide, ventilation, and volatile organic compound exposures in office workers: a controlled exposure study of green and conventional office environments. *Environ Health Perspect* 124:805–812
- Allen JG, Macnaughton P, Cedeno Laurent JG et al (2018) Airplane pilot flight performance on 21 maneuvers in a flight simulator under varying carbon dioxide concentrations. *J Expo Sci Environ Epidemiol* 29(4):457–468. <https://doi.org/10.1038/s41370-018-0055-8>
- Andersen I, Lundqvist GR, Mølhave L et al (1983) Human response to controlled levels of toluene in six-hour exposures. *Scand J Work Environ Health* 9:405–418. <https://doi.org/10.5271/sjweh.2393>
- Bælum J, Andersen I, Lundqvist G et al (1985) Response of solvent-exposed printers and unexposed controls to six-hour toluene exposure. *Scand J Work Environ Health* 11:271–280
- Bælum J, Lundqvist GR, Mølhave L, Andersen NT (1990) Human response to varying concentrations of toluene. *Int Arch Occup Environ Health* 61:65–71. <https://doi.org/10.1007/BF00397850>
- Bakó-Biró Z (2004) Human Perception, SBS Symptoms and Performance of Office Work during Exposure to Air Polluted by Building Materials and Personal Computers. Technical University of Denmark
- Bakó-Biró Z, Wargocki P, Weschler CJ, Fanger PO (2004) Effects of pollution from personal computers on perceived air quality, SBS symptoms and productivity in offices. *Indoor Air* 14: 178–187. <https://doi.org/10.1111/j.1600-0668.2004.00218.x>
- Bekö G, Clausen G, Weschler CJ (2007) Further studies of oxidation processes on filter surfaces: evidence for oxidation products and the influence of time in service. *Atmos Environ* 41: 5202–5212. <https://doi.org/10.1016/j.atmosenv.2006.07.063>
- Cedeno Laurent JG, Macnaughton P, Jones E et al (2021) Associations between acute exposures to PM_{2.5} and carbon dioxide indoors and cognitive function in office workers: a multicountry longitudinal prospective observational study. *Environ Res Lett* 16. <https://doi.org/10.1088/1748-9326/ac1bd8>
- Fadeyi MO, Weschler CJ, Tham KW (2009) The impact of recirculation, ventilation and filters on secondary organic aerosols generated by indoor chemistry. *Atmos Environ* 43:3538–3547. <https://doi.org/10.1016/j.atmosenv.2009.04.017>
- Fang L, Wyon DP, Clausen G, Fanger PO (2004) Impact of indoor air temperature and humidity on perceived air quality, SBS symptoms and performance. *Indoor Air* 14:74–81. <https://doi.org/10.1111/j.1600-0668.2004.00276.x>
- Fedderspiel C, Fisk WJ, Price PN et al (2004) Worker performance and ventilation in a call center: analyses of work performance data for registered nurses. *Indoor Air* 14(Suppl 8):41–50. <https://doi.org/10.1111/j.1600-0668.2004.00299.x>
- Heschong Mahone Group (2003) Windows and Offices: A Study of Office Worker Performance and the Indoor Environment. California, USA
- Johnson CHL (2016) Effect size measures in a two-independent-samples case with nonnormal and nonhomogeneous data. *Behav Res Methods* 48:1560–1574. <https://doi.org/10.3758/s13428-015-0667-z>
- Kajtár L, Herczeg L (2014) Influence of carbon-dioxide concentration on human well-being and intensity of mental work. *Q J Hungarian Meteorol Serv* 116:145–169
- Klepeis NE, Nelson WC, Ott WR et al (2001) The National Human Activity Pattern Survey (NHAPS): A resource for assessing exposure to environmental pollutants. *J Expo Anal Environ Epidemiol* 11(3):231–252. <https://doi.org/10.1038/sj.jea.7500165>
- Lakens D (2013) Calculating and reporting effect sizes to facilitate cumulative science: a practical primer for t-tests and ANOVAs. *Front Psychol* 4:1–12. <https://doi.org/10.3389/fpsyg.2013.00863>
- Liu W, Zhong W, Wargocki P (2017) Performance, acute health symptoms and physiological responses during exposure to high air temperature and carbon dioxide concentration. *Build Environ* 114:96–105. <https://doi.org/10.1016/j.buildenv.2016.12.020>

- MacNaughton P, Satish U, Cedeño Laurent JG et al (2017) The impact of working in a green certified building on cognitive function and health. *Build Environ* 114:178–186. <https://doi.org/10.1016/j.buildenv.2016.11.041>
- Maddalena R, Mendell MJ, Eliseeva K et al (2015) Effects of ventilation rate per person and per floor area on perceived air quality, sick building syndrome symptoms, and decision-making. *Indoor Air* 25:362–370. <https://doi.org/10.1111/ina.12149>
- Maula H, Hongisto V, Naatula V et al (2017) The effect of low ventilation rate with elevated bioeffluent concentration on work performance, perceived indoor air quality, and health symptoms. *Indoor Air* 27:1141–1153. <https://doi.org/10.1111/ina.12387>
- Mishra AK, Schiavon S, Wargocki P, Tham KW (2020) Carbon dioxide and its effect on occupant cognitive performance: A literature review Carbon dioxide and its effect on occupant cognitive performance : A literature review. In: Proceedings of the Windsor Conference. London, UK
- Mishra AK, Schiavon S, Wargocki P, Tham KW (2021) Respiratory performance of humans exposed to moderate levels of carbon dioxide. *Indoor Air* 1–13. <https://doi.org/10.1111/ina.12823>
- Mølhave L, Bach B, Pedersen OF (1986) Human reactions to low concentrations of volatile organic compounds. *Environ Int* 12:167–175. [https://doi.org/10.1016/0160-4120\(86\)90027-9](https://doi.org/10.1016/0160-4120(86)90027-9)
- Myhrvold AN, Olsen E (1997) Pupil's Health and Performance Due to Renovation of Schools. Healthy Buildings/IAQ, Washington DC
- National Research Council (1981) (US) Committee on Indoor Pollutants. *Indoor Pollutants*. Washington (DC): National Academies Press (US). PMID: 25121329
- Nickerson RS (2000) Null hypothesis significance testing: a review of an old and continuing controversy. *Psychol Methods* 5:241–301. <https://doi.org/10.1037/1082-989X.5.2.241>
- Otto DA, Hudnell HK, House DE et al (1992) Exposure of humans to a volatile organic mixture. I. Behavioral assessment. *Arch Environ Health* 47:23–30. <https://doi.org/10.1080/00039896.1992.9935940>
- Park JS, Yoon CH (2011) The effects of outdoor air supply rate on work performance during 8-h work period. *Indoor Air* 21:284–290. <https://doi.org/10.1111/j.1600-0668.2010.00700.x>
- Porras-Salazar JA, Schiavon S, Wargocki P et al (2021) Meta-analysis of 35 studies examining the effect of indoor temperature on office work performance. *Build Environ* 203. <https://doi.org/10.1016/j.buildenv.2021.108037>
- Rodeheffer CD, Chabal S, Clarke JM, Fothergill DM (2018) Acute exposure to low-to-moderate carbon dioxide levels and submariner decision making. *Aerospace Med Hum Perform* 89:520–525. <https://doi.org/10.3357/AMHP.5010.2018>
- Satish U, Mendell MJ, Shekhar K et al (2012) Concentrations on human decision-making performance. *Environ Health Perspect* 120:1671–1677
- Sayers JA, Smith REA, Holland RL, Keatinge WR (1987) Effects of carbon dioxide on mental performance. *J Appl Physiol* 63:25–30. <https://doi.org/10.1152/jappl.1987.63.1.25>
- Scully RR, Basner M, Nasrini J et al (2019) Effects of acute exposures to carbon dioxide on decision making and cognition in astronaut-like subjects. *NPJ Microgravity* 5:1–15. <https://doi.org/10.1038/s41526-019-0071-6>
- Seppänen O, Fisk WJ, Lei QH (2006) Ventilation and performance in office work. *Indoor Air* 16: 28–36. <https://doi.org/10.1111/j.1600-0668.2005.00394.x>
- Snow S, Boyson AS, Paas KHW et al (2019) Exploring the physiological, neurophysiological and cognitive performance effects of elevated carbon dioxide concentrations indoors. *Build Environ* 156:243–252. <https://doi.org/10.1016/j.buildenv.2019.04.010>
- Tham KW (2004) Effects of temperature and outdoor air supply rate on the performance of call center operators in the tropics. *Indoor Air* 14:119–125. <https://doi.org/10.1111/j.1600-0668.2004.00280.x>
- Tham KW, Willem HC (2004) Effects of reported neurobehavioral symptoms on call center operator performance in the tropics. In: Proceeding of Room Vent 2004 Conference. Coimbra, Portugal

- Tham KW, Willem HC (2005) Temperature and ventilation effects on performance and neurobehavioral-related symptoms of tropically acclimatized call center operators near thermal neutrality. ASHRAE Trans 111 PART 2:687–698
- Wargocki P, Wyon DP, Baik YK et al (1999) Perceived air quality, Sick Building Syndrome (SBS) symptoms and productivity in an office with two different pollution loads. Indoor Air:165–179
- Wargocki P, Wyon DP, Sundell J et al (2000) The effects of outdoor air supply rate in an office on perceived air quality, Sick Building Syndrome (SBS). Indoor Air 10:222–236
- Wargocki P, Lagercrantz L, Witterseh T et al (2002) Subjective perceptions, symptom intensity and performance: a comparison of two independent studies, both changing similarly the pollution load in an office. Indoor Air 12:74–80. <https://doi.org/10.1034/j.1600-0668.2002.01101.x>
- Wargocki P, Wyon DP, Fanger PO (2004) The performance and subjective responses of call-center operators with new and used supply air filters at two outdoor air supply rates. Indoor Air 14: 7–16
- WHO (1979) Health aspects related to indoor air quality. Denmark, Copenhagen
- Zhang X, Wargocki P, Lian Z (2016a) Human responses to carbon dioxide, a follow-up study at recommended exposure limits in non-industrial environments. Build Environ 100:162–171. <https://doi.org/10.1016/j.buildenv.2016.02.014>
- Zhang X, Wargocki P, Lian Z (2016b) Physiological responses during exposure to carbon dioxide and bioeffluents at levels typically occurring indoors. Indoor Air 27:65–77. <https://doi.org/10.1111/ina.12286>
- Zhang X, Wargocki P, Lian Z, Thyregod C (2017) Effects of exposure to carbon dioxide and bioeffluents on perceived air quality, self-assessed acute health symptoms, and cognitive performance. Indoor Air 27:47–64. <https://doi.org/10.1111/ina.12284>



Effects of Classroom Air Quality on Learning in Schools 49

Pawel Wargocki

Contents

Introduction	1448
The Effects on the Performance of Schoolwork and Absence Rates	1448
The Effects on Psychological and Neurobehavioral Tests	1448
The Effects on Typical School Tasks	1450
The Effects on National and Aptitude Tests and Examination Results	1451
The Effects on Absence Rates	1452
Sleep and Learning	1453
The Relationships Between Learning and IAQ	1453
Conclusions	1456
References	1457

Abstract

This chapter describes the evidence of the effects of indoor air quality (IAQ) on learning of children and gives an overview of the size of the effects expected. The results from the published experiments on the effects of classroom air quality on the performance of schoolwork do confirm that these effects are systematic and show that improving classroom air quality will have a significant positive effect on some aspects of learning, both on cognitive skills and academic attainment, as well as academic achievements and absence rates. Present studies show that to ensure classroom IAQ conducive to learning, CO₂ levels (indicating the adequacy of ventilation) should be kept below 900 ppm at all times. It should be ensured that windows can be opened when needed, to improve classroom IAQ, and CO₂ sensors should be installed to indicate when windows must be open (or any other

P. Wargocki ()

International Centre for Indoor Environment and Energy, Department of Civil Engineering,
Technical University of Denmark, Kongens Lyngby, Denmark
e-mail: paw@byg.dtu.dk

measure to improve IAQ must be executed) if the CO₂ concentration is too high and when they should be closed to conserve energy.

Keywords

Schools · Learning · Absence rate · Ventilation · Carbon dioxide · Sleep

Introduction

Poor air quality in classrooms has been shown to occur frequently (Angell and Daisy 1997). In addition to increasing the risks of adverse health effects and discomfort, it has been shown to reduce schoolwork performance.

Classroom air quality was mainly examined by either monitoring outdoor air supply rates or changing them and observing the subsequent effects; only in a few cases, particle levels, ozone, and semivolatile organic compounds (SVOCs) in classrooms were measured and associated with learning outcomes.

CO₂ concentrations were used to assess classroom ventilation rates because CO₂ is emitted at a known rate by every occupant; thus, CO₂ levels are a convenient indicator of the outdoor air supply rate and ventilation efficiency. In this chapter, CO₂ should therefore be considered such an indicator and not a pollutant even though pure CO₂ was shown in a few studies to affect adults' cognitive performance though the effects were not consistent (Fisk et al. 2019; Du et al. 2020). No research was done in which pure CO₂ has been shown to affect the performance of tasks resembling schoolwork.

Different methods for measuring the effects on the learning performance of pupils were used in the published reports. Children's ability to perform schoolwork was assessed by simple cognitive tests examining different skills needed for proper learning, such as the ability to concentrate and to memorize and recall information, typical school tasks examining arithmetical and language-based skills, the tests developed by educational departments, the number of pupils passing public exams, and the rate of absenteeism. Most of the studies examining the effects of indoor air quality and ventilation on the performance of schoolwork and learning used psychological and neurobehavioral tests.

The studies were mainly carried out in schools.

The Effects on the Performance of Schoolwork and Absence Rates

The Effects on Psychological and Neurobehavioral Tests

Cross-Sectional Studies

Myhrvold et al. (1996) found a weak association between CO₂ levels and simple reaction time that suggested a positive effect of increased ventilation on performance when CO₂ was reduced from 1500–4000 ppm to <1000 ppm. Ribic (2008) observed

improved performance on the d2 test, a standard test for measuring concentration and attention when the CO₂ concentration was reduced from around 3800 ppm to 870 ppm (absolute level). Sarbu and Pacuraru (2015) found that students' performance on two psychological tests requiring concentration, and cue-utilization (Kraepelin test and Prague test) improved linearly when CO₂ levels were reduced from about 2000 ppm to 500 ppm.

Intervention Studies

Coley et al. (2007) and Bakó-Biro et al. (2012) improved the air quality in classrooms by either allowing students to open the windows or retrofitting the classrooms with an external ventilation system specially designed for the experiments, installed in the window and making it possible to either deliver outdoor air or to recirculate the air already in the classroom. In the former study, the levels of CO₂ were reduced from about 2900 ppm to 690 ppm, and this had a positive and significant effect on tests measuring reaction time; the authors concluded that the power of attention was improved. In the latter study, the ventilation rate was increased from about 1 L/s per person to 8 L/s per person (CO₂ levels were reduced from about 1500–5000 ppm to <1000 ppm). This intervention significantly improved the performance of tests examining reaction time, concentration and attention, recognition, and memory. The effects were from about 3% to 15%. None of these studies identified the level of ventilation for optimal performance, but they showed that improving the air quality in classrooms would provide benefits, and no threshold effect was identified.

Matsson and Hygge (2005) installed electrostatic air cleaners operated or disabled in two pairs of classrooms. Five tests similar to schoolwork were applied. The air cleaners reduced the concentration of airborne particles found in classroom air and tended to reduce the amount of cat allergen, but the effect did not reach statistical significance. When the air cleaners were operated, children "stating themselves to be sensitive to airborne particulate contaminants" experienced a significantly more significant reduction in eye and airway irritation. These pupils scored about 25% higher on one of the five performance tests (finding synonyms). However, the authors themselves cite "multiple testing" (i.e., chance) as a possible reason for the apparent significance of this isolated effect.

Effects of Specific Pollutants

Hutter et al. (2013) showed that the cognitive performance of about 600 pupils in the first and second grade in nine elementary schools improved with reduced levels of tris(2-chlorethyl)-phosphate (TCEP) in PM10, PM2.5, and dust; they also found an association between a polycyclic aromatic hydrocarbon and cognitive performance. This is one of the few studies reporting the effects of specific pollutants on the cognitive performance of children in schools. Hutter et al. (2013) observed that lower CO₂ levels (indicating a higher ventilation rate) were associated with improved performance in parallel to these observations. Cognitive performance was measured using the Standard Progressive Matrices test, a nonverbal assessment tool used to measure the reasoning component of general intelligence. The pupils

performed it for about 45 min. TCEP is a phosphor-organic compound used widely in plasticizers, flame retardants, and floor sealing and is currently a substance of serious concern in terms of its long-term health effects.

The Effects on Typical School Tasks

Intervention Studies

Many studies used shorter tests examining the ability to read, comprehend, and calculate (e.g., Wargocki and Wyon 2013). In studies reported by Wargocki and Wyon (2013), pupils performed arithmetical calculations and language-based tasks under different air quality conditions achieved by changing the outdoor air supply rate between 3 and about 10 L/s per person. The existing mechanical ventilation system was used after increasing the fan capacity and re-balancing the system to direct more outdoor air to one of the two classrooms in which performance was being compared. The children's usual teachers administered parallel versions of language-based and numerical performance tasks representing different aspects of schoolwork, from reading to mathematics. The presentation of tasks was distributed relatively evenly during each experimental week, and the teachers were asked to apply the same task always on the same weekday. The speed at which the tasks were solved was improved with increased ventilation, but there were no effects on errors. Similar results were observed in studies reported by Bakobiro et al. (2012), Petersen et al. (2015), and Hviid et al. (2020), who used research protocols very similar to those of Wargocki and Wyon. In the study by Bakobiro et al. (2012), the air quality in classrooms was improved by retrofitting the classrooms with an external ventilation system specially designed for the experiments, as described above. They showed that the time needed to solve simple mathematics tests was reduced when the ventilation rate was increased from about 0.3–0.5 to 13–16 L/s per person. Petersen et al. (2015) performed a double-blind 2x2 crossover intervention in four classrooms with 10–12-year-old children. The outdoor air supply rate was modified by the decentralized ventilation units installed in each classroom that did not change the background noise level, which was about 35 dB(A). They showed that increasing outdoor air supply rate from 1.7 L/sp. to 6.6 L/sp. improved performance for tasks involving addition, number comparison, grammatical reasoning, and reading and comprehension. No effects on the % errors were seen. Hviid et al. (2020) also used a crossover design in elementary school classrooms and measured the performance of 10–12-year-old pupils. They examined the effect of artificial light and ventilation rate and found that when the outdoor air supply rate was changed from 3.9 L/s per person to 10.6 L/s per person, and at the same time the lighting was changed from 450 lux (color temperature 2900 K) to a dynamic cool light (4900 K) at 750 lux, processing speed and concentration improved, as well as mathematical processing.

Wargocki et al. (2008) installed electrostatic air cleaners in 6 classrooms in 3 schools. The experiments were carried out in winter and early spring. The classrooms in which the experiments were conducted were mechanically ventilated with 100% outdoor air. The interventions were implemented in a crossover design in parallel classrooms. The electrostatic air cleaners had their intended effect on airborne

particle concentrations, which were substantially reduced by operating the air cleaners in all size ranges. Airborne particle concentrations were lower in all size ranges the more outdoor air a given school provided to its classrooms (as would be expected if there were significant indoor sources of particles) and were reduced more markedly in the smaller size ranges. Operating electrostatic air cleaners also reduced settled dust on horizontal surfaces. However, there were no effects on the performance of a wide range of tasks selected to be characteristic of schoolwork, including the language-based and mathematics tasks used by Wargocki and Wyon (2007). Since in the other experiments Wargocki and Wyon (2007) showed that increasing outdoor air supply rate improved the performance of pupils, it was inferred that the effects on the performance of schoolwork should be attributed to gaseous pollutants and not to the particles, since the operation of electrostatic air cleaners recirculating classroom air will not have changed the gaseous pollutants in the air (unless some gaseous pollutants such as semivolatile organic compounds (SVOCs) could permanently adsorb on the deposition plates and did not desorb).

The Effects on National and Aptitude Tests and Examination Results

Cross-Sectional Studies

Haverinen-Shaughnessy et al. (2011) measured CO₂ levels in 100 fifth grade classrooms in 100 schools and showed that poor ventilation reduced the number of pupils managing to pass language and mathematics examinations. A linear relationship was found suggesting 3% more pupils passed the tests for every 1 L/s per person increase in ventilation up to 7 L/s per person. In another study in 140 fifth grade classrooms in 70 schools, Haverinen-Shaughnessy and Shaughnessy (2015) showed that mathematics scores improved by about 0.5% for every 1 L/s per person increase in ventilation rate in the range from 0.9 to 7 L/s per person. Mendell et al. (2016) performed 2-year-long measurements in 150 classrooms in 28 schools and showed that increasing ventilation rates had positive effects on mathematics and English scores, although only in the latter case did the effects reach statistical significance: a 10% increase in ventilation resulted in a 0.6 point increase in the score obtained in the English test. This was a very small effect, as the average scores for this test were about 350–380 points. Toftum et al. (2015) evaluated academic achievement using scores from a standardized Danish test scheme, adjusted for a socioeconomic reference score; the scheme includes mainly language-based and mathematics tests and tests examining fluency in other subjects (for the higher grades only). The lowest national test scores were generally found for pupils in classes with CO₂ concentrations above 2000 ppm, although the association was insignificant. Pupils in schools with some means of mechanical ventilation scored on average higher in the national tests than pupils in schools with natural ventilation, probably because the efficacy of ventilation was higher. In contrast to these studies, Gaihre et al. (2014) did not find any relation between air quality approximated by the levels of CO₂ and educational attainment measured as the % of class attaining the average level expected for the group. The absence of an effect could be due to the choice of performance measure or the season when the measurements were performed: The measurements were made in 60 naturally ventilated classrooms

in 30 schools during the non-heating season (May–June). The range of CO₂ measured was quite large (between 600 ppm and 2100 ppm), but it is unclear whether the CO₂ levels measured for 3–5 days were representative of typical exposure levels experienced in the classrooms over the whole school year. Kabirikopaei et al. (2021) performed measurements in 220 classrooms in schools and found associations between higher ventilation rates and higher reading scores but no mathematical scores; seasonal dependence was observed in the effects observed in fall. Fine particle counts, but not coarse, were associated with mathematics scores, while ozone with reading scores. They also observed that the presence of unit ventilators was associated with lower mathematics scores compared with multizone systems; the presence of unit ventilators was associated with higher coarse particle counts, lower ventilation rates, and higher background noise (Lau et al. 2020).

Experimental Studies

Murakami et al. (2006) examined whether changing air quality affects learning by college students taking courses preparing them for architectural examinations. A recorded lecture was played from a DVD so that each class received the same amount and type of education and the same information from the same teacher, creating a reproducible learning environment. Indoor air quality was modified by changing the outdoor air supply rate between 0.4 h⁻¹ and 3.5 h⁻¹. Air temperatures also changed between conditions, from about 24–25 °C at the higher ventilation rate to 27–28 °C at the lower rate, so the observed effects of improved air quality on learning were confounded with a temperature change; it was not possible to disconnect the two effects. The results of experiments showed the positive effect of improving air quality on learning. Ito et al. (2006) performed laboratory experiments that were similar to the studies by Murakami et al. (2006), the difference being the students sitting in a climate chamber where the same conditions were created as in the field intervention experiment by Murakami et al. All other experimental aspects were the same. They obtained very similar results to those in the intervention experiments of Murakami et al.

The Effects on Absence Rates

Some studies measured illness absence and associated it with poor air quality or poor classroom ventilation to examine the effects indirectly on learning outcomes, although there is no clear evidence that short-term absence affects the academic performance of students (Mendell and Heath 2005).

Cross-Sectional Studies

Piloto et al. (1997) showed in a cohort study that air pollutants from gas heaters had a negative effect on attendance at school, which was presumed to be due to a negative effect on children's health. Berner (1993) showed an association between poor maintenance of schools and the children's poor academic achievement. Ervasti et al. (2012) found increased short-term sick leave among teachers in schools with poor perceived air quality. Shendell et al. (2004) found that student absence decreased by 10–20% when the CO₂ concentration decreased by 1000 ppm in 434 American

classrooms. A study of Gaihre et al. (2014) in Scottish schools showed that an increase of 100 ppm of CO₂ corresponds only to a 0.2% increase in absence rates (roughly one order of magnitude lower than the data of Shendell et al. (2004)) corresponding roughly to 0.5 days a year in the 190-day school year. Simons et al. (2010) found high student absenteeism associated with poor ventilation in 2751 New York schools. A study performed in day-care centers equipped with a balanced mechanical ventilation system found that increasing the air change rate by 1 h⁻¹ would reduce the number of sick days by 12% even though the ventilation rates were relatively high, high enough for the CO₂ levels to remain below 1000 ppm, and on average around 640 ppm (Kolarik et al. 2015). A very comprehensive study in 162 Californian classrooms observed that illness absence decreased by as much as 1.6% for each additional 1 L/s per person of the ventilation rate (Mendell et al. 2016); this is again lower than the data of Shendell et al. (2004) but higher than the data of Gaihre et al. Deng and Lau (2018) monitored conditions in 85 elementary school classrooms (ca. 1900 pupils) and correlated them with student illness-related absenteeism. They observed that the presence of fine particles during the cooling season increased absence rates, while the increased absenteeism during the heating season was caused by reduced ventilation (indicated by the increased CO₂ levels).

Sleep and Learning

Indoor air quality in homes can disturb sleep quality and next-day performance, as shown in studies that examined the correlation between sleep quality and next-day concentration (Tynjälä et al. 1999; Meijer et al. 2000). Disturbed sleep is a widespread problem, but insufficient data are documenting whether indoor air quality in bedrooms plays an important role in these outcomes. Akimoto et al. (2021) summarized studies reporting the effects of bedroom IAQ on sleep quality and showed that when CO₂ concentration in bedrooms is below 800 ppm, no disturbance to sleep is expected. Effects on sleep quality are likely between 800 and 1000 ppm and were seen to occur above 1000 ppm. At CO₂ levels at and above 2600 ppm, sleep quality and next-day performance are affected. The latter results were obtained in experiments in dormitories where students slept with high and low outdoor air supply rates that were achieved by a simple fan mounted in the air-intake aperture (Strøm-Tejsen et al. 2016). They reported that the air in their room was fresher, they felt more refreshed, and their mental state was better when the fan was in operation. Their objectively measured sleep efficiency (time spent asleep) was higher, and their performance on a concentration test taken in the morning was better when the fan was on.

The Relationships Between Learning and IAQ

Wargocki et al. (2020) summarized published studies on the effects of indoor air quality in classrooms on children's performance in schools. Using the published data, they created relationships between CO₂ (as a marker of ventilation efficiency

and the outdoor air supply rate) and the measured performance of schoolwork, national and aptitude tests and exams, and absenteeism; the performance of schoolwork was characterized by performance on tests measuring cognitive abilities and skills and school tasks including mathematical and language-based tasks.

Figure 1 shows the relationship between schoolwork performance (speed or reaction time) and the concentration of classroom CO₂ or ventilation rate; ventilation rate was estimated using CO₂ concentration. There were negligible effects on schoolwork performance regarding the precision (accuracy) with which the tests were performed, and these results are not shown. The results show that children perform schoolwork 12% faster (and 2% more accurately, not shown) when the outdoor air supply rate is such that the resulting CO₂ concentration in a typical classroom is 900 ppm instead of 2100 ppm.

Figure 2 shows the relationship between the performance of national and aptitude tests and examination results and the concentration of classroom CO₂ or the ventilation rate as estimated from the resulting CO₂ concentration. The results show that school test and examination results are 5% better when the outdoor air supply rate is such that the resulting CO₂ concentration in a typical classroom is 900 ppm instead of 2400 ppm. This demonstrates that the effects of classroom air quality on schoolwork performance do predict its effects on examination results, although the magnitude of the effect is only half as large. They also show that classroom air quality effects on school test and examination results predict national test results, widely regarded as the most reliable indicator of overall learning.

Figure 3 shows the relationship between absence rates and the concentration of classroom CO₂. The results show that reducing CO₂ from 4100 ppm to 1000 ppm

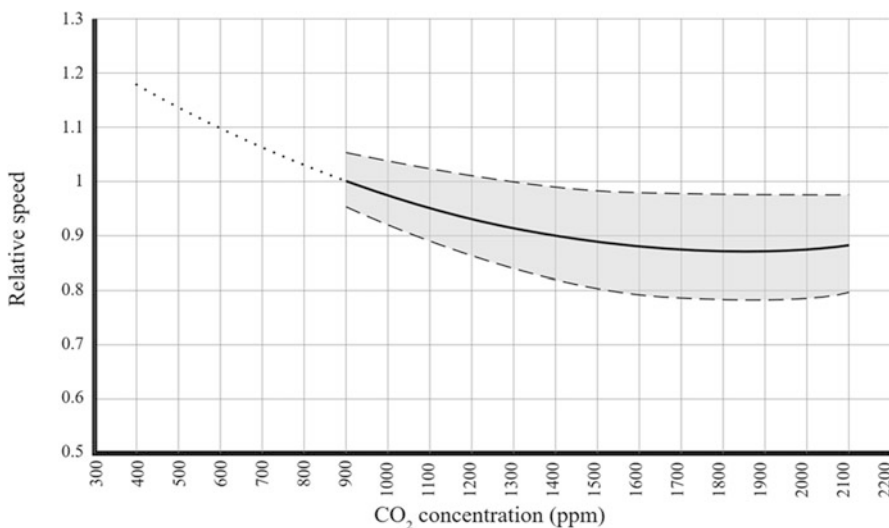


Fig. 1 Performance of schoolwork as a function of CO₂

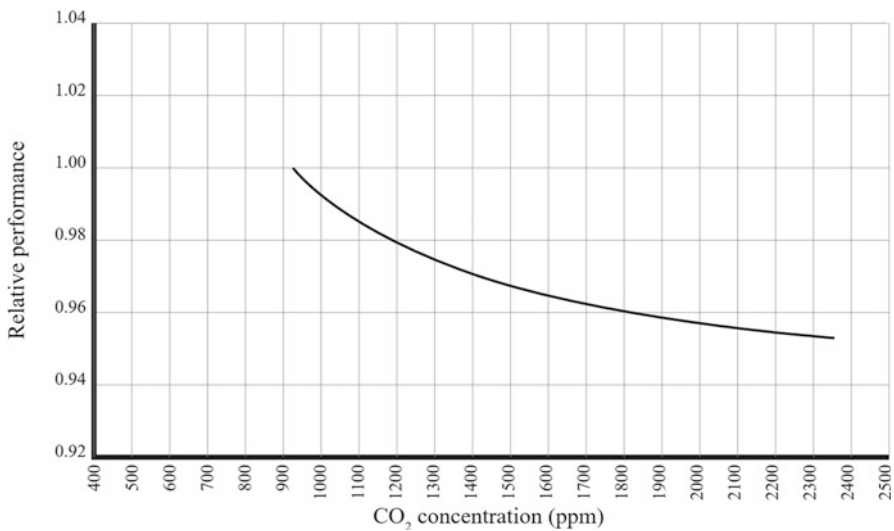


Fig. 2 The results of national and aptitude tests and examination results as a function of CO₂ indicating ventilation efficiency (left) and ventilation with outdoor air (right)

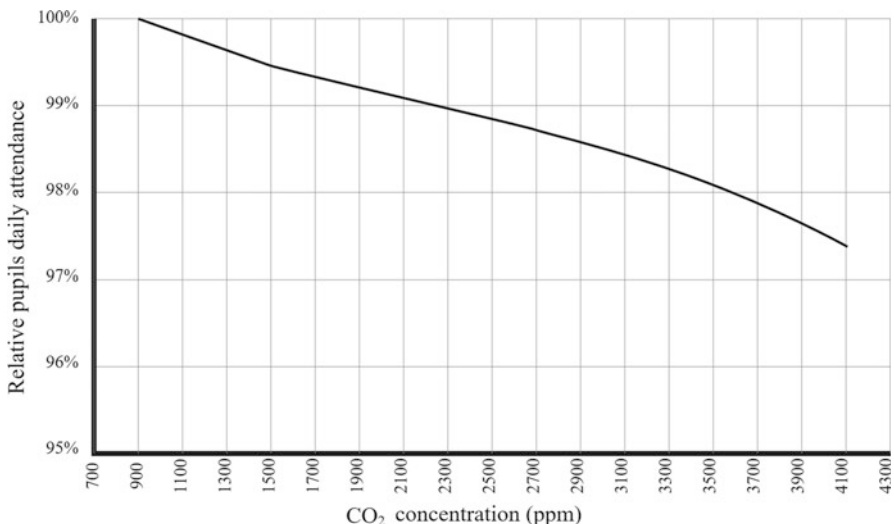


Fig. 3 Absence rates of pupils in a school as a function of CO₂

would increase daily attendance by 2.5%. They suggest that an increased outdoor air supply rate can reduce cross-infection between children or mitigate pre-existing conditions that cause absenteeism. An increased outdoor air supply rate removes and dilutes airborne pathogens as well as gas-phase air pollutants and the

concentration of airborne particles (Li et al. 2007), and to the extent that absenteeism is due to children staying home while sick, this must be presumed to be the mechanism for the observed effect on absenteeism. Therefore, to reduce the impact of future pandemics on learning in school, maintaining a high outdoor air supply rate must be viewed as a viable strategy. However, recirculation through filters that remove very fine particles from indoor air may remove some pathogens. Even recirculation through coarser filters will benefit pupils suffering from allergies during the season when pollen is present in classroom air.

Conclusions

The results from the published experiments on the effects of classroom air quality on the performance of schoolwork do confirm that these effects are systematic and show that improving classroom air quality will have a significant positive effect on some aspects of learning, both on cognitive skills and academic attainment, as well as academic achievements and absence rates. The level of this effect is not the same across different studies as might be expected since learning can also be affected by the IAQ conditions in homes.

Although long-term learning outcomes are expected to be affected by the absence of abilities to perform simple psychological tests and the ability to read, calculate, and comprehend, the connection between the progress in learning and these abilities is not very well documented. Therefore, some studies measured IAQ effects on long-term learning using standardized tests, which national education departments often develop. These tests monitor progress in learning, benchmark individual pupils and schools, and evaluate teaching methods and curricula effectiveness over time. The studies described did not use interventions to classroom conditions. However, they used a cross-sectional approach, i.e., they monitored classroom ventilation in many schools and related these measurements to the results obtained by the children in those classrooms in standardized tests adjusting the results for numerous confounders, including socioeconomic factors. These studies showed that long-term learning outcomes are affected by the poor air quality in classrooms in the same way as the ability to perform simple psychological tests and the ability to read, calculate, and comprehend. They thus validate the use of simple tests to predict progress in learning.

The results of studies examining the effects on absence rates in schools are quite systematic and suggest that increasing classroom ventilation may substantially decrease illness absence. This may affect the learning experience though there is no clear evidence linking the short-term absence of pupils and academic performance. It is also worth mentioning that many other factors not necessarily related to school environments can influence the absence rates.

Learning can also be affected by the effects of bedroom air quality on sleep quality, but the studies published to date are only a few and inconsistent.

Summarized results suggest that increasing the ventilation rate in classrooms estimated using measured CO₂ concentrations from 2 L/s-person to 10 L/s-person

(see also Wargocki et al. 2020) can bring significant benefits in terms of learning performance and pupil attendance; no data are available for higher ventilation rates. However, there are still many unanswered questions, for example, the extent to which classroom occupant density and a low outdoor air supply rate affect cross-infection, whether there are any negative indoor air quality effects on teachers that affect teaching quality, and whether thermal effects interact with the effects of air quality; the latter was not explicitly explored in the previous studies. The mechanisms for the negative effects of air quality on cognition and the physiological processes by which this occurs should be examined, and it has already been shown that lung capacity is temporarily reduced by exposure to poor indoor air quality (Shriram et al. 2019; Mishra et al. 2021). If the mechanisms were known, it might be possible to identify the airborne molecules responsible for these negative effects and somehow eliminate them from indoor air. This evidence would also help in developing an IAQ metric from studies attributing the effects to gaseous pollutants.

Present studies show that to ensure classroom IAQ conducive to learning, CO₂ levels should be kept below 900 ppm at all times, it should be ensured that windows can be opened when needed, to improve classroom IAQ, and CO₂ sensors should be installed to indicate when windows must be open (or any other measure to improve IAQ must be executed) if the CO₂ concentration is too high and when they should be closed to conserve energy, i.e., when CO₂ has reached the intended low level, e.g., below 900 ppm or even lower. To ensure good sleep quality, bedroom CO₂ should be kept below 800 ppm, but the data is scarce. These recommendations are tentative and should be revised when new research evidence is published. At the time of publication of the present Handbook of Indoor Air Quality (December 2021), it is unknown what ventilation rates and CO₂ levels should be provided in classrooms to reduce the risk of infection with airborne viruses.

References

- Akimoto M, Sekhar C, Bivolarova MP, Liao C, Fan X, Laverge J, Lan L, Wargocki P (2021) Reviewing how bedroom ventilation affects IAQ and sleep quality. *ASHRAE J* 63(4):56–60
- Angell WJ, Daisey J (1997) Building factors associated with school indoor air quality problems: a perspective, *Proc. of Healthy Buildings/IAQ'97*, Vol 1, Virginia Polytechnic Institute and State University, Washington, DC, pp 143–8
- Bakó-Biró Z, Clements-Croome DJ, Kochhar N, Awbi HB, Williams MJ (2012) Ventilation rates in schools and pupils' performance. *Build Environ* 48:215–223
- Berner M (1993) Building conditions, parental involvement, and student achievement in the District of Columbia public school system. *Urban Educ* 28:1:6–29
- Coley D, Greeves R, Saxby B (2007) The effect of low ventilation rates on the cognitive function of a primary school class. *Int J Vent* 62:107–112
- Deng S, Lau J (2018) Preliminary results: different indoor classroom conditions during different seasons in the US midwestern region and their associations with student absenteeism. In 15th Conference of the International Society of Indoor Air Quality and Climate, INDOOR AIR 2018. International Society of Indoor Air Quality and Climate

- Du B, Tandoc MC, Mack ML, Siegel JA (2020) Indoor CO₂ concentrations and cognitive function: a critical review. *Indoor Air* 30(6):1067–1082
- Ervasti J, Kivimäki M, Kawachi I, Subramanian S, Pentti J, Oksanen T, Puusniekka R, Pohjonen T, Vahtera J, Virtanen M (2012) School environment as predictor of teacher sick leave: data-linked prospective cohort study. *BMC Pub Health* 12:770
- Fisk W, Wargocki P, Zhang X (2019) Do indoor CO₂ levels directly affect perceived air quality, health, or work performance? *ASHRAE J* 61(9)
- Gaihre S, Semple S, Miller J, Fielding S, Turner S (2014) Classroom carbon dioxide concentration, school attendance, and educational attainment. *J School Health* 84(9):569–574
- Haverinen-Shaughnessy U, Shaughnessy RJ (2015) Effects of classroom ventilation rate and temperature on students' test scores. *PLoS One* 10(8):e0136165
- Haverinen-Shaughnessy U, Moschandreas DJ, Shaughnessy RJ (2011) Association between sub-standard classroom ventilation rates and students' academic achievement. *Indoor Air* 21(2): 121–131
- Hutter H, Haluza D, Piegler K, Hohenblum P, Fröhlich M, Scharf S, Uhl M, Damberger B, Tappler P, Kundi M, Wallner P, Moshammer H (2013) Semi-volatile compounds in schools and their influence on cognitive performance of children. *Int J Occup Med Environ Health* 26(4): 628–635
- Hviid CA, Pedersen C, Dabelsteen KH (2020) A field study of the individual and combined effect of ventilation rate and lighting conditions on pupils' performance. *Build Environ* 171:106608
- Ito K, Murakami D, Kaneko T, Fukao H (2006) Study on the productivity in classroom Part 2. Realistic simulation experiment on effects of air quality/thermal environment on learning performance. In: Proceedings of Healthy Buildings 2006, ISIAQ, Lisbon, Portugal, pp 207–212
- Kabirikopaei A, Lau J, Nord J, Bovaird J (2021) Identifying the K-12 classrooms' indoor air quality factors that affect student academic performance. *Sci Total Environ* 786
- Kolarik B, Andersen ZJ, Ibfelt T, Engelund EH, Møller E, Bräuner EV (2015) Ventilation in day care centers and sick leave among nursery children. *Indoor Air*. <https://doi.org/10.1111/ina.12202>
- Lau J, Liu YW, Johnson K (2020) Associating different indoor air contaminant levels with various ventilation systems in K-12 classrooms. In 16th conference of the International Society of Indoor Air Quality and Climate: Creative and Smart Solutions for Better Built Environments, Indoor Air 2020. International Society of Indoor Air Quality and Climate
- Li Y, Leung GM, Tang JW, Yang X, Chao CYH, Lin JZ, Lu JW, Nielsen PV, Niu J, Qian H, Sleigh AC, Su H-JJ, Sundell J, Wong TW, Yuen PL (2007) Role of ventilation in airborne transmission of infectious agents in the built environment – a multidisciplinary systematic review. *Indoor Air* 17(2):18
- Mattsson M, Hygge S (2005) Effect of articulate air cleaning on perceived health and cognitive performance in school children during pollen season. In: Yang X, Zhao B, Zhao R (eds) Proc. indoor air 2005, vol I2. Tsinghua University Press, Beijing, pp 1111–1115
- Meijer AM, Habekothé HT, van den Wittenboer GL (2000) Time in bed, quality of sleep and school functioning of children. *J Sleep Res* 9:45–153
- Mendell MJ, Heath GA (2005) Do indoor pollutants and thermal conditions in schools influence student performance? A critical review of the literature. *Indoor Air* 15:27–52
- Mendell MJ, Eliseeva EA, Davies MM, Lobscheid A (2016) Do classroom ventilation rates in California elementary schools influence standardized test scores? Results from a prospective study. *Indoor Air* 26(4):546–557
- Mishra AK, Schiavon S, Wargocki P, Tham KW (2021) Respiratory performance of humans exposed to moderate levels of carbon dioxide. *Indoor Air*
- Murakami S, Kaneko T, Ito K, Fukao H (2006) Study on the productivity in classroom part 1. Field survey on effects of air quality/thermal environment on learning performance. In: Proceedings of Healthy Buildings 2006, ISIAQ, Lisbon, Portugal, pp. 271–276
- Myhrvold AN, Olsen E, Lauridsen Ø (1996) Indoor environment in schools – pupils' health and performance in regard to CO₂ concentration. In: Yoshizawa S, Kimura K, Ikeda K, Tanabe S,

- Iwata T (eds) Proc Indoor Air '96, Nagoya, 7th Int Conf Indoor Air Quality and Climate, Vol 4, pp. 369–74
- Petersen S, Jensen KL, Pedersen AL, Smedegaard Rasmussen H (2015) The effect of increased classroom ventilation rate indicated by reduced CO₂-concentration on the performance of schoolwork by children. *Indoor Air*. <https://doi.org/10.1111/ina.12210>
- Pilotto LS, Douglas RM, Attewel RG, Wilson SR (1997) Respiratory effects associated with indoor nitrogen dioxide exposure in children. *Internat J Epidemiol* 264:788–796
- Ribic W (2008) Nachweis des Zusammenhangs zwischen Leistungsfähigkeit und Luftqualität, HLHLU 'ftung/Klima –Heizung/Sanitär – Gebäudetechnik 59:43–46
- Sarbu I, Pacurar C (2015) Experimental and numerical research to assess indoor environment quality and schoolwork performance in university classrooms. *Build Environ* 93:141–154
- Shendell DG, Prill R, Fisk WJ, Apte MG, Blake D, Faulkner D (2004) Associations between classroom CO₂ concentrations and student attendance in Washington and Idaho. *Indoor Air* 145:333–341
- Shriram S, Ramamurthy K, Ramakrishnan S (2019) Effect of occupant-induced indoor CO₂ concentration and bioeffluents on human physiology using a spirometric test. *Build Environ* 149:58–67
- Simons E, Hwang SA, Fitzgerald EF, Kielb C, Lin S (2010) The impact of school building conditions on student absenteeism in Upstate New York. *Am J Public Health* 100:1679–1686
- Strøm-Jeisen P, Zukowska D, Wargocki P, Wyon DP (2016) The effects of bedroom air quality on sleep and next-day performance. *Indoor air* 26(5):679–686
- Toftum J, Kjeldsen BU, Wargocki P, Menå HR, Hansen EMN, Clausen G (2015) Association between classroom ventilation mode and learning outcome in Danish schools. *Build Environ*. <https://doi.org/10.1016/j.buildenv.2015.05.017>
- Tynjälä J, Kannas L, Levälahti E, Välimäki R (1999) Perceived sleep quality and its precursors in adolescents. *Health Promot Int* 14:155–166
- Wargocki P, Wyon DP (2007) The effects of outdoor air supply rate and supply air filter condition in classrooms on the performance of schoolwork by children (RP-1257). *Hvac&r Res* 13(2): 165–191
- Wargocki P, Wyon DP (2013) Providing better thermal and air quality conditions in school classrooms would be cost-effective. *Build Environ* 59:581–589
- Wargocki P, Wyon DP, Lynge-Jensen K, Bornehag CG (2008) The effects of electrostatic particle filtration and supply-air filter condition in classrooms on the performance of schoolwork by children (RP-1257). *Hvac&R Res* 14(3):327–344
- Wargocki P, Porras-Salazar JA, Contreras-Espinoza S, Bahnfleth W (2020) The relationships between classroom air quality and children's performance in school. *Build Environ* 173:106749



Sleep and Indoor Air Quality

50

Li Lan and Zhiwei Lian

Contents

Introduction	1462
The Importance of Good Sleep	1462
Measurement of Sleep Quality	1462
Sleep Functions	1464
IAQ in the Bedroom	1464
CO ₂ Levels in Bedroom	1465
Other Pollutants in Bedroom	1466
Air Pollution Exposure and Sleep	1467
Ambient Exposure and Sleep	1467
IAQ and Sleep	1469
Possible Mechanisms	1471
Interactions with Temperature	1472
Aromatherapy and Sleep	1472
Possible Solutions to Improve IAQ in Bedrooms	1473
Conclusion	1473
Cross-References	1473
References	1474

Abstract

Sleep is essential for our mental and physical health. People typically sleep 8 h and consume 26.8% of total air inhaled per day when sleeping. Indoor air quality (IAQ) in bedrooms may influence sleep quality. Many IAQ problems, including high CO₂ and fine particulate matter (PM2.5) levels, have been observed in studies on bedrooms. Considering the CO₂ level as an indicator of indoor air pollution caused mainly by human bioeffluents, these findings indicate that the studied bedrooms were poorly ventilated. Although current studies are limited, they suggest that poor IAQ may result in poor sleep quality, indicating the

L. Lan (✉) · Z. Lian

Department of Architecture, School of Design, Shanghai Jiao Tong University, Shanghai, China
e-mail: lanli2006@sjtu.edu.cn; zwlian@sjtu.edu.cn

necessity to improve IAQ in bedrooms. However, most of the current studies measured sleep quality with sleep trackers or subjective questionnaires, resulting in a wide range of associations and no clear mechanisms. Future studies should use a more accurate assessment of sleep quality, such as polysomnography (PSG), and control air pollution exposure to examine the exact effects and mechanisms of IAQ on sleep quality. As people tend to close windows/doors during the sleeping period, which decreases the air exchange rate and accumulates pollutants in the bedroom, specific alternative solutions to improve the IAQ in bedrooms should be researched.

Keywords

Sleep quality · Bedroom · Pollution · Fine particulate matter · Ventilation

Introduction

For young adults and adults (18–64 years), a sleep duration of 7–9 h per night is recommended (Hirshkowitz et al. 2015), which corresponds to one-third of a total lifetime. It is estimated that the air inhaled during sleep accounts for approximately 26.8% of the total air inhaled per day if the total sleep time is 8 h (Sekhar et al. 2020). Hence, the air quality in bedrooms is important in contributing to both acute and chronic exposure to indoor air pollutants. Because insufficient sleep impairs the immune system, disrupts blood sugar levels, increases cardiovascular disease, and decreases next-day work performance, such exposures are a particular concern if the sleep quality of occupants is affected. However, it is evident in some recent review articles that bedrooms are not as studied as other parts of houses in this regard (Liu et al. 2020). Among the hundreds of articles on semi-volatile organic compounds (SVOCs) and indoor air quality (IAQ), very few refer to concentrations of air pollutants in bedrooms. In this chapter, the current situation of IAQ in bedrooms and the possible consequences of both outdoor and indoor air quality on sleep quality are summarized. Additionally, mechanisms that mediate the effects of air pollution on sleep are indicated, and finally, some possible solutions for improving IAQ in bedroom are suggested.

The Importance of Good Sleep

Measurement of Sleep Quality

Normal human sleep is comprised of two states – rapid eye movement (REM) and non-REM (NREM) sleep – that alternate cyclically across a sleep episode. Sleep begins in NREM (usually stage N1) and progresses through deeper NREM stages (stages N2 and N3) before the first episode of REM sleep occurs approximately 80–100 min later (Carskadon and Dement 2011). Light sleep is the term for sleep that

falls into the categories of stage N1 and stage N2. The stage N3 sleep is characterized by slow wave activity (brain waves of frequency 0.5 Hz–2 Hz), thus is referred as slow wave sleep (SWS) or deep sleep. REM sleep is characterized by random rapid movement of the eyes, accompanied by low muscle tone throughout the body, and the propensity of the sleeper to dream vividly.

To provide the basic information requisite for classification of the above sleep stages, polysomnography (PSG) is usually used, which records signals on brain wave, eye movements, and chin muscle tension (Fig. 1). Table 1 shows the sleep

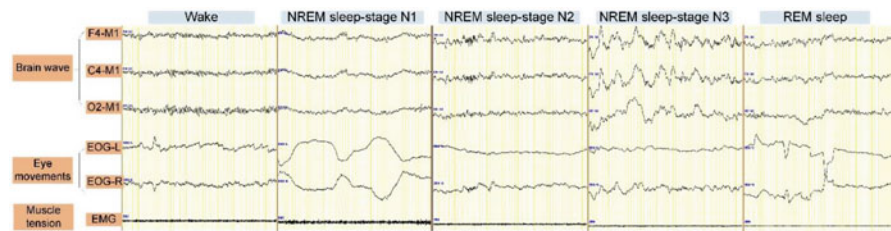


Fig. 1 Stages of wake, nonrapid eye movement (NREM) sleep, and rapid eye movement (REM) sleep. The tracings of brain wave were records from three electrodes at right frontal lobe (F4), right central lobe (C4), and right occipital lobe (O2) referenced to left mastoid (M1). Eye movements are recorded from the left (L) eye and right (R) eye. Muscle tension is recorded by two leads which are placed on the chin with one above the jawline and one below

Table 1 Parameters derived from objective measurements of sleep quality

Parameter	Explanation	Normative values of good sleep ^a
Lights out clock time	The clock time (in hh:mm) when the subject was instructed to allow himself or herself to fall asleep	/
Lights on clock time	The clock time (in hh:mm) when the subject was awakened	/
Total recording time, TRT	Elapsed time with lights out (in minutes)	/
Total sleep time, TST	Total time scored as sleep (in minutes)	>420 min
Sleep efficiency, SE	Percentage of time in bed actually spent sleeping, i.e., TST as a percentage of TRT (%)	90–96%
Sleep onset latency, SOL	Elapsed time from lights out to the first occurrence of Stage N1 sleep (the start of sleep) (in minutes)	<20 min
Wake time after sleep onset, WASO	Total time of wakefulness recorded from the start of sleep to lights on (in minutes)	<25 min
Duration of each sleep stage	Total number of minutes scored as N1, N2, N3, and REM sleep	/
Percentage of each sleep stage	Time scored as N1, N2, N3, and REM as a percentage of TST	N1: 2–5% N2: 45–55% N3: 13–23% REM: 20–25%

^aThe suggested normative values of good sleep are for young adults

quality statistics that are calculated based on PSG measurement. Lower sleep efficiency (SE), lower duration of N3 or REM stage, longer sleep onset latency (SOL), and/or higher wake time indicate poorer sleep quality. In recent years, more and more sleep trackers are commercially available. These trackers have the advantages of long-time recording and cause less disturbance to sleep, thus is commonly used in field study or large-scale survey. However, the reliability and validity of the trackers need further confirmation. Self-evaluated sleep quality on questionnaires is also usually adopted. There are two types of assessments, one examines sleep quality or habits in the previous month, e.g., the Pittsburgh Sleep Quality Index (PSQI), the other evaluates daily sleep quality, e.g., the Groningen Sleep Quality Scale (GSQS).

Sleep Functions

Sleep is essential for the body to recover from both physical and psychological fatigue throughout the day and to restore energy to maintain bodily functions. Without sleep, cognitive and emotional abilities are markedly disrupted. Sleep is an important requirement before learning, to prepare specific brain networks for the initial encoding of information, and after learning, for the subsequent consolidation and enhancement of procedural memories (Walker 2010). Moreover, sleep may offer the ability to test and build common informational schemas of knowledge, providing increasingly accurate statistical predictions about the world and allowing for the discovery of novel, even creative next-day solution insights (Walker 2010).

Sleep loss has been linked to heart disease, diabetes, obesity, and cancer. Sleep is also related to neurodegenerative disorders, such as Alzheimer's disease. The data presented by Fultz et al. (2019) suggest that the cerebrospinal fluid flow oscillations during SWS may contribute to the disposal of waste products, including toxic brain proteins that cause Alzheimer's disease (Fultz et al. 2019).

In summary, sleep problems can play a causal role in the development of mental and physical health morbidities. The benefits of good sleep affect a wide range of critical health outcomes and next-day work performance. The sleeping environment is expected to significantly affect the sleep quality, thus improving the sleeping environment including the IAQ in the bedroom is a necessary step toward achieving healthy sleep.

IAQ in the Bedroom

Indoor CO₂ concentration has been used as an indicator of air quality in buildings, indicating the quantity and effectiveness of ventilation with outdoor air. It has not been confirmed whether CO₂ is an air pollutant. Thus, in this section, reports on CO₂ levels and other indoor air pollutants in bedrooms are discussed separately.

CO₂ Levels in Bedroom

Studies usually observed higher CO₂ level during cooling and heating season owing to closed window and door for the need of energy conservation. The most comprehensive review of this topic was recently made by Sekhar et al. (2020). Figure 2 shows the CO₂ concentrations of some studies reviewed in Sekhar et al. (2020).

Liu et al. (2015) measured 454 children's bedrooms in Shanghai over one year and reported that the mean CO₂ level \pm standard deviation was 1123 ± 741 ppm (range: 367–4595 ppm) (Liu et al. 2015). Hou et al. (2018) measured CO₂ levels in 399 homes in Tianjin and Cangzhou (Hou et al. 2018). The median bedroom CO₂ levels during spring, summer, autumn, and winter were 1146, 575, 1313, and 1407 ppm, respectively. Lei et al. (2017) measured four bedrooms (two with four occupants each and two having six occupants each) in a naturally ventilated dormitory with radiant water heating during the heating season in Beijing and reported that the CO₂ levels ranged between 1057 and 5150 ppm (Lei et al. 2017).

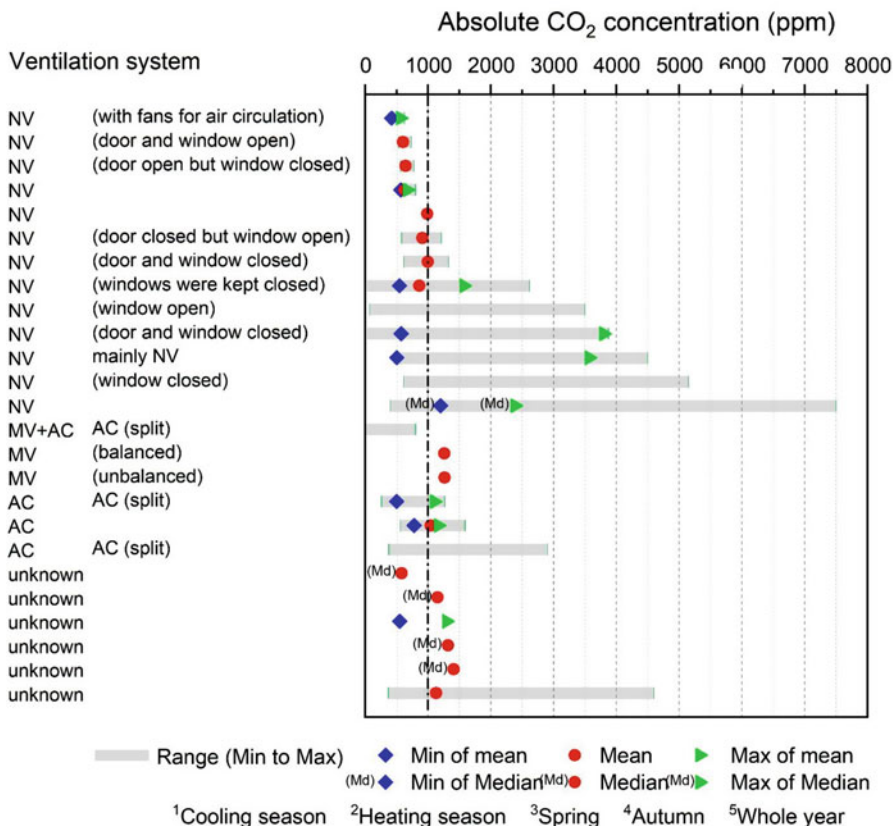


Fig. 2 Summary of CO₂ measured in bedrooms. For ventilation system, NV refers to natural ventilation, MV refers to mechanical ventilation, and AC refers to air conditioner

Wong and Huang (2004) carried out measurements in three residential buildings in Singapore and observed that the CO₂ levels in bedrooms using AC were consistently higher than those using natural ventilation (NV) (Wong and Huang 2004). The CO₂ levels built up and could reach approximately 1600 ppm in bedrooms using AC without ventilation, while they were approximately 550–600 ppm in bedrooms using NV. Sekhar and Goh (2011) reported CO₂ levels of around 420–560 ppm in bedrooms with NV in Singapore, which was around half that observed in bedrooms using AC (Sekhar and Goh 2011). Bedroom CO₂ levels can reach 2900 ppm with an occupancy of two adults and a child in approximately 8 h (Sekhar 2004).

High CO₂ concentrations have also been reported in many residential buildings in Europe. Batoga and Badura (2013) observed that when the windows and doors closed, the CO₂ levels of most tested sleeping rooms significantly exceeded the recommended hygienic standards (Batoga and Badura 2013). The CO₂ concentrations measured in bedrooms in Poland were 857 ± 217 ppm, with highest value of 1570 ppm (Kozielska et al. 2020). Bekö et al. (2010) performed measurements in 500 bedrooms during spring in Denmark, showing that Danish bedrooms were poorly ventilated: 23% of bedrooms exceeded 2000 ppm and 6% exceeded 3000 ppm in 20 min (Bekö et al. 2010). Fernandez-Aguera et al. (2019) measured the IAQ in naturally ventilated dwellings for one year in the south of Spain and found that in the bedrooms the CO₂ concentrations were above 3000 ppm, with peaks above 7500 ppm (Fernández-Agüera et al. 2019). Canha et al. (2017) performed three studies in Portugal to measure the IAQ in bedrooms. In one study, the lowest mean CO₂ level (550 ± 36 ppm, ranging between 484 and 672 ppm) was found in rooms with open windows and open doors, whereas the highest mean level was observed in rooms with closed windows and closed doors (911 ± 183 ppm, ranging between 565 and 1216 ppm) (Canha et al. 2017). In the second study, they observed that the mean CO₂ levels were significantly different between rooms of smokers and nonsmokers, 2029 ± 429 ppm and 1123 ± 479 ppm, respectively (Canha et al. 2019). In the third study, they measured CO₂ levels in bedrooms of ten couples and found that the mean CO₂ level during sleep was 1751 ± 819 ppm, ranging from 611 ± 107 ppm to 3466 ± 336 ppm (Canha et al. 2020).

The above studies indicate that, compared with mechanically ventilated rooms, in naturally ventilated rooms with closed windows and doors the CO₂ levels are higher, usually exceeding 1000 ppm; when the rooms were occupied by multiple person the CO₂ levels were increased and could be higher than 7500 ppm. Using of split air conditioners in the rooms also increased the indoor CO₂ level.

Other Pollutants in Bedroom

Fernandez-Aguera et al. (2019) reported the levels of total volatile organic compounds (TVOC) and PM_{2.5} in three dwellings with NV in the south of Spain (Fernández-Agüera et al. 2019). The annual average PM_{2.5} values were 16.09 ug m^{-3} , 7.1 ug m^{-3} , and 9.66 ug m^{-3} in the three dwellings. For 15–45% of the hours the PM_{2.5} levels exceeded the threshold of 10 ug m^{-3} . Indoor average

TVOC concentration is usually below the 1200 ppb threshold with uneven distribution. The indoor concentrations are higher in winter than in summer.

Canha et al. (2017) observed that the concentrations of several pollutants, including volatile organic compounds (VOCs), formaldehyde, and PM_{2.5}, exceeded the established Portuguese guidelines (Canha et al. 2017). They also observed that smokers were exposed to higher levels of PM, carbon monoxide (CO), and formaldehyde than nonsmokers while sleeping (Canha et al. 2019). Low compliance with guideline on VOCs (10%), bacteria (20%), and fungi (44%) were found (Canha et al. 2020). In 70% of cases, the PM_{2.5} concentrations ($15.3 \pm 9.1 \text{ mg m}^{-3}$) exceeded the WHO guideline of 10 mg m^{-3} . Notably, all bedrooms presented air change rates above the recommended minimum value of 0.7 h^{-1} , highlighting that good IAQ during sleep is not guaranteed.

Fan et al. (2018) measured the IAQ in five urban and five rural houses of elderly people in Beijing, China, during the heating season (Fan et al. 2018). They observed CO₂ levels higher than 1000 ppm in the bedroom during sleeping time. They also found that indoor fuel combustion resulted in extremely high PM_{2.5} (up to 550 ug m^{-3}) and CO level (up to 70 ppm) in rural houses.

Winkens et al. (2017) reported perfluoroalkyl acids (PFAAs) and their precursors from children's bedrooms in Finland: Higher PFAA concentrations were found in rooms with plastic floors than in those with wood or laminate (Winkens et al. 2017).

In summary, it was not until recent 10 years that researchers paid attention to the IAQ in bedrooms. Most studies found CO₂ levels that exceeded the limits stipulated in standards of each country. Considering the CO₂ level as an indicator of indoor air pollution caused mainly by human bioeffluents, these findings indicate that the studied bedrooms were poorly ventilated. Other pollutants including VOCs, formaldehyde, and PM_{2.5} have also been reported in bedrooms. However, these pollutants are caused by various sources, such as smoking and cooking in the room, furniture and bedding, the use of polluted materials, and poor ventilation.

Air Pollution Exposure and Sleep

While most studies have focused on ambient air pollutants and showed that air pollution resulted in poor sleep health, only a few have investigated the associations between bedroom IAQ and sleep. In this section, the effects of ambient exposure and IAQ on sleep are summarized, respectively.

Ambient Exposure and Sleep

Particulate Matter and Sleep

One major component of air pollution is particulate matter, which is composed of both solid and liquid particles found in the air and classified by aerodynamic diameter. Exposure to ambient particulate matter has been shown to reduce sleep quality.

Zanobetti et al. (2010) found that, in summer, increases in the respiratory disturbance index (RDI) and percentage of sleep time at less than 90% O₂ saturation, as well as decreases in sleep efficiency, were associated with increases in short-term variation in PM₁₀ (Zanobetti et al. 2010). This study is one of the very few that have examined the effects of particulate matter on sleep quality with objective PSG measurements.

Chen et al. (2019) performed a cohort study during 2015–2017 in rural areas of Henan Province, China, and observed that the odds ratios of poor sleep quality associated with per interquartile range (IQR) increase in PM_{2.5}, PM₁₀, and NO₂ were 1.15, 1.11, and 1.14, respectively (Chen et al. 2019). The authors concluded that long-term exposure to PM_{2.5}, PM₁₀, and NO₂ was associated with poor sleep quality in rural China.

Chuang et al. (2018) investigated the effects of personal exposure to metal fume fine particulate matter (PM_{2.5}) on lung function, urinary biomarkers, and sleep quality in shipyard welding workers (Chuang et al. 2018); the welding workers had longer waking times than did office workers, suggesting that exposure to heavy metals in metal fume PM2.5 may disrupt sleep quality in welding workers.

Two studies observed the negative effects of particulate matters on sleep in children (Abou-Khadra 2013; Nosetti et al. 2016). More significantly, the effects of particulate air pollution exposure on sleep disruption persist even during pregnancy; exposure during weeks 1–8 was associated with decreased sleep efficiency, during weeks 31–35 was associated with decreased sleep duration, and during weeks 39–40 was associated with increased sleep duration (Bose et al. 2019).

Multiple Air Pollutants and Sleep

Some studies have examined the effects of exposure to multiple air pollutants from ambient air on sleep.

Tang et al. (2020) conducted a study among the elderly in Ningbo, China, and found that short-term exposure to multiple air pollutants was associated with hospital visits for sleep disorders, with the strongest associations occurring 2–3 days prior to a clinic visit for traffic-related pollutants including the PM_{2.5}, PM₁₀, and NO₂, and for SO₂ and O₃ for 5 days prior to the clinic visit (Tang et al. 2020).

Yu et al. (2019) performed a five-year study among freshmen in Beijing, China; they observed that air pollution was associated with a reduction in sleep duration among freshman students living in Beijing: One standard deviation increase in air pollution concentration in PM_{2.5}, PM₁₀, and NO₂ was associated with a reduction in daily sleep of 0.68 h, 0.55 h, 0.70 h, and 0.51 h, respectively (Yu et al. 2019).

Lawrence et al. (2018) performed a large-scale study in children in seven northeastern cities in China (Lawrence et al. 2018). They found that sleep disorders were generally associated with all air pollutants, including PM₁, PM_{2.5}, PM₁₀, SO₂, NO₂, and O₃, with the highest odds found for PM₁ exposure. The strongest association was between exposure to PM₁ and disorders of excessive somnolence.

Kheirandish-Gozal et al. (2014) examined the association between habitual snoring of children and exposure to air pollutants, including PM₁₀, NO₂, SO₂, CO, and O₃ in five districts of Iran (Kheirandish-Gozal et al. 2014). Among the 4322

children aged 6–12 years, those living in regions with higher levels of pollutant exposure were more likely to show habitual snoring. This effect remained after controlling for other risk factors, such as family history of snoring, wheezing, respiratory problems, and parental smoking status.

IAQ and Sleep

Ventilation and Sleep

The studies on ventilation and sleep were recently summarized by Akimoto et al. (2021), Fig. 3. They used measured CO₂ as a marker of ventilation.

Strøm-Tejsen et al. (2016) conducted two field intervention studies in Denmark during the heating season: one pilot experiment in naturally ventilated dormitory rooms and one experiment in dormitory rooms with balanced MV (Strøm-Tejsen et al. 2016). In the pilot experiment, the mean bedroom CO₂ level was 2585 ppm (range: 1730–3900 ppm) with windows closed and 660 ppm (range: 525–840 ppm) with open windows. In the second experiment, the mean bedroom CO₂ level was 2395 ppm (range: 1620–3300 ppm) when the fan was disabled and 835 ppm (range: 795–935 ppm) when it was in operation. The lower CO₂ concentration resulted in improved sleep quality, both as rated by the subjects and measured by Actigraphy and improved next-day performance.

Mishra et al. (2018) changed the bedroom ventilation by opening or closing windows and doors (Mishra et al. 2018). The mean measured CO₂ levels were 717 ppm with the window and door open, 658 ppm with only the window open, 791 ppm with only the door open, and 1150 ppm with the window or door closed; it was noted that levels could exceed 3000 ppm when both the door and window were closed. Self-evaluated sleep depth and length, objectively measured sleep efficiency, and the number of awakenings measured using actigraphy correlated well with the measured CO₂ levels – the lower the CO₂, the better sleep quality.

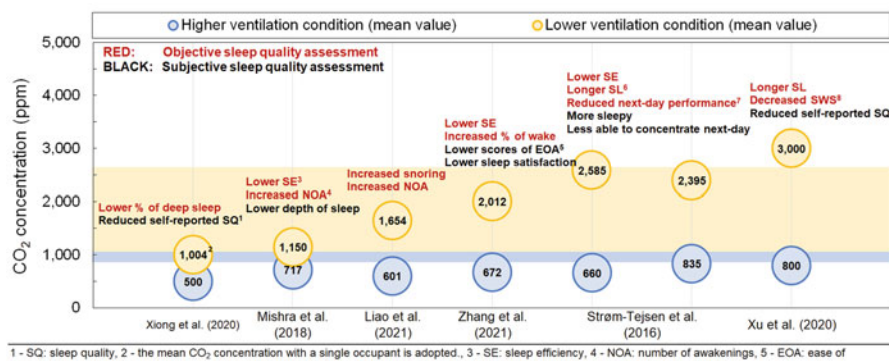


Fig. 3 Summary of studies investigating the effects of ventilation on sleep. (Modified from (Akimoto et al. 2021))

Xiong et al. (2020) conducted a field study during the Australian summer between January and early March 2019 in Sydney (Xiong et al. 2020). The bedroom CO₂ levels under different scenarios were as follows: fan 955 ± 721 ppm; AC 889 ± 521 ppm; and open window or door 542 ± 84 ppm. A 4.3% decrease in deep sleep was observed for every 100 ppm increase in the overnight average CO₂ concentration, with adjustments made for the other variables. However, few high CO₂ cases were observed in this study, and thus the results cannot represent those for typical bedrooms in hot summer areas.

Liao et al. (2021) examined the effects of open windows in the bedroom on sleep (Liao et al. 2021). The CO₂ levels were approximately 600 ppm with open windows and 1600 ppm with closed windows. The results showed that the poorer ventilation increased snoring and the number of awakenings.

Xu et al. (2021) investigated the impact of indoor CO₂ levels on sleep quality in climate chambers furnished and decorated as bedrooms for three CO₂ concentration conditions (800 ppm, 1900 ppm, and 3000 ppm) (Xu et al. 2021). Sleep quality was measured with PSG. The results showed that sleep onset latency increased and SWS decreased with the increase of CO₂ concentration.

Zhang et al. (2021) conducted a field study in bedrooms during spring and autumn (Zhang et al. 2021). Two groups with bedroom CO₂ concentrations of less than and more than 1000 ppm were compared, with an average of 672 ppm and 2012 ppm, respectively. The results showed that the wake stage percentage was lower and the sleep efficiency, ease of awakening, and sleep satisfaction were higher with higher ventilation (indicated by lower CO₂ levels).

Lan et al. (2013) and Zhou et al. (2014) proposed a personalized ventilation system that supplied clean air directly to the breathing zone of a sleeping person while cooling/warming the face (Lan et al. 2013; Zhou et al. 2014). The results showed that providing outdoor air directly to a sleeping person's breathing zone resulted in better sleep quality, as indicated by improved subjective evaluation, skin temperature, heart rate, and heart rate variability.

In general, poor bedroom ventilation, as indicated by increased levels of CO₂, has negative effects on several aspects of sleep and can also result in poor cognitive performance the next day.

Other Indoor Pollutants and Sleep

The studies investigating the effects of other indoor pollutants on sleep quality are scarce.

Wei et al. (2017) conducted a population-based cross-sectional study to examine the association between sleep quality and cooking oil fumes (COFs) in Chinese households (Wei et al. 2017). Individual sleep quality assessments were completed for 2197 participants with an average age of 37.52 years, using PSQI. Additionally, urine samples were collected and analyzed for 1-hydroxypyrene (1-HOP), a urinary biomarker of polycyclic aromatic hydrocarbons in COFs. The results showed that subjective poor kitchen ventilation, preheating oil to smoking, and cooking for over 30 min were positively associated with overall poor sleep quality (global PSQI score > 5). High urinary 1-HOP levels were also positively associated with overall poor sleep quality.

An intervention study was conducted to investigate the effects of biomass pollution on sleep of Peruvian children under the age of 14 years (Accinelli et al. 2014). Household exposure to biomass pollution was reduced by replacing highly polluting stoves with less-polluting Inkawasi stoves. Using parent reports of child sleep habits, improvements in sleep and respiratory-related symptoms (such as snoring and nighttime awakening) were found with decreased biomass pollution. Furthermore, lower levels of pollutant exposure were associated with increased willingness to sleep and ease of falling asleep and waking up for both exclusive and partial use of the improved stoves.

The limited number of studies published to date have consistently shown that poor IAQ in bedrooms has negative effects on sleep quality. A recent study investigated the effects of ventilation and ventilation noise on sleep quality, as measured objectively using PSG (Lan et al. 2021). This study confirmed that poor ventilation in bedroom resulted in poorer sleep quality, as indicated by a lower sleep efficiency and longer wake time after sleep onset. However, ventilation noise was perceived to be less acceptable, disrupt sleep, and cancel the positive effects of ventilation. It is expected that occupants will not operate the ventilation system as required if the ventilation noise is high. These results suggest that ventilation system for bedroom should be appropriately designed with low noise.

Possible Mechanisms

Mechanisms explaining the effect of air pollution on sleep are not fully understood and have only been studied minimally. Liu et al. (2020) reviewed the present evidence and summarized two potential mechanisms (Liu et al. 2020), as shown in Fig. 4; the pollutants affect regulation of sleep by central nervous system and changes in the physiology of the respiratory system. The causal models and

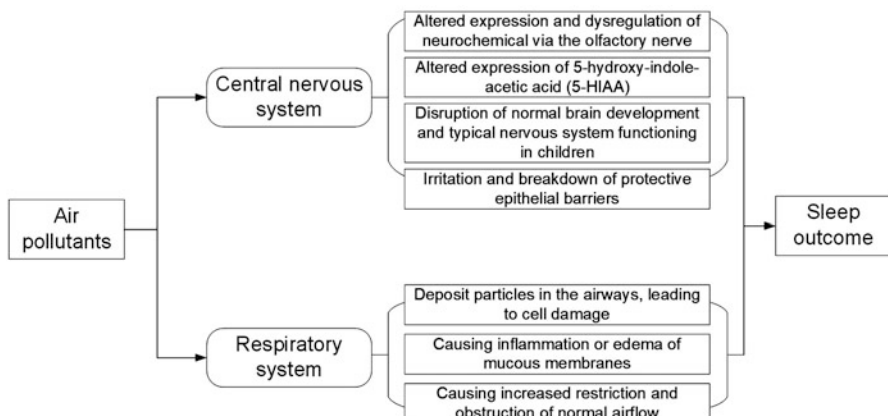


Fig. 4 Potential mechanisms by which sleep is affected by air pollutants

mechanisms linking air pollutants and sleep are currently limited; more fundamental research and epidemiological studies are needed to elucidate potential biological mechanisms underlying the association between air pollutants and sleep outcomes.

Interactions with Temperature

A comfortable thermal environment is crucial for good sleep quality. Studies have observed that when the air temperature deviates from a neutral temperature of 26 °C (higher or lower) by 3 °C, the subjects' sleep quality decreased; the sleep onset latency increased by 33 min and the duration of SWS decreased by 50 min, which corresponds to about one-third of the total SWS in healthy people (Lan et al. 2014, 2017).

Temperature may confound the effects of air pollutants on sleep. Weinreich et al. (2015) examined the relationships between PM₁₀, temperature, ozone levels, and relative humidity and sleep-disordered breathing (SDB) in middle-aged to elderly population (Weinreich et al. 2015). Positive associations between AHI and both temperature and ozone levels were observed and found to be strongest in summer. Conversely, using PSG and air monitoring stations to estimate exposure, Cassol et al. (2012) observed more SDB events in winter than in other seasons, and reported that AHI was inversely correlated with ambient temperature and directly correlated with atmospheric pressure, RH, and carbon monoxide levels (Cassol et al. 2012). These contradictory findings regarding the relationship between sleep outcomes and temperature emphasize that more studies are needed to understand both the relationship and the mechanism involved.

Aromatherapy and Sleep

As an adjunctive therapy to improve sleep problems, aromatherapy has been gaining popularity since the 1990s. Aromatherapy entails the absorption of oils extracted from the flowers, stems, leaves, roots, and fruits of various plants into the body through the skin or respiratory system to improve mental and bodily health.

Aromatherapy was found to be effective in reducing stress and improving depression and sleep quality in healthy adults. Lin et al. (2019) conducted a systematic review and meta-analysis and reported that aromatherapy effectively improves sleep quality (Lin et al. 2019).

Aromatherapy is suggested to be applied to special groups with a high incidence of sleep disorders, such as college students, shift workers, and elderly people. Nematolahi et al. (2018) reported that the use of rosemary significantly enhanced memory, reduced anxiety and depression, and improved sleep quality in college students (Nematolahi et al. 2018). Aromatherapy massage was shown to improve sleep quality in nurses with monthly rotating night shifts (Chang et al. 2017).

However, most studies on the influence of aromatherapy on sleep quality use subjective evaluation methods. It is recommended to include measurements of physiological indicators to increase the generalizability of the study results.

Possible Solutions to Improve IAQ in Bedrooms

With few exceptions, existing ventilation standards do not prescribe specific ventilation requirements for bedrooms; ventilation in bedrooms is merely the result of the ventilation requirements for the entire dwelling (Sekhar et al. 2020). Very few studies have specifically investigated ventilation technology in bedrooms.

Free-standing filters, also called room air filters or purifiers, may help to reduce pollutants in bedrooms. A study evaluated the long-term effectiveness of high-efficiency particulate air filters in Baltimore, MD, and found PM10 reductions of up to 39% compared to a control group (Eggleson et al. 2005). More sophisticated air cleaning/ventilating units can further improve IAQ, but expensive building modifications may be required (Xu et al. 2010).

During the sleeping period, people are immobile and occupy a relatively small space, which is a favorable condition for the use of local ventilation. A bedside personalized ventilation (PV) system that supplies fresh and cool/warm air to the head and face of a sleeping person was proposed by Lan et al. (2013). This PV system was applied to human subjects of different ages (including children, adults, and the elderly), for whole nights, in both winter and summer seasons and was shown to potentially improve sleep quality (Lan et al. 2013; Zhou et al. 2014).

Conclusion

Many IAQ problems, including high CO₂ and PM_{2.5} levels, have been observed in studies on bedrooms. During sleep, people may breathe passively and are exposed to air pollutants for several hours. Although current studies are limited, these evidences suggest that poor IAQ may result in poor sleep quality, indicating the necessity to improve IAQ in bedrooms. However, most of the above studies measured sleep quality with sleep trackers or subjective questionnaires, resulting in a wide range of associations and no clear mechanisms. Future studies should use a more accurate assessment of sleep quality, such as PSG, and control air pollution exposure to examine the exact effects and mechanisms of IAQ on sleep quality. As people tend to close windows/doors during the sleeping period, which decreases the air exchange rate and accumulates pollutants in the bedroom, specific alternative solutions to improve the IAQ in bedrooms should be researched.

Cross-References

- ▶ [Appliances for Cooking, Heating, and Other Energy Services](#)
- ▶ [Control of Airborne Particles: Filtration](#)
- ▶ [Epidemiology for Indoor Air Quality Problems](#)
- ▶ [Evaluating Ventilation Performance](#)

- IAQ Requirements in Green Building Labeling Systems and Healthy Building Labeling Systems
- Influence of Ventilation on Indoor Air Quality
- Occupant Emissions and Chemistry

References

- Abou-Khadra MK (2013) Association between PM10 exposure and sleep of Egyptian school children. *Sleep Breath* 17:653–657
- Accinelli RA, Llanos O, Lopez LM et al (2014) Adherence to reduced-polluting biomass fuel stoves improves respiratory and sleep symptoms in children. *BMC Pediatr* 14:12
- Akimoto M, Sekhar C, Bivolarova M, Liao CX, Fan XJ, Lan L, Wargocki P (2021) Reviewing how bedroom ventilation affects IAQ and sleep quality. *ASHRAE J* 4:56–60
- Batoga P, Badura M (2013) Dynamic of changes in carbon dioxide concentration in bedrooms. *Procedia Eng* 57:175–182
- Bekö G, Lund T, Nors F et al (2010) Ventilation rates in the bedrooms of 500 Danish children. *Build Environ* 45:2289–2295
- Bose S, Ross KR, Rosa MJ et al (2019) Prenatal particulate air pollution exposure and sleep disruption in preschoolers: windows of susceptibility. *Environ Int* 124:329–335
- Canha N, Lage J, Candeias S et al (2017) Indoor air quality during sleep under different ventilation patterns. *Atmos Pollut Res* 8:1132–1142
- Canha N, Lage J, Coutinho JT et al (2019) Comparison of indoor air quality during sleep in smokers and non-smokers' bedrooms: a preliminary study. *Environ Pollut* 249:248–256
- Canha N, Alves AC, Marta CS et al (2020) Compliance of indoor air quality during sleep with legislation and guidelines – a case study of Lisbon dwellings. *Environ Pollut* 264:114619
- Carskadon MA, Dement WC (2011) Normal human sleep: an overview. In: Kryger MH, Roth T, Dement WC (eds) *Principles and practice of sleep medicine*, 5th edn. Elsevier, Philadelphia, pp 16–26
- Cassol CM, Martinez D, da Silva FABS et al (2012) Is sleep apnea a winter disease? Meteorologic and sleep laboratory evidence collected over 1 decade. *Chest* 142:1499–1507
- Chang YY, Lin CL, Chang LY (2017) The effects of aromatherapy massage on sleep quality of nurses on monthly rotating night shifts. Evidence-based Complementary and Alternative Medicine, paper no. 3861273
- Chen GB, Xiang H, Mao ZX et al (2019) Is long-term exposure to air pollution associated with poor sleep quality in rural China? *Environ Int* 133:105205
- Chuang HC, Su TY, Chuang KJ et al (2018) Pulmonary exposure to metal fume particulate matter cause sleep disturbances in shipyard welders. *Environ Pollut* 232:523–532
- Eggleston PA, Butz A, Rand C et al (2005) Home environmental intervention in inner-city asthma: a randomized controlled clinical trial. *Ann Allergy Asthma Immunol* 95:518–524
- Fan G, Xie JC, Yoshino H et al (2018) Indoor environmental conditions in urban and rural homes with older people during heating season: a case in cold region, China. *Energ Buildings* 167: 334–346
- Fernández-Agüera J, Dominguez-amarillo S, Fornaciari M, Orlandi F (2019) TVOCs and PM2.5 in naturally ventilated homes: three case studies in a mild climate. *Sustainability* 11:6225
- Fultz NE, Bonmassar G, Setsompop K et al (2019) Coupled electrophysiological, hemodynamic, and cerebrospinal fluid oscillations in human sleep. *Science* 366:628–631
- Hirshkowitz M, Whiton K, Albert SM et al (2015) National sleep foundation's sleep time duration recommendations: final reports. *Sleep Health* 1:233–243
- Hou J, Zhang Y, Sun Y et al (2018) Air change rates at night in northeast Chinese homes. *Build Environ* 132:273–281

- Kheirandish-Gozal L, Ghalebandi M, Salehi M et al (2014) Neighbourhood air quality and snoring in school-aged children. *Eur Respir J* 43:824–832
- Kozielska B, Mainka A, Źak M et al (2020) Indoor air quality in residential buildings in Upper Silesia, Poland. *Build Environ* 177:106914
- Lan L, Lian Z, Zhou X et al (2013) Pilot study on the application of bedside personalized ventilation to sleeping people. *Build Environ* 67:160–166
- Lan L, Lian ZW, Huang HY, Lin YB (2014) Experimental study on thermal comfort of sleeping people at different air temperatures. *Build Environ* 73:24–31
- Lan L, Tsuzuki K, Liu YF, Lian ZW (2017) Thermal environment and sleep quality: a review. *Energ Buildings* 149:101–113
- Lan L, Sun YX, Wargocki P, Wyon DP (2021) Pilot study on the effects of ventilation and ventilation noise on sleep quality in the young and elderly. *Indoor Air*. <https://doi.org/10.1111/ina.12861>
- Lawrence WR, Yang M, Zhang C et al (2018) Association between long-term exposure to air pollution and sleep disorder in Chinese children: the Seven Northeastern Cities study. *Sleep* 41: 1–10
- Lei Z, Liu C, Wang L, Li N (2017) Effect of natural ventilation on indoor air quality and thermal comfort in dormitory during winter. *Build Environ* 125:240–247
- Liao C, Delghust M, Wargocki P, Laverge J (2021) Effects of windows opening on the sleep environment and quality. *Sci Technol Built Environ* 27:995–1015
- Lin PC, Lee PH, Tseng SJ, Lin YM, Chen SR, Hou WH (2019) Effects of aromatherapy on sleep quality: a systematic review and meta-analysis. *Complement Ther Med* 45:156–166
- Liu W, Huang C, Shen L et al (2015) Associations between natural ventilation for the child's bedroom during night and childhood asthma in Shanghai, China. *Procedia Eng* 121:501–505
- Liu JH, Wu T, Liu Q et al (2020) Air pollution exposure and adverse sleep health across the life course: a systematic review. *Environ Pollut* 262:114263
- Mishra AK, van Ruitenbeek AM, Loomans MGLC, Kort HSM (2018) Window/door opening-mediated bedroom ventilation and its impact on sleep quality of healthy, young adults. *Indoor Air* 28:339–351
- Nematolahi P, Mehrabani M, Karami-Mohajeri S, Dabaghzadeh F (2018) Effects of *Rosmarinus officinalis* L. on memory performance, anxiety, depression, and sleep quality in university students: a randomized clinical trial. *Complement Ther Clin Pract* 30:24–28
- Nosetti LM, Montomoli C, Tentoni S et al (2016) Is PM10 air pollution a risk factor for sleep-disordered breathing in children? A study in the province of Varese. *Am J Respir Crit Care Med* 193:A1213
- Sekhar SC (2004) Enhancement of ventilation performance of a residential split-system air-conditioning unit. *Energ Buildings* 36:273–279
- Sekhar SC, Goh SE (2011) Thermal comfort and IAQ characteristics of naturally/mechanically ventilated and air-conditioned bedrooms in a hot and humid climate. *Build Environ* 46: 1905–1916
- Sekhar C, Akimoto M, Fan XJ et al (2020) Bedroom ventilation: review of existing evidence and current standards. *Build Environ* 184:107229
- Strøm-Tejsen P, Zukowska D, Wargocki P, Wyon DP (2016) The effects of bedroom air quality on sleep and next-day performance. *Indoor Air* 26:679–686
- Tang ML, Li D, Liew ZY et al (2020) The association of short-term effects of air pollution and sleep disorders among elderly residents in China. *Sci Total Environ* 708:134846
- Walker MP (2010) Chapter 4 sleep, memory and emotion. In: Kerkhof GA, Van Dongen HPA (eds) *Progress in brain research*, vol 185. Elsevier, pp 49–68
- Wei F, Nie G, Zhou B et al (2017) Association between Chinese cooking oil fumes and sleep quality among a middle-aged Chinese population. *Environ Pollut* 227:543–551
- Weinreich G, Wessendorf TE, Pundt N et al (2015) Association of short-term ozone and temperature with sleep disordered breathing. *Eur Respir J* 46:1361–1369
- Winkens K, Koponen J, Schuster J et al (2017) Perfluoroalkyl acids and their precursors in indoor air sampled in children's bedrooms. *Environ Pollut* 222:423–432

- Wong NH, Huang B (2004) Comparative study of the indoor air quality of naturally ventilated and air-conditioned bedrooms of residential buildings in Singapore. *Build Environ* 39:1115–1123
- Xiong J, Lan L, Lian Z, De Dear R (2020) Associations of bedroom temperature and ventilation with sleep quality. *Sci Technol Built Environ* 26:1274–1284
- Xu Y, Raja S, Ferro AR et al (2010) Effectiveness of heating, ventilation and air conditioning system with HEPA filter unit on indoor air quality and asthmatic children's health. *Build Environ* 45:330–337
- Xu X, Lian Z, Shen J et al (2021) Experimental study on sleep quality affected by carbon dioxide concentration. *Indoor Air* 31(2):440–453
- Yu HJ, Chen PP, Gordon SP et al (2019) The association between air pollution and sleep duration: a cohort study of freshmen at a university in Beijing, China. *Int J Environ Res Public Health* 16: 3362
- Zanobetti A, Redline S, Schwartz J et al (2010) Associations of PM10 with sleep and sleep-disordered breathing in adults from seven U.S. urban areas. *Am J Respir Crit Care Med* 182: 819–825
- Zhang X, Luo G, Xie J, Liu J (2021) Associations of bedroom air temperature and CO₂ concentration with subjective perceptions and sleep quality during transition seasons. *Indoor Air*. <https://doi.org/10.1111/ina.12809>. (in press)
- Zhou X, Lian Z, Lan L (2014) Experimental study on a bedside personalized ventilation system for improving sleep comfort and quality. *Indoor Built Environ* 23(2):313–323



Economic Consequences

51

Jerzy Sowa, Shin-Ichi Tanabe, and Paweł Wargocki

Contents

The Costs and Benefits Related to IAQ	1478
Health Costs	1479
The Costs of Reduced Work Performance	1481
The Costs of Reduced Learning	1481
Other Costs	1482
Green Buildings	1482
Working from Home	1483
An Example of a Model Used to Estimate the Costs	1483
Conclusion	1485
References	1485

Abstract

Indoor air quality (IAQ) affects the quality of life by increasing the risks for health problems and reduced work performance. Consequently, different societal costs are incurred. By reducing pollutants elevating exposures indoors, and improving IAQ, these costs can be reduced or avoided. This chapter attempts to summarize the evidence and the methods for estimating the costs and economic

J. Sowa (✉)

Faculty of Building Services, Hydro, and Environmental Engineering, Warsaw University of Technology, Warsaw, Poland

e-mail: jerzy.sowa@pw.edu.pl

S.-I. Tanabe

Department of Architecture, Waseda University, Tokyo, Japan

e-mail: tanabe@waseda.jp

P. Wargocki

International Centre for Indoor Environment and Energy, Department of Civil Engineering, Technical University of Denmark, Kongens Lyngby, Denmark

e-mail: paw@byg.dtu.dk

consequences of poor IAQ affecting work performance. The value of lost work is discussed considering discomfort and health, absence from work (absenteeism), or working with limitations due to illness (presenteeism). The impact of air quality and other environmental factors on work performed at home is also presented as a hypothesis, but this evidence is limited.

Keywords

Absenteeism · Benefits · Costs · Environment and public health · Indoor air quality · Learning · Productivity · Presenteeism, · Respiratory disease · Societal consequences · Work performance

The Costs and Benefits Related to IAQ

Air quality in buildings affects financially mainly not only occupants, building owners, and employers, but also other stakeholders such as insurance companies, thereby affecting societal costs. The societal costs at the community and national levels can increase insurance claims, workers' compensation claims, litigation, and increased payments for sick leave with potential consequences for the gross domestic product (GDP).

For *occupants*, the costs associated with exposures to indoor air pollution may include, among others, reduced salary or wages due to lost days at work and minor restricted activity days, medical costs associated with visits for medical assistance, including visits to general practitioners, specialists as well as emergency room visits and hospital admissions, and the costs of health insurance policies. Moreover, adverse health effects can result in the loss of productive years owing to premature disability. Increased sick leave or suboptimal performance can also result in less diligent work, less care of customers, etc., which may also have consequences in the form of increased costs. In addition to absenteeism, so-called presenteeism needs also to be considered, i.e., coming to work when ill because of previous exposures to poor IAQ and despite poor IAQ, which is expected to generate considerably higher costs than taking sick leave or holidays. However, these estimations are not accurate (Lohaus and Habermann 2019).

The increased costs for individuals may be expected in up to 10% of buildings where building-related illnesses (BRI) have been observed. Additionally, some costs may be expected in up to 20% of buildings where sick building syndrome (SBS) has been observed. These data suggest that the increased costs due to poor IAQ can be expected in up to 30% of the buildings. However, it must be recognized that BRI and SBS have multifactorial etiology, poor IAQ being one of the factors. In addition, although the definition of SBS assumes the relief of symptoms when leaving the school or office, this relief may not occur because the contaminants in homes causing SBS symptoms may be the same as in the workplaces.

The costs for *building owners* include those related to sharing of rented or leased space in the building, utility costs including energy costs associated with controlling the building environment, maintenance, cleaning and operating costs, capital assets including costs of capital equipment, furniture, and other interior furnishings, and

construction costs (first costs) including those of planning, designing, and constructing nonindustrial buildings. Especially, the operating, cleaning, and maintenance costs can be strongly affected by poor IAQ.

Wargocki and Djukanovic (2005) performed a simulation comparing the life-cycle costs of investments improving IAQ in a hypothetical office building with the expected revenues from increased work performance. The benefits from improved IAQ were estimated to be up to 60 times higher than the necessary investments, which were shown to be generally recovered in no more than 2 years, the rate of return being up to 7 times higher than the minimum acceptable interest rate. Furthermore, the estimations suggested that the total costs of installing and running the building can be offset by productivity gains of just 10% (Wargocki et al. 2006).

The costs for *employers* include salaries and wages, some of which can be paid by the insurance companies in case of prolonged morbidity or mortality. They also cover the costs of staff turnover. When customers, visitors, or guests choose to stay away from retail stores, restaurants, hotels, and other public facilities because of the fear of exposure to poor air quality, the employer's revenue is lower also because the company's image is somewhat compromised.

A 1% increase in productivity would correspond to reduced sick leave of 2 days per year, fewer breaks from work, improved effective time at work of 5 minutes per day, or a 1% increase in the effectiveness of physical and mental work (Wargocki et al. 2006). Considerable benefits can thus be achieved by employers when IAQ is improved. These benefits stem from employees' improved productivity and health status, resulting from general satisfaction from the working environment, lower staff turnover, and more satisfied customers.

In summary, all stakeholders benefit from improved IAQ. These benefits outweigh potential energy and investment costs if only the effects of improved performance are included in the calculations (Wargocki et al. 2006). Despite the possible high economic premiums and rewards, health and productivity benefits are not yet regularly included in conventional financial analyses used during the design and operation of buildings. One reason could be inadequate communication and lack of confidence regarding the benefits of improving air quality, as well as low willingness to pay for these improvements. This is nicely demonstrated by Hamilton et al. (2016), who documented opinions of the US building industry. Their analysis showed that less than half of respondents expected that improving ventilation and filtration of buildings would improve productivity and even less associated these interventions with lower absence rates and health risks. Respondents attributed high costs to the interventions aiming to improve IAQ, which were more significant than the estimated actual costs. In addition, green building owners were less likely to pay for the upgrades.

Health Costs

There are limited estimations regarding the health costs related to poor IAQ. One of the key publications by Fisk and Rosenfeldt (1997) was published nearly 25 years ago. Its summary supplemented by the more recent analyses is presented below.

Fisk and Rosenfeldt (1997) estimated that savings due to reduced respiratory illnesses as a result of improved IAQ could in the US amount to \$6–14 billion annually, assuming that they constitute 10–30% of the total costs of these illnesses estimated to be \$64 billion annually (1990s figures). Using the work of Milton et al. (2000), it may be assumed that the direct costs of respiratory diseases also include the costs of absence from work estimated in the USA to be \$400 per employee per year (2000 figures).

Fisk and Rosenfeldt (1997) estimated that savings due to reduced costs of allergies and asthma as a result of improved IAQ in the USA could amount to \$2–4 billion annually, assuming that they constitute 10–30% of their total costs estimated to be \$12.8 billion annually (1990s figures). A significant portion of these costs reflected the burden of disease in children, including mainly health care and lost school days. In 2016, the new estimate of direct medical costs and wage-related losses in the USA for selected allergy-induced health conditions, including exposure to damp and mold in homes, showed that direct medical expenses related to allergic rhinitis were \$2.26 billion, to asthma were \$ 880 million, and to bronchitis were \$287 million (Mudarri 2016). \$335 million was estimated as the total loss due to sick days (including care for sick children) and reduced labor productivity caused by allergic rhinitis. The corresponding losses were estimated to be \$156 million for asthma and \$56 million for acute bronchitis. These figures do not differ much from the estimates of Fisk and Rosenfeldt (1997).

Fisk and Rosenfeldt (1997) also produced an estimate for the cost of reduced productivity in the USA due to SBS yielding \$50 billion per year (1990 figures). This estimate corresponded to about \$400 per worker annually, being about 2–3 lost working days of each worker per year. In the Finnish offices, similar estimates were obtained: A reduction in the prevalence of SBS symptoms was estimated to result in savings of ca. €330 per worker annually, corresponding to about 1–2 lost working days for each worker per year (Seppänen 1999). However, it must be underlined that some of these costs are not related directly to poor IAQ and are associated with job satisfaction, psychosocial conditions, or personal issues. Nevertheless, assuming that only 10% are attributable to poor IAQ, they would yield nonnegligible costs of \$0.75–2 billion annually.

Recently, the health impact of air pollution was estimated in Europe and the USA using the Disability-Adjusted Life Years (DALYs). DALY estimates the lost healthy life years and combines the effects on premature mortality and morbidity. In economic terms, the cost of one DALY is estimated to be around \$100 k but can vary by a factor of one or two (Boulanger et al. 2017). Logue et al. (2012) estimated that 1.3 to 3.5 million healthy life years could be lost due to premature death or disability to perform work each year in the USA due to poor IAQ in homes. Similar estimations in Europe (EU-26), though for the entire building stock, including public and residential buildings but excluding secondhand tobacco smoke, led to a very similar figure of ca. two million healthy life years lost (Jantunen et al. 2011; Asikainen et al. 2016). For comparison, the estimated DALYs caused by exposure to air pollutants are about seven times lower than DALYs for all noncommunicable nonpsychiatric diseases combined independently of the etiology. Nevertheless, the

two cited estimations clearly illustrate that indoor exposures contribute significantly to the burden of disease in the population and create significant challenges for public health with considerable economic consequences. Such estimations are rare. Those that exist confirm that the socioeconomic costs of poor indoor air quality are very high. For example, a recent estimation of health consequences of exposures to selected indoor air pollutants in France yielded the cost of €20 billion annually (Boulanger et al. 2017).

In estimations of DALYs, PM2.5 was shown to account for a majority of lost healthy life years. The potential health benefits due to installation of particle filtration were estimated to amount annually \$5–\$15/person for the human capital loss and as much for the minor restricted activity days, \$5–\$20/person for work loss days, \$10–\$35/person for the total morbidity, and \$40–\$160/person for the lost value of the statistical life year (Bekö et al. 2008), the size of the benefits depending on the reduction of the exposure to PM indoors. The potential annual total benefits from the reduced adverse effects on health can be estimated to be as high as \$250 per person. This figure is much lower than the potential benefit from the productivity, which can reach a few thousand dollars annually per person depending on productivity (estimated to be $\leq 5\%$) and salary.

The Costs of Reduced Work Performance

Fisk and Rosenfeldt (1997) estimated that direct improvements in worker performance unrelated to illness and health symptoms could be \$12–125 billion per year (1990 figures); this estimate included mainly lighting quality affecting vision and thermal effects and is only partially caused by poor IAQ. Fisk et al. (2011) postulated that up to 20% reduction in SBS could be obtained by improved ventilation resulting in savings of \$5 billion annually. Other estimates more closely related to poor IAQ were presented by Fisk et al. (2012). They simulated the effects of changing ventilation rates in the US offices and showed that benefits due to improved productivity could amount to \$13 billion by increasing minimum ventilation rates to 10 L/s per person, \$38 billion when increased to 15 L/s per person. Filtration can also bring substantial benefits, but they can be offset due to pollutants emitted from used filters that can cause poor IAQ (Bekö et al. 2008).

The Costs of Reduced Learning

Wargocki et al. (2014) presented economic calculations showing that students performing better in primary schools would have higher income in adult life. Using the Danish data, they showed that the socioeconomic consequences of improved air quality in primary schools in Denmark would produce the benefit corresponding to about 1 per million of the Danish GDP (€240 billion in 2011). The benefits were attributed to improved ventilation in schools, improved learning, and shortened stay in school – fewer children took tenth grade in the ninth-grade schooling system in

Denmark and started work earlier, and lower teacher sick leave. However, the most significant effect was seen for improved productivity resulting in the annual growth of €104 million (measured in 2011 prices); the effect is expected to increase steadily with the increasing number of pupils graduating earlier from school.

Another way of estimating the potential benefits of improved IAQ on learning is to relate schoolwork performance with the expenses needed to cover salaries for teachers assuming that any performance improvement can be expected to reduce overtime and extra teaching hours. Simple estimations for Danish conditions suggest that renovations of primary schools leading to improved performance of school performance by 5% and subsequent 5% reduction in the expenses for wages for teachers would result in the net benefit of €0.10 per child per day (2011 data) after deducting the costs of renovations. The breakeven would occur if renovations resulted in the improved performance of schoolwork by 3% and thus a 3% reduction in teachers' wages (Marxen et al. 2011). Studies show that the effects of improved IAQ in schools can be expected to be much higher (Wargocki and Wyon 2013; Wargocki et al. 2020).

Mendell et al. (2013) estimated the benefits of improved ventilation in schools resulting in decreased illness absence in school districts, i.e., increased revenue from the student attendance and reduced costs to families from the lost caregiver wages. These benefits yielded \$33 to \$66 million annually from the increased revenue and \$80 to \$160 million from the reduced losses to caregivers.

Other Costs

In health care facilities, the adverse effects of poor IAQ can be exemplified by a negative impact on the hospital staff, increased risk for nosocomial infections, and extended hospital patient stays (patient recovery time); the 1990s estimates in the USA conditions suggested that they can amount to \$2 billion annually.

In the hospitality industry, including restaurants, bars, lodgings, and casinos, the costs for health and productivity were estimated to be as high as \$19.6 billion per year in the USA (2000s figures); \$1.46 billion were the productivity costs, \$1.65 billion employee medical costs, \$11.37 billion lost sales, and the remaining \$5.12 billion absenteeism, training, sick leave, and dealing with complaints (Dorgan and Dorgan 2006).

The costs in other buildings such as supermarkets, department stores, and fast-food outlets have not been estimated. Still, they can be approximated by the daily turnover resulting from customer behavior and staff performance.

Green Buildings

Recent studies examining the green office buildings' asset value have shown that these buildings generally have a higher market value considering their sale and leasing value than conventional buildings (Harrison and Seiler 2011; Chegut et al.

2013; Eichholtz et al. 2013). The evidence exists of leasing premiums being up to 17% in green buildings compared to conventional buildings (Wiley et al. 2008); the evidence in selling prices shows a bonus of up to 30% (Eichholtz et al. 2013; Newell et al. 2011). In addition, there is supporting evidence of higher sale yields (Sayce et al. 2010), higher occupancy rates, and lower operating expenses in green buildings than conventional buildings (Wiley et al. 2008; Eichholtz et al. 2013).

Working from Home

Working from home (teleworking or telecommuting) has become an increasingly popular work mode, boosting significantly during the COVID-19 pandemic in 2020–2021. Before the pandemic, it was estimated at the level of 3% for EU workers (Eurofound 2016). Dingel and Neiman (2020) estimated that 37% of all US jobs could be performed from home.

Working from home may result in a radical change of the working environment, including ergonomic aspects and communication and other conditions related, among others, to IAQ. For example, Morawska et al. (2017) suggested that, in general, office air is less polluted with particles than the air in homes (and schools). Zhao et al. (2015) estimated the economic consequences of improved air filtration in US homes and showed that application of filters with an efficiency higher than MERV5 would reduce premature mortality by 0.002–2.5% and extend life expectancy by 0.02–1.6 months, yielding annual economic benefits ranging from \$1 to \$1348; the benefits increased with a higher filtration class. The earlier presented estimates of Logue et al. (2012) can also be recalled here, showing 1.3 to 3.5 million healthy life years lost potentially due to poor IAQ in homes which could cost the society an astronomical \$1.3–3.5 trillion annually.

An Example of a Model Used to Estimate the Costs

When the economic estimates are made, different approaches are used, including:

- Simple balance methods
- Optimization methods
- Methods based on Bayesian Network

The applied model should include the costs of building and productivity of the company staff and the changes in the monetary value over time. In addition, models contain some constraints such as boundary conditions for thermal comfort or indoor air quality. For example, Petersen and Knudsen (2017) described yearly productivity loss with work performance treated as an indicator of productivity using two components: overall thermal comfort sensation and perceived air quality. Jensen et al. (2009) presented a Performance Index (P) determined with a Bayesian Network that can be used to compare different building designs in terms of their estimated

economic consequences when the effects on occupant performance and energy use are taken into account. The overview of the various methods of calculation of economic costs used in practice is presented in the REHVA Guidebook 6 (Wargocki et al. 2006).

From the company perspective, the annual profit depends on annual production revenues decreased by annual labor costs and costs related to a building (Skåret 1992; Hanssen 1997). The annual profit can be calculated from the simplified equation that also considers the variable value of the money over time.

$$G = P - S - (B \cdot a + E + M + C)$$

where:

G = annual profit

P = annual production revenue

B = investment capital cost-related building, furnishing, equipment, and installations per floor area

a = annuity factor

E = annual energy costs

M = annual operation and maintenance cost

C = annual cleaning costs

S = annual salaries including related costs

The annuity factor that allows converting the investment cost over n years when the annual interest rate is r can be calculated using the following formula

$$a = \frac{r \cdot (1 + r)^n}{(1 + r)^n - 1}$$

It is more convenient to analyze the profitability of the investment in improving indoor environmental quality in slightly modified form by relating some costs to the floor area (subscript F) or the number of employees (subscript P). The average floor area per person is denoted as y.

$$G_F = \frac{P_p}{y} - S_F - (B_F \cdot a + E_F + M_F + C_F)$$

The investment can be regarded as profitable when the increase of production revenue (due to increased productivity) exceeds the increase of costs related to buildings.

$$\Delta P_P \geq y \cdot (\Delta B_F \cdot a + \Delta E_F + \Delta M_F + \Delta C_F)$$

Generally, in the methods presented above, due to the predominating share of annual salaries (with the related costs), even a slight increase in productivity by a few percent increases the company profit.

Conclusion

Poor IAQ has been shown to result in considerable economic costs related to health, reduced productivity, absence from work, and the presence when sick. The benefits from improved IAQ will significantly outweigh the costs necessary for achieving high IAQ. The estimates suggest the returns being 3–6 times higher than the costs for increased ventilation, 8 times higher for increased filtration, and up to 60 times higher when all improvements and related benefits are taken into account (Hawkins et al. 2020).

Crude estimates suggest that 2 million healthy life years can be saved in Europe by improving IAQ in nonindustrial buildings while up to 3.5 million in the USA when residential buildings are considered. This will result in massive economic benefits considering that one healthy life year costs about \$100k.

The potential annual savings and productivity gains from the improved IAQ were estimated to be \$168 billion in the USA (1997 data) and €330 per worker in Europe (2000 data); reduced absenteeism was estimated to be \$400 per employee per year (2000 data). There are also significant economic benefits of improved learning when IAQ in schools is improved.

Despite the obvious economic and societal benefits, the effects of improved IAQ have not yet been integrated into the conventional financial calculations pertaining to building design and operation.

References

- Asikainen A, Carrer P, Kephalopoulos S, de Oliveira Fernandes E, Wargocki P, Hänninen O (2016) Reducing burden of disease from residential indoor air exposures in Europe (HEALTHVENT project). *Environ Health* 15(1):61–72
- Bekö G, Clausen G, Weschler CJ (2008) Is the use of particle air filtration justified? Costs and benefits of filtration with regard to health effects, building cleaning, and occupant productivity. *Build Environ* 43(10):1647–1657
- Boulanger G, Bayeux T, Mandin C, Kirchner S, Vergriette B, Pernelet-Joly V, Kopp P (2017) Socio-economic costs of indoor air pollution: a tentative estimation for some pollutants of health interest in France. *Environ Int* 104:14–24
- Chegut AM, Eichholtz PM, Rodrigues P (2013) The London commercial property price index. *J Real Estate Financ Econ* 47(4):588–616
- Dingel JI, Neiman B (2020) How many jobs can be done at home? *J Public Econ* 189:104235
- Dorgan CE, Dorgan CB (2006) Assessment of link between productivity and indoor air quality. In: Creating the productive workplace. Taylor & Francis, pp 141–163
- Eichholtz P, Kok N, Quigley JM (2013) The economics of green building. *Rev Econ Stat* 95(1):50–63
- Eurofound. (2016) Sixth European working conditions survey – overview report. Publications Office of the European Union, Luxembourg
- Fisk WJ, Rosenfeld AH (1997) Estimates of improved productivity and health from better indoor environments. *Indoor Air* 7(3):158–172
- Fisk WJ, Black D, Brunner G (2011) Benefits and costs of improved IEQ in US offices. *Indoor Air* 21(5):357–367
- Fisk WJ, Black D, Brunner G (2012) Changing ventilation rates in US offices: implications for health, work performance, energy, and associated economics. *Build Environ* 47:368–372

- Hamilton M, Rackes A, Gurian PL, Waring MS (2016) Perceptions in the US building industry of the benefits and costs of improving indoor air quality. *Indoor Air* 26(2):318–330
- Hanssen SO (1997) Economical consequences of poor indoor air quality and its relation to the total building operation costs. Proc. EuroFM/IFMA Conference & Exhibition. Torino, Italy, pp 1–21, International Facility Management Association
- Harrison D, Seiler M (2011) The political economy of green office buildings. *J Prop Invest Financ* 29:551
- Hawkins VR, Marcham CL, Springston JP, Miller J, Braybrooke G, Mauder C, Feng L, Kollmeyer B (2020) The value of IAQ: a review of the scientific evidence supporting the benefits of investing in better indoor air quality. Retrieved from <https://commons.erau.edu/publication/1500>
- Jantunen M, Fernandes EO, Carrer P, Kephalaopoulos S (2011) Indoor air risks and impacts of alternative policy interventions in the EU countries—the IAIAQ study. Project Funded by European Commission, DG Sanco EAHC, 2
- Jensen KL, Toftum J, Friis-Hansen P (2009) A Bayesian network approach to the evaluation of building design and its consequences for employee performance and operational costs. *Build Environ* 44(3):456–462
- Logue JM, Price PN, Sherman MH, Singer BC (2012) A method to estimate the chronic health impact of air pollutants in US residences. *Environ Health Perspect* 120(2):216–222
- Lohaus D, Habermann W (2019) Presenteeism: a review and research directions. *Hum Resour Manag Rev* 29(1):43–58
- Marxen C, Knorborg RB, Hviid CA, Wargocki P (2011) Hvad koster et godt indeklima på folkeskoler? *HVAC Magasinet* 9:40–42
- Mendell MJ, Eliseeva EA, Davies MM, Spears M, Lobscheid A, Fisk WJ, Apte MG (2013) Association of classroom ventilation with reduced illness absence: a prospective study in California elementary schools. *Indoor Air* 23(6):515–528
- Milton K, Glenross P, Walters M (2000) Risk of sick leave associated with outdoor air supply rate, humidification, and occupant complaint. *Indoor Air* 10:211–221
- Morawska L, Ayoko GA, Bae GN, Buonanno G, Chao CYH, Clifford S, Fu SC, Hanninen O, He C, Isaxon C, Mazaheri M, Saltherammer T, Warring MS, Wierzbicka A (2017) Airborne particles in the indoor environment of homes, schools, offices, and aged care facilities: the main routes of exposure. *Environ Int* 108:75–83
- Mudarri DH (2016) Valuing the economic costs of allergic rhinitis, acute bronchitis, and asthma from exposure to indoor dampness and mold in the US. *J Environ Public Health* 2016
- Newell G, McFarlane J, Kok N (2011) Building better returns. A study of the financial performance of green office buildings in Australia – (Research by the University of Western Sydney Australia and the University of Maastricht Netherlands in conjunction with Jones Lang LaSalle and CBRE)
- Petersen S, Knudsen MD (2017) Method for including the economic value of indoor climate as design criterion in optimization of office building design. *Build Environ* 122:15–22
- Sayce S, Sundberg A, Clements B (2010) Is sustainability reflected in commercial property prices: an analysis of the evidence base. RICS, London
- Seppänen O (1999) Estimated cost of indoor climate in finnish buildings. Proceedings of the 8th international conference on Indoor Air Quality and Climate, Edinburgh, Scotland
- Skåret JE (1992) Indoor environment and economics. Project no. 6405 The Norwegian Institute for Building Research (NBI-Byggforsk), Oslo February 1992, (in Norwegian)
- Wargocki P, Djukanovic R (2005) Simulations of the potential revenue from investment in improved indoor air quality in an office building. *ASHRAE Trans* 111(2)
- Wargocki P, Wyon DP (2013) Providing better thermal and air quality conditions in school classrooms would be cost-effective. *Build Environ* 59:581–589
- Wargocki P, Seppänen O, Andersson J, Clements-Croome D, Fitzner K, Hanssen SO (2006) Indoor climate and productivity in offices. REHVA guidebook, 6

- Wargocki P, Foldbjerg P, Eriksen KE, Videbæk LE (2014) Socio-economic consequences of improved indoor air quality in Danish primary schools. Proc Indoor Air:2014
- Wargocki P, Porras-Salazar JA, Contreras-Espinoza S, Bahnfleth W (2020) The relationships between classroom air quality and children's performance in school. Build Environ 173:106749
- Wiley J, Benefield JD, Johnson KH (2008) Green design and the market for commercial office space. J Real Estate Financ Econ 41(2):228–243
- Zhao D, Azimi P, Stephens B (2015) Evaluating the long-term health and economic impacts of central residential air filtration for reducing premature mortality associated with indoor fine particulate matter (PM_{2.5}) of outdoor origin. Int J Environ Res Public Health 12(7):8448–8479

Part X

Standards and Guidelines



WHO Health Guidelines for Indoor Air Quality and National Recommendations/Standards

52

Lidia Morawska and Wei Huang

Contents

Introduction	1492
WHO Indoor Air Quality Guidelines	1495
WHO Guidelines Related to Indoor Environment: Background	1495
Criteria for Inclusion and Exclusion of the Specific Pollutants	1496
Summary of the IAQ Numerical Guideline Values	1498
National Standards	1498
Summary	1509
References	1509

Abstract

This chapter reviews and discusses the World Health Organization (WHO) guidelines related to indoor air quality (IAQ). The WHO IAQ health guidelines are developed and published after systematic reviews of evidence from medical and public health studies, and through extensive panel discussion and expert consultation, which provide an important basis for countries to develop your national indoor air standards. First, a general background is provided for establishing health-based air quality guidelines, followed by a summary of the criteria for the inclusion and exclusion of specific pollutants in these documents and a summary of the values of the numerical guidelines for IAQ. The following

L. Morawska (✉)

International Laboratory for Air Quality and Health, Queensland University Technology, Brisbane, QLD, Australia

Global Centre for Clean Air Research, Department of Civil and Environmental Engineering, Faculty of Engineering and Physical Sciences, University of Surrey, Guildford, UK
e-mail: l.morawska@qut.edu.au

W. Huang

Department of Occupational and Environmental Health, School of Public Health, and Institute of Environmental Medicine, Peking University, Beijing, China
e-mail: w.huang@bjmu.edu.cn

is a summary of existing or planned national standards or guidelines for IAQ management, including monitoring, in countries around the world, and discussed in the context of the WHO IAQ guidelines. Globally, only several countries have enacted national indoor air quality standards or health guidelines. The importance of developing a national standard or guideline for indoor air quality based on health evidence is discussed as a measure to reduce indoor exposure.

Keywords

Indoor air quality · Indoor air quality guidelines · Indoor air quality standards · WHO indoor air quality guidelines

Introduction

In this chapter, guidelines and standards for indoor air quality are reviewed and discussed. While the terms “guidelines” and “standards” are often used interchangeably, these are different types of documents, which we explain first. Secondly, we define indoor air quality for the purpose of this discussion. Finally, we outline the scope of this chapter.

An air quality health guideline is any kind of recommendation or guideline on the protection of a human population or receptors in the environment from the adverse effects of air pollution. The guidelines, which are globally considered to be the foundation for the prevention of health effects in relation to air pollution, are those developed by the World Health Organization (WHO). In 1979, the WHO published a criteria document focused on sulfur dioxide (SO_2) and particulate matter (WHO 1979), but the first edition of the guidelines was published by the WHO European Office in 1987 (WHO 1987). Following this, a global edition of the guidelines was published in 2000 (WHO 2000), with the most recent update published in 2021 (WHO 2021). The first edition of the guidelines (1987) included carbon monoxide (CO), lead, nitrogen dioxide (NO_2), ozone (O_3), sulfur dioxide (SO_2), and total suspended particulate (TSP) matter. The Global and European guidelines published in 2000, as well as the Global guidelines published in 2006, included the same pollutants; however, in 2000, TSP was replaced by $\text{PM}_{2.5}$ and PM_{10} , (particulate matter with aerodynamic diameter $<2.5\ \mu\text{m}$ and $10\ \mu\text{m}$, respectively), albeit without the provision of numerical guideline levels. In addition, the 2000 Global and European guidelines also included the following pollutants: cadmium, carbon disulfide, carbon monoxide, 1,2-dichloroethane, dichloromethane, formaldehyde, hydrogen sulfide, manganese, mercury, platinum, styrene, tetrachloroethylene, toluene, and vanadium. These pollutants were not included in the 2006 updated WHO AQG due to the limited resources available for the project, and therefore their values from the 2000 remain in effect. The new edition of the guidelines includes particulate matter: ($\text{PM}_{2.5}$ and PM_{10}), ozone, nitrogen dioxide, sulfur dioxide, and carbon monoxide (WHO 2021). As a general comment, the concept in WHO air quality guidelines has evolved over the years, to include in terms of the method used and environmental protection considerations (WHO 2017).

Health guidelines published by WHO are adopted based on expert panel agreements, following consideration of evidence from medical and public health studies. As stressed in the latest edition of the guidelines, “*The overall objective of these guidelines is to offer quantitative health-based recommendations for air quality, expressed as long- or short-term concentrations of a number of key air pollutants*” (WHO 2021).

Health guidelines are exclusively based on exposure (concentration)-response relationships found in epidemiological, toxicological, and environment-related studies. In general, they are not restricted to a numerical value but can be expressed in different ways. However, air quality guideline values are fixed numerical values corresponding to a defined averaging time. They could be expressed as: pollutant concentration in ambient air, a pollutant deposition level, other physical-chemical value, or a unit risk. In relation to human health, the air quality guideline is a concentration below which no adverse effects are expected, albeit a small individual risk always exists.

Over decades, there have been continued improvements to the meaning of the term “adverse health effects,” and improved in the understanding of the distinction between adverse and nonadverse effects (WHO 1972, 1978). These improvements came with the expansion of medical knowledge, including a higher sensitivity of research approaches and the application of biomarkers that can detect even the most subtle perturbation in the human biological system resulting from exposure to air pollution. These expansions were discussed and utilized in the Official Statement of the American Thoracic Society as to “What Constitutes an Adverse Health Effect of Air Pollution,” released in 2000 (Samet et al. 2000), thus modifying the previous statement of the Society released in 1985 (Andrews et al. 1985).

The above example illustrates many steps, which need to be taken before initiating the process of establishing air quality health guidelines – which are “*rigorous scientific tool that can be used by regulatory authorities as a basis for setting standards, taking into account local sociopolitical and economic conditions and prevailing ambient concentrations of air pollutants*” (WHO 2017) – as discussed in section “**National Standards**,” below. The quantification of risk due to environmental exposure to a particular pollutant is always a complex process, since there are numerous other pollutants and environmental factors, which have an impact on the individual at the same time, and the particular exposure investigated is only one of those factors. Such a process is normally initiated when evidence emerges that exposure to the pollutant constitutes a risk to human health. Some of the key subsequent steps in the process include the quantification of both the exposure-response relationship, as well as the impact of the proposed regulations or policy measures on the actual reduction in exposure. The entire process of risk assessment, for the purpose of risk management, encompasses several more steps, in particular, establishing the exposure-dose and dose-response relationships (these two are not always conducted, instead concertation-response is considered), the lifetime individual risk, and the risk to the exposed population (Naugle and Pierson 1991).

By contrast to air quality health guideline, an air quality standard is a level of air pollution (concentration, deposition, etc.), which is promulgated by a regulatory

authority and adopted as enforceable. The key elements in formulation of a standard are: (i) effect-based level, (ii) averaging time, (iii) measurement procedure, (vi) definition of compliance parameters corresponding to the averaging times, and (vii) permitted number of exceeding. Ideally, national (state, provincial, etc.) standards should be set at the level (or below) recommended by WHO guidelines. For a range of reasons this is often not possible and a higher-standard values are decided upon and set. Unlike WHO air quality guidelines that are exclusively based on exposure-response relationships, there are two key aspects that are considered by public health regulators when setting standards, which are acceptability of risk and cost-benefits analysis. Acceptability of the risk and thus the standard value selected depend on: (i) the expected incidence and severity of the potential health effects; (ii) the size of the population at risk; and (iii) the degree of scientific uncertainty that the health effect will occur at any given level of air pollution. The acceptability of risk may vary among countries (or even among administrative regions within the countries), because of differences in social norms, degree of adversity, risk perception in the general population and various stakeholders, and how the risk associated with air pollution compares with other risks. Therefore, approaches to derivation of air quality standards from air quality guideline have the objectives of: (i) reducing the risk of adverse effects to a socially acceptable level and (ii) identification of the control actions that achieve greatest net economic benefit or is most economically efficient.

It is important to keep in mind these broad aspects characterizing indoor air quality (IAQ) guidelines and standards when considering these two types of documents. In principle, we compare different national standards and discuss how they relate to WHO IAQ guidelines.

IAQ is an element of indoor environment quality (IEQ) and is characterized in terms of concentration of pollutants that affect health (discussed in more detail below). IEQ is concerned, in addition to airborne pollutant concentrations, with several other factors, including thermal comfort, lighting, and acoustics. Another critical factor characterizing IEQ is ventilation for acceptable IAQ. Its role in the first instance is to remove from indoor air, and thus lower below acceptable levels (set by guidelines or standards), pollutants generated within the indoor environment. The pollutants are generated by the occupants and sources existing within the indoor environment (for example, mould or wall paint) or operating there (for example, combustion sources). Carbon dioxide (CO_2) requires a specific mention, as it is produced by combustion processes in indoor and outdoor environments but is a by-product of the natural metabolism of living organisms. Sampling for CO_2 is often used as a means for screening areas where potential IEQ problems may exist. Importantly, CO_2 , that is an indoor pollutant generated by humans, is commonly considered as a measure of perceived air quality, or a proxy for ventilation (Khovalyg et al. 2020).

Considering the above background, the scope of this chapter is:

1. WHO IAQ guidelines: (i) WHO guidelines related to indoor environment – background: (i) criteria for inclusion and exclusion of the specific pollutants and (ii) a summary of the IAQ numerical guideline values.

-
2. National IAQ standards: summary of the existing numerical national IAQ standards available in English language; (ii) summary of the rationale for selecting specific pollutants and their numerical values by the national health authorities; and (iii) discussion on the relation between national standards and WHO IAQ guidelines.

Outside the scope of the chapter are: (i) any qualitative IAQ guidelines or recommendations; and (ii) analysis of any broader IEQ aspects, in particular ventilation guidelines or standards. The later are critically reviewed, by, for example (Khovalyg et al. 2020).

WHO Indoor Air Quality Guidelines

WHO Guidelines Related to Indoor Environment: Background

There is an added complexity to indoor air pollution, compared to outdoor air pollution, since indoor air contains a mix of pollutants that penetrated from outside and those that were emitted inside; it is the mix of the pollutants that affects human health. This added complexity of relating indoor air quality and health, when compared to the impact of outdoor air, reflected in the WHO approach to develop health guidelines related to both of these environments. While, in relation to the outdoor air, there are two current documents, *WHO Global Air Quality Guidelines: particulate matter (PM_{2.5} and PM₁₀), ozone, nitrogen dioxide, sulfur dioxide, and carbon monoxide* (WHO 2021) and for some pollutant and averaging times (WHO 2006), indoor air is covered by three documents. Recommendation for developing separate indoor air quality guidelines came from the working group of the *WHO Air Quality Guidelines: Global Update 2005: particulate matter, ozone, nitrogen dioxide, and sulfur dioxide* (WHO 2006), in recognition that the management of indoor air quality requires approaches different from those used for outdoor air. In the subsequent work, it was acknowledged that while the existing WHO air quality guidelines are applicable to indoor air, a number of chemical substances were also identified for which specific indoor air guidelines were recommended. This led to the development of *WHO Guidelines for Indoor Air Quality, Selected Pollutants* (WHO 2010) – discussed below. In addition, guidelines on two other categories of health risk in indoor environments were also developed: biological agents and indoor combustion of solid fuels. The WHO guidelines on *Dampness and Mould* were published in 2009 (WHO 2009) and later, the *WHO Guidelines for Indoor Air Quality: Household Fuel Combustion* (WHO 2014). These two sets of WHO guidelines do not, however, provide limit values in indoor air but provide qualitative recommendations to manage mould and dampness in buildings and best approaches to reducing household air pollution, respectively. Given our objective is to provide to the reader an overview of existing numerical guideline values for indoor air (regulatory or voluntary), the WHO guidelines on dampness and combustion of solid fuels are out of the scope of this chapter.

Criteria for Inclusion and Exclusion of the Specific Pollutants

The criteria, which were defined for selecting the compounds to be included in the WHO guidelines for indoor air were:

- The existence of indoor sources.
- The availability of toxicological and epidemiological data.
- Indoor levels exceeding the levels of health concern (NOAEL – no observed adverse effect level and/or LOAEL – lowest observed adverse effect level).

The substances initially selected based on these criteria as requiring specific attention in relation to the indoor environment were: benzene, carbon monoxide, formaldehyde, naphthalene, nitrogen dioxide, particulate matter ($PM_{2.5}$ and PM_{10}), polycyclic aromatic hydrocarbons (especially benzo-[*a*]-pyrene), radon, tetrachloroethylene, and trichloroethylene. Later, however, particulate matter – $PM_{2.5}$ and PM_{10} – was included in the list of the pollutants covered by the same outdoor and indoor air quality guidelines. In this chapter we discuss all these pollutants, including particulate matter, since exposure to particulate matter is one of the most significant environmental risks factors (GBD 2019).

The pollutants covered by the WHO *Air Quality Guidelines: Global Update 2005: particulate matter, ozone, nitrogen dioxide, and sulfur dioxide* (WHO 2006) are regarded as not requiring specific attention in regard to indoor air: O₃, lead, and SO₂. Therefore, the same numerical health guidelines apply to both outdoor and indoor environments in relation to these pollutants (now provided by [WHO 2021]). While all three of these pollutants also originate from indoor sources, outdoor air is typically their main source in indoor environments, and the chemical structure of their molecules is the same, whether originating from indoor or outdoor sources.

Organic Indoor Air Pollutants

In relation to the impact of the organic air pollutants (benzene, formaldehyde, naphthalene, and polycyclic aromatic hydrocarbons, including especially benzo-[*a*]-pyrene, tetrachloroethylene, and trichloroethylene), the list of effects includes: carcinogenicity, co-carcinogenicity, mucus coagulation, cilia toxicity, increased allergic sensitization, increased airway reactivity, eye, throat or nose irritation, headache, cough, and fatigue. While it is outside the scope of this chapter to discuss these effects in more detail, they are comprehensively covered by the guideline document. The indoor sources of these pollutants include – *benzene*: tobacco smoke, solvents used for hobbies or cleaning, or using building materials that off-gas benzene; *formaldehyde*: particleboard, insulation, furnishing, tobacco smoke, gas stoves, and consumer products; *naphthalene*: naphthalene mothballs, but also the combustion of biomass; *polycyclic aromatic hydrocarbons*: mainly combustion, including cooking smoking, candle burning, etc; *trichloroethylene*: using wood stains, varnishes, lubricants, paint removers, etc; and *tetrachloroethylene*: cleaning solvent and dry cleaning agents.

Inorganic Indoor Gaseous Pollutants: CO and NO₂ and Radon

In contrast, CO was included in the WHO Air Quality Guidelines for Europe, 2nd ed. (WHO 2000), and NO₂ was included in the WHO *Air Quality Guidelines: Global Update 2005: particulate matter, ozone, nitrogen dioxide, and sulfur dioxide* (WHO 2006). The two pollutants were in turn included in the WHO *Guidelines for Indoor Air Quality, Selected Pollutants* (WHO 2010), considering the different nature of exposure to these gases in indoor environments. Briefly, exposure to CO results in a reduction of oxygen delivery to tissues, owing to the formation of carboxyhemoglobin, and its indoor sources include tobacco smoke, faulty appliances (e.g., furnaces and hot water heaters), clogged chimneys, and automobile exhaust in houses with attached garages. Chronic health effects may be present for low concentrations of CO and sudden death can occur at high levels of the gas. Nitrogen dioxide exposure may lead to the occurrence of respiratory health effects, including short-term effects due to peak concentrations, particularly in susceptible individuals (asthmatics), as well as long-term effects on the incidence and prevalence of respiratory disease, primarily among children. Its indoor sources mainly include unvented combustion appliances, such as gas stoves, kerosene heaters, etc.

Radon, mainly ²²²Rn, is a naturally occurring noble radioactive gas which is classified by the International Agency for Research on Cancer (IARC) as a human carcinogen, which emanates and penetrates to indoor air from rocks, soil, groundwater, and also building materials. The radiation released, mainly from alpha decay of short-lived decay products within the lungs, imparts on the lung a dose to which an increased risk of lung cancer can be attributed. The WHO has identified radon as the highest priority area for reducing environmental radiation risk and in 2009 they launched the *WHO Radon Handbook* which gives a comprehensive overview on the radon problem (Zeeb et al. 2009).

Particulate Matter: PM_{2.5} and PM₁₀

There are still many questions remaining regarding PM, with one of them being whether there is convincing evidence for a difference in risk caused by PM from indoor sources, as compared with those from outdoors. One complexity is that ambient air is a significant contributor to indoor PM, whereby indoor concentrations are of the order of 50% of ambient concentrations, in the absence of any indoor sources. However, when indoor sources are present, the indoor levels of PM are usually higher than the outdoor levels. A large number of indoor particle sources were identified and emissions from these sources were investigated by many studies reported in the literature, e.g., He et al. (2004). Combustion processes are the main indoor sources of smaller particles, with the majority of them (in terms of number) in the ultrafine size range (<0.1 µm), containing a host of organic and inorganic material (Morawska and Zhang 2002). Other sources or human activities contributing to elevated levels of indoor ultrafine particles include vacuuming, cleaning using detergents, showering, operation of electric motors, and operation of printing and photocopying devices (Monn et al. 1995; Tucker 2000). Resuspension of particles by human movement, on the other hand, contributes to the coarse mode of indoor

particles, usually in the supermicrometer size (He et al. 2004). Contributions of different sources to different particle metrics (particle mass or particle number concentration), and different particle size ranges, were reviewed and summarized by Morawska et al. (2017). The analysis of the data available in literature showed that the key source contribution varies between different indoor environments. In particular, the main source of residential PM₁₀ and PM_{2.5} is outdoor; ultrafine particles (measured as particles number concentration) are generated predominantly by indoor sources, which is opposite to schools and day cares, for which ultrafine particles originate from outside, but PM₁₀ and PM_{2.5} originate from indoor sources, and for offices, particles of all sizes originate mainly from outdoors.

Health effects due to exposure to particulate matter include: decreased lung function, increased respiratory symptoms, increased chronic obstructive pulmonary disease, increased cardiovascular and cardiopulmonary disease, and increased all cause and cause-specific mortality. A large body of evidence on health effects associated with exposure to PM₁₀ and PM_{2.5} since publication of WHO *Air Quality Guidelines: Global Update 2005: particulate matter, ozone, nitrogen dioxide, and sulfur dioxide* (WHO 2006), which was used in the current update of the WHO *Global Air Quality Guidelines: particulate matter (PM_{2.5} and PM₁₀), ozone, nitrogen dioxide, sulfur dioxide, and carbon monoxide* (WHO 2021).

Summary of the IAQ Numerical Guideline Values

Table 1 summarizes WHO IAQ guideline values based on WHO *Guidelines for Indoor Air Quality, Selected Pollutants* (WHO 2010). Included in the table are also guideline values for PM_{2.5} and PM₁₀, NO₂, and CO based on the WHO *Global Air Quality Guidelines: particulate matter (PM_{2.5} and PM₁₀), ozone, nitrogen dioxide, sulfur dioxide, and carbon monoxide* (WHO 2021), as well as NO₂ and CO for the averaging times that are covered by WHO *Air Quality Guidelines: Global Update 2005: particulate matter, ozone, nitrogen dioxide, and sulfur dioxide* (WHO 2006).

National Standards

National air quality standards are enacted based on the potential for health and economic effects of the identified pollutants. We conducted a comprehensive Internet search to identify any existing indoor air quality national standards or guidelines. Unlike literature searches for referred journal papers, we could not use databases such as Web of Science, Scopus, etc. to identify national standards. Our search was also limited to English and Chinese language published documents; countries in which English is not spoken will not necessarily have their standards published in English (but some European Union [EU] countries have). While our search was comprehensive, we cannot exclude that we missed some countries' national regulations due to, for example, different terminology used or the indoor air regulations being imbedded into other types of broader regulations.

Table 1 Guideline values, as well as critical health outcomes of the indoor air pollutants included in the WHO *Guidelines for Indoor Air Quality, Selected Pollutants* (WHO 2010)⁽¹⁾, on particulate matter, NO₂, and CO averaging times based on the WHO Global Air Quality Guidelines: particulate matter ($PM_{2.5}$ and PM_{10}), ozone, nitrogen dioxide, sulfur dioxide, and carbon monoxide (WHO 2021)⁽²⁾, and on NO₂ and CO that are covered by WHO Air Quality Guidelines: Global Update 2005: particulate matter, ozone, nitrogen dioxide, and sulfur dioxide (WHO 2006)⁽³⁾

Pollutant	Guideline value	Critical outcome ^a
Benzene ⁽¹⁾	No safe level of exposure can be recommended Unit risk of leukaemia per 1 $\mu\text{g}/\text{m}^3$ air concentration is 6×10^{-6} The concentrations of airborne benzene associated with an excess lifetime risk of 1/10,000, 1/100,000 and 1/1,000,000 are 17, 1.7, and 0.17 $\mu\text{g}/\text{m}^3$, respectively	Acute myeloid leukemia (sufficient evidence on causality) Genotoxicity
Carbon ⁽¹⁾ monoxide Carbon ⁽²⁾ monoxide	15 min – 100 mg/m^3 1 h – 35 mg/m^3 8 h – 10 mg/m^3	Acute exposure-related reduction of exercise tolerance and increase in symptoms of ischemic heart disease (e.g., ST-segment changes)
	24 h – 4 mg/m^3	Association with hospital admissions and mortality from myocardial infarction
Formaldehyde ⁽¹⁾	0.1 mg/m^3 –30-min average	Sensory irritation
Naphthalene ⁽¹⁾	0.01 mg/m^3 – annual average	Respiratory tract lesions leading to inflammation and malignancy in animal studies
Nitrogen dioxide ⁽³⁾ Nitrogen dioxide ⁽²⁾	200 $\mu\text{g}/\text{m}^3$ –1 h average	Respiratory symptoms, bronchoconstriction, increased bronchial reactivity, airway inflammation, and decreases in immune defence, leading to increased susceptibility to respiratory infection
	10 $\mu\text{g}/\text{m}^3$ – annual average 25 $\mu\text{g}/\text{m}^3$ –24-h average	Nonaccidental mortality, cause-specific, and respiratory mortality
Polycyclic aromatic hydrocarbons ⁽¹⁾	No threshold can be determined, and all indoor exposures are considered relevant to health Unit risk for lung cancer for PAH mixtures is estimated to be 8.7×10^{-5} per ng/m^3 of B[a]P The corresponding concentrations for lifetime exposure to B[a]P producing excess lifetime cancer risks of 1/10,000, 1/100,000, and 1/1,000,000 are approximately 1.2, 0.12, and 0.012 ng/m^3 , respectively	Lung cancer

(continued)

Table 1 (continued)

Pollutant	Guideline value	Critical outcome ^a
Radon ⁽¹⁾	The excess lifetime risk of death from radon-induced lung cancer (by the age of 75 years) is estimated to be 0.6×10^{-5} per Bq/m ³ for lifelong nonsmokers and 15×10^{-5} per Bq/m ³ for current smokers (15–24 cigarettes per day); among ex-smokers, the risk is intermediate, depending on time since smoking cessation The radon concentrations associated with an excess lifetime risk of 1/100 and 1/1000 are 67 and 6.7 Bq/m ³ for current smokers and 1670 and 167 Bq/m ³ for lifelong nonsmokers, respectively	Lung cancer suggestive evidence of an association with other cancers, in particular leukemia and cancers of the extra thoracic airways
Trichloroethylene ⁽¹⁾	Unit risk estimate of 4.3×10^{-7} per µg/m ³ The concentrations of airborne trichloroethylene associated with an excess lifetime cancer risk of 1:10,000, 1:100,000, and 1:1,000,000 are 230, 23, and 2.3 µg/m ³ , respectively	Carcinogenicity (liver, kidney, bile duct, and non-Hodgkin's lymphoma), with the assumption of genotoxicity
Tetrachloroethylene ⁽¹⁾	0.25 mg/m ³ – annual average	Effects in the kidney indicative of early renal disease and impaired performance
PM _{2.5} ⁽²⁾	1 year, 5 µg/m ³ 24 h, 15 µg/m ³	All-cause, cardiovascular, respiratory, and lung cancer mortality
PM ₁₀ ⁽²⁾	1 year, 15 µg/m ³ 24 h, 45 µg/m ³	All-cause, cardiovascular, respiratory, and lung cancer mortality

^aBesides these outcomes, there are other health effects of the exposure to each of the considered pollutants. The critical outcomes were selected for the risk assessment of the exposure to given pollutant with the assumption (based on available evidence) that the reduction of exposure to prevent this critical health outcome prevents other health outcomes of the exposure as well

Based on the Internet search, we found that not all countries have their own national standards or guidelines. There is no directive guideline or standard at the EU level, but there are national guidelines in some European countries, including the guideline or target values in the UK (Shrubsole et al. 2019), France (France 2020), Germany (Bundesamt 2021), and Belgium (De Brouwere et al. 2020). Table 2 presents a summary of national standards or guidelines for IAQ management or monitoring and Table 3 tabulates pollutants and their limit values for the countries that have national standards, guidelines, or targets.

We have also separately listed the countries which state that they do not have national standards. Those countries in alphabetic order include: Albania, Algeria, Andorra, Angola, Argentina, Armenia, Australia, Austria, Azerbaijan, Bahrain, Bangladesh, Bahamas, Barbados, Belarus, Benin, Bhutan, Bolivia, Bosnia and Herzegovina, Botswana, Brunei, Bulgaria, Burkina Faso, Burundi, Cambodia, Cameroon, Capo Verde, Central African Republic, Chad, Chile, Colombia, Comoros, Congo, Cote d'Ivoire, Croatia, Cyprus, Czech Republic, Democratic Republic of Congo, Denmark, Djibouti, Ecuador, Egypt, Equatorial Guinea, Eritrea, Estonia, Eswatini, Ethiopia, Falkland Islands, Finland, French Guiana, Gabon, Gambia, Georgia, Ghana, Greece, Guinea, Guyana, Iceland, Iran, Ireland, Italy, Jamaica, Jordan, Kazakhstan, Kenya, Kyrgyzstan, Latvia, Laos, Lebanon, Lesotho, Liberia, Libya, Liechtenstein, Lithuania, Luxembourg, Madagascar, Malawi, Maldives, Mali, Malta, Mauritania, Mauritius, Mayotte, Moldova, Monaco, Mongolia, Montenegro, Morocco, Mozambique, Myanmar, Namibia, the Netherlands, New Zealand, Niger, Nigeria, North Macedonia, Oman, Pakistan, Paraguay, Peru, Philippines, Qatar, Réunion, Romania, Rwanda, Saint Helena, San Marino, Sao Tome and Principe, Senegal, Serbia, Seychelles, Sierra Leone, Singapore, Slovakia, Slovenia, Somalia, South Africa, South Sudan, Sri Lanka, State of Palestine, Sudan, Suriname, Switzerland, Syria, Tajikistan, Tanzania, Thailand, Timor-Leste, Togo, Trinidad and Tobago, Tunisia, Turkmenistan, Turkey, Uganda, Ukraine, United Arab Emirates, Uruguay, Venezuela, Vietnam, Western Sahara, Zambia, Zimbabwe, etc.

Although there are no specific policies in these countries, in some of the countries actions are being taken to comply with other countries' air quality standards or other type of indoor air regulations. For example, in Singapore, building owners, facility managers, and occupants all have liability in maintaining indoor air quality for the health and comfort of occupants in buildings. In Bahamas, the government regularly compare local air quality levels with the US air quality index values.

Different environments in different countries, as well as different factors considered in health and economic assessments of the impact of indoor air pollution, can result in different pollutants to be included in national standards or guidelines across countries. Most national guideline or standard threshold values are enacted in consideration with exposure level that is undesirable for health; however, the numerical values for the same pollutant can be different across countries. For example, in Germany, Guide value II (RW II) is an effect-related value based on current toxicological and epidemiological evidence of a substance's effect threshold with uncertainty factors considered. Guide value I (RW I) represents the concentration of a substance in indoor air for which, when considered individually, there is no evidence at present that even lifelong exposure is expected to bear any adverse health impacts. In India, three levels of threshold values have been defined as aspirational (Class A), acceptable (Class B), and marginally acceptable (Class C).

An important question is how the national indoor air quality guideline or standard values for individual pollutants relate to the WHO guideline values for these pollutants. To answer this question, in Fig. 1a, b, we compare national threshold values to the WHO ones, for PM ($PM_{2.5}$ and PM_{10}) and CO, respectively. An interesting observation from Fig. 1a is that while for PM_{10} the regulatory threshold

Table 2 Summary of National Standards or Guidelines for Indoor Air Quality Management or Monitoring in individual countries, or indicated as potential standards/guidelines(*)

Country	Document title	Links to the document
Belgium	Establishing target and intervention guidance values for indoor air in dwellings and publicly accessible buildings: The Flemish approach	https://doi.org/10.1016/j.ijheh.2020.113579
Brazil*	Guidelines for Indoor Air Quality (IAQ) in Nonindustrial and Nonspecialized Settings	https://www.semanticscholar.org/paper/GUIDELINES-FOR-INDOOR-AIR-QUALITY-IN-OFFICES-IN-Neto-Siqueira/b8e2fe3fbe093c81542947377ef0caecf8682e29
Canada	Residential Indoor Air Quality Guidelines	https://www.canada.ca/en/health-canada/services/air-quality/residential-indoor-air-quality-guidelines.html
China	Indoor Air Quality Standard (GB/T 1883—2002)	http://www.mee.gov.cn/image20010518/5295.pdf (in Chinese)
France	Indoor Air Quality Action Plan	https://www.ecologie.gouv.fr/sites/default/files/Plan_QAI_23_10_2013.pdf (in French)
German	German Committee on Indoor Guide Values	https://www.umweltbundesamt.de/en/topics/health/commissions-working-groups/german-committee-on-indoor-guide-values
Hong Kong China	Indoor Air Quality Monitoring Guideline for Office and Public Buildings (2003)	https://www.iaq.gov.hk/media/8688/certguide-chi.pdf (in Chinese)
Hungary	National Indoor Air Quality Action Plan (Version 1, 2018)	https://www.interreg-central.eu/Content.Node/InAirQ/National-IAQ-Action-Plan-Hungary.pdf
India	Indoor Environmental quality Standard(2nd Version:2018–2019)	https://ishrae.in/Content/Download/ISHRAE_IEQ_Feb_26_2019_public_draft.pdf
Japan	Law of Maintenance of Sanitation in Building	To be found
Korea	Issues on indoor air quality in Korea	http://www.zyaura.com/quality/Archives/Recently%20issues%20on%20Indoor%20air%20quality%20in%20Korea%5B1%5D.pdf
Kuwait	Indoor air pollution and exposure assessment of the gulf cooperation council countries: A critical review	https://www.sciencedirect.com/science/article/pii/S0160412018318142
Norway*	Guidelines for indoor air in Norway – a practical approach Recommended Guidelines for Indoor Air Quality	http://lodel.irevues.inist.fr/pollutionatmospherique/docannexe/file/3772/245_becher.pdf
Poland	Indoor Air Quality Action Plan – School Environment (Version 5.0, 2019)	https://www.interreg-central.eu/Content.Node/InAirQ/National-IAQ-Action-Plan-Poland.pdf
Portugal*	Indoor Air Quality in Portugal: Technical, Institutional, and Policy Challenges in the	https://www.witpress.com/Secure/elibrary/papers/AIR07/AIR07056FU1.pdf

(continued)

Table 2 (continued)

Country	Document title	Links to the document
	Implementation of the Directive on the Energy Performance of Buildings (work in progress)	
Russia*	Standards and Laws for Indoor Air Quality in Russia	https://doi.org/10.1159/000463337
Spain*	Indoor air quality regulations: The Spanish case	https://www.aiev.org/resource/indoor-air-quality-regulations-spanish-case
Sweden*	Sweden Air Quality Policies	https://wedocs.unep.org/bitstream/handle/20.500.11822/17118/Sweden.pdf?sequence=1&isAllowed=y
UK	Indoor Air Quality Guidelines for selected volatile organic compounds (VOCs) in the UK	https://assets.publishing.service.gov.uk/government/uploads/system/uploads/attachment_data/file/831319/VO_statement_Final_12092019_CS_1_.pdf

for four out of six countries that have regulations, significantly exceed the WHO values, for PM_{2.5} by contrast, only in one out of six countries the national threshold value exceeded this of WHO, while in four countries, the national thresholds are lower than the WHO ones. However, CO national guideline/standard values are all one (out of nine countries) higher than WHO guideline levels.

Another important question is the enforcement of indoor air quality national regulations. The first element of enforcement is compliance monitoring of the concentration levels of the regulated pollutants. Compliance monitoring of ambient air pollution is conducted at networks of air monitoring stations, usually operated by the relevant authorities, or by organizations mandated to do so. Measurements from a set number of central monitoring stations are considered for this purpose as representative of the entire area the network covers. In contrast, compliance monitoring of indoor air quality would require monitoring to be conducted in every building or in several locations within the building, as no central indoor monitoring would be representative of air quality in the entire local building stock. Therefore, indoor air monitoring is usually not conducted on a routine manner, which means there is no enforcement of indoor air quality regulations (UNEP 2021). A particularly difficult case regarding enforcement is, if the pollutant in question is generated predominantly outdoors, from where it penetrates indoors. This is the case in relation to PM_{2.5} and PM₁₀, in homes, and offices, as discussed above, based on a review by Morawska et al. (2017). This is also the case in many air pollution episodes, such as bushfires are haze episodes. In such situations controlling indoor air quality may be difficult or impossible, if the building does not have an efficient mechanical ventilation system.

It is somewhat easier to compare regulatory values and the averaging times for the so-called criteria pollutants (PM and gaseous pollutants: CO, NO_x, O₃, and SO₂), then for organic compounds. Due to the complex structure and toxicity of organic matter in indoor environments, we have summarized national standards of major

Table 3 Summary on threshold or guideline values for common pollutants in National Indoor Air Quality Standards or Guidelines^a

Country	PM _{2.5}	Ozone, O ₃	Nitrogen dioxide, NO ₂	Sulfur dioxide, SO ₂	Carbon dioxide, CO ₂	Carbon monoxide, CO
Belgium	Lifetime exposure – 10 µg/m ³	Lifetime exposure – 40 µg/m ³	Lifetime exposure – 20 µg/m ³			24 h – 8 mg/m ³ intervention value
Canada	As low as possible	8 h – 40 µg/m ³	24 h – 20 µg/m ³ 1 h – 170 µg/m ³			24 h – 11.5 mg/m ³ 1 h – 28.6 mg/m ³
China	24 h – 150 µg/m ³	1 h – 160 µg/m ³	1 h – 240 µg/m ³	1 h – 500 µg/m ³	24 h – 0.10%	1 h – 10 mg/m ³
German			1 h – GVI: 80 µg/m ³ ; GVI: 250 µg/m ³			
Hong Kong China	8 h – 180 µg/m ³	8 h – 120 µg/m ³	8 h – 150 µg/m ³		8 h – 1000 ppm	8 h – 10 mg/m ³
Hungary	24 h – 25 µg/m ³	24 h – 50 µg/m ³	7 days – 80 µg/m ³ 24 h – 50 µg/m ³	7 days – 40 µg/m ³ 24 h – 100 µg/m ³ 1 h – 200 µg/m ³	7 days – 1500 ppm	7 days – 80 mg/m ³ 24 h – 30 mg/m ³

India	Class A: 15 µg/m ³ Class B: 25 µg/m ³ Class C: 25 µg/m ³	Class A: 50 µg/m ³ Class B: 100 µg/m ³ Class C: 100 µg/m ³	Class A: 50 µg/m ³ Class B: 100 µg/m ³	Class A: 40 µg/m ³ Class B: 80 µg/m ³	Class A: 40 µg/m ³ Class B: 80 µg/m ³	Class A: Ambient +350 ppm Class B: Ambient +500 ppm Class C: Ambient +700 ppm	Class A: 2 ppm Class B: 9 ppm Class C: 9 ppm
Japan		150 µg/m ³	120 µg/m ³	0.06 ppm	0.05 ppm	1000 ppm	10 ppm
Korea		150 µg/m ³				1000 ppm	10 ppm
Kuwait	8 h – 40 µg/m ³	1 h – 235 µg/m ³ 8 h – 200 µg/m ³ 24 h – 120 µg/m ³ 1 year – 60 µg/m ³	30 min – 660 µg/m ³ 1 h – 200 µg/m ³ 24 h – 100 µg/m ³	8 h – 50 µg/m ³	1 h – 9689 mg/m ³ 24 h – 2713 mg/m ³ 1 year – 581 mg/m ³	30 min – 60 mg/m ³ 1 h – 30 mg/m ³ 8 h – 10 mg/m ³	
Norway	24 h – 20 µg/m ³						
Poland	10 µg/m ³						
						1200 ppm	

a The units are listed exactly as they are provided in the National Standards

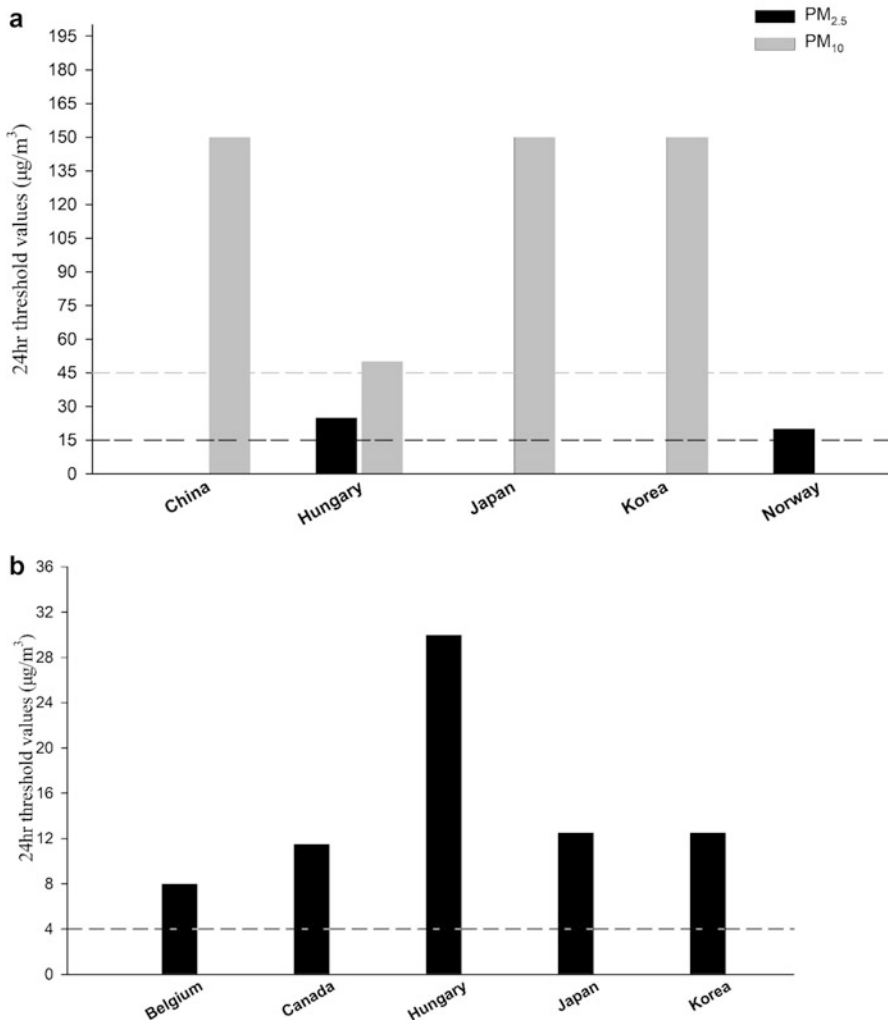


Fig. 1 (a) The 24 h threshold or guideline values for PM_{2.5} and PM₁₀ in several national indoor air quality standards in comparison with WHO guidelines of 15 µg/m³ for PM_{2.5} and 45 µg/m³ for PM₁₀. (b) The 24 h threshold or guideline values for CO in several national indoor air quality standards in comparison with WHO guidelines of 4 mg/m³

organic compounds considered by WHO indoor guidelines in Table 4. As radon has been identified as the highest priority for reducing indoor environmental radiation risk in many countries, we have also included the threshold values of radon in Table 4.

Reviewing the information presented in Table 4, it can be seen firstly that only a relatively small number of 14 countries has national regulations regarding indoor organic airborne pollutants. Secondly, the threshold values differ significantly

Table 4 Summary on threshold or guideline values for organic and radioactive pollutant of national indoor air quality standards or guidelines

Country	Benzene 0.4 µg/m ³ Intervention value	Formaldehyde 100 µg/m ³ Intervention value	Naphthalene 3 µg/m ³	Trichloroethylene 0.2 µg/m ³	Tetrachloroethylene 4 µg/m ³	PAHs 0.012 ng/m ³	TVOCs 300 µg/m ³	Radon 200 Bq/m ³
Belgium								
Canada	As low as possible	8 h – 50 µg/m ³ 1 h – 123 µg/m ³			40 µg/m ³			200 Bq/m ³
China	1 h – 110 µg/m ³	1 h – 100 µg/m ³					8 h – 600 µg/m ³	400 Bq/m ³
Germany		GVI: 100 µg/m ³			GVI: 100 µg/m ³ ; GVII: 1000 µg/m ³		GVI: 200–300 µg/m ³ ; GVII: 1000–3000 µg/m ³	250
Hong Kong China	16.1 µg/m ³	8 h – 100 µg/m ³		770 µg/m ³	250 µg/m ³		8 h – 600 µg/m ³	200
Hungary	7 days – 5 µg/ m ³ 24 h – 10 µg/m ³	7 days – 30 µg/m ³ 24 h – 50 µg/m ³		7 days – 10 µg/m ³	7 days – 250 µg/m ³			400
India	3 µg/m ³	30 µg/m ³	9 µg/m ³	600 µg/m ³	35 µg/m ³		Class A: 200 µg/m ³ Class B: 400 µg/m ³ Class C: 500 µg/m ³	

(continued)

Table 4 (continued)

Country	Benzene	Formaldehyde	Naphthalene	Trichloroethylene	Tetrachloroethylene	PAHs	TVOCs	Radon
Japan	0.08 ppm						400 µg/m ³	
Korea	0.1 ppm						500 µg/m ³	
Kuwait	30 min – 120 µg/m ³					1 h – 5000 ppm		
	8 h – 52.9 µg/m ³					24 h – 1400 ppm		
Norway								200
Poland	1.7 µg/m ³	10 µg/m ³						
United Kingdom	As low as possible	30 m – 100 µg/m ³	1 year – 10 µg/m ³	1 year – 10 µg/m ³	As low as possible	24 h – 40 µg/m ³		200

between countries. However, it is outside the scope of this work to analyze in detail the differences and the rationale of different countries to select specific values.

Summary

Health guidelines for indoor air quality that developed and published by WHO following systematic reviews on evidence from medical and public health studies and through extensive expert panel discussion and consultation have provided an important foundation for countries to develop their national indoor air standards. Nevertheless, globally, only several countries have promulgated national indoor air quality standards or health guidelines, and in many cases the threshold values are higher than the current WHO guideline levels. Given the importance of air quality in indoor environments where people spend most of their time, developing health evidence-based national indoor air quality standard or guideline development to reduce indoor exposure is of paramount significance in terms of public health protection, particularly in low- and middle-income countries (LIMCs) with poorer indoor air quality.

References

- Andrews C, Buist AS, Ferris B (1985) Guidelines as to what constitutes an adverse respiratory health effect, with special reference to epidemiologic studies of air pollution. American Thoracic Society. Am Rev Respir Dis 131:666–668
- Bundesamt U (2021) German committee on indoor guide values
- De Brouwere K, Bautmans B, Benoy S, Geerts L, Stranger M, Van Holderbeke M (2020) Establishing target and intervention guidance values for indoor air in dwellings and publicly accessible buildings: the Flemish approach. Int J Hyg Environ Health 230:113579
- France EGd (2020) Qualité de l'air intérieur
- GBD (2019) Global Burden of Disease (GBD) visualization hub. Institute for Health Metrics and Evaluation (IHME)
- He C, Morawska L, Hitchins J, Gilbert D (2004) Contribution from indoor sources to particle number and mass concentrations in residential houses. Atmos Environ 38:3405–3415
- Khvalyag D, Kazanci OB, Halvorsen H, Gundlach I, Bahmfleth WP, Toftum J, Olesen BW (2020) Critical review of standards for indoor thermal environment and air quality. Energ Buildings 213:109819
- Monn C, Fuchs A, Kogelschatz D, Wanner H-U (1995) Comparison of indoor and outdoor concentrations of PM-10 and PM-2.5. J Aerosol Sci 26:S515–S516
- Morawska L, Zhang JJ (2002) Combustion sources of particles. 1. Health relevance and source signatures. Chemosphere 49:1045–1058
- Morawska L, Ayoko G, Bae G, Buonanno G, Chao C, Clifford S, Fu SC, Hänninen O, He C, Isaxon C (2017) Airborne particles in indoor environment of homes, schools, offices and aged care facilities: the main routes of exposure. Environ Int 108:75–83
- Naugle DF, Pierson TK (1991) A framework for risk characterization of environmental pollutants. J Air Waste Manage Assoc 41:1298–1307
- Samet J, Buist S, Bascom R, Garcia J, Lipsett M, Mauderly J, Mannino D, Rand C, Romieu I, Utell M (2000) What constitutes an adverse health effect of air pollution? American Thoracic Society. Am J Respir Crit Care Med 161:665–673

- Shrubsole C, Dimitroulopoulou S, Foxall K, Gadeberg B, Doutsi A (2019) IAQ guidelines for selected volatile organic compounds (VOCs) in the UK. *Build Environ* 165:106382
- Tucker WG (2000) An overview of PM_{2.5} sources and control strategies. *Fuel Process Technol* 65: 379–392
- UNEP (2021) Regulating air quality: the first global assessment of air pollution legislation. Air pollution series. UN Environmental Program (UNEP), Nairobi
- WHO (1972) Definition of adverse effect according to the report of the WHO: air quality criteria and guides for urban air pollutants. Technical report series no. 506. World Health Organization, Geneva
- WHO (1978) Distinctions between adverse and non-adverse effects according to EHC 6: principles and methods for evaluating the toxicity of chemicals. World Health Organization, Geneva
- WHO (1979) Sulfur dioxides and suspended particulate matter, environmental health criteria no. 8. World Health Organization, Geneva
- WHO (1987) Air quality guidelines for Europe, European series no. 23. World Health Organization, Copenhagen
- WHO (2000) Air quality guidelines for Europe, 2nd edn. World Health Organisation, Regional Office for Europe
- WHO (2006) Air quality guidelines: global update 2005: particulate matter, ozone, nitrogen dioxide and sulfur dioxide. World Health Organization. Regional Office for Europe
- WHO (2009) Guidelines for indoor air quality: dampness and mould. World Health Organization for Europe
- WHO (2010) Guidelines for indoor air quality, selected pollutants. World Health Organization, Geneva
- WHO (2014) Guidelines for indoor air quality: household fuel combustion. World Health Organization
- WHO (2017) Evolution of WHO air quality guidelines: past, present and future. World Health Organization. Regional Office for Europe
- WHO (2021) WHO global air quality guidelines: particulate matter (PM_{2.5} and PM₁₀), ozone, nitrogen dioxide, sulfur dioxide and carbon monoxide. World Health Organization, Geneva
- Zeeb H, Shannoun F, WHO (2009) WHO handbook on indoor radon: a public health perspective. World Health Organization



ASTM and ASHRAE Standards for the Assessment of Indoor Air Quality

53

Xiaoyu Liu

Contents

Introduction	1512
IAQ Test Standards	1515
Overview	1515
ASTM Methods Developed by Subcommittee on Indoor Air	1515
ASTM Methods Developed by Other Subcommittees	1518
ISO Methods Developed by ISO TC 146/SC 6 Indoor Air Subcommittee	1519
US EPA Methods	1521
Government Regulations	1521
Other Frequently Used Standards	1522
ASTM Test Standards	1523
ASHRAE Standards	1527
ASHRAE 62.1	1528
ASHRAE 62.2	1533
Applications	1536
Priority Areas for Future Standardization Related to IAQ Testing	1536
Conclusions	1541
Cross-References	1541
References	1542

Abstract

With the rapid development of high technology and indoor health problems in the modern world, indoor air quality (IAQ) becomes a matter of great concern to building occupants, building industry, manufacturers, national, state, and local government agencies, and other relevant entities. Utilizing harmonized consensus test standards is essential to characterize indoor pollutants and investigate indoor environmental conditions for assessing and improving IAQ and reducing occupants' risk of exposure and adverse health effects. This chapter elaborates on

X. Liu (✉)

Office of Research and Development, Center for Environmental Measurement & Modeling,
U.S. Environmental Protection Agency, Research Triangle Park, NC, USA
e-mail: liu.xiaoyu@epa.gov

consensus test standards that are widely used in the USA to assess IAQ-related issues, specifically highlighting the standards from ASTM International and Standard 62.1 and 62.2 of the American Society of Heating, Refrigerating, and Air-Conditioning Engineers (ASHRAE). ASTM methods help source control of indoor air pollutants for IAQ, whereas ASHRAE standards address the control and assessment of IAQ and ventilation of commercial and residential buildings for IAQ management. Primary focuses of this chapter are ASTM methods for indoor air sampling and analysis, emission and material testing, IAQ evaluation and exposure assessment, and the ventilation calculation methods and procedures in ASHRAE Standards 62.1 and 62.2. The IAQ acceptable limits and ventilation requirements are out of the scope of this chapter. Other standards discussed include US Environmental Protection Agency methods, International Organization for Standardization standards, and others. Recommendations of future standardization efforts comprises standards for exposure test protocols, new and advanced sampling and analysis methods, emerging contaminant measurements, indoor air modeling, and updates of ASHRAE standards.

Keywords

ASTM standard · ASHRAE standard · Consensus standards · Emission testing · Ventilation

Introduction

In the modern world, green building movements to improve energy efficiency, advances in construction technology using synthetic materials, and increase use of varied chemicals in building materials and consumer products have contributed to a more comfortable life while at the same time potentially producing high concentrations of indoor air pollutants (Liu 2018). Indoor air pollutants and indoor environment have significant impacts on human health since people spend nearly 90% of their time indoors. Human exposure to indoor air pollution has the potential to cause acute and chronic adverse health effects, especially for sensitive populations like children and the elderly. In addition, poor indoor air quality (IAQ) directly affects occupant quality of life and productivity. IAQ includes consideration of both indoor air pollution levels and thermal environmental parameters (ASHRAE 2009). This potential increase on indoor pollution and its greater health impact invokes the desire for better IAQ through control of temperature, humidity, ventilation, and airborne contaminants in the indoor environment. Emissions from building materials, furnishings, consumer products, and indoor equipment, and entry of outdoor contaminants along with human activities, airborne particles, settled dust, and indoor radon are all major causes of IAQ problems. Poor air ventilation and inadequate supply of outdoor air to the indoor environment increase indoor pollution. Extreme temperature and humidity could elevate air pollution levels and accelerate growth of bacteria and viruses. During the development of relevant IAQ regulations, guidelines, and

labeling systems, consensus standards play an important role in helping understand the indoor environments in buildings, improving IAQ, and ensuring greener and healthier buildings and indoor environments. This chapter provides an overview of indoor air test standards with the focus on standards of ASTM International and guidance on ventilation from the American Society of Heating, Refrigerating, and Air-Conditioning Engineers (ASHRAE) used by the indoor air research community for the assessment and control of IAQ.

The word “consensus” is defined by the US Office of Management and Budget (OMB) in the OMB Circular A-119 Section 5e as “*general agreement, but not necessarily unanimity. During the development of consensus, comments and objections are considered using fair, impartial, open, and transparent processes*” (OMB 2016). This definition aligns closely to the definition given by American National Standards Institute (ANSI), which is “*substantial agreement reached by directly and materially affected interest categories. This signifies the concurrence of more than a simple majority, but not necessarily unanimity. Consensus requires that all views and objections be considered, and that an effort be made toward their resolution*” (ANSI 2020a). Measurements undertaken using consensus test standards ensure that the data is collected based upon agreed best practice with data quality and uncertainty taken into account, such that they be used nationally and internationally by product manufacturers, consumers, and researchers allowing data comparability. Consensus test standards can help business and industry manufacture safe, reliable, and good quality products while also safeguarding consumers and the end users to minimize potential harm, hazardous exposure, and adverse health effects. Consensus test standards are not mandatory for regulatory compliance, but they could become mandatory if they are incorporated by the government or law enforcement for technical details into a legislation. There are a few voluntary consensus standards bodies in the USA and around the world that oversee or develop voluntary consensus test standards related to IAQ. The following organizations and institutions (in alphabetical order) are well recognized in the development, use, and distribution of test standards related to IAQ issues in the USA.

American Conference of Governmental Industrial Hygienists (ACGIH), (ACGIH 2020a), founded in 1938, is an organization whose members are industrial hygienists or other occupational health and safety professionals. ACGIH is not a standards-setting body. It publishes guidelines based on scientific literature review, known as threshold limit values (TLVs) and biological exposure indices (BEIs), for use by industrial hygienists each year. TLVs for over 700 chemical substances and physical agents and BEIs for more than 50 selected chemicals are currently available for use. TLVs and BEIs are not consensus standards per se, but they are guidelines for safe levels of chemical and physical agents’ exposure in the workplace (ACGIH 2020b).

American Industrial Hygiene Association (AIHA), (AIHA 2020), founded in 1939, is the association for scientists and professionals of occupational and environmental health and safety in the workplace and community. AIHA supports the development and harmonization of national and international industrial/occupational hygiene-related standards.

American National Standards Institute (ANSI), (ANSI 2020b), founded in 1918, oversees the development of voluntary consensus standards for products, services, processes, systems, and personnel in the USA. ANSI itself does not develop standards but accredits the procedures of standards developing organizations (SDOs) and approve documents developed by SDOs as American National Standards. ANSI coordinates US standards with international standards and plays an important role in the US voluntary standards community.

American Society of Heating, Refrigerating, and Air-Conditioning Engineers (ASHRAE), (2020a), was founded in 1894. The current name and organization came from the 1959 merger of the American Society of Heating and Air-Conditioning Engineers (ASHAE) and the American Society of Refrigerating Engineers (ASRE). The society develops and publishes standards and guidelines relating to heating, ventilation, and air-conditioning (HVAC) systems to improve building service engineering, energy efficiency, and IAQ.

ASTM International (ASTM), (2020a), founded in 1898, was formerly known as American Society for Testing and Materials. It is an international standards organization that develops and publishes over 12,000 voluntary consensus technical standards for a variety of systems, services, materials, and products. There are over 140 technical committees within ASTM, among which D22 is the air quality committee with 13 subcommittees including D22.05, the indoor air subcommittee.

Business and Institutional Furniture Manufacturers Association (BIFMA), (2020), founded in 1973, is the not-for-profit trade association for business and institutional furniture manufacturers, which develops, maintains, and publishes safety and performance standards for commercial furniture products.

California Department of Public Health (CDPH), (2020), is a subdivision of the California Health and Human Services Agency. CDPH developed a standard test method, known as the CDPH Standard Method, V1.2-2017. This test method expanded on requirements of the California 01350 Specification developed by the State of California to address IAQ problems related to emissions from building materials (California Department of Resources Recycling and Recovery (CalRecycle) 2019).

US Consumer Product Safety Commission (CPSC), (2020), formed in 1972, is a US federal regulatory agency for consumer product safety. CPSC collaborates with other standard bodies such as Underwriters Laboratories Inc. (UL), ASTM, and others to develop safety standards for consumer products.

International Organization for Standardization (ISO), (2020a), founded in 1947, is the world's largest developer of voluntary international standards composed of 165 national standards bodies and headquartered in Geneva, Switzerland. ISO standards are developed by ISO technical committees (TC) and subcommittees (SC). The organization has published more than 20,000 international standards covering almost every industry.

National Institute for Occupational Safety and Health (NIOSH), (2018) established in 1971, is part of the Centers for Disease Control and Prevention (CDC) within the US Department of Health and Human Services. The institute is a research agency focusing on the study of worker safety and health. NIOSH

publishes the Manual of Analytical Methods (NMAM), which is a frequently updated living document that provides evaluated methods for sampling and analysis of contaminants at workplaces (NIOSH 2020)

Underwriters Laboratories Inc. (UL), (2020a) established in 1894, is an accredited standards developer in the USA and Canada. It has produced over 1500 standards that are used to test and evaluate products, systems, and innovative technologies (UL 2020b).

United States Environmental Protection Agency (US EPA), (2020a) established in 1972, is a US federal agency whose mission is to protect human health and the environment. EPA offices and laboratories develop test methods for the analysis of various environmental media. EPA developed Test Methods for Evaluating Solid Waste: Physical/Chemical Methods, also known as SW-846 (US EPA 2020b), which includes over 200 analytical methods for hazardous and environmental pollutants. EPA also published Compendium of Methods for the Determination of Toxic Organic (TO) Compounds in Ambient Air, which include a set of 17 peer-reviewed, standardized methods for the determination of volatile, semivolatile, and selected toxic organic pollutants in the air (US EPA 2020c).

IAQ Test Standards

Overview

Poor IAQ is often considered to result in human exposure to adverse levels or mixtures of indoor air pollutants or adverse indoor environmental conditions. Indoor air pollutants can be categorized by (1) organic chemicals, including volatile organic compounds (VOCs) and semivolatile organic compounds (SVOCs), emitted from building materials, furnishings, consumer products, and human activities such as cooking, smoking, and cleaning; (2) inorganic gases and other chemicals, e.g. carbon monoxide, nitrogen oxides, and lead; (3) airborne particles and dust; (4) microorganisms such as bacteria, fungi, and viruses; and (5) outdoor sources, such as radon and chemicals entering through vapor intrusion and penetration. Additional environmental conditions contributing to IAQ include temperature, humidity, building pressures induced by air infiltration and/or stack effect, and the presence of natural and/or mechanical ventilation. The IAQ consensus test standards summarized in this section are used by government regulators, industry, consumer groups, and others for IAQ assessment and/or potential remediation. They are also effective tools used for building codes and product labeling.

ASTM Methods Developed by Subcommittee on Indoor Air

The standards listed below were developed by the ASTM Subcommittee D22.05 on Indoor Air (ASTM 2020b). All the ASTM standards cited in this chapter are reprinted with permission from ASTM, copyright ASTM International, 100 Barr

Harbor Drive, and West Conshohocken, PA 19428. A copy of the complete standard may be obtained from ASTM international, <http://www.astm.org>.

- D4861 Standard Practice for Sampling and Selection of Analytical Techniques for Pesticides and Polychlorinated Biphenyls in Air
- D5075 Standard Test Method for Nicotine and 3-Ethenylpyridine in Indoor Air
- D5116 Standard Guide for Small-Scale Environmental Chamber Determinations of Organic Emissions from Indoor Materials/Products
- D5157 Standard Guide for Statistical Evaluation of Indoor Air Quality Models
- D5197 Standard Test Method for Determination of Formaldehyde and Other Carbonyl Compounds in Air (Active Sampler Methodology)
- D5438 Standard Practice for Collection of Floor Dust for Chemical Analysis
- D5466 Standard Test Method for Determination of Volatile Organic Compounds in Atmospheres (Canister Sampling Methodology)
- D5791 Standard Guide for Using Probability Sampling Methods in Studies of Indoor Air Quality in Buildings
- D5955 Standard Test Methods for Estimating Contribution of Environmental Tobacco Smoke to Respirable Suspended Particles Based on UVPM and FPM
- D6177 Standard Practice for Determining Emission Profiles of Volatile Organic Chemicals Emitted from Bedding Sets
- D6178 Standard Practice for Estimation of Short-Term Inhalation Exposure to Volatile Organic Chemicals Emitted from Bedding Sets
- D6196 Standard Practice for Choosing Sorbents, Sampling Parameters and Thermal Desorption Analytical Conditions for Monitoring Volatile Organic Chemicals in Air
- D6245 Standard Guide for Using Indoor Carbon Dioxide Concentrations to Evaluate Indoor Air Quality and Ventilation
- D6271 Standard Test Method for Estimating Contribution of Environmental Tobacco Smoke to Respirable Suspended Particles Based on Solanesol
- D6306 Standard Guide for Placement and Use of Diffusive Samplers for Gaseous Pollutants in Indoor Air
- D6327 Standard Test Method for Determination of Radon Decay Product Concentration and Working Level in Indoor Atmospheres by Active Sampling on a Filter
- D6330 Standard Practice for Determination of Volatile Organic Compounds (Excluding Formaldehyde) Emissions from Wood-Based Panels Using Small Environmental Chambers Under Defined Test Conditions
- D6332 Standard Guide for Testing Systems for Measuring Dynamic Responses of Carbon Monoxide Detectors to Gases and Vapors
- D6333 Standard Practice for Collection of Dislodgable Pesticide Residues from Floors
- D6399 Standard Guide for Selecting Instruments and Methods for Measuring Air Quality in Aircraft Cabins
- D6485 Standard Guide for Risk Characterization of Acute and Irritant Effects of Short-Term Exposure to Volatile Organic Chemicals Emitted from Bedding Sets
- D6669 Standard Practice for Selecting and Constructing Exposure Scenarios for Assessment of Exposures to Alkyd and Latex Interior Paints

- D6670 Standard Practice for Full-Scale Chamber Determination of Volatile Organic Emissions from Indoor Materials/Products
- D6803 Standard Practice for Testing and Sampling of Volatile Organic Compounds (Including Carbonyl Compounds) Emitted from Architectural Coatings Using Small-Scale Environmental Chambers
- D7034 Standard Guide for Deriving Acceptable Levels of Airborne Chemical Contaminants in Aircraft Cabins Based on Health and Comfort Considerations
- D7143 Standard Practice for Emission Cells for the Determination of Volatile Organic Emissions from Indoor Materials/Products
- D7297 Standard Practice for Evaluating Residential Indoor Air Quality Concerns
- D7339 Standard Test Method for Determination of Volatile Organic Compounds Emitted from Carpet Using a Specific Sorbent Tube and Thermal Desorption/Gas Chromatography
- D7706 Standard Practice for Rapid Screening of VOC Emissions from Products Using Microscale Chambers
- D7859 Standard Practice for Spraying, Sampling, Packaging, and Test Specimen Preparation of Spray Polyurethane Foam (SPF) Insulation for Testing of Emissions Using Environmental Chambers
- D7911 Standard Guide for Using Reference Material to Characterize Measurement Bias Associated with Volatile Organic Compound Emission Chamber Test
- D8141 Standard Guide for Selecting Volatile Organic Compounds (VOCs) and Semivolatile Organic Compounds (SVOCs) Emission Testing Methods to Determine Emission Parameters for Modeling of Indoor Environments
- D8142 Standard Test Method for Determining Chemical Emissions from Spray Polyurethane Foam (SPF) Insulation Using Microscale Environmental Test Chambers
- D8283 Standard Practice for Cleaning and Certification of Specially Prepared Canisters

There are currently seven proposed new standards under the jurisdiction of D22.05:

- WK52095 Determination of an Emission Parameter for Phthalate Esters and Other Non-Phthalate Plasticizers from Planar Polyvinyl Chloride Indoor Materials for Use in Mass Transfer Modeling Calculations
- WK58354 Measuring Chemical Emissions from Spray Polyurethane Foam (SPF) Insulation Samples in a Large-Scale Spray Room
- WK58356 Conducting Emission and Fate Modeling for Spray Polyurethane Foam (SPF) Insulation in An Indoor Environment
- WK72782 Environmental Odor Assessment Using Odorant Prioritization with Solid Phase Microextraction (SPME) Air Sampling, Multidimensional Gas Chromatography-Mass Spectrometry (MDGC-MS) Olfactometry Analysis, and Synthetic Odor-Matching Validation
- WK62732 Evaluating PM_{2.5} Sensors or Sensor Systems Used in Indoor Air Applications

WK71196 Measurement Techniques for Formaldehyde in Indoor Air
WK74360 Evaluating CO₂ Indoor Air Quality Sensors or Sensor Systems Used in Indoor Applications

ASTM Methods Developed by Other Subcommittees

The ASTM standards listed below are regularly used for IAQ testing and assessments but were generated by subcommittees other than Subcommittee D22.05, such as Subcommittee D22.01 on Quality Control (ASTM 2020c), Subcommittee D22.08 on Assessment, Sampling, and Analysis of Microorganisms (ASTM 2020d), Subcommittee E06.41 on Air Leakage and Ventilation Performance (ASTM 2020e), Subcommittee D07.03 on Panel Products (ASTM 2020f), Subcommittee D01.28 on Biodeterioration (ASTM 2020g), and Subcommittee C16.31 on Chemical and Physical Properties (ASTM 2020h).

- D1356 Standard Terminology Relating to Sampling and Analysis of Atmospheres (Subcommittee D22.01)
- D6329 Standard Guide for Developing Methodology for Evaluating the Ability of Indoor Materials to Support Microbial Growth Using Static Environmental Chambers (Subcommittee D22.08)
- D7338 Standard Guide for Assessment of Fungal Growth in Buildings (D22.08)
- D7391 Standard Test Method for Categorization and Quantification of Airborne Fungal Structures in an Inertial Impaction Sample by Optical Microscopy (D22.08)
- D7658 Standard Test Method for Direct Microscopy of Fungal Structures from Tape (D22.08)
- D7788 Standard Practice for Collection of Total Airborne Fungal Structures via Inertial Impaction Methodology (D22.08)
- D7789 Standard Practice for Collection of Fungal Material from Surfaces by Swab (D22.08)
- D7910 Standard Practice for Collection of Fungal Material from Surfaces by Tape Lift (D22.08)
- D3273 Standard Test Method for Resistance to Growth of Mold on the Surface of Interior Coatings in an Environmental Chamber (Subcommittee D01.28)
- C1338 Standard Test Method for Determining Fungi Resistance of Insulation Materials and Facings (Subcommittee C16.31)
- E741 Standard Test Method for Determining Air Change in a Single Zone by Means of a Tracer Gas Dilution Active Standard (Subcommittee E06.41)
- E1333 Standard Test Method for Determining Formaldehyde Concentrations in Air and Emission Rates from Wood Products Using a Large Chamber (Subcommittee D07.03)
- D6007 Standard Test Method for Determining Formaldehyde Concentrations in Air from Wood Products Using a Small-Scale Chamber (D07.03)
- E241 Standard Guide for Limiting Water-Induced Damage to Buildings (E06.41 Subcommittee)

-
- E779 Standard Test Method for Determining Air Leakage Rate by Fan Pressurization (E06.41)
- E1827 Standard Test Methods for Determining Airtightness of Buildings Using an Orifice Blower Door (E06.41)

ISO Methods Developed by ISO TC 146/SC 6 Indoor Air Subcommittee

ISO TC 146 (air quality) and specifically subcommittee (SC) 6 (indoor air) have published 50 standards, nine of which (ISO12219:1 to 12219:9) are standards about emission testing for interior parts and materials of road vehicles. The ISO 16000 standards listed here are the standards focusing on indoor air quality issues only (ISO 2020b). They are measurement methods for characterizing emissions in indoor air and procedures for quality assurance/quality control (QA/QC).

- ISO16000-1:2004 Indoor Air – Part 1: General Aspects of Sampling Strategy
- ISO16000-2:2004 Indoor Air – Part 2: Sampling Strategy for Formaldehyde
- ISO16000-3:2011 Indoor Air – Part 3: Determination of Formaldehyde and Other Carbonyl Compounds in Indoor Air and Test Chamber Air – Active Sampling Method
- ISO16000-4:2011 Indoor Air – Part 4: Determination of Formaldehyde – Diffusive Sampling Method
- ISO16000-5:2007 Indoor Air – Part 5: Sampling Strategy for Volatile Organic Compounds (VOCs)
- ISO16000-6:2011 Indoor Air – Part 6: Determination of Volatile Organic Compounds in Indoor and Test Chamber Air by Active Sampling on Tenax TA Sorbent, Thermal Desorption and Gas Chromatography using MS or MS-FID
- ISO16000-7:2007 Indoor Air – Part 7: Sampling Strategy for Determination of Airborne Asbestos Fiber Concentrations
- ISO16000-8:2007 Indoor Air – Part 8: Determination of Local Mean Ages of Air in Buildings for Characterizing Ventilation Conditions
- ISO16000-9:2006 Indoor Air – Part 9: Determination of the Emission of Volatile Organic Compounds from Building Products and Furnishing – Emission Test Chamber Method
- ISO16000-10:2006 Indoor Air – Part 10: Determination of the Emission of Volatile Organic Compounds from Building Products and Furnishing – Emission Test Cell Method
- ISO16000-11:2006 Indoor Air – Part 11: Determination of the Emission of Volatile Organic Compounds from Building Products and Furnishing – Sampling, Storage of Samples, and Preparation of Test Specimens
- ISO16000-12:2008 Indoor Air – Part 12: Sampling Strategy for Polychlorinated Biphenyls (PCBs), Polychlorinated Dibenz-p-dioxins (PCDDs), Polychlorinated Dibenzofurans (PCDFs), and Polycyclic Aromatic Hydrocarbons (PAHs)
- ISO16000-13:2008 Indoor Air – Part 13: Determination of Total (gas and particle-phase) Polychlorinated Dioxin-like Biphenyls (PCBs) and Polychlorinated

- Dibenzo-p-dioxins/dibenzofurans (PCDDs/PCDFs) – Collection on Sorbent-backed Filters
- ISO16000-14:2009 Indoor Air – Part 14: Determination of Total (gas and particle-phase) Polychlorinated Dioxin-like Biphenyls (PCBs) and Polychlorinated Dibenzo-p-dioxins/dibenzofurans (PCDDs/PCDFs) – Extraction, Clean-up, and Analysis by High-resolution Gas Chromatography and Mass Spectrometry
- ISO16000-15:2008 Indoor Air – Part 15: Sampling Strategy for Nitrogen Dioxide (NO_2)
- ISO16000-16:2008 Indoor Air – Part 16: Detection and Enumeration of Moulds – Sampling by Filtration
- ISO16000-17:2008 Indoor Air – Part 17: Detection and Enumeration of Moulds – Culture-based Method
- ISO16000-18:2011 Indoor Air – Part 18: Detection and Enumeration of Moulds – Sampling by Impaction
- ISO16000-19:2012 Indoor Air – Part 19: Sampling Strategy for Moulds
- ISO16000-20:2014 Indoor Air – Part 20: Detection and Enumeration of Moulds – Determination of Total Spore Count
- ISO16000-21:2013 Indoor Air – Part 21: Detection and Enumeration of Moulds – Sampling from Materials
- ISO16000-23:2018 Indoor Air – Part 23: Performance Test for Evaluating the Reduction of Formaldehyde and Other Carbonyl Compounds Concentrations by Sorptive Building Materials
- ISO16000-24:2018 Indoor Air – Part 24: Performance Test for Evaluating the Reduction of Volatile Organic Compound Concentrations by Sorptive Building Materials
- ISO16000-25:2011 Indoor Air – Part 25: Determination of the Emission of Semivolatile Organic Compounds by Building Products – Microchamber Method
- ISO16000-26:2012 Indoor Air – Part 26: Sampling Strategy for Carbon Dioxide (CO_2)
- ISO16000-27:2014 Indoor Air – Part 27: Determination of Settled Fibrous Dust on Surfaces by SEM (scanning electron microscopy) (direct method)
- ISO16000-28:2012 Indoor air – Part 28: Determination of Odor Emissions from Building Products using Test Chambers
- ISO16000-29:2014 Indoor Air – Part 29: Test Methods for VOC Detectors
- ISO16000-30:2014 Indoor Air – Part 30: Sensory Testing of Indoor Air
- ISO16000-31:2014 Indoor Air – Part 31: Measurement of Flame Retardants and Plasticizers Based on Organophosphorus Compounds – Phosphoric Acid Ester
- ISO16000-32:2014 Indoor Air – Part 32: Investigation of Buildings for the Occurrence of Pollutants
- ISO16000-33:2017 Indoor Air – Part 33: Determination of Phthalates with Gas Chromatography/Mass Spectrometry (GC/MS)
- ISO16000-34:2018 Indoor Air – Part 34: Strategies for the Measurement of Airborne Particles
- ISO16000-36:2018 Indoor Air – Part 36: Standard Method for Assessing the Reduction Rate of Culturable Airborne Bacteria by Air Purifiers using a Test Chamber

- ISO16000-37:2019 Indoor Air – Part 37: Measurement of PM_{2.5} Mass Concentration
- ISO16000-38:2019 Indoor Air – Part 38: Determination of Amines in Indoor and Test Chamber Air – Active Sampling on Samplers Containing Phosphoric Acid Impregnated Filters
- ISO16000-39:2019 Indoor Air – Part 39: Determination of Amines – Analysis of Amines by (ultra-) High-performance Liquid Chromatography Coupled to High-resolution or Tandem Mass Spectrometry
- ISO16000-40:2019 Indoor Air – Part 40: Indoor Air Quality Management System

US EPA Methods

US EPA has developed the well-known compendium of methods for characterizing organic pollutants in the ambient air (US EPA 2020c) and for sampling and analysis of organic and inorganic chemicals in waste and other metrics in the environment (US EPA 2020b). The EPA methods presented here are closely related to indoor air sampling and analysis and have been widely accepted and employed by the IAQ community.

EPA Compendium Method TO-1 Method for the Determination of Volatile Organic Compounds in Ambient Air Using Tenax® Adsorption and Gas Chromatography/Mass Spectrometry (GC/MS)

EPA Compendium Method TO-11A Determination of Formaldehyde in Ambient Air Using Adsorbent Cartridge Followed by High Performance Liquid Chromatography (HPLC) (Active Sampling Methodology)

EPA Compendium Method TO-14A Determination of Volatile Organic Compounds (VOCs) in Ambient Air Using Specially Prepared Canisters with Subsequent Analysis by Gas Chromatography

EPA Compendium Method TO-15A Determination of Volatile Organic Compounds (VOCs) In Air Collected in Specially-prepared Canisters and Analyzed by Gas Chromatography/Mass Spectrometry (GC/MS)

EPA Compendium Method TO-17 Determination of Volatile Organic Compounds in Ambient Air Using Active Sampling onto Sorbent Tubes

EPA SW-846 Test Methods for Evaluating Solid Waste Physical Chemical Methods

Government Regulations

The Code of Federal Regulations (CFR) is frequently referenced in the test standards. CFR is the codification of the federal regulations published in the Federal Register by the US federal government (GPO 2020). CFR Title 29 (29 CFR) – Labor and CFR Title 40 (40 CFR) – Protection of Environment are 2 of 50 titles comprising CFRs. Twenty-nine CFR includes federal rules and regulations regarding labor,

including occupational safety and health. Forty CFR are environmental regulations that are promulgated by the US EPA. The following CFR items are cited in the ASTM methods listed previously:

- 29 CFR Part 1910 Occupational Safety and Health Standards
- 29 CFR 1910.1450 Occupational Exposure to Hazardous Chemicals in Laboratories
- 40 CFR Part 50 National Primary and Secondary Ambient Air Quality Standards
- 40 CFR Part 53 Ambient Air Monitoring Reference and Equivalent Methods
- 40 CFR Part 60 Standards of Performance for New Stationary Sources – Appendix A: Test Methods
- 40 CFR Part 136 Guidelines Establishing Test Procedures for the Analysis of Pollutants
- 40 CFR Part 136 Guidelines Establishing Test Procedures for the Analysis of Pollutants Appendix B: Definition and Procedure for the Determination of the Method Detection Limit

Other Frequently Used Standards

Standards developed by other government agency and standard bodies not listed above and commonly used for compliance with regulations include below. It is to point out that ASHRAE Standard 52.2 is not generally used for compliance with regulations, but it prescribes the test method forming the basis of the minimum efficiency reporting values (MERVs) rating system to address particulate matter for the majority of centrally ducted HVAC systems.

CDPH Standard Method v1.2 ([CDPH 2017](#)), Standard Method for the Testing and Evaluation of Volatile Organic Chemicals Emission from Indoor Sources using Environmental Chamber (Emission Testing Method for California Specification 01350) ([CDPH 2017](#))

California 01350 Specification, a special environmental requirements standard specification developed by the State of California to cover key environmental performance issues related to the selection and handling of building materials (California Department of Resources Recycling and Recovery (CalRecycle) [2019](#)).

ANSI/BIFMA M7.1-2011(R2016), Standard Test Method for Determining VOC Emissions from Office Furniture Systems, Components, and Seating ([BIFMA 2016a](#))

ANSI/BIFMA X7.1-2011(R2016), Standard for Formaldehyde and TVOC Emissions of Low-emitting Office Furniture and Seating ([BIFMA 2016b](#))

ANSI/ASHRAE Standard 52.2-2017, Method of Testing General Ventilation Air-Cleaning Devices for Removal Efficiency by Particle Size ([ASHRAE 2017a](#))

ANSI/ASHRAE Standard 55-2017, Thermal Environmental Conditions for Human Occupancy ([ASHRAE 2017b](#))

ANSI/ASHRAE Standard 62.1-2019, Ventilation for Acceptable Indoor Air Quality ([ASHRAE 2019a](#))

ANSI/ASHRAE Standard 62.2-2019, Ventilation and Acceptable Indoor Air Quality in Residential Buildings (ASHRAE 2019b)

ANSI/ASHRAE Standard 189.1-2017, Standard for the Design of High-Performance Green Buildings (ASHRAE 2017c)

CAN/ULC-S774-09 (R2014), Standard Laboratory Guide for the Determination of Volatile Organic Compound Emssions from Polyurethane Foam (ULC 2020)

CPSC-CH-C1001-09.4, Standard Operating Procedure for Determination of Phthalates (CPSC 2018)

ASTM Test Standards

ASTM standards are classified into three types: test method, guide, and practice. By ASTM definitions (2018), test method is “*a definitive procedure that produces a test result,*” guide is “*a compendium of information or series of options that does not recommend a specific course of action,*” and practice is “*a set of instructions for performing one or more specific operations that does not produce a test result.*” In general, ASTM standards prescribe procedures in sufficient detail for users to perform tests and collect data successfully and at the same time with flexibility through informative notes and annexes. The existing ASTM standards are reviewed and updated as needed and at a minimum every 5 years.

ASTM D22.05 Indoor Air Subcommittee currently maintains 34 active standards and is developing several new standards as listed above. The standards are on topics related to indoor air and dust sampling and analysis, emission testing for air pollutants from consumer products and building materials, ventilation, determination of uncertainty in chamber testing and indoor air modeling, and IAQ evaluation and exposure. They exclude the establishment of IAQ limit values. It is notable that these ASTM standards measure IAQ parameters in buildings and chemical emissions from materials, but not for automobiles. For individual pollutants there may be different sampling and analytical procedures in separate standards. The ASTM D22.08 Assessment, Sampling, and Analysis of Microorganisms Subcommittee also maintains and develops standards related to IAQ and focuses on indoor microorganisms. The ASTM standards and other relevant standards are categorized in Table 1.

In addition to the test standards, the ASTM standard terminology D1356 developed by Subcommittee D22.01 on Quality Control harmonizes definitions of terms commonly used in the air quality standards. There are also definitions of terms specific to individual ASTM standards when applicable. The following listing contains most frequently used terminologies that are not only referenced in the ASTM standards but also very often cited in other IAQ standards and publications. These terminologies are alphabetically adopted from ASTM D22 standards. The numbers in the parentheses are the ASTM standard numbers. All the ASTM terminology cited in this chapter are reprinted with permission from ASTM, copyright ASTM International.

Table 1 ASTM indoor air test standards by field applications

Field	Subfield	ASTM standard	Other relevant standard
Samplings/ Analysis	Microorganism	D7391, D7658, D7788, D7789, D7910	ISO16000-16, 17, 18, 19, & 20
	Pesticides and SVOCs	D4861, D5075, D6333	ISO16000-12, 13, 14, 31, & 33; TO-11A, SW-846, NIOSH Method, CPSC-CH-C1001-09.4
	Formaldehyde	D5197	ISO16000-2, 3, & 4; TO-11A
	Dust and particles	D5438	ISO16000-27, 34, & 37
	VOCs	D5466, D6196, D6306, D8283	ISO16000-5, 6, 38, & 39; TO-14A, 15A, &17;
	Tobacco smoke	D5955, D6271	
	Radon	D6327	
	Inorganic gas	D6332	ISO16000-15 & 26
Emission and material test	General	D5116, D6670, D7143, D7706, D7911, D8141	ISO16000-9, 10, 11, 23, 24, & 25; CDPH Standard Method v1.2
	Bedding set	D6177	
	Wood products	D6330, E1333, D6007	ANSI/BIFMA M7.1 & X7.1
	Coating	D6803	
	Carpet	D7339	
	SPF	D7859, D8142	CAN/ULC-S774-09
	Microbial ^a	D6329, D3273, C1338	ISO16000-21,
	Odor	Under development	ISO16000-28 & 30
Ventilation	Air change	E741, E779, E1827	
	Evaluation	D6245	ISO16000-8, ASHRAE Standard 62.1& 62.2
Indoor air modeling	Evaluation	D5157	
IAQ evaluation and exposure	Exposure	D6178, D6485, D6669	
	Aircraft cabins	D6399, D7034	
	IAQ	D5791, D7297	ISO16000-32
	Microorganism	D7338	ISO16000-36
	Moisture	E241	

^aD6329, D3273, and C1338 are not emission or material test standards of microbial, they are standards of material testing for microbial growth

Air change rate, the volumetric flow rate (volume per unit time) of air entering a space or enclosure divided by the net volume of air in that space or enclosure (1/s, 1/h) (D1356, D6177).

Chamber loading ratio, the total amount of test specimen exposed in the chamber divided by the net or corrected internal air volume of the chamber (D5116, D6670).

Clean air, air that does not contain any airborne contaminants in excess of defined limits (D6803).

Emission factor, the mass of a VOC or total VOC emitted per unit time and per unit amount of source tested. Depending on the type of source, the amount of source may be expressed by its exposed surface area (that is, an area source such as a painted gypsum wallboard surface), its dominant dimension (that is, a line source such as a caulk or sealant), its mass, or its standard setup (that is, a “unit” source such as a predefined work station system). As a result, the unit for the emission factor will be mg/h, mg/(m² h), mg/(m³ h), mg/(kg h), and mg/(m³ h) for the “unit,” line, area, mass, and volume emission sources, respectively (D6670).

Emission profile, a time series of emission rates of one or more chemicals (D6177, D6669, D6485).

Emission rate, the mass emitted per unit of time from a source or, alternatively, per unit of material or energy produced or consumed by a process (D1356).

Nonvolatile organic chemical, an organic compound with a saturation vapor pressure less than 10⁻⁸ kPa at 25 °C (D1356, D6177).

Semivolatile organic chemical (SVOC), an organic compound with a saturation vapor pressure between 10⁻² and 10⁻⁸ kPa at 25 °C (D1356).

Test chamber, an enclosed test volume constructed of chemically inert materials with a clean air supply and exhaust (D5116).

Total volatile organic compounds (TVOC), the summed concentration of all the individual volatile organic compounds (VOCs) quantifiable in an air sample by both a precisely specified sampling protocol and a precisely defined analytical method (D1356).

Tracer gas, a gaseous compound that can be used to determine the mixing characteristics of the test chamber and be a cross-check of the air change rate. The tracer gas must not be emitted by the test specimen and must not be contained in the supply air (D6670).

Volatile organic chemical (VOC), an organic compound with a saturation vapor pressure greater than 10⁻² kPa at 25 °C (D1356).

There are also commonly used terms and definitions for IAQ health, exposure, and risk assessment in ASTM D22.05 standards. They are:

Acute exposure guideline levels (AEGLs), represent short-term threshold or ceiling exposure values intended for the protection of the general public, including susceptible or sensitive individuals, but not hypersusceptible or hypersensitive individuals (D6485).

Ceiling limit, a maximum allowable air concentration, established by the Occupational Safety and Health Administration (OSHA), that must not be exceeded during any part of the workday (D6399, D6485).

Inhalation reference concentration (RfC), an estimate (with uncertainty spanning an order of magnitude) of the daily exposure to the human population (including sensitive subgroups) that is likely to be without an appreciable risk of deleterious effects (D6485).

Lethal concentration 50 (LC_{50}), a calculated concentration of a chemical in air to which exposure for a specific length of time is expected to cause death in 50% of a defined experimental animal population (D6485).

Lethal concentration low (LCL_o), the lowest calculated concentration of a chemical in air to which exposure over any period of time is reported to have caused death in humans or animals (D6485).

Level of concern, an exposure level or concentration that is not to be exceeded by regulation or, for unregulated pollutants, an exposure level or concentration that is believed to be associated with odor, sensory irritation, and other adverse health or toxic effects (D6399).

Lowest-observed-adverse-effect level (LOAEL), the lowest dose of a chemical in a study or group of studies that produce statistically or biologically significant increases in frequency or severity of adverse effects between the exposed population and its appropriate control (D6399, D6485).

Minimal risk level (MRL), an estimate of the daily human exposure to a hazardous substance that is likely to be without appreciable risk of adverse noncancer health effects over a specified duration of exposure (D6485).

No-observed-adverse-effect level (NOAEL), the dose of chemical at which there are no statistically or biologically significant increases in frequency or severity of adverse effects seen between the exposed population and its appropriate control (D6399, D6485).

Permissible exposure limit (PEL), an OSHA defined term meaning the limit of OSHA permitted exposure to a specific contaminant as required in the applicable regulation. This limit is an 8 h time weighted average (TWA), determined in the worker's breathing zone, and is expressed in a number of units of measure (D1356).

Potential inhaled dose, the estimated dose of an airborne chemical that an individual is likely to have inhaled within a specified period of time (D6485).

Short-term exposure limit (STEL), the airborne concentration of a substance in a continuous 15-min time period which should not be exceeded at any time during a workday (D1356).

Threshold limit value (TLV), Threshold limit value-time weighted average (TLV-TWA), the time-weighted average concentration for a conventional 8-h workday and 40-h workweek, to which it is believed that nearly all workers may be repeatedly exposed, day after day, without adverse effect (D1356).

Toxic concentration low (TCL_o), the lowest air concentration of a substance introduced by the inhalation route over any period of time that is reported to have produced any significant toxic effects in animals or humans (D6485).

As mentioned at the beginning of this chapter, even though these standards are a consensus on test methods and measurement practices, they do not provide specific criteria on concentrations and limits of material and product emissions. Nevertheless, they could be appropriate or adaptable by regulatory agencies in the laws or regulations. The Public Law 104-113 National Technology Transfer and Advancement Act (NTTAA) of 1995 (NIST 2019) was signed into law on March 7, 1996. The law supports interaction and cooperation between the private and public sectors

in developing and adopting standards that serve the government's purposes and support trade. The NTTAA § 12(d)(1) directs federal agencies and departments to use voluntary consensus standards with the two exceptions in bold below:

[A]ll Federal agencies and departments shall use technical standards that are developed or adopted by voluntary consensus standards bodies, using such technical standards as a means to carry out policy objectives or activities determined by agencies and departments . . . [except where] **inconsistent with applicable law or otherwise impractical.** [emphasis added]

Also, Section 12(d)(2) of the NTTAA directs federal agencies and departments to participate in the development of voluntary consensus standards:

[F]ederal agencies and departments shall consult with voluntary, private sector, consensus standards bodies and shall, when such participation is in the public interest and is compatible with agency and departmental missions, authorities, priorities, and budget resources, participate with such bodies in the development of technical standards.

As an example, ASTM D6007 (secondary method) and E1333 (primary method) are compliance test methods for chamber testing of composite wood products in the US Formaldehyde Standards for Composite Wood Products Act (GovTrack.us 2020). California (which is not subject to NTTAA) has also elected to base the California regulation 17 CCR §93120 Airborne Toxic Control Measure to Reduce Formaldehyde Emissions from Composite Wood Products (CARB 2007) on ASTM D6007 and E1333, which have many benefits to regulators and their stakeholders. These regulations limit formaldehyde emissions from composite wood products, e.g., hardwood plywood, particleboard, and medium-density fiberboard panels, and finished goods, manufactured domestically or imported into the USA. The CDPH Standard Method v1.2 is the emission test method for California Specification 01350. It incorporates ANSI/BIFMA M7.1, ASTM D5116 for small chamber testing procedures and data analysis, ASTM Standards D5197, D6196, D6345, D7339, and EPA methods TO-1 and TO 17 for sampling and analysis. Of note, California Specification 01350 is the only health-based building material specification and one of the most widely recognized US standards for restricting VOC emissions from building materials and products in the indoor environment. It has been referenced or required in criteria by numerous manufacturers and various certification and labeling schemes, such as US Green Building Council's (USGBC) Leadership in Energy and Environmental Design (LEED) program, EPA Indoor airPLUS program, UL GREENGUARD certification, the National Green Building Standard (NGBS), and Carpet and Rug Institute (CRI) Green Label Plus program.

ASHRAE Standards

Ventilation plays an important role in IAQ. Inadequate ventilation poses health-related problems due to increased levels of indoor air pollutants. This section addresses ANSI/ASHRAE Standard 62.1, ventilation for acceptable indoor air

quality, and Standard 62.2, ventilation and acceptable indoor air quality in residential buildings, which are consensus standards of practice regarding ventilation and IAQ in commercial buildings (62.1) and residential buildings (62.2). These two standards focus on IAQ and specify the ventilation criteria and other measurements to minimize adverse occupant health effects. ANSI/ASHRAE 62.1-2019 defines acceptable IAQ as: “air in which there are no known contaminants at harmful concentrations, as determined by cognizant authorities, and with which a substantial majority (80% or more) of the people exposed do not express dissatisfaction.” Both standards are accredited by ANSI and serve the building industry and the public as the most prescriptive standards on ventilation for IAQ.

In 1973, ASHRAE published Standard 62 for the first time to help engineers and other professionals on ventilation system design and operation practices for buildings with the IAQ procedure (IAQP) being initiated (ASHRAE 1973). The standard was then revised in 1981, 1989, 1999, and 2001, and split into Standards 62.1 and 62.2 in 2004 with significant modifications. The original edition of the standard was renamed to ASHRAE 62.1 in the 2004 edition. Since then the two standards have been continually reviewed and updated every 3 years. The latest versions of the standards are ASHRAE Standard 62.1-2019 and ASHRAE Standard 62.2-2019. ASHRAE standards are dynamic documents. A noteworthy foreword in each version of the standards informs the historical perspective on the development of the standards and describes the detailed changes compared to the previous version. In addition to the review process, official and unofficial interpretation documents for some of the editions exist (Standard 62-1989, 1999, 2001; Standard 62.1-2004, 2007, 2010, 2013, 2016, 2019; Standards 62.2-2004, 2007, 2010, 2013, 2016, 2019) (ASHRAE 2020b). An official interpretation is a written response to a request for an explanation of the meaning of a standard by the cognizant project committee or interpretation committee, whereas an unofficial interpretation is addressed by the manager of technical services, the chair of the cognizant project committee, or the manager of standards (ASHRAE 2020b).

ASHRAE 62.1

ASHRAE 62.1 is best recognized for its ventilation airflow requirements for the design of ventilation systems in various commercial and institutional buildings, which includes new buildings and additions and renovations to existing buildings. It is also used as a guide to improve IAQ in existing buildings. Over the years, most notable revisions to this standard included:

- Reducing the minimum outdoor-air rates; introducing performance-based IAQP (1981 edition)
- Formalizing IAQP; introducing “sick building syndrome” terminology and the requirement for multizone recirculating systems; increasing the minimum outdoor-air rates, removing thermal comfort (1989 edition)

- Recognizing the harm of cigarette smoking; clarifying CO₂ as ventilation metric (1999 edition)
- Minor revision (2001 edition)
- Substantially modifying the IAQP and the ventilation rate procedure (VRP) (2004 edition)
- Adding Appendix H (2007 edition)
- Adding Section 6.4 for the natural ventilation procedure (NVP) and requirements for demand-control ventilation (2010 edition)
- Making changes to exhaust air requirements; clarifying the requirements for the quality of water used in humidification system and building level pressurization (2013 edition)
- Moving all residential spaces to Standard 62.2 (2016 edition)
- Significantly modifying the NVP; adding a new simplified version of VRP (2019 edition)

The outlines of the standards in different editions have had little changes over the years. The 2019 edition is divided into nine sections, including the purpose, scope, definitions, outdoor air quality, system and equipment, procedures, construction and system start-up, normative references, and 15 appendices. The definitions section provides definitions of terms used throughout the standard. The standards also serve as disciplines for terminology and concepts in building design and building code communities as well as for educators, public officials, and building owners. Additionally, ASHRAE also provides over 3700 searchable terms and definitions used in the fields of HVACs design, engineering, and commissioning as a free online resource (ASHRAE 2020c). The important feature of ASHRAE 62.1-2019 is its three procedures, the ventilation rate procedure (Fig. 1), the indoor air quality procedure (Fig. 2), and the natural ventilation procedure (Fig. 3) in Section 6. These procedures are methods for determining outdoor air intake flow through the HVAC system(s). In addition, the standard incorporates information relevant to a certain number of contaminants and their indoor sources. Other factors that contribute to IAQ, such as thermal comfort, noise, lighting, etc. are not within the scope of Standard 62.1. The mold growth and humidity tests of materials are referenced to the standardized test methods, UL 181 (UL 2013), ASTM C1338, and ASTM D3273. Thermal comfort is covered in ANSI/ASHRAE 55, Thermal Environmental Conditions for Human Occupancy.

The VRP is very often cited and widely used for compliance. It provides the prescriptive approaches for the ventilation calculations and tabulates the minimum ventilation rates in breathing zone, minimum exhaust rates, and zone air distribution effectiveness for a wide range of scenarios, such as different spaces and occupant density, etc. The acceptable air quality is achieved by specifying those parameters. In Standard 62.1-2019, the breathing zone outdoor airflow is given by Eq. 1 below (Copyright notice for ASHRAE Standards ©ASHRAE, <http://www.ashrae.org>. Used with permission from (2019) ASHRAE Standard-62.1 & ASHRAE Standard-62.2):

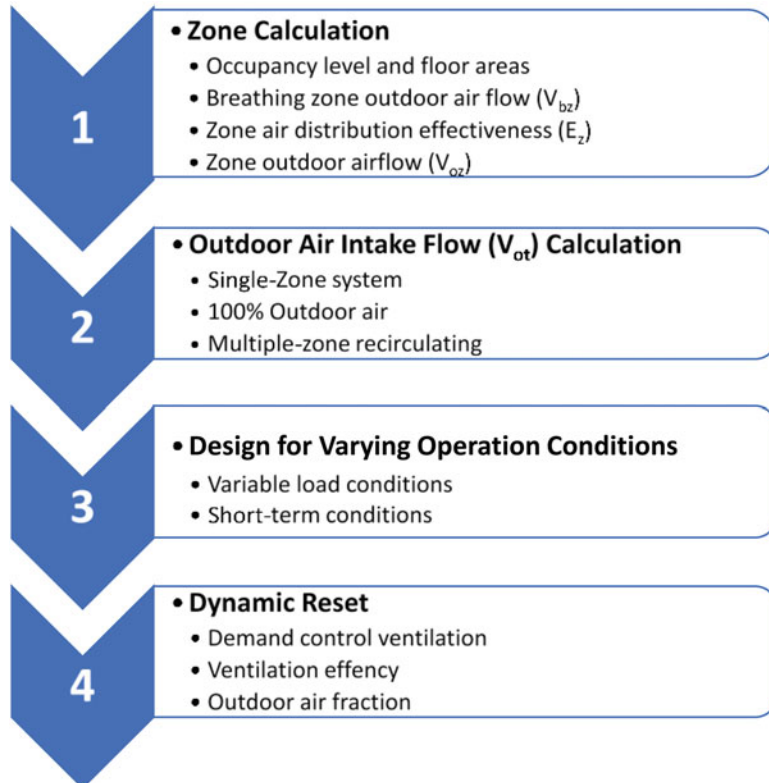


Fig. 1 ASHRAE Standard 62.1-2019, ventilation rate procedure (VRP)

$$V_{bz} = R_p \times P_z + R_a \times A_z \quad \text{ASHRAE 62.1} \quad (1)$$

where, V_{bz} is the breathing zone outdoor airflow, A_z is the zone floor area (ft^2, m^2), P_z is the zone population, R_p is outdoor airflow rate required per person, and R_a is the outdoor airflow rate required per unit area. The zone outdoor airflow (V_{oz}) is calculated by:

$$V_{oz} = V_{bz}/E_z \quad \text{ASHRAE 62.1} \quad (2)$$

where E_z is the zone air distribution effectiveness. For a single-zone system, the outdoor air intake flow (V_{ot}) is determined by:

$$V_{ot} = V_{oz} \quad \text{ASHRAE 62.1} \quad (3)$$

If the air handler supplies only outdoor air to the zones, the V_{ot} value shall be the sum of the zone outdoor airflows for all zones as:

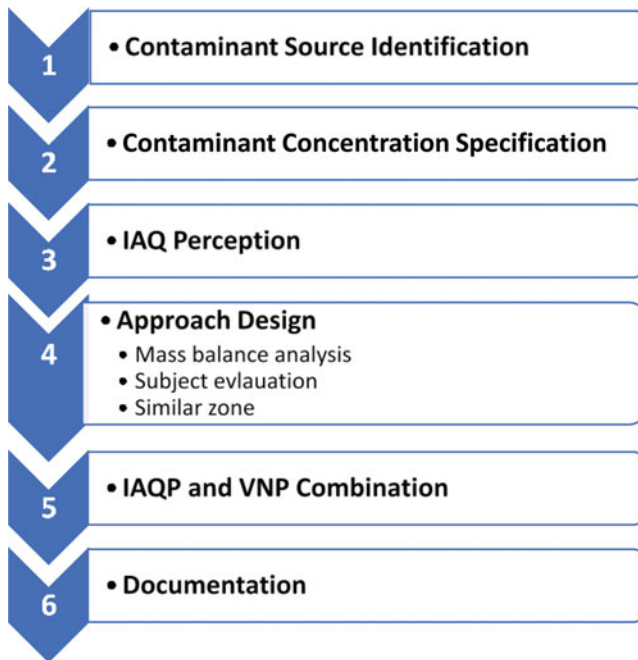


Fig. 2 ASHRAE Standard 62.1-2019, indoor air quality procedure (IAQP)

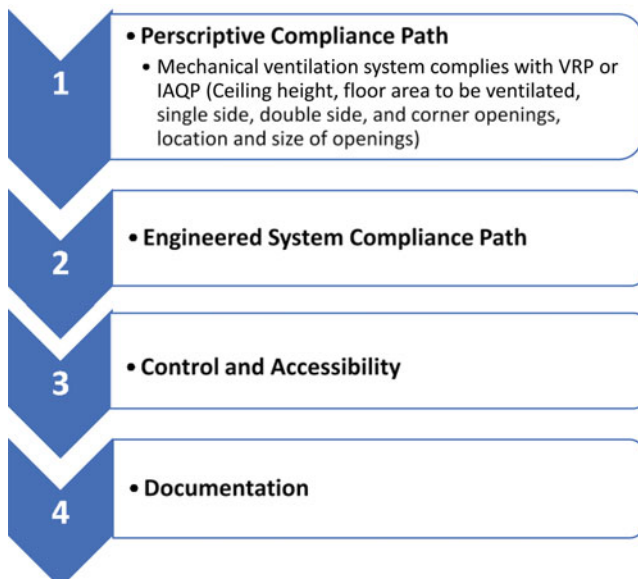


Fig. 3 ASHRAE Standard 62.1-2019, natural ventilation procedure (NVP)

$$V_{ot} = \sum_{\text{all zones}} V_{oz} \quad \text{ASHRAE 62.1} \quad (4)$$

For multiple-zone recirculating systems, the uncorrected outdoor air intake (V_{ou}) is calculated by:

$$V_{ou} = D \sum_{\text{all zones}} (R_p \times P_z) + \sum_{\text{all zones}} (R_a \times A_z) \quad \text{ASHRAE 62.1} \quad (5)$$

where the occupant diversity ratio (D) is determined by:

$$D = P_s / \sum_{\text{all zones}} P_z \quad \text{ASHRAE 62.1} \quad (6)$$

The VRP also offers calculations for a simplified procedure through Eqs. (6–7) to (6–10):

$$E_v = 0.88 \times D + 0.22 \text{ for } D < 0.60 \quad \text{ASHRAE 62.1} \quad (7)$$

$$E_v = 0.75 \text{ for } D \geq 0.60 \quad \text{ASHRAE 62.1} \quad (8)$$

$$E_{pz-\min} = V_{oz} \times 1.5 \quad \text{ASHRAE 62.1} \quad (9)$$

$$V_{ot} = \frac{V_{ou}}{E_v} \quad \text{ASHRAE 62.1} \quad (10)$$

where, E_v is the system ventilation efficiency and V_{pz-min} is the minimum primary airflow.

When the VRP is applied, it is important to evaluate and determine whether outdoor air treatment is necessary. For instance, particulate matter with a maximum diameter of 10 µm (PM10), particulate matter with a maximum diameter of 2.5 µm (PM2.5), ozone, and other outdoor contaminants are to be considered (Standard 62.1-2019 Section 6.1.4). Also note that ASHRAE provided an online Excel spreadsheet (62MZCalc.xls), and more recently, developed and updated a smart phone application for comprehensively calculating ventilation rates for simple and complicated ventilation systems of various buildings exclusively through Carmel Software Corporation (ASHRAE 2020d). The application is user friendly with features of being flexible with multiple projects, calculations in the field and the office, and full online help support. The latest application was developed based on Standard 62.1-2013. Trane Air Conditioning Economics (TRACE™) 700 commercial software developed by TRANE Technologies also integrated the VRP of Standard 62.1 in its design-and-analysis program (Trane 2020).

The IAQP is a performance specification based on acceptable concentrations of indoor air contaminants for protecting the health of the occupants in buildings. The factors to be considered include the contaminant sources, concentrations, and emission rates and IAQ acceptable limits. Mass balance equations for a single-zone system under the steady-state condition are provided in Appendix E of Standard 62.1-2019. It is worth mentioning that the criteria for acceptable IAQ may be different among IAQ experts and thus performing the IAQP is challenging.

The NVP includes mechanical ventilation systems in accordance with the VRP and/or IAQP. It defines the requirements for conditions such as ceiling height, floor space, opening locations, and size, etc.

ASHRAE 62.2

The ASHRAE Standard 62.2 Committee first approved and released the standard in 2004 as the only nationwide standard for low-rise residential buildings in the USA. Low-rise residential building refers to buildings with one to three stories. In the standard, the acceptable IAQ in residential buildings is achieved by controlling dwelling unit ventilation, local demand-controlled exhaust, and contaminant sources. The standard primarily applies to new construction but provides an alternative compliance path for existing buildings in its Appendix A. Standard 62.2 is reviewed and revised in 3-year cycles with interpretations and addenda being published between each edition. The contemporary version is ANSI/ASHRAE Standard 62.2-2019.

The 2019 edition has ten sections: purpose, scope, definitions, dwelling-unit ventilation, local exhaust, other requirements, air-moving equipment, climate data, references, and five appendices. The foreword and Appendix E of Standard 62.2-2019 detail the changes of the edition compared to its 2016 version. The updated scope and title of Standard 62.2-2019 is no longer limited to low-rise residential buildings. It applies to residential buildings in which occupants are nontransient. An important aspect of ASHRAE 62.2-2019 is the dwelling-unit ventilation in Section 4, which provides methods to calculate whole dwelling-unit ventilation rates and is summarized in Fig. 4. The local exhaust system with the option of demand-controlled mechanical exhaust or continuous mechanical exhaust discussed in Section 5 addresses kitchen and bathroom ventilation.

Other noteworthy facts about Standard 62.2 are that it does not address indoor activities that potentially cause high indoor contaminations such as painting, cleaning, smoking, etc., as well as concentration limits of contaminants. Standard 62.2 also does not address thermal comfort conditions and refers users to ANSI/ASHRAE 55.

In Section 4, the total ventilation rate is calculated using Eq. 11 or 12 with the parameters in different units:

$$Q_{\text{tot}} = 0.03A_{\text{floor}} + 7.5(N_{br} + 1) \quad \text{ASHRAE 62.2} \quad (11)$$

where Q_{tot} is the total required ventilation rate (cubic feet per minute, cfm), A_{floor} is the dwelling-unit floor area (ft^2), and N_{br} is the number of bedrooms (not to be less than 1).

$$Q_{\text{tot}} = 0.15A_{\text{floor}} + 3.5(N_{br} + 1) \quad \text{ASHRAE 62.2} \quad (12)$$

where Q_{tot} is expressed in units of L/s, and A_{floor} in units of m^2 .

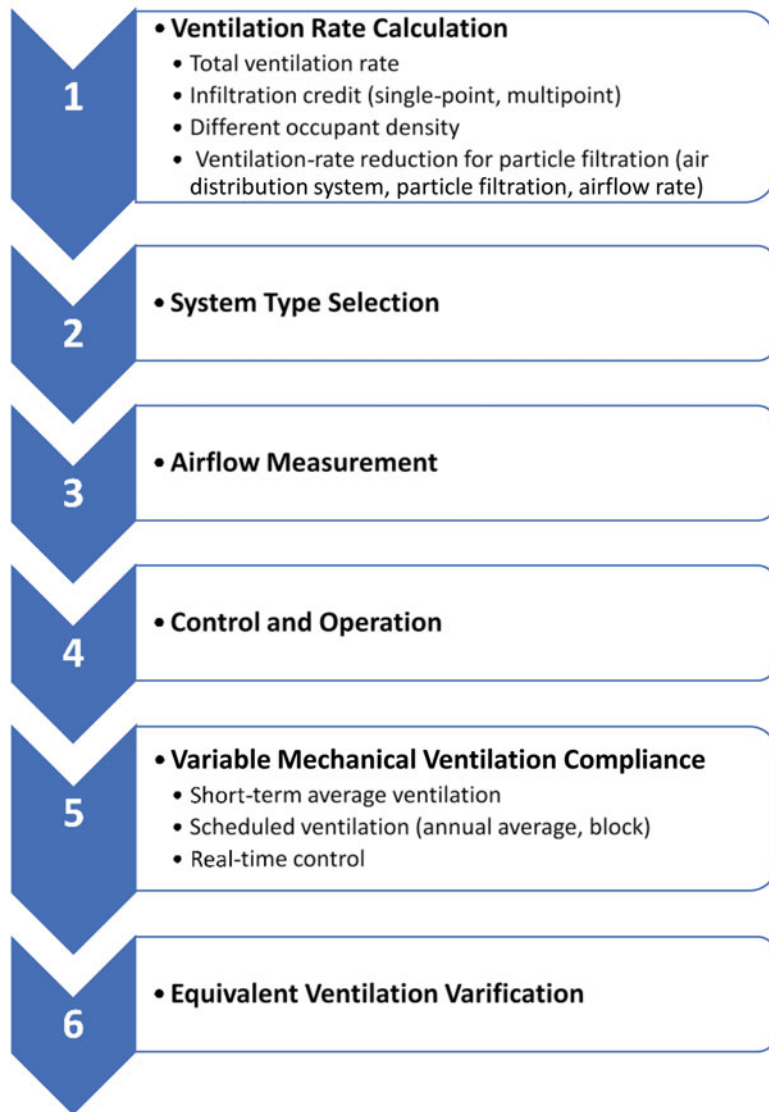


Fig. 4 ASHRAE Standard 62.2-2019, dwelling-unit ventilation process

The required mechanical ventilation rate (Q_{fan}) is calculated by:

$$Q_{fan} = Q_{tot} - \Phi(Q_{inf} \times A_{ext}) \quad ASHRAE\ 62.2 \quad (13)$$

where Q_{fan} is the required mechanical ventilation rate (cfm, L/s); Q_{inf} is the infiltration rate (cfm, L/s); $A_{ext} = 1$ for detached dwelling units, otherwise, for horizontally attached dwelling units, it is the ratio of exterior envelope surface area that is not

attached to garages or other dwelling units to total envelope surface area; $\phi = 1$ for balanced ventilation system, and $Q_{\text{inf}}/Q_{\text{tot}}$ otherwise.

The effective annual average infiltration rate, Q_{inf} , using a single-point envelope leakage test can be calculated via:

$$Q_{\text{inf}} = 0.052 \times Q_{50} \times wsf \times \left(\frac{H}{H_r} \right)^z \quad \text{ASHRAE 62.2} \quad (14)$$

where Q_{50} is the leakage rate at 50 Pa depressurization or pressurization (cfm, L/s), wsf is the weather and shielding factor, H is the vertical distance between the lowest and highest above-grade points within the pressure boundary (ft, m), H_r is the reference height, 8.2 ft. (2.5 m), and z is equal to 0.4 for the purpose of calculating the effective annual average infiltration rate.

For Q_{inf} using a multipoint envelope leakage test, the effective leakage area is used for the calculations. The effective leakage area can be calculated by the ASTM procedure:

$$ELA = \frac{L_{\text{press}} + L_{\text{dpress}}}{2} \quad \text{ASHRAE 62.2} \quad (15)$$

where ELA is the effective leakage area (ft^2 , m^2), L_{press} is the leakage area from pressurization (ft^2 , m^2), and L_{dpress} is the leakage area from depressurization (ft^2 , m^2). ELA can also be calculated by the Canadian General Standards Board (CGSB) procedure:

$$ELA = 0.61 \times (0.4)^{n-0.5} \times L_{\text{cgsb}} \quad \text{ASHRAE 62.2} \quad (16)$$

where n is the exponent measured from the CGSB 149.10 Standard, determination of the airtightness of building envelopes by the fan depressurization method, referenced in the Standard 62.2; and L_{cgsb} is the CGSB leakage area (ft^2 , m^2).

Then the normalized leakage is calculated using Equation:

$$NL = 1000 \times \frac{ELA}{A_{\text{floor}}} \times \left[\frac{H}{H_r} \right]^z \quad \text{ASHRAE 62.2} \quad (17)$$

where NL is the normalized leakage. Thus, the Q_{inf} is calculated using the following equations in different units:

$$Q_{\text{inf}}(\text{cfm}) = \frac{NL \times wsf \times A_{\text{floor}}}{7.3} \quad \text{ASHRAE 62.2} \quad (18)$$

where A_{floor} is ft^2 .

$$Q_{\text{inf}}(\text{L/s}) = \frac{NL \times wsf \times A_{\text{floor}}}{1.44} \quad \text{ASHRAE 62.2} \quad (19)$$

where A_{floor} is m^2 .

There are also available tools to make the calculations easier. For example, Robert Bean has developed the ASHRAE Standard 62.2 calculator, a free tool for Standard 62.2 calculations for home designers. It works for both 2011 and 2013 editions of the standard (Rossetti 2014). In addition, RED Calc software developed by Residential Energy Dynamics includes both free and “pro” versions of a calculation tool based on 2010 to 2019 editions (RED 2020a, b).

Applications

Standard 62.2 applying to residential buildings in which occupants are nontransient and Standard 62.1 applying to essentially all other buildings, largely commercial, have served as the most prominent standards to specify minimum ventilation rates for acceptable IAQ. These standards have provided a reference point for many building and energy codes and regulations as well as various green building certification schemes for US homes and buildings. Their major applications in the USA are summarized in Table 2. As we can see, different editions of the standards are adopted in different applications. One of the reasons behind this is that controversies exist among IAQ acceptable limits and ventilation requirements in different editions.

Standards 62.1-2016 and 62.2-2016 serve as the prescriptive compliance for the ventilation and IAQ requirements in California 2019 Building Energy Efficiency Standards, which took effect on January 1, 2020, for the zero net energy (ZNE) target (California Energy Commission 2018). Standard 62.2-2013 was adopted by Building Performance Institute, Inc (BPI) in their standard ANSI/BPI-1200-S-2017 (BPI 2017), which has been used for energy audits and related diagnostic tests by professionals nationwide. The approaches of Standards 62.1 and 62.2 have also been included in national model codes and well-known rating and labeling green building certification schemes as listed in Table 2. In the table, the year marked in parenthesis is the edition of the ASHRAE 62 standards referenced in the application when the information is available.

Priority Areas for Future Standardization Related to IAQ Testing

The consensus standards discussed above provide procedures and protocols to address air pollutant issues and to assure an energy-efficient and healthy IAQ environment for building occupants. It is to point out that before standardized procedures are to be developed, a good understanding about exposure and risk assessments of indoor air pollutants are needed. Nevertheless, with the advances in technology in building energy efficiency, rapid market changes of consumer products and building materials, and consumers’ demand driven by health effects, new standards will be developed to further facilitate addressing the risk of indoor air pollution from emerging contaminants and improve IAQ.

Tens of thousands of chemicals are in use daily and hundreds more are introduced into the market every year. In the USA, EPA regulates new or already existing

Table 2 Applications of ASHRAE Standard 62.1 and 62.2 in the USA

ASHRAE 62.1	ASHRAE 62.2	Reference
ASTM D6670 (2010), D6245	ASTM D6670 (2010)	
USGBC LEED V4.1 (2010 to 2016)	USGBC LEED V4.1 (2016)	USGBC 2019
California 2019 Building Energy Efficiency Standards, Title 24 (2016)	California 2019 Building Energy Efficiency Standards, Title 24 (2016)	California Energy Commission 2018
RESNET Guideline for Multifamily Energy Ratings (2007)	RESNET Guideline for Multifamily Energy Ratings	RESNET 2014
NREL Standard Work Specifications Tool, Topic 6.62 (2010)	NREL Standard Work Specifications Tool, Topic 6.62 (2010)	NREL 2020
NAHB ICC 700-2020 National Green Building Standard (2016)	NAHB ICC 700-2020 National Green Building Standard (2010, 2007)	NAHB 2020
US EPA Energy Savings Plus Health Guidelines for Multifamily Building Upgrades (2013)	US EPA Energy Savings Plus Health Guidelines for Multifamily Building Upgrades (2013)	US EPA 2016
US EPA ENERGY STAR Multifamily New Construction National HVAC Design Report, Version 1/1.1/1.2 (Rev.02) (2010, 2013)	US EPA ENERGY STAR Multifamily New Construction National HVAC Design Report, Version 1/1.1/1.2 (Rev.02) (2010, 2013)	US EPA 2020e
IAQ Tools for School Program (2001)	US EPA Healthy Indoor Environment Protocols for Home Energy Upgrades (2010)	US EPA 2009 , US EPA 2011
CHPS National Core Criteria, Version 3.0 (2016)	US EPA ENERGY STAR Single-family New Home HVAC Design Report, Version 3/3.1 (Rev.11) (2010 to 2016)	CHPS 2019 , US EPA 2020f
US EPA IAQ Building Education and Assessment Model (I-BEAM) (1989)	US EPA Indoor airPLUS Construction Specifications Version 1 (Rev.04) (2010)	US EPA 2017 , US EPA 2018
	ANSI/RESNET/ICC 301-2019 (2016)	ANSI/RESNET/ICC 301 2019
	RESNET Home Evaluation and Performance Improvement ANSI/ACCA 12 QH-2018 (2016)	ACCA 2018
	DOE Zero Energy Ready Home National Program Requirements (Rev. 07) (2010)	DOE 2019
	Building Performance Institute (BPI), ANSI/BPI-1200-S-2017 (2013)	BPI 2017

chemicals under the Toxic Substances Control Act (TSCA) and its amendment, the Frank R. Lautenberg Chemical Safety for the Twenty-First Century Act. Ten chemicals have undergone risk evaluation since they were identified and initiated

in December 2016. Twenty more chemicals were further identified as priority chemicals in December 2019 (Table 3) (US EPA 2020d). These chemicals are predominantly VOCs or SVOCs with different chemical-physical properties and widely used in consumer products, furniture, and building materials in the indoor environment. The risk evaluation process includes hazard and exposure assessment for risk characterization and determination of chemicals. There is an essential need to develop consensus test protocols to inform and refine estimates of indoor exposures, especially standards for characterizing indoor SVOC sources, fate and transport of emissions, and exposure to people through inhalation, ingestion, and dermal contact. The majority of the existing test standards focus on VOC emissions as opposed to SVOCs but there are few standards for indoor exposure testing and assessment for both VOCs and SVOCs. One of the reasons for the lack of SVOC protocols is that SVOC testing is very experimentally challenging due to their low volatilities. There is an increasing interest and demand for the development of consensus standards for the measurement of SVOCs, such as flame retardants, phthalates, per- and poly-fluoroalkyl substances (PFAS), and polychlorinated biphenyls (PCBs), in support of indoor exposure assessment.

Although IAQ is often assessed by standards involving chemical testing, microbial populations (molds, bacteria, and viruses) in the indoor environment can also cause serious health problems for building occupants. Moisture-related microbial contaminants of indoor air have brought lots of attention during IAQ evaluation practice. Standards for characterizing moisture-related pollutants, including microbial and chemical emissions, and for assessing microbial contaminated building environments and exposures of occupants are greatly needed (Stetzenbach et al. 2004).

Existing test standards for IAQ assessments are limited to target pollutants with specifically optimized off-line analytical procedures, which determine trace concentrations in complex environmental and biological matrices using conventional methods. There are new technical sampling and analytical methodologies that have notably progressed in recent years. The nontargeted analysis (NTA) method is a new technology that screens a large number of environmental pollutants using databases and libraries, which allows rapid characterization of many chemicals simultaneously (Sobus et al. 2018). With the increase of chemical usage in the indoor environment and demand for rapid exposure assessment, nontargeted screening of indoor environmental pollutants provides the possibility to collect analytical information efficiently. This analytical approach can be adapted to the assessment of IAQ.

Another technology that is currently evolving is real-time air sensors (Kumar et al. 2016; Zhang and Srinivasan 2020). There are many different air sensors developed in a wide variety of capacities for detecting gases and particles, such as PM2.5, carbon monoxide (CO), carbon dioxide (CO₂), and some VOCs, in the air. They can be used in indoor air monitoring and provide instantaneous measurement data for IAQ assessment and management, especially under emergency circumstances, such as indoor pollutant monitoring during wildfire events. Standards for using air sensors to detect indoor air pollutants and for evaluating the performance of

Table 3 Priority chemicals under EPA TSCA review

Category	Chemicals	CASRN
First ten chemicals	1,4-Dioxane	123-91-1
(2016)	1-Bromopropane	106-94-5
	Asbestos	1332-21-4
	Carbon tetrachloride	56-23-5
	Cyclic aliphatic bromide cluster	25637-99-4; 3194-55-6; 3194-57-8
	Methylene chloride	75-09-2
	N-methylpyrrolidone (NMP)	872-50-4
	Pigment violet 29	81-33-4
	Tetrachloroethylene	127-18-4
	Trichloroethylene (TCE)	79-01-6
Second 20 chemicals	p-Dichlorobenzene	106-46-7
(2019)	1,2-Dichloroethane	107-06-2
	trans-1,2- Dichloroethylene	156-60-5
	o-Dichlorobenzene	95-50-1
	1,1,2-Trichloroethane	79-00-5
	1,2-Dichloropropane	78-87-5
	1,1-Dichloroethane	75-34-3
	Dibutyl phthalate	84-74-2
	Butyl benzyl phthalate	85-68-7
	Bis(2-ethylhexyl) phthalate	117-81-7
	Diisobutyl phthalate	84-69-5
	Dicyclohexyl phthalate	84-61-7
	Diisodecyl phthalate (DIDP)	26761-40-0, 68515-49-1
	4,4'-(1-Methylethylidene)bis[2, 6-dibromophenol] (TBBPA)	79-94-7
	Tris(2-chloroethyl) phosphate (TCEP)	115-96-8
	Phosphoric acid, triphenyl ester (TPP)	115-86-6
	Ethylene dibromide	106-93-4
	1,3-Butadiene	106-99-0
	1,3,4,6,7,8-Hexahydro-4,6,6,7,8,8-hexamethylcycllopenta [g]-2-benzopyran (HHCB)	1222-05-5
	Formaldehyde	50-00-0
	Octamethylcyclotetra- siloxane (D4)	556-67-2

this blooming technology, especially low-cost air sensors emerging in the market, could help the IAQ community identify best practices and obtain comparable data for detecting indoor air pollutants.

Currently, as COVID-19 continues to spread across the USA and around the world, there are numerous efforts to better manage IAQ. Urgent questions remain

regarding how to prevent the spread of airborne diseases in indoor environments (Morawska et al. 2020). There is a consensus among the majority of engineers, building professionals, and researchers around the globe that changes in ventilation and filtration provided by HVAC systems can reduce the airborne concentration of severe acute respiratory syndrome coronavirus 2 (SARS-CoV-2) (Schoen 2020). As such, there is a growing demand for mechanical improvements, utilizing ASHRAE Standard 62.1 and 62.2, to address the effectiveness of engineering control methods such as ventilation and air cleaning in buildings to reduce exposure risk. Surface cleaning and disinfecting, handwashing, and air cleaner usage (e.g., ultraviolet (UV) disinfection systems) are other straightforward steps that people can take to reduce the potential exposure to the virus (Raeiszadeh and Adeli 2020). Not surprisingly, widespread use of these cleaning agents and disinfection products has raised questions about generating potential air pollutants leading to a broad range of exposure scenarios that could adversely affect people's health and can sometimes be associated with respiratory symptoms, asthma, and other sick building syndrome symptoms (Atolani et al. 2020). To address these concerns, test standards for antimicrobial chemicals used in consumer products and building materials are expected to be fast developing.

Indoor air modeling for source characterization and exposure assessment is also an important tool for IAQ management. Consensus models will allow the prediction of the pollutants' concentrations and the evaluation of their behaviors in indoor settings (Eichler et al. 2020). However, the existing standards on this topic are scarce. To effectively conduct indoor air modeling, there are two components that are equally important: (i) physically based models of emissions and their dynamics based on scale and nature of chemicals indoors and (ii) the parameters used as inputs of models, which can be determined by experimental approaches or estimated by empirical methods. Standardizing these methods and protocols could benefit building communities and IAQ managers in predicting and reducing exposures.

In short, consensus IAQ standards development should consider the rapid changing market of consumer products, emerging materials, advanced analytical tools, environmental emergency, and pandemic outbreaks. With this under consideration, future standardization efforts should focus on:

- Determining SVOCs (e.g., flame retardants, phthalates, PFAS, and PCBs) sources, fate and transport in the indoor environment.
- Exposure tests for regulatory use. These standards could include test methods or guidance for indoor existing and new chemicals, including antimicrobial chemicals, emitting from materials and products, migrating to indoor exposure media, such as dust and airborne particle formation, and transferring from sources to dust, and dermal and oral exposure routes.
- New and advanced indoor air sampling and analytical methods.
- Characterizing moisture-related pollutants, including microbial and chemical emissions.
- Indoor air modeling, including indoor sources and exposures.
- ASHRAE 62.1 and 62.2 updates to highlight the control methodology of ventilation for effectively reducing the aerosol generation and infectious transmission.

Conclusions

In summary, consensus standards play an essential role in environmental risk assessment and management. The standards discussed in this chapter comprise harmonized procedures and protocols to address indoor air pollutants and IAQ issues from different perspectives. ASTM standards and other test standards, including sampling and analysis, emission and product testing, IAQ evaluation, and exposure assessment, can help to identify contaminant sources in the indoor environment and inform the need for risk evaluation and source control strategies. ASHRAE Standards 62.1 and 62.2 provide effective measures for mitigating the air pollutants in practice through ventilation. These two standards are widely used in combination by professionals, industry, public, and governmental regulators to assure that minimum ventilation rates are achieved to provide IAQ that is acceptable for building occupants in order to minimize adverse health effects. There have been years of determined efforts developing comprehensive up-to-date standards to comply with government regulations and keep up with product development and manufacturing in the twenty-first century. Future IAQ standards development should reflect the dynamic changes and needs on the market from the environmental viewpoint.

Cross-References

- ▶ [Analytical Tools in Indoor Chemistry](#)
- ▶ [Evaluating Ventilation Performance](#)
- ▶ [IAQ Requirements in Green Building Labeling Systems and Healthy Building Labeling Systems](#)
- ▶ [Influence of Ventilation on Indoor Air Quality](#)
- ▶ [Reference Materials for Building Product Emission Characterization](#)
- ▶ [Sampling and Analysis of Semi-volatile Organic Compounds \(SVOCs\) in Indoor Environments](#)
- ▶ [Sampling and Analysis of VVOCs and VOCs in Indoor Air](#)
- ▶ [Source/Sink Characteristics of SVOCs](#)
- ▶ [Source/Sink Characteristics of VVOCs and VOCs](#)
- ▶ [WHO Health Guidelines for Indoor Air Quality and National Recommendations/Standards](#)

Acknowledgments The author expresseses her gratitude to Libby Nessley and Doris Betancourt at US EPA Center for Environmental Measurement and Modeling, Elise Owen at US EPA Office of Policy, Laureen Burton and Nicholas Hurst at US EPA Office of Radiation and Indoor Air for their assistance in reviewing this manuscript, and to Emily Vorhies, EPA Electronic Resources and Cataloging Librarian, UNC Contract Staff for helping format the reference and addressing standards' copyright and license issues in the manuscript.

Disclaimer The views expressed in this publication are those of the authors and do not necessarily represent the views or policies of the US EPA. Mention of trade names or commercial products does not constitute endorsement or recommendation for use by the US EPA. The authors declare no competing financial interest.

References

- ACCA (2018) ANSI/ACCA 12 QH-2018 ACCA Standard 12 Home evaluation and performance improvement. <https://www.acca.org/HigherLogic/System/DownloadDocumentFile.ashx?DocumentFileKey=1898c981-0cf8-5b71-8e79-c5d88aacfae3&forceDialog=0>. Accessed 19 Dec 2020
- ACGIH (2020a) About ACGIH. <https://www.acgih.org/about-us/about-acgih>. Accessed 19 Dec 2020
- ACGIH (2020b) TLV/BEI guidelines. <https://www.acgih.org/tlv-bei-guidelines/policies-procedures-presentations/overview>. Accessed 19 Dec 2020
- AIHA (2020) About AIHA. <https://www.aiha.org/about-aiha>. Accessed 19 Dec 2020
- ANSI (2020a) ANSI essential requirements: due process requirements for American National Standards. <http://www.ansi.org/essentialrequirements>. Accessed 19 Dec 2020
- ANSI (2020b) About ANSI. <https://www.ansi.org/>. Accessed 19 Dec 2020
- ANSI/RESNET/ICC 301 (2019) Standard for the calculation and labeling of the energy performance of dwelling and sleeping units using an energy rating index. Residential Energy Service Network, Oceanside. <https://codes.iccsafe.org/content/RESNETICC3012019>. Accessed 5 Jan 2021
- ASHRAE (1973) ANSI/ASHRAE Standard 62-1973 Standards for natural and mechanical ventilation. American Society of Heating, Refrigerating and Air – Conditioning Engineers, Georgia
- ASHRAE (2009) Indoor air quality guide: best practices for design, construction, and commissioning. American Society of Heating, Refrigerating and Air – Conditioning Engineers. ISBN 978-1-933742-59-5. <https://www.ashrae.org/technical-resources/bookstore/indoor-air-quality-guide>. Accessed 14 June 2021
- ASHRAE (2017a) ANSI/ASHRAE Standard 52.2-2017 method of testing general ventilation air-cleaning devices for removal efficiency by particle size. American Society of Heating, Refrigerating and Air – Conditioning Engineers, Georgia
- ASHRAE (2017b) ANSI/ASHRAE standard 55-2017 thermal environmental conditions for human occupancy. American Society of Heating, Refrigerating and Air – Conditioning Engineers, Georgia
- ASHRAE (2017c) ANSI/ASHRAE standard 189.1-2017 standard for the design of high-performance green buildings. American Society of Heating, Refrigerating and Air – Conditioning Engineers, Georgia
- ASHRAE (2019a) ANSI/ASHRAE standard 62.1-2019 ventilation for acceptable indoor air quality. American Society of Heating, Refrigerating and Air – Conditioning Engineers, Georgia
- ASHRAE (2019b) ANSI/ASHRAE standard 62.2-2019 ventilation and acceptable indoor air quality in residential buildings. American Society of Heating, Refrigerating and Air – Conditioning Engineers, Georgia
- ASHRAE (2020a) About ASHRAE. <https://www.ashrae.org/about>. Accessed 19 Dec 2020
- ASHRAE (2020b) Standards interpretations. <https://www.ashrae.org/technical-resources/standards-and-guidelines/standards-interpretations>. Accessed 19 Dec 2020
- ASHRAE (2020c) ASHRAE terminology. <https://xp20.ashrae.org/terminology/>. Accessed 19 Dec 2020
- ASHRAE (2020d) ASHRAE 62.1 App. <https://www.ashrae.org/technical-resources/bookstore/standard-62-1-app>. Accessed 19 Dec 2020
- ASTM (2018) Form and style for ASTM standards. https://www.astm.org/FormStyle_for_ASTMDTDS.html#definitions. Accessed 19 Dec 2020
- ASTM (2020a) About us. <https://www.astm.org/>. Accessed 19 Dec 2020
- ASTM (2020b) Subcommittee D22.05 on indoor air. <https://www.astm.org/COMMIT/SUBCOMMIT/D2205.htm>. Accessed 19 Dec 2020
- ASTM (2020c) Subcommittee D22.01 on quality control. <https://www.astm.org/COMMIT/SUBCOMMIT/D2201.htm>. Accessed 19 Dec 2020
- ASTM (2020d) Subcommittee D22.08 on assessment. <https://www.astm.org/COMMIT/SUBCOMMIT/D2208.htm>. Accessed 19 Dec 2020
- ASTM (2020e) Subcommittee E06.41 on air leakage and ventilation performance. <https://www.astm.org/COMMIT/SUBCOMMIT/E0641.htm>. Accessed 19 Dec 2020

- ASTM (2020f) Subcommittee D07.03 on panel products. <https://www.astm.org/COMMIT/SUBCOMMIT/D0703.htm>. Accessed 19 Dec 2020
- ASTM (2020g) Subcommittee D01.28 on biodeterioration. <https://www.astm.org/COMMIT/SUBCOMMIT/D0128.htm>. Accessed 19 Dec 2020
- ASTM (2020h) Subcommittee C16.31 on chemical and physical properties. <https://www.astm.org/COMMIT/SUBCOMMIT/C1631.htm>. Accessed 19 Dec 2020
- Atolani O, Baker MT, Adeyemi OS et al (2020) COVID-19: critical discussion on the applications and implications of chemicals in sanitizers and disinfectants. EXCLI J 19:785–799
- BIFMA (2016a) ANSI/BIFMA M7.1–2011 (R2016) Standard test method for determining VOC emissions from office furniture systems, components, and seating. BIFMA, Grand Rapids
- BIFMA (2016b) ANSI/BIFMA X7.1-2011 (R2016) Standard for formaldehyde & TVOC emission of low-emitting office furniture and seating. BIFMA, Grand Rapids
- BIFMA (2020) The office furniture industry voice for workplace solutions. <https://www.bifma.org/page/about>. Accessed 19 Dec 2020
- BPI (2017) ANSI/BPI-1200-S-2017 Standard practice for basic analysis of buildings. BPI, Malta. <http://www.bpi.org/sites/default/files/ANSI%20BPI-1200-S-2017%20Standard%20Practice%20for%20Basic%20Analysis%20of%20Buildings.pdf>. Accessed 19 Dec 2020
- California Department of Resources Recycling and Recovery (CalRecycle) (2019) Section 01350. <https://www.calrecycle.ca.gov/greenbuilding/specs/section01350>. Accessed 19 Dec 2020
- California Energy Commission (2018) 2019 Building energy efficiency standards for residential and nonresidential building, Title 24, Part 6 and associated administrative regulations in Part 1. December 2018, CEC-400-2018-020-CMF. <https://ww2.energy.ca.gov/2018publications/CEC-400-2018-020/CEC-400-2018-020-CMF.pdf>. Accessed 19 Dec 2020
- CARB (2007) California code of regulation 17 CCR §93120 Airborne toxic control measure to reduce formaldehyde emissions from composite wood products. California Air Resources Board (CARB). https://ww3.arb.ca.gov/regact/2007/compwood07/fro-final.pdf?_ga=2.134163404.332868379.1605828868-986791758.1600721279. Accessed 19 Dec 2020
- CDPH (2017) CDPH standard method v1.2 Standard method for the testing and evaluation of volatile organic chemicals emission from indoor sources using environmental chamber, (Emission testing method for California Specification 01350). Indoor Air Quality Section, Environmental Health Laboratory Branch, Division of Environmental and Occupational Disease Control, California Department of Public Health https://www.cdph.ca.gov/Programs/CCDPHP/DEODC/EHLB/IAQ/CDPH%20Document%20Library/CDPH-IAQ_StandardMethod_V1_2_2017_ADA.pdf. Accessed 19 Dec 2020
- CDPH (2020) Indoor air quality (IAQ) section. California Department of Public Health (CDPH). <https://www.cdph.ca.gov/Programs/CCDPHP/DEODC/EHLB/IAQ/Pages/Main-Page.aspx>. Accessed 19 Dec 2020
- CHPS (2019) Collaborative for high performance schools, Inc. (CHPS) National Core Criteria Version 3.0. <https://chps.net/criteria/chps-core-criteria-template-local-adaptation>. Accessed 19 Dec 2020
- CPSC (2018) Test method CPSC-CH-C1001-09.4 Standard operating procedure for determination of Phthalates. United States Consumer Product Safety Commission (CPSC) Directorate for Laboratory Sciences Division of Chemistry, Rockville. https://cpsc.gov/s3fs-public/CPSC-CH-C1001-09.4_Standard_Operating_Procedure_for_Determination_of_phthalates.pdf?Uaxl4iIPOM6FkTpqgas9ffFKWLRsOCue0t. Accessed 19 Dec 2020
- CPSC (2020) About CPSC. <https://www.cpsc.gov/About-CPSC>Contact-Information>. Accessed 19 Dec 2020
- DOE (2019) Department of Energy (DOE) Zero Energy Ready Home national program requirements (Rev. 07). <https://www.energy.gov/sites/prod/files/2019/04/f62/DOE%20ZERH%20Specs%20Rev07.pdf>. Accessed 19 Dec 2020
- Eichler CMA, Hubal EAC, Xu Y et al (2020) Assessing human exposure to SVOCs in materials, products, and articles: a modular mechanistic framework. Environ Sci Technol. <https://doi.org/10.1021/acs.est.0c02329>

- GovTrack.us (2020) S. 1660-111th congress: formaldehyde standards for composite wood products act. <https://www.govtrack.us/congress/bills/111/s1660>. Accessed 19 Dec 2020
- GPO (2020) Code of federal regulations. <https://www.govinfo.gov/help/cfr#about>. Accessed 19 Dec 2020
- ISO (2020a) About us. <https://www.iso.org/about-us.html>. Accessed 19 Dec 2020
- ISO (2020b) Standards by ISO/TC 146/SC 6. <https://www.iso.org/committee/52822/x/catalogue/p/1/u/0/w/0/d/0>. Accessed 19 Dec 2020
- Kumar P, Skouloudis AN, Dell M et al (2016) Real-time sensors for indoor air monitoring and challenges ahead in deploying them to urban buildings. *Sci Total Environ* 560–561:150–159
- Liu X (2018) Characterise sources for exposure assessment of chemicals in indoor environment. *Indoor Built Environ* 27(3):291–295
- Morawska L, Tang JW, Bahnfleth W et al (2020) How can airborne transmission of COVID-19 indoors be minimised? *Environ Int* 105832:142
- NAHB (2020) ICC 700-2020 National green building standard. <https://www.nahb.org/advocacy/industry-issues/sustainability-and-green-building/sustainability-and-green-building/ICC-700-National-Green-Building-Standard>. Accessed 19 Dec 2020
- NIOSH (2018) About NIOSH. <https://www.cdc.gov/niosh/about/default.html>. Accessed 19 Dec 2020
- NIOSH (2020) NIOSH manual of analytical methods (NMAM), 5th edn, Andrews R, Fey O'Connor PF (ed). https://www.cdc.gov/niosh/nmam/pdf/NMAM_5thEd_EBook-508-final.pdf. Accessed 19 Dec 2020
- NIST (2019) National technology transfer and advancement act of 1995. <https://www.nist.gov/standardsgov/national-technology-transfer-and-advancement-act-1995>. Accessed 19 Dec 2020
- NREL (2020) National Renewable Energy Laboratory, U.S. Department of Energy Standard work specifications tool, Topic 6.62 Whole building ventilation. <https://sws-2017.nrel.gov/spec/662>. Accessed 19 Dec 2020
- OMB (2016) U.S. Office of Management and Budget, Executive Office of the President, OMB Circular A-119, Federal participation in the development and use of voluntary consensus standards and in conformity assessment activities. https://www.nist.gov/system/files/revised_circular_a-119_as_of_01-22-2016.pdf. Accessed 30 Dec 2020
- Raeiszadeh M, Adeli B (2020) A critical review on ultraviolet disinfection systems against COVID-19 outbreak: applicability, validation, and safety considerations. *ACS Photon* 7(11):2941–2951
- RED (2020a) Residential energy dynamics, LLC (RED) Calc Free Tools. <https://www.redcalc.com/red-calc-free/>. Accessed 19 Dec 2020
- RED (2020b) Residential energy dynamics, LLC (RED) Calc Pro. <https://www.redcalc.com/red-calc-pro/>. Accessed 19 Dec 2020
- RESNET (2014) RESNET guidelines for multifamily energy ratings. https://www.resnet.us/wpcontent/uploads/Adopted_RESNET_Guidlines_for_Multifamily_Ratings_8-29-14.pdf. Accessed 19 Dec 2020
- Rossetti G (2014) Two free tools: ASHRAE standards 55 and 62.2 calculators. *Heatspring Magazine*, September 14, 2014. <https://blog.heatspring.com/two-free-tools-ashrae-standards-55-62-2-calculators/>. Accessed 19 Dec 2020
- Schoen LJ (2020) Guidance for building operations during the COVID-19 pandemic. *ASHRAE J* 62(5):72–74
- Sobus JR, Wambaugh JF, Isaacs KK et al (2018) Integrating tools for non-targeted analysis research and chemical safety evaluations at the US EPA. *J Expo Sci Environ Epidemiol* 28:411–426. <https://doi.org/10.1038/s41370-017-0012-y>
- Stetzenbach LD, Amman H, Johanning E, King G, Shaughnessy RJ (2004) Microorganism, mold, and indoor air quality. <https://asm.org/ASM/media/docs/laq.pdf>. Accessed 19 Dec 2020
- Trane (2020) TRACE™ 700. <https://www.trane.com/commercial/north-america/us/en/products-systems/design-and-analysis-tools/trace-700.html>. Accessed 19 Dec 2020
- UL (2013) UL 181 Standard for factory-made air ducts and air connectors, 11th edn. Underwriters Laboratories Inc. (UL), Northbrook

- UL (2020a) About UL. <https://www.ul.com/about>. Accessed 19 Dec 2020
- UL (2020b) Standards. <https://ulstandards.ul.com/>. Accessed 19 Dec 2020
- ULC (2020) CAN/ULC-S774-09 (R2014) standard laboratory guide for the determination of volatile organic compound emissions from polyurethane foam. Underwriters Laboratories of Canada (ULC), Toronto
- US EPA (2009) Indoor air quality tools for schools. <https://www.epa.gov/sites/production/files/2014-08/documents/ventchklstbkgd.pdf>. Accessed 19 Dec 2020
- US EPA (2011) Healthy indoor environment protocols for home energy upgrades. Office of Air and Radiation (6609J), EPA 402/K-11/003. https://www.epa.gov/sites/production/files/2014-12/documents/epa_reetrofit_protocols.pdf. Accessed 19 Dec 2020
- US EPA (2016) Energy savings plus health: indoor air quality guidelines for multifamily building upgrades, publication no. EPA 402/K-16-01. https://www.epa.gov/sites/production/files/2016-02/documents/esh_multifamily_building_upgrades_508c_02_09_2016.pdf. Accessed 4 Jan 2021
- US EPA (2017) Indoor air quality building education and assessment model. https://19january2017snapshot.epa.gov/indoor-air-quality-iaq/indoor-air-quality-building-education-and-assessment-model_.html. Accessed 19 Dec 2020
- US EPA (2018) Indoor airPLUS construction specifications version 1 (REV.04) https://www.epa.gov/sites/production/files/2018-03/documents/indoor_airplus_construction_specifications.pdf. Accessed 19 Dec 2020
- US EPA (2020a) About EPA. <https://www.epa.gov/aboutepa>. Accessed 19 Dec 2020
- US EPA (2020b) The SW-846 compendium. <https://www.epa.gov/hw-sw846/sw-846-compendium>. Accessed 19 Dec 2020
- US EPA (2020c) Compendium of methods for the determination of toxic organic compounds in ambient air. <https://www.epa.gov/amtic/compendium-methods-determination-toxic-organic-compounds-ambient-air>. Accessed 19 Dec 2020
- US EPA (2020d) Risk evaluation for existing chemicals under TSCA. <https://www.epa.gov/assessing-and-managing-chemicals-under-tscas/risk-evaluations-existing-chemicals-under-tscas>. Accessed 19 Dec 2020
- US EPA (2020e) National HVAC design report ENERGY STAR multifamily new construction, version 1/1.1/1.2 (Rev. 02). https://www.energystar.gov/sites/default/files/asset/document/ENERGY%20STAR%20MFNC%20HVAC%20Design%20Report%20Version%201_1_Rev02.pdf. Accessed 5 Jan 2021
- US EPA (2020f) ENERGY STAR single-family new homes national HVAC design report, version 3/3.1 (Rev. 11) https://www.energystar.gov/sites/default/files/National%20HVAC%20Design%20Report_Rev%2011.pdf. Accessed 5 Jan 2021
- USGBC (2019) U.S. Green Building Council (USGBC) LEED v4.1. https://www.cagbc.org/CAGBC/Programs/LEED/LEEDv4/LEED_v4.1.aspx. Accessed 19 Dec 2020
- Zhang H, Srinivasan R (2020) A systematic review of air quality sensors, guideline, and management studies for indoor air quality management. Sustainability 12(21):9045



IEC/ISO Standards of Air Cleaners

54

Dejun Ma and Shanshan Li

Contents

Introduction	1548
IEC Standards of Air Cleaners	1549
IEC Profile (https://www.iec.ch/who-we-are)	1549
IEC/TC 61 and Air Cleaner Safety Standards	1552
IEC/TC 59 and Air Cleaner Performance Standards	1553
ISO Standards of Air Cleaners	1558
ISO Profile (https://www.iso.org/about-us.html)	1558
ISO/TC 142 (https://www.iso.org/committee/52624.html)	1560
Standards of ISO/TC 142 (https://www.iso.org/committee/52624.html)	1560
Conclusion	1561
References	1564

Abstract

At no time in the history over the past century have so many media and consumer concerns been centered on the health of our breathing space as we have seen in 2020 and 2021. COVID-19 has a profound effect on helping us to recognize the importance of the air we breathe. As a very effective household appliance to improve indoor air quality, air cleaners have been used a lot in recent years for cleaning indoor particulate, gaseous, and microbial pollutants. Different levels of relevant standards also got widespread attention from regulatory agencies, testing laboratories, enterprises, and consumers. However, as is known to all, international standards are more effective in gauging all the good features and serving consumers worldwide.

This chapter aims to introduce the international standards of air cleaners and the corresponding IEC (International Electrotechnical Committee) and ISO (International Organization for Standardization) development organizations,

D. Ma (✉) · S. Li

China Household Electric Appliance Research Institute (CHEARI), Beijing, China
e-mail: madj@cheari.com; liss@cheari.com

including their basic information, structure, technical committees and the way of participation. Both the two standardization organizations have technical committees responsible for standardization of air treatment appliances or equipment. In total, there are about 25 published standards and 16 standards under development for air cleaners and air cleaning equipment till the end of 2020. Furthermore, this chapter gives a detailed introduction of IEC 63086 series, especially the published IEC 63086-1: 2020 and the two underdeveloped standards on microbe reduction and fresh-air air cleaners.

In conclusion, the international standard organizations have realized the importance of air cleaner standards and their role in improving indoor air quality, and encouraged the technical committees to carry out a lot of preliminary research and standard development work, to lead the development of industries and protect people's health and lives all over the world.

Keywords

Air cleaners · International standards · IEC · ISO

Introduction

Statistics show that humans spend at least 70% of their time indoors, while the urban population spends more than 90% of their time indoors, especially infants and young children, the elderly, the weak, and the disabled (Morris 2020). However, the concentrations of indoor air pollutants are generally several times that of outdoor pollutants, and in some cases tens or even hundreds of times that of outdoor pollutants (Yinping 2013). The pollutions may come from the human body's metabolism, kitchen fume, electrical appliances, smoking, decoration, microorganisms, etc., which may cause respiratory diseases and damage the human hematopoietic system or central nervous system (Morris 2020).

In 2020, we have all felt the effects of significant interest in the health and well-being of the indoor environment. At no time in history over the last 100 years have so many media and consumer concerns been centered on the health of our breathing space as we have seen in the last year. COVID-19 has a profound effect on helping us to recognize the importance of the air we breathe. Not only that, but in many countries and regions, citizens were forced to spend long hours quarantined in their private dwellings and the role of indoor air quality became vitally important.

None of existing methods could work in all cases and certainly no invention could prevent all illness. However, there are many ways to improve indoor air quality. One of the methods is the use of electrical appliances such as an air cleaner in the residential space. Air cleaners were first introduced in the 1970s and 1980s with basic filter and fan functions to reduce allergens and other external pollutants. In the next 50 years since the widespread introduction of air cleaners, many countries have developed standards to measure the safety and performance of air cleaners with

different features including the United States, China, Japan, Korea, and so on. Several of these countries have had performance test method standards for more than 20 years. Differences in these standards revolve around the differences in pollutants, but also the technologies which have developed.

However, an international standard is more effective in gauging all the good features and serving consumers worldwide. IEC and ISO, the two international standardization organizations, both have technical committees responsible for standardization of air treatment appliances or equipment, including IEC/TC61 (Safety of household and similar electrical appliances), IEC/TC59 (Performance of household and similar electrical appliances), and ISO/TC142 (Cleaning equipment for air and other gases). Furthermore, IEC/TC59 and ISO/TC142 have established a joint work group (JWG) to develop standards concerning the performance of air treatment appliances.

IEC Standards of Air Cleaners

IEC Profile (<https://www.iec.ch/who-we-are>)

The IEC is a worldwide, not-for-profit membership standardization organization. It aims to facilitate technical innovation, affordable infrastructure development, efficient and sustainable energy access, smart urbanization and transportation systems, climate change mitigation, and increase the safety of people and the environment through its work in electrical and electronic fields.

Membership

The IEC members are composed of IEC National Committees (NC). They provide the management expertise and send experts to represent national needs in the global IEC standardization and conformity assessment arena. Upon admission, every IEC Member – one National Committee per country – promises to fully represent all private and public national interests in the field of electrotechnology at the global level in IEC standardization and conformity assessment activities.

For membership levels, IEC members are divided into Full Member and Associate Member. Any country which can demonstrate that its National Committee has been constituted in accordance with the **IEC Statutes and Rules of Procedure** may apply to become an IEC Full Member. IEC Full Members, after paying their yearly membership fee, have the possibility to send experts to participate actively in any technical committee/subcommittee according to their choice. They are also able to apply for management positions and functions in the IEC and have voting rights in the IEC Council. Some countries can opt to become an IEC Associate Member. IEC Associate Members can access all working documents and opt to send experts to participate in a limited number of technical committees/subcommittees. They cannot occupy management positions and functions within the IEC and do not have voting rights in the IEC Council.

Structure

The IEC brings together more than 170 countries and provides a global, neutral, and independent standardization platform to 20,000 experts globally. It administers four Conformity assessment systems whose members certify that devices, systems, installations, services, and people work as required.

Figure 1 shows the IEC management structure (till the end of 2020), where we can find that the Council is the supreme governing body of the IEC. Management is

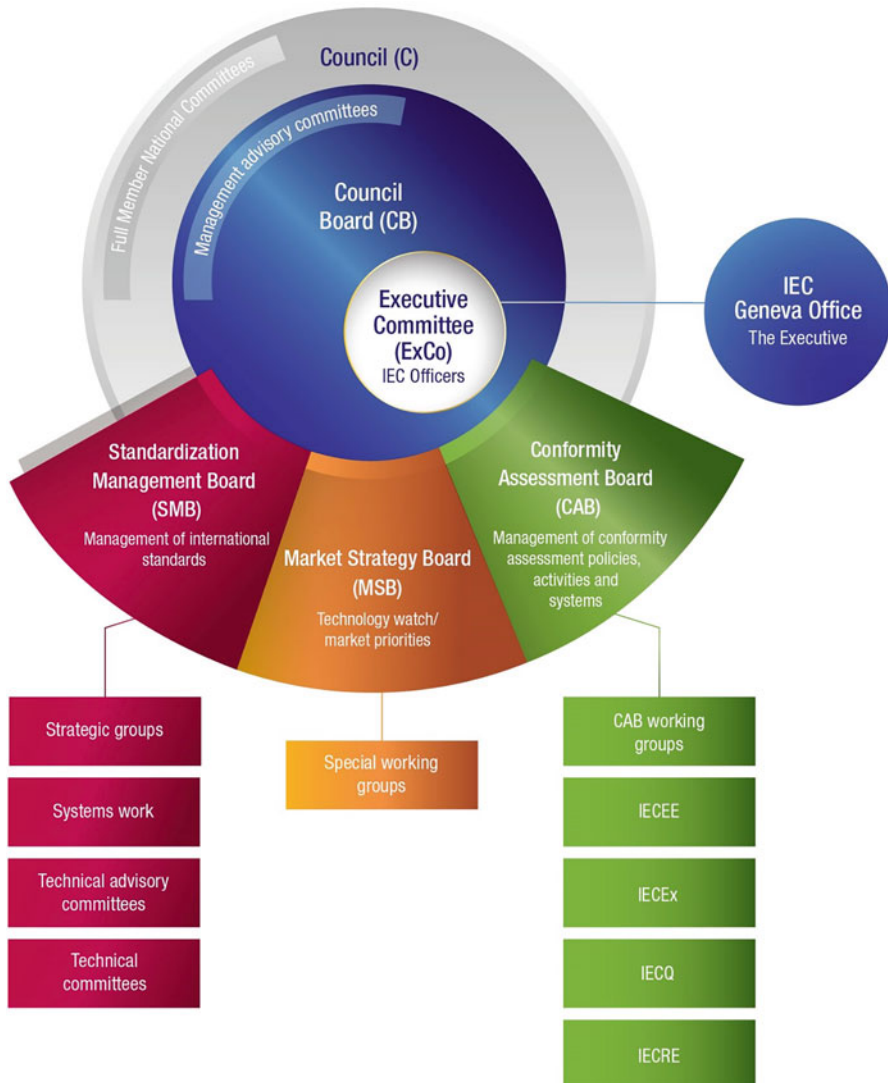


Fig. 1 IEC management structure. (Source: IEC website. <https://www.iec.ch/management-structure>)

delegated to the Council Board, the SMB (Standardization Management Board), MSB (Market Strategy Board), and CAB (Conformity Assessment Board). For the development of most standards, the direct responsible groups are Technical Committees under SMB.

Technical Committees

As an important outcome, IEC publishes International Standards, Technical Specifications, Technical Reports, Publicly Available Specifications (PAS) and Guides. Their preparation is entrusted to technical committees. Any NC interested in the subject may participate in this preparatory work. International governmental and nongovernmental organizations liaising with the IEC also participate in this preparation. IEC collaborates closely with the International Organization for Standardization (ISO) in accordance with conditions determined by agreement between the two organizations.

The IEC publishes around 10,000 IEC International Standards which together with conformity assessment provide the technical framework that allows governments to build national quality infrastructure and companies of all sizes to buy and sell consistently safe and reliable products in most countries of the world. IEC International Standards serve as the basis for risk and quality management and are used in testing and certification to verify that manufacturer promises are kept.

Thousands of experts participate in IEC standardization work in IEC technical committees and subcommittees (TC/SCs). They are chosen by their National Committee (NC) to share their technical expertise and represent the national requirements of industry, government, test and research laboratories, academia or user groups at the global level in the IEC.

The IEC offers these experts a neutral and independent platform where they can discuss and agree on state-of-the-art technical solutions with global relevance and reach. These are published as voluntary, consensus-based international standards. Each TC defines its scope and area of activity, which it submits to the IEC Standardization Management Board (SMB) for approval. A TC can form one or more SCs depending on the extent of its work program. Each SC defines its scope and reports directly to the parent TC. Till the end of December 2020, there are 109 TCs, 101 SCs, 707 WGs, 194 project teams, and 645 maintenance teams within IEC.

IEC/TC61 and IEC/TC59 are technical committees under IEC responsible for the safety and performance of household and similar electrical appliances. The standards they develop involve more than 100 household and similar electrical appliances, for example, washing machines, dishwashers, room air conditioners, range hoods, fans, air cleaners, etc. Here gives the introduction about the safety and performance standards for air cleaners and the responsible development institutions.

Participation

If you want to contribute to IEC work and are located in one of the IEC member countries, you need to reach out to your IEC National Committee (NC). They can tell you more about how you can get involved at the national level and/or the global

level in the IEC. The NC is responsible for nominating experts to participate in the development of IEC work and in the IEC Confirmation Assessment Systems.

If travelling to face-to-face working meetings is a hurdle for you, you can participate in the IEC work from the national level. Share your needs with the NC and help to make the standard more relevant for your industry.

IEC/TC 61 and Air Cleaner Safety Standards

IEC/TC 61 (https://www.iec.ch/dyn/www/f?p=103:7:0::::FSP_ORG_ID:1236)

The title of IEC/TC 61 is safety of household and similar electrical appliances. It is responsible for preparing safety requirements for electrical appliances primarily for household purposes, but also for other equipment and appliances in similar fields where there is no IEC Technical Committee in existence. The Secretariat is the United States of America.

For working structure, there are 5 SCs, 9 working groups, 3 project teams, 10 maintenance teams, 1 joint working group, 1 advisory group, and 1 editing group under TC61.

Till the end of 2020, IEC/TC61 and its subcommittees have developed 103 safety standards, among which 101 are IEC 60335 series standards.

IEC 60335 series deal with safety of household and similar electrical appliances, including 1 Part 1 standard of general requirements and more than 100 Part 2 standards of particular requirements for different kinds of household appliances. Every Part 2 standard shall be used in conjunction with IEC 60335-1. With the aim of protecting the personal and property safety of consumers, the IEC 60335 series put forward safety requirements and testing methods for household and similar electrical appliances mainly in terms of anti-shock, anti-fire, anti-scald, anti-mechanical, anti-radiation, and anti-toxicity hazard.

IEC 60335-2-65

IEC 60335-2-65, Household and similar electrical appliances – Safety – Part 2-65: Particular requirements for air-cleaning appliances is a Part 2 particular requirement standard for air cleaners. IEC 60335-2-65 has experienced two whole number editions, three amendments, and one corrigendum, and its current edition is IEC 60335-2-65:2015 (Ed2.2), see Table 1 for its evolution. IEC 60335-2-65 consists of 32 Clauses and several Annexes covering Classification; Marking and instructions; Protection against access to live parts; Starting of motor-operated appliances; Power input and current; Heating; Leakage current and electric strength at operating temperature; Transient overvoltages; Moisture resistance; Leakage current and electric strength; Overload protection of transformers and associated circuits; Endurance; Abnormal operation; Stability and mechanical hazards; Mechanical strength; Construction; Internal wiring; Components; Supply connection and external flexible cords; Terminals for external conductors; Provision for earthing; Screws and connections; Clearances, creepage distances, and solid

Table 1 Different editions of IEC 60335-2-65

No.	Editions	Title
Ed 1.0	IEC 60335-2-65: 1993	Household and similar electrical appliances – Safety – Part 2-65: Particular requirements for air-cleaning appliances
Amendment 1	IEC 60335-2-65: 1993/AMD1:2000	
Ed 2.0	IEC 60335-2-65: 2002	
Corrigendum 1	IEC 60335-2-65: 2002/COR1:2004	
Amendment 1	IEC 60335-2-65: 2002/AMD1:2008	
Amendment 2	IEC 60335-2-65: 2002/AMD2:2015	

insulation; Resistance to heat and fire; Resistance to rusting; Radiation, toxicity, and similar hazards; etc.

You can find the detailed information of this standard at IEC website <https://webstore.iec.ch/publication/1695>.

IEC/TC 59 and Air Cleaner Performance Standards

IEC/TC 59 (https://www.iec.ch/dyn/www/f?p=103:14:13818013144838:::FSP_ORG_ID,FSP_LANG_ID:19691,25)

The title of IEC/TC 59 is performance of household and similar electrical appliances. It is responsible for preparing International Standards on methods of measurement of characteristics which are of importance to determine the performance of electrical appliances for household use or of electrical appliances for commercial use and that are of interest for the user. This may include associated aspects related to the use of the appliances and aspects such as the classification, accessibility, and usability of appliances, ergonomic characteristics, and conditions for the information provided at the point of sale. The Secretariat is Germany.

For working structure, there are 7 SCs, 5 working groups, 1 project team, 1 maintenance team, 1 joint working group, 1 advisory group, 1 ad hoc group, and 1 editing group under TC 59.

Till the end of 2020, IEC/TC 59 have developed 79 performance standards.

IEC 63086 Series

IEC 63086 series standards, Household and similar electrical air cleaning appliances – Methods for measuring the performance, have a much shorter history. They are the first performance standards for air cleaners proposed by China in 2016 to develop a single performance standard and then derived into a series standard due to a strong desire of participating members to deal with different

types of pollutants. The first edition, IEC 63086-1:2020, was published on April 9, 2020.

Background

As is known to all, indoor air quality is a huge issue in many countries. With the increase of natural and man-made pollution items at home, many people, especially for vulnerable groups like children and elderly people, are experiencing health-related issues from poor indoor air quality. In many cases, consumers are now choosing to use air cleaners as the method to reduce pollutants in their own homes and apartments. This has given rise to a huge increase in these appliances and to the numbers of manufacturers worldwide. Along with this huge increase in products, also comes an increase in the claims of reduction of pollutants without a unified means of performing testing and certification. In several countries, national standards have been developed. These include standards in the United States, China, Japan, and Korea, to name a few. All of these standards share many features in testing, but there is no one international standard to gauge the performance. China has also encountered similar pollution problems in its development process and saw this need to solve the global problem. Chinese National Committee proposed to IEC/TC 59 in May 2016 to develop a performance standard for air cleaners based on its national standard GB/T 18801 Air cleaners.

Summary of Development Process or Plans

The Chinese proposal was approved by IEC/TC59 and a project team PT 63086 was formed in September 2016 with Mr. Dejun Ma from China as convenor and six original registered member experts from the Netherlands, Korea, Germany, Italy, and the UK. PT 63086 immediately launched its work through regular web meetings and face-to-face meetings in Washington, DC, Venice, Busan, Aix-en-Provence, etc. They carried out in-depth review of the scientific literature on indoor air quality, technologies on pollutant reduction and relative test methods, prepared its own draft, and organized round robin tests. Many countries showed interest and applied to join in the standardization work during its progress. Till the end of 2020, more than 80 experts from at least 11 member countries are involved, including scientists, university professors, testing lab specialists, and manufacturers. The countries include China, the United States, Germany, France, Italy, Japan, Korea, Belgium, the UK, the Netherlands, and Sweden.

Performance of air cleaners is a very complex subject. It involves testing different types of pollutants, testing chambers, energy efficiency, advanced electronic controls, remote communication through public networks, along with several types of air delivery. In 2018, PT 63086 made an important decision to develop a series standard, including one Part 1 standard with general requirements and multiple Part 2 standards for different pollutant reduction and characteristics for testing, which was then approved by IEC/TC59 in October 2018, and this PT was upgraded to a working group (WG 17). WG 17 firstly focused on Part 1 standard IEC 63086-1 and would proceed to Part 2 standards step-by-step.

Table 2 Stages of developing IEC 63086-1:2020

	Stage	Decision date
1	NP – New Proposal	May 2016
2	CD – Committee Draft	June 2018
3	CDV – Committee Draft for Voting	March 2019
4	FDIS – Final Draft of International Standard	February 2020
5	IS – International Standard	April 2020

For IEC 63086-1:2020, before its final publication early this year, WG 17 had experienced many WG meetings and several tough official stages for comments or voting from all IEC/TC59 member countries, see Table 2.

For Part-2 standards, WG 17 has mapped out a detailed plan and formed 12 sub-working groups to develop Technical Reports or Part 2 standards:

- SWG 1 – Develop a Part 2 Standard for Reduction of Particles
- SWG 2 – Develop a Part 2 Standard for Reduction of Chemical Gases
- SWG 3 – Develop a Part 2 Standard for Reduction of Microbes
- SWG 4 – Develop a Technical Report on Air Cleaners with Automatic Mode
- SWG 5 – Develop a Technical Report on Air Cleaners for Measurement of Power and Energy
- SWG 6 – Develop a Part 2 Standard for Fresh-Air, Air Cleaners
- SWG 7 – Develop a Part 2 Standard for Automobile Passenger Air Cleaners
- SWG 8 – Manage Round Robin Testing
- SWG 9 – Develop a Technical Report on Mobile/Robotic Air Cleaners
- SWG 10 – Develop a Part 2 Standard for Measuring Performance Over Time
- SWG 11 – Working with IEC TC 59 WG 2, Develop test method for measurement of Acoustical Noise
- SWG 12 – Develop a Part 2 Standard for Reduction of Ozone

Not all SWGs are active at the moment. Till December of 2020, there are three standards under development by SWG1, SWG6, and SWG11, and some others are still under preparation (Ma et al. 2020).

- IEC 63086-2-1 ED1 (NP)
Household and similar electrical air cleaning appliances – Methods for measuring the performance – Part 2-1: Particular requirements for determination of reduction of particles
- IEC 63086-2-6 ED1(NP)
Household and similar electrical air cleaning appliances – Methods for measuring the performance – Part 2-6: Particular requirements for fresh-air air cleaners
- IEC 60704-2-19 ED1(NP) (SWG11 experts join TC59/WG2 for development of this standard)

Household and similar electrical appliances – Test code for the determination of airborne acoustical noise – Part 2-19: Particular requirements for air cleaners

Joint Work Together with ISO/TC 142

WG 17 became aware of the work of ISO TC 142 in 2017. Much of the work of ISO/TC 142 has been on filters, pollutants, and special media. One of its working groups (WG 11) was interested in writing a test method for air cleaners and has long been preparing. After communication between ISO/TC142 and IEC/TC59, WG 17 was renamed JWG 17 in October 2019 as a joint working group of IEC/TC 59 and ISO/TC 142. Mr. Dejun Ma from IEC side and Mr. Tim Johnson from ISO side act as co-convenors (Ma et al. 2020).

Projects under the responsibility of JWG 17 will be developed as dual logo.

Information of IEC 63086-1:2020

IEC 63086-1:2020, Household and similar electrical air cleaning appliances – Methods for measuring the performance – Part 1: General requirements, consists of eight clauses and three annexes, see Table 3, specifying the terms and definitions, classification, test conditions, test chamber conditions, instrumentation and equipment, determination of the air exchange rate of test chamber, noise, energy efficiency, etc.

You can find the detailed information of this standard at IEC website <https://webstore.iec.ch/publication/33044>.

Work Plan and Progress of SWGs on Microbe Reduction and Fresh-Air Air Cleaners

SWG 3 on Microbe Reduction

SWG 3 started work from November 2020. It aims to develop a Part 2 standard of IEC 63086 series on determination of reduction of microbes.

Table 3 The structure of IEC 63086-1

Clauses and annexes	Title
Clause 1	Scope
Clause 2	Normative references
Clause 3	Terms and definitions
Clause 4	Classification
Clause 5	Conditions, instrumentation, and equipment for measurement
Clause 6	Determination of the air exchange rate of the test chamber
Clause 7	Measurement of noise
Clause 8	Energy efficiency
Annex A	Determination of the test chamber mixing level
Annex B	Standardization of calculation
Annex C	Test stand for wall and direct plug-in type air cleaners

During preliminary research, the group leader Ms. Xiao Zhang and her team investigated related standards and literatures from all countries and organizations, especially the literatures on the pathogen analysis of respiratory diseases in hospitals, and screened out the bacteria and molds closely related to respiratory diseases, like *Staphylococcus aureus*, *Streptococcus pneumoniae*, *Escherichia coli*, *Klebsiella pneumonia*, MS2, and *Aspergillus fumigatus*. Although viruses are also the main cause of respiratory diseases, considering the strict restriction on laboratory biosafety levels and the difficulty of virus test operation, bacteriophages are often used in many medical device standards instead of animal viruses. Most air cleaners rely on filtration technology for microbial removal, the effect of which is closely related to the size of the microorganism, so although the pathogenicity of different kinds of microorganisms vary greatly, their size difference is not so much and thus there is no big difference of the microbe removal result of air cleaners. Therefore, considering the test cost and restrictions, it is not recommended to choose too many kinds of microorganisms for the test, but to select the typical types, such as MS2 and phi X 174 for virus. Test bacteria and molds can also be treated the same way.

Since Chinese and Japanese national standards GB 21551.3 and JEM 1467, as well as international standard ISO 16000-36 have developed test methods to remove microbes such as *Staphylococcus albus*, *Micrococcus luteus*, Phi-X174/MS2, and H1N1/H3N2, SWG3 will make full reference to the existing standards and achieve one common-consensus international standard.

According to the workplan of SWG 3, the Part 2 standard will be progressed according to the workplan listed in Table 4.

SWG 6 on Fresh-Air Air Cleaners

SWG 6 started work from April 2019. It aims to develop a Part 2 standard for fresh-air air cleaners.

In the last 10 years, air cleaners have become popular worldwide due to people's pursuit of a healthy life and the increasing air pollution problems, but longtime operation of air cleaners may result in lack of oxygen and increase of carbon dioxide in a confined space, which will affect the health and comfort of indoor users. In response to this, fresh-air air cleaners appeared and are accepted in the market. They help to remove indoor particles, VOCs, disinfect and introduce the outdoor fresh air, preventing indoor and outdoor particle pollution. They are very useful household fresh-air products.

Table 4 Workplan of SWG 3 for a Part 2 standard of IEC 63086 series

	Stage	Decision date
1	NP – New Proposal	April 2021
2	CD – Committee Draft	December 2022
3	CDV – Committee Draft for Voting	June 2023
4	FDIS – Final Draft of International Standard	December 2023
5	IS – International Standard	March 2024

From the market perspective, taking China as an example, in 2018, the sales volume of fresh-air air cleaners was 1.06 million units, a year-on-year increase of 39%, with sales of 10.2 billion yuan, a year-on-year increase of 27%. While compared to the 44.5% increase in 2017, the speed has slowed significantly (https://mp.weixin.qq.com/s/TzFpGgZRz1_PutMDVq_KA). In 2019, the sales volume of the fresh-air air cleaner industry exceeded 1.46 million units, a year-on-year increase of 39%, and sales reached 13.9 billion yuan annually (<https://mp.weixin.qq.com/s/kN3Q39I6Dxq66Yqmbiw0Bg>).

Due to a different construction, the test methods are totally different between fresh-air air cleaners and room air cleaners. For example, test chamber for fresh-air air cleaners may operate at a pressure slightly above ambient. From installation perspective, this product is intended to be installed by a professional individual or company, which may enhance the ventilation and air cleaning of the HVAC system, and it is intended to be installed in the residential dwelling, which can be used to treat the indoor environment of multiple rooms.

The NP document was put forward in June 2019 and got approved as IEC 63086-2-6 Household and similar electrical air cleaning appliances – Methods for measuring the performance – Part 2-6: Particular requirements for fresh-air air cleaners, in August the same year by IEC/TC 59.

This standard aims to include methods to measure the performance of a fresh-air air cleaner to improve the indoor environment, and is applicable to those appliances which are connected to the external environment, which provides pollutant reduced outdoor air into an indoor space but are not connected to the HVAC system of the dwelling or building. It intends to specify release of harmful substances, standby power, air volume and outlet full pressure, fresh air cleaning efficiency, clean fresh air volume, internal circulation clean air volume, air cleaning efficiency, fresh cumulate clean mass, air exchange efficiency, etc.

It is estimated that this standard will be published in December 2024.

ISO Standards of Air Cleaners

ISO Profile (<https://www.iso.org/about-us.html>)

ISO is an independent, nongovernmental membership international standardization organization. It brings together experts to share knowledge and develop voluntary, consensus-based, market relevant International Standards that support innovation and provide solutions to global challenges, covering almost all aspects of technology and manufacturing except electric and electronic aspects.

Membership

ISO is a global network of national standards bodies. Its members are the foremost standards organizations in their countries and there is only one member per country. Each member represents ISO in its country.

There are three-member categories including full members, corresponding members, and subscriber members. Each enjoys a different level of access and influence over the ISO system. This helps ISO to be inclusive while also recognizing the different needs and capacity of each national standards body.

Full members (or member bodies) influence ISO standards development and strategy by participating and voting in ISO technical and policy meetings. Full members sell and adopt ISO International Standards nationally. Correspondent members observe the development of ISO standards and strategy by attending ISO technical and policy meetings as observers. Correspondent members that are national entities sell and adopt ISO International Standards nationally. Correspondent members in the territories that are not national entities sell ISO International Standards within their territory. Subscriber members keep up to date on ISO's work but cannot participate in it. They do not sell or adopt ISO International Standards nationally.

Structure

ISO is an independent, nongovernmental organization made up of members from the national standards bodies of 165 countries.

Figure 2 shows the ISO governance structure, where we can find that the General Assembly is the overarching organ and ultimate authority of the organization. The ISO Council is the core governance body of the organization and reports to the General Assembly. The Council has direct responsibility over a number of bodies reporting to Council including President's Committee, Council Standing Committees, Advisory groups, and Policy development committees. The management of the technical work is taken care of by the Technical Management Board, which reports to Council. This body is also responsible for the technical committees that lead standards development and any strategic advisory boards created on technical matters.

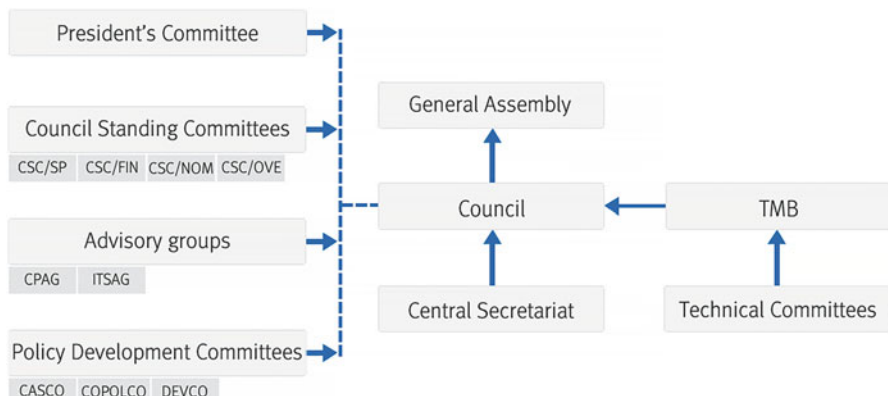


Fig. 2 ISO governance structure. (Source: <https://www.iso.org/structure.html>)

Technical Committees

Till the end of 2020, there are 254 technical committees and 539 subcommittees under ISO to take care of standards development covering food and agriculture, chemicals, building and construction, business management and innovation, energy, sustainability and environment, health, medicine and laboratory equipment, nonmetallic materials, information technology, services, and so on. The first technical committee, TC1, deals with screw threads and was created back in 1947. ISO has developed 23626 international standards covering almost all aspects of technology and manufacturing.

Participation

Individuals or companies cannot become ISO members, but there are ways that you can take part in standardization work. Please see the list below for information about the ISO member in your country.

ISO/TC 142 (<https://www.iso.org/committee/52624.html>)

The title of ISO/TC142 is Cleaning equipment for air and other gases. It is responsible for standardization in the fields of terminology, classification, characteristics, and test and performance methods for **air and gas cleaning and disinfecting equipment** for general ventilation and industrial applications with the following exclusion:

- Exhaust gas cleaners for gas turbines and IC engines in mobile equipment, this being within the scope of other ISO technical committees.
- Filters for personal protection equipment which are the field of work of technical committee ISO/TC 94.
- Cabin filters in mobile equipment covered by ISO/TC 22, 23, and 127.

Its secretariat is UNI (Ente Italiano di Normazione) with the current Chair Mr. Riccardo Romanò and Committee manager Mrs. Anna Martino. There are 12 working groups under ISO/TC142 with the following specific and detailed responsibilities, see Table 5, where **ISO/TC 142/JWG 11** is the joint working group with IEC/TC 59.

Standards of ISO/TC 142 (<https://www.iso.org/committee/52624.html>)

There are in total 22 published standards and 16 standards under development till December 2020 under the direct responsibility of ISO/TC 142, see Tables 6 and 7.

Table 5 Twelve WGs under ISO/TC142

WGs	Title
ISO/TC 142/WG 1	Terminology
ISO/TC 142/WG 2	UV-C technology
ISO/TC 142/WG 3	General ventilation filters
ISO/TC 142/WG 4	HEPA and ULPA filters
ISO/TC 142/WG 5	Dust collectors, droplet separators, and purifiers
ISO/TC 142/WG 7	Cleanable filter media used in industrial applications
ISO/TC 142/WG 8	Gas-phase air cleaning devices
ISO/TC 142/WG 9	Particulate air filter intake systems for rotary machinery and stationary internal combustion engines
ISO/TC 142/JWG 10	Joint ISO/TC 142 – ISO/TC 85/SC 2 WG: Aerosol filters for nuclear applications
ISO/TC 142/JWG 11	Joint ISO/TC 142 – IEC/TC 59 WG: Portable room air cleaners for comfort applications
ISO/TC 142/WG 12	Sustainability of air cleaning equipment and media
ISO/TC 142/WG 13	Biological equipment for waste gas treatment

Conclusion

In the internationalization practice, international standards have received more and more attention from countries all over the world as they are playing an increasingly important role in the world's economic and social development. The implementation of international standards is conducive to eliminating technical barriers in international trade, facilitating technological progress, improving product quality and efficiency, and promoting international economic and technological exchanges and cooperation.

As introduced in the above contents, for air cleaners, existing international standards have covered safety, performance, and parameters of key components, air filters, and formed a relatively complete international standard system. As many test reports and research show, air cleaners in accordance with these international standards can significantly improve indoor air quality through filtration and retention, activated carbon adsorption, ultraviolet sterilization, lysozyme and chemical fungicides, ozone, and other biological aerosol removal methods in accordance. Furthermore, it is reported that due to the impact of this epidemic and people's growing awareness of health, the standards related to microbe removal, especially virus removal, will be developed or reviewed to better solve the problems of particulate matter, gaseous and microbial pollutants in the indoor air.

Table 6 Twenty-two published standards under ISO/TC142

No.	Standard number	Title
1	ISO 10121-1: 2014	Test method for assessing the performance of gas-phase air cleaning media and devices for general ventilation – Part 1: Gas-phase air cleaning media
2	ISO 10121-2: 2013	Test methods for assessing the performance of gas-phase air cleaning media and devices for general ventilation – Part 2: Gas-phase air cleaning devices (GPACD)
3	ISO 15714: 2019	Method of evaluating the UV dose to airborne microorganisms transiting in-duct ultraviolet germicidal irradiation devices
4	ISO 15727: 2020	UV-C devices – Measurement of the output of a UV-C lamp
5	ISO 15858: 2016	UV-C Devices – Safety information – Permissible human exposure
6	ISO 15957: 2015	Test dusts for evaluating air cleaning equipment
7	ISO 16170: 2016	In situ test methods for high-efficiency filter systems in industrial facilities
8	ISO 16890-1: 2016	Air filters for general ventilation – Part 1: Technical specifications, requirements, and classification system based upon particulate matter efficiency (ePM)
9	ISO 16890-2: 2016	Air filters for general ventilation – Part 2: Measurement of fractional efficiency and air flow resistance
10	ISO 16890-3: 2016	Air filters for general ventilation – Part 3: Determination of the gravimetric efficiency and the air flow resistance versus the mass of test dust captured
11	ISO 16890-4: 2016	Air filters for general ventilation – Part 4: Conditioning method to determine the minimum fractional test efficiency
12	ISO 16891: 2016	Test methods for evaluating degradation of characteristics of cleanable filter media
13	ISO 21083-1: 2018	Test method to measure the efficiency of air filtration media against spherical nanomaterials – Part 1: Size range from 20 nm to 500 nm
14	ISO/TS 21083-2:2019	Test method to measure the efficiency of air filtration media against spherical nanomaterials – Part 2: Size range from 3 nm to 30 nm
15	ISO 29461-1: 2013	Air intake filter systems for rotary machinery – Test methods – Part 1: Static filter elements
16	ISO 29462: 2013	Field testing of general ventilation filtration devices and systems for in situ removal efficiency by particle size and resistance to airflow
17	ISO 29463-1: 2017	High-efficiency filters and filter media for removing particles from air – Part 1: Classification, performance, testing, and marking
18	ISO 29463-2: 2011	High-efficiency filters and filter media for removing particles in air – Part 2: Aerosol production, measuring equipment and particle-counting statistics
19	ISO 29463-3: 2011	High-efficiency filters and filter media for removing particles in air – Part 3: Testing flat sheet filter media
20	ISO 29463-4: 2011	High-efficiency filters and filter media for removing particles in air – Part 4: Test method for determining leakage of filter elements – Scan method

(continued)

Table 6 (continued)

No.	Standard number	Title
21	ISO 29463-5: 2011	High-efficiency filters and filter media for removing particles in air – Part 5: Test method for filter elements
22	ISO 29464: 2017	Cleaning of air and other gases – Terminology

Table 7 Sixteen standards under development under ISO/TC142

No.	Standard Number	Title
1	ISO/CD 10121-3	Test method for assessing the performance of gas-phase air cleaning media and devices for general ventilation – Part 3: Classification system for treatment of make-up air
2	ISO/AWI 15957	Test dusts for evaluating air cleaning equipment
3	ISO/AWI 16313-1	Laboratory test of dust collection systems utilizing porous filter media online cleaned using pulses of compressed gas – Part 1: Systems not utilizing integrated fans
4	ISO/DIS 16890-2	Air filters for general ventilation – Part 2: Measurement of fractional efficiency and air flow resistance
5	ISO/DIS 16890-4	Air filters for general ventilation – Part 4: Conditioning method to determine the minimum fractional test efficiency
6	ISO/AWI 16890-5	Air filters for general ventilation – Part 5: Measurement of fractional efficiency and air flow resistance for flat sheet filter media
7	ISO/FDIS 22031	Sampling and test method for cleanable filter media taken from filters of systems in operation
8	ISO/AWI 23137-1	Requirements for aerosol filters used in nuclear facilities against specified severe conditions – Part 1: General requirements
9	ISO/AWI 23138	Biological equipment for treating air and other gases – General requirements
10	ISO/AWI 23139	Biological equipment for treating air and other gases – Application guidance for deodorization in wastewater treatment plants
11	ISO/DIS 29461-1	Air intake filter systems for rotary machinery – Test methods – Part 1: Static filter elements
12	ISO/CD 29461-7	Air filter intake systems for rotary machinery – Test methods – Part 7: Filter element endurance test in fog and mist environments
13	ISO/DIS 29462	Field testing of general ventilation filtration devices and systems for in situ removal efficiency by particle size and resistance to airflow
14	ISO/CD 29463-5	ISO 29463-5 High-efficiency filters and filter media for removing particles in air – Part 5: Test method for filter elements
15	IEC/AWI 63086-2-1	Household and similar electrical air cleaning appliances – Methods for measuring the performance – Part 2-1: Particular requirements for determination of reduction of particles
16	IEC/AWI 63086-2-6	Household and similar electrical air cleaning appliances – Methods for measuring the performance – Part 2-6: Particular requirements for fresh-air air cleaners

References

- 2018 Fresh Air Industry Annual Report, Beijing All View Cloud Data Technology Co. Ltd, https://mp.weixin.qq.com/s/TzFpGgIZRz1_PutMDVq_KA
- 2019 Fresh Air Industry Annual Report, Beijing All View Cloud Data Technology Co. Ltd, <https://mp.weixin.qq.com/s/kN3Q39I6Dxq66Yqmhiw0Bg>
- Ma D, Johnson T, Morris W (2020) IEC/TC59/JWG17 report to TC59. Online, Oct 2020
- Morris W (2020) The role of technical standards in improving IAQ. Draft Presentation at Indoor Air 2020[R], Korea, November 2020
- Yinping Z (2013) Indoor air quality control: the challenges and responsibilities of HVAC researchers in the new century. HV&AC 43(12):1–7



IAQ Requirements in Green Building Labeling Systems and Healthy Building Labeling Systems

55

Li Jingguang, Wei Jingya, and Ji Siyu

Contents

Introduction	1566
Green and Health Building Labeling Systems	1567
China Assessment Standard for Green Building (CASGB)	1567
LEED	1567
BREEAM	1567
China Assessment Standard for Healthy Building (CASHB)	1568
WELL	1568
Environmental Index	1568
Environmental Index in CASGB	1568
Environmental Index in LEED	1569
Environmental Index in BREEAM	1569
Environmental Index in CASHB	1569
Environmental Index in WELL	1569
Formaldehyde, VOC, and SVOC Control in Labeling Systems	1571
CASGB	1572
LEED	1573
BREEAM	1574
CASHB	1574
WELL	1576
Particulate Matter (PM) Control in Labeling Systems	1578
CASGB	1578
LEED	1581
BREEAM	1582

L. Jingguang (✉) · J. Siyu

Shanghai Research Institute of Building Sciences (Group) Co. Ltd, Shanghai, China
e-mail: lijingguang@sribs.com; jisiyu@sribs.com

W. Jingya
Tsinghua University, Beijing, China
e-mail: weixxjulia9148@163.com

CASHB	1582
WELL	1583
Conclusion	1584
References	1585

Abstract

Green and healthy buildings are currently an important goal for the construction industry. To achieve this goal, developing and implementing green building labeling systems and healthy building labeling systems is important. At present, many countries and regions have developed individual green building labeling systems and healthy building labeling systems. Leadership in Energy and Environmental Design (LEED), Building Research Establishment Environmental Assessment Methodology (BREEAM), and China Assessment Standard for Green Building (CASGB) are representative green building labeling systems. The China Assessment Standard for Healthy Building (CASHB) and the International WELL Building Institute building standard (WELL) are representative healthy building labeling systems. In these standards, the assessment of IAQ is crucial. This chapter details: (1) systematic description of the IAQ-related provisions in each system; (2) systematic analysis according to the perspective of engineering and materials control; (3) deficiencies in current IAQ management; and (4) main tasks for the future.

Keywords

CASGB · LEED · BREEAM · CASHB · WELL

Introduction

With the promotion of sustainable development goals, green and healthy procedures in the construction industry are vital. In the construction industry, green building labeling systems and healthy building labeling systems have provided direction for improved construction practices and building performance.

Many countries have developed green building labeling systems. These include Leadership in Energy and Environmental Design (LEED) from the USA, Building Research Establishment Environmental Assessment Methodology (BREEAM) from the UK, Comprehensive Assessment System for Built Environment Efficiency (CASBEE) from Japan, Deutsche Gesellschaft für Nachhaltiges Bauen (DGNB) from Germany, Haute Qualité Environnementale (HQE) from France, GBTool from Canada, and China Assessment Standard for Green Building (CASGB). The healthy building labeling systems include the International WELL Building Institute building standard (WELL) and China Assessment Standard for Healthy Building (CASHB). In this chapter, CASGB, LEED, and BREAM are introduced in detail as representative green building labeling systems and CASHB and WELL are introduced as representative healthy building labeling systems.

Green and Health Building Labeling Systems

China Assessment Standard for Green Building (CASGB)

CASGB is a Chinese national standard by which the green performance of civil buildings can be evaluated. It was first published in 2006 and was updated in 2015 and 2019 (SAMR 2019). It defines a green building as one which has high-quality performance in saving energy, reducing pollution, and consequently protecting the environment. A CASGB building provides people with healthy, flexible use, and efficient spaces and maximizes harmonious coexistence between humans and nature. There are six main aspects evaluated in the CASGB system: Safety and Durability; Health and Comfort; Occupant Convenience; Resources Saving; Environment Livability; and Promotion and Innovation. The indoor air quality requirements are defined in the Health and Comfort section (SAMR 2019).

LEED

LEED is a rating scheme developed by The US Green Building Council (USGBC) for the design, construction, and operation of high-performance green buildings. LEED has evaluation guides for different building types and different building phases, including new construction, interior fit outs, operations and maintenance, and core and shell. It was first developed as LEED v1.0 in 1998 and began its pilot program testing. Following the success of the pilot program, LEED formally launched LEED v2.0 in 2001 and then updated to LEED v2019, v4.0, and v4.1 in 2009, 2015, and 2019 separately. In this chapter, LEED v4.1 BUILDING DESIGN AND CONSTRUCTION is considered and cited (USGBC 2021). The rating system has 7 categories of requirements: Integrative Process (IP), Location and Transportation (LT), Sustainable Sites (SS), Water Efficiency (WE), Energy and Atmosphere (EA), Materials and Resources (MR), and Indoor Environmental Quality (EQ). The EQ section gives the indoor air quality environment index limitations and control requirements.

BREEAM

BREEAM is a rating system with a series of measures and associated criteria related to environmental issues, which functions as an evaluating tool to help buildings perform in a more energy-efficient and environmental-friendly way. Developed by the British Building Research Establishment (BRE), the first BREEAM scheme is launched in 1990, being one of the earliest green building-rating system in the world. It considers the sustainability in building design, construction, and use in the UK (BRE 2016). BREEAM International New Construction 2016 is discussed here. It consists of 11 sections (Management, Health and Well-Being, Hazards, Energy, Transport, Water, Materials, Waste, Land Use and Ecology, Pollution, and Innovation). Specifically, issues related to indoor air quality are addressed in the Health and Well-Being section.

China Assessment Standard for Healthy Building (CASHB)

CASHB is a social organization standard widely used in China, first published in 2016 and updated in 2021. It evaluates fully furnished and decorated buildings. CASHB is divided into pre-evaluation and operation evaluation. Pre-evaluation is carried out after the construction drawing design documents of the construction project are reviewed and approved. Operational evaluation is performed after the construction project is completed and the building is put into operation. The various building performances are quantified by evaluating a range of criteria from six perspectives, including air, water, comfort, exercise, humanity, service, and promotion and innovation (ASC 2017). Indoor air quality requirements are described in three sections (Air, Service, and Promotion and Innovation).

WELL

The WELL Building Standard is another widely used assessment system. Developed by International WELL Building Institute (IWBI), the WELL Building Standard® Version 1 (WELL v1) was launched on 2014 for the Commercial and Institutional Office building sector. The version introduced here is WELL v2 (launched in 2018) that covers all project types and sectors (IWBI 2020). To ensure the health performance of an evaluated building, WELL v2 lists both precondition requirements and optimization features for ten elements: air, water, nourishment, light, movement, thermal comfort, sound, materials, mind, and community. The indoor air quality requirements are described in the Air section. Various strategies such as source control, design and operation strategies, and human behavior interventions are presented here.

Environmental Index

Environmental Index in CASGB

The indoor air quality index in CASGB consists of mandatory prerequisites and optimization evaluation.

Mandatory Prerequisites The indoor concentration of formaldehyde, benzene, and total volatile organic compounds must meet the requirement of current national “indoor air quality standard” (GB/T 18883) (SAMR 2002). A list of the VOCs and their limit values is given in Table 1.

Optimization Evaluation

- Indoor concentrations of ammonia, formaldehyde, benzene, TVOC, and radon 10% lower than the limit value of current national standard “indoor air quality standard” (GB/T 18883), 3 points; 20% lower than the limit value, 6 points.

Table 1 Environmental requirements in GB/T 18883

Contaminant	Concentration limitation	Comments
Formaldehyde (HCHO)	$\leq 0.10 \text{ mg/m}^3$	1 h average
Benzene (C ₆ H ₆)	$\leq 0.11 \text{ mg/m}^3$	1 h average
Total volatile organic compounds (TVOC)	$\leq 0.6 \text{ mg/m}^3$	8 h average
Ammonia (NH ₃)	$\leq 0.2 \text{ mg/m}^3$	1 h average
Radon ²²² Rn	$\leq 400 \text{ Bq/m}^3$	Annual average (reference level)

Annual average concentration of PM_{2.5} does not exceed 25 $\mu\text{g}/\text{m}^3$; annual average PM₁₀ concentration does not exceed 50 $\mu\text{g}/\text{m}^3$, 6 points.

Environmental Index in LEED

The specific requirements of LEED indoor air quality for particulate matter, inorganic gases, and volatile organic compounds are listed in Table 2.

Environmental Index in BREEAM

The BREEAM requirements for indoor air quality are shown in Table 3. These include limits for formaldehyde and TVOC. They also set limits for CO₂, VOCs, PM₁₀, SO₂, NO₂, and O₃. Also, they ensure that room-conditioning systems have adequate ventilation, according to EN 13779:2007 (EN 2007).

Environmental Index in CASHB

The CASHB system standard requires that indoor air quality meet the current Chinese national “indoor air quality standard” (GB/T 18883). Although the CASHB and CASGB use the same standard (GB/T 18883), there are a few differences in these two systems because of the different objectives and edit time. The requirements with respect to indoor air quality are shown in Table 4.

Environmental Index in WELL

The WELL requirements for indoor air quality are listed in Table 5. They include standards for PM, VOCs, and inorganic gases.

Tables 1, 2, 3, 4 and 5 show that the target contaminants and concentration limits under different labeling system guidelines. Moreover, the test methods for contaminants differ based on various nations’ local standards, so the limit values are very

Table 2 Environmental requirements in LEED

Contaminant	Concentration limitation	Allowed test methods
Carbon monoxide (CO)	9 ppm; no more than 2 ppm above outdoor levels	ISO 4224 (ISO 2000a) EPA Compendium Method IP-3 (EPA 1999a) GB/T 18883-2002 for projects in China (SAMR 2002) Direct calibrated electrochemical instrument with accuracy of $\pm 3\%$ of reading and resolution of 0.1 ppm NDIR CO sensors with accuracy of 1% of 10 ppm full scale and display resolution of less than 0.1 ppm
PM ₁₀	ISO 14644-1:2015 (ISO 2015), cleanroom class of 8 or lower: 50 $\mu\text{g}/\text{m}^3$ Healthcare only: 20 $\mu\text{g}/\text{m}^3$	Particulate monitoring device with accuracy greater of 5 $\mu\text{g}/\text{m}^3$ or 20% of reading and resolution (5 min average data) $\pm 5 \mu\text{g}/\text{m}^3$
PM _{2.5}	12 $\mu\text{g}/\text{m}^3$ or 35 $\mu\text{g}/\text{m}^3$ (projects in areas with high ambient levels of PM _{2.5} (known EPA nonattainment areas for PM _{2.5} , or local equivalent) must meet the 35 $\mu\text{g}/\text{m}^3$ limit; all other projects should meet the 12 $\mu\text{g}/\text{m}^3$ limitation)	
Ozone	0.07 ppm	Monitoring device with accuracy greater of 5 ppb or 20% of reading and resolution (5 min average data) $\pm 5 \text{ ppb}$ ISO 13964 (ISO 1998) ASTM D5149-02 (ASTM 2016a) EPA designated methods for Ozone (EPA 2021)
Formaldehyde 50-00-0	20 $\mu\text{g}/\text{m}^3$ (16 ppb)	ISO 16000-3, 4 (ISO 2011, ISO 2004a);
Acetaldehyde 75-07-0	140 $\mu\text{g}/\text{m}^3$	EPA TO-11a (EPA 1999b), EPA comp. IP-6A (EPA 1990) ASTM D5197-16 (ASTM 2016b)
Benzene 71-43-2	3 $\mu\text{g}/\text{m}^3$	ISO 16000-6 (ISO 2004b);
Hexane (n-) 110-54-3	7000 $\mu\text{g}/\text{m}^3$	EPA IP-1 (EPA 1990);
Naphthalene 91-20-3	9 $\mu\text{g}/\text{m}^3$	EPA TO-17 (EPA 1999c);
Phenol 108-95-2	200 $\mu\text{g}/\text{m}^3$	EPA TO-15 (EPA 2002);
Styrene 100-42-5	900 $\mu\text{g}/\text{m}^3$	ISO 16017-1, 2 (ISO 2000b, ISO 2003);
Tetrachloroethylene 127-18-4	35 $\mu\text{g}/\text{m}^3$	ASTM D6196-15 (ASTM 2015)
Toluene 108-88-3	300 $\mu\text{g}/\text{m}^3$	
Vinyl acetate 108-05-4	200 $\mu\text{g}/\text{m}^3$	

(continued)

Table 2 (continued)

Contaminant	Concentration limitation	Allowed test methods
Dichlorobenzene (1,4-) 106-46-7	800 µg/m ³	
Xylenes-total 108-38-3, 95-47-6, and 106-42-3	700 µg/m ³	

Table 3 Environmental requirements in BREEAM

Contaminant	Concentration limitation	Comments
Formaldehyde (30 minutes)	100 µg/m ³ , be measured postconstruction (but preoccupancy)	
TVOC (8 h)	300 µg/m ³ , be measured postconstruction (but preoccupancy)	
Sulfur dioxide SO ₂ (24 h)	125 µg/m ³	WHO (1999)
Sulfur dioxide SO ₂ (1 year)	50 µg/m ³	WHO (1999)
Ozone O ₃ (8h)	120 µg/m ³	WHO (1999)
Nitrogen dioxide NO ₂ (1 year)	40 µg/m ³	WHO (1999)
Nitrogen dioxide NO ₂ (1 h)	200 µg/m ³	WHO (1999)
Particulate matter PM ₁₀ (24 h)	50 µg/m ³ Max. 35 days exceeding	99/30/EC
Particulate matter PM10 (1 year)	40 µg/m ³	99/30/EC

different. We note that some contaminant limitation values are set for “health” but others for commercially advantageous objectives that lack scientific evidence.

Formaldehyde, VOC, and SVOC Control in Labeling Systems

There are two ways to control indoor volatile chemical pollutants. The Prescriptive Index Method addresses the composition of materials and furniture. This method is often used in product manufacture and covers both emission parameters and content parameters. The second method is the Performance Index Method, which addresses how materials and furnishings will meet environmental requirements in a given building environment. The performance limits are based on emission parameters.

Table 4 Environmental requirements in CASHB

Contaminant	Concentration limitation	Comments
Carbon dioxide (CO ₂)	≤ 0.09% (optimization)	24 h average
Formaldehyde (HCHO)	≤ 0.01 mg/m ³ (precondition)	1 h average
	≤ 70% of limit value (innovation)	
Benzene (C ₆ H ₆)	≤ 0.11 mg/m ³ (precondition)	1 h average
	≤ 90% of limit value (innovation)	
Toluene (C ₇ H ₈)	≤ 0.2 mg/m ³ (precondition)	1 h average
Xylene (C ₈ H ₁₀)	≤ 0.2 mg/m ³ (precondition)	1 h average
	≤ 70% of limit value (innovation)	
TVOC	≤ 0.6 mg/m ³ (precondition)	8 h average
	≤ 90% of limit value (innovation)	
Ozone(O ₃)	≤ 70% of limit value: 0.11 mg/m ³ (innovation)	1 h average
PM ₁₀	≤ 70 µg/m ³ (precondition)	Annual average
	75 µg/m ³ (optimization)	Daily average (while 18 exceptional days is allowed each year)
PM _{2.5}	≤ 35 µg/m ³ (precondition)	Annual average
	≤ 37.5 µg/m ³ (optimization)	Daily average (while 18 exceptional days is allowed each year)
	≤ 25 µg/m ³ (innovation)	Daily average (while 18 exceptional days is allowed each year)
Radon ²²² Rn	≤ 200 Bq/m ³ (optimization)	Annual average (reference level)

CASGB

The CASGB standard uses the Performance Index Method and Prescriptive Index Method to regulate the performance of material and furniture. The Performance Index Method uses the standards JGJ/T 436 (technical specifications for indoor decoration pollution control of residential buildings) (MOHURD 2018) and JGJ/T 461 (Design Standard for Controlling Indoor Air Quality in Public Building) (MOHURD 2019). The Prescriptive Index Method uses some national mandatory standards and some national green product assessment standards, as shown in Table 6.

Table 5 Environmental requirements in WELL

Contaminant	Concentration limitation	Optimization requirement
	Precondition requirements	
Carbon monoxide (CO)	<ul style="list-style-type: none"> • $\leq 10 \text{ mg/m}^3$ • $\leq 34 \text{ mg/m}^3$, commercial kitchen spaces and industrial 	$\leq 7 \text{ mg/m}^3$
PM ₁₀	<ul style="list-style-type: none"> • $\leq 50 \text{ } \mu\text{g/m}^3$ or lower (acceptable thresholds for occupiable spaces) • $\leq 50 \text{ } \mu\text{g/m}^3$ or lower (modified thresholds in polluted regions. For projects where the annual average outdoor PM_{2.5} level is 35 $\mu\text{g/m}^3$ or higher) 	<ul style="list-style-type: none"> • $\leq 30 \text{ } \mu\text{g/m}^3$ (1 point) • $\leq 20 \text{ } \mu\text{g/m}^3$ (2 point)
PM _{2.5}	<ul style="list-style-type: none"> • $\leq 15 \text{ } \mu\text{g/m}^3$ or lower (acceptable thresholds for occupiable spaces) • $\leq 25 \text{ } \mu\text{g/m}^3$ or lower (modified thresholds in polluted regions. For projects where the annual average outdoor PM_{2.5} level is 35 $\mu\text{g/m}^3$ or higher) 	<ul style="list-style-type: none"> • $\leq 12 \text{ } \mu\text{g/m}^3$ (1 point) • $\leq 10 \text{ } \mu\text{g/m}^3$ (2 point)
TVOC (monitoring)	<ul style="list-style-type: none"> • $\leq 500 \text{ } \mu\text{g/m}^3$ • data covering at least the previous 1 month, at least 90% of regularly occupied hours for all sensors 	/
Ozone	$\leq 100 \text{ } \mu\text{g/m}^3$	/
Formaldehyde	$\leq 50 \text{ } \mu\text{g/m}^3$	$\leq 9 \text{ } \mu\text{g/m}^3$
Benzene	$\leq 10 \text{ } \mu\text{g/m}^3$	$\leq 3 \text{ } \mu\text{g/m}^3$
Toluene	$\leq 300 \text{ } \mu\text{g/m}^3$	$\leq 300 \text{ } \mu\text{g/m}^3$ or lower.
Acetaldehyde	/	$\leq 140 \text{ } \mu\text{g/m}^3$
Acrylonitrile	/	$\leq 50 \text{ } \mu\text{g/m}^3$
Caprolactam	/	$\leq 2.2 \text{ } \mu\text{g/m}^3$
Radon	$\leq 150 \text{ Bq/m}^3$	/
Naphthalene	/	$\leq 9 \text{ } \mu\text{g/m}^3$
Nitrogen dioxide	/	$\leq 40 \text{ } \mu\text{g/m}^3$

LEED

This guideline uses both methods. One is the Prescriptive Index Method which in practice is to use interior building materials (everything within the waterproofing membrane) that meet the low-emitting criteria. These requirements are shown in Table 7.

The LEED guideline requires experimental VOC emission evaluation. Laboratories that conduct the tests must be accredited under ISO/IEC 17025 (ISO 2007) for the selected test methods. Products used in any setting other than schools and classrooms must be modeled according to a private office scenario. For school projects, modeling as office and/or school scenario is permitted. This method is a Performance Index Method. It does not calculate or design according to the mathematical model but tests the products as a whole.

Table 6 Sources requirements in CASGB

1	Wood-based panels and finishing product	Indoor decorating and refurbishing materials – limit of formaldehyde emission of wood-based panels and finishing product (GB 18580) (SAMR 2017g)
2	Woodenware coatings	Limit of harmful substances of woodenware coatings (GB 18581) (SAMR 2020c)
3	Architectural coatings	Indoor decorating and refurbishing materials – limit of harmful substances of interior architectural coatings (GB 18582) (SAMR 2020b)
4	Adhesives	Indoor decorating and refurbishing materials – limit of harmful substances of adhesives (GB 18583) (SAMR 2008b)
5	Wood-based furniture	Indoor decorating and refurbishing materials – limit of harmful substances of wood-based furniture (GB 18584) (SAMR 2001b)
6	Wood-based panels and wooden flooring	Green product assessment – wood-based panels and wooden flooring (GB/T 35601) (SAMR 2017h)
7	Coating material	Green product assessment – Coating material (GB/T 35602)
8	Furniture	Green product assessment – furniture (GB/T 35607) (SAMR 2017b)
9	Waterproof materials sealants	Green product assessment – waterproof materials sealants (GB/T 35609) (SAMR 2017e)
10	Ceramics tiles	Green product assessment – ceramics tiles (board) (GB/T 35610) (SAMR 2017a)
11	Textile products	Green product assessment – textile products (GB/T 35611) (SAMR 2017d)
12	Wood plastic composites product	Green product assessment – wood plastic composites product (GB/T 35612) (SAMR 2017f)
13	Paper and paper product	Green product assessment – paper and paper product (GB/T 35613) (SAMR 2017c)

BREEAM

BREEAM approval requires that at least four of five product types listed in Table 8 have been tested according to standards and meet the emission limits. Exemplary-level mission criteria are listed in Table 9. Maximum TVOC content for paints and coatings are in the guideline. This is a Prescriptive Index Method.

CASHB

This standard uses both the Performance Index Method and Prescriptive Index Method. The Performance Index Method requirements are that the concentrations of formaldehyde, benzene, toluene, xylene, TVOC, and other pollutants in indoor air should be pre-evaluated, such that the indoor air quality meets the requirements of

Table 7 Sources requirements in LEED

Inherently no emitting sources	No binders, surface coatings, or sealants that include organic chemicals
Salvaged and reused materials	Meet the VOC emissions evaluation AND VOC content evaluation requirements
VOC emissions evaluation	<ul style="list-style-type: none"> • product has been tested according to California Department of Public Health (CDPH) standard method v1.2–2017 and complies with the VOC limits in Table 4-1 of the method • Laboratories that conduct the tests must be accredited under ISO/IEC 17025 (ISO 2017) for the test methods they use. Products used in any setting other than schools and classrooms must be modeled to private office scenario
VOC content evaluation	<ul style="list-style-type: none"> • statement of product compliance must be made by the manufacturer or a USGBC-approved third party • if the applicable regulation requires subtraction of exempt compounds, any content of intentionally added exempt compounds larger than 1% weight by mass (total exempt compounds) must be disclosed • paints and coatings: <ul style="list-style-type: none"> – California air resource board (CARB) 2007 suggested control measure (SCM) for architectural coatings – South Coast Air Quality Management District (SCAQMD) Rule 1113, effective February 5, 2016 • adhesives and sealants: <ul style="list-style-type: none"> – SCAQMD Rule 1168, October 6, 2017
Formaldehyde emissions evaluation	<p>Product meets one of the following:</p> <ul style="list-style-type: none"> • certified as ultralow-emitting formaldehyde (ULEF) product under EPA toxic substances control act, formaldehyde emission standards for composite wood products (TSCA, title VI) (EPA TSCA title VI), or California air Resources Board (CARB) airborne toxic control measure (ATCM) • certified as no added formaldehyde resins (NAF) product under EPA TSCA title VI or CARB ATCM • wood structural panel manufactured according to PS 1–09 or PS 2–10 (or one of the standards considered by CARB to be equivalent to PS 1 or PS 2) and labeled bond classification exposure 1 or exterior • structural wood product manufactured according to ASTM D 5456 (for structural composite lumber), ANSI A190.1 (for glued laminated timber), ASTM D 5055 (for I-joists), ANSI PRG 320 (for cross-laminated timber), or PS 20–15 (for finger-jointed lumber)
Furniture emissions evaluation	<ul style="list-style-type: none"> • product has been tested in accordance with ANSI/BIFMA standard method M7.1–2011 (R2016) and complies with ANSI/BIFMA e3–2014e or e3–2019e furniture sustainability standard, Sections 7.6.1 (for half credit, by cost) OR 7.6.2 (for full credit, by cost), OR 7.6.2 AND 7.6.3 for one and a quarter credit, by cost • Laboratories that conduct the tests must be accredited under ISO/IEC 17025 for the test methods they use

the current national standard “indoor air quality standard” (GB/T 18883). The Prescriptive Index Method consists of emission evaluation and content evaluation. Emission evaluation depends on the national standard and IAQ design. Content standards and some emission standards are shown in Table 10.

WELL

The WELL guideline uses a Performance Index Method to minimize exposure to certain chemicals, such as orthophthalates, halogenated flame retardants (HFR), and per-fluorinated compounds (PFCs) by limiting their presence in products and limiting the percent fraction of volatile organic compounds (VOCs) emitted by products in indoor air. The specific requirements are described in Table 11.

From Table 6 to Table 11, all labeling systems provide certain criteria that restrict the main sources of formaldehyde, VOCs, and SVOCs (PAEs, PCBs, PAHs, etc.), including wet-applied materials and dry-applied materials. These materials can also be divided into ceiling materials, floor materials, wall materials, and furniture. Evaluation is based on either emission or content. Emissions evaluation is the main method for restricting formaldehyde and VOC, while content evaluation is used for restricting SVOC. Developing methods to quickly evaluate SVOC emission parameters has been an important task.

Up till now, the Performance Index Method is still applied in a few guidelines to evaluate environmental concentrations and regulate material and furniture emissions. However, scenarios, material and furniture, and environmental concentration limitations are inconsistent among different standards. Moreover, without building performance evaluation, how to deal with engineering design, engineering pre-evaluation, and engineering operation will become a severe problem. Therefore,

Table 8 Emission criteria by product type in BREEAM

Product type	Emission limit* formaldehyde	Total volatile organic compounds (TVOC)	Category 1A and 1B carcinogens
Interior paints and coatings	$\leq 0.06 \text{ mg/m}^3$	$\leq 1.0 \text{ ma/m}^3$	$\leq 0.001 \text{ mg/m}^3$
Wood-based products (including wood flooring)	$\leq 0.06 \text{ mg/m}^3$ (non-MDF) $\leq 0.08 \text{ mg/m}^3$ (MDF)	$\leq 1.0 \text{ mg/m}^3$	$\leq 0.001 \text{ mg/m}^3$
Flooring materials (including floor-leveling compounds and resin mooring)	$\leq 0.06 \text{ mg/m}^2$	$\leq 1.0 \text{ mg/m}^3$	$\leq 0.001 \text{ mg/m}^3$
Ceiling, wall, and acoustic and thermal insulation materials	$\leq 0.06 \text{ mg/m}^3$	$\leq 1.0 \text{ mg/m}^3$	$\leq 0.001 \text{ mg/m}^3$
Interior adhesives and sealants (including flooring adhesives)	$\leq 0.06 \text{ mg/m}^3$	$\leq 1.0 \text{ mg/m}^3$	$\leq 0.001 \text{ mg/m}^3$

Table 9 Exemplary-level mission criteria by product type in BREEAM

Product type	Emission limit Formaldehyde (mg/m ³)	TVOC (mg/m ³)	Total semivolatile organic compounds (TSVOC) (mg/m ³)	Category 1A and 1B carcinogens (mg/m ³)	Testing requirement
Interior paints and coatings	≤ 0.01	≤0.3	≤0.1	≤0.001	<ul style="list-style-type: none"> • EN 16402 (EN 2019) • ISO 16000-9 (ISO 2019) • CEN/TS 16516 (EN 2017) • CDPH Standard Method v1.1 (CDPH 2010)
Wood-based products (including wood flooring)	≤ 0.01	≤0.3	≤0.1	≤0.001	<ul style="list-style-type: none"> • ISO 16000-9 CEN/TS 16516 • CDPH standard method v1.1 • EN 717-1 (EN 2004)
Flooring materials (including floor-leveling compounds and resin mooring)	≤0.01	≤0.3	≤0.1	≤0.001	<ul style="list-style-type: none"> • ISO 10580 (ISO 2010) • ISO 16000-9 • CEN/TS 16516 • CDPH standard method v1.1
Ceiling, wall, and acoustic and thermal insulation materials	≤0.01	≤0.3	≤0.1	≤0.001	<ul style="list-style-type: none"> • ISO 10580 • ISO 16000-9 CEN/TS 16516 • CDPH standard method v1.1

(continued)

Table 9 (continued)

Product type	Emission limit Formaldehyde (mg/m ³)	TVOC (mg/m ³)	Total semivolatile organic compounds (TSVOC) (mg/m ³)	Category 1A and 1B carcinogens (mg/m ³)	Testing requirement
Interior adhesives and sealants (including flooring adhesives)	≤0.01	≤0.3	≤0.1	≤0.001	<ul style="list-style-type: none"> • EN 13999 (Parts 1–4) (EN 2013) • ISO 16000-9 • CEN/TS 16516 • CDPH standard method v1.1

improving and promoting Performance Index Method will become an important issue in this field.

Particulate Matter (PM) Control in Labeling Systems

The architectural engineering control chain consists of plan, design, construction, acceptance, maintenance and operation, and monitoring. Some guidelines describe the control chain differently: Design, Construction, Before Occupancy, During Occupancy, and Monitoring. In general, the Design and Monitoring stages focus on PM control. At present, there are qualitative and quantitative methods for indoor PM control design.

CASGB

Design

The instructions in JGJ/T 461 (MOHURD 2019) provide a quantitative design method to select suitable particle filters or air-cleaning devices for outdoor air PM₁₀ and PM_{2.5} concentration so as to meet indoor environmental PM concentration requirements. During the design process, architecture base parameters are input. These include indoor air PM concentration requirements, outdoor air quality conditions, indoor PM contaminant sources, penetration coefficient, infiltration ratio, and minimum fresh air rate. Then a design model is selected to calculate PM. Air filters and cleaners can be selected based on the calculations.

Table 10 Sources requirements in CASHB

Product type		Content limit
Floor, carpet, floor coatings, wallpaper, rolling shutter, awnings, and other products	di (2-ethyl) hexyl phthalate (DEHP)	$\leq 0.01\%$
	di-n-butyl phthalate (DBP)	
	Butyl benzyl phthalate (BBP)	
	di-iso-nonyl phthalate (DINP)	
	di-iso-sunyl phthalate (DIDP)	
	di-n-octyl phthalate (DNOP)	
Carpet ^a	TOVC	$\leq 0.500 \text{ mg/m}^2\cdot\text{h}$
	Formaldehyde	$\leq 0.050 \text{ mg/m}^2\cdot\text{h}$
	Styrene	$\leq 0.400 \text{ mg/m}^2\cdot\text{h}$
	4-Phenyleylohexene	$\leq 0.050 \text{ mg/m}^2\cdot\text{h}$
Carpet cushions ^a	TOVC	$\leq 1.000 \text{ mg/m}^2\cdot\text{h}$
	Formaldehyde	$\leq 0.050 \text{ mg/m}^2\cdot\text{h}$
	BHT-butylated hydroxytoluene	$\leq 0.030 \text{ mg/m}^2\cdot\text{h}$
	4-Phenyleylohexene	$\leq 0.050 \text{ mg/m}^2\cdot\text{h}$
Carpet adhesive ^a	TOVC	$\leq 10.000 \text{ mg/m}^2\cdot\text{h}$
	Formaldehyde	$\leq 0.050 \text{ mg/m}^2\cdot\text{h}$
	2-ethyl-1-hexanol	$\leq 3.000 \text{ mg/m}^2\cdot\text{h}$
Fiberboard, particleboard, plywood, and blockboard ^b	Formaldehyde	$\leq 0.072 \text{ mg/m}^2\cdot\text{h}$
	TVOC	$\leq 0.15 \text{ mg/m}^2\cdot\text{h}$ (24 h)
Chloride floor ^c	Vinyl chloride monomer	$\leq 3.5 \text{ mg/kg}$
Foaming chloride floor ^c	Glass fiber substrate	TVOC $\leq 52.5 \text{ g/m}^2$
	Other substrate	$\leq 24.5 \text{ g/m}^2$
Nonfoaming chloride floor ^c	Glass fiber substrate	$\leq 28 \text{ g/m}^2$
	Other substrate	$\leq 7 \text{ g/m}^2$
Woodware coatings and caseosa products ^d	VOCs	$\leq 350 \text{ g/L}$
Fire-retardant coatings	VOCs	$\leq 100 \text{ g/L}$
Polyurethane waterproof coatings	VOCs	
Special functional porous materials (such as sound absorption board) installed in the main functional rooms	Formaldehyde	$\leq 0.05 \text{ mg/(m}^2\cdot\text{h)}$

(continued)

Table 10 (continued)

Product type			Content limit
Furniture and interior furnishings	Upholstered furniture	Formaldehyde	$\leq 0.05 \text{ mg}/(\text{m}^2 \cdot \text{h})$
	More than 70% purchase cost of wood furniture products ⁱ	Formaldehyde emission rate	$\leq 0.9 \text{ mg/L}$ (GB/T 17657–2013) (SAMR 2013)
Textile and leather products	Meet the requirements of the current industry standard “Technical requirement for environmental labeling products: Textile products” (HJ 2546)		
Interior furnishings	PFCs		$\leq 0.01\%$ (mass ratio)
	PAEs		$\leq 0.01\%$ (mass ratio)
	Polyurethane		$\leq 0.01\%$ (mass ratio)
	Urea formaldehyde resin		$\leq 0.01\%$ (mass ratio)
Plastic furniture and products ^j	Phthalate esters	DBP	$\leq 0.1\%$
		BBP	$\leq 0.1\%$
		DEHP	$\leq 0.1\%$
		DNOP	$\leq 0.1\%$
		DINP	$\leq 0.1\%$
		DIDP	$\leq 0.1\%$
	Polycyclic aromatic hydrocarbons	Benzo (ASTM) pyrene	$\leq 1.0 \text{ mg/kg}$
		Total amount of 16 polycyclic aromatic hydrocarbons (PAHs)	$\leq 10 \text{ mg/kg}$
		Polybrominated biphenyls (PBB)	$\leq 1000 \text{ mg/kg}$
	Polybrominated diphenols (PBDE)		$\leq 1000 \text{ mg/kg}$

^a“Indoor decorating and refurbishing materials—Limitations of harmful substances emitted from carpets, carpet cushions and adhesives” (GB 18587) (SAMR 2001c)

^b“Technical requirement for environmental labeling products: Wood based panels and finishing products” (HJ 571) (MEE, PRC 2010)

^c“Indoor decorating and refurbishing materials—Limit of harmful substances of polyvinyl chloride floor coverings” (GB 18586) (SAMR 2001a)

^d“Limit of harmful substances of woodware coatings” (GB 18581) (SAMR 2020c)

^e“Indoor decorating and refurbishing materials – Limit of harmful substances of adhesives” (GB 18583) (SAMR 2008b)

^f“Water-based interior wall coating with low-emission volatile organic compounds (VOC)” (JG/T 481) (MOHURD 2015)

^gCoatings and putty meet the highest limit requirement of the current industry standard.

^hMore than 40% of the procurement cost of indoor woodware coatings products is water-based woodware coatings.

ⁱ“Indoor decorating and refurbishing materials—Limit of harmful substances of wood-based furniture” (GB 18584) (SAMR 2001b)

^j“Limit of harmful substances of plastic furniture” (GB 28481) (SAMR 2013)

Table 11 Sources requirements in WELL

Product type	Contaminant	Limitation
Furniture, millwork, and fixtures	<ul style="list-style-type: none"> • HFR • per- and polyfluoroalkyl substances (PFAS) 	≤0.01%
Flooring products	<ul style="list-style-type: none"> • HFR • PFAS • Orthophthalates 	≤0.01%
Insulation products	HFR	≤0.01%
Ceiling and wall panels	<ul style="list-style-type: none"> • HFR • Orthophthalates 	≤0.01%
Plastic plumbing	Orthophthalates	≤0.01%
Wet-applied paints, coatings, adhesives, sealants, and finished poured floorings	VOCs	<ul style="list-style-type: none"> • CAQMD Rule 1168 (adhesives and sealants, 2017) • GB 33372–2020 (adhesives) (SAMR, S. A. 2020d) • 2019 CARB SCM for architectural coatings • EU ecolabel for indoor and outdoor paints and varnishes • HJ 2537–2014 (paints) (MEE, PRC 2014) • “low-emitting materials” credit of the LEED v4.1 standard
Furniture, architectural and interior products	VOCs	<ul style="list-style-type: none"> • California Department of Public Health (CDPH) standard method v1.2 • AgBB • European Union LCI VOC thresholds following EN 16516–1: 2018 testing methods • ANSI/BIFMA e3–2014, sections 7.6.1 or 7.6.2 (furniture)

Monitoring

An indoor air quality-monitoring system with PM₁₀ and PM_{2.5} concentration monitoring function is installed in the building. The system records and stores the indoor particle concentration data for at least one year.

LEED

Design

The LEED guideline uses a qualitative design method to select different particle filters or air-cleaning devices. Each ventilation system that supplies outdoor air to occupied spaces must have particle filters to filter both outdoor air and recirculated air or air-cleaning devices which meet at least one of the following filtration media requirements:

- Minimum efficiency reporting value (MERV) of 13 or higher, in accordance with ASHRAE Standard 52.2–2017 (ASHRAE 2017).
- Equivalent filtration media class of ePM1 50% or higher, as defined by ISO 16890-2016, Particulate Air Filters for General Ventilation, Determination of the Filtration Performance (ISO 2016).
- Projects in East Asia may use filtration media classified as high efficiency or higher as defined by Chinese standard GB/T 14295–2008 (SAMR 2008a).

Monitoring

Monitoring systems with sensors designed to detect the specific contaminants should be installed. An alarm must give an alert for any unusual or unsafe condition. The particulate monitoring device must have an accuracy greater than 5 micrograms/m³ or 20% of reading, and resolution (5 min average data) of +/– 5 µg/m³.

BREEAM

There are no requirements for monitoring in the BREEAM guideline. For the design period, the guideline uses a qualitative design method. HVAC systems must incorporate suitable filtration to minimize external air pollution, as defined in EN 13779: 2007 Annex A3, shown in Table 12.

CASHB

Design

CASHB uses a quantitative design method to select different particle filters or air-cleaning devices for various outdoor air PM₁₀ and PM_{2.5} concentrations in order to meet the environmental concentration requirements for PM₁₀ and PM_{2.5}. The processes are similar to the processes described for CASGB.

Table 12 Recommended minimum filter classes per filter section in BREEAM

Outdoor air quality	Indoor air quality			
	IDA 1 (high)	IDA 1 (medium)	IDA 1 (moderate)	IDA 1 (low)
ODA1	(pure air) F9	F8	F7	F5
ODA 2 (dust)	F7 + F9	F6 + F8	F5 + F7	F5 + F6
ODA 3 (very high concentration of dust or gases)	F7 + GF ^a + F9	F7 + GF + F9	F5 + F7	F5 + F6

^aGF = Gas filter (carbon filter) and/or chemical filter

Monitoring

An indoor air quality monitoring system for PM₁₀ and PM_{2.5} should be installed. The system records and stores indoor particle concentration data for at least one year. The particulate monitoring device should have accuracy greater than 25% at 50 µg/m³. In addition, the monitoring system should connect with the HVAC and air purifier system to achieve auto control of indoor air quality.

WELL

Design

WELL uses a qualitative design method. The filter operation requirements are listed below:

- (a) Media filters are used in the ventilation system to filter outdoor air supplied to the space, in accordance with thresholds specified in Table 13.
- (b) Partially recirculated air is treated with the following:
 - 1. Activated carbon filter.
 - 2. At least one of the following: (i) media filter with PM removal of $\geq 90\%$ (e.g., MERV 14 or F8), (ii) UVGI within the ducts to treat the moving air, or (iii) upper-room UVGI.
- (c) For partially recirculated air, air purification/cleaning devices are required (with a quantity appropriate to the room volume or area, based on manufacturer specifications) and must include the following:
 - 1. Activated carbon filter.
 - 2. Media filter with PM removal of $\geq 90\%$ (e.g., MERV 14 or F8) or UVGI.

Monitoring

- (a) The air quality monitoring system must have a concentration monitoring function for PM₁₀, PM_{2.5}, and CO₂. The system must store monitoring data for at least one year and have a real-time display function.
- (b) The air quality monitoring system and all indoor air quality control equipment are automatically controlled. The system sets the limit for the main pollutant concentration parameters and gives an alarm when the limit is exceeded.

Table 13 filter requirements for outdoor air in WELL

Annual average outdoor PM threshold	Minimum air filtration level (PM removal)
23 µg/m ³ or less	$\geq 80\%$ (e.g., MERV 12 or M6)
24–39 µg/m ³	$\geq 90\%$ (e.g., MERV 14 or F8)
40 µg/m ³ or greater	$\geq 95\%$ (e.g., MERV 16 or E10)

There are both qualitative and quantitative methods included in the above-mentioned guidelines. The latest WHO air quality guidelines (WHO 2006) call for an annual PM_{2.5} level of 5 µg/m³ and 24 h mean level of 15 µg/m³. Thus, whether quantitative method can still meet the increasing precision requirements of current WHO requirements needs to be further verified. Meanwhile, because of counting efficiency and weight efficiency, filter classification will become more and more complex. Clearly, quantitative methods will be required more and more and improving quantitative methods is therefore an important task.

In addition, as informatization progresses in society, PM sensor engineering will progress. Presently, some PM_{2.5} sensors from industry can be used for monitoring. In the future, it might be widely used as other sensors, for example, temperature sensors, and will be integrated in the HVAC system or elsewhere in the building.

Conclusion

1. Green, healthy buildings have taken on great importance in building construction. IAQ improvement is of prime importance in green, healthy buildings.
2. Basic scientific research in IAQ as related to human health will continue. International organizations like WHO will continue to develop guidelines for IAQ. Local indoor environmental standards are optimally based on disease burdens as they differ among various regions and countries. IAQ standards must emphasize human health.
3. Predicting pollutant concentrations in a building during acceptance and operation is for the purpose of controlling formaldehyde, VOCs, and SVOCs. The technologies need to be improved so as to (1) quantify SVOC emissions parameters quickly; (2) strengthen the Performance Index Method; and (3) develop performance sensors.
4. Controlling PM is a key task. We can anticipate that concentration limitations will become stricter. Filter classifications and the control requirements for building operation will become more complex. Thus, quantitative planning and evaluation methods for both design and operation must advance in step with increasing complexities.
5. Controlling microbial contaminants will also be an engineering task. Currently, the mainstream control methods are sterilization and disinfection. While microbial contaminants are mentioned in various guidelines, no systematic control methods have been included from Plan & Design to Maintenance & Operation.

Acknowledgments The authors acknowledge the substantial contribution of Louise B. Weschler to this chapter.

References

- ASC (2017) Assessment standard for healthy building (T/ASC 02–2016)
- ASHRAE (2017) ANSI/ ASHRAE standard 52.2–2017 method of testing general ventilation air-cleaning devices for removal efficiency by particle size
- ASTM (2015) ASTM D6196–15 standard practice for choosing sorbents, sampling parameters and thermal desorption analytical conditions for monitoring volatile organic chemicals in air
- ASTM (2016a) ASTM D5149–02(2016) standard test method for ozone in the atmosphere: continuous measurement by ethylene chemiluminescence
- ASTM (2016b) ASTM D5197–16 standard test method for determination of formaldehyde and other carbonyl compounds in air (Active Sampler Methodology)
- BRE (2016) BREEAM international new construction 2016 technical manual SD233 2.0. United Kingdom
- CDPH (2010) Component of the general emissions evaluation. EN 2004. EN 717–1: 2004 Wood-based panels – Determination of formaldehyde release – Part 1: Formaldehyde emission by the chamber method
- EN (2007) EN 13779:2007 ventilation for non-residential buildings – performance requirements for ventilation and room-conditioning systems
- EN (2013) EN 13999–1 adhesives – short term method for measuring the emission properties of low-solvent or solvent-free adhesives after application – Part 1: General procedure
- EN (2017) EN 16516 Construction products: assessment of release of dangerous substances – Determination of emissions into indoor air
- EN (2019) EN 16402 paints and varnishes – assessment of emissions of substances from coatings into indoor air – sampling, conditioning and testing
- EPA (1990) Compendium of methods for the determination of air pollutants in indoor air. Project Summary. IP-6A
- EPA (1999a) Compendium of methods for the determination of inorganic compounds in ambient air
- EPA (1999b) Compendium of methods for the determination of toxic organic compounds in ambient air—Compendium method TO-11A determination of formaldehyde in ambient air using adsorbent cartridge followed by high performance liquid chromatography (HPLC) [Active Sampling Methodology]
- EPA (1999c) Compendium of methods for the determination of toxic organic compounds in ambient air—compendium method TO-17 determination of volatile organic compounds in ambient air using active sampling onto sorbent tubes
- EPA (2002) Method TO-15 supplement analysis of 1,1-DCE at pptv concentrations
- EPA (2021) List of designated reference and equivalent methods
- ISO (1998) ISO 13964:1998(en) air quality — determination of ozone in ambient air — ultraviolet photometric method
- ISO (2000a) ISO 4224:2000 ambient air – determination of carbon monoxide – non-dispersive infrared spectrometric method
- ISO (2000b) ISO 16017-1:2000 Indoor, ambient and workplace air — Sampling and analysis of volatile organic compounds by sorbent tube/thermal desorption/capillary gas chromatography — Part 1: Pumped sampling
- ISO (2003) ISO 16017-2:2003 Indoor, ambient and workplace air — Sampling and analysis of volatile organic compounds by sorbent tube/thermal desorption/capillary gas chromatography — Part 2: Diffusive sampling
- ISO (2004a) ISO 16000-4:2004 Indoor air — Part 4: determination of formaldehyde — diffusive sampling method
- ISO (2004b) ISO 16000-6:2004 indoor air — Part 6: determination of volatile organic compounds in indoor and test chamber air by active sampling on Tenax TA sorbent, thermal desorption and gas chromatography using MS/FID

- ISO (2010) ISO 10580:2010 Resilient, textile and laminate floor coverings — Test method for volatile organic compound (VOC) emissions
- ISO (2011) ISO 16000-3:2011 Indoor air—Part 3: Determination of formaldehyde and other carbonyl compounds in indoor air and test chamber air — Active sampling method
- ISO (2015) ISO 14644-1:2015 Cleanrooms and associated controlled environments — Part 1: Classification of air cleanliness by particle concentration
- ISO (2016) ISO 16890-1:2016 Air filters for general ventilation — Part 1: Technical specifications, requirements and classification system based upon particulate matter efficiency (ePM_{2.5})
- ISO 2016b. ISO 16890-2-2016 Air filters for general ventilation – Part 2: Measurement of fractional efficiency and air flow resistance
- ISO (2017) ISO/IEC 17025:2017 General requirements for the competence of testing and calibration laboratories
- ISO (2019) ISO 16000-9:2006 Indoor air — Part 9: Determination of the emission of volatile organic compounds from building products and furnishing — emission test chamber method
- IWBI (2020) WELL v2
- MEE, PRC, M (2010) Technical requirement for environmental labeling products: wood based panels and finishing products (HJ 571–2010)
- MEE, PRC, M (2014) Technical requirement for environmental labeling products: water based coatings (HJ 2537–2014)
- MOHURD (2015) Water-based interior wall coating with low-emission volatile organic compounds (VOC) (JG/T 481–2015);
- MOHURD (2018) Technical standard for interior decoration pollution control of residential buildings (JGJ/T 436–2018). China
- MOHURD (2019) Design standard for controlling indoor air quality in public building (JGJ/T 461–2019)
- SAMR (2001a) Indoor decorating and refurbishing materials—Limit of harmful substances of polyvinyl chloride floor coverings (GB 18586–2001)
- SAMR (2001b) Indoor decorating and refurbishing materials—Limit of harmful substances of wood based furniture (GB 18584–2001)
- SAMR (2001c) Indoor decorating and refurbishing materials—Limitations of harmful substances emitted from carpets, carpet cushions and adhesives (GB 18587–2001)
- SAMR M (2002) Indoor air quality standard (GB/T 18883–2002). China
- SAMR (2008a) Air Filters (GB/T 14295–2008)
- SAMR (2008b) Indoor decorating and refurbishing materials – Limit of harmful substances of adhesives (GB 18583–2008). SAMR 2012. Limit of harmful substances of plastic furniture (GB 28481–2012)
- SAMR (2013) Test methods of evaluating the properties of wood-based panels and surface decorated wood-based panels (GB/T 17657–2013)
- SAMR (2017a) Green product assessment—Ceramics tiles(Board) (GB/T 35610–2017)
- SAMR (2017b) Green product assessment—Furniture (GB/T 35607–2017)
- SAMR (2017c) Green product assessment—Paper and paper products (GB/T 35613–2017)
- SAMR (2017d) Green product assessment—Textile products (GB/T 35611–2017)
- SAMR (2017e) Green product assessment—Waterproof materials and sealants (GB/T 35609–2017)
- SAMR (2017f) Green product assessment—Wood plastic composites products (GB/T 35612–2017)
- SAMR (2017g) Indoor decorating and refurbishing materials—Limit of formaldehyde emission of wood-based panels and finishing products (GB 18580–2017)
- SAMR (2017h) Green product assessment-Wood-based panels and wooden flooring (GB/T 35601)
- SAMR M (2019) Assessment standard for green building (GB/T50378–2019). China
- SAMR SA (2020b) Limit of harmful substances of architectural wall coatings (GB 18582–2020)

- SAMR SA (2020c) Limit of harmful substances of woodware coatings (GB 18581–2020)
SAMR SA (2020d) Limit of volatile organic compounds conten in adhesive (GB 33372–2020)
USGBC (2021) LEED v 4.1 buiding design and construction
WHO (1999) The WORLD HEALTH REPORT 1999 —— making a difference
WHO (2006) Air quality guidelines: global update 2005: particulate matter, ozone, nitrogen dioxide and sulfur dioxide. WHO 2021. WHO global air quality guidelines: particulate matter (PM2.5 and PM10), ozone, nitrogen dioxide, sulfur dioxide and carbon monoxide

Part XI

Indoor Air Quality Control



Testing and Reducing VOC Emissions from Building Materials and Furniture 56

Jianshun Jensen Zhang, Wenhao Chen, Ningrui Liu,
Bing Beverly Guo, and Yiping Zhang

Contents

Introduction	1592
Standard Environmental Chamber Testing Methods and Procedure	1593
Overview	1593
Principles	1594
Air Sampling and Chemical Analysis	1605
Test Procedure	1610
Data Analysis and Interpretation	1613
Establishing the Link Between Chamber Testing and Real Applications	1618
Overview of the Process	1618
Standard Methods, Evaluation Criteria, and Labeling Schemes	1619
Product Labeling Programs	1626
Application in Building Rating Systems	1626
Whole Building Approach for Modeling the Impact of Product Emission on IAQ	1627
Application Examples	1628
ANSI/BIFMA e3 Furniture Sustainability Standard and ANSI/BIFMA M7.1 and X7.1	1628

J. J. Zhang (✉)

Building Energy and Environmental Systems Laboratory, Department of Mechanical and Aerospace Engineering, Syracuse University, Syracuse, NY, USA

School of Architecture and Urban Planning, Nanjing University, Nanjing, China
e-mail: jszhang@syr.edu

W. Chen

Environmental Health Laboratory Branch, California Department of Public Health, Richmond, CA, USA

N. Liu · Y. Zhang

Department of Building Science, School of Architecture, Tsinghua University, Beijing, China
Beijing Key Laboratory of Indoor Air Quality Evaluation and Control, Beijing, China

B. B. Guo

Building Energy and Environmental Systems Laboratory, Department of Mechanical and Aerospace Engineering, Syracuse University, Syracuse, NY, USA

CDPH Standard Method v1.2	1628
EN 16516 Test Method with EU-LCI Values or German AgBB Evaluation Scheme	1629
VOC Emission Testing and Labeling Systems in China	1629
Eco Mark Labeling System in Japan	1630
Concluding Remarks and Future Outlook	1631
References	1632

Abstract

Labeling and certification for low-emission building materials and furniture is an effective source control strategy for reducing indoor air pollution. The labeling and certification programs rely on the results from standardized environmental chamber tests to measure the emission rates of volatile organic compounds (VOCs) and assess their impact on indoor air quality (IAQ). In this chapter, we first introduce the fundamental principles, methods, and procedures of environmental chamber testing of VOC emissions and then discuss how the chamber test results are applied in various labeling and certification programs including the process, criteria, and the corresponding standard environmental chamber testing methods. Examples are drawn from widely used material emission testing and labeling programs. Sufficient details on the emission test methods and procedures are provided for readers to develop practical applications as well as a comprehensive understanding and appreciation of the principles and processes of material emission testing and labeling. For detailed implementation, readers are referred to product-specific testing methods and labeling programs that match their interests and needs.

Keywords

Volatile organic compounds (VOCs) · Source control · Environmental chamber · Emission test standard · Labeling programs · Green buildings

Introduction

Volatile organic compounds (VOCs) are a major type of pollutants found indoors, and many of them are emitted from building and furnishing materials. Many of these VOCs are mucous membrane irritants and some (e.g., formaldehyde and acetaldehyde) are carcinogenic in humans, and hence are of great indoor air quality (IAQ) concern. In order to understand and reduce indoor pollution loads caused by VOCs emissions, environmental chamber testing methods and procedures have been developed to determine the emission characteristics including: (1) identification of the VOCs emitted by different materials and (2) determination of their emission rates over time (e.g., ASTM 5116 (ASTM International 2017), ASTM 6670 (ASTM International 2018a)). Understanding the emission characteristics is an important step in developing standard testing methods and procedures for specific building materials and furnishings. The standard test methods and procedures are developed through a consensus development process involving diverse stakeholders from academic or research institution, testing laboratories, material manufactures/suppliers,

and IAQ consultants (e.g., ANSI/BIFMA 7.1 (BIFMA International 2011a)), which take into account the emission characteristics, product usage conditions, sensitivity of analytical instruments, repeatability and reproducibility, and quality assurance measures.

The standard environmental chamber testing methods and procedures provide the basis for many labeling, certification, or compliance programs that are aimed at limiting VOC emissions indoors. For example, green or healthy building rating systems such as LEED (U. S. Green Building Council 2020) and WELL (International WELL Building Institute 2020) use the emission test results to determine if the materials/products qualify for receiving credits related to indoor pollution source control. Architects, interior designers, building managers, and homeowners use emission test data and labeling/certification/compliance programs to specify low emission materials and furniture. Manufacturers use the testing and labeling/certification/compliance programs to obtain product certification and qualify their products as low-emission materials or furniture. A labeling, certification, or compliance program specifies the intended applications, emission criteria, and the standard test method and procedure that generate the data for comparison with the emission criteria.

In this chapter, we first introduce the fundamental principles, methods, and procedure of environmental chamber testing of VOC emissions (section “[Standard Environmental Chamber Testing Methods and Procedure](#)”) and then discuss how the chamber test results are applied in various labeling and certification programs including the process and criteria (section “[Establishing the Link Between Chamber Testing and Real Applications](#)”). Examples will be drawn from widely used material emission testing and labeling programs. Several examples are provided in section “[Application Examples](#)”. For detailed applications, readers are referred to the specific testing methods and labeling programs that match their interests and needs. Section “[Concluding Remarks and Future Outlook](#)” provides a summary of the current state and an outlook on future development.

Standard Environmental Chamber Testing Methods and Procedure

Overview

Environmental chamber testing methods for material emissions include small, mid-size, and large chamber test methods. The size of small chambers is typically less than 1 m³ in volume with 50 L chambers being most popularly used. They are often used for testing individual materials such as carpet, composite wood boards, vinyl flooring, paints, varnishes, adhesives, and sealants, etc. Mid-size chambers typically range between 4 and 8 m³ and are used for testing individual components or assemblies such as a chair, sofa, desk, cabinet, mid-size wall assembly, printer, computer, etc. Large or room-size chambers range from 24 to 55 m³ in volume, and are used for testing full-scale office workstations, full-scale wall sections and large equipment. Regardless of the chamber volume, they are made of inert materials such as stainless steel and glass with Teflon gasket for sealing in order to minimize

the background contamination and VOC adsorption and reemission by the chamber surfaces. The chamber is contained in a temperature-controlled enclosure, supplied with clean and conditioned air and equipped with fittings for air sampling at chamber air exhaust or inside the chamber. All materials and components in contact with the specimen, or the air stream from the chamber inlet to the sample collection point, are chemically inert and accessible for cleaning. Suitable materials include stainless steel and glass. All gaskets and flexible components are made from chemically inert materials. Example small chamber testing systems can be found in ASTM D5116 (ASTM International 2017). Examples of full-scale chamber test facilities can be found in Zhang's study (Zhang et al. 1999b), ASTM D6670 (ASTM International 2018a), and Herrmann's study (Herrmann et al. 2003).

The quantity of materials tested in the chamber is typically scaled in terms of the ratio between the emitting surface area (A , m^2) and chamber volume (V , m^3), which is called loading ratio, L in m^2/m^3 whose value is intended to mimic the typical material usage conditions. The chamber is supplied with clean/filtered air at a constant flow rate (Q , m^3/h) that is typically scaled in terms of the ratio between the supply airflow rate and the chamber volume (called air change rate, $N = Q/V$, in air changes per hour, ach, or h^{-1}) simulating typical ventilation conditions in the room space. The ratio between the air change rate (N) and loading ratio (L) is the area specific airflow rate (N/L , $(\text{m}^3/\text{h})/\text{m}^2$). Air samples are typically taken at the chamber exhaust air outlet to determine the concentrations of VOCs (C , ug/m^3) of interest. Depending on the VOCs of interest to be measured, the air samples are either taken with sorbent tubes and/or 2,4-dinitrophenylhydrazine (DNPH) cartridges, followed by thermal desorption-gas chromatography/mass spectrometry (TD-GC/MS) analysis, and/or High Performance Liquid Chromatography (HPLC) analysis, respectively, or with online sampling instruments. The measured concentration data are then used to determine the emission rates (R , ug/h) or the emission factor (E , $\text{ug}/\text{h}/\text{m}^2$) as a function of time or at specific time points of interests required by given labeling, certification, or compliance programs or as input to estimate the contribution of the materials to the indoor concentrations of interest.

In the following sections, we focus our discussions on the test principles, air sampling and chemical analyses, test procedure, and data analysis and interpretation. Readers are referred to product-specific test methods for more detailed specifications and requirements of chamber test conditions, test specimen collection and storage, specimen preparation and conditioning, air sampling intervals, selection of target VOCs for analysis, quality assurance and quality control (QA/QC), and reporting requirements.

Principles

Determination of Emission Factor

Emission factor is defined as the emission rate per unit quantity of emission source. For a chamber with a volume of V , supply airflow rate of Q , and a test specimen with exposed area A (see Fig. 1), assuming that the air is perfectly mixed inside the

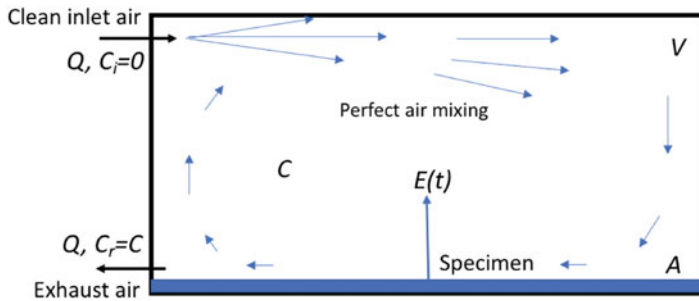


Fig. 1 Schematic of an emission test chamber containing a test specimen (a material, component/assembly or furniture system)

chamber, and the VOC concentration inside the chamber is the same as the concentration at the exhaust outlet (C_r). It is governed by the following mass balance equation:

$$V \frac{dC(t)}{dt} = AE(t) - QC(t) \quad (1)$$

where, V is air volume of the chamber excluding air volume taken by test specimens, m^3 ; t is time, h ; $C(t)$ is concentration of the emitted VOC in the air exhausted from the chamber (can be measured in chamber air or at the exhaust air duct), ug/m^3 ; A is amount of the source(s), 1, m , m^2 , kg , and m^3 , for “unit,” line, area, mass, and volume emission sources, respectively; $E(t)$ is emission factor of the source(s) in the chamber, ug/h , $\text{ug}/\text{h}/\text{m}$, $\text{ug}/\text{h}/\text{m}^2$, $\text{mg}/\text{h}/\text{kg}$, and $\text{mg}/\text{h}/\text{m}^3$ for “unit,” line, area, mass, and volume emission sources, respectively; and Q is clean air flow rate supplied to the chamber (measured at inlet air supply duct or determined by a tracer gas test), m^3/h .

Equation (1) states that the rate of change in mass of a VOC in the chamber is equal to the rate of emission from the source minus the rate at which the VOC is removed by ventilation. With the concentrations measured at pre-specified sampling time $C(t_i, i = 1, 2, 3, \dots, n)$, the emission factors can be calculated directly as follows:

$$E(t_i) = \frac{V}{2A} \left[\frac{C(t_i) - C(t_{i-1})}{t_i - t_{i-1}} + \frac{C(t_{i+1}) - C(t_i)}{t_{i+1} - t_i} \right] + \frac{Q}{A} C(t_i) \quad (2)$$

At steady-state or when the emission rate changes very slowly with time (which is the case for dry or dried building materials or furniture after a certain initial emission/conditioning period), the first term on the right is negligible, resulting in:

$$E(t_i) \approx \frac{Q}{A} C(t_i) = q_A C(t_i) \quad (3)$$

where, $q_A = Q/A$ is the source specific ventilation rate, m^3/h , $\text{m}^3/\text{h}/\text{m}$, $\text{m}^3/\text{h}/\text{m}^2$, $\text{m}^3/\text{h}/\text{kg}$, $\text{m}^3/\text{h}/\text{m}^3$ for “unit,” line, area, mass, and volume emission sources, respectively. It is also equal to the clean air change rate divided by the chamber loading ratio (N/L).

The validity of Eq. (1) depends on how well the chamber's actual operation meets the perfect mixing assumption. Therefore, the performance of the chamber must be evaluated against established criteria to obtain reliable and reproducible test results.

Material Emission Characteristics

Material emission characterization starts with the identification of VOCs emitted and selection of compounds of interests. This is often done with headspace analysis in which a material specimen is placed inside a completely sealed chamber or Teflon bag, and air samples are taken from the air space (“headspace”) above or surrounding the material when steady state is reached. The air samples are analyzed by GC/MS or HPLC to identify the VOCs emitted from the material using established protocols (e.g., U.S. EPA TO-1, TO-11, TO-15 and TO-17 (U. S. EPA 1995a, b). Target VOCs are selected for testing in accordance with their potential impact on human exposure and health or based on the requirements of labeling or certification programs. Formaldehyde and BTEX compounds (i.e., benzene, toluene, ethylbenzene, and xylene) are among the targeted VOCs in most labeling programs (see Table 3 in section “[Establishing the Link Between Chamber Testing and Real Applications](#)”). Other target VOCs differ among different labeling or certification programs and in different published studies. Table 1 shows an example list of target VOCs taken from commonly used standard methods in North America for VOC emission testing of building materials and furniture (CDPH Standard Method v1.2 (CDPH 2017), ANSI/BIFMA e3 (BIFMA International 2019), and ANSI/BIFMA X7.1 (BIFMA International 2011b)).

The VOC emission rates vary with the time, properties of VOCs, material types, and environmental conditions. Under a standard environmental chamber test condition (e.g., 23 °C, 50% RH, and 1 ach, which is typical of small chamber testing), the emission rates exhibit different patterns over time (Fig. 2). “Wet” coating materials such as paints and varnishes generally have a high initial emission rate immediately after application due to evaporation of the liquid solution. The emission rate then decreases quickly with time as the material “dries” (Chang and Guo 1992a, b; Zhang et al. 1996). The duration of the initial period is relatively short. Depending on the coating material and substrate used, it can vary from a few hours to about 10–20 h. The amount of VOC mass emitted during the initial emission period relative to the total VOC mass that can be emitted also depends on the material and substrate. The initial emission period is primarily controlled by evaporation and hence is largely affected by air velocity and turbulence over the surface. The later emission period is primarily controlled by VOC diffusion in the material and substrate, and thus is not significantly affected by the air velocity over the surface (Zhang et al. 1996), a behavior of dry or “dried” materials. The emission characteristics also differ among different VOCs, which depend on the vapor pressure and molecular weight of the VOC and its mass amount relative to other VOCs in the material (Guo et al. 1998). “Wet” installation material such as adhesives, caulk, and sealants have similar emission rate pattern as the “wet” coating materials except that the transition from the initial evaporative controlled to the in-material diffusion-controlled emission period takes a longer time to complete due to a thicker layer of the material. Dry or

Table 1 Example list of target individual VOCs

Chemical name	CAS No.	Chemical class	Maximum allowable concentrations (ug/m ³)*	IARC group 1 or 2A [§]	Reference standard or labeling program
2-Propanol (Isopropanol)	67-63-0	Alcohol	3500		a, b
Phenol	108-95-2	Alcohol	100		a, b
Acetaldehyde	75-07-0	Aldehyde	70		a, b
Formaldehyde	50-00-0	Aldehyde	9 or 62.5 ⁺	1	a, b, c ⁺
<i>n</i> -Hexane	110-54-3	Aliphatic HC	3500		a, b
Benzene	71-43-2	Aromatic HC	1.5	1	a, b
Ethylbenzene	100-41-4	Aromatic HC	1000		a, b
Naphthalene	91-20-3	Aromatic HC	4.5		a, b
Styrene	100-42-5	Aromatic HC	450		a, b
Toluene	108-88-3	Aromatic HC	150		a, b
Xylenes ((<i>m</i> -, <i>o</i> -, <i>p</i> -xylene))	108-38-3 95-47-6 106-42-3	Aromatic HC	350		a, b
4-Phenylcyclohexene	4994-16-5	Aromatic HC	6.5		b, c
2-Ethoxyethyl acetate	111-15-9	Ester	150		a, b
Ethylene glycol monomethyl ether acetate	110-49-6	Ester	45		a, b
Vinyl acetate	108-05-4	Ester	100		a, b
1,4-Dioxane	123-91-1	Ether	1500		a, b
Methyl t-butyl ether	1634-04-4	Ether	4000		a
1,2-Ethanediol (Ethylene glycol)	107-21-1	Glycol/Glycol Ether	200		a, b
1-Methoxy-2-propanol	107-98-2	Glycol/Glycol Ether	3500		a, b
2-Ethoxyethanol	110-80-5	Glycol/Glycol Ether	35		a, b
2-Methoxyethanol	109-86-4	Glycol/Glycol Ether	30		a, b
1,1-dichloroethylene	75-35-4	Halocarbon	35		a

(continued)

Table 1 (continued)

Chemical name	CAS No.	Chemical class	Maximum allowable concentrations ($\mu\text{g}/\text{m}^3$)*	IARC group 1 or 2A [§]	Reference standard or labeling program
1,4-Dichlorobenzene	106-46-7	Halocarbon	400		a, b
Carbon tetrachloride	56-23-5	Halocarbon	20		a
Chlorobenzene	108-90-7	Halocarbon	500		a, b
Chloroform	67-66-3	Halocarbon	150		a, b
Dichloromethane	75-09-2	Halocarbon	200		a, b
Epichlorohydrin	106-89-8	Halocarbon	1.5		a, b
Methyl chloroform	71-55-6	Halocarbon	500		a, b
Tetrachloroethylene	127-18-4	Halocarbon	17.5	2A	a, b
Trichloroethylene	79-01-6	Halocarbon	300	1	a, b
Isophorone	78-59-1	Ketone	1000		a
Carbon disulfide	75-15-0	Other	400		a, b
<i>N,N</i> -Dimethylformamide	68-12-2	Other	40		a, b
1-Methyl-2-Pyrrolidinone	872-50-4	Other	350		b

Taken from CDPH Standard Method v1.2 (2017)^a, ASNI/BIFMA e3 (2019)^b, and X7.1 (2011 (R2016)^c

*Maximum allowable concentrations are one-half of the corresponding Chronic Reference Exposure Level (CREL) adopted by California Office of Environmental Health Hazard Assessment (OEHHA) except for formaldehyde, 4-Phenylcyclohexene, and 1-Methyl-2-Pyrrolidinone. For furniture, the listed maximum allowable concentrations are for workstations; the maximum allowable concentrations are one-half of those listed in the table for seating

^aThe maximum allowable concentration of 9 $\mu\text{g}/\text{m}^3$ for formaldehyde is based on full CREL. It is required in CDPH Standard Method v1.2. For furniture, the maximum allowable formaldehyde emission concentration is 62.5 $\mu\text{g}/\text{m}^3$ (50 ppb) for workstations in ANSI/BIFMA X7.1. The requirements in ASNI/BIFMA e3 depend on the credit level; the maximum allowable concentrations for workstations are 62.5 $\mu\text{g}/\text{m}^3$ (50 ppb), 16.9 $\mu\text{g}/\text{m}^3$ (13.5 ppb), and 9 $\mu\text{g}/\text{m}^3$ for Section 7.6.1, 7.6.2, and 7.6.3, respectively

^bCompounds that are listed by the International Agency for Research on Cancer (IARC) as Group 1 or 2A carcinogen are marked in this column

“dried” materials such as carpets, vinyl flooring, composite wood products (particleboards, plywood boards, and oriented strand boards), painted gypsum wallboards, ceiling tiles, desktop and cabinet panels, etc.) have low initial emission rates that also decay slowly as an in-material diffusion-controlled process.

Many empirical and mechanistic emission source models have been developed to predict the rate of emissions over time for the three different types of building and furnishing materials (Chang and Guo 1992a, b; Hu et al. 2007; Little et al. 1994; Xu and Zhang 2003; Yang et al. 2001a; Yang et al. 2001b; Zhang et al. 1999c). Interior building and furnishing materials and furniture are typically used under dry or “dried” conditions. Following an initial period of preconditioning, their emission rates decay slowly. Equation (3) can be used to determine the

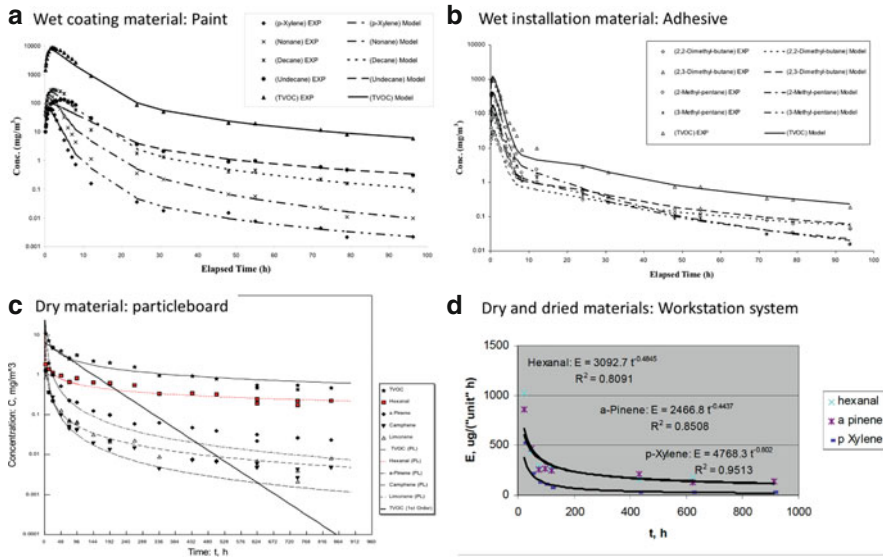


Fig. 2 Emission patterns of different material types: **a**, **b**, and **c** are measured concentrations over time from small chamber testing, Zhang et al. 1999; **d** is emission factor over time from ANSI/BIFMA M7.1)

emission factor at a given time point of chamber testing based on the measured concentration without appreciable error (Zhang et al. 1997). The measured emission factor as a function of time can be well represented by the power law model (Zhang et al. 1999c, 2006):

$$E(t) = at^b \quad (4)$$

where, a and b are model parameters to be determined from the emission test data. A decaying emission factor is reflected by $b < 0$.

Variables Affecting Emission Rates

Variables affecting emission rates include those related to the materials/products themselves (emitting source variables), those related to the environment within which they are used or tested (environmental variables) as described in ASTM D6670 (ASTM International 2018a), and those associated with VOC sampling and analysis. The environmental variables are standardized and controlled in order to reduce uncertainty. For example, for estimating the impact of the workstation systems or seating on the VOC concentration in an office environment, assumptions are made regarding the size and volume of the office environment containing the workstation, the size of the workstation and the number of seating units, clean air flow rate per system, temperature, relative humidity, and air velocities over emitting surfaces (BIFMA International 2011a).

Effect of Product Age

Since VOC emission rates of building materials and furniture typically decrease with time, the age of the specimen to be tested needs to be controlled considering the typical timelines for delivery and occupancy. For example, it is assumed 10 days typically are required between manufacturing and onsite delivery of office workstation and seating systems. Seven and fourteen days following delivery and on site assembly of the workstation and seating system are defined as the times of interest for early occupancy in furniture testing (BIFMA International 2011a).

Estimation of the Contribution of the Materials to the VOC Concentrations in Buildings

A standard reference conditions should first be defined for a specific type of building accounting for the quantity of materials used, ventilation rate, and environmental conditions. For example, for the purpose of estimating the impact of furniture on the VOC concentrations in office spaces, a standard open plan office environment and a standard private office environment are defined based on research (Table 2). These standard open plan and private office conditions define representative “worst case” conditions and combine high density (90th percentile) furniture loading conditions with minimum allowable outdoor (clean) air ventilation rates (Carter and Zhang 2007). Each accommodates one workstation system for a single occupant. The areas include traffic area and support space for copiers, files, storage, etc. The outdoor or clean air ventilation rate for each environment is the minimum required outdoor ventilation rate per ASHRAE Standard 62.1-2007 (ASHRAE 2007), which specifies a minimum ventilation rate of 2.36 L/s per person or 5 cfm per person plus 0.3 L/s per square meter of floor area (or 0.06 cfm per square foot of floor area).

For residential houses, a reference house with quantities of floor, wall, and ceiling materials and ventilation rate has been defined for evaluating the baseline indoor VOC pollution loads and the effects of various IAQ strategies on indoor

Table 2 Standard office environment parameters per ANSI/BIFMA M7.1

Parameter	Open plan workstation	Private office workstation	Seating
Floor area per workstation with common area (m^2)	5.95	23.78	24.8 ^a
Modeled building/room volume (m^3)	16.3	65	
Modeled air flow, Q_o , (m^3/h)	15.02	34.59	
Workstation components	11.08	7.63	
Panel vertical area (m^2)			
Work surface horizontal area (m^2)	6.10	6.73	
Storage external surface area (m^2)	4.57	10.55	
Total potential emitting surface area (m^2)	21.75	24.91	Largest of represented product(s)

^aCalculated as the average for open plan and private office workstations

VOC concentrations. In both office and residential house applications, 23 °C and 50% RH have been selected as the reference conditions consistent with the standard environmental chamber test conditions, and hence the emission factors determined from the chamber tests can be directly applied to estimate the pollution loads in IAQ design.

For example, assuming that the emission factor only changes very slowly with time, the following equation is used to estimate the concentrations in a standard office environment at the time of interest for early occupancy [e.g., $t = 168$ or 336 h (7 or 14 days) after the workstation is installed]:

$$C(t) \approx \frac{A_o E(t)}{Q_o} \quad (5)$$

where, $C(t)$ is concentration in the defined office environment at the time of early occupancy ($t = 7$ or 14 days after the installation), ug/m³; A_o is source amount in the office environment (e.g., number of workstation units, and is equal to 1 in this case); $E(t)$ is estimated emission factor at $t = 168$ or 336 h (7 or 14 days) from Time Zero based on chamber testing, mg/h per workstation unit; Q_o = clean air ventilation rate in the office environment for the standard open plan or private office environments as defined in ANSI/BIFMA 7.1. (BIFMA International 2011a, b)

For the residential reference house application, the concentration of a VOC emitted by multiple materials is calculated by:

$$C(t) \approx \frac{1}{Q_o} \sum_j^n [A_j E_j(t)] \quad (6)$$

where, subscript j represents a material that emits the specific VOC, A_j is the quantity of material j , and E_j is the emission factor determined from the chamber testing.

Other Important Considerations

The goal of a standard test method is to achieve consistent, accurate, reliable, and repeatable test results while making the test procedure practical for implementation. Several important considerations are discussed below:

1. Standard Test Conditions. Chamber conditions of 23 ± 0.5 °C and $50 \pm 5\%$ RH are commonly used in small, mid-size, and large-scale chamber testing methods (ASTM International 2017, 2018a) as they represent typical indoor thermal condition that are well within the thermal comfort zone for occupants. Small-scale chamber test methods commonly adopt an air change rate of 1.0 ACH and a specimen loading ratio of 0.3 to 0.7. Mid-size and large-scale chamber test methods have a broader range of air change rate and specimen loading, depending on the purposes and applications of testing (e.g., office spaces or residential houses). Mimicking the usage conditions also leads to a realistic VOC concentration range in the test chamber, which helps specify the requirements for air sampling and chemical analysis.

2. Requirements for Environmental Chamber Control. A test chamber should have inner interior surfaces with minimal adsorption effects. Polished 304 or 316 stainless steel sheets are often used for chamber construction. They are electropolished for small chambers to further reduce the sorption on chamber surfaces. Test chambers should also be airtight with an air leakage less than 1% of the supply air flow rate. They should be kept at a slightly positive air pressure during testing (e.g., about 10 Pa above the ambient air in the lab space) to avoid any possible contamination by the air in the laboratory. The chamber needs to be supplied with clean/filtered air and the chamber background concentrations should satisfy the following criteria:

- TVOC $\leq 10 \mu\text{g}/\text{m}^3$ for small chamber, and $\leq 50 \mu\text{g}/\text{m}^3$ for mid- and full-scale chambers
- Any individual compound to be measured $\leq 0.5 \mu\text{g}/\text{m}^3$ for small chamber, and $\leq 2.0 \mu\text{g}/\text{m}^3$ for mid- and full-scale chambers
- Particulate $\leq 100 \text{ particles}/\text{m}^3$ of $0.5 \mu\text{m}$ diameter or larger, which is the Class M2 clean room requirement for $>0.5 \mu\text{m}$ diameter particles (ASHRAE 1995)
- Ozone and other potentially reactive species (NO_x, SO_x, etc.) $\leq 3 \mu\text{g}/\text{m}^3$ for small chamber, and $\leq 10 \mu\text{g}/\text{m}^3$ for mid- and full-scale chambers

Good air mixing should be achieved via air diffusers or mixing fans to ensure that the concentration difference between the chamber exhaust outlet and chamber air is less than 5%. Table 3 shows the required control accuracy and precision for the temperature, RH, pressure, and airflow rate. More detailed guidance on the requirements and methods to evaluate the chamber's performance against the established criteria can be found in ASTM 5116, 6670 and Herrmann's study (ASTM International 2017, 2018a; Herrmann et al. 2003).

3. Test Specimen Collection and Storage. Different product-specific test methods may have different requirements. For example, ANSI/BIFMA M7.1 (BIFMA International 2011a) includes the following requirements:

- The complete test item – all components or component assemblies of a workstation system, workstation component, or seating unit – must be

Table 3 Required accuracy and precision limits parameters

Parameter	Accuracy (as bias)	Precision
Temperature (°C)	± 0.5	± 1.0
Relative humidity (%)	± 5	± 5
Air flow rate (%)	± 3	± 5
Area of the testing surface of the specimen (%)	± 1.0	± 1.0
Time (%)	± 1.0	± 2.0
Organic concentration (% RSD ^a)	—	± 15.0
Emission factor (% RSD ^a)	—	± 20.0

^aRSD = Relative standard deviation = $(s/m) \times 100\%$, where, s = estimate of the standard deviation; and m = mean

received by the testing laboratory not more than 15 days after the date of manufacture of the first workstation component. The manufacturer should attempt to minimize the total elapsed time from manufacture to receipt of the sample at the lab in a way that best represents their standard manufacturing, packaging and shipping processes. The manufacturer's most air-tight packaging option for that workstation component, component assembly, or seating unit should be used unless the manufacturer prefers to use a more airtight means of packaging (Typically the most airtight packaging will fully encase the product in plastic coverings (polybags, shrink-wrap, etc.). Corrugated (cardboard) packaging materials, even if combined with shrink-wrap that does not fully enclose the product, are generally less airtight than fully encasing plastic materials. Blanket wrapping is generally not considered to be airtight and is discouraged for use as a packaging material for emissions testing. More airtight packaging may be preferred to prevent the potential for cross-contamination during shipping if such contamination is suspected).

- When testing component materials for screening purposes, the material samples should be packaged at the time of sample collection, and should be sealed or packed in a fashion to limit emissions (e.g., double-layer aluminum foil wrap with shiny side out and placed in a polyethylene bag, or directly placed in a Mylar or Tedlar bag and sealed). Samples should remain in their packaging until prepared and placed in a test chamber. Sample collection should occur within 24 h of manufacture.
 - Each system, component, or material shipped must be accompanied by a chain-of-custody (COC) form that contains the full identification of the item, the dates of manufacture, collection and shipping, and individuals handling the item.
 - Upon receipt, the test specimen should be stored in a conditioned and ventilated room of 23 ± 3 °C and not to exceed 60% RH without unpacking, or unpacked and immediately installed in the conditioned chamber for testing. The test specimen must be unpacked and installed for testing within 25 days of the manufacture date of the first sample. The concentrations of TVOC, individual VOCs, and particles in the storage room should be controlled by limiting indoor sources using appropriate filtering (e.g., granulated activated carbon filter and high efficiency particle filter) on the HVAC system. Compliance with the following criteria should be verified at the initial commissioning and again if the storage area or surrounding environment changes in a way that may affect these values.
 - $\text{TVOC}_{\text{Toluene}} \leq 100 \mu\text{g}/\text{m}^3$
 - Any individual compound to be measured in the chamber $\leq 10.0 \mu\text{g}/\text{m}^3$
 - Particulates $\leq 35,200 \text{ particles}/\text{m}^3$ of $0.5 \mu\text{m}$ diameter or larger, and $<0.5 \mu\text{g}/\text{m}^3$ in mass concentration and
 - Ozone and other potentially reactive species (NO_x , SO_x , etc.) $<10 \mu\text{g}/\text{m}^3$
4. Testing Period and Air Sampling Time Points. Testing period and air sampling time points should be selected to either represent the complete emission rate patterns of individual VOCs of interest or the pollution load at the beginning of

product usage or early occupancy stage for the purpose of IAQ design and management as required in the relevant labeling or certification criteria. As an example, Fig. 3 shows the different testing periods and air sampling time points for furniture emission testing in relation to the emission criteria set in relevant labeling or certification programs for formaldehyde. The Greengard Test required 4 days of testing and extrapolated the test results to estimate the emission rate on day 7. The Zhang/BIFMA Test relied on duplicate air samples at 72 and 168 h (day 3 and 7) to determine the coefficients of the power-law model and use the model to predict the emission rate at 14th day for comparing with the LEED-CI limit at 7th day and CA-1350 limit at 14th day, respectively.

- Scaling. Emission test data for individual materials from small chamber testing can be scaled up per the emission surface area to estimate the emission factor of a workstation system or component. The direct scaling approach (i.e., based on the emitting surface area) tends to be conservative in predicting the emission rates of a workstation system or component (Hodgson et al. 2009). The data indicate that small chamber tests should focus on the measurement of VOC emissions from component assemblies rather than from isolated surfaces because sealing of a primary face can alter the emission characteristics of some compounds. Also, relatively detailed knowledge of material construction is required to select the most appropriate items for testing at small scale. Using such techniques, the study

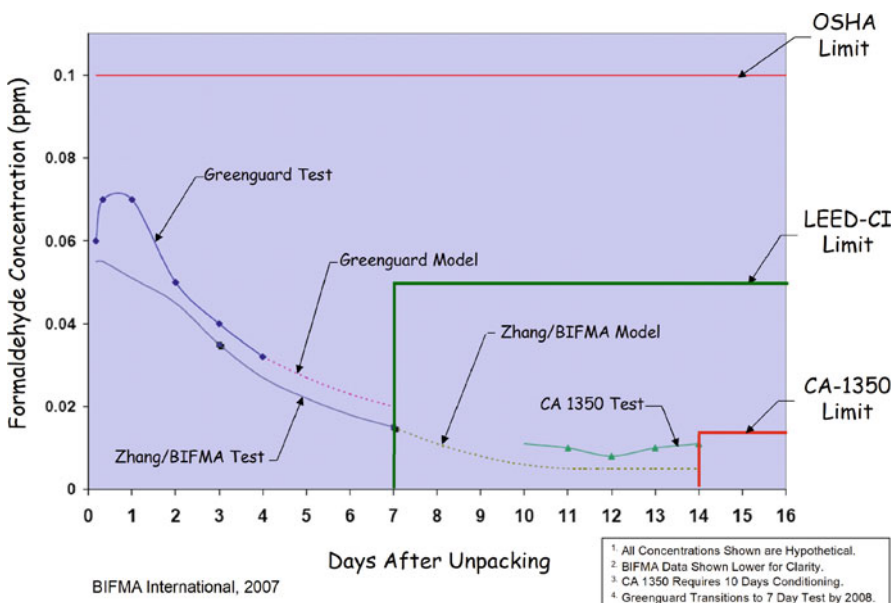


Fig. 3 Testing periods and sampling time points in relation to relevant labeling and certification programs

demonstrated that the scaling of VOC emissions from the small-scale tests to the full system and to its major components either produced comparable projections or overpredicted the emissions for the system and units tested in the mid-scale and large-scale chambers.

6. Quality Control and Quality Assurance. Due to the complexity of source emissions testing, careful planning is usually required to ensure meaningful data. A quality assurance plan identifies the critical data needed to meet testing goals and provides a framework for collecting data that will help ensure that the data are of sufficient quantity and quality to meet the goals of the testing program. Certain kinds of quality control data are necessary to assess the performance of sampling and analysis systems. These data include results of periodic flow rate checks of sampling systems, analysis of replicate samples, analysis of field and lab blanks, spiked field control samples, daily tuning criteria for MS systems, and results of daily mid-range calibration check samples. Guidance on developing a quality assurance and quality control program (QA/QC) plan is available from several sources (USEPA QA/R-5 (U. S. EPA 2001), ASTM D5116 (ASTM International 2017) and ASTM D6670 (ASTM International 2018a)). The QA/QC plan should be based on established data quality objectives and acceptance criteria, which are specified in product-specific test methods such as ANSI/BIFMA M7.1 (BIFMA International 2011a).

Air Sampling and Chemical Analysis

Air sampling and chemical analysis is a vital part of environmental chamber testing and evaluation of product emissions.

Sampling Methods

VOC emissions from sources that impact IAQ include very volatile, volatile, semi-volatile, polar, nonpolar, oxygenated, and other species of organic compounds. Sampling systems include syringes, sampling loops, sorbent traps, cryogenic traps, whole air canisters, and other devices that collect and concentrate analytes of interest. The choice of sampling systems depends upon the nature and concentration of the analytes as well as testing goals. Very volatile compounds may be sampled with whole air canisters, sampling loops, or adsorbents such as Carbosieve SIII[®]. Many VOCs emitted from solvents or oil-based products may be collected on adsorbents or combination of adsorbents such as Tenax[®], charcoal, or Carbotrap[®]. Semi-volatile VOCs may be collected on adsorbent media such as XAD[®] resin or Carbotrap C[®]. Oxygenated compounds may be collected on silica gel coated with DNPH, or other suitable adsorbent. Traps to remove particles or reactive compounds such as ozone may be required upstream of the adsorbent. Whenever a sampling line or probe is placed upstream of the sample collection device, it may be necessary to demonstrate quantitative recovery of analytes to make sure that no adsorption takes place in the sampling line. Several methods are generally applicable to the collection and analysis of VOC emissions from products in chamber tests:

- *Collection on sorbent media:* Collection on sorbent media is currently the most commonly used approach for indoor air source sampling and in standard environmental chamber testing. Sorbents such as Tenax® or graphitic carbon are packed in glass or metal tubes and known volumes of air are drawn through them. Analytes collected on these traps may be thermally desorbed to a concentrator unit or extracted with appropriate solvent for liquid injection. Thermal desorption is the most common approach due to ease of use and lower method detection limits. For selected low molecular weight aldehydes and ketones, compounds are collected and derivatized on cartridges containing silica gel coated with 2,4-dinitrophenylhydrazine (DNPH). The derivatized compounds are solvent extracted and determined by HPLC with UV or photo diode array detection. The air sampling system should include a sorbent tube (or cartridge), an air sampling pump, and an airflow controller, which can measure and control the air flow rate through the sampling system to within $\pm 5\%$ of a specified value. All system components between the chamber and the sorbent tube (or cartridge) should be constructed of chemically inert materials. The sorbent tube or cartridge should be connected directly to the sampling location at the chamber return/exhaust or inside the chamber by using a short (<0.4 m) stainless steel or Teflon tube/connector. The pump should be operated in suction mode downstream of the sorbent tube or cartridge to avoid contamination of air samples by the pump.
- *Online sampling* can be achieved by using near-real-time sampler and analyzer such as proton-transfer mass spectrometer (PTR-MS) with quantitation limit at 1 ppb or less depending on the compounds. Automated systems consisting of a concentrator (i.e., sorbent media as VOC traps) and a GC configured with a gas sampling valve, actuator, sample loops, and detector can also be developed for online sampling. In a typical online concentration system, there are two VOC traps. The sample air is pulled through one trap during the desorption/analysis phase of the other trap. Each trap may contain a single adsorbent or combination of materials (glass beads, Tenax, carbon adsorbents). The range of analytes that can be collected and recovered from the traps will depend upon the composition of the traps and efficiency of transfer of analytes from the traps to the GC. Online sampling methods are mostly used in research where fine time resolution is needed to capture the change of emissions over time and secondary emissions resulting from chemical reactions. They are rarely used in standard material emission tests due to the high cost of equipment.
- *Whole air samples:* Whole air samples may be collected for subsequent off-line analysis using gas sampling syringes, Tedlar or Teflon bags, or stainless steel Summa® polished canisters. Whole air samples permit sample storage and repeated analyses of the same sample. Gas sampling syringes have limited applicability to emission source testing due to their relatively small volume capacity, poor reproducibility, and potential for losses to syringe surfaces. Tedlar® and Teflon® bags provide an adequate volume of air for concentration but analytes may diffuse through the bag or be lost to bag surfaces. Canister technology has been proven to be effective for many volatile compounds at ambient concentrations. Source testing often generates atmospheres with high concentrations of

pollutants and generates pollutants of less volatility than those for which the canister technology has been developed and demonstrated. Therefore, as with any sampling system, it may be necessary to determine the appropriate application of the technique for a particular source.

Sampling Volume and Flow Rates

Sampling volumes and flow rates for sorbent traps used to collect VOCs are selected based on analytical detection limits and breakthrough volumes of compounds of interest, acceptable pressure drop across the sampling traps, and time resolution required for calculation of emission rates from chamber concentration data. Recommendations of the sorbent tube or cartridge manufacturer/supplier should be followed. The lowest concentration to be measured quantitatively should be higher than three times the detection limit of the analytical method. For example, if the detection limit of a GC/MS analytical system is 0.001 µg per tube sample for a VOC of interest, and the lowest concentration to be measured is 1.0 µg/m³, a minimum of 0.003 m³ or 3 L (i.e., $0.001 \times 3/1.0$) air sample should be obtained. A proper sampling volume should be determined through a pre-screening analysis for specific materials or products. In standard chamber testing methods for VOC emissions, typical sampling airflow rates are 100–200 mL/min for VOC sorbent tubes, and 500–1000 mL/min for DNPH cartridges. For a 5 L air sample collected by a VOC sorbent tube, the sampling time would be 25 min if sampling at 200 mL/min.

Chemical Analysis Systems

The appropriate instrumentation for the determination of emissions from products and processes depends upon the nature of the emissions and testing goals. A GC equipped with capillary column and flame ionization (FID) or mass spectral detector (MSD) is commonly employed for identification and quantification of VOC emissions. Due to the complexity of emissions from many types of sources, a GC MS system may be considered essential for identification of VOC emissions from the majority of sources. A GC FID system is often useful for quantification of emissions due to the sensitivity and broad linear dynamic range of the detector. Other GC detectors such as electron capture (ECD) or photo ionization detector (PID) are useful for specific types of compounds. Low molecular weight aldehydes and ketones, collected on silica gel coated with DNPH, may be determined by liquid chromatography with ultraviolet or photo diode array detectors. Additional guidance is provided in product-specific test methods for analyzing VOCs of interest. For example, ANSI/BIFMA M7.1 (BIFMA International 2011a) included the following directions based on the experience gained from an inter-lab comparison study (Zhang et al. 2009):

1. Thermal Desorption-Gas Chromatograph/Mass Spectrometer (TD-GC/MS) System and Methods.

Analytical System Optimization. The TD-GC/MS system and associated analytical method should be optimized for the quantitative recovery and analysis of individual VOCs of interest within a volatility range bounded, at a minimum,

by *n*-hexane and *n*-hexadecane (C6-C16). Note that some criteria may require the analysis of VOCs over a different volatility range. The MS should be an electron impact ionization (70 eV) instrument operated in the scanning mode over a mass range of at least m/z 35–450 at ≤ 0.5 Hz. The system and method should have sufficient sensitivity to quantify chamber concentrations of target analytes $\geq 2 \mu\text{g m}^{-3}$. ASTM D7339 (ASTM International 2018b) and US EPA Methods TO-1 and TO17, or equivalent methods, are used as the basis for configuring the instrument and establishing instrument operating parameters.

Identification of Individual VOCs by TD-GC/MS. An individual VOC is identified by comparing the chromatographic retention time and mass spectrum of the unknown peak to the corresponding parameters for the pure compound analyzed using the same instrument and method. For a confirmed identification, the retention times of the unknown and the standard must agree within 0.25%, or better, of the total run-time and the match quality of mass spectrum of the unknown to the mass spectrum of the standard must be $\geq 90\%$. All VOCs specifically named in an acceptance criterion and present in samples should be positively identified. If confirmation is not obtained, the unknown spectrum is compared to spectra contained in the NIST electronic library. A trained analyst should decide if the identification is likely based on the match quality and the reasonableness of the retention time. Typically, a match quality $\geq 85\%$ is sufficient for tentative identification. If no such identification is obtained, the compound is designated as unknown.

Tuning of TD-GC/MS System. Tuning and mass standardization of the MS is performed using perfluorotributylamine (PFTBA) as the calibrant. The instrument parameters should be adjusted to achieve target relative ion abundances such as given in ASTM D7339. The MS should be tuned as needed to achieve relative ion abundances that are repeatable from day to day.

Internal Standard. The use of one or more internal standard is recommended. An internal standard serves to adjust the MS instrument response for small run-to-run and day-to-day variations. Toulene-d8 and 1-bromo-4-fluorobenzene are commonly used as internal standards. An identical amount of the internal standard is added at the time of analysis to both samples and standards.

Calibration of TD-GC/MS System for Target VOCs. Standard calibration curves are required for all VOCs specifically named in an acceptance criterion. Initially, the TD-GC/MS system should be calibrated using pure compounds with a minimum of five calibration levels spanning the anticipated mass ranges of the individual target VOCs. Prepare calibration levels by injecting aliquots of standard solutions or known volumes of calibration gas mixtures onto clean VOC sorbent samplers. The calibration standards should not exceed the capacities of the sorbent sampler, the analytical column, or the MS detector. Analyze the spiked samplers using parameters identical to be used for the analysis of chamber air samples. If using an internal standard, analyze at least one calibration check standard with each batch of samples analyzed. If not using an internal standard, perform at least a three-level calibration with each batch of samples. Processing of calibration standard and sample data files

requires the extraction of characteristic ions from the total ion-current (TIC) chromatograms for each VOC. Use one quantitative (i.e., primary) ion and at least one confirming (i.e., secondary) ion for each compound including any internal standard. The extracted ion peaks are integrated. The ratio of the area of each confirming ion peak to the area of the quantitative ion peak for a VOC is determined. These ratios and peak retention times serve to provide positive identification of target VOCs. Refer to USEPA TO-15 (U. S. EPA 1995a), Table 2 for characteristic primary and secondary ions for some common air contaminants. The calibration curve for a VOC is constructed using the peak area responses of its quantitative ion in the standards. Apply a linear least squares fit or an average response factor fit to a plot of peak area versus mass of compound injected. If the response is not linear, a quadratic fit may be required. Assuming a zero intercept and linear response, the slope of the plot is the response factor in area/mass injected. When using an internal standard, the response factor is normalized by the internal standard mass and the peak area response of the quantitative ion for the internal standard.

Quantification of Nontarget VOCs. If reporting of nontarget VOCs is required by an acceptance criterion, such VOCs that can be positively identified should be quantified using pure compound calibrations. If a VOC cannot be positively identified, its Total Ion Current (TIC) peak area response should be quantified using toluene as the surrogate standard. Initially, construct a multipoint (\geq five points) calibration for toluene using the TIC areas of toluene in the standards as the response. For routine control, analyze a single-point calibration for toluene for every batch of air samples. Normalize the calibration if an internal standard is used. Calculate the response factor and use this to make semiquantitative estimates of the masses of tentatively identified and unidentified peaks in a sample. VOCs quantified by this surrogate method should be clearly reported.

Quantification of TVOC_{Toluene}. For the purposes of this method, TVOC_{Toluene} is defined as the combined, toluene-equivalent mass of all VOCs in a sample eluting on a nonpolar polydimethylsiloxane analytical column over a volatility range bounded by *n*-hexane and *n*-hexadecane. If a more polar analytical column is used, the equivalent volatility range should be utilized. First, determine the TIC areas of all chromatographic peaks within the defined range using appropriate parameters that achieve baseline-to-baseline integration and then sum these areas. Using a toluene TIC response factor, estimate the toluene-equivalent mass represented by this summed area.

2. High Performance Liquid Chromatography (HPLC) System and Methods.

Analytical System Optimization. The HPLC system and associated analytical method should be optimized for the quantitative recovery and analysis of formaldehyde and other low molecular weight aldehydes of interest. Base the method on ASTM D5197 (ASTM International 2016), or an equivalent method. The HPLC system should be equipped with a UV detector operating at 360 nm and a C18 reverse phase analytical column providing full resolution of the formaldehyde hydrazone derivative from unreacted DNPH in a sample.

The system and method should have sufficient sensitivity to quantify chamber concentrations of analytes $\geq 2 \mu\text{g m}^{-3}$. Note that unsaturated low molecular weight aldehydes such as acrolein are not accurately determined by this method unless special procedures are used. Higher molecular weight aldehydes approximately beginning with butanal can be analyzed by TD-GC/MS.

Identification of Individual Aldehydes by HPLC. The aldehydes in a sample are identified by comparing their retention times with those of standard DNPH derivatives analyzed using the same instrument and method. The retention times of the unknown and the standard must agree within 0.25%, or better, of the total run-time.

Calibration of HPLC System for Target Aldehydes. A calibration standard stock solution is prepared with accurately weighed amounts of each individual DNPH-aldehyde derivative. Purified crystals or solutions of DNPH-aldehyde derivatives are available from commercial sources. Calculate stock solution concentrations as the mass of free aldehyde per unit volume. Prepare calibration standards (at least five levels) spanning the anticipated response ranges of interest by dilution of the stock solution. Construct the calibration curve for an aldehyde by plotting the peak area responses of the standards versus their DNPH aldehyde concentrations. Apply a linear least squares fit to the plot to obtain the response factor. Analyze at least one mid-level standard with each batch of samples.

Quantification of Total Aldehydes. The criteria specified in ANSI/BIFMA X7.1 (BIFMA International 2011b) require the measurement of Total Aldehydes. For the purposes of this method, Total Aldehydes is defined as the sum of the molar volume concentrations of all normal aldehydes from formaldehyde through nonanal plus benzaldehyde. Analyze formaldehyde and acetaldehyde by HPLC. The remaining aldehydes should be analyzed by TD-GC/MS as this method has the advantage of providing positive peak identification. For individual compounds that can be clearly identified and accurately quantified by HPLC those values can be used in place of the corresponding values measured by GC/MS.

Test Procedure

A logical and practical test procedure is critical to ensuring accurate, reliable, and repeatable test results. Test procedures may vary among different product-specific standard test methods, but should generally include the following components as exemplified in ANSI/BIFMA M7.1 (BIFMA International 2011a):

Chamber Operation

All tests should be conducted under tightly controlled and constant environmental conditions typically at 23.0 ± 1.0 STD °C, $50\% \pm 5\%$ STD RH, and 10.0 to 25.0 ± 5 STD Pa of positive pressure relative to the surrounding area. These control parameters should be monitored and maintained throughout the test period.

The ventilation air flow rate depends upon the scale of the chamber that is used to perform the test. Specifications in product specific test methods should be followed.

Measurement of Background VOC Concentrations

Chamber background VOC concentrations should be measured within 1 week prior to the initiation of a test. The chamber should be configured and operated exactly as it will be operated for the corresponding test, but without the test specimen. Before collecting the background samples, the chamber should be operated at the specified test conditions for a minimum of three full air changes. This removes approximately 95% of the background contamination that may have been introduced when the chamber door was open, stabilizes test parameters, and creates a near-steady-state condition for the collection of air samples. Following this purge, air samples for the analysis of VOCs and aldehydes should be collected using procedures identical to those used for the collection of test samples except that it is acceptable to use single samples rather than duplicate samples. The samples should be analyzed to confirm that chamber background VOC concentrations meet the criteria. If background concentrations exceed these criteria, investigate the cause, eliminate the source(s) of contamination, and repeat the background measurement before proceeding with the test. The measured background concentration of any component is denoted as C_{bk} , and is used in data analysis. The chamber should be operated continuously after the background sample is collected and prior to initiating the test. Chamber conditions should be monitored with the data acquisition system throughout this period.

Unpackaging and Transfer of Test Piece to Chamber

The objective is to remove the test piece from its factory packaging, perform any specimen preparation and assembly operations, and transfer the test piece into the chamber as quickly as possible. Supply airflow into the chamber should be maintained during transfer to reduce intrusion of laboratory air. The required dimensional measurements may be made at this time if they can be accomplished within the specified time limit or the measurements may be made at the conclusion of the test. The sequence and details of these operations depend upon the scale of the test:

- For a workstation system, unpack the workstation components outside the chamber and then immediately move them into the chamber for assembly. Complete the entire assembly process within 6 h or less. During this time, operate the chamber at the specified air flow rate and temperature/humidity conditions recognizing that opening of the chamber door and the presence of workers in the chamber will alter these conditions. Installers should not use greasy tools and should wear disposable clean room booties to minimize contamination.
- For workstation components, individual furniture items, and seating, unpack the test piece outside the chamber. Perform all required assembly operations within one hour or less and then immediately place the piece into the chamber.

- Prepare the specimen of a component assembly or component material within 1 h including sealing the edges of the boards.

Place Test Specimen in Chamber

For workstations, workstation components, individual furniture items, component assembly, component material, and seating units, the test piece should be assembled following the manufacturer's instructions so that its components and parts are in their correct orientations and relative positions. The test piece should be located in the center of the full- or mid-scale chamber so that air inlets and outlets are not obstructed and there is at least a 0.4-m air space between the piece and chamber walls. Adjustable feet on components should be set so the bottom edges are approximately 2 cm above the chamber floor. Seating should be placed in an upright position with feet resting on the chamber floor. All workstation and component doors and drawers should be closed for testing. For small-scale chamber tests, the prepared specimen should be placed inside chamber and supported on a stainless steel stand (e.g., three supports each 0.64 cm diameter or less) or rack to minimize the contact area so that all intended emitting surfaces are exposed to chamber air. Photographically recording the installation is recommended.

Record Time Zero

The chamber door should be closed and sealed immediately after installing/loading the test piece. This marks the initiation of the test and the time should be recorded as Time Zero for the test.

Collect Air Samples

Duplicate VOC samples and duplicate aldehyde samples should be collected at 72 and 168 h elapsed time after the initiation of a test. Additional air samples may be taken during or beyond the 7-day elapsed time period to meet other objectives. For example, if a test is conducted to determine if a workstation system would comply with emission criteria specified at day 14, one may extend the test period to 14 days. Two different methods for air sampling and chemical analysis of VOCs are utilized. Air samples for the analysis of TVOC and individual VOCs including higher molecular weight aldehydes are collected on sorbent tubes and are analyzed by thermal desorption (TD)-GC/MS. Air samples for the analysis of low molecular weight aldehydes (e.g., formaldehyde and acetaldehyde) are collected on chemically treated cartridges and are analyzed by HPLC. Refer to ANSI/BIFMA M7.1 (BIFMA International 2011a) for more specific guidance on VOC and aldehyde samplers, sampling flow rates and volumes, and sampling procedure.

Perform Chemical Analysis

VOC sorbent samplers are analyzed for individual VOCs and total VOCs (TVOC) by two-stage, thermal desorption GC/MS (TD-GC/MS). Aldehyde samplers are analyzed for formaldehyde, other individual aldehydes, and total aldehydes by HPLC. Generally, the VOCs (including aldehydes) of interest are those organic chemicals in the volatile range that either are used in the production of furniture or

are present as residuals in component materials. Selection of the specific chemicals or chemical classes to be measured is dictated by acceptance criteria for furniture VOC emissions, for example the criteria specified in ANSI/BIFMA X7.1 (BIFMA International 2011b). Other criteria may be established by government agencies, certification bodies, customers, etc., as discussed in section “[Establishing the Link Between Chamber Testing and Real Applications](#)”. Refer to ANSI/BIFMA M7.1 (BIFMA International 2011a) for more specific directions on TD-GC/MS and HPLC analyses.

Unloading and Background Verification

The test specimen should be removed after the last air sample has been taken, and the chamber air be purged for three air changes. An air sample should be taken from the chamber exhaust. If the concentration of the selected VOCs exceeds 15% of the minimum concentration measured during the test, the problem should be identified and corrected, and the test should be repeated.

Data Analysis and Interpretation

It usually includes the calculation of concentration of chamber air and emission rates of the test specimen (also called chamber source emission rates), and the quantities required for compliance of the established criteria in relevant labeling and certification programs. For example, ANSI/BIFMA M7.1 (BIFMA International 2011a) includes multiple paths to qualify for low-emission product labels, and requires the following data analyses:

Chamber Concentration

Individual VOCs (including individual aldehydes) and TVOC chamber concentrations are calculated by:

$$C_{\text{chamber}}(t_i) = \frac{m(t_i)}{V_s} - C_{bk} \quad (7)$$

where, $C_{\text{chamber}}(t_i)$ is chamber concentration of the compound at time t_i , $\mu\text{g}/\text{m}^3$; $m(t_i)$ is mass amount measured, μg ; t_i is elapsed time from Time Zero; V_s is sampling volume (equal to the air sampling airflow rate times the air sampling period), m^3 ; and C_{bk} is background concentration of the compound in the chamber measured before the test, $\mu\text{g}/\text{m}^3$. In the BIFMA M7.1, the concentrations at $t_1 = 72$ h and $t_2 = 168$ h are calculated as the averages of the duplicate air samples, and denoted as $C(t_1)$ and $C(t_2)$, respectively.

Chamber Source Emission Rate

Workstation systems, workstation components, individual furniture items (including seating units) and their materials can be treated as sources with a constant or near-

constant emission rate after the initial (72 h) conditioning period. The chamber source emission rates are calculated by:

$$R_{\text{chamber}}(t_i) = Q_{\text{chamber}} \times C_{\text{chamber}}(t_i) \quad (8)$$

where, $R_{\text{chamber}}(t_i)$ is chamber source emission rate at time t_i , $\mu\text{g}/\text{h}$; Q_{chamber} is chamber clean air supply flow rate, m^3/h ; and $C_{\text{chamber}}(t_i)$ is concentration of the compound at time t_i , $\mu\text{g}/\text{m}^3$. This calculation applies to individual aldehydes, including formaldehyde.

Chamber Emission Factor

Individual VOC (including individual aldehydes) and TVOC chamber emission factors are calculated by:

$$E(t_i) = \frac{R_{\text{chamber}}(t_i)}{A_{\text{chamber}}} \quad (9)$$

where, $E(t_i)$ is emission factor at time t_i , $\mu\text{g}/(\text{unit h})$, $\mu\text{g}/(\text{m h})$, $\mu\text{g}/(\text{m}^2 \text{ h})$, $\mu\text{g}/(\text{m}^3 \text{ h})$, and $\mu\text{g}/(\text{kg h})$ for unit, line, area, volume, and mass sources, respectively; $R_{\text{chamber}}(t_i)$ is chamber source emission rate at time t_i , $\mu\text{g}/\text{h}$; and A_{chamber} is amount of materials/products tested in the chamber, unit, m, m^2 , m^3 , and kg for unit, line, area, volume, or mass emission sources, respectively.

Calculation of Power-Law Model Coefficients

The emission factors for individual VOCs (including individual aldehydes) from $t_1 = 72$ h and $t_2 = 168$ h may be used to determine the two coefficients of a power-law model, which describes the emission factor as a function of time at any point from 72 h to 336 h (14 days):

$$b = \frac{\ln E(t_1) - \ln E(t_2)}{\ln t_1 - \ln t_2} \quad (10)$$

$$a = E(t_1)t_1^b = E(t_2)t_2^b \quad (11)$$

where, $E(t_i)$ is emission factor at time t_i ($i = 1, 2$), $\mu\text{g}/(\text{unit h})$, $\mu\text{g}/(\text{m h})$, $\mu\text{g}/(\text{m}^2 \text{ h})$, $\mu\text{g}/(\text{m}^3 \text{ h})$, and $\mu\text{g}/(\text{kg h})$ for unit, line, area, volume, and mass sources, respectively; $t_1 = 72$, h; and $t_2 = 168$, h. The procedure described above is adopted because it is simpler to use and provides sufficient accuracy. If more air samples are taken between 72 and 168 h, regression analysis can also be used to determine a and b . Users should refer to ASTM Guide D6670 (ASTM International 2018a) for the detailed calculation procedure.

Determinations of Compliance

Determinations of compliance for workstations, workstation components, or individual furniture items should be made using the open plan and/or private office standard

environments, depending on the product type, application, and intended use. Determinations of compliance for seating units should be made using the seating standard environment. The choice of which standard environment(s) to use for compliance is specified by the requestor (typically the product manufacturer). The parameters of the standard office environments for estimating the impact of workstations, workstation components (including seating units), and individual furniture items on the VOC concentrations in office spaces are summarized in Table 2. BIFMA M7.1 (BIFMA International 2011a) includes three approaches to determine compliance:

1. Estimated Building Concentration Compliance Approach.
 - For a complete standard workstation or complete seating unit tested in whole, the estimated building concentration of each relevant VOC (including individual aldehydes, total aldehydes, and TVOC) should be calculated by:

$$C_{\text{bldg}}(t) = \frac{A_o E(t)}{Q_o} \quad (12)$$

where $C_{\text{bldg}}(t)$ is estimated building concentration of the compound at time t , $\mu\text{g}/\text{m}^3$; t is any time point between 72 h and 336 h, including 72 and 336 h; A_o is 1 workstation or seating unit; $E(t)$ is the emission factor calculated from the direct measurements (Eq. 9) or by the power-law model (Eqs. 4, 10, and 11); $Q_o = 15.0 \text{ m}^3/\text{h}$ (i.e., 4.17 L/s or 8.84 cfm) for the standard open plan office environment, or $Q_o = 34.6 \text{ m}^3/\text{h}$ (i.e., 9.63 L/s or 20.4 cfm) for the standard private office environment, or $Q_o = 24.9 \text{ m}^3/\text{h}$ (i.e., 6.89 L/s or 14.6 cfm) for a seating unit as defined in Table 2.

- For a standard workstation, where several workstation components are tested independently, the estimated building concentration of each relevant VOC (including individual aldehydes, total aldehydes, and TVOC) should be calculated by:

$$C_{\text{bldg}}(t) = \frac{\sum_i^n A_i E_i(t)}{Q_o} \quad (13)$$

where n is the number of workstation components in the standard workstation; A_i is the number of i workstation components used in the standard workstation system (e.g., one file cabinet is tested but workstation contains two identical file cabinets, so $A_i = 2$ “units”); $E_i(t)$ is the emission factor i workstation component; and Q_o is the ventilation rate for the standard open plan office environment, or the standard private office environment, as defined in Table 2.

2. Emission Factor Compliance Approach. When VOC emissions compliance requirements are specified as maximum concentration limits under standard

conditions (i.e., airflow rates and standard source quantities in “units,” surface area, volume, or mass), the concentration limits may be converted to emission factor limits by:

$$E_{\max}(t) = \frac{Q_{\text{std}}}{A_{\text{std}}} C_{\max}(t) \quad (14)$$

where $E_{\max}(t)$ is Emission Factor Limit at time t , $\mu\text{g}/(\text{“unit” h})$, $\mu\text{g}/(\text{m h})$, $\mu\text{g}/(\text{m}^2 \text{ h})$, $\mu\text{g}/(\text{m}^3 \text{ h})$, and $\mu\text{g}/(\text{kg h})$ for unit, line, area, volume, and mass sources, respectively; Q_{std} is standard airflow (ventilation) rate defined with $C_{\max}(t)$, m^3/h ; $C_{\max}(t)$ is maximum allowable concentration of the compound under the standard conditions at time t , $\mu\text{g}/\text{m}^3$; and A_{std} is standard source amount defined with $C_{\max}(t)$, “unit,” m , m^2 , m^3 , and kg for “unit,” line, area, volume, and mass sources, respectively. The emission factors directly measured from the chamber testing (Eq. 9) or predicted by the power-law model (Eqs. 4, 10, and 11) are then compared with $E_{\max}(t)$ used to determine if compliance is achieved for the workstations, workstation components, or individual furniture items tested in whole.

3. Scaling from Component Assemblies. Small-scale (or larger) chamber test results of component assemblies may be used to determine if a workstation system, workstation components, or individual furniture items (including seating units) are compliant with the VOC emissions concentration or emission factor requirements of a given standard such as ANSI/BIFMA X7.1 (BIFMA International 2011b). The following procedure should be used:

- (a) Analyze the design, materials, and construction of the product to identify all component assemblies of the product and the exposed material area, A_i , source amount of each component assembly in the finished product state. When demonstrating compliance for a workstation using the building concentration approach, the material areas should be for the workstation components identified when establishing the standard workstation(s) (refer to ANSI/BIFMA M7.1 (BIFMA International 2011a) for specific definitions of typical types of workstations).
- (b) Test a representative sample of each component assembly and determine the emission factor, $E(t)$ for each compound and for the identified source type (i.e., face, edge, etc.) of each component assembly.
- (c) Calculate the emission rate for each component assembly in the fully assembled product state by:

$$R_i(t) = A_i E_i(t) \quad (15)$$

where $R_i(t)$ is emission rate of the component assembly in the fully assembled product state for the compound of interest at time t , $\mu\text{g}/\text{h}$ or $\mu\text{mol}/\text{h}$.

- (d) For each compound of interest, calculate the sum of the emission rates from all component assemblies in the product (i.e., workstation, workstation component, individual furniture item, or seating unit), as the total emission rate of the product, R_{tot} ; in $\mu\text{g}/\text{h}$ or $\mu\text{mol}/\text{h}$, i.e.,

$$R_{\text{tot}}(t) = \sum_i^n R_i(t) \quad (16)$$

- (e) Determine compliance for a workstation, workstation component, or seating unit by calculating the estimated building concentration for each compound of interest by:

$$C_{\text{bldg}}(t) = \frac{R_{\text{tot}}(t)}{Q_o} \quad (17)$$

where $C_{\text{bldg}}(t)$ is estimated building concentration for the compound of interest at time t , $\mu\text{g}/\text{m}^3$ to be compared with the limits set in relevant labeling or certification programs for compliance.

4. Substitution of Component Assemblies or Materials. Emission test results for component assemblies may be used to assess if an alternative component assembly would result in a significant change of the emissions from a product (i.e., workstation, workstation component, individual furniture item, or seating unit). Assuming that a product has an original/reference emission factor of $E_{\text{original}}(t)$, and a component assembly with an emission factor of $E_{i_original}(t)$ is replaced by an alternative component assembly with an emission factor of $E_{i_alternative}(t)$, the VOC concentrations due to emissions from the revised product with the alternative assembly may be calculated by:

$$C(t) = \frac{E_{\text{original}}(t) - A_{i_original}E_{i_original} + A_{i_alternative}E_{i_alternative}}{Q_o} \quad (18)$$

where $A_{i_original}$ and $A_{i_alternative}$ are, respectively, the amount of the original and alternative component assembly material used in complete furniture or seating unit, m^2 . Application of this method requires that the original component assembly be tested separately, ideally at the same time the product is tested to minimize material variations. It may be tested at a later time if the materials have not changed. The approach may be used for screening of component materials (such as fabric, fiberglass, foam, particleboard with or without surface finish, etc.) to identify the relative potential impact of alternative component materials on the emissions of the product or component assembly. The results of this approach may be used to identify which component material may be tested as part of a product or component assembly to represent more than one possible alternative material.

Establishing the Link Between Chamber Testing and Real Applications

Overview of the Process

Low VOC-emitting product criteria are included in many green or healthy building rating systems, purchasing programs, and sometimes government regulations. Multiple steps are involved for designating compliant products based on chamber testing of a single or group of product samples. Figure 4 shows a schematic program that highlights this process.

Guidance documents or standards are developed first by governmental bodies or standard development organizations, which specify the selection of representative product samples, the chamber (or other laboratory) testing method, the exposure modeling scenario, and the acceptance criteria for chemicals of concern and their maximum allowable concentrations. They also often include the quality assurance and accreditation requirements of testing laboratories (i.e., accredited to ISO 17025 (ISO 2017)) and certification bodies (i.e., accredited to ISO 17065 (ISO 2012)). Not all components are required in a single guidance or standard. The requirements on chamber testing and the evaluation schemes (or acceptance criteria) can be integrated into one document or be kept separately. Additionally, some standard set the acceptance criteria directly based on the VOC emissions factors (EFs, in units of mg/h·m²) obtained from chamber testing without defining a modeling scenario.

Based on a guidance or standard chosen depending on the region and product category, companies (or manufacturers) can test representative samples of their products to demonstrate they meet the acceptance criteria and then make product claims. This is most often accomplished by participating in a third-party labeling/

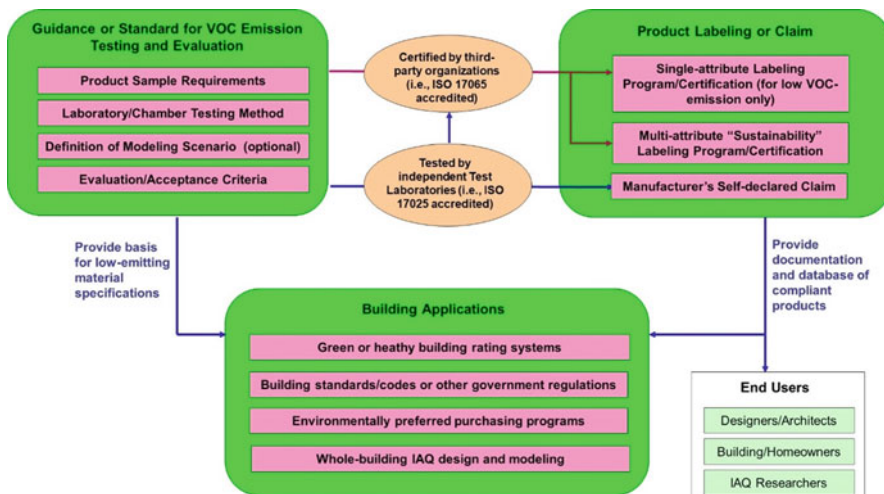


Fig. 4 Schematic diagram for designating low-emitting products in building applications

certification program. Alternatively, the manufacturers can also make their own first-party declaration if they assume full responsibility for their product claims (i.e., based on ISO 14021 (ISO 2016)). Regardless of the type of labeling or claim, a big challenge is always to keep the process (or information) transparent and to make the documentation (including actual emission test data) of low-emitting products more readily accessible to architectural projects and other end users.

Finally, the low VOC-emitting products need to be specified for use in real building applications and their IAQ benefits need to be demonstrated and documented. Although participation is voluntary, the green or healthy building rating systems that provide low-emitting material (LEM) credits for using such products seem to be the largest market-driven force for this purpose (McArthur and Powell 2020). Most of these rating systems directly specify the guidance/standards used for VOC testing and evaluation in their credit language. Some LEM requirements have also been written into government regulations, purchasing programs, and building codes, making the compliance mandatory. For example, many countries have established regulatory formaldehyde emission requirements for composite-wood-based products.

Standard Methods, Evaluation Criteria, and Labeling Schemes

Various standards and guidance documents have been developed in different regions/countries and for different product categories. The environmental chamber testing methodology and the method for determining VOC EFs are similar in these documents and have been discussed thoroughly in section “[Standard Environmental Chamber Testing Methods and Procedure](#)”. However, the target VOCs differ and the time points specified for reporting VOC EFs also vary. As for the evaluation criteria, some guidance and labeling schemes directly compare the reported VOC EFs to acceptable EF levels. Others convert the measured EFs into estimated airborne VOC concentrations by applying a mass balance for a defined modeling scenario. The modeling scenario here refers to a standardized single room (or a house if it can be considered as a single well-mixed zone) with a set of defined parameters (e.g., room dimensions, air change rate, and product loadings) that are typical or representative for the products being considered. These estimated VOC concentrations are then compared to existing occupant inhalation exposure reference values where such guidance is available. Both the modeling scenario definition and the inhalation exposure reference values can vary among different guidance and labeling schemes. Table 4 compares major standards and labeling schemes in the USA, Europe, and Asia and illustrates how they differ in the above-discussed features. Although not included in Table 4, other types of standards that are not based on environmental chamber testing (e.g., flask, perforator, or desiccator method) are also available for quantifying formaldehyde emissions from wood-based products. The formaldehyde emissions measured with these test methods have shown some correlations with chamber testing results. The variations can be explained by differences in test conditions and sample treatments (Rishholm-Sundman et al. 2007).

Table 4 Examples of VOC emission testing and evaluation methods and labeling schemes in the USA, Europe, and Asia

		Descriptions		If criteria based on estimated VOC concentrations		Applicable product category	
Document title	Region or country	Target chemicals of concern	Time point for reporting EFs	Acceptable EF levels if criteria directly based on VOC EFs	Modeling room definition	Acceptable reference exposure levels	
CDPH SM v1.2, 2017 (CDPH 2017)	USA	A list of 35 individual VOCs with CRELs; additionally, ten VOCs having the highest EFs (most abundant VOCs) need to be quantified	At day 14 (including 10-day conditioning period)	N/A	Private office (30.6 m ³ , 0.68 ACH) or school classroom (231 m ³ , 0.82 ACH); voluntary whole-house (547 m ³ , 0.23 ACH)	≤CREL (9 µg/m ³ or 7.3 ppb) for formaldehyde; ≤1/2 of the CREL for all other VOCs	Building materials (general)
ANSI/BIFMA M7.1, 2011 (R2016) (BIFMA International 2011a)	USA	N/A	At day 3 (72 h) and day 7 (168 h)	N/A	Open plan workstation (16.3 m ³ , 0.92 ACH); Private office (34.68 m ³ , 0.53 ACH)	N/A	Furniture and seating

ANSI/BIFMA X7.1, 2011 (R2016) (BIFMA International 2011b)	USA	Formaldehyde, 4-Phenylcyclohexene (PCH), total aldehydes, TVOC	At day 7 (168 h)	N/A	Reference room defined in ANSI/BIFMA M7.1, 2011 (R2016)	Workstation Systems: formaldehyde ≤ 50 ppb, 4-PCH ≤ 0.0065 mg/m ³ , total aldehydes ≤ 100 ppb, TVOC ≤ 0.5 mg/m ³ ; Seating: one half of the above threshold values	Furniture and seating
ANSI/BIFMA e3, 2019 (BIFMA International 2019)	USA	A list of 30 individual VOCs (including formaldehyde), 4-PCH, total aldehydes, TVOC	At day 7 and day 14 (modeled)	N/A	Reference room defined in ANSI/BIFMA M7.1, 2011 (R2016)	Workstation Systems: Credit 7.6.1: same as BIFMA X7.1; Credit 7.6.2: same as CDPH SM v1.2 (except formaldehyde ≤ 13.5 ppb plus 1-Methyl-2-pyrrolidinone ≤ 350 μ g/m ³ ; Credit 7.6.3: formaldehyde ≤ 7.3 ppb; Seating: one half of the above threshold values	Furniture and seating
EN 16516:2018 (European Collaborative Action 2018)	EU	N/A	At day 28 or at both day 3 and 28	N/A	Reference room (30 m ³ , 0.5 ACH)	N/A	Building materials (general)

(continued)

Table 4 (continued)

Document title	Region or country	Target chemicals of concern	Time point for reporting EFs	Descriptions		If criteria based on estimated VOC concentrations	Applicable product category
				Acceptable EF levels if criteria directly based on VOC EFs	Modeling room definition		
AgBB, 2018 (Committee for Health-related Evaluation of Building Products 2018)	Germany	TVOC, TSVOC, carcinogenic substances in EU categories 1A and 1B, a list of individual VVOC, VOC, and SVOC with LCIs, odorous VOCs subject to sensory testing (optional)	At day 3 and 28	N/A	Reference room defined in EN 16516: 2018	At day 3: TVOC $\leq 10 \text{ mg/m}^3$; carcinogenic substances in EU categories 1A and 1B $\leq 0.01 \text{ mg/m}^3$. At day 28: TVOC $\leq 1 \text{ mg/m}^3$, TSVOC $\leq 0.1 \text{ mg/m}^3$, carcinogenic substances in EU categories 1A and 1B $\leq 0.001 \text{ mg/m}^3$; individual VVOC, VOC, and SVOC with listed LCIs: $R = \text{sum of } (C_i / LCI_i) \leq 1$; sum of VOCs with unknown LCIs $\leq 0.1 \text{ mg/m}^3$	Building materials (general)

M1 (The Building Information Foundation RTS 1996)	Finland	TVOC, formaldehyde, ammonia, carcinogenic compounds (IARC category 1), odor (dissatisfaction with odor below 15% is deemed as “no odor”)	At day 28	TVOC (mg/m ² ·h): <0.2 for M1, <0.4 for M2, and >0.4 for M3; formaldehyde (mg/m ² ·h): <0.05 for M1, <0.125 for M2, and >0.125 for M3; ammonia (mg/m ² ·h): <0.03 for M1, <0.06 for M2, and >0.06 for M3; carcinogenic compounds (mg/m ² ·h): <0.005 for M1 and M2; no odor for M1 and M2.	N/A	N/A	Building materials (general)
French VOC Label (ANSES 2016)	France	A list of ten individual VOCs and TVOC	At day 28	N/A	Reference room defined in EN 16516: 2018	VOC emissions classes are categorized as “A+,” “A,” “B,” and “C” (see the regulation document for details of allowable concentrations of individual VOCs and TVOC for each class)	Building materials (general)
GB 18580-2017 (Standardization Administration of China 2017a)	China	Formaldehyde	After reaching steady state, at most 28 days	Formaldehyde (mg/m ² ·h): <0.124 ^a in GB 18580, <0.12 ^a in China environmental label	N/A	N/A	Building material (wood-based panels and products)

(continued)

Table 4 (continued)

Document title	Region or country	Target chemicals of concern	Time point for reporting EFs	Descriptions		Acceptable EF levels if criteria directly based on VOC EFs	Modeling room definition	Acceptable reference exposure levels	If criteria based on estimated VOC concentrations	Applicable product category
				If criteria based on estimated VOC concentrations	Acceptable reference exposure levels					
GB/T 35601-2017 (Standardization Administration of China 2017b)	China	Formaldehyde	After reaching steady state, at most 28 days	Formaldehyde (mg/m ² ·h): <0.05 ^a	N/A	N/A	N/A	N/A	Building material (wood-based panels)	
		Benzene, toluene, xylenes, and TVOC	At day 3 (72 h)	Benzene (mg/m ² ·h): <0.010 ^a ; toluene (mg/m ² ·h): <0.020 ^a ; xylenes (mg/m ² ·h): <0.020 ^a ; TVOC (mg/m ² ·h): <0.100 ^a	N/A	N/A	N/A	N/A	Building material (wood-based panels and floors)	
GB/T 35607-2017 (Standardization Administration of China 2017c)	China	Formaldehyde, benzene, toluene, xylenes, and TVOC	At 20 h	Formaldehyde (mg/m ³ ·h): <0.03 ^b ; benzene (mg/m ³ ·h): <0.03 ^b , toluene (mg/m ³ ·h): <0.07 ^b ; xylenes (mg/m ³ ·h): <0.07 ^b ; TVOC (mg/m ³ ·h): <2.00 ^b	N/A	N/A	N/A	N/A	Wooden furniture	
Eco Mark (according to JIS A 1901) (Japan Environmental Association 2019)	Japan	Formaldehyde	At day 28	Formaldehyde (mg/m ² ·h): <0.005	N/A	N/A	N/A	N/A	Furniture and wooden materials	

Eco Mark (according to JIS A 1901) (Japan Environmental Association 2019)	Japan	Benzene, toluene, ethylbenzene, styrene	At day 28	Benzene (mg/m ² ·h): <0.038, toluene (mg/m ² ·h): <0.12, ethylbenzene (mg/m ² ·h): <0.55, styrene (mg/m ² ·h): <0.32	N/A	N/A	Adhesives and coatings/ paints
Eco-label 172 (according to KS I ISO 16000-9) (Ministry of Environment of Korea 2017)	Korea	Formaldehyde, toluene, VOCs	At day 7	Formaldehyde (mg/m ² ·h): <0.12, toluene (mg/m ² ·h): <0.080, VOCs (mg/m ² ·h): <0.4	N/A	N/A	Furniture
Green Label (Singapore Environment Council 2013)	Singapore	Formaldehyde, TVOC	After reaching steady state	Formaldehyde (mg/m ² ·h): <0.063 ^a for hardwood plywood wall paneling, 0.141 ^a for particleboard panel, 0.229 ^a for medium density fiberboard, 0.462 ^a for particleboard door core, TVOC (mg/m ² ·h): <0.5	N/A	N/A	Furniture and wood products

^aThe standard for building materials directly specifies the allowable VOC concentration in the test chamber and the reported EF is calculated based on $EF = Q \times C/A$, where Q is the ventilation rate (m³/h), C is the allowable concentration in the chamber (mg/m³), A is the emission area (m²)

^bThe standard for wooden furniture directly specifies the allowable VOC concentration in the test chamber and the reported EF is calculated based on $EF = Q \times C/V$, where Q is the ventilation rate (m³/h), C is the allowable concentration in the chamber (mg/m³), V is the volume of furniture (m³)

Product Labeling Programs

Numerous labeling programs exist. The first labeling program that focused on VOC emission from indoor materials was Blue Angel in Germany initiated in 1978 (Federal Ministry for the Environment 2021). In the 1990s, various labeling programs began to appear in Europe, such as M1 and AgBB. (Committee for Health-related Evaluation of Building Products 2018; The Building Information Foundation RTS 1996) The labeling programs in the USA started from 2000, such as BIFMA. (BIFMA International 2011a) Recently, labeling programs also developed very quickly in Asian countries, including Japan, Korea, China, and Singapore. Some labeling programs mentioned above are single attribute, focusing only on VOC emission, while others are multi-attribute “environmentally preferable” (or “sustainability”) programs with more comprehensive health and environment components including VOC emission evaluation as prerequisites or credit options. A labeling program can be owned or managed by government agencies, nonprofit environmental advocacy organizations, or private sector entities, while the testing and certifications for VOC content or emission are often provided by third-party organizations and independent testing laboratories.

The labeling programs and the availability of products that are evaluated and certified by these programs mostly depend on the region/country. The national product evaluation and certification programs for low-emitting materials in the USA, Europe, and Asia have been summarized in previous research (Levin 2010; Willem and Singer 2010). Although these programs continue to evolve, the general process and underlying principles remain similar over the past decade.

Application in Building Rating Systems

Many green or healthy building rating systems provide LEM credits for products with low VOC contents or emissions. McArthur and Powell (McArthur and Powell 2020) systematically reviewed these rating systems available in today's market. They found that almost all rating systems prohibit or prescribe strict limits of VOCs within the indoor environment, with a strong focus on source elimination through the selection of low-emitting products.

The LEED rating system, which is probably the most widely used globally today, is analyzed here. In the latest version of LEED v4.1 (U. S. Green Building Council 2020), there are eight product categories eligible for LEM credits, including Paints & Coatings, Adhesives & Sealants, Flooring, Wall panels, Ceilings, Insulation, Furniture, and Composite wood. The general VOC emissions evaluations for building materials are all based on the CDPH Standard Method v1.2 (2017) (CDPH 2017). The furniture VOC emission evaluations are based on ANSI/BIFMA M7.1–2011 (R2016) (BIFMA International 2011a) and ANSI/BIFMA e3-2019e (BIFMA International 2019). The criteria for formaldehyde emission from composite wood products are based on EPA Toxic Substances Control Act, Formaldehyde Emission Standards for Composite Wood Products (U. S. EPA 2016) or California Air Resources Board (CARB) Airborne Toxic

Control Measure (CARB 2008). Besides VOC emissions, the VOC content requirements for paints, coatings, adhesives, and sealants are also included, which are based on California regulations (CARB 2007; SCAQMD 2016, 2017). Without more complex IAQ modeling, the number of credits given is then simply determined based on the quantity of products in compliance with the above specified standards/regulations, either as the percent of cost or surface area (for dry materials and furniture) or as the percent of volume or surface area (for web-applied products). Considering the feasibility of implementation, the threshold ranges for compliance are set as $\geq 75\text{--}\geq 90\%$ of total product quantities depending on the product category. Overall, the LEED system provides a good example of how to specify LEM credits based on the standard methods and government regulations for product evaluation.

Whole Building Approach for Modeling the Impact of Product Emission on IAQ

In the above-mentioned labeling and green building rating systems, product emission data are obtained under standardized test conditions and the indoor air VOC concentrations are estimated based on a simplified single room model (e.g., the reference room defined in EN 16516 (European Collaborative Action 2018) or the private office and classroom scenarios defined in CDPH Standard Method v1.2 (CDPH 2017)). The actual impact of product VOC emissions on IAQ in real buildings, however, can be much more complex due to the use of multiple materials with different loading factors, the building source/sink characteristics, and the variation of environmental conditions such as temperature and relative humidity. Predicting such impacts will need a whole building/house approach using appropriate IAQ simulation tools and with accessible VOC emission database of various types of products. An example implementation of this approach using either prescriptive index or performance index has been demonstrated in a recently published Chinese technical standard for interior decoration pollution control of residential buildings (Ministry of Housing and Urban-Rural Development of China 2018).

Various IAQ simulation programs have been developed over the last 30 years. Some programs (e.g., MEDB-IAQ) focus only on modeling the impact of VOC emission and include embedded material emission data base (Zhang et al. 1999a). Others are more comprehensive models that are able to estimate building concentration levels of various contaminants (e.g., CONTAM) (Dols and Polidoro 2015) or combine further with building energy modeling. However, they often require additional effort from the user to identify appropriate material emission rates (for empirical models) or derived characteristic emission parameters (for mechanistic VOC emission models) as inputs. Although product emission tests are common practice today, detailed information on VOC emission rates and emission parameters is generally not publicly available due to the nondisclosure agreements between the testing laboratories/labeling programs and product manufacturers (Willem and Singer 2010). Efforts of developing openly accessible product emission database

have been made by multiple research groups. A series of databases were identified in the International Energy Agency's Annex 68 (Rode et al. 2019). Further efforts are needed to establish more comprehensive and regularly maintained databases and to better assess the effectiveness of source control strategies on whole-building IAQ starting from the design stage.

Application Examples

A few more commonly used standards or guidance procedures are briefly discussed below:

ANSI/BIFMA e3 Furniture Sustainability Standard and ANSI/BIFMA M7.1 and X7.1

ANSI/BIFMA e3 Furniture Sustainability Standard (BIFMA International 2019) is a voluntary standard intended to provide measurable market-based definitions of progressively more sustainable furniture by establishing performance criteria addressing environmental and social impacts throughout the supply chain. It addresses product-based characteristics in the general areas of environmental, health and wellness, and social impacts. The standard was designed to allow for multiple levels of achievement and to provide an open alternative to proprietary protocols. It references ANSI/BIFMA M7.1 and X7.1 standards (BIFMA International 2011a, b) for testing and determining compliance regarding VOC emissions from office furniture systems, components, and seating.

CDPH Standard Method v1.2

In the USA, the CDPH Standard Method V1.2 (2017) (also known as Section 01350) is a widely used voluntary guideline for testing and evaluation of VOC emissions for building materials in the USA (CDPH 2017). It applies to all major building material categories including paints and coatings, adhesives and sealants, flooring (i.e., hard surface flooring and carpet), wall panels, ceilings, and insulation. This standard method covers all the steps necessary for a product evaluation, including selection of representative product samples, description of environmental chamber testing method, definition of modeling scenarios and acceptance criteria, and establishment of claims for compliant products. In this standard, the VOC measurements after 14 days (including a 10-day precondition period in a conditioning chamber followed by a 96-h test period in a test chamber at more precisely controlled conditions) are used to determine the acceptance of a product. The maximum allowable concentrations for chemicals of concern are based on the CRELs developed by OEHHA, which are solely based on health considerations. A list of certifications and labeling programs that use this method can be found on the website of CDPH IAQ program (CDPH 2019).

EN 16516 Test Method with EU-LCI Values or German AgBB Evaluation Scheme

In Europe, different countries have different guidance documents and labeling schemes (see Table 4). As part of the European Collaborative Action (ECA), efforts have been made to harmonize the chamber emission testing method (European Collaborative Action 2018), the indoor material labeling schemes (Kephalaopoulos et al. 2005), and the health-based evaluation using the European Union (EU) Lowest Concentration of Interest (LCI) concept (Kephalaopoulos et al. 2013). The EN 16516 testing method together with the EU-LCI values or German AgBB evaluation scheme seem to be the most widely used and recognized by building rate systems such as LEED and WELL for projects out of the USA. EN 16516 measures VOC emissions after 28 days (or after both 3 and 28 days depending on the legislation) in an environmental test chamber and defines a reference room for modeling indoor air VOC concentrations. The EU-LCI values are then used for assessing the acceptance of a product based on its emissions after 28 days. These EU-LCI values are health-based and are considered likely not to cause adverse effects over the longer term by use of the model room as a reference. German AgBB uses the same LCI values, but includes additional evaluation criteria on TVOC, TSVOC, as well as carcinogenic substances in EU categories 1A and 1B (Committee for Health-related Evaluation of Building Products 2018).

VOC Emission Testing and Labeling Systems in China

There are three important voluntary labeling systems concerning building materials and furniture in China: environmental labeling, ecolabeling, and green product labeling. The environmental labeling is the most widely used. It applies China's national standard GB 18580 (Standardization Administration of China 2017a) to test the formaldehyde emission from wooden panels and products (Ministry of Ecology and Environment of China 2010), which requires that the material be conditioned in a ventilated chamber until stable (usually very slowly decreasing) concentrations in the chamber are achieved to measure the concentrations of formaldehyde. Additionally, the environmental labeling requires that the material be conditioned in a ventilated chamber for 72 h before measuring the concentrations of TVOC. The measured concentrations are multiplied by the clean air supply flow rate to the chamber to obtain the emission rates for TVOC and formaldehyde, respectively. The limit of emission rate in this labeling is stricter than the national standard itself. Content-based limits are also provided in this labeling for wallpapers, coatings, and adhesives. Additionally, this labeling system requires that wooden furniture use the wooden panels, coatings, and adhesives that meet the above requirements, instead of directly testing the emission from furniture in the chamber as a whole (Ministry of Ecology and Environment of China 2016).

The ecolabeling system is established by China Quality Certification Centre. This label regulates that wooden furniture should satisfy China's national standard GB 18584 (Standardization Administration of China 2001), which employs the

desiccator method (China Quality Certification Center 2018). The formaldehyde concentration absorbed into water after 24-h emission in a closed desiccator is used to determine whether the furniture is acceptable. Unlike environmental chamber testing, the desiccator method only tests the emission characteristics of small pieces of materials cut from the whole furniture and cannot provide the emission rate of the whole furniture. Therefore, GB 18584 is under revision and will be changed into emission chamber test method as well. Other new national standards for furniture in China, such as GB/T 38723 (Standardization Administration of China 2020), are also based on chamber method to acquire the emission rate of furniture.

The last labeling system is the China green product labeling proposed in 2018. The green product labeling conforms to another Chinese national standard GB/T 35601 (Standardization Administration of China 2017b) to limit the VOC emission from building materials. The testing method for formaldehyde is the same as that in China environmental labeling, but this label additionally focuses on benzene, toluene, xylene, and TVOC emitted from building materials. The final concentrations of these four pollutants in the chamber after 72 h are used to evaluate the emission rates of building materials. For furniture, the green product label demands that the furniture is directly exposed in a ventilated chamber for 20 h after 120-h pre-conditioning, according to GB/T 35607. (Standardization Administration of China 2017c) This is the only label for furniture in China that tests the emission characteristic of the whole furniture directly.

Unlike the USA and Europe, there have been no available testing standards and labels based on the estimated VOC concentration in a modeling room in China. To overcome this shortcoming, Liu et al. (Liu et al. 2013) proposed a labeling system for VOC emission from furniture based on reference rooms. Via a survey of 1500 homes in Beijing, they established a reference bedroom and a reference living room with the information of furniture type and loading factor. Later, C-history method (Xiong et al. 2011; Zhang et al. 2018) is recommended to obtain the emission characteristic parameters of the furniture rapidly. At last, the predicted VOC concentration in the reference room due to emission from furniture is compared with the national standard on indoor air quality in China, GB/T 18883 (National Health Commission of China 2002), to evaluate whether this furniture can qualify for the label. This labeling method takes the association between furniture and realistic indoor environment into account. It suggests a new direction for developing standard and labeling system in China.

Eco Mark Labeling System in Japan

In Japan, Eco Mark is one of the most widely used labeling system for building materials and furniture (Japan Environmental Association 2019). This label limits the formaldehyde emission from furniture and wood materials via two methods. The first is the desiccator method, which requires placing the material or part of the furniture in a closed desiccator for 24 h and then measuring the amount of formaldehyde absorbed into water at the bottom of the desiccator (Japanese Standards

Association 2021). The allowable limit value for this label (i.e., 0.3 mg/L average and 0.4 mg/L maximum) is much stricter than China (<1.5 mg/L) (Standardization Administration of China 2001). Another method is the chamber method, which allows the material to emit formaldehyde in a ventilated chamber for 28 days (Japanese Standards Association 2015). The limit of formaldehyde emission rate is set as 5 $\mu\text{g}/\text{m}^2\cdot\text{h}$. Applying the same chamber method, Eco Mark also restricts the emission rate of benzene, toluene, ethylbenzene, and styrene from adhesives or coatings used in furniture. Similarly, an alternative content-based standard is given for these four VOCs in the adhesives or coatings.

Concluding Remarks and Future Outlook

The environmental chamber test method for testing VOCs emissions from building materials and furniture has been well established. It has been applied to various labeling, certification, and compliance programs to significantly reduce the indoor pollution loads resulting from material emissions over the last 30 years. The threshold values of area-specific emission rates (either directly specified or derived from the specified concentration threshold values, ventilation rate, and surface area) in various emission standards or labeling and certification programs can be used as the upper limit of indoor pollution loads for IAQ design of green buildings and healthy buildings.

The target VOCs and their threshold values are expected to change over time as the understanding of the impact of VOC mixtures as well as individual VOCs improves or as product formulations or manufacturing processes change. Retesting of products (e.g., every 2–3 years when no changes are made in the manufacturing process) is necessary for keeping low-emission certification up-to-date.

While the principles of environmental chamber testing are universal, the way they are applied in product-specific testing standards and labeling and certification programs vary among countries. Harmonization of the test methods and programs or establishing equivalencies or correlations among them will help international collaboration and trading on low-emitting products.

Standard chamber testing of material emissions generates useful data for design and helps drive the development and application of low-emitting products. However, it does not provide sufficient information to estimate the impact of environmental conditions (temperature, humidity, and airflows) on the pollution loads, nor does it provide long-term predictions on the impact of the VOC emissions on IAQ. A model-based testing and evaluation approach is needed. In such an approach, mechanistic models of emissions are established with their parameters determined by standardized tests (Zhang et al. 2019). For example, the VOC emissions from dry or dried building materials can be represented by in-material diffusion to material surface and then by convective mass transfer to the air. Assuming uniform distribution of VOCs in the material, the diffusion and convective mass transfer processes are governed by the Fick's Law of diffusion and convective mass transfer principle with four model parameters: the initial concentration in the material (C_{m0}), the

diffusion coefficient (D_m), the partition coefficient (i.e., the ratio between material phase and air phase concentration at equilibrium, K_{ma}), and the convective mass transfer coefficient (k_m) (Zhang et al. 1999c). k_m depends on the airflow conditions above the material surface, which is a constant for a given chamber or room condition. C_{m0} , D_m , and K_{ma} can hence be used to fully characterize an emission source. China Healthy Building Assessment Standard adopted an apparent C_{m0} , D_m , and K_{ma} approach and used software (Hu et al. 2007; Xu and Zhang 2003) to determine if the VOC emissions are below the established criteria. As part of the IEA Annex 68 effort, a procedure has been developed to estimate the apparent C_{m0} , D_m , and K_{ma} from the emission data obtained from the standard environmental chamber tests (Liu et al. 2021). The mechanistic models for predicting emissions under material usage conditions should also account for the effects of local air temperature, relative humidity, airflow, and material aging on the emission rates. Further efforts are needed to establish universal guidance/standards for the model-based testing and evaluation and to apply it for better assessing the effectiveness of source control strategy in real applications.

In addition to VOCs emissions from building materials and indoor furnishings, IAQ analysis and design are needed to consider chemical emissions from occupants (bio-effluents) and occupant activities, and secondary emissions resulting from ozone initiated indoor air and surface chemistries, which can also be investigated using environmental chambers. In such investigations, it is necessary to include realistic settings of ventilation, material usage, and environmental conditions to test the combined effects of primary and secondary emissions on IAQ.

References

- ANSES (2016) Labelling of building and decoration products with respect to VOC emissions. <https://www.anses.fr/en/content/labelling-building-and-decoration-products-respect-voc-emissions>. Accessed 20 Apr 2021
- ASHRAE (1995) ASHRAE handbook: HVAC applications, Chapter 15. In: ASHRAE, 1791 Tullie Circle, N.E., Atlanta, GA 30329
- ASHRAE (2007) ASHRAE standard 62.1: ventilation for acceptable indoor air quality. <https://www.ashrae.org/technical-resources/standards-and-guidelines/standards-interpretations/interpretations-for-standard-62-1-2007>. Accessed 20 Apr 2021
- ASTM International (2016) ASTM D5197, test method for determination of formaldehyde and other carbonyl compounds in air (active sampler methodology). https://compass.astm.org/EDIT/html_annot.cgi?D5197+16. Accessed 20 Apr 2021
- ASTM International (2017) ASTM D5116, standard guide for small scale environmental chamber determinations of organic emissions from indoor materials/products. https://compass.astm.org/EDIT/html_annot.cgi?D5116+17. Accessed 20 Apr 2021
- ASTM International (2018a) ASTM D6670, standard practice for full-scale chamber determinations of volatile organic emissions from indoor materials/products. https://compass.astm.org/EDIT/html_annot.cgi?D6670+18. Accessed 20 Apr 2021
- ASTM International (2018b) ASTM D7339, standard test method for determination of volatile organic compounds emitted from carpet using a specific sorbent tube and thermal desorption/gas chromatography. https://compass.astm.org/EDIT/html_annot.cgi?D7339+18. Accessed 20 Apr 2021

- BIFMA International (2011a) ANSI/BIFMA M7.1, standard test method for determining VOC emissions from office furniture systems, components and seating
- BIFMA International (2011b) ANSI/BIFMA X7.1, standard for formaldehyde & TVOC emissions of low-emitting office furniture and seating.
- BIFMA International (2019) ANSI/BIFMA e3 furniture sustainability standard
- CARB (2007) Suggested control measure for architectural coatings. <https://ww2.arb.ca.gov/our-work/programs/coatings/architectural-coatings/suggested-control-measure>. Accessed 29 Apr 2021
- CARB (2008) Final regulation order: airborne toxic control measure to reduce formaldehyde emissions from composite wood products. <https://www.arb.ca.gov/regact/2007/compwood07/fro-atcmfin.pdf>. Accessed 29 Apr 2021
- Carter RD, Zhang JSS (2007) Definition of standard office environments for evaluating the impact of office furniture emissions on indoor VOC concentrations. *ASHRAE Trans* 113:466–477
- CDPH (2017) Standard method for the testing and evaluation of volatile organic chemical emissions from indoor sources using environmental chambers. <https://www.cdpb.ca.gov/Programs/CCDPHP/DEODC/EHLB/IAQ/Pages/VOC.aspx>. Accessed 20 Apr 2021
- CDPH (2019) List of certifications and programs that use CDPH standard method v1.2. <https://www.cdpb.ca.gov/Programs/CCDPHP/DEODC/EHLB/IAQ/Pages/VOC.aspx>. Accessed 20 Apr 2021
- Chang JCS, Guo ZS (1992a) Characterization of organic emissions from a wood finishing product – wood stain. *Indoor Air* 2:146–153
- Chang JCS, Guo ZS (1992b) Modeling of the fast organic emissions from a wood-finishing product – floor wax. *Atmos Environ* 26(13):2365–2370. [https://doi.org/10.1016/0960-1686\(92\)90366-S](https://doi.org/10.1016/0960-1686(92)90366-S)
- China Quality Certification Center (2018) CQC 5109, environmental friendly certification technical specification for furniture.
- Committee for Health-related Evaluation of Building Products (2018) AgBB, evaluation procedure for VOC emissions from building products. <https://www.umweltbundesamt.de/en/document/agbb-evaluation-scheme-2018-1>. Accessed 20 Apr 2021
- Dols W, Polidoro B (2015) CONTAM user guide and program documentation: version 3.2. <https://nvlpubs.nist.gov/nistpubs/TechnicalNotes/NIST.TN.1887.pdf>. Accessed 20 Apr 2021
- European Collaborative Action (2018) EN 16516, construction products: assessment of release of dangerous substances – determination of emissions into indoor air
- Federal Ministry for the Environment NCaNS (2021) Low-emission furniture and slatted frames made of wood and wood-based materials (Version 7). <https://produktinfo.blauer-engel.de/uploads/criteriafile/en/DE-UZ%202038-201301-en-Criteria-V1-7.pdf>. Accessed 29 Apr 2021
- Guo ZS, Sparks LE, Tichenor BA, Chang JCS (1998) Predicting the emissions of individual VOCs from petroleum-based indoor coatings. *Atmos Environ* 32(2):231–237
- Herrmann TJ, Zhang JS, Zhang Z, Smith J, Gao X, Li H, Chen W, Wang S (2003) Performance test results for an innovative full-scale indoor environmental quality and climate simulator. *ASHRAE Trans* 110(2)
- Hodgson AT, Zhang JS, Guo B, Xu J (2009) Development and validation of a scaling method for environmental chamber determination of VOC emissions from office furniture. In: Santanam S, Bogucz EA, Peters C, Benson T (eds) Proceedings of the 9th international healthy buildings conference and exhibition. Syracuse
- Hu HP, Zhang YP, Wang XK, Little JC (2007) An analytical mass transfer model for predicting VOC emissions from multi-layered building materials with convective surfaces on both sides. *Int J Heat Mass Tran* 50(11–12):2069–2077
- International WELL Building Institute (2020) WELL building standard – WELL v2. <https://v2.wellcertified.com/>. Accessed 20 Apr 2021
- ISO (2012) ISO/IEC 17065, conformity assessment – requirements for bodies certifying products, processes and services. International Organization for Standardization. <https://www.iso.org/obp/ui/#iso:std:iso-iec:17065:ed-1:v1:en>. Accessed 20 Apr 2021
- ISO (2016) ISO 14021, environmental labels and declarations – self-declared environmental claims (Type II environmental labelling). <https://www.iso.org/obp/ui/#iso:std:iso:14021:ed-2:v1:en>. Accessed 20 Apr 2021

- ISO (2017) ISO/IEC 17025, general requirements for the competence of testing and calibration laboratories. International Organization for Standardization. <https://www.iso.org/obp/ui/#iso:std:iso-iec:17025:ed-3:v1:en>. Accessed 20 Apr 2021
- Japan Environmental Association (2019) Eco Mark label No. 130 Furniture Version 2.4. <https://www.ecomark.jp/nintei/130.html>. Accessed 20 Apr 2021
- Japanese Standards Association (2015) JIS A 1901, determination of the emission of volatile organic compounds and aldehydes by building products – small chamber method. https://webdesk.jsa.or.jp/books/W11M0090/index/?bunsyo_id=JIS+A+1901%3A2015. Accessed 29 Apr 2021
- Japanese Standards Association (2021) JIS A 1460, determination of the emission of formaldehyde from building boards – desiccator method. https://webdesk.jsa.or.jp/books/W11M0090/index/?bunsyo_id=JIS+A+1460%3A2021. Accessed 29 Apr 2021
- Kephalaopoulos S, Koistinen K, Kotzias D (2005) Harmonisation of indoor material emissions labelling systems in EU: inventory of existing schemes. European Collaborative Action Report No. 24. Athens University, Athens
- Kephalaopoulos S, Geiss O, Annys E (2013) Harmonisation framework for health based evaluation of indoor emissions from construction products in the European Union using the EU-LCI concept. European Collaborative Action Report No. 29. Publications Office of the European Union, Luxembourg. <https://doi.org/10.2788/016992>
- Levin H (2010) National programs to assess IEQ effects of building materials and products. Indoor Environment Division Office of Radiation and Indoor Air UEPA, USA
- Little JC, Hodgson AT, Gadgil AJ (1994) Modeling emissions of volatile organic-compounds from new carpets. *Atmos Environ* 28(2):227–234
- Liu WW, Zhang YP, Yao Y (2013) Labeling of volatile organic compounds emissions from Chinese furniture: consideration and practice. *Chin Sci Bull* 58(28–29):3499–3506
- Liu ZL, Nicolai A, Abadie M, Qin MH, Grunewald J, Zhang JS (2021) Development of a procedure for estimating the parameters of mechanistic VOC emission source models from chamber testing data. *Build Simul-China* 14(2):269–282
- McArthur JJ, Powell C (2020) Health and wellness in commercial buildings: systematic review of sustainable building rating systems and alignment with contemporary research. *Build Environ* 171:106635
- Ministry of Ecology and Environment of China (2010) HJ 571, technical requirement for environmental labeling products – wood based panels and finishing products. <http://www.mee.gov.cn/ywgz/fgbz/bz/bzwb/other/hjbz/201005/W020130204567628160066.pdf>. Accessed 20 Apr 2021
- Ministry of Ecology and Environment of China (2016) HJ 2547, technical requirement for environmental labeling products – furniture. Ministry of Ecology and Environment of China. <http://www.mee.gov.cn/ywgz/fgbz/bz/bzwb/other/jjbz/201701/W020170123561883132984.pdf>. Accessed 20 Apr 2021
- Ministry of Environment of Korea (2017) Eco-label 172, Korea Eco-label certification standard – furniture. <http://el.keiti.re.kr/enservice/enpage.do?mMenu=2&sMenu=1>. Accessed 20 Apr 2021
- Ministry of Housing and Urban-Rural Development of China (2018) JGJ/T 436, technical standard for interior decoration pollution control of residential buildings
- National Health Commission of China (2002) GB/T 18883, indoor air quality standard. <http://c.gb688.cn/bzgk/gb/showGb?type=online&hcno=59392CE8FD442291D711459014EA4A7>. Accessed 20 Apr 2021
- Risholm-Sundman M, Larsen A, Vestin E, Weibull A (2007) Formaldehyde emission – comparison of different standard methods. *Atmos Environ* 41(15):3193–3202
- Rode C, Abadie M, Qin M, Grunewald J, Kolarik J, Lavergne J (2019) Key findings of IEA EBC Annex 68-indoor air quality design and control in low energy residential buildings. Paper presented at the IOP conference series: materials science and engineering
- SCAQMD (2016) Rule 1113 for architectural coatings. <http://www.aqmd.gov/home/rules-compliance/compliance/vocs/architectural-coatings>. Accessed 29 Apr 2021
- SCAQMD (2017) Rule 1168 for adhesive and sealant applications. <https://www.aqmd.gov/home/rules-compliance/compliance/vocs/adhesive-and-sealants>. Accessed 29 Apr 2021

- Singapore Environment Council (2013) Singapore green labelling scheme certification guide, home furniture & fittings
- Standardization Administration of China (2001) GB 18584, indoor decorating and refurbishing materials – limit of harmful substances of wood based furniture. <http://c.gb688.cn/bzgk/gb/showGb?type=online&hcno=E88676C207C5B252708CAE16A182BF7E>. Accessed 20 Apr 2021
- Standardization Administration of China (2017a) GB 18580, indoor decorating and refurbishing materials – limit of formaldehyde emission of wood-based panels and finishing products. <http://c.gb688.cn/bzgk/gb/showGb?type=online&hcno=3345334EB620CE121DCDEB82C603349>. Accessed 20 Apr 2021
- Standardization Administration of China (2017b) GB/T 35601, green product assessment – wood-based panels and wooden flooring. <http://c.gb688.cn/bzgk/gb/showGb?type=online&hcno=A6213DFC946CE2BC9A29EEC667F0002C>. Accessed 20 Apr 2021
- Standardization Administration of China (2017c) GB/T 35607, green product assessment – furniture. <http://c.gb688.cn/bzgk/gb/showGb?type=online&hcno=CE5011CE8A9A5AAB7407980015332201>. Accessed 20 Apr 2021
- Standardization Administration of China (2020) GB/T 38723, determination of emission rate of volatile organic compounds from wooden furniture – concentration history method. <http://c.gb688.cn/bzgk/gb/showGb?type=online&hcno=57AF6CF9DC7BD209E2321EF1FA520BC9>. Accessed 29 Apr 2021
- The Building Information Foundation RTS (1996) M1-emission classification of building materials. <https://www.greenbuildingsupply.com/core/media/media.nl?id=411494&c=772072&h=d447753ebd140a0896b3&xt=.pdf>. Accessed 20 Apr 2021
- U. S. EPA (1995a) Compendium method TO-15, determination of volatile organic compounds (VOCs) in air collected in specially-prepared canisters and analyzed by gas chromatography/mass spectrometry (GC/MS). US Environmental Protection Agency, USA
- U. S. EPA (1995b) Compendium of methods for the determination of toxic organic compounds in ambient air: TO-1, TO-11, and TO-17. US Environmental Protection Agency, USA
- U. S. EPA (2001) EPA QA/R-5, EPA requirements for quality assurance project plans. United States Environmental Protection Agency OoEI, Washington, DC 20460
- U. S. EPA (2016) Formaldehyde emission standards for composite wood products. <https://www.epa.gov/formaldehyde/formaldehyde-emission-standards-composite-wood-products>. Accessed 29 Apr 2021
- U. S. Green Building Council (2020) LEED v4.1 interior design and construction rating system. <https://www.usgbc.org/leed/v41>. Accessed 20 Apr 2021
- Willem H, Singer BC (2010) Chemical emissions of residential materials and products: review of available information. Lawrence Berkeley National Laboratory, Berkeley
- Xiong JY, Yao Y, Zhang YP (2011) C-history method: rapid measurement of the initial emittable concentration, diffusion and partition coefficients for formaldehyde and VOCs in building materials. Environ Sci Technol 45(8):3584–3590
- Xu Y, Zhang YP (2003) An improved mass transfer based model for analyzing VOC emissions from building materials. Atmos Environ 37(18):2497–2505
- Yang X, Chen Q, Zeng J, Zhang JS, Shaw CY (2001a) A mass transfer model for simulating volatile organic compound emissions from ‘wet’ coating materials applied to absorptive substrates. Int J Heat Mass Tran 44(9):1803–1815
- Yang X, Chen Q, Zhang JS, Magee R, Zeng J, Shaw CY (2001b) Numerical simulation of VOC emissions from dry materials. Build Environ 36(10):1099–1107
- Zhang J, Shaw CY, Kanabus-Kaminska J, MacDonald R, Magee R, Lustyk E, Weichert H (1996) Study of air velocity and turbulence effects on organic compound emissions from building materials/furnishings using a new small test chamber. In: Characterizing sources of indoor air pollution and related sink effects. ASTM International, West Conshohocken, pp 184–199. <https://doi.org/10.1520/STP15621S>
- Zhang JS, Wang J, Shaw CY (1997) Theoretical examination of a simplified procedure for data analysis in small chamber testing of material emissions. Internal Report No. IRC-733. National Research Council, Canada

- Zhang JS, Shaw CY, Sander D, Zhu JP, Huang Y (1999a) MEDB-IAQ: a material emission database and single-zone IAQ simulation program – a tool for building designers, engineers and managers. CMEIAQ Report 4.2. National Research Council, Canada
- Zhang JS, Shaw CY, Zhu JP, Mason M, Howard B, Brown S (1999b) A standard guide for full-scale chamber determination of VOC emissions from indoor materials/products. CMEIAQ Report 2.1. National Research Council, Canada
- Zhang JS, Zhu JP, Shaw CY, Plett E, Bodalal A, Chen Q, Yang X (1999c) Models for predicting volatile organic compound (VOC) emissions from building materials. CMEIAQ Report 3.1. National Research Council, Canada
- Zhang JS, Li H, Mason M, Zhang Z, Salomaa M (2006) On the power-law model for predicting the VOC emissions from office workstation systems. In: Proceedings of international specialty conference: indoor environmental quality – problems, research and solutions. Durham
- Zhang JS, Mason M, Hodgson AT, Guo B, Krebs K, Barry A, Peters B (2009) An inter-laboratory comparison study of the ANSI/BIFMA standard test method M7.1 for furniture. In: Santanam S, Bogucz EA, Peters C, Benson T (eds) Proceedings of the 9th international healthy buildings conference and exhibition. Syracuse
- Zhang X, Cao JP, Wei JY, Zhang YP (2018) Improved C-history method for rapidly and accurately measuring the characteristic parameters of formaldehyde/VOCs emitted from building materials. *Build Environ* 143:570–578
- Zhang JS, Liu Z, Guo B (2019) Model-based testing and evaluation of VOC emission sources and sinks in the indoor environment: theory and applications. In: Proceedings of IAQVEC2019 – 10th international conference on indoor air quality, ventilation and energy conservation in buildings. Bari



Influence of Ventilation on Indoor Air Quality

57

Mengqiang Lv, Sumei Liu, Qing Cao, Tengfei Zhang, and Junjie Liu

Contents

Introduction	1638
Residential Building	1640
Natural Ventilation	1640
Mechanical Ventilation	1644
Hybrid Ventilation	1647
Office Building	1649
Natural Ventilation	1650
Mechanical Ventilation	1650
Transportation Vehicle Cabin	1661
Mixing Ventilation	1661
Displacement Ventilation	1664
Personalized Ventilation	1666
Conclusion	1670
Cross-References	1671
References	1671

M. Lv · S. Liu · J. Liu

Tianjin Key Laboratory of Indoor Air Environmental Quality Control, School of Environmental Science and Engineering, Tianjin University, Tianjin, China
e-mail: lvmq@tju.edu.cn; smliu@tju.edu.cn; jjliu@tju.edu.cn

Q. Cao

School of Civil Engineering, Dalian University of Technology, Dalian, China
e-mail: caoqing@dlut.edu.cn

T. Zhang (✉)

Tianjin Key Laboratory of Indoor Air Environmental Quality Control, School of Environmental Science and Engineering, Tianjin University, Tianjin, China

School of Civil Engineering, Dalian University of Technology, Dalian, China
e-mail: timzhang@tju.edu.cn

Abstract

Ventilation is to provide unconditioned outdoor air or conditioned, combined, outdoor, and recirculated air for suitable indoor comfort and acceptable air quality. Ventilation can be categorized into natural ventilation, mechanical ventilation, and their hybrid form. Due to the pros and cons of each ventilation mode, a ventilation mode may suit to a pertinent indoor space in a specific climate region or location. The purpose of this chapter is to examine the impacts of ventilation modes on indoor air quality in different indoor spaces, such as residential buildings, office buildings, and transportation vehicle cabins with the dense commercial aircraft cabin as an example. The evaluated ventilation modes include natural ventilation, mechanical ventilation, and the occasional hybrid ventilation. The mechanical ventilation is further divided into mixing ventilation, displacement ventilation, stratum ventilation, and personalized ventilation in an office building or aircraft cabin. Ventilation of residential buildings in the situation with outdoor PM_{2.5} pollution has been systematically addressed. The indoor air quality performance in terms of ventilation rate, concentrations of CO₂, formaldehyde, TVOC, and PM_{2.5} was evaluated. In addition to indoor air quality, the possible airborne infection transmission, thermal comfort, energy consumption, and affordability of each ventilation mode have also been examined.

Keywords

Natural ventilation · Mechanical ventilation · Residential building · Office building · Transportation vehicle cabin

Introduction

Ventilation is to displace the polluted air indoors to the outside and deliver fresh air into indoor space to maintain a healthy and comfortable environment. Generally, ventilation can be classified as “natural ventilation,” “mechanical ventilation,” or their combination as “hybrid ventilation.” Natural ventilation relies on natural forces like the wind from the surrounding environment as well as buoyancy forces that develop due to temperature gradients within the building. In natural ventilation, outdoor air flows into a building through planned openings (such as louvers, doors, and windows) or unplanned cracks or holes. Mechanical ventilation is driven by fans. Mechanical ventilation systems may include supply fans (which push outdoor air into a building), exhaust fans (which draw air out of the building), or a combination of both (which thereby cause equal ventilation flow into a building).

Natural ventilation is generally thought to be able to reduce energy usage in buildings, benefiting from passive cooling. The acceptable thermal comfort range for naturally ventilated buildings is significantly larger than that for buildings with mechanical heating, ventilating, and air-conditioning (HVAC) systems (De and Brager 2002; Yu et al. 2012). Furthermore, natural ventilation has been shown

being able to reduce sick building syndrome (SBS). However, natural ventilation is nearly uncontrollable and thus unable to provide ventilation at an exact demanding rate and in the expected time. The natural ventilation is subject to the climate region, terrain, surrounding buildings, the studied building geometry, ventilation opening shape, size, and direction, as well as the occupant behaviors (Lai et al. 2018a, b). Note that natural ventilation is unsuited to noisy, polluted, or harsh climate regions.

In contrast, mechanical ventilation is robust and can nearly be applied where power is available. Mechanical ventilation rates are nearly independent of outdoor climates. Most mechanical ventilation systems are designed with fixed ventilation rates that shall satisfy the typical ventilation demand. Except for simplified mechanical ventilation for providing only the unconditioned outdoor air or only exhausting the internal air, a more advanced mechanical ventilation system or HVAC system is welcomed in recent years, which can simultaneously heat, cool, humidify, or dehumidify the ventilated air and even filtrate particles or deodorize. The HVAC system requires devices and thus involves certain initial investment. The running expense of an HVAC system is not trivial for both operating energy consumption and dis-functional component replacement.

Even if a building is installed with mechanical ventilation systems, the mechanical ventilation can also be turned off during the transitional seasons for energy conservation if the windows are openable. This forms switching between natural and mechanical ventilation and hence constitutes hybrid ventilation (Cho et al. 2020). Either the manual or automatic switch of the ventilation mode can be used. The automatic switch requires sophisticated sensors and actuators. The hybrid ventilation may help reduce building energy consumption without sacrificing indoor air quality (Rey-Hernández et al. 2020; Gomis et al. 2020). Hybrid ventilation can set natural ventilation as the priority mode. Once the natural ventilation cannot assure indoor air quality or thermal comfort, then the mechanical ventilation is turned on. It was claimed that hybrid ventilation in residential buildings can reduce the cooling load but not cut much the utility costs (Zhang et al. 2018).

The purpose of this chapter is to evaluate the impacts of ventilation on indoor air quality in residential buildings, office buildings, and transportation vehicle cabins. Most residential buildings adopt natural ventilation by infiltration and opening windows/doors. Some residential buildings also use mechanical ventilation for the rigorous demand of outdoor air. The residents may sometimes switch the mechanical ventilation and natural ventilation for hybrid use. Hence, the impacts of three different ventilation modes on indoor air quality are evaluated in residential buildings. Most office buildings use mechanical ventilation, though natural ventilation may occasionally be utilized in some countries. Various forms of mechanical ventilation modes are examined in office buildings. Transportation vehicles such as trains and airplanes use only mechanical ventilation, and thus only mechanical ventilation is addressed in transportation vehicle cabins. In addition to indoor air quality, the airborne infection risk, thermal comfort, energy consumption, running expense, and the initial investment of each ventilation mode have also been examined.

Residential Building

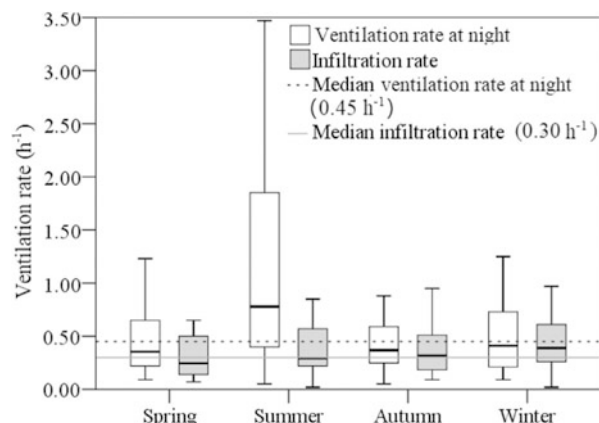
According to ANSI/ASHRAE Standard 62.2-2014 (ASHRAE 2014), single, detached residential buildings are required to meet a whole-house ventilation rate based on the number of bedrooms in the house, the number of occupants, in addition to the infiltration. There are a variety of ways to meet this standard, either by natural ventilation or mechanical systems.

Natural Ventilation

Natural ventilation is the most widely used ventilation in residential buildings. Many homes rely on infiltration for background ventilation and open windows to provide increased ventilation when needed. Note that the discussion is limited to natural ventilation by infiltration and opening windows/doors. It does not include designed natural ventilation with designed variable openings. Infiltration means that outdoor air enters the room through gaps in the building envelope due to the difference in the sum of the wind and stack pressures between the indoor and outdoor. No window or door is opened when evaluating the infiltration rate. The residents tend to close windows and doors when encountering harsh climate or heavy outdoor air pollution. A recent survey (Sun et al. 2019) shows that the median infiltration rate of 294 apartments in China was only 0.30 h^{-1} , as shown in Fig. 1, which is lower than the recommended air change per hour (ACH) of 0.5 h^{-1} (Dimitroulopoulou 2012) for sufficient ventilation of homes. Because most residents tend to close windows during the nighttime with only the infiltration allowed, 90% of the surveyed Chinese bedrooms were found with insufficient ventilation rate (Dai et al. 2018). This implies that the infiltration may not assure acceptable indoor air quality.

On average, residents in China keep their windows open for one-third of the time. The occupants use natural ventilation when the outdoor air temperature is between

Fig. 1 Ventilation rates at night (without intervention regarding windows and doors opening) and infiltration rates (with closed windows and doors) in bedrooms (Sun et al. 2019)



15 °C and 26 °C (Lai et al. 2018a, b). When the outdoor air temperature is out of this range, people tend to close windows (Hou et al. 2018). Figure 2 illustrates the association between outdoor air temperature and opened windows at night in different climate zones in China. The window opening varies greatly with the outdoor air temperatures and climate zones. According to Liddament (2001), windows are most likely to be opened under the following conditions: sunny days, higher occupant density, higher outdoor temperature, low wind speed, during cleaning or cooking activities, and when smoking. That is, the windows are opened when residents feel they need ventilation. However, there are many circumstances when opening a window is not practical, such as with noise, rain or high winds, outdoor pollutants, cold drafts, privacy, security and safety issues, and energy loss, or the window may be difficult to operate. This suggests that window opening or closing is not always in response to ventilation needs. Even with the opened windows, natural ventilation may still not provide sufficient outdoor air to dilute the hourly average indoor CO₂ concentration below 1000 ppm. Song et al. (2019) claimed that the indoor hourly average CO₂ concentration was above 1000 ppm in 40–54% of the total occupied time and varied with the city in different climate zones, as shown in Table 1. The outdoor air rate will be further insufficient once the window is closed due to a couple of reasons (Zhao et al. 2018). The high CO₂ concentration is very common in bedrooms in China, especially in the cold climate zone. In winter,

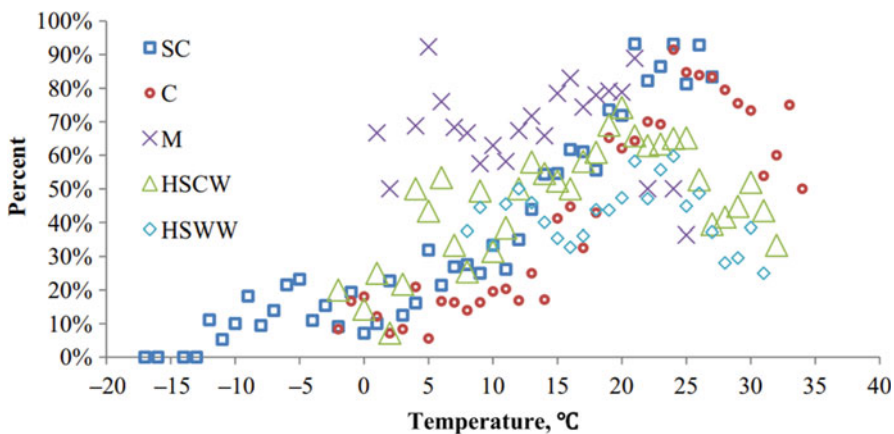


Fig. 2 Percentage of opened windows at night in 46 homes versus the outdoor air temperatures (C, cold zone; HSCW, hot summer, and cold winter zone; HSWW, hot summer, and warm winter zone; M, mild zone; and SC, severe cold zone) (Lai et al. 2018a, b)

Table 1 Time ratios of the hourly average indoor CO₂ concentrations above 1000 ppm for the apartment in a city with different climate zones when adopting natural ventilation (Song et al. 2019)

Item	Shenyang	Tianjin	Chengdu	Shenzhen	Kunming
Time ratio of CO ₂ ≥ 1000 ppm (%)	54	53	43	44	40

severe outdoor environmental conditions prevent occupants from opening windows at night. When occupants sleep with only the infiltration, the CO₂ concentration often reaches extremely high levels in the morning.

Note that the metabolic CO₂ is innocuous. However, the high concentration of CO₂ may indicate insufficient ventilation to dilute chemical pollutants, because unqualified building materials and furniture may emit poisonous gases, such as formaldehyde and other harmful volatile organic compounds (VOCs) (Yin et al. 2019). The formaldehyde was found to contribute to increased risk of asthma, allergies, airway diseases, and sick building syndrome symptoms as well (Doi et al. 2003; Garrett et al. 1999; Wieslander et al. 1996). The maximum allowable formaldehyde concentration was 0.10 mg/m³ for the Chinese threshold (GB/T 18883-2002, 2002). The survey showed that more than 69.4% of all the newly built or decorated housing from 2002 to 2004 in China had indoor formaldehyde concentrations exceeding the Chinese-specified value (Tang et al. 2009). The median indoor formaldehyde concentration after renovation from 2002 to 2015 in homes of Chinese cities was 125 µg/m³, which is still above the Chinese threshold (Huang et al. 2017). Generally, low ventilation rates in residential buildings would result in elevated concentrations of formaldehyde and VOCs, and an increased prevalence of SBS symptoms (Sun et al. 2019).

Figure 3 illustrates the indoor formaldehyde concentrations in 25 residential buildings in different seasons under normal daily conditions and the condition with closed doors and windows (Yin et al. 2019). The daily median formaldehyde

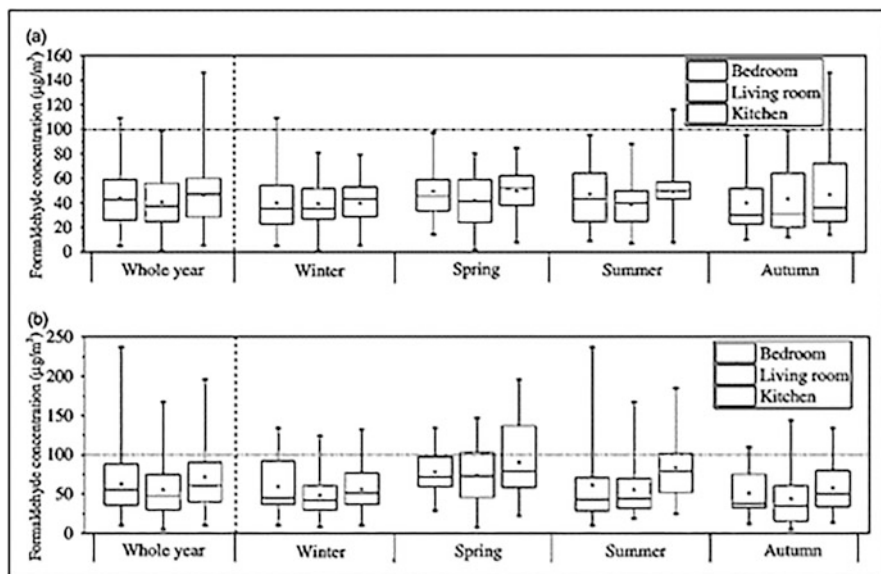


Fig. 3 Indoor formaldehyde concentration of 25 residential buildings in different seasons (the order of the three box plots for each season: bedrooms, living rooms, and kitchen): (a) under the normal daily condition; (b) under the condition with doors and windows closed (modified from Yin et al. 2019)

concentrations in bedrooms, living rooms, and kitchens monitored over four seasons were $42.5 \mu\text{g}/\text{m}^3$, $37.5 \mu\text{g}/\text{m}^3$, and $47.0 \mu\text{g}/\text{m}^3$, respectively. The indoor formaldehyde concentration under the normal daily condition in most naturally ventilated residential buildings in northwestern China can meet the Chinese formaldehyde threshold of $0.10 \text{ mg}/\text{m}^3$ (GB/T 18883-2002, 2002). The ratio of the indoor formaldehyde concentrations between daily and closed conditions in three room types were 0.77, 0.78, and 0.77, respectively. The main difference between these two conditions was that the residents may open windows under the normal daily condition. Natural ventilation with opened windows normally can remove approximately 23% of indoor formaldehyde. Hence, daily natural ventilation is a straightforward approach to reduce indoor formaldehyde exposure.

The indoor formaldehyde concentrations were measured in over 2000 residential buildings (Ye et al. 2017), which included newly decorated homes and not in 22 cities of China. The measured formaldehyde concentration ranges within the first 3 months, 3–6 months, and 6–12 months are $10\text{--}33,300 \mu\text{g}/\text{m}^3$, $10\text{--}1420 \mu\text{g}/\text{m}^3$, and $10\text{--}1620 \mu\text{g}/\text{m}^3$, respectively. Most of the formaldehyde concentrations within the first 6 months exceed the 30-minute average concentration guideline of $100 \mu\text{g}/\text{m}^3$ by the Chinese standard (GB/T 18883-2002, 2002). The peak concentrations keep appearing even for the buildings decorated one year ago. Pei et al. (2020) measured the total VOCs (TVOCs) concentrations in 251 Chinese homes in different seasons. The average TVOCs concentration in China is within the range of $104\text{--}1151 \mu\text{g}/\text{m}^3$. As compared with the specified Chinese TVOCs threshold of $600 \mu\text{g}/\text{m}^3$ (GB/T 18883-2002, 2002), 20% of the residences were over the limit. However, as compared with the $300 \mu\text{g}/\text{m}^3$ limit by ISO17772-1 (2017) for very low pollution buildings, up to 48% of the residences were unqualified (Fig. 4).

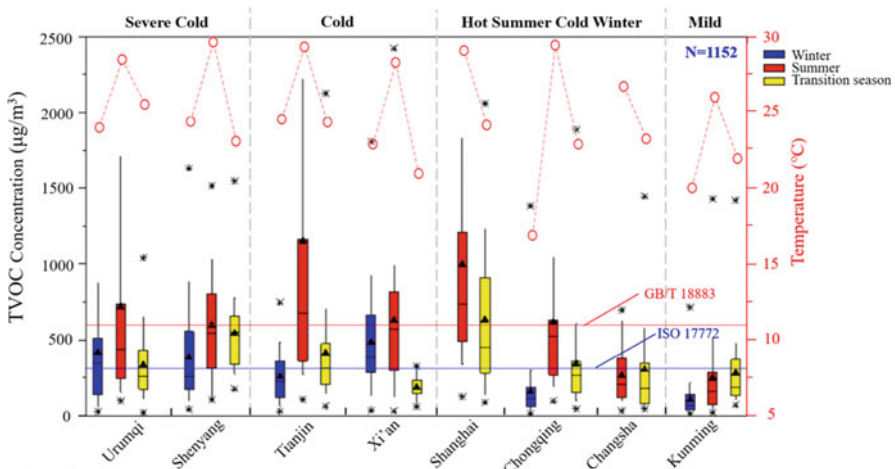


Fig. 4 TVOCs concentrations and average temperatures of surveyed Chinese cities in different seasons. Note: Each boxplot represents the minimum, 10th, 25th, 50th, 75th, 90th, and maximum concentration (Pei et al. 2020)

The outdoor air in developing countries, such as in China, is sometimes polluted with exceeding PM_{2.5} concentrations in the last decade. On severely polluted days, the outdoor PM_{2.5} concentrations in several major cities in China could be three to ten times that in cities of developed countries, such as London, Tokyo, and New York (Cao et al. 2016). In situations with outdoor PM_{2.5} pollution, the outdoor air cannot be directly introduced to residential buildings for ventilation. An onsite monitoring study (Dai et al. 2018) shows that only approximately 2% of the Chinese homes in 2017 maintained indoor PM_{2.5} concentrations below 75 µg/m³. In about half of the homes, more than 10% of days exhibited whole-day averaged PM_{2.5} concentrations higher than 75 µg/m³. No homes maintained indoor PM_{2.5} concentrations below 25 µg/m³. Another study (Zhao et al. 2018) shows that nearly half of the time in winter from 2017 to 2018, the outdoor PM_{2.5} concentrations in Tianjin, China, were above 35 µg/m³. During this period, natural ventilation cannot be used.

Natural ventilation is theoretically unhealthy to use in areas with severe outdoor pollution unless the indoor air has been properly cleaned. Taking PM_{2.5} pollution in China in 2016 as an example, without indoor particulate filtration, the indoor PM_{2.5} concentrations were above 35 µg/m³ in more than 39% of the total occupied time in Shenyang, Tianjin, and Chengdu in China (Song et al. 2019). Indoor particle filtration is an affordable solution to indoor PM_{2.5} pollution. A combination of natural ventilation and portable demand-controlled particulate filtration has the lowest operating cost (Zhao et al. 2018). The ratio of clean air delivery rate (CADR) to room volume (h⁻¹), which can be considered as an equivalent air change rate, has an impact on the indoor particle concentrations (Ye et al. 2017). The CADR-to-room volume ratio (an “equivalent air change rate”), together with the CADR, needs both to be accounted for when selecting air cleaners or implementing natural ventilation of residential buildings.

Pros and Cons of Natural Ventilation

Natural ventilation is simple, energy-saving, and economic. In addition, natural ventilation can provide a high ventilation rate to displace indoor pollutants if the outdoor air is clean, the outdoor wind is strong enough, and buildings have large openings. Therefore, it is suggested to utilize natural ventilation when the outdoor environment is favorable.

However, natural ventilation is varied and depends on outside climatic conditions. It is unstable and not fully under control. The ventilation cannot be provided with the exact demanding rate at the expected time. Furthermore, in the situation with outdoor PM_{2.5} pollution, the natural ventilation may bring too much outdoor particulate matters to indoor space, which worsens indoor air quality. Therefore, pure natural ventilation cannot completely guarantee good indoor air quality.

Mechanical Ventilation

There are a variety of mechanical ventilation systems for the residential building, including exhaust ventilation, supply ventilation, and balanced ventilation systems,

as shown in Fig. 5. Any of these may be in continuous operation or operated intermittently, they may have single-port or multiports, or the system may be integrated into an existing HVAC system. A properly designed mechanical ventilation system in a residential building provides a reliable, controllable, and probably comfortable indoor environment. However, the operation of mechanical ventilation consumes energy and may generate noise. It also has a much higher initial investment cost and would involve nontrivial expense for dis-functional component replacement.

Generally, mechanical ventilation can maintain relatively good indoor air quality. The PM_{2.5} concentration was measured by Zhao et al. (2018) in a naturally ventilated dwelling, a naturally ventilated dwelling with an air cleaner, and a mechanically ventilated dwelling, respectively. They found that pure natural ventilation could not maintain acceptable indoor air quality when the outdoor PM_{2.5} concentration is high, as shown in Fig. 6. An air cleaner must be in operation to filtrate the indoor PM_{2.5}. The finding is consistent with the conclusion by Zhang et al. (2018) that indoor particulate filtration must be utilized in northern Chinese dwellings during the outdoor PM_{2.5} pollution season. The mechanical ventilation system with particle filtration in ducts prevented the entry of outdoor particles, but it could not remove the cooking-generated pollution well. Filtrating the recirculated air inside the home is more energy-efficient, because of lower pressure resistance when recirculating air than introducing the outdoor air. There is no substantial difference in the indoor PM_{2.5} concentrations with the same CADR between the introduced outdoor air filtration and the recirculated air filtration.

Although the indoor air quality in the dwellings with mechanical ventilation is generally better than those in the naturally ventilated dwellings, residents may not

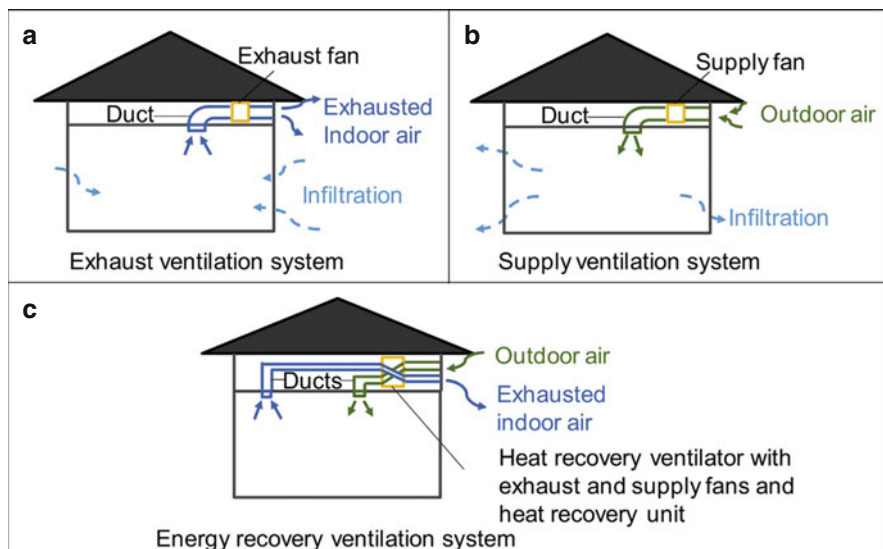


Fig. 5 Schematics of mechanical ventilation for residential buildings: (a) exhaust ventilation; (b) supply ventilation; and (c) balanced ventilation (Lai et al. 2018a, b)

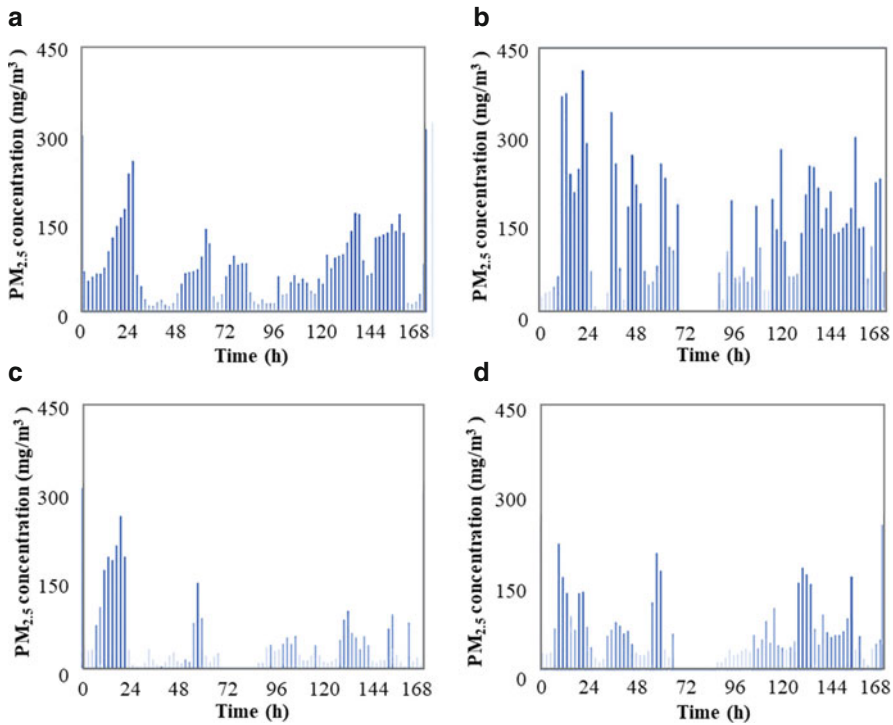


Fig. 6 Two-hour average PM_{2.5} concentration of: (a) the outdoor air; (b) the indoor air with natural ventilation; (c) the indoor air with natural ventilation plus air purifier; and (d) the indoor air with mechanical ventilation (Zhao et al. 2018)

continuously run the mechanical ventilation due to the energy costs and thermal comfort concerns (Lai et al. 2018a, b). The average daily running duration of mechanical ventilation generally decreases with the daily average outdoor air temperature. Energy saving is a possible reason for the reduction of the running hours of mechanical ventilation. When the outdoor air temperature is mild, people prefer natural ventilation over mechanical ventilation. There are large differences in the running time of the mechanical ventilation among different climate regions and seasons. From north to south in China, the running hour of mechanical ventilation decreases. The mechanical ventilation running duration is the longest in winter and the shortest in summer. Generally, occupants prioritized their thermal comfort needs over indoor air quality. The type of mechanical ventilation system also impacts the running hours. The occupants would turn off the simple outdoor air blower without temperature conditioning or set it to the minimum air rate in the bedroom during nighttime. The noise is another reason to make it hard to be accepted (Zhao et al. 2018).

Most current household mechanical ventilation uses the so-called centralized system, i.e., a single system to ventilate the whole family. That is, if any of the rooms is occupied, the system must be turned on to ventilate all of the rooms.

Contrarily, the decentralized mechanical ventilation operates only during the occupied period for a specific room so that it has a great potential to cut utility costs (Zhang et al. 2018). Furthermore, the mechanical ventilation in demand-controlled operation and its hybrid with natural ventilation can reduce energy consumption. Most household mechanical ventilation has indoor air overfiltrated because the CADR is usually designed to handle the most polluted situations. Song et al. (2019) compared the energy consumption, and utility bill, using different ventilation modes in nearly the same residential apartments located in five cities in different climatic zones of China, as shown in Table 2. They found that natural ventilation without indoor particulate filtration uses the least energy and is the cheapest. Indoor particulate filtration does not consume much energy. Mechanical ventilation together with indoor particulate filtration uses the most energy and is the most expensive. Similarly, Zhao et al. (2018) reported that the daily energy consumption of mechanical ventilation is about 1.5 times that of the natural ventilation with a portable air cleaner.

Pros and Cons of Mechanical Ventilation

Mechanical ventilation is robust to deliver the designed airflow rate and varies little with the outdoor climate. In addition, filtration can be embedded in mechanical ventilation to filtrate airborne particles and dilute indoor chemical pollutants. Furthermore, mechanical ventilation can be nearly applied anywhere with electricity.

However, mechanical ventilation may often work in compromised performance or may occasionally be interrupted due to equipment failure, maintenance, or even poor design, or incorrect management. Initial investment and maintenance costs of mechanical ventilation are high, which may be unaffordable especially in developing countries. Therefore, it is beneficial to combine mechanical ventilation with natural ventilation.

Hybrid Ventilation

Hybrid ventilation has been long recommended to benefit from both natural ventilation and mechanical ventilation. Well-operated hybrid ventilation may help reduce building energy consumption without sacrificing indoor air quality. The hybrid ventilation may set the natural ventilation as the prior mode. Once the natural ventilation cannot assure indoor air quality or thermal comfort, then the mechanical ventilation is turned on, and vice versa.

Hybrid ventilation can provide adequate ventilation rates even when weather conditions are unfavorable due to the use of mechanical ventilation as a backup (Yoshino et al. 2003). However, sophisticated hybrid ventilation requires a controller to switch modes between natural and mechanical ventilation. Thus, an elaborate control system, such as CO₂ sensors, room temperature thermostats, airflow sensors, motorized windows, and even a weather station, may have to be adopted. The rationality of the control logic and accuracy of the intelligent control system have a large influence on the performance of this system.

Table 2 The energy consumption and running cost for the apartment in cities of different climate zones (Song et al. 2019)

City	Ventilation	Heating/kWh	Cooling/kWh	Filtration/kWh	Fan/kWh	Appliances/kWh	Running cost/CNY
Shenyang	NV only	4777	563	0	43	3088	2878
	MV+ filtration	4560	567	341	43	3088	3113
	MV+ filtration	10,726	1663	1532	185	3088	5267
Tianjin	NV only	3314	778	0	43	3088	2670
	NV+ filtration	3130	826	383	43	3088	2861
	MV+ filtration	5963	2912	1697	184	3088	4676
Chengdu	NV only	400	1796	0	43	3088	2279
	NV+ filtration	335	1785	260	43	3088	2471
	MV+ filtration	1044	2941	941	196	3088	3665
Shenzhen	NV only	17	4378	0	43	3088	3216
	NV+ filtration	17	4381	16	43	3088	3229
	MV+ filtration	74	7607	263	199	3088	4349
Kunming	NV only	83	428	0	43	3088	1345
	NV+ filtration	83	428	7	43	3088	1348
	MV+ filtration	322	1604	181	183	3088	1726

NV natural ventilation; MV mechanical ventilation; and CNY currency of Chinese Yuan

Table 3 Comparison of annual energy consumption and running cost (Zhang et al. 2018)

Ventilation	Heating/ kWh	Cooling/ kWh	Particle filtration/kWh	Fan/ kWh	Appliances/ kWh	Running cost/CNY
NV0	2264	1887	0	43	3073	2844
NV1	2133	2135	651	43	3073	3223
MV0	3647	4174	2561	163	3073	5481
MV1	2708	2965	1286	103	3073	3985
HV0	3647	3614	2317	151	3073	5131
HV1	2708	2522	1166	97	3073	3769

NV0 natural ventilation without filtration; *NV1* natural ventilation with filtration; *MV0* mechanical ventilation with fixed and central supply; *MV1* mechanical ventilation with fixed airflow rate and decentralized supply; *HV0* same as MV0 in the MV submode and same as NV0 in the NV submode; *HV1* same as MV1 in the MV submode and same as NV1 in the NV submode; and *CNY* currency of Chinese Yuan

Comparing with mechanical ventilation, hybrid ventilation consumes less energy and saves utility costs. However, it may not be always the case for residential buildings. One investigation (Zhang et al. 2018) compared the annual energy consumption and utility bills of natural ventilation, mechanical ventilation, and hybrid ventilation in a northern city in China. The hybrid ventilation was found to have approximately the same heating load, but lower cooling load and mechanical fan energy consumption. This is because hybrid ventilation benefited from the passive cooling of natural ventilation in transitional seasons or nighttime in summer. However, the utility bills of hybrid ventilation were only slightly lower than those of mechanical ventilation. The hybrid ventilation in northern Chinese residential buildings reduces the cooling load but does not cut much the utility costs, as shown in Table 3.

Pros and Cons of Hybrid Ventilation

Hybrid ventilation takes advantage of both natural ventilation and mechanical ventilation. Therefore, hybrid ventilation has the potential to reduce energy consumption without sacrificing indoor air quality.

However, the control system of hybrid ventilation is complex. This adds an extra cost to the system's initial investment and maintenance. In addition, the effectiveness of hybrid ventilation depends on the control logic and accuracy of the sensor. Furthermore, hybrid ventilation in residential buildings may reduce the cooling load but not cut much the utility cost.

Office Building

Office buildings mainly adopt mechanical ventilation. However, in developing countries, natural ventilation may also be used in office buildings. In this section, natural ventilation is discussed a little bit first, while putting a major focus to address

mechanical ventilation in terms of mixing ventilation, displacement ventilation, stratum ventilation, and personalized ventilation, accordingly.

Natural Ventilation

Natural ventilation is also used in office buildings, especially in developing countries. When the outdoor climates are benign, windows and/or doors may be opened for natural ventilation. Otherwise, both windows and doors are closed and heating, cooling, or air-cleaning devices may have to be run to condition the indoor air. The windows and doors may occasionally be opened for intermittent ventilation if the infiltration rate is not sufficient. Natural ventilation has been well summarized in the literature (Chen 2009; Chen et al. 2010). The advantages and disadvantages of natural ventilation in office buildings are similar to those of residential buildings. These have been discussed in section of “[Residential Building](#)” and are thus not repeated here.

Mechanical Ventilation

Comparing with residential buildings, the office building is commonly more crowded. For a continuous and robust ventilation supply, more and more office buildings adopt mechanical ventilation. Like mechanical ventilation for residential buildings, the mechanical ventilation in an office building may also be divided into extract ventilation, supply ventilation, and balance (combined of extract and supply) ventilation (Russell et al. 2007). Modern offices use balance ventilation because airflow patterns between the supply and the extract are controllable. The mechanical balance ventilation can be classified into mixing, displacement, stratum, and personalized ventilation according to the different airflow patterns. Their basic principles and impacts on indoor air quality are addressed as follows.

Mixing Ventilation

Mixing ventilation is one of the earliest mechanical ventilation types. As shown in Fig. 7, conditioned air in mixing ventilation is normally supplied from ceiling diffusers at a relatively high velocity (typically ≥ 1.5 m/s) with a suitable temperature for heating or cooling. The air-supply jet mixes with the ambient room air through entrainment, and the jet speed is reduced. Meanwhile, the conditioned air dilutes the indoor contaminants.

Contaminant concentrations in the occupied zone are relatively uniform in mixing ventilation. In an office, as shown in Fig. 8, the formaldehyde concentration was found relatively uniform in the room with the ceiling-supply and floor-exhaust mixing ventilation (Zhang et al. 2020), though the complete mixing had not reached. Note that the mixing is favorable to thermal comfort but may result in cross mixing of airborne contaminants. There are a couple of standards (CEN Standard 1998; ISO EN 7730 Standard 2005; EN 15251 Standard 2007) and guidebooks (Muller et al. 2013) that addressed mixing ventilation performance.

Fig. 7 Diagram of mixing ventilation in an office

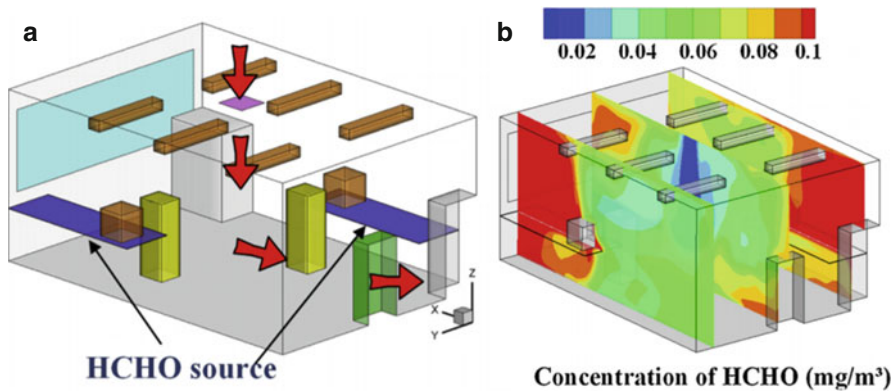
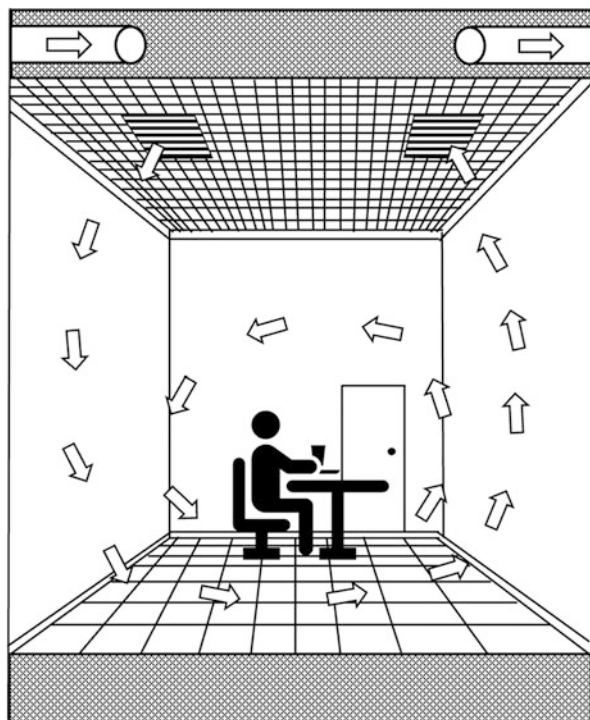
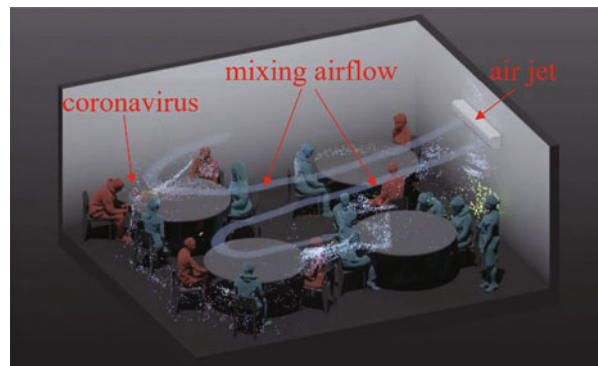


Fig. 8 Simulated formaldehyde concentration in an office with mixing ventilation: (a) office geometry; (b) formaldehyde concentrations on three vertical sections (Zhang et al. 2020)

More critically, mixing ventilation may induce a certain risk of airborne infection transmission. Figure 9 shows the potential spread of coronavirus in a restaurant with an air conditioner (Tom et al. 2020), which somewhat resembles an office case. The computational modeling showed that the exhaled virus particles can move over a

Fig. 9 The potential spread of coronavirus in mixing ventilation (modified from Tom et al. 2020)



long distance in the room, with the infected particles circulating everywhere in the room. The particles might cause inhalation exposure or induce surface touch risk once some particles were deposited to tables or chairs that had high chances for hand touch. To minimize the airborne infection risk, a large ventilation rate of cleaned air is required, so that the virus can be quickly diluted to a sufficiently low concentration. It was claimed that a dilution ratio of over 10,000 is required to prevent airborne infection (Jiang et al. 2009), which may be unaffordable in most operations.

Pros and Cons of Mixing Ventilation

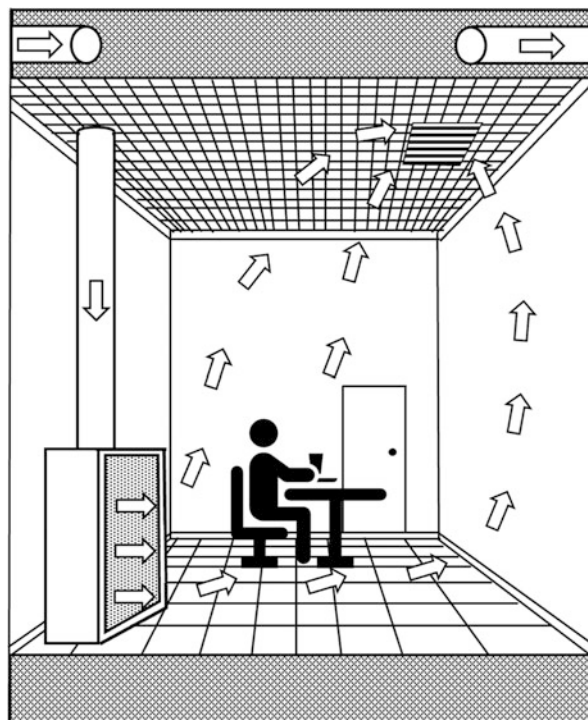
Mixing ventilation promotes a uniform indoor environment. This means the vertical temperature difference between the head and ankles is small, which is welcomed from the perspective of thermal comfort. Additionally, mixing ventilation has a large cooling or heating capacity.

However, mixing ventilation also has some limitations. The conditioned air is mixed before being delivered to the breathing zone, meaning low ventilation effectiveness. Besides, the conditioned air jets with high speed may cause draft risk to occupants.

Displacement Ventilation

Different from mixing ventilation, displacement ventilation supplies conditioned air from a low position while extracting the room air from a high position. Figure 10 shows the diagram of displacement ventilation in an office. Conditioned air is supplied into the room from a wall-mounted diffuser near the floor. The supply air temperature is slightly lower than the desired room air temperature, and the supply air velocity is low (typically $< 0.5 \text{ m/s}$). Due to the low temperature of the supplied air, the supplied air is spread over the floor and then rises as it is heated by some heat sources in the occupied zone. These heat sources (e.g., persons and computers) create upward buoyancy flows toward the exhaust located at or close to the ceiling. Consequently, both air temperature and concentration of airborne pollutants released

Fig. 10 Diagram of displacement ventilation in an office



from the middle height, such as the exhaled pollutant, are stratified. If the indoor space needs heating, a separate heating system, such as baseboard heaters, must be used to allow for a slightly lower temperature of the supplied air than the indoor air. Otherwise, the upward displacement flow would be destroyed. That is, displacement ventilation can only be adopted for cooling rather than heating.

Figure 11 presents the flow path lines of the supplied air in an office with displacement ventilation (Zhang et al. 2010a, b). The supplied air goes downward from the wall-mounted diffuser to the floor, as shown in Fig. 11a. It moves forward until the heat sources or walls, and then goes upward to the ceiling exhaust. Even with the underfloor grilles as shown in Fig. 11b, the upward supplied air goes down first due to the high density of the low-temperature supplied air. The air then moves to the sides and finally goes upward by thermal buoyancy. Figure 12 shows the tracer gas concentration profiles along the height, where the SF₆ gas is released from the head of an occupant. Both CFD simulation and the measurement results show that the tracer gas concentration is stratified with a relatively low concentration in the seated occupational zone and a high concentration near the ceiling. Such concentration stratification is very helpful for reducing airborne pollutant exposure to the occupants. The high concentration near the ceiling improves the pollutant exhaust efficiency. Therefore, from the perspective of indoor air quality, displacement ventilation prevails over mixing ventilation.

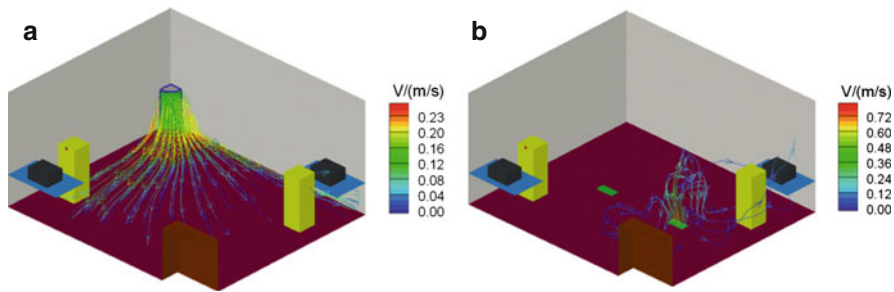


Fig. 11 Flow path lines of displacement ventilation in an office: (a) with a wall-mounted diffuser; (b) with underfloor grilles (Zhang et al. 2010a, b)

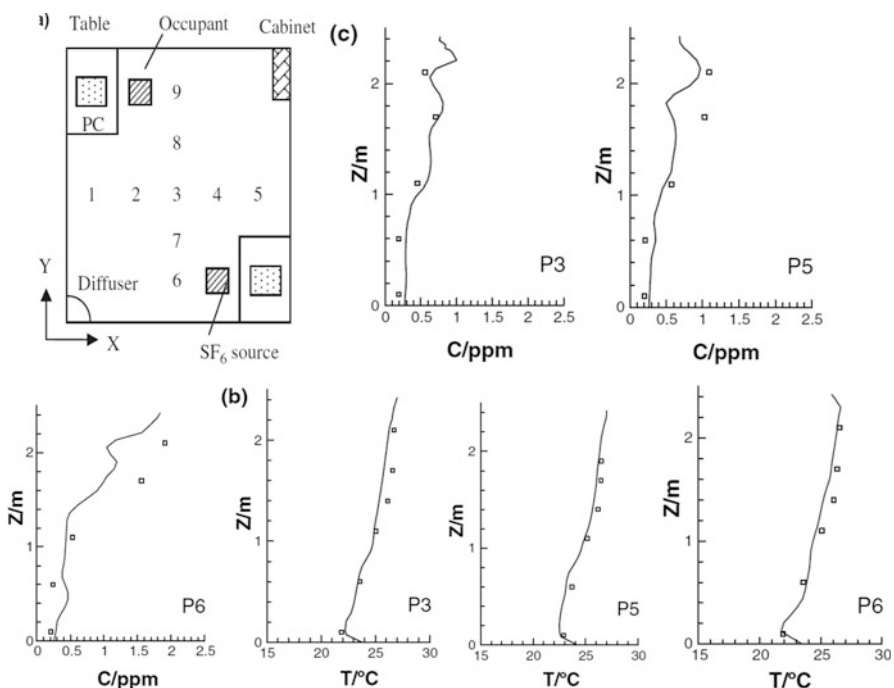
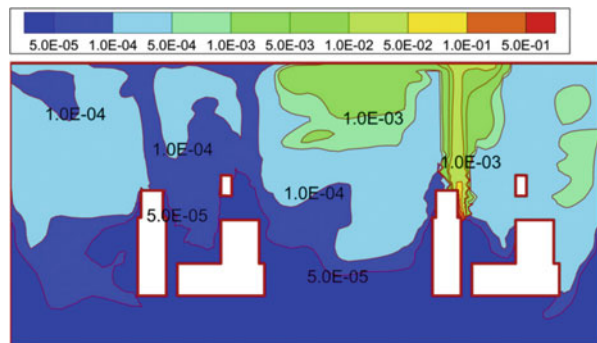


Fig. 12 Vertical profiles of tracer gas concentrations and air temperatures in an office with wall-mounted displacement ventilation, lines for CFD-simulated results, and symbols for the measurement data (Zhang et al. 2010a, b)

Displacement ventilation has also a good performance in reducing airborne infection. Figure 13 shows the concentrations of particles in 0.8 μm in an office with displacement ventilation, in which one patient and one uninfected person shared the office. The exhaled particles from the patient moved upward, which formed a high concentration near the ceiling but a low concentration in the breathing zone. The stratification of particle concentration helps to protect the uninfected

Fig. 13 Particle concentration in a vertical slice in an office with displacement ventilation (He et al. 2011)



person. Thus, the displacement ventilation prevails over the mixing ventilation in minimizing infection from the airborne route.

However, displacement ventilation also creates temperature stratification, with a low temperature near the floor and high temperature near the ceiling. Figure 12 shows that the air temperature profiles resemble the concentration profiles. Indeed, most occupants prefer warm feet and slightly cool head, especially people from east Asia. The temperature gradient along height is one of the most criticized points for displacement ventilation. The ASHRAE Standard 161 (2007) has circumscribed the temperature gradient within 2 °C/m to make displacement ventilation acceptable.

Pros and Cons of Displacement Ventilation

If properly designed, displacement ventilation can take advantage of the contaminants carried by the thermal plumes and thus has a high ventilation efficiency. Furthermore, displacement ventilation maintains a relatively low concentration in the occupied zone for pollutants released from the middle to high heights and thus has a great potential to minimize airborne infection. Moreover, displacement ventilation has also high efficiency in removing heat because of air temperature stratification. The slightly high temperature of the supplied air is also helpful for reducing cooling energy in summer.

The temperature gradient along height is one of the most criticized points of displacement ventilation. In addition, special attention should be paid to the pollutants that are released from the low height or floor, since the displacement ventilation may create mixing similar to the mixing ventilation. Besides, displacement ventilation does not have a large cooling capacity as the mixing ventilation. In heating seasons, separate heating devices are needed to allow for a cool air supply in order not to destroy the upward displacement flow.

Stratum Ventilation

Different from the mixing ventilation with the air supply near or at the ceiling, displacement ventilation with the air supply near or on the floor, the stratum

ventilation supplies air in the middle height and usually near the human breathing zone. Figure 14 shows the diagram of stratum ventilation in an office. Conditioned air is supplied into the room at a high speed (typically 1.2 m/s) from a side wall diffuser in the middle height. The air flows through the working zone and finally to the air exhaust.

Different from displacement ventilation, stratum ventilation can be adopted for either cooling or heating. Figure 15 shows the airflow patterns for heating in an office with stratum ventilation (Zhang et al. 2019). The warm air was directly supplied at a proper downward direction to the occupied zone by configuring the air-supply terminal on walls/columns slightly above the head of occupants. The high-speed conditioned air reaches the occupied zone and then circulates inside the room. The air exhaust outlet is located below the air supply inlet and avoids short-circuiting of warm supply air. Figure 15b shows the CO₂ concentration on a vertical section. The plume flow around the human body is effectively disrupted by the air supply jet. As a result, the exhaled CO₂ is rapidly diluted with a low concentration in the inhaling zone.

Figure 16 presents a case for the stratum ventilation in removing airborne particles in a classroom (Zhang et al. 2012a, b). The air supply was located on the front wall, and the air exhaust was on the back wall. Figure 16b shows the concentration of particles released by one infected student seated in the first row.

Fig. 14 Diagram of stratum ventilation in an office

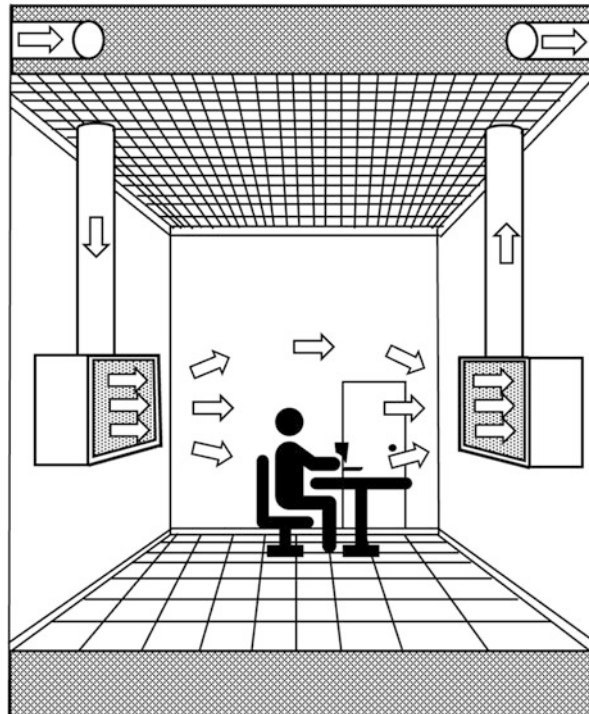


Fig. 15 Air temperature and CO₂ concentration in an office with stratum ventilation: (a) flow path lines and air temperature; (b) CO₂ concentration (Zhang et al. 2019)

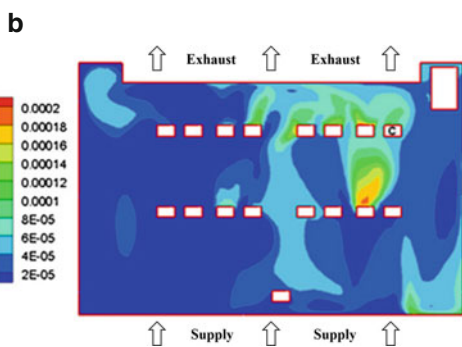
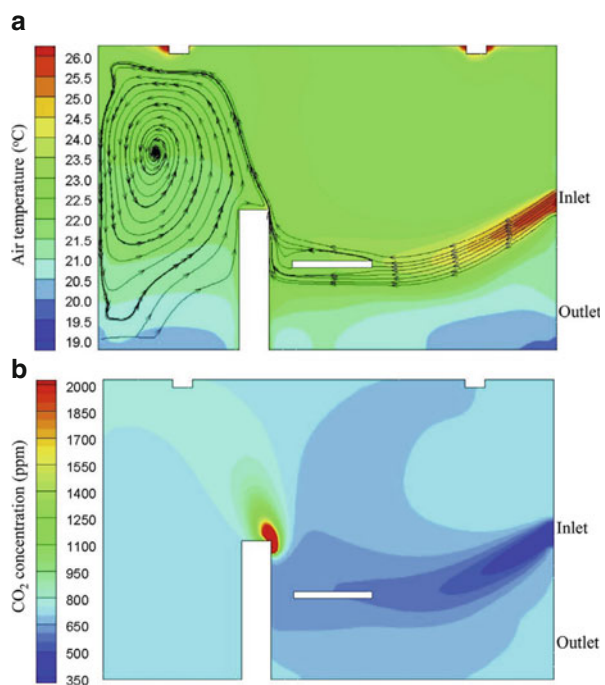


Fig. 16 Droplets concentration in a classroom with stratum ventilation: (a) the investigated classroom; (b) droplet concentration distributions at a horizontal direction near the breathing zone (Zhang et al. 2012a, b)

The whole classroom has a relatively low particle concentration except for the downstream region of the infected student. This indicates that the stratum ventilation may still result in a certain risk of cross-infection unless the infected person sits near the air exhaust.

Because conditioned air is directly delivered to the breathing zone in stratum ventilation, a higher temperature of supply air is required than the mixing ventilation to prevent draft risk. There may be reversed temperature gradient in the occupied zone when cooling the office, i.e., with the low air temperature at the head-chest level but the high temperature at the ankle level.

Pros and Cons of Stratum Ventilation

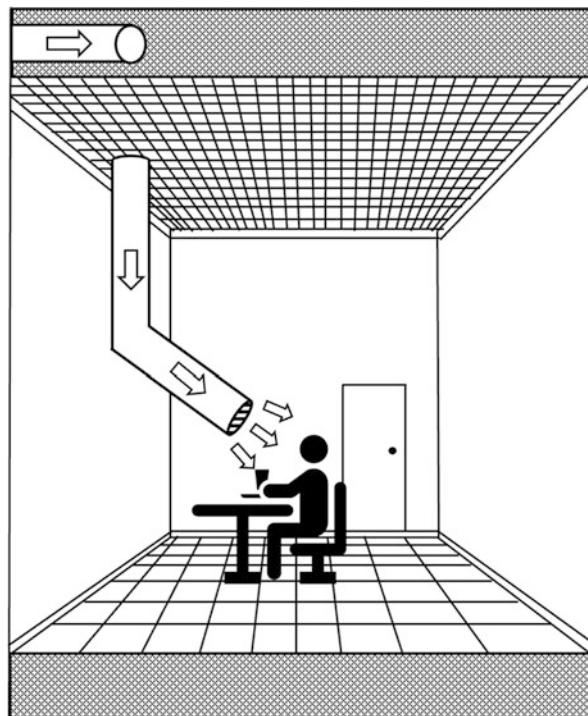
Stratum ventilation supplies conditioned air directly to the breathing zone, which lowers the inhaled pollutant concentrations and improves indoor air quality. The high ventilation efficiency is also beneficial for heat removal.

However, the stratum ventilation may induce cross-contamination in offices with many occupants, because the horizontally supplied-air sweeps the breathing zone of all the occupants. If inappropriately controlled, the stratum ventilation may also create draft risk. Additionally, the stratum ventilation does not provide cooling capacity as high as the mixing ventilation.

Personalized Ventilation

For many years, attempts have been performed to improve the air quality of a person's microenvironment via personalized ventilation. As shown in Fig. 17, in personalized ventilation, conditioned air is directly supplied to the proximity of an

Fig. 17 Diagram of personalized ventilation in an office



occupant. Personalized ventilation creates a microclimate in the context of a macroclimate (entire indoor space). The building occupants can regulate the air supply device to achieve a desired thermal comfort and indoor air quality performance.

Personalized ventilation can be applied for either cooling or heating. Figure 18 shows the airflow patterns for cooling the microenvironment with personalized ventilation (Douaa et al. 2017). The slightly low-temperature air is directly supplied at a mild speed by the terminals near the occupant. The air jet sweeps the thermal plume boundary flow for delivering the conditioned air for inhalation and facial comfort. The short distance between the air-supply terminal and occupant avoids much the mixing of conditioned air with the surrounding air for the microenvironment control. Figure 19 presents the CO₂ concentration in a vertical section (Douaa et al. 2018). Even though the surrounding air has a CO₂ concentration above 1000 ppm, the CO₂ concentration in the inhalation zone is maintained below 750 ppm, which shows superior performance to improve the inhaling indoor air quality.

Personalized ventilation can also reduce airborne infection risk. Even in a situation with coughs by an infected person, personalized ventilation can protect the uninfected person with a properly designed ventilation rate (Elvire et al. 2021). Figure 20a shows the maximum particle concentration exposure to the right person after the left patient released particles by coughs. The cleaned air jet of the personalized ventilation successfully shielded away from the particle plume to the right uninfected person. Figure 20b further shows that the particle plume could be cleaned after a short while, with the residual plume of particles released by only the breath from the left patient. Imagine that the right person was not equipped with personalized ventilation, the particles would be spread to their breathing zone considering the very short distance between these two persons. This shows that personalized ventilation may protect uninfected persons no matter when an infected person releases virus particles by coughing or breathing.

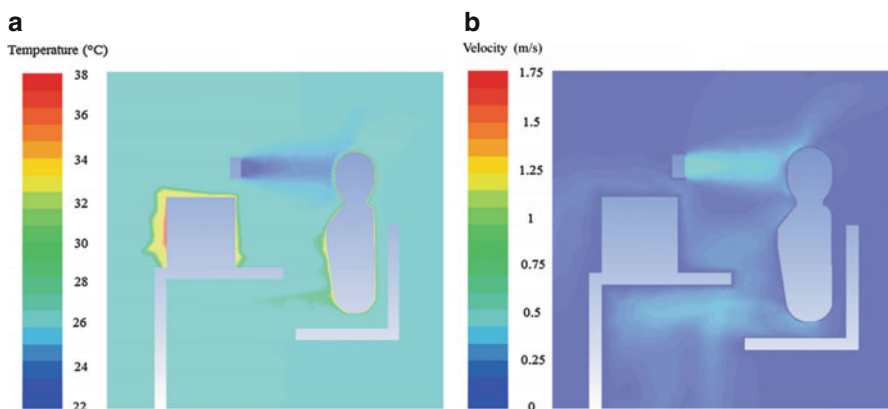


Fig. 18 Temperature and velocity distribution in an office with personalized ventilation (Douaa et al. 2017)

Fig. 19 CO₂ concentration in an office with personalized ventilation (Douaa et al. 2018)

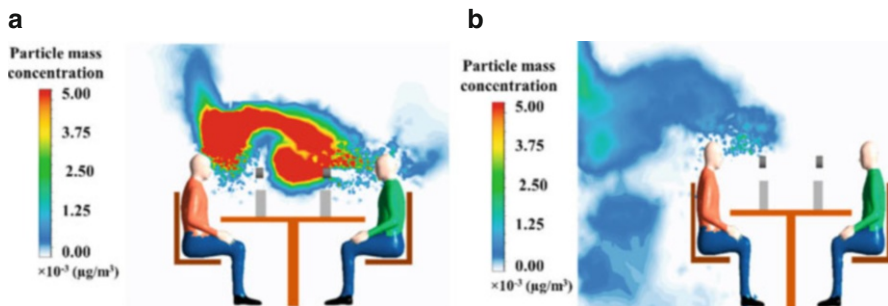
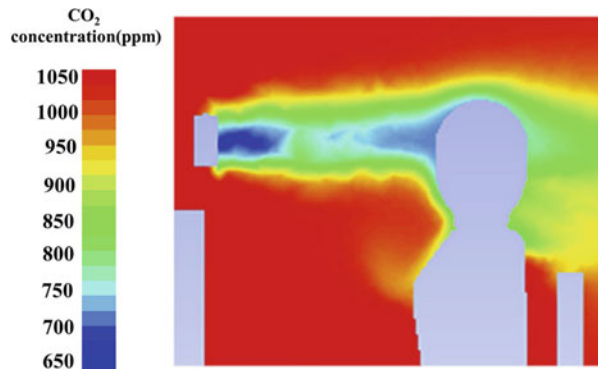


Fig. 20 Particle mass concentration contour in an office with personalized ventilation: (a) maximum particle exposure to the right person once the particles were released from the left person by coughs; (b) particle concentration distribution a short while after the coughs (Elvire et al. 2021)

In contrast to one setting for an entire space with total ventilation, the personalized ventilation is individually controlled, which allows individual occupant to adjust the air to their desired conditions. However, this means that multiple air supply terminals must be used so that the initial investment is high. In addition, the short distance between the ventilation system and occupants means the noise may not be trivial. Meanwhile, the air-supply jets may result in draft complaints.

Pros and Cons of Personalized Ventilation

The personalized ventilation improves air delivery efficiency and perceivable air quality and consequently creates an individual preferred comfortable environment. Another advantage is that the system targets a local microenvironment, and thus has a great potential for energy saving.

However, personalized ventilation is more expensive than total ventilation. In addition, the ventilation devices close to the working zone occupy space and may interrupt working activity. The draft risk may also be a problem if the air-supply jets are not well controlled.

Transportation Vehicle Cabin

Commonly, mechanical ventilation is the only ventilation mode for transportation vehicles such as trains and airplanes. The air ventilation system plays roles including distributing air appropriately, cleaning up contaminated air, and minimizing cross airborne disease transmission, toward creating a comfortable, healthy, and safe cabin environment for passengers and crews. Among transportation vehicles, a commercial aircraft cabin is a mostly confined space. In this section, the aircraft cabin is thus selected to illustrate various forms of mechanical ventilation in transportation vehicles. The mixing ventilation, displacement ventilation, and personalized ventilation are addressed in the following sections, with the schematics shown in Fig. 21 (modified from Elmagraby et al. 2018).

Mixing Ventilation

Currently, mixing ventilation is prevalently used on commercial aircraft. The supplied conditioned air is a mixture of approximately half outdoor air and half filtered recirculated air. The conditioned air is commonly supplied into the aircraft cabin from slot openings located above or below the luggage compartment, as shown in Fig. 21a. The air circulates in the cabin under the combined inertial, viscous, and body (such as buoyancy induced by thermal plumes from the occupants' bodies) forces (Liu et al. 2013) and exits from the grilles at the floor level on both sides of the cabin. Each passenger is provided with the air mixture at a flow rate of approximately 9.4 L/s (20 cfm). Due to the compact size of the cabin, the internal air is displaced roughly 2–3 mins, though the ventilation rate is much smaller than that in buildings.

The mixing ventilation creates an extensively mixed air environment on airplanes. The air temperature is highly uniform, which is welcomed from the perspective of thermal comfort. However, to promote air mixing, the conditioned air has to be supplied at a relatively high speed at approximately 2.5 m/s (Hunt et al. 1995). The high momentum jets near the occupied zone may induce draft complaints

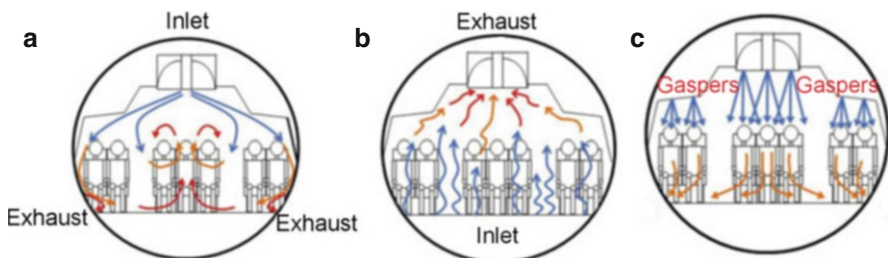


Fig. 21 Schematics of different modes for mechanical ventilation of aircraft cabin: (a) mixing ventilation; (b) displacement ventilation; and (c) overhead individual personalized ventilation (modified from Elmagraby et al. 2018)

(Hinninghofen and Enck 2006). The mixed air not only spawns numerous complaints regarding cabin air quality (Nagda and Hodgson 2001; Spengler and Wilson 2003) but also imposes threats to physical health (Lindgren and Norbäck 2005). More critically, it may result in risks of airborne infectious disease transmission (Leder and Newman 2005).

As shown in Fig. 22, the CO₂ concentration in a Boeing 767 aircraft cabin with mixing ventilation is very uniform (Zhang et al. 2010a, b). Due to the air-supply jets near the ceiling, the region near the ceiling and windows has a slightly lower CO₂ concentration. The strong air motion inside the cabin has refrained the CO₂ plumes from rising far away except for the middle passenger who is seated in the air recirculation zone. Generally, within a small region after CO₂ release, the gas has been diluted immediately. As shown in Fig. 22b, the concentration in the inhaling region or above the passengers has no significant difference. It reveals that the highly mixed air is formed in the mixing ventilation.

Figure 23 shows temporal distributions of the released particles from an index patient during a single cough in a seven-row B767 cabin (Cao, 2010). The particles reach the window seats in about 10–12 s after being released. The passengers near windows in the same row of the index patient have a higher risk of infection for this aircraft model. The particles could be transported to the entire seven-row cabin within 1 min, but most particles were confined to the three rows surrounding the index patient, i.e., in the same row of the patient, in one row ahead, and in one row behind the patient. The risk of infection for the passengers sitting in these three rows can be significantly higher than those sitting in the other rows. Approximately 88% of the released particles were exhausted out of the cabin within 4 min.

The aerosol dispersion and deposition were measured on flights of two twin-aisle aircraft (B767 and B777) using fluorescent and DNA-tagged microspheres (Silcott et al. 2020). The particles were released and measured in multiple rows of seats throughout each aircraft. It was found that the longitudinal spread of particles was subjected to the utilized tracer and the tracer released location. The exposure risk of widespread aerosol is minimal on long-haul flights but not zero. The exposure risk is notably highest in the row of an index patient, while the rows in front and behind the index patient have the next highest risk. Such finding is consistent with that reported by Gupta et al. (2011) and Cao (2010).

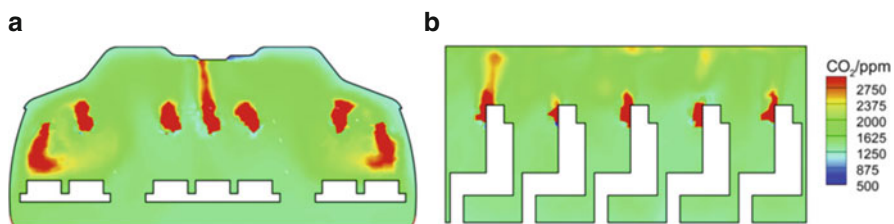


Fig. 22 Distribution of CO₂ concentration in mixing ventilation: (a) in a cross section of the cabin; (b) in the midlongitudinal section (Zhang et al. 2010a, b)

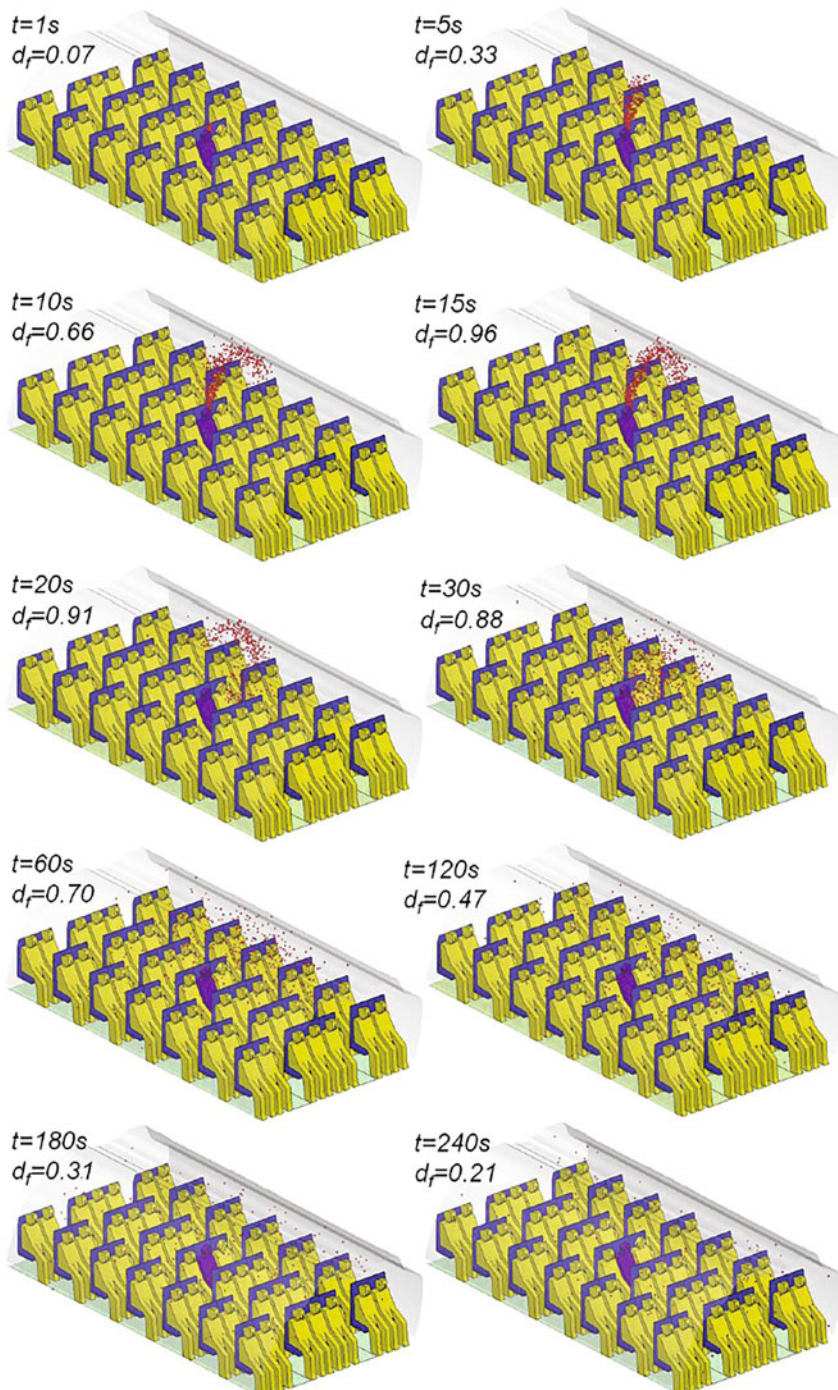


Fig. 23 Temporal distributions of droplets due to a single cough from the index patient (Cao, 2010)

Pros and Cons of Mixing Ventilation

The mixing ventilation creates an extensively mixed air context, in which the air temperature can be quite uniform. Besides, the mixing ventilation has a large cooling and heating capacity.

However, the mixing ventilation forms a large-scale circulation around the passengers in the cross section, which spawns risks of airborne infectious disease transmission. In addition, the high-speed air supply near the occupied zone may cause draft complaints.

Displacement Ventilation

Displacement ventilation was developed as an alternative ventilation mode for the aircraft cabin. Displacement ventilation with sidewall air supply near the floor (Zhang et al. 2017), underaisle-perforated panel air supply (Zhang et al. 2010a, b), and underseat downward air supply (Maier et al. 2017) have been proposed. The supplied cool air at low momentum heats as it rises in the cabin due to thermal buoyancy. The heat is from occupants and electric appliances. Consequently, air temperature stratification is formed and the warm air is extracted by the overhead exhaust vents on the ceiling. Meanwhile, airborne contaminants are trapped by this rising air toward the air exhausts.

Figure 24a presents displacement ventilation with sidewall air supply near the floor and the air exhaust at the central ceiling in a single-aisle aircraft cabin mock-up (Liu et al. 2021). The cabin mock-up contained seven rows of seats. The DEHS particles in 1 μm were released with very low momentum from the head of the manikin seated in the middle seat of the fourth row in the right half cabin. Figure 24b shows that the high concentration in the cross section was just concentrated above the manikins seated in the middle and near the aisle. Once the particles were released from the source, they were spread away along with the uprising flow. These particles were finally discharged out by the outlet in the middle ceiling. The particle

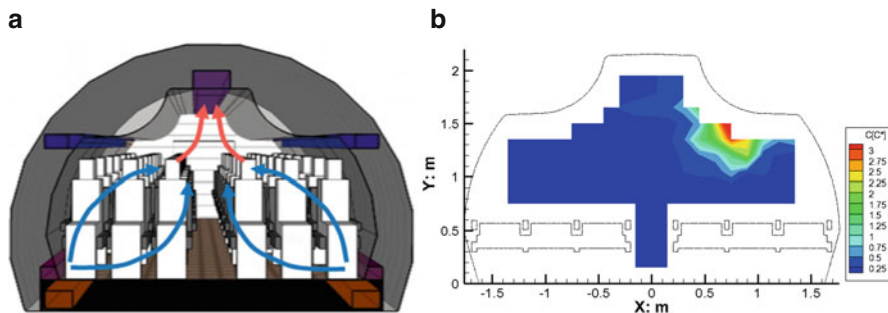


Fig. 24 Particle distribution in an aircraft cabin mock-up with displacement ventilation: (a) schematics of the ventilation mode; (b) dimensionless particle concentration (Liu et al. 2021)

concentrations in the breathing zone of the passengers seated adjacent to the particle source were quite low. Few particles enter the left half cabin.

Figure 25a presents underaisle air-supply displacement ventilation for a twin-aisle Boeing767 aircraft cabin (Zhang et al. 2010a, b). This modified underaisle displacement ventilation supplies a warm air mixture of conditioned outdoor air and recirculated air from the underaisle-perforated panels. It also supplies fully conditioned outdoor air through a narrow channel passage along both side walls to the middle height of the internal cabin just beneath the stowage bins. The air channel warms the cabin to decrease the draft complaints for passengers seated near windows. The contaminated air is extracted by both ceiling exhausts. Figure 25b and c show the CO₂ concentration distribution in a cross section and the midlongitudinal section, respectively. With the rising air streams, the plumes of CO₂ go up to the ceiling and are diluted by the surrounding air. Below the exhalation height, the CO₂ is maintained at a relatively low level without being contaminated by the passengers. Above the head level, the CO₂ concentration rises rapidly. The cross mixing among the passengers in the same row, or in the longitudinal section containing different rows, is very weak. The conditioned, outside air supply from both channel inlets helps somewhat dilute the CO₂ concentration on both sides of the cabin. Comparing with the mixing ventilation, the displacement system was found to decrease the CO₂ concentration in the cabin by 30%.

Similar to CO₂ concentration stratification, the air temperature inside the cabin as shown in Fig. 25d is also stratified. Near the floor, the air temperature is relatively low at approximately 23 °C, while the air temperature is close to 27 °C near the ceiling. The stratified air temperature shall be precisely controlled to prevent draft

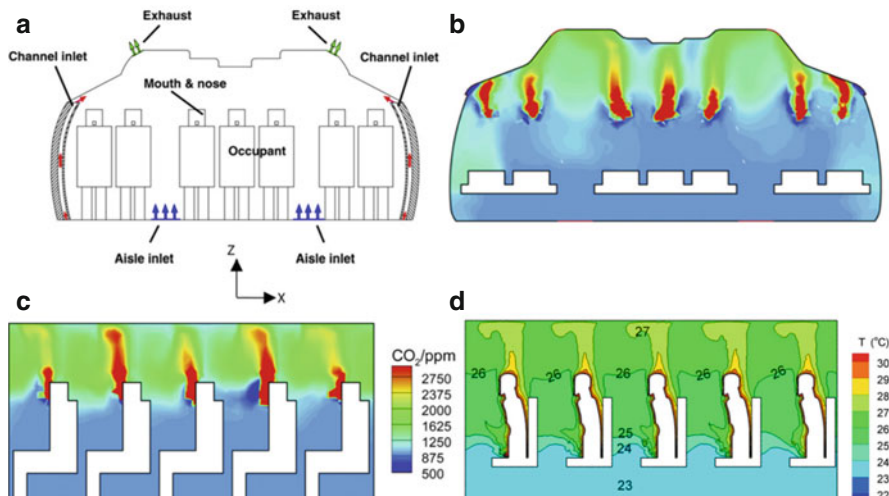


Fig. 25 Improved displacement ventilation for aircraft cabin: (a) schematics of ventilation schemes; (b) CO₂ concentration in a cross section; (c) CO₂ concentration in the midlongitudinal section; and (d) air temperature in the midlongitudinal section (Zhang et al. 2010a, b)

complaints. The acceptable air temperature gradient according to the ASHRAE standard 161 (2007) is less than 2 °C/m.

Pros and Cons of Displacement Ventilation

The displacement ventilation mode generally maintains the uprising flow, so it helps minimize air mixing and cross-transmission of airborne diseases. Compared with the mixing ventilation, the displacement ventilation has a higher ventilation efficiency, pertinently for expired airborne pollutants.

However, due to weak airflow in displacement ventilation, the human motion may occasionally destroy the uprising flow. The high concentration region is still very close to the inhalation zone. Moreover, the displacement ventilation leads to temperature stratification, in which the temperature gradients must be carefully controlled to prevent draft risk.

Personalized Ventilation

Personalized ventilation has been employed in various forms to shield away contaminants entering into the inhalation zone or protect from airborne infection. Most commercial airplanes are designed with overhead gaspers, i.e., the small, circular, and adjustable vents above passengers. When the gaspers are turned on, strong air jets are created toward the passenger's upper body. You et al. (2017) investigated the impacts of gasper ventilation on the airborne infection risk in a Boeing 767 aircraft cabin as shown in Fig. 26a. The mean airborne infection risk for the 49 passengers when they turned their gaspers on and off is shown in Fig. 26b. The horizontal axis indicates the mean infection risk when the gasper was off, while the vertical axis indicates the risk when the gasper was on. The solid line represents the diagonal,

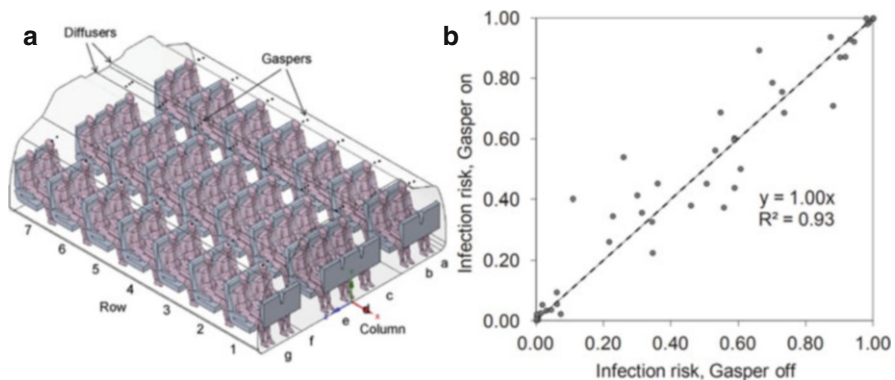


Fig. 26 Impact of overhead gasper ventilation on the calculated airborne infection risk: (a) schematic of a Boeing 767 aircraft cabin; (b) infection risk with and without gasper ventilation for each passenger with the index patient seated at 4E (You et al. 2017)

while the dashed line is the linear regression. Each point represents the case for a passenger. If a point is located exactly on the diagonal, it means that there was no difference in the mean airborne infection risk for that passenger between gasper on and off. If a point is above the diagonal, it means that the gasper ventilation increases the mean infection risk for that passenger, and vice versa. It can be seen that most of the points are close to the diagonal, which indicates that the overall impact of personalized gasper ventilation does not minimize the airborne infection risk. The reason is ascribed to the strong jets from the overhead gaspers, which entrains the surrounding air and promotes mixing of the cabin air. Because thermal plume goes up, strong jets at a typical speed of 15–20 m/s (Tang et al. 2017) are required to press the uprising flow to allow for the jets into the passenger. Such strong jets may probably cause draft risk complaints, especially for those who are sensitive to cool air motion.

To prevent strong jets, attempts were carried out to supply air adjacent to the breathing zone. One of the attempts is to supply fully conditioned outdoor air from the rectangular air terminal on the seatback in front of each passenger in a Boeing 767 aircraft cabin as shown in Fig. 27a (Zhang and Chen 2007). The supplied conditioned air was at 0.35 m/s and 19.5 °C, with a CO₂ concentration of 350 ppm. Figure 27b and c show that the CO₂ concentrations in the inhalation zone of two typical passengers with the personalized ventilation are much lower than those using the mixing ventilation and underaisle displacement ventilation. The reason is that the conditioned outdoor air was directly supplied into the breathing zone. Figure 27b and c also show that the displacement ventilation maintains the CO₂ concentration lower than the mixing ventilation. Note that the personalized ventilation in this research adopted the underaisle displacement ventilation as the background ventilation. Due to generally weak airflow in the background displacement ventilation, the low-moment air supply from the personalized air terminal is sufficient to deliver the conditioned air into the breathing

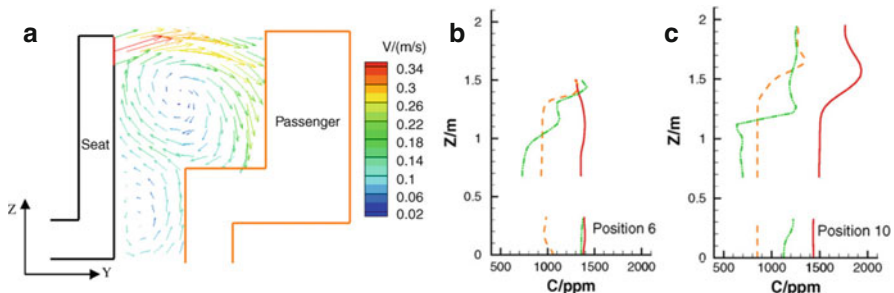


Fig. 27 Personalized ventilation with conditioned air supplied from the seatback air terminal in front of each passenger: (a) CFD-simulated airflow pattern; (b) CFD simulated CO₂ concentration profiles on a vertical pole in front of passenger 4A; and (c) CFD simulated CO₂ concentration profiles on a vertical pole in front of passenger 4D, where mixing ventilation is in red solid lines, displacement ventilation in orange dashed lines, and personalized ventilation in green dash-dot-dot lines (Zhang and Chen 2007)

zone. In general, the air speeds near the occupants are lower than 0.25 m/s, which would not cause much draft risk.

To further reduce draft risk around passengers, personalized ventilation with chair armrest air supply was proposed (Zhang et al. 2012a, b), and also using the underaisle displacement ventilation as the background system. This design delivers conditioned, warm, humid, outdoor air directly from the air terminal devices embedded within both chair armrests, as shown in Fig. 28a. To assure thermal comfort, the personal supply air is conditioned to about 25 °C, so the cabin is mainly cooled down by the air from the underaisle-perforated panels (around 22.5 °C). Figure 28b shows the flow pattern in one cross section across the personal air terminal devices. Although the air terminal devices supply air at medium momentum (around 0.65 m/s), on benefiting from the rising thermal plume near the human body, the supplied air is efficiently delivered into the inhalation zone. Figure 28c presents the CFD-simulated dimensionless tracer gas concentration for the pollutant released from the underaisle air supply. Note that the pollutant release from the underaisle air supply is the worst case of pollutant spreading for the background displacement ventilation. However, with the personal air supply, at least 40% of pollutants can be shielded off around the passenger. It is thus concluded that such personalized ventilation is robust to prevent the contaminants released at any height from imposing exposure to the passenger's breathing zone. Though there is temperature stratification in the aircraft cabin as shown in Fig. 28d, the system is acceptable in perspective of percent dissatisfied (PD) for draught risk as illustrated in Fig. 28e.

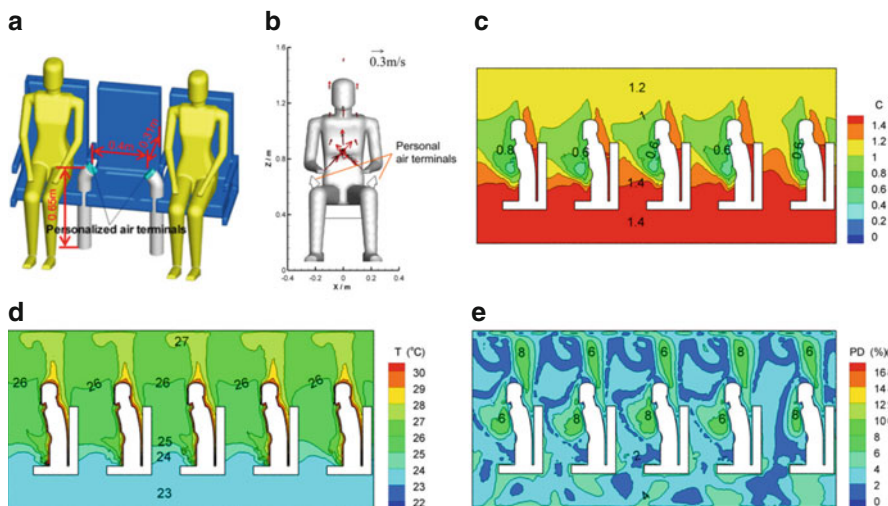


Fig. 28 Personalized ventilation with individual air terminals embedded in armrests: (a) schematics of the personalized ventilation; (b) measured (red arrows) and simulated (black arrows) flow pattern in one cross section; (c) CFD-simulated dimensionless concentration in the midlongitudinal section for pollutant released from the underaisle air supply; (d) temperature distribution; and (e) percentage of draft risk (Zhang et al. 2012a, b)

Personalized displacement ventilation is also proposed to be utilized in the aircraft cabin (You et al. 2019), as shown in Fig. 29a. Each passenger is provided with individual diffusers on the floor, just under the seats in front of the passengers, and the cabin air is extracted at the ceiling. The supplied air together with the uprising thermal plume carries exhaled contaminants from the passengers to the exhausts. Figure 29b-d compares airborne infection risk among the personal displacement ventilation, the mixing ventilation, and the conventional displacement ventilation with side-wall air supply, assuming the index passenger was seated in 4D. The computed average infection risks among all of the passengers were 0.23, 0.09, and 0.15, respectively, for the mixing ventilation, conventional displacement ventilation, and personalized displacement ventilation. From the perspective of average PD, personalized displacement ventilation prevails over conventional displacement ventilation. The highest PD among the passengers was 32%, 43%, and 31% for the mixing ventilation, conventional displacement ventilation, and personalized displacement ventilation, respectively. Though the above, the personal displacement ventilation also creates temperature stratification. If feet are adjacent to the personal displacement air terminals, one may complain about the possible draft feeling.

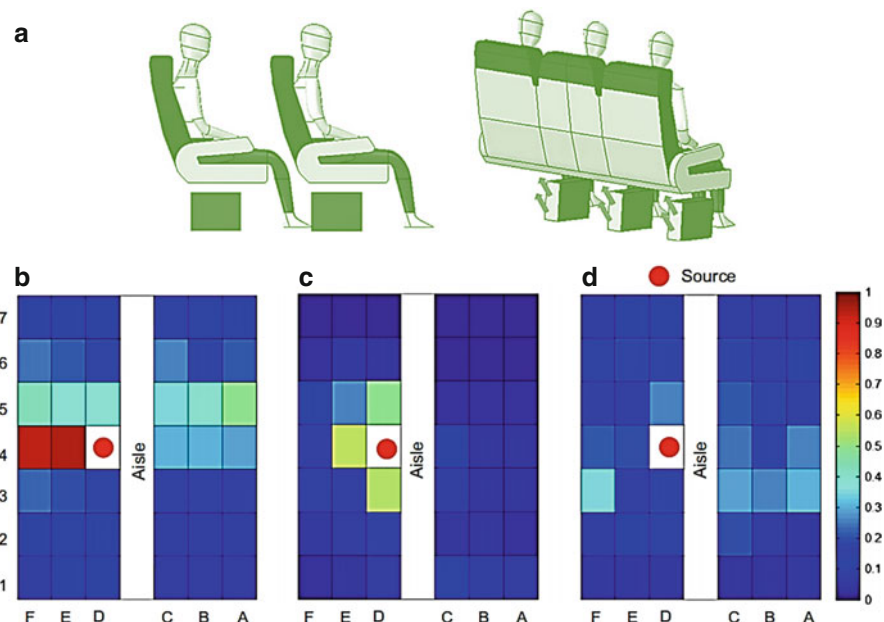


Fig. 29 Personalized displacement ventilation in a Boeing 737 aircraft cabin: (a) schematics of the personal underseat air supply; (b) CFD-simulated airborne infection risk in mixing ventilation for the index passenger at 4D; (c) airborne infection risk in conventional displacement ventilation; and (d) airborne infection risk in personalized displacement ventilation (modified from You et al. 2019)

Pros and Cons of Personalized Ventilation

The personalized air supply with displacement ventilation as the background system prevails substantially over the mixing ventilation and displacement ventilation in terms of lowering the inhaled pollutant concentration and minimizing airborne infection risk.

However, the high-speed gasper ventilation entrains the surrounding air and promotes air mixing and does not show favorable performance in improving cabin air quality and reducing airborne infection risk. In addition, the personalized ventilation with displacement ventilation as the background systems also creates temperature stratification, which must be carefully designed to prevent the draft risk. Besides, the personalized ventilation may have a higher initial investment expense than the remaining two systems because individual air terminals and connecting ducts are needed.

Conclusion

Natural ventilation is the most widely used in residential buildings in developing countries. Natural ventilation is simple, energy-saving, and affordable but may occasionally result in an insufficient ventilation rate. In situations with outdoor PM_{2.5} pollution, a combination of natural ventilation and portable demand-controlled particulate filtration has the lowest operating cost. The outdoor air supply and indoor particle filtration are suggested for decoupled, independent consideration. Among the mechanical ventilation modes, decentralized systems operating only during the occupied period have great potential to minimize utility costs. Mechanical ventilation in demand-controlled operation and its hybrid with natural ventilation can further reduce energy consumption.

In modern office buildings, mechanical ventilation is more preferred because of its robustness and continuity. Among the commonly used mechanical ventilation systems, mixing ventilation has a significant advantage in creating a relatively uniform indoor environment. However, the mixing ventilation may create cross-contamination and induce airborne infectious risk. In contrast, displacement ventilation, stratum ventilation, and personalized ventilation are showed to provide better indoor air quality than traditional mixing ventilation. However, temperature gradients or draft risks must be well controlled to prevent possible discomfort feeling.

For aircraft cabins, the currently used mixing ventilation mode creates an extensively mixed air environment, which has a lower ventilation efficiency than displacement ventilation mode. Personalized ventilation has been employed in various forms to create the preferred microenvironment for each passenger. Displacement ventilation combining with personalized ventilation can substantially improve cabin air quality and minimize airborne infection risk. However, temperature stratification and draft risks must be paid significant attention to when designing and running displacement ventilation and/or personalized ventilation.

Cross-References

- [Evaluating Ventilation Performance](#)
- [Indoor Air Quality in Commercial Air Transportation](#)
- [Indoor Air Quality in Offices](#)

Acknowledgments The presented work was supported by the National Key R&D Program of the Ministry of Science and Technology, China, on “Green Buildings and Building Industrialization” through Grant No. 2016YFC0700500 and by the National Natural Science Foundation of China through Grant No. 51978450.

References

- ASHRAE (2007) ANSI/ASHRAE standard 161-2007, air quality within commercial aircraft, American Society of Heating, Refrigerating and Air-Conditioning Engineers
- ASHRAE (2014) ANSI/ASHRAE standard 62.2-2014, ventilation and acceptable indoor air quality in low-rise residential buildings. American Society of Heating, Refrigerating and Air-Conditioning Engineers, Atlanta
- Cao Q (2010) Respiratory exhalation/inhalation models and prediction of airborne infection risk in an aircraft cabin. Ph.D Thesis Purdue University
- Cao Q, Liu Y, Liu W et al (2016) Experimental study of particle deposition in the environmental control systems of commercial airliners. *Build Environ* 96:62–71
- CEN Standard TR 1752. 1998. Ventilation for buildings: design criteria for the indoor environment; CEN
- Chen Q (2009) Ventilation performance prediction for buildings: a method overview and recent applications. *Build Environ* 44(4):848–858
- Chen Q, Lee K, Mazumdar S et al (2010) Ventilation performance prediction for buildings: model assessment. *Build Environ* 45(2):295–303
- Cho H, Cabrera D, Sardy S et al (2020) Evaluation of performance of energy efficient hybrid ventilation system and analysis of occupants’ behavior to control windows. *Build Environ* 107434
- Dai X, Liu J, Li X et al (2018) Long-term monitoring of indoor CO₂ and PM2.5 in Chinese homes: concentrations and their relationships with outdoor environments. *Build Environ* 144:238–247
- De M, Brager G (2002) Thermal comfort in naturally ventilated buildings: revisions to ASHRAE standard 55. *Energ Buildings* 34(6):549–561
- Dimitroulopoulou C (2012) Ventilation in European dwellings: a review. *Build Environ* 47:109–125
- Doi S, Suzuki S, Morishita M et al (2003) The prevalence of IgE sensitization to formaldehyde in asthmatic children. *Allergy* 58(7):668–671
- Douaa A, Kamel G, Nesreen G et al (2017) Mixing ventilation coupled with personalized sinusoidal ventilation: optimal frequency and flow rate for acceptable air quality. *Energ Buildings* 154: 569–580
- Douaa A, Kamel G, Nesreen G et al (2018) Effectiveness of intermittent personalized ventilation assisting a chilled ceiling for enhanced thermal comfort and acceptable indoor air quality. *Build Environ* 144:9–22
- Elmaghraby H, Chiang Y, Aliabadi A (2018) Ventilation strategies and air quality management in passenger aircraft cabins: A review of experimental approaches and numerical simulations. *Sci Technol Built Environ* 24:160–175
- Elvire K, Nesreen G, Kamel G et al (2021) Effect of individually controlled personalized ventilation on cross-contamination due to respiratory activities. *Build Environ* 107719

- EN 15251 (2007) Indoor environmental input parameters for design and assessment of energy performance of buildings addressing indoor air quality, thermal environment, lighting and acoustics. CEN, Brussels
- Garrett M, Hooper M, Hooper B et al (1999) Increased risk of allergy in children due to formaldehyde exposure in homes. *Allergy* 54(4):330–337
- GB/T 18883-2002 (2002) Indoor air quality standard. Beijing: standardization Administration of China
- Gomis L, Fiorentini M, Daly D (2020) Potential and practical management of hybrid ventilation in buildings. *Energ Buildings* 110597
- Gupta J, Lin C, Chen Q (2011) Transport of expiratory droplets in an aircraft cabin. *Indoor Air* 21 (1):3–11
- He Q, Niu J, Cao N et al (2011) CFD study of exhaled droplet transmission between occupants under different ventilation strategies in a typical office room. *Build Environ* 46(2):397–408
- Hinninghofen H, Enck P (2006) Passenger well-being in airplanes. *Auton Neurosci Basic Clin* 129: 80–85
- Hou J, Zhang Y, Sun Y et al (2018) Air change rates at night in northeast Chinese homes. *Build Environ* 132:273–281
- Huang S, Wei W, Weschler L et al (2017) Indoor formaldehyde concentrations in urban China: preliminary study of some important influencing factors. *Sci Total Environ* 590:394–405
- Hunt E, Reid D, Space D, et al (1995) Commercial airliner environmental control system. Aerospace Medical Association Annual Meeting, May 7–11, Anaheim, CA
- ISO EN 7730 (2005) Ergonomics of the thermal environment e analytical determination and interpretation of thermal comfort using calculation of the PMV and PPD indices and local thermal comfort criteria. [Published in Switzerland]
- Jiang Y, Zhao B, Li X et al (2009) Investigating a safe ventilation rate for the prevention of indoor SARS transmission: an attempt based on a simulation approach. *Build Simul*
- Lai D, Jia S, Qi Y et al (2018a) Window-opening behavior in Chinese residential buildings across different climate zones. *Build Environ* 142:234–243
- Lai D, Qi Y, Liu J et al (2018b) Ventilation behavior in residential buildings with mechanical ventilation systems across different climate zones in China. *Build Environ* 143:679–690
- Leder K, Newman D (2005) Respiratory infections during air travel. *Intern Med J* 35:50–55
- Liddament M (2001) Occupant impact on ventilation, AIVC technical note 53, Air Infiltration and Ventilation Center, UK
- Lindgren T, Norbäck D (2005) Health and perception of cabin air quality among Swedish commercial airline crew. *Indoor Air* 15:65–72
- Liu S, Xu L, Chao C et al (2013) Thermal environment around passengers in an aircraft cabin. *HVAC & R Res* 19(5):627–634
- Liu M, Chang D, Liu J et al (2021) Experimental investigation of air distribution in an airliner cabin mockup with displacement ventilation. *Build Environ* 191:107577
- Maier J, Marggraf-Micheel C, Dehne T et al (2017) Thermal comfort of different displacement ventilation systems in an aircraft passenger cabin. *Build Environ* 111:256–264
- Muller D, Kandzia C, Kosonen R et al (2013) Mixing ventilation-guidebook on mixing air air distribution design. No. 19, REHVA guidebook
- Nagda N, Hodgson M (2001) Low relative humidity and aircraft cabin air quality. *Indoor Air* 11: 200–214
- Pei J, Yin Y, Liu J et al (2020) An eight-city study of volatile organic compounds in Chinese residences: compounds, concentrations, and characteristics. *Sci Total Environ* 698:134137
- Rey-Hernández J, José-Alonso J, Velasco-Gómez E et al (2020) Performance analysis of a hybrid ventilation system in a near zero energy building. *Build Environ* 185:107265
- Russell M, Sherman M, Rudd A (2007) Review of residential ventilation technologies. *HVAC & R Res* 13(2):235–248
- Silcott D, Kinahan S, Santarpia J et al (2020) TRANSCOM/AMC commercial aircraft cabin aerosol dispersion tests

- Song R, Zhang T, Wang S (2019) Numerical evaluation of residential ventilation accompanied with particle filtration in different climatic zones of China. Proceedings of Healthy Buildings 2019 Asia, ID: 1396178, pp. 1–4, Changsha, China, Oct. 22–25
- Spengler J, Wilson D (2003) Air quality in aircraft. Proc Inst Mech Eng Part E J Process Mech Eng 217(4):323–336
- Sun Y, Hou J, Cheng R et al (2019) Indoor air quality, ventilation and their associations with sick building syndrome in Chinese homes. Energ Buildings 197:112–119
- Tang X, Bai Y, Duong A et al (2009) Formaldehyde in China: production, consumption, exposure levels, and health effects. Environ Int 35(8):1210–1224
- Tang Z, Guo Y, Cui X et al (2017) Turbulent characteristics in the near fields of gasper jet flows in an aircraft cabin environment: intermittently energetic coherent structures. Build Environ 117: 73–83
- Tom L, Darem A, Nicolas S et al (2020) Review of ventilation strategies to reduce the risk of disease transmission in high occupancy buildings. Int J Thermofluids 7:100045
- Wieslander G, Norbäck D, Björnsson E et al (1996) Asthma and the indoor environment: the significance of emission of formaldehyde and volatile organic compounds from newly painted indoor surfaces. Int Arch Occup Environ Health 69(2):115–124
- Ye W, Zhang X, Gao J et al (2017) Indoor air pollutants, ventilation rate determinants and potential control strategies in Chinese dwellings: a literature review. Sci Total Environ 586:696–729
- Yin H, Liu C, Zhang L et al (2019) Measurement and evaluation of indoor air quality in naturally ventilated residential buildings. Indoor Built Environ 28(10):1307–1323
- Yoshino H, Liu J, Wada J (2003) Performance analysis of hybrid ventilation system for residential buildings using a test house. Indoor Air 13(6):28–34
- You R, Chen J, Lin C et al (2017) Investigating the impact of gaspers on cabin air quality in commercial airliners with a hybrid turbulence model. Build Environ 111:110–122
- You R, Lin C, Wei D et al (2019) Evaluating the commercial airliner cabin environment with different air distribution systems. Indoor Air 29(5):840–853
- Yu J, Ouyang Q, Zhu Y et al (2012) A comparison of the thermal adaptability of people accustomed to air-conditioned environments and naturally ventilated environments. Indoor Air 22(2): 110–118
- Zhang T, Chen Q (2007) Novel air distribution systems for commercial aircraft cabins. Build Environ 42(4):1675–1684
- Zhang T, Lee K, Chen Q (2010a) A simplified approach to describe complex diffusers in displacement ventilation for CFD simulations. Indoor Air 19(3):255–267
- Zhang T, Yin S, Wang S (2010b) An under-aisle air distribution system facilitating humidification of commercial aircraft cabins. Build Environ 45(4):907–915
- Zhang L, Wang J, Yao T et al (2012a) Investigation into anti-airborne infection performance of stratum ventilation. Build Environ 54:29–38
- Zhang T, Li P, Wang S (2012b) A personal air distribution system with air terminals embedded in chair armrests on commercial airplanes. Build Environ 47:89–99
- Zhang Y, Liu J, Pei J et al (2017) Performance evaluation of different air distribution systems in an aircraft cabin mockup. Aerosp Sci Technol 70:359–366
- Zhang T, Su Z, Wang J et al (2018) Ventilation, indoor particle filtration, and energy consumption of an apartment in northern China. Build Environ 143:280–292
- Zhang S, Lin Z, Ai Z et al (2019) Effects of operation parameters on performances of stratum ventilation for heating mode. Build Environ 148(15):55–66
- Zhang T, Li X, Rao Y et al (2020) Removal of formaldehyde in urban office building by the integration of ventilation and photocatalyst-coated window. Sustain Cities Soc 55:102050
- Zhao L, Liu J, Ren J (2018) Impact of various ventilation modes on IAQ and energy consumption in Chinese dwellings: first long-term monitoring study in Tianjin, China. Build Environ 143: 99–106



Evaluating Ventilation Performance

58

Andrew Persily

Contents

Introduction	1676
Terminology	1677
Reasons for Evaluating Ventilation	1679
Building and System Impacts on Ventilation Evaluation	1680
Performance Issues and Parameters	1682
Building and System Design Information	1686
Measurement Methods	1690
System Status	1690
Envelope Air Leakage	1691
Ventilation System Airflow	1694
Outdoor Air Change Rate	1696
Interzone Airflow	1699
Air Distribution	1700
Other Considerations	1701
Deviations from Design Intent	1705
Conclusions	1707
Cross-References	1709
References	1709

Abstract

The evaluation of building ventilation performance is critical to understanding indoor contaminant transport dynamics and interpreting indoor contaminant measurements. However, ventilation performance involves many different issues and metrics that can make such evaluations challenging. Also, many indoor air quality research studies have not included adequate evaluation of building ventilation and its impacts on indoor contaminant concentrations. There are several reasons for this history of neglect; they include the complexity of ventilation, the

A. Persily (✉)

National Institute of Standards and Technology, Gaithersburg, MD, USA

e-mail: andrew.persily@nist.gov

© This is a U.S. Government work and not under copyright protection in the U.S.;
foreign copyright protection may apply 2022

Y. Zhang et al. (eds.), *Handbook of Indoor Air Quality*,
https://doi.org/10.1007/978-981-16-7680-2_20

1675

cost associated with the measurements, and the lack of guidance on how to conduct such evaluations. This chapter explains what is involved in evaluating and understanding ventilation performance in buildings, with a focus on the parameters involved, how building configuration and ventilation system type impact how such evaluations are conducted, and the connection between the reasons for ventilation evaluations and the strategies employed. Among the ventilation performance parameters that are covered are whole building outdoor air change rates, ventilation system outdoor air and supply air delivery rates, and envelope infiltration rates. Some of the key points stressed in this chapter include the following: actual ventilation performance often does not match design intent; ventilation rates vary significantly with weather and system operation and therefore a single value is not particularly useful without information on the conditions during the measurement; multiple repeated measurements under different conditions are required in order to fully understand ventilation in a building; and, while indoor carbon dioxide concentrations can be a useful tool in evaluating ventilation, its application is based on multiple assumptions that must be valid.

Keywords

Airflow · Building performance · Indoor air quality · Infiltration · Ventilation

Introduction

Building ventilation performance is important for several reasons, including impacts on indoor air quality (IAQ), energy use, thermal comfort, occupant health and safety, and degradation of building materials and furnishings. In some respects, the impacts are relatively straightforward. For example, the energy required for heating and cooling is based primarily on the amount of outdoor airflow into a building, the indoor-outdoor air temperature difference, and air properties such as specific heat and humidity ratio. However, the details of energy and other impacts are often more complex as they depend on the details of the relevant airflows, the heating, ventilating and air-conditioning (HVAC) equipment in the building, building and equipment operating strategies, and other factors.

Building ventilation performance cannot be characterized by a single metric but involves a range of performance issues and parameters. The next section of this chapter discusses ventilation performance in more detail, with a focus on ventilation systems and building characteristics. These performance issues include system status, envelope air leakage, ventilation system airflow rates, outdoor air change rates, interzone airflow, and air distribution. A key step in understanding the significance of ventilation performance is to understand how the system is intended to perform, sometimes referred to as the design intent. To that end, building and system design information is discussed after the section on performance issues. The next section covers measurement methods to quantify performance, accounting for building configuration and system design in making these measurements, as well as

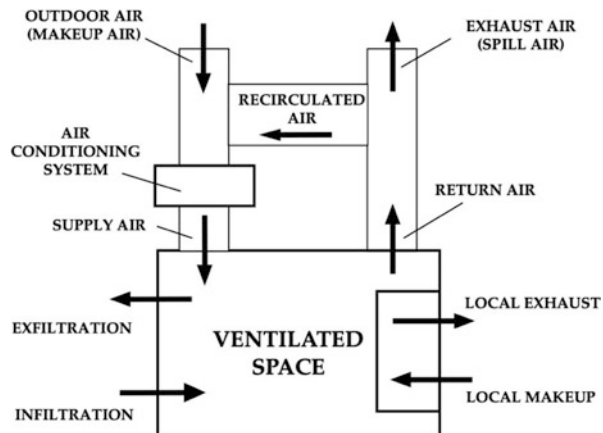
capturing variations in performance over time and as a function of weather. Comparison of measurement results to the system design, as well as to relevant standards and guidelines, is also discussed.

It is important to note that many IAQ studies of buildings have done a poor job of evaluating ventilation. This is demonstrated by an analysis of the ventilation characterization approaches in a key review of 26 peer-reviewed papers on the relationship of ventilation rates and occupant health outcomes (Sundell et al. 2011). A number of different techniques were used to assess ventilation rates in these papers, and there was a range of detail included in the description of these techniques. However, an analysis of the ventilation assessment approaches in these studies revealed that about half of them do not mention the instrumentation used to make the measurements and only four report a value for the measurement uncertainty (Persily and Levin 2011). More than 10% of the papers do not describe how the ventilation rates were determined, and about 75% do not describe the time scale over which the measurements were made. Other common problems with the treatment of ventilation in IAQ studies is a lack of sufficient description of how the building is intended to be ventilated, information on the HVAC equipment in the building including design ventilation rates, or data on weather and equipment operation during the ventilation measurements. This chapter describes how to evaluate ventilation in buildings with different ventilation system types, and what information needs to be provided with ventilation measurement results to support their interpretation and use.

Terminology

While this chapter discusses ventilation performance parameters in some detail, it is important to note that the relevant terms are not always used consistently by researchers, practitioners, and others. Figure 1 shows a mechanically ventilated building with a ventilation approach that is typical of many commercial buildings in the USA, with several key terms displayed. Note that many of these terms are defined in ASHRAE Standard 62.1 (ASHRAE 2019a). (While a US commercial building perspective exists for much of the discussion in this chapter, much of this material also applies to residential buildings and non-US buildings.) Sometimes outdoor air is referred to as makeup air, often when it is needed for combustion or exhaust ventilation equipment. In many systems, outdoor air is mixed with recirculated air that flows from the ventilated space as return air. In general, a portion of the return air leaves the building as exhaust air or spill air. Some ventilation systems, sometimes referred to as 100% dedicated outdoor air systems (DOAS), do not recirculate any air. The mixture of outdoor air and recirculated air flows through an air conditioning system where it is heated/cooled, humidified/dehumidified, and filtered. The air then flows to the space as supply air, where it serves the needs of that space for outdoor air ventilation and in many cases also provides thermal conditioning. The figure does not show local mixing boxes such as variable-air-volume (VAV) boxes that are sometimes used to mix supply air (sometimes referred to primary air in

Fig. 1 Schematic of ventilated building



such systems) with room air drawn to meet local thermal requirements. Figure 1 also shows local exhaust airflow, which is often used to remove locally generated contaminants before they mix with air in the rest of the building. Local makeup air is sometimes provided rather than drawing air from elsewhere in the building.

It is important to note that some individuals consider ventilation to be outdoor air and others consider it to be supply air; the term "air change rate" also does not specify the type of air. To avoid confusion, it is important to clarify the air source as outdoor or supply air when discussing ventilation. ASHRAE Standard 62.1 defines ventilation as follows: the process of supplying air to or removing air from a space for the purpose of controlling air contaminant levels, humidity, or temperature within the space. This definition does not mention outdoor air but focuses on air treatment (e.g., heating, cooling, and filtration), delivery, and exhaust. In this chapter, when the term ventilation appears without a qualifier, it is being used in this general sense to cover outdoor and supply air delivery, air treatment, and exhaust air removal.

One issue that is often not fully appreciated in considering the impacts of ventilation is the distinction between infiltration and outdoor air ventilation. Infiltration refers to uncontrolled entry of outdoor air through unintentional openings in the building envelope, i.e., leakage. Infiltration is driven by indoor-outdoor air pressure differences due to weather (wind and temperature) and the operation of building systems (e.g., exhaust fans and vented combustion equipment). Exfiltration refers to airflow from the building interior to the outdoors, again through unintentional leaks. The term infiltration is often used to describe the combined processes of infiltration and exfiltration. It is important to note that infiltration rates are not controlled, nor is the distribution of infiltration air within a building. Additionally, infiltration can have negative impacts on IAQ (since infiltration air is unfiltered), indoor moisture management, and material durability. Outdoor air ventilation refers to outdoor airflow into a building through intentional openings such as intakes, vents, and open windows. Mechanical ventilation is outdoor air ventilation induced by powered equipment, i.e., fans, while natural

ventilation is driven by weather. Ventilation systems, mechanical or natural, that are well designed, installed, operated, and maintained are preferable to infiltration for meeting building ventilation requirements since they can provide the desired ventilation rate where it is needed, avoiding both under- and overventilation. Ventilation systems also provide opportunities to reduce energy impacts, such as by recovering heat or moisture from the outgoing air.

Reasons for Evaluating Ventilation

When conducting any measurement, it is essential to consider why it is being done and what will be done with the results. When deciding what to measure as part of a building ventilation evaluation, one must start with the reason for the evaluation, as well as the configuration of the building and the ventilation system design. Building and system issues are discussed later in the chapter, but the reason for the ventilation evaluation is critical. There are multiple reasons that one might evaluate ventilation in a building or a space within a building, and the reasons will impact the approach that is used including the timing of the evaluation and the financial resources and expertise required. Reasons for evaluating ventilation include: a research study of ventilation or IAQ, an effort to understand the reasons for an IAQ problem, and a commissioning effort to ensure the building and system are operating as intended. Research can range from an intense, long-term study of a single building to a survey of dozens to hundreds of buildings involving short-term (hours to days) measurements. Long-term ventilation studies of a building may be designed to characterize ventilation and infiltration rates and other performance parameters as a function of weather conditions, system operation, and occupant activities, and therefore require many real-time measurements over days, weeks, and perhaps seasons. To facilitate long-term, real-time measurements, automated measurement and data acquisition systems are very helpful if not essential, perhaps involving a temporarily installed tracer gas measurement system or anemometers in HVAC ductwork. Long-term research studies of indoor contaminant levels would involve similar (long-term, real-time) ventilation measurements, though they may focus on a limited number of ventilation performance parameters. At a minimum, the interpretation of long-term indoor contaminant measurements requires outdoor air change rates to understand variations in contaminant concentrations, often employing mass balance analysis.

For short-term IAQ research studies, which may involve only a single or a small number of indoor contaminant concentration measurements, it generally does not make sense to install instrumentation and data acquisition systems that may be justified in a longer term study. However, air change rates and perhaps other ventilation performance parameters still need to be quantified to interpret indoor contaminant concentration measurements. Such analyses may also need system supply airflows to account for contaminant removal by filtration and air cleaning equipment and infiltration rates to account for outdoor contaminant penetration (i.e., the removal of outdoor contaminants as they flow through building envelope leaks). A special case of short-term IAQ studies are building surveys, in which

dozens of buildings or more are studied to capture a range of performance parameters including the concentrations of different contaminants, thermal comfort conditions, nonthermal indoor environmental parameters (e.g., lighting and acoustics), and occupant symptoms and perceptions of the indoor environment. Several IAQ surveys have been conducted over the years, most of which have included some measurements of ventilation performance (EPA 2006; Bluyssen et al. 1996; Offermann 2009; Bennett et al. 2011, 2012). In these studies, the cost of the measurements is critical and difficult choices often have to be made about which parameters will be measured and the level of sophistication for the various measurements. But given the first-order relationship of ventilation and IAQ, these studies need to include reliable ventilation measurements to be useful.

Short-term IAQ studies are also conducted to understand the cause(s) of occupant IAQ complaints or health problems. Such forensic investigations generally include an assessment of the potential role of the ventilation system and how its performance may be contributing to the problem being studied. Most of these studies are done using approaches determined by the investigator, but there is an ASTM standard for investigating residential IAQ issues that includes some aspects of ventilation performance (ASTM 2014). The specific parameters included in IAQ investigations and the manner in which they are assessed are generally a function of the building and its HVAC systems, the nature of the IAQ problem being investigated, and the contaminant sources that could be causing the problems. These investigations may require measurement of outdoor air change rates, supply airflow rates, and infiltration rates. They may also merit assessment of interzone airflows that can transport contaminants from zones where key sources are located to the zones where the occupants are experiencing symptoms. This chapter does not cover the measurement of interzone airflows in detail, but it does discuss their measurement and describes some qualitative tools that can be useful.

Another reason for evaluating building ventilation is as part of a commissioning effort to ensure the system is operating as intended. Commissioning is becoming increasingly common and is in fact required by high-performance building standards and rating systems (ASHRAE 2020). HVAC system commissioning has been part of normal practice for decades, where it is referred to as testing and balancing (TAB) (ASHRAE 2008). As noted in the foreword to ASHRAE Standard 111, “Field test results are considered essential to designers, manufacturers, and installers to better enable them to evaluate the results of their design, equipment performance, and installation techniques under actual operating conditions.” TAB is typically done for new buildings and systems, but there is value in recommissioning systems at various points in the life of a building to ensure that it is still performing as intended given the likelihood that control sensors and hardware may have degraded over time or building space use has changed.

Building and System Impacts on Ventilation Evaluation

In addition to the reasons for conducting an evaluation, the building configuration and the ventilation system design and layout are key to how a ventilation evaluation

is conducted, specifically what is measured and how. Buildings and systems are extremely variable, and these variations must be considered when planning and conducting ventilation evaluations. Key building configuration parameters include building size, how the building is divided into zones, how zones are connected in terms of airflow (e.g., doorways, common hallways), and ventilation approach (es) employed. In describing the size of a building, one needs to include the building height, the number of stories, and floor area and height of each story. Zoning covers how the building is laid out into different sections or sometimes wings, which portions are handled by which ventilation systems, and how space use and occupancy vary among zones. These latter factors will determine how much outdoor air is required by ventilation standards and regulations. Other relevant building features that should be considered in the assessment include information on the climate of the building location, e.g., annual heating and cooling degree days, monthly average outdoor air temperature and wind speed, and wind exposure of the building.

The approach used to ventilate the building is key to planning a ventilation evaluation effort and involves the following questions: Is there a mechanical ventilation system that brings in outdoor air, or is the building ventilated only by infiltration and natural ventilation? Does the ventilation system provide space conditioning (heating and cooling) only with no outdoor air intake? Does the system provide 100% outdoor air with no recirculation? Are there local exhausts in kitchens and toilet rooms? If natural ventilation is used to ventilate the building, is it a designed system (e.g., thermal stacks and designed air inlets), or simply operable windows? If mechanically ventilated, does the building contain a central, ducted system that serves multiple rooms or zones? Or do the systems serve single zones, e.g., using through-the-wall fan coil units. When are these systems intended to operate, i.e., is operation based on time of day, controlled by a thermostat or manual? If the system provides outdoor air intake, is that intake rate varied based on weather conditions, indoor contaminant concentrations (e.g., CO₂ demand control ventilation), time of day, or some other approach? These questions must be answered in order to understand how the building is intended to be ventilated, which ventilation performance parameters are relevant, and how they should be measured.

This chapter is organized into three primary sections. The following section describes performance issues that need to be covered in conducting ventilation assessments, as well as the specific parameters used to characterize each issue. That section is followed by a description of the system design information that needs to be collected as part of ventilation assessments to support interpretation of the results. The third section focuses on the measurement methods used to determine the performance parameters described previously. The chapter concludes with some key points regarding building ventilation assessment. Note that this chapter is not a detailed guide on how to conduct such assessments, including how to make the often-challenging decisions on exactly what to measure in a specific building and how to do so. It might be considered as a heavily annotated menu rather than a how-to cookbook. The author is planning to expand this material into a much longer guidance document (the cookbook) that will contain those operational details. The reader can access a great deal of useful information on building ventilation and its measurement via the AIVC (Air Infiltration and Ventilation Centre) bibliographic

database Airbase, which contains 22,000 references and 16,000 documents, at <https://www.aivc.org/resources/airbase>.

Performance Issues and Parameters

This section describes the performance issues that are relevant to ventilation evaluations and specific parameters under each. As noted above, the parameters that are assessed as part of a building ventilation evaluation and the manner in which they are assessed depend on the purpose of the evaluation and the details of the building and its ventilation systems. Table 1 lists key ventilation performance issues and parameters, with methods for their measurement or assessment covered later in this chapter.

The first performance issue in Table 1 is system status, which is fairly broad and mostly qualitative but extremely important. It includes whether the system is operating and the condition of the system and its components, including cleanliness and moisture damage, whether there are clearly dysfunctional or broken components (e.g., dampers) and filter condition. Another important aspect of system status is maintenance, including the intended system maintenance schedule and records of maintenance activities. Since maintenance is critical for keeping systems performing as intended, this information is key to evaluating ventilation systems. The last

Table 1 Ventilation performance issues and parameters

Performance issue	Relevant parameters
System status	Operation Condition Maintenance Design documentation
Envelope air leakage	Envelope airtightness Building infiltration rate Indoor-outdoor pressure difference
Ventilation system airflow	Outdoor air intake rate Percent outdoor air Supply airflow rate (system and space level) Return airflow rate (system and space level) Exhaust airflow rate (system and space level) Operating status and mode of operation
Outdoor air change rate	Whole building Room or other building zone
Interzone airflow	Airflow rates ^a Interzone partition airtightness Interzone pressure differences
Air distribution	Ventilation efficiency or effectiveness ^a

^aMeasurement methods not described in this chapter

parameter under system status in Table 1 is the existence of system design documentation, the specifics of which are described in more detail in the next section of this chapter. It is unfortunate, but in many buildings, such design documentation is nonexistent or at least not current. For example in the EPA BASE study of 100 randomly selected office spaces in the USA, design values of minimum outdoor air intake rates were not available for roughly half of the buildings studied (Persily and Gorfain 2008).

The second performance issue in Table 1, envelope air leakage, is important because infiltration is the only outdoor air ventilation mechanism in many buildings, particularly residential buildings and some older commercial and institutional buildings. In fact, infiltration is generally a significant portion of the total outdoor air change rate in all buildings, even buildings with relatively tight envelopes (Ng et al. 2015). Infiltration impacts heating and cooling energy use and provides a path for outdoor contaminants to enter a building. As noted earlier, infiltration is not a good way to ventilate a building since the rates and air distribution are not controlled, the incoming air is not filtered, and infiltrating air can lead to indoor moisture problems and material degradation. Envelope airtightness, measured with a fan pressurization test, is a key parameter for understanding the potential for infiltration. It is usually expressed as a volumetric airflow rate or effective leakage area at a reference indoor-outdoor pressure differential and is typically normalized by the building volume or the envelope surface or floor area. Airtightness measurements can be completed relatively quickly (compared with infiltration rate measurements) and provide a single parameter that is useful for comparing buildings and for predicting airflows using computer models and other calculation tools (Dols and Polidoro 2020; ASHRAE 2021; Breen et al. 2014). There is a significant body of work on field studies of building airtightness in residential and commercial buildings that can be useful for comparing test results (Chan et al. 2012a, b; Emmerich and Persily 2014). However, envelope airtightness measurements are conducted under imposed indoor-outdoor pressure differences to override pressures due to weather effects. Infiltration rates, on the other hand, are the rate of outdoor air entry through leaks in the envelope due to normal weather effects and the operation of local exhaust fans and vented building equipment (e.g., combustion appliances), and therefore provide a measure of the airflows that are actually occurring in the building. Infiltration rates are therefore more relevant to real-time performance, but the values still vary with weather and equipment operation and only indicate the rates for the conditions during the measurement.

Infiltration rates are typically expressed in air changes per hour or h^{-1} , which is the volumetric airflow rate of the infiltrating air divided by the building volume. These units are commonly used for air change rates, whether they are outdoor, supply or some other airflow. Some people use ACH, ACPH, or other nonstandard units, or refer to these airflows as air exchange rates. The author of this chapter objects to using invented units like ACH, noting that the pure SI unit for air change rate is actually s^{-1} . The term “air exchange rate” is also flawed because it implies that air is simply exchanged between the outdoors and indoors when, in fact, airflow into and out of buildings often takes very indirect and circuitous routes involving

intermediary spaces such as crawl spaces, attics, wall cavities, and plenums. Air change rate is preferred as simply a unit, with the type of airflow described using modifiers such as outdoor air intake, supply air, or infiltration.

In discussing air change rates, including infiltration, it is important to note that if a space has an outdoor air ventilation rate of one air change per hour, it does not mean all of the air is replaced in 1 h. One air change per hour means that a volume of air equal to the space volume enters every hour, but that entering air mixes with the air already in the space such that the air leaving is a mixture of air that entered recently and air that has been in the space for a longer time. If there is a uniform contaminant concentration in the space, the concentration decays exponentially with a time constant equal to the inverse of the air change rate. Therefore, after one time constant (1 h for one air change per hour), the contaminant concentration is reduced to 63% of its initial value.

Measured indoor-outdoor air pressure differences across the building envelope can also be a useful indicator of envelope leakage, as their sign and magnitude provide information on where air may leak into and out of a building over its exterior surface. These pressures are not readily convertible to actual infiltration rates, but they can be helpful for understanding the direction of infiltration airflows, particularly at key locations such as entrances and areas where there are strong outdoor sources, e.g., loading docks. Indoor-outdoor pressure differences vary with location and time, and therefore they should be measured under a range of conditions to better understand the airflow dynamics. In some cases, pressurization testing or infiltration rate measurements may not be feasible, and indoor-outdoor air pressure measurements can be quick and useful even though they provide less information.

The next performance issue listed in Table 1 is ventilation system airflow, along with the parameters that can be used to characterize these airflows. Note that many of these are displayed in Fig. 1. These parameters include: outdoor air intake rate – how much outdoor air is brought in by the system; supply air flow rate – how much air the system delivers to the occupied portion of building or to a specific room or zone; percent outdoor air intake of the system – the ratio of the outdoor air intake to the supply airflow rate; return airflow rate – how much air the system removes from the occupied portion of building or from a specific room or zone; and exhaust airflow rate – the amount of air exhausted by a central system or local exhaust. Not all of these parameters apply to all ventilation systems, e.g., some systems do not have any return airflow but rather supply only outdoor air to occupied spaces, and some systems do not have any outdoor air intake. The latter is the case for most space conditioning systems in US homes, although that is changing in newer housing. The last listed parameter for ventilation system airflow (operating status and mode of operation) is actually a number of different parameters using the overarching term operating status (e.g., is the system on or off?) and what mode of operation is currently in effect. For instance, many systems in commercial buildings have several modes of operation including minimum outdoor air intake and economizer operation.

The outdoor air change rate performance issue in Table 1 refers to the sum of the airflow rate due to infiltration and the outdoor air intake, i.e., the total rate at which

outdoor air enters a building. This is the outdoor airflow rate relevant to heating and cooling loads as well as contaminant mass balance analysis. When considering contaminants with nonzero outdoor concentrations, the total outdoor air change will generally need to be considered separately for the outdoor air intake by the system and for the infiltration through the envelope. Outdoor contaminants entering via the system intake may need to account for removal due to filtration and air cleaning, and contaminant entry via infiltration may need to account for penetration losses. Infiltration is sometimes assumed to be negligible, relative to outdoor air intake rates, but in the absence of measurements or sound calculations, this assumption cannot be supported and may lead to the neglect of important air and contaminant entry into a building. Building outdoor air change rates include all of the outdoor airflows at all infiltration entry points on the envelope and the system intakes for all systems. If there are many systems, it can be challenging to measure at all of the intakes, but conceptually, whole building outdoor air change rates are clearly defined. Outdoor air change rates can be expressed as volumetric airflow rates or air changes per hour, which is the volumetric rate divided by the interior volume of the building being considered. In many cases, it can be challenging to define the interior volume given that many buildings are divided into conditioned spaces, unconditioned spaces (e.g., attached garages), and semi-conditioned spaces (e.g., attics and basements), which often have significant airflows to and from the occupied and conditioned spaces. The interactions of these volumes can also complicate tracer gas measurements of air change rates as discussed below.

In many cases, researchers and practitioners are interested in outdoor air change rates for individual rooms. However, rooms in buildings exist as part of multizone building airflow systems, with airflows between rooms, and therefore room outdoor air change rates are not straightforward to define and less so to measure. The outdoor air change rate for a room would include outdoor air infiltration directly into the room and outdoor air delivered to the room by a ventilation system. The influence of airflow from other rooms on contaminant concentrations are more complex, and their measurement involves multizone tracer gas techniques. These techniques are mentioned in the section “[Measurement Methods](#)” but are not described in detail. In some studies, CO₂ concentrations in individual rooms, often bedrooms, are used to estimate outdoor ventilation rates to the rooms. However, as discussed in the section “[Measurement Methods](#),” these techniques generally neglect interzone transport of CO₂ from other rooms, resulting in uncertainties that are difficult to characterize. Note that CO₂ concentrations are not listed as a metric of ventilation in Table 1, despite their common use. As explained below and in more detail elsewhere (ASTM 2018b), CO₂ concentrations are not direct measures of ventilation. Under some circumstances they can be used to estimate per person ventilation rates using well-established tracer gas methods, but this application requires the validity and verification of several key assumptions.

The next performance issue in Table 1, interzone airflow, is important for contaminant mass balance analyses, particularly when building zones are at different concentrations, and for achieving an overall understanding of the airflow dynamics in a building. They are difficult to measure as they require the use of multizone tracer

gas techniques, which are not typically employed except in research studies. In lieu of measuring interzone airflows directly, one can measure the airtightness of the partitions and the pressure differences between zones. Airtightness of interzone partitions can be assessed using fan pressurization methods and have been conducted to quantify the air leakage between attached garages and the living spaces of residences (Offermann 2009; Nirvan et al. 2012) and between rooms in low-energy homes (Guyot et al. 2016; Ng et al. 2018). Interzone pressure differences can be helpful in understanding the direction of these airflows. As in the case of indoor-outdoor pressure differences, interzone pressure differences are not easily converted to actual airflow rates, but they can be helpful for understanding the potential for contaminant transport from zones containing sources of interest to other zones. Interzone pressures vary with location and time, and therefore need to be repeated under a range of conditions to understand airflow dynamics.

The last performance issue listed in Table 1 is air distribution, which refers to the manner and uniformity with which ventilation air is delivered to a space. Some air distribution systems, for example in many US office buildings, are designed to mix the supply air with air in the occupied space and are often referred to as mixing systems. Other air distribution systems are designed to ventilate a space in a manner resembling plug flow, e.g., operating rooms, in which air enters and “sweeps” through the space in an approximately one-dimensional airflow pattern. Air distribution can be quantified using various measures of ventilation effectiveness, such as age of air, which are described briefly in the section “[Measurement Methods](#).”

Building and System Design Information

As noted earlier, a key factor in determining how to assess building ventilation is the design of the building and its ventilation system(s), including how the building is configured, how ventilation is intended to occur, system design airflows, and the assumptions on which the design is based. Gathering system design information is an essential part of assessing ventilation in a building, as such information is critically important as a basis for comparing the results of ventilation measurements. Field studies have shown that building ventilation performance is too often inconsistent with design intent (Persily 2016; Persily and Gorfain 2008), and such discrepancies can increase energy use and degrade IAQ. Examples of performance not matching design intent are noted later in this chapter, but the important message is that one should never assume a building is performing as intended. Measured data are essential to determining what is actually occurring regarding ventilation and airflow. It is interesting to note that many building and IAQ surveys contain entries for an HVAC description that are only a line or two. Ventilation systems are more complex than can be captured in a small amount of space and require some detail in order to document important design information. Several previous survey studies of multiple buildings have collected system design information. The EPA BASE study is of particular note, as it had detailed protocols and checklists for collecting information on the building, the portion of the building being studied, and the

system serving that space (EPA 2003). A modified version of the BASE protocol was employed in a study of 37 small and medium commercial buildings in California (Bennett et al. 2011). A number of other studies of large numbers of buildings have collected building and system information (Derbez et al. 2018; Ramalho et al. 2013; Offermann 2009; Pigg et al. 2014; Weisel et al. 2005). However, standardized protocols for collecting building and system design information have not been developed, but they could be quite useful in future studies.

Table 2 contains information needed to describe a ventilation system. The items in bold font might be considered the most critical, but all of them are important. The first entry to Table 2 relates to the system status, which in the context of design involves determining whether the design documentation exists and is up-to-date. Building use and applicable standards and regulations change over time, and the design should be updated to reflect these changes, but that does not always happen. System maintenance schedules are also an important aspect of system design given the importance of maintenance in keeping systems performing as intended.

The next aspect of system design that needs to be captured is the approach used to ventilate the building of interest. Is the building ventilated by unintentional infiltration only? Or is there a designed mechanical or natural ventilation system? Designed natural ventilation systems are those that include elements that are arranged and sized based on engineering principles, e.g., thermal stacks and inlet vents, which are described elsewhere (CIBSE 2005; Dols et al. 2012). The term hybrid or mixed-mode ventilation is used when a building uses both mechanical and natural ventilation. Local exhaust systems are typically located in buildings zones, such as kitchens and bathrooms, with high contaminant generation rates (including moisture) in order to remove those substances before they have a chance to mix with the rest of the building air. Mechanically and naturally ventilated buildings may also have local exhausts, although they often have central exhaust systems with a single fan connected to a duct system that removes air from multiple spaces, such as toilet rooms throughout a building. Whether a building has operable windows, which would fall under natural ventilation but are typically not a designed natural ventilation system, is also part of a building's ventilation approach.

The next section of Table 2 lists information that describes mechanical ventilation systems, the first being the type of system: supply or exhaust only, 100% outdoor air, or having the ability to recirculate return air. There are many terms used to describe ventilation systems in terms of how they perform heating and cooling and how they distribute air to spaces, such as variable-air-volume, dual-duct and others, but those details are not covered here. Rigorous system taxonomies do not yet exist to capture this information, although EPA (2003) contains a comprehensive approach to HVAC system description that merits updating. For each air handling unit (AHU) in the mechanical ventilation system, the design will typically include fan specifications with the design supply airflow rate, the minimum outdoor air intake rate, and in some cases a maximum outdoor air intake rate that would apply when the system is operating under economizer mode. (Economizer operation refers to increased outdoor air intake to cool a building rather than using mechanical cooling equipment, i.e., chillers, as an energy efficiency option.) However, economizer operation is only

Table 2 Ventilation system design information (with most essential information in bold font)

System category	Design information
System status	Design documentation Maintenance schedule
Ventilation approach	Infiltration only
	Mechanical ventilation
	Natural ventilation
	Hybrid ventilation
	Local or central exhaust
	Operable windows
Mechanical ventilation	Type: supply or exhaust only, 100% outdoor air, recirculation
	Supply airflow rate
	Minimum and maximum outdoor air intake rate
	Basis for minimum outdoor air intake rate (which standard or building regulation; calculations and assumptions employed)
	Particular filter locations and efficiencies
	Exhaust airflow rate: system and space level
	Space-level air distribution, e.g., use of mixing boxes and description of their controls.
	Sequence of operations
	System maintenance schedules by component
Natural ventilation	Operable windows (location, size of openable area)
	Purpose-provided vents (location, size)
	Engineered system, description of major elements and intended airflow patterns , primarily where air is intended to enter and leave the building and the occupied spaces, <i>and assumed operating conditions</i>
	Controls: occupant-based, automated (describe)
	Estimated ventilation rates and method of estimation
Hybrid or mixed-mode ventilation	Design concept: when would mechanical system operate (e.g., based on season, time of day, weather)
	Above information for both mechanical and natural

feasible if the outdoor air is cool and dry enough and if elevated outdoor pollutants can be effectively removed by filtration or air cleaning. Outdoor air ventilation rates are specified during building design to comply with building regulations and standards that contain requirements for minimum ventilation rates, typically on a per occupant and per-unit floor area basis. For example, ASHRAE Standard 62.1 contains such requirements for commercial and institutional buildings, while ASHRAE Standard 62.2 contains requirements for residential buildings (ASHRAE 2019a, b). Ventilation standards exist around the world, based on the priorities and expectations of the country or region in which they are developed (CEN 2007; Limb 2001). Fan specifications or other design documentation should include the basis for the minimum outdoor air intake rates including the standard or building regulation used to determine these rates, key assumptions (e.g., floor areas and design

occupancies of the spaces, occupancy category), and a record of the calculations of the minimum intake rate. However, the existence of these details is more common in commercial buildings than in residential. ASHRAE Standard 62.1 actually requires that this information be provided in writing; the standard also contains an informative appendix (not an official part of the standard) with sample tables for preparing design documentation (ASHRAE 2019a).

Other information needed to describe mechanical ventilation systems listed in Table 2 include the location of particulate filters and their removal efficiencies, e.g., MERV ratings. Exhaust airflow rates for central exhaust systems and exhaust vents in spaces feeding these central systems, and airflow rates for local exhaust systems are also listed. Information on space level air distribution is next, which can be quite detailed but at a minimum the existence of mixing and VAV boxes should be noted, along with a description of how they are controlled. The latter information is often contained in the so-called sequence of operations for a system, which explains how the system is intended to operate, how it will respond to outdoor weather and internal thermal loads, and other aspects of system control (The ASHRAE Terminology Glossary (www.ashrae.org/ashraeterms) definition of sequence of operations includes the following: an organized narration specifying how the integrated functions of a device, system, or facility will perform. It should incorporate energy efficiency and environmental concerns with detailed, comprehensive control strategies, i.e., how each individual piece of equipment will be controlled and what information and adjustment will be available to the user. These may be provided in a combination of narratives, diagrams, and point lists for every unique type of equipment and for each system.). The sequence of operation is critical to understanding how a system is intended to operate and then to determining whether it is operating as intended. The final entry under mechanical ventilation is system maintenance, which includes schedules for visual inspection of different components, filter changing, and sensor calibration. ASHRAE Standard 62.1 contains a table of minimum ventilation system equipment maintenance activities that is useful in identifying items to record under this category.

Describing natural ventilation systems involves identifying the locations and sizes of operable windows and any purpose-provided inlet and outlet vents. If the system is engineered, rather than just providing these openings and assuming the resulting ventilation is adequate and well-distributed, the system description should include information on the major elements of the system, (e.g., inlet vents, thermal stacks) and the intended airflow patterns (e.g., where air is intended to enter and leave the building, and how it is expected to move through the building). The latter should be provided under different weather conditions, such as cold and windy, warm and mild, or other prevalent weather patterns for the climate. The manner in which the components of the natural ventilation system are controlled is also key to its design. Specifically, are the vents controlled based on occupant preferences and actions? If the system is automated based on weather conditions, indoor air temperatures, indoor contaminant concentrations, or other parameters, the manner in which these controls are intended to operate needs to be described. Finally, if the design has an estimate of the expected ventilation rates in the building or in individual spaces,

these rates, including the assumed weather conditions on which the estimate is based and the method used for their estimation, should be noted.

For hybrid or mixed-mode ventilation systems, in addition to the previously described information for mechanical and natural ventilation systems, the system description should include the design concept: When would the mechanical system operate? Is that based on season, time of day, weather conditions, or some other approach? Is there an interlock that prevents the mechanical ventilation system from operating when windows or vents are opened?

While the information in Table 2 may appear to be very detailed, understanding the ventilation system design is key to building ventilation assessment. Measured ventilation rates or other performance parameters are extremely difficult to interpret without such design information.

Measurement Methods

Building ventilation performance assessment methods have been available for decades and have been reviewed previously. The AIVC bibliographic database Airbase, mentioned earlier, is a helpful resource for identifying previous reviews and other relevant material. McWilliams (2002) provides a thorough bibliography of publications covering multiple measurement techniques. Nazaroff (2021) discusses several means of characterizing residential air change rates in a review of available measurement results. There is not space in this chapter for a detailed description of available assessment methods; instead, this section reviews methods of assessing the performance parameters listed in Table 1, providing references (particularly standard methods of test where available) and highlighting some key issues in their application. This section also discusses other important issues including variations in ventilation rates and deviations from design intent. As noted earlier, buildings and systems are extremely variable, and the specific features of each must be considered when planning and conducting ventilation measurements. Also, the interpretation of measurement results requires that they be compared with a baseline value, which would typically be based on the design information discussed in the previous section and results from similar buildings, as well as relevant standards and regulations.

System Status

There is no standard approach to assessing system status, although the BASE protocols mentioned earlier thoroughly cover system condition, operation, and maintenance (EPA 2003). These protocols contain detailed checklists for documenting system condition and maintenance schedules. The inspection checklist (C-12) covers the operation and condition of many system components including fans, filters, drain pans, controls, and terminal units. The information covered under operation includes simple matters such as whether the fan is on or off and if air is moving in the intended direction through the outdoor air intake. The system condition questions cover the presence of dirt and moisture, and the state of dampers, linkages, and sensors.

Assessing system operation and condition is primarily conducted by visual inspection of the system and its components using these checklists or other resources, as well as accessing information available from building automation system (BAS) interfaces. However, as useful as BAS information can be, visual inspection is essential to confirm BAS indications of system operation and to assess the condition of the system and its components, as BAS systems do not necessarily monitor cleanliness, moisture damage, dysfunctional or broken components, and filter condition. The BASE protocol maintenance checklist (C-11) is useful for recording information on system maintenance procedures and schedules. The maintenance information covered by this checklist includes the frequency of air handler inspections, filter replacement, control system inspection and sensor calibration, ventilation system testing and balancing, and the inspection, cleaning, and treatment of a range of specific system components. Whether one uses these detailed checklists or some other approach, system condition and maintenance are extremely important to understanding ventilation in a building. Information on maintenance practices can be obtained through discussions with building managers and operators as well as examining manuals on system operation that should be provided with the design documentation. Note that in larger buildings, the operations staff can vary in their familiarity with these procedures, and it is important to identify knowledgeable staff members.

A key aspect of assessing system status is locating the design documentation, determining if it is up-to-date, and identifying any key gaps or updates required to reflect current building use and compliance with current standards and regulations. Similarly, maintenance schedules and logs need to be identified, either hard copies or electronic. These records should be evaluated as to whether they are current and for thoroughness in covering all the building systems and components. As noted earlier, in some buildings, design and maintenance records can be hard to find and may not exist at all, although this should be less common as building and system information is increasingly in digital form. The EPA BASE protocol contains checklists (C-1 through C-10) for documenting HVAC system design information including air handlers, perimeter units, unitary systems, and exhaust fans. Among these system design descriptions, minimum outdoor air intake rates are one of the most important for assessing ventilation system performance. Along with this value, the design should also describe how this minimum rate was determined, which standard or building regulation was used, the activities assumed to be taking place in the spaces served by the system, the design occupancy, and the floor area served. These assumptions are key to determining if the design outdoor air rate is still applicable to the space as it is currently being used and if a more recent ventilation standard or regulation is relevant. The previous section of this section, “[Building and System Design Information](#),” discussed system design information in more detail, with reference to Table 2.

Envelope Air Leakage

As discussed earlier, infiltration is the only ventilation mechanism in many buildings, and even in tight buildings, infiltration rates are comparable to mechanical ventilation rates. Characterization of air leakage involves three parameters: envelope

airtightness, building infiltration rates, and indoor-outdoor pressure differences. Envelope airtightness is measured with a fan pressurization test, which involves using a fan (either brought to the building or the existing air handling equipment) to temporarily impose a uniform indoor-outdoor pressure difference across the envelope and then measuring the airflow required to induce this pressure difference. Often a series of pressure differences are induced to generate an airflow versus pressure curve, which can reduce the uncertainty in the reported test result. Fan pressurization testing has been employed for about 50 years, and several standards exist that describe the equipment and instrumentation, test protocols, data reduction, and reporting. There are three ASTM fan pressurization standards, with E779 (ASTM 2019) being the most general. E1827 (ASTM 2017) describes the use of an orifice blower door to conduct the test, and E3158 (ASTM 2018a) is specific to larger buildings. ISO 9972 (ISO 2015) is also a fairly general test method, while CGSB 149.15 (CGSB 1995) discusses the use a building's air handling equipment to conduct the test. Using existing air handlers has advantages over bringing a fan to the building, assuming one is able to accurately measure the airflow supplied by the system using the ventilation system airflow methods described below. Envelope airtightness is typically expressed as a volumetric airflow rate, e.g., m^3/s , at a reference indoor-outdoor pressure differential that is typically normalized by the building volume or the envelope surface area, or as an effective leakage area, which may be normalized by the building envelope or floor area (ASHRAE 2021).

In conducting whole building fan pressurization tests, it is important that all points on the exterior envelope of the building are subject to the same indoor-outdoor pressure difference. This condition can be facilitated by opening all interior doors and running tests when outdoor temperatures are mild and wind speeds are calm. The impact of indoor-outdoor air temperature differences becomes more critical as buildings get taller, since stack- or buoyancy-induced pressures increase with building height. The referenced test methods have criteria for weather conditions and pressure difference uniformity and describe the management of interior doors and other partitions to support achieving uniform pressure difference. Another important issue in fan pressurization testing is the need to clearly define the pressure boundary of the building that is being tested. In buildings with attics, basements, and other unconditioned or partially conditioned spaces, the definition of the pressure boundary can be complex. Some of these spaces are not well-connected with either the outdoors or the building interior, leading to significant pressure differences to the outdoors or interior, interfering with the goal of a uniform indoor-outdoor pressure difference. These standards describe how to deal with such spaces, but tests in these buildings can be more complex than in simpler single zone buildings. Multizone buildings, in which the interior spaces are not well-connected in terms of airflow, may require more than one fan pressurization device in the different zones to meet the pressure uniformity test requirement. Another important issue in conducting fan pressurization tests is the position of vents and dampers in the exterior envelope, which is covered by the standards referenced above. If all such vents and dampers are closed and sealed, the test results provide a measure of the envelope construction quality in terms of airtightness. If those vents and dampers are open, the results are a

more useful measure of the airtightness in determining infiltration rates under normal conditions of weather and building operation.

Infiltration rates, in units of air changes per hour or h^{-1} , quantify the amount of outdoor air that enters a building through unintentional openings in the building envelope. In buildings that are ventilated only by infiltration (no mechanical ventilation or open windows or doors), the tracer gas methods for measuring outdoor air change rate described below can be used to measure these rates. Given the strong dependence of infiltration rates on indoor-outdoor temperature difference, wind speed and direction, and the operation of building equipment (e.g., vented combustion appliances), multiple measurements under a range of these variables are required to characterize infiltration in a building. (Examples of such detailed measurements are shown below.) At a minimum, a reported infiltration rate must be accompanied by information on weather conditions and building equipment operation to be meaningful. In large buildings, particularly those with large horizontal footprints or otherwise divided into sections of different ages and envelope construction, different portions of the building may have different envelope leakage values and different indoor-outdoor pressure differences due to variations in wind exposure and other factors. These differences can result in different infiltration rates in these various sections of the building, which can be difficult to measure with standard tracer gas techniques but which can have significant effects on energy use, thermal conditions, and indoor contaminant levels.

In buildings with outdoor air mechanical ventilation, infiltration rates can be estimated by subtraction; one measures the whole building outdoor air change rate using a tracer gas dilution method and subtracts the system outdoor air intake rate measured using the system airflow rate measurement techniques described below. This approach is not common, but was applied in a commercial building by Persily and Norford (1987), who studied the variation in infiltration and intake rates as a function of weather and ventilation system control mode. However, ventilation system operation can induce indoor-outdoor pressure differences that will impact the infiltration rate. Even if the ventilation system is balanced, i.e., the system outdoor air intake and exhaust rates are equal, operating the system can induce local pressure effects that will impact infiltration rates. Infiltration rates in mechanically ventilated buildings can also be measured by conducting a tracer gas test with the system off, as was done in a very, tight residential building by Ng et al. (2015). However, conducting tracer gas tests with the system off can interfere with achieving uniform tracer concentrations, which are required for accurate measurements as discussed below.

As noted earlier, measuring indoor-outdoor air pressure differences across the building envelope can be useful in understanding envelope leakage. There are no standards that describe how to make these measurements and interpret the results, although there have been some useful articles in building industry trade publications. Standards exist that describe air pressure measurements and instrumentation in detail (ASHRAE 2014, 1988). Indoor-outdoor pressure differences can be measured at key locations over the building envelope, either one-time or periodically with a handheld device or automatically over an extended period of time to capture inevitable

variations in these pressure differences. Since these pressures will vary with location and time, they should be measured under a range of weather and system operation conditions to understand the airflow dynamics of the building being studied. Consistent pressure difference values over the entire building envelope or locally can be an indication that a specific building or system operating mode is inducing higher infiltration rates than others, or that there is an airflow imbalance between the supply and exhaust airflows for a space. The latter conclusion should be confirmed by measuring those system flows and comparing them to their design values.

Ventilation System Airflow

Depending on the type and configuration of a ventilation system, it will be associated with several different airflows as described in Table 1 and shown in Fig. 1: outdoor air intake, supply, return, and exhaust. For systems serving multiple spaces, the latter three are relevant at both the system level and in individual rooms or ventilated spaces. As noted earlier, not all of these parameters apply to all ventilation systems, e.g., some have no return airflow and some have no outdoor air intake. The rate at which outdoor air is brought into the ventilation system can also be characterized by the percent outdoor air or outdoor air fraction, which is the outdoor air intake rate divided by the supply airflow rate. Percent outdoor air values vary from 0% (no intake) to 100% (no return air being recirculated). Exhaust airflow rates, both at the system and space level, are relevant to systems whose sole function is to draw air from single or multiple spaces, e.g., toilet rooms, and exhaust that air to the outdoors. As noted earlier, system airflow rates depend on the system operating status and mode of operation, which need to be considered in planning these measurements and included with reported measurement results.

System airflow rates can be measured in ducts or at outdoor air intakes using standard air speed traverse methods employing pitot tubes or hot-wire anemometers (ASHRAE 2008; NEBB 2005; SMACNA 2002). Traverse measurements involve multiple air speed measurements across a cross section of a duct, with the number of measurement points depending on the duct size. The average air speed is then multiplied by the cross-sectional area of the duct to yield the volumetric airflow rate in units of L/s or cfm. Accurate traverse measurements require uniform velocity profiles in the ducts, and the referenced standards and guides contain criteria for evaluating whether the profile is acceptable. These documents typically claim a measurement accuracy of $\pm 10\%$ under good conditions, but the basis of these accuracy estimates is not provided. In order to meet the requirements for a uniform velocity profile, there needs to be a sufficient number of lengths of ductwork downstream of transitions (as a multiple of duct diameter) upstream of the measurement plane. However, in many system configurations, such lengths do not exist, making these measurements less accurate. This is especially true at outdoor air intakes, where there may be very few duct diameters before the outdoor airstream mixes with the return air (Fisk et al. 2002). Some ventilation systems have permanently installed airflow monitoring stations, which include an array of thermal

anemometers or other sensors to provide a continuous airflow rate measurement, which is often accessible via the BAS. While these systems can be fairly accurate under ideal conditions, they should be calibrated as installed as every system installation is unique and may affect the measurements. Technologies exist to measure outdoor air intake rates by incorporating air speed or pressure sensors into outdoor air intake louvers. Studies into the performance of such devices show promise, with potential measurement errors from 10% to 30%, but each louver and sensor configuration needs to be tested to verify its accuracy, which tends to degrade at lower airflow rates (Fisk et al. 2004, 2008).

Outdoor air intake rates can be determined by separately measuring the supply airflow rate (using a duct traverse) and multiplying it by the percent outdoor air intake rate. Percent outdoor air can be estimated based on measurements of the air temperature in the return, supply, and outdoor airstreams of the air handler (ASHRAE 2008). Accurate measurements using this approach requires that the three air temperatures are sufficiently different relative to the air temperature measurement uncertainty and that there is no heating or cooling of the air between these temperature measurement locations. Alternately, one can estimate the percent outdoor air based on the CO₂ concentration in these three airstreams, which is discussed in ASTM Standard D6245 (ASTM 2018b). This method also requires that the three CO₂ concentrations are sufficiently different relative to the concentration measurement uncertainty, with the referenced standard describing how to estimate the associated measurement error.

Airflow rates in ducts can also be measured with tracer gas methods as described in ASTM E2029 (ASTM 2011a). This method involves injecting tracer gas into a duct at a constant rate and measuring the concentration upstream and downstream of the injection point. The airflow rate is equal to the tracer gas injection rate divided by the increase in tracer gas concentration from upstream of the injection to the downstream location. As described in the referenced standard, care must be exercised in injecting the tracer gas to facilitate good mixing with the duct airstream, and the downstream concentration measurements must provide a good estimate of the average downstream concentration.

Supply airflow rates into, and return and exhaust airflow rates out of, individual ventilated spaces can be measured using flow hoods. These devices use a conical or other shaped hood to collect all of the air from a supply vent and guide it over an airflow measuring device that employs vane anemometers or pressure difference based gauges (ASHRAE 2008; SMACNA 2002; NEBB 2005). Flow hoods can also be used in reverse at return and exhaust vents. The referenced standard and manufacturers' literature provide limits on air speeds, calibration requirements, cautions on directional effects related to supply air discharge patterns, and potential impacts of pressure drops associated with the flow measurement device itself.

Ventilation system operating status and mode of operation needs to be checked and recorded whenever measuring system airflow rates. This involves more than just whether the system is on or off but also the outdoor air intake mode, e.g., morning warm up during the heating season when outdoor air fractions will be reduced or even zero, or economizer operation when outdoor air intake is maximized for

cooling the building without using mechanical cooling equipment. Modern ventilation systems in commercial building typically have multiple modes of operation, and describing their operating status requires an understanding of the system design and sequence of operation as described earlier.

Ventilation system airflow measurements must be planned based on the building layout, the number of systems and an understanding of which portions of the building are served by each. Part of this planning relates to logistics, scheduling, and instrumentation deployment, as these systems can be located at significant distances from each other in different mechanical rooms throughout a large building. If system airflow rate measurements are going to be related to airflow measurements at supply, return, or exhaust vents in the occupied space, the spaces served by the system must be identified prior to making the measurements through the examination of the building mechanical drawings and floor plans. Situations in which this can be useful include comparisons of the supply airflow rate at the system to the sum of all the supply airflow rates at the individual vents, which can help to verify the supply airflow rate value and perhaps also to provide an indication of duct leakage between the air handler and the vents. Another example is multiplying the percent outdoor air fraction at the air handler by local supply airflow rate measurements to estimate the outdoor air delivery to the ventilated space.

When evaluating buildings with multiple air handling systems, ventilation measurements in the different systems need to be coordinated to ensure that they are conducted under sufficiently similar weather, occupancy, and operation conditions such that the results can be combined in a meaningful way to yield total supply and outdoor air intake rates for the building. For example, measuring outdoor air intake in some systems during the cool part of a morning when outdoor air intake fractions are high, and other systems during warmer periods in the afternoon when outdoor air intake are more likely to be at minimum values, will not allow a meaningful determination of the total outdoor air intake of the building.

Outdoor Air Change Rate

Outdoor air change rates, envelope infiltration plus outdoor air intake, impact the amount of energy required for heating and cooling a building and indoor contaminant concentrations. Infiltration is often assumed to be negligible, but in the absence of measurements or physics-based analysis, this assumption cannot be supported. Also, as noted earlier, infiltration is the only means of outdoor air ventilation in many buildings.

Total outdoor air change rates can be measured using tracer gas dilution methods as described in ASTM Standard E741 and ISO 12569 (ASTM 2011b; ISO 2017). In fact, tracer gas methods are the only way to measure building outdoor air change rates except in the unusual case in which a building is so extremely tight that all of the airflows into and out of the building are known to take place via the ventilation system ductwork. In these cases, the system airflows can be measured using duct airflow measurement techniques described above. Both referenced tracer gas standards are single-zone techniques, which means the tracer gas concentration

throughout the building being tested can be characterized by a single value. Some discussions refer to this as perfect mixing, but the key issue is actually tracer gas concentration uniformity. The referenced ASTM standard requires that concentrations in the test space differ by less than 10% of the average concentration to achieve a test precision and bias of 10%. There are three tracer gas dilution methods: decay, constant concentration, and constant injection. In the decay method, a quantity of tracer gas is released directly into the test space or supplied via the ventilation system and allowed to mix with the interior air until the concentration is sufficiently uniform. Sometimes portable mixing fans are installed in the space to enhance mixing, but these should not be relied on to mix the air and tracer between rooms in a building. Air handling systems can be used to enhance distribution and mixing of the tracer gas between rooms. However, if these systems are left on during the actual decay, they can create indoor-outdoor pressure differences across the building envelope that impact the infiltration rates. Once the tracer gas concentration is sufficiently uniform, the concentration decay over time is monitored and used to estimate the air change rate, with ASTM E741 providing detail on sampling, analysis, and reporting. Some tracer gas decay studies have been conducted by monitoring the decay rate in a single room, such as a bedroom, and referring to that as the air change rate of that room. However, this approach ignores air and tracer transport from adjoining spaces, and unless there is explicitly accounting for interzone transport in the tracer gas mass balance analysis, single-room decay rates in multizone buildings should not be referred to as outdoor air change rates. They can be informative but should only be referred to as room decay rates as they generally do not provide accurate outdoor air change rates for a test space or the whole building.

Another tracer gas dilution approach, also described in ASTM E741, is the constant concentration tracer technique, which involves varying the tracer gas injection rate to maintain a constant indoor tracer gas concentration using automated feedback control. This approach can be advantageous in multizone buildings where zones have different outdoor air change rates, in which a decay test would not be able to maintain a uniform tracer gas concentration throughout the building. However, this approach requires more complex instrumentation than the decay method and is not used often except in research studies (Takaki et al. 2005).

The third single-zone tracer gas dilution method is the constant injection method, which involves injecting tracer gas at a constant rate into the space being tested and monitoring the concentration response. Assuming the outdoor concentration is zero and the injection rate is constant, the single-zone mass balance can be integrated to yield an expression for the outdoor air change rate that requires the average of the inverse of the tracer gas concentration. If the airflow rate is constant, the tracer gas concentration will eventually reach steady state, at which point the outdoor airflow rate equals the tracer gas injection rate divided by the steady-state tracer gas concentration. The constant injection approach can be useful for measuring airflow rates in ducts per ASTM E2029 as discussed earlier, and the steady-state formulation serves as the basis for the use of peak CO₂ concentrations for estimating ventilation rates, which is discussed below.

The constant injection tracer approach is the basis of the so-called perfluorocarbon tracer (PFT) method, in which a PFT is injected using passive devices, typically over measurement periods of days to weeks or longer. Passive samplers are then deployed throughout the building being tested to determine the average tracer gas concentration during the sampling period. This approach has the advantage of being relatively inexpensive since the samplers are analyzed in a laboratory facility after the field test, and it has been used in a number of residential field surveys (Offermann 2009; Yamamoto et al. 2010). This technique employs a transient tracer gas mass balance, since the air change rate cannot be assumed to be constant over typical sampling periods given variations in weather, equipment operation, and occupant activities. The fact that the sampling technique determines the average concentration, not the average of the inverse concentration, introduces bias into the measurement results. Specifically, there is a tendency to overestimate the average air change rate, which has been shown to be as high as 15–35% for seasonal average air change rates (Sherman 1989). In tight buildings with very low infiltration rates and fairly constant mechanical ventilation rates, this bias is less of a concern. In those cases, a short-term tracer gas measurement may suffice.

The peak CO₂ approach has been used for decades, purportedly as an inexpensive and simple means of estimating outdoor air change rates in buildings and sometimes spaces within buildings. However, it has been misapplied in many cases due to a lack of recognition that it is fundamentally a single-zone, constant injection steady-state tracer technique and thus must abide by several key assumptions to yield valid air change rates. These assumptions include: the CO₂ generation rate is known, constant, and uniform throughout the building being tested; the CO₂ concentration is uniform throughout the building and has achieved steady state; the outdoor CO₂ concentration is known and constant; and the outdoor air ventilation rate is constant (ASTM 2018b). Also, because it is a single-zone approach, it can only be used to determine the air change rate of an entire building with a uniform CO₂ concentration. If the CO₂ concentration varies among rooms, the single-zone mass balance is no longer valid and one must employ a multizone mass balance of CO₂ that accounts for the airflows between zones. The assumption that the CO₂ generation rate is known, constant, and uniform throughout the building translates to the occupancy level also being known, constant, and uniform. It also requires that the occupant levels of physical activity are relatively constant as physical activity impacts CO₂ generation rates (Persily and de Jonge 2017). The requirement for the CO₂ concentration to be at steady state translates to conditions being constant for long enough that a steady-state concentration is achieved. As described in ASTM D6245 (ASTM 2018b), the time required to achieve steady state depends on the air change rate of the building. For a given air change rate, the concentration will be within 95% of steady state after three time constants, where the time constant is the inverse of the air change rate. For an air change rate of 1 h⁻¹, it will therefore take 3 h to reach 95% of the steady-state concentration. For an air change rate of 0.5 h⁻¹, it will take 6 h. During this time, the ventilation rate, occupancy, and outdoor CO₂ concentration must all be constant, which will not be the case in some buildings. Using a CO₂ concentration before

steady state has been achieved will overestimate the air change rate, in some cases by significant amounts.

As noted above in the discussion of the tracer gas decay technique, the peak CO₂ approach has also been applied in single rooms, such as bedrooms, with the result being referred to as the air change rate of that room. However, the tracer gas methods on which this approach is based apply only to single zones. Using peak CO₂ in bedrooms ignores interzone air and CO₂ transport from other indoor spaces such as adjoining rooms and hallways. The impacts of such transport on the measurement results are difficult to characterize unless interzone transport is explicitly accounted for in the tracer gas mass balance analysis. Only then can CO₂ concentrations in a bedroom be used to calculate outdoor air change rates. Several studies have converted peak CO₂ concentrations in bedrooms to outdoor air change rates without speaking to the issue of interzone transport and the inaccuracies in this approach. Maximum CO₂ concentrations in bedrooms and other spaces in multizone buildings can be informative, but they are not outdoor air change rates.

It needs to be noted that single-zone, tracer gas dilution methods for measuring outdoor air change rates are challenging in naturally ventilated buildings. Specifically, when there are large openings, e.g., open windows, the large and localized airflows into the building at zero outdoor tracer gas concentrations will interfere with the tracer gas concentration uniformity requirements of these test protocols (Jones and Kirby 2010; Nikolopoulos et al. 2012). Some studies have measured air speeds in ventilation openings, but these approaches have not been well studied nor will they capture infiltration through unintentional leaks.

The tracer gas dilution methods discussed so far are for measuring building outdoor air change rates. In some circumstances, one is also interested in airflow rates between zones, commonly referred to as interzone airflows. Also, as noted earlier, larger buildings with sections that are different in terms of construction, wind exposure, or ventilation system design or operation can have different air change rates. The single-zone tracer decay and constant injection methods are not able to quantify differences between building sections and may be challenging to implement given the lack of tracer gas concentration uniformity that is likely to exist. Measuring airflows in such situations requires multizone tracer techniques that are discussed briefly below.

Interzone Airflow

Interzone airflows are an important aspect of ventilation assessment in many applications, particularly when one needs to perform a contaminant mass balance analysis for building zones at different contaminant concentrations or to understand the overall airflow dynamics in a building. Interzone airflows, as well as differences in airflows to and from outdoors in different sections of a building, become more important as buildings are larger and configured such that different portions of the building vary in their construction and ventilation systems. The constant concentration

method discussed above can be used to determine the outdoor airflow rate into individual zones but not interzone airflow rates. Multizone tracer gas methods exist for estimating interzone airflows, but they are complex and have typically only been used in research studies going back four decades (T'Anson et al. 1982). More recent applications of multizone tracer techniques (Dodson et al. 2007; Du et al. 2012, 2015; Bekö et al. 2016) are discussed by Nazaroff (2021). These references involve studies to estimate airflows to and from basement zones or garages to the living space, or bedrooms to and from the rest of the building. Interzone airflow measurements are scarce in commercial buildings, with one study conducted by the author almost 30 years ago (Persily and Axley 1990). In contrast to the single-zone tracer gas techniques discussed above, multizone tracer gas techniques have not been standardized, are more complex and costly, and are subject to potentially large uncertainties, which are some of the reasons they have not been widely applied.

As alternatives to tracer gas measurements of interzone airflows, the airtightness of partitions between zones and pressure differences between zones can be measured more easily. The former can be measured using fan pressurization methods, while the latter can be measured with differential pressure gauges, but neither approach has been standardized and general guidance on their application is lacking. Measurement of the airtightness of interzone partitions can be useful for understanding the potential for interzone airflows, but without values of the pressure difference across the partitions, they cannot be related to actual airflow rates. However, these interzone airtightness values can be used for airflow modeling.

As noted above in the discussion of indoor-outdoor pressure differences, standards exist that describe air pressure measurements and instrumentation (ASHRAE 1988, 2014). Again, the concept is to measure interzone pressure differences at locations of interest in the building to better understand the direction of these airflows, and more specifically the pressure relationships between zones. The measurement locations should relate to the goals of the building study being carried out, which might include concerns regarding airflows to and from zones with elevated contaminant concentrations (e.g., toilet rooms and attached garages) or stack-driven pressures within a building via stairwells and other vertical stacks. These pressures can be measured one-time with a handheld device or automatically over an extended period of time to capture variations. They should be measured under a range of weather and system operation conditions as they will vary with location and time.

Air Distribution

Air distribution refers to the manner and uniformity with which ventilation air is delivered to a space, specifically the portions of the space where occupants are located. A variety of metrics and definitions have been employed over the years to quantify air distribution including age of air, pollutant removal efficiency, ventilation effectiveness, and ventilation efficiency. The specific terms and definitions are not always used consistently, but published experimental and simulations studies are

generally clear on what is being measured or calculated. Most air distribution measurements involve tracer gas methods, though some are based on air speed, temperature, and contaminant levels (Fisk et al. 2005; Rim and Novoselac 2010; Karimipanah et al. 2007; Zhai 2005; Faulkner et al. 2004; Chao and Wan 2004). The air diffusion performance index (ADPI) is used to characterize the performance of air diffusers in spaces based on air speed and temperature distribution in the context of thermal comfort and depends on the geometry and cooling load of the space, but it does not characterize outdoor air distribution (ASHRAE 2013). An ASHRAE standard for measuring air change effectiveness using a tracer gas to quantify the effectiveness of outdoor air distribution was approved in 1997, and reaffirmed in 2002, but has not been updated since (ASHRAE 1997).

Other Considerations

Variation in Ventilation

As noted earlier, many of the performance parameters listed in Table 1 vary with weather, system operation, and occupant activities. The existence and extent of these variations in ventilation performance have been seen in multiple building studies of infiltration rates, mechanical ventilation system airflows, and total outdoor air change rates (Persily 2016). Given these variations, one needs to understand the building and its system before planning a ventilation measurement effort, and multiple measurements under a range of conditions are needed to characterize ventilation in a building. Even if one is only interested in the outdoor air change during a specific period of time, for example in conjunction with indoor contaminant measurements, it is critical to report weather, system status, and other factors along with the outdoor air change rate measurement. Space does not permit an extensive discussion of the many studies showing these variations, but three examples are highlighted here.

One example is a study involving multiple measurements of outdoor air change rates in a three-bedroom manufactured house used for IAQ research, before and after an airtightening retrofit (Nabinger and Persily 2011). The retrofits included sealing of ducts and floor penetrations over a vented crawlspace and installation of a house wrap under the exterior siding, resulting in an overall reduction of 24% in the envelope airtightness based on whole building pressurization tests. Figures 2 and 3 are plots of the air change rate versus indoor-outdoor temperature difference with the forced-air heating and cooling fan off and on, respectively. Each plot distinguishes between the measurements before and after the airtightening retrofit. Note in Fig. 2 that the air change rate varies over a range of about 5 to 1 based on temperature difference with the fan off; the range of variation with wind speed is similar in magnitude. Also, the dependence on temperature difference has an entirely different form with the fan on in Fig. 3, and this dependence changes dramatically after the retrofit. These data highlight the importance of accounting for weather, system operation, and building status when measuring and reporting air change rates.

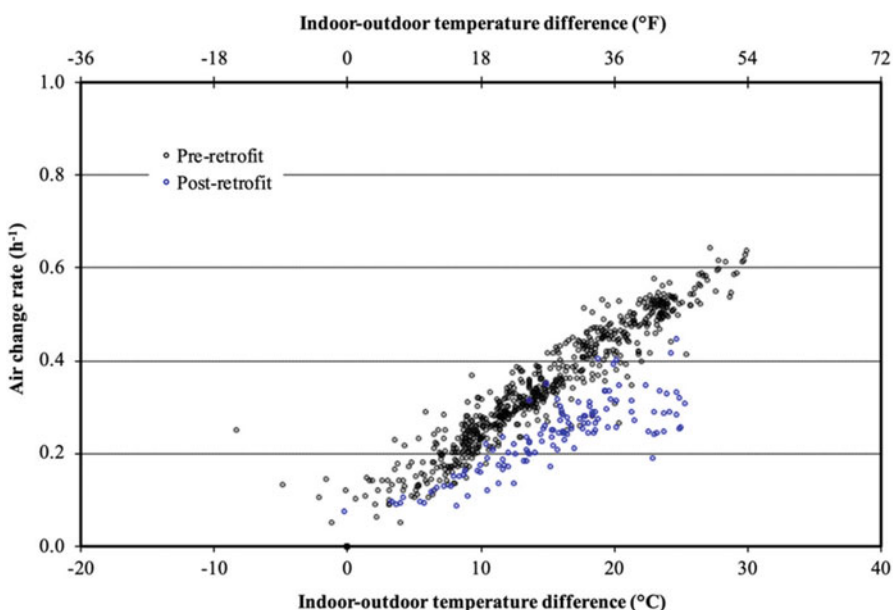


Fig. 2 Air change rates versus indoor–outdoor temperature in manufactured house, forced-air system off

An earlier, year-long study of air change rates in an occupied townhouse also shows variations with weather and occupant actions, specifically exhaust and attic fan operation and window opening (Wallace et al. 2001). About 4500 hourly average air change rates were measured, with a mean air change rate of 0.65 h^{-1} and a standard deviation of 0.56 h^{-1} . Figure 4 is a frequency distribution of the measured rates, revealing a lognormal distribution, which is typical for air change rates in single buildings and collections of buildings. Once again, we see a roughly 5 to 1 variation in air change rates. Window opening had a strong influence on the air change rates, with operation of an attic fan having a smaller influence. The indoor–outdoor air temperature difference impacted the air change rates, but wind speed had very little effect on this house due in part due to its location in a wooded area.

Another example is a long-term study of 14 mechanically ventilated office buildings in the USA (Persily 1989). These studies involved automated tracer gas decay measurements over multiple seasons of the year to get a fairly complete picture of air change rate variations with weather and system operation in each building. Figure 5 shows whole building air change rates for one of those buildings with the mechanical ventilation system operating over a wide range of outdoor air temperatures (Persily et al. 1992). These data exhibit the economizer cycle common in US commercial buildings, in which the system operates at minimum outdoor air intake during warm weather (about 20°C and higher) when mechanical cooling is required. At cooler temperatures, the outdoor air intake rate is increased dramatically to use outdoor air to cool the building rather than the mechanical cooling equipment

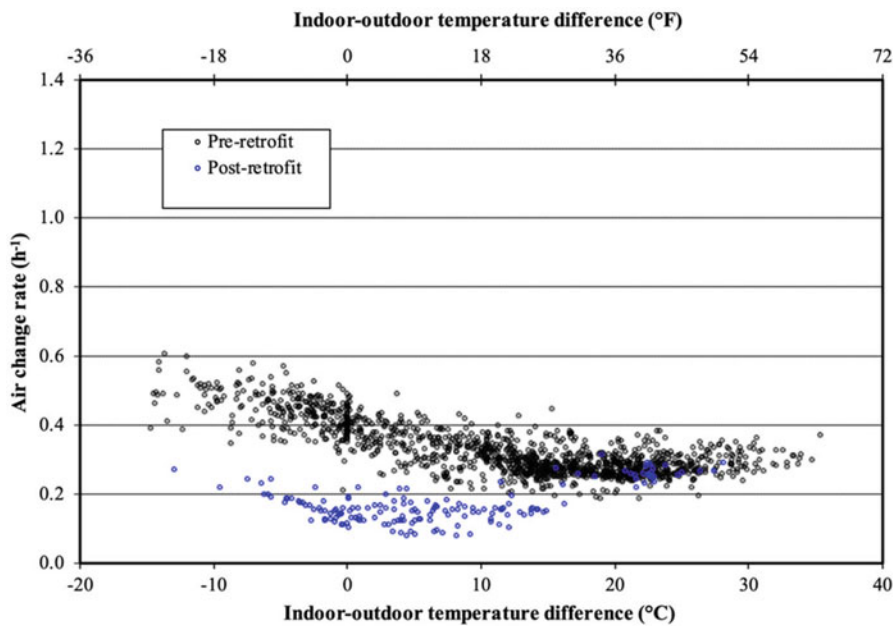


Fig. 3 Air change rates versus indoor–outdoor temperature in manufactured house, forced-air system on

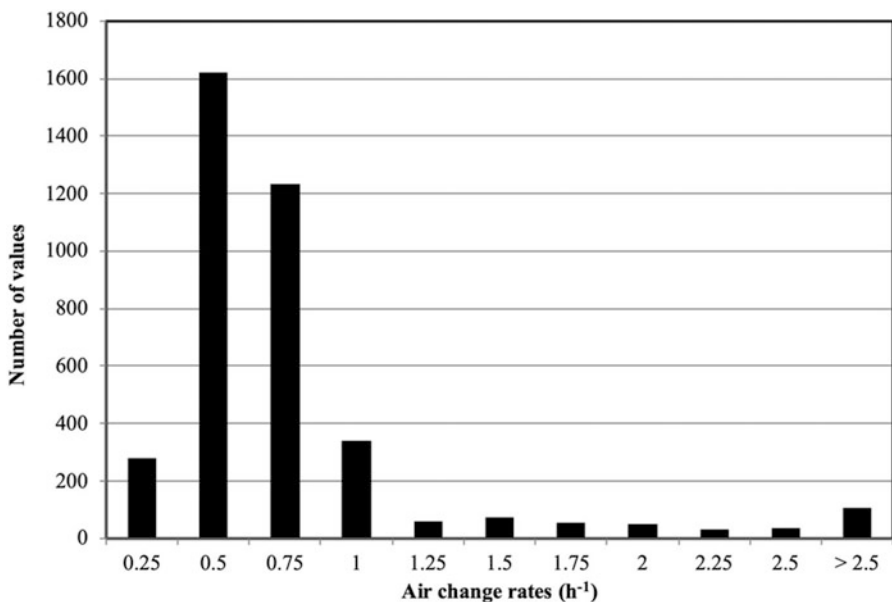


Fig. 4 Distribution of air change rates over 1 year in an occupied town house

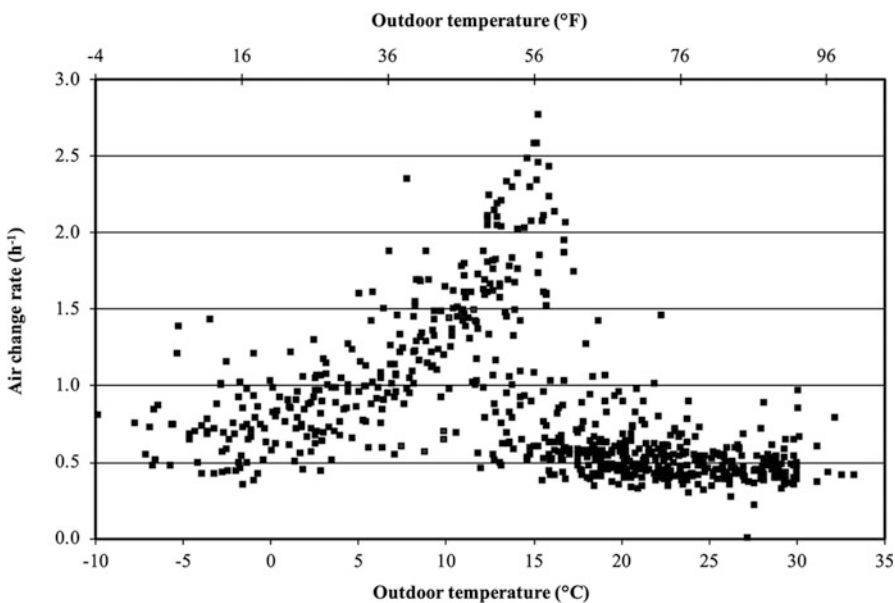


Fig. 5 Air change rates versus indoor–outdoor temperature in an office building (Persily et al. 1992)

as an energy efficiency measure. At lower outdoor air temperatures, the HVAC control system reduces the outdoor air fraction as less outdoor air is needed to cool the building. The outdoor air rate varies over a range of 5 to 1 based on the control system function, with a range of about 2 to 1 at a single outdoor temperature, presumably due to wind effects, measurement error, and other factors.

Figure 6 is a frequency distribution of outdoor air change rate measurements in 14 US office buildings (Persily 1989). This plot shows more than 3000 individual measurements, each corresponding to a tracer gas decay test lasting an hour or two, conducted over a wide range of weather and system operating conditions. The air change rates vary over a range of 10 to 1, with the rates in the individual buildings typically covering a narrower range depending on the weather during each building's tests and its individual characteristics such as airtightness. It is important to note that about 40% of the measured values were below the outdoor air ventilation requirement of 10 L/s per person for office buildings in ASHRAE Standard 62-1989, which was in effect at the time. Also, about 50% of the measurements were below the minimum outdoor air intake specification in the respective building's design documentation. This deviation from design is more notable since these air change rates include infiltration through envelope leakage, while the requirements in the standard and the design value are only for intentional intake. Presumably, if the system outdoor air intake rates were measured separately, even a higher fraction would be below the design value.

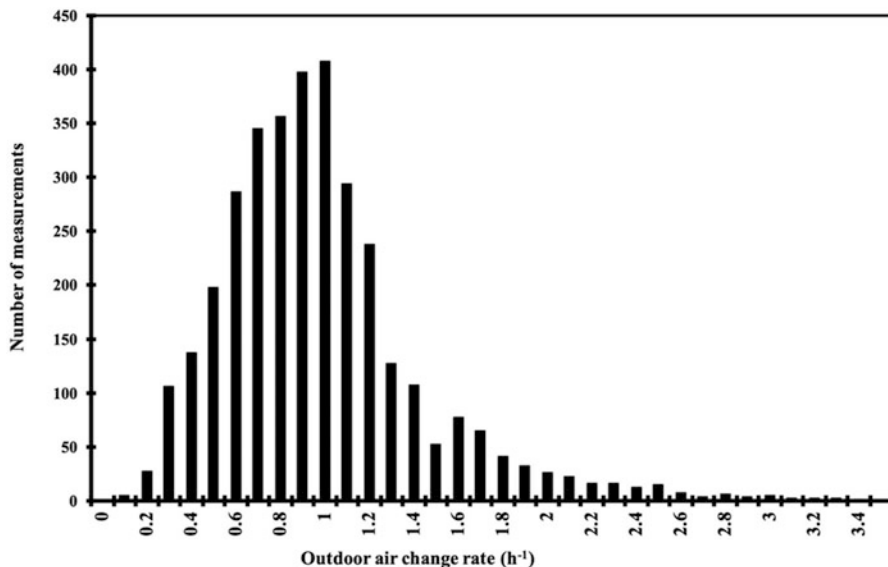


Fig. 6 Frequency distribution of outdoor air change rates in 14 US office buildings (Persily 1989)

Deviations from Design Intent

As noted above, actual ventilation performance can be significantly different from design intent. Such deviations in ventilation performance have been seen in studies of mechanical ventilation system airflows and total outdoor air change rates (Persily 2016). One example of that deviation is from the EPA BASE study of 100 US office buildings mentioned earlier. That study included ventilation measurements during a 1-week study period in each building (Persily and Gorfain 2008). The mean measured outdoor air ventilation rate was 49 L/s per person based on volumetric airflow measurements at the air handlers and measured occupant densities, which is high relative to the minimum outdoor air requirements in almost all ventilation standards. However, these high air change rates were due in part to frequent operation in economizer mode and the actual space occupancies being on average 80% of the design occupancy. Nevertheless, about 17% of the ventilation measurements were still below the 10 L/s per person requirement in ASHRAE Standard 62-1999, the version of the standard that was in effect at the time of the analysis (ASHRAE 1999). Considering only measurements made under minimum outdoor air intake and accounting for the actual occupancy levels, the mean ventilation rate was roughly 11 L/s per person and about one-half of the values were below the minimum requirement in Standard 62-1999. These results demonstrate the need to consider building occupancy and system operation when interpreting ventilation measurement results, as well as the deviation of measured ventilation rates from expectations based on design values or standard requirements.

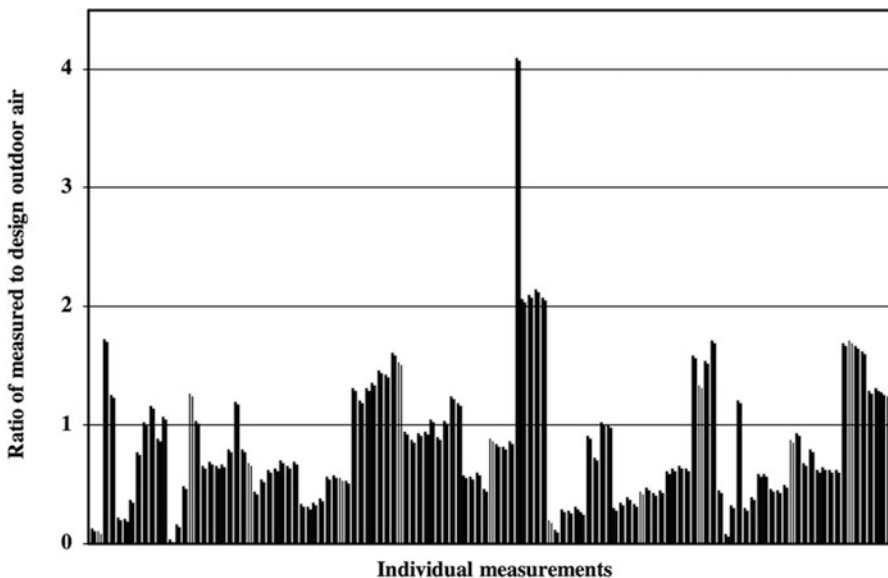


Fig. 7 Ratio of measured minimum outdoor air intake to design value (Persily 2016)

Another finding of the BASE ventilation study, highlighted in Fig. 7, is the deviation of the measured outdoor air intake rate from the corresponding design value, shown here exclusively for measurements conducted when systems were running at minimum outdoor air intake. The horizontal axis is simply the individual measurement result, and the vertical axis is the ratio of the measured value to the design value. If the systems were operating as designed, the ratios would all equal 1.0, subject to some variation due to measurement error. However, many values are less than one, reflecting systems operating with less outdoor air intake than intended, which can have a negative impact on IAQ. There are also many values greater than one, indicating higher outdoor air intake rates than intended, which leads to unplanned energy cost and potentially other problems, e.g., excessive indoor moisture.

Another field study in 108 new, single-family homes in California included measurements of air change rates using the steady-state PFT approach and outdoor air intake measurements using flow hoods or hot wire anemometers (Offermann 2009). This study evaluated the performance of ducted outdoor air ventilation systems, which typically operated intermittently in conjunction with the forced air space conditioning system fan, and of heat recovery ventilators that typically ran 24 h per day. Sixty-four percent of the ducted outdoor air systems failed to meet the California Energy Commission's 2008 Building Energy Efficiency Standards, which was attributed to a combination of low airflow rates and short operating times. All of the heat recovery ventilator systems met the 2008 standards. The median 24-h outdoor air change rate was 0.26 h^{-1} , with a range of $0.09\text{--}5.3 \text{ h}^{-1}$, and 67% of the homes had outdoor air change rates below the minimum California Building

Code requirement of 0.35 h^{-1} . The report attributed the lower air change rates to relatively tight envelope construction and limited window use by the building occupants. This study again highlights the impacts of system operation and occupant action, as well as the deviation of performance from design standards.

Conclusions

Assessing building ventilation performance, including the measurement of ventilation rates, is essential for interpreting indoor contaminant concentrations, accounting for the impacts of outdoor air entry on energy use, and understanding building airflow dynamics. This chapter has stressed that building ventilation assessment is not about a single quantity but covers several parameters, some of which are qualitative but still important. The quantitative parameters include but are not limited to outdoor air intake rates, system supply and exhaust airflow rates, envelope infiltration rates, and indoor-outdoor and interzone pressure differences, while the qualitative features include building design information, operational status and condition, and maintenance schedules. While ventilation assessment is important in field studies of IAQ and other building performance issues, it is not always obvious how to best characterize ventilation performance in any given building. Ultimately, the approaches employed will depend on the reasons for the measurements, the characteristics of the building and its system(s), the available time and resources, the required level of accuracy, and how the measurement results will be used. Buildings and systems are extremely variable, and these variations must be considered when planning and conducting ventilation assessments. Examples of important building characteristics affecting ventilation assessment include building size, how the building is divided into zones, how zones are connected in terms of airflow, the ventilation approach(es) employed in the building, and the ventilation system design. While this summary does not repeat all of the discussion of ventilation performance parameters and measurement methods, the critical points are that they be measured, that the measurement methods be well-described, and that the measurements be repeated to establish uncertainty of the results and to capture temporal and seasonal changes.

This chapter makes several important points about ventilation performance assessment, which are reiterated here:

- Ventilation rates vary significantly with weather and system operation, with weather effects easily leading to variations on the order of 5 to 1 for an individual building. Therefore a single value is not particularly informative without additional information on the conditions during the measurement. In order to fully understand ventilation in a building, multiple repeated measurements under different conditions are required. Also, a single value will be subject to unknown measurement errors unless the measurements are repeated, or otherwise planned and conducted to provide a sound uncertainty estimate. Extrapolating ventilation measurements from one set of conditions to another is potentially associated with

significant uncertainty, but can be performed with reasonable accuracy using models, especially if the model predictions have been validated using other measured data.

- Ventilation performance often does not match design intent due to the realities of building construction, system installation, operation, and maintenance. Interpretation of measurement results requires an understanding of how the system is intended to perform, e.g., when it is supposed to be operating and design outdoor air intake rates. Rather than reporting a measured ventilation rate as low or high, it is much more informative to say it is below the design value or the outdoor air requirements in a specific ventilation standard.
- Many of the measurement methods described in this chapter can be challenging to apply in the field given the complexities of real buildings and systems. Therefore, it can be helpful to use more than one measurement method to increase one's confidence in the results, i.e., air speed traverse in a supply duct combined with measurements of supply airflow rates out of individual diffusers. While indoor CO₂ concentrations can be a useful tool in evaluating ventilation, using peak CO₂ (which is in essence a steady-state, constant injection tracer gas method) to estimate per person outdoor air ventilation rates must be done with a full understanding of the assumptions involved.

The discussion in this chapter leads to suggestions for the development of standards and guidance. One such need is a standardized approach to describing buildings and systems. As described in this chapter, the EPA BASE protocol is the only such approach that currently exists, but it is quite detailed and bears updating given that it was developed more than 25 years ago (EPA 2003). Another area where additional guidance, or even standardization is needed, is the measurement and interpretation of indoor-outdoor and interzone pressure differences. Also, while tracer gas and building pressurization measurement standards include reporting requirements, standards or guidance for reporting the results of a ventilation assessment would be helpful. The following list includes some suggestions on what should be reported when documenting the results of ventilation assessments and measurements:

- *Building*: Age, height, measured envelope airtightness, activities in building and occupancy levels, geographical location
- *System*: Type(s), ventilation approach(es), availability of design documentation, design outdoor air ventilation rate, design exhaust airflow rate (with the latter two at both the system and space level)
- *Space*: Floor area and ceiling height, activity and occupancy levels, system (s) serving it
- *Assessments performed*: Quantities measured, measurement method(s), instrumentation employed including its measurement uncertainty, number of measurements, conditions during measurement (e.g., weather, system operating status)
- *Results*: Values including the test conditions and their overall measurement uncertainty

A standard or guideline on reporting ventilation assessments might present different levels of detail from the minimum essential in all cases to more comprehensive.

Building ventilation performance is important, and while it can be difficult to measure, that is not a valid reason not to perform these assessments or not to do them properly. IAQ researchers and others need to do a better job characterizing ventilation of the buildings and spaces they are studying to understand their measurement results and to report them thoroughly enough to allow comparability between studies and enable others to interpret their results. This chapter has described just a portion of the large amount of knowledge available on building ventilation assessment that has been generated over the years. As the building community strives for improved understanding of IAQ in buildings and overall better building performance, the role of ventilation must be addressed through the use of sound approaches to ventilation assessment.

Cross-References

- ▶ [Influence of Ventilation on Indoor Air Quality](#)
 - ▶ [Visualization and Measurement of Indoor Airflow by Color Sequence Enhanced Particle Streak Velocimetry](#)
-

References

- ASHRAE (1988) Standard 111-1988, Practices for measurement, testing, adjusting, and balancing of building heating, ventilation, airconditioning, and refrigeration systems. American Society of Heating, Refrigerating and Air-Conditioning Engineers, Inc., Atlanta
- ASHRAE (1997) ANSI/ASHRAE Standard 129, Measuring air-change effectiveness. American Society of Heating, Refrigerating, and Air-Conditioning Engineers, Inc.,
- ASHRAE (1999) ANSI/ASHRAE Standard 62-1999, ventilation for acceptable indoor air quality. American Society of Heating, Refrigerating and Air-Conditioning Engineers, Inc., Atlanta
- ASHRAE (2008) ANSI/ASHRAE Standard 111-2008, measurement, testing, adjusting, and balancing of building HVAC systems. American Society of Heating, Refrigerating and Air-Conditioning Engineers, Inc., Atlanta
- ASHRAE (2013) ANSI/Standard 113-2005, Method of testing for room air diffusion. American Society of Heating, Refrigerating and Air-Conditioning Engineers, Inc., Atlanta
- ASHRAE (2014) ANSI/ASHRAE Standard 41.3-2014, standard methods for pressure measurement. American Society of Heating, Refrigerating and Air-Conditioning Engineers, Inc., Atlanta
- ASHRAE (2021) Fundamentals Handbook. American Society of Heating, Refrigerating and Air-Conditioning Engineers, Inc., Atlanta
- ASHRAE (2019a) ANSI/ASHRAE Standard 62.1-2019 ventilation for acceptable indoor air quality. American Society of Heating, Refrigerating and Air-Conditioning Engineers, Inc., Atlanta
- ASHRAE (2019b) ANSI/ASHRAE Standard 62.2-2019 ventilation and acceptable indoor air quality in low-rise residential buildings. American Society of Heating, Refrigerating and Air-Conditioning Engineers, Inc., Atlanta

- ASHRAE (2020) ANSI/ASHRAE/ICC/USGBC/IES Standard 189.1-2020, standard for the design of high-performance green buildings. American Society of Heating, Refrigerating and Air-Conditioning Engineers
- ASTM (2011a) E2029 Standard test method for volumetric and mass flow rate measurement in a duct using tracer gas dilution. American Society for Testing and Materials, West Conshohocken
- ASTM (2011b) E741, Standard test method for determining air change in a single zone by means of a tracer gas dilution, American Society for Testing and Materials
- ASTM (2014) D7297, Standard practice for evaluating residential indoor air quality concerns, ASTM International
- ASTM (2017) E1827, Standard test method for determining airtightness of buildings using an orifice blower door, American Society for Testing and Materials, Philadelphia
- ASTM (2018a) E3158, Standard test method for measuring the air leakage rate of a large or mulitzone building. American Society for Testing and Materials, West Conshohocken
- ASTM (2018b) D6245, Standard guide for using indoor carbon dioxide concentrations to evaluate indoor air quality and ventilation, ASTM International
- ASTM (2019) E779, Standard test method for determining air leakage rate by fan pressurization. American Society for Testing and Materials, West Conshohocken
- Bekö G, Gustavsen S, Frederiksen M, Bergsøe NC, Kolarik B, Gunnarsen L, Toftum J, Clausen G (2016) Diurnal and seasonal variation in air exchange rates and interzonal airflows measured by active and passive tracer gas in homes. *Build Environ* 104:178–187. <https://doi.org/10.1016/j.buildenv.2016.05.016>
- Bennett D, Wu X, Trout A, Apte M, Faulkner D, Maddalena R, Sullivan D (2011) Indoor environmental quality and heating, ventilating, and air conditioning survey of small and medium size commercial buildings. California Energy Commission
- Bennett D, Fisk W, Apte MG, Wu X, Trout A, Faulkner D, Sullivan D (2012) Ventilation, temperature, and HVAC characteristics in small and medium commercial buildings in California. *Indoor Air* 22:309–320
- Bluyssen PM, Fernandes EO, Groes L, Clausen G, Fanger PO, Valbjorn O, Bernhard CA, Roulet CA (1996) European indoor air quality audit project in 56 office buildings. *Indoor Air* 6(4): 221–238
- Breen MS, Schultz BD, Sohn MD, Long T, Langstaff J, Williams R, Isaacs K, Meng QY, Stallings C, Smith L (2014) A review of air exchange rate models for air pollution exposure assessments. *J Expo Sci Environ Epidemiol* 24(6):555–563. <https://doi.org/10.1038/jes.2013.30>
- CEN (2007) Ventilation for non-residential buildings – performance requirements for ventilation and room-conditioning systems. European Committee for Standardization, Brussels
- CGSB (1995) The spillage test. Method to determine the potential for pressure-induced spillage from vented, fuel-fired, space heating appliances, water heaters and fireplaces. Canadian General Standards Board, Ottawa
- Chan WR, Carrié R, Novák J, Kitvak A, Richieri F, Solcher O, Pan W, Emmerich S (2012a) Building air leakage databases in energy conservation policies: analysis of selected initiatives in 4 European countries and the USA. TightVent Europe
- Chan WR, Joh J, Sherman MH (2012b) Analysis of air leakage measurements from residential diagnostics database. Lawrence Berkeley National Laboratory, Berkeley
- Chao CY, Wan MP (2004) Experimental study of ventilation performance and contamination of underfloor ventilation systems vs. traditional ceiling-based ventilation system. *Indoor Air* 14(5): 306–316
- CIBSE (2005) Natural ventilation in non-domestic buildings. Chartered Institution of Building Services Engineers, London
- Derbez M, Wyart G, Le Ponner E, Ramalho O, Riberon J, Mandin C (2018) Indoor air quality in energy-efficient dwellings: levels and sources of pollutants. *Indoor Air* 28:318–338
- Dodson RE, Levy JI, Shine JP, Spengler JD, Bennett DH (2007) Multi-zonal air flow rates in residences in Boston, Massachusetts. *Atmos Environ* 41(17):3722–3727. <https://doi.org/10.1016/j.atmosenv.2007.01.035>

- Dols WS, Polidoro BJ (2020) CONTAM user guide and program documentation. Version 3.4. National Institute of Standards and Technology, Gaithersburg
- Dols WS, Emmerich SJ, Polidoro BJ (2012) LoopDA 3.0 – natural ventilation design and analysis software user guide. National Institute of Standards and Technology
- Du L, Batterman S, Godwin C, Chin JY, Parker E, Breen M, Brakefield W, Robins T, Lewis T (2012) Air change rates and interzonal flows in residences, and the need for multi-zone models for exposure and health analyses. *Int J Environ Res Public Health* 9(12):4639–4661. <https://doi.org/10.3390/ijerph9124639>
- Du L, Batterman S, Godwin C, Rowe Z, Chin JY (2015) Air exchange rates and migration of VOCs in basements and residences. *Indoor Air* 25(6):598–609. <https://doi.org/10.1111/ina.12178>
- Emmerich SJ, Persily AK (2014) Analysis of U.S. commercial building envelope air leakage database to support sustainable building design. *Int J Vent* 12(4):331–343
- EPA (2003) A standardized EPA protocol for characterizing indoor air quality in large office buildings. U.S. Environmental Protection Agency,
- EPA (2006) BASE data on indoor air quality in public and commercial buildings. United States Environmental Protection Agency
- Faulkner D, Fisk WJ, Sullivan DP, Lee SM (2004) Ventilation efficiencies and thermal comfort results of a desk-edge-mounted task ventilation system. *Indoor Air* 14(8):92–97
- Fisk WJ, Faulkner D, Sullivan DP, Delp W (2002) Measuring rates of outdoor airflow into HVAC systems. Lawrence Berkeley National Laboratory, Berkeley
- Fisk WJ, Faulkner D, Sullivan DP (2004) An evaluation of three commercially available technologies for real-time measurement of rates of outdoor airflow into HVAC systems. Lawrence Berkeley National Laboratory
- Fisk WJ, Faulkner D, Sullivan D, Chao C, Wan M, Zagreus L, Webster T (2005) Results of a field study of underfloor air distribution. *Indoor Air* 15(11):1016–1021
- Fisk WJ, Sullivan DP, Cohen S, Han H (2008) Measuring outdoor air intake rates using electronic velocity sensors at louvers and downstream of airflow straighteners. Lawrence Berkeley National Laboratory, Berkeley
- Guyot G, Ferllay J, Gonze E, Woloszyn M, Planet P, Bello T (2016) Multizone air leakage measurements and interactions with ventilation flows in low-energy homes. *Build Environ* 107:52–63. <https://doi.org/10.1016/j.buildenv.2016.07.014>
- I'Anson SJ, Irwin C, Howarth AT (1982) Air flow measurement using three tracer gases. *Build Environ* 17(4):245–252
- ISO (2015) ISO 9972:2015 thermal performance of buildings – determination of air permeability of buildings – fan pressurization method. International Standards Organization
- ISO (2017) Thermal performance of buildings and materials – determination of specific airflow rate in buildings – tracer gas dilution method, 12569: 2017, International Standards Organization
- Jones BM, Kirby R (2010) The performance of natural ventilation windcatchers in schools – a comparison between prediction and measurement. *Int J Vent* 9(3):273–286
- Karimipanah T, Awbi HB, Sandberg M, Blomqvist C (2007) Investigation of air quality, comfort parameters and effectiveness for two floor-level air supply systems in classrooms. *Build Environ* 42(2):647–655
- Limb MJ (2001) A review of international ventilation, airtightness, thermal insulation and indoor air quality criteria. Air Infiltration and Ventilation Centre, Coventry
- McWilliams J (2002) Review of airflow measurement techniques. Lawrence Berkeley National Laboratory, Berkeley
- Nabinger S, Persily A (2011) Impacts of airtightening retrofits on ventilation rates and energy consumption in a manufactured home. *Energ Build* 43(11):3059–3067
- Nazaroff WW (2021) Residential air-change rates: a critical review. *Indoor Air* 31(2):282–313. <https://doi.org/10.1111/ina.12785>
- NEBB (2005) Procedural standards for testing adjusting balancing of environmental systems, 5th edn. National Environmental Balancing Bureau, Gaithersburg

- Ng L, Persily A, Emmerich S (2015) Infiltration and ventilation in a very tight, high performance home. Paper presented at the 36th AIVC conference effective ventilation in high performance buildings, Madrid
- Ng LC, Kindser L, Emmerich SJ, Persily AK (2018) Estimating Interzonal leakage in a net-zero energy house. In: Weston T, Nelson K, Wissink KS (eds) Whole building air leakage: testing and building performance impacts. ASTM STP 1615. American Society for Testing and Materials, West Conshohocken, pp 211–229
- Nikolopoulos N, Nikolopoulos A, Larsen TS, Nikas K-SP (2012) Experimental and numerical investigation of the tracer gas methodology in the case of a naturally cross-ventilated building. *Build Environ* 56:379–388
- Nirvan G, Haghigat F, Wang L, Akbari H (2012) Contaminant transport through the garage – house interface leakage. *Build Environ* 56:176–183
- Offermann F (2009) Ventilation and indoor air quality in new homes. California Air Resources Board and California Energy Commission
- Persily AK (1989) Ventilation rates in office buildings. In: IAQ '89 the human equation: health and comfort. American Society of Heating, Refrigerating and Air-Conditioning Engineers, Inc., San Diego, pp 128–136
- Persily AK (2016) Field measurement of ventilation rates. *Indoor Air* 26(1):97–111. <https://doi.org/10.1111/ina.12193>
- Persily AK, Axley JW (1990) Measuring airflow rates with pulse tracer techniques. In: Sherman MH (ed) Air change rate and airtightness in buildings, ASTM STP 1067, American Society for Testing and Materials, Philadelphia, pp 31–51
- Persily AK, de Jonge L (2017) Carbon dioxide generation rates of building occupants. *Indoor Air* 27(5):868–879. <https://doi.org/10.1111/ina.12383>
- Persily A, Gorfain J (2008) Analysis of ventilation data from the U.S. Environmental Protection Agency building assessment survey and evaluation (BASE) study. National Institute of Standards and Technology, Gaithersburg
- Persily A, Levin H (2011) Ventilation measurements in IAQ studies: problems and opportunities. Paper presented at the 12th international conference on indoor air quality and climate, Austin
- Persily AK, Norford LK (1987) Simultaneous measurements of infiltration and intake in an office building. *ASHRAE Trans* 93(2):942–956
- Persily AK, Dols WS, Nabinger SJ (1992) Environmental evaluation of the Federal Records Center in Overland Missouri. National Institute of Standards and Technology, Gaithersburg
- Pigg S, Cautley D, Francisco P, Hawkins B, Brennan T (2014) Weatherization and indoor air quality: measured impacts in single-family homes under the weatherization assistance program. Oak Ridge National Laboratory,
- Ramalho O, Mandin C, Riberon J, Wyart G (2013) Air stuffiness and air exchange rate in French schools and day-care centres. *Int J Vent* 12(2):175–180
- Rim D, Novoselac A (2010) Ventilation effectiveness as an indicator of occupant exposure to particles from indoor sources. *Build Environ* 45:1214–1224
- Sherman MH (1989) Analysis of errors associated with passive ventilation measurement techniques. *Build Environ* 24(2):131–139
- SMACNA (2002) HVAC systems testing, adjusting & balancing. Sheet Metal and Air Conditioning Contractors' National Association, Chantilly
- Sundell J, Levin H, Nararoff WW, Cain WS, Fisk WJ, Grimsrud DT, Gyntelberg F, Li Y, Persily AK, Pickering AC, Samet JM, Spengler JD, Taylor ST, Weschler CJ (2011) Ventilation rates and health: multidisciplinary review of the scientific literature. *Indoor Air* 21(3):191–204
- Takaki R, et al. (2005) Measurement of ventilation rates of occupied houses by three different methods: measurement results by constant concentration method. Indoor Air 2005, 10th International Conference on Indoor Air Quality and Climate, Paper 1.6–17

- Wallace LA, Emmerich SJ, Howard-Reed C (2001) Continuous measurements of air change rates in an occupied house for 1 year: the effect of temperature, wind, fans, and windows. *J Expo Anal Environ Epidemiol* 12(4):296–306
- Weisel CP, Zhang J, Turpin BJ, Morandi MT, Colome S, Stock TH, Spektor DM, et al. (2005) Relationships of indoor, outdoor, and personal air (RIOPA). Part I. collection methods and descriptive analyses. Health Effects Institute, Boston MA
- Yamamoto N, Shendell DG, Winer AM, Zhang J (2010) Residential air exchange rates in three major US metropolitan areas: results from the relationship among indoor, outdoor, and personal air study 1999–2001. *Indoor Air* 20:85–90
- Zhai J (2005) A new building ventilation effectiveness index. *Indoor Air* 15(11):3195–3199



Control of Airborne Particles: Filtration

59

Brent Stephens, Andrew Maynard, and Philip K. Hopke

Contents

Introduction	1716
Filtration Theory	1718
Single Fiber Collection Efficiency	1718
Overall Filter Efficiency	1719
Selecting Filters: Test Methods and Rating Systems	1721
Filter Applications in Buildings	1722
Portable and Room-Level Systems	1722
In-Duct Filters	1727
Impacts of Filters in Real Buildings	1731
Conclusions	1733
References	1734

Abstract

The control of airborne particulate matter (PM) in indoor air is important for improving the health and well-being of the building inhabitants. Indoor PM arises from both infiltration of ambient particulate pollution and from multiple indoor sources. Given the large amount of time people spend indoors, reducing exposure

B. Stephens

Department of Civil, Architectural, and Environmental Engineering, Illinois Institute of Technology, Chicago, IL, USA

A. Maynard

Arizona State University College of Global Futures, Arizona State University, Tempe, AZ, USA

P. K. Hopke (✉)

Institute for a Sustainable Environment, Clarkson University, Potsdam, NY, USA

Department of Public Health Sciences, University of Rochester School of Medicine and Dentistry, Rochester, NY, USA

e-mail: phopke@clarkson.edu

to PM is an important contribution to better indoor air quality. The most common approach to PM reduction is through filtration. Filtration systems can be designed at various scales from room air cleaners to large-scale building HVAC systems. This chapter provides an introduction to filtration theory and then describes applications of filtration systems at various levels of scale.

Keywords

Filtration · Clean air delivery rate · Efficiency · Pressure drop

Introduction

Removal of airborne particles from indoor air is an important way to improve indoor air quality and protect the health and well-being of the occupants. As described elsewhere in this handbook, particles in indoor air arise from multiple sources including infiltration of the ambient aerosols (Chen and Zhao 2022), indoor sources of particles (e.g., ► [Chap. 14, “Cooking Aerosol”](#)), and the formation of particles through reactions of hydrocarbons and oxidants such as ozone. The resulting particulate matter (PM) can produce adverse health effects (Samet et al. 2022) and damage or soil materials such as furniture, draperies, and artwork (Grau-Bové and Strlič 2013). The indoor atmosphere is a dynamic environment such that particles are constantly infiltrating, depositing, resuspending, being emitted from indoor sources, and/or forming from indoor chemistry. A wide variety of air cleaning and filtration technologies designed to remove particles from indoor environments are available for use (ASHRAE 2018; US EPA 2018). Thus, it is important to understand their mechanisms of action, their impacts on indoor particle removal rates, and ultimately their impacts on reducing indoor particle concentrations.

The most common approach to PM reduction is through filtration. Fibrous media filters are what most people envisage when they think of a filter. The filter is composed of a woven or nonwoven mat of fibers. In most filters used to control indoor air quality, the fibers are derived from wood (paper), glass, or synthetic polymer fibers. These may be held together with a binder material that may be as high as 10% of the filter material. Fibers of a wide range of diameters are used (ranging from less than 1 μm to over 100 μm) – often in the same filter. Figure 1 presents scanning electron micrographs of typical paper and glass fiber filters.

Depending on the nature of the structure and the volume of air to be cleaned, different approaches to filtration are employed ranging from room air cleaners to filters within central forced air heating/air conditioning systems to filtration of large volumes of air in heating, ventilating, and air-conditioning (HVAC) systems for large buildings (offices, schools, etc.). This chapter will begin with an introduction to the theory of air filtration and then examine filter use for different application scales.

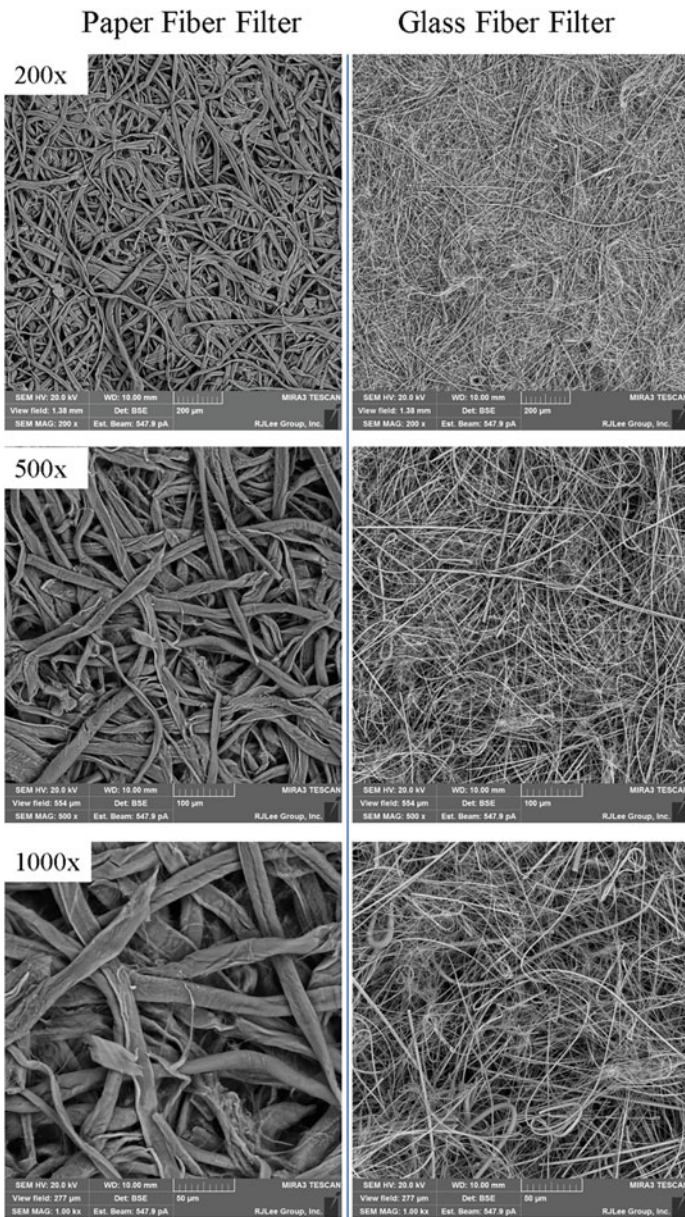


Fig. 1 SEM micrographs of a paper (left) and glass fiber filter (right) at different magnifications: top: 200x; middle: 500x; bottom: 1000x. (SEM images provide courtesy of R.J. Lee Group, Monroeville, PA)

Filtration Theory

Particle sizes of interest in indoor air quality extend from nanometers to tens of micrometers. Sizes above 100 μm have sufficiently high gravitational settling velocities that they do not remain airborne for very long given that a unit density spherical particle with a diameter of 100 μm has a settling velocity of 25 cm/s. A critical aspect of air filtration is that the fluid supporting the particles is a gas having much lower viscosity than particles suspended in a liquid. Because of this, air filtration does not depend on a sieving mechanism where the hole through which the fluid flows is smaller than the particle. Rather, air filters utilize an arrangement of fibers designed to allow air to flow through them while capturing a portion of the particles suspended in the air stream using a variety of mechanisms.

Single Fiber Collection Efficiency

The theoretical efficiency of a fibrous filter may be approached starting with the collection efficiency of a single fiber (Davies 1973). As an aerosol particle moves in the vicinity of a filter fiber, multiple mechanisms control its fate, depending on the particle size and fiber characteristics. Primary mechanisms include inertial impaction, interception, and diffusion, as depicted in Fig. 2. Other mechanisms, including gravitational settling and electrostatic attraction, may also contribute to single fiber collection efficiency.

In addition, there is an interaction term that accounts for the interception of diffusing particles.

The total single fiber collection efficiency, η_T , is then the sum of the collection by impaction (η_I), interception (η_R), diffusion (η_D), and diffusional interception (η_{DR}) (Hinds and Zhu 2022).

$$\eta_T \approx \eta_I + \eta_R + \eta_D + \eta_{DR} \quad (1)$$

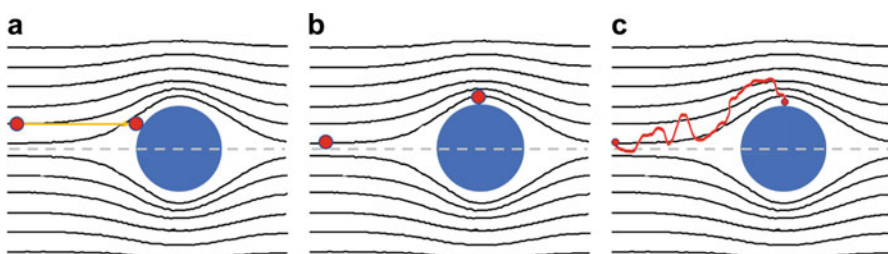


Fig. 2 Illustration of the mechanisms of particle collection by a single cylindrical fiber-oriented perpendicular to the flow through the filter

$$\eta_T = (2\kappa)^{-2} I * Stk + \frac{(1 - \alpha)R^2}{\kappa(1 + R)} + 2Pe^{-\frac{2}{5}} + 1.24 * R^{\frac{2}{5}}(\kappa * Pe)^{-1/2} \quad (2)$$

where

α = solid volume fraction of the filter = (fiber volume)/(total volume) = 1 - porosity.
 a = fiber radius.

a_p = particle radius.

$$I = (29.6 - 28\alpha^{0.62})R^2 - 27.5R^{2.8} \text{ for } R < 0.4$$

$$\kappa = -\frac{\ln \alpha}{2} - \frac{3}{4} + \alpha - \frac{\alpha^2}{4}$$

$$R = a_p/a; Pe = 2aU_0/D; Stk = \frac{\rho_p d_p^2 C U_0}{18 \xi d_f}$$

U_0 = face velocity = volumetric flow rate through the filter/filter area.

D = particle diffusion coefficient.

ϵ = kinematic viscosity.

d_f = $2a$ = fiber diameter.

d_p = $2a_p$ = particle diameter.

Under some circumstances would require inclusion of gravitational settling and electrostatic attraction for charged filter fibers. Details are provided in Hinds and Zhu (2022).

Overall Filter Efficiency

The efficiency of the filter is defined by how many particles of a given size penetrate the filter relative to the initial upstream concentration. Assuming that all fibers have the same diameter, the total length of fibers in a filter is given by:

$$L = \frac{4\alpha}{\pi d_f^2} \quad (3)$$

The number of particles collected from a unit volume of air passing through a unit cross-sectional area of the filter which have a thickness of dt (dN) is given by:

$$n_c = N\eta_T d_f L dt = N\gamma dt \quad (4)$$

where

$$\gamma = \frac{4\alpha\eta_T}{\pi d_f^2}$$

$$dN = -N\gamma dt \quad (5)$$

$$\int_{N_{in}}^{N_{out}} \frac{dN}{N} = \int_0^t -\gamma dt \quad (6)$$

$$\ln \frac{N_{out}}{N_{in}} = -\gamma t \quad (7)$$

The ratio of N_{out}/N_{in} represents the penetration (P) of particles through the filter. Thus,

$$P = e^{-\gamma t} = \exp \left(-\frac{4\alpha\eta_T}{\pi d_f} \right) \quad (8)$$

The efficiency of a filter is then the fraction of particles retained in the filter ($E = 1 - P$). The qualitative plot of filter efficiency based on single fiber collection efficiency compares well to real filters (Fig. 3). ***Thus, the efficiency depends only on diffusion and inertia, and NOT the size of the holes in the filter.*** Large particles are collected by inertial deposition and interception, and the collection efficiency decreases with decreasing size. However, for small, diffusional particles ($d_p < 0.1 \mu\text{m}$), the filter efficiency increases with decreasing size. Therefore, filter efficiency characterizations should include the particle diameter that will represent the highest penetration (typically around $0.3 \mu\text{m}$), since the collection efficiency will increase as particle size either increases or decreases. This size range with the lowest removal efficiency is commonly referred to as the most penetrating particle size (MPPS).

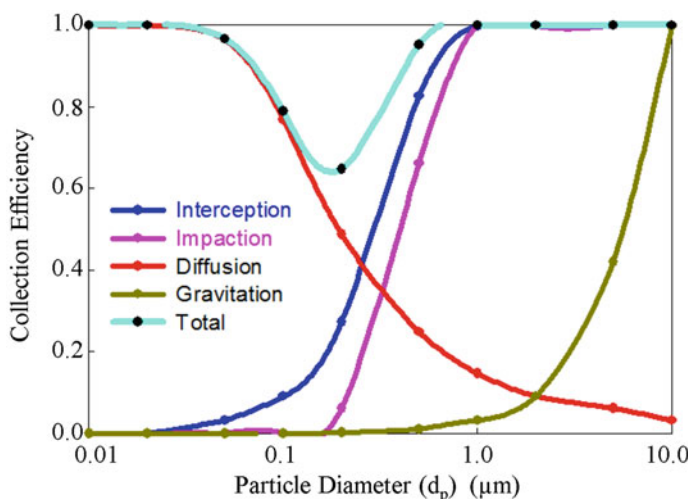


Fig. 3 Filter efficiency as a function of particle diameter showing the effects of the various deposition mechanisms

Selecting Filters: Test Methods and Rating Systems

Filters are tested for their size-resolved particle removal efficiency and other performance characteristics, including pressure drop and dust-loading capacity in test ducts following industry consensus test standards, such as ASHRAE Standard 52.2 (ASHRAE 2017) and/or ISO 16890 (ISO 2016). In all filter-testing approaches, the single-pass removal efficiency of a filter is a fractional measure of its ability to reduce the concentration of particles in air that passes through it:

$$\text{Efficiency} = \left(1 - \frac{C_{\text{downstream}}}{C_{\text{upstream}}} \right) \times 100\% \quad (9)$$

In ASHRAE Standard 52.2, the removal efficiency of particles 0.3 to 10 µm in diameter is measured under a range of dust-loading conditions and reported as a minimum efficiency-reporting value (MERV). MERV ranges from 1 to 20 based on the average removal efficiency across three particle size ranges (0.3–1 µm, 1–3 µm, and 3–10 µm), although MERV 17 to 20 are not commonly used in standard building applications but rather in clean room and surgical room environments. In general, higher MERV values represent higher filtration efficiency for most particle sizes, although it should be noted that the test standard does not characterize the removal efficiency of particles smaller than 0.3 µm that make up the vast majority of particles in any indoor or outdoor environment by number (Azimi et al. 2014; Fazli et al. 2019). The MERV ratings and particle efficiency are presented in Table 1.

Table 1 ASHRAE Standard 52.2 MERV table

MERV	Composite average particle size efficiency 0.3–1 µm	Composite average particle size efficiency 1–3 µm	Composite average particle size efficiency 3–10 µm	Types of particles captured
1	—	—	Less than 20%	Pollen, dust mites, standing dust, spray paint dust, and carpet fibers
2	—	—	Less than 20%	
3	—	—	Less than 20%	
4	—	—	Less than 20%	
5	—	—	20% or better	Mold spores, hair spray, fabric protector, and cement dust
6	—	—	35% or better	
7	—	—	50% or better	
8	—	20% or better	70% or better	
9	—	35% or better	75% or better	Humidifier dust, lead dust, auto emissions, and milled flour
10	—	50% or better	80% or better	
11	20% or better	65% or better	85% or better	
12	35% or better	80% or better	90% or better	
13	50% or better	85% or better	90% or better	Bacteria, most tobacco smoke, and droplet nuclei (sneeze)
14	75% or better	90% or better	95% or better	
15	85% or better	90% or better	95% or better	
16	95% or better	95% or better	95% or better	

The ISO 16890 standard similarly characterizes size-resolved removal efficiency of filters and also estimates removal efficiency for mass-based metrics of ePM₁, ePM_{2.5}, and ePM₁₀ for the mass of particles less than 1 μm , 2.5 μm , and 10 μm in diameter, respectively. Estimates of ePM are made using assumptions for ambient (outdoor) particle size distributions, making them most directly relevant for understanding filtration efficiency for particles of outdoor origin (such as those entering the HVAC system via the outdoor air intake).

Other common test metrics for filters also include the proprietary MPR (Micro-particle Performance Rating) and FPR (Filter Performance Rating) systems. There is less publicly available information on these proprietary test standards because they are used by commercial manufacturers and distributors of filters, but they are increasing in use, especially for residential and light-commercial applications. Last, for critical particle cleaning applications, as well as for many stand-alone in-room devices, the highest efficiency filters available can achieve “**high efficiency particulate air [filter]**” (HEPA) designation. HEPA filters remove at least 99.97% of dust, pollen, mold, bacteria, and any 0.3 μm airborne particles. Thus, they should also remove any larger or smaller particle with at least this efficiency. More details on testing and rating of filters are provided by ASHRAE (2020).

Filter Applications in Buildings

There are two main approaches to implementing filtration systems in buildings: 1) portable or room-level air-cleaning devices and 2) in-duct filters mounted inside HVAC systems.

Portable and Room-Level Systems

To reduce particle concentrations within a space via filtration, it is possible to use a room air cleaner. These systems include an air moving system (fan) and a filter coupled together such that the air passing through the fan must pass through the filter. There are many commercially available systems that are commonly sized based on the room square footage, determined by a combination of the flow rate through the system and the removal efficiency of the filter used within the system.

Clean Air Delivery Rate

Room air cleaners are commonly characterized in terms of the **clean air delivery rate (CADR)** or the **effective cleaning rate (ECR)** (Offermann et al. 1985). Although both terms are used interchangeably in the scientific literature, CADR is most commonly used on product labeling, as both a CADR test standard and the resulting test metric are maintained by the Association of Home Appliance Manufacturers (AHAM). The CADR represents the volume flow (cubic feet per minute, CFM) of air that has all given sized particles filtered from it. In other words: It is a measure of an air cleaner’s delivery of relatively clean air. There are separate CADR

values for particles of different sizes generated by tobacco smoke ($0.09\text{--}1\ \mu\text{m}$), dust ($0.5\text{--}3\ \mu\text{m}$), and pollen ($5\text{--}11\ \mu\text{m}$). The higher the CADR for a given particle size, the faster the unit filters the air; the faster the unit filters the air, the lower the resulting concentration will be in the space.

While the CADR can be measured as the product of flow rate times removal efficiency, it is actually measured by comparing loss rates in a test chamber with and without the air cleaner operating. In the ANSI/AHAM AC-1-2006 (ANSI 2006) test standard, the CADR is defined as “the rate of contaminant reduction in the test chamber when the unit is turned on, minus the rate of natural decay when the unit is not running, multiplied by the volume of the test chamber as measured in cubic feet” (Eq. 10).

$$\text{CADR} = V(L_{\text{on}} - L_{\text{off}}) \quad (10)$$

Where L_{on} and L_{off} are the first-order particle loss rates measured in a test chamber with an air cleaner on and off, respectively (min^{-1}), and V is the volume of the test chamber (ft^3). The standard is based on a $1008\ \text{ft}^3$ test chamber used to compare among different air cleaners in a uniform manner. The rating is for the combination of a new filter in a specific air cleaner design used in a 20-minute test.

AHAM provides a database of air cleaners that have registered results from CADR testing (<https://www.ahamdir.com/room-air-cleaners>). In general, reported CADRs for the three particle size ranges tested are within about 10% of each other, depending on the device. CADRs of in-room or portable devices – which are most commonly tested and reported at an in-room air cleaner’s highest fan speed setting – commonly range from less than 50 CFM to over 450 CFM, with most products falling between about approximately 100 and 250 CFM. Lower fan speed settings will typically reduce the CADR. AHAM recommends that filters should be chosen such that the CADR for smoke is equal to or greater than two-third of the room area for rooms with ceiling heights $<8\ \text{ft}$. CADR is now widely used to characterize in-room air cleaners.

Practical Considerations for Portable and Room-Level Filtration Systems

There are several practical factors to consider in portable or room-level filtration system applications. These include power demands, noise and comfort, and operation and maintenance, all of which affect trade-offs between flow rates and filter efficiency.

Pressure Drop and Power Demands There are trade-offs between filter efficiency and the ability of air to flow through the filter. As the solid volume fraction, α , increases, there are more fibers in the path of the flow. Thus, using an HEPA filter results in a higher differential in pressure between the inlet and outlet of the filter to yield the same flow rate as a lower efficiency, lower pressure drop filter. The pressure drop through a filter (ΔP) is given by (Davies 1973):

$$\Delta P = \frac{\epsilon t U_0 f(\alpha)}{d_f^2} \quad (11)$$

where:

$$f(\alpha) = 64\alpha^{1.5}(1 + 56\alpha^3) \text{ for } 0.006 < \alpha < 0.3$$

With higher pressure drop, it takes a more powerful fan (or, if using a variable speed fan, a higher fan speed) to draw the air through the filter to maintain the same flow rate. There are three “fan” laws that cover flow, pressure differential, and power use. Fan Law 1 relates the change in air flow rate of a fan to the change in speed of the propeller. If the propeller speed is increased by 10%, the air flow rate will also increase by 10%. Fan Law 2 tells us that the change in total static pressure across the filter will increase by the square of the change in propeller speed of the fan. If the propeller speed is increased by 10%, the total static pressure increases by 21%. Fan Law 3 tells us that the change in horsepower required by the fan to turn the propeller will increase by the cube of the change in propeller speed of the fan. If the propeller speed is increased by 10%, the horsepower required to turn the propeller will increase by 33.1%. Thus, filter systems with higher efficiency filters with higher resistance to airflow will often require a higher fan speed (and thus higher fan power, meaning more electricity usage) to produce the same flow rate through the system, and thus the unit will be more costly to operate.

Noise and Comfort There are often trade-offs between air cleaning rates and livability in the space. If the fan speed is too high, then the excess air velocity in the room might make it uncomfortable to use. Moreover, the CADR of an in-room air cleaner is usually highest at the highest airflow rate, which is also usually the loudest setting. If an in-room air cleaner is too loud, occupants might choose to switch off the unit or operate it at a lower fan speed setting (with a lower CADR). Unfortunately, noise is not routinely quantified or reported on consumer packaging, so it can be difficult to compare one device to another based on noise ratings. One can look for noise ratings provided voluntarily on product packaging or alternative sources of noise ratings such as consumer test reports websites.

Operation and Maintenance A given room with an air cleaner will be exchanging air with other spaces. If there is an exterior wall, there can be infiltration of ambient aerosol particles. Open doors or passageways allow movement of air from other locations where particles could be generated such as a kitchen. Forced air heating/cooling will move air with their particle concentrations around the dwelling and bring particles to the room with the cleaner. Thus, sealing around windows or outside doors and closing interior doors will make the room air cleaner more effective for the given space in which it resides. It may be obvious, but it is worth noting that in-room air cleaners only filter air when they are operating. Therefore, air cleaners should run frequently, even continuously, to deliver maximum effect. Running air cleaners continuously come with added costs including electricity costs to run the device and costs to replace filters as they become loaded. In considering selection of portable and in-room air cleaners, it is useful to conduct a life cycle cost assessment that factors in upfront costs, ongoing energy costs for operation, and filter

replacement costs for maintenance. New innovations in portable and in-room air cleaners include those that are using low-cost particle sensors to determine the fan speed to use to achieve a given particle concentration. Units now may also include pressure-differential sensors to monitor filter clogging and provide a warning that it is time to change the filter. As these technologies continue to decline in cost, more of these “smart” air cleaners will become available.

Trade-Offs: Flow Rates, Filter Efficiency, and Effectiveness These combined factors of pressure drop, power demands, noise, comfort, and operation and maintenance issues combine to result in sometime counterintuitive trade-offs between flow rates and filter efficiency. For example, a compromise between filter efficiency (which affects the replacement cost of the filter and the cost of the electricity to operate) and flow rate (which affects air speeds in the space and also the electricity costs to operate) can be found to maximum occupant comfort, subject to the level of contamination, size of the room, and tolerance of the occupants to air movement and noise.

As an example, it may be more practical to use a 95% efficient filter with lower pressure drop compared to an HEPA (99.97%) to meet particle removal goals in the space. Figures 4 and 5 show the results of an unpublished study conducted in a rectangular ($2.24\text{ m W} \times 3.91\text{ m L} \times 2.44\text{ m H}$) experimental chamber built using typical residential construction materials with an air-cleaning unit operating with two

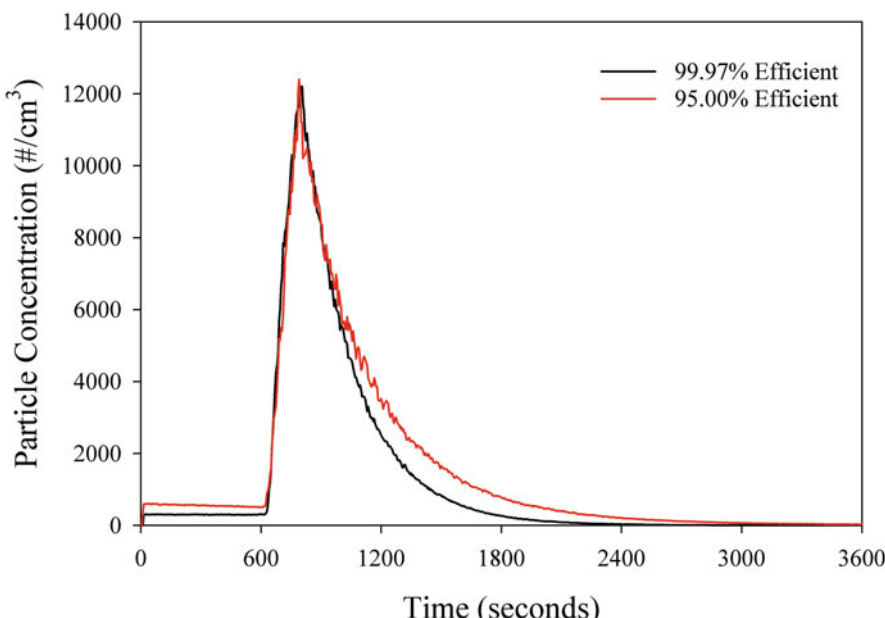


Fig. 4 Particle concentration decay for the 99.97% and 95% efficient filters on high fan speed

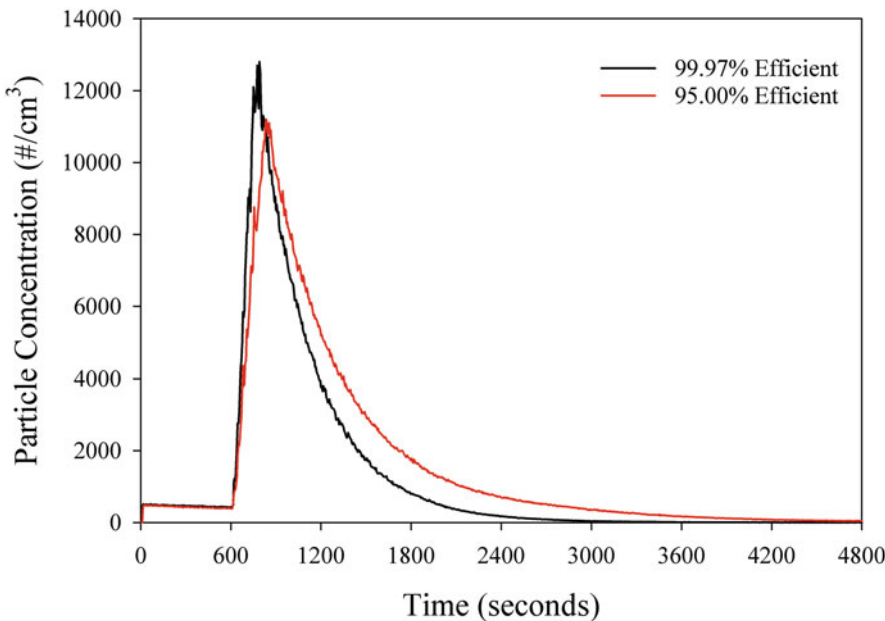


Fig. 5 Particle concentration decay for the 99.97% and 95% efficient filters on low fan speed

possible fan speeds. The airflows were: 207 cfm and 142 cfm for a 95% efficient filter installed with the fan operating on high speed and low speed, respectively, and 171 cfm and 119 cfm for a 99.97% efficient filter installed with the fan operating on high and low speed, respectively. It can be seen that the performance difference is relatively small, as the product of flow rate and efficiency (i.e., calculated CADR, Eq. 12) is similar between the two devices, but there can be substantial savings in energy when using the 95% filter due to lower power draw requirements for moving air through the lower resistance filter.

$$CADR = \dot{V} \times \eta \quad (12)$$

Where \dot{V} is the flow rate through the filter (CFM) and η is the removal efficiency of the filter.

Considerations of trade-offs between flow rates and efficiency, as well as concerns for upfront costs of many portable air-cleaning devices, have led to the development of do-it-yourself solutions for in-room air cleaning. A prime example is the Corsi-Rosenthal box fan filter, which combines low-cost box fans with relatively low-cost MERV 13 filters (or higher, but not as high as HEPA) to yield a cost-effective high-CADR in-room air-cleaning solution, without needing HEPA filters and controlled manufacturing. While the minimum average removal efficiency of a MERV 13 filter is only 50% or higher for particles in the most penetration particle size (MPPS) range (0.3–1 μm) in the 52.2 test, the flow rate through box fans

can be as high as 2500 CFM (unobstructed). Installing five MERV 13 filters in a cube with the sixth side being a box fan could result in a CADR of as high as 1000 CFM, assuming flow is reduced to 2000 CFM and the removal efficiency of the filters is 50% (i.e., $2000 \text{ CFM} \times 0.5 = 1000 \text{ CFM}$).

In-Duct Filters

For residential, commercial, and institutional buildings with dedicated forced-air heating, cooling, and/or ventilating (HVAC) systems, in-duct filters are widely used, originally to protect equipment (e.g., heat exchangers and fans) from large particles, but now increasingly to protect people from exposure to airborne particulate matter. In all cases, filters are placed such that the air flow within the HVAC system passes through to capture particles. There are some important practical differences in filtration between smaller residential systems and larger commercial and institutional systems that influence what types of filters can be installed, what the energy and airflow consequences of higher efficiency filtration might be, and how effective filters are in reducing particle concentrations. As such, two scales of in-duct HVAC filtration applications are considered here: residential and nonresidential (i.e., commercial and institutional).

Residential In-Duct Air Filters

In homes with forced air heating and/or cooling systems, a filter is placed such that the flow from the house to the air handler (often referred to as a furnace in heating-dominated climates) passes through the filter (Fig. 6). The filtered air then passes through the heat exchanger, and the conditioned and filtered air is distributed to the house through central ductwork. Filters are often located in a filter slot on the upstream side of the furnace or may be located at return grille(s) farther from the air handler.

Most existing homes typically use MERV 8 or lower in-duct air filters (El Orch et al. 2014), and even newer homes built to ASHRAE Standard 62.2, “Ventilation and Acceptable Indoor Air Quality in Residential Buildings,” which is not universally adopted across the USA but is required in some jurisdictions, which are required to have only a minimum of MERV 6 air filters in their forced air mechanical systems (ASHRAE 2019). From Table 1, it can be seen that MERV 8 and lower filters have limited effectiveness in removing many of the particle types and sizes that are important for occupant health. Among higher efficiency residential filters that are readily available, homeowners commonly upgrade to MERV 11 or MERV 13 but rarely venture beyond MERV 13 (Stephens 2019). Conversely, the US EPA recommends using filters with an MERV 13 or higher to capture at least 50% of the smallest particles that contribute most to indoor fine particulate matter ($\text{PM}_{2.5}$) concentrations (US EPA 2018). There remain many opportunities to improve residential filtration, as well as practical challenges.

Historically, the use of higher efficiency (i.e., higher MERV or equivalent) filters in residences has been limited by the prevailing conception that they have higher

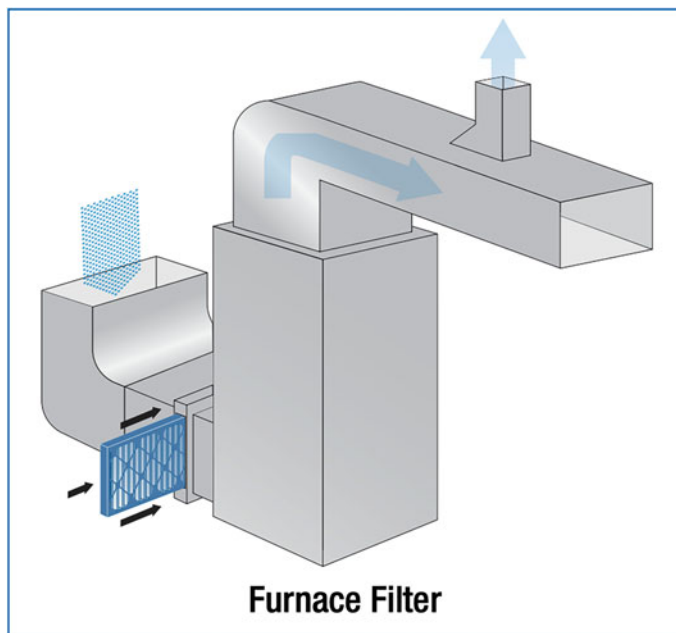


Fig. 6 Schematic of a home-forced air furnace showing the location of the air filter. Figure taken from https://www.epa.gov/sites/default/files/2018-07/documents/residential_air_cleaners_-_a_technical_summary_3rd_edition.pdf

pressure drops and thus higher resistance to airflow, which makes heating and cooling systems “work harder” to overcome the pressure drop, using more fan energy (Figure 7). However, most residential forced air heating and cooling systems in existing homes utilize permanent split capacitor (PSC) blower motors, which do not adjust speeds to compensate for additional airflow resistance but rather respond to a higher pressure drop by moving less air (and often drawing less power). Therefore, in most existing homes, the concern for higher efficiency (and higher pressure drop) filters is: How much will they reduce airflow, and how will the reduced airflow impact system performance and energy use (e.g., runtime and heating/cooling capacity)? To date, most research suggests that the impacts on these performance metrics are relatively small (Fazli et al. 2015; Stephens et al. 2010a, b; Walker et al. 2012), except for systems that have not been properly designed or maintained and may already be on the verge of failure; in these systems, the additional pressure drop of higher efficiency filters could decrease airflow to the point where system performance issues such as frozen cooling coils can arise. It is also worth noting that many newer forced air heating and cooling systems utilize electronically commutated motors (ECMs) that will adjust fan speeds to overcome additional resistance encountered in the system. In these systems, adding a higher pressure drop filter will tend to lead to increased fan power draws to overcome the

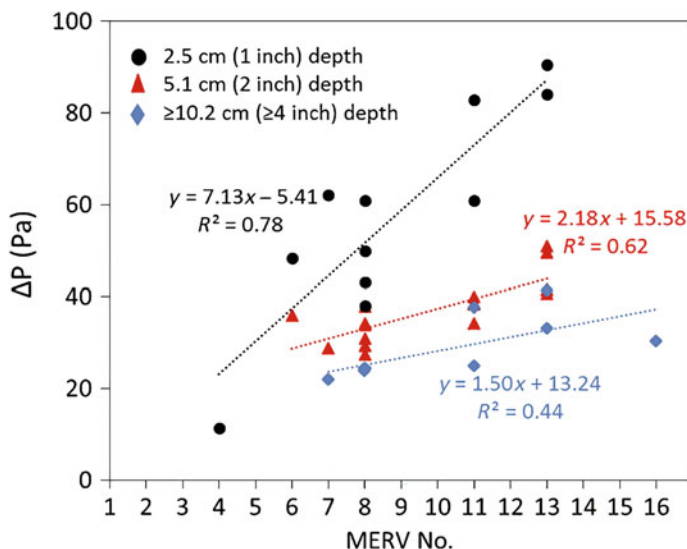


Fig. 7 Initial pressure drop for new filters as a function of the manufacturer's reported MERV ratings. (Figure taken from Fazli et al. 2019)

added resistance and maintain a relatively constant airflow rate, but with no other meaningful impacts.

Given these issues with pressure drop, some strategies that manufacturers use to enable higher efficiency filtration in residential forced air systems are increasing filter thickness and utilizing electrostatically charged (sometimes called electret) filter media (Wang and Hofacre 2008; Liu et al. 2017). The use of electrostatically charged media allows for higher initial particle removal efficiency than relying on mechanical capture mechanisms alone, although it should be noted that as the filter loads with particles over time, the electrostatic charge will diminish and reduce removal efficiency (Lehtimäki et al. 2002; Owen et al. 2013). Conversely, dust loading can increase the removal efficiency of lower MERV mechanical media filters. The use of extended depth filters allows for spreading the filter media out over a larger surface area and reduces the filter pressure drop; research shows that there are now 2-inch and 4-inch depth MERV 13 and MERV 16 filters available with initial pressure drops that are below MERV 6–8 1-inch filters (Fazli et al. 2019). One challenge of deeper filters is that modifications to existing HVAC systems are often required to accommodate their wider thickness.

It is also worth noting that while there are commercially available options for improving residential air filtration in central forced air systems, there are fewer options for high efficiency filtration in mechanical ventilation systems that intentionally bring in outdoor air (e.g., energy and heat recovery ventilators) and for heating and cooling systems that do not utilize centralized ductwork for air distribution (e.g., mini-split heat pump systems).

Commercial and Institutional In-Duct Air Filters

Larger commercial and institutional buildings utilize heating, ventilation, and air conditioning (HVAC) systems to provide occupant comfort and meet ventilation needs for occupied spaces. Ventilation is described in detail elsewhere in this handbook (Lv et al. 2022; Persily 2022).

Figure 8 shows a schematic view of a typical central HVAC system. Outdoor air and return air are mixed – at variable fractions ranging from 100% outdoor air to the code minimum amount of outdoor air, depending on factors such as occupancy and climate conditions – and then filtered, conditioned, and supplied to the occupied space. Whether ambient or returned indoor air, particulate matter will be introduced into the system either as part of the ambient makeup air or from indoor sources (or both). These particles need to be removed, and filters are commonly employed so that the design problem is similar to residential in-duct filter issues, but on a much larger scale. The design problem is how much filtration is needed to provide air quality sufficient for the purposes of utilizing the occupied space. There is again the trade-off between filtration efficiency and pressure drop/energy use, as many commercial and institutional systems utilize fans that adjust speed to maintain airflow rates in the fact of added resistance from a higher pressure drop filter (Azimi and Stephens 2013; Bekö et al. 2008; Montgomery et al. 2012). Thus, in many cases,

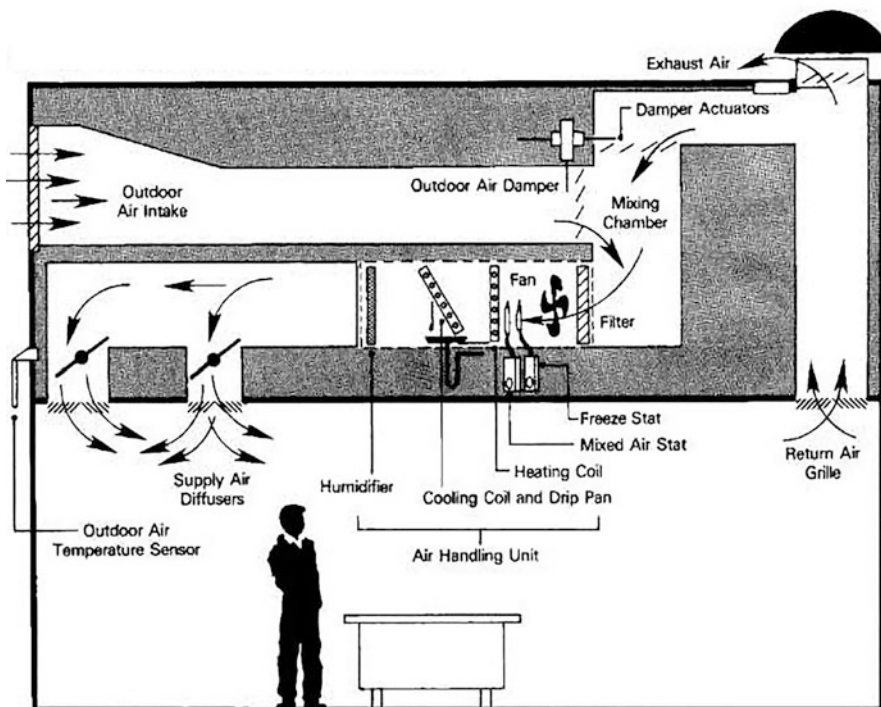


Fig. 8 Diagram of the components of a typical HVAC system. (Figure taken from USEPA 1991)



Fig. 9 Actual installation using MERV 8 box filters (left) and MERV 13 bag filters (right) to provide high-filtration efficiency at a lower total pressure drop

lower-efficiency (MERV 8) filters were often used to remove large particle dust, but not significant amounts of fine particles. In fact, ASHRAE Standard 62.1 “Ventilation for Acceptable Air Quality,” which is widely adopted in building codes across the USA, requires a minimum of MERV 8 filters in all buildings except those located in an area where the national standard for PM_{2.5} is exceeded (these buildings should improve to MERV 11 filters).

However, during the COVID-19 pandemic beginning in 2020, many buildings were upgraded to MERV 13 filtration, led by the convening of an ASHRAE Epidemic Task Force, which adopted core recommendations for reducing airborne infectious aerosol exposure, including using combinations of filters and air cleaners that achieve MERV 13 or better levels of performance for air recirculated by HVAC systems. Commercial and institutional systems also differ from residential systems in that they can also use larger bag filters, as well as prefilters. Prefilters are lower efficiency (and lower cost) that are installed upstream of a higher efficiency (higher cost) filter, extending the lifetime of the higher-efficiency filter and lowering filter replacement costs. Figure 9 shows this type of configuration with MERV 8 box filters (left) that are placed in front of MERV 13 bag filters. The bag filters provide significantly more surface area than would be possible in a box filter and, thus, lower pressure drop for the same filtration performance (Fig. 9).

Impacts of Filters in Real Buildings

Regardless of the type of building (i.e., residential or commercial), filter installation (i.e., in-duct or in-room), or filter type (i.e., MERV 2 through HEPA), there exist useful performance metrics that can be used to evaluate (through measurements) or predict (through models) the impacts of filters on indoor particulate matter in

buildings. There are also several practical factors that affect how a filtration system performs in a real building.

The effectiveness of an air filtration device or system is a dimensionless measure of its ability to remove pollutants from the spaces it serves in real-world situations (Miller-Leiden et al. 1996; Zhang et al. 2020). It is simply a comparison of pollutant concentrations in a space with and without an air filtration device/system operating, assuming other parameters like emission rates, ventilation/infiltration rates, deposition rates, and any other source and loss mechanisms are held constant (Eq. 13).

$$\text{Effectiveness} = 1 - \frac{C_{\text{on}}}{C_{\text{off}}} \quad (13)$$

where C_{on} and C_{off} are the contaminant concentrations in a space with the filtration device/system on and off, respectively (#/m³ or equivalent). The terms C_{on} and C_{off} can be expanded to include common loss terms of ventilation, deposition, and CADR, assuming other factors such as source strengths are held constant (Waring et al. 2008):

$$\text{Effectiveness} = 1 - \frac{\text{ACH} + k_{\text{dep}}}{\text{ACH} + k_{\text{dep}} + \text{CADR}/V} \quad (14)$$

where ACH is the air change rate in the space (h⁻¹), k_{dep} is the deposition loss rate constant in the space (h⁻¹), and CADR/V (ft³/min) is the CADR divided by the volume of the space (ft³) and multiplied by a conversion factor of 60 mins per hour. For stand-alone in-room air cleaner applications, the effectiveness can be measured easily (Eq. 13) or readily calculated using the CADR of the unit (Eq. 14). For in-duct devices that operate continuously, as long as the removal efficiency of the filter and the flow rate through the filter is known, an effective CADR can be calculated (Eq. 12) and incorporated into estimates of effectiveness (Eq. 14). For both in-duct and in-room devices that operate intermittently, such as portable air cleaners that are switched on and off by occupants and residential in-duct filters in heating and cooling systems that operate only intermittently to meet heating and cooling loads, a fractional runtime term (f) can be introduced into Eq. 15 to predict effectiveness:

$$\text{Effectiveness} = 1 - \frac{\text{ACH} + k_{\text{dep}}}{\text{ACH} + k_{\text{dep}} + f \text{CADR}/V} \quad (15)$$

It is also worth noting that it is possible to measure the effective CADR of both in-room and in-duct filtration systems operating in real spaces (MacIntosh et al. 2008; Stephens and Siegel 2012). The procedure is similar to the AHAM CADR test procedure described previously, except that it takes place in a real building operating under relatively tightly controlled conditions (e.g., minimal occupancy or at least constant occupancy, consistent or at least measured ventilation rates, etc.). Particles are injected and allowed to decay to background levels while monitoring, repeated with and without an air filtration device/system operating. The data are used to

estimate loss rate constants under each condition, which can be used to estimate an in situ CADR (Eq. 10). Particle concentration measurements can also be conducted within HVAC systems to measure the in situ removal efficiency of in-duct filtration systems (ASHRAE 2008; Ben-David et al. 2018), although this is generally easier to accomplish in large commercial systems than in smaller residential systems (Li and Siegel 2020).

Finally, several practical factors also impact how a filtration system performs in a real building. The runtime fraction, or the fraction of time a filtration system operates, has a large impact on the effectiveness of filtration systems. Typical residential heating and cooling systems operate less than 25% of the time in most locations, which limits how effective even the best in-duct filter can be (Touchie and Siegel 2018). Systems can instead be run in continuous fan-only mode, but there are energy penalties for doing so, as well as comfort and maintenance considerations. Studies of portable air cleaner use have also noted that occupants frequently turn off devices and/or turn them down to lower fan speed settings with lower CADR. Other factors that affect primarily in-duct systems include how the filter performs as installed (compared to lab-tested performance), including whether or not there is any bypass airflow around the filter, which can diminish performance by allowing essentially unfiltered air into the air stream (VerShaw et al. 2009; Ward and Siegel 2005). The timing and nature of indoor particle sources relative to when filtration systems operate also affects their effectiveness in real buildings. For example, if indoor emission sources occur at time when filtration systems are off, obviously the effect of filtration diminishes (Li and Siegel 2021). Occupants can also open windows in buildings with operable windows, which may introduce outdoor pollutants when ambient concentrations are elevated higher than indoors. There is also the issue of proximity effects, especially for in-duct systems, whereby point sources of indoor pollutants (such as cooking) may lead to occupant exposures for those in proximity to sources prior to pollutants being mixed in the space and encountering a central filter; locating in-room devices closer to known sources can help mitigate this effect.

Conclusions

Filtration is a well-developed and universally employed technique for removing particles from air that is forced to move through the filter. The efficiency of removal depends on filter design and particle size. The minimum efficiency typically occurs for particles with aerodynamic diameters around 0.3 μm . As particles increase in size, they become more inertial and can be more effectively collected by the filter. As particle size decreases, the particles become more diffusional and are more effectively collected. The flow through the filter depends on its efficiency of filtration and the pressure differential across the filter. Higher filtration efficiency filters require a higher pressure differential to drive the same flow rate and, thus, require more

energy. Choosing the appropriate filter for a given situation involves trade-offs between efficiency, flow rates, and energy use, and care is needed to ensure that the particle removal is sufficient to protect the inhabitants of the indoor spaces as well as the objects like furniture or art work onto which those particles might deposit.

References

- American National Standards Institute (ANSI) (2006) Method for measuring performance of portable household electric room air cleaners, Standard No. ANSI/AHAM AC-1-2006, <https://webstore.ansi.org/standards/aham/ansiahamac2006>
- American Society of Heating, Refrigerating and Air-Conditioning Engineers (ASHRAE) (2008) Guideline 26: guideline for field testing of general ventilation devices and systems for removal efficiency in-situ by particle size and resistance to flow
- American Society of Heating, Refrigerating and Air-Conditioning Engineers (ASHRAE) (2017) Standard 52.2: method of testing general ventilation air-cleaning devices for removal efficiency by particle size
- American Society of Heating, Refrigerating and Air-Conditioning Engineers (ASHRAE) (2018) ASHRAE position document on filtration and air cleaning
- American Society of Heating, Refrigerating and Air-Conditioning Engineers (ASHRAE) (2019) ANSI/ASHRAE standard 62.2–2019: ventilation and acceptable indoor air quality in residential buildings
- American Society of Heating, Refrigerating and Air-Conditioning Engineers (ASHRAE) (2020) Air cleaners for particulate contaminants, 2020 ASHRAE Handbook-HVAC systems and equipment (I-P), Chapter 29, available from: <https://www.ashrae.org/technical-resources/ashrae-handbook/description-2020-ashrae-handbook-hvac-systems-and-equipment>
- Azimi P, Stephens B (2013) HVAC filtration for controlling infectious airborne disease transmission in indoor environments: predicting risk reductions and operational costs. *Build Environ* 70: 150–160. <https://doi.org/10.1016/j.buildenv.2013.08.025>
- Azimi P, Zhao D, Stephens B (2014) Estimates of HVAC filtration efficiency for fine and ultrafine particles of outdoor origin. *Atmos Environ* 98:337–346. <https://doi.org/10.1016/j.atmosenv.2014.09.007>
- Bekö G, Clausen G, Weschler C (2008) Is the use of particle air filtration justified? Costs and benefits of filtration with regard to health effects, building cleaning and occupant productivity. *Build Environ* 43:1647–1657. <https://doi.org/10.1016/j.buildenv.2007.10.006>
- Ben-David T, Wang S, Rackes A, Waring MS (2018) Measuring the efficacy of HVAC particle filtration over a range of ventilation rates in an office building. *Build Environ* 144:648–656. <https://doi.org/10.1016/j.buildenv.2018.08.018>
- Carslaw N (2022) Indoor gas-phase chemistry. In: Zhang Y, Mandin C, Hopke PK (eds) *Handbook of indoor air quality*. Springer. 18 pp
- Chen C, Zhao B (2022) Impact of outdoor particles on indoor air. In: Zhang Y, Mandin C, Hopke PK (eds) *Handbook of indoor air quality*. Springer. 23 pp
- Davies CN (1973) *Air filtration*. Academic Press, New York
- El Orch Z, Stephens B, Waring MS (2014) Predictions and determinants of size-resolved particle infiltration factors in single-family homes in the U.S. *Build Environ* 74:106–118. <https://doi.org/10.1016/j.buildenv.2014.01.006>
- Fazli T, Yeap RY, Stephens B (2015) Modeling the energy and cost impacts of excess static pressure in central forced-air heating and air-conditioning systems in single-family residences in the U.S. *Energ Buildings* 107:243–253. <https://doi.org/10.1016/j.enbuild.2015.08.026>
- Fazli T, Zeng Y, Stephens B (2019) Fine and ultrafine particle removal efficiency of new residential HVAC filters. *Indoor Air* 1a.12566. <https://doi.org/10.1111/ina.12566>

- Grau-Bové J, Strli M (2013) Fine particulate matter in indoor cultural heritage: a literature review. *Herit Sci* 1:8. <https://doi.org/10.1186/2050-7445-1-8>
- Hinds WC, Zhu Y (2022) Aerosol technology: properties, behavior, and measurement of aerosol particles, 3rd edn. Wiley, New York
- ISO (2016) ISO 16890: Air filters for general ventilation
- Lehtimäki M, Säämänen A, Taipale A (2002) ASHRAE RP-1189: investigation of mechanisms and operating environments that impact the filtration efficiency of charged air filtration media. American Society of Heating, Refrigerating, and Air-Conditioning Engineers.
- Li T, Siegel JA (2020) In situ efficiency of filters in residential central HVAC systems. *Indoor Air* 30:315–325. <https://doi.org/10.1111/ina.12633>
- Li T, Siegel JA (2021) Assessing the impact of filtration systems in indoor environments with effectiveness. *Build Environ* 187:107389. <https://doi.org/10.1016/j.buildenv.2020.107389>
- Liu G, Xiao M, Zhang X, Gal C, Chen X, Liu L, Pan S, Wu J, Tang L, Clements-Croome D (2017) A review of air filtration technologies for sustainable and healthy building ventilation. *Sustain Cities Soc* 32:375–396
- Lv M, Liu S, Cao Q, Zhang T, Liu J (2022) Influence of ventilation on indoor air quality. In: Zhang Y, Mandin C, Hopke PK (eds) *Handbook of indoor air quality*. Springer. 38 pp
- MacIntosh DL, Myatt TA, Ludwig JF, Baker BJ, Suh HH, Spengler JD (2008) Whole house particle removal and clean air delivery rates for in-duct and portable ventilation systems. *J Air Waste Manag Assoc* 58:1474–1482
- Miller-Leiden S, Lohascio C, Nazaroff WW, Macher JM (1996) Effectiveness of in-room air filtration and dilution ventilation for tuberculosis infection control. *J Air Waste Manag Assoc* 46:869–882. <https://doi.org/10.1080/10473289.1996.10467523>
- Montgomery JF, Green SI, Rogak SN, Bartlett K (2012) Predicting the energy use and operation cost of HVAC air filters. *Energ Buildings* 47:643–650. <https://doi.org/10.1016/j.enbuild.2012.01.001>
- Offermann FJ, Sextro RG, Fisk WJ, Grimsrud DT, Nazaroff WW, Nero AV, Revzan KL, Yater J (1985) Control of respirable particles in indoor air with portable air cleaners. *Atmos Environ* 19: 1761–1771. [https://doi.org/10.1016/0004-6981\(85\)90003-4](https://doi.org/10.1016/0004-6981(85)90003-4)
- Owen K, Pope R, Hanley J (2013) ASHRAE RP-1360: how do pressure drop, weight gain, and loaded dust composition change throughout filter lifetime. American Society of Heating, Refrigerating, and Air-Conditioning Engineers
- Persily A (2022) Evaluating ventilation performance. In: Zhang Y, Mandin C, Hopke PK (eds) *Handbook of indoor air quality*. Springer. 39 pp
- Samet J, Holguin F, Buran M (2022) The health effects of indoor air pollution. In: Zhang Y, Mandin C, Hopke PK (eds) *Handbook of indoor air quality*. Springer. 47 pp
- Stephens B (2019) Analyzing a database of over 6 million online sales of residential HVAC filters from 2008 to 2017. Built Environ Res Group URL <http://built-envi.com/analyzing-a-database-of-over-6-million-online-sales-of-residential-hvac-filters-from-2008-to-2017/>
- Stephens B, Siegel JA (2012) Comparison of test methods for determining the particle removal efficiency of filters in residential and light-commercial central HVAC systems. *Aerosol Sci Technol* 46:504–513. <https://doi.org/10.1080/02786826.2011.642825>
- Stephens B, Novoselac A, Siegel JA (2010a) The effects of filtration on pressure drop and energy consumption in residential HVAC systems. *HVACR Res* 16:273–294
- Stephens B, Siegel JA, Novoselac A (2010b) Energy implications of filtration in residential and light-commercial buildings (RP-1299). *ASHRAE Trans* 116:346–357
- Touchie MF, Siegel JA (2018) Residential HVAC runtime from smart thermostats: characterization, comparison, and impacts. *Indoor Air* 28:905–915. <https://doi.org/10.1111/ina.12496>
- U.S. Environmental Protection Agency (USEPA) (1991) Building air quality: a guide for building owners and facility managers. EPA document # 402-F-91-102, December 1991. Available from: <https://epa.gov/indoor-air-quality-iaq/building-air-quality-guide-guide-building-owners-and-facility-managers>.
- US EPA (2018) Residential air cleaners: a technical summary, 3rd
- VerShaw J, Siegel J, Chojnowski D, Nigro P (2009) Implications of filter bypass. *ASHRAE Trans* 115:191–198

- Walker IS, Dickerhoff DJ, Faulkner D, Turner WJN (2012) Energy implications of in-line filtration in California (No. LBNL-6143E). Lawrence Berkeley National Laboratory, Berkeley
- Wang A, Hofacre KC (2008) Assessment of advanced building air filtration systems, Report No. EPA/600/R-08/032. Available from: https://cfpub.epa.gov/si/si_public_record_report.cfm?dirEntryId=189523&Lab=NHSRC
- Ward M, Siegel JA (2005) Modeling filter bypass: impact on filter efficiency. ASHRAE Trans 111: 1091–1100
- Waring MS, Siegel JA, Corsi RL (2008) Ultrafine particle removal and generation by portable air cleaners. Atmos Environ 42:5003–5014. <https://doi.org/10.1016/j.atmosenv.2008.02.011>
- Zhang Y, Li T, Siegel JA (2020) Investigating the impact of filters on long-term particle concentration measurements in residences (RP-1649). Sci Technol Built Environ 26:1037–1047. <https://doi.org/10.1080/23744731.2020.1778402>



PCO and TCO in Air Cleaning

60

Jinhan Mo and Enze Tian

Contents

Introduction	1738
Photocatalytic Oxidation	1738
Principal	1738
Enhancement of the Removal Effectiveness	1739
Identification of PCO By-Products	1748
Thermal Catalytic Oxidation	1757
Formaldehyde Removal by TCO	1759
Kinetic Reaction Model	1763
Conclusions	1768
References	1769

Abstract

Indoor air cleaning has been proved to be an efficient way to reduce indoor harmful VOCs. Many advanced technologies have been studied for the quick and economical removal of VOCs from indoor air. This chapter introduced photo-catalytic oxidation (PCO) and room-temperature thermal catalytic oxidation (TCO). The principle of PCO was introduced, and then a general model was developed for analyzing the VOCs removal performance by PCO. The enhancement of PCO performance was analyzed based on the general model. The unwanted by-products during the PCO reaction process were observed online and qualitatively identified. We also introduce various kinetic models for TCO. The experimental results show that a kinetic model with a bimolecular Langmuir-Hinshelwood mechanism and temperature effect best fit the data. The activation energy of the TCO reaction for formaldehyde was then obtained. In summary, the great potential of the combination of PCO, TCO, and adsorption will advance indoor air cleaning in the future.

J. Mo (✉) · E. Tian

Department of Building Science, School of Architecture, Tsinghua University, Beijing, China
e-mail: mojinhan@tsinghua.edu.cn; tez18@tsinghua.org.cn

Keywords

Photocatalytic oxidation · Room temperature · Thermal catalyst · Formaldehyde · Kinetic parameters

Introduction

Indoor air pollutants impact human health, comfort, and productivity. Volatile organic compounds (VOCs) are among the most abundant chemical pollutants in the indoor air that we breathe (USEPA 1990; WHO 1989). Some of these compounds are associated with sick building syndrome (SBS), including mucous membrane irritation, headache, and fatigue (Wang et al. 2007; Meininghaus et al. 1999; Kim et al. 2001; WHO 1989; USEPA 1990); others are known carcinogens (e.g., formaldehyde and acrolein [Oehha 2007]). Millions of people are currently suffering from the consequences of poor indoor air quality and billions of dollars are lost in the world each year due to poor indoor air quality (Fisk and Rosenfeld 1997).

Because indoor air quality is an important determinant of human health, comfort, and productivity, high-quality indoor air is desirable. Air cleaning technologies are of increasing importance, especially when building ventilation rates are being reduced to conserve energy. Commonly used technologies for indoor air purification include adsorption, catalytic oxidation, and photocatalytic oxidation (PCO) (Zhang et al. 2011; Gallego et al. 2013; Mo et al. 2009a).

Photocatalytic Oxidation**Principal**

As the pioneers in this field, Fujishima and Honda (1972) discovered the phenomenon of photoinduced water cleavage to TiO₂ electrodes. In the subsequent three decades, a wide range of potential applications of PCO to air purification has been reported.

The air purification technique of PCO commonly uses nano-semiconductor catalysts and ultraviolet (UV) light to convert organic compounds in indoor air into benign and odorless constituents – water vapor (H₂O) and carbon dioxide (CO₂) (Tompkins 2001). Most PCO reactors use nano-titania (TiO₂) as the catalyst that is activated by UV light. Figure 1 shows the schematic of the UV-PCO process of VOCs using TiO₂ as the catalyst. An electron in an electron-filled valence band (VB) is excited by photoirradiation to a vacant conduction band (CB), leaving a positive hole in the VB. These electrons and positive holes drive reduction and oxidation, respectively, of compounds adsorbed on the surface of a photocatalyst (Ohtani 2008).

The activation equation can be written as:



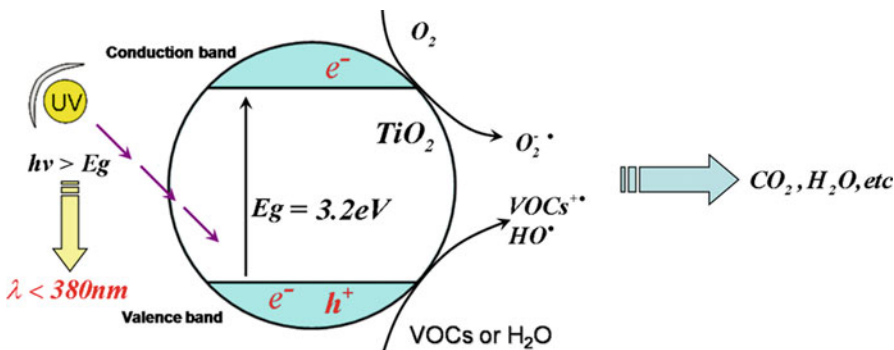
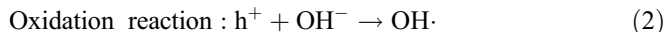
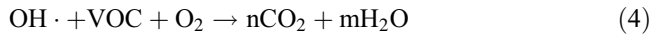


Fig. 1 Schematic of TiO_2 UV photocatalytic oxidation process of VOCs (Mo et al. 2009a)

In this reaction, h^+ and e^- are powerful oxidizing and reducing agents, respectively. The oxidation and reduction reactions can be expressed as:



When organic compounds are chemically transformed by a PCO device, the hydroxyl radical ($\text{OH}\cdot$), derived from the oxidation of adsorbed water or adsorbed OH^- , is the dominant strong oxidant. Its net reaction with a VOC can be expressed as:



The process of PCO has several advantages (Ollis 2000): (1) GRAS (generally recognized as safe): the common photocatalyst is anatase TiO_2 , an n-type semiconductor oxide which is also a component of some toothpaste and pharmaceutical suspensions; (2) mild oxidant: kinetic studies demonstrate that the ultimate source of oxygen during oxidation is molecular oxygen, a far milder oxidant than hydrogen peroxide or ozone, etc.; (3) ambient temperature: photocatalysis appears to be active at room temperature; and (4) general: while several mechanistic pathways for oxidation have been proposed, the dominant view is that the hydroxyl radical (or some other equally strong oxidant) is photogenerated on the titania surface; the potency of this oxidant is responsible for the titania's broad activity toward various contaminants (such as aromatics, alkanes, olefins, halogenated hydrocarbons, odor compounds, etc.).

Enhancement of the Removal Effectiveness

Much research has been performed on how different factors affect the PCO reactor performance (Obie and Brown 1995; Obie 1996; Obie and Hay 1997; Dreyer et al.

1996; Hall et al. 1998; Yoneyama and Torimoto 2000). It is difficult to know what influence the various factors have on the VOC removal performance of PCO reactors only through experiments. Modeling and simulation are powerful methods for determining the relationship between VOC removal performance and the influencing factors. Hossain et al. (1999) developed a three-dimensional convection-diffusion reaction model for analyzing the VOC removal performance of honeycomb PCO reactors under steady-state conditions, which fitted very well with the experiments. Chen and Zhang (Chen and Zhang 2008; Chen 2007) involved both a model and experimental investigation on the interference between multiple VOCs. It indicated that the interference effects among test VOCs were generally small in the 2-VOC and 3-VOC mixture tests performed on toluene, ethylbenzene, octane, decane, and dodecane with the initial concentration of approximately 1 mg/m^3 for each compound. However, there were still few studies on the interaction effects between PCO reactor structure and environmental factors.

Based on a few suitable assumptions, many physical models of PCO reactors were developed. Tronconi and Forzatti (1992) developed a lumped parameter model for a honeycomb structure reactor decomposing NO_x . They derived dimensionless numbers to express the reaction rate and convective mass transfer rate and demonstrated the application of the model to different geometries and boundary conditions. Hall et al. (1998) described a reduced-order model for photocatalytic honeycomb reactors and discussed mass transport and reaction rate limits. He found that the product of volumetric flow rate and conversion rate, which represent the overall rate of VOC removal, reaches an asymptote with the velocity increasing. Zhang et al. (2003) developed a PCO reactor model. They found that two parameters, the number of the mass transfer unit, NTU_m , and the fractional conversion, ε , were the main parameters influencing the photooxidation performance of a PCO reactor. In Zhang's model, it was assumed that the photocatalytic reaction was a first-order reaction with a constant reaction rate coefficient and a constant convective mass transfer coefficient along the flow direction. Yang et al. (2004) developed an improved model considering the variable apparent reaction rate coefficient, K , and the variable convective mass transfer coefficient, h_m , along the flow direction. Three new parameters, the ideal reaction number of mass transfer units, $\text{NTU}_{m,ir}$, the ideal reaction fractional conversion, ε_{ir} , and the reaction effectiveness, η , were defined. The latter is useful in evaluating the upper limit and the bottleneck of VOC removal performance of PCO reactors.

Mo et al. (2005) developed a general PCO reactor model that takes account of the variable apparent reaction rate coefficient and convective mass transfer coefficient on the reaction surface (not only in the axial but also in the perimetric direction). It provides a novel insight into the analysis of VOC removal performance of PCO reactors. In practical applications, three types of PCO reactors (plate, honeycomb, and light in tube) are often applied (Fig. 2). These reactors can be summarized as shown in Fig. 3b, which describes the mass transfer balance of a finite element in the cross-section.

Based on the general channel shown in Fig. 3, the following assumptions are made: (1) the cross-sectional shape remains the same along the airflow direction; (2) there is only one species of VOC in indoor air or the VOCs can be treated as one

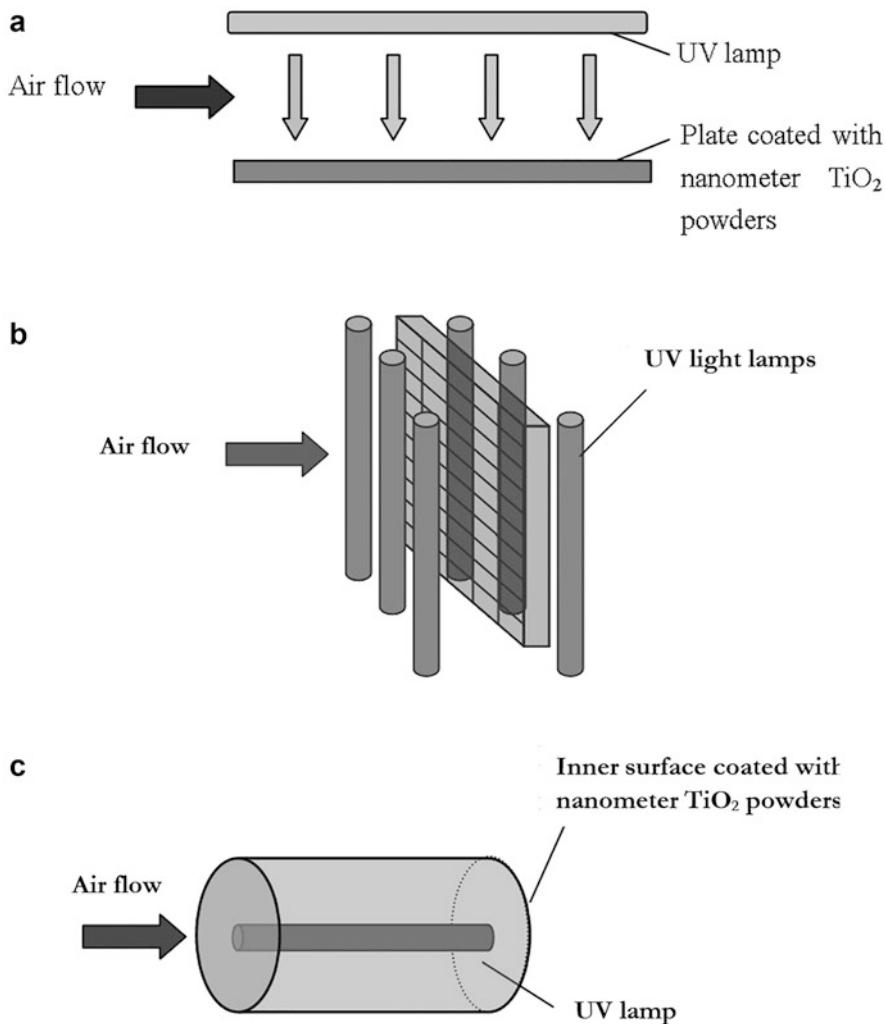
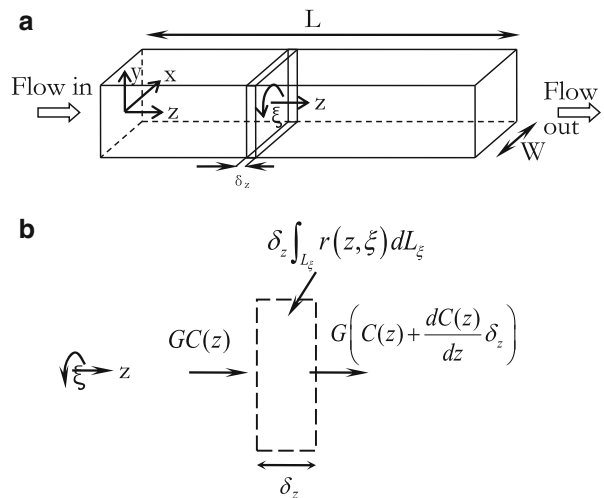


Fig. 2 Schematic of several PCO reactors. (a) Plate-type reactor; (b) honeycomb-type reactor; (c) light-in-tube reactor (Mo et al. 2005)

species. The photocatalytic reaction rate is expressed as the product of the VOC concentration adjacent to the reaction surface and the apparent reaction rate coefficient. Thus, for the PCO reactor shown in Fig. 3b, the mass conservation equation and boundary condition can be written as:

$$-G \frac{dC(z)}{dz} = \int_{L_\xi} r(z, \xi) d\xi \quad (5)$$

Fig. 3 Schematic of a channel of a monolith PCO reactor: (a) coordinates of the channel; (b) mass balance of the finite cross-sectional element (Mo et al. 2005)



$$r(z, \xi) = K(z, \xi)C_s(z, \xi) = h_m(z, \xi)(C(z) - C_s(z, \xi)) \quad (6)$$

$$z = 0, \quad C(z) = C_{in} \quad (7)$$

where z is the distance in the axial direction, m; ξ is the distance in the perimetric direction, m; L is the length of the channel, m; L_ξ is the perimeter of the cross-sectional area of the reaction surface path, m; G is the volumetric airflow rate, m^3s^{-1} ; $C(z)$ is the mass-rate-averaged VOC concentration on the cross-section at location z , that is:

$$C(z) = \frac{\int_{A_c} (u \cdot C) dA_c}{\int_{A_c} u dA_c} \quad (8)$$

where u is the velocity compound in z direction, A_c is the cross-sectional area, m^2 ; $C_s(z, \xi)$ is the local VOC concentration in the air adjacent to the air-solid interface at location (z, ξ) , mol m^{-3} ; C_{in} is the inlet VOC concentration, mol m^{-3} ; $r(z, \xi)$ is the local reaction rate at location (z, ξ) , $\text{mol m}^{-2} \text{s}^{-1}$; $K(z, \xi)$ is the local apparent reaction rate coefficient at location (z, ξ) , m s^{-1} , which is the function of intensity and wavelength of UV light, the physical properties of photocatalyst, and the humidity concentration and VOC concentration (based on the Langmuir-Hinshelwood kinetic rate formula in Obee (1996)); and $h_m(z, \xi)$ is the local convective mass transfer coefficient at location (z, ξ) , m s^{-1} .

Defining the local total VOC removal factor:

$$K_t(z, \xi) = \frac{1}{1/K(z, \xi) + 1/h_m(z, \xi)} \quad (9)$$

The solution of Eq. (5) gives:

$$\ln C_{out} - \ln C_{in} = -\frac{1}{G} \int_0^L \int_0^{L_\xi} K_t(z, \xi) d\xi dz \quad (10)$$

where C_{out} is the outlet VOC concentration, mol m⁻³.

Define the average total VOC removal factor K_t as follows:

$$K_t = \frac{\int_0^L \int_0^{L_\xi} K_t(z, \xi) d\xi dz}{\int_0^L \int_0^{L_\xi} d\xi dz} = \frac{\int_0^L \int_0^{L_\xi} K_t(z, \xi) d\xi dz}{A_r} \quad (11)$$

where A_r is the reaction surface area, m². Combining Eqs. (10) and (11) yields

$$C_{out} = C_{in} \cdot e^{-\frac{K_t A_r}{G}} \quad (12)$$

The number of the mass transfer unit, NTU_m, the fractional conversion, ε , and removal rate, \dot{m} , for a PCO reactor are expressed as follows:

$$NTU_m = \frac{K_t A_r}{G} \quad (13)$$

$$\varepsilon = \frac{C_{in} - C_{out}}{C_{in}} = 1 - e^{-NTU_m} \quad (14)$$

$$\dot{m} = G\varepsilon = G(1 - e^{-NTU_m}) \quad (15)$$

When $h_m(z, \xi)$ and $K(z, \xi)$ are independent of location ξ , this model can be simplified to the model of Yang et al. (2004); when independent of both z and ξ , this model can be simplified to the model of Zhang et al. (2003). The advantage of the present model is that it can be used to analyze the VOC removal performance of three-dimensional PCO reactors, in particular to those with inner extended surfaces and spatially dependent mass transfer rate coefficient and reaction rate coefficient.

From Eq. (13), the fractional conversion, ε , monotonically increases with increasing NTU_m. Thus, in order to improve the fractional conversion of a PCO reactor, it is very important to analyze how to increase NTU_m.

The Number of the Mass Transfer Unit, NTU_m

NTU_m can be rewritten as follows:

$$NTU_m = \frac{K_t A_r}{G} = \frac{K_t A_r}{u_a A_c} = \frac{1}{A_c} \int_0^L \int_0^{L_\xi} \frac{1/u_a}{1/K(z, \xi) + 1/h_m(z, \xi)} d\xi dz \quad (16)$$

where u_a is the average air velocity of the cross-sectional flow area, m s⁻¹.

Applying the Reynolds number, Re; Schmidt number, Sc; local Sherwood number, $Sh(z, \xi)$; and local Damkohler number (Tronconi and Forzatti 1992), $Da(z, \xi)$:

$$\begin{aligned}\text{Re} &= \frac{u_a d_e}{\nu}, \quad Sc = \frac{\nu}{D} \\ Sh(z, \xi) &= \frac{h_m(z, \xi) d_e}{D} \\ Da(z, \xi) &= \frac{K(z, \xi) d_e}{D}\end{aligned}\tag{17}$$

where d_e is the equivalent diameter of the airflow channel, m; ν is the kinematic viscosity, $\text{m}^2 \text{s}^{-1}$; and D is the diffusion coefficient of the VOC species in air, $\text{m}^2 \text{s}^{-1}$. Equation (16) can be rewritten as:

$$\text{NTU}_m = \frac{1}{A_c} \int_0^L \int_0^{L_\xi} \left(\frac{Sh(z, \xi)}{\text{Re} Sc} \cdot \frac{1}{Sh(z, \xi)/Da(z, \xi) + 1} \right) d\xi dz\tag{18}$$

Applying the local Stanton number of mass transfer:

$$St_m(z, \xi) = \frac{Sh(z, \xi)}{\text{Re} Sc}\tag{19}$$

and defining the local reaction effectiveness:

$$\eta(z, \xi) = \frac{1}{Sh(z, \xi)/Da(z, \xi) + 1}\tag{20}$$

Equation (18) can be rewritten as:

$$\text{NTU}_m = \frac{1}{A_c} \int_0^L \int_0^{L_\xi} St_m(z, \xi) \eta(z, \xi) d\xi dz\tag{21}$$

The average St_m and η for the whole reactor can be expressed as follows:

$$St_m = \frac{\int_0^L \int_0^{L_\xi} St_m(z, \xi) d\xi dz}{\int_0^L \int_0^{L_\xi} d\xi dz} = \frac{\int_0^L \int_0^{L_\xi} St_m(z, \xi) d\xi dz}{A_r}\tag{22}$$

$$\eta = \frac{\int_0^L \int_0^{L_\xi} (St_m(z, \xi) \eta(z, \xi)) d\xi dz}{\int_0^L \int_0^{L_\xi} St_m(z, \xi) d\xi dz} = \frac{\int_0^L \int_0^{L_\xi} (St_m(z, \xi) \eta(z, \xi)) d\xi dz}{A_r St_m}\tag{23}$$

Finally, the NTU_m is

$$\begin{aligned}\text{NTU}_m &= A^* \cdot St_m \cdot \eta, \\ A^* &= \frac{A_r}{A_c},\end{aligned}\tag{24}$$

where A^* is the area ratio of the reaction area to the cross-sectional area. NTU_m is the linear product of three parts, A^* , St_m , and η .

Applying the Taylor series yields

$$(1 - e^{-NTU_m}) = \sum_{n=1}^{\infty} (-1)^{n-1} \frac{(NTU_m)^n}{n!} = \sum_{n=1}^{\infty} (-1)^{n-1} \frac{(A^* \cdot St_m \cdot \eta)^n}{n!} \quad (25)$$

Thus, the VOC removal rate is expressed as:

$$\begin{aligned} \dot{m} &= G\varepsilon = u_a A_c \cdot \sum_{n=1}^{\infty} (-1)^{n-1} \frac{(A^* \cdot St_m \cdot \eta)^n}{n!} \\ &= A_r \cdot h_m \cdot \eta - \frac{(A_r \cdot h_m \cdot \eta)^2 (u_a A_c)^{-1}}{2!} + \frac{(A_r \cdot h_m \cdot \eta)^3 (u_a A_c)^{-2}}{3!} \dots \end{aligned} \quad (26)$$

If u_a is high enough,

$$\dot{m} \approx A_r \cdot h_m \cdot \eta \quad (27)$$

Therefore, when the averaged velocity, u_a , increases, at some point it reaches an asymptote, which is accordant with Hall's conclusion (Hall et al. 1998). Furthermore, the limit value of \dot{m} is a linear product of A_r , h_m , and η .

In summary, the VOC removal performance of PCO reactors improves with increasing values of the aforementioned dimensionless parameters. The influence of geometry and configuration, convective mass transfer rate, and PCO reaction rate on the VOC removal performance of a PCO reactor can be analyzed by applying the above model.

Discussion on A^*

A^* is a very useful parameter in optimizing a PCO reactor geometric configuration. Considering that $0 \leq \eta \leq 1$ and $0 \leq St_m \leq 1$, the maximal value of NTU_m is A^* , theoretically. If taking NTU_m as A^* , the fractional conversion is still not satisfactory, and it means that no matter how much the mass transfer and reaction rate are enhanced, the VOC removal performance cannot reach the desired level. For this case, the geometric configuration design or selection should not be accepted. Therefore, A^* can be regarded as a reactor geometric configuration evaluation parameter with which any unreasonable reactor geometric design or selection can easily be found.

Discussion on St_m

The mass transfer is the precondition of a PCO reaction. That is to say, it has to make sure that the mass transfer rate is high enough to guarantee a high reaction rate. If the value of A^* is high enough, the value of St_m will determine the VOC removal performance. Assuming η equal to 1, the maximal value of NTU_m is $(A^* St_m)$. Only when the value of $(A^* St_m)$ is high, the VOC removal performance of the reactor is promising. Otherwise, the reactor design is failed. Therefore, St_m can be regarded as the mass transfer evaluation parameter with which the mass transfer bottleneck of any unreasonable reactor can be found.

St_m shows the synergistic degree of fluid and mass flow fields. The field synergy between flow and heat transfer was analyzed by Guo et al. (Guo et al. 1998; Guo 2001), based on the parabolic fluid flow. Tao et al. (2002a, b) extended the concept to elliptic fluid flow and other heat transfer problems. This concept was well used in heat transfer enhancement but not in the mass transfer field. Similarly, from the analogy between heat transfer and mass transfer, the synergy of fluid and mass flow fields presents a new insight into the physical meaning of St_m . Based on Guo's concept, Mo et al. (2005) derived how to enhance the mass transfer in a PCO reactor.

For two-dimensional steady boundary flow, the mass balance equation is written as:

$$u \frac{\partial C}{\partial x} + v \frac{\partial C}{\partial y} = D \frac{\partial^2 C}{\partial y^2} \quad (28)$$

where x is the coordinate along with the flow, and y is normal to x ; u and v are the velocity components in x and y directions, respectively, m s^{-1} ; and C is mole concentration, mol m^{-3} .

Defining the vector:

$$\mathbf{U}_\infty = 0 \cdot \mathbf{i} - u_\infty \cdot \mathbf{j}, \quad (29)$$

and the following dimensionless variables,

$$\begin{aligned} \bar{\mathbf{U}} &= \frac{\mathbf{U}}{u_\infty}, \quad \bar{\mathbf{U}}_\infty = \frac{\mathbf{U}_\infty}{u_\infty}, \quad \bar{x} = \frac{x}{\delta_m(x)}, \quad \bar{y} = \frac{y}{\delta_m(x)}, \\ \bar{\nabla} \bar{C} &= \frac{\nabla C}{(C_s(x) - C_\infty)/\delta_m(x)}, \end{aligned} \quad (30)$$

where $\delta_m(x)$ is the mass boundary layer thickness at x location, m ; u_∞ is the velocity components in x in free-stream flow, m/s ; C_∞ is the VOC mole concentration in free-stream flow, mol m^{-3} ; and $C_s(x)$ is the VOC mole concentration in the air adjacent to the surface at y location, mol m^{-3} .

St_m is finally expressed as:

$$St_m(x) = \frac{Sh(x)}{Re Sc} = \frac{\int_0^1 (|\bar{\mathbf{U}}| |\nabla \bar{C}| \cos \beta) d\bar{y}}{\int_0^1 (|\nabla \bar{C}|) d\bar{y}} \quad (31)$$

where Sh , Re , and Sc represent the Sherwood number, the Reynolds number, and the Schmidt number, respectively. β is the intersection angle between $\bar{\mathbf{U}}$ and $\nabla \bar{C}$.

It is evident from Eq. (31) that: (1) St_m depends not only on the values of the velocity and concentration gradient of fluid flow, but also on the intersection angle between them; (2) $St_m \leq 1$, only when there is $|\bar{\mathbf{U}}| = 1$ and $\beta = 0$ everywhere, $St_m = 1$, that is, the vector $\bar{\mathbf{U}}$ has to be the same with $\bar{\mathbf{U}}_\infty$, not only the value but also the vector direction; obviously, when β equals to 0 everywhere, $|\bar{\mathbf{U}}|$ must be equal to

1; and (3) β plays an important role in describing the synergistic degree of fluid and mass flow fields.

β is in the range of 0 to π . If β is equal to $\pi/2$, the mass flux on the reaction surface is zero. Thus, the fractional conversion of the reactor is 0%. If β is equal to 0 (or π), $St_m = 1$, which means that $NTU_m = A^* \cdot 1 \cdot \eta$. Thus, in this case, the fractional conversion depends only on A^* and η . β is important to analyze the value of St_m . The average St_m is proportional to the cosine value of the average angle. For example, if the average angle reduces from 89 degree to 88 degree, the cosine value of the average angle increases about 100%.

From Eq. (19) and the definition of the convective mass transfer coefficient, it yields

$$St_m = \frac{h_m}{u_a} = -D \frac{\nabla C|_{wall}}{(C_m - C_s)} \frac{1}{u_a} \quad (32)$$

where $\nabla C|_{wall}$ is the concentration gradient on the reaction surface and C_m is the mass-rate-averaged concentration of the cross-sectional area. Thus, if the term $(\frac{\nabla C|_{wall}}{(C_m - C_s)})$ is not equal to constant (as is the case in most practical situations), St_m is the function of the concentration distribution. Tronconi and Forzatti (1992) found that the Sherwood number, Sh , varies with the value of the Damkohler number, Da . That is to say, St_m depends on η . Thus, it implies that η influences the concentration distribution and then affects St_m indirectly.

However, if the VOC concentration difference in the PCO reactor is not high, the influence of VOC concentration to St_m can be neglected, just as the situation of the influence of temperature to the heat transfer. Zhang et al. (2003) found that when the VOC concentration is low (lower than 2 ppmv), NTU_m remains almost constant in a series of experiments with various VOC concentrations. Therefore, it is justified to assume that St_m is independent of the VOC concentration if the concentration is low (as is the case in most practical situations).

Discussion on η

Equation (20) can be changed into:

$$\eta(z, \xi) = \frac{1}{h_m(z, \xi)/K(z, \xi) + 1} \quad (33)$$

If the mass transfer rate is much greater than the reaction rate, i.e., $h_m(z, \xi) \gg K(z, \xi)$, $\eta(z, \xi)$ approaches its minimum, 0. If the reaction rate is much greater than the mass transfer rate, i.e., $K(z, \xi) \gg h_m(z, \xi)$, $\eta(z, \xi)$ approaches its maximum, 1. Therefore, η , the averaged value of $\eta(z, \xi)$ for the whole reaction surface, can be regarded as a PCO reaction evaluation parameter. If η is near 0, it implies that the bottleneck of VOC removal by a PCO reactor is reaction rate. For this case, applying a high-performance photocatalyst or improving the reaction condition may obviously increase VOC removal performance.

Determination of A^* , St_m , η , and β_a for a Given PCO Reactor

A^* can be calculated by the geometric size of the PCO reactor. St_m can be calculated by using the computational fluid dynamic (CFD) method or by using suitable empirical correlations. NTU_m is calculated by using the measured fractional conversion, ε of a PCO reactor. When A^* , St_m , and NTU_m are known, η can be calculated by using Eq. (24). In addition, η also can be calculated by using Eq. (23) and CFD method.

Illustrative Examples: Honeycomb-Type Reactors

Hossain et al. (1999) developed a mathematical model to describe the VOC removal performance of a titania-coated honeycomb monolith PCO reactor for air purification (Fig. 2b). In the experiment, they employed two-monolith/one-UV-lamp-bank configuration. Monolith lengths were 0.5, 1.0, and 1.5 in. (12.7, 25.4 and 38.1 mm). Each monolith contained 64 cells per square inch (CPSI). The flow rate was 55 cubic feet per min (CFM), with mean UV intensities on the 12" \times 12" monolith face of 6.5 mW/cm². The inlet formaldehyde concentration was 2.1 ppm_v and the water concentration was 2700 ppmv. Applying Hossain's model, Mo et al. (2005) solved the conservation equations, including the convection, diffusion, and reaction for each component in the monolith, using Phoenics 3.3 (Commercial CFD software). Thus, NTU_m , A^* , St_m , η , and β were obtained by using Eqs. (22), (23), and (24). Table 1 lists the CFD-simulated and experimental results for the formaldehyde conversion tests. Compared with Hossain's experimental data, a statistical best-fit result was obtained, with a slope of 1.045 and R^2 of 0.972. Thus, the CFD method is capable of predicting the experimental results with a high level of confidence.

According to the discussion above, the VOC removal performance can be evaluated step by step. From Table 1, A^* values are always much greater than 1. Thus the geometry design for this type PCO reactor is satisfactory. In addition, the products ($A^* St_m$) are also greater than 2 except for Test 1. However, the final fractional conversions are less than 85% because of low η values. It implies that the bottleneck for honeycomb type PCO reactor is the reaction rate. From Hossain's paper (1999), it is known that the UV radiation intensity drops sharply with increasing distance into the channel. This is the main reason for a small value of η . From Table 1, it is also seen that St_m is much smaller than its maximum, 1. The intersection angle, β , is close to 90 degrees, resulting in low St_m values. Hence, for this typical PCO reactor, A^* offsets the low St_m values, which makes the product ($A^* St_m$) satisfactory.

Identification of PCO By-Products

The resultant of complete PCO for VOCs should be CO₂ and water. However, many reactants form partial oxidation products (Blanco et al. 1996; Augugliaro et al. 1999), which may be relatively more harmful to people's health. As one of the typical organic compounds indoors, toluene was used as the target pollutant in the

Table 1 The simulated and experimental results for formaldehyde removal (Mo et al. 2005)

Test	Lamp number/number of surface radiated	Monolith length (in.)	Measured ε (%)	Simulated ε (%)	Diff. (%)	$\dot{m} = G\varepsilon \times 10^{-3}$ m ³ /h	NTU _m ($\times 10^{-2}$)	A*	S _{Tm} ($\times 10^{-2}$)	η(%)	β (degree)
1	4/1	0.5	35.0	36.1	-3.17	3.32	4.48	16.0	9.67	29.0	98.0
2	4/2	0.5	52.5	57.4	-9.35	5.28	8.53	32.0	7.73	34.5	95.4
3	4/1	1.0	42.5	40.5	4.80	3.73	5.18	32.0	7.73	21.0	96.9
4	4/2	1.0	60.5	64.2	-6.12	5.91	10.30	64.0	6.90	23.3	95.6
5	4/1	1.5	43.5	46.4	-6.55	4.27	6.23	48.0	7.18	18.1	95.1
6	4/2	1.5	66.0	68.3	-3.50	6.28	11.50	96.0	6.66	18.0	94.9

PCO studies. Gas Chromatograph-Flame Ionization Detector (GC-FID), GC-MS, High-Performance Liquid Chromatography (HPLC), Fourier-Transform Infrared spectroscopy (FTIR), Temperature-Programmed Oxidation (TPO), and Temperature-Programmed Hydrogenation (TPH) are often used to characterize the by-products of toluene PCO (Blanco et al. 1996; Luo and Ollis 1996; d'Hennezel et al. 1998; Augugliaro et al. 1999; Blount and Falconer 2001, 2002; Marci et al. 2003; Irokawa et al. 2006; Guo et al. 2008; Chen and Zhang 2008; Martra et al. 1999). It appears that no significant by-products of toluene were identified using GC-FID (Luo and Ollis 1996). Combined with GC/FID/MS, GC/MS/HPLC, GC/FTIR, or TPH and TPO, some by-products were found on the PCO reaction surface. However, the only gas-phase by-product found was CO. FTIR has been widely used to analyze the surface by-products of toluene. However, it seems that FTIR is only suited to situations where the toluene concentration is high, from 30 to 13,000 ppm in the published articles (Mendez-Roman and Cardona-Martinez 1998; Martra et al. 1999; Augugliaro et al. 1999; Maira et al. 2001). Benzaldehyde, benzyl alcohol, benzoic acid, and phenol were the main by-products (Maira et al. 2001; Blount and Falconer 2001, 2002; Blanco et al. 1996). Since the concentration of toluene in indoor air is ppb or sub-ppm levels, it is doubted whether the investigation conclusions from these high concentration experiments could be used in indoor air cases. However, very little research concerning low-concentration, gas-phase by-products is reported in the literature. Sleiman et al. (2008) found that benzaldehyde and benzene were the main gaseous by-products of toluene at indoor air levels. Proton transfer reaction mass spectrometer (PTR-MS) has been proved to be a powerful device for online detecting transient by-products (Wisthaler et al. 2007). Several studies used PTR-MS to study PCO gas-phase by-products of a continuous flow of toluene over TiO₂ (Mo et al. 2009b, 2013).

Mo et al. (2009b) used a stainless steel plate-type UV-PCO reactor (as shown in Fig. 4) to study the PCO by-products. The experiments were all performed at a typical indoor air conditioning level with temperatures of 24.0–26.0 °C, and relative humidity (RH) of 47–50%. Two photocatalyst-coated glass plates (76.0 × 25.0 × 1.0 mm³) were placed in the reactor. The photocatalyst powders (Degussa P25) were deposited on the glass plate as a film using the dip-coating method (Yang et al. 2007) with a net weight of 22 mg loading on the reaction side. Two UV-C lamps were used to irradiate the photocatalyst film from the top of the reactor through a quartz glass. The lamps (Philips Hg-Lamp, TUV 15 W G15T8 UV-C, made in Holland) with 98% of the UV lamp radiation emitted at 254 nm and the UV radiation intensities were in the range of 0.43–0.95 mW/cm² on the reaction surface. Compressed air from a gas cylinder was divided into two streams. One stream passed through a mass flow controller and the other passed through a bottle-wash humidifier to control the humidity concentration. Pure toluene gas was mixed with the compressed air and then was supplied to the plant-type PCO reactor. All the airflow rates were controlled by two mass flow controllers. The total airflow rate was kept at 0.55 l/min with a contact time of 0.2 s in the reactor.

In the PTR-MS measurement, mass-scan and mass-identification-detection (MID) modes were used during the research. MID was used to continuously trace

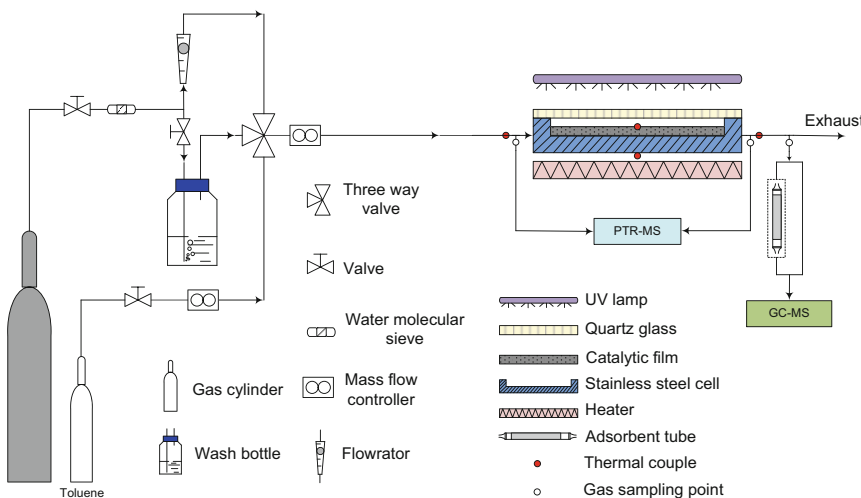
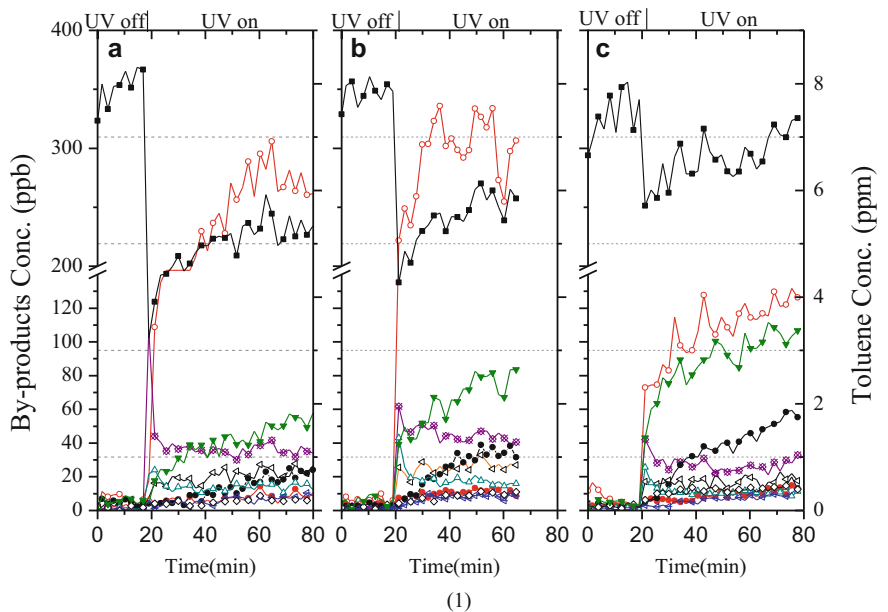


Fig. 4 Schematic of the experimental system, including the gas preparation part and UV-PCO reaction cell (Mo et al. 2009b)

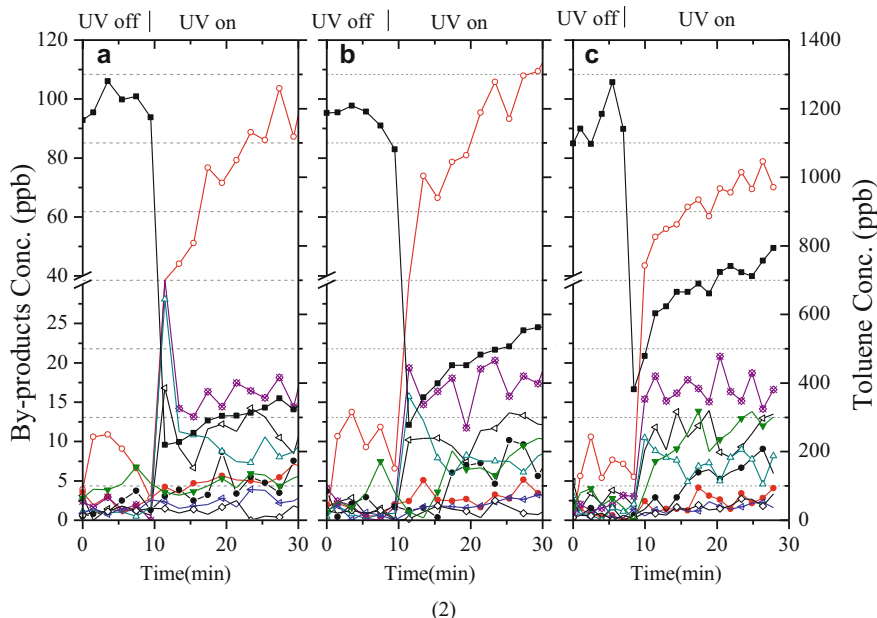
some specific compounds found from the mass-scan mode. In the experiments, the compounds with molecular mass 30, 32, 42, 44, 46, 58, 60, 78, and 106 were found to be the by-products. The concentrations of molecular mass 30, 32, 42, 44, 46, 58, and 60 always increased after UV irradiation. The concentrations of molecular mass 78 and 106 were only found to increase when inlet toluene concentrations of 1200 and 8000 ppb. The by-products with molecular mass 30, 32, 42, 44, and 58 have not previously been reported in the literature.

In order to observe the instant changes of by-products, the compounds identified in the mass scan process were traced continually in MID process. No adsorption effect of molecular mass 30, 32, 42, 44, 58, 60, 78, and 106 on the interior surface of the reactor cell was observed before and after the UV light irradiated on the blank glass without TiO₂ film. Figure 5 shows the conversions versus time before and after UV light irradiated on the glass with TiO₂ film at different inlet concentrations and UV intensities. Under the experimental condition, the concentrations of molecular mass 44 and 58 increased sharply at the beginning of UV-PCO reaction (UV on) and trended to be steady state. The concentration peaks of molecular mass 44 and 58 were much high under high inlet toluene levels and high UV intensity (Fig. 5a1, b1). Simultaneously, the compounds with molecular mass 32, 46, and 106 were generated, but the increases were slower compared with the compounds of molecular mass 44 and 58. Molecular mass 78 was only found to have slight and regular change when the inlet concentration of toluene was 8000 ppb (Fig. 5a).

Under the instant concentration pulse of water vapor, the by-products adsorbed on TiO₂ surface were replaced by water vapor due to their completed adsorption effect. These by-products were released into the gas phase. Figure 6 shows the



(1)



(2)

Fig. 5 (continued)

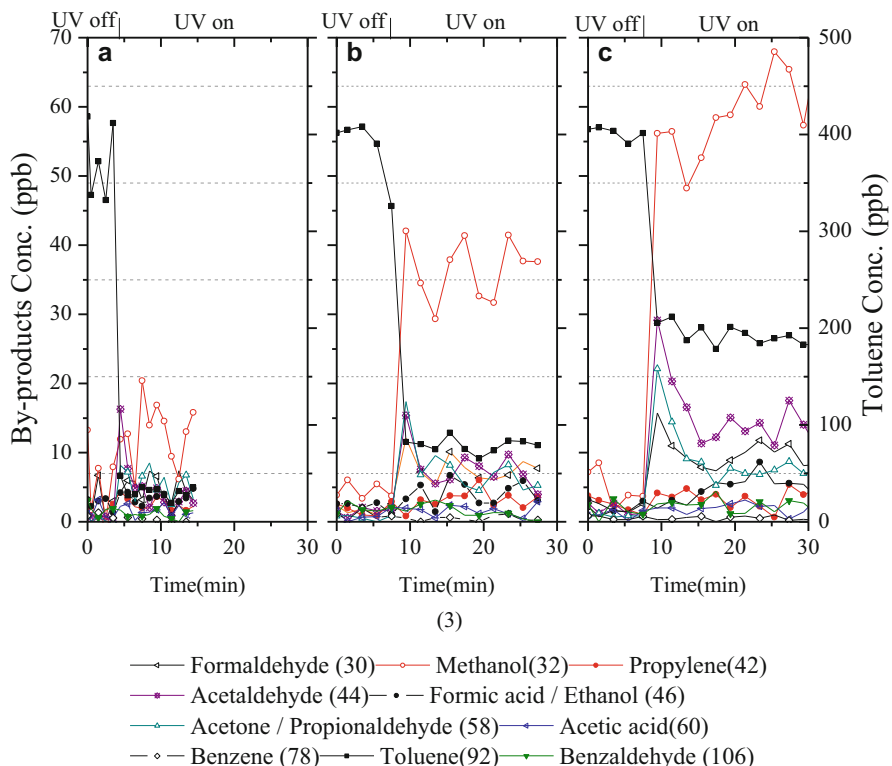


Fig. 5 Toluene and its by-products conversions vs. time with inlet toluene concentration of (a) 8 ppm, (b) 1200 ppb, and (c) 450 ppb; $T = 24\text{--}26\text{ }^{\circ}\text{C}$; RH = 47–50%; 254 nm: (1) UV intensity = 0.95 mW/cm^2 ; (2) UV intensity = 0.78 mW/cm^2 ; (3) UV intensity = 0.43 mW/cm^2 (The numbers in brackets are their molecular mass values.) (Mo et al. 2009b)

concentration changes of the by-products. Under UV irradiation and lack of water vapor (RH: 1.1%), the inlet and outlet concentrations of toluene were almost the same. It means that the PCO reaction of toluene was inhibited without water vapor. With the instant increase of water vapor and UV off, the concentration peaks (Fig. 6a) of molecular mass of 42, 46, 60, 78, and 106 were detected by PTR-MS. In addition, PTR-MS also detected some other gas-phase by-products with very low concentrations (less than 15 ppb) during the water vapor pulse (Fig. 6b). They were molecular mass 54, 56, 72, 86, and 122. It indicated that these by-products were generated under a lack of water vapor. They were strongly adsorbed on TiO_2 surface and made the deactivation of photocatalyst (Fig. 6). The by-products with molecular mass 32, 42, 44, 58, and 60 were generated if keeping UV on with abundant water vapor (RH: 84%). It shows that the adsorbed by-products on TiO_2 surface should be continuously decomposed into compounds with small molecular mass. The by-products with molecular mass 42 and 60 were both generated under high and low concentrations of water vapor.

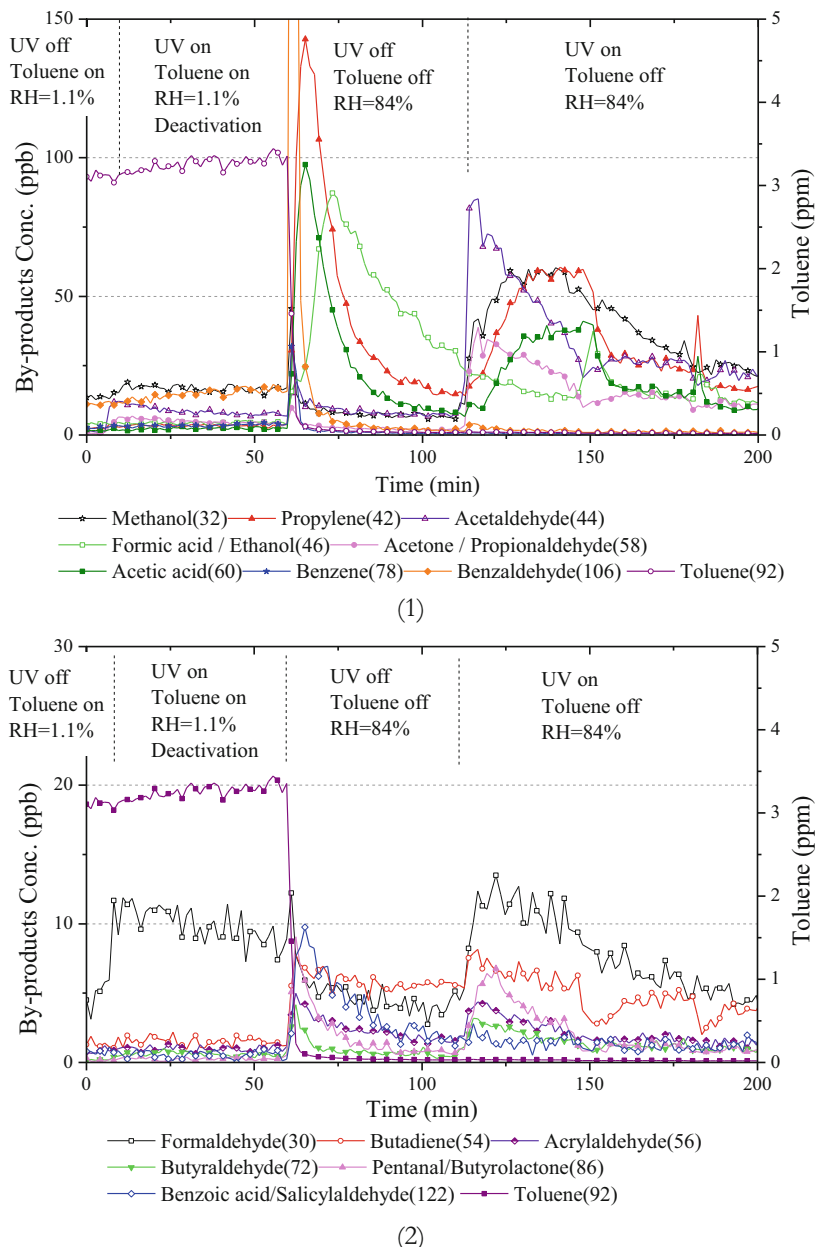


Fig. 6 Toluene and its by-products conversions vs. time under water vapour pulse from 1.1–84% with inlet toluene concentration of 3200 ppb, $T = 24\text{--}26\text{ }^{\circ}\text{C}$; UV intensity = 0.43 mW/cm^2 . **(a)** By-products with high concentrations; **(b)** by-products with low concentrations (The numbers in brackets are their molecular mass values.) (Mo et al. 2009b)

By-Products Detected via GC-MS

The gas phase by-products were concentrated from the outlet gas by an adsorption tube packed with Tenax TA. Due to the low concentration of by-products, the concentration process was performed to be over 10 h. The compounds with molecular mass 58, 60, 72, 78, 86, 106, and 122 were respectively identified to be acetone, acetic acid, butyraldehyde, benzene, pentanal, benzaldehyde, and benzoic acid. Some by-products found in Mo's study (2009b) agreed with the literature (Table 2). d'Hennezel et al. (1998) and Irokawa et al. (2006) reported that benzaldehyde was the main by-products on the reaction surface. Benzene (molecular mass 78) was identified on the solid surface by Blanco et al. (1996) and Martra et al. (1999) at very high inlet toluene concentrations after PCO process. In addition, acetic acid (molecular mass 60) and formic acid (molecular mass 46) were also found from PCO decomposition of toluene by d'Hennezel et al. (1998).

Possible PCO Pathways of Toluene

Most previous studies believed that the primary pathway in toluene photocatalytic oxidation is the hydrogen abstraction from the methyl group leading to a benzyl radical and then forming benzaldehyde, benzoic acid, and benzyl alcohol (d'Hennezel et al. 1998; Van Durme et al. 2007; Guo et al. 2008). d'Hennezel et al. (1998) gave a detailed photocatalytic oxidation pathway from toluene to benzoic acid. However, the further pathways of the aromatic ring were still not clear enough.

Frankcombe and Smith (2007) presented that the first step of toluene oxidation was the addition of an OH radical to the toluene ring followed by donation of the hydrogen atom of the added OH fragment to an O₂ molecule, which leaded to the corresponding hydroxylated isomers (phenol, -methyl-). Finally, the aromatic ring was opened and formed two carbonyl groups (O=C-R-C=O) at the attacked position, respectively. Based on this mechanism proposed by Frankcombe and Smith (2007), it is believed that toluene and its three initial by-products (benzaldehyde, benzoic acid, and benzyl alcohol) were attacked by a OH radical addition to the aromatic ring, which resulted in the opening of the aromatic ring. The compounds generated after ring opening contained several carbonyl bonds (C=O) and alkenyl bonds (C=C). In this study, the main by-products identified in the gas phase were all with small molecular mass, which indicated the carbonyl and alkenyl bonds were synchronously or continuously attacked by OH radical and adsorbed oxygen O₂. It implies that the toluene might react through the pathways: toluene → benzaldehyde → benzoic acids → ring broken → O=C-R-C=C-R'-C=O → shorter-carbon-chain aldehydes and alcohols. This results in the main photocatalytic oxidation pathways of toluene (Mo et al. 2009b). The compounds enclosed by full frame were identified in this study. In addition, the by-products: oxalic acid, pyruvic acid, propionic acid, isovaleric acid, and succinic acid reported in Mo's study (2009b) were also detected by Irokawa et al. (2006).

The concentration of water vapor has both active and inhibiting effects on the photocatalytic oxidation process (Mo et al. 2013). It has already been proved that the

Table 2 By-products identified by PTR-MS/GC-MS and their health-related information (Mo et al. 2009b)

Identified by-products		Probable by-products	NIOSH REL (ppm)	IARC carcinogenic classification
PTR-MS (molecular weight)	GC-MS			
Gas phase				
30	—	Formaldehyde	0.016	Group 2A, probably carcinogenic to humans
32	—	Methanol	200	—
42	—	Propylene	None established	—
44	—	Acetaldehyde	None established	Group 2B, possibly carcinogenic to humans
46	—	Formic acid	5	—
		Ethanol	1000	—
58	Acetone	Acetone	250	—
		Propionaldehyde	None established	—
60	Acetic acid	Acetic acid	10	—
78	Benzene	Benzene	0.1	Group 1, carcinogenic to humans
106	Benzaldehyde	Benzaldehyde	None established	—
—	Benzyl alcohol	Benzyl alcohol	—	—
—	Phenol, —methyl—	Phenol, —methyl—	—	—
On surface				
54	—	Butadiene	—	—
56	—	Acrylaldehyde	0.1	Group 3, not classifiable as to its carcinogenicity to humans
72	Butyraldehyde	Butyraldehyde	None established	—
86	Pentanal	Pentanal	50	—
	Butyrolactone	Butyrolactone	—	—
122	Benzoic acid	Benzoic acid	None established	—
	Salicylaldehyde	Salicylaldehyde	—	—
Reactant				
92	Toluene	—	100	—

NIOSH National Institute for Occupational Safety and Health (USA), *REL* Recommended Exposure Limit, IARC International Agency for Research on Cancer

photogenerated positive holes will drive the oxidation of compounds adsorbed on the surface of a photocatalyst (Ohtani 2008). But the holes will react with adsorbed water and generate hydroxyl radical (OH^\bullet), which is the dominant strong oxidant (Einaga

et al. 2002). Therefore, water plays a key positive role on PCO reaction. However, another function of water is the competitive adsorption effect with other compounds (Einaga et al. 2002; Raillard et al. 2004). When the concentration of water vapor is extremely high, competitive adsorption with water reduces the residence time of the by-products on the surface of the photocatalyst. Both low and high molecular weight by-products quickly release from the surface and are detected in the gas phase.

When the concentration of water vapor decreases, this competitive adsorption is inhibited. More and more toluene and its by-products are adsorbed on the photocatalytic surface, resulting in the higher toluene-decomposed efficiency and lower generation of by-products. There is a balance between the active and inhibiting effects of water. If the formation of HO[•] radicals is exactly consumed by adsorbed toluene and its by-products, a minimal quantity of by-products is obtained. If the OH[•] only matches the demand of toluene decomposition but not its by-products simultaneously, a maximum efficiency of toluene removal is obtained, but more by-products will release into the gas phase due to the lack of HO[•] radicals. Thus, the maximum efficiency and minimal by-product generation do not occur at the same water vapor concentration.

However, when the water vapor level approaches 0, the by-products accumulated on the reaction surface and blocked the photocatalyst (Mo et al. 2009b; Sleiman et al. 2009), resulting in a deactivation of the photocatalyst. In Mo's study (2013), acetaldehyde was the main by-product at low water vapor levels. This is consistent with the results of Sleiman et al. (2009), who found that some small aldehydes were produced in the gas phase at low water vapor concentrations. In addition, many high molecular weight by-products were adsorbed on the surface (Mo et al. 2009b). However, Sleiman et al. (2009) found there were fewer high molecular weight by-products, such as benzaldehyde at low water vapor concentration, compared with that at high water vapor concentration after 1 or 3 days reaction time. The reason may be that the photocatalyst deactivates very early at low water vapor concentration and does not generate any by-products later, thus the high molecular weight by-products adsorbed on the surface or in the gas phase were finally less than that found with high water vapor concentrations.

Figure 7 summarizes the photocatalytic oxidation efficiencies of toluene versus water vapor levels with the inlet toluene concentrations of 90, 145, 250, 400, 600, 700, and 800 ppb_v. It shows that the profiles of toluene oxidation efficiency varied significantly with water vapor concentrations. When the inlet toluene concentrations were lower than 250 ppb_v, the efficiencies always decreased with increasing humidity. When the inlet toluene concentrations were higher than 250 ppb_v, the oxidation efficiency increased first and then dropped down with the increase of water vapor levels. Maximum efficiency was obtained at optimal humidity.

Thermal Catalytic Oxidation

Recently, thermal catalytic oxidation (TCO) by specific catalysts was reported to remove formaldehyde efficiently. TCO does not require ultraviolet (UV) light or plasma, and the catalytic reaction occurs in the entire bulk of the catalyst rather than

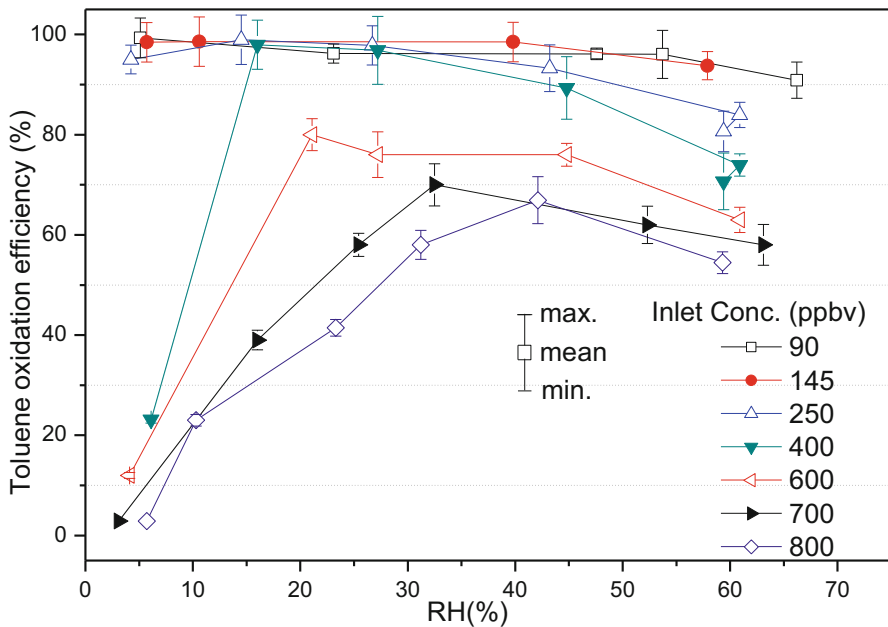


Fig. 7 Toluene oxidation efficiency versus relative humidity at inlet toluene concentrations of 90–800 ppbv with UV intensity of 0.43 mW/cm^2 (Mo et al. 2013)

only on the surface activated by UV. Such advantages make it more suitable than other techniques for indoor formaldehyde removal.

Various TCO catalysts have been investigated for their formaldehyde removal performance, including metal oxides (Sekine 2002), supported non-noble metals (Peng and Wang 2007), and supported noble metals on metal oxides (Zhang et al. 2006; Shen et al. 2008). Peng and Wang (2007) investigated the activities of a series of metals (Pt, Pd, Rh, Cu, and Mn) supported on TiO_2 for the catalytic oxidation of formaldehyde. It was found that supported noble metals on metal oxides have much better low-temperature activeness, and the activities were correlated with the dispersion of the noble metal on the supporting material. Foster and Masel (1986) studied the formaldehyde oxidation rate on nickel oxide at 220°C using the rate equation derived from Conner and Bennett's mechanism. Imamura et al. (1991) found that Ru/CeO_2 completely oxidized formaldehyde at 200°C . The complete removal temperature for formaldehyde and methanol on Pd–manganese oxide catalyst was found to be about 88°C (O'Shea et al. 2005). These studies showed high formaldehyde removal performance; however, their operating temperatures were much higher than the normal room temperature range. The Pt/TiO_2 catalyst by Zhang et al. (2005) and the $\text{Pt}/\text{MnO}_x\text{--CeO}_2$ catalyst by Tang et al. (2008) were proved to be efficient for formaldehyde decomposition at room temperature. Formaldehyde of 102 ppm through the Pt/TiO_2 catalyst was found to be totally oxidized into CO_2 (Zhang et al. 2005). Tang et al. (2008) found that formaldehyde of 30 ppm was

completely decomposed into CO₂ and H₂O on Pt/MnO_x–CeO₂ without deactivation over a 120 h reaction period, and the humidity has a negligible influence on the activity of a MnO_x–CeO₂ catalyst (Tang et al. 2006). However, there were few studies concerned with the reaction's kinetic mechanism, the relevant parameters, and the influencing factors for TCO, especially for concentrations below 1 ppm (Sekine 2002; Zhang et al. 2005; Tang et al. 2008). This limited the design and development of TCO air cleaners for removing indoor formaldehyde.

Formaldehyde Removal by TCO

This section introduced the formaldehyde removal performance by room-temperature TCO. The catalyst Pt/MnO_x–CeO₂ was prepared by a conventional impregnation process (Tang et al. 2008). The ratio of Mn and Ce in the catalyst was 1:1. The platinum loading was about 1.0 wt%. Excess water was removed in a rotary evaporator at 50 °C until dry. The resulting sample was dried at 110 °C for 12 h and then further thermally processed at 400 °C for 4 h. The physical properties of the catalyst are listed in Table 3.

The experiments were performed in a stainless steel once-through fixed-bed reactor (Fig. 8). The reactor was located in a steel chamber with temperature control in the range of 20–200 °C. Gaseous formaldehyde was generated by bubbling a formaldehyde solution using a nitrogen gas flow. The flow rate was controlled by a mass flow controller. The gaseous formaldehyde was diluted by synthetic air (O₂ 20 vol%, N₂ balance). The total flow rate through the reactor was 2.5 l/min and the gas hourly space velocity (GHSV) was $4.43 \times 10^6 \text{ h}^{-1}$. The inlet formaldehyde concentration was controlled by adjusting the flow ratio of formaldehyde gas. The concentration range was between 280 and 3000 ppb, which was a compromise for minimizing the test error and close to the indoor concentration level. The water vapor in the airflow was controlled at 7500 ppm by a water bubbling bottle. The concentrations of the inlet and outlet were monitored by a PTR-MS. A steady-state condition was achieved after several minutes to several hours, depending on the temperature. The final outlet concentration was determined under steady-state conditions.

Table 3 Physical properties of the catalyst

Particle parameters		Bed parameters	
Particle size (mesh)	40–60	Weight (mg)	26.2
Average pore diameter (nm) ^a	24.6	Bed depth (mm)	4.2
BET area (m ² /g) ^a	60.6	Bed diameter (mm)	3
Particle porosity ^a	0.48	Bulk density (kg m ⁻³)	874.4
Particle density (kg m ⁻³) ^b	1287		

^a Measured by nitrogen adsorption BET method

^b Measured by mercury porosimeter method

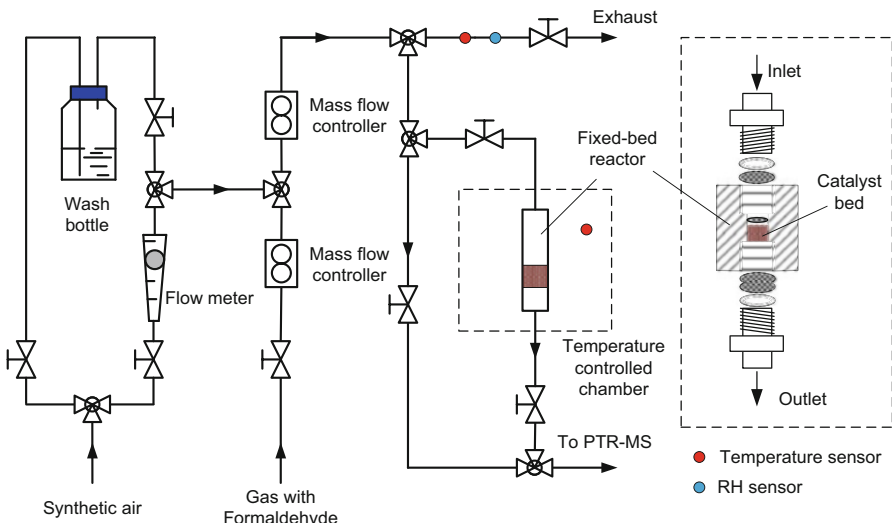


Fig. 8 Schematic of the experimental setup and fixed-bed reactor (Xu et al. 2011)

Data analysis. The once-through formaldehyde conversion, ε , is written as follows:

$$\varepsilon = \frac{C_{\text{in}} - C_{\text{out}}}{C_{\text{in}}} \quad (34)$$

where C_{in} and C_{out} are the steady-state inlet and outlet formaldehyde concentrations, ppb, respectively.

The average reaction rate was obtained from the mass balance in the reactor

$$r = \frac{G(C_{\text{in}} - C_{\text{out}})}{A_{\text{BET}}} \quad (35)$$

where r was the average reaction rate per BET surface area, ppb m s^{-1} ; G the gas flow rate, 1 min^{-1} ; and A_{BET} the total BET surface area, m^2 .

The apparent reaction factor K_{app} , m s^{-1} , was defined as the reaction rate divided by the surface concentration

$$K_{\text{app}} = \frac{r}{C_s} \quad (36)$$

Generally, the reaction takes place on the catalyst surface, so the mass transfer from bulk air to the surface needs to be considered (Yang et al. 2007). At the steady-state condition, the reaction rate in the reactor equals the external mass transfer rate,

$$K_{\text{app}} C_s(x) = \frac{h_m A_s}{A_{\text{BET}}} \Delta C(x) \quad (37)$$

where h_m was the mean external mass transfer coefficient, m s^{-1} ; ΔC the concentration difference between the bulk flow and the surface, ppb; A_s the total external surface area, m^2 ; and x the location in flow direction, m. h_m can be estimated by an empirical correlation (Wakao et al. 1979).

h_m and K_{app} were assumed as lumped parameters along the reactor. By deriving Eq. (37), the following equation was obtained:

$$\frac{\bar{C}_s}{\Delta \bar{C}} = \frac{C_s(0)}{C_{\text{in}} - C_s(0)} = \frac{C_s(L)}{C_{\text{out}} - C_s(L)} \quad (38)$$

where $\Delta \bar{C}$ was the logarithmic mean concentration difference between the bulk flow and the surface.

$$\Delta \bar{C} = \frac{(C_{\text{in}} - C_s(0)) - (C_{\text{out}} - C_s(L))}{\ln(C_{\text{in}} - C_s(0)) - \ln(C_{\text{out}} - C_s(L))} \quad (39)$$

The average surface concentration was obtained by solving Eqs. (37), (38), (39):

$$\bar{C}_s = \frac{C_{\text{in}} - C_{\text{out}}}{\ln(C_{\text{in}}) - \ln(C_{\text{out}})} \cdot f_m \quad (40)$$

where f_m was the external mass transfer correction factor

$$f_m = \frac{h_m A_s}{h_m A_s + K_{\text{app}} A_{\text{BET}}} \quad (41)$$

The value of f_m stands for the ratio of the reaction resistance in the series process of external mass transfer and the surface reaction.

There are three unknown parameters (K_{app} , f_m and \bar{C}_s) in Eqs. (36), (40), and (41). By solving these three equations, K_{app} and f_m can be obtained. To avoid the influence of external mass transfer, a high flow rate condition is necessary, which results in f_m being closer to 1. The reaction kinetics was studied by analyzing the variation of the reaction rate with the average surface concentration.

Once-through formaldehyde conversion. Figure 9 shows the result of ε at different temperatures. At inlet formaldehyde concentrations of 280–500 ppb, ε achieved 35.4%, 39.5%, 55.4%, 79.0%, and 96.3% at 25 °C, 40 °C, 60 °C, 100 °C, and 180 °C (GHSV $4.43 \times 10^6 \text{ h}^{-1}$), respectively. The formaldehyde conversion showed a significant decrease with decreasing temperature and increasing concentration. The mass scan result of PTR-MS showed that no significant increases of any signals were detected by PTR-MS in the effluent air. The impact of external mass transfer was studied by measuring the reaction rates at flow rates between 1.0 and 3.0 l/min. The measured apparent reaction coefficient and the external mass transfer correction factor are shown in Fig. 10. From the result, f_m was more than 0.95 when GHSV reached $4.43 \times 10^6 \text{ h}^{-1}$ (flow rate 2.5 l/min). Based on Eq. (41), the external mass transfer effect can be neglected, which was necessary to obtain the kinetic mechanism.

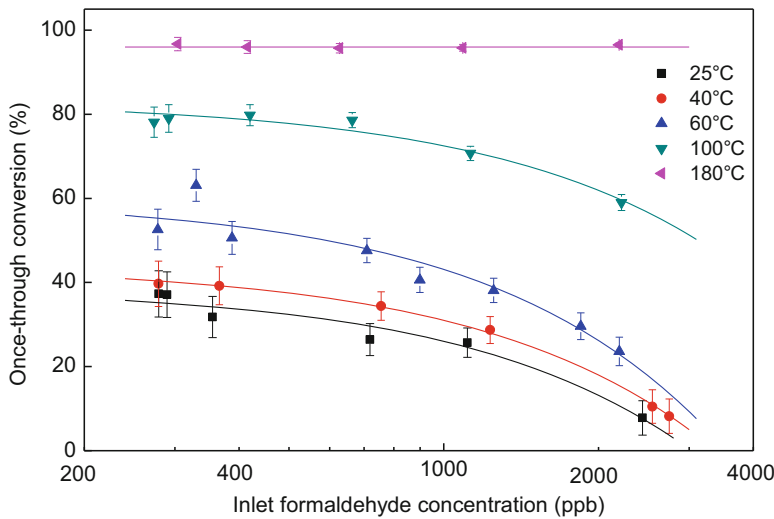


Fig. 9 Once-through formaldehyde conversion at different temperatures with GHSV $4.43 \times 10^6 \text{ h}^{-1}$; O₂ 20 vol%, N₂ balance; water vapor concentration 7500 ppm (Xu et al. 2011)

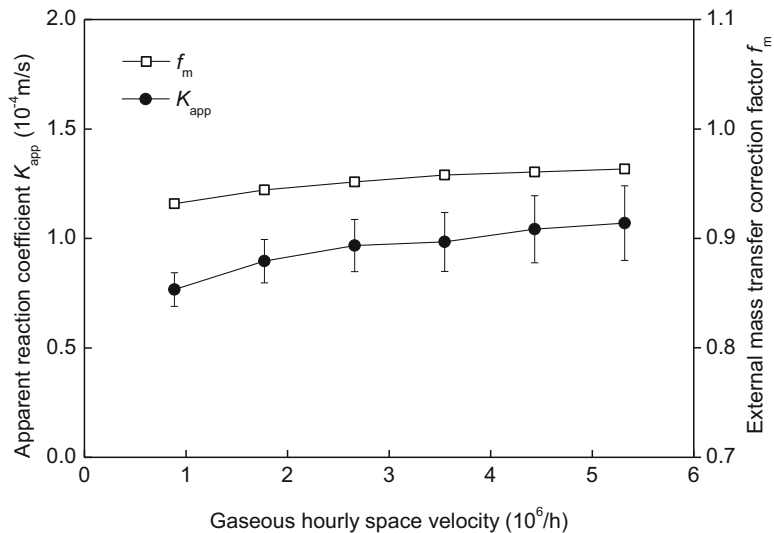


Fig. 10 The apparent reaction coefficient in the reactor: impact of external mass transfer; 700 ppb inlet formaldehyde; O₂ 20 vol%, N₂ balance; water vapor concentration 7500 ppm; reaction temperature 60 °C (Xu et al. 2011)

Effect of temperature and oxygen concentration. The reaction rate is related to the surface formaldehyde concentration. Figure 11 shows the reaction rate of different surface formaldehyde concentrations under different reaction temperatures.

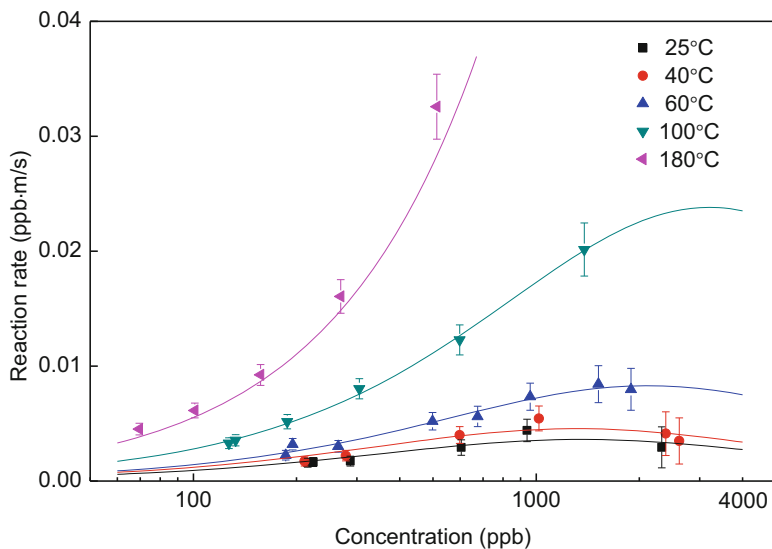


Fig. 11 The reaction rate at different surface formaldehyde concentrations under temperatures of 25 °C, 40 °C, 60 °C, 100 °C, and 180 °C. GHSV $4.43 \times 10^6 \text{ h}^{-1}$; O₂ 20 vol%, N₂ balance; water vapor concentration 7500 ppm. Points: experimental data; solid lines: nonlinear regression by bimolecular L-H model (Xu et al. 2011)

The reaction rate increased with increasing temperature and increasing concentration (below ppm levels). As the formaldehyde concentration kept increasing, the reaction rate peaked and began to decrease. The concentration at the turning point was higher at higher temperatures. The influence of oxygen concentration on the reaction rate was not very significant (Fig. 12). The decrease of oxygen concentration by a factor of 10 changes the reaction rate by less than 40%.

Kinetic Reaction Model

The kinetic reaction model is important for designing and developing TCO air cleaners for removing indoor formaldehyde. A recent study on Au/Co₃O₄–CeO₂ catalyst supposed a reaction route of formaldehyde oxidation (Ma et al. 2011), where HCOOH was found to be an intermediate on the catalyst surface during oxidation formaldehyde into CO₂. According to the results in section “Formaldehyde Removal by TCO,” no gaseous HCOOH yields (m/z 47) were detected. It indicated that the rate of HCOOH further oxidizing into CO₂ is higher than that of its generation. It may be due to the low product generation rate caused by low inlet concentration. And the effect of product desorption rate also can be ignored.

Several kinetic models (Yang et al. 2007; Chuang et al. 1994; Zhang et al. 2003; Obree 1996; Zhou and Akgerman 1995) (see Table 4 for the details) were assumed for the reaction. The experimental data were fit into those models to regress the kinetic

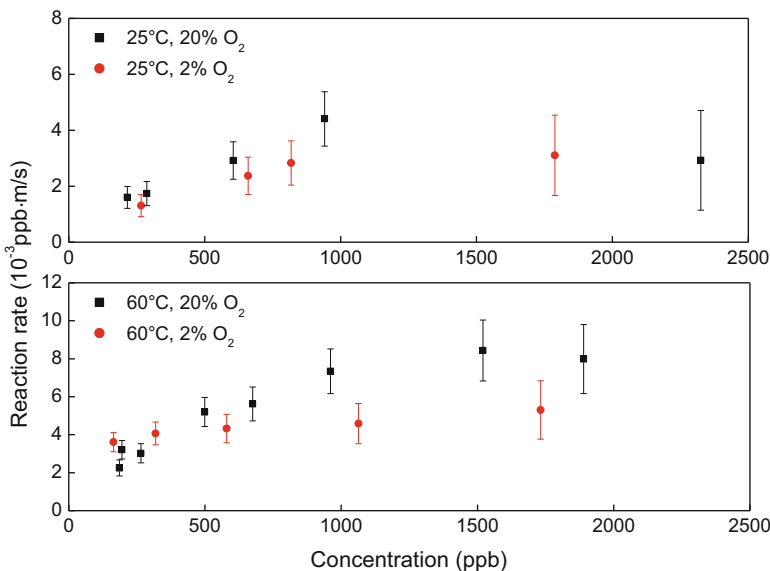


Fig. 12 The reaction rate of different surface formaldehyde concentrations under O₂ 20 vol% and O₂ 2 vol%; N₂ balance; GHSV 4.43×10^6 h⁻¹; and water vapor concentration 7500 ppm (Xu et al. 2011)

constants at each reaction temperature. The fitting results are also shown in Table 4. These results show that the model with bimolecular L-H kinetics, based on the competitive adsorption mechanism, provided the best fit to the data (with the highest R^2 value). The fitting parameters for bimolecular L-H kinetics are shown in Table 5.

The bimolecular L-H kinetics implies that two reactants in the rate-determining step compete with one another for adsorption sites. According to the reaction mechanism, the reactants were probably formaldehyde and oxygen (both in adsorbed phase). Tang et al. (2008) has reported the importance of the surface active oxygen in the reaction. In addition, from the experimental result (Fig. 12), there was little impact of gaseous oxygen concentration on the overall reaction rate. It indicated the surface active oxygen in the rate-determining step was not directly from the air oxygen, but from the metal oxide. CeO₂ is reported as a good oxygen storage material, which may help to store and provide the surface active oxygen (Campbell and Peden 2005). Under conditions of high formaldehyde concentration, adsorbed formaldehyde prevented surface active oxygen from transferring to the adsorption sites, so that the reaction rate decreased. At indoor formaldehyde concentrations (usually lower than 500 ppb), the effect of competitive adsorption appears to be negligible (Fig. 11), and the model also can be reduced to a unimolecular L-H model by neglecting the square term of concentration in the denominator.

Temperature impact. The Arrhenius equation can describe the temperature dependence of a specific reaction coefficient and adsorption coefficient

Table 4 Experimental data fitting using different kinetic models

Ref.	Kinetic model	Form of reaction rate	Principle and rate-determine step	k^a (ppb m s ⁻¹)	K^a (ppb ⁻¹)	A^a (ppb ⁻¹ m ⁻¹ s)	Variance ^b (ppb m s ⁻²)	R^{2b}
Yang et al. (2007)	Unimolecular Langmuir-Hinshelwood mechanism	$r = \frac{kKC_s}{1+kC_s}$	Adsorbed formaldehyde reacted with O ₂ , no competitive adsorption	4.2×10^{-3}	3.5×10^{-3}	—	4.42×10^{-7}	0.83
Obee (1996)	Bimolecular Langmuir-Hinshelwood mechanism	$r = \frac{kKC_s}{(1+kC_s)^2}$	Adsorbed formaldehyde reacted with adsorbed O ₂ , with competitive adsorption	1.45×10^{-2}	7.4×10^{-4}	—	3.07×10^{-7}	0.92
Zhou and Akgerman (1995)	Dissociated adsorption Langmuir-Hinshelwood mechanism	$r = \frac{kKC_s^{1/2}}{(1+kC_s^{1/2})^2}$	Dissociation adsorbed formaldehyde reacted with adsorbed O ₂ , with competitive adsorption	1.55×10^{-2}	1.19×10^{-2} (ppb ^{-0.5})	—	9.91×10^{-6}	0.73
Chuang et al. (1994)	Mars-van Krevelen mechanism	$r = \frac{k'C_s}{1+k'A'C_s}$	Electronic balance between formaldehyde and O ₂	—	1.44×10^{-5}	239.8	4.42×10^{-7}	0.83
Zhang et al. (2003)	First-order reaction model	$r = k'C_s$	Gaseous formaldehyde reaction	—	2.04×10^{-6}	—	3.79×10^{-6}	-0.30

^aValues were estimated at 25 °C; k the reaction constant, ppb m s⁻¹; K in unimolecular and bimolecular L-H mechanism, the adsorption constant, ppb⁻¹; K in dissociated adsorption L-H mechanism, the adsorption constant, ppb^{-0.5}; k' the reaction constant, m s⁻¹; A the constant of Mars-van Krevelen mechanism, ppb⁻¹ m⁻¹ s

^bMean fitting result of five temperatures

Table 5 Parameters of formaldehyde catalytic oxidation in bimolecular L-H form

Temperature (°C)	k (ppb m s ⁻¹)	K (ppb ⁻¹)
25	(1.45 ± 0.14) × 10 ⁻²	(7.4 ± 1.8) × 10 ⁻⁴
40	(1.82 ± 0.13) × 10 ⁻²	(7.6 ± 1.5) × 10 ⁻⁴
60	(3.32 ± 0.14) × 10 ⁻²	(4.7 ± 0.5) × 10 ⁻⁴
100	(9.53 ± 0.37) × 10 ⁻²	(3.1 ± 0.2) × 10 ⁻⁴
180	3.66 ± 14.58	(2.0 ± 7.0) × 10 ⁻⁵

$$\ln k = \ln A - E/RT \quad (42)$$

where A was frequency factors for the specific reaction coefficient, the same unit as k ; E the activation energy, J mol⁻¹; T the absolute temperature, K; and R the universal gas constant, J mol⁻¹ K⁻¹. By applying the Arrhenius equation to correlate the reaction coefficient and adsorption coefficient at different temperatures, the bimolecular L-H kinetics were expressed as:

$$r = \frac{k_0 \exp\left(\frac{-E_1}{RT}\right) K_0 \exp\left(\frac{-E_2}{RT}\right) C_s}{(1 + K_0 \exp\left(\frac{-E_2}{RT}\right) C_s)^2} \quad (43)$$

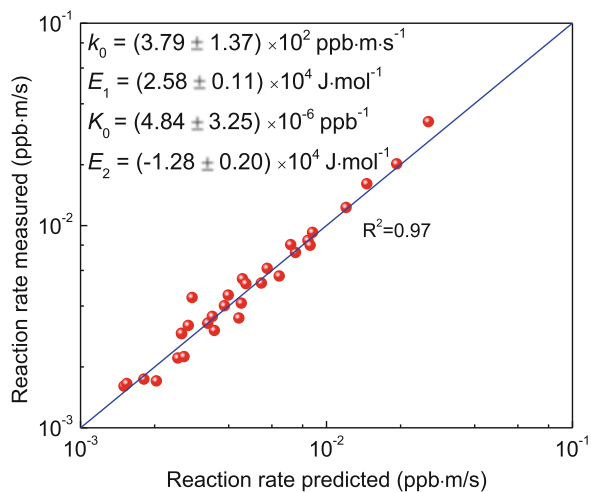
where k_0 and K_0 were frequency factors for the reaction coefficient and the adsorption coefficient, ppb m s⁻¹ and ppb⁻¹, respectively, E_1 the activation energy of the reaction, J mol⁻¹; and E_2 the activation energy of adsorption, J mol⁻¹. The activation energy is the minimum energy required to overcome the potential barrier to start the reaction. In a thermal catalytic oxidation reaction, the energy of the reactant molecule is expressed as the reaction temperature. The activation energy reflects the influence of temperature on the reaction rate. When the activation energy is higher, the influence of temperature is larger.

The parameter values and the fitting results are shown in Fig. 13. The coefficient of determination R^2 is 0.97, which indicates the model fits well with the experimental data. The apparent activation energy of oxidation was estimated as 25.8 kJ mol⁻¹. It is clear that pollutant-removal efficiency and energy costs are taken into account in practical air cleaners. Through Eq. (43), the performance and energy cost of the TCO technique can be evaluated when it is used in a practical honeycomb-type reactor.

A simulated honeycomb reactor of 100,000 channels, channel size 1 × 1 mm, length 2 cm, catalyst coating thickness 10 μm, and flow rate 360 m³/h, was used in this calculation. The reactor was assumed to be thermally insulated, so the auxiliary heating energy was equal to the heating energy removed by the airflow. A heat and mass transfer correlation for honeycomb reactors (Hawthorn 1974) was applied for the calculation. The environment temperature was 20 °C, and the formaldehyde concentration was 200 ppb.

The performance of an air reactor is evaluated by its clean air delivery rate (CADR), which is defined as the volume of fresh air generated per hour (ANSI/AHAM AC-1988 1988). CADR can be expressed by the following equation:

Fig. 13 The predicted versus experimental reaction rates for the catalytic oxidation of formaldehyde (Xu et al. 2011)



$$\text{CADR} = \varepsilon G \quad (44)$$

The clean air delivery rate per power input (CADR/P) has been considered as part of the present analysis to evaluate the energy consumption of air purifiers with a certain CADR, where P is the energy consumption rate, including fan power and any auxiliary heating rate. The energy of auxiliary heating is zero when the reaction occurs at room temperature. Figure 14 shows that the CADR value of this reactor increases with the temperature almost linearly, while CADR/P decreases with temperature exponentially. So the catalyst needs much more energy input to increase the same amount of output at a higher temperature.

In a real indoor environment, when the reactor is connected to an indoor heating device (such as the heating radiation surface or system), the heating can help to increase the efficiency of the catalyst; otherwise, it needs extra heating energy to first heat the air (or heat the catalyst), then cool the air. In addition, based on the kinetic parameters from Fig. 13, such a simulated reactor has a CADR of about $118 \text{ m}^3/\text{h}$ at room temperature, which shows good performance compared with other commonly used indoor air cleaners ($1.4\text{--}40 \text{ m}^3/\text{h}$) (Chen et al. 2005). Thus, operating at room temperature without auxiliary heating is the favorable mode for the catalyst operation.

Comparison of TCO and PCO for indoor air purification. Catalytic oxidation reactors are suitable for solving chronic emission problems such as formaldehyde in indoor air since they are expected to have a longer effective life than various adsorption methods. A comparison was made between TCO and PCO for the removal of formaldehyde. Since the reaction with PCO also has bimolecular L-H kinetics, the parameters in the equation are comparable. For the conditions of temperature at 25°C , water vapor concentration of 7500 ppm, and UV intensity of $330 \mu\text{W}/\text{cm}^2$, the k and K of PCO were estimated to be 138 ppb m s^{-1} and

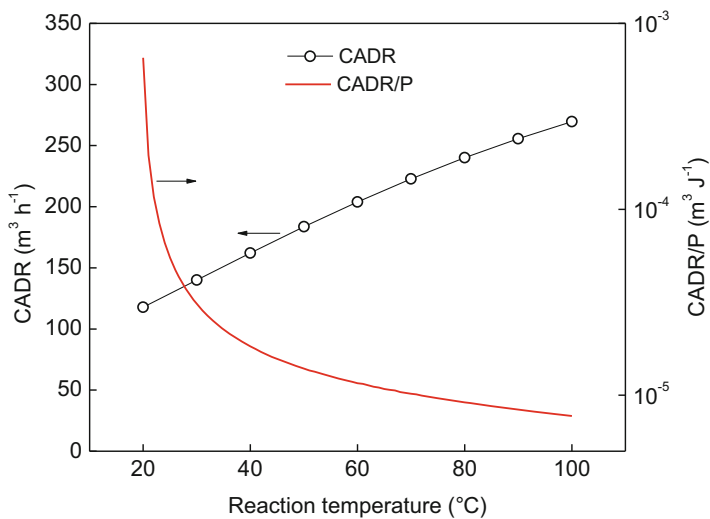


Fig. 14 The influence of temperature on clean air delivery rate (CADR) and clean air delivery rate per power input (CADR/P). Honeycomb reactor with 100,000 channels, length 2 cm, channel size $1 \times 1 \text{ mm}$, catalyst thickness $10 \mu\text{m}$, flow rate $360 \text{ m}^3/\text{h}$, formaldehyde 200 ppb, and environmental temperature 20°C (Xu et al. 2011)

$4.2 \times 10^{-4} \text{ ppb}^{-1}$, respectively (Obee 1996). The value of k represents the reaction rate per reaction area. The result indicates that k for PCO was four orders of magnitude larger than that for TCO (Table 5). However, these k s have different respective reaction areas. The reaction area of PCO is limited to its irradiated surface (about $0.1 \text{ m}^2/\text{g}$) (Mo et al. 2009a), while the reaction area of TCO is the total BET surface ($60.6 \text{ m}^2/\text{g}$). Accounting for the reaction area, by coating more catalysts to the surface within reasonable thickness limits, the reaction rate of TCO would be larger than PCO. The value of the equivalent adsorption constant K represents the adsorption ability of the catalyst. The K of TCO is about 1.8 times that of PCO, so it tends to perform better than PCO at low formaldehyde concentrations. Although the cost will be greater when using noble metals in the TCO catalyst, it can be made acceptable by distributing the catalyst more efficiently in the reactors. The good performance shown by the honeycomb reactor calculated above (Fig. 5) only needs about 100 g of the TCO catalysts (including 1 g Pt). This is not too costly and is economically feasible when compared with other on-sell air cleaners.

In real indoor environments, the influence of humidity, particles, and other VOCs on the performance of the TCO needs to be considered.

Conclusions

In summary, PCO and room-temperature TCO are promising technologies to reduce indoor VOCs. The VOC removal bottleneck of the PCO reactor can be determined by analyzing the dimensionless parameters. The lack of coordination of the reaction

structure and the UV sources makes it difficult to design a high-efficiency PCO reactor. Another challenging point for PCO is the various and unwanted by-products. The room-temperature TCO can only decompose formaldehyde but not other compounds, which limits its application indoors. It may be the trend to combine PCO, TCO, and adsorption to solve the indoor VOC problem.

References

- ANSI/AHAM AC-1988 (1988) Portable household electric cord-connected room air cleaners. Association of Home Appliance Manufacturers, Chicago
- Augugliaro V, Coluccia S, Loddo V, Marchese L, Martra G, Palmisano L, Schiavello M (1999) Photocatalytic oxidation of gaseous toluene on anatase TiO₂ catalyst: mechanistic aspects and FT-IR investigation. *Appl Catal B Environ* 20(1):15–27
- Blanco J, Avila P, Bahamonde A, Alvarez E, Sanchez B, Romero M (1996) Photocatalytic destruction of toluene and xylene at gas phase on a titania based monolithic catalyst. *Catal Today* 29(1–4):437–442
- Blount MC, Falconer JL (2001) Characterization of adsorbed species on TiO₂ after photocatalytic oxidation of toluene. *J Catal* 200(1):21–33. <https://doi.org/10.1006/jcat.2001.3174>. ISSN 0021-9517
- Blount MC, Falconer JL (2002) Steady-state surface species during toluene photocatalysis. *Appl Catal B Environ* 39(1):39–50
- Campbell CT, Peden CHF (2005) Chemistry – oxygen vacancies and catalysis on ceria surfaces. *Science* 309(5735):713–714. <https://doi.org/10.1126/science.1113955>
- Chen W (2007) Experimental evaluation of indoor air cleaning technologies and modeling of UV-PCO (photocatalytic oxidation) air cleaners under multiple VOCs conditions. PhD dissertation, Department of Mechanical and Aerospace Engineering, Syracuse University, Syracuse
- Chen W, Zhang JS (2008) UV-PCO device for indoor VOCs removal: investigation on multiple compounds effect. *Build Environ* 43:246–252. <https://doi.org/10.1016/j.buildenv.2006.03.024>
- Chen WH, Zhang JS, Zhang ZB (2005) Performance of air cleaners for removing multiple volatile organic compounds in indoor air. *ASHRAE Trans* 111:1101–1114
- Chuang KT, Zhou B, Tong SM (1994) Kinetics and mechanism of catalytic-oxidation of formaldehyde over hydrophobic catalysts. *Ind Eng Chem Res* 33(7):1680–1686
- d'Hennezel O, Pichat P, Ollis DF (1998) Benzene and toluene gas-phase photocatalytic degradation over H₂O and HCl pretreated TiO₂: by-products and mechanisms. *J Photochem Photobiol A* 118(3):197–204
- Dreyer M, Newman G, Lobban L, Kersey S, Wang R, Harwell J (1996) Enhanced oxidation of air contaminants on an ultra-low density UV-accessible aerogel photocatalyst. *Mater Res Soc Symp Proc* 454:141
- Einaga H, Futamura S, Ibusuki T (2002) Heterogeneous photocatalytic oxidation of benzene, toluene, cyclohexene and cyclohexane in humidified air: comparison of decomposition behavior on photoirradiated TiO₂ catalyst. *Appl Catal B Environ* 38(3):215–225
- Fisk WJ, Rosenfeld AH (1997) Estimates of improved productivity and health from better indoor environments. *Indoor Air* 7(3):158–172
- Foster JJ, Masel RI (1986) Formaldehyde oxidation on nickel-oxide. *Ind Eng Chem Res* 25(4): 563–568
- Frankcombe TJ, Smith SC (2007) OH-initiated oxidation of toluene. 1. Quantum chemistry investigation of the reaction path. *J Phys Chem A* 111(19):3686–3690. <https://doi.org/10.1021/jp067112i>. ISSN 1089-5639
- Fujishima A, Honda K (1972) Electrochemical photolysis of water at a semiconductor electrode. *Nature* 238(5358):37–38

- Gallego E, Roca FJ, Perales JF, Guardino X (2013) Experimental evaluation of VOC removal efficiency of a coconut shell activated carbon filter for indoor air quality enhancement. *Build Environ* 67:14–25
- Guo ZY (2001) Mechanism and control of convective heat transfer – coordination of velocity and heat flow fields. *Chin Sci Bull* 46(7):596–599
- Guo ZY, Li DY, Wang BX (1998) A novel concept for convective heat transfer enhancement. *Int J Heat Mass Transf* 41(14):2221–2225
- Guo T, Bai ZP, Wu C, Zhu T (2008) Influence of relative humidity on the photocatalytic oxidation (PCO) of toluene by TiO₂ loaded on activated carbon fibers: PCO rate and intermediates accumulation. *Appl Catal B Environ* 79(2):171–178. <https://doi.org/10.1016/j.apcatb.2007.09.033>
- Hall RT, Bendfeldt P, Obee TN, Sangiovanni JJ (1998) Computational and experimental studies of UV/titania photocatalytic oxidation of VOCs in honeycomb monoliths. *J Adv Oxid Technol* 3: 243–251
- Hawthorn RD (1974) Afterburner catalysts – effects of heat and mass transfer between gas and catalyst surface. *AIChE Symp Ser* 70(137):428–438
- Hossain MM, Raupp GB, Hay SO, Obee TN (1999) Three-dimensional developing flow model for photocatalytic monolith reactors. *AICHE J* 45(6):1309–1321
- Imamura S, Uematsu Y, Utani K, Ito T (1991) Combustion of formaldehyde on ruthenium cerium (IV) oxide catalyst. *Ind Eng Chem Res* 30(1):18–21
- Irokawa Y, Morikawa T, Aoki K, Kosaka S, Ohwaki T, Taga Y (2006) Photodegradation of toluene over TiO₂-xNx under visible light irradiation. *Phys Chem Chem Phys* 8(9):1116–1121. <https://doi.org/10.1039/b517653k>. ISSN 1463-9076
- Kim YM, Harrad S, Harrison RM (2001) Concentrations and sources of VOCs in urban domestic and public microenvironments. *Environ Sci Technol* 35(6):997–1004
- Luo Y, Ollis DF (1996) Heterogeneous photocatalytic oxidation of trichloroethylene and toluene mixtures in air: kinetic promotion and inhibition, time-dependent catalyst activity. *J Catal* 163 (1):1–11
- Ma CY, Wang DH, Xue WJ, Dou BJ, Wang HL, Hao ZP (2011) Investigation of formaldehyde oxidation over Co₃O₄-CeO₂ and Au/Co₃O₄-CeO₂ catalysts at room temperature: effective removal and determination of reaction mechanism. *Environ Sci Technol* 45(8):3628–3634. <https://doi.org/10.1021/es104146v>
- Maira AJ, Coronado JM, Augugliaro V, Yeung KL, Conesa JC, Soria J (2001) Fourier transform infrared study of the performance of nanostructured TiO₂ particles for the photocatalytic oxidation of gaseous toluene. *J Catal* 202(2):413–420. <https://doi.org/10.1006/jcat.2001.3301>. ISSN 0021-9517
- Marci G, Addamo M, Augugliaro V, Coluccia S, Garcia-Lopez E, Loddo V, Martra G, Palmisano L, Schiavello M (2003) Photocatalytic oxidation of toluene on irradiated TiO₂: comparison of degradation performance in humidified air, in water and in water containing a zwitterionic surfactant. *J Photochem Photobiol A* 160(1–2):105–114. [https://doi.org/10.1016/s1010-6030\(03\)00228-4](https://doi.org/10.1016/s1010-6030(03)00228-4). ISSN 1010-6030
- Martra G, Coluccia S, Marchese L, Augugliaro V, Loddo V, Palmisano L, Schiavello M (1999) The role of H₂O in the photocatalytic oxidation of toluene in vapour phase on anatase TiO₂ catalyst – a FTIR study. *Catal Today* 53(4):695–702
- Meininghaus R, Salthammer T, Knoppel H (1999) Interaction of volatile organic compounds with indoor materials – a small-scale screening method. *Atmos Environ* 33(15):2395–2401. [https://doi.org/10.1016/s1352-2310\(98\)00367-7](https://doi.org/10.1016/s1352-2310(98)00367-7)
- Mendez-Roman R, Cardona-Martinez N (1998) Relationship between the formation of surface species and catalyst deactivation during the gas-phase photocatalytic oxidation of toluene. *Catal Today* 40(4):353–365
- Mo J, Zhang Y, Yang R (2005) Novel insight into VOC removal performance of photocatalytic oxidation reactors. *Indoor Air* 15(4):291–300. <https://doi.org/10.1111/j.1600-0668.2005.00374.x>
- Mo JH, Zhang YP, Xu QJ, Lamson JJ, Zhao RY (2009a) Photocatalytic purification of volatile organic compounds in indoor air: a literature review. *Atmos Environ* 43(14):2229–2246. <https://doi.org/10.1016/j.atmosenv.2009.01.034>

- Mo JH, Zhang YP, Xu QJ, Zhu YF, Lamson JJ, Zhao RY (2009b) Determination and risk assessment of by-products resulting from photocatalytic oxidation of toluene. *Appl Catal B Environ* 89(3–4):570–576. <https://doi.org/10.1016/j.apcatb.2009.01.015>
- Mo JH, Zhang YP, Xu QJ (2013) Effect of water vapor on the by-products and decomposition rate of ppb-level toluene by photocatalytic oxidation. *Appl Catal B Environ* 132:212–218. <https://doi.org/10.1016/j.apcatb.2012.12.001>
- O’Shea V, Alvarez-Galvan MC, Fierro JLG, Arias PL (2005) Influence of feed composition on the activity of Mn and PdMn/Al₂O₃ catalysts for combustion of formaldehyde/methanol. *Appl Catal B Environ* 57(3):191–199. <https://doi.org/10.1016/j.apcatb.2004.11.001>
- Obee TN (1996) Photooxidation of sub-parts-per-million toluene and formaldehyde levels an titania using a glass-plate reactor. *Environ Sci Technol* 30(12):3578–3584
- Obee TN, Brown RT (1995) TiO₂ photocatalysis for indoor air applications: effects of humidity and trace contaminant levels on the oxidation rates of formaldehyde, toluene, and 1,3-butadiene. *Environ Sci Technol* 29(5):1223–1231
- Obee TN, Hay SO (1997) Effects of moisture and temperature on the photooxidation of ethylene on Titania. *Environ Sci Technol* 31(7):2034–2038
- Oehha (2007) California’s Office of Environmental Health Hazard Assessment. <http://www.oehha.ca.gov/air.html>
- Ohtani B (2008) Preparing articles on photocatalysis – beyond the illusions, misconceptions, and speculation. *Chem Lett* 37(3):217–229. <https://doi.org/10.1246/cl.2008.216>
- Ollis DF (2000) Photocatalytic purification and remediation of contaminated air and water. *C R Acad Sci Ser IIc Chim* 3(6):405–411
- Peng JX, Wang SD (2007) Performance and characterization of supported metal catalysts for complete oxidation of formaldehyde at low temperatures. *Appl Catal B Environ* 73(3–4): 282–291. <https://doi.org/10.1016/j.apcatb.2006.12.012>
- Raillard C, Hequet V, Le Cloirec P, Legrand J (2004) Kinetic study of ketones photocatalytic oxidation in gas phase using TiO₂-containing paper: effect of water vapor. *J Photochem Photobiol A* 163(3):425–431. <https://doi.org/10.1016/j.jphotochem.2004.01.014>. ISSN 1010-6030
- Sekine Y (2002) Oxidative decomposition of formaldehyde by metal oxides at room temperature. *Atmos Environ* 36(35):5543–5547
- Shen YN, Yang XZ, Wang YZ, Zhang YB, Zhu HY, Gao L, Jia ML (2008) The states of gold species in CeO₂ supported gold catalyst for formaldehyde oxidation. *Appl Catal B Environ* 79 (2):142–148. <https://doi.org/10.1016/j.apcatb.2007.09.042>
- Sleiman M, Conchon P, Ferronato C, Chovelon J-M (2008) Photocatalytic oxidation of toluene at indoor air levels (ppbv): towards a better assessment of conversion, reaction intermediates and mineralization. *Appl Catal B Environ*. <https://doi.org/10.1016/j.apcatb.2008.1008.1003>
- Sleiman M, Conchon P, Ferronato C, Chovelon JM (2009) Photocatalytic oxidation of toluene at indoor air levels (ppbv): towards a better assessment of conversion, reaction intermediates and mineralization. *Appl Catal B Environ* 86(3–4):159–165. <https://doi.org/10.1016/j.apcatb.2008.08.003>
- Tang XF, Li YG, Huang XM, Xu YD, Zhu HQ, Wang JG, Shen WJ (2006) MnOx-CeO₂ mixed oxide catalysts for complete oxidation of formaldehyde: effect of preparation method and calcination temperature. *Appl Catal B Environ* 62(3–4):265–273. <https://doi.org/10.1016/j.apcatb.2005.08.004>
- Tang XF, Chen JL, Huang XM, Xu Y, Shen WJ (2008) Pt/MnOx-CeO₂ catalysts for the complete oxidation of formaldehyde at ambient temperature. *Appl Catal B Environ* 81(1–2):115–121. <https://doi.org/10.1016/j.apcatb.2007.12.007>
- Tao W-Q, Guo Z-Y, Wang B-X (2002a) Field synergy principle for enhancing convective heat transfer – its extension and numerical verifications. *Int J Heat Mass Transf* 45(18):3849–3856. [https://doi.org/10.1016/S0017-9310\(02\)00097-2](https://doi.org/10.1016/S0017-9310(02)00097-2)
- Tao WQ, He YL, Wang QW, Qu ZG, Song FQ (2002b) A unified analysis on enhancing single phase convective heat transfer with field synergy principle. *Int J Heat Mass Transf* 45(24):4871–4879
- Tompkins DT (2001) Evaluation of photocatalytic air cleaning capability: a literature review and engineering analysis. ASHARE research project RP-1134

- Tronconi E, Forzatti P (1992) Adequacy of lumped parameter models for SCR reactors with monolith structure. *AICHE J* 38(2):201–210
- USEPA (1990) Reducing risk: setting priorities and strategies for environmental protection. US Environmental Protection Agency, Washington, DC
- Van Durme J, Dewulf J, Sysmans W, Leys C, Van Langenhove H (2007) Abatement and degradation pathways of toluene in indoor air by positive corona discharge. *Chemosphere* 68(10):1821–1829
- Wakao N, Kaguei S, Funazkri T (1979) Effect of fluid dispersion coefficients on particle-to-fluid heat transfer coefficients in packed beds: correlation of nusselt numbers. *Chem Eng Sci* 34(3): 325–336. [https://doi.org/10.1016/0009-2509\(79\)85064-2](https://doi.org/10.1016/0009-2509(79)85064-2)
- Wang SB, Ang HM, Tade MO (2007) Volatile organic compounds in indoor environment and photocatalytic oxidation: state of the art. *Environ Int* 33(5):694–705. <https://doi.org/10.1016/j.envint.2007.02.011>
- WHO (1989) Indoor air quality: organic pollutants. Report on a WHO meeting. EURO report and studies 111:1–70
- Wisthaler A, Strøm-Tejsen P, Fang L, Arnaud TJ, Hansel A, Märk TD, Wyon DP (2007) PTR-MS assessment of photocatalytic and sorption-based purification of recirculated cabin air during simulated 7-h flights with high passenger density. *Environ Sci Technol* 41:229–234. <https://doi.org/10.1021/es060424e>. ISSN 0013-936X
- Xu QJ, Zhang YP, Mo JH, Li XX (2011) Indoor formaldehyde removal by thermal catalyst: kinetic characteristics, key parameters, and temperature influence. *Environ Sci Technol* 45(13):5754–5760. <https://doi.org/10.1021/es2009902>
- Yang R, Zhang YP, Zhao RY (2004) An improved model for analyzing the performance of photocatalytic oxidation reactors in removing volatile organic compounds and its application. *J Air Waste Manag Assoc* 54(12):1516–1524
- Yang R, Zhang Y, Xu Q, Mo J (2007) A mass transfer based method for measuring the reaction coefficients of a photocatalyst. *Atmos Environ* 41(6):1221–1229. <https://doi.org/10.1016/j.atmosenv.2006.09.043>
- Yoneyama H, Torimoto T (2000) Titanium dioxide/adsorbent hybrid photocatalysts for photo-destruction of organic substances of dilute concentrations. *Catal Today* 58(2–3):133–140
- Zhang YP, Yang R, Zhao RY (2003) A model for analyzing the performance of photocatalytic air cleaner in removing volatile organic compounds. *Atmos Environ* 37(24):3395–3399. [https://doi.org/10.1016/s1352-2310\(03\)00357-1](https://doi.org/10.1016/s1352-2310(03)00357-1)
- Zhang CB, He H, Tanaka K (2005) Perfect catalytic oxidation of formaldehyde over a Pt/TiO₂ catalyst at room temperature. *Catal Commun* 6(3):211–214. <https://doi.org/10.1016/j.catcom.2004.12.012>
- Zhang CB, He H, Tanaka K (2006) Catalytic performance and mechanism of a Pt/TiO₂ catalyst for the oxidation of formaldehyde at room temperature. *Appl Catal B Environ* 65(1–2):37–43. <https://doi.org/10.1016/j.apcatb.2005.12.010>
- Zhang YP, Mo JH, Li YG, Sundell J, Wargocki P, Zhang J, Little JC, Corsi R, Deng Q, Leung MH (2011) Can commonly-used fan-driven air cleaning technologies improve indoor air quality? A literature review. *Atmos Environ* 45(26):4329–4343
- Zhou L, Akgerman A (1995) Catalytic oxidation of ethanol and acetaldehyde in supercritical carbon dioxide. *Ind Eng Chem Res* 34(5):1588–1595. <https://doi.org/10.1021/ie00044a011>



Managing IAQ at Multiple Scales: From Urban to Personal Microenvironments

61

Jianshun Jensen Zhang, Jialei Shen, and Zhi Gao

Contents

Introduction	1774
Motivation and Challenge	1774
Multi-scale Nature of the Built Environmental System	1775
Multitudes of Pollutants Indoors and Their Sources	1776
IAQ Control Principles and Strategies	1777
A 3-D View of IAQ Engineering	1777
Approach and Model for Assessing the Effectiveness of IAQ Control Strategies	1779
Overview	1779
A Simplified Multi-scale IAQ Model	1779
Definition of Baseline Cases	1781
Assessment Procedure	1785
Potentials and Limits of Source Control, Ventilation and Air Purification at Different Scales	1785
Urban Scale	1785
Building Scale	1790
Room Scale	1793
Personal Microenvironments	1797
Integration of IAQ Strategies	1799
Case Study: IAQ Design and Control Strategies for a LEED Platinum Building: SyracuseCOE Headquarters	1805

J. J. Zhang (✉)

Building Energy and Environmental Systems Laboratory, Department of Mechanical and Aerospace Engineering, Syracuse University, Syracuse, NY, USA

School of Architecture and Urban Planning, Nanjing University, Nanjing, China

e-mail: jszhang@syr.edu

J. Shen

Building Energy and Environmental Systems Laboratory, Department of Mechanical and Aerospace Engineering, Syracuse University, Syracuse, NY, USA

Z. Gao

School of Architecture and Urban Planning, Nanjing University, Nanjing, China

Concluding Remarks and Future Outlook	1808
Cross-References	1809
References	1810

Abstract

Indoor air quality (IAQ) is vital to human health, comfort, performance, and wellbeing as people typically spend over 80% of their time indoors. The indoor pollutants people are exposed to originate from both indoors and outdoors. In order to devise an energy-efficient and cost-effective approach to improve IAQ, it is necessary to consider strategies across multiple scales—from the outdoor environment around buildings to inside buildings, to rooms, and to the microenvironment around the occupants that directly affect the human exposure and intake of the pollutants. In this chapter, we present a 3-dimensional view of the IAQ engineering: the scales (of environments), the species (of pollutants), and strategies (of IAQ control). The objective is to improve the understanding of and assess the potential and limits of the various source control, ventilation, and air purification strategies across the different scales so that an integrated approach can be developed for managing IAQ. Existing data from previous research on the effectiveness of various IAQ strategies at the different environmental scales are discussed along with an outlook to the future work and challenges.

Keywords

Indoor air quality · IAQ control strategies · Multiscale built environmental systems · Ventilation · Source control · Air purification

Introduction

Motivation and Challenge

Good indoor air quality (IAQ) is vital to human health, comfort, performance and wellbeing for several reasons: (1) people spent vast majority of their time indoors (as high as 80–90%); (2) people's exposure to air pollutants in their lifetime takes place primarily indoors, and this is not only the case for pollutants of indoor origin, but also for some pollutants of outdoor origin; (3) air pollutants found indoors can be odorous, cause irritations to skins, eyes and membranes, respiratory diseases, cardiovascular diseases, and cancer; (4) poor IAQ has been associated with increased sick leaves, significant productivity loss as well as sick building syndrome and building related illnesses; and (5) good IAQ provides a solid foundation for reducing the risk of infectious diseases such as COVID-19 since most IAQ control strategies are also effective for reducing the dose exposure of building occupants to the virus-containing aerosols (Zhang 2020; Shen et al. 2021). Since buildings account for about 40% of the total energy consumed, it is also vitally important to devise energy-efficient and cost-effective IAQ strategies to save energy and minimize the

associated carbon emissions in an effort to combat the global climate change. Providing good IAQ while saving energy and reducing carbon emissions remains a significant challenge.

Multi-scale Nature of the Built Environmental System

A built environmental system involves multiple scales in space and time (Fig. 1). Spatially, it ranges from the microenvironment around an occupant, to a cubical, a room, a floor, a whole building, and the building's surrounding airshed. Temporally, its state variables such as temperature, relative humidity and pollutant concentrations vary with time scales ranging from seconds to hours, days, months, seasons, and years depending on the perturbing events and the response times of the environmental scale. Different management and control strategies can be applied at different scales to improve the indoor environmental quality (IEQ including IAQ, thermal comfort, acoustic, lighting and visual quality), energy efficiency, and safety and security of the occupants. As we refine the management and control from a larger scale to a smaller and smaller scale with an occupant-centered approach, it is possible to significantly improve the satisfaction of building occupants from the acceptable level (80%) to near 100% satisfaction level. In this chapter, we focus on strategies for improving IAQ, which alone is affected by a multitude of factors including the media/materials where pollutants reside, the

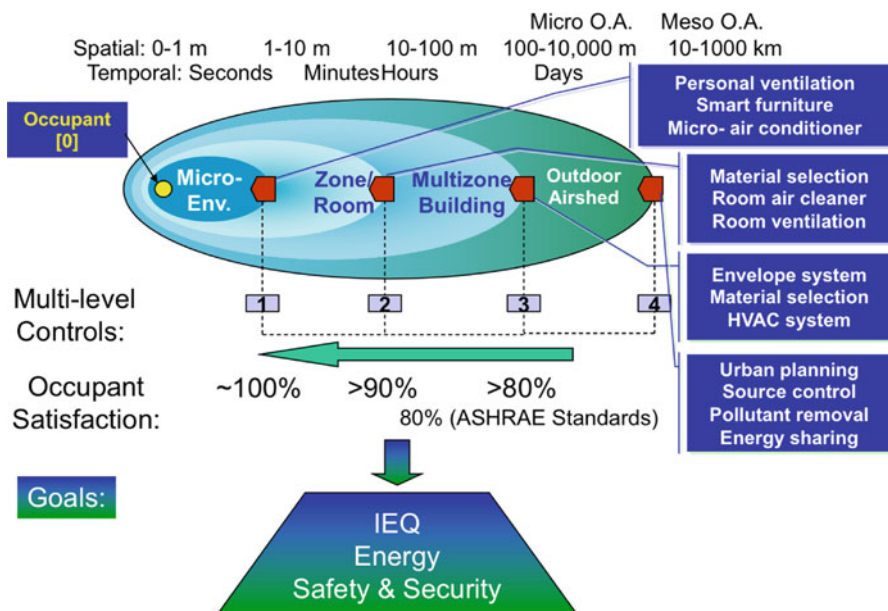


Fig. 1 Managing IEQ and energy of a built environmental system across multiple scales (Zhang 2005)

environmental conditions, and the species of pollutants—i.e., the media, environment, and species (MES) in short.

Multitudes of Pollutants Indoors and Their Sources

IAQ is a complex problem largely because it involves many types of pollutants (Fig. 2): (1) inorganic compounds (e.g., CO, CO₂, SO₂, NO_x, and O₃); (2) organic compounds including volatile organic compounds (i.e., VOCs such as formaldehyde, acetaldehyde, benzene, toluene, styrene, 1,4-dichlorobenzene, and 4-phenyl cyclohexene or 4-PC) and semi-volatile organic compounds (i.e., SVOCs such as di-n-butyl phthalate or DnBP, butyl benzyl phthalate or BBP, and di(2-ethylhexyl), Phthalate or DEHP); (3) radioactive gases (e.g., radon); (4) particulate matters (PM10, PM2.5, and ultrafine particles); (5) bioaerosols derived from virus, bacteria, fungi, protozoa, dust mites, and pollen; and (6) Ozone-initiated oxidation products (e.g., methacrolein, methyl vinyl ketone, nitrogen dioxide, acetone, 6-MHO, geranyl acetone, 4-OPA, formaldehyde, nonanal, decanal, 9-oxo-nonanoic acid, azelaic acid, and nonanoic acid). Some indoor pollutants mainly come from indoors (e.g., CO₂, VOCs and SVOCs emitted from building materials and furnishings); some mainly from outdoors (e.g., SO₂ and NO_x); some from both indoors and outdoors (e.g., PM2.5 from outdoor air pollution and indoor emission from occupant activities, and O₃ from outdoor air pollution or due to indoor emissions from printers, copiers and some ionization-based electronic air purifiers); and some from the interaction between the pollutant from the outdoor air and the indoor air and indoor surfaces (e.g., O₃-initiated chemical reaction products). As a result, different source control and removal strategies or technologies are needed for effective reduction of different target pollutants. The effects of the co-existence of multiple pollutants on the

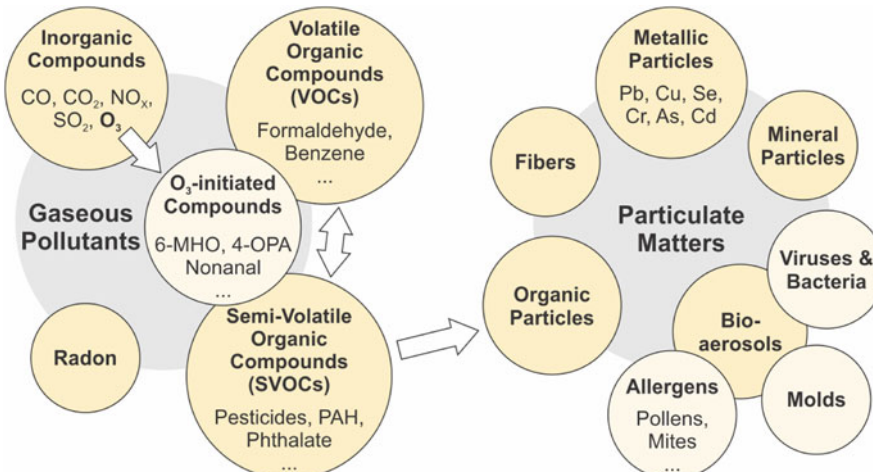


Fig. 2 Classification of indoor pollutants. (Adapted from Abadie and Wargocki 2017)

effectiveness and efficacy of IAQ strategies or technologies should be considered. For example, a particular air purification technology may have very different pollutant removal efficiencies for different gaseous pollutants. Dilution by ventilation is non-discriminative to different gaseous pollutants.

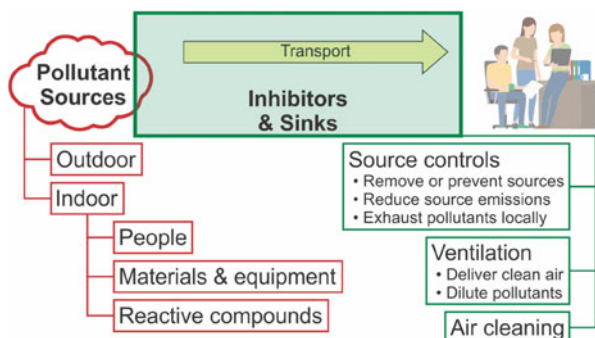
IAQ Control Principles and Strategies

Air pollution takes place when the pollutants emitted from sources transport to the space where occupants reside. IAQ control means providing inhibitors or sinks to reduce the exposure. This can be achieved by various source control, ventilation, or air purification strategies (Fig. 3). Source control is often the most effective approach and should always be considered first. Ventilation is a non-discriminative approach applicable for diluting all types of pollutants in the space. It however has an energy implication as more outdoor air needs to be conditioned to maintain the desired thermal condition in the space. In order to reduce the energy consumption while meeting the IAQ requirements, air purification can be used to remove specific compounds of interests (target compounds) so that the ventilation rate for pollutant dilution can be reduced. In addition, moisture and temperature control and management is also vital for IAQ control, especially for reducing the bio-contamination. For example, the formation and growth of mold heavily relies on prolonged access to favorable moisture and temperature conditions (WHO 2009).

A 3-D View of IAQ Engineering

IAQ engineering can be viewed as a dynamic “3-D” process in which the various management and control *strategies* are applied over *time* to the different *spaces* of different scales to reduce the occupant’s exposure to various pollutant *species* of health concern (Fig. 4). In this chapter, we focus the discussion on source control, ventilation, and air purification strategies. Hygrothermal control requires the understanding of the water vapor sorption/desorption and moisture retention

Fig. 3 Air pollution process and control strategies



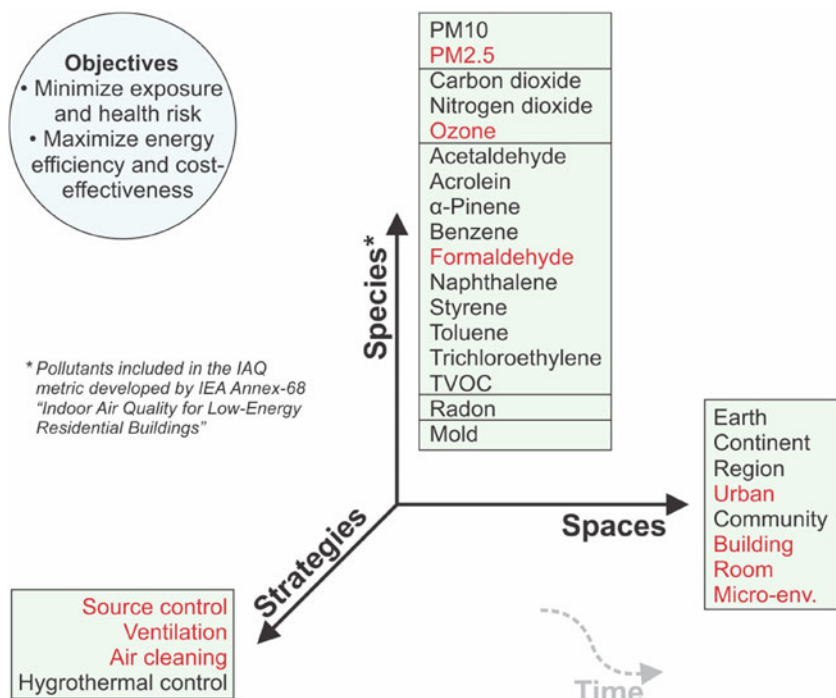


Fig. 4 “3-D” view of indoor air quality engineering

characteristics of various building and indoor materials as well as mechanical systems for humidification and dehumidification, which deserves a dedicated chapter. In the remaining discussion, we make the assumption that space air is maintained within the thermal comfort zone as defined by the ASHRAE standard 55, and the applications of the other three strategies are discussed under such hygrothermal condition unless explicitly stated otherwise. The discussion on the spaces is limited to the microenvironment around the occupant, room, building, community and urban scales with the understanding that the regional, continental and global/earth scales have significant impact on the boundary conditions of urban, community, and building environment (e.g., regional wildfires directly impact the air quality in nearby urban, community and building environment). For the pollutant species, we limit the discussion to a few representative compounds including formaldehyde (a carcinogen and a typical VOC found indoors with a low allowable concentration), PM2.5, and O₃ and SARS CoV-2 as examples to illustrate the 3-D IAQ engineering process. The goal is to understand and quantify the potential and limit of various IAQ control strategies across the different scales of the built environmental system (BES), and discuss how they can be integrated to improve IAQ while saving energy and reducing carbon emissions.

Approach and Model for Assessing the Effectiveness of IAQ Control Strategies

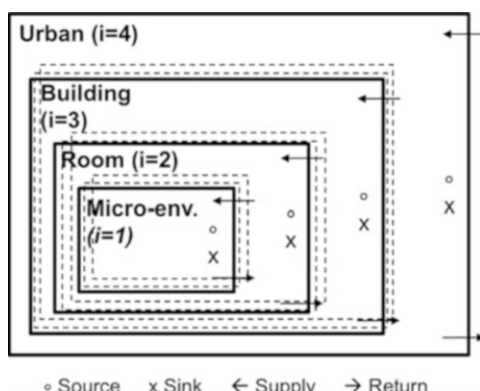
Overview

For the purpose of assessing the effectiveness of various IAQ control strategies, we first consider a simplified multi-scale IAQ model that can account for the interactions between different scale levels as well as between the zones within the same scale level. The model is then further simplified to focus on the effects of IAQ strategies at the different scales on the air quality in the breathing zone of occupants (i.e., in the microenvironment). Pollutant concentrations at a higher scale level are considered as the boundary condition (input) to the immediate lower scale level. A baseline IAQ condition is established based on ASHRAE standard 62.1 and 62.2 considering typical range of building operating conditions for heating, ventilating, and air conditioning of specific building types. Various IAQ strategies and their combinations are then evaluated relative to the baseline conditions. A similar approach has been developed and applied for estimating the effectiveness of various mitigation strategies for reducing the risk of COVID-19 infection in different types of buildings (Shen et al. 2021).

A Simplified Multi-scale IAQ Model

Consider a multiscale built environment system with four nested scales: microenvironment, room, building, and urban air surrounding the building (Fig. 5). Each scale level provides supply air to the level below and returns air to the level above. Each scale level can contain multiple zones, with each having its own sources and sinks. A zone receives a fraction of the total supply air from the upper scale level and returns air to the upper scale level as well as exchanges air with zones in the same scale level (represented by dashed blocks). As a simplified model, we assume that:

Fig. 5 A simplified model of multiscale pollutant transport in built environmental system (dashed lines indicate multiple zones in the same scale)



1. Air within each zone is perfectly mixed.
2. Exchange between the scale levels take place in an aggregated way. That is, a scale level receives the total airflow rate ($m'_{i+1 \leftrightarrow i, sa}$) from the upper level and distributes them to the zones with the scale according to the fractions required by each zone. The return/exhaust air from each zone is mixed and return to the upper scale level with a total airflow rate and an equivalent concentration of the mixed air ($m'_{i \leftrightarrow i+1, ra}$).
3. The total airflow rate supplied to and returned from a lower scale level is balanced at all times (i.e., $m'_{i+1 \leftrightarrow i, sa} = m'_{i \leftrightarrow i+1, ra} = m'_{i+1 \leftrightarrow i, a}$).

Under the above assumptions, the mass conservation of pollutant species k in zone j of scale level i can be represented by

$$\begin{aligned} \frac{\partial}{\partial t} (M_{i,j,a} C_{i,j,k}) &= R'_{i,j,k} - S'_{i,j,k} + \sum_{l(l \neq j)}^{n_i} \left[m'_{l \rightarrow j,k} C_{i,l,k} - m'_{j \rightarrow l,k} C_{i,j,k} \right] \\ &\quad + f_{i+1 \rightarrow i,j} m'_{i+1 \leftrightarrow i,a} (C_{i+1,sa,k} - C_{i,j,k}) \\ &\quad - m'_{i \leftrightarrow i-1,a} (C_{i,sa,k} - C_{i-1,ra,k}) \end{aligned} \quad (1)$$

where,

$C_{i,j,k}$ = mass concentration, kg/(kg of air)

$f_{i+1 \rightarrow i,j}$ = fraction of mass flow rate that zone j receives from the adjacent upper scale level

$M_{i,j,a}$ = air mass in zone j of scale level i

m' = mass flow rate of air mixture, kg/s

n_i = number of zones at the scale level i

R' = source's emission rate, kg/s

S' = sink's removal rate, kg/s

Subscripts: i = scale level ($i = 1, 2, 3, 4$), j = zone number ($j = 1, 2, \dots, n_i$),

k = species, sa = supply air, ra = return air.

Equation (1) states that the rate of mass change for a pollutant k in zone j of scale level i is balanced by the source and sink rates in the zone, the exchange rate between zones within the same scale level, and the exchange with the upper and lower scale levels.

The source rate is the summation of emissions of pollutant k from all sources in the zone (e.g., formaldehyde emissions from building materials, indoor furniture, and office equipment and releases from O₃-initiated oxidation processes). The sink rate is the summation of the rates of removal of pollutant k from the air by all processes taking place in the zone (e.g., adsorption/deposition on surfaces, removal by air cleaners and chemical reactions). The supply air flow rate along with its pollutant concentration represents the input from the upper scale level. For a building space, it includes the outdoor ventilation rate and the infiltration rate.

The return air flow rate and its pollutant concentration represent the aggregated impact of the current scale level on the upper scale level. The microenvironment inside a room is affected by the source and sink strengths and distributions, room and local air distributions, and space partitioning. For a given space configuration, the combined effect can be represented by the *relative room ventilation effectiveness* defined as

$$\eta_v = \frac{C - C_s}{C_\mu - C_s} \quad (2)$$

where C , C_s and C_μ represent the concentrations in the room under perfect mixing condition, room supply air and the air in the microenvironment, respectively. For a perfectly mixed room air, $C_\mu = C$, so that $E_v = 1$. For displacement and personal ventilation, $C_\mu < C$, so that $E_v > 1$. Note that definition of the E_v is different from the conventional definition of ventilation efficiency or contaminant removal effectiveness where C is replaced by the C_e , the concentration in the room exhaust air. The pollutant concentration in the microenvironment in a room space can then be determined by first solving the mass conservation for a room zone using Eq. (1) to obtain C under the perfect mixing condition, and then be estimated with Eq. (2).

Considering a single zone/room space with outdoor ventilation rate of Q_o , recirculation flow rate of Q_r , pollutant filtration efficiency in the recirculated airflow $\varepsilon_{\text{filter}}$, outdoor pollutant concentration C_o , pollutant penetration factor P , space volume V , net indoor pollutant emission rate R , and first-order deposition/removal rate constant of the pollutant k_d , Eq. (1) can be simplified to Eq. (3) for calculating the indoor pollutant concentration C :

$$\frac{dC}{dt} = \frac{PQ_o}{V}C_o - \frac{Q_o}{V}C - \varepsilon_{\text{filter}} \frac{Q_r}{V}C + \sum \frac{R}{V} + \sum k_dC \quad (3)$$

Definition of Baseline Cases

The specification in the prescriptive procedure for acceptable IAQ in the ASHRAE standard 62.1 and 62.2 can be used to define the baseline ventilation conditions for commercial and residential buildings. The baseline ventilation conditions for several space types of commercial buildings are presented in Table 1 (Shen et al. 2021).

The pollution loads for a baseline case should be specified based on the material/product emission test data, the quantity of materials/products used and occupant activities in the space type of interest. When such data are not available, the emission loads can be specified as the product of the maximum allowable concentrations of target compounds and the specified ventilation rate in the baseline case. The second approach is used here because it can be more universally applied in comparing different studies. The maximum allowable concentrations are defined as the chronic Exposure Limit Values (ELVs) of the reference compounds for quantifying IAQ (Table 2) (Abadie and Wargocki 2017).

Table 1 Configurations of baseline cases. (Adapted from Shen et al. 2021)

Scenario		Space layout		Occupant status		Minimum ventilation requirement (per ASHRAE 62.1)		
	Space type	Area [m ²]	Height [m]	Density [#/100 m ²]	Number [person]	Requirement per person [L/s p]	Requirement per floor area [L/s m ²]	Required ventilation rate [L/s]
Long-term care facility	Nursing home	Bedroom (double resident)	36.8	3.0	/	2	2.5	0.3
	Dining room		70.0	3.0	/	20	3.8	0.9
	Living room		50.0	3.0	10	5	2.5	0.3
	Physical therapy room		23.2	3.0	20	5	5	0.3
	Classroom		99.0	4.0	35	5	0.6	234.4
	Library		840.1	4.0	10	84	2.5	0.6
Educational	Cafeteria/dining room	Gym	624.0	4.0	100	624	3.8	0.9
	Classroom (small)		1976.2	8.0	7	138	10	0.9
	Classroom (large)		51.5	3.0	/	25	5	0.6
	Library (public study area)		150.0	4.0	/	96	5	0.6
	Auditorium		338.6	6.0	/	96	2.5	0.6
	Computer lab		1134.0	14.6	/	1500	3.8	0.3
College	Dining hall	Gym (fitness area)	573.5	4.0	100	574	3.8	0.6
	Study lounge		84.3	4.0	/	21	2.5	0.6
	Gym		256.0	8.0	/	60	10	0.9
	Classroom		155.9					
	Library		103.1					
	Auditorium		830.4					

		Resident hall (bedroom)	21.5	3.0	/	2	2.5	0.3	11.5
		Greek house (social gathering)	50.0	3.0	/	20	2.5	0.3	65.0
Manufacturing facility	Meat plant	Processing room (dense)	434.0	4.0	/	108	5.0	0.9	930.6
		Processing room (sparse)	434.0	4.0	/	27	5.0	0.9	525.6
Retail	Standalone	Core shopping space	1600.4	6.0	1.5	240	3.8	0.6	1872.2
		Store (large)	348.4	5.2	8	28	3.8	0.3	210.9
		Store (small)	174.2	5.2	8	14	3.8	0.3	105.5
Healthcare facility	Hospital	Operating room	55.7	4.3	/	3	/	/	198.2
		Patient room	20.9	4.3	/	2	/	/	49.6
		Physical therapy room	487.6	4.3	/	26	/	/	186.0
		Dining room	696.5	4.3	/	75	/	/	902.4
		Lobby	1474.3	4.3	/	21	/	/	499.3
Office	Medium	Open plan office	191.9	2.7	5	10	2.5	0.3	82.6
		Enclosed office	42.3	2.7	5	2	2.5	0.3	17.7
		Conference room	43.2	2.7	50	22	2.5	0.3	68.0
		Lounge	89.6	2.7	50	45	2.5	0.6	166.3
Correctional facility	Prison	Housing (double resident cell)	10.0	3.0	/	2	2.5	0.6	11.0

(continued)

Table 1 (continued)

		Space layout			Occupant status			Minimum ventilation requirement (per ASHRAE 62.1)		
Scenario	Space type	Area [m ²]	Height [m]	Density [#/ 100 m ²]	Number [person]	Requirement per person [L/s p]	Requirement per floor area [L/s m ²]	Required ventilation rate [L/s]	Required ventilation rate [L/s m ²]	
Lodging	Housing (dormitory)	160.0	3.0	25	40	2.5	0.6	196.0		
	Dayroom	160.0	6.0	30	48	2.5	0.3	168.0		
	Guest room/bedroom	39.0	3.0	/	2	2.5	0.3	16.7		
	Banquet/dining room	331.7	3.0	70	232	3.8	0.9	1180.1		
Other public facilities	Lobby	1308.2	4.0	30	392	3.8	0.3	1882.1		
	Restaurant	371.7	3.0	70	260	3.8	0.9	1322.5		
	Dining room (ordinary)									
	Dining room (fast-food)	116.1	3.0	70	81	3.8	0.9	412.3		
Religious	Worship hall	204.0	4.0	/	200	2.5	0.3	561.2		
	Casino	253.1	4.0	120	304	3.8	0.9	1383.0		

Table 2 Exposure limit values (ELVs, chronic effects) of the reference compounds for quantifying IAQ (Abadie and Wargocki 2017)

Compound	ELV ^a
PM10	20
PM2.5	10
Nitrogen dioxide	20
Ozone	100
Acetaldehyde	48
Acrolein	0.35
α -Pinene	200
Benzene	0.2
Formaldehyde	9
Naphthalene	2
Styrene	30
Toluene	250
Trichloroethylene	2
Radon	200
Mold	200

^aELV concentration in $\mu\text{g}/\text{m}^3$ except for radon in Bq/m^3 and mold in CFU/m^3 . These values are adopted in this study for the purpose of defining the pollution loads in the baseline case

Assessment Procedure

Once the ventilation and pollution load for a baseline case are defined, the simplified multi-scale IAQ model can be used to first calculate the concentrations of the target compounds under the baseline conditions, and then determine the potential and limits of individual and combined strategies in improving the IAQ relative to the baseline case.

Potentials and Limits of Source Control, Ventilation and Air Purification at Different Scales

Urban Scale

The major atmospheric pollutants include particulate matter (PM), ozone (O_3), carbon monoxide (CO), nitrogen oxides (NO_x), sulfur dioxide (SO_2), and volatile organic compounds (VOCs), which can originate from industry emissions, vehicle exhausts, chemical products, construction dusts, household stove combustions, and the reactions between these compounds and the compounds on material surfaces. Considering the heavy traffic and construction activities in urban areas that generate more pollutant emissions, as well as the high density of buildings that can enhance the accumulation of pollutants in urban areas, the air quality in urban areas, particularly densely populated areas, is likely worse than other areas in the city. Urban air quality can impact the health of people who are directly exposed to the ambient air. Outdoor pollutants may also enter the indoor environments through ventilation or

infiltration and affect the indoor air quality. Therefore, managing the air quality on the urban scale can benefit both outdoor and indoor environments and people's health.

Source control One approach to control the urban air quality is to control the emission sources of the concerned pollutants (Fig. 6). Pollutants generated by industry emission, vehicle exhaust, chemical products, construction dust, household stove combustion, and other potential sources should be controlled and limited. High-level air quality and pollutant emission standards/policies need to be developed and strictly implemented by the public agencies. It can promote relevant entities to upgrade their pollutant-producing facilities to reduce emissions to the atmosphere. Tremendous efforts and resources are required for mitigating emissions from various sources, but it has been proven to be effective for improving outdoor air quality. For example, the significant concentration declines in some air pollutants (e.g. SO₂, NO_x, and PM2.5) in China during the past few years is closely correlated with the implementation of the strict policies and actions on air quality, e.g. enhancing and enforcing industrial emission standards, upgrading industrial boilers, phasing out outdated industrial capacity, promoting clean fuels in the residential sector, phasing out small and polluting factories, and strengthening vehicle emission standards (Zhang et al. 2019).

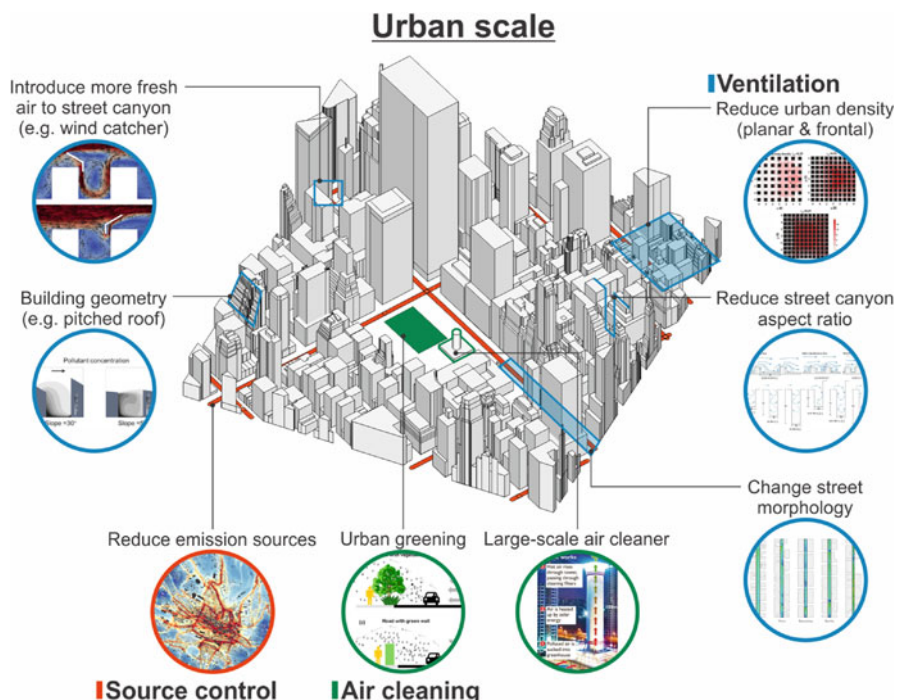


Fig. 6 Schematic of urban-scale air quality control strategies

Pollutant sources in the urban area should be managed to meet or exceed the national ambient air quality standards established by the respective government agencies. For example, in U.S. the ambient air quality standard established by the US Environmental Protection Agency (EPA) has been used as the criteria to determine if the outdoor air is sufficiently clean for ventilation or additional filtration is needed.

Ventilation Urban air quality can also be affected by urban ventilation. Wind from rural and suburban areas is usually believed to be clean and fresh for purging the pollutants emitted by vehicle exhaust and other activities in urban areas. However, the building density in urban areas impacts the urban ventilation. In-street pollutants can be accumulated within the street canyon in high-density compact urban areas due to the poor airflow patterns. Poor ventilation and unfavorable pollutant dispersion in the urban canopy result in poor air quality.

Pollutants generated in the urban canopy layer can be purged by horizontal air exchanges through street openings and vertical air exchanges through street roofs. Urban density, including planar density λ_p and frontal density λ_f (i.e., the ratios of the plan area and frontal area of buildings to the lot area, respectively) are key parameters that can significantly impact the airflow and pollutant dispersion in the urban canopy. Compact urban areas with higher planar and frontal density typically slow down the airflow velocity in the urban canopy, particularly at the pedestrian level. The mean wind velocity at the pedestrian level in urban areas can be decreased by over 35% when increasing the urban planar density from 10 to 35% (Kubota et al. 2008). The decreased wind velocity may reduce the pollutant removal and result in the accumulation of pollutants in the street canyon. It was observed that for a compact city with over 44% planar density, the city itself responds as a single obstacle, and the city breathability is greatly weakened and the pollutants tend to accumulate in the street canyon (Buccolieri et al. 2010). Increasing frontal urban density (i.e. building heights) causes pollutant accumulation in the urban canopy likely due to weaker air exchanges through the urban roof. Poor urban ventilation can be observed in urban areas with a frontal density of over 40% (Mei et al. 2017). Therefore, to improve the ventilation in the urban canopy, urban design with lower planar and frontal density is preferred. Urban heterogeneity, including planar urban non-uniformity and building height variation, can also affect the airflow pattern in the urban canopy. But its effect on urban ventilation is highly dependent on the specific urban morphology (Li et al. 2021a). The non-uniform planar building configuration may weaken the channeling flow inside the street canyon, which was supposed to purge in-street pollutants but can also decrease the vortices behind buildings, which was supposed to cause pollutant accumulation. The non-uniform building height arrangement can enhance the urban ventilation at the high-rise level of the urban canopy due to the improved vertical and horizontal air exchanges but may deteriorate the ventilation at the low-rise level because of more turbulent dissipation at the high-rise level. Thus, it requires professional designs and analyses before performing urban heterogeneity strategies to improve the urban ventilation potential.

The ventilation and pollutant dispersion in the urban canopy are determined by the airflow patterns in the street canyon, which is dependent on both direction and aspect ratio (i.e. the ratio of street height and width, H/W) of the street canyon. When the approaching airflow is parallel to the street, the airflow inside the street canyon can be accelerated due to the channelization effect, which can help to purge the pollutants and improve the street ventilation. A higher aspect ratio may reduce the pollutant removal due to less vertical air exchanges through the street roof, although stronger channeling flow can be observed. Higher street continuity and closure (reduced building setbacks and lateral openings) can lead to a stronger channeling flow, but it reduces the pollutant removal through lateral openings of the street (e.g. intersected streets) and street roofs (Ng and Chau 2014; Shen et al. 2017). When the approaching airflow is perpendicular to the street, the airflow pattern is closely related to the street aspect ratio. If the buildings are well apart ($0.05 < H/W < 0.3$), the airflow fields around buildings do not interact but act as isolated roughness flows. If buildings are too close ($H/W > 0.7$), a skimming flow pattern is formed and a stable vortex is developed within the street canyon, which is not beneficial for removing in-street pollutants (Oke 1988). More vertical vortices are developed inside the street canyon as the street aspect ratio increases, and the wind velocity near the ground becomes weaker, which further deteriorates the air exchanges and pollutant dispersion. Typically, a street canyon with an aspect ratio of 2 (i.e. $H/W = 2$) can form two vertical vortices, and three vortices are formed when the aspect ratio reaches 3 (i.e. $H/W = 3$). In many high-density compact cities, the aspect ratios of street canyons can be higher than 5, so that the ground-level airflow is mostly in calm conditions, and there are very few vertical air changes (He et al. 2019a). Therefore, street orientations are preferred to be designed parallel to the prevailing wind from the perspective of urban ventilation and pollutant dispersion. The aspect ratios of streets are suggested to be lower for improving the vertical air exchanges. The shape of buildings along the street also affects the airflow in the street canyon. For example, sloped/pitched building roofs can improve the pollutant dispersion in the street canyon compared to flat roofs (Li et al. 2021b). Building lift-up design can also improve the local air distribution. The first-floor lift-up design may result in a 34–50% reduction in the building intake fraction and daily pollutant exposure (Sha et al. 2018).

Ventilation in the street canyon can also be enhanced by introducing more wind into the street canyon using technologies such as street wind catchers (Chew et al. 2017), and pedestrian ventilation systems (Mirzaei and Haghhighat 2010). More fresh air can be introduced to the pedestrian level through wind pressure or thermal pressure gradient. But the practical effects of these potential technologies still require more studies and validations.

Air cleaning Air cleaning technologies at the urban scale aim to remove urban pollutants through sorption, deposition, or filtration. Urban greenings such as trees, shrubs, and grasslands, as well as green envelopes, play a significant role in mitigating urban pollutants (Nowak et al. 2006). The effectiveness of greenings

on air quality improvement depends on the plant species, the configuration of greening infrastructure, and the greening layouts. Trees can mitigate urban pollutants mainly through the deposition of gaseous and particulate matters onto leaf surfaces, and pollutant dispersion by the dilution with clean air. However, trees can also increase the flow resistance and reduce the airflow velocity, which likely results in local pollutant accumulation. Previous studies revealed that trees in the street canyon can result in a nearly 20–58% increase in the average concentration of in-canyon pollutants, owing to the reduced air exchanges between the air above the street roof and within the street canyon (Li et al. 2021b). However, in open areas, trees have a positive impact on air quality. Vegetation barriers with thick, dense, and tall trees can remove considerable pollutants when they are planted closer to the pollutant source and plume's maximum concentration. A reduction of over 50% was observed with a 10 m thick vegetation barrier for numerous pollutants in open roads (Abhijith et al. 2017). Parks with trees and shrubs can remove traffic pollutants at ground level by over 20% compared to the surrounding areas (Yin et al. 2011). Hedges consist of shrubs and usually grow smaller than trees, but they may have higher leaf density than trees. Hedges can also hinder airflow and air exchange, but not as significant as trees. Hedges can generally reduce pollutant concentrations and improve the air quality in both street canyons and open areas. Reduced pollutant exposure by 24–61% at the footpath areas in street canyons with hedges was observed in studies (Abhijith et al. 2017). Besides, green envelopes such as green walls and green roofs have been developed as sustainable building strategies providing benefits for urban environments, which play a significant role in mitigating pollutants in the street canyon without consuming spaces at street level. Pollution mitigation by green envelopes is dominated by deposition, as green envelopes are less likely to change the airflow within the street canyon. Green walls are generally more effective than green roofs for improving in-canyon air quality. However, their ability to remove pollutants is lesser compared to trees and vegetation barriers (Abhijith et al. 2017). In addition to possible air pollution reduction, urban greenings are also beneficial for urban heat island mitigation, potential reduction in energy consumption and noise pollution, better storm water management, urban biodiversity, and climate change mitigation (Abhijith et al. 2017).

Some other approaches for air cleaning at urban/street scale have also been proposed and implemented, e.g. large-scale air cleaning system. Traditionally, air cleaners are designed to clean the indoor air by filtering particles and gaseous pollutants. A large-scale air cleaning system is proposed to purify the urban air with a similar filtration mechanism as indoor air cleaners (Cao et al. 2015; Zhou et al. 2015). A solar-driven large-scale air cleaning system with a 60 m high solar chimney was built and tested in China (Cyranoski 2018). Experiments showed that this system reduced the PM_{2.5} concentration by 11–19% within a 10 km area around the system. However, its practical effectiveness has been questioned by many researchers, considering its limited effective area and, particularly, its high investment and maintenance costs (Cyranoski 2018).

Building Scale

Outdoor pollutants can be introduced to the indoor environment through building openings and cracks or enter through the HVAC system. Building materials (including construction and surface materials) also produce considerable pollutants, particularly VOCs. Some reactive pollutants (e.g. O₃) readily react with VOCs or building materials, which produce hazardous by-products. As people spend over 80% of their time indoors, properly managing the indoor air quality is essential for people's health, performance, and wellbeing.

Source control Building materials can be a major source of indoor pollutant emissions if not controlled properly. To control the potential sources of indoor pollutants, it is necessary to use the materials with less emissions during building design, construction, and decoration periods. Building materials such as plywood, carpet, and some painting materials can typically generate many VOCs of concern for human health and comfort (Won et al. 2003). Reactions between O₃ and these materials or the VOCs they emitted may also result in considerable oxidized by-product yields, including C1-C13 carbonyls, dicarbonyls, and hydroxycarbonyls (Shen and Gao 2018). Therefore, it is suggested to use materials with less emissions for constructing, flooring, and painting of the building (Fig. 7).

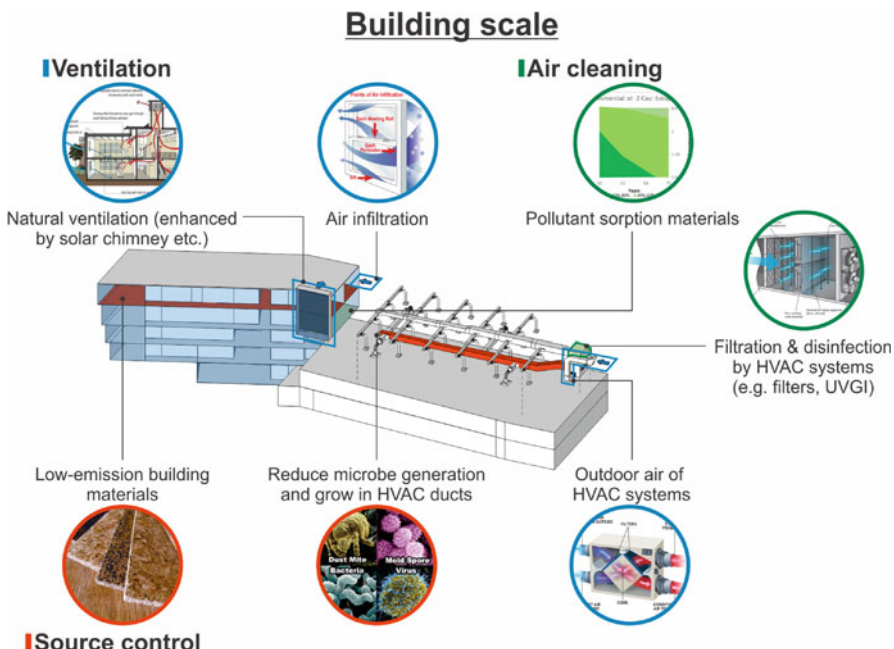


Fig. 7 Schematic of building-scale IAQ control strategies

HVAC system introduces outdoor air to ensure required ventilation of fresh air for occupants indoors. However, outdoor air may contain some pollutants that can be introduced to the indoor environment by the HVAC system. For buildings without significant indoor particle and O₃ emission sources, outdoor air is likely the primary source of indoor particle and O₃ pollution. Therefore, filters that can remove ambient pollutants (particularly the pollutants with considerable concentrations in the outdoor air, e.g. particles and O₃) are required in the HVAC system for controlling the outdoor sources of indoor pollution. Besides, due to poor control of humidity or inadequate maintenance of filters, microbes may generate and grow in the HVAC ducts or on the filters in the presence of moisture, and bioaerosols can be introduced to the indoor environment through the supply air (Batterman and Burge 1995). Elevated concentrations of VOCs such as formaldehyde and acetone may also be observed after the filters of HVAC systems, which are probably initiated from the microbes on filters (Schleibinger and Rüden 1999). Therefore, HVAC systems can also be possible sources of bioaerosols and VOCs in indoor environments. It is necessary to clean and maintain HVAC systems and their filters regularly.

Ventilation Proper ventilation can dilute indoor pollutants and improve indoor air quality. There are multiple standards or guidelines that define the minimum ventilation requirements in different buildings to keep CO₂ levels at an acceptably low level, e.g. 800 ppm or 1000 ppm (ASHRAE 2019a, b; IWBI 2019). Air infiltration through envelope cracks, natural ventilation through building openings, and mechanical ventilation by HVAC systems can contribute to the building air exchanges. Air infiltration is usually unintentional and uncontrolled and can result in heat loss and introduce outdoor pollutants and moisture condensation in building enclosures. It can be responsible for over 10% of the total annual heating and cooling energy consumption while it can even account for more than 40% of heating/cooling load in some scenarios (Han et al. 2015). Therefore, air infiltration should be minimized during construction or retrofitting. Data revealed that the average infiltration rate in buildings is generally below 0.5 h⁻¹ (Persily et al. 2010; Shi et al. 2015; Cheng and Li 2018; Ji et al. 2020). Natural ventilation provides air changes by thermal, wind, or diffusion effects through doors, windows, or other intentional openings in the building. When outdoor weather and air quality conditions allow, natural ventilation can be an effective approach to increase the indoor air changes and pollutant dilution. The effect is determined by factors like opening area, ambient wind direction and velocity, and temperature difference. It was found that more openings can result in the enhanced natural ventilation. Data showed the average air change rate in a residence to change from 0.76 h⁻¹ for no openings to 1.51 h⁻¹ for one opening, 2.30 h⁻¹ for two openings, and 2.75 h⁻¹ for three or more openings (Johnson et al. 2004). Besides, opening windows is a more effective method of increasing natural residential ventilation rates compared to the impact of continuously opening doors (Marr et al. 2012). Natural ventilation can introduce more outdoor air to the building incorporating with fans. Some passive technologies have been developed to improve the efficiency of ventilation, e.g. windcatcher and solar chimney. A windcatcher is a unit installed on the roof of the building, which

captures outdoor air through its openings and directs it toward the indoor space. It has been widely used in the Middle East to provide natural ventilation and passive cooling inside the building. A well-designed one-sided windcatcher can provide up to 4 h^{-1} ventilation of outdoor air to a dwelling while a configuration with two one-sided windcatchers can provide up to 5.6 h^{-1} ventilation (Jomehzadeh et al. 2020). A solar chimney uses solar energy to generate airflow movements that could be used for building ventilation, and it is usually attached to the south façade of the building to maximize the solar gain. A well-designed solar chimney can typically provide relatively consistent air change rates of about $2\text{--}5 \text{ h}^{-1}$ on average (He et al. 2021). But the effectiveness of windcatchers and solar chimneys is closely related to the local climate and to their designs. Their effects on building natural ventilation vary significantly case to case. However, natural ventilation also introduces ambient pollutants along with the outdoor air, which is not practical to filter or remove during the natural ventilation.

HVAC system is designed to control the indoor thermal comfort, but it also needs to introduce outdoor air to meet the ventilation requirement for occupants. Based on the ASHRAE 62.1 standard (ASHRAE 2019a), each person in a typical office with 5 persons per 100 m^2 requires approximately 8.5 L/s minimum outdoor air, which accounts for around 0.6 h^{-1} air changes. This requirement is based on the minimum accepted level of indoor CO_2 . Higher air change rates are preferred for improving the indoor air quality. The outdoor air fraction of the supply air in the HVAC system is typically 25% (Persily and Gorfain 2004). Increasing the fraction of outdoor air can elevate the ventilation rate but also require more energy for heating/cooling the outdoor air. Increasing the total supply air flow rate can provide more outdoor air but require more energy consumption as well. The extend to which the outdoor air supply can be increased is also limited by the HVAC system capacity. Considering that most HVAC systems have filters installed, the ambient pollutants in the outdoor air are probably not a significant risk for indoor air quality. If the filters in HVAC systems are not well-designed or maintained, the outdoor pollutants become a potential risk.

Air cleaning HVAC systems incorporated with in-duct air cleaning units can significantly improve the indoor air quality in the building scale. Typically, MERV 8 filter and activated carbon filter are installed in the HVAC system. A MERV 8 filter can remove approximately 50% of particles and bioaerosols $>0.3 \mu\text{m}$ in diameter. Higher MERV-rating filters can remove particles more efficiently, e.g. over 99.9% particle removal efficiency for HEPA filter, but also increase the flow resistance, resulting in higher energy consumption for delivering the same amount of air. Overall effectiveness of reducing particle concentrations depends on several factors, including filter efficiency, airflow rate through the filter, size of the particles, and location of the filter in the HVAC system. Activated carbon filters remove odors and some VOCs and can decompose O_3 readily without significant by-product yields. Other common in-duct filtration/disinfection components include UVGI lights (which is typically used for inactivating viruses, bacteria and fungi, but may also have O_3 leakage), and bipolar ionization units (which high voltage electrodes create

reactive ions in air that react with airborne contaminants, including viruses, but may emit O₃ as well) (ASHRAE 2020). Some units may intentionally generate O₃ in the duct to react with unsaturated VOCs. But the by-products become a new challenge for indoor air quality and they must be removed before recirculating the air to the room. The effectiveness of these in-duct air cleaning units may vary greatly.

Some building materials can also be considered to be air cleaning technologies due to the effects of sorption and deposition on the building surface. For example, some inorganic materials, e.g. bricks, clay-based plasters, perlite-based ceiling tiles, and activated carbon cloth, are usually considered as the most promising passive removal materials (PRMs) for indoor O₃, since they can remove substantial O₃ while yielding negligible by-products (Gall et al. 2011; Shen and Gao 2018). The use of these PRMs in the building construction/renovation may result in a lower level of O₃ and by-products, hence a better air quality, while they do not consume additional energy for ventilation or air cleaning. In addition, some sorption materials embedded in gypsum wall and ceiling boards have been developed as an effective solution on the market to reduce the formaldehyde concentration levels indoors (Pétigny et al. 2021). A formaldehyde deposition velocity of 2.08 m/h has been tested in commercial buildings and 1.02 m/h in residential settings, with a high level of formaldehyde removal (70–80% reduction in concentration) even after 50 years, which has a high potential for long-term IAQ improvement (Pétigny et al. 2021).

Room Scale

Source control The indoor pollutants in a room not only originate from the construction materials (i.e. constructing, flooring, painting materials), but also from indoor furnishing and equipment, as well as occupants and their activities. Indoor furnishing, equipment, and occupancy depend on the room function and settings. For example, an office has totally different settings of furnishing, equipment, and occupancy as compared to a residential space such as a bedroom. A typical office has multiple workstations (likely cubicles with partitions) with desktop computers, and some office devices such as printers and photocopiers. It may contain several occupants working from 9 am to 5 pm during the weekdays. A typical bedroom can have a bed, a table, and a closet with large areas covered by fabrics. Commonly, there are commonly two people sleeping during the night. Therefore, the potential indoor pollutant sources are in great differences for various spaces. Household furniture may generate considerable VOCs. Workstations or partitions in offices may also release pollutants. Some air cleaning/disinfection devices, e.g. portable UVGI lights and ionization-based air cleaners, and printing devices such as printers and photocopiers may generate abundant O₃ (Guo et al. 2019). Occupant activities like smoking and cooking generate a large number of particles and VOCs, which is hazardous for people's health. In order to control the emission sources, furnishing with less emissions are encouraged (Fig. 8). Emission devices should be used less frequently, in separated rooms or when nobody occupying the room. Smoking should be prohibited in indoor environment, especially when other people are

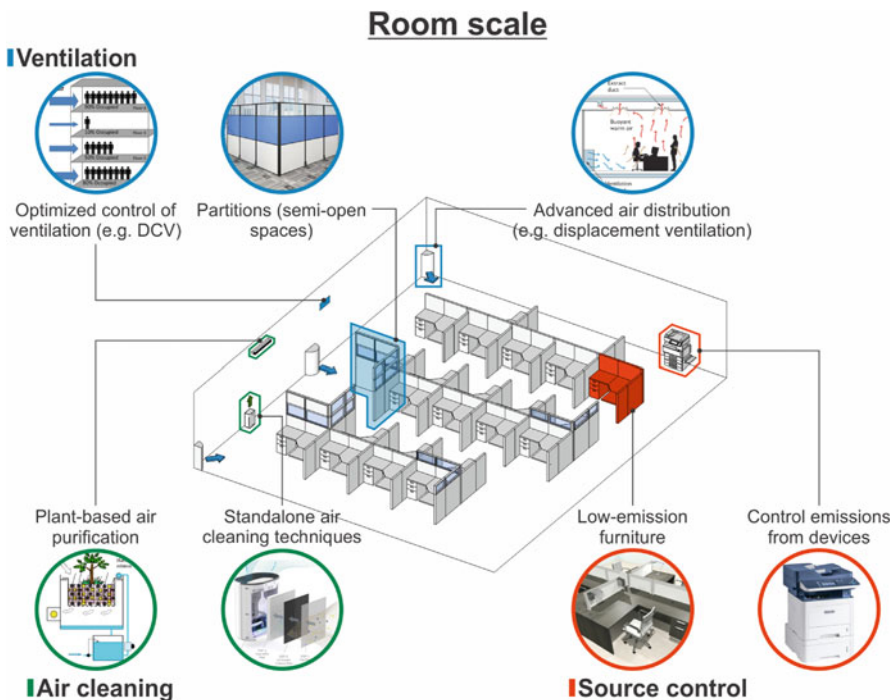


Fig. 8 Schematic of room-scale IAQ control strategies

sharing the same room. Cooking exhaust should be removed immediately and an efficient hood should be used.

Ventilation The design of diffuser and exhaust of the HVAC system can have an impact on the air distribution in the room. The air distribution affects the efficiency of ventilation and pollutant dilution in the room and people's exposure to pollutants. Typical HVAC systems provide mixing ventilation for the room, which is designed to supply sufficient conditioned fresh air to the whole space. The air circulation due to supply and return air can help to mix and dilute the pollutants. It ideally distributes the pollutants from emission sources to the room air uniformly, although the room air may not be perfectly mixed in real conditions. Ideally, the room air pollutant concentration equals the pollutant level in the return air, which is not a very efficient approach for mitigating pollutants and has the possibility of increasing the local pollutant concentration in some areas in the room and resulting in cross contamination. In terms of the control of airborne transmission for respiratory diseases, the mixing ventilation can cause cross contamination between the patients and other healthy people and increase the infection risk for susceptible people in the room.

Therefore, improved air distribution strategies are suggested for improving the ventilation efficiency. Displacement ventilation is a room air distribution strategy where conditioned air is supplied at a low velocity from air supply diffusers located

near floor level and extracted above the occupied zone, usually at ceiling height (Chen and Glicksman 2003). Displacement ventilation is typically used for cooling. The near-floor clean air is delivered to the breathing zone by the thermal plume around the human body, which ideally would not result in pollutant mixing in the room and reduce the risk of cross contamination. It can improve the clean air delivery efficiency with a typical ventilation effectiveness of 1.2–2 compared to the well-mixing ventilation (Chen and Glicksman 2003). But displacement ventilation requires professional design and implementation to maximize its performance. Underfloor air distribution (UFAD) system is also widely used in many commercial buildings like offices. Air can be delivered through a variety of supply outlets located at floor level (most common), or as part of the furniture and partitions. It usually exhibits better performance in removing indoor pollutants compared to conventional overhead (ceiling-based) systems. A well-designed UFAD system can provide as much IAQ efficiency improvement as a displacement ventilation system (Cermak and Melikov 2016). However, both displacement ventilation system and UFAD system are often claimed to bring contaminants at floor level to the breathing zone, resulting in an equivalent removal efficiency for floor pollutants as a mixing ventilation system (Cermak and Melikov 2016). For example, resuspended particles at the floor level can cause problems in an UFAD system (Zhang and Chen 2006). But both of them are highly effective in removing exhaled pollutants and reducing cross-contamination (Cermak and Melikov 2016).

The room air distribution can also be affected by the furnishing and partitions in the room, which may block the air flow. Partition screens have been widely used during the COVID-19 pandemic since they can ideally reduce the transmission of droplets. In terms of the transmission of airborne pollutants (including viruses), well-designed partitions can reduce the risk of cross contamination while poor designs may increase the risk in some locations (Rooney et al. 2021). Cubical workstations in open office plan settings are a common scenario with many partitions. The partitions can typically reduce cross contamination between cubicles with a typical ventilation effectiveness of 1.1–3.6 (require well-designed ventilation and air distribution) (Haghigat et al. 1996). When partitions are incorporated with other strategies such as displacement ventilation, the ventilation efficiency can be even higher (Halvoňová and Melikov 2010). But all these strategies require professional design of partition layouts in coordination with room air distribution and proper operation control to maximize their effectiveness. Poor design can lead to a worse performance than the conventional mixing ventilation.

The advanced/intelligent control of ventilation system also has the potential in improving IAQ and energy efficiency. Demand control ventilation (DCV) system estimates the occupant number in the room based on CO₂ detection or occupant detection, and then signals the system controller to change the ventilation volume, which is mainly designed for reducing energy consumed by heating/cooling outdoor air when less people occupying the room. But it also works for providing sufficient/required clean air to all occupants in the room when more people enter the room (within the system capacity). Some advanced control algorithms have been developed to optimize the effectiveness of DCV system, including PID control, model predictive control (MPC), or data-driven control. As an example, the application of

machine-learning-based CO₂ concentration prediction in DCV can reduce the HVAC energy consumption by 51.4% and provide ventilation as needed (Taheri and Razban 2021). The optimization of ventilation system control has been proved to have a high potential for IAQ improvement and energy efficiency.

Air cleaning Standalone air cleaning technologies can usually work efficiently for indoor pollutant removal. They have been widely used in indoor environments, which can typically improve IAQ through catalytic oxidation, filtration, ozone oxidation, plasma, sorption, or UVGI. Most catalytic oxidation air cleaning studies focus on UV or visible light photocatalytic oxidation (PCO). UVPCO technology has the potential to degrade organic contaminants efficiently with low airflow resistance (Chen et al. 2005). But it is not yet ready to be applied in practice due to potential byproduct formation and short service life. Other PCO technologies currently have low efficiency in pollutant removal (Zhang et al. 2011). Filtration is the most used technology in air cleaners. Particles can be filtered readily using high-efficiency filters such as HEPA filters (over 99.9% removal efficiency). Other filters such as activated carbon filter can remove some VOCs and O₃. In general, mechanical filters can efficiently remove particles, but are not as effective for organic and inorganic chemical pollutants. The main problem with mechanical filters is that they act as a pollution source if they are not properly used (Zhang et al. 2011). Therefore, filters are usually recommended to be replaced every 6–12 months. Ozone is an oxidant that can react with some indoor pollutants, and therefore, has been used in some air cleaners for oxidizing some organic chemical pollutants and disinfection. However, considering that ozone and ozone-initiated by-products are quite harmful for people, caution should be taken when using ozone-emitting air cleaning techniques. Plasma air cleaners have been reported to remove particles at high efficiency, e.g., within the range of 76–99% (Zhang et al. 2011). But it is not efficient at removing gas-phase pollutants. The production of secondary pollutants such as NO_x and O₃ is a major drawback of plasma technology. Sorption is good for gas pollutant removal (such as VOCs and O₃), while its efficiency depends on sorption mechanism, specific sorbent surface area, porosity, and diffusion characteristics of target pollutants. UVGI technique in standalone air cleaners is typically used for disinfection (e.g. inactivating viruses, bacteria, and fungi). Upper-room UVGI system has been developed to kill airborne pathogens, which refers to a disinfection zone located above people (the upper area of the room) preventing direct UV exposures to people. Proper use of upper-room UVGI system can typically provide an equivalent 6.7–33 ACH ventilation to the room, depending on its operating conditions and circumstance (Riley and Nardell 1989; Xu et al. 2003; U.S. CDC and NIOSH 2009). Its efficiency also relies on the room air distribution. For example, displacement ventilation may reduce the efficiency (around 78% of the efficiency incorporating with mixing ventilation (Kanaan and Abou Moughabay 2018)) as it decreases the residence time of pathogens in the disinfection zone. Some UVGI systems may produce unintended O₃, which also need certain caution.

The combined application of multiple air cleaning technologies in standalone air cleaners typically has elevated efficiency. For example, the combination of plasma

and UV-catalytic technology can provide improved removal efficiencies for formaldehyde, benzene, toluene, and xylene (Zhang et al. 2011). According to a market survey, a common room air cleaner can typically supply a median clean air delivery rate (CADR) of 361 m³/h to the room (Zhao et al. 2020). The CADR per square meter of room is roughly between 6 and 16 m³/h (Liu et al. 2017). The Association of Home Appliance Manufacturers (AHAM) recommended a minimum CADR of 12 m³/h per square meter when selecting an air cleaner for home use (AHAM 2021), which is in accordance with the U.S. EPA's guide (U.S. EPA 2018).

Potted plants have demonstrated abilities to remove VOCs indoors. However, the efficiency may not be very significant in real scenarios. The distribution of single-plant CADR spanned orders of magnitude, with a median of 0.023 m³/h, necessitating the placement of 10–1000 plants/m² of a building's floor space for the combined VOC-removing ability by potted plants to achieve the same removal rate that outdoor-to-indoor air exchange already provides in typical buildings (~1 ACH) (Cummings and Waring 2019). It is impractical to directly use potted plants for improving IAQ. One solution might be to integrate plants and mechanical air cleaning or ventilation system. Dynamic botanical air filtration (DBAF) system is therefore developed. It consists of an activated-carbon/hydroculture-based root bed for potted-plant, a fan for driving air through the root bed for purification, and an irrigation system for maintaining proper moisture content in the root bed. A well-designed DBAF system is effective for removing formaldehyde and toluene over a long period, and has the ability to supply an equivalent CADR of 476 m³/h (Wang and Zhang 2011).

Personal Microenvironments

Pollutant concentration and air quality in personal microenvironments, such as the space around a person or the breathing zone, are closely associated with people's exposure to air pollutants and health. A personalized environmental control system or micro-environmental control system has the potential to restore people's thermal comfort as well as provide fresh outdoor air to the people directly and hence save energy (Khalifa 2017; Kong 2017).

Source reduction Human body can produce considerable particles and VOCs through primary emission due to respiratory activities or sweating (Žitnik et al. 2016; Shen et al. 2021), or secondary emission caused by the reactions between O₃ and skin oil (Shen and Gao 2018). The average emission rate of total VOC (TVOC) from the whole-body was 742.8 µg/h, while the average TVOC emission rate from the breath samples was 41.4 µg/h (He et al. 2019b). People's movement can raise the floor dust and resuspend particles in the air. The thermal plume around the human body may introduce some pollutant-like particles from the floor level to the breathing zone and increase people's inhalation. Personalized/localized air exhaust aims to remove as much contaminants as possible directly from the occupants who produce pollutants before it can significantly mix with the bulk flow (Dygert and Dang 2010).

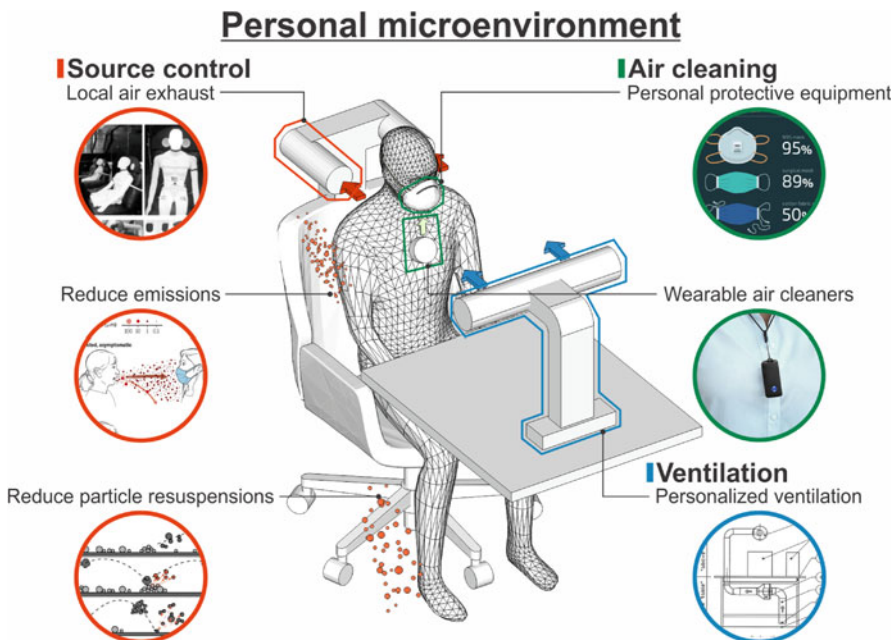


Fig. 9 Schematic of personal-scaled IAQ control strategies

The pollutant removal process is accomplished using localized suction orifices near and around the source occupant to unobtrusively ingest the individual's thermal plume and filter it or exhaust it from the occupied space. A well-designed local air exhaust system can reduce the cross-contamination with typical ventilation effectiveness of 1.4–10 (Dygert and Dang 2012). Source control can be performed in personal microenvironments by reducing the near-person emissions and chemical reactions or particle resuspension (Fig. 9).

Ventilation Personal ventilation increases clean air supply to the personal micro-environment and has the potential to improve the air quality by a typical factor of 1.7, depending on diffuser location and airflow rate (Melikov et al. 2007), which is close to the air distribution effectiveness in ASHRAE Standard 62.1 (ASHRAE 2019a). Local air exhaust ventilation is designed to remove the pollutants near the emission sources, which is usually used to reduce the exhaled pollutants by occupants and mitigate the cross contamination between occupants. It can reduce the cross contamination with a typical ventilation effectiveness of 1.4–10, depending on the local partition configuration, exhaust location and airflow rate (Dygert and Dang 2012).

Air cleaning There are some air cleaning technologies for personal microenvironment. Wearable air cleaner is a technique similar to portable room air cleaner but can directly deliver filtered/clean air to the breathing zone. It can provide corresponding

mass removal rates of PM 2.5 between approximately 0.5–5.4 h⁻¹. But some models with ionization units may produce a number of O₃ (up to 670 µg/h), which need to be considered in practice.

A low-cost air cleaning technique that protects the breathing zone is wearing masks, which can efficiently filter the inhaled air and remove particles. A cloth mask can provide an overall 30% particle filtration efficiency considering leakage from gaps caused by improper fit (Konda et al. 2020), while a surgical mask has an overall 50% particle removal efficiency and a N95 mask can provide over 95% particle reduction (Rothamer et al. 2020; Konda et al. 2020). Conventional masks can only remove particles through filtration, but some novel masks (e.g. with activated carbon cloth) can also remove reactive gaseous compounds (e.g. O₃) and/or some VOCs. Masks are also very useful for mitigating infection risk of respiratory diseases through airborne transmission, which has been highly recommended since the COVID-19 pandemic (Shen et al. 2021).

Integration of IAQ Strategies

To demonstrate the analysis for the potential of source control, ventilation, and air cleaning strategies at different scales, the standard open plan office environment (ANSI/BIFMA M7.1) presented in ► Chap. 56, “Testing and Reducing VOC Emissions from Building Materials and Furniture” of this book section (Testing and reducing VOC emissions from building materials and furniture to improve indoor air quality) is adopted to define the example case. An open plan office with ten workstations (ten occupants) is defined based on the information in Chap. 1. The space configuration parameters of the reference office are shown in Table 3. The total floor area is 59.5 m² since the standard floor area per workstation with common area is 5.95 m² and there is an assumption of ten workstations in the reference case. Four typical indoor pollutants are simulated to study the indoor air quality of the reference office, including PM 2.5, O₃, formaldehyde, and virus-laden aerosols (considering the serious situation of pandemic). The average pollutant concentrations of PM2.5, O₃, formaldehyde, and infectious aerosols in outdoor air in the U.S. are 8 µg/m³,

Table 3 Configuration parameters of the reference open plan office (per ANSI/BIFMA M7.1)

Parameter	Open plan office
Room information	
Total floor area (m ²)	59.5 (5.95 × 10)
Room height (m)	2.7
Room volume (m ³)	162.8
Total wall area (m ²)	93.5
Workstation/occupant number (#)	10
Workstation components	
Total panel vertical area (m ²)	110.8 (11.08 × 10)
Total work surface horizontal area (m ²)	61.0 (6.10 × 10)
Total storage external surface area (m ²)	45.7 (4.57 × 10)

135 $\mu\text{g}/\text{m}^3$, 7.2 $\mu\text{g}/\text{m}^3$, and 0 quanta/ m^3 , respectively (WHO 2010; U.S. EPA 2021a, b; Chirizzi et al. 2021). The infiltration rate for the reference office case is assumed to be 0.2 h^{-1} . The penetration factor for O_3 and formaldehyde through building envelope is typically 1, while the penetration factor for particles is assumed to be 0.9 (Chen and Zhao 2011). The indoor emission source of PM 2.5 is assumed to be 600 $\mu\text{g}/\text{h}$ per occupant (due to generation or resuspension through occupant activities) (Qian et al. 2014), while no significant O_3 source exists in the reference case. For infection risk analysis, only one infector is assumed to be in the office, which can exhale 58 infectious quanta of virus-laden particles (one quantum in the inhalation risk estimation model represents an infectious dose that would infect 63% of the population with the exposure) (Shen et al. 2021). Formaldehyde is released from building materials (Salthammer 2019) and workstation components (Carter and Zhang 2007), as well as through the oxidation reactions between O_3 and building materials (Gall et al. 2013), workstation components, and occupant surfaces (e.g. skin or clothes) (Rai et al. 2014). The reactions between the chemicals on these surfaces and O_3 can remove considerable O_3 due to irreversible oxidation, resulting in O_3 deposition on surfaces (Di et al. 2016; Shen and Gao 2018), and yield secondary by-product emissions, which can be quantified by the molar yield factor (Gall et al. 2013; Rai et al. 2014). The O_3 deposition and formaldehyde production by different materials are illustrated in Table 4, which are from the literature data (Carter and Zhang 2007; Gall et al. 2013; Rai et al. 2014; Di et al. 2016; Shen and Gao 2018; Salthammer 2019). The particle deposition relies on an approximate

Table 4 Ozone deposition and formaldehyde production by different materials

	Ozone deposition factor	Formaldehyde emission factor	
	Deposition velocity, v_d (m/h)	Primary emission rate ($\mu\text{g}/\text{m}^2 \text{ h}$)	Secondary molar yield factor (ozone oxidation reactions)(–)
Room surfaces			
Floor (carpet)	3.4	3.9	0.01
Wall (painted drywall)	1.4	2.3	0.01
Ceiling (painted drywall)	1.4	2.3	0.01
Workstation components			
Panel	1.5	50	0.01
Work surface	0.2	15	0.01
Storage	0.2	0	0.01
Occupant surfaces			
Occupant Skin/Clothes	10.8	0	0.02

estimate of gravitational settling (Nicas et al. 2005), while the deposition of formaldehyde is not considered. The inactivation rate of the virus-laden particles is defined based on the data for SARS-CoV-2 (i.e. 0.63 h^{-1}) (van Doremalen et al. 2020). The pulmonary rate for occupants is $0.3 \text{ m}^3/\text{h}$, while the exposure time is 8 h (U.S. EPA 2011). The ventilation rate of outdoor air provided through the HVAC system is defined to be 0.9 h^{-1} based on the ANSI/BIFMA M7.1 standard (Carter and Zhang 2007). Considering that the average outdoor air fraction for building ventilation system is around 25% (Persily and Gorfain 2004), the total supply airflow rate of the HVAC system in this simulation is 3.6 h^{-1} . A MERV 8 filter is included in the HVAC duct, which can remove approximately 20% of PM2.5 particles and 50% of infectious particles (Shen et al. 2021). Mixing ventilation is used in the reference case (ventilation effectiveness = 1).

The simulation through the simplified multiscale pollutant transport model (Eq. 3) revealed that the steady-state concentrations in the breathing zone for the reference open plan office case are $23.1 \mu\text{g}/\text{m}^3$, $25.2 \mu\text{g}/\text{m}^3$, $48.1 \mu\text{g}/\text{m}^3$, and $0.1 \text{ quanta}/\text{m}^3$ for PM 2.5, O₃, formaldehyde (HCHO), and infectious aerosols, respectively. The infection risk for the susceptible occupants is 20.4%, which is estimated by the inhaled dose of infectious quanta through the Wells-Riley model (Shen et al. 2021). Several selected IAQ control strategies at different scales are applied in the reference office case (Table 5). The effectiveness of each strategy is analyzed comparing to the IAQ metrics of the reference case (reduction percentage).

Reducing ambient pollutant concentrations by 50% can improve indoor PM 2.5, O₃, and formaldehyde concentrations by 8.2%, 50.0%, and 8.9%, respectively. But it does not impact the indoor infection probability due to the exposure to viral particles exhaled by the infector. Using green building materials (ceiling, wall, and floor materials) with 50% less primary and secondary formaldehyde emissions can reduce the formaldehyde concentration by around 4%, while using green furniture (workstations) can reduce formaldehyde exposure by 37.8%. Improving building ventilation by using 100% outdoor air improve indoor PM 2.5 level by 34.6%, formaldehyde level by 59.3%, and infection risk by 24.0%, but also increase the indoor O₃ concentration since it is mainly from the ambient air and there is no O₃ filtration for the HVAC system. Increasing building airtightness (reducing building air infiltration) can reduce indoor O₃ (by 11.5%) but increase other indoor pollutants. Natural ventilation that provides 0.5 h^{-1} more indoor ventilation also introduces more O₃ indoors (by 34.1%) while it reduces concentrations of other pollutants of indoor origin. Upgrading HVAC system filter to HEPA filter at the building scale can reduce indoor PM2.5 level by over 59% and infection probability by 24% but has no effects on improving indoor O₃ and formaldehyde levels. It has a high potential for reducing indoor particle exposure and infection risk. Using additional activated carbon filter in the HVAC system that has 80% efficiency on O₃ reduction has a high potential on decreasing indoor O₃ exposure, which has a 74.6% O₃ reduction and 2.3% formaldehyde reduction due to reduced secondary emission. Replacing wall and ceiling materials by depolluting materials that can absorb formaldehyde with a deposition velocity of 2.08 m/h can greatly improve the indoor formaldehyde level (by 93.1%), indicating a high potential for indoor formaldehyde improvement.

Table 5 Effectiveness of selected IAQ control strategies in the reference office case

Scale	Category	Strategy	Description	IAQ metrics				Effectiveness on IAQ improvement			
				PM2.5 ($\mu\text{g}/\text{m}^3$)	O_3 ($\mu\text{g}/\text{m}^3$)	HCHO ($\mu\text{g}/\text{m}^3$)	Infection probability (%)	PM2.5 (%)	O_3 (%)	HCHO (%)	Infection (%)
Outdoor air				8.0	135.0	7.2	0				
Reference open plan office				23.1	25.2	48.1	20.4				
Urban	Source control	Reducing emissions	50% reduced ambient pollutant level	21.2	12.6	43.8	20.4	8.2	50.0	8.9	0
	Ventilation	Higher ventilation	20% reduced ambient pollutant level	22.4	20.2	46.3	20.4	3.0	19.8	3.7	0
	Air cleaning	Urban greenings	10% reduced ambient pollutant level	22.8	22.7	47.2	20.4	1.3	9.9	1.9	0
Building	Source control	Low-emission building materials	50% less primary and secondary formaldehyde emissions	23.1	25.2	46.1	20.4	0	0	4.2	0
	Ventilation	Higher ventilation	20% more total supply airflow rate of HVAC system	20.6	28.5	42.5	18.5	10.8	-13.1	11.6	9.3
			50% outdoor air fraction of HVAC	19.0	39.7	30.1	18.5	17.7	-57.5	37.4	9.3

		100% outdoor air fraction of HVAC	15.1	59.7	19.6	15.5	34.6	-136.9	59.3	24.0
Higher airtightness	Reduced air infiltration (0.05 h^{-1})	24.5	22.3	54.3	21.2	-6.1	11.5	-12.9	-3.9	
Natural ventilation	0.5 h^{-1} more ventilation	19.8	33.8	35.6	18.3	14.3	-34.1	26.0	10.3	
Air cleaning system	Upgrading filter of HVAC	10.3	25.2	48.1	18.6	55.4	0	0	8.8	
	Using HEPA filter	9.4	25.2	48.1	15.5	59.3	0	0	24.0	
	Adding activated carbon filter (80% efficiency on O ₃ reduction)	23.1	6.4	47.0	20.4	0	74.6	2.3	0	
Formaldehyde absorption material	Deposition velocity for HCHO = 2.08 m/h (area = wall and ceiling area)	23.1	25.2	3.3	20.4	0	0	93.1	0	
Room	Source control	Low-emission furniture	23.1	25.2	29.9	20.4	0	0	37.8	0

(continued)

Table 5 (continued)

Scale	Category	Strategy	Description	IAQ metrics				Effectiveness on IAQ improvement			
				PM2.5 ($\mu\text{g}/\text{m}^3$)	O ₃ ($\mu\text{g}/\text{m}^3$)	HCHO ($\mu\text{g}/\text{m}^3$)	Infection probability (%)	PM2.5 (%)	O ₃ (%)	HCHO (%)	Infection (%)
Ventilation	Displacement ventilation	Ventilation effectiveness = 1.5	17.9	33.0	36.5	16.1	22.5	-31.0	24.1	21.1	
Air cleaning	Portable air cleaner	CADR = 361 m ³ /h (HEPA filter and activated carbon filter)	10.7	19.4	47.7	13.4	53.7	23.0	0.8	34.3	
Personal control	Local air exhaust	Reduced viral particle exhalation (ventilation effectiveness = 5)	23.1	25.2	48.1	6.5	0	0	0	68.1	
Ventilation	Personal ventilation	Ventilation effectiveness = 1.7	16.5	35.8	33.5	14.9	28.6	-42.1	30.4	27.0	
Air cleaning	Wearing mask	50% on particle filtration	11.6	25.2	48.1	5.5	49.8	0	0	73.0	

Displacement ventilation (ventilation effectiveness = 1.5) can improve indoor PM2.5, formaldehyde, and infection risk levels but also increase the indoor O₃ concentration owing to less O₃ deposition because of imperfect air mixing. Portable air cleaner that has a CADR of 361 m³/h (with HEPA filter and activated carbon filter) can reduce indoor PM2.5, O₃, formaldehyde, and infection probability by 53.7%, 23.0%, 0.8%, and 34.3%, respectively. Improving the IAQ in personal microenvironments by using local air exhaust technique that can remove viral particle exhalation with a ventilation effectiveness of 5 can reduce the infection risk by 68.1%, which has a high potential on reducing the infection risk. Personal ventilation (effectiveness = 1.7) can improve indoor PM2.5, formaldehyde, and infection risk levels but also increase the indoor O₃ concentration. Masks can remove 50% particles (including PM2.5 and infectious particles). Wearing masks can reduce PM2.5 inhalation by almost 50% and infection risk by 73% (reduction on both infectious particle exhalation and inhalation).

It can be found that most IAQ control strategies cannot remove all indoor pollutants effectively. They may be effective against certain pollutants, but ineffective against others. Some strategies may even introduce some pollutants when working against other pollutants. To meet certain IAQ criteria, the integrated implementation of multiple IAQ control strategies in indoor environments are usually necessary. Like the optimization of HVAC system control, the optimal control of other strategies (e.g. standalone air cleaners and local air exhaust) also has great potential of IAQ improvement. Especially, the coordination of different strategies can be optimized through optimal control algorithms, e.g. the combination of UFAD, personal ventilation, and partitions in office settings (Kong et al. 2015). Intelligent/optimized control of IAQ strategies has great potential in improving IAQ while saving energy.

Case Study: IAQ Design and Control Strategies for a LEED Platinum Building: SyracuseCOE Headquarters

The Syracuse Center of Excellence (SyracuseCOE) Headquarters is a five-story building located at the southeastern corner of the intersection between two interstate highways (I-81 and I-690), near the downtown of Syracuse, NY (Fig. 10). This LEED Platinum certified office building was built for environmental and energy technologies and building research, development and demonstration, equipped with the facilities such as green roof, geothermal system, natural ventilation, personal ventilation systems, advanced building heat recovery/reuse systems, air quality monitoring of outside air and integrated controls for improving/protecting indoor air, etc. The HVAC system in the building uses 100% outdoor air and can coordinate with natural ventilation (window opening). The narrow-shape design is good for the application of natural ventilation as well as for maximizing the benefit of daylighting. High-efficiency filters are used to filtrate outdoor air before supplying it to indoor spaces. Low-emission materials and furniture (per ANSI/BIFMA M7.1) are selected and used in the building to minimize indoor pollutant sources.



Fig. 10 SyracuseCOE case study

The Total Indoor Environmental Quality (TIEQ) Lab is located on the fourth floor of SyracuseCOE. The lab space spans two floors. There is an open mechanical space on the fourth floor and two configurable suites with raised floor systems on the fifth floor, directly above. The configurable spaces can be used for simulating multi-zone office and classroom settings, testing various ventilation, air distribution, and environmental control technologies, and studying the control of the micro-environments around individual occupants. When the configurable spaces are used for office settings, each space can typically contain up to 12 workstations (cubicles) (Fig. 10). The building management system of the lab is isolated from the building's main HVAC system. The main air handler and 12 individual air treatment modules are combined to control the relative humidity (RH), temperature and CO₂ levels. Temperature, RH, CO₂, and VOCs can be monitored at the supply, room, or the individual level at each workstation. Demand-controlled underfloor air distribution (UFAD) ventilation system can be applied in the space. Personal ventilation system is mounted on the desk of each cubicle and can be used to control the micro-environments around occupant. The major IAQ control strategies at different scales used in the SyracuseCOE case are illustrated in Table 6.

At the urban scale, the I-81 highway on the west side of the SyracuseCOE building is planned to be rerouted in a few years. Though this is primarily from the urban transportation and community interaction planning point of view, it can also reduce the pollutant emissions from traffic. It has been found that traffic is the primary source of the particles near the highway. According to the field measurement near I-81, the traffic on I-81 has a significant impact on the particle level in nearby communities (Kong et al. 2016). Particularly, the particle level in the downstream area is much larger than the particle level in the upstream area. Considering that the prevailing wind in Syracuse is from the west, traffic emissions from I-81 can very likely have a considerable impact on the local air quality surrounding the SyracuseCOE building.

Table 6 Major IAQ control strategies at different scales used in the SyracuseCOE case

	Source control	Ventilation	Air cleaning
Urban scale	Removing traffic emissions by I-81 (planned)	First-floor lift-up design	Green roof
Building scale	Low-emission building materials (per ANSI/BIFMA criteria)	100% outdoor air mechanical ventilation Natural ventilation (potential strategy)	High-efficiency filters in HVAC (MERV 13 + activated carbon)
Room scale	Low-emission furniture (per ANSI/BIFMA criteria)	Underfloor air distribution system Demand control ventilation	Standalone air cleaner (potential strategy)
Personal scale		Personal ventilation	

Therefore, rerouting I-81 is assumed to have the ability to reduce the outdoor particle level around the SyracuseCOE building by 50%. First-floor lift-up design of the building can ideally improve the local ventilation and reduce the pollutant accumulation in local areas. But its effectiveness on air quality improvement is questioned since the building is located in the downstream side of the pollutant source. Green roof is mainly used for improving local thermal and hydrologic environment. However, due to the limited area of the green roof on the SyracuseCOE building, its impact on pollutant removal is probably very little. Thus, first-floor lift-up design and green roof are assumed to have insignificant impacts on local pollutant reduction.

Building materials and furniture in the SyracuseCOE building were selected per ANSI/BIFMA criteria (see Chap. 1). They are assumed to have 50% lower emissions than regular materials and furniture. The HVAC system in the building uses 100% outdoor air and MERV 13 and activated carbon filters for filtration. The demand controlled UFAD system is assumed to improve the ventilation by an equivalent effectiveness as the displacement ventilation (ventilation effectiveness = 1.5). A field test in the TIEQ lab revealed that the studied personal ventilation system can improve the IAQ in the breathing zone by a factor of 3–5 (Kong et al. 2015). In this study, its ventilation effectiveness is assumed to be 3.

In addition, natural ventilation can also be utilized by opening windows. However, currently, windows can only be opened manually, which means natural ventilation probably cannot be utilized very well. An optimal control that coordinates mechanical and natural ventilation has the potential for enhancing indoor ventilation and improving IAQ. It can be assumed that the use of natural ventilation can provide additional 0.5 h^{-1} outdoor air to the room. Standalone air cleaner is another potential strategy that can further improve IAQ of the building. The studied air cleaner is assumed to use a HEPA filter (99.9% removal efficiency on particles) and an activated carbon filter (80% removal efficiency on ozone), which can provide a CADR of $361 \text{ m}^3/\text{h}$.

The TIEQ lab ($6.3 \text{ m} \times 10.5 \text{ m} \times 3.2 \text{ m}$) is defined as the studied case, with 12 cubicles arranged in 2 rows. A reference case with same dimensions and

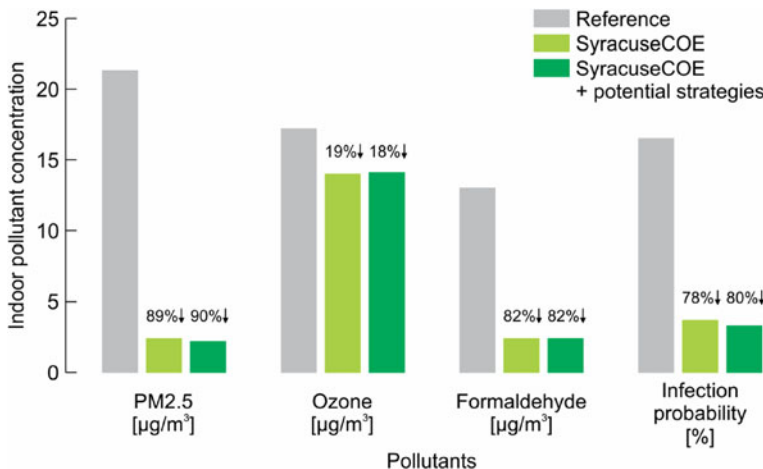


Fig. 11 IAQ metrics in studied cases

occupancy settings is also defined. The reference settings defined in the previous section are adopted to define the building systems of this reference case. The total supply airflow rate of the HVAC system is assumed to be 3.6 h^{-1} (25% outdoor air for the reference case while 100% outdoor air for the SyracuseCOE case). The potential strategies, including controlled natural ventilation and standalone air cleaner, are used to define a case with potential improvement. The outdoor concentrations of PM2.5, O₃, and formaldehyde in Syracuse are around 6.4 µg/m³, 84 µg/m³, and 2.6 µg/m³, respectively (Han et al. 2014; U.S. EPA 2020).

Based on the analysis approach introduced in the previous section, it can be observed that the current strategies used in the SyracuseCOE case (TIEQ lab) can significantly improve IAQ compared to the baseline case (Fig. 11), particularly for pollutants that are mainly generated indoors (such as PM2.5, from occupants activities, formaldehyde, and infectious particles; see the reference settings in the previous section). Potential strategies can further reduce these pollutants but with minimal effect on the O₃ concentration, because more outdoor air is introduced through natural ventilation while outdoor air is the main source of indoor O₃. Therefore, the LEED Platinum certified SyracuseCOE building can provide quite a good IAQ for occupants with the existing control strategies, while the potential strategies, including controlled natural ventilation and standalone air cleaner would only have small further improvement (1–2% reduction comparing to the baseline condition).

Concluding Remarks and Future Outlook

In the foregoing sections, we introduced a simplified IAQ model and used it to assess the effectiveness of source control, ventilation, and air purification at urban, building, room, and personal microenvironment scales in reducing the occupant's exposure to various pollutants with indoor or outdoor origins. Baseline cases were

defined for various commercial and institutional building spaces so that the various IAQ strategies can be evaluated as relative percent of improvement against the defined baselines. In particular, results for typical open plan office spaces were obtained and a case study analysis was presented for a LEED Platinum-certified building. The same approach can be extended to other types of buildings such as residential buildings.

The analysis has been limited to several individual pollutants of indoor or outdoor origins, and to the reduction of concentrations. Future work should include an analysis of the combined effects of major indoor pollutants on the overall IAQ and of how the various IAQ improvement strategies at different scales can be integrated and optimized in building design and urban planning. Such analysis would require the development and use of more comprehensive IAQ metrics such as the DALY (Disability-Adjusted Life Years) metric or the ELV method that accounts for a pre-defined set of indoor pollutants (Abadie and Wargocki 2017).

The analysis has also been limited to steady state conditions. It can be extended to dynamic conditions in which both indoor and outdoor pollution loads can vary over time, and building occupancy also changes over time. Analysis for dynamic conditions also offers additional opportunity for further optimizing the implementation and integration of the various IAQ strategies. For example, outdoor ventilation rate and air purification at the building scale can be optimized to improve indoor air quality while saving energy (Han et al. 2014). Model predictive control method can be applied to further optimize the application of the various IAQ strategies in real or near real time (Woldekidan 2015). The arrival of Internet of Things (IOT) technologies is expected to make the implementation of the dynamic control and optimization more convenient and at a lower cost as it would depend less on initial infrastructure setup. It would make it easier to install and operate a plug and play system with the different products/IAQ strategies that communicate and coordinate with each other for whole system optimization.

Energy and cost implications of the various IAQ strategies at the different scales have not been discussed in detail. Future work should include the quantification of energy consumption, cost, and carbon emissions of the IAQ strategies. Such data are needed to perform multi-objective optimizations of the built environmental systems (BES) as pertaining to IEQ improvement, energy saving and reduction of carbon emissions and building safety (Fig. 1).

Cross-References

- ▶ [ASTM and ASHRAE Standards for the Assessment of Indoor Air Quality](#)
- ▶ [Control of Airborne Particles: Filtration](#)
- ▶ [Deposition](#)
- ▶ [IAQ Requirements in Green Building Labeling Systems and Healthy Building Labeling Systems](#)
- ▶ [Indoor Air Quality in the Context of Climate Change](#)
- ▶ [Influence of Ventilation on Indoor Air Quality](#)
- ▶ [Occupant Emissions and Chemistry](#)

- Resuspension
- Simulations for Indoor Air Quality Control Planning
- Source/Sink Characteristics of SVOCs
- Source/Sink Characteristics of VVOCs and VOCs
- WHO Health Guidelines for Indoor Air Quality and National Recommendations/Standards

References

- Abadie MO, Wargocki P (2017) Annex-68 subtask 1 final report: International Energy Agency Indoor Air Quality Design and Control in Low-energy Residential Buildings—Annex 68 | Subtask 1: defining the metrics | In the search of indices to evaluate the Indoor Air Quality of low-energy
- Abhijith KV, Kumar P, Gallagher J et al (2017) Air pollution abatement performances of green infrastructure in open road and built-up street canyon environments—a review. *Atmos Environ* 162:71–86. <https://doi.org/10.1016/j.atmosenv.2017.05.014>
- AHAM (2021) Air filtration standards & sustainability. In: AHAM. <https://ahamverifide.org/ahams-air-filtration-standards/>. Accessed 15 Jan 2021
- ASHRAE (2019a) ASHRAE Standard 62.1-2019, ventilation for acceptable indoor air quality. https://ashrae.iwrapper.com/ViewOnline/Standard_62.1-2019. Accessed 10 Feb 2020
- ASHRAE (2019b) ASHRAE Standard 62.2-2019, ventilation and acceptable indoor air quality in low-rise residential buildings. https://ashrae.iwrapper.com/ViewOnline/Standard_62.2-2019. Accessed 10 Feb 2020
- ASHRAE (2020) Filtration/disinfection. <https://www.ashrae.org/technical-resources/filtration-disinfection>. Accessed 5 Sept 2020
- Batterman SA, Burge H (1995) HVAC systems as emission sources affecting indoor air quality: a critical review. *HVAC&R Res* 1:61–78. <https://doi.org/10.1080/10789669.1995.10391309>
- Buccolieri R, Sandberg M, Di Sabatino S (2010) City breathability and its link to pollutant concentration distribution within urban-like geometries. *Atmos Environ* 44:1894–1903. <https://doi.org/10.1016/j.atmosenv.2010.02.022>
- Cao Q, Pui DYH, Lipinski W (2015) A concept of a novel solar-assisted large-scale cleaning system (SALSCS) for urban air remediation. *Aerosol Air Qual Res* 15:1–10. <https://doi.org/10.4209/AAQR.2014.10.0246>
- Carter RD, Zhang JS (2007) Definition of standard office environments for evaluating the impact of office furniture emissions on indoor VOC concentrations. *ASHRAE Trans* 113(Part 2):466–477
- Cermak R, Melikov A (2016) Air quality and thermal comfort in an office with underfloor. Mix Displace Ventil 5:323–332. <https://doi.org/10.1080/14733315.2006.11683749>
- Chen Q, Glicksman LR (2003) System performance evaluation and design guidelines for displacement ventilation. In: Ashrae. <https://subscriptions-techstreet-com.libezproxy2.syr.edu/products/172794>. Accessed 7 Aug 2020
- Chen C, Zhao B (2011) Review of relationship between indoor and outdoor particles: I/O ratio, infiltration factor and penetration factor. *Atmos Environ* 45:275–288. <https://doi.org/10.1016/j.atmosenv.2010.09.048>
- Chen W, Zhang JS, Zhang Z (2005) Performance of air cleaners for removing multiple volatile organic compounds in indoor air. *ASHRAE Trans* 111(Part 1):1101–1114
- Cheng PL, Li X (2018) Air infiltration rates in the bedrooms of 202 residences and estimated parametric infiltration rate distribution in Guangzhou, China. *Energ Buildings* 164:219–225. <https://doi.org/10.1016/J.ENBUILD.2017.12.062>
- Chew LW, Nazarian N, Norford L (2017) Pedestrian-level urban wind flow enhancement with wind catchers. *Atmosphere* 8:159. <https://doi.org/10.3390/ATMOS8090159>

- Chirizzi D, Conte M, Feltracco M et al (2021) SARS-CoV-2 concentrations and virus-laden aerosol size distributions in outdoor air in north and south of Italy. *Environ Int* 146:106255. <https://doi.org/10.1016/j.envint.2020.106255>
- Cummings BE, Waring MS (2019) Potted plants do not improve indoor air quality: a review and analysis of reported VOC removal efficiencies. *J Expo Sci Environ Epidemiol* 30(30): 253–261. <https://doi.org/10.1038/s41370-019-0175-9>
- Cyranoski D (2018) China tests giant air cleaner to combat smog. *Nature* 555:152–153. <https://doi.org/10.1038/d41586-018-02704-9>
- Di Y, Mo J, Zhang Y, Deng J (2016) Ozone deposition velocities on cotton clothing surface determined by the field and laboratory emission cell. *Indoor Built Environ* 26:631–641. <https://doi.org/10.1177/1420326X16628315>
- Dygert RK, Dang TQ (2010) Mitigation of cross-contamination in an aircraft cabin via localized exhaust. *Build Environ* 45:2015–2026. <https://doi.org/10.1016/j.buildenv.2010.01.014>
- Dygert RK, Dang TQ (2012) Experimental validation of local exhaust strategies for improved IAQ in aircraft cabins. *Build Environ* 47:76–88. <https://doi.org/10.1016/j.buildenv.2011.04.025>
- Gall ET, Corsi RL, Siegel JA (2011) Barriers and opportunities for passive removal of indoor ozone. *Atmos Environ* 45:3338–3341. <https://doi.org/10.1016/j.atmosenv.2011.03.032>
- Gall E, Darling E, Siegel JA et al (2013) Evaluation of three common green building materials for ozone removal, and primary and secondary emissions of aldehydes. *Atmos Environ* 77: 910–918. <https://doi.org/10.1016/j.atmosenv.2013.06.014>
- Guo C, Gao Z, Shen J (2019) Emission rates of indoor ozone emission devices: a literature review. *Build Environ* 158:302–318. <https://doi.org/10.1016/J.BUILDENV.2019.05.024>
- Haghhighat F, Huo Y, Zhang J, Shaw C (1996) The influence of office furniture, workstation layouts, diffuser types and location on indoor air quality and thermal comfort conditions at workstations. *Indoor Air* 6:188–203. <https://doi.org/10.1111/j.1600-0668.1996.t01-1-00006.x>
- Halvoňová B, Melikov AK (2010) Performance of “ductless” personalized ventilation in conjunction with displacement ventilation: impact of intake height. *Build Environ* 45:996–1005. <https://doi.org/10.1016/j.buildenv.2009.10.007>
- Han K, Zhang JS, Guo B (2014) A novel approach of integrating ventilation and air cleaning for sustainable and healthy office environments. *Energ Buildings* 76:32–42. <https://doi.org/10.1016/J.ENBUILD.2014.02.055>
- Han G, Srebric J, Enache-Pommer E (2015) Different modeling strategies of infiltration rates for an office building to improve accuracy of building energy simulations. *Energ Buildings* 86: 288–295. <https://doi.org/10.1016/J.ENBUILD.2014.10.028>
- He B-J, Ding L, Prasad D (2019a) Enhancing urban ventilation performance through the development of precinct ventilation zones: a case study based on the Greater Sydney, Australia. *Sustain Cities Soc* 47:101472. <https://doi.org/10.1016/j.scs.2019.101472>
- He J, Zou Z, Yang X (2019b) Measuring whole-body volatile organic compound emission by humans: a pilot study using an air-tight environmental chamber. *Build Environ* 153:101–109. <https://doi.org/10.1016/J.BUILDENV.2019.02.031>
- He G, Wu Q, Li Z et al (2021) Ventilation performance of solar chimney in a test house: field measurement and validation of plume model. *Build Environ* 193:107648. <https://doi.org/10.1016/J.BUILDENV.2021.107648>
- IWBI (2019) WELL building projects. <https://www.wellcertified.com/about-iwbi/>. Accessed 20 Feb 2020
- Ji Y, Duanmu L, Liu Y, Dong H (2020) Air infiltration rate of typical zones of public buildings under natural conditions. *Sustain Cities Soc* 61:102290. <https://doi.org/10.1016/J.SCS.2020.102290>
- Johnson T, Myers J, Kelly T et al (2004) A pilot study using scripted ventilation conditions to identify key factors affecting indoor pollutant concentration and air exchange rate in a residence. *J Expo Sci Environ Epidemiol* 14(14):1–22. <https://doi.org/10.1038/sj.jea.7500294>
- Jomehzadeh F, Hussein HM, Calautit JK et al (2020) Natural ventilation by windcatcher (Badgir): a review on the impacts of geometry, microclimate and macroclimate. *Energ Buildings* 226: 110396. <https://doi.org/10.1016/J.ENBUILD.2020.110396>

- Kanaan M, Abou Moughlbay A (2018) Comparative CFD investigation of upper room UVGI efficacy with three different ventilation systems
- Khalifa HE (2017) Micro environmental control system
- Konda A, Prakash A, Moss GA et al (2020) Aerosol filtration efficiency of common fabrics used in respiratory cloth masks. *ACS Nano* 14:6339–6347. <https://doi.org/10.1021/acsnano.0c03252>
- Kong M (2017) Semi-open space and micro-environmental control for improving thermal comfort, indoor air quality, and building energy efficiency
- Kong M, Zhang J, Wang J (2015) Air and air contaminant flows in office cubicles with and without personal ventilation: a CFD modeling and simulation study. *Build Simul* 8:381–392. <https://doi.org/10.1007/s12273-015-0219-6>
- Kong M, Chen R, Chen D et al (2016) Fine and ultrafine particle concentrations close to a highway and potential impact on IAQ in nearby residences. In: *IndoorAir*
- Kubota T, Miura M, Tominaga Y, Mochida A (2008) Wind tunnel tests on the relationship between building density and pedestrian-level wind velocity: development of guidelines for realizing acceptable wind environment in residential neighborhoods. *Build Environ* 43:1699–1708. <https://doi.org/10.1016/J.BUILDENV.2007.10.015>
- Li Z, Ming T, Liu S et al (2021a) Review on pollutant dispersion in urban areas-part A: effects of mechanical factors and urban morphology. *Build Environ* 190:107534. <https://doi.org/10.1016/j.buildenv.2020.107534>
- Li Z, Ming T, Shi T et al (2021b) Review on pollutant dispersion in urban areas-part B: local mitigation strategies, optimization framework, and evaluation theory. *Build Environ* 198: 107890. <https://doi.org/10.1016/j.buildenv.2021.107890>
- Liu G, Xiao M, Zhang X et al (2017) A review of air filtration technologies for sustainable and healthy building ventilation. *Sustain Cities Soc* 32:375–396
- Marr D, Mason M, Mosley R, Liu X (2012) The influence of opening windows and doors on the natural ventilation rate of a residential building. *HVAC&R Res* 18:195–203
- Mei S-J, Hu J-T, Liu D et al (2017) Wind driven natural ventilation in the idealized building block arrays with multiple urban morphologies and unique package building density. *Energ Buildings* 155:324–338. <https://doi.org/10.1016/j.enbuild.2017.09.019>
- Melikov A, Grønbæk H, Nielsen JB (2007) Personal ventilation: from research to practical use
- Mirzaei PA, Haghhighat F (2010) A novel approach to enhance outdoor air quality: pedestrian ventilation system. *Build Environ* 45:1582–1593. <https://doi.org/10.1016/j.buildenv.2010.01.001>
- Ng WY, Chau CK (2014) A modeling investigation of the impact of street and building configurations on personal air pollutant exposure in isolated deep urban canyons. *Sci Total Environ* 468–469:429–448. <https://doi.org/10.1016/J.SCITOTENV.2013.08.077>
- Nicas M, Nazaroff WW, Hubbard A (2005) Toward understanding the risk of secondary airborne infection: emission of respirable pathogens. *J Occup Environ Hyg* 2:143–154. <https://doi.org/10.1080/15459620590918466>
- Nowak DJ, Crane DE, Stevens JC (2006) Air pollution removal by urban trees and shrubs in the United States. *Urban For Urban Green* 4:115–123. <https://doi.org/10.1016/j.ufug.2006.01.007>
- Oke TR (1988) Street design and urban canopy layer climate. *Energ Buildings* 11:103–113. [https://doi.org/10.1016/0378-7788\(88\)90026-6](https://doi.org/10.1016/0378-7788(88)90026-6)
- Persily A, Gorfain J (2004) Analysis of ventilation data from the U.S. Environmental Protection Agency Building Assessment Survey and Evaluation (BASE) Study. *Environ Prot Indoor Air* 20:473–485. <https://doi.org/10.1111/J.1600-0668.2010.00669.X>
- Pétigny N, Zhang J, Horner E et al (2021) Indoor air depolluting material: combining sorption testing and modeling to predict product's service life in real conditions. *Build Environ* 202: 107838. <https://doi.org/10.1016/J.BUILDENV.2021.107838>
- Qian J, Peccia J, Ferro AR (2014) Walking-induced particle resuspension in indoor environments. *Atmos Environ* 89:464–481

- Rai AC, Guo B, Lin CH et al (2014) Ozone reaction with clothing and its initiated VOC emissions in an environmental chamber. *Indoor Air* 24:49–58. <https://doi.org/10.1111/ina.12058>
- Riley R, Nardell E (1989) Clearing the air: The theory and application of ultraviolet air disinfection. *Am Rev Respir Dis* 139:1286–1294. <https://doi.org/10.1164/AJRCCM/139.5.1286>
- Rooney CM, McIntyre J, Ritchie L, Wilcox MH (2021) Evidence review of physical distancing and partition screens to reduce healthcare acquired SARS-CoV-2. *Infect Prev Pract* 3:100144. <https://doi.org/10.1016/j.infpip.2021.100144>
- Rothamer DA, Sanders S, Reindl D et al (2020) Strategies to minimize SARS-CoV-2 transmission in classroom settings: combined impacts of ventilation and mask effective filtration efficiency. *medRxiv*. <https://doi.org/10.1101/2020.12.31.20249101>
- Salthammer T (2019) Data on formaldehyde sources, formaldehyde concentrations and air exchange rates in European housings. *Data Brief* 22:400–435. <https://doi.org/10.1016/J.DIB.2018.11.096>
- Schleibinger H, Rüden H (1999) Air filters from HVAC systems as possible source of volatile organic compounds (VOC)—laboratory and field assays. *Atmos Environ* 33:4571–4577. [https://doi.org/10.1016/S1352-2310\(99\)00274-5](https://doi.org/10.1016/S1352-2310(99)00274-5)
- Sha C, Wang X, Lin Y et al (2018) The impact of urban open space and ‘lift-up’ building design on building intake fraction and daily pollutant exposure in idealized urban models. *Sci Total Environ* 633:1314–1328. <https://doi.org/10.1016/J.SCITOTENV.2018.03.194>
- Shen J, Gao Z (2018) Ozone removal on building material surface: a literature review. *Build Environ* 134:205–217. <https://doi.org/10.1016/J.BUILDENV.2018.02.046>
- Shen J, Gao Z, Ding W, Yu Y (2017) An investigation on the effect of street morphology to ambient air quality using six real-world cases. *Atmos Environ* 164:85–101. <https://doi.org/10.1016/J.ATMOSENV.2017.05.047>
- Shen J, Kong M, Dong B et al (2021) A systematic approach to estimating the effectiveness of multi-scale IAQ strategies for reducing the risk of airborne infection of SARS-CoV-2. *Build Environ* 200:107926. <https://doi.org/10.1016/j.buldenv.2021.107926>
- Shi S, Chen C, Zhao B (2015) Air infiltration rate distributions of residences in Beijing. *Build Environ* 92:528–537. <https://doi.org/10.1016/J.BUILDENV.2015.05.027>
- Taheri S, Razban A (2021) Learning-based CO₂ concentration prediction: application to indoor air quality control using demand-controlled ventilation. *Build Environ* 205:108164. <https://doi.org/10.1016/J.BUILDENV.2021.108164>
- U.S. CDC, NIOSH (2009) Basic upper-room ultraviolet germicidal irradiation guidelines for healthcare settings Department of Health and Human Services Centers for Disease Control and Prevention National Institute for Occupational Safety and Health
- U.S. EPA (2011) Exposure factors handbook 2011 Edition (Final Report). Washington, DC
- U.S. EPA (2018) Guide to air cleaners in the home
- U.S. EPA (2020) Air quality statistics report, air data: air quality data collected at outdoor monitors across the US, U.S. EPA. In: U.S. Environ. Prot. Agency. <https://www.epa.gov/outdoor-air-quality-data/air-quality-statistics-report>. Accessed 5 Sept 2021
- U.S. EPA (2021a) Particulate matter (PM2.5) trends | US EPA. In: U.S. Environ. Prot. Agency. <https://www.epa.gov/air-trends/particulate-matter-pm25-trends>. Accessed 14 Aug 2021
- U.S. EPA (2021b) Ozone trends | US EPA. In: U.S. Energy Inf. Adm. <https://www.epa.gov/air-trends/ozone-trends>. Accessed 14 Aug 2021
- van Doremalen N, Bushmaker T, Morris DH et al (2020) Aerosol and surface stability of SARS-CoV-2 as compared with SARS-CoV-1. *N Engl J Med* 382:1564–1567. <https://doi.org/10.1056/nejmcm2004973>
- Wang Z, Zhang JS (2011) Characterization and performance evaluation of a full-scale activated carbon-based dynamic botanical air filtration system for improving indoor air quality. *Build Environ* 46:758–768. <https://doi.org/10.1016/J.BUILDENV.2010.10.008>
- WHO (2009) WHO guidelines for indoor air quality: dampness and mould
- WHO (2010) WHO guidelines for indoor air quality: selected pollutants. WHO Guidel Indoor Air Qual Sel Pollut

- Woldekidan K (2015) INDOOR ENVIRONMENTAL QUALITY (IEQ) AND BUILDING ENERGY OPTIMIZATION THROUGH MODEL PREDICTIVE CONTROL (MPC). Diss—ALL
- Won D, Magee RJ, Lusztyk E et al (2003) A comprehensive VOC emission database for commonly-used building materials
- Xu P, Peccia J, Fabian P et al (2003) Efficacy of ultraviolet germicidal irradiation of upper-room air in inactivating airborne bacterial spores and mycobacteria in full-scale studies. *Atmos Environ* 37:405–419. [https://doi.org/10.1016/S1352-2310\(02\)00825-7](https://doi.org/10.1016/S1352-2310(02)00825-7)
- Yin S, Shen Z, Zhou P et al (2011) Quantifying air pollution attenuation within urban parks: an experimental approach in Shanghai, China. *Environ Pollut* 159:2155–2163. <https://doi.org/10.1016/j.envpol.2011.03.009>
- Zhang JJ (2005) Combined heat, air, moisture, and pollutants transport in building environmental systems. *JSME Int J Ser B* 48:182–190. <https://doi.org/10.1299/JSMEB.48.182>
- Zhang J (2020) Integrating IAQ control strategies to reduce the risk of asymptomatic SARS CoV-2 infections in classrooms and open plan offices. *Sci Technol Built Environ* 26:1013–1018. <https://doi.org/10.1080/23744731.2020.1794499>
- Zhang Z, Chen Q (2006) Experimental measurements and numerical simulations of particle transport and distribution in ventilated rooms. *Atmos Environ* 40:3396–3408. <https://doi.org/10.1016/j.atmosenv.2006.01.014>
- Zhang Y, Mo J, Li Y et al (2011) Can commonly-used fan-driven air cleaning technologies improve indoor air quality? A literature review. *Atmos Environ* 45:4329–4343. <https://doi.org/10.1016/J.ATMOSENV.2011.05.041>
- Zhang Q, Zheng Y, Tong D et al (2019) Drivers of improved PM_{2.5} air quality in China from 2013 to 2017. *Proc Natl Acad Sci U S A* 116:24463–24469. <https://doi.org/10.1073/pnas.1907956116>
- Zhao B, Liu Y, Chen C (2020) Air purifiers: a supplementary measure to remove airborne SARS-CoV-2. *Build Environ* 177:106918
- Zhou X, Xu Y, Yuan S et al (2015) Performance and potential of solar updraft tower used as an effective measure to alleviate Chinese urban haze problem. *Renew Sust Energ Rev* 51:1499–1508. <https://doi.org/10.1016/j.rser.2015.07.020>
- Žitnik M, Bučar K, Hiti B et al (2016) Exercise-induced effects on a gym atmosphere. *Indoor Air* 26:468–477. <https://doi.org/10.1111/INA.12226>



Simulations for Indoor Air Quality Control Planning

62

Mengqiang Lv, Weihui Liang, Xudong Yang, and
Jianshun Jensen Zhang

Contents

Introduction	1816
Principle of the Performance-Based Approach	1818
Identification of Purpose	1820
Model Assumptions	1820
Governing Equations	1820
Determination of Model Inputs	1820
Specification of Model Outputs	1820
Simulation Case Design	1821
Simulation Running	1821
Analysis of Simulation Results	1821
Single-Zone Modeling and Simulation	1821
Purpose Identification and Model Selection	1822
Model Assumptions and Governing Equations	1822
Model Input Parameters and Their Determination	1823
Model Output and Analysis of Cases	1831
Example Software Tools	1833

M. Lv

Tianjin Key Laboratory of Indoor Air Environmental Quality Control, School of Environmental Science and Engineering, Tianjin University, Tianjin, China

e-mail: lvmq@tju.edu.cn

W. Liang

School of Architecture and Urban Planning, Nanjing University, Nanjing, China

e-mail: liangwh@nju.edu.cn

X. Yang (✉)

Department of Building Science, School of Architecture, Tsinghua University, Beijing, China

e-mail: xyang@tsinghua.edu.cn

J. J. Zhang

Building Energy and Environmental Systems Laboratory, Department of Mechanical and Aerospace Engineering, Syracuse University, Syracuse, NY, USA

School of Architecture and Urban Planning, Nanjing University, Nanjing, China

e-mail: jszhang@syr.edu

Multi-Zone Modeling and Simulation	1834
Purpose Identification and Model Selection	1834
Model Assumptions and Governing Equations	1835
Model Input Parameters and their Determination	1835
Model Output and Analysis of Typical Cases	1836
Example Software Tools	1839
Computational Fluid Dynamics Modeling and Simulation	1841
Purpose Identification and Model Selection	1841
Governing Equations and Solving Methods	1842
Model Inputs and their Determinations	1842
Model Output and Analysis of Typical Cases	1843
Example Software Tools	1845
Data-Driven Models	1846
Conclusions and Future Perspectives	1847
Conclusions	1847
Future Perspectives	1848
References	1849

Abstract

Indoor air pollution has become a broad problem due to various indoor or outdoor pollutant sources and limited ventilation. A performance-based approach, which is built upon accurate modeling and simulation of indoor air pollutant characteristics, has obvious advantages over the prescription-based method to achieve a better indoor environment. Moreover, the simulation could play a key role in actively preventing indoor air pollution from happening in the first place. In this Chapter, we introduce the working procedures of the performance-based approach including identification of purpose, model assumptions, governing equations, determination of model inputs, specification of model outputs, simulation case design, simulation running, and analysis of simulation results for indoor air quality (IAQ) design. Single-zone, multi-zone, and detailed computational fluid dynamics (CFD) models are discussed along with a brief review of example software tools available for implementing the simulation models. Discussions are focused on modeling volatile organic compound (VOC) sources, sinks, ventilation, and their impact on the concentrations indoors. As for the public concerned SARS and SARS-CoV-2 virus, a brief discussion is provided based on the real cases.

Keywords

Indoor air quality (IAQ) · Simulation · Model · Design · Volatile organic compound (VOC)

Introduction

Modern built environments are filled with various natural or man-made air contaminants, leading to the increased sensitivity of the public to indoor air quality (IAQ). Investigations on IAQ have demonstrated that indoor pollutant concentrations such

as volatile organic compound (VOC) and particulate matter 2.5 (PM_{2.5}) may reach a high level (Shin and Jo 2012; Weschler and Nazaroff 2012). The prescription-based approach has been adopted to eliminate indoor pollutants (JGJ/T 436-2018 2018). In this approach, control strategies, such as material using area and ventilation rate, were proposed mainly based on experience. However, such an approach is not reliable all the time. Once the pollution occurs, a huge cost is needed to remedy the pollution.

Recently, the performance-based approach has attracted public attention (Liang et al. 2012). Compared with the prescription-based method, this approach is characterized by active design rather than passive repairment. Rough estimates of the effectiveness of active prevention indicate that it is at least 4 times less costly than remediation of damage after the fact to achieve comparable IAQ (Hal 2016). Even so, performance-based design for IAQ has not been widely adopted in practice due to a much larger number of parameters than thermal comfort analysis, because pollutant mass transfer within buildings is an extremely complex process.

Taking VOC as an example, its emissions from building materials to indoor air is a dynamic process, involving mass transfer inside the material, at the material-air interface, and in the bulk air (Little et al. 1994). The processes are likely to be affected by environmental conditions, such as temperature, humidity, and velocity of air flow, leading to more challenges in an accurate description of pollutant emissions (Liang et al. 2016). Meanwhile, some porous building materials can act as sinks. Therefore, VOC emitted from one material can be adsorbed by other materials and then gradually released into the air under suitable conditions, affecting the indoor concentrations in the long term (Won et al. 2001). The airflow exchange between a building and outdoors plays a key role in diluting indoor-generated pollutants. In addition, the internal airflows determine the pollutant inter-exchange between zones. Both external and internal airflows vary with outdoor meteorological and indoor environment conditions (Caron et al. 2020). The possible uses of air cleaning devices, such as portable air cleaners can reduce indoor pollutant load to some extent, including the adsorption process of pollutant molecules from the air to inside of the activated filter (Pei and Ji 2018).

The key point of the performance-based approach is to accurately assess the impact of these influencing factors on indoor pollutant concentration. Two main research methods are available for this purpose: experimental investigation and computer simulation. In principle, direct measurements give the most realistic information for concerned problems. However, the experimental method requires full-scale, well-controlled facilities (e.g., a test house), meaning a high initial investment. In addition, direct measurements of the pollutant distributions in a full-scale room are time-consuming and technically difficult. In this case, simulation becomes a more efficient option.

Simulation is a technique for implementing various hypotheses over time even those that cannot be tested experimentally. It is most likely the only opportunity that the designer can improve the design before its final implementation (Sokolowski and Banks 2010). Problems and flaws can be avoided in advance, not only saving time and money but also probably saving lives if we are dealing with life safety building services. If reasonably designed, a simulation is fully capable of obtaining the same

results as an experiment, but with significantly less cost and time. Therefore, simulation is regarded as a time- and cost-effective technology, and can be advanced enough to be applied to daily design and operation. Successful simulation is of course inseparable from the support of the predictive models.

Predictive modeling is the art of developing a set of equations that faithfully represent the complex mass transfer phenomena and then solving the equations to predict the pollutant behaviors (Sokolowski and Banks 2010). Modeling is a powerful tool that is being used extensively by scientists to design IAQ in modern buildings. A model can be physical, mathematical, or otherwise logical representations, determined by the concerned IAQ problems. However, it should be noted that a model is not required to represent all aspects of the issues being studied. That would be too timely, expensive, and complex – even impossible. Instead, the model should be developed as simply as possible, representing only the key aspects that affect the performance of the system being investigated. Generally speaking, modeling is full of challenges. Modelers need to have not only a professional background but also mathematical and analytical ability.

The purpose of this chapter is to introduce the performance-based approach in IAQ design and evaluate its effectiveness. The principle is presented in section “[Principle of the performance-based approach](#)” to show how to use the performance-based approach to deal with an IAQ problem at the design stage. Then, typical models and their simulation processes in the performance-based approach, including single-zone model, multi-zone model, computational fluid dynamic (CFD) model, and date-driven model, are summarized, respectively. Finally, a conclusion and future perspectives are presented.

Principle of the Performance-Based Approach

The key point of the performance-based method is to accurately predict various indoor pollutant concentrations at the design stage. Different pollutants require different models and simulation processes, which should be determined in advance. Pollutants that attract public concern in recent years may include PM_{2.5}, VOC, severe acute respiratory syndrome coronavirus (SARS), and corona virus disease (SARS-CoV-2) (Paterson et al. 2021; Baboli et al. 2021; Wu and Weng 2021; Shen et al. 2021). Their sources are shown in Fig. 1. Most indoor PM_{2.5} comes from the outdoor atmosphere, and others are contributed by human activities (Long et al. 2021; Yang et al. 2020). Indoor VOC is mainly from building material and furniture (Liang et al. 2014). VOC emitted from interior materials to indoor air involves a series of mass transfer processes. Mechanism of VOC emission and transmission has been studied for over 20 years, and some novel conclusions have been drawn (Yang 1999). Both SARS and SARS CoV-2 belong to viruses and are derived from infected people. Up to now, their transmitted behaviors have been realized by the public, but generation and pathogenicity are yet to be well addressed (Shen et al. 2021; Tang et al. 2022). Considering the urgency of the problem and maturity of current research, VOC is selected as the target pollutant to show the principle of the



Fig. 1 Indoor pollutants and their sources

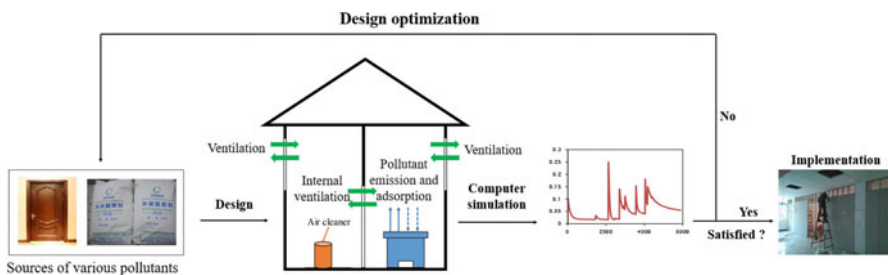


Fig. 2 Schematic of using the performance-based approach to prevent indoor VOC pollution

performance-based method. For the public concerned SARS and SARS-CoV-2, a brief discussion is provided based on real case studies.

Figure 2 shows the schematic of the performance-based approach to prevent indoor VOC pollution. Before interior construction, the pollutant-concentration goal, i.e., the level that must not exceed at a certain time, should be set. Some may choose “meeting the minimum indoor air-quality standard requirement two weeks after the indoor decoration is complete” as their goal, while others may select a higher standard (lower concentration levels). Then, indoor VOC concentration will be previewed using a computer, according to the construction plan. If the simulation finds that a design cannot achieve satisfactory results, optimization work will be performed until the requirement is achieved. A key feature of the aforementioned approach is that a prescient result will be provided at the design stage, it would not be too late to propose necessary correctional actions before the plan is finalized or implemented if a potential problem is foreseen.

The principle of the performance-based approach is not difficult to understand, but its application in engineering is not simple, involving complex and rigorous procedures:

Identification of Purpose

A clear understanding of the design purpose is the first step. Different purposes require different modeling and simulation methods. For example, the model used in a small room may not be suitable in a large space. This requires the designers to collect data and knowledge of the studied issues in advance. The abundant information will improve the designer's insight, and help to make the correct choice when modeling.

Model Assumptions

As noted previously, a model should not be required to reflect all aspects but should focus on using mathematics and logic to describe the expected behavior. Therefore, only those significant behaviors to the study or research need to be represented in the model, others could be assumed or simplified based on the studied issues to ensure a fast and efficient solving process.

Governing Equations

With clear purpose and necessary assumptions, the pollutants transmission (physical behavior or phenomena related to IAQ) within buildings can be described by models. Models can be mathematical or any other logical expressions. Normally, models based on mathematical expressions are concise and convenient to use, and are thus welcomed by users. One or more mathematical expressions for the concerned problems constitute the model governing equations.

Determination of Model Inputs

Mathematics-based model governing equations usually contain a series of letters or symbols, which are so-called model parameters. These parameters can be classified into input parameters and output parameters. Normally, the model input parameters are related to various control strategies in an IAQ problem. They can be determined by the experimental method, simulation method, or combination of both, depending on their complexity.

Specification of Model Outputs

Corresponding to the model inputs, model outputs are related to the control results and typically represent a dynamic response of a given set of inputs and conditions. Model outputs should be specified before simulations depending on the study

purpose. Model outputs are often the parameters that the designers are most concerned, and cannot be directly obtained through experiments.

Simulation Case Design

The purpose of a simulation is to compare the influence of various control strategies (model inputs) on the results (model outputs). Before this, a good design for the simulation case is needed, which may be a challenging job. It requires the designer to comprehensively consider all feasible control strategies, and then provide a series of logical and operable conditions to ensure a more correct and representative simulation result.

Simulation Running

The next procedure is running the simulation. When the simulation technology was first applied in the IAQ field, the designer was required to write the code in the computer and manually complete the calculation process. With the improvement of computer power, a variety of commercial software has been developed. When the designers provide model inputs according to the requirements of the program, computers can rapidly give the expected results. These significant advancements provide convenience for the users, which are beneficial for the wide spread of simulation technology in the IAQ field.

Analysis of Simulation Results

After the simulation step, computers will output a series of data. Simulation analysis is converting these data into meaningful information that describes the effectiveness of control strategies on IAQ. One optimal design will undoubtedly take several iterations of the simulation cycle. The first iteration often provides information for modifying the model. It is a good practice to repeat the cycle as often as needed until the simulation results are close enough to the designer's expectation.

Almost any IAQ case can be designed through the above-mentioned procedures but may require different types of models depending on the characteristics of the designed case. Typical models and their applications will be introduced as follows.

Single-Zone Modeling and Simulation

VOC mass transfer in the indoor environment is a dynamic and complex process. The theory behind the transfer phenomena has been established and mathematically documented over the years by the scientific community. The single-zone model, as

one typical physics-based model, can be used to describe this physical process taking place in the building environment. Its principle and application are discussed in this section.

Purpose Identification and Model Selection

Single-zone model is the simplest IAQ model. The purpose of single-zone modeling and simulation is to predict and/or analyze the average concentrations of target pollutants in a space of interest. The space can be the microenvironment around an occupant (e.g., in an office cubical), a room, or an entire building. The entire space is represented by a single zone in which the spatial concentration gradients are not considered. The single-zone model is useful for providing an overall estimation of the indoor air quality in the space under a given building condition, and for predicting the effectiveness of various IAQ control strategies including pollutant source reduction, ventilation, and air purification at building design stage (Zhang and Shaw 1999; Liang et al. 2012). Single-zone model can also be used to simulate the dynamic behavior of pollutant concentrations in the space to devise optimized IAQ control strategies considering the variations of the indoor and outdoor pollution loads, weather conditions, and the building occupancy in an effort to minimize energy consumption while maintain the pollutant concentrations below the acceptable threshold values (Woldekidan et al. 2013).

The single-zone model is one typical physics-based model. It is established based on first principles, also known as the mass balance model (Liang et al. 2012). The building is considered as one whole space, represented by a single node, as shown in Fig. 3 (Abdalla and Peng 2021), and the average VOC concentration is thus of interest. It is particularly suitable for IAQ design in buildings with uniform indoor VOC concentrations, such as:

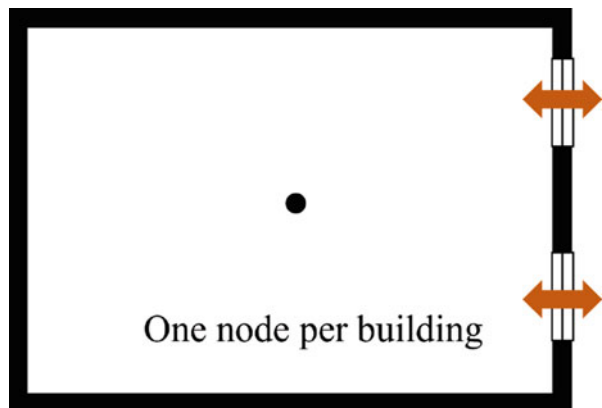
- Small office
- Classroom

In terms of a small office, the limited interior space facilitates the rapid mixing of gaseous pollutants. As for the classroom, the regular source (desk and chair) distribution helps to eliminate the VOC concentration gradient. Both of these features help to create a uniform concentration and ensure the good performance of the single-zone model.

Model Assumptions and Governing Equations

Despite the good performance of the single-zone model, it is based on assumptions that simplify the building representation, which also constrain the use of the model. One major assumption for the single-zone model is that the investigated zone or zones are well mixed (Liang et al. 2012). Besides the above-mentioned limited interior space and regular source distribution, the well-mixed assumption may also include the following aspects (Sparks 2016):

Fig. 3 Schematic of VOC mass transfer by single-zone model: Plan view of a one-store building. (Modified from Abdalla and Peng 2021)



- Time scales of interest are several minutes or longer.
- Concentrations very close to large sources are not of interest.
- There are no local airflow disturbances close to the location of interest.

With the well-mixed assumption, the single-zone model for VOC concentration prediction can be characterized by the following ordinary differential equation:

$$V \frac{dC_{in}}{dt} = Q_{out} \cdot C_{out} - Q_{in} \cdot C_{in} + \sum R - \sum S \quad (1)$$

where V is the zone volume (m^3), C_{in} is the indoor VOC concentration (mg/m^3), t is the simulation time (s), Q_{out} is the ventilation rate introduced into the zone (m^3/s), C_{out} is the VOC concentration introduced into the zone (mg/m^3), Q_{in} is the ventilation rate escaped out of the zone (m^3/s), R is the source term, S is the sink term.

Normally, indoor pressure is a constant value for most building types, meaning a balanced ventilation rate between indoor and outdoor. Therefore, the single-zone model can be simplified as:

$$V \frac{dC_{in}}{dt} = Q(C_{out} - Q_{in}) + \sum R - \sum S \quad (2)$$

where Q is the ventilation rate between indoor and outdoor (m^3/s), and other parameters have the same meanings as those in Eq. (1).

Model Input Parameters and Their Determination

The quality of model predictions depends on not only the correct mathematical expression but also the adequacy of the input parameters. From a broad view, input parameters in the single-zone model include the source, sink, and ventilation terms.

For most cases of interest, they are not constants and may be determined by additional models or eqs. A summary is given below.

Emission Source

Emission sources are the original cause of VOC pollution in a building and can affect indoor concentrations especially during the early days, weeks, and months after their installation. In modern buildings, VOC sources are everywhere and of numerous types, including but not limited to building materials and furniture, various appliances, cooking devices, office equipment, lighting, and occupants (Philip 2016). Among these, building materials and furniture contribute a considerable part (Zhang et al. 2018), and a major focus is putting to address their emission mechanism. While others are summarized in the research (Lee et al. 2001; Ahn et al. 2015; He et al. 2019b) and are not repeated here.

Based on the emission characteristics, building materials can be broadly classified into dry material, “wet” material, and assembled one (Zhang et al. 1999a). Their emissions behavior and representative models are summarized below.

Dry Material

Dry materials contribute a considerable part for indoor VOC pollution. Dry materials commonly used in buildings include plywood, particleboard, medium density fiberboard, wood paneling, carpets, etc. (Jia et al. 2020; Katsogiannis et al. 2008). Normally, VOC diffusions from interior material to indoor air is a slow process, resulting in a long emission life. Emissions of formaldehyde from medium density fiberboard have been measured more than 3 years after the products were installed (Liang et al. 2015). Accurate prediction of material emissions in such a long period is usually difficult.

One challenge is how to cognize the complex mass transfer mechanism. Little et al. (1994) pioneered that VOC mass transfer inside the material is dominated by molecular diffusion and follows Fick’s law as shown in Fig. 4. Later, focuses have been paid to the improvement of Little’s model (Yang 1999; Huang and Haghightat 2002; Xu and Zhang 2003; Kumar and Little 2003; Wang et al. 2006; Hu et al. 2007), so that material emissions with more complicated boundary conditions can be predicted. Up to now, the improved Little’s model has been widely used to simulate VOC emission from various dry building materials and achieve satisfied prediction results in the laboratory.

Another challenge is how to evaluate the impact of environmental conditions such as temperature and humidity on the VOC emission process. The improved Little’s model performed well under constant temperature and humidity conditions but was downgrade once the environmental parameters change. Liang et al. (2016) proposed a physics-based model to describe formaldehyde emissions influenced by coupling temperature and humidity (shown in Fig. 5). The model makes it possible to predict dry material emissions under varied and realistic environmental conditions.

Fig. 4 Schematic of VOC mass transfer from dry building materials (Little, 1994)

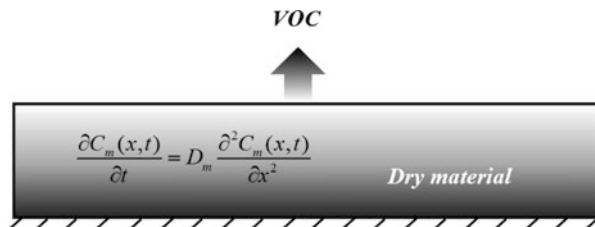
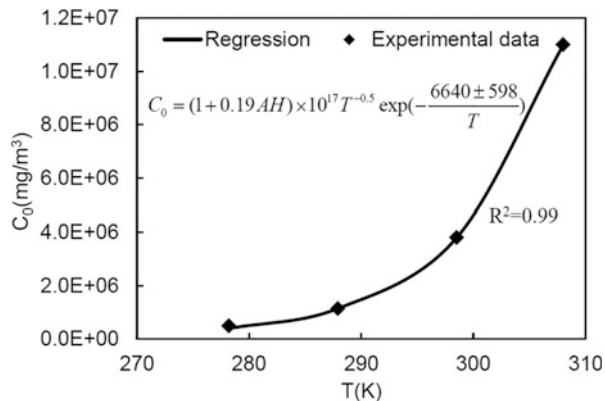


Fig. 5 Correlation between initial emittable concentration (C_0) and the combined effects of temperature and absolute humidity (Liang et al. 2016)



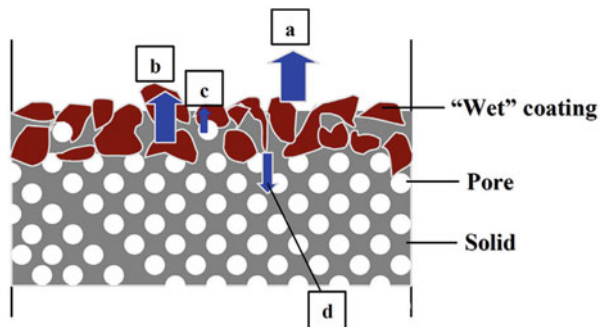
“Wet” Material

Materials like paints, adhesives, wood stains, vanishes are widely used in buildings (Yang 1999). These materials are generally named “wet” materials because they are in wet conditions when initially applied. Normally, “wet” materials cure quickly and emit the majority of their VOC during the first few days, weeks, or months of their service life. Compared to dry materials, the emission mechanism of “wet” materials is much more complicated.

A previous study (Zhang et al. 1998) has indicated that the “wet” material appears to have three emission phases as shown in Fig. 6. The first phase represents the period shortly after the material is applied but is still relatively wet. VOC emissions in this phase are characterized by high emission rates but fast decay. It appears that emissions are related to evaporation at the surface of the material. In the second phase, the material dries as emissions transition from an evaporation-dominant phase to an internal-diffusion controlled phase. In the third phase, the material becomes relatively dry. The VOC off-gassing rate decreases and so does the decay rate. The dominant emission mechanism in this phase is just like dry material.

At the beginning of model development, attention was paid to the first phase of “wet” material emissions. Guo and Tichenor (1992) initially developed the Vapor pressure and Boundary layer (VB) model to simulate VOC emissions from “wet” materials. This model focused on the evaporation dominant process but ignored the

Fig. 6 Schematic representation of the emission mechanisms of a “wet” material embedded in a porous substrate. (a) evaporation; (b) movement of free and bound VOC; (c) vapor flow; (d) diffusion to the substrate (Yang 1999)



diffusion process in the material film. Therefore, the model performed well at the early emission stage but accuracy decreases as time went by.

Yang (1999) proposed a physics-based model to describe VOC emission from a “wet” coating material based on the theory of stratified convection and diffusion. Compared with the VB model, one improvement of Yang’s model is that all the above-mentioned three emission phases are considered so that the model shows good performance in the entire prediction phase. Additionally, using one equation to describe the entire emission process (from “wet” to dry) provides convenience for model users and is usually welcomed in practical engineering.

Currently, “wet” material with a more complex emission mechanism can be considered with the maturity of modeling. One example is the silicone adhesive, whose major VOC is generated by a chemical reaction during the curing process. In addition, the continuously moving interface of chemical reactions makes modeling more challenging. He et al. (2019a) developed a one-dimensional curing model to describe such a complex process and achieved satisfying prediction results. The model helps to accurately interpret the emission behavior of silicone adhesive and is of significance for correctly providing the inputs for concentration simulation.

Assembled Material

In practice, different individual materials are usually used together to form material systems/assemblies. Examples are:

- carpet // adhesive // concrete,
- paint // gypsum wallboard // vapor barrier,
- carpet // under-pad // plywood (or OSB) sub-floor // wood joists,
- wax // vinyl sheet // adhesive // concrete,
- polyurethane floor varnish // wood stain // hardwood strip flooring// plywood (or OSB) // wood joists.

In order to estimate the actual contributions of each individual material to the VOC concentrations in a building, it is necessary to understand the emission

characteristics of these material systems/assemblies as well as the associated individual materials.

Normally, “wet” materials are rarely used alone, but in combination with dry materials to form assembled materials. According to the spatial location of “wet” materials, assembled materials can be divided into two categories. One is to apply the wet material on the dry material, and another is to cover the dry material on the wet material.

In terms of the former, the surface to which “wet” materials are applied will considerably affect their emission life cycle. For example, when wall paint is applied to the gypsum board, a part of VOC will directly release into the air, while others will move into the gypsum board and then re-emit to indoor air once environmental conditions permit. In contrast, a sealant applied to smooth glass will not result in much adsorption and most of VOC will directly emit into the air. VOC mass transfer process for a “wet” material applied on a solid substrate has been well analyzed and summarized in the literature (Yang 1999).

As for the latter, VOC emissions from “wet” materials are considerably affected by the materials that cover them. One example is to apply wooden floor or carpet on the adhesives. The coverings change the emissions from adhesives by providing a mass transfer barrier. This can reduce the VOC exposure at the early emission stage but may result in long-term indoor pollution (Dong et al. 2013).

Although the assembled materials behave differently from a single material, their emission behaviors can be deduced based on the emission model of dry and “wet” materials if the assembling and using conditions are adequate. When a material assembly involves complex sources such as adhesives, the complex source layer may be modeled by the diffusion model with diffusivities varying as a function of the VOC concentration (Zhang et al. 1999a, b). This approach was used to predict the concentrations of VOCs emitted from an adhesive in a “vinyl tile // adhesive // stainless steel” assembly. Stainless steel was used as a backing to simplify the emission scenario. The predicted results agreed reasonably well with those measured in a small chamber test (Bodalal 1999). For assemblies involving only dry material layers, the fundamental Fick’s law of diffusion can be applied to each individual material layer with their respective diffusion and partition coefficients plus the equilibrium partition coefficients at the interface between two adjacent material layers (Zhang et al. 1999a, b). This approach was applied to model the VOC emissions from a large wall assembly of typical wood-framed residential houses, which including gypsum wallboard, fiberglass insulation, oriented strained board (OSB), and vinyl siding (Li et al. 2005). The study also investigated the effects of infiltration on the VOC emissions and transport to the indoor space.

Adsorption Sink

From a broad view, any material or device which can absorb or capture VOC molecules from indoor air can be regarded as a sink. Based on adsorption characteristics, sinks can be classified into chemical sinks and physical sinks.

Chemical sinks are to use specific methods or technologies (photocatalysis, negative ions, and catalytic oxidation, etc.) to capture indoor VOC molecules

(Filho et al. 2019; Saoud et al. 2019). Then the adsorbed molecules are degraded or eliminated through chemical reactions, consequently reducing indoor VOC concentrations. The chemical sinks usually have a high removal efficiency for specific VOC, but the by-products pollution associated with chemical reactions limits its popularity in the building environment (Xu et al. 2018).

In contrast, physical adsorption is usually safe and reliable. Physical adsorption has a considerable removal efficiency on both high and low VOC concentrations (Zhu et al. 2018). Moreover, the relatively low cost also makes it welcomed in engineering. Physical sinks in the indoor environment mainly include two types. One is VOC adsorbed by building materials, which can be called adsorbed materials. Another is VOC adsorbed by equipment, such as air cleaners. The mechanisms and models of these two types of sinks are introduced separately.

Adsorbed Material

Adsorbed materials are characterized by pore structures and rough surfaces, such as sofa cushions, and carpets. VOC moves from air to the specific sites within these adsorbed materials to complete the so-called adsorption behavior. Mass transfer in such a process includes interfacial diffusion in the gas phase, adsorption at the material-air interface, and diffusion inside the material for a permeable material (Yang et al. 2001). Note that, VOC adsorption by building material is usually a reversible process. The adsorbed VOC can re-emit into the air when indoor condition permits, and elevate indoor concentrations even long after the original source is depleted or removed. Therefore, materials capable of depositing, adsorbing, and/or accumulating VOC can influence IAQ during the entire service life of a building (Yang et al. 2001).

Researchers initially used equilibrium models to describe the material adsorbed behavior (Axley 1991). The equilibrium models assume that the adsorption and desorption simultaneously occur on the material surface and an equilibrium is achieved at the material-air interface. One commonly used equilibrium model is the Langmuir model (Axley 1991). Despite the simple principle, neglecting both the interfacial mass transfer and the material-phase diffusion may result in a doubtful model prediction.

The kinetic model is another type of adsorption model (Axley 1991; Dunn and Chen 1993; Little and Hodgson 1996). Different from the equilibrium model, VOC diffusion in the material phase is considered in the kinetic model. Additionally, the model parameters are the physical characteristics of materials, which can be obtained independently from experimental data. However, the kinetic model is based on a few assumptions, and its usage is limited to some simple cases.

Yang et al. (2001) subsequently proposed a “wall function” model to describe the material adsorbed behavior. Different from the equilibrium model and kinetic model, the “wall function” model has clear physical meanings for the entire adsorption process and is thus suitable for more general conditions. The validation results indicate that the model can achieve promising predictions if the diffusion coefficient and partition coefficient are accurately provided, which needs the support of necessary measurement data.

Zhang et al. (2002), Zhang and Chen (2002, 2003) provided a comprehensive review of the physical sorption models and how they compare with experimental data for a variety of building materials under different temperature, humidity, temperature and air velocity conditions.

It should be mentioned that VOC adsorbed by building materials is driven by the concentration gradient, which can be regarded as a passive adsorption process. The adsorption rate in this process is usually slow, especially compared with active adsorption.

Air Cleaner

VOC captured by air cleaners is a typical active adsorption process. Dirty air flows through the filters under the running of fans. Then the cleaned air return back to the room to dilute indoor VOC concentration. Models and performance data are available for filters packed with adsorbents (Pei and Zhang 2010, 2011). According to a survey in literature, activated-carbon-based technology is widely used in household air cleaners (Zhu et al. 2019a). These devices normally have a robust and stable working efficiency at the initial running time, and the performance will gradually decay as time goes by. If VOC adsorption efficiency at the initial few hours is focused, the clean air delivery rate (CADR) could be an effective indicator, which represents the equivalent fresh air volume flow rate that the air cleaners can provide. If long-term working performance is desired, the actual physical mass transfer process needs to be well addressed.

VOC adsorbed by air cleaners involves three physical processes as shown in Fig. 7: (1) Convection mass transfer from the bulk air to the outer surface of the activated carbon; (2) Diffusion mass transfer from the outer surface to the interior pore of the activated carbon; (3) Adsorption process by the inner wall of the pore. Zhu et al. (2019a) proposed a physical model to describe the above-mentioned mass transfer processes. The model has been proved to be capable of giving accurate responses to the dynamic operation of air cleaners. Agreements were observed between model predictions and measurements in both laboratory and actual rooms.

Adsorb-based air cleaners can easily reach saturation under long-term running. If the filters are not replaced in time, they will become pollution sources. To avoid

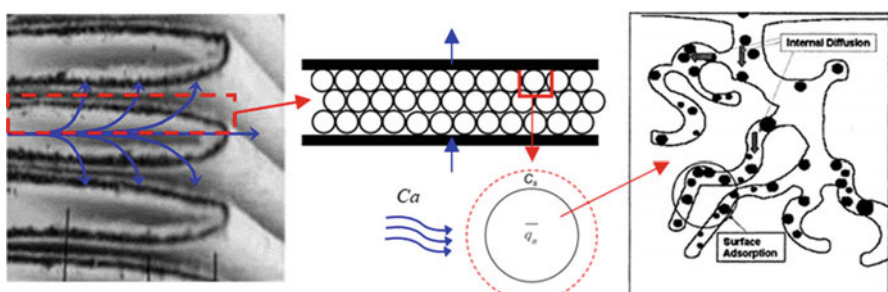


Fig. 7 VOC mass transfer process in an adsorptive air cleaner (Zhu et al. 2019a)

this, it is necessary to estimate their service life and replace the filter before saturation to ensure a continuous and stable purified capacity. These can also be accurately evaluated with the proposed model (Zhu et al. 2019b).

More recently, sorbent materials have also been integrated into building materials such as gypsum wallboard to take advantage the large surface area available in the space and the high adsorption capacity of the sorbents. A model was developed to predict the product's formaldehyde removal performance over its service life (Pentigny et al. 2021).

Ventilation

Ventilation is to provide unconditioned outdoor air or conditioned, combined, outdoor, and recirculated air for diluting pollutant concentrations and achieving acceptable IAQ. Ventilation can be broadly categorized into mechanical ventilation and natural ventilation. Generally, mechanical ventilation is driven by fans and can provide ventilation at the exact demanding rate and in the expected time. The ventilation rate is robust when the system is running and can be estimated by cross-sectional area and air velocity in the pipeline.

Natural ventilation depends on natural forces like the wind from the surrounding environment as well as buoyancy forces that develop due to temperature differences between inside and outside the building. Compared to mechanical ventilation, natural ventilation is almost uncontrollable. Many factors can affect behaviors of natural ventilation, such as climate region, terrain, surrounding buildings, the studied building geometry, ventilation opening shape, size, and direction, as well as the occupant activities (Lai et al. 2018). Therefore, estimating the natural ventilation rate is usually difficult.

Many buildings rely on infiltration for basic fresh air demand and open windows to provide increased ventilation when needed. Infiltration means no window or door is opened so that outdoor air enters the rooms through leakages in the building envelope under the drive of wind and thermal pressure between indoor and outdoor. The tracer gas decay method is usually used for evaluating the infiltration rate (Reardon and Zhang 1995; Kabirikopaei and Lau 2020). Previous studies show that the infiltration rate varied in a limited range within a few hours but shows obvious changes with the seasons (Shi et al. 2015). This means that a constant infiltration assumption is acceptable when considering the ventilation effect in a few hours. However, infiltration rate changed with time needs to be evaluated once a few months simulation is focused.

When the door or window is opened, the outdoor air enters the room through the large opening driven by wind pressure. In this case, even slight fluctuations of the outdoor environment will rapidly transmit to the indoor space, consequently resulting in a rapid change of ventilation rate. The uncontrollable ventilation behavior also brings challenges for ventilation rate assessment. Field investigation is rough in this situation. Simulation based on accurate model evaluation then becomes a choice. Up to now, different types of software, including CONTAMW, EnergyPlus, and VentSim, have been developed to predict ventilation rates under various complex conditions (Han et al. 2014; Zhang et al. 2013; Wei et al. 2011).

Model Output and Analysis of Cases

With the input parameters of source, sink, and ventilation, defining the model output becomes the next task. In the single-zone model, the average concentration curve is one of the desired outputs. It can be obtained by simultaneously solving the mass balance and additional source, sink, and ventilation model equations. Due to the complexity of these models, pursuing an accurate analytical solution is unrealistic. The numerical method, therefore, becomes an alternative choice. First, the ordinary differential equations are discretized in time and then converted into computer code. Computer code must be written to algorithmically represent the mathematical statements of the models. Next, the code is typed into a computer for the iterative calculation to complete the so-called simulation running process. The computer then gives a large amount of calculating data. Data analysis is then performed to convert the data into meaningful information. With this knowledge, improvement suggestions can be provided to ensure the achievable design purpose.

A recent study was conducted to verify the long-term performance of the single-zone simulation model (Liang et al. 2021). A full-scale experimental room was built with a single formaldehyde source of medium density board inside the room. Interior temperature and humidity, as well as the air change rate between outdoor and indoor, were allowed to vary naturally with the ambient environment. Indoor environmental monitoring data indicated that the temperature varied from $-10.9\text{ }^{\circ}\text{C}$ to $31.4\text{ }^{\circ}\text{C}$, while that of relative humidity fell into a range between 46.5% and 83.6%, almost covering the range of indoor environmental parameters commonly observed in buildings. In such a complex environment, time-varying indoor formaldehyde concentration was simulated, and the results indicated the concentrations varied seasonally with peak values decreasing with year (shown in Fig. 8). Meanwhile, frequent field sampling (ranging from a few days to 4 weeks) of actual indoor formaldehyde concentration was conducted from October 2012 to February 2015, and the results agreed well with that of simulations. Such a long-term model verification, especially in an actual room with environmental conditions changing sharply, gives a certain level of confidence to the simulation model.

Another study intended to test the feasibility of the simulation tool in predicting potential IAQ problems in an actual apartment (Lv and Yang 2019). In this case, the block-board is planned to use in the interior decoration of an apartment. The model predicts that its installation will significantly elevate the indoor formaldehyde concentration (the 0–72 h curve in Fig. 9). Although not shown in the figure, the simulation results showed that such a high level of formaldehyde concentration would last years before decreasing to an acceptable level. Hence, the suggestion of using another low-emitting material instead of the block-board was put forward to the owner. Unfortunately, it was not adopted and the block-board was introduced into the apartment. This led to the generation of indoor formaldehyde pollution as expected. The field concentration results (measurement point at 72 h) confirmed the correctness of the model predictions. This prompted the owner to admit that the block-board is a strong source of formaldehyde. However, the owner still hesitated to dismantle the installed block-board in a hope that the problem would not last long.

Fig. 8 Comparison between simulation and measurement (Liang et al. 2021)

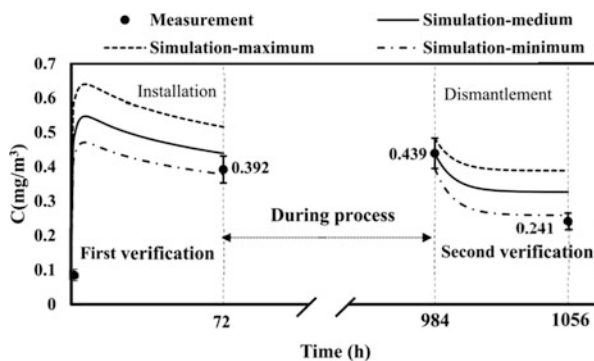
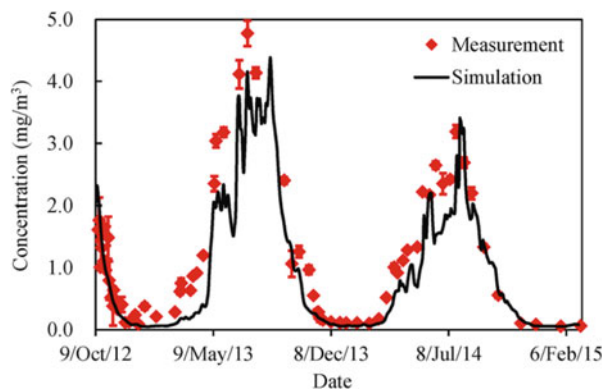


Fig. 9 Comparison of formaldehyde concentrations between measurement and simulation, in the apartment. The first part (0–72 h) represents the introduction of the blockboard indoors. The middle part (72–984 h) is the duration between the material introduction and removal. The third part (984–1056 h) represents the removal of the blockboard (Lv and Yang 2019)

Hence, the board remained inside the apartment and other decoration work continued. After approximately 40 days, another field measurement result (measurement point at 984 h) indicated that indoor formaldehyde was still at a high level, and this prompted the decision to remove the block-board. The concentration change resulting from the blockboard removal was simulated again using the single-zone model (the 984–1056 h curve in Fig. 9). Indoor formaldehyde concentration was tested 3 days after the material was removed, and the result was close to the predicted result, which verified the accuracy of the model predictions for the second time. From the IAQ control point of view, this is not a successful case because of the failure in preventing the formaldehyde emission source in the first place. Despite the lesson learned from such a mistake, an unexpected “benefit” was that the rigorous simulation exercise is a useful tool for IAQ design, and can help prevent VOC pollution from occurring initially.

The single-zone model has many advantages, including concise mathematical expression, easy-to-understand mechanism, relatively fast calculation, and clear physical meaning, etc. These characteristics provide the convenience for applying the single-zone model in engineering. However, the single-zone model predictions heavily depend on the accuracy of the input parameters, which requires a professional background. This undoubtedly brings challenges to modelers. Additionally, the well-mixed assumption for the whole zone leads to lumped parameters for simulations, and the flow conditions among rooms are neglected in the model. Therefore, a single-zone model may not be adequate when pollutants are not perfectly mixed throughout the building.

Example Software Tools

The example computer software tools based on the single-zone model are MEDB-IAQ (Zhang 1999), IA-Quest (Magee et al. 2002; Won 2008). Descriptions of both software are given below.

MEDB-IAQ

The Materials Emission DataBase and Indoor Air Quality (MEDB-IAQ) simulation program was developed by the Institute for Research in Construction (IRC) of the National Research Council of Canada (Zhang 1999). It is characterized by using the single-zone model to simulate the indoor VOC concentration contributed by building materials. Input parameters of the software involve source, sink, and ventilation terms. VOC mass transfer for source and sink is described by a material emission database in which VOC emission rates of typical building materials are represented by empirical or semi-empirical models such as the power-law model for dry materials and the vapor evaporation and boundary layer model (VB) for wet materials, respectively. Key parameters in both models are determined by the environmental chamber method. Space volume, ventilation rates and schedule, and quantity and time of materials used in the space are specified by users. The program output is the time-varying indoor VOC concentrations. The MEDB-IAQ provides a convenient platform for evaluating the influence of building materials on IAQ.

IA-Quest

The Indoor Air Quality Emission Simulation Tool (IA-Quest) was developed by National Research Council Canada, as an extension to the MEDB-IAQ. A database and a simulation component are included in IA-Quest. The database provides information on the emission of health-relevant “target” VOC, abundant VOC, and TVOC (total VOC). The material emission database currently consists of about 2,300 data sets of emission characteristics based on emission testing of 69 building materials commonly used in Canada. For the simulation component, IA-Quest used empirical models to describe the material emission characteristics, such as the power-law model and the peak model. Emission coefficients in models are based on environmental chamber tests conducted at conditions of 23 °C and 50% and a

period of 120 h on average. Other program inputs include the volume of a space, ventilation schedule, material emission area, in-time, and out-time of materials, simulation duration, time step for calculation. The IA-Quest could be used for evaluating the impact of material selection choices and ventilation schedules on IAQ.

Mult-Zone Modeling and Simulation

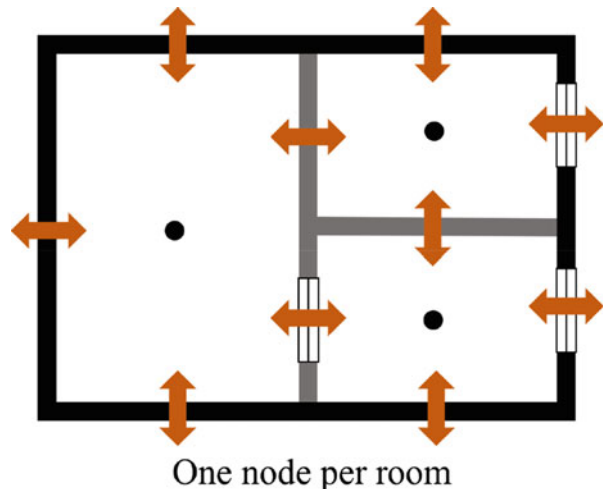
As the name implies, a multi-zone model is used to describe pollutant mass transfer in different regions. Compared with the single-zone model, it is a more general IAQ prediction model. Its principle and application are introduced in this section.

Purpose Identification and Model Selection

The multi-zone model also belongs to the physics-based model. It is established based on the mass balance theory. Compared with the single-zone model, the multi-zone model still focuses on average concentration, but can separately give average concentration in each zone (as shown in Fig. 10). Hence, it is suitable to describe the pollutant transport among rooms. Such an improvement is due to the introduction of inter-zonal airflows as model input. The multi-zone model is particularly suitable for solving IAQ problems in the following buildings:

- Residence
- Hotel
- Library

Fig. 10 Schematic of VOC mass transfer by multi-zone model: Plan view of a one-store building. (Modified from Abdalla and Peng 2021)



- Fitness room
- Prison
- Comprehensive office building

These buildings usually contain more than one room, and source characteristics are different among zones due to various uses. However, interior volume for each space is limited, and a well-mixed assumption is still acceptable. Therefore, VOC concentration in each room can be replaced by an average value.

Model Assumptions and Governing Equations

In the multi-zone model, a building is represented by several connected spaces. It can essentially be regarded as a combination of several single-zone models. Therefore, model assumptions in each room are the same as the single-zone model.

The multi-zone model can be deduced by applying the same mass balance concept for every zone. The general equation for the mass balance of room i in a building with N zones can be written as:

$$V_i \frac{dC_i}{dt} = Q_{out-i} \cdot C_{out} - Q_{i-out} \cdot C_i + \sum_N Q_{j-i} \cdot C_j - \sum_N Q_{i-j} \cdot C_i + \sum R_i - \sum S_i \quad (3)$$

where V_i is the volume of zone i (m^3), C_i is the average VOC concentration in zone i (mg/m^3), t is the simulation time (s), Q_{out-i} is the ventilation rate from outdoor to zone i (m^3/s), C_{out} is the outdoor VOC concentration (mg/m^3), Q_{i-out} is the ventilation rate from zone i to outdoor (m^3/s), Q_{j-i} is the airflow rate from zone j to zone i (m^3/s), C_j is the average VOC concentration in zone j (mg/m^3), Q_{i-j} is the airflow rate from zone i to zone j (m^3/s), R_i is the source term in zone i , S_i is the sink term in zone i .

When the air is well mixed among all zones, the multi-zone model can be simplified as the single-zone model. Hence, the single-zone model is a special condition of the multi-zone model.

Model Input Parameters and their Determination

As can be seen from Eq. (3), room VOC concentration is a function of room-to-room airflow, airflow between indoor and outdoor, sources, and sinks. Among these, source and sink terms have the same meaning as those in the single-zone model. Therefore, the major focus is paid on the inter-zonal flow rate term.

Inter-zonal airflow is normally dominated by the forced airflow provided by a mechanical ventilation system or by naturally driven airflow resulted from the

temperature differences. The tracer gas decay method can still be used for determining multi-zone ventilation rates. A recent study has proved that the airflow rate in two zones can be estimated by monitoring the dynamic CO₂ concentration changes (Remion et al. 2020). The feasibility of the tracer gas decay method heavily depends on the number of investigated rooms. If the zone number is more than two, increasing demand for both trace gas type and corresponding monitoring facility will be found. This will not only increase the test uncertainty but also increase the initial investment. Due to these notable flaws, more efforts have been paid to modeling multi-zone ventilation (Pan et al. 2019; Zhuang et al. 2021). Up to now, commercial software has been developed to calculate the multi-zone ventilation rate (Walton and Denton 2000; Chen et al. 2015). The typical one is the CONTAM, which can be used for calculating airflows if sufficient data on openings, wind speed and direction, temperature differences, mechanical ventilation parameters, and so forth, are provided (Walton and Denton 2000).

Model Output and Analysis of Typical Cases

Although the multi-zone model adds the airflow among rooms as model input, it is essentially a lumped parameter model. Average VOC concentration is normally the primary concern. Besides, the model output can also include material emission rate, pollution load rate, and source contribution rate, etc., depending on the user's demands. The abundant outputs can provide designers with more useful information to finally make an optimal technical route.

IAQ problem has been designed using the multi-zone model in a comprehensive office building (Liang 2015). The focused building has 11 rooms. Formaldehyde concentration in each region at the delivery phase is simulated, and the results are shown in Fig. 11a. The model predicted that the office located in the northwest corner (called head office) has a significantly higher formaldehyde concentration than other rooms due to insufficient ventilation. This brings a challenge for material selection if a comparable concentration level is to be achieved. Further analysis is performed based on another model output, that is dynamic source contribution rate shown in Fig. 11b. At the initial decoration stage (2112–2880 h), room formaldehyde mainly comes from wet materials, such as wall paint. As time goes by (2880–5040 h), the added dry materials replaced the wet materials to became the main sources. At the time of building delivery (5040 h), emissions from furniture and carpets are significantly more than other materials, contributing more than 90% of the indoor formaldehyde. Hence, an improvement suggestion is to replace furniture and carpets with other low-emission materials indoors. Although not shown in the figure, the model predictions show that the improved design can significantly decrease formaldehyde concentration in the head office. Subsequently, interior decoration was carried out according to the improved design. The field investigations at the delivery time showed that formaldehyde concentration in the head office was comparable with those in other offices. Besides, formaldehyde concentrations in all the rooms were lower than the standard recommended value of 0.1 mg/m³ (GB/T

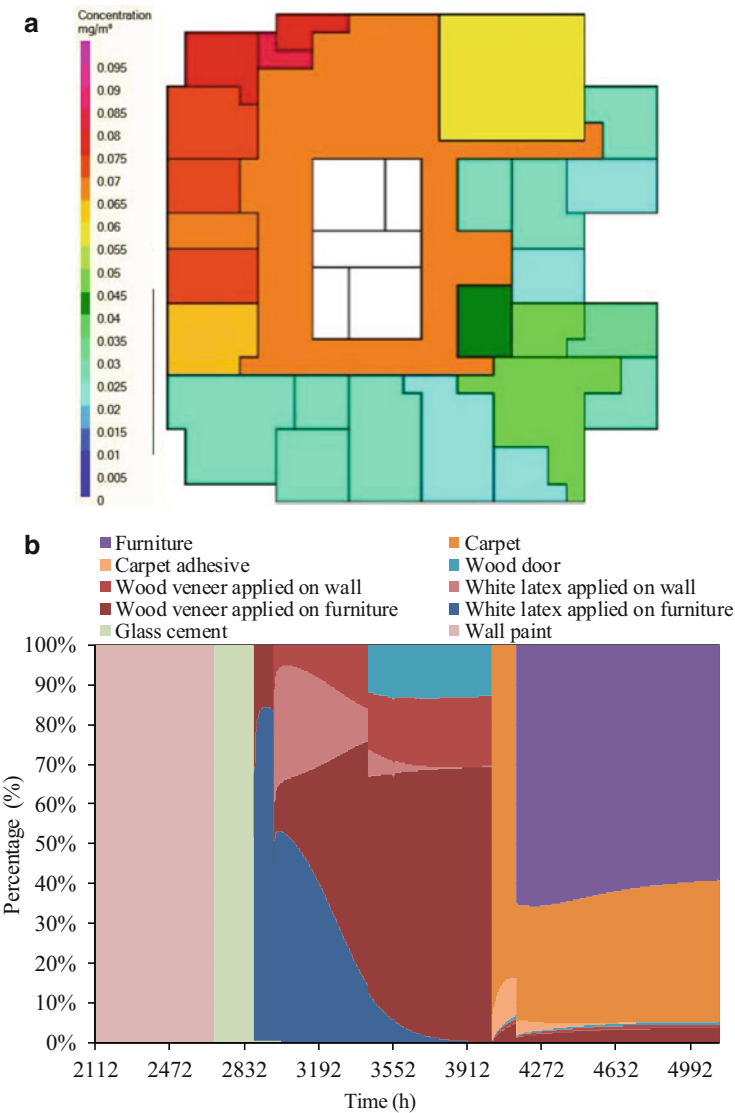
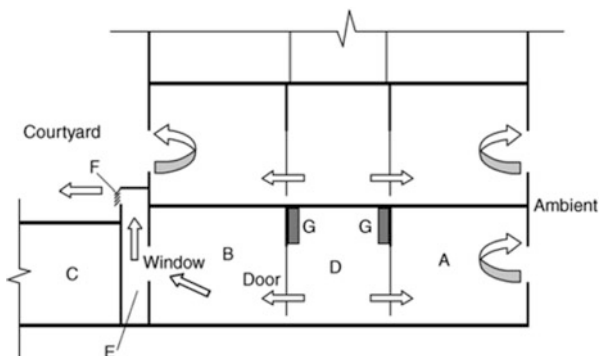


Fig. 11 Application of the multi-zone model in an office building: (a) Simulated formaldehyde concentration at the building delivery time; (b) Dynamic source contribution rate for the head office (Liang 2015)

18883-2002 2002). The good agreement between measurement and simulations indicates that the multi-zone model can prevent possible VOC pollution from initial occurring.

The multi-zone model can also help to analyze the transmission of respiratory infectious diseases, such as SARS. One previous study has reported a cross-infected

Fig. 12 The layout of the corridor and adjacent rooms with possible flow directions (plan view). A-orthopedic clinic room A; B-orthopedic clinic room B; C-critical care room; D-corridor; E-interlayer; F-grille; G-patient beds (Jiang et al. 2010)



incident occurred in an actual hospital (Jiang et al. 2010). Figure 12 is the layout of the focused building. The corridor near the emergency treatment center was where the infections occur. A total of 12 SARS patients were hospitalized here from April 17 to 22, 2003. Rooms A and B were offices with four orthopedic physicians working in each room. Room A was connected to the outside through a window, which was open for most of the 6 days. Room B was connected through a chimney that only enabled air to exit the room as the outside temperature was cooler than the inside temperature during that period. A few days later, all four physicians in Room B were diagnosed with SARS while none of the physicians in Room A was infected. All the 8 orthopedic physicians in Room A and Room B had never direct contact with SARS patients and their daily routines were very similar. The only identified difference was their office rooms' ventilation. Room A was well ventilated with outside air through a window while Room B was ventilated with air from the corridor where the 12 SARS patients were hospitalized.

Jiang et al. (2010) simulated the virus concentration in Room B to expect to find the infected reason. Trace gas SF₆ was released in the same locations as the SARS patients' bed to simulate the SARS virus exhaled by infectors. Combined with field ventilation, the average SF₆ concentration in Room B was calculated using the multi-zone model. As the red line shown in Fig. 13, the SF₆ concentration in Room B was predicted to reach 800 ppm, which resulted high infective risk. To validate the simulation results, SF₆ concentration at a series of points along the corridor and different locations in Room B were sampled, and the results are shown in Fig. 13. Good agreements were observed between the simulation and the measurement, indicating that the multi-zone model is capable of predicting the transmission of SARS before the virus actually spreads. In addition, the study also reproduced the SARS infected cases in another two hospitals in Beijing. By comparing the released SF₆ concentrations with those measured in the room in these typical cases, Jiang et al. (2010) concluded that a 10,000 times dilution can significantly reduce the risk of SARS infection. These findings show that reproducing actual infective and non-infective cases with simulation is a valid method for determining safe

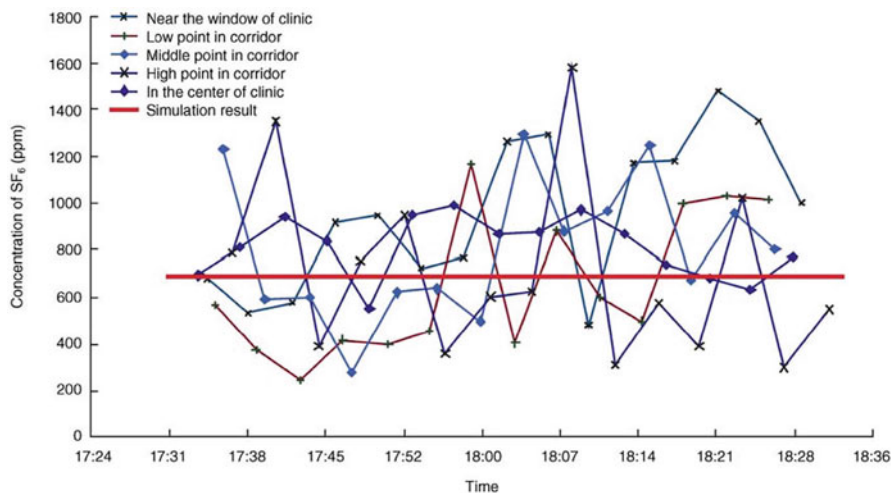


Fig. 13 Comparison of measured and simulated results of the SF₆ concentration in the corridor (Jiang et al. 2010)

ventilation rates for the purpose of maintaining an infection-free building environment. Further, simulation and modeling provide a methodology for preventing respiratory infective diseases and designing a safe building environment.

The multi-zone model is established based on the mass balance theory. It thus has some similar characteristics as the single-zone model, including concise mathematical expression, easy-to-understand mechanism, and clear physical meaning. Besides, the ability to distinguish concentration differences among zones enables broader application of the multi-zone. For example, it has been applied to predict the dynamic variations of chemical concentrations in 73 different zones of an educational building as a result of chemical release inside a zone or at outdoor air supply inlet, and use the information in an evaluation planning model to minimize the exposure of occupants to the pollutant (Zhang et al. 2005). However, the multi-zone models cost more computer power than the single-zone model and require accurate knowledge or modeling of the inter-zonal airflows. Additionally, no information is provided on the spatial distribution of the contaminants, and local VOC exposure cannot be evaluated using this type of model.

Example Software Tools

Compared with the program based on the single-zone model, existing multi-zone contaminant simulation software are more abundant, including IAQX, RISK, MCCEM, CONTAMW, and COMIS. Their simulation procedures and applications have been well summarized in the literature (Guo 2000; Sparks 1996; Koontz and Nagda 1991; Dols and Walton 2002; Feustel 1999). However, the limitation of these

programs is that source and sink models are either simplified or empirical, making these tools perform well only for certain specific conditions. To explore general use, more integrated tools have been developed including CHAMPS-Multizone and PACT-IAQ (Zhang 2005; Wei et al. 2012; Liang et al. 2017).

Champs

Syracuse University developed a Coupled Heat, Air, Moisture, and Pollutant Simulation (CHAMPS-Multizone) software in collaboration with the Technical University of Dresden of Germany. Models used in the tool are physics-based. Identifications of model input and their determinations have been well summarized in the literature (Zhang 2005). The program output includes not only the VOC concentration but also the airflow, moisture, and energy consumption. Therefore, CHAMPS is a comprehensive simulation tool. Applications of the CHAMPS may include, but are not limited to:

- Understanding and predicting the material emission characteristic and their impact on IAQ;
- Locating pollutant sources;
- Optimal placement of distributed sensors for intelligent control of building environmental system;
- Development of new materials for the built environment that have the required transport properties for heat, air, moisture, and pollutant control in buildings.

Pact-IAQ

PACT-IAQ was jointly developed by Tsinghua University and Shenzhen Institute of Building Research Co., Ltd. It is characterized by estimating the dynamic pollutant loads and concentration variations by considering the coupled effects of source, sink, and ventilation. Models used in the program are physical-based. Compared with other programs, one obvious improvement is that the PACT-IAQ can give accurate responses to dynamic environmental changes, and model predictions have been examined by a series of actual engineering applications. Such an advantage extends the IAQ predictions from the laboratory to real buildings. More importantly, the PACT-IAQ develops a comprehensive database containing hundreds of materials and provides sufficient support for IAQ design. Required inputs include key parameters, applying areas, and installed schedules of sources and sinks, ventilation among zones, ventilation between indoor and outdoor, hourly indoor temperature and humidity, and room volume. The user has a wide selection of simulation output including:

- Hourly indoor VOC concentration;
- Hourly pollutant load or emission rate contributed by each building material;
- Optimal material selection based on the designed concentration;
- Suggested check-in time based on exposure assessment;
- Effectiveness evaluation for various ventilation modes.

Computational Fluid Dynamics Modeling and Simulation

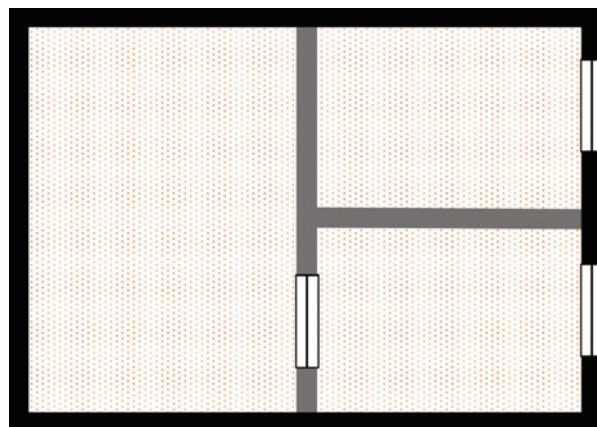
Both single-zone and multi-zone models focus on average in-room VOC concentrations. However, there are situations where the local concentration is of interest instead of the average in-room concentration. For this type of application, the CFD model may provide the desired predictions. Its principle and application are summarized in this section.

Purpose Identification and Model Selection

CFD model is also one physics-based model which can be used for predicting airflow distributions or air movement within buildings (as shown in Fig. 14). Coupled with the source and sink models, the CFD model can give the spatial distribution of pollutant concentration. Therefore, it is particularly welcomed for IAQ problems where the airflow parameters or the local personal exposures are needed. Buildings that are suitable for applying CFD models include:

- Shopping mall
- Factory
- Theater
- Gym
- Hospital
- Cleanroom
- Chemical laboratory

Fig. 14 Schematic of VOC mass transfer by CFD model: Plan view of a one-store building. (Modified from Abdalla and Peng 2021)



Multiple nodes per room

The first four types of buildings usually have enormous interior volumes. In these buildings, IAQ control for the whole space is expensive and sometimes unaffordable. Creating a locally healthy and comfortable environment through reasonable airflow design becomes a more realistic choice. In contrast, the last three types of buildings have limited space, but pollutants in rooms may cause serious health problems. Personal exposure becomes an important design parameter in these buildings. Both demands can be realized with the help of CFD models.

Governing Equations and Solving Methods

CFD model is developed based on the Navier-Stokes equation, which is for describing viscous fluid flow. It was developed first by Navier in 1827 and extended later by Stokes in 1845. One general expression of the Navier-Stokes equation can be written as:

$$\frac{\partial \vec{v}}{\partial t} + (\vec{v} \cdot \nabla) \vec{v} = \vec{f} - \frac{1}{\rho} \nabla p + \frac{\mu}{\rho} \nabla^2 \vec{v} \quad (4)$$

where \vec{v} is the velocity vector (m/s), t is the time (s), \vec{f} is the external force per unit volume of fluid (N/m^3), ρ is the fluid density (kg/m^3), p is the pressure (N/m^2), μ is the dynamic viscosity coefficient (m^2/s).

As known, the Navier-Stokes equation is used for analyzing flow characteristics of the laminar viscous fluid. However, most of the real-life engineering problems, including indoor airflows, are not laminar but turbulent flows. To make turbulence prediction possible, more effort has been paid to the improvement of the Navier-Stokes equation, and a series of turbulence models were then developed. The well-known turbulent models for indoor airflows include the Prandtl mixing length model, the Spalart-Allmaras model, the Standard k-e model, the RNG k-e model, the Realizable k-e model, the Standard k-w model, the SST k-w model, and the Reynolds stress model (Obermeier 2010; Paciorri and Sabetta 2003; Cheng and Wang 1997; Sun et al. 2017; Thompson and Hassan 2015).

Note that, these models include a series of partial differential equations, meaning that they do not have an analytical solution in the full form. Hence, the numerical solution becomes the prior choice. The flow domain is divided into small computational cells or finite control volumes. For each cell, an algebraic set of the conservation equation can be developed based on the finite difference method, finite volume method, finite element method, or finite analytic method. The algebraic equation is then solved in each computational cell using an iterative manner. In this regard, the CFD method is a numerical approximation of the Navier-Stokes governing equation.

Model Inputs and their Determinations

Input parameters of the CFD models involve basic physical parameters and boundary conditions of the fluid. Physical parameters represent the basic characteristics of

fluids, and generally include fluid density, molecular weight, and viscosity, etc. They can be determined once the fluid being studied is confirmed. Boundary conditions are the physical conditions that variables should meet on the computational boundary, which can be divided into the following categories:

- Fluid inlet and outlet parameters: including inlet and outlet pressure, speed, and mass flow, etc.
- Surface boundary conditions: including parameters or equations at the outer boundary of the calculation domain and the solid walls within the calculation domain.
- Internal unit partition: including fluid partition and solid partition.

Determination of boundary conditions depends on actual engineering problems or design requirements so that a desired fluid flow prediction result can be obtained. If the spatial distribution of VOC concentration is going to be evaluated, input parameters of source and sink are also needed.

Model Output and Analysis of Typical Cases

Output parameters of CFD models include airflow velocity, temperature, pressure, and pollutant concentration, etc. The various types of output parameters and detailed spatial distributions provide designers with more useful information than single-zone mass balance models. Such an advantage makes CFD methods welcomed in IAQ design where spatial distributions of pollutants are of concern.

An important application of the CFD model is to design airflow patterns, usually by means of mechanical ventilation. Normal airflow modes include mixing ventilation, displacement ventilation, stratum ventilation, and personalized ventilation, etc. Zhang et al. (2020) compared the effect of mixing ventilation (Fig. 15a) and displacement ventilation (Fig. 15b) on the removal of formaldehyde in the office. CFD simulation results show the formaldehyde concentration is relatively uniform in the room with the ceiling-supply and floor-exhaust mixing ventilation, which may cause the cross mixing of airborne contaminants. In contrast, formaldehyde concentration is stratified by floor-supply and ceiling-exhaust displacement ventilation, with a relatively low concentration in the seated occupational zone and a high concentration near the ceiling. Such concentration stratification is very helpful for reducing airborne pollutant exposure to the occupants. The high concentration near the ceiling also improves the pollutant exhaust efficiency. Therefore, if IAQ at the occupational zone is concerned, airflow design should refer to displacement ventilation rather than mixing ventilation. Note that, airflow design based on CFD simulation is particularly suitable for the occupied apartments or new buildings where the decorations have been completed.

Evaluation of personal exposure is another important use of CFD models. This is especially important for the prevention and control of respiratory infective diseases. Fig. 16 shows the simulation results of SARS-CoV-2 spread in a restaurant using the

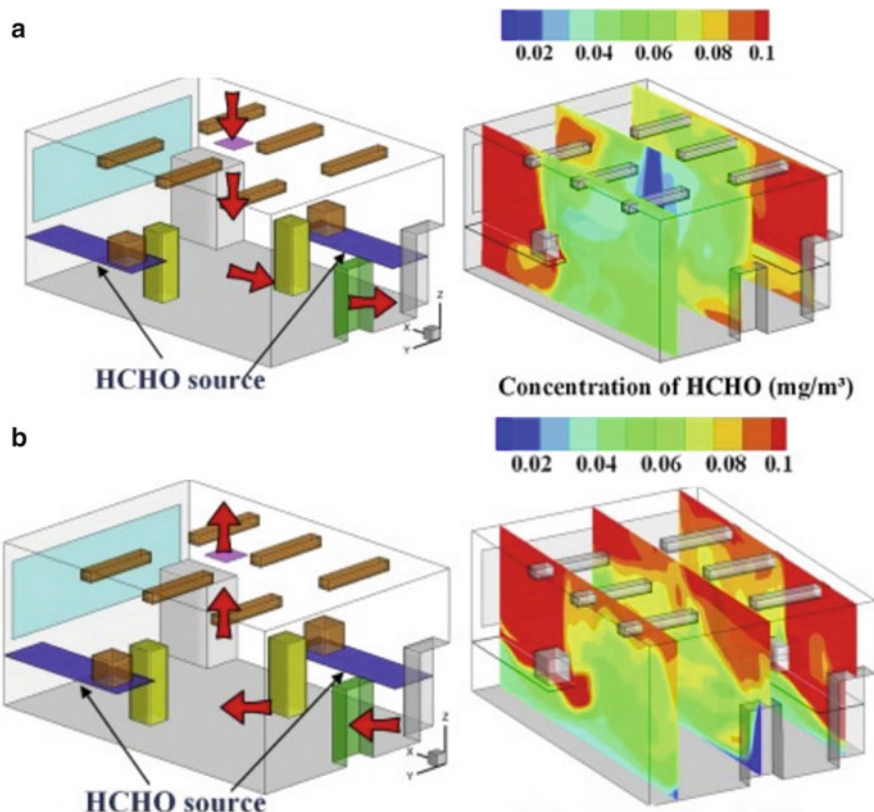
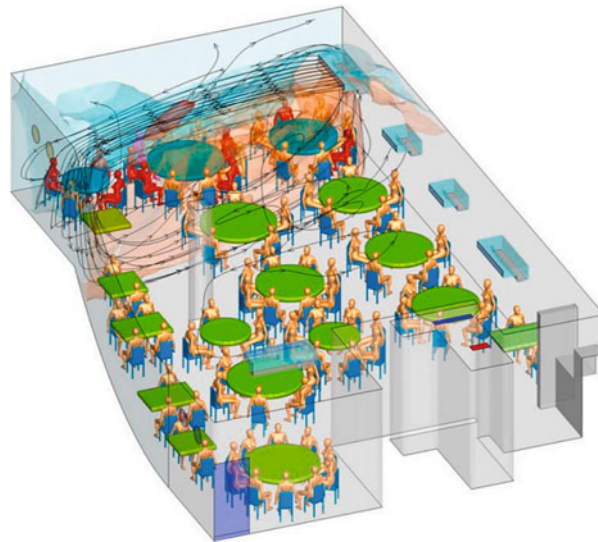


Fig. 15 Simulation of formaldehyde removal efficiency: (a) Mixing ventilation; (b) Displacement ventilation (Zhang et al. 2020)

CFD method (Li et al. 2021). A vortex zone is created due to the jet of the air conditioner. The virus is exhaled by the patients and then moves up to the vortex zone under the driven thermal plume. This will significantly increase the individual exposure of SARS-CoV-2 in the vortex zone. The model predicts that humans marked red color are possibly infected. Others, even in the same restaurant, have relatively low infection risk by staying away from the vortex zone. The model predictions successfully reproduced the SARS-CoV-2 infected event in a restaurant in Guangzhou. The good agreement between simulation and reality shows that the CFD model is capable of assessing individual exposure, which is of great significance for preventing the possible occurrence of respiratory infective diseases.

Compared with the single-zone mass balance model, the CFD models have the following advantages. CFD model predicts pollutant concentration at individual points in a room instead of the average concentration, which provides considerably more information for IAQ designers. More importantly, the CFD model considers the flow parameters of the bulk air when solving the equation, which means more robust and accurate prediction results. However, CFD models need to solve a set of

Fig. 16 The potential spread of coronavirus in a restaurant (Li et al. 2021)



partial differential equations instead of the ordinary differential equations, which requires significantly more computing power. It also requires good knowledge of the boundary conditions, which sometimes are difficult to obtain especially with regard to their spatial distributions (e.g., air velocity distribution across a diffuser outlet, spatial distribution of wall temperature). Therefore, the CFD method is more expensive. Besides, the abundant output will cost more time on results examination, and a high level of engineering background for the users is thus required.

Example Software Tools

With the improvement of CFD technology, more and more commercial software was developed to solve IAQ problems. Typical tools include Fluent, Phoenix, CFX, etc. (You et al. 2021; Stathopoulou and Assimakopoulos 2008; Majid et al. 2013).

Fluent

Fluent can simulate the complex flows ranged from incompressible fluid to highly compressible fluid, and therefore has a wide applying range. Uses include evaluation of the airflow efficiency for mechanical ventilation and natural ventilation, calculation of point pollutant concentrations, and assessment of individual exposure, etc. The programming language of the software is C++, which consumes less computer memory. Besides, Fluent contains advanced turbulence models, which can be used to analyze various engineering airflow problems. Moreover, Fluent adopts progressive solving methods and multi-grid convergent technologies, which significantly improve the prediction accuracy and calculation speed. Fluent has a user-friendly interface and provides a secondary input port for its users. This means that the

user-defined source and sink modules can be simultaneously solved in the Fluent program, and satisfy the individual needs to the greatest extent. These improvements enhance the competitiveness of Fluent in dealing with IAQ problems. Despite its indisputable strengths, strong engineering background, and a high level of computer skills are required for its users.

Phonics

Phonics is short for “Parabolic Hyperbolic Or Elliptic Numerical Integration Code Series,” and is the commercial software for computational fluid and computational heat transfer. Phonics provides three coordinate systems including right angles, cylinders, and spheres, which can analyze compressible or incompressible, single-phase or multi-phase, steady-state, or transient flow in three-dimensional space. Phonics has excellent openness, and allows users to modify the existing models or add new models in the software using the FORTRAN language. In addition, Phonics has good communications with external tools, such as the CAD program. Graphics files in the CAD can be directly imported into Phonics for use, which greatly facilitates the modeling process. Similar to Fluent, Phonics also contains a series of turbulence models, providing wide options for engineering problems.

CFX

CFX is a practical tool used to analyze flow problems in aerospace, energy, petrochemical industry, mechanical manufacturing, automobiles, biotechnology, water treatment, and environmental protection, etc. CFX uses the finite volume method to discretize the computational domain. Combined with the fully implicit and multi-grid coupled solving technology, both prediction accuracy and calculation speed of the software have greatly improved, but also consume more computer memory.

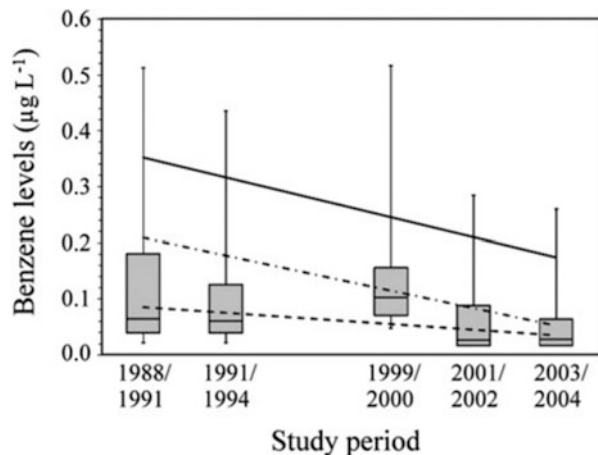
Data-Driven Models

Physical models are always trusted in IAQ design because they are developed based on the mass transfer mechanism. However, the physical model may suffer troubles in the following situations. One is that the mass transfer mechanism is too complicated or not well understood so that it is difficult to find a suitable mathematical description. Another is that the design process based on physical models is too time-consuming or expensive. In these situations, data-driven models become an alternative choice.

The data-driven model, also known as an empirical model or black-box model, is characterized by data causality and developed with advanced research or data collection. Data sources for this type of model can include actual measurement experience via laboratory tests or field investigations, available results from literature or reports, and even suggestions from the industry experts. Data used for this type of model is usually required to be large in quantity so that the potential associations behind the data can be discovered. Statistical analyses are also needed to give a correct mathematical expression.

Su et al. (2011) analyzed toluene personal exposures in the United States using the data-driven model. Data in the research come from the National Health and

Fig. 17 Box plot of benzene concentrations showing 0.05, 0.25, 0.50, 0.75 and 0.95 quantiles for each NHANES cohort. Linear QR trend lines for 0.5, 0.75, and 0.95 quantiles are shown as dashed, dashed and dotted, and solid lines, respectively (Su et al. 2011)



Nutrition Examination Survey (NHANES), which has collected tens of thousands of samples in 15 years. Figure 17 is a box diagram of toluene exposure, showing 0.05, 0.25, 0.50, 0.75 and 0.95 quantile distributions. The investigations show that overall toluene exposure decreases over time. Further, the statistical analysis found that 0.5, 0.75, and 0.95 quantiles follow a linearly decreasing trend, and corresponding mathematical equations are then provided. With these regressed mathematical equations, toluene individual exposures can be approximately estimated in the next few years. The prediction can help to improve policies or national standards and are of great significance for maintaining a safe exposure to indoor pollutants.

The data-driven model is more user-friendly compared with the physical model. Its development is independent of pollutant mass transfer mechanism, and thus has a lower requirement for professional skills. However, a data-driven model cannot provide insight into the physical processes, making it incapable of discovering some general conclusions. In addition, the data-driven model does not allow separation of influencing factors (sources, sinks, and ventilation, etc.), and special attention should be paid when the result scaling from one situation to another (from environmental chamber to actual buildings). Moreover, a data-driven model performs its best when large quantities of high-precision data are provided, which undoubtedly have more rigorous requirements for the data source.

Conclusions and Future Perspectives

Conclusions

This chapter introduces the performance-based IAQ control method that is based on modeling and simulation to accurately predict indoor air pollution characteristics at the design stage. It enables early intervention to prevent the possible occurrence of indoor air pollution. This performance-based approach is conducted without the

expense of large field experiments, and thus could prevent indoor air pollution in a time- and cost-effective way. The successful implementation of this method relies on models, which are built upon physical mechanism or experimental data to accurately predict the behavior of pollutants under key influencing factors including source, sink, ventilation, temperature, and humidity. For IAQ problems, commonly used models include physics-based and data-driven models.

The physics-based models include the single-zone, multi-zone, and CFD model. Single-zone and multi-zone models can provide the tools best suited for studying general IAQ problems in offices or residences with limited interior volumes. These models have an easy-to-understand mechanism. The numerical solution is recommended because of the complex differential equations for source and sink. A typical engineering case has confirmed that the mass balance model can give good predictions even under complex environmental conditions.

When indoor airflow characteristics or personal exposures are desired, the CFD model is a good choice. CFD model usually works together with the source and sink models in an IAQ problem. The numerical solution has become the only option due to the extremely complex mathematical expression of the Navier-Stokes equation. CFD model can provide point concentration rather than average concentration. Such an improvement makes it welcomed for local IAQ control or personal exposure assessment.

The data-driven model is independent of physical mechanisms and is developed upon abundant available data. Normally, statistical analysis is a good assistant for the data-driven model, which can help extract a mathematical description. A data-driven model is often simple and easy to use. If the data is sufficient and credible enough, the data-driven model can be tried in any type of buildings. However, the lack of communication with the mass transfer mechanism limits the flexibility of the data-driven model in data transfer, and a non-negligible deviation may be introduced once the environmental conditions are different. In this regard, the data-driven model is not as robust and scalable as the physics-based model.

Future Perspectives

Although the performance-based method based on modeling and simulation has been proved to be able to prevent possible air pollution, a lot more efforts are still required to make IAQ simulations readily useful in actual engineering applications, including:

Various Source Emission Models

With the improvement of living standards, more types of building materials may be installed indoors to satisfy the occupants' yearning for a comfortable life. The corresponding source emission model should be developed so that the pollutant transmitted behavior within buildings can be accurately predicted. This chapter has limited the discussion to primary emissions from building materials and furnishings. Emissions from occupant activities and secondary emissions due to chemical

reactions (e.g., ozone initiated indoor air and surface chemistry) should also be considered in the future.

Health Effect

Since different pollutants may have various effects on health even if they have the same concentration levels, and a health index of individual compounds and their interactions should be considered.

Occupant Behavior

Humans can be considered an important part of buildings. On the one hand, occupant behaviors can determine IAQ. On the other hand, the IAQ could influence occupant behaviors. The interrelation between occupant behaviors and IAQ needs to be considered.

Smart Sensors and Big Data

On-line air pollutant monitoring technology should be considered, which provides an extended “eye” to reach out to remote sites at a larger scale and collecting “big data.” Advanced simulation technologies combining these online monitors provide an effective tool to predict the indoor contaminant levels and optimize the control strategies.

Various Control Strategies

In terms of the new building, source control may be the most effective way to prevent air pollution. However, this strategy may face limitations in buildings where the interior decoration has been finished. In such cases, the focus may be paid to comprehensive control strategies combining source control, ventilation, and air cleaning.

Combined IAQ and Energy Modeling and Simulations

This chapter has focused on modeling and simulation of pollutant concentrations in buildings. As IAQ and energy efficiency strategies can affect each other. Combined IAQ and energy modeling and simulation methods and tools need to be further developed to evaluate tradeoffs and devise most energy-efficient and cost-effective strategies for improving IAQ.

References

- Abdalla T, Peng C (2021) Evaluation of housing stock indoor air quality models: a review of data requirements and model performance. *J Build Eng* 43:102846
- Ahn J, Kim K, Kim Y et al (2015) Characterization of hazardous and odorous volatiles emitted from scented candles before lighting and when lit. *J Hazard Mater* 286:242–251
- Axley J (1991) Adsorption modeling for building contaminant dispersal analysis. *Indoor Air* 1: 147–171
- Baboli Z, Neisi N, Babaei A et al (2021) On the airborne transmission of SARS-CoV-2 and relationship with indoor conditions at a hospital. *Atmos Environ* 3:118563

- Bodalal A (1999) A fundamental study of volatile organic emissions from building materials. Ph.D. Thesis, Carleton University. Ottawa
- Caron F, Guichard R, Robert L et al (2020) Behavior of individual VOCs in indoor environments: how ventilation affects emission from materials. *Atmos Environ* 234:117713
- Chen Y, Gu L, Zhang J (2015) EnergyPlus and CHAMPS-Multizone co-simulation for energy and indoor air quality analysis. *Build Simul* 8:371–380
- Cheng L, Wang X (1997) Numerical simulation of junction flow by an RNG K-E model
- Dols S, Walton G (2002) CONTAMW 2.0 user manual
- Dong H, Dong H, Seong Y et al (2013) A numerical simulation of VOC emission and sorption behaviors of adhesive-bonded materials under floor heating condition. *Build Environ* 68: 193–201
- Dunn J, Chen T (1993) Critical evaluation of the diffusion hypothesis in the theory of porous media VOC sources and sinks. In: Modeling Indoor Air Quality and Exposure, ASTM STP-1205. American Society of Testing and Materials, Philadelphia, pp 64–80
- Feustel H (1999) COMIS – an international multizone air-flow and contaminant transport model. *Energ Buildings* 30:3–18
- Filho B, Silva G, Boaventura R et al (2019) Ozonation and ozone-enhanced photocatalysis for VOC removal from air streams: process optimization, synergy and mechanism assessment. *Sci Total Environ* 687:1357–1368
- GB/T 18883-2002 (2002) Indoor Air Quality Standard; Chinese National Standard. [in Chinese]
- Guo Z (2000) Simulation tool kit for indoor air quality and inhalation exposure (IAQX) version 1.0. United States Environmental Protection Agency
- Guo Z, Tichenor B (1992) Fundamental mass transfer models applied to evaluating the emissions of vapor-phase organics from interior architectural coatings. Proceedings of EPA/AWMA Symposium, Durham
- Han K, Zhang J, Guo B (2014) A novel approach of integrating ventilation and air cleaning for sustainable and healthy office environments. *Energ Buildings* 76:32–42
- He J, Lv M, Yang X (2019a) A one-dimensional VOC emission model of moisture-dominated cure adhesives. *Build Environ* 156:171–177
- He J, Zou Z, Yang X (2019b) Measuring whole-body volatile organic compound emission by humans: a pilot study using an air-tight environmental chamber. *Build Environ* 153:101–109
- Hu H, Zhang Y, Wang X et al (2007) An analytical mass transfer model for predicting VOC emissions from multi-layered building materials with convective surfaces on both sides. *Int J Heat Mass Transf* 50:2069–2077
- Huang H, Haghigat F (2002) Modelling of volatile organic compounds emission from dry building materials. *Build Environ* 37:1349–1360
- JGJ/T 436-2018 (2018) Specifications for Indoor Decoration Pollution Control in Residential Buildings; [in Chinese]
- Jia L, Chu J, Li J et al (2020) Formaldehyde and VOC emissions from plywood panels bonded with bio-oil phenolic resins. *Environ Pollut* 263:114819
- Jiang Y, Zhao B, Li X et al (2010) Investigating a safe ventilation rate for the prevention of indoor SARS transmission: an attempt based on a simulation approach. *Build Simul* 3:179–179
- Kabirikopaei A, Lau J (2020) Uncertainty analysis of various CO₂-based tracer-gas methods for estimating seasonal ventilation rates in classrooms with different mechanical systems. *Build Environ* 197:107003
- Katsogiannis A, Leva P, Kotzias D (2008) VOC and carbonyl emissions from carpets: a comparative study using four types of environmental chambers. *J Hazard Mater* 152:669–676
- Koontz M, Nagda N (1991) A multichamber model for assessing consumer inhalation exposure. (605):593–605
- Kumar D, Little J (2003) Characterizing the source/sink behavior of double-layer building materials. *Atmos Environ* 37:5529–5537
- Lai D, Qi Y, Liu J et al (2018) Ventilation behavior in residential buildings with mechanical ventilation systems across different climate zones in China. *Build Environ* 143:679–690

- Lee S, Lam S, Fai H (2001) Characterization of VOCs, ozone, and PM10 emissions from office equipment in an environmental chamber. *Build Environ* 36:837–842
- Hal L (2016) Preventing indoor environmental problems. *Indoor Air Quality Handbook* Chapter 60. 1–21
- Li H, Zhang J, Yang M (2005) Measurement and modeling of VOC emissions from a large wall assembly of typical wood-framed residential houses. *Trans ASHRAE* 112
- Li Y, Qian H, Hang J et al (2021) Probable airborne transmission of SARS-CoV-2 in a poorly ventilated restaurant. *Build Environ* 196:107788
- Liang W (2015) VOC Pre-assessment modeling and application in real buildings. Ph.D. Thesis, Tsinghua University. [in Chinese]
- Liang W, Gao P, Guan J et al (2012) Modeling volatile organic compound (VOC) concentrations due to material emissions in a real residential unit. Part I: methodology and a preliminary case study. *Build Simul* 5:351–357
- Liang W, Chao W, Yang C et al (2014) Volatile organic compounds in different interior construction stages of an apartment. *Build Environ* 81:380–387
- Liang W, Yang S, Yang X (2015) Long-term formaldehyde emissions from medium-density fiberboard in a full-scale experimental room: emission characteristics and the effects of temperature and humidity. *Environ Sci Technol* 49:10349–10356
- Liang W, Lv M, Yang X (2016) The combined effects of temperature and humidity on initial emittable formaldehyde concentration of a medium-density fiberboard. *Build Environ* 98:80–88
- Liang W, Yang X, Chen F et al (2017) A pre-assessment and control tool for indoor air quality (PACT-IAQ) simulation in actual buildings. *Proc Eng* 205:219–225
- Liang W, Lv M, Yang X (2021) Development of a physics-based model for analyzing formaldehyde emissions from building material under coupling effects of temperature and humidity. *Build Environ* 203:108078
- Little J, Hodgson A (1996) A strategy for characterizing homogeneous, diffusion-controlled, indoor sources and sinks. In: *Characterizing Sources of Indoor Air Pollution and Related Sink Effects*, Vol. ASTM STP-1287. American Society of Testing and Materials, Philadelphia, pp 294–304
- Little J, Hodgson A, Gadgil A (1994) Modeling emissions of volatile organic compounds from new carpets. *Atmos Environ* 28:227–234
- Long K, Lidia M, Tran N et al (2021) The impact of incense burning on indoor PM 2.5 concentrations in residential houses in Hanoi, Vietnam. *Build Environ* 205:108228
- Lv M, Yang X (2019) Improving material selection for residences using volatile organic compound simulation at design stage: field verifications from a unique case study. *Build Environ* 157:277–283
- Magee R, Bodalal A, Biesenthal T, et al (2002) Prediction of VOC concentration profiles in a newly constructed house using samll chamber data and an IAQ simulation program. 9th international conference on IAQ and climate, pp 298–303
- Majid A, Yan C, Sun Z et al (2013) CFD simulation of dust particle removal efficiency of a venturi scrubber in CFX. *Nucl Eng Des* 256:169–177
- Obermeier F (2010) Prandtl's mixing length model – revisited. *PAMM* 6:577–578
- Paciорri R, Sabetta F (2003) Compressibility correction for the Spalart-Allmaras model in free-shear flows. *J Spacecr Rocket* 40:326–331
- Pan W, Liu S, Wang Y et al (2019) Measurement of cross-ventilation rate in urban multi-zone dwellings. *Build Environ* 158:51–59
- Paterson C, Sharpe R, Taylor T et al (2021) Indoor PM2.5, VOCs and asthma outcomes: a systematic review in adults and their home environments. *Environ Res* 202:111631
- Pei J, Ji L (2018) Secondary VOCs emission from used fibrous filters in portable air cleaners and ventilation systems. *Build Environ* 142:464–471
- Pei J, Zhang J (2010) Modeling of sorbent based gas filters: development, verification and experimental validation. *Build Simul* 3:75–86
- Pei J, Zhang J (2011) On the performance and mechanisms of formaldehyde removal by chemisorbents. *Chem Eng J* 167:59–66

- Pentigny N, Zhang J, Elliott H et al (2021) Indoor air depolluting material: combining sorption testing and modeling to predict product's service life in real conditions. *Build Environ* 202: 107838
- Philip D (2016) Modeling IAQ and building dynamic. *Indoor Air Quality Handbook* Chapter 57. 1–21
- Reardon J, Zhang J (1995) A comparison of three models of air infiltration in houses against field measurement. Second international conference on indoor air quality, ventilation and energy conservation in buildings, Montréal, pp 377–384
- Remion G, Moujalled B, Mankibi M (2020) Dynamic measurement of the airflow rate in a two-zones dwelling, from the CO₂ tracer gas-decay method using the Kalman filter. *Build Environ* 188:107493
- Saoud W, Assadi A, Kane A et al (2019) Integrated process for the removal of indoor VOCs from food industry manufacturing: elimination of Butane-2,3-dione and Heptan-2-one by cold plasma-photocatalysis combination. *J Photochem Photobiol A Chem* 386:112071
- Shen J, Meng K, Bing D et al (2021) Airborne transmission of SARS-CoV-2 in indoor environments: a comprehensive review. *Sci Technol Built Environ* 1977693
- Shi S, Chen C, Zhao B (2015) Air infiltration rate distributions of residences in Beijing. *Build Environ* 92:528–537
- Shin S, Jo W (2012) Volatile organic compound concentrations, emission rates, and source apportionment in newly-built apartments at pre-occupancy stage. *Chemosphere* 89:569–578
- Sokolowski J, Banks C (2010) *Modeling and Simulation Fundamentals (Theoretical Underpinnings and Practical Domains)*. 25–56
- Sparks L (1996) IAQ model for windows RISK version 1.0 user manual. U.S. Environmental Protection Agency, National Risks Management Research Laboratory, Research Triangle Park
- Sparks L (2016) Indoor air quality modeling. *Indoor Air Quality Handbook* Chapter 58. 1–21
- Stathopoulou O, Assimakopoulos V (2008) Numerical study of the indoor environmental conditions of a large athletic hall using the CFD code PHOENICS. *Environ Model Assess* 13:449–458
- Su F, Mukherjee B, Batterman S (2011) Trends of VOC exposures among a nationally representative sample: analysis of the NHANES 1988 through 2004 data sets. *Atmos Environ* (45):4858–4867
- Sun E, Hongguo L, Wang M (2017) Study on numerical simulation of ammonia leakage based on realizable k- ε turbulence model. *J Saf Sci Technol*
- Tang L, Liu M, Ren B et al (2022) Transmission in home environment associated with the second wave of COVID-19 pandemic in India. *Environ Res* 204:111910
- Thompson K, Hassan H (2015) Simulation of a variety of wings using a reynolds stress model. *Aiaa Atmospheric Flight Mechanics Conference*
- Walton G, Denton (2000) CONTAMW 10 user manual: multizone airflow and contaminant transport analysis software. National Institute of Standards and Technology (U.S.)
- Wang X, Zhang Y, Zhao R (2006) Study on characteristics of double surface VOC emissions from dry flat-plate building materials. *Chin Sci Bull* 51:2287–2293
- Wei F, Zhu F, Lv H (2011) The use of 3D simulation system in mine ventilation management. *Proc Eng* 26:1370–1379
- Wei F, Grunewald J, Nicolai A et al (2012) CHAMPS-multizone – a combined heat, air, moisture and pollutant simulation environment for whole building performance analysis. *HVAC&R Res* 18:1–2
- Weschler C, Nazaroff W (2012) SVOC exposure indoors: fresh look at dermal pathways. *Indoor Air* 22:356–377
- Woldekidan K, Zhang J, Lu Y (2013) A novel energy efficient demand-based ventilation system for critical contaminant and overall IAQ control. *Proceedings of IAQ 2013: environmental health in low energy buildings*, Vancouver
- Won D (2008) IA-QUEST (indoor air quality emission simulation tool). National Research Council Canada
- Won D, Sander D, Shaw C et al (2001) Validation of the surface sink model for sorptive interactions between VOCs and indoor materials. *Atmos Environ* 35:4479–4488

- Wu J, Weng W (2021) COVID-19 virus released from larynx might cause a higher exposure dose in indoor environment. Environ Res 199:111361
- Xu Y, Zhang Y (2003) An improved mass transfer-based model for analyzing VOC emissions from building materials. Atmos Environ 37:2497–2505
- Xu T, Zheng H, Zhang P (2018) Performance of an innovative VUV-PCO purifier with nanoporous TiO₂ film for simultaneous elimination of VOCs and by-product ozone in indoor air. Build Environ 142:379–387
- Yang X (1999) Study of building material emissions and indoor air quality. Ph.D Thesis Massachusetts Institute of Technology, September
- Yang X, Chen Q, Zhang J et al (2001) A mass transfer model for simulating VOC sorption on building materials. Atmos Environ 35:1291–1299
- Yang K, Teng M, Luo Y et al (2020) Human activities and the natural environment have induced changes in the PM2.5 concentrations in Yunnan Province, China, over the past 19 year. Environ Pollut 265:114878
- You Y, Wang S, Lv W et al (2021) A CFD model of frost formation based on dynamic meshes technique via secondary development of ANSYS fluent. Int J Heat Fluid Flow 89:108807
- Zhang J (1999) MEDB-IAQ user's manual and software. CMEIAQ report 4.3. IRC/NRC, Ottawa
- Zhang J (2005) Combined heat, air, moisture, and pollutants transport in building environmental systems. JSME Int J 48:182–190
- Zhang J, Chen Q (2002) Effects of environmental conditions on the VOC sorption by building materials – Part I: experimental results. Trans ASHRAE 108:273–282
- Zhang J, Chen Q (2003) Effects of environmental conditions on the VOC sorption by building materials – Part II: model evaluations. Trans ASHRAE 109
- Zhang J, Shaw C (1999) MEDB-IAQ: material emission database and a single-zone IAQ model – a tool for building designers, engineers and managers. CMEIAQ report 4.2. IRC/NRC, Ottawa
- Zhang J, Nong G, Shaw C et al (1998) Measurements of volatile organic compound (VOC) emissions from wood stains using an electronic balance. ASHRAE Trans 105:279–288
- Zhang J, Shaw C, Yan A (1999a) MEDB-IAQ: a material emission database and indoor air quality simulation program. 8th international conference on indoor air quality and climate, Edinburgh, pp 1–6
- Zhang J, Zhu J, Shaw C et al (1999b) Models for predicting volatile organic compound (VOC) emissions from building materials. CMEIAQ report 3.1. IRC/NRC, Ottawa
- Zhang J, Chen Q, Yang X (2002) A critical review on VOC sorption models. Trans ASHRAE 108: 162–174
- Zhang J, Mohan C, Varshney P et al (2005) Coupling of airflow and pollutant dispersion models with evacuation planning algorithms for building system controls. Trans ASHRAE 112
- Zhang R, Lam K, Yao S et al (2013) Coupled EnergyPlus and computational fluid dynamics simulation for natural ventilation. Build Environ 68:100–113
- Zhang X, Cao J, Wei J et al (2018) Improved C-history method for rapidly and accurately measuring the characteristic parameters of formaldehyde/VOCs emitted from building materials. Build Environ 143:570–578
- Zhang T, Li X, Rao Y et al (2020) Removal of formaldehyde in urban office building by the integration of ventilation and photocatalyst-coated window. Sustain Cities Soc 55:102050
- Zhu X, Lv M, Yang X (2018) Performance of sorption-based portable air cleaners in formaldehyde removal: laboratory tests and field verification. Build Environ 136:177–184
- Zhu X, Lv M, Yang X (2019a) A predictive model for the formaldehyde removal performance of sorption-based portable air cleaners with pleated composite filter. Build Environ 147:517–527
- Zhu X, Lv M, Yang X (2019b) A test-based method for estimating the service life of adsorptive portable air cleaners in removing indoor formaldehyde. Build Environ 154:89–96
- Zhuang C, Shan K, Wang S (2021) Coordinated demand-controlled ventilation strategy for energy-efficient operation in multi-zone cleanroom air-conditioning systems. Build Environ 191: 107588

Part XII

Air Quality in Various Indoor Environments



Indoor Air Quality in Day-Care Centers

63

Shuo Zhang, Elizabeth Cooper, Samuel Stamp, Katherine Curran,
and Dejan Mumovic

Contents

Introduction	1858
Building Typologies	1859
Occupancy	1860
Function/Uses of Space in Day-Care Centers	1861
Air Temperature and Relative Humidity	1862
Ventilation	1864
Air Cleaning	1866
Indoor Air Pollutants	1868
NO ₂	1868
Carbon Monoxide (CO)	1869
Ozone (O ₃)	1870
Allergens	1871
Particulate Matter	1872
Infectious Diseases	1875
Dampness and Mold	1877
VOCs	1878
Radon	1880
Emerging Hazards	1880
Conclusions	1881
Cross-References	1883
References	1883

S. Zhang · E. Cooper (✉) · S. Stamp · D. Mumovic

Institute for Environmental Design and Engineering, University College London, London, UK
e-mail: ucbqsz0@ucl.ac.uk; elizabeth.l.cooper@ucl.ac.uk; samuel.stamp@ucl.ac.uk;
d.mumovic@ucl.ac.uk

K. Curran

Institute for Sustainable Heritage, University College London, London, UK
e-mail: k.curran@ucl.ac.uk

Abstract

Considering the alarming rise in the rate of asthma and respiratory diseases among school children, it is of great importance to investigate all probable causes. Outside of the home, children spend most of their time in school. Many studies have researched the indoor air quality of elementary and secondary school buildings to determine the exposure of school children to indoor air pollution. However, studies of exposures to very young children in day-care centers are scarce. Unlike at elementary schools or universities, children in day-care centers are more vulnerable due to their physiology, inability to articulate discomfort, or to adapt their behavior to avoid exposures. This chapter reviews current studies on the indoor environment in day-care centers. It summarizes air pollution levels and related environmental and behavioral factors in day-care centers that have been reported in the literature. Additionally, exposure to indoor air pollution and related potential health outcomes are examined. This chapter concludes that indoor air pollution in day-care centers often exceeds current guidelines, and designers and policymakers should be made aware of the impact on the health and wellbeing of children in day-care centers. Proper interventions and guidelines should be considered to create a healthy indoor environment for children in day-care centers.

Keywords

Indoor air quality (IAQ) · Day-care center · Health impacts

Introduction

Day-care centers, also called kindergartens, nurseries, or preschools, offer children from 6 weeks to 6 years old daily care and early education before they attend elementary school. The age ranges of the children who attend day-care centers vary internationally. Day-care centers are not categorized by a specific building type. The variety and complexity of building characteristics pose a challenge when trying to assess the indoor air quality in a comprehensive and cohesive way. Some day-care centers are purpose-built structures, while others are repurposed commercial or residential buildings. Compared to the uses for which these retrofitted buildings were designed, day-care center classrooms tend to have higher occupant densities (Singh et al. 2019), which can make the indoor environment in day-care centers worse due to inadequate ventilation to meet the occupant load.

Children, especially those under 6 years old, are more vulnerable than adults to environmental pollutants because their immune and respiratory systems are not fully developed. Children have a larger surface area to volume ratio; and a faster rate of respiration. Furthermore, children spend more time indoors, averaging 7–11 h/weekday in classrooms alone (Almeida et al. 2011). It has been shown that indoor air pollutants have the potential to damage children's central nervous systems

(Calderón-Garcidueñas et al. 2014) and that exposure to air pollutants before the age of 1 year may contribute to the development of childhood asthma (Deng et al. 2015). The evidence that has been gathered for these observed outcomes has been primarily focused on offices and residential buildings. What research there is on schools tends to be on elementary and secondary schools. There is a substantial and important lack of data and guidance about the indoor air quality of day-care centers.

A lack in evidence is compounded by a large range in types of buildings, their activities, and occupancy. Context changes drastically between countries and education systems. Yet there are no large-scale studies to create a comprehensive picture. This gap in the research means there is significant difficulty in understanding underlying trends and key factors influencing IAQ in day-care centers. Many published findings are contradictory or inconsistent, in part due to the difficulties of monitoring and comparing across different measuring periods, climates, countries, and building characteristics.

Studies focusing on indoor air quality in nursery environments were conducted in Europe, including Portugal, France, and Poland, as well as in South Korea, Singapore, and Canada. Only a few studies were available from developing countries. Many studies focused solely on a single parameter of indoor air quality. Temperature, humidity, CO₂, particulate matter (PM), and volatile organic compounds (VOCs) were the parameters most often studied. The number of nurseries monitored varied from 1 to 310, and classroom sizes also varied between studies. Most of the investigated classrooms were naturally ventilated, and the age of children was mainly older than 3 years. For studies conducted in a location with a varied climate, few included any observed seasonal differences. Most studies only measured for 1 day during occupied hours. Few studies measured for more than 1 day, and for those that did the measurement periods lasted from 2 to 9 days. The environmental monitoring methods used in the studies also varied between studies.

This chapter documents the state-of-the-art in research on the indoor air quality of day-care centers. The aims of this chapter are: first, to explore the perception of thermal comfort of children in day-care centers; second, to describe current ventilation strategies in day-care centers; third, to identify the type and scale of exposure of children to pollutants in day-care center environments. An extensive review of the literature on IAQ in day-care centers can be found in Zhang et al. (2021). In the future, day-care centers should be designed and built with a comprehensive approach that integrates physical characteristics, occupant behavior patterns, and avoidance of harmful microbial and chemical exposures in their design and operation (Chatzidiakou et al. 2012).

Building Typologies

Day-care centers offer children from 6 weeks to 6 years old daily care and early education before they attend elementary schools. They can be either publicly funded and operated, or privately run. Dudek (2007) identifies three main design approaches for day-care centers. First, newly designed buildings which focus upon a strictly

codified room schedule. In this approach, a series of quasi-functional zones with predetermined floor areas are designed for a certain number of children. This approach is widely used, with the safety and security of children as its first concern. In the second approach, spaces in the day-care center are adapted for new forms of teaching. In this circumstance, architects may be inspired by the work of pedagogy, and spaces can keep changing to match the evolving curriculum. The third is a child-orientated design approach. This approach is more subjective and may be driven by architects' personal experiences of childhood (Dudek 2007).

Within the published IAQ research, day-care centers were categorized based on different factors including their location (urban or rural day-care centers), and the type of ventilation used (naturally or mechanically ventilated). Other factors that can impact IAQ are the types of building and furniture material provided, cleaning and personal care products used, and classroom activities (such as arts and crafts). These and other influencing factors will be discussed later in the chapter.

Occupancy

While practices vary substantially, day-care centers typically offer early education for children under 6 years old, with children often grouped by age and allocated to different grades. Normally, there are three categories: infants less than 1-year-old, toddlers between the ages of 1 and 3, and children older than 3 years. As over-crowded classrooms are associated with high indoor air pollutant concentrations, proper child/staff ratios and floor space per child are often a requirement of local governments/authorities (Table 1).

Table 1 Recommended child/staff ratio and floor space per child

Age	Maximum child: staff ratio		Indoor space requirements US ^a	UK ^b
	US ^a	UK ^b		
≤12 months	3:1	3:1	42 sq. ft (3.9 m^2) of usable floor space per child; 50 sq. ft (4.6 m^2) per child is preferred	$3.5\text{ m}^2/\text{child}$
1-year-olds	4:1	3:1		$3.5\text{ m}^2/\text{child}$
2-year-olds	4:1	3:1		$2.5\text{ m}^2/\text{child}$
3-year-olds	7:1	8:1		$2.3\text{ m}^2/\text{child}$
4-year-olds	8:1	8:1		$2.3\text{ m}^2/\text{child}$
5-year-olds	8:1	8:1		$2.3\text{ m}^2/\text{child}$

^aRecommended by National Resource Center for Health and Safety in Child Care and Early Education, USA

^bRecommended by Department for Education, UK

Typical operating hours of day-care centers are around 9:00 am to 3:00 pm, Monday to Friday except for holidays. Opening hours can vary for different day-care centers. Studies have demonstrated that occupants have a significant influence on IAQ. One study reported that the PM concentrations in a day-care center started to rise from the beginning of the occupancy period and started decreasing after the end of the occupancy period (Branco et al. 2014). Another study reported an average PM_{10} level of 97.0 $\mu\text{g}/\text{m}^3$ during the occupied period and 58.2 $\mu\text{g}/\text{m}^3$ during the unoccupied period, and the PM_{10} concentrations were much higher when children were entering or leaving the classroom (Alves et al. 2013). Based on their conclusions, the rise in indoor PM levels are most likely caused by resuspension (Resuspension is covered in depth in ► Chap. 12, “Resuspension,” in this book by Ferro) and other internal activities.

The activities in day-care centers, and the corresponding effects, need further study. The table below (Table 2) shows the arrangement of the school day of a typical day-care center in the UK. The time periods for different activities are comparatively shorter than for elementary schools or higher institutions. The high frequency of activity changes may make it difficult for researchers to trace the associations between occupant activities and change in indoor air quality.

Function/Uses of Space in Day-Care Centers

In general, the main spaces of a day-care center include baby home bases (4 months to 2 year-olds), toddler home bases (2–3 year-olds), pre-school home bases (3–4 year-olds), garden, toilets, kitchen, laundry, staffrooms, storage, reception,

Table 2 Typical schedule of a day-care-center in the UK

Time (AM)	Activity	Time (PM)
Half day		
8:30	Children Arrive	12:15
8:45	Free flow & focus activity inside/outside	12:30
10:20	Snack time	2:00
10:45	Tidy up time	2:30
10:55	Group time	2:40
11:10	Singing Goodbye song	2:55
11:15	Home time	3:00
Full day		
8:30	Welcome	Settle in from lunch
9:00	Dialogic reading group	Dialogic group time
9:20	Snack within group	Free flow and focus time
9:30	Free flow and focus time	Tidy
10:55	Tidy	Snack within group
11:10	Group time	Group time
11:30	Children's lunch	Home time

manager's office, medical room, and external facilities (Dudek 2013). Home bases are the most commonly used space in the day-care center, where children spend most of their time. There are many functions of home bases, e.g., for sleeping, learning, and playing.

One thing that sets day-care centers apart from other education buildings is the predominance of sleeping as a daily activity. Day-care centers typically have either sleeping-only rooms or offer mattresses for children to sleep on in the classroom. In Poland, a study measured two classrooms in one day-care center and found the highest CO₂ concentrations were measured in the afternoon nap time at the classroom of younger children (Mainka et al. 2015a). A similar conclusion was also reported by a study in the USA. Ferng and Lee (2002) found a high CO₂ concentration in sleeping-only rooms (a closed space without enough ventilation). Additional analysis of the relationship between the CO₂ peaks and sleeping activity was not provided. However, one explanation is that windows tend to be closed during naptime to keep the noise level down which leads to insufficient ventilation. More research is needed to further explain these findings.

The age of occupants is another element that may affect IAQ performance. In general, classrooms with older children tend to have higher PM levels. In Portugal, a study concluded that classrooms occupied by older children had the highest PM concentrations due to their greater mobility (increasing PM resuspension) when compared with the classrooms of younger children (Branco et al. 2014). Another study with a similar conclusion reported that PM (PM₁, PM_{2.5}, PM₁₀, and TSP) concentrations were higher in older children's (5–6 years old) classrooms due to the intensive activities of older children (Mainka and Zajusz-Zubek 2015).

Children's activities during classes are also important sources of pollutants in day-care centers (PMs, VOCs, etc.). Activities like painting, sculpting, other arts and crafts activities, and the use of do-it-yourself products may have an effect on air quality (Morawska et al. 2009; Fonseca et al. 2014). Additionally, some staff activities should also be noted. For example, high PM concentrations were reported during cleaning and cooking activities (Alves et al. 2013; Branco et al. 2014). In Portugal, a study concluded that canteens had the highest ultra-fine particulate matter (UFP) concentrations (especially during the children's lunch time) as they were connected to the kitchens using gas-fueled appliances for cooking (Fonseca et al. 2014). Cleaning solvents may also be the source of air pollutants, e.g., toluene, xylenes, and other VOCs (Mainka et al. 2018).

Air Temperature and Relative Humidity

According to ASHRAE (American Society of Heating, Refrigeration and Air Conditioning Engineers), Standard 55-2017, the recommended indoor temperature range for buildings in general is around 19–27 °C, and the recommended indoor relative humidity is between 30% and 60% (EPA 2012). Several studies from across the globe have measured the indoor air temperature and relative humidity in day-care centers and compared the results with current guidelines. Temperature and relative

humidity in most day-care centers lie within the comfort range. However, some studies reported thermal conditions outside this range (Daneault et al. 1992; Ruotsalainen et al. 1993; Zuraimi and Tham 2008; Kamaruzzaman and Razak 2011; Roda et al. 2011; St-Jean et al. 2012; Branco et al. 2015a; Zender-Swiercz and Telejko 2019).

One study measuring four day-care centers in Portugal reported a situation with lower temperature and higher relative humidity values compared with the guidelines recommended by ASHRAE. These conditions may be due to a poorly constructed or ageing building (e.g., insufficient thermal insulation and water intrusion), and the inappropriate use of heaters or air conditioning systems (Branco et al. 2015b). Another study investigated 26 day-care centers in the western United States. They reported that 42% of the monitored day-care centers were outside of the temperature comfort zone (34.6% lower and 7.7% higher), and during naptime, 26.1% of the day-care centers had a higher relative humidity than the comfort zone (Ferng and Lee 2002). In Poland, a study found high indoor temperatures, ranging from 24.0 °C to 29.6 °C during the daytime. The author explained this situation as the overheating due to reduced heat loss following increased insulation (Zender-Swiercz and Telejko 2019).

In addition to collecting temperature and relative humidity data from day-care centers, researchers assessed the thermal comfort of the children. Fanger's model is typically used to evaluate thermal comfort in school classrooms (Fanger 1973). It includes two indices, which are: Predicted Mean Vote (PMV) and Predicted Percentage of Dissatisfied (PPD). Adaptive models have also been developed to evaluate naturally ventilated buildings. These models adjust for occupant behavior, physiological, and psychological factors (Conceição et al. 2012). However, studies addressing thermal comfort of children in day-care centers are scarce, and it is difficult to get accurate feedback from children using traditional methods like questionnaires and interviews. Children have higher metabolic rates than adults, and when they are dissatisfied with the thermal conditions, they do not necessarily behave like adults to adapt to the environment (e.g., take off/add clothes, open/close windows). One study did focus on the thermal comfort of day-care centers in winter and spring (Mendes et al. 2014). They reported PMV between "neutral" (0) and "slightly cool" (≤ -1), on the thermal sensation scale. In Japan, Yoshida et al. (2000) used an indirect method of assessment by administering a questionnaire to teachers and observing the thermal responses of disabled day-care center children. They reported that about 40% of the children had thermo-regulatory disorders. Another study reported that children prefer lower temperatures (about 3 °C lower) than adults and girls prefer temperature about 1 °C lower than boys of day-care center age (Yun et al. 2014).

In summary, temperature and humidity are important elements in the study of indoor air quality. It has been well demonstrated that temperature and humidity have a strong influence on the perception of indoor air quality and on volatilization of chemicals used indoors (Fang et al. 1998, 2004; Haghhighat and De Bellis 1998). Notably, according to the available studies, day-care centers generally performed within temperature and relative humidity guidelines.

Ventilation

Ventilation moves outdoor air into a space to replace indoor air. It can be categorized into three types: mechanical ventilation, natural ventilation, and hybrid (or mixed-mode) ventilation. Natural ventilation can provide a high air-change rates at a low cost, but it is affected by the outdoor environment and might introduce other problems, such as outdoor air pollution, noise, and security issues. With mechanical ventilation, temperature, relative humidity, and air flow rate can be easily controlled, but limitations are maintenance and energy use. In most reported studies, the classrooms in day-care centers were naturally ventilated, with mixed evidence on the advantages and dis-advantages of mechanically and naturally ventilated spaces. In Canada, a study investigated 21 day-care centers, and 18 of them had mechanical ventilation systems. They concluded that mechanical ventilation systems were significantly associated with lower indoor CO₂, formaldehyde, and acetaldehyde levels due to higher ventilation rates. However, in this same study, 85% of the classrooms had mean CO₂ levels that exceeded 1000 ppm, which indicated that many day-care centers have insufficient ventilation (St-Jean et al. 2012). In another study, 83 predominantly naturally ventilated rooms and 40 predominantly mechanically ventilated rooms in day-care centers were sampled. Here, indoor CO₂ and human-related bacteria levels were significantly lower in naturally ventilated rooms. The air exchange rates, O₃, and fungal concentrations were significantly lower in mechanically ventilated rooms (Zuraimi and Tham 2008).

The indoor concentration of CO₂ can be used as an indicator of ventilation rate and indoor air quality. However, it is a poor indicator of outdoor-associated pollutants (e.g., traffic-related pollutants and fungi species). Indoors, CO₂ is mainly produced by respiration of occupants. Several factors can affect the concentration of CO₂ in indoor environments, including the ventilation rate, occupant density, activity level of occupants, and the occupied time (BB101 2018). The ASHRAE Standard 62.1-2016 (Ventilation for Acceptable Indoor Air Quality) recommends that indoor CO₂ concentrations should not exceed 700 ppm above the outdoor concentration (typically around 400 ppm), and when mechanical ventilation is used, indoor CO₂ concentrations in schools should be maintained at/or below 1000 ppm according to UK guidelines for schools (BB101 2018). The guidelines do not specify a difference between schools and nurseries.

Studies commonly report that CO₂ concentrations in day-care centers are high. Published results from several studies found 75% (out of 6 schools), 89.3% (out of 28 samples) and 90% (out of 91 schools) of the measured indoor CO₂ concentrations exceeded 1000 ppm (Daneault et al. 1992; Stankevica and Lesinskis 2017; Rejc et al. 2019). In France, one study reported that 75% of monitored day-care centers had mixed-mode ventilation; mechanical ventilation and operable windows with an opening frequency at least one time per day. However, 46.4% of these day-care centers still had CO₂ concentrations that exceeded 1000 ppm (Roda et al. 2011). Across numerous studies (see Fig. 1), measured indoor CO₂ concentrations ranged from 377 to 2750 ppm (Daneault et al. 1992; Yang et al. 2009; Roda et al. 2011; Yoon et al. 2011; Kabir et al. 2012; St-Jean et al. 2012; Mendes et al. 2014;

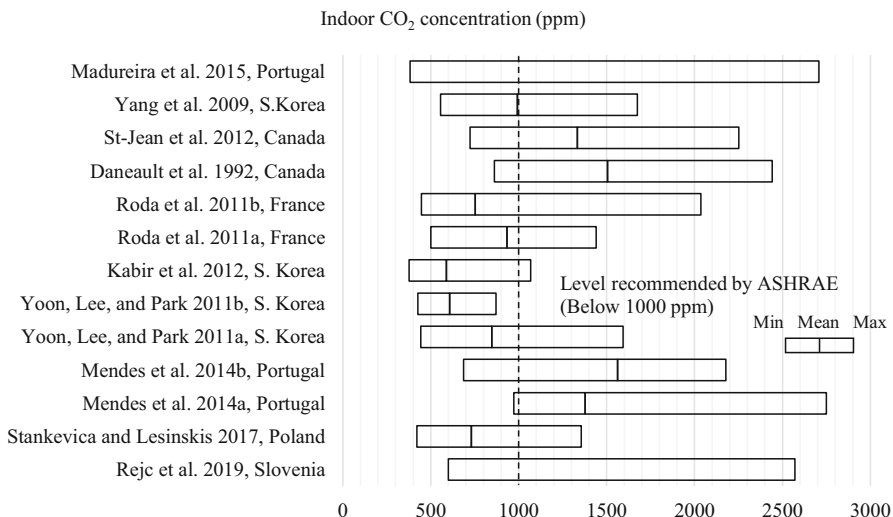


Fig. 1 Summary of reported indoor CO₂ concentration means and ranges (Zhang et al. 2021)

Madureira et al. 2015; Stankevica and Lesinskis 2017; Rejc et al. 2019). However, as monitoring methods (e.g., monitoring periods) used in the studies were different, comparing the results is tricky. Therefore, this range provides a snapshot of the CO₂ concentration published in the current research. As shown in Fig. 1, indoor CO₂ concentrations are relatively high in most studies. Canha et al. (2016) monitored seven day-care centers in France and reported a mean CO₂ concentration of 1200 ppm (Canha et al. 2016). However, low CO₂ concentrations (below 1000 ppm) do not guarantee acceptable indoor air quality. As one study done in South Korea reported, 41% of rural schools exceeded the South Korean IAQ standard for TVOC concentrations (400 µg/m³), even though the average CO₂ concentration was 607.8 ppm in these same day-care centers (Yoon et al. 2011).

Studies have reported that classrooms of younger children tend to have a higher CO₂ concentration than classrooms of older children. Additionally, higher CO₂ concentrations often occur during nap-time, about 104 ppm higher than non-nap-times (Ferng and Lee 2002; Mendes et al. 2014; Mainka et al. 2018). This finding was not explained, but could be due to less window opening, or higher occupant densities during nap times. The effect of inadequate ventilation on human health and performance includes: respiratory illnesses, allergies and asthma, sick building syndrome symptoms (SBS), reductions in performance and productivity and perceived air quality (Seppänen and Fisk 2004). Previous meta-analyses have reported that low ventilation rates might have adverse effects on the health of school children (Daisey et al. 2003). Sundell et al. (2011) and Smedje and Norbäck (2000) reported that increasing the outdoor air flow rate from 1.3 to 12.8 l/s·p (corresponding to a decreased mean indoor CO₂ concentration of 1050–780 ppm) and reduced asthma symptoms in pupils from 11.1% to 3.4% over a 2-year period. In addition to health

outcomes, a study in elementary and secondary schools reported that a 1000 ppm increase in indoor CO₂ related to a 10–20% increase in student absenteeism (Shendell et al. 2004). These studies were from school-age children, and work to confirm similar effects in younger children needs to be confirmed by more research.

Air Cleaning

There are three main approaches to improving indoor air quality: (1) eliminate sources of indoor air pollution, (2) improve ventilation, and (3) providing some form of air cleaning (Siegel 2016). Many studies attempted to track the sources of indoor air pollutants to suggest means of reducing the levels, and ventilation is recognized as an efficient method of diluting pollutants from indoor sources. However, these approaches are not always feasible, leaving air cleaning as an additional strategy to improve indoor air quality.

Air cleaners are designed to remove pollutants of different types. They may be integrated into the ventilation system to serve multiple spaces within a building, or they can be a portable or fixed (wall, window, or ceiling) device installed in one room or area. Current air filtration technologies were reviewed by Luengas et al. (2015) and Kelly and Fussell (2019), and are presented in ► Chap. 59, “Control of Airborne Particles: Filtration,” in this book by Stephens. The pollutants typically targeted in air cleaning are PM, VOCs, and bioaerosols. Studies reported efficient removal rates in many circumstances (Kelly and Fussell 2019). However, there are still limitations for each technology, including unwanted and potentially harmful by-products such as O₃, and NO_X. The literature review by Luengas et al. (2015) investigated various types of indoor air treatment and reported that “mechanical filtration is a simple and extensively used technique for removing suspended particles from indoor air.”

The use of air cleaning technology to reduce particulate pollutants in homes has been demonstrated to be effective in improving indoor air quality (Cooper et al. 2021). In the USA, a study found that an air cleaner intervention (using HEPA filtration) in homes substantially decreased the indoor PM_{2.5} levels, from 38 to 24 µg/m³ over a 12-month period (Eggelston et al. 2005). However, research on school and nursery environments is scarce, with relevant information from the few available studies in Table 3. One study selected 18 classrooms (9 control, 9 intervention) in 3 urban elementary schools. They reported that the PM_{2.5} levels in the intervention classrooms with HEPA filters were substantially reduced compared with control classrooms, with mean PM_{2.5} concentrations reduced from 6.2 to 2.4 µg/m³ (Jhun et al. 2017).

Two recent studies also reported the efficiency of air cleaners to improve indoor air quality in day-care centers. In South Korea, PM₁₀, PM_{2.5}, airborne bacteria, and fungi were measured for 5 days in ten nurseries before the use of air cleaners. The authors then took the same measurements with the air cleaners operating. The researchers reported that all pollutants were substantially reduced over the 3 weeks of air cleaner use. Concentrations dropped from 39.9 to 5.6 µg/m³ for PM_{2.5}, and

Table 3 Studies using air purifiers in day-care center environments

Study	No. of nurseries	Targeted pollutants	Filtration technology	Reference classroom	Outdoor levels	Study design	Conclusion/effectiveness
Rosén and Richardson (1999), Sweden	2	Particulate matter (0.3–7 µm)	Electrostatic Air Cleaning (EAC system)	No	Taken into consideration	Over 3 years, the EAC systems were turned on year 2, then turned off and left in place throughout year 3. Indoor particle counts were recorded for 24-h periods in one center only	Reductions of 78% for fine particles ($PM_{3.7}$) from outdoors. The very fine particles ($PM_{0.3-3}$) produced indoors were reduced by 45% compared with rooms without air cleaners, a substantial reduction from 428 to 232 particles/liter of air
Oh et al. (2014), S. Korea	10	$PM_{2.5}$, PM_{10} , airborne bacteria and fungi	Air purifier (LA-R119SWF, Korea)	No	Not taken into consideration	(1) $PM_{2.5}$, PM_{10} , airborne bacteria and fungi were measured with air purifier off (2) Air purifier was on for 5 days (3) Measured for 20 days. Concentrations compared before and after air purifier use	The concentration went from 39.9 to 5.6 $\mu\text{g}/\text{m}^3$ for $PM_{2.5}$ and from 81.3 to 15.0 $\mu\text{g}/\text{m}^3$ for PM_{10} . The bio-aerosol concentration went from 794.1 to 304.4 CFU/m ³ , and from 94.4 to 42.5 CFU/m ³ for airborne bacteria and fungi, respectively
Gayer et al. (2018), Poland	4	$PM_{2.5}$	HEPA filters	One in each nursery	Taken into consideration	In each of the selected classrooms where routine work was performed the air purifier was turned on for 24 h, 7 days a week, and in the other room the air purifier was turned off. Measurements of $PM_{2.5}$ concentration were taken over 5 days (3 working days and weekend)	Two classrooms were measured (one with an air cleaner and one without) in each nursery, the measured mean $PM_{2.5}$ concentrations were 20.9 and 33.0 $\mu\text{g}/\text{m}^3$; 13.3 and 7.3 $\mu\text{g}/\text{m}^3$; 17.8 and 8.4 $\mu\text{g}/\text{m}^3$; 17.1 and 13.0 $\mu\text{g}/\text{m}^3$ for the classroom with and without an air cleaner respectively

from 81.3 to 15.0 $\mu\text{g}/\text{m}^3$ for PM_{10} . The bio-aerosol concentrations decreased from 794.1 to 304.4 CFU/m^3 and from 94.4 to 42.5 CFU/m^3 for airborne bacteria and fungi, respectively (Oh et al. 2014). Another pilot study tested the efficiency of HEPA filtration in four day-care centers, they selected two classrooms (one with an air purifier and one without) in each nursery building. The measured $\text{PM}_{2.5}$ concentrations were respectively, nursery (A) 33.0 and 20.9 $\mu\text{g}/\text{m}^3$; nursery (B) 13.3 and 7.3 $\mu\text{g}/\text{m}^3$; nursery (C) 17.8 and 8.4 $\mu\text{g}/\text{m}^3$; nursery (D) 17.1 and 13.0 $\mu\text{g}/\text{m}^3$. Outdoor $\text{PM}_{2.5}$ concentrations were 35.5, 18.6, 26.9 and 21.9 $\mu\text{g}/\text{m}^3$, respectively. Although air cleaning appears to be an effective method of removing some indoor air pollutants, the links between their use and health improvements need further development (Gayer et al. 2018).

Indoor Air Pollutants

There are many kinds of indoor air pollutants, including PM, NO_2 , CO, and VOCs, and it is difficult to trace the sources of all indoor air pollutants. Pollutants can be from outdoor sources, via ventilation or infiltration, as well as from indoor sources, such as the use of cleaning products and emissions from building materials. Additionally, occupants may carry harmful pollutants from other environments into indoor spaces. This chapter presents common indoor air pollutants, including NO_2 , CO, O_3 , allergens, PM_{10} , $\text{PM}_{2.5}$, ultrafine particles, infectious diseases, fungi, VOCs, and radon.

NO₂

Compared to other indoor environments, day-care centers tend to have higher indoor NO_2 levels. Indoor levels are strongly influenced by outdoor levels associated with road traffic. For convenience, day-care centers are often located on the ground floor and close to main roads making them vulnerable to this pollutant (Roda et al. 2011; Villanueva et al. 2018). Reported indoor NO_2 levels in day-care centers (Fig. 2) ranged from below the limit of detection to 138.0 $\mu\text{g}/\text{m}^3$. Most studies did not report concentrations exceeding the previous annual mean value of 40 $\mu\text{g}/\text{m}^3$ recommended by the World Health Organization (WHO 2010), but the majority would now all exceed the latest annual limit (WHO 2021) of 10 $\mu\text{g}/\text{m}^3$ (Kamaruzzaman and Razak 2011; Roda et al. 2011; Villanueva et al. 2018). However, high indoor NO_2 levels in day-care centers in Portugal were reported with mean NO_2 concentrations in ten urban and five rural classrooms ranging from below the limit of detection to 136 $\mu\text{g}/\text{m}^3$ and 16.67–125.17 $\mu\text{g}/\text{m}^3$, respectively. The classroom with the highest NO_2 concentration was the one located on the ground floor with windows in the front (roadside) façade of the building (Nunes et al. 2016).

Contradictory findings have been reported for the relationship between occupancy and NO_2 concentrations. One study reported higher NO_2 levels in classrooms with more students (Villanueva et al. 2018). However, in another study, a classroom was measured both fully occupied and partially occupied for NO_2

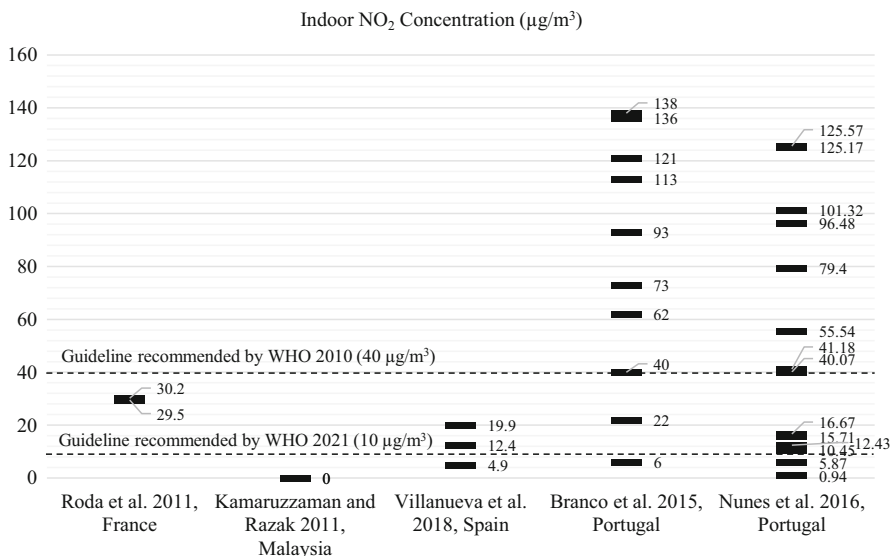


Fig. 2 Summary of reported indoor NO₂ concentration averages (Zhang et al. 2021)

concentrations, and the outcomes were 16.67 and 41.18 $\mu\text{g}/\text{m}^3$, respectively, indicating lower NO₂ levels with more students (Nunes et al. 2016). The relationship between indoor NO₂ levels and occupant density, or intermediately factors, warrants further exploration.

The health impact of NO₂ is primarily on the respiratory system, increasing the risk of lung infection and causing problems such as wheezing, coughing, colds, flu and bronchitis. A meta-analysis (the age range of children in the panel studies was 5–19 years) found that with an increase of 10 $\mu\text{g}/\text{m}^3$ of NO₂, there was an increase in asthma symptoms of 3.1% (Weinmayr et al. 2010). However, compared with other pollutants, the adverse impact of NO₂ on health may have a longer lag period, which contributes to the difficulty in studying the relationship between NO₂ exposure and health outcomes (Mukala et al. 1999).

Carbon Monoxide (CO)

One study in day-care centers reported that the CO found indoors was mainly from outdoor sources, and generally traffic related (Nunes et al. 2016). As a result, day-care centers located in urban and naturally ventilated buildings tend to have higher indoor concentrations (Zuraimi and Tham 2008; Nunes et al. 2016). However, there are still indoor sources that should be considered such as gas-fired heating systems, water heaters, dryers, and stoves as well as wood-burning stoves and fireplaces (Kabir et al. 2012).

Studies investigating CO levels in day-care center environments reported an average concentration range from 4.2 to 2786.0 $\mu\text{g}/\text{m}^3$ (Zuraimi and Tham 2008; Yang et al. 2009; Kabir et al. 2012; Cano et al. 2012; Alves et al. 2013; Mendes et al. 2014; Branco et al. 2015a; Oliveira et al. 2016). In Greece, a study investigated two elementary schools and one kindergarten in their research. They reported that during the heating season, one kindergarten that included kitchen facilities had an extremely high CO concentration of 4.2 ppm (approximately 4900 $\mu\text{g}/\text{m}^3$) (Kalimeri et al. 2016).

The health effects of breathing CO include headache, dizziness, vomiting, and nausea. If levels are high enough, people can become unconscious or die. The CO concentrations in the reviewed studies do not exceed the 6.1 ppm for 24-h exposure (approximately 7015 $\mu\text{g}/\text{m}^3$) set up by WHO (2010) guidelines. However, it should be noted that a study on elementary schools showed that with each 1.0 ppm increase in CO levels, the rate of absenteeism increased by 3.79% (Chen et al. 2000).

Ozone (O_3)

Indoor O_3 concentrations are mainly influenced by outdoor air. In most day-care centers indoor O_3 levels are significantly lower than outdoor levels because there are typically few indoor sources (e.g., printers, electronic air purifiers), and O_3 is highly reactive with products commonly used in nurseries (e.g., ozone/terpene reactions) (Kalimeri et al. 2016). One study investigated ten classrooms in four urban day-care centers, the mean O_3 concentrations in classrooms ranged from 9 to 24 $\mu\text{g}/\text{m}^3$. Higher mean O_3 concentrations ranging from 19 to 38 $\mu\text{g}/\text{m}^3$ in lunchrooms were reported, with no identifiable indoor sources. The author explained that this might be caused by the higher ventilation from outdoors in lunchrooms (Branco et al. 2015a). In another study, the authors compared O_3 levels in rural and urban day-care centers. Higher O_3 levels were reported in rural day-care centers, and the highest concentrations were associated with window opening (Nunes et al. 2016). They also concluded that O_3 concentrations were lower on weekends than on weekdays due to lower ventilation rates (less frequent window opening). In Singapore, a study focused on the difference between mechanically and naturally ventilated day-care center classrooms. Naturally ventilated classrooms had a mean O_3 concentration of 71.0 $\mu\text{g}/\text{m}^3$, which was significantly higher than the mechanically ventilated classrooms which had a mean concentration of 31.5 $\mu\text{g}/\text{m}^3$ (Zuraimi and Tham 2008).

A study from Portugal reported a mean O_3 concentration of 119 $\mu\text{g}/\text{m}^3$ (20–30 min sampling periods during mornings as well as in the afternoons for 5 working days) which exceeds the 100 $\mu\text{g}/\text{m}^3$ (over an 8-h period) recommended by WHO (2010). The outdoor mean O_3 concentration was 188 $\mu\text{g}/\text{m}^3$. The authors did not provide a reason for the high concentrations, but reported that the studied day-care center was located on streets with moderate levels of traffic (Oliveira et al. 2016). A list of studies and their reported findings on O_3 concentration can be found in Fig. 3. Based on the results of these studies, outdoor O_3 concentration and total

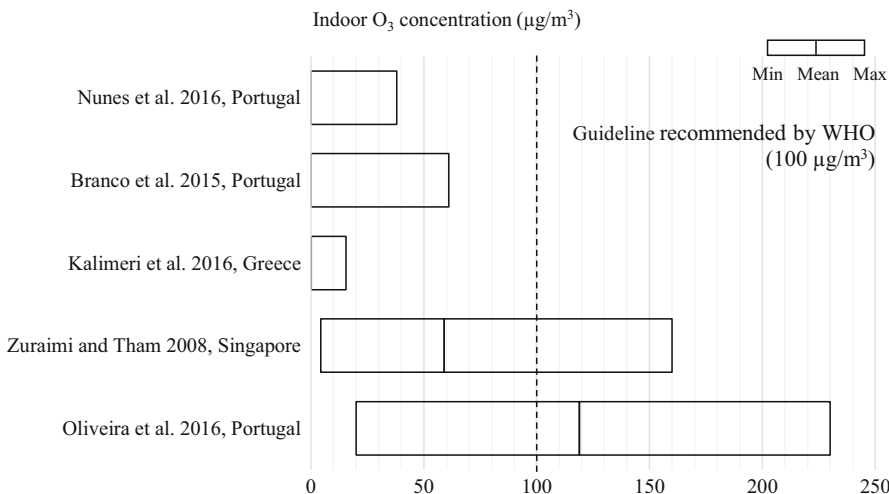


Fig. 3 Summary of study reported indoor O₃ concentration means and ranges (Zhang et al. 2021)

area cleaned are important elements that influence indoor O₃ concentration (Zuraimi and Tham 2008).

Exposure to O₃ is associated with various respiratory symptoms including coughing, wheezing, dyspnea, and other symptoms such as nausea and headaches (Carlisle and Sharp 2001). In Mexico, a study reported that when day-care center children were exposed for 2 consecutive days to relatively high O₃ levels (>0.13 ppm or 278.4 μg/m³), there was a 20% increased risk of respiratory illness (Romieu et al. 1992). Another study focused on primary schools estimated that an increase of 0.02 ppm (42.8 μg/m³) of O₃ was associated with an 82.9% increase in upper respiratory illnesses, 173.9% for lower respiratory illness with wet cough, and 62.9% for illness-related absence (Gilliland et al. 2001). A separate study, with similar outcomes, estimated that relative risks of illness-related absenteeism for O₃ were 1.08 (95% CI, 1.06–1.11) per 0.016 ppm (34.1 μg/m³) (Park et al. 2002).

Allergens

Studies have demonstrated that indoor allergens are common in day-care centers, and allergens can be different due to different geographic, climatic, and cultural factors (Salo et al. 2009). Higher concentrations of allergens were reported in the heating season than in the non-heating season (Roda et al. 2011). Most studies in day-care center environments reported a low concentration of allergens which did not exceed recommended levels; however, low levels of exposure still have the potential to cause allergic reactions (Grant et al. 2019).

Based on current studies, cat (*Fel d 1*) and dog (*Can f 1*) allergens were the dominant allergens found in day-care centers. Measured cat allergen (*Fel d 1*) ranged

from undetectable to 1.48 µg/g (Rullo et al. 2002; Instanes et al. 2005; Gülbahar et al. 2012; Cyprowski et al. 2013). Measured dog allergen (Can f 1) ranged from undetectable to 3.3 µg/g (Rullo et al. 2002; Instanes et al. 2005; Cyprowski et al. 2013). The concentrations of both dog and cat allergens were substantially higher on samples collected from mattresses and curtains than from pillows and soft toys. Cat allergens were reported up to 4.5 µg/g and dog allergens up to 10.0 µg/g on samples from mattresses (De Andrade et al. 1995; Instanes et al. 2005).

Dust mite (Der f 1 and Der p 1) and cockroach (Bla g 1 and Bla g 2) allergens were also detected in some studies. Dust mite allergens (Der f 1 and Der p 1) ranged from 0.13 to 5.40 µg/g and 0.05 to 21.8 µg/g (Fernández-Caldas et al. 2001; Roda et al. 2011; Gülbahar et al. 2012; Mendes et al. 2014). In Brazil, a study reported that dust mite allergens were greater than 2 µg/g in 67% of samples collected from day-care centers and preschools, and the highest levels were seen in a preschool bed with a mean Der 1 (Der p 1 + Der f 1) concentration of 6.3 µg/g (Rullo et al. 2002). Cockroach allergen levels were comparatively low or undetectable in other studies (De Andrade et al. 1995; Cyprowski et al. 2013).

The common reservoirs for allergens were carpeting, upholstered furnishings, and clothing (Salo et al. 2009). Animals were not allowed in almost all day-care centers, so the indoor allergens were mainly from the shedding of hair and clothing worn by occupants with pets at home. It should be noted that day-care center children are more likely to play on the floor than school children and therefore may be exposed to higher allergen levels. Cleaning was beneficial at reducing indoor allergens as reported by Smedje and Norback (2001).

Particulate Matter

PM is a complicated mixture of solid and liquid particles suspended in the air. It can vary continuously by location with a wide variety of physical and chemical characteristics (WHO 2013). Particulate matter is defined by its aerodynamic diameter, the USEPA (United States Environmental Protection Agency) has classified it mainly into two size categories: PM₁₀ and PM_{2.5}. Indoor PM is described in detail in the indoor air particles section of this book. Indoor PM concentrations are strongly influenced by outdoor sources (mainly from traffic emissions), and urban day-care centers tend to have higher PM levels than rural day-care centers (Oh et al. 2014; Nunes et al. 2015). There are also indoor determinants that strongly influence the PM level. In indoor environments, particles can be generated from human-related activities like cooking, activities of children (playing/walking), cleaning activities, shedding of skin cells, emission of clothing fibers, and from construction-related activities like renovation and reconstruction (Zuraimi and Tham 2008; Yang et al. 2009; Patel et al. 2020). Studies also find that higher indoor PM levels are associated with high occupant density and PM₁₀ concentrations are more sensitive to occupancy than PM_{2.5} (Alves et al. 2013; Branco et al. 2014; Rim et al. 2017). However, a small number of children in the classroom is enough to increase PM concentrations through re-suspension (Nunes et al. 2015). Indoor PM levels have been found to be

higher in the classrooms of older children, due to the high level of activity of older children (Branco et al. 2014; Mainka and Zajusz-Zubek 2015).

Particulate matter is a known cause of death and disability worldwide (Kim et al. 2015). Studies have demonstrated that PM has a negative impact on human health (e.g., respiratory and cardiovascular systems) and this impact is also true for children (McCormack et al. 2011; Kim et al. 2015). Particles can penetrate into the respiratory tract (Varghese and Gangamma 2009) posing a great threat to human health. Studies show that large-scale international or national interventions, as well as personal prevention approaches, might help to reduce particulate matter and improve indoor air quality (Kelly and Fussell 2019). In an example of one intervention study, two Swedish day-care centers used electrostatic cleaning systems, and reported reductions of 78% and 45% for fine particles (PM_{3-7}) and ultra-fine particles ($PM_{0.3-3}$), respectively. Additionally, illness-related absenteeism was reduced by 55% (Rosén and Richardson 1999).

PM₁₀

The reported PM₁₀ levels in indoor day-care center environments ranged from 6.8 to 216 $\mu\text{g}/\text{m}^3$ (Yang et al. 2009; Cano et al. 2012; Kabir et al. 2012; Oh et al. 2014; Mainka and Zajusz-Zubek 2015; Oliveira et al. 2016; Kaczmarek et al. 2017; Rim et al. 2017). As shown in Fig. 4, almost all the studies report indoor PM₁₀ levels that exceed the 50 $\mu\text{g}/\text{m}^3$ 24-h mean guidelines recommended by WHO (2013). Some studies find higher PM₁₀ concentrations during the heating season and lower concentration in the non-heating season (Oliveira et al. 2016; Kaczmarek et al. 2017). While others reported a higher PM₁₀ level in the non-heating seasons (Kabir et al. 2012; Mendes et al. 2014). In general, higher PM₁₀ levels in the heating season may be caused by solid fuel combustion and higher average outdoor concentrations. Higher PM₁₀ levels in the non-heating season might be influenced by increased

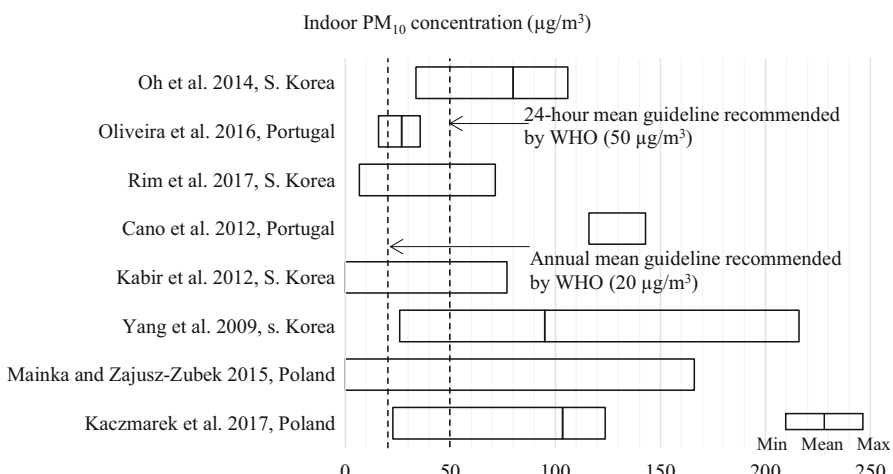


Fig. 4 Summary of reported indoor PM₁₀ concentration means and ranges (Zhang et al. 2021)

frequency of open windows (greater contributions from outdoor air). A meta-analysis reported that with an increase of $10 \mu\text{g}/\text{m}^3$ of PM_{10} , there was an increase of 2.8% in asthma symptoms and 1.2% in cough (Weinmayr et al. 2010). Exposure to air pollutants such as PM_{10} was associated with illness-related absenteeism in a 3-year study, with estimated relative illness-related absenteeism risks of 1.06 (95% confidence interval, 1.04–1.09) per $42.1 \mu\text{g}/\text{m}^3$ increase in PM_{10} (Park et al. 2002).

PM_{2.5}

The reported $\text{PM}_{2.5}$ levels in day-care center environments ranged from 3.2 to $177.2 \mu\text{g}/\text{m}^3$ (Zuraimi and Tham 2008; Wichmann et al. 2010; Oh et al. 2014; Mainka and Zajusz-Zubek 2015; Mainka et al. 2015b; Canha et al. 2016; Oliveira et al. 2016; Rim et al. 2017). The authors concluded that $\text{PM}_{2.5}$ was positively correlated with CO_2 levels and ventilation rates (the correlation were weaker for ventilation rates) (Canha et al. 2016). Outdoor $\text{PM}_{2.5}$ concentration (mainly derive from traffic emission), carpeted floor, presence of curtains and soft toys, recent renovation, shelf area, and fan cleaning are the key elements that could influence indoor $\text{PM}_{2.5}$ level (Zuraimi and Tham 2008).

$\text{PM}_{2.5}$ is a pollutant of significant concern worldwide due to its recognized association with negative health impacts such as cardiovascular disease and cancer. Due to the varied health risks of $\text{PM}_{2.5}$ exposure, WHO (2021) has established both long-term and short-term limit guidelines (5 and $15 \mu\text{g}/\text{m}^3$ respectively). As shown in Fig. 5, almost all the studies reported substantially higher indoor $\text{PM}_{2.5}$ levels than the $15 \mu\text{g}/\text{m}^3$. One study measured seven day-care centers and ten elementary schools and reported an average $\text{PM}_{2.5}$ level of $21.0 \mu\text{g}/\text{m}^3$ in day-care centers. In their research, all investigated classrooms exceeded the long-term limit of $5 \mu\text{g}/\text{m}^3$, and 31% of the classrooms exceeded the short-term limit. One study found that children exposed to an excess level of $\text{PM}_{2.5}$ have a greater risk of respiratory symptoms and reduced lung function (Gold et al. 1999). An epidemiological study

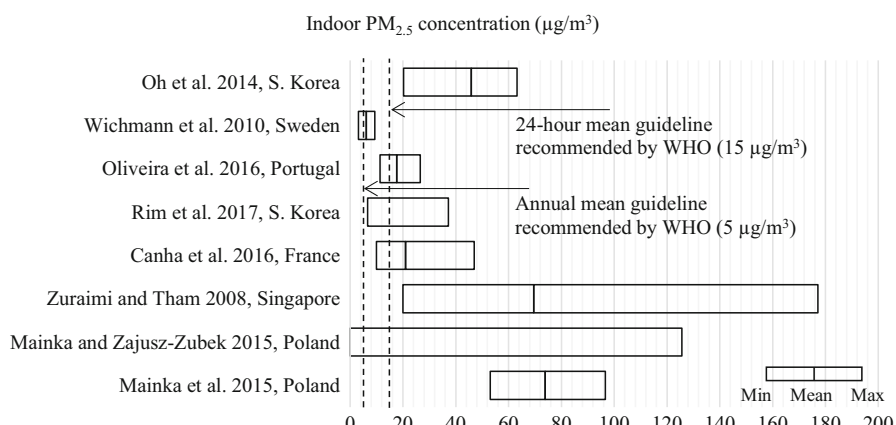


Fig. 5 Summary of reported indoor $\text{PM}_{2.5}$ concentration means and ranges (Zhang et al. 2021)

reported that a $10 \mu\text{g}/\text{m}^3$ increase in $\text{PM}_{2.5}$ was correlated with a 15% rise in hospital admissions for asthma (Tecer et al. 2008). Studies in school-aged children have found several health symptoms associated with $\text{PM}_{2.5}$, such as cough, eczema, dermatitis, headache, and nausea.

Ultra-Fine Particulates (UFPs)

Limited data are available on the concentration of ultrafine particles (particulate matter of nanoscale size; less than $0.1 \mu\text{m}$ or 100 nm in diameter) in day-care centers. The main elements influencing UFP level are summarized as: children's activities during classes (e.g., painting and other arts and crafts activities), combustion sources (e.g., candles on a birthday cake), and classroom cleaning (e.g., dusting and wood polishing) (Morawska et al. 2009).

In Portugal, a study investigated three day-care centers and reported a mean concentration of 1.82×10^4 and $1.32 \times 10^4 \text{ particle}/\text{cm}^3$ in urban day-care centers, and $1.15 \times 10^4 \text{ particle}/\text{cm}^3$ in a rural day-care center. They concluded that canteens have the highest UFP level, likely because they were directly connected to a kitchen with a gas stove. Also, they mentioned that UFP levels in playrooms were about two times higher than in school classrooms. During two activities (candles burning on a birthday cake and clay grinding), the concentrations were 13 times higher than the estimated mean value (Fonseca et al. 2014). Due to the small size of UFPs, they can penetrate biological membranes and translocate into the systemic circulation, and eventually get into organ systems including the brain and nervous system. Studies about independent health effects of UFP are scarce. A review study identified 85 studies and reported that there were inflammatory and cardiovascular changes associated with short-term UFP exposure (Ohlwein et al. 2019).

Infectious Diseases

Children who attend day-care centers may have increased infectious diseases risks. Infections like enteric infection (e.g., diarrhea, hepatitis A), respiratory tract infections (e.g., pharyngitis, pneumonia), invasive bacterial disease (e.g., *Hemophilus influenzae* type b, *streptococcus pneumonia*), herpesvirus infection (e.g., cytomegalovirus, varicella zoster) and other types of diseases should be noted (Holmes et al. 1996). Although guidelines (e.g., caring for our children-CFOC, USA) have been developed to help protect children from infectious diseases, eliminating these risks is impossible. A birth cohort study reported a rapid increase of respiratory infections after children started to attend day-care center with 3.79 mean sick days/month before the start of day-care to 10.57 mean sick days/month during the second month of attendance (Schuez-Havupalo et al. 2017).

During the COVID-19 pandemic, indoor air quality has become even more critical. Qian et al. (2020) investigated 318 outbreaks in China and reported that they all occurred in indoor environments. Respiratory droplets (generally $>5 \mu\text{m}$) and aerosol droplets (generally $<5 \mu\text{m}$) that can carry the SARS-CoV-2 virus (the causative agent for COVID-19) are the means of airborne transmission of

COVID-19 (Christopherson et al. 2020). Respiratory droplets deposit on the ground or surface rapidly, but aerosol droplets may remain suspended in indoor air for one or more hours. Knibbs et al. (2011) suggested that increased air exchange rates could decrease the risk of airborne disease transmission through dilution with outdoor air. In addition to, or in lieu of, increased ventilation, air filtration could also be used to help reduce the transmission risk by reducing the concentration of virus-laden droplets. One recent review reported that air purifiers with HEPA filters which have a high removal rate for indoor particles larger than $0.3\text{ }\mu\text{m}$, may be an effective method for reducing viral load in hospital environments (Mousavi et al. 2020). Previous experiments on SARS-CoV-1 (the causative agent of the SARS outbreak) demonstrated the efficacy of HEPA filters in the “capture and containment of diseases of similar particle size” (Schentag et al. 2004). However, since no direct studies have been conducted to validate this assumption, more specific studies on the impact of using air purifiers on indoor viral load of SARS-CoV-2 are needed (Christopherson et al. 2020).

Studies about indoor airborne bacteria in day-care centers mainly focused on the total bacterial concentrations. It is difficult to determine if indoor bacteria have a specific influence on health, because of a lack of speciation information. However, long exposure time in an environment with high levels of bacteria was shown to have adverse health effects (Daisey et al. 2003). It is worth noting that day-care centers tended to have higher bacterial concentrations compared with other indoor environments that were tested. These high levels may be due to higher occupancy densities, activities of children, and poor ventilation. A study in South Korea focused on bacteria levels in public buildings found the highest concentrations in a kindergarten in a hospital, a kindergarten, an elderly welfare facility, and a postpartum nursing center that were tested (Kim and Kim 2007). A study done in Portugal investigated four environments including homes, child day-care centers, primary schools, and elderly care centers. They reported the highest bacterial concentration with a median of 3870 CFU/m^3 in 50 rooms of 9 day-care centers, and found that children have at least two times the dose rates of bacteria than older people (Madureira et al. 2015).

Most studies reported significantly higher indoor total bacterial concentration than outdoor, with results that ranged from 1596 to 4630 CFU/m^3 (Cano et al. 2012; Mendes et al. 2014; Mainka et al. 2015a, 2018; Carreiro-Martins et al. 2016). Based on these higher indoor concentrations, the main airborne-bacteria sources are likely from indoors. Human oral and respiratory droplets emitted during coughing, sneezing, talking, breathing, and skin shedding are likely sources (Carreiro-Martins et al. 2016).

The reported bacteria concentrations were much lower in some locations. Researchers in South Korea studied 43 child care facilities and the mean total suspended bacteria was 418 CFU/m^3 (Kabir et al. 2012). Another study in South Korea reported that the mean concentrations of total and respirable airborne bacteria were 931 and 358 CFU/m^3 in childcare centers (Kim and Kim 2007). The indoor concentrations they reported were lower than outdoor concentrations, and the I/O ratios were below 1.0. The author concluded that the primary bacterial contamination was of outdoor origin. The explanation they provided was that the measuring

periods of their study were spring and autumn, which are the highest periods of outdoor concentrations of airborne bacteria.

In addition to studies of total bacteria concentrations, a few studies focused on determining the size distribution and the genera of indoor bacteria in day-care center environments. One study reported that *Staphylococcus spp.*, *Micrococcus spp.*, *Corynebacterium spp.*, and *Bacillus spp.* were the dominant genera and accounted for over 95% of the total airborne bacteria (Kim and Kim 2007). In Poland, a study investigated one urban day-care center and identified *Micrococcus spp.* as the dominant indoor bacteria. They also analyzed the size distribution of bacterial aerosols and concluded that small particles ($<4.7\text{ }\mu\text{m}$) contributed up to 85% of the total bacterial aerosols in indoor air. In this study, they developed a day-care center exposure dose equation and reported that the highest inhaled values happen in the winter (Brągoszewska et al. 2016).

For the determinants that influence indoor bacterial concentration, studies have concluded that increased indoor bacteria levels were associated with high occupant densities, low ventilation rates, and irregular floor cleaning, but frequent table cleaning frequencies (table cleaning activities resuspend bacteria from surfaces) (Zuraimi and Tham 2008; Cano et al. 2012; Mendes et al. 2014).

Dampness and Mold

Issues of moisture and mold damage in structures have been reported in many countries. An increase in fungal levels in the indoor environment is associated with mold/water damage in the building structure. Exposure to fungi can cause adverse human health effects from three aspects: immune response, infection by the organism, or toxic-irritant effects from by-products of mold (mycotoxins, MVOCs, etc.) (Bush et al. 2006). It has also been reported that mold and other fungi are sources of VOCs (Bennett and Inamdar 2015). However, little is known about the relationship between inhalation and response, and there are no unified sampling or analytical methods for mold exposure (Salonen et al. 2015).

Studies in South Korea and Portugal reported that day-care centers tend to have higher fungi concentrations compared to homes, hospitals, postpartum nursing centers, primary schools and elderly care centers (Kim and Kim 2007; Madureira et al. 2015). The fungi found in the indoor environment were mainly from outdoor sources. *Penicillium* and *Cladosporium* were the two main fungi genera found in indoor environments (Aydogdu and Asan 2008; Roda et al. 2011; Madureira et al. 2015; Rejc et al. 2019). Studies investigating total indoor fungi concentrations reported results ranging from 69.2 to 707 CFU/m³, with a higher concentration in summer (Kim and Kim 2007; Roda et al. 2011; Cano et al. 2012; Mendes et al. 2014; Madureira et al. 2015; Carreiro-martins et al. 2016; Mainka et al. 2015a, 2018).

In tropical countries, the indoor fungi concentrations in day-care centers tended to be much higher. In Singapore, a study reported that the total fungi concentration was 1424.2 CFU/m³ on dry days and 2930.5 CFU/m³ on rainy days (Zuraimi et al. 2009). They also reported that most of the indoor airborne culturable fungi had a size range

between 1.1 and 3.3 μm . However, another study reported a dominant size range of 3.3–4.7 μm (Kim and Kim 2007). Further studies are needed to explain this inconsistency. In addition to outdoor air (the main determinant), occupant density, cleaning, pets, plants, plumbing systems, heating, ventilation, air-conditioning systems, mold and dust resuspension all had an impact on the fungi concentrations indoors (Zuraimi and Tham 2008; Rejc et al. 2019).

VOCs

In many studies on the indoor air quality of day-care centers, total VOCs (TVOCs) are used to report the indoor organic chemical compounds level. As shown in Fig. 6, reported indoor TVOCs ranged from below the limit of detection to 6440 $\mu\text{g}/\text{m}^3$ (with mean concentrations that ranged from 114 to 642.11 $\mu\text{g}/\text{m}^3$). Some high TVOC peaks are included in this range, but further studies that may explain those high peaks have not been conducted (Ruotsalainen et al. 1993; Yang et al. 2009; Yoon et al. 2011; Cano et al. 2012; Mendes et al. 2014; Oliveira et al. 2016).

Some detailed research on indoor concentrations of specific VOCs in day-care center environments has been conducted, with BTEX (benzene, toluene, ethylbenzene and xylenes) some of the most commonly reported compounds. The ranges of reported mean concentrations for benzene (1.4–2.93 $\mu\text{g}/\text{m}^3$), toluene (2.2–7.9 $\mu\text{g}/\text{m}^3$), ethylbenzene (0.6–2.2 $\mu\text{g}/\text{m}^3$), m,p-xylenes (1.6–5 $\mu\text{g}/\text{m}^3$), and o-xylenes (1.3–1.6 $\mu\text{g}/\text{m}^3$). As reported in the UK school guidance document, BB101 (2018), trichloroethylene, tetrachloroethylene, naphthalene, and d-Limonene are also important chemicals in indoor environments. However, there is limited information about indoor concentrations of those pollutants in day-care center

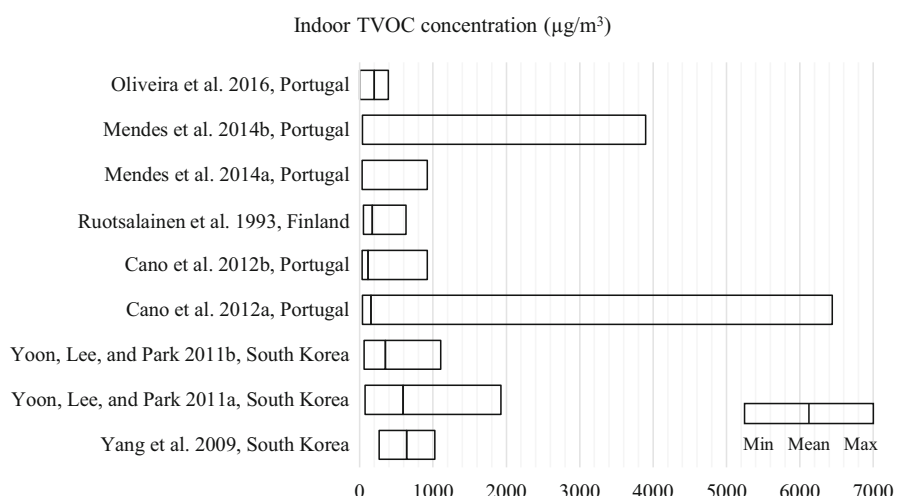


Fig. 6 Summary of reported indoor TVOC concentration means and ranges (Zhang et al. 2021)

environments. One study investigated seven day-care centers and ten primary schools in France and reported a mean trichloroethylene concentration of $2.3 \mu\text{g}/\text{m}^3$ with a range of $0\text{--}28.3 \mu\text{g}/\text{m}^3$ and mean tetrachloroethylene concentrations of $1.1 \mu\text{g}/\text{m}^3$ with a range of $0\text{--}11.5 \mu\text{g}/\text{m}^3$ (Canha et al. 2016). Two studies reported a naphthalene concentration that ranged from 0.3 to $3.1 \mu\text{g}/\text{m}^3$ (St-Jean et al. 2012; Mainka et al. 2015a). Studies on indoor d-Limonene levels in day-care centers were not found.

Due to the relative complexity of individuals' susceptibilities to TVOCs, only indicators of sensory effects are reported (Chatzidiakou et al. 2012). The complex mixture of chemicals in TVOCs can cause eye, nose, and throat irritation, shortness of breath, headaches, fatigue, nausea, dizziness, and skin problems. Higher concentrations may cause irritation of the lungs, as well as damage to the liver, kidney, or central nervous system. The estimated change in the odds ratio for chronic lower respiratory symptoms associated with a $2 \mu\text{g}/\text{m}^3$ change in process-related (industrial) compounds was 1.08 (95% CI 1.02–1.14) (McCloskey 1996).

Since indoor materials can emit formaldehyde including plywood, particleboard, carpets, and foam insulation that are frequently used indoors, many studies focus on the indoor level of this compound (Gilbert et al. 2008). As shown in Fig. 7, mean indoor formaldehyde levels reported are relatively low. However, high concentration peaks were reported in many studies. One study found those peaks corresponded

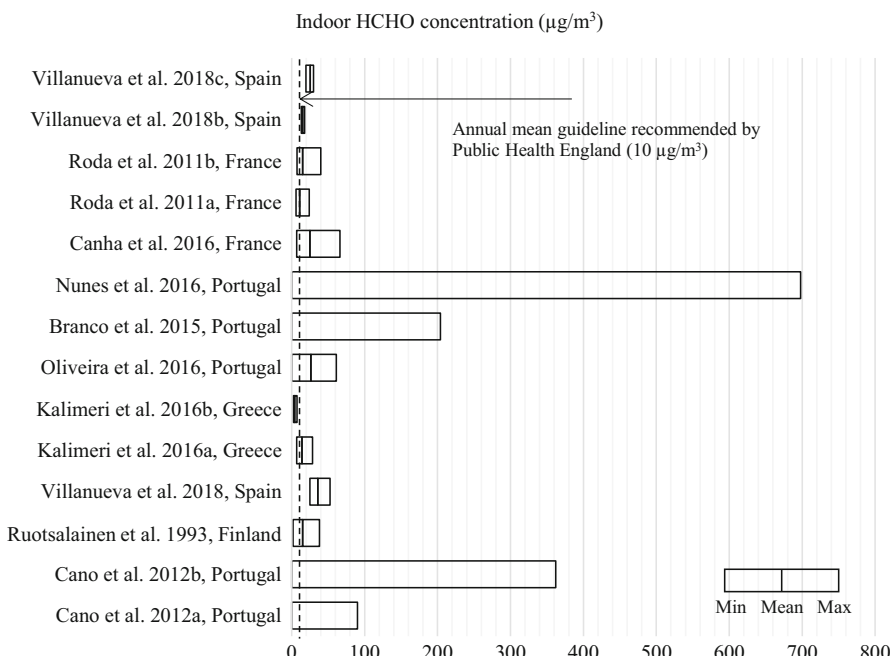


Fig. 7 Summary of reported indoor formaldehyde (HCHO) concentration means and ranges (Zhang et al. 2021)

with poor ventilation and the activities of cleaning and moving furniture (i.e., scraping the floor) (Ramalho et al. 2015; Nunes et al. 2016). Most studies report high formaldehyde during the hot/non-heating season (Kabir et al. 2012; Ramalho et al. 2015; Kalimeri et al. 2016). It is worth noting that there was a strong correlation between benzene and CO with formaldehyde, which could suggest they may occur from common sources (Kabir et al. 2012; Ramalho et al. 2015).

Radon

Radon is a naturally occurring radioactive gas produced from the decay of uranium in soil and rocks. It can penetrate buildings through cracks in the foundation. When its decay products are inhaled, they can release ionizing radiation that damages tissue (National Research Council 1999; WHO 2009).

Most studies that looked at the radon levels in day-care center environments reported acceptable average indoor values, below the 100 Bq/m³ recommended by WHO (Planinić et al. 1993; Al-Ghamdi et al. 2011; Bem et al. 2013; Jónsson et al. 2015). Other studies reported ranges of 100–300 Bq/m³ recommended by ICRP (The International Commission on Radiation Protection) (Kullab 2005; Fojtikova and Navratilova Rovenska 2014; Ivanova et al. 2014; Sousa et al. 2015; Branco et al. 2016).

However, in some high radon areas, relatively high levels were reported. In Slovenia, a study investigated ten high radon level kindergartens. The average indoor air radon concentration ranged from 264 to 1700 Bq/m³ (Vaupotič 2002). Studies have reported high radon levels in other countries (Italy; Slovenia; Bulgaria), with results ranging as following: 50–1047 Bq/m³ (Trevisi et al. 2012); 145–794 Bq/m³ (Vaupotič et al. 2012); 104–1761 Bq/m³ (Vuchkov et al. 2013). Although in many places radon is not a serious pollutant, in high-risk locations, radon should be taken into consideration in the indoor environments of day-care centers. Mitigation systems, such as active soil depressurization that remove the radioactive gas from the soil below the structure are recommended when radon levels are high.

Emerging Hazards

Recently, semi-volatile organic compounds (SVOCs) have drawn the attention of researchers, as they may have adverse effects on human health. The endocrine and respiratory systems of humans could be affected by SVOCs that are used in buildings, such as phthalic acid esters (phthalates or PAEs), polycyclic aromatic hydrocarbons (PAHs) and polybrominated diphenyl ethers (PBDEs). SVOCs have a higher molecular weight and boiling point temperature and are more stable than VOCs and therefore can remain in the indoor environment for years. There are three routes of exposure to SVOCs: inhalation, dermal and oral (Wang et al. 2010).

In day-care center environments, the presence of phthalates has been reported in many studies. Phthalates are used as a plasticizer in many consumer products and

industrial goods. Many studies have revealed an association between phthalate exposure and reproductive and developmental effects, and it is one of the risk factors for atopic diseases in children. Flooring, wire, cables, toys and children's products are reported as main sources of indoor phthalates. Di(2-Ethylhexyl) phthalate (DEHP), Di-isobutyl phthalate (DiNP), and Di-n-butyl phthalate (DnBP) are the most commonly reported phthalate esters (Fromme et al. 2005; Kim et al. 2013; Gaspar et al. 2014).

Measurable levels of a number of SVOCs, or their metabolites, have been found in children. One study noted that phthalates are rapidly absorbed and metabolized after inhalation or oral administration (Kavlock et al. 2006). Higher concentrations of phthalate metabolites in children compared with their parents and day-care center teachers have been reported (Koch et al. 2004). In Germany, a study investigating 63 day-care centers, collected indoor air samples, indoor dust samples, and urine samples of children. For some phthalates, they reported "significant correlations between the concentrations in the indoor air and dust and their corresponding metabolites in the urine specimens," and mentioned that a further reduction in phthalates exposure is necessary (Fromme et al. 2013). Additional studies are needed to better understand the sources, transportation, intake, and exposure risks of SVOCs in day-care center environments.

Conclusions

This chapter focused on indoor air quality in day-care center environments. The current research on IAQ in day-care centers includes a wide range of building types, activities, and occupancy. In addition, context changes drastically between countries, climates, and education systems. These differences pose a challenge when trying to assess the indoor air quality in a comprehensive and cohesive way, and many of the published findings are contradictory or inconsistent. As a result, more comprehensive studies considering building typologies and characteristics are needed. The overall evidence indicates that the indoor air quality in day-care centers is poor, and poor indoor air quality can lead to negative health outcomes. Key findings are as follows:

- Regarding thermal conditions in day-care centers, most reported temperature and relative humidity levels were within the comfort range. However, both lower and higher temperatures occurred due to poor building facilities. HVAC systems should be properly operated and maintained, which may require appropriate training or additional personnel. Also, it was reported that children prefer lower temperatures than adults, and that there is a difference between the preferences of boys and girls. The methods of collecting accurate feedback on the thermal comfort of children, and guidelines based on the needs of children warrants further development.
- Ventilation in many studied nurseries appears inadequate based on CO₂ concentrations which commonly exceeded recommended standards (mean

concentrations: 377–2750 ppm). The main reasons for high CO₂ levels were overcrowding and poor ventilation of the classrooms. Higher ventilation rates, reducing occupant density, and additional mechanical ventilation are recommended. Additionally, sleep time and sleeping-only rooms should be of special consideration because higher CO₂ concentrations were often reported during naptime.

- Particulate matter of both indoor and outdoor origin was reported in studies. PM levels in day-care centers often exceeded current guidelines. Air cleaning systems, such as HEPA filtration, may be useful in improving indoor air quality. High intensity activities of children, as well as activities that produce indoor particles (e.g., cooking, burning candles, clay grinding), should be considered in the design and operation of day-care centers.
- Indoor NO₂, O₃, and CO levels were generally influenced by outdoor levels, and although limited information was available, most measurements exceeded the 2021 WHO guidelines (10 µg/m³). Urban day-care centers, or day-care centers adjacent to high traffic areas, should be aware of these pollutants. When ambient air quality is not ideal (e.g., during peak traffic periods), ventilation from outdoor air without adequate filtration may not be advisable.
- High peaks in VOC concentration were reported in most studies, the mean concentrations, however, were generally low. The effect of short-term exposures to VOCs on children's health needs further study. Construction materials, interior decoration, cleaning and office products should be carefully selected and used in areas with proper ventilation.
- Bioaerosols like allergens, fungi species and bacteria were reported in some studies. Day-care centers could be potential important sources of exposures to those contaminants. Low levels of exposure might still cause adverse health outcomes. Well-defined thresholds, as well as methods for cleaning or removal, of biological contaminants are needed.
- In areas known to be at high-risk for radon, indoor levels should be measured, and appropriate remediation actions taken if standards are exceeded.
- Air purifiers may be a useful tool to help improve indoor air quality when source control and ventilation alone cannot achieve the necessary levels. The filtration technology should be carefully selected as some air cleaning technologies produce unwanted by-products. Currently, HEPA filters are recommended as one of the best options (especially for reducing PM levels). However, it should be noted that the costs of purchasing and maintaining air purifiers could exacerbate existing health inequalities (Cheek et al. 2020).

Studies reported in this review originate from different countries with different climates. Also, the methods used were different, for instance, monitoring devices, monitoring periods, and monitored parameters varied in different studies. It is therefore difficult to directly compare results, and we can only gain a general understanding about the current IAQ performance in day-care center environments. More comprehensive studies with longer monitoring campaigns and more considered confounders are needed to help us further understand the issues.

Additionally, more research from developing countries, where approximately 70% of the world's population lives, is needed. Studies have found that poor indoor air quality in homes in developing countries has a fundamental impact on health (Bruce et al. 2000; Gall et al. 2013). However, it is noteworthy that most of the studies cited in this chapter were from developed countries, and yet the overall IAQ performance was unacceptable. The authors express concern, therefore, that the air quality in nurseries in developing countries may be even more precarious, especially where outdoor pollution is high, and the structural fabric of buildings is poor.

The present chapter highlights the poor indoor air quality in day-care center and its potential effect on the health of children. When it comes to day-care centers, designers should take ambient pollution levels, ventilation, filtration, decoration and construction materials, and occupant density and activities into consideration to design for healthier indoor environments in the future.

Cross-References

- [Control of Airborne Particles: Filtration](#)
 - [Resuspension](#)
-

References

- Al-Ghamdi SS, Al-Garawi MS, Al-Mosa TM, Baig MR (2011) Investigating indoor radon levels and influencing factors in primary schools of Zulfi City, Saudi Arabia. AIP Conf Proc 1370: 294–298. <https://doi.org/10.1063/1.3638115>
- Almeida SM, Canha N, Silva A et al (2011) Children exposure to atmospheric particles in indoor of Lisbon primary schools. Atmos Environ 45:7594–7599. <https://doi.org/10.1016/j.atmosenv.2010.11.052>
- Alves C, Nunes T, Silva J, Duarte M (2013) Comfort parameters and particulate matter (PM_{10} and $PM_{2.5}$) in school classrooms and outdoor air. Aerosol Air Qual Res 13:1521–1535. <https://doi.org/10.4209/aaqr.2012.11.0321>
- Aydogdu H, Asan A (2008) Airborne fungi in child day care centers in Edirne City, Turkey. Environ Monit Assess 147:423–444. <https://doi.org/10.1007/s10661-007-0130-4>
- Bem H, Bem EM, Krawczyk J et al (2013) Radon concentrations in kindergartens and schools in two cities: Kalisz and Ostrów Wielkopolski in Poland. J Radioanal Nucl Chem 295:2229–2232. <https://doi.org/10.1007/s10967-012-2272-2>
- Bennett JW, Inamdar AA (2015) Are some fungal volatile organic compounds (VOCs) mycotoxins? Toxins 7:3785–3804. <https://doi.org/10.3390/toxins7093785>
- Bragoszewska E, Mainka A, Pastuszka JS (2016) Bacterial aerosols in an urban nursery school in Gliwice, Poland: a case study. Aerobiologia 32:469–480. <https://doi.org/10.1007/s10453-015-9419-x>
- Branco PTBS, Alvim-Ferraz MCM, Martins FG, Sousa SIV (2014) Indoor air quality in urban nurseries at Porto city: particulate matter assessment. Atmos Environ 84:133–143. <https://doi.org/10.1016/j.atmosenv.2013.11.035>
- Branco PTBS, Alvim-Ferraz MCM, Martins FG, Sousa SIV (2015a) Children's exposure to indoor air in urban nurseries-part I: CO_2 and comfort assessment. Environ Res 140:1–9. <https://doi.org/10.1016/j.envres.2015.03.007>

- Branco PTBS, Nunes RAO, Alvim-Ferraz MCM et al (2015b) Children's exposure to indoor air in urban nurseries – part II: gaseous pollutants' assessment. *Environ Res* 142:662–670. <https://doi.org/10.1016/j.envres.2015.08.026>
- Branco PTBS, Nunes RAO, Alvim-Ferraz MCM et al (2016) Children's exposure to radon in nursery and primary schools. *Int J Environ Res Public Health* 13:1–16. <https://doi.org/10.3390/ijerph13040386>
- Bruce N, Perez-Padilla R, Albalak R (2000) Indoor air pollution in developing countries: a major environmental and public health challenge. *Bull World Health Organ* 78:1078–1092
- Bush RK, Portnoy JM, Saxon A et al (2006) The medical effects of mold exposure. *J Allergy Clin Immunol* 117:326–333. <https://doi.org/10.1016/j.jaci.2005.12.001>
- Calderón-Garcidueñas L, Torres-Jardón R, Kulesza RJ et al (2014) Air pollution and detrimental effects on children's brain. The need for a multidisciplinary approach to the issue complexity and challenges. *Front Hum Neurosci* 8:613. <https://doi.org/10.3389/fnhum.2014.00613>
- Canha N, Mandin C, Ramalho O et al (2016) Assessment of ventilation and indoor air pollutants in nursery and elementary schools in France. *Indoor Air* 26:350–365. <https://doi.org/10.1111/ina.12222>
- Cano M, Nogueira S, Papoila AL et al (2012) Indoor air quality in Portuguese day care centers – ENVIRH project. In: COBEE conf proc, pp 1–4
- Carlisle AJ, Sharp NCC (2001) Exercise and outdoor ambient air pollution. *Br J Sports Med* 35: 214–222. <https://doi.org/10.1136/bjsm.35.4.214>
- Carreiro-martins P, Papoila AL, Caires I et al (2016) Effect of indoor air quality of day care centers in children with different predisposition for asthma. *Pediatr Allergy Immunol* 27:299–306. <https://doi.org/10.1111/pai.12521>
- Chatzidiakou L, Mumovic D, Summerfield AJ (2012) What do we know about indoor air quality in school classrooms? A critical review of the literature. *Intell Build Int* 4:228–259. <https://doi.org/10.1080/17508975.2012.725530>
- Cheek E, Guercio V, Shrubsole C, Dimitroulopoulou S (2020) Portable air purification: review of impacts on indoor air quality and health. *Sci Total Environ* 2020:142585. <https://doi.org/10.1016/j.scitotenv.2020.142585>
- Chen L, Jennison BL, Yang W, Omaye ST (2000) Elementary school absenteeism and air pollution. *Inhal Toxicol* 12:997–1016. <https://doi.org/10.1080/08958370050164626>
- Christopherson DA, Yao WC, Lu M et al (2020) High-efficiency particulate air filters in the era of COVID-19: function and efficacy. *Otolaryngol Head Neck Surg* 163:1153–1155. <https://doi.org/10.1177/0194599820941838>
- Conceição EZE, Gomes JMM, Antão NH, Lúcio MMJR (2012) Application of a developed adaptive model in the evaluation of thermal comfort in ventilated kindergarten occupied spaces. *Build Environ* 50:190–201. <https://doi.org/10.1016/j.buildenv.2011.10.013>
- Cooper E, Wang Y, Stamp S et al (2021) Use of portable air purifiers in homes: operating behaviour, effect on indoor PM_{2.5} and perceived indoor air quality. *Build Environ* 191:107621. <https://doi.org/10.1016/j.buildenv.2021.107621>
- Cyprowski M, Buczyńska A, Szadkowska-Stańczyk I (2013) Indoor allergens in settled dust from kindergartens in city of Łódź, Poland. *Int J Occup Med Environ Health* 26:890–899. <https://doi.org/10.2478/s13382-013-0153-8>
- Daisey JM, Angell WJ, Apte MG (2003) Indoor air quality, ventilation and health symptoms in schools: an analysis of existing information. *Indoor Air* 13:53–64. <https://doi.org/10.1034/j.1600-0668.2003.00153.x>
- Daneault S, Beausoleil M, Messing K (1992) Air quality during the winter in Quebec day-care centers. *Am J Public Health* 82:432–434. <https://doi.org/10.2105/AJPH.82.3.432>
- De Andrade AD, Charpin D, Birnbaum J, Lanteaume A, Chapman M, Vervloet D (1995) Indoor allergen levels in day nurseries. *Journal of allergy and clinical immunology*, 95(6), 1158–1163
- Deng Q, Lu C, Ou C, Liu W (2015) Effects of early life exposure to outdoor air pollution and indoor renovation on childhood asthma in China. *Build Environ* 93:84–91. <https://doi.org/10.1016/j.buildenv.2015.01.019>

- Dudek M (2007) Schools and kindergartens: a design manual. Walter de Gruyter, Berlin
- Dudek M (2013) Nurseries: a design guide. Routledge, New York
- Education and Skills Funding Agency. BB 101: Guidelines on ventilation, thermal comfort, and indoor air quality in schools, <https://www.gov.uk/government/publications/building-bulletin-101-ventilation-for-school-buildings> (2018, accessed 10 May 2022).
- Eggleston PA, Butz A, Rand C et al (2005) Home environmental intervention in inner-city asthma: a randomized controlled clinical trial. Ann Allergy Asthma Immunol 95:518–524. [https://doi.org/10.1016/S1081-1206\(10\)61012-5](https://doi.org/10.1016/S1081-1206(10)61012-5)
- EPA (United States Environmental Protection Agency). A brief guide to mold, moisture, and your home, 2012. <https://www.epa.gov/mold/brief-guide-mold-moisture-and-your-home> (2012, accessed 10 May 2022)
- Fang L, Clausen G, Fanger PO (1998) Impact of temperature and humidity on perception. Indoor Air 8:80–90. <https://doi.org/10.1111/j.1600-0668.1998.t01-2-00003.x>
- Fang L, Wyon DP, Clausen G, Fanger PO (2004) Impact of indoor air temperature and humidity in an office on perceived air quality, SBS symptoms and performance. Indoor Air 14:74–81. <https://doi.org/10.1111/j.1600-0668.2004.00276.x>
- Fanger PO (1973) Assessment of man's thermal comfort in practice. Occup Environ Med 30:313–324
- Fernández-Caldas E, Codina R, Ledford DK et al (2001) House dust mite, cat, and cockroach allergen concentrations in daycare centers in Tampa, Florida. Ann Allergy Asthma Immunol 87: 196–200. [https://doi.org/10.1016/S1081-1206\(10\)62225-9](https://doi.org/10.1016/S1081-1206(10)62225-9)
- Ferng S-F, Lee L-W (2002) Indoor air quality assessment of daycare facilities with carbon dioxide, temperature, and humidity as indicators. J Environ Health 65:14–22
- Fojtikova I, Navratilova Rovenska K (2014) Influence of energy-saving measures on the radon concentration in some kindergartens in the Czech Republic. Radiat Prot Dosim 160:149–153. <https://doi.org/10.1093/rpd/ncu073>
- Fonseca J, Slezakova K, Morais S, Pereira MC (2014) Assessment of ultrafine particles in Portuguese preschools: levels and exposure doses. Indoor Air 24:618–628. <https://doi.org/10.1111/ina.12114>
- Fromme H, Lahrz T, Piloty M et al (2005) Occurrence of phthalates and musk fragrances in indoor air and dust from apartments and kindergartens in Berlin (Germany). Indoor Air 14:188–195. <https://doi.org/10.1046/j.1600-0668.2003.00223.x>
- Fromme H, Lahrz T, Kraft M et al (2013) Phthalates in German daycare centers: occurrence in air and dust and the excretion of their metabolites by children (LUPE 3). Environ Int 61:64–72. <https://doi.org/10.1016/j.envint.2013.09.006>
- Gall ET, Carter EM, Earnest CM, Stephens B (2013) Indoor air pollution in developing countries: research and implementation needs for improvements in global public health. Am J Public Health 103:67–72. <https://doi.org/10.2105/AJPH.2012.300955>
- Gaspar FW, Castorina R, Maddalena RL et al (2014) Phthalate exposure and risk assessment in California child care facilities. Environ Sci Technol 48:7593–7601. <https://doi.org/10.1021/es501189t>
- Gayer A, Mucha D, Adamkiewicz Ł, Badyda A (2018) Children exposure to PM_{2.5} in kindergarten classrooms equipped with air purifiers – a pilot study. MATEC Web Conf 247:00016. <https://doi.org/10.1051/matecconf/201824700016>
- Gilbert NL, Guay M, Gauvin D et al (2008) Air change rate and concentration of formaldehyde in residential indoor air. Atmos Environ 42:2424–2428. <https://doi.org/10.1016/j.atmosenv.2007.12.017>
- Gilliland FD, Berhane K, Rappaport EB et al (2001) The effects of ambient air pollution on school absenteeism due to respiratory illnesses. Epidemiology 12:43–54. <https://doi.org/10.1097/0001648-200101000-00009>
- Gold DR, Damokosh AI, Dockery DW et al (1999) Particulate and ozone pollutant effects on the respiratory function of children in southwest Mexico City. Epidemiology 10:8–16
- Grant T, Rule AM, Koehler K et al (2019) Sampling devices for indoor allergen exposure: pros and cons. Curr Allergy Asthma Rep 19:0833. <https://doi.org/10.1007/s11882-019-0833-y>

- Gülbahar O, Korkmaz M, Erdem N et al (2012) An important source for cat and house dust mite allergens: day-care centers. *Turk Klin J Med Sci* 32:750–758. <https://doi.org/10.5336/medsci.2011-26355>
- Haghghat F, De Bellis L (1998) Material emission rates: literature review, and the impact of indoor air temperature and relative humidity. *Build Environ* 33:261–277. [https://doi.org/10.1016/S0360-1323\(97\)00060-7](https://doi.org/10.1016/S0360-1323(97)00060-7)
- Holmes SJ, Morrow AL, Pickering LK (1996) Child-care practices: effects of social change on the epidemiology of infectious diseases and antibiotic resistance. *Epidemiol Rev* 18:10–28. <https://doi.org/10.1093/oxfordjournals.epirev.a017913>
- Instanes C, Hetland G, Berntsen S et al (2005) Allergens and endotoxin in settled dust from day-care centers and schools in Oslo, Norway. *Indoor Air* 15:356–362. <https://doi.org/10.1111/j.1600-0668.2005.00381.x>
- Ivanova K, Stojanovska Z, Tsanova M et al (2014) Measurement of indoor radon concentration in kindergartens in Sofia, Bulgaria. *Radiat Prot Dosim* 162:163–166. <https://doi.org/10.1093/rpd/neu251>
- Jhun I, Gaffin JM, Coull BA et al (2017) School environmental intervention to reduce particulate pollutant exposures for children with asthma. *J Allergy Clin Immunol Pract* 5:154–159.e3. <https://doi.org/10.1016/j.jaip.2016.07.018>
- Jónsson G, Theodórrsson ÓHP, Karlsson SMMRK (2015) Indoor and outdoor radon levels in Iceland. In: Conf proc NSFS XVII, pp 128–134
- Kabir E, Kim KH, Sohn JR et al (2012) Indoor air quality assessment in child care and medical facilities in Korea. *Environ Monit Assess* 184:6395–6409. <https://doi.org/10.1007/s10661-011-2428-5>
- Kaczmarek K, Zajusz Zubek E, Mainka A (2017) PM₁₀ composition in urban and rural nursery schools in Upper Silesia, Poland: a trace elements analysis. *Int J Environ Pollut* 61:98. <https://doi.org/10.1504/ijep.2017.10006759>
- Kalimeri KK, Saraga DE, Lazaridis VD et al (2016) Indoor air quality investigation of the school environment and estimated health risks: two-season measurements in primary schools in Kozani, Greece. *Atmos Pollut Res* 7:1128–1142. <https://doi.org/10.1016/j.apr.2016.07.002>
- Kamaruzzaman S, Razak R (2011) Measuring indoor air quality performance in Malaysian government kindergarten. *J Build Perform* 2:70–79
- Kavlock R, Barr D, Boekelheide K et al (2006) NTP-CERHR expert panel update on the reproductive and developmental toxicity of di(2-ethylhexyl) phthalate. *Reprod Toxicol* 22:291–399. <https://doi.org/10.1016/j.reprotox.2006.04.007>
- Kelly FJ, Fussell JC (2019) Improving indoor air quality, health and performance within environments where people live, travel, learn and work. *Atmos Environ* 200:90–109. <https://doi.org/10.1016/j.atmosenv.2018.11.058>
- Kim KY, Kim CN (2007) Airborne microbiological characteristics in public buildings of Korea. *Build Environ* 42:2188–2196. <https://doi.org/10.1016/j.buildenv.2006.04.013>
- Kim W, Choi I, Jung Y et al (2013) Phthalate levels in nursery schools and related factors. *Environ Sci Technol* 47:12459–12468. <https://doi.org/10.1021/es4025996>
- Kim KH, Kabir E, Kabir S (2015) A review on the human health impact of airborne particulate matter. *Environ Int* 74:136–143. <https://doi.org/10.1016/j.envint.2014.10.005>
- Knibbs LD, Morawska L, Bell SC, Grzybowski P (2011) Room ventilation and the risk of airborne infection transmission in 3 health care settings within a large teaching hospital. *Am J Infect Control* 39:866–872. <https://doi.org/10.1016/j.ajic.2011.02.014>
- Koch HM, Drexler H, Angerer J (2004) Internal exposure of nursery-school children and their parents and teachers to di(2-ethylhexyl)phthalate (DEHP). *Int J Hyg Environ Health* 207:15–22. <https://doi.org/10.1078/1438-4639-00270>
- Kullab M (2005) Assessment of radon-222 concentrations in buildings, building materials, water and soil in Jordan. *Appl Radiat Isot* 62:765–773. <https://doi.org/10.1016/j.apradiso.2004.10.010>
- Luengas A, Barona A, Hort C, Gallastegui G, Platel V, Elias A (2015) A review of indoor air treatment technologies. *Reviews in Environmental Science and Bio/Technology* 14(3):499–522. <https://doi.org/10.1007/s11157-015-9363-9>

- Madureira J, Paciência I, Rufo JC et al (2015) Assessment and determinants of airborne bacterial and fungal concentrations in different indoor environments: homes, child day-care centres, primary schools and elderly care centres. *Atmos Environ* 109:139–146. <https://doi.org/10.1016/j.atmosenv.2015.03.026>
- Mainka A, Zajusz-Zubek E (2015) Indoor air quality in urban and rural preschools in Upper Silesia, Poland: particulate matter and carbon dioxide. *Int J Environ Res Public Health* 12:7697–7711. <https://doi.org/10.3390/ijerph120707697>
- Mainka A, Brągoszewska E, Koziełska B et al (2015a) Indoor air quality in urban nursery schools in Gliwice, Poland: analysis of the case study. *Atmos Pollut Res* 6:1098–1104. <https://doi.org/10.1016/j.apr.2015.06.007>
- Mainka A, Zajusz-Zubek E, Kaczmarek K (2015b) PM_{2.5} in urban and rural nursery schools in Upper Silesia, Poland: trace elements analysis. *Int J Environ Res Public Health* 12:7990–8008. <https://doi.org/10.3390/ijerph120707990>
- Mainka A, Zajusz-Zubek E, Koziełska B, Brągoszewska E (2018) Investigation of air pollutants in rural nursery school – a case study. *E3S Web Conf* 28:01022. <https://doi.org/10.1051/e3sconf/20182801022>
- McCloskey WW (1996) American Journal of Therapeutics. *JAMA J Am Med Assoc* 276:504. <https://doi.org/10.1001/jama.1996.03540060080044>
- McCormack MC, Breyssse PN, Matsui EC et al (2011) Indoor particulate matter increases asthma morbidity in children with non-atopic and atopic asthma. *Ann Allergy Asthma Immunol* 106: 308–315. <https://doi.org/10.1016/j.anai.2011.01.015>
- Mendes A, Aelenei D, Papoila AL et al (2014) Environmental and ventilation assessment in Child Day Care Centers in Porto: the Envirh Project. *J Toxicol Environ Health A* 77:931–943. <https://doi.org/10.1080/15287394.2014.911134>
- Morawska L, He C, Johnson G et al (2009) Ultrafine particles in indoor air of a school: possible role of secondary organic aerosols. *Environ Sci Technol* 43:9103–9109. <https://doi.org/10.1021/es902471a>
- Mousavi ES, Kananizadeh N, Martinello RA, Sherman JD (2020) COVID-19 outbreak and hospital air quality: a systematic review of evidence on air filtration and recirculation. *Environ Sci Technol* 55:4134–4147. <https://doi.org/10.1021/acs.est.0c03247>
- Mukala K, Pekkanen J, Tiittanen P et al (1999) Personally measured weekly exposure to NO₂ and respiratory health among preschool children. *Eur Respir J* 13:1411–1417. <https://doi.org/10.1034/j.1399-3003.1999.13f30.x>
- National Research Council (US) Committee on Health Risks of Exposure to Radon (BEIR VI) (1999) Health effects of exposure to radon: BEIR VI. National Academies Press, Washington, DC. <https://doi.org/10.17226/5499>
- Nunes RAO, Branco PTBS, Alvim-Ferraz MCM et al (2015) Particulate matter in rural and urban nursery schools in Portugal. *Environ Pollut* 202:7–16. <https://doi.org/10.1016/j.envpol.2015.03.009>
- Nunes RAO, Branco PTBS, Alvim-Ferraz MCM et al (2016) Gaseous pollutants on rural and urban nursery schools in Northern Portugal. *Environ Pollut* 208:2–15. <https://doi.org/10.1016/j.envpol.2015.07.018>
- Oh HJ, Nam IS, Yun H et al (2014) Characterization of indoor air quality and efficiency of air purifier in childcare centers, Korea. *Build Environ* 82:203–214. <https://doi.org/10.1016/j.buildenv.2014.08.019>
- Ohlwein S, Kappeler R, Kutlar Joss M et al (2019) Health effects of ultrafine particles: a systematic literature review update of epidemiological evidence. *Int J Public Health* 64:547–559. <https://doi.org/10.1007/s00038-019-01202-7>
- Oliveira M, Slezáková K, Delerue-Matos C et al (2016) Assessment of air quality in preschool environments (3–5 years old children) with emphasis on elemental composition of PM₁₀ and PM_{2.5}. *Environ Pollut* 214:430–439. <https://doi.org/10.1016/j.envpol.2016.04.046>
- Park H, Lee B, Ha EH et al (2002) Association of air pollution with school absenteeism due to illness. *Arch Pediatr Adolesc Med* 156:1235–1239. <https://doi.org/10.1001/archpedi.156.12.1235>

- Patel S, Sankhyan S, Boedicker EK et al (2020) Indoor particulate matter during HOMEChem: concentrations, size distributions, and exposures. *Environ Sci Technol* 54:7107–7116. <https://doi.org/10.1021/acs.est.0c00740>
- Planinić J, Vaupotić J, Kobal I (1993) Indoor radon concentrations in kindergartens. *J Environ Radioact* 19:167–171
- Qian H, Miao T, Liu L et al (2020) Indoor transmission of SARS-CoV-2. *Indoor Air* 2020:1–7. <https://doi.org/10.1111/ina.12766>
- Ramalho O, Wyart G, Mandin C et al (2015) Association of carbon dioxide with indoor air pollutants and exceedance of health guideline values. *Build Environ* 93:115–124. <https://doi.org/10.1016/j.buildenv.2015.03.018>
- Rejc T, Kukec A, Bizjak M, Godič Torkar K (2019) Microbiological and chemical quality of indoor air in kindergartens in Slovenia. *Int J Environ Health Res* 00:1–14. <https://doi.org/10.1080/09603123.2019.1572870>
- Rim D, Gall ET, Kim JB, Bae GN (2017) Particulate matter in urban nursery schools: a case study of Seoul, Korea during winter months. *Build Environ* 119:1–10. <https://doi.org/10.1016/j.buildenv.2017.04.002>
- Roda C, Barral S, Ravelomanantsoa H et al (2011) Assessment of indoor environment in Paris child day care centers. *Environ Res* 111:1010–1017. <https://doi.org/10.1016/j.envres.2011.06.009>
- Romieu I, Lugo MC, Velasco SR et al (1992) Air pollution and school absenteeism among children in Mexico City. *Am J Epidemiol* 136:1524–1531. <https://doi.org/10.1093/oxfordjournals.aje.a116474>
- Rosén KG, Richardson G (1999) Would removing indoor air particulates in children's environments reduce rate of absenteeism – a hypothesis. *Sci Total Environ* 234:87–93. [https://doi.org/10.1016/S0048-9697\(99\)00266-1](https://doi.org/10.1016/S0048-9697(99)00266-1)
- Rullo VEV, Rizzo MC, Karla LA et al (2002) Daycare centers and schools as sources of exposure to mites, cockroach, and endotoxin in the city of São Paulo, Brazil. *J Allergy Clin Immunol* 110: 582–588. <https://doi.org/10.1067/mai.2002.127511>
- Ruotsalainen R, Jaakkola N, Jaakkola JJK (1993) Ventilation and indoor air quality in Finnish daycare centers. *Environ Int* 19:109–119
- Salo PM, Sever ML, Zeldin DC (2009) Indoor allergens in school and day care environments. *J Allergy Clin Immunol* 124:185–192. <https://doi.org/10.1016/j.jaci.2009.05.012>
- Salonen H, Duchaine C, Mazaheri M et al (2015) Airborne viable fungi in school environments in different climatic regions – a review. *Atmos Environ* 104:186–194. <https://doi.org/10.1016/j.atmosenv.2015.01.012>
- Schentag JJ, Akers C, Campagna P, Chirayath P (2004) SARS: clearing the air. In: Learning from SARS: preparing for the next disease outbreak: workshop summary. National Academies Press, Washington, DC. <https://www.ncbi.nlm.nih.gov/books/NBK92445>. Accessed 11 May 2021
- Schuez-Havupalo L, Toivonen L, Karppinen S et al (2017) Daycare attendance and respiratory tract infections: a prospective birth cohort study. *BMJ Open* 7:1–8. <https://doi.org/10.1136/bmjopen-2016-014635>
- Seppänen OA, Fisk WJ (2004) Summary of human responses to ventilation. *Indoor Air* 14(Suppl 7):102–118. <https://doi.org/10.1111/j.1600-0668.2004.00279.x>
- Shendell DG, Prill R, Fisk WJ, Apte MG, Blake D, Faulkner D (2004) Associations between classroom CO₂ concentrations and student attendance in Washington and Idaho. *Indoor Air* 14: 333–341. <https://doi.org/10.1111/j.1600-0668.2004.00251.x>
- Siegel JA (2016) Primary and secondary consequences of indoor air cleaners. *Indoor Air* 26:88–96. <https://doi.org/10.1111/ina.12194>
- Singh MK, Ooka R, Kumar A et al (2019) Progress in thermal comfort studies in classrooms over last 50 years and way forward. *Energy Build* 188–189:149–174. <https://doi.org/10.1016/j.enbuild.2019.01.051>
- Smedje G, Norbäck D (2000) New ventilation systems at select schools in Sweden—effects on asthma and exposure. *Arch Environ Heal An Int J* 55:18–25

- Smedje G, Norback D (2001) Irritants and allergens at school in relation to furnishings and cleaning. *Indoor Air* 11:127–133. <https://doi.org/10.1034/j.1600-0668.2001.110207.x>
- Sousa SIV, Branco PTBS, Nunes RAO et al (2015) Radon levels in nurseries and primary schools in Bragança District – preliminary assessment. *J Toxicol Environ Health A* 78:805–813. <https://doi.org/10.1080/15287394.2015.1051171>
- Stankevica G, Lesinskis A (2017) Indoor air quality and thermal comfort evaluation in Latvian daycare centers with carbon dioxide, temperature and humidity as indicators. *J Civ Eng Archit* 6:633–638. <https://doi.org/10.17265/1934-7359/2012.05.012>
- St-Jean M, St-Amand A, Gilbert NL et al (2012) Indoor air quality in Montréal area day-care centres, Canada. *Environ Res* 118:1–7. <https://doi.org/10.1016/j.envres.2012.07.001>
- Strachan DP, Sanders CH (1989) Damp housing and childhood asthma; respiratory effects of indoor air temperature and relative humidity. *J Epidemiol Community Health* 43:7–14
- Sundell J, Levin H, Nazaroff WW, et al (2011) Ventilation rates and health: multidisciplinary review of the scientific literature. *Indoor Air* 21:191–204
- Tecer LH, Alagha O, Karaca F et al (2008) Particulate matter ($PM_{2.5}$, $PM_{10-2.5}$, and PM_{10}) and children's hospital admissions for asthma and respiratory diseases: a bidirectional case-crossover study. *J Toxicol Environ Health A* 71:512–520. <https://doi.org/10.1080/15287390801907459>
- Trevisi R, Leonardi F, Simeoni C et al (2012) Indoor radon levels in schools of South-East Italy. *J Environ Radioact* 112:160–164. <https://doi.org/10.1016/j.jenvrad.2012.05.030>
- Varghese SK, Gangamma S (2009) Particle deposition in human respiratory system: deposition of concentrated hygroscopic aerosols. *Inhal Toxicol* 21:619–630. <https://doi.org/10.1080/08958370802380792>
- Vaupotić J (2002) Search for radon sources in buildings – kindergartens. *J Environ Radioact* 61: 365–372. [https://doi.org/10.1016/S0265-931X\(01\)00134-5](https://doi.org/10.1016/S0265-931X(01)00134-5)
- Vaupotić J, Bezek M, Kávási N et al (2012) Radon and thoron doses in kindergartens and elementary schools. *Radiat Prot Dosim* 152:247–252. <https://doi.org/10.1093/rpd/ncs232>
- Villanueva F, Tapia A, Lara S, Amo-Salas M (2018) Indoor and outdoor air concentrations of volatile organic compounds and NO_2 in schools of urban, industrial and rural areas in Central-Southern Spain. *Sci Total Environ* 622–623:222–235. <https://doi.org/10.1016/j.scitotenv.2017.11.274>
- Vuchkov D, Ivanova K, Stojanovska Z et al (2013) Radon measurement in schools and kindergartens (Kremikovtsi Municipality, Bulgaria). *Romanian Rep Phys* 58:S328–S335
- Wang L, Zhao B, Liu C et al (2010) Indoor SVOC pollution in China: a review. *Chin Sci Bull* 55: 1469–1478
- Weinmayr G, Romeo E, de Sario M et al (2010) Short-term effects of PM_{10} and NO_2 on respiratory health among children with asthma or asthma-like symptoms: a systematic review and meta-analysis. *Environ Health Perspect* 118:449–457. <https://doi.org/10.1289/ehp.0900844>
- Wichmann J, Lind T, Nilsson MAM, Bellander T (2010) $PM_{2.5}$, soot and NO_2 indoor–outdoor relationships at homes, pre-schools and schools in Stockholm, Sweden. *Atmos Environ* 44: 4536–4544. <https://doi.org/10.1016/j.atmosenv.2010.08.023>
- World Health Organization (2009) WHO handbook on indoor radon: a public health perspective. World Health Organization
- World Health Organization (2010) WHO guidelines for indoor air quality: selected pollutants. World Health Organization. Regional Office for Europe
- World Health Organization (2013) Global tuberculosis report 2013. World Health Organization
- World Health Organization (2021) WHO global air quality guidelines: particulate matter ($PM_{2.5}$ and PM_{10}), ozone, nitrogen dioxide, sulfur dioxide and carbon monoxide. World Health Organization, Geneva
- Yang W, Sohn J, Kim J et al (2009) Indoor air quality investigation according to age of the school buildings in Korea. *J Environ Manag* 90:348–354. <https://doi.org/10.1016/j.jenvman.2007.10.003>

- Yoon C, Lee K, Park D (2011) Indoor air quality differences between urban and rural preschools in Korea. *Environ Sci Pollut Res* 18:333–345. <https://doi.org/10.1007/s11356-010-0377-0>
- Yoshida JA, Nomura M, Mikami K, Hachisu H (2000) Thermal comfort of severely disabled children in nursery schools in Japan. In: Proceedings of the Human Factors and Ergonomics Society Annual Meeting. SAGE Publications Sage CA: Los Angeles, CA, pp 712–715
- Yun H, Nam I, Kim J et al (2014) A field study of thermal comfort for kindergarten children in Korea: an assessment of existing models and preferences of children. *Build Environ* 75:182–189. <https://doi.org/10.1016/j.buildenv.2014.02.003>
- Zender-Swiercz E, Telejko M (2019) Indoor air quality in kindergartens in Poland. *IOP Conf Ser Mater Sci Eng* 471:092066. <https://doi.org/10.1088/1757-899X/471/9/092066>
- Zhang S, Mumovic D, Stamp S et al (2021) What do we know about indoor air quality of nurseries? A review of the literature. *Build Serv Eng Res Technol* 2021:014362442110098. <https://doi.org/10.1177/01436244211009829>
- Zuraimi MS, Tham KW (2008) Indoor air quality and its determinants in tropical child care centers. *Atmos Environ* 42:2225–2239. <https://doi.org/10.1016/j.atmosenv.2007.11.041>
- Zuraimi MS, Fang L, Tan TK et al (2009) Airborne fungi in low and high allergic prevalence child care centers. *Atmos Environ* 43:2391–2400. <https://doi.org/10.1016/j.atmosenv.2009.02.004>



Indoor Air Quality in Schools

64

Chryssa Thoua, Elizabeth Cooper, Samuel Stamp,
Anna Mavrogianni, and Dejan Mumovic

Contents

Introduction	1892
What Is Unique About Schools?	1892
Review of the School Building Archetypal Forms	1893
Classroom IAQ	1894
IAQ Variables	1894
Empirical Evidence and Key Monitoring Studies	1894
Health Outcomes and Limits	1895
Ventilation Rates	1898
Effect on Health and Academic Performance	1898
Ventilation Rates Requirements and Limits	1901
Ventilation Rates: Levels	1902
The Assessment of IAQ	1904
Carbon Dioxide	1906
Effects of CO ₂ on Health and Cognitive/Academic Performance	1906
Limits for CO ₂ and Required Ventilation Rates in Schools	1906
CO ₂ Levels from Existing Studies	1908
Influencing Factors and Correlations	1912
Nitrogen Dioxide	1912
NO ₂ Limits, Link to Health	1912
NO ₂ Levels from Existing Studies	1913
Influencing Factors	1914
Particulate Matter (PM)	1914
PM _x Limits, Link to Health	1914
PM _x Levels from Existing Studies	1916
Influencing Factors	1917
VOCs	1919
VOC Limits, Link to Health	1919
VOC Levels from Existing Studies	1921
Influencing Factors	1923

C. Thoua · E. Cooper (✉) · S. Stamp · A. Mavrogianni · D. Mumovic

Institute for Environmental Design and Engineering, University College London, London, UK

e-mail: c.thoua.12@ucl.ac.uk; elizabeth.l.cooper@ucl.ac.uk; samuel.stamp@ucl.ac.uk;

a.mavrogianni@ucl.ac.uk; d.mumovic@ucl.ac.uk

Summary and Conclusions	1925
The Evidence Gap	1925
Influencing Factors and Correlations	1925
Ventilation Strategy	1926
Air Exchange Rates	1926
Building Envelope Airtightness	1926
Classroom Occupancy	1927
Seasonal Effects	1927
Building Better Schools	1927
Cross-References	1928
References	1928

Abstract

Schools are tasked with providing a safe and healthy place in which children can learn and grow, and it is very important that schools do not contribute to children's exposure to air pollution. Not only do children spend much of their time in school classrooms, but they are also more vulnerable than adults to airborne pollutants because of their developing lungs, narrower airways, and greater air breathed to body weight. Childhood exposure to air pollution can result in reduced lung function that is persistent into adulthood, and may lead to greater susceptibility to respiratory and cardiovascular diseases as adults. Additionally, exposure to poor indoor air quality can lead to increased absenteeism and poorer cognitive or academic performance. Studies from around the world have demonstrated that many schools fail to provide adequate indoor air quality in terms of particulate matter (PM), volatile organic compounds (VOCs), and ventilation rates to reduce indoor generated pollutants.

Keywords

Schools · Classrooms · IAQ · Ventilation · Cognitive performance

Introduction

What Is Unique About Schools?

The primary purpose of schools is to provide a safe and healthy place in which children can learn and grow. Schools present a unique and complex building type for several reasons. First, outside of the home, children spend most of their time indoors at school, roughly 30% of the time. Second, occupant densities are typically higher than for other building types. Third, there are a wide range of pollutant types associated with the wide range of activities common in schools (e.g., arts, gym). Finally, children's different physiologies and developing bodies may make them more vulnerable to different environmental exposures than adults. Specifically, children breathe more air relative to their body weight, have narrower airways, and their actively developing lungs, and other organs, may be less able to repair

themselves from injury (Bateson and Schwartz 2008). Failure to respond appropriately to indoor air quality (IAQ) problems can lead to long- and short-term health problems for the occupants, negatively impact the attendance and performance of students, and impair staff performance. Therefore, it is important to provide optimal indoor air conditions that support the education, health, and well-being of children.

Over the past few decades, problems with the indoor air in schools have come to the attention of both researchers and the public. Issues that affect the quality of air in schools include: increasingly airtight building envelopes, reduced ventilation rates, an increase in the use of harmful compounds in products such as pesticides and cleaning products employed indoors, and the use of synthetic building materials, finishes, and furnishings. This chapter introduces some of the key factors associated with the indoor air quality in schools. First, the chapter will provide a brief review of some of the common school building typologies and influences. Second, there is an introduction to key IAQ variables and monitoring studies in schools. Then the chapter will review what has been reported about IAQ in schools and the health and cognitive performance of students. Next, some of the most commonly occurring indoor air pollutants will be discussed, including existing levels in classrooms from recent studies, and finally a synthesis of the evidence and a discussion of the current knowledge gaps will be provided.

Review of the School Building Archetypal Forms

Understanding the drivers that encourage persistence or change of the school archetypal forms requires a consideration of the historical context of educational activities. Examples of drivers are technological, scientific, and social advances, and crucially through perception of the functional failure or success. The perception of failure or success of a building, and the criteria for this evaluation evolve through research, which influences guideline documents and practice. The emergence, persistence, or replacement of different building typologies are influenced in multiple ways by factors that include interpretation of emerging evidence, and of architectural trends that change the criteria for the evaluation of the success or failure of buildings. Another factor is advancement in construction technology that influences the construction methods and ultimately the different characteristics of buildings. These are reflected in building practice and building standards and regulations. Conversely, these regulations and performance targets can drive technological advances and innovation. Funding streams and procurement methods are traditionally also recognized as a factor. These are historically linked to the evolution of the education system, current pedagogy, and curriculum. In addition to these, in some places, listing and heritage value criteria continue to shape today's school building stock.

From an IAQ perspective, existing literature recognizes building design as an overarching determinant (Ashmore and Dimitroulopoulou 2009; de Gennaro et al. 2014). Factors such as airtightness, air exchange rates, and materials of construction can all contribute to improved or poor air quality.

Emerging evidence is likely to influence building characteristics on a wide scale, leading to new typologies directly and indirectly, through guidelines, changes in building regulations, large-scale adoption of voluntary standards, and guidance documents. An example is the requirement for energy efficient and low-carbon school building structures, e.g., through standards such as Passivhaus or the European Union's Energy Performance of Buildings Directive (EPBD). Additionally, a changing climate will require that our buildings be more resilient and adaptive to new ambient environmental conditions. Most recently, knowledge on how the indoor environment impacts children's health and performance is leading to changes in design guidelines.

Classroom IAQ

IAQ Variables

Acceptable levels for IAQ in classrooms are determined through criteria, ranges, and limits/thresholds for different variables in existing standards and guidelines. These are based on available evidence on their likely effect on health, comfort, and academic or cognitive performance. Indoor air quality in the classroom is directly indicated by the measured indoor air pollutant concentrations or by proxy measures such as ventilation rates.

Indoor air quality variables, investigated because of their relevance to health, include:

- (i) Temperature and thermal comfort indices
- (ii) Ventilation rates and CO₂ levels, and indoor air pollutants including:
 - (a) Particulate matter (PM_x)
 - (b) Nitrogen dioxide (NO₂)
 - (c) A range of volatile organic compounds (VOCs)

Not all known contaminants are presented in this chapter, which focuses instead on pollutants listed in the ambient air quality regulations (PM_x, NO₂, and VOCs), and pollutants with potential indoor sources in classrooms (for example, PM₁₀ and the VOCs formaldehyde, limonene, α-pinene, and toluene). Uncertainty around the chemical composition of the indoor air matrix of pollutants means that variables relevant to IAQ are not fixed and are not universal for all buildings. This result is especially true for VOCs and the chemical components of PM_x in indoor air.

Empirical Evidence and Key Monitoring Studies

Empirical evidence from monitoring studies in schools is important for research in order (i) to identify correlations between IAQ variables in indoor air and health

outcomes, (ii) to link building characteristics to levels of IAQ variables, and (iii) to include more potentially harmful chemical IAQ variables, achieving a holistic assessment of IAQ.

Comprehensive IAQ studies reviewed in this section are included with other indoor environmental studies in schools in Table 1. Among the key IAQ monitoring studies in schools was the comprehensive SINPHONIE study (Schools Indoor Pollution and Health Observatory Network in Europe) with monitoring in 2010–2012 in 114 schools, in 23 countries (Csobod 2014); the SEARCH study (School Environment and Respiratory Health of Children) between 2006–2009 and 2010–2013 in 10 countries (Csobod 2014); and the AIRMEX study (Geiss et al. 2011) which included other building types focused on VOCs. The SEARCH project (2006–2009) explored the relationship between school environments and health with the aim of drafting recommendations. Other review studies include the European Commission's Pilot Indoor Air monitoring study (Kephalopoulos et al. 2014) and the French six cities project (Annesi-Maesano et al. 2013a).

Health Outcomes and Limits

The influence of IAQ in classrooms on children's health, well-being, comfort, attendance, academic achievement, and productivity was explored in a number of studies. The classroom indoor environment was shown to be important for children's health again and again (Bakó-Biró et al. 2012; Mendell and Heath 2005; Wargocki and Wyon 2007) and is noted in regulatory and guidance documents (Kephalopoulos et al. 2014; WHO 2015). The adverse health effects from exposure to poor indoor air quality in classrooms can be both short- and long-term since children spend a large amount of time in the school classroom. The wealth of the available evidence and the complexity of the involved parameters are evident from a series of literature review studies on the correlation of health symptoms to poor IAQ in school classrooms (Annesi-Maesano et al. 2013a; Bluyssen et al. 2018; Daisey et al. 2003; de Gennaro et al. 2014). The review by Daisey et al. (2003) investigated the correlations between a set of IAQ parameters in schools (including ventilation rates, CO₂ concentrations, and concentrations of indoor air pollutants including VOCs, formaldehyde, microbiological factors, and allergens) and a number of adverse health effects on children: asthma, acute and chronic irritation symptoms, and cancer.

Another review (Mendell and Heath 2005) focused on the influence of IAQ and thermal conditions on academic performance and attendance of children in schools. It found evidence to link higher nitrogen dioxide (NO₂) levels to reduced school attendance and inadequate ventilation rates to reduced performance. The study suggested asthma and respiratory infections associated with dampness and microbiological factors are likely influencing performance and attendance. Key studies that investigated the correlation between classroom indoor environment and cognitive or academic performance are summarized in Table 2.

Table 1 Key monitoring studies of indoor environmental quality in schools in different countries

Study name and reference	Sample (country, numbers), years	Monitored parameters
The AIRMEX study Geiss et al. (2011)	Included school buildings, monitoring between 2003 and 2008 In nonresidential buildings: including schools, public buildings and offices, in EU cities	Monitored parameters VOCs
EXPOLIS-UK Lai et al. (2004)	1998–2000, Oxford, UK Measured locations: home indoor, home outdoor, work indoor concentrations, and personal exposure	NO ₂ , CO ₂ , CO, PM _{2.5} , 37 elements in PM _{2.5} , 30 VOCs
WHO Schools Survey WHO (2015)	2012–2014, monitoring in Croatia, Albania, Latvia, Estonia, and Lithuania, 233 schools	NO ₂ , CO ₂ , CO, formaldehyde, benzene, ventilation rates, mold
SEARCH (School Environment and Respiratory Health of Children) Csobod (2014)	2006–2009 (phase I), monitoring in 6 countries: Albania, Bosnia and Herzegovina, Hungary, Italy, Serbia, and Slovakia 2010–2013 (phase II) In 10 countries in addition: Belarus, Kazakhstan, Tajikistan, and Ukraine	CO, CO ₂ , NO ₂ , formaldehyde, benzene, toluene, xylenes, PM ₁₀
HESE (Health Effects of the School Environment) Csobod (2014)	2004–2005, monitoring in 21 schools, 5 European countries (Italy, France, Norway, Sweden, Denmark)	Ventilation, lighting, PM, NO ₂ , CO ₂ , O ₃ , formaldehyde, dust/air allergens, molds, bacteria.
SINPHONIE Csobod (2014)	2010–2012, monitoring in 114 primary schools across 23 countries in Europe Countries included the UK	CO, NO ₂ , CO ₂ , O ₃ , PM ₁₀ , PM _{2.5} , dust allergens, dust/air bacteria, mold, formaldehyde, benzene, α-pinene, D-limonene, naphthalene, trichloroethylene, tetrachloroethylene, PAHs (B[a]P)
SINPHONIE-UK Chatzidiakou, Mumovic, Summerfield, Hong, and Altamirano-Medina (2014)	5 primary schools and 1 nursery, UK	PM, NO ₂ , O ₃ , TVOCs monitored over 5 consecutive days
BRE-ODPM Ajiboye, White, Graves, and Ross (2006)	8 primary schools, England, UK. Post-1995 buildings 2 classrooms in each school, duration 1 working week Measurements September 2002–February 2003 and October–November 2003	Monitored over 2 weeks in each school: air exchange rates, temperature, RH, CO ₂ , VOCs, TVOCs, CO, NO ₂ , PM ₁₀ , PM _{2.5} , aldehydes, fungi and bacteria, dust mites

(continued)

Table 1 (continued)

Study name and reference	Sample (country, numbers), years	Monitored parameters
CEHAP-E-WHO-Austria Wallner et al. (2012)	Elementary schools, Austria 2 classrooms per school, both seasons, 1-week periods	34 pollutants Temperature, RH, CO ₂ , PM Chemical groups: alcohols, chlorinated hydrocarbons, aliphatic hydrocarbons, terpenes, aldehydes, other including NO ₂ , VOCs in PM/dust, perfumes, phenols, phthalates, trisphosphates, PAHs, PCBs, and other Spirometry on children
Zhong, Su, and Batterman (2017)	144 classrooms in 37 conventional and high-performance schools recently built or renovated (last 15 years) in the USA. Monitoring took place in 2015–2016.	Temperature, RH, CO ₂ , PM, noise. Indoor and outdoor concentrations of 94 VOCs were determined (using thermal desorption, gas chromatography-mass spectroscopy) Only those compounds, 24 were detected in over 15% of the samples were included in the analysis. Duplicates in 3 schools
PRIMEQUAL Blondeau, Iordache, Poupard, Genin, and Allard (2005) Poupard, Blondeau, Iordache, and Allard (2005)	France 8 primary schools 1 classroom in a MV school. 5 classrooms total. 2-week periods, repeated in winter and in summer	O ₃ , nitrogen oxides (NO and NO ₂), PM, temperature, RH, CO ₂ concentration
EC ISAAC II Annesi-Maesano et al. (2013a), Annesi-Maesano et al. (2012) (International Survey of Asthma and Allergy in Childhood)	France, 6 cities, 108 schools, 401 classrooms	PM _{2.5} , formaldehyde, NO ₂ , O ₃
Stranger, Potgieter-Vermaak, and Van Grieken (2008) reported on a subset in Belgium of the ISAAC III Project schools in 56 countries ISAAC monitoring took place in 2001	Antwerp, Belgium, in 2001, 27 primary schools, children ages 6–7 and 13–14 years (older than primary school ages in the UK) Heating (December 2002 and non-heating season (June 2003)	PM _{2.5} (elemental content of PM) NO ₂ , SO ₂ , O ₃ BTEX
de Gennaro et al. (2014)	8 school buildings, both middle and elementary, Southeast Italy	The study provided quantitative information on 14 compounds including formaldehyde

(continued)

Table 1 (continued)

Study name and reference	Sample (country, numbers), years	Monitored parameters
Rovelli et al. (2014)	7 schools (of which 3 primary schools), Milan, Italy, three classrooms in each school, monitoring over a week in winter, 2011–2013. Naturally ventilated only	PM, CO ₂ , temperature
Sofuoğlu, Aslan, Inal, and Sofuoğlu (2011)	3 primary schools, Turkey	The method was optimized for quantitative determination of 51 compounds, and an average of 16 compounds were found in the samplers. Active sampling, repeated 6–9 times each season, repeated in fall, winter, and spring. Monitoring in a classroom, a kindergarten, and outdoor playground site
Ye, Won, and Zhang (2017)	A practical method and its applications to prioritize volatile organic compounds emitted from building materials based on ventilation rate requirements and ozone-initiated reactions	List of priority VOCs and assessment based on combined effect
Kim et al. (2007)	8 primary schools, Sweden	Plasticizers MVOCs
Fromme et al. (2013) LUPE 2 study	Germany, 14 classrooms over 20 consecutive days, 1 classroom over 83 days	PM, endotoxins, CO ₂

Ventilation Rates

Effect on Health and Academic Performance

Many studies have found a positive correlation between ventilation rates and measures of academic, cognitive performance and productivity. The following provides some of the key findings.

Wargocki and Wyon (2013) found that numerical test performance (in terms of speed) increased with ventilation rates and in the same paper proposed a dose-response relationship between classroom ventilation rates and student performance. An earlier study, by the same authors (Wargocki and Wyon 2007), reported on findings from the investigation of the influence of outdoor airflow rate on academic performance and found significant improvements in the speed of completing tasks with increased outdoor airflow.

Table 2 Existing evidence on effects of classroom IEQ on health, comfort, academic and cognitive performance of children

Study	Method	Sample	Environmental variable	Health or performance variable	Nr/ages of children	Findings/limitations
Wyon (1970) from review	Intervention study		Temperature (20, 27, 30 °C)	School exercises: Numerical (addition, multiplication, number checking) Language (reading and comprehension, supplying synonyms and antonyms)	9–10-year-old 3 classes	Numerical exercises, a decrease in speed was seen with higher temperatures. Reading comprehension as well as reading speed was reduced. Significant changes in afternoon not in morning.
Schoer (1973) from reviews	Timed with stopwatch, maximum effort conditions		Temperature	19 tests from simple-repetitive tests to school exercises	10–12-year-old, 2 groups, over 6–8 weeks	Finding: cooler classroom, higher performance Limitations: increasing difference between groups with time
Wargocki and Wyon (2007)	Field intervention experiments, summer, double crossover, 1 week	Denmark, 1 school, 2 classrooms	Air temp. and Air temp. plus outdoor air supply	Timed tests for academic performance Language and numerical, incorporated in normal lesson	10–12-year-old	
Petersen, Jensen, Pedersen, and Rasmussen (2016)	Field intervention, double-blind crossover	Denmark, 2 schools, 4 classrooms	Ventilation rates (measured through CO ₂ concentration)		10–12-year-old	
Haverinen-Shaughnessy, Moschandreas, and	Intervention, monitoring 1 day, closed conditions, winter/spring months	USA south west, 104 classrooms /schools	Ventilation rates from CO ₂ levels	Academic achievement, standardized tests, curriculum aligned	Fifth grade 10–11 years	A correlation was found between ventilation rates and percentages of children passing the math and reading tests

(continued)

Table 2 (continued)

Study	Method	Sample	Environmental variable	Health or performance variable	Nr/ages of children	Findings/limitations
Shaughnessy (2011)						
Twardella et al. (2012)		6 schools MV, 20 classrooms, 417 children, Germany	Median CO ₂ levels	Concentration, using a test	9–10 years	Accuracy decreased when median CO ₂ concentration increased but concentration was unaffected
Hutter et al. (2013)	Monitoring, 1 week winter one in summer	9 primary schools, 436 children, in Austria	Semi-volatile organic compounds (including phosphorganic compound TCEP) and CO ₂	Cognitive performance of children, using SPM tests	6–8 years	A negative correlation was found between CO ₂ and concentrations of CO ₂ and a SVOC and a PAH with cognitive performance in children
Wallner et al. (2012)	LuKi Study: Air and Children					
Bakó-Biró et al. (2012)	Field intervention		Ventilation rates (1 l/s/p to 9 l/s/p)	VisCoPe tests on laptops: Simple reaction time, choice reaction time, color word vigilance, addition reaction time, digit span memory, digit classification, digit symbol matching, picture memory	200 pupils 53 groups of children in 8 school	Faster and more accurate responses for choice reaction, color word vigilance, picture memory, word recognition at higher ventilation rates

A study in the USA explored correlations between classroom ventilation rates and student academic achievement (Haverinen-Shaughnessy et al. 2011). The authors measured ventilation rates in 104 schools (one fifth-grade classroom in each school) in the southwestern USA. Academic achievement was assessed using the national multiple choice standardized tests aligned with the curriculum for that year for subjects of mathematics, reading, social studies, science, and writing. The study concluded that ventilation rates explained an additional 3–6% of the variation of academic achievement (in addition to other explanatory variables including race/ethnicity, type of school, home environment). Within the ventilation range $0.9\text{--}7.1\text{ l s}^{-1}$ per person, an increase of 1 l s^{-1} per person corresponded to an additional 2.9% and 2.7% children passing the math and reading tests, respectively.

A double-blind two-by-two intervention experiment in Denmark, which took place in two schools and four classrooms, investigated the effect of ventilation rate as indicated by CO₂ levels on schoolwork performance (short-term concentration and logical thinking) for children aged 10–12 years (Petersen et al. 2016). The study found an increase in correct answers (but not an increase in wrong answers) as the ventilation rate increased from an average 1.7 l s^{-1} per person to 6.6 l s^{-1} per person (Petersen et al. 2016).

A study in England explored ventilation rates and performance of school children in a field intervention study in 8 primary schools involving 200 pupils (Bakó-Biró et al. 2012; Clements-Croome et al. 2008). Two classrooms in each school (a total of 16 classrooms) were monitored over 3 weeks, and ventilation rates were increased from 1 l s^{-1} per person to 8 l s^{-1} per person while the temperature was maintained within acceptable levels. The study used tests to assess 9–10-year-old children's performance. The results showed improved performance in terms of speed and accuracy for tasks requiring attention, vigilance, memory, and concentration, when ventilation rates increased.

Ventilation Rates Requirements and Limits

Required ventilation rates in classrooms are determined both through performance-based criteria (that is, requirements are based upon how the building, or building systems, meets measurable outcomes) and prescriptive criteria. The prescribed methods, however, should be derived from performance-based considerations.

The 2018 UK guidance for schools (BB101, 2018) requires a minimum 3 L s^{-1} per person and a minimum daily average 5 L s^{-1} per person. The occupants should be able to achieve a recommended 8 L s^{-1} per person in mixed mode ventilation or naturally ventilated school buildings. The UK guidelines suggest that ventilation levels above the minimum may be determined necessary based on the CO₂ requirements (ESFA 2018). Ventilation levels equivalent to 8 L s^{-1} per person, regardless of ventilation strategy, were associated with levels below 1000 ppm (Santamouris et al. 2008).

Similarly, the ANSI/ASHRAE Standard 62.1 2016 requires a minimum of 5 L s^{-1} per person and a 0.6 L per m^2 floor area in primary school classrooms occupied by

children. For a classroom of typical floor area 60 m^2 , and 30 occupants, this amounts to 6.2 L s^{-1} per person (ANSI/ASHRAE 2016).

The Australian building regulations require a 7.5 L s^{-1} per person to achieve acceptable levels of CO₂ concentration (Luther et al. 2018). This value is a steady state estimation, suggesting that it corresponds to the daily average. In Sweden, regulatory requirement of ventilation in schools requires $0.35 \text{ L s}^{-1} \text{ m}^{-2}$ plus 7 L s^{-1} per person.

While mainly based on office buildings, an outdoor air supply rate of 10 L s^{-1} per person is recommended for occupant health, also satisfying the 8 L s^{-1} per person to limit odor dissatisfaction due to bio-effluent emissions when entering an occupied space. These requirements may not suffice for addressing “occasional occupant controlled” sources of pollution such as cleaning and painting. Ventilation per occupant for limiting CO₂ levels to below 1000 ppm may not be adequate to limit other pollutants (Apte 2000; Daisey et al. 2003). A summary of requirements in standards and guidelines for rates of ventilation in schools is found in Table 3.

Ventilation Rates: Levels

Ventilation rates in primary school classrooms vary greatly with studies finding many classrooms do not achieve the recommended rate, which is typically about

Table 3 Requirements for ventilation rates in classrooms in standards and guidance

Standard or guidance document	Required ventilation rates
BB101 U.K. (ESFA 2018)	Minimum ventilation rate: 3 L s^{-1} per person Minimum average ventilation rate: 5 L s^{-1} per person Achievable ventilation rate (and for bio-effluents): 8 L s^{-1} per person
ADF U.K. (HM Government 2010)	For human health: 10 L s^{-1} per person
ANSI/ASHRAE Standard 62.1 2016 for classrooms with children (ANSI/ASHRAE 2016)	5 L s^{-1} per person plus 0.6 L s^{-1} per m^2 floor area $= 6.2 \text{ L s}^{-1}$ per person (assuming 60 m^2 classroom 30 occupants)
Australian Building Code (Luther et al. 2018)	7.5 L s^{-1} per person
BS EN ISO 16798-1: 2019 (BSI 2019)	10 L s^{-1} per person plus $1 \text{ L s}^{-1} \text{ m}^{-2}$ floor area (Cat. 1) 7 (Cat. 2.) 4 (Cat. 3) Minimum during occupancy 4 L 4, 7, or 10 L per person Plus 1 , 0.7 , or 0.4 L per m^2 Total 12 , 8.4 , 4.8 L per person

8 L s⁻¹ per person average (Blondeau et al. 2005; Chatzidiakou et al. 2012, 2015a, b, c; Daisey et al. 2003; Fromme et al. 2007). A number of studies estimated or measured ventilation rates under normal operation of the occupied classroom or under controlled conditions during interventions for the evaluation of infiltration and purge/maximum achievable ventilation rates, and found them to be inadequately ventilated (e.g., Chatzidiakou et al. 2014; Mendell et al. 2016).

A European study calculated ventilation rates from monitored CO₂ levels (Csobod 2014). The study found average ventilation rates of 1.8 L s⁻¹ per person, and a minimum to maximum range of 0.1–13.3 L s⁻¹ per person, highlighting that the large majority (86%) of the classrooms achieved less than 4 L s⁻¹ per person, which was cited as the minimum required average. The UK, Belgium, Germany, France, and Austria were among those countries for which even lower ventilation rates were reported (average 0.9 L s⁻¹ per person, range 0.2–2.9 L s⁻¹ per person).

A study of schools in Greece reported ventilation rates from a database generated from a literature review across different countries that included over 1,000 classrooms. Median ventilation rates were 8.3 L s⁻¹ per person for mechanically ventilated school buildings and 3.0 L s⁻¹ per person for naturally ventilated schools in the database (Santamouris et al. 2008). According to the review, 81% of the naturally ventilated and 45% of the mechanically ventilated classrooms failed to achieve ventilation levels at or better than the recommended minimum of 8 L s⁻¹ per person.

In the UK, Chatzidiakou et al. (2014) estimated infiltration, usual, and purge ventilation rates in 18 primary school classrooms in the UK and reported these as air changes per hour and L s⁻¹ per person, and found higher typical ventilation rates in the non-heating season. The usual ventilation rates during occupancy in the heating season ranged from 2.3 to 5.1 L s⁻¹ per person and in the non-heating season ranged 2.8–6.3 L s⁻¹ per person (Chatzidiakou et al. 2014). The average ventilation rate requirement of 5 L s⁻¹ per person (per UK regulations) was not achieved in most classrooms.

Studies in mild to warm climates found higher ventilation rates than studies in colder climates under normal operation, which could be due to more frequent window opening as well as design and construction characteristics allowing for larger opening areas. Santamouris et al. (2008) measured ventilation rates in 61 classrooms in naturally ventilated schools in Greece. The infiltration rates, determined with closed windows, were on average about 1.5 L s⁻¹ per person, increasing to 4.5 L s⁻¹ per person (range 2–11 L s⁻¹ per person) during teaching and further increasing during breaks, with a median of 7 L s⁻¹ per person and a range of 2–20 L s⁻¹ per person. The study found that ventilation rates were consistently higher in Greek schools during teaching hours, and that ventilation rates were highly variable during both teaching and break periods. In California, USA, Mendell et al. (2016) investigated the influence of ventilation rates in primary school classrooms on children's performance on standardized tests. The study estimated daily ventilation rates in 150 classrooms of 28 schools from measured occupant generated CO₂ concentrations over equilibrium periods, over a 2-year period. The sample consisted of naturally ventilated, mechanically ventilated, and air-conditioned mechanically ventilated classrooms. The ventilation rates were compared to the requirements in

California, of 7.1 L s^{-1} per person and the now superseded ASHRAE 62 Standard $6.7\text{--}7.4 \text{ L s}^{-1}$ per person (ANSI/ASHRAE 2013). The study found median school-year ventilation rates of 6.8 L s^{-1} per person for naturally ventilated schools, 7.7 L s^{-1} per person for mechanically ventilated schools, and 2.9 for air-conditioned classrooms. The averages and standard deviation (σ) were respectively $7.0 (2.4) \text{ L s}^{-1}$ per person, $8.0 (2.2) \text{ L s}^{-1}$ per person, and $3.3 (1.7) \text{ L s}^{-1}$ per person. Findings from Mendell et al. are not consistent with the wide differences between naturally ventilated and mechanically ventilated schools found in Santamouris et al. (2008) but revealed that air-conditioned classrooms were likely to experience lower ventilation rates.

Mumovic et al. (2009) monitored 18 classrooms in 9 contemporary secondary schools in England, UK. The study found that ventilation rates under normal operation in the heating season in secondary classrooms were lower in naturally ventilated classrooms compared to four mechanically or mixed mode ventilation classrooms. Average ventilation rates in 12 naturally ventilated classrooms were 3.3 L s^{-1} per person, and 7.2 L s^{-1} per person in 4 classrooms with mechanical ventilation. The 8 L s^{-1} per person was only achieved through window opening even in mechanically ventilated classrooms. Higher natural ventilation rates were observed in classrooms with cross and stack airflow or fully openable windows.

Across the reviewed studies, average ventilation rates during usual operation were 4.9 L s^{-1} per person. A summary of findings from investigations in ventilation in classrooms can be found in Table 4.

The Assessment of IAQ

Existing guidelines and standards, regulatory documents, and academic studies provide different interpretations of the definition of good indoor air quality, which are reflected in the assessment procedures and relevant criteria.

The ANSI/ASHRAE standard provides a comprehensive procedure for the assessment of indoor air quality and the provision of measures, such as ventilation, for providing acceptable indoor air quality without adverse health effects for occupants. More specifically, compliance with requirements is assessed with one of, or a combination of, the three procedures: the *Ventilation Rate Procedure* and the *IAQ Procedure* for the mechanical ventilation systems, and the *Natural Ventilation Procedure* for the natural ventilation systems of a building. The “*IAQ Procedure*” includes identification of main sources for contaminants of concern and determination of individual contaminant concentration limits. This method is a knowledge-based approach, not only relying on source identification but also suggesting that exhaustive IAQ assessment is required. It also suggests that the IAQ indicators need to reflect a different list of contaminants in each building, thus any comparison cannot rely on individual contaminant concentrations but on a cumulative metric, e.g., a version of the total VOC metric. In the following sections, the most common indoor pollutants, their effects, sources, and influencing factors are explored in greater detail.

Table 4 Monitoring studies which investigated classroom air exchange and ventilation rates in schools

Study	Country	Length of monitoring	Sample size	Conditions of operation	Ventilation rates (units vary)
SINPHONIE (Csobod et al. 2014)	European countries including the UK	One week in each season	300 primary schools	Normal operation	Average 1.8 L s^{-1} per person, range $0.1\text{--}13.3 \text{ L s}^{-1}$ per person
Santamouris et al. (2008) database from literature review	International database			Mediannally ventilated schools	Mediannally ventilated schools Median 8.3 L s^{-1} per person in mechanically ventilated schools Median 3 L s^{-1} per person in naturally ventilated schools
Chatzidiakou et al. (2014)	UK, primary schools	One week in each season	18 primary school classrooms	Normal operation, usual	Range $2.3\text{--}6.3 \text{ L s}^{-1}$ per person
Mendell et al. (2016)	California, USA	Longitudinal, average daily VRs, average of 30 days, medians over 2 years	150 classrooms, 28 schools	Heating season average 3.8 L s^{-1} per person Non-heating season average 5.2 L s^{-1} per person	

Carbon Dioxide

Effects of CO₂ on Health and Cognitive/Academic Performance

Existing literature provides evidence on correlations between increased CO₂ levels and health and cognitive performance of adults and children. High CO₂ levels were associated with several metrics for asthma, absenteeism, and poor cognitive performance in children (Annesi-Maesano et al. 2013a; Daisey et al. 2003). Azuma et al. (2018) found that exposure to indoor CO₂ levels influenced health and psychomotor performance. The correlation between CO₂ and attendance and academic performance was investigated by Gaihre et al. (2014) in Scottish primary schools. The study found a negative correlation between CO₂ levels and attendance records, but found no correlation between CO₂ concentrations and measures of academic performance. An increase of 100 ppm in CO₂ concentration was associated with a 0.2% drop in attendance, which is equivalent to 1 half day per year. From the Csobod et al. (2014) investigation of the effect of indoor air on attention and concentration levels, increased CO₂ levels were found to have a negative correlation with performance in morning logical tests as well as with attendance, with asthma being the most common reason for missing school among chronic diseases. Increased CO₂ levels were associated with reduced cognitive performance in children according to Hutter et al. (2013) in a study in Austrian schools.

Since CO₂ levels in classrooms are strongly correlated with ventilation rates and other occupant-related pollutants (Chatzidiakou et al. 2015a, b, c), some studies have challenged the implied causal relationship between exposure to CO₂ and health effects due to confounding effects from covariates (Azuma et al. 2018; Carreiro-Martins et al. 2014). Zhang et al. (2017) suggested that bio-effluents, rather than CO₂, were responsible for effects on performance tasks. Addressing these concerns around methodological limitations of existing studies, a review by Azuma et al. (2018) concluded that CO₂ exposure can have effects on health and physiological performance. Nevertheless, further research is required to understand the effects of a wide range of CO₂ levels (500–3000 ppm) on children who may be more susceptible than adults (Azuma et al. 2018).

Limits for CO₂ and Required Ventilation Rates in Schools

Since CO₂ is generated by the occupants through exhaled air, its concentration in indoor air is often used for the performance-based determination of ventilation requirements in classrooms. This approach is in addition to sufficient ventilation for satisfying cooling requirements and for limiting pollutants from indoor sources other than occupants.

Slight variations in guidance exist between countries, and a summary of several standards can be found in Table 5. Azuma et al. (2018) reported that upper limits for indoor CO₂ concentrations are set at 1000 ppm in a number of countries including Germany, Norway, South Korea, Japan, and Canada. In Portugal, the

Table 5 Recommended limits for indoor CO₂ levels in nonresidential buildings in existing standards

Standard/publication year	Category/description	CO ₂ levels limit or target value (ppm)	CO ₂ levels assuming outdoor levels 400 ppm
ANSI-ASHRAE 62.1 Standard (ANSI/ASHRAE 2016)	Maximum Limit	Outdoor +700	1100
2018 BB101 (ESFA 2018)	Achievable levels most of the occupied time in new buildings	Outdoor +800	1200
	Achievable levels most of the occupied time in existing buildings	Outdoor +1350	1750
BS EN ISO 16798-1: 2019 (BSI 2019)	Category 1	Outdoor +550	950
	Category 2	Outdoor +800	1200
	Category 3	Outdoor +1350	1750

limit for average CO₂ concentration in classrooms is higher at 1250 ppm. The national regulations for school buildings in the Netherlands, according to Teeuwen et al. (2015), require a maximum 95th percentile of 1200 ppm, allowing for the limit to be exceeded up to 5% of the time while defining three bands of performance. The performance is acceptable if the 95th percentile is between 1000 and 1200 ppm, good if between 800 and 1000 ppm, and very good if less than 800 ppm. The influential American National Standard Institute (ANSI) Standard *ANSI/ASHRAE 62.1 2016 Ventilation for Acceptable Indoor Air Quality* recommends concentrations of CO₂ not to exceed 700 ppm over outdoor levels (1,100 ppm, assuming outdoor levels 400 ppm) (ANSI/ASHRAE 2016). The World Health Organization recommended levels of 1,000 ppm above outdoor levels, while a study found 25% predicted percentage of dissatisfied (PPD) at these levels (~1,400 ppm) (Luther et al. 2018).

In the UK, the regulatory requirements for CO₂ concentrations in classrooms are intertwined with ventilation rate requirements in the Approved Document F Ventilation of the UK Building Regulations (HM Government 2010) and the supplementing guidance document Building Bulletin 101 (BB101) Guidelines on ventilation, thermal comfort, and indoor air quality in schools (ESFA 2018). The CO₂ concentration requirements were differentiated for schools that operate on mechanical/mixed and natural ventilation modes. Therefore, two different thresholds are given for maximum daily averages (1000 ppm and 1500 ppm) and for 20-min-long peaks (1500 ppm and 2000 ppm) for mechanically ventilated and naturally ventilated classrooms, respectively. In new naturally ventilated school buildings, BB01 states that concentrations below 1200 ppm (assuming outdoor concentrations at 400 ppm) must be achievable for most of the occupied hours. Similarly, BB101 recommends that mechanical ventilation set points should be set to achieve levels of CO₂ less than 1000 ppm.

CO₂ Levels from Existing Studies

As carbon dioxide is considered as a proxy for indoor air quality in classrooms, it is among the most monitored and investigated pollutants in classrooms. It should be noted, however, that CO₂ may not be a useful proxy for all indoor air pollutants, particularly those from traffic-related sources. Studies that report results from continuous monitoring of CO₂ concentrations in school classrooms generally focus on assessing ventilation rates, indoor air quality, and correlations of CO₂ to pollutants and other variables of environmental performance and children's health or attendance.

A literature review of CO₂ levels in classrooms collated results from studies from several countries (Santamouris et al. 2008). Their literature review of 36 papers reported median levels across naturally ventilated schools of approximately 1420 ppm and for mechanically ventilated schools 910 ppm. Average concentrations exceeded 1500 ppm in 46% of the naturally ventilated schools and 15% of the mechanically ventilated schools. The exceedance percentages over 1000 ppm were 75% and 48%, respectively. Finally, exceedance percentages over 2000 ppm were 18% and 5%, respectively. The study did not distinguish between seasons and primary or secondary schools. Results of this comprehensive review by Santamouris et al. are often used as a reference across studies.

Carbon dioxide concentration levels monitored under the SINPHONIE framework in primary school buildings in Europe were collated in the final report (Csobod et al. 2014). The average CO₂ concentration across the 300 primary school classrooms was 1433 (σ : 856) ppm and the median was 1257 ppm. However, classrooms which featured mechanical ventilation (11% of the classrooms) averaged considerably lower concentrations at 1087 ppm. This compares to the average for naturally ventilated classrooms of 1500 ppm (Csobod et al. 2014). In 20 countries out of a total of 22 participating in the SIPHONIE study, the reported overall median CO₂ concentrations exceeded 1000 ppm (1490 ppm), with the exceptions of Sweden and Norway (with 657 ppm and 686 ppm, respectively). The SINPHONIE study provided a comparison between countries, highlighting that occupancy densities in different countries can play a significant role.

Several studies in the UK have found similar CO₂ levels to those found in the SINPHONIE project. Bako-Biro et al. (2012) monitored CO₂ levels in 16 classrooms in 8 schools for 1 week before an intervention that increased ventilation rates to investigate potential correlations with children's health and cognitive performance. Average CO₂ concentrations during occupied hours ranged from 644 ppm to 2833 ppm (average 1426 ppm, σ : 624). Peaks reported averaged 3132 ppm and reached the 5000 ppm limit. In another UK study, Korsavi et al. (2020) investigated the influence of occupants on indoor air quality and monitored CO₂ levels in 29 classrooms in 8 naturally ventilated primary school buildings. Of these classrooms, 14 were monitored over a day in the heating season and 15 over a day in the non-heating season in 2017–2018. The study found average CO₂ levels of 1208 (σ : 427) ppm in the heating season and 1050 (σ : 444) ppm in the non-heating season (values referred to nominal occupied hours). A summary of some of the studies investigating CO₂ levels in classrooms can be found in Table 6.

Table 6 Monitoring studies which investigated classroom CO₂ levels in schools

Study with continuous monitoring of CO ₂ in classrooms	Country	Length of monitoring	Year of monitoring	Sample size	Seasons	Results on CO ₂ levels (ppm)
SINPHONIE Csobod et al. (2014)	European countries including the UK	One week in each season	2012–2013	300 primary schools	Heating and non-heating	Average 1433 ppm, median 1257 ppm
Bako-Biro et al. (2012)	UK	Week (before intervention)	2006–2008	8 primary schools, 16 classrooms	Mix of seasons	
Korsavi, Montazami and Mumovic (2020)	UK, England	One day, random	2016–2017	29 classrooms in 8 schools, 14 in the heating season, 15 in the non-heating season	Heating and/or non-heating	
Gaihre et al. (2014)	UK, Scotland	3–5 days	2010	60 classrooms, 30 primary schools, Aberdeen	Non-heating, May–June	Median of daily averages: 1086 ppm Median of peak values: 2167 ppm
Dorizas et al. (2018)	UK, London, England	Long-term monitoring over 15 months and seasonal week-long monitoring	2006–2007	1 primary school, 2 classrooms, naturally ventilated with Monodraught	Heating and non-heating	
Beisterner and Coley (2003)	UK	Continuous at 5 min intervals over 1 week approximately	2002	4 classrooms, 2 primary schools	Non-heating: May and June Heating	Non-heating: average during occupied period 1570 ppm, maximum 3750 ppm Heating: average during occupied period

(continued)

Table 6 (continued)

Study with continuous monitoring of CO ₂ in classrooms	Country	Length of monitoring	Year of monitoring	Sample size	Seasons	Results on CO ₂ levels (ppm)
Fromme et al. (2007)	Munich, Germany	One day (during occupied hours), 1 min interval	2004–2005	64 schools, 92 classrooms in winter, 75 classrooms in summer	Heating, non-heating	1957 ppm, max over 4000 ppm
WHO-CEHAPe, Lukis Study Air and Children, Austria (Wallner et al. 2012; Hutter et al. 2013)	Austria	1-week period per season		18 classrooms, 9 primary schools	Autumn and spring	Daily average: from 500 to 1400 ppm Median: 850 ppm Maximum of 1 h moving average: 3300 ppm
Teeuwen et al. (2015)	The Netherlands	Continuous monitoring, 1 week, mechanically ventilated school buildings including 2 Passivhaus schools		4 schools	Heating season	Average 1066 (300) Norm. average 1655 (467) 95th percentile averaged at 1281 (412), 90th percentiles ~2300 ppm

Rovelli et al. (2014)	Italy, Milan	Naturally ventilated only	7 schools (of which 3 primary schools), 3 classrooms in each school	Over a week in winter, two monitoring campaigns 2011–2013.	Averages from two campaigns: 1423 (σ : 562) 1428 (σ : 609) Medians: 1333, 1271
Pegas et al. (2011)	Lisbon, Portugal	Primary schools. 1 day per season	3 classrooms in 3 primary schools (one classroom per school)	Spring, autumn, and winter	Average 1109 (σ : 499) ppm
Heudorf, Neitzert, and Spark (2009)	Germany	2 schools, 4 classrooms	February	1 week of normal operation	Average 1437 (994) ppm Median 1100 ppm Max 4840 ppm
Fronnme et al. (2013) LUPE 2 study	Germany	14 classrooms over 20 consecutive days, 1 classroom over 83 days.			Mean 1329 ppm, median 1211 ppm Range 267–4247 ppm Daily medians ranged 423–3135 ppm

Influencing Factors and Correlations

From the previously listed studies, factors affecting CO₂ concentrations in the classroom included:

- Number of occupants
- Occupant metabolic rates (occupant activities)
- Air exchange rates
- Ventilation type (natural ventilation vs. mechanical or mixed move ventilation)
- Ventilation rate control type (fixed rate vs. dynamic control).

Nitrogen Dioxide

NO₂ Limits, Link to Health

Nitrogen dioxide is one the few selected pollutants in the 2010 WHO Guidelines for indoor air due to its recognized impacts on health (WHO 2010). The recommended limits for both short- and long-term exposure to indoor air NO₂ are listed in Table 7. WHO Air Quality Guidelines (2021) recommended a short-term limit of 25 µg m⁻³ (13.3 ppb) for hourly average concentrations. This recommendation was based on evidence presented in the systemic review by Orellano et al. (2020). A chronic exposure limit at 10 µg m⁻³ (5.3 ppb) is recommended for annual average concentrations. The long-term limit was based on a systematic review by Huangfu and Atkinson (2020). The guidelines, however, acknowledge that there is a lack of

Table 7 Levels of NO₂ in schools in existing literature

Study	Levels (µg m ⁻³)	HRQ, level-over-limit ratios (WHO 2010) long-term limit of 40 µg m ⁻³	IORs
SINPHONIE, Csobod et al. (2014)	Average 14 µgm ⁻³ (7.5 ppb), median 11 µg m ⁻³ (5.9 ppb) (range: below detection limit – 88 µg m ⁻³)	<1.0	
Chatzidiakou et al. (2015d)	Averaged over 2 weeks. Heating season: 23.0 (9.7) Non-heating season: 14.7 (5.4) Urban heating season: 31.2 Suburban heating season 14.9 Urban non-heating: 19.1 Suburban non-heating: 10.2	Long-term limit: >1.0 (except suburban in the non-heating season)	>1
Wichmann et al. (2010) Sweden			Average ~ 1 (0.96) Range 0.44–2.17
Blondeau et al. (2005)			0.88–1.00

evidence on the exposure-response effect for NO₂, and the certainty of the evidence from the review was only considered moderate (Huangfu and Atkinson 2020).

Exposure to NO₂, mainly from outdoor sources in schools, is associated with respiratory health effects, and high concentrations can affect lung growth in children and low attendance rates in schools (Annesi-Maesano et al. 2013a; WHO 2006). The WHO guidelines note that an increase of 28 µg m⁻³ over 15 µg m⁻³ associated with indoor sources led to an increase by 20% of respiratory health risk in children. Exposure to indoor air NO₂ was consistently linked to respiratory symptoms, and respiratory infections resulting from impaired immune response, bronchoconstriction, increased bronchial reactivity, and airway inflammation (Kephalopoulos et al. 2014).

NO₂ Levels from Existing Studies

The WHO Schools Survey including more than 150 schools across 5 countries found that median NO₂ levels in classrooms were below the 40 µg m⁻³ annual average WHO limit. The SINPHONIE-EU study average classroom indoor concentration ($n = 300$) was 14 µg m⁻³ (SD = 8), with a range from below the detection limit to 88 µg m⁻³. Only a few classrooms exceeded the annual exposure limit as outlined by the 2006 WHO guidelines, with 90% of the classrooms below 26.4 µg m⁻³ (Csobod et al. 2014). However, more than half of the classrooms exceeded the revised WHO guideline of 10 µg m⁻³ annual average (50th percentile, 11.4 µg m⁻³).

The PRIMEQUAL study covered eight schools in France and found that NO₂ indoor to outdoor ratios (IORs) were within the range of 0.88–1.00, suggesting that little removal of the pollutant from outdoor air introduced to the building occurs (Blondeau et al. 2005). The ventilation type and airtightness were not found to correlate with NO₂ infiltration.

Nitrogen dioxide concentrations were monitored with passive sampling over 2 weeks in the UK primary school classrooms by Chatzidiakou et al. (2015b, c). Average classroom concentrations in the heating season were 23.0 (σ : 9.7) µg m⁻³ and 14.7 (σ : 5.4) µg m⁻³ in the non-heating season. The difference is influenced by ambient concentration variation across the seasons. Twofold higher concentrations were observed in urban environments and in schools close to major roads in both seasons (Ferguson et al. 2021). Urban outdoor concentrations in Chatzidiakou et al. (2015d) ranged from 40.2 to 49.4 µg m⁻³ and were higher than ambient concentrations in suburban school locations. The authors reported IORs ranging from 0.3 to 0.5 in more airtight buildings and from 0.6 to 0.8 to leakier buildings in the heating season. Higher IORs were observed in the non-heating season, ranging from 0.8 to 0.9, commensurate with more window opening.

Time-averaged NO₂ levels monitored with passive samplers over occupied hours ranged from 2.9 to 47.0 µg m⁻³ with an average of 17.3 (σ : 12.5) µg m⁻³ and a median of 14.1 µg m⁻³ in Swedish schools with IORs ranging 0.44–2.17 and averaging 0.96 (σ : 0.36). (Wichmann et al. 2010). Levels found in the literature are summarized in Table 7.

Influencing Factors

Nitrogen dioxide in schools is primarily introduced from the external environment and is associated with traffic-related sources and proximity to roads. Therefore, average classroom NO₂ concentrations in schools are primarily influenced by outdoor levels (Chatzidiakou et al. 2015d; Poupart et al. 2005). However, potential indoor sources, such as school kitchens, should be noted.

The relationship between NO₂, ventilation rates and building airtightness is complicated. An intervention study by Rosbach et al. (2013) introduced CO₂ controlled ventilation in naturally ventilated classrooms, increasing ventilation rates during occupied hours, reflected in the reduced CO₂ concentrations, but found that NO₂ levels remained the same before and after the intervention.

In an effort to investigate the effect of school building airtightness on indoor air pollutants, Poupart et al. (2005) monitored eight naturally and mechanically ventilated school buildings in France. The investigation of the correlation between indoor and outdoor concentrations of the nitrogen oxides (NO and NO₂) showed that indoor concentrations followed outdoor concentrations, but this was not influenced by the building envelope airtightness levels. The IORs of NO₂ were consistently close to 1, suggesting that an airtight envelope does not protect from outdoor NO₂.

Findings from IORs investigations in Chatzidiakou et al., however, contradicted the Poupart et al. findings, suggesting that infiltration of NO₂ to the indoor environment was influenced by the airtightness of the building envelope (Chatzidiakou et al. 2015d). A study by Wichmann et al. (2010) on personal microenvironments, school, and home NO₂ and PM_{2.5} concentrations in Sweden found that indoor and outdoor NO₂ concentrations were strongly correlated. They reported that ventilation type and air exchange rates did not influence the infiltration rate of NO₂. More evidence is required from continuous real-time monitoring to investigate these differences.

Particulate Matter (PM)

PM_x Limits, Link to Health

Particulate matter (PM) includes all suspended solid and liquid phase material in the air. PM can be grouped into subcategories by size (particle aerodynamic diameter) and can vary in terms of chemical composition depending upon the sources (WHO 2021). Both size and chemical composition matter in terms of the toxicity of PM. Chemical composition grouping of ambient PM is comprised of sulfates, nitrates, diesel smoke, and soil/road dust (a more comprehensive discussion of which can be found in the ► Chap. 8, “Introduction to Particles in Indoor Air”). There are relationships between particle size and chemical composition categories. For example, diesel smoke particles are likely smaller than nitrate particles and soil dust or road dust. Exposure limits are differentiated by broad size categories for PM_{2.5} and PM₁₀ (Table 8).

Table 8 Acceptable concentrations of PM_{2.5} and PM₁₀ according to existing standard and guidelines

Air pollutant	Upper limit, criterion ($\mu\text{g m}^{-3}$)	Type of exposure	Based on outcomes	Reference
PM _{2.5}	5	Long-term, mean annual exposure	Cardiovascular and respiratory functions	WHO Ambient Air Quality Guidelines (2021)
	15	Short-term exposure, 24-h mean	Cough, eczema, dermatitis, headache, and nausea	WHO Ambient Air Quality Guidelines (2021)
	25	Long-term, mean annual exposure		EU Ambient Air Quality Directives
	12	Long-term, annual average (primary)		USEPA NAAQS
	35	Short-term, 24- h average (98th percentile, averaged over 3 years)		USEPA NAAQS
PM ₁₀	15	Long-term, mean annual exposure		WHO Ambient Air Quality Guidelines (2021)
	45	Short-term exposure, 24-h mean		WHO Ambient Air Quality Guidelines (2021)
	40	Long-term, mean annual exposure		EU Ambient Air Quality Directives
	150	24-h maximum (not to be exceeded more than once per year on average over 3 years)		USEPA NAAQS

Oeder et al. (2012) reported that the chemical composition, particle numbers, and particle mass concentration for the coarse size fraction in indoor air are typically different compared to outdoor air. The study found that indoor PM₁₀ levels were not only higher (six times higher in this study) than outdoor levels but could also be qualitatively different (more biologically active), causing stronger health effects per unit concentration. Oeder et al. found that particle bound endotoxin and polycyclic aromatic hydrocarbons (PAHs) were higher in classroom air than outdoor air due to the presence of indoor sources. Investigating the chemical composition of different size fractions can further support the source apportionment of PM in indoor air. Some studies argue that PM_{2.5} in schools is introduced substantially through outdoor sources (e.g., road traffic), primarily due to lack of well-defined indoor sources in

schools. However, in other indoor environments, particles are reported to arise from human-related activities such as cooking, resuspension of particles from the activities of occupants (e.g., walking), cleaning, shedding of skin flakes, and from construction projects (Zuraimi and Tham 2008; Patel et al. 2020). Studies also find that indoor PM levels are associated with occupant density, with PM_{10} concentrations more sensitive to occupancy than $\text{PM}_{2.5}$ (Alves et al. 2013; Branco et al. 2014; Rim et al. 2017). Even a small number of children in the classroom is enough to increase PM concentrations through resuspension (Nunes et al. 2015). Indoor PM levels have been found to be higher in the classrooms of older children, due to higher activity levels (Branco et al. 2014; Mainka and Zajusz-Zubek 2015). Other sources include secondary formation from ozone and terpenes for smaller sizes (Madureira et al. 2016; WHO 2021; Morawska et al. 2009).

Exposure of children to $\text{PM}_{2.5}$ and PM_{10} has been demonstrated to be associated with adverse health effects by many studies (e.g., Annesi-Maesano et al. 2012; Daisey et al. 2003; Morawska et al. 2013). Both long- and short-term exposure to $\text{PM}_{2.5}$ are of concern to health according to the United States Environmental Protection Agency (USEPA) and the WHO. Annesi-Maesano et al. (2012) found that asthma prevalence in school children increased with exposure to $\text{PM}_{2.5}$ levels over $17.5 \mu\text{g m}^{-3}$. $\text{PM}_{2.5}$ in classrooms is associated with several health symptoms such as cough, eczema, dermatitis, headache, and nausea (Annesi-Maesano et al. 2013b). The long-term exposure limit for $\text{PM}_{2.5}$ of $5 \mu\text{g m}^{-3}$ aims at protecting against effects on cardiovascular and respiratory function (WHO 2021). PM_{10} concentrations were associated with lung disorders and reduced lung function. Madureira et al. (2016) investigated indoor air quality in schools and its relation to childhood respiratory health in Portugal. The study found that $\text{PM}_{2.5}$ and PM_{10} were positively correlated to increased risk for asthma-like symptoms, such as wheezing and irritating cough. PM_{10} showed a stronger association than $\text{PM}_{2.5}$ to this short-term health effect.

PM_x Levels from Existing Studies

The levels of fine particulate matter ($\text{PM}_{2.5}$) exceeded the long-term limit for annual average concentration of $5 \mu\text{g m}^{-3}$ as well as the $15 \mu\text{g m}^{-3}$ for 24-h average set out in WHO Ambient Air guidelines (WHO 2021) in primary school classrooms across European countries participating in the SINPHONIE study. $\text{PM}_{2.5}$ concentrations averaged $43 \mu\text{g m}^{-3}$ (median of $37 \mu\text{g m}^{-3}$) and ranged from 4 to $185 \mu\text{g m}^{-3}$. Levels of PM_{10} were reported by country average in the WHO Schools Study; country averages ranged between 28 and $102 \mu\text{g m}^{-3}$ (WHO 2015). A review of PM levels in classrooms in several countries found average PM_{10} concentrations in classrooms across northern Europe and the USA of $23 \mu\text{g m}^{-3}$ (Fischer et al. 2015).

In a study of six schools in Munich, Germany, PM_{10} concentrations were higher in classrooms than in both dwellings and outdoor air (Oeder et al. 2012). Oeder et al. found indoor classroom PM_{10} concentrations of $117 \pm 48 \mu\text{g m}^{-3}$ and outdoor concentrations were at least five times less at $21 \pm 15 \mu\text{g m}^{-3}$. In a study in French primary school classrooms, Tran et al. (2014) found PM_{10} during occupied hours between 70 and $99 \mu\text{g m}^{-3}$, although $\text{PM}_{2.5}$ concentrations were lower at less than $25 \mu\text{g m}^{-3}$.

Continuous measurements by Fromme et al. (2007) in classrooms in 64 schools in Munich in winter and summer 2004–2005 found daily median concentrations from the classroom were $19.8 \mu\text{g m}^{-3}$ in winter and $12.7 \mu\text{g m}^{-3}$ in summer. Median PM_{10} concentrations were $91.5 \mu\text{g m}^{-3}$ in winter and $64.9 \mu\text{g m}^{-3}$ in summer. Gravimetrically determined $\text{PM}_{2.5}$ median concentrations were slightly higher than from continuous measurements, $36.7 \mu\text{g m}^{-3}$ in winter and $20.2 \mu\text{g m}^{-3}$ in summer. Wallner et al. (2012) determined $\text{PM}_{2.5}$ and PM_{10} averages in spaces adjacent to 18 Austrian classrooms, using gravimetric measurements. They found PM_{10} concentrations of a median of $29 \mu\text{g m}^{-3}$ while $\text{PM}_{2.5}$ concentrations had a median of $12 \mu\text{g m}^{-3}$. A summary of study findings of PM levels in schools can be found in Table 9.

Influencing Factors

Resuspension of particles in classrooms is an important factor in the concentration of PM in classrooms. Larger particles are especially influenced by occupancy and resuspension, as they deposit more quickly on surfaces (Blondeau et al. 2005; Chatzidiakou et al. 2015a). Occupant density has been found to influence indoor levels of PM_{10} (Chatzidiakou et al. 2015b, c). The influence of occupancy is confirmed by findings in Tran et al. (2014), again reporting much lower PM_{10} concentrations during unoccupied hours, a difference that could not be explained by a much smaller decrease in outdoor concentrations across unoccupied periods. In line with these findings, higher occupant densities were associated with increased median PM_{10} concentrations in Fromme et al. (2007). Similarly, Fischer et al. (2015) found that larger particles concentrations increased when children were in the classroom due to resuspension of material deposited on surfaces leading to marked peaks. Resuspension of PM_{10} is consistent with findings in Wallner et al. (2012) where indoor $\text{PM}_{2.5}/\text{PM}_{10}$ ratios were higher than the outdoor ones. Primary schools and classrooms with younger children have higher PM levels compared to secondary schools (Fischer et al. 2015). This finding was attributed to activity types and levels of younger children. Resuspension related PM_{10} peaks can be addressed by cleaning. Fischer et al. (2015) suggest that cleaning in the morning before the start of the day reduces PM levels and that surface cleaning frequency and thoroughness may play a role in reducing PM concentrations. However, cleaning during occupied hours was found to increase fine and coarse PM during occupied hours through resuspension (Chatzidiakou et al. 2015d).

Smaller particles, including PM_1 , are heavily influenced by generation from occupants, including skin flakes, squalene, and other reactive hydrocarbons and secondary formation (Weschler 2004). For example, the ozonolysis of terpenes is likely to cause the secondary formation of ultrafine PM (PM_1) (Blondeau et al. 2005; Fischer et al. 2015; Morawska et al. 2009). This process is influenced by ventilation rates. Increasing ventilation rates lowers terpene concentrations but introduces ozone in indoor air. Fischer et al. found that further increasing ventilation rates could prevent this process, but that intermittent ventilation could increase the efficiency of PM_1 production through the ozonolysis of terpenes. The presence of terpenes in classroom indoor air is influenced by cleaning activities (terpenes are often used in cleaning products) but

Table 9 Levels of $\text{PM}_{2.5}$ and PM_{10} in schools

Study	Monitoring method	Sample	Optical results	Gravimetric results	Level-over-limit ratios
SEARCH				PM_{10} country averages 28–102 $\mu\text{g m}^{-3}$	
Csobod et al. (2014) SINPHONIE				$\text{PM}_{2.5}$ Average 44 $\mu\text{g m}^{-3}$, median 37 $\mu\text{g m}^{-3}$ (range: 4–250 $\mu\text{g m}^{-3}$)	<1 Average exceeded limit 65% classrooms exceeded WHO limit
Wallner et al. (2012) Austrian CEHAPE	Gravimetric (sampling on filters)	Austria, 18 classrooms in 9 schools		$\text{PM}_{2.5}$ averages ranged 1–34 $\mu\text{g m}^{-3}$ (median 12 $\mu\text{g m}^{-3}$) PM_{10} averages ranged 2–62 $\mu\text{g m}^{-3}$ (median 29 $\mu\text{g m}^{-3}$)	$\text{PM}_{2.5}$ averages ranged 1–34 $\mu\text{g m}^{-3}$ (median 12 $\mu\text{g m}^{-3}$) PM_{10} averages ranged 2–62 $\mu\text{g m}^{-3}$ (median 29 $\mu\text{g m}^{-3}$)
Fronnme et al. (2007)	Gravimetric and continuous measurement with laser aerosol spectrometer, and particle number concentration using scanning mobility particle sizer	64 schools in Munich, Germany	$\text{PM}_{2.5}$: median 19.8 $\mu\text{g m}^{-3}$ in winter and 12.7 $\mu\text{g m}^{-3}$ in summer PM_{10} : median 91.5 $\mu\text{g m}^{-3}$ in winter and 64.9 $\mu\text{g m}^{-3}$ in summer	$\text{PM}_{2.5}$ median 36.7 $\mu\text{g m}^{-3}$ in winter and 20.2 $\mu\text{g m}^{-3}$ in summer	Gravimetric measurements of $\text{PM}_{2.5}$ exceeded short-term limits in winter. Continuous measurements $\text{PM}_{2.5}$ exceeded long-term limits. Continuous PM_{10} concentrations exceeded limits
Tran et al. (2014)	Continuous, optical particle counter (GRIMM) spectrometer and gravimetric measurements		Average 8-h PM_{10} 70–89.3 $\mu\text{g m}^{-3}$ during occupied periods.		

also fruit consumption. Citrus fruit pealing during breaks led to peaks of PM₁, through the secondary process described above (Fischer et al. 2015).

Poupard et al. (2005) reported that the building envelope airtightness did not have an effect on the correlation between indoor and outdoor PM₁ levels or fine PM (2–3 um). Poupard et al. also noted IORs for PM₁ decreased with increasing outdoor concentrations, hypothesizing that an increase of outdoor PM₁ levels at night coincided with decreased indoor generation from occupancy. Fischer et al. (2015) reported that when mechanical ventilation is on, infiltration through the building envelope had a proportionately small effect on indoor concentrations of PM.

Seasonal variations investigated in Fromme et al. (2007) showed that a significant decreases of indoor PM_{2.5} and PM₁₀ concentrations is likely to occur in summer. The seasonal variation was attributed to different ventilation practices and therefore, different primary sources in winter and in summer. Chatzidiakou et al. (2015d) also found that classroom PM_{2.5} and PM₁₀ levels were higher in the heating season compared to the non-heating season, commensurate with ambient concentrations. However, lower air exchange rates with outdoor air in the non-heating season means that indoor sources are likely still important (Morawska et al. 2017).

Madureira et al. (2016) found PM₁₀ levels were influenced by the number of windows open during the heating season (with levels reducing with more open windows). Similarly, Chatzidiakou et al. (2015d) noted inadequate ventilation rates correlated with higher PM concentrations in classrooms. Chatzidiakou et al. also found that lower wind-driven natural ventilation rates (wind direction parallel to classroom window wall) were associated with higher PM levels. The location of air intake for mechanical systems is also an important factor as they are often located near loading docks, or areas where school buses or other vehicles idle, leading to the contribution of diesel exhaust to indoor PM concentrations.

In terms of internal finishes, higher PM_{2.5} were found in classrooms with carpet compared to classrooms with hard flooring material (Shaughnessy et al. 2002). This finding is consistent with those in laboratory studies (Tian et al. 2014) and more recent findings in the UK; Chatzidiakou et al. (2015d) found considerably higher indoor coarse and fine PM in classrooms with carpet flooring versus classrooms with hard flooring. Other indoor sources of PM in schools included visible damp spots and mold growth (Madureira et al. 2016), and in schools which prepare meals, cooking of hot food for lunches (Weichenthal et al. 2008).

VOCs

VOC Limits, Link to Health

Adverse health effects from inhalation of the wide range of indoor air VOCs are known to result in acute and chronic adverse health effects including irritation of the mucous membrane and lower respiratory irritation, neurological, allergic, developmental, reproductive, and carcinogenic effects. The presence of VOCs in indoor air

has been specifically associated with discomfort, sensory irritation, and cancer (Sofuoğlu et al. 2011).

A number of studies investigated the influence of VOCs on children specifically. One study found there was a correlation between levels of a semi-volatile organic compounds (SVOCs) and children's concentration performance (Hutter et al. 2013). The VOCs formaldehyde and benzene were found to have a negative correlation with morning and afternoon mathematical test results by Csobod et al. (2014). Additionally, Csobod et al. (2014) found that attendance was negatively influenced by increased concentrations of the VOCs limonene and naphthalene in classrooms. Reduced school attendance is considered to negatively impact academic performance.

A few studies discussed the relationships of total VOC (TVOCs) in indoor air and health (e.g., Daisey et al. 2003). Predictors of TVOCs include cleaning products, fleecy materials, and occupancy density. Common sources include paints, furniture, and air fresheners. Exposure to increased TVOCs was associated with an increased risk of asthma in children in a study in primary schools in Portugal (Madureira et al. 2016).

The influence of levels of SVOCs in dust in primary schools and the cognitive performance of children, aged 6–8 years was investigated in the Austrian LuKi study: "Air and Children" which included nine schools (Hutter et al. 2013). The study found a negative correlation between cognitive performance and indoor concentrations of the semi-volatile organic phosphor-organic compound (POC), tris(2-chlorethyl)-phosphate (TCEP) in dust and air samples. POCs are used as flame retardants, plasticizers, and floor adhesives. TCEP is a carcinogenic substance of very high concern due to its reproduction toxicity. In addition, cognitive performance of children was found to have a negative correlation with the polycyclic aromatic hydrocarbon (PAH), phenanthrene.

Limiting values for indoor air concentrations of different lists of individual compounds have been developed by different organizations in various countries. Additionally, studies reported on current efforts to derive limiting values for 95 more compounds (Harrison et al. 2011; Ye et al. 2014). Limits for indoor air concentrations of VOCs applicable to all building types from both building regulations and the WHO Guidelines are listed in Table 10. The compounds are listed in hierarchical order as they appear in documents in hierarchical order. On an international level and applicable to all four building types, the WHO guidelines for indoor air quality: selected pollutants (WHO 2010) provide limiting values for VOCs including benzene, formaldehyde, naphthalene, trichloroethylene (T3CE), tetrachloroethylene (T4CE), 1,3-butadiene, polycyclic aromatic hydrocarbons (PAHs) and their indicator benzo[a]pyrene (BaP). A number of additional air pollutants for which exposure limits were not determined due to insufficient evidence are also listed in the WHO Guidelines and include acetaldehyde, biocides and pesticides, flame retardants, glycol ethers, hexane, phthalates, styrene, toluene, and xylenes.

Limiting values for all indoor air pollutants, including VOCs, take into consideration toxicological and epidemiological data, the levels of exposure linked to adverse effects on health, and the likelihood of presence of indoor sources and current levels. Despite the well-established health risks of specific air pollutants

Table 10 WHO and UK DEFRA limits for VOCs in primary school building classrooms

Pollutants	WHO	UK Air Quality Objectives (DEFRA, 2007)
VOCs		
Benzene ($\mu\text{g}/\text{m}^3$)	No safe level	5 (1 year) England and Wales 3.25 (running annual mean) Scotland and N. Ireland
T3CE ($\mu\text{g}/\text{m}^3$)	No safe level	—
T4CE ($\mu\text{g}/\text{m}^3$)	250 (1 year)	—
Formaldehyde ($\mu\text{g}/\text{m}^3$)	100 (30 min)	
Naphthalene ($\mu\text{g}/\text{m}^3$)	10 (1 year)	
PAHs (ng/m^3 B[a]P)	No safe level	0.25 (1 year)
1,3-butadiene ($\mu\text{g}/\text{m}^3$)		2.25 (running annual mean)
a-pinene ($\mu\text{g}/\text{m}^3$)		
n-limonene ($\mu\text{g}/\text{m}^3$)		
m-, p-xylene (<i>o</i> -xylene) ($\mu\text{g}/\text{m}^3$)	870 (1 week)	
Styrene ($\mu\text{g}/\text{m}^3$)	260 (1 week)	
Toluene ($\mu\text{g}/\text{m}^3$)	260 (1 week)	

found in classrooms, and the guidelines addressing these, there is currently little evidence available on the actual levels in classrooms, as collecting it can be complex, expensive, labor intensive, and time consuming, and requires technical expertise. Evidence that is available is described in the following section.

VOC Levels from Existing Studies

There are several comprehensive indoor air quality studies in school buildings identified in Csobod et al. (2014). The reviewed studies, de Gennaro et al. (2013) in Italy, Zhong et al. (2017) in the USA in 2015–2016, and Sofuoğlu et al. (2011) in Turkey, are summarized in Table 11 and further described below.

A sample of 144 mechanically ventilated classrooms in 37 school buildings in a 2015–2016 air quality monitoring in US school classrooms in Ohio, Indiana, Michigan, and Illinois reported concentrations of the 94 most frequently detected (detection frequency over 15%) VOCs (Zhong et al. 2017). All schools were built or renovated between 2001 and 2012 and were Energy Star and LEED-certified. Most of the detected compounds were aromatic hydrocarbons, alkanes, and terpenes. Benzene, toluene, xylenes, n-tetradecane, and n-limonene were found in most classrooms. While formaldehyde, methyl-cyclohexane, methylene-chloride, and n-limonene had the highest median concentrations.

A monitoring study in classrooms of eight naturally ventilated middle and elementary school buildings in southeastern Italy determined concentrations for different classes of VOCs, including alkanes, aliphatic hydrocarbons (alkanes, cycloalkanes), aromatic hydrocarbons, terpenes, ketones, aldehydes, alcohols, and

Table 11 Comprehensive indoor air quality studies that determined a range of VOC concentration levels in school buildings

Study	Sample	Method/limitations	Key findings
Zhong et al. (2017)	144 classrooms in 37 conventional and high-performance schools recently built or renovated (last 15 years) in the USA Monitoring took place in 2015–2016.	Indoor and outdoor concentrations of 94 VOCs were determined (using thermal desorption, gas chromatography-mass spectroscopy) Only those compounds detected in more than 15% of the samples were included in the analysis (24 VOCs in total)	24/94 compounds with a detection frequency >15%. Most of the detected VOCs fell into classes of aromatic hydrocarbons, alkanes, and terpenes. Average concentrations below 5 µg m ⁻³ .
de Gennaro et al. (2013)	8 school buildings, both middle and elementary, South each Italy	The study provided quantitative information on 14 compounds including formaldehyde	Passive sampling using radial samplers over a week, in 3 classrooms and an outdoor site. Limonene, pinene, and toluene were at highest concentrations in schools in Italy (of 14 compounds measured)
Sofuoğlu et al. (2011)	3 primary schools, Turkey	The method was optimized for quantitative determination of 51 compounds, and an average of 16 compounds were found in the samplers. Active sampling, repeated 6–9 times each season, repeated in fall, winter, and spring. Monitoring in a classroom, a kindergarten, and outdoor playground site	Benzene, toluene, and formaldehyde were the most abundant compounds with 95th percentile indoor air concentrations of 29, 87, and 106 µg/m ³ , respectively

halocarbons as reported by de Gennaro et al. (2013). de Gennaro monitored VOCs in three classrooms and one outdoor site in each school building using passive sampling. The most abundant compounds were determined to be *a*-pinene, *D*-limonene, and toluene. The study discussed potential sources and health-risk associated limits of specific compounds.

Concentrations of VOCs and formaldehyde in three primary school buildings in Turkey were evaluated in Sofuoğlu et al. (2011). Benzene, toluene, and formaldehyde were confirmed as the most abundant compounds in indoor classroom air with 29, 87,

and $106 \mu\text{g m}^{-3}$ 95th percentile concentrations, respectively. The importance of indoor sources is highlighted in Sofuođlu et al. (2011) since results showed greater variation between urban schools compared to variation between urban and suburban schools. A summary of key pollutants, and their target levels, in schools can be found in Table 12.

Influencing Factors

Likely sources of commonly targeted VOCs have been identified in the literature. Madureira et al. (2016) found that 21% of the variation of indoor VOC concentrations were explained by factors including: main flooring material, number of windows open in the cooling season, number of windows usually open before the start of teaching, and the presence of graphic arts materials in the classroom. Surface materials are important influencing factors of indoor air quality in classrooms as they function as primary indoor sources, sinks, and secondary sources of pollution. Poulhet et al. (2014), in a source apportionment study in eight primary schools in France, showed that a surface material with high loading factor can be responsible for 87–98% of the formaldehyde emissions in classrooms even though 29 different sources of formaldehyde were identified (see ► Chap. 2, “Very Volatile Organic Compounds (VVOCs)”). Temperature, relative humidity, and air exchange rates influence the emission rates of compound/source couples. Other processes also play a role, including deposition and chemical reactions.

Many VOCs have strong indoor sources, including T3CE, limonene, and pinene with the last two mainly from cleaning products (Chatzidiakou et al. 2015d; de Gennaro et al. 2013, 2014). Toluene is emitted from traffic as well as being a solvent, and therefore both indoor and outdoor sources can be present. Benzene is predominantly traffic related but can also be emitted from art supplies (Chatzidiakou et al. 2014). As with particulate matter, if the air intake for mechanical HVAC systems is located near areas where vehicles stand idling (such as in bus queues or loading docks), the exhaust can contribute substantially to indoor VOC concentrations. Formaldehyde is mainly emitted from furnishing and construction materials containing resins and adhesives. Emissions from these sources are persistent and gradually decline over the years. Sources of α -limonene and α -pinene are cleaning products and fragrances, and sources of 2-butoxyethanol include latex paints, paint thinners, and varnishes. Many compounds were found to have significant indoor sources including: α -limonene, hexanal (I/O ratio 14.3), formaldehyde, acetone, 1-butoxy-2-propanol, acetaldehyde, propanol, 1-butanol, *n*-undecane, methylcyclohexane, and *n*-dodecane (Geiss et al. 2011).

Compounds with high IORs in the AIRMEX monitoring study in offices, public buildings, and schools included: formaldehyde, hexanal, α -limonene, α -pinene, 2-butoxyethanol, acetaldehyde, acetone, 1-butoxy-2-propanol, *n*-undecane, propanol, methyl-cyclohexane, *n*-dodecane, and 1-butanol. Ye et al. (2017) created a priority list of VOCs that were most likely to contribute to ventilation rate requirements that included pinene, hexanal, and 2-ethyl-1-hexanol (but not formaldehyde or phthalates).

Table 12 Levels of target VOCs in schools in reviewed studies

Key pollutants	Levels	Study	Limits ^a	Level-over-limit ratios
Total volatile organic compounds (TVOCs)		SINPHONIE-UK Chatzidiakou et al. (2014)	300 µg m ⁻³ (UK building regulations)	Exceeded limit
Formaldehyde	SEARCH: country averages 1.7–33.1 µg m ⁻³ SINPHONIE average 12 µg m ⁻³ (range: 1–66 µg m ⁻³) WHO country median range: 6.6–10.7 µg m ⁻³	HESE, SINPHONIE, SEARCH, WHO	100 µg m ⁻³ (30-min average) ^a	<1 Limit not exceeded in SINPHONIE study
Benzene	SINPHONIE: median 2 µg m ⁻³ (range: below detection limit – 38 µg m ⁻³) SEARCH: country averages 2–7.4 µg m ⁻³ Croatia median 0.7, 1 µg m ⁻³ 90th Percentile 2, 11.4 µg m ⁻³ (WHO) WHO country median range: 0.7–4.5 µg m ⁻³	SINPHONIE, SEARCH, WHO	No safe level	Detection frequency can be used as a measure
Ethylbenzene	SEARCH: country averages 0.8–1.8 µg m ⁻³	SEARCH		
Naphthalene	SINPHONIE: median below detection limit, maximum 31 µg m ⁻³	SINPHONIE	10 µg m ⁻³	Limit exceeded in some countries
T3CE	SINPHONIE: median below detection limit, max 126 µg m ⁻³	SINPHONIE	23 µg m ⁻³	>1 Median exceeded limit
T4CE	SINPHONIE: median below detection limit, max 81 µg m ⁻³	SINPHONIE	250 µg m ⁻³	<1 Median below limit
Xylenes	SEARCH: country averages 4.3–9.1 µg m ⁻³	SINPHONIE, SEARCH		
Toluene	SEARCH: country averages 4.6–29.5 µg m ⁻³	SINPHONIE, SEARCH		
o-limonene	SINPHONIE: Average 38 µg m ⁻³ (range: detection limit – 672 µg m ⁻³)	SINPHONIE	20 (short-term, French ANSES) 450 (long-term)	>1 Average exceeds short-term limit

^aWHO guidelines for indoor air quality: selected pollutants (2010)

Higher ventilation rates were associated with lower TVOC concentrations in classrooms (Madureira et al. 2016). Increasing ventilation levels to 7–10 L s⁻¹ per person was found to reduce TVOC concentrations in classrooms to acceptable levels (Daisey et al. 2003) and in the review by Luther et al. (2018).

Summary and Conclusions

The Evidence Gap

More empirical evidence from classrooms is needed for assessing IAQ in schools. Modelling approaches for determining indoor air pollution from building characteristics and sources are limited by the many unknowns in complex physicochemical processes and cannot substitute for monitoring (Poupard et al. 2005). Analysis of monitoring results using statistical modelling techniques can help identify and verify potential relationships between building physical and operational characteristics that influence indoor air quality. These techniques can facilitate determination of population-level environmental exposures of children to be used for policymaking and school building design. There is a need for a holistic understanding of actual indoor air quality in school classrooms and the role of heating, cooling, and ventilation systems, as well as finishing and furnishing materials, on air quality of classrooms. Comprehensive indoor air pollution monitoring evidence is limited in schools. Despite their importance for the determination of health risks, the chemical composition of PM and qualitative description of the matrix of VOCs in schools is understudied. This information is greatly needed since the types of VOCs present in indoor air is heavily influenced by indoor sources, which can vary between countries, and building types.

Influencing Factors and Correlations

The physical characteristics that distinguish the indoor environment from the outdoor environment are (as listed in the review by Abbatt and Wang (2020)): air exchange rates and mixing rates, volume to surface ratios, sunlight, limited temperature and relative humidity variation, absence of moisture deposition, and occupancy density. The processes that determine indoor concentrations, and thus exposure to pollutants, are indoor primary sources, infiltration, and secondary processes (generation or depletion). Indoor sources are linked to design and delivery decisions (building materials), cleaning and occupancy, and can be pulse or continuous, persistent or transient. Infiltration of outdoor sourced compounds relate to the building envelope and the age of air (air infiltration, air exchange rates and patterns) and can be influenced by different factors for different pollutants.

IAQ is evaluated with many different methodologies. The investigation of proxies of IAQ demonstrate that existing proxies such as CO₂ and ventilation rates are not likely to provide a holistic description of IAQ in classrooms. Therefore, IAQ

studies with comprehensive monitoring of IAQ are important. As school building characteristics evolve with changes in building practices and building regulations, in particular high-performance buildings and retrofits, a better understanding of IAQ is increasingly important.

Ventilation Strategy

The ventilation strategy, broadly classified as natural ventilation only, mechanical ventilation only, and mixed mode ventilation, was found to influence average ventilation rates in school classrooms. Santamouris et al. (2008) found that median ventilation rates in classrooms in naturally ventilated schools were considerably lower compared to those in mechanically ventilated school ($3.0 \text{ vs. } 8.3 \text{ L s}^{-1} \text{ p}^{-1}$). This is corroborated by findings in Mumovic et al. (2009) that average heating season ventilation rates under normal operation in 12 naturally ventilated classrooms were lower compared to 4 mechanically or mixed mode ventilation classrooms ($3.28 \text{ vs. } 7.15 \text{ L s}^{-1} \text{ p}^{-1}$). In addition, while mixed mode ventilated schools have wider fluctuations than mechanical ventilation, similar to naturally ventilated schools, on average they provide higher ventilation rates than naturally ventilated schools (Mumovic et al. 2009).

Air Exchange Rates

Air exchange rates in school classrooms are often estimated from CO_2 concentration as these variables are strongly and inversely correlated. While increasing ventilation rates will reduce CO_2 concentrations in the occupied classroom, this is not the case for the concentrations of all other pollutants. Evidence from several monitoring studies agreed that increasing ventilation rates during occupied hours decreased indoor PM_{10} classroom concentrations. Findings on the relationship between ventilation rates and $\text{PM}_{2.5}$ were contradictory, and more work needs to be done to reach consensus on the relationship between $\text{PM}_{2.5}$ and ventilation rates. NO_2 has no indoor sources in schools, and a number of studies suggested that higher ventilation rates increased NO_2 levels in classrooms. However, in at least one study, increasing ventilation rates with a CO_2 control system in a classroom did not influence NO_2 . A number of studies found that higher ventilation rates were associated with lower TVOC.

Building Envelope Airtightness

Infiltration, due to leakage through the building envelope, has a smaller impact on overall air exchange rates the higher the ventilation rates are, and in densely populated classrooms, required ventilation rates are quite high. Findings from existing literature reviewed in this chapter found that airtightness influenced indoor thermal conditions and air quality parameters in classrooms, as follows.

The literature reviewed in this chapter identified contradictory findings with regards to the influence of building envelope air permeability on classroom NO₂ concentrations, but that NO₂ IORs did not appear to be influenced by outdoor concentration levels.

Airtightness was not found to influence the correlation between indoor and outdoor PM. Indoor followed outdoor concentrations no matter the airtightness. However, it is noted that findings mostly represent PM₁ particle size fraction.

Classroom Occupancy

The role of occupants in the generation of pollutants is a significant factor in the concentration of, and exposure to, indoor air contaminants in schools. Occupants shed skin flakes, and produce squalene, which contributes to PM. Occupants also (especially active children) play a major role in the resuspension of particles through activities such as walking and playing. They also produce a number of bio-effluents, including CO₂ and VOCs, that impact indoor air quality (Béko et al., 2020). It is, therefore, critically important to consider both occupant density and activities in the evaluation and assessment of air quality in classrooms.

The lower limits of 1.5 m² per child and 2 m² per child (or equivalent upper limits of 0.7 and 0.5 children per m²) are set in the SINPHONIE final report as associated with increased CO₂ levels (above 1500 ppm) and associated risk for health and academic performance. Additionally, smaller classroom volumes per occupant were associated with increased median PM₁₀ concentrations.

Seasonal Effects

Several parameters that define the classroom air quality are found to vary across the heating (cold) and non-heating (warm) seasons. A considerable decrease of classroom ventilation rates during occupied hours, and CO₂ levels from winter to summer is a frequent finding. Lower ventilation rates are anticipated in cold weather in naturally and mixed mode ventilated schools. While NO₂ IORs are lower in the heating season compared to the non-heating season (due to its correlation with ventilation rates), indoor classroom concentrations are not lower in summer than winter. This result is because ambient NO₂ concentrations are lower in summer compared to winter. Higher ventilation rates also contributed to lower concentrations of terpenes in the warm season compared to the cold season. Higher ventilation rates increased the reaction of terpenes with O₃.

Building Better Schools

Current practices for building design optimization in both new construction and retrofit projects involve iterative processes (optioneering) for meeting targets of

environmental and energy performance. These targets are regulatory requirements or optional requirements from guidance documents. Within these limits, there is room for prioritization of certain criteria through trade-offs. In school buildings, designing for the minimization of energy use and the optimization of the indoor environment involves such trade-offs. Bernardo et al. (2018) investigated the issues that influence energy performance of school buildings in a methodological framework for multi-criteria decision analysis.

As discussed in the “Influencing Factors” section of this chapter, different physical and operational features of the building (airtightness, surface materials, ventilation strategy and rates) and surrounding area can impact IAQ. Several of these may also impact other outcomes: energy efficiency, carbon footprint, and cost of the building. It is worth noting also that there is little evidence for the IAQ impact of new net-zero and other high-performance building types. Furthermore, IAQ is linked to a number of outcomes including health and academic performance. From these correlations, the building/classroom characteristics are indirectly linked to the health and performance outcomes (for example, this is directly studied in Bluyssen et al. (2018)). A building performance assessment that takes into consideration these outcomes for children, in a comparable manner, can help decision-making beyond the existing regulatory framework where conflicts and requirements for trade-offs can arise in the procurement process.

Cross-References

- [Very Volatile Organic Compounds \(VVOCs\)](#)
-

References

- Abbatt JP, Wang C (2020) The atmospheric chemistry of indoor environments. *Environ Sci Process Impacts* 22(1):25–48
- Ajiboye P, White M, Graves H, Ross D (2006) Ventilation and indoor air quality in schools—GUIDANCE REport 202825. Building Research Establishment, London
- Alves C, Nunes T, Silva J, Duarte M (2013) Comfort Parameters and Particulate Matter (PM10 and PM2.5) in School Classrooms and Outdoor Air. *Aerosol and Air Quality Research* 13(5):1521–1535. <https://doi.org/10.4209/aaqr.2012.11.0321>
- ASHRAE, American Society of Heating, Refrigeration and Air-conditioning Engineers (2016) ASHRAE standard: standards for natural and mechanical ventilation. The Society, New York [2016] ©2016
- Annesi-Maesano I, Hulin M, Lavaud F, Raherison C, Kopferschmitt C, de Blay F, ... Denis C (2012) Poor air quality in classrooms related to asthma and rhinitis in primary schoolchildren of the French 6 Cities Study. *Thorax* 67(8):682–688. <https://doi.org/10.1136/thoraxjnl-2011-200391>
- Annesi-Maesano I, Baiz N, Banerjee S, Rudnai P, Rive S, Group, S (2013a) Indoor air quality and sources in schools and related health effects. *J Toxicol Environ Health B Crit Rev* 16(8): 491–550. <https://doi.org/10.1080/10937404.2013.853609>

- Annesi-Maesano I, Baiz N, Banerjee S, Rudnai P, Rive S, Group, S (2013b) Indoor air quality and sources in schools and related health effects. *J Toxicol Environ Health, Part B* 16(8):491–550
- Apte MG (2000) Associations between indoor CO₂ concentrations and sick building syndrome symptoms in US office buildings: an analysis of the 1994–1996 BASE study data. *Indoor Air* 10(4)
- Ashmore MR, Dimitroulopoulou C (2009) Personal exposure of children to air pollution. *Atmos Environ* 43(1):128–141. <https://doi.org/10.1016/j.atmosenv.2008.09.024>
- Azuma K, Kagi N, Yanagi U, Osawa H (2018) Effects of low-level inhalation exposure to carbon dioxide in indoor environments: a short review on human health and psychomotor performance. *Environ Int* 121:51–56
- Bakó-Biró Z, Clements-Croome DJ, Kochhar N, Awbi HB, Williams MJ (2012) Ventilation rates in schools and pupils' performance. *Build Environ* 48:215–223
- Bateson TF, Schwartz J (2008) Children's response to air pollutants. *J Toxicol Environ Health A* 71 (3):238–243. <https://doi.org/10.1080/15287390701598234>
- Beisteiner A, Coley DA (2003) Carbon dioxide levels and summertime ventilation rates in UK schools. *Int J Vent* 1(3):181–187
- Bekö G, Wargocki P, Wang N, Li M, Weschler CJ, Morrison G, . . . Williams J (2020) The Indoor Chemical Human Emissions and Reactivity (ICHEAR) project: overview of experimental methodology and preliminary results. *Indoor Air* 30:1213
- Bernardo H, Gaspar A, Henggeler Antunes C (2018) A combined value focused thinking-soft systems methodology approach to structure decision support for energy performance assessment of school buildings. *Sustainability* 10(7):2295
- Blondeau P, Iordache V, Poupard O, Genin D, Allard F (2005) Relationship between outdoor and indoor air quality in eight French schools. *Indoor Air* 15(1):2–12
- Bluyssen PM, Zhang D, Kurvers S, Overtoom M, Ortiz-Sánchez M (2018) Self-reported health and comfort of school children in 54 classrooms of 21 Dutch school buildings. *Build Environ* 138: 106–123
- Branco PTBS, Alvim-Ferraz MCM, Martins FG, Sousa SIV (2014) Indoor air quality in urban nurseries at Porto city: Particulate matter assessment. *Atmospheric Environment* 84:133–143
- BSI (2019) Energy performance of buildings. British Standards Institute
- Carreiro-Martins P, Viegas J, Papoila AL, Aelenei D, Caires I, Araújo-Martins J, . . . Virella D (2014) CO₂ concentration in day care centres is related to wheezing in attending children. *Eur J Pediatr* 173(8):1041–1049
- Chatzidiakou L, Mumovic D, Summerfield A (2012) What do we know about indoor air quality in school classrooms? A critical review of the literature. *Intell Build Int* 4(4):228–259. <https://doi.org/10.1080/17508975.2012.725530>
- Chatzidiakou L, Mumovic D, Summerfield A, Hong S, Altamirano-Medina H (2014) A Victorian school and a low carbon designed school: comparison of indoor air quality, energy performance, and student health. *Indoor Built Environ* 23(3):417–432. <https://doi.org/10.1177/1420326x14532388>
- Chatzidiakou E, Mumovic D, Summerfield AJ, Altamirano HM (2015a) Indoor air quality in London schools. Part 1: 'Performance in use'. *Intelligent Build Int* 7(2–3):101–129
- Chatzidiakou L, Mumovic D, Summerfield A (2015b) Is CO₂ a good proxy for indoor air quality in classrooms? Part 1: The interrelationships between thermal conditions, CO₂ levels, ventilation rates and selected indoor pollutants. *Build Serv Eng Res Technol* 36(2):129–161. <https://doi.org/10.1177/0143624414566244>
- Chatzidiakou L, Mumovic D, Summerfield A (2015c) Is CO₂ a good proxy for indoor air quality in classrooms? Part 2: Health outcomes and perceived indoor air quality in relation to classroom exposure and building characteristics. *Build Serv Eng Res Technol* 36(2):162–181. <https://doi.org/10.1177/0143624414566245>
- Chatzidiakou L, Mumovic D, Summerfield A, Täubel M, Hyvärinen A (2015d) Indoor air quality in London schools. Part 2: Long-term integrated assessment. *Intell Build Int* 7(2–3):130–146
- Clements-Croome DJ, Awbi H, Bakó-Biró Z, Kochhar N, Williams M (2008) Ventilation rates in schools. *Build Environ* 43(3):362–367

- Csobod EA-M, Carrer P, Kephalopoulos S, Madureira J, Rudnai P, Fernandes EdO, Barrero-Moreno J, Beregszaszi T, Hyvarinen A, Moshammer H, Norback D, Paldy A, Pandics T, Sestini P, Stranger M, Taubel M, Varro MJ, Gabriela-Ventura E, Viegi G (2014) SINPHONIE – Schools Indoor Pollution and Health Observatory Network in Europe – final report. Retrieved from
- Daisey JM, Angell WJ, Apte MG (2003) Indoor air quality, ventilation and health symptoms in schools: an analysis of existing information. *Indoor Air* 13:53–64
- de Gennaro G, Farella G, Marzocca A, Mazzone A, Tutino M (2013) Indoor and outdoor monitoring of volatile organic compounds in school buildings: indicators based on health risk assessment to single out critical issues. *Int J Environ Res Public Health* 10(12):6273–6291
- de Gennaro G, Dambruoso PR, Loiotile AD, Di Gilio A, Giungato P, Tutino M, ... Porcelli F (2014) Indoor air quality in schools. *Environ Chem Lett* 12(4):467–482. <https://doi.org/10.1007/s10311-014-0470-6>
- DEFRA (2007) UK Air Quality Limits. Retrieved from <https://uk-air.defra.gov.uk/air-pollution/uk-eu-limits>
- Dorizas PV, Samuel S, Dejan M, Keqin Y, Dimitris M-M, Tom L (2018) Performance of a natural ventilation system with heat recovery in UK classrooms: an experimental study. *Energ Build* 179:278–291. <https://doi.org/10.1016/j.enbuild.2018.09.005>
- ESFA (2018) Building Bulletin 101 (BB101) Guidance Document for Indoor Air Quality in School Buildings
- Ferguson L, Taylor J, Zhou K, Shrubsole C, Symonds P, Davies M, Dimitroulopoulou S (2021) Systemic inequalities in indoor air pollution exposure in London, UK. *Build Cities* 2(1)
- Fischer A, Ljungström E, Hägerhed Engman L, Langer S (2015) Ventilation strategies and indoor particulate matter in a classroom. *Indoor Air* 25(2):168–175. <https://doi.org/10.1111/ina.12133>
- Fromme H, Twardella D, Dietrich S, Heitmann D, Schierl R, Liebl B, Rüden H (2007) Particulate matter in the indoor air of classrooms – exploratory results from Munich and surrounding area. *Atmos Environ* 41(4):854–866
- Fromme H, Bischof W, Dietrich S, Lahrz T, Schierl R, Schwegler U (2013) Airborne allergens, endotoxins, and particulate matter in elementary schools, results from Germany (LUPE 2). *J Occup Environ Hyg* 10(10):573–582
- Gaihre S, Semple S, Miller J, Fielding S, Turner S (2014) Classroom carbon dioxide concentration, school attendance, and educational attainment. *J Sch Health* 84(9):569–574
- Geiss O, Giannopoulos G, Tirendi S, Barrero-Moreno J, Larsen BR, Kotzias D (2011) The AIRMEX study – VOC measurements in public buildings and schools/kindergartens in eleven European cities: statistical analysis of the data. *Atmos Environ* 45(22):3676–3684. <https://doi.org/10.1016/j.atmosenv.2011.04.037>
- Harrison P, Crump D, Kephalopoulos S, Yu C, Däumling C, Rouselle C (2011) Harmonised regulation and labelling of product emissions—a new initiative by the European commission. Sage, London
- Haverinen-Shaughnessy U, Moschandreas D, Shaughnessy R (2011) Association between standard classroom ventilation rates and students' academic achievement. *Indoor Air* 21(2):121–131
- Heudorf U, Neitzert V, Spark J (2009) Particulate matter and carbon dioxide in classrooms—the impact of cleaning and ventilation. *Int J Hyg Environ Health* 212(1):45–55
- HM Government (2010) Approved Document F (AD F) F1 Means of Ventilation of the UK Building Regulations for all Building Types in the UK. Retrieved from <https://www.gov.uk/government/publications/ventilation-approved-document-f>
- Huangfu P, Atkinson R (2020) Long-term exposure to NO₂ and O₃ and all-cause and respiratory mortality: a systematic review and meta-analysis. *Environ Int* 144:105998
- Hutter H-P, Haluza D, Piegl K, Hohenblum P, Fröhlich M, Scharf S, ... Kundi M (2013) Semivolatile compounds in schools and their influence on cognitive performance of children. *Int J Occup Med Environ Health* 26(4):628–635
- Kephalopoulos S, Csobod E, Bruinen de Bruin Y, Oliveira Fernandes E (2014) Guidelines for healthy environments within European schools. Retrieved from <https://www.um.edu.mt/library/oar/handle/123456789/22916>

- Kim J-L, Elfman L, Mi Y, Wieslander G, Smedje G, Norbäck D (2007) Indoor molds, bacteria, microbial volatile organic compounds and plasticizers in schools: associations with asthma and respiratory symptoms in pupils. *Indoor Air* 17(2):153–163
- Korsavi SS, Montazami A, Mumovic D (2020) Indoor air quality (IAQ) in naturally-ventilated primary schools in the UK: occupant-related factors. *Build Environ* 180:106992
- Lai HK, Kendall M, Ferrier H, Lindup I, Alm S, Hänninen O, ... Ashmore M (2004) Personal exposures and microenvironment concentrations of PM_{2.5}, VOC, NO₂ and CO in Oxford, UK. *Atmos Environ* 38(37):6399–6410
- Luther MB, Horan P, Tokede O (2018) Investigating CO₂ concentration and occupancy in school classrooms at different stages in their life cycle. *Archit Sci Rev* 61(1–2):83–95
- Madureira J, Paciência I, Cavaleiro-Rufo J, de Oliveira Fernandes E (2016) Indoor pollutant exposure among children with and without asthma in Porto, Portugal, during the cold season. *Environ Sci Pollut Res* 23(20):20539–20552. <https://doi.org/10.1007/s11356-016-7269-x>
- Mainka A, Brągoszewska E, Kozielska B, Pastuszka JS, Zajusz-Zubek E (2015) Indoor air quality in urban nursery schools in Gliwice Poland: Analysis of the case study. *Atmospheric Pollution Research* 6(6):1098–1104. S1309104215000239. <https://doi.org/10.1016/j.apr.2015.06.007>
- Mendell MJ, Heath GA (2005) Do indoor pollutants and thermal conditions in schools influence student performance? A critical review of the literature. *Indoor Air* 15(1):27–52
- Mendell M, Eliseeva E, Davies M, Lobscheid A (2016) Do classroom ventilation rates in California elementary schools influence standardized test scores? Results from a prospective study. *Indoor Air* 26(4):546–557
- Morawska L, He C, Johnson G, Guo H, Uhde E, Ayoko G (2009) Ultrafine particles in indoor air of a school: possible role of secondary organic aerosols. *Environ Sci Technol* 43(24):9103–9109
- Morawska L, Afshari A, Bae GN, Buonanno G, Chao CYH, Hänninen O, ... Wierzbicka A (2013) Indoor aerosols: from personal exposure to risk assessment. *Indoor Air* 23(6):462–487. <https://doi.org/10.1111/ina.12044>
- Morawska L, Ayoko GA, Bae GN, Buonanno G, Chao CYH, Clifford S, ... Wierzbicka A (2017) Airborne particles in indoor environment of homes, schools, offices and aged care facilities: the main routes of exposure. *Environ Int* 108:75–83
- Mumovic D, Palmer J, Davies M, Orme M, Ridley I, Oreszczyn T, ... Way P (2009) Winter indoor air quality, thermal comfort and acoustic performance of newly built secondary schools in England. *Build Environ* 44(7):1466–1477. <https://doi.org/10.1016/j.buildenv.2008.06.014>
- Nunes RAO, Branco PTBS, Alvim-Ferraz MCM, Martins FG, Sousa SIV (2015) Particulate matter in rural and urban nursery schools in Portugal. *Environmental Pollution* 202:7–16.
- Oeder S, Jörres RA, Weichenmeier I, Pusch G, Schober W, Pfab F, ... Nowak D (2012) Airborne indoor particles from schools are more toxic than outdoor particles. *Am J Respir Cell Mol Biol* 47(5):575–582
- Orellano P, Reynoso J, Quaranta N, Bardach A, Ciapponi A (2020) Short-term exposure to particulate matter (PM₁₀ and PM_{2.5}), nitrogen dioxide (NO₂), and ozone (O₃) and all-cause and cause-specific mortality: systematic review and meta-analysis. *Environ Int* 142. <https://doi.org/10.1016/j.envint.2020.105876>
- Patel S, Sankhyan S, Boedicker EK, DeCarlo PF, Farmer DK, Goldstein AH, ... Vance ME (2020) Indoor particulate matter during HOMEChem: Concentrations, size distributions, and exposures. *Environmental science & technology* 54(12):7107–7116
- Pegas P, Alves C, Evtyugina M, Nunes T, Cerqueira M, Franchi M, ... Freitas M (2011) Seasonal evaluation of outdoor/indoor air quality in primary schools in Lisbon. *J Environ Monit* 13(3):657–667
- Petersen S, Jensen K, Pedersen A, Rasmussen HS (2016) The effect of increased classroom ventilation rate indicated by reduced CO₂ concentration on the performance of schoolwork by children. *Indoor Air* 26(3):366–379
- Poulhet G, Dusanter S, Crunaire S, Locoge N, Gaudion V, Merlen C, ... Coddeville P (2014) Investigation of formaldehyde sources in French schools using a passive flux sampler. *Build Environ* 71:111–120

- Poupard O, Blondeau P, Iordache V, Allard F (2005) Statistical analysis of parameters influencing the relationship between outdoor and indoor air quality in schools. *Atmos Environ* 39(11): 2071–2080
- Rim D, Gall ET, Kim JB, Bae GN (2017) Particulate matter in urban nursery schools: A case study of Seoul, Korea during winter months. *Building and Environment* 119:1–10.
- Rosbach JT, Vonk M, Duijm F, Van Ginkel JT, Gehring U, Brunekreef B (2013) A ventilation intervention study in classrooms to improve indoor air quality: the FRESH study. *Environ Health* 12(1):1–10
- Rovelli S, Cattaneo A, Nuzzi CP, Spinazzè A, Piazza S, Carrer P, Cavallo DM (2014) Airborne particulate matter in school classrooms of northern Italy. *Int J Environ Res Public Health* 11(2): 1398–1421
- Santamouris M, Synnefa A, Asssimakopoulos M, Livada I, Pavlou K, Papaglastra M, ... Assimakopoulos V (2008) Experimental investigation of the air flow and indoor carbon dioxide concentration in classrooms with intermittent natural ventilation. *Energ Buildings* 40(10): 1833–1843
- Schoer L (1973) A combined evaluation of three separate research projects on the effects of thermal environment on learning and performance
- Shaughnessy RJ, Turk B, Evans S, Fowler F, Casteel S, Louie S (2002) Preliminary study of flooring in school in the US: airborne particulate exposure in carpeted vs. uncarpeted classrooms. *Proceedings of Indoor Air* 974–979.
- Sofuoğlu SC, Aslan G, Inal F, Sofuoğlu A (2011) An assessment of indoor air concentrations and health risks of volatile organic compounds in three primary schools. *Int J Hyg Environ Health* 214(1):36–46
- Stranger M, Potgieter-Vermaak S, Van Grieken R (2008) Characterization of indoor air quality in primary schools in Antwerp, Belgium. *Indoor Air* 18(6):454–463
- Teeuwen S, Bruggema H, Zeiler W (2015) Highly sustainable Dutch schools: what about IAQ? *ASHRAE Trans* 121:1Q
- Tian Y, Sul K, Qian J, Mondal S, Ferro AR (2014) A comparative study of walking-induced dust resuspension using a consistent test mechanism. *Indoor Air* 24(6):592–603
- Tran DT, Alleman LY, Coddeville P, Galloo J-C (2014) Indoor–outdoor behavior and sources of size-resolved airborne particles in French classrooms. *Build Environ* 81:183–191. <https://doi.org/10.1016/j.buildenv.2014.06.023>
- Twardella D, Matzen W, Lahrz T, Burghardt R, Spegel H, Hendrowarsito L, ... Fromme H (2012) Effect of classroom air quality on students' concentration: results of a cluster-randomized cross-over experimental study. *Indoor Air* 22(5):378–387
- Wallner P, Kundt M, Moshammer H, Piegl K, Hohenblum P, Scharf S, ... Hutter H-P (2012) Indoor air in schools and lung function of Austrian school children. *J Environ Monit* 14(7): 1976–1982
- Wargocki P, Wyon DP (2007) The effects of moderately raised classroom temperatures and classroom ventilation rate on the performance of schoolwork by children (RP-1257). *Hvac&R Res* 13(2):193–220
- Wargocki P, Wyon DP (2013) Providing better thermal and air quality conditions in school classrooms would be cost-effective. *Build Environ* 59:581–589. <https://doi.org/10.1016/j.buildenv.2012.10.007>
- Weichenthal S, Dufresne A, Infante-Rivard C, Joseph L (2008) Characterizing and predicting ultrafine particle counts in Canadian classrooms during the winter months: model development and evaluation. *Environ Res* 106(3):349–360
- Weschler CJ (2004) Chemical reactions among indoor pollutants: what we've learned in the new millennium. *Indoor Air* 14(s 7):184–194
- WHO (2010) WHO guidelines for indoor air quality: selected pollutants (9289002131). Retrieved from
- WHO (2015) School environment: policies and current status. Retrieved from Copenhagen

- Wichmann J, Lind T, Nilsson MAM, Bellander T (2010) PM_{2.5}, soot and NO₂ indoor–outdoor relationships at homes, pre-schools and schools in Stockholm, Sweden. *Atmos Environ* 44(36): 4536–4544. <https://doi.org/10.1016/j.atmosenv.2010.08.023>
- World Health Organization (2021) WHO global air quality guidelines: particulate matter (PM_{2.5} and PM₁₀), ozone, nitrogen dioxide, sulfur dioxide and carbon monoxide. World Health Organization. <https://www.apps.who.int/iris/handle/10665/345329>. License: CC BY-NC-SA 3.0 IGO
- Wyon D (1970) Studies of children under imposed noise and heat stress. *Ergonomics* 13(5): 598–612
- Ye W, Little JC, Won D, Zhang X (2014) Screening-level estimates of indoor exposure to volatile organic compounds emitted from building materials. *Build Environ* 75:58–66
- Ye W, Won D, Zhang X (2017) A practical method and its applications to prioritize volatile organic compounds emitted from building materials based on ventilation rate requirements and ozone-initiated reactions. *Indoor Built Environ* 26(2):166–184
- Zhang X, Wargocki P, Lian Z, Thyregod C (2017) Effects of exposure to carbon dioxide and bioeffluents on perceived air quality, self-assessed acute health symptoms, and cognitive performance. *Indoor Air* 27(1):47–64
- Zhong L, Su F-C, Batterman S (2017) Volatile organic compounds (VOCs) in conventional and high performance school buildings in the US. *Int J Environ Res Public Health* 14(1):100
- Zuraimi MS, Tham KW (2008) Indoor air quality and its determinants in tropical child care centers. *Atmospheric Environment* 42(9):2225–2239



Indoor Air Quality in Offices

65

Andrea Cattaneo, Andrea Spinazzè, and Domenico M. Cavallo

Contents

Introduction	1936
Background	1936
Problem Statement: IAQ in Office Buildings	1937
Strategic Considerations	1938
Indoor Air Pollutants of Concern for Offices	1939
Sources and Determinants of IAPs in Offices	1940
Assessment Methods and Strategies for IAQ in Offices	1943
IAQ Monitoring Approaches	1944
IAQ Perception and Health Symptoms	1948
IAQ and Health Outcomes in Office Workers	1952
IAQ Management and Risk Mitigation Measures in Offices	1954
Conclusions	1955
References	1956

Abstract

Since multiple studies have addressed IAQ and associated exposure-related symptoms in office workers, a careful assessment and management of indoor air quality (IAQ) in office-like environments is important for the protection of human health and to ensure optimal comfort and well-being for office workers. For this purpose, the development of appropriate monitoring strategies is crucial to properly characterize the chemical and physical complexity of IAQ dynamics and subsequent potential impacts on office occupants. To obtain comprehensive and representative conclusions about IAQ problems in office-like environments, and to prioritize the order of management interventions, a multilevel approach should be implemented. The assessment process should include a general survey of the building and of the offices, occupants' questionnaire surveys (concerning

A. Cattaneo (✉) · A. Spinazzè · D. M. Cavallo

Department of Science and High Technology, Università degli Studi dell'Insubria, Como, Italy
e-mail: andrea.cattaneo@uninsubria.it; andrea.spinazze@uninsubria.it;
domenico.cavallo@uninsubria.it

IAQ, symptoms, and psychosocial working aspects), and environmental measurements. IAQ monitoring and assessment, combined with source identification and control and adjustment of ventilation rates, has been recognized as the prioritized strategy for improving IAQ in office-like environments and reducing the combined health risks associated with indoor exposures.

Keywords

IAQ · Indoor air pollutants · Office-like environments · Comfort · Symptoms

Introduction

Background

Indoor environmental quality (IEQ), which is related both to indoor air quality (IAQ) and to other environmental characteristics (such as temperature, noise, and light), may affect occupants' health, comfort, and well-being (Wolkoff 2013). The IAQ of confined nonindustrial environments is considered as a priority interest for both the general population and for a large part of the workforce. Indoor air contains a wide variety of physical (e.g., alpha ionizing radiation deriving from radon), biological (e.g., fungi, bacteria, mites, algae, etc.), and chemical contaminants (e.g., volatile organic compounds (VOCs), formaldehyde, ozone (O_3), particulate matter (PM), asbestos and man-made fibers, environmental tobacco smoke), arising from several sources, and presenting wide spatial and temporal variations. The sources of pollution consist mainly of infiltration of air from outdoors, heating, ventilation, and air-conditioning (HVAC) systems, humidifiers, building materials, furniture and furnishings, electronic equipment (including computers and photocopiers), and activities carried out by the occupants and the occupants themselves, who represent a source of many bioeffluents (e.g., skin flakes, carbon dioxide (CO_2), squalene, acetaldehyde). Overall, the contribution of IAQ to personal exposure to pollutants could be more relevant than the contribution of outdoor exposure. The indoor concentration of some pollutants is often equal to (e.g., for PM_{2.5} and nitrogen oxides (NO_x)) or much greater than (formaldehyde, radon, fungi) the corresponding outdoor concentrations, but the duration of exposure indoors is far greater than that outdoors. Overall, indoor chemical air pollutants can be divided into two general categories: (1) pollutants most commonly associated with occupant discomfort or acute illness (e.g., carbon monoxide (CO), formaldehyde, petroleum-derived solvents, halogenated solvents, and a variety of other VOCs) and (2) pollutants that can also cause chronic or carcinogenic illnesses (some VOCs, NO_x , airborne fibers, and airborne PM). There are also physical agents relevant to the field of IAQ assessment such as alpha ionizing radiations, emitted mainly by radon and its decay products. Radon exposure is the most relevant source of exposure to ionizing radiations in the general population and the primary risk factor for lung cancer in never smokers, with an almost linear increase in risk with increasing long-term exposure in indoor

spaces. Specific regulatory measures have therefore been adopted in various countries for preventive purposes (e.g., in Europe, the 2013/59/EURATOM directive laying down basic safety standards for protection against the dangers arising from exposure to ionizing radiation). Further, a mixture of biological pollutants can be present in indoor living and working environments. Viruses, bacteria (and their endotoxins), fungal spores, mites, algae, amoebas can proliferate in hydraulic and HVAC systems and in furnishings (carpets, upholstered furniture, rugs, wallpaper). High humidity and temperature facilitate the growth of molds and fungi and their presence is quite common and affecting, according to some estimates, between 18% and 50% of buildings. Biological agents can cause allergic diseases (e.g., rhinitis and conjunctivitis, bronchial asthma, hypersensitivity pneumonias) and infectious diseases (e.g., “Legionnaires’ disease,” Pontiac fever, Q fever), including viral diseases and miosis (Menzies and Kreiss 2006). HVAC systems can facilitate both the spread of infectious agents (influenza viruses, measles viruses, bacteria, fungi) and their proliferation, since they often represent a good growth environment. The World Health Organization has defined that exposure to mold in indoor environments involves an increased risk of respiratory symptoms for occupants (cough, wheezing), respiratory infections, new asthma onset, and exacerbations of preexisting bronchial asthma. There is also clinical evidence of an increased risk of less common diseases such as hypersensitive pneumonia, chronic rhinosinusitis, and allergic sinusitis.

Problem Statement: IAQ in Office Buildings

Overall, IAQ has been identified as a major concern in terms of its potential impact on human health: indoor exposures have been estimated to cause a substantial loss of health (Asikainen et al. 2016). The burden of disease is dominated by airborne PM, but also includes a contribution from long-term exposure to the most common air pollutants (e.g., nitrogen dioxide (NO_2), volatile organic compounds (VOCs) – this last group also include aldehydes which, however, are often named separately from other VOCs). Exposure to these indoor air pollutants (IAPs), even at low concentrations, may affect human health, causing or aggravating diseases, such as sensory irritation, cardiovascular diseases, chronic obstructive pulmonary disease, allergic and asthma symptoms, and lung cancer (Carrer et al. 2015). Overall, multifactorial causality of IAQ-related symptoms have been found, suggesting that a given symptom may arise from a combination of individual, occupational, and environmental risk factors (Wolkoff 2013, 2017). On the other hand, some relationships have been found between building characteristics and self-reported health complaints (Bluyssen et al. 2016). Generally, diseases and uncomfortable situations mainly reported in office workers find their origin in a condition of nonoptimal IAQ, especially if associated with unfavorable microclimatic conditions. Further, other factors such as the exposure to noise, the prolonged use of equipment with monitor (especially for some workers such as designers, journalists, brokers, computer scientists, web designers, graphic designers, etc.), inadequate working space and a

tight work organization can take on considerable importance in specific cases (Steinemann et al. 2017).

From these considerations and considering that people spend approximately 90% of their time indoors, IAQ may considerably affect human health and well-being (World Health Organization 2010). In this context, nonindustrial built work environments such as offices are of particular concern, as they represent the most common occupational environment in developed countries. In industrialized countries, about 67% of the employed population works in environments in the tertiary sector and in offices (while 27% and 6% are employed in industry and agriculture, respectively). In developing countries, about 46% of the employed work in the tertiary sector (while 19% work in industry and 35% in agriculture). Different sources may emit pollutants in office indoor environments directly (e.g., emissions from consumer products, building materials, office equipment, indoor combustion sources, etc.) or indirectly (i.e., primary pollutants may react with each other, with pollutants from other sources, or with surface materials, creating secondary compounds) (Trantallidi et al. 2015). IAQ in office buildings can be affected by several parameters such as inappropriate selection of indoor materials, emissions from electronic equipment and performance of the heating, ventilation, and air-conditioning (HVAC) systems, the use of carpets as floor covering, recently painted walls, and is related with other workplace conditions (crowded offices and presence of unpleasant odors, dust, and dirt). Further, office environments involve some other specific characteristics leading to the presence of typical pollutants sources (e.g., printers and photocopiers, computers, solvents, adhesives, cleaners, air fresheners, etc.). Finally, office employees spend a significant part of their time in environments that in recent years are typically characterized by complex building systems (e.g., mechanical, electrical, plumbing, controls, and fire protection systems) designed to reduce energy costs through controlled indoor environment conditions. Beside central control, a certain degree of personal control (local thermostats, windows, personal lights etc.) over the indoor environment should be allowed to office occupants, since personal control has a crucial role in achieving a healthy, comfortable, and productive environment (Sakellaris et al. 2019).

In summary, also considering the specific peculiarities of office environments, inadequate IAQ in office building could influence the perceived IAQ, comfort, health, but also indirectly impacts office work performance (Wyon 2004; Wolkoff et al. 2021).

Strategic Considerations

A careful assessment and management of IAQ in offices is important for the protection of human health and to ensure optimal comfort and IAQ perception for office workers. For this purpose, the development of appropriate monitoring strategies is crucial to properly characterize the chemical and physical complexity of the IAQ dynamics. Chemical and physical transformation of the pollutants can occur with high spatial and temporal variability. A proper IAQ assessment strategy should

consider the wide variety of indoor pollutants, as well as their temporal and spatial inhomogeneity. Further, several of monitoring methods and techniques are available, and the choice of the most appropriate method must be based on both the target constituent and the objective of field investigation. The aim of this chapter is to provide insight to carry out a comprehensive and accurate assessment of IAQ in a general office exposure scenario. Obviously, when considering a given specific scenario, further insights (which are impossible to report here extensively) should be considered. Independently of the methods of the evaluation, it is generally important to develop a multidisciplinary evaluation process based on a manifold know-how of air sampling, analytical chemistry, occupational hygiene, and toxicology and occupational medicine. It is also crucial to properly inform and interact with the employer, HSE (health, safety, and environment) and/or building managers, and last but not least workers and building occupants.

Indoor Air Pollutants of Concern for Offices

When setting up an IAQ study, the selection of proper parameters to be evaluated is of fundamental importance and needs to be aligned with traditional risk assessment paradigms whose first step is “hazard identification.” This choice clearly depends on the specific objectives of the study to be conducted, but in general, the aim should be to identify the chemical, biological, and/or physical agents that represent the highest priority for research, surveillance, or intervention due to their potential risks for occupant health (Sérafin et al. 2021). Among the most important and most widely considered reference documents, the World Health Organization (WHO) published IAQ-specific guidelines for the protection of public health from risks due to exposure to selected pollutants commonly present indoors and in particular, O₃, NO₂, PM (PM_{2.5} and PM₁₀), sulfur dioxide (SO₂), CO (World Health Organization 2021) and benzene, formaldehyde, naphthalene, benzo[a]pyrene, radon, trichloroethylene, and tetrachloroethylene (World Health Organization 2010). These are known to have indoor sources, can be found indoors in concentrations of health concern, and are considered of key importance due to their hazardous nature. These guidelines are certainly useful, but they refer to a limited number of key pollutants, compared to those that can be identified in indoor environments. Thus, some studies have considered different pollutants or have sought to define prioritization criteria for a wider number of air pollutants monitoring in indoor environments (Logue et al. 2011). As an example, in the OFFICAIR study (Mandin et al. 2017), a combination of physical (temperature, relative humidity, air change rate) and chemical parameters were measured. These parameters included PM_{2.5}, O₃, NO₂, aldehydes (formaldehyde, acetaldehyde, acrolein, propanal, benzaldehyde, glutaraldehyde, hexanal), and VOCs (benzene, toluene, xylenes, ethylbenzene, n-hexane, trichloroethylene, tetrachloroethylene, α -pinene, d-limonene, 2-butoxyethanol, 2-ethylhexanol, styrene). These selected chemicals were chosen since most of them were known to be emitted from building materials, cleaning products, and office equipment, and had potential

associations with adverse health outcomes (e.g., sensory irritation symptoms, cardiovascular and pulmonary effects) (Wolkoff 2013).

A WHO publication (World Health Organization 2020) also provides a list of most common chemical pollutants of indoor air in public settings for children, as they are also considered of particular concern (priority pollutants) for the assessment of risk of combined exposure in indoor environments. The same document also lists other common pollutants of indoor air in public settings that should be measured for the control of IAQ.

A method was developed to identify priority IAPs in office buildings (Sérafín et al. 2021) using both a chronic risk assessment approach and a hazard classification method based on carcinogenic, mutagenic, reprotoxic, and endocrine disruptive effects. The study evaluated 342 chemicals for which indoor air concentrations had been previously measured in office buildings and identified 71 of these as priority pollutants. These were further divided into five priority classes, ranging from “non-priority” or “unclassifiable” to “very high priority.” Among these, 16 pollutants (i.e., formaldehyde, acetaldehyde, glutaraldehyde, acrolein, benzene, dichloropropane, 1,2,4-trichlorobenzene, NO₂, SO₂, PM_{2.5}, PM₁₀, antimony, nickel, cadmium, manganese, and chlorine) were considered as pollutants of particular concern. Interestingly, 123 additional chemicals are proposed for future monitoring surveys to update the prioritization of IAPs in offices, since these could be present in office indoor air but could not be assessed with the proposed criteria due to the lack of measured data in the scientific literature (Sérafín et al. 2021). Table 1 presents a list of chemical pollutants considered as being of relevance for IAQ assessment in office buildings. However, there is no definitive consensus concerning the prioritizing method for IAPs based on health concerns and as knowledge of health hazards evolves, both well-known and emerging pollutants may present potential risks for building occupants. Thus, regular assessment and prioritization of indoor pollutants is essential to guide research, policies, IAQ surveys, and product development.

Sources and Determinants of IAPs in Offices

IAP concentrations are affected by several factors, including infiltration from the outdoors, indoor emission rates, indoor reaction and deposition dynamics, air change rates, room volume, and indoor temperature and humidity. In countries where effective anti-smoking policies have not been promulgated, environmental tobacco smoke (ETS) could be a significant source of indoor pollutants. Further, due to the presence of these sources and the confined air volume, indoor air concentrations in some indoor environments, such as offices, can be higher than in the outdoor air (Katsoyiannis et al. 2012). This problem is especially true for modern buildings, which have very different characteristics from traditional ones, such as energy-efficient structure and the interior fittings’ design and construction (i.e., the growing adoption of nonsmoking policies, “low-emitting” materials, synthetic heat-insulating and sound-absorbing materials, electronic equipment, air-conditioning and mechanical ventilation systems, and open-plan offices in place of cellular

Table 1 List of chemical pollutants to be considered as of relevance for IAQ assessment in office buildings

Reference	Guideline/project	Relevant pollutants
World Health Organization (2010)	WHO guidelines for indoor air quality: selected pollutants	Benzene, CO, formaldehyde, naphthalene, NO ₂ , polycyclic aromatic hydrocarbons (especially benzo[a]pyrene), radon, trichloroethylene, and tetrachloroethylene
Mandin et al. (2017)	OFFICAIR Project	PM (PM _{2.5} , O ₃ , NO ₂ , aldehydes (formaldehyde, acetaldehyde, acrolein, propanal, benzaldehyde, glutaraldehyde, hexanal), and VOCs (benzene, toluene, xylenes, ethylbenzene, n-hexane, trichloroethylene (TCE), tetrachloroethylene (PCE), α -pinene, d-limonene, 2-butoxyethanol, 2-ethylhexanol, styrene)
World Health Organization (2020)	Methods for sampling and analysis of chemical pollutants in indoor air	Priority pollutants: Oxygenated VOCs – aldehydes (formaldehyde and acetaldehyde); VOCs (aromatic hydrocarbons (benzene, ethylbenzene, o-xylene, m,p-xylenes, styrene, toluene, 1,2,3-trimethylbenzene and 1,4-dichlorobenzene), esters (butyl acetate), terpenes (limonene and α -pinene), chlorinated hydrocarbons (tetrachloroethylene and trichloroethylene)); SVOCs (PAHs (naphthalene and benzo(a)pyrene); inorganic compounds (NO ₂)) Other pollutants: PM, O ₃ , CO, phthalates, musks, BFRs, organophosphate flame retardants (OPFRs), and chlorinated paraffins (CPs)
Sérafin et al. (2021)	Indoor air pollutant health prioritization in office buildings	$n = 71$ priority pollutants [of which $n = 16$ pollutants of particular concern (formaldehyde, acetaldehyde, glutaraldehyde, acrolein, benzene, dichloropropane (DCP), 1,2,4-trichlorobenzene, NO ₂ , SO ₂ , PM _{2.5} , PM ₁₀ , antimony nickel, cadmium, manganese, and chlorine)] $n = 123$ chemicals are proposed for future monitoring surveys
World Health Organization (2021)	WHO global air quality guidelines	PM (PM _{2.5} and PM ₁₀), O ₃ , NO ₂ , SO ₂ , and CO

offices) have resulted in temporal changes of the factors driving the presence of IAPs and the resulting IAQ. Microclimatic conditions can affect IAQ differently: high temperatures and humidity affects volatile species emissions including the emissions

of VOCs from building materials and furnishings. Humidity may also influence aerosol formation by condensation and coagulation processes, as well as its chemical composition. Ventilation (i.e., the rate of air exchange with outdoor air) has a strong relationship with the concentrations of indoor pollutants. High concentrations of VOCs are generally related to low air exchange rates. Nevertheless, some pollutants are associated with outdoor sources (e.g., vehicular traffic). Thus, high air exchange rates may lead to higher indoor concentrations due to higher infiltration from outdoor but depending on the effectiveness of the HVAC system's filtration system. IAP concentrations can also significantly vary in different locations of the same indoor environment. This variation can be due to (i) the different types of sources and sinks in various locations, (ii) different activities performed by occupants in different locations (and at different times), and (iii) the effect of ventilation and air flows (mechanical and natural) that distribute contaminants from a given emission point throughout the indoor environment. A non-negligible temporal variability in concentrations can be also observed in office indoor environments, reflecting the intermittent nature of their sources (e.g., for contaminants associated to specific activities, such as printing, cleaning, etc.), interferences, and/or incursion of outdoor air or other temporal dynamics. Since emissions from construction materials and furnishings are important sources for indoor pollutants, newly constructed, remodeled, or furnished environments are expected to produce highly contaminated indoor air (Baek 2011). Seasonality could also play a major role in defining IAPs, with particular emphasis on VOC emissions from building materials (Campagnolo et al. 2017) and O₃-related indoor chemistry, which plays a major role in the summer period. The greater ultraviolet radiation, higher temperatures, and higher biogenic VOC emission rates in summer cause high O₃ concentrations outdoors that after infiltration, leads to the formation of oxidation products from O₃-initiated reactions involving common VOCs such as limonene and squalene (Nørgaard et al. 2014). Primary sources (traffic emissions, indoor product emissions, cleaning products, transport from other microenvironments, and air fresheners) of 30 target VOCs in residential interiors and workplace microenvironments were defined in the EXPOLIS study (Edwards et al. 2001). Two studies, conducted as part of the Officair project, were aimed at the source identification (Campagnolo et al. 2017) and assessment of IAP determinants (Spinazzè et al. 2020) specifically in office buildings, accounting also for seasonal variability. The dominant source of chemical IAPs in both summer and winter periods was linked to the infiltration of contaminated outdoor air into indoor environments, which was particularly relevant for benzene, toluene, ethylbenzene, xylenes, and n-hexane (Campagnolo et al. 2017). The other identified sources were individually attributed to wooden-based material emissions (α -pinene, formaldehyde, acetaldehyde, propanal, and hexanal), flooring emissions (α -pinene, 2-butoxyethanol, 2-ethylhexanol, and propanal), and printer emissions (styrene). In summer, O₃-initiated oxidation reactions were identified as important sources of formaldehyde and acetaldehyde. Further, sources directly linked to paint emissions (acrolein and benzaldehyde) and cleaning products (2-butoxyethanol) were defined for the winter period. Beyond these identified sources, several associations between IAPs concentrations and buildings' structural characteristic or

occupants' activity patterns were identified. Aldehydes and VOCs determinants in office buildings include building and furnishing materials, indoor climate characteristics (room temperature and relative humidity), the use of consumer products (e.g., cleaning and personal care products, office equipment), as well as the presence of outdoor sources in the proximity of the buildings (i.e., vehicular traffic) (Spinazzè et al. 2020).

Assessment Methods and Strategies for IAQ in Offices

A prerequisite for the assessment of IAQ and associated conditions in offices and office-like environments should be a detailed knowledge of building characteristics and possible pollution sources as well as the indoor activities, which are often collected by trained personnel making use of checklists. Besides those lists developed on a building-level basis, checklists at room level and time-activity diaries coupled with real-time measurements of IAPs allow the collection of higher-level information to gain a more detailed picture of the microenvironmental characteristics and exposure determinants (Spinazzè et al. 2020). The methods and strategies for the assessment of IAQ and associated factors in offices can vary substantially depending on the purposes of IAQ surveys. For instance, source identification and apportionment of IAPs are of great relevance to develop risk management strategy and to steer the choice of technological controls for IAQ improvement. For this purpose, a large number of repeated measurements with proper temporal resolution are typically needed to make inferences about the relationship between the monitored IAPs and continuous emission sources rather than intermittent or sporadic emission events. In parallel, reliable methods to assess IAQ or occupants' exposures should be thoughtfully identified based on the reference periods upon which IAQ guideline values are defined and to ensure good data quality. Although offices are classified as workplaces from the legal point of view, the traditional air sampling methods and occupational exposure limit values developed for occupational risk assessment are not directly applicable in office environments.

IAQ experts can be asked for advice on a problem building or building area in which there is a high prevalence of complaints or reported health symptoms by office workers. In this case, the reason behind the study is the identification of the causal agents and their sources for evidence-based and effective risk management. Thus, a recommendable study design is first to perform an assessment of symptoms and IAQ perception by standardized questionnaires followed by an IAQ monitoring campaign specifically focused on some targeted IAPs. As an example, a high prevalence of mucous membrane irritation and itching can be indeed associated with high concentrations of O₃ and some VOCs such as ethylbenzene and n-hexane (Sakellaris et al. 2021). Possible interventions must be focused on their possible emission sources or increasing air change rates, although the impact of the latter option can be somewhat overestimated (Rackes and Waring 2016).

In some other cases, a periodic IAQ assessment can be required by occupational risk prevention programs planned by the management system of private companies

or required by public authorities. If that is the case, the focus should be on the identification of priority IAPs to be monitored for an IAQ assessment based on testing the compliance of measured concentrations against guideline values. This should include, as a complement, an assessment of other IEQ stressors that could impact on occupants' health, comfort, and well-being.

A new frontier in this context is the application of sensor networks allowing a real-time monitoring of IAPs with good spatial coverage for an immediate and efficient energy, risk assessment, and risk management (Kumar et al. 2016).

IAQ Monitoring Approaches

There are many aspects of IAQ that have a potential impact on the sampling and analysis strategies adopted for its assessment. IAQ is determined by a complex series of processes, and thus, no single sampling and analysis system is completely appropriate for all the constituents of IAQ. For this reason, the monitoring protocol must be optimized to consider different compounds and classes of pollutants (Spinazzè et al. 2021). The constituents of IAQ components comprise gases and lower molecular weight organic compounds, which reside predominantly in the vapor phase, and higher molecular organic species and inorganic PM constituents that can be found predominantly in the particulate phase. Therefore, a sampling protocol for many IAQ constituents that emphasizes only the vapor or the particle phases could result in an incomplete understanding of the ambient levels of the target components. IAPs concentrations vary both spatially and temporally to a large extent relative to common outdoors pollutants. This variation is due to the large variety of sources, the intermittent operation of some of these sources, and the different types and quantities of sinks present at various locations. Mechanical ventilation and atmospheric diffusion tend to distribute contaminants from a given source throughout the indoor environment. By way of example, the high temporal variability in concentrations of combustion products reflects the intermittent nature of their sources. Thus, the time resolution and duration of sampling is a key factor affecting the concentrations and variability found in any study (Baek 2011).

The sampling strategy design is a fundamental step in IAQ assessment surveys to ensure representativeness of the assessment. A proper IAQ monitoring strategy should be based on several preliminary critical choices. First, the compounds to be investigated should be selected based on their possible impacts on human health or if they are known to be prominent substances emitted in the office environment by specific sources. Some insights were previously reported in *this chapter*. A prerequisite for the assessment of IAQ in offices and office-like environments should be a detailed knowledge of building characteristics. A preliminary step is a general survey of the building and of the office environments to allow the collection of technical information and to obtain a detailed picture of the environment (Spinazzè et al. 2020). All factors that may affect IAQ should be identified, analyzed, and reported, including activities in offices, HVAC systems, furnishings, fittings, cleaning routines, cleaning products, and potential outdoor sources of pollutants

(Kalimeri et al. 2016). Recommendations about the information to be recorded during indoor air measurement can be found in ISO 16000-1 (2004).

As said, the methods and strategies for the assessment of IAQ and associated factors in offices can vary substantially depending on the reasons for and purposes of the IAQ surveys; however, an overview of potentially useful approaches and instrumentation is reported in Spinazzè et al. (2021). Generally, for each building, the field campaigns should consist of multiple measurements performed in different indoor locations and, possibly outdoors for a proper period. An outdoor sampling site is optional but could be useful to identify the contribution of outdoor sources to the indoor air pollution. Outdoor samplers should be located close to the investigated building but no closer than 1.0 m (ISO 16000-1:2004 2004), protected from direct sunlight and precipitation and, when possible, from people; distance sources of emissions should be recorded for outdoor sampling site. If the building has a HVAC system, ambient air should be sampled close to the air intake (World Health Organization 2020).

Any sampling equipment should allow office workers to perform their work without being affected by the ongoing IAQ monitoring, also in terms of productivity and ability to stay focused. Thus, compact and silent methods using portable equipment should be preferred. In some cases, an effective noise reduction can be achieved using noise-reducing enclosures.

The number of sampling locations per building should be a compromise between extensive IAQ characterization for the whole building, the budget, and other feasibility issues (power supply, accessibility, etc.). The indoor locations should be selected as diverse as possible to represent IAQ at different workplaces in the building. Thus, for example, the locations should be selected on different floors and their position on each floor could be defined to have different orientations (North, South, East, and West). Moreover, if the office building had both types of working spaces, measurement should be performed in both in open-plan and cellular offices. The samplers should be placed in the center of each room, not close to the wall, at the height of the breathing zone of seated occupants (i.e., approximately 110 cm); ventilation channels and heating sources, including the sun, should be avoided. ISO 16000-1 (2004) recommends placing samplers in the center of a room. If this is not possible, the sampler should be placed 1.0–2.0 m from a wall and 1.0–1.5 m from the floor.

The general principles for IAQ monitoring in offices are similar to those already defined for the assessment of IAQ in the general living environments. The monitoring of IAPs in office building is typically carried out using active or passive samplers and/or real-time monitors placed in a fixed position (in the center of the room) away from door and windows. IAQ problems have multifactorial causes, and multi-pollutant measurement systems are generally used to account for the different chemical, biological, and physical agents, and quantify their contamination levels in indoor air. For this reason, multipollutant IAQ monitoring stations have also been developed and used in IAQ research studies (Spinazzè et al. 2021; Villanueva et al. 2021). Besides the already mentioned interaction between microclimatic parameters and IAPs, T and RH should also be monitored because of their possible influence

(e.g., uptake rates of passive samplers) or interference with air sampling (e.g., electrochemical sensors).

Concerning monitoring strategies, ISO 16000-1 (2004) provides recommendations about sampling of IAPs (i.e., duration, period, and location of sampling) with parallel measurements of concentrations of outdoor air pollutants. Basically, two different approaches can be considered for sampling duration: (i) 24-h measurements for 5 consecutive working days (24 h/5 days) and/or (ii) measurements during periods when workers are physically present indoors (typically 5–8 h for the workday). The first option may result in overestimation of exposure to certain pollutants which typically have indoor sources and could accumulate during the night (due to windows closed and mechanical systems turned off). Obviously, the contrary could be observed for pollutants typically emitted outdoors or IAPs having short atmospheric lifetimes. For example, a study outlined that by including unoccupied periods in the sampling interval, some VOC concentrations were overestimated (namely acetaldehyde, formaldehyde, tetrachloroethylene), while other VOCs were underestimated (i.e., toluene, ethylbenzene, xylenes, styrene, 1,2,3-trimethylbenzene, and 1,4-dichlorobenzene). In another case, an underestimation of formaldehyde concentration was observed when unoccupied periods were included (Mishra et al. 2015). Measuring during periods when workers are present in offices requires measurement techniques that can be activated or deactivated at specific times, and/or direct-reading measurements methods. Overall, passive sampling over a 5-working day (i.e., a working week) can be recommended for assessing combined exposure to chemicals in indoor air. In practice, different measurement techniques could be combined with each other to optimize the monitoring strategy based on pollutants characteristics and for the specific aims of the study. For example, the SINPHONIE and Officair projects applied this strategy in schools and offices, respectively. The SINPHONIE project applied different approaches for different pollutants: samples of PM ($PM_{2.5}$) were collected for gravimetric analysis for 8 h/day (due to the relationship between $PM_{2.5}$ and occupancy density and for reasons of detection limit). CO was continuously measured by a low-cost direct-reading instrument (short-term assessment is more suitable since CO causes acute health effects). CO_2 was measured by direct-reading instruments to calculate ventilation rates. $PM_{2.5}$ and PM_{10} were measured by optical light scattering (Kalimeri et al. 2016). In the OFFICAIR study, sampling was carried out over 5 days from Monday morning (approximately 9 a.m.) to Friday afternoon (approximately 5 p.m.) at four locations in each building, except for $PM_{2.5}$ (one location per building). The duration of the sampling was a compromise between the interest in characterizing the average concentrations in office buildings to assess long-term worker exposure and technical feasibility. Both passive and active sampling techniques were adopted for measurement of VOCs, aldehydes, NO_2 , O_3 , and $PM_{2.5}$ over the work-week period (Mandin et al. 2017), but also short-term active sampling and direct-reading methods were adopted for specific measurement (Nørgaard et al. 2014).

Further, concentration of some pollutants (e.g., emissions of formaldehyde from materials and products) can vary significantly, depending on the season and on several other factors (i.e., temperature, relative humidity, ventilation rate). For this

reason, analysis of indoor air pollution in the cold (“heating”) season (November to March in the northern hemisphere) would likely find higher levels for certain compounds, such as benzene, NO₂, and D-limonene (Mandin et al. 2017). To evaluate the seasonal variation of pollutant concentrations in indoor air, measurements during both in the cold (heating) and in the warm (non-heating) season are highly recommended, with periodicity and periods to be defined depending on the geographical location of the country (World Health Organization 2020).

In most cases, samples for IAQ investigations are collected in the field and returned to the laboratory for subsequent chemical analysis. However, for some IAPs, real-time monitors can be also used. Active sampling involves drawing air into a collection media by means of a pump, whereas passive sampling places a material that irreversibly adsorbs, absorbs, or immobilizes the chemical of interest in the target substrate. Active sampling is used to sample large volumes of air or to sample small volumes of air over short durations. Passive sampling is primarily used to sample small volumes of air over long periods of time. Passive systems offer the advantages of being relatively simple and inexpensive without pumping apparatus. Being noiseless and low cost are other advantages. Passive sampling has some disadvantages, for instance, it can be affected by ambient humidity. However, active sampling requires the mass transport of material to the collection device, thus requiring a sampling pump and electric power, and making the monitoring systems more complex (Baek 2011).

A WHO publication (World Health Organization 2020) discusses the advantages and drawbacks of some methods for sampling and analysis that have been used to characterize chemical pollution of indoor air. The methods were selected from among (i) those recommended by the International Organization for Standardization (ISO) and (ii) the most commonly used for sampling and analysis of IAPs in public settings. The document presents both passive (also called diffusive) and active sampling method. These are discontinuous methods: the pollutants are collected on a filter or sorbent for further analysis in a laboratory. Laboratory analysis usually consists of extraction, clean-up (when necessary), and the chemical characterization using appropriate analytical equipment. The extraction can be carried out using thermal desorption or solvent extraction. Analysis can be performed by means of different analytical systems depending on the pollutant to be analyzed (such as gas chromatography (GC) and liquid chromatography (LC) coupled to different detectors and an ultraviolet-visible (UV-Vis) spectrophotometer or mass spectrometer) (World Health Organization 2020).

Other than those mentioned above, the number of instrumental systems commercially available for the real-time measurement of IAPs has increased considerably. In many cases, a given constituent can be determined by a variety of instrumental techniques. The choice of the best approach can be a complex decision, which is influenced by several factors, including cost, system portability, selectivity and sensitivity, and the number and influence of potential interferences. Direct-reading instruments could provide substantial benefits (including lower efforts at lower cost) when applied in IAQ monitoring compared to traditional exposure assessment methods, which rely on active or passive sampling, collection substrates (e.g.,

sampling filters, adsorbent substrates), and offline analyses (e.g., gravimetric determination, chemical characterization, microscopic analysis). More in detail, one of the advantages of direct-reading techniques is to provide new insights on exposure dynamics due to their ability in collecting data at high spatiotemporal resolutions (Gao et al. 2015). Further, direct-reading instruments can report and process the data as soon as they are collected and while the instrument is still deployed (i.e., near real time analysis). Then, due to their features (reduced cost, ease of deployment, potential to be used in wireless networks), newer direct-reading sensor technologies (i.e., placeable, wearable, and implantable devices) (Howard et al. 2022) represent new ways of collecting and sharing environmental and occupational exposure information. For these reasons, not only the need for accurate evaluation of exposure to airborne pollutants is confirmed and reiterated, but a step forward is required as regards the methods, the techniques, and the technologies to be used for this purpose. Despite the advantages related to the use of newer direct-reading sensor technologies, these are generally less reliable (in terms of accuracy, sensitivity, precision, and specificity to the chemical/variable of interest) if compared to high-end devices (Fanti et al. 2021; Howard et al. 2022) and should be carefully evaluated before use. Overall, newer direct-reading sensors are being successfully used complementary to reference device monitoring, but they are not yet validated as alternative techniques for (or to replace) reference instruments (especially for purposes of mandatory monitoring). Further, unlike what happens for reference-grade instruments that are subjected to comprehensive regulatory standards and processes for evaluation and certification, only few standards exist for direct-reading techniques (Williams et al. 2018). Further, biases in the acquisition and interpretation of the data obtained with direct-reading techniques can derive from different sources of measurement error and interference, which arise once operating in the field and which cannot be completely covered in the development and calibration phases carried out in the laboratory. For these reasons, direct-reading techniques should be operated applying rigorous quality assurance and quality control protocols.

IAQ Perception and Health Symptoms

Complaints about deteriorated air quality that may be related to the building or a part of it are common in office workers (Rios et al. 2009). The existence of excessive complaints related to IAQ can be temporary and related to building renovation or adaptation. However, some buildings can be affected by long-term problems that require ad-hoc mitigation measures. In parallel, a high prevalence of complaints about health symptoms is commonly found in office buildings but it is not generally possible to attribute them to single causal factors.

Sick building syndrome (SBS) is somehow a semantically incorrect and outmoded wording used to describe work-related nonspecific symptom complexes occurring in buildings in which more than 20% of occupants report one or more symptoms that may be associated with IEQ and to the time spent by subjects in the building (Wolkoff 2013). SBS symptoms include mental fatigue and headache,

nausea and dizziness, eye, nose, and throat symptoms (i.e., dryness and irritation of the eyes, upper and lower airways symptoms, high frequency of airway infection, respiratory irritations, difficulty in breathing, coughing, tight chest, wheezing, etc.), skin symptoms (e.g., erythema, dry skin sensation, itching), and nonspecific hypersensitivity (World Health Organization 1983, 1986). The most common symptoms reported by office workers fall within the categories of mucosal irritation in eyes and upper airways, lower respiratory symptoms, central nervous system symptoms, and fatigue (Wolkoff 2013). These symptoms are characterized by multiple causality and IAQ is only one of them. SBS symptoms causes are not always known, but a common feature is that the majority of the occupants reports relief soon after leaving the building. SBS symptoms can be influenced by both personal (e.g., age, gender, allergy medical history, smoking status, anxiety, interpersonal conflicts, type of occupation, amount of work, and psychosocial work stress) and environmental factors (Azuma et al. 2015). The SBS symptoms are also related to physical environment and to IAQ. More in detail, among the causes of SBS in offices, chemical and biological contamination as well as poor ventilation (Finnegan et al. 1984; Hedge et al. 1989) were recognized as of primary importance since the early studies, but later on it became mostly regarded as a multifactorial health problem (Norback et al. 1990) viewed as a medical, psychological, and social phenomenon (Thörn 2000).

The assessment of perceived IAQ is typically based on questionnaire surveys. In the Audit project, questions were rated on seven-point scales and were focused on the perception of air dryness, stuffiness, and odors (Bluyssen 1996), further divided by perception type (mold or unpleasant odor) (Tähtinen et al. 2020). IAQ perception is time dependent and can be separated into immediate (e.g., when entering a building) and delayed perception that may build up during the workday. The immediate perception of IAQ is mainly driven by the olfactory sense via stimuli of the olfactory nerve (Wolkoff 2013). Smelly air is not of direct relevance to health risks, because there is no direct association between the odor thresholds of chemical compounds and those of toxicological concern. Taking aldehydes as an example, the odor thresholds for octanal and decanal are two to three orders of magnitude lower than formaldehyde. Occupants' complaints have been very frequent in office buildings constructed in the 1970s and 1980s, when ventilation was reduced for economic reasons in response to the oil crises. All self-reported data are intrinsically subjective and influenced by many possible factors, first and foremost those of psychosocial nature, and probably IAQ perception above all. Complaints by office workers as regards air quality are typically dominated by stuffy and dry air (Wargocki et al. 1999), being the perception of odors less frequent and correlated to specific odor sources. Large-scale studies in offices showed that office employees reported frequent complaints about stuffy and dry air (25–30% of respondents), and personal control of the indoor environment resulted in occupants being more satisfied with the overall air quality (Sakellaris et al. 2019).

For over 40 years, measurements of IAPs and their possible association with self-reported symptoms and health effects related to building-related problems have been made in offices to assess acute health symptoms related to short-term exposures.

Most of the studies are based on a cross-sectional design (data gathered at the same point in time) and the collection of self-reported symptoms and IEQ perception using self-administered questionnaire. In some cases, the focus was specifically on “sick” buildings (Thörn 2000), otherwise in nonproblem buildings (Muzi et al. 1998) or on the comparison of these two situations (Sunesson et al. 2006), sometimes with randomly selection of buildings/occupants to ensure representativeness (Finnegan et al. 1984), with some insights on building sealing (Rios et al. 2009) and building renovation. Surveys done in the late 1980s and 1990s on SBS and building-related illnesses (BRIs) were aimed to provide a standardized approach for the estimation of the prevalence of symptoms and IEQ perception, which should be tested for reliability and reproducibility to provide an unbiased assessment. The reliability of self-reported symptoms can be tested based on the judgment of a medical expert (occupational physicians for office workers) or against objective measurements of health effects. In the same way, the reliability of IEQ factors such as IAPs, noise, and microclimate indexes can be evaluated via expert judgment by IAQ experts or occupational hygienists or against objective measurements by environmental monitoring (see the next paragraph).

Questionnaires were initially based on a short list of basic and simple questions in which the intensity of factors/symptoms was not usually considered, and whose common core topics regarded health-related symptoms and IEQ perception including IAQ, microclimate, noise, and light. Later, it was found that general questions were not sufficient to obtain good validity, but specific questions on perceptions and observations were needed, as well as some contextual information about personal history, medical history, and family history of atopic diseases (Engvall et al. 2004). Psychological factors should be also carefully assessed as potential modifiers of perception and responses (Lu et al. 2018). Other factors like noise, distance from window, and privacy also may influence the overall perception of IAQ and the prevalence of symptoms.

Some examples of standardized questionnaires for the assessment of indoor environment and health can be found in Ooi et al. (1998) and Engvall et al. (2004). Recommendations for the optimal design of questionnaire-based surveys in offices, e.g., to increase the response rate, ensure anonymity, select the best administration mode, can be found elsewhere (Wolkoff 2013; Carrer and Wolkoff 2018). Questionnaire surveys are also recommended as a first step to assess work-related risks and monitor the health status of office workers (Carrer and Wolkoff 2018). Results from the questionnaire survey are useful to assess the occupant’s perceptions of IAQ and indoor climate, other than their psychosocial aspects. This information is fundamental to prioritize the hierarchy of potential interventions. Some important issues should be considered when assessing questionnaires data: (i) to distinguish whether the reported symptoms are specifically associated with the indoor working place and not with other outdoor/external issues (e.g., home, transport, or nearby industry); (ii) to determine if an alternative causality may prevail in occupants’ answers (Brauer et al. 2006).

Productivity of office workers can be also assessed by text-typing speed and errors tests (Wargocki et al. 1999; Bakó-Biró et al. 2004), as well as calculation

(Wargocki et al. 1999), addition (Lan et al. 2011), and proofreading (Bakó-Biró et al. 2004) tasks. Open-ended tests of creative thinking, memory, and recall can also be assessed (Wyon 2004). Another way to assess the health impacts in office-like environments is the analysis of number of days of sickness absence (Steensma 2011), which should be done using a longitudinal study design and have been correlated to the number of occupants in open-plan offices (Pejtersen et al. 2011). Several experimental studies have demonstrated deteriorated workers' performance caused by poor IAQ, but general conditions of the office (e.g., lighting and noise) should also be considered. A complete understanding of the causal link behind the loss of work productivity and performance is complex. Chemical pollutants and bioeffluents, rather than CO₂ itself, have been suggested to cause mental distraction and stress by perceived poor IAQ (Zhang et al. 2017), but other mechanisms are also in play (Zhang et al. 2017). The overall concern about work performance is not only related to absenteeism and associated diseases due to the work environment (IAQ), but it may result in less comfortable working conditions (Wyon 2004).

Among the IAPs postulated to be associated with office workers symptoms, a particular attention was paid to VOCs from the 1990s onwards, despite an association with airborne particles and SBS cannot be discarded (Apter et al. 1994). Some VOCs and semi-VOCs are indeed well known for their sensory irritation and neurotoxic potential at high doses from the accumulated knowledge in the field of toxicology and industrial hygiene, while the relevance of total VOCs as a risk index for health and discomfort effects in buildings was somewhat refuted by the scientific literature (Andersson 1997). The detail on specific airborne chemicals and biological agents in relation to perceived symptoms in office buildings grew over time, so that in more recent studies a variety of VOCs were monitored (Sakellaris et al. 2016) to test the hypothesis that health symptoms could derive by exposure to an air mixture of many chemicals at low concentration rather than only one or a few highly concentrated compounds. As a complete analysis and identification of all the compounds present in the indoor air mixture is almost impossible, and there are reasons to argue that compounds that are difficult to be collected and analyzed can play a role on the onset of health-related symptoms (Wolkoff et al. 1997). Parallelly, a growing attention was paid toward individual microbial species and their products (e.g., endotoxins, mycotoxins) rather than total bioaerosol contamination (Straus 2009).

Large-scale research has analyzed a dataset of more than 20 IAPs collected in 37 office buildings across 8 European countries (Sakellaris et al. 2016). Here, frequently reported symptoms were eye irritation (mostly dry eyes and watering or itchy eyes), respiratory symptoms (mostly blocked or stuffy nose), and general ones (mostly headache). Although IAP concentrations were generally below guideline values, the multivariate analysis showed significant associations between ethylbenzene and eye irritation as well as respiratory symptoms, xylenes with general symptoms (e.g., headache), formaldehyde, acrolein, and alpha-pinene with respiratory symptoms and styrene with skin symptoms. O₃ was associated with almost all symptom groups. Besides, there are some indications that several acids are more concentrated in problem buildings, probably due to their high reactivity, e.g., with O₃ and hydroxyl radicals to form secondary organic pollutants (Sunesson et al. 2006).

On the other hand, some studies aimed at addressing the correlation between IAPs concentrations and SBS symptoms in office workers did not confirm these supposed associations (Rios et al. 2009), and in some cases, psychosocial factors seem to play the biggest role in determining perceived symptoms (Eriksson 1996).

In the case of the California Healthy Building study, the focus was moved to sources as independent variables affecting IAQ-related perceived symptoms rather than to single chemicals. In short, 39 individual VOCs were measured in 12 offices, and data analysis was based on exposure metrics defined by a preliminary principal component analysis to account for the irritant potency of VOC mixtures. Among the principal component vectors obtained, the one represented by cleaning products and water-based paints showed the highest correlations with the vector representative of irritant symptoms prevalence, in particular for eye, skin, and mucous membranes (Brinke et al. 1998), and 2-butoxyethanol was the compound with the highest contribution on this factor.

Still about the relationship between sources and self-reported symptoms in offices, the early studies of the 1980s and 1990s indicated the use of photocopiers and work in crowded areas (Taylor et al. 1984), handling of paper (Skov et al. 1989), visual display terminal work (Hedge et al. 1989; Skov et al. 1989), and mechanical ventilation and/or air-conditioning (Finnegan et al. 1984; Hedge et al. 1989) as SBS risk indicators. More recently, one study concluded that the time/frequency of exposure to carbonless copy paper, paper dust, and emissions from photocopiers and printers increases the risk for respiratory, eye, and skin symptoms, as well as middle ear infections (Jaakkola et al. 2007). Within the context of offices, it is worth noting that intensive video display terminal work can cause ocular symptoms by altering blinking behavior and disturbing the tear film (Wolkoff 2008), but it can be regarded as a cause of psychosocial distress as well (Kubo et al. 2006). It was also argued that the presence of PCs could increase dissatisfaction with the perceived air quality and office workers performance, probably due to indoor air contamination at low levels by the so-called and supposed “stealth chemicals” effect (Bakó-Biró et al. 2004).

It is well known that indoor settled dust has a relevant allergenic and inflammatory potential, and this was confirmed also in relationship with SBS symptoms (Allermann et al. 2007). There is a quite large body of literature demonstrating the causal relationship between indoor dampness and molds and perceived health symptoms, in particular mucosal symptoms (Zhang et al. 2012). These could be, at least partially, attributed to the increased chemical emissions by wet polyvinyl chloride floor materials from the alkaline degradation of acrylate polymers in water-based glue or plasticizers (Campagnolo et al. 2017).

IAQ and Health Outcomes in Office Workers

Exposure to poor IAQ can cause or exacerbate a series of short- and long-term health outcomes (allergic symptoms and asthma, chronic obstructive and pulmonary diseases, airways infections, cardiovascular effects, and lung cancer) (Jantunen et al.

2011). Studies in the 1960s to the 1980s were focused on serious office-related illness such as hypersensitivity pneumonitis, Legionnaires' disease, and cancer due to asbestos exposure. Radon is also risk factor to be assessed for lung cancer prevention especially among people working in underground rooms, which sometimes can happen in some indoor work settings such as banks.

The so-called BRIs (Seltzer 1994) are characterized by the onset of a disease with clear diagnosis (e.g., legionellosis) and well associated to a specific risk factor and the time spent in a specific building.

Health effects potentially related to exposure to IAPs in office environments include acute and semi-acute effects and longer-term based effects. Acute effects are referred to into immediate perceived IAQ that is related to odor perception (olfactory nerve), while semi-acute effects (like sensory irritation in eyes and airways (trigeminus nerve), and symptoms related to the central nervous system (e.g., headache and fatigue)) are characterized by some latency (Jaakkola et al. 2007). Long-term effects (i.e., due to continuous or repeated exposure to IAPs) may be associated with aggravation of asthma exacerbation and allergic responses, oxidative stress and inflammation, chronic obstructive and pulmonary disease, lung cancer, and cardiovascular diseases. However, studies in office buildings have focused primarily on acute health symptoms (unspecific symptoms of irritation of eyes, nose, and mucous membranes, fatigue, and headache) experienced by office worker. Long-term effects are generally not evaluated in office workers due to the complexity and required resources for clinical testing, which seem unrealistic in view of occupants' mobility and the inhomogeneity of exposures (Carrer et al. 2015).

As several diseases can be associated to office working, a medical evaluation (focused on occupants) should guide environmental surveys and monitoring, especially when the indoor environmental and air quality measurements suggest compliance with air quality guidelines (Lukcsó et al. 2016). In the framework of IAQ assessments and management actions, individual health surveillance or individual clinical examination should be proposed only when periodical health surveillance is already being performed for other risks factors or when the occurrence of symptoms such as sensorial disturbances, eyes infections, respiratory and inflammatory effects in upper and lower airways appears to be clearly associated with inadequate IAQ. The examination of individuals must encompass (Carrer and Wolkoff 2018):

- (i) Workplace description (building and offices, ventilation, lighting, cleaning, mold growth, smells, thermal climate (e.g., such as experience of cold feet, cold/warm air, dry or stuffy air, static electricity), and noise).
- (ii) Description of symptoms and signs. Special regard should be reserved for mucous membrane (sensory) irritation, skin and general symptoms, and relationship with work (symptom development). The typical time of symptom onset during the week (morning/afternoon, working days/weekend), and seasonal variations should be also addressed. Routine physical examination generally implies a particular focus on eyes, nose, throat, skin, and lungs.

- (iii) Allergy (atopy) evaluation, when indicated; for example, in case of asthma and/or rhinitis, where allergens are suspected at the workplace, e.g., mold growth, animal fur, and plants.
- (iv) Other risk factors: for instance, transport conditions, use of medication, and use of contact lenses. Furthermore, it should be considered that the worker may be affected by an unrecognized disease that influences the overall perception of the IAQ and symptom reporting.

More in detail, some specific physiological methods have been applied to study health effects of the indoor environment. Ocular methods include measurement of tear film break-up time, blink frequency, detection of corneal damage by vital staining of cells or inflammatory markers in tear fluid. Nasal methods include acoustic rhinometry, rhino stereometry, and nasal peak expiratory flow. In addition, the concentrations of biomarkers of inflammation can be measured in the nasal lavage fluid. Field studies have demonstrated associations between ocular and nasal physiological response and the indoor environment (Bakke et al. 2008).

Oxidative stress has been in focus as an important mechanism behind health effects of outdoor air pollution, but it has been also shown that it can be an important biological factor for SBS symptoms in relation to indoor chemical indoor exposure.

Risk factors in the office environment could be heterogeneous. Eye symptoms were associated with proximity to outdoor pollution like traffic, portable humidifiers, and crowded spaces (Wolkoff 2017), visual display unit work, inadequate ventilation (Sundell et al. 2011), low humidity (Wolkoff 2018), or high temperature (Wolkoff 2017). Mold in moisture-damaged buildings is another risk that may have an impact on the IAQ and susceptible people (e.g., with asthma symptoms) (Zhang et al. 2012). Other office-related factor could have an impact in symptoms and occupants' health: for example, generally, more dissatisfaction and increase of adverse health effects are reported in crowded offices (Bergström et al. 2015; Leder et al. 2016).

Then, potential synergies between indoor air and psychosocial stress on health and comfort of office workers have been explored (Azuma et al. 2015). Odor annoyance and exposure to unpleasant odors influence general comfort (fatigue, impaired power of concentration, headache, nausea, and insomnia, including possible mood disorders) (Hurraß et al. 2017); psychic reactions with nonspecific symptoms are plausible, but they would not induce direct physiological reactions like sensory irritation in eyes and upper airways (Hurraß et al. 2017). Susceptible people, with high distress or being diagnosed with asthma or multiple diagnoses of asthma/allergy, may react more intensely to poor IAQ than people with low distress or without asthma (Claeson et al. 2016).

IAQ Management and Risk Mitigation Measures in Offices

IAQ monitoring and assessment, combined with source identification and control (e.g., using low-emitting materials and products as well as control of some indoor activities such as smoking, use of candles, and of air fresheners, etc.), has been

increasingly recognized as the prioritized strategy for improving IAQ and reducing the combined health risks associated with indoor exposures. Other management measures, such as the adjustment of ventilation rates, should be implemented after source control to account for any residual pollution (Carrer et al. 2018). However, the identification of sources and determinants of IAPs is particularly complex: researches have examined several specific factors (e.g., temperature, various chemical compounds, or mold), sources of pollution (e.g., environmental tobacco smoke, occupational activities such as manufacturing, combustion of fuels, consumer cleaning products), and control technologies (e.g., ventilation systems) in order to define the determinants of major IAPs, as well as the effect of seasonal variations and environmental conditions on indoor air pollution (Campagnolo et al. 2017; Spinazzè et al. 2020).

Evidence from intervention studies is also available: for example, after the replacement of scented cleaning agents in modern office buildings, substantially lower concentrations of IAPs and some oxidation products (secondary pollutants) were also reduced in line with limonene (Nørgaard et al. 2014).

The deployment of networks of heterogeneous devices based on wireless communication infrastructures and equipped with smart devices and IAQ sensors allowing increased spatial resolution of real-time IAPs concentrations offer unprecedented opportunities for planning and controlling a new generation of office buildings. Due also to their miniaturization and affordability, low-cost sensor systems are increasingly used for the monitoring of air contamination and can be applied in intelligent and autonomous control systems for a real-time and long-term optimized management of IAQ, energy consumption, and microclimate. On the one hand, this would provide building managers with integrated and adaptive management systems for a nearly real-time energy and IAQ control (Kumar et al. 2016). On the other hand, some critical issues and challenges for their large-scale deployment remain, such as the manipulation and analysis of the big amount of data obtained and the need of affordable services for sensor-network maintenance.

Conclusions

Since different studies have addressed IAQ and associated exposure-related symptoms in office workers, a careful assessment and management of IAQ in office-like environments is of key importance for the protection of human health and to ensure optimal comfort and well-being for office workers. For this purpose, the development of appropriate monitoring strategies is crucial to properly characterize the chemical and physical complexity of IAQ dynamics and subsequent potential impact on office occupants. To obtain comprehensive and representative conclusions about IAQ problems in office-like environments, and to prioritize the order of management interventions, a multilevel approach should be implemented. This should include a general survey of the building and of the offices, occupants' questionnaire surveys (concerning IAQ, symptoms, and psychosocial working aspects), and environmental measurements. IAQ monitoring and assessment, combined with source identification

and control, and adjustment of ventilation rates as well, has been recognized as the prioritized strategy for improving IAQ in office-like environments and reducing the combined health risks associated with indoor exposures to IAPs.

Whatever the objectives and methods of the evaluation, it is important to combine multiple expertise in the process and properly inform the employer, HSE (health, safety and environment) managers, and last but not least workers and building occupants in active collaboration with other prevention professionals.

In summary, when there is the need to achieve a comprehensive understanding of IAQ and its related determinants or effects, it is recommended to collect integrated information about the building and its occupants by inspection visits to offices, questionnaire surveys (concerning perceived IAQ, symptoms, and psychosocial working aspects) and environmental monitoring, to reach sound conclusions about IAQ or exposure assessment, source identification and/or apportionment, and the most effective risk management options.

References

- Allermann L, Pejtersen J, Gunnarsen L, Poulsen OM (2007) Building-related symptoms and inflammatory potency of dust from office buildings. *Indoor Air* 17:458–467. <https://doi.org/10.1111/j.1600-0668.2007.00493.x>
- Andersson K (1997) TVOC and health in non-industrial indoor environments report from a Nordic scientific consensus meeting at Långholmen in Stockholm, 1996. *Indoor Air* 7:78–91. <https://doi.org/10.1111/j.1600-0668.1997.t01-2-00002.x>
- Apter A, Bracker A, Hodgson M et al (1994) Epidemiology of the sick building syndrome. *J Allergy Clin Immunol* 94:277–288
- Asikainen A, Carrer P, Kephalopoulos S et al (2016) Reducing burden of disease from residential indoor air exposures in Europe (HEALTHVENT project). *Environ Health* 15:S35. <https://doi.org/10.1186/s12940-016-0101-8>
- Azuma K, Ikeda K, Kagi N et al (2015) Prevalence and risk factors associated with nonspecific building-related symptoms in office employees in Japan: relationships between work environment, indoor air quality, and occupational stress. *Indoor Air* 25:499–511. <https://doi.org/10.1111/ina.12158>
- Baek SO (2011) Assessing indoor air quality. In: Encyclopedia of environmental health. Elsevier, Amsterdam/London, pp 213–220. ISBN 978-0-444-52272-6
- Bakke JV, Norbäck D, Wieslander G, Hollund B-E, Florvaag E, Haugen EN, Moen BE (2008) Symptoms, complaints, ocular and nasal physiological signs in university staff in relation to indoor environment – temperature and gender interactions. *Indoor Air* 18:131–143
- Bakó-Biró Z, Wargocki P, Weschler CJ, Fanger PO (2004) Effects of pollution from personal computers on perceived air quality, SBS symptoms and productivity in offices. *Indoor Air* 14: 178–187. <https://doi.org/10.1111/j.1600-0668.2004.00218.x>
- Bergström J, Miller M, Horneij E (2015) Work environment perceptions following relocation to open-plan offices: a twelve-month longitudinal study. *Work* 50:221–228. <https://doi.org/10.3233/WOR-131798>
- Bluyssen PM (1996) European indoor air quality audit project in 56 office buildings. *Indoor Air* 6: 221–238. <https://doi.org/10.1111/j.1600-0668.1996.00002.x>
- Bluyssen PM, Roda C, Mandin C et al (2016) Self-reported health and comfort in “modern” office buildings: first results from the European OFFICAIR study. *Indoor Air* 26:298–317. <https://doi.org/10.1111/ina.12196>
- Brauer C, Kolstad H, Ørbæk P, Mikkelsen S (2006) The sick building syndrome: a chicken and egg situation? *Int Arch Occup Environ Health* 79:465–471. <https://doi.org/10.1007/s00420-005-0075-2>

- Brinke JT, Selvin S, Hodgson AT et al (1998) Development of new volatile organic compound (VOC) exposure metrics and their relationship to “sick building syndrome” symptoms. *Indoor Air* 8:140–152
- Campagnolo D, Saraga DE, Cattaneo A et al (2017) VOCs and aldehydes source identification in European office buildings – the OFFICAIR study. *Build Environ* 115:18–24. <https://doi.org/10.1016/j.buildenv.2017.01.009>
- Carrer P, Wolkoff P (2018) Assessment of indoor air quality problems in office-like environments: role of occupational health services. *Int J Environ Res Public Health* 15:741. <https://doi.org/10.3390/ijerph15040741>
- Carrer P, Wargocki P, Fanetti A et al (2015) What does the scientific literature tell us about the ventilation-health relationship in public and residential buildings? *Build Environ* 94:273–286. <https://doi.org/10.1016/J.BUILDENV.2015.08.011>
- Carrer P, de Oliveira Fernandes E, Santos H et al (2018) On the development of health-based ventilation guidelines: principles and framework. *Int J Environ Res Public Health* 15:1360. <https://doi.org/10.3390/ijerph15071360>
- Claeson AS, Palmquist E, Lind N, Nordin S (2016) Symptom-trigger factors other than allergens in asthma and allergy. *Int J Environ Health Res* 26:448–457. <https://doi.org/10.1080/09603123.2015.1135314>
- Engvall K, Norrby C, Sandstedt E (2004) The Stockholm Indoor Environment Questionnaire: a sociologically based tool for the assessment of indoor environment and health in dwellings. *Indoor Air* 14:24–33. <https://doi.org/10.1111/j.1600-0668.2004.00204.x>
- Eriksson N (1996) Psychosocial factors and the “sick building-syndrome”. A case-referent study. *Indoor Air* 6:101–110. <https://doi.org/10.1111/j.1600-0668.1996.t01-2-00006.x>
- Fanti G, Borghi F, Spinazzè A et al (2021) Features and practicability of the next-generation sensors and monitors for exposure assessment to airborne pollutants: a systematic review. *Sensors* 21(13):4513. <https://doi.org/10.3390/s21134513>
- Finnegan MJ, Pickering CAC, Burge PS (1984) The sick building syndrome: prevalence studies. *Br Med J* 289:1573–1575. <https://doi.org/10.1136/bmj.289.6458.1573>
- Gao M, Cao J, Seto E (2015) A distributed network of low-cost continuous reading sensors to measure spatiotemporal variations of PM_{2.5} in Xi'an, China. *Environ Pollut* 199:56–65. <https://doi.org/10.1016/j.envpol.2015.01.013>
- Hedge A, Burge PS, Robertson AS et al (1989) Work-related illness in offices: a proposed model of the “sick building syndrome”. *Environ Int* 15:143–158. [https://doi.org/10.1016/0160-4120\(89\)90020-2](https://doi.org/10.1016/0160-4120(89)90020-2)
- Howard J, Murashov V, Cauda E, Snawder J (2022) Advanced sensor technologies and the future of work. *Am J Ind Med* 65(1):3–11. <https://doi.org/10.1002/ajim.23300>
- Hurraß J, Heinzow B, Aurbach U et al (2017) Medical diagnostics for indoor mold exposure. *Int J Hyg Environ Health* 220:305–328
- ISO 16000-1:2004 (2004) Indoor air – part 1: general aspects of sampling strategy. International Organisation for Standardisation, Geneva, Switzerland
- Jaakkola MS, Yang L, Ieromnimon A, Jaakkola JJK (2007) Office work exposures and respiratory and sick building syndrome symptoms. *Occup Environ Med* 64:178–184
- Jantunen M, Fernandes EO, Carrer P (2011) Promoting actions for healthy indoor air (IAIAQ). European Commission Directorate General for Health and Consumers, Luxemburg. ISBN 978-92-79-20419-7
- Kalimeri KK, Saraga DE, Lazaridis VD et al (2016) Indoor air quality investigation of the school environment and estimated health risks: two-season measurements in primary schools in Kozani, Greece. *Atmos Pollut Res* 7:1128–1142. <https://doi.org/10.1016/j.apr.2016.07.002>
- Katsoyiannis A, Leva P, Barrero-Moreno J, Kotzias D (2012) Building materials. VOC emissions, diffusion behaviour and implications from their use. *Environ Pollut* 169:230–234. <https://doi.org/10.1016/j.envpol.2012.04.030>
- Kubo T, Mizoue T, Ide R et al (2006) Visual display terminal work and sick building syndrome – the role of psychosocial distress in the relationship. *J Occup Health* 48:107–112
- Kumar P, Martani C, Morawska L et al (2016) Indoor air quality and energy management through real-time sensing in commercial buildings. *Energy Build* 111:145–153

- Lan L, Wargocki P, Lian Z (2011) Quantitative measurement of productivity loss due to thermal discomfort. *Energy Build* 43:1057–1062
- Leder S, Newsham GR, Veitch JA et al (2016) Effects of office environment on employee satisfaction: a new analysis. *Build Res Inf* 44:34–50. <https://doi.org/10.1080/09613218.2014.1003176>
- Logue JM, McKone TE, Sherman MH, Singer BC (2011) Hazard assessment of chemical air contaminants measured in residences. *Indoor Air* 21:92–109. <https://doi.org/10.1111/j.1600-0668.2010.00683.x>
- Lu C-Y, Tsai M-C, Muo C-H et al (2018) Personal, psychosocial and environmental factors related to sick building syndrome in official employees of Taiwan. *Int J Environ Res Public Health* 15(1):7. <https://doi.org/10.3390/ijerph15010007>
- Lukcso D, Guidotti TL, Franklin DE, Burt A (2016) Indoor environmental and air quality characteristics, building-related health symptoms, and worker productivity in a federal government building complex. *Arch Environ Occup Health* 71:85–101. <https://doi.org/10.1080/19338244.2014.965246>
- Mandin C, Trantallidi M, Cattaneo A et al (2017) Assessment of indoor air quality in office buildings across Europe – the OFFICAIR study. *Sci Total Environ* 579:169–178. <https://doi.org/10.1016/j.scitotenv.2016.10.238>
- Menzies D, Kreiss K (2006) Building-related illnesses. In: Bernstein DI, Chan-Yeung M, Malo J-L, Bernstein IL (eds) *Asthma in the workplace*, 3rd edn. Taylor and Francis, New York
- Mishra N, Bartsch J, Ayoko GA et al (2015) Volatile organic compounds: characteristics, distribution and sources in urban schools. *Atmos Environ* 106:485–491. <https://doi.org/10.1016/j.atmosenv.2014.10.052>
- Muzi G, Dell'omo M, Abbritti G et al (1998) Objective assessment of ocular and respiratory alterations in employees in a sick building. *Am J Ind Med* 34:79–88. [https://doi.org/10.1002/\(SICI\)1097-0274\(199807\)34:1<79::AID-AJIM11>3.0.CO;2-1](https://doi.org/10.1002/(SICI)1097-0274(199807)34:1<79::AID-AJIM11>3.0.CO;2-1)
- Norback D, Michel I, Widstrom J (1990) Indoor air quality and personal factors related to the sick building syndrome. *Scand J Work Environ Health* 16:121–128. <https://doi.org/10.5271/sjweh.1808>
- Nørgaard AW, Kofoed-Sørensen V, Mandin C et al (2014) Ozone-initiated terpene reaction products in five European offices: replacement of a floor cleaning agent. *Environ Sci Technol* 48(22): 13331–13339. <https://doi.org/10.1021/es504106j>
- Ooi PL, Goh KT, Phoon MH et al (1998) Epidemiology of sick building syndrome and its associated risk factors in Singapore. *Occup Environ Med* 55:188–193. <https://doi.org/10.1136/oem.55.3.188>
- Pejtersen JH, Feveile H, Christensen KB, Burr H (2011) Sickness absence associated with shared and open-plan offices – a national cross sectional questionnaire survey. *Scand J Work Environ Health* 37:375–382. <https://doi.org/10.5271/sjweh.3167>
- Rackes A, Waring MS (2016) Do time-averaged, whole-building, effective volatile organic compound (VOC) emissions depend on the air exchange rate? A statistical analysis of trends for 46 VOCs in U.S. offices. *Indoor Air* 26:642–659. <https://doi.org/10.1111/ina.12224>
- Rios JL, Boechat JL, Gioda A et al (2009) Symptoms prevalence among office workers of a sealed versus a non-sealed building: associations to indoor air quality. *Environ Int* 35(8):1136–1141. <https://doi.org/10.1016/j.envint.2009.07.005>
- Sakellaris I, Saraga D, Mandin C et al (2016) Perceived indoor environment and occupants' comfort in European "modern" office buildings: the OFFICAIR study. *Int J Environ Res Public Health* 13(5):444. <https://doi.org/10.3390/ijerph13050444>
- Sakellaris I, Saraga D, Mandin C et al (2019) Personal control of the indoor environment in offices: relations with building characteristics, influence on occupant perception and reported symptoms related to the building – the OFFICAIR project. *Appl Sci* 9(16):3227. <https://doi.org/10.3390/app9163227>
- Sakellaris I, Saraga D, Mandin C et al (2021) Association of subjective health symptoms with indoor air quality in European office buildings: The OFFICAIR project. *Indoor air* 31(2):426–439. <https://doi.org/10.1111/ina.12749>

- Seltzer JM (1994) Building-related illnesses. *J Allergy Clin Immunol* 94:351–361. [https://doi.org/10.1016/0091-6749\(94\)90096-5](https://doi.org/10.1016/0091-6749(94)90096-5)
- Sérafín G, Blondeau P, Mandin C (2021) Indoor air pollutant health prioritization in office buildings. *Indoor Air* 31:646–659. <https://doi.org/10.1111/ina.12776>
- Skov P, Valbjørn O, Pedersen BV et al (1989) Influence of personal characteristics, job-related factors and psychosocial factors on the sick building syndrome. *Scand J Work Environ Health* 15:286–295. <https://doi.org/10.5271/sjweh.1851>
- Spinazzè A, Campagnolo D, Cattaneo A et al (2020) Indoor gaseous air pollutants determinants in office buildings – the OFFICAIR project. *Indoor Air* 30(1):76–87. <https://doi.org/10.1111/ina.12609>
- Spinazzè A, Borghi F, Rovelli S et al (2021) Combined and modular approaches for multi-component monitoring of indoor air pollutants. *Appl Spectrosc Rev* 2021:1–37. <https://doi.org/10.1080/05704928.2021.1995405>
- Steensma H (2011) Sickness absence, office types, and advances in absenteeism research. *Scand J Work Environ Health* 37:359–362. <https://doi.org/10.5271/sjweh.3185>
- Steinemann A, Wargocki P, Rismanni B (2017) Ten questions concerning green buildings and indoor air quality. *Build Environ* 112:351–358. <https://doi.org/10.1016/j.buildenv.2016.11.010>
- Sundell J, Levin H, Nazaroff WW et al (2011) Ventilation rates and health: multidisciplinary review of the scientific literature. *Indoor Air* 21:191–204. <https://doi.org/10.1111/j.1600-0668.2010.00703.x>
- Sunesson AL, Rosén I, Stenberg B, Sjöström M (2006) Multivariate evaluation of VOCs in buildings where people with non-specific building-related symptoms perceive health problems and in buildings where they do not. *Indoor Air* 16(5):383–391
- Tähtinen K, Remes J, Karvala K et al (2020) Perceived indoor air quality and psychosocial work environment in office, school and health care environments in Finland. *Int J Occup Med Environ Health* 33:479–495. <https://doi.org/10.13075/ijomeh.1896.01565>
- Taylor PR, Dell'Acqua BJ, Baptiste MS et al (1984) Illness in an office building with limited fresh air access. *J Environ Health* 47(1):24–27
- Thörn Å (2000) Emergence and preservation of a chronically sick building. *J Epidemiol Community Health* 54:552–556. <https://doi.org/10.1136/jech.54.7.552>
- Trantallidi M, Dimitroulopoulou C, Wolkoff P et al (2015) EPHECT III: health risk assessment of exposure to household consumer products. *Sci Total Environ* 536:903–913. <https://doi.org/10.1016/j.scitotenv.2015.05.123>
- Villanueva F, Ródenas M, Ruus A et al (2021) Sampling and analysis techniques for inorganic air pollutants in indoor air. *Appl Spectrosc Rev* 2021:1–49. <https://doi.org/10.1080/05704928.2021.2020807>
- Wargocki P, Wyon DP, Baik YK et al (1999) Perceived air quality, sick building syndrome (SBS) symptoms and productivity in an office with two different pollution loads. *Indoor Air* 9:165–179
- Williams R, Nash D, Hagler G et al (2018) Peer review and supporting literature review of air sensor technology performance targets. EPA 600/R-18/324, September 2018
- Wolkoff P (2008) “Healthy” eye in office-like environments. *Environ Int* 34:1204–1214
- Wolkoff P (2013) Indoor air pollutants in office environments: assessment of comfort, health, and performance. *Int J Hyg Environ Health* 216:371–394. <https://doi.org/10.1016/j.ijeh.2012.08.001>
- Wolkoff P (2017) External eye symptoms in indoor environments. *Indoor Air* 27:246–260. <https://doi.org/10.1111/ina.12322>
- Wolkoff P (2018) Indoor air humidity, air quality, and health – an overview. *Int J Hyg Environ Health* 221:376–390
- Wolkoff P, Clausen PA, Jensen B et al (1997) Are we measuring the relevant indoor pollutants? *Indoor Air* 7:92–106
- Wolkoff P, Azuma K, Carrer P (2021) Health, work performance, and risk of infection in office-like environments: the role of indoor temperature, air humidity, and ventilation. *Int J Hyg Environ Health* 233:113709

- World Health Organization (1983) Indoor air pollutants: exposure and health effects. Report on a WHO meeting, EURO reports and studies no. 78. WHO Regional Office for Europe, Copenhagen, pp 1–42
- World Health Organization (1986) Indoor air quality research. World Health Organization, Regional Office for Europe, Copenhagen
- World Health Organization (2010) WHO guidelines for indoor air quality – selected pollutants. WHO, Copenhagen
- World Health Organization (2020) Methods for sampling and analysis of chemical pollutants in indoor air: supplementary publication to the screening tool for assessment of health risks from combined exposure to multiple chemicals in indoor air in public settings for children. World Health Organization, Geneva
- World Health Organization (2021) Global air quality guidelines. Particulate matter (PM_{2.5} and PM₁₀), ozone, nitrogen dioxide, sulfur dioxide and carbon monoxide. World Health Organization, Geneva. ISBN 978-92-4-003422-8 (electronic version)
- Wyon DP (2004) The effects of indoor air quality on performance and productivity. *Indoor Air* 14 (Suppl 7):92–101. <https://doi.org/10.1111/j.1600-0668.2004.00278.x>
- Zhang X, Sahlberg B, Wieslander G et al (2012) Dampness and moulds in workplace buildings: associations with incidence and remission of sick building syndrome (SBS) and biomarkers of inflammation in a 10 year follow-up study. *Sci Total Environ* 430:75–81. <https://doi.org/10.1016/j.scitotenv.2012.04.040>
- Zhang X, Wargocki P, Lian Z (2017) Physiological responses during exposure to carbon dioxide and bioeffluents at levels typically occurring indoors. *Indoor Air* 27:65–77. <https://doi.org/10.1111/ina.12286>



Indoor Air Quality in Elderly Care Centers

66

Joana Madureira and João Paulo Teixeira

Contents

Introduction	1962
A Paradigm Shift to Address Indoor Air Quality	1963
Major Chemical Pollutants, Source Signatures, and Health Relevance	1964
Particulate Matter	1965
Volatile Organic Compounds	1968
Nitrogen Dioxide	1971
Ozone	1972
Carbon Dioxide	1973
Indoor Air Quality Health-Based Guidelines	1974
Current Guidelines	1975
Future Perspectives	1976
The Challenges of Making Indoors Healthy	1976
Conclusions	1978
Cross-References	1979
References	1979

Abstract

A growing body of literature indicates that concentrations of indoor particulate matter and gaseous pollutants in elderly care centers (ECCs) often exceed those recorded in nearby outdoor environment. At present, unlike the outdoors, indoor air quality (IAQ) in ECCs is not regulated and is seldom monitored. Elderly citizens commonly spend most of their day indoors where they are exposed to indoor air pollutants, even at low concentrations, for long periods of time. Given that many ECCs residents, especially those of advanced age, are more susceptible to the effects of air pollutants, this prolonged exposure may adversely impact their

J. Madureira (✉) · J. P. Teixeira

Environmental Health Department, National Institute of Health, Porto, Portugal

EPIUnit, Institute of Public Health, University of Porto, Porto, Portugal

Laboratory for Integrative and Translational Research in Population Health (ITR), Porto, Portugal
e-mail: jvmadureira@gmail.com; jpft12@gmail.com

health. Despite these facts, there are few data among older adults and their exposure to IAQ pollutants in ECCs. In the current pandemic situation, IAQ has become an even more prominent research topic, encompassing issues such as the need of good ventilation of indoor spaces. Thus, this chapter presents the highlights of the existing knowledge on IAQ in ECCs. It summarizes the most recent findings related to: (i) major indoor air pollutants, its source signatures, levels and health relevance; (ii) current and future perspectives on IAQ health-based guidelines; and, finally, (iii) strategies to assure a healthy indoor environment. This overview underlines that indoor air pollution in ECCs represents a major global public health problem requiring further efforts in research that can inform evidence-based risk management and public health interventions to reduce current and future risks associated with poor IAQ in ECCs in line with the 2030 Agenda for Sustainable Development.

Keywords

Aging · Air exposure · Particulate matter · Source control · Health effects

Introduction

The built environment is undergoing constant changes driven by global megatrends such as global warming and urbanization, resulting in increased ambient (outdoor) air pollution that inevitably impacts indoor air quality (IAQ). The relationship between the outdoor environment and IAQ is well known, being evident from several research works that the concentration of indoor air pollutants are two to four times higher than those of outdoor air pollutants (Campagnolo et al. 2017; Madureira et al. 2016). Nevertheless, unlike the outdoors, IAQ is not regulated and is seldom monitored. With higher concentrations of pollutants inside buildings, IAQ is one of the world's highest environmental health risks (WHO 2017) that cannot be neglected.

While prior studies of indoor environments have focused mostly on office buildings (e.g., Campagnolo et al. 2017), homes (e.g., Madureira et al. 2016, 2020a), or school facilities (e.g., Madureira et al. 2016), recent scientific studies on elderly care centers (ECCs) have found that poor IAQ may adversely affect both cardiorespiratory systems and that the elderly are at higher risk of suffering from such health problems than other age groups due to the progressive decline of their body' function leading to increased vulnerability, frailty, or sensitivity (Mendes et al. 2018; Maio et al. 2015).

According to the European Commission, by 2050, the number of people aged 65 and above in the EU is projected to rise more than twice and the number of persons aged over 80 is expected to grow by 170% (UN 2017). This inevitable increase in the share of older persons that results from the decline in fertility and enhancement in survival constitutes a new demographic reality and a major societal challenge common to all European countries to fulfill the pledge of the 2030 Agenda for Sustainable Development that “no one will be left behind.” With these trends, it is

anticipated that many more elderly will live in ECCs, and because most of older citizens in industrialized countries typically spend a significantly larger number of hours (19–20 h/day) indoors compared to the general population (Almeida-Silva et al. 2015; WHO 2010), the need to ensure they are not unnecessarily exposed to indoor pollutants becomes crucially important.

While the volume of aging research output has increased in the last decade, knowledge about the indoor air conditions of older people living in ECCs remains limited. The expansion of such knowledge is critical to enable policy-makers, ECCs staff, and other key stakeholders to anticipate health risks among the most susceptible and proactively implement policies and programs needed to respond to the challenges and opportunities of coming decades. Beginning in 2020, the rapid spread of SARS-CoV-2/COVID-19 (severe acute respiratory syndrome coronavirus-2/coronavirus disease 2019) pandemic and the related containment measures has led to “tragic” consequences in ECCs’ residents and has revealed several weaknesses in monitoring, preparedness, and resources to mitigate the transmission of airborne infectious diseases, such as improved ventilation (Morawska et al. 2020). Therefore, it is both timely and necessary to integrate the environmental and human health aspects to improve indoor environments and provide healthy conditions for elderly people that occupied them.

Thus, the purpose of this chapter is to highlight the existing knowledge on IAQ in ECCs. It summarizes the most recent findings related to the major indoor air pollutants, its source signatures, levels, and health relevance. Following this, an overview of existing and future perspectives on IAQ health-based guidelines is also presented considering the most recent state-of-the-art on this field. Finally, a separate section is devoted to strategies for control and mitigation of indoor pollutant concentrations in line with the 2030 Agenda for Sustainable Development.

A Paradigm Shift to Address Indoor Air Quality

Outdoor air pollution has been recognized as a serious problem in many urban places worldwide, and has being investigated over the years from economic, social, and legislative as well as lifestyle habits perspectives (EEA 2018). The primary outdoor air pollutants are particulate matter (PM), volatile organic compounds (VOCs), nitrogen dioxide (NO_2), ozone (O_3), carbon monoxide, and sulfur dioxide(SO_2) (EEA 2018). In urban areas, the increase in emission of these air pollutants is largely due to fossil fuel burning, automobile emissions (Morawska et al. 2017), which in turn is affected by global warming and urbanization levels. Several long-term policies, programs, and interventions across different sectors (i.e., transport, housing, energy, and industry) have been implemented for public health purposes (EEA 2018). The 2005 World Health Organization (WHO) air quality guidelines (AQGs) offer global guidance on thresholds and limits for key outdoor air pollutants that pose health risks (WHO 2006) including PM, O_3 , NO_2 , and SO_2 . This guidance was revised on September 2021 (WHO 2021) and updated recommendations, produced based on stronger body of evidence that shows how air pollution affects different

health outcomes, resulted in almost all the AQG levels being strengthened in comparison to the AQG established in 2005. In addition, the WHO's new guidelines highlight good practices for the management of certain types of PM, as black carbon/elemental carbon, ultrafine particles (UFP), particles from sand and dust storms, for which there is currently insufficient evidence to establish AQG values. To be noticed that the updated recommendations are applicable to both outdoor and indoor environments globally, and cover all settings, including ECCs (WHO 2021).

In the last decades, IAQ has become a relevant area of concern and has received increasing attention from the scientific community. The US Environmental Protection Agency (USEPA) defines IAQ as "the air quality within and around buildings and structures, especially as it relates to the health and comfort of building occupants." The indoor air monitoring can be challenging due to several factors and its interrelationship, such as pollutants coming from outdoor sources, building features, and, to a large extent, occupants' behavior. Building features include, geographic variations and climate; building age; building design, construction and maintenance; and ventilation rates. With such a wide variety of building types and characteristics, establishing rigorous and repeatable protocols for monitoring indoor air pollutants is a challenging task. In addition, the occupants' behavior has nearly as many varieties and activities as there are occupants, and includes, for example, cooking, cleaning, pet ownership, smoking habits, frequency of opening window, as well as patterns of use (e.g., time spent indoors). The contribution of each of these factors to indoor air pollutants concentrations is difficult to estimate due to not only the specific characteristics of each location and building use, but also due to the variability over time of indoor concentrations and chemical reactivity leading to the formation of secondary pollutants. However, many studies have confirmed that IAQ is highly influenced by outdoor air quality and can be more polluted than outdoor environment (Campagnolo et al. 2017; Madureira et al. 2016). Poor IAQ has been linked to adverse health effects as described in the section of this handbook on IAQ and human health.

Indoor air quality does not affect everyone in the same way: older persons are considered particularly at risk for detrimental health effects from indoor air pollution (Mendes et al. 2018; Maio et al. 2015) due their reduced immunological defenses and multiple chronic diseases. The quality of air inside ECCs is an essential determinant of a healthy life. Improvements of the indoor environment may be the most cost-effective way to reduce the burden of indoor exposure. However, little research has been conducted in regard to older adults and their exposure to IAQ pollutants in ECCs.

Major Chemical Pollutants, Source Signatures, and Health Relevance

Indoor air of ECCs contains numerous pollutants, such as airborne particles of complex composition and widely differing sizes and VOCs. Other pollutants, such as NO_2 and O_3 are classical pollutants of outdoor air that penetrate indoor

environments in different ways in addition to releases from indoor sources (Wichman et al. 2010). According to Annesi-Maesano et al. (2013), high temperatures and relative humidity levels might contribute to the increase of concentrations of some of these pollutants.

The relevance of measuring the concentrations of these pollutants indoors has been recognized (WHO 2010, 2021) since many chemical pollutants that are hazardous to human health are present in concerning concentrations. Within this chapter, information about PM, VOCs, NO₂, and O₃ will be presented taken into account the likelihood of their presence in ECCs and their potential contribution to elderly's health. According to Carrer et al. (2018), it is estimated that indoor air pollution is responsible for a loss of over 700,000 healthy life-years within the EU.

Despite the large number of pollutants present in indoor environments, only a few of them are typically measured. In addition to the four chemical pollutants previously mentioned, information about carbon dioxide (CO₂) will be also considered since this gas is an important parameter to monitor and control given the evidence of their presence in indoor air and their common use as proxy of ventilation rate.

Particulate Matter

Particulate matter is a complex mixture of organic and inorganic chemicals, including sulfates, nitrates, polycyclic aromatic hydrocarbons (PAHs), and metals (cooper, zinc, iron) (Hamanaka and Mutlu 2018).

Airborne PM span a range of diameters from a few nanometers to tens of micrometers, such as PM₁₀, PM_{2.5} (PM with aerodynamic diameter <10 µm and <2.5 µm, respectively), and PM_{0.1} (PM with aerodynamic diameter ≤0.1 µm), called UFP; being their composition and toxicity very complex and variable, with similarities but also differences to outdoor PM (Leikauf et al. 2020). PM_{0.1} are also called nanoparticles because of their size, although many authors use the word "nanoparticles" to the 100 nm or smaller PM manufactured through controlled engineering processes, in contrast to ambient or indoor PM, which are incidentally derived from natural or fossil fuel combustion processes (Li et al. 2016a).

Indoor particles are comprised of ambient PM of different size fractions that infiltrate from outdoors, and particles that are generated indoors. Ambient PM in the urban environment originate mostly from fossil fuel burning, automobile emissions, resuspension, or chemical and thermodynamic processes, but also from long range transport since they can travel large distances (>100 km) (Rivas et al. 2020; Morawska et al. 2017). Outdoor air is a major PM_{2.5} source in roadside buildings (Rivas et al. 2020). Cooking, fireplaces, fossil fuels combustion activities, smoking, secondary formation processes, and dust resuspension (Stabile et al. 2021; Almeida-Silva et al. 2014) are the main possible sources of PM inside ECCs.

In a study developed with elder living in Amsterdam and Helsinki, the authors found indoor PM_{2.5} average concentrations of 16 µg/m³ and 11 µg/m³, respectively (Lanki et al. 2007). In both European cities, the main determinants of PM_{2.5} were environmental tobacco smoke (ETS) and cooking; although outdoor air concentrations

were also strongly associated with indoor levels. Previous studies have demonstrated that ETS is a major source of exposure to PM_{2.5} among nonsmokers' homes (Ferro et al. 2004) and that cooking has often been associated with episodic peaks in PM_{2.5} concentrations (Amouei Torkmahalleh et al. 2017; Li et al. 2016b; Lanki et al. 2002) because high-temperature can lead to water vapor and other solid and liquid particles emissions. However, it is possible to find studies with higher particles concentrations, such as the one developed by Chao and Wong (2002) where PM_{2.5} (mean) levels of 45 µg/m³ were measured due to smoking, cooking, and burning incense practices. Lin et al. (2008) showed that incense burning generates PM>45 mg/g compared to 10 mg/g from cigarette burning. A review study revealed relationships between PM emissions and some important cooking variables as cooking method, cooking oil employed, cooking pan, food being cooked, cooking temperature, energy source, additives, and source surface area (Amouei Torkmahalleh et al. 2017). This review also concluded that: (1) cooking on gas burners produce higher PM compared to electric stoves and changing in cooking manner may reduce the cooking PM emissions; and (2) increased ventilation rates were efficient in reducing indoor PM concentrations during and after cooking. Hopke et al. (2003) reported that in a retirement facility in Baltimore, MA (USA) the average indoor PM_{2.5} level was significantly lower than outdoors (7.9 µg/m³ vs. 21.7 µg/m³) showing the influence of the outdoor air quality. By contrast, Kim et al. (2014) stated that mean indoor PM_{2.5} levels (23.3 µg/m³) was slightly higher than outdoors (21.2 µg/m³) in four ECCs in South Korea. In another Korean study, the mean PM₁₀ concentration was 58 µg/m³ in facilities for susceptible populations (Hwang et al. 2018). The same study indicated that indoor PM₁₀ concentrations were higher than outdoor concentrations at all ECCs studied and exhibited a significant weak positive correlation with CO₂ concentration, which is influenced by human density and movement (Hwang et al. 2018). Similarly, Segalin et al. (2017) investigated PM in 59 elderly residences in metropolitan area of São Paulo, Brazil. The authors obtained mean values of measured PM₁₀ and PM_{2.5} of 35.2 µg/m³ and 27.4 µg/m³, respectively. They further report that about 77% and 40% of the residences had higher PM_{2.5} and PM₁₀ indoors than those in outdoor environments, mainly due to smoking and cooking. PM_{2.5} levels were also studied in four French ECCs by Baudet et al. (2021). The authors reported median PM_{2.5} levels of 9.0 µg/m³ associated with human activity, including the resuspension of deposited particles due to human movements and also affected by PM_{2.5} outside. Mixed results were reported in Portugal by Almeida-Silva et al. (2015) who conducted measurements in four ECCs. The study found that the average living room PM₁₀ concentration was slightly lower than outdoors (19 µg/m³ vs. 21 µg/m³), but the average bedroom concentration was significantly lower than outdoors (11 µg/m³ vs. 24 µg/m³). According to the same authors, the higher levels of PM₁₀ found in the living rooms than the bedrooms were attributed to the density of occupation of the former, as well as the higher ingress of the outdoor pollution through the doors and windows that were frequently opened were occupied (Almeida-Silva et al. 2015). A study developed in Hong-Kong residences (Chau et al. 2002) reported that indoor microenvironments contributed to 38.7%, and 32.1% of the PM₁₀ exposure for adult and elderly, respectively. Likewise, in China and for the same age groups, Wang et al. (2008) estimated

that PM₁₀ in indoor microenvironments contributed to higher percentages of PM₁₀ exposure (54%, and 80%, respectively). In 2016, PM composition and sources influencing elderly exposure was investigated by Almeida-Silva et al. (2016) in an urban ECC. This study suggests that the proximity of highways and the airport (located less than 500 m from the ECC) have a great importance for both indoor and outdoor PM₁₀ levels; whereas organic carbon concentration was significantly higher indoors, being associated with the sub-micrometer fragments of paper, skin debris, clothing fibers, cleaning products, and waxes (Almeida-Silva et al. 2016). Hopke et al. (2003) postulated that personal care products, such as a Zn oxide powder that might include talc (Conner et al. 2001), represent a source of indoor PM exposure among a population with a mean age of 84 in Baltimore.

A rich body of literature has demonstrated significant adverse health implications following the exposure to PM, namely, PM_{2.5} such as the fact that increased concentrations of PM_{2.5} were associated with increased rates of hospitalization and emergency department visits (Hopke et al. 2019). Morawska et al. (2013) concluded that 10–30% of the total burden of disease from PM exposure resulted from indoor-generated particles. Bentayeb et al. (2015) carried out a study on geriatric health effects of air quality in nursing homes in Europe (GERIE study) among 600 individuals 65 years of age and older who resided in 50 nursing homes in different 7 European countries. The indoor mean level of PM₁₀ concentrations was higher than 50 µg/m³ in 12% of the nursing homes (mean value 29.8 µg/m³) (Bentayeb et al. 2015). The authors reported that exposure to elevated concentrations of indoor PM₁₀ in the main common rooms of these facilities was associated with breathlessness and cough. Mendes et al. (2016) conducted a similar study in 22 ECCs, Portugal. The authors obtained a relatively high prevalence of respiratory symptoms among ECCs residents. In the frame of the same study, Mendes et al. (2016) found a higher risk of allergic rhinitis in those elderly that were exposed to high concentrations of PM₁₀, even at concentrations lower than 50 µg/m³. Consistent with these results, higher risks for respiratory symptoms with increasing indoor PM₁₀ concentrations was reported in a study of Chinese older adults (Venners et al. 2001). Chen et al. (2019) also observed that the decline of lung function in the elderly (≥ 65 years) was related to PM exposure. Other epidemiological studies indicate that exposure to PM is associated with low bone mineral density and osteoporosis-related fractures (Prada et al. 2020); whereas Calderon-Garciduenas et al. (2013) described an association with cognitive deficits, oxidative stress, neuroinflammation, and neurodegeneration. Saenz et al. (2021) also suggested that household air pollution from the use of polluting cooking fuel may play an important role in shaping cognitive outcomes of older adults in India, Mexico, and China where reliance on polluting fuels for domestic energy needs still prevails. According to Pohl et al. (2011), several metals present in the PM, including aluminum, arsenic, cadmium, lead, manganese, and mercury, have been shown to affect the nervous system, while the general accumulation of metal ions in the brain can exacerbate oxidative stress and neuronal damage. Bentayeb et al. (2015) reported that wheeze in the past year was associated with PM_{0.1} exposure among elderly living in nursing homes. In addition, chronic obstructive pulmonary disease (COPD), defined on the basis of

the Forced Expiratory Volume in the first second (FEV1)/forced vital capacity (FVC) ratio, was highly related to PM_{0.1}. Because of the absence of data, it is not possible to compare these results with previous epidemiological studies, despite the fact that UFP are more dangerous than larger PM since when inhaled they may reach the peripheral regions of the bronchioles and interfere with gas exchange inside the lungs (Madureira et al. 2020b; Li et al. 2016a; WHO 2013). Moreover, UFP may lead to an increase in oxidative stress, exacerbating asthma and other respiratory symptoms (Li et al. 2016a).

To reduce exposure to indoor PM and its adverse health outcomes, WHO have formulated updated guidelines for PM_{2.5} and PM₁₀ with values of 5 µg/m³ and 15 µg/m³ for annual and 24 h for PM_{2.5}, respectively; and 15 µg/m³ annual averages and 45 µg/m³ for 24 h for PM₁₀ (WHO 2021). These guidelines can guide the development of effective mitigation strategies to mitigate exposure to indoor PM and have a key role in the support government's making decisions on IAQ regulation. Furthermore, substantial reductions in exposure to PM can be achieved by using existing ventilation guidelines that aim to maintain good IAQ irrespective of sources and activities (ASHRAE 2016; EN 15251 2007), which, in addition to increasing the supply of fresh air, include controlling pollution from emission sources, cleaning the air, and improving the efficiency of ventilation. Thus, ventilation practices and interventions can reduce the airborne concentrations and reduce the overall exposure of occupants. This is particularly relevant for elderly homes or geriatric centers, which, although not subject to specific regulatory requirements, are buildings that require appropriate air-conditioning and ventilation systems essential to enable the elderly people who live in these facilities to achieve a good standard of living in terms of their personal well-being, due to their special needs in terms of health and comfort. For instance, in a study of elderly (60–75 years) people, an 8% improvement in microvascular function was detected following 48 h of air filtration in their homes (Bräuner et al. 2008).

Volatile Organic Compounds

The term VOCs includes a large set of chemical substances emitted from liquids or solids, many of those known or expected to be irritating or even carcinogenic (Wolkoff 2017; Weschler 2006). Based on the categorization provided by ISO 16000-6 (2011), VOCs and very volatile organic compounds (VVOCs) are indoor organic compounds with a boiling point range of 50–100 °C and 240–260 °C; and <0 °C to 50–100 °C, respectively. They differ from the family of semi-volatile organic compounds (SVOCs) that present boiling point range of 240–260 °C and 380–400 °C.

Volatile organic compounds are emitted from a very wide range of indoor and outdoor sources (Lee et al. 2018; Madureira et al. 2016, 2020a; Annesi-Maesano et al. 2013), through human activities, including cooking, smoking, and the use of cleaning and cosmetic/personal care products; building materials, new furnishings, and decoration products; indoor chemical reactions; and penetration of outdoor air nearby

traffic and industrial emissions (Bonnet et al. 2018; Annesi-Maesano et al. 2013). Typical VOCs found in the indoor environment include benzene, toluene, ethylbenzene, and xylenes from fuel combustion and building renovations; benzene and styrene from cigarette smoking; alkanes from natural gas; formaldehyde and terpenes such as α -pinene from wood-based building materials, and limonene from fragranced cleaning and laundry products (WHO 2013; Kotzias et al. 2005). Cleaning solutions, detergents and disinfecting are largely used and have particular significance for the emission of broad spectrum of VOC indoors ECCs because of the need for maintaining infection control (Baudet et al. 2021; Pereira et al. 2021; Bonnet et al. 2018; Su et al. 2018; Almeida-Silva et al. 2014; Bessonneau et al. 2013). Furthermore, the recent pandemic (COVID-19) has seen a sweeping and surging use of products intended to clean and disinfect, such as air sprays, hand sanitizers, and surface cleaners, many of which contain fragrance. Additionally, personal care products are generally used for personal hygiene, grooming, and beautification in ECCs. These include hair and skin care products, perfumes, soap, and shampoos that contribute to the indoor levels of VOCs and SVOCs at ECCs (Khalid and Abdollahi 2021). Some studies were identified to have investigated total and specific VOCs in the indoor air of ECCs as described below. Hwang et al. (2018) investigated the total VOCs in 62 ECCs facilities. The mean total VOC ($126.1 \mu\text{g}/\text{m}^3$) concentrations reported by the authors was higher than in other indoor environments used by children, including classrooms ($114.0 \mu\text{g}/\text{m}^3$) in an elementary school in Seoul (Yang et al. 2015) and elderly people in 21 Portuguese ECCs ($110.0 \mu\text{g}/\text{m}^3$) (Mendes et al. 2016). Hwang et al. (2018) also revealed that total VOC concentrations may be attributed less to emissions sources and more to poor ventilation of ECCs indoor spaces; while Mendes et al. (2016) identified that VOCs were emitted from indoor sources in their building materials. In Korea, Lee and colleagues performed a study to characterize the indoor and outdoor levels of VOCs in 30 ECCs (Lee et al. 2018). Findings of this study showed that indoor total VOC levels were significantly higher than those of their outdoor levels ($230.7 \mu\text{g}/\text{m}^3$ vs. $137.8 \mu\text{g}/\text{m}^3$; $p < 0.05$) and that indoor/outdoor (I/O) ratio for formaldehyde was 2.48. These results suggest that both total VOC and formaldehyde are mainly emitted from indoor sources at ECCs, such as such as carpets, paints, and new wooden furniture. Sim et al. (2010) reported that the elderly who live in newly constructed residences could be exposed to high concentrations of VOCs and formaldehyde from construction materials. Under the framework of the GERIE study, the mean concentration of formaldehyde was $7.21 \mu\text{g}/\text{m}^3$ while the maximum indoor level (weekly average) was $21 \mu\text{g}/\text{m}^3$ (Bentayeb et al. 2015). These findings are in agreement with Almeida-Silva et al. (2014) that found low indoor levels of formaldehyde in ten Portuguese ECCs. Nevertheless, the authors also underlined the importance of the time activity patterns of elderly and the IAQ in different microenvironments for the daily exposure and inhaled dose estimation. Walgraeve et al. (2011) measured 25 VOCs in 6 elderly homes in Antwerp, Belgium. Overall the indoor total VOC concentration ranges from $12 \mu\text{g}/\text{m}^3$ to $311 \mu\text{g}/\text{m}^3$. The main contributor to the high total VOC concentration is limonene, but also increased levels of aromatic hydrocarbons were found. Toluene, with a mean concentration of $60.8 \mu\text{g}/\text{m}^3$, accounted for more than half of the aromatic hydrocarbons (69%), representing 25% of the total VOC

indoor concentration. Alcohols (ethanol, isopropanol), ketones (acetone), and aldehydes were the three VOCs with the highest concentrations in French ECCs as reported by Baudet et al. (2021), where cleaning activities were indicated as the main sources of these pollutants. Su et al. (2018) reported that cleaning tasks, using products containing chlorine, resulted in elevated exposures to chloroform, α -pinene, and limonene. Likewise, Singer et al. (2006) reported a concentration of 200 ppb of limonene following cleaning indoors. According to Nematollahi et al. (2019), a chemical analyses and comparisons of fragranced and fragrance-free cleaning products showed that all of the fragranced products emitted terpenes (e.g., α -pinene, β -pinene, limonene), but none of the fragrance-free products emitted terpenes that can act as both primary pollutants as well as react with O_3 to generate a range of secondary pollutants, such as formaldehyde.

The assessment of human exposure to SVOCs in indoor environment and respective risk assessment is an emerging research topic, since limited studies were performed due to analytical challenges (Weschler and Nazaroff 2008). Nonetheless, ECCs may have elevated exposure concentrations to many SVOCs due to the frequent use of several cosmetics, health care and household cleaning products (Bonnet et al. 2018; Annesi-Maesano et al. 2013). Arnold and colleagues were the first to report indoor concentrations of a large range of SVOCs in senior care facilities in the USA and in Portugal (Arnold et al. 2018). The authors found that organophosphate esters (OPEs), PAHs, and brominated flame retardants (BFRs) were the most prevalent, and organochlorine pesticide (OCPs) and polychlorinated biphenyls (PCBs) were the least abundant SVOC groups in these indoor environments. Furthermore, the levels of OPEs, PAHs, and BFRs were significantly higher in USA buildings compared to Portuguese facilities, reflecting the widespread use of some of these chemicals. More recently, Baudet et al. (2021) found that diisobutylphthalate, diethylphthalate, and dibutylphthalate were the three most quantified phthalates in a French investigation including four ECCs, with median concentration levels of 270, 240, and 77 ng/m³, respectively. Thus it is crucial to use low-emitting and non-absorbent consumer products and building materials in order to minimize pollutant exposure-related risk.

Findings by studies in various countries suggest that the exposure to VOCs, primarily emitted from indoor sources, was associated with adverse health outcomes, such as headaches, upper and lower respiratory symptoms (e.g., irritation of the nose and eyes), and may contribute to the worsening of the respiratory diseases, namely, asthma attacks and exacerbations (Hulin et al. 2012; WHO 2010) and additional health problems related to neurological gastrointestinal, dermatological, and immune systems (e.g., WHO 2010). An excess of asthma was observed among French school children exposed to concentrations of formaldehyde higher than the established standards in their classrooms (Annesi-Maesano et al. 2012) or dwellings (Hulin et al. 2012). In a longitudinal study performed in Sweden between 1989 and 1992, the prevalence of self-reported asthma was higher among subjects living in newly painted dwellings compared to others (Wieslander et al. 1997). In an adult population, a significant association was showed between asthma and exposure of VOCs, especially aromatic compounds (Arif and Shah 2007). A recent review of

epidemiological studies highlighted that the use of cleaning and disinfecting products is harmful to respiratory health and increases the risk of asthma (Folletti et al. 2017).

Despite the fact that elderly is likely more exposed to indoor air pollutants, very few studies targeted the respiratory effects of VOCs in this age group. In one study conducted in elder people, the urinary levels of hippuric acid and methyl-hippuric acid (metabolites of toluene and xylene, respectively) were significantly associated with a harmful effect on pulmonary function due to the reduction of FEV1, FEV1/FVC, and forced expiratory flow at 25–75% of FVC (Yoon et al. 2010). Another study, carried out in France, explored the relationship between exposure to VOCs and respiratory health outcomes in the elderly population (Bentayeb et al. 2013). The findings revealed a significant relationship between toluene and o-xylene levels and breathlessness among the elderly participants. These results are in agreement with those from Yoon et al. (2010), under the hypothesis that breathlessness and dyspnea are a proxy of lung function deterioration. A relationship between increased indoor concentrations of VOCs and pulmonary infection was noted by Belo et al. (2019).

Nitrogen Dioxide

Another common indoor pollutant is NO₂. Since NO₂ is a traffic- and industrial emissions-related pollutant (EEA 2018), concentrations of NO₂ are commonly higher in urban than in rural environments, and generally higher in outdoor air compared to indoor air, if no specific indoor sources are available, such as gas appliances like stoves, ovens, or water heaters, fireplaces and tobacco smoke (WHO 2010). Moreover, as indoor concentrations of NO₂ are modulated by ventilation, optimized ventilation is an important factor in the prevention of adverse effects of NO₂ pollution (Bentayeb et al. 2015).

The evidence from epidemiological studies for a threshold for long-term exposure to NO₂ is inconsistent, with some large studies suggesting that the threshold for increased symptoms it is likely to lie below 19 µg/m³ among asthmatic children (Belanger et al. 2013). In addition, a concentration–response relation has been determined between long-term NO₂ concentration and mortality, with most concentrations below 20 µg/m³ among adults (Raaschou-Nielsen et al. 2012).

However, little is known about exposures to NO₂ in indoor environments such as in ECCs. The results from Hwang and Park (2020) study indicated that NO₂ concentrations were significantly higher in the four facilities with susceptible occupants (19.9 µg/m³) than in the general facilities (11.8 µg/m³); however, in all the studies facilities, the respective I/O ratio was less than one, which suggest that the outdoor traffic generated origin of NO₂, rather than indoor sources. Similar mean indoor NO₂ concentrations (20.1 µg/m³) were reported by Bentayeb et al. (2015) who documented that elevated indoor NO₂ concentrations was associated with decreased lung function and COPD. This association was observed for NO₂ levels below 40 µg/m³ and was amplified in ECCs with poor ventilation and in elderly residents over the age of 80 (Bentayeb et al. 2015). In a previous Italian study

(Simoni et al. 2002), highest weekly indoor NO₂ levels were found in a rural area when compared with urban area (54.5 µg/m³ vs. 62.0 µg/m³, $p < 0.05$ in winter and 41.4 µg/m³ vs. 37.6 µg/m³, $p < 0.01$ in the summer for urban and rural areas, respectively). This population-based study also indicated an association between low doses of indoor NO₂ and acute respiratory symptoms and reduced peak expiratory flow in adults, while bronchitis and asthmatic symptoms were significantly more prevalent in the presence of high NO₂ levels. High NO₂ exposure was also associated with greater symptom duration.

Other research works have also indicated NO₂ as a cause of adverse effects on health. A study of British adults showed a significantly reduced FEV1 in study participants who currently used gas for cooking compared to those who used electricity (Moran et al. 1999). The principal indoor source of NO₂ in Australian homes was also the use of gas heaters (Pilotto et al. 1997). The authors showed that the presence of gas heaters at home was significantly associated with increased prevalence of asthma (Pilotto et al. 1997). Gas cooking was associated with increased risk of respiratory problems and impaired lung function in nonsmoking adults in Singapore as reported by Ng and co-authors (Ng et al. 1993).

Ozone

Ozone is a secondary pollutant formed by a complex reaction chain where VOCs, oxides of nitrogen (NOx), mainly comprised of NO₂ and nitric oxide, and solar irradiation are the key actors (Hwang and Park 2020; EEA 2018). This formation mechanism explains why elevated O₃ concentrations are found in several large urban and industrial agglomerations where anthropogenic emissions of its two main precursors (NOx and VOCs) have been increasing (Zhang et al. 2019; EEA 2018). Precursors can be transported by local/regional air mass flows away from the urban areas and toward suburban and rural areas, which are impacted by O₃ episodes. At the same time, O₃ are strongly linked to other factors such as weather conditions (i.e., season, time of day) as well as geographical region; higher temperatures can promote the formation of O₃ and also accelerate the reaction among different precursors and their intermediate products (EEA 2018; Coates et al. 2016).

Indoor O₃ concentrations generally fluctuate from 30% to 70% of the outdoor levels (Zhang et al. 2019) according to the air exchange rate and O₃ removal rate and where specific indoor sources, e.g., air purifiers, laser printers, photocopiers, are not present (Nicolas et al. 2007).

Ozone is a pollutant of concern in any type of indoor environment and elderly is considered a sensitive group of population such as children. By this reason and because studies performed in ECCs are scarce, research developed in schools will also be presented. The average indoor levels of O₃ found in school environments from ten European cities were 8.50 µg/m³ and much lower than the average outdoor levels (HESE 2006). More recently, Dimakopoulou et al. (2017) evaluated O₃ levels in different school buildings in Greece and concluded that: (i) outdoor to indoor transport of O₃ is significant; and (ii) the length of time windows were open was

significantly associated with exposure to O₃. In line with these results, Blondeau et al. (2005) also reported that all I/O ratios <1, suggesting that O₃ indoors derives from the O₃ transport from outdoors rather than internal sources.

In comparison to school buildings, indoor O₃ concentrations were low in European nursing homes (Bentayeb et al. 2015), a finding that corroborates earlier observations in ten Portuguese ECCs (Almeida-Silva et al. 2014), which reported O₃ levels below 0.2 µg/m³ or, in some cases, below the detection limit. Higher indoor O₃ concentrations were reported in 66 ECCs in Korea (Hwang and Park 2020). These authors observed that mean indoor O₃ concentrations were lower in ECCs (26.2 µg/m³) than in museums facilities (32.6 µg/m³); even the highest mean concentrations were observed in summer months compared to the winter months in multiple facilities despite indoor environments not having any identified source of O₃. This suggest that indoor O₃ are influenced by outdoor concentrations and that seasonal variations in O₃ levels might be caused by limited or decreased photochemical reactivity of O₃ during winter (EEA 2018).

Most epidemiological studies published on the health effects have repeatedly reported decrements in lung function associated with O₃ exposure in infants and children; however, estimated individual exposures were obtained from outdoor measurements (Triche et al. 2006). Largely unexplored is the association between indoor ECCs O₃ concentrations and elderly health. According to Brauner et al. (2014) no significant changes in lung function were observed in association with increased levels of residential O₃ among 39 healthy elderly nonsmokers; nevertheless, among the seven study participants with asthma or obstructive airway disease, the authors detected a significant inverse association between residential O₃ and FEV1/FVC.

Carbon Dioxide

Carbon dioxide, a colorless and odorless gas, is a well-known constituent of the Earth's atmosphere contributing to the greenhouse effects and accelerating global warming (EEA 2018; Azuma et al. 2018). Outside levels of CO₂ are relatively constant. Outdoor CO₂ concentration is currently at nearly 412 ppm and rising (NASA 2019), which is primarily the result of the combustion of fossil fuels (EEA 2018). In a usual indoor environment, concentrations of CO₂ range from outdoor levels up to several thousand parts per million (e.g., Madureira et al. 2016). Indoor CO₂ concentrations are commonly used as a good indicator for the concentrations of occupant-generated pollutants, particularly bioeffluents emissions including PM and VOCs, as well as of poor ventilation (Madureira et al. 2016). According to the ASHRAE standard, it is recommended that indoor CO₂ concentrations are maintained below 700 ppm to ensure human health (ASHRAE 2016).

Hwang and Park (2020) evaluated CO₂ levels in multiple ECCs and the mean measured concentration was 598 ppm. In the same study, indoor CO₂ concentrations showed a significant correlation with indoor NO₂ and O₃ levels suggesting that CO₂ can be used as a surrogate for indoor concentrations of other pollutants and housing

factors, since indoor CO₂ concentrations are strongly correlated with indoor ventilation. The GERIE study analyzed CO₂ levels, showing that only 19% of the elderly individuals had an adequate ventilation system in nursing home where they live (Bentayeb et al. 2015). Likewise, Almeida-Silva et al. (2014) reported that in 60% of the studied bedrooms, CO₂ levels exceed 1800 mg/m³ for almost 15 h/day. More recently, Hwang et al. (2018) observed significantly higher mean CO₂ concentrations in facilities for susceptible populations (638 ppm) than those obtained in other general facilities (542 ppm) and subway station platforms (563 ppm) in Seoul. Also in Korea, Park et al. (2010) found that in several ECCs, indoor levels of CO₂ were significantly higher than those in other residences or public facilities. The authors concluded that robust air cleaning and mechanical ventilation systems should be used to reduce indoor pollution levels because indoor levels of CO₂ exceeded 1000 ppm (Park et al. 2010). In Portugal, ventilation in ECCs, based on CO₂ concentrations, which commonly exceed 1000 ppm, appears inadequate (Mendes et al. 2016). Mendes et al. (2016) refers that the main reasons for the high CO₂ levels were elevated density of occupation and poor ventilation of the ECCs' rooms.

In previous epidemiological and intervention studies, CO₂ concentrations have been shown to be related with adverse health outcomes. According to the study performed by Azuma et al. (2018), nonspecific symptoms including headache and dizziness among 107 participants from 11 offices were positively associated with a 100 ppm increase in CO₂ concentration (range from 549 ppm to 1318 ppm), although the correlation was not significant. Prior research has shown that a 100 ppm increase in CO₂ concentration (range from 674 ppm to 1450 ppm) found inside university classrooms was significantly associated with headache among 355 students and this association was independent of temperature, relative humidity, and air exchange rate (Norbäck and Nordström 2008). In Taiwan, Tsai et al. (2012) found a significant increase of eye irritation and upper respiratory symptoms when 111 office workers were exposed to indoor CO₂ concentrations higher than 800 ppm. Nocturnal symptoms related to asthma were associated with higher CO₂ levels in dwellings in Sweden (Norbäck et al. 1995). According to the same authors, the inadequate outdoor air supply, or the indoor concentration of CO₂, leads to increased levels of VOCs and other indoor pollutants. It is postulated that the relationship between indoor CO₂ concentrations and specific adverse health effects exist because the higher indoor CO₂ levels at lower ventilation rates are likely correlated with higher levels of other coexisting indoor generated pollutants that directly cause adverse effects. Thus, further epidemiological studies are advised.

Indoor Air Quality Health-Based Guidelines

The population is evolving, i.e., changing its lifestyle and modifying its consumer product uses due to development of novel household products and building materials. These changes bring a great variety of sources and wide range of indoor air pollutants, even at low concentrations, within the building environment with potential health risks. Therefore, it is essential for the protection of occupant's health the

continuing monitoring and the development of IAQ health-based guidelines. In this context, member states need to adopt and implement measures to ensure adequate air quality in indoor environments in line with the priorities of both national and European prevention plans, such as the programs from the United Nations Sustainability Development Agenda, since, there is no specific European legislation for IAQ so far, except in what regards the ban of tobacco smoke in public buildings and commercial establishments (EC 2007).

Current Guidelines

In recent years, the scientific communities as well as worldwide organizations have attempted to develop and implement IAQ guidelines since there is a common recognized need for a horizontal policy framework, which spans safety, health, energy efficiency, and sustainability aspects across existing legislative instruments and standardization activities related to the indoor built environment. DG SANCO undertook a relevant breakthrough promoting a number of high-grade projects such as Promoting actions for healthy indoor air (IAIAQ), HealthVent (Health-based ventilation guidelines for Europe), EPHECT (Emissions, Exposure Patterns and Health Effects of Consumer Products in the EU), while from the European Commission side, Joint Research Center (JRC) has been for the last 25 years a true leader in what regards IAQ through the European Collaborative Action on Urban Air, Indoor Environment and Human Exposure (http://ihcp.jrc.ec.europa.eu/our_activities/publichealth/indoor_air_quality/eca/eca-publications).

Since 1987, the WHO has developed guidelines, provided technical support and tools to facilitate assessment and quantification of the health impacts of air pollution (WHO 1987). The AQGs are addressed to the whole world in an attempt to produce a set of reference values grounded on the results of scientific studies and from practical experience or consensus based on available knowledge. In September 2021, the WHO updated its 2005 AQGs reflecting the large impact that air pollution has on global public health burden (WHO 2021). They recommend aiming for annual mean concentrations of PM_{2.5} not exceeding 5 µg/m³ and NO₂ not exceeding 10 µg/m³, and the peak season mean 8-h O₃ concentration not exceeding 60 µg/m³ (WHO 2021). For reference, the corresponding 2005 WHO AQGs values for PM_{2.5} and NO₂ were, respectively, 10 µg/m³ and 40 µg/m³ with no recommendation issued for long-term O₃ concentrations. While the guidelines are not legally binding, several countries, such as UK (PHE 2019), Belgium (HGR 8794 2017), France (Décret 2011-1727, 2011; Décret 2011-1728, 2011), and Portugal (DL 60, 2013) have started efforts to design and adopt guideline/reference values for IAQ to protect human health; in some cases, enforced in the legislative acts of these countries while in other the recommended guideline values have no legal value, even though in practice they have reached considerable importance, since these actions will facilitate the detection of problems and the formulation of effective control strategies. Please find all the information related with guidelines/regulations in the dedicated chapter to this topic in this handbook.

Future Perspectives

Indoor air quality is an important determinant of public health and will continue to be a priority topic in the future, namely, within environmental and health programs. Existing IAQ guidelines are based on assessments carried out on individual pollutants and taking into account a single route of exposure. Since in reality humans are continuously exposed to a large set and combination of indoor air pollutants, there is increasing concern about the potential adverse health risks of the interactions between those pollutants. In addition, there are multiple routes of exposure for specific indoor pollutants (Kienzler et al. 2016) and when there are multiple exposures to indoor pollutants, combined health effects (e.g., dose addition, response addition, synergism, and antagonism) are often a cause for concern (Azuma et al. 2016). In light of the above considerations, to reduce the health risks due to chemical pollutants via multi-route exposures, human risk management based on estimates of the total body burden of the pollutants and the relative contributions of these exposures to the total body burden is required. At present at the EU level, there is not a consistent, comprehensive, and integrated recommended approach to conduct risk assessment for chemical mixtures or for combined effects due to co-exposure to different chemicals via different routes (Kienzler et al. 2016).

A novel approach that integrates the contribution of the different routes and pollutants exposure using multi-environmental biomarkers (e.g., oxidative stress markers) to evaluate biological and potential health risks is essential. They can contribute to improve the knowledge on the link between air pollution and human health in a more global and future perspective.

The Challenges of Making Indoors Healthy

According to the last WHO estimates, more than 80% of people living in the urban context are subjected to air quality levels above the concentration limits regarding outdoor air pollution due to the rapid industrialization and urbanization in these areas (EEA 2018). The assessment of outdoor air quality is frequently driven often for regulatory targets compliance purposes. Unlike outdoors, IAQ is not regulated by legislation and seldom monitored. Whereas improving outdoor air quality leads to general improvements of IAQ as well, certain sources of air pollution not covered by ambient air quality regulations/standards can dominate in some indoor environments leading to an indoor environment with poor air quality that can cause potential adverse health effects particularly relevant among the most susceptible groups of the population, such as the elderly. The current pandemic situation placed IAQ under a bright spotlight and emphasized the need to prioritize effective strategies to promote healthy indoor spaces and buildings. However, the success of any IAQ strategy or approach strongly depends on targeted policy changes across the public health, urban planning, and architectural design sectors.

Increased emphasis has been placed in the residential environment for older people as the number of ECCs increases as well as on identifying the relationship between health and the residential environment for older people. The older population risk assessment may require the design of a specific strategy and intervention plan with specific recommendations for controlling, mitigating, and/ or solving risk factors to protect them from exposure to indoor air pollutants. Indoor air quality in ECCs can be improved in three ways: source control, improved ventilation, and using technologies for indoor air treatment. An overview of existing studies performed on ECCs is displayed below; please see chapter on strategies to ensure a healthy IAQ for further details.

The most cost-effective IAQ control strategy is to remove/replace the individual sources of pollution or to reduce their emissions. A reduction in outdoor air pollution will reduce indoor pollution as a flow-on effect. The selection of low emission products and materials with “clean” or “ecological” labels like improved plastics and paints (phenol resins instead of urea resins, polyurethane coatings, etc.) are another example of source control strategy (ECA 27 2012; Kotzias et al. 2005) since some VOCs emissions can be prevented. Mendes et al. (2018) established a set of recommendations and good practices to improve IAQ in ECCs. Among others, the authors have suggested to avoid the use of: sprays, air fresheners, and detergents with intense smell; and carpets, fitted carpeting, plaids on the sofas and draperies, as well as excessive decorative items that make it difficult for cleaning. Moreover, the cleaning processes should be done when there are no occupants in the divisions, being in other microenvironments. Smoking ban measures are also a very effective measure since tobacco smoke is a source of multiple harmful chemicals in elevated concentrations. The suppression of tobacco smoke in indoor places has resulted in consistent IAQ improvements (Kotzias et al. 2005).

In the past few years, the advance on portable and inexpensive sensors and systems has emerged as an additional strategy for the real-time, even remote, monitoring and control IAQ. In this context, it is predicted that the progress on development of materials for IAQ sensors and IAQ-monitoring systems is a promising strategy for control and enhancement of IAQ in the future, namely, in ECCs (Tran et al. 2020).

Another strategy that is used for controlling IAQ in buildings is ventilation. Ventilation is the process of providing fresh and clean outdoor air to a room or building via natural systems or mechanical equipment, such as fans and blowers, to reduce exposure (Carrer et al. 2018). Most recently, researchers have highlighted the role of proper ventilation of indoor spaces as a means to reduce exposure to SARS-CoV-2 (Morawska et al. 2020). Similarly, other entities, such as the Federation of European Heating, Ventilation and Air Conditioning Associations (REHVA), and the American Society of Heating, Ventilating, and Air-Conditioning Engineers (ASHRAE), have recognized the potential airborne hazard indoors and recommended ventilation control measures accordingly (ASHRAE 2020; REHVA 2020), since ventilation plays a crucial role in relation to the indoor pollution levels and minimizing the possibility of health problems as a consequence. The capacity to increase ventilation rates to ensure good IAQ may differ, and may be somewhat limited by their original design specifications and implementation.

Mendes et al. (2018) suggested that combination of controlling the indoor air sources and selecting appropriate ventilation rate was the most effective to reduce health risks in ECCs. In that context, if the indoor emission source cannot be removed or their emissions cannot be reduced to an accepted level, higher ventilation rates, reduced occupant density, and additional mechanical ventilation are recommended to ensure good IAQ. The ventilation rate should differ for different building facilities and rooms according to the occupancy and activities conducted there.

Indoor air pollutants can be removed by place filters in a building's heating, ventilation, and air conditioning (HVAC) system or operate as portable units. There are many HVAC filters that have been developed and used in various buildings, namely, schools and office buildings. It was reported that adsorptive HVAC filters, designed in different shapes, may effectively remove several noxious pollutants, including PM, VOCs, and O₃ (Zhao et al. 2007). According to a review carried out by Kelly and Fussell (2019) there is substantial evidence HVAC filters reduce indoor PM_{2.5} concentrations by at least 50%. Similarly, another study showed that 72-h use of inexpensive, portable air cleaners placed in a low-income senior facility in Detroit, MI (USA) was associated with significant reductions in indoor PM_{2.5} levels (Morishita et al. 2018). Fisk and Chan (2017) suggest that the economic benefits of reduced mortality among elderly during the 2003 California wildfires outweighed costs for HVAC filtration. Despite these facts, this technology has demonstrated several limitations in terms of the adsorption efficiency (Kelly and Fussell 2019), which is remarkably reduced in the presence of humidity, proliferation of molds and germs, limiting their overall role in public health. Therefore, advanced technologies, such as photocatalysis, and other physical-chemical technologies for indoor air treatment, such as electronic filtration or membrane separation, are emerging (González-Martín et al. 2021).

Conclusions

Although few studies have been carried out so far, the current literature confirms that ECCs' indoor environments may play a special role in the elderly health, emphasizing the importance of ensuring good IAQ, as COVID-19 has further demonstrated the need for rapidly developing and deploying IAQ solutions in ECCs. The development of new portable, inexpensive sensors and systems to measure certain air pollutants can be a useful tool to tackle poor IAQ event.

More than ever, more epidemiological research on indoor pollution and elderly health is needed, with a focus on emerging indoor pollutants given that building techniques are constantly evolving and new questions are being raised due to new occupant lifestyle, uses, and products on daily basis. More research is also needed in relation to exposure assessment, various types of short-term and long-term health outcomes. At the same time, further identification of subgroups among the elderly who are susceptible to the adverse effects of air pollutants would also be an important help in the definition of effective preventive and mitigation strategies for

healthy aging. Although various international agencies have continuously developed quantitative IAQ guidelines, it is also of high importance that future studies are conducted on multi-route and combined exposures, including interactions between pollutants, reactions occurring between pollutants and all potential transformation, to close existing knowledge gaps. This requires interdisciplinary studies in which the interactions between IAQ in ECCs toward elderly's health are investigated. Lastly, it is a challenging task for public authorities to embed air quality standards in legislation. They must make social and economic choices to meet air quality standard levels, beyond assessment and information requirements. Nevertheless, there is no doubt that enforceable regulations that require better air quality with the responsibility of governments to monitor, control, and implement regulations are needed in order to mitigate the adverse effects on human health, namely, among the more sensitive to air pollution impacts such as the elderly.

Cross-References

- [ASTM and ASHRAE Standards for the Assessment of Indoor Air Quality](#)
- [Control of Airborne Particles: Filtration](#)
- [PCO and TCO in Air Cleaning](#)
- [WHO Health Guidelines for Indoor Air Quality and National Recommendations/Standards](#)

Acknowledgments This work was supported by the Foundation for Science and Technology-FCT (Portuguese Ministry of Science, Technology and Higher Education) under the project UIDB/04750/2020. Joana Madureira is also supported by FCT (SFRH/BPD/115112/2016).

References

- Almeida-Silva M, Wolterbeek HT, Almeida SM (2014) Elderly exposure to indoor air pollutants. *Atmos Environ* 85:54–63
- Almeida-Silva M, Almeida SM, Pegas PN, Nunes T, Alves CA, Wolterbeek HT (2015) Exposure and dose assessment to particle components among an elderly population. *Atmos Environ* 102: 156–166
- Almeida-Silva M, Faria T, Saraga D, Maggos T, Wolterbeek HT, Almeida SM (2016) Source apportionment of indoor PM10 in Elderly Care Centre. *Environ Sci Pollut Res Int* 23(8):7814–7827
- Amouei Torkmahalleh M, Gorjinezad S, Unluevcek HS, Hopke PK (2017) Review of factors impacting emission/concentration of cooking generated particulate matter. *Sci Total Environ* 586:1046–1056
- Annesi-Maesano I, Norback D, Zielinski J, Bernard A, Gratziou C, Sigsgaard T, Sestini P, Viegi G, GERIE Study (2013) Geriatric study in Europe on health effects of air quality in nursing homes (GERIE study) profile: objectives, study protocol and descriptive data. *Multidiscip Respir Med* 8(1):71
- Annesi-Maesano I, Lavaud F, Raherison C, Kopferschmitt C, Blay F, Charpin D, Caillaud D (2012) Poor air quality in classrooms related to asthma and rhinitis in primary schoolchildren of the French 6 Cities Study. *Thorax* 67:682–688

- Arif AA, Shah SM (2007) Association between personal exposure to volatile organic compounds and asthma among US adult population. *Int Arch Occup Environ Health* 80(8):711–719
- Arnold K, Teixeira JP, Mendes A, Madureira J, Costa S, Salamova A (2018) A pilot study on semivolatile organic compounds in senior care facilities: implications for older adult exposures. *Environ Pollut* 240:908–915
- ASHRAE Standard 62.1-2016 (2016) Ventilation for acceptable indoor air quality. American Society of Heating, Refrigerating and Air-Conditioning Engineers, Inc., Atlanta
- ASHRAE (2020) COVID-19 (CORONAVIRUS) Preparedness resources. American Society of Heating, Ventilating, and Air-Conditioning Engineers
- Azuma K, Uchiyama I, Uchiyama S, Kunugita N (2016) Assessment of inhalation exposure to indoor air pollutants: screening for health risks of multiple pollutants in Japanese dwellings. *Environ Res* 145:39–49
- Azuma K, Ikeda K, Kagi N, Yanagi U, Osawa H (2018) Physicochemical risk factors for building-related symptoms in air-conditioned office buildings: ambient particles and combined exposure to indoor air pollutants. *Sci Total Environ* 616–617:1649–1655
- Baudet A, Baurès E, Guegan H, Blanchard O, Guillaso M, Cann L, Gangneux JP, Florentin A (2021) Indoor air quality in healthcare and care facilities: chemical pollutants and microbiological contaminants. *Atmosphere* 12:1337
- Belanger K, Hol福德 TR, Gent JF, Hill ME, Kezik JM, Leaderer BP (2013) Household levels of nitrogen dioxide and pediatric asthma severity. *Epidemiology* 24(2):320–330
- Belo J, Carreiro-Martins P, Papoila AL, Palmeiro T, Caires I, Alves M, Nogueira S, Aguiar F, Mendes A, Cano M, Botelho MA, Neuparth N (2019) The impact of indoor air quality on respiratory health of older people living in nursing homes: spirometric and exhaled breath condensate assessments. *J Environ Sci Health A Tox Hazard Subst Environ Eng* 54:1153–1158
- Bentayeb M, Norback D, Bednarek M, Bernard A, Cai G, Cerrai S, Eleftheriou KK, Gratziosi C, Holst GJ, Lavaud F, Nasilowski J, Sestini P, Samo G, Sigsgaard T, Wieslander G, Zielinski J, Viegi G, Annesi-Maesano I, GERIE Study (2015) Indoor air quality, ventilation and respiratory health in elderly residents living in nursing homes in Europe. *Eur Res J* 45(5):1228–1238
- Bentayeb M, Billionnet C, Baiz N, Derbez M, Kirchner S, Annesi-Maesano I (2013) Higher prevalence of breathlessness in elderly exposed to indoor aldehydes and VOCs in a representative sample of French dwellings. *Respir Med* 107(10):1598–1607
- Bessonneau V, Mosqueron L, Berrubé A, Mukensturm G, Buffet-Bataillon S, Gangneux JP, Thomas O (2013) VOC contamination in hospital, from stationary sampling of a large panel of compounds, in view of healthcare workers and patients exposure assessment. *PLoS One* 8: e55535
- Blondeau P, Iordache V, Poupart O, Genin D, Allard F (2005) Relationship between outdoor and indoor air quality in eight French schools. *Indoor Air* 15(1):2–12
- Bonnet P, Achille J, Malingre L, Duret H, Ramalho O, Mandin C (2018) VOCs in cleaning products used in age care and social facilities: identification of hazardous substances. *AIMS Environ Sci* 6(6):402–417
- Bräuner EV, Forchhammer L, Møller P, Barregard L, Gunnarsen L, Afshari A, Wählén P, Glasius M, Dragsted LO, Basu S, Raaschou-Nielsen O, Loft S (2008) Indoor particles affect vascular function in the aged: an air filtration-based intervention study. *Am J Respir Crit Care Med* 177(4):419–425
- Bräuner EV, Karottki DG, Frederiksen M, Kolarik B, Spilak M, Andersen ZJ, Vibenholt A, Ellermann T, Gunnarsen L, Loft S (2014) Residential ozone and lung function in the elderly. *Indoor Built Environ* 25(1):93–105
- Calderon-Garcidueñas L, Serrano-Sierra A, Torres-Jardón R, Zhu H, Yuan Y, Smith D, Delgado-Chavez R, Cross JV, Medina-Cortina H, Kavanaugh M et al (2013) The impact of environmental metals in young urbanites' brains. *Exp Toxicol Pathol* 65:503–511
- Campagnolo D, Saraga DE, Cattaneo A, Spinazzè A, Mandin C, Mabilia R, Perreca E, Sakellaris I, Canha N, Mihucz VG, Szegedi T, Ventura G, Madureira J, Fernandes EO, Kluizenaar Y, Cornelissen E, Hänninen O, Carrer P, Wolkoff P, Cavallo DM, Bartzis JG (2017) VOCs and

- aldehydes source identification in European office buildings-the OFFICAIR study. *Build Environ* 115:18–24
- Carrer P, de Oliveira FE, Santos H, Hänninen O, Kephalopoulos S, Wargocki P (2018) On the development of health-based ventilation guidelines: principles and framework. *Int J Environ Res Public Health* 15(7):1360
- Chao CY, Wong KK (2002) Residential indoor PM10 and PM2.5 in Hong Kong and the elemental composition. *Atmos Environ* 36(2):265–277
- Chau C, Tu EY, Chan D, Burnett J (2002) Estimating the total exposure to air pollutants for different population age groups in Hong Kong. *Environ Int* 27:617–630
- Chen CH, Wu CD, Chiang HC, Chu DC, Lee KY, Lin WY, Yeh JI, Tsai KW, Guo YLL (2019) The effects of fine and coarse PM on lung function among the elderly. *Sci Rep* 9:14790
- Coates J, Mar KA, Ojha N, Butler TM (2016) The influence of temperature on ozone production under varying NO_x conditions – a modelling study. *Atmos Chem Phys* 16(18):11601–11615
- Conner TL, Norris GA, Landis MS, Williams RW (2001) Individual particle analysis of indoor, outdoor, and community samples from the 1998 Baltimore Particulate Matter Study. *Atmos Environ* 35:3935–3946
- Décret n° 2011–1727 du 2 décembre 2011 relatif aux valeurs-guides pour l'air intérieur pour le formaldéhyde et le benzene. J. Officiel République Française 2011. Available online: <https://www.legifrance.gouv.fr/affichTexte.do?cidTexte=JORFTEXT000024909119&categorieLien=id>. Accessed 23 Mar 2021
- Décret n° 2011–1728 du 2 décembre 2011 relatif à la surveillance de la qualité de l'air intérieur dans certains établissements recevant du public. J. Officiel République Française. 2011. Available online: <https://www.legifrance.gouv.fr/affichTexte.do?cidTexte=JORFTEXT000024909128>. Accessed 23 Mar 2021
- Dimakopoulou K, Grivas G, Samoli E, Rodopoulou S, Spyros D, Papakosta D, Karakatsani A, Chaloulakou A, Katsouyanni K (2017) Determinants of personal exposure to ozone in school children. Results from a panel study in Greece. *Environ Res* 154:66–72
- DL n. 60/2013 de 5 de fevereiro de 2013 (2013) Diário da República, 2a Série n. 25; Ministérios das Finanças e da Economia e do Emprego: Lisboa, Portugal, 2013
- EC (2007) Green Paper towards a Europe free from tobacco smoke: policy options at EU level. [gp_smoke_en.pdf \(europa.eu\)](http://ec.europa.eu/green_smoke_en.pdf)
- ECA 27 2012 Report nr 27 of European Collaborative Action (ECA), Harmonisation framework for indoor products labelling schemes in the EU. Ispra. Environment and Quality of Life, EC Joint Research Centre, Italy
- EEA (2018) Air quality in Europe – 2018 report. ISBN: 978-92-9213-990-2. Air quality in Europe – 2018 – European Environment Agency (europa.eu). Accessed 12 Mar 2021
- EN 15251 (2007) Indoor environmental input parameters for design and assessment of energy performance of buildings addressing indoor air quality, thermal environment, lighting and acoustics; EN 15251; CEN: Brussels, Belgium
- Ferro AR, Kopperud RJ, Hildemann LM (2004) Elevated personal exposure to particulate matter from human activities in a residence. *J Expo Sci Environ Epidemiol* 14:S34–S40
- Fisk WJ, Chan WR (2017) Health benefits and costs of filtration interventions that reduce indoor exposure to PM2.5 during wildfires. *Indoor Air* 27:191–204
- Folletti I, Siracusa A, Paolocci G (2017) Update on asthma and cleaning agents. *Curr Opin Allergy Clin Immunol* 17(2):90–95
- HESE (2006) Health Effects of School Environment (HESE). Final Scientific Report. http://ec.europa.eu/health/ph_projects/2002/pollution/pollution_2002_04_en.htm. Accessed 12 Mar 2021
- HGR 8794 (2017) Indoor air quality in Belgium. HGR: Brussel. 2017; Advies nr. 8794. Available online: https://www.health.belgium.be/sites/default/files/uploads/fields/fpshealth_theme_file/hgr_8794_advice_iaq.pdf. Accessed 9 Mar 2021
- González-Martín J, Kraakman NJR, Pérez C, Lebrero R, Munoz R (2021) A state-of-the-art review on indoor air pollution and strategies for indoor air pollution control. *Chemosphere* 262: 1238376

- Hamanaka RB, Mutlu GM (2018) Particulate matter air pollution: effects on the cardiovascular system. *Front Endocrinol* 9:680
- Hopke PK, Ramadan Z, Paatero P, Norris GA, Landis MS, Williams RW, Lewis CW (2003) Receptor modeling of ambient and personal exposure samples: 1998 Baltimore Particulate Matter Epidemiology-Exposure Study. *Atmos Environ* 37:3289–3302
- Hopke PK, Croft D, Zhang W, Lin S, Masiol M, Squizzato S, Thurston SW, van Wijngaarden E, Utell MJ, Rich DQ (2019) Changes in the acute response of respiratory diseases to PM_{2.5} in New York State from 2005 to 2016. *Sci Total Environ* 10(677):328–339
- Hulin M, Simoni M, Viegi G, Annese-Maesano I (2012) Respiratory health and indoor air pollutants based on quantitative exposure assessments. *Eur Respir J* 40:1033–1045
- Hwang SH, Roh J, Park WM (2018) Evaluation of PM₁₀, CO₂, airborne bacteria, TVOCs, and formaldehyde in facilities for susceptible populations in South Korea. *Environ Pollut* 242 (Pt A):700–708
- Hwang SH, Park WM (2020) Indoor air concentrations of carbon dioxide (CO₂), nitrogen dioxide (NO₂), and ozone (O₃) in multiple healthcare facilities. *Environ Geochem Health* 42(5): 1487–1496
- ISO 16000-6:2011: Indoor air – Part 6: determination of volatile organic compounds in indoor and test chamber air by active sampling on Tenax TA sorbent, thermal desorption and gas chromatography using MS or MS-FID
- Khalid M, Abdollahi M (2021) Environmental distribution of personal care products and their effects on human health. *Iran J Pharm Res* 20(1):216–233
- Kelly FJ, Fussell JC (2019) Improving indoor air quality, health and performance within environments where people live, travel, learn and work. *Atmos Environ* 200:90–109
- Kienzler A, Bopp SK, van der Linden S, Berggren E, Worth A (2016) Regulatory assessment of chemical mixtures: requirements, current approaches and future perspectives. *Regul Toxicol Pharmacol* 80:321–334
- Kim H-H, Lee G-W, Yang J-Y, Jeon J-M, Lee W-S, Lim J-Y, Lee H-S, Gwak Y-K, Shin D-C, Lim Y-W (2014) Indoor exposure and health risk of polycyclic aromatic hydrocarbons (PAHs) via public facilities PM2.5, Korea (II). *Asian J Atmos Environ* 8:35–47
- Kotzias D et al (2005) The INDEX project. Critical appraisal of the setting and implementation of indoor exposure limits in the EU. Ispra, European Commission Joint Research Centre
- Lanki T, Alm S, Ruuskanen J, Janssen NAH, Jantunen M, Pekkanen J (2002) Photometrically measured continuous personal PM_{2.5} exposure: levels and correlation to a gravimetric method. *J Expo Anal Environ Epidemiol* 12:172–178
- Lanki T, Ahokas A, Alm S, Janssen NA, Hoek G, De Hartog JJ, Brunekreef B, Pekkanen J (2007) Determinants of personal and indoor PM_{2.5} and absorbance among elderly subjects with coronary heart disease. *J Expo Sci Environ Epidemiol* 17(2):124–133
- Lee K, Choi JH, Lee S, Park HJ, Oh YJ, Kim GB, Lee WS, Son BS (2018) Indoor levels of volatile organic compounds and formaldehyde from emission sources at elderly care centers in Korea. *PLoS One* 13(6):e0197495
- Leikauf GD, Kim SH, Jang AS (2020) Mechanisms of ultrafine particle-induced respiratory health effects. *Exp Mol Med* 52(3):329–337
- Li N, Georas S, Alexis N, Fritz P, Xia T, Williams MA, Horner E, Nel A (2016a) A work group report on ultrafine particles (American Academy of Allergy, Asthma & Immunology): why ambient ultrafine and engineered nanoparticles should receive special attention for possible adverse health outcomes in human subjects. *J Allergy Clin Immunol* 138(2):386–396
- Li T, Cao S, Fan D, Zhang Y, Wang B, Zhao X, Leaderer BP, Shen G, Zhang Y, Duan X (2016b) Household concentrations and personal exposure of PM_{2.5} among urban residents using different cooking fuels. *Sci Total Environ* 548:6–12
- Lin TC, Krishnaswamy GH, Chi DS (2008) Incense smoke: clinical, structural and molecular effects on airway disease. *Clin Mol Allergy* 6:3
- Madureira J, Paciência I, Cavaleiro-Rufo J, de Oliveira FE (2016) Indoor pollutant exposure among children with and without asthma in Porto, Portugal, during the cold season. *Environ Sci Pollut Res Int* 23(20):20539–20552

- Madureira J, Slezakova K, Costa C, Pereira MC, Teixeira JP (2020a) Assessment of indoor air exposure among newborns and their mothers: levels and sources of PM₁₀, PM_{2.5} and ultrafine particles at 65 home environments. *Environ Pollut* 264:114746
- Madureira J, Slezakova K, Silva AI, Lage B, Mendes A, Aguiar L, Pereira MC, Teixeira JP, Costa C (2020b) Assessment of indoor air exposure at residential homes: inhalation dose and lung deposition of PM₁₀, PM_{2.5} and ultrafine particles among newborn children and their mothers. *Sci Total Environ* 717:137293
- Maio S, Sarno G, Baldacci S, Annesi-Maesano I, Viegi G (2015) Air quality of nursing homes and its effect on the lung health of elderly residents. *Expert Rev Respir Med* 9(6):671–673
- Mendes A, Teixeira-Gomes A, Costa S, Laffon B, Madureira J, Teixeira JP (2018) Indoor environments and elderly health. In: *Elderly care: options, challenges and trends*. Nova Science Publishers, Inc. ISBN: 978-1-53613-463-6 (e-Book); 978-1-53613-462-9
- Mendes A, Papoila AL, Carreiro-Martins P, Bonassi S, Caires I, Palmeiro T, Aguiar L, Pereira C, Neves P, Mendes D, Botelho MA, Neuparth N, Teixeira JP (2016) The impact of indoor air quality and contaminants on respiratory health of older people living in long-term care residences in Porto. *Age Ageing* 45(1):136–142
- Moran SE, Strachan DP, Johnston ID, Anderson HR (1999) Effects of exposure to gas cooking in childhood and adulthood on respiratory symptoms, allergic sensitization and lung function in young British adults. *Clin Exp Allergy* 29:1009–1013
- Morawska L, Tang JW, Bahnfleth W, Bluyssen PM, Boerstra A, Buonanno G, Cao J, Dancer S, Floto A, Franchimont F, Haworth C, Hogeling J, Isaxon C, Jimenez JL, Kurnitski J, Li Y, Loomans M, Marks G, Marr LC, Mazzarella L, Melikov AK, Miller S, Milton DK, Nazaroff W, Nielsen PV, Noakes C, Peccia J, Querol X, Sekhar C, Seppänen O, Tanabe SI, Tellier R, Tham KW, Wargocki P, Wierzbicka A, Yao M (2020) How can airborne transmission of COVID-19 indoors be minimised? *Environ Int* 142:105832
- Morawska L, Ayoko GA, Bae GN, Buonanno G, Chao CYH, Clifford S, Fu SC, Hänninen O, He C, Isaxon C, Mazaheri M, Salthammer T, Waring MS, Wierzbicka A (2017) Airborne particles in indoor environment of homes, schools, offices and aged care facilities: the main routes of exposure. *Environ Int* 108:75–83
- Morawska L, Afshari A, Bae GN, Buonanno G, Chao CY, Hänninen O, Hofmann W, Isaxon C, Jayaratne ER, Pasanen P, Salthammer T, Waring M, Wierzbicka A (2013) Indoor aerosols: from personal exposure to risk assessment. *Indoor Air* 23(6):462–487
- Morishita M, Adar SD, D'Souza J, Ziembra RA, Bard RL, Spino C, Brook RD (2018) Effect of portable air filtration systems on personal exposure to fine particulate matter and blood pressure among residents in a low-income senior facility: a randomized clinical trial. *JAMA Intern Med* 178(10):1350–1357
- NASA (2019) <https://climate.nasa.gov/news/2915/the-atmosphere-getting-a-handle-on-carbon-dioxide/>
- Nematollahi N, Kolev S, Steinemann A (2019) Volatile chemical emissions from 134 common consumer products. *Air Qual Atmos Health* 12(11):1259–1265
- Nicolas M, Ramalho O, Maupetit F (2007) Reactions between ozone and building products: Impact on primary and secondary emissions. *Atmos Environ* 41(15):3129–3138
- Ng TP, Hui KP, Tan WC (1993) Respiratory symptoms and lung function effects of domestic exposure to tobacco smoke and cooking by gas in non-smoking women in Singapore. *J Epidemiol Community Health* 47(6):454–458
- Norbäck D, Nordström K (2008) Sick building syndrome in relation to air exchange rate, CO₂, room temperature and relative air humidity in university computer classrooms: an experimental study. *Int Arch Occup Environ Health* 82(1):21–30
- Norbäck D, Björnsson E, Janson C, Widström J, Boman G (1995) Asthmatic symptoms and volatile organic compounds, formaldehyde, and carbon dioxide in dwellings. *Occup Environ Med* 52 (6):388–395
- Park H, Oh Y, Lee H, Woo W, Sohn J (2010) A study of indoor air quality of public facilities in Incheon city. *J Korean Soc Environ Admin* 16(2):53–61

- Pereira EL, Madacussengua O, Baptista P, Feliciano M (2021) Assessment of indoor air quality in geriatric environments of southwestern Europe. *Aerobiologia* 37:139–153
- Pilotto LS, Douglas RM, Attewell RG, Wilson SR (1997) Respiratory effects associated with indoor nitrogen dioxide exposure in children. *Int J Epidemiol* 26:788–796
- PHE (Public Health England) (2019) Indoor Air Quality Guidelines for Selected Volatile Organic Compounds (VOCs) in the UK. Available online: <https://www.gov.uk/government/publications/air-quality-uk-guidelines-for-volatile-organic-compounds-in-indoor-spaces>. Accessed 10 May 2021
- Pohl HR, Roney N, Abadin HG (2011) Metal ions affecting the neurological system. *Met Ions Life Sci* 8:247–262
- Prada D, Lopez G, Solleiro-Villavicencio H, Garcia-Cuellar C, Baccarelli AA (2020) Molecular and cellular mechanisms linking air pollution and bone damage. *Environ Res* 185:109465
- Raaschou-Nielsen O, Andersen ZJ, Jensen SS, Ketzel M, Sorensen M, Hansen J, Loft S (2012) Traffic air pollution and mortality from cardiovascular disease and all causes: a Danish cohort study. *Environ Health* 11:60
- REHVA (2020) COVID-19 Guidance [REHVA_COVID-19_guidance_document_V3_03082020.pdf](#). Accessed 14 May 2021
- Rivas I, Beddows DCS, Amato F, Green DC, Järvi L, Hueglin C, Reche C, Timonen H, Fuller GW, Niemi JV, Pérez N, Aurela M, Hopke PK, Alastuey A, Kulmala M, Harrison RM, Querol X, Kelly FJ (2020) Source apportionment of particle number size distribution in urban background and traffic stations in four European cities. *Environ Int* 135:105345
- Saenz JL, Adar SD, Zhang YS, Wilkens J, Chattopadhyay A, Lee J, Wong R (2021) Household use of polluting cooking fuels and late-life cognitive function: a harmonized analysis of India, Mexico, and China. *Environ Int* 156:106722
- Segalin B, Kumar P, Micadei K, Fornaro A, Gonçalves FLT (2017) Size-segregated particulate matter inside residences of elderly in the Metropolitan Area of São Paulo, Brazil. *Atmos Environ* 148:139–151
- Singer BC, Coleman BK, Destaillats H, Hodgson AT, Lunden MM, Weschler CJ, Nazaroff WW (2006) Indoor secondary pollutants from cleaning product and air freshener use in the presence of ozone. *Atmos Environ* 40(35):6696–6710
- Sim S, Moon J, Kim Y, Tae J (2010) Emission rates of selected volatile organic compounds and formaldehyde in newly constructed apartment. *Toxicol Environ Heal Sci* 2(4):263–267
- Simoni M, Carrozzi L, Baldacci S, Scognamiglio A, Di Pede F, Sapigni T, Viegi G (2002) The Po River Delta (north Italy) indoor epidemiological study: effects of pollutant exposure on acute respiratory symptoms and respiratory function in adults. *Arch Environ Health* 57(2):130–136
- Stabile L, De Luca G, Pacitto A, Morawska L, Avino P, Buonanno G (2021) Ultrafine particle emission from floor cleaning products. *Indoor Air* 31(1):63–73
- Su FC, Friesen MC, Stefaniak AB, Henneberger PK, LeBouf RF, Stanton ML, Liang X, Humann M, Virji MA (2018) Exposures to volatile organic compounds among healthcare workers: modeling the effects of cleaning tasks and product use. *Ann Work Expo Health* 62 (7):852–870
- Tsai DH, Lin JS, Chan CC (2012) Office workers' sick building syndrome and indoor carbon dioxide concentrations. *J Occup Environ Hyg* 9(5):345–351
- Tran VV, Park D, Lee YC (2020) Indoor air pollution, related human diseases, and recent trends in the control and improvement of indoor air quality. *Int J Environ Res Public Health* 17(8):2927
- Triche EW, Gent JF, Holford TR, Belanger K, Bracken MB, Beckett WS, Naehler L, McSharry JE, Leaderer BP (2006) Low level ozone exposure and respiratory symptoms in infants. *Environ Health Perspect* 114:911–916
- UN (United Nations) (2017) Department of Economic and Social Affairs, Population Division (2017). World Population Ageing 2017 – Highlights (ST/ESA/SER.A/397). [WPA2017_Highlights.pdf\(un.org\)](#). Accessed 5 Apr 2021
- Venners SA, Wang B, Ni J, Jin Y, Yang J, Fang Z, Xu X (2001) Indoor air pollution and respiratory health in urban and rural China. *Int J Occup Environ Health* 7(3):173–181

- Walgraeve C, Demeestere K, Dewulf J, Huffel V, Langenhove HV (2011) Diffusive sampling of 25 volatile organic compounds in indoor air: uptake rate determination and application in Flemish homes for the elderly. *Atmos Environ* 45:5828–5836
- Wang S, Zhao Y, Chen G, Wang F, Aunan K, Hao J (2008) Assessment of population exposure to particulate matter pollution in Chongqing, China. *Environ Pollut* 153:247–256
- Weschler CJ, Nazaroff WW (2008) Semivolatile organic compounds in indoor environments. *Atmos Environ* 42(40):9018–9040
- Weschler CJ (2006) Ozone's impact on public health: contributions from indoor exposures to ozone and products of ozone-initiated chemistry. *Environ Health Perspect* 114:1489–1496
- Wolkoff P (2017) External eye symptoms in indoor environments. *Indoor Air* 27:246–260
- Wieslander G, Norback D, Edling C (1997) Airway symptoms among house painters in relation to exposure to volatile organic compounds (VOCs) – a longitudinal study. *Ann Occup Hyg* 41: 155–166
- Wichman J, Lin T, Nilsson MA-M, Bellander T (2010) PM2.5, soot and NO₂ indoor-outdoor relationships at homes, pre-schools and schools in Stockholm, Sweden. *Atmos Environ* 44: 4536–4544
- WHO (World Health Organization) (2017) Public Health, Environmental and Social Determinants of Health (PHE). World Health Organization, Geneva
- WHO (World Health Organization) (2013) Review of evidence on health aspects of air pollution—REVIHAAP project. WHO Regional Office for Europe, Copenhagen. Available online at: http://www.euro.who.int/_data/assets/pdf_file/0004/193108/REVIHAAP-Final-technical-report.pdf. Accessed 13 May 2021
- WHO (World Health Organization) (2010) WHO guidelines for indoor air quality: selected pollutants. Available online at: http://www.euro.who.int/_data/assets/pdf_file/0009/128169/e94535.Pdf. Accessed 13 May 2021
- WHO (World Health Organization) (1987) Air quality guidelines for Europe. World Health Organization Regional Office for Europe, Copenhagen
- WHO (World Health Organization) (2006) WHO air quality guidelines for particulate matter, ozone, nitrogen dioxide and sulfur dioxide: global update 2005 (Summary of risk assessment) Genova, Switzerland. Available online at: http://whqlibdoc.who.int/hq/2006/WHO_SDE_PHE_OEH_.pdf. Accessed 13 May 2021
- WHO (World Health Organization) (2021) WHO global air quality guidelines: particulate matter (PM2.5 and PM10), ozone, nitrogen dioxide, sulfur dioxide and carbon monoxide. World Health Organization. Available online at: <https://apps.who.int/iris/handle/10665/345329>. Accessed 24 Jan 2022
- Yang J, Nam I, Yun H, Kim J, Oh H-J, Lee D, Jeon S-M, Yoo S-H, Sohn J-R (2015) Characteristics of indoor air quality at urban elementary schools in Seoul, Korea: assessment of effect of surrounding environments. *Atmos Pollut Res* 6(6):1113–1122
- Yoon HI, Hong YC, Cho SH, Kim H, Kim YH, Sohn JR, Kwon M, Park SH, Cho MH, Cheong HK (2010) Exposure to volatile organic compounds and loss of pulmonary function in the elderly. *Eur Respir J* 36(6):1270–1276
- Zhang JJ, Wei Y, Fang Z (2019) Ozone pollution: a major health hazard worldwide. *Front Immunol* 31(10):2518
- Zhao P, Siegel JA, Corsi RL (2007) Ozone removal by HVAC filters. *Atmos Environ* 41:3151–3160



Inhalation and Skin Exposure to Chemicals in Hospital Settings

67

M. Abbas Virji, Lauren N. Bowers, and Ryan F. LeBouf

Contents

Introduction	1988
Exposure and Health Hazards in Hospital Settings	1989
Exposure to Chemicals Used for Cleaning, Disinfection, Sterilization, and Skin	
Antiseptics	1990
Exposure to Other Hospital Products and Chemicals	2008
Conclusions	2016
Cross-References	2017
References	2017

Abstract

Healthcare is one of the largest and fastest growing industries worldwide. It is complex and comprises different occupations directly providing healthcare services, and occupations providing other supporting services. The industry is changing rapidly with advances in medical science and new technologies. It faces new challenges stemming from changing demographics, migration, environmental and geopolitical instability, increased demand and cost of health services, and new disease outbreaks, all contributing to new hazards or exacerbating existing ones. A healthy healthcare workforce is central to sustain healthcare systems and for a prosperous society and economy. However, healthcare workers are exposed to a mixture of hazards that can include chemical (anesthetic gases), biological (pathogens), physical (radiation), ergonomic (musculoskeletal), psychosocial (stress), and safety hazards (violence). Chemical hazards arise from sources, such as cleaning, disinfecting, and sterilizing agents, solvents, glues, metals, hazardous drugs, laboratory chemical reagents, waste

M. A. Virji (✉) · L. N. Bowers · R. F. LeBouf

Respiratory Health Division, National Institute for Occupational Safety and Health, Morgantown, WV, USA

e-mail: MVirji@cdc.gov; Mju3@cdc.gov; RLeBouf@cdc.gov; igu6@cdc.gov

© This is a U.S. Government work and not under copyright protection in the U.S.; foreign copyright protection may apply 2022

1987

Y. Zhang et al. (eds.), *Handbook of Indoor Air Quality*,
https://doi.org/10.1007/978-981-16-7680-2_60

anesthetic gases, surgical smoke, and other indoor air contaminants. Working in healthcare is associated with a spectrum of adverse health outcomes including respiratory, reproductive, dermatologic, neurologic, other systemic outcomes, and cancer. These exposures and health hazards are preventable but continue to occur among healthcare workers in part because industry attention is focused on preventing healthcare-associated infections in patients caused by pathogens. Healthcare workers' exposures to chemicals is consequently not well recognized and disease prevention or exposure mitigation measures are not fully implemented. The focus of this review is to highlight inhalation and dermal exposures to chemicals among various occupations and units in healthcare and identify opportunities for exposure mitigation and disease prevention.

Keywords

Healthcare · Hospital · Chemical exposures · Health effects · Cleaning products

Introduction

Healthcare is one of the largest and fastest growing industries worldwide, especially in many developed countries. An estimated 59 million workers were employed in the healthcare and social sector worldwide in 2006, accounting for over 12% of the working population; over 70% were women (WHO 2006). In the USA in 2020, 20.7 million workers were employed in the healthcare industry, accounting for 14% of the US working population, of which 77.8% were women (BLS 2020). Within this industry, about 6.6 million employees (31.6%) worked in ambulatory care, 7.3 million (35.2%) in hospitals, 3.1 million (15.1%) in social assistance, and 3.7 million (18.0%) in skilled nursing, residential, or home care facilities. The healthcare industry is rapidly changing with advances in medical science, new technologies and products, and enhancement in worker and patient protection leading to improved working conditions and patient safety. At the same time, new challenges are creating new hazards, such as exposure to new chemicals and hazardous drugs, or exacerbating existing ones, such as increased workloads and stress. These challenges stem from aging population and workforce, population growth, gender dynamics, increased demand and cost of health services and products, push toward universal health coverage, globalization and migration, environmental and geopolitical instability, shortages of healthcare professionals and healthcare funding, privatization of hospitals and health services, health inequalities, and new disease outbreaks (ILO 2019). The demand for health services is expected to create 40 million new jobs worldwide by the year 2030. However, this growth is mostly expected to occur in developed countries with projected shortages of 18 million jobs in developing countries (ILO 2019). The healthcare industry is complex and comprises different occupations, some directly providing healthcare services while others indirectly supporting health or other services. Occupations in healthcare settings include physicians, nurses, midwives, therapists, social workers, a variety of technicians in

laboratories and research, pharmacists, and other personnel such as cleaners, administrative staff, dietary staff, laundry workers, medical equipment maintenance workers, and facilities and maintenance workers (NIOSH 2017a). Healthcare workers provide services that occur in a variety of work settings including hospitals, clinics, dental offices, out-patient surgery and care centers, birthing centers, emergency medical care, home healthcare, and nursing homes (OSHA 2021).

A healthy healthcare workforce is central to sustain healthcare systems and for society to prosper and the economy to thrive. It is most critical for the safety and well-being of patients, workers, and the population in general. Although the core mission of the healthcare industry is to care for and promote healing in patients, healthcare workers themselves are exposed to a myriad of health and safety hazards that cause numerous illnesses and injuries. The healthcare industry is among the most hazardous workplaces in the USA; healthcare workers experienced the highest number of nonfatal injuries and illnesses in 2017 (BLS 2018). Healthcare workers are potentially exposed to a mixture of hazards that can include chemical (e.g., anesthetic gases), biological (e.g., pathogens), physical (e.g., radiation), ergonomic (e.g., musculoskeletal), psychosocial (e.g., stress, shift work, and work organization), and safety hazards (e.g., violence). Chemical hazards include well recognized as well as some not-so-well known exposure to gases, vapors, and aerosols resulting in a spectrum of adverse health outcomes including respiratory, reproductive, dermatologic, neurologic, other systemic outcomes, and cancer (Weaver 1997). These exposures and health hazards are preventable, but they nevertheless continue to occur among healthcare workers (NIOSH 2017a). Although a great deal of attention has focused on minimizing biological hazards to prevent healthcare-associated infections (HAI) in patients caused by pathogens, healthcare workers' exposures to chemicals is often not well recognized or controlled. This lack of focus is in part due to hospitals being perceived as clean, hazard-free workplaces, and the selfless nature of the healthcare workforce whose first instinct is to place patient care needs above their own health and safety concerns. Consequently, hazard recognition is lacking, and disease prevention or exposure mitigation measures are not fully implemented. The focus of this review is to highlight the chemical products used by healthcare workers, their ingredients and potential for inhalation and dermal exposures among various hospital occupations in various units, and identify opportunities for exposure mitigation and disease prevention.

Exposure and Health Hazards in Hospital Settings

Hospital workers are exposed to a complex mixture of chemicals simultaneously and sequentially, mostly via inhalation and dermal routes of exposure. These exposures arise from multiple sources, such as sterilizing agents, cleaning and disinfecting products, detergents, solvents, glues, heavy metals, hazardous drugs, laboratory chemical reagents, waste anesthetic gases, surgical smoke, and other indoor air contaminants from products and building and construction materials (Gorman et al. 2013). Some exposures such as cleaning chemicals are pervasive throughout

the hospital potentially affecting patients and workers in all occupations; certain occupations such as housekeepers have among the highest exposures to these cleaning and disinfecting chemicals (Weaver 1997). Many other exposures are unique to specific departments or units affecting selected occupations such as high exposure to solvents (e.g., xylenes) among laboratory technicians (Weaver 1997). Thus, exposure to chemicals in hospital settings can vary considerably by department or unit and occupation, and most workers are exposed to a mixture of chemicals either directly or indirectly as bystanders.

Exposure to Chemicals Used for Cleaning, Disinfection, Sterilization, and Skin Antiseptics

Cleaning, disinfection, and sterilization has special significance in hospital settings, where intensive cleaning and disinfection is performed in an effort to prevent HAIs (Rutala et al. 2008). Hospitals use a rational approach to clean and disinfect surfaces and equipment devised by Spaulding, which places surfaces or items to be cleaned into three categories based on the risk of infection conferred if these surfaces are contaminated.

1. Critical surfaces are those that come into contact with sterile tissue and must be sterile because any contamination could result in infection. These surfaces include items such as surgical instruments that are cleaned using sterilizers such as ethylene oxide gas or high-level disinfectants such as ortho-phthalaldehyde (OPA).
2. Semi-critical surfaces are those that come into contact with mucous membranes or nonintact skin such as respiratory therapy devices and are cleaned using high-level disinfectants.
3. Noncritical surfaces are those that come into contact with intact skin such as blood pressure cuffs and are cleaned using intermediate-level disinfectants such as a strong bleach solution or low-level disinfectants such as quaternary ammonium compounds (QACs).

Table 1 summarizes the chemical ingredients of cleaning, disinfecting, and sterilizing chemicals and antiseptic products as well as their purpose or function, and hospital units and occupations where they are frequently used.

Cleaning and Disinfecting Environmental Surfaces

Environmental surfaces include building surfaces, equipment, and patient care items. Environmental surfaces that only come in contact with intact skin are classified as noncritical surfaces and are cleaned using intermediate-level disinfectants, which are effective against vegetative bacteria, some spores, fungi, and some viruses, or low-level disinfectants which are effective against vegetative bacteria, fungi, enveloped viruses, and some nonenveloped viruses (Rutala et al. 2008). Cleaning and disinfection of environmental surfaces is complex and involves physical action

Table 1 Summary of products and chemical exposure to cleaning, disinfecting, and sterilizing chemicals and antiseptics among healthcare occupations and hospital units

Unit/Occupation	Product or chemical class	Purpose or function	Chemical ingredients
All units and occupations, exposed directly or indirectly as a bystander	Cleaners and disinfectants to disinfect surfaces	Active disinfection ingredients	Alcohols (e.g., ethanol and isopropyl alcohol), sodium hypochlorite (bleach), QACs (e.g., see Table 2), phenolics (e.g., <i>o</i> -phenylphenol and benzoyl-p-chlorophenol), acetic acid, peracetic acid, hydrogen peroxide and their mixture
		Additives to add functional properties, e.g., surfactant or aesthetic or fragrance properties	Terpenes (e.g., pinene, <i>d</i> -limonene), and linalool
		Solvents and propellants	Toluene, alcohols, and glycol ethers (e.g., 2-butoxyethanol)
		Complexing agents to dissolve cations and regulate pH	Ethylenediaminetetraacetic acid (EDTA), nitrilotriacetic acid (NTA), and tripolyphosphates
		Preservatives	Formaldehyde, isothiazolines, and QACs
		Degreasers to remove fatty substances	Alkaline agents (e.g., ammonium hydroxide, sodium hydroxide, silicates, and carbonates)
		Scale removers	Various acids (e.g., acetic, phosphoric, citric, sulphamic, and hydrochloric acids)
Patient care occupations including all nursing occupations, e.g., LPN, RN, NA in different units, and occupations in OR/surgery	Antiseptics and skin disinfectants	Preoperative skin preparation and wound dressings	Ethanolamines
			Alcohols (e.g., ethanol and isopropyl alcohol), chlorhexidine, hexachlorophene, iodophores (povidone-iodine), octenidine, polyhexanide, hexamidine diisethionate, QACs, chlorhexidine gluconate, triclosan, chloroxylenol, and silver-based wound dressing

(continued)

Table 1 (continued)

Unit/Occupation	Product or chemical class	Purpose or function	Chemical ingredients
All occupations	Hand sanitizers	Hand sanitizers	Alcohols (e.g., ethanol and isopropyl alcohol), triclosan
Central supply, surgical suites, endoscopy, procedure rooms, dental clinics, radiology, and pathology	Sterilizers and high-level disinfectants	Sterilizing and disinfecting medical instruments	Ethylene oxide, orthophthalaldehyde, glutaraldehyde, hydrogen peroxide, peracetic acid, formaldehyde, chloramine-T, and chlorhexidine
	Detergents and cleaners	Clean and remove soils	Subtilisin (enzymatic cleaner), fatty acid salts, organic sulphonates, and VOCs (e.g., acetone, formaldehyde, and halogenated alkanes)
Housekeeping	Surface strippers	Floor preparation for waxing and polishing, paint remover	Ethanolamines (e.g., monoethanolamine and triethanolamine), ammonia, phthalates, potassium hydroxide, sodium hydroxide, methylene chloride, 2-butoxyethanol, d-limonene, xylene, and <i>n</i> -methylpyrrolidone
	Surface disinfectants, e.g., furniture and floors	Disinfecting floor and other surfaces	QACs, chloramine T, phenol, chlorine bleach, etc. (see above)
	Polishes and waxes	Polish or wax different surfaces, e.g., wood, metal, etc.	Film formers, polishes (wax, acryl polymers, and polyethylene), and acrylics
	Glass cleaners	Clean windows and mirrors	Ethanolamines and ammonia
	Ceramics cleaners	Clean bathroom surfaces	Acids (e.g., hydrochloric, sulfuric, and acetic acid)

to remove organic material and gross contaminants, followed by disinfection using sprays, wipes soaked in disinfectants, textile, or microfiber cloth, or premoistened wipes (Leas et al. 2015). Cleaning and disinfection can also be done in one step using products that contain ingredients to remove soils and disinfect. Noncritical surfaces that are touched on average > 3 times per interaction are classified as high-touch surfaces and are targeted for cleaning and disinfection (Huslage et al. 2010). Common high-touch surfaces include bed rails, bed surfaces, overbed table supply or medicine carts, intravenous pumps, doorknobs, light switches, and edges of

privacy curtains; the classification of a high-touch surface can vary by unit/location (Suleyman et al. 2018). Low-touch surfaces include walls, ceilings, mirrors, windows, and flooring in patient areas. Patient care items and equipment include oximeters, glucometers, mobility aids, electrocardiogram (EKG/ECG) monitors, respiration machines and spirometers, blood pressure cuffs, stethoscopes and scopes, thermometers, infusion pumps, dialysis machines, ultrasound transducers, and venipuncture tourniquets (Suleyman et al. 2018). A mixture of pathogens may be present on different environmental surfaces, as some pathogens, such as *Pseudomonas* sp., persist in damp places like bathroom surfaces, while others, such as *C. difficile* and vancomycin-resistant enterococci (VRE), are frequently found around toilet surfaces. Methicillin-resistant *Staphylococcus aureus* (MRSA) and *Acinetobacter* sp. are often present in dusty, inaccessible places (Dancer 2011). Thus, a product with a broad spectrum of antimicrobial activity may be needed to disinfect different surfaces. Interventions aimed at reducing surface contamination through enhanced cleaning procedures, change of disinfection products, education of healthcare workers, and evaluation of compliance with cleaning procedures can reduce microbial contamination and lower prevalence of HAI (Rutala et al. 2018). Thus, cleaning and disinfecting environmental surfaces is effective in reducing the levels of pathogens on surfaces and is a critical and integral component of an infection control program.

Cleaning and disinfection of environmental surfaces is performed multiple times daily to reduce the buildup of microbial burden on surfaces, and a more thorough cleaning and disinfection, terminal cleaning is performed when a patient is discharged to ensure the safety of the next patient. Housekeepers are primarily engaged in cleaning and disinfecting noncritical building surfaces and fixed equipment throughout the hospital. Housekeepers have some of the longest durations of cleaning and disinfecting tasks as well as some of the highest exposures to cleaning and disinfecting chemicals and solvents in surface maintenance products (Weaver 1997; Saito et al. 2015; LeBouf et al. 2014). However, almost all healthcare occupations perform some cleaning and disinfecting tasks at least once per shift with endoscopy technicians, dental assistants, nursing staff, and central supply workers spending the highest amounts of time on cleaning tasks after housekeepers (Saito et al. 2015). These occupations mostly clean and disinfect medical instruments and equipment, patient care items, and surfaces touched by patients. Performance of cleaning and disinfection tasks is variable by units with the greatest amount of cleaning done in central supply (sterilization), followed by wards, operating rooms, and emergency rooms.

Cleaning and Disinfecting Products for Environmental Surfaces

There are a multitude of disinfectants that can be used to clean and disinfect environmental surfaces and patient care items with different composition, biocidal capabilities, and application requirements summarized in Table 1. Most products are one-step cleaners and contain multiple functional ingredients: soft water; detergents and soaps as emulsifying agents; alkali to remove protein, fats, and carbohydrates; surfactants to help penetrate soils; water conditioners to prevent formation of scales;

solvents to cut grease; enzymes to remove biofilms; and the active disinfectant ingredient (Stewart and Smith 2017). Numerous factors influence the choice of a disinfectant including the types of microorganisms targeted, surface characteristics, and product toxicity. Antimicrobial characteristics, toxicity, and effectiveness of some common disinfectants are summarized below. Chlorine-releasing products such as bleach or hypochlorite are widely used and are effective against bacteria, fungi, viruses, and some spores. However, they are corrosive to some surfaces, are affected by organic matter, and cause skin and respiratory irritation. Peracetic acid, another commonly used disinfectant, is effective against a wide range of microbes including spores but can corrode metals. Accelerated hydrogen peroxide is effective against bacteria, fungi, viruses, and spores, does not affect surfaces, and is not affected by organic matter. QACs are effective against a wide range of gram-positive bacteria with persistent biocidal effect, but ineffective against spores and non-enveloped viruses, are affected by water hardness, and some QACs are associated with allergic asthma and skin sensitization. Alcohols are broad-spectrum disinfectants but cannot be used as a cleaner and are ineffective against spores. Phenolics are the oldest disinfectants but also have strong adverse health effects, their efficacy is impacted by organic material, and they are ineffective against spores. Finally, aldehydes have a wide range of antimicrobial activity but can cause sensitization (Stewart and Smith 2017; Leas et al. 2015; Rutala et al. 2008). A panel of experts emphasized the importance of proper implementation of cleaning and disinfecting strategy at the local level over the choice of disinfectant used (Leas et al. 2015). Key factors affecting proper implementation include inappropriate preparation (e.g., dilution), or application (e.g., contact time of disinfectants or failure to decontaminate reusable items), interruption of cleaning by patient and other healthcare staff, room turnaround time, inadequate training of housekeepers, lack of cleaning checklists or procedures, hospital safety culture, and low priority given to hiring cleaning staff and purchasing cleaning supplies (Leas et al. 2015).

Ingredients of Cleaning and Disinfecting Products for Environmental Surfaces

Several studies have identified ingredients of cleaning and disinfecting products through headspace analysis of cleaning products or review of safety data sheets (SDSs). Bleach products were found to emit a variety of aliphatic and aromatic halogenated hydrocarbons in the headspace, e.g., chloroform, carbon tetrachloride, and chlorobenzene, of which 13 were quantified (Odabasi 2008). When these products were diluted and applied to various types of surface cleaning tasks such as bathroom, kitchen, or floor, 16 emitted volatile organic compounds (VOCs) were quantified. More varied VOCs may be emitted when bleach products react with organic material in soiled surfaces that are being cleaned. Consumer cleaning products and air fresheners were found to emit a range of terpene hydrocarbons (e.g., α -limonene), terpene alcohols (e.g., 1-terpineol), glycol ethers (e.g., 2-butoxyethanol), and a variety of other VOCs (e.g., eucalyptol, benzyl acetate, and linalool); 2-butoxyethanol was present in most products (Singer et al. 2006). Emissions from the use of these products for various applications to clean and disinfect hard surfaces generated peak concentrations of these VOCs that could

reach mg/m³ level concentrations. Headspace analysis of 37 commonly used consumer spray products identified 156 unique VOCs many of which are classified as hazardous air pollutants (Steinemann 2015). The most common ingredients were terpenes used as fragrances; a vast majority (97%) of the ingredients were not disclosed in the SDS. The study found little difference in hazardous air pollutants emitted from the various labeling of these products such as “green” or “fragrance-free” products, except for the fragrance-free products which did not contain terpenes. Whereas these studies are of consumer products and not professional hospital cleaners, many of the products used in hospitals are formulated similarly and will likely result in similar emission profiles. A survey of 27 hospitals was conducted in Germany to quantify the consumption of 11 classes of biocides for disinfection and human hygiene including alcohols (e.g., benzyl alcohol), aldehyde-releasing agents (e.g., ethylenedioxy dimethanol), aldehydes (e.g., glutaraldehyde), alkyamines (e.g., aminoalkylglycine), glycol derivatives (e.g., propylene glycol), guanidines and pyridines (e.g., chlorhexidine), iodine-releasing compounds (e.g., povidone-iodine), peroxy-compounds (e.g., hydrogen peroxide), phenols (e.g., chlorocresol), QACs (e.g., benzalkonium chloride), and other compounds (e.g., acetic acid) (Tluczkiewicz et al. 2010). Emission estimates were compiled on mass-per-bed-per-day and mass-per-nurse-per-day for hand and skin disinfection, surface disinfection, and instrument disinfection for the 11 chemical classes which can be used to estimate hospital exposures.

A review of the SDSs of 105 common professional cleaning products identified over 132 different chemical ingredients with an average of 3.5 chemicals per product. The most common chemicals found in products were fragrances, glycol ethers, surfactants, solvents, and, to a lesser extent, phosphates, salts, detergents, pH stabilizers, acids, and bases. Over 75% of the ingredients were classified as irritants (Gerster et al. 2014). These products were classified into ten categories of cleaning application: floor, general purpose, carpet, scale removing, bathroom, glass, kitchen, surface, disinfection, and polishing products. Glycol ethers were present in most products for most cleaning applications; ethanolamines, which are surfactants known for their sensitizing properties, were present in kitchen, floor, and general-purpose cleaning products. Another study reviewed 185 SDSs of products used by hospital workers and grouped the product ingredients into 27 chemical classes based on their common physical (e.g., phases) and chemical properties (e.g., functional groups): acid, acrylate, alcohol, aldehyde, alkane, amide, amine, ammonia, aromatic, base, carboxylic acid, enzyme, ester, ether, fragrance, glycol ether, halogenated compound, metal, metal salt, metalloid, oxidizer, phenolic, QACs, salt, surfactant, terpene, and others (Saito et al. 2015). The chemical composition of products used varied by occupations, with housekeepers using products with the most complex and widest number of ingredients, followed by instrument disinfection occupations, laboratory occupations, and patient care occupations. Many of these frequently present ingredients are classified as asthmagens by the Association of Occupational and Environmental Clinics (AOEC), which also includes many sensitizers (Quirce and Barranco 2010; AOEC 2012). A study of chemicals in 101 commonly used spray products found most products contained organic solvents (ethanol, isopropyl alcohol [IPA]), fragrances, disinfectants, nonionic surfactants, acids, bases, and salts

(Clausen et al. 2020). Ingredients of concern included ammonia, hypochlorite, QACs, glycols, and glycol ethers.

A review of 299 SDSs of cleaning products used in age care facilities identified 212 chemical ingredients, of which 41 were classified as carcinogenic, mutagenic, toxic to reproductive or other organs, endocrine disrupters, skin sensitizers, and respiratory sensitizers (Bonnet et al. 2018). The ingredients ranged from volatile to semi-volatile and nonvolatile organic compounds used as solvents, disinfectants, detergent, surfactants, scenting agents, and chelating agents. The semi-volatile and nonvolatile ingredients may pose dermal as well as respiratory hazards when these components are aerosolized through the use of spray products, or by adsorbing onto particles on surfaces that are disturbed and particles are re-entrained into the air stream (LeBouf et al. 2017). Although the list of chemical ingredients generated from review of the SDSs is helpful, SDSs do not constitute a complete list of product ingredients because many chemical components are indicated as proprietary and not listed (e.g., fragrances and surfactants) while many others whose concentrations are below the target value for reporting on SDSs are excluded (Steinemann 2015).

Exposure to Cleaning and Disinfecting Chemicals

Exposure to chemicals in cleaning products in hospitals has not been well studied because of the chemical complexity of cleaning products and the difficulty in conducting personal exposure monitoring for multiple chemicals in this work environment. As such, current knowledge of the types of tasks performed, products used, and exposures among occupations is incomplete. The few quantitative exposure assessment studies done in hospitals that report exposure measurements related to cleaning and disinfecting chemicals are summarized in Table 2. The measured chemicals are summarized by ranges of means, geometric means, or measurements for specific chemicals and various occupations, locations, tasks, or activities in each study. These limited data show complex chemical exposure profiles, which are highly variable within and between occupation/unit. These primary ingredients may also react with one another, such as bleach and acid to release chlorine gas or QACs with ozone in the air to generate secondary oxidation reaction products such as carbonyls, carboxylic acids, nitrates, and possibly amines that may not be monitored and can pose additional health hazards.

Modeling factors affecting exposure to cleaning and disinfecting chemicals are essential to explain sources of exposure variability but are also rare in studies conducted in healthcare settings. One study identified product type, task, room volume and ventilation, and product concentration as significant predictors of 2-butoxyethanol exposures in a quasi-experimental study (Bello et al. 2013). A recent study of several healthcare occupations evaluated the determinants of exposure to TVOCs, ethanol, 2-propanol, acetone, α -limonene, α -pinene, and chloroform, focusing on tasks, product application, amount of product, background activities, product ingredients, and local exhaust ventilation (LEV) as predictors (Su et al. 2018). A study of factors affecting real-time TVOC exposure in hospitals identified use of sprays to be associated with increasing exposures, while presence of LEV, large room volume, and automatic sterilizer use were all associated with

Table 2 Quantitative exposures to cleaning and disinfecting chemicals and their ingredients in hospital settings

Occupation/Unit/Tasks	Chemical	Exposure summary (ppb)*
LeBouf et al. 2017: Hospitals: housekeeper/all areas/ regular cleaning duties	Benzethonium chloride	Mean: 0.46 ^b
	Benzylidimethyldodecylammonium chloride	Mean: 0.011–3.5 ^b Range: 6.9–21.8 ^c
	Benzylidimethylhexadecylammonium chloride	Mean: 0.006–0.96 ^b Range: 10.5–28.8 ^c
	Benzylidimethyltetradecylammonium chloride	Mean: 0.028–1.5 ^b Range: 23.8–76.6 ^c
Hawley et al. 2017: Hospital: cleaning staff/multiple locations/regular cleaning duties	Acetic acid	Mean: 122 GM: 13–145 P95: 39–307
	Hydrogen peroxide	Mean: 25 GM: 10–167 P95: 19–511
	Hydrogen peroxide and peracetic acid	Mean: 29 GM: 12–191 P95: 31–522
	Hydrogen peroxide, peracetic acid, and acetic acid	Mean: 151 GM: 26–335 P95: 70–701
	Peracetic acid	Mean: 5 GM: 2–30 P95: 7–48
Teschke et al. 2002: All facilities: radiographers/X-ray film processing facilities/film processing	Acetic acid	GM: 0.06 ^d Mean: 0.088 ^d Range: 0.031–0.8 ^d
	Glutaraldehyde	GM: 0.0008 ^d Mean: 0.0009 ^d Range: 0.0006–0.0023 ^d
	Sulfur dioxide	GM: 0.04 ^d Mean: 0.078 ^d Range: 0.02–0.41 ^d
Hospitals: radiographers/X-ray film processing facilities/film processing	Acetic acid	GM: 0.048 ^d Mean: 0.053 ^d Range: 0.031–0.12 ^d
	Glutaraldehyde	GM: 0.0007 ^d Mean: 0.0007 ^d Range: 0.0006–0.002 ^d
	Sulfur dioxide	GM: 0.027 ^d Mean: 0.041 ^d Range: 0.024–0.32 ^d
Clinical facilities: radiographers/X-ray film	Acetic acid	GM: 0.089 ^d Mean: 0.12 ^d Range: 0.042–0.8 ^d

(continued)

Table 2 (continued)

Occupation/Unit/Tasks	Chemical	Exposure summary (ppb)*
processing facilities/film processing	Glutaraldehyde	GM: 0.0009 ^d Mean: 0.0011 ^d Range: 0.0008–0.0023 ^d
	Sulfur dioxide	GM: 0.08 ^d Mean: 0.11 ^d Range: 0.02–0.41 ^d
All facilities no general room ventilation: radiographers/X-ray film processing facilities/film processing	Acetic acid	GM: 0.035 ^d Mean: 0.071 ^d
	Glutaraldehyde	GM: 0.0008 ^d Mean: 0.0009 ^d
	Sulfur dioxide	GM: 0.059 ^d Mean: 0.063 ^d
All facilities general room ventilation; room air volumes/hour <10: radiographers/X-ray film processing facilities/film processing	Acetic acid	GM: 0.048 ^d Mean: 0.086 ^d
	Glutaraldehyde	GM: 0.0008 ^d Mean: 0.0008 ^d
	Sulfur dioxide	GM: 0.062 ^d Mean: 0.081 ^d
All facilities general room ventilation; room air volumes/hour ≥10: radiographers/X-ray film processing facilities/film processing	Acetic acid	GM: 0.035 ^d Mean: 0.069 ^d
	Glutaraldehyde	GM: 0.0007 ^d Mean: 0.0008 ^d
	Sulfur dioxide	GM: 0.059 ^d Mean: 0.051 ^d
All facilities no local exhaust ventilation: radiographers/X-ray film processing facilities/film processing	Acetic acid	GM: 0.061 ^d Mean: 0.01 ^d
	Glutaraldehyde	GM: 0.0009 ^d Mean: 0.001 ^d
	Sulfur dioxide	GM: 0.086 ^d Mean: 0.094 ^d
All facilities local exhaust ventilation; volumetric flow rate < 20 cfm: radiographers/X-ray film processing facilities/film processing	Acetic acid	GM: 0.038 ^d Mean: 0.079 ^d
	Glutaraldehyde	GM: 0.0007 ^d Mean: 0.0007 ^d
	Sulfur dioxide	GM: 0.05 ^d Mean: 0.051 ^d
All facilities local exhaust ventilation; volumetric flow rate ≥ 20 cfm: radiographers/X-ray film processing facilities/film processing	Acetic acid	GM: 0.033 ^d Mean: 0.053 ^d
	Glutaraldehyde	GM: 0.0007 ^d Mean: 0.0008 ^d
	Sulfur dioxide	GM: 0.049 ^d Mean: 0.066 ^d

(continued)

Table 2 (continued)

Occupation/Unit/Tasks	Chemical	Exposure summary (ppb)*
Bessonneau et al. 2013: Hospital: all sties/disinfection	1,1,1-Trichloroethane	Mean: 0.6 ^b Range: 0.1–6.7 ^b
	1,2,4-Trimethylbenzene	Mean: 0.5 ^b Range: 0.1–1.1 ^b
	1,4-Dichlorobenzene	Mean: 0.2 ^b Range: 0.1–1.1 ^b
	2-Butanone	Mean: 8.7 ^b Range: 0.1–174 ^b
	2-Ethoxyethanol	Mean: 0.8 ^b Range: 0.6–1.6 ^b
	2-Ethyl-1-hexanol	Mean: 3.1 ^b Range: 0.1–8.8 ^b
	2-Phenoxyethanol	Mean: 1.4 ^b Range: 0.1–11.6 ^b
	Acetaldehyde	Mean: 5.7 ^b Range: 1–16.2 ^b
	Acetone	Mean: 22.6 ^b Range: 0.1–82.3 ^b
	Acrolein	Mean: 4.7 ^b Range: 0.1–18.1 ^b
	Benzene	Mean: 1.6 ^b Range: 0.5–5.1 ^b
	Chloroform	Mean: 6.3 ^b Range: 0.2–23.8 ^b
	Cyclohexane	Mean: 0.9 ^b Range: 0.6–2.6 ^b
	Cyclohexanone	Mean: 3.3 ^b Range: 0.1–20.1 ^b
	Ethanol	Mean: 928 ^b Range: 0.3–3956 ^b
	Ether	Mean: 75.6 ^b Range: 0.6–678 ^b
	Ethylbenzene	Mean: 1.8 ^b Range: 0.1–6.6 ^b
	Formaldehyde	Mean: 5.8 ^b Range: 1.5–14.8 ^b
	Hexaldehyde	Mean: 1.9 ^b Range: 1–4.2 ^b
	Isopropanol	Mean: 47.9 ^b Range: 0.7–174 ^b
	Isovaleraldehyde	Mean: 2.2 ^b Range: 1–5.9 ^b
	Limonene	Mean: 8.7 ^b Range: 2.9–113 ^b

(continued)

Table 2 (continued)

Occupation/Unit/Tasks	Chemical	Exposure summary (ppb) [*]
Gerster et al. 2014: Private or state-owned cleaning companies: cleaners/emptied rooms and corridors, apartments, construction sites, public spaces, and patient rooms/intensive floor cleaning, general surface cleaning	<i>m,p</i> -Xylene	Mean: 3.6 ^b Range: 1–10.6 ^b
	Naphthalene	Mean: 0.3 ^b Range: 0.2–0.6 ^b
	<i>n</i> -Hexane	Mean: 1.9 ^b Range: 0.6–39 ^b
	<i>n</i> -Heptane	Mean: 0.9 ^b Range: 0.6–6.1 ^b
	<i>n</i> -Undecane	Mean: 3.8 ^b Range: 2.9–5.5 ^b
	<i>o</i> -Xylene	Mean: 1.6 ^b Range: 0.5–6.2 ^b
	Phenol	Mean: 2.3 ^b Range: 0.2–5.9 ^b
	Propan-1-ol	Mean: 5.9 ^b Range: 0.5–24.9 ^b
	Styrene	Mean: 0.6 ^b Range: 0.1–2.3 ^b
	Toluene	Mean: 4.7 ^b Range: 0.5–16.5 ^b
	Trichloroethylene	Mean: 0.3 ^b Range: 0.1–1.7 ^b
Bello et al. 2013: Hospitals and university: researcher/bathrooms/bathroom cleaning	Benzyl alcohol	GM: 2.561 ^d
	Butoxypropanol	GM: 0.005–0.513 ^d
	Ethylene glycol mono- <i>n</i> -butyl ether	GM: 54.532 ^d
	Diethylene glycol monoethyl ether	GM: 0.019–0.083 ^d
	Diethylene glycol mono- <i>n</i> -butyl ether	GM: 0.031–1.201 ^d
	Monoethanolamine	GM: 0.014–0.055 ^d
	Phenoxyethanol	GM: 0.026 ^d
Wieslander et al. 2010: Hospital: cleaners/cleaning department/during polish removal, application, and after application (2, 7, and 17 days)	2-Butoxyethanol	Mean: 0.1–8.7 ^a
	Diethylene glycol monobutyl ether	Mean: <5–71 ^b
	Diethylene glycol monoethyl ether	Mean: <5–13650 ^b
	Dipropylene glycol monomethyl ether	Mean: <5–7000 ^b
	Ethylene glycol monobutyl ether	Mean: <5–666 ^b
	Ethylene glycol monoethyl ether	Mean: <5–103 ^b
LeBouf et al. 2014: US Veterans Affairs: nursing staff, laboratory staff, respiratory therapists,	Ethylene glycol phenyl ether	Mean: <5–63 ^b
	2-Propanol	Personal: GM: 70.4–4566 ^b Area: GM: 66.8–9014 ^b

(continued)

Table 2 (continued)

Occupation/Unit/Tasks	Chemical	Exposure summary (ppb)*
pharmacists, housekeepers, dental staff/general cleaning, patient cleaning, hand cleaning, sterilizing, and high-level disinfection	α -Pinene	Personal: GM: <0.28–0.43 ^b Area: GM: <0.28–0.81 ^b
	Acetone	Personal: GM: 43.9–160 ^b Area: GM: 23.8–75.1 ^b
	Benzene	Personal: GM: <0.083–4.2 ^b Area: GM: 0.42–1.1 ^b
	Chloroform	Personal: GM: <0.14–2.1 ^b Area: GM: 0.38–2.5 ^b
	β -limonene	Personal: GM: <0.53–232.6 Area: GM: 2.1–67.8
	Ethanol	Personal: GM: 0.41–4899 ^b Area: GM: <0.13–4591 ^b
	Ethylbenzene	Personal: GM: <0.16–4.7 ^b Area: GM: <0.16–4.1 ^b
	Hexane	Personal: GM: <0.11–3.9 ^b Area: GM: 0.12–1.7 ^b
	<i>m,p</i> -Xylene	Personal: GM: <0.18–28.6 ^b Area: GM: 0.39–14.1 ^b
	Methylene chloride	Personal: GM: <0.36–4.5 ^b Area: GM: <0.36–0.72 ^b
<i>o</i> -Xylene	Methyl methacrylate	Personal: GM: <0.17–2.1 ^b Area: GM: <0.17–36.5 ^b
	<i>o</i> -Xylene	Personal: GM: <0.19–7.0 ^b Area: GM: <0.19–3.9 ^b

(continued)

Table 2 (continued)

Occupation/Unit/Tasks	Chemical	Exposure summary (ppb)*
	Toluene	Personal: GM: 5.1–162.0 ^b Area: GM: 2.0–17.3 ^b
Su et al. 2018: US Veterans Affairs: nursing staff, laboratory staff, respiratory therapists, pharmacists, housekeepers, dental staff/general cleaning, patient cleaning, hand cleaning, sterilizing, and high-level disinfection	2-Propanol	Personal: GM: 20.1–1310 Area: GM: 20.2–3667
	α-Pinene	Personal: GM: 0.04–0.16 Area: GM: 0.14–0.19
	Acetone	Personal: GM: 18.5–70.6 Area: GM: 10.0–32.5
	Chloroform	Personal: GM: 0.09–0.57 Area: GM: 0.04–0.22
	δ-limonene	Personal: GM: 0.12–4.23 Area: GM: 0.37–12.2
	Ethanol	Personal: GM: 1.54–2594 Area: GM: 2.31–2241
Adisesh et al. 2011: Hospital: sterile services department/ technician/clean surgical instruments	Subtilisin	Inhalation: Mean: <10–10.22 ^f Surfaces: Mean: 2.98–199403 ^e
Jachuck et al. 1989: Hospital: endoscopy unit/nurse/ disinfection	Glutaraldehyde	Mean: 5–20 ^a
Koda et al. 1999: Hospital: pathology division/ sterilization and dissection	Ethylene oxide	Mean: 0.3–300 ^a
	Formaldehyde	Mean: 0.3–8.6 ^a ; Range: 0.2–5 ^a
	Glutaraldehyde	Mean: 0.2–2.6 ^a Range: 0.1–0.8 ^a
Leinster et al. 1993: Hospital: endoscopy unit/cleaning and filling and emptying tanks	Glutaraldehyde	Mean: 0.005–0.17 ^d ; Range: 0.002–0.23 ^d

(continued)

Table 2 (continued)

Occupation/Unit/Tasks	Chemical	Exposure summary (ppb)*
Norback 1988: hospital/sterilization of instruments	Glutaraldehyde	Mean: <0.01–0.57 ^d
Pisaniello et al. 1997: Hospital: operating theaters, endoscopy areas/nurse/ disinfection	Glutaraldehyde	GM: 0.008–0.093 ^a
Wellons et al. 1998: Hospital: cysto room, ultrasound, physical therapy/nurse/ mixing base solution, and activator of glutaraldehyde- based sterilant	Glutaraldehyde	Mean: 0.004–0.128 ^a
Hori et al. 2002: Hospital: sterilizer operators and other workers/hospital A, B, C, D, and E/sterilization	Ethylene oxide	Mean: 0.033–200 ^a ; Range: 0.035–5.7 ^a
Puskar and Hecker 1989: Hospital: location 1, 2, 3, and 4/sterilization	Ethylene oxide	Mean: <0.02–3.2 ^a
Yoshida et al. 1989: Hospital: sterilizer operator/opening door to sterilizer and unloading	Ethylene oxide	Range: 1–23.5 ^a

*All units in ppb except where noted otherwise; a = parts per million; b = $\mu\text{g}/\text{m}^3$; c = $\mu\text{g}/100\text{cm}^2$; d = mg/m^3 ; e = $\text{ng}/100\text{ cm}^2$; f = ng/m^3 ; Nursing staff = nursing assistant, licensed practical nurse, registered nurse; Laboratory staff = medical equipment preparer, surgical technologists, endoscopy technicians, clinical laboratory technicians, medical appliance technicians; Dental staff = dental assistants, dental laboratory technician; Housekeepers = floor strippers and waxers; All sites = patient room, nursing care, post-anesthesia care unit, endoscope disinfection unit, parasitology laboratory, reception hall; GM = Geometric Mean; P95 = 95th percentile

decreasing exposures (Virji et al. 2019). These studies of exposure determinants identify factors associated with increasing exposures to target exposure control strategies and factors associated with decreasing exposures to encourage implementation of control measures.

Exposure to cleaning and disinfecting products occurs during routine product use, as well as during preparation such as mixing or diluting products, inappropriate mixing or dilution, spills, cleanup of spills and contaminants, and as a bystander to cleaning and disinfecting activities. Approaches to reduce exposures include avoiding use of spray products, ordering ready-to-use cleaners, using automated

mixing stations, removing soils with water and detergents and only using disinfectants where needed, adequately ventilating various spaces where or when disinfectants are used, spacing out cleaning and disinfection across multiple shifts where appropriate, and, lastly, appropriate use of personal protective equipment (PPE) (Gorman et al. 2013). Whereas there is a trend toward the use of “green cleaning products,” these products do not necessarily contain less hazardous ingredients, and the criteria for their claims vary widely by manufacturers (Saito et al. 2015). The eco-friendly labels are often based on minimizing environmental impact and not necessarily the prevention of respiratory disease, and not well regulated in the USA or the European Union.

Skin Exposure to Disinfectants and Antiseptics

Healthcare workers may be exposed to cleaning chemicals through direct application of hand sanitizers and disinfectants to their skin, unprotected application of skin antiseptics on patients, or application of surface cleaning products. Transmission of pathogens is related to contaminated hands of healthcare providers as well as contaminated surfaces, equipment, and patient care items. Hand hygiene is an integral component of infection control and compliance with hand hygiene recommendations being essential for HAI prevention. Thus, hospitals are constantly promoting hand hygiene programs to achieve higher compliance with hand hygiene guidelines (Boyce and Pittet 2002). A variety of skin antiseptics are used in hospitals (Table 1). Use of alcohol-based hand sanitizers is common practice among most hospital occupation but may result in deterioration of the skin barrier (dryness, cracking, etc.). Chlorhexidine (chlorhexidine gluconate) solution is another extensively used antiseptic for preoperative skin preparation, hand hygiene, medical instrument disinfection, and mouth rinse (Barnes et al. 2019). Other antiseptics used in hospitals include hexachlorophene (used in handwash and surgical scrub), iodophores (e.g., povidone-iodine, with widespread use throughout the world), octenidine (used on chronic wounds and burns to prevent bacterial infections), polyhexanide (used for pressure wounds), hexamidine diisethionate (used widely in some countries), QACs (used for burns, ointments, and mouth and hand washes), chloroxylenol (used in personal care products), triclosan (used mostly in personal care products), and silver-based wound dressing (Barnes et al. 2019). Workers may also be exposed to cleaning and disinfecting chemicals when cleaning surfaces without appropriate skin protection. One study reported that most workers engaged in cleaning and disinfecting occupations wore gloves during their cleaning tasks, while a lower proportion of workers in noncleaning and disinfecting occupations wore gloves during their cleaning tasks. Glove use itself may lead to occlusion of skin and possibly dermatitis if moisture builds up in the glove or allergic reactions to glove materials such as latex and other natural proteins occur (Jungbauer et al. 2005). Quantitative exposure measurements for use of these antiseptic products are not available.

Exposure to High-Level Disinfectants and Sterilizing Chemicals

High-level disinfectants and sterilizers such as glutaraldehyde, OPA, hydrogen peroxide and peracetic acid mixture, ethylene oxide, and hydrogen peroxide

plasma gas are used throughout hospitals to disinfect and sterilize critical and semi-critical medical and dental devices and instruments. Whereas sterilization is performed in central supply and is time consuming, instrument disinfection is performed throughout the hospital wherever there is a need for quick turnaround of disinfected instruments (Gorman et al. 2013). Several occupations in healthcare can be exposed to high-level disinfectants including central supply workers, surgical technologists and assistants, X-ray technicians, pathology/histology laboratory technicians, dental assistants in clinics, nurses and technologists in endoscopy and other surgical/procedural units, and staff in dialysis and intensive care units (González Jara et al. 2013). Several studies have quantified glutaraldehyde exposure in a variety of units such as radiology, endoscopy, and central supply during various jobs, procedures, and tasks, summarized in Table 2. These exposures vary within the activity monitored as well as across the activities with measurements ranging from very low levels to above exposure limit. OPA was introduced as a safer alternative to glutaraldehyde, however exposure measurements are lacking but cases of asthma and dermatitis have been reported in endoscopy nurses (Henn et al. 2015; Mazurek and Weissman 2016). A mixture of peracetic acid and hydrogen peroxide is widely used as a high-level disinfectant for reprocessing endoscopes and other medical instruments but resulting exposure and health data are lacking. A less concentrated version of this product, also containing acetic acid, is used as an intermediate-level disinfectant for cleaning noncritical surfaces and instruments and is associated with higher prevalence of asthma as well as upper and lower respiratory symptoms (Hawley et al. 2017). Exposures to this product are summarized in Table 2, which shows variable exposures by unit and activity.

Guidelines exist on the use of LEV and enclosures, as well as other safe use and handling of high-level disinfectants especially glutaraldehyde in multiple settings including endoscopy suites (NIOSH 2017a). In a 2011 NIOSH national survey of nurses, technologists, dental professionals, and respiratory therapists who completed a module on high-level disinfection, responders reported using glutaraldehyde most frequently followed by peracetic acid, OPA, hydrogen peroxide, and mixtures of peracetic acid and hydrogen peroxide (Henn et al. 2015). A large proportion of the respondents reported not receiving training or not having standard procedures for safe handling of high-level disinfectants or had received training over a year prior to the survey. Less than 50% of responders reported using automated systems and less than 25% reported having a LEV system while manually disinfecting instruments. Other activities that increase exposure include manually pouring disinfectant into automated systems, using manual immersion trays for disinfection, and manually draining disinfectant from automated processing systems. While PPE such as gloves were frequently worn, other gear such as protective gowns or eye protection were not. Workers also reported spills occurring in the last 7 days that were not always cleaned up. In this large national survey of healthcare professionals engaged in high-level instrument disinfection, safety practices and procedures were lacking despite existing guidelines on safe handling of these chemicals.

Ethylene oxide is widely used for sterilizing medical instrument in hospitals, with exposure mostly occurring in central supply workers and to a lesser extent in end users who may come in contact with improperly aerated or packaged equipment (Weaver 1997). In ethylene oxide gas sterilization, items are packaged before sterilization and the gas diffuses through the packaging material during sterilization (Hori et al. 2002). After sterilization, residual gas in the sterilization unit is removed and the packaged items are aerated in a ventilated area to let the gas diffuse out of the packaging. Lack of appropriate equipment or procedures to allow for adequate aeration time can result in high exposure to ethylene oxide (Hori et al. 2002). Several studies have quantified exposure to ethylene oxide in various hospital locations near the sterilizing unit or during certain tasks summarized in Table 2. The exposures are highly variable within and between locations/activities and range from very low levels to levels above the exposure limit. An important determinant of exposure is allowing adequate time to air out the unit after sterilization and before opening the unit door (Hori et al. 2002).

Health Effects Associated with Cleaning, Disinfecting, and Sterilizing Chemicals

Healthcare workers are at an increased risk of asthma, rhinitis, respiratory symptoms, and dermatitis, related to cleaning and disinfecting products. Work-related asthma (WRA) is common among healthcare workers and places a substantial health and economic burden on society but is preventable. WRA includes occupational asthma (OA) that is caused by work, and work-exacerbated asthma (WEA) that is a worsening of existing asthma due to workplace conditions. Based on the 2004–2011 National Health Interview Survey, the prevalence of current and lifetime asthma in healthcare occupations were 9.5% and 13.7%, respectively, for nursing and residential care facilities, 9.3% and 14.7% for social assistance, 8.1% and 12.1% for hospitals, and 7.7% and 12.7% for ambulatory care (NIOSH 2017b). Among all current occupational categories, the category of nursing, psychiatric, and home health aides had among the highest prevalence of lifetime asthma at 14.6% (NIOSH 2017b). Data from the 2013 adult Behavioral Risk Factor Surveillance System (BRFSS) report the highest prevalence of current asthma for the healthcare and social assistance industry (10.6%) and healthcare support occupation (12.4%) among all industries and occupations in 21 reporting states (Dodd and Mazurek 2016). The 2006–2007 Asthma Call-Back Survey, part of BRFSS, further reports that 47.5% of ever-employed adults with asthma potentially have WRA, which is a preventable disease (Knoeller et al. 2011). Among the putative agents, cleaning products were the third most commonly reported agent (15.3%) associated with WRA in the four states reporting asthma cases to the NIOSH Sentinel Event Notification System for Occupational Risks (SENSOR), behind miscellaneous chemicals and materials (22.4%) and mineral and inorganic dusts (16.3%) (NIOSH 2017b).

Epidemiologic studies continue to report increased risk of asthma, rhinitis, respiratory symptoms, and dermatitis in healthcare occupations that perform cleaning or disinfecting tasks (Folletti et al. 2014; NIOSH 2017b; Arif and Delclos

2012; Garrido et al. 2021; Su et al. 2019). Studies have reported associations of asthma symptoms with most major classes of cleaning and disinfecting products including chlorine-based compounds (Arif and Delclos 2012), ammonia (Arif and Delclos 2012), QACs (Gonzalez et al. 2014), peroxygen compounds (Hawley et al. 2017), enzymatic cleaners (Adisesh et al. 2011), detergents (Arif and Delclos 2012), high-level disinfectants and sterilizers (Arif and Delclos 2012), chemicals used for floor stripping and waxing (Wieslander and Norbäck 2010), groups/classes of chemicals such as VOCs, construction dust, and poor indoor air quality (Arif and Delclos 2012; Wieslander and Norbäck 2010), and their functional or aesthetic additives (DeLeo et al. 2018) such as surfactants, preservatives, and fragrances, e.g., ethanolamines and terpenes. Relevant tasks include cleaning instruments or surfaces, patient care, using spray products, washing instruments manually, using aerosol products, cleaning operating rooms, cleaning sanitary rooms, preparing disinfectants, filling devices with cleaning products, waxing floors, spot-cleaning floors, stripping wax floors, and cleaning tiles (Garrido et al. 2021). While the mechanism of asthma related to cleaning and disinfecting is not clear, it is thought to include both irritant- and sensitizer-induced asthma (Tarlo et al. 2017). Many cleaning products are complex mixtures of chemicals that contain both irritants (e.g., chlorinated compounds) and sensitizers (e.g., QACs) (Quirce and Barranco 2010; AOEC 2012; Nazaroff and Weschler 2004).

The outbreaks of communicable diseases beginning in 2020 have resulted in the widespread use of cleaning and disinfecting products to disinfect homes, public spaces, and workplaces. Whereas the effects of increased use of cleaning and disinfecting products on hospital workers has not been evaluated, a study of the general population demonstrated increased use of such products at home is associated with an increase in the risk of uncontrolled asthma (Eldeirawi et al. 2021). The effect on hospital workers is likely to be similar.

Cleaning and disinfecting activities in hospitals are critical for preventing HAIs and transmissions of other respiratory diseases; thus, the need for and efficacy of preventive measures for asthma need to be clearly demonstrated. Although the risk factors for respiratory symptoms associated with cleaning in healthcare and other settings have been identified (Folletti et al. 2014), quantitative exposure metrics and their direct impact on asthma and respiratory symptoms through exposure-response relationships remain unclear. Knowledge of exposure-response relationships is critical for the design of effective preventive measures. To date, only one epidemiologic study has demonstrated longitudinal declines in lung function associated with the use of cleaning products, but quantitative exposure-response relationships with specific products or chemicals were not assessed (Svanes et al. 2018). Additionally, most of the epidemiologic studies of the health effects of exposure to cleaning and disinfection products have investigated a single product or ingredient at a time, however, workers are exposed to a complex mixture of chemicals which may have synergistic effects. The health effects observed are likely due to certain mixtures of these components and not to all or any single component. A study of hospital workers performed hierarchical cluster analysis of exposures and health and observed various combinations of product applications, like using alcohols, bleach,

high-level disinfectants, and enzymes to clean and disinfect instruments, and clean surfaces were identified as risk factors for different asthma symptom clusters, indicating that prevention efforts may require targeting multiple products or ingredients simultaneously (Su et al. 2019).

Glutaraldehyde has been classified as a skin and respiratory sensitizer and associated with dermatitis and asthma (Mazurek and Weissman 2016; Weaver 1997). OPA and the mixture of peracetic acid and hydrogen peroxide were introduced as alternatives to glutaraldehyde, but are also associated with irritant dermatitis and upper and lower airway symptoms (Rideout et al. 2005). Ethylene oxide is associated with central and peripheral nervous systems effects such as headache, vertigo, sleeplessness, dullness, and numbness (Yahata et al. 2001), a variety of respiratory effects such as irritation, upper and lower airway symptoms (Weaver 1997), and irritant dermatitis as well as reproductive effects (NIOSH 2017a). Ethylene oxide is also classified as a group 1 known human carcinogen by the International Agency for Research on Cancer (Weaver 1997).

Healthcare workers are reported to have the highest prevalence of dermatitis compared to workers in other industries, and healthcare providers had the third highest prevalence of dermatitis compared to other occupations (Luckhaupt et al. 2013); nurses in particular often report work-related rash and dermatitis that could be from direct irritant effects or via sensitization and have a high prevalence of work-related dermatitis (Luckhaupt et al. 2013). Use of antiseptics, such as iodoform, iodine tincture, and chlorhexidine, on skin is known to cause irritant and allergic reactions. In a study of nurses and midwives at one hospital, use of hand hygiene products containing chlorhexidine, a commonly used disinfectant in hand hygiene products, was associated with asthma, contact dermatitis, allergy to chlorhexidine, and self-reported dry skin, eczema, and dermatitis (Barnes et al. 2019). Increased risk of uncontrolled asthma has also been reported among nurses who use antiseptics on hands and arms suggesting a link between skin exposure and respiratory health (Dumas et al. 2018). Use of cleaning products, especially bleach products, among healthcare workers conducting disinfection tasks is associated with an increased risk of skin symptoms (Garrido et al. 2021). Aldehyde-based disinfectants such as glutaraldehyde and formaldehyde as well as QACs are associated with dermatitis and sensitization (Mazurek and Weissman 2016). Hand dermatitis is also a concern among healthcare workers due to “wet work” because they frequently perform wet cleaning tasks (i.e., activities involving wet hands or glove use), which is shown to vary by occupation and unit (Jungbauer et al. 2005).

Exposure to Other Hospital Products and Chemicals

In addition to cleaning and disinfection products, hospital workers are also directly or indirectly (as bystanders) exposed to a variety of other chemical substances used or found in different areas of a hospital such as formaldehyde in laboratory technicians, methyl methacrylates (MMA) and isocyanates in dental and orthopedics, aerosolized medications and other pharmaceuticals in respiratory therapy and

pharmacy, high-level disinfectants and biological enzymes in endoscopy and central supply, animal allergens in animal laboratory workers, allergenic proteins from latex gloves, as well as emissions from building materials and products, and mold contamination of building surfaces which are reviewed and summarized in subsequent sections (Mazurek and Weissman 2016).

Exposures to Chemical Hazards in Operating Rooms (OR)/Surgical Units and Orthopedics

In 2015 an estimated 36 million surgeries were performed in the USA and 266 million worldwide under general anesthesia (Varughese and Ahmed 2021). The main chemical hazards of concern during surgery in OR include waste anesthetic gases, surgical smoke, and cleaning and disinfecting chemicals (Table 3). A study of VOCs measured in the air in OR during surgeries, and in breath samples of workers before and after surgeries, reported elevated levels of certain VOCs in air and in breath samples after surgery (Cheng et al. 2019). Specifically, the study reported elevated

Table 3 Exposures in surgical rooms/OR, endoscopy, and procedure rooms

Product/Class and occupation/unit	Exposures
Anesthetic gases – during various procedures among surgeons, anesthesiologists, technicians, nurses, dental surgery in OR, and postsurgical recovery units	Nitrous oxide, nitric oxide, desflurane, enflurane, halothane, isoflurane, methoxyflurane, sevoflurane, and trichlorethylene
Surgical smoke – during cutting, laser, and electrosurgery	Particulates and bioaerosols, acetone, acetonitrile, acetylene, acrolein, acrylonitrile, alkyl benzene, alpha-methyl styrene, benzaldehyde, benzene, benzonitrile, butadiene, butanone, butene, 3-butenenitrile, carbon monoxide, chlorodifluoromethane, chloromethane, creosol, 1-decene, 1,3-dichlorobenzene, dichlorodifluoromethane, 2,3-dihydro indene, <i>n</i> -dodecane, ethane, ethene, ethylbenzene, ethylene, <i>m</i> -ethyltoluene, ethynyl benzene, formaldehyde, furfural, hexadecenoic acid, hydrogen cyanide, indole, isobutene, isopropylbenzne, methane, methanol, 3-methyl butenal, 6-methyl indole, 4-methyl phenol, 2-methyl propanol, methylene chloride, phenol, propane, propene, 2-propylene nitrile, pyridine, pyrrole, styrene, toluene, trichlorodifluoromethane, 1,2,4-trimethylbenzene, <i>n</i> -undecane, 1-undecene, (<i>m,p</i>)-xylene, and <i>o</i> -xylene
Casts	Isocyanates (methylene diphenyl diisocyanate) and acrylics
Acrylates – bone cement, orthopedic prosthesis implantation, tissue repair, and reconstructive surgery	Methyl methacrylate, polymethylmethacrylate, and cyanoacrylate

levels of sevoflurane, anesthetic gas that was measured across surgeries; methyl methacrylate, a component of bone cement after orthopedic surgery; and hexamethyldisiloxane, a marker of electrosurgery. In another study, upper respiratory symptoms and skin reactions among OR staff were associated with elevated levels of VOC exposure (Rautiainen et al. 2019).

In 2015, over 25 million US healthcare workers were potentially exposed to anesthetic gases that leaked out during procedures (Varughese and Ahmed 2021). Surgical personnel, including surgeons, anesthesiologists, nurses, technicians, dentists, and dental technicians, are potentially exposed to a variety of chemicals and gases during surgical procedures in multiple hospital units where surgeries and procedures are performed, such as operating and recovery rooms, labor and delivery rooms, dental surgery rooms, endoscopy suites, and during dermatological and many other procedures (NIOSH 2017a). Additionally, recovery room or post-anesthesia care unit (PACU) staff can be exposed to high levels of anesthetic gases (Norton et al. 2020), while technicians and cleaning staff can be exposed to these chemicals after the procedure during breakdown and cleanup tasks. Several anesthetic gases may be used, including nitrous oxide, diethyl ether, and halogenated or fluorinated anesthetic gases such as enflurane, desflurane, halothane, isoflurane, and sevoflurane (Boiano and Steege 2016). The halogenated anesthetic gases are used alone or in combination with nitrous oxide. Several studies show that exposure to anesthetic gases is associated with reproductive effects especially among female workers in operating rooms, neurobehavioral changes, hematologic, hepatic, immune, and renal effects, as well as various cancers and acute effects, such as headache, dizziness, lethargy, fatigue, memory problems, and upper airway irritation (Boiano and Steege 2016; Van Den Berg-Dijkmeijer et al. 2011).

Leakage of anesthetic gases from equipment, inappropriate equipment and practices, nonautomatic ventilation and scavenging system, and escape of gases from the patients' mouths in OR or recovery room are the main sources of emission into the room, with the latter contributing most to the anesthetist's and surgeon's breathing zone exposure (NIOSH 2017a). Emissions into the room can be minimized by ensuring joints are well connected and sealed, and an appropriately designed face mask, laryngeal mask airway, or tracheal tube is used to connect the patient to the anesthesia machine to minimize escape of gases (Boiano and Steege 2016); any remaining fugitive emissions can be controlled by ventilation and scavenging systems. Government agencies and professional organizations have developed guidelines to minimize worker exposures to anesthetic gases including training, having SDS, labeling, information on safety plans and exposure hazards, appropriate ventilation and scavenging systems, medical monitoring, and record keeping (NIOSH 2017a). Regular monitoring of waste gases enables early detection of leaks and ensures timely equipment maintenance. Exposure measurements for various anesthetic gases in the OR as well as PACU have shown variable concentration ranging from below detection to much higher exposures (Norton et al. 2020).

Surgical smoke generated by lasers, ultrasonic scalpels, power tools, and electro-surgical devices during electrosurgical procedures contains numerous organic chemicals such as benzene, hydrogen cyanide, polycyclic aromatic hydrocarbons

(PAHs), and formaldehyde and particulate matter in the respirable size range (Table 3) (Lester et al. 2012; Gorman et al. 2013). Electrosurgical tools are used for cutting, cauterizing, and burning tissue in a variety of procedures such as wart ablation, LASIK, and laparoscopic cholesteectomy performed in hospital ORs or other clinical settings (Gorman et al. 2013). The chemical composition of VOCs in the surgical smoke plume is complex and various studies have identified different mixtures of VOCs and PAHs present at highly variable concentrations (Limchantra et al. 2019; Benson et al. 2019). There are numerous factors that could affect the generation and levels of chemicals in the smoke plume such as surgery and tissue type, tools used, and controls present, which have not been evaluated making meaningful synthesis of exposure data quite difficult (Benson et al. 2019). Exposure to surgical smoke is associated with ocular and upper respiratory airway irritation, and some components have mutagenic potential (NIOSH 2017a). Surgical smoke can be effectively controlled by: (1) LEV, such as a portable smoke evacuator, which consists of a nozzle, hose, filter, or scrubber to remove contaminants, and a vacuum pump, and (2) general room ventilation, although this system is not sufficient to capture particles (Lee et al. 2018; NIOSH 2017a). Suctioning smoke at the source is the most efficient way to eliminate the hazard (Lester et al. 2012). A laboratory study demonstrated significant reduction in aerosol concentrations generated from electrosurgical devices through the combined use of filtration, suction, and irrigation (Schramm et al. 2021). In addition, recent advances in air cleaning technology can easily be integrated into existing controls equipment to reduce air contaminants in the OR; evaluation of such technologies suggest that the technology is effective in reducing exposures.

Methacrylates are present in surgical cements and adhesives used in orthopedics (Table 3). Surgeons mix the cement before applying and the use of mixing trays with vacuum, local suction during applying or surgical helmets can result in significant reduction in exposure (Gorman et al. 2013). Exposure to MMA is associated with asthma, dermatitis, irritation, respiratory symptoms, and acute neurological effects. Options to reduce exposure include using existing systems for mixing products connected to exhaust devices, installation of LEV, or working in negative pressure hoods (Darre et al. 1992). In one study, use of local suction and PPE during a cementation procedure reduced MMA concentration to less than detectable, however, exposures can vary depending on the type of procedure, the tool used to apply the cement, and the surface area of the exposed cement (Darre et al. 1992). Orthopedic surgeons and nurses have an increased risk of exposure to not only polymethylmethacrylate but also to methylene diphenyl diisocyanate when working with plaster or fiberglass casts (Lester et al. 2012; Suojalehto et al. 2011). Exposure to diisocyanates is associated with asthma and skin dermatitis and sensitization (Mazurek and Weissman 2016).

Exposure to Chemicals and Dust in Dental Clinics and Laboratories

Dental personnel, including dental assistants, hygienists, technicians, and dentists, perform a variety of tasks and are potentially exposed to a wide range of chemicals from multiple sources including cleaning and disinfecting products, anesthetic gases, adhesives, and various materials used in dental applications, e.g., dentures and

amalgams, gases, vapors, and dusts (Table 4), associated with adverse respiratory effects and allergic contact dermatitis (Gambhir et al. 2011). As in other patient care occupations, exposure to biological agents including bioaerosols is a constant hazard of concern in dental clinics and a great deal of attention is given to sterilizing or high-level disinfection of instruments, and cleaning and disinfecting surfaces after each patient (Leggat et al. 2007). Additionally, disinfection of hands is frequently done with alcohol-based hand sanitizers and/or QACs. In developed countries, dental personnel generally sterilize dental instruments using steam autoclaves instead of high-level disinfectants (Leggat et al. 2007).

Acrylates are commonly used by dental personnel for prostheses and tooth fillings. The handling of acrylate monomers and methyl methacrylate can cause adverse health effects from inhaling vapors and dusts, including irritation, respiratory hypersensitivity, asthma, and numbness in the fingers (Gambhir et al. 2011; Leggat et al. 2007; Hong et al. 2015; Nayeb zadeh and Dufresne 1998). In a Finnish study, methacrylate and natural rubber latex exposures were very low (Henriks-Eckerman et al. 2001) ranging from not detected to 0.01 mg/m^3 for methyl methacrylate and a median of $0.12\text{ arbitrary units/m}^3$ to a maximum of $1.1\text{ arbitrary units/m}^3$ for latex allergen in dust collected from air (Henriks-Eckerman et al. 2001). These same researchers also measured personal exposures to isobutylmethacrylate (infrequently detected to 0.12 mg/m^3), 2-hydroxymethylmethacrylate (maximum 0.033 mg/m^3), and triethyleneglycol dimethacrylate (maximum 0.015 mg/m^3). Several studies have quantified exposures of dental personnel to various acrylates,

Table 4 Exposures in dental occupations and units including dentists, dental assistants, hygienist, and laboratory technicians

Products/Class	Function	Exposures
Metals	Amalgams and composite resin fillings	Mercury, beryllium, zinc oxide, silver, and eugenol
Particles	Dust during grinding	Dust, silica, metals, and acrylates
Acrylic paste, cements and resins, polymers, and monomers	Bonding dental composites, prosthetics resin used to make dentures	Glass ionomers, methyl methacrylates, cyanoacrylate, ethylene glycol dimethacrylate, triethylene glycol dimethacrylate, bisphenol A diglycidyl methacrylate, 2-hydroxyethyl methacrylate, and polymethylmethacrylate
Solvents	Developing solutions, neutralizers, and preservatives in medical imaging	Acetic acid, diethyl glycol, glutaraldehyde, hydroquinone, potassium hydroxide, sulfur dioxide, ammonia, and formaldehyde
Anesthetic gases	Dental surgeries and procedures	Nitrous oxide, halothane, and lidocaine
Other exposures including cleaners and disinfectants, and natural rubber latex	Sterilizing, cleaning, and disinfecting	See previous tables for detailed ingredients and exposures

aldehydes, and VOCs during different procedures (Santarsiero et al. 2009; Hagberg et al. 2005). Others have found in laboratory studies that respirable composite dust emitted during grinding with a dental burr can release unpolymerized methacrylate, which could be available for inhalation exposure (Cokic et al. 2017). Other potential sources of exposure are the use of amalgam containing mercury or beryllium, nitrous oxide gas used for anesthesia, ethylene oxide used for sterilization, glutaraldehyde used for high-level disinfection, cleaning and disinfecting chemicals, and latex gloves (Gambhir et al. 2011; Leggat et al. 2007; OSHA 2002).

Dental laboratory technicians can be exposed to a variety of metals from working with precious and nonprecious alloys. Technicians cast and finish dental alloys creating potential exposures to metallic fumes and dusts, which when not well controlled can pose both inhalation and dermal hazards. Metals include both non-precious (cobalt, chromium, nickel, molybdenum, and beryllium) and precious (palladium, platinum, silver, and gold) metals (Nayeb zadeh and Dufresne 1998). Exposure to silica during finishing and polishing is also of concern. Kim et al. 2002 found a threefold increase in respiratory symptoms among dental technicians (76.5%) compared to controls (28.6%). Respiratory protection was not used and dental technicians performed cutting, grinding, and polishing tasks that generated dust close to their breathing zone (Kim et al. 2002). Neurological effects from methyl methacrylate and solvent exposure, pneumoconiosis and asthma from metal and porcelain dust exposure, allergic contact dermatitis from latex allergies and methyl methacrylate exposure, and IPF are some of the main health effects of concern.

Exposures to Chemicals in Other Hospital Occupations and Departments

Patient care occupations are exposed to chemicals in almost all departments in the hospital. In addition to surface cleaning and disinfecting products, patient care workers apply antiseptics to patients (e.g., chlorhexidine), use glues containing acrylates to apply bandages, and use various solvents to remove glue from the skin (Table 5). Exposure to mercury, mostly from thermometers and blood pressure machines, was previously of concern in nursing stations, but there is a trend away from using mercury-containing patient care items (Gorman et al. 2013). Exposure to mercury occurs during equipment repair and spills from breakage. Chronic exposure to mercury is associated with neurologic and neurobehavioral outcomes, while acute exposure is associated with bronchitis and pneumonitis (Weaver 1997).

Respiratory therapists, nurses, or physicians may administer a variety of aerosolized medications using a nebulizer or other aerosol generating system to treat various respiratory diseases and infections. During treatment, healthcare personnel may be chronically exposed to low levels of these aerosolized medications that escape/leak from the delivery system. These medicines include ribavirin (antiviral), pentamidine (antiprotozoal), amikacin, colistin, and tobramycin (antibiotic), which are associated with adverse reproductive effects, kidney toxicity, respiratory irritation, asthma, and asthma symptoms (Tsai et al. 2015). Because there are no less toxic substitutes for these medications, exposure control should follow the hierarchy of control scheme starting with engineering controls, administrative controls, and PPE.

Table 5 Exposures in other hospital occupations and departments

Unit/Occupation	Product or chemical class	Purpose or function	Chemical ingredients
Patient care occupations including all nursing occupations, e.g., LPN, RN, and NA in different units	Antiseptics and skin disinfectants	Skin disinfection	Alcohol, chlorhexidine, and hexachlorophene
	Glues	Applying bandages, wound dressing, and plasters	Acrylates (e.g., cyanoacrylate)
	Solvents and adhesive removers	Removing bandages and adhesives	Acetone, dipropylene glycol methyl ether, ethanol, isoparaffinic hydrocarbons, and isopropanol
	Metals	Thermometers and blood pressure devices	Mercury
Respiratory therapists and pulmonologist and nurses	Aerosolized medications	Antiprotozoal	Pentamidine
		Antibiotics	Amikacin, colistin, and tobramycin
		Antiviral	Ribavirin
Clinical, histology, and pathology laboratories, and morgue	Laboratory chemicals and reagents	Solvents	Toluene, xylene, acetone
		fixative solutions	Formaldehyde, and glutaraldehyde
Pharmacy and oncology	Medications and drugs	Antineoplastic, antibiotics, and cytotoxic drugs	Alpha-fluoro-beta-alanine, amoxycillin, amoxicillin + clavulanate, ampicillin, budiastase, biperiden, bleomycin, bortezomib, carboplatin, cecisplatin, cefepime, cefoperazone, cefotiam, cefotaxime, cefoxitin, cefazolin, ceftazidime, ceftizoxime, ceftriaxone, chlorhexidine, chlorpromazine, ciprofloxacin, clindamycin, cyclophosphamide, cytarabine, daunorubicin, dicloxacillin, 2',2'-diflurorodeoxyuridine, doxorubicin, docetaxel, Empynase®, epirubicin, etoposide, flomoxef, flucloxacillin, 5-fluorouracil, gemcitabine, gentamycin, idarubicin, ifosfamide, irinotecan, meropenem, methotrexate, nitrogen

(continued)

Table 5 (continued)

Unit/Occupation	Product or chemical class	Purpose or function	Chemical ingredients
			mustard, omeprazole, oxaliplatin, paclitaxel, pantoprazole, pantothenine, propacetamol, pemetrexed, penicillin, penicillin G, perphenazine, phenobarbital, piperacillin, piperacillin + tazobactam, propercizaine, psyllium, sodium benzylpenicillin, sucralfate, sulfamethoxazole + trimethoprim, taxol, tazobactam, thioridazine, topotecan, vinblastine, and vincristine
Radiology	Chemical mixture	Film processing and development chemicals	Hydroquinone, glutaraldehyde, formaldehyde, glycols, acetic acid, sulfur dioxide, ammonium chloride, and silver compounds
ICU and emergency	Nitrates and nitric oxide, treatment for cardiovascular stabilization	Escape from ventilators	Nitric oxide and nitrogen dioxide
Laundry workers	Mixed exposure	Contaminated clothing or linen	Various biohazards and drugs
Maintenance and construction	Mixed exposure	Repair and construction of building, grounds maintenance	Dusts, VOCs, formaldehyde, molds and moisture, material off-gassing, phthalates, and pesticides

Laboratory personnel and technicians may be exposed to formaldehyde, and previously glutaraldehyde, tissue preservatives, and fixative solutions. Additionally, they are exposed to a variety of solvents containing VOCs such as acetone, xylene, and toluene that are used in pathology, histology, other laboratories, and autopsy suites (Table 5). Laboratory technicians and other workers in these areas have some of the highest inhalation and skin exposure to these VOCs (Weaver 1997). A study of VOCs in histology laboratories reported high levels of ethanol, isopropanol, 2-butanone, ethyl acetate, thiophene, toluene, ethylbenzene, limonene, xylene, and ethylbenzene (Cipolla et al. 2017). Formaldehyde is a confirmed human carcinogen and a skin sensitizer and is associated with irritation and upper airway symptoms (Gorman et al. 2013). Exposure to solvents is associated with central nervous system effects (Weaver 1997).

About eight million U.S. healthcare workers are potentially exposed to drugs, in various occupations and departments such as pharmacy, nursing professionals, and physicians (e.g., in oncology), OR personnel, and research laboratory personnel as they prepare, handle, or administer a multitude of drugs daily some of which are hazardous (NIOSH 2020). Maintenance, shipping, laundry, and housekeeping staff are also at risk of exposure to these drugs through contaminated work surfaces, linen and clothing, or shipping packages (NIOSH 2020). These hazardous drugs include some antibiotics, antineoplastic drugs, hormone agents, and bioengineered drugs. NIOSH maintains a list of common hazardous antineoplastic drugs, which was last updated in 2016 (NIOSH 2020). Exposure primarily occurs through inhalation and dermal routes of exposure, but accidental ingestion through hand to mouth contact and accidental injection through needle stick injury can also occur. Numerous studies have conducted surface contamination and skin exposure assessments for hazardous drugs in pharmacy and different hospital locations among staff who handle these drugs at various stages from preparation to delivery (Crul et al. 2020; Poupeau et al. 2018). Exposure to these drugs can cause acute and chronic effects including respiratory and skin irritation, reproductive problems, and cancer (NIOSH 2020). Antibiotics, including penicillin, amoxicillin, and dicloxacillin, are known to cause allergic dermal reactions (exanthema, eczema, and erythema) (Pinheiro et al. 2018). Exposure to frequently used antineoplastic drugs, such as cyclophosphamide, 5-fluorouracil, and paclitaxel, are associated with increased risk of allergic respiratory and dermal reactions, nasal sores, loss of hair, carcinogenicity, and irritant contact dermatitis (Ivanova and Avota 2016). There is mixed evidence for reproductive effects of exposure to antineoplastic drugs among nurses in various departments. Various guidance from government and professional societies exist to minimize opportunities for exposure.

Numerous chemical hazards exist in radiology from using chemicals for film processing and development, such as hydroquinone, glutaraldehyde, formaldehyde, glycols, acetic acid, sulfur dioxide, ammonium chloride, silver compounds, and many others (Teschke et al. 2002; Byrns et al. 2000). However, the current trend is toward digital imaging that eliminates these hazards. Exposure to aldehydes is associated with asthma. Increased risk of asthma has been reported for radiographers and technicians who process films. Approaches to minimize these hazards include recognizing their presence, installing appropriate LEV controls, and moving toward digital imaging.

Maintenance workers may be exposed to vapors and dusts from various repairs to the building or mechanical systems, building materials, and exposures prevalent in any areas where they work. Laundry workers may be exposed to detergents from laundry, biological hazards, and hazardous drugs that contaminate linen and clothing. Maintenance and laundry workers may also be exposed to cleaning and disinfecting chemicals.

Conclusions

Hospital workers are exposed to complex mixtures of chemicals mostly via inhalation and dermal routes of exposure. These exposures arise from multiple sources, such as cleaners and disinfectants, sterilizing agents, detergents, solvents, heavy

metals, hazardous drugs, laboratory chemical reagents, waste anesthetic gases, surgical smoke, and other indoor air contaminants from products, building, and construction materials. Exposures to these gases, vapors, and aerosols result in a spectrum of health outcomes including respiratory, dermatologic, reproductive, neurologic, other systemic outcomes, and cancer. A great deal of attention is focused on preventing HAIs, and consequently exposure to chemicals is often not well recognized or controlled and prevention measures are lagging. This review highlights the chemical products used by healthcare workers in different occupations and units, their ingredients and potential for inhalation and dermal exposures, and opportunities for exposure mitigation and disease prevention. In particular, preventing HAI through cleaning and disinfecting surfaces creates chemical hazards that are associated with asthma, rhinitis, dermatitis, and sensitization, presenting a significant challenge. There is thus a need for a more integrated approach to infection control and asthma prevention, requiring cooperation among professional organizations in infection control, industrial hygiene, and occupational medicine in formulating guidelines. Additionally, the numerous health and safety hazards present in hospital setting need to be recognized, monitored, and mitigated.

Cross-References

- [FrAGRANCED CONSUMER PRODUCTS AS SOURCES](#)
- [FUNDAMENTALS OF EXPOSURE SCIENCE](#)
- [INDOOR AIR QUALITY IN ELDERLY CARE CENTERS](#)
- [INDOOR GAS-PHASE CHEMISTRY](#)
- [INFLUENCE OF VENTILATION ON INDOOR AIR QUALITY](#)
- [PREDICTING VOC AND SVOC CONCENTRATIONS IN COMPLEX INDOOR ENVIRONMENTS](#)
- [SAMPLING AND ANALYSIS OF VVOCs AND VOCs IN INDOOR AIR](#)
- [THE HEALTH EFFECTS OF INDOOR AIR POLLUTION](#)
- [VOLATILE ORGANIC COMPOUNDS \(VOCs\)](#)

Disclaimer The findings and conclusions in this report are those of the author(s) and do not necessarily represent the official position of the National Institute for Occupational Safety and Health, Centers for Disease Control and Prevention.

References

- Adisesh A, Murphy E, Barber CM, Ayres JG (2011) Occupational asthma and rhinitis due to detergent enzymes in healthcare. *Occup Med (Lond)* 61(5):364–369
- AOEC (2012) Exposure code lookup. <http://www.aoedata.org/ExpCodeLookup.aspx>. Accessed 23 July 2013
- Arif AA, Delclos GL (2012) Association between cleaning-related chemicals and work-related asthma and asthma symptoms among healthcare professionals. *Occup Environ Med* 69(1):35–40
- Barnes S, Stuart R, Redley B (2019) Health care worker sensitivity to chlorhexidine-based hand hygiene solutions: a cross-sectional survey. *Am J Infect Control* 47(8):933–937
- Bello A, Quinn MM, Milton DK, Perry MJ (2013) Determinants of exposure to 2-butoxyethanol from cleaning tasks: a quasi-experimental study. *Ann Occup Hyg* 57(1):125–135

- Benson SM, Maskrey JR, Nembhard MD, Unice KM, Shirley MA, Panko JM (2019) Evaluation of personal exposure to surgical smoke generated from electrocautery instruments: a pilot study. *Ann Work Expo Health* 63(9):990–1003
- Bessonneau V, Mosqueron L, Berrubé A, Mukensturm G, Buffet-Bataillon S, Gangneux J-P et al (2013) VOC contamination in hospital, from stationary sampling of a large panel of compounds, in view of healthcare workers and patients exposure assessment. *PLoS One* 8(2): e55535
- BLS (2018) 2017 Survey of occupational injuries & illnesses charts package. <https://www.bls.gov/iif/osch0062.pdf>. Accessed 13 June 2021
- BLS (2020) Current population survey. Characteristics of the employed. <https://www.bls.gov/cps/cpsaat18.htm>. Accessed 13 June 2021
- Boiano JM, Steege AL (2016) Precautionary practices for administering anesthetic gases: a survey of physician anesthesiologists, nurse anesthetists and anesthesiologist assistants. *J Occup Environ Hyg* 13(10):782–793
- Bonnet P, Achille J, Malingre L, Duret H, Ramalho O, Mandin C (2018) VOCs in cleaning products used in age care and social facilities: identification of hazardous substances. *AIMS Environ Sci* 5(6):402–417
- Boyce JM, Pittet D (2002) Guideline for hand hygiene in health-care settings: recommendations of the Healthcare Infection Control Practices Advisory Committee and the HICPAC/SHEA/APIC/IDSA Hand Hygiene Task Force. *Am J Infect Control* 30(8):S1–S46
- Byrns G, Palatianos KC, Shands L, Fennelley K, McCammon C, Boudreau A et al (2000) Chemical hazards in radiology. *Appl Occup Environ Hyg* 15(2):203–208
- Cheng NY, Chuang HC, Shie RH, Liao WH, Hwang YH (2019) Pilot studies of VOC exposure profiles during surgical operations. *Ann Work Expo Health* 63(2):173–183
- Cipolla M, Izzotti A, Ansaldi F, Durando P, Piccardo MT (2017) Volatile organic compounds in anatomical pathology wards: comparative and qualitative assessment of indoor airborne pollution. *Int J Environ Res Public Health* 14(6):609
- Clausen PA, Frederiksen M, Sejbæk CS, Sørli JB, Hougaard KS, Frydendall KB et al (2020) Chemicals inhaled from spray cleaning and disinfection products and their respiratory effects. A comprehensive review. *Int J Hyg Environ Health* 229:113592
- Cokic SM, Duca RC, Godderis L, Hoet PH, Seo JW, Van Meerbeek B et al (2017) Release of monomers from composite dust. *J Dent* 60:56–62
- Crul M, Hilhorst S, Breukels O, Bouman-d'Onofrio JRC, Stubbs P, van Rooij JG (2020) Occupational exposure of pharmacy technicians and cleaning staff to cytotoxic drugs in Dutch hospitals. *J Occup Environ Hyg* 17(7–8):343–352
- Dancer SJ (2011) Hospital cleaning in the 21st century. *Eur J Clin Microbiol Infect Dis* 30(12): 1473–1481
- Darre E, Jørgensen LG, Vedel P, Jensen JS (1992) Breathing zone concentrations of methylmethacrylate monomer during joint replacement operations. *Pharmacol Toxicol* 71(3 Pt 1):198–200
- DeLeo PC, Ciarlo M, Pacelli C, Greggs W, Williams ES, Scott WC et al (2018) Cleaning product ingredient safety: what is the current state of availability of information regarding ingredients in products and their function? *ACS Sustain Chem Eng* 6(2):2094–2102
- Dodd KE, Mazurek JM (2016) Asthma among employed adults, by industry and occupation – 21 states, 2013. *MMWR Morb Mortal Wkly Rep* 65(47):1325–1331
- Dumas O, Varraso R, Boggs KM, Descatha A, Henneberger PK, Quinot C et al (2018) Association of hand and arm disinfection with asthma control in US nurses. *Occup Environ Med* 75(5): 378–381
- Eldeirawi K, Huntington-Moskos L, Nyenhuis SM, Polivka B (2021) Increased disinfectant use among adults with asthma in the era of COVID-19. *J Allergy Clin Immunol Pract* 9(3):1378–1380.e2
- Folletti I, Zock JP, Moscato G, Siracusa A (2014) Asthma and rhinitis in cleaning workers: a systematic review of epidemiological studies. *J Asthma* 51(1):18–28
- Gambhir RS, Singh G, Sharma S, Brar R, Kakar H (2011) Occupational health hazards in the current dental profession-a review. *Mercury* 81:82

- Garrido AN, House R, Lipszyc JC, Liss GM, Holness DL, Tarlo SM (2021) Cleaning agent usage in healthcare professionals and relationship to lung and skin symptoms. *J Asthma* 1–14. <https://doi.org/10.1080/02770903.2021.1871740>
- Gerster FM, Vernez D, Wild PP, Hopf NB (2014) Hazardous substances in frequently used professional cleaning products. *Int J Occup Environ Health* 20(1):46–60
- González Jara MA, Mora Hidalgo A, Avalos Gulin JC, López Albiach M, Muñoz Ortiz L, Torán Monserrat P et al (2013) Exposure of health workers in primary health care to glutaraldehyde. *J Occup Med Toxicol* 8(1):31
- Gonzalez M, Jégu J, Kopferschmitt MC, Donnay C, Hedelin G, Matzinger F et al (2014) Asthma among workers in healthcare settings: role of disinfection with quaternary ammonium compounds. *Clin Exp Allergy* 44(3):393–406
- Gorman T, Dropkin J, Kamen J, Nimbalkar S, Zuckerman N, Lowe T et al (2013) Controlling health hazards to hospital workers. *New Solut* 23(Suppl):1–167
- Hagberg S, Ljungkvist G, Andreasson H, Karlsson S, Barregård L (2005) Exposure to volatile methacrylates in dental personnel. *J Occup Environ Hyg* 2(6):302–306
- Hawley B, Casey M, Virji MA, Cummings KJ, Johnson A, Cox-Ganser J (2017) Respiratory symptoms in hospital cleaning staff exposed to a product containing hydrogen peroxide, Peracetic acid, and acetic acid. *Ann Work Expo Health* 62(1):28–40
- Henn S, Boiano JM, Steege AL (2015) Precautionary practices of healthcare workers who disinfect medical and dental devices using high-level disinfectants. *Infect Control Hosp Epidemiol* 36(2):180–185
- Henriks-Eckerman ML, Alanko K, Jolanki R, Kerosuo H, Kanerva L (2001) Exposure to airborne methacrylates and natural rubber latex allergens in dental clinics. *J Environ Monit* 3(3):302–305
- Hong Y-J, Huang Y-C, Lee I-L, Chiang C-M, Lin C, Jeng HA (2015) Assessment of volatile organic compounds and particulate matter in a dental clinic and health risks to clinic personnel. *J Environ Sci Health A* 50(12):1205–1214
- Hori H, Yahata K, Fujishiro K, Yoshizumi K, Li D, Goto Y et al (2002) Personal exposure level and environmental ethylene oxide gas concentration in sterilization facilities of hospitals in Japan. *Appl Occup Environ Hyg* 17(9):634–639
- Huslage K, Rutala WA, Sickbert-Bennett E, Weber DJ (2010) A quantitative approach to defining “high-touch” surfaces in hospitals. *Infect Control Hosp Epidemiol* 31(8):850–853
- ILO (2019) The future of work in the health sector. Working paper no 325. ILO, Geneva
- Ivanova K, Avota M (2016) Antineoplastic drugs: occupational exposure and side effects. *Proc Latv Acad Sci Sect B* 70(5):325–329
- Jachuck SJ, Bound CL, Steel J, Blain PG (1989) Occupational hazard in hospital staff exposed to 2 per cent glutaraldehyde in an endoscopy unit. *Occup Med* 39(2):69–71. <https://doi.org/10.1093/occmed/39.2.69>
- Jungbauer FHW, Steenstra FB, Groothoff JW, Coenraads PJ (2005) Characteristics of wet work in nurses. *Int Arch Occup Environ Health* 78(3):248–251
- Kim TS, Kim HA, Heo Y, Park Y, Park CY, Roh YM (2002) Level of silica in the respirable dust inhaled by dental technicians with demonstration of respirable symptoms. *Ind Health* 40(3):260–265
- Knoeller GE, Mazurek JM, Moorman JE (2011) Work-related asthma among adults with current asthma in 33 states and DC: evidence from the Asthma Call-Back Survey, 2006–2007. *Public Health Rep* 126(4):603–611
- Koda S, Kumagai S, Ohara H (1999) Environmental monitoring and assessment of short-term exposures to hazardous chemicals of a sterilization process in hospital working environments. *Acta Med Okayama* 53(5):217–223
- Leas BF, Sullivan N, Han JH, Pegues DA, Kaczmarek JL, Umscheid CA (2015) Environmental cleaning for the prevention of healthcare-associated infections. Agency for Healthcare Research and Quality, Rockville
- LeBouf RF, Virji MA, Saito R, Henneberger PK, Simcox N, Stefaniak AB (2014) Exposure to volatile organic compounds in healthcare settings. *Occup Environ Med* 71(9):642–650
- LeBouf RF, Virji MA, Ranpara A, Stefaniak AB (2017) Air and surface sampling method for assessing exposures to quaternary ammonium compounds using liquid chromatography tandem mass spectrometry. *Ann Work Expo Health* 61(6):724–736

- Lee T, Soo JC, LeBouf RF, Burns D, Schwegler-Berry D, Kashon M et al (2018) Surgical smoke control with local exhaust ventilation: experimental study. *J Occup Environ Hyg* 15(4):341–350
- Leggat PA, Kedjarune U, Smith DR (2007) Occupational health problems in modern dentistry: a review. *Ind Health* 45(5):611–621
- Leinster P, Baum JM, Baxter PJ (1993) An assessment of exposure to glutaraldehyde in hospitals: typical exposure levels and recommended control measures. *Occup Environ Med* 50(2): 107–111
- Lester JD, Hsu S, Ahmad CS (2012) Occupational hazards facing orthopedic surgeons. *Am J Orthop (Belle Mead NJ)* 41(3):132–139
- Limchantra IV, Fong Y, Melstrom KA (2019) Surgical smoke exposure in operating room personnel: a review. *JAMA Surg* 154(10):960–967
- Luckhaupt SE, Dahlhamer JM, Ward BW, Sussell AL, Sweeney MH, Sestito JP et al (2013) Prevalence of dermatitis in the working population, United States, 2010 National Health Interview Survey. *Am J Ind Med* 56(6):625–634
- Mazurek JM, Weissman DN (2016) Occupational respiratory allergic diseases in healthcare workers. *Curr Allergy Asthma Rep* 16(11):77
- Nayeb zadeh A, Dufresne A (1998) Chemical hazards in dental laboratories. *Indoor Built Environ* 7 (3):146–155
- Nazaroff WW, Weschler CJ (2004) Cleaning products and air fresheners: exposure to primary and secondary air pollutants. *Atmos Environ* 38(18):2841–2865
- NIOSH (2017a) Healthcare workers: chemical hazards. <https://www.cdc.gov/niosh/topics/healthcare/chemical.html>. Accessed 27 June 2021
- NIOSH (2017b) Work-related lung disease surveillance system (eWoRLD). 2015/2017-866, 870, 882, 923. April 2, 2018. U.S. Department of Health and Human Services, Centers for Disease Control and Prevention, National Institute for Occupational Safety and Health, Respiratory Health Division, Morgantown. Available at: <https://www.cdc.gov/eworld/Data/923>
- NIOSH (2020) Hazardous drug exposures in healthcare. <https://www.cdc.gov/niosh/topics/hazdrug/default.html>. Accessed 27 June 2021
- Norback D (1988) Skin and respiratory symptoms from exposure to alkaline glutaraldehyde in medical services. *Scand J Work Environ Health* 14(6):366–371
- Norton P, Pinho P, Xará D, Pina F, Norton M (2020) Assessment of anesthetic gases in a central hospital. *Porto Biomed J* 5(4):e076
- Odabasi M (2008) Halogenated volatile organic compounds from the use of chlorine-bleach-containing household products. *Environ Sci Technol* 42(5):1445–1451
- OSHA (2002) OSHA Hazard Information Bulletin: preventing adverse health effects from exposure to beryllium in dental laboratories. www.osha.gov/dts/hib/hib_data/hib20020419.pdf. Accessed 27 June 2021
- OSHA (2021) Healthcare. <https://www.osha.gov/healthcare>. Accessed 15 June 2021
- Pinheiro V, Pestana C, Pinho A, Antunes I, Gonçalo M (2018) Occupational allergic contact dermatitis caused by antibiotics in healthcare workers – relationship with non-immediate drug eruptions. *Contact Dermatitis* 78(4):281–286. <https://doi.org/10.1111/cod.12960>
- Pisaniello DL, Gun RT, Tkaczuk MN, Nitshcke M, Crea J (1997) Glutaraldehyde exposures and symptoms among endoscopy nurses in South Australia. *Appl Occup Environ Hyg* 12(3):171–177
- Poupeau C, Tanguay C, Caron NJ, Bussières JF (2018) Multicenter study of environmental contamination with cyclophosphamide, ifosfamide, and methotrexate in 48 Canadian hospitals. *J Oncol Pharm Pract* 24(1):9–17
- Puskar MA, Hecker LH (1989) Field validation of passive dosimeters for the determination of employee exposures to ethylene oxide in hospital product sterilization facilities. *Am Ind Hyg Assoc J* 50(1):30–36
- Quirce S, Barranco P (2010) Cleaning agents and asthma. *J Investig Allergol Clin Immunol* 20(7): 542–550
- Rautiainen P, Hyttinen M, Ruokolainen J, Saarinen P, Timonen J, Pasanen P (2019) Indoor air-related symptoms and volatile organic compounds in materials and air in the hospital environment. *Int J Environ Health Res* 29(5):479–488

- Rideout K, Teschke K, Dimich-Ward H, Kennedy SM (2005) Considering risks to healthcare workers from glutaraldehyde alternatives in high-level disinfection. *J Hosp Infect* 59(1): 4–11
- Rutala WA, Weber DJ, Control, C. f. D (2008) Guideline for disinfection and sterilization in healthcare facilities. Centers for Disease Control (US). <https://stacks.cdc.gov/view/cdc/47378>
- Rutala WA, Kanamori H, Gergen MF, Knelson LP, Sickbert-Bennett EE, Chen LF et al (2018) Enhanced disinfection leads to reduction of microbial contamination and a decrease in patient colonization and infection. *Infect Control Hosp Epidemiol* 39(9):1118–1121
- Saito R, Virji MA, Henneberger PK, Humann MJ, LeBouf RF, Stanton ML et al (2015) Characterization of cleaning and disinfecting tasks and product use among hospital occupations. *Am J Ind Med* 58(1):101–111
- Santarsiero A, Fuselli S, Piermattei A, Morlino R, De Blasio G, De Felice M et al (2009) Investigation of indoor air volatile organic compounds concentration levels in dental settings and some related methodological issues. *Ann Ist Super Sanita* 45(1):87–98
- Schramm MWJ, Sheikh AJ, Chave-Cox R, McQuaid J, Whitty RCW, Ilyinskaya E (2021) Surgically generated aerosol and mitigation strategies: combined use of irrigation, respirators and suction massively reduces particulate matter aerosol. *Acta Neurochirurgica* 163:1819–1827. Accession Number: 34031774 PMCID: PMC8143442. <https://doi.org/10.1007/s00701-021-04874-4>
- Singer BC, Destaillats H, Hodgson AT, Nazaroff WW (2006) Cleaning products and air fresheners: emissions and resulting concentrations of glycol ethers and terpenoids. *Indoor Air* 16(3): 179–191
- Steinemann A (2015) Volatile emissions from common consumer products. *Air Qual Atmos Health* 8(3):273–281
- Stewart E, Smith R (2017) Guidelines for selection and use of environmental surface disinfectants in healthcare. American Industrial Hygiene Association, Falls Church
- Su FC, Friesen MC, Stefaniak AB, Henneberger PK, LeBouf RF, Stanton ML et al (2018) Exposures to volatile organic compounds among healthcare workers: modeling the effects of cleaning tasks and product use. *Ann Work Expo Health* 62(7):852–870
- Su FC, Friesen MC, Humann M, Stefaniak AB, Stanton ML, Liang X et al (2019) Clustering asthma symptoms and cleaning and disinfecting activities and evaluating their associations among healthcare workers. *Int J Hyg Environ Health* 222(5):873–883
- Suleyman G, Alangaden G, Bardossy AC (2018) The role of environmental contamination in the transmission of nosocomial pathogens and healthcare-associated infections. *Curr Infect Dis Rep* 20(6):12
- Suojaelehto H, Linström I, Henriks-Eckerman ML, Jungewelter S, Suuronen K (2011) Occupational asthma related to low levels of airborne methylene diphenyl diisocyanate (MDI) in orthopedic casting work. *Am J Ind Med* 54(12):906–910
- Svanes O, Bertelsen RJ, Lygre SHL, Carsin AE, Anto JM, Forsberg B et al (2018) Cleaning at home and at work in relation to lung function decline and airway obstruction. *Am J Respir Crit Care Med* 197(9):1157–1163
- Tarlo SM, Malo JL, de Blay F, Le Moual N, Henneberger P, Heederik D et al (2017) An official American Thoracic Society workshop report: presentations and discussion of the sixth Jack Pepys workshop on asthma in the workplace. *Ann Am Thorac Soc* 14(9):1361–1372
- Teschke K, Chow Y, Brauer M, Chesson E, Hirtle B, Kennedy SM et al (2002) Exposures and their determinants in radiographic film processing. *AIHA J* (Fairfax, Va) 63(1):11–21
- Tluczkiewicz I, Bitsch A, Hahn S, Hahn T (2010) Emission of biocides from hospitals: comparing current survey results with European Union default values. *Integr Environ Assess Manag* 6(2): 273
- Tsai RJ, Boiano JM, Steege AL, Sweeney MH (2015) Precautionary practices of respiratory therapists and other health-care practitioners who administer aerosolized medications. *Respir Care* 60(10):1409–1417
- Van Den Berg-Dijkmeijer ML, Frings-Dresen MHW, Sluiter JK (2011) Risks and health effects in operating room personnel (Review). *Work* 39(3):331–344

- Varughese S, Ahmed R (2021) Environmental and occupational considerations of anesthesia: a narrative review and update. *Anesth Analg* 133:826–835
- Virji MA, Liang X, Su F-C, LeBouf RF, Stefaniak AB, Stanton ML et al (2019) Peaks, means, and determinants of real-time TVOC exposures associated with cleaning and disinfecting tasks in healthcare settings. *Ann Work Expo Health* 63(8):759–772
- Weaver VM (1997) Chemical hazards in health care workers. *Occupational Medicine* (Philadelphia, Pa.), 01 Oct 1997, 12(4):655–667. PMID: 9353815
- Wellons SL, Trawick EG, Stowers MF, Jordan SLP, Wass TL (1998) Laboratory and hospital evaluation of four personal monitoring methods for glutaraldehyde in ambient air. *Am Ind Hyg Assoc J* 59(2):96–103
- WHO (2006) Healthcare workers: a global profile. In: *World health report*, 2006. WHO, Geneva
- Wieslander G, Norbäck D (2010) A field study on clinical signs and symptoms in cleaners at floor polish removal and application in a Swedish hospital. *International Archives of Occupational and Environmental Health* 83(5):585–91. Accession Number: 202581312; 20407787. <https://doi.org/10.1007/s00420-010-0531-5>
- Yahata K, Fujishiro K, Hori H, Higashi T (2001) An investigation of symptoms in ethylene oxide sterilization workers in hospitals. *J Occup Health* 43(4):180–184
- Yoshida K, Bryant HE, Visser ND, Atiemo MA (1989) Determination of worker exposure to instantaneously emitted ethylene oxide in sterilization facilities. *Appl Ind Hyg* 4(7):166–170



Exposure to Air Pollutants in Ground Transport Microenvironments

68

S. M. Almeida and V. Martins

Contents

Introduction	2024
Most Important In-Cabin Pollutants	2025
Methods to Assess the Exposure During Commuting	2029
Measuring	2029
Factors Affecting the Personal Exposure During Commuting	2032
Transport Characteristics	2033
Road and Traffic Conditions	2037
Meteorological Variables	2038
Individual Behavior	2040
Impacts on Health	2042
Measures to Reduce Exposure During Commuting	2043
Optimizing Driving Behavior	2043
Transition to Active Transportation	2044
Healthier Routes Planning	2045
Conclusions	2046
Cross-References	2047
References	2047

Abstract

Although commuters spend a small proportion of their time in vehicles, transport microenvironments (TME) are a significant contributor to their total daily air pollution exposure, thereby affecting the citizens' health and well-being. The vehicle interior is a specific environment of small volume, affected by traffic-related air pollutants, and by the emissions from a variety of building materials, some of them harmful to the human health. The aim of this chapter is to identify the key factors affecting the exposure in TME. It identifies the principal pollutants influencing the air quality inside vehicle cabins, discusses advantages and

S. M. Almeida (✉) · V. Martins

Centro de Ciências e Tecnologias Nucleares, Instituto Superior Técnico, Bobadela, Portugal
e-mail: smartaa@ctn.tecnico.ulisboa.pt; vania.martins@ctn.tecnico.ulisboa.pt

disadvantages of the main measuring and modelling approaches used to assess these pollutants, and presents control measures. It is difficult to compare and rank the exposures experienced in buses, cars, motorcycles, trams, trains, subways, cycling, or walking. The exposure varies considerably within and between the different modes of transport, due to disparities in the measurement protocols, vehicle characteristics, ventilation settings, road typology, atmospheric conditions, temporal variations, and user habits. Considering public health, efforts should be made to prioritize active travel, optimize vehicle ventilation and filtration, avoid heavily trafficked roads and rush hours, and maintain indoor cabin hygiene. The information in this chapter can contribute to develop transport and planning policies in urban areas.

Keywords

Transport mode · Commuting · Personal monitoring · Traffic-related air pollutants · Vehicle cabin

Introduction

The study of commuter exposure to air pollutants is not a new field of research. Indeed in 1966, Haagen-Smit (1966) made a series of carbon monoxide measurements on heavily traffic roads in Los Angeles. Since then, the importance of the topic increased as a consequence of population growth, the increased number of motor vehicles, and the higher degree of proximity to vehicular emissions.

Personal exposure to environmental substances is largely determined by time-activity patterns while moving across locations or microenvironments (Duan et al. 2022). Time-activity pattern studies performed in European (Cunha-Lopes et al. 2019), North America (Klepeis et al. 2001), and Asian (Chau et al. 2002) cities have reported that time spent commuting varies between 3.4% and 10% of the day. However, although people only spend a reduced fraction of time in-transit, commuting lead to a substantial contribution to their total daily exposure and inhalation of air pollution, especially in high vehicle-density metropolitan areas.

Transport microenvironments (TME) have higher air pollutant concentrations than other settings most people occupy in their daily routines. Aboveground transports are affected by the exhaust emissions from nearby cars, trucks, and buses, the evaporative emissions from the fuel system, and the abrasion emissions from brakes, clutch, and tires. The underground systems are mainly influenced by the mechanical abrasion between wheels, brakes, and rails. The concentrations of most traffic-related air pollutants are particularly high along busy roads, which often do not meet air quality standards, principally during morning commute hours. During the commuting time, drivers and passengers are also exposed to high pollutant concentrations emitted by the cabin materials. The volatile organic compounds concentrations in a vehicle cabin could be much higher than normal ambient levels. According to Mandalakis et al. (2008), the inhalation intake exposure to polybrominated

diphenyl ethers (PBDEs), which is a flame retardant, during an 80-min drive is approximately equivalent to 16.5-h exposure at home.

Consequently, commuters are exposed to short periods of high pollutant concentrations. Indeed, a study conducted in Barcelona showed that commuting contributed to 11% of the daily exposure to nitrogen dioxide (NO_2) (de Nazelle et al. 2013). In Los Angeles, Fruin et al. (2008) estimated that the influence of measured in-automobile ultrafine particles (UFP) on daily exposure ranged between 33% and 45%. Moreover, the personal exposure to BC during commuting showed to contribute in 21%, 19%, and 12% to the total daily exposure in Belgium (Dons et al. 2012), Lisbon (Cunha-Lopes et al. 2019), and Paris (Paunescu et al. 2017), respectively.

Several reviews have been published in the last years about the factors affecting the exposure in different travel modes and about the associated health impacts (Cepeda et al. 2017; de Nazelle et al. 2017; Hachem et al. 2019; Karanasiou et al. 2014; Knibbs et al. 2011; Kumar et al. 2018; Ma et al. 2020; Xu et al. 2018). These works have flagged the exposure while commuting as a priority topic of further investigations.

The objective of this chapter is to better understand personal exposure during commuting by different modes of transport and under different conditions and to contribute for making informed decisions to manage and reduce the health risks in cities.

Most Important In-Cabin Pollutants

TME have become a significant source of exposure to several air pollutants. The wide range of commuting modes, vehicle cabin designs, and modes of operation result in a large variation in the occurrence of pollutants species, concentrations, and personal exposure levels. The sources of air pollutants in-cabin can be classified, as in other indoor environments, as outdoor air, interior materials and finishes, and human behavior (Fig. 1).

Particles ($\text{PM}_{2.5}$, aerodynamic diameter $<2.5\ \mu\text{m}$; PM_{10} , aerodynamic diameter $<10\ \mu\text{m}$) emissions from road vehicles include emissions from the tailpipe and non-exhaust emissions due to tear and wear of vehicle parts such as clutch, brake, and tire and resuspension of dust (Padoan and Amato 2018). As stringent policies and technological upgrades have led to sizeable reductions in exhaust emissions, the contribution of non-exhaust emissions is becoming more important. Rexeis and Hausberger (2009) estimated that the contribution of non-exhaust PM to the total PM emissions will increase from about 50% up to some 80–90% by the end of the decade. Non-exhaust emissions are usually characterized by trace metals, such as Ba, Cu, Mn, Sb, Zn, although organic markers, such as polycyclic aromatic hydrocarbons (PAHs) and n-alkanes, have also been used as markers (Pant and Harrison 2013). Exposure to PM increases the risk of cardiovascular diseases and stroke (Lee et al. 2018a), central nervous system diseases (Babadjouni et al. 2017),

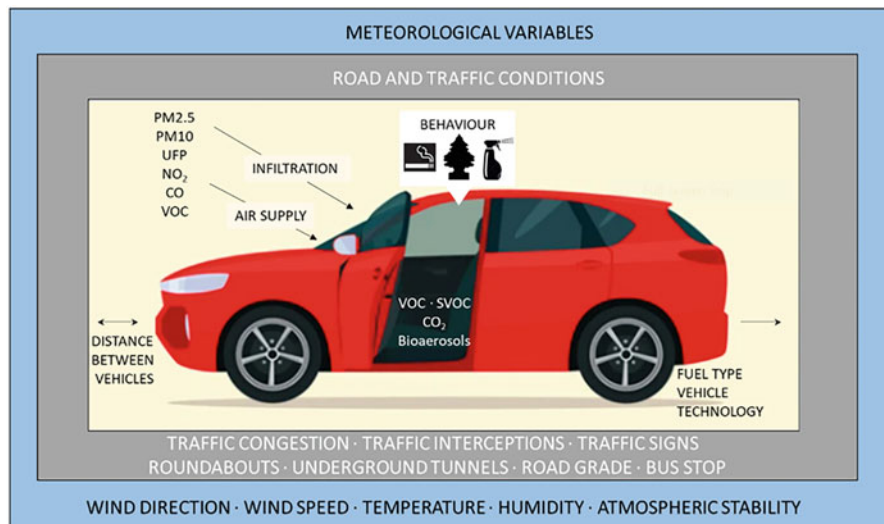


Fig. 1 Principal pollutants influencing the air quality inside vehicle cabins and key factors affecting the exposure in TME

neurodevelopmental and neurodegenerative diseases (Chen et al. 2017), and mortality (Pun et al. 2017).

Ultrafine Particles (UFP, mobility diameter <100 nm) typically constitute more than 90% of particle number concentrations in polluted roadside environments (Morawska et al. 2008). Although there are several natural sources of UFP, the combustion of fossil fuel for heating and transportation is the principal source in congested urban environments with heavy-duty diesel powered vehicles the dominant contribution to UFP concentrations (Morawska et al. 2008). UFP from vehicles can be emitted as primary particles or generated as a secondary aerosol, such as following homogenous nucleation of SO₂, NH₃, and NOx into SO₄²⁻, NH₄⁺, and NO₃⁻ (Morawska et al. 2008). Ambient UFP number concentrations are typically elevated on and near busy roads, and decay to background within 500 m of the edge of the road (Padró-Martínez et al. 2012). Previous studies have demonstrated cardiovascular and respiratory health effects of UFP, which likely have different and partly independent effects from larger particles, due to their small size, large surface area, high number concentration, different chemical composition, greater bioavailability of reactive compounds, content of redox-active compounds, ability to penetrate deep into the alveolar system, and increased lung retention (Araujo and Nel 2009).

Black Carbon (BC), a component of PM_{2.5}, originates from the incomplete combustion of wood and diesel engine exhaust (Dons et al. 2013), and is a suitable indicator of traffic-related air pollution (Janssen et al. 2011). Transportation is a major source of BC in urban areas where road vehicles contribute to ~58% of total BC emissions (Kumar et al. 2018) and lead to high BC concentrations on and near

busy roads (Padró-Martínez et al. 2012). BC is considered a better indicator of harmful particulate substances from combustion sources (principally traffic) than undifferentiated PM mass (Janssen et al. 2011) and has been associated with adverse cardiovascular effects (Gan et al. 2011), respiratory diseases (Patel et al. 2013), decreases in childhood cognition (Suglia et al. 2008), and mortality (Gan et al. 2011).

Nitrogen Dioxide (NO_2) is formed through the rapid reaction of NO, which is primarily emitted by the combustion of fossil fuels by vehicles, with O_3 . NO_2 is a well-established indicator of air pollution stemming from motor vehicle sources. The health impacts associated to exposure to NO_2 have been discussed because NO_2 and PM usually occurs in the same environment, and the relative contribution of individual components of the mixture is difficult to disentangle (Ackermann-Liebrich et al. 2019). However, recent works have dedicated to NO_2 as a possible independent contributor to adverse health impacts, and reported associations of long-term exposure to NO_2 with increased all-causes, cardiovascular, respiratory, cancer, ischemic heart, cerebrovascular, and pneumonia mortality (Do Eum et al. 2019), and associations of short-term exposure to NO_2 with risk of all-cause, cardiovascular and respiratory mortality (Mills et al. 2015).

Carbon Monoxide (CO) results from incomplete combustion of diesel or gasoline in traffic engines. High concentrations of CO generally occur in areas with heavy traffic intensity affecting the health of people who work or live nearby these areas. CO concentrations are spatially heterogeneous within a city, with higher levels on busy roads and especially in street canyons. Multisite studies performed in 19 European cities (Samoli et al. 2007) and in 126 US urban counties (Bell et al. 2009) found significant associations of CO with total and cardiovascular mortality and with risk of cardiovascular disease hospitalizations, respectively.

Volatile Organic Compounds (VOC) are emitted by vehicle exhaust, the most abundant of which include benzene, toluene, ethylbenzene and m-, p-, and o-xylene isomers, ethane, ethylene, acetylene, 1-butene, isobutene, propane, propene, isopentane, n-pentane, i-pentane, 2,2-dimethylbutane, 2-methylpentane, n-hexane, 3-methylhexane, ethylbenzene, m-ethyltoluene, and various trimethylbenzene isomers (Watson et al. 2001). For benzene, toluene, and xylene, a comparison between concentrations measured in the car with those determined immediately outside showed little difference (I/O ratio = 1.17) indicating their outdoor origin (Leung and Harrison 1999). However, organic compounds are also emitted from interior materials inside vehicle cabins. Yoshida et al. (2006) measured the concentrations of organic compounds in the interior air of 101 different types of Japanese domestically produced private-use cars and identified a total of 275 organic compounds, including many aliphatic and aromatic hydrocarbons, demonstrating that the air inside vehicle cabins is contaminated by high concentrations of a large variety of organic compounds emitted by the interior materials. Benzene, emitted by vehicle exhaust, and formaldehyde, the most familiar organic compounds affecting indoor air quality in transports, are classified as carcinogen by the International Agency for Research on Cancer.

Semi-volatile Organic Compounds (SVOC) are ubiquitous components of indoor environment. Some SVOC, such as PAHs originating from combustion, are

well-known pollutants contributing to human exposure, while other SVOC are less studied because they have been produced in large amounts only within the last half-century (Weschler and Nazaroff 2008). Since SVOC account for a large quantity of the material weight and their emission rates are relatively slow, they tend to exist in new and old vehicles for a long time (Xu et al. 2018). SVOC occur as active ingredients in personal care products and cleaning agents, and as main additives in materials such as electronic components, furnishings, and floor coverings (Weschler and Nazaroff 2008). Some SVOC are known to be toxic (e.g., dioxins, benzo[a]pyrene, pentachlorophenol), and for others, there are emerging indicators of concern. Phthalate esters have been associated with the change of the semen quality (Hauser et al. 2007) and with allergic symptoms in children (Bornehag et al. 2004). Certain SVOC are linked to endocrine disrupting activity such as brominated flame retardants (Birnbaum and Staskal 2004) and di-2-ethylhexyl phthalate (Sharpe 2005).

Carbon Dioxide (CO_2) concentrations can build up due to exhaust emissions and human exhalation. According to Gladyszewska-Fiedoruk (2011), a car driver exhales as much CO_2 as during physical exercise, due to the needed focused attention and concentration that affect the human metabolism, while a passenger exhales approximately the same quantity of CO_2 as a person taking a rest. The rate of increase of the CO_2 concentration is dependent on the occupation and several vehicle-specific parameters, such as the vehicle volume, and the air ventilation rate. CO_2 is considered a nonpoisonous gas; however, when concentrations in the air are too high, headaches, sore eyes, breathing difficulties, and declining concentration can occur, which can be unsafe while driving.

Bioaerosols refer to aerosols containing biological particles, such as fungi, bacteria, and viruses, and have allergenicity, infectivity, and pathogenicity (Wen et al. 2020). Microbes are ubiquitous in the TME and can enter inside vehicle cabins through the ventilation system, attached to people and objects, among other pathways (Buitrago et al. 2021). The vehicles' cabins provide the conditions for growth and propagation of wide range of pathogens, due to crowded population, foods and garbage produced by passengers, limited ventilation, and thermal environment (Wen et al. 2020). The infection transmission depends on several parameters, such as the load and proximity of the biological agent, host susceptibility, and exposure time (Nasir et al. 2016). The exposure to high concentrations of microorganisms is frequently associated with inflammatory reactions, asthma, pneumonitis, and hypersensitivity (Jo and Lee 2008). Worldwide field research focuses on concentrations, diversity, sources, and virulence – and survival – associated characteristics. Existing research shows that the most common microbes include aspergillus, alternaria, bacillus, cladosporium, chrysosporium, geotrichum, micrococcus, propionibacterium, penicillium, and staphylococcus (Wen et al. 2020). Most of these microbes are associated with the human body and activity (Buitrago et al. 2021). Nowadays, the possibility of SARS-CoV-2 infection while travelling in public transport is a huge concern for all the commuters and transport companies. The scientific evidence related to COVID-19 transmission on public transportation is very limited. However, the spread of COVID-19 in transports follow the same routes of transmission of respiratory viral diseases: through small airborne microdroplets,

via larger respiratory droplets, which fall close to where they are expired, and through contact with contaminated surfaces. Hadei et al. (2021) investigated the presence of SARS-CoV-2 RNA in the air of transports in Tehran and concluded that 67% of samples collected were positive (100% in subway trains and 50% in buses). Moreno et al. (2021) evaluated the presence of traces of SARS-CoV-2 RNA in the air, surfaces, and air-conditioning systems of subway trains and buses and found that from a total of 82 samples, 30 showed evidence for the presence of one or more of the 3 target RNA gene regions of SARS-CoV-2 virus. This work showed that positive results were more common in surface swab samples from support bars than in ambient air inside the vehicles and that there was a notable decrease in RNA traces detected after the bus cleaning.

Methods to Assess the Exposure During Commuting

Measuring

Fix Monitoring Stations

Measurements from fixed monitoring stations (FMS) have been commonly used to estimate the personal and community exposure levels to air pollutants. The most relevant advantage of FMS is the ability to provide highly accurate air quality measurements. Nevertheless, the high operation costs associated with the FMS maintenance means that only a few stations are available within the whole city, assuming that the air quality is homogenous within several kilometers around. A more accurate assessment of exposure during transportation needs the spatial distribution of air pollutants along the commute route, which is impossible to be fulfilled from FMS measurements. Several studies showed that urban background FMS significantly underestimate the exposure of the commuters. Asmi et al. (2009) assessed the relationship between UFP concentrations in the drivers' cabin of buses to that measured at an urban background site and reported ratios between 1.2 and 6.9, depending on the route, time of the day, and age of the bus. Zuurbier et al. (2010) found ratios between background and vehicle between 1.6 (diesel car, electric bus) and 2.5 (diesel bus), and reported correlations between 0.01 (diesel bus) and 0.87 (bicycle on low-traffic route). The roadside FMS appear to better represent the traveler's exposure although the concentrations recorded are still lower. Kaur et al. (2005) obtained ratios of 1.5 (bus), 1.6 (car), and 1.8 (taxi) when the personal measurements of PM_{2.5} were compared with roadside FMS, while ratios of 3.4 (bus), 3.8 (car), and 4.2 (taxi) were found for the comparison with the background FMS. These studies highlight the need for direct personal measurements to assess the personal exposure experienced during commuting.

Portable Devices and Low-Cost Sensors

Personal monitoring is the most direct approach to assess the individuals' exposure during commuting, and it can provide detailed information about short-term exposure in a specified area (Steinle et al. 2015). With the development of novel

Table 1 Instruments used for measurement of PM_{2.5}, PM₁₀, UFP, BC and CO

	Measuring principle	Equipment
PM	Light scattering	Grimm (model 1.101, 1.108, 1.109); Thermo (pDR 1200, pDR 1500); Turnkey (OSIRIS, DUSTMATE), TSI DustTrak (models 8520, 8530, 8533, 8534); TSI OPS (model 3330)
	Laser particle counter	TSI AeroTrak (model 9306); Lighthouse Handheld (model 3016)
	Gravimetry	Micro-Vol sampler, SKC pump, OSIRIS, Casella Vortex Ultraflow
UFP	Light scattering	TSI P-Trak (model 8525), TSI CPC (models 3007, 3775, 3785), TSI NanoScan (model 3910)
	Diffusion charging	Philips Aerasense NanoTracer
	Electrical charging/conductivity measurement, Faraday cup electrometer	GRIMM NanoCheck (model 1.320)
	Electrical charging	Testo DiSCmini
	Electrometer sensing	ELPI
	Spectrometer with particle detection by electrometer	TSI FMPS (model 3091)
BC	Light absorption	AethLabs Micro-aethalometer (models AE51, MA200, MA300, MA350)
CO	Electrochemical monitor	Langan DataBear (models T15, T15v), Draeger Industry PAC II CO, TSI IAQ-track (model 7545), Graywolf (610 IAQ probe), Draeger PAC II CO

observation technologies, portable instruments enable the measurement of air quality data at a higher spatial resolution and have been widely used in the assessment of the individual exposure inside vehicles along the commute route. The main air pollutants measured with personal equipment include PM_{2.5}, PM₁₀, UFP, BC, and CO, and the most frequently used equipment are listed in Table 1.

Portable instruments can be installed in travelers' backpacks, carried in hand, worn over the waist, or mounted inside the vehicles. The devices used to characterize the exposure inside the different transport modes have differences in terms of concentration range, measurement frequency, particle size resolution (for UFP monitors), battery life, clock drift, and portability. Therefore, the selection of the monitoring device can affect the quality of the assessment and the comparability between studies. For example, the P-Trak only detects UFP greater than 20 nm diameter, while TSI CPC 3007 or 3785, Philips NanoTracer and testo DiSCmini count particles as small as 10 nm, which is relevant considering that fresh emissions from vehicular traffic can have a large fraction of particle number below 20 nm. One disadvantage of using portable PM monitors, based on light scattering, is that the optical properties of PM are known to be affected by factors such as particle size, composition, and age. Moreover, optical PM monitors are commonly sensitive to ambient temperature and humidity, and therefore monitors must be checked against

reference instruments (Wang et al. 2009). The instrument microAeth AE51 measures the rate of change of light absorption (880 nm) due to the accumulation of BC on a filter. Nevertheless, the accumulation of BC on the filter reduces the effective optical path resulting in a loading-dependent relationship between the measured absorption and BC mass. Therefore, correction factors must be applied during post-processing of the data to compensate this measurement artifact (Park et al. 2010; Virkkula et al. 2007). Furthermore, in metro, the main sources of PM – the mechanical abrasion between wheel, brakes, and rails – produce high concentrations of particulate iron that result in a BC overestimation by the microAeth AE51 since iron absorbs light at 880 nm.

One of the disadvantages of using these portable devices is that they can only be applied to small-scale studies due to the cost and time required to undertake the fieldwork (Ma et al. 2020). However, the air pollution monitoring paradigm is quickly changing thanks to the fast evolution of the available small sensors technologies, increased computational and visualization capabilities, and wireless communication infrastructure (Morawska et al. 2018). These sensors have two main advantages over classical devices. First, some of these sensors are relatively low cost, which allows the simultaneous monitoring of a large number vehicles with different operating conditions. Secondly, sensor units are small, battery powered, and therefore are easy to worn by people or install inside the cabins. The most promising tool for future exposure assessment during commuting is the development low-cost microsensors that could be integrated in a mobile phone circuit board, allowing seamless tracking of the individuals. Currently, smartphones have been used in Barcelona to track person-level time, geographic location, and physical activity patterns, and showed to be more accurate and efficient than the conventional method using GPS tracker (Donaire-Gonzalez et al. 2016). On the other hand, these sensors present disadvantages such as the selectivity in the case of PM measurements. PM sensors are based on light scattering so they cannot measure properly PM smaller than 0.3 μm .

Exposure Modelling Techniques

The ability to accurately model in-transit exposure has numerous applications in urban planning, transport, and policy development. Modelling techniques avoid the limitations of personal monitoring by extending the studies to wider areas and by scaling sampling sizes to the population level. The exposure models estimate the time-averaged concentration for the exposed individual based on the variation in air pollutant levels over time and space, and the time-activity pattern of the individual. Several exposure models have emerged in the last years aiming at predicting interindividual variability in exposure levels taking into account: (1) the time that each individual spends in each microenvironment over the day, (2) ambient air quality, (3) infiltration of ambient air to indoor microenvironment, (4) characteristics of the indoor microenvironment such as air exchange rates, and (5) population demographics at high spatial resolution such as from census data (Kumar et al. 2018).

The increased availability of population-based information regarding time-location patterns allowed the development of a new generation of exposure models that simulate interindividual variability in exposure, thanks to the increasing use of mobile electronic devices such as smartphones, which often have imbedded GPS receivers, and dedicated GPS dataloggers to collect personal time-location information (Duan et al. 2022; Breen et al. 2014).

The exposure models include temporally and spatially resolved ambient monitoring data and/or predictions of air quality models. Two frequently used air quality modelling techniques are air dispersion models and land use regression (LUR) models. Air dispersion models simulate air pollutant concentrations by using pollutant source information, meteorology, and the underlying surface. The LUR is an application of geographic information system (GIS) that is gaining momentum as a tool to predict exposure to a multiplicity of pollutants. The LUR models estimate the ambient pollutant concentrations at un-sampled points of interest by considering the influence of the land use and the environmental features of the surrounding area. This is based on the construction of a multiple linear regression with explanatory variables, such as distance from the road, altitude, and population density (Gressent et al. 2020). More recently, other methods are used for mapping such as machine learning techniques (Support Vector Regression, Decision Tree Regression, Random Forest Regression, or Extreme Gradient Boosting) (Gressent et al. 2020).

Concurrently, exposure models are also based on the relationship between ambient air quality and pollutant concentrations in indoor microenvironments, which is usually based on mass balance or statistical models. The mass balance approach quantifies infiltration considering air exchange rate, penetration factor, and deposition rates. Several recent studies adopted a more mechanistic, mass-balance modelling approach for automobiles. These works have been based on measurements of the effects of cabin ventilation, filtration, particle penetration, or deposition on in-cabin concentrations (Knibbs et al. 2011). The statistical methods typically estimate the ratio of indoor-to-outdoor concentrations as a single parameter or as part of a linear regression model in which the intercept term accounts for non-ambient pollution of indoor origin. For instance, Correia et al. (2020) measured ambient and in-vehicle concentrations in multiple transport microenvironments in Lisbon to quantify the ratio of in-vehicle to ambient concentrations.

As an example, the Stochastic Human Exposure and Dose Simulation (SHEDS) model has been used by Liu and Frey (2011) to model in-vehicle human exposure to ambient fine particulate matter.

Factors Affecting the Personal Exposure During Commuting

Various studies have focused on personal pollutant exposure in diverse transport modes, such as bus, car, motorcycle, tram, train, subway, cycling, and walking (Buitrago et al. 2021; Correia et al. 2020; de Nazelle et al. 2012; Kaur and Nieuwenhuijsen 2009; Kumar et al. 2021; Martins et al. 2016, 2021). The exposure has been found to vary considerably within and between the different modes of

transport, which can be associated with disparities in the measurement protocols, vehicle characteristics, road typology, and temporal variations. In this review chapter, the several factors that affect the personal exposure were broadly classified into four categories, including (i) transport characteristics; (ii) road and traffic conditions; (iii) meteorology variables; and (iv) individual behaviors.

Transport Characteristics

Several studies have reported that the traffic-related pollutant concentrations inside the vehicles are lower than those in the respective ambient air, evidencing that the vehicle cabin may offer a protective effect (Alameddine et al. 2016; Correia et al. 2020; Leavey et al. 2017; Matthaios et al. 2020; Vijayan and Kumar 2010; Zuurbier et al. 2010). However, vehicles are not built to be airtight and pollutants enter the cabin through leaks in door and window seals and other openings (Martins et al. 2021). Alameddine et al. (2016) attributed the differences in-cabin PM_{2.5} concentrations among car **brands** and **models** to possible distinct penetration factors of the car shells.

Type of Fuel, Vehicle Category, and Emission Standards

The vehicle exhaust emissions are not only affected by **fuel type** but also by **vehicle category** (transport mode) and **vehicle emission standards**. The emission standards are in different stages of development around the world. For example, the European Union is imposing increasingly stringent requirements on exhaust emissions since 1992. The vehicle manufacturers have continually improved engine technologies and have introduced various emission-control systems to comply with the European legislation. Clean fuels, such as lower sulfur content gasoline and diesel fuel, compressed natural gas (CNG), liquefied natural gas (LNG), and hydrogen, are associated to much less pollutant emissions than the traditional ones (gasoline and diesel) due to their physical or chemical properties.

Most of the studies reported that the exposure to traffic-related pollutants during commuting is mainly affected by the emissions from the surrounding vehicles, rather than from the vehicle the individual is commuting in (Karanasiou et al. 2014 and references therein). In a short experiment conducted in Barcelona, particle number concentration (PNC) and BC concentration inside an electric vehicle were higher than in a gasoline vehicle both under traffic and stable conditions (cars parked side by side with the engines off and no passengers inside) (Karanasiou et al. 2014). The indoor concentrations were highly dependent on the outdoor levels, evidencing that the electric car had higher infiltration rate than the gasoline car, which should be related to the vehicle structure and the building materials (Karanasiou et al. 2014).

Other studies have related fuel type of the vehicle with self-pollution. Zuurbier et al. (2010) found that PNC and soot levels in diesel-fueled buses were higher than in electric buses. In diesel buses, a percentage of the existing exhaust pollutants was associated with vehicle self-pollution (Zuurbier et al. 2010). The PM₁₀ concentrations in-cabin of diesel and electric buses were not significantly different, probably

due to the resuspension of particles, created by the passengers' movement and the air flowing when doors open (Martins et al. 2021; Zuurbier et al. 2010). Targino et al. (2020) reported in-cabin of a diesel-fueled buses higher BC concentrations but less particles with smaller diameters than in a biodiesel bus, which was related to the different emission factors of diesel and biodiesel engines. Recently, Zheng et al. (2021) also found that the type of fuel used can influence the PM concentrations inside cars and buses. They observed that PM_{2.5} concentrations inside gasoline-fueled cars were higher than those powered by CNG and even higher compared to those powered by methanol. PM₁₀ concentrations were comparable inside electric and CNG buses (Zheng et al. 2021).

Ventilation Settings

Vehicle cabin ventilation can occur by four different modes, namely natural ventilation, mechanical ventilation, hybrid ventilation, and infiltration (Tong et al. 2019). In natural ventilation, the air enters intentionally into the vehicle' cabin through apertures due to outdoor air movement and pressure differences (e.g., windows open). Mechanical ventilation uses fans to move air into vehicle' cabin; this air can be recirculated inside the cabin or be introduced from outside into vehicle. In these two mechanical modes, the air passes through the cabin filter before (re-) entering the in-vehicle environment. The hybrid ventilation occurs when natural and mechanical forces are used simultaneously, providing a comfortable internal environment. During the vehicle' motion, outside air can also infiltrate into the cabin through leaks due to pressure differences because vehicles are not built to be airtight.

The ventilation control and cabin air filters are capable of improving thermal comfort and indoor air quality (Buitrago et al. 2021; Kumar et al. 2021; Martins et al. 2016; Matthaios et al. 2020). Different air pollutants are affected differently by the ventilation and the filter used. The **filtration** efficiency is dependent on the filter type used in the ventilation system. For instance, cabin air filtration system equipped with a particle filter is efficient to remove pollen, spores, dust, and soot, while the activated carbon filter, besides the function of the particulate filter, also absorbs odors, harmful gases, ozone, benzene, and nitrogen dioxide.

Several authors have assessed the air pollution exposure of vehicle occupants under different ventilation modes, and their results are consistent, demonstrating that the lowest particle exposure occurs when the **air recirculation** is on with the **windows closed** (e.g., Correia et al. 2020; Kumar et al. 2021; Matthaios et al. 2020). The air recirculation reduces the particle concentrations by moving the air inside the vehicle through the cabin filter multiple times. Moreover, other authors have observed that complementing the recirculation with **air-conditioning** mode, the concentrations of particles can be further reduced (Alameddine et al. 2016; Matthaios et al. 2020). In-cabin pollutant concentrations tend to track those existing outdoor when windows are open (Leavey et al. 2017). Particles are dominantly coarse with windows open, while under recirculation or fan on (outdoor air intake), the particles are mainly fine, evidencing the effectiveness of filters removing coarser particles (Kumar et al. 2021). Alameddine et al. (2016) found no statistical difference in PM_{2.5} concentrations between windows half open and air-conditioning with fresh

air intake. Buitrago et al. (2021) verified that the concentrations of VOC, CH₂O, fungi, and bacteria were lower when the ventilation was on. These pollutants were mostly associated with indoor sources and the ventilation promotes dilution.

The **position of the ventilation air intake** also have shown to influence the exposure to air pollutants in-vehicles due to the vertical pollution gradient. For example, Limasset et al. (1993) reported that when the air intake is from the roof of bus, the in-vehicle pollutant concentrations are significantly lower than under the typical front air admission.

Matthaios et al. (2020) evaluated the effect of protection of vehicle structure to outdoor air pollutants, conducting measurements with mechanical ventilation switched off and windows closed. They observed that the personal exposure to UFP, NO₂, and PM2.5 in-vehicle was approximately 63%, 30%, and 20% lower than outdoor, respectively. However, under this lack of ventilation or using recirculation mode, the CO₂ exhaled by vehicle occupants tends to accumulate inside the cabin, which may impair cognitive function, and cause drowsiness and anxiety (Matthaios et al. 2020).

In subway system, the mechanical ventilation also improves air quality, removing more efficiently coarse particles (Lee et al. 2018b; Martins et al. 2015). Martins et al. (2015) tested several ventilation protocols to evaluate PM concentrations differences and observed that the ventilation intensity is very important in the control of air quality. Weak ventilation enhanced the accumulation of PM in the Barcelona subway stations (Martins et al. 2015). Inside the subway trains, the ventilation system provides a clear abatement of PM concentrations due to the particle deposition and filtration (Martins et al. 2015; Van Ryswyk et al. 2017). In trains where the windows are usually open, such as in Athens (carriage windows can be open by the passengers), the concentrations can increase when passing through tunnels (Martins et al. 2016), due to the entrance of polluted air from tunnels and platforms into the trains.

Interior Materials

Different manufacturers design vehicles with different characteristics such as interior volume, ventilation settings, and building materials, which highly influence the commuters' exposure (Xu et al. 2018). VOC constitute the biggest proportion of pollutants in vehicle cabin (Geiss et al. 2009). Yoshida et al. (2006) measured air pollution in 101 cars due to organic compounds diffusing from the interior materials and found 275 VOC and SVOC being the sum of the aliphatic and aromatic hydrocarbons 45% of all compounds identified.

The **main sources** of VOC in cabins are the plastics (such as polystyrene, polyethylene, polypropylene, polyamide, polyester, polyacetal, acrylonitrile-butadiene-styrene), fibers, textiles, natural or artificial leather, rubber, polyurethane foams, coatings, and adhesives, which are used to produce components in the cabin interior: steering wheel, wrapping of the steering wheel, dashboard, insulations, seats and couch, upholstery, soundproofing, roof ceiling, floor mats, and seat covers (Faber and Brodzik 2017). Chien (2007) analyzed interior parts of domestic cars and verified that 2,6-di-tert-butyl-4-methylphenol, a common antioxidant in plastics, rubbers, and petroleum products, was the most frequent chemical in the interior

parts, followed by aliphatic hydrocarbons, such as heptadecane, hexadecane, and tetradecane. Long-chain aliphatic hydrocarbons, namely tetradecane, pentadecane, hexadecane, and heptadecane, respectively, were found in most grease samples. Other long-chain aliphatics, such as eicosane (C₂₀) and docosane (C₂₂), which are commonly applied as synthesis materials or plasticizers, were found in rear panel and carpet samples. The adhesives, which are used to attach the various components of interior parts, are probably the major sources of toluene and xylene (Chien 2007). Among all the materials, it was verified that leather is an important source of VOC. According to Yoshida et al. (2006), the content of VOC increased in luxury cars where the concentrations of aromatic hydrocarbons, alcohols, ethers, furans, and nitrogen-containing compounds increased with price of the cars. Results of this work showed that the contents of alcohols and 1-methyl-2-pyrrolidone were higher in cars with leader seats than in those with fabric seats, and the concentrations of ketones, furans, styrene, and 1-methyl-2-pyrrolidone were higher in cars with leader steering wheels instead of polyurethane steering wheels.

VOC emissions can be divided into **primary and secondary emissions**. Primary emissions are emissions of non-bound or free VOC within building materials, which takes place during the first year after material production date, and are mostly low-molecular organic compounds. The secondary emissions refer to VOC that were originally chemically or physically bound, takes place over 1 year after material manufacture and is mostly connected with organic compounds which are products of degradation, hydrolysis, or oxidation reaction, and others (Kataoka et al. 2012). The concentration of the compounds resulting from the secondary emission is usually several orders lower than from the primary emission (Faber and Brodzik 2017). Therefore, the interior air inside the cabins of new cars immediately after the delivery can be always considered contaminated with very high concentrations of contaminants diffusing from interior materials that tend to decay in the following months. Yoshida et al. (2006) observed that 1 month after the delivery, the TVOC concentrations decreased to about one-fourth. Along with the time of vehicle usage, emission of organic compounds from materials is gradually replaced by emission from external sources, such as the fuel leakages and combustion of fuel. According to Bakhtiari et al. (2018), the vehicle's age increases fugitive emissions of exhaust fumes as gaskets age or joints in the exhaust train become loose. These emissions can penetrate into the cabin through gaps and lead to increased air pollutant concentrations.

Some attempts are being made to establish **indoor air quality guidelines** for passenger cars. The Japan Automobile Manufacturers Association (JAMA) launched the "Voluntary Approach to Vehicle Cabin VOC Reduction" to satisfy government demands for 13 VOC. In July 2007, the Chinese government introduced a vehicle cabin VOC regulation including buses and trucks. In Europe, several German Original Equipment Manufacturers (OEM) have set VOC targets based on VDA (Verband der Automobilindustrie) test methods. The big step to harmonization of test procedures were the ISO 12219, which outlines a method of measuring the types and concentrations of VOC in vehicle cabin air under controlled conditions, and the Mutual Resolution No. 3 (Nations 2018) that outlined the provisions and

harmonized test procedure for the measurement of interior emissions, taking into account existing standards, aiming at encouraging the reduction of the use of materials and chemicals, which can be unsafe to humans, and the increased use of emission-friendly materials, improving the air quality inside the vehicles.

Road and Traffic Conditions

Several studies have identified **horizontal pollution gradients** along traffic roads (Amato et al. 2019 and references therein). Generally, pollutant concentrations decrease with increasing distance from the road edge, being typically elevated on and near heavily trafficked roads. Recently, Amato et al. (2019) found that traffic pollutants decay to urban background concentrations on average within 67 m of the road edge, with higher distances for more busy roads. High commuters' exposure to traffic-related air pollutants are mainly associated to their close proximity to the mobile sources. Short **distance between vehicles** allows the infiltration of pollutants emitted by the neighboring vehicles, resulting in high exposures. McNabola et al. (2009) concluded that keeping a 2 m distance from the preceding vehicle can reduce the exposure to PM and VOC of 30–40% in comparison with vehicles that only keep 1 m distance.

Road traffic conditions – **light or heavy traffic congestion** – can affect the personal exposure during commuting. Commuters can reduce their exposure by travelling in low-traffic roads (Kaur and Nieuwenhuijsen 2009; Zuurbier et al. 2010). Traffic density does not affect significantly the PM10 and PM2.5 concentrations, but it has a greater influence on PNC, BC, and CO levels (Kaur and Nieuwenhuijsen 2009; Zuurbier et al. 2010). Dons et al. (2013) verified that the in-vehicle BC exposure is positively correlated with the traffic intensity.

At **traffic intersections**, there are restrictions laid by **traffic signals**, which affect the traffic flow due to the changes of driving conditions (i.e., idle, acceleration, deceleration, and cruise). At signalized traffic intersections, vehicles frequently stop with idling engines during the red-light period and accelerate rapidly when the traffic signal change to green, which produces higher emission rates. For instance, spending only 2% of commuting time at signalized traffic intersections may account for up to ~25% of the PNC total commuting exposure doses in certain situations (Goel and Kumar 2015). During typical delay conditions at traffic intersections, Goel and Kumar (2015) measured PNC during acceleration up to ~6 times higher than those during idling conditions. Moreover, they also observed that average PNC at traffic intersections during congested conditions can be up to 29 times higher in comparison with **free-flowing conditions**. Similarly, Matthaios et al. (2020) also measured high concentrations of air pollutants close to junctions and **roundabouts**.

The highest concentrations were observed in an **underground tunnel** due to the limited air dispersion (Matthaios et al. 2020). De Vlieger et al. (2000) showed that generally city journeys resulted in higher CO, total hydrocarbons (HC) and NOx emissions than in rural and ring road journeys. **Road grade** also affects vehicle pollutant emissions due to the change in the engine power demand (Zhou et al.

2016). The pollutant emissions during uphill driving increase due to the high demand of engine power (Goel and Kumar 2014 and references therein).

Traffic density varies over time. This variation influences traffic-related emissions and consequent pollutant exposures (Batterman et al. 2015). Brand et al. (2019) measured higher BC concentrations in the morning peak hours in São Paulo and Rotterdam, while in London, higher BC concentrations were recorded during the evening peak hours. In Brussels, the average CO and HC emissions during the rush hours were 80% higher than in smooth-flowing traffic, and 50% for NOx (De Vlieger et al. 2000). During rush hours (at around 13.5 km/h), CO₂ emissions doubled compared to driving at 50 km/h (De Vlieger et al. 2000).

On subway systems, PM concentrations depend largely on the operation and frequency of trains (Martins et al. 2016; Van Ryswyk et al. 2017; Woo et al. 2018).

Meteorological Variables

Meteorological conditions affect the personal exposure to pollutants during commuting. The most important variables to consider are wind speed and direction, temperature, and relative humidity.

Several commute studies have reported negative linear correlations between **wind speed** and in-vehicle air pollutants (e.g., Alameddine et al. 2016; Gómez-Perales et al. 2004; Kaur and Nieuwenhuijsen 2009; Onat et al. 2019; Rivas et al. 2017), since wind speed affects the dispersion and dilution of pollutants and thus atmospheric mixing. For example, Onat et al. (2019) found that wind speed was a significant factor influencing UFP, BC, and PM2.5 in-vehicle concentrations on four travel modes (bus, metrobus, car, and light rail) and explained up to 29%, 20%, and 11% of their variability, respectively. Gómez-Perales et al. (2004) observed reductions in PM2.5 concentrations of 22% and 24% for every 1 m/s increase in wind speed for minibuses and buses, respectively. For CO, the reductions were slightly lower, 18% and 12% for every 1 m/s increase in wind speed for minibuses and buses, respectively (Gómez-Perales et al. 2004). **Wind direction** also proved to have a considerable impact mainly when it comes to street canyons (Kumar et al. 2018).

Diverse studies found negative correlation between **temperature** and outdoor air pollutants concentrations (de Nazelle et al. 2012; Du et al. 2020; Kaur and Nieuwenhuijsen 2009; Leavey et al. 2017). Kaur and Nieuwenhuijsen (2009) verified that temperature is a significant determinant of UFP and CO exposure levels, which explained approximately 12% and 11% of the variability in the respective pollutants. When the vehicle hot exhaust gases mixes with cold ambient air results in optimal conditions to occur particle nucleation (Morawska et al. 2008). At higher temperatures, the nucleation is limited due to temperature dependence of saturation vapor pressure, resulting in lower PNC (Morawska et al. 2008). Vehicle engine operate less efficiently when cold resulting in higher emissions of products of incomplete combustion, such as CO and HC (Du et al. 2020). The cold ambient

temperatures can enhance the cold-start emissions due to the longer warm-up time (Du et al. 2020).

A strong temperature-dependent increase in the concentrations of indoor origin VOC has been reported in several studies (Chien 2007; Yoshida and Matsunaga 2006). Parking in sunlight in summer can increase the interior temperature up to 89 °C, with dashboard temperature reaching 120 °C (Mandalakis et al. 2008). A high temperature promotes the emission of VOC and may also induce photochemical reactions and the production of degradation by-products, which can be more harmful than their precursors. For example, labile decabrominated diphenyl ether, which is the main component of the widely produced flame retardant deca-BDE, can be photodegraded to more toxic tetra- and penta-brominated diphenyl ethers and brominated dibenzofurans (PBDFs) (Söderström et al. 2004). Moreover, through the hydrolysis and thermal degradation, the phthalates, which have been identified in door-panel and adhesive samples from cars (Chien 2007), can result in 2-ethyl-1-hexanol (Wolkoff 1999), a compound whose in-cabin concentrations increase with days lapsed after delivery and with temperature (Yoshida and Matsunaga 2006).

Therefore, the compounds which increase in winter are typically produced during combustion processes and are not predominantly released from equipment parts used inside the vehicle (Geiss et al. 2009). This can occur because the lowest ventilation rate inside the car during the cold period can concentrate pollutants inside the vehicle. Chien (2007) showed that the use of air-conditioning generally reduced the in-cabin VOC concentrations by reducing the interior temperature or dilution but the reduction was not statistically significant probably due to the interference from outdoor VOC.

The analysis of the UFP concentrations in London showed that **humidity** also has a positive correlation with the personal exposure levels (Kaur and Nieuwenhuijsen 2009). The relative humidity affects largely the nucleation mode particles, existing high concentrations during high humidity periods (Morawska et al. 2008). High atmospheric water content favors the formation of new particles (nuclei mode) and also the growth of particles (nuclei mode and primary particles) (Jamriska et al. 2008).

de Nazelle et al. (2012) evaluated the effect of weather variables (wind speed and direction, relative humidity, temperature) on commuters' exposure, and indicated that the only significant variables were wind speed for BC, CO₂, and CO (explaining 6.2%, 1.5%, and 1.2% of the variability, respectively), and humidity for UFP (3.6%). They did not find any significant influence of weather conditions on PM2.5 exposure levels. However, the authors mentioned that the low variance in commuters' exposure explained by weather conditions may be related with low meteorological variations during measurements. Rivas et al. (2017) indicated that among the meteorological predictor variables explored in the study (temperature, relative humidity, and wind speed), the wind speed had the strongest significant linear associations with pollutant concentrations. Comparing transport modes, the wind speed had a higher influence on bus concentrations than on car and walking (Rivas et al. 2017).

Moreover, **atmospheric stability** can also influence the personal exposure to traffic-related air pollutants over the day. Typically, mornings are characterized by stable atmospheric conditions, which favor the accumulation of air pollutants, and in afternoons occurs unstable conditions with greater dispersion (Batterman et al. 2015). Such patterns emphasize the importance of the morning traffic peak.

The impact of meteorological variables on air pollutants varied across studies, because it is dependent on location and transport mode. Although the meteorological factors can influence the ambient pollutant concentrations, the commuters can do little to reduce their personal exposure, especially those travelling by active transport or motorcycle. In subway systems, the weather conditions do not have direct effect in the indoor air quality, and it depends on the existing ventilation in these confined spaces.

Individual Behavior

Driving modes such as speed, acceleration, deceleration, cruise, and idling have an important impact on fuel consumption and vehicle pollutant emissions (Birrell et al. 2014; Sanguinetti et al. 2020). Adopting an **aggressive driving** style (i.e., sudden and frequent acceleration and braking events, late gear changes, and high driving speeds) can be responsible for reducing the fuel economy by 20–40% (Birrell et al. 2014; De Vlieger et al. 2000). De Vlieger et al. (2000) found that aggressive driving resulted in increases of CO up to a factor of 8 compared to **normal driving**. The HC and NOx emissions increased by 15–400% and 20–150%, respectively. Air resistance increases with the vehicle velocity, reducing the fuel efficiency and generating more pollution (Gonder et al. 2011). An experimental test conducted by Lee et al. (2015) indicated that UFP infiltration into passenger vehicles is location-specific and driving-speed dependent. The higher speeds favor the infiltration of UFP due to increased surface pressure. The in-vehicle BC concentrations are elevated at lower speeds (up to 30 km/h) and at speeds above 80 km/h (Dons et al. 2013). At lower speeds, the influence of the emissions from neighboring vehicles is higher. Gonder et al. (2011) verified that reducing accelerations and decelerations together (i.e., stop/start cycles) saves a larger amount of fuel in city trips, while reducing high speeds seems to be the dominant factor for improving highway driving efficiency.

The in-vehicle pollutant concentrations showed to be highly dependent on **window condition** (open vs. closed) and **ventilation setting** (in-cabin recirculation vs. outside air intake), being considerably lower with windows closed and air recirculation on (Correia et al. 2020; Kumar et al. 2021; Matthaios et al. 2020). Drivers should travel with windows closed when commuting in heavy traffic conditions to avoid the entrance of outdoor pollutants into the vehicle (Leavey et al. 2017).

Buitrago et al. (2021) evaluated the influence of **cleaning** on the air quality inside the cars. They observed that cleaning process decreased the concentrations of VOC, CH₂O, fungi, and bacteria inside the cabin.

The use of specific products in cars or by the users had been found to affect the air quality inside the cabins. Yoshida et al. (2006) analyzed the volatile components from 25 **fresheners** and found that the major components were terpenes (β -pinene, limonene, 1,8-cineole, β -linalool, dihydromyrcenol) and esters (ethylacetate, ethylbutyrate, isopentylacetate, and 4-tert-butylcyclohexyl-acetate). Limonene was the compound with maximum concentration in 11 air fresheners.

Smoking cigarettes in car generated high concentrations of several hazardous pollutants, putting occupants at increased health risk (Savdie et al. 2020 and references therein). Even under realistic ventilation conditions in cars, the tobacco smoke pollution can reach unhealthy levels (Sendzik et al. 2009). Airborne nicotine was detected in cars in which drivers or passengers smoked (Yoshida et al. 2006) and significant higher values of formaldehyde were measured in the same cars (Yoshida et al. 2006). The fabric ceiling, seats, and floor mats of the cars are likely to be major sources of nicotine and formaldehyde from tobacco, and esters and terpenes from air fresheners because textiles serve as storage media and as a reversible interim store for chemical substances due to their strong sorption ability (Yoshida et al. 2006).

Other key personal factors that have shown to affect exposure in-buses are: doors opening frequently, bus stop locations, vehicle occupancy (number of passengers), and seating location. In-bus pollutant concentrations are affected by the frequent **door openings**, because the outdoor polluted air can enter the cabin when doors open for passengers to get on and off (Zuurbier et al. 2010). Inside the subway trains, Martins et al. (2016) also observed the occurrence of short-term peaks in PM concentrations after the train doors closed, related to the turbulence and resuspension created by the passengers' movement.

Bus stops are typically located near intersections, which are characterized by high concentrations of air pollution due to the changes of driving conditions (i.e., deceleration, idle and acceleration) (Goel and Kumar 2015; Matthaios et al. 2020). For instance, Choi et al. (2018) estimated that the exposure to UFP can be reduced in 38% if the bus stop is moved from 20 to 40 m after the intersection.

Several studies have shown the **seating location** (i.e., front, middle, or back) can potentially influence the exposure of bus travelers (Vijayan and Kumar 2010; Zuurbier et al. 2010). Vijayan and Kumar (2010) measured at the back area of bus PM concentrations up to 2–7 times higher than in the front. When the driver area has a protective barrier, the driver is exposed to lower PM, BC, and PNC concentrations than the passengers (Zuurbier et al. 2010).

Some air pollutants are highly affected by the **vehicle occupancy**. A number of studies conducted inside vehicles have illustrated that the CO₂ concentrations can increase rather rapidly principally in crowded public transports and during rush hours (Martins et al. 2016; Ramos et al. 2016). Airborne microbiota is also highly influenced by the occupancy of the vehicles and consequently, the bacterial and fungi loads were found to be higher in buses and trains than in cars (Buitrago et al. 2021).

Impacts on Health

Findings from previous studies indicate that commuters inside transport cabins from private or public car, metro, train, or bus are exposed to high concentrations of air pollutants, impacting on healthy individuals but principally on health of vulnerable cohorts of the population such as children, elders, asthmatic, diabetics, and specific professional groups.

Healthy individuals commuting in roadway experienced a decrease in lymphocytes and increase in levels of red blood cell indices, neutrophils, exhaled nitric oxide, C-reactive-protein, and exhaled malondialdehyde, which indicated pulmonary and systemic inflammation and increased oxidative stress (Riediker et al. 2004; Sarnat et al. 2014). A large case-crossover study, with a total of 1459 cases, suggested that exposure during commuting increase the risk of acute myocardial infarction (Peters et al. 2013). In vitro studies indicate that underground particulate matter, as a result of its metal-rich nature, may be more toxic than urban particulate matter, principally in terms of endpoints related to oxidative stress and reactive oxygen species generation (Loxham and Nieuwenhuijsen 2019). Nevertheless, although there are quantifiable impacts on a variety of endpoints following exposure *in vivo*, there is a lack of evidence for these impacts being clinically significant (Loxham and Nieuwenhuijsen 2019).

Children are more vulnerable to the adverse effects of air pollution because they are continually growing, and their defense mechanisms are still immature. The exposure of children during commutes is linked with adverse cognitive outcomes and severe wheeze in asthmatic children (Ma et al. 2020). Among a cohort of 4741 children, McConnell et al. (2010) found that severe wheeze is linked with commuting periods for asthmatic children.

Elderly volunteers that rode for 2 h in a van modified with high-efficiency filtration system, which delivered filtered or unfiltered air to the cabin, experienced a 30% decrease in cardiopulmonary stress biomarkers and 20% decrease in the incidence of atrial ectopic heartbeats when the air was filtered (Hinds 2010). This work indicates a cardiac and vascular response of elders associated with freeway travel. Adar et al. (2007) also showed that fine particle exposures during trips aboard a diesel bus resulted in increased levels of exhaled nitric oxide in elderly adults, suggesting increased airway inflammation.

Type 2 diabetics exposed to pollutants in automobile highway trips during 1.5–1.8 h experienced a decrease in high-frequency heart rate variability the day after exposure, which was more associated with the interquartile range of UFP concentration compared to those of PM2.5, NO₂, and CO (Laumbach et al. 2010).

Professional drivers could be at risk regarding their respiratory health due to the constant exposure to traffic-related air pollutants inside vehicles (Hadei et al. 2019). Several works have showed that professional groups whose workday is constituted by long periods in TME had a higher prevalence/incidence of respiratory symptoms, such as cough, phlegm, wheezing, short breath, throat unwell, chest pain, nose discomfort, and rhino sinusitis (Hachem et al. 2019).

Measures to Reduce Exposure During Commuting

Policy makers and urban planners should make concerted efforts to reduce traffic pollutant emissions by effective implementation and enforcement of stringent policies. Glazener and Khreis (2019) conducted a systematic review of the best policies and practices to improve air quality and support active transportation in cities. They highlighted that implementing a variety of policies simultaneously, such as vehicle use restrictions, vehicle technologies improvements, emission standards, integrated public transportation, urban design interventions, and green space provision, the results are more effective. A study by Wen et al. (2020) formulated mitigation strategies to reduce pollutant concentrations in subway stations based on existing literature findings. The identified strategies are focused on preventing external filtration, limiting internal sources, and eliminating or diluting pollutants, and should be considered by subway system managers. While public policies and practices have a crucial role in improving air quality, individual actions can also be effective in reducing exposure and health risks. For instance, commuters can reduce their exposure by:

- Avoiding heavily trafficked roads and major intersections
- Keeping a distance from the preceding vehicle
- Optimizing vehicle filtration/ventilation
- Maintaining indoor cabin hygiene
- Enhancing the driving-related behavior
- Shifting from motorized to active transport
- Walking and cycling in designated paths
- Using health-optimal routing service

A deliberate effort of the population to practice mitigation measures is crucial to reduce the emission of air pollutants and therefore decrease the health effects and economic costs associated to the air pollution exposure.

Optimizing Driving Behavior

Techniques aimed at changing driving behavior such as eco-driver training, eco-routing, and on-board eco-driving feedback technologies have been demonstrating to be an effective way to reduce fuel consumption and pollutant emissions (Chen et al. 2018; Sanguinetti et al. 2020; Zhou et al. 2016). In the study by Sanguinetti et al. (2020), the use of **on-board eco-driving feedback** showed to improve the fuel economy by 6.6% on average. Chen et al. (2018) established an eco-driving behavior based on vehicle operating and fuel consumption data and provided several driving advice. The **eco-driving behavior** can be achieved by: (i) starting smoothly; (ii) accelerating moderately and evenly until desired speed; (iii) keeping steady speed (cruise mode); (iv) minimizing the brake events by keeping a proper following distance; (v) reducing the number of instances of sharp acceleration and

deceleration, (vi) using engine braking, and (vii) minimizing idling (Birrell et al. 2014; Sanguinetti et al. 2020).

Transition to Active Transportation

World Health Organization (WHO) recommends that adults get at least 150 min of **physical activity** weekly to reduce the risk of early death, cardiovascular diseases, hypertension, type 2 diabetes, and several cancers (WHO 2020). Replacing daily trips from motorized to active transport could enable commuters to achieve the daily-recommended levels of physical activity. The most common modes of active transport are walking and cycling. Proximity to motorized traffic has been associated with high cyclist and pedestrian exposure to traffic-related air pollutants (Dons et al. 2013). Nevertheless, studies have shown that active commuters' exposure can be reduced by increasing the **distance** of walk and cycle paths from traffic (Correia et al. 2020; MacNaughton et al. 2014). MacNaughton et al. (2014) observed that in cycle paths adjacent to road traffic the BC and NO₂ concentrations were around 33% higher than in cycle paths away from the vehicle traffic. They also found that the existence of a **vegetation barrier** affects the pollution concentrations; increasing vegetation density, the levels of air pollution in cycle path decrease. Urban planners should prioritize the selection of off-road walking and cycle paths and/or the inclusion of vegetation barriers whenever possible. Separated paths not only increase safety but also enhance the public perception of safety from the point of view of traffic injury, which may promote active travels (Hull and O'Holleran 2014). Thus, the creation of comprehensive and dedicated **active transport infrastructures** can therefore be an effective policy to promote population behavioral changes, leading to environmental, health, social, and equity benefits (de Nazelle et al. 2011; Mueller et al. 2015). Hull and O'Holleran (2014) makes several recommendations for improving cycling infrastructure provision.

In the past decade, health impact assessment (HIA) has been frequently used as a practical approach to evaluate potential health effects of policies, programs, and projects in the non-health sector. These potential health risks and benefits are considered during the decision-making process. Programs to change travel behaviors are crucial to incentive people to use sustainable modes of commuting. Encouraging active transportation is an effective means of promoting a more active and healthier lifestyle (Mueller et al. 2015). A shift from motorized to active transport contributes to a reduction in traffic volume and consequent reduction of air pollution emissions.

Active commuters may inhale more air pollutants than motorized commuters when travelling the same distance/route due to both longer journey times and higher inhalation rates (de Nazelle et al. 2012, 2017; Martins et al. 2021; Zheng et al. 2021; Zuurbier et al. 2010). Authors of a systematic review (Cepeda et al. 2017) calculated the motorized-to-active travel dose ratios of pollutants based on 12 studies; they obtained the following median ratios: 0.22 for car, 0.38 for motorcycle, 0.49 for rail transport, and 0.72 for bus. Nevertheless, HIA studies have stated that the **health benefits** from physical activity during active transportation largely **outweigh the**

risks associated with the high inhaled dose of traffic-related pollutants (Mueller et al. 2015 and references therein). Andersen et al. (2015) indicated beneficial effects of physical activity on mortality even in high air pollution areas.

Several studies have been estimating the overall impact of switching commutes from motorized to active transport. Cepeda et al. (2017) calculated differences in terms of years of life expectancy (YLE) according to differences in fine particulate inhaled dose and physical activity when commuting, and they concluded that motorized commuters lost up to 1 year more in YLE than cyclists. A Swedish study estimated the potential effects on mortality by shifting commuting from car to bicycle of 111,000 people in Stockholm County area. In annual terms, the reduction of population exposure to NOx related to this modal shift can avoid 63 premature deaths and save 449 years of life (Johansson et al. 2017). The extensive study conducted by Rojas-Rueda et al. (2016) assessed the potential health impacts of reaching two active transportation targets (35% cycling and 50% walking) in six European cities (Barcelona, Basel, Copenhagen, Paris, Prague, and Warsaw), considering the changes in physical activity, exposure to PM2.5, and traffic fatalities. These targets are based on the real levels of cycling in Copenhagen and walking in Paris. The highest benefits can be achieved with the increment of cycling trips to 35%, which can avoid annually around 113 deaths in Warsaw, 61 in Prague, 38 in Barcelona, 37 in Paris, and 6 in Basel. Increasing the walking trips to 50% can avoid approximately 20 deaths per year in Warsaw, 11 in Prague, 6 in Basel, 4 in Copenhagen, and 3 in Barcelona (Rojas-Rueda et al. 2016). Moreover, recent findings reported by Dinu et al. (2019) support the evidence that active commuters can reduce in 8% the risk of all-cause mortality, 9% the cardiovascular disease incidence, and 30% the risk of diabetes. Commuting by cycling was associated with a significant lower risk of all-cause mortality (-24%) and a reduction of 25% of total cancer incidence. The associated environmental benefits from active transportation include the reduction of energy consumption and greenhouse gas emissions (Rabl and de Nazelle 2012).

Healthier Routes Planning

Commuters' exposure may vary substantially depending on the selected route (Hertel et al. 2008). Typically, the commuters tend to choose the route based on the shortest time duration or the shortest distance. **Route planner** incorporating air pollution information may encourage the population to choose the lowest exposure route (Hertel et al. 2008).

Several studies have shown that the mobile air pollution monitoring systems can effectively be used to derive **accurate pollution maps** with high spatiotemporal resolution (Devarakonda et al. 2017; Santana et al. 2021). Using large quantities of sensors in wireless networks can increase the coverage area and spatial distribution of the monitoring systems, especially if mounted on mobile platforms. The deployment of sensor nodes on vehicles, enables the automated collection of large, spatially resolved data sets. Recently, the ExpoLIS project developed a novel and affordable vehicle-mounted sensor system to obtain accurate and fine-grained air pollution road

maps (Santana et al. 2021). A **health-optimal routing service** was developed to help users to reduce their exposure to air pollution by not taking the shortest path between origin and destination but a healthier and slightly longer alternative route, based on multi-criteria optimization techniques.

The online route plan tool “Route2School” provides schoolchildren with indication of less polluted routes to-and-from school (Ahmed et al. 2020). In a study area context (in Antwerp, Belgium), **cleaner alternative routes** have been found for nearly 34% of the commuting trips, with a difference of NO₂ concentration of around 10 µg/m³ between the alternative and the current choice of route. In similar study conducted in Montreal (Canada), the alternative routes were estimated based on the shortest distance and less polluted route; approximately 57% of the cycling trips can be changed by cleaner alternative routes (Hatzopoulou et al. 2013).

Zou et al. (2020) proposed an innovative healthier route planning method that estimates the potential adverse health effects associated to the PM2.5 exposure in routes located in Beijing-Tianjin-Hebei (China). While the other studies consider the distance length, time duration, and pollution exposure, this study also introduces the exposure-response relationship, enabling the identification of routes with lower potential health effects.

In contrast to the previous studies, Vamshi and Prasad (2018) proposed a dynamic route planning algorithm to divert the traffic from busy junctions to low traffic junctions in real time. Thus, the algorithm provides the shortest route with smallest number of busy junctions and therefore reducing the existence of air pollution hotspots at traffic junctions. This algorithm tries to avoid amount and time of air pollution exposure to the commuters travelling from a source to destination.

All these studies suggest that commuters can reduce significantly their exposure to air pollutants and consequent health risks by adopting the suggested less polluted routes.

Conclusions

Transport is a ubiquitous component of life, and the scientific community findings suggest that exposures incurred during commuting can contribute substantially to daily exposure and be associated with adverse health effects in healthy people and susceptible population. Although commuters typically spend less than 10% of their time in vehicles, the emissions from various interior materials of vehicles and the exhaust emissions carried by ventilation supply air are significant sources of air pollutants, which can lead to unhealthy human exposure due to their high concentrations inside vehicles’ cabins. The measures to lower the in-cabin exposure levels of air pollutants include optimizing vehicle ventilation and filtration, avoiding trafficked roads and rush hours, maintaining indoor cabin hygiene, and pre-bake-out of interior materials prior to installation to vehicles.

There are no specific regulations to control air quality within TME, even in public transports systems. Various regulatory bodies have defined limit values for several ambient air pollutant, but these are meant to control ambient pollutant concentrations

and do not represent the human exposure during commuting that varies considerably between different TME and different conditions in each transport mode. Besides that, regulatory levels for important transport related pollutants, such as BC and UFP, are still nonexistent. Therefore, the results reported by the scientific community about the concentrations of pollutants in different TME, factors influencing the exposure while commuting and health impacts are very useful for exposure analyses and may inform planners and decision makers on urban policies. Policy makers need to recognize that commuting contributes substantially to overall pollutant intake and can lead to detrimental health impact and help address air pollution while promoting active travel to yield substantial health benefits in the population.

Cross-References

► [Time-Activity Patterns](#)

Acknowledgments This study was developed in the scope of the project ExpoLIS funded by FEDER, through Programa Operacional Regional de Lisboa (LISBOA-01-0145-FEDER-032088), and by national funds (OE), through FCT - Fundação para a Ciência e Tecnologia, I.P. (PTDC/EAM-AMB/32088/2017). Authors also acknowledge the support of FCT through the strategic project UIDB/04349/2020+UIDP/04349/2020 and the contract CEECIND/04228/2018.

References

- Ackermann-Liebrich U, Felber Dietrich D, Joss MK (2019) Respiratory and cardiovascular effects of NO₂, in: reference module in Earth systems and environmental sciences. Elsevier. <https://doi.org/10.1016/b978-0-12-409548-9.02128-x>
- Adar SD, Adamkiewicz G, Gold DR, Schwartz J, Coull BA, Suh H (2007) Ambient and microenvironmental particles and exhaled nitric oxide before and after a group bus trip. Environ Health Perspect 115:507–512. <https://doi.org/10.1289/EHP.9386>
- Ahmed S, Adnan M, Janssens D, Wets G (2020) A route to school informational intervention for air pollution exposure reduction. Sustain Cities Soc 53:101965. <https://doi.org/10.1016/j.scs.2019.101965>
- Alameddine I, Abi Esber L, Bou Zeid E, Hatzopoulou M, El-Fadel M (2016) Operational and environmental determinants of in-vehicle CO and PM 2.5 exposure. Sci Total Environ 551–552: 42–50. <https://doi.org/10.1016/j.scitotenv.2016.01.030>
- Amato F, Pérez N, López M, Ripoll A, Alastuey A, Pandolfi M, Karanasiou A, Salmatoniadis A, Padoan E, Frasca D, Marcoccia M, Viana M, Moreno T, Reche C, Martins V, Brines M, Mingüillón MC, Ealo M, Rivas I, van Drooge B, Benavides J, Craviotto JM, Querol X (2019) Vertical and horizontal fall-off of black carbon and NO₂ within urban blocks. Sci Total Environ 686:236–245. <https://doi.org/10.1016/j.scitotenv.2019.05.434>
- Andersen ZJ, de Nazelle A, Mendez MA, Garcia-Aymerich J, Hertel O, Tjønneland A, Overvad K, Raaschou-Nielsen O, Nieuwenhuijsen MJ (2015) A study of the combined effects of physical activity and air pollution on mortality in elderly urban residents: the Danish Diet, Cancer, and Health Cohort. Environ Health Perspect 123:557–563. <https://doi.org/10.1289/ehp.1408698>
- Araujo JA, Nel AE (2009) Particulate matter and atherosclerosis: role of particle size, composition and oxidative stress. Part Fibre Toxicol 6:1–19. <https://doi.org/10.1186/1743-8977-6-24>

- Asmi E, Antola M, Yli-Tuomi T, Jantunen M, Aarnio P, Mäkelä T, Hillamo R, Hämeri K (2009) Driver and passenger exposure to aerosol particles in buses and trams in Helsinki, Finland. *Sci Total Environ* 407:2860–2867. <https://doi.org/10.1016/j.scitotenv.2009.01.004>
- Babadjouni RM, Hodis DM, Radwanski R, Durazo R, Patel A, Liu Q, Mack WJ (2017) Clinical effects of air pollution on the central nervous system; a review. *J Clin Neurosci* 43:16–24. <https://doi.org/10.1016/j.jocn.2017.04.028>
- Bakhtiari R, Hadei M, Hopke PK, Shahsavani A, Rastkari N, Kermani M, Yarahmadi M, Ghaderpoori A (2018) Investigation of in-cabin volatile organic compounds (VOCs) in taxis; influence of vehicle's age, model, fuel, and refueling. *Environ Pollut* 237:348–355. <https://doi.org/10.1016/j.envpol.2018.02.063>
- Batterman S, Cook R, Justin T (2015) Temporal variation of traffic on highways and the development of accurate temporal allocation factors for air pollution analyses. *Atmos Environ* 107:351–363. <https://doi.org/10.1016/j.atmosenv.2015.02.047>
- Bell ML, Peng RD, Dominici F, Samet JM (2009) Emergency hospital admissions for cardiovascular diseases and ambient levels of carbon monoxide results for 126 United States urban counties, 1999–2005. *Circulation* 120:949–955. <https://doi.org/10.1161/CIRCULATIONAHA.109.851113>
- Birnbaum LS, Staskal DF (2004) Brominated flame retardants: cause for concern? *Environ Health Perspect*. <https://doi.org/10.1289/ehp.6559>
- Birrell S, Taylor J, McGordon A, Son J, Jennings P (2014) Analysis of three independent real-world driving studies: a data driven and expert analysis approach to determining parameters affecting fuel economy. *Transp Res Part D: Transp Environ* 33:74–86. <https://doi.org/10.1016/j.trd.2014.08.021>
- Bornehag CG, Sundell J, Weschler CJ, Sigsgaard T, Lundgren B, Hasselgren M, Hägerhed-Engman L (2004) The association between asthma and allergic symptoms in children and phthalates in house dust: a nested case-control study. *Environ Health Perspect* 112:1393–1397. <https://doi.org/10.1289/ehp.7187>
- Brand VS, Kumar P, Damascena AS, Pritchard JP, Geurs KT, Andrade M d F (2019) Impact of route choice and period of the day on cyclists' exposure to black carbon in London, Rotterdam and São Paulo. *J Transp Geogr* 76:153–165. <https://doi.org/10.1016/j.jtrangeo.2019.03.007>
- Breen MS, Long TC, Schultz BD, Crooks J, Breen M, Langstaff JE, Isaacs KK, Tan YM, Williams RW, Cao Y, Geller AM, Devlin RB, Batterman SA, Buckley TJ (2014) GPS-based microenvironment tracker (MicroTrac) model to estimate time-location of individuals for air pollution exposure assessments: model evaluation in Central North Carolina. *J Expo Sci Environ Epidemiol* 24:412–420. <https://doi.org/10.1038/jes.2014.13>
- Buitrago ND, Savdie J, Almeida SM, Verde SC (2021) Factors affecting the exposure to physico-chemical and microbiological pollutants in vehicle cabins while commuting in Lisbon. *Environ Pollut* 270:116062. <https://doi.org/10.1016/j.envpol.2020.116062>
- Cepeda M, Schoufour J, Freak-Poli R, Koolhaas CM, Dhana K, Bramer WM, Franco OH (2017) Levels of ambient air pollution according to mode of transport: a systematic review. *Lancet Public Health* 2:e23–e34. [https://doi.org/10.1016/S2468-2667\(16\)30021-4](https://doi.org/10.1016/S2468-2667(16)30021-4)
- Chau CK, Tu EY, Chan DWT, Burnett J (2002) Estimating the total exposure to air pollutants for different population age groups in Hong Kong. *Environ Int* 27:617–630. [https://doi.org/10.1016/S0160-4120\(01\)00120-9](https://doi.org/10.1016/S0160-4120(01)00120-9)
- Chen H, Kwong JC, Copes R, Tu K, Villeneuve PJ, van Donkelaar A, Hystad P, Martin RV, Murray BJ, Jessiman B, Wilton AS, Kopp A, Burnett RT (2017) Living near major roads and the incidence of dementia, Parkinson's disease, and multiple sclerosis: a population-based cohort study. *Lancet* 389:718–726. [https://doi.org/10.1016/S0140-6736\(16\)32399-6](https://doi.org/10.1016/S0140-6736(16)32399-6)
- Chen C, Zhao X, Yao Y, Zhang Y, Rong J, Liu X (2018) Driver's eco-driving behavior evaluation modeling based on driving events. *J Adv Transp*. <https://doi.org/10.1155/2018/9530470>
- Chien YC (2007) Variations in amounts and potential sources of volatile organic chemicals in new cars. *Sci Total Environ* 382:228–239. <https://doi.org/10.1016/j.scitotenv.2007.04.022>

- Choi W, Ranasinghe D, DeShazo JR, Kim JJ, Paulson SE (2018) Where to locate transit stops: cross-intersection profiles of ultrafine particles and implications for pedestrian exposure. *Environ Pollut* 233:235–245. <https://doi.org/10.1016/j.envpol.2017.10.055>
- Correia C, Martins V, Cunha-Lopes I, Faria T, Diapouli E, Eleftheriadis K, Almeida SM (2020) Particle exposure and inhaled dose while commuting in Lisbon. *Environ Pollut* 257:113547. <https://doi.org/10.1016/j.envpol.2019.113547>
- Cunha-Lopes I, Martins V, Faria T, Correia C, Almeida SM (2019) Children's exposure to sized-fractioned particulate matter and black carbon in an urban environment. *Build Environ* 155. <https://doi.org/10.1016/j.buildenv.2019.03.045>
- de Nazelle A, Nieuwenhuijsen MJ, Antó JM, Brauer M, Briggs D, Braun-Fahrlander C, Cavill N, Cooper AR, Desqueyroux H, Fruin S, Hoek G, Panis LI, Janssen N, Jerrett M, Joffe M, Andersen ZJ, van Kempen E, Kingham S, Kubesch N, Leyden KM, Marshall JD, Matamala J, Mellios G, Mendez M, Nassif H, Ogilvie D, Peiró R, Pérez K, Rabl A, Ragettli M, Rodríguez D, Rojas D, Ruiz P, Sallis JF, Terwoert J, Toussaint J-F, Tuomisto J, Zuurbier M, Lebret E (2011) Improving health through policies that promote active travel: a review of evidence to support integrated health impact assessment. *Environ Int* 37:766–777. <https://doi.org/10.1016/j.envint.2011.02.003>
- de Nazelle A, Fruin S, Westerdahl D, Martinez D, Ripoll A, Kubesch N, Nieuwenhuijsen M (2012) A travel mode comparison of commuters' exposures to air pollutants in Barcelona. *Atmos Environ* 59:151–159. <https://doi.org/10.1016/j.atmosenv.2012.05.013>
- de Nazelle A, Seto E, Donaire-Gonzalez D, Mendez M, Matamala J, Nieuwenhuijsen MJ, Jerrett M (2013) Improving estimates of air pollution exposure through ubiquitous sensing technologies. *Environ Pollut* 176:92–99. <https://doi.org/10.1016/j.envpol.2012.12.032>
- de Nazelle A, Bode O, Orjuela JP (2017) Comparison of air pollution exposures in active vs. passive travel modes in European cities: a quantitative review. *Environ Int* 99:151–160. <https://doi.org/10.1016/j.envint.2016.12.023>
- De Vlieger I, De Keukeleere D, Kretzschmar JG (2000) Environmental effects of driving behaviour and congestion related to passenger cars. *Atmos Environ* 34:4649–4655. [https://doi.org/10.1016/S1352-2310\(00\)00217-X](https://doi.org/10.1016/S1352-2310(00)00217-X)
- Devarakonda S, Liu R, Nath B (2017) On providing healthy routes: a case for Fine-grained pollution measurements using mobile sensing. In: UBICOMM 2017: the eleventh international conference on Mobile ubiquitous computing, systems, services and technologies
- Dinu M, Pagliai G, Macchi C, Sofi F (2019) Active commuting and multiple health outcomes: a systematic review and meta-analysis. *Sports Med* (Auckland, NZ) 49:437–452. <https://doi.org/10.1007/s40279-018-1023-0>
- Do Eum K, Kazemiparkouhi F, Wang B, Manjourides J, Pun V, Pavlu V, Suh H (2019) Long-term NO₂ exposures and cause-specific mortality in American older adults. *Environ Int* 124:10–15. <https://doi.org/10.1016/j.envint.2018.12.060>
- Donaire-Gonzalez D, Valentín A, de Nazelle A, Ambros A, Carrasco-Turigas G, Seto E, Jerrett M, Nieuwenhuijsen MJ (2016) Benefits of Mobile Phone Technology for Personal Environmental Monitoring. *JMIR Mhealth Uhealth*, 4(4), e126. <https://doi.org/10.2196/mhealth.5771>
- Dons E, Int Panis L, Van Poppel M, Theunis J, Wets G (2012) Personal exposure to Black Carbon in transport microenvironments. *Atmos Environ* 55:392–398. <https://doi.org/10.1016/j.atmosenv.2012.03.020>
- Dons E, Temmerman P, Van Poppel M, Bellermans T, Wets G, Int Panis L (2013) Street characteristics and traffic factors determining road users' exposure to black carbon. *Sci Total Environ* 447:72–79. <https://doi.org/10.1016/j.scitotenv.2012.12.076>
- Du B, Zhang L, Geng Y, Zhang Y, Xu H, Xiang G (2020) Testing and evaluation of cold-start emissions in a real driving emissions test. *Transp Res Part D: Transp Environ* 86:102447. <https://doi.org/10.1016/j.trd.2020.102447>
- Duan X, Wang B, Cao S (2022) Time-activity patterns. In: Zhang Y, Hopke PK, Mandin C (eds) *Handbook indoor air quality*. Springer

- Faber J, Brodzik K (2017) Air quality inside passenger cars. *AIMS Environ Sci* 4:112–133. <https://doi.org/10.3934/environsci.2017.1.112>
- Fruin S, Westerdahl D, Sax T, Sioutas C, Fine PM (2008) Measurements and predictors of on-road ultrafine particle concentrations and associated pollutants in Los Angeles. *Atmos Environ* 42: 207–219. <https://doi.org/10.1016/j.atmosenv.2007.09.057>
- Gan WQ, Koehoorn M, Davies HW, Demers PA, Tamburic L, Brauer M (2011) Long-term exposure to traffic-related air pollution and the risk of coronary heart disease hospitalization and mortality. *Environ Health Perspect* 119:501–507. <https://doi.org/10.1289/ehp.1002511>
- Geiss O, Tirendi S, Barrero-Moreno J, Kotzias D (2009) Investigation of volatile organic compounds and phthalates present in the cabin air of used private cars. *Environ Int* 35:1188–1195. <https://doi.org/10.1016/j.envint.2009.07.016>
- Gladyszewska-Fiedoruk K (2011) Concentrations of carbon dioxide in a car. *Transp Res Part D: Transp Environ* 16:166–171. <https://doi.org/10.1016/j.trd.2010.07.003>
- Glazener A, Khreis H (2019) Transforming our cities: best practices towards clean air and active transportation. *Curr Environ Health Rep* 6:22–37. <https://doi.org/10.1007/s40572-019-0228-1>
- Goel A, Kumar P (2014) A review of fundamental drivers governing the emissions, dispersion and exposure to vehicle-emitted nanoparticles at signalised traffic intersections. *Atmos Environ* 97: 316–331. <https://doi.org/10.1016/j.atmosenv.2014.08.037>
- Goel A, Kumar P (2015) Characterisation of nanoparticle emissions and exposure at traffic intersections through fast-response mobile and sequential measurements. *Atmos Environ* 107: 374–390. <https://doi.org/10.1016/j.atmosenv.2015.02.002>
- Gómez-Perales JE, Colvile RN, Nieuwenhuijsen MJ, Fernández-Bremauntz A, Gutiérrez-Avedoy VJ, Páramo-Figueroa VH, Blanco-Jiménez S, Bueno-López E, Mandujano F, Bernabé-Cabanillas R, Ortiz-Segovia E (2004) Commuters' exposure to PM_{2.5}, CO, and benzene in public transport in the metropolitan area of Mexico City. *Atmos Environ* 38:1219–1229. <https://doi.org/10.1016/j.atmosenv.2003.11.008>
- Gonder J, Earleywine M, Sparks W (2011) Final report on the fuel saving effectiveness of various driver feedback approaches. United States. <https://doi.org/10.2172/1010863>
- Gressent A, Malherbe L, Colette A, Rollin H, Scimia R (2020) Data fusion for air quality mapping using low-cost sensor observations: feasibility and added-value. *Environ Int* 143:105965. <https://doi.org/10.1016/j.envint.2020.105965>
- Haagen-Smit AJ (1966) Carbon monoxide levels in city driving. *Arch Environ Health*. <https://doi.org/10.1080/00039896.1966.10664429>
- Hachem M, Saleh N, Paunescu AC, Momas I, Bensefa-Colas L (2019) Exposure to traffic air pollutants in taxicabs and acute adverse respiratory effects: a systematic review. *Sci Total Environ* 693:133439. <https://doi.org/10.1016/j.scitotenv.2019.07.245>
- Hadei M, Shahsavani A, Hopke PK, Kermani M, Yarahmadi M, Mahmoudi B (2019) Comparative health risk assessment of in-vehicle exposure to formaldehyde and acetaldehyde for taxi drivers and passengers: effects of zone, fuel, refueling, vehicle's age and model. *Environ Pollut* 254: 112943. <https://doi.org/10.1016/j.envpol.2019.07.111>
- Hadei M, Mohebbi SR, Hopke PK, Shahsavani A, Bazzazpour S, Alipour M, Jafari AJ, Bandpey AM, Zali A, Yarahmadi M, Farhadi M, Rahmatinia M, Hasanzadeh V, Nazari SSH, Asadzadeh-Aghdaei H, Tanhaei M, Zali MR, Kermani M, Vaziri MH, Chobineh H (2021) Presence of SARS-CoV-2 in the air of public places and transportation. *Atmos Pollut Res* 12:302–306. <https://doi.org/10.1016/j.apr.2020.12.016>
- Hatzopoulou M, Weichenthal S, Barreau G, Goldberg M, Farrell W, Crouse D, Ross N (2013) A web-based route planning tool to reduce cyclists' exposures to traffic pollution: a case study in Montreal, Canada. *Environ Res* 123:58–61. <https://doi.org/10.1016/j.envres.2013.03.004>
- Hauser R, Meeker JD, Singh NP, Silva MJ, Ryan L, Duty S, Calafat AM (2007) DNA damage in human sperm is related to urinary levels of phthalate monoester and oxidative metabolites. *Hum Reprod* 22:688–695. <https://doi.org/10.1093/humrep/dej428>

- Hertel O, Hvidberg M, Ketzel M, Storm L, Stausgaard L (2008) A proper choice of route significantly reduces air pollution exposure – a study on bicycle and bus trips in urban streets. *Sci Total Environ* 389:58–70. <https://doi.org/10.1016/j.scitotenv.2007.08.058>
- Hinds W (2010) Cardiovascular health effects of Fine and ultrafine particles during freeway travel. California Environmental Protection Agency, Air Resources Board, Research Division
- Hull A, O'Holleran C (2014) Bicycle infrastructure: can good design encourage cycling? *Urban Plann Transp Res* 2:369–406. <https://doi.org/10.1080/21650020.2014.955210>
- Jamriska M, Morawska L, Mergersen K (2008) The effect of temperature and humidity on size segregated traffic exhaust particle emissions. *Atmos Environ* 42:2369–2382. <https://doi.org/10.1016/j.atmosenv.2007.12.038>
- Janssen NAH, Hoek G, Simic-Lawson M, Fischer P, van Bree L, Ten Brink H, Keuken M, Atkinson RW, Ross Anderson H, Brunekreef B, Cassee FR (2011) Black carbon as an additional indicator of the adverse health effects of airborne particles compared with pm 10 and pm2.5. *Environ Health Perspect* 119:1691–1699. <https://doi.org/10.1289/ehp.1003369>
- Jo WK, Lee JH (2008) Airborne fungal and bacterial levels associated with the use of automobile air conditioners or heaters, room air conditioners, and humidifiers. *Arch Environ Occup Health* 63: 101–107. <https://doi.org/10.3200/AEOH.63.3.101-107>
- Johansson C, Lövenheim B, Schantz P, Wahlgren L, Almström P, Markstedt A, Strömgren M, Forsberg B, Sommar JN (2017) Impacts on air pollution and health by changing commuting from car to bicycle. *Sci Total Environ* 584–585:55–63. <https://doi.org/10.1016/j.scitotenv.2017.01.145>
- Karanasiou A, Viana M, Querol X, Moreno T, de Leeuw F (2014) Assessment of personal exposure to particulate air pollution during commuting in European cities-recommendations and policy implications. *Sci Total Environ* 490:785–797. <https://doi.org/10.1016/j.scitotenv.2014.05.036>
- Kataoka H, Ohashi Y, Mamiya T, Nami K, Saito K, Ohcho K, Takigaw T (2012) Indoor air monitoring of volatile organic compounds and evaluation of their emission from various building materials and common products by gas chromatography-mass spectrometry. In: Advanced gas chromatography – progress in agricultural, biomedical and industrial applications. InTech. <https://doi.org/10.5772/31659>
- Kaur S, Nieuwenhuijsen MJ (2009) Determinants of personal exposure to PM 2.5, ultrafine particle counts, and CO in a transport microenvironment. *Environ Sci Technol* 43:4737–4743. <https://doi.org/10.1021/es803199z>
- Kaur S, Nieuwenhuijsen M, Colvile R (2005) Personal exposure of street canyon intersection users to PM2.5, ultrafine particle counts and carbon monoxide in Central London, UK. *Atmos Environ* 39:3629–3641. <https://doi.org/10.1016/j.atmosenv.2005.02.046>
- Klepeis NE, Nelson WC, Ott WR, Robinson JP, Tsang AM, Switzer P, Behar JV, Hern SC, Engelmann WH (2001) The National Human Activity Pattern Survey (NHAPS): a resource for assessing exposure to environmental pollutants. *J Expo Anal Environ Epidemiol* 11:231–252. <https://doi.org/10.1038/sj.jea.7500165>
- Knibbs LD, Cole-Hunter T, Morawska L (2011) A review of commuter exposure to ultrafine particles and its health effects. *Atmos Environ* 45:2611–2622. <https://doi.org/10.1016/j.atmosenv.2011.02.065>
- Kumar P, Patton AP, Durant JL, Frey HC (2018) A review of factors impacting exposure to PM2.5, ultrafine particles and black carbon in Asian transport microenvironments. *Atmos Environ* 187: 301–316. <https://doi.org/10.1016/j.atmosenv.2018.05.046>
- Kumar P, Hama S, Nogueira T, Abbass RA, Brand VS, Andrade M d F, Asfaw A, Aziz KH, Cao SJ, El-Gendy A, Islam S, Jeba F, Khare M, Mamuya SH, Martinez J, Meng MR, Morawska L, Muula AS, Shiva Nagendra SM, Ngowi AV, Omer K, Olaya Y, Osano P, Salam A (2021) In-car particulate matter exposure across ten global cities. *Sci Total Environ* 750:141395. <https://doi.org/10.1016/j.scitotenv.2020.141395>
- Laumbach DRJ, Rich DDQ, Gandhi DS, Amorosa DL, Schneider DS, Zhang DJ, Ohman-Strickland DP, Gong MJ, Lelyanov MO, Kipen DHM (2010) Acute changes in heart rate variability in subjects with diabetes following a highway traffic exposure. *J Occup Environ Med/Am Coll Occup Environ Med* 52:324. <https://doi.org/10.1097/JOM.0B013E3181D241FA>

- Leavey A, Reed N, Patel S, Bradley K, Kulkarni P, Biswas P (2017) Comparing on-road real-time simultaneous in-cabin and outdoor particulate and gaseous concentrations for a range of ventilation scenarios. *Atmos Environ* 166:130–141. <https://doi.org/10.1016/j.atmosenv.2017.07.016>
- Lee ES, Stenstrom MK, Zhu Y (2015) Ultrafine particle infiltration into passenger vehicles. Part I: Experimental evidence. *Transp Res Part D: Transp Environ* 38:156–165. <https://doi.org/10.1016/j.trd.2015.04.025>
- Lee KK, Miller MR, Shah ASV (2018a) Air pollution and stroke. *J Stroke*. <https://doi.org/10.5853/jos.2017.02894>
- Lee Y, Lee Y-C, Kim T, Choi JS, Park D (2018b) Sources and characteristics of particulate matter in Subway tunnels in Seoul, Korea. *Int J Environ Res Public Health* 15:2534. <https://doi.org/10.3390/ijerph15112534>
- Leung PL, Harrison RM (1999) Roadside and in-vehicle concentrations of monoaromatic hydrocarbons. *Atmos Environ* 33:191–204. [https://doi.org/10.1016/S1352-2310\(98\)00147-2](https://doi.org/10.1016/S1352-2310(98)00147-2)
- Limasset J-C, Diebold F, Hubert G (1993) Assessment of bus drivers' exposure to the pollutants of urban traffic. *Sci Total Environ* 134:39–49. [https://doi.org/10.1016/0048-9697\(93\)90337-6](https://doi.org/10.1016/0048-9697(93)90337-6)
- Liu X, Frey HC (2011) Modeling of in-vehicle human exposure to ambient fine particulate matter. *Atmos Environ* 45:4745–4752. <https://doi.org/10.1016/j.atmosenv.2011.04.019>
- Loxham M, Nieuwenhuijsen MJ (2019) Health effects of particulate matter air pollution in underground railway systems- a critical review of the evidence. Part Fibre Toxicol 16:1–24. <https://doi.org/10.1186/s12989-019-0296-2>
- Ma X, Longley I, Gao J, Salmond J (2020) Assessing schoolchildren's exposure to air pollution during the daily commute – a systematic review. *Sci Total Environ* 737:140389. <https://doi.org/10.1016/j.scitotenv.2020.140389>
- MacNaughton P, Melly S, Vallarino J, Adamkiewicz G, Spengler JD (2014) Impact of bicycle route type on exposure to traffic-related air pollution. *Sci Total Environ* 490:37–43. <https://doi.org/10.1016/j.scitotenv.2014.04.111>
- Mandalakis M, Stephanou EG, Horii Y, Kannan K (2008) Emerging contaminants in car interiors: evaluating the impact of airborne PBDEs and PBDD/fs. *Environ Sci Technol* 42:6431–6436. <https://doi.org/10.1021/es7030533>
- Martins V, Moreno T, Minguillón MC, Amato F, de Miguel E, Capdevila M, Querol X (2015) Exposure to airborne particulate matter in the subway system. *Sci Total Environ* 511:711–722. <https://doi.org/10.1016/j.scitotenv.2014.12.013>
- Martins V, Moreno T, Mendes L, Eleftheriadis K, Diapouli E, Alves CA, Duarte M, de Miguel E, Capdevila M, Querol X, Minguillón MC (2016) Factors controlling air quality in different European subway systems. *Environ Res* 146:35–46. <https://doi.org/10.1016/j.envres.2015.12.007>
- Martins V, Correia C, Cunha-Lopes I, Faria T, Diapouli E, Manousakas MI, Eleftheriadis K, Almeida SM (2021) Chemical characterisation of particulate matter in urban transport modes. *J Environ Sci* 100:51–61. <https://doi.org/10.1016/j.jes.2020.07.008>
- Matthaios VN, Kramer LJ, Crilley LR, Sommariva R, Pope FD, Bloss WJ (2020) Quantification of within-vehicle exposure to NO_x and particles: variation with outside air quality, route choice and ventilation options. *Atmos Environ* 240:117810. <https://doi.org/10.1016/j.atmosenv.2020.117810>
- McConnell R, Liu F, Wu J, Lurmann F, Peters J, Berhane K (2010) Asthma and school commuting time. *J Occup Environ Med* 52:827–829. <https://doi.org/10.1097/JOM.0b013e3181ebf1a9>
- McNabola A, Broderick BM, Gill LW (2009) The impacts of inter-vehicle spacing on in-vehicle air pollution concentrations in idling urban traffic conditions. *Transp Res Part D: Transp Environ* 14:567–575. <https://doi.org/10.1016/j.trd.2009.08.003>
- Mills IC, Atkinson RW, Kang S, Walton H, Anderson HR (2015) Quantitative systematic review of the associations between short-term exposure to nitrogen dioxide and mortality and hospital admissions. *BMJ Open*. <https://doi.org/10.1136/bmjopen-2014-006946>
- Morawska L, Ristovski Z, Jayaratne ER, Keogh DU, Ling X (2008) Ambient nano and ultrafine particles from motor vehicle emissions: characteristics, ambient processing and implications on human exposure. *Atmos Environ*. <https://doi.org/10.1016/j.atmosenv.2008.07.050>

- Morawska L, Thai PK, Liu X, Asumadu-Sakyi A, Ayoko G, Bartonova A, Bedini A, Chai F, Christensen B, Dunbabin M, Gao J, Hagler GSW, Jayaratne R, Kumar P, Lau AKH, Louie PKK, Mazaheri M, Ning Z, Motta N, Mullins B, Rahman MM, Ristovski Z, Shafei M, Tjondronegoro D, Westerdahl D, Williams R (2018) Applications of low-cost sensing technologies for air quality monitoring and exposure assessment: how far have they gone? *Environ Int* 116:286–299. <https://doi.org/10.1016/j.envint.2018.04.018>
- Moreno T, Pintó RM, Bosch A, Moreno N, Alastuey A, Minguillón MC, Anfruns-Estrada E, Guix S, Fuentes C, Buonanno G, Stabile L, Morawska L, Querol X (2021) Tracing surface and airborne SARS-CoV-2 RNA inside public buses and subway trains. *Environ Int* 147: 106326. <https://doi.org/10.1016/j.envint.2020.106326>
- Mueller N, Rojas-Rueda D, Cole-Hunter T, de Nazelle A, Dons E, Gerike R, Götschi T, Int Panis L, Kahlmeier S, Nieuwenhuijsen M (2015) Health impact assessment of active transportation: a systematic review. *Prev Med* 76:103–114. <https://doi.org/10.1016/j.ypmed.2015.04.010>
- Nasir ZA, Campos LC, Christie N, Colbeck I (2016) Airborne biological hazards and urban transport infrastructure: current challenges and future directions. *Environ Sci Pollut Res* 23 (15):15757–66. <https://doi.org/10.1007/s11356-016-7064-8>
- Nations, U. (2018) Economic Commission for Europe Inland Transport Committee of the 1958 and the 1998 agreements concerning Vehicle Interior Air Quality (VIAQ) contents
- Onat B, Şahin ÜA, Uzun B, Akin Ö, Özkaya F, Ayvaz C (2019) Determinants of exposure to ultrafine particulate matter, black carbon, and PM2.5 in common travel modes in Istanbul. *Atmos Environ* 206:258–270. <https://doi.org/10.1016/j.atmosenv.2019.02.015>
- Padoan E, Amato F (2018) Chapter 2 – Vehicle non-exhaust emissions: impact on air quality. In: Amato F (ed) Non-exhaust emissions: an urban air quality problem for public health; impact and mitigation measures. Academic, pp 21–65. <https://doi.org/10.1016/B978-0-12-811770-5.00002-9>
- Padrón-Martínez LT, Patton AP, Trull JB, Zamore W, Brugge D, Durant JL (2012) Mobile monitoring of particle number concentration and other traffic-related air pollutants in a near-highway neighborhood over the course of a year. *Atmos Environ* 61:253–264. <https://doi.org/10.1016/j.atmosenv.2012.06.088>
- Pant P, Harrison RM (2013) Estimation of the contribution of road traffic emissions to particulate matter concentrations from field measurements: a review. *Atmos Environ* 77:78–97. <https://doi.org/10.1016/j.atmosenv.2013.04.028>
- Park SS, Hansen ADA, Cho SY (2010) Measurement of real time black carbon for investigating spot loading effects of Aethalometer data. *Atmos Environ* 44:1449–1455. <https://doi.org/10.1016/j.atmosenv.2010.01.025>
- Park J, Jo W, Cho M, Lee J, Lee H, Seo S, Lee C, Yang W (2020) Spatial and temporal exposure assessment to PM2.5 in a community using sensor-based air monitoring instruments and dynamic population distributions. *Atmosphere*. <https://doi.org/10.3390/atmos11121284>
- Patel MM, Chillrud SN, Deepti KC, Ross JM, Kinney PL (2013) Traffic-related air pollutants and exhaled markers of airway inflammation and oxidative stress in New York City adolescents. *Environ Res* 121:71–78. <https://doi.org/10.1016/j.envres.2012.10.012>
- Paunescu AC, Attoui M, Bouallala S, Sunyer J, Momas I (2017) Personal measurement of exposure to black carbon and ultrafine particles in schoolchildren from PARIS cohort (Paris, France). *Indoor Air* 27:766–779. <https://doi.org/10.1111/ina.12358>
- Peters A, Von Klot S, Mittleman MA, Meisinger C, Hörmann A, Kuch B, Erich Wichmann H (2013) Triggering of acute myocardial infarction by different means of transportation. *Eur J Prev Cardiol* 20:750–758. <https://doi.org/10.1177/2047487312446672>
- Pun VC, Kazemiparkouhi F, Manjourides J, Suh HH (2017) Long-term PM2.5 exposure and respiratory, cancer, and cardiovascular mortality in older US adults. *Am J Epidemiol* 186: 961–969. <https://doi.org/10.1093/aje/kwx166>
- Rabl A, de Nazelle A (2012) Benefits of shift from car to active transport. *Transp Policy* 19:121–131. <https://doi.org/10.1016/j.tranpol.2011.09.008>

- Ramos CA, Wolterbeek HT, Almeida SM (2016) Air pollutant exposure and inhaled dose during urban commuting: a comparison between cycling and motorized modes. *Air Qual Atmos Health* 9. <https://doi.org/10.1007/s11869-015-0389-5>
- Rexeis M, Hausberger S (2009) Trend of vehicle emission levels until 2020 – prognosis based on current vehicle measurements and future emission legislation. *Atmos Environ* 43:4689–4698. <https://doi.org/10.1016/j.atmosenv.2008.09.034>
- Riediker M, Cascio WE, Griggs TR, Herbst MC, Bromberg PA, Neas L, Williams RW, Devlin RB (2004) Particulate matter exposure in cars is associated with cardiovascular effects in healthy young men. *Am J Respir Crit Care Med* 169:934–940. <https://doi.org/10.1164/rccm.200310-1463oc>
- Rivas I, Kumar P, Hagen-Zanker A, Andrade M d F, Slovic AD, Pritchard JP, Geurs KT (2017) Determinants of black carbon, particle mass and number concentrations in London transport microenvironments. *Atmos Environ* 161:247–262. <https://doi.org/10.1016/j.atmosenv.2017.05.004>
- Rojas-Rueda D, de Nazelle A, Andersen ZJ, Braun-Fahrländer C, Bruha J, Bruhova-Foltynova H, Desqueyroux H, Praznocy C, Ragettli MS, Tainio M, Nieuwenhuijsen MJ (2016) Health impacts of active transportation in Europe. *PLoS One* 11:e0149990
- Samoli E, Touloumi G, Schwartz J, Anderson HR, Schindler C, Forsberg B, Vigotti MA, Vonk J, Košník M, Skorkovsky J, Katsouyanni K (2007) Short-term effects of carbon monoxide on mortality: an analysis within the APHEA project. *Environ Health Perspect* 115:1578–1583. <https://doi.org/10.1289/ehp.10375>
- Sanguinetti A, Queen E, Yee C, Akanesuvan K (2020) Average impact and important features of onboard eco-driving feedback: a meta-analysis. *Transport Res F: Traffic Psychol Behav* 70:1–14. <https://doi.org/10.1016/j.trf.2020.02.010>
- Santana P, Almeida A, Mariano P, Correia C, Martins V, Almeida SM (2021) Air quality mapping and visualisation: an affordable solution based on a vehicle-mounted sensor network. *J Clean Prod* 315:128194. <https://doi.org/10.1016/j.jclepro.2021.128194>
- Sarnat JA, Golan R, Greenwald R, Raysoni AU, Kewada P, Winquist A, Sarnat SE, Dana Flanders W, Mirabelli MC, Zora JE, Bergin MH, Yip F (2014) Exposure to traffic pollution, acute inflammation and autonomic response in a panel of car commuters. *Environ Res* 133:66–76. <https://doi.org/10.1016/j.envres.2014.05.004>
- Savdie J, Canha N, Buitrago N, Almeida SM (2020) Passive exposure to pollutants from a new generation of cigarettes in real life scenarios. *Int J Environ Res Public Health* 17:3455. <https://doi.org/10.3390/ijerph17103455>
- Sendzik T, Fong GT, Travers MJ, Hyland A (2009) An experimental investigation of tobacco smoke pollution in cars. *Nicotine Tob Res* 11:627–634. <https://doi.org/10.1093/ntr/ntp019>
- Sharpe RM (2005) Phthalate exposure during pregnancy and lower anogenital index in boys: wider implications for the general population? *Environ Health Perspect*. <https://doi.org/10.1289/ehp.113-a504>
- Söderström G, Sellström U, De Wit CA, Tysklind M (2004) Photolytic debromination of decabromodiphenyl ether (BDE 209). *Environ Sci Technol* 38:127–132. <https://doi.org/10.1021/es034682c>
- Steinle S, Reis S, Sabel CE, Semple S, Twigg MM, Braban CF, Leeson SR, Heal MR, Harrison D, Lin C, Wu H (2015) Personal exposure monitoring of PM_{2.5} in indoor and outdoor microenvironments. *Sci Total Environ* 508:383–394. <https://doi.org/10.1016/j.scitotenv.2014.12.003>
- Suglia SF, Gryparis A, Wright RO, Schwartz J, Wright RJ (2008) Association of black carbon with cognition among children in a prospective birth cohort study. *Am J Epidemiol* 167:280–286. <https://doi.org/10.1093/aje/kwm308>
- Targino AC, Kreel P, Cipoli YA, Oukawa GY, Monroy DA (2020) Bus commuter exposure and the impact of switching from diesel to biodiesel for routes of complex urban geometry. *Environ Pollut* 263:114601. <https://doi.org/10.1016/j.envpol.2020.114601>
- Tong Z, Li Y, Westerdahl D, Adamkiewicz G, Spengler JD (2019) Exploring the effects of ventilation practices in mitigating in-vehicle exposure to traffic-related air pollutants in China. *Environ Int* 127:773–784. <https://doi.org/10.1016/j.envint.2019.03.023>

- Vamshi B, Prasad RV (2018) Dynamic route planning framework for minimal air pollution exposure in urban road transportation systems. In: 2018 IEEE 4th world forum on internet of things (WF-IoT). pp 540–545. <https://doi.org/10.1109/WF-IoT.2018.8355209>
- Van Ryswyk K, Anastasopoulos AT, Evans G, Sun L, Sabaliauskas K, Kulka R, Wallace L, Weichenthal S (2017) Metro commuter exposures to particulate air pollution and PM_{2.5}-associated elements in three Canadian cities: the urban transportation exposure study. *Environ Sci Technol* 51:5713–5720. <https://doi.org/10.1021/acs.est.6b05775>
- Vijayan A, Kumar A (2010) Experimental and statistical analyses to characterize in-vehicle fine particulate matter behavior inside public transit buses operating on B20-grade biodiesel fuel. *Atmos Environ* 44:4209–4218. <https://doi.org/10.1016/j.atmosenv.2010.07.012>
- Virkkula A, Mäkelä T, Hillamo R, Yli-Tuomi T, Hirsikko A, Hämeri K, Koponen IK (2007) A simple procedure for correcting loading effects of aethalometer data. *J Air Waste Manage Assoc* 57:1214–1222. <https://doi.org/10.3155/1047-3289.57.10.1214>
- Wang X, Chancellor G, Evenstad J, Farnsworth JE, Hase A, Olson GM, Sreenath A, Agarwal JK (2009) A novel optical instrument for estimating size segregated aerosol mass concentration in real time. *Aerosol Sci Technol* 43:939–950. <https://doi.org/10.1080/02786820903045141>
- Watson JG, Chow JC, Fujita EM (2001) Review of volatile organic compound source apportionment by chemical mass balance. *Atmos Environ*. [https://doi.org/10.1016/S1352-2310\(00\)00461-1](https://doi.org/10.1016/S1352-2310(00)00461-1)
- Wen Y, Leng J, Shen X, Han G, Sun L, Yu F (2020) Environmental and health effects of ventilation in subway stations: a literature review. *Int J Environ Res Public Health*. <https://doi.org/10.3390/ijerph17031084>
- Weschler CJ, Nazaroff WW (2008) Semivolatile organic compounds in indoor environments. *Atmos Environ* 42:9018–9040. <https://doi.org/10.1016/j.atmosenv.2008.09.052>
- WHO (2020) WHO guidelines on physical activity and sedentary behaviour. World Health Organization, Geneva
- Wolkoff P (1999) How to measure and evaluate volatile organic compound emissions from building products. A perspective. *Sci Total Environ* 227:197–213. [https://doi.org/10.1016/S0048-9697\(99\)00019-4](https://doi.org/10.1016/S0048-9697(99)00019-4)
- Woo S-H, Kim JB, Bae G-N, Hwang MS, Tahk GH, Yoon HH, Yook S-J (2018) Investigation of diurnal pattern of generation and resuspension of particles induced by moving subway trains in an underground tunnel. *Aerosol Air Qual Res* 18:2240–2252. <https://doi.org/10.4209/aaqr.2017.11.0444>
- Xu B, Chen X, Xiong J (2018) Air quality inside motor vehicles' cabins: a review. *Indoor Built Environ* 27:452–465. <https://doi.org/10.1177/1420326X16679217>
- Yoshida T, Matsunaga I (2006) A case study on identification of airborne organic compounds and time courses of their concentrations in the cabin of a new car for private use. *Environ Int* 32:58–79. <https://doi.org/10.1016/j.envint.2005.04.009>
- Yoshida T, Matsunaga I, Tomioka K, Kumagai S (2006) Interior air pollution in automotive cabins by volatile organic compounds diffusing from interior materials: I. Survey of 101 types of Japanese domestically produced cars for private use. *Indoor Built Environ* 15:425–444. <https://doi.org/10.1177/1420326X06069395>
- Zheng J, Qiu Z, Gao HO, Li B (2021) Commuter PM exposure and estimated life-expectancy loss across multiple transportation modes in Xi'an, China. *Ecotoxicol Environ Saf* 214:112117. <https://doi.org/10.1016/j.ecoenv.2021.112117>
- Zhou M, Jin H, Wang W (2016) A review of vehicle fuel consumption models to evaluate eco-driving and eco-routing. *Transp Res Part D: Transp Environ* 49:203–218. <https://doi.org/10.1016/j.trd.2016.09.008>
- Zou B, Li S, Zheng Z, Zhan BF, Yang Z, Wan N (2020) Healthier routes planning: a new method and online implementation for minimizing air pollution exposure risk. *Comput Environ Urban Syst* 80:101456. <https://doi.org/10.1016/j.compenvurbsys.2019.101456>
- Zuurbier M, Hoek G, Oldenwening M, Lenters V, Meliefste K, van den Hazel P, Brunekreef B (2010) Commuters' exposure to particulate matter air pollution is affected by mode of transport, fuel type, and route. *Environ Health Perspect* 118:783–789. <https://doi.org/10.1289/ehp.0901622>



Indoor Air Quality in Commercial Air Transportation

69

Florian Mayer, Richard Fox, David Space, Andreas Bezold, and Pawel Wargocki

Contents

Introduction	2059
Air Supply in Means of Air Transportation: The Environmental Control System (ECS)	2060
Commercial Aircraft	2060
Business Jets and Helicopters	2064
Requirements	2064
Regulations	2064
Mandatory Standards	2066
Voluntary Guidelines	2066
Outside Air Supply Rate	2068
Relative Humidity	2068

F. Mayer (✉)

Department Environment, Hygiene, Sensor Technology, Fraunhofer Institute for Building Physics
IBP, Valley, Germany

e-mail: florian.mayer@ibp.fraunhofer.de

R. Fox

Aircraft Environment Solutions Inc., San Tan Valley, AZ, USA

e-mail: richardfox@acenvinc.com

D. Space

Environmental Control Systems, Retired, Boeing, Everett, WA, USA

e-mail: davidrspace@gmail.com

A. Bezold

Environmental Control Systems, Airbus Operations GmbH, Hamburg, Germany

e-mail: andreas.bezold@airbus.com

P. Wargocki

International Centre for Indoor Environment and Energy, Department of Civil Engineering,
Technical University of Denmark, Kongens Lyngby, Denmark

e-mail: paw@byg.dtu.dk

Selected Pollutants in the Aircraft Cabin	2068
Carbon Dioxide (CO ₂)	2068
Carbon Monoxide (CO)	2069
Ozone (O ₃)	2069
Volatile Organic Compounds (VOCs)	2070
Total Volatile Organic Compounds (TVOC)	2075
Semivolatile Organic Compounds (SVOCs)	2075
Particles	2078
Selected Sources of Some Typical Cabin Air Contaminants	2078
Engine Oils	2079
Hydraulic Fluids	2079
Exhaust	2080
Deicing Liquids	2080
Possible Unlikely Failure Cases That May Compromise Cabin Air Quality	2081
Pathogens	2081
Physiological Response	2084
Conclusion	2084
Cross-References	2085
References	2086

Abstract

This chapter deals with the air quality in means of air transportation. Since air travel in large passenger aircraft represents the vast majority of travel, the air quality in commercial aircraft cabins is vitally important to the public.

At typical cruising altitudes between 31,000 and 41,000 ft (about 9,500 and 12,500 m), ambient conditions of very low temperature and pressure, elevated ozone concentrations, and dry air constitute a hostile environment to human beings. To create a life-supporting atmosphere inside the aircraft, environmental control systems provide appropriate regulation of pressure, temperature, and ventilation in the cabin. As aircraft cabins increasingly become part of the normal habitat for humans, passenger and crew expectations for the cabin environment are rising, leading to additional requirements for environmental control systems.

Air pollution sources in aircraft cabins can be attributed to passengers and their personal hygiene, activities in the cabin, carry-on luggage, cabin equipment and materials, outside air contaminants, and very rarely, to abnormal conditions or pollution of system components like compressors, ducting, or fans in the air supply path.

Many volatile organic compounds (VOCs) found in aircraft cabins do not differ from compounds found in residential buildings and offices, and concentrations are in the same range or even lower. Some semivolatile organic compounds (SVOCs) from, e.g., flame-retardants or operational fluids are more specific for the aircraft environment but only occur in trace concentrations. Environmental ozone can be reliably reduced in high-temperature sections of the air supply system and by employing converters. Average carbon dioxide concentrations are higher than in other environments but are kept well below regulatory limits for aircraft cabins.

Keywords

Aircraft · Environmental control system · Cabin air quality · Contaminants · Pollutants

Introduction

Commercial air traffic has significantly increased over the past seven decades with cabin air quality becoming a topic of interest during the same period of time (Crump 2016). In 2019, more than 4.5 billion passengers traveled on board commercial airplanes (Mazareanu 2021). The continuous growth of air travel during the last decades was abruptly interrupted by the SARS-CoV-2 pandemic in early 2020. However, a recovery to prepandemic passenger numbers is expected by 2023–2024 (Airports Council International 2021).

Aircraft cabins represent a special indoor environment for both mainly sedentary passengers and more active cabin crew, and also sedentary pilots in the cockpit. They all encounter high daytime solar loads, reduced pressure (depending on the flight altitude down to 755 hPa), high air change rates, low relative humidity (5–15% r. h.), high occupant density, continuous noise, and three-dimensional motion (Space et al. 2000). Moreover, limited mobility while flying across multiple time zones affects one's circadian rhythm. Cabin conditions may influence the perception of the cabin environment, comfort, and well-being.

Air quality investigations in the past focused on passenger cabins in commercial aircraft with passengers and flight attendants as their occupants. Some studies also addressed cockpits with regard to pilots' working environment. Consequently, several studies investigated cabin air quality and its effect on passengers (Nagda and Rector 2003; Spicer et al. 2004; Lindgren and Norbäck 2005; Spengler et al. 2012; Ahmadpour et al. 2014; Harshada and Mirabelle 2017; Rosenberger 2018) and crew (Griffiths and Powell 2012; McNeely et al. 2014; Wolkoff et al. 2016).

The air quality in the aircraft cabin is mainly controlled by ventilation. The ventilation of aircraft cabins is controlled by an Environmental Control System (ECS). The main tasks of the ECS on board of an aircraft are to ensure proper pressurization of the cabin, to maintain a comfortable thermal environment and air quality for the health and well-being of passengers as well as the working conditions for crew members. The ECS also provides air for other features such as cargo ventilation and air conditioning, potable water, hydraulic reservoir pressurization, and anti-icing for wings and engines.

The ECS provides the necessary amount of air and mixes the cabin-recirculated air with fresh (outside) air. During flight, the air outside of the aircraft is very cold (-56°C), dry (<1% relative humidity at cabin conditions), and low in pressure and hence in oxygen partial pressure (comparable to <5% oxygen on ground), i.e., hostile to human life (ASHRAE 161 2018). The outside air is normally taken from the jet engine compressors before the combustion chamber. Since the withdrawal of already pressurized air from the compressors negatively affects the energy balance of the engine, this air is called bleed air (Hunt et al. 2000). Only one type of aircraft (Boeing 787) currently does not use bleed air but uses separate electric compressors to provide outside air to the cabin (bleed less air). Besides removing contaminants generated in the cabin, ventilation is used to remove the heat generated by the occupants and electrical systems such as inflight entertainment.

The air change rate in the aircraft cabin is about 15 to 20 times per hour with outside air. This air change rate is much higher than in residential or office buildings and even higher than in a surgical or critical care facility (AIA 2001). During ground operations, the air from outside may bring in contaminants such as exhaust from ground support equipment and other aircraft. At cruise altitudes, ozone from the troposphere can be brought into the aircraft cabin (ASHRAE 161 2018; SAE 4766/2A 2021). Particles are removed in the recirculated air path by high efficiency particulate air (HEPA) filters, but bio-effluents from occupants and other pollutants generated in the cabin will be recirculated back to the cabin. These pollutants are diluted with outside air.

Volatile organic compounds (VOCs) can partially be removed on aircraft equipped with carbon-based air purification systems, which are available as standard or optional features on selected aircraft (Donaldson 2018; Simpson et al. 2019). Aircraft are equipped or can be equipped upon airline request with optional personal air outlets (PAOs) above each aircraft cabin seat allowing an adjusted direct air flow to the head/body of the passengers for enhanced personal control of thermal comfort.

Rarely, abnormal events inside or outside the cabin may compromise cabin air quality.

Air Supply in Means of Air Transportation: The Environmental Control System (ECS)

Commercial Aircraft

Introduced in 1918 (and retired in 1931), the British USD.9A was the first attempt at pressurizing an aircraft crew compartment to enable higher altitude flights while providing a life-sustaining environment for the pilots. Most commercial airliners were pressurized by the 1950s enabling high-altitude flights, which were subject to less air turbulence, with improved comfort, range, and fuel efficiency.

Early jet airplanes did not have cabin air recirculation systems and provided 100% outside air for pressurization and ventilation. Bleed air-driven cabin air compressors were used in the first commercial pressurized cabins, such as the Boeing Stratoliner (1938–1945), 707 family (produced 1956–1978), and McDonnell Douglas DC-8 Family (produced 1955–1972). Early jets were powered by highly inefficient turbojet engines in which all the air entering the engine went through the core to provide thrust. Fuel consumption was very high. A small percentage of the total core flow was used to provide outside air to the cabin. Engine technology progress resulted in turbofan engines with a core bypass ratio of about 2 to 1. Fuel consumption for outside air supply was still small enough to make 100% bleed air provision to the cabin cost effective. At that time, average flight lengths were shorter and a lower percentage of direct operating costs was attributable to fuel. Modern turbofan engines have a high 5 to 1 bypass ratio and are much more fuel-efficient. With that, the percentage of fuel needed for outside/bleed air supply significantly increased, almost proportional to higher bypass ratios (Hunt et al. 2000).

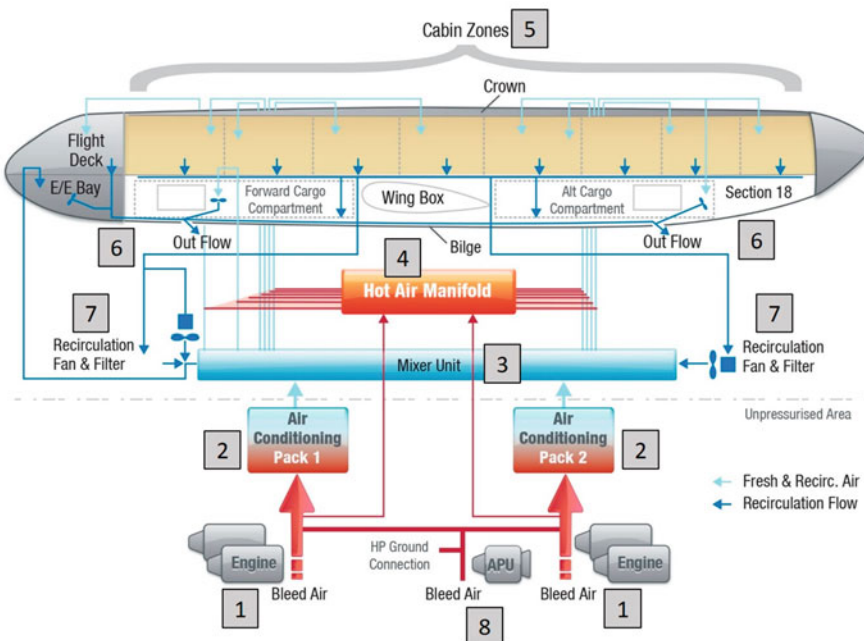


Fig. 1 Simplified Environmental Control System (ECS) on board of commercial aircraft (with exception of B787) – air path for cabin ventilation (© Airbus SAS 2021. All rights reserved)

In the 1960s, increasing needs for more air supply with increasing aircraft size, and the continuous increase in engine bypass ratios with newer engines, resulted in a change in the utilization of the engine compressors and cooled bleed air (through air conditioning packs) to improve efficiency and to eliminate the added weight of external cabin air compressors.

The working principle of a commercial aircraft ECS is shown in Fig. 1. For air supply to the cabin during flight, compressed air is taken from the jet engines compressors before the combustion chamber (#1). An exception is the B787, which does not use engine bleed air per se but an electric compressor to provide outside air. Bleed air has a pressure of up to 40 bar and due to adiabatic compression temperatures may exceed 649 °C (1200 °F) (SAE ARP1796B 2020) depending on the compression ratio during takeoff on limited occasions. Typical takeoff bleed air temperatures are about 350 °C (662 °F) and cruise bleed air temperatures are about 250 °C (482 °F) (NRC 2002). The fraction of air for the ECS cannot be used for thrust, consumes about 2–5% (Rosero et al. 2007) to 3–5% (Zavaglio et al. 2019) of fuel, and contributes to the CO₂ footprint of an aircraft.

On some aircraft, the bleed air is led through an ozone converter to deplete atmospheric ozone especially on polar routes. Bleed supply air is guided from the engine compressors to the air conditioning packs (#2) by which it is cooled down in several steps to typically less than room temperature using outside air as cooling

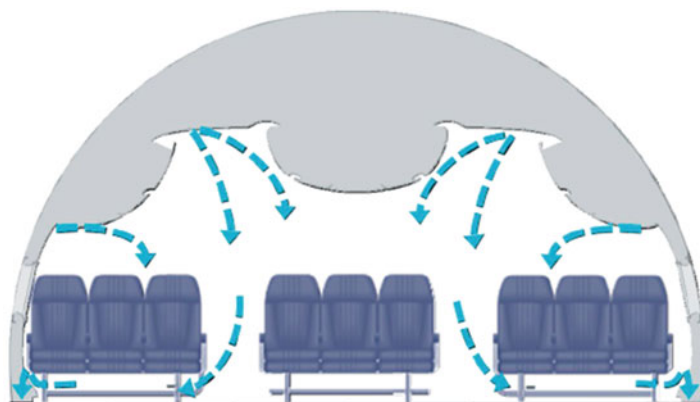


Fig. 2 Cabin cross section with typical airflow from ceiling/lateral outlets to floor dado panels exhaust (© Airbus SAS 2020. All rights reserved)

medium and air cycle machines for compression and expansion cooling. The conditioned outside air then enters the Mixer Unit (#3) where it is mixed with the recirculated air from the cabin. The resulting supply air is typically composed of 40–60% outside air and 60–40% recirculated air depending upon the aircraft model and derivative, the cabin layout, and the actual number of occupants under normal operating conditions (Bezold 2009).

The outside and recirculation airflow split to the flight deck can vary depending upon airplane model and requirements for solar and electronic heat loads (NRC 1986). Some aircraft models supply outside air only to the flight deck under normal operating conditions. A portion of the hot bleed air – the so-called trim air – bypasses the air-conditioning packs to the hot air manifold (#4) for temperature control. The air leaving the Mixer Unit is ducted to each individual temperature control zone in the aircraft (#5, typically 3 to 9, up to 16 zones (A380) in the occupied cabin, including flight deck); if necessary, hot trim air (small amount of bleed air) is used to adjust the air mix to each temperature control zone to provide the desired temperature and then supplied to the cabin from ceiling outlets typically located above and/or below the overhead bins (see Fig. 2).

The airflow in the cabin is generally from top to bottom, either from the ceiling supply outlets above and/or below the overhead bins (lateral) or the personal air outlets above each seat (if equipped) to the cabin return air outlets at floor level at the lower part of the sidewall lining (dado panel). The return air grilles at floor level run the length of the cabin on both sides. The airflow along the cabin from zone to zone is limited.

Approximately 50% of the cabin return air leaves the aircraft by the outflow valves (#6) that are also used to regulate the cabin pressure. The other portion of the cabin return air is guided through HEPA filters (#7), back to the Mixer Unit, and is used again. Recirculation filters may contain additional carbon-based adsorption layers. They are standard on B787 and available as an option for several other aircraft platforms.

Highly efficient recirculation systems were enabled from studies conducted with the National Aeronautics and Space Administration (NASA), the McDonnell Douglas Aircraft Company, and American Airlines in the 1970s. Results indicated that the use of recirculating air allowed a corresponding decrease of bleed air and subsequent fuel savings when applying HEPA filters without compromising cabin air quality (Hunt et al. 2000). The Boeing 757 and 767, brought into service in 1982, and Airbus A300 in 1988 provided cabin air by mixing outside air with filtered recirculated air.

HEPA filters can remove at least 99.95% (ISO 29463-1 2017) or 99.97% (NASA 2016) of particles from air, including spores, bacteria, and viruses. The filters can provide essentially particle-free air through the recirculation system (Strøm-Tejsen et al. 2008; NASA 2016). Additional activated carbon-based filters, offered as optional feature, can effectively reduce the concentration of VOCs in the recirculated air (Schuchardt et al. 2017, 2019; Rosenberger 2018; Destaillats et al. 2018). Air purification was found to be a more important factor than increased humidity for addressing many aspects of passenger and crew complaints including eye, nose, and throat irritation and general dryness (ASHRAE 1999; Strøm-Tejsen et al. 2008; Spengler et al. 2012; Weisel et al. 2017).

The volume of outside air corresponding to the cabin volume is added to an aircraft cabin about every 3 min, so the air change rate with outside air is about 20 h^{-1} . Aircraft are typically overventilated to ensure that minimum regulated airflow requirements are met (see requirements section). In 1986, the NRC found that if the lowest rate of ventilation permitted by current equipment design had been used under nearly full or full occupant loads, the air quality would have been acceptable for nonsmoking flights (NRC 1986).

On ground, supply air may be generated by the auxiliary power unit (APU, #8) drawn in at the back of the aircraft and supplied to the air-conditioning packs or is provided by fixed or mobile air-conditioning units at the airports. An industry standard is currently being drafted that will require ground cart air to be purified (filtered) prior to provision to the air-conditioning packs (high-pressure ground connection) or the mixing manifold (low-pressure ground connection). Ozone converters with VOC reduction capabilities for use during ground operation are also available. The APU may also provide air supply during flight up to a certain flight level.

The ECS must deliver a minimum of 0.28 m^3 (0.55 pounds, 0.25 kg) per minute per person outside air during normal operation to maintain pressurization, thermal control, and avionics cooling (EASA 2020; FAA 2021, see requirements section). For a probable failure condition, the amount of air supplied should not be less than 0.18 kg (0.4 pounds, 0.2 m^3) per minute per person for any period exceeding 5 min (EASA 2020; FAA 2021).

Air-conditioning pack hybrid systems that utilize a combination of air cycle and vapor cycle systems to improve system efficiency are currently under research. Additionally, variable airflow systems that utilize outside and purified airflow to enable improved air quality, airplane economics, and lessen engine emissions are installed on selected aircraft today and currently investigated as well.

New optimized ECS units have the potential for reducing fuel consumption and engine emissions by reducing the outside ventilation rate while increasing filtered/purified airflow to improve overall air quality and comfort. It is estimated that an optimized ECS aircraft could potentially save nearly 0.8%–2% of the fuel in comparison with traditional ECS if the outside air supply rate could be reduced with commensurate increase in filtered/purified airflow (Newman and Viele 1980; Zavaglio et al. 2019).

Business Jets and Helicopters

Business jets and helicopters have similar regulatory requirements for cabin air environment as larger commercial airliners. However, due to weight, cost constraints, and mission profiles, they often do not utilize recirculated cabin air but utilize 100% outside / bleed air to provide air to the cabin and cockpit. In addition, some of these systems may be equipped with vapor cycle, rather than air cycle air-conditioning systems. Vapor cycle systems utilize compressed refrigerant for cooling (SAE ARP 292D 2020). They have traditionally been used because of their high heat capacity and small size. More recently, air cycle machines have been developed that meet the requirements for conditioning business jets and helicopters and are being employed for cooling. Some more complex business jet ECS systems utilize a jet pump to extract cabin air and mix it with incoming air from the ECS pump. Filtration and humidification are also provided as an option on some business jet air supply systems.

Helicopters fly at much lower elevations than jets and do not have a pressurized cabin. Because of the low number of people (crew and passengers) and the low heat load on board, outside air supplied to the cabin of helicopters and business jets is not cooled as much as in commercial aircraft.

Requirements

Regulations

Large airplanes (20 or more passengers) have to fulfill certification requirements of authorities such as Federal Aviation Administration (FAA) in the US or European Aviation Safety Agency (EASA) in Europe. These requirements contain limited regulations on cabin air quality for minimum ventilation rates, sufficient outside air supply to enable the crew members to perform their duties without undue discomfort or fatigue, and limit maximum concentrations for carbon dioxide (CO_2), carbon monoxide (CO), and ozone (O_3) (FAR, CS 25.831 and 25.832, Table 1). The Chinese CCAR has adopted FAA and EASA requirements. In addition, the Russian AP-25 regulation lists maximum values for nitrogen oxides (NOx), selected volatile organic compounds (VOCs), and semi volatile organic compounds (SVOCs) that shall not be exceeded.

Table 1 Air quality regulations for aircraft

	Mandatory				Voluntary
Country	USA	EU	China	Russia	USA
Regulation	FAA FAR 14 CFR § 25.831 and 25.832	CS 25.831 and 25.832	CCAR	AP-25	ASHRAE 161
Ventilation rate	0.55 pounds/ min per person (3.5–4.7 L/s per person, 0–8000 ft. pressure)	4.7 L/s per person (min. outside)	0.55 pounds/ min per person (3.5–4.7 L/s per person, 0–8000 ft. pressure)	0.28 m ³ /min per person (4.7 L/s per person)	7.5 cfm per person (3.5 L/s per person) (min. outside) 15 cfm per person (7.1 L/s per person) (min. total) 20 cfm per person (9.4 L/s per person) (recommended total)
CO	50 ppm	50 ppm	50 ppm	50 ppm	9 ppm TWA 10 min 50 ppm 1-min peak
CO ₂	5000 ppm	5000 ppm	5000 ppm	5000 ppm	—
O ₃	100 ppb TWA 3 h 250 ppb any time	100 ppb TWA 3 h 250 ppb any time	100 ppb TWA 3 h 250 ppb any time	100 ppb TWA 3 h 250 ppb any time	100 ppb TWA 3 h 250 ppb any time
NO _x	—	—	—	5 mg/m ³	—
VOCs	—	—	—	Fuel vapor 300 mg/m ³ Mineral oil vapor and aerosols 5 mg/m ³ Synthetic oil vapor and aerosols 2 mg/m ³ Acrolein 0.2 mg/m ³ Phenol 0.3 mg/m ³ Formaldehyde 0.5 mg/m ³ Benzene 5 mg/m ³	—

(continued)

Table 1 (continued)

Country	Mandatory				Voluntary
	USA	EU	China	Russia	USA
SVOCs	–	–	–	Tricresyl phosphate 0.5 mg/m ³ Diocetyl sebacate 5 mg/m ³	–

The major source of CO₂ within the aircraft are occupants; during the SARS-CoV-2 pandemic, another temporary source was introduced by additional carriage of dry ice to keep COVID 19 vaccines cold. Since the ban of on board smoking, the major source for CO is incomplete combustion from aircraft and ground support vehicles exhaust that may be ingested into the bleed air supply. For O₃, the main source is air outside the aircraft during ground operations and during high altitude, high latitude flights that may be ingested by the engine systems.

The oxygen (O₂) partial pressure on commercial aircraft is set by regulation FAR 25.841 that limits the cabin altitude to a maximum of 8,000 feet (2438 m, 753 hPa), only reached at the highest certification flight altitude of the airplane. Airplanes typically fly with a cabin altitude between 5500 feet (1676 m, 827 hPa) and 7000 feet (2134 m, 782 hPa).

Mandatory Standards

Current airworthiness standards (FAA) or certification specifications (EASA) require that each passenger and crew compartment be ventilated with a sufficient amount of uncontaminated (fresh) outside air (at least 0.55 lb./min per occupant) to enable crew members to perform their duties without undue discomfort or fatigue and to provide reasonable passenger comfort (EASA 2020; FAA 2021).

Regulators may permit alternative variable flow systems in future designs if the system designers can ensure that air quality is equivalent or better than that provided by current system designs. An equivalency approach to control air quality in buildings is being addressed by ASHRAE Commercial Building Standard 62.1 (ASHRAE 2019a) through its Indoor Air Quality Procedure, which is further detailed in a future Guideline 42P that is currently under development and will likely be published in 2022. No such solution has been applied in aircraft so far.

Voluntary Guidelines

Besides the mandatory air quality requirements from certification authorities, some voluntary documents suggest additional limits for environmental parameters related to the aircraft cabin. Among these, ASHRAE Standard 161 Air Quality within Commercial Aircraft (2018) provides guidance for factors affecting air quality

such as temperature, humidity, pressure, and ventilation, including contaminants, (counter-) measures, and measurement procedures. The standard is accompanied by Guideline 28: Air Quality within Commercial Aircraft (ASHRAE 2016), which gives supporting information.

Additional documents addressing air quality in aircraft and possible contamination sources have been and are being elaborated by SAE Aerospace Council:

- SAE ARP 4418B 2018 describes a Procedure for Sampling and Measurement of Aircraft Propulsion Engine and APU Generated Contaminants in Bleed Air. It outlines recommended practices to quantify the concentrations of a subset of bleed air-contaminant marker compounds on an aircraft propulsion engine or APU prior to delivery and installation on civil and military aircraft.
- SAE AIR 7521 2018 provides Measurement Data and Reference Values for Compounds Potentially Found in Aircraft Engine Bleed and summarizes published measurement data and reference values for marker chemical compounds listed in ARP 4418 potentially found in aircraft engine bleed air.
- SAE AIR 4766 2018 provides information on Air Quality for Commercial Aircraft Cabins and some of the factors affecting the perception of cabin air quality in commercial aircraft cabin air.
- SAE AIR 4766/2A 2021 provides information on Airborne Chemicals in Aircraft Cabins, including origins of chemical airborne contaminants during routine operating and failure conditions as well as exposure control measures.
- SAE AIR 1539C 2020 provides information on liquid and particulate contaminants as well as gaseous contaminants such as ozone or fuel vapors, etc. which may enter the aircraft through the Environmental Control System (ECS) from outside.
- SAE AIR 6418, under development since 2016 and to be published in 2022, will detail Sampling and Measurement of Bleed Air Supplies from Engines or APUs and will consider a broader range of contaminants than ARP 4418.

Whereas US standardization groups within ASHRAE and SAE have made progress in elaborating voluntary standards and informative guidelines on cabin air quality, the European Union has been struggling to develop a European cabin air quality standard with concrete requirements since the withdrawal of EN 4618:2009 (Aerospace series – aircraft internal air quality standards, criteria, and determination methods) in 2013. prEN 17436:2021 (Cabin air quality on civil aircraft – chemical compounds) was rejected by national standardization bodies in the 2nd enquiry in 2021 and may now be downgraded from a standard to a Technical Specification (TS) or Technical Report (TR) or the work will be stopped completely because the responsible Technical Committee within CEN (Comité Européen de Normalisation, European Committee for Standardization) did not come to an agreeable wording that is acceptable for sufficient positive votes from national standardization bodies. EN 4618:2009 was a performance-based standard providing health, safety, and comfort limit values for selected possible contaminants of cabin air. The current draft prEN 17436:2021 in contrast is written as a descriptive standard giving – similar to abovementioned US Standards – no clear pass/fail criteria for cabin air quality parameters.

Outside Air Supply Rate

Outside air supply rates for aircraft cabins reported in the literature ranged from 1.7 to 39.5 L/s per person with an average of 6.0 ± 0.8 L/s/p and a median of 5.8 L/s/p, respectively (Wieslander et al. 2000; Lindgren and Norbäck 2002; Spicer et al. 2004; Spengler et al. 2012; Giaconia et al. 2013; Li et al. 2014; Guan et al. 2015; Cao et al. 2019; Liu et al. 2020). All of the reported average values exceeded the minimum required outside air supply rate of 0.55 lb./min/p (3.5–4.7 L/s/p, 0–8000 ft. pressure) (ASHRAE 2018; FAA 2021; CCAC 2016); most even reached the recommended value of 4.7 L/s/p (EASA 2020) or 5 L/s/p stated by the ASHRAE Handbook (2019b).

Relative Humidity

The main sources of humidity in an aircraft cabin during flight are exhaled air and perspiration from the occupants and beverage service. For some aircraft models, humidification systems are available as an option for dedicated cabin areas or crew rest compartments.

Relative humidity measured in aircraft cabins ranges between 0.9% and 77% (Nagda et al. 1992; ASHRAE 1999; Lee et al. 1999; Haghigat et al. 1999; Dumyahn et al. 2000; Ree et al. 2000; Wieslander et al. 2000; Nagda et al. 2000; Lindgren and Norbäck 2002; Waters et al. 2002; Spicer et al. 2004; MacGregor et al. 2008; Spengler et al. 2012; Gladyszewska-Fiedoruk 2012; Giaconia et al. 2013; Schuchardt et al. 2017). The lowest levels most likely occur in cabins during cruise with very few passengers on board and the maximum levels likely on ground at airports in humid climates shortly after closing the doors. The average reported relative humidity was $16\% \pm 5.0\%$; the median was 17%. Reported measurements are from all flight phases, and it is difficult to separate the measurements reported in different studies according to the flight phase.

Standards do not give guideline values for the relative humidity in aircraft cabins; however, for buildings, levels around $40\% \pm 20\%$ (CEN EN 16798-1:2019 recommends a range from 20 to 70%) are considered comfortable. Such humidity levels cannot be reached on aircraft because of the dry outside supply air (< 1% during cruise) used for air conditioning and would require substantial additional weight for humidification with increased risk of water condensation or icing on the cold fuselage during cruise and subsequent moisture damage to aircraft structures or electric systems.

Selected Pollutants in the Aircraft Cabin

Carbon Dioxide (CO₂)

CO₂ created by metabolism is exhaled by the crew and passengers on board, and the level depends on the number of people present and the dilution by ventilation rate, and it is therefore an indicator of outside ventilation per occupant. Dry ice carriage can also influence the CO₂ level in the cabin.

Several studies measured CO₂ concentrations in aircraft cabins (Chen et al. 2021). Some studies mentioned that values were automatically or manually corrected for pressure changes (ASHRAE 1999; Dumyahn et al. 2000; Nagda et al. 2000; Lindgren and Norbäck 2002; Waters et al. 2002; Spicer et al. 2004; Li et al. 2014; Guan et al. 2015; Cao et al. 2019; Liu et al. 2020), whereas some did not report whether a pressure correction was applied (Nagda et al. 1992; Lee et al. 1999; Haghigheh et al. 1999; Wieslander et al. 2000; Spengler et al. 2012; Gladyszewska-Fiedoruk 2012; Giaconia et al. 2013; Schuchardt et al. 2017; Rosenberger 2018). For the first group, the minimum measured CO₂ concentrations were in the range of 410 to 874 ppm, and the maximum in the range of 1485 to 3374 ppm with an average concentration of 1315 ± 232 ppm and a median of 1387 ppm. For the second group, the minimum measured CO₂ concentrations were in the range of 293 to 1100 ppm, and the maximum in the range between 1190 and 5177 ppm, the average CO₂ concentration was 1320 ± 302 ppm, and the median was 1404 ppm. The differences of mean and median between the two study groups are only marginal. However, in the second study group the lowest values reported were lower than the CO₂ concentration in outdoor air, ranging then between 365 and 390 ppm (Sawa et al. 2004; Foucher et al. 2011; Tuzson et al. 2011; ASHRAE 2019b).

All measured CO₂ concentrations were below the regulatory, standard maximum level, occupational health and workplace exposure limit of 5000 ppm (EASA 2020; FAA 2021; CCAC 2016; IAC 2005) with one exception. All average and minimum CO₂ concentrations measured were lower than 2000 ppm, and the reported average CO₂ concentrations were mostly above 1000 ppm, which is generally considered the target for achieving acceptable air quality in low-density occupied buildings for control of building-generated contaminants and odor perception of visitors (Fisk et al. 2019). CO₂ concentrations were usually highest during boarding and deplaning (deboarding) and lowest during cruise. CO₂ concentrations showed a slightly decreasing trend over the last 30 years (He et al. 2021).

Carbon Monoxide (CO)

The source of CO is mostly outside the aircraft, incomplete combustion from vehicles on ground, and enters by ingestion.

CO concentrations measured on board of aircraft (Nagda et al. 1992; ASHRAE 1999; Lee et al. 1999; Nagda et al. 2000; Waters et al. 2002; Spicer et al. 2004; Spengler et al. 2012; Schuchardt et al. 2017; Rosenberger 2018) were in the range of below the limit of detection (LOD) to 9.4 ppm with a median of 1 ppm and a mean of 0.8 ± 0.3 ppm and below standard limits, the maximum value however came close to the 9 ppm 10 min TWA limit (Table 1) during ground operation.

Ozone (O₃)

O₃ may enter the aircraft cabin from outside during cruise, especially on high-altitude polar routes and at some airports during ground operations. Aircraft fly in

the troposphere at elevations generally up to 41,000 feet (Spengler et al. 2004; Yates et al. 2017); some aircraft are even certified for levels up to 43 or 45,000 ft. (B777, B767, B747). At these altitudes, the ambient concentrations of O₃ range between 25 and 900 ppb (WHO 2005; Weisel et al. 2013; Bhangar and Nazaroff 2013) and up to 1800 ppb at 45,000 ft. in winter on polar routes (AC 120-38, FAA 1980). Tropospheric ozone levels have been steadily increasing since AC 120-38 issued guidance on meeting ozone destruction efficiency requirements in 1980 (Cooper et al. 2014).

When entering the cabin, O₃ will decompose on surfaces and may also react with other pollutants in air and on surfaces and may generate new compounds (Weisel et al. 2013). Ozone can be removed from outside air. Ozone removal efficiency in aircraft systems considers the ozone destruction potential of the entire system, including the high temperature areas in engine and bleed air systems, the ozone converter itself, and the other surfaces within the air supply and distribution system.

The levels of O₃ measured in aircraft cabins were between 0 and 275 ppb. The average concentration of O₃ reported was 38 ± 30 ppb, and the median was 33 ppb. Most levels were below 250 ppb, which is the peak regulatory limit for O₃ in aircraft cabins, but some peak measurements exceeded 100 ppb. Regulations limit ozone to 250 ppb peak and 100 ppb three-hour time-weighted average (EASA 2020; FAA 2021; CCAC 2016; IAC 2005). All mean levels reported were below 100 ppb. However, on selected flights average concentration exceeded the recommended airborne exposure levels averaged over 8 h for heavy workloads by the American Conference of Governmental Industrial Hygienists (ACGIH) of 50 ppb. Since ozone is an irritant, on routes where high outside O₃ concentrations are expected, NRC (2002) and ASHRAE 161 (2018) recommended that O₃ converters should be employed and O₃ should be monitored continuously. However, the current certification regarding O₃ rather aims at a robust design of O₃-converter efficiency to reduce O₃ sufficiently until the end of its useful life since an O₃-monitoring concept can be complex and error-prone.

O₃ levels reported in many studies (ASHRAE 1999; Dumyahn et al. 2000; Spicer et al. 2004; Spengler et al. 2004, 2012; Bhangar et al. 2008; Weisel et al. 2013; Ji and Zhao 2014; Gao et al. 2015; Schuchardt et al. 2017; Rosenberger 2018) have been decreasing over time, as more attention has been paid to ozone in aircraft cabins and the utilization of catalytic ozone converters on flights where elevated ozone levels may occur (Chen et al. 2021).

Volatile Organic Compounds (VOCs)

Previous investigations of cabin air quality measured VOC contamination by different sampling methods: active sampling on adsorbent tubes, or passive sampling by diffusion samplers, or (vacuum) canister sampling. Most studies (Dechow et al. 1997; ASHRAE 1999; Waters et al. 2002; Crump et al. 2011a, b; Spengler et al. 2012; Weisel et al. 2013; Ji and Zhao 2014; Guan et al. 2014; Wang et al. 2014a, b; Gao et al. 2015; Rosenberger et al. 2016; Schuchardt et al. 2017) used active

sampling. By that method, a total of 140 VOCs were detected and measured. Passive sampling was only used in a few studies (Wieslander et al. 2000; Lindgren and Norbäck 2002; Spicer et al. 2004; MacGregor et al. 2008) and resulted in 48 detected VOCs. Five studies used canister sampling (Nagda et al. 2000; Spicer et al. 2004; Spengler et al. 2012) to measure 96 VOCs.

The concentrations of VOCs detected by active sampling ranged from 0 to 3 mg/m³ with the highest levels often obtained during meal service (ASHRAE, 1999, Schuchardt et al. 2017) and with average concentrations between 0.1 and 100 µg/m³. Table 2 shows the main chemical compound groups measured on nonsmoking flights in 12 studies (Chen et al. 2021). The most frequently detected compounds were alcohols (57.8%) followed by aldehydes (6.4%), alkanes (4.8%), terpenes (4.5%), aromatics (3.5%), and ketones (3.4%); all other VOC groups accounted for less than 3% of compounds.

Table 3 shows compounds that were most frequently detected in cabin air quality studies.

As shown in Table 3, the compounds most frequently measured in cabin air were the aromatic compounds toluene, xylenes, benzene, ethylbenzene, and styrene, the terpene limonene, aldehydes such as benzaldehyde, nonanal, formaldehyde, acrolein, hexanal, decanal, acetaldehyde, and octanal, the ketones acetone and 6-methyl-5-hepten-2-one, the alkanes undecane, dodecane, hexane, nonane, decane, and heptane, the organochloro compounds tetrachloroethene, trichloroethene, and 1,4-dichlorobenzene, the alkene isoprene, the ester ethyl acetate, and acetic acid (Chen et al. 2021).

Toluene, xylenes, benzene, ethylbenzene, and styrene are fuel-related and engine combustion-related compounds (Knighton et al. 2009), which likely penetrated into the cabin from ground-level emissions. The average benzene concentration of

Table 2 Compound groups and their percentage found in 12 cabin air quality-monitoring studies on nonsmoking flights (Chen et al. 2021, modified, based on data from ASHRAE 1999; Crump et al. 2011a, b; Spengler et al. 2012; Weisel et al. 2013; Ji and Zhao 2014; Guan et al. 2014; Wang et al. 2014a, b; Gao et al. 2015; Rosenberger et al. 2016; Schuchardt et al. 2017)

Compound group	Percentage
Alcohols	57.8
Aldehydes	6.4
Alkanes	4.8
Terpenes	4.5
Aromatics	3.5
Ketones	3.4
Acids	2.8
Siloxanes	2.4
Nitrogenous	2.3
Esters	1.7
Chlorocarbons	1.4
Ethers	1.2
Alkenes	0.8
Phthalates	0.2
Phosphates	0.2
Others	6.8

Table 3 Concentration ranges of VOCs most frequently measured in aircraft cabins (Chen et al. 2021, modified)

Compound	CAS No.	Concentration [$\mu\text{g}/\text{m}^3$]				
		Min	Median	Max	Mean	SD
Toluene	108-88-3	2.5	12	123	15	12
Limonene	138-86-3	1.4	12	276	24	31
m&p-Xylene	108-38-3, 106-42-3	0.6	1.6	21	2.5	2.3
Benzene	71-43-2	0.1	0.6	57	5.9	5.5
Benzaldehyde	100-52-7	0.0	2.0	14	>2.5	2.0
Undecane	1120-21-4	0.0	2.2	13	2.9	1.6
o-Xylene	95-47-6	0.3	1.0	14	2.5	2.8
Ethylbenzene	100-41-4	0.2	0.7	23	2.3	2.9
Styrene	100-42-5	0.0	0.5	6.1	1.0	0.9
Nonanal	124-19-6	1.9	5.4	24	7.8	5.6
Formaldehyde	50-00-0	2.7	5.9	7.1	5.4	1.5
Acrolein	107-02-8	<LOD	0.4	3.2	<0.8	1.0
Hexanal	66-25-1	1.7	2.8	14	5.2	4.8
Tetrachloroethene	127-18-4	0.6	3.8	16	7.3	5.7
Decanal	112-31-2	2.7	15	36	14	5.0
Acetone	4468-52-4	0.5	16	49	14	5.6
Dodecane	93685-81-5	0.0	1.9	13	3.1	1.8
6-Methyl-5-hepten-2-one	129085-68-3	0.2	8.5	16	7.0	3.5
Trichloroethene	79-01-6	0.1	0.3	0.7	0.4	0.2
Acetaldehyde	75-07-0	5.2	5.3	7.7	6.4	1.2
Isoprene	78-79-5	0.8	9.0	14	6.8	4.9
Ethyl acetate	141-78-6	3.9	4.9	16	6.5	4.4
1,4-Dichlorobenzene	106-46-7	0.1	1.0	6.9	2.4	2.9
Hexane	110-54-3	0.0	0.5	68	20	31
Octanal	124-13-0	1.3	2.9	10	4.2	1.8
Nonane	111-84-2	0.0	1.8	2.0	>1.4	0.7
Decane	124-18-5	0.0	1.0	1.7	1.1	0.6
Heptane	142-82-5	0.0	0.9	0.9	>0.7	0.3
Acetic acid	64-19-7	1.1	12	16	11	2.7
Butanal	123-72-8	0.8	0.9	1.3	1.0	0.2
2-Butanone	78-93-3	1.2	2.9	2.9	2.4	0.8
2,2,4-Trimethylpentane dioldiisobutyrate	NO	0.2	1.0	1.3	1.1	0.3
2-Propanol	67-63-0	3.5	13	13	10	3.4
Dichloromethane	75-09-2	0.0	1.1	2.8	1.4	1.0
Methylcyclohexane	108-87-2	0.1	0.6	1.1	0.6	0.5
Heptanal	111-71-7	0.7	2.3	4.6	3.2	1.3
N,N-Dimethyl formamide	68-12-2	0.0	7.7	7.7	<6.8	3.9

(continued)

Table 3 (continued)

Compound	CAS No.	Concentration [$\mu\text{g}/\text{m}^3$]				
		Min	Median	Max	Mean	SD
2-Ethyl-1-hexanol	104-76-7	2.9	4.0	5.9	4.7	1.0
Menthol	15356-70-4, 491-02-1	1.0	12	12	9.6	3.6
Ethanol	64-17-5	81	82	3009	386	899
Tridecane	629-50-5	0.0	1.7	1.7	1.5	0.4
Pentane	109-66-0	0.4	1.4	4.7	1.4	0.4
3-Carene	13466-78-9	0.0	1.3	1.3	1.1	0.5
alpha-Pinene	80-56-8	0.0	1.2	1.2	1.1	0.3
beta-Pinene	127-91-3	0.0	0.6	0.6	0.5	0.2
Octane	111-65-9	0.0	0.5	0.6	>0.5	0.1

$5.9 \pm 5.5 \mu\text{g}/\text{m}^3$ measured exceeded the 8-h recommended exposure levels (RELS) and the Chronic RELs (WHO 2010). Benzene is a genotoxic carcinogen in humans, and no safe level of exposure can be recommended.

Limonene can be emitted by many sources, e.g., fragrances, deodorants, cleaning agents, wet napkins, fruits, or soft drinks (Singer et al. 2006; Sun 2007; Orth et al. 2013; Simpson et al. 2019). Limonene may react with ozone to form secondary organic aerosols (SOAs) (Langer et al. 2008; Rai et al. 2014) as well as oxygenated VOCs and SVOCs including aldehydes like formaldehyde or acetaldehyde (Singer et al. 2006; Sun 2007).

Formaldehyde and acetaldehyde are products of O_3 chemistry occurring in aircraft (Wisthaler et al. 2005; Singer et al. 2006; Weschler et al. 2007; Norgaard et al. 2014), combustion products (Knighton et al. 2009), and associated with lubricant and hydraulic oils as well as fuel (ASHRAE 161 2018).

Benzaldehyde is contained in almonds (Franklin and Mitchell 2019) and used as flavoring in cosmetics (<https://www.whatsinproducts.com/chemicals/view/1/1461/000100-52-7>). It may also be a degradation product of the commonly used adsorbent Tenax TA for VOC sampling for chemical analysis (Kleno et al. 2002).

Nonanal, hexanal, decanal, and octanal were also detected frequently in aircraft cabins. These aldehydes can be associated with the presence of humans as a result of reactions of ozone with human skin oil (squalene) on the skin, on clothing, and on all surfaces that were in contact with human skin such as seats, armrests, and headrests (Wisthaler et al. 2005; Weisel et al. 2013; Gao et al. 2015; Tsushima et al. 2018). Decanal, nonanal, and octanal have very low odor thresholds (Abraham et al. 2012) which are often exceeded in aircraft cabins, so they may contribute to an odor nuisance if the concentrations get too high. Their odor qualities are soapy, citrus-like while hexanal smells rather grassy, green. Also, 6-methyl-5-hepten-2-one is a product of skin reactions.

Acrolein is a combustion product not only from fuels or oils but also of tobacco. Acrolein can also be formed by reactions of hydrocarbons with ozone (Nazaroff and

Weschler 2010). Acrolein is not only toxic but also very reactive; because of the conjugated double bond to the aldehyde group, it can polymerize or react with many compounds to form secondary products (Stevens and Maier 2008).

Acetone is not only a common solvent but also a major bioeffluent. Together with ethanol and isoprene, they are products of human metabolism (Perry 1995), and exhaled in significant amounts. Ethanol is the compound measured at highest concentrations on some flights also because of alcohol consumption by passengers before and during flights.

Alkanes including undecane, dodecane, hexane, nonane, decane, and heptane are common fuel constituents and likely ingested during ground operation. The alkane range in jet fuel is from heptane (C7) to pentadecane (C15); of those, the largest fraction are decane, undecane, and dodecane. Usually hexane is only present in small amounts. Hexane is an organic solvent and may have other origins such as adhesives, cleaners, and lacquers (<https://www.whatsinproducts.com/chemicals/view/1/284/000110-54-3>).

Tetrachloroethene was and still is widely used for dry cleaning (<https://www.whatsinproducts.com/chemicals/view/1/177/000127-18-4>); however, it is considered harmful, even toxic and possibly carcinogenic, and should not be used anymore (Ceballos et al. 2021).

Trichloroethene is also a chloro-organic solvent, which is used as degreaser or stain remover (<https://www.whatsinproducts.com/chemicals/view/1/316/000079-01-6>).

1,4-Dichlorobenzene is hardly degradable in the environment and was/is used as toilet deodorant and insecticide (<https://www.whatsinproducts.com/chemicals/view/1/1464/000106-46-7>).

Ethyl acetate is a common solvent and is contained in nail polish remover, glues (<https://www.whatsinproducts.com/chemicals/view/1/196/000141-78-6>), and also a fruit ester formed by yeast in alcoholic beverages (Saerens et al. 2010).

Acetic acid can be a reaction product of O₃ and squalene (Wisthaler et al. 2005; Gao et al. 2015). It can also be exhaled or be emitted from vinegar-containing foods such as salads or pickles.

A number of compounds have been found less frequently in aircraft cabins, but sometimes at higher concentrations (Chen et al. 2021):

- 1-Propanol (0.6–81 µg/m³) is used as solvent and disinfectant (<https://www.whatsinproducts.com/chemicals/view/1/480/000071-23-8>).
- Isoalkanes C14-C20 (25–62 µg/m³) may originate from lubricants or anti-corrosive agents.
- 1,2-Propanediol (11–45 µg/m³) residues may originate from deicing liquid (Ritter 2001) or from cleaners, hand soap, detergents, dish washer soap, shower gel, hair care products, shaving creams, toothpaste, makeup, deodorants, air fresheners, insect repellent, and paint (<https://www.whatsinproducts.com/chemicals/view/1/47/000057-55-6>).
- Acetonitrile (19–27 µg/m³) from smokers – it can be found in breath up to 1 week after smoking the last cigarette (Jordan et al. 1995).

- Cyclopentasiloxane (9.8–18 µg/m³) from deodorants or hair care products (<https://www.whatsinproducts.com/chemicals/view/1/3705/000000-79-7>).
- Diocylether (0.4–6.4 µg/m³) from sunscreen or hair care products (<https://www.whatsinproducts.com/chemicals/view/1/3774/000629-82-3>).
- Benzoic acid (3.3–5.3 µg/m³) widely used as a preservative (<https://www.whatsinproducts.com/chemicals/view/1/1031/000065-85-0>), but also a degradation product of Tenax TA, often used for VOC sampling (Kleno et al. 2002).

All compounds listed above can be found in other indoor environments with human occupancy as well.

Typical levels of VOCs found in aircraft are similar to or lower than those commonly found in other environments such as office buildings and schools (Spicer et al. 2004; Spengler et al. 2012; Schuchardt et al. 2017; AGÖF 2013). They are also well below indoor air guideline values (MHLW 2002, Chinese standard 2002; WHO 2010; OEHHA 2019; ACGIH 2021; baua 2021; Health Canada 2021, NIOSH 2021; UBA 2021). Measured VOC levels were lower in flight on aircraft equipped with carbon-based air purification (Schuchardt et al. 2017; Rosenberger 2018).

Several compounds are regulated by airworthiness standards such as IAC 2005. Maximum concentrations of compounds measured are below these limits. There are currently no guideline limits set for other VOCs in cabin air.

Total Volatile Organic Compounds (TVOC)

Some cabin air quality studies monitored the TVOC content by online monitors such as flame ionization detector (FID, Lee et al. 1999) or photoionization detector (PID, Crump et al. 2011a, b; Guan et al. 2015; Schuchardt et al. 2017). Average TVOC concentration measured by FID was about 8 mg/m³, and average TVOC concentration measured by PID was 277 µg/m³ with a range from 0 to 38 mg/m³. The average PID TVOC level fits well to TVOC levels measured in other indoor environments such as residential and office buildings, often even lower. AGÖF 2013, e.g., states as TVOC mean value of more than 2500 measurements in residential and office buildings between 2006 and 2012 a concentration of 360 µg/m³ – determined as sum of concentrations of compounds eluting between hexane and hexadecane from the nonpolar column used for VOC analyses according to ISO 16000-6:2011 (ISO 2011).

Semivolatile Organic Compounds (SVOCs)

SVOCs in aircraft cabins and cockpits have been measured and reported in several studies (CAA 2004; Maddalena and Mckone 2008; Denola et al. 2011; Marsillach et al. 2011; Solbu et al. 2011; Spengler et al. 2012; Ree et al. 2014; Rosenberger et al. 2016; Howard et al. 2018; Schuchardt et al. 2019). Of those measured, especially

organophosphates have been in discussion to be potentially neurotoxic and therefore potentially responsible for negative effects on health of passengers and crew (UK Parliament, House of Lords 2000; Civil Aviation Authority CAA 2004; UK Committee on Toxicology 2007; UK Committee on Toxicology 2013; EASA 2009–10 A-NPA Ree et al. 2014; Wolkoff et al. 2016). Measurement of SVOCs at low concentrations is a challenge, and only in recent years, analytical technologies improved and limits of detection decreased. In 2003, Nagda and Rector reported SVOC concentrations below their LODs (under normal operating conditions), except for tricresyl phosphates (TCPs) from engine oils, and tributyl phosphate (TBP) from hydraulic oil.

Table 4 provides a summary of the SVOCs and concentration ranges in cabin air previously detected and reported.

On flights on which a smell was perceived or a leak in an aircraft system suspected that allowed operating fluids to enter the bleed air system, a special focus had been put on the determination of SVOCs, especially organophosphorus compounds. Smell events were documented in nine studies (Nagda et al. 2000; Spicer et al. 2004; Muir et al. 2008; Solbu et al. 2011; Crump et al. 2011a, b; Spengler et al. 2012; Ree et al. 2014; Schuchardt et al. 2017), but a correlation to SVOCs is difficult since event concentrations were not higher than ranges reported from other studies, with two exceptions.

Tris (butoxy-ethyl) phosphate (TBEP) was found by Rosenberger 2018 at a maximum level of up to 2370 ng/m³ on 1 of 17 flights including event flights. Trixyl phosphate (TXP) was only detected by Schuchardt et al. (2019) at levels between 30 and 39 ng/m³ on 2 of 196 samples drawn on A380 and on 2 of 207 samples drawn on A321 flights.

SVOCs in cabin air were frequently measured and reported; their concentrations ranged from below the limit of detection (LOD) to 49 µg/m³. The SVOCs with highest concentrations and high frequency of detection were naphthalene, tris (chloro-isopropyl) phosphate (TCPP), tributyl phosphate (TBP), tri-n-butyl phosphate (TnBP), and triisobutyl phosphate (TiBP).

Naphthalene was used in mothballs; it is also contained in pesticides, varnish, stain remover, or fuel additives (<https://www.whatsinproducts.com/chemicals/view/1/289/000091-20-3>). TCPP is a common flame retardant in many polymer products, e.g., polyurethane foams. TBP, TnBP (likely the same compound with a different name in different studies), and TiBP are major constituents of hydraulic oil.

Tri-o-cresyl phosphate (ToCP) concentrations were reported from 0 to 22,800 ng/m³ with an average of 50 ± 14 ng/m³; in other studies, ToCP was below the LOD (Schuchardt et al. 2019). Wolkoff et al. (2016) observed that the level of 22,800 ng/m³ was a single reading out of 1000 readings, and the level of ToCP that had been reported in that study (Crump et al. 2011b) could have been overestimated because of its chromatographic overlap of other more prevalent ortho isomers. In fact, the methodology used in the study with this extraordinary finding was not specifically designed for TCP and can be considered inferior to the methods used in later studies related to TCP. Based on the isomeric composition of TCP formulations used in engine oils, ToCP is the isomer that can be least expected (Denola et al. 2008). Among SVOCs for which regulations exist, maximum levels of

Table 4 SVOCs ranges measured in aircraft cabins (Chen et al. 2021, modified)

Compound	CAS No.	Concentration [ng/m ³]			
		Min	Max	Mean	SD
Naphthalene	91-20-3	0	49,100	1241	166
Tris (chloro-isopropyl) phosphate (TCPP)	13674-84-5	23	9977	506	0.4
Tributyl phosphate (TBP)	126-73-8	37	9100	495	59
Tri-n-butyl phosphate (TnBP)	NO	20	4100	330	421
Triisobutyl phosphate (TiBP)	126-71-6	3	1610	92	9.3
Tris (butoxy-ethyl) phosphate (TBEP)	78-51-3	0	642	71	4.4
Tri-o-cresyl phosphate (ToCP)	78-30-8	0	22,800	50	14
Tricresyl phosphates (TCP)	1330-78-5	0.3	14,900	35	7.7
Tris (chloroethyl) phosphate (TCEP)	115-96-8	1	324	15	1.0
Diphenyl-2-ethylhexyl phosphate (DPEHP)	1241-94-7	0	282	15	0.2
Triphenyl phosphate (TPP)	115-86-6	1	119	8.7	0.3
Tris (1,3-dichloro-isopropyl) phosphate (TDCPP)	13674-87-8	1	49	7.7	0.3
Tri-mmp-cresyl phosphate (T-mmp-CP)	NO	1	691	6.5	0.4
Acenaphthene	83-32-9	17	24	5.7	4.7
Phenanthrene	85-01-8	13	21	4.9	3.7
Tri-m-cresyl phosphate (T-m-CP)	563-04-2	1	428	4.4	0.3
Tri-mpp-cresyl phosphate (T-mpp-CP)	NO	1	339	4.2	0.2
Tris (ethyl-hexyl) phosphate (TEHP)	78-42-2	0	88	3.5	0.4
Fluorene	86-73-7	8.8	12	3.0	2.2
Pyrene	129-00-0	3.6	15	2.6	1.9
Tri-p-cresyl phosphate (T-p-CP)	563-04-2	1	57	2.1	0.1
trans-Permethrin	61949-77-7	1.1	2.0	1.5	—
Retene	483-65-8	0.8	2.0	1.4	—
cis-Permethrin	61949-76-6	ND	0.9	0.9	—
Acenaphthylene	208-96-8	2.6	3.3	0.8	0.6
Fluoranthene	206-44-0	0.0	1.9	0.5	0.4
Anthracene	120-12-7	0.8	1.1	0.3	0.2
Hexachlorobenzene	118-74-1	0.4	2.3	0.2	0.2

cresyl phosphate mixture and dioctyl sebacate (which is an older oil base stock formulation) are stipulated in IAC AP-25 (2005) but have not been measured as such in the studies included in the present review.

Generally, the concentration of SVOCs measured in aircraft cabins was lower than the statutory limits for the compounds, if available, in buildings (MHLW 2002; Chinese standard 2002; WHO 2010, OEHHA 2019; ACGIH 2021; baua 2021; Health Canada 2021; NIOSH 2021; UBA 2021).

A joint study conducted by Kansas State University for ASHRAE and the FAA currently (2021) underway will gain further information on SVOC, VOC, and particulate matter released from contamination of a bleed air heat exchanger; when bleed air inlet temperatures are elevated, results will be published within the next few years.

Particles

Particulate matter has been measured and reported in several cabin air quality studies (Lindgren and Norbäck 2002; Nagda et al. 1992; Lee et al. 1999; Wieslander et al. 2000; Nagda et al. 2000; Waters et al. 2002; Spicer et al. 2004; Cao et al. 2017), some of which referred to them as Respirable Suspended Particulates (RSP). Respirable particles (RSP or PM₄) have a 50% cut point at 4 µm (US EPA 2004; ACGIH 2021). PM₁₀ have a 50% cut point at 10 µm (US EPA 2004). What particulate fraction the authors measured is indicated as subscript number giving the upper particle diameter recorded. Nagda et al. 2000; Spicer et al. 2004, and Cao et al. 2017 reported PM₁₀ and PM_{2.5} in the cabin at concentrations below 10 µg/m³. Lee et al. 1999 reported RSP concentrations from 1 up to 3159 µg/m³ with an average of 57 µg/m³. Waters et al. 2002 reported PM₅ at 38–300 µg/m³ with an average of 120 µg/m³, and Nagda et al. 1992 reported PM_{3.5} at 31–176 µg/m³ with an average of 62 µg/m³. Lindgren and Norbäck 2002 and Wieslander et al. 2000 reported PM_{0.3} at 1 to 253 µg/m³ with an average of 16 and 24 µg/m³, respectively.

Average concentrations are below residential indoor air quality guideline level concentrations (WHO 2005; EU 2008). In September 2021 the WHO published new air quality guideline levels for PM₁₀ and PM_{2.5} that are 10 to 25% and 40 to 50%, respectively, stricter. Particulates are removed from cabin air by dilution with outside air and the HEPA filters installed in the recirculating air path. These filters also are highly effective at removal of spores, bacteria, and viruses from recirculated cabin air. However, particles and microorganisms may be present initially when the source is in the cabin or when they are ingested from outside, e.g., from exhaust plumes on the airport tarmac.

Hydraulic fluids undergo pyrolysis at around 177 °C (e.g., Eastman Technical Data Sheets of Skydrol LD-4 or Skydrol PE-5), which is lower than bleed air temperatures found during main engine idle and APU operation (about 200 °C, NRC 1986, 2002).

Heated oil, on the other hand, pyrolyzes at around 300 °C at the pressure levels found within the bleed air system. At temperatures around 200 °C, if oil is present, it will be primarily in the form of ultrafine particle droplets. Hydraulic fluids at the same temperature would be present as particulate matter and VOCs. Particle size of bleed air contaminants is predominantly in the ultrafine particle size range, with the greatest presence in the 60 to 300 nanometer size range. The particle size range extends up to around 1 micron (Jones et al. 2017).

ASHRAE and the FAA are currently (2021) performing a study on particle size range of ultrafine particles and PM that are generated when oil, hydraulic fluid, or deicing fluid are ingested into an engine. Results will be available by 2022.

Selected Sources of Some Typical Cabin Air Contaminants

Low-level contaminants typical for an aircraft environment include organophosphorus compounds. They are widely used as flame-retardants, hydraulic fluids, or antiwear additives. Trace concentrations of organophosphates are frequently found

in aircraft cabin air. They may enter cabin air via the bleed air system through possible leaks. However, they can also be released from cabin materials, polluted surfaces, or equipment in the cabin or can be ingested into the cabin from outside air on ground on the airport tarmac. Sources for organophosphates may include the following:

Engine Oils

Engine oil is one of the contaminants that is often addressed as a major concern. Engine oil may enter the bleed air system by a leaking seal in the engine. It may also infiltrate into the cabin from outside. However, whether a base constituent of engine oil or a degradation product may enter cabin air, it has not been shown that leaking engine oil may cause any long-term negative health effects that were hypothesized in connection with odor events (UK Parliament, House of Lords 2000; Civil Aviation Authority CAA 2004; UK Committee on Toxicology 2007; UK Committee on Toxicology 2013; EASA A-NPA 2009–10 A-NPA; Ree et al. 2014; Wolkoff et al. 2016). Engine oils are classified based on MIL-PRF-23699G (2014) into four classes, Standard (STD), Corrosion Inhibiting (C/I), Enhanced Ester (EE), and High Thermal Stability (HTS). In commercial aircraft engines, mostly EE and recently HTS engine oils are used. Widely used EE oils are based on esters such as pentaerythritol (PE) esters or trimethylolpropane (TMP) esters. The acidic compounds used are linear or branched saturated organic acids with 5 to 10 carbon atoms, predominantly pentanoic and heptanoic acid, followed by octanoic acid, nonanoic acid, decanoic acid, 2–3-methyl butanoic acid, 3,3-dimethylheptanoic acid, or 3,5,5-trimethylhexanoic acid (Mair et al. 2015; Johnson 2016; Johnson 2018). The type and distribution of acids used vary between brands. In addition, the amounts of additives used to increase the load carrying or oxidative and thermal stability vary from one manufacturer to the next (Sniderman 2020).

Tri-m-and tri-p-cresyl phosphate is most widely used. Triphenyl phosphate (TPP) and isopropylated triphenyl phosphate (TIPP) have also come into use in one brand of oil to reduce potential exposure to tricresyl phosphates. Over the years, there has been much discussion on the types of isomers of tricresyl phosphates used. Tri-orthocresyl phosphate and all other ortho-isomers of TCP, which were originally thought to cause health issues in people who came into contact with aircraft turbine oils, have been almost virtually removed from all additive packages used in the entire industry after the specific toxicity of these particular isomers was recognized in the last century (Henschler 1958). Trimethyl propane phosphate was also proposed by some to be a potential decomposition product from oils based on TMP-Esters but had not been found during any engine or aircraft cabin air tests.

Hydraulic Fluids

On some aircraft, bleed air is used to pressurize the hydraulic fluid reservoir and freshwater tank. The hydraulic pressurization systems that use bleed air to pressurize

the reservoir use dual check valves to prevent backflow of hydraulic fluid into the bleed air. In the rare case of a dual check valve failure, hydraulic fluid could enter the bleed air system.

Hydraulic fluids generally consist of base stocks of tributyl phosphate (TBP) or triisobutyl phosphate (TiBP). TBP is frequently detected in cabin air. Triisobutyl phosphate has a lower density than tributyl phosphate and may offer weight reduction that in turn translates into fuel savings. Generally, the breathing of hydraulic fluid mist should be avoided, and protective breathing apparatus and eye protection worn when working around these fluids. Traces of hydraulic fluids may enter cabin air by outside air ingestion on the airport tarmac on ground. Contaminated surfaces or equipment stored in the pressurized cabin may also be a source for trace contamination.

Exhaust

During ground operation, at the gate, during push back, during taxiing, and during line-up for takeoff, aircraft may ingest exhausts from other vehicles and aircraft. This is common occurrence. By that also, carbon monoxide and nitrogen oxides may infiltrate into cabin air supply. Other major constituents of exhaust that may get into the cabin that way include formaldehyde, acetaldehyde, acrolein, and benzene (Knighton et al. 2009).

Oil aerosol, which may contain organophosphates like tricresyl phosphate (TCP), may be present in aircraft engine exhaust (Cheng 2013; Schuchardt et al. 2019) and may enter cabin air. Also, exhaust particles, in a size range around 10 nm in diameter, can travel to the aircraft cabin, as they behave more like gas than particles.

Deicing Liquids

In winter, airport runways as well as aircraft surfaces, especially the wings and engine cowlings, have to be clear of snow and ice before takeoff. Deicing fluids used for runway applications typically consist of a potassium chloride salt that is distributed on the runway after snow removal. Aircraft deicing utilizes one or more of four types of deicing, depending on the aircraft ground hold-time that is necessary following deicing, and which conform to SAE AMS 1424R/2020 for Aircraft Deicing/Anti-icing Fluid. Primary fluid base stocks include ethylene glycol, diethylene glycol, and propylene glycol mixed with water, corrosion inhibitors, wetting agents, and a dye. Ethylene glycol is used by some operators but is more infrequently used because of environmental toxicity. Propylene glycol is the most prevalent base stock for aircraft deicing and is typically mixed 50/50 with water. Liquid-deicing fluid that is sprayed onto aircraft surfaces must be done with proper procedures such as nozzle orientation to minimizing spraying the liquid into the engines/APU inlet and closing bleed air supply valves during deicing. If deicing liquid is ingested into the ECS, it is vaporized.

Rosenberger et al. (2014) detected high amounts of propylene glycol (up to 2.5 mg/m³) in cabin air on flights after aircraft deicing – with running APU. They also reported up to 1.5 mg/m³ of 1-hydroxyacetone, a degradation product of propylene glycol. Other contaminants such as organophosphates were not detected in this study at elevated levels after deicing.

A joint study being conducted by Kansas State University for ASHRAE and the FAA is underway. It will publish further information on VOC and particulate matter generated during the ingestion of deicing fluid after the study has been completed by the end of 2021.

Possible Unlikely Failure Cases That May Compromise Cabin Air Quality

Contaminants mentioned before may enter cabin air during normal operation by ingestion from outside while on the ground, often without being particularly noticed or concerned. In addition, each year hundreds of reports on fume and smell events causing discomfort to either crew or passengers on board an aircraft are filed with authorities. For one-third of them, the source is unknown, and one-quarter of them has its source in the air-conditioning system, mostly fan failures that generate odor when failed bearing allows the impeller to contact the inside of the fan housing, which is a focus of current investigations. Almost another fifth of reports is sourced to the APU and ingestion of contaminants from outside. With much lower frequency, events are sourced to the hydraulic power or other cabin systems. If events happen to be prominent in the news, they are often said to be caused by engine oil in the bleed air system; however, only 0.3–0.4% of all reported events can be related to engine oil or engine air. Number of events reported to FAA by Airlines for America (A4A) between 2012 and 2017 are shown in Table 5 by source and the respective aircraft part or system (ATA Chapter number, ATA Spec. 100, 1999).

Pathogens

The SARS-CoV-2 pandemic has documented the profound economic impact of infectious pathogens on the aviation industry. Many airlines suspended operations or canceled a significant proportion of flights. Airports have closed or shut one or more terminals. Airlines stopped and/or altered routes and frequency, with the number of seats offered by airlines in 2020 50% less and the overall number of passengers 60% less compared to 2019 levels (ICAO, 2021). Still, given the volume of daily commercial flights, carrying millions of passengers worldwide, the number of documented incidents of infectious disease transmission occurring on board remains infrequent (HSPH 2020). There have been few reports of SARS-CoV-1 and SARS-CoV-2 transmissions on board of aircraft during flights (Olsen et al. 2003; Khanh et al. 2020). Based on previous investigations of tuberculosis transmissions on (long-haul) flights, the distance from an infected passenger with high likelihood

Table 5 Events reported by Airlines for America to FAA between 2012 and 2017 by source, ATA chapter number

ATA chapter	ATA title	Number	Frequency (%)
	Unknown	438	33.64
21	AIR CONDITIONING AND PRESSURIZATION (primarily fan failures)	335	25.73
49	AIRBORNE AUXILIARY POWER (Primarily APU-ingested contaminants)	229	17.59
25	EQUIPMENT	71	5.45
33	LIGHTS	50	3.84
24	ELECTRICAL POWER	40	3.07
29	HYDRAULIC POWER	22	1.69
12	SERVICING-ROUTINE MAINTENANCE	17	1.31
44	CABIN SYSTEMS	17	1.31
36	PNEUMATIC	16	1.23
23	COMMUNICATIONS	15	1.15
52	DOORS	9	0.69
38	WATER / WASTE	7	0.54
73	ENGINE FUEL AND CONTROL	6	0.46
79	ENGINE OIL	5	0.38
28	FUEL	4	0.31
71	POWER PLANT	4	0.31
75	ENGINE AIR	4	0.31
30	ICE AND RAIN PROTECTION	3	0.23
78	ENGINE EXHAUST SYSTEM	3	0.23
26	FIRE PROTECTION	2	0.15
5	TIME LIMITS / MAINTENANCE CHECKS	1	0.08
22	AUTO FLIGHT	1	0.08
27	FLIGHT CONTROLS	1	0.08
77	ENGINE INDICATING	1	0.08
80	ENGINE STARTING	1	0.08
	Total	1302	100

to catch the infection is two rows forward and backward (CDC, 1995). However, SARS transmissions were also reported to passengers sitting as far as 7 rows to the front or 5 rows to the back (Olsen et al. 2003) or even two zones apart; however, transmission may have also occurred at the gate, during boarding, via a crew member as transmitter or during deplaning (deboarding), baggage claim, or immigration (Khanh et al. 2020). Transmission becomes possible across the whole cabin when the ECS is not operational as, e.g., happened on a grounded aircraft in Alaska with an influenza outbreak with ECS off for 3 h (Moser et al. 1979). Consequently, for transmission avoidance the ECS should always be operational when people (passengers, crew, or ground personnel) are on board.

The aircraft ventilation offers enhanced protection for diluting and removing airborne contagions in comparison to other indoor spaces with conventional mechanical ventilation being substantially better than residential situations. This level of ventilation effectively counters the proximity travelers are subject to during flights. Based on the available scientific evidence, it is the view of Harvard APHI that a very low number of infections only could be attributed to exposure on aircraft during travel (HSPH 2020).

The significant advantages of aircraft cabin environment in controlling pathogens and limiting the spread of disease compared to other indoor spaces are related to air change rates, filtration, passenger position, and airflow direction. Air change rates in the cabin are high compared to other indoor spaces, with about 15 to 20 air changes per hour with outside air and commensurate air changes with hospital grade HEPA-filtered recirculation air resulting in an equivalent total air change rate of up to 35 to 40 per hour. Air supply is predominantly downward, enters the cabin at the top through the air supply nozzles, and exists through return air grilles at floor level (Fig. 2). The ventilation system is designed to minimize airflow between the different temperature control zones along the cabin. Additionally, airplane seat configurations (forward facing, high-back seating) help to isolate occupants from each other and contribute to a reduction in passenger exposure to particles compared to other indoor environments (Freeman 2020).

The United States Transportation Command (USTRANSCOM) conducted tracer particle releases to simulate an infected passenger in multiple rows and seats on wide body and standard body commercial aircraft, to determine the exposure risk via penetration into breathing zones in that row and numerous rows ahead and behind the index case (40+ seats measured). The cough scenarios were conducted on ground and inflight with over 65 releases of 180,000,000 florescent particles and utilized real-time optical sensors, coupled with DNA-tagged tracers for aerosol deposition. Measured inhaled mass in the breathing zones of occupants adjacent to the simulated infected passenger showed the maximum inhaled mass was 0.46% of the exhaled mass, with medium inhaled mass of 0.009% (Kinahan et al. 2021).

The results from detailed CFD analysis and ground/inflight measurements (USTRANSCOM) are complimentary and further demonstrate that the airplane cabin is a mixed flow system and shows more characteristics of a plug flow system than a uniformly mixed system for particulates. The flow regime results in higher concentrations of particles near the infected individual and lower concentrations in the seats at a greater distance. As a result of the ventilation system design, inhaled masses in the cabin are low especially compared to other indoor spaces (HSPH 2020; Davis et al. 2021a, b; Kinahan et al. 2021).

Besides transmission by air, transmission by contact is also a possible way of spreading. Contact transmission may occur by touching of commonly used surfaces such as seat backs, armrests, tables, or door handles. Disinfection of such surfaces by disinfecting liquids containing, e.g., quaternary ammonium salts, hydrogen peroxide, phenols, sodium chlorite, sodium hypochlorite, isopropyl alcohol, ethanol, peroxyacetic acid, citric acid, and lactic acid, or by UVC radiation is appropriate means of transmission risk reduction (Pradhan et al. 2020; EPA List N 2021).

In addition to the existing solutions to control risk of infection, other solutions have been implemented (during SARS-CoV-2 pandemic) in a multilayered approach to keep passengers and flight crews healthy. They include physical distancing during boarding, deplaning (deboarding), and jet bridge, masking, providing appropriate ventilation gate-to-gate, vaccinations, washing hands, avoiding travel for individuals feeling unwell, and thorough cleaning/disinfecting the airplane cabin and flight deck between flights (HSPH 2020).

Physiological Response

Although it is not the main objective of the present chapter, it is worth mentioning studies that investigated the effects of exposures to pollutants in the aircraft cabins on human responses.

Human subject testing was performed with different CO₂ and VOC loads / different outside and recirculation air rates with and without air purification to evaluate comfort, health, and physiological responses. Air purification was found to be a more important factor than increased humidity for addressing the most prevalent and highest intensity passenger and crew health-related symptoms including eye, nose, and throat irritation and general dryness (ASHRAE, CSS 1999; Rankin et al. 2000; Strøm-Tejsen et al. 2008; Spengler et al. 2012; Weisel et al. 2017).

Most recent human subject testing has taken place shortly before the SARS-CoV-2 pandemic (January 2020): “CO₂ and VOC requirements for aircraft cabins / occupied spaces based on cognitive performance, comfort responses and physiological changes depending on pressure level” (CognitAir, 2018–2021) and “Investigation of cabin ventilation strategies impact on aircraft cabin air quality and passengers’ comfort and wellbeing through subject study in realistic aircraft environment” (ComAir 2018–2021, <https://cordis.europa.eu/project/id/820872>). Results of increased recirculation air rates on cabin environment parameters have been published (Norrefeldt et al. 2021), so have preliminary results on subjects’ wellbeing and health under the traditional air ventilation regime (Herbig et al. 2020). Results on subject responses and performance under non-traditional ventilation regimes with increased recirculation air rates have not been available before the completion of this chapter but will be published within the next two years.

Conclusion

The air in commercial aircraft cabins is generally of very good quality, usually better than in other means of mass transport operating on ground. The range of VOCs detected in cabin air is similar to other indoor environments such as offices or residential buildings (e.g., AGÖF 2013), and their levels are often at lower concentrations. Permissible levels, if existing, or levels recommended for other indoor environments are usually not exceeded. One exception – according to some

publications – is benzene. There are no particular limits or guideline values that are exclusive for aircraft cabins, and it is debatable if this was useful.

Many of the compounds found in occupied aircraft cabins originate from passengers (bioeffluents), their belongings, or their activities. Ethanol and sometimes also acetone concentrations are often elevated in aircraft cabins compared to offices or residential buildings, or other means of mass transport on ground (Dumyahn et al. 2000; Nagda and Rector 2003). Both compounds are typical human bioeffluents. Ethanol is also released by alcoholic beverages served on board, and contained in consumer products (cosmetics, cleaners).

CO₂ levels increase during boarding and deplaning (deboarding) – typically because the ECS is not always fully operated during these phases – and quickly decrease during flight. Average levels are comparable to other means of mass transport on ground (train, subway, and bus) and are within the recommended levels.

During ground operations, contaminations from outside the aircraft such as diesel exhaust from ground vehicles or engine exhaust from other aircraft or uncombusted fuel vapor can enter the cabin air. These trace contaminants may contribute to odors during boarding, push back, and taxiing. Traces of aircraft operational fluids in the bleed air and ECS systems may contribute particularly odorous pollutants. Though the initial air entering the cabin is not filtered, the high air change rate, the operation in very clean environment, and filtration of recirculated air contribute to the general good air quality on board of commercial aircraft. Most odors perceived in the cabin are not bleed air related (Table 5). Also, SVOC levels, including aviation typical organophosphates, are only found in trace concentrations and below the limits prescribed for indoor environments.

The likelihood of catching an infection on board of an aircraft is low provided the ECS is operational and additional required hygiene measures are obeyed. The risk increases if the ECS is turned off or an infected person is sitting in the immediate proximity and hygiene measures are neglected.

Maintaining adequate air quality through proper ventilation, filtration, and purification of the aircraft cabin air is important not only from the passenger and crew member point of view but also for the airline because economically significant fuel savings can be achieved if the systems for maintaining cabin environmental quality are operated and controlled according to the actual pollution loads while not exceeding the permissible levels of the parameters defining the quality of air in the aircraft cabin. Recently published and ongoing studies provide additional data that will aid design of systems that can optimize passenger and crew comfort and health while maximizing fuel efficiency leading to less emissions and hence reducing the environmental impact of air travel.

Cross-References

- ▶ [Analytical Tools in Indoor Chemistry](#)
- ▶ [Control of Airborne Particles: Filtration](#)
- ▶ [Influence of Ventilation on Indoor Air Quality](#)

- Occupant Emissions and Chemistry
- Sampling and Analysis of Semi-volatile Organic Compounds (SVOCs) in Indoor Environments
- Sampling and Analysis of VVOCs and VOCs in Indoor Air
- Semi-Volatile Organic Compounds (SVOCs)
- Volatile Organic Compounds (VOCs)

References

- Abraham MH, Sanchez-Moreno R, Cometto-Muniz JE, Cain WS (2012) An algorithm for 353 odor detection thresholds in humans. *Chem Senses* 37(3):207–218. <https://doi.org/10.1093/chemse/bjr094>
- ACGIH (2021) TLV/BEI guidelines. <https://www.acgih.org/science/tlv-bei-guidelines/>
- AGÖF Arbeitsgemeinschaft Ökologischer Forschungsinstitute e. V. (Association of Ecological Research Institutes e.V.), Guidance Values for Volatile Organic Compounds in Indoor Air, 2013 Edition, https://www.agof.de/fileadmin/user_upload/dokumente/orientierungswerte/AGOEF-VOC-GuidanceValues-2013-11-28.pdf
- Ahmadpour N, Lindgaard G, Robert J-M, Pownall B (2014) The thematic structure of passenger comfort experience and its relationship to the context features in the aircraft cabin. *Ergonomics* 57(6):801–815. <https://doi.org/10.1080/00140139.2014.899632>
- AIA American Institute of Architects, Academy of Architecture for Health (2001) Guidelines for design and construction of hospital and health care facilities, table 7.2, Washington, DC
- Airports Council International (ACI), Montreal, 25 March 2021. <https://aci.aero/news/2021/03/25/the-impact-of-covid-19-on-the-airport-business-and-the-path-to-recovery/>
- ASHRAE (2016) ASHRAE Guideline 28-2016, Air quality within commercial aircraft, Atlanta
- ASHRAE (2018) ANSI/ASHRAE Standard 161-2018, air quality within commercial aircraft, Atlanta
- ASHRAE (2019a) ANSI/ASHRAE Standard 62.1-2016, ventilation for acceptable indoor air quality, Atlanta
- ASHRAE (2019b) ASHRAE Handbook – HVAC applications, Atlanta
- ASHRAE, CSS (1999) RP-957 – relate air quality and other factors to symptoms reported by passengers and crew on commercial aircraft. <http://atp.iengineering.com/Report/Detail/500>
- ATA Spec (1999) 100: Manufacturers' technical data, A4A publications department, Washington, DC. <https://publications.airlines.org/CommerceProductDetail.aspx?Product=33>
- Bezold A (2009) Environmental control systems. Proceedings of the ICE – Ideal Cabin Environment International Aviation Conference, 9–10 March, Munich, Germany, ICE consortium
- Bezold A (2021) Cabin air quality – key to a comfortable flight. FAST technical magazine. <https://services.airbus.com/content/dam/corporate-topics/publications/fast/fast-articles/FAST-article-Cabin-air-Jan-2021.pdf>
- Bhangar S, Nazaroff WW (2013) Atmospheric ozone levels encountered by commercial aircraft on transatlantic routes. *Environ Res Lett* 8(1):014006. <https://doi.org/10.1088/1748-9326/8/1/014006>
- Bhangar S, Cowlin SC, Singer BC, Sextro RG, Nazaroff WW (2008) Ozone levels in passenger cabins of commercial aircraft on north American and transoceanic routes. *Environ Sci Technol* 42(11):3938–3943. <https://doi.org/10.1021/es702967k>
- Bundesanstalt für Arbeitsschutz und Arbeitsmedizin baua (Federal Institute for Occupational Safety and Health). TRGS 900 Arbeitsplatzgrenzwerte, Technische regel für Gefahrstoffe (workplace limit values, Technical Rules for Hazardous Substances), 2006–2021. <https://www.baua.de/DE/Angebote/Rechtstexte-und-Technische-Regeln/Regelwerk/TRGS/pdf/TRGS-900.pdf?blob=publicationFile&v=21>

- CAAC (2016) Chinese civil aviation regulations Part 25 airworthiness standards for transport aircraft, Order of CAAC no. 19 of 2016
- Cao Q, Xu Q, Liu W et al (2017) In-flight monitoring of particle deposition in the environmental control systems of commercial airliners in China. *Atmos Environ* 154:118–128. <https://doi.org/10.1016/j.atmosenv.2017.01.044>
- Cao X, Zevitas CD, Spengler JD et al (2019) The on-board carbon dioxide concentrations and ventilation performance in passenger cabins of US domestic flights. *Indoor Built Environ* 28(6): 761–771. <https://doi.org/10.1177/1420326X18793997>
- Ceballos DM, Fellows KM, Evans AE, Janulewicz PA, Lee EG, Whittaker SG (2021) Perchloroethylene and dry cleaning: it's time to move the industry to safer alternatives. *Front Public Health* 9:638082. Published online 2021 Mar 5. <https://doi.org/10.3389/fpubh.2021.638082>
- Centers for Disease Control and Prevention (1995) Exposure of passengers and flight crew to mycobacterium tuberculosis on commercial aircraft, 1992–1995. *MMWR Morb Mortal Wkly Rep* 44:137–140. <http://www.cdc.gov/mmwr/preview/mmwrhtml/00036502.htm>
- Chen R, Fang L, Liu J, Herbig B, Norrefeldt V, Mayer F, Fox R, Wargocki P (2021) Cabin air quality on non-smoking commercial flights: a review of published data on airborne pollutants. *Indoor Air* 31(4):926–957. <https://doi.org/10.1111/ina.12831>
- Cheng MD (2013) Classification of volatile engine particles. *Aerosol Air Qual Res* 13(5): 1411–1422. <https://doi.org/10.4209/aaqr.2013.01.0011>
- Chinese Standard GB/T 18883–2002: Indoor air quality standards, 2002
- Civil Aviation Authority CAA (2004) Cabin air quality-CAA paper 2004/04. https://publicappscaa.co.uk/docs/33/CAPAP2004_04.PDF
- Comité Européen de Normalisation CEN. EN 16798-1: 2019 Energy performance of buildings. Ventilation for buildings. Indoor environmental input parameters for design and assessment of energy performance of buildings addressing indoor air quality, thermal environment, lighting and acoustics. Module M1-6. CEN, 01-05-2019
- Cooper OR, Parrish DD, Ziemke J, Balashov NV, Cupeiro M, Galbally IE, Gilge S, Horowitz L, Jensen NR, Lamarque JF, Naik V, Oltmans SJ, Schwab J, Shindell DT, Thompson AM, Thouret V, Wang Y, Zbinden RM (2014) Global distribution and trends of tropospheric ozone: an observation-based review. *Elementa Sci Anthropolocene* 2:000029. <https://doi.org/10.12952/journal.elementa.000029>
- Crump D (2016) Air quality in aircraft: a continuing debate. *Indoor Built Environ.* 25:725–727. <https://doi.org/10.1177/1420326X16654756>
- Crump D, Harrison P, Walton C (2011a) Aircraft cabin air sampling study; part 1 of the final report. Institute of Environment and Health report
- Crump D, Harrison P, Walton C (2011b) Aircraft cabin air sampling study; part 2 of the final report. Institute of Environment and Health report
- Davis A, Menard D, Clark A, Cummins J, Olson N. Comparison of cough particle exposure for indoor commercial and aircraft cabin spaces. MedRxiv, March 2021a, online. <https://doi.org/10.1101/2021.03.24.21254275>
- Davis A, Zee M, Clark D, Wu T, Menard D, Jones S, Waite L, Atmuri R, Cummins J, Olson N. Computational fluid dynamics modeling and the transport of cough particles in an aircraft cabin; BioRxiv, June 2021b, online, <https://doi.org/10.1101/2021.02.15.431324>
- Dechow M, Sohn H, Steinhanses J (1997) Concentrations of selected contaminants in cabin air of airbus aircrafts. *Chemosphere* 35(1–2):21–31. [https://doi.org/10.1016/s0045-6535\(97\)00135-5](https://doi.org/10.1016/s0045-6535(97)00135-5)
- Denola G, Kibby J, Mazurek W (2008) Determination of ortho-cresyl phosphate isomers of tricresyl phosphate used in aircraft turbine engine oils by gas chromatography and mass spectrometry. *J Chromatogr A* 1200(2):211–216. <https://doi.org/10.1016/j.chroma.2008.05.035>
- Denola G, Hanhela PJ, Mazurek W (2011) Determination of tricresyl phosphate air contamination in aircraft. *Ann Occup Hyg* 55(7):710–722. <https://doi.org/10.1093/annhyg/mer040>
- Destaillats H, Russell ML, Tang X, Hotchi T, Trent SM, Space DR, Scheer DA, Maddalena RL. Evaluating air purification technologies for the aircraft cabin environment. In: Proceedings of Indoor Air Conference 2018, Philadelphia, USA, Paper 502

- Donaldson (2018) Understanding carbon-based chemical filtration systems for aircraft cabins. <https://www.donaldson.com/content/dam/donaldson/aerospace-defense/literature/north-america/f112271/Air-Purification-System-APS-White-Paper.pdf>
- Dumyahn TS, Spengler JD, Burge HA, Muilenburg M (2000) Comparison of the environments of transportation vehicles: results of two surveys. In: Nagda NL (ed) Air quality and comfort in airliner cabins: ASTM STP 1393. American Society for Testing and Materials, West Conshohocken, pp 3–23
- EASA, ADVANCE NOTICE OF PROPOSED AMENDMENT (A-NPA) 2009–10 and COMMENT RESPONSE DOCUMENT (CRD) TO ADVANCE NOTICE OF PROPOSED AMENDMENT (A-NPA) 2009–10 “Cabin Air Quality onboard Large Aeroplanes”. <https://www.easa.europa.eu/document-library/notices-of-proposed-amendments/npa-2009-10>
- EASA, Certification specifications and acceptable means of compliance for large Aeroplanes CS-25, amendment 26, 15 December 2020. <https://www.easa.europa.eu/document-library/certification-specifications/cs-25-amendment-26-0>
- Eastman Technical Data Sheet Skydrol® LD4 Fire Resistant Hydraulic Fluid. https://productcatalog.eastman.com/tds/ProdDatasheet.aspx?product=71093409&pn=Skydrol+LD-4#_ga=2.196390956.1832617528.1625337023-1796466.1625337023
- Eastman Technical Data Sheet Skydrol® PE-5. https://productcatalog.eastman.com/tds/ProdDatasheet.aspx?product=71093410&pn=Skydrol+PE-5#_ga=2.136615728.1832617528.1625337023-1796466.1625337023
- Environmental Protection Agency EPA, 2021, List N tool: COVID-19 disinfectants, <https://cfpub.epa.gov/wizards/disinfectants/>
- European Commission. Horizon 2020 research project, Investigation of cabin ventilation strategies impact on aircraft cabin air quality and passengers' comfort and wellbeing through subject study in realistic aircraft environment ComAir, 2018–2021. <https://cordis.europa.eu/project/id/820872>
- European Union. EU Directive 2008/50/EC on ambient air quality and cleaner air for Europe. <https://eur-lex.europa.eu/legal-content/EN/TXT/PDF/?uri=CELEX:32008L0050&from=en>
- FAA (2021) Federal Aviation Regulations (FAR) part 25 airworthiness standards: transport category airplanes (Code of Federal Regulations (CFR) title 14, chapter I, subchapter C, part 25), Washington. <https://www.ecfr.gov/cgi-bin/text-idx?node=14:1.0.1.3.11>
- FAA AC 120-38. Transport Category Airplanes Cabin Ozone Concentrations 1980. https://www.faa.gov/regulations_policies/advisory_circulars/index.cfm/go/document.information/documentID/22760
- Fisk W, Wargocki P, Zhang X (2019) Do indoor CO₂ levels directly affect perceived air quality, health, or work performance? ASHRAE J 61(9):70–77
- Foucher PY, Chédin A, Armante R, Boone C, Crevoisier C, Bernath P (2011) Carbon dioxide atmospheric vertical profiles retrieved from space observation using ACE-FTS solar occultation instrument. Atmos Chem Phys 11(6):26473–26512. <https://doi.org/10.5194/acp-11-2455-2011>
- Franklin LM, Mitchell AE (2019) Review of the sensory and chemical characteristics of almond (*Prunus dulcis*) flavor. J Agric Food Chem 67(10):2743–2753. <https://doi.org/10.1021/acs.jafc.8b06606>
- Freeman D (2020) COVID-19 and beyond: a brief introduction to passenger aircraft cabin air quality. ASHRAE J 62:8–12
- Gao K, Xie J, Yang X (2015) Estimation of the contribution of human skin and ozone reaction to volatile organic compounds (VOC) concentration in aircraft cabins. Build Environ 94 (pt 1):12–20. <https://doi.org/10.1016/j.buildenv.2015.07.022>
- Giaconia C, Orioli A, Gangi AD (2013) Air quality and relative humidity in commercial aircrafts: an experimental investigation on short-haul domestic flights. Build Environ 67(3):69–81. <https://doi.org/10.1016/j.buildenv.2013.05.006>
- Gladyszewska-Fiedoruk K (2012) Indoor air quality in the cabin of an airliner. J Air Trans Manage 20:28–30. <https://doi.org/10.1016/j.jairtraman.2011.10.009>
- Griffiths RF, Powell DM (2012) The occupational health and safety of flight attendants. Aviat Space Environ Med 83(5):514–521

- Guan J, Wang C, Gao K, Yang X, Lin CH, Lu C (2014) Measurements of volatile organic compounds in aircraft cabins. Part II: target list, concentration levels and possible influencing factors. *Build Environ* 75:170–175. <https://doi.org/10.1016/j.buildenv.2014.01.023>
- Guan J, Li Z, Yang X (2015) Net in-cabin emission rates of VOCs and contributions from outside and inside the aircraft cabin. *Atmos Environ* 111:1–9. <https://doi.org/10.1016/j.atmosenv.2015.04.002>
- Haghhighat F, Allard F, Megri AC, Blondeau P, Shimotakahara R (1999) Measurement of thermal comfort and indoor air quality aboard 43 flights on commercial airlines. *Indoor Built Environ* 8(1):58–66. <https://doi.org/10.1177/1420326X9900800106>
- Harshada P, Mirabelle DC (2017) Passenger-centric factors influencing the experience of aircraft comfort. *Transp Rev* 38(2):252–269. <https://doi.org/10.1080/01441647.2017.1307877>
- Harvard TH Chan School of Public Health HSPH (2020) Assessment of risks of SARS-CoV-2 transmission during air travel and non-pharmaceutical interventions to reduce risk phase one report: gate-to-gate travel onboard aircraft. <https://cdn1.sph.harvard.edu/wp-content/uploads/sites/2443/2020/10/HSPH-APHI-Phase-One-Report.pdf>
- He J, Yin Y, Yang X, Pei J, Sun Y, Cui X, Chen Q (2021) Carbon dioxide in passenger cabins: spatial temporal characteristics and 30-year trends. *Indoor Air*. <https://doi.org/10.1111/ina.12874>
- Health Canada (2021) Residential indoor air quality guidelines
- Henschler D (1958) Die Trikresylphosphatvergiftung – experimentelle Klärung von Problemen der Ätiologie und Pathogenese. *Klin Wochenschr* 36:663–674. <https://doi.org/10.1007/BF01488746>
- Herbig B, Ströhlein R, Ivandic I, Norrefeldt V, Mayer F, Wargocki P, Lei F (2020) Impact of different ventilation strategies on aircraft cabin air quality and passengers' comfort and wellbeing – the ComAir study, 50th International Conference on Environmental Systems, Paper 2020-156. <https://ttu-ir.tdl.org/handle/2346/86254>
- House of Lords, select sub-committee on science and technology, Fifth report, November 2000. <https://publications.parliament.uk/pa/ld199900/ldselect/ldsctech/121/12101.htm>
- Howard CV, Johnson DW, Morton J, Michaelis S, Supplee D, Burdon J (2018) Is a cumulative exposure to a background aerosol of nanoparticles part of the causal mechanism of aerotoxic syndrome? *J Nanomed Nanosci* 2018(1):1–8
- Hunt EH, Reid DH, Space DR, Tilton FE (2000) Commercial airliner environmental control system – engineering aspects of cabin air quality. http://www.smartcockpit.com/docs/Engineering_Aspects_of_Cabin_Air_Quality.pdf
- IAC (2005) Aviation regulations (AP) part 25 airworthiness standards for transport category airplanes (in Russia)
- International Civil Aviation organization ICAO (2021) Economic development of air transport, economic impacts of COVID-19 on civil aviation. <https://www.icao.int/sustainability/Pages/Economic-Impacts-of-COVID-19.aspx>
- International Organization for Standardization ISO (2011) ISO 16000-6: Indoor air – Part 6: Determination of volatile organic compounds in indoor and test chamber air by active sampling on Tenax TA sorbent, thermal desorption and gas chromatography using MS or MS-FID
- International Organization for Standardization ISO (2017) ISO 29463-1: High efficiency filters and filter media for removing particles from air – Part 1: Classification, performance, testing and marking
- Ji W, Zhao B (2014) Estimation of the contribution of secondary organic aerosol to PM_{2.0} concentration in aircraft cabins. *Build Environ* 82:267–273. <https://doi.org/10.1016/j.buildenv.2014.08.025>
- Johnson DW (2016) Lubricants for turbine engines. In: Agarwal RK (ed) Recent progress in some aircraft technologies. Washington University, St. Louis., InTech. <https://doi.org/10.5772/62394>
- Johnson DW (2018., InTech) Turbine engine lubricant and additive degradation mechanisms. In: Dekoulis G (ed) Aerospace engineering. Aerospace Engineering Institute, Cyprus. <https://doi.org/10.5772/intechopen.82398>

- Jones B, Amiri SN, Roth JW, Hosni M (2017) The nature of particulates in aircraft bleed air resulting from oil contamination. ASHRAE Winter Conference – Papers, LV-17-C046, 1–8
- Jordan A, Hansel A, Holzinger R, Lindinger W (1995) Acetonitrile and benzene in the breath of smokers and non-smokers investigated by proton transfer reaction mass spectrometry (PTR-MS). *Int J Mass Spectrom Ion Process* 148(1–2):L1–L3. [https://doi.org/10.1016/0168-1176\(95\)04236-E](https://doi.org/10.1016/0168-1176(95)04236-E)
- Khanh NC, Thai PQ, Quach HL, Thi NAH, Dinh PC, Duong TN, Mai LTQ, Nghia ND, Tu TA, Quang LN, Quang TD, Nguyen TT, Vogt F, Anh DD (2020) Transmission of SARS-CoV-2 during long-haul flight. *Emerg Infect Dis* 26(11):2617–2624. <https://doi.org/10.3201/eid2611.203299>
- Kinahan SM, Silcott DB, Silcott BE, Silcott RM, Silcott PJ, Silcott BJ, Distelhorst SL, Herrera VL, Rivera DN, Crown KK, Lucero GA, Santarpia JL. Aerosol tracer testing in Boeing 767 and 777 aircraft to simulate exposure potential of infectious aerosol such as SARS-CoV-2, MedRxiv, January 2021, online. <https://doi.org/10.1101/2021.01.11.21249626>
- Kleno JG, Wolkoff P, Clausen PA, Wilkins CK, Pedersen T (2002) Degradation of the adsorbent Tenax TA by nitrogen oxides, ozone, hydrogen peroxide, OH radical, and limonene oxidation products. *Environ Sci Technol* 36:4121–4126. <https://doi.org/10.1021/es025680f>
- Knighton WB, Herndon SC, Miake-Lye RC (2009) Aircraft engine speciated organic gases: speciation of unburned organic gases in aircraft exhaust. EPA-420-R-09-902, May 2009
- Langer S, Moldanová J, Arrhenius K, Ljungström E, Ekberg L (2008) Ultrafine particles produced by ozone/limonene reactions in indoor air under low/closed ventilation conditions. *Atmos Environ* 42(18):4149–4159. <https://doi.org/10.1016/j.atmosenv.2008.01.034>
- Lee SC, Poon CS, Li XD, Luk F (1999) Indoor air quality investigation on commercial aircraft. *Indoor Air* 9(3):180–187. <https://doi.org/10.1111/j.1600-0668.1999.t01-1-00004.x>
- Li Z, Guan J, Yang X, Lin C-H (2014) Source apportionment of airborne particles in commercial aircraft cabin environment: contributions from outside and inside of cabin. *Atmos Environ* 89: 119–128. <https://doi.org/10.1016/j.atmosenv.2014.01.042>
- Lindgren T, Norbäck D (2002) Cabin air quality: indoor pollutants and climate during intercontinental flights with and without tobacco smoking. *Indoor Air* 12(4):263–272. <https://doi.org/10.1034/j.1600-0668.2002.01121.x>
- Lindgren T, Norbäck D (2005) Health and perception of cabin air quality among Swedish commercial airline crew. *Indoor Air* 15(S10):65–72. <https://doi.org/10.1111/j.1600-0668.2005.00353.x>
- Liu M, Liu J, Ren J, Liu L, Chen R, Li Y (2020) Bacterial community in commercial airliner cabins in China. *Int J Environ Health Res* 30(3):284–295. <https://doi.org/10.1080/09603123.2019.1593329>
- MacGregor IC, Spicer CW, Buehler SS, Spicer C, Dean SW (2008) Concentrations of selected chemical species in the airliner cabin environment. *J ASTM Int* 5(8):101639. <https://doi.org/10.1520/JAI101639>
- Maddalena RL, McKone TE (2008) Insecticide exposures on commercial aircraft – a literature review and screening level assessment. Lawrence Berkeley National Laboratory, pp 1–43
- Mair S, Scherer C, Mayer F (2015) Emissionsverhalten eines Flugzeugmotorenöls bei thermischer Belastung. *Gefahrstoffe – Reinhaltung der Luft* 75(7/8):295–302
- Marsillach J, Richter RJ, Kim JH et al (2011) Biomarkers of organophosphorus (OP) exposures in humans. *Neurotoxicology* 32(5):656–660. <https://doi.org/10.1016/j.neuro.2011.06.005>
- Mazareanu E (2021) Air transportation – statistics & facts. <https://www.statista.com/statistics/564717/airline-industry-passenger-traffic-globally/>
- McNeely E, Gale S, Tager I, Kincl L, Bradley J, Coull B, Hecker S (2014) The self-reported health of U.S. flight attendants compared to the general population. *Environ Health* 13(1):13. <https://ehjournal.biomedcentral.com/articles/10.1186/1476-069X-13-13>
- MHLW (2002) Committee on sick house syndrome: indoor air pollution progress report no. 4. <http://www.nihs.go.jp/mhlw/chemical/situnai/kentoukai/rep-eng4.pdf>

- MIL-PRF-23699G (2014) Performance specification: lubricating oil, aircraft turbine engine, synthetic base, NATO Code Numbers: O-152, O-154, O-156, and O-167
- Moser MR, Bender TR, Margolis HS, Noble GR, Kendal AP, Ritter DG (1979) An outbreak of influenza aboard a commercial airline. *Am J Epidemiol* 110:1–6. <https://doi.org/10.1093/oxfordjournals.aje.a112781>
- Muir H, Walton C, McKeown R (2008) Cabin air sampling study functionality test. Cranfield University School of Engineering. <http://hdl.handle.net/1826/2389>
- Nagda NL, Rector HE (2003) A critical review of reported air concentrations of organic compounds in aircraft cabins. *Indoor Air* 13:292–301. <https://doi.org/10.1034/j.1600-0668.2003.00202.x>
- Nagda NL, Koontz MD, Konheim AG, Hammond SK (1992) Measurement of cabin air quality aboard commercial airliner. *Atmos Environ* 26(12):2203–2210. [https://doi.org/10.1016/0960-1686\(92\)90409-E](https://doi.org/10.1016/0960-1686(92)90409-E)
- Nagda NL, Rector HE, Li Z, Hunt EH (2000) RP-959 – determine aircraft supply air contaminants in the engine bleed air supply system on commercial aircraft. ASHRAE, Atlanta
- NASA-2016-218244. Submicron and nanoparticulate matter removal by HEPA-rated media filters and packed beds of granular materials J.L. Perry Marshall Space Flight Center, Huntsville, Alabama
- National Research Council NRC (1986) The airliner cabin environment: air quality and safety. The National Academies Press, Washington, DC, p 320. <https://doi.org/10.17226/913>
- National Research Council NRC (2002) The airliner cabin environment and the health of passengers and crew. The National Academies Press, Washington, DC, 344. <https://doi.org/10.17226/10238>
- Nazaroff W, Weschler C. Ozone in passenger cabins: concentrations and chemistry. August 2010, Final Report. Report No. RITE-ACER-CoE-2010-2. https://www.faa.gov/data_research/research/med_humanfac/cer/media/OzonePassengerCabins.pdf
- Newman WH, Viele MR (1980) Engine bleed air reduction in DC-10. NASA technical report. <https://ntrs.nasa.gov/citations/19800023870>
- NIOSH (2021) NIOSH pocket guide to chemical hazards. <https://www.cdc.gov/niosh/npg/default.html>
- Nørgaard AW, Kudal JD, Kofoed-Sørensen V, Koponen IK, Wolkoff P (2014) Ozone-initiated VOC and particle emissions from a cleaning agent and an air freshener: risk assessment of acute airway effects. *Environ Int* 68:209–218. <https://doi.org/10.1016/j.envint.2014.03.029>
- Norrefeldt V, Mayer F, Herbig B, Ströhlein R, Wargocki P, Fang L (2021) Effect of increased cabin recirculation airflow fraction on relative humidity, CO₂ and TVOC. *Aerospace* 8(1):15. <https://doi.org/10.3390/aerospace8010015>
- OEHHA (2019) OEHHA Acute, 8-hour and chronic reference exposure level (REL) Summary. <https://oehha.ca.gov/air/general-info/oehha-acute-8-hour-and-chronic-reference-exposure-level-rel-summary>
- Olsen SJ, Chang HL, Cheung TY et al (2003) Transmission of severe acute respiratory syndrome on aircraft. *N Engl J Med* 349:2416–2422. <https://doi.org/10.1056/nejmoa031349>
- Orth AM, Lu Y, Engel KH (2013) Assessment of dietary exposure to flavouring substances via consumption of flavoured teas. Part 1: occurrence and contents of monoterpenes in Earl Grey teas marketed in the European Union. *Food Addit Contaminants: Part A* 30(10):1701–1714. <https://doi.org/10.1080/19440049.2013.817687>
- Perry JL (1995) NASA technical memorandum 108497: trace chemical contaminant generation rates for spacecraft contamination control system design. <https://ntrs.nasa.gov/citations/19960003343>
- Pradhan D, Biswasroy P, Naik PK, Ghosh G, Ratha G (2020) A review of current interventions for COVID-19 prevention. *Arch Med Res* 51(5):363–374. <https://doi.org/10.1016/j.arcmed.2020.04.020>
- Rai AC, Guo B, Lin CH, Zhang J, Pei J, Chen Q (2014) Ozone reaction with clothing and its initiated VOC emissions in an environmental chamber. *Indoor Air* 24(1):49–58. <https://doi.org/10.1111/ina.12058>

- Rankin W, Space D, Nagda N (2000) Passenger comfort and the effect of air quality. In: Nagda N (ed) Air quality and comfort in airliner cabins. ASTM International, West Conshohocken, pp 269–290. <https://doi.org/10.1520/STP14499S>
- Ree HD, Bagshaw M, Simons R, Brown RA (2000) Ozone and relative humidity in airline cabins on polar routes measurements and physical symptoms. Air quality and comfort in airliner cabins. KLM Royal Dutch Airlines, Schiphol, The Netherlands, pp 243–258
- Ree HD, van den Berg M, Brand T et al (2014) Health risk assessment of exposure to tricresyl phosphates (TCPs) in aircraft: a commentary. *Neurotoxicology* 45:209–215. <https://doi.org/10.1016/j.neuro.2014.08.011>
- Ritter S (2001) What's that stuff? Aircraft deicers. *Cenear* 79(1):30
- Rosenberger W (2018) Effect of charcoal equipped HEPA filters on cabin air quality in aircraft. A case study including smell event related in-flight measurements. *Build Environ* 143:358–365. <https://doi.org/10.1016/j.buildenv.2018.07.031>
- Rosenberger W, Wrbitzky R, Elend M, Schuchardt S (2014) Untersuchungen zur Emission organischer Verbindungen in der Kabinenluft nach dem Enteisen von Verkehrsflugzeugen - Determination of organic compounds in cabin air after aircraft de-icing of commercial aircraft. *Gefahrstoffe, Reinhaltung der Luft* 74(11–12):467–475
- Rosenberger W, Beckmann B, Wrbitzky R (2016) Airborne aldehydes in cabin-air of commercial aircraft: measurement by HPLC with UV absorbance detection of 2,4-dinitrophenylhydrazones. *J Chromatogr B* 1019:117–127. <https://doi.org/10.1016/j.jchromb.2015.08.046>
- Rosero JA, Ortega JA, Aldabas E, Romeral L (2007) Moving towards a more electric aircraft. *IEEE A&E Syst Magazine* 22(3):3–9. <https://ieeexplore.ieee.org/document/4145070>
- SAE AIR 1539C (2020) Environmental control system contamination. SAE, 2020-05-29
- SAE AIR 4766 (2018) Air quality for commercial aircraft cabins. SAE, 2018-08-23
- SAE AIR 4766/2A (2021) Airborne Chemicals in Aircraft Cabins. SAE, 2021-06-22
- SAE AIR 6418, under development. Sampling and measurement of bleed air supplies from engines or APUs. SAE, 2021
- SAE AIR 7521 (2018) Measurement data and reference values for compounds potentially found in aircraft engine bleed air. SAE, 2018-10-09
- SAE AMS 1424R (2020) Fluid, aircraft deicing/anti-icing, SAE Type I SAE, 2020-11-18
- SAE ARP 1796B (2020) Engine bleed air systems for aircraft. SAE, 2020-05-12
- SAE ARP 292D (2020) Environmental control systems for rotorcraft. SAE, 2020-05-12
- SAE ARP 4418B (2018) Procedure for sampling and measurement of aircraft propulsion engine and APU generated contaminants in bleed air. SAE, 2018-11-12
- Saerens SMG, Delvaux FR, Verstrepen KJ, Thevelein JM (2010) Production and biological function of volatile esters in *Saccharomyces cerevisiae*. *Microb Biotechnol* 3(2):165–177. <https://doi.org/10.1111/j.1751-7915.2009.00106.x>
- Sawa Y, Matsueda H, Makino Y et al (2004) Aircraft observation of CO₂, CO, O₃ and H₂ over the North Pacific during the PACE-7 campaign. *Tellus Ser B Chem Phys Meteorol* 56(1):2–20. <https://doi.org/10.3402/tellusb.v56i1.16402>
- Schuchardt S, Bitsch A, Koch W, Rosenberger W (2017) CAQ Preliminary cabin air quality measurement campaign. https://www.easa.europa.eu/sites/default/files/dfu/EASA%20CAQ%20Study%20Final%20Report_21.03.2017.pdf
- Schuchardt S, Koch W, Rosenberger W (2019) Cabin air quality-quantitative comparison of volatile air contaminants at different flight phases during 177 commercial flights. *Build Environ* 148: 498–507. <https://doi.org/10.1016/j.buildenv.2018.11.028>
- Simpson S, Roux P, Dinca M (2019) The science behind sensing and filtering cabin air. AST 2019, February 19–20, Hamburg, Germany. ISBN 978-3-8440-6470-4
- Singer BC, Coleman BK, Destaillats H et al (2006) Indoor secondary pollutants from cleaning product and air freshener use in the presence of ozone. *Atmos Environ* 40(35):6696–6710. <https://doi.org/10.1016/j.atmosenv.2006.06.005>

- Sniderman D (2020) What it takes to be a commercial Aviation jet engine lubricant. *Machine Design*, Feb 28th. <https://www.machinedesign.com/mechanical-motion-systems/article/21124388/what-it-takes-to-be-a-commercial-aviation-jet-engine-lubricant>
- Solbu K, Daae HL, Olsen R et al (2011) Organophosphates in aircraft cabin and cockpit air-method development and measurements of contaminants. *J Environ Monit* 13(5):1393–1403. <https://doi.org/10.1039/c0em00763c>
- Space DR, Johnson RA, Rankin WL, Nagda NL (2000) The airplane cabin environment: past, present and future research. In: Nagda N (ed) Air quality and comfort in airliner cabins. ASTM International, West Conshohocken, pp 189–214. <https://doi.org/10.1520/STP14495S>
- Spengler JD, Ludwig S, Weker RA (2004) Ozone exposures during trans-continental and trans-pacific flights. *Indoor Air* 14(s7):67–73. <https://doi.org/10.1111/j.1600-0668.2004.00275.x>
- Spengler JD, Vallarino J, McNeely E, Estephan H (2012) In-flight/onboard monitoring: ACER's component for ASHRAE 1262, Part 2. final report, 2005–2010
- Spicer CW, Murphy MJ, Holdren MW, Myers JD, MacGregor IC, Holloman C, James RR, Tucker K, Zaborski R (2004) Relate air quality and other factors to comfort and health symptoms reported by passengers and crew on commercial transport aircraft (Part I) (ASHRAE Project 1262-TRP)
- Stevens JF, Maier CS (2008) Acrolein - sources, metabolism, and biomolecular interactions relevant to human health and disease. *Mol Nutr Food Res* 52(1):7–25. <https://doi.org/10.1002/mnfr.200700412>
- Strøm-Tejsen P, Zukowska D, Fang L, Space DR, Wyon DP (2008) Advantages for passengers and cabin crew of operating a gas-phase adsorption air purifier in 11-h simulated flights. *Indoor Air* 18(3):172–181. <https://doi.org/10.1111/j.1600-0668.2007.00511.x>
- Sun J (2007) D-limonene: safety and clinical applications. *Altern Med Rev* 12(3):259–264. <http://archive.foundationalmedicinereview.com/publications/12/3/259.pdf>
- Tsushima S, Wargozi P, Tanabe S (2018) Sensory evaluation and chemical analysis of exhaled and dermally emitted bioeffluents. *Indoor Air* 28(1):146–163. <https://doi.org/10.1111/ina.12424>
- Tuzson B, Henne S, Brunner D et al (2011) Continuous isotopic composition measurements of tropospheric CO₂ at Jungfraujoch (3580 m a.s.l.), Switzerland: real-time observation of regional pollution events. *Atmos Chem Phys* 11(4):1685–1696. <https://doi.org/10.5194/acp-11-1685-2011>
- U.S. Environmental Protection Agency (US EPA). Air Quality Criteria for Particulate Matter, Volume I of II, National Center for Environmental Assessment-RTP Office, Office of Research and Development, U.S. Environmental Protection Agency, Research Triangle Park, NC, Report No. EPA/600/P-99/002aF, October 2004. <https://cfpub.epa.gov/ncea/risk/recordisplay.cfm?deid=87903>
- UK Committee on Toxicology (2007) Review of the cabin air environment, ill-health in aircraft crews and the possible relationship to smoke/fume events in aircraft
- UK Committee on Toxicology (2013) Review of possible adverse health effects in the crew of commercial aircraft
- UK Parliament, House of Lords. Session 1999–2000. Publications on the internet. Science and technology committee publications. Science and technology - fifth Report <https://publications.parliament.uk/pa/ld199900/ldselect/ldstech/121/12101.htm>
- Umweltbundesamt UBA (2021) German environment agency, German Committee on Indoor Guide Values; Guide values I and II for indoor air pollutants
- Wang C, Yang X, Guan J, Gao K, Li Z (2014a) Volatile organic compounds in aircraft cabin: measurements and correlations between compounds. *Build Environ* 78:89–94. <https://doi.org/10.1016/j.buildenv.2014.04.016>
- Wang C, Yang X, Guan J, Li Z, Gao K (2014b) Source apportionment of volatile organic compounds (VOCs) in aircraft cabins. *Build Environ* 81:1–6. <https://doi.org/10.1016/j.buildenv.2014.06.007>
- Waters MA, Bloom TF, Grajewski B, Deddens J (2002) Measurements of indoor air quality on commercial transport aircraft. *Proceedings: Indoor Air* 4:782–787

- Weisel C, Weschler CJ, Mohan K, Vallarino J, Spengler JD (2013) Ozone and ozone byproducts in the cabins of commercial aircraft. *Environ Sci Technol* 47(9):4711–4717. <https://doi.org/10.1021/es3046795>
- Weisel CP, Fiedler N, Weschler CJ, Ohman-Strickland PA, Mohan KR, McNeil K, Space DR (2017) Human symptom responses to bioeffluents, short-chain carbonyls/ acids, and long-chain carbonyls in a simulated aircraft cabin environment. *Indoor Air* 27(6):1154–1167. <https://doi.org/10.1111/ina.12392>
- Weschler CJ, Wisthaler A, Cowlin S et al (2007) Ozone-initiated chemistry in an occupied simulated aircraft cabin. *Environ Sci Technol* 41(17):6177–6184. <https://doi.org/10.1021/es0708520>
- WHO (2005) WHO Air quality guidelines for particulate matter, ozone, nitrogen dioxide and sulfur dioxide
- WHO (2010) WHO guidelines for indoor air quality: selected pollutants
- WHO (2021) WHO global air quality guidelines. Particulate matter (PM_{2.5} and PM₁₀), ozone, nitrogen dioxide, sulfur dioxide and carbon monoxide
- Wieslander G, Lindgren T, Norbäck D, Venge P (2000) Changes in the ocular and nasal signs and symptoms of aircrews in relation to the ban on smoking on intercontinental flights. *Scand J Work Environ Health* 26(6):514–522. <https://doi.org/10.5271/sjweh.576>
- Wisthaler A, Tamás G, Wyon D, Strøm-Tejsen P, Space D, Beauchamp J, Hansel A, Märk T, Weschler C (2005) Products of ozone-initiated chemistry in a simulated aircraft environment. *Environ Sci Technol* 39(13):4823–4832. <https://doi.org/10.1021/es047992j>
- Wolkoff P, Crump DR, Harrison PTC (2016) Pollutant exposures and health symptoms in aircrew and office workers: is there a link? *Environ Int* 87:74–84. <https://doi.org/10.1016/j.envint.2015.11.008>
- Yates EL, Johnson MS, Iraci LT et al (2017) An assessment of ground level and free tropospheric ozone over California and Nevada. *J Geophys Res Atmos* 122(18):10089–10102. <https://doi.org/10.1002/2016jd026266>
- Zavaglio E, Le Cam M, Thibaud C, Quartarone G, Zhu Y, Franzini G, Roux PD, Dinca M, Walte A, Rothe P (2019) Innovative environmental control system for aircraft, 49th international conference on environmental systems, 7–11 July 2019, Boston, MA, Paper 2019–171. <https://ttu-ir.tdl.org/handle/2346/84939>



Indoor Air Quality in Industrial Buildings

70

Yi Wang, Tengfei Zhang, Zhixiang Cao, and Zhichao Wang

Contents

Introduction	2096
Industrial Pollutants	2097
High-Temperature Particles	2098
Droplets	2103
Gaseous Pollutants	2106
Industrial Ventilation	2109
General Ventilation with Zoning Environmental Control Strategy	2109
Local Exhaust Ventilation Technology	2112
Assessment of Industrial Building Environment with High-Pollution Sources	2115
Divisional Principles for Environmental Assessment	2116
Environmental Parameters	2116
Prediction Methods of Environmental Parameter Values	2118
Conclusions	2121
References	2122

Y. Wang (✉) · Z. Cao

School of Building Services Science and Engineering, Xi'an University of Architecture and Technology, Xi'an City, China

State Key Laboratory of Green Building in Western China, Xi'an University of Architecture and Technology, Xi'an City, China

e-mail: wangyi@xauat.edu.cn; caozx@xauat.edu.cn

T. Zhang

Tianjin Key Laboratory of Indoor Air Environmental Quality Control, School of Environmental Science and Engineering, Tianjin University, Tianjin, China

School of Civil Engineering, Dalian University of Technology, Dalian, China

e-mail: timzhang@tju.edu.cn

Z. Wang

China Academy of Building Research, Beijing, China

e-mail: wangzc@emcsco.com

Abstract

This chapter discusses the indoor air quality of industrial buildings with high pollution sources. Firstly, the basic characteristics of indoor air quality in industrial buildings and the differences between industrial buildings and civil buildings in indoor source and control demand are briefly introduced. Then it discusses the emission and diffusion characteristics of three kinds of typical pollutants in industrial buildings with high pollution sources: high-temperature particles, droplets, and harmful gases, and introduces the analysis methods and research conclusions of these pollutants in the indoor environmental control of industrial buildings. On this basis, the refined ventilation control methods for indoor air pollution in industrial buildings in recent years are presented, including zoning environmental control strategy for overall indoor air quality and novel local ventilation technology for centralized pollution sources. Finally, the assessment indexes of high pollution industrial buildings in different industrial sectors in China and three prediction methods for indoor air quality schemes are introduced.

Keywords

Industrial building · High pollution sources · Industrial ventilation · Assessment indexes · Prediction method

Introduction

The primary purpose of industrial buildings is to meet the needs of production, leading to significant differences in indoor air quality compared with human-oriented commercial and residential buildings. In addition to the environmental issues common to all buildings discussed previously, the indoor air quality of industrial buildings needs additional attention to meet the increasingly stringent occupational health, environmental protection, and carbon emission reduction requirements. Distinct differences exist between industrial and civil buildings indoor air quality in terms of indoor sources and control demand (Wang and Cao 2017).

Indoor Sources. In industrial buildings, source terms often exist, producing large amounts of waste heat, excess humidity, and pollutants. Based on different production processes, many types of pollutants exist, having significant differences in their physical parameters. The emissions may be dozens of times greater than those of civil buildings, mainly including high-temperature flue gas, acid mist droplets, and harmful gases.

In commercial and residential buildings, the major heat sources include the human body, electronic equipment, and lighting equipment, and the major pollution sources are human activities. The heat and pollution sources in industrial buildings usually come from the industrial production process, and the release process of heat and pollutants is often instantaneous and periodic (Goodfellow et al. 2021). As industrial plants are mostly tall space buildings, pollutants will diffuse in large

spaces based on their properties, and may be deposited near the ground, suspended in the air, or accumulated at the top of the workshop (Han et al. 2020; Zhang et al. 2019). The effective elimination of these fugitive pollutants in industrial buildings has always been a difficult problem to ensure the indoor air quality of industrial buildings, as discussed below.

Control Demand. The indoor environmental control of industrial buildings needs to consider both the production process and the health and safety of workers, whereas the purpose of environmental control in civil buildings mainly satisfies the health and well-being requirements of residents. Many forms of industrial buildings exist, such as a clean plant with high requirements for temperature and humidity, and general plants that produce waste heat and other pollutants. Some of these are labor-intensive processing plants, high-level automation plants, totally enclosed plants, and open plants. Based on the different needs of production processes, the demand for industrial environmental control on indoor environmental parameters such as temperature, humidity, cleanliness, and airflow velocity would vary significantly, and may even require several orders of magnitude, much higher than that required in civil buildings. In addition, significant differences exist between industrial and civil buildings in terms of human demand. In civil buildings, the primary consideration is to create a comfortable and healthy environment for occupants, whereas in industrial buildings, the principal consideration is to create an acceptable work environment. Therefore, the difference in environmental control demand for these two types of buildings demonstrates not only their control index but also the assessment index. Workers in industrial buildings can perform high intensity labor leading to thermal stress irrespective of the environment. Thus, the evaluation of indoor thermal environment must aim to reduce its impact on human health. Various thermal stress indices can be used to evaluate thermal health and safety issues in workplaces (Belding and Hatch 1955; Wyndham et al. 1967; Yaglou and Minard 1957). Thus, this difference in the levels of physical exertion produces great differences in the need for environmental control between industrial and civil buildings due to their different control requirements to provide safe and productive workspaces.

Owing to the significant difference between industrial buildings and commercial and residential buildings, this chapter first introduces the characteristics and prediction methods of pollutants in industrial buildings, and then briefly introduce efficient industrial ventilation methods to improve the indoor air quality, and to improve the understanding of readers on the current situation and solutions of indoor air quality problems in industrial buildings.

Industrial Pollutants

Compared with civil buildings, the pollutants in high pollution industrial buildings are mainly the pollutants emitted in the production process, mainly including high-temperature particulate matter (flue gas), droplets, and gaseous pollutants. The emission mode and transmission mode of pollutants are significantly related to the process, with the characteristics of large emission and high concentration.

High-Temperature Particles

High-temperature particles are common contaminants in industrial plants. They are generated from various production processes, such as the liquid-metal pouring process, welding process, and sand-casting process. High-temperature particles with large concentrations can cause significant harm to the health of workers and indoor air quality. The dispersion of high-temperature particles in industrial plants is of great interest for chronic obstructive pulmonary disease and pneumoconiosis. Chronic obstructive pulmonary disease progresses slowly and is characterized by a gradual loss of lung function.

Based on World Health Organization statistics, chronic obstructive pulmonary disease accounts for 2.7% of all diseases globally (WHO 2017), and this percentage could be higher in developing countries with large populations. For example, by the end of 2020, over 17,064 cases of occupational diseases were reported in China, 84% of which were occupational pneumoconiosis (National Health Commission of the PRC 2020). Therefore, it is necessary to develop an energy-saving ventilation system to capture high-temperature particles and provide a solid understanding of the emission and migration characteristics of high-temperature particles.

Emission Characteristics of High-Temperature Particles

The high temperatures and gaseous and particulate pollutants generated in the metallurgy workshop can harm the health of workers. Contaminated airflows are frequently generated during various liquid-metal pouring processes. This airflow induced by liquid-metal pouring processes is generated intensely and dynamically. Commonly used ventilation design manual practices simplify the dynamic process of pollutants generation to a steady state. This results in either poor control of the polluted airflow or wastage of a large amount of the exhaust flow rate in the actual process. An accurate understanding of the flow field characteristics of the induced airflow during the pouring process can help match the exhaust flow rate in local exhaust ventilation with the dynamic generation of pollutants to refine the design of the ventilation system. The flow field characteristics of the induced airflow include flow velocity distribution, temperature distribution, and the distribution of polluted airflow found using the color schlieren image. Among these, the distribution of polluted airflow should be the primary focus because its identification can define the pollutant generation locations and estimate pollutant emission rates.

An illustration of the contaminated airflow generation during the pouring process is shown in Fig. 1. It was found that an eddy current composed of non-isothermal airflow was formed on the side near the pouring cup below the liquid column, which is called the air mass. The formation of air mass is related to the air pocket formed by the geometry of the fluid chain flow at the pouring cup outlet. Numerous contaminated airflows can be formed in the air pocket, which becomes the primary source of the air mass. When the air mass cannot remain stable, some contaminated airflow is emitted into the ambient environment. The air mass releases an enormous amount of contaminated air, which is the primary source of pollution during pouring. Throughout the pouring period, air masses will be formed in 60% of the entire period

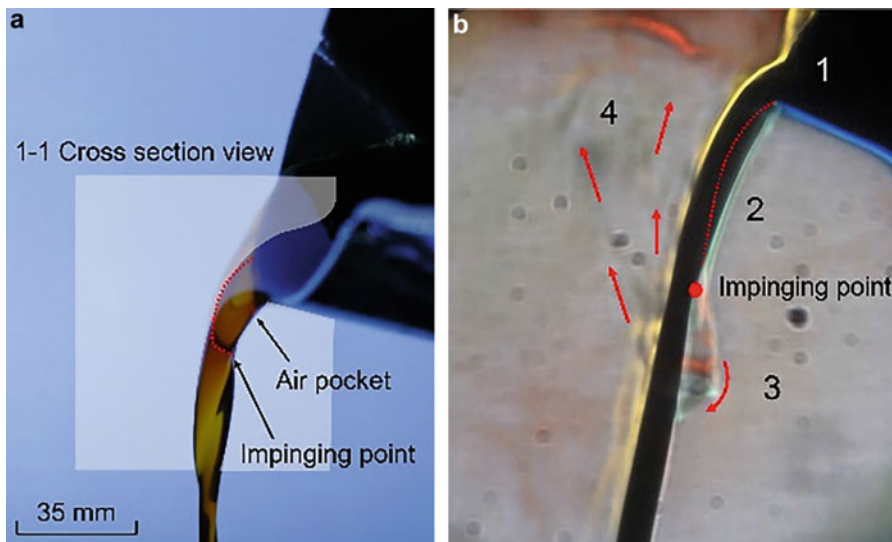


Fig. 1 Images of contaminated airflow generation during the pouring process ((1) Pouring liquid, (2) air pocket, (3) air mass, (4) contaminated airflow). (a) Image of the air pocket formed around the pouring cup outlet. (b) Schlieren image of contaminated airflow generation process (2-2 cross-sectional view)

(Huang et al. 2021a). Subsequently, the position and diameter of the air mass and the flow direction of the contaminated airflow released by the air mass during the entire liquid-metal pouring process were investigated.

Based on the quantitative analysis of the position and diameter of the air mass during the entire pouring process, it was found that the function types of the air mass position and diameter with the pouring time are approximately consistent with the variations of the trigonometric function, which rises first and then decreases rapidly. When the pouring flow rate is at its maximum, the air mass position and diameter reach a maximum (Huang et al. 2021a). Based on the position of the maximum air mass, it is suggested to strengthen the contaminated airflow control at a position 0.45 times the outlet radius of the pouring cup in the liquid column flow direction. Finally, when the pouring flow rate was the largest, the contaminated airflow released by the air mass flowed upward along the syncline away from the pouring cup at an angle of 85° in the horizontal direction (Huang et al. 2021a). This phenomenon differs from the vertical upward flow direction of an ideal thermal plume. In summary, the relevant conclusions can assist in the design of high-efficiency ventilation systems and in reducing energy consumption in industrial plants.

Some industrial processes, such as welding and spraying of large concentrations of high-temperature particles (Zimmer and Biswas 2001; Zimmer et al. 2002), result in significant harm to both indoor air quality and worker health. Therefore, an accurate understanding of the emission characteristics of high-temperature particles is important for achieving high-efficiency ventilation system design in industrial plants.

The transient discharge of high-temperature particles from industrial processes is usually accompanied or followed by high-temperature airflow; the initial airflow temperature significantly differs from the surroundings. Because high-temperature particles usually have small diameters, most studies have concluded that particles completely follow the airflow when moving. Here, airflow variations were considered, whereas the particle properties have not been studied. However, some recent studies (Duan et al. 2017; Huang et al. 2022) have shown that particles with different diameters are distributed differently in the same airflow field and may not always follow the airflow during the dispersion process. Along with the movement of high-temperature particles, the surrounding ambient air is heated. This leads to changes in the airflow field, which influences the particle dispersion mode.

Research has shown that ambient air is heated as high-temperature particles move; the variation in airflow velocity around the particles results in a nonuniform velocity across particles (Duan et al. 2017). The particle velocities near the centerline were larger than those far away from it. In addition, the dispersion mode of the particle population is determined based on the temperature and velocity variations in the airflow field and particles. Particles with higher initial temperatures and smaller particle diameters are associated with significant horizontal diffusion. This includes the movement of most particles within the upper space. Particles with either a larger diameter and higher initial temperature, or smaller diameter and lower initial temperature, experienced the least horizontal diffusion. Upward transport was limited, with most of the particles remaining at lower levels. Particles with moderate diameters and initial temperatures exhibited moderate horizontal diffusion. Most particles moved in the upper-middle space and spent the longest time in the vertical direction. These conclusions are necessary for future studies on the design of human protection and ventilation systems. Meanwhile, this will provide more reliable boundary conditions for future simulations and may reveal more parameters that impact particle dispersion modes.

Migration Characteristics of High-Temperature Particles

During the sand-casting process, the high-temperature molten metal liquid poured into a sand mold instantly heats the air in the cavity. This heated air volume expands and is then ejected at the sand exhaust port. This airflow, with a certain initial velocity and high initial temperature, can be regarded as a high-temperature buoyant jet. High-temperature buoyant jets usually contain dust particles; therefore, in industrial ventilation, to protect the health of workers, the canopy hood is often used to capture high-temperature buoyant jets.

Based on the recommendations in the industrial ventilation design manual, the installation position of the canopy hood should be set at the contracted section of the high-temperature buoyant jet. The contracted section had the smallest cross-sectional area and the largest flow velocity in the high-temperature buoyant jet. However, these industrial ventilation design manuals only provide the approximate location of the contracted section based on empirical formulas and do not discuss the formation of the contracted section, the temporal evolution process of the contracted section, or the influence of the initial temperature of the buoyant jet on the position of

the contracted section. Therefore, it is necessary to study these topics to improve the design guidelines for the installation of exhaust hoods at a suitable height, which can be used in high-temperature buoyant jets to achieve energy savings.

In the case of the high-temperature buoyant jet generated in industrial processes such as pouring and smelting, the emission characteristics of the high-temperature buoyant jet with an initial temperature of 303–473 K were introduced (Huang et al. 2021b). The initial temperature is an important factor that affects the transport characteristics of high-temperature buoyant jets. Because the diffusion angle and penetration distance of high-temperature buoyant jets increase with an increase in the initial temperature, the installation position of the local exhaust system for high-temperature buoyant jets should be as close as possible to the pollution source.

When the initial temperature is greater than or equal to 373 K, the flow field of the high-temperature buoyant jet produced a contracted section. The position of the contracted section was within two times the source diameter from the outlet of the pollution source. When the initial temperature increased, the position of the contracted section was closer to the outlet of the pollution source.

The contracted section is caused by the rupture of the vortex ring at the outlet of the pollution source, as shown in Fig. 2. The vortex ring is continuously generated within the range of 0.7 times the source diameter from the outlet. Outside this range, the vortex ring is broken and reorganized into a spiral vortex structure. The vortex ring can restrict the flow field diffusion of the high-temperature buoyant jet before the vortex ring ruptures, and the spiral vortex structure formed after the vortex ring ruptures and entrains a large amount of ambient air and expands. Therefore, it is suggested that the installation height of the canopy hood is within 0.7–2 times the source diameter from the outlet without affecting the operation process.

High-temperature buoyant jets usually carry particles of different diameters, and these particles driven by high-temperature buoyant jets exhibit different transport behaviors. In the case of the pulsating high-temperature particles produced in industrial processes such as forging and casting, the transport characteristics of pulsating high-temperature particles with an initial temperature of 1273 K and particle diameter of 5–30 μm are introduced. The pulsating high-temperature particles are driven by a high-temperature buoyant jet with a pulsed initial velocity and a short duration. The transportation process includes the supply, thermal energy attenuation, and kinetic energy attenuation stages.

Particles of different diameters present similar heating effects on the airflow at the edge of the flow field during the thermal energy attenuation stage. Therefore, the different distributions of particles in the horizontal direction are not mainly caused by the edge airflow heated by particles at the thermal energy attenuation stage but by the influence of the vortex structure on the particles at the kinetic energy attenuation stage.

During the transport of pulsating high-temperature particles, the vortex structure in the flow field was dominated by spiral vortex structures. The spiral vortex structure includes the vortex core regions, boundary regions at the edge of the vortex structure, and vortex braid regions between adjacent vortex structures. The vorticity of the vortex structure was transmitted to both sides, and a new vortex core was generated around the original vortex core. The attenuation of the vorticity leads to

Q Level=0.01

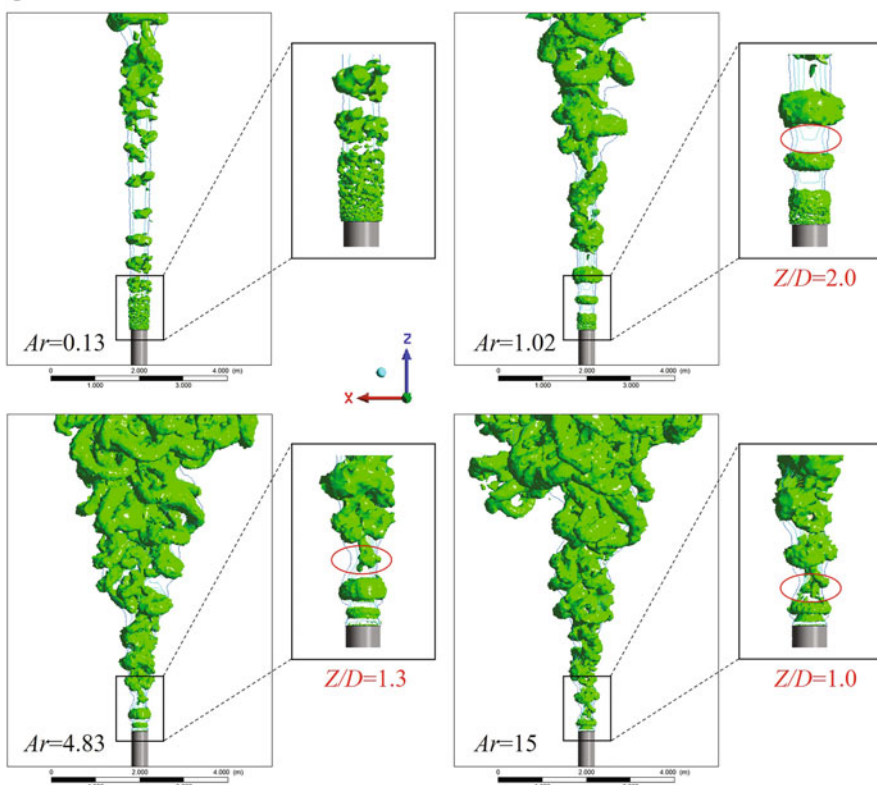


Fig. 2 Comparison between iso-surface of vorticity magnitude and streamline variations of the high-temperature buoyant jets when $t = 10$ s with different initial temperature: (a) 303 K, (b) 373 K, (c) 673 K, and (d) 1473 K. (Reprinted from Huang et al. (2021b), Copyright (2022), with permission from Elsevier)

the horizontal transport of particles in the spiral vortex structure. In addition, the horizontal transport of particles leads to variations in the particle concentration in the boundary regions of the vortex structure, which affects the shape of the small-scale vortex structure in the boundary regions. The increase in the particle concentration in the boundary regions increases the complexity and concentration of the small-scale vortex structure.

When the particle diameter is 5–30 μm , particles are transported from the inside to the outside of the work area, and 99% of the particles are suspended in the upper space outside the work area (Huang et al. 2022). The key capture area of the particles should be located in the upper space outside the work area. When the particle diameter is 50–70 μm , the particles suspended outside the work area are transported to the inside of the work area (Huang et al. 2022). The key capture areas of the particles should be located in the work area.

Droplets

Droplets, such as acid mist, oil mist, and water mist, are typical airborne contaminants in industrial indoor environments (Yang et al. 2019b). Their escape into indoor environments can harm human health or thermal comfort and cause equipment corrosion and construction damage (Wang et al. 2019). Field studies report that mist comprising droplets may severely hinder normal production and worker operation. The emission sources of the droplets are mainly from industrial processes (Fan et al. 2021). The surface treatment processes of steel and nonferrous metals mainly emit acid droplets, metal surface spraying mainly emits oil droplets, and water/spray cooling mainly emits water droplets. Although many industrial processes are involved in the emission of different droplet types, four main emission mechanisms exist, including direct spray, condensation, mechanical actions, and bubble burst, as shown in Fig. 3. Different emission mechanisms may generate droplets with different diameters and velocities.

Droplet transport may differ significantly from that of solid particles because evaporation changes their diameters (Yang et al. 2019a). Dispersion, deposition, and human exposure may exhibit more complex characteristics. When droplets are emitted into indoor environments, with the influence of the temperature and relative humidity of the ambient air, droplets evaporate during the motion. Evaporation leads to a constant change in the diameter of the droplets. As the diameter changes, forces such as gravity and drag force acting on the droplet also change, as shown in Fig. 4.

Different droplets have different diameter-variation tendencies owing to evaporation. Generally, pure water droplets evaporate rapidly. When it is a solution droplet, such as an acid droplet, the solute causes the water vapor pressure at the

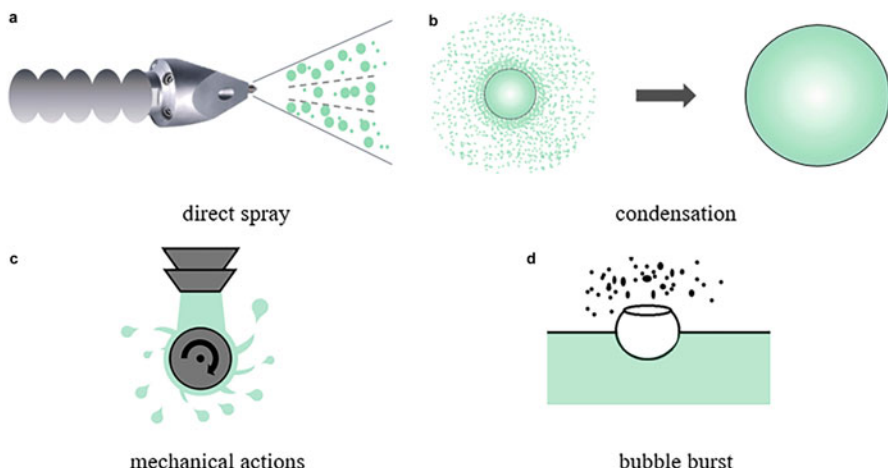


Fig. 3 Droplet emission mechanisms in industrial environments. (a) Direct spray. (b) Condensation. (c) Mechanical actions. (d) Bubble burst

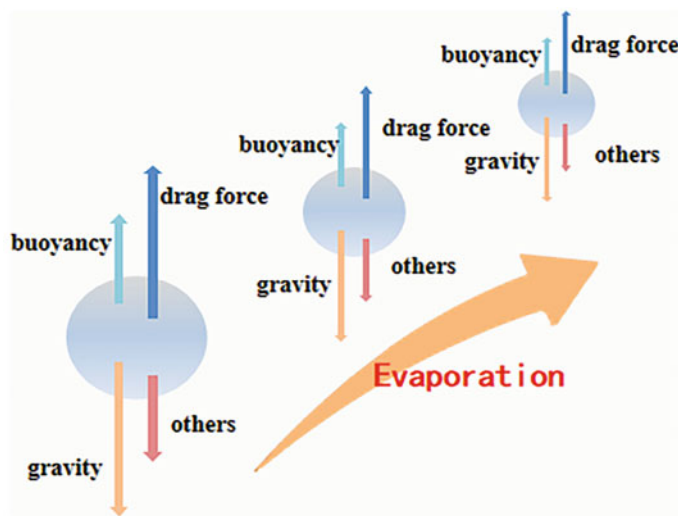


Fig. 4 Forces acting on the droplets change with evaporation

droplet to be lower than that of a pure water droplet, which is the solution effect. Thus, the evaporation of the solution droplet was slower. The strength of the solution effect on the water vapor pressure at the droplet surface mainly depends on the number of ions and the number of charges ionized by the solute.

Sulfuric acid (H_2SO_4) droplets and hydrochloric acid (HCl) droplets generated from the surface treatment processes of steel, such as pickling, electrolysis, and electroplating, are two common acid droplets in industrial environments. The evaporation of these two types of droplets differs from that of pure water droplets. For instance, at an ambient temperature and relative humidity of 25 °C and 50%, respectively, a pure water droplet of 100 μm needs approximately 12 s to evaporate completely, as shown in Fig. 5. For a sulfuric acid droplet, the diameter change owing to evaporation quite differs from that of a pure water droplet. It evaporates when the mass fraction of the solute is low. When the mass fraction of the solute is much higher owing to water loss, the evaporation almost stops, and it remains at a balanced diameter for a long time. The diameter evolution curve of a hydroelectric droplet is similar to that of a pure water droplet. As the mass fraction of a solute would not be much higher because HCl volatilized, it could evaporate completely. However, the duration of complete evaporation for a hydroelectric droplet is much longer than that of a pure water droplet under the same conditions (Yang et al. 2019a). This could be an important reason the acid mist could remain in industrial environments for a long time. With an increase in relative humidity, the sulfuric acid droplets evaporate more slowly, and the “balance diameter” of the sulfuric acid droplets increases. This is because the vapor pressure difference between the droplet surface and the ambient air decreases as the relative humidity increases, and the evaporation rate then slows down. With an increase in relative humidity, the evaporation rate of the hydrochloric acid droplets decreased. A longer time is

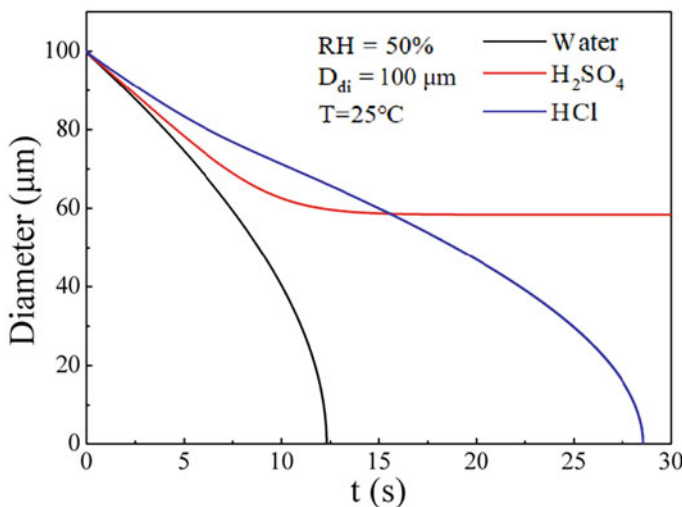


Fig. 5 Diameter variation of different droplets

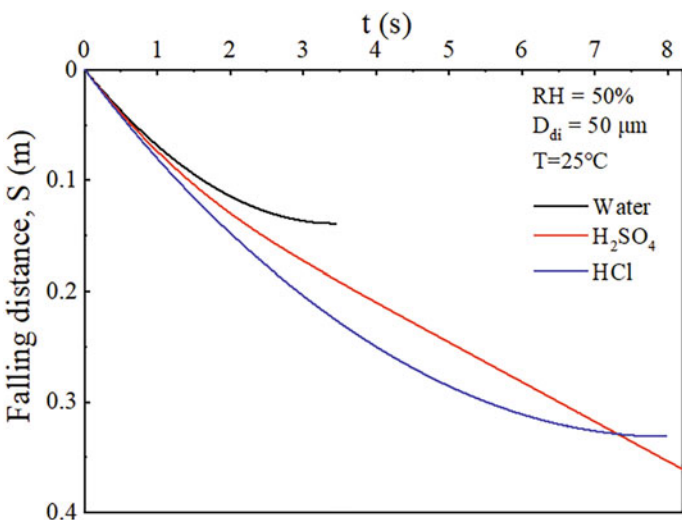


Fig. 6 Comparison of the falling distances of sulfuric and hydrochloric acid droplets

required for a hydrochloric acid droplet to evaporate completely in a higher-RH environment.

Different diameter variations lead to different droplets with different motion behaviors. As shown in Fig. 6, during the sedimentation process of a droplet, a pure water droplet quickly disappears after falling in a short time. A hydrochloric acid droplet with the same initial diameter could fall down a long distance and then disappear. In the case of a sulfuric acid droplet, because it could maintain a certain

diameter for a long time, it would fall to a very long distance. Initially, a hydrochloric acid droplet falls faster than a sulfuric acid droplet.

Gaseous Pollutants

Many types of gaseous contaminants are present in buildings. Many types of industries emit large amounts of hazardous gases. For example, the rubber industry emits pollutants such as vulcanizing heating fumes, toluene, and xylene. Dangerous hydrogen cyanide gas is emitted from the open surface tank processes in plating and metal-finishing shops. Harmful pollutants, such as tungsten fluoride and octafluorocyclobutane, are emitted by the semiconductor industry. Hydrogen leaks in the air can cause fires or explosions.

The concentration buoyancy is caused by density variations resulting from concentration differences. Gaseous pollutants are often considered as “passive” (Li et al. 1997; Liu et al. 2012) owing to their low concentration in civil building ventilations. However, in industrial facilities, the contaminant emission rates may be 10–100 times higher than those in civil building environments. Thus, concentration buoyancy should be considered in some circumstances.

Many studies have shown that concentration buoyancy may play an important role in the flow field and contaminant (or tracer) distributions. Ricciardi et al. (2008) and Gelain and Prevost (2015), both experimentally and computationally, showed that even in low quantities, the injection of gas of high density or low density compared with air can lead to stratification phenomena and thus create areas of high concentration. Many studies show similar results: the heavy gas may be deposited at the lower part of a space, whereas the light gas may be gathered in the upper region by the negative and positive concentration buoyancy. Niemela et al. (1991) revealed a difference in behavior between the three tracer gases of different densities using an experimental method. Zhou et al. (2018) showed that the concentration buoyancy effect is significant for tracer distribution with different tracer gases at a low velocity under isothermal conditions. In their investigation, three tracer gas concentrations were used, that is, the mass fractions of tracer gases were $Y_{0, \text{tracer}} = 0.001, 0.005$, and 0.01 . CH_4 represents a “light” tracer gas, and CO_2 represents a “heavy” tracer gas. Figure 7 shows the relative mass fraction distributions (Y/Y_0) of the supply air and tracer gases with different tracer gas concentrations under isothermal conditions with $u_0 = 1$ m/s. The tracer distributions were compared with the exact reference without a tracer. The comparison shows that the tracer distributions deviate from the exact reference as the tracer concentration increases. Moreover, even under isothermal conditions, the distributions of the tracer gas are up for the light tracer gas CH_4 and down for the heavy tracer gas CO_2 . This is because the density of CH_4 is lighter than that of air, causing a positive concentration buoyancy force and affecting the tracer gas distribution. However, the heavy tracer CO_2 causes a negative buoyancy force. Moreover, the tracer distribution deviation increased with an increase in the concentration of the tracer gas.

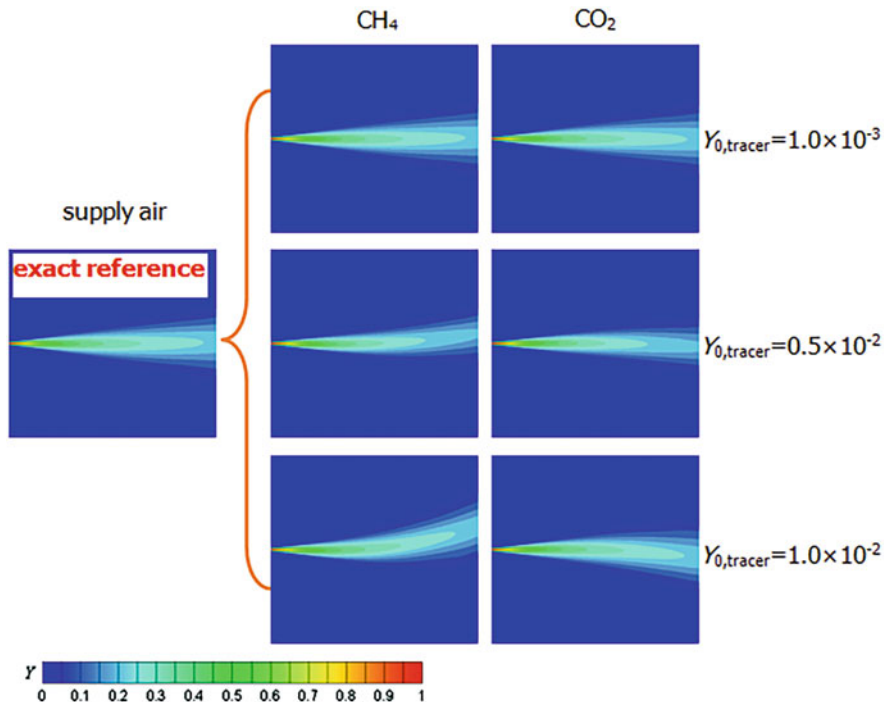


Fig. 7 Relative mass fraction distributions (Y/Y_0) of the supply air without tracer and the tracer gases with different tracer concentrations under isothermal conditions with $u_0 = 1 \text{ m/s}$

To quantitatively compare the effect of the tracer gas concentration on the tracer gas error, the relative tracer gas error is defined as:

$$Er = \frac{(Y/Y_0)_{\text{tracer}} - (Y/Y_0)_{\text{exact}}}{(Y/Y_0)_{\text{exact}}} \times 100\% \quad (1)$$

where Y/Y_0 is the relative mass fraction of the supply air, $(Y/Y_0)_{\text{tracer}}$ is the Y/Y_0 using the tracer method, and $(Y/Y_0)_{\text{exact}}$ is the Y/Y_0 using the self-label method.

Figure 8 shows the effect of the tracer gas concentration on the tracer gas deviation at the centerline of the jet under isothermal conditions. For $Y_{0,\text{tracer}} = 0.001$, and for both tracer gases, the tracer gas errors were close to zero. For $Y_{0,\text{tracer}} = 0.01$, and for both tracer gases, the tracer gas deviation is significantly larger. Moreover, the tracer gas deviation of CH₄ was much higher than that of CO₂. This is because the change in the density of CH₄ is larger than that of CO₂, thus increasing the additional concentration buoyancy force. The corresponding changes in the density are shown in Table 1.

Except for the concentration and contaminant (or tracer) type (light or heavy), flow velocity notably affects the distribution of concentration owing to the relative concentration buoyancy. Figure 9 shows the mass fraction distributions of the supply

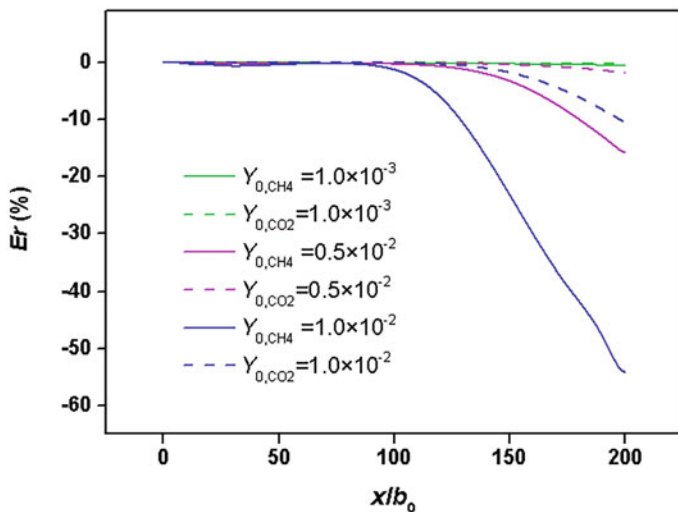


Fig. 8 Effect of tracer gas concentration on tracer gas deviation at the centerline of the jet under isothermal conditions with $u_0 = 1 \text{ m/s}$

Table 1 Parameters values related to the mixture density at the supply inlet

Tracer	Mass fraction, Y	Mole fraction, x_t	Tracer-mixture density, $\rho_{\text{mix-t}}$ (kg/m^3)	Change in density, $\delta\rho = \rho_{\text{mix-t}} - \rho_{\text{air}}$ (kg/m^3)	Ratio, $\delta\rho/\rho_{\text{air}} (\%)$
CH ₄	1.0×10^{-3}	1.80×10^{-3}	1.17573	-0.94×10^{-3}	-0.08
	0.5×10^{-2}	0.90×10^{-2}	1.17195	-4.72×10^{-3}	-0.40
	1.0×10^{-2}	1.79×10^{-2}	1.16727	-9.40×10^{-3}	-0.80
CO ₂	1.0×10^{-3}	0.66×10^{-3}	1.17708	0.41×10^{-3}	0.03
	0.5×10^{-2}	0.33×10^{-2}	1.17869	2.02×10^{-3}	0.17
	1.0×10^{-2}	0.66×10^{-2}	1.18071	4.04×10^{-3}	0.34

Note: $\rho_{\text{air}} = 1.17667 \text{ kg/m}^3$

air and tracer gases ($Y_{0, \text{tracer}} = 0.02$) with different air velocities under isothermal conditions. It can be seen that the mass fraction distributions deviate less from the exact reference as the air velocity increases for both CH₄ and CO₂. The tracer gas deviation decreased with an increase in supply air velocity. This is because with an increase in supply air velocity, the inertial force increases, thus decreasing the relative concentration of the buoyancy force.

In building environments, pollutants are often distributed under non-isothermal conditions. Thus, fluid motion and contaminant (or tracer) distribution may be induced not only by the concentration buoyancy but also by the thermal buoyancy, that is, double buoyancy owing to temperature and concentration differences. Laporte et al. (2001) found that differences in the stratifications of the tracer gas in hot air and cold air trials exist, indicating the heating or cooling conditions may affect the tracer gas distribution. Concentration buoyancy is positive for light

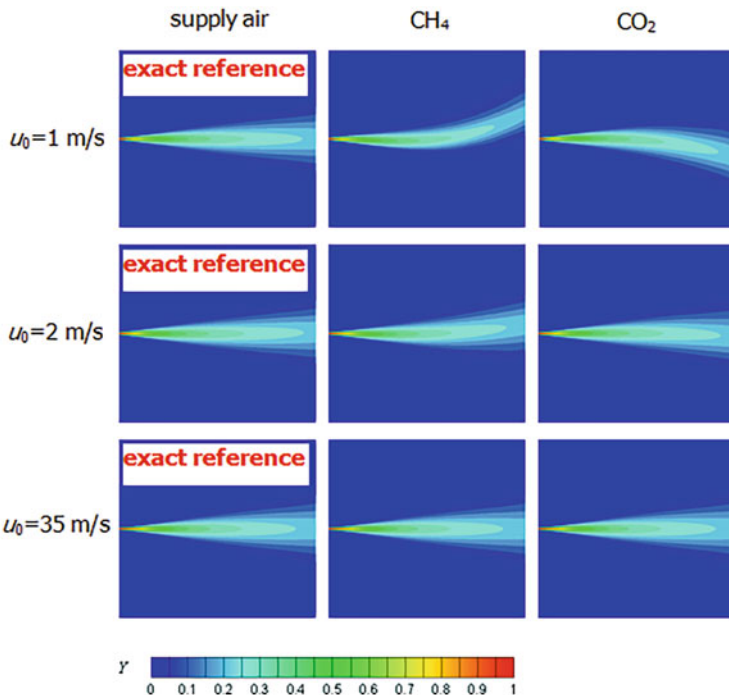


Fig. 9 Mass fraction distributions of the supply air and tracer gases ($Y_{0, \text{tracer}} = 0.02$) with different air velocities under isothermal conditions

contaminants and negative for heavy contaminants, and thermal buoyancy is positive under heating conditions and negative under cooling conditions. Therefore, the double buoyancy force was positive or negative. These factors still need to be investigated further.

Industrial Ventilation

General Ventilation with Zoning Environmental Control Strategy

Several production processes often exist simultaneously in an industrial workshop, and the emission of pollutants varies with location and environment in the workshop. For areas comprising a pollution source, it is necessary to capture as many pollutants as possible and avoid their spread. Owing to the huge volume of industrial plants, it is uneconomical and difficult to achieve the goal of increasing the airflow and improving the ventilation rate throughout the workshop. Consequently, it is necessary to divide the workshop into several parts based on the release location and diffusion characteristics of the pollutants and use different

ventilation strategies in different areas to use the minimum energy consumption to achieve the best indoor air quality. Generally, three modes for the zoning control of industrial buildings exist: natural zoning, physical partition, and airflow partition.

Natural Zoning

Natural zoning is a mode of zoning that fully utilizes the diffusion characteristics of pollutants. This mode does not need to consume too much energy; it only needs to set the vents as close to the pollutant deposition as possible, making zoning environmental control efficient. When the pollutant density is significantly higher than that of air and the pollutant release is not accompanied by thermal processes, the pollutants deposit near the ground. The best way to achieve this is to set the exhaust outlet near the ground, which not only ensures the safety of the working area but also ensures the highest pollutant concentration near the exhaust outlet and achieves the highest efficiency, as shown in Fig. 10a. When the release of pollutants is accompanied by a thermal process, the diffusion of pollutants becomes more intense and complex. Driven by buoyancy, pollutants move upward into the large space, then diffuse around the roof and accumulate in the upper part of the workshop, which is similar to the distribution of displacement ventilation. It is worth mentioning that when the temperature of pollutants accumulated in the upper part of the room decreases, pollutants may resettle and enter the work area, resulting in a wide range of pollution. Therefore, for the natural zoning control of pollutants in the upper part, it is necessary to set the exhaust outlet in the upper part of the room to remove the pollutants accumulated in the upper part of the room, as shown in Fig. 10b.

Physical Partition

The most efficient method of zoning is to use physical methods such as walls and partitions to divide industrial buildings into rooms, successively. This is difficult to achieve in industrial buildings, and some obstacles exist: production lines need to be set continuously, cranes are often set above industrial buildings, and the frequent handling of production materials also makes the setting of physical partitions difficult. Nevertheless, some physical isolation methods that minimize the impact on the process exist.

First, the partition can be set according to the deposition characteristics of the pollutants. For the lower deposition pollutants generated by grinding, spraying, and other processes, the working area can be surrounded by a semi-open grid to prevent the further diffusion of deposition pollutants in the room. For high-temperature pollutants driven by buoyancy, a continuous partition can be set on the roof directly above the pollution source, similar to the smoke vertical wall to prevent fire, to delay the horizontal diffusion of pollutants in the upper part of the room, and realize zoning, as shown in Fig. 11.

The other method is to use movable physical partitions, such as rolling shutters, automatic doors, and other devices that can be opened when they do not affect the

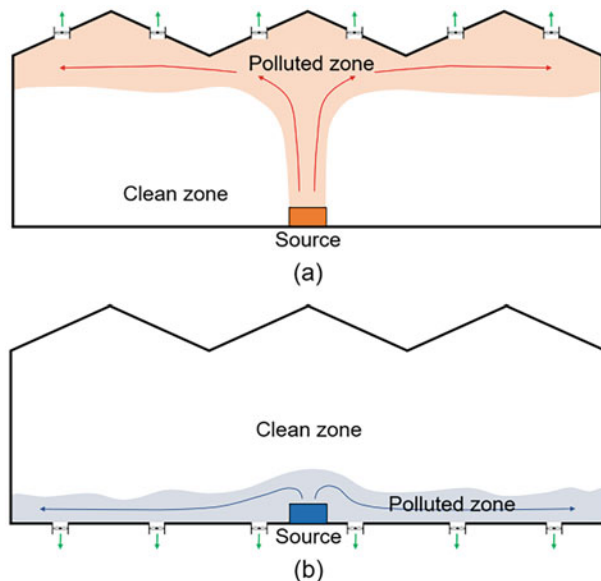


Fig. 10 Ventilation system setting under natural zoning

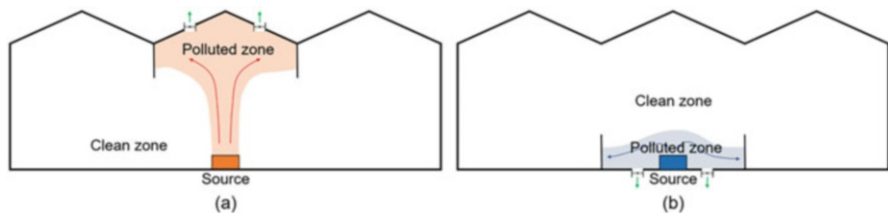


Fig. 11 Mode of ventilation system associated with physical partition: (a) upper partition and (b) lower partition

process to play the role of partition, while closing when they do, which can shorten the diffusion time of pollutants as much as possible.

Airflow Partition

When setting a physical partition is inconvenient, the airflow can also realize the partition function. The function of the airflow partition can be divided into two types: air curtain partition zoning and vortex airflow zoning.

The air curtain partition is widely used, which mainly blocks the airflow on both sides of itself through high-speed air, such as a gate air curtain. In an industrial plant, a wide range of air curtains can also be set to partition the space on both sides to maintain the difference in temperature, humidity, and pollutant concentration on both sides of the air curtain, as shown in Fig. 12.

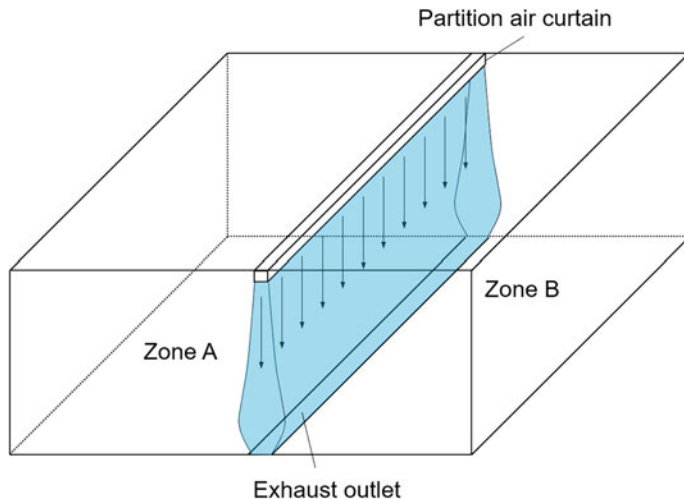


Fig. 12 Industrial workshop separated by an air curtain

The vortex airflow zoning mode is new and uses a tornado-like columnar air vortex to partition industrial buildings. The principle is that after generating vortex airflow in a large space, it mainly sucks pollutants inside the vortex zone, whereas less airflow movement occurs between the vortex ventilation system, the surrounding environment, and adjacent vortex ventilation systems. Thus, the effect of the zoning control was realized. When the pollution source is inside the vortex zone, the emitted pollutants are entrained by the vortex flow and transported to the roof exhaust outlet through the vortex pipe for elimination, as shown in Fig. 13. In industrial buildings with a large aspect ratio, multiple vortex ventilation systems can be set simultaneously to ensure the pollutants in each vortex ventilation system will not diffuse to other areas, as shown in Fig. 14.

Local Exhaust Ventilation Technology

Local exhaust is a common form of ventilation in industrial buildings. When concentrated pollution sources exist, first, we should consider setting local exhaust near the pollution sources to capture and control pollutants at the highest concentration just released, thus preventing pollutants from spreading into industrial buildings. The relevant contents of the local exhaust hood have been introduced in design handbooks (ACGIH 2010; HSE 2017). This section introduces several high-efficiency local exhaust modes suitable for industrial building environmental control.

Adjustable Exhaust Hoods

For local exhaust, the minimization of the contact area between the pollution source and the environment by enclosing as much as possible can not only reduce the

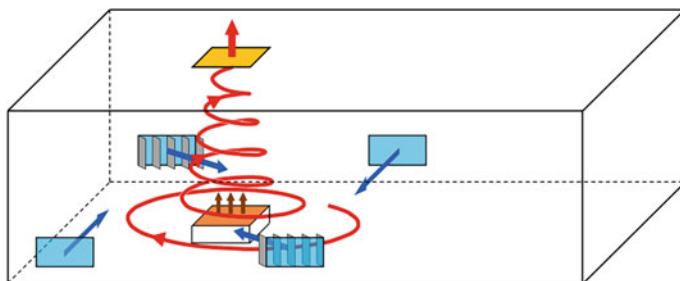


Fig. 13 Scheme of vortex ventilation in buildings with large space

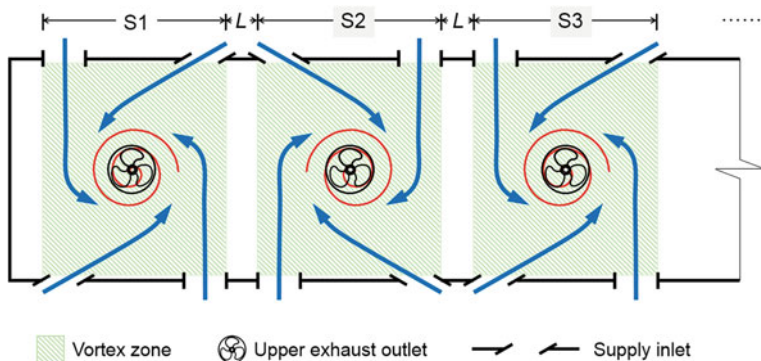


Fig. 14 Multi-vortex ventilation

possibility of pollutant diffusion but also reduce the entrainment of clean ambient air through the exhaust system, thus reducing the exhaust air rate. However, the setting of this enclosed hood is often limited by this process. Some production processes require frequent operations near the pollution source, resulting in an inability to effectively enclose the pollution source. Setting an adjustable exhaust hood is an effective alternative. The adjustable exhaust hood is often equipped with movable baffles, and the location of these baffles can be adjusted by the motor driving device to minimize the impact on the production process, as shown in Fig. 15. With an increase in the manufacture of cheap and accurate sensors in recent years, the adjustable exhaust hood can realize automatic operation, further reduce the operation cost, and improve work efficiency.

Movable Exhaust Hoods

In industrial buildings, sometimes the emission location of pollution sources is not fixed, such as cutting and grinding of large parts, welding, and spraying of large equipment. This challenges the setting of the local exhaust hood. If the local exhaust hood covers every location where pollutants may be released, the size of the exhaust

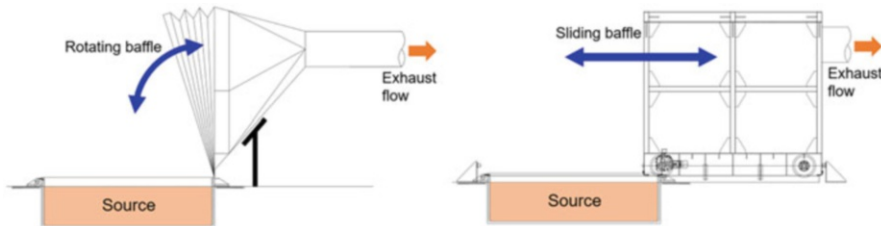


Fig. 15 Different types of adjustable exhaust hoods



Fig. 16 Multi-duct integrated movable exhaust hood used for spraying of a large airplane

hood is too large and the required air rate will be large; however, the efficiency is very low. Therefore, to solve the abovementioned pollutant capture problem of movable pollution sources, a movable exhaust hood can be used.

A movable exhaust hood means the air duct connected to the exhaust hood can move within a certain range through joints or hoses to adapt to the locations of pollution sources. The movable exhaust hood has been used in many chemical laboratories and automatic welding production lines, which significantly improves safety and operational convenience. For some extra-large movable pollution sources, such as surface spraying of large airplanes, setting a new integrated movable exhaust hood can effectively reduce the concentration of volatile organic compounds (VOCs) in the workshop through economical air rate without affecting the spraying operation, and effectively improve the indoor air quality of industrial buildings, as shown in Fig. 16.

Parallel-Flow Push-Pull Ventilation

Parallel-flow push-pull ventilation is an efficient local ventilation method that uses an air supply curtain with low turbulence intensity to shield the pollution source from the outside environment and prevent pollutants from escaping; it also uses the supply airflow to transport pollutants to the exhaust hood simultaneously. Owing to the low turbulence intensity of the supply airflow, the amount of mixing with the ambient air is very low in the process of transporting pollutants. Therefore, a good pollutant control effect can be achieved with a low air rate. Parallel-flow push-pull ventilation

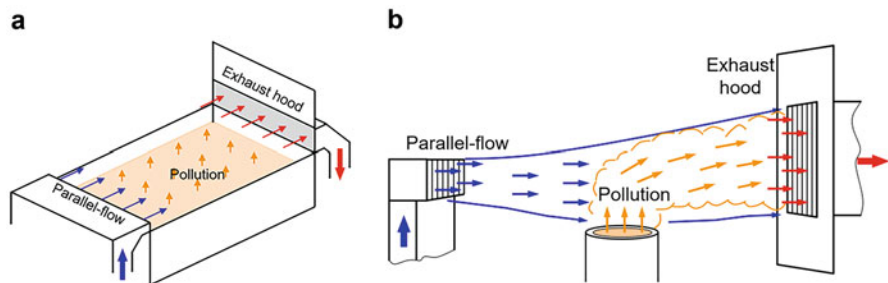


Fig. 17 Two types of parallel-flow push-pull ventilation: (a) above the open tank and (b) long-distance transportation of pollutants

systems are generally used in two application fields. One is used above the liquid surface of an open tank, and the other is to transport pollutants over a large range and long distance, as shown in Fig. 17.

Vortex Ventilation Hoods

The use of tornado columnar air vortex flow can achieve high-efficiency capture and control of pollutants in a certain indoor area. The vortex exhaust hood is a local exhaust hood that utilizes the vortex airflow, which can efficiently and quickly capture the pollutants released from pollution sources using tornado airflow. Owing to the strong control ability of vortex airflow, the vortex exhaust hood has strong adaptability to pollutants and has high capture and control performance for pollutants with high initial momentum and buoyancy flux.

The basic elements of the vortex airflow are the angular momentum air supply, the bottom plane, and the updraft. In the vortex exhaust hood, the angular momentum air supply can be provided by setting the air supply fan, and the updraft can be provided by the exhaust hood. The different control distances of the vortex exhaust hood can generally be divided into two types: bottom air supply type and total process air supply type. The angular momentum air supply devices of the bottom air supply type vortex exhaust hood are only arranged near the ground pollution source, whereas the total process air supply type vortex exhaust hood is equipped with angular momentum air supply devices between the pollution source and the exhaust hood, which can achieve a more stable vortex flow and a longer air supply distance, as shown in Fig. 18.

Assessment of Industrial Building Environment with High-Pollution Sources

For representative industrial buildings with high-pollution sources in the production process, including nonferrous metal smelting and calendaring, ferrous smelting and calendaring, and rubber products, a special Chinese building environmental assessment standard (CECS 2021) has been developed to assess the indoor environment of single industrial buildings.

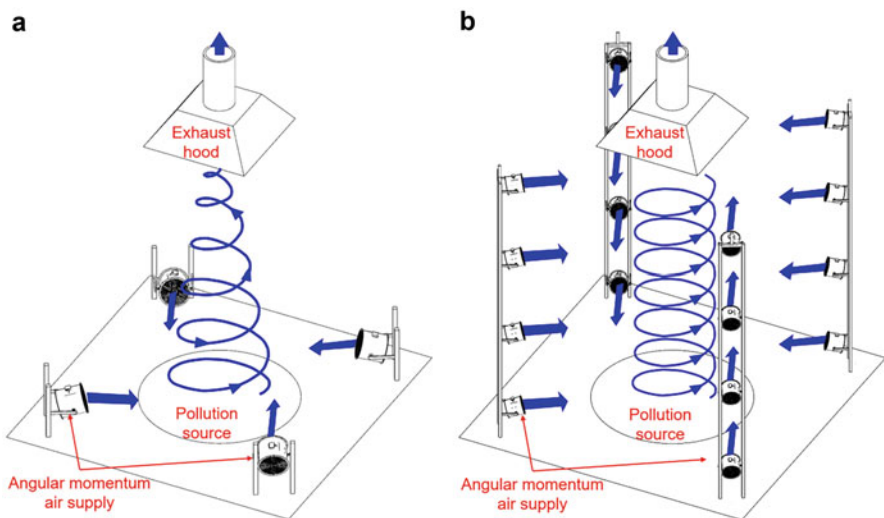


Fig. 18 Two types of vortex exhaust hood: (a) bottom air supply type and (b) total process air supply type

Divisional Principles for Environmental Assessment

Industrial buildings with high-pollution sources generally integrate many parts for different uses, including the parts for process production, offices, rest, etc. Each part has different environmental conditions, personnel residence times, and personnel health needs for the environment. In addition, to achieve precise control of the environment and industrial building energy conservation, it is necessary to design a reasonable cleaning and dust removal system for different environmental needs. Therefore, the standard divides single industrial buildings into three areas, including working, clean, and emissions areas, which would be more reasonable to assess the environment quality. The working area refers to the area where staffs often or quantitatively stay to observe and manage the production process, including the direct operation area of staff and the area of management, control, or scheduling. The clean area refers to the auxiliary office, rest, and other non-production areas. The emissions area refers to the unorganized emission area, excluding the working area and the clean area.

Environmental Parameters

The environmental parameters of industrial buildings with high pollution sources include common parameters and specific parameters. Common parameters refer to the indexes that all industrial buildings should meet the requirements of the indoor environment, such as temperature, humidity, and particle concentration. The

specific parameters proposed in the standard (CECS 2021) are based on the industry characteristics and the production situation of industrial buildings. The specific parameters should be assessed based on common parameters that meet the requirements.

Common Parameters

The common indexes in the working area include temperature, relative humidity, airflow velocity, and total particle concentration. Temperature, relative humidity, and airflow velocity should meet the current Chinese national health standards, and the total particle concentration should not be higher than 8 mg/m^3 (PC-TWA, permissible concentration-time weighted average). The common indexes of clean area include temperature, humidity, airflow velocity, and particle concentration, and each environment index should meet the requirements of Table 2. The common index of indoor emission area of industrial buildings with high pollution sources is the concentration of total suspended particles, which should not be higher than 5 mg/m^3 (time average value in 1 h).

Specific Parameters

The indoor specific parameter of nonferrous metal (lead-zinc) industrial buildings include sulfur dioxide, sulfur trioxide (sulfuric acid mist), lead and its compounds, and mercury and its compounds. The permissible concentrations of each parameter should meet the requirements of Fig. 19.

Table 2 Common parameters and the permissible values in indoor clean areas

Number	Parameters	Unit	Standard value	Seasons	Remark
1	Temperature	$^{\circ}\text{C}$	18~24	Winter heating	Time average value, time interval less than 30 min
			25~28	Summer air conditioning	
2	Relative humidity	%	/	Winter heating	
			40~70	Summer air conditioning	
3	Airflow velocity	m/s	0.2	Winter heating	
			0.3	Summer air conditioning	
4	PM _{2.5}	mg/m^3	0.075	/	Daily average value, time interval less than 1 min
5	PM ₁₀	mg/m^3	0.15	/	
6	Total suspended particles	mg/m^3	0.30	/	

Source: China Nonferrous Metal Industry Association (2015)

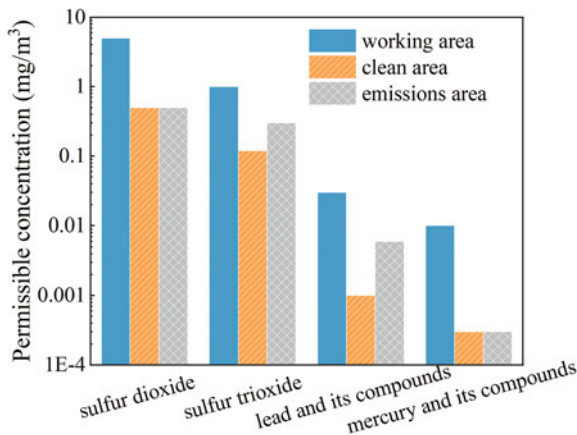


Fig. 19 Permissible indoor concentrations for specific parameters in different areas of nonferrous metal industrial building. Note: (a) Sulfur dioxide and sulfur trioxide are used as specific parameters in working area, sulfuric acid mist is used as specific parameters in clean area and emissions area. (b) Permissible concentrations for working area refer to PC-TWA, permissible concentrations for clean area refer to the time average value in 1 h, and permissible concentrations for emissions area refer to the time average value in 1 h. (Source: National Health Commission of the People's Republic of China (2019), National Institute of Environmental Health, China CDC et al. (2002), and CINF Engineering Co., Ltd et al. (2010))

The permissible concentrations of some indoor specific parameters of ferrous metal (calendering) industrial buildings, such as sulfur trioxide (sulfuric acid mist), hydrogen chloride, benzene, toluene, xylene, should meet the requirements of Fig. 20.

The permissible concentrations of some indoor specific parameters of rubber products industrial buildings, such as benzene, toluene, xylene, hydrogen sulfide, and ammonia, should meet the requirements of Fig. 21.

The principles for formulating the permissible indoor concentrations generally consider factors such as human health effects, economic feasibility, and technical feasibility. Some permissible concentrations only consider human health effects, while in some countries and regions, the determination of permissible concentrations should consider the overall level and economy of the industry at the same time. Thus, for a given environmental parameter, the value is not always the same and not comparable between different standards.

Prediction Methods of Environmental Parameter Values

Different methods can be used to obtain the value of environment parameters of industrial buildings with high pollution sources at different stages. For the existing industrial buildings with high pollution sources, the measurement method that determines the values through site tests and can truly reflect the

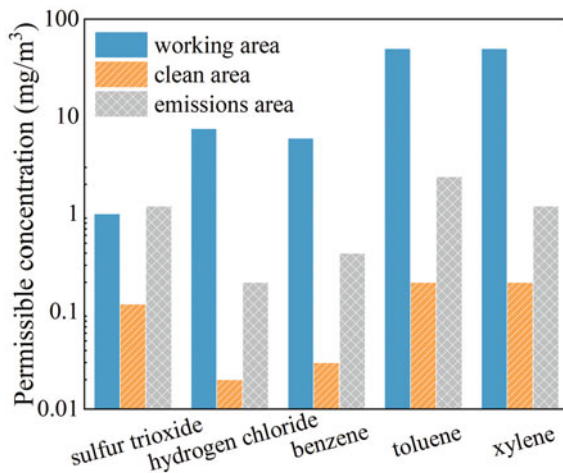


Fig. 20 Permissible indoor concentrations for specific parameters in different areas of ferrous metal smelting industrial building. Note: (a) Sulfur trioxide is used as specific parameters in working area, sulfuric acid mist is used as specific parameters in clean area and emissions area. (b) Production processes or facilities applicable to sulfur trioxide and hydrogen chloride as specific parameters: pickling machine and waste acid regeneration. (c) Production processes or facilities applicable to benzene, toluene, and xylene as specific parameters: coating units. (d) Permissible concentrations of hydrogen chloride for working area refer to MAC (maximum allowable concentration), permissible concentrations of other pollutions for working area refer to PC-TWA, permissible concentrations for clean area refer to the time average value in 1 h, and permissible concentrations for emissions area refer to the time average value in 1 h. (Source: National Health Commission of the People's Republic of China (2019), National Institute of Environmental Health, China CDC et al. (2002), and Baoshan Iron and Steel Co., Ltd et al. (2012))

indoor environment. For the industrial building environments in the design stage, the environmental indexes can be predicted to access whether the environments meet the requirements by analogy method, model experiment, or numerical simulation.

Analogy Method

The analogy method is commonly used in the prediction of occupational hazards (CECS 2021). It predicts the environment of to-be-assessed buildings by field investigation and indoor environmental parameter tests of the production process and indoor environment of the same or similar projects. When the analogy method is adopted, appropriate analogy items and data should be selected, and the feasibility analysis of the analogy between the two items should be performed.

When the industrial building to be assessed is an extension project, the original industrial building project can be selected as an analogy project. If the industrial building to be assessed is the expansion project of the original industrial building, the design scale, production process, production equipment, raw and auxiliary materials, protection facilities, and occupational health management of the industrial building

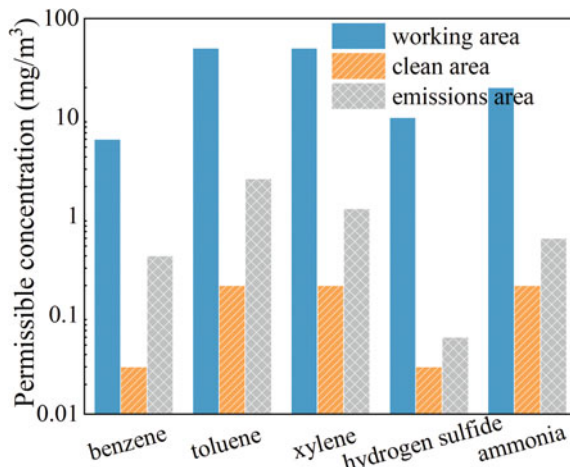


Fig. 21 Permissible indoor concentrations for specific parameters in different areas of rubber products industrial building. Note: Permissible concentrations for working area refer to PC-TWA, permissible concentrations for clean area refer to the time average value in 1 h, and permissible concentrations for emissions area refer to the time average value in 1 h. (Source: National Health Commission of the People's Republic of China (2019), National Institute of Environmental Health, China CDC et al. (2002), and Tianjin Academy of Environmental Sciences et al. (2011))

are probably completely or basically the same as those of the original industrial building. Here, the analogy project has strong comparability and is more suitable for the analogy method.

When the industrial building to be assessed is a new project, similar enterprises in the same industry and industrial buildings with similar processes can be selected. If the project and the project to be assessed are in the same province or city, and the assessment of the analogy project is also completed by the same institution, the environmental parameter data can be obtained from those of previous industrial buildings. If the project is in another province, city, or abroad, but belongs to the same owner as the construction project, the information required for assessment can be provided by the owner. If the project is in other provinces, cities, or abroad, and belongs to different owners of the construction project, it is necessary to obtain analogy information through group companies, industry associations, or other assessment agencies.

Model Experiment

It is a method to restore the airflow and characteristics of the indoor environment of the building in the actual project under laboratory conditions, based on the similarity theory (Huang et al. 2021c). It should be based on the process and environmental conditions of industrial buildings to determine the appropriate number of similarity criteria. The model design should be based on geometric similarities. The determination of an appropriate geometric scale should consider the scale of industrial buildings, test sites, equipment, and other conditions. The boundary conditions of

the model experiment should be set according to the conversion results of the wind tunnel test or design parameters based on the similarity criteria. In the model experiment, if different velocities and temperature differences are involved, the values with large changes in the dimensionless criterion number should be selected. When the initial temperature of the airflow in the model is high, the initial velocity can be adjusted to reduce the initial temperature of the airflow while ensuring the same number of criteria. To avoid large measurement errors, the adjusted initial velocity must be significantly greater than the ambient airflow velocity. The results of the model experiment should be converted to actual values based on the similarity criteria.

Numerical Simulation

Numerical simulation is an environmental prediction method based on computational fluid dynamics (ANSYS 2011). It should be performed based on the basic idea of “analysis of actual industrial building environments – proposal of the physical problems – selection of a mathematical model to describe.” The geometric model, including the shape, size, relative position of the space, and relative position of each component in the space, should be determined based on practical projects. The established model can be simplified based on the actual situation of industrial buildings, and a simplified basis should be provided. The mesh division, initial and boundary conditions, calculation methods, and convergence criteria should meet the corresponding requirements to ensure the accuracy of the calculation. Meanwhile, the calculation model and calculation method used in the numerical simulation should be verified experimentally.

Conclusions

The indoor air quality of industrial buildings with high pollution sources is closely related to the production process, which needs to be controlled through efficient industrial ventilation technology based on the characteristics of pollution sources. With the continuous emergence of new environmental requirements and production processes, the indoor air quality control of industrial buildings is facing new problems, which are mainly reflected in the expansion of industrial buildings and their indoor production scale, the reduction of emission capacity, and the improvement of healthy environmental requirements, which pose a higher challenge to ventilation technology.

In recent years, industrial ventilation technology has made great progress. A series of research results on refined industrial building ventilation technology have been proposed and have been successfully used in industrial buildings with high pollution sources, such as the new ventilation air distribution model based on parallel flow and vortex flow, the efficient control and cleaning technology of high-temperature particles, droplets, and harmful gases. The research on ventilation technology of industrial buildings also shows that with the progress of experiment and numerical simulation technology, it has great potential to improve the effect of

pollutant control and reduce energy consumption and carbon emission by deepening the level of cognition. Facing the low-carbon goal and ultra-low emission demand, there is a long way to go to improve the indoor air quality of industrial buildings with high pollution sources. Meanwhile, it also provides a good opportunity for the significant improvement of relevant technical development. The indoor air quality of many industrial sectors needs to be further improved, and more in-depth and systematic basic research is urgently needed to make a new breakthrough in efficient and low consumption industrial ventilation technology.

References

- ACGIH (2010) Industrial ventilation: a manual of recommended practice for design, 27th edn. ACGIH, Cincinnati
- ANSYS (2011) ANSYS fluent user's guide. ANSYS, Inc, Canonsburg
- Baoshan Iron and Steel Co., Ltd et al (2012) Emission standard of air pollutants for steel rolling industry. China Environmental Science Press, Beijing
- Belding HS, Hatch TF (1955) Index for evaluating heat stress in terms of resulting physiological strains. Heat Piping Air Cond 52:35
- China Association for Engineering Construction Standardization (CECS) (2021) Standard for environment assessment of high-pollution industrial building (T/CECS 980-2021). China Association for Engineering Construction Standardization (CECS), Beijing
- China Nonferrous Metal Industry Association (2015) Design code for heating ventilation and air conditioning of industrial buildings. China Planning Press, Beijing
- CINF Engineering Co., Ltd et al (2010) Emission standards of pollutants for lead and zinc industry. China Environmental Science Press, Beijing
- Duan M et al (2017) Modeling dispersion mode of high-temperature particles transiently produced from industrial processes. Build Environ 126:457–470
- Fan J-N et al (2021) Emission and local ventilation control of droplets generated by condensation and bubble-bursting during pickling. Sustain Cities Soc 76:103491
- Gelain T, Prevost C (2015) Experimental and numerical study of light gas dispersion in a ventilated room. Nucl Eng Des 293:476–484
- Goodfellow H et al (2021) Industrial ventilation design guidebook. Academic Press, Cambridge, MA
- Han O, Zhang Y, Li AG et al (2020) Experimental and numerical study on heavy gas contaminant dispersion and ventilation design for industrial buildings. Sustain Cities Soc 55:102016
- HSE (2017) Controlling airborne contaminants at work: a guide to local exhaust ventilation (LEV). Series code HSG258, health and safety executive
- Huang Y et al (2021a) Experimental study of induced airflow characteristics during liquid metal pouring process through PIV, thermography, and color schlieren imaging. Int J Therm Sci 170: 107–144
- Huang Y et al (2021b) Flow-field evolution and vortex structure characteristics of a high-temperature buoyant jet. Build Environ 187:107–407
- Huang Y et al (2021c) Chapter 4. Experimental techniques. In: Industrial ventilation design guidebook, 2nd edn. Academic Press, Cambridge, MA, pp 185–277
- Huang Y et al (2022) Transport characteristics of pulsating high-temperature particles based on vortex structure analysis by large-eddy simulation. Build Environ 209:108679
- Laporthe S, Virgone J, Castanet S (2001) A comparative study of two tracer gases: SF₆ and N₂O. Build Environ 36:313–320
- Li YG, Delsante A, Symons J (1997) Residential kitchen range hoods-buoyancy-capture principle and capture efficiency revisited. Indoor Air 7:151–157

- Liu D, Zhao FY, Wang HQ (2012) History recovery and source identification of multiple gaseous contaminants releasing with thermal effects in an indoor environment. *Int J Heat Mass Transf* 55:422–435
- National Health Commission of the People's Republic of China (2019) Occupational limits for hazardous agents in the workplace – part 1: chemical hazardous agents. National Health Commission of the People's Republic of China, Beijing
- National Health Commission of the People's Republic of China (2020) Statistical bulletin of health development in China in 2020 – material from China government network. <http://www.nhc.gov.cn/guihuaxxs/s10743/202107/af8a9c98453c4d9593e07895ae0493c8.shtml>
- National Institute of Environmental Health, China CDC et al (2002) Indoor air quality standard
- Niemela R, Lefevre A, Muller JP, Aubertin G (1991) Comparison of three tracer gases for determining ventilation effectiveness and capture efficiency. *Ann Occup Hyg* 4:405–417
- Ricciardi L, Prévost C, Bouilloux L, Sestier-Carlin R (2008) Experimental and numerical study of heavy gas dispersion in a ventilated room. *J Hazard Mater* 152(2):493–505
- Tianjin Academy of Environmental Sciences et al (2011) Emission standard of pollutants for rubber products industry. China Environmental Science Press, Beijing
- Wang Y, Cao ZX (2017) Industrial building environment: old problem and new challenge. *Indoor Built Environ* 26:1035–1039
- Wang Y, Cao Y, Meng X (2019) Energy efficiency of industrial buildings. *Indoor Built Environ* 28 (3):293–297
- WHO (2017) Global Health Observatory (GHO). Available at: <http://www.who.int/gho/en/>
- Wyndham CH, Allan AM, Bredell GAG, Andrew R (1967) Assessing the heat stress and establishing limits for work in a hot mine. *Br J Ind Med* 24:255
- Yaglou CP, Minard D (1957) Control of heat casualties at military training centers. *AMA Arch Ind Health* 16:302
- Yang Y, Song B, Wang Y, Fan J-N, Karkrī M, Wei Y (2019a) Numerical investigation of motion of sulfuric and hydrochloric droplets with phase change in free-falling process. *Build Environ* 157: 16–23
- Yang Y, Wang Y, Song B, Fan J, Cao Y, Duan M (2019b) Transport and control of droplets: A comparison between two types of local ventilation airflows. *Powder Technology* 345:247–259
- Zhang Y, Wang L, Li A et al (2019) Performance evaluation by computational fluid dynamics modelling of the heavy gas dispersion with a low Froude number in a built environment. *Indoor Built Environ* 29(5):1420326X1985604
- Zhou Y, Wang MY, Wang Y, Cui HH, Wang JL (2018) Development of self-label method to distinguish supply air from room air without tracer in numerical simulations. *Build Environ* 145: 223–233
- Zimmer AT, Biswas P (2001) Characterization of the aerosols resulting from arc welding processes. *J Aerosol Sci* 32:993–1008
- Zimmer AT, Baron PA, Biswas P (2002) The influence of operating parameters on number-weighted aerosol size distribution generated from a gas metal arc welding process. *J Aerosol Sci* 33: 519–531



Household Air Pollution in Rural Area

71

Zhihan Luo and Guofeng Shen

Contents

Introduction	2126
Household Air Pollution (HAP) Definition	2126
Household Air Pollution (HAP) Sources	2127
Indoor Combustion Emissions and Air Quality	2128
Indoor Combustion Emissions	2128
Indoor Fugitive Emission	2129
Household Air Pollution	2131
Indoor-Outdoor Ratio	2133
Exposure and Influencing Factors	2133
Quantification of Exposure	2133
Contribution of Indoor Exposure	2134
Influencing Factors	2135
Health Risks Associated with HAP	2136
Estimates of HAP-Related Health Impacts	2136
Amplified Contribution and Clean Household Energy Transition	2137
Conclusions	2139
Cross-References	2139
References	2140

Abstract

Solid fuels like coal and biomass fuels are still frequently used for daily cooking, heating, and lighting, especially in rural areas of developing countries. Low-efficient burning of these solid fuels in residential stoves produce significant amounts of air pollutants into not only ambient but also indoor air, resulting in high air pollution exposure and various diseases associated with household air pollution (HAP) exposure. With longer time spent indoors, indoor air pollution contributes significantly to the total air pollution exposure and related adverse

Z. Luo · G. Shen (✉)

Laboratory of Earth Surface Processes, College of Urban and Environmental Sciences, Peking University, Beijing, China

e-mail: gfshen12@pku.edu.cn

health outcomes. The HAP issue has been attracting growing interests and high concern. This chapter focuses on main research progresses in HAPs in developing countries. Pollutant emissions, exposures, health risks, and needs in future studies are analyzed and discussed. Fugitive emission from home stoves is one main source of indoor air pollution. Due to influencing factors like different stove-fuel combinations and highly variable operational behaviors, both pollutant emissions and indoor air pollutant levels have very high inter- and intra-variations uncertainties in residential pollutant emissions and the associated impact assessment results are relatively high. Significant differences in the inhalation exposure dose were generally observed among different fuel-stove users and gender difference is often found. Contributions of household solid fuels on the energy consumption, pollutant emission, air pollution exposure, and health risks amplified, indicating obvious health benefits in reducing air pollution from household solid fuel use in rural areas.

Keywords

Household air pollution · Solid fuels · Indoor combustion · Fugitive emission · Exposure · Clean intervention

Introduction

It was estimated that globally there were nearly 2.8 billion people relying on traditional solid fuels like biomass and coals for daily cooking, with most from less developed or developing countries with relatively low socioeconomic status (Bonjour et al. 2013). Besides cooking, solid fuels are important energy sources for heating, resulting more people exposing to air pollutants from the solid fuel combustion (Chen and Zhao 2022; Du et al. 2018a). Solid fuel burning in residential stoves often has low efficiencies and produces high emissions of products of incomplete combustion (PICs) such as carbon monoxide (CO), PM_{2.5} (particles with a diameter of <2.5 μm), black carbon, and polycyclic aromatic hydrocarbons (Du et al. 2018a; Garland et al. 2017). Indoor solid fuel combustion affects not only ambient air pollution but also directly to severe indoor (household) air pollution (Smith et al. 2014; Shen et al. 2019). Since most people spend ~80% or more time indoors, serious indoor air pollution and long residence time indoors cause high exposures to PICs associated with solid fuel use. Exposure to household air pollution (HAP) from solid fuel use has been recognized as one leading environmental risk factor causing more than 1.6 million premature deaths globally in 2017, including ~0.27 million in China and 0.48 million in India (GBD 2019).

Household Air Pollution (HAP) Definition

The problem of air pollution associated with residential combustion has been widely recognized as household air pollution (HAP). The concept of indoor air pollution

(IAP) is well-known and studied. According to the US EPA (2021), IAP refers to air pollution within and around buildings and structures, caused by various sources like fuel-burning combustion, tobacco products, building materials and furnishings, products for household cleaning and maintenance, personal care, or hobbies, central heating and cooling systems and humidification devices, excess moisture, and some outdoor sources. That is, besides solid fuel combustion sources, IAP has other sources including non-combustion processes. Meanwhile, HAP is defined as air pollution arising from inefficient combustions of solid or nonsolid fuels used for domestic cooking, lighting, and/or heating (Smith et al. 2014). The term involves not only indoor but also near residences and in the ambient air (Clark et al. 2013; Du et al. 2018a). When household ventilation is poor or absent, indoor HAP could be more serious than outdoor air. Note that in some studies, HAP is used as the abbreviation of hazardous air pollutants, which is different from the issue discussed here.

Therefore, the differences between IAP and HAP, from their definitions, are obvious (Smith et al. 2014). Compared to IAP, HAP sources are more specific and explicit. The term “HAP” emphasizes the health risk of the exposure to the definite source from cooking, lighting, and heating, not food, spreading to any space. While the term “IAP” covers the health risk of exposure to all sources contributing to the indoor. Some researches use the term “indoor air pollution from household use of solid fuel” to express the air pollution from domestic cooking fuel burning (Smith et al. 2014). However, this term *“neglects the near-household environment, which is the main site of health-relevant air pollution exposure”* and *“the term indoor implies that an effective chimney or other venting would solve the problem entirely, when the basic problem is dirty combustion, thus confusing the attribution of risk and assessment of appropriate interventions unless it is specified which household uses are being considered.”* In rural areas, there are also indoor air pollution issues like hazardous pollutants from furniture, decorations, building materials, and cleaning products that are not limited to urban homes. IAP issues associated with other common indoor sources like cooking fume, furniture, and building materials have been covered in other chapters (Bond 2022; Torkmahalleh 2022; Zhang et al. 2022), and in this chapter, we focus on household air pollution associated with indoor energy use.

Household Air Pollution (HAP) Sources

As mentioned above, HAP here refers to air pollution associated with household fuel use. Therefore, major sources of HAPs are indoor combustion processes and outdoor air pollution via indoor-outdoor air exchange (Chen and Zhao 2022). Efforts have been made to alleviate HAP by promoting clean household energy such as natural gas, liquid petroleum gas, propane, and electricity (Anenberg et al. 2013). Installation of vented facilities like chimney and fans and optimization of stove designs are also purposed as effective countermeasures to lower HAP, especially before utilization of modern energies like electricity and gaseous fuels. Emission smokes from unvented stoves enter indoor environment directly contributing HAP. Some field

studies revealed health benefits after the adoption of improved stoves with chimney (Guarnieri et al. 2015), but some did not find significant improvements (Mortimer et al. 2017). Although chimneys can effectively remove indoor smokes to outdoor, the emission contributes to neighborhood or village pollution, which in turn would influence indoor air quality to some extent. High indoor levels of PICs are still often reported in households burning coal or biomass in chimney stoves (Hartinger et al. 2013; Jiang and Bell 2008; Qi et al. 2019; Qiu et al. 2019). For instance, the kitchen PM_{2.5} in rural Peru homes using improved chimney stoves was as high as 148 (88–208 as 95% confidence interval) $\mu\text{g}/\text{m}^3$ (Hartinger et al. 2013). The wintertime kitchen PM₁₀ concentrations in a rural village were reported at about $100 \pm 203 \mu\text{g}/\text{m}^3$, with a maximum concentration of $1570 \mu\text{g}/\text{m}^3$, though stoves used were equipped with outdoor chimneys (Jiang and Bell 2008). A recent study in rural southern China found that daily average kitchen PM_{2.5} concentration in homes burning solid fuels in brick chimney stoves was $101 \pm 56 \mu\text{g}/\text{m}^3$ (Qi et al. 2019).

High indoor pollution levels in homes with vented stoves are thought to be associated with reasons like leakages (also known as fugitive emissions from stoves) into indoor air, and/or short-circuiting resulting from improper design (Smith et al. 2011). These are two important sources of household air pollution (Johnson et al. 2011; Ruiz-Garcia et al. 2018; Smith et al. 2011). While outdoor air pollution impacts via indoor–outdoor air exchange has been recognized and discussed extensively, fugitive emissions are significantly underappreciated (Shen et al. 2020; Luo et al. 2021). The proportion of fugitive emissions into indoor environment in the total emissions from the combustion process is defined as the fugitive emission fraction. There are significant gaps in data and understanding for this important parameter as very few experiments and modeling studies are available.

Indoor Combustion Emissions and Air Quality

Indoor Combustion Emissions

Emissions of air pollutants can be estimated based on emission factors (EFs) and fuel consumptions. Reported EFs in literature often vary several orders of magnitude and most used to be from tests in developed countries rather than the real-world conditions in rural developing countries, leading to high uncertainties and potential biases in emission inventory development (Lei et al. 2011; Wang et al. 2012). Significant differences are reported between the EFs from laboratory chamber tests and those measured in real kitchens, and between the EFs under controlled conditions and those in field (Roden et al. 2009; Zhang et al. 2011). For example, a study from uncontrolled in-field measurements in Ghana (Coffey et al. 2017) showed the fuel-mass-based carbon monoxide (CO) and particulate matter (PM) emission factors were generally higher in field compared with in laboratory. Roden et al. (2009) found that PM emissions measured in field were on average three times higher than those measured in laboratory tests. Garland et al. (2017) reported that laboratory tests generally had lower black carbon (BC) emission factors but higher BC/PM ratios

compared with field tests. Laboratory experiments allow investigators to repeat the process under controlled conditions to assess influencing factors, pollutant formation kinetics, and mechanisms (Jetter et al. 2012; Zhang et al. 2011). As such, laboratories are suitable for testing a variety of stove/fuel combinations operated under different conditions. Even so, direct field measurements are preferable in developing inventories, because they are more realistic and may cover emissions from stoves operated at random conditions that are difficult to reproduce in laboratory. However, field measurements are much more difficult in sampling and financially expensive compared with the laboratory tests. In recent years, with the development of portable emission testing system, more and more field tests and important data are available. There are more studies in developing countries including China and India.

Indoor Fugitive Emission

While short-circuiting of air pollution is recognized as one source of indoor air pollution from solid fuel combustion, the source of fugitive emissions has been underappreciated. There are very few experimental measurements of fugitive emissions nowadays. Four studies evaluated fugitive emissions, and two of them were laboratory-based tests. At the US Environmental Protection Agency (US EPA) household energy research facility, a well-built system has been developed to evaluate efficiency performance and emissions for stoves with or without chimneys (Jetter et al. 2012; Shen et al. 2017). The facility can quantify chimney and fugitive emissions separately by fully capturing emission exhaust in two separate fume hoods. For a 60 L institutional stove fueled with wood, a study found that fugitive emissions were approximately 2.0–2.7% and 1.0–1.9% of the total emissions for PM_{2.5} and CO, respectively (Jetter 2016). In another laboratory study, Ruiz-Garcí'a et al. (2018) found that fugitive emissions from Plancha-type chimney stoves were only $5 \pm 3\%$ and $1 \pm 1\%$ for PM_{2.5} and CO, respectively.

In the development of the World Health Organization (WHO 2010a) guidelines for indoor air quality (IAQ): household fuel combustion, because of the absence of direct measurement of fugitive emissions prior to that time, it was assumed that for vented stove emissions, the fraction of PM_{2.5} and CO into the kitchen was approximately $25 \pm 10\%$ (range of 1–50%) of those for unvented stoves. This assumption was conservatively based on comparison of the decrease in the concentration of indoor air pollution between homes using stoves with or without chimneys from the two field campaigns (Cynthia et al. 2008; Johnson et al. 2011; Smith et al. 2010). The assumed 25% and the normal distribution were further adopted in models to simulate and to set indoor emission rate targets (Johnson et al. 2011). The value of 25% was far different from the results of the two laboratory studies mentioned above. It has been widely recognized in pollutant emission studies that due to factors like different operator behaviors and burning conditions, there are substantial differences between lab- and field-based pollutant emission factors, with usually higher values and larger variations in the latter (Roden et al. 2009). Given the importance of fugitive emissions and recognizing gaps in data and knowledge, researchers are calling for

evidence-based experiments on fugitive emission characterization, especially under real-world conditions.

Shen et al. (2020) developed a new field fugitive emission study method and quantified field-based fugitive emission fractions (Luo et al. 2021; Shen et al. 2020). The fraction of fugitive CO emissions to the total emissions ranged from $10.9 \pm 9.2\%$ for corn cob burning to $21.6 \pm 17.1\%$ for wood combustion, with an average fraction of $13.5 \pm 10.3\%$. For PM_{2.5}, the average fugitive emission fraction was $27.9 \pm 13.7\%$, ranging from $12.1 \pm 4.0\%$ for corn cob burning to $36.7 \pm 15.0\%$ for wood combustion. An ANOVA result showed that differences among fuel types were statistically insignificant. The fugitive fractions of PM_{2.5} were significantly higher than those of CO ($p < 0.05$), as found in past laboratory tests (Jetter 2016; Ruiz-Garcia et al. 2018). Ruiz-Garcia et al. (2018) thought that the higher fractions for PM_{2.5} may be due to greater fractions of PM_{2.5} escaping during lighting or due to emissions from larger fuel pieces sticking out of the fuel chamber (Ruiz-Garcia et al. 2018). Different dispersion and transport abilities between fine particles and gases like CO may also result in the fugitive fraction difference.

The field-based fugitive fractions presented here are much higher than those in the previous two lab studies, which were $<5\%$. Besides the stove and fuel differences, different testing conditions and quantitative approaches may have caused the discrepancy. There may be similar differences in fugitive emissions and the fraction of fugitive to total emissions between lab- and field-based measurements (Fig. 1). In comparison with the default value of 25% used in the development of WHO guidelines for IAQ: Household fuel combustion, the CO fugitive fraction found ($13.5 \pm 10.3\%$) was much lower ($p < 0.001$), but the fugitive fraction for PM_{2.5}

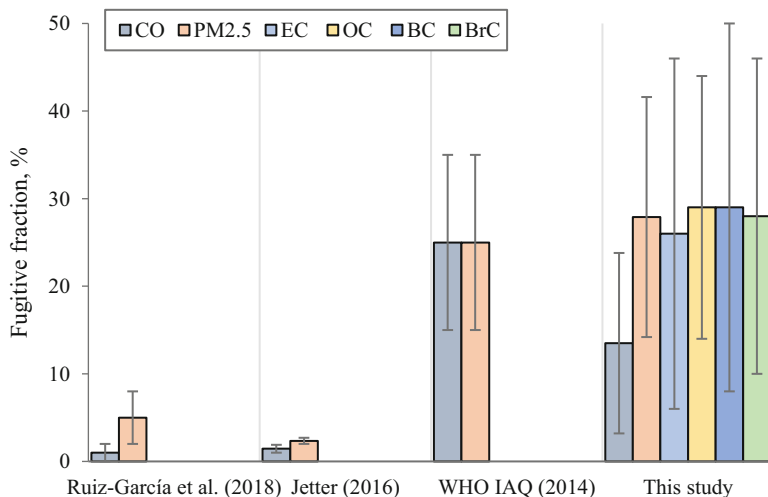


Fig. 1 Comparison of fugitive fractions in two previous lab studies, the default values used in the development of guidelines for IAQ: Household fuel combustion, and values from the field-based study presented here

($27.9 \pm 13.7\%$) was not significantly different from 25% ($p > 0.05$). There was no significant correlation between CO and PM_{2.5} fugitive fractions. The fractions of fugitive emissions of EC and OC were recorded as $26 \pm 20\%$ and $29 \pm 15\%$, respectively, with no significant differences found across different biomass fuels. Average fractions of fugitive values for BC (black carbon) and BrC (brown carbon) were $29 \pm 21\%$ and $28 \pm 18\%$, respectively.

Using a single-zone model (Johnson and Chiang 2015) and assuming that cooking activities occur 3 times a day (for 30 min in the morning and at noon and for 1.0 h in the evening), modelled increments for 24-h-averaged PM_{2.5}, EC, and OC concentrations reached as high as 342 (interquartile range of 251–623), 9.46 (3.59–18.4), and 42.4 (23.9–96.1) $\mu\text{g}/\text{m}^3$ with peak concentrations of 5880, 163, and 728 $\mu\text{g}/\text{m}^3$, respectively. Noted that these indoor concentrations estimates are highly variable, depending on the emission rates and indoor-outdoor air exchange rates. The results here were only semi-quantitatively, but show the high indoor pollution concentrations from the fugitive emissions from vented stoves. While the modelled results are associated with relatively large variations, a few previous field monitoring studies have reported hundreds of $\mu\text{g}/\text{m}^3$ in daily PM_{2.5} with peaks of tens of mg/m^3 for rural households (Qiu et al. 2019), indicating strong indoor air quality contributions and consequently significant adverse health impacts of solid fuel combustion. These studies clearly demonstrate that the simultaneous measurement of indoor and outdoor emissions and air quality is crucial to understanding mechanisms of the environmental impacts of indoor combustion sources. It is necessary and important to evaluate the fugitive emission impacts on indoor air quality in future work.

Household Air Pollution

For most air pollutants in rural homes using solid fuels, HAP in kitchen is often more severe than that in living room and ambient air. Utilization of clean modern energies can reduce HAP effectively for most air pollutants. However, large variations in pollutant concentrations are often reported from the different household structures, various stove-fuel types, meteorological factors, and spatiotemporal conditions (Du et al. 2018a).

CO is one typical gaseous pollutant from incomplete combustion processes. Most HAP studies measured CO. CO was generally higher in winter than that in summer, although the difference might be statistically not significant in some cases (Du et al. 2018a) due to high variations. The kitchen CO in literature ranged from 0.1 to 35 mg/m^3 in summer in homes using solid fuels, and from 0.4 to 30 mg/m^3 in winter. The concentration was generally lower in bedroom than that in kitchen. However, Edwards et al. (2007) observed higher CO concentrations in the bedroom than the CO in the kitchen in the winter of 2002–2003 in rural Shanxi Province, northern China. Data compiled from the literature showed that the difference between homes using solid and nonsolid fuels was statistically not significant, when the comparison was not adjusted for other influencing factors. For homes using gaseous fuels, the

kitchen CO ranged from 2.8 to 12 mg/m³, while in homes using traditional solid fuels, CO had a larger variation across different studies (Du et al. 2018a).

SO₂ contamination is a serious issue particularly in homes burning coal. Indoor SO₂ concentration in rural areas vary largely in 2–3 orders of magnitude, ranging from several to a few thousand µg/m³. The contamination is considerably higher in kitchen compared to the bedroom and outdoor air. The wintertime SO₂ was often reported to be higher than that in summer, and explained by more coal uses for space heating in cold days. SO₂ was also detected in homes using nonsolid fuels, with relatively lower levels compared to that in solid fuel use homes.

TSP or PM₁₀ are often studied in early years, and now, there are more concerns on fine particles (PM_{2.5}, PM_{1.0}) and even ultrafine particles. High wintertime levels, in both indoor and outdoor air, were often reported. For the site difference, there were generally higher concentrations in kitchen than that in bedroom, and lower concentrations in outdoor air. Studies from China showed that the outdoor PM₁₀ in rural areas ranged from 23 to 770 µg/m³, with an arithmetic mean of 261 µg/m³, which was nearly 1.7 times the China National Air Quality Standard of 150 µg/m³, and more than 17 times the new standard of 15 µg/m³ (WHO 2021). The PM_{2.5} ranged from 10 to 460 µg/m³, often exceeding the standards of 15 µg/m³ (WHO 2021). The indoor levels from homes using clean fuels like gas and electricity were lower than those using solid fuels, but serious HAP issue with PM_{2.5} exceeding the standard by several times did still exist in many gas-use households, due to the neighboring effect, unignorable emissions from gas burning, and short-circuiting of air pollution.

Polycyclic aromatic hydrocarbons (PAHs) consist of numerous individual compounds with multiple aromatic rings, existing in either gaseous or particulate phases, but a number of studies reported only particulate PAHs. High indoor pollution levels than the outdoor concentration appeared to be much more significant for PAHs compared to other pollutants, as well as the difference between winter and summer. PAHs are largely produced from the burning of solid fuels, and residential coal and biomass burning is a major source of PAHs globally in many developing countries. The indoor BaP concentration was significantly lower in homes burning LPG compared to that in homes burning solid fuels, but even in those using clean household energies, the indoor BaP levels can exceed the standard of 1.2 ng/m³ set by the WHO (2000), causing adverse health outcomes. Most studies are confined to only the US EPA's designated 16 priority PAHs, or 15 priority PAHs excluding naphthalene as it is volatile and has large measurement uncertainties compared to other PAHs. Chen et al. (2016) measured 28 PAHs including 16 priority PAHs and 12 non-priority ones, in rural Shanxi Province, northern China. Although the mass concentrations of the 12 non-priority ones comprised only about 16%, 8%, and 1% of targeted 28 PAHs in the kitchen, bedroom, and outdoors, respectively. Some of the non-priority compounds are more toxic than the priority ones. Besides parent PAHs, there are concerns on PAHs derivatives like nitrated and oxygenated PAHs which might be more toxic compared to the parent ones. Contamination, transformation, and impacts of these toxic non-priority PAHs in rural areas should be investigated.

Measurements of other pollutants, including but not limited to OC, BC, EC, fluoride, heavy metals, and NOx, led to the following conclusions: higher

concentrations in summer than in winter; higher in indoor than in outdoor; higher in bad ventilation than in good ventilation; more severe in kitchen than in bedroom; and coal > fuelwood > LPG/biogas.

Indoor-Outdoor Ratio

The indoor/outdoor ratio (I/O) is often calculated as an indicator to exchange direction and strength of the exchange between indoor and ambient environments (Chen and Zhao 2011). The I/O value is influenced by many factors, such as stove/fuel combinations, ventilation, the type of air pollutants, and so on.

Studies on I/O ratios of PMs indicated strong impacts of internal sources in rural areas (Huang et al. 2017). The PM that leaked from the cookstoves increased the indoor PM concentrations, which then became concentrated due to the low air exchange rates between the indoor and outdoor air during the local cold winter. Alternatively, diffusion and dilution of particles in outdoor air were usually much stronger than that in indoor air, leading to lower outdoor concentrations of PM. In urban areas, however, the concentrations of indoor PM were generally lower than those outdoors, and a few cases with elevated indoor concentrations were mainly attributed to the infiltration of outdoor PM (Diapouli et al. 2011), which supports the role of rural indoor burning of solid fuels to produce higher concentrations of PM indoors. Du et al. (2017a) reported that for homes using clean fuels, outdoor air pollution is an important contributor to indoor air pollution, while for homes using traditional solid fuels, indoor combustion sources are the main sources of both indoor and outdoor pollution.

I/O ratios larger than 1.0 were also reported for other pollutants including OC, EC, and PAHs. For example, Du et al. (2017b) reported the indoor/outdoor ratios (I/O) for EC, OC, PM_{2.5}, and TSP in homes burning coal were 4.1 (1.1–10 as range), 3.3 (1.9–6.0), 4.6 (1.6–12), and 4.5 (1.9–10), respectively, while for homes burning wood, they were 1.7 (0.93–3.1), 2.5 (0.85–4.4), 2.2 (1.9–3.5), and 2.4 (1.5–4.0), respectively, suggesting significant contributions from indoor sources. The average I/O value for PAH in rural Shanxi, north China, was reported to be 1.8 (0.5–3.8), and was 2.6 (0.9–7.1) in Guizhou, south China (Du et al. 2018b). Although in many studies, stoves were equipped with outdoor chimneys, fugitive emissions may still lead to considerable amounts of air pollutants into indoor air directly.

Exposure and Influencing Factors

Quantification of Exposure

Inhalation exposure is one main pathway of the air pollution. The overall exposure depends on not only outdoor air pollution, but indoor air quality and exposure activities like time spent in different microenvironments and respiratory rates. Some studies estimate time-weighted exposure concentrations based on measured

indoor and outdoor air pollutant concentrations and the time spent in these environments (Mestl et al. 2007). Despite relatively high price of individual samplers and the need of high levels of cooperation from the residents, personal portable samplers are expected to have a more accurate assessment on daily inhalation exposure and have gained popularity in more recent studies. Because of temporal variations in area concentrations (e.g., peak concentrations during a cooking period) and numbers of different microenvironments, there are considerable biases and uncertainties in this indirect estimation approach compared to the direct measurement using personally carried samplers. For instance, a summertime study in rural Shanxi Province by Huang et al. (2017) found that the calculated time-weighted PM average was generally positively correlated with the direct measurement, but the former was ~30% lower. Shen et al. (2014) also found that the inhalation exposure to BaPeq calculated from area concentrations was underestimated by 31–65% compared to the concentration from the personal samplers.

Contribution of Indoor Exposure

As mentioned above, there could be large differences in air pollutant concentrations between the indoor and outdoor air. In the case of no strong internal sources, outdoor air pollution could be a significant source of indoor air pollution, which is known as ambient-originated indoor pollution. In this case, if only using the outdoor pollution concentration in assessing exposure and health risks, the overall exposure would be overestimated. Xiang et al. (2019) estimates that indoor exposures accounted for 66–87% of the total exposure to PM_{2.5} originating outdoors and consequently contributed up to three-quarters of the PM_{2.5}-associated premature deaths in urban China in 2015. Li et al. (2016) reported in an urban area from the northwest China, where coal, gas, and electricity are used for cooking and heating, 75% of the total exposure was attributed to indoor PM_{2.5} exposure. High indoor levels and indoor exposure contributions were observed in the heating period compared to the non-heating period. In case of strong internal sources like solid fuel combustion in rural areas, high indoor pollution concentrations and longer time spent indoors result in high contributions of indoor exposure to the total exposure. For example, in Shanxi Province, Huang et al. (2017) reported that the kitchen PM_{2.5} was the highest ($376 \pm 573 \mu\text{g}/\text{m}^3$), nearly 3 times of the bedroom concentration of $114 \pm 81 \mu\text{g}/\text{m}^3$, and significantly higher than that outdoors at $64 \pm 28 \mu\text{g}/\text{m}^3$. In another study in rural southwestern China, the PM_{2.5} difference between kitchens ($101 \pm 56 \mu\text{g}/\text{m}^3$) and living rooms ($99 \pm 46 \mu\text{g}/\text{m}^3$) was not significant, but both were much higher than the ambient air pollution (Qi et al. 2019). The field study by Huang et al. (2021) reported that the indoor PM_{2.5} exposure for the population using biomass fuels contributed to over 80% to the total exposure in the Eastern Tibetan Plateau area. Recently, a nationwide modeling study in rural China demonstrated that indoor PM_{2.5} inhalation exposure ($80 \mu\text{g}/\text{m}^3$) occupied 95% of the total exposure ($84.5 \mu\text{g}/\text{m}^3$). The higher contribution was more significant for the rural population (94%) where the indoor PM_{2.5} concentration ($95 \pm 34 \mu\text{g}/\text{m}^3$) was much higher than

that in urban areas ($58 \pm 23 \mu\text{g}/\text{m}^3$) because of the strong dependence on solid fuels as household energy sources (Yun et al. 2020). Therefore, compared to outdoor exposure, indoor inhalation exposure contributes largely to the weighted total exposure.

Influencing Factors

Personal exposures varied largely depending on various factors like fuel-stove systems used, activity patterns like time spent indoors and outdoors, and indoor-outdoor air exchanges which are affected by factors like household structure, window-opening, etc. In countries like China and Mongolia, the highest exposure concentrations were generally in cold seasons when home heating was needed and solid fuels like coal and wood are burned. For example, Du et al. (2017a), using personal carried samplers, estimated that the daily exposure to PM_{2.5} were $451 \pm 301 \mu\text{g}/\text{m}^3$ for the population from the north where traditional solid fuels were used for daily cooking and heating, and the concentrations were twice the exposure to PM_{2.5} among the population who do not heat homes by burning solid fuels. Compiled data on HAP exposure in rural China showed that the overall geometric means of exposure to PM_{2.5} among the rural residents of northern and northeastern China in summer ($121 \mu\text{g}/\text{m}^3$) were nearly one-third of that in winter ($359 \mu\text{g}/\text{m}^3$), and in the southwestern regions, the daily exposure concentrations were 160 and $69 \mu\text{g}/\text{m}^3$ in winter and other seasons (spring, summer, and fall), respectively (Du et al. 2018a).

The gender difference in HAP exposure was observed in rural areas. In many developing countries, women often undertake housework, such as cooking, and spend more time in kitchen. Exposure concentrations for the children are also high because of longer time indoors. Therefore, the exposure concentrations are generally in the sequence of women > children > men (Li et al. 2017). The wintertime study by Pan et al. (2001) in rural Anhui Province, eastern China, also found that the daily inhalation exposure to PM₁₀ for males ($556 \pm 535 \mu\text{g}/\text{m}^3$) was lower than that for the females ($659 \pm 646 \mu\text{g}/\text{m}^3$). The exposure to BaP eq was nearly twice as high for the cook compared to the non-cook (Shen et al. 2014).

Exposure could vary largely among the population using different fuel-stove systems. Shen et al. (2016) reported the inhalation exposure concentrations to air pollutants for the rural residents using wood gasifier burners were significantly lower than those burning wood in traditional built-in brick stoves, and comparable to those using LPG and electricity.

Recently, Shupler et al. (2020) measured household and personal PM_{2.5} exposures in 120 communities in 8 countries (including Bangladesh, Chile, China, Colombia, India, Pakistan, Tanzania, and Zimbabwe). As seen from Fig. 2, the exposure concentration for the population using clean energies (e.g., gas and electricity) is much lower than those using dirty fuels (e.g., coal, crop waste, wood, animal dung, and shrubs/grass). However, there were no significant differences between males and females in their PM_{2.5} and black carbon exposures across the

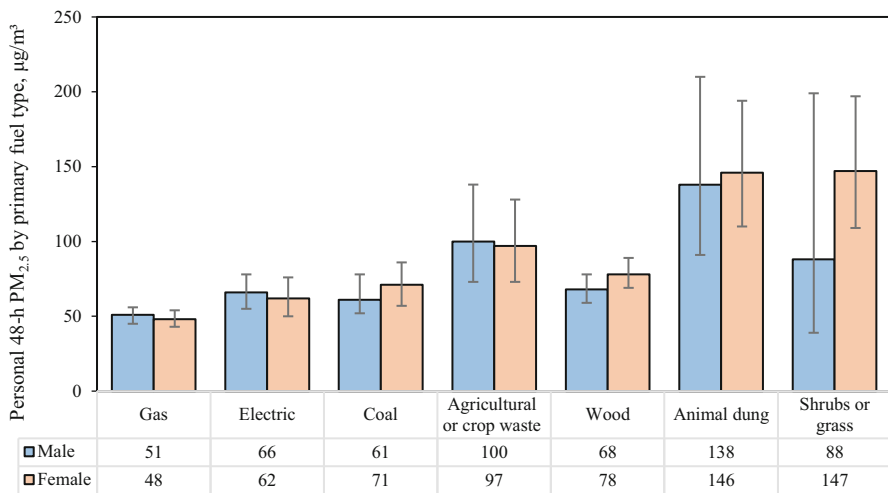


Fig. 2 Summary of 48-h average $\text{PM}_{2.5}$ personal exposures by the primary fuel type. Data was from a study in 120 communities in 8 countries by Shupler et al. (2020)

eight countries. In Bangladesh and Pakistan, where biomass fuels are widely used, females had higher $\text{PM}_{2.5}$ and black carbon exposure were much higher compared to the exposure for males. In populations using clean energies like gas and electricity, the exposure differences between the male and the female are small.

Health Risks Associated with HAP

Estimates of HAP-Related Health Impacts

Adverse health outcomes associated with household air pollution have been reported in mounting empirical studies, and some provides valuable exposure-dose relationship which is critical in accurately quantifying the outcomes. For example, Alim et al. (2014) conducted a cross-sectional survey in Bangladesh and compared the occurrence of respiratory symptoms between adult women using biomass fuels in rural areas and adult women using gas fuels in urban areas. The prevalence of respiratory symptoms and diseases investigated in biomass users was significantly higher than that among the gas fuel users. Albers et al. (2019) studied the association between latent tuberculosis infection (LTBI) and household fuel use in Nepal. Among the population aged 18–70 years, cooking with biogas reduced LTBI compared to cooking with wood and LPG. Kerosene is still used for cooking or lighting in some developing countries. Arku et al. (2020) found the risk of cardiovascular and respiratory mortality for kerosene users was 20–47% higher than that for solid fuel users.

Using low-cost sensors and cause-specific mortality database in China, Dong et al. (2020) found that an increase of $10 \mu\text{g}/\text{m}^3$ in the time-averaged $\text{PM}_{2.5}$ exposure was associated with increased daily mortality estimates of approximately 0.44–0.69% for the total non-accidental causes, cardiovascular diseases, coronary heart disease, stroke, respiratory diseases, chronic obstructive pulmonary disease, respectively. The study also showed that the risk would be underestimated if only ambient $\text{PM}_{2.5}$ exposure was considered.

Premature deaths and disability-adjusted life years (DALYs) are usually estimated to quantitatively evaluate the burden of disease. DALYs for a disease or health condition are the sum of the years of life lost (YLL) due to premature mortality in the population and the years lost due to disability (YLD) for incident cases of the health condition: $\text{DALY} = \text{YLL} + \text{YLD}$ (WHO 2010b). The Global Burden of Disease Study shows that in 2019 (GBD 2019), premature deaths associated with exposure to $\text{PM}_{2.5}$ from solid fuel use were 2.3 million. The DALY was 91,474,469 that was nearly 9 times of that caused by exposure to ambient particulate matter pollution (18,215,374). Adverse health outcomes were mostly in developing countries, including China, India, and the African countries, attributed to dirty fuels, stoves with low thermal efficiency, poor indoor ventilation, and large populations using solid fuels.

The health impacts of HAP exposures for the sensitive group like the infants, children, pregnant women, and the old requires more attention. Bates et al. (2013) found the increase in acute lower respiratory infection (ALRI) in the childhood was associated with the use of biomass stoves, kerosene stoves, and gas stoves, as opposed to electric cooking. Compared with no heating or clean heating (gas or electricity), the use of dirty fuels like wood, kerosene, or coal for heating was also associated with higher ALRI. Persistent cough in the first year of infant life are related to gas stoves and wood-burning stoves (Belanger et al. 2003). Alexander et al. (2017) investigated the influence of clean cookstoves intervention on blood pressure for the pregnant women, in which they found that before the intervention, 8.8% of the kerosene users had hypertension, while 1.8% of the ethanol users ($p = 0.029$). After the intervention, ethanol cookstoves reduced diastolic blood pressure and hypertension during pregnancy.

Amplified Contribution and Clean Household Energy Transition

Based on the updated emissions from on-site emission measurements and a new database of household energy, Yun et al. (2020) estimated that in China, although the residential sector contributed only 7.5% of total energy consumption, the sector contributed 27% of primary $\text{PM}_{2.5}$ emissions; 23% and 71% of the outdoor and indoor $\text{PM}_{2.5}$ concentrations, respectively; 68% of $\text{PM}_{2.5}$ exposure; and 67% of $\text{PM}_{2.5}$ -induced premature deaths in 2014, showing a progressive order of magnitude increases from sources to receptors. The study also found that biomass fuels and coal had comparable contributions to the adverse health impacts. Rural populations are suffering more from severe household air pollution compared to urban populations.

To reduce adverse health outcomes, also in response to climate impacts of climate-relevant pollutants like BC from the residential sector, clean household energies like electricity and gas fuels are being promoted for cooking or heating. Shen et al. (2017) evaluated PM_{2.5} and UFP emissions for 11 fuel-stove combinations, finding that LPG and alcohol combustion emitted $\sim 10^{11}$ particles per useful energy delivered (particles/MJ_d), and burning of kerosene had $\sim 10^{13}$ particles/MJ_d, while solid fuels, including pellet, wood, charcoal, and rice hulls, had higher UFP emissions by 2–3 orders of magnitude (10^{14} – 10^{15} particles/MJ_d). PM_{2.5} EFs, on the basis of useful energy delivered, are also much lower for the liquid and gas fuels: alcohol < LPG < kerosene < solid fuels. For EC and PAHs, the emissions from clean fuels are also lower (Shen 2015).

However, in some studies, the use of clean fuels did not always reduce health risks. A case-control study by Bates et al. (2019) showed that the women using LPG stoves had higher pulmonary tuberculosis risks than those who used wood or biogas stoves, which might be explained by more ultrafine particle emissions. Amaral et al. (2014) suggested that the gas cooking may cause the increase of bronchial responsiveness compared with electricity.

Generally, with the socioeconomic development, many households are switching to clean energies, but fuel and stove stacking are common since one single fuel or stove cannot meet all household energy consumption demands. Zhu et al. (2019), based on a national survey of household energy, pointed out that the stacking phenomena is more and more obvious. The number of household energy types increased significantly between 1992 and 2012, especially in northern areas where there is a need for heating. The number of household energy types was positively correlated with the heating degree days, and negatively with the household income. The mixed use of fossil fuels and biomass may result in more energy consumption (about 20–40%). Because of the common “stacking” approach, the proportion of coal use may be underestimated if only the main energy source was counted in household survey. In addition, the transition rates are different between the cooking energy and heating energy, and there are large spatial differences. Clean transitions first appear in more developed areas, followed by a clean transition in inland provinces after 5–10 years in rural China.

To fight against high wintertime air pollution from widespread space heating burning coals in northern China, China launched a clean heating campaign (CHC) in “2 + 26” cities. Although CHC-1 aims to reduce outdoor air pollution, it had a positive impact on improving indoor air quality (Meng et al. 2020). It was estimated that if the goal of clean heating was achieved by 60%, the primary PM_{2.5} emissions and outdoor PM_{2.5} concentration will be reduced by 70% and 60%, respectively, and meanwhile indoor PM_{2.5} concentrations would be reduced from 209 $\mu\text{g}/\text{m}^3$ to 125 $\mu\text{g}/\text{m}^3$. Consequently, the overall exposure would decrease from 140 $\mu\text{g}/\text{m}^3$ to 78 $\mu\text{g}/\text{m}^3$. If the clean substitution targets were all met, the population exposure concentration would be further reduced to 61 $\mu\text{g}/\text{m}^3$. The clean heating campaign usually requires a fixed proportion of clean heating in each region, but in fact, the realization of the situation in each city is very different. The differences are related to

socioeconomic differences as well as geographical conditions across the region. If differentiated clean heating goals were set according to the actual situation in different places, there would be greater health benefits. The differentiated target could have prevented 30,000 (23,000–34,000) premature deaths in the region, compared to 26,000 (21,000–31,000) premature deaths averted by a fixed clean heating ratio (Meng et al. 2020).

Conclusions

Indoor solid fuel use is an important source of indoor air pollution, especially in many rural areas. Though transition to cleaner modern household energies like electricity and gaseous fuels did occur in many places, especially for cooking, high indoor pollution levels and adverse health outcomes associated with indoor exposure are still often reported. In homes relying on traditional solid fuels, high indoor-outdoor ratios indicated significant impacts of internal combustion sources on indoor air quality and human health. Indoor air pollutant concentrations in literature vary largely across different studies, because of various influencing factors like fuel-stove systems, household characteristics, and meteorological conditions.

Indoor exposure can account for >80% of the total exposure, due to high indoor pollution levels and longer time spent indoors for most population. Exposure to PM_{2.5} associated with indoor solid fuel use causes millions of premature deaths every year, with high deaths in developing countries in east and south Asia, and Africa. Adoption of cleaner household energy and improved low-emission stoves has been demonstrated to lower health risks.

Access to affordable modern household energy is an important part of sustainable development. Indoor air pollution in rural areas, not only from indoor solid fuel use but also other indoor sources, is also concerned in environmental health equality. Adoption of cleaner energies and improved stoves should be encouraged, but it is always not just a technical issue. Future studies are called to evaluate enablers and barriers in clean fuel and stove adoption and sustainable use. Consequent impacts on health and regional climate need to be assessed. It would be also interesting and vitally important to link the health outcomes associated with HAP exposure with unique biomarkers and epidemiological studies. Such studies would enrich our understanding on the adverse impacts of HAP in support of decision-making (Samet et al. 2022; Kinney 2022).

Cross-References

- [Appliances for Cooking, Heating, and Other Energy Services](#)
- [Cooking Aerosol](#)
- [Impact of Outdoor Particles on Indoor Air](#)
- [Indoor Air Quality in the Context of Climate Change](#)

References

- Albers AE, Pope K, Sijali TR, Subramanya SH, Verma SC, Bates MN (2019) Household fuel use and latent tuberculosis infection in a Nepali population. *Environ Res* 173:69–76
- Alexander D, Northcross A, Wilson N, Dutta A, Pandya R, Ibigbami T et al (2017) Randomized controlled ethanol cookstove intervention and blood pressure in pregnant Nigerian women. *Am J Respir Crit Care Med* 195:1629–1639
- Alim MA, Sarker MAB, Selim S, Karim MR, Yoshida Y, Hamajima N (2014) Respiratory involvements among women exposed to the smoke of traditional biomass fuel and gas fuel in a district of Bangladesh. *Environ Health Prev* 19:126–134
- Amaral AFS, Ramasamy A, Castro-Giner F, Minelli C, Accordini S, Sorheim I-C et al (2014) Interaction between gas cooking and gstm1 null genotype in bronchial responsiveness: results from the European community respiratory health survey. *Thorax* 69:558–564
- Anenberg SC, Balakrishnan K, Jetter J, Masera O, Mehta S, Moss J et al (2013) Cleaner cooking solutions to achieve health, climate, and economic cobenefits. *Environ Sci Technol* 47: 3944–3952
- Arku RE, Brauer M, MyLinh D, Wei L, Hu B, Tse LA et al (2020) Adverse health impacts of cooking with kerosene: a multi-country analysis within the prospective urban and rural epidemiology study. *Environ Res* 188:109851
- Bates MN, Chandyo RK, Valentiner-Branth P, Pokhrel AK, Mathisen M, Basnet S et al (2013) Acute lower respiratory infection in childhood and household fuel use in Bhaktapur, Nepal. *Environ Health Perspect* 121:637–642
- Bates MN, Pope K, Sijali TR, Pokhrel AK, Pillarisetti A, Lam NL et al (2019) Household fuel use and pulmonary tuberculosis in western Nepal: a case-control study. *Environ Res* 168: 193–205
- Belanger K, Beckett W, Triche E, Bracken MB, Holford T, Ren P et al (2003) Symptoms of wheeze and persistent cough in the first year of life: associations with indoor allergens, air contaminants, and maternal history of asthma. *Am J Epidemiol* 158:195–202
- Bond T (2022) Indoor air chemical pollutants: cooking, heating appliances. In: Zhang Y, Hopke PK, Mandin C (eds) *Handbook of indoor air quality*. Springer, Singapore
- Bonjour S, Adair-Rohani H, Wolf J, Bruce NG, Mehta S, Pruess-Ustuen A et al (2013) Solid fuel use for household cooking: country and regional estimates for 1980–2010. *Environ Health Perspect* 121:784–790
- Chen C, Zhao B (2011) Review of relationship between indoor and outdoor particles: I/O ratio, infiltration factor and penetration factor. *Atmos Environ* 45:275–288
- Chen C, Zhao B (2022) Indoor air particles: impact of outdoor particles on indoor air. In: Zhang Y, Hopke PK, Mandin C (eds) *Handbook of indoor air quality*. Springer, Singapore
- Chen Y, Shen G, Huang Y, Zhang Y, Han Y, Wang R et al (2016) Household air pollution and personal exposure risk of polycyclic aromatic hydrocarbons among rural residents in Shanxi, China. *Indoor Air* 26:246–258
- Clark ML, Peel JL, Balakrishnan K, Breyssse PN, Chillrud SN, Naeher LP et al (2013) Health and household air pollution from solid fuel use: the need for improved exposure assessment. *Environ Health Perspect* 121:1120–1128
- Coffey ER, Muvandimwe D, Hagar Y, Wiedinmyer C, Kanyomse E, Piedrahita R et al (2017) New emission factors and efficiencies from in-field measurements of traditional and improved cookstoves and their potential implications. *Environ Sci Technol* 51:12508–12517
- Cynthia AA, Edwards RD, Johnson M, Zuk M, Rojas L, Jimenez RD et al (2008) Reduction in personal exposures to particulate matter and carbon monoxide as a result of the installation of a patsari improved cook stove in michoacan Mexico. *Indoor Air* 18:93–105
- Diapouli E, Eleftheriadis K, Karanasiou AA, Vratolis S, Hermansen O, Colbeck I et al (2011) Indoor and outdoor particle number and mass concentrations in Athens. Sources, sinks and variability of aerosol parameters. *Aerosol Air Qual Res* 11:632–642

- Dong Z, Wang H, Yin P, Wang L, Chen R, Fan W et al (2020) Time-weighted average of fine particulate matter exposure and cause-specific mortality in China: a nationwide analysis. *Lancet Planet Health* 4:E343–E351
- Du W, Shen GF, Chen YC, Zhuo SJ, Xu Y, Li XY et al (2017a) Wintertime pollution level, size distribution and personal daily exposure to particulate matters in the northern and southern rural Chinese homes and variation in different household fuels. *Environ Pollut* 231:497–508
- Du W, Shen GF, Chen YC, Zhu X, Zhuo SJ, Zhong QR et al (2017b) Comparison of air pollutant emissions and household air quality in rural homes using improved wood and coal stoves. *Atmos Environ* 166:215–223
- Du W, Li X, Chen Y, Shen G (2018a) Household air pollution and personal exposure to air pollutants in rural China – a review. *Environ Pollut* 237:625–638
- Du W, Chen Y, Zhu X, Zhong Q, Zhuo S, Liu W et al (2018b) Wintertime air pollution and health risk assessment of inhalation exposure to polycyclic aromatic hydrocarbons in rural China. *Atmos Environ* 191:1–8
- Edwards RD, Li Y, He G, Yin Z, Sinton J, Peabody J et al (2007) Household CO and PM measured as part of a review of China's national improved stove program. *Indoor Air* 17:189–203
- Garland C, Delapena S, Prasad R, L'Orange C, Alexander D, Johnson M (2017) Black carbon cookstove emissions: a field assessment of 19 stove/fuel combinations. *Atmos Environ* 169: 140–149
- Global Burden of Disease Collaborative Network. Global Burden of Disease Study 2019 (GBD) (2019) Results. Institute for Health Metrics and Evaluation (IHME), Seattle, 2020. <http://ghdx.healthdata.org/gbd-results-tool>
- Guarnieri M, Diaz E, Pope D, Eisen EA, Mann J, Smith KR et al (2015) Lung function in rural Guatemalan women before and after a chimney stove intervention to reduce wood smoke exposure results from the randomized exposure study of pollution indoors and respiratory effects and chronic respiratory effects of early childhood exposure to respirable particulate matter study. *Chest* 148:1184–1192
- Hartinger SM, Commodore AA, Hattendorf J, Lanata CF, Gil AI, Verastegui H et al (2013) Chimney stoves modestly improved indoor air quality measurements compared with traditional open fire stoves: results from a small-scale intervention study in rural Peru. *Indoor Air* 23:342–352
- Huang Y, Du W, Chen YC, Shen GF, Su S, Lin N et al (2017) Household air pollution and personal inhalation exposure to particles (TSP/PM_{2.5}/PM_{1.0}/PM_{0.25}) in rural Shanxi, north China. *Environ Pollut* 231:635–643
- Huang Y, Wang J, Fu N, Zhang S, Du W, Chen Y et al (2021) Inhalation exposure to size-segregated fine particles and particulate pahs for the population burning biomass fuels in the eastern Tibetan Plateau area. *Ecotoxicol Environ Saf* 211:111959
- Jetter J (2016) Test report – in stove 60-liter institutional stove with wood fuel – air pollutant emissions and fuel efficiency. Report EPA/625/R-16/003. U.S. Environmental Protection Agency, Washington, DC
- Jetter J, Zhao Y, Smith KR, Khan B, Yelverton T, DeCarlo P et al (2012) Pollutant emissions and energy efficiency under controlled conditions for household biomass cookstoves and implications for metrics useful in setting international test standards. *Environ Sci Technol* 46:10827–10834
- Jiang R, Bell ML (2008) A comparison of particulate matter from biomass-burning rural and non-biomass-burning urban households in northeastern China. *Environ Health Perspect* 116:907–914
- Johnson M, Edwards R, Morawska L, Smith K, Nicas M (2011) WHO Indoor air quality guideline: household fuel combustion. Review 3: model for linking household energy use with indoor air quality. <https://www.who.int/airpollution/guidelines/household-fuelcombustion>. Assessed Nov 2021
- Johnson M, Chiang R (2015) Quantitative guidance for stove usage and performance to achieve health and environmental targets. *Environ Health Perspect* 123:820–826
- Kinney P (2022) Special indoor environments: Indoor Air Quality in the Context of Climate Change. In: Zhang Y, Hopke PK, Mandin C (eds) *Handbook of indoor air quality*. Springer, Singapore

- Lei Y, Zhang Q, He KB, Streets DG (2011) Primary anthropogenic aerosol emission trends for China, 1990–2005. *Atmos Chem Phys* 11:931–954
- Li T, Cao S, Fan D, Zhang Y, Wang B, Zhao X et al (2016) Household concentrations and personal exposure of PM_{2.5} among urban residents using different cooking fuels. *Sci Total Environ* 548: 6–12
- Li Q, Jiang J, Wang S, Rumchev K, Mead-Hunter R, Morawska L et al (2017) Impacts of household coal and biomass combustion on indoor and ambient air quality in China: current status and implication. *Sci Total Environ* 576:347–361
- Luo Z, Zhang L, Li G, Du W, Chen Y, Cheng H et al (2021) Evaluating co-emissions into indoor and outdoor air of EC, OC, and BC from in-home biomass burning. *Atmos Res* 248:105247
- Meng W, Shen H, Yun X, Chen Y, Zhong Q, Zhang W et al (2020) Differentiated-rate clean heating strategy with superior environmental and health benefits in northern China. *Environ Sci Technol* 54:13458–13466
- Mestl HES, Aunan K, Seip HM, Wang S, Zhao Y, Zhang D (2007) Urban and rural exposure to indoor air pollution from domestic biomass and coal burning across China. *Sci Total Environ* 377:12–26
- Mortimer K, Ndamala CB, Naunje AW, Malava J, Katundu C, Weston W et al (2017) A cleaner burning biomass-fuelled cookstove intervention to prevent pneumonia in children under 5 years old in rural Malawi (the cooking and pneumonia study): a cluster randomised controlled trial. *Lancet* 389:167–175
- Pan X, Dong Z, Jin X, Wang B, Wang L, Xu X (2001) Study on assessment for exposure to air pollution in rural areas. *J Environ Health* 18:323–325. (In Chinese)
- Qi M, Du W, Zhu X, Wang W, Lu C, Chen Y et al (2019) Fluctuation in time-resolved PM_{2.5} from rural households with solid fuel-associated internal emission sources. *Environ Pollut* 244:304–313
- Qiu Y, Tao S, Yun X, Du W, Shen G, Lu C et al (2019) Indoor PM_{2.5} profiling with a novel side-scatter indoor lidar. *Environ Sci Technol Lett* 6:612–616
- Roden CA, Bond TC, Conway S, Pinel ABS, MacCarty N, Still D (2009) Laboratory and field investigations of particulate and carbon monoxide emissions from traditional and improved cookstoves. *Atmos Environ* 43:1170–1181
- Ruiz-Garcia VM, Edwards RD, Ghasemian M, Berrueta VM, Princevac M, Vazquez JC et al (2018) Fugitive emissions and health implications of plancha-type stoves. *Environ Sci Technol* 52: 10848–10855
- Samet J, Deng F, Li R, Yang X, Zhang J, Zheng X et al (2022) Health Effects and Health Risk Assessment. In: Zhang Y, Hopke PK, Mandin C (eds) *Handbook of indoor air quality*. Springer, Singapore
- Shen G (2015) Quantification of emission reduction potentials of primary air pollutants from residential solid fuel combustion by adopting cleaner fuels in China. *J Environ Sci* 37:1–7
- Shen G, Zhang Y, Wei S, Chen Y, Yang C, Lin P et al (2014) Indoor/outdoor pollution level and personal inhalation exposure of polycyclic aromatic hydrocarbons through biomass fuelled cooking. *Air Qual Atmos Health* 7:449–458
- Shen G, Chen Y, Du W, Lin N, Wang X, Cheng H et al (2016) Exposure and size distribution of nitrated and oxygenated polycyclic aromatic hydrocarbons among the population using different household fuels. *Environ Pollut* 216:935–942
- Shen G, Gaddam C, Ebersviller S, Wal RLV, Williams C, Faircloth JW et al (2017) A laboratory comparison of emission factors, number size distributions, and morphology of ultrafine particles from 11 different household cookstove-fuel systems. *Environ Sci Technol* 51:6522–6532
- Shen G, Ru M, Du W, Zhu X, Zhong Q, Chen Y et al (2019) Impacts of air pollutants from rural Chinese households under the rapid residential energy transition. *Nat Commun* 10:1
- Shen G, Du W, Luo Z, Li Y, Cai G, Lu C et al (2020) Fugitive emissions of CO and PM_{2.5} from indoor biomass burning in chimney stoves based on a newly developed carbon balance approach. *Environ Sci Technol Lett* 7:128–134

- Shupler M, Hystad P, Birch A, Miller-Lionberg D, Jeronimo M, Arku RE et al (2020) Household and personal air pollution exposure measurements from 120 communities in eight countries: results from the pure-air study. *Lancet Planet Health* 4:E451–E462
- Smith KR, McCracken JP, Thompson L, Edwards R, Shields KN, Canuz E et al (2010) Personal child and mother carbon monoxide exposures and kitchen levels: methods and results from a randomized trial of woodfired chimney cookstoves in Guatemala (respire). *J Expo Sci Environ Epidemiol* 20:406–416
- Smith KR, McCracken JP, Weber MW, Hubbard A, Jenny A, Thompson LM et al (2011) Effect of reduction in household air pollution on childhood pneumonia in Guatemala (RESPIRE): a randomised controlled trial. *Lancet* 378:1717–1726
- Smith KR, Bruce N, Balakrishnan K, Adair-Rohani H, Balmes J, Chafe Z et al (2014) Millions dead: how do we know and what does it mean? Methods used in the comparative risk assessment of household air pollution. *Annu Rev Public Health* 35:85–206
- Torkmahalleh MA (2022) Indoor air particles: cooking aerosol. In: Zhang Y, Hopke PK, Mandin C (eds) *Handbook of indoor air quality*. Springer, Singapore
- United States Environmental Protection Agency (U.S. EPA). <https://www.epa.gov/indoor-air-quality-iaq/introduction-indoor-air-quality#sources>. Assessed Nov 2021
- Wang R, Tao S, Wang W, Liu J, Shen H, Shen G et al (2012) Black carbon emissions in China from 1949 to 2050. *Environ Sci Technol* 46:7595–7603
- World Health Organization (WHO) (2000) Air quality guidelines for Europe, 2nd edn. World Health Organization
- World Health Organization (WHO) (2010a) WHO guidelines for indoor air quality: selected pollutants. ISBN 978-92-890-0213-4
- World Health Organization (WHO) (2010b) Global burden of disease (GBD), 2010. http://www.who.int/healthinfo/global_burden_disease/en/index.html
- World Health Organization (WHO) (2021) WHO global air quality guidelines. Particulate matter ($PM_{2.5}$ and PM_{10}), ozone, nitrogen dioxide, sulfur dioxide and carbon monoxide. World Health Organization, Geneva
- Xiang J, Weschler CJ, Wang Q, Zhang L, Mo J, Ma R et al (2019) Reducing indoor levels of “outdoor $PM_{2.5}$ ” in urban China: impact on mortalities. *Environ Sci Technol* 53:3119–3127
- Yun X, Shen G, Shen H, Meng W, Chen Y, Xu H et al (2020) Residential solid fuel emissions contribute significantly to air pollution and associated health impacts in China. *Science Advances* 6:eaba7621
- Zhang H, Hu D, Chen J, Ye X, Wang SX, Hao JM et al (2011) Particle size distribution and polycyclic aromatic hydrocarbons emissions from agricultural crop residue burning. *Environ Sci Technol* 45:5477–5482
- Zhang J, Chen W, Liu N, Guo B, Zhang Y (2022) Control: testing and reducing VOC emissions from building materials and furniture to improve indoor air quality. In: Zhang Y, Hopke PK, Mandin C (eds) *Handbook of indoor air quality*. Springer, Singapore
- Zhu X, Yun X, Meng W, Xu H, Du W, Shen G et al (2019) Stacked use and transition trends of rural household energy in mainland China. *Environ Sci Technol* 53:521–529



Indoor Air Quality in the Context of Climate Change 72

Patrick L. Kinney

Contents

Introduction	2146
Key Aspects of the Changing Climate	2147
Impacts of CC on the Indoor Environment	2149
Changes in Activity Patterns Due to and in Parallel with Climate Change	2155
Vulnerability	2155
Implications for IAQ of Climate Adaptation and Mitigation Actions	2156
Conclusions	2160
References	2160

Abstract

There is now unequivocal evidence that the climate is rapidly changing due to the accumulation of anthropogenic warming pollutants (e.g., carbon dioxide, methane) in the Earth's atmosphere. Climate change may affect indoor air quality and associated health impacts via increases in indoor temperatures, higher or lower emissions of pollutants from indoor sources, changes in ambient air pollution driven by climate change, changes in building construction and operations that alter ventilation rates, and changing activity patterns and behaviors, including use of windows and air-conditioning. These changes will be driven not only by climate change itself, but also by efforts to adapt to or mitigate climate change, and will occur in parallel with other societal trends, such as population growth and urbanization, that could impact the built environment and IAQ. Those most vulnerable to climate-related changes in the indoor environment likely include the poor, the elderly, and children. While the challenges posed by climate change for IAQ are not qualitatively new, the pace and complexity of future changes will offer new challenges, as will the societal transformations needed to transition to a

P. L. Kinney (✉)

Department of Environmental Health, Boston University School of Public Health, Boston, MA,
USA

e-mail: pkinney@bu.edu

net zero carbon if we are to avert more severe climate change. Since the residential indoor environment is where individuals who are most vulnerable to climate change are and will continue to be found in the largest numbers, it is critical that policy makers and technology developers focus their efforts on finding ways to keep those places as healthy as possible to all members of society in the face of climate change.

Keywords

Climate change · Adaptation · Mitigation · Ambient pollution · Penetration · Sources · Ventilation · Air exchange · Extreme events

Introduction

Substantial changes in the global climate have been evident since about 1960, and evidence from the past few decades demonstrates accelerating warming and increasing intensity of heat waves, extreme precipitation events, and periods of extreme draught. While the trends are clear on a global basis, these changes exhibit strong regional differences. Models tell us that climate change will continue to accelerate over the next several decades, regardless of societal efforts to mitigate, due to the long-term increase of carbon dioxide (CO_2) in the atmosphere and the inherent inertia in the climate system. This highlights the need for large-scale efforts to adapt to the changing climate. It is important to note that the extent of future climate change depends critically on mitigation actions we take now to reduce societal impact on the climate. Strategies to adapt to or mitigate climate change will likely to be important implications for indoor air quality. For example, in addition to their long-term benefits for reducing climate change, mitigation strategies will likely alter indoor and outdoor air pollution sources, as well as building ventilation characteristics. Finally, it is important to recognize that vulnerability to climate change, as well as the benefits of adaptation and mitigation efforts, will vary substantially across populations due to such factors as income, age, the built environment, and social/governance structures (IOM 2011).

Because we spend most of our time indoors, the majority of people will experience climate change to a large extent through its impacts on the indoor environment. This is especially true for the elderly, infants, and those with chronic illnesses, who spend more time at home and are highly vulnerable to environmental health risks. In addition to direct effects of climate change on rising temperatures, humidity, and precipitation, there are several ways in which climate change could affect indoor air quality and associated health impacts. These include increased indoor temperatures, higher emissions of volatile organic compounds (VOCs) from indoor materials, changes in ambient air pollution driven by climate change and/or by efforts to mitigate it, changes in building construction and operations that alter exchanges between indoor and outdoor air, and changing activity patterns and behaviors, including use of windows and air-conditioning. Some of these changes will be

driven by efforts to adapt to higher temperatures and more intense precipitation events, and others will be driven by efforts to become more energy efficient as society transitions to a low-carbon future. In addition to climate change and society responses to it, there will be simultaneous challenges related to increases in population and urbanization, and related changes in the built environment, particularly in developing countries. Figure 1 illustrates the main drivers and linkages among these diverse factors.

While climate change is likely already affecting the indoor environment, there has been relatively little empirical research so far on IAQ in the context of climate change. Nazaroff notes that the question of how IAQ will be affected by climate change involves a complex system (Nazaroff 2013). While the system as a whole has not been studied, he notes that we do have a good understanding of individual system components and their connections with each other. Based on that understanding, we can make useful inferences about how the system may continue to evolve in a changing climate. In this chapter, we make use of several recent reviews and reports which have explored this complex but important topic (IOM 2011; Spengler 2012; Nazaroff 2013; Vardoulakis et al. 2015).

We begin by summarizing some of the key aspects of climate change, drawing from the 2021 report of the IPCC (IPCC 2021). This is followed by a series of subsections summarizing key pathways by which climate change may impact IAQ. Finally, we consider climate change adaptation and mitigation from the perspective of IAQ.

Key Aspects of the Changing Climate

The fact that the global climate is changing due to anthropogenic drivers is no longer in doubt. In its 2021 report on the physical science basis of climate change, IPCC stated that “It is unequivocal that human influence has warmed the atmosphere, ocean and land,” the most definitive statement ever from this body comprised of leading climate experts from around the world (IPCC 2021). Widespread and rapid changes have occurred, including a rise in global mean surface temperature of 1.09 °C for 2011–2020 as compared to 1850–1900, with substantially larger increases over land than water. From 1970 to 2020, global temperature rose faster than in any other 50-year period for at least the past 2000 years. In addition to temperature change, heavy precipitation events have become more frequent as well as intense. Compound climate events where more than one climate-rated extreme occurs in close proximity in space and/or time have also increased in recent decades. The magnitude of these myriad climate changes is unprecedented over many centuries to many thousands of years, based on the best available science.

Along with climate change, rising CO₂ concentrations in the atmosphere are also striking. IPCC concludes that CO₂ concentrations are higher now than at any time in the last 800K years at least, and the amount of change since 1750 is similar in magnitude to the variations observed between glacial and interglacial periods over that time frame. Given the rate of GHG emissions and the inertia of the earth/climate

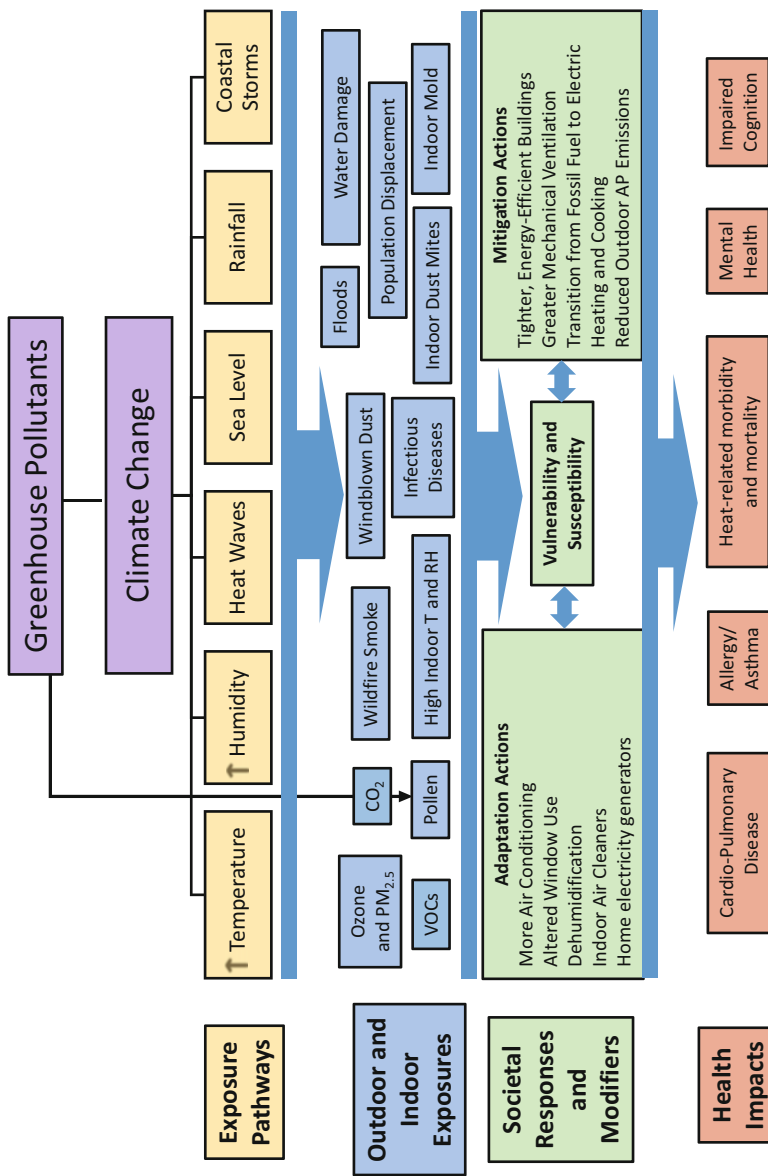


Fig. 1 Key pathways linking climate change to indoor air quality and health

system, scientists expect that temperatures will continue to rise rapidly for several decades this century, with the rate of change and end point being determined by the ability of countries to adhere to ambitious carbon reduction targets. IPCC anticipates additional global warming through 2100 of between 1.4 and 4.4 °C, depending on emission reduction policies. Many of the other climate events, e.g., heat waves, intense storms, droughts, flooding will increase in proportion to the temperature change. Similarly, sea level is virtually certain to continue to rise, by between 0.3 and 1.0 m by 2100 depending on the global GHG emissions trajectory. Unlike temperature, sea level rise is now committed to rise for several centuries to millennia due to the inertia in the earth/ocean/ice systems. We usually talk about climate change in terms of changes in the average state of the system. Superimposed on these gradual trends will be substantial variability across years and decades due to natural drivers and internal variability in the climate system, for example, due to the El Nino Southern Oscillation (the magnitude of which is itself expected to be enhanced by climate change). This is important because many of the effects of climate change on human society are felt most significantly in connection with extreme events in the tails of the distributions of extreme climate events.

Impacts of CC on the Indoor Environment

Climate change involves a long-term trend towards higher temperatures as well as more intense and longer duration heat events in summer, larger and more intense storms and droughts, altered patterns of large-scale atmospheric circulation, and rising sea levels. These direct impacts lead to a range of downstream changes, including higher humidity and declining soil moisture, rising risk of wildfires, higher concentrations of ambient ozone and fine particles (in the absence of emission changes), longer pollen seasons, and more intense dust storms. All of these changes in outdoor environmental conditions have implications for IAQ. We review some of the most well documented in the following sections.

Climate Extremes: Climate change involves both gradual changes in average conditions as well as increases in the frequency and/or severity of extreme events such as heat waves and storms. Extreme climate events, made more intense and in some cases more frequent by climate change, can put people at risk via a range of pathways. In particular, extreme climate events often lead to infrastructure disruption, including loss of power due to floods, wind/tree damage, or the effects of extremes of temperature. Climate extremes can damage homes so severely that families become displaced. When this happens, there can be a wide range of adverse effects due to the living conditions in the new or temporary housing, with potential adverse impacts on several health outcomes including mental health.

Loss of power can lead to greater reliance on portable generators to supply backup power. Portable generators burn liquid fuels such as gasoline or diesel fuel and emit a range of harmful pollutants including carbon monoxide gas (CO), PM, and others. If used in or near enclosed spaces, use of portable generators can lead to deadly exposures to CO (Hampson and Stock 2006; Damon et al. 2013). While the

transition to a low-carbon economy should eventually lead to greater reliance on batteries for backup power, in the near term, it is likely that CO exposure from fuel-based backup generators will continue to be common following power failures. Resulting indoor exposures are more likely in high-density neighborhoods where homes are closely spaced and yards are small, as is common in low-income urban communities. Indoor space heating using fuel-based stoves or heaters poses similar risks, as can indoor cooking with charcoal or wood stoves. People with limited financial resources can be expected to be at higher risk of these effects. During power outages, household exposures to air pollution can also occur due to cooking with gas or charcoal grills. Chen and colleagues found a large and significant increase in CO-related exposures and poisonings reported to the NYC poison control center in the 2 weeks following Hurricane Sandy in 2012, compared to years 2008–2011 (Chen et al. 2013). Most were due to indoor grilling or use of generators.

Moisture Changes: Climate change will result in higher moisture levels in the atmosphere, as well as changing patterns of precipitation, with more rain in some areas and less in others. Higher moisture, alone or in combination with climate-induced sea level rise and coastal flooding, could cause IAQ problems. The 2011 IOM report highlighted the extensive literature linking indoor moisture to adverse respiratory health effects (IOM 2011). For example, Fisk et al. (2007) estimated that one in five of asthma cases in the USA could be attributed to indoor moisture. Moisture-related building material damage promotes bacterial and mold growth, and can release chemical contaminants, such as phthalates from vinyl floor coverings (IOM 2011). Higher temperatures and relative humidity both can affect off-gassing emissions from building materials. Many studies and reports have highlighted the importance of indoor mold (fungi) as a source of health risk indoors (WHO 2009; Brambilla and Sangiorgio 2020). Tighter building envelopes without ventilation and moisture management to keep water activity of surfaces below thresholds for spore germination can lead to IAQ problems.

Many biological agents that are sensitive to temperature or humidity can have profound impacts on human health. Respiratory viruses in particular are of special concern. For example, seasonal respiratory viruses like influenza contribute to morbidity and mortality throughout the world. In the USA, influenza outbreaks occur mostly in the winters. Evidence suggests that low absolute humidity promotes higher infection rates and may be at least partially responsible for observed seasonality (Shaman and Kohn 2009). Low vapor pressure may hasten the evaporation of exhaled respiratory droplets, allowing virus particles to remain airborne for longer periods. The COVID-19 pandemic also exhibited seasonality but was not limited to the cold season. Rising ambient temperatures and humidity may influence future transmission of respiratory viruses; however, those changing ambient conditions will mainly be relevant for human exposure and health to the extent that they influence indoor conditions, where people spend the vast majority of their time. More time spent indoors in air conditioned spaces in a warmer, more humid world could promote spread of disease even if ambient conditions would appear unfavorable for virus survival.

Ambient Air Quality: Climate change and outdoor air quality are closely related. Many GHG sources, such as power plants and motor vehicles, are also key emitters of health-relevant pollutants and/or precursors for PM and ozone. At the same time, warming temperatures and changing weather patterns can alter air pollution emissions, transport, and atmospheric chemistry. Since IAQ is influenced in part by ambient AQ, if outdoor concentrations change, indoor concentrations may too.

Over the past two decades, research has shown how climate change can make it more difficult to achieve ambient air quality objectives. Higher temperatures and changing weather patterns tend to make ozone pollution worse in places where it is already a problem, with adverse consequences for human health (Knowlton et al. 2004; Bell et al. 2007; Kinney 2018). This is of concern both due to direct health effects of ozone on health, as well as from the potential for ozone to oxidize indoor co-pollutants such as VOCs. Recent work has shown that both PM_{2.5} and ozone concentrations in the continental USA could worsen over the current century due to climate change, even with further air pollution emission controls (Fann et al. 2021). Evidence shows that anthropogenic emissions of ozone and PM_{2.5} precursors play a dominant role in future trajectories of ambient AQ, and suggest that the “climate penalty” could be surmounted by more stringent emission controls. However, because ozone chemistry is complex, and depends on the ratio of VOC to nitrogen dioxide (NO₂) in the atmosphere, there are some regions and regimes in which ozone control is especially challenging. The ozone challenge is compounded by potential increases in biogenic VOC emissions as temperatures rise. Indeed, while ambient PM_{2.5} has shown improving trends in recent years, ozone is trending upwards in many locations, including in China (Li et al. 2020) and the eastern USA (Squizzato et al. 2018; Blanchard et al. 2019).

Penetration of outdoor pollutants indoors depends on air exchange between the indoor and outdoor environment. If, in response to a changing climate, homes become tighter and more energy efficient, this may lead to decreased ventilation by outdoor air and reduced penetration of ambient pollution. Mechanical ventilation with air cleaning can enable higher ventilation by clean outdoor air, counteracting the negative consequences of tighter buildings for exposures to pollutants of indoor origin, including CO₂. Recent studies have explored the potential impacts of climate-driven changes in ambient air quality to affect IAQ, with or without changes in building ventilation. For example, Dionisio and colleagues used the EPA APEX exposure model to simulate future ozone exposures for people living in each of 12 large US metro areas (Dionisio et al. 2017). Under a climate change scenario, personal exposures to ozone were predicted to rise, especially for a high climate change scenario. These changes were driven by climate-induced increases in ambient ozone. This study did not take into account changes in home ventilation changes that might occur as a function of climate, which should be included in future studies. Salthammer and colleagues evaluated scenarios of climate change and ambient and indoor air quality in Germany (Salthammer et al. 2018). They concluded that there will likely be higher ambient background concentrations of ozone, but decreasing concentrations of NO₂ and PM_{2.5}, and that with “intelligent manual ventilation behavior, adjusted to suit the conditions of the day, it is unlikely that concentrations

which are critical in terms of health aspects will be attained in indoor areas through infiltration.” On the other hand, they anticipate significant challenges related to keeping indoor temperature and humidity within healthy limits (Salthammer et al. 2018). See the section “[Implications for IAQ of Climate Adaptation and Mitigation Actions](#)” on adaptation responses for related research findings.

Anthropogenic PM_{2.5} is likely to continue to decline in coming decades in the USA and many other parts of the world, following current trends, and accelerated by the transition to a low carbon energy system. This will be especially true for motor vehicle related PM in more urbanized areas, which has a disproportionate impact on local PM exposure, including indoors near roadways, and will be highly sensitive to the trend towards electrification of the vehicle fleet, a trend that is already accelerating. However, “natural” sources of PM, including from wildfires, dust storms, and pollen, are expected to rise with climate change, though with strong regional and temporal heterogeneity. This could change the size and chemical characteristics of PM, its dosimetry, and potential effects on different adverse health outcomes. For example, an increase in secondary organic aerosol could enhance oxidative stress and inflammation leading to both respiratory and cardiovascular morbidity. Also, dust and pollen are risk factors for asthma and other respiratory diseases.

Climate change promotes wildfire risk for several reasons. Higher temperatures draw water vapor into the atmosphere, lowering available soil moisture, which increases the likelihood of fire. Temperature, water, and insect stress in a warming climate also increases the risk of disease-related morbidity and mortality of trees. In a 2008 study, Westerling and Bryant modeled how fire risk in California may be influenced by climate change through this century (Westerling and Bryant 2008). Their analysis suggested that higher temperatures would increase fire risk in wetter, forested regions, but could decrease fire risk in places where lower precipitation might reduce the amount of fuel available to burn in the longer run. More recently, Neumann et al. modeled the potential future impacts of climate change on wildfire-related PM_{2.5} and mortality across the continental USA (Neumann et al. 2021). They found that climate change could increase wildfire pollution emissions by about 38% between 2006 and 2100 under a lower GHG emission scenario, and about 67% over the same period under a high GHG emission scenario. Their model further showed that wildfire PM_{2.5} concentrations could more than double by the end of the century, with substantial impacts on premature mortality among exposed populations.

In addition to PM_{2.5}, wildfires also increase ambient concentrations of ozone, CO, NO₂, formaldehyde, acetaldehyde, and other pollutants. Fisk (2015) estimates, based on a 50% infiltration rate, 90% of time indoors, and typical at-rest breathing rates, that adults may receive about 65% of total wildfire smoke exposure indoors and children about 50%. To protect people from exposure and health risks from wildfires when they occur, he recommends spending more time indoors with windows and doors closed, and to operate particle filtration systems. The latter can reduce indoor PM by 50% or more, which would reduce risks from wildfire smoke as well as from general PM for people living in high pollution areas.

As large-scale regional smoke exposure becomes more common due to persistent fires, there will be a growing need for information on how best to mitigate IAQ

impacts in affected areas. Burke and colleagues analyzed a range of social media and other data sources to shed light on current impacts of wildfire smoke on household behaviors and exposures (Burke et al. 2021). The authors noted that protection from wildfire smoke is currently treated as a private responsibility in the USA – i.e., encouraging staying indoors, closing windows, and/or using air filtration devices. However, there are likely large differences in the ability of people to implement protective measures. Using cell phone location records, the authors showed that fire smoke days with PM_{2.5} concentrations above 50µg/m³ lead to about a 10% increase in average time spent indoors. This effect was higher for high income versus low income populations, potentially because lower income people have less options to work from home and/or less ability to control IAQ. The study also analyzed data from indoor low-cost PurpleAir sensors used in the San Francisco Bay area and compared the PM_{2.5} to outdoors when fire smoke is present. The average I/O ratio was about 0.15, but was lower at higher ambient concentrations, probably due to protective behaviors. Infiltration varied substantially across households. The highest quartile infiltration versus lowest had 3.5x higher indoor PM_{2.5} concentrations, meaning that population exposure to wildfire smoke varies markedly across the population. Interestingly, the study observed no income gradient in penetration, but the authors note that users of low-cost sensors tend to be more wealthy than average.

Results from this study make the point that exposures to fire smoke depend only partially on outdoor airborne pollutant concentrations, but also on such factors as knowledge about risks, ability to shelter at home, and the ability to modify the indoor environment in ways that reduce exposure and risk. Those attributes will likely vary across the population. Education can help with the first part. Government assistance programs can help with the second. However, there is likely to be a dichotomy in agency between owners and renters.

Rising CO₂: CO₂ concentrations outdoors have risen steadily for several decades, as clearly demonstrated by the continuous series of CO₂ measurements at the Mona Loa observatory since 1958. As of December 1, 2021, CO₂ concentrations there had reached 416 ppm. Rising CO₂ concentrations (as well as warmer temperatures) are leading to longer and potentially more severe pollen seasons in North America, with adverse impacts on allergy and asthma (Anenberg et al. 2017; Neumann et al. 2018; Anderegg et al. 2021). Laboratory studies in which common ragweed was grown under different CO₂ concentrations demonstrated dose-related increases in both the amount, and the potency, of the pollen generated (see, e.g., USGCRP 2016). Similar findings were reported for ragweed grown in downtown Baltimore, where mean CO₂ concentrations were 30% higher than in a comparison plot grown in a rural location (Ziska et al. 2003). Authors reported that “ragweed grew faster, flowered earlier, and produced significantly greater above-ground biomass and ragweed pollen at urban locations than at rural locations.” Recent analyses of ambient pollen trends demonstrate that pollen seasons are getting longer in response to climate change (Anderegg et al. 2021). Although pollen grains tend to have large physical diameters, their low density gives them much smaller aerodynamic diameters, which enhances their penetration into indoor spaces.

In addition to its impacts on plant biology, CO₂ can be problematic indoors for human health and well-being. CO₂ can reach very high concentrations indoors due to respiration of human occupants. Concentrations well above 1000 ppm are routinely observed in conference and classrooms. Studies have shown a range of adverse effects of concentrations about 1000 ppm, including reduced cognitive performance on standardized tests. Tighter buildings and reduced interior volumes aimed at efficient use of energy will make it difficult to keep CO₂ at healthy concentrations.

While CO₂ is often used as a tracer for poor ventilation, evidence on the direct health effects of CO₂ itself remains sparse. Since CO₂ indicates inadequate ventilation, health effects observed in field studies may also be due to the increases in concentration of indoor contaminants as a consequence of a poor ventilation. However, emerging evidence from carefully controlled studies suggests a range of direct effects at CO₂ concentrations of 1000 ppm and above (Jacobson et al. 2019). The American Society of Heating and Air-Conditioning Engineers (ASHRAE) recommends indoor CO₂ below 700 above ambient to ensure comfort, which would translate to an indoor concentration in the neighborhood of 1100 ppm. However, ambient concentrations are rising, and urban areas are already higher than the global mean, and more people are moving to urban areas. In the future, the urban CO₂ dome will diminish in intensity as we transition to renewable energy sources for transportation and building energy needs. Like other indoor-source pollutants, smaller spaces and lower ventilation as energy savings measures will tend to increase CO₂ concentrations resulting from occupant respiration. Satish and colleagues carried out an experimental study in which 22 subjects were exposed to CO₂ for 2.5 h at each of three CO₂ concentrations: 600, 1000, and 2500 ppm in an enclosed office-like space. Performance on decision-making tasks (assessed by computer) diminished modestly but significantly at 1000 ppm compared to 600 ppm, and quite substantially at 2500 ppm, for most of the decision-related sub-domains (Satish et al. 2012). Implications are uncertain but reinforce the target of staying below 1000 ppm indoors.

Household Air Pollution from Solid Fuel Combustion: Cooking and/or heating with biomass fuels such as wood, dung, charcoal is a daily reality in much of the world where access to clean fuels is limited by cost and/or technical constraints (see chapter “Cooking/Heating”). Biomass fuel use is highly prevalent in rural regions of Africa, Asia, and South America. This combustion leads to very high concentrations of PM, CO, and many carbonaceous compounds in the indoor environment, and presents substantial health risks, especially for women and children. Climate change could influence biomass-related IAQ through several mechanisms. Heating demand would likely go down with warmer winters, lowering indoor impacts. Also, higher ambient temperatures and dry conditions could lead to more cooking outdoors or in better-ventilated structures, potentially leading to lower personal exposures. However, other trends not directly related to climate change could have more profound impacts, including urban migration, economic development, and national clean-fuel initiatives aimed at providing greater access to LPG, electricity, or other clean options. While there have been substantial efforts over several decades to develop cleaner-burning stoves using biomass fuels, and some have shown promising results,

in general they have proven unable to sustainably reduce exposures sufficiently to avoid adverse health impacts (Chillrud et al. 2021).

Changes in Activity Patterns Due to and in Parallel with Climate Change

Another important trend affecting exposures to IAQ is time spent indoors in various microenvironments: home, work, transit, and school. All are likely to change as society transitions to a zero-net-carbon future. Historically, people spent 60–70% of time at home and 80–90% of time indoors (IOM 2011) (see ► Chap. 37, “Time-Activity Patterns”). The COVID-19 pandemic in 2019–2021 led to major shifts in allocation of time across these modes, with substantial increases time spent indoors at home. After the pandemic receded, there is evidence of some shift back part way in the direction of pre-pandemic time allocation. However, it is unclear to what extent society will fully return to the old way of life. Moreover, zero-net-carbon implies reducing unnecessary energy use for commuting and climate control in office buildings, which will be an added pressure in that direction. An additional relevant factor, not directly related to climate, is the shift away from brick and mortar commerce as online retail continues its rising dominance. This will reduce the need for in-person shopping and favor time spent at home. It is unclear though whether climate change itself will result in addition pressure to shift spent at home versus other locations (see p. 43 of (IOM 2011)).

Vulnerability

Effects of climate on IAQ likely vary for different segments of the population due to differences in housing type and quality, owner versus renter, economic resources, knowledge of the issue, language, local microclimates, location in relation to the urban heat island, baseline health status, age, etc. (Fisk 2015; Vardoulakis et al. 2015). This diversity of impacts calls for extra effort on the part of policy makers to level the playing field by targeting interventions to those most affected and/or unable to take action on their own. Groups vulnerable to climate-related extremes affecting the indoor environment include the poor (low energy security; poor housing quality; lack of resources and/or knowledge to respond to extreme events; lower baseline health status), the elderly (chronic illnesses; limited mobility/homebound; cognitive deficits; limited social and economic resources; less physiologically able to acclimate to heat waves), and children (more time spent at home, especially for infants). Lower income individuals are less likely to be homeowners. Renters have less control over their indoor environment. They may be more likely to rely on windows for ventilation, and also more exposed and less able to protect from extreme heat or storm events. Also, income gradients lead to differential ability to respond to extreme events including heat waves and storms, and the ability to repair damage and get back to normal versus being displaced and/or exposed to mold or chemicals

for longer periods. What little is known about vulnerability and IAQ is mainly based on research in North America and Europe. Fisk (2015) points out that this makes it difficult to draw conclusions for other, potentially more vulnerable, world regions.

Implications for IAQ of Climate Adaptation and Mitigation Actions

IAQ is likely to be affected not only by climate change itself but also by societal responses to climate change, including strategies to both adapt to climate change and/or mitigate (reduce or eliminate) GHG emissions. Adaptations are actions taken to reduce the impacts of a changing climate, for example, to maintain indoor thermal comfort in response to higher ambient temperature, or to avoid penetration by water in the event of floods or extreme rainfall. Mitigation involves actions to reduce GHG emissions, or enhance sinks, in an effort to minimize our impact on the future climate. Since the building sector is a major contributor to carbon emissions, it will also be an important target of mitigation actions aimed at improved energy performance and for shifting from fossil-fuel based fuels to renewably generated electricity.

Indoor air quality depends on the joint influence of indoor sources, ventilation with outdoor air, and concentrations of pollutants in outdoor air. Both adaptation and mitigation efforts in buildings are likely to result in tighter buildings with less natural ventilation. Thus, along with energy efficiency and thermal comfort measures, it will be important to identify and reduce indoor pollution sources related to building materials, consumer products, and cooking, and, where necessary to incorporate air cleaning or local ventilation to reduce impacts of indoor sources. Meanwhile, mitigation of GHG emissions more broadly, as well as air quality regulations, should lead to a continued trend towards lower ambient air pollution concentrations.

There is increasing recognition that the climate is changing at an accelerating rate, and that both adaptation and mitigation responses will be necessary to both build resilience to climate extremes in the near term and to limit our impact on future climate change. Rising temperatures will have important implications for indoor thermal comfort. As ambient temperature rises, the seasonal and geographic patterns of window use and air-conditioning will evolve to maintain internal thermal comfort. While hard to predict, and very location specific, these changes are likely to affect indoor concentrations of pollutants of both indoor and outdoor sources.

A recent study in Atlanta illustrates how warming temperatures could affect home ventilation and indoor/outdoor penetration of ambient PM over the course of the seasons (Liang et al. 2021). The researchers measured I/O infiltration ratios for PM_{2.5} sulfate in 60 Atlanta homes between 2016 and 2017. They observed seasonal variations in I/O infiltration ratios, with ~20% lower values in summer when A/C use was highest compared to spring and fall (see Fig. 2). The seasonal pattern was stronger in homes without HVAC systems. They then developed prediction models for infiltration ratio based on ambient temperature, and then used those models to

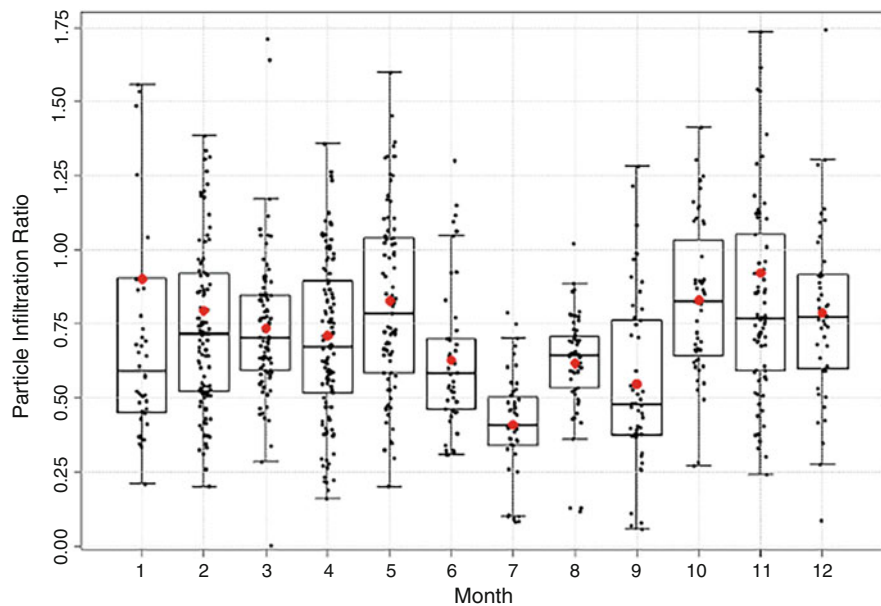


Fig. 2 Distribution of particle infiltration ratio by month in 60 houses in Atlanta. (From Liang et al. 2021)

estimate future I/O infiltration ratios under climate change scenarios in 2046–2065 as compared to a baseline climate period of 1981–2000. With 2.1 °C warming in Atlanta, they estimated there could be a 4% *increase* in infiltration ratio during cooler months and a 6% *decrease* in warmer months. While these results for Atlanta cannot be generalized directly to other locations, they do illustrate the bidirectional impact of seasonal changes in ventilation on indoor exposures to PM of outdoor origin and how those could shift in a future, warmer climate. Figure 2 shows the distribution of particle infiltration ratios by month from that study.

Ilacqua and colleagues used a model for building infiltration that is driven by indoor versus outdoor temperature differences, which partly drives infiltration, for nine US metro areas (Ilacqua et al. 2017). By mid-century, annual mean infiltration went down about 5% based on T output from eight climate models. But seasonal differences were noted, with some locations experiencing increases of 20–30% in summer.

Air-conditioning is an effective way to reduce indoor exposure to heat and to protect from adverse health effects during heat waves. However, prolonged use of A/C among inactive residents prevents physiological adaptation to even moderate increases in heat, putting people at greater risk if they must leave the A/C space for whatever reason or during power outage. Also, extensive A/C use increases load on grid and can be a reason for blackouts, contribute to the urban heat island, and lead to higher CO₂ emissions if the electricity comes from a power plant fueled by coal, oil, or gas.

On the mitigation side, increasing commitments by local and regional government bodies to achieve a net zero carbon economy by mid-century implies that we are embarking on a rapid trend towards an all-electric energy system based on renewable energy sources like solar and wind (Steinemann et al. 2017). This in turn implies lower ambient air pollution (at least for NO₂ and PM), no indoor gas cooking emissions or space heating emissions, and tighter building envelopes for energy efficiency.

Mitigation-related efforts to reduce energy use in buildings could lead to lower volume structures with less ventilation with outdoor air, leading to higher impacts of indoor sources, including cooking and heating, emissions from materials, furniture, cleaning products, etc. As indoor volume and air exchange are reduced, indoor sources will have a larger impact on IAQ unless the sources themselves are mitigated through elimination, substitution, or focused ventilation. Because exhaust fans have a more difficult time drawing air outdoors when there is high back pressure due to a tight building envelope, this tendency would need to be counteracted with engineered retrofits. As a general matter, space heating energy needs will gradually diminish worldwide as mean global temperature rises. There could also be pressure for greater use of renewably sourced wood-based fuels, which could have adverse impacts in IAQ if not burned efficiently and fully ventilated outdoors. In addition, it is possible that there will be some northward migration of populations as new communities are established in cooler regions closer to the poles.

There will be strong pressure to maximize energy efficiency as we transition to a net-zero carbon economy. Conditioning of indoor temperature and humidity is a major factor in building energy use and will thus be an important target for energy efficiency measures. These could lead to lower ventilation rates, which might in turn lead to higher concentrations of pollutants generated indoors (CO₂, combustion-related PM and gases, VOCs and semi-volatile VOCs), while also reducing penetration of ambient pollution.

There is a growing literature examining the interplay between energy efficiency, climate change, and IAQ. For example, based on a systematic review of literature since 2000, Levasseur and colleagues recommend a holistic approach to IAQ management, incorporating knowledge about how to reduce contaminants at the source (referring to both indoor sources and infiltration of ambient), ensuring adequate ventilation, and purifying indoor air if needed, taking into account ambient conditions (Levasseur et al. 2017). They note that because buildings are getting tighter due to concerns of energy and carbon emissions, there is a growing need for complementary ventilation to maintain adequate IAQ. Heat recovery and energy recovery ventilators are increasingly being used to deliver fresh air while maintaining indoor thermal and moisture comfort, without introducing condensation problems. However, to operate effectively, proper calibration and ongoing maintenance are needed. Natural ventilation is another option and is modifiable via window opening by occupants. There is a potential interaction of hot weather, window opening, and the presence of high outdoor pollution due to climate-related ozone, pollen, or wildfire pollution. Encouraging more natural ventilation at night could help since pollution concentrations tend to be lower (at least for ozone and

anthropogenic PM) and temperatures tend to be cooler (though less so in a warming climate).

A potentially important new direction in IAQ under climate change will be development and application of adaptive, active intelligent control ventilation systems which monitor occupancy, indoor/outdoor T, RH, CO₂, and possibly PM, and adjust infiltration of fresh air to maximize comfort and IAQ as well as being as energy efficient as possible (Laverge et al. 2011). During extreme air pollution episodes, whether from wildfires or other sources, the ability to minimize infiltration, accompanied by some filtration could help to preserve IAQ while the event is ongoing. Based on their analysis, Laverge et al. suggest that demand-controlled mechanical exhaust ventilation in residences can reduce indoor CO₂ concentrations and save 25–60% of heat loss during the heating season as compared with conventional systems. In another study, Carbonare and colleagues evaluated a ventilation system that learns based on user behavior and adjusts indoor CO₂ and RH (Carbonare et al. 2021). The idea is to provide comfort and IAQ where and when it is needed, rather than in all places at all times, providing good IAQ at reduced energy cost.

Improved source controls or elimination will also be critical in tighter, more energy-efficient homes to maintain adequate IAQ. Air cleaning may be needed when IAQ problems cannot be addressed with ventilation or source controls. Air cleaners can be effective, but may require frequent maintenance to be most efficient, and need to be scaled to the volume of the space, taking into account air exchange (Davison et al. 2021). Cleaning close to the source of indoor pollution is usually most effective.

Fisk (2015) suggested that we should prioritize indoor environmental quality in residential settings, where vulnerable people are most likely to be exposed. He highlights the value of passive thermal control measures – insulation, window shading, better windows, reflective roofs – because they do not result in ongoing CO₂ emissions, unlike A/C use. However, A/C use with the windows closed substantially reduces indoor concentrations of ozone. Ozone episodes often coincide with heat waves, so air-conditioning can provide a double benefit. Evidence also suggests that health effect associations for ambient air pollution are lower for homes with A/C, likely due to lower exposures indoors.

Moreno-Rangel and colleagues note that the building sector is responsible for a substantial amount of energy use and GHG emissions currently, and thus will be an important target for mitigation actions on the path to a zero-carbon future (Moreno-Rangel et al. 2020). This paper surveyed the literature on IAQ characteristics of passivhaus dwellings. These are highly energy-efficient buildings that provide thermal comfort using mechanical ventilation to supply fresh air from outdoors with heat recovery. They found relatively little data on IAQ in relation to energy efficiency, but what is available suggests that homes meeting passivhaus standards have generally better IAQ than conventional homes, including new energy-efficient homes, probably because of the greater supply of fresh air. However, this finding points out the need for filtration of inlet air stream using appropriate methods, in locations or at times when ambient pollution concentrations are high, as well as the

importance of indoor source elimination or controls to maximize IAQ. They reinforce the value of keeping ventilation rates above 0.5 h^{-1} along with indoor source controls and air cleaning where needed. This review suggests that highly energy-efficient dwellings, when properly designed and maintained, have the potential to provide good IAQ while also achieving substantial energy reductions. But proper functioning requires adequate knowledge among building occupants.

Conclusions

Climate change is and will have increasing impacts on society, including via the indoor environment. Impacts, both negative and beneficial, may be felt due to longer and more intense heat waves, milder winters, more intense storm events, coastal flooding, rising concentrations of ambient pollen and smoke from wildfires, reduced anthropogenic air pollution, the low-carbon energy transition, energy efficiency measures, and other direct or indirect pathways related to climate change. The mechanisms by which IAQ may change due to these factors are ones that building scientists have been studying for decades: changes in indoor sources; technology for air cleaning; impacts of ventilation by fresh air, etc. Thus, the toolkit available to confront these changes will be similar to what we are already familiar with. However, the pace and complexity of changes will offer new challenges, as will the societal transformations needed to transition to a net zero carbon if we are to avert more severe climate change. Since the residential indoor environment is where individuals who are most vulnerable to climate change are and will continue to be found in the largest numbers, it is critical that policy makers and technology developers focus their efforts on finding ways to keep those places as healthy as possible to all members of society in the face of climate change.

References

- Anderegg WRL, Abatzoglou JT, Anderegg LDL, Bielory L, Kinney PL, Ziska L (2021) Anthropogenic climate change is worsening North American pollen seasons. *Proc Natl Acad Sci* 118(7):e2013284118
- Anenberg SC, Weinberger KR, Roman H, Neumann JE, Crimmins A, Fann N, Martinich J, Kinney PL (2017) Impacts of oak pollen on allergic asthma in the United States and potential influence of future climate change. *GeoHealth* 1(3):80–92
- Bell ML, Goldberg R, Hogrefe C, Kinney PL, Knowlton K, Lynn B, Rosenthal J, Rosenzweig C, Patz JA (2007) Climate change, ambient ozone, and health in 50 US cities. *Clim Chang* 82(1–2):61–76
- Blanchard CL, Shaw SL, Edgerton ES, Schwab JJ (2019) Emission influences on air pollutant concentrations in New York State: I. ozone. *Atmos Environ X* 3:100033
- Brambilla A, Sangiorgio A (2020) Mould growth in energy efficient buildings: causes, health implications and strategies to mitigate the risk. *Renew Sust Energ Rev* 132:110093
- Burke M, Heft-Neal S, Li J, Driscoll A, Baylis PW, Stigler M, Weill J, Burney J, Wen J, Childs M, Gould C (2021) Exposures and behavioral responses to Wildfire Smoke. National Bureau of Economic Research Working paper series no. 29380

- Carbonare N, Pflug T, Bongs C, Wagner A (2021) Design and implementation of an occupant-centered self-learning controller for decentralized residential ventilation systems. *Build Environ* 206:108380
- Chen BC, Shawn LK, Connors NJ, Wheeler K, Williams N, Hoffman RS, Matte TD, Smith SW (2013) Carbon monoxide exposures in New York City following Hurricane Sandy in 2012. *Clin Toxicol (Phila)* 51(9):879–885
- Chillrud SN, Ae-Ngibise KA, Gould CF, Owusu-Agyei S, Mujtaba M, Manu G, Burkart K, Kinney PL, Quinn A, Jack DW, Asante KP (2021) The effect of clean cooking interventions on mother and child personal exposure to air pollution: results from the Ghana Randomized Air Pollution and Health Study (GRAPHS). *J Exposure Sci Environ Epidemiol* 31(4):683–698. <https://doi.org/10.1038/s41370-021-00309-5>. Epub 2021 Mar 3.
- Damon SA, Poehlman JA, Rupert DJ, Williams PN (2013) Storm-related carbon monoxide poisoning: an investigation of target audience knowledge and risk behaviors. *Soc Mark Q* 19(3):188–188
- Davison G, Barkjohn KK, Hagler GSW, Holder AL, Coefield S, Noonan C, Hassett-Sipple B (2021) Creating clean air spaces during Wildland Fire Smoke Episodes: web summit summary. *Front Public Health* 9:508971–508971
- Dionisio KL, Nolte CG, Spero TL, Graham S, Caraway N, Foley KM, Isaacs KK (2017) Characterizing the impact of projected changes in climate and air quality on human exposures to ozone. *J Exposure Sci Environ Epidemiol* 27(3):260–270
- Fann NL, Nolte CG, Sarofim MC, Martinich J, Nassikas NJ (2021) Associations between simulated future changes in climate, air quality, and human health. *JAMA Netw Open* 4(1):e2032064–e2032064
- Fisk WJ (2015) Review of some effects of climate change on indoor environmental quality and health and associated no-regrets mitigation measures. *Build Environ* 86:70–80
- Fisk WJ, Lei-Gomez Q, Mendell MJ (2007) Meta-analyses of the associations of respiratory health effects with dampness and mold in homes. *Indoor Air* 17(4):284–296
- Hampson NB, Stock AL (2006) Storm-related carbon monoxide poisoning: lessons learned from recent epidemics. *Undersea Hyperb Med* 33(4):257–263
- Ilacqua V, Dawson J, Breen M, Singer S, Berg A (2017) Effects of climate change on residential infiltration and air pollution exposure. *J Expo Sci Environ Epidemiol* 27(1):16–23
- IOM (2011) Climate change, the indoor environment, and health. The National Academies Press, Washington, DC
- IPCC (2021) Climate change 2021: the physical science basis. Contribution of Working Group I to the sixth assessment report of the Intergovernmental Panel on Climate Change. [Masson-Delmotte V, Zhai P, Pirani A, Connors SL, Péan C, Berger S, Caud N, Chen Y, Goldfarb L, Gomis MI, Huang M, Leitzell K, Lonnoy E, Matthews JBR, Maycock TK, Waterfield T, Yelekçi O, Yu R, Zhou B (eds)]
- Jacobson TA, Kler JS, Hernke MT, Braun RK, Meyer KC, Funk WE (2019) Direct human health risks of increased atmospheric carbon dioxide. *Nat Sustain* 2(8):691–701
- Kinney PL (2018) Interactions of climate change, air pollution, and human health. *Curr Environ Health Rep* 5(1):179–186
- Knowlton K, Rosenthal J, Hogrefe C, Lynn B, Gaffin S, Goldberg R, Rosenzweig C, Civerolo K, Ku J, Kinney P (2004) Assessing ozone-related health impacts under a changing climate. *Environ Health Perspect* 112(15):1557–1563
- Laverge J, Van Den Bossche N, Heijmans N, Janssens A (2011) Energy saving potential and repercussions on indoor air quality of demand controlled residential ventilation strategies. *Build Environ* 46(7):1497–1503
- Levasseur ME, Poulin P, Campagna C, Leclerc JM (2017) Integrated management of residential indoor air quality: a call for stakeholders in a changing climate. *Int J Environ Res Public Health* 14(12):1455
- Li K, Jacob DJ, Shen L, Lu X, De Smedt I, Liao H (2020) Increases in surface ozone pollution in China from 2013 to 2019: anthropogenic and meteorological influences. *Atmos Chem Phys* 20(19):11423–11433

- Liang D, Lee W-C, Liao J, Lawrence J, Wolfson JM, Ebelt ST, Kang C-M, Koutrakis P, Sarnat JA (2021) Estimating climate change-related impacts on outdoor air pollution infiltration. *Environ Res* 196:110923
- Moreno-Rangel A, Sharpe T, McGill G, Musau F (2020) Indoor air quality in Passivhaus dwellings: a literature review. *Int J Environ Res Public Health* 17(13):4749
- Nazaroff WW (2013) Exploring the consequences of climate change for indoor air quality. *Environ Res Lett* 8(1):015022
- Neumann JE, Anenberg SC, Weinberger KR, Amend M, Gulati S, Crimmins A, Roman H, Fann N Kinney PL (2018) Estimates of Present and Future Asthma Emergency Department visits associated with exposure to Oak, Birch, and Grass Pollen in the United States. *GeoHealth*
- Neumann JE, Amend M, Anenberg S, Kinney PL, Sarofim M, Martinich J, Lukens J, Xu J-W, Roman H (2021) Estimating PM_{2.5}-related premature mortality and morbidity associated with future wildfire emissions in the western US. *Environ Res Lett* 16(3):035019
- Salthammer T, Schiewek A, Gu J, Ameri S, Uhde E (2018) Future trends in ambient air pollution and climate in Germany – implications for the indoor environment. *Build Environ* 143:661–670
- Satish U, Mendell MJ, Shekhar K, Hotchi T, Sullivan D, Streufert S, Fisk WJ (2012) Is CO₂ an indoor pollutant? Direct effects of low-to-moderate CO₂ concentrations on human decision-making performance. *Environ Health Perspect* 120(12):1671–1677
- Shaman J, Kohn M (2009) Absolute humidity modulates influenza survival, transmission, and seasonality. *Proc Natl Acad Sci U S A* 106(9):3243–3248
- Spengler JD (2012) Climate change, indoor environments, and health. *Indoor Air* 22(2):89–95
- Squizzato S, Masiol M, Rich DQ, Hopke PK (2018) PM_{2.5} and gaseous pollutants in New York State during 2005–2016: spatial variability, temporal trends, and economic influences. *Atmos Environ* 183:209–224
- Steinemann A, Wargoocki P, Rismanchi B (2017) Ten questions concerning green buildings and indoor air quality. *Build Environ* 112:351–358
- USGCRP (2016) The impacts of climate change on human health in the United States: a scientific assessment. Crimmins A, Balbus J, Gramble JL, Beard CB, Bell JE, Dodgen JE, Eisen RJ, Fann N, Hawkins MD, Herring SC, Jantarasami L, Mills DM, Saha S, Sarofim MC, Trtanj J, Ziska L. Washington, DC
- Vardoulakis S, Dimitroulopoulou C, Thornes J, Lai K-M, Taylor J, Myers I, Heaviside C, Mavrogianni A, Shrubsole C, Chalabi Z, Davies M, Wilkinson P (2015) Impact of climate change on the domestic indoor environment and associated health risks in the UK. *Environ Int* 85:299–313
- Westerling AL, Bryant BP (2008) Climate change and wildfire in California. *Clim Chang* 87(1): 231–249
- WHO (2009) WHO Guidelines approved by the Guidelines Review Committee. WHO guidelines for indoor air quality: dampness and mould. World Health Organization, Geneva. Copyright © 2009, World Health Organization
- Ziska LH, Gebhard DE, Frenz DA, Faulkner S, Singer BD, Straka JG (2003) Cities as harbingers of climate change: common ragweed, urbanization, and public health. *J Allergy Clin Immunol* 111(2):290–295

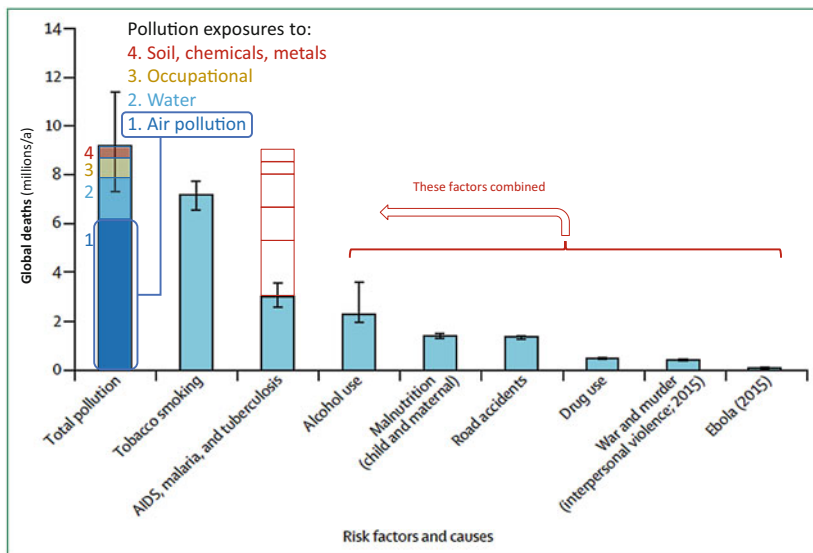


Correction to: Disease Burden of Indoor Air Pollution

Otto Hänninen, Corinne Mandin, Wei Liu, Ningrui Liu, Zhuohui Zhao, and Yingping Zhang

**Correction to: Disease Burden of Indoor Air Pollution in
Y. Zhang et al. (eds.), *Handbook of Indoor Air Quality*,
https://doi.org/10.1007/978-981-16-7680-2_48**

Owing to an oversight on the part of Springer, this chapter was initially published with missing details in figure 1 of the chapter. This has been now corrected.



The updated original version for this chapter can be found at
https://doi.org/10.1007/978-981-16-7680-2_48

Index

A

- Absenteeism, 1478, 1482
Accelerated solvent extraction (ASE), 453–454
Acceleration, particle motion, 267
 curvilinear motion, 269–270
 relaxation time, 268
 stopping distance, 268–269
Acceleration sensors, 1065
Acceptability ratings, 625
Acceptability scale, 619
Accuracy verification
 HWA verification, 588–591
 rotating board test, 586–587
 wind tunnel, 587–588
Accurate pollution maps, 2045
Acetaldehyde, 74
Acetic acid, 918
Acetone, 74, 619, 2074
Acetylacetone method, 495
Acid-base chemistry, 893–895
Acrolein, 2073
Acrylates, 2012
Active air sampling, 447–450
Active sampling, 432–433, 468
Active transportation, 2044–2045
Active transport infrastructures, 2044
Activity diary application, 1066
Activity recognition methods, 1066
Acute exposure guideline levels (AEGLs), 1525
Acute lethality, 41
Acute lower respiratory infection (ALRI), 1199, 2137
Acute myeloid leukemia, 1228
Acute respiratory infections (ARIs), 1199
Adaptations, climate, 2156–2160
Adhesion, 343
Adjustable fan network (AFN), 591
Adsorbed materials, 1828–1829
Adsorption/desorption model, 780
Adsorption sink, 1827–1830
Adverse health effects, 131, 1493
Aerodynamic diameter, 266–267, 944
Aerosol, 815, 816
 indoor inorganic, 969–970
 indoor organic, 967–969
 mass spectrometry, 947
 secondary organic, 964–967
Aerosol dynamics
 gas behavior, 248–261
 particle motion, in air, 262
Aerosol particle deposition
 boundary layer thickness, 316–317
 Brownian/turbulent diffusion, 308–309
 comparison of aerosol chamber
 measurements, 320
 energy dissipation, 317–318
 turbulent nature of indoor air flow, 306–308
 wall deposition (*see* Wall deposition)
Aerosol time of flight mass spectrometer (ATOFMS), 946
Age-care facilities, 1996
Agricultural wastes, 1153
Airborne bacteria, 1876
Airborne emission testing, 742
Airborne particles, 891, 1121
Air change rate, 870, 1678
Air cleaners, 1829–1830
 IEC standards, 1549–1552
 IEC/TC 59, 1553–1558
 IEC/TC 61, 1552–1553
 indoor air quality, 1548
 ISO standards, 1558–1563
 statistics, 1548
Air cleaning, 1866
 building scale, 1790–1792
 for personal microenvironment, 1798
 room scale, 1794–1796
 urban scale, 1786–1788

- Aircraft cabins, 2059
 Air diffusion performance index (ADPI), 1701
 Air distribution, 1700–1701
 Air exchange, 2151, 2158, 2159
 Air exchange rates, 1926
 Airflow
 interzone, 1685, 1699–1700
 multi-zone building, 1685
 partition, 2111, 2112
 rate measurement techniques d, 1693
 ventilation system, 1684, 1694–1696
 Airflow pattern
 AFN, 603–605
 chamber setup, 592–593
 flow patter, MV, 602–603
 imaging settings, 593
 MV (*see* Mixing ventilation (MV))
 results, 592–593
 Air pollutants, 2024
 Air Pollution Exposure Distributions of Adult
 Urban Populations in Europe
 (EXPOLIS), 1099
 Air purification technique, 1738,
 1777, 1808
 Air purifiers, 1882
 Air quality standard, 1493
 Air sensors, 1538
 Air temperature, 1862–1863
 Airtightness, 1926
 Air ventilation, 1512
 Airway inflammation, 1191
 Aldehyde based disinfectants, 2008
 Aldehyde-releasing agents, 1995
 Aldehydes, 395, 911
 Alkanes, 395, 2074
 Allergens, 1871–1872
 Allergic alveolitis, 1179
 Allergy, 622
 Allylic hydroperoxides, 394
 α -linolenic acid metabolism, 1227
 Alternative Extended U (maximal adaptability)
 model, 1402
 Alzheimer's disease (AD), 1225, 1291
 Ambient exposure
 multiple air pollutants/sleep, 1468
 particulate matter/sleep, 1467, 1468
 Ambient particles, 239, 518
 Ambient pollution, 991, 995–996, 2151,
 2158, 2159
 American Conference of Governmental
 Industrial Hygienists (ACGIH), 1513
 American Industrial Hygiene Association
 (AIHA), 1513
 American National Standards Institute (ANSI),
 1513, 1514
 American Society for Testing and Materials
 (ASTM), 134
 American Society of Heating, Refrigerating
 and Air-Conditioning Engineers
 (ASHRAE), 8, 284, 1513, 1514,
 1862, 1863
 applications, 1536, 1537
 standard 62.1, 1528–1532
 standard 62.2, 1533, 1534
 American Society of Heating and
 Air-Conditioning Engineers
 (ASHAE), 1514
 American Society of Refrigerating Engineers
 (ASRE), 1514
 American Standard Code for Information
 Interchange (ASCII), 1062
 American Thoracic Society (ATS), 1191
 4-Amino-3-hydrazino-5-mercapto-4H-
 1,2,4-triazole (AHMT), 48
 Ammonia, 911
 Analyte absorbance spectra, 860
 Analytical chemistry, 933, 936–937
 Anecdotal report, 1412
 Aniline, 74
 Animal test
 controversy and principles, 1221
 definition of, 1221
 history of, 1221
 limitations of, 1240–1242
 particulate matter pollution, 1235–1240
 radon, 1233–1235
 SVOCs, 1228–1233
 VOC pollution (*see* Indoor VOC pollution)
 ANSI/BIFMA e3 Furniture Sustainability
 Standard, 1628
 ANSI/BIFMA X7.1, 1610
 Anti-Müllerian hormone (AMH), 1285, 1287
 Antioxidants, 1231
 Aplastic anemia, 1228
 Apocrine glands, 908
 Aromatherapy, 1472
 Arousal (inverted U) theory, 1401
 Arterial blood pressure (ABP), 1192
 Aryl hydrocarbon receptor
 (AhR), 1195
 ASHRAE Standard 62.2, 189
 Asphyxiation, 1151

- Association of Home Appliance Manufacturers (AHAM), 1722, 1723
- Asthma, 622, 1166
- ASTM E 544-2004(2004) standard, 630
- Atmospheric stability, 2040
- Atomic emission detectors (AEDs), 81
- Atomic emission spectroscopy (ICP/AES), 524
- Attributable incidence (AI), 1337
- Audio sensors, 1065
- Audit project, 1949
- Augmentation index (AI), 1266
- Automated gas-chromatography systems, 510
- Automated tracer gas decay measurements, 1702
- B**
- Bacteria concentrations, 1876
- Badge-type samplers, 469
- Barrier discharge ionization detector (BID), 436
- BASE protocol maintenance checklist, 1691
- BASE ventilation study, 1706
- Basset-Boussinesq-Oseen equation of motion, 309
- Bayesian Kernel Machine Regression (BKMR), 1198
- Beck Anxiety Inventory (BAI), 1195
- Beck Depression Inventory-II (BDI-II), 1195
- Behavioral Assessment and Research System (BARS), 1195
- Benzaldehyde, 2073
- Benzene (BZ), 74–77, 486, 1163, 1212, 1227–1228, 2010
- Benzene-induced hematopoietic toxicity, 1228
- Benzylbutylphthalate (BBP), 1017
- Benzyl chloride, 74
- Berge equation, 64
- Beta attenuation monitors (BAMs), 527
- Big data, 1849
- Bioaerosols, 1164, 1882, 2028–2029
- asthma, 1166
 - mitigation, 1166–1167
 - risk, 1164–1166
 - source and exposure, 1164
- Bioeffluents, 921
- Biological Exposure Indices (BEIs), 1513
- Biomarkers, 1305
- cardiovascular system, 1260
 - hematologic health, 1268–1273
 - immune system, 1279–1280
- indoor air pollution, 1253–1254
- indoor environmental conditions, 1252
- physiologic systems, 1288–1291
- reproductive system, 1284
- respiratory system, 1253
- systemic inflammation, 1273–1277
- Biot number, 362
- Black carbon (BC), 186, 522, 529, 947, 1261, 2026
- Bladder cancer, 1204
- Blinding, 458
- Blood coagulation biomarkers
- fibrinogen, 1272
 - sP-selectin, 1272
 - VWF, 1272–1273
- Blood pressure (BP), 1192, 1266–1268
- Blood related parameters
- Hb, 1268
 - platelet count, 1271
 - RBC, 1271
 - WBC, 1271
- Boilers, 164, 173, 174, 176
- combustion, 174
 - Wood, 174
- Boltzmann constant, 270
- Boundary-layer theory, 257, 308
- Boundary layer thickness, 316–317
- Box model, indoor air pollutants, 956–958
- Boyle's law, 252
- Breast cancer, 1205
- Breath emissions, 907–909
- British Petroleum, 169
- Brominated flame retardants (BFRs), 102, 109–110
- Bronchoalveolar lavage fluid (BALF), 1224, 1230
- Brown carbon (BrC), 523
- Brownian motion, 270, 271
- diffusion, 270
 - mean free path, 272
 - mean particle velocity, 271
 - relative deposition velocities, 272
- Brunauer-Emmett-Teller (BET) isotherm, 352
- Building assessment survey and evaluation (BASE) study, 137
- Building automation system (BAS) interfaces, 1691
- Building Bulletin 101 (BB101), 1907
- Building materials, 78
- Building owners, 1478
- Building Performance Institute, Inc (BPI), 1536

- Building product reference materials
definition, 750
inter-laboratory studies, 750–751
- Building-related illnesses (BRI), 1478
- Building Research Establishment
Environmental Assessment
Methodology (BREEAM), 1567
emission criteria, product type, 1576
environmental Index, 1569
exemplary level mission criteria, product type, 1577
PM control, 1582
prescriptive index method, 1574
- Building ventilation performance evaluation, 1676
air distribution, 1700
building and system design information, 1686–1690
building and system impacts on, 1680–1682
deviation from design intent, 1705–1707
envelope air leakage, 1691–1694
interzone airflows, 1699–1700
long-term ventilation studies, 1679
measurement methods, 1690–1701
outdoor air change rates, 1696–1699
performance issues and parameters, 1682–1686
reasons for evaluation, 1679–1680
short-term IAQ research studies, 1679
system status, 1690–1691
variation in ventilation, 1701–1705
ventilation system airflow, 1694–1696
- Built environmental system, 1775–1776
- Built environment and public health (BEPH), 8
- Burden of disease (BoD), indoor air pollution characteristics, 1328
China, 1356–1361
EBD, 1332–1334
European EBoDE Study, 1340–1345
France, 1351–1356
GBD, 1327–1330
HealthVent study, 1345–1351
HIA, 1334–1335
methods, 1335–1337
PAF, 1337–1339
risk assessment, 1330–1332
toxicological databases, 1339
- Business and Institutional Furniture Manufacturers Association (BIFMA), 1514
- Business jets/helicopters, 2064
- Bus stops, 2041
- 2-Butanone, 623
- 2-Butoxyethanol, 623
- Butylbenzyl phthalate, 1302, 1307
- C**
- California activity pattern survey, 1076
auto repair shops/gas station/parking garage, 1080
heating time, 1080, 1081
indoor, 1076
kitchen smoke, 1080
smoking, 1079
- California children's activity patterns, 1081, 1082
- California Department of Public Health (CDPH), 1514
- Canadian General Standards Board (CGSB), 1535
- Canadian Human Activity Pattern Survey II (CHAPS II), 1086, 1098
- Canadian population-based national indoor air quality survey, 136
- Canister technology, 1606
- Capillary bundle model, 682
- Capillary electrophoresis-electrochemical detection (CEED), 49
- Capture of exhaust, 180
- Carbograph 4, 484
- Carbon-balance method, 180
- Carbon dioxide (CO₂), 1494, 1973–1974, 2068, 2208
on cognitive performance, 1410–1412
concentration occurring indoors, 1410–1411
concentrations higher than PEL, 1411
effect of human bioeffluents with, on cognitive performance, 1408–1409
health and cognitive/academic performance, 1906
influencing factors and correlations, 1908–1912
levels, 1907–1908
limits, 1906–1907
long-term exposures, 1412
physiologically impact cognitive performance, 1412–1414
ventilation rates in schools, 1906–1907
- Carbon monoxide (CO), 170, 1150–1152, 1197, 1497, 1869–1870, 2027, 2069
- Carbon tetrachloride, 74

- Carbonyl, 430–432, 436
Carboxylic acids, 395
Carcinogenicity, 42–43
Cardiac autonomic function, 1192, 1261–1265
Cardiovascular health effects, *see* Indoor air pollution
Cardiovascular system, 1238
Carpet and Rug Institute (CRI), 1527
CDPH Standard Method V1.2, 1628
Cellphone networks, 1064
Centers for Disease Control and Prevention (CDC), 1514
Central heating, 173
Centrifugation, 457, 458
Certified reference material (CRM), 749
Chamber background VOC concentrations, 1611
Chamber for laboratory investigations of materials, pollution and air quality (CLIMPAQ) method, 669
Chamber studies, VOCs in, 133–135
Chamber test, 700
Chemical analysis, SVOCs, 1612
 chromatography, 459
 MS, 459–460
Chemical composition, 1203
 e-cig aerogels, 214–219
 particles, 185
Chemical exposures
 abiotic particles, 1029, 1039
 antimicrobial agents, 1050
 clothing as a mediator, 1050
 clothing-associated exposure, 1030
 clothing harbors, 1028
 clothing-mediated particle, 1029
 dermal transfers/absorption, 1036–1038
 factors affecting, 1049
 ingestion, 1038, 1039
 inhalation, 1038
 occurrence/persistence/accumulation, 1033–1036
 particles, 1049
Chemical ionization, 936, 940
Chemical ionization mass spectrometry (CIMS), 497, 500–502, 509, 935, 938, 940, 941
Chemical mass balance (CMB), 526
Chemical processing, 1116
Chemical sensitivity scale (CSS), 623
Chemical sinks, 1828
Chemical transformations, occupant-related, 911–916
Chemiluminescence, 934, 936
China, IAP-BD, 1360–1361
 estimation, 1358–1360
 health outcomes, 1358–1359
 indoor exposure assessment, 1356–1358
China Assessment Standard for Green Building (CASGB), 1567
 environmental index, 1568–1569
 performance index method, 1572
 PM control, 1578–1581
 prescriptive index method, 1572
 sources requirements in, 1574
China Assessment Standard for Healthy Building (CASHB), 1568
 environmental index, 1569
 performance index method, 1574
 PM control, 1582–1583
 prescriptive index method, 1574
 sources requirements in, 1579
Chinese Environmental Exposure-Related Human Activity Patterns Survey for Children (CEERHAPS-C), 1069
Chinese/Indian cooking styles, 397
C-history method, 58–60, 674–676, 781
Chlorhexidine, 2004
Chlorinated paraffins (CPs), 373
Chlorine bleach, 865
Chlorine chemistry, 893
Chlorine monoxide (ClO), 849
Chlorine radical, reactions, 848–850
Chloroxylenol, 2004
Chromatographic method, 48–49
Chromatography, 459
Chromotropic acid, 48
Chronic CO poisoning, 1151
Chronic Hazard Advisory Panel (CHAP), 1129
Chronic kidney disease (CKD), 1196
Chronic lower respiratory disease (CLRD), 1199
Chronic lymphocytic leukemia, 1209
Chronic non-communicable disease, 1199
Chronic obstructive pulmonary disease (COPD), 1155, 1196, 1202, 1237, 1253, 1967
Classroom air quality
 learning vs. IAQ, 1453–1455
 schoolwork and absence rates, 1448–1453
 sleep and learning, 1453
Classrooms
 empirical evidence, 1894–1895
 health outcomes and limits, 1895
 IAQ variables, 1894
 key monitoring studies, 1894–1895

- Clean air delivery rate (CADR),
1722–1723, 1829
- Clean Cooking Alliance, 187
- Clean heating campaign (CHC), 2138
- Climate change
changes in activity patterns due to, 2155
extreme events, 2149, 2155
impact on indoor environment, 2149–2155
and indoor air quality, 2158
pathways linking to indoor air quality and health, 2148
physical science basis of, 2147
- CLIMPAQ method, 699
- Clothes drying appliances, 178
- Clothing, 919, 920
- Clothing-associated exposures
airborne chemicals, 1031, 1032
allergens, 1040
health effects, 1032
nanomaterials, 1041
para-occupational, 1042
pathogenic microbes, 1040
personal cloud, 1042
skin/blood/urine, 1030
- Clothing-mediated particle exposures,
1043–1049
- CNS Vital Signs battery (CNS), 1195
- Coagulation indicators, 1194
- Coal, 1153
- CO₂ concentration
on cognitive abilities, effects of, 1433–1435
on office work performance, effects of, 1433–1435
on work performance, effects of, 1433–1435
- Code of Federal Regulations (CFR), 1521
- Coefficient of investment (COI), 24
- Cognitive abilities, 1433–1435
- Cognitive abilities tests, 1437
- Cognitive Drug Research (CDR), 1195
- Cognitive function, 1290–1291
- Cognitive health, 1195
- Cognitive performance, 1373, 1392, 1398, 1401, 1402, 1430, 1434–1440, 1893, 1894, 1898, 1906, 1920
- CO₂, effects of, 1433–1435
- pollution sources/sinks, effects of adding or removing, 1438
- ventilation rates, effects of modifying, 1436–1438
- VOCs, effects of, 1435
- Color sequence enhanced particle streak velocimetry (CSPSV)
accuracy verification, 585–591
- CSIS, 577–579
- digital image processing, 582–583
- operational procedure, 579–580
- quad-view, 579–582
- Color sequence illumination system (CSIS), 577–579
- Combustion by-products, 373
- Comfort, 1936, 1938, 1954, 1955
- Commercial aircraft, 2060–2064
- Commercial aircraft ECS, 2061
- Commercial air traffic, 2059
- Commercial air transportation
acetone, 2074
acrolein, 2073
aircraft cabins, 2059
aircraft ventilation, 2083
air quality investigations, 2059
air quality regulations, 2065
alkanes, 2074
benzaldehyde, 2073
cabin air contaminants, 2078–2081
cabin air quality, 2081
carbon monoxide (CO), 2069
CO₂, 2068
ECS, 2059–2064
formaldehyde, 2073
HEPA filters, 2060
limonene, 2073
mandatory standards, 2066
naphthalene, 2076
outside air supply rates, 2068
Ozone (O₃), 2069
particles, 2078
pathogens, 2081–2084
physiological response, 2084
regulations, 2064–2066
relative humidity, 2068
SVOCs, 2075, 2077
TVOC, 2075
VOCs, 2071
voluntary guidelines, 2066–2067
- Commercial and institutional in-duct air filters, 1730–1731
- Commuting
exposure modelling techniques, 2031
FMS, 2029
low-cost sensors, 2029–2031
personal exposure (*see* Personal monitoring)
portable devices, 2029–2031
- Comparative risk factor assessment, 1329
- Compliance, 1614, 1615
- Comprehensive smoke-free policies, 1150
- Computational fluid dynamics (CFD) model, 7, 656, 814, 829, 977, 978

- Computational fluid dynamics (CFD) modeling and simulation, IAQ control, 1848
CFX, 1846
Fluent, 1845–1846
governing equations and solving methods, 1842
model inputs and determinations, 1842–1843
model output and analysis of typical cases, 1843–1845
Phonics, 1846
purpose identification and model selection, 1841
Computer-assisted telephone follow-up system (CATI), 1083
Computer-assisted telephone interviewing technology, 1082
Computerized Neurocognitive Battery (CNB), 1195
Computer Managed Auxiliary Telephone Survey Access (CATI) technology, 1076
Concentration, 433, 434, 436, 458
Concentration-response (C-R) relationships, 1358
Condensation particle counter (CPC), 536
Confidence interval (CI), 1438, 1439
Consensus test standards, 1513
Constant emission factor model, 85
Constant vapor pressure model, 87
Consumer Product Safety Commission (CPSC), 1514
CONTAM, 958
Contaminant concentrations, 180
Continuous automatic encoder (CAE), 1063
Control Questionnaire (CCQ), 1192
Convective mass transfer coefficient, 82, 1747
Convergent thinking, 1382
Cooking aerosol
 additives, 413–414
 carbohydrates/sugars, 395
 chemical properties of particles, 390
 citizen science, 419
 cooking oils, 411–413
 cooking pans, 409–411
 cooking style/method/habit, 397–405
 emission rate, 397
 energy source, 398–408
 food, 415
 frying process, 392
 hydrolysis, 394
 lipid oxidation, 394
 methods, 392
 particle loss, 417
 particle mode diameter values, 389
 particle morphology, 418
 particle number emission rates, 389
 particulate matter, 389
 POA, 395
 SOA, 396–397
 solid fuels, 389
 surface area of pan, 416
 temperature, 415
 thermal alteration, 395
Cooking appliances, 170
Cooking fumes, 1074
Cooking oil fumes (COFs), 391, 1470
Cooking oils, 411–413
Cooking pans, 409–411
Cooking stoves, 171, 172, 174, 177, 178, 180, 181, 187, 188, 1152
Cooking style, 397–405
Cooktops, 170, 171, 180, 181
COPD Assessment Test (CAT), 1192
Coronary heart disease (CHD), 1149, 1193
Coronavirus, 1845
Cost benefit analysis, 1376–1383
Coupled Heat, Air, Moisture, and Pollutant Simulation (CHAMPS-Multizone), 1840
COVID-19 pandemic, 1483, 1548, 1875
C-reactive protein (CRP), 1273–1276
Criegee mechanism, 813, 913, 960
Croup, 1306
Cryogen-free cooling devices, 510
Cryogenic milling (CM), 57
Cup method, 668
Curvilinear motion, 269–270
Cyclic volatile methylsiloxanes (cVMS)
 emission of, 778
 models for prediction, 779
Cyclization, 394
Cytokines, 1283
Czech uranium miners, 1209
- D**
- Daily diary, 1081
Dampness, 1877–1878
Data-driven models, 1846–1847
Day-care centers
 air cleaning, 1866
 building typologies, 1859–1860
 children, 1858
 function/uses of space, 1861–1862
 IAQ, 1859
 indoor air pollutants, 1866
 occupancy, 1860
 purpose-built structures, 1858
 ventilation, 1864–1866

- Decamethylcyclopentasiloxane (D5), 778
 emission from skin lipids, 781
 modeling for emission, 779
 parameter determination in the model, 781–782
 validation of physics-based model, 782–783
- Decipol, 615, 616
- Dedicated outdoor air systems (DOAS), 1677
- Deicing fluids, 2080
- Demographic and Health Surveys (DHS), 1200
- Dendritic cells (DC), 1280
- Deposition, 241, 301
- Depression Anxiety Stress Scales (DASS), 1195
- Depuration compounds (DCs), 444
- Dermal exposure processes, 786
- Desiccator method, 47
- Detachment, 333, 337, 343, 345
- Diabetes, 1233
- Diastolic blood pressure (DBP), 1197
- Dibutyl phthalate (DBP), 1018, 1231
- Dichlorodiphenyltrichloroethane (DDT), 1031
- 1,2-Dichloroethane, 74
- Di(2-ethylhexyl) phthalate (DEHP), 1018, 1229, 1232
- Diethyl phthalate (DEP), 1031
- Differentially methylated regions (DMRs), 1288
- Differential mobility analyzer (DMA), 407, 537
- Diffusion, 250, 270–271
- Diffusion-based dynamic model, 362
- Diffusion coefficient, 254, 270, 272, 725
 CLIMPAQ method, 669
 cup method, 668
 inverse method, 670
 mesoscale structure, 681
 microbalance method, 670
 pore size distribution, 681
 two chamber method, 670
- Diffusive passive sampling method, 705
- Digital image processing, 582–583
- Diheptyl phthalate (DHP), 1231
- Di-isodecyl phthalate (DIDP), 1018, 1230, 1231
- Diisonyl phthalate (DINP), 1229
- Dimensionless analysis, 683–684
- Dimethylamine, 74
- Di-n-butyl phthalate (DnBP), 1118, 1119
- 2,4-Dinitrophenyl-hydrazine (DNPH), 48, 431, 495
- Direct exposure assessment, 990–992
- Direction sensors, 1065
- Direct measurement campaigns
 field campaigns, 993–994
 personal (breathing zone), 994–995
 sensor networks, 994
- Direct methods, 1058
- Direct olfactometry, 636, 637
- Direct sunlight, 868
- Dirichlet boundary condition, 310
- Disability-adjusted life years (DALYs), 24, 1329, 1330, 1333, 1335, 1344, 1347, 1349, 1351, 1356, 1358, 1360, 1361, 2137
- Displacement ventilation, 1652–1655
- D-limonene, 147, 148, 154–157
- Door open condition, 209
- Double exponential model, 86
- DPC coefficients (DPC), 1231
- Drag coefficient, 262
- Drag force, 262
- Driving modes, 2040
- Droplets, 2103–2105
- Drying/curing reference material, 752–753
- Dry materials, 1598
- Dual-scale calculation model, 683
- DuPont™ bags, 635
- Dust mites, 1872
- Dust/ surface sampling, 451–452
- Dust-to-breathing zone transport efficiency, 342
- Dynamic emission chamber test systems, 746–747
- Dynamic olfactometry, 631, 632, 634
- Dynamic shape factor, 265
- E**
- E-cig or vaping product use-associated lung injury (EVALI), 202
- Eco-driving behavior, 2043
- Ecolabeling system, 1629
- Eco Mark labeling system, 1630
- Economic costs
 Bayesian Network, 1483
 and benefits, 1478
 health, 1479–1481
 hospitality industry, 1482
 optimization methods, 1483
 reduced learning, 1481, 1482
 reduced work performance, 1481
 simple balance methods, 1483
 working from home, 1483
- Eddy diffusivity, 317
- Effective cleaning rate (ECR), 1722
- Effect size (ES), 1439
- Efficiency, 179, 1718–1734

- Elderly care centers (ECCs), IAQ
 carbon dioxide, 1973–1974
 challenges, 1976–1978
 nitrogen dioxide, 1971–1972
 ozone, 1972–1973
 particulate matter, 1965–1968
 volatile organic compounds, 1968–1971
- Electrical mobility diameter, 944
- Electric burners, 406
- Electron capture detector (ECD), 81, 436
- Electronically commutated motors
 (ECMs), 1728
- Electronic cigarettes, 200
 cardiovascular effects, 221
 chemical profiles of e-cig aerosols, 214–216
 e-cig emissions, to passive exposures/
 potential health, 202
 factors affecting chemical compositions,
 217–219
 factors affecting particle concentration,
 204–206
 generations of, 201
 human studies, 222
 in vivo/in vitro studies, 219–220
 particle concentration and size distribution,
 203–204
 particulate matter in e-cig aerosols, 203–206
 respiratory effects, 220–221
 thirdhand exposure, 219
- Electrostatic precipitator (ESP), 418
- Elemental carbon (EC), 525
- Elemental composition, 390
- Emission characteristics, 181
- Emission factor compliance approach, 1615
- Emission factors (EFs), 179, 182, 183, 2128
- Emission rates, 180
- Emissions, 130, 132–134, 137–140, 143–146,
 148, 153, 154, 156–158, 697–699
 chamber studies, 145–146
 formaldehyde, 49–56
 and listed ingredients, 144–145
- Emission source, 1824
 assembled material, 1826–1827
 dry material, 1824–1825
 wet material, 1825–1826
- Emission standards, 2033–2034
- Emission testing, VOC
 chemicals in, 743–746
 dynamic emission chamber test systems,
 746–747
 dynamic emission testing variability, 747
 examples of emission regulation, 743
 extractor/perforator methods, 746
- reference material (*see* Reference material)
 static methods, 746
 testing standards examples, 744–745
- Emission test standards
 ANSI/BIFMA e3 Furniture Sustainability
 Standard, 1628
 CDPH Standard Method V1.2, 1628
 Eco Mark labeling in Japan, 1630
 EN 16516 test method, 1629
 VOC emission testing and labeling system
 in China, 1629–1630
- Empirical models, 650, 1114
- Endocrine disruptors chemicals (EDCs), 1284
- End-use data, 169, 170
- Energy and Environment of Residential
Buildings (EERB), 8
- Energy conservation laws, 304
- Energy intensity, 179
- Energy Performance of Buildings Directive
(EPBD), 1894
- Energy services, 167, 168
- Energy sources, 165, 389
- Engine oil, 2079
- EN 16516 test method, 1629
- Entrainment zone, 595
- Envelope airtightness, 1691–1694
- Environmental burden of disease (EBD),
 1332–1334
- Environmental Burden of Disease in European
Countries (EBoDE), 1340
 exposure assessment, 1341
 exposure-response relationship modelling,
 1341–1345
 stressor selection, 1340–1341
- Environmental chamber testing method,
 1593–1595
 air sampling/ chemical analysis, 1605–1610
 data analysis/ interpretation, 1613–1617
 effect of product age, 1600
 emission factor, 1594–1596
 HPLC system, 1609–1610
 material emission characterization,
 1596–1599
 principles, 1594–1605
 and real applications, 1618–1628
 TD-GC/MS, 1607–1609
 test procedure, 1610–1613
 variables affecting emission rates, 1599
- Environmental Control System (ECS),
 2059–2064
- Environmental index
 in BREEAM, 1569–1571
 in CASGB, 1568–1569

- Environmental index (*cont.*)
 in CASHB, 1569–1572
 in LEED, 1569
 in WELL, 1569–1573
- Environmental Protection Agency (EPA), 1060, 1082, 1125
- Environmental surfaces, 1990–1996
- Environmental tobacco smoke (ETS), 6, 528, 1034, 1145, 1202
- Eosinophil cationic proteins (ECP), 1230
- EPA BASE protocol, 1691
- Epidemiology, 987
- Epigenetics, 1194
- Epithelial mesenchymal transition (EMT), 1234
- Equilibrium method, 445, 446
- estimated glomerular filtration rate (eGFR), 1195
- Ethanol, 1996
- Ethyl acrylate, 74
- Ethylene glycol, 2080
- Ethylene oxide, 2006
- European EBoDE Study, 1340–1345
- European Respiratory Society (ERS), 1191
- European Union (EU), 1629
- Exfiltration, 1678
- Exhaled breath condensate (EBC), 1258
- Exhaled gases, 907
- Exhaust, 2080
- Existing work performance outcomes, 1439
- Experiment protocols, 1391–1395
- Exposome, 988, 989
- Exposure
 assessment strategies, 1114
 biological agents, 1013
 contribution of indoor, 2134–2135
 dermal, 1012
 formaldehyde, 1016
 goods/personal, 1018–1021
 house dust, 1018
 indoor air, 1006, 1007, 1015
 indoor chemistry, 1018
 influencing factors, 2135–2136
 inhalation, 1009
 modelling techniques, 989, 2031
 non-dietary/indirect ingestion, 1013
 penetration vapors, 1015
 quantification, 2133–2136
 radon, 1016
 reduction, 186
 routes, 1007, 1008
 SVOCs, 1017
 VOCs, 1015
- Exposure assessment, 1058, 1059, 1062, 1063, 1096, 1098, 1099, 1110, 1341
- Exposure Research Group (ERG), 1063
- Exposure-response relationship modelling, 1341–1345
- Exposure science
 core elements, 987
 definitions, 988–989
 description, 986
 direct vs. indirect assessment, 990
 in environmental epidemiology, 988
 epidemiology, 987
 indoor air quality, 987
 toxicology, 987
- External convective mass transfer, 658
- Extractive electrospray ionization mass spectrometer (EESI-MS), 947
- Eye symptoms, 1954
- F**
- Face to face interviews, 1067
- Fanger's comfort model, 626
- Fan-induced airflow, 596
- Fan-jet stoves, 1153
- Fan pressurization testing, 1692
- Fibrinogen, 1272
- Fick's diffusion law, 669
- Fick's first law of diffusion, 254, 270
- Fick's law, 90, 473, 704, 718
- Fick's second law, 697
- Field intervention experiments, 1377
- Film reference materials, 753–755, 759
- Filter inlet, for gases/aerosols, 947
- Filter performance rating (FPR), 1722
- Filtration, 458, 1718, 2034
 buildings, filter applications in, 1722–1731
 impacts of filters, in real buildings, 1731–1733
 in-duct filters, 1727–1731
 overall filter efficiency, 1719–1720
 portable and room-level systems, 1722–1727
 single fiber collection efficiency, 1718–1719
 test methods and rating systems, 1721–1722
- Fireplaces, 169, 173, 175, 176, 180, 181
- First-order decay model, 86, 650
- Fixed Monitoring Stations (FMS), 2029
- Flame ionization detector (FID), 435, 1607
- Flask method, 46
- FLEC chamber method, 699
- Fluent, 1845–1846

- Fluidized-bed desorption (FBD) method, 57, 668
Fluorinated ethylene propylene(FEP), 635
Follicle-stimulating hormone (FSH), 1285
Food and Agriculture Organization, 169
Food contact materials (FCMs), 1117
Formaldehyde, 133, 135, 137–139, 145–148, 150, 152, 153, 156, 495–497, 746, 751, 754, 757, 763, 1163, 1211, 2008, 2073
acute lethality, 41
carcinogenicity, 42–43
chromatographic method, 48–49
desiccator method, 47
developmental/reproductive toxicity, 42
3-dimensional structure, 41
environmental factors on, 60–65
flask method, 46
gas analysis method, 47
genotoxicity, 42
hazards, 41–43
indoor and outdoor formaldehyde concentrations, 45
international guideline values, 44
key emission parameters of, 57–60
long-term emission model, 53–56
neurotoxicity, 42
nonlethal toxicity, 41
perforator method, 46
physical and chemical properties, 42
properties, 38–41
relative humidity, impact of, 64
sensors, 49
short-term emission models, 49–53
spectrophotometric method, 47–48
standard test methods, 46–47
structure of, 41
temperature and humidity, emission rate, 64–65
temperature on C_0 , impact of, 62–63
temperature on D_m , impact of, 62–63
temperature on K , impact of, 63
usages and pollution levels, 43–46
worldwide annual production, 43
Formaldehyde (FA), 1223–1228
Formaldehyde multimode monitor, 496
Formaldehyde removal, TCO
catalyst properties, 1759
formaldehyde conversion, 1761
temperature and oxygen concentration effect, 1763
Formalin, 41
Fractional exhaled nitric oxide (FeNO), 1191, 1254–1257
Fragranced consumer products, 130, 131, 133, 134, 137–140, 144–148, 158
Fragrance-free environments, 157
Fragrance-free policies and practices, 152–157
Fragrance-free products, 154–155
France, indoor air pollution
evaluation of yearly morbidity, 1353–1354
evaluation of yearly mortality, 1352–1353
pollutants, 1351–1352
socio-economic cost evaluation, 1354–1355
Freundlich isotherm, 714
Fuels
consumption, 2060
homogeneous, 189
processing, 189
switching, 190
type, 2033–2034
Fugacity models, 792
Fugitive emissions, 2128–2131, 2133
Full chain model, 1303
environmental exposure, 1303
human exposure, 1304–1305
human health, 1305
SELMA study to, 1308–1316
Furnishings, 886, 887
- G**
Gas analysis method, 47
Gas behavior, 248–249
kinetic theory of gases, 249–256
macroscopic properties of gases, 256–261
properties of gases, 249
Gas burners, 171, 176
Gas chromatography-flame ionization detection (GC-FID), 7
Gas chromatography-mass spectrometry (GC/MS), 7, 132, 133, 136, 137, 140, 143, 144, 1521
Gas chromatography-olfactometry (GC-O), 629
Gas chromatography-olfactometry-mass spectrometry (GC-O-MS), 629
Gaseous pollutants, 2106–2109
Gas flame, 406
Gas-particle equilibrium, 370
Gas-phase chemicals, 350
Gas-phase chemistry, 958–963
chlorine radical, reactions of, 848–850
hydroxyl radical reactions, 842–846
nitrate radical reactions, 846–848
oxidants, 850
ozone reactions, 839–842
particle formation, 850–851

- Gas phase photochemical reactions indoors, 864–866
- Gas-phase pollutants/airborne particles
- adsorption-based approach, 354–356
 - adsorption-based model, 366
 - BET isotherm, 352
 - deposition rate of airborne particles, 372
 - diffusion-based model, 358–361
 - equilibrium interaction, 353, 354
 - equilibrium model, 357
 - gas-phase concentration, 351
 - increase emission rate, 351
 - intraparticle diffusion coefficient, 371–372
 - intraparticle reaction of SVOCs, 364–366
 - Langmuirian sorption, 352
 - lumped parameter method, 361–364
 - mass accommodation coefficient, 369–371
 - particle-gas partition coefficient (K_p), 367–369
 - poly parameter approach, 356–357
- Gas-phase pollutants/settled dust
- aerosol dynamics, 375–376
 - diffusion-based model, 376–379
 - dust-gas partition coefficient, 379
 - dynamic models, 374
 - equilibrium model, 374
 - indoor materials or consumer products, 373
 - indoor pollutants, 373
- Gas-phase reaction models, 816
- Gas-phase semi-volatile organic compounds, 698
- Gas-phase SVOCs, 351
- Gas-surface partition coefficient, 720
- Gas-surface partitioning behavior, 827
- Gas viscosity, 262
- Genetics/omics, 1198
- Genotoxicity, 42
- Geographic information systems (GIS), 1061
- Geriatric Depression Scale (GDS), 1195
- Global and European guidelines, IAQ, 1492
- Global burden of disease studies (GBD), 1327–1330
- Global Navigation Satellite System (GNSS), 1061
- Global Positioning System (GPS), 1062
- Global warming, 26, 1962, 1973
- Glutaraldehyde, 2005, 2008
- Glutathione (GSH), 1231
- Glycocholic acid, 921
- Graphitic carbon, 1606
- Gravitational force, 263
- Green building movements, 1512
- Greengard test, 1604
- Groningen Sleep Quality Scale (GSQS), 1464
- Guidance documents, 1618
- H**
- Halo effect, 1386
- Halogenated flame retardants (HFR), 1576
- Halons, 74
- Hantzsch method, 495
- The HAPIN Trial, 1156
- Harvard School of Public Health Personal Exposure Monitor (H-PEM), 521
- Hazard index, 1332
- Head-down tilt bed rest (HDBR), 1412
- Headspace analysis techniques, 133
- Headspace method, 670–671
- Health, 5, 7, 12, 14, 16–18, 22, 23, 25
- Healthcare-associated infections (HAI), 1989, 1993, 2004
- Health costs, 1479, 1480
- Health effects, 131, 137, 147, 157, 1849, 1953, 1964, 1967, 1973, 1974, 1976
- Health effects of e-cigs
- cardiovascular effects, 221
 - in vivo and in vitro studies, 219–220
 - passive exposures to SHV aerosols, 222
 - respiratory effects, 220
- Healthier routes planning, 2045–2046
- Health impact assessment (HIA), 1334–1335, 2044
- Health impacts, 1869, 1874
- Health risk assessment (HRA), 1330
- Health risks, 830
- amplified contribution, 2137–2139
 - characterization, 1327
 - clean household energy transition, 2137–2139
 - HAP-related, 2136–2139
- HealthVent study, 1345–1351
- Heart disease, 1202
- Heart rate variability (HRV), 1192
- Heating and air conditioning (HAC) fan, 417
- Heating, ventilation, and air conditioning (HVAC), 866, 1514, 1716, 1730, 1938
- Helium-filled soap bubbles (HFSB), 574
- Hematologic health, blood coagulation biomarkers, 1271–1273
- Hemoglobin (Hb), 1268
- Henry's law, 75, 894
- Hesperidin (HP), 1226

- Heterogeneous adsorption theory, 679
Heterogenous photochemistry, 814
Hexabromocyclododecanes (HBCDs), 110–112, 1036
High efficiency particulate air (HEPA) filters, 1014, 1722, 2060, 2062, 2063
Higher-order decay models, 650
Highly oxygenated organic molecules, 826
High-performance liquid chromatography (HPLC), 49, 80, 81, 431, 432, 436, 1521, 1609–1610
High-sensitivity CRP (hsCRP), 1273
High-speed ring, 600
High-temperature particles
 emission characteristics, 2098–2100
 migration characteristics, 2100–2102
High-touch surfaces, 1992
History, indoor air quality research
 early stage development, 5–6
 financial support, 23
 modern developments, 6–10
 multidisciplinary co-operation, 23
 quantitative analysis of general information, in Web of Science, 10–22
 targeting health effects, 23
Homeostasis, 1398, 1399
Homogeneous reference materials, 764
Honeycomb monolith PCO reactor, 1748
HONO photolysis, 863, 864, 871
Hospital Anxiety and Depression Scale (HADS), 1195
Hospital products and chemicals
 dust in dental clinics and laboratories, 2011–2013
 hospital occupations and departments, 2013–2016
 operating rooms (OR)/surgical units and orthopedics, 2009–2011
Hossain’s model, 1748
Household air pollution (HAP), 1152
 definition, 2126–2127
 exposure and influencing factors, 2133–2136
 health risks, 1154–1155, 2136–2139
 indoor combustion, 2128–2133
 management, 1155–1157
 social-economic status, 2126
 sources/exposure, 1152–1154, 2127–2128
House Observations of Microbial and Environmental Chemistry (HOMEChem), 500, 506, 512, 934
Human activity, 332, 334, 338, 340, 342
Human activity patterns, 1085
Human bioeffluents, 626
 on cognitive performance, 1408–1409
 physiological pathways, impact cognitive performance, 1412
Human emissions
 breath emissions, 907–909
 diffusion, 254
 health effects of, 922–923
 skin emissions, 908–911
Human exposure, 1085
Human generated particle emissions, 342
Human malodor, 815
HuMAN’s system, 1066
Humidity, 613, 918
Hybrid ventilation, 1647, 1649
Hydraulic fluids, 2078, 2080
Hydrocarbons (HC), 915
Hydrochloric acid (HCl) droplets, 2104, 2105
Hydrochlorofluorocarbons (HCFC), 74
Hydrogen cyanide, 2010
Hydrogen peroxide, 865
Hydrolysis, 895–896
Hydroperoxy radical, 844
1-hydroxypyrene (1-HOP), 1470
Hydroxyl radical reactions, 842–846
Hypermethylation, 1288
Hypersensitivity pneumonitis, 1179
- ## I
- IAQ control strategies
 assessment procedure, 1785
 baseline cases, 1781–1785
 multiscale IAQ model, 1779–1781
- IEC profile
 membership, 1549
 participation, 1551–1552
 structure, 1550–1551
 technical committees, 1550–1551
- IEC 63086 series standards, 1553
- IEC/TC 59
 development process or plans, 1554–1556
 IEC 63086 series standards, 1553
 man-made pollution items, 1554
 testing and certification, 1554
 with ISO/TC 142, 1556
- IEC/TC 61, 1552–1553
- Immune cells
 cytokines, 1283
 DC, 1280
 lymphocytes, 1280
- Immune system, 1229, 1237
- Immunoglobulin E (IgE), 1283

- Immunoglobulins (Igs), 1280–1283
Immunotoxicity, 1223, 1227
Impermeable surfaces, 713
Improved C-history method, 678–679
Improved cook stoves, 1152
In-cabin environment, VOC emission, 776–778
In-cabin pollutants, 2025–2029
Incidence, 1329, 1333, 1335
Indirect assessment method, 1058, 1059
Indirect exposure assessment
 airborne pollutant, 995
 ambient pollution, 995–996
Indirect olfactometry, 635, 636
Indoor
 activities, 276
 concentration, 277
 particles, 276
Indoor airborne particles, 351
Indoor air environments
 fragrance-free environments, preferences for, 157
 fragrance-free policies and practices, 152–157
Indoor air flow
 airflow measurement system, 574
 PTV, 571
 room-scale air flow measurement, 574
 smoke/colored gases, 570
Indoor air modeling, 1540
Indoor air pollutants (IAPs), 1085, 1512, 1937
 allergens, 1871–1872
 categories, 1515
 chemical pollutants, 1940, 1941
 chronic risk assessment approach, 1940
 CO, 1869–1870
 dampness and mold, 1877–1878
 exposure, 1059
 IAQ-specific guidelines, 1939
 infectious diseases, 1875–1877
 NO₂, 1868–1869
 O₃, 1870–1871
 OFFCAIR study, 1939
 PM, 1872–1873
 radon, 1880
 sources and determinants, 1940–1943
 VOCs, 1877–1878
Indoor air pollution, 1202
 bioaerosols, 1164–1167
 blood coagulation biomarkers, 1271–1273
 blood related parameters, 1268–1271
 carbon monoxide, 1150–1152
 cardiovascular health effects, 1261
 cardiovascular system, 1265
 AI, 1266
 BP, 1266
 cardiac autonomic function, 1261–1265
 PWV, 1265
 RHI, 1265
 vascular function, 1265
 household air pollution, 1152–1157
 oxidative stress, 1278–1279
 radon, 1157–1160
 respiratory health, 1253–1254–1260
 respiratory infections, 1167–1171
 secondhand smoke exposure, 1145–1150
 systemic inflammation, 1273–1277
 volatile and semi-volatile organic compounds, 1161–1164
Indoor air quality emission simulation tool (IA-Quest), 1833–1834
Indoor air quality health-based guidelines, 1974–1976
Indoor air quality (IAQ), 130–132, 136, 137, 147, 152, 156, 158, 204, 210, 217, 987, 1373, 1375, 1420–1431, 1478, 1512, 1676, 1774, 1786, 1792, 1799, 2129
 air cleaning, 1864–1866
 air pollutants/sleep, 1470, 1471
 air temperature, 1862–1863
 ANSI/ASHRAE standards, 1528
 aromatherapy, 1472
 assessment, 1904
 ASTM standards, 1523, 1524
 ASTM standards Subcommittee D01.28, 1518
 ASTM standards Subcommittee D07.03, 1518
 ASTM standards Subcommittee D22.01, 1518
 ASTM standards Subcommittee D22.05, 1515–1517
 ASTM standards Subcommittee D22.08, 1518
 ASTM standards Subcommittee E06.41, 1518
 bedroom, 1464
 classroom IAQ, 1894–1900
 CO₂, 1904–1912
 CO₂ level, 1465, 1466
 day-care center (*see* Day-care center)
 environmental conditions, 1515
 EPA TSCA, 1539
 evidence gap, 1925
 government regulations, 1521
 guidelines, 1492

- health outcomes in office workers, 1952–1954
humidity and temperature, 1937
HVAC systems, 1522, 1937
improve sleep, improve, 1473
indoor air pollutants, 1866
influencing factors and correlations, 1925–1926
ISO TC 146, 1519, 1521
long-term studies, 1679
management and risk mitigation, 1955
mechanisms, 1471
microenvironmental characteristics, 1943
monitoring approaches, 1944–1948
 NO_2 , 1912–1914
non-industrial environments, 1936
occupational risk prevention programs, 1943
office buildings, 1937–1938
office work performance (*see* Office work performance, IAQ)
perception/ health symptoms, 1948–1952
personal exposure, 1936
PM, 1914–1919
pollutants, bedroom, 1466, 1467
problem building, 1943
relative humidity, 1862–1863
in schools (*see* Schools)
short-term studies, 1679
sleep quality, 1473
strategic considerations, 1938–1939
temperature, 1472
US EPA, 1521
ventilation, 1469, 1470, 1528, 1864–1866
ventilation rates, 1898–1904
voluntary consensus standards, 1527
- Indoor air quality (IAQ) control
computational fluid dynamics modeling and simulation, 1841–1846
data-driven models, 1846–1847
multi-zone modeling and simulation, 1834–1840
occupant behavior, 1849
performance-based approach, principle of, 1818–1821
single-zone modeling and simulation, 1821–1834
smart sensors and big data, 1849
- Indoor air quality problems
adverse health effects, 1190
bladder cancer, 1204
breast cancer, 1205
cardiovascular effects, 1205–1206
- cardiovascular health, 1192–1194
chemical composition, 1203
cognitive health, 1195
effect on respiratory system, 1196–1197
effects on cardiovascular system, 1197–1198
ETS, 1202
ETS/sinus cancer, 1204
eye diseases and symptoms, 1195
formaldehyde, 1211
indoor VOCs, 1212
kidney health, 1195
long-term health effects, 1199–1202
lung cancer, 1203, 1207–1208
mental health, 1195
mortality, 1190
 NO_2 , 1209, 1210
NOAEL, 1212
non-cancer respiratory health effects, 1205
poor indoor air quality, 1190
radon, 1207
respiratory system, 1190–1192
short-term exposure, 1198
skin diseases and symptoms, 1194
VOCs, 1211
- Indoor Air Quality Procedure (IAQP), 1532
- Indoor air quality related papers
annual number of peer-reviewed papers, 20
average citations, 19–22
institutions, 19–21
international journals, 19
specific indoor air pollutants, 10–20
- Indoor air quality research
academy of ISIAQ Fellows, 8–9
annual number of peer-reviewed papers, 20
burden of disease, 24
early stage development, 5–6
financial support, 23
Indoor Air Conferences, 7–8
indoor air quality problems, 26
ISIAQ, 9–10
machine learning system and big data analysis technology, 24–25
modern developments, 6–19
multidisciplinary co-operation, 23
public health, 26
quantitative analysis of general information, in Web of Science, 10–22
representative events/works, 10–19
targeting health effects, 23
- Indoor air quality, ventilation and energy conservation (IAQVEC), 8
- Indoor air sources, 79

- Indoor analytical chemistry
 analytical chemistry approaches, 936–937
 bulk vs. compound-specific measurement, 934–935
 chemical vs. physical analysis, 935–936
 instrumental analysis, 933–934
 low cost sensors vs. research
 instrumentation, 936
 off-line vs. on-line measurements, 935
 on-line measurement of gases, 937–942
 on-line measurement of particles, 942–948
 surface measurements, 948
- Indoor chemical emission, 1115
- Indoor chemicals, 350
- Indoor chemistry modelling, 812
 analytical tools in, 815–816
 box model for indoor air pollutants, 956–958
 gas-phase chemistry, 958–963
 indoor air gas phase chemistry, 813
 indoor particulate matter concentration, 963–970
 modeling of gas-, particle-and surface-phase processes, 816–817
 vs. outdoor chemistry, 812
 photochemistry, 813
 surface chemistry modeling, 814, 970–977
- Indoor combustion
 emissions, 2128
 fugitive emission, 2129–2131
 HAP, 2131–2133
 I/O, 2133
- Indoor environmental quality (IEQ), 1374, 1438, 1439, 1494, 1936
 cost-benefit analysis, 1376–1383
 goals, 1373
 productivity belief, 1374
 simulation, 1375
- Indoor environments, 350, 389, 1077
 assumption, 1117
 calculation of concentrations, 1123
 clothing-air partitioning, 1128
 DnBP, 1123, 1127
 exposure calculations, 1123–1125, 1132
 exposure estimation, 1129, 1130
 impact of clothing, 1128
 modeling, 1118
 model parameters, 1123
 model selection, 1120, 1121, 1131
 parameterization, 1118, 1122
 TCEP, 1130, 1132, 1133
 uncertainties, 1127
- Indoor exposure, 1119, 1311, 1312, 2134–2135
- Indoor formaldehyde concentration levels, 44
- Indoor gas-phase chemistry
 chlorine radical, reactions of, 848–850
 hydroxyl radical reactions, 842–846
 nitrate radical reactions, 846–848
 oxidants, 850
 ozone reactions, 839–842
 particle formation, 850–851
- Indoor ingorganic aerosol, 969–970
- Indoor location, 1078
 age/gender, 1079
 gender/employment station, 1079
 region, 1079
 season, 1079
- Indoor organic aerosol, 967–969
- Indoor-outdoor air pressure differences, 1684, 1693
- Indoor/outdoor ratio (I/O), 2133
- Indoor particle dynamics, 240
 deposition, 241
 infiltration, 240
 resuspension, 241
- Indoor photochemistry, 863–864
 aqueous phase chemistry, 874
 condensed phase and heterogeneous, 871–874
 in dust and on surface films, 873–874
 factors controlling gas phase, 866–870
 photochemical formation of oxidants on painted surfaces, 872
 solar photon flux, 867–868
- Indoor photolabile species, 865
- Indoor positioning system (IPS), 1063
- Indoor surface chemistry
 acid-base chemistry, 893–895
 chlorine chemistry, 893
 hydrolysis, 895–896
 nitrogen oxides, 891–892
 ozone initiated chemistry, 888–891
- Indoor VOC concentration
 constant emission factor model, 85
 constant vapor pressure model, 87
 double exponential model, 86
 emission source models, 84
 first-order decay model, 86
 influential factors of, 92–93
 interfacial mass transfer models, 87
 internal diffusion mass transfer models, 89
 mass transfer related models, 90
 non-surface source, 84
 nth order decay model, 87
 second-order decay model, 86
 semi-empirical model, 89

- vapor pressure and boundary layer model, 88
VBX model, 88
- Indoor VOC pollution benzene, 1227–1228 formaldehyde and toxic effects, 1223–1227
- Induced sputum, 1191
- In-duct filters commercial and institutional, 1730–1731 residential, 1727–1729
- Inductively couple plasma (ICP), 524
- Industrial building airflow partition, 2111, 2112 analogy method, 2119, 2120 control demand, 2097 droplets, 2103–2105 environmental assessment, 2116 environmental parameters, 2116–2118 gaseous pollutants, 2106–2109 human-oriented commercial/residential buildings, 2096 indoor sources, 2096, 2097 model experiment, 2120, 2121 natural zoning, 2110, 2111 numerical simulation, 2121 physical partition, 2110, 2111
- Inertial forces, 259, 260, 262, 266
- Infectious diseases, 1875–1877
- Inferential statistics, 1384
- Infiltration, 240, 888, 1678
- Infiltration factor, 287, 290 equilibrium approach, 286 modeling methods, 287 rates, 1683, 1693 regression approach, 285, 286 tracer element, 286, 287
- Inflammatory cytokines, 1276–1277
- Inflammatory/oxidative indicators, 1193
- Inhalation reference concentration (RfC), 1525
- Inhalation/skin exposure chemical exposure to cleaning, disinfecting, 1991 cleaning/disinfecting activities, 2007 cleaning/disinfecting chemicals, 1996–2004 cleaning/disinfecting products, 1989 demand for health services, 1988 dental occupations and units, 2012 detergents, 1989 disinfectants/antiseptics, 2004 disinfectants/sterilizing chemicals, 2004–2006 environmental surfaces, 1990–1996 glues, 1989
- glutaraldehyde, 2008 hazardous drugs, 1989 heavy metals, 1989 hospital occupations and departments, 2014 hospital products and chemicals (see Hospital products and chemicals) laboratory chemical reagents, 1989 non-fatal injuries and illnesses, 1989 solvents, 1989 sterilizing agents, 1989 sterilizing chemicals and antiseptics, 1991 surgical rooms/OR, endoscopy, procedure rooms, 2009 surgical smoke, 1989 waste anesthetic gases, 1989 work-related dermatitis, 2008
- Initial emittable concentration fluidized-bed desorption method, 668 multi-flushing extraction method, 668 non-fitting method, 668
- Inorganic ions, 390
- Inorganic trace gases, 938
- Institute for Health Metrics and Evaluation (IHME), 1330
- Institute for Research in Construction (IRC), 1833
- Instrumental analysis, 933–934
- Intake fraction (iF), 996–998
- Interfacial mass transfer models, 87
- Interior materials, 2035–2037
- Inter-laboratory studies building product reference materials, 750–751 designed reference materials for chamber testing, 759–760 film reference material, 759 lacquer reference material, 761 procedure variability, 768 RSDs for, 762–763
- Interleukin-17 (IL-17), 1195
- Interleukin 17A (IL-17A), 1236
- Internal diffusion mass transfer models, 89
- International Academy of Indoor Air Sciences (IAIAS), 8
- International Agency for Research on Cancer (IARC), 1223, 1233
- International Conference on Indoor Air, 7
- International Energy Agency, 169
- International Organization for Standardization (ISO), 1514
- ISO/TC 142, 1560
- membership, 1558–1559
- participation, 1560

- International Organization for Standardization (ISO) (*cont.*)
 standards of ISO/TC 142, 1560
 structure, 1559
 technical committees, 1560
- International Society of Indoor Air Quality and Climate (ISIAQ), 9–10
- International standards, 1549, 1551, 1553, 1557, 1559, 1561
- International Symposium of Heating, Ventilating and Air-Conditioning (ISHVAC), 8
- Inter-zonal airflow, 1835
- Inverse method, 670
- Iodophores, 2004
- Ionic liquid SPMD (IL-SPMD), 473
- Irradiance, 859
- Isobutylmethacrylate, 2012
- Iso-prostaglandin F2 α (8-isoPGF2 α), 1278
- ISO TC 142, 1556
- J**
- Jet core zone, 595
- Junge-Pankow model, 732, 800
- K**
- Kerosene, 1153
- Key emission parameters, of formaldehyde, 56–60
- Key parameters, 38, 50, 55, 61, 66
- Kidney health, 1195
- Kidneys, 1288
- Kinetic gas theory, 249–251
 diffusion, 254
 mean free path, 253–254
 mean velocity, 253
 pressure, 251–252
 viscosity, 254–256
- Kinetic model, 1828
- Kinetic multilayer (KM-SUB-Skin) model, 784–785
- Kinetic reaction model, 1763–1768
- Kitchen smoke, 1080
- Kitchen ventilation systems, 417
- Koble-Corrigan model, 714
- L**
- Labeling programs, 1626–1628
- Labeling systems, PM control
 BREEAM, 1582
 CASGB, 1578–1581
 CASHB, 1582–1583
 LEED, 1582
 WELL, 1583–1584
- Lacquer reference materials, 752, 759
- Lagrangian approach, 284, 309
- Laminar flow, 259
- Land use regression (LUR), 996, 2032
- Langmuir isotherm, 352
- Laplace transformation, 52, 776
- Laser Doppler anemometry (LDA), 570
- Latent tuberculosis infection (LTBI), 2136
- Leadership in Energy and Environmental Design (LEED), 1527, 1567
 environmental index, 1569
 performance index method, 1573
 PM control, 1581–1582
 prescriptive index method, 1573
 sources requirements in, 1575
- LEED rating system, 1626
- Legionnaires' disease, 1169–1170
- Levulinic acid, 918
- Leydig cell tumor, 1212
- Life expectancy (LE), 1335
- Lifetime Achievement Award, 9
- Light absorbing carbon (LAC), 529
- Lighting appliances, 176, 177
- Light sources, 866, 869
- Limit of detection (LOD), 933
- Limonene, 2073
- Linear curve fitting, 685
- Linear isotherm, 713
- Lipid oxidation, 394
- Lipid ozonolysis, 890
- Liquid deicing fluid, 2080
- Liquid diffusion-film-emission (LiFE)
 reference material, 756–757
- Local exhaust ventilation (LEV), 1996
 adjustable exhaust hoods, 2112
 movable exhaust hoods, 2113, 2114
 parallel-flow push-pull ventilation, 2114
 vortex ventilation hoods, 2115, 2116
- Long-term emission model, 53–56
- Long-term ventilation studies, 1679
- Low-concentration benzene, 76
- Low-cost sensors, 948, 949, 2029–2031
- Low-density polyethylene (LDPE), 473
- Low emitting cooking oil, 413
- Low-emitting products, 1618
- Lower respiratory infection (LRI), 1199
- Lowest concentration of interest (LCI), 1629
- Lowest-observed-adverse-effect level (LOAEL), 1526
- Low-touch surfaces, 1993
- LPM-based model, 363
- Lumped parameter model, 1740
- Lung cancer, 1159, 1202, 1207

- Lung function parameters, 1258–1260
Luteinizing hormone (LH), 1285
Lymphocyte micronucleus, 76
- M**
- Machine learning, 24, 25
Machine learning methods, 1198
Macroscopic properties, of gases, 256
 boundary layers, 257
 flow separation, 261
 flow stagnation, 260
 gas flow, tube, 258
 laminar and turbulent flow, 259
 Reynolds number, 259
 streamlines, 256
Maleic anhydride, 74
Malondialdehyde (MDA), 1231, 1258, 1278
Markov network, 1065
Masonry heaters, 175
Mass balance theory, 1839
Mass-identification-detection (MID), 1750
Mass spectral detector (MSD), 1607
Mass spectrometry (MS), 459–460, 526
Mass transfer, 51
 Biot number, 683
 fourier number, 683
 source/sink models for dry building materials, 652–664
 source/sink models for wet building materials, 661
Mass transfer-based model, 90, 91, 793–797
Mass-transfer model, SVOC emission, 708
Material-air-material (M-A-M) open-ended cylinder micro chamber, 701
Material emission testing, 619
Materials Emission DataBase and Indoor Air Quality (MEDB-IAQ), 1833
Matrix metalloproteinase-9 (MMP-9), 1284
Maximal mid-expiratory flow (MMEF), 1259
Mean arterial blood pressure
 (MABP), 1192
Mean free path, 253–254, 272
Mean particle velocity, 271
Mean velocity, 253
Mechanical ventilation, 1650–1660
 displacement ventilation, 1652–1655
 mixing ventilation, 1650–1652
 residential building, 1644–1647
Mechanistic models, 1114
Mediated exposure pathways, 1117
Melatonin (MT), 1224
Membership levels, 1549, 1558–1559
Mercury intrusion porosimetry (MIP) experiments, 681
Metabolic Equivalent (MET), 1010
Metabolic indicators, 1193
Metabolic system, 1289–1290
Metabolomics, 1194
Meteorological variables, 2038–2040
Methacrylates, 2011
Methicillin-resistant *Staphylococcus aureus* (MRSA), 1993
3-Methyl-2-benzothiazolinone hydrazine (MBTH), 48, 431, 432
Methyl methylacrylates (MMA), 2008
4-(Methylnitrosamino)-1-(3-pyridyl)-1-butanone, 217
Metrics, 1373–1375
Microbalance method, 670
Micro emission cell (μ EC) chamber, 703
Microenvironment, 993
Microgasifier cook stoves, 1153
Micro-level activity time series (MLATS), 1062
Micro-particle Performance Rating (MPR), 1722
MicroPEM, 522
MicroRNAs (miRNAs), 1194, 1198, 1283
MicroTrac, 1062
Microvascular function (MVF), 1265
Microwave-assisted extraction (MAE), 453, 455–456
Minimal risk level (MRL), 1526
Minimum efficiency reporting value (MERV), 1522, 1721
MIRA Pico formaldehyde analyzer, 497
Mitigation, 2146, 2156, 2159
Mitochondrial DNA (mtDNA), 1194
Mixing ventilation (MV), 1650–1652
Mobile phone method, 1064
Mobility patterns, 1065
Modular mechanistic modeling, 1114
Mold, 1877–1878
Molecular diffusion, 255
Molecular signatures, 920
Momentum conservation laws, 303
Monoacylglycerol (MAG), 1232
Monocyte chemoattractant protein-1 (MCP-1), 1277
Monolith PCO reactor, 1742
Monoterpenes, 840–842
Multi-attribute task battery (MATB) tasks, 1410
Multi-emission/flush regression method, 671
Multi-flushing extraction method, 668
Multi-layer source models, 657–658
Multi-objective optimization, 788
Multi-pathway exposure model, 779
Multi-phase approach, 659

- Multiphase chemistry, 824, 825
- Multiple chemical sensitivity, 1143, 1172
 clinical and epidemiological picture, 1173–1174
 definition, 1173
 etiology, 1173
 management, 1174–1177
- Multiple functional ingredients, 1993
- Multiple organ systems toxicity, 1238
- Multiple sink residential rooms, 774–775
- Multiplex assays, 1276
- Multiscale built environment system, 1779
- Multi-sorption/emission process, 674
- Multi-source emission model, 777
- Multistage series-connection fractal capillary-bundle (MSFC) model, 683
- Multi-zone modelling/simulation, IAQ control
 CHAMPS, 1840
 model assumptions and governing equations, 1835
 model input parameters and determination, 1835–1836
 model output and analysis of typical cases, 1836–1839
 PACT-IAQ, 1840
 purpose identification and model selection, 1834
- Multizone tracer gas methods, 1685, 1700
- Myelodysplastic syndrome, 1228
- Myeloperoxidase (MPO), 1277
- Myrcia*, 414
- N**
- N-Alcanoic acid emission, 390
- NanoTracer, 409
- Naphthalene, 390, 2076
- National Aeronautics and Space Administration (NASA), 2063
- National air quality standards, 1498–1500
 guideline values for common pollutants, 1504
 guideline values for organic and radioactive pollutants, 1507–1508
 24hr threshold/guideline values for CO, 1506
 24hr threshold/guideline values for particulate matter, 1506
 for IAQ management, 1502–1503
- National Ambient Air Quality Standard (NAAQS), 519
- National Green Building Standard (NGBS), 1527
- National Human Activity Pattern Survey (NHAPS), 1060, 1082, 1083, 1085, 1097
- National Institute for Occupational Safety and Health (NIOSH), 48, 1514
- National Statistical Office Life Time Survey, 1099
- National Technology Transfer and Advancement Act (NTTAA), 1526
- Natural/native immunity, 1279
- Natural ventilation procedure (NVP), 1529, 1533, 2158
 office building, 1650
 residential building, 1640–1644
- Natural zoning, 2110, 2111
- Navier-Stokes equation, 256, 1842
- n-butanol, 623
- Needle trap device (NTD), 448, 450
- Nervous system, 1230
- Neurobehavioral tests, 1427
- Neurological pathways, 1399–1402
- Neuropeptide S receptor 1 (NPSR1), 1283
- Neurotoxicity, 42, 1223
- Newtonian drag, 262
- Newton's law of viscosity, 255
- Nicotine, 212
- Night sleep, 1082
- Nitrate radical reactions, 846–848
- Nitrate radicals, 75
- Nitric acid, 860
- Nitric oxide, 839
- Nitrogen dioxide (NO₂), 1209, 1210, 1497, 1868–1869, 1895, 1971–1972, 2027
 influencing factors, 1913–1914
 levels, 1913
 limits, 1912
 photolysis, 865
- Nitrogen oxides (NO_x), 891–892, 2064
- Nitrous acid, 864, 891
- N-methyl-D-aspartic acid receptor (NMDA2R), 1225
- N'-Nitrosonornicotine (NNN), 217
- Nondispersive Infrared (NDIR) analyzer, 633
- Non-fitting method, 668
- Non-intrusive measurement, 571, 572, 591
- Nonlethal toxicity, 41
- Non-rapid eye movement (NREM), 1462, 1463
- Non-regulatory networks, 991
- Non-sensory analysis methods, 628

- Non-targeted analysis (NTA) method, 1538
Non-volatile species, 239
No-observed-adverse-effect-level (NOAEL),
 1212, 1526
No observed effect level (NOEL), 1332
*n*th order decay model, 87
Null hypothesis (NH), 1390
Null hypothesis significance test method
 (NHST), 1439
- O**
- Occupancy, 1860
Occupant emissions and chemistry
 health effects of human emissions, 922–923
 microbial population, role of, 920–921
 modifying factors, 917–920
 occupant-related chemical transformations,
 911–916
 perceived air quality, 921–922
 primary emissions from humans, 907–911
 SOA, 916–917
Occupational asthma (OA), 2006
Occupational exposure limits (OEL), 46
Octafluorocyclobutane, 2106
Octamethylcyclotetrasiloxane, 778
Octenidine, 2004
Ocular methods, 1954
Odor intensity, 618–621
Odor persistency, 621
OFFICAIR study, 136
Office building, 1649–1660
 mechanical ventilation, 1650–1655
 displacement ventilation, 1652–1655
 mixing ventilation, 1650–1652
 personalized ventilation, 1658–1660
 stratum ventilation, 1655–1658
 natural ventilation, 1650
 stratum ventilation, 1655–1658–1660
Office-like environments, 1943, 1944, 1951,
 1955
Office of Management and Budget
 (OMB), 1513
Office work performance, IAQ, 1420
 call-centers, 1436–1437
 CO₂, effects of, 1433–1435
 limitations, 1439–1440
 modifying ventilation rates, 1436–1438
 pollution source/sink, 1438
 ventilation rates, effects of modifying,
 1436–1438
 VOCs, effects of, 1435
- OH reactivity, 918
Olfactometer calibration technique, 633
Olfactometry method, 629
 calibration of, 633
 direct olfactometry, 636, 637
 dynamic olfactometry, 630–632, 634
 indirect olfactometry, 635, 636
Olive oils, 419
Online
 formaldehyde measurements, 497
 GC systems, 511
 VOC measurements, 495
On-line air pollutant monitoring
 technology, 1849
On-line measurement of gases
 inert gases, 937
 reactive gases, 937–942
 VOCs, 939–942
On-line measurement of particles
 black carbon, 947
 bulk aerosol composition measurements,
 946–947
 chemical measurement techniques, 945–946
 particle size distributions, 942–945
 speciated aerosol composition
 measurements, 947
Optical diameter, 944
Organic carbon (OC), 239, 525
Organic indoor air pollutants, 1496
Organization for Economic Co-operation and
 Development (OECD), 1208
Organochlorine pesticide (OCPs), 1970
Organophosphate esters (OPEs),
 112, 1970
Organophosphate flame retardants
 (OPFRs), 102, 112–117, 701, 717,
 1018, 1116, 1131
Outdoor air pollution, 1963
Outdoor air ventilation, 1678
Outdoor atmospheric chemistry, 830
 dynamics, 828–829
 partitioning, 826–828
 primary chemical sources, 821–824
 reactivity, 824–826
Outdoor photochemistry, 862
Ovalbumin (OVA), 1224, 1230
Ovens, 172
 gas, 172
 microwave, 190
Oxidants, 850, 937–938
Oxidative stress, 907, 1954

- Oxides of nitrogen (NO_x), 170
 Oxidized low-density lipoprotein (ox-LDL), 1278
 Ozone chemistry, indoor, 960–963
 Ozone initiated chemistry, 888–891
 kinetic multilayer model, 784–785
 models for predicting, 784
 physical-chemical coupling model, 785–788
 in realistic indoor environments, 783–784
 transient-state mass transfer model, 784
 validation of physical-chemical model, 788–789
 Ozone (O₃), 75, 1197, 1870–1871, 1972–1973, 2069
 Ozone reactions, 839–842
 Ozone/squalene reactions
 Ozonolysis, 842, 913, 919
- P**
- PACT-IAQ, 1840
 Parallel pore model, 681
 Pararosaniline method, 47, 48
 Parkinson's disease, 1241
 Particle approach, 309
 Particle deposition, 300
 Particle diameter, 944
 Particle formation, 850–851
 Particle image velocimetry (PIV), 570
 Particle-laden air, 368
 Particle mobility, 263
 Particle motion, in air, 261
 acceleration, 267–270
 aerodynamic diameter, 266–267
 Brownian motion, 270–272
 drag, 261
 particle mobility, 263
 particle shape, 264–265
 slip correction, 263
 Stokes' law, 262
 tranquil and stirred settling, 265–266
 Particle-phase phthalates, 794
 Particle shape, 264–265
 Particle size distributions, 182
 accumulation mode, 182
 nucleation/Aitken mode, 182
 Particles mass measurements
 aerosol measurement, 519
 fixed location samplers, 521
 methods, 519, 520
 portable and/or personal samplers, 521, 522
- Particle streak velocimetry (PSV)
 illumination system, 573
 limitations, 576–577
 operation and typical image, 573
 theory, 575–576
 Particle surface loading, 340–341
 Particle Total Exposure Assessment Methodology (PTEAM), 526
 Particle tracking velocimetry (PTV)
 exposure time, 573
 measurements, 571
 small-scale model, 572
 speed, 571
 3D flow data, 571
 trade-off parameters, 572
 Particulate compositions
 non-volatile species, 239
 semi-volatile species, 239–240
 Particulate matter (PM), 6, 11, 19, 203, 1005, 1252, 1497–1498, 1716, 1859, 1963, 1965–1968, 2128
 aerodynamic particle sizers, 527
 defined, 1872
 influencing factors, 1917–1919
 limits, 1914–1915
 low-cost monitors, 530, 532
 monitors, 527
 optical, 528
 PM10, 1873–1874
 PM2.5, 1874–1875
 pollution, 1197, 1235–1240
 semicontinuous composition
 measurements, 529
 source identification/apportionment, 526
 UFPs, 1875
 Partition coefficient
 Arrhenius relation, 687
 CTR-VVL method, 673
 headspace method, 670–671
 multi-emission/flush regression
 method, 671
 and vapor pressure, 683
 variable volume loading
 method, 672
 Partitioning, 822, 826–828
 Passive air sampling (PAS), 443–446
 Passive flux sampler method, 704
 Passive sampling, 433–434
 diffusion-based model, 474
 diffusion-based sampler, 475
 environmental monitoring, 468
 exposure evaluation, 468
 external mass transfer resistance, 482

- sampling flux, 474
VOC concentration, 481
wind velocity, 480, 482
Patient Health Questionnaire-9 (PHQ-9), 1195
PCO, *see* Photocatalytic oxidation
Peak CO₂ approach, 1698
Penetration factors
 concentration approach, 278, 279
 error analysis approach, 279, 280
 laboratory methods, 280
 outdoor pollutants, 2151, 2156
 regression approach, 278
Peracetic acid, 1994
Per-and polyfluorinated alkyl substances (PFAS), 117–120
Perceived indoor air quality
 chemical compounds, 610
 comparison of assessments, 616–617
 complex compound-by-compound approach, 611
 GC-O-MS, 629
 impact of temperature, 624–628
 non-sensory analysis methods, 628
 odor intensity, 618–621
 odor persistency, 621
 olfactometry (*see* Olfactometry method)
 relative humidity, 624–628
 selection of human observers, 622–624
 sensory effects, 611
 sensory pollution load, 617
 trained panels/decipol scale, 615–616
 untrained panels/acceptability scale, 613–615
Perfluorinated alkyl substances (PFASs), 373
Per-fluorinated compounds (PFCs), 1576
Perfluoroalkyl acids (PFAAs), 1467
Perfluoroalkyl substances (PFAS), 1017
Perfluorooctane sulfonic acid (PFOS), 121
Perfluorooctanoic acid (PFOA), 121
Perfluorotributylamine, 1608
Perforator method, 46
Performance-based approach, 1818–1819
 analysis of simulation results, 1821
 determination of model inputs, 1820
 governing equations, 1820
 identification of purpose, 1820
 model assumptions, 1820
 simulation case design, 1821
 simulation running, 1821
 specification of model outputs, 1820
Performance index method, 1571–1574, 1576, 1578, 1584
Permanent split capacitor (PSC), 1728
Permeable surfaces, 716
Permissible airborne exposure limit (PEL), 80
Permissible exposure limit (PEL), 1526
Peroxyacetyl nitrate (PAN), 75
Peroxybenzoyl nitrate (PBN), 75
Peroxy radicals, 841–845, 847, 848, 851
Persian (Iranian) style cooking, 398
Personal (breathing zone), 994–995
Personal care products, 773, 778–783
Personal Cascade Impactor Sampler (PCIS), 521
Personal Environmental Monitor (PEM), 522
Personalized ventilation, 1658–1660, 1666–1670
Personal monitoring
 individual behavior, 2040–2041
 meteorological variables, 2038–2040
 road and traffic conditions, 2037–2038
 scaling sampling, 2031
 transport characteristics, 2033–2037
Personal protective equipment (PPE), 2004
Pesticides, 373
Phenolics, 1994
Phonics, 1846
Photocatalytic oxidation
 advantages, 1739
 air purification technique, 1738–1739
 by-product identification, 1748–1754
 gas phase by-products, 1755–1756
 honeycomb monolith PCO reactor, 1748
 number of the mass transfer unit, 1743–1745
 pathway in toluene, 1755–1758
 reactor types, 1740, 1741
 removal effectiveness, 1739–1743
 synergistic degree of fluid and mass flow fields, 1746
Photochemically-generated species, 874–875
Photochemistry, 813
 condensed phase and heterogeneous, 860–861
 description, 856
Photographic images, 574
Photoionization detector (PID), 80, 435
Photolysis, 856
 Cl₂, 863
 direct, 856
 HONO, 863, 876
 nitrate, 871
 nitrogen dioxide, 865
 O₃, 863
 quantum yield, 857
 rate constants, 857, 861, 863, 877

- Photometric calibration factor (PCF), 528
Photon flux, 859–860
from light bulbs, 868–870
measurements and predictions, 875–876
solar, 867–868
Photosynthetically active radiation (PAR)
sensors, 876
Phthalate esters (PAEs), 102–109, 1231
Phthalates, 1302
in dust, 1315–1316
exposure to human health, 1306
intake from dust ingestion, 1311–1313
metabolites in urine/PVC flooring,
1309–1310
prenatal exposure, 1313
sources of indoor emission, 1308
total daily external exposure, 1310
in urine and dust, 1310
Physical appliances, 170
Physical-chemical coupling model, 785–789
Physically-based model of particles, 727
Physical partition, 2110, 2111
Physical sinks, 1828
Physics-based emission model, 776–778
Physics-based semi-analytical model, 777
Pittsburgh Sleep Quality Index
(PSQI), 1464
Plastic additives, 373
Platelet count, 1271
Plateout, 300, 318
Pliofilm cohort studies, 77
PM composition measurements
analytical strategy, 522
elemental analyses, 524
inductively coupled plasma
methods, 524
light absorption, 522, 523
organic compound analysis, 526
organic/elemental carbon, 525
water soluble ions, 524
PM10 levels, 1873–1874
PM2.5 levels, 1239, 1240, 1874–1875
Polyaromatic hydrocarbons (PAHs), 1017,
1050
Polybrominated diphenyl ethers (PBDEs), 102,
110–111, 442, 873, 1880, 2025
Polychlorinated biphenyls (PCBs), 102, 373,
1030, 1519, 1538, 1970
Polychlorinated Dibenz-p-dioxins/
dibenzofurans (PCDDs/PCDFs),
1030, 1520
Polychlorinated dioxin-like biphenyls (PCB),
1519, 1520
Polycyclic aromatic hydrocarbons (PAHs), 102,
389, 390, 1116, 1257, 1519, 1880,
2011, 2132
Polydimethylsiloxane (PDMS), 443
Polyfluoroalkyl substances (PFAS), 1117, 1538
Polyhexanide, 2004
Polymer components, 373
Poly parameter-linear free energy relationships
(pp-LFER), 720, 735, 800
Polysomnography (PSG), 1463
Polyurethane foam (PUF), 443, 448
Polyvinyl chloride (PVC), 895, 1118
Population attributable fraction (PAF),
1337–1339
Population-based studies, 137, 146–148
Porous solid materials, 90
Portable/room-level systems
CADR, 1722–1723
flow rates, filter efficiency/effectiveness,
1725–1727
noise/comfort, 1724
operation/maintenance, 1724–1725
practical considerations, 1723
pressure drop/power demands, 1723–1724
Position-Aware Multi-Sensor (PAMS), 1066
Position sensors, 1065
Positive matrix factorization (PMF), 526
Post-anesthesia care unit (PACU), 2010
Postulated pathways
cognitive performance, 1398
physiological and neurological pathways,
1399–1402
psychological pathways, 1402–1403
Power-law model coefficients, 1614
pp-LFER approach, 356, 357
Predicted Mean Vote (PMV), 1863
Predicted Percentage of Dissatisfied (PPD),
1863
Prediction methods, 2097, 2121
Predictive modeling, 1818
Prescriptive index method, 1571–1574, 1576
Presenteeism, 1478
Pressure, 251–252
Pressure drop, 1721, 1723, 1725, 1728–1731
pressurized liquid extraction (PLE), 453
Pressurized solvent extraction (PSE), 453
Pretreatment
cleanup, 457
concentration, 458
solvent extraction, 452–457
TD, 458
Preventative maintenance, 188
Primary chemical sources, 821–824

Primary organic aerosol (POA), 395
Product labeling programs, 1626
Products of incomplete combustion (PICs), 170
Proinflammatory cytokine, 1277
Project Surya in India, 1156
Propylene glycol, 216
Proton transfer reaction mass spectrometer (PTR-MS), 498, 1756–503, 940, 1606
Pseudo-first-order rate constant, 54, 861
Psychological and neurobehavioral tests, 1448–1450
Psychological tests, 1427
PTFE-coated aluminum pans, 410
Publicly Available Specifications (PAS), 1551
Puffing topography, 206, 218
Pulse wave velocity (PWV), 1254, 1265
Pumping/pouring gasoline, 1080
Pyroglutamic acid, 911

Q

Quality Assurance/Quality Control (QA/QC), 1519
Quantitative Structure Property Relationships (QSPRs), 357, 800
Questionnaire survey method, 1059, 1061, 1109

R

Radicals, 856, 864, 869
Radiello sampler, 478
Radon, 1016, 1157, 1207, 1233–1235, 1497, 1880
decay products, 1233
management, 1160
risks, 1159
sources and exposure, 1158
Random digit dial (RDD), 1083
Rapeseed oils, 412
Rapid eye movement (REM), 1462, 1463
Ratio method, 180
Reactive hyperemia index (RHI), 1265
Reactive oxygen species (ROS), 1231, 1277
Reactivity, 824–826
Real-time logging, 1060
Recirculation zones, 595
Recommended airborne exposure limit (REL), 80
Recreational appliances, 178
Rectification, 584–585
Red blood cells (RBC), 1271
Referenced test methods, 1692

Reference material

analytical measurement variability, 767–768
building product, 750–751
consensus values, 749
definition, 748
designed material, 751–759
drying/curing, 752–753
film, 753–755, 759
inter-laboratory proficiency testing studies, 759–760
lacquer, 759
liquid diffusion-film-emission, 756–757
reference material variability, 763–765
temperature controlled diffusive evaporator, 757–759
test system variability, 765–767
thermoplastic polyurethane, 755–756
traceability, 749
true values, 749
types of, 749
uncertainties in emission testing, 763–768

Refrigeration

Regulatory monitoring networks, 991, 992
Relative deposition velocities, 272
Relative humidity (RH), 63–64, 92, 918, 1862–1863, 2068
Relaxation time, 268
Repeated-measures design, 1390
Reproductive system, 1232, 1239

DNA damage, 1287
DNA methylation, 1283, 1287–1288
hormones, 1284
oocyte, 1285
semen parameter, 1285

Reproductive toxicity

Research strategy
cost benefit analysis of IEQ, 1376–1383
missing data, 1389–1391

Residential building, 1640–1649
hybrid ventilation, 1647–1649
mechanical ventilation, 1644–1647
natural ventilation, 1640–1644

Residential in-duct air filters

Respiratory diseases, 1480

Respiratory disturbance index (RDI)

Respiratory infections

Legionnaires' disease, 1169–1170
management, 1170–1171
SARS-CoV-2, 1170
symptoms, 1192
tuberculosis, 1169

Respiratory system

1190–1192, 1234,

1236, 1253

- Respiratory therapists, 2013
 Resuspension, 1917
 by crawling infants, 342
 definition, 333
 dust components of concern, 341
 emission rate estimates, 337–338
 fraction estimate, 338–340
 human generated particle emissions, 342
 particle surface loading, 340–341
 single particle, 343–345
 two-compartment material balance model, 335
 typical bulk aerosol resuspension experiments, 334–335
 uniform mixing assumption, 343
 Reynolds number, 258–259, 269, 316
 Risk assessment (RA), 1330–1332
 Road and traffic conditions, 2037–2038
 Rocket stoves, 1153
 Rotating board
 accuracy verification, 586–589
 experimental setup, 586–587
 Route planner, 2045
 Runge-Kutta methods, 957
- S**
 SAE Aerospace Council, 2067
 Salivary lysozyme, 1284
 Sample, age/season, 1078
 Sampling
 active air sampling, 446–450
 dust and surface, 451–452
 PAS, 443–446
 VOCs, 432–436
 VVOCs, 431–432
 weights, 1070
 Sandwich-like chamber method, 700, 730–731
 SARS-CoV-2 pandemic, 1170, 2059, 2066, 2081
 Satellite data, 992
 Scanning mobility particle sizer (SMPS), 389, 943, 945
 Schools
 assessment of IAQ, 1904
 building archetypal forms, 1893–1894
 building better schools, 1927–1928
 building envelope airtightness, 1926
 classroom occupancy, 1927
 classroom IAQ, 1894–1900
 CO₂, 1904–1912
 IAQ, 1893
 NO₂, 1912–1914
 PM, 1914–1919
 ventilation rates, 1898–1904
 Schools Indoor Pollution and Health Observatory Network in Europe (SINPHONE), 1895
 Sealed chamber method, 718–720
 Seasonal effects, 1927
 Sea surface microlayer (SSML), 824
 Sebaceous glands, 910
 Secondary organic aerosols (SOAs), 134, 395–397, 845, 851, 916–917, 964–967
 Secondhand smoke (SHS) exposure, 204, 1145
 management, 1149
 risk, 1148–1149
 sources, 1146–1148
 Secondhand vaping (SHV) aerosols, 202
 effects of proximity on, 206–208
 exposures to, 204
 transport in in multiunit indoor environment, 209–213
 Second-order decay model, 86
 Self-cleaning, 872
 Self-collected fuels, 167
 Self-estimated productivity, 1374
 Semi-analytical model, 656, 664
 Semiconductor sensor, 80
 Semi-critical surfaces, 1990
 Semi-empirical model, 89
 Semi-permeable membrane devices (SPMD), 473
 Semivolatile organic compounds (SVOCs), 11, 15, 17, 18, 341, 406, 430, 442, 448, 495, 511, 512, 696, 916, 939, 1009, 1017, 1114, 1228–1233, 1356–1360, 1515, 1517, 1880, 1920, 1968, 1970, 2027, 2064, 2075
 aerosols, 729–730
 chemical analysis, 459–460
 CLIMPAQ and FLEC chamber methods, 699
 in complex indoor environments, 788–803
 diffusion coefficient, 725
 dynamic model, 726
 emission model, 697
 emission parameter, 710–711
 equilibrium model, 726
 equilibrium relationship between source materials and air, 709
 flow chart to predict indoor concentration, 802
 framework for predicting indoor, 791
 fugacity models, 792

- gas-particle partition coefficient, 732
gas-surface partition coefficient, 720
impermeable surfaces, 713
in indoor environments, 696
indoor fate, 790
influence of environmental factors on indoor, 791
Junge-Pankow method, 732
mass transfer-based model, 793–797
mass transfer in chamber, 697
methods for measuring emission values, 699
methods for measuring sorption parameters, 716–720
parameters for surface sorption, 721–726
partition coefficients of, 796–801
partitioning, 802
passive flux sampler method, 704
permeable surfaces, 716
poly-parameter linear free energy relationship, 733–735
sample pretreatment (*see* Pretreatment) sampling, 443–452
sandwich-like chamber method, 700, 730
sealed chamber method, 718–720
sorption by particles and dust, 726
sorption by sink materials, 713
SPMЕ-based sealed chamber, 707
tube chamber, 731–732
ventilated dual chamber method, 716–718
ventilation, 801
- Semi-volatile thermal desorption aerosol gas chromatograph (SV-TAG), 511, 512, 947
- Sensitivity, 933
- Sensor acceleration signal, 1067
- Sensor data mining methods, 1063
- Sensor method, 1063, 1064
- Sensor networks, 994
- Sensors, 49
- Sensory assessments, 612, 613, 622
- Sensory discomfort, 626
- Sensory measurements, 612
- Sensory pollution load, 617
- Severe Acute Respiratory Syndrome Coronavirus 2 (SARS-CoV-2) virus, 1540
- Short-term emission models, 49–53
- Short-term exposure limit (STEL), 1526
- Sick-building syndrome, 1177
clinical picture, 1178–1179
etiology, 1177–1178
management, 1179
- Sick building syndrome (SBS), 1378, 1948
- Silver-based wound dressing, 2004
- Simulated office work tasks, 1423, 1424, 1427, 1432
- Single fiber collection efficiency, 1718–1719
- Single-layer source models, 654–657
- Single parameter model, 798
- Single particle resuspension measurement, 343–345
- Single-zone modeling and simulation, IAQ control
- adsorption sink, 1827–1830
 - emission source, 1824–1827
 - IA-Quest, 1833–1834
 - MEDB-IAQ, 1833
 - model assumptions and governing equations, 1822–1823
 - model input parameters and determination, 1823
 - model output and analysis of cases, 1831–1833
 - purpose identification and model selection, 1822–1823
 - ventilation, 1830
- Sink-diffusion model, 660–661, 774–775
- Sink surface/air partition coefficient, 698
- Sinus cancer, 1204
- Sips model, 714
- Skin emissions, 908–911
- Skin-permeation coefficient, 780
- Sleep
 - air pollution exposure, 1467
 - ambient exposure (*see* Ambient exposure) functions, 1464
 - parameters, 1463
 - quality, 1462, 1463
- Sleep disordered breathing (SDB), 1472
- Sleep efficiency (SE), 1464
- Sleep Onset Latency (SOL), 1464
- Slip correction, 263–264
- Slow wave sleep (SWS), 1463
- Smartphones, 1065
- Smoking, 1079, 2041
- Social development index (SDI), 1201
- Social media, 419
- Sociodemographic characteristics, 1081
- Solar photon flux, 867–868
- Solid fuels, 166, 167, 169–171, 173, 174, 176, 182, 187, 189, 190, 388
in brick chimney stoves, 2128
burning, 2126
- Coal, 166
- combustion, 2126
- HAP, 2132

- Solid fuels (*cont.*)
 household energy sources, 2135
 indoor air pollution, 2139
 waste, 166
 wood, 166
- Solid particles, 2103
- Solid-phase extraction (SPE), 434
- Solid-phase microextraction (SPME), 431, 432, 434–436, 444–445, 488, 702
- Soluble CD40 ligand (sCD40L), 1273
- Soluble P-selectin (sP-selectin), 1272
- Solvent-based adhesives, 76
- Solvent extraction
 ASE, 453–454
 MAE, 455–456
 Soxhlet, 452–454
 USE, 453–456
- Soot/ black carbon, 186
- Sorption saturation degree (SSD), 661
- Source control, 1593, 1628, 1977
 building scale, 1790–1791
 room scale, 1793–1794
 urban scale, 1786
- Source emission categories (SECs), 1116
- Source models for porous materials, 658–660
- Soxhlet extraction, 452
- Space cooling, 174, 178
- Space heating appliances, 173–176
 free-standing, 174, 175
 hydronic, 174
 ventless, 176
- Spectrophotometric method, 47–48
- Spiral vortex structure, 2101
- Spirometry, 1190
- SPME-based sealed chamber, 707
- Spray Polyurethane Foam (SPF), 1517
- Spreading zone, 595
- Stacking, 188
- Standardization Management Board (SMB), 1551
- Standardized tests, 1451–1452
- Standards developing organizations (SDO), 1514
- Standards of ISO/TC 142, 1560
- Staphylococcus aureus*, 1045
- State-Trait Anxiety Inventory (STAI), 1195
- Statistical modeling, 996
- Steady-state concentration, 861
- Steady-state PFT approach, 1706
- Stealth chemicals, 1952
- St. George's Respiratory Questionnaire (SGRQ), 1192
- Stokes' law, 262–264
- Stopping distance, 268–269
- Strategic management simulation (SMS), 1410, 1433, 1434
- Stratum ventilation, 1655–1658
- Streptozotocin (STZ), 1233
- Stressor selection, 1340–1341
- Subcommittees (SC), 1514
- Suction zone, 595
- Sudden infant death syndrome, 1148
- Sulfuric acid (H₂SO₄) droplets, 2104, 2105
- Superoxide dismutase (SOD), 1279
- Surface-air partition coefficients, 801
- Surface chemistry, 814
 byproduct formation, 970–971
 modeling transport within boundary layer, 971–973
 skin chemistry, example, 976–977
 surface processes, 973–976
- Surface diffusion, 681
- Surface dust loading, 337, 340
- Surface measurements, 948
- Surface-phase reactions, 816
- Surfaces and chemical transformations
 acid-base chemistry, 893–895
 chlorine chemistry, 893
 hydrolysis, 895–896
 indoor surfaces, 886–888
 nitrogen oxides, 891–892
 ozone initiated chemistry, 888–891
- Survey method, 1059
- Swedish Building Research Institute, 6
- Swedish Environmental Longitudinal Mother and child Asthma and allergy (SELMA) study, 1305
 airway outcomes, 1306–1307
 chemical exposure, 1305–1306
 environmental exposure, 1308–1309
 health effects, 1313–1315
 human exposure, 1309–1313
- Swedish Radiation Protection Institute, 6
- SWG 3 on microbe reduction, 1556–1557
- SWG 6 on fresh-air air cleaners, 1557–1558
- Symmetrical sealed chamber, 718
- Symptoms, IAQ in offices, 1937, 1943, 1949, 1950, 1953, 1954
- Systolic blood pressure (SBP), 1197

T

- Tapered element oscillating microbalance (TEOM), 527
- Target VOCs, 1596
- Taurocholic acid, 921

- TCO, *see* Thermal catalytic oxidation
Technical committees and subcommittees (TC/SCs), 1550–1551, 1560
Tedlar® bags, 636
Teflon/granitium pans, 409, 411
Telephone survey, 1060, 1088
Temperature controlled diffusive evaporator reference material, 757–759
Temperature sensors, 1065
Tenax®, 1606
Terpenes, 152
Terpenoids, 152
Tetrachloroethene, 1021
T-helper 17 (Th17) cell, 1195
Thermal catalytic oxidation, 1757
 formaldehyde removal, 1759–1764
 kinetic reaction model, 1763–1768
Thermal conductivity detectors (TCDs), 81
Thermal desorption/gas chromatography/mass spectrometry (TD/GC/MS), 458, 526, 1607–1609
Thermal desorption (TD) sampling tubes, 777
Thermionic detectors (TIDs), 81
Thermoplastic polyurethane (TPU) reference material, 755–756
Thiohydrocarbons, 74
Three-dimensional convection-diffusion-reaction model, 1740
3D stereo reconstruction algorithm, 584–585
Threshold limit value-time weighted average (TLV-TWA), 1526
Threshold limit value (TLV), 1513, 1526
Thymic stromal lymphopoietin (TSLP), 1230, 1283
Thyroid, 1289
Time-activity, 990, 995, 996
Time-activity patterns survey, 1058, 1063, 1064, 1086, 1099, 1110
 adults, 1067
 Africa, 1106, 1108
 children, 1069
 China, 1067–1077
 Europe, 1106
 factors, 1067, 1070
 Korea, 1096, 1098
Time-activity survey methods, 1061
Time-consuming activity, 1076
Time diaries, 1076
Time indoors, 1069, 1073
Time-integrated exposure, 989
Time Microenvironment Activity (TMA), 1106
Time-of-flight (TOF) detectors, 499, 941
Time-resolved indoor source strength, 506
Time weighted average (TWA), 1526
TiO₂ UV photocatalytic oxidation, 1739
Titanium dioxide, 872
Tobacco smoke, 1081, 1146
Toluene, PCO, 74, 77–79, 1755–1758
Total antioxidant capacity (TAOC), 1231
Total Exposure Assessment Methodology (TEAM), 1005
Total suspended particles (TSP), 519
Total volatile organic compound (TVOC), 1197, 1525, 1878, 2075
Toxicokinetics, 1304
Toxicology, 987
Toxic Organic (TO) Compounds, 1515
Toxic Substances Control Act (TSCA), 1537
Trace gas sources, 824
Tracer gas dilution method, 1693
Traffic intersections, 2037
Traffic-related air pollutants, 2037, 2040, 2044
Traffic-related air pollution (TRAP), 1257
Traffic signals, 2037
Transdermal permeability coefficient, 1129
Transient-state mass transfer model, 784
Transportation vehicle cabin
 displacement ventilation, 1664–1666
 mixing ventilation, 1661–1664
 personalized ventilation, 1666–1670
Transport microenvironments (TME)
 health impacts, 2042
 in-cabin pollutants, 2025–2029
 optimizing driving behavior, 2043
Transport modes, 2030, 2032, 2039, 2047
Travel activities, 1061
Triangle bag method, 631
“Triangle test” method, 631
Tributyl phosphate (TBP), 2076
1,1,1-Trichloroethane, 74
Trichloroethylene (ACE), 74, 1163, 1212
Tri(chloropropyl)phosphate (TCP), 896
Trichlorotoluene, 74
Triclosan, 2004
Tri(dichloropropyl)phosphate (TCCPP), 896
Trisobutyl phosphate (TiBP), 2076
Trilinolein, 392
Trim air, 2062
Trimethylpentane containing passive samplers (TRIMPS), 473
Tri-n-butyl phosphate (TnBP), 2076
Tri-o-cresyl phosphate (ToCP), 2076
Triolein, 392
Triolein-embedded cellulose acetate membrane (TECAM), 473
Triphenyl phosphate (TPP), 2079

- Triple adsorbent cartridge, 433
 Trip-level traffic mode prediction model, 1061
 Tris (butoxy-ethyl) phosphate (TBEP), 2076
 Tris(2-chloroethyl) phosphate (TCEP), 1130
 Tsinghua Passive Diffusive Sampler (THPDS), 486, 487
 Tube chamber, 731–732
 Tube chamber method, 370
 Tuberculosis, 1169
 Tube-type samplers, 469
 Tungsten fluoride, 2106
 Turbulence, 260, 308, 314–315
 Two chamber method, 670
 Two-compartment material balance model, 335
 Two-dimensional gas chromatography, 436
 2-D mass transfer model, 707
 Typical school tasks, 1450, 1451
- U**
 Ultrafine particles (UFP), 389, 1875, 1964, 1965, 1968, 2025
 candle burning, 539
 CPC, 536
 definition, 531
 DMA, 537
 electric monitors, 539
 electric stoves, 538
 emission rates, 540, 541
 gas burning appliance emissions, 538
 health effects, 531
 indoor concentrations/sources/emission rates, 542, 556
 1-nm instruments, 537
 source identification/measurement, 540
 Ultra-high performance liquid chromatography (UHPLC), 138
 Ultrasonic anemometry (UA), 570
 Ultrasonication extraction (USE), 453–456
 Ultrasonic bath system, 455
 Ultraviolet-visible (UV-Vis), 1947
 Ultra Wide Band (UWB), 1063
 Underwriters Laboratories Inc. (UL), 1514, 1515
 United States Environmental Protection Agency (US EPA), 1515
 Upper respiratory infection (URI), 1199
 Uptake rate (UR), 433
 US Environmental Protection Agency (US EPA), 6, 72, 1330, 1331
 U.S. Green Building Council (USGBC), 1527, 1567
 US Occupational Safety and Health Administration (OSHA), 6
- V**
 Vacuum aerodynamic diameter, 944, 945
 Vancomycin-resistant Enterococci (VRE), 1993
 Vape shops, 210
 Vapor pressure and boundary layer model, 88
 Variable volume loading method, 672
 Varied ventilation rate (VVR) method, 702
 Vascular function, 1265
 Vector air-driven modules (VADM), 602–603
 Vegetable glycerine (VG), 216
 Vegetation barrier, 2044
 Vehicle category, 2033–2034
 Vehicle occupancy, 2041
 Velocity contour, 598
 Ventilated building, 1678
 Ventilated-chamber-history method, 677, 777
 Ventilated chamber method, 716–718
 Ventilation, 180, 188, 189, 888, 919, 1527, 1777, 1830, 1864–1866, 1881, 1942, 2151, 2156, 2158
 building scale, 1791–1792
 and cognitive performance, 1438
 health and academic performance, 1898–1901
 personal, 1798
 rates, 1901–1904
 room scale, 1794–1796
 settings, 2034–2035
 strategy, 1926
 urban scale, 1787–1788
 Ventilation rate procedure (VRP), 1529
 Ventilation rates (VRs)
 call-centres, 1436–1437
 on cognitive abilities, effects of modifying, 1436
 office-like controlled environments, 1436
 on office work performance, effects of modifying, 1436–1438
 on work performance, effects of modifying, 1432
 Very volatile organic compounds/volatile organic compounds (VVOCs/VOCs), 7, 12–16, 38, 39, 66, 430, 431, 1968
 characteristic parameters
 diffusion coefficient, 687
 dimensionless analysis, 683–684
 experimental techniques, 668
 health consequences of, 1162
 influencing factors on, 685–688
 initial emittable concentration, 685–686
 mass transfer (*see* Mass transfer)
 model parameters and physical/chemical properties, 679–683

- partition coefficient, 687–688
risks, 1162–1164
sample analysis, 432
sampling treatment, 431
source control for emission control, 684–685
Videotaping, 1062
Vinyl chloride, 74
Vinyl flooring, 1118
Viscosity, 255–256
Vision sensors, 1065
Visual-analogue (VA) scales, 1379
Volatile organic compound (VOC) emissions
application in building rating systems, 1626–1627
emission test standards, 1628–1631
environmental chamber testing methods (*see* Environmental chamber testing method)
from multiple sources in indoor settings, 774–778
from occupants due to personal care products, 778–783
ozone/squalene reactions, 783–789
product labeling programs, 1626
physics-based emission model, 776–778
sink-diffusion model, 774–775
testing/evaluation methods, Europe and Asia, 1620
Volatile organic compounds (VOCs), 131, 139, 140, 350, 430, 468, 495, 518, 628, 772, 838, 839, 841–843, 845, 846, 849–852, 861, 904, 905, 907, 908, 910–913, 917–920, 938–942, 1005, 1015, 1117, 1211, 1264, 1356, 1357, 1359, 1360, 1467, 1515, 1517, 1521, 1576, 1819, 1821, 1822, 1859, 1937, 1963, 1968–1971, 1994, 2060, 2070–2072, 2114
active sampling, 432–433
benzene, 75–77
boiling point and vapor pressure, 73
in chamber studies, 133–135
classes of, 72
on cognitive abilities, effects of, 1435
common car air freshener, 143
common essential oil, 143
common fragranced baby product, 143
common fragranced product, 140
concentration prediction, 83–85, 1823
consumer products, emitted from, 132–133
defined, 72
detectors, 82
emission models for, 81–85
existing studies, 1921–1923
exposure assessment, 509
hazards, 74–75
headspace analysis techniques, 133
HPLC, 81
indoor environment, 72
within indoor environments, 137–139
indoor VOC concentration (*see* Indoor VOC concentration)
influencing factors, 1923–1925
integrated sampling/analysis, 80
large population-based IAQ studies, 135–137
limits, 1919–1921
mass transfer, 1823, 1825, 1829, 1841
median indoor to outdoor concentration ratios, 149–151
on office work performance, effects of, 1435
organic compounds, 74
passive sampling, 433–434
population-based studies, 146–148
from product use indoors, 146–152
properties of, 73
PTR-MS, 498–499
real time monitoring, 80
sample analysis, 435–436
sampling treatment, 435
spatial variation, 505
speciation, 502
SPME, 434–435
temporal variation, 503–505
toluene, 77–79
types and compositions of, 73
whole-air sampling, 434
on work performance, effects of, 1432
xylene, 79–80
Volatility basis set (VBS) approach, 965–969
Voluntary consensus standards, 1527
Von Willebrand Factor (VWF), 1272–1273
Vortex flow test, 591–592
Vorticity, 596, 597
Vulnerability, 2155

W

- Wall deposition, 300, 304, 306, 308
dimensional analysis, 313–314
fractal nature of turbulence, 314–315
model adjustment, experiments, 312–313
turbulent, 309–311
Wall function model, 1828
Water heating appliances, 176

- Waterproof materials, 76
Water-soluble organic compounds, 874
Water soluble organic gases (WSOG), 939
Web surveys, 1060
Weighted quantile sum (WQS) regression, 1198
WELL, 1568
 environmental index, 1569
 performance index method, 1576
PM control, 1583–1584
 sources requirements in, 1581
Western style cooking, 398
Wet coating materials, 1596
Wheeze, 1306
White blood cells (WBC), 1271
WHO indoor air quality guidelines, 1493
 criteria for inclusion and exclusion of
 pollutants, 1496–1498
 indoor environment, 1495
 inorganic indoor gaseous pollutants, 1497
 numerical values, 1498–1500
 organic indoor air pollutants, 1496
 particulate matter, 1497–1498
Whole-air sampling, 434
Wind speed, 2038
Wind tunnel, 587–588
Wireless Sensor Network (WSN), 1063
Wood fuel, 1153
Wood heating stoves, 175
Work performance, IAQ, 1420
 call-centres, 1436–1437
 CO₂, effects of, 1433–1435
 limitations, 1439–1440
 modifying ventilation rates, effects of, 1435,
 1438
 office-like controlled environments, 1436
 pollution source/sink, 1438
 VOCs, effects of, 1435
Work related asthma (WRA), 2006
World Health Organization (WHO), 1327, 1939
- X**
X-ray fluorescence (XRF), 524, 527
Xylene, 79–80
- Y**
Years lived with disability (YLD), 1335
Years of life lost (YLL), 1335, 1362
- Z**
Zanthoxylum piperitum, 414
Zero Net Energy (ZNE), 1536
Zhang's model, 1740